ACTA CHEMICA SCANDINAVICA 12 (1958) 1—7

Anomalous Reactions of 2-Naphthylmethylmagnesium Bromide

SVEN-OLOV LAWESSON*

Department of Organic Chemistry, Chemical Institute, University of Uppsala, Sweden

2-Naphthylmethylmagnesium bromide has been prepared with a "cyclic reactor" and its reactions with ethyl chlorocarbonate, formaldehyde, ethylene oxide and acetyl chloride have been shown to give rearrangement products. Exclusively normal products were isolated only in the reactions with carbon dioxide and tributyl borate.

Organomagnesium halides with the $-CH=CH-CH_2-MgX$ grouping often give abnormal products and since Grignard [1] himself initially conducted such a rearrangement reaction (which he did not know at that time), many investigations have been made in this field. Kharasch and Reinmuth [2] have recently summarized the situation until 1952. In connection with the preparation and study of 2-napththylmethylboronic acid as a plant growth regulator [3] it was neeessary to find out if rearrangement occurred or not and we have now further studied this and similar reactions.

The preparation of Grignard reagents from halides of the benzylic type is generally troublesome and the yields are often very low. The reason is, that under the usual conditions some metathesis will always occur between the Grignard reagent formed and the later added halide thus giving coupling products. Various strategies to avoid coupling have been tried: high dilution, excess of magnesium, etc., but the best way was introduced by Rowlands, Greenlee and Boord, who used a so called cyclic reactor [4]. By this method we have, contrary to earlier reports [3,5,6] obtained good yields of 2-naphthylmethylmagnesium bromide.

In Scheme 1, six reactions of 2-naphthylmethylmagnesium bromide are represented. 2-Naphthylmethyl bromide (I) was easily converted to the corresponding Grignard reagent (II) in the cyclic reactor (Fig. 1). In all experiments, however, small amounts of the coupling product, 1,2-di(2-naphthyl)-ethane were also isolated. The reagent II was treated with carbon dioxide, tributyl from 2-methyl-1-naphthyllithium reagent and ethylene oxide and by reduction of 2-methyl-1-naphthylacetic acid.

* Present address: Department of Organic Chemistry, University of Chicago, Chicago 37, Ill.

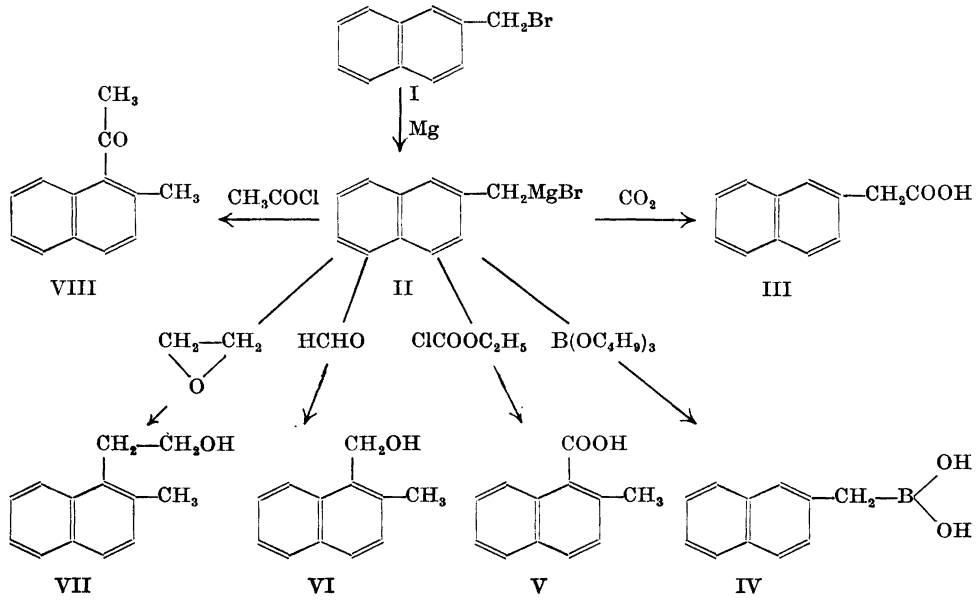

Scheme 1.

borate, ethyl chlorocarbonate, formaldehyde, ethylene oxide and acetyl chloride. "Normal" products were isolated only in the reactions with carbon dioxide and tributyl borate.

2-Naphthylacetic acid, prepared *via* the nitrile [7] was identical with III, obtained by carbonation of II. The hypothetical rearrangement product, 2-methyl-1-naphthylcarboxylic acid was shown by mixed meltingpoint test to be non-identical with III.

The non-identity of 2-naphthylmethylboronic acid [3] (IV) with the possible rearrangement product, 2-methyl-1-naphthylboronic acid [8] was confirmed by infrared investigation and by melting point differences.

The acid V was obtained if the reagent II was treated with ethyl chlorocarbonate and hydrolysis of the ester. The identity of V with 2-methyl-1-naphthylcarboxylic acid [9], was confirmed in this case by infrared analysis as well.

Gaseous formaldehyde gives with the reagent II exclusively 2-methyl-1-naphthylcarbinol (VI). The same compound was prepared from V by reduction with lithium aluminiumhydride or by treating 2-methyl-1-naphthylmagnesium bromide with gaseous formaldehyde [10]. For comparison the normal product was also prepared by reduction of 2-naphthylacetic acid with lithium aluminium hydride.

The abnormal product VII was formed by treating II with ethylene oxide. A review [11] of reactions between Grignard reagents and the oxirane (epoxide) ring was published some years ago. The compound VII was also prepared from 2-methyl-1-naphthyllithium reagent and ethylene oxide and by reduction of 2-methyl-1-naphtylacetic acid.

The product VIII was formed upon treating II with acetylchloride. Its hydrazone was shown by infrared analysis and by mixed melting point to be identical with the corresponding derivative of methyl-(2-methyl-1-naphthyl) ketone.

No rearrangement to the open 3-position has been observed in any of our experiments; consequently this constitutes another manifestation of the symmetrical bond fixation in the naphthalene nucleus. Furthermore our results agree with those of Gaertner [12] concerning the reactions of 2-thianaphthenylmethylmagnesium chloride with different substances. In both cases *exclusively* abnormal products were isolated (except with carbon dioxide) and these two examples show that rearrangement will occur more extensively to a position which is attacked preferentially in electrophilic substitution. There are exceptions, however, and our results might be only an indication.

EXPERIMENTAL

Apparatus and procedure

The cyclic reactor is sketched in Fig. 1. The condenser is topped by a funnel for slow addition of the halide. The magnesium turnings are amalgamated by mixing the magnesium and $HgBr_2$ in the column and then adding dry ether. The apparatus is then allowed to stand overnight, and after the ether has been swept down into the pot and renewed,

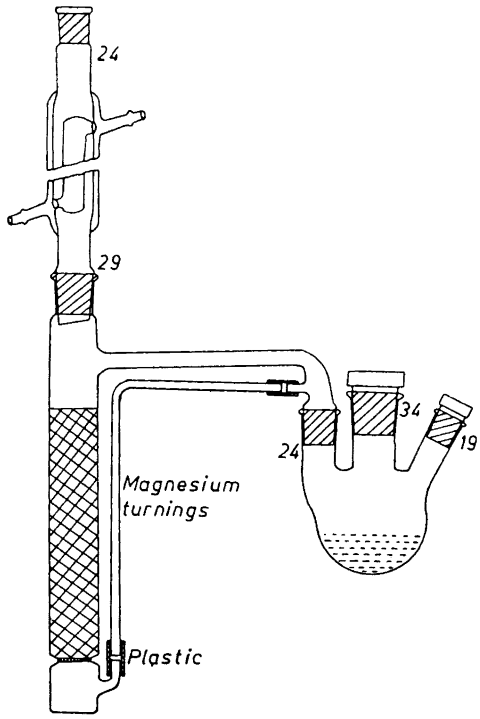

Fig. 1.

the "cycling" can start. The reactor is operated under nitrogen or at least the apparatus is swept free from oxygen before the experiment. It is furthermore important to start the column with allyl bromide or the like and then "cycle" until all the Grignard reagent is swept into the flask. Anhydrous conditions are always essential and it is also important that the addition of the halide is slow, that gentle boiling is maintained in the upper part of the Mg-column with a good ether cycling rate. High dilution must be maintained in the column (200—300 ml of ether per 0.1 mole of halide) at all times. Otherwise this method is no better than the usual pot method. Once the Grignard reagent is formed and swept into the pot it is stable against coupling.

Preparation of 2-naphthylmethylmagnesium bromide

In all experiments 0.05 mole (11 g) of I [13] was used, dissolved in 125 ml of dry ether. Hydrolysis of the Grignard reagent formed gave 2-methylnaphthalene (b.p. 108—110°C/16 mm Hg, m.p. 33—35°C) and the yield could thus be determined. The best yield was 84 % when the method of Greenlee and coworkers was used. The conventional method gave only 39 % of the theoretical, the remainder being mostly coupling products.

Carbonation of 2-naphthylmethylmagnesium bromide

The Grignard reagent II, prepared from 11 g of I, was cooled to about 0°C and then poured slowly into crushed dry ice in absolute ether. The mixture was allowed to warm to room temperature and then was hydrolyzed with water. The organic layer was separated off, the water solution extracted with ether and the combined ether layers extracted with dilute sodium hydroxide. Upon acidification of the alkaline solution, a white powder precipitated, which after recrystallisation from water-ethanol gave white needles. M.p. 140—142°C. Weight 6.9 g. Yield 74 % . With an authentitc sample [7], m.p. and mixed m.p. 139—141°. From the ether phase 0.3 g of a substance was separated, which after recrystallisation from ethanol gave white plates with m.p. 183—185°; presumably 1,2-di(2-naphthyl)-ethane [14]: m.p. 182°C.

Reaction of the Grignard reagent II with tributyl borate

The Grignard reagent, prepared from 11 g of I, was added with stirring over a two-hour period, to 15 g of tributyl borate [15] in 100 ml of dry ether at —60°C. After standing overnight it was treated with 1 M hydrochloric acid, the organic portion separated and the aqueous phase extracted with ether. The combined ether layers were extracted with 1 M sodium hydroxide. The alkaline aqueous layer was acidified with hydrochloric acid precipitating 4.5 g of the crude moist acid (Yield ≈48 %). The diethanolamine ester was prepared in the usual way [3]; m.p. 229—231°C.

Reaction of the Grignard reagent II with ethyl chlorocarbonate

The Grignard reagent, prepared from 11 g of I, was added during half an hour to a well-stirred solution of 50 ml of redistilled ethyl chlorocarbonate, cooled to —20°C in an ice-water bath. After standing with stirring overnight during which time the temperature rose to room temperature, water and 25 g of sodium hydroxide were added under gentle reflux. The alkaline solution was then acidified, liberating carbon dioxide, and then the aqueous layer was repeatedly shaken with ether. The ether was evaporated and the

residual oil was saponified by alcoholic sodium hydroxide. Upon acidifying the solution, a white powder was precipitated, which after recrystallisation from water gave fine needles. M.p. 125—127°C. Weight 6.6 g. Yield 71 %. With an authentic sample of 2-methyl-1-naphthylcarboxylic acid [9] no depression of the melting point was observed. (Found: Equiv.wt. 187.7. Calc.: Equiv.wt. 186.20.)

Reaction of the Grignard reagent II with formaldehyde

Gaseous formaldehyde [16] from 90 g of dry paraformaldehyde was carried by dry oxygen-free nitrogen into a solution of II, prepared from 11 g of I. The reaction took place at room temperature. A white precipitate was formed at once and after the solution had been cooled in an ice bath, saturated ammonium chloride was added to dissolve the magnesium compound. The solution was shaken with ether repeatedly, the organic extracts shaken free from acid and after being dried over sodium sulphate and freed from ether, the residue was distilled. The main fraction, b.p. 140—144°C/10—11 mm Hg, consisted of a heavy yellow liquid. Weight 4.4 g. Yield 51 %. The liquid was dissolved in petroleum ether and after some time faintly yellow plates were precipitated. Recrystallisation from ligroin + ether gave white plates with m.p. 114—116°C. (Found: C 84.0; H 7.24. Calc. for $C_{12}H_{12}O$(172.21): C 83.7; H 7.03.)

Reduction of 2 methyl-1-naphthylcarboxylic acid

A solution of 1.9 g of 2-methyl-1-naphthylcarboxylic acid in 50 ml of dry ether was added to an ethereal solution of lithium aluminium hydride (in excess) at such a rate that the reaction mixture boiled gently. When the reaction was over, an excess of cold water was added and then the mixture was poured into ice-cold dilute sulphuric acid. The solution was shaken repeatedly with ether, the organic layer separted, dried over sodium sulphate and evaporated. The white powder was then recrystallized from ligroin + ether, giving an almost quantitative yield of white plates. M.p. 114—116°C. Mixed m.p. with VI: 114—116°C.

Reduction of 2-naphthylacetic acid

Addition of an ethereal solution of 1.9 g of the acid to a stirred suspension of 1 g of lithium aluminium hydride in 50 ml of ether, followed by usual procedures, gave white plates of β-(2-naphthyl)-ethanol. M.p. 72—73°C. Weight 1.7 g. Yield: almost quantitative. (Found: C 83.8; H 7.00. Calc. for $C_{12}H_{12}O$ (172.21): C 83.7; H 7.03.)

Reaction of the Grignard reagent II with ethylene oxide

A solution of II, prepared from 11 g of I, was stirred in an ice-salt bath under nitrogen while excess of ethylene oxide in dry ether was added during one hour. Vigorous reaction occurred at first with each drop and a white precipitate separated. The bath was removed and stirring continued until escape of gas subsided, then ether and excess oxide were removed by distillation. Dilute hydrochloric acid was added and stirring continued until dissolution of the precipitate was complete. The ether layer was separated, the water layer shaken with ether and the organic solution combined, dried and distilled. The main fraction, boiling at 185—195°C/9 mm Hg, was a viscous colourless liquid. Weight 4.5 g. Phenylurethan, m.p. 230—232°C. (Found: C 79.1; H 6.41. Calc. for $C_{20}H_{19}O_2N$ (305.36): C 78.7; H 6.28 %.)

Preparation of β-(2-methyl-1-naphthyl)-ethanol

To 11 g of 1-bromo-2-methylnaphthalene [17], cooled to 0°C, 0.05 mole of butyllithium [18] in 50 ml of ether was added. After the spontaneous lithium-halogen exchange reaction was complete, excess of ethylene oxide in ether was added dropwise and then the usual procedure followed as above. B.p. 190–195°C/9–10 mm Hg. Weight 6.3 g. Yield 67 %. Phenylurethan m.p. 230–232°C. Mixed m.p. with the phenylurethan of VII: 230–232°C.

2-Methyl-1-chloromethylnaphthalene

This compound has been prepared before but no yields were given [19]. By repeating the experiments, low yields were obtained and mostly tarry products. A modified method is given here:

Into a 2–l flask, fitted with a reflux condenser and a teflon stirrer, were placed 65 g of 2-methylnaphthalene, 30 g of paraformaldehyde, 65 g of glacial acetic acid, 45 ml of 85 % phosphoric acid and 90 ml of concentrated hydrochloric acid. The mixture was heated at 100°C with stirring for 5 h. After the mixture had been cooled it was washed twice with cold water, then with potassium carbonate solution and finally with cold water. The organic layer was dissolved in ether, thoroughly dried over sodium sulphate and distilled. The main fraction was obtained at 165–170°C/9–10 mm Hg. Recrystallisation from ethanol gave white needles. M.p. 62–63°C. Weight 64 g. Yield 75 %.

2-Methyl-1-naphthylacetonitrile

9.5 g of 2-methyl-1-chloromethylnaphthalene and 5 g of sodium cyanide in 50 ml of aceton and 4 ml of water was refluxed for 4 h. The acetone was evaporated and water and ether were added. Excess of sodium cyanide was removed by repeated extractions with water. The ether layers were dried and the ether evaporated. The residue recrystallized from formic acid gave fine, white needles. M.p. 77–79°C. Weight 7.4 g. Yield 81 %. (Found: C 86.6; H 5.95. Calc. for $C_{13}H_{11}N$ (181.23): C 86.2; H 6.12.)

2-Methyl-1-naphthylacetic acid

a) via the nitrile. 7 g of 2-methyl-1-naphthylacetonitrile was refluxed for 12 h with excess of sodium hydroxide in a water-ethanol solution. The alcohol was distilled off and the residue extracted with ether in order to remove unsaponified nitrile. When the water solution was acidified with hydrochloric acid, the organic acid precipitated as a white powder. The acid was recrystallized from water-ethanol forming small, white needles. M.p. 176–168°C. Weight 6.5 g. Yield 84 %. (Found: Equiv.wt. 199.6; C 78.7; H 6.21. Calc. for $C_{13}H_{12}O_2$ (200.23): Equiv.wt. 200.2; C 78.0; H 6.05 %.)

b) via the Grignard reagent. 9.5 g of 2-methyl-1-chloromethylnaphthalene in 50 ml of dry ether was dropped to 1.7 g of magnesium turnings in 75 ml of ether. The reaction was initiated with a few drops of bromine. After carbonation with dry ice the reaction mixture was treated with hydrochloric acid, the ether layer was separated, the water phase extracted repeatedly with ether and the combined extracts shaken with sodium hydroxide solution. The alkaline solution was acidified with hydrochloric acid, precipitating the acid as a white powder. After recrystallisation from water-ethanol the acid was obtained as small, white needles. M.p. 176–178°C. Weight 7.1 g. Yield 71 %.

The ether phase was evaporated and the residue recrystallized, giving a white powder. M.p. 173–175°C (from ethanol). This compound seems to be 1,2-di(2-methyl-1-naphthyl)-ethane. (Found: C 93.4; H 7.15. Calc. for $C_{24}H_{22}$ (310.42): C 92.9; H 7.10.)

The same compound was formed almost exclusively when by a mistake a mechanical stirrer of *copper* was used and bromine was added as an activator. The chlorides of copper which formed apparently made the coupling product predominate and very little acid was isolated after carbonation.

Reduction of 2-methyl-1-naphthylacetic acid

The acid (2 g) was reduced with lithium aluminium hydride in the usual way. Quantitative yields. Phenyluretan, m.p. 231—233°C.

Reaction of the Grignard reagent II with acetyl chloride

The Grignard reagent (II), prepared from 11 g of I was added dropwise during one hour to a solution of 25 g of acetyl chloride in 100 ml of ether, cooled in an ice-water bath. The bath was removed and the mixture allowed to warm to room temperature, when water and ice were added to hydrolyze the excess of acetyl chloride. The water phase was shaken repeatedly with ether, the organic portions combined, washed with sodium carbonate and water, dried and distilled. The main fraction boiled at 160—170°/10 mm Hg. This was a yellow, heavy liquid, whose 2,4-dinitrophenylhydrazone melted at 236—238°C. This derivative was identical with that of an authentic sample of methyl-2(2-methyl-1-naphthyl) ketone, prepared as above from 2-methyl-1-naphthylmagnesium bromide and acetyl chloride. (Found: C 63.0; H 4.72. Calc. for $C_{19}H_{16}O_4N_4$ (364.35): C 62.6; H 4.43.)

Thanks are due to Professor A. Fredga for his keen interest in this work. A grant from the *Swedish Natural Science Research Council* is gratefully acknowledged.

REFERENCES

1. Grignard, M. V. *Bull. soc. chim* [3], **29** (1903) 953.
2. Kharasch, M. S. and Reinmuth, O. *Grignard reactions of Nonmetallic Substances*, Prentice Hall. Inc. N.Y. 1954, p. 1133.
3. Lawesson, S.-O. *Arkiv Kemi* **10** (1956) 171.
4. Rowlands, D. C., Greenlee, K. W. and Boord, C. E. *Abstracts of Papers, 117th Meeting, Am. Chem. Soc.*, Philadelphia, Pa. April 9—13, 1950, p. 8 L.
5. Gilman, H. and Kirby, J. E. *J. Am. Chem. Soc.* **51** (1929) 3475.
6. Sontag, D. *Ann. chim.* [11] **1** (1934) 359.
7. Mayer, F. and Schnecko, O. *Ber.* **56** (1923) 1408.
8. Lawesson, S.-O. *Acta Chem. Scand.* **11** (1957) 1075.
9. Rule, H. G., Spence, J. and Bretscher, E. *J. Chem. Soc.* **1929** 2516.
10. Ziegler, K. and Tiemann, P. *Ber.* **55** (1922) 3406.
11. Gaylord, N. G. and Becker, E. I. *Chem. Rev.* **49** (1951) 413.
12. Gaertner, R. *J. Am. Chem. Soc.* **74** (1952) 766.
13. Chapman, N. B. and Williams, J. F. A., *J. Chem. Soc.* **1952** 5044.
14. Friedmann, W. *Ber.* **49** (1916) 1352.
15. *Org. Syntheses*, Coll. vol. II, p. 106.
16. *Org. Syntheses*, Coll. vol. I, p. 188.
17. Mayer, F. and Sieglitz, A. *Ber.* **55** (1922) 1835.
18. Wittig, G. *Angew. Chem.* **53** (1940) 241.
19. Darzens, G. and Lévy, A. *Compt. rend.* **202** (1936) 73.

Received September 9, 1957

ACTA CHEMICA SCANDINAVICA 12 (1958) 8—23

The Photochemical Reaction between Nitric Oxide and *Iso*propanol, Sensitized by Benzophenone

HANS L. J. BÄCKSTRÖM and ALVAR STENERYR

Institutionen för fysikalisk kemi, Chalmers Tekniska Högskola, Göteborg, Sweden

PETER PERLMANN*

Institutet för oorganisk och fysikalisk kemi, Stockholms Högskola, Stockholm, Sweden

The photochemical reaction between *iso*propanol and nitric oxide with benzophenone as sensitizer has been studied at 25°C using light of wavelength 366 mμ. The results indicate that, in the main reaction, one molecule of acetone, one of nitrogen, one of nitrous oxide, and two of *iso*propyl nitrite are formed for every six molecules of nitric oxide reacting. A slight side-reaction seems to be connected with the formation of a light-absorbing by-product.

The number of molecules of nitric oxide reacting per light quantum absorbed is given approximately by: $\varphi = \frac{3.5}{1+252\,c}$, where c is the concentration of NO in mole/l. The retardation of the reaction by nitric oxide must be connected with the fact that a metastable biradical state of benzophenone has to be assumed as an intermediate in the reaction. This biradical state may be identified with the triplet state responsible for the phosphorescence shown by carbonyl compounds in solid solution at low temperatures. Apparently, molecules in this state may be deactivated on collision with nitric oxide molecules before they have time to react with the alcohol. A similar deactivating effect of oxygen has been reported previously.

The mechanism of deactivation is discussed. It is concluded that nitric oxide and oxygen owe their specific deactivating power to their unpaired electrons. In a collision with the biradical, the presence of unpaired electrons in both collision partners must give rise to strong exchange forces that may lead to the formation of a bond. The complex formed, on losing its excitation energy, must be assumed to dissociate again, regenerating the original molecules in their ground states. It is pointed out that the assumed mechanism is in accord with the Wigner spin conservation rule for collisions.

A large number of photochemical reactions of carbonyl compounds are known that can best be interpreted [1, 2] by assuming that the molecule on light absorption is transformed into a biradical: $R'R''C{=}O \rightarrow R'R''\dot{C}{-}O\cdot$.

* Preliminary experiments, carried out in 1946—47. Present address: Wenner-Grens Institut, Stockholm, Sweden.

Due to the odd electron on oxygen, this biradical will react with many substances by hydrogen abstraction, the free radicals thus formed subsequently undergoing dimerization or disproportionation. Thus, a solution of benzophenone in *iso*propanol, when irradiated in the absence of oxygen, gives acetone and benzopinacol, $(C_6H_5)_2C(OH)C(OH)(C_6H_5)_2$. In the presence of oxygen, on the other hand, the reaction takes a different course, the free radicals instead reacting with oxygen, with regeneration of benzophenone and formation of acetone and hydrogen peroxide, the net result being a photosensitized oxidation of the alcohol.

As found by Berthoud [3], the rate of this photosensitized oxidation decreases with increasing oxygen pressure. This can be explained [4] by assuming that excited benzophenone molecules in the biradical state may be deactivated on collision with oxygen molecules before they have time to react with the alcohol. Since this specific deactivating power of oxygen might be connected with its paramagnetism it seemed of interest to investigate whether a similar deactivating action is exercised by another paramagnetic gas, nitric oxide.

EXPERIMENTAL

Preliminary work

In the preliminary experiments, essentially the same experimental technique was used as in the earlier work [4] on the benzophenone-sensitized reaction between alcohols and oxygen. Solutions of benzophenone in 95 % ethanol were shaken with nitric oxide at atmospheric pressure, using a glass shaking tube connected to a gas burette by means of rubber tubing. Irradiation with a mercury arc caused rapid absorption of NO, the main reaction products identified being N_2, N_2O, and acetaldehyde. Some acetic acid was also formed. The solutions soon turned slightly yellow owing to the formation of small quantities of a coloured by-product which could only be isolated as a brown tar giving a positive test for nitrogen.

The technique employed was not suitable for quantitative determinations. Owing to the formation of gaseous reaction products, one of them highly soluble in the alcohol, there was no simple relation between the measured rate of volume decrease and the rate of nitric oxide absorption. The results of experiments where the nitric oxide was diluted with nitrogen indicated, however, that the rate of reaction increased with decreasing partial pressure of NO. A corresponding effect was to be expected in runs with pure NO, as the partial pressure of NO decreased during the run owing to the accumulation of gaseous reaction products. Such an effect was, indeed, observed, but it was rather weak. Apparently it was masked by a decrease in the rate caused by the formation of the above-mentioned coloured by-product, which acted as an internal light filter. In accordance with this, successively lower rate values were obtained when the same solution was shaken repeatedly with fresh portions of pure NO. In one such experiment, where the total amount of NO absorbed by 15 ml of ethanol +2.75 mmole of benzophenone was estimated at approximately 80 mmole, 97 % of the benzophenone could be recovered as 2,4-dinitrophenylhydrazone. Thus, benzophenone was not consumed in the reaction but acted merely as a sensitizer.

As in the corresponding reaction with oxygen [4], *iso*propanol gave about the same rate as ethanol whereas with methanol the rate was definitely lower (<50 %).

When pure liquid benzophenone was shaken with NO at 60°C in the light of the mercury arc for 2 h, no perceptible reaction took place.

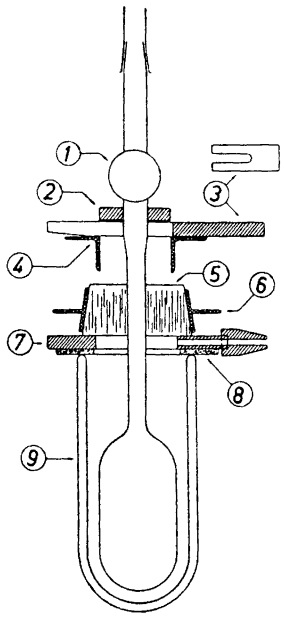

Fig. 1. Shaking tube connected to Töpler system, with arrangements for cooling with liquid oxygen under reduced pressure. (1) Stop-cock. (2) Plexiglas plate, glued on to neck of shaking tube. (3) Plexiglas wedge with groove for neck. (4) Angle-bars attached to vacuum rack. (5) Split rubber stopper with hole fitting neck, held in position by (6) metal ring. (7) Plexiglas ring with evacuation channel. (8) Rubber ring. (9) Dewar vessel with liquid oxygen. When evacuation began, the Dewar with rings 8 and 6 was forced by hand against the rubber stopper, but was soon held in position by the external pressure.

Present work

The alcohol selected for the final experiments was *iso*propanol. In principle, the experimental method employed consisted in allowing the reaction to take place in a closed shaking tube of sufficient size so that a measureable change in composition caused only a moderate decrease in the partial pressure of NO. Remaining nitric oxide as well as the quantities of N_2 and N_2O formed in the reaction were determined by isolating the different gases in the pure state by fractionation at suitable low temperatures and measuring their volumes under standard conditions.

The shaking tube, shown in Fig. 1, was made of thick-walled Pyrex tubing and carried a ground glass joint by means of which it could be attached to the vacuum system, and a stop-cock of such dimensions (bore 11 mm) as to permit the solution to be introduced into the tube by means of a pipette without danger of contamination by stop-cock grease. The wider part of the tube had a diameter of 50 mm and a length of 75 mm, the length of the neck below the stop-cock being 210 mm. The volume was 144.4 ml.

The vacuum system was of conventional type [6]. The arrangements for measuring gas volumes were:

1. A condensation trap connected to a Töpler pump and a calibrated gas burette. This "Töpler system" was connected with the main vacuum line by way of a stop-cock.
2. Another trap connected with a mercury manometer of calibrated bore. This trap-manometer system, also connected to the main line by way of a stop-cock, was used in certain cases for determining larger quantities of condensable gases. It was calibrated

against the gas burette by moving a condensable gas from one system to the other. Its volume at zero pressure was 58.4 ml.

The whole vacuum system was mounted on a rigid stand, made of angle iron. It was evacuated by a two-stage mercury diffusion pump and a fore pump. Vacuum was measured with a Pirani gauge or a McLeod gauge. All stop-cocks were lubricated with Apiezon N *. Removal of NO from the system for discarding was accomplished by adsorption on silica gel at liquid oxygen temperature in a removable trap. This arrangement was also found useful for over-night pumping-off of adsorbed gases from the system. A side-tube with a stop-cock and a ground glass joint enabled the shaking tube to be attached to the Töpler system.

The vapour pressure of nitric oxide at the temperature of liquid oxygen (90°K) is 3.3 mm. For a satisfactory separation of this gas from nitrogen it was therefore necessary to reach lower temperatures by cooling with liquid oxygen under reduced pressure. Arrangements for accomplishing this without strain on the glass parts are shown in Fig. 1. A similar arrangement was used for cooling the manometer trap. A copper gauze immersed in the liquid oxygen served to increase thermal conduction. Using pumps of sufficient capacity, temperatures of 63—65°K, as indicated by the equilibrium oxygen pressure, were reached without difficulty, corresponding to a nitric oxide pressure of about 5×10^{-4} mm.

The shaking experiments were performed at 25°C in a thermostat with a quartz window. The light source was a vertical 220 V AC mercury arc (LK 700) from Lumalampan, Stockholm, burned in series with a regulating resistance. Voltage variations were eliminated by means of a Sorensen constant voltage regulator. Relative values of the radiation intensity at 366 mμ (the only mercury line transmitted by the wall of the shaking tube and absorbed by the solution) were obtained with the aid of a thermopile and galvanometer as described earlier [4].

Materials

Nitric oxide was prepared in a special vacuum system from potassium nitrite, potassium iodide and sulfuric acid by the method of Winkler. It was freed from iodine vapour and higher oxides by passage through two large wash bottles with 50 % potassium hydroxide solution in which it was finely dispersed by means of fritted glass disks, and dried by passing through a trap at −79°C. It was then condensed at 90°K and freed from N_2O and N_2 by fractionation according to Gray [6]. The purified gas was collected in an evacuated glass bulb with stop-cock, which was later sealed to the main vacuum system.

Nitrogen was prepared by heating sodium azide in an evacuated glass system as described by Justi [7]. It was stored in the same way as NO.

Nitrous oxide. The commercial product was introduced into the vacuum system and dried by passing through a trap at −79°C. Volatile impurities were removed by pumping at 90°K.

Iso*propanol.* C.P. *iso*propanol was fractionally distilled at atmospheric pressure. Only the middle fractions were used.

Benzophenone. Merck's benzophenone, "M.P. *ca.* 48°C", previously found to be of satisfactory purity [4], was freed from traces of volatile impurities by melting in a vacuum.

Experimental procedure

In starting an experiment, 2 g of benzophenone were dissolved in 26 ml of *iso*propanol, and 25 ml of the solution introduced into the shaking tube. The tube was then attached to the Töpler system and cooled to 90°K and the air removed by pumping. With the stop-cock closed, the tube was then allowed to warm to room temperature, again cooled to 90°K, the pumping repeated, and so on, until pressure readings indicated that dissolved gases had been completely removed. Generally three such pumpings sufficed. An accurately measured quantity of NO was then condensed in the tube, whereupon the stop-cock was closed and the tube disconnected from the vacuum system.

* Much time was wasted in trying to use commercial silicone grease. No satisfactory vacuum could be maintained with this lubricant.

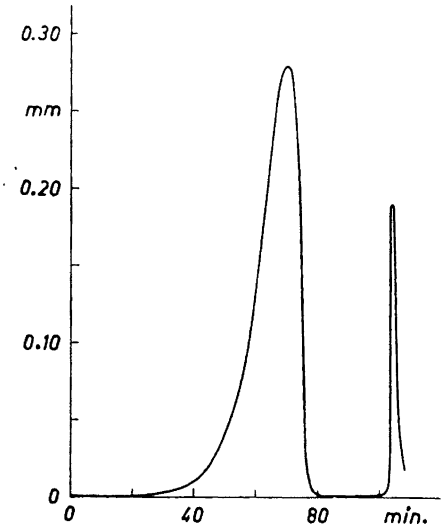

Fig. 2. Change of pressure with time during low-temperature distillation of a nitrous oxide-*iso*propanol mixture.

After an experiment, the shaking tube was again attached to the Töpler system and cooled to 64°K whereupon uncondensed gas (nitrogen) was pumped into the gas burette by means of the Töpler pump. This was repeated twice, with intermediate thawing of the solution, after which the nitrogen was recirculated through the Töpler trap, kept at −79°C, to remove alcohol vapour, and its volume again measured.

With the shaking tube at 90°K, unreacted NO was then sublimed into the manometer trap, kept at 64°K. This was repeated several times with intermediate thawing of the solution. The gas was freed from alcohol vapour by recirculation and its volume determined.

The determination of N_2O presented difficulties because of its high boiling point (−89°C) and its high solubility in the alcohol. The method finally arrived at was as follows.

With the shaking tube at about −25°C, the Dewar vessel was removed and a brass container in two parts, lined with asbestos, was placed around the neck of the tube and filled with pulverized CO_2-ice. The length of the cooled part of the tube was about 8 cm. The tube was then opened to the evacuated Töpler system (volume about 425 ml). The heating action of the surrounding air caused the solution to boil with reflux under a pressure which increased as nitrous oxide collected in the Töpler system. Approximate values of the pressure were obtained by observing the mercury levels in the two limbs of the gas burette. When after some hours no further increase in pressure was observed, the stop-cock of the shaking tube was closed, the Töpler system opened to the main line, and the gas obtained condensed in the manometer trap with liquid oxygen. The process was repeated twice, using a smaller volume (about 70 ml) to receive the gas, the shaking tube being connected only to the gas burette.

Attempts to separate the nitrous oxide from admixed alcohol vapour by recirculation through a trap at −79°C were unsuccessful. A satisfactory separation was, however, obtained in the following manner.

The bottom of the Töpler trap was covered with mercury (weight about 20 g). The gas was carefully condensed in the lowest part of this trap by cooling only the bottom with liquid oxygen. The whole trap was then brought to liquid oxygen temperature, the Dewar vessel rapidly replaced by an empty Dewar precooled to the same temperature, and the neck covered with cotton wool. The Töpler system was opened to the manometer trap, which was immersed in liquid oxygen, and the pressure read at regular intervals on the Pirani gauge.

The result of one of the model experiments, using a mixture of 216 μmole N_2O and 8 μmole *iso*propanol vapour, is shown graphically in Fig. 2. After the first pressure maximum, caused by distillation of N_2O, the pressure soon dropped to 1 or 2×10^{-3} mm. When this pressure had been maintained for 19 min, the Dewar vessel was, in this case, removed (at "100 min") in order to speed up the process. The second maximum, caused by distillation of the alcohol, appeared shortly after the mercury had melted.

The good separation obtained is ascribed to the heat capacity and thermal conductivity of the mercury lump, slowing down the heating process and causing evaporation to take place from a surface of more uniform temperature. When the method was used for the determination of N_2O, the stop-cock of the manometer trap was closed as soon as the pressure, after passing the first maximum, had reached a level of 1 or 2×10^{-3} mm. The Dewar vessel was removed, the trap allowed to reach room temperature, and the quantity of N_2O determined by reading the manometer.

The whole procedure for determining N_2O was tested by condensing measured quantities in the shaking tube. Before starting the analysis, the gas was allowed time to dissolve in the alcohol at room temperature. The following results were obtained. Throughout this paper, gas volumes are given in ml at 20°C and 760 mm.

Quantity of N_2O used, ml	5.44	9.71
» » » found, ml	5.43	9.71

After completing the analyses for the above-mentioned reaction products, any volatile constituents that might have escaped into the vacuum system and become adsorbed on the walls were again collected in the shaking tube by cooling the latter with liquid oxygen for a sufficient length of time. The solutions were then analyzed for acetone as described earlier [4], except that a photoelectric spectrophotometer, Beckman Model DU, was used. They were then stored in glass-stoppered bottles in the dark for further examination on a later occasion.

RESULTS

As shown by Table 1, nitrogen and nitrous oxide are formed in equimolar quantities irrespective of experimental conditions. Further details in connection with the experiments are given in Table 2.

Table 1. The relation between the quantities of nitrogen and nitrous oxide formed in the reaction.

Experiment No.	5	6	7	9	10
N_2 formed, ml	3.73	0.74	2.71	4.94	7.54
N_2O » »	3.73	0.73	2.70	5.13	7.36

In Table 2, the experiments are arranged in chronological order. In the first five experiments (series I), that were of an orientating nature, the current through the lamp was kept constant at 5.00 A but no intensity measurements were made. The rate of reaction was inconveniently high. The rest of the experiments were therefore made at lower intensities, corresponding to galvanometer deflections of about 2.6 cm in experiments 6—12 (series II), and 6.0 cm in experiments 13—20 (series III). Column 3 gives the average galvanometer deflection during the run in cm.

Table 3 summarizes derived values for runs in presence of nitric oxide. Column 2 gives the average quantity of NO present in ml, columns 3 and 4 moles of nitrogen and acetone formed per mole of NO consumed, and column 5 the rate of reaction expressed as μmoles of NO consumed per minute. The

Table 2. Results of systematic experiments as regards nitric oxide consumed and nitrogen and acetone formed under different experimental conditions.

1 Expt. No.	2 Time, min	3 Light intensity	4 NO added, ml	5 NO consumed, ml	6 Nitrogen, ml	7 Acetone, μmole
1	15	—	—	—	—	1 050
2	7	—	112.3	26.3	3.59	169
3	3	—	36.90	22.15	5.36	146
4	1	—	18.25	8.76	1.20	73
5	5	—	74.63	27.69	3.73	169
6	3	2.62	20.84	4.55	0.74	31
7	32	2.59	111.00	19.71	2.71	110
8	25	2.56	80.10	20.16	2.70	119
9	45	2.61	79.88	37.08	4.94	239
10	65	2.62	80.11	52.42	7.54	350
11	30	2.62	—	—	—	396
12	30	2.62	—	—	—	398
13	9	6.00	—	—	—	293
14	9.5	6.00	—	—	—	295
15	1.5	6.00	19.62	5.40	0.82	34
16	15	6.00	115.86	20.65	2.94	131
17	10	6.00	94.53	17.05	2.36	102
18	6	6.00	67.66	12.29	1.75	76
19	3	6.00	42.92	7.58	1.15	52
20	10	6.00	96.78	15.57	2.35	—

strongly deviating values within brackets may probably be ascribed to experimental errors and are left out of consideration. In Fig. 3, the remaining values in columns 3 and 4 are plotted against consumed NO in ml. The points show considerable scattering but nevertheless an unmistakable trend, especially as regards the nitrogen values. The conclusion seems justified that the main

Table 3. 1) Nitrogen and acetone formed in the reaction in relation to nitric oxide consumed (mole/mole); 2) rate of nitric oxide absorption in μmole min^{-1}.

1 Expt. No.	2 NO ml	3 $\frac{N_2}{NO}$	4 $\frac{\text{Acetone}}{NO}$	5 NO consumed μmole/min
2	99.1	0.137	0.155	156
3	25.8	(0.242)	0.159	307
4	13.9	0.137	(0.200)	364
5	60.8	0.135	0.147	230
6	18.6	0.163	0.164	63.1
7	101.0	0.138	0.134	25.6
8	70.0	0.134	0.142	33.5
9	61.3	0.133	0.155	34.3
10	53.9	0.144	0.161	33.5
15	16.9	0.152	0.151	149.7
16	105.5	0.142	0.153	57.2
17	86.0	0.138	0.144	70.9
18	61.5	0.142	0.149	85.2
19	39.1	0.152	0.165	105.1
20	89.0	0.151	—	64.7

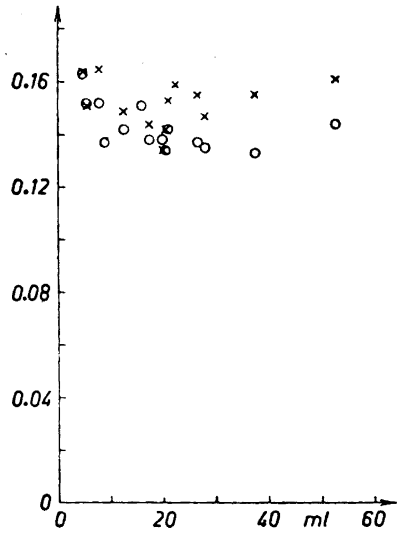

Fig. 3. Yields of nitrogen (O) and acetone (×) (mole per mole of NO) as a function of total NO absorbed (ml).

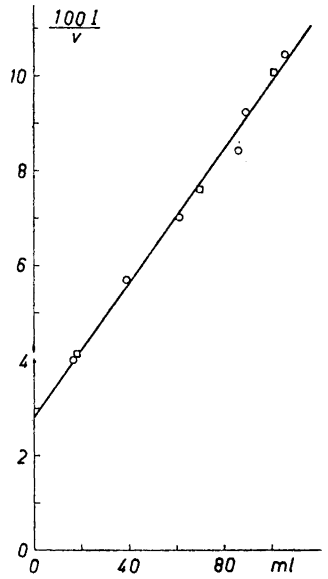

Fig. 4. Plot of $\frac{100\ I}{v}$ against initial nitric oxide in ml. I = average galvanometer deflection during run in cm, v = rate of nitric oxide absorption in μmole min^{-1}. □ Series II, O Series III. The straight line corresponds to the calculated rate equation (see text).

reaction gives rise to one molecule of acetone, one of nitrogen, and one of nitrous oxide, for every 6 molecules of nitric oxide reacting, but that the yields of nitrogen and nitrous oxide are markedly reduced as the reaction proceeds, in connection with a side-reaction. As in the preliminary work on ethanol, the solutions turned slightly yellow. In runs 6—10 the increase in light absorption at 366 mμ was followed spectrophotometrically by diluting 1-ml samples with 2 ml of *iso*propanol, and measuring the extinction in a layer-thickness of 1 mm. The values found were 0.667, 0.680, 0.680, 0.695, 0.722, as against 0.645 in a blank determination, thus increasing regularly with the amount of NO absorbed (see Table 2).

As shown by Table 3, the rate of nitric oxide absorption at constant light intensity generally decreases with increasing NO concentration, as measured by the average quantity of NO present during the run. However, runs 8, 9, and 10, show that the decrease in NO concentration taking place as a result of the reaction does not lead to a corresponding increase in reaction rate. In runs 9 and 10, the amount of NO initially present was the same as in run 8, but the percentage conversion was considerably increased by increasing the time of irradiation. The results indicate that the increase in rate normally

associated with decreasing NO concentration is here very nearly compensated by a decrease caused by the change in light absorption, an increasing fraction of the active light being absorbed by the coloured by-product formed. Under these circumstances it seems correct to relate the observed reaction rate to the quantity of NO initially present rather than to the average during the run. This has been done in Fig. 4.

In calculating the best straight line through the points by the method of least squares, runs 9 and 10 were excluded. The equation found was $\frac{100\ I}{v} = 2.73(1+0.0239[\mathrm{NO}])$.

The observed rates of acetone formation in the runs without nitric oxide, recalculated to a galvanometer deflection of 1 cm and expressed in μmole/min, were as follows:

Run No.	11	12	13	14	Average
Rate of acetone formation	5.04	5.07	5.43	5.18	5.18

Assuming a quantum efficiency of 0.5 (see page 18), the number of quanta absorbed by the solution per minute becomes $1.04 \times I \times N \times 10^{-5}$, where I represents the galvanometer deflection in cm, and N Avogadro's number. On this basis, the following formula is obtained for the quantum efficiency of nitric oxide absorption:

$$\varphi_{NO} = \frac{3.5}{1+0.0239[\mathrm{NO}]} \quad *$$

Nitrite determinations

The quantities of nitrogen and nitrous oxide formed in the reaction will account for at most 2/3 of the nitric oxide consumed. A search was therefore made for other nitrogenous reaction products. A qualitative test revealed the presence of nitrite. Attempts were accordingly made to obtain a method for determining nitrites in the reaction mixture, based on the usual spectrophotometric method for nitrite determination in water.

In the procedure of Rider and Mellon [8], nitrite is made to react with sulfanilic acid in strongly acidic solution and the resulting diazonium salt coupled with α-naphthylamine after buffering with sodium acetate in order to speed up the coupling reaction. As alkyl nitrites are very rapidly hydrolyzed in acid solution [9], this method can also be used for determining alkyl nitrites. In view of the presence of benzophenone in the reaction mixtures, we tried to work in alcoholic solutions. Experiments with pure sodium nitrite showed that the coupling process, when performed in 50 % ethanol, was completed in less than 10 min at room temperature even without buffering the solution. The addition of sodium acetate was therefore omitted. The presence of the alcohol greatly increased the stability of the resulting dyestuff solution, the extinction remaining unchanged for more than 3 h. Whether the diazotization was carried out in water or in 95 % ethanol was without influence on the final result. A diazotization time of 10 min was sufficient.

* A possible source of error in the runs without nitric oxide, which was not realized at the time, is the different behaviour of the solution when shaken with or without added gas. It would have been better to add an inert gas like nitrogen. As it is, light absorption may have been less complete than in the other runs which would lower the rate of acetone formation and cause the calculated values of φ_{NO} to come out too high.

The molar decadic extinction coefficient of the dyestuff at 520 mμ was found to be 4.30×10^4 l mole^{-1}cm^{-1}.

In studying the application of the method to alkyl nitrites, model experiments were made with redistilled amyl nitrite of 88.9 % purity, as determined by the method of van Itallie, Steenhauer and Harmsma [10]. No entirely satisfactory method was obtained. Results in the presence of benzophenone tended to be low and were not very reproducible. In the method finally adopted, the nitrite was therefore separated from the benzophenone by distillation. A sample of the reaction mixture was suitably diluted with ethanol. 1 ml of the resulting solution was rapidly introduced into a distillation apparatus of special design where it was subsequently mixed with 5 ml of 25 % ethanol and the nitrite distilled off as ethyl nitrite [11] in a current of oxygen at 70—75°C. The vapours were absorbed in 25 ml of ice-cold 95 % ethanol mixed with 1 ml of sulfanilic acid solution (0.6 g of sulfanilic acid +20 ml of concentrated hydrochloric acid + water to 100 ml). The distillation was continued for 20 min, after which the alcoholic sulfanilic acid solution was transferred to a measuring flask, mixed with 1 ml of naphthylamine reagent (0.6 g of α-naphthylamine + 1 ml of concentrated hydrochloric acid + water to 100 ml) and diluted with water to 50 ml. After standing at least 10 min, the extinction was measured at 520 mμ, using a layer-thickness of 1 cm.

In model experiments, the results obtained by this method were fairly reproducible but they were consistently about 10 % low (90.5±1 % of the theoretical value). In Table 4, the experimental values have therefore been multiplied by a factor of 1.1. They are given in moles of nitrite per mole of nitric oxide absorbed.

Table 4. Quantities of nitrite found in relation to nitric oxide consumed in the reaction (mole/mole).

Expt. No.	6	7	8	9	10	15	16	17	18	19	20
$\frac{\text{Nitrite}}{\text{NO}}$	0.116	0.088	0.097	0.262	0.239	0.131	0.293	0.234	0.306	0.168	0.273

*Iso*propyl nitrite is highly volatile (B.P. 45°C) and losses by evaporation may therefore have taken place during the long time of storing the reaction mixtures (from 2 to more than 6 months). This was definitely the case with the solution from experiment No. 15, for which determinations made 2 months previously by a preliminary method, without distillation, had given values of 0.264 and 0.266. Taken as a whole, the evidence seems to support the assumption that, in the main reaction, one third of the nitric oxide reacts to form *iso*propyl nitrite.

Solubility of nitric oxide in *iso*propanol

The solubility of nitric oxide in *iso*propanol at 25°C was determined, using an apparatus similar to the shaking tube (Fig. 1), except that it had two bulbs above each other. The lower bulb, containing the alcohol, was furnished with a magnetic stirrer. The stop-cock connecting the bulbs had a bore of 11 mm to facilitate gas diffusion. After greasing the stop-cocks, the apparatus was connected to the vacuum system, and dissolved air was removed as described earlier. Because of the large quantity of *iso*propanol used, 8 successive pumping operations were required. To avoid cracking of the glass tube surrounding the magnetic stirring rod, on solidification of the alcohol, the tube had to be made of thick glass, and with pointed ends. Starting at these points, cracks were formed in the solidified alcohol, thus relieving the strain on the tube.

After condensing a measured volume of NO in the apparatus, it was disconnected from the vacuum system, surrounded by a polythene bag and immersed in a water thermostat at 25.0°C. After 5 h, with the magnetic stirrer operated at such speed that a marked indentation was observed in the alcohol surface, the stop-cock between the bulbs was closed and the apparatus again connected to the vacuum system. The NO in the upper bulb was condensed in the manometer trap at 64°K, freed from alcohol by trap to trap distillation, and measured in the gas burette. All gas volumes were measured at three different pressures to diminish the effect of calibration errors.

The following results were obtained.

Total nitric oxide used, ml	17.46	6.425
Nitric oxide in upper bulb, ml	11.035	4.05

The volumes, as determined by weighing, were: upper bulb, 143.3 ml; both bulbs including the stop-cock but excluding the magnetic stirrer, 333.6 ml; *iso*propanol, 149.9 ml. The values calculated for the Ostwald solubility coefficient are 0.287 and 0.291, respectively. Mean value 0.289.

In the experimental formula for φ_{NO} (p. 16) the concentration of NO is given as the quantity of NO initially present in the reacting system, expressed in ml at 20°C and 760 mm of mercury. Knowing the volume of the shaking tube (144.4 ml), the volume of the solution (25 ml), and the partition coefficient, (0.289), the corresponding concentration of NO in the solution in mole/l c_{NO}, can be calculated. The formula then becomes

$$\varphi_{NO} = \frac{3.5}{1+252\ c_{NO}}$$

DISCUSSION

The following mechanism, similar to the one proposed for the corresponding reaction with oxygen [4], will account for the main features of the results obtained.

$$(C_6H_5)_2CO + h\nu \rightarrow (C_6H_5)_2CO^* \rightarrow (C_6H_5)_2\dot{C}-O\cdot \quad (1)$$

$$(C_6H_5)_2\dot{C}-O\cdot + (CH_3)_2CHOH \rightarrow (C_6H_5)_2COH + (CH_3)_2\dot{C}OH \quad (2)$$

$$2(C_6H_5)_2\dot{C}OH \rightarrow (C_6H_5)_2C(OH)C(OH)(C_6H_5)_2 \quad (3)$$

$$2(CH_3)_2\dot{C}OH \rightarrow (CH_3)_2CHOH + (CH_3)_2CO \quad (4)$$

$$(C_6H_5)_2\dot{C}-O\cdot + NO \rightarrow (C_6H_5)_2CO + NO \quad (5)$$

$$(C_6H_5)_2\dot{C}OH + (CH_3)_2\dot{C}OH + n\ NO \rightarrow \text{reaction products} \quad (6)$$

The reaction in the absence of nitric oxide is determined by steps (1)—(4), giving a quantum efficiency of 0.5 for the formation of benzopinacol and acetone *. In the presence of nitric oxide, the reaction is determined by steps (1), (2), (5), and (6). Assuming stationary state concentration for the intermediate

* Preliminary results obtained by C. Åquist in this laboratory indicate that the true value is between 0.47 and 0.57. The investigation is being continued.

radicals, and on condition that n is constant, the following expression is obtained for the quantum efficiency of nitric oxide absorption:

$$\varphi_{NO} = \frac{n}{1 + \frac{k_5 c_{NO}}{k_2 c_A}}$$

where c_A denotes the concentration of *iso*propanol.

The most important steps in the reaction mechanism will now be discussed separately.

The activation of benzophenone by light absorption

The biradical state of benzophenone appearing in the reaction scheme may be identified with the metastable triplet state responsible for the phosphorescence exhibited by carbonyl compounds in solid solution at liquid air temperatures [12]. Absorption of long-wave ultraviolet light raises the molecules to the lowest excited singlet state, from which they pass, by a process of radiationless internal conversion, to a slightly lower lying triplet level, the energy given out in the process being taken up by the surrounding solvent molecules as vibrational energy. In accordance with the selection rule prohibiting intercombinations between levels of different multiplicity, the radiative return from the triplet to the ground (singlet) level is a slow process. The rate of decay of phosphorescence under the conditions specified gives an approximate measure of the natural mean life-time of the triplet state. The value found for benzophenone [13] is 0.008 sec.

A change from a singlet to a triplet state means the unpairing of two electrons in the molecule, *i.e.* the formation of a biradical. As the structure of the triplet state of carbonyl compounds Lewis and Kasha [12] suggested a molecule in which one member of the double bond of the carbonyl group had been broken. Apparently, they were not aware of the wealth of photochemical evidence which had caused one of us [1] to postulate the existence of a biradical of this kind as an intermediate in a large group of photochemical reactions of carbonyl compounds.

In fluid solvents at ordinary temperatures the same process of internal conversion to the triplet state may be expected to take place, but the life-time of the biradicals will normally be shortened by deactivating collisions with solvent molecules to such an extent that no phosphorescence is observed under these conditions. This is the case with benzophenone. Apparently, however, the life-time is long enough for photochemical reactions to take place with suitable reaction partners.

Substances showing phosphorescence in solid solution at liquid air temperatures generally also show normal fluorescence, *i.e.* the much more short-lived radiation connected with the return from the excited singlet to the ground state. According to Kasha [14], however, fluorescence is scarcely to be observed in the case of carbonyl compounds, showing that the "forbidden" conversion to the triplet state is essentially complete. He gives the ratio of the yield of fluorescence to that of phosphorescence as $\leq 10^{-3}$. Since the natural life-time of the

excited singlet state is probably of the order of 10^{-8} sec, this means that the time required for its conversion to the triplet state under the conditions of the experiments is of the order of 10^{-11} sec.

The quantum efficiency of phosphorescence of benzophenone dissolved in EPA glass (a mixture of ether, pentane, and alcohol) at 77°K has been determined by Gilmore, Gibson and McClure [13], who found a value of 0.84 ± 10 %. There is reason to believe, however, that this is less than the natural value since it has been found [15, 16] that phosphorescent substances react photochemically with the ethanol in the solvent even at these low temperatures.

The assumption underlying step (1) in the reaction mechanism that one biradical is formed for every light quantum absorbed, thus seems to be in accord not only with the photochemical evidence [4] but also with the results of phosphorescence studies.

The reaction products

The analytical results indicate that, in the main reaction, 1 molecule of nitrogen, 1 of nitrous oxide, 1 of acetone, and 2 of *iso*propyl nitrite are formed for every 6 molecules of nitric oxide taken up by the solution. The experimental formula for φ_{NO} (p. 18), when extrapolated to zero nitric oxide concentration, gives 3.5 molecules of NO reacting for every light quantum absorbed. A value of 3.0 would make the extrapolated quantum yields for the reaction products 0.5 and 1, respectively. We accordingly assume n in step (6) to be $= 3$.

If step (6) is written for 2 light quanta absorbed and in such a way that it will account for the analytical results of the present investigation as well as for the fact, established in the preliminary experiments, that benzophenone is not consumed in the reaction, it becomes:

$$2(C_6H_5)_2\dot{C}OH + 2(CH_3)_2\dot{C}OH + (CH_3)_2CHOH + 6NO = 2(C_6H_5)_2CO + (CH_3)_2CO + 2(CH_3)_2CHONO + N_2 + N_2O$$

This equation is not balanced, 4 hydrogen atoms and 3 oxygen atoms remaining to be accounted for. The formation of one molecule of water seems likely, but the complete elucidation of the stoichiometry will require further work. We have searched the literature in vain for reactions of NO giving N_2 and N_2O in equimolar quantities. For the present we are not prepared to make any suggestions as to the probable course of the reaction. One point should be mentioned, however. The fact that nitrites are formed in the reaction might suggest that the radical formed from the alcohol in step (2) is not $(CH_3)_2\dot{C}OH$ but the alcoxy radical $(CH_3)_2CHO\cdot$, since alcoxy radicals are known to add on nitric oxide to form nitrites [17]. In several cases it has been proved definitely, however, that free radicals react with alcohols by abstracting a hydrogen atom from the α-carbon atom [18]. A case which is of particular interest in the present connection is the one reported by Symons and Townsend [16].

For the purpose of the present investigation, however, the only important question is whether the value of n in step (6) is constant or not. The results indicate that this is true for the main reaction and, as explained earlier (p. 16),

the method of correlating the observed reaction rate with the initial concentration of NO rather than with the average during the run should have largely eliminated the effect of the side reaction on the rate equation.

The formula previously found for the rate of the corresponding reaction with oxygen at 25°C under the experimental conditions used [4], as a function of the oxygen pressure, when recalculated using the known Ostwald solubility coefficient of oxygen in *iso*propanol [19], 0.2463, becomes

$$v = \frac{43.5}{1 \times 95 c_{ox}}$$

where c_{ox} is the concentration of oxygen in mole/l. The denominator in this expression is $= 1 + \frac{k_7 c_{ox}}{k_2 c_A}$, where k_7 is the rate constant for the reaction:

$$(C_6H_5)_2\dot{C}{-}O \cdot + O_2 = (C_6H_5)_2CO + O_2 \qquad (7)$$

Comparison with the expression for φ_{NO} shows that the rate constants of reactions (5) and (7) are of the same order of magnitude. This was to be expected since both reactions may be presumed to be so rapid as to be essentially diffusion-controlled [20]. This means that the rate constants in *iso*propanol at 25°C should approach a calculated limiting value [21] of about 3.5×10^9 l mole^{-1}sec^{-1}. On this basis it is found that the mean life of the biradical in pure *iso*propanol is about 10^{-7} sec and that only one collision with *iso*propanol molecules in about 10^6 leads to reaction [22].

The mechanism of deactivation by NO and O_2

The analogy between the deactivation process represented by step (5) of the proposed reaction mechanism and the phenomenon of fluorescence quenching was emphasized in an earlier paper [4]. In recent studies of the fluorescence of organic compounds in the vapour state it has been found that O_2 and NO are, without exception, equally effective as quenchers. The substances studied were, anthraquinone and a number of its derivatives [23], anthracene and two related hydrocarbons [24], and β-naphthylamine [25]. The results are interpreted in terms of a theory advanced by Karyakin, Terenin and Kalenichenko [23]. The quenching is assumed to be "paramagnetic", collisions with the paramagnetic quencher molecules enabling an otherwise forbidden transition of the singlet excited fluorescer molecule to a somewhat lower lying triplet level to take place. It is an essential feature of the theory that, for the paramagnetic mechanism to be effective, the energy difference between the excited singlet and the triplet levels should be small. In cases where this difference was of the order of 0.2 *e*V the efficiency of the quenching collisions was found to be = 1 for both O_2 and NO whereas no quenching was observed by either gas when it amounted to 0.8 *e*V.

The present case is, however, altogether different from the one discussed above. What we are dealing with is the interaction between a molecule of nitric oxide or oxygen and an excited benzophenone molecule which is not in a singlet but in a triplet state. The energy of the triplet state is 3.0 *e*V above

the ground (singlet) level[12]. Transition to the ground state by a paramagnetic mechanism appears to be a highly improbable event.

There can be little doubt, however, that the unpaired electrons of NO and O_2, that cause their paramagnetism, are also responsible for their deactivating power. In a collision with a benzophenone molecule in the biradical state, the presence of unpaired electrons in both collision partners must give rise to strong exchange forces that may lead to bond formation. The property of NO and O_2 of undergoing addition reactions with free radicals is well known. To explain the experimental results, the reaction product must be assumed only to be stable in the excited state (*cf.* Förster and Kasper [26]) and to dissociate into the original molecules in their ground states when the excitation energy is lost through collisions with neighbouring molecules *. The assumption of a quenching mechanism of this kind receives support from theoretical considerations of the ways in which electronic energy may be transformed into thermal energy [27]. It is also in accord with the Wigner spin-conservation rule for collisions [28] and thus involves no forbidden transitions. It should therefore have a high intrinsic probability.

Not every collision between the biradical and a molecule of O_2 or NO may be expected to lead to bond formation. For this to happen, the spins must be favourably oriented and presumably also other steric requirements have to be met. In addition, an energy of activation may be involved, although this can hardly be expected to be large [29]. However, the influence of these factors on the rate of the quenching reaction should be much less in solution than in the gas phase. In solution, the rate of reaction is governed primarily by the rate of diffusion of the reactants toward each other. As shown by Rabinowitch [30], the diffusion process leads to an "encounter", a set of collisions. These repeated collisions, in conjunction with molecular rotation, should markedly increase the probability of reaction. It seems significant that the rate of quenching by oxygen of the long-lived fluorescence of biacetyl in the vapour state [31] corresponds to a steric factor of about 0.1, whereas the rate in benzene solution [32] approches 50 % of the limiting value for a diffusion-controlled reaction.

In view of the above considerations, the most probable explanation of the lower deactivating efficiency of O_2 as compared to NO, which cannot be due to a difference in diffusion rate, would seem to be a difference in activation energy.

Acknowledgement. The authors gratefully acknowledge the support of this work by *Statens Naturvetenskapliga Forskningsråd.*

REFERENCES

1. Bäckström, H. L. J. *Z. physik. Chem.* **B25** (1934) 99.
2. Hirschberg, Y. and Farkas, L. *J. Am. Chem. Soc.* **59** (1937) 2453.
3. Berthoud, A. *Helv. Chim. Acta* **16** (1933) 592.

* In the analogous case of the long-lived fluorescence of biacetyl vapour, which according to Lewis and Kasha (*J. Am. Chem. Soc.* **67** (1945) 1000) is a triplet → singlet transition, quenching by oxygen leads to a permanent oxidation of the fluorescer (Almy, G. M., Fuller, H. Q. and Kinzer, G. D. *Phys. Rev.* **55** (1939) 238).

4. Bäckström, H. L. J. *The Svedberg 1884—1944*, Almquist & Wiksells Boktryckeri, Uppsala, 1944, p. 45.
5. Sanderson, R. T. *Vacuum Manipulation of Volatile Compounds*, John Wiley & Sons, Inc., New York 1948.
6. Gray, R. W. *J. Chem. Soc.* **87** (1905) 1605.
7. Justi, E. *Ann. Physik* [5] **10** (1931) 985.
8. Rider, B. F. and Mellon, M. G. *Ind. Eng. Chem. Anal. Ed.* **18** (1946) 96.
9. Fischer, W. M. *Z. physik. Chem.* **65** (1909) 61.
10. van Itallie, L., Steenhauer, A. J. and Harmsma, A. *Pharm. Weekblad* **66** (1929) 15; *Chem. Zentr.* **1929:I**, 1245.
11. Bertoni, G. *Gazz. chim. ital.* **12** (1882) 438.
12. Lewis, G. N. and Kasha, M. *J. Am. Chem. Soc.* **66** (1944) 2100.
13. Gilmore, E. H., Gibson, G. E. and McClure, D. S. *J. Chem. Phys.* **20** (1952) 829; **23** (1955) 399.
14. Kasha, M. *Discussions Faraday Soc.* **No. 9** (1950) 14.
15. Gibson, G. E., Blake, N. and Kalm, M. *J. Chem. Phys.* **21** (1953) 1000.
16. Symons, C. R. and Townsend, M. *Ibid.* **25** (1956) 1299.
17. Levy, J. B. *J. Am. Chem. Soc.* **75** (1953) 1801; **76** (1954) 3790.
18. Kharasch, M. S., Rowe, J. L. and Urry, W. H. *J. Org. Chem.* **16** (1951) 905; Urry, W. H., Stacey, F. W., Huyser, E. S. and Juveland, O. O. *J. Am. Chem. Soc.* **76** (1954) 450.
19. Kretschmer, C. B., Nowakowska, J. and Wiebe, R. *Ind. Eng. Chem.* **38** (1946) 506.
20. Förster, Th. *Fluoreszenz organischer Verbindungen*, Vandenhoeck & Ruprecht, Göttingen 1951, p. 209.
21. Debye, P. *Trans. Electrochem. Soc.* **82** (1942) 265.
22. Moelwyn-Hughes, E. A. *Trans. Chem. Soc.* **1932**, 95.
23. Karyakin, A. W., Terenin, A. N. and Kalenichenko, Y. I. *Doklady Akad. Nauk S.S.S.R.* **67** (1949) 305.
24. Stevens, B. *Trans. Faraday Soc.* **51** (1955) 610.
25. Dubois, J. T. *J. Chem. Phys.* **25** (1956) 178.
26. Förster, Th. and Kasper, K. *Z. Elektrochem.* **59** (1955) 976.
27. Franck, J. and Levi, H. *Z. physik. Chem.* **B 27** (1934) 409; Franck, J. and Sponer, H. Volume commemoratif Victor Henri: "*Contribution à l'Étude de la Structure Moléculaire*", 1948, p. 169.
28. Laidler, K. J. *The Chemical Kinetics of Excited States*, Oxford University Press, Oxford 1955, p. 32, 100.
29. Williamson, B. and La Mer, V. K. *J. Am. Chem. Soc.* **70** (1948) 717.
30. Rabinowitch, E. *Trans. Faraday Soc.* **33** (1937) 1225.
31. Coward, N. A. and Noyes, W. A. *J. Chem. Phys.* **22** (1954) 1207.
32. Bäckström, H. L. J. and Sandros, K. *J. Chem. Phys.* **23** (1955) 2197.

Received September 11, 1957.

ACTA CHEMICA SCANDINAVICA 12 (1958) 24—30

The Magnetic Properties of $[Co(NH_3)_5(NO)]Cl_2$ (black) and $[Co(NH_3)_5(NO)](NO_3)_2 \cdot \frac{1}{2}H_2O$ (red)

Studies in Magnetochemistry 21 *

R. W. ASMUSSEN, OLE BOSTRUP and J. POTTS JENSEN

The Chemical Laboratory B, Technical University of Denmark, Copenhagen, Denmark

Magnetic susceptibility measurements of 6 independent preparates of the black $[Co(NH_3)_5(NO)]Cl_2$ show that the compound does not contain unpaired electrons. Our best samples give $\chi_g = +0.17 \times 10^{-6}$ at room temperature. It has been verified that the red $[Co(NH_3)_5(NO)](NO_3)_2 \cdot \frac{1}{2}H_2O$ is diamagnetic having $\chi_g = -0.20 \times 10^{-6}$. The absorption spectrum of this compound in aqueous solution has been measured. The similarity between this spectrum and the known absorption spectra of the ordinary Co(III)-pentammineacido complexes is evident. The possible structures of the compounds are discussed. The black pentahydrate $[Co(NH_3)_5(NO)]Cl_2 \cdot 5H_2O$ does not seem to exist.

In 1903 Sand and Genssler [1,2] showed that the action of NO(g) on $[Co(NH_3)_6]^{+2}$ solutions can result in two series of salts, "red salts" and "black salts". The empirical formula of both types of compounds is $[Co(NH_3)_5(NO)]X_2$. Later the preparation and the chemical properties of these compounds were critically studied and discussed by Werner and Karrer [3] and the magnetic properties were investigated by several authors [5–9].

These puzzling complexes have received great interest and many discussions concerning the possible structures, in particular their electronic structures on basis of the above mentioned chemical and magnetic investigations, have been published [3,7,10–12,19].

On account of the attention these compounds have received and the many contradictions concerning the experimental results and their interpretations, which are stated in the literature, we found it worth while to study thoroughly a typical example from each of the two series of salts, *viz.* "the black chloride" $[Co(NH_3)_5(NO)]Cl_2$ and the "red nitrate" $[Co(NH_3)_5(NO)](NO_3)_2 \cdot \frac{1}{2}H_2O$.

* No. 20 of this series: *Acta Chem Scand.* 11 (1957) 1534.

1. The black chloride

Previously the magnetic susceptibility of this compound has been measured several times and effective magnetic moments μ_{eff} can be calculated. Thus Ray, and Bahr [6] obtained the value $\mu_{eff} = 2.78\ \mu_B$, Bose [5] found $\mu_{eff} = 2.81\ \mu_B$, Milward *et al.* [8] $\mu_{eff} = 1.63\ \mu_B$, Ghosh and Ray [7] $\mu_{eff} = 1.44\ \mu_B$, and Mellor and Craig [9] $\mu_{eff} = 1.60\ \mu_B$ (mean value).

Our examinations of the preparation-methods described in the literature [1-3,7,13] revealed that a contamination of the black chloride with the strongly paramagnetic [14] cobalt(II)hexamminechloride is very difficult to avoid. We have modified the preparation-method (compare the results in the experimental part) and have then obtained samples of $[Co(NH_3)_5(NO)]Cl_2$ which under the microscope did not reveal even traces of reddish crystals of $[Co(NH_3)_6]Cl_2$. Some data from our measurements of the magnetic gram susceptibility at 295°K, 195°K and 85°K of 6 independent preparations are given in Table 1.

Table 1. The magnetic gram susceptibility χ_g of independent samples of $[Co(NH_3)_5(NO)]Cl_2$ (black). Analyses.

Sample No.	Analysis		$\chi_g \cdot 10^6$		
	Calc. %	Found %	295°K	195°K	85°K
17	28.94 Cl 34.75 NH_3		0.171	0.316	0.526
19	28.94 Cl 34.75 NH_3	29.06 Cl 34.79 NH_3	0.262	0.417	0.730
20	28.94 Cl 34.75 NH_3	28.89 Cl 34.90 NH_3	0.198	0.373	0.485
22	28.94 Cl 34.75 NH_3	28.75 Cl 34.63 NH_3	0.367	0.634	
23	28.94 Cl 34.75 NH_3	28.83 Cl 34.91 NH_3	0.173	0.366	0.807
25	28.94 Cl 34.75 NH_3 24.06 Co	28.77 Cl 34.50 NH_3 23.95 Co	0.277	0.508	1.26

It will be seen from Table 1 that we have succeeded in obtaining the compound in a higher and better reproducible magnetic purity than hitherto reported. The reproducibility of the magnetic measurements from sample to sample is far from the usual requirements. Our experiences prove, however, that it is very difficult to eliminate the last traces of paramagnetic impurities. The temperature dependence of the susceptibility can be explained as being due to such impurities still present even in our best samples.

We conclude from Table 1 that the expressions

$$\chi_g = +0.17 \times 10^{-6} \qquad (295°K) \tag{1}$$

$$\chi_M = 245 \times 0.17 \times 10^{-6} = +41 \times 10^{-6} \qquad (295°K) \tag{2}$$

give the best statement of the present measurements of the gram and the molar susceptibility, respectively. Since a compound with one unpaired electron ($\mu = 1.73\ \mu_B$) has the molar susceptibility

$$\chi_M = 1\,260 \times 10^{-6} \tag{3}$$

at room temperature, it follows from (2) and (3) that no unpaired electrons are present. We consider this result more reasonable for a compound with an even number of electrons than the old values for the magnetic moment, which roughly correspond to — and also have been interpreted as originating from — one unpaired electron.

Concerning the chemical properties of the black chloride we shall mention the following facts: The chloride cannot be dissolved in water (even at 0°C) without decomposition to basic Co(II)-chlorides; treatment with conc. HCl or conc. NH_3 (in a N_2-atmosphere) yields $[CoCl_4]^{-2}$ and $[Co(NH_3)_6]^{+2}$-solutions, respectively, but on the other hand Nast and Rohmer [19] have shown recently that treatment of $[Co(NH_3)_5(NO)]Cl_2$ with aqueous KCN yields the yellow, diamagnetic $K_3[Co(CN)_5(NO)] \cdot 2H_2O$ which, as pointed out by Nast, very probable contains the unstable, diamagnetic [4,18] nitroxylate ion NO^- as a ligand. *I.e.*, in some reactions the black chloride behaves like a Co(II)- in other as a Co(III)-complex. The conversion from one oxidation state to another seems only to require a rather small energy.

It is, however, not only the chemical properties but also the magnetic properties and the intense black colour which may be interpreted on the basis of a structure formula represented as

$$(H_3N)_5\overset{+3}{Co}\,NO^-$$

together with the further assumption of near lying Co(II)-states. We must, however, point out that further experimental investigations on other physical properties of the compound are necessary before further advance in the discussions of the structure of the black chloride can be expected.

2. *The red nitrate (semihydrate)*

The magnetic susceptibility of this compound has been measured several times previously. The first published values of χ_g were given by Ray and Bahr[6], who found $\chi_g = -0.109 \times 10^{-6}$. Later Milward *et al.*[8] published the

Table 2. The magnetic gram susceptibilities χ_g of independent samples of $[Co(NH_3)_5(NO)](NO_3)_2 \cdot \frac{1}{2}H_2O$ (red). Analyses.

Sample No.	Analyses		$\chi_g \cdot 10^6$		
	Calc. %	Found %	295°K	195°K	85°K
1	19.19 Co 27.72 NH_3	19.11 Co 27.84 NH_3	−0.180		
2	19.19 Co 27.72 NH_3	19.21 Co 27.72 NH_3	−0.197	−0.156	−0.10
3	27.72 NH_3	27.75 NH_3	−0.159	−0.161	−0.03

value $\chi_g = -0.19 \times 10^{-6}$, and Ghosh and Ray [7] found $\chi_g = -0.201 \times 10^{-6}$. In the papers by Bose [5] and Mellor and Craig [9] it is mentioned that they have measured χ_g and found diamagnetism, but no values are given.

The results of our measurements on different preparations are given in Table 2. The agreement with the data quoted above is obvious and the slight temperature dependence of χ_g can be explained as being due to small amounts of paramagnetic impurities.

The chemical properties of the red nitrate $[Co(NH_3)_5(NO)](NO_3)_2 \cdot \frac{1}{2}H_2O$ are very different from those of the black $[Co(NH_3)_5(NO)]Cl_2$. The former salt is remarkably more stable and can, *e.g.*, be recrystallized from water with only slight decomposition. Therefore it is possible to measure a reliable absorption-spectrum and this is given in Fig. 1. The great similarity between this absorption-curve and the corresponding curves for ordinary Co(III)-pentammine complexes is evident. (Compare, *e.g.*, the spectra measured by Linhard *et al.*[15]).

It is not only these physical properties (magnetism and absorption spectrum) which indicate that the compound is a Co(III)-complex, also the chemical properties are in accordance with this assumption: The action of conc. HCl, conc. HBr or 80 % HNO_3 on the red nitrate yields chloro-, bromo-, and nitrato-pentammine salts, respectively, whereas treatment with a KCN-solution yields [16,19] $K_3[Co(CN)_6]$. We are therefore of the opinion that the red nitrate is either a pentammine Co(III) complex or a binuclear decammine Co(III)-complex.

3. The black chloride (penta-hydrate)

Frazer and Long [4] have published data (preparation and magnetic measurements) for a pentahydrate of the black chloride. We are, however, not convinced of the existence of this hydrate. We have never been able to isolate a hydrate of the black chloride. The procedure of Frazer and Long gives impure

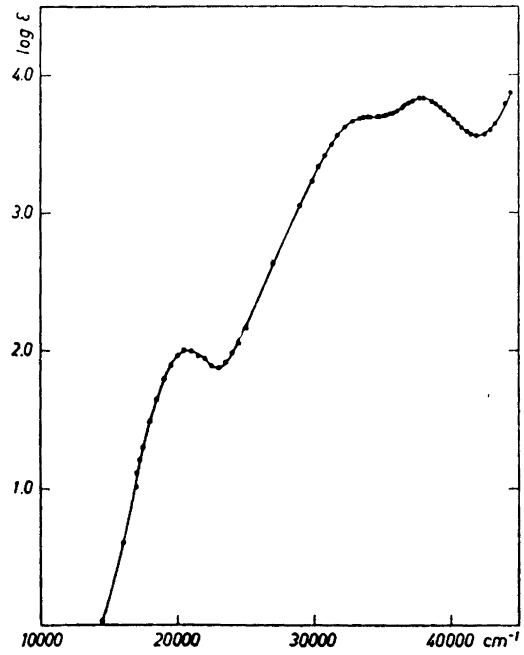

Fig. 1. Absorption spectrum of $[Co(NH_3)_5(NO)](NO_3)_2$ in aqueous solution.

samples of the anhydrous complex; furthermore we consider the analytical methods used to be unnecessarily complicated. The susceptibility was measured in rather weak fields (300 Ørsted). The value given by Frazer and Long corresponds to between 2 and 4 unpaired electrons.

EXPERIMENTAL

Preparation of the compounds

$[Co(NH_3)_5(NO)]Cl_2$. 1 000 ml of 12 % ammonia placed in the apparatus shown in Fig. 2 is cooled to 0°C by immersion of the apparatus in an ice-water bath. After the apparatus has been freed from oxygen by passing a stream of purified nitrogen through A, 50 ml of 2.50 M $CoCl_2$ is introduced at H maintaining a vigorous stream of nitrogen in order to prevent oxydation of the cobaltoammine solution formed. This solution is now treated with nitric oxide at 0°C for 5 h. Nitric oxide is then replaced by nitrogen and suction is applied at C in order to get rid of the original liquor. The crystals are purified by careful flotation with alcohol in a nitrogen atmosphere and are finally washed with alcohol and ethyl ether and dried by evacuating the apparatus. The hard, black, octahedral crystals are stored in a nitrogen atmosphere. The yield is approximately 20 % of the cobalt used.

$[Co(NH_3)_5(NO)](NO_3)_2 \cdot \frac{1}{2}H_2O$ was prepared according to Werner and Karrer [3] and recrystallized from water containing ammonia [8].

NO was prepared in an ordinary Kipp-apparatus from $NaNO_2$ (p.a. *in rotulis*) and 20 % H_2SO_4 and purified by passing through a 30 % NaOH solution and four U-tubes with solid NaOH (p.a. *in bacillis*).

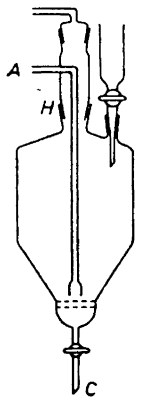

Fig. 2. Apparatus for the preparation of $[Co(NH_3)_5(NO)]Cl_2$, black.

Quantitative analysis. Co was determined as $CoSO_4$ after destruction of the complex by means of H_2SO_4. Cl was estimated as AgCl by weighing. NH_3 was determined acidimetrically (distillation of the complex with 30 % NaOH solution). The results of the analyses are given in Tables 1 and 2. In this connection it may be of interest to point out that the theoretical Co-, Cl-, and N-contents of the black chloride and those of $Co(NH_3)_6Cl_2$ do not differ very much, which will be seen from Table 3.

Table 3. Comparison of the analytical composition of $[Co(NH_3)_6]Cl_2$, $[Co(NH_3)_5(NO)]Cl_2$ and a mixture of these containing 10 % $[Co(NH_3)_6]Cl_2$.

Substance	% Co	% Cl	% NH_3	% N
$Co(NH_3)_5(NO)Cl_2$	24.06	28.94	34.75	34.31
$Co(NH_3)_6Cl_2$	25.40	30.56	44.04	36.22
Mixture of the composition: 10 % $Co(NH_3)_6Cl_2$ 90 % $Co(NH_3)_5(NO)Cl_2$	24.19	29.10	35.70	34.50

In Table 3 is furthermore given the calculated Co-, Cl-, NH_3-, and N per cents for a mixture of the composition: 10 % $[Co(NH_3)_6]Cl_2$ and 90 % $[Co(NH_3)_5(NO)]Cl_2$. The presence of as much as 10 % $[Co(NH_3)_6]Cl_2$ in a black chloride sample has, as will be seen, practically no influence upon the composition compared to that of chemical pure $[Co(NH_3)_5(NO)]Cl_2$. The magnetic gram susceptibility of this 10 % mixture is 4.6×10^{-6} and the magnetic moment is $\mu_{eff} = 1.73\ \mu_B$. The gram susceptibilities for $[Co(NH_3)_6]Cl_2$ and $[Co(NH_3)_5(NO)]Cl_2$ are 47.0×10^{-6} and 0.17×10^{-6} respectively, at 22°C. The following diamagnetic corrections were applied for Cl^-, NO^- and NH_3 [18,20], respectively: -21×10^{-6}, -18×10^{-6} and -15×10^{-6} (gram ion susceptibilities).

Magnetic measurements

The measurements were carried out as described previously [17].

Absorption spectrum

In the region below 800 mμ the measurements were carried out by means of a Cary MS recording spectrophotometer kindly placed at our disposal by professor Jannik Bjerrum. In the region 800—1 250 mμ the measurements were carried out by means of a Beckman DU spectrophotometer.

REFERENCES

1. Sand, J. and Genssler, O. *Ber* **36** (1903) 2083.
2. Sand, J. and Genssler, O. *Ann.* **329** (1903) 197.
3. Werner, A. and Karrer, P. *Helv. Chim. Acta* **1** (1918) 54.
4. Frazer, J. H. and Long, N. O. *J. Chem. Phys.* **6** (1938) 462.
5. Bose, D. M. *Z. Physik.* **65** (1930) 677.
6. Ray, P. and Bahr, *J. Indian Chem. Soc.* **5** (1928) 497.
7. Ghosh, S. P. and Ray, P. *J. Indian Chem. Soc.* **20** (1943) 409.
8. Milward, J. L., Wardlaw, W. and Way, W. J. R. *J. Chem. Soc.* **1938** 233.
9. Mellor, D. P. and Craig, D. P. *J. Proc. Roy. Soc. N. S. Wales* **78** (1944) 25.
10. Nyholm, R. S. *Quart. Rev.* **7** (1953) 377.
11. Pauling, L. *The Nature of the Chemical Bond*, 2nd Ed., 3 Impr. Cornell Univ. Press. Ithaca 1952, p. 269.
12. Hückel, W. *Structural Chemistry of Inorg. Compounds* **II** (1951) 516.
13. Moeller, Th. and King, G. L. *Inorg. Syntheses* **IV** (1953) 168.
14. Klemm, W. and Schüth, W. *Z. anorg. Chem.* **210** (1933) 33.
15. Linhard, M., Siebert, H. and Weigel, M. *Z. anorg. Chem.* **278** (1955) 287.
16. Müller, H. *Ueber Ammoniak-Verbindungen des zweiwertigen Eisens. (Dissertation)*, Rössner, Merseburg 1926, p. 8.
17. Asmussen, R. W. and Soling, H. *Acta Chem. Scand.* **8** (1954) 558, 563.
18. Asmussen, R. W. *Acta Chem. Scand.* **11** (1957) 1435.
19. Nast, R. and Rohmer, M. *Z. anorg. Chem.* **285** (1956) 271.
20. Asmussen, R. W. *Studies in the Magnetochemistry of Inorganic Complex Compounds* (in Danish). Copenhagen 1944.

Received September 12, 1957.

ACTA CHEMICA SCANDINAVICA 12 (1958) 31—37

The Crystal Structure of Mo_5SiB_2

B. ARONSSON

Institute of Chemistry, University of Uppsala, Uppsala, Sweden

The result of an investigation of the Mo-rich corner of the Mo—Si—B system is in accordance with the phase diagram recently given by Nowotny *et al.*[1] The crystal structure of the ternary phase, Mo_5SiB_2, has been determined from single crystal data. There is definite evidence for an ordered distribution of the Si and B atoms. The Mo_5SiB_2-structure is described and discussed in comparison to similar phases, especially the ternary $Me_5Si_3(X')$-phases of the $D8_8$-type, (X′ = B, C, N, O).

After the intensive research during the last few years the binary borides and silicides of the transition metals are so well known that studies on ternary systems containing both these nonmetals have been started. It seems as if metal rich ternary (MeSiB)-phases are not uncommon and the determination of the crystal structures of these should be of a considerable crystallographic interest.

Such a ternary phase was found to exist in the Mo-Si-B system and an investigation of this system was started.* From powder photographs it was concluded that the ternary phase had a composition around Mo_5SiB_2 and that it was bodycentered tetragonal (probably isomorphous [2] with Cr_5B_3). Parthé *et al.*[3] have reported the same structure for Nb_5Si_3 and Ta_5Si_3 and call it the $T2$-structure, a notation that will be used in the following.

Before presenting the results of the refinement of the Mo_5SiB_2-structure some data are given for the Mo-Si-B system.

I. PRELIMINARY SURVEY OF THE Mo—Si—B SYSTEM

Experimental. Some alloys in the Mo—MoB—Mo_5Si_3 region were prepared from Mo powder (99.7 %), Si powder (99.9 %) and B powder of 94 % purity.** Weighed amounts

* In an early stage of this work Prof. Nowotny in Vienna kindly informed me that the same system was being studied at his institute. Therefore this investigation has been mainly devoted to the determination of the crystal structure of the ternary phase from single crystal data. Nowotny *et al.*[1] have later given a report on the Mo—Si—B system in which they stated this ternary phase to have the composition Mo_5SiB_2 and to be of the $T2$-type .

** Some boron was donated by the Borax Consolidated Ltd.

of the elements were melted twice in an arc-furnace. Powder photographs were taken in cameras of the Guinier-type, using Cu$K\alpha$-radiation. The lattice dimensions could be determined with an accuracy of ± 0.1 %.

Results. The phases observed in the powder photographs are consistent with the phase diagram of Nowotny *et al.*[1] The ternary phase was found to be in equilibrium with Mo, Mo_2B, MoB, Mo_3Si and Mo_5Si_3. The lattice parameters (l.p.) of the boundary phases differed very little ($\sim$0.1—0.2 %) from those reported for the binary compounds, indicating that the substitution of Si for B and vice versa is very limited. The smallest l.p. of Mo_5SiB_2 were observed in the Mo_2B-MoB-Mo_5SiB_2 region ($a = 5.99_8$ Å, $c = 11.02_7$ Å) and the largest in the MoB-Mo_5SiB_2-Mo_5Si_3 region ($a = 6.02_8$ Å, $c = 11.07_0$ Å). The results of the chemical analysis indicated that the atomic Si/B ratio of the ternary phase did not exceed 0.5. If the l.p.-variations depend on a variation of this ratio, the homogeneity range of Mo_5SiB_2 should be about $MoSi_{0.14}B_{0.46}$—$MoSi_{0.20}B_{0.40}$ under the applied conditions.

II. REFINEMENT OF THE CRYSTAL STRUCTURE OF Mo_5SiB_2

Experimental. A small single crystal was picked out of an alloy of the approximate composition $MoSi_{0.27}B_{0.36}$ (MoB—Mo_5SiB_2—Mo_5Si_3 region). Weissenberg photographs were taken with MoK-radiation around the a-axis. The layer lines 0—7 were recorded and the intensities of 200 reflexions were visually estimated using the multiple film technique. By plotting log I_o/I_c against $(\sin \Theta/\lambda)^2$ an empirical correction for Θ-dependent adsorption and thermal movement was obtained. Because of the adsorption, log I_o/I_c did not decrease linearly with $(\sin \Theta/\lambda)^2$. The refinement was repeated until the parameters used in the I_c-calculation differed less from the final parameters of the I_o-synthesis than the estimated standard deviation. The Fourier summations were made on the Hägg-Laurent machine [4].

As mentioned the unit cell of Mo_5SiB_2 was similar [2] to that of Cr_5B_3. Bertaut and Blum [2] found that the latter was bodycentered tetragonal ($a = 5.46$ Å, $c = 10.64$ Å) and contained four formula units. The spacegroup was D_{4h}^{18}—$I4/m\,c\,m$ with 16 Cr in 16 (l) ($x = 1/6$, $z = 0.15$) and 4 Cr in 4(c). From spatial considerations the B atoms were placed in 4(a) and 8(h) with $x = 0.375$. (The value of 0.125 given in the paper by Bertaut and Blum is probably due to a misprint.)

From the l.p. of Mo_5SiB_2 it was concluded that there were four formula units in the cell, that is 20 Mo, 4 Si and 8 B atoms. The systematic absences were consistent with the space group D_{4h}^{18}—$I\,4/m\,c\,m$. The preliminary electron density calculations confirmed this spacegroup and showed that 16 Mo atoms were situated in 16 (l) and 4 Mo atoms in 4 (c).

Starting from the parameters of Bertaut and Blum the atomic parameters of the Mo atoms were refined by carrying out successive $\varrho_o(x\,z)$ and ϱ_c $(x\,z)$ projections. (48 $h0l$ reflections were used.) The backshift corrections determined from the last synthesis were less than the standard deviations, computed with Cruickshank's formula [5].

The number of electrons found in the different maxima of the two final syntheses were counted in exactly the same way and a backshift correction

was applied to the scattering parameters obtained from the last $\varrho_o(x\,z)$ synthesis. The final atomic and scattering parameters are

	atomic par.	scattering par.
4 Mo_I in 4 (c)		42.0
16 Mo_{II} in 16 (l)	$x = 0.165_3 \pm 0.0008$	41.9
	$z = 0.138_8 \pm 0.0004$	
4 Si(?) in 4 (a)		14.0

As seen, the $\varrho(x\,z)$ projections strongly suggest that the four Si atoms of the unit cell are situated in the 4(a)-positions. In that case the 8 B atoms which are not revealed by the projection should be found in the 8 (h)-positions.

A three-dimensional F_o—F_c synthesis which was carried out in the $xy0$-section supports this hypothesis. The only significant maximum found in this section had a position corresponding to an atom in 8(h) with $x = 0.37_5$. Electron counts in the $xy0$-section gave the ratio 3.1/42 between the mentioned maximum and that of the Mo atom in origo.

It is difficult to appreciate the reliability of electron counts when atoms of widely different scattering powers are involved. The various formulæ given by Lipson and Cochran [6] suggest a standard deviation of somewhat less than 2 e per peak. The flat background of the final $\varrho(x\,z)$ and $D(xy0)$ syntheses (the background did not exceed 1/3 of the Si or B peakheight, respectively) makes this accuracy seem reasonable. Therefore, the result of the Fourier summations is taken as an evidence for an ordered distribution of the B and Si atoms in Mo_5SiB_2, the Si atoms mainly occupying the 4 (a)- and the B atoms the 8 (h)-positions.

DESCRIPTION OF THE STRUCTURE

Most of the transition metal atoms in the $T2$ phases are arranged in layers of the type shown in Fig. 1 a. Metal atom layers of this type have been called A-layers by Black [7] in his discussion of alloys of Al and transition elements. The simplest way to build up a structure of A-layers is to place successive layers exactly above each other. With this stacking of A-layers (A—A—A— . . .) there will be large cubic and smaller trigonal prismatic holes between the layers. A better packing of A-layers is obtained if every second layer is translated half the base diagonal of the unit cell. (Fulldrawn and dotted A-layers of Fig. 1 c alternate.) With this stacking (A—$A_{\frac{1}{2}\frac{1}{2}}$—$A$—$A_{\frac{1}{2}\frac{1}{2}}$— . . .) the layers fit better in each other and only one type of holes is found between the layers, namely cubic antiprismatic holes.

While the A-layer skeleton in the Al-transition metal alloys [7] consists of Al atoms, it is the transition metal atoms that form layers of this type in the structures of some borides and silicides. In Mo_5SiB_2 the sequence of A-layers (consisting of Mo atoms) is A—A—$A_{\frac{1}{2}\frac{1}{2}}$—$A_{\frac{1}{2}\frac{1}{2}}$— . . . (Two fulldrawn and two dotted layers of Fig. 1 c alternate.) Thus, there are holes of all the three mentioned types: cubic, antiprismatic and trigonal prismatic, filled by Mo, Si and B atoms respectively. The Mo atoms in the cubic holes and the B atoms are in contact and form what can be called subsidiary layers in $z = 0$ and $z = \frac{1}{2}$ (Fig. 1b). The Si atoms are situated between Mo atoms of successive subsidiary layers.

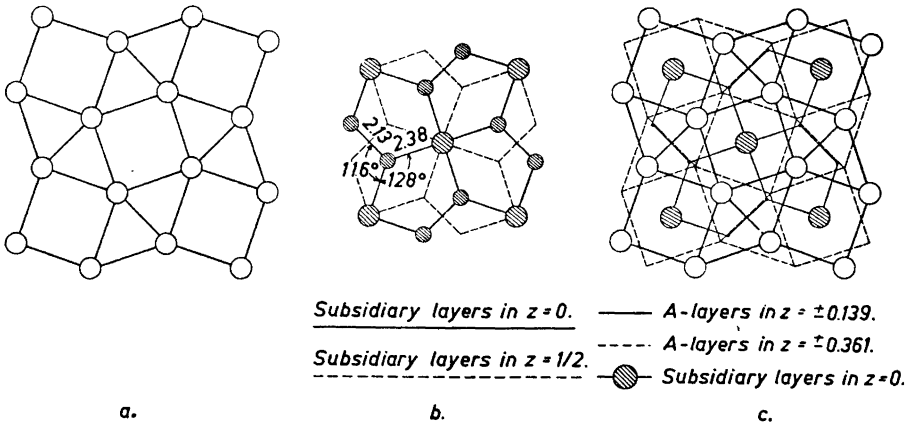

Fig. 1. a) *A*-type layer: b) Subsidiary layers of Mo and B atoms in $z = 0, \frac{1}{2}$; c) The Mo_5SiB_2-structure, projected along the *c*-axis.

As pointed out in Refs. [1,2], the atomic environments in Mo_5SiB_2 are similar to those found in related phases. The ninefold coordination around the B atoms (6 neighbours situated at the corners of a trigonal prism and 3 outside the square faces of this prism) has been found in a number of borides [8]. The ninth neighbour is a B atom at a distance of 2.13 Å. This points to a weak interaction but is another manifestation of the tendency towards B—B bonding revealed in a number of boride structures [8]. The Mo—B—Mo angle in the subsidiary layers is the same as the B—B—B angle in the boron chains of MoB (128°). The antiprismatic environment of the Si atoms (with two additional remote contacts outside the square faces of the prism) has earlier been found in the silicides of the $CuAl_2$- and W_5Si_3-types.

Table 1. Interatomic distances in Å (Estimated accuracy ±0.03 Å)

	In Mo_5SiB_2	In Mo_2B	In Mo_5Si_3*
B	— 2 Mo_I 2.38 (2)	B — 8 Mo 2.37 (8)	
	— 6 Mo_{II} 2.34 (4) 2.36 (2)	— 2 B 2.37 (2)	
	— 1 B 2.13		
Si	— 2 Mo_I 2.77 (2)		Si — 2 Si 2.45 (2)
	— 8 Mo_{II} 2.56 (8)		— 8 Mo 2.56 (8)
Mo_I	— 4 B 2.38 (4)		
	— 2 Si 2.77 (2)		
	— 8 Mo_{II} 2.72 (8)		
Mo_{II}	— 2 B 2.34, 2.36		
	— 2 Si 2.56 (2)		
	— 2 Mo_I 2.72 (2)		
	— 9 Mo_{II} 2.82, 2.85, 3.07, 3.17 (2), 3.18 (4)		

* The l.p. given in Ref.[11] have been used. Less accurate l.p. of Mo_5Si_3 have earlier been reported by this author. A redetermination has confirmed the values of Dauben, Templeton and Myers [11] within 0.05 %.

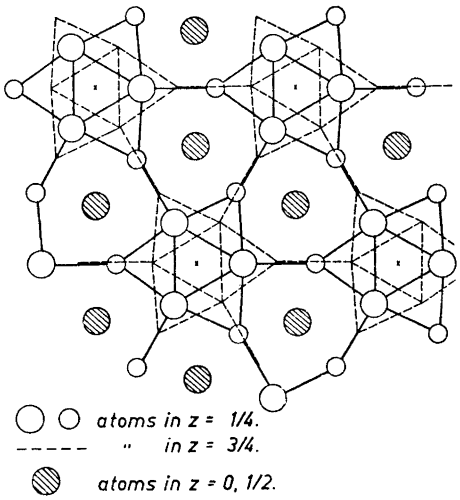

Fig. 2. The $D8_a$-structure. The position of the octahedral holes are marked with **x**.

Table 1 shows that an ordered distribution of the Si and B atoms gives Mo—B and Mo—Si distances that agree much better with those observed in Mo_2B [9] and Mo_5Si_3 [10, 11] than a disordered one. The Mo—Si distances especially would be abnormally short in a disordered structure. The fact that the atomic Si/B ratio in Mo_5SiB_2 does not exceed 0.5 probably indicates that the Si atoms can not occupy the positions giving such short distances.

DISCUSSION

As evident from the preceding paragraph the structural details of Mo_5SiB_2 are in accordance with the crystal chemical principles which have emerged from earlier studies on metal rich compounds between the transition metals and small nonmetals.

It seems as if the size factor is quite important in determining the structures in which these compounds crystallize. Hägg [12] has shown that a large number of borides, carbides, nitrides and hydrides can be classified from spatial considerations. When $r_X/r_{Me} < 0.59$ (X = nonmetal, Me = transition metal) the nonmetals are conveniently accommodated in the holes (tetrahedral, octahedral or trigonal prismatic) of simple metal lattices. When the radius ratio exceeds 0.59 these simple structures do not permit a good packing of the atoms and other structures are formed where the transition metal atoms are arranged so as to give the nonmetals larger "holes" to occupy.

The trigonal prismatic and cubic antiprismatic holes found in metal skeletons built up from *A*-type metal layers, would be suitably sized for nonmetals with r_X/r_{Me} in the range 0.65—0.85. Thus, it is not surprising that metal lattices of this type have been found among borides and silicides, *e.g.* in the

$T2$ structure. The occurrence of these structures may to a considerable extent depend on the fact that they permit a good packing of atoms with radius ratio in the above mentioned range. As pointed out by Nowotny *et al.*[1] the known $T2$ phases (Ta_5Ge_3[13], Ta_5Si_3[3], Nb_5Si_3[3], $W_5(Si, B)_3$[1], Mo_5SiB_2,[1] Cr_5B_3[2]) do indicate that the radius ratio is important for the stability of this structure. The ordered distribution of the Si and B atoms in Mo_5SiB_2 means that the B atoms occupy the smaller and the Si atoms the large holes in the Mo lattice and this also points to an influence from the size factor.

From the spatial discussion of the interstitial phases we would expect the holes in an A-type metal skeleton to be too large for carbon and nitrogen atoms (X'atoms) — especially with metal atoms from the IVa—VIa groups. Consequently we would not expect to find ternary (MeSiX') phases of the $T2$ type but rather that such phases had structures in which the Me—Si skeleton should contain octahedral holes where the X' atoms could be accommodated and thus obtain the same environment as in the wellknown stable carbides and nitrides of MeX' ($B1$ type) and Me_2X' types. (Boron and oxygen may also behave as X' elements in special cases.)

A number of ternary (MeSiX') phases have been found [14–17] for the IVa—VI a groups metals. All these phases have the composition $Me_5Si_3(X')$ and crystallize in the $D8_8$-structure [18]. They often contain quite small amounts of the X' element. It has been hinted [14, 15] that the small atoms might function interstitially but no comprehensive discussion of this possibility seems to have appeared. I think that the "stabilization" of the $D8_8$-silicides by X' atoms to some extent depends on the filling up of the octahedral holes in the $D8_8$ structure [18]. This would account for the increasing l.p. of Zr_5Si_3 (C) and Nb_5Si_3 (C) [14] with increasing carbon content and it would give some explanation to the fact that the $D8_8$-silicides have a much greater ability to dissolve X' atoms than have silicides with other structures.

It seems reasonable to assume that the interstitial solubility of X' atoms in the $D8_8$-silicides is most important for the group IV a metals and that the carbon-silicon substitution as found by Nowotny *et al.* in Mo_5Si_3 (C) will be of increasing importance with increasing group number of the metal.

The size factor has evidently a considerable influence on the occurrence of the structures mentioned in this paper and discussion from size considerations may still be of some value for the description and classification of the compounds formed by the transition metals and the small nonmetals.

Acknowledgements. I wish to thank professor Hägg for his kind interest in this work and *Statens tekniska forskningsråd* for financial support. Thanks are also due to Mr Rundqvist for many valuable discussions and Dr Lilly Gustafsson for analytical assistance.

REFERENCES

1. Nowotny, H., Dimakopoulou, E. and Kudielka, H. *Monatsh.* **88** (1957) 180.
2. Bertaut, F. and Blum, P. *Compt. rend.* **236** (1953) 1055.
3. Parthé, E., Lux, B., and Nowotny, H. *Monatsh.* **86** (1955) 859.
4. Hägg, G. and Laurent, T. *J. Sci. Instr.* **23** (1946) 155.
5. Cruickshank, D. W. J. *Acta Cryst.* **2** (1949) 65.
6. Lipson, H. and Cochran, W. *The Determination of Crystal Structures*, London 1953.

7. Black, P. J. *Acta Met.* **4** (1956) 172.
8. Kiessling, R. *Acta Chem. Scand.* **4** (1950) 209.
9. Kiessling, R. *Ibid.* **1** (1947) 893.
10. Aronsson, B. *Ibid.* **9** (1955) 1107.
11. Dauben, C. H., Templeton, D. H. and Myers, C. E. *J. Phys. Chem.* **60** (1956) 443.
12. Hägg, G. *Z. physik. Chem. B* **12** (1931) 33.
13. Nowotny, H., Searcy, A. W. and Orr, J. E. *J. Phys. Chem.* **60** (1956) 677.
14. Nowotny, H., Lux, B. and Kudielka, H. *Monatsh.* **87** (1956) 447.
15. Brewer, L. and Krikorian, O. *UCRL* — 2544 (1954).
16. Knapton, A. G. *Nature* **175** (1955) 730.
17. Nowotny, H., Parthé, E., Kieffer, R. and Benesovsky, F. *Monatsh.* **85** (1954) 255.
18. Åmark, K., Borén, B. and Westgren, A. *Metallwirtschaft* **15** (1936) 835.

Received September 20, 1957.

ACTA CHEMICA SCANDINAVICA 12 (1958) 38—43

Quantitative Micro-Determination of Proteins and Peptides

HERMAN NIELSEN

Dr. med.h.c. Herman Nielsen's Laboratory, Aabyhøj, Denmark

The spectrophotometric measurement of the colour, produced by the biuret reaction of proteins and peptides, can be replaced by measurement of the colour, produced by the copper salt of diethyldithiocarbamic acid. In this way microgram of proteins and peptides can be determined with the same accuracy as milligram by Kjeldahl. The method is easy and rapid and suitable for hospital laboratories.

The proteins and peptides in biological fluids are continuously built up and broken down, and they never maintain the same pattern. Nevertheless, their quantitative estimation is of practical importance. We have to resort to indirect analyses, and by determination of the amount of nitrogen some idea of the quantity of proteins or peptides can be obtained when other nitrogen-containing sources are removed beforehand. Native proteins can be precipitated by trichloroacetic acid or sulfosalicylic acid. Amino-acids can be removed from polypeptides by dialysis. For more than half a century the Kjeldahl method has been and still is the classical procedure for determination of proteins by multiplying the nitrogen found by an empirical factor, most often 6.25. That does not tell us anything about the structural distribution of the nitrogen atoms in the protein molecules. As the number of N in one amino-acid may be different from those of another and because of the inconstant distribution of the individual amino-acids in proteins and peptides it is impossible to calculate the number of amino-acids from the number of N-atoms, found by the Kjeldahl analysis.

Other difficulties arise when small amounts of proteins have to be examined, *e.g.* in the cerebrospinal fluid (CSF) where often less than 10 mg/100 ml has to be measured. A reliable micro-Kjeldahl analysis cannot be performed as routine in the clinical laboratories unless many precautions are taken. That is why the analytical accuracy is often replaced by some easy but very inexact method.

The extensive literature about the Kjeldahl method and its numerous modifications shows us the difficulties, and it is the scope of the present publication to find a way out of the uncertainty and try to obtain some more accurate results and propose a new method which is easy to perform and suitable for application in the clinical laboratories of the hospitals.

THE BIURET REACTION AND ITS MODIFICATION

This new method is based upon the biuret reaction in which a red-violet colour appears when a cupric salt is mixed with substances containing more than one —$CONH_2$ or —CONH—radical in their molecules. Consequently, the reaction is also given by proteins and peptides.

We are dealing here with the formation of a copper complex, established by chelation and ring closure with the metallic ion. The development of the chemistry of complex formation and the importance of ligands as donors of a lone pair of electrons for coordinative bonds is thoroughly explained in two excellent monographs by American authors [1, 2] that may be consulted for proper understanding of the structural explication to follow. Schwarzenbach [3, 4] has described the practical utilization of this knowledge for many purposes.

Fig. 1 shows a schematic structural design of the biuret reaction and the way in which peptide chains combine with cupric ions by chelation to form a multinuclear complex. The figure represents the glycyl backbone of the molecular structure of a protein, and it shows how four nitrogen atoms from the peptide bonds, —CONH—, can establish four coordinative bonds to the cupric ion. R represents the non-glycyl moiety of the individual amino-acids. All the nitrogen atoms in R are too far away from the metallic ion to produce an electrostatic field. The size of the cupric ion is small enough to be wedged between four glycyl-N, and a strong electrostatic field is established hereby stabilizing the compound.

In a strong alkaline solution uncoiling of peptide chains is effected in such a way that two peptide chains with four nitrogen atoms can be placed in coplanar position. An electronic explanation is put forward by Rây and Sen [5] and cited in the monograph by Martell and Calvin [1]. It is evident that there exists a correlation of colour and bond type, and when $3d^9$ in the lower orbit is the unpaired electron a blue colour is produced, but when $4p^5$ is occupied a red-violet colour prevails. The 4 nitrogen ligands with their 8 electrons approximate the electron configuration of Cu to that of Kr (36). They give a purely covalent coordination and 2 five-rings are established when 4 peptide bonds take part in the formation of the complex. In this way a great stability is obtained. In glycine and glycylglycine the ionic bond from Cu^{++} to the carboxyl group produces a salt-like compound with blue colour because the $4p$-orbit is not occupied.

Cox, Wardlaw and Webster [6] have pointed out that the 4 nitrogen atoms from the ligands must be coplanar with the copper ion and have proved it by X-ray analysis. The continuity of the peptide chain is not broken by the chelation and a multinuclear complex is formed. The length of the chain decides the numbers of copper ions.

From these stoichiometric considerations it appears that the ratio $4N/Cu^{++}$ or $4(—CONH—)/Cu^{++}$ can be calculated from the amount of complexed copper. The picture of a vertebral column of glycyl radicals with R representing the ribs, attached to the backbone, and the row of cupric ions, placed as a *medulla spinalis*, gives us an idea of the structural edification of the biuret compound.

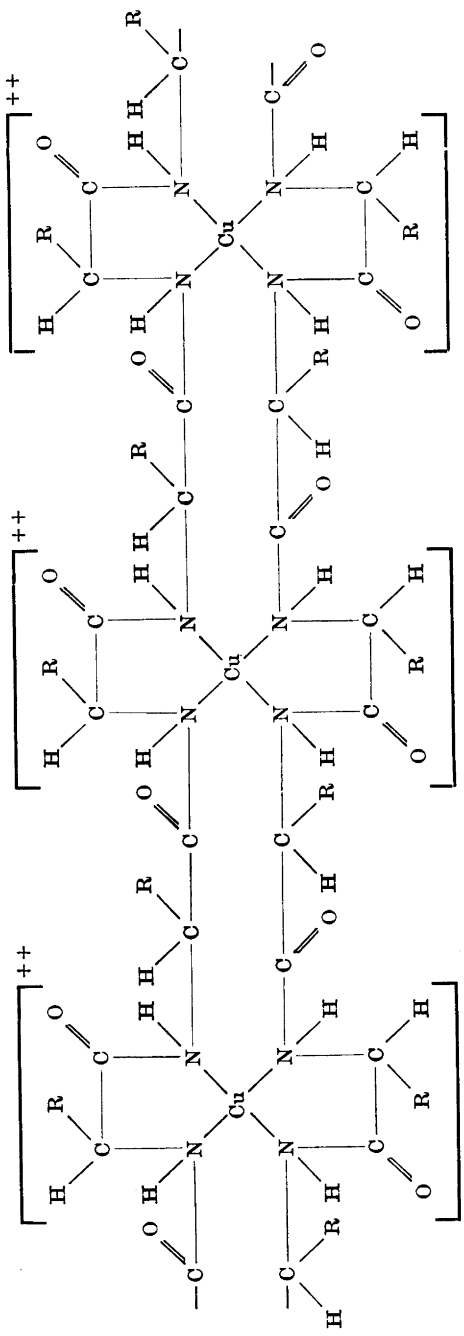

Fig. 1

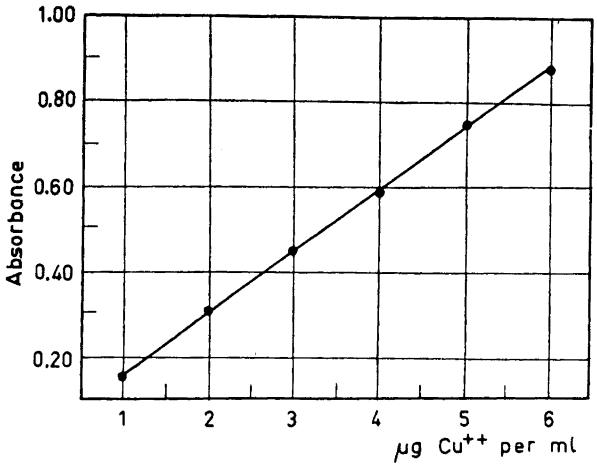

Fig. 2.

The colour of the biuret reaction compound is too faint for quantitative determination of small differences by measurement of the extinction. Moreover, there is another inconvenience which is often overlooked. A small part of the precipitated cupric hydroxide is dissolved in the strong alkaline solution of NaOH and imparts to the solution a bluish tint which moves the maximum of spectrophotometric absorbancy to lower wave-length.

PROCEDURE

Reagents. Trichloroacetic acid, 10 % aqueous sol.
Trisodiumphosphate (Na_3PO_4,$12H_2O$), 5 % aqueous sol.
Cupric sulphate ($CuSO_4$,$5H_2O$), 4 % aqueous sol.
Sodium diethyldithiocarbamate, solid. (DDTC).

Equipment. Conical centrifuge tubes
Sintered glass disc filters (3G5, Jena)
Spectrophotometer, Beckman B.

Procedure for plasma and serum. Dilute 1 ml of the sample with 49 ml of normal saline sol. Mix 1 ml of the diluted sample with at least 2 ml of the trichloroacetic reagent in a conical centrifuge tube. After centrifugation for 10 min at 3 000 r.p.m. the supernatant fluid is discarded and drained off the inside of the tube. Dissolve the precipitate in 5 ml of the phosphate reagent and add 1 drop of the copper reagent. Place the tube in a mechanical device for gentle shaking for 30 min. The excess of copper is precipitated as cupric phosphate and brought down by centrifugation for 10 min. The supernatant fluid is poured upon a sintered glass filter and by suction the complexed copper compound is collected. Mix 1 ml of the filtrate with 5 ml of the phosphate reagent and add a few crystals of DDTC. The yellow colour is fully developed in 15 min and the extinction is measured in the Beckman B against the phosphate reagent at 440 mμ.

Fig. 2 shows the absorbancy, plotted against the amount of copper, as a linear function from 1 to 6 μg of Cu++. Taking account of the dilution, here 1 500 times, and by introduction of an experimental factor of 9.80 for the ratio protein/Cu++ the percentage of protein is found directly. For instance, an extinction of 0.72 corresponds to 4.87 μg of Cu++ and 7.15 % of protein ($4.87 \times 1\,500 \times 9.80$).

Procedure for CSF. 1 ml of CSF is mixed with 1 ml of the trichloroacetic reagent in a centrifuge tube and treated as above. The filtrate from the sintered glass filter is diluted 1:1 with the phosphate reagent. Now the dilution is only 10 times, and by multiplication by the factor 9.80 the content of protein is found directly in mg/100 ml.

Since a reagent blank, carefully performed, never shows a transmission less than 98 % it can be replaced by the phosphate reagent. Cleaning of the sintered glass filters must be made by suction through the filters in the inverted position, first with 0.85 % NaCl, next with 2 N HCl and finally twice with water.

DISCUSSION

In order to separate the native proteins from peptides which also form copper complexes, we have preferred the use of trichloroacetic acid instead of sulphosalicylic acid. The latter has the inconvenience that the precipitate may adhere to the inside of the tubes. Stiff [7] has introduced cupric phosphate for reaction with the protein, but we consider cupric sulphate to be more suitable, for the reactivity of cupric ions with protein proceeds easier and more completely when the precipitation of cupric phosphate occurs at the same time. Mehl, Pacowska and Winzler [8] have found it feasible to calculate the amount of protein, bound by 1 g of copper atom in the complex. The most consistent investigations are perhaps made by Plekhan [9] who has tried to depict the structural relationship between copper and proteins. Beauchene *et al.*[10] determine the copper by flame photometry. Recently Kingsley and Getchell [11] have developed a method for quantitative estimation of small amounts of proteins in serum and in CSF by use of tetrabromophenolphthalein ethylester which in form of the blue potassium salt is absorbed to protein. They find, however, a marked difference in the binding capacity of the dye by proteins in CSF and by those of serum. With the present copper chelation method no such dissimilarity of the proteins exists.

THE ACCURACY OF THE METHOD

As already mentioned not only the native proteins but also polypeptides and oligopeptides down to tripeptides can be measured by this copper test, and the accuracy of the method can be demonstrated by the following example.

Glycylglycylglycine (GGG) was examined *. The sample was accompanied by the statement that the GGG had $2H_2O$, but had lost part of the water. 4 mg is calculated to contain 0.746 mg of N, but 0.773 mg was found. In my laboratory we determined the water content by the Karl Fischer method, according to the procedures described in detail in the monograph by Mitchell and Smith [12]. We used a micro-method where an end-point-stop device, equipped with a double triode and a magic eye as indicator, permits exact measurement. We have also examined the GGG sample by the copper chelation method and found complete accordance.

Found by	Kjeldahl	0.193	mg	of	N	per	mg	of	GGG
»	» Karl Fischer	0.194	»	»	»	»	»	»	»
»	» Cu-Chelation	0.194	»	»	»	»	»	»	»

* The author wishes to thank Professor K. Linderström-Lang and the Carlsberg Laboratories for generously providing the peptides, used in this study.

The amount of N in the water analysis is computed as follows. There is

0.222 mg of N in 1 mg of GGG, (mol.-weight 189)
0.186 » » » » 1 » » » $2H_2O$ (mol.-weight 225)

We soon found that the copper chelation method yields more accurate results than the Kjeldahl procedure when we made both kind of tests as a routine *in duplo*. Yet, by painstaking performance of the Kjeldahl analyses the deviations are in mg almost the same as are in μg those of the copper chelation method.

REFERENCES

1. Martell, A. E. and Calvin, M. *Chemistry of the Metal Chelate Compounds.* Prentice-Hall. Inc., New York 1952.
2. Bailar, J. C. jr. (Ed.). *The Chemistry of the Coordination Compounds.* Reinhold, New York 1956.
3. Schwarzenbach, G. *Analyst.* **80** (1955) 713.
4. Schwarzenbach, G. *Die Komplexometrische Titration.* Ferdinand Enke, Stuttgart 1955.
5. Rây, P. and Sen, D. N. *J. Indian Chem. Soc.* **25** (1948) 473.
6. Cox, E. G., Wardlaw, W. and Webster, K. C. *J. Chem. Soc.* **1935** 1475.
7. Stiff, H. *J. Biol. Chem.* **177** (1949) 1798.
8. Mehl, J. W., Pacowska, E. and Winzler, R. J. *J. Biol. Chem.* **177** (1949) 13.
9. Plekhan, M. I. *J. gen. Chem.* (in Russian). **21** (1952) 347, 635; **22** (1952) 1633; **23** (1953) 512.
10. Beauchene, R. E. et al. *J. Biol. Chem.* **214** (1955) 731.
11. Kingsley, G. R. and Getchell, G. *J. Biol. Chem.* **225** (1956) 545.
12. Mitchell, J. jr. and Smith, D. M. *Aquametry.* Interscience, New York 1948.

Received August 15, 1957.

ACTA CHEMICA SCANDINAVICA 12 (1958) 44—51

Structure of a Solvate of Barium Pentathionate with Acetone

OLAV FOSS and OLAV TJOMSLAND

Chemical Institute, University of Bergen, Bergen, Norway

The solvate, $BaS(S_2O_3)_2 \cdot (CH_3)_2CO \cdot H_2O$, is monoclinic with $a = 5.04$ Å, $b = 10.47$ Å, $c = 13.61$ Å, $\beta = 104°$, space group $C_{2h}^2 - P2_1/m$ and $Z = 2$. Fourier projections along the a and b axes show that the crystals are built up of layers which have the same internal structure as in the dimorphs of barium pentathionate dihydrate, but for the substitution of a water molecule by an acetone molecule.

The barium ion, the middle sulphur atom of the chain, and the water and acetone molecule lie in a crystallographic mirror plane. The values obtained for sulphur-sulphur bond lengths and angles agree within the experimental errors with those found in the dihydrates. The mean values in the three salts are: $S_1-S_2 = S_4-S_5 = 2.12 \pm 0.02$ Å, $S_2-S_3 = S_3-S_4 = 2.04 \pm 0.02$ Å, $\angle S_1-S_2-S_3 = \angle S_3-S_4-S_5 = 105 \pm 1.5°$, $\angle S_2-S_3-S_4 = 106 \pm 2°$, and the dihedral angles, $S_1S_2S_3/S_2S_3S_4 = S_2S_3S_4/S_3S_4S_5 = 108 \pm 1.5°$.

The data indicate that the outermost sulphur-sulphur bonds in the pentathionate ion are single bonds, while the middle bonds possess some double-bond character.

It was shown recently [1] that barium pentathionate, selenopentathionate and telluropentathionate when crystallized from aqueous acetone or tetrahydrofuran, occur as solvates containing one mole of water and one mole of the organic solvent per mole of salt. The crystals of the solvates are isomorphous. The solvate of barium pentathionate with acetone has now been studied by two-dimensional Fourier methods, and the pentathionate ion found to have the same configuration and dimensions as in the orthorhombic [2] and triclinic [3] dimorphs of the dihydrate.

CRYSTAL DATA

The crystals of $BaS(S_2O_3)_2 \cdot (CH_3)_2CO \cdot H_2O$ were obtained as thin, rhomb-shaped plates {001}, bounded by {110}. There is perfect cleavage along (001) and a rather pronounced tendency of twinning on the same plane. The crystals are monoclinic, with the unit cell dimensions [1]: $a = 5.04$ Å, $b = 10.47$ Å, $c = 13.61$ Å (± 0.5 %), $\beta = 104°$. There are two formula units per unit cell;

density, calc. 2.24, found 2.25 g/cm³. The only systematic absences are in the $0k0$ reflections when k is odd. Of the two monoclinic space groups compatible with these absences, the centrosymmetric one, C_{2h}^2—$P2_1/m$, was assumed to be the correct one, and this choise seems justified through the outcome of the structure analysis.

The intensities of the $0kl$ and $h0l$ reflections were estimated visually from Weissenberg photographs taken with CuK radiation. The crystals used had cross-sections of 0.09×0.06 mm and 0.11×0.07 mm, respectively, in the case of the a and b axis photographs. They were transparent and apparently unchanged after the exposures. Some difficulties were experienced in finding untwinned crystals, and in cutting the crystals because of the ready cleavage, but relatively good intensity photographs were at last obtained. A double-film, multiple-exposure technique was used; the a axis photographs, except for the strongest-exposure ones, were taken on a Nonius integrating Weissenberg camera. 158 out of 186 $0kl$ reflections and 152 out of 171 $h0l$ reflections attainable with CuK_α radiation were observed. The intensities were corrected for the Lorentz and polarization factors, but not for absorption; with $\mu = 311$ cm^{-1} for CuK_α radiation the absorption may introduce a serious error. The F_o^2 and F_o summations were made with Beevers-Lipson strips, at 6° intervals along the b and c axes and at 12° intervals along the a axis.

ANALYSIS OF THE STRUCTURE

The space group, $P2_1/m$, has fourfold general positions, and symmetry centres and mirror planes as special, twofold positions. With two formula units per unit cell, the middle sulphur atom of the pentathionate ion, the water molecule and the acetone molecule lie in mirror planes, as does also the barium ion.

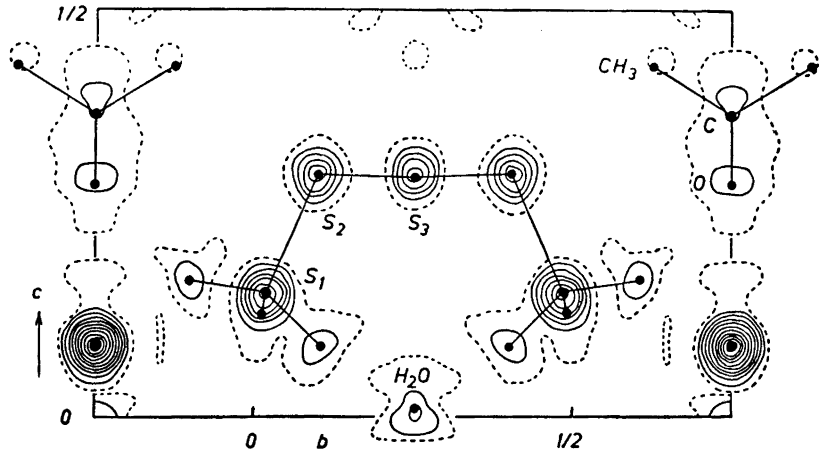

Fig. 1. Electron density projection of the acetone solvate along the a axis. The 3-electron line is dashed. Contour intervals: 10 e · Å^{-2} for the barium ion, 5 e · Å^{-2} for sulphur and oxygen atoms, and 2 e · Å^{-2} for carbon atoms.

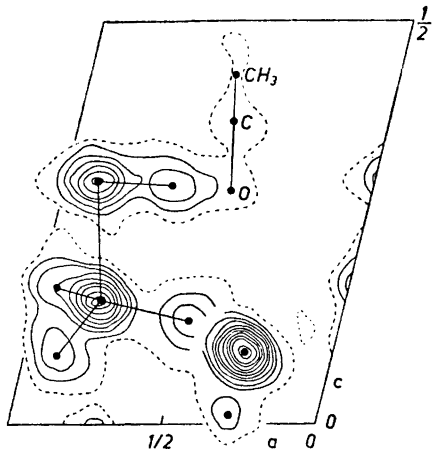

Fig. 2. Electron density projection along the *b* axis. The 5-electron line is dashed, and contours are at intervals of 8 e · Å^{-2} for the barium ion, otherwise as in Fig. 1.

The y and z coordinates of the barium ion and the three sulphur atoms of the asymmetric unit were first derived from a F_o^2 synthesis of the $0kl$ data. They differed on the average only 0.003 (maximum 0.006) from the final values. A F_o synthesis of about 60 of the largest $0kl$ terms, with signs based on the barium and sulphur contributions, gave approximate coordinates of the lighter atoms and permitted successive F_o refinements to be carried out. The *b*-axis projection was solved and refined by F_o^2 and F_o syntheses in the same way.

The $0kl$ and $h0l$ electron density maps are reproduced in Figs. 1 and 2, and the atomic coordinates are listed in Table 1. In the Table, x, y and z are in fractions of monoclinic cell edges, and x', y' and z' are orthogonal coordinates in Å referring to the same origin and to the a, b and c' axes, where c' is normal to a and b. The z coordinates from the two projections were the same for the barium ion and differed on the average 0.025 Å for the sulphur and for the oxygen atoms; the values of Table 1 are means of the two, weighted according to their apparent reliability.

The reliability index, $R = \Sigma||F_o|-|F_c||/\Sigma|F_o|$, with reflections not observed included when $|F_c|$ exceeds the observable limit, is 0.15 for the $0kl$ reflect-

Table 1. Atomic coordinates. Origin at a centre of symmetry.

	x	y	z	x'	y'	z'
Ba	0.711	0.250	−0.088	3.87	2.62	−1.16
S_1	0.798	0.015	0.153	3.52	0.16	2.02
S_2	0.903	0.097	0.299	3.57	1.02	3.95
S_3	0.655	0.250	0.294	2.33	2.62	3.88
O_1	0.495	0.010	0.127	2.08	0.10	1.68
O_2	0.953	−0.105	0.169	4.25	−1.10	2.23
O_3	0.897	0.102	0.085	4.24	1.07	1.12
H_2O	0.292	0.250	0.010	1.44	2.62	0.13
O_c	0.459	0.250	−0.285	3.67	2.62	−3.77
C_1	0.510	0.250	−0.372	3.69	2.62	−4.91
C_2	0.539	0.125	−0.430	3.74	1.31	−5.68

ions and 0.21 for the *h0l* reflections. A list of calculated and observed structure factors is available from the authors on request. The calculated values were based on the Thomas-Fermi atomic scattering curve for xenon in the case of the barium ion, and on the Hartree curves for sulphur, oxygen and carbon. The hydrogen contributions were ignored. In the temperature factor exp $[-B(\sin^2\Theta/\lambda^2)]$ finally chosen B was 2.0 Å^2 and 4.0 Å^2, respectively, for the $0kl$ and $h0l$ reflections, except for the carbon atoms where the values, 4.0 Å^2 and 5.0 Å^2, respectively, were found to give better agreement.

DESCRIPTION OF THE STRUCTURE

The structure is built up of layers parallel to the *c* plane. The layers have the same internal structure as in the orthorhombic [2] and triclinic [3] dihydrates, but for the substitution of a water molecule by an acetone molecule. The orthogonal coordinates of Table 1, included to allow a comparison with the corresponding coordinates for the dihydrate structures [3], show close correspondence with the latter. Apart from the presence of the acetone molecule, the structures differ only in the way the layers are arranged relative to each other, as discussed earlier [1].

The pentathionate ion has mirror plane symmetry, required by the space group. The dimensions of the sulphur chain, from the coordinates of Table 1, are listed in Table 2. The standard deviations of the bond lengths and angles are probably not less than 0.04 Å and 3°, respectively. Primes are used to denote the equivalent of an atom across the mirror plane.

Table 2. Sulphur-sulphur bond lengths and angles.

S_1-S_2	= 2.11 Å	$\angle S_1-S_2-S_3$	= 106°
S_2-S_3	= 2.02	$\angle S_2-S_3-S_2'$	= 105°

$S_1S_2S_3/S_2S_3S_2'$ (dihedral angle) = 108°

The non-bonded distances within the chain are $S_1—S_3$ = 3.31 Å, $S_2—S_2'$ = 3.20 Å, $S_1—S_2'$ = 4.49 Å, $S_1—S_1'$ = 4.92 Å. The sulphur-oxygen bond lengths are $S_1—O_1$ = 1.48 Å, $S_1—O_2$ = 1.47 Å, $S_1—O_3$ = 1.47 Å, and the angles, $\angle O_1—S_1—O_2$ = 119°, $\angle O_1—S_1—O_3$ = 111°, $\angle O_2—S_1—O_3$ = 112°.

Within the experimental errors the above dimensions are the same as in the dihydrates. Also, the barium-oxygen coordination is the same, the barium ion being surrounded by nine oxygen atoms at an average distance of 2.78 Å. Six are sulphonate oxygen atoms and two are water oxygen atoms as in the dihydrates, and one is the oxygen atom of an acetone molecule. The water molecule is coordinated to two barium ions, at distances of 2.76 Å and 2.91 Å and an angle of 126°, and forms hydrogen bonds to the sulphonate oxygen atoms O_1 and O_1', at distances of 3.02 Å and an angle of 113°. This water molecule is firmly held in the lattice; it is the other water molecule of the dihydrates which in the solvate is replaced by acetone.

The carbon peaks in the electron density maps are low and diffuse, and the coordinates of these atoms are approximate only. Inclusion of the carbon

contributions with half their weight in the calculated structure factors, with the same temperature factors as for the other atoms, gave about the same R index as when they were included with full weight and the larger temperature corrections. From the coordinates of Table 1 the closest approach between methyl carbon atoms of different acetone molecules, across symmetry centres at $z = \frac{1}{2}$ and $-\frac{1}{2}$, is 3.3 Å, which is rather short. As indicated earlier [1], there appears to be a possibility that the acetone content of the solvates is non-stoechiometric, in the sense that some of the acetone positions are, statistically, occupied by water. This might leave better space for the methyl groups. On the other hand, the large c spacing, *i.e.*, layer thickness, namely 13.21 Å as compared with 10.78 Å and 10.89 Å in the dihydrates [2, 3], is caused by the acetone molecules, and complete substitution of acetone by water would lead to collapse of the structure. The layers are held together through methyl-methyl contacts, the closest methyl-sulphur approach across a layer interface being 4.1 Å, which exceeds the sum of the van der Waals radii. Sulphur-sulphur contacts across the interface, which are 3.5—3.8 Å in the dihydrates [2, 3] and there hold the layers together, do not occur in the solvate, the shortest such distance being 5.3 Å.

THE NATURE OF BONDING IN THE SULPHUR CHAIN OF THE PENTATHIONATE ION

The objective of the structure determinations of the dimorphs of barium pentathionate dihydrate and of the solvate with acetone, has been more to establish the structure of the pentathionate ion than to obtain accurate dimensional data. However, each distance and angle has in the three structures been determined independently four times, once in each half of the ion in the triclinic dihydrate and once in each of the two other structures where mirror plane symmetry is crystallographically required. Taking the standard deviation of the individual measurements as 0.04 Å for S—S bond lengths and 3° for S—S—S bond angles, the standard deviation of the arithmetical mean of the four values should be 0.02 Å for bond lengths and 1.5° for angles *. The individual and mean values are listed in Table 3, and a drawing of the pentathionate ion, with the mean bond lengths and angles indicated, is shown in Fig. 3.

Table 3. Dimensions of the sulphur chain of the pentathionate ion in barium salts.

Bond or angle	Orthorhombic dihydrate	Triclinic dihydrate	Acetone solvate	Mean value
S_1-S_2	2.14 Å	2.13, 2.11 Å	2.11 Å	2.12 Å
S_2-S_3	2.04 Å	2.04, 2.04 Å	2.02 Å	2.04 Å
$\angle S_1-S_2-S_3$	103°	106, 105°	106°	105°
$\angle S_2-S_3-S_4$	106°	107°	105°	106°
$S_1S_2S_3/S_2S_3S_4$ (dihedral angle)	110°	108, 107°	108°	108°

* The $S_2—S_3—S_4$ angle occurs only once also in the triclinic dihydrate, and the mean value of this angle should thus have a standard deviation of 2°.

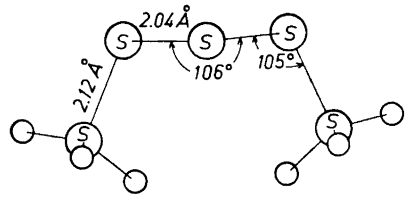

Fig. 3. The pentathionate ion as it occurs in the barium salts.

The difference, Δ, between the outermost S—S bonds, 2.12 Å, of the pentathionate ion, and the middle bonds, 2.04 Å, both with e.s.d. $\sigma = 0.02$ Å, gives $\Delta/\sqrt{2}\sigma = 2.8$ and should thus be significant. Variations in bond lengths along sulphur chains have been reported also for cesium hexasulphide [4], barium tetrasulphide monohydrate [5], barium tetrathionate dihydrate [6], and dimethanesulphonyl disulphide [7].

The middle S—S bonds in the pentathionate ion are between divalent sulphur atoms, and correspond formally to the S—S bonds of trisulphides, X—S—S—S—X. Data are available for dimethyl trisulphide [8] (S—S = 2.05±0.02 Å), *bis*(trifluoromethyl) trisulphide [9] (2.065±0.016 Å) and 2,2′-diiododiethyl trisulphide [10, 11] (2.05±0.04 Å). In disulphides, X—S—S—X, the S—S bond length is 2.05±0.02 Å in hydrogen disulphide [12], 2.04±0.03 Å in dimethyl disulphide [12], 2.053±0.019 Å in *bis*(trifluoromethyl) disulphide [9], 2.04±0.005 Å in N,N′-diglycyl-L-cystine dihydrate [13], and 2.04±0.02 Å and 2.04±0.01 Å, respectively, in the monohydrates of formamidinium disulphide diiodide [14] and dibromide [15]. The weighted mean of these nine values, if they are assumed to be equal, is 2.045 Å, as compared with 2.04 Å for the short bonds in pentathionate. In orthorhombic sulphur [16], the S—S bonds are 2.037 ±0.005 Å.

The outermost S—S bonds in pentathionate are between a divalent sulphur atom and a sulphonate sulphur atom. Bonds of this type are 2.13±0.04 Å in barium selenopentathionate dihydrate [17], 2.12±0.03 Å in ammonium telluropentathionate [18], 2.10±0.02 Å in monoclinic barium telluropentathionate dihydrate [19], and 2.12±0.03 Å in barium tetrathionate dihydrate [6]. The weighted mean is 2.115 Å, again not significantly different from the length of the corresponding bond in pentathionate.

A -S—SO_3 bond should be expected to be close to a single bond, or possibly a little shorter if some of the *pd* π-bond character of the S—S bond in the thiosulphate ion [20] is retained when two such ions combine with divalent sulphur to give pentathionate. There does not appear to be any reason for the bond to be longer than a single bond. The S—S single-bond length is somewhat uncertain; the Pauling value [21] is 2.08 Å, and Abrahams first [4] proposed 2.11 Å and later [5, 22] 2.08 Å. A S—S double-bond length of [4, 21, 22] 1.89 Å, as in the S_2 molecule in the ground state, leads, with 0.21 Å as the difference between single- and double-bond length [21, 23], to 2.10 Å, and the same value is obtained from 1.82 Å as the length of a S—C single bond [22], and the C—C single-bond radius of 0.77 Å. The data indicate that Abrahams' first proposal [4], 2.11 Å, is closer to the S—S single-bond length than is 2.08 Å. A discussion of

so small differences in bond lengths may be meaningless unless the hybridization ratio of the bond orbitals is defined, more *s* character in a σ bond leading to shorter bond lengths; however, for sulphur little information is available on this point. It appears that the 2.12 ± 0.02 Å S—S bonds of pentathionate are, at least, fairly close to single bonds.

The middle S—S bonds, of lengths 2.04 ± 0.02 Å, like the S—S bonds of the same length in di- and trisulphides and in orthorhombic sulphur, probably possess some double-bond character, arising from overlap of the $p\pi$ electron pair of one divalent sulphur atom with available 3*d* orbitals of a bond partner. Pauling's relation [23], $R = R_1 - 0.706 \log n$, leads to 22 % π-bond character, if R_1 is taken as 2.10 Å. Abrahams' curves [4,5] give about 25 %. In view of the uncertain nature of the bond order and bond length data, the figures serve only to indicate orders of magnitude.

The sulphur-sulphur bonds of the pentathionate ion readily undergo heterolysis in reactions with nucleophilic reagents [24, 25]. The principal reaction type involves a nucleophilic attack on the middle sulphur atom of the chain, and leads to the elimination of one or both of the thiosulphate groups as anions. The pentathionate thus behaves as a thiosulphate of divalent sulphur. This has been interpreted [24] as due to a certain amount of ionic character, or polarity of the σ bond, in the direction of heterolysis, on the ground that ionic character, or polarity already present, ordinarily serves to facilitate the further polarizability of the bond in the direction of polarity. The degree of ionic character can hardly be more than a few per cent; it would, however, leave a fractional positive charge on the middle sulphur atom, if the bonds from this atom were pure σ bonds.

It has been argued [26], on the basis of the K_α X-ray emission spectra from sulphur in solid potassium pentathionate, that the divalent sulphur atoms, including the middle one, have not a positive, but a negative charge. The interpretation of X-ray emission spectra in terms of charge distributions may not be quite clear-cut, and a net negative charge on the divalent sulphur atoms appears unlikely in view of the, presumably *, positive charge on the sulphur atom of the terminal sulphonate groups. However, if the middle S—S bonds of pentathionate, of lengths 2.04 Å, possess π-bond character, electroneutrality of the middle sulphur atom may not be in disagreement with ionic character, as indicated, of the σ bonds. The π-bonding, if involving for each bond to a higher degree the 3*d* orbitals of the middle sulphur atom than of the adjacent sulphur atoms, will tend to neutralize the positive charge on the middle sulphur atom due to ionic character of the σ bonds. This would not contradict the formulation, on a reactivity basis, of pentathionate as a thiosulphate of divalent sulphur, it being the direction of polarity of the σ bond, notwithstanding neutralizing charges due to π-bonding, which is indicative of the preferred direction of heterolysis of a bond, and *vice versa*.

The work has been financially supported by *Norges almenvitenskapelige forskningsråd.*

* A positive charge (though less than one) on the sulphur atom of an ionized sulphonate group, $-SO_3^-$, may be inferred from its Hammett σ values [27-30], its acidifying effect on aliphatic acids [31], and the dipole moment of sulphur-oxygen bonds [32].

REFERENCES

1. Foss, O. and Tjomsland, O. *Acta Chem. Scand.* **10** (1956) 424.
2. Foss, O. and Zachariasen, H. *Acta Chem. Scand.* **8** (1954) 473.
3. Foss, O. and Tjomsland, O. *Acta Chem. Scand.* **10** (1956) 288.
4. Abrahams, S. C. and Grison, E. *Acta Cryst.* **6** (1953) 206.
5. Abrahams, S. C. *Acta Cryst.* **7** (1954) 423.
6. Foss, O., Furberg, S. and Zachariasen, H. *Acta Chem. Scand.* **8** (1954) 459.
7. Sörum, H. *Acta Chem. Scand.* **7** (1953) 1.
8. Donohue, J. and Schomaker, V. *J. Chem. Phys.* **16** (1948) 92.
9. Bowen, H. J. M. *Trans. Faraday. Soc.* **50** (1954) 452.
10. Dawson, I. M. and Robertson, J. M. *J. Chem. Soc.* **1948** 1256.
11. Donohue, J. *J. Am. Chem. Soc.* **72** (1950) 2701.
12. Stevenson, D. P. and Beach, J. Y. *J. Am. Chem. Soc.* **60** (1938) 2872.
13. Yakel, H. L. and Hughes, E. W. *Acta Cryst.* **7** (1954) 291.
14. Foss, O. and Johnsen, J. *Acta Chem. Scand.* **11** (1957) 189.
15. Foss, O. and Tvedten, O. *Unpublished work.*
16. Abrahams, S. C. *Acta Cryst.* **8** (1955) 661.
17. Foss, O. and Tjomsland, O. *Acta Chem. Scand.* **8** (1954) 1701.
18. Foss, O. and Larssen, P. A. *Acta Chem. Scand.* **8** (1954) 1042.
19. Foss, O. and Tjomsland, O. *Acta Chem. Scand.* **12** (1958) 52.
20. Foss, O. and Hordvik, A. *Acta Chem. Scand.* **11** (1957) 1443.
21. Pauling, L. *The Nature of the Chemical Bond,* Cornell University Press, Ithaca, New York 1945.
22. Abrahams, S. C. *Quart. Rev. London* **10** (1956) 407.
23. Pauling, L. *J. Am. Chem. Soc.* **69** (1947) 542.
24. Foss, O. *Kgl. Norske Videnskab. Selskabs Skrifter* **1945** No. 2.
25. Foss, O. *Acta Chem. Scand.* **4** (1950) 404.
26. Faessler, A. and Goehring, M. *Naturwiss.* **39** (1952) 169.
27. Zollinger, H., Büchler, W. and Wittwer, C. *Helv. Chim. Acta* **36** (1953) 1711.
28. Zollinger, H. and Wittwer, C. *Helv. Chim. Acta* **39** (1956) 347.
29. McCoy, R. D. and Swinehart, D. F. *J. Am. Chem. Soc.* **76** (1954) 4708.
30. Heppolette, R. L. and Miller, J. *J. Chem. Soc.* **1956** 2329.
31. Banks, C. V. and Zimmerman, J. *J. Org. Chem.* **21** (1956) 1439.
32. Cumper, C. W. and Walker, S. *Trans. Faraday Soc.* **52** (1956) 193.

Received September 15, 1957.

ACTA CHEMICA SCANDINAVICA 12 (1958) 52—62

The Crystal Structure of Monoclinic Barium Telluropentathionate Dihydrate

OLAV FOSS and OLAV TJOMSLAND

Chemical Institute, University of Bergen, Bergen, Norway

The monoclinic dimorph of the salt, $BaTe(S_2O_3)_2 \cdot 2H_2O$, crystallizes in a four-molecule unit cell based on the space group, C_{2h}^3-A2/m, with $a = 4.99$ Å, $b = 10.59$ Å, $c = 23.61$ Å, $\beta = 98°$. The structure has been determined by two-dimensional X-ray methods. With mirror plane symmetry crystallographically required, the telluropentathionate ion occurs in the *cis* form in this salt. The S—S—Te—S—S chain has the dimensions, S—S = 2.10 ± 0.02 Å, S—Te = 2.34 ± 0.02 Å, ∠S—S—Te = 106 ± 1°, ∠S—Te—S = 101 ± 1°. These values are within the experimental errors the same as found earlier for the *trans* form in the ammonium salt. The dihedral angle, SSTe/STeS = 103°.

The crystals have a layer structure and differ from the triclinic and orthorhombic barium pentathionate dihydrates and the acetone and tetrahydrofuran solvates only in the way of packing of the parallel layers.

Solvates of barium pentathionates with dioxane are described, containing one mole of water and half a mole of dioxane per mole of salt. The barium selenopentathionate solvate, $BaSe(S_2O_3)_2 \cdot H_2O \cdot \frac{1}{2}C_4H_8O_2$, crystallizes in the space group, C_{2h}^3-A2/m with $Z = 4$, and $a = 5.02$ Å, $b = 10.59$ Å, $c = 22.72$ Å, $\beta = 102°$, and is isostructural with monoclinic barium telluropentathionate dihydrate.

A recent study of the crystal chemistry of barium salts of telluropentathionic acid [1] led to the characterization of a trihydrate and of a triclinic and a monoclinic dihydrate. Unit cell and space group data indicated that the triclinic dihydrate is isomorphous with triclinic barium pentathionate dihydrate [2], and that the *a*-axis projection of the monoclinic dihydrate has the same symmetry as the *a*-axis projections of orthorhombic barium pentathionate [3] and selenopentathionate [4] dihydrates. A solvate of barium telluropentathionate with tetrahydrofuran furthermore exists [5], isomorphous with the solvates of barium pentathionate and selenopentathionate with tetrahydrofuran and acetone [5,6]. In the barium salts the telluropentathionate ion thus occurs in the *cis* form, with mirror-plane symmetry, like the pentathionate and selenopentathionate ions in the barium salts. This is different from the conditions

in the ammonium salt, where the telluropentathionate ion has been found to occur in enantiomorphous *trans* forms [7]. No crystal structure determination of an alkali pentathionate or selenopentathionate has been made; however, it appears likely that in alkali salts also these anions have *trans* forms, the occurrence of the *cis* form in the barium salts being due to the oxygen-coordinating powers of the barium ion, and favourable lattice conditions for the mirror-plane *cis* coordination complex.

The crystal structure of monoclinic barium telluropentathionate dihydrate has now been determined, and data obtained for a comparison of the *cis* and *trans* forms of the telluropentathionate ion. Apart from the rotational isomerism, the dimensions of the ion were found to be the same in the two forms. A further objective of the structure determination was to inquire more thoroughly into the indicated relationship [1] between the monoclinic dihydrate structure and the structures of the triclinic [1,2] and orthorhombic [3,4] dihydrates and the solvates [5,6]. As discussed earlier [1,5] and confirmed in the present work, monoclinic barium telluropentathionate dihydrate is built up of layers having the same internal structure as in the three other structure types. The layers are parallel to the *c* plane, and the structure types differ only in the way the layers are arranged relative to each other. In the triclinic dihydrates [1,2], of space group C_i^1—$P\bar{1}$ with $Z = 2$, the oblique β and α angles lead to relative displacements of successive layers in the directions of the *a* and *b* axes, while in the solvates [5,6], of space group C_{2h}^2—$P2_1/m$ with $Z = 2$, displacements occur in the *a*-axis direction only. In the orthorhombic dihydrates [3,4] of space group D_{2h}^{16}—*Pnma* with $Z = 4$, adjacent layers are related through glide planes *a* in the layer interface, and in the monoclinic dihydrate, through two-fold rotation axes in the interface.

The present structure is the fifth to be described for a telluropentathionic compound, and the first in which the S—S—Te—S—S chain has been found to have the *cis* instead of the *trans* configuration. Beside ammonium telluropentathionate [7], the earlier structures are those of tellurium dimethanethiosulphonate [8], dibenzenethiosulphonate [9] and di-*p*-toluenethiosulphonate [10].

CRYSTAL DATA

The monoclinic dimorph of barium telluropentathionate dihydrate, $BaTe(S_2O_3)_2 \cdot 2H_2O$, has the unit cell dimensions [1], $a = 4.99$ Å, $b = 10.59$ Å $c = 23.61$ Å, $\beta = 98°$. There are four formula units per unit cell; density, calc. 2.82, found 2.80 g/cm^3. The crystals occur as prisms along the *a* axis, with {001} dominant. There is a pronounced tendency of cleavage along the *c* plane.

On the basis of the systematic absences, *hkl* when $k+l$ is odd, and a comparison of the 0*kl* zone of reflections with the 0*kl* zones of orthorhombic barium pentathionate and selenopentathionate dihydrate, the space group, C_{2h}^3—$A2/m$, was originally chosen [1], and no later observations contradict this choise. The barium ion and the tellurium atom are thereby required to lie in special positions, and were found to lie in the mirror planes, as do also the water molecules.

The intensities of the 0*kl* and *h*0*l* reflections were estimated visually from Weissenberg photographs, taken with CuK_α radiation using a double-film,

multiple-exposure technique. The crystals employed had cross-sections of 0.09×0.05 mm and 0.08×0.06 mm, respectively, in the case of the *a*- and *b*-axis photographs. 156 out of 172 $0kl$ reflections and 148 out of 156 $h0l$ reflections attainable with CuK_α radiation were observed and measured. The intensities were corrected for the Lorentz and polarization factors and converted to relative structure factors in the usual way, and were ultimately brought to an approximately absolute scale by comparison with the calculated values. Although the absorption coefficient for CuK_α radiation is 531 cm^{-1}, no correction for absorption was made, mainly because of the large amount of work it would involve, but reflections likely to be most heavily influenced by absorption were omitted from the $(F_o - F_c)$ syntheses in the final stages of refinement.

Summations were made by means of Beevers-Lipson strips, at 12°, 6° and 3° intervals, respectively, along the *a*, *b* and *c* axes, except for the F_o^2 and first F_o syntheses where the summations were made at 6° intervals also along the *c* axis.

The atomic scattering curves used in the calculation of structure factors were that of Berghuis *et al.*[11] and of Viervoll and Ögrim [12], respectively, for oxygen and sulphur, and the Thomas-Fermi curve [13] for tellurium. For the barium ion a curve was constructed based on the Thomas-Fermi values [13] for xenon at small scattering angles and for electroneutral barium at intermediate and larger scattering angles.

ANALYSIS OF THE STRUCTURE

The *y* and *z* coordinates of the barium ion and tellurium atom, and also of the two sulphur atoms of the asymmetric unit, were derived from a F_o^2 synthesis of the $0kl$ data. These first coordinates gave the signs of 117 of the largest $0kl$ terms, which were used for a F_o synthesis. The resulting electron density map revealed the approximate positions of the sulphonate oxygen atoms and water molecules, and allowed F_o refinement to be carried out. Finally, a series of $(F_o - F_c)$ refinements were made.

The *b*-axis projection was solved and refined in essentially the same way. Here, however, $(F_o - F_c)$ refinement did not proceed quite satisfactorily and was therefore abandoned at a relatively early stage. One reason may be that in this projection the water molecule $(H_2O)_2$ is obscured by the tellurium atom and therefore cannot be located with any certainty; also, the overlapping makes the tellurium *x* coordinate less reliable.

The difference maps indicated individual and partly anisotropic temperature vibrations of the atoms. In temperature factor $\exp[-B(\sin^2\Theta/\lambda^2)]$ the following values of *B* were adopted in the last stages: For the $0kl$ data, 3.0 Å^2 for tellurium, 2.8 Å^2 for the sulphur and oxygen atoms except for $(H_2O)_2$ where $B = 5.0$ Å^2, and $(2.6+0.8\cos^2\varphi)$ Å^2 for the barium ion, where φ is the angle between the normal of the reflecting plane and the direction of maximum vibration of the ion. This direction is parallel to the *c* axis. For the $h0l$ data, $B = 2.8$ Å^2 for the sulphur and oxygen atoms, and $(2.6+1.0\cos^2\varphi)$ Å^2 and $(3.0+2.0\cos^2\varphi)$ Å^2, respectively, for the barium ion and tellurium atom. Here, the directions of maximum vibration make angles of 34° and 45°, respectively,

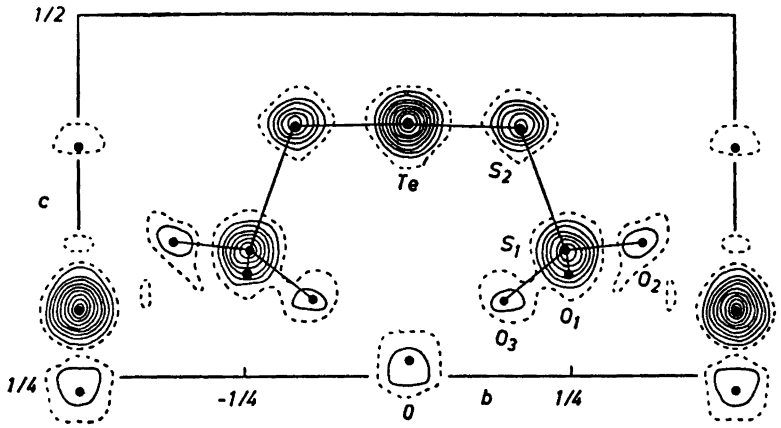

Fig. 1. Electron density projection of monoclinic barium telluropentathionate dihydrate along the *a* axis. Contour intervals: 10 e · Å^{-2} for the barium ion and tellurium atom, and 5 e · Å^{-2} for the sulphur and oxygen atoms and water molecules. The 5-electron line is dashed.

with the *c* axis in the acute angle. The temperature factors may have little physical reality in terms of thermal motions of the atoms; rather, they also represent absorption and other errors in the observed structure factors.

The final electron density maps are shown in Figs. 1 and 2, and the final atomic coordinates are listed in Table 1. The *z* coordinates are from the *a*-axis projection, since attempts to establish independent *z* coordinates from the *b*-axis projection were not made. One exception is that of O_1. It should be noted that the *b*-axis projection did not indicate changes in the *z* coordinates of the heavier atoms including sulphur.

In Table 2, observed and calculated values of structure factors are compared for all 0*kl* and *h*0*l* reflections within the range of CuK_α radiation. The strong reflections 002, 004, 006, 008, 011, 013, 015, 026 in the 0*kl* zone and 002, 004, 006, 008, 108, $\bar{1}08$, $\bar{3}04$, $\bar{3}$ 0 12 in the *h*0*l* zone have observed values markedly

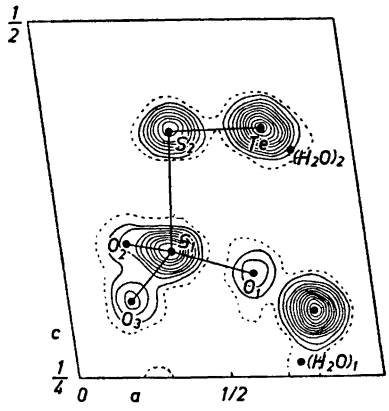

Fig. 2. Electron density projection along the *b* axis. Contours are at intervals of 8 e · Å^{-2} for the barium ion and tellurium atom, and the 8-electron line is dashed; otherwise as in Fig. 1. Each sulphur and sulphonate oxygen peak represents two exactly overlapping atoms, one on each side of the mirror plane.

lower than the calculated ones, probably due to absorption and extinction effects. These reflections were omitted from the (F_o—F_c) syntheses and from the calculation of scale factors for the respective zones, and were included in the final F_o syntheses with their calculated values. The relatively weak reflections 0 0 28, 031, 062, 0 10 2 in the 0*kl* zone and 0 0 28, 1 0 24, 206, $\bar{2}$ 0 28, 300, 304, $\bar{3}$ 0 26, 408, 4 0 16, $\bar{4}$08, 602, 606, $\bar{6}$ 0 12 in the *h*0*l* zone have small calculated values and therefore uncertain signs, and were not included in the F_o or (F_o—F_c) syntheses.

Table 1. Atomic coordinates, in fractions of monoclinic cell edges. Origin at a centre of symmetry (2/*m*).

	x	*y*	*z*		*x*	*y*	*z*
Ba	0.802	0	0.2045	S_1	0.365	0.240	0.3382
Te	0.712	0	0.4238	S_2	0.413	0.171	0.4224
$(H_2O)_1$	0.739	0	0.262	O_1	0.623	0.241	0.322
$(H_2O)_2$	0.200	0	0.091	O_2	0.240	0.360	0.343
				O_3	0.211	0.146	0.303

The reliability index, $R = \Sigma||F_o|-|F_c||/\Sigma|F_o|$, with non-observed reflections included when $|F_c|$ exceeds the observable limit, is 0.082 for the 0*kl* reflections and 0.170 for the *h*0*l* reflections, if the above-mentioned groups of strong reflections with high calculated values are omitted. With these reflections included, the R values become 0.108 and 0.190, respectively.

ASSESSMENT OF ACCURACY

The standard deviations of the coordinates of the heavier atoms were estimated from the root-mean-square gradients of the difference maps and the curvatures of the electron density peaks [14,15]. The gradients were 2.3 e · Å^{-3} in the y and z directions of the 0*kl* difference map, and 5.8 e · Å^{-3} in the x direction of the less refined *h*0*l* map. The derived standard deviations are: $\sigma(x) = 0.005$ Å, $\sigma(z) = 0.002$ Å for the barium ion; $\sigma(x) = 0.006$ Å, $\sigma(z) = 0.003$ Å for the tellurium atom; $\sigma(x) = 0.010$ Å, $\sigma(y) = 0.007$ Å, $\sigma(z) = 0.008$ Å for the sulphur atoms. The y coordinates of barium and tellurium are fixed by symmetry relations. $\sigma(x)$ for sulphur is relatively low despite the large gradient because in the *b*-axis projection exact overlapping of two and two sulphur atoms (and likewise of sulphonate oxygen atoms) occurs. $\sigma(z)$ and $\sigma(x)$ for S_1 may be larger than the given values due to overlapping with oxygen atoms in both projections. The s.d. for resolved oxygen atoms may be taken as about three times those of the sulphur atoms, except for the x coordinate of $(H_2O)_1$ and particularly $(H_2O)_2$ where the uncertainties are larger.

The above values give s.d. of 0.009 Å and 0.011—0.014 Å, respectively, for S—Te and S—S distances, and 0.3—0.4° for angles involving these atoms. Considering uncertainties in the estimates due to overlapping in some cases, and non-random errors in the observed structure factors due to absorption and other effects, s.d. of about 0.02 Å for S—S and S—Te distances and about 1° for the angles may be more realistic. Similar estimates lead to s.d. of about 0.04 Å for S—O bond lengths, 2—3° for S—S—O and O—S—O bond angles, and 0.03 Å for distances from barium to sulphonate oxygen atoms.

Table 2. Observed and calculated 0*kl* and *h*0*l* structure factors for monoclinic barium telluropentathionate dihydrate.

l	F_o	F_c	*l*	F_o	F_c	*l*	F_o	F_c
	0*kl* zone		5	213	+231	14	149	+163
	00*l*		7	110	−110	16	22	+ 24
2	87	−176	9	96	+118	18	114	−123
4	57	−120	11	16	+ 14	20	18	− 12
6	44	− 74	13	139	−147	22	57	− 58
8	316	−372	15	75	+ 79	24	51	+ 48
10	119	+117	17	97	− 91	26	33	+ 36
12	139	+145	19	86	+ 80			
14	209	+189	21	18	+ 11		07*l*	
16	40	− 37	23	<16	− 5	1	40	− 44
18	100	− 92	25	23	+ 17	3	122	−127
20	42	− 29	27	53	− 52	5	184	+170
22	130	−127	29	12	+ 15	7	51	+ 49
24	102	+104				9	45	+ 43
26	61	+ 54		04*l*		11	36	− 36
28	26	+ 1	0	350	+364	13	81	− 86
30	13	+ 16	2	103	− 93	15	19	− 13
			4	11	− 5	17	41	− 39
	01*l*		6	48	− 56	19	103	+107
1	109	−140	8	160	−171	21	<14	+ 9
3	134	−177	10	68	+ 80	23	<12	− 7
5	239	+291	12	30	+ 41	25	<8	− 3
7	85	+ 81	14	86	+ 91			
9	107	+129	16	24	− 18		08*l*	
11	75	− 75	18	28	− 31	0	243	+235
13	190	−185	20	20	− 15	2	88	− 90
15	15	+ 4	22	82	− 74	4	16	− 6
17	70	− 67	24	70	+ 62	6	19	+ 13
19	163	+155	26	<12	+ 5	8	110	−110
21	40	+ 36	28	<8	+ 7	10	48	+ 48
23	<16	− 11				12	20	+ 11
25	16	− 20		05*l*		14	56	+ 59
27	78	− 72	1	121	−119	16	19	− 19
29	<9	+ 12	3	98	− 93	18	19	− 19
			5	236	+222	20	<13	+ 12
	02*l*		7	19	+ 12	22	60	− 61
0	205	+189	9	121	+138	24	31	+ 42
2	<7	− 8	11	61	− 60			
4	137	+120	13	177	−182		09*l*	
6	218	−268	15	29	+ 34	1	<16	− 19
8	96	−108	17	51	− 54	3	41	− 43
10	153	+181	19	113	+113	5	97	+ 87
12	105	−100	21	43	+ 43	7	55	− 54
14	154	+157	23	16	− 11	9	71	+ 71
16	29	+ 33	25	20	− 22	11	21	− 10
18	115	−111	27	55	− 60	13	69	− 72
20	17	+ 18				15	49	+ 50
22	52	− 49		06*l*		17	51	− 51
24	33	+ 33	0	278	+281	19	39	+ 37
26	<13	+ 10	2	13	− 1	21	20	+ 12
28	24	+ 26	4	36	+ 31			
			6	200	−203		0,10,*l*	
	03*l*		8	160	−158	0	79	+ 73
1	9	+ 2	10	131	+141	2	18	− 4
3	142	−161	12	22	− 17	4	35	+ 35

l	F_o	F_c
	0,10,l	
6	75	− 84
8	55	− 49
10	68	+ 67
12	31	− 37
14	60	+ 64
16	12	+ 15
18	45	− 47
20	<7	0
	0,11,l	
1	31	− 32
3	69	− 68
5	119	+109
7	16	+ 14
9	31	+ 36
11	16	− 18
13	72	− 73
15	<10	+ 4
17	18	− 20
	0,12,l	
0	126	+130
2	20	− 19
4	<13	− 8
6	27	− 33
8	68	− 73
10	36	+ 35
12	10	+ 20
14	41	+ 53
	0,13,l	
1	21	− 26
3	18	− 17
5	46	+ 49
7	<8	− 5
	$h0l$ zone	
	00l	
2	87	−176
4	64	−120
6	51	− 72
8	307	−375
10	113	+124
12	132	+135
14	203	+186
16	44	− 38
18	108	− 96
20	46	− 18
22	139	−120
24	112	+ 97
26	65	+ 48
28	26	− 6
30	15	+ 17
	10l	
0	129	−121
2	148	−180
4	65	+ 37
6	148	−160
8	278	+323
10	84	+ 90
12	145	−163
14	56	+ 53
16	146	−126
18	24	− 13
20	80	+ 79
22	49	+ 33
24	26	+ 2
26	41	− 39
28	<10	+ 16
	$\bar{1}0l$	
2	36	+ 25
4	156	+187
6	202	+230
8	144	−200
10	56	+ 56
12	129	−143
14	85	− 88
16	141	+136
18	18	+ 8
20	73	+ 58
22	22	− 20
24	45	− 29
26	26	− 23
28	19	− 33
30	43	+ 56
	20l	
0	292	−327
2	45	+ 22
4	74	+ 72
6	14	+ 2
8	151	+161
10	94	− 92
12	17	+ 19
14	116	−108
16	20	− 27
18	128	+121
20	52	− 58
22	73	+ 75
24	19	− 12
26	53	− 54
	$\bar{2}0l$	
2	191	+192
4	80	− 79
6	70	+ 77
8	113	+118
10	77	− 86
12	<15	− 8
14	73	− 74
16	41	+ 64
18	<18	− 21
20	27	+ 14
22	40	+ 46
24	68	− 73
26	31	+ 36
28	15	− 4
30	<6	− 16
	30l	
0	38	+ 5
2	211	+223
4	39	+ 2
6	44	+ 46
8	103	−113
10	168	−179
12	95	+ 94
14	23	+ 17
16	82	+ 92
18	34	+ 32
20	58	− 61
22	35	− 30
24	38	− 49
	$\bar{3}0l$	
2	22	− 31
4	127	−171
6	86	− 91
8	104	+126
10	38	− 45
12	169	+199
14	47	− 56
16	75	− 98
18	20	+ 24
20	79	− 81
22	59	+ 62
24	35	+ 41
26	13	− 4
28	<9	+ 4
	40l	
0	19	+ 15
2	19	− 23
4	92	−107
6	20	− 7
8	19	− 6
10	105	+107
12	19	+ 14
14	18	− 21
16	16	+ 4
18	101	− 96
20	21	+ 38
	$\bar{4}0l$	
2	22	+ 18
4	145	+163
6	101	− 90
8	18	− 1
10	24	− 47
12	69	− 83
14	74	+ 78

l	F_o	F_c	l	F_o	F_c	l	F_o	F_c
	$\bar{4}0l$		14	14	− 6		$60l$	
16	20	+ 22	16	<4	− 7	0	13	− 7
18	30	+ 41				2	11	− 5
20	18	− 12		$\bar{5}0l$		4	38	+ 46
22	15	− 26	2	51	− 57	6	8	− 3
24	15	− 21	4	24	+ 10			
26	17	− 21	6	40	+ 28		$\bar{6}0l$	
			8	24	− 32	2	30	− 36
	$50l$		10	34	+ 43	4	33	− 25
0	67	+ 77	12	51	− 42	6	43	+ 50
2	105	− 77	14	35	+ 38	8	27	− 21
4	19	+ 13	16	<15	− 28	10	31	+ 41
6	56	+ 43	18	<14	− 16	12	9	0
8	25	− 45	20	29	+ 36	14	22	− 42
10	55	+ 54	22	20	− 28			
12	37	− 27						

DESCRIPTION OF THE STRUCTURE

The telluropentathionate ion consists of a divalent tellurium atom to which are attached two thiosulphate groups, through Te—S bonds. The S—S—Te—S—S chain thus resulting has the dimensions listed in Table 3. The ion possesses mirror plane symmetry, and a prime is used to denote the equivalent of an atom across the mirror plane.

Table 3. S—S and S—Te bond lengths and angles.

S_1-S_2 = 2.10 Å	$\angle S_1-S_2-Te$ = 105.7°	S_1S_2Te/S_2TeS_2'
S_2-Te = 2.34	$\angle S_2-Te-S_2'$ = 101.2°	(dihedral angle) = 103°

Non-bonded S—S and S—Te distances.

S_1-S_1' = 5.08 Å	S_1-Te = 3.55 Å
S_1-S_2' = 4.78	S_2-S_2' = 3.62

The bond lengths and angles found in ammonium telluropentathionate [7], where the two halves of the ion are not related by symmetry, are: S—S = 2.11 Å and 2.12 Å, S—Te = 2.35 Å and 2.36 Å, ∠ S—S—Te = 105° and 104°, ∠ S—Te—S = 103°, and the non-bonded distances not dependent on rotation about the S—Te bonds: S_1—Te = 3.57 Å, S_5—Te = 3.52 Å, S_2—S_2' = 3.68 Å. The differences between these values and those of Table 3 are not significant.

Whereas the telluropentathionate ion in the ammonium salt occurs in the *trans* form, with the two terminal sulphur atoms located on different sides of the plane of the tellurium and two middle sulphur atoms, the ion in the barium salt has the *cis* form, with the terminal sulphur atoms on the same side of the plane. This is reflected in the shorter S_1—S_1' separation, 5.08 Å, in the barium salt as compared with 6.11 Å in the ammonium salt. In the latter the SSTe/STeS dihedral angles are 86° and 95°, and thus smaller than in the barium salt.

The sulphonate groups have S_1-O_1 = 1.39 Å, S_1-O_2 = 1.43 Å, S_1-O_3 = 1.45 Å, $\angle O_1-S_1-O_2$ = 117°, $\angle O_1-S_1-O_3$ = 107°, $\angle O_2-S_1-O_3$ = 117°.

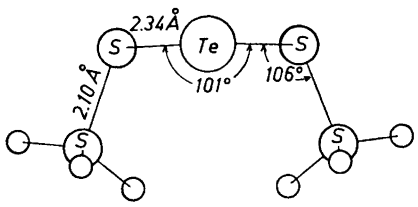

Fig. 3. The *cis* form of the telluropentathionate ion, with principal bond lengths and angles.

The small value of the second angle may be due to maximum error in the y coordinate of O_1, since this atom in the a-axis projection is overlapped by S_1.

The barium-oxygen coordination is as in the four structures of barium pentathionates determined earlier [2-4,6]. The barium ion is surrounded by nine oxygen atoms, at an average distance of 2.82 Å. The extreme values are 2.68 Å and 2.98 Å. The arrangement has been described in detail earlier [3,4] and shall not be repeated here. As in the other structures, the water molecule $(H_2O)_1$ probably forms hydrogen bonds to the sulphonate oxygen atoms O_1 and O_1'; the distances are in the present structure 3.01 Å and the $O_1—(H_2O)_1—O_1'$ angle 116°.

The structure within layers parallel to the c plane is the same as in the triclinic [2] and orthorhombic [3,4] dihydrates and, apart from the replacement of a water molecule by an organic molecule, as in the acetone and tetrahydrofuran solvates [5,6]. In the present space group, adjacent layers are related through twofold rotation axes which run parallel to the b axis in the layer interfaces at $z = 0$ and $\frac{1}{2}$. The layers are held together through non-bonded contacts between atoms of the $S_2—Te—S_2'$ groups across the interfaces. The closest approaches are: Te—Te = 4.28 Å over twofold axis at $(1,y,\frac{1}{2})$, and Te—Te = 4.42 Å, Te—S = 4.18 Å, S—S = 3.65 Å over twofold axis at $(\frac{1}{2},y,\frac{1}{2})$.

It may be noted that the origin chosen in the present work (at $2/m$ in accordance with the *International Tables* [16]) lies in a layer interface and in a mirror plane, and not in the middle of a layer and midway between mirror planes as in the earlier structure determinations [2-4,6]. To make the present b-axis projection correspond with those of the triclinic dihydrate [2] and the solvate [6] structures, another c axis should, furthermore, be chosen. The new cell, still A-centered, would have $c = 24.32$ Å, $\beta = 106°$ and be derived from the first by means of the transformation matrix, $\bar{1}00/010/201$.

SOLVATES WITH DIOXANE

In the crystals of the acetone solvate [5,6], $BaS(S_2O_3)_2 \cdot H_2O \cdot (CH_3)_2CO$, the internal layer structure differs from the dihydrate structures only in the substitution of an acetone molecule for one of the water molecules of the dihydrates. The oxygen atom of the acetone molecule is coordinated to the barium ion, like the oxygen atom of the replaced water molecule, and is located between the barium ion and the nearest layer interface, with the methyl groups directed towards the interface. A symmetrical molecule with two oxygen atoms, like dioxane, might be thought to be able to extend across the layer interfaces and replace two water molecules, one in each of two adjacent layers. Crystal symmetry and layer structure would permit such a replacement in the triclinic dihydrate structure, space group $C_i^1—P\bar{1}$ with $Z = 2$, and in the

monoclinic dihydrate structure, space group C_{2h}^3—$A2/m$ with $Z = 4$, but not in the orthorhombic dihydrate structure or in the acetone and tetrahydrofuran solvate structure. In the two permitted space groups, $P\bar{1}$ and $A2/m$, the molecular symmetries, $\bar{1}$ and $2/m$, respectively, would be required for the dioxane molecule.

Experiments have shown that barium pentathionate, selenopentathionate and telluropentathionate readily give solvates with dioxane. The seleno- and telluropentathionate solvates have been analyzed and found to have the expected composition, *i. e.*, one mole of water and half a mole of dioxane per mole of salt. The solvates are relatively stable, more so than the acetone and tetrahydrofuran solvates, and the perfect cleavage displayed by the latter crystals and those of the dihydrates is absent, in agreement with the idea that dioxane molecules extend across the layer interface and hold the layers more firmly together.

The solvate of barium selenopentathionate with dioxane, $BaSe(S_2O_3)_2 \cdot H_2O \cdot \frac{1}{2}C_4H_8O_2$, was studied crystallographically. The pale green crystals are monoclinic, and formed relatively large, short prisms extended along the a axis and bounded by {011} and {001}. The specimens examined were all persistently twinned. From oscillation and Weissenberg photographs taken with copper radiation, $\lambda(CuK_\alpha) = 1.542$ Å, the unit cell dimensions are: $a = 5.02$ Å, $b = 10.59$ Å, $c = 22.72$ Å (all ± 0.5 %), $\beta = 102°$. There are four formula units per unit cell; density, calc. 2.83, found 2.81 g/cm^3. Systematic absences, hkl when $k+l$ is odd. The $0kl$ zone of reflections has the same symmetry and intensity distribution as the $0kl$ zone of orthorhombic barium selenopentathionate dihydrate [4], of space group D_{2h}^{16}—$Pnma$, and the a-axis projections of the two salts have also very like dimensions. The unit cell dimensions and systematic absences indicate that the solvate is isostructural with monoclinic barium telluropentathionate dihydrate. These analogies leave little doubt that the space group of the dioxane solvate is the centrosymmetric one, C_{2h}^3—$A2/m$, and that replacement of two crystallographically equivalent water molecules, one in each of two adjacent layers, by one dioxane molecule occurs as indicated above.

EXPERIMENTAL

Solutions of about 1 g of barium pentathionate [2], selenopentathionate [4] and telluropentathionate [1] hydrates in 12 ml of 0.2 N perchloric acid were filtered, when necessary, then warmed to about 40 °C, and about 3 ml of 1,4-dioxane was added. On standing, the solvates crystallized, and were filtered off, washed with dioxane and then with ether, and dried for a short time in a vacuum over sulphuric acid.

The dioxane solvates are less soluble and crystallize more rapidly than the acetone and tetrahydrofuran solvates [5]. As usual, the solubilities decrease in the order, pentathionate, selenopentathionate and telluropentathionate. The crystals of the latter were very small and not suited for single-crystal X-ray work.

For analysis, the selenopentathionate was oxidized with potassium bromate and subsequently analyzed iodometrically by means of the Norris and Fay method, as described earlier [17]. The telluropentathionate was titrated directly with iodine [18].

0.2850 g substance: 22.71 ml of 0.09954 N sodium thiosulphate.
$BaSe(S_2O_3)_2 \cdot H_2O \cdot \frac{1}{2}C_4H_8O_2$ (502.7). Mol. weight found, 504.3.
0.2557 g substance: 18.31 ml of 0.1001 N iodine.
$BaTe(S_2O_3)_2 \cdot H_2O \cdot \frac{1}{2}C_4H_8O_2$ (551.3). Mol. weight found, 558.1.

The work has been aided by grants from *Norges almenvitenskapelige forskningsråd*.

REFERENCES

1. Foss, O. and Tjomsland, O. *Acta Chem. Scand.* **10** (1956) 416.
2. Foss, O. and Tjomsland, O. *Acta Chem. Scand.* **10** (1956) 288.
3. Foss, O. and Zachariasen, H. *Acta Chem. Scand.* **8** (1954) 473.
4. Foss, O. and Tjomsland, O. *Acta Chem. Scand.* **8** (1954) 1701.
5. Foss, O. and Tjomsland, O. *Acta Chem. Scand.* **10** (1956) 424.
6. Foss, O. and Tjomsland, O. *Acta Chem. Scand.* **12** (1958) 44.
7. Foss, O. and Larssen, P. A. *Acta Chem. Scand.* **8** (1954) 1042.
8. Foss, O. and Vihovde, E. H. *Acta Chem. Scand.* **8** (1954) 1032.
9. Øyum, P. and Foss, O. *Acta Chem. Scand.* **10** (1956) 279.
10. Foss, O. and Øyum, P. *Acta Chem. Scand.* **9** (1955) 1014.
11. Berghuis, J., Haanappel, I. M., Potters, M., Loppstra, B. O., MacGillavry, C. H. and Veenendaal, A. L. *Acta Cryst.* **8** (1955) 478.
12. Viervoll, H. and Ögrim, O. *Acta Cryst.* **2** (1949) 277.
13. *Internationale Tabellen zur Bestimmung von Kristallstrukturen*, Borntraeger, Berlin 1935.
14. Cruickshank, D. W. *Acta Cryst.* **2** (1949) 65.
15. Cochran, W. *Acta Cryst.* **4** (1951) 81.
16. *International Tables for X-ray Crystallography*, Kynoch Press, Birmingham 1952, Vol. I, p. 95.
17. Foss, O. *Acta Chem. Scand.* **3** (1949) 435.
18. Foss, O. *Acta Chem. Scand.* **3** (1949) 708.

Received September 30, 1957.

ACTA CHEMICA SCANDINAVICA 12 (1958) 63—67

Cis- and *Trans*-2,5-Dimethoxy-2,5-dihydrofuran *

JØRGEN TORMOD NIELSEN, NIELS ELMING ** and NIELS CLAUSON-KAAS

Centrallaboratoriet, Sadolin & Holmblad A/S, Copenhagen, Denmark

2,5-Dimethoxy-2,5-dihydrofuran was separated into the *cis* and the *trans* isomer by fractional distillation. Hydrogenation gave the corresponding *cis* and *trans* isomers of 2,5-dimethoxytetrahydrofuran.

The two isomers of 2,5-dimethoxy-2,5-dihydrofuran were *cis*-hydroxylated. Only one *cis*-3,4-dihydroxy-2,5-dimethoxytetrahydrofuran was isolated in each case. The corresponding diacetates were prepared. Attempts to resolve *d,l-cis*-3,4-dihydroxy-*trans*-2,5-dimethoxytetrahydrofuran into the *d*- and the *l*-form by chromatography failed. Attempts to carry out the optical resolution *via* the *l*-menthoxyacetates were also unsuccessful.

2,5-Dimethoxy-2,5-dihydrofurans, prepared by methoxylation of furans, are usually mixtures of the *cis* and the *trans* isomers [1,2]. The same applies to 2,5-dimethoxytetrahydrofurans, which are prepared from the dihydrofurans by catalytic hydrogenation. In one case, *viz.* the derivatives of 2-acetamidomethylfuran, the pair of isomers has been separated [2]. In general, however, these cyclic acetals are used as intermediates for the preparation of 1,4-dicarbonyl compounds and are therefore not separated since both isomers give the same dicarbonyl compounds on acid hydrolysis.

The parent 2,5-dimethoxy-2,5-dihydrofuran has now been separated into the pure isomers by fractional distillation. Hydrogenation gave the corresponding pure 2,5-dimethoxytetrahydrofurans. *Cis*-hydroxylation with potassium permanganate gave only one *cis*-3,4-dihydroxy-2,5-dimethoxytetrahydrofuran from each isomer. The hydroxylation reaction therefore gives no information as to the *cis-trans* relationship between the isomers. Neither did an investigation of the infrared spectra, dipole measurements of the dimethoxydihydrofurans, chromatography of the *cis*-glycols on D-lactose and on starch or the preparation of acetates and *l*-menthoxyacetates of the *cis*-glycols enable us to solve the problem of the *cis-trans* relationship. The reactions are shown in Fig. 1.

* Presented (N.E.) before the Division of Organic Chemistry at the XVIth International Congress of Pure and Applied Chemistry, Paris, France, August 1957.

** Present address: A/S PHARMACIA, Copenhagen, Denmark.

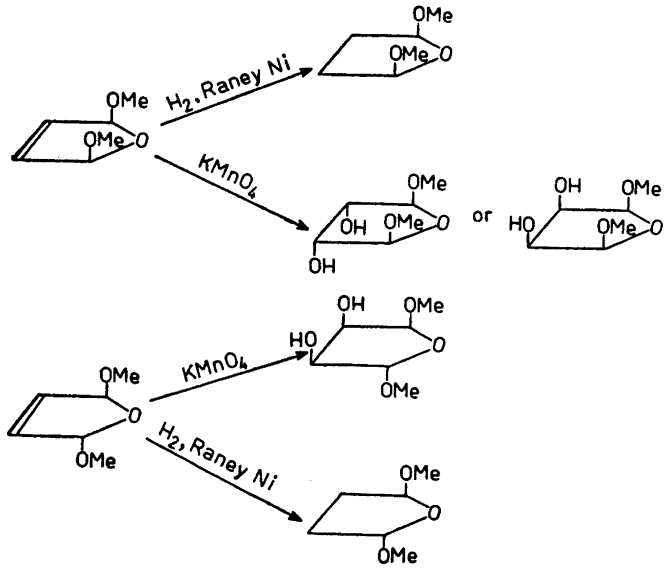

Fig. 1.

It is interesting to observe that there is a marked difference in the yields (44 and 17 %, respectively) of the two *cis*-glycols. Actually the present experiments were initiated by the desire to improve the yields of the hydroxylation reaction of dimethoxydihydrofurans, since a good general procedure for this reaction might open a simple route for the preparation of certain carbohydrates from furans.

Data of all compounds prepared during this investigation are given in Tables 1—5 of the experimental part. It will be noted that the low boiling isomer of 2,5-dimethoxy-2,5-dihydrofuran on hydrogenation gives the high boiling isomer of 2,5-dimethoxytetrahydrofuran.

EXPERIMENTAL

Microanalyses by E. Boss, K. Glens and P. Hansen

2,5-Dimethoxy-2,5-dihydrofurans (I and II). Technical 2,5-dimethoxy-2,5-dihydrofuran (175 g, n_D^{25} 1.4321), prepared by electrolysis [3], was separated into the two isomers by distillation through a 50 cm packed column [4] under 90 mm. It was inferred from the infrared spectra that the purity of the isomers was higher than 95 %. Data of the two isomers are given in Table 1.

Table 1. Data of 2,5-dimethoxy-2,5-dihydrofurans.

	C	H	OCH_3	B.p.$_{90}$ °C	n_D^{25}	Yield, % of distilland
$C_4H_4O(OCH_3)_2$ (130.1) requires	55.4	7.8	47.7			
I	55.6	7.7	47.2	96.0	1.4318	54
II	55.5	7.8	47.6	98.5	1.4331	40

The dielectric constants of dilute benzene solutions of identical concentrations of the isomers were found to be identical within the experimental error.

2,5-Dimethoxytetrahydrofurans (III and IV). This pair of isomers was prepared by catalytic hydrogenation of the pure *cis-* and *trans*-2,5-dimethoxy-2,5-dihydrofurans as described previously [5]. Their data (Table 2) were in agreement with those recorded on samples obtained by fractional distillation of technical 2,5-dimethoxytetrahydrofuran through a 50 cm packed column under 100 mm.

Table 2. Data of 2,5-dimethoxytetrahydrofurans.

	C	H	OCH_3	B.p.$_{760}$ °C	n_D^{25}	Yield %
$C_4H_6O(OCH_3)_2$ (132.2) requires	54.5	9.2	47.0			
III (prepared from I)	54.6	9.2	46.3	147	1.4148	80
IV (prepared from II)	54.7	9.2	46.7	144	1.4158	81

Cis-*3,4-dihydroxy-2,5-dimethoxytetrahydrofurans (V and VI).* I and II were *cis*-hydroxylated by a modification of the method previously described [6]. Powdered potassium permanganate (30.0 g, 0.19 mole) was added in small portions during 1.3 h with vigorous stirring to a solution of 2,5-dimethoxy-2,5-dihydrofuran (26.0 g, 0.20 mole) in water (100 ml) and acetone (100 ml). The temperature was kept at −18° to −21°. The resultant suspension was stirred for 1 h at −20° and the manganese dioxide removed by centrifugation and washed twice with water. The turbid solution was filtered and the filtrate concentrated in a vacuum to about 50 ml. Potassium carbonate (10 g) was added and the solution continuously extracted with ether overnight. The reaction products were isolated by distillation in a vacuum. Their data are given in Table 3.

Table 3. Data of *cis*-3,4-dihydroxy-2,5-dimethoxytetrahydrofurans.

	C	H	OCH_3	B.p.$_{0.1}$ °C	n_D^{25}	M.p. °C	Yield %
$C_4H_6O_3(OCH_3)_2$ (164.2) requires	43.9	7.4	37.8				
V (prepared from I)	43.9	7.4	37.9	109−110	1.4569	34-36	44
VI (prepared from II)	43.9	7.4	37.9	85−87	1.4600	67-69	17

V and VI were crystallized from ether [m.p's 34−36° and 67−69°, respectively (Hershberg apparatus, corr.)]. Another crystallization did not change the m.p's. By evaporation of the mother liquors white crystalline residues having the same m.p's were obtained.

V and VI are therefore believed to be pure isomers. This was also indicated by the infrared spectra.

VI is apparently identical with the product (b.p.$_2$ 130°, n_D^{25} 1.4600, m.p. 65−67°) obtained by Sheehan and Bloom [7] by distillation through a semi-micro fractionating column of their crude product (b.p.$_2$ 106−132°).

Since V or VI must be *d,l-cis*-3,4-dihydroxy-*trans*-2,5-dimethoxytetrahydrofuran it was attempted to resolve V and VI by chromatography on D-lactose using the technique described by Prelog and Wieland [8], but no resolution was observed. Experiments using starch as the adsorbing agent as described by Krebs, Wagner and Diewald [9] were also unsuccessful.

Diacetates of cis-*3,4-dihydroxy-2,5-dimethoxytetrahydrofurans (VII and VIII).* V (328 mg) was dissolved in a mixture of pyridine (3 ml) and acetic anhydride (3 ml) and

the mixture left standing overnight. Evaporation followed by crystallization from ether gave 346 mg of VII (white crystals).

VI (1.26 g) was acetylated as described above and the reaction product isolated by distillation. The yield was 1.47 g of VIII (colorless, viscous liquid, which did not crystallize on standing or by treatment with various solvents). Data of the two isomers are given in Table 4.

Table 4. Data of diacetates of *cis*-3,4-dihydroxy-2,5-dimethoxytetrahydrofurans.

	C	H	OCH_3	$COCH_3$	B.p.$_{0.1}$ °C	n_D^{25}	M.p. °C	Yield %
$C_4H_4O_3(OCH_3)_2(COCH_3)_2$ (248.2) requires	48.4	6.5	25.0	34.7				
VII (prepared from V)	48.5	6.7	24.7	34.5			97–98	70
VIII (prepared from VI)	48.2	6.7	24.7	34.4	90–92	1.4431		77

VII is apparently identical with the diacetate (m.p. 97–99°) reported by Zeile and Heusner [10].

l-Menthoxyacetates of cis*-3,4-dihydroxy-2,5-dimethoxytetrahydrofurans (IX, X and XI).* When treated with one mole of *l*-menthoxyacetyl chloride in pyridine V gave 33 % of a mono-*l*-menthoxyacetate (IX) and 53 % of its di-*l*-menthoxyacetate (X). Under the same conditions VI gave only its di-*l*-menthoxyacetate (XI) (yield 83 %).

Cis-3,4-dihydroxy-2,5-dimethoxytetrahydrofuran (1.35 g, 0.0082 mole) was dissolved in pyridine (10 ml) and *l*-menthoxyacetyl chloride (1.92 g, 0.0082 mole) was added dropwise with cooling at 10–15°. The mixture was left standing at room temperature overnight. Water (5 ml) was added and the mixture continuously extracted with ether for 2 h. The ether extract was washed once with a little water, dried with magnesium sulfate and distilled in a vacuum. Data of the *l*-menthoxyacetates are given in Table 5.

Table 5. Data of *l*-menthoxyacetates of *cis*-3,4-dihydroxy-2,5-dimethoxytetrahydrofurans.

	C	H	OCH_3	B.p.$_{0.05}$ °C	n_D^{25}	Yield %
$C_{16}H_{26}O_5(OCH_3)_2$ (360.4) requires	60.0	9.0	17.2			
IX (prepared from V)	59.5	9.0	17.2	175–185	1.4699	33
$C_{28}H_{46}O_7(OCH_3)_2$ (556.7) requires	64.7	9.4	11.2			
X (prepared from V)	64.3	9.4	11.8	230–235	1.4712	53
XI (prepared from VI)	64.7	9.3	11.5	222–226	1.4731	83

IX, X and XI did not crystallize on standing or by treatment with various solvents. Attempts to prepare a crystalline acetate of IX failed. Only an oil was obtained. It was therefore not possible to separate any diastereomeric forms by fractional crystallization.

Acknowledgment. We are indebted to our colleagues, Professor Børge Bak and Mr. Daniel Christensen for measuring and interpreting the infrared spectra and the dielectric constants.

REFERENCES

1. Clauson-Kaas, N. and Limborg, F. *Acta Chem. Scand.* **6** (1952) 551.
2. Clauson-Kaas, N. and Tyle, Z. *Acta Chem. Scand.* **6** (1952) 667.
3. Clauson-Kaas, N., Limborg, F. and Glens, K. *Acta Chem. Scand.* **6** (1952) 531.
4. Clauson-Kaas, N. and Limborg, F. *Acta Chem. Scand.* **8** (1954) 1579.
5. Clauson-Kaas, N., Li, S. O. and Elming, N. *Acta Chem. Scand.* **4** (1950) 1233.
6. Clauson-Kaas, N. (to Kemisk Værk Køge A/S). Danish patent 78381 (filed July 5, 1951).
7. Sheedan, J. C. and Bloom, B. M. *J. Am. Chem. Soc.* **74** (1952) 3825.
8. Prelog, V. and Wieland, P. *Helv. Chim. Acta* **27** (1944) 1127.
9. Krebs, H., Wagner, J. A. and Diewald, J. *Chem. Ber.* **89** (1956) 1875.
10. Zeile, K. and Heusner, A. *Chem. Ber.* **87** (1954) 439.

Received September 19, 1957.

ACTA CHEMICA SCANDINAVICA 12 (1958) 68—78

On the Biosynthesis of some Recently Discovered Derivatives of Glutamic Acid in Plants

PEKKA LINKO* and ARTTURI I. VIRTANEN

Laboratory of the Foundation for Chemical Research, Biochemical Institute, Helsinki, Finland

1- and 2-^{14}C-pyruvates, respectively, were fed to excised leaves of *Asplenium septentrionale* and *Phlox decussata* by different methods, and the incorporation of radioactivity into the amino compounds was followed as a function of time. No significant differences in the metabolic pattern could be found in these plants containing "new" amino acids as compared to the other plants examined. Transaminase activity is very high, alanine being most rapidly labelled. Already after a few minutes from the beginning of infiltration amino compounds contained up to 75 % of the total in 70 % ethanol soluble activity. After about 15 h glutamine was the major labelled product.

γ-Methyl-γ-hydroxyglutamic acid is shown to exist free in *Phlox decussata* by means of isotopic techniques. Hence this amino acid may be a normal metabolite in plants. The main biosynthetic route to γ-methyl-γ-hydroxyglutamic acid is most probably an aldol condensation of two pyruvate molecules, following transamination. γ-Hydroxyglutamic acid is not noticeably synthesized in the leaves of *Phlox decussata*.

The role of γ-aminobutyric acid in relation to glutamine is discussed. The most probable route from γ-AB to glutamic acid seems to be *via* glutamine.

The results indicate that glycine is not the main precursor of serine in these plants.

A great number of previously unknown amino compounds have been detected in living organisms during the last few years. Most of these compounds are found only in the 70 % ethanol soluble part, but some are thought to be protein components, too. Though it appears probable that these amino derivatives are not central metabolites in plants, it seems to be quite possible that many of them occur widely distributed in the plant kingdom.

Very little is still known about the metabolism of most of these "new" compounds. Not much could be done to solve this problem before the techniques using radioactive isotopes as tracers were available. It will be of great impor-

* Present address: Kansas State College, Department of Flour and Feed Milling Industries, Manhattan, Kansas, U.S.A.

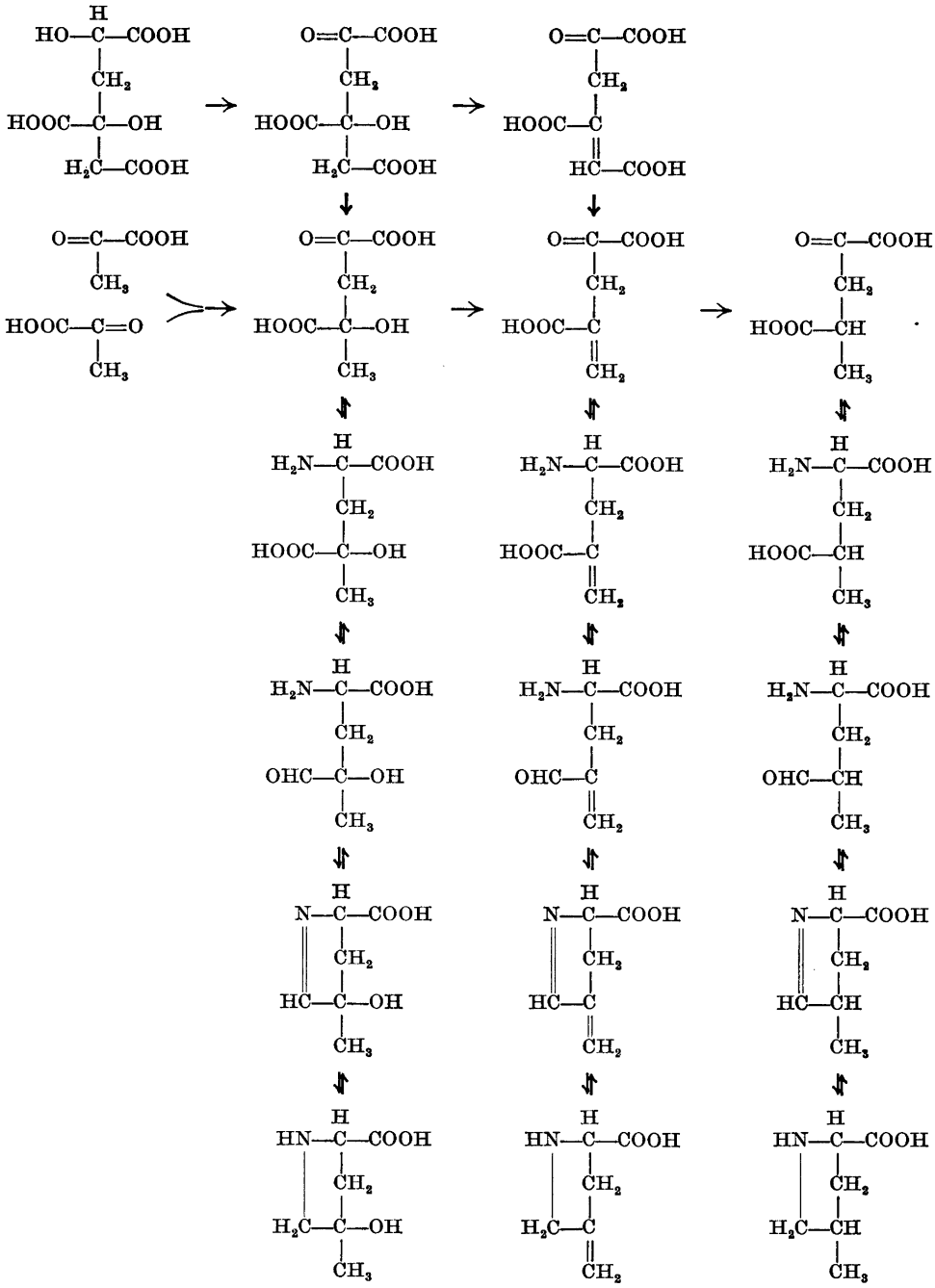

Fig. 1. Scheme of the possible biosynthetic reactions leading to γ-derivatives of glutamic acid.

tance to discover whether the metabolism of plants containing large amounts of these compounds is entirely different from that of others or if there is merely a simple enzyme block present. The latter hypothesis would explain the fact that some of these compounds, when present, are predominant among the free amino acids. In other cases they would be only very short lifetime intermediates and therefore not detectable without tracer techniques.

Already eleven monoaminodicarboxylic acids have been found to exist in plants. Four of them are derivatives of glutamic acid: γ-methyleneglutamic acid and the corresponding amide [1], γ-methylglutamic acid [2], γ-methyl-γ-hydroxyglutamic acid, γ-MHGA [2,3], and γ-hydroxyglutamic acid, γ-HGA [4]. All of these, as well as the known derivatives of γ-aminoadipic and pimelic acids [5], contain the substituents in γ-position. This has led to the assumption [6] that the primary reaction of the biosynthesis of these compounds would be an aldol condensation of either two molecules of pyruvate or one pyruvate molecule and one molecule of some other oxo compound as glyoxylic acid. Transamination would then result to the corresponding amino acid. Many of these keto acids are now known to exist free in plants [7–10].

A different possibility has been postulated by Bentley and Thiessen [11]. According to them, 2,4-dihydroxy-1,2,4-butanetricarboxylic acid, which is known to exist in dog's liver [12] and in bacteria [13], would be oxidized and dehydrated to 4-oxo-1-butene-1,2,4-tricarboxylic acid. The carboxyl group in position 1 would then be decarboxylated by means of a specific decarboxylase. Oxalocitramalic acid, which is a postulated intermediate in this scheme, is, however, not a normal metabolite [14].

A third possibility would be the biosynthesis from the corresponding proline derivatives. This hypothesis seems to be quite possible at least when γ-HGA is in question. A summary of all these reactions is shown in Fig. 1.

To test the aldol condensation hypothesis sodium 1- and 2-^{14}C-pyruvates were fed to *Asplenium septentrionale* [15] and *Phlox decussata*. In the former γ-MHGA [16] and in the latter γ-HGA [4] were known to occur.

MATERIALS AND METHODS

Plant material. *Asplenium septentrionale* was harvested in September and October. Most experiments were performed with freshly picked plants, but in some cases *Asplenium*, kept up to several months at +4°C in an open jar, was used. The results in different cases did not markedly differ from each other. *Phlox decussata* was grown in the greenhouse from a piece of root picked early in the spring under snow. Plants were used for experiments when about 10 cm high.

Radiochemicals were obtained from the Radiochemical Centre, Amersham, England.

Experiments of two different types were performed. I. 25 *Asplenium* plants (*ca.* 700 mg fresh wt.) were put in each of a series of small test tubes containing 4 ml of water. Half a cm of the plants was cut off under water, and 3 ml of the liquid was carefully pipetted away. To each of the test tubes 100 μl of sodium pyruvate solution (0.067 mg = 2.7 μC ml of water was added mixing carefully. After 2, 6 and 13 h 0.5 ml of water was added to each tube. Samples were collected after ½, 1, 2, 4, 6, 12, 24 and 48 h. The uptake of radioactivity was much higher when plants stored (and dried) at +4°C were used. II. Most of the experiments were performed by the vacuum infiltration method. About 500 —700 mg fresh wt. of plants were cut to pieces, *ca.* 1 cm long, and put into small glass jars each containing 2 ml of radioactive pyruvate solution (2—4 μC in different experiments). Samples were then subjected to a small vacuum by means of a vacuum desicca-

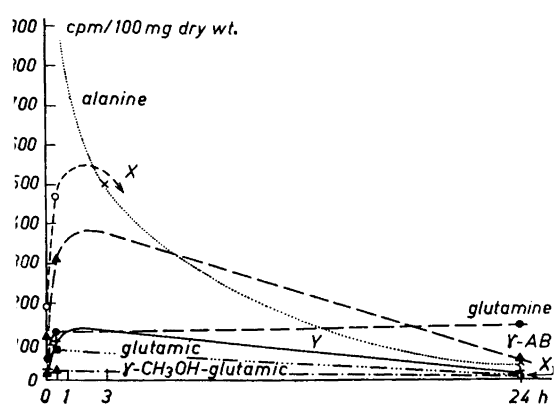

Fig. 2. Total radioactivity changes in the amino compounds of *Asplenium septentrionale* after 2-^{14}C-pyruvate infiltration.

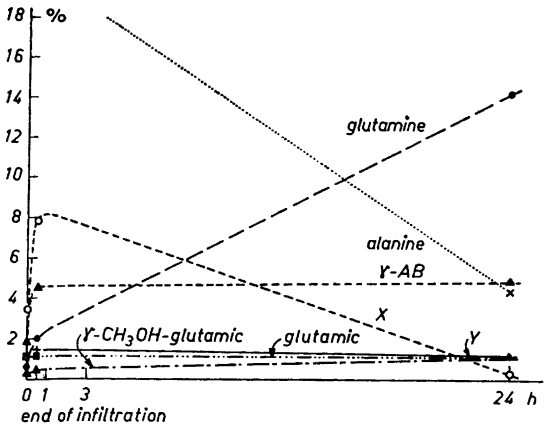

Fig. 3. Percentage of radioactivity in the individual amino compounds calculated from the total ethanol soluble activity in *Asplenium septentrionale* after 2-^{14}C-pyruvate infiltration.

tor several times after each other. The time of infiltration varied from 5 to 30 min. During this period practically all of the solution was taken up by the plants. Samples were dried lightly between filter papers and put on moist filter papers into light for different periods of time. Sometimes all of the plant material was subjected to infiltration simultaneously, and aliquots were taken after certain time intervals. All experiments with *Phlox decussata* were performed by this method.

The extraction was done with 70 % ethanol until the residue was practically colorless. Extracts were purified from salts and other materials, disturbing in paper chromatography, by passing through an Amerberlite IR-120 cation exchange resin, the extract thus being divided into the amino compound and "peptide" fractions. The amino compounds were eluted from the resin with 1 N NH_4OH. Both fractions were evaporated to a small volume *in vacuo* at 40°C. It was noticed using algae, from which good chromatograms can be made even without ion exchange treatment, that the "peptide" fraction does not continue to give a correct picture of the "anionic" compounds [17]. This is largely due to decomposition of phosphates and some other easily hydrolysable compounds including even some amino derivatives.

For chromatography Whatman No. 4 paper was used without prewashing. First solvent: phenol (Merck, "für Chromatographie", without distillation) saturated with water in ammonia atmosphere. Ammonia was omitted for chromatography of the "peptide" fraction. Second solvent: *n*-butanol: acetic acid: water (63:10:27). In both solvent systems HCN was used to prevent the "pink front" on ninhydrin sprayed amino acids.

Radioautograms were taken either on Ilford Ilfex X-Ray film or on Kodak's single coated Medical X-Ray tinted back film.

Radioactivity measurements of the spots on paper chromatograms were first done by extracting the spots with small amounts of water and counting the evaporated extracts on aluminium discs with Friesecke & Hoepfner, G.m.b.H., Erlangen-Bruck, scaler using Geiger tube FHZ 15/5716 (window -2.1 mg/cm^2). Later, spots were counted directly on chromatograms with a Tracerlab Autoscaler using a self made gasflow counter (DuPont mylar window). If found necessary, the results were corrected for the self absorption and coincidence.

Only semiquantitative paperchromatographical estimations were made in cases when the specific activity was determined.

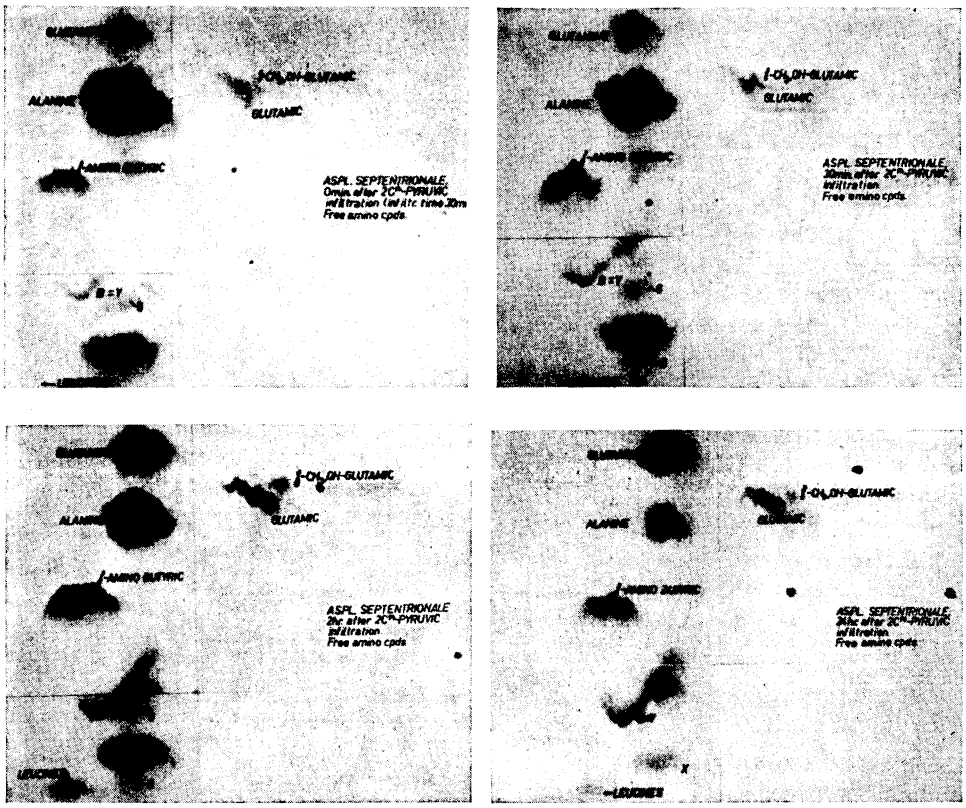

Fig. 4. Radioautograms of the amino compound fraction of *Asplenium septentrionale*. After 2-^{14}C-pyruvate infiltration.

RESULTS AND DISCUSSION

Radioactive pyruvate was readily metabolised in all experiments performed with *Asplenium septentrionale* (Figs. 2, 3 and 4). When excised shoots were allowed to take up active pyruvate solution the activity of the nutrient solution dropped to about 30 % in 2 h and to 4 % in 24 h (Table 1). A slightly higher percentage of the 70 % ethanol soluble radioactivity was incorporated into the amino compounds when pyruvate was infiltrated into the detached plants. The amino compounds contained relatively more activity after 2-^{14}C-pyruvate infiltration than when 1-^{14}C-pyruvate was used. Though pyruvate itself is found in the "peptide" fraction already after a few minutes amino compounds contained more than 50 % of the soluble activity. This amount dropped to about 10 % in 20 h when 1-^{14}C-pyruvate was given, but on 2-^{14}C-pyruvate infiltration after 24 h the amino compound fraction still contained 46 % of the activity (Table 2). The rapid labelling of this fraction was largely due to a very high transaminase activity, hence alanine being formed most

Table 1. Percentage of activity of 1-^{14}C-pyruvate in the nutrient solution when pyruvate was given to the excised shoots of *Asplenium septentrionale.*

Time, h	%
2	28.3
4	12.2
12	6.5
24	4.2

rapidly and with a rather high specific activity. When 1-^{14}C-pyruvate is used part of the active alanine may also be formed secondarily from the refixed carbon dioxide *via* 3-phosphoglyceric acid and the tricarboxylic acid cycle. The initially high activity of alanine then decreased rapidly.

Generally, 2-^{14}C-pyruvate was much more effectively utilized for the synthesis of labelled amino acids than was 1-^{14}C-pyruvate (Figs. 5 and 6). The latter is readily decarboxylated in the plant, the active CO_2 then being

Table 2. Percentage of activity in amino compounds from the total 70 % ethanol soluble in *Asplenium septentrionale.*

Time	1-^{14}C-pyruvate, no infiltration	1-^{14}C-pyruvate, infiltration	2-^{14}C-pyruvate, infiltration
h	%	%	%
½	42	55	75
1	36	45	67
2	26	—	65
3	—	37	—
20	—	11	—
24	—	—	46
70	—	6	—

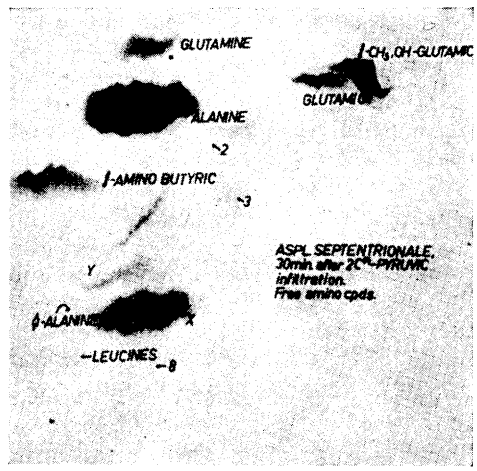

Fig. 5. Radioautogram of the amino compound fraction of *Asplenium septentrionale.* 30 min after 2-^{14}C-pyruvate infiltration.

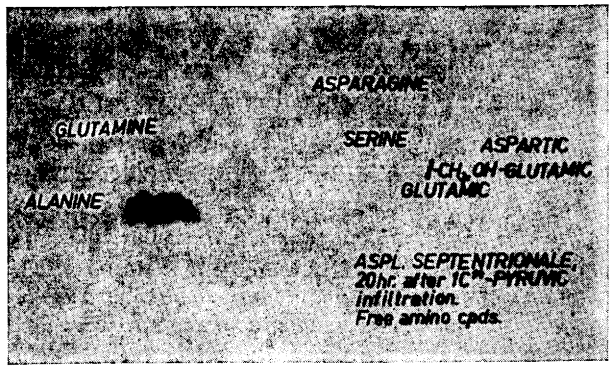

Fig. 6. Radioautogram of the amino compound fraction of *Asplenium septentrionale.* 20 h after 1-^{14}C-pyruvate infiltration.

reutilized to a great extent for carbohydrate synthesis etc. In this case most of the amino acids were rapidly found labelled with a low specific activity. This indicates that decarboxylation to acetyl-CoA is probably more important in the plant than is the carboxylation of pyruvate to oxalacetic acid. The relatively highest specific activity was found in the γ-MHGA. The results confirm those obtained by Miettinen [18] who showed that carboxyl labelled alanine was taken up with out breakdown by a shoot of the pea plant *(Pisum sativum)* detached from the root but was then immediately decarboxylated. On the contrary, no active CO_2 was primarily lost from 2-^{14}C-pyruvate.

An unknown amino compound X was also very rapidly labelled reaching its peak within one hour. Its activity then decreased very rapidly as did that of alanine. After 24 h almost no more activity could be found in this compound. The spot did not give a positive ninhydrin reaction, but this does not exclude the possibility that X is present in only such a low concentration that it cannot be detected by ninhydrin spray. In this case compound X would have had the highest specific activity.

It was of interest to notice that after 2-^{14}C-pyruvate infiltration no activity could be found in either aspartic acid or its amide. If aspartic acid is mainly formed by transamination from oxalacetic acid formed in turn either by the Wood-Werkman reaction or *via* the tricarboxylic acid cycle the resulting aspartate would be radioactive. Both aspartic acid and its amide were readily labelled when 1-^{14}C-pyruvate was given to the plant. Aspartic acid is known to be among the first radioactive compounds formed during photosynthetic $^{14}CO_2$ fixation by algae [17]. This agrees very well with the fact that carboxyl labelled pyruvate is rapidly decarboxylated in plants, carbon dioxide then being reutilized. Several observations have shown that the main biosynthetic route to aspartic acid in plants is not *via* transamination from oxalacetic acid [19,20]. Nelson and Krotkov [20] postulate a condensation for its formation. It now looks very probable that the two-carbon pieces possibly involved in this reaction are not directly derived from pyruvate.

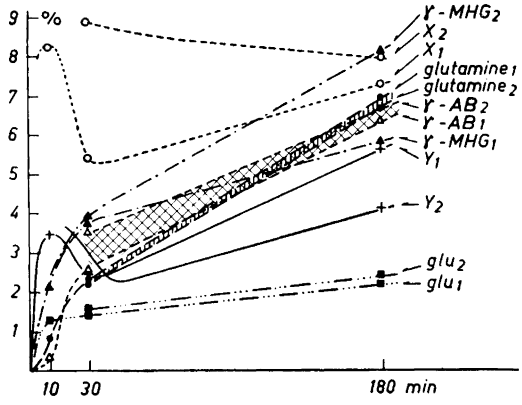

Fig. 7. The relative radioactivity changes of the individual amino compounds in *Asplenium septentrionale* after 2-^{14}C-pyruvate infiltration with (2) and without (1) inactive γ-AB addition.

In all experiments serine was labelled before glycine, which clearly indicates that it is not synthesized from the latter in *Asplenium septentrionale*. Similar results have been obtained by Tolbert and Gailey with wheat leaves [21]. In animal tissues [22,23] and in yeast [24] serine is found to be the precursor of glycine.

The radioactivity of glutamic acid rises rapidly to a certain level remaining then at a constant value. The same thing happens also with γ-aminobutyric acid (γ-AB). The specific activities of both of them are about the same. The activity of glutamine rises rapidly after a short lag period, being after about 15 h the major active compound. It is thought that the main route to γ-AB should be decarboxylation of glutamic acid [25,26]. Steward *et al.* [27,28] found only a slight activity of L-glutamic acid decarboxylase in potato tubers, which contain a high concentration of γ-AB. They suggested therefore that γ-AB was merely a precursor of glutamic acid and not its decarboxylation product. Miettinen and Virtanen [29] detected a considerable glutamic acid decarboxylase activity both in pea and alder but found no direct correlation between the concentration of γ-AB and the enzyme activity in plant tissues. According to Baptist [30] γ-AB may arise as a result of some reaction connected with protein synthesis. This is specially interesting because glutamine is thought to have some important role in protein synthesis [31,32]. Hence the role of γ-AB in relation to glutamine becomes an important question. Glutamate is known to be rapidly metabolised to glutamine and γ-ketoglutaric acid but not much to γ-AB in higher plants [33,34].

To try to trace the role of γ-AB, two experiments were performed with *Asplenium septentrionale*, in which 2-^{14}C-pyruvate only and 2-^{14}C-pyruvate with inactive γ-AB, respectively, were infiltrated to the plants (Fig. 7). The activity of the γ-AB itself was slightly increased in the latter case. This was probably due to the fact that while the rate of synthesis of active γ-AB remains the same, the γ-AB pool is diluted with the added inactive product, and hence less of the active molecules react further in a given time. This results in the enrichment of active γ-AB. The primary metabolic products from γ-AB should have slightly lowered the relative activity when inactive γ-AB is added. This

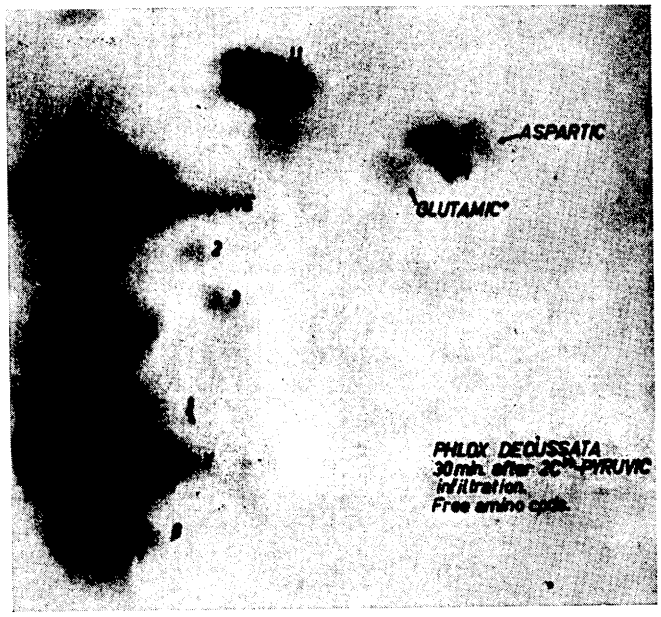

Fig. 8. Radioautogram of the amino compound fraction of *Phlox decussata*. 30 min after 2-^{14}C-pyruvate infiltration. The numbered spots are unknown. No. 1 is identified as γ-MHGA.

was found only in the case of glutamine and an unknown amino compound Y. The radioactivity of compound Y had a minimum after about 30 min, which could be explained under the assumption that two different metabolic pools of the precursor of Y exist, one of these two becoming much more slowly active. Because the radioactivity of glutamic acid was slightly increased in the latter experiment it may not be a primary carboxylation product of γ-AB. It seems much more probable that glutamic acid arises from γ-AB *via* glutamine. However, the increase of radioactivity of glutamic acid can at least be partly explained by the fact that the addition of inactive γ-AB increases the amount of nitrogen available for transamination reactions. The enzyme catalysing transamination between γ-AB and α-ketoglutaric acid is known to exist in pea [35].

γ-MHGA is rapidly labelled both with 1- and 2-^{14}C-pyruvates. In both cases the amount of radioactivity increases all the time resulting in a high specific activity as compared to other amino compounds. If the aldol condensation hypothesis is correct, pyruvic acid should be incorporated intact into the γ-derivative of glutamic acid. If this is the fact, 1-^{14}C-pyruvate would give a relatively high activity in γ-MHGA compared with the activities of glutamate and aspartate, since in this case the active carbon atom would enter directly into the molecule of γ-MHGA. Because the pyruvate molecules would undergo decarboxylation to give inactive acetyl-CoA, the only way labelled aspartic acid could be formed were the Wood-Werkman reaction of the liberated active

CO_2. From this labelled glutamic acid could then be formed. Therefore only a slight labelling of glutamic and aspartic acids would be expected. If the carbon chain of pyruvate would not enter intact into γ-MHGA, the radioactive compound could only arise from the reutilized carbon dioxide produced by decarboxylation. In such a case the Wood-Werkman reaction is probably the most important fixation mechanism, and the relative specific activities of aspartic and glutamic acids would be expected to be much higher than that of γ-MHGA. However, when 1-^{14}C-pyruvate was infiltrated to the plant γ-MHGA gained much greater specific activity than did the other amino acids. The observed difference was greater than what can be expected to arise from the possible dilution of the activities of the latter compounds during hydrolysis of inactive protein.

Active pyruvate, active pyruvate + inactive glycine, and active pyruvate + inactive glyoxylic acid, respectively, were infiltrated to the leaves of *Phlox decussata* to study whether γ-hydroxyglutamic acid would arise by a similar type of aldol condensation. In no experiments could any activity be incorporated into γ-HGA. Since the activity was rapidly incorporated into most of the other amino acids including a number of unknown amino compounds (Fig. 8) it seems very probable that γ-HGA is synthesized very slowly in the leaves, if at all. Even if this compound were to be synthesized *via* any intermediates of the tricarboxylic acid cycle in the leaves at least some radioactivity would be expected in it. However, synthesis from the protein amino acid hydroxyproline would result in an inactive product during short time experiments. It is also possible that the main site of the synthesis of γ-HGA is located elsewhere. This assumption is in good agreement with Fowden's [36] discovery that γ-methyleneglutamic acid and its amide arise during the early stages of seedling growth.

A spot with a very high specific activity was found on the place of γ-MHGA on paper chromatograms of the extracts of *Phlox decussata*. When isolated, it could indeed be shown to be identical with γ-MHGA isolated from *Asplenium*. This compound was not previously known to exist in *Phlox* and it could not even in this case be found by ninhydrin spray. The infiltration of inactive glycine did not have any significant effect on the labelling of this compound.

An interesting finding was that serine was rapidly labelled when inactive glycine was also infiltrated, but practically no formation of active serine was obtained with pyruvate infiltration alone.

All these experiments show that the most probable biosynthetic pathway of γ-MHGA in higher plants is *via* an aldol condensation from two pyruvate molecules. The final proof of this hypothesis would require a stepwise degradation of the γ-MHGA molecule and the determination of the radioactivities of each of the six carbon atoms, using pyruvate labelled in all three different positions, respectively. However, the total activity obtained in this compound was not great enough for such an experiment. The experiments with *Phlox decussata* showed in addition that γ-MHGA may be a normal metabolite in higher plants, but usually present in such a low concentration that the detection by the usual methods is not possible. This may be due to most of the newly discovered amino acids.

That no radioactivity could be incorporated into γ-HGA did not rule out the possibility of the existence of an aldol condensation with pyruvate and glyoxylate, but merely showed that this compound is not an active metabolite in the leaves of *Phlox decussata*. Generally, no significant differences in the metabolic pattern could be found in these plants containing "new" amino acids as compared to the other plants examined.

REFERENCES

1. Done, J. and Fowden, L. *Biochem. J.* **49** (1951) xx; **51** (1952) 451.
2. Virtanen, A. I. and Berg, A.-M. *Acta Chem. Scand.* **9** (1955) 553.
3. Grobbelaar, N., Pollard, J. K. and Steward, F. C. *Nature* **175** (1955) 703.
4. Virtanen, A. I. and Hietala, P. K. *Acta Chem. Scand.* **9** (1955) 175.
5. Virtanen, A. I., Uksila, E. and Matikkala, E. J. *Acta Chem. Scand.* **8** (1954) 1091.
6. Virtanen, A. I. Festschrift Arthur Stoll, Basel 1957, p. 565.
7. Virtanen, A. I. and Alfthan, M. *Acta Chem. Scand.* **8** (1954) 1720; **9** (1955) 188.
8. Towers, G. H. N. and Steward, F. C. *J. Am. Chem. Soc.* **76** (1954) 1959.
9. Fowden, L. and Webb, J. A. *Biochem. J.* **59** (1955) 228.
10. Wickson, M. E. and Towers, G. H. N. *Can. J. Biochem. & Physiol.* **34** (3) (1956) 502.
11. Bentley, R. and Thiessen, C. P. *Science* **122** (1955) 330.
12. Rapoport, S. and Wagner, R. H. *Nature* **168** (1951) 295.
13. Umbreit, W. W. *J. Bacteriol.* **66** (1953) 74.
14. Martius, C. *Hoppe-Seyler's Z. physiol. Chem.* **279** (1943) 96.
15. The yearly report (1956) of the Laboratory of the Foundation for Chemical Research, Biochemical Institute, Helsinki, Finland (in Finnish).
16. Bramesfeld, B. and Virtanen, A. I. *Acta Chem. Scand.* **10** (1953) 688.
17. Experiments done by one of us (P.L.) at the Radiation Laboratory, University of California, Berkeley.
18. Miettinen, J. K. *Suomen Kemistilehti* **B 30** (1957) 30.
19. Towers, G. H. N. and Martinus, D. C. *Can. J. Biochem. & Physiol.* **34** (3) (1956) 511.
20. Nelson, C. D. and Krotkov, G. *Can. J. Botany* **34** (1956) 423.
21. Tolbert, N. E. and Gailey, F. B. *Plant Physiol.* **30** (1955) 491.
22. Shemin, D. *J. Biol. Chem.* **162** (1946) 297.
23. Nyc, J. F. and Zabin, I. *J. Biol. Chem.* **215** (1955) 35.
24. Dawis, J. W., Cheldelin, V. H., Christensen, B. E. and Wang, C. H. *Biochem. et Biophys. Acta* **21** (1956) 101.
25. Wingo, W. J. and Awapara, J. *J. Biol. Chem.* **187** (1950) 267.
26. Roberts, E. and Frankel, S. *J. Biol. Chem.* **187** (1950) 55.
27. Steward, F. C., Thompson, J. F. and Dent, C. E. *Science* **110** (1948) 439.
28. Steward, F. C. and Thompson, J. F. *Ann. Rev. Plant Physiol.* **1** (1950) 233.
29. Miettinen, J. K. and Virtanen, A. I. *Acta Chem. Scand.* **7** (1953) 289.
30. Baptist, N. G. *Nature* **178** (1956) 1403.
31. Steward, F. C., Bidwell, R. G. S. and Yemm, E. W. *Nature* **178** (1956) 698.
32. Adelberg, E. A. and Rabinowitz, M. *Ann. Rev. Biochem.* **25** (1956) 349.
33. Webster, G. C. *Plant Physiol.* **29** (1954) 382.
34. Steward, F. C. and Bidwell, R. G. S. *Nature* **178** (1956) 734.
35. Miettinen, J. K. and Virtanen, A. I. *Acta Chem. Scand.* **7** (1953) 1243.
36. Fowden, L. *Biochem. J.* **48** (1954) 327.

Received September 16, 1957.

ACTA CHEMICA SCANDINAVICA 12 (1958) 79—88

The Crystal and Molecular Structure of Ethylene Thiocyanate

RASMUS BRINGELAND and OLAV FOSS

Chemical Institute, University of Bergen, Bergen, Norway

The structure of NCS · H_2C-CH_2 · SCN has been determined from single-crystal X-ray data. The crystals belong to the space group, $D_{2h}^{15}-Pbca$, with four molecules in a unit cell of dimensions: $a = 7.39$ Å, $b = 7.81$ Å, $c = 11.48$ Å. The molecules have a centrosymmetric, *trans* form, with the cyanide groups rotated out of the SCCS plane.

The bond lengths and angles are: C—C = 1.51 ± 0.03 Å, C—S = 1.80 ± 0.01 Å, S—C = 1.63 ± 0.01 Å, C—N = 1.18 ± 0.02 Å, ∠C—C—S = 110.7 ± 0.9°, ∠C—S—C = 99.4 ± 0.7°. The results indicate that the thiocyanate group is a hybrid of the structures $\diagup S-C\equiv N$ and $\diagup \overset{+}{S}=C=\overline{N}$. A value of 172° was found for the S—C—N angle, but the deviation from linearity is probably not significant.

In the course of preliminary work on the crystal structure of sulphur dithiocyanate [1], one of the present authors became interested in the nature of bonding in the thiocyanate group and its configuration and dimensions in other covalent compounds. Ethylene thiocyanate, NCS · H_2C—CH_2 · SCN, was chosen for study because of its simple formula and since the molecules, from literature data on other symmetrically disubstituted ethanes, might be expected to lie in crystallographic centres of symmetry.

CRYSTAL DATA

Ethylene thiocyanate (1,2-dithiocyanato-ethane) was prepared from ethylene bromide by heating in ethanol solution with a slight excess of potassium thiocyanate [2]. The compound melts at 90°C and vaporizes slowly in open air at room temperature. From chloroform, it crystallized as orthorhombic plates {010}, or as bipyramids {111} with in most cases {010} more or less developed. Buff [2], in 1856, described it as crystallizing from ethanol in rhombic plates.

From Weissenberg photographs, the axial lengths are: $a = 7.39$ Å, $b = 7.81$ Å, $c = 11.48$ Å. They are based on $\lambda(CuK_\alpha) = 1.542$ Å and are

believed to be accurate to better than 0.5 %. There are four molecules per unit cell; density, calc. 1.45, found 1.42 g/cm^3. The space group, from systematic absences, is D_{2h}^{15}—*Pbca*, which has eightfold general positions, and fourfold sets of symmetry centres as special positions. It follows that the molecules are centrosymmetric in the crystals.

The intensities of the 0*kl* and *h*0*l* reflections were estimated visually from Weissenberg photographs, taken with CuK_α radiation for which the absorption coefficient of the crystals is 63.2 cm^{-1}. Crystals with small, nearly uniform diameters were used in order to minimize absorption and spot shape effects. Out of 58 possible 0*kl* reflections within the range sin $\Theta < 0.985$ (CuK_α radiation) 53 were recorded with measurable intensity, the corresponding figures for *h*0*l* being 50 out of 59. The intensities were corrected in the usual way to give sets of relative structure amplitudes; these were eventually put to an approximately absolute scale by comparison with the calculated values.

The latter were based on the atomic scattering curves of Viervoll and Ögrim [3] for sulphur and hydrogen, and of Berghuis *et al.*[4] for nitrogen and carbon.

All summations were performed by means of Beevers-Lipson strips, at 6° intervals.

DETERMINATION AND REFINEMENT OF THE STRUCTURE

There is one sulphur, one nitrogen and two carbon atoms in the asymmetric unit, apart from two hydrogen atoms, and conditions should thus be favourable for use of the heavy atom method in the initial stages.

From the *a*-axis Patterson projection, the coordinates, $y = 0.02$, $z = 0.075$ were derived for sulphur. A F_o synthesis based on 35 of the largest 0*kl* terms, with signs corresponding to the sulphur contributions alone, gave an electron density map where the general outline of the molecule could be recognized, but extensive overlapping occurred and further work on this projection was postponed until use could be made of *z* coordinates obtained from the *h*0*l* data.

The *b*-axis Patterson projection gave $x = 0.25$, $z = 0.078$ for sulphur, and these coordinates were used to derive the signs of 42 of the largest *h*0*l* terms for a subsequent F_o synthesis. Although overlapping of atoms was evident also here, the electron density map, together with considerations of probable bond lengths and the assumption of a linear thiocyanate group, allowed approximate coordinates for the nitrogen and carbon atoms to be determined. Signs were then calculated for all observed *h*0*l* structure factors, and none of these signs changed later. The electron density map thus obtained is shown in Fig. 1.

The refinement of this projection proceeded as follows. With $x = 0.25$, the sulphur atom lies in or close to the glide plane *b* at $x = \frac{1}{4}$, and overlaps with another sulphur atom belonging to a different molecule. The shape of the composite peak indicated that the sulphur atom should be slightly removed from the glide plane, and on changing *x* from 0.25 to 0.26 and then to 0.267 the reliability index *R* (using at this stage an overall, isotropic temperature correction with $B = 5.0$ Å^2) dropped from 0.135 over 0.123 to 0.115. Small adjustments in the nitrogen and carbon coordinates led to a further improve-

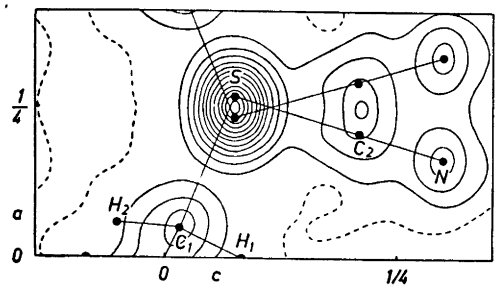

Fig. 1. Electron density projection of ethylene thiocyanate along the *b* axis. The 1-electron line is dashed, and the first full contour line is at 3 e · Å^{-2}. Intervals thereafter: 3 e · Å^{-2} for the sulphur atom and 2 e · Å^{-2} for the nitrogen and carbon atoms. The final atomic positions are marked with dots.

ment in R of about 0.01; from then on, refinement was carried out by means of (F_o—F_c) syntheses. In the first difference map, peaks appeared which were taken to indicate the positions of the two hydrogen atoms. When the hydrogen contributions were included in the calculated structure factors, with hydrogen coordinates chosen within the peaks on the basis of C—H = 1.1 Å and tetrahedral carbon, the value of R dropped by 0.02 to 0.085. Five more difference refinements were made.

Work on the *a*-axis projection was then resumed. The *z* coordinates were here, until after the fourth difference synthesis, kept equal to those found from the *h0l* data. Trial calculations on *y* coordinates relatively soon led to the determination of the correct signs of all observed *0kl* structure factors; the corresponding electron density map is shown in Fig. 2. The reliability index, using $B = 5.0$ Å^2 in the temperature factor as above, was at this stage 0.20. By trial and error, this figure was reduced to 0.13. At that stage the hydrogen contributions were included, based on the same *z* coordinates as in the *b*-projection and *y* coordinates derived by taking C—H = 1.1 Å. R then dropped to 0.115. Finally, extensive (F_o—F_c) refinement was carried out.

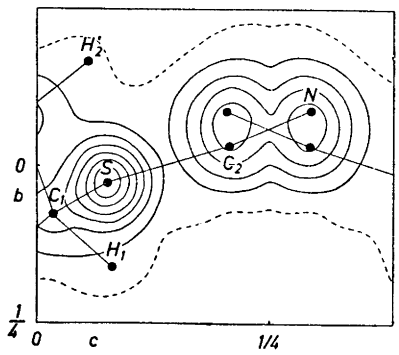

Fig. 2. Electron density projection along the *a* axis. All full contour lines are at intervals of 3 e · Å^{-2}, otherwise as in Fig. 1.

In both projections the difference maps indicated individual and partly anisotropic temperature corrections. In the temperature factor $\exp[-B(\sin^2\Theta/\lambda^2)]$ finally chosen the values of B were: For the $h0l$ data, $B = 4.6$ Å^2 and 5.5 Å^2 for the carbon atoms C_1 and C_2, respectively, 5.2 Å^2 for the nitrogen atom and $(4.3 + 0.4 \cos^2 \varphi)$ Å^2 for the sulphur atom, where φ is the angle between the normal of the reflecting plane and the direction of maximum vibration of the atom, the a axis. For the $0kl$ data, $B = 5.0$ Å^2 for C_1 and 5.7 Å^2 for C_2, and $(5.2 + 1.2 \cos^2 \varphi)$ Å^2 and $(4.5 + 1.2 \cos^2 \varphi)$ Å^2 for the nitrogen and the sulphur atom, respectively. Here, the direction of maximum vibration was for both atoms taken to be that of the b axis, although in the case of sulphur a slightly different direction was indicated in the last maps. For the hydrogen atoms, $B = 5.0$ Å^2 in both zones. The large thermal parameters are in agreement with the relatively low melting point and high sublimation pressure of the substance.

The final atomic coordinates are given in Table 1. Two independent sets of z coordinates were obtained, namely, $z(S) = 0.0770$ and 0.0765, $z(N)=0.299$ and 0.297, $z(C_1) = 0.016$ and 0.017, $z(C_2) = 0.208$ and 0.206, from the $h0l$ and $0kl$ data, respectively. The mean values are listed in the Table. The hydrogen coordinates, which of course are approximate only, are for H_1: $x = 0.056$, $y = 0.168$, $z = -0.056$, and for H_2: $x = -0.019$, $y = 0.155$, $z = 0.082$.

Table 1. Atomic coordinates, in fractions of corresponding cell edges. Origin at a centre of symmetry.

	x	y	z
S	0.268	0.027	0.0768
N	0.165	−0.088	0.298
C_1	0.051	0.080	0.016$_5$
C_2	0.205	−0.029	0.207

Observed and calculated $h0l$ and $0kl$ structure factors are listed in Table 2. The reliability index, $R = \Sigma||F_o|-|F_c||/\Sigma|F_o|$, with non-observed reflections included when $|F_c|$ exceeds the observable limit, is 0.047 for the $h0l$ data and

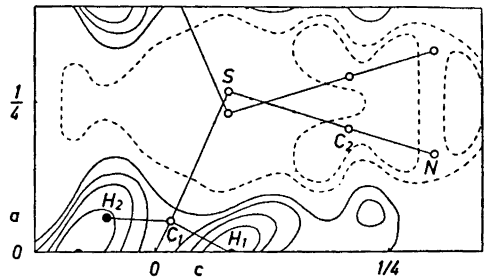

Fig. 3. Difference projection along the b axis, with hydrogen atoms *not* subtracted. Their positions are marked with dots, those of the other atoms with rings. Contour lines at −0.4, −0.2, 0.2, 0.4 ... e · Å^{-2}, with negative lines dashed.

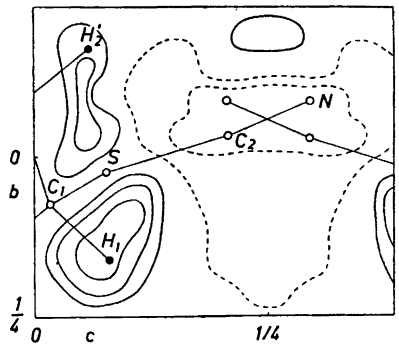

Fig. 4. Difference projection as in Fig. 3, along the *a* axis.

0.056 for the 0*kl* data. If the hydrogen contributions to F_c are omitted, the R values increase to 0.078 and 0.081, respectively. The effect is thus quite large. The difference maps of Figs. 3 and 4, calculated after ended refinement on the basis of F_c values with hydrogen contributions not included, are reproduced to show the hydrogen peaks and the assumed hydrogen positions.

The extent to which the projections could be refined was in the last stages felt to be limited by lack of accuracy of the experimental data. An estimate of random errors in the F_o, made by comparing values from different quadrants of a film, and scaled values from different films in the multiple-exposure series, led to reliability indexes of 2.5—3.0 % for the F_o for both zones.

ASSESSMENT OF ACCURACY

The standard deviation in electron density, evaluated as the root-mean-square of the figures in the difference maps, is slightly above 0.2 e · Å^{-2} for both zones, and the r.m.s. gradient of the difference maps is about 0.7 e · Å^{-3} in both axial directions of each map. The estimation of standard deviations in atomic coordinates on the basis of the gradients and the curvatures of the electron density peaks [5,6] is rendered uncertain by the rather extensive overlapping which occurs in both projections. Use of the method on the relatively well resolved nitrogen atom in the *b*-axis projection gave $\sigma(x) = 0.013$ Å, $\sigma(z) = 0.010$ Å for this atom. Assuming that the errors are the same for all three coordinates of an atom, and that they are inversely proportional to the atomic number, one gets $\sigma = 0.005$ Å for the sulphur coordinates and 0.011—0.015 Å for the nitrogen and carbon coordinates. The figures are relatively large despite the good agreement between observed and calculated structure factors, owing to the large thermal vibrations of the atoms and correspondingly low curvature of the electron density peaks. Because of the overlapping, the errors may be considerably larger than should be expected from the calculated standard deviations; however, the correspondence between the two independently determined sets of z coordinates, one from each zone, indicates that the estimates are of a reasonable order of magnitude. The difference between the z coordinates is 0.006 Å for sulphur, 0.01 Å for C_1 and 0.02 Å for C_2 and N.

Table 2. Observed and calculated *h0l* and *0kl* structure factors for ethylene thiocyanate.

l	F_o	F_c
	h0l zone	
	00*l*	
2	34	+35
4	20	+21
6	38	−36
8	36	−37
10	17	+17
12	9	+10
14	12	+11
	10*l*	
2	78	−77
4	75	−75
6	13	−13
8	26	+24
10	21	+21
12	8	+ 8
14	7	− 6
	20*l*	
0	93	−99
2	16	+19
4	26	+24
6	51	+51
8	37	+36
10	7	− 7
12	7	− 9
14	9	− 9
	30*l*	
2	54	+55
4	36	+34
6	13	+12
8	26	−27
10	24	−21
12	8	− 8
14	<1	+ 2
	40*l*	
0	52	+49
2	33	+33
4	12	−11
6	29	−29
8	14	−14
10	<4	+ 2
12	10	+ 9
	50*l*	
2	37	−33
4	19	−19
6	15	−15
8	10	+10
10	8	+ 8
12	<2	+ 1
	60*l*	
0	16	−16
2	19	−21
4	6	+ 7
6	14	+15
8	5	+ 5
10	<3	+ 1
	70*l*	
2	11	+12
4	7	+ 8
6	<3	+ 2
8	7	− 7
	80*l*	
0	<3	+ 2
2	<3	+ 4
4	6	− 6
6	7	− 7
8	<1	− 3
	90*l*	
2	<2	− 3
4	3	− 4
	0kl zone	
	00*l*	
2	37	+35
4	23	+22
6	39	−36
8	39	−37
10	17	+16
12	7	+ 9
14	10	+11
	02*l*	
0	153	+153
1	27	+28
2	25	+20
3	60	−56
4	2	+ 3
5	15	−16
6	35	−33
7	6	+ 5
8	28	−28
9	3	− 3
10	9	+10
11	6	+ 7
12	8	+ 8
13	5	− 4
14	8	+ 8
	04*l*	
0	31	+31
1	6	+ 9
2	13	+13
3	45	−47
4	14	−14
5	18	−18
6	26	−26
7	5	+ 4
8	15	−15
9	<3	+ 2
10	<3	0
11	7	+ 8
12	6	+ 6
13	4	− 3
	06*l*	
0	3	+ 3
1	5	− 6
2	5	+ 4
3	23	−23
4	9	−11
5	10	−11
6	14	−14
7	3	+ 3
8	7	− 6
9	7	+ 7
10	2	− 2
11	5	+ 6
	08*l*	
0	<3	0
1	5	− 5
2	<3	0
3	10	−10
4	2	− 3
5	4	− 5
6	3	− 3
7	3	+ 2
8	<2	− 2
9	3	+ 5

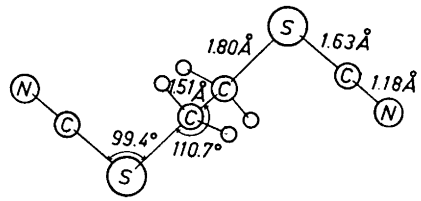

Fig. 5. The ethylene thiocyanate molecule as it appears in projection along the *b* axis.

DESCRIPTION AND DISCUSSION OF THE STRUCTURE

The dimensions of the ethylene thiocyanate molecule were calculated from the coordinates of Table 1 and are listed in Table 3. A prime is used to denote the equivalent of an atom in the other half of the molecule across the centre of symmetry.

The ethane carbon and the sulphur valency angles are normal, and the lengths of bonds involving the ethane carbon atoms correspond within the errors to single bonds, as should be expected. In the thiocyanate group the value, 172.3 ± 1.3°, obtained for the S—C—N angle indicates that the group may not be linear. Least squares straight lines through the projected atoms, with the sulphur coordinates given three times the weight of the carbon and nitrogen coordinates, pass at shortest distances of 0.011 Å, 0.064 Å and 0.031 Å, respectively, from S, C and N in the *a*-projection, and at 0.002 Å, 0.012 Å and 0.007 Å in the *b*-projection. The largest deviation occurs for C in the *a*-projection, in which this atom is subject to heavy overlapping and may well have larger coordinate errors than corresponding to the e.s.d. of about 0.015 Å. Thus, the deviation from linearity of the thiocyanate group is probably not significant.

Table 3. Bond lengths and angles.

$C_1'-C_1 = 1.51 \pm 0.03$ Å	$\angle C_1'-C_1-S = 110.7 \pm 0.9°$
$C_1-S = 1.80 \pm 0.01$	$\angle C_1-S-C_2 = 99.4 \pm 0.7°$
$S-C_2 = 1.63 \pm 0.01$	$\angle S-C_2-N = 172.3 \pm 1.3°$
$C_2-N = 1.18 \pm 0.02$	

Some non-bonded distances within the molecule.

$C_1-C_2 = 2.61$ Å	$S-N = 2.80$ Å	$S-S' = 4.36$ Å
$C_1-N = 3.59$	$S-C_1' = 2.72$	$N-N' = 8.47$

The lengths found for the S—C and C—N bonds of the thiocyanate group, namely 1.63 ± 0.01 Å and 1.18 ± 0.02 Å respectively, can be interpreted in terms of the structures:

$$\diagup S-C\equiv N \qquad \text{and} \qquad \diagup \overset{+}{S}=C=\overline{N}$$

(I) (II)

The lengths of pure single, double and triple bonds are taken to be:

S—C = 1.78 Å	C=N = 1.26 Å
S=C = 1.59	C≡N = 1.16

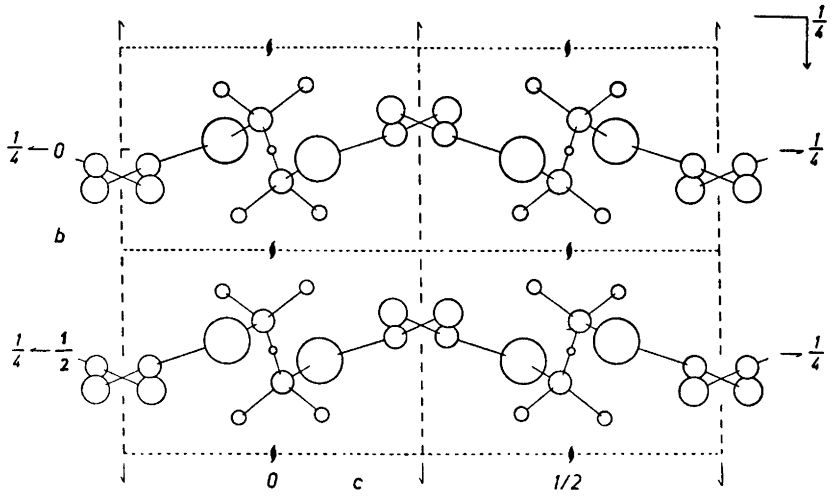

Fig. 6. The arrangement of molecules in the unit cell as seen along the *a* axis. In order of decreasing size the circles mark sulphur, nitrogen, carbon and hydrogen atoms.

In arriving at these figures, the single- and double-bond radii of carbon, 0.771 Å and 0.677 Å which are valid for sp^3 and sp^2 hybridization, respectively, of the carbon σ-bond orbitals, have been reduced by about 0.035 Å and 0.015 Å, respectively, to account for the *sp* state of hybridization of the carbon σ-bond orbitals in the thiocyanate group. The shortenings *cf.* [7,8] are based on evidence from C—H bonds with carbon in the appropriate valency states.

The found bond lengths indicate that structures I and II both contribute. The length of the thiocyanate group, *i. e.*, the S—N distance, is 2.80 Å whereas the calculated length is 2.94 Å for structure I and 2.85 Å for structure II. In view of the magnitude of the probable errors, and uncertainties in the bond order-bond length data, the results do hardly permit any conclusion beyond the one that structure II appears to be at least as important as structure I.

No structural data are available for other organic thiocyanates. Beard and Dailey [9] have made a microwave study of gaseous methyl thiocyanate, but did not determine the bond lengths. Assuming S—C = 1.61 Å and C—N=1.21 Å and a linear thiocyanate group, they arrived at 142° for the C—S—C angle, a value which appears unreasonable. Lindqvist's recent crystal structure determination of silver thiocyanate [10] led to S—C = 1.64 ± 0.03 Å and C—N = 1.19 ± 0.07 Å, and a not significant deviation from linearity of the thiocyanate group. The sulphur valency angle was here 180°, and also the nitrogen atom was covalently bonded to silver, so that the conditions are not quite comparable. The same applies to thiocyanic acid, which has the tautomeric structure H—NCS [11]. In the thiocyanate ion, from a crystal structure determination of the ammonium salt [12], the S—C and C—N bonds are 1.58 ± 0.02 Å and 1.24 ± 0.02 Å, and the ion linear. This corresponds to structure II above:

$S=C=\bar{N}$. More contribution of structure I is expected in a covalent thiocyanate, in agreement with the findings in ethylene thiocyanate.

The cyanogen halides, X—CN, are analogues of covalent thiocyanates in the respect that they contain a cyanide group linked to an atom with lone electron pairs. Particularly in the chloride, where X has nearly the same size as sulphur, conditions should be comparable, apart from the higher electronegativity of chlorine and thereby larger ionic character of the Cl—C bond relative to S—C. From microwave studies of the gases [13,14] the bond lengths in the linear cyanogen halide molecules are:

	ICN	BrCN	ClCN
X—C	1.995 Å	1.790 Å	1.630 Å
C—N	1.159	1.159	1.163

The C—N bond has in all three compounds close to triple-bond length, while the X—C bonds are about 0.1 Å shorter than single bonds. From nuclear quadropole coupling constants, estimates of the relative importance of structures corresponding to I and II were made for gaseous cyanogen iodide and bromide [15–17]. The data indicated 13 % contribution of II, X=C=N, in the iodide and 26 % in the bromide. In the chloride the percentage of II should be still higher, judging from the relative importance of $p\pi$-bonding from I, Br and Cl in aromatic compounds. Bonding conditions in the thiocyanate group thus appear to be about the same as in cyanogen chloride.

The ethylene thiocyanate molecule occurs in the *trans* configuration in the crystals, a molecular centre of symmetry being crystallographically required. This agrees with the finding from infrared measurements [18] that the compound exists in the *trans* form in the solid state, and with observations [19] that the stable form in the solid state of molecules of the types $X \cdot H_2C—CH_2 \cdot X$ and $X \cdot H_2C—CH_2 \cdot Y$ is, with few exceptions, the *trans* form. The cyanide groups are rotated out of the SCCS plane.

The arrangement of molecules in the unit cell as seen along the *a* axis is shown in Fig. 6. There are no particularly close intermolecular contacts.

REFERENCES

1. Foss, O. *Acta Chem. Scand.* **10** (1956) 136.
2. Bufi, H. L. *Ann.* **100** (1856) 219, p. 242.
3. Viervoll, H. and Ögrim, O. *Acta Cryst.* **2** (1949) 277.
4. Berghuis, J., Haanappel, I. M., Potters, M., Loopstra, B. O., MacGillavry, C. H. and Veenendal, A. L. *Acta Cryst.* **8** (1955) 478.
5. Cruickshank, D. W. J. *Acta Cryst.* **2** (1949) 65.
6. Cochran, W. *Acta Cryst.* **4** (1951) 81.
7. Coulson, C. A. *Victor Henri Memorial Volume*, Desoer, Liége 1948, p. 15.
8. Maccoll, A. *Trans. Faraday Soc.* **46** (1950) 369.
9. Beard, C. I. and Dailey, B. P. *J. Am. Chem. Soc.* **71** (1949) 929.
10. Lindqvist, I. *Acta Cryst.* **10** (1957) 29.
11. Beard, C. I. and Dailey, B. P. *J. Chem. Phys.* **18** (1950) 1437.
12. Zvonkova, Z. V. and Jdanov, G. S. *Zhur. fiz. Khim.* **23** (1949) 1495.

13. Townes, C. H., Holden, A. N. and Merritt, F. R. *Phys. Rev.* **74** (1948) 1113.
14. Smith, A. G., Ring, H., Smith, W. V. and Gordy, W. *Phys. Rev.* **74** (1948) 370.
15. Townes, C. H. and Dailey, B. P. *J. Chem. Phys.* **20** (1952) 35.
16. Geller, S. and Schawlow, A. L. *J. Chem. Phys.* **23** (1955) 779.
17. Heiart, R. B. and Carpenter, G. B. *Acta Cryst.* **9** (1956) 889.
18. Quagliano, J. V. and Mizushima, S.-I. *J. Am. Chem. Soc.* **75** (1953) 6084.
19. Mizushima, S.-I. *Structure of Molecules and Internal Rotation*, Academic Press Inc., New York 1954, Chapters II and III.

Received September 15, 1957.

ACTA CHEMICA SCANDINAVICA 12 (1958) 89—94

Crystalline Myeloperoxidase

KJELL AGNER

Department of Clinical Chemistry, Serafimerlasarettet, Stockholm, Sweden *

A modified method for the preparation of myeloperoxidase, MPO, from pus of infected dog uteri is described. The most significant improvement is the use of a chromatographic procedure where the MPO is adsorbed on kieselguhr and later eluated from it by ammoniacal ammonium formate solution.

The myeloperoxidase has been obtained as a crystalline preparation with an iron content of 0.074 %. The enzyme behaved as would be expected for a single component in chemical and physical tests. Two atoms of porphyrin bound iron per enzyme molecule are indicated by chemical splitting of the enzyme.

The isolation of myeloperoxidase, MPO, in quantities, that will suffice for studies of the structure and properties of the enzyme, requires a starting material enriched in leucocytes or methods and equipments for separation of leucocytes from large quantities of blood.

The peroxidase preparation, described 1941 [1], was isolated from empyema fluid from tuberculous patients. This starting material has become progressively more scarce because of general medical progress. The separation of large quantities of leucocytes from blood presents certain difficulties. It has therefore been found necessary to search for another suitable starting material.

Infected dog uteri have proved appropriate. These uteri have been obtained as surgical specimens from the dog clinic at the Veterinary Institute. They have contained hemorrhagic or sometimes green coloured pus in varying amounts up to 1.5 liter. It has been possible to use the earlier published method of preparation [1] as a fractionation procedure for the purification of the MPO from this initial material. However, certain modifications have proved appropriate. The most significant of these is the adsorption of the MPO to kieselguhr and eluating the enzyme by ammoniacal ammonium formate solution.

* Present address: Department of Clinical Chemistry, S:t Görans sjukhus, Stockholm, Sweden.

PREPARATION PROCEDURE

Immediately after the operations the uteri have been taken to the laboratory and opened.

After step 3 in the preparation procedure given below the preparations usually have become purified to such an extent that it has been possible to determine the concentration of the MPO, the degree of purity, and the yield, by measurements of the absorbancy values at different wavelengths. At 430 mμ 1.0 mg of the crystalline MPO per ml has an absorbancy value of 1.2. The values for the ratios

$$\frac{\text{absorbancy}_{430\ m\mu}}{\text{absorbancy}_{280\ m\mu}} \quad \text{and} \quad \frac{\text{absorbancy}_{430\ m\mu}}{\text{absorbancy}_{390\ m\mu}}$$

has been the guidance for an approximate evaluation of the degree of purity of the preparations. The values of these ratios for the crystalline peroxidase are 0.82 and 2.0, respectively. Lower ratio values imply an admixture of impurities — proteins, heme components, etc. The figures for the amounts of MPO given for each step in the preparative procedure relate to the over-all yield from 100 ml starting material. The values are means of determinations from seven separate preparations. The variations between these values for different preparations lie within ± 35 %.

Step 1. Addition of ammoniacal ammonium sulphate solution. To every 100 ml of pus 10 ml of ammoniacal ammonium sulphate solution (800 ml of saturated ammonium sulphate solution + 100 ml ammonia) were added under stirring. At first there was a considerable gel-formation, which however, gradually disaggregated. The preparation was left at room temperature under stirring for 15—18 h.

Step 2. Precipitation with barium acetate. About 15 ml of saturated barium acetate solution were added for every 10 ml of the ammoniacal ammonium sulphate solution in the preceding step. The exact amount had to be checked for every preparation in order to avoid an excess of barium. After centrifugation the precipitate was discarded.

Step 3. Precipitation with ethyl alcohol at +5°C. The precipitate obtained at +5°C after addition of ethyl alcohol up to a concentration of 40 vol.% was discarded. The peroxidase was thereafter precipitated at about 65 vol.% ethyl alcohol. After centrifugation the precipitate was dissolved in saline.

Amount: 75 mg MPO per 100 ml of pus. Ratio: A_{430}/A_{280} = *ca.* 0.1.

Step 4. Precipitation of impurities with cadmium. Cadmium chloride solution (prepared from anhydrous powder) was added up to a concentration of about 0.02 M. The amount, which gave the optimum purification, had to be checked for every preparation. The precipitate formed was discarded after centrifugation.

Amount: 65 mg MPO per 100 ml of pus. Ratio: A_{430}/A_{280} = 0.22.

Step 5. Ammonium sulphate precipitation. The MPO was precipitated by ammonium sulphate at a concentration of 40—45 % saturation and thereafter dialysed against distilled water.

Amount: 55 mg MPO per 100 ml of pus. Ratio: A_{450}/A_{280} = 0.30.

Step 6. Adsorption on kieselguhr. Prior to its use, the commercial kieselguhr preparation was heated at 70—80°C in a large volume of 4 N hydrochloric acid solution, strained first with hot hydrochloric acid on a Büchner funnel until a negative qualitative test for iron in the wash water, and thereafter with distilled water until neutral reaction. The preparation was dried at 80°C.

For every 100 mg of MPO to be processed, 50—60 g of the dried kieselguhr powder were suspended in distilled water and packed in a chromatogram glass tube. The MPO preparation was then filtered through the column. In doing this the preparation was adsorbed on the powder in the two third upper parts of the column. The column was washed with saline and thereafter with an ammoniacal ammonium formate solution (prepared from a stock solution — equal amounts of 2 M ammonium formate and 1 M ammonium hydroxide — by adding 2 volumes of distilled water) until the eluate was free from substances absorbing at the wavelength of 280 mμ. Thereafter the MPO was eluated by the ammoniacal ammonium formate stock solution cited above.

The MPO in the eluate was precipitated with ammonium sulphate at 50 % saturation and thereafter dialysed against distilled water.

Fig. 1. MPO, recrystallized from ammoniacal ammonium sulphate solution. Dark field illumination. 300 × magnification.

Amount: 40 mg MPO per 100 ml of pus. Ratio: $A_{430}/A_{280} = 0.80$; $A_{430}/A_{390} = 1.95$.

Step 7. Crystallization from ammonium sulphate solution. Ammoniacal ammonium sulphate solution (50 volumes of saturated ammonium sulphate solution + 1 volume of ammonia) was added to the MPO solution up to a degree of saturation of about 0.40. Thereafter very small quantities of the ammonium sulphate solution were added with intervals of 2—3 h until thyxotropy was observed. After two or three days the greater part of the MPO had crystallized. The MPO-crystals separated as needles and displayed double refraction; Fig. 1.

ANALYSIS

The crystalline preparation obtained by the described procedure has been checked for homogeneity by ammonium sulphate solubility test, Fig. 2, electrophoresis at different pH-values, ultracentrifugation and diffusion. In

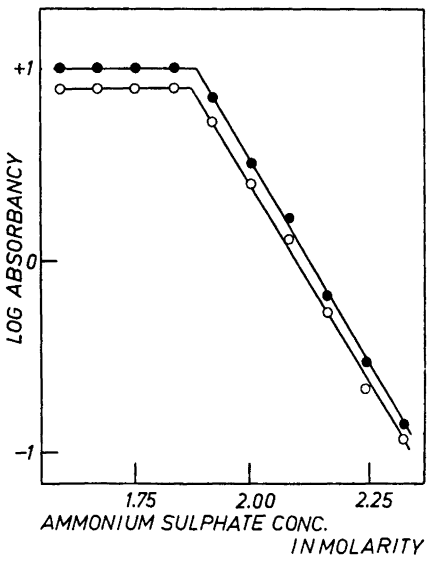

Fig. 2. Solubility of recrystallized MPO in solutions of increasing ammonium sulphate concentrations determined by spectrophotometric readings at 430 and 280 mμ. The MPO conc.: 7 mg/ml.

●—●—● log absorbancy, 280 mμ
○—○—○ log absorbancy, 430 mμ

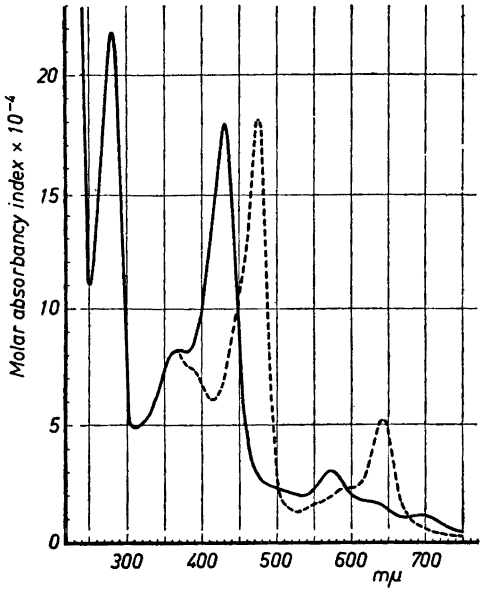

Fig. 3. Molar absorbancy index of oxidized and reduced MPO.

———— MPO oxidized
– – – – – MPO reduced

all these experiments the preparation behaved as expected for a single component. The results from the ultracentrifugation and diffusion experiments, as well as the estimation of the molecular weight, 149 000, will be described in a separate paper [2].

The molar absorbancy index values [3], A_μ, for the MPO at different wavelengths have been calculated from the absorbancy readings obtained in a Beckman spectrophotometer, model DU and are summarized in Fig. 3.

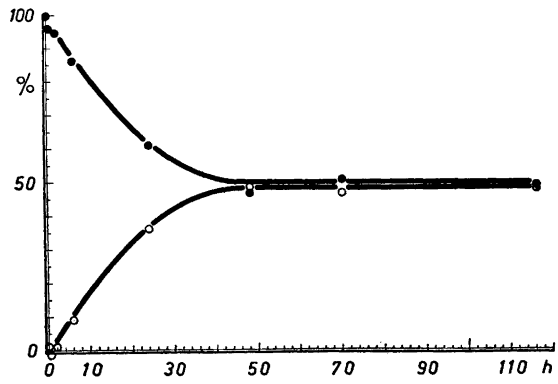

Fig. 4. Distribution of the iron after fractionation by methyl alcohol from 50 % pyridine solution after varying time.

O—O—O percentage of iron, "soluble in methanol"
●—●—● percentage of iron, "insoluble in methanol"

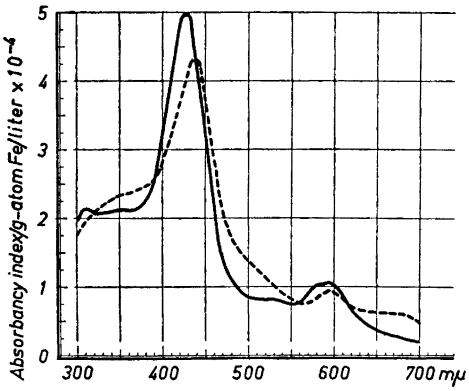

Fig. 5. Absorbancy index/g-atom Fe/liter for
the iron compound "soluble in methanol" ————
» » » "insoluble in methanol" — — — — —

The iron content of the MPO has been analysed by a modification of the method described by Lorber [4]. It was found to be 0.74 μg per mg of dry weight.

After addition of concentrated sulphuric acid and perchloric acid (0.2 ml of each) the preparation (2—8 mg) was combusted in test tubes (140 × 15 mm) at about 250°C. The heating was extinguished when the white heavy vapour had disappeared. The sample was diluted, 0.2 ml of a 20 % solution of sulphosalicylic acid was added, followed by ammonia until a yellow colour was produced. After dilution of the sample up to 5 ml the colour intensity was determined at 455 mμ in a Beckman spectrophotometer, model B, equipped with a special adapter for 50 mm long and 4 mm wide cuvettes. Absorbancy = 0.100 per μg of iron in the sample.

Procedures described for a fission of the linkages between the iron-porphyrin structures and their protein moieties by treatment with acid acetone or with some metals, e.g. silver ions, have been found to be unsuitable for breaking the bonds between the iron-porphyrin compound and the protein of the MPO. The effect of some other substances upon the MPO has been studied. It has been found that MPO splits into two parts in 50 % pyridine solution. The separation of the two fragments has been achieved by precipitation of one of them by adding 4 volumes of methyl alcohol. The second fragment is soluble in methyl alcohol. Fig. 4 demonstrates the velocity of this reaction at room temperature (about 22°C).

The reaction is a rather slow one at room temperature. The velocity increases at higher temperature. At 70°C the fission was completed within 60 min.

The absorbancy index values per g-atom of iron per liter have been determined for the two split products dissolved in 50 % pyridine solution, Fig. 5.

DISCUSSION

The crystalline MPO obtained from dog leucocytes by the procedure described above has proved to behave as would be expected for a homogeneous substance in ammonium sulphate solubility tests, ultracentrifugation, and

electrophoretic experiments at different pH-values. The molecular weight for the dog MPO calculated from the sedimentation and diffusion constants and the value for the specific volume is found to be 149 000 [2]. The iron content of the enzyme is 0.074 %. The theoretical value for the iron content, when assuming two atoms of iron per molecule of MPO, is 0.075 %. The experimental results suggest that the preparation is homogeneous and can be characterized as »pure».

The absorbtion spectrum and other properties investigated are very similar to those found for the preparations from the human starting material in 1941. The figure for the iron content given for the earlier preparation (1941) from human leucocytes was 0.1 %. However, according to the analyses, mentioned above, the iron content is found as 0.074 %. The molar absorbancy index calculated for the MPO from dog leucocytes is about 25 % higher than the values found for the preparation in 1941 *. These differences may reflect a diversity in characteristics of the MPO from the two different species. However, it cannot be excluded that the explanation for the differences might be a misinterpretation of the iron content in the previous experiments due to a shortage of material.

When acid acetone is added to hemoglobin, myoglobin, catalases, horse radish peroxidase, cytochrome a and b, the prosthetic group is released from the protein part which precipitates, while the prosthetic group remains in the dissolved state. Likewise the cysteine-porphyrin bonds in cytochrome c have been found to be broken by treatment with $AgNO_3$ and some other metal salts. If these procedures be applied to the MPO the whole molecule is precipitated without fission; therefore, the linkages between the porphyrin and the protein are more stable in this respect. By treatment with pyridine the MPO molecule is split into two parts. Each of them contain almost exactly 50 % of the original amount of iron and, thus, one atom of iron. The two components, when dissolved in 50 % pyridine solution, have absorbtion spectra, which indicate that both of the iron atoms are incorporated in porphyrin structures.

At present it is not possible to ascertain whether the two prosthetic groups are linked to the protein differently or if the findings are due to a splitting of the protein moiety into two parts.

Acknowledgement. This investigation has been aided by a grant from "*Stiftelsen Gustaf och Tyra Svenssons Minne*".

REFERENCES

1. Agner, Kj. *Acta Physiol. Scand.* **2** (1941) Suppl. VIII.
2. Ehrenberg, A. and Agner, Kj. *Acta Chem. Scand.* **12** (1958) **95.**
3. *Natl. Bur. Standards, Letter Circ.* LC-857, 1947.
4. Lorber, F. *Biochem. Z.* **181** (1927) 1927.
5. Paul, K-G. *Acta Chem. Scand.* **4** (1950) 239.

Received October 2, 1957.

* Recalculated from the values expressed as the absorption coefficients cm^2/g-atom of iron (logarithmic base e).

ACTA CHEMICA SCANDINAVICA 12 (1958) 95—100

The Molecular Weight of Myeloperoxidase

ANDERS EHRENBERG and KJELL AGNER*

Biochemical Department, Nobel Medical Institute, Stockholm, Sweden

The molecular weight of myeloperoxidase with an iron content of 0.074 % has been determined to be 149 000, which means that there are two atoms of iron per enzyme molecule. The calculations are based upon experimental results indicating a sedimentation coefficient at infinite dilution of 7.93 *S*, a diffusion coefficient of 4.81 *F* and a partial specific volume of 0.731 ml/g.

Myeloperoxidase [1] (MPO) has recently been obtained as a highly purified and crystalline preparation with an iron content of 0.074 % [2]. Therefore, it has been of interest to determine the sedimentation and diffusion coefficients of the enzyme as well as its partial specific volume and by means of these values to calculate the molecular weight.

METHODS

Sedimentation. The sedimentation studies were carried out in a Spinco analytical ultracentrifuge, model E, at a rotor speed of 59 780 rpm. The centrifuge was equipped with an automatic rotor temperature control. The inclined bar was used as schlieren diaphragm in most of the experiments; in a few cases the bar was replaced by a phase-plate [3], that facilitated the evaluation of the exposures but did not effect the results.

The sedimentation velocity was determined for enzyme concentrations from 0.8 up to 30 mg per ml. Temp. 20°C. The MPO was in these experiments as well as in the diffusion experiments stated below dissolved in phosphate buffer, 0.05 N, pH 7.0, containing also 1 % NaCl.

Diffusion. The diffusion experiments were made in a Spinco diffusion and electrophoresis instrument at a temperature of 1.17° C. Boundary sharpening was obtained by suction with a long hypodermic syringe needle cut perpendicular to its axes, and the diffusion process was followed over a period of 43 h. The optics were adjusted for studying the Rayleigh-Calvet-Philpot-interferogram at 546 mμ, and the number of fringes and the position of maxima and minima were measured out visually by means of the optical arrangements of a Hilger densitometer for spectrograms, using the slit plane as a projection screen. The cell magnification was 1.007. The diffusion coefficients were evaluated according to the "height-area" method as described by Svensson [4] and according to the moment method also described by Svensson [5] but slightly modified here.

Partial specific volume. The partial specific volume was determined for solutions of MPO, extensively dialysed against distilled water. The density was determined in a pycnometer of Sprengel-Ostwald type at 24°C.

* Present address: Department of Clinical Chemistry, S:t Görans Sjukhus, Stockholm, Sweden.

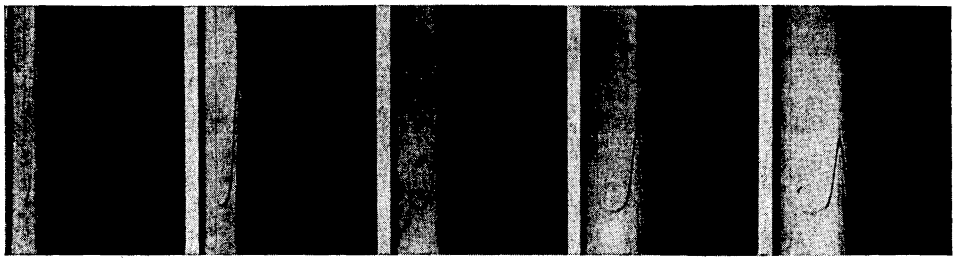

Fig. 1. Photographs taken in the ultracentrifuge during sedimentation of a myeloperoxidase solution of 10 mg/ml. First exposure taken 7 min after full speed was attained. Exposure intervals 8 min.

RESULTS

Sedimentation coefficient. The enzyme appeared to be homogeneous as far as could be judged from the photographs of the ultracentrifuge experiments, Fig. 1. The sedimentation coefficients were evaluated both from drawings made from magnified pictures and from measurements made directly on the plates in the Hilger densitometer. By means of the least square method the two sets of data were separately fitted to the equation

$$S^0_{20} = S_\infty - \beta a$$

where S_∞ is the sedimentation coefficient extrapolated to infinite dilution and a is the mean concentration of myeloperoxidase during the sedimentation in

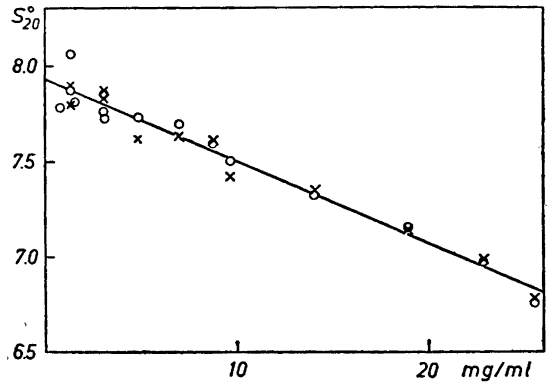

Fig. 2. Concentration dependence of the sedimentation coefficient of myeloperoxidase. Abscissa: mean protein concentration during observation in the ultracentrifuge. Ordinate: Sedimentation coefficients S^0_{20} calculated from enlarged drawings of the photographs O, and from comparator readings directly on the photographs, ×. The drawn line has been fitted to the points by the least square method.

Table 1. Diffusion data obtained by the "height area" method.

Conc.	t_0	$D_{1.17}$	D^0_{20}
mg/ml	sec	F	F
2.50	−2 170	2.467	4.813
1,30	−2 000	2.474	4.826

mg/ml. S_∞ was found to be 7.935 and 7.915 S, respectively, and β was 0.04359 and 0.04215 S ml.mg^{-1}, respectively. The following equation

$$S^0_{20} = 7.93 - 0.0429 \cdot a$$

may thus be accepted as the equation of the line that best fits the experimental data, Fig. 1.

Diffusion coefficient. Two concentrations were studied, 2.50 and 1.30 mg/ml, corresponding to the total fringe numbers of 38.50 and 20.31. When the "height-area" method was applied, the fringe interval Δn used in calculating the maximum fringe density, n'_{max}, was accordingly chosen as 10 and 5, respectively [4]. In the former experiment 6 exposures were evaluated and in the latter 8. In Fig. 3 plots have been made of $(1/n'_{max})^2$ *versus* the time and the best fitting lines, as calculated by the least square method, have been drawn. The numerical data are given in Table 1. The apparent starting time, t_0, is slightly negative because of the impossibility to produce a completely sharp boundary.

Three exposures from each experiment were also evaluated according to the moment method. The equation to be used has the following form [5]

$$D_m = \frac{\int_{n_0}^{n_c} x^2 dn}{2(t-t_0)(n_c-n_0)} = \frac{a}{t-t_0} \qquad (1)$$

where n denotes the refractive index increment measured in fringe numbers ($n_0 = 0$ and $n_c = n_{tot}$), x is the fringe coordinate measured from the center of the boundary, and t is the time of the exposure. Since the myeloperoxidase is strongly coloured, only dilute solutions could be studied, and n_{tot} was small. It thus appeared difficult to estimate the limiting parts of the integral, since x approaches infinity when n approaches zero or n_{tot} and it had to be extrapolated over relatively large intervals. This difficulty was avoided by taking the integral only over the interval that really was covered by the fringes that could be measured in the comparator. For instance, if the first minimum, $n = 0.5$, could be read, and Simpsons formula was used for the numerical integration, the lower limit, μ, of the integral equals 0.5; if instead the trapets

formula was used, $\mu = 0.25$. The same is valid for the upper limit. To compensate for the smaller interval of integration, a of eqn. (1) must be changed into the form

$$a = \frac{\int_{\mu}^{\nu} x_2 \mathrm{d}n}{2n_{tot} \int_{z_\mu}^{z_\nu} z^2 \frac{1}{\sqrt{2\pi}} \cdot e^{-\frac{1}{2}z^2} \mathrm{d}z} \qquad (2)$$

The two integrals are proportional as long as the diffusion is ideal. In the denominator integral the normalized error function $f(z) = \frac{1}{\sqrt{2\pi}} e^{-\frac{1}{2}z^2}$ has been used. The corresponding limits of integration are readily found from any table of that function including its integral, since $\int_0^{z_n} f(z)dz = \frac{n_{tot} - 2n}{2n_{tot}}$. A table of the integral $\int_{-\infty}^{z} z^2 f(z)\, dz$ is easily constructed from the data of the error function table, and the denominator integral of eqn. (2) is calculated by means of the formula

$$\int_{z_\mu}^{z_\nu} z^2 f(z)dz = 1 - \int_{-\infty}^{z_\mu} z^2 f(z)dz - \int_{z_\nu}^{+\infty} z^2 f(z)dz$$

after interpolation of the values of the two later integrals in the constructed table.

Table 2. Diffusion data obtained by the moment method. t_o is taken from Table 1.

Conc.	t	$t-t_o$	$a \times 10^2$	$D_{1.17}$	D°_{20}
mg/ml	sec	sec	cm²	F	F
2.50	23 640	25 810	0.6406	2.482	4.84
	66 840	69 010	1.696	2.457	4.79
	154 200	156 370	3.845	2.459	4.80
			Mean value		4.81
1.30	20 820	22 820	0.5643	2.473	4.82
	64 020	66 020	1.644	2.490	4.86
	93 120	95 120	2.302	2.420	4.72
			Mean value		4.80

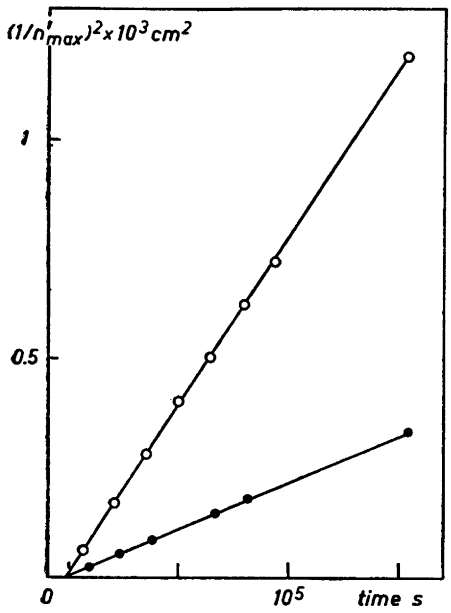

Fig. 3. Graphs from which the diffusion coefficients have been calculated according to the "height-area" method. Abscissa: time of exposure measured from end of boundary sharpening procedure. Ordinate: inverted square of maximum fringe density. Protein concentrations 2.50 mg/ml, ●, and 1.30 mg/ml, O.

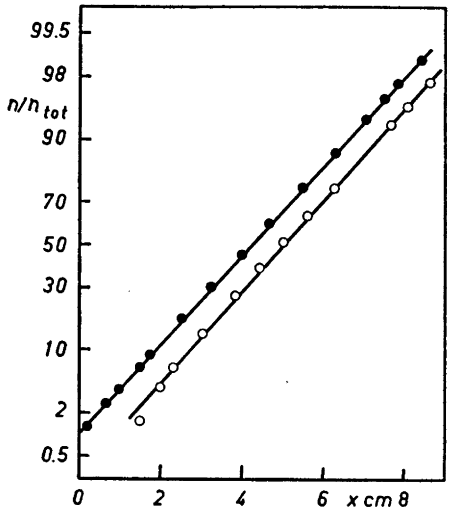

Fig. 4. Plots on a normal distribution graph showing the fit of boundary shape to that required by the ideal law of diffusion. Abscissa: measured fringe coordinates. Ordinate: relative fringe numbers. Exposures for 2.50 mg/ml at 66 840 sec, ●, and for 1.30 mg/ml at 64 020 sec, O. The drawn lines correspond to $D^{\circ}_{20} = 4.81\ F$.

The results obtained by the moment method are collected in Table 2. The zero time corrections as found by the "height-area" method have been used. For the protein concentration 2.50 mg/ml the mean value of D°_{20} is 4.81 F and for 1.30 mg/ml it is 4.80 F. It is not necessary to use the zero time corrections obtained by the "height-area" method, since according to eqn. (1) a plot of α *versus* time directly would give D_m as the slope of the line. This would, however, necessitate the evaluation of several exposures, which is rather time consuming.

The close agreement between the values obtained by the two methods might be considered as indicating that the diffusion is ideal and follows Fick's law. No dependence on protein concentration could be detected, and the mean value of all the data, $D^{\circ}_{20} = 4.81\ F$, is taken as the best value of the diffusion coefficient for the concentration range studied.

How closely the concentration distribution of the boundary fits the requirements of the law of ideal diffusion can be studied in detail in the way that has been described by Svensson [4]. A convenient and rapid method, that was

suggested to us by Lindqvist *, makes use of commercially available normal distribution graphs. On these graphs the ordinate is adjusted so that a straight line is obtained, when the integral

$$\int_{-\infty}^{z} \frac{1}{\sqrt{2\pi}} e^{-\frac{1}{2}z^2} dz$$

is plotted as a function of z. In Fig. 4 the relative fringe numbers n/n_{tot} have been plotted *versus* the fringe coordinates for two exposures, one for each concentration. The drawn lines correspond to $D^{\circ}_{20} = 4.81\ F$, and minor deviations of the points from the line is only seen in case of the lower concentration.

Partial specific volume. The apparent partial specific volume was determined in three experiments at the protein concentrations 26.17, 36.39 and 27.90 mg/ml. The following values were found: 0.732, 0.730 and 0.730. Mean value 0.731 ml/g.

DISCUSSION

Insertion of $S^{\circ}_{20} = 7.93\ S$, $D^{\circ}_{20} = 4.81\ F$ and $V = 0.731$ ml/g in the Svedberg formula yields a molecular weight of 149 000 for myeloperoxidase. The iron content of the enzyme has been determined to be 0.074 % which corresponds to an equivalent weight of 75 500 per iron atom. Each molecule of myeloperoxidase contains thus two atoms of iron — in contrast to other hitherto analyzed heme proteins which contain either one or four iron atoms per molecule.

The fricitional ratio f/f_0 is calculated to be 1.26. If the molecule is an unhydrated rotational ellipsoid the axial ratio would thus be about 5: 1.

Acknowledgements. The authors wish to thank Professor T. Storgårds and Mr. B. Lindqvist at Mjölkcentralen Laboratories, for making their Spinco diffusion and electrophoresis instrument available. Special thanks are due to Mr. B. Lindqvist for making the diffusion experiments and for helpful discussions. It is a pleasure to thank Mr. J. Grabosch, Mr. K. Ingebrigtsen and Mr. N. Ekman for valuable technical assistance. Financial support was obtained from *Stiftelsen Gustaf och Tyra Svenssons Minne* and *Knut och Alice Wallenbergs Stiftelse.*

REFERENCES

1. Agner, Kj. *Acta Physiol. Scand.* **2** (1941) Suppl. VIII.
2. Agner, Kj. *Acta Chem. Scand.* **12** (1958) 89.
3. Ehrenberg, A. *Acta Chem. Scand.* **11** (1957) 1257.
4. Svensson, H. *Acta Chem. Scand.* **5** (1951) 72.
5. Svensson, H. *Acta Chem. Scand.* **5** (1951) 1410.

Received October 2, 1957.

* Lindqvist, B., Mjölkcentralen, Laboratories, Stockholm, personal communication.

ACTA CHEMICA SCANDINAVICA 12 (1958) 101—109

On the Reactions and Biosynthesis of Azetidine-2-carboxylic Acid

PEKKA LINKO*

Laboratory of the Foundation for Chemical Research, Biochemical Institute, Helsinki, Finland

The hydrolysis of azetidine-2-carboxylic acid is studied.

β-Naphthoquinone sulphonate is presented as a sensitive and specific reagent for compounds containing the =CH—NH—CH= group.

Homoserine, which does not occur free in *Convallaria majalis*, is found in the acid hydrolysates of the "peptide fraction".

Uniformly labelled aspartic acid is infiltrated into the leaves of *Convallaria majalis* and the incorporation of radioactivity is followed. No activity is found in azetidine-2-carboxylic acid. Aspartic acid is readily decarboxylated to both α- and β-alanine. From the other compounds glutamic acid is primarily labelled. The activity accumulates in asparagine, glutamine and an unknown glutamic acid derivative. In the "peptide" fraction hydrolysates aspartic acid, glutamic acid and serine are labelled, whereas in the protein hydrolysates only aspartic acid is found to be labelled.

The metabolic role of azetidine-2-carboxylic acid is discussed.

Only a few years ago Miettinen *et al.*[1] for the first time isolated and identified homoserine as a free amino acid in pea *(Pisum sativum)*. According to earlier experiments [2] based only on chromatographical evidence it was known to occur in *Neurospora*. Later homoserine has been found to be widely distributed in the plant kingdom [3].

Though homoserine is rather a "newcomer" among the free amino acids in plants, some of its derivatives have been known for a long time. Kitagawa and Tomita [4] as far back as 1929 isolated canavanine, α-amino-γ-guanidinoxybutyric acid, from *Canavalia ensiformis*. Recently canavanine was also found in *Colutea arborescens* [5]. Pantonine, another homoserine derivative, was isolated from *Escherichia coli* [6]. Because there was already strong evidence for the importance of homoserine and its derivatives in the metabolism of plants, the recent discovery of azetidine-2-carboxylic acid in some *Liliaceae* plants

* Present address: Kansas State College, Department of Flour and Feed Milling Industries, Manhattan, Kansas, U.S.A.

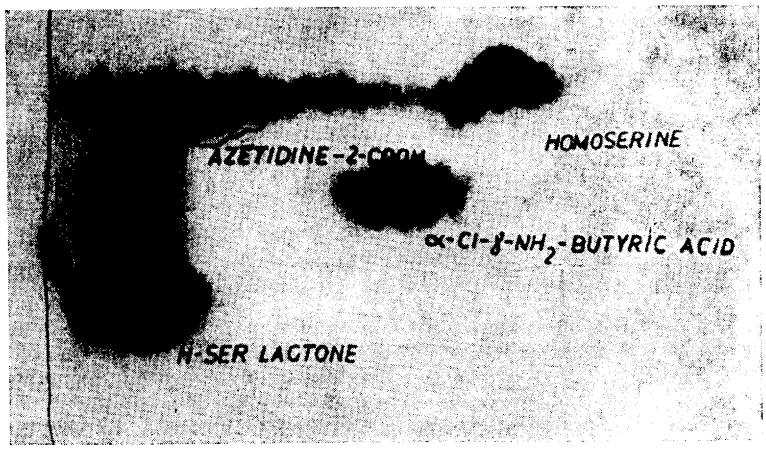

Fig. 1. The products of hydrolysis of azetidine-2-carboxylic acid by means of 6 N hydrochloric acid (sealed tube, 20 h, 100°C).

was very interesting [7–9]. This imino acid may be related to α,γ-diaminobutyric acid [10,11] or to its deamination product, aspartic-α-semialdehyde. This known intermediate in the reduction of aspartic acid to homoserine [12,13] is found to occur in yeast [14]. Hence the possibility that azetidine-2-carboxylic acid may be formed from aspartic acid in the leaves of *Convallaria majalis* was examined.

HYDROLYSIS OF AZETIDINE-2-CARBOXYLIC ACID

When azetidine-2-carboxylic acid is subjected to hydrolysis with hydrochloric acid three new spots on the chromatograms are observed in addition to that corresponding to the small amount of unchanged compound (Fig. 1) [15,7]. Two of these spots were identified as homoserine and γ-amino-α-chlorobutyric acid [9], the relative amount of the latter being [15] only about 5 %. The third compound, homoserine lactone [15], formed secondarily from homoserine, is evidently identical with spot S_3 of Fowden, which he in turn describes as α-amino-γ-chlorobutyric acid but which could not, however, be synthesized. This compound was isolated in crystalline form as the hydrochloride. It gave the typical lactone reaction with ferric chloride and hydroxylamine, could easily be hydrolysed to homoserine by barium hydroxide and was finally found identical with the synthetic product of Armstrong [16]. The optical rotation determined as a function of time (Fig. 2) was in good agreement with Armstrong's results. In contrast to the observation of Fowden that azetidine-2-carboxylic acid is stable against alkalies it was found that 4 N sodium hydroxide caused some decomposition already on standing at room temperature. Only homoserine was formed during alkaline hydrolysis. Ammonia and acids, however, did not cause decomposition at this temperature.

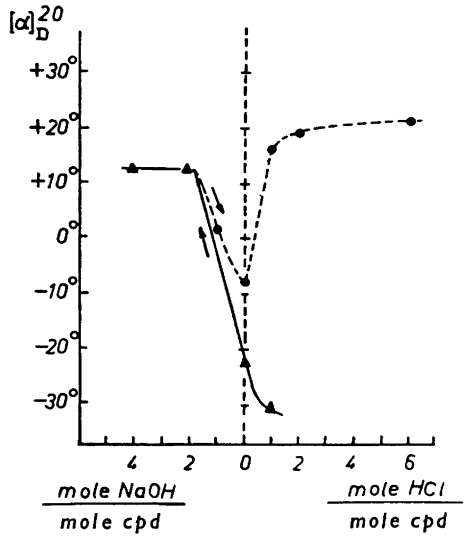

Fig. 2. The optical rotation of homoserine (---) and its lactone (———) as a function of pH.

β-NAPHTHOQUINONESULPHONATE REAGENT

Müting [17] and Giri and Nagabushanan [18] detected that α-naphthoquinonesulphonate gives, with most of the amino acids and their derivatives, colors varying from green to bluish when the paper chromatogram is dipped into the reagent. Only proline was found to give a red color reaction. Because azetidine-2-carboxylic acid also gave an intensive red color reaction, several other secondary amines were studied in respect to this reagent. Hydroxyproline, piperidine-4-carboxylic acid, sarcosine and N-phenylglycine developed a strong red color, whereas the red color caused by piperidine-2-carboxylic acid and its 5-hydroxyderivative was somewhat weaker. With peptides and N-acetylderivatives of amino acids the normal bluegreen color was obtained. The reaction is about as sensitive to secondary amines as ninhydrin and therefore seems to be a good specific reagent for the compounds containing the = CH—NH—CH= group. As the only exception so far known 1-amino-*cyclo*propane-1-carboxylic acid developed a weak red color [19].

ON THE BIOSYNTHESIS OF AZETIDINE-2-CARBOXYLIC ACID

The amount of azetidine-2-carboxylic acid in young *Convallaria majalis* plants was about 20 % or even more of the ethanol soluble nitrogen compounds. When the plants started to turn yellow in the fall, the relative amounts of most of the free amino acids increased (Fig. 3). The only noticeable exception was azetidine-2-carboxylic acid which had almost disappeared from the completely yellow plants. This is in good agreement with the results of Kemple and Macpherson [20] who noticed that the amount of all protein amino acids increased in the ethanol soluble fraction during the drying of grass. All the nitrogen

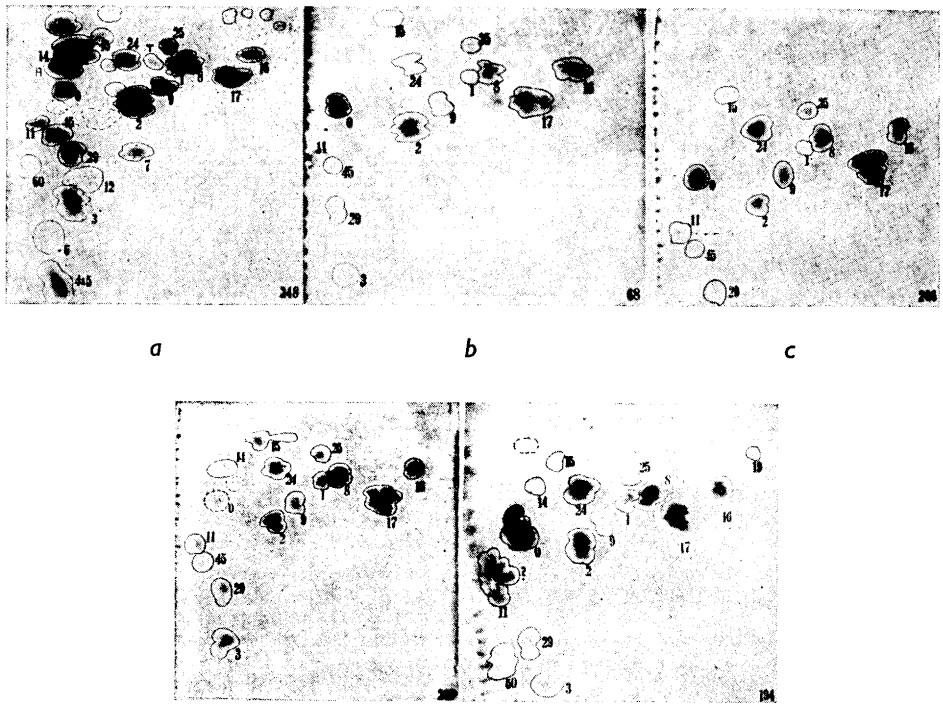

Fig. 3. Free amino acids of *Convallaria majalis*. *a*, Seeds; *b*, young leaves; *c*, partly yellow leaves; *d*, completely yellow leaves; *e*, soft part of ripe berries. 1 = gly, 2 = ala, 3 = val, 4 & 5 = leu + ileu, 6 = β-ala, 8 = ser, 9 = threo, 11 = prol, 12 = tryptophane, 14 = arg, 15 = lys, 16 = asp, 17 = glu, 24 = glu-NH_2, 25 = asp-NH_2, 29 = γ-AB, 45 = ethanolamine, 60 = piperidine-2-carboxylic acid, 0 = azetidine-2-carboxylic acid, ? = unknown compound.

liberated from proteins could be found in the free amino acids, amides, peptides and volatile bases.

During the disappearance of azetidine-2-carboxylic acid no homoserine or other "new" amino compounds were formed. However, great amounts of the imino acid were detected in the soft parts of ripe berries, while almost none was found in the seeds. It may be of interest to mention here that 1-aminocyclopropane-1-carboxylic acid also exists only in ripe fruits [19,21]. Two unknown amino compounds, which could not be detected in the other parts of the plants, were also found in the berries of *Polygonatum officinale*. One of them was isolated by fractionation on a Dowex 50 cation exchange resin column and identified as tyramine. This amine was found [22] in *Viscum album* already 1916. Later it was isolated from *Sarothamnus* [23,24] and chromatographically identified in some other plants [24,25]. The other unknown compound

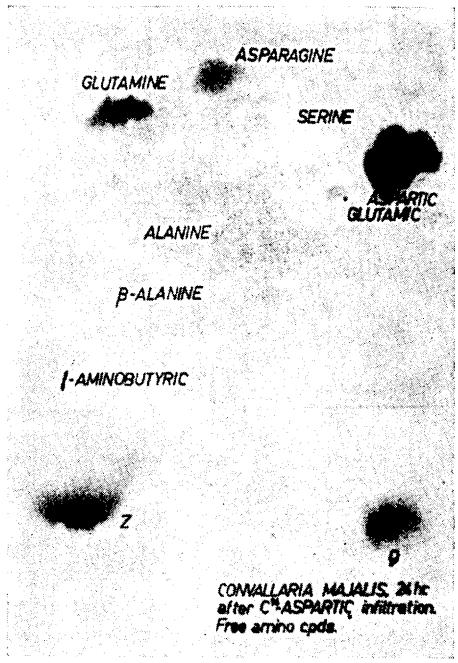

Fig. 4. Radioautogram of the amino compound fraction of *Convallaria majalis*. 24 h after uniformly labelled aspartic acid infiltration.

marked with a question mark in Fig. 3 e has not yet been identified. Both the place on the chromatogram and the graybluish color reaction with ninhydrin are characteristic to many amines.

Virtanen *et al.*[26] noticed that homoserine, which did not occur either in free state or bound in pea seeds, was rapidly formed during germination. Already after 72 h this compound was the most abundantly appearing free amino acid. After five days the relative amount of homoserine had still increased while glutamic acid and serine had decreased. The young stem and root now contained far greater amounts of homoserine than did the seed. Examination of *Convallaria* in this respect was very difficult because the seeds do not easily germinate. With a few seeds it could, however, be shown that azetidine-2-carboxylic acid behaved like homoserine during the germination of seeds.

The observation of Fowden and Steward[27] that azetidine-2-carboxylic acid was found in all parts of *Convallaria*, but in some other species only in leaves or in seeds, respectively, may be due to the changes in concentration of this compound in different parts of plants during various stages. It is interesting that in the leaves of *Fritillaria meleagris* γ-methyleneglutamic acid but no azetidine-2-carboxylic acids was found whereas in the seeds of *Fr. imperialis* the situation was quite the opposite.

The phosphorylation of the β-carboxyl group of aspartic acid is now known to be the primary reaction in threonine biosynthesis in yeast. β-Aspartyl-

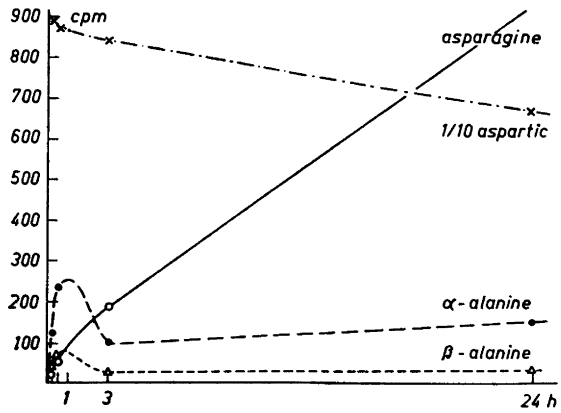

Fig. 5. Relative activities of aspartic acid and its direct biosynthetic products in *Convallaria majalis* after uniformly labelled aspartic acid infiltration.

phosphate can quantitatively be reduced to homoserine by means of a specific enzyme isolated from baker's yeast [13]. A few years later [28] it was noticed that incubation of rat liver homogenate with DL-2-^{14}C-homoserine induced labelling into α-ketobutyrate, α-hydroxybutyrate, α-aminobutyrate and propionate, but no labelling was found in threonine, methionine, alanine and α-keto-γ-hydroxybutyrate. Therefore, in this case the primary reaction would be identical with the dehydration of threonine and serine. However, α-keto-γ-hydroxybutyric acid is now known to occur in higher plants [29].

The cyclization of aspartic β-semialdehyde is the most likely reaction leading to azetidine-2-carboxylic acid. A similar type of reaction is known in the conversion of δ-aminolaevulinic acid to the porphyrin ring [30]. 4-Carb-

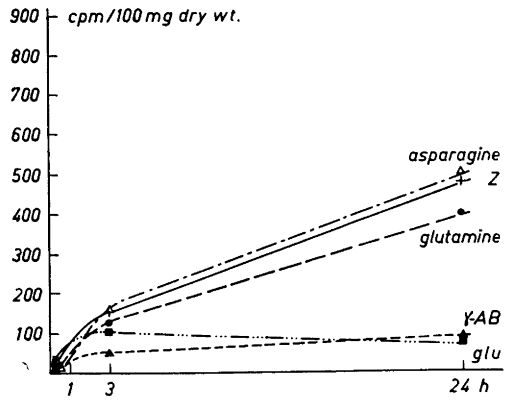

Fig. 6. Total radioactivity changes in *Convallaria majalis* after uniformly labelled aspartic acid infiltration.

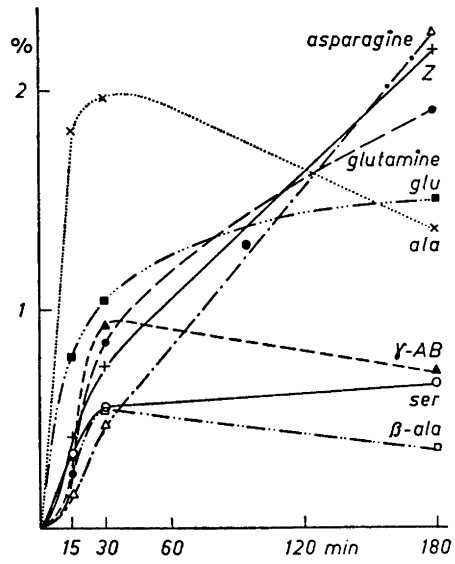

Fig. 7. The percentage of radioactivity in the individual amino compounds calculated from the total ethanol soluble activity in *Convallaria majalis* after uniformly labelled aspartic acid infiltration.

oxyl-azetidinone is also known to be formed synthetically from asparagine in phosphate buffer[31] (pH 6.7; 100°C). Uniformly labelled aspartic acid was therefore infiltrated into the leaves of young *Convallaria majalis* plants grown in the greenhouse. Similar methods were used as described earlier[32]. After half an hour there was a slight minimum in the percentage of activity of the amino compound fraction as compared to the total ethanol soluble activity. After 24 h the activity of this fraction was still 90 % of the total soluble one. No radioactivity could be found in azetidine-2-carboxylic acid (Fig. 4). Both carboxyl groups of aspartic acid were readily decarboxylated α- and β- alanine respectively, being formed (Fig. 5). The β-carboxyl was more rapidly removed. The activity of both decarboxylation products had a peak after about one hour showing that they were rapidly metabolised further. From the other compounds glutamic acid was primarily formed. After short lag periods activities in both asparagine and glutamine increased countinuously. The same was due to an unknown compound, Z, which yielded glutamic acid as the only active component on acid hydrolysis (Figs. 6 and 7).

In the acid hydrolysates of the proteins only aspartic acid was found labelled, but when the "peptide" fraction was subjected to acid hydrolysis aspartic acid, glutamic acid and serine were found to be labelled (Fig. 8). Practically all the amino acids, except azetidine-2-carboxylic acid, were found to occur in the hydrolysates. The percentage of the activity of aspartic acid had a peak after half an hour, glutamic acid being the main labelled product after 24 h. It was very interesting to find that though azetidine-2-carboxylic acid was absent in this fraction, inactive homoserine was always found in the hydrolysates. This cannot arise from azetidine-2-carboxylic acid during hydrolysis, because no α-chloro-γ-aminobutyric acid could be detected on

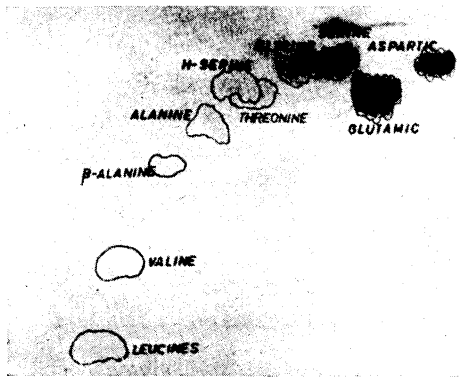

Fig. 8. A ninhydrin sprayed chromatogram of amino acids arising from the "peptide" fraction of *Convallaria majalis* in acid hydrolysis. The darkened spots were labelled after uniformly labelled aspartic acid infiltration.

the chromatograms. The experiments performed in order to show the synthesis of azetidine-2-carboxylic acid from inactive homoserine by the method of Miettinen and Virtanen [33] failed, but this could be due to the great amount of azetidine-2-carboxylic acid originally present, making comparisons very difficult. Recently, bound homoserine was found in the ethanol insoluble fraction of cowberries and cranberries [34]. Even in this case no free homoserine was found, but the berries of cowberries contained a cyclic four-carbon amino acid, 1-amino-*cyclo*propane-1-carboxylic acid [19]. It may also be mentioned here that strains of *Neurospora* requiring homoserine for growth also grow with canavanine [35].

That no radioactivity was found in azetidine-2-carboxylic acid after ^{14}C-aspartic acid infiltration may partly be due to the small amount of labelled aspartate available as compared to the relatively great amount of azetidine-2-carboxylic acid originally present in the plant thus causing great dilution of the possible active synthetic product with inactive material. However, it is most evident that the rate of synthesis of azetidine-2-carboxylic acid is much lower in the leaves than in young sprouts and that this compound may arise from the compound present in the "peptide" fraction which yields homoserine on acid hydrolysis and which in turn may be formed from aspartic acid *via* aspartic-β-semialdehyde.

I am greatly indebted to Professor Artturi I. Virtanen for his keen interest in this work and for the excellent working facilities put at my disposal. I am also indebted to Dr. Armstrong who kindly supplied samples of some synthetic homoserine derivatives.

This paper belongs to the group of investigations for which the *Rockefeller Foundation* has awarded a grant to the Foundation for Chemical Research.

REFERENCES

1. Miettinen, J. K., Kari, S., Moisio, T., Alfthan, M. and Virtanen, A. I. *Suomen Kemistilehti* **B 2** (1953) 26.
2. Fling, M. and Horowitz, N. H. *J. Biol. Chem.* **190** (1951) 277.
3. Berg, A-M., Kari, S., Alfthan, M. and Virtanen, A. I. *Acta Chem. Scand.* **8** (1954) 358.
4. Kitagawa, M. and Tomita, T. *J. Biol. (Japan)* **11** (1929) 265.
5. Fearon, W. R. and Bell, E. A. *Biochem. J.* **59** (1955) 221.
6. Ackermann, W. W. and Kirby, H. *J. Biol. Chem.* **175** (1948) 483.
7. Virtanen, A. I. and Linko, P. *Acta Chem. Scand.* **9** (1955) 551.
8. Virtanen, A. I. *Nature* **176** (1955) 989.
9. Fowden, L. *Nature* **176** (1955) 347.
10. Catch, J. R., Jones, T. S. G. and Wilkinson, S. *Ann. N. Y. Acad. Sci.* **51** (1949) 917.
11. Peterson, D. H. and Reineke, L. M. *J. Biol. Chem.* **181** (1949) 95.
12. Black, S. and Wright, N. G. *J. Am. Chem. Soc.* **75** (1953) 5766.
13. Black, S. and Wright, N. G. *J. Biol. Chem.* **213** (1955) 51.
14. Black, S. and Wright, N. G. *J. Biol. Chem.* **218** (1955) 39.
15. Linko, P. Licentiate Dissertation (1955), Univ. of Helsinki (in Finnish).
16. Armstrong, M. D. *J. Am. Chem. Soc.* **71** (1949) 3399.
17. Müting, D. *Naturwiss.* **39** (1952) 303.
18. Giri, K. V. and Nagabushanan, A. *Naturwiss.* **39** (1952) 548.
19. Vähätalo, M-L. and Virtanen, A. I. *Acta Chem. Scand.* **11** (1957) 741.
20. Kemple, A. R. and Macpherson, H. T. *Biochem. J.* **58** (1954) 46.
21. Burroughs, L. F. *Nature* **179** (1957) 360.
22. Crawford, A. H. and Watanabe, W. K. *J. Biol. Chem.* **24** (1916) 169.
23. Schmalfus, H. and Heider, A. *Biochem. J.* **236** (1931) 226.
24. Correale, P. and Cortese, I. *Naturwiss.* **40** (1953) 57.
25. Erspamer, V. and Falconieri, G. *Naturwiss.* **39** (1952) 431.
26. Virtanen, A. I., Berg, A.-M. and Kari, S. *Acta Chem. Scand.* **7** (1953) 1423.
27. Fowden, L. and Steward, F. C. *Ann. of Botany, N. S.* Vol. **XXI**, No. 81 (1957) 53.
28. Matsuo, Y., Rothstein, M. and Greenberg, D. M. *J. Biol. Chem.* **221** (1956) 679.
29. Virtanen, A. I. and Alfthan, M. *Acta Chem. Scand.* **9** (1956) 188.
30. Shemin, D. and Russel, C. S. *J. Am. Chem. Soc.* **75** (1953) 4873.
31. Talley, E. A., Fitzpatrick, T. J. and Porter, W. L. *J. Am. Chem. Soc.* **78** (1956) 5877.
32. Virtanen, A. I. and Linko, P. *Acta Chem. Scand.* **12** (1958) 68.
33. Miettinen, J. K. and Virtanen, A. I. *Acta Chem. Scand.* **7** (1953) 1243.
34. Vähätalo, M.-L. and Virtanen, A. I. *Acta Chem. Scand.* **11** (1957) 747.
35. Teas, H. J. *J. Biol. Chem.* **190** (1951) 369.

Received September 16, 1957.

ACTA CHEMICA SCANDINAVICA 12 (1958) 110—118

Fractionation of the Lipids of Eye Lenses by Gradient Elution on Activated Silicic Acid Columns

SVEN ELOV BROLIN

Histological Department, University of Uppsala, Sweden

Dried and powdered eye lenses were extracted with chloroform and the extract was fractionated by gradient elution from activated silicic acid columns. The elution of the phospholipids was studied and several peaks with different properties were obtained. Some figures are given for the composition of the lipids from a sample of cattle eyes obtained from a Swedish abattoir.

Chloroform extracts of lens tissue contain fluorescent substances and during the present investigation attempts have been made to fractionate these. The methods previously available were not suitable for the requirements of this separation. The usefulness of silicic acid columns was demonstrated by Borgström [1] and it has been used successfully in lipid chromatography by Lea and Rhodes [2]. The theory and application of gradient elution has been described by Tiselius and coworkers (for references see Lederer and Lederer [3]).

The chemical composition of the lipids of the eye lens has been described in detail and a survey of the literature has been given by Bellows [4]. However as in other branches of lipid research the application of chromatography should provide further information on the separation and determination of the various components. The fluorescent material in the different chromatographic fractions will be described in a later paper.

MATERIAL AND METHODS

Preparation of the lipid sample. The lenses from 3 500 cattle eyes were smeared on glass plates and dried at 37°. This material was scraped off, ground in a porcelain ball mill and then extracted with chloroform in a Soxhlet for 72 h. After evaporation under reduced pressure the lipid sample was redissolved in chloroform and filtered again.

Chromatographic procedure. The columns were prepared mainly following the directions of Borgström [1]. Silicic acid (Baker) was washed with chloroform and ethanol until no further fluorescent matter was removed and then activated at 120°C for 24 h. 20 mm columns were packed with a mixture of this silicic acid powder (10 g) and filter aid (Hyflo supercel, 5 g) suspended in chloroform. A solution of the lipid extract (300 mg) in chloroform (50 ml) was poured onto each column and the column was then washed

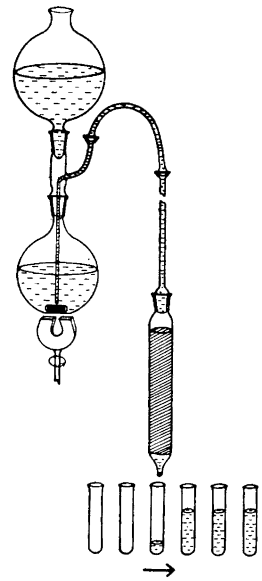

Fig. 1. The gradient elution apparatus. The solvent in the mixing chamber is mixed with a magnetic stirrer. Gradient elution is started by replacing the top vessel containing chloroform with one containing the chloroform-methanol mixture.

with pure chloroform; about 225 ml seemed to be the optimum quantity. The column was then eluted with chloroform-methanol using a gradient elution method as shown in Fig. 1. A mixture of methanol and chloroform (1:2) flowed continuously into the mixing vessel which contained about 100 ml of chloroform. Fractions were collected over 20 min intervals and the elution curves were therefore plotted against the time.

Paper chromatography. Each fraction was hydrolysed with sulphuric acid and then neutralised with baryta. The paper (Whatman No. 1) was equilibrated over the solvent in the development tank; ascending development was used; solvent composition is given in Table 3.

Spot tests on paper. Spot tests were made by dropping 0.2 ml from each fraction onto paper placed over a hot air stream. Ethanolamine and serine were made visible by spraying with 0.1 % ninhydrin in *n*-butanol and then heating at 95° for 10 min. Choline was tested for by the method of Bevan, Gregory, Malkin and Poole [5].

Quantitative determination. Phospholipids were calculated as 25 P following the method of Brante [6] which is a modification of the methods of Teorell [7] and Fiske-Subbarow [8].

Cerebrosides and gangliosides were estimated by the methods elaborated by Svennerholm [9].

Cholesterol was estimated by a routine photometric method. The sample was dissolved in chloroform (5 ml), and then acetic anhydride (2 ml) and concentrated sulphuric acid (0.2 ml) were added, the mixture was shaken mechanically in the dark for 5 min and the absorption was measured at 630 mμ.

Glycerol was determined by the method of Blix [10].

The distribution of plasmalogens in different fractions was estimated by the method described by Feulgen and Grünberg [11]. The absorption was measured directly without extraction by amyl alcohol.

The lipid fractions were weighed after evaporation of the solvent under reduced pressure.

Purification of solvents. Only analytical grade reagents were used. It was necessary to remove small amounts of fluorescent impurities because of the experimental method to be used. Distillation under water pump vacuum from a large flask immersed in a water bath at 45° gave satisfactory purification. The separation was poor unless the condenser joint was heated strongly with an electrical heating tape. No rubber connections were used.

RESULTS

General composition of the lipids. The lens powder was extracted only with chloroform but the denaturation of the proteins by drying and the long extraction period should permit sufficient release of the lipids.

It is possible to outline the composition of the lipid sample without considering the effect of the gradient elution. As stated by Borgström [1], chloroform elution will give a good separation of the phospholipids from the cholesterol esters and glycerides and the free fatty acids. Phosphorus determination on the chloroform eluate confirmed the retention of the phospolipids on the column provided the recommended volume of chloroform was not exceeded by too much. This separation is of assistance in several analytical determinations.

The amounts of glycerol and cholesterol in the lipids eluted by chloroform were determined on the material from four columns and gave mean values of 0.53 % of the original sample for glycerol and 27.5 % for cholesterol. The chloroform eluate may contain various esters but for the sake of simplicity can be regarded as containing glycerides, cholesterol and cholesterol esters. The possibility of free fatty acids being present is neglected. If the glycerides have a molecular weight as high as that of tristearin, 891, they will amount to 5.1 % of the original sample and the corresponding mean value for cholesterol and its esters will be 34.9 %. A molecular weight as low as 700 will give values of 3.6 and 36, respectively. The percentage figures are thus not influenced to any great extent by errors in the molecular weight assumed for the glycerides. A mean molecular weight lower than that of tristearin was assumed in estimating the approximate values given in Table 1.

Table 1. Constituents of the lipids.

	%
Glycerides	4.5
Cholesterol and its esters	35.5
Phospholipids	48.0
Cerebrosides	0.8
Gangliosides	(0 < 0.5)
Undefined material	11.0

Before chromatography the sample contained 48 % phospholipids. This could also be determined from the amount of phospholipid fraction obtained by chromatography. The results from 8 columns are given in Table 2 with the percentage of phospholipid worked out in three different ways. In each case they are higher than the values determined from the original sample. The 25 × P formula thus does not apply to some of the lipids remaining on the column after elution with chloroform. The gradient elution was intended to concentrate these lipids into definite fractions.

Gradient elution. The material in the fractions eluted by chloroform methanol was weighed and the phospholipids present were estimated. These values when plotted gave a reproducible pattern. There were some variations but the characteristic peaks of the curves were always recognisable. There

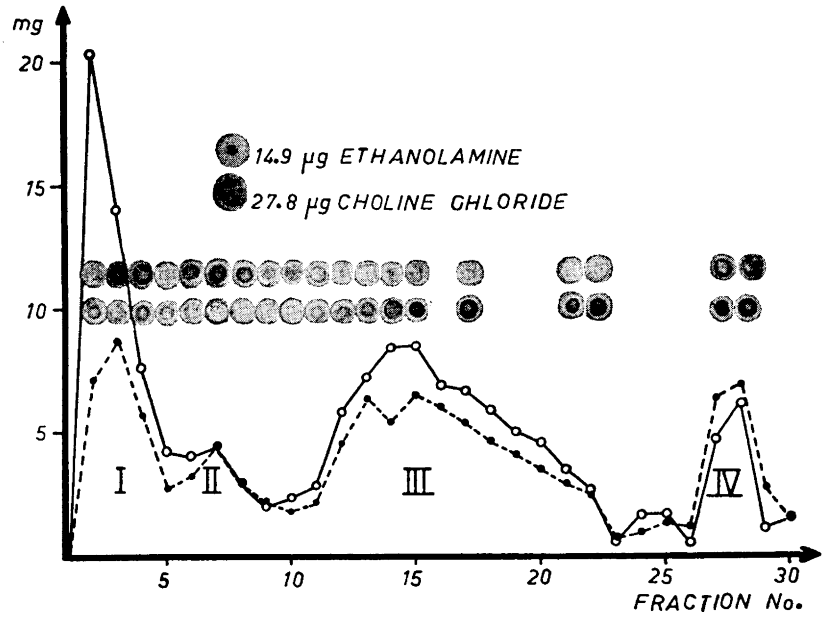

Fig. 2. Fractions obtained by elution with chloroform methanol. The unbroken line represents the lipid amount of each fraction and the dotted line the calculated weight of phospholipids. The spots show ninhydrin reactions and choline tests made on paper with material from the corresponding fractions. The four phospholipid peaks are marked I—IV.

were three phospholipid peaks designated I, II and III in Figs. 2, 3 and 4 with a further peak, IV, in the material stripped from the column with methanol. There were sometimes signs of a slightly smaller peak in front of peak I, see Figs. 3 and 4.

Spot tests for cephalins and lecithin were made on paper using the ninhydrin and choline reactions. The ninhydrin reaction was strong for peaks I and II but very weak for peak III, while the lecithin choline reaction was strong only for peak III. The cephalins should therefore be eluted in front of the lecithin (see Fig. 2). Since the cephalins can be divided into phosphatide ethanolamine and phosphatide serine peaks I and II were investigated to see whether they differed in this way. After hydrolysis the nitrogeneous constituents were separated by chromatography on paper as shown in Fig. 3. The results are shown in Table 3.

The elution curves showing also the spot tests and the paper chromatographic results indicate that the phosphatidyl ethanolamine, the phosphatidyl serine and the phosphatidyl choline are eluted in that order and correspond to the peaks I, II and III. It is also evident that the chromatogram does not give a complete separation especially for peaks I and II. The ninhydrin reaction showed only a single weak spot with an R_F value different from those of ethanolamine and serine. There can be only very little of other strongly reacting amino groups.

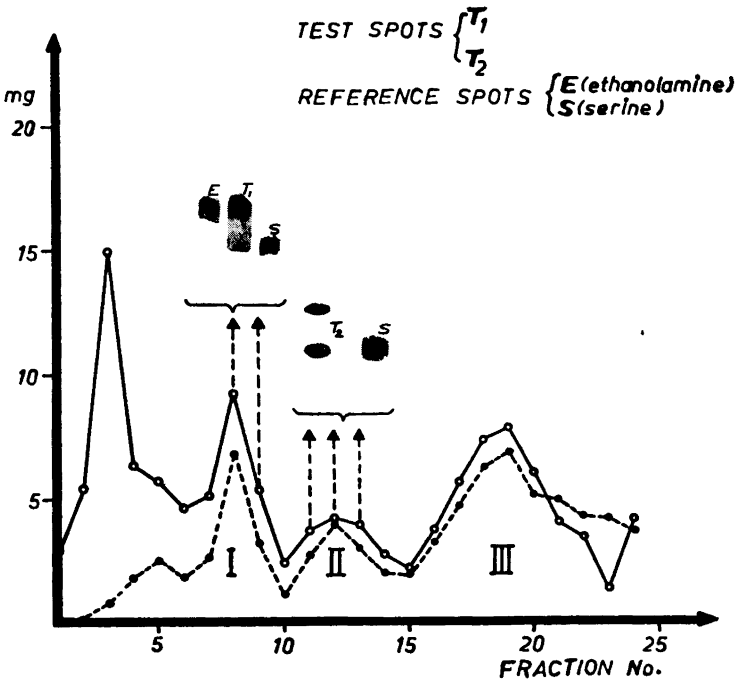

Fig. 3. Fractions obtained by gradient elution with chloroform methanol; same scale as in Fig. 2. The paper chromatograms shown were run on hydrolysed material.

Table 2. Phospholipid fractions from a series of columns.

Initial elution with chloroform ml	a Eluted by chloro-form mg	300—a	b Eluted by chloro-form/ methanol mg	a + b Total wt. of eluates mg	Number of fractions	300—a as % of 300	b as % of 300	b as % of a + b
135	119	181	171	290	50	60	57	59
135	121	179	176	297	60	60	59	59
135	130	170	178	307	60	57	59	58
135	108	193	200	308	60	64	67	65
450	147	153	165	312	80	51	55	53
270	106	194	223	329	89	65	74	68
150	128	172	154	282	55	57	51	55
225	125	175	135	261	44	58	45	52
	122.9	177.1	175.3	298.6		59.0	58.4	58.6

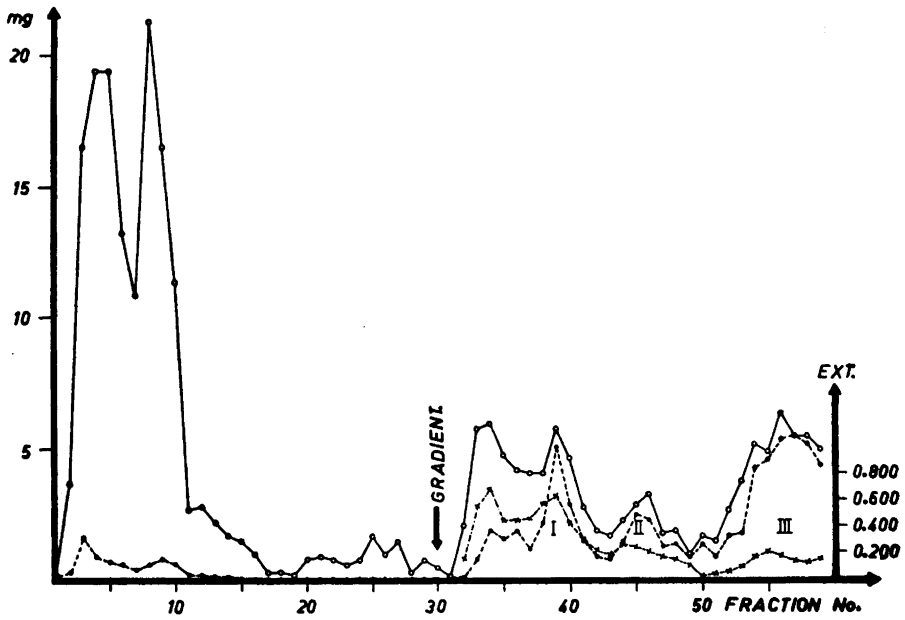

Fig. 4. Chromatogram including the fractions eluted by chloroform; scale as in Fig. 2. The distribution of Feulgen material positive is shown by the curve with crosses; scale as extinction, on the right. In this chromatogram the chloroform eluate had a higher phosphorus content than usual.

Solubility tests permit only rough conclusions to be drawn if the fractions do not contain pure compounds but seemed to accord with the elution sequence given above. The solubility in ethanol was higher for the lecithin fractions than for the first fractions while the material of peak IV was almost insoluble in ether and was preceded by fractions with low ether solubility.

The residue stripped from the column with methanol was designated peak IV and was almost solely phospholipids calculated as 25 × P. To ascertain

Table 3. Paper chromatography of hydrolysed fractions. The R_F values in brackets indicate weaker spots.

	Time of development	Solvent (% v/v) *n*-Butanol:acetic acid:water	R_F values of reference spots		R_F values of hydrolysed compounds
			Serine	Ethanolamine	
PEAK I	9 h	40:10:50	—	0.31	(0.18), 0.31, (0.63)
PEAK II	6 h 20 min	40:10:50	0.17, (0.29)	0.27	0.27, (0.60)
	9 h 35 min	66:17:17	0.16	0.33	(0.16), 0.33
PEAK III	8 h 15 min	66:17:17	0.13	—	0.13, 0.29
	10 h	40:10:50	0.19	0.28	0.16, 0.29, (0.60)

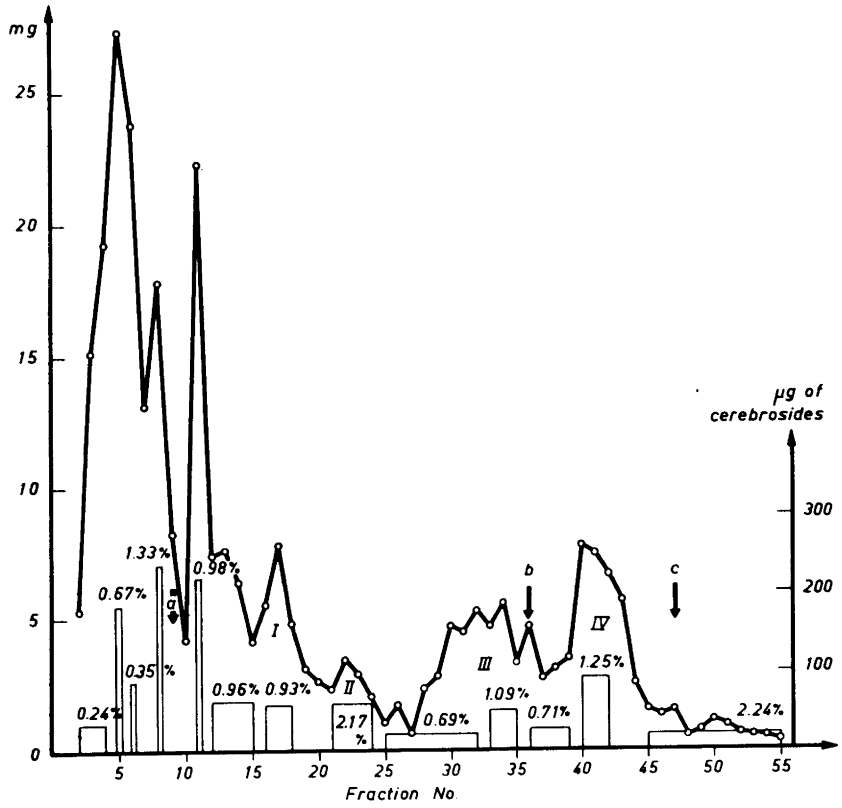

Fig. 5. Elution of the cerebrosides. The curve shows the weight eluted. The height of the columns shows the total cerebroside content of the corresponding fractions; scale on the right. The figures on the columns give the cerebroside contents of each combined fraction as a percentage of total material eluted. Phosphorus determinations were not made in this case but the position of the peaks can be deduced from the shape of the curve. The arrows indicate: a) the start of chloroform methanol elution, b) methanol in the top vessel, c) stripping with methanol. A more prolonged elution with chloroform would have given a better separation of the first fractions eluted by chloroform methanol.

whether sphingomyelin or other glycerol-free phospholipids were present the phosphatide content was calculated from the result of glycerol determinations. The mean value of four determinations was 6.3 % corresponding to 53 % glycerophosphatides using the factor 8.4. This factor should possibly be reduced to allow for the presence of compounds such as lysolecithin; small amounts of cerebrosides may also cause a slight increase. It can however be concluded that sphingomyelin or some similar compound is eluted in the peak IV region.

Lea and Rhodes [2] separated the lipids of egg yolk on silicic acid columns and found lysolecithin in the strongly adsorbed residue on the column. The possibility of this being present in the peak IV material does not invalidate the conclusions above since different phosphatidyl compounds have the same

P:glycerol ratio. The high value given by calculation with 25 × P may however obscure the presence of undefined material. Lea and Rhodes rejected the material insoluble in cold ether before chromatography and therefore would not have found sphingomyelin.

No attempts were made to follow the elution of the plasmalogens quantitatively. The Feulgen reaction was used in one case and the densities were plotted on the weight curve; see Fig. 4. High values were recorded at the beginning of the curve but further along the reaction was weaker. It might be expected that the plasmalogens and the cephalins would be eluted together. This assumption was not entirely refuted by the experimental results but was incompatible with the first part of the curve. The initial hump of peak I corresponded to a peak in the plasmalogen curve. It is therefore possible that a plasmalogen fraction was eluted just in front of the cephalins but was incompletely separated from them.

The cerebrosides amount to 0.8 % of the original lipid sample. The chromatographic fractions were grouped to give sufficient material for study, see Fig. 5. The largest amounts of cerebrosides were eluted by chloroform although some of the later fractions contained slightly higher proportions of cerebrosides. Because of the small quantities present, no attempt was made to find whether the differences in chemical composition of the cerebrosides influenced the order of elution.

The fractions eluted by chloroform methanol gave more material than that shown by phosphorus determinations on the original material. The phospholipid content in the first part of the gradient elution curve is apparently low as can be seen in Figs. 2 and 3. Cholesterol determinations were made to check the separation, but only low and insignificant values were obtained even when the preceding elution was brief.

The first fractions eluted by chloroform methanol had a low phosphorus content even after prolonged elution with pure chloroform, see Fig. 4. Taurog, Enteman, Fries and Chaikoff [12] found that magnesium oxide retains cephalins and a preliminary test showed that the undefined material eluted with the cephalins could be separated using this adsorbent.

Work on further purification of the fractions is in progress and will be published later.

This investigation was carried out with the financial assistance of the *Swedish Medical Research Council (Statens Medicinska Forskningsråd)*. The assistance of Mr. R. Kikas and Fil.kand. R. Lundquist is gratefully acknowledged. I am much indebted to Docent L. Svennerholm for the cerebroside estimations.

REFERENCES

1. Borgström, B. *Acta Physiol. Scand.* **25** (1952) 101.
2. Lea, C. H. and Rhodes, D. N. *Biochem. J.* **57** (1954) xxii.
3. Lederer, E. and Lederer, M. *Chromatography, a Review of Principles and Applications*, Elsevier, Amsterdam 1953.
4. Bellows, J. G. Henry Kimpton, *Cataract and Anomalies of the Lens*, London 1944.
5. Bevan, T. H., Gregory, G. I., Malkin, T. and Poole, A. G. *J. Chem. Soc.* **1951** 841.
6. Brante, G. *Acta Physiol. Scand.* **18** (1949) Suppl. 63.

7. Teorell, T. *Biochem. Z.* **230** (1931) 1; **232** (1931) 485.
8. Fiske, C. H. and Subbarow, Y. *J. Biol. Chem.* **66** (1925) 375.
9. Svennerholm, M. L. *J. Neurochem.* **1** (1956) 42.
10. Blix, G. *Mikrochim. Acta* **1** (1937) 75.
11. Feulgen, R. and Grünberg, H. *Hoppe-Seylers Z. physiol. Chem.* **257** (1938) 161.
12. Taurog, A., Enteman, C., Fries, B. A. and Chaikoff, I. L. *J. Biol. Chem.* **155** (1944) 19.

Received July 5, 1957.

ACTA CHEMICA SCANDINAVICA 12 (1958) 119—123

The Quantitative Determination of 2(3)-Benzoxazolinone from Rye Seedlings

PENTTI K. HIETALA and ARTTURI I. VIRTANEN

Laboratory of the Foundation for Chemical Research, Biochemical Institute, Helsinki, Finland

A method for the quantitative determination of the antifungal substance, benzoxazolinone (BOA), found in rye seedlings, is described. The method is based on the determination of the absorption at 275 mμ in an ethanol solution in which BOA shows a strong maximum. Before the determination of the absorption a fraction has to be prepared from the rye extract where BOA is found in its entirety, and from which disturbing substances are removed. The purification is performed in a cellulose powder column using *cyclo*hexane-ethanol-water as solvent.

After we had discovered the occurrence of benzoxazolinone as an antifungal factor in rye seedlings [1] it was important to develop a quantitative method for its determination. The method developed by us and used in this laboratory since the beginning of 1956 is reported in this paper.

PRINCIPLE

2(3)-Benzoxazolinone (BOA) is extracted from a homogenized sample with boiling water, shaken into ether, the ether is evaporated, the evaporation residue is chromatographed on a cellulose powder column using *cyclo*hexane-ethanol-water as a solvent. The fraction containing BOA is diluted with absolute ethanol to a fixed volume, and its ultraviolet absorption spectrum is measured. The 275 mμ extinction of the maximum is compared with an extinction curve determined with known amounts of BOA, by which procedure the BOA content of the sample to be investigated is obtained.

Reagents: Absolute ethanol. *Cyclo*hexane (Merck's or May & Baker's *cyclo*hexane): The ultraviolet absorption spectra of different batches of *cyclo*hexane differed noticeably. When necessary, *cyclo*hexane was purified by silica gel-aluminum oxide treatment [2]. Several batches could, however, be used as such without special purification. Ether: The ether was purified by shaking with acid ferrosulphate solution 4 to 5 times, by washing with water, and finally by distillation. Cellulose powder (Whatman, "Ashless",

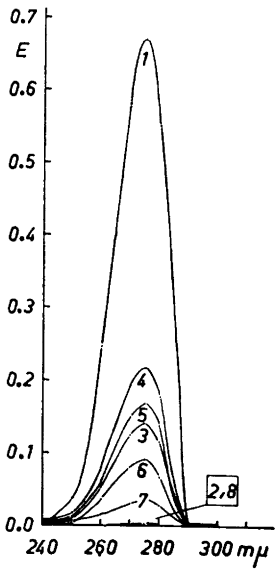

Fig. 1. Elution of BOA from the cellulose powder column with *cyclo*hexane-ethanol-water (*cf.* text). 200 μg pure BOA was used in the experiment.

Curve	1.	Fraction	between	5.6	and	9.0	cm	206	μg	BOA
»	2.	»	»	5.6	»	6.0	»	~0	»	»
»	3.	»	»	6.0	»	6.5	»	44	»	»
»	4.	»	»	6.5	»	7.0	»	68	»	»
»	5.	»	»	7.0	»	7.5	»	52	»	»
»	6.	»	»	7.5	»	8.0	»	28	»	»
»	7.	»	»	8.0	»	8.5	»	11	»	»
»	8.	»	»	8.5	»	9.0	»	~0	»	»
								203	μg	BOA

W. & R. Balston & Co.). Benzoxazolinone: The product used for determination of the extinction curve was synthesized from *o*-aminophenol and urea; m. p. 141°C. Glass-wool: Merck's *pro analysi* glass-wool or ordinary glass-wool washed with acid, ethanol, and water.

Preparation of cellulose powder columns: The columns used in chromatography were prepared from cellulose powder in glass tubes, 20 cm high and 9 mm in diameter. The lower end was drawn into a short beak. The diameter of the tube should not deviate much from 9.0 mm.

Glass-wool is placed into the lower end of the tube and stopped as tight as possible with a glass rod. Cellulose powder (1.70 g) is placed on the top of the wool in 5 or 6 portions. After each addition the tube is shaken in vertical position until the powder ceases to sink, and then it is packed tight with a glass rod. The height of the finished cellulose powder column has been 5.0 ± 0.2 cm. Distilled water is absorbed through the column from below, after which distilled water is placed on top of the column and sucked through with a vacuum pump. The column should not be allowed to dry. The column is now washed once with ethanol (94 %), and twice with the solvent *cyclo*hexane-absolute ethanol-water (400:80:1). Even cellulose powder columns are obtained more quickly when using centrifugation.

PROCEDURE OF THE DETERMINATION

0.3 to 4 g of rye seedlings, homogenized in a mortar, is weighed in a Pyrex-glass centrifuge tube, 15 ml of distilled water is added, and the suspension is mixed. The tube is kept in boiling water for 20 min under occasional shaking. After that the tube is immediately centrifuged and the separated solution is filtered into a 250 ml centrifuge tube. The residue is treated four times in the same way. The combined water extract in the centrifuge tube is shaken four times with peroxide free ether. The ether solution, separated by centrifugation, if necessary, is evaporated to dryness in a glass bowl, and the residue

is transferred to a 4 ml test tube by small amounts of ether. The ether is evaporated to dryness, and the residue dissolved in *cyclo*hexane-ethanol-water solution (1.00 ml) in which it dissolved completely. 0.200 ml of the solution obtained is placed on top of the column when there is no more solvent. The solution is allowed to run into the column, 3 drops of solvent are carefully added with a pipette, and when these drops have run into the column the tube is filled to the 0 mark on a centimetre scale fastened behind the tube. A small glass tube is placed upside down on the column to prevent evaporation. When the surface of the solvent has sunk 5.6 cm, the liquid emerging from the column is collected into a 10 ml volumetric flask. BOA emerges from the column between 5.6 and 9.0 cm as could be shown in experiments with pure BOA (Fig. 1). This fraction is taken up in a volumetric flask which is then filled to the mark with absolute ethanol, and the ultraviolet absorption spectrum is measured in a Beckman spectrophotometer.

EXTINCTION CURVE

The BOA content of the solution measured is obtained from the extinction curve, or by using multiplication by a coefficient calculated from the curve. The extinction curve was obtained with the following amounts of BOA: 50, 100, 200, and 400 μg/10 ml. The same amount of solvent was placed in a 10 ml volumetric flask as when chromatographing the proper samples to be investigated. The above-mentioned amounts of BOA, dissolved in absolute ethanol, were pipetted into this solution and the flasks were filled to the mark with absolute ethanol. The blank, made by simply running the solvent through the column, showed that if the *cyclo*hexane used is pure, the effluent has no absorption, and that the measurements can as well be made using absolute ethanol in the blank.

The extinction at 275 mμ follows Lambert-Beer's law. The extinction using 1 cm quartz cells has to be multiplied by 317.0 to establish the amount of BOA contained in 10 ml solution. The logarithm of the molar extinction of the substance is 3.63. The spectrum in the region 240—300 mμ is always measured in order to find out if there is an absorption caused by foreign substances. From young rye seedlings, the BOA content of which is high, a curve nearly corresponding to that of the pure substance is generally obtained, the absorption at 245—255 mμ and 285—300 mμ being, however, somewhat higher than with pure BOA solution. Especially at 245—255 mμ this absorption has every now and then become considerably high. The BOA content has been calculated by subtracting the calculated unknown absorption from the extinction measured at the absorption maximum at 275 mμ. If the foreign absorption is high, the accuracy of the method is low.

Control of the method: 1) In order to find out if BOA in the extract from rye seedlings emerges completely from the column at the range 5.6—9.0 cm, the following experiment was performed with the rye-varieties Ensi and Kungsråg II, which in regard to winter hardiness represent extreme types among the varieties used:

Ensi, 20 seedlings, 7 days old, fresh weight 2.138 g
Kungsråg II, 21 seedlings, 7 days old, fresh weight 2.380 g

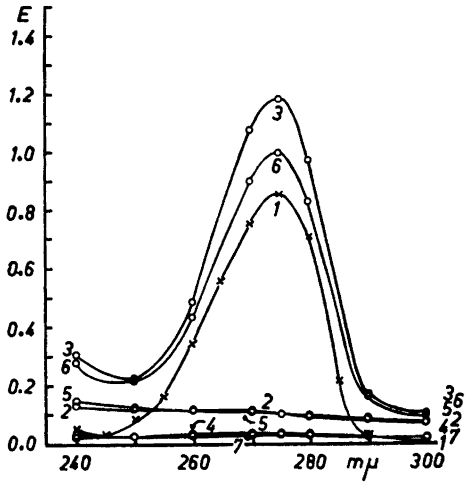

Fig. 2. BOA-Determination of Ensi and Kungsråg II rye seedlings. BOA-fraction (5.6—9.0 cm), prefraction (4.6—5.6 cm), and afterfraction (9.0—10.0 cm). E = E/g fresh weight. 1. Pure BOA. 2. Prefraction (Ensi rye). 3. BOA-fraction (Ensi rye). 4. Afterfraction (Ensi rye). 5. Prefraction (Kungsråg II rye). 6. BOA-fraction (Kungsråg II rye). 7. Afterfraction (Kungsråg II rye).

Determination and chromatography were performed in the usual way. In addition to the proper fraction containing BOA, 1 cm of solvent was taken before and after this fraction. Fig. 2 shows the spectra of pre- and afterfractions as well as the spectrum of the fraction containing BOA. The absorption maximum of BOA is completely lacking in pre- and after-fractions. It can thus be concluded that BOA has emerged entirely at the range mentioned.

Table 1. Recovery of BOA added to the rye extract.

Run	Extinction 275 mμ	μg BOA found	Recovery %
200 μl (1 μg BOA/μl)	0.628	199	99.5
100 μl BOA solution + 100 μl rye solution	0.596	189	102.5
200 μl rye solution	0.551	173	

Table 2.

Determination	BOA μg/g fresh weight	Deviation % from mean value
1	467	2
2	442	3
3	438	5
4	455	0
5	480	5
	Mean value 456	

Table 3. Parallel determinations of BOA from different varieties of rye (field experiments).

Variety of rye	BOA μg/g fresh weight	Mean value	Deviation % from mean value
Ensi 1	334	323	3
2	312		
Onni 1	456	486	6
2	516		
Pekka 1	490	476.5	3
2	461		
Visa 1	211	211	0
2	211		
Toivo 1	458	438.5	4
2	419		

This is in accordance with the results obtained with pure BOA (*cf.* Fig. 1). Similar curves were also obtained with Pekka, Visa, and Greus rye.

2) Recovery of BOA added to the plant extract. 70 g of rye was extracted. The residue of the ether extract was dissolved into 8.00 ml solvent. The determinations were carried out as described above; details of the experiments and results in Table 1.

3) Differences between parallel determinations. The following determinations were made on August 16, from young rye seedlings (Pekka variety) cultivated in pot cultures in sand. The same solution was used in all determinations (Table 2). Some results obtained in parallel determinations on rye seedlings from field experiments are shown in Table 3.

The authors are indebted to Miss Terttu Ettala and Miss Aino Aura for determinations of BOA, and to Professor O. Pohjakallio, from the Department of Plant Pathology, University of Helsinki, for samples of rye obtained from his field experiments.

The support given by the *Rockefeller Foundation* is gratefully acknowledged.

REFERENCES

1. Virtanen, A. I. and Hietala, P. K. *Acta Chem. Scand.* **9** (1955) 1543.
2. Hesse, G. and Schildknecht, H. *Angew. Chem.* **67** (1955) 737.

Received September 24, 1957.

ACTA CHEMICA SCANDINAVICA 12 (1958) 124—128

On the Antifungal Effect of Benzoxazolinone and 6-Methoxybenzoxazolinone, Respectively, on *Fusarium nivale*

Ö. WAHLROOS and ARTTURI I. VIRTANEN

Laboratory of the Foundation for Chemical Research, Biochemical Institute, Helsinki, Finland

The decomposition of benzoxazolinone and 6-methoxybenzoxazolinone by *Fusarium nivale*, the adaptation of this fungus to benzoxazolinone, and the fungistatic or fungicidic action of benzoxazolinone on it has been investigated. The mode of inhibition of growth of *F. nivale* in media containing benzoxazolinone is discussed in relation to the results. The results suggest that benzoxazolinone has a fungistatic influence in a concentration < 0.5 mg per ml. In a concentration > 0.6 mg per ml the fungicidic influence is already prevailing and the growth of *Fusarium* is totally inhibited.

The growth curves, shown in Fig. 1, are obtained when the biological activity of benzoxazolinone (BOA), the antifungal substance found in rye seedlings, is determined in an oat-glycerol solution or on agar plates, using different BOA concentrations and *F. nivale* as test organism.

A pronounced lag period is thus observed which is the longer the higher the BOA content. Even after a long period of time no growth was observed when the BOA concentration was higher than 0.5 mg/ml.

Some experiments were performed in order to find out if the influence of BOA and 6-methoxybenzoxazolinone (MBOA) is fungistatic or fungicidic and to study the reactions underlying the lag period. In this paper these experiments and the results are described and discussed.

DECOMPOSITION OF BOA BY *F. nivale*

40 mg of BOA were added to 100 ml of Czapek's nutrient solution containing 0.63 g of glycerol per litre and sterilized for 15 min under 0.8 atm pressure. Subsequently an amount corresponding to about 7 mg dry weight of the mycelium of *F. nivale*, grown for 7 days at 20°C on oat-glycerol-agar, was added aseptically. The suspension in a 1 litre Erlenmeyer flask, closed by a cotton

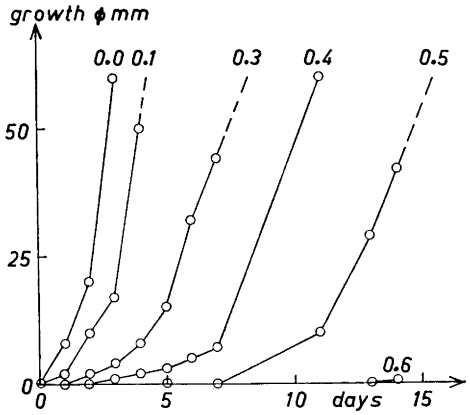

Fig. 1. Growth of the mycelium of *F. nivale* in a BOA containing oat-glycerol-medium. Curve numbers indicate the BOA content, mg/ml.

plug, was shaken in an automatical shaker at a frequency of 50 oscillations per min. A corresponding suspension without BOA was used as control. At intervals 1 ml samples were taken with a sterile pipette. The samples were diluted to 100 ml, and the absorption at 230 to 300 mμ was determined with a Beckman spectrophotometer. The BOA content was calculated from the

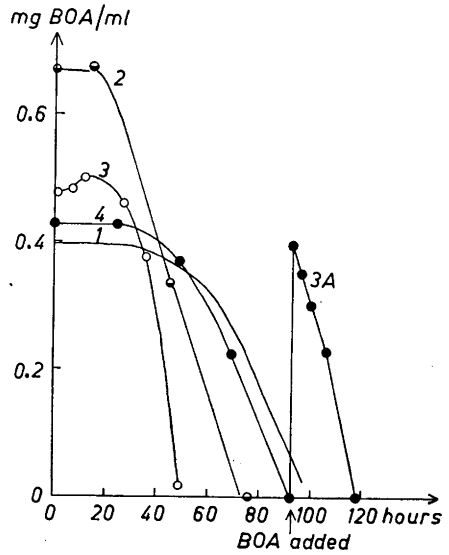

Fig. 2. Decomposition of BOA in a suspension of *F. nivale* in: 1 and 2 : Czapek solution ; 3 and 4 : oat-glycerol solution. The numbers of curves 3 and 4 have changed places.

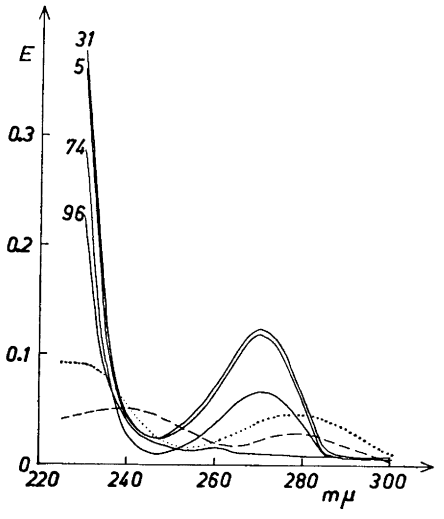

Fig. 3. UV-Spectra of the suspension of *F. nivale* in a Czapek solution containing BOA. Solid lines: vigorously shaken suspension. Curve numbers indicate test time in hours. Broken line: The spectrum of an unshaken suspension after decomposition of BOA. Dotted line: The spectrum of *o*-aminophenol in the same suspension.

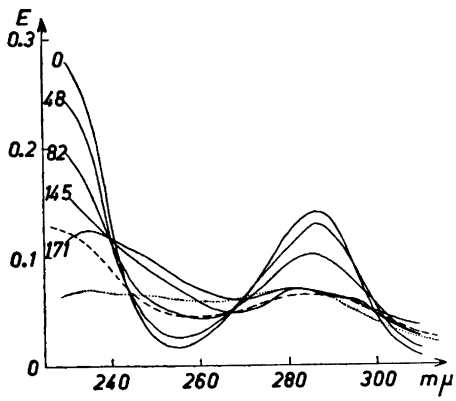

Fig. 4. Solid lines: The breakdown of MBOA effected by the mycelium of *F. nivale* in a vigorously shaken Czapek solution. Curve numbers indicate test time in hours. Broken line: 2-amino-5-methoxyphenol, partly oxidized in air. Dotted line: 2-amino-5-methoxyphenol, further oxidized in air.

absorption maximum at 270 mμ. The weight of the mycelium was determined in 5 ml samples. The results are shown in Fig. 3 and curve 1 in Fig. 2.

In another experiment, in which the BOA content was 0.67 mg per ml, and the amount of mycelium corresponded to about 70 mg dry weight per 100 ml solution, the BOA content decreased by 50 % in 45 h; after 76 h no BOA could be found in the test solution (Fig. 2, curve 2).

After 120 h a determination of BOA was made on the mycelium in 50 ml test solution; 0.041 mg of BOA was found, which is about 1/500 of the amount of BOA added at the beginning of the experiment.

It is noticeable that in all experiments it took 20 to 30 h before the decomposition of BOA started. Does this lag period depend on an adaptive formation of a BOA-decomposing enzyme? To test this possibility a new portion of BOA was added to a suspension in which the originally added BOA was decomposed. As can be seen from curve 3 A in Fig. 2 the decomposition of BOA has now started immediately.

DECOMPOSITION OF 6-METHOXYBENZOXAZOLINONE BY *F. nivale*

The experiment was performed as above. The MBOA content of the solution was 0.4 mg per ml, and the amount of mycelium corresponded to about 90 mg dry weight per 100 ml solution.

After 170 h practically all MBOA had disappeared from the solution.

CHANGES IN THE UV SPECTRUM DURING THE DECOMPOSITION OF BOA AND MBOA BY *F. nivale*

The UV spectrum of the BOA solution with the mycelium of *F. nivale* had during the experiment the same shape as the spectrum of pure BOA solution, from which fact it can be concluded that aromatic decomposition products of BOA, possibly formed during the experiment, were hardly enriched in the solution (Fig. 3). When practically all BOA had disappeared a very weak maximum at 260 mμ could be noticed. It disappeared rapidly, however.

On performing the experiment without shaking, two new maxima (at 240 and 280 mμ) were observed when BOA had disappeared (Fig. 3).

In the MBOA solution with *F. nivale* mycelium two new maxima were observed at 235 mμ and 282 mμ after 125 h as well as an inflexion point at 295 mμ which disappeared after 170 h when all MBOA was already decomposed (Fig. 4). In addition there was a maximum at 460 mμ. The change in the spectrum cannot be due to pH-variations, since the pH remained constant during the experiment. It thus seems that one or more new compounds containing a benzene ring had been formed from MBOA by *F. nivale*.

In Figs. 3 and 4 are also seen the spectra of *o*-aminophenol and 2-amino-5-methoxyphenol oxidized in the air. The latter compound also showed a maximum at 460 mμ. It is seen that the spectra do not quite correspond to the maxima observed in *F. nivale* suspensions during and after the disappearance of BOA and MBOA though there are certain similarities.

The rate of decomposition seems to depend on the amount of mycelium as well as on the original BOA concentration of the solution. MBOA seems to decompose slower than BOA. It ought to be mentioned that in an unshaken mycelium suspension BOA was no longer decomposed in a concentration of 0.5 to 0.6 mg/ml.

ADAPTATION OF *F. nivale* TO BOA

The lag period might thus be the time required by *F. nivale* to decompose BOA around the inoculate. Another possibility might be the adaptation of *F. nivale* to BOA. Therefore the following experiment was performed.

F. nivale mycelium was transferred to 20 oat-glycerol-agar plates containing 0.6 mg of BOA per ml. After 9 days growth could be seen on 12 plates. The mycelium grown on these plates was cultivated during 4 transfers on plates containing 0.6, 1.0, and 1.25 mg of BOA per ml. As early as during the second transfer *F. nivale* grew in the concentration 1 mg per ml. Even after the fourth transfer *F. nivale* did not grow in a higher concentration than this.

The observed length of the lag period at concentrations of 0.1 to 0.5 mg BOA per ml can be supposed to depend on this weak adaptation.

THE FUNGICIDIC INFLUENCE OF BOA AND MBOA ON *F. nivale*

Nine days old mycelium of *F. nivale* was transferred to sterile 0.9 % NaCl solutions containing different amounts of BOA. Each test tube contained 5 ml solution and about 5 mg dry weight of mycelium. At the contact times, shown in Table 1, samples of the mycelium were separated, washed three times with sterile 0.9 % NaCl solution and then transferred to an oat-glycerol-agar. Growth was followed during 7 days.

The results shown in Table 1 indicate that BOA has a fungicidic influence on *F. nivale* from a concentration of 0.5 mg per ml upwards. In concentrations higher than this the fungicidic influence is comparatively rapid. MBOA also exerts a fungicidic influence on *F. nivale* at least in the concentration 0.5 mg per ml (contact time 6 days).

Table 1. Growth of the mycelium of *F. nivale* after contact times of 1 to 33 days. Substrate in the growth tests oat-glycerol-agar.

mg BOA/ml	Growth Contact time, days 1	2	3	4	8	17	33
0 (control)	+	+	+	+	+	+	(+)
0.3	+	+	+	+	+	+	+
0.5	+	+	+	+	(+)	(+)	−
0.75	+	(+)	−	−	−	−	−
1.0	+	(+)	−	−	−	−	−
1.4	+	−	−	−	−	−	−

Marking of growth: + = normal growth, (+) = poor growth, − = no growth.

DISCUSSION

On the basis of the observations reported above the growth of *F. nivale* in a nutrient solution or on agar plates containing BOA or MBOA could perhaps be explained in the following way: in a concentration up to 0.4 mg per ml the influence is fungistatic, and the lag period depends on the adaptation of *F. nivale* to these substances. When growth has started, it at first proceeds slowly, and then accelerates to reach about the same rate as in a solution without BOA (Fig. 1). BOA determinations from growth flasks indicate that at this point BOA had practically disappeared from the media. In 0.5 mg per ml there is already a weak fungicidal influence, the fungistatic one still prevailing, however. When the concentration rises to 0.6 or 0.7 mg per ml, the fungicidic influence prevails, and growth is totally inhibited.

The chemical mechanism of the fungistatic and fungicidic influence of BOA and MBOA is still unknown.

As regards the way of the decomposition of BOA and MBOA by *F. nivale* it is possible that the corresponding aminophenols occur among the products, though, at least in the case of BOA, the decomposition probably goes further.

The support given by the *Rockefeller Foundation* is gratefully acknowledged.

Received September 25, 1957.

ACTA CHEMICA SCANDINAVICA 12 (1958) 129—146

Short Communications

On Some Unknown Metabolic Intermediates in Plants

PEKKA LINKO*

Laboratory of the Foundation for Chemical Research, Biochemical Institute, Helsinki, Finland

In an earlier paper [1] from this laboratory it was reported that several unknown compounds were rapidly labelled with ^{14}C after infiltration of radioactive pyruvate into the leaves of *Phlox decussata* and *Asplenium septentrionale* (Figs. 1 and 2). When these compounds were subjected to acid hydrolysis (6 N HCl, 20 h, 105°C, sealed tube, except in case of compound No. 11, 1 N HCl, 2 h) the following results were obtained:

Spot No. 5. The only hydrolysis product detected was active alanine.

Spot No. 6. Active glutamic acid and a ninhydrin positive inactive compound, probably identical with glucosamine, were formed. It is likely that this compound may be a derivative of glutamic acid and glucosamine. It is interesting to notice that the amino group of glucosamine-6-phosphate is known to be derived from the amide-group of glutamine [2,3].

Spot No. 7. This is probably identical with compound X in *Asplenium septentrionale*. Both compounds are rapidly and heavily labelled in the beginning of the experiment, the activity decreasing soon thereafter. As the other unknown compounds in question it was first thought to be ninhydrin negative, but in one case a slight brownish-violet color developed after some hours. Therefore it is thought that

* Present address: Kansas State College, Department of Flour and Feed Milling Industries, Manhattan, Kansas, U.S.A.

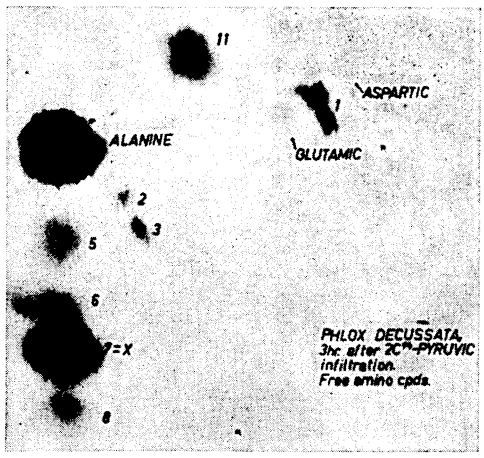

Fig. 1. Radioautogram of free amino compounds 3 h after 2—^{14}C-pyruvate infiltration into *Phlox decussata*.

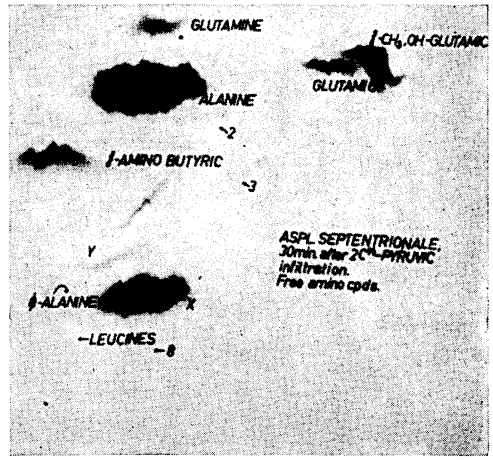

Fig. 2. Radioautogram of free amino compounds 30 min after 2—^{14}C-pyruvate infiltration into *Aspl. septentrionale*.

these compounds in general may be present only at very low concentrations, hence the specific activity being very high. On hydrolysis only one heavily active spot, again ninhydrin negative, was found. This unknown product travelled with the phenol frontier at the level of the leucines in butanol acetic acid solvent. The same result was obtained both on strong and mild hydrolysis.

Spot No. 8. Only spot found on hydrolysis was active alanine.

Spot No. 11. This compound was subjected only to mild hydrolysis and it seemed to be unaffected under these conditions. The spot was, however, most probably superimposed by an inactive spot, because great amounts of inactive γ-hydroxyglutamic acid were formed. The other possibility would be that the compound should have been only partially hydrolysed, the active carbon atom being split off. Such a case, where only one carbon atom becomes labelled after a short time, has been detected during photosynthetic $^{14}CO_2$ assimilation by blue-green algae [4]. In this case only the carbamyl group of the heavily labelled citrulline was found active.

No attempts have so far been made to identify the possible carbohydrates or other ninhydrin negative compounds which

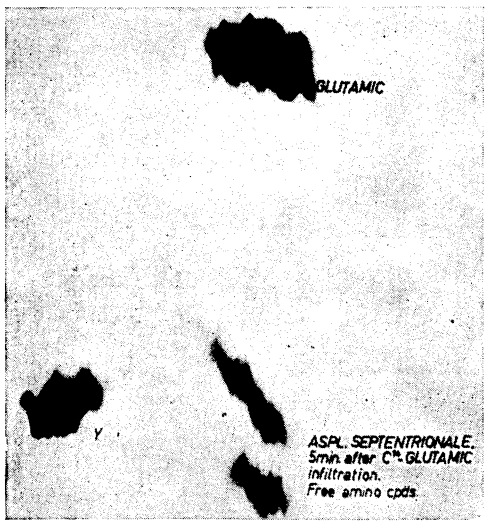

Fig. 3. Radioautogram of free amino compounds 5 min after 1—^{14}C-glutamate infiltration into *Aspl. septentrionale.*

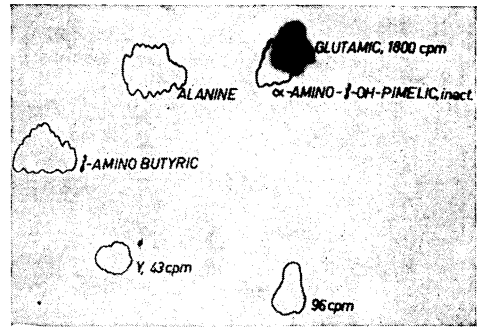

Fig. 4. Radioautogram of the products of hydrolysis of compound Y. Drawn spots are inactive ninhydrin positive compounds. Inactive glutamic acid, alanine and γ-aminobutyric acid were added on the chromatogram.

may arise during the hydrolysis of these unknown compounds.

When 1—^{14}C-glutamic acid was infiltrated into *Asplenium septentrionale* plants only three unknown compounds were found (Fig. 3). On acid hydrolysis of the major spot Y, active glutamic acid was formed in addition to inactive α-amino-γ-hydroxypimelic acid (Fig. 4) which was identified by means of paperchromatography. Even though the nature of this compound is unknown it is of great interest that α-amino-γ-hydroxypimelic acid is found bound to a compound formed as early as during a few minutes. Most of the glutamic acid is evidently readily decarboxylated thus losing its active carbon atom. If the primary reaction would be transamination to γ-ketoglutaric acid, at least some activity would be expected in other amino acids arising *via* the tricarboxylic acid cycle. It was of great interest to notice, too, that no active glutamine was found though glutamine was heavily labelled after 2—^{14}C-pyruvate and slightly labelled even after 1—^{14}C-pyruvate infiltration [1]. This is in good agreement with the assumption that glutamine may arise *via* γ-aminobutyric acid.

It has been known for a few years that the fraction of the 70 % ethanol extract of plant tissues, which passes through a cation exchange resin column, contains bound amino acids liberated on acid hydrolysis [5]. When hydrolysed after 2—^{14}C-pyruvate infiltration into *Asplenium septentrionale* mainly glutamic acid, alanine,

Table 1. The incorporation of activity into the amino acids in the hydrolysates of the "peptide" fraction after 2—^{14}C-pyruvate infiltration into *Aspl. septentrionale*.

Time, h	½	1	2	24
Glutamic, cpm	140	493	266	60
Alanine, cpm	243	175	94	
γ-Aminobutyric, cpm	94	163	—	—
Valine, cpm	15	—	—	—

and α-aminobutyric acid were found labelled in this fraction. Alanine was the major labelled compound after half an hour, but already after one hour the activity of glutamic acid was greater (Table 1). Whereas alanine decreased from the "peptide" fraction it increased in the proteins. However, the activity of compounds 5, 6, 7, 8 and 11 also had a peak within 10 to 30 min when 2—^{14}C-pyruvate alone was infiltrated. Glutamine was not labelled in this case. Inactive glycine, when infiltrated together with active pyruvate, caused a great inhibition of the labelling of these compounds during the first minutes after infiltration, whereafter the activity of compounds 6 and 7 as well as that of glutamic acid greatly increased, showing again the relationship of compound 6 to glutamic acid. In this case even glutamine was slightly labelled after 3 h. Glycine had only a slight inhibitory effect to the alanine containing compounds 5 and 8, while the activity of alanine itself increased due to the greater amount of nitrogen available for transamination reactions.

1. Linko, P. and Virtanen, A. I. *Acta Chem. Scand.* **12** (1958) 68.
2. Leloir, L. F. and Cardini, C. E. *Biochim. et Biophys. Acta* **12** (1953) 15.
3. Pogell, B. M. *Biochim. et Biophys. Acta* **21** (1956) 204.
4. Linko, P., Holm-Hansen, O., Bassham, J. A. and Calvin, M. *J. Exptl. Botany* **8** (1957) 147.
5. Virtanen, A. I. and Miettinen, J. K. *Biochim. et Biophys. Acta* **12** (1953) 181.

Received September 16, 1957.

The Influence of Anharmonicity upon the Vibrational Probability Density and Mean Amplitudes in Diatomic Molecules

ARNE REITAN

Institutt for teoretisk kjemi, N.T.H., Trondheim, Norway

The influence of anharmonicity upon the vibrational probability density and mean amplitudes in diatomic molecules has been investigated by using two different models to describe the molecular vibrations:

a) an anharmonic oscillator with perturbation terms of first and second order in the potential function,

b) an anharmonic oscillator described by a Morse potential function.

For case a) the probability density $w(r)$, where $r = R - R_e$ is the deviation of the interatomic distance R from its equilibrium value R_e, has been calculated by two different methods. In the first place, an expression for $w(r)$ has been developed by a superposition of probability densities for the different stationary states, according to the equation

$$w(r) = \sum_v |\psi_v(r)|^2 \exp(-E_v/kT) / \sum_v \exp(-E_v/kT)$$

where E_v and ψ_v are the corresponding eigenvalues and normalized eigenfunctions for the vibrational state v, k is Boltzmann's constant, and T is the absolute temperature. The eigenvalues E_v and eigenfunctions ψ_v have been obtained by a second order perturbation calculation similar to that performed by Hutchisson [1] (the results given by this author are, however, somewhat erroneous), and the sums have been evaluated by using well known properties of the Hermite orthogonal functions.

In the second place, the probability density $w(r)$ has been calculated by making use of an analogy to the solution of the time-dependent Schrödinger equation for the system (compare Bloch [2] and Kennard [3]).

In both cases the calculations are somewhat tedious, the result is, however, quite simple:

$$w(r) = (a_0 + a_1 r + a_2 r^2 + a_3 r^3 + a_4 r^4 + a_6 r^6) w^\circ(r)$$

Table 1. The incorporation of activity into the amino acids in the hydrolysates of the "peptide" fraction after 2—^{14}C-pyruvate infiltration into *Aspl. septentrionale*.

Time, h	½	1	2	24
Glutamic, cpm	140	493	266	60
Alanine, cpm	243	175	94	
γ-Aminobutyric, cpm	94	163	—	—
Valine, cpm	15	—	—	—

and α-aminobutyric acid were found labelled in this fraction. Alanine was the major labelled compound after half an hour, but already after one hour the activity of glutamic acid was greater (Table 1). Whereas alanine decreased from the "peptide" fraction it increased in the proteins. However, the activity of compounds 5, 6, 7, 8 and 11 also had a peak within 10 to 30 min when 2—^{14}C-pyruvate alone was infiltrated. Glutamine was not labelled in this case. Inactive glycine, when infiltrated together with active pyruvate, caused a great inhibition of the labelling of these compounds during the first minutes after infiltration, whereafter the activity of compounds 6 and 7 as well as that of glutamic acid greatly increased, showing again the relationship of compound 6 to glutamic acid. In this case even glutamine was slightly labelled after 3 h. Glycine had only a slight inhibitory effect to the alanine containing compounds 5 and 8, while the activity of alanine itself increased due to the greater amount of nitrogen available for transamination reactions.

1. Linko, P. and Virtanen, A. I. *Acta Chem. Scand.* **12** (1958) 68.
2. Leloir, L. F. and Cardini, C. E. *Biochim. et Biophys. Acta* **12** (1953) 15.
3. Pogell, B. M. *Biochim. et Biophys. Acta* **21** (1956) 204.
4. Linko, P., Holm-Hansen, O., Bassham, J. A. and Calvin, M. *J. Exptl. Botany* **8** (1957) 147.
5. Virtanen, A. I. and Miettinen, J. K. *Biochim. et Biophys. Acta* **12** (1953) 181.

Received September 16, 1957.

The Influence of Anharmonicity upon the Vibrational Probability Density and Mean Amplitudes in Diatomic Molecules

ARNE REITAN

Institutt for teoretisk kjemi, N.T.H., Trondheim, Norway

The influence of anharmonicity upon the vibrational probability density and mean amplitudes in diatomic molecules has been investigated by using two different models to describe the molecular vibrations:

a) an anharmonic oscillator with perturbation terms of first and second order in the potential function,

b) an anharmonic oscillator described by a Morse potential function.

For case a) the probability density $w(r)$, where $r = R - R_e$ is the deviation of the interatomic distance R from its equilibrium value R_e, has been calculated by two different methods. In the first place, an expression for $w(r)$ has been developed by a superposition of probability densities for the different stationary states, according to the equation

$$w(r) = \sum_v |\psi_v(r)|^2 \exp(-E_v/kT) / \sum_v \exp(-E_v/kT)$$

where E_v and ψ_v are the corresponding eigenvalues and normalized eigenfunctions for the vibrational state v, k is Boltzmann's constant, and T is the absolute temperature. The eigenvalues E_v and eigenfunctions ψ_v have been obtained by a second order perturbation calculation similar to that performed by Hutchisson [1] (the results given by this author are, however, somewhat erroneous), and the sums have been evaluated by using well known properties of the Hermite orthogonal functions.

In the second place, the probability density $w(r)$ has been calculated by making use of an analogy to the solution of the time-dependent Schrödinger equation for the system (compare Bloch [2] and Kennard [3]).

In both cases the calculations are somewhat tedious, the result is, however, quite simple:

$$w(r) = (a_0 + a_1 r + a_2 r^2 + a_3 r^3 + a_4 r^4 + a_6 r^6) w^\circ(r)$$

where $w^\circ(r)$ is the probability density for the harmonic case, and the a_k's are explicitly given as functions of the temperature T, the vibrational frequency ω_e for the corresponding harmonic oscillator, and the spectroscopic anharmonicity constant x_e.

If the most probable value of R is denoted by R_m, and the values of R corresponding to a probability density equal to one half of the maximum value are denoted by $R_{h,1}$ and $R_{h,2}$, it is found that to terms of second order

$$R_{h,1} - R_m = r_h^\circ(1 + x_e^{1/2}b_1 + x_e b_2),$$
$$R_m - R_{h,2} = r_h^\circ(1 - x_e^{1/2}b_1 + x_e b_2),$$

where r_h° is the half width for the harmonic case, and the b_k's are functions of the temperature T and the vibrational frequency ω_e. The probability density curve is, as it is seen, unsymmetric, the unsymmetry appearing already in a first order treatment.

Furthermore, explicit expressions have been developed for the mean amplitudes

$$u_e = [\overline{(R-R_e)^2}]^{1/2},$$
$$u_a = [\overline{(R-\bar{R})^2}]^{1/2},$$
$$u_m = [\overline{(R-R_m)^2}]^{1/2},$$

where the reference values of the interatomic distance in the three cases are the equilibrium value R_e, the mean value $\bar{R}$, and the most probable value R_m, respectively.

In case b) of the Morse-potential approximation the calculations have been carried out in a straightforward manner, considering only the lower vibrational states. However, the numerical results obtained by the two methods seem to be in very good agreement, as indicated by the values for the hydrogen molecule listed in Table 1. The necessary spectroscopic data have been obtained from Herzberg [4]. The values obtained when assuming harmonic vibrations are also given.

Table 1. Numerical data for hydrogen in Å units at $T = 300$ °K.

	Harm. osc.	Pert. meth.	Morse pot.
u_e	0.0872	0.0915	0.0917
u_a	0.0872	0.0890	0.0891
u_m	0.0872	0.0893	0.0894
$R_{h,1}-R_m$	0.1027	0.1075	0.1075
$R_m-R_{h,2}$	0.1027	0.1009	0.1008

A more detailed report on the calculations performed is to be published in *Kgl. Norske Videnskab. Selskab Skrifter.*

1. Hutchisson, E. *Phys. Rev.* **37** (1931) 45.
2. Bloch, F. *Z. Physik* **74** (1932) 295.
3. Kennard, E. H. *Z. Physik* **44** (1927) 326.
4. Herzberg, G. *Molecular Spectra and Molecular Structure*, Vol. I, *Spectra of Diatomic Molecules*, 2. Ed. Nostrand, New York 1950.

Received October 29, 1957.

N-Terminal Amino Acids of Human Pituitary Growth Hormone

F. HEIJKENSKJÖLD

Department of Clinical Chemistry, Karolinska Sjukhuset, Stockholm, Sweden

Analyses of the N-terminal amino acids of growth hormone prepared from ox pituitaries have been carried out by means of two methods. The dinitrofluorobenzene-technique (DNFB) of Sanger [1] has been applied by Li [2], who found two amino acids (phenylalanine and alanine) in equal molar proportions. These results were confirmed by the phenylthiohydantoin (PTH) method of Edman [3]. The latter method proved to be better since it was clearly demonstrable that the two amino acids were present as one mole each per mole of protein hormone [4].

This suggests a constitution formula of the ox hormone of two peptide chains linked together by SH-groups and ending in phenylalanine and alanine as N-terminal amino acids.

The following experiments were carried out to analyse the N-terminal amino acid of human pituitary growth hormone [5].

Material and methods. Growth hormone was prepared from human pituitaries by means of a method of Li and Papkoff [6]. 4 to 10 mg samples of the protein hormone were dissolved in 0.5—2.0 ml of phosphate buffer pH 9.0, ionic strength 0.1. An equal volume of 0.5 % phenylthio*iso*cyanate (Eastman Kodak) in ethanol was added and the mixture stirred for 2 h. The pH was maintained at 8.8 by the addition of small portions of 0.01 N sodium

where $w^\circ(r)$ is the probability density for the harmonic case, and the a_k's are explicitly given as functions of the temperature T, the vibrational frequency ω_e for the corresponding harmonic oscillator, and the spectroscopic anharmonicity constant x_e.

If the most probable value of R is denoted by R_m, and the values of R corresponding to a probability density equal to one half of the maximum value are denoted by $R_{h,1}$ and $R_{h,2}$, it is found that to terms of second order

$$R_{h,1} - R_m = r_h^\circ(1 + x_e^{1/2}b_1 + x_e b_2),$$
$$R_m - R_{h,2} = r_h^\circ(1 - x_e^{1/2}b_1 + x_e b_2),$$

where r_h° is the half width for the harmonic case, and the b_k's are functions of the temperature T and the vibrational frequency ω_e. The probability density curve is, as it is seen, unsymmetric, the unsymmetry appearing already in a first order treatment.

Furthermore, explicit expressions have been developed for the mean amplitudes

$$u_e = [\overline{(R-R_e)^2}]^{1/2},$$
$$u_a = [\overline{(R-\bar{R})^2}]^{1/2},$$
$$u_m = [\overline{(R-R_m)^2}]^{1/2},$$

where the reference values of the interatomic distance in the three cases are the equilibrium value R_e, the mean value $\bar{R}$, and the most probable value R_m, respectively.

In case b) of the Morse-potential approximation the calculations have been carried out in a straightforward manner, considering only the lower vibrational states. However, the numerical results obtained by the two methods seem to be in very good agreement, as indicated by the values for the hydrogen molecule listed in Table 1. The necessary spectroscopic data have been obtained from Herzberg [4]. The values obtained when assuming harmonic vibrations are also given.

Table 1. Numerical data for hydrogen in Å units at $T = 300$ °K.

	Harm. osc.	Pert. meth.	Morse pot.
u_e	0.0872	0.0915	0.0917
u_a	0.0872	0.0890	0.0891
u_m	0.0872	0.0893	0.0894
$R_{h,1}-R_m$	0.1027	0.1075	0.1075
$R_m-R_{h,2}$	0.1027	0.1009	0.1008

A more detailed report on the calculations performed is to be published in *Kgl. Norske Videnskab. Selskab Skrifter.*

1. Hutchisson, E. *Phys. Rev.* **37** (1931) 45.
2. Bloch, F. *Z. Physik* **74** (1932) 295.
3. Kennard, E. H. *Z. Physik* **44** (1927) 326.
4. Herzberg, G. *Molecular Spectra and Molecular Structure*, Vol. I, *Spectra of Diatomic Molecules*, 2. Ed. Nostrand, New York 1950.

Received October 29, 1957.

N-Terminal Amino Acids of Human Pituitary Growth Hormone

F. HEIJKENSKJÖLD

Department of Clinical Chemistry, Karolinska Sjukhuset, Stockholm, Sweden

Analyses of the N-terminal amino acids of growth hormone prepared from ox pituitaries have been carried out by means of two methods. The dinitrofluorobenzene-technique (DNFB) of Sanger [1] has been applied by Li [2], who found two amino acids (phenylalanine and alanine) in equal molar proportions. These results were confirmed by the phenylthiohydantoin (PTH) method of Edman [3]. The latter method proved to be better since it was clearly demonstrable that the two amino acids were present as one mole each per mole of protein hormone [4].

This suggests a constitution formula of the ox hormone of two peptide chains linked together by SH-groups and ending in phenylalanine and alanine as N-terminal amino acids.

The following experiments were carried out to analyse the N-terminal amino acid of human pituitary growth hormone [5].

Material and methods. Growth hormone was prepared from human pituitaries by means of a method of Li and Papkoff [6]. 4 to 10 mg samples of the protein hormone were dissolved in 0.5—2.0 ml of phosphate buffer pH 9.0, ionic strength 0.1. An equal volume of 0.5 % phenylthio*iso*cyanate (Eastman Kodak) in ethanol was added and the mixture stirred for 2 h. The pH was maintained at 8.8 by the addition of small portions of 0.01 N sodium

hydroxide. A Beckman autotitrator apparatus was used for the checking of pH and addition of alkali. When the alkali consumption had ceased three volumes of ethanol were added and the pH was lowered to 4 by addition of hydrochloric acid. After centrifugation the PTC-protein was washed three times with ethanol and lyophilized.

10 ml of N hydrochloric acid was added to the dry PTC-protein powder and the mixture was refluxed on a sandbath for 2 h. After cooling the PTH-amino acids were extracted with three 10 ml portions of ethyl acetate. The combined extracts were evaporated to dryness *in vacuo*. The dry residue was dissolved in a small volume of ethyl acetate and applied for chromatography on formamide-buffered Whatman No. 1 papers and developed with descending chromatography using xylene as a solvent [7].

Standard PTH-amino acids were always run together with the unknown. Indication of the spots was made by means of ultraviolet absorption with the aid of a fluorescence screen. For quantitative estimation of the N-terminal amino acid various amounts of the PTH-amino acid were run together with the preparations. The spots were eluated with 70 % ethanol, the volume made up to 10 ml and samples thereof read against ethanol in a Beckman spectrophotometer model DU at 269 mμ. Care was taken to make the paper pieces of exactly the same area since extracts from the formamide-buffered paper has a high blank absorption. The area of filter paper used usually had an absorption value of 0.2 (See Fig. 1).

Parts of the PTH-amino acid extracts were boiled in 2 N sodium hydroxide for 3 h in order to transform them into the original amino acid. Identification of the amino acid was made by two-dimensional paper chromatography using Whatman No. 4 paper, water-saturated phenol and collidine-lutidine according to Dent [8]. The standard PTH-amino acids used were synthetisized according to Edman [3] and the purity was checked with melting point determination and paper chromatography.

Results. Only one N-terminal amino acid was demonstrable as a PTH-preparation by the method used. The identification of this amino acid proved to be rather troublesome. Use of xylene as a solvent in the paper chromatography showed a spot with a R_F-value in the vicinity of PTH-valine or PTH-phenylalanine. Other solvents (formic acid, *n*-butanol and hexane in various proportions according to Sjöquist [9]) did not give a reliable identification though the results of chromatography

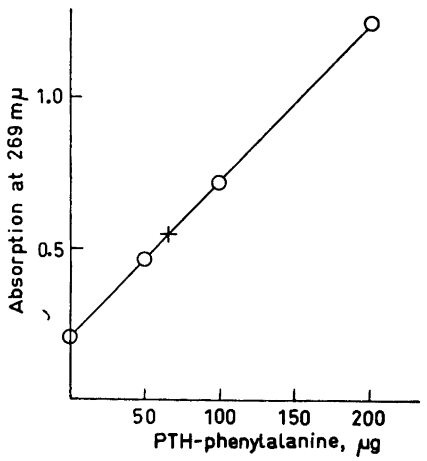

Fig. 1. Absorption at 269 mμ of a PTH-preparation from 10.0 mg of growth hormone and a standard PTH-phenylalanine preparation.

The PTH-phenylalanine from 10.0 mg of growth hormone had an absorption value of 0.550 which corresponds to 65 μg of PTH-phenylalanine (+) or 35.9 μg of phenylalanine. Thus one protein molecule contains 10 000/35.9 = 278 amino acids which means a molecular weight of about 30 600.

with xylene were confirmed. Breaking down the PTH-amino acid to the original amino acid by alkali and chromatography according to Dent [8] clearly showed the presence of phenylalanine. Quantitative determination of the PTH-phenylalanine showed that one mole of phenylalanine was present as N-terminal amino acid per mole of protein hormone.

Discussion. This study shows the presence of phenylalanine as N-terminal amino acid of human pituitary growth hormone. In contrast to the growth hormone of ox pituitaries this indicates the possibility that only one N-terminal amino acid per mole of protein is present. Thus the structure of the human growth hormone seems to differ from that of ox hormone. As already has been pointed out the ox hormone consists of two peptide chains. The human hormone, however, seems to be built up as a single peptide chain ending in phenylalanine as N-terminal amino acid. By means of the DNFB-technique phenylalanine has been demon-

strated in the human growth hormone [6]. The molecular weight calculated on basis of the quantitative analysis of N-terminal amino acid gave a value of 30 600 which is in accordance with previously reported values [10] (See Fig. 1).

1. Sanger, F. *Biochem. J.* **39** (1945) 507.
2. Li, C. H. and Ash, L. *J. Biol. Chem.* **203** (1953) 419.
3. Edman, P. *Acta Chem. Scand.* **4** (1950) 277; **4** (1950) 283.
4. Levy, A. and Li, C. H. *J. Biol. Chem.* **217** (1955) 355.
5. Gemzell, C. A. and Heijkenskjöld, F. *Endocrinology* **59** (1956) 681.
6. Li, C. H. and Papkoff, H. *Science* **124** (1956) 1293.
7. Edman, P. and Sjöquist, J. *Acta Chem. Scand.* **10** (1956) 1507.
8. Dent, C. E. *Biochem. J.* **43** (1948) 169.
9. Sjöquist, J. *Acta Chem. Scand.* **7** (1953) 447.
10. Ehrenberg, A. and Heijkenskjöld, F. *Acta Chem. Scand.* **10** (1956) 1675.

Received November 25, 1957.

On the Crystal Structure of $POCl_3 \cdot SbCl_5$

INGVAR LINDQVIST and
CARL IVAR BRÄNDÉN

Institute of Chemistry, University of Uppsala, Uppsala, Sweden

Single crystals of $POCl_3 \cdot SbCl_5$ were prepared in capillary tubes by a method of zone melting. Rotation and Weissenberg photographs were taken around the *c*-axes with Mo-*K* and Cu-*K* radiation. The orthorhombic unit cell has the dimensions $a = 8.06 \pm 0.01$ Å, $b = 16.42 \pm 0.01$ Å and $c = 8.93 \pm 0.02$ Å. These values are in agreement with the preliminary values found earlier [1] ($a = \frac{1}{2} = 8.1$ Å, $b = 16.2$ Å and $c = 8.8$ Å). The extinctions $h0l$ for $h + l$ odd, and $hk0$ for k odd are in agreement with the centrosymmetric space-group $P\,m\,n\,b$ which has been confirmed by the structure determination. (This space group was by mistake not found in the earlier investigation [1]).

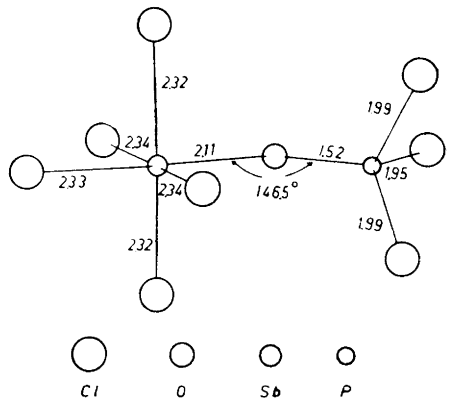

Fig. 1.

The number of molecules in the unit cell has been shown [1] to be 4.

The structure was determined from three-dimensional Patterson functions and confirmed by a three-dimensional electron density calculation. The unrefined parameters are:

4 Sb	in	$x = 0.250$	$y = 0.145$	$z = 0.079$
4 Cl	in	$x = 0.250$	$y = 0.257$	$z = 0.919$
4 Cl	in	$x = 0.250$	$y = 0.021$	$z = 0.207$
4 Cl	in	$x = 0.250$	$y = 0.226$	$z = 0.294$
8 Cl	in	$x = 0.538$	$y = 0.143$	$z = 0.070$
4 O	in	$x = 0.250$	$y = 0.073$	$z = 0.884$
4 P	in	$x = 0.250$	$y = 0.073$	$z = 0.714$
4 Cl	in	$x = 0.250$	$y = 0.464$	$z = 0.871$
8 Cl	in	$x = 0.054$	$y = 0.133$	$z = 0.633$

The shape of the $POCl_3 \cdot SbCl_5$ molecule and the interatomic distances within the molecule are given in Fig. 1. The structure is built up by the packing of such molecules. The complete structure determination will be published after refinement of the parameters.

This work was supported by the *Swedish Natural Science Research Council* whose support is gratefully acknowledged.

1. Gutmann, V., Wittman, A. and Nahringbauer, G. *Monatsh.* **88** (1957) 403.

Received December 3, 1957.

strated in the human growth hormone [6]. The molecular weight calculated on basis of the quantitative analysis of N-terminal amino acid gave a value of 30 600 which is in accordance with previously reported values [10] (See Fig. 1).

1. Sanger, F. *Biochem. J.* **39** (1945) 507.
2. Li, C. H. and Ash, L. *J. Biol. Chem.* **203** (1953) 419.
3. Edman, P. *Acta Chem. Scand.* **4** (1950) 277; **4** (1950) 283.
4. Levy, A. and Li, C. H. *J. Biol. Chem.* **217** (1955) 355.
5. Gemzell, C. A. and Heijkenskjöld, F. *Endocrinology* **59** (1956) 681.
6. Li, C. H. and Papkoff, H. *Science* **124** (1956) 1293.
7. Edman, P. and Sjöquist, J. *Acta Chem. Scand.* **10** (1956) 1507.
8. Dent, C. E. *Biochem. J.* **43** (1948) 169.
9. Sjöquist, J. *Acta Chem. Scand.* **7** (1953) 447.
10. Ehrenberg, A. and Heijkenskjöld, F. *Acta Chem. Scand.* **10** (1956) 1675.

Received November 25, 1957.

On the Crystal Structure of $POCl_3 \cdot SbCl_5$

INGVAR LINDQVIST and
CARL IVAR BRÄNDÉN

Institute of Chemistry, University of Uppsala, Uppsala, Sweden

Single crystals of $POCl_3 \cdot SbCl_5$ were prepared in capillary tubes by a method of zone melting. Rotation and Weissenberg photographs were taken around the *c*-axes with Mo-*K* and Cu-*K* radiation. The orthorhombic unit cell has the dimensions $a = 8.06 \pm 0.01$ Å, $b = 16.42 \pm 0.01$ Å and $c = 8.93 \pm 0.02$ Å. These values are in agreement with the preliminary values found earlier [1] ($a = \frac{1}{2} = 8.1$ Å, $b = 16.2$ Å and $c = 8.8$ Å). The extinctions $h0l$ for $h + l$ odd, and $hk0$ for k odd are in agreement with the centrosymmetric space-group $P\,m\,n\,b$ which has been confirmed by the structure determination. (This space group was by mistake not found in the earlier investigation [1]).

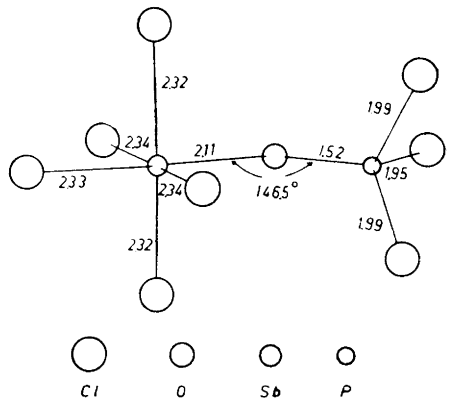

Fig. 1.

The number of molecules in the unit cell has been shown [1] to be 4.

The structure was determined from three-dimensional Patterson functions and confirmed by a three-dimensional electron density calculation. The unrefined parameters are:

4 Sb	in	$x = 0.250$	$y = 0.145$	$z = 0.079$
4 Cl	in	$x = 0.250$	$y = 0.257$	$z = 0.919$
4 Cl	in	$x = 0.250$	$y = 0.021$	$z = 0.207$
4 Cl	in	$x = 0.250$	$y = 0.226$	$z = 0.294$
8 Cl	in	$x = 0.538$	$y = 0.143$	$z = 0.070$
4 O	in	$x = 0.250$	$y = 0.073$	$z = 0.884$
4 P	in	$x = 0.250$	$y = 0.073$	$z = 0.714$
4 Cl	in	$x = 0.250$	$y = 0.464$	$z = 0.871$
8 Cl	in	$x = 0.054$	$y = 0.133$	$z = 0.633$

The shape of the $POCl_3 \cdot SbCl_5$ molecule and the interatomic distances within the molecule are given in Fig. 1. The structure is built up by the packing of such molecules. The complete structure determination will be published after refinement of the parameters.

This work was supported by the *Swedish Natural Science Research Council* whose support is gratefully acknowledged.

1. Gutmann, V., Wittman, A. and Nahringbauer, G. *Monatsh.* **88** (1957) 403.

Received December 3, 1957.

On the Reactions in Solutions of Phosphorus Oxychloride

INGVAR LINDQVIST

Institute of Chemistry, University of Uppsala, Uppsala, Sweden

The acid-base concept suggested by Gutmann and Lindqvist [1] has already been applied in a discussion [2] of solutions in arsenic trichloride, $AsCl_3$. This short communication will deal with the differences in behaviour, compared with that in $AsCl_3$, which might be expected in phosphorus oxychloride, $POCl_3$. The main difference between these two solvents is that only $POCl_3$ contains oxygen. The reaction between bases like $(CH_3)_4NCl$ and the solvent cannot be much influenced by the presence of an oxygen atom, but it may be mentioned that $POCl_3$ has a very small tendency to react with bases, that is, to function as an acid (a detailed comparison will be made in a subsequent paper [3]). The reason for this is probably that the phosphorus atom in $POCl_3$ cannot easily increase its coordination. This is possible for As in $AsCl_3$ and Se in $SeOCl_2$, and those solvents react much better with bases.

With chlorides like $SbCl_5$, $SnCl_4$ and $TiCl_4$ which are acids in $AsCl_3$ there are certain changes in the reactions with oxychlorides. The important factor is always the increase in coordination. In $AsCl_3$ this increase can only take place in this way:

$$AsCl_3 + SbCl_5 \rightleftharpoons Cl_2AsClSbCl_5 \rightleftharpoons AsCl_2^+ + SbCl_6^- \quad (1)$$

The analogous reaction in $POCl_3$ is:

$$POCl_3 + SbCl_5 \rightleftharpoons Cl_2OPClSbCl_5 \rightleftharpoons POCl_2^+ + SbCl_6^- \quad (2)$$

The dissociations to $AsCl_2^+$ or $POCl_2^+$ and $SbCl_6^-$ have been established through potentiometric measurements [4,5].

In $POCl_3$ a competing reaction is possible, however:

$$POCl_3 + SbCl_5 \rightleftharpoons Cl_3POSbCl_5 \quad (3)$$

The further dissociation to PCl_3^{2+} and $SbOCl_5^{2-}$ is very improbable because it would require the breaking of the strong P—O bond and would lead to the formation of bivalent ions in a solvent with a very low dielectric constant.

Reaction (3) would not change the chloride ion activity but the occurrence of the reaction would decrease the apparent strength of $SbCl_5$ as an acid in $POCl_3$.

The structure of the solid compound $POCl_3 \cdot SbCl_5$ which has recently been determined [6], is built up by $Cl_3POSbCl_5$ molecules (contrary to the conclusions drawn from Raman spectroscopic work [7]). This is not in conflict with the assumption of different competitive equilibria in solution, because the equilibrium system can easily be shifted by the precipitation of the energetically most favourable solid phase.

The ionic compounds obtained by reactions (1) and (2) do not seem to have very favourable lattice energies compared with the compound found by reaction (3) and $SbCl_5$, $SnCl_4$ and $TiCl_4$ give crystalline compounds with $POCl_3$ and $SeOCl_2$ while only eutectic points are obtained with $AsCl_3$[3].

The reactions discussed so far involve only *addition* of solvent molecules, giving increased coordination. With an excess of solvent *substitution* reactions of the type:

$$Cl_3POSbCl_5 + POCl_3 \rightleftharpoons (Cl_3PO)_2SbCl_4^+ + Cl^- \quad (4)$$

cannot be quite excluded. It is true that potentiometric measurements have shown that reaction (4) does not take place [5] with $SbCl_5$ but it remains to be seen whether reactions of type (2), (3) or (4) are most important for other chlorides, *e. g.* $SnCl_4$ and $TiCl_4$.

It is obvious that investigations along the same lines as earlier drawn up for $AsCl_3$[2] are also of importance for the study of $POCl_3$ as a solvent.

1. Gutmann, V. and Lindqvist, I. *Z. physik. Chem.* **203** (1954) 250.
2. Lindqvist, I. *Acta Chem. Scand.* **9** (1955) 73.
3. Agerman, M., Andersson, L. H., Lindqvist, I. and Zackrisson, M. *Acta Chem. Scand.* **12** (1958). *In press.*
4. Andersson, L. H. and Lindqvist, I. *Acta Chem. Scand.* **9** (1955) 79.
5. Gutmann, V. and Mairinger, F. *Z. anorg. Chem.* **289** (1957) 279.
6. Lindqvist, I. and Brändén, C. I. *Acta Chem. Scand.* **12** (1958) 134.
7. Maschka, A., Gutmann, V. and Sponer, R. *Monatsh.* **86** (1955) 52.

Received December 3, 1957.

Oxidation of Phenolphthalein with Alkaline Hydrogen Peroxide

HAKON LUND

Chemical Institute, Aarhus University, Denmark

Some time ago it was pointed out [1] that the so-called phenolphthalein oxime cannot possess the structure hitherto assigned to it (I), but is a derivative of 2,3,1-benzoxazine (II).

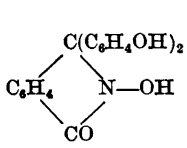

I

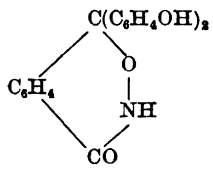

IIa

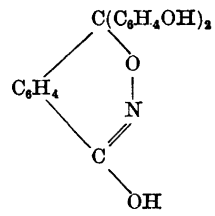

IIb

It can be rearranged and hydrolyzed to *p*-aminophenol and 2-*p*-hydroxybenzoyl benzoic acid.

When in the preparation of the "oxime" an excess of hydroxylamine is present a side reaction occurs with formation of *p*-aminophenol and N-*p*-hydroxyphenyl phthalimide [1]. The final products after hydrolysis are thus 2 moles of *p*-aminophenol and one of phthalic acid.

Due to the structural similarity between hydroxylamine and hydrogen peroxide it was thought worth while to examine the behaviour of the latter towards phenolphthalein in alkaline solution. It is known [2] that triphenylmethyl hydroperoxide can rearrange to benzophenone and phenol, so it was thought possible that a similar rearrangement might take place in a reaction with phenolphthalein:

(It could hardly be expected to be possible to isolate a cyclic compound corresponding to phenolphthalein oxime.)

Preliminary experiments showed that the red colour of the alkaline solution of phenolphthalein faded rapidly after addition of hydrogen peroxide. Addition of sodium hydroxide to a suspension of phenolphthalein in 10 % hydrogen peroxide caused a rise in temperature, at first fairly slow, but suddenly extremely rapid, and most of the reaction mixture was thrown out of the flask. In order to get a controlled reaction it was necessary to keep the temperature rather low.

Only the red form of the phenolphthalein anion seems to react with hydrogen peroxide at room temperature. A solution in a large excess of 10 % sodium hydroxide brought to the fading equilibrium was left overnight at 10° after addition of an excess of hydrogen peroxide. On acidification the phenolphthalein could be recovered almost quantitatively.

When carried out under suitable conditions the reaction gave a good yield of hydroquinone; the other product was not, however, the expected hydroxybenzoyl benzoic acid, but phthalic acid, and the yield of hydroquinone could be raised to about 120 % of that calculated for the expected reaction. Obviously the reaction proceeds in a similar way as the side reaction observed with an excess of hydroxylamine:

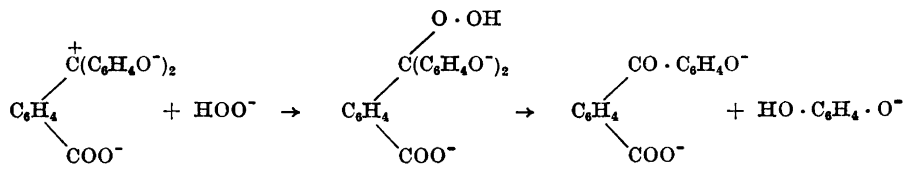

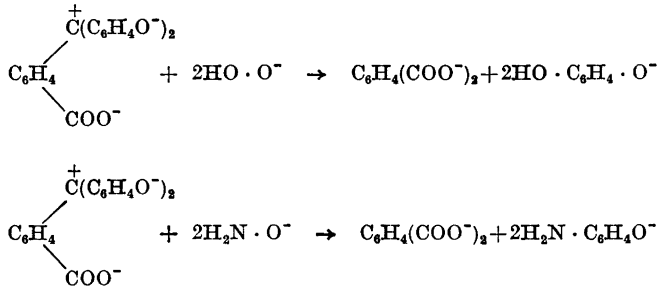

It is noteworthy that neither hydrogen peroxide nor hydroxylamine reacts with *p*-hydroxybenzoyl benzoic acid in alkaline solution. Obviously the attack of the second molecule of hydrogen peroxide or hydroxylamine sets in at some intermediate stage, the first one having a high and the latter a lower rate of reaction as compared with the rearrangement reaction proper.

The very violent reaction observed in the preliminary experiments seems to be an oxidation of hydroquinone: addition of hydrogen peroxide to an alkaline solution of hydroquinone results in a quite similar phenomenon. How far the oxidation goes has not been ascertained, but at least some carbonic acid is formed.

Other phthaleins react similarly, although with very different velocities. Fluorescein, thymolphthalein, and α-naphtholphthalein react very slowly and the corresponding polyvalent phenols could not be isolated, but were oxidized further. At higher temperatures thymolphthalein gave, besides phthalic acid, fatty acids with the rancid odour of butyric acids.

Experimental: 1. *Phenolphthalein.* In a 3-necked flask provided with a stirrer, a thermometer, and a dropping funnel, phenolphthalein (20 g) is suspended in water (40 ml) and 30 % hydrogen peroxide (10 ml). The flask is placed in a cooling bath. Stirring is started and a 30 % sodium hydroxide solution is added dropwise at such a rate that the temperature is kept at 15 ± 2°. After about 15 ml have been added, three 5 ml portions of hydrogen peroxide are added during the addition of some 15 ml of sodium hydroxide more. It may be necessary to add one more portion of hydrogen peroxide when all solid phenolphthalein has been dissolved. After some standing the red colour of the solution turns brown (due to some oxidation of hydroquinone). The solution is acidified with conc. hydrochloric acid and cooled. A mixture of phthalic acid and hydroquinone separates and is filtered off. The filtrate is extracted twice with ether (100 ml). The ether extract combined with the mass of crystalline material is treated with aqueous potassium hydrogen carbonate. From this extract phthalic acid (9.5 g) separates on acidification. From the ether solution hydroquinone is isolated, yield 8.2 g (59 %).

2. *Fluorescein.* Fluorescein (5 g) is dissolved in 10 % sodium hydroxide (30 ml) and 30 % hydrogen peroxide (10 ml) is added. The flask is cooled under the tap and the temperature is kept at 30—35°. More portions (5 ml) of hydrogen peroxide are added when no spontaneous rise of temperature is noticed, until the orange colour of the solution changes to pure yellow. If necessary, sodium hydroxide is added to keep the solution alkaline. Addition of hydrochloric acid causes strong effervescence, indicating the oxidation of the tervalent phenol to carbon dioxide. Phthalic acid (2.1 g), yellow, but otherwise pure can be isolated.

3. *Hydroquinone and hydrogen peroxide.* Hydroquinone (1 g) is dissolved in 10 % sodium hydroxide (15 ml) and 30 % hydrogen peroxide (5 ml) is added. The temperature rises and in less than a minute the liquid boils vigorously.

1. Lund, Hakon *Acta Chem. Scand.* **8** (1954) 1307.
2. Wieland, H. and Maier, J. *Ber.* **64** (1931) 1205.

Received November 29, 1957.

The Isolation of a Green Pigment from Yeast

W. J. RUTTER* and BRITA ROLANDER

Medicinska Nobelinstitutet, Biokemiska Avdelningen, Stockholm, Sweden

In connection with attempts to find efficient means of extraction of various oxidative enzymes, yeast cells were subjected to various treatments with non-aqueous solvents. After certain preextraction conditions deep green solutions were obtained. The green pigment has been concentrated and partially purified. A colorless material present as a contaminant these purified green preparations has been crystallized.

The primary observations, together with certain of the chemical properties of the compounds are presented in this communication.

Results and discussion. Fresh bottom yeast kindly furnished by Stockholm's Hamburgerbryggeriet was washed by decantation several times with cold water and finally when the washes were almost colorless, the yeast was collected by centrifugation. The yeast cake was then extracted twice with 2 volumes ethylene glycol at −12°C. Short-time homogenization with a blendor in the cold was useful at this point. 2 volumes of acetone were added, and the very dark brown solution was filtered off at −12°. The next acetone extract was noticeably green, but was usually discarded. Extraction with ethyl ether then gave a deep green or in some cases a yellowish green solution.

If the ethylene glycol preextraction step was omitted, the procedure was much less successful. Preextraction with other agents, for example glycerol, was also less satisfactory.

All subsequent steps were carried out in the dark. The first extract was concentrated to an oil *in vacuo* at 10°C.; the oil was then dissolved in a minimum amount of acetone. A 5 ml aliquot of the green solution (equivalent to a total of 5—10 O.D. units at 650 μ) was then placed on a powdered cellulose column (3.7 × 30 cm). After washing the column with 10 volumes methanol, the green pigment remained as a narrow band at the top, while much of the yellow contaminants migrated down the column. Gradient elution with increasing concentrations of ether in acetone yielded a sharp fraction containing the green compound(s). The green material was concentrated to an oil and dissolved in acetone. Addition of methanol with cooling produced a heavy crop of colorless crystals which were removed by filtration and washed with cold methanol.

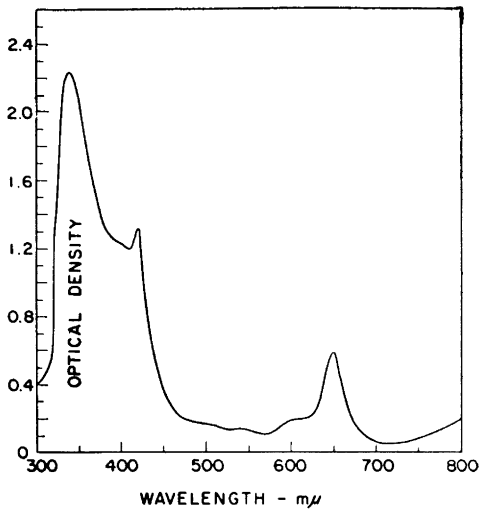

Fig. 1. Absorption spectrum of purified green pigment obtained from yeast.

The remaining deeply green solution was then concentrated and stored as an oil in the dark. The absorption spectrum of the purified green pigment is shown in Fig. 1. The spectrum is similar in form to certain hematin compounds, especially the chlorophylls [1,2]. However, no pyridine hemochromogen could be obtained under the usual conditions. Analysis of the preparation by chemical and spectroscopic means showed the presence of low concentrations of iron, and rather more magnesium. No other metals were detected. Addition of $FeCl_3$ to the green compound produced an immediate conversion to a yellow compound. The green material fluoresces intensely when irradiated with ultraviolet light, but solutions

* Postdoctoral fellow of United States Public Health Service, 1954—55; present address, Division of Biochemistry, University of Illinois, Urbana, Illinois.

are also self-quenching. The colorless crystals did not fluoresce.

The spectrum of the white crystals ($CHCl_3$) in the infra red region showed prominent absorption peak at 2 940 with a shoulder at 2 870 cm^{-1}. Less prominent peks are at 1 725, 1 605, 1 467, 1 380, 1 060, 1 035, 985 and 842 cm^{-1}. The purified green material exhibited the same prominent peak at 2 920 cm^{-1} and the shoulder at 2 860 cm^{-1}, and in addition, the absorption at 1 730 cm^{-1} was very much intensified. There was a great deal of generalized absorption from 900—1 500 cm^{-1}, with two distinct peaks at 1 465 cm^{-1} and 1 385 cm^{-1}. The spectra are not overly informative, but do suggest the possible presence of aldehyde or COOH groups in the green compound, while the white crystals could be a saturated lipid having comparatively few functional groups.

The question whether the green compound is a natural constituent with a role in the physiology of the yeast cell cannot be answered unequivocally. It can be stated that the green compound was consistently obtained from each of five different air-dried brewers yeast preparations in this laboratory. This procedure, however, did not yield a green product from bakers yeast. It is pertinent, however, that Keilin [3] reported a green fraction in initial attempts at the isolation of cytochrome c from brewers yeast in 1931. Efforts to obtain the present green compound by a suitable modification of Keilin's procedure have not proved successful.

There is some evidence which suggests that some of the efficiency of extraction of the green compound is very closely related to the state of the cells. Thus it has not been possible to obtain the green compound by extraction of fresh yeast cells, nor of cells which have been autolyzed even for short periods. It has also not been possible to obtain the green compound from freeze-dried preparations. Suitable experiments indicate that the green color is not due to an artifact of the reagents used.

The actual chemical structure of the green compound and its role in biological systems awaits clarification. It would be particularly interesting to know if present compounds have a relation to any of the physiologically important green compounds known.

Acknowledgment. The authors wish to express appreciation to Professor Theorell for his active interest in this work, and W. J. Rutter wishes to express his thanks for the gracious hospitality extended by Professor Theorell and other members of the Biochemical Department.

1. Lemberg, R. *Hematin Compounds and Bile Pigments*, Interscience Publishers, New York 1949.
2. Rabinowitch, E. I. *Photosynthesis*, Interscience Publishers, New York 1945—1951.
3. Keilin, D. *Proc. Roy. Soc. London* **B 106** (1930) 418.

Received December 19, 1957.

Examination of the Behaviour of Liquid Mixtures in the Critical Region

HANS LUDVIG LORENTZEN and BJØRN BERGSNOV HANSEN

Universitetets Kjemiske Institutt, Blindern-Oslo, Norway

In order to investigate the shape of the co-existence curves close to the critical point, the two systems of partly miscible liquids, triethylamine-water (at the lower critical point) and succinonitrile-ethanol have been examined. The results are shown in Fig. 1, where the co-existence curves are seen to follow the "cubic rule" [1,2]

$$\Delta c = k \cdot \sqrt[3]{\Delta T} \qquad (1)$$

Δc being the composition of the individual phases measured from the critical, and ΔT the temperature distance from the critical.

It will be observed from Fig. 1 that in the case of triethylamine-water the plotted results follow the straight line as close as 1 mdeg to the critical. However, uncertainties regarding the fixation of the critical temperature involve uncertainty as regards the plots from the critical temperature to about $\Delta T = 2$ mdeg. Nevertheless, the visually obtained information about the initiation of the two phases when passing the critical temperatures

are also self-quenching. The colorless crystals did not fluoresce.

The spectrum of the white crystals ($CHCl_3$) in the infra red region showed prominent absorption peak at 2 940 with a shoulder at 2 870 cm^{-1}. Less prominent peks are at 1 725, 1 605, 1 467, 1 380, 1 060, 1 035, 985 and 842 cm^{-1}. The purified green material exhibited the same prominent peak at 2 920 cm^{-1} and the shoulder at 2 860 cm^{-1}, and in addition, the absorption at 1 730 cm^{-1} was very much intensified. There was a great deal of generalized absorption from 900—1 500 cm^{-1}, with two distinct peaks at 1 465 cm^{-1} and 1 385 cm^{-1}. The spectra are not overly informative, but do suggest the possible presence of aldehyde or COOH groups in the green compound, while the white crystals could be a saturated lipid having comparatively few functional groups.

The question whether the green compound is a natural constituent with a role in the physiology of the yeast cell cannot be answered unequivocally. It can be stated that the green compound was consistently obtained from each of five different air-dried brewers yeast preparations in this laboratory. This procedure, however, did not yield a green product from bakers yeast. It is pertinent, however, that Keilin [3] reported a green fraction in initial attempts at the isolation of cytochrome c from brewers yeast in 1931. Efforts to obtain the present green compound by a suitable modification of Keilin's procedure have not proved successful.

There is some evidence which suggests that some of the efficiency of extraction of the green compound is very closely related to the state of the cells. Thus it has not been possible to obtain the green compound by extraction of fresh yeast cells, nor of cells which have been autolyzed even for short periods. It has also not been possible to obtain the green compound from freeze-dried preparations. Suitable experiments indicate that the green color is not due to an artifact of the reagents used.

The actual chemical structure of the green compound and its role in biological systems awaits clarification. It would be particularly interesting to know if present compounds have a relation to any of the physiologically important green compounds known.

Acknowledgment. The authors wish to express appreciation to Professor Theorell for his active interest in this work, and W. J. Rutter wishes to express his thanks for the gracious hospitality extended by Professor Theorell and other members of the Biochemical Department.

1. Lemberg, R. *Hematin Compounds and Bile Pigments*, Interscience Publishers, New York 1949.
2. Rabinowitch, E. I. *Photosynthesis*, Interscience Publishers, New York 1945—1951.
3. Keilin, D. *Proc. Roy. Soc. London* **B 106** (1930) 418.

Received December 19, 1957.

Examination of the Behaviour of Liquid Mixtures in the Critical Region

HANS LUDVIG LORENTZEN and BJØRN BERGSNOV HANSEN

Universitetets Kjemiske Institutt, Blindern-Oslo, Norway

In order to investigate the shape of the co-existence curves close to the critical point, the two systems of partly miscible liquids, triethylamine-water (at the lower critical point) and succinonitrile-ethanol have been examined. The results are shown in Fig. 1, where the co-existence curves are seen to follow the "cubic rule" [1,2]

$$\Delta c = k \cdot \sqrt[3]{\Delta T} \qquad (1)$$

Δc being the composition of the individual phases measured from the critical, and ΔT the temperature distance from the critical.

It will be observed from Fig. 1 that in the case of triethylamine-water the plotted results follow the straight line as close as 1 mdeg to the critical. However, uncertainties regarding the fixation of the critical temperature involve uncertainty as regards the plots from the critical temperature to about $\Delta T = 2$ mdeg. Nevertheless, the visually obtained information about the initiation of the two phases when passing the critical temperatures

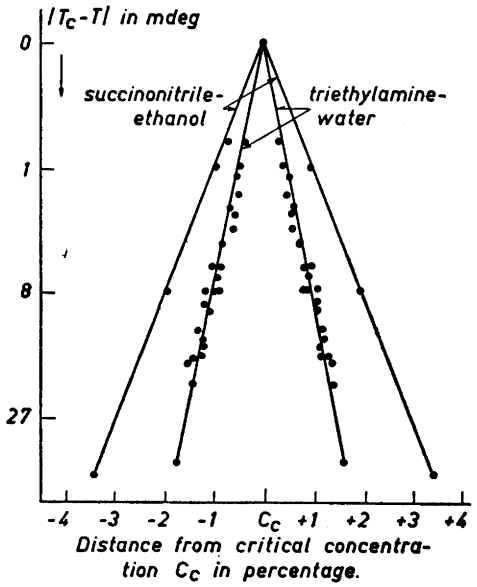

Fig. 1. Top of co-existence curves. C_c is the critical concentration. T_c is the critical temperature. Curves are obtained for the critical systems succinonitrile-ethanol and triethylamine-water. The co-existence curve for the latter is obtained through series of experiments, each series giving four to eight points on the curve.

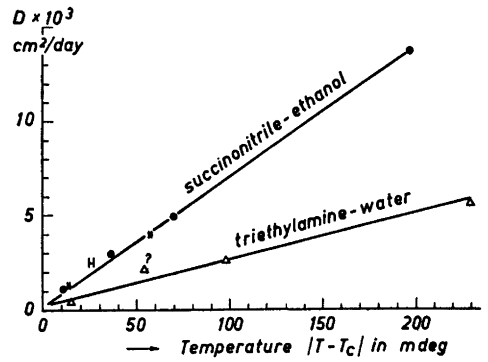

Fig. 2. Diffusion constant as a function of the temperature. For the critical system succinonitrile-ethanol the curve is obtained through two different series of experiments. The point marked ? on the critical system triethylamine-water may be due to the difficulties regarding the determination of the critical temperature — see text.

allows the assumption that the co-existence curve is regular to ΔT, this being only a fraction of a millidegree.

It should be noted that the critical temperature was not found to be constant. In the triethylamine-water system the critical temperatures seemed to have some connection with the initial concentration gradient in the sample. Impurities inside the sample may or may not be the cause of the fluctuations of the critical temperature.

The co-existence curve was determined in a large number of series, showing the critical temperature to be constant for each series. Because of the fluctuation of the critical temperature between the individual series, the critical temperature for each series had to be extrapolated from the determined concentrations of the two phases formed; in the case of the succinonitrile-ethanol system, at temperatures below the critical, and in the case of the triethylamine-water system, at temperatures above the critical.

The critical temperature, *i.e.*, the temperature at which the first sign of the development of the two phases appeared, was not observed with the requisite accuracy in most of the series. This left an element of doubt regarding the form of the co-existence curve at temperatures closer to the critical, as mentioned above.

The measurement of diffusion constants for the triethylamine-water mixture was carried out in the same way as already reported,[3] for the mixture of succinonitrile-ethanol at different temperatures from the critical. In Fig. 2 the diffusion constants found are plotted against temperature differences from the critical for both the systems examined. The two figures may permit the assumption that some correlation exists between the dD/dT of Fig. 2 and the $d\Delta c/d\sqrt[3]{\Delta T}$ of Fig. 1, the latter being the cube root of the constant of formula (1). It must, however, be remembered that the diffusion constants determined concern critical composition, whereas the two phases formed are naturally of compositions different from the critical.

The abscissa scale of Fig. 1 can be determined with greater accuracy than has been done here. However, the primary

aim of the investigations was to study the validity of the "cubic rule" [1,2] close to the critical point. The determination of the co-existence curves themselves, and the constant of formula (1) for the two mixtures was regarded as being of secondary importance.

The investigation of the triethylamine-water system was complicated by the fact that, at temperatures above, but closer to the critical, the two phases formed did not show the homogeneous composition which is to be expected. Furthermore, at temperatures below the critical, fog was occasionally seen to form inside the prism. After about an hour the fog would disappear, and the section of the concentration curve previously veiled by fog was then seen to have attained an arched form different from the arched concentration curves obtained by diffusion.

The author wishes to thank Professor O. Hassel of the University of Oslo for the interest he has shown in this work.

1. Guggenheim, E. A. *J. Chem. Phys.* **13** (1945) 253.
2. Zimm, B. H. *J. Chem. Phys.* **20** (1952) 538.
3. Lorentzen, H. L. and Bergsnov Hansen, B. *Acta Chem. Scand.* **11** (1957) 893.

Received December 16, 1957.

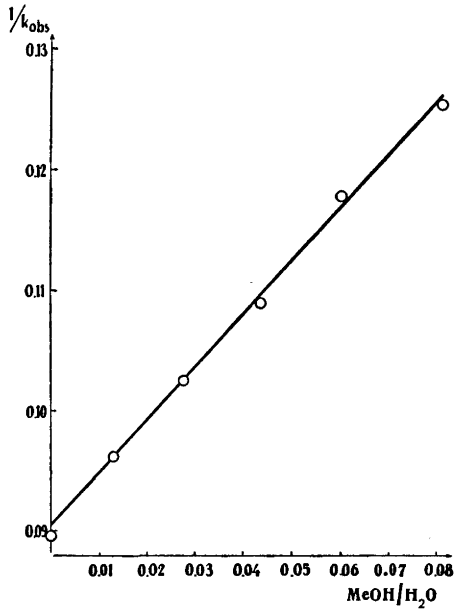

Fig. 1. Weight ratio of methanol and water in the resin phase *versus* $1/k_{obs}$ at the concentration range of 0 to 5 % methanol in the outside solution.

Reaction Kinetic Determination of the Hydroxyl-Alkoxide Equilibrium in Anion Exchangers

EERO SJÖSTRÖM and LALLI NYKÄNEN

Lääketehdas Orion Oy, Pharmaceutical Manufacturers, Helsinki, Finland

As a sequel to a previous work on the reaction mechanism between estradiol benzoate and an anion exchange resin [1], a kinetic method was developed which is reported here. This method makes it possible to follow the rate of hydrolysis (or alcoholysis) at very low ester concentrations. The method has been used for the investigation of the hydrolysis of methyl benzoate in water and in water-methanol mixtures of low methanol content. The experiments were carried out at 25 ± 0.02°C, by a batch-wise technique with constant stirring. At suitable time intervals samples were taken from the reaction mixture by means of a constant pressure apparatus. The amount of unreacted ester was estimated spectrophotometrically in the ultraviolet region.

According to Samelson and Hammet [2], the alkaline hydrolysis by anion exchangers in ethanol-water mixtures is a second order reaction. The present results show that when the hydroxyl ion concentration (the resin) is high compared with the ester, the rate constant can be calculated from the first order equation.

On adding methanol to the resin-water mixture the hydroxyl ions are in part converted into alkoxide ions owing to the reaction:

$$MeOH + HO^- \rightleftharpoons MeO^- + H_2O$$

and the hydroxyl ion concentration in the resin phase is decreased. If this reaction is the dominant factor in reducing the hydrolysis rate, it should be possible in theory to calculate the state of this equilibrium from the observed kinetic data. In fact, it was found that at low methanol

aim of the investigations was to study the validity of the "cubic rule" [1,2] close to the critical point. The determination of the co-existence curves themselves, and the constant of formula (1) for the two mixtures was regarded as being of secondary importance.

The investigation of the triethylamine-water system was complicated by the fact that, at temperatures above, but closer to the critical, the two phases formed did not show the homogeneous composition which is to be expected. Furthermore, at temperatures below the critical, fog was occasionally seen to form inside the prism. After about an hour the fog would disappear, and the section of the concentration curve previously veiled by fog was then seen to have attained an arched form different from the arched concentration curves obtained by diffusion.

The author wishes to thank Professor O. Hassel of the University of Oslo for the interest he has shown in this work.

1. Guggenheim, E. A. *J. Chem. Phys.* **13** (1945) 253.
2. Zimm, B. H. *J. Chem. Phys.* **20** (1952) 538.
3. Lorentzen, H. L. and Bergsnov Hansen, B. *Acta Chem. Scand.* **11** (1957) 893.

Received December 16, 1957.

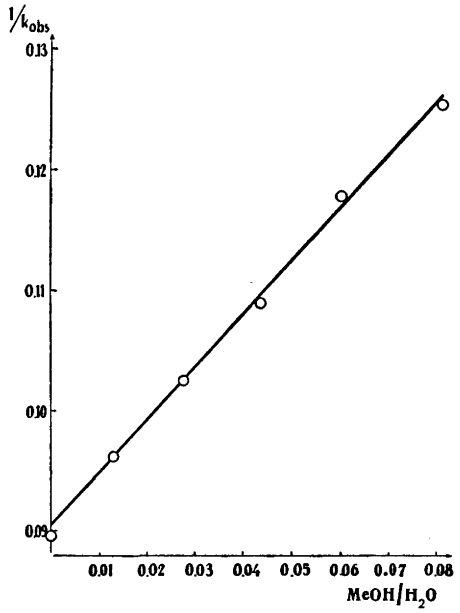

Fig. 1. Weight ratio of methanol and water in the resin phase *versus* $1/k_{obs}$ at the concentration range of 0 to 5 % methanol in the outside solution.

Reaction Kinetic Determination of the Hydroxyl-Alkoxide Equilibrium in Anion Exchangers

EERO SJÖSTRÖM and LALLI NYKÄNEN

Lääketehdas Orion Oy, Pharmaceutical Manufacturers, Helsinki, Finland

As a sequel to a previous work on the reaction mechanism between estradiol benzoate and an anion exchange resin [1], a kinetic method was developed which is reported here. This method makes it possible to follow the rate of hydrolysis (or alcoholysis) at very low ester concentrations. The method has been used for the investigation of the hydrolysis of methyl benzoate in water and in water-methanol mixtures of low methanol content. The experiments were carried out at 25 ± 0.02°C, by a batch-wise technique with constant stirring. At suitable time intervals samples were taken from the reaction mixture by means of a constant pressure apparatus. The amount of unreacted ester was estimated spectrophotometrically in the ultraviolet region.

According to Samelson and Hammet [2], the alkaline hydrolysis by anion exchangers in ethanol-water mixtures is a second order reaction. The present results show that when the hydroxyl ion concentration (the resin) is high compared with the ester, the rate constant can be calculated from the first order equation.

On adding methanol to the resin-water mixture the hydroxyl ions are in part converted into alkoxide ions owing to the reaction:

$$MeOH + HO^- \rightleftharpoons MeO^- + H_2O$$

and the hydroxyl ion concentration in the resin phase is decreased. If this reaction is the dominant factor in reducing the hydrolysis rate, it should be possible in theory to calculate the state of this equilibrium from the observed kinetic data. In fact, it was found that at low methanol

concentrations, up to about 10% (w/w), the equilibrium constant

$$K = \frac{[MeO^-][H_2O]}{[MeOH][HO^-]}$$

can be calculated from the following equation:

$$\frac{[MeOH]}{[H_2O]} \cdot K + 1 = \frac{k}{k_{obs}}$$

where k is the true rate constant, *i.e.*, the same as in aqueous solution, k_{obs} the observed rate constant, and [MeOH] and [H_2O] the molar concentrations of methanol and of water, respectively, in the resin phase. The linear relationship between the values of [MeOH]/[H_2O] and $1/k_{obs}$ was verified by the data obtained from Fig. 1, and the resulting value for K was found to be 11.1. This equilibrium in anion exchangers has thus been determined for the first time.

A detailed description of the procedure as well as of the mathematical treatment will be published in the near future. Investigations on the hydrolysis of ethyl benzoate in water-ethanol mixtures are still in progress. Furthermore, the study of the saponification of several phenolic esters by this method has been started.

Acknowledgement: Appreciation is expressed to the *Finnish State Scientific Board* for financial support of this research.

1. Sjöström, E. and Nykänen, L. *J. Org. Chem.* **21** (1956) 1321.
2. Samelson, H. and Hammet, L. P. *J. Am. Chem. Soc.* **78** (1956) 524.

Received December 18, 1957.

Action of Group Blocking Agents and Enzymes on Intrinsic Factor Preparations

RALPH GRÄSBECK*

Biochemical Department, Nobel Medical Institute, Stockholm, Sweden, and Fourth Medical University Clinic, Maria Hospital, Helsingfors, Finland

The binding of vitamin B_{12} appears to be of importance for the physiological action of intrinsic factor [1,2]. It therefore seemed of interest to study the mode of binding of B_{12} to the B_{12}-binding principle contained in intrinsic factor preparations. This was performed by subjecting hog intrinsic factor concentrates and pepsin-inactivated [1] human gastric juice to group blocking agents. During the course of attempts to break down the B_{12}-binding principle with proteolytic enzymes some data were obtained bearing upon the mode of binding of B_{12}, and these results are included in the following together with some data on the physiological activities of the chemically modified preparations.

Vitamin B_{12}-binding was assayed by adding radioactive ^{60}Co labeled B_{12}, whereupon the free and bound vitamin was separated with dialysis [1] or ultrafiltration [3].

The action of the group blocking agents is apparent from Table 1. A clearcut effect is observed with fluorodinitrobenzene, iodine, and monochromatic (280 mμ) ultraviolet light, whereas treatment with *p*-chloromercuribenzoate, acetic anhydride, and nitrous acid lacked effect. The absence of effect of the three last mentioned compounds makes the involvement of SH- and NH_2-groups less likely, whereas the involvement of phenol or imidazole groups seems more probable. An active tyrosinase preparation (Worthington) lacked effect, however. This does not eliminate the possibility of a phenolic group being involved, because tyrosinase has been found to lack effect on tyrosine groups of several proteins [4]. The mode of binding of B_{12} to intrinsic factor preparations seems to be much the same as in the cobalamin protein of sow's milk [3].

When both gastric juice and hog stomach preparations were subjected to thorough digestion with crystalline pepsin, trypsin, and highly purified chymotrypsin and mucinase [5] preparations, addition of B_{12} prior to digestion was found to have a marked protective action against chymotrypsin. A slight similar effect was observed in the case of pepsin, whereas B_{12} did not influence the effect of trypsin and mucinase. The latter were found not to have any effect on B_{12}-binding.

The protective action of B_{12} against chymotrypsin seemed to be limited to very few components of the intrinsic factor preparations. This was shown by digesting two identical samples, one in presence of B_{12}, and the other one in its absence. After digestion, vitamin B_{12} was added to the second sample and both samples

* Present address: Department of Medical Chemistry, Helsingfors University, Finland.

concentrations, up to about 10% (w/w), the equilibrium constant

$$K = \frac{[MeO^-][H_2O]}{[MeOH][HO^-]}$$

can be calculated from the following equation:

$$\frac{[MeOH]}{[H_2O]} \cdot K + 1 = \frac{k}{k_{obs}}$$

where k is the true rate constant, *i.e.*, the same as in aqueous solution, k_{obs} the observed rate constant, and [MeOH] and [H_2O] the molar concentrations of methanol and of water, respectively, in the resin phase. The linear relationship between the values of [MeOH]/[H_2O] and $1/k_{obs}$ was verified by the data obtained from Fig. 1, and the resulting value for K was found to be 11.1. This equilibrium in anion exchangers has thus been determined for the first time.

A detailed description of the procedure as well as of the mathematical treatment will be published in the near future. Investigations on the hydrolysis of ethyl benzoate in water-ethanol mixtures are still in progress. Furthermore, the study of the saponification of several phenolic esters by this method has been started.

Acknowledgement: Appreciation is expressed to the *Finnish State Scientific Board* for financial support of this research.

1. Sjöström, E. and Nykänen, L. *J. Org. Chem.* **21** (1956) 1321.
2. Samelson, H. and Hammet, L. P. *J. Am. Chem. Soc.* **78** (1956) 524.

Received December 18, 1957.

Action of Group Blocking Agents and Enzymes on Intrinsic Factor Preparations

RALPH GRÄSBECK*

Biochemical Department, Nobel Medical Institute, Stockholm, Sweden, and Fourth Medical University Clinic, Maria Hospital, Helsingfors, Finland

The binding of vitamin B_{12} appears to be of importance for the physiological action of intrinsic factor [1,2]. It therefore seemed of interest to study the mode of binding of B_{12} to the B_{12}-binding principle contained in intrinsic factor preparations. This was performed by subjecting hog intrinsic factor concentrates and pepsin-inactivated [1] human gastric juice to group blocking agents. During the course of attempts to break down the B_{12}-binding principle with proteolytic enzymes some data were obtained bearing upon the mode of binding of B_{12}, and these results are included in the following together with some data on the physiological activities of the chemically modified preparations.

Vitamin B_{12}-binding was assayed by adding radioactive ^{60}Co labeled B_{12}, whereupon the free and bound vitamin was separated with dialysis [1] or ultrafiltration [3].

The action of the group blocking agents is apparent from Table 1. A clearcut effect is observed with fluorodinitrobenzene, iodine, and monochromatic (280 mμ) ultraviolet light, whereas treatment with *p*-chloromercuribenzoate, acetic anhydride, and nitrous acid lacked effect. The absence of effect of the three last mentioned compounds makes the involvement of SH- and NH_2-groups less likely, whereas the involvement of phenol or imidazole groups seems more probable. An active tyrosinase preparation (Worthington) lacked effect, however. This does not eliminate the possibility of a phenolic group being involved, because tyrosinase has been found to lack effect on tyrosine groups of several proteins [4]. The mode of binding of B_{12} to intrinsic factor preparations seems to be much the same as in the cobalamin protein of sow's milk [3].

When both gastric juice and hog stomach preparations were subjected to thorough digestion with crystalline pepsin, trypsin, and highly purified chymotrypsin and mucinase [5] preparations, addition of B_{12} prior to digestion was found to have a marked protective action against chymotrypsin. A slight similar effect was observed in the case of pepsin, whereas B_{12} did not influence the effect of trypsin and mucinase. The latter were found not to have any effect on B_{12}-binding.

The protective action of B_{12} against chymotrypsin seemed to be limited to very few components of the intrinsic factor preparations. This was shown by digesting two identical samples, one in presence of B_{12}, and the other one in its absence. After digestion, vitamin B_{12} was added to the second sample and both samples

* Present address: Department of Medical Chemistry, Helsingfors University, Finland.

Table 1. Effect of group blocking agents on B_{12}-binding capacity. GJ = Gastric juice. HS = Hog stomach preparation *.

Treatment before binding assay	Effect on binding capacity
GJ or HS + 32 mg fluorodinitrobenzene/ml, pH 8.6, stirring 3 1/2 h	66 % inactivation
GJ or HS at pH 8.6, alcoholic I_2 solution added to final concentration 2.5×10^{-4} M, afterwards dialysis 21 h to remove I_2	96 % inactivation **
Same, 5×10^{-4} M I_2	beginning inactivation
HS (BFS 209) irradiated 3 h with 280 mμ UV light 4×10^{19} quanta/16 mg, O_2 supplied	25 % inactivation
HS pH 7, 1.7 mg *p*-chloromercuribenzoate/ml	None
HS in half saturated Na-acetate, 0.12 ml acetic anhydride/ml, 0°C, stirring 1 h ***	None
HS in 1 M $NaNO_2$, pH 4.6, 0°C, samples taken up to 82 h	None ****
Tyrosinase 0.2 mg/mg HS, 10^{-6} M $CuCl_2$, pH 6—7, 24 h, O_2 supplied	None

* In all experiments an Organon preparation BFS 209 was used, in many cases also other preparations. BFS 209 bound 0.27 μg B_{12}/mg and was active in the Schilling test [6] in 16.6 mg dose.
** Also complete loss of intrinsic factor activity as observed on two patients.
*** The intensity of the color produced by ninhydrin reaction dropped with 88 %.
**** 10 % inhibition was observed after 82 h. This could be due to direct diazotization of tyrosyl groups.

were dialyzed in order to remove the small molecular material. There was no observable difference in the dry weight of the two dialyzed samples. The possibility that B_{12} had a direct inhibitory action on chymotrypsin was eliminated by the failure to find any inhibition of the chymotryptic digestion of casein by similar concentrations of B_{12}.

A few samples of gastric juice were digested with chymotrypsin with and without B_{12} as described above. Afterwards both the B_{12}-binding capacity and the intrinsic factor activity were assayed, the latter using the urinary radioactivity test [6] employed in previous studies [1]. As is apparent from Fig. 1, B_{12} also protected the intrinsic factor activity. This may indicate that the B_{12}-binder is identical with intrinsic factor or a part of it. The simultaneous loss of B_{12}-binding capacity and intrinsic factor activity after iodination also points in this direction.

The explanation of the protective action of B_{12} against chymotryptic digestion is probably that the cyanocobalamin molecule covers up a chymotrypsin-sensitive bond in the molecule. In view of the above findings with group blocking agents, it is interesting to note that chymotrypsin hydrolyzes, *inter alia*, peptide bonds in which the carbonyl group is supplied by tyrosine [7].

The rate of hydrolysis of the bond which can be protected with B_{12} appears to be slow, because even in the absence of B_{12}

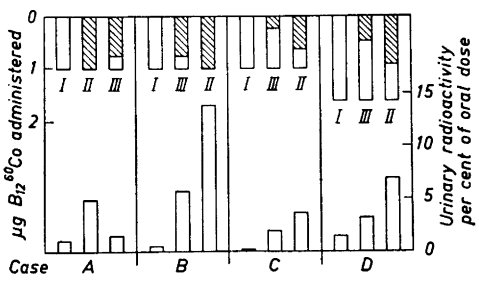

Fig. 1. Intrinsic factor assay of chymotrypsin digested gastric juice. Upper columns: Material administered. White columns: Free B_{12}. Shaded columns: Bound B_{12}. I = Basal test without intrinsic factor, II = Sample digested in presence of B_{12}, III = Sample digested in absence of B_{12}. Lower columns: Patient's response in the Schilling test [6]. *N.B.* In cases A and B sample II was not saturated with B_{12}.

some B_{12}-binding and intrinsic factor activity is retained after 20 h of digestion with high concentrations of chymotrypsin (Fig. 1).

As regards the action of chymotrypsin the present study confirms similar observations made during the preparation of commercial intrinsic factor preparations [8].

Preliminary ultracentrifugal studies [9] indicate that the B_{12}-binder — vitamin B_{12} complex remains a relatively large molecule after trypsin-chymotrypsin digestion (mol.wt. 52 000 both before and after digestion for cobalamin complex from pepsin-inactivated gastric juice). It therefore appears that the B_{12}-binder (and apparently also intrinsic factor) contains only a few bonds sensitive to the action of these enzymes.

The author is greatly indebted to Professor H. Theorell for valuable advice, to Dr. K. Yamashina for the chymotrypsin, to Dr. J. Gad Andresen for the mucinase, to Dr. H. Wijmenga for the intrinsic factor preparations, and to Dr. B. Josephson for arrangements in connection with the collection of gastric juice. Dr. J. Schuberth was kind to assist in the UV studies, and the Schilling-tests were carried out by Dr. G. Amnell. The investigation was supported by generous grants from *N. V. Organon* and *Sigrid Jusélius Stiftelse.*

1. Gräsbeck, R. *Acta Med. Scand.* Suppl. **314** (1956).
2. Schilling, R. F. and Schloesser, L. L. in *Vitamin B_{12} und Intrinsic Factor*, Enke, Stuttgart 1957, p. 194.
3. Gregory, M. E. and Holdsworth, E. S. *Biochem. J.* **59** (1955) 335.
4. Haas, W. J., Sizer, I. W. and Loofbourow, J. R. *Biochim. et Biophys. Acta* **6** (1951) 589.
5. Ada, G. L. and French, E. L. *Australian J. Sci.* **13** (1950) 82.
6. Schilling, R. F. *J. Lab. Clin. Med.* **42** (1953) 860.
7. Neurath, H. and Schwert, G. W. *Chem. Revs.* **46** (1950) 69.
8. Wijmenga, H. G. in *Vitamin B_{12} und Intrinsic Factor*, Enke, Stuttgart 1957, p. 156.
9. Gräsbeck, R. and Ehrenberg, A. *Unpublished data.*

Received December 22, 1957.

Barium Hydroxide as a Selective Precipitating Agent for Hemicelluloses

HANS MEIER

Wood Chemistry Department, Swedish Forest Products Research Laboratory, Stockholm, Sweden

A widely applied method of fractionating and purifying hemicelluloses is by precipitating them as their insoluble copper complexes. The separation of acidic hemicelluloses from neutral ones has been achieved by fractional precipitation using long-chain quaternary ammonium salts (*e. g.* "cetavlon") [1].

Another method has now been found which on its own, or in conjunction with known methods, may enable a more efficient fractionation to be achieved. We have observed that barium ions readily form insoluble complexes with mannans and glucomannans, probably by reaction with the vicinal *cis*-hydroxyl groups on carbon atoms 2 and 3 of the mannose units. Those complexes are precipitated from aqueous solutions on the addition of small quantities of barium hydroxide.

Ivory nut mannan A and spruce glucomannans were both precipitated comple-

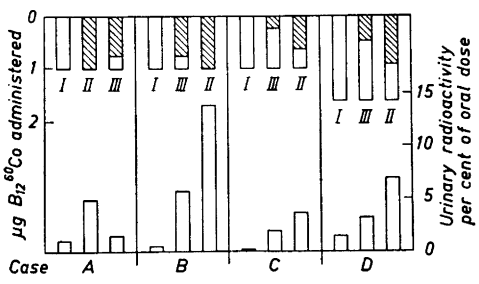

Fig. 1. Intrinsic factor assay of chymotrypsin digested gastric juice. Upper columns: Material administered. White columns: Free B_{12}. Shaded columns: Bound B_{12}. I = Basal test without intrinsic factor, II = Sample digested in presence of B_{12}, III = Sample digested in absence of B_{12}. Lower columns: Patient's response in the Schilling test [6]. *N.B.* In cases A and B sample II was not saturated with B_{12}.

some B_{12}-binding and intrinsic factor activity is retained after 20 h of digestion with high concentrations of chymotrypsin (Fig. 1).

As regards the action of chymotrypsin the present study confirms similar observations made during the preparation of commercial intrinsic factor preparations [8].

Preliminary ultracentrifugal studies [9] indicate that the B_{12}-binder — vitamin B_{12} complex remains a relatively large molecule after trypsin-chymotrypsin digestion (mol.wt. 52 000 both before and after digestion for cobalamin complex from pepsin-inactivated gastric juice). It therefore appears that the B_{12}-binder (and apparently also intrinsic factor) contains only a few bonds sensitive to the action of these enzymes.

The author is greatly indebted to Professor H. Theorell for valuable advice, to Dr. K. Yamashina for the chymotrypsin, to Dr. J. Gad Andresen for the mucinase, to Dr. H. Wijmenga for the intrinsic factor preparations, and to Dr. B. Josephson for arrangements in connection with the collection of gastric juice. Dr. J. Schuberth was kind to assist in the UV studies, and the Schilling-tests were carried out by Dr. G. Amnell. The investigation was supported by generous grants from *N. V. Organon* and *Sigrid Jusélius Stiftelse.*

1. Gräsbeck, R. *Acta Med. Scand.* Suppl. **314** (1956).
2. Schilling, R. F. and Schloesser, L. L. in *Vitamin B_{12} und Intrinsic Factor*, Enke, Stuttgart 1957, p. 194.
3. Gregory, M. E. and Holdsworth, E. S. *Biochem. J.* **59** (1955) 335.
4. Haas, W. J., Sizer, I. W. and Loofbourow, J. R. *Biochim. et Biophys. Acta* **6** (1951) 589.
5. Ada, G. L. and French, E. L. *Australian J. Sci.* **13** (1950) 82.
6. Schilling, R. F. *J. Lab. Clin. Med.* **42** (1953) 860.
7. Neurath, H. and Schwert, G. W. *Chem. Revs.* **46** (1950) 69.
8. Wijmenga, H. G. in *Vitamin B_{12} und Intrinsic Factor*, Enke, Stuttgart 1957, p. 156.
9. Gräsbeck, R. and Ehrenberg, A. *Unpublished data.*

Received December 22, 1957.

Barium Hydroxide as a Selective Precipitating Agent for Hemicelluloses

HANS MEIER

Wood Chemistry Department, Swedish Forest Products Research Laboratory, Stockholm, Sweden

A widely applied method of fractionating and purifying hemicelluloses is by precipitating them as their insoluble copper complexes. The separation of acidic hemicelluloses from neutral ones has been achieved by fractional precipitation using long-chain quaternary ammonium salts (*e. g.* "cetavlon") [1].

Another method has now been found which on its own, or in conjunction with known methods, may enable a more efficient fractionation to be achieved. We have observed that barium ions readily form insoluble complexes with mannans and glucomannans, probably by reaction with the vicinal *cis*-hydroxyl groups on carbon atoms 2 and 3 of the mannose units. Those complexes are precipitated from aqueous solutions on the addition of small quantities of barium hydroxide.

Ivory nut mannan A and spruce glucomannans were both precipitated comple-

Table 1.

Sample	Galactose %	Glucose %	Mannose %	Arabinose %	Xylose %
Hemicellulose mixture from spruce	7.1	10,4	19.8	6.6	56.1
Fraction I: $Ba(OH)_2$-precipitate	12.9	17.1	51.8	3.8	14.4
Fraction II: material left in solution	1.8	3.6	1.4	9.8	83.4

tely from aqueous solutions at barium hydroxide concentrations below 0.03 M. The barium complexes of the mannans and glucomannans are easily soluble in dilute acids and even in water, but are insoluble in organic solvents and in copper ethylene diamine.

Although the use of barium hydroxide did not lead to the precipitation of a larch arabo-galactan it caused a spruce galactan to be precipitated. This may be attributed to the fact that galactose, when present either as an end-group, or as a 1,6-linked residue in a polysaccharide, contains the requisite vicinal *cis*-hydroxyl groups on carbon atoms 3 and 4. As the hemicellulose galactans are highly branched molecules they will possess a high percentage of end-groups.

A birch xylan (2.5 % glucose + galactose, 85.6 % xylose, 11.9 % uronic acids) was also precipitated from aqueous solution when the barium hydroxide concentration was made up to 0.15 M. This may be due to the formation of an insoluble barium salt by the acidic xylan.

When barium hydroxide was added to a hemicellulose mixture (extracted from spruce holocellulose with 14 % potassium hydroxide) the glucomannans were precipitated almost completely. They were, however, contaminated by other polysaccharides containing galactose, xylose and arabinose residues. The precipitation of a galactan can be attributed to the presence of vicinal *cis*-hydroxyl groups as mentioned above. If precipitation is due only to them, then it would be difficult to explain why a xylan or an arabo-xylan should be precipitated by barium hydroxide as readily as were the glucomannans. When fraction I (*cf.* Table 1) was dissolved in water and "cetavlon" was added, xylose and arabinose together with galactose and minor amounts of glucose and mannose were detected in the hydrolysate of the precipitate whereas a pure glucomannan was left in solution. The presence of a galacto-arabo-xylan may therefore be suspected. However, the xylose residues in fraction I could also be parts of a very acidic xylan. The hemicellulose fraction II (*cf.* Table 1) which had not precipitated with barium hydroxide and which accounted for nearly two thirds of the recovered material was shown to be mainly an arabo-xylan with an arabinose : xylose ratio of 1:8.5 and an uronic acid content of 19 %. Even with a high excess of barium hydroxide (more than 0.2 M) no precipitation occurred. Two explanations might be possible. Either the barium salt of this acidic arabo-xylan is soluble in barium hydroxide concentrations up to 0.2 M or the branches of arabinose residues sterically hinder salt formation of neighbouring chains.

It is evident from these preliminary experiments that the use of barium hydroxide as a precipitant will provide a complement to previous methods of fractionating polysaccharides even if the scope and limitation of the method have not yet been fully explored.

Experimental. The hemicelluloses were dissolved in water or in dilute sodium hydroxide and then saturated barium hydroxide solution was added. If a precipitate formed it was centrifuged and was purified by dissolving it in water and reprecipitating it with barium hydroxide. After centrifugation the precipitate was dissolved in 2 N acetic acid and from this solution the hemicelluloses were precipita-

ted with ethanol and were washed successively with ethanol/water, with ethanol and with ether.

The quantitative paper chromatography of the samples was carried out according to Saeman *et al.*[2] using the solvent systems ethyl acetate-acetic acid-water (3:1:3) and, for the separation of glucose and galactose, ethyl acetate-pyridine-water (2:1:2).

1. Scott, J. E. *Chem & Ind. London* **1955** 168.
2. Saeman, J. F., Moore, W. E., Mitchell, R. L. and Millet, M. A. *Tappi* **38** (1954) 336.

Received January 4, 1958.

Preparation of Thiotaurine (Aminoethanethiosulfonic Acid)

BO SÖRBO

Research Institute of National Defence, Dept. 1, Sundbyberg, and Nobel Medical Institute, Biochemical Dept., Stockholm, Sweden

Recently [1] an enzymatic transsulfuration product from β-mercaptopyruvate and hypotaurine (2-aminoethanesulfinic acid) was identified as 2-aminoethanethiosulfonic acid, for which the shorter name thiotaurine was suggested. Thiotaurine has now been synthesized with taurine as starting material. Taurine was first transformed into phthalimidoethanesulfonyl chloride [2] and the latter then converted to hypotaurine by a novel method. The sulfonyl chloride was first reacted with phenylhydrazine to give phthalimidoethanesulfonyl phenylhydrazide which was not isolated but instead heated with an excess of phenylhydrazine and tri-*n*-butylamine in ethanol, in order to remove the phthaloyl group [3]. During this treatment it was found that the sulfonylphenylhydrazide decomposed to the corresponding sulfinic acid [4]. Hypotaurine was thus formed (yield 80 %) and precipitated with methyl ethyl ketone. Thiotaurine was then obtained from hypotaurine through treatment of the latter with ammonium polysulfide [5] and crystallized from ethanol-water (yield 40 %). Colourless crystals, m.p. about 213° (decomp.), were obtained and found to contain 22.5 % cyanide labile sulfur [6] (calc. for $NH_2C_2H_4S_2O_3H$: 22.7 %). Paper chromatography of the compound in 4 different solvent systems demonstrated only the presence of one single component. It was previously suggested that thiotaurine might be identical with an unknown sulfur containing compound from human blood, first detected by Smith and Tuller [7] by paper chromatography and reported to behave as taurine. This possibility could now be excluded, as the synthetic thiotaurine was found to be clearly resolved from taurine in the solvent system used by Smith and Tuller.

Details of this work will be published later.

1. Sörbo, B. *Biochim. et Biophys. Acta* **24** (1957) 324.
2. Winterbottom, R., Clapp, J. W., Miller, W. H., English, J. P. and Roblin, R. O. Jr. *J. Am. Chem. Soc.* **69** (1947) 1393.
3. Schumann, I. and Boissonas, R. A. *Helv. Chim. Acta* **35** (1952) 2235.
4. Escales, R. *Chem. Ber.* **18** (1885) 893.
5. Limpricht, H. *Ann.* **278** (1894) 239.
6. Sörbo, B. H. *Acta Chem. Scand.* **7** (1953) 1137.
7. Smith, E. L. and Tuller, E. F. *Arch. Biochem. Biophys.* **54** (1955) 114.

Received January 8, 1958.

ted with ethanol and were washed successively with ethanol/water, with ethanol and with ether.

The quantitative paper chromatography of the samples was carried out according to Saeman *et al.*[2] using the solvent systems ethyl acetate-acetic acid-water (3:1:3) and, for the separation of glucose and galactose, ethyl acetate-pyridine-water (2:1:2).

1. Scott, J. E. *Chem & Ind. London* **1955** 168.
2. Saeman, J. F., Moore, W. E., Mitchell, R. L. and Millet, M. A. *Tappi* **38** (1954) 336.

Received January 4, 1958.

Preparation of Thiotaurine (Aminoethanethiosulfonic Acid)

BO SÖRBO

Research Institute of National Defence, Dept. 1, Sundbyberg, and Nobel Medical Institute, Biochemical Dept., Stockholm, Sweden

Recently [1] an enzymatic transsulfuration product from β-mercaptopyruvate and hypotaurine (2-aminoethanesulfinic acid) was identified as 2-aminoethanethiosulfonic acid, for which the shorter name thiotaurine was suggested. Thiotaurine has now been synthesized with taurine as starting material. Taurine was first transformed into phthalimidoethanesulfonyl chloride [2] and the latter then converted to hypotaurine by a novel method. The sulfonyl chloride was first reacted with phenylhydrazine to give phthalimidoethanesulfonyl phenylhydrazide which was not isolated but instead heated with an excess of phenylhydrazine and tri-*n*-butylamine in ethanol, in order to remove the phthaloyl group [3]. During this treatment it was found that the sulfonylphenylhydrazide decomposed to the corresponding sulfinic acid [4]. Hypotaurine was thus formed (yield 80 %) and precipitated with methyl ethyl ketone. Thiotaurine was then obtained from hypotaurine through treatment of the latter with ammonium polysulfide [5] and crystallized from ethanol-water (yield 40 %). Colourless crystals, m.p. about 213° (decomp.), were obtained and found to contain 22.5 % cyanide labile sulfur [6] (calc. for $NH_2C_2H_4S_2O_3H$: 22.7 %). Paper chromatography of the compound in 4 different solvent systems demonstrated only the presence of one single component. It was previously suggested that thiotaurine might be identical with an unknown sulfur containing compound from human blood, first detected by Smith and Tuller [7] by paper chromatography and reported to behave as taurine. This possibility could now be excluded, as the synthetic thiotaurine was found to be clearly resolved from taurine in the solvent system used by Smith and Tuller.

Details of this work will be published later.

1. Sörbo, B. *Biochim. et Biophys. Acta* **24** (1957) 324.
2. Winterbottom, R., Clapp, J. W., Miller, W. H., English, J. P. and Roblin, R. O. Jr. *J. Am. Chem. Soc.* **69** (1947) 1393.
3. Schumann, I. and Boissonas, R. A. *Helv. Chim. Acta* **35** (1952) 2235.
4. Escales, R. *Chem. Ber.* **18** (1885) 893.
5. Limpricht, H. *Ann.* **278** (1894) 239.
6. Sörbo, B. H. *Acta Chem. Scand.* **7** (1953) 1137.
7. Smith, E. L. and Tuller, E. F. *Arch. Biochem. Biophys.* **54** (1955) 114.

Received January 8, 1958.

ACTA CHEMICA SCANDINAVICA 12 (1958) 147—164

Studies on the Chemistry of Lichens

XI.* Structure of Picrolichenic Acid **

CARL AXEL WACHTMEISTER

Institutionen för organisk kemi, Kungl. Tekniska Högskolan, Stockholm, Sweden

Picrolichenic acid, $C_{25}H_{30}O_7$, a bitter compound from *Pertusaria amara* (Ach.) Nyl., has been shown to contain a carboxyl group, a lactone ring, a phenolic hydroxyl group, a methoxyl group and two *n*-amyl groups. It reacts with piperidine forming a piperidide $C_{30}H_{41}O_7N$. Mild alkaline hydrolysis followed by acidification causes decarboxylation with formation of a monocarboxylic acid (A), $C_{24}H_{32}O_6$. On decarboxylation and demethylation acid (A) affords a phenol (C), $C_{12}H_4(C_5H_{11})_2(OH)_4$, identified as 2,2′-di-*n*-amyl-4,6,4′,6′-tetrahydroxydiphenyl (XII) by dehydration to 3,7-dihydroxy-1,9-di-*n*-amyldibenzofuran (XIV), methylated and oxidised to the known 3,7-dimethoxydibenzofuran-1,9-dicarboxylic acid. These results are in harmony with a structure (XXIII) for picrolichenic acid which is further supported by infra-red and ultra-violet absorption spectra.

The crustose lichen *Pertusaria amara* (Ach.) Nyl. is widely spread in Europe, occurring on the bark of broadleaf trees such as oak and beech. It has an intense, bitter taste similar to that of quinine. This attracted early chemical investigation, and a paper by Alms on "Picrolichenin" from *Variolaria amara* Ach., a synonym of *P. amara*, appeared in 1832 in the first volume of *Annalen der Pharmacie* [1]. According to Alms, picrolichenin showed promising results in the treatment of malaria.

Zopf [2,3] obtained the bitter principle which he called "Pikrolicheninsäure", in a state of reasonable purity (m.p. 178°, decomp.) and suggested the empirical composition $C_{17}H_{20}O_5$.

For the present investigation some hundred grams of *P. amara* were collected from beech trees in Blekinge, Southern Sweden. The powdery lichen was extracted with large volumes of cold ether and a concentrated solution was left in the refrigerator to crystallise. The crude acid, isolated in 5—7 % yield from the dry lichen, was purified by treatment with aluminium oxide and

* Part X. *Acta Chem. Scand.* **10** (1956) 1404.
** Preliminary communication: *Chem. & Ind.* London **1954** 1042.

crystallisation from benzene or aqueous acetic acid. When pure, the acid forms colourless prisms, m.p. about 180° with decomposition. It is optically inactive and contains carbon, hydrogen and oxygen only. The analytical values for picrolichenic acid and a number of its derivatives and degradation products indicate the empirical composition $C_{25}H_{30}O_7$, including a carboxyl group, a methoxyl group and two C-methyl groups.

Picrolichenic acid is readily soluble in most common solvents except benzene and light petroleum. It dissolves slowly with the evolution of gas in aqueous sodium bicarbonate to give a colourless solution from which it can be recovered unchanged on acidification [3]. The solution in alkali turns brownish red when exposed to the air [1].

The acid gives an intense violet colour with ferric chloride in ethanol [2] but no coloration with 2,6-dichloroquinone-monochloroimide (Gibbs' reagent[4]), *bis*-diazotised benzidine [5] or bleaching powder [6]. However, after short treatment with cold aqueous alkali it gave a dark red colour with the benzidine reagent and a red colour with bleaching powder. This resembles the behaviour of certain easily hydrolysed depsides and depsidones. Phenolic groups were also liberated very rapidly when paper chromatographic spots of the acid were exposed to ammonia vapour.

On heating to the melting point the acid decomposed with the evolution of a gas containing carbon dioxide. A crystalline decomposition product, m. p. 153—155°, was isolated but this has not yet been subjected to thorough studies.

Short treatment of picrolichenic acid with diazomethane in the cold furnished methyl picrolichenate, m. p. 102—103,5° which was soluble in cold 0.05 N sodium hydroxide solution and gave a brownish ferric chloride reaction. Prolonged methylation with diazomethane yielded neutral methyl O-methylpicrolichenate $C_{23}H_{25}O_3(OCH_3)_2COOCH_3$, m. p. 80—82°.

Picrolichenic acid reacted in the cold with piperidine yielding a piperidide which gave a violet ferric test and was obtained in two interconvertible forms, m. p. 169—172° and 187—190° (decomp.) respectively. The piperidide titrated as a monobasic acid and gave analytical values which agreed with the composition $C_{30}H_{41}O_7N$ and thus contained all the atoms of the reacting components. On methylation with diazomethane a dimethyl derivative was formed which as shown by its low solubility in alkali and by its colour reactions contained a phenolic hydroxyl group.

Because of the sensitivity of picrolichenic acid to alkali and amines, tests for carbonyl functions were carried out with the piperidide instead of the acid itself. No positive results were obtained with carbonyl reagents under ordinary conditions.

On oxidation with permanganate picrolichenic acid afforded about 1.5 moles of volatile acids. The main component was *n*-caproic acid as indicated by paper chromatography and confirmed by the identity of the purified *p*-bromophenacyl ester with an authentic sample of *n*-caproic acid *p*-bromophenacyl ester. Paper chromatography also revealed the presence of small amounts of lower fatty acids but no spots corresponding to acids with more than six carbon atoms were observed.

These results indicate the presence in picrolichenic acid of a free carboxyl group, a lactone group, a phenolic hydroxyl group *ortho* to a carboxyl function,

a methoxyl group and two *n*-pentyl chains. Assuming the presence of two six-membered carbocyclic rings, all the carbon atoms and six of the seven oxygen atoms are accounted for.

The presence of *n*-pentyl chains in picrolichenic acid points to a relationship with the orcinol-homologue, olivetol, a fairly widespread unit in lichen acids. The empirical composition, $C_{25}H_{30}O_7$, agrees with that of a dehydrogenation product of a monomethylated depside $C_{25}H_{32}O_7$ derived from two molecules of olivetol carboxylic acid. A depside of this type, perlatolinic acid (II, R = *n*-C_5H_{11}) has been isolated from a *Parmelia*-species by Asahina and Fuzikawa [7] and picrolichenic acid might be a related depsidone such as (IV). This possibility could be ruled out by the following observations.

Picrolichenic acid after treatment with cold N sodium hydroxide solution and then acidification gave a gum which rapidly expanded to a spongy mass due to the evolution of carbon dioxide. The purified crystalline product (A) gave a violet ferric test and was found to be a monocarboxylic acid containing a methoxyl group, $C_{22}H_{28}O_3(OCH_3)COOH$ (= $C_{25}H_{30}O_7 + H_2O—CO_2$).

The acid (A) melted at about 145° with decomposition, losing one mole of carbon dioxide and forming an oily phenol (B) which was characterised by paper chromatography. It was very sensitive towards oxygen in alkaline solution and rapidly developed a brown-red colour.

On simultaneous decarboxylation and demethylation with hydrobromic acid, the acid (A) furnished a phenol m. p. 180—181°, identical with a phenol (C), $C_{22}H_{30}O_4$, obtained directly from picrolichenic acid under similar conditions. Like phenol (B) it gave no colour with ferric chloride.

On methylation the phenols (B) and (C) afforded the same tetramethyl ether $C_{12}H_4(C_5H_{11})_2(OCH_3)_4$, m. p. 34.5—35.5°, which on bromination furnished di-, tri- and tetrabromoderivatives. The composition of the tetramethyl ether and its bromination products clearly shows that the phenol (C) and its monomethyl ether (B) are diphenyl derivatives. The U.V. spectrum of the tetramethyl ether was very similar to that of 2,2′-dimethyl-4,6,4′,6′-tetramethoxydiphenyl, the tetramethyl ether of a symmetrical diorcinol.

The acid (A) which gives a violet ferric test is obviously a carboxy derivative of phenol (B) with the carboxyl group in the *ortho*-position to a free hydroxyl group. The very facile decarboxylation of the acid indicates that there is also a free hydroxyl group in the *para*-position to the carboxyl group.

The above results indicate that picrolichenic acid contains two six-membered rings joined by a carbon-carbon bond as well as by an ester linkage. This brings to mind compounds of the ellagic acid and alternariol [8] (I) type. Such compounds, however, in contrast to picrolichenic acid do not lose carbon dioxide on acidification after alkaline hydrolysis. Moreover, structures of this type cannot be derived from orcinol derivatives.

It has been suggested [9,10] that depsidones are formed in Nature by dehydrogenation of depsides such as (II) with a mesomeric diradical (IIIa ⟷ IIIb ⟷ IIIc) as an intermediate. Coupling oxygen-carbon (IIIa → IV) would yield a depsidone. Coupling carbon-carbon (IIIb → V; IIIc → VI), however, would yield products of a structural type so far not encountered in lichens, γ-lactones containing a 2,4-*cyclo*hexadien-1-one structure (V, VI).

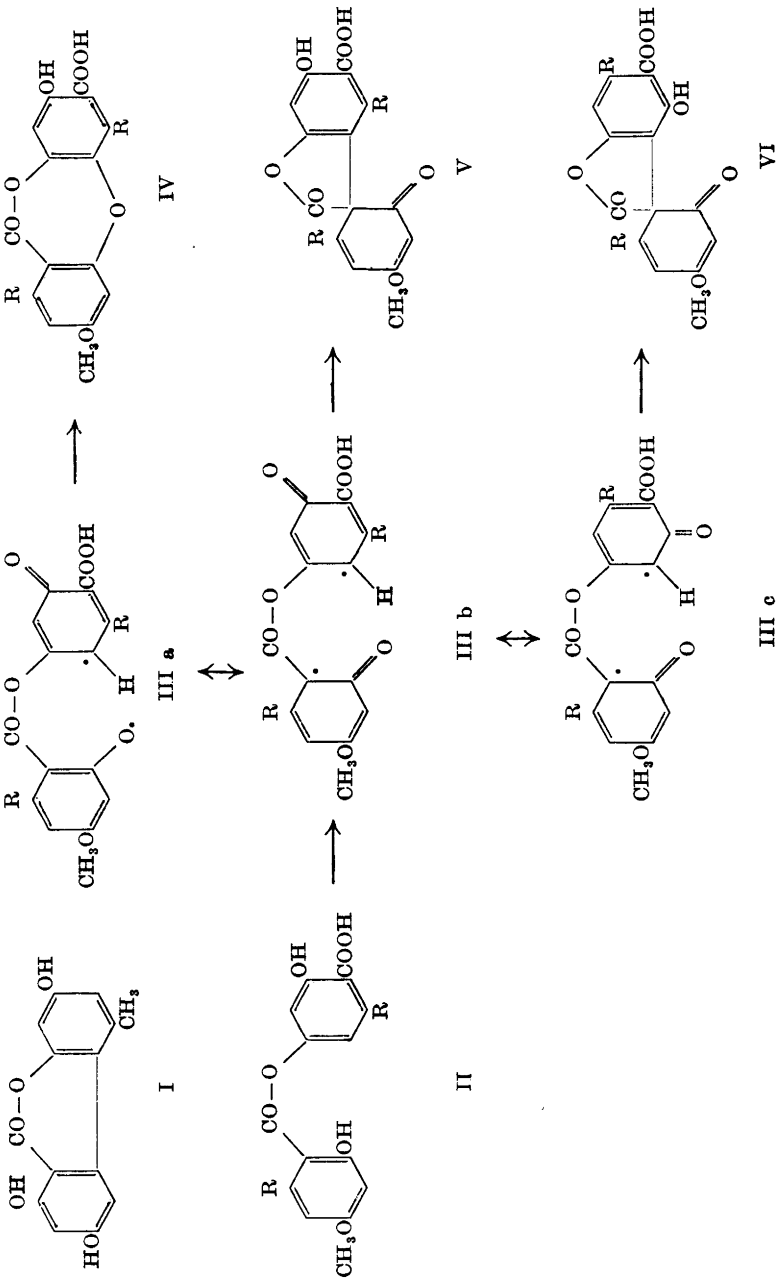

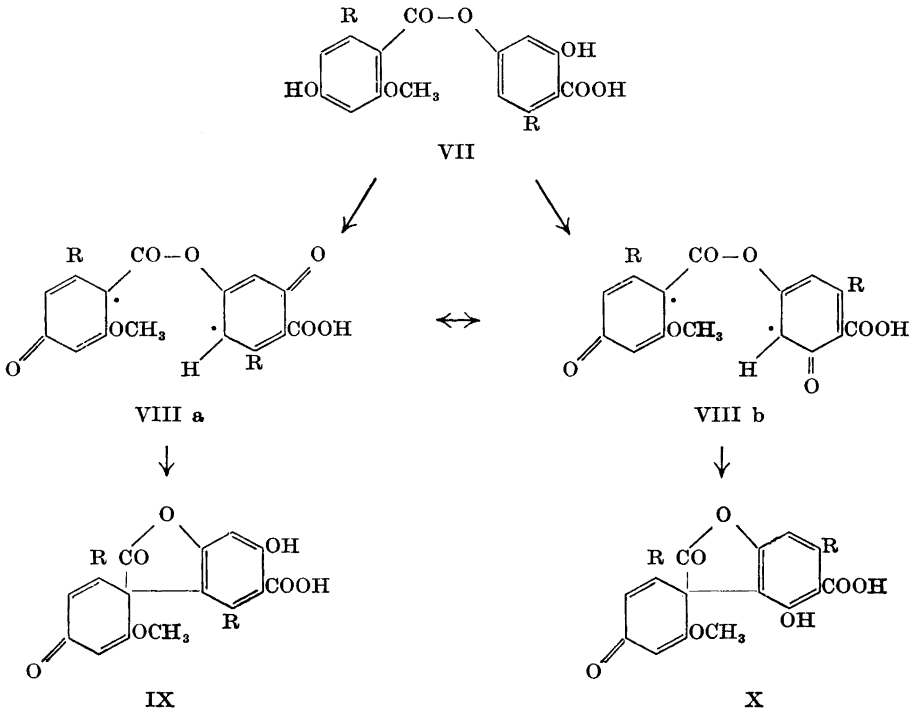

A depside precursor (VII) in which the phenolic hydroxyl group *ortho* to the ester group is methylated (or protected in some other way) would yield a diradical (VIIIa, VIIIb) which could stabilise by carbon-carbon coupling with the formation of γ-lactones (IX, X) containing a 2,5-*cyclo*hexadien-1-one structure [11].

The properties expected for γ-lactones of these types are compatible with the known chemical behaviour of picrolichenic acid. Alkaline hydrolysis of for example a lactone (IX) would yield a dicarboxylic acid (IX a) which, being a vinylogue of a β-keto-acid, should be easily decarboxylated and aromatised to a monocarboxylic acid (IX b) with a diphenyl structure. On the other hand, the dienone structure would be expected to be retained if the lactone ring opens on aminolysis to form an amide. This is exactly what was observed when picrolichenic acid was treated with piperidine. On this basis (V), (VI), (IX) and (X) (R = n-C_5H_{11}) would appear to be plausible structures for picrolichenic acid and a structure like (XI) for the piperidide.

Two alternative structures would then be possible for the phenolic degradation product, (C): 2,2′-di-n-amyl-4,6,4′,6′-tetrahydroxydiphenyl (XII) and 2,4′-di-n-amyl-4,6,2′,6′-tetrahydroxydiphenyl (XIII). Tetrahydroxydiphenyls of this type undergo acid catalysed cyclisation to dibenzofuran derivatives. (XII) and (XIII) would yield homologues of 3,7- and 1,7-dihydroxydibenzofuran respectively and it would be possible to distinguish between these iso-

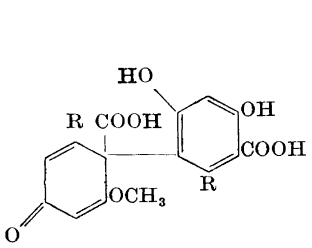

IX a

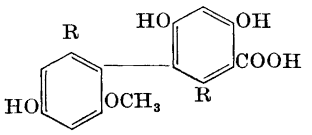

IX b

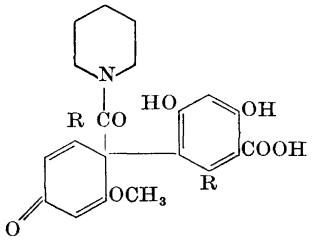

XI

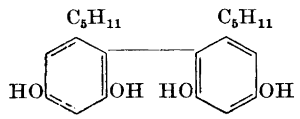

XII

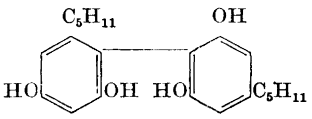

XIII

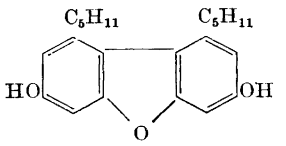

XIV

mers by their behaviour with Gibbs' reagent [4]. The 1,7-dihydroxy-derivative, containing a methine group in the *para*-position to a hydroxyl group, should give a blue colour with this reagent while the 3,7-derivative should give only a greyish colour [12].

When treated with zinc chloride for a few minutes at 240—250°, phenol (C) gave a phenol (D), $C_{12}H_4O(C_5H_{11})_2(OH)_2$, m. p. 124—125°, which on methylation gave a dimethyl ether. Phenol (D) gave a greyish colour with Gibbs' reagent and the solution in alkali exhibited an intense bluish fluorescence in ultra-violet light. The U.V. spectrum of the dimethyl ether was very similar to that of 3,7-dimethoxy-1,9-dimethyldibenzofuran which was synthesised essentially by a method described by Shibata [13]. This indicates strongly that phenol (D) is 3,7-dihydroxy-1,9-di-*n*-amyldibenzofuran (XIV).

The structure (XIV) of phenol (D) was definitely settled by oxidation of its dimethyl ether with permanganate. The crude oxidation product was, paper chromatographically, identical with 3,7-dimethoxydibenzofuran-1,9-dicarboxylic acid [13] and on methylation afforded a dimethyl ester $C_{18}H_{16}O_7$, m. p. 191—193.5°, identical with 3,7-dimethoxy-1,9-dicarbomethoxydibenzofuran [13].

Accordingly phenol (C) is 2,2′-di-*n*-amyl-4,6,4′,6′-tetrahydroxydiphenyl (XII), a structure which is also supported by the U.V. spectrum of its tetramethyl ether. Lower homologues show very similar properties and give oily tetramethyl ethers [13].

It follows that two structures, (XV) and (XVI), are possible for phenol (B), the monomethyl ether of (C). Two alternative structures, (XVII) and (XVIII), remain for the monocarboxylic acid (A) in view of its violet ferric reaction and easy decarboxylation. These alternatives are also biogenetically plausible, being related to orsellinic acid.

It may thus be concluded that the structures (V) and (IX) (R = n-C_5H_{11}) for picrolichenic acid are in accordance with observed facts while the alternatives (VI) and (X) are ruled out.

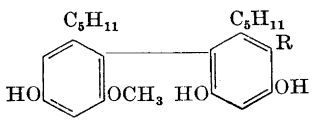

XV : R=H
XVII : R=COOH

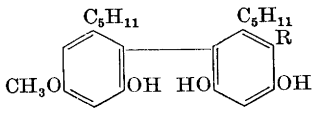

XVI : R=H
XVIII : R=COOH

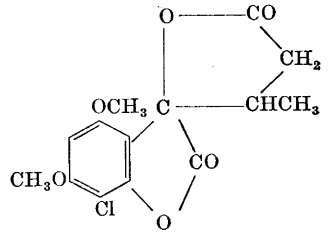

XIX

Additional evidence in favour of a dienone-γ-lactone structure is provided by the infra-red spectra of picrolichenic acid and its derivatives (Figs. 1—4).

Picrolichenic acid (Fig. 1), methyl picrolichenate (Fig. 2) and methyl O-methylpicrolichenate (Fig. 3) all show strong absorption at 1 820—1 825 cm^{-1} but the piperidide (Fig. 4) shows no absorption in this region. Aliphatic β,γ-unsaturated γ-lactones are known [14] to absorb at about 1 800 cm^{-1} but picrolichenic acid should be compared with β,γ-unsaturated γ-lactones in which the double bond forms part of an aromatic ring. Two recent examples are 4,6-diacetoxy-7-acetyl-3,5-dimethylcoumaran-2-one (1 822, 1 780 and 1 698 cm^{-1} in the carbonyl region; $CHCl_3$-solution) [15] and the spirane γ-lactone (XIX) (1 815 and 1 795 cm^{-1}) [16]. The 1 820 cm^{-1} band of picrolichenic acid and its methyl derivatives is therefore strong support for the presence of a γ-lactone carbonyl group.

The two remaining carbonyl functions of picrolichenic acid give rise to a single band at 1 665—1 670 cm^{-1}. Methyl O-methylpicrolichenate (Fig. 3), however, shows two strong bands at 1 725—1 730 cm^{-1} and 1 665—1 670 cm^{-1} which may be ascribed to the carboxymethyl group and the dienone carbonyl group, respectively [14]. As is shown by examples from steroid chemistry [17], cross conjugated as well as linear conjugated dienones absorb strongly in a narrow region at 1 660—1 670 cm^{-1}.

Methyl picrolichenate, containing a hydroxyl group in the *ortho*-position to a carboxymethyl group, would be expected to show an ester band in the frequency range characteristic for chelated aromatic esters (1 670—1 690 cm^{-1}) [14]. Hence, the strong band at 1 665—1 670 cm^{-1} shown by the methyl ester (Fig. 2) may be due to an ester band overlapping a dienone carbonyl band. The unexpected medium intensity band at 1 725 cm^{-1} shown by this compound may indicate that chelation is weak. It should perhaps be mentioned that substituents such as methyl or bromine in the *ortho*-position to the carboxyl group of salicylic acid have recently been regarded as the cause of a decrease in the strength of chelation between the hydroxyl and the carboxyl group [18].

The infra-red spectrum of the piperidide of picrolichenic acid (Fig. 4) shows a broad absorption in the 1 650—1 725 cm^{-1} region with a maximum at 1 690—1 700 cm^{-1}, indicating overlapping of the carbonyl bands.

Picrolichenic acid and its piperidide show broad absorption in the 2 500—2 800 cm^{-1} region, indicating strongly hydrogen bonded hydroxyl groups [14]. These compounds as well as methyl picrolichenate also show a broad hydroxyl band at about 3 450 cm^{-1}. Methyl O-methylpicrolichenate has no hydroxyl absorption.

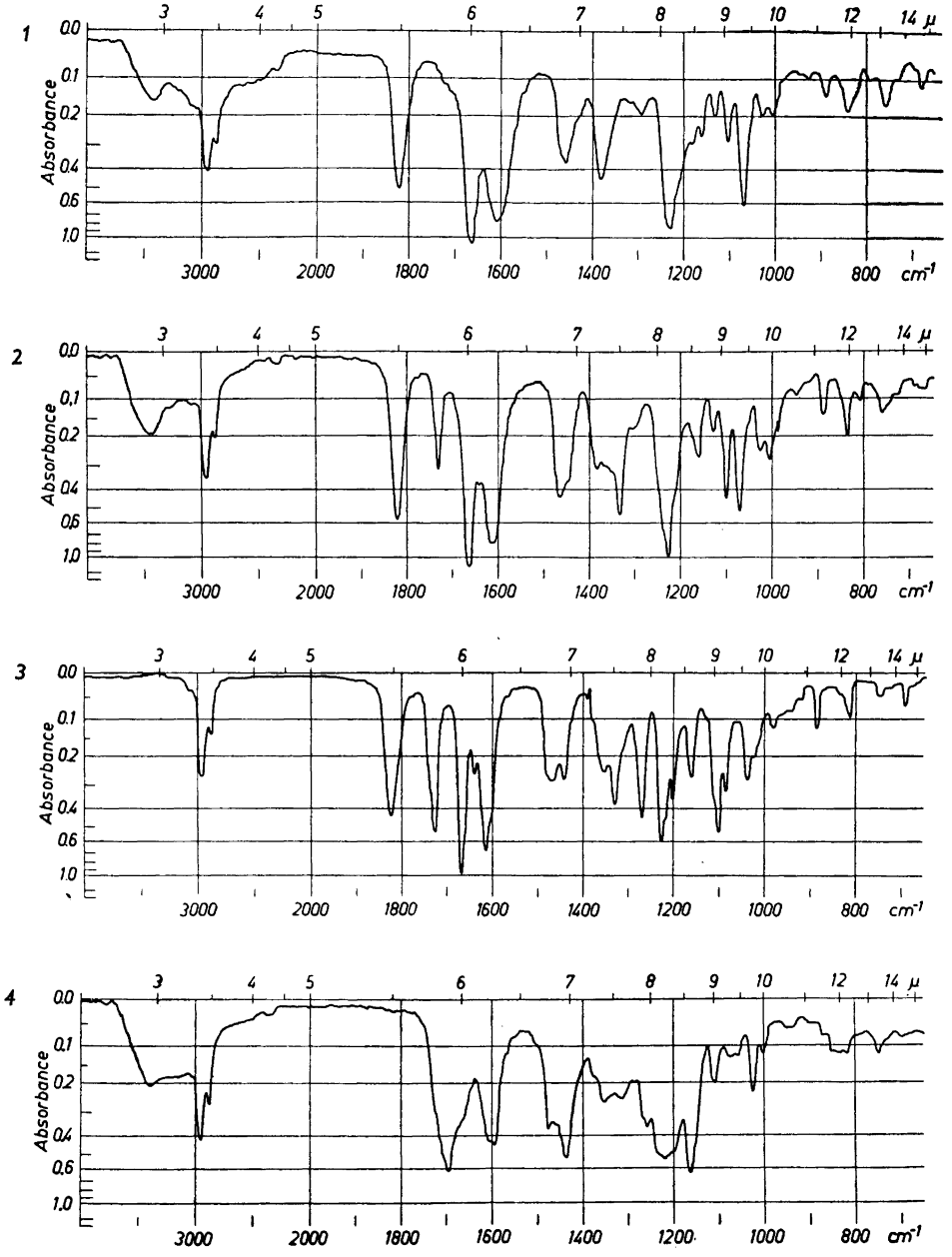

Fig. 1—4. Infra-red absorption spectra (in potassium bromide) of picrolichenic acid (XXIII) (Fig. 1), methyl picrolichenate (XXIV) (Fig. 2), methyl O-methylpicrolichenate (XXV) (Fig. 3) and picrolichenic acid piperidide (XI, R = n-C_5H_{11}) (Fig. 4).

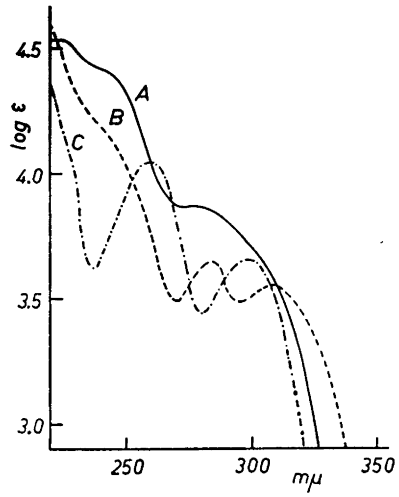

Fig. 5. Ultra-violet absorption spectra (in ethanol) of picrolichenic acid (XXIII) (A ————), picrolichenic acid piperidide (XI, R = *n*-C_5H_{11}) (B - - -) and orsellinic acid (C —.—.—.—).

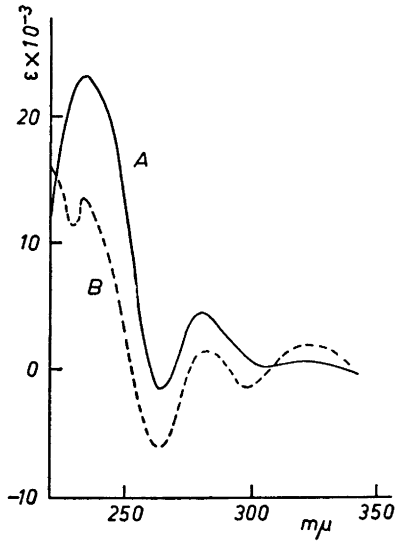

Fig. 6. Difference curves; A: Picrolichenic acid — orsellinic acid; B: Picrolichenic acid piperidide — orsellinic acid

While the main skeleton of picrolichenic acid as in (V) or (IX) (R = *n*-C_5H_{11}) appears well established, the choice between the two alternatives remains. From a biological point of view the structure (IX) derived from (VII) appears far more likely than (V). The widespread occurrence of depsidones in lichens indicates that the dehydrogenation of depsides such as (II) usually proceeds with oxygen-carbon coupling. In the case of depsides methylated as in (VII), however, oxygen-carbon coupling cannot occur and only carbon-carbon coupling is possible. A few depsides of this type are known, one example being umbilicaric acid[19], a tridepside derived from orsellinic acid.

The stability of the piperidide of picrolichenic acid may also be taken as an indication of the correctness of the structure (IX) for the acid. A piperidide derived from (V) would be expected to undergo ready *cyclo*-acetalisation and aromatisation to a dibenzofuran.

However, a final choice between the alternatives (V) and (IX) requires a knowledge of the exact position of the methoxyl group in phenol (B), the monomethyl ether of (XII). A strong indication in favour of structure (XV) for this phenol — and hence structure (IX) for picrolichenic acid — is its great sensitivity to oxygen in alkaline solution. Similar easy oxidation is characteristic of for example 2,4,2′,4′-tetrahydroxydiphenyl but not of 2,4,2′,6′-tetrahydroxydiphenyl which possesses only one hydroxyl group in a 4-position.

Since no direct conjugation exists between the two moieties of picrolichenic acid, information about the structure of the *cyclo*hexadienone part could be

obtained by subtracting the U.V. spectrum of the aromatic part from the spectrum of the acid itself. The difference curves obtained by subtracting the U.V. curve for orsellinic acid (Fig. 5:C) — used as a model for the aromatic part of the molecule — from the curves for picrolichenic acid (Fig. 5:A) and picrolichenic acid piperidide (Fig. 5:B) are shown in Fig. 6. The two curves, of course, give only a rough idea of the spectral type of the methoxy *cyclo*hexadienone chromophore of picrolichenic acid.

2,4- and 2,5-*cyclo*hexadien-1-ones differ considerably in spectral properties, the former absorbing at a longer wavelength in the U.V. region. Wessely and Sinwel [20] report unspecific absorption in the short U.V. region for 4-methyl-4-hydroxy-2,5-*cyclo*hexadien-1-one, 2,4,6-trimethyl-4-hydroxy-2,5-*cyclo*hexadien-1-one and their acetates whereas 6-methyl-6-acetoxy-2,4-*cyclo*hexadien-1-one and related compounds which are linear conjugated showed well-defined maxima in the 290—310 mμ region (log ε 3.6—3.7).

Jeger, Rüegg and Ruzicka [21] studied a system with a more direct bearing upon the present problem. A pyrolysis product of α-amyrin containing the partial structure (XX) afforded two isomeric monomethyl ethers, one of which showed a very broad maximum at 330 mμ (log ε about 3.8) and was alloted the linear conjugated formula (XXI). The isomer which showed maxima at 250 and 278 mμ (log ε 4.2 and 3.7, respectively) was given the cross-conjugated partial structure (XXII).

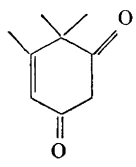

XX

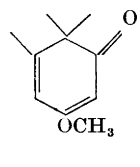

XXI

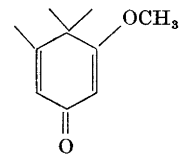

XXII

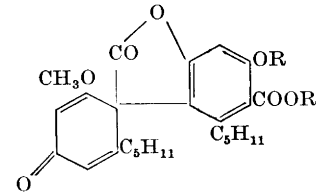

XXIII : R=R'=H
XXIV : R=H, R'=CH_3
XXV : R=R'=CH_3

One of the two difference curves mentioned above (Fig. 6) shows a distinct maximum at about 325 mμ, but this maximum is less intense (log ε 3.25) and much narrower than the broad maximum of the compound containing the structure (XXI). Both curves, however, show maxima near 235 mμ (log ε 4.4; 4.1) and 280 mμ (log ε 3.8; 3.15) corresponding roughly to the two maxima of the cross-conjugated compound (XXII) which again supports the structure (IX) for picrolichenic acid.

The chemical and physical evidence so far discussed appears to be in harmony with a structure (XXIII) (IX, R = *n*-C_5H_{11}) for picrolichenic acid. The structure of the piperidide $C_{30}H_{41}O_7N$ would then be (XI) (R = *n*-C_5H_{11}) and that of the monocarboxylic acid (A), (XVII).

There is, however, one observation which could be taken as evidence against structure (XXIII); the lack of optical activity in the compound. Several explanations could be offered to explain this inactivity, but a successful resolution of picrolichenic acid would constitute a valuable confirmation of the

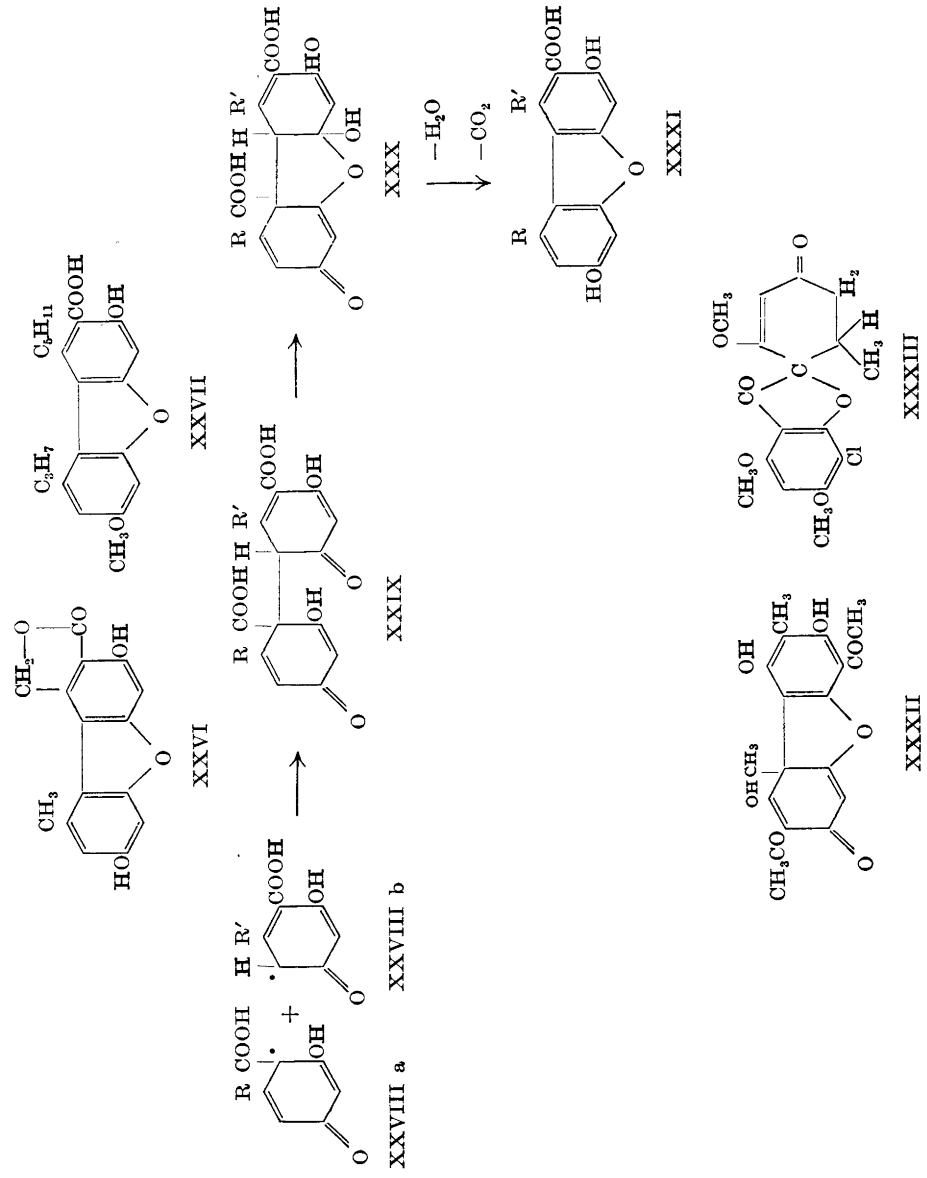

structure. Work is in progress in this direction, and attempts are also being made to obtain a more direct proof of the position of the methoxyl group in phenol (B) and to elucidate the structure of the thermal decomposition product of picrolichenic acid.

The lichen acids strepsilin [22] (XXVI) and didymic acid [13] (XXVII) are dibenzofurans which unlike most depsides and depsidones contain only one carboxyl group. It appears reasonable to suggest that their biosynthesis has proceeded essentially along the same lines as picrolichenic acid (XXVIII a, b → XXXI) but that, owing to the presence of a free hydroxyl group in the *ortho*-position to the carbon-carbon linkage between the two nuclei of the radical coupling product (XXIX), a *cyclo*acetalisation to (XXX) has taken place followed by elimination of water and carbon dioxide with formation of (XXXI).

Essentially the same scheme has recently been proposed by Barton and Cohen [9]. However, the above scheme differs in details which are also of importance for an understanding of the structure of related dibenzofurans such as porphyrilic acid [12]. A full discussion of these questions will be presented elsewhere.

The unique structure (XXIII) of picrolichenic acid combines features of the depsidones and of usnic acid (XXXII) [23-25] and it may also be compared with the fungal metabolite griseofulvin [26] (XXXIII) which contains a similar spirane structure. These compounds like the dibenzofurans contain a heterocyclic ring system and it is obvious that the theory of oxidative coupling of phenols provides a common basis for a rational interpretation of their possible biosynthesis from simple phenolic progenitors.

EXPERIMENTAL

Unless otherwise stated the melting points were determined on the Kofler-Block. Whatman No. 1 paper was used for paper chromatography. The U.V. spectra were measured with a Beckman spectrophotometer, model DU. The infra-red spectra were recorded with a Perkin-Elmer double beam spectrophotometer, model 21, using the potassium bromide technique.

Isolation of picrolichenic acid (XXIII). The powdery lichen material (250 g) was extracted with cold ether (2 500 ml) in several portions and the combined extracts were concentrated to 30 ml. On standing in the refrigerator, the solution deposited a crystallisate which was collected and washed with cold ether (yield, 11.0 g). The mother liquor on evaporation in air and treatment with benzene/light petroleum (2:1) gave a second crop (6 g), contaminated by resinous material. The resulting mother liquor was not further investigated.

The first fraction (11.0 g) was dissolved in hot benzene (50 ml) and the insoluble residue was filtered off. The solution deposited a yellowish crystallisate of crude picrolichenic acid (7.4 g); a second crop (2.3 g) was obtained from the mother liquor. The fraction 6.0 g gave crude picrolichenic acid (3.0 g) on treatment with ice-cold ether and crystallisation from benzene.

The acid was purified by passing a benzene solution through a small column of alumina to adsorb some of the coloured impurities. The analytical samples crystallised (I) from benzene as prisms, m. p. 184—187° (decomp.) or (II) from aqueous acetic acid as prisms, m. p. 187—190° (decomp.) (m.p:s uncorrected, measured in a capillary tube; rate of temperature increase, 4°/min). The samples were dried *in vacuo* at 120°.

The acid, dissolved in aqueous acetone, titrated sharply with bromothymol blue as indicator. (Found: I. C 68.3; 68.6; H 6.74; 6.70; OCH_3 6.91; $C-CH_3$ 4.0; 4.0; equiv. wt. 443. II. C 67.9; H 7.15. $C_{25}H_{30}O_7$ requires C 67.9; H 6.83; OCH_3 7.01; $(C-CH_3)_2$ 6.8; equiv. wt. (as a monobasic acid) 442.5.)

The acid in ethanol ($c = 5$) or chloroform ($c = 5$) showed $[\alpha]_D^{20} \pm 0$ as measured in a 1 dm tube.

U.V. spectrum (in ethanol): Fig. 5 A; I.R. spectrum, Fig. 1.

Picrolichenic acid (0.01 % in ethanol) gave a violet colour with ferric chloride. The acid gave no colour with bleaching powder in aqueous methanol but gave a red colour when treated with bleaching powder and aqueous alkali. It gave no colour with *bis*-diazotised benzidine when tested on neutral filter paper but an intense red colour with this reagent after pretreatment with 0.1 N sodium hydroxide solution for a few minutes. As shown by spot tests on filter paper, phenolic groups were also liberated by exposure of the acid for a few seconds to ammonia vapour. Picrolichenic acid gave no colour with Gibbs' reagent when tested in a borate buffer (pH 9.0).

Thermal decomposition of picrolichenic acid. The acid (200 mg) in a test tube was heated for a few minutes in a salt bath to 210°; a gas containing carbon dioxide was evolved. The residue when distilled in high vacuum gave a yellowish, viscous oil which crystallised as prisms, m. p. 153—155° from 90 % acetic acid. The compound gave a yellowish-brown colour with *bis*-diazotised benzidine but no colour with ferric chloride.

Methyl picrolichenate (XXIV). An excess of ethereal diazomethane was added to an ice-cold solution of picrolichenic acid in ether, followed after one minute by a drop of acetic acid. Evaporation afforded the ester as an oil, which crystallised from methanol as needles, m. p. 102—103.5°. (Found: C 68.1; H 7.16; OCH_3 13.8. $C_{26}H_{32}O_7$ requires C 68.4; H 7.06; $(OCH_3)_2$ 13.6.) $[\alpha]_D^{20} \pm 0$ (ethanol, $c = 1$). I.R. spectrum, Fig. 2.

The ester was soluble in cold 0.05 N sodium hydroxide solution and gave a brownish ferric test.

Methyl O-methylpicrolichenate (XXV). Picrolichenic acid (150 mg) was treated overnight with an excess of ethereal diazomethane containing methanol. The methyl derivative (90 mg) crystallised from a solution of the oily reaction product in light petroleum (b.p. 40—60°; 70 ml) and was finally obtained from hexane as needles, m. p. 80—82°. (Found: C 68.4; H 7.21; OCH_3 20.0. $C_{27}H_{34}O_7$ requires C 68.9; H 7.28; $(OCH_3)_3$ 19.8.) I.R. spectrum, Fig. 3.

The compound was insoluble in 0.1 N sodium hydroxide solution in the cold and gave no colour with phenol reagents.

Piperidide of picrolichenic acid (XI, R = n-C_5H_{11}). The acid (720 mg) in dry piperidine (10 ml) was set aside at room temperature in an atmosphere of nitrogen. After a few days, the solution was poured with stirring into 2 N hydrochloric acid (500 ml) containing ice. The crude piperidide (800 mg) separated as a brownish precipitate which crystallised from benzene as prisms m.p. 168—172° (I); a second form (II) was obtained as prisms, m. p. 187—190° (decomp.) from 80 % acetic acid. A benzene solution of the higher melting form gave the lower melting form on seeding with it.

The piperidide in aqueous acetone titrated sharply as a monobasic acid (bromothymol blue). (Found: (I) N 2.58; OCH_3 6.29; equiv. wt 527. (II) C 68.8; H 8.09; N 2.76. $C_{30}H_{41}O_7N$ requires C 68.3; H 7.80; N 2.66; OCH_3 5.88; equiv. wt. 527.6.) $[\alpha]_D^{20} \pm 0$ (c 5.0, ethanol or chloroform.) U.V. spectrum (in ethanol), Fig. 5 B; I.R. spectrum, Fig. 4.

Colour reactions: Ferric chloride-ethanol, violet; *bis*-diazotised benzidine, yellowish brown; bleaching powder, no colour.

Prolonged methylation of the piperidide with ethereal diazomethane in the presence of methanol gave a dimethyl derivative which crystallised from methanol as prisms, m.p. 163—165°. (Found: N 2.62; OCH_3 17.0. $C_{32}H_{45}O_7N$ requires N 2.52; $(OCH_3)_3$ 16.8.) The compound gave no colour with ferric chloride but gave a yellowish-brown colour with *bis*-diazotised benzidine when tested on buffered paper (Na_3PO_4). It was slightly soluble in 1 N sodium hydroxide solution.

Permanganate oxidation of picrolichenic acid. A 1 % aqueous solution of potassium permanganate (200 ml) was added dropwise with stirring to a solution of picrolichenic acid (192 mg, 0.435 mmole) in 0.05 N sodium hydroxide solution (50 ml). After 2 h at 20°, the temperature was kept at 45° for 30 min to complete the oxidation. Excess permanganate was destroyed, the solution was acidified with sulphuric acid and the manganese sludge was dissolved by passing sulphur dioxide through the solution. The solution was extracted with ether (600 ml) and the ether phase was shaken with 1 N sodium hydroxide solution (50 ml). The alkaline solution was acidified with sulphuric acid, saturated with

sodium sulphate and steam distilled. The distillate (250 ml) contained 0.64 mmole of volatile acids, as estimated by titration.

A sample of the distillate was extracted with ether and the ether phase was analysed by chromatography using paper impregnated with dimethyl sulphoxide and a mobile phase of ether-light petroleum (b.p. 65—75°) 1:1 [27]. A reference sample containing the normal saturated acids with 2, 3, 4, 5, 6 and 8 carbon atoms was run on the same chromatogram. The spots were detected by spraying the paper with a mixed indicator solution as recommended by Duncan and Porteous [28]. The main component of the ether extract appeared as a spot with the same R_F-value as *n*-caproic acid. Faint spots of the lower fatty acids were also observed but no spots corresponding to acids with more than six carbon atoms.

The main part of the distillate, neutralised with standard alkali, was evaporated to dryness and the *p*-bromophenacylester prepared in the usual way. The crude ester (102 mg, m. p. 55—63°) on crystallisation from aqueous methanol yielded blades (50 mg), m. p. 68.5—69.5, undepressed on admixture with an authentic sample of *p*-bromophenacyl caproate, m. p. 71—72°.

Alkaline hydrolysis of picrolichenic acid. The acid (2.7 g) in 1 N sodium hydroxide solution (50 ml) was left for 40 min at 20° in a nitrogen atmosphere. The reddish solution poured into 1 N hydrochloric acid (100 ml) gave the hydrolysis product as a voluminous precipitate which changed to a gum and rapidly expanded to a spongy mass due to the evolution of gas. The product was taken up in ether and the ether solution was washed, dried and evaporated *in vacuo*. The oily residue (2.1 g) was dissolved in benzene (30 ml) and the solution was filtered through a small column of alkali-free alumina. The monocarboxylic acid (A) (XVII) separated from the filtrate as needles (1.2 g) and was recrystallised from benzene. To avoid decarboxylation which was noticeable even below the melting point of the acid the analytical sample, m. p. 145—148° (decomp.) was dried *in vacuo* at 100° for only a short time. (Found: C 68.9; H 7.55; OCH_3 7.52; equiv. wt. 419. $C_{24}H_{32}O_6$ requires C 69.2; H 7.75; OCH_3 7.45; equiv. wt. 416.5.) U.V. absorption (in ethanol): λ_{max} 264 mμ (log ε 4.06); 306 mμ (3.67). λ_{min} 254 mμ (4.01); 294 mμ (3.61).

Colour reactions: Ferric chloride, violet; *bis*-diazotised benzidine, red; bleaching powder, red-violet, changing to brown-red.

Decarboxylation of acid (A). A small sample of the acid in a test tube was heated in an oil bath for a few minutes to 150—160°; carbon dioxide was evolved. (Loss of weight, 10.5 %. Calculated for decarboxylation of a monocarboxylic acid $C_{24}H_{32}O_6$, 10.6 %). The decarboxylation product (B) (XV), obtained as a colourless oil by distillation *in vacuo*, did not crystallise. It gave a negative ferric test but otherwise gave colour reactions similar to those given by the acid (A). Paper chromatography, using the solvent system benzene-water, gave a single, somewhat elongated spot, $R_F = 0.4—0.5$. Phenol (B) in alkaline solution was rapidly oxidised in the air with the formation of a brown-red colour.

Methylation of phenol (B). The phenol (150 mg) in dry acetone (50 ml) was boiled under reflux for 8 h with potassium carbonate (5 g) and dimethyl sulphate (2.5 g). The oily reaction product, isolated in the usual way, was distilled under reduced pressure and crystallised on seeding with the tetramethyl ether of the phenol (C), described below. The crude methyl ether (m. p. 30—34°) on bromination in glacial acetic acid for 30 min afforded a dibromide which crystallised from acetic acid as prisms, m. p. 119—120°, undepressed on admixture with the dibromide of the tetramethyl ether of the phenol (C), described below. (Found: Br 29.1. $C_{26}H_{36}O_4Br_2$ requires Br 27.9.)

Demethylation and decarboxylation of acid (A). The acid (2 g) was boiled under reflux for 2 h with hydrobromic acid (20 ml, $d = 1.5$) and glacial acetic acid (25 ml) in an atmosphere of nitrogen. The reaction mixture when poured into water (300 ml) gave a voluminous, brownish precipitate which was collected, washed and dried (1.7 g). The crude phenol was dissolved in hot benzene (300 ml) and filtered through a small column of alkali-free alumina. The filtrate afforded a crystallisate (0.9 g), m. p. 175—178°. A second crop (0.5 g) was obtained from the mother liquor. Crystallisation from glacial acetic acid furnished the phenol as needles, m. p. 180—181°, undepressed on admixture with the phenol (C), obtained directly from picrolichenic acid as described below.

Degradation of picrolichenic acid with hydrobromic acid. Picrolichenic acid (5 g) was refluxed for 2.5 h with hydrobromic acid (20 ml, $d = 1.5$) and glacial acetic acid (25 ml)

in an atmosphere of nitrogen. The dark-brown reaction mixture was poured into water (500 ml) yielding a precipitate which was collected, washed and dried (4.0 g). Crystallisation from glacial acetic acid (30 ml) afforded the phenol (C) (XII) as greyish needles (1.1 g), m. p. 176–179°. The analytical sample, colourless needles from the same solvent, had m. p. 180–181°. (Found: C 73.0; H 8.61. $C_{32}H_{30}O_4$ requires C 73.7; H 8.44.)

Colour reactions: Ferric chloride, no colour; *bis*-diazotised benzidine, wine-red; bleaching powder, violet-red, changing to brown-red. Like phenol (B), the phenol (C) in alkaline solution was rapidly oxidised by air.

Paper chromatography, using the solvent system benzene-water, showed an elongated spot, $R_F = 0-0.2$ or higher, depending upon the amount of substance applied.

Methylation of phenol (C). The phenol (2.3 g) in dry acetone was boiled under reflux for 10 h with an excess of dimethyl sulphate and potassium carbonate. The tetramethyl ether was obtained as an oil which crystallised from methanol on cooling with liquid ammonia (yield, 1.9 g). After recrystallisation from methanol at −30° and distillation *in vacuo* it crystallised spontaneously, m. p. 34.5–35.5°. (Found: C 75.0; H 9.22; OCH_3 29.8; 30.2. $C_{36}H_{38}O_4$ requires C 75.3; H 9.24; $(OCH_3)_4$ 29.9.) U.V. absorption (in ethanol): λ_{max} 282 mμ (log ε 3.73); λ_{min} 261 mμ (3.34). λ = 220 mμ, log ε 4.35.

The tetramethyl ether was brominated in glacial acetic acid at room temperature. The first two moles of bromine were consumed rapidly and the excess of bromine was destroyed after 30 min by pouring the solution into water containing sulphur dioxide; the crude dibromide separated as an oil that crystallised rapidly. It was obtained from glacial acetic acid as prisms, m. p. 119.5–120.5°. (Found: Br 27.9. $C_{36}H_{36}O_4Br_2$ requires Br 27.9.)

A tribromide was obtained as the main product when the reaction time was extended to 24 h. Prisms, m. p. 106–107° from glacial acetic acid. (Found: C 47.9; H 5.63; Br 38.0; OCH_3 19.5. $C_{36}H_{35}O_4Br_3$ requires C 47.9; H 5.42; Br 36.8; $(OCH_3)_4$ 19.1.)

Prolonged bromination for 7 days gave a tetrabromide, which crystallised from glacial acetic acid as prisms, m. p. 97–98°. (Found: Br 44.0. $C_{36}H_{34}O_4Br_4$ requires Br 43.8.)

Dehydration of phenol (C). Zinc chloride (12 g) mixed with the phenol (C) (600 mg) in a test tube was heated in a salt bath to 240–250° and stirred continuously with a glass rod. The melt solidified after 4–5 min and was then cooled and extracted with water. The undissolved residue was collected, dried and dissolved in benzene (25 ml). Paper chromatography (solvent system, benzene-water) showed the main component as a spot, $R_F = 0.6-0.7$, characterised by a brownish-yellow colour with *bis*-diazotised benzidine and a greyish colour with Gibbs' reagent. A spot due to unreacted phenol (C) was also observed. The benzene solution was filtered through a small column of alkali-free alumina and the column was washed with further benzene. The absence of phenol (C) in the eluates was established by paper chromatography. Evaporation of the combined benzene solutions yielded the crude phenol (D) (XIV) (550 mg), m. p. 114–118°. It was recrystallised from benzene-light petroleum (40–60°) and showed m. p. 124–125° after sublimation *in vacuo*. (Found: C 77.3; H 8.16. $C_{32}H_{28}O_3$ requires C 77.6; H 8.29.)

The phenol (D) gave a green colour with bleaching powder but no colour with ferric chloride. An alkaline solution of the phenol showed an intense bluish fluorescence in ultra-violet light.

Methylation of phenol (D). The crude phenol (190 mg) was treated for two days with an excess of ethereal diazomethane containing methanol. Acetic acid was then added and the solution was shaken with 0.5 N sodium hydroxide solution, washed with water, dried and evaporated yielding an oil (200 mg) which crystallised on treatment with methanol. It was purified by chromatography on alumina. The material eluted by benzene was recrystallised from ethanol and from aqueous acetic acid to give the dimethylether of phenol (D) as needles, m. p. 72–73°. (Found: C 77.8; H 8.54; OCH_3 16.6. $C_{34}H_{32}O_3$ requires C 78.2; H 8.76; $(OCH_3)_2$ 16.8.) U.V. absorption (in ethanol): λ_{max} 229.5 mμ (log ε 4.37); 240.5 mμ (4.31); 255 mμ (4.07); 262 mμ (4.12); 300 mμ (shoulder, 4.24); 307 mμ (4.30). λ_{min} 238.5 mμ (4.30); 251 mμ (4.02); 257 mμ (4.06); 271 mμ (3.28).

Permanganate oxidation of the dimethyl ether of phenol (D). A solution of crude dimethyl ether (240 mg, m. p. 63–70°) in pyridine (75 ml, purified by treatment with selenium dioxide) [29] was boiled with stirring under reflux and a hot, 20 % aqueous solution of potassium permanganate was added in 5 ml portions until a total of 16 g had been added in 10 h. The solution was boiled for another 2 h, the manganese sludge was filtered

off and washed with pyridine and the combined filtrates were evaporated to dryness under reduced pressure. The residue was taken up in water and insoluble products removed from the alkaline solution by extraction with ether. For chromatography, a sample of the aqueous phase was acidified and extracted with ether. The presence in the ether phase of a number of acids was established using *n*-butanol-water and paper impregnated with trisodium phosphate [12,30]. The spots were visible in ultra-violet light. To effect complete oxidation, the main part of the aqueous phase was heated on a water bath and a 10 % permanganate solution (20 ml) was added dropwise with stirring over a 6 h period. The excess permanganate was destroyed and the manganese sludge was filtered off and washed with 0.1 N sodium hydroxide solution. The crude oxidation product (25 mg) separated from the concentrated filtrate on acidification with hydrochloric acid. The main component was chromatographically identical with 3,7-dimethoxydibenzofuran-1,9-dicarboxylic acid [13] synthesised as described below. The R_F-values on phosphate impregnated papers [12,30] were 0.05 (Na_3PO_4); 0.10 (Na_2HPO_4); 0.80 (NaH_2PO_4) (solvent system, *n*-butanol-water). The spots showed a very intense blue fluorescence in ultra-violet light.

The crude acid on methylation with diazomethane afforded a dimethyl ester, sparingly soluble in ethanol and crystallising from this solvent as needles (16 mg), m. p. 187—194°. The analytical sample, sublimed *in vacuo* and crystallised from ethanol, melted at 191—193.5° after slight sintering above 187°. The melting point was undepressed on admixture of 3,7-dimethoxy-1,9-dicarbomethoxydibenzofuran [13], m. p. 192—194°, described below. (Found: C 62.9; H 4.61. $C_{18}H_{16}O_7$ requires C 62.8; H 4.68.)

2-Iodo-3,5-dimethoxytoluene [31]. Iodine (84 g, 0.33 mole) and yellow mercuric oxide (66 g, 0.30 mole) was added in portions with stirring to orcinol dimethyl ether (45.8 g, 0.30 mole) and care was taken to keep the temperature below 50°. The solidified reaction mixture was extracted with ether (700 ml) and the ether solution was filtered and evaporated to dryness. The residue was dissolved in benzene (400 ml) and the solution was repeatedly extracted with a saturated aqueous solution of potassium iodide. The benzene solution was evaporated to dryness and the residue was distilled under reduced pressure to give 2-iodo-3,5-dimethoxytoluene (66 g, b.p. 155—170°/8 mm). It crystallised from ethanol as prisms, m. p. 84—85°. (Found: I 46.3. $C_9H_{11}O_2I$ requires I 45.6.)

The non-volatile residue from the distillation was crystallised from acetone to give (probably) 2,6-di-iodo-3,5-dimethoxytoluene as prisms, m. p. 203—204°. (Found: I 61.9. $C_9H_{10}O_2I_2$ requires I 62.8.)

The structure of the mono-iodide of orcinol dimethyl ether, not discussed in the available referate of the Japanese paper [31], follows clearly from its non-identity with 4-iodo-3,5-dimethoxytoluene [32], m. p. 96—97°.

2,2′-Dimethyl-4,6,4′,6′-tetramethoxydiphenyl [13]. 2-Iodo-3,5-dimethoxytoluene (20 g) was mixed with copper bronze (60 g) and heated in a salt bath to 200—210° for 15 min and then to 220—230° for a further 20 min. The reaction mixture was extracted with chloroform, the extract was evaporated to dryness and the residue was crystallised from ethanol (yield, 7.7 g). Distillation *in vacuo* and crystallisation from ethanol gave 2,2-dimethyl-4,6,4′,6′-tetramethoxydiphenyl as prisms, m. p. 106—107°. (Shibata [13] reports m.p. 103—104°.) U.V. absorption (in ethanol): λ_{max} 282 mμ (log ε 3.75); λ_{min} 261 mμ (3.36). λ = 220 mμ, log ε = 4.38.

Shibata [13] reports λ_{max} 282 mμ (3.7); 274 mμ (3.6); λ_{min} 262 mμ (3.4).

3,7-Dimethoxy-1,9-dimethyldibenzofuran [13]. 2,2′-Dimethyl-4,6,4′,6′-tetramethoxydiphenyl (2.5 g) was boiled under reflux for 24 h with hydrobromic acid (40 ml, d = 1.50) in an atmosphere of carbon dioxide. The material obtained from the solution on cooling was collected (1.8 g) and methylated with dimethyl sulphate and alkali to give 3,7-dimethoxy-1,9-dimethyldibenzofuran, which was distilled *in vacuo* and crystallised from ethanol as blades, m. p. 159—160°. (Shibata [13] reports m.p. 157°.) U.V. absorption (in ethanol): λ_{max} 226 mμ (4.46); 239 mμ (shoulder, 4.36); 257 mμ (shoulder, 4.10); 263 mμ (4.15) 299 mμ (4.26); 309 mμ (4.33). λ_{min} 250 mμ (4.00); 272 mμ (3.61); 302 mμ (4.25).

3,7-Dimethoxy-1,9-dicarbomethoxydibenzofuran [13]. 3,7-Dimethoxy-1,9-dimethyldibenzofuran (440 mg) in pyridine (25 ml) was boiled under reflux and a solution of potassium permanganate (5 g) in water (100 ml) was added dropwise with stirring over a period of 10 h after which the heating was continued for another 4 h. The solution was acidified

with sulphuric acid, the manganese sludge was dissolved and the crude oxidation product was collected (340 mg). It was dissolved in 5 % sodium carbonate solution and the solution was filtered and acidified with hydrochloric acid. The crude acid separated as a yellowish precipitate which was collected (220 mg). A sample was recrystallised from dioxan, yielding 3,7-dimethoxydibenzofuran-1,9-dicarboxylic acid as yellowish needles, m. p. about 300 (decomp.), characterised by paper chromatography as described above. (Shibata [13] reports m. p. 321—322° (decomp.)). The main part of the crude acid was methylated with diazomethane to give 3,7-dimethoxy-1,9-dicarbomethoxydibenzofuran, crystallised from ethanol as needles, m. p. 192—194° (Shibata [13] gives m. p. 188.5—189.5°). (Found: C 62.9; H 4.50; OCH_3 35.0. $C_{18}H_{16}O_7$ requires C 62.8; H 4.68; $(OCH_3)_4$ 36.0.)

Air oxidation of hydroxydiphenyls. 2,4,2′,6′-Tetramethoxydiphenyl [33] (20 mg) was boiled for 1.5 h with hydrobromic acid (d = 1.50; 0.5 ml) and glacial acetic acid (0.5 ml). The solution was evaporated to dryness *in vacuo*. The residue was shown by paper chromatography to contain only traces of 1,7-dihydroxydibenzofuran [33]. 2,4,2′,4′-Tetramethoxydiphenyl [34] was demethylated in the same way. Spots of 1 % solutions in acetone of the crude tetrahydroxydiphenyls and of the phenol (B) were applied to filter paper moistened with 1 N sodium hydroxide solution. The spots of phenol (B) and of 2,4,2′,4′-tetrahydroxydiphenyl turned brown-red within a few minutes but the spot for 2,4,2′,6′-tetrahydroxydiphenyl darkened only after about 30 min.

The author is indebted to Dr. J. F. Grove, Herts, England, for valuable information on the infra-red spectra of lactones.

Grants from *Hierta-Rezius fond för vetenskaplig forskning* and from *Sigrid Arrhenius fond* are gratefully acknowledged.

REFERENCES

1. Alms. *Ann. der Pharmacie* **I** (1832) 61.
2. Zopf, W. *Liebigs Ann.* **313** (1900) 335.
3. Zopf, W. *Ibid.* **321** (1902) 38.
4. Gibbs, H. D. *J. Biol. Chem.* **72** (1927) 649.
5. Koch, J. E. and Krieg, W. *Chem. Ztg* **62** (1938) 140.
6. Asahina, Y. and Shibata, S. *Chemistry of Lichen Substances*, Tokyo 1954; p. 7.
7. Asahina, Y. and Fuzikawa, F. *Ber.* **68** (1935) 634.
8. Raistrick, H., Stickings, C. E. and Thomas, R. *Biochem. J.* **55** (1953) 421.
9. Barton, D. H. R. and Cohen, T. *Festschrift Arthur Stoll*, Basel 1957, p. 117.
10. Erdtman, H. and Wachtmeister, C. A. *Ibid., p. 144.*
11. Erdtman, H. and Wachtmeister, C. A. *Chem. & Ind. London* **1957** 1042.
12. Wachtmeister, C. A. *Acta Chem. Scand.* **10** (1956) 1404.
13. Shibata, S. *Acta Phytochim. Japan* **14** (1944) 9.
14. Bellamy, L. J. *The infra-red Spectra of Complex Molecules*, Methuen, London 1954.
15. Barton, D. H. R. and Bruun, T. *J. Chem. Soc.* **1953** 604.
16. Grove, J. F., Mac Millan, J., Mulholland, T. P. C. and Zealley, J. *J. Chem. Soc.* **1952** 3970.
17. Jones, R. N., Humphries, P. and Dobriner, K. *J. Am. Chem. Soc.* **72** (1950) 956.
18. Bray, L. G., Dippy, J. F. J., Hughes, S. R. C. and Laxton, L. W. *J. Chem. Soc.* **1957** 2405.
19. Koller, G. and Pfeiffer, G. *Monatsh.* **62** (1933) 324.
20. Wessely, F. and Sinwel, F. *Ibid.* **81** (1950) 1055.
21. Jeger, O., Rüegg, R. and Ruzicka, L. *Helv. Chim. Acta* **30** (1947) 1296.
22. Shibata, S. *Acta Phytochim. Japan* **14** (1944) 177.
23. Curd, F. H. and Robertson, A. *J. Chem. Soc.* **1957** 894.
24. Schöpf, C. and Ross, F. *Liebigs Ann.* **546** (1941) 1.
25. Barton, D. H. R., Deflorin, A. M. and Edwards, O. E. *J. Chem. Soc.* **1956** 530.
26. Grove, J. F., MacMillan, J., Mulholland, T. P. C. and Rogers, M. A. T. *J. Chem. Soc.* **1952** 3977.
27. Wickberg, B. *Svensk Kem. Tidskr.* **69** (1957) 402.
28. Duncan, R. E. B. and Porteous, J. W. *Analyst* **78** (1953) 641.

29. Jerchel, D. and Bauer, E. *Angew. Chem.* **68** (1956) 61.
30. Wachtmeister, C. A. *Acta Chem. Scand.* **6** (1952) 818.
31. Asahina, Y. and Aoki, M. *J. Pharm. Soc. Japan* **64** (1944) 50; *Chem. Abstr.* **45** (1951) 2929.
32. Posternak, T., Ruelius, H. W. and Tcherniak, J. *Helv. Chim. Acta* **26** (1943) 2036.
33. Wachtmeister, C. A. *Acta Chem. Scand.* **8** (1954) 1433.
34. Späth, E. and Gibian, K. *Monatsh.* **55** (1930) 342.

Received November 9, 1957.

ACTA CHEMICA SCANDINAVICA 12 (1958) 165—181

On the Complex Chemistry of the Tervalent Rare Earth Ions

I. The Acetate Systems of Lanthanum, Cerium, Neodymium, and Gadolinium

ARTUR SONESSON

Department of Inorganic and Physical Chemistry, Chemical Institute, University of Lund, Lund, Sweden

The complexity constants of the acetate complexes of La^{3+}, Ce^{3+}, Nd^{3+}, and Gd^{3+} have been determined. The values of the complexity constants $\beta_n = \frac{[MA_n]}{[M]\cdot[A]^n}$ that are given in Table 8 have been found in perchlorate medium of ionic strength 2 M at 20°C. The fourth constant must be considered only as a quantity formally computed from the potentiometric measurements, as an ion exchange investigation (Fronæus [1,17]) has shown that the cerium acetate system most probably does not contain anionic complexes to a detectable amount at acetate concentrations <500 mM.

The value of β_1 increases from La^{3+} to Nd^{3+}, which is expected on account of the decreasing ionic radius. The gadolinium acetate system, however, has a smaller β_1 than the neodymium system.

The fifteen elements with the atomic numbers 57 to 71 are called rare earths or lanthanons *. As all the terpositive rare earth ions have the same electron configuration $5s^2\ 5p^6$ of the outermost shell, they show great similarity with regard to their chemical properties. The decrease of the ionic radius from lanthanum to lutetium (*cf.* Herlinger [2]) leads, however, gradually to a slight change in the chemical properties. Thus, we can expect that the terpositive ions will form complexes of the same structure and of about the same strength, but that the strength of the complexes will increase from lanthanum to lutetium. Such a change has also been found by Schwarzenbach [3,4], Spedding [3,5], Vickery [6] and their coworkers. They have investigated the complex formation with some very strong complexing agents, such as ethylenediamine tetra-acetic acid and some of its derivatives, which all give chelates. These

* Spectroscopists usually do not count lanthanum among the rare earths as it has no electrons in the 4f subshell. Chemically, however, lanthanum belongs to the rare earths.

investigations also show that the increase in the stability of the complexes is not quite uniform. If the complexity constants are plotted as a function of the atomic number or the ionic radius of the rare earth, the curve will show a distinct break at gadolinium.

So far the variation of the complexity constants in the rare earth series has been studied only for polydentates. For an examination of the different steps of the complex formation, a monodentate ligand must be chosen that gives complexes of at least moderate strength. The acetate ion has proved a suitable ligand, especially as the acetate complexes are easy to investigate by potentiometric measurements. The only rare earth acetate system that has been investigated so far is the cerium(III) acetate system, the complexity constants of which Fronæus [1] has determined by the cation exchange method. In the present investigation a series of rare earth acetate systems will be examined by potentiometric measurements. In some cases the potentiometrically obtained results will be controlled by other investigations.

Calculation of the complexity constants in measurements of the free ligand concentration

By the potentiometric measurements the concentration of free ligand ([A]) has been determined in solutions with a known total concentration of the central ion (C_M) and of the ligand (C_A). The calculations are performed according to the method elaborated by Fronæus [7] (earlier works by Bjerrum [8] and Leden [9]). In the present paper only definitions of the symbols and a summary of the equations used are given.

If only mononuclear complexes MA_1, MA_2, ... MA_N are formed, we have the following equilibrium for the formation of the complex MA_n

$$MA_{n-1} + A \rightleftharpoons MA_n$$

The corresponding complexity constant β_n is defined

$$\beta_n = \frac{[MA_n]}{[M] \cdot [A]^n}$$

With β_n we can express C_M and C_A as functions of [A] and [M].

$$C_M = [M] \cdot X \tag{1a}$$

$$C_A = [A] + [M] \cdot X' \cdot [A] \tag{1b}$$

where $X = X([A])$ is defined by the equation

$$X = 1 + \sum_{n=1}^{N} \beta_n \cdot [A]^n$$

and

$$X' = \frac{d\ X([A])}{d\ [A]}$$

The ligand number $\bar{n}$ is defined according to Bjerrum [8]

$$\bar{n} = \frac{C_A - [A]}{C_M} \tag{2}$$

By plotting $\bar{n}$ as a function of log [A] we get the complex formation curve. Combination of the eqns. (1) and (2) and elimination of [M] will give

$$\frac{\bar{n}}{[A]} = \frac{X'}{X} \tag{3}$$

and after integration

$$\ln X([A]_j) = \int_0^{[A]_j} \frac{\bar{n}}{[A]} \cdot d[A] \tag{4}$$

Thus, this integration gives us corresponding values of X and [A].

The complexity constants $\beta_1, \beta_2, \ldots$ can now be calculated by successive extrapolation to [A] = 0 of the functions $X_1, X_2, \ldots$

$$\begin{aligned} X_1 &= \frac{X-1}{[A]} = \beta_1 + \beta_2 \cdot [A] + \beta_3 \cdot [A]^2 + \ldots . \\ X_2 &= \frac{X_1 - \beta_1}{[A]} = \beta_2 + \beta_3 \cdot [A] + \ldots . \end{aligned} \tag{5}$$

and so on for the following constants.

The composition of the complex system at a known [A] can be computed from the following equations.

$$\begin{aligned} \alpha_0 &= \frac{[M]}{C_M} = \frac{1}{1 + \beta_1 \cdot [A] + \beta_2 \cdot [A]^2 + \ldots .} \\ \alpha_n &= \frac{[MA_n]}{C_M} = \frac{\beta_n \cdot [A]^n}{1 + \beta_1 \cdot [A] + \beta_2 \cdot [A]^2 + \ldots .} \end{aligned} \tag{6}$$

When the complexity constants are known we can check our calculations by computing the ligand number $\bar{n}_c$ at some values of [A].

$$\bar{n}_c = \sum_{n=1}^{N} \frac{n\beta_n [A]^n}{1 + \beta_n [A]^n} \tag{7}$$

If polynuclear complexes are formed, we cannot directly use the $\bar{n}$/[A]-function for the computation of the constants of the mononuclear complexes. We assume here that the solution contains only mono- and dinuclear complexes. β'_n denotes the constant for the n:th dinuclear complex

$$\beta'_n = \frac{[M_2A_n]}{[M]^2 \cdot [A]^n}$$

We mean by Y the following function (Fronæus [7 p. 14])

$$Y([A]) = \sum_{n=1}^{L} \beta'_n \cdot [A]^n$$

Then we get for the total concentration of central ion and ligand

$$C_M = [M] \cdot X + 2[M]^2 \cdot Y$$

and

$$C_A = [A] + [M] \cdot X' \cdot [A] + [M]^2 \cdot Y' \cdot [A]$$

The expression corresponding to eqn. (3) will now be

$$\frac{\bar{n}}{[A]} = \frac{X' + [M] \cdot Y'}{X + 2[M] \cdot Y} \tag{8}$$

Thus, for a system with both mono- and dinuclear complexes $\bar{n}/[A]$ is a function of both [A] and [M]. When $C_M \rightarrow 0$, we get

$$\lim_{C_M \rightarrow 0} \frac{\bar{n}}{[A]} = \frac{X'}{X} \tag{9a}$$

Consequently, it is possible to compute the constants of the mononuclear complexes in the ordinary way by the aid of (9a).

If $C_A \rightarrow 0$, eqn. (8) will give (as $[M] \rightarrow C_M$, when $C_A \rightarrow 0$)

$$\lim_{C_A \rightarrow 0} \frac{\bar{n}}{[A]} = \beta_1 + C_M \cdot \beta_1' \tag{9b}$$

Thus, the $\bar{n}/[A]$-values at low [A] must increase with C_M if the complex system contains both mono- and dinuclear complexes.

Calculation of [A] and $\bar{n}$ from experimental data

If C'_{HA} and C'_A signify the stoichiometric concentrations of acetic acid and sodium acetate, respectively, and $[H^+]'$ the hydrogen ion concentration in a buffer solution free from rare earth ions, the following equation is valid

$$K_c = \frac{[H^+]' (C'_A + [H^+]')}{C'_{HA} - [H^+]'} \tag{10}$$

For a solution with the concentration C_M of rare earth ions and with the same stoichiometric concentration of acetate buffer as above, we denote by $[H^+]$ the concentration of hydrogen ions, by [A] the concentration of free acetate ions and by [HA] the concentration of unprotolysed acetic acid. If the rare earth perchlorate contains some free acid, its concentration $C_H = \nu \cdot C_M$ must be accounted for. Then we get

$$[HA] = C'_{HA} + C_H - [H^+]$$

and

$$K_c = \frac{[H^+] \cdot [A]}{C'_{HA} + C_H - [H^+]} \tag{11}$$

[A], which is the concentration sought, can be derived from eqns. (10) and (11). If $C'_{HA}/C'_A = \delta$ we get

$$[A] = \frac{[H^+]'}{[H^+]} \cdot \frac{(C'_A + [H^+]') (\delta C'_A + C_H - [H^+])}{\delta C'_A - [H^+]'} \tag{12}$$

This expression can (Ahrland [10]) be simplified to

$$[A] = \frac{[H^+]'}{[H^+]} \left[C'_A + \frac{C_H - [H^+] + (1 + \delta) \cdot [H^+]'}{\delta} \right] \tag{13}$$

Eqn. (13) can be used for the computation of [A] except at the very lowest [A]-values.

As the total acetate concentration in the complex solution is $C_A = C'_A + [H^+] - C_H$, we get for the ligand number

$$\bar{n} = \frac{C'_A + [H^+] - C_H - [A]}{C_M}$$

The hydrogen ion concentration has been determined by a quinhydrone electrode. If E denotes the emf of the element in (15) and E' the emf of the same element when $C_M = 0$, we have at 20°C

$$E' - E = E_A = 58.16 \log \frac{[H^+]}{[H^+]'} \qquad (14)$$

CHEMICALS USED

Rare earth perchlorates. The perchlorates were prepared from *perchloric acid* (Baker's analyzed) and lanthanum chloride *puriss.*, cerium(III) chloride *puriss.*, neodymium oxide (quality "Specpure" from Johnson, Matthey and Co, London) and gadolinium nitrate (from A. D. Mackay, New York), respectively. The nitrate and the chlorides were evaporated several times with perchloric acid until no nitrate or chloride ions could be detected. The oxide was dissolved by heating with the acid. The greatest part of the excess of perchloric acid was removed by evaporation and the residue was determined by a potentiometric pH-titration.

The stock solutions were examined in a Beckman DU Spectrophotometer. No foreign elements with absorption in the wavelength range 2 000—9 000 Å could be detected. Cerium(IV) ions could not be found in the cerium(III) perchlorate.

The concentrations of lanthanum, neodymium and gadolinium were determined according to Berl-Lunge [11] by precipitating the rare earth as oxalate, igniting the precipitate and weighing the residue as oxide. The concentrations of lanthanum and neodymium were controlled by precipitation with 8-hydroxychinoline according to Pirtea [12]. The agreement between the values obtained by the oxalate and the hydroxychinoline method was very good. The cerium content was determined volumetrically according to Weiss and Sieger [13].

Sodium perchlorate with less than 0.01 % Cl^- and ClO_3^- was prepared from the quality *purum* by two recrystallizations according to Fronæus [7, p. 31].

Calculated amounts of *acetic acid (p. a.)* and *sodium acetate* (Baker's analyzed) were used for preparation of the buffer solutions. The concentrations of acid and acetate were controlled.

Quinhydrone was prepared according to Biilman and Lund [14].

EXPERIMENTAL

By potentiometric measurements the emf of elements of the following composition was determined.

Au	Quinhydrone 10.2 mM $HClO_4$ $NaClO_4$ to I = 2.0 M	2.0 M $NaClO_4$	Quinhydrone C_M mM $Me(ClO_4)_3$ $C_H = \nu \cdot C_M$ mM $HClO_4$ C'_A mM NaAc $C'_{HA} = \delta \cdot C'_A$ mM HAc $NaClO_4$ to I = 2.0 M	Au	(15)

Here Me^{3+}, Ac^- and I denote, respectively, rare earth ions, acetate ions and the ionic strength of the solution. The concentration of perchloric acid in the left half-cell was not quite the same in all series, but the exact value did not differ very much from 10.2 mM.

The solution in the right half-cell was prepared by adding a known volume of a buffer solution S_2 to a known volume of a solution S_1 with rare earth perchlorate.

	Solution S_1	Solution S_2	
$Me(ClO_4)_3$	C_M^0	0	mM
$HClO_4$	$C_H^0 = \nu \cdot C_M^0$	0	mM
NaAc	0	$C_A^0 = 1\,000$	mM
HAc	0	$C_{HA}^0 = \delta \cdot C_A^0$	mM
$NaClO_4$	$2\,000 - 6\ C_M^0 - C_H^0$	1 000	mM

The mixing of the solutions to be measured was brought about by a stream of nitrogen, free from oxygen but containing water vapour of the pressure prevailing over a 2 M solution of sodium perchlorate. During the experiments the solutions were kept in a thermostat at a constant temperature of 20°C. Every titration series was repeated at least once. For the potentiometric measurements a Leeds-Northrup »Students Potentiometer» was used. The emfs were stable and could be reproduced within 0.2 mV with very few exceptions. The uncertainty of the E_A-values is estimated to $\pm$ 0.2 mV.

MEASUREMENTS

As a check of the applicability of the quinhydrone electrode for pH-measurements in solutions with rare earth ions, a quinhydrone element with C_H = 90 mM ($HClO_4$) and C_M = 0 mM (I = 2.0 M) was mixed with different volumes of a neodymium perchlorate solution with very nearly the same content of acid as above (I = 2.0 M). A slight deviation, increasing with C_M, was found between the calculated and the measured emfs. At C_M = 15 mM the deviation was 0.3 mV and at C_M = 100 mM as high as 1.0 mV. The direction of the deviation was such that the hydrogen ion concentration of the neodymium solution became too high. This may indicate a slight complex formation between neodymium and hydroquinone. However, a positive conclusion cannot be drawn, because at least a part of the deviation may depend on a salt error of the quinhydrone electrode and on variations of f_{H^+} and the liquid junction potentials, caused by the medium changes.

In order to obtain another check of the E_A-values obtained by the quinhydrone electrode, two titration series were repeated using a hydrogen gas electrode. If hydroquinone complexes are formed, the hydrogen gas electrode should give lower E_A-values (E_A^H) than the quinhydrone electrode (E_A^Q). The difference $E_A^Q - E_A^H$ ought to be particularly significant at high C_M and low C_A. Tables 3 D and 5 E show that generally E_A^Q is greater than E_A^H, even at such high acetate concentrations that the hydroquinone complexes must have disappeared. This confirms that the formation of hydroquinone complexes is not the only reason for the disagreement between the two sets of E_A-values.

The plausible conclusion seems to be that if rare earth-hydroquinone complexes exist, they are so weak that they cannot cause serious errors in the complexity constants computed form E_A^Q.

In order to check the tendency of the unprotolyzed acetic acid to form complexes with the rare earth ions, the solutions I and II in the table below were examined extinctiometrically.

	Solution I	Solution II	
$Nd(ClO_4)_3$	50	50	mM
$HClO_4$	100	100	mM
$NaClO_4$	1 600	1 600	mM
HAc	0	2 500	mM

The two solutions gave extinction curves that were practically identical in the wave length range 3 000—9 000 Å. Therefore, complexes with the unprotolyzed acetic acid can be excluded.

The hydrated rare earth ions (at least up to gadolinium) have only a very slight tendency to give off protons at pH <5 as shown by Moeller [15] and Fronæus [16]. This conclusion must be drawn also from the investigations related to in the present paper. The concentration of acetic acid of the buffer solutions used in the titration series has been varied widely, but the $\bar{n}/[A]$-functions of the acetate systems show no tendency to depend on the pH of the complex solutions.

On account of the complex formation the ionic strength of the solutions we measure decreases considerably at higher C_M. This causes a certain error in E_A and then also in $\bar{n}/[A]$. We can eliminate this error by determining $\bar{n}/[A]$-functions for different C_M and extrapolating them to $C_M = 0$. This method, however, is rather time-consuming as it requires several series of measurement, and, moreover, it cannot be used if we want to determine complexity constants for dinuclear complexes. In the present investigation the decrease of ionic strength has been compensated by addition of a calculated amount of sodium perchlorate. The change of emf, ΔE_A, obtained in this way, has then been plotted in a diagram against ΔI, the decrease in ionic strength. The increase in volume caused by the added perchlorate requires only a slight correction of ΔE_A. Measurements of this kind have been carried out with some rare earth acetate systems at different C_M. They have given practically the same connection between ΔE_A and ΔI.

$$\Delta E_A = 5.0 \cdot \Delta I \tag{16}$$

(ΔE_A in mV and ΔI in M). ΔI has been computed according to formula (17) from $\bar{n}$, calculated with the aid of uncorrected E_A-values.

$$\Delta I = 0.5\ C_M \cdot \bar{n}\ (7 - \bar{n}) \tag{17}$$

This formula is derived with the assumption that the solution contains only the complex $MA_{\bar{n}}^{3-\bar{n}}$ ($\bar{n}$ is the ligand number). However, assuming that four complexes are formed, the correct expression for ΔI is

$$\Delta I = C_M(3\alpha_1 + 5\alpha_2 + 6\alpha_3 + 6\alpha_4) \tag{18}$$

α is the distribution of the central ions between the particular complexes (eqn. 6). In order to be able to use eqn. (18), we must know at least approximate values of the complexity constants. However, calculations have shown

Table 1. Determination of E' as a function of C'_A for the different acetate buffers used.

↓ Buffer	C'_A mM →	9.90	29.1	74.1	130.4	230.7	333	444	546	$K_c \times 10^{+5}$ at $C'_A \approx$ 100 mM
$\delta = 0.5$	E' mV →	180.2	180.1	180.0	180.0	179.9	179.9	179.9	179.9	1.64
$\delta = 2.0$	E' mV →	145.1	145.0	144.9	144.8	144.6	144.6	144.6	144.7	1.65
$\delta = 5.0$	E' mV →	121.8	121.6	121.3	121.1	120.9	120.8	120.9	121.0	1.68

that the eqns. (17) and (16) give ΔE_A-values, which at most are only 0.2 mV higher than ΔE_A computed with ΔI from eqn. (18). As there are probably other errors in E_A on account of the medium changes, which we have no possibility of making corrections for, eqn. (17) gives a value of ΔI that is accurate enough.

The emf E' in eqn. (14) has been determined at different C'_A by measuring the emf of the element (15) with $C_M = 0$. The E'-values for the buffers used are shown in Table 1. The measurements show that the emf varies slightly when the perchlorate is gradually exchanged for acetate buffer. Additions of the most acid buffer have an especially great influence. The reason for the change of emf may be that the medium changes cause variations of the liquid junction potentials and of the activity coefficients of the hydrogen ions and the quinhydrone components. Under the presumption that E' is changed in the same way when rare earth ions are present in the solution, the variation of E' does not affect the results, as only the E_A-values are used for the computations (except for determination of the correction terms of eqn. (12)).

1. The lanthanum acetate system

The experimentally obtained values of E_A and the values of [A] and $\bar{n}$/[A] calculated from $E_A - \Delta E_A$ are collected in Tables 2A-D. The second term in the E_A-columns is the correction term ΔE_A in eqn. (16), which must be subtracted from the first term, the experimentally determined E_A-value to compensate for the reduction of the ionic strength.

Fig. 1 shows that the agreement between the $\bar{n}$/[A]-values from series with different C_M is so good that polynuclear complexes can be formed only to a very slight extent.

For the lanthanum acetate system, as for the following complex systems in this paper, the $\bar{n}$/[A]-values are independent of the ratio C'_{HA}/C'_A of the buffer solutions.

By graphical integration of the fulldrawn curve in Fig. 1, the function X in Table 4A has been computed and after that the functions $X_1 \ldots X_4$ and the complexity constants. As the lanthanum acetate system, like the other

Table 2. Determination of corresponding values of [A] and $\bar{n}$/[A] for the lanthanum acetate system.

$C_M = C_M^\circ(1 - C'_A \times 10^{-3})$ mM

	A C_M° = 50.6 mM $C_H = 4.25 \times 10^{-3} \times C_M$ mM Buffer ½ : 1 Sign □			B C_M° = 75.5 mM $C_H = 2.12 \times 10^{-3} \times C_M$ mM Buffer ½ : 1 Sign △		
C'_A mM	E_A mV	[A] mM	$\frac{\bar{n}}{[A]}$ M^{-1}	E_A mV	[A] mM	$\frac{\bar{n}}{[A]}$ M^{-1}
9.90	26.9	3.55	34.6	33.3	2.73	34.6
19.61	24.9—0.1	7.50	32.0	31.8—0.2	5.69	32.7
38.5	22.4—0.3	16.21	27.9	29.5—0.4	12.24	29.4
56.6	20.5—0.4	25.7	25.0	27.7—0.6	19.46	26.7
90.9	17.6—0.6	46.6	20.6	24.6—0.8	35.5	22.7
122.8	15.4—0.7	68.9	17.6	22.0—1.0	53.6	19.5
152.5	13.7—0.8	91.8	15.4	19.9—1.1	72.6	17.2
200.0	11.5—0.9	131.7	12.8	17.0—1.2	107.1	14.3
285.7	8.6—0.9	210.9	9.8	12.9—1.3	180.6	10.8
375	6.5—0.8	299.5	8.0	9.8—1.2	267	8.6
500	4.5—0.7	430	6.4	6.7—1.0	399	6.7
	C C_M° = 50.6 mM $C_H = 4.25 \times 10^{-3} \times C_M$ mM Buffer 2:1 Sign ■			D C_M° = 75.5 mM $C_H = 2.12 \times 10^{-3} \times C_M$ mM Buffer 2:1 Sign ▲		
C'_A mM	E_A mV	[A] mM	$\frac{\bar{n}}{[A]}$ M^{-1}	E_A mV	[A] mM	$\frac{\bar{n}}{[A]}$ M^{-1}
9.90	25.7	3.62	34.0	32.7	2.73	34.8
29.13	23.0—0.2	11.86	29.5	30.5—0.3	8.84	31.2
47.6	21.2—0.3	20.85	26.5	28.4—0.5	15.81	27.9
74.1	18.8—0.5	36.0	22.5	26.1—0.7	27.1	24.7
107.1	16.4—0.6	57.4	19.1	23.2—0.9	44.4	21.0
166.7	12.9—0.8	103.3	14.5	18.8—1.2	83.1	16.0
230.7	10.3—0.9	159.1	11.6	15.3—1.3	132.6	12.7
333	7.3—0.8	258	8.7	11.1—1.3	226	9.4
444	5.2—0.7	372	6.9	7.9—1.1	340	7.4
546	3.8—0.6	481	5.9	5.8—0.9	449	6.2
583	3.4—0.5	520	5.8	—	—	—

systems of this paper, shows no tendency to stop its complex formation at $\bar{n} = 3$ (*cf.* Fig. 2), four constants have been computed.

In Table 9 the experimentally determined ligand number $\bar{n}_{exp}$, the computed ligand number $\bar{n}_c$ and the distribution of the central ion between the particular complexes are given for some values of [A].

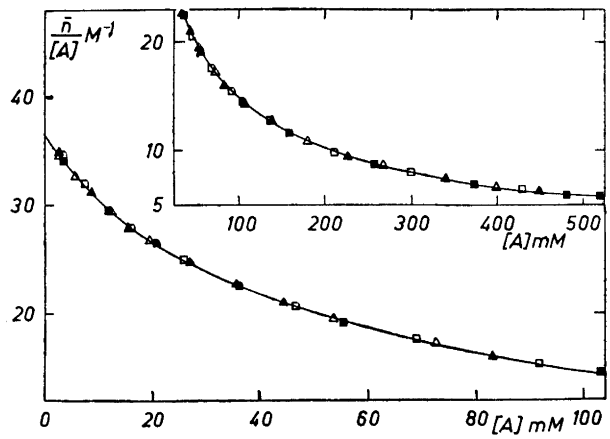

Fig. 1. $\bar{n}/[A]$ as a function of [A] for the lanthanum acetate system. The signs refer to the corresponding series in Table 2.

2. The cerium(III) acetate system

Experiments and calculations for the cerium acetate system were performed in the same way as for the preceding system. The results are to be found in Tables 3A—D and 4B. The complex formation curve is shown in Fig. 2.

Also for this system the coincidence between the $\bar{n}/[A]$-curves of the different series is so good that polynuclear complexes can be formed only to a very slight extent.

In order to check the applicability of the quinhydrone electrode, the quinhydrone series in 3D was repeated with a hydrogen gas electrode, which gave the E_A^H-values in the same table. The maximum discrepancy between uncorrected E_A^Q and E_A^H is 0.5 mV. A possible cause of this difference has been discussed on page 170.

3. The neodymium acetate system

The results obtained for this system are collected in Tables 5A-E and 7A. For this system, too, we can exclude formation of polynuclear complexes.

The series 5E was performed with both quinhydrone electrode and hydrogen gas electrode. The maximum difference $E_A^Q - E_A^H$ is + 0.8 mV.

4. The gadolinium acetate system

Measurements and calculations for this system were performed in the same way as in the foregoing systems. The results are shown in Tables 6A—D and 7B and in Fig. 3.

Table 3. Determination of corresponding values of [A] and $\bar{n}$/[A] for the cerium(III) acetate system.

$C_M = C^\circ_M(1 - C'_A \times 10^{-3})$ mM

	A C°_M = 25.0 mM C_H = 5.24 × 10^{-2} × C_M mM Buffer 5 : 1 Sign ○			B C°_M = 50.0 mM C_H = 5.24 × 10^{-2} × C_M mM Buffer 2 : 1 Sign ■		
C'_A mM	E_A mV	[A] mM	$\frac{\bar{n}}{[A]}$ M^{-1}	E_A mV	[A] mM	$\frac{\bar{n}}{[A]}$ M^{-1}
9.90	22.3	4.23	43.6	40.5	2.25	46.8
19.61	18.8—0.1	9.51	38.5	33.8—0.2	5.52	43.0
38.5	15.1—0.3	21.6	30.3	28.2—0.3	13.16	36.1
56.6	12.9—0.3	34.6	25.6	24.8—0.4	22.0	31.0
90.9	10.2—0.4	61.9	19.8	20.6—0.6	41.7	24.7
130.4	8.2—0.4	96.0	16.0	16.7—0.8	70.1	19.9
200.0	5.9—0.4	161.1	11.7	12.4—0.9	127.6	13.8
285.7	4.3—0.4	245.1	9.1	8.9—0.9	208.9	10.1
375	3.3—0.4	334.5	7.6	6.6—0.8	299	8.0
500	2.2—0.3	464	6.1	4.4—0.7	433	6.1
546	1.9—0.3	512	5.6	—	—	—

	C C°_M = 50.0 mM C_H = 5.24 × 10^{-2} × C_M mM Buffer ½ : 1 Sign □			D C°_M = 75.0 mM C_H = 5.24 × 10^{-2} × C_M mM Buffer 5 : 1 Sign △			
C'_A mV	E_A mV	[A] mM	$\frac{\bar{n}}{[A]}$ M^{-1}	E^0_A mV	E^H_A mV	[A] mM	$\frac{\bar{n}}{[A]}$ M^{-1}
9.90	48.2	2.23	46.5	49.9	50.0	1.480	46.6
29.13	33.6—0.2	9.12	39.6	39.3—0.3	38.9	6.39	41.5
47.6	28.5—0.3	17.23	34.0	35.2—0.5	35.0	12.26	36.4
74.1	23.7—0.5	31.5	27.5	30.9—0.7	30.6	22.65	30.5
107.1	19.7—0.7	52.7	22.1	26.8—0.9	26.3	38.7	25.1
166.7	14.8—0.8	98.3	16.1	21.1—1.2	20.5	76.2	18.4
230.7	11.4—0.9	155.0	12.4	16.4—1.3	16.2	127.3	13.7
333	7.9—0.8	254	9.1	11.5—1.3	11.7	223	9.7
444	5.7—0.8	368	7.3	8.0—1.1	8.3	339	7.3
546	4.0—0.7	481	5.7	5.6—0.9	5.5	453	5.9
583	—	—	—	5.0—0.9	—	496	5.5

For this system the values of $\bar{n}$/[A] at low [A] show a slight tendency to increase with C_M. This may indicate a slight formation of polynuclear complexes. However, the value of β'_1 computed according to eqn. (9b) will be as low as 30 ± 20, and therefore the existence of dinuclear complexes must be considered as rather uncertain. The $\bar{n}$/[A]-function used for the computation of the complexity constants has been drawn in accordance to the lower $\bar{n}$/[A]-values at low [A].

Table 4. The X-functions of the lanthanum (A) and the cerium (B) acetate systems, obtained by graphical integrations of the $\bar{n}$/[A]-functions.

[A] mM	A The lanthanum acetate system					B The cerium acetate system				
	X ([A])	X_1 M^{-1}	X_2 M^{-2}	X_3 M^{-3}	X_4 M^{-4}	X ([A])	X_1 M^{-1}	X_2 M^{-2}	X_3 M^{-3}	X_4 M^{-4}
0	*1*	*36.3*	*296*	*950*	*850*	*1*	*48.4*	*485*	*1 350*	*1 600*
2	1.0740	37.0				1.0987	49.4			
6	1.230	38.2				1.310	51.6			
12	1.481	40.1				1.658	54.8			
20	1.853	42.7				2.178	58.9			
30	2.384	46.1	327			2.926	64.2	525		
50	3.688	53.8	350			4.81	76.2	556		
70	5.365	62.4	373			7.24	89.2	585		
100	8.67	76.7	404			12.14	111.4	630		
140	14.87	99.1	449			21.55	147	705		
200	29.2	141	523	1 135		43.4	212	820	1 670	1 600
300	71.1	234	655	1 200	840	108.8	359	1 040	1 840	1 630
400	144.9	360	810	1 280	830	226	563	1 290	2 000	1 620
500	266	529	985	1 380	860	414	826	1 560	2 140	1 580

DISCUSSION OF THE RESULTS

The complexity constants of the systems investigated are collected in Table 8. Table 9 gives for all four systems a comparison between determined and calculated ligand numbers ($\bar{n}_{exp}$ resp. $\bar{n}_c$) and information about the calculated distribution of the central ion between the particular complexes at some [A]-values (eqns. 6 and 7).

The limits of error given in Table 8 refer to the maximum random errors. For the four acetate systems so far examined, the potentiometric measurements have given a fourth complexity constant, the random error of which may be

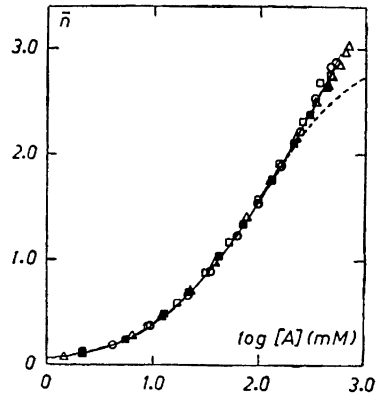

Fig. 2. The complex formation curve of the cerium acetate system. The fulldrawn curve is computed by use of β_1—β_4 and the broken curve by use of β_1—β_3 only.

Table 5. Determination of corresponding values of [A] and $\bar{n}$/[A] for the neodymium acetate system.

$C_M = C^\circ_M\ (1 - C'_A \times 10^{-3})$ mM

	A C°_M = 25.0 mM $C_H = 1.40 \times 10^{-3} \times C_M$ mM Buffer ½ : 1			B C°_M = 50.0 mM $C_H = 1.40 \times 10^{-3} \times C_M$ mM Buffer ½ : 1			C C°_M = 75.5 mM $C_H = 1.40 \times 10^{-3} \times C_M$ mM Buffer ½ : 1		
C'_A mM	E_A mV	[A]mM	$\frac{\bar{n}}{[A]}$ M^{-1}	E_A mV	[A]mM	$\frac{\bar{n}}{[A]}$ M^{-1}	E_A mV	[A]mM	$\frac{\bar{n}}{[A]}$ M^{-1}
9.90	27.5—0.1	3.58	67.7	42.9—0.1	2.06	70.4	54.9—0.1	1.36	74.5
19.61	23.5—0.1	8.04	57.1	38.4—0.2	4.61	63.5	49.7—0.2	3.05	69.2
38.5	18.4—0.3	19.11	41.5	33.0—0.4	10.95	51.0	44.2—0.4	7.14	58.6
56.6	15.2—0.3	31.7	32.8	28.8—0.5	18.89	41.6	40.1—0.6	12.26	49.7
90.9	11.5—0.4	59.0	23.6	22.9—0.7	38.3	29.8	33.6—0.9	25.4	37.0
130.4	8.9—0.5	93.9	17.7	18.1—0.8	66.4	22.0	27.4—1.2	46.9	26.8
200.0	6.3—0.5	159.5	12.6	13.1—0.9	124.1	15.2	20.0—1.4	96.6	17.6
285.7	4.5—0.4	243.3	9.7	9.4—0.9	204.8	10.5	14.3—1.4	172.4	12.1
375	3.3—0.4	334.5	7.7	6.9—0.8	295	8.6	10.5—1.3	261	9.2
500	2.3—0.4	464	6.2	4.5—0.7	431	6.4	7.0—1.1	397	6.9
546	1.9—0.3	512	5.7	3.7—0.6	483	5.7	5.9—1.0	450	6.1

	D C°_M = 75.5 mM $C_H = 1.40 \times 10^{-2} \times C_M$ mM Buffer 5 : 1			E C°_M = 100.0 mM $C_H = 1.40 \times 10^{-2} \times C_M$ mM Buffer 5 : 1			
C'_A mM	E_A mV	[A] mM	$\frac{\bar{n}}{[A]}$ M^{-1}	E^Q_A mV	E^H_A mV	[A] mM	$\frac{\bar{n}}{[A]}$ M^{-1}
9.90	49.3—0.1	1.44	74.1	56.7—0.2	56.1	1.091	75.8
29.13	44.5—0.3	5.10	62.8	52.3—0.4	51.8	3.76	67.4
47.6	40.6—0.5	9.78	53.0	48.9—0.6	48.3	7.08	59.0
74.1	35.5—0.8	18.81	41.5	44.1—0.9	43.5	13.45	48.0
107.1	30.1—1.0	33.9	31.7	38.7—1.3	37.9	24.4	37.5
166.7	22.7—1.3	71.5	21.0	30.2—1.6	29.7	53.8	25.0
230.7	17.4—1.4	122.6	15.1	23.4—1.8	23.0	98.2	17.4
333	12.0—1.4	219.2	10.3	16.2—1.8	15.8	188.7	11.2
444	8.3—1.2	336	7.7	11.1—1.6	11.0	305	8.2
546	5.8—1.0	451	6.1	7.9—1.3	8.1	420	6.5
630	—	—	—	6.0—1.1	—	519	5.8

estimated to about 40 %. Thus, it seems to be possible to give at least the order of magnitude of the fourth constant.

As to the systematic errors, they apparently do not affect the determination of the lower constants, as the three first complexity constants of the cerium(III) acetate system found by Fronæus [1] in a cation exchange investigation are in good agreement with the constants obtained by the author. The two sets of constants are given in Table 10. The constants published by Fron-

Table 6. Determination of corresponding values of [A] and $\bar{n}$/[A] for the gadolinium acetate system.

$C_M = C_M^\circ\ (1 - C_A' \times 10^{-3})$ mM						
	A C_M° = 23.6 mM C_H = 8.30 × 10^{-2} × C_M mM Buffer ½ : 1 Sign ○			B C_M° = 47.2 mM C_H = 6.37 × 10^{-2} × C_M mM Buffer ½ : 1 Sign □		
C_A' mM	E_A mV	[A] mM	$\frac{\bar{n}}{[A]}$ M^{-1}	E_A mV	[A] mM	$\frac{\bar{n}}{[A]}$ M^{-1}
9.90	36.6	3.23	63.1	56.5 − 0.1	1.69	67.1
19.61	28.2 − 0.1	7.74	55.6	45.2 − 0.2	4.29	62.6
38.5	21.6 − 0.3	18.17	44.7	37.3 − 0.4	10.26	54.4
56.6	17.9 − 0.4	30.2	36.6	32.8 − 0.6	17.68	45.8
90.9	13.5 − 0.4	56.2	27.2	26.3 − 0.8	35.1	35.1
122.8	10.8 − 0.5	83.9	21.4	21.6 − 0.9	56.5	27.2
152.5	8.9 − 0.5	111.7	17.5	18.2 − 0.9	79.5	22.2
200.0	7.0 − 0.5	157.0	14.0	14.3 − 1.0	121.0	16.7
285.7	4.8 − 0.4	242.4	10.2	9.8 − 0.9	203.8	11.6
375	3.5 − 0.4	334	8.1	6.9 − 0.8	298	8.6
500	2.2 − 0.3	466	6.1	4.5 − 0.7	433	6.4
	C C_M° = 23.6 mM C_H = 8.30 × 10^{-2} × C_M mM Buffer 5 : 1 Sign ●			D C_M° = 47.2 mM C_H = 3 × 10^{-5} × C_M mM Buffer 5 : 1 Sign ■		
C_A' mM	E_A mV	[A] mM	$\frac{\bar{n}}{[A]}$ M^{-1}	E_A mV	[A] mM	$\frac{\bar{n}}{[A]}$ M^{-1}
9.90	28.9	3.29	63.9	34.9 − 0.1	2.51	65.9
29.13	21.8 − 0.2	12.58	51.3	32.3 − 0.3	8.22	56.2
47.6	17.9 − 0.3	23.9	40.8	29.4 − 0.5	15.18	47.9
74.1	14.3 − 0.4	43.0	31.3	25.3 − 0.7	27.9	38.0
107.1	11.2 − 0.5	70.4	23.6	21.2 − 0.8	47.8	29.5
137.9	9.2 − 0.5	98.0	19.2	17.9 − 0.9	70.4	23.6
166.7	7.8 − 0.5	125.2	16.2	15.4 − 1.0	94.3	19.6
230.7	5.7 − 0.5	188.1	12.0	11.2 − 1.0	153.4	13.9
333	3.9 − 0.4	290.5	9.1	7.6 − 0.9	255.5	9.7
444	2.7 − 0.4	406	7.0	5.1 − 0.8	375	7.1
546	1.9 − 0.3	512	5.9	3.6 − 0.6	485	5.9

æus as obtained potentiometrically by the present author are those calculated without correction for the decrease of the ionic strength, and therefore they differ somewhat from the figures given below.

The fourth constant, however, seems to be rather dubious, as Fronæus found that anionic complexes are not formed to a detectable amount at acetate ion concentrations < 500 mM. This result is, moreover, supported by anion exchange measurements, Fronæus [17]. It is possible that the small

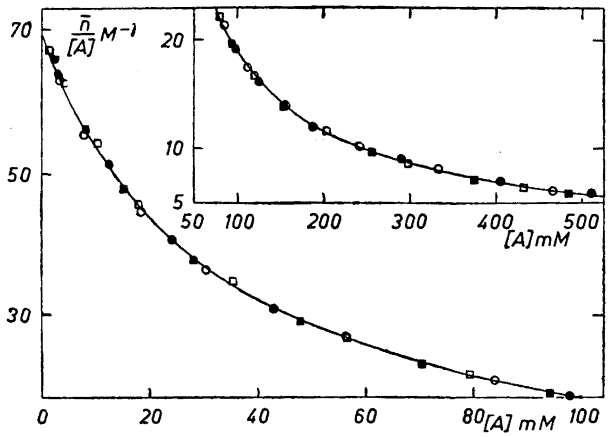

Fig. 3. The connection between $\bar{n}$/[A] and [A] for the gadolinium acetate system, according to the titration series in Table 6.

E_A-values at high ligand concentrations contain so great systematic errors that the fourth complexity constant is only imaginary. If so the complex formation curve for the cerium acetate system is represented by the broken curve in Fig. 2.

In order to exclude the dubious fourth complex, the composition of the complexity systems has been given in Table 9 only at low ligand concentrations.

Table 7. The X-functions of the neodymium (A) and the gadolinium (B) acetate systems.

	A The neodymium acetate system					B The gadolinium acetate system				
[A] mM	X ([A])	X_1 M^{-1}	X_2 M^{-2}	X_3 M^{-3}	X_4 M^{-4}	X ([A])	X_1 M^{-1}	X_2 M^{-2}	X_3 M^{-3}	X_4 M^{-4}
0	*1*	*79.7*	*1 020*	*2 850*	*3 600*	*1*	*69.3*	*1 320*	*5 200*	*5 000*
2	1.1635	81.8				1.1439	72.0			
6	1.518	86.3				1.465	77.5			
12	2.112	92.6				2.036	86.3			
20	3.028	101.4	1 085			2.972	98.6	1 460		
30	4.395	113.2	1 115			4.440	114.7	1 510		
50	7.92	138.5	1 170			8.53	150.7	1 630		
70	12.65	166.5	1 240			14.43	191.8	1 750		
100	22.45	214.5	1 350			27.3	263	1 940		
140	41.6	290	1 500			53.6	376	2 190		
200	86.5	428	1 740	3 600		118.2	586	2 580	6 300	
300	223	740	2 200	3 930	3 600	322	1 070	3 330	6 700	5 000
400	471	1 175	2 740	4 300	3 630	700	1 750	4 200	7 200	5 000
500	882	1 760	3 360	4 690	3 680	1 32	2 640	5 130	7 650	4 900

Table 8. The complexity constants of the systems investigated.

System	β_1 M^{-1}	β_2 M^{-2}	β_3 M^{-3}	β_4 M^{-4}
$La^{3+} - Ac^-$	36 ± 1	300 ± 30	950 ± 200	~ 900
$Ce^{3+} - Ac^-$	48 ± 1	490 ± 50	1 350 ± 250	~ 1 500
$Nd^{3+} - Ac^-$	80 ± 3	1 020 ± 100	2 900 ± 500	~ 3 500
$Gd^{3+} - Ac^-$	69 ± 2	1 320 ± 150	5 200 ± 1 000	~ 5 000

Table 9. Experimentally determined ligand numbers ($\bar{n}_{exp}$), calculated ligand numbers ($\bar{n}_c$), and the composition of the acetate systems with the assumption that only three complexes are formed.

[A] mM	Rare earth	$\bar{n}_{exp}$	$\bar{n}_c$	100 α_0	100 α_1	100 α_2	100 α_3
10	La^{3+}	0.30	0.30	72.0	25.9	2.1	—
	Ce^{3+}	0.39	0.38	65.4	31.4	3.2	—
	Nd^{3+}	0.53	0.53	52.5	42.0	5.4	0.1
	Gd^{3+}	0.54	0.53	54.7	37.8	7.2	0.3
50	La^{3+}	1.00	1.00	27.3	49.1	20.4	3.2
	Ce^{3+}	1.12	1.12	20.8	50.1	25.6	3.5
	Nd^{3+}	1.29	1.27	12.5	49.9	33.1	4.5
	Gd^{3+}	1.46	1.43	11.9	41.1	39.3	7.7
100	La^{3+}	1.48	1.46	11.7	42.1	35.1	11.1
	Ce^{3+}	1.57	1.55	8.3	39.8	40.7	11.2
	Nd^{3+}	1.72	1.68	4.5	36.2	46.2	13.1
	Gd^{3+}	1.92	1.86	3.8	26.2	50.2	19.8

Table 10. The complexity constants of the cerium(III) acetate system determined by

	the potentiometric method	the cation exchange method
β_1	48 ± 1 M^{-1}	48 ± 2 M^{-1}
β_2	490 ± 50 M^{-2}	450 ± 80 M^{-2}
β_3	1 350 ± 250 M^{-3}	1 700 ± 500 M^{-3}
β_4	1 600 ± 600 M^{-4}	—

At [A] = 100 mM β_4 would give 100 . α_4 = 1.0 and 1.6 for the lanthanum and the gadolinium systems, respectively.

Table 8 shows that the stability of the first complex increases from lanthanum to neodymium, as is to be expected from the decreasing ionic radius, whereas gadolinium gives a considerably weaker first complex than neodymium. The gadolinium complexes number two and three, however, are stronger than the corresponding neodymium complexes.

A more detailed discussion must be postponed until other acetate systems have been examined.

Professor Sven Bodforss, who has been my teacher in chemistry, suggested this investigation to me. I am very indebted to him for the valuable aid he has given me in different respects and for the interest he has always shown in my work.

Moreover, I wish to thank Dr. Sture Fronæus and Dr. Sten Ahrland for many fruitful discussions and valuable suggestions.

REFERENCES

1. Fronæus, S. *Svensk Kem. Tidskr.* **65** (1953) 19.
2. Herlinger, E. *Z. Krist.* **93** (1936) 399; *cf.* Templeton, D. H. and Dauben, C. H. *J. Am. Chem. Soc.* **76** (1954) 5237.
3. Wheelwright, E. J., Spedding, F. H. and Schwarzenbach, G. *J. Am. Chem. Soc.* **75** (1953) 4196.
4. Schwarzenbach, G., Gut, R. and Anderegg, G. *Helv. Chim. Acta* **37** (1954) 937.
5. Spedding, F. H., Powell, J. E. and Wheelwright, E. J. *J. Am. Chem. Soc.* **78** (1956) 34.
6. Vickery, R. C. *J. Chem. Soc.* **1952** 421, 1895.
7. Fronæus, S. *Komplexsystem hos koppar* (Diss.) Lund 1948.
8. Bjerrum, J. *Metal Ammine Formation in Aqueous Solution* (Diss.) Copenhagen 1941.
9. Leden, I. *Potentiometrisk undersökning av några kadmiumsalters komplexitet.* (Diss.) Lund 1943.
10. Ahrland, S. *Acta Chem. Scand.* **5** (1951) 199.
11. Berl-Lunge, *Chemisch-technische Untersuchungsmethoden* 8th Ed., Berlin 1932, Vol. II:2, p. 1631.
12. Pirtea, Th. *Z. anal. Chem.* **107** (1936) 191.
13. Weiss, L. and Sieger, H. *Z. anal. Chem.* **113** (1938) 305, p. 314.
14. Biilmann, E. and Lund, H. *Ann. chim.* (9) **16** (1921) 339.
15. Moeller, Th. *J. Phys. Chem.* **50** (1946) 242.
16. Fronæus, S. *Svensk Kem. Tidskr.* **64** (1952) 317, p. 319.
17. Fronæus, S. *Svensk Kem. Tidskr.* **65** (1953) 1.

Received October 12, 1957.

ACTA CHEMICA SCANDINAVICA 12 (1958) 182—187

On Ion Exchange Equilibria

V. An Approximate Method for Calculating the Partial Molar Volumes of the Species in Ion Exchangers *

ERIK HÖGFELDT**

Brookhaven National Laboratory, Upton, L.I., N.Y., U.S.A.

By formally regarding an ion exchange system as a binary mixture of the two resin forms, partial molar volumes can be determined using the intercept method of Roozeboom. This method has been applied to the potassium-tetramethylammonium exchange on resins with DVB content 2, 10 and 26 %, reported by Gregor, Gutoff and Bregman. It is surprising to find that, to a first approximation all three systems have an ideal volume of mixing over the large range of variation, 1.3 to 18, in total molality of the resin.

Boyd *et al.* [1,2] have recently calculated equilibrium quotients for ion exchange equilibria using rigorous thermodynamics. In these calculations there is need for evaluation of a term $p(Z_B\overline{V}_A - Z_A\overline{V}_B)$ where p is the swelling pressure. $\overline{V}_A$ and $\overline{V}_B$ are the partial molar volumes of the two ionic resin forms, and Z_A, Z_B are their respective charges. Methods for calculating the swelling pressure have been described [3,4]. A method for obtaining the partial molar volume *difference* using cross differentiation relationships has recently been given by Myers and Boyd[1].

It is the aim of this paper to show how the partial molar volumes themselves can be obtained, by using the approximation that the partial molar volume of water is a constant.

The volume, V, of a resin (in this case a cation exchanger exchanging monovalent ions) is made up of three components:

$$\overline{V} = N_{AR}\overline{V}_{AR} + N_{BR}\overline{V}_{BR} + N_{WR}\overline{V}_{WR} \qquad (1)$$

* Research performed under the auspices of the U.S. Atomic Energy Commission.

** On leave of absence from the Department of Inorganic Chemistry, Royal Institute of Technology, Stockholm, Sweden.

where N_{AR}, N_{BR} and N_{WR} are the number of moles of the three components A^+R^-, B^+R^- and water and $\overline{V}_{AR}$, $\overline{V}_{BR}$, $\overline{V}_{WR}$ their partial molar volumes. By dividing all terms with the capacity of the resin (S_o) (1) is transformed to:

$$V_e = \frac{V}{S_o} = X_{AR}\overline{V}_{AR} + X_{BR}\overline{V}_{BR} + X_{WR}\overline{V}_{WR} \quad (2)$$

where V_e = the equivalental volume

X_{AR}, X_{BR} are the mole fractions of the resin forms A^+R^- and B^+R^-

X_{WR} = the number of moles of water per equivalent of resin; no water is assumed to belong to the ions as water of hydration.

Now, Gregor *et al.*[5] as well as Boyd *et al.*[1,2] have shown that the partial molar volume of water is constant for each ionic form provided the water content of the resin is not too small. According to Boyd *et al.* $\overline{V}_{WR}$ remains constant down to $X_{WR} = 4$. Water contents as low as $X_{WR} = 4$ are never encountered when one deals with moderately cross-linked ion exchange resins in equilibrium with a water phase. Even a 26% DVB resin [6] contains more than 6 moles of water per equivalent of resin, so that on the basis of these results the constancy of $\overline{V}_{WR}$ is a good approximation even for this rather extreme case. Thus in view of the fact that the partial molar volume of water is practically the same for several different ions [5], it is reasonable to assume that the partial molar volume of water is constant. Using this assumption eqn. (2) can be rearranged to give:

$$V_e - X_{WR}\overline{V}_{WR} = \Delta V = X_{AR}\overline{V}_{AR} + X_{BR}\overline{V}_{BR} \quad (3)$$

ΔV can now be calculated using a known value for V_{WR}. According to eqn. (3) we can formally regard the resin as a binary mixture of A^+R^- and B^+R^-. By plotting ΔV against the mole fractions of the resin species, the partial molar volumes can be obtained from the intercepts of the tangent to the curve with the axes $X_{AR} = 1$ and $X_{BR} = 1$ [7,8].

In order to illustrate the method, we apply it to the data for the potassium-tetramethylammonium exchange on resins with DVB contents 2, 10 and 26 %, reported by Gregor, Gutoff and Bregman [6]. For V_{WR} we adopt the value 17.20, the mean of the two values, 17.15 for tetramethylammonium resin and 17.25 for potassium resin, reported by Gregor, Sundheim, Held and Waxman [5]. The resins used by the latter were not the same as those used by Gregor, Gutoff and Bregman. However, the resins were of the same type, being polystyrene sulfonic acid resins, and the assumption that the partial molar volume of water is the same for both sets of resins is a reasonable one. It is also assumed that the partial molar volume of water is independent of swelling pressure, which is a good approximation, since the difference between the partial molar volumes of water at 100 and 1 000 atmospheres is only 4 % [4].

In Figs. 1—3 V_e and ΔV are plotted against X_{KR} for the three different crosslinkings. It is interesting to note that straight lines are obtained in the ΔV-plots. This behavior implies, that to a first approximation all three systems behave ideally over a range between ~1.3 and ~18 in total molality of the resins.

The values obtained of the partial molar volumes obtained from the ΔV *vs* X plots are given in Table 1.

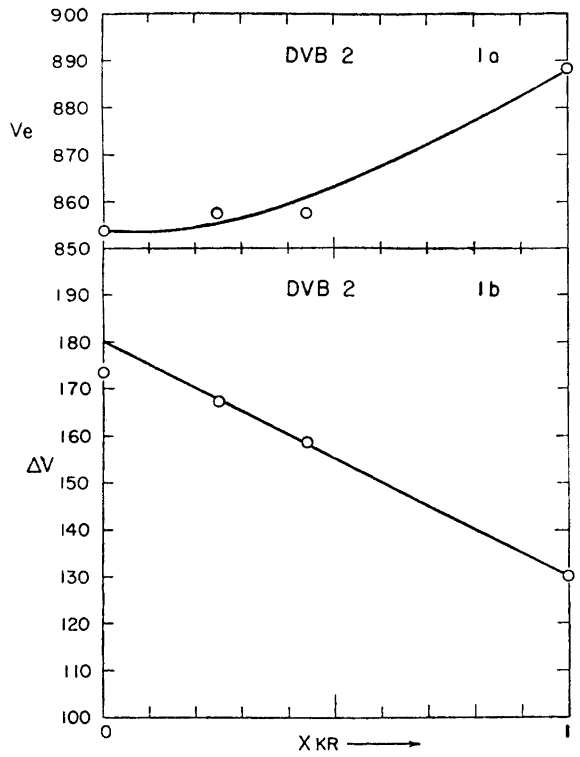

Fig. 1 a. The equivalental volume, V_e, plotted against the mole fraction of potassium, X_{KR}, in the DVB 2 resin.
Fig. 1 b. The function ΔV plotted against mole fraction of potassium, X_{KR}, in the DVB 2 resin.

Table 1. Partial molar volumes of potassium and tetramethylammonium forms in different resins; ml/equiv. of resin.

Method of evaluation	DVB 2		DVB 10		DV
	$\overline{V}_{KR}$	$\overline{V}_{(CH_3)_4NR}$	$\overline{V}_{KR}$	$\overline{V}_{(CH_3)_4NR}$	$\overline{V}_{KR}$
Extrapolation	130	180	114	154	140
Direct measurement	151	—	—	—	—

These values should be compared with directly determined volumes of pure moisture-free resinates. The measured value in Table 1 is that of Gregor *et al.*[6] who report only the dry volume for potassium saturated DVB 2.

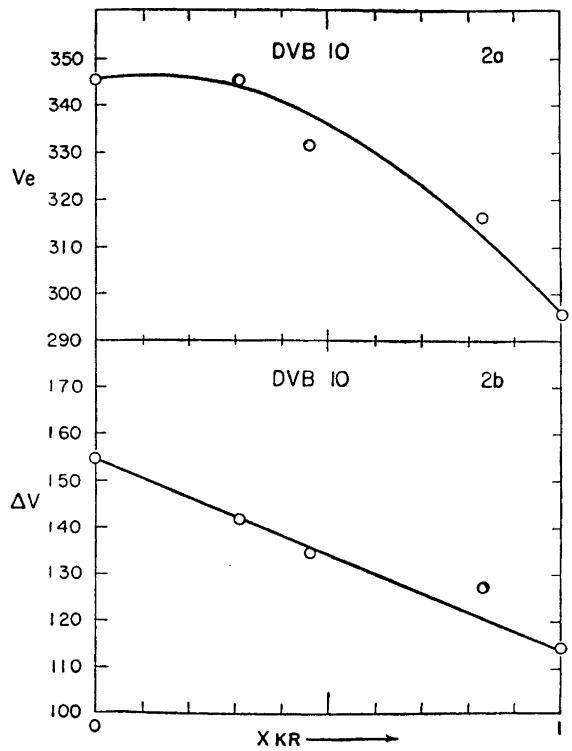

Fig. 2 a. The equivalental volume, V_e, plotted against the mole fraction of potassium, X_{KR}, in the DVB 10 resin.
Fig. 2 b. The function ΔV plotted against mole fraction of potassium, X_{KR}, in the DVB 10 resin.

As is seen from Table 1 the extrapolated volume is smaller than the directly measured volume, an effect previously noted by Gregor *et al.*[5,6] and Boyd and Soldano [4]. The latter authors ascribed it to a contraction in the total volume when the resin is allowed to swell in water. It is also seen from Table 1 that little correlation seems to exist between individual $\overline{V}$-values and degree of crosslinking or water content. However, the difference between the two partial molar volumes decreases with increasing DVB content. In Fig. 4 the partial molar volume difference is plotted against DVB content and average molality ($\overline{m}$) of resin. $\overline{m}$ is equal to the average value of the molalities for the two pure resinates. As is seen from Fig. 4 no straight line is obtained when the difference is plotted against DVB content, but a fairly good straight line is obtained when plotted against the average molality of the resin. The extrapolated value down to $\overline{m} = 0$ is 52 ml/equiv. which has no correlation with the atomic volume difference 76.1 ml/mole, given in Table VII in Ref.[6] No values for the partial molal volume difference at infinite dilution for potassium and

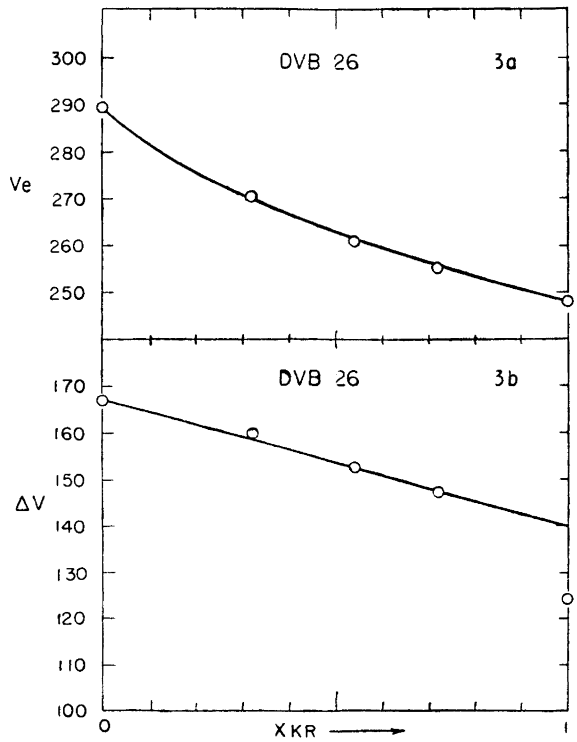

Fig. 3 a. The equivalental volume, V_e, plotted against the mole fraction of potassium, X_{KR} in the DVB 26 resin.
Fig. 3 b. The function ΔV plotted against the mole fraction of potassium, X_{KR}, in the DVB 26 resin.

tetramethylammonium salts with a common anion have been found, so no such comparison can be made. The ideal volume behavior of the potassium-tetramethylammonium system shows that the interaction between water and resin is independent of ionic composition.

If we make another choice of components such as $A^+R^-(H_2O)_m$ and $B^+R^-(H_2O)_n$ and water in order to split up the water content in water of hydration belonging to the ions and "free" water, again straight lines are obtained in the ΔV *vs* X_{KR} plots as this only means that we add the constant quantity $(n + m)\overline{V}_{WR}$ to the original ΔV.

More measurements are needed to show how far the concept of ideal volume of mixing is valid for other systems and at what molalities deviations start to occur.

Acknowledgments. The author is indebted to Dr. William Rubinson for valuable discussions and for correcting the English text.

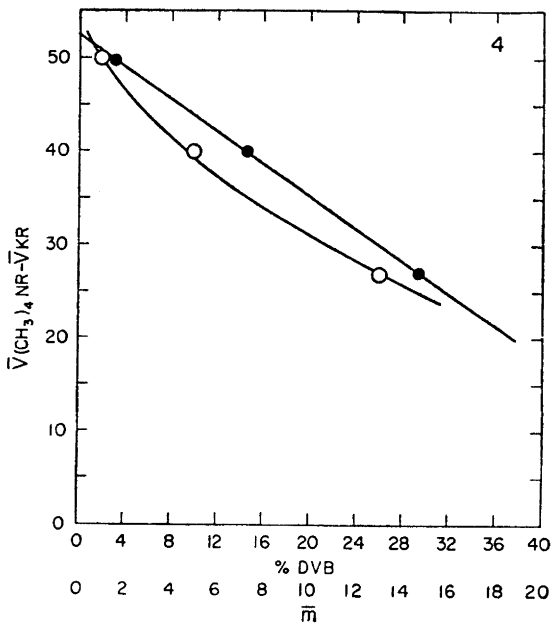

Fig. 4. The partial molar volume difference, $\overline{V}_{(CH_3)_4NR}-\overline{V}_{KR}$ plotted against: (a) DVB content of resins, O, (b) Average molality of resins, ●.

REFERENCES

1. Myers, G. E. and Boyd, G. E. *J. Phys. Chem.* **60** (1956) 521.
2. Boyd, G. E., Myers, G. E. and Lindenbaum, S. *ORNL-2159* (1956) 43; Boyd, G. E. *132nd Meeting, Am. Chem. Soc.* September 1957.
3. Glueckauf, E. *Proc. Roy. Soc. London* **A214** (1952) 207.
4. Boyd, G. E. and Soldano, B. A. *Z. Elektrochem.* **57** (1953) 162.
5. Gregor, H. P., Sundheim, B. R., Held, K. M. and Waxman, M. H. *J. Colloid Sci.* **7** (1952) 511.
6. Gregor, H. P., Gutoff, F. and Bregman, J. I. *J. Colloid Sci.* **6** (1951) 245.
7. Roozeboom, H. B. *Die heterogenen Gleichgewichte*, II—1, Braunschweig 1904, p. 288.
8. Lewis, G. N. and Randall, M. *Thermodynamics and the free energy of chemical substances*, McGraw-Hill Book Co., New York 1923, p. 38.

Received October 14, 1957.

ACTA CHEMICA SCANDINAVICA 12 (1958) 188—192

Phenol Dehydrogenations

VIII.* Synthesis of Magnolol

J. RUNEBERG

Institutionen för organisk kemi, Kungl. Tekniska Högskolan, Stockholm, Sweden

2,2′-Dimethoxy-5,5′-dibromo-diphenyl (IV) reacted with magnesium in the presence of ethylmagnesium bromide to give the corresponding Grignard compound. This, on treatment with allyl bromide, furnished 2,2-dimethoxy-5,5′-diallyl-diphenyl (III) which on demethylation with methylmagnesium iodide afforded magnolol (II). Application of the Tschugajew reaction to 2,2′-dimethoxy-5,5′-bis-(ω-hydroxy-*n*-propyl)-diphenyl also furnished magnolol but in this case the product was difficult to obtain in a pure state. Thermal rearrangement of 2,2′-diallyloxy-diphenyl yielded 2,2′-dihydroxy-3,3′-diallyl-diphenyl as the sole identifiable product.

Magnolol, dehydrodichavicol, (II) is a constituent of the bark of some *Maynolia* species [1], and it is interesting to note that chavicol methylether occurs in other species of the same genus [2]. Magnolol was recently [3] prepared by dehydrogenation of chavicol (I) with ferric chloride and has now been synthesised by ordinary methods.

2,2′-Dihydroxy-diphenyl was easily brominated to 2,2′-dihydroxy-5,5′-dibromo-diphenyl [4]. This was methylated and the dimethylether (IV) converted into 2,2′-dimethoxy-5,5′-diallyl-diphenyl (magnolol dimethylether) (III) in good yield, using ethylmagnesium bromide as a catalyst according to a method by Short and Wang [5]. It was found necessary, however, to carry out the allylation in tetrahydro-furan solution; in diethylether no reaction took place. 2,2′-Dimethoxy-5,5′-dicarbomethoxy-diphenyl, prepared from magnolol dimethylether [1] was found to be identical with a sample prepared from 2,2′-dimethoxy-5,5′-bis-(ω-carbomethoxy-ethyl)-diphenyl (*cf.* experimental part). Demethylation of magnolol dimethylether with methylmagnesium iodide [6] furnished crude magnolol which was purified *via* its bis-phenylurethan. When the pure urethan was heated in a vacuum it dissociated into phenyl*iso*cyanate and magnolol.

* Part VII: *Acta Chem. Scand.* **11** (1957) 1060.

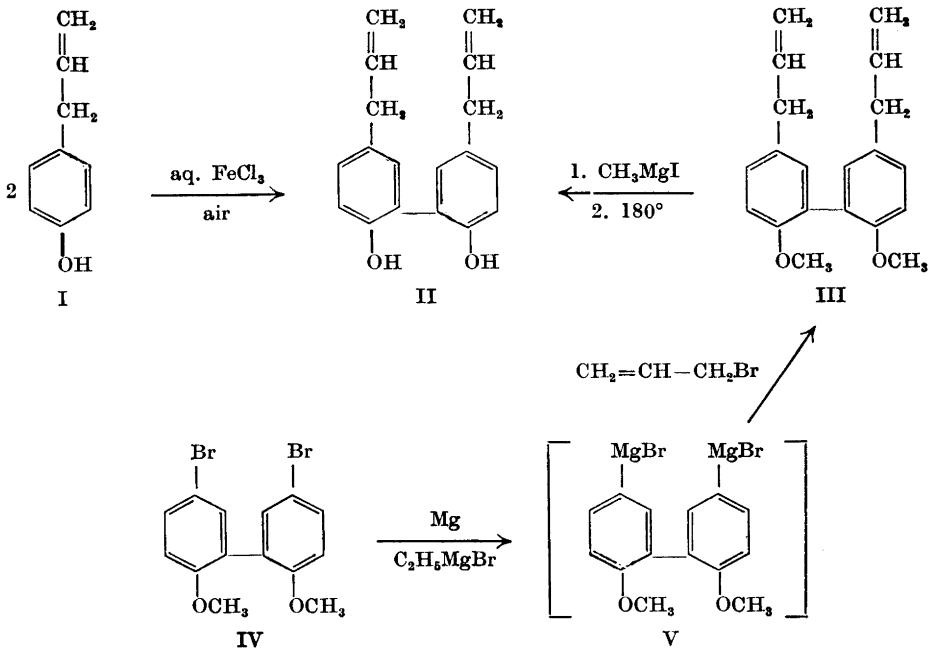

Following an observation that β-(4-methoxy-phenyl)-propanol on dehydration by the Tschugajew method furnished chavicol methylether, although in poor yield, an attempt was made to synthesise magnolol in a similar way. β-(4-Hydroxy-phenyl)-propanoic acid was iodinated in ammonia to β-(4-hydroxy-3-iodo-phenyl)-propanoic acid which was converted into its methyl-ether-methylester. This was then coupled by the Ullman procedure to give 2,2′-dimethoxy-5,5′-bis-(ω-carbomethoxy-ethyl)-diphenyl, which was reduced with lithium aluminum hydride to the corresponding diol. This product was converted into its bis-methylxanthate, which on heating furnished oily, crude 2,2′-dimethoxy-5,5′-diallyl-diphenyl. On demethylation with methylmagnesium iodide this material yielded a phenol which, however, failed to crystallise. The paper chromatographic behaviour of the product indicated that it consisted essentially of magnolol.

Finally, the di-allylether of 2,2′-dihydroxy-diphenyl was subjected to thermal rearrangement. The resulting phenolic product, on paper chromatographic examination, appeared to be rather inhomogeneous but it obviously contained no magnolol. Methylation of the crude rearrangement product followed by oxidation with permanganate furnished a fair yield of 2,2′-dimethoxy-3,3′-dicarboxy-diphenyl. The rearrangement obviously proceeds essentially in the normal way to give the bis-*ortho* allylated product.

EXPERIMENTAL

Melting points are uncorrected

2,2′-Dihydroxy-5,5′-dibromo-diphenyl: A solution of bromine (120 g) in chloroform (700 ml) was added dropwise with stirring at room temperature to a solution of 2,2′-dihydroxy-diphenyl (70 g) in chloroform (700 ml). After concentration to about 200 ml and cooling, a first crop of crystals (112 g) was obtained. A second crop (8 g) was recovered from the mother liquors. Yield 120 g (93 %). After one recrystallisation from ethanol-water the product melted at 186—189° (lit.[7] m. p. 188—189°).

2,2′-Dimethoxy-5,5′-dibromo-diphenyl: Dimethyl-sulphate (25 g) was added in portions with stirring to a solution of 2,2′-dihydroxy-5,5′-dibromo-diphenyl (23 g) in 10 % sodium hydroxide (100 ml). A white crystalline product precipitated. Yield 22.1 g (89 %). The product was recrystallised from 95 % ethanol, m. p. 127—129° (lit.[4] m. p. 129—130°).

2,2′-Dimethoxy-5,5′-diallyl-diphenyl (Magnolol dimethylether): Ethyl bromide (29.2 g) was added in portions to magnesium turnings (13.1 g) in tetrahydrofuran (250 ml) dried over sodium. The formation of the Grignard compound was initiated by adding a crystal of iodine and heating gently. When all the ethyl bromide (and half of the magnesium present) had reacted, the mixture was chilled in ice and a solution of 2,2′-dimethoxy-5,5′-dibromo-diphenyl (50 g) in dry tetrahydrofuran (250 ml) was added drop by drop with stirring. The reaction mixture was then stirred at room temperature for another 24 h. Allyl bromide (97 g) was now added with stirring. The reaction mixture was refluxed for 3 h, chilled, and then 2 N hydrochloric acid (300 ml) was added in portions. The tetrahydrofuran phase was separated and the water phase extracted with ether. The nonaqueous phases were combined, washed with water, dried and evaporated yielding a yellow oil (37 g). This was distilled in a nitrogen atmosphere, the main fraction (27.8 g) boiling at 165°/0.7 mm. Yield 70 % (lit.[1] b.p. 186°/5 mm).

2,2′-Dimethoxy-5,5′-dicarbomethoxy-diphenyl from magnolol dimethylether: On oxidation with potassium permanganate, magnolol dimethylether furnished 2,2′-dimethoxy-5,5′-dicarboxy-diphenyl, m. p. above 310°. Treatment with diazomethane afforded the dimethylester, m. p. 174—175° (lit.[4] m. p. 173—174°). Mixed with 2,2′-dimethoxy-5,5′-dicarbomethoxy-diphenyl obtained from 2,2′-dimethoxy-5,5′-bis-(ω-carbomethoxy-ethyl)-diphenyl (*cf.* below) the product melted at 173—175°.

2,2-Dihydroxy-5,5′-diallyl-diphenyl (Magnolol): A solution of magnolol dimethylether (10 g) in absolute ether (50 ml) was added with stirring to a solution of methylmagnesium iodide made from magnesium turnings (1.6 g) and methyl iodide (9.7 g) in absolute ether (100 ml). The ether was then removed by distillation and the temperature of the reaction flask slowly raised to 180° and kept at this level for 1 h. During the heating, gas was evolved. Small portions of water were then cautiously added to the glassy residue, followed by 2 N hydrochloric acid (75 ml). The mixture was then extracted with ether and the ether solution shaken with 2 N sodium hydroxide. Starting material (3.4 g) was recovered from the ether phase. The alkaline solution was acidified and extracted with ether. The ether extract was washed with water, dried and evaporated yielding a red-brown syrup (5.0 g). This was dissolved in benzene (50 ml) and filtered through a thin layer of aluminum oxide. The solution was evaporated and the remaining syrup distilled in a nitrogen atmosphere, yielding a main fraction (2.2 g) which boiled at 178—180°/1.0 mm. This material did not readily crystallise when scratched but crystallised immediately on seeding with magnolol obtained by dehydrogenation of chavicol[3]. Allowing for recovered starting material the yield was 37 %.

Purification of magnolol: Magnolol was purified *via* its bisphenylurethan (m. p. 143—144°) as described in a previous paper[3]. On thermal decomposition the phenylurethan afforded magnolol which was resublimed twice, m. p. 100.5—101.5° (lit.[1] m. p. 103°).

β-(3-Iodo-4-hydroxy-phenyl)-propanoic acid: Potassium iodide (400 g) and iodine (127 g) were dissolved in water and diluted to 1 000 ml. This solution (230 ml) was added drop by drop with stirring to a solution of β-(4-hydroxy-phenyl)-propanoic acid (20 g) in conc. ammonia (2 400 ml). The ammonia was evaporated in a vacuum and the volume of the solution reduced to about 400 ml. This solution was acidified stepwise with 10 N hydrochloric acid. The strongly discoloured material (2 g) precipitated first was discarded. The main fraction (26.9 g) consisted of reddish crystals. Extraction of the mother

liquor with ether gave additional material (4 g). The combined products were digested with hot benzene (150 ml) and the solution was filtered. On cooling, crystals (25.2 g), m. p. 103—108°, were obtained and concentration of the mother liquor yielded a second crop (2.7 g). Yield 79 %. For analysis a sample was extracted four times with hot ligroin and the residue was recrystallised from the same solvent, m. p. 112—113° (with sintering at 104°). (Found: I 43.30; equiv. wt. 291 (titration). Calc. for $C_9H_9O_3I$: I 43.45; equiv. wt. 292).

Methyl-β-(3-iodo-4-methoxy-phenyl)-propanoate: β-(3-Iodo-4-hydroxy-phenyl)-propanoic acid (21 g) was treated overnight with an excess of diazomethane in ether. Excess reagent was then destroyed with acetic acid, the solution was evaporated and the residue recrystallised from methanol, m. p. 42—43°. (Found: I 39.29. Calc. for $C_{11}H_{13}O_3I$: I 39.64.)

2,2'-Dimethoxy-5,5'-bis-(ω-carbomethoxy-ethyl)-diphenyl: Methyl-β-(3-iodo-4-methoxy-phenyl)-propanoate (20 g) was heated with copper bronze (60 g). At 225° a sudden reaction took place and the temperature rose to 285°. After cooling, the mixture was exhaustively extracted with acetone. The acetone was evaporated and the remaining syrup distilled in a vacuum. The main fraction, boiling at 234°/1.0 mm, crystallised on standing. Yield: 7.0 g (58 %). Recrystallised from 95 % ethanol, the product melted at 66—67°. (Found: C 68.10; H 6.99. Calc. for $C_{22}H_{26}O_6$: C 68.37; H 6.78.)

Reduction, dehydration and demethylation: Reduction of 2,2'-dimethoxy-5,5'-bis-(ω-carbomethoxy-ethyl)-diphenyl with lithium aluminum hydride afforded a viscous oil boiling at 252°/3.7 mm. A sample was converted into the bis-methylxanthate by the Tschugajew procedure (*cf.* Ref.[8]). On pyrolysis at 250°, an oil (b. p. 165—175°/1 mm) was obtained which on treatment with methyl magnesium iodide (*cf.* magnolol above) furnished an alkali soluble syrup [2.4 g from 10 g 2,2'-dimethoxy-5,5'-bis-(ω-carbomethoxy-ethyl)-diphenyl]. Samples of this product were chromatographed in the same way as the rearrangement product of 2,2'-diallyloxy-diphenyl (*cf.* below) and a spot was obtained with the same R_F-value (0.76) and colour reaction with diazotised benzidine as a blank of 2,2'-dihydroxy-5,5'-diallyl-diphenyl (magnolol). The product obviously contained magnolol but refused to crystallise.

2,2'-Dimethoxy-5,5'-dicarbomethoxy-diphenyl: On alkaline hydrolysis, 2,2'-dimethoxy-5,5'-bis(ω-carbomethoxy-ethyl)-diphenyl afforded the corresponding dicarboxylic acid, m. p. 221—222° which on oxidation with permanganate gave 2,2'-dimethoxy-5,5'-dicarboxy-diphenyl, m. p. above 310°. Dimethylester, m. p. 174—175° (lit.[1] 172°).

2,2'-Diallyloxy-diphenyl: 2,2'-Dihydroxy-diphenyl (13 g) in dry xylene (200 ml) was added to metallic potassium (5.5 g) suspended in the same solvent (100 ml) with vigorous stirring under reflux. A pale yellow salt was formed. The mixture was refluxed for 2 h and then potassium carbonate (5 g) was added. Allyl bromide (34 g) was added drop by drop and the reaction mixture was refluxed for a further 2 h. The filtered solution was extracted with 2 N sodium hydroxide, washed with water and evaporated. The residual oil was distilled in a vacuum, the main fraction (11.8 g) boiling at 142°/0.8 mm. Yield 64 %. (Found: C 80.46; H 6.91. Calc. for $C_{18}H_{18}O_2$: C 81.17; H 6.81).

Rearrangement of 2,2'-diallyloxy-diphenyl: 2,2'-Diallyloxydiphenyl (4 g) was heated at 250° for 10 min. The alkali soluble reaction product (3.8 g) was analysed by paper chromatography. A Whatman No. 1 filter paper was immersed in a solution of dimethylsulphoxide (10 %) in benzene and dried at room temperature for 15 min. A mixture of benzene (10 parts), ligroin (10 parts) and dimethylsulphoxide (0.5 parts) was used as the mobile phase. The chromatogram was run against a blank of magnolol prepared from 2,2'-dimethoxy-5,5'-diallyl-diphenyl (*cf.* above) and developed with diazotised benzidine [9]. The crude product gave the following spots: I (R_F 0.90, yellowish-brown, main spot), II (R_F 0.64, red-brown), III (R_F 0.43, red-brown), IV (R_F 0.15, red-brown). No trace of magnolol (R_F 0.76, yellowish-brown) was obtained.

On methylation with dimethyl sulphate and alkali the product yielded a neutral oil b. p. 155—156°/1.0 mm. This crude material was oxidised with potassium permanganate yielding an acid, m. p. 207—208° in agreement with the reported [4] melting point for 2,2'-dimethoxy-3,3'-dicarboxy-diphenyl (208—209°). (2,2'-Dimethoxy-5,5'-dicarboxy-diphenyl melts [1] above 300°.)

REFERENCES

1. Sugi, Y. *J. Pharm. Soc. Japan* **50** (1930) 23.
2. Fujita, Y. *J. Jap. Bot.* **30** (1955) 188.
3. Erdtman, H. and Runeberg, J. *Acta Chem. Scand.* **11** (1957) 1060.
4. Gilman, H., Swiss, J. and Cheney, L. C. *J. Am. Chem. Soc.* **62** (1940) 1966.
5. Short, W. F. and Wang, H. *J. Chem. Soc.* **1950** 993.
6. Grignard, V. and Ritz, J. *Bull. soc. chim. France* (5) **3** (1936) 1181.
7. Diels, O. and Bibergeil, A. *Ber.* **35** (1902) 306.
8. Whitmore, F. C. and Simpson, C. T. *J. Am. Chem. Soc.* **55** (1933) 3809.
9. Koch, J. E. and Krieg, W. *Chem. Ztg.* **62** (1938) 140.

Received October 17, 1957.

ACTA CHEMICA SCANDINAVICA 12 (1958) 193—197

An Application of Condensation Polymerization in Solid Phase

SVEN SÖNNERSKOG

AB Svenskt Konstsilke, Borås, Sweden

A series of model filaments showing successively increasing molecular weights were prepared by hydrolytic polymerization of ε-caprolactam (in some cases with hexamethylenediammoniumdiadipate as a co-reactant) according to an easily reproducible schedule. The molten polymer was extruded as monofilament, quenched in cold water, washed, cold drawn and subjected to a hot stretching at 190°C. A change in tenacity and viscosity number was observed at prolonged heating in an inert atmosphere. Favourable conditions for reaching a high mechanical strength were found already at a *medium* molecular weight of the treated specimen (viscosity number 1.0—1.2 in formic acid). A further increase of molecular weight did not improve the tensile properties, probably due to unfavourable flow conditions in the spinnerette at high melt viscosities, or an increased degree of entanglement at high degrees of polymerization. This limitation can be avoided by extruding the primary polymer at a stage of medium molecular weight and subjecting the hot stretched filament to a continued polymerization in solid phase. The said operation causes a significant increase of the tensile strength if carried out in an inert atmosphere at a high permanent stress. The time of reaction should not exceed two hours at 190°C.

As repeatedly emphasized by Carothers [1], orientability and fibreforming properties in high polymeric systems are distintive features of the linear molecules, intimately connected with their average absolute size. This means, among other things, that the average chain length should exceed a certain minimum (approximately 800 Å in the case of linear polyamides and polyesters). As a consequence, in polymer homologous series, the degree of polymerization has a marked influence on solubility and mechanical properties. Thus in 66 nylon [2] the tensile strength is known to increase in relation to the molecular weight, the increments being large in the region representing low and medium molecular weights but fairly low at higher ones. This saturation phenomenon is found in most linear macromolecular systems, for instance in fibres of polyethylene, polyvinyl chloride, polyacrylonitrile, polyamides, polyesters and cellulose acetate, but its physical significance is difficult to elucidate.

Table 1. Tenacity and viscosity number of cold drawn filaments, obtained from a polymerizing system of caprolactam, water and coreactant. (The hydrolytic reaction step is not included in the schedule but found in the experimental part below.)

Sample index	Time of reaction, min.	Viscosity number (in formic acid) * of polymer **				Tenacity, g/denier (aver. denier ~500)			
		I	II	III	IV	I	II	III	IV
1	0	part. sol.	0.48	0.50	0.48	NOT FIBRE-FORMING			
2	15	0.48	0.53	0.56	0.50				
3	30	0.62	0.61	0.68	0.63				
4	45	0.88	0.94	0.98	0.77	4.5	4.5	4.8	4.0
5	60	1.00	1.07	1.07	0.95	5.2	5.7	4.8	4.3
6	75	1.08	1.15	1.17	1.19	6.4	5.8	5.3	5.1
7	90	1.18	1.26	1.21	1.31	5.6	5.8	5.9	5.3
8	105	1.26	1.31	1.28	1.34	5.6	5.5	5.4	5.3
9	120	1.28	1.38	1.32	1.41	4.8	5.7	5.6	4.9
10	135	1.30	1.40	1.42	1.49	4.2	5.1	5.0	4.9
11	150	1.32	1.47	1.46	1.47	4.6	4.6	4.5	4.6

* Conc. of acid: 85 %
Conc. of polymer: 1.00 %
** Polymer I: pure poly ε-caproamide
II: 2 % coreactant
III: 5 % coreactant
IV: 7.5 % coreactant

The present paper deals with the tensile properties of homologous polymer series of ε-caprolactam and some copolymers with hexamethylenediammoniumdiadipate. Model filaments of the different polymers have been obtained by melt extrusion into cold water, followed by a "cold" stretching at room temperature. The latter operation is generally considered to develop a high mechanical strength in the direction of the fibre axis due to an increased orientation with subsequent formation of crystalline regions between adjacent molecules. It seems apparent, however, that a saturation effect enters at medium molecular weights, as shown in Table 1. As the possibility *a priori* must be precluded that the strength of oriented molecules rises to a maximum and then falls off, it appears reasonable to seek for an explanation of the actual discrepancy in some imperfections of the fibre, inherently connected with the molecular weight.

In the case of polyamides and polyesters it has generally been stated [3] that molecular weight and melt viscosity are unambigously dependent according to the formula:

$$\ln \eta = A + B M_w^{\frac{1}{2}} + E/RT$$

where η indicates the melt viscosity in arbitrary units, A and B constants, M_w the weight average molecular weight, E the activation energy of flow, R the gas constant and T the temperature in Kelvin units. The expression emphasizes that the viscosity of the molten polymer rapidly increases at increasing degrees of polymerization. Its numerical value may well be above 10^6 cps

Table 2. A comparison, showing the ultimate strength and elongation at break for two types of fibres after rapid hot stretching at 190°C. (Fibres I:7—IV:7 are labeled as *medium* viscosity polymers, I:11—IV:11 as *high* viscosity polymers, in accordance with the preceding table.)

Fibre	Denier after stretching	Breaking load, kg (Scott tester)	Tenacity, g/denier	Ultimate elongation, %
I:7	420	2.75	6.6	11.8
II:7	442	3.02	6.8	12.7
III:7	469	3.21	6.8	12.0
IV:7	386	2.43	6.3	13.1
I:11	483	2.60	5.4	12.1
II:11	445	2.58	5.8	11.6
III:11	415	2.27	5.5	12.9
IV:11	501	2.81	5.6	13.7

at equilibrium in a polymerizing system. Such a dope shows a rheology similar to glass. On extrusion through a cylindrical orifice, especially at a low shear stress, all essential features of the liquid polymer will remain in the subcooled state, obtained by quenching in cold water. The behavior of this specimen at subsequent cold stretching will largely depend upon the internal friction. This magnitude has the same characteristics as viscosity and can also be estimated according to the cited formula. It leaves no doubt that a low temperature and a high degree of polymerization can cooperate in such a manner, that rupture occurs before cold flow ("necking") sets in.

Such a filament can be subjected to stretching at elevated temperature, even in the vicinity of its melting point ("hot stretching"), but experience shows that such an operation alone is insufficient to develop a high mechanical strength. Due to an increased molecular mobility above the second order transition temperature a hot stretching enhances the effect of cold drawing, as seen from Table 2, but is inefficious to impart a high degree of orientation upon the chain molecules directly from the isotropic state.

Another influence of molecular weight arises from the change in shape of the weight distribution function of the polymer at increasing extent of reaction. In the case of most probable distribution the weight fraction w_n showing a degree of polymerization n at an extent of reaction p is given by [4]

$$w_n = n \cdot p^{n-1} \cdot (1-p)^2$$

This function shows a distinct maximum already at $p = 0.9$, corresponding to an average degree of polymerization $n = 1/(1-p) = 10$, but is very broad at $p = 0.98$ ($n = 50$). The internal friction between single chain molecules can hardly be independent of this change of distribution, as it predicts the presence of an increasing number of *very* long molecules at high extents of reaction. This would increase the probability of chain rupture at cold drawing. In fact such a degradation has frequently been observed to judge from a slight but significant change of viscosity number.

Table 3. Tenacity and viscosity number of polyamide fibres on prolonged heating in an inert atmosphere at 190°C under stress (2 g/denier). Polymer I: homopolymer of caprolactam, polymer IV: copolymer (cf. Table 1).

Time of heating, min.	Type of fibre							
	Homopolymer				Copolymer			
	I : 7		I : 11		IV : 7		IV : 11	
	Tenacity g/denier	Visc. number	Tenacity g/denier	Visc. number	Tenacity g/denier	Visc. number	Tenacity g/denier	Visc. number
0	5.6	1.18	4.6	1.32	5.3	1.31	4.6	1.47
15	5.9	1.22	5.4	1.34	6.4	1.33	5.8	1.47
30	6.4	1.22	6.5	1.36	7.4	1.34	7.1	1.49
45	7.1	1.25	6.7	1.36	7.8	1.36	7.6	1.49
60	7.1	1.24	6.8	1.36	8.3	1.38	7.9	1.50
75	8.2	1.26	6.8	1.36	8.6	1.38	7.9	1.50
90	8.3	1.31	6.9	1.37	8.8	1.41	7.8	1.49
120	8.1	1.30	6.8	1.34	8.9	1.42	7.8	1.51
150	8.3	1.32	—	—	8.7	1.40	7.7	1.48
180	8.1	1.26	6.6	1.34	8.3	1.34	7.4	1.49
240	8.1	1.26	6.3	1.34	8.1	1.34	7.3	1.48

Chain rupture at cold stretching might also occur by a high degree of molecular entanglement (irreversible looping). Recent calculations [5] on simplified models indicate that in polymerhomologous series this phenomenon increases in relation to the degree of polymerization. It is obviously also connected with the internal friction. Its influence on physical properties is wellknown from the theory of rubber elasticity and needs no discussion here. The absence of a network structure in the actual polymers does not principally prevent a qualitative comparison. At rapid plastic deformation (400—450 % elongation) of a polyamide fibre the internal friction acts in a similar manner as crosslinks in a network. In other words the time available for a long molecule to extricate itself from entanglements with adjacent ones is too short, resulting in chain rupture.

To sum up, the observed maximum of tenacity at medium molecular weights, observed in Table 1, appears to be a superposed effect due to gradually increasing imperfections of the fibre. Most of these can be avoided by selective choice of molecular weight and stretching temperature(s).

When the second stretching was carried out at 190° C on unstabilized polymer, an increase of viscosity number was observed on prolonged heating (Table 3), indicating that a continued polymerization in solid phase takes place. This statement is also valid for copolymers. Under carefully controlled conditions it gives a considerable increase of tenacity (Table 3) provided it is carried out at high stress (2 g/denier) in an inert atmosphere. This reactivity of polyamides below their melting point is known from previous investigations [6] and considered to be a consequence of the accumulation of end groups in the amorphous phase, where chain mobility is high. A number of important appli-

cations of this effect seem to have been overlooked, before all its usefulness of eliminating imperfections in the weakest, most disordered regions of the polymer structure.

EXPERIMENTAL

Model filaments were prepared by hydrolytic condensation polymerization of ε-caprolactam and water. In some cases 66 nylon salt was added as a coreactant to increase the plasticity of the polymer on stretching (reducing the melting point and the second order transition temperature). The reaction was carried out in the absence of a chain stopper.

Apparatus: An autoclave of stainless steel, volume approximately 1 000 ml, fitted with a surrounding jacket (a cylinder of aluminium) serving as heat transfer medium from an electrically heated plate. Samples of the molten polymer were extruded during the reaction through a horisontally directed needle valve and a cylindrical orifice. As a mantle for heat control in the valve served an aluminium block, electrically heated by a copper-bolt, placed in a bore. This arrangement for extrusion proved to work very satisfactory by applying different pressures (carbon dioxide or water vapour) in the autoclave. At the beginning, *e. g.* when the melt is mobile and non-filogenic, great care must be exercised to avoid sprinkling of the hot liquid.

Chemicals: Caprolactam, recrystallized from ethyl acetate and dried in a slow current of carbon dioxide at room temperature. Added to the autoclave as a saturated (80 % by wt.) aqueous solution.

Nylon salt. The commercial grade was purified by dissolving in distilled water to give a 40 % (by wt.) aqueous solution, filtered and precipitated in a large excess of methanol, analytical grade. The alcohol was removed in a current of dry carbon dioxide at room temperature.

Schedule of reaction: The autoclave was charged with 750 ml aqueous solution of monomer(s). A first, hydrolytic reaction step was carried out at 260°C during 120 min. After release of pressure to 4 atm, polymerization was continued for another 2 h, when samples were drawn every 15 min from the heated bottom valve.

Purification: Rapid cooling of the model filaments in a water bath between extrusion nozzle and bobbin, followed by washing in water for 15 min and cold stretching to at draw ratio of 4.5. After a further extraction with water at room temperature the fibre was subjected to hot stretching at 190°C. Part of the cold drawn fibres were used also for measurements of primary tensile strength.

REFERENCES

1. *Collected Papers of W. H. Carothers on Polymerization*, Edited by Mark, H. and Whitby, G. S. Interscience Publishers, New York 1940, pp. 129—136, 197—200.
2. Mark, H. *Ind. Eng. Chem.* **34** (1942) 1343.
3. Flory, P. J. *J. Am. Chem. Soc.* **62** (1940) 1057.
4. Flory, P. J. *Principles of Polymer Chemistry*, Cornell University Press, Ithaca, New York 1953, p. 322.
5. Bueche, F. *J. Polymer Sci.* **25** (1957) 243.
6. Flory, P. J. *J. Chem. Phys.* **17** (1949) 223.

Received October 17, 1957.

ACTA CHEMICA SCANDINAVICA 12 (1958) 198—223

Studies on the Hydrolysis of Metal Ions

21. The Hydrolysis of the Tin(II) Ion, Sn^{2+}

R. STUART TOBIAS

Department of Inorganic Chemistry, Royal Institute of Technology, Stockholm 70, Sweden

The hydrolysis of Sn(II) has been studied in a constant ionic medium (3 M ClO_4^-) at 25°C by two series of electrometric titrations. In one series, $[H^+] = h$ was measured with a glass electrode, and in the other $[Sn^{2+}] = b$ was measured with a tin amalgam electrode.

A mathematical analysis has been made of the two families of curves $Z(\log h)_B$ and $\eta(\log h)_B$, where Z is the average number of ligands (hydroxyl groups) bound per tin(II), B is the total Sn concentration, and $\eta = \log B/b$. The main product of the hydrolysis reaction is $Sn_3(OH)_4^{2+}$, and the equilibrium constant of the reaction $3\,Sn^{2+} + 4\,H_2O \rightleftharpoons Sn_3(OH)_4^{2+} + 4\,H^+$ was found to be $\log K_{43} = -6.77 \pm 0.03$. Deviations at low values of Z, η, and B indicate the presence of $Sn_2(OH)_2^{2+}$ and $SnOH^+$. The following equilibrium constants were found: $2\,Sn^{2+} + 2\,H_2O \rightleftharpoons Sn_2(OH)_2^{2+} + 2\,H^+$, $\log K_{22} = -4.4_5 \pm 0.15$; $Sn^{2+} + H_2O \rightleftharpoons SnOH^+ + H^+$, $\log K_{11} = -3.9_2 \pm 0.15$.

The first attempt to determine the products of the hydrolysis of tin(II) solutions and the equilibrium constants for their formation was made by Prytz [1] in 1928. Solutions of tin(II) salts were prepared in various ionic media and titrated at 25° C with NaOH. A hydrogen electrode was used to follow the change in the hydrogen ion concentration; an attempt was also made to follow the change in $[Sn^{2+}]$ using a tin electrode. The data could not be explained by a simple reaction giving $SnOH^+$, but equilibrium constants were calculated on the basis of the following reaction

$$2\,Sn^{2+} + 2\,H_2O \rightleftharpoons Sn_2(OH)_2^{2+} + 2\,H^+ \quad \text{or}$$
$$2\,Sn^{2+} + H_2O \rightleftharpoons Sn_2O^{2+} + 2\,H^+$$

since such measurements cannot determine the number of solvent molecules involved. The following values of the equilibrium constant ($= K_{22}$ below) were given. $SnCl_2$ in 0.5 M KCl, 8×10^{-5}, in water, 2×10^{-3}; $SnBr_2$ in 0.5 M KBr, 5.8×10^{-4}, in water, 8.3×10^{-3}; $Sn(ClO_4)_2$ in water and 0.5 M $NaClO_4$, 1.8×10^{-3}.

Randall and Murakami [2] studied the hydrolysis of Sn^{2+} in chloride solution. The equilibrium constant for the reaction $Sn^{2+} + 2\,H_2O + Cl^- \rightleftharpoons$

$Sn(OH)ClH_2O(s) + H^+$ was obtained from solubility measurements. The constant was given as $\log K = 2.75$.

In 1939, Gorman [3] titrated tin(II) perchlorate solutions with NaOH and measured the hydrogen ion concentration with a hydrogen electrode at 25° C. The data were interpreted in terms of the reaction

$$Sn^{2+} + H_2O \rightleftharpoons SnOH^+ + H^+$$

The data were extrapolated to zero ionic strength to obtain the equilibrium constant, and a value $\log K_{11} = -1.70$ was given for 25°C.

Garrett and Heiks [4] measured the solubility of SnO in HCl solutions and interpreted the results in terms of the mononuclear species Sn^{2+}, $SnOH^+$, and $Sn(OH)_2(aq)$. From their data, we may obtain the following constants: $\log K_{11} = -2.1$, $\log K_{21} = -7.06$.

More recently, Vanderzee and Rhodes [5,6] have estimated equilibrium constants for the reaction giving $SnOH^+$ at 0°, 25°, 35°, and 45°C, assuming this to be the only hydrolysis reaction occurring in solutions with high concentrations of halide ions. The values for $\log K_{11}$ range from −1.8 at 0° to −1.6 at 40°C.

Since the hydrolysis of many metal ions has been found to yield polynuclear complexes, it is essential to study the equilibria at a number of different total tin concentrations. The aim of this work was, therefore, to investigate the hydrolysis of tin(II) by the methods developed in this laboratory [7–10] in order to elucidate the mechanism of the hydrolysis and to calculate the various equilibrium constants.

Symbols and formulas

The symbols adopted are mainly those used in the previous papers in this series.

b	concentration of free Sn^{2+}
B	total concentration of Sn(II)
$\boldsymbol{B}$	normalized value of B (27)
E_A	-emf, $E°_A$-constant, E_{jA}-liquid junction potential, all for cell A (3)
E_B	-emf, $E°_B$-constant, E_{jB}-liquid junction potential, all for cell B (4)
F_q	function of experimental data defined by (22)
$g(u) =$	$\Sigma_n k_n u^n$
h	concentration of free H^+
j_A, j_B	constants in $E_j = jh$
k_n	equilibrium constant for $(n+1)Sn^{2+} + nt\,H_2O \rightleftharpoons Sn[(OH)_tSn]_n^{(2n+2-tn)+} + nt\,H^+$
k, k_0	constants in $k_n = k^N$, hypothesis II; $k_n = k_0k^n$, hypothesis IIIa; $k_n = k_0nk^n$, hypothesis IIIb; $k_n = k_0k^n\,(n!)^{-1}$, hypothesis IIIc (AB II 28a, b, c) [8]
K_{pq}	equilibrium constant for the reaction $qSn^{2+} + pH_2O \rightleftharpoons Sn_q(OH)_p^{(2q-p)+} + pH^+$
n	number of links per complex
$\bar{n}$	average number of links per complex (11)

N	number of $Sn(OH)_t$ links in a unique complex
P_1, P_2	normalizing constants (28), (29)
p	number of OH^- in $Sn_q(OH)_p$
q	number of Sn^{2+} in $Sn_q(OH)_p$
R	ratio K_{43}/K_{22}^2
t	number of hydroxyl groups per link
u	$= h^{-t}b$
x	$= \log B - t \log h$
$x_{½}$	value of x at $y = ½$
X	normalized $x = x + \log 2 - x_{½}$ (AB II 10) [8]
y	$= Z/t$
Z	average number of (OH) bound per Sn(II)
α	normalized h (29)
β	normalized b (28)
γ_+, γ_{2+}	activity factors of H^+ and Sn^{2+}
δ	residual integral in (17)
η	$= \log B/b$
ξ	normalized x

All species may be combined with the medium ions, Na^+ and ClO_4^-, or with the solvent. The mole l^{-1}, M, is the standard unit of concentration used in all equilibrium constants. In some cases, the convenient mM unit is used in the text and headings.

METHOD

The hydrolysis of tin(II) was studied by two series of potentiometric titrations at 25°C. These will be referred to, in the following discussion, as the Z and η titrations. The free concentrations of H^+ and Sn^{2+} will be denoted by

$$[H^+] = h \qquad [Sn^{2+}] = b$$

B is the total concentration of tin in the solution, and H is the analytical excess of hydrogen ion, assuming no hydrolysis, *i. e.* all tin(II) in the form Sn^{2+}. H is therefore negative in the latter parts of the titrations. The quantities B and H are known from the analytical data.

In each Z and η titration, B was maintained constant while H was varied and h measured. The average number of OH^- bound per Sn(II), Z, could then be calculated.

$$Z = (h - H) / B \tag{1}$$

The data are most conveniently plotted in the form $Z(\log h)_B$.

In the η titrations, the free tin concentration, $[Sn^{2+}] = b$, was also measured. One can then calculate

$$\eta = \log B/b \tag{2}$$

These data are presented in the form η $(\log h)_B$.

The acidity of the solutions was increased by adding $H^+ClO_4^-$ and decreased by adding $Na^+HCO_3^-$. The use of $Na^+HCO_3^-$ as a base has been recommended

by Hedström [11] to avoid the formation of a precipitate which would be only slowly redissolved to give true equilibrium.

In both types of cells used, the reference electrode was

$$SE| = Ag|AgCl|10\ mM\ Ag^+, 2\,990\ mM\ Na^+, 3\,000\ mM\ ClO_4^-|3\,000\ mM\ Na\ ClO_4.$$

The hydrogen ion concentration was determined with the cell

$$-\ \text{glass electrode}\ |\ \text{solution S}\ |\ SE+ \qquad (A)$$

Solution S had the initial composition

$$(Sn(II),\ B\ M;\ H^+,\ H\ M;\ Na^+,\ (3 - 2B - H)\ M;\ ClO_4^-,\ 3\ M)$$

The measured emf is related to h by the following equation

$$E_A = E_A^\circ - 59.16\ \log\ h - E_{jA} - 59.16\ \log\gamma_+ \qquad (3)$$

The equilibrium tin(II) concentration was measured using the following cell.

$$-Sn,\ Hg\ (sat'd)\ |\ Solution\ S\ |\ SE+ \qquad (B)$$

The equilibrium tin (II) concentration, b, is related to the emf of cell (B) by the equation

$$E_B = E_B^\circ - \frac{59.16}{2}\log\ b - \frac{59.16}{2}\log\frac{\gamma_{2+}}{a_{Sn}} - E_{jB} \qquad (4)$$

In the two cells (A) and (B), E_A° and E_B° are constants characteristic of each cell. $NaClO_4$ was added to make all solutions 3 M in ClO_4^- with no other anions present. The activity coefficients, γ_+ and γ_{2+}, are defined so that $\lim_{c\to 0} a/c = 1$ in the solvent 3 M $NaClO_4$. Since the concentrations of tin(II) and hydrogen ions were quite low compared to the 3 000 mM ClO_4^- (Sn(II)-maximum 40 mM; H^+-maximum 70 mM), it can be assumed to a close approximation that activity factors remain constant and can be included in the E° for the cell [12] so that true stoichiometric equilibrium constants are obtained. The tin activity in the amalgam is maintained constant by the use of the mercury-rich phase of the 2-phase amalgam. At these low concentrations E_{jA} and E_{jB} are linear functions of the hydrogen ion concentration. If these junction potentials are written in the form $j_A h$ and $j_B h$, j_A has a value of -0.017 ± 0.001 mV/mM as reported earlier [12]. The value of j_B varied somewhat between titrations with different B, and the value was determined for each titration by measurements in a region where no hydrolysis occurred. j_B varied from -0.022 to -0.028 mV/mM. It seems probable that the liquid junction potentials are the same and that the difference between E_{jA} and E_{jB} is caused by the inclusion of a small correction term for minute deviations of the amalgam electrode from the Nernst equation. At any rate, the magnitude of the effect is so small that it has no significant influence on the amalgam electrode data.

When E_A° and j_A are known and E_A is measured, h may be obtained using equation (3). Similarly, b is obtained from E_B°, j_B, and measured values of E_B applying eqn. (4).

EXPERIMENTAL DETAILS

One especially difficult problem encountered during the study of the hydrolysis of tin(II) solutions is that the tin(II) ion is very easily oxidized in solution to the 4-valent state. It is almost impossible to store and handle tin(II) solutions for any length of time without having small amounts of tin(IV) formed by reaction with atmospheric oxygen, a reaction that is greatly accelerated by light. Since the reduction of tin(IV) to tin(II) by metallic tin is a very slow process, it is quite difficult to reduce tin(IV) to the +2 state quantitatively. Halide ions are also particularly undesirable when the hydrolysis of tin(II) is to be investigated, since strong complexes are formed between these ions and Sn^{2+}. The following experimental procedure was developed to circumvent these experimental difficulties.

Tin(II) perchlorate solutions were prepared by a modification of the method first described by Noyes and Toabe[13]. Standard copper(II) perchlorate solutions were prepared by dissolution of Merck (p.a.) CuO in warm dilute perchloric acid. No traces of Cl^- could be found in the solutions which were then filtered and diluted.

The copper(II) content of the solutions was determined by electrodeposition of Cu using HNO_3 as a depolarizing agent and adding a small excess of urea just before the completion of the electrolysis to destroy any accumulated nitrous acid. The accuracy was better than ± 0.1 %.

The total ClO_4^- content of the stock solution was determined by passing a definite volume through the cation exchange resin Duolite C 3 and titrating the eluate with standard NaOH. The analytical excess of H^+ in the stock solution was calculated from $[H^+] = [ClO_4^-] - 2[Cu^{2+}]$.

Standard solutions for the titrations were prepared by dilution of the stock solution with standard $NaClO_4$ and $HClO_4$.

The tin(II) solutions were prepared just before each titration to the concentration $2B$ in a modification of the apparatus described by Lingane and Pecsok [14] for the production of solutions of strong reducing agents. Hopkins and Williams' "Analar" metallic tin was used to displace copper(II) from the solutions. It was found that the hydrogen overvoltage on a pure tin surface was sufficient to prevent any reduction of H^+ so long as the solutions were free of any dissolved oxygen. Dissolved oxygen was flushed from the solutions by bubbling N_2 through them for about one hour. The tin was cleaned with dilute HCl before use, washed with water and ethanol, and dried under vacuum. Iodometric determinations of the tin(II) content of the most concentrated solution prepared (80 mM) agreed within $\pm$ 0.3 % of the value calculated on the basis of the copper displaced.

Tin amalgams were prepared in the two-limbed vessel described by Biedermann [15] by warming freshly cleaned Merck (p.a.) tin and triple distilled mercury in an atmosphere of CO_2. The two phase amalgam formed was thermostated at 25° $\pm$ 0.1 °C for about 20 h before use. Since the liquid phase of the tin amalgam contains 1.263 mole % tin at 25°C[16], amalgams with a constant tin activity could be easily prepared. The two phases were separated by passing the amalgam through a capillary tube just before the amalgam was introduced into the titration vessel.

Perchloric acid solutions were prepared by dilution of Kebo (p.a.) $HClO_4$ and standardized against $KHCO_3$ dried under CO_2 and also against standard NaOH solutions. The *sodium hydroxide solutions* were in turn standardized against potassium acid phthalate. The determinations agreed to $\pm$ 0.1 %.

Sodium hydrogen carbonate solutions were prepared from Merck (p.a.) $NaHCO_3$ containing less than 0.01 % Cl^-.

Sodium perchlorate solutions were prepared by neutralizing a solution of $HClO_4$ (p.a.) with Merck (p.a.) $NaHCO_3$. The solutions were filtered to remove silicates and analyzed by evaporation and drying to a constant weight. The analysis was checked by passing portions of the solution through the hydrogen form of an ion exchanger and titrating the perchloric acid with NaOH. Good agreement was found between the two methods. No chloride, chlorate, or iron could be detected in the final product.

Silver perchlorate solutions were prepared by evaporating Merck (p.a.) $AgNO_3$ with a large excess of $HClO_4$ until no nitrate could be detected in the product. The remaining $HClO_4$ was neutralized with Ag_2O, the solution filtered, and the silver determined gravimetrically as AgCl.

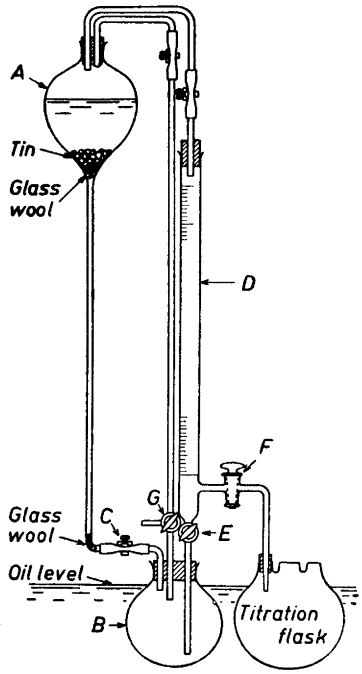

Fig. 1. Arrangement for the preparation of tin(II) solutions.

Nitrogen gas was purified by washing with 10 % H_2SO_4, 10 % NaOH, distilled water, and finally 3 M $NaClO_4$. Both the nitrogen and carbon dioxide gases were freed of oxygen by passage over hot activated copper.

Apparatus

A titration cell of the "Wilhelm" type as described by Forsling, Hietanen, and Sillén [7] was used. All measurements were made in a paraffin oil thermostat at 25° ± 0.1°C which was located in a room thermostated at approximately 25°C.

The silver reference electrode was prepared as described by Brown [17] and was coated with AgCl by electrolysis for half of an hour with a current of 0.3 mA.

The glass electrode was a Radiometer, Copenhagen, type G-102 AK. The potential of the cell

$$-\text{Glass electrode} \mid H^+ \mid \text{quinhydrone} \mid Pt+$$

was constant to ±0.1 mV indicating that eqn. (3) is valid. The emf values of the glass electrode cell (A) were read to 0.1 mV using a Radiometer PHM3 valve potentiometer. The emf values of the amalgam cell (B) were read to 0.01 mV with a Leeds and Northrup K-2 potentiometer.

The solution in the titration vessel was agitated with nitrogen gas while CO_2 was introduced over the surface of the liquid to prevent the entry of any atmospheric oxygen.

Titration procedure

Almost all of the titrations were carried out in the following manner. The preparation train illustrated in Fig. 1 was flushed with carbon dioxide for about 2 h. Approximately 100 ml of standard Cu(II) solution was introduced into the reservoir A containing the metallic tin. A strong flow of CO_2 was maintained during the addition to prevent the

entry of oxygen into the system. The flask was gently agitated for 10 – 15 min after which samples of the solution were withdrawn at C and tested for Cu^{2+}. When the solution gave no test for copper using $Fe(CN)_6^{4-}$ in dilute HCl, it was transferred to the reservoir B. The burette D could be filled by pressing the solution up with CO_2 admitted through the 3-way stopcock G. The tin solution was thus completely protected from the atmosphere during the preparation. Stopcock F was used to meter the solution during the titration.

25.00 ml of 3 M $NaClO_4$ solution was pipetted into the titration flask. About 100 g of tin amalgam was introduced into the cell from the two limbed vessel. A strong stream of CO_2 was passed over the surface of the $NaClO_4$ solution, while N_2 was bubbled into the solution. A platinum needle was used to make electrical contact with the amalgam. 25.00 ml of the tin solution T_1 (concentration 2 B) was then added. This mixture, solution S, was titrated with equal volumes v_1 of $NaHCO_3$ solution (T_2) and solution T_1. In this way, the total concentration of tin was maintained constant at B. The values of the cell constants E_A° and E_B° were obtained as illustrated in Table 1 by titration at hydrogen ion concentrations where hydrolysis was negligible.

The one exception to the above procedure was for the titration with B = 2.5 mM. In this case T_1 had a concentration of 4 B. Therefore, 75.00 ml of $NaClO_4$ (3 M) was added together with 25.00 ml of T_1. Titration was with equal volumes v_1 of T_1 and T_2 plus $2v_1$ ml of 3 M $NaClO_4$.

At the end of the titrations with 5 and 2.5 mM Sn(II), the emf values of both cells were noted. CO_2 was passed into the solution for one hour and N_2 bubbled through the solution again for 2 min. No change in either the glass or amalgam electrode potentials was observed, so that it can be assumed that there was no significant formation of complexes between tin(II) and carbonate ion even at the lowest value of $h \simeq 1.0$ mM.

Steady values of both potentials were attained rapidly, usually within 15 min, and remained constant for 10 h. At $\eta > 0.3$ the amalgam surface apparently became contaminated, since variations of 0.1 mV could be obtained by agitation of the amalgam. The glass electrode potentials were reproducible within ±0.2 mV and the amalgam potentials within ±0.05 mV.

A back titration was performed at the lowest value of B, and the points for both $Z(\log h)$ and η ($\log h$) fell on the same curve, indicating that true equilibria had been obtained even in this region.

At tin(II) concentrations of less than 2.5 mM, the amalgam electrode potentials became very sensitive to agitation of the amalgam pool even at low values of η, and hence no measurements were made for $B < 2.5$ mM.

Table 1. Standardization of electrodes for B = 20 mM.

B = 20.00 mM, H = 60.00 mM, $[ClO_4]$ = 3 M 50.00 ml
B = 40.00 mM, H = 120.00 mM, $[ClO_4]$ = 3 M v_1 ml
$[NaHCO_3]$ = 272.5 mM, $[ClO_4]$ = 3 M v_1 ml
E_A° = 316.1 ± 0.05 mV
E_B° = 777.26 ± 0.01 mV

v_1 ml	E_A mV	E_B mV	H mM	$E_A^{\circ\prime}$	E_B°	E_{jA}	E_{jB}
0.00	211.9	740.10	60.00	316.1	777.30	1.00	1.28
0.50	213.0	740.00	57.33	316.0	777.25	0.96	1.23
1.00	241.1	739.94	54.77	316.1	777.25	0.91	1.17
1.75	215.8	739.88	51.08	316.0	777.27	0.85	1.09
2.50	217.7	739.80	47.62	316.2	777.26	0.79	1.02
3.00	218.8	739.74	45.39	316.0	777.25	0.76	0.97
3.50	220.0	739.70	43.26	316.1	777.26	0.72	0.92
4.00	221.3	739.65	41.21	315.9	777.25	0.69	0.88
5.00	223.6	739.57	37.30	316.4	777.25	0.62	0.80
6.00	226.7	739.53	33.63	316.0	777.29	0.56	0.72
7.00	229.0	739.43	30.19	316.0	777.26	0.50	0.65
8.00	231.8	739.38	26.97	316.1	777.28	0.45	0.58

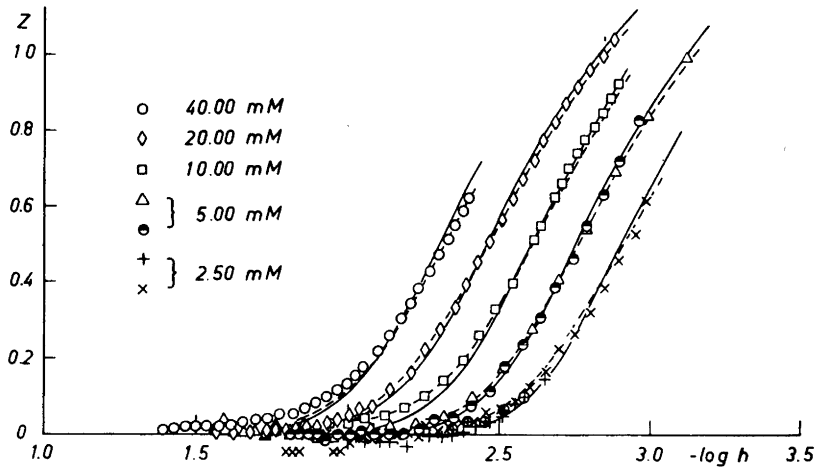

Fig. 2. Data from glass electrode measurements. Average number, Z, of OH bound per Sn as a function of log h (molar scale), B as a parameter. Full curves calculated for $K_{11} = K_{22} = 0$, log $K_{43} = -6.69$. Broken curves calculated for log $K_{11} = -3.92$, log $K_{22} = -4.45$, log $K_{43} = -6.77$. Points ◓ adjusted upward by 0.02 units.

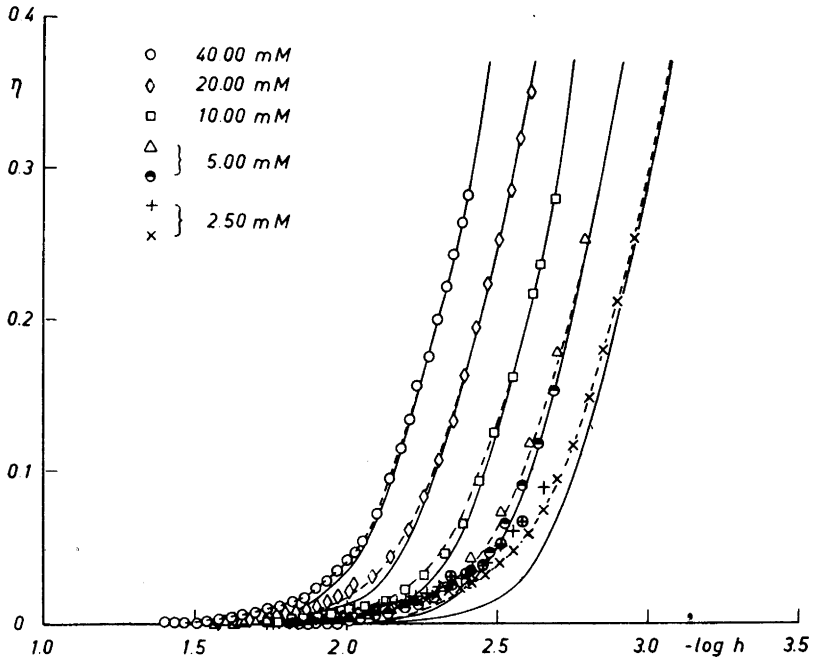

Fig. 3. Data from amalgam electrode measurements, $\eta = \log B/b$ as a function of log h (molar scale), B as a parameter. Curves calculated for the same sets of constants as in Fig. 2.

THE MAIN PRODUCTS OF HYDROLYSIS

Fig. 2 gives the data $Z(\log h)_B$ as calculated from the emf values of the cell (A), using eqns. (1) and (3). Fig. 3 gives the data η $(\log h)_B$ calculated using eqns. (2) and (4) together with the emf values of cells (A) and (B). Table 2 gives the values of log h, Z, and η for each titration.

It is seen from Figs. 2 and 3 that Z and η are functions of both B and h, which indicates that at least one polynuclear species is formed during the hydrolysis of tin(II) solutions. If only mononuclear complexes were formed, Z and η would be functions of the single variable h.

In order to evaluate the data, several different approaches will be tried in the following discussion.

"Core + links" approach

The systematic treatment developed by Sillén [8,18] will be closely followed in this discussion. It has frequently been observed that the products formed by the hydrolysis of metal ions can be described by a general "core + links"

Table 2. Experimental data Z, η, log h.

Titration 1. B = 40 mM			*Titration 2.* B = 20 mM		
Z	η	$-\log h$	Z	η	$-\log h$
0.01	0.0000	1.391	0.001_5	0.0008	1.569
0.01_5	0.0000	1.425	0.002	0.0025	1.622
0.01_8	0.0003	1.460	0.001_5	0.0028	1.675
0.02	0.0014	1.496	0.01	0.0038	1.731
0.02_2	0.0014	1.533	0.01	0.0049	1.761
0.02_2	0.0024	1.573	0.01	0.0066	1.795
0.025	0.0034	1.612	0.01	0.0072	1.830
0.032	0.0058	1.650	0.02	0.0092	1.861
0.038	0.0071	1.693	0.02	0.0116	1.898
0.042	0.0098	1.732	0.03	0.0140	1.932
0.054	0.0108	1.771	0.04	0.0174	1.966
0.054	0.0145	1.817	0.052	0.0211	2.003
0.068	0.0173	1.856	0.066	0.0258	2.037
0.085	0.0227	1.893	0.074	0.0312	2.080
0.10	0.0277	1.930	0.119	0.0437	2.140
0.115	0.0341	1.964	0.164	0.0616	2.204
0.135	0.0412	1.996	0.220	0.0836	2.256
0.157	0.0470	2.021	0.276	0.1076	2.305
0.177	0.0538	2.048	0.333	0.1332	2.351
0.219	0.0720	2.097	0.392	0.1627	2.390
0.261	0.0950	2.138	0.452	0.1942	2.427
0.304	0.1143	2.173	0.506	0.2229	2.469
0.344	0.1342	2.204	0.562	0.2523	2.506
0.384	0.1559	2.229	0.616	0.2851	2.544
0.429	0.1748	2.268	0.670	0.3189	2.579
0.473	0.1995	2.295	0.722	0.3477	2.611
0.513	0.2208	2.324	0.772	—	2.645
0.552	0.2421	2.348	0.820	—	2.681
0.587	0.2634	2.375	0.867	—	2.719
0.622	0.2813	2.935	0.912	—	2.758

Table 2. Continued

0.956	—	2.799
0.998	—	2.841
1.040	—	2.880

Titration 3. B = 10 mM

Z	η	$-\log h$
0.00	0.0000	1.731
0.01	0.0007	1.768
0.00	0.0024	1.812
0.02	0.0027	1.852
0.01	0.0037	1.900
0.03	0.0054	1.945
0.028	0.0085	2.001
0.041	0.0108	2.057
0.050	0.0145	2.121
0.069	0.0220	2.187
0.102	0.0314	2.251
0.143	0.0477	2.317
0.195	0.0646	2.380
0.261	0.0926	2.432
0.329	0.1248	2.484
0.396	0.1616	2.544
0.511	0.2164	2.611
0.548	0.2360	2.637
0.625	0.2782	2.682
0.661	—	2.709
0.700	—	2.730
0.738	—	2.757
0.776	—	2.780
0.810	—	2.814
0.847	—	2.841
0.885	—	2.866
0.922	—	2.894

Titration 4. B = 5 mM

Z	η	$-\log h$
0.01	−0.0008	1.563
0.04	0.0002	1.592
0.00	−0.0001	1.628
0.00	−0.0004	1.660
0.00	0.0002	1.695
−0.01	0.0002	1.732
0.02	0.0002	1.768
0.00	0.0009	1.813
0.02	0.0009	1.854
−0.02	0.0022	1.905
−0.02	0.0029	1.957
0.01_4	0.0039	2.010
0.01_4	0.0043	2.074
0.024	0.0087	2.143
0.026	0.0141	2.226
0.046	0.0232	2.317
0.096	0.0425	2.412
0.172	0.0729	2.512
0.274	0.1179	2.610
0.402	0.1780	2.699
0.542	0.2524	2.792
0.690	—	2.887
0.838	—	2.992
0.986	—	3.118

Titration 5. B = 5 mM

Z	η	$-\log h$
−0.02	0.0016	1.808
−0.02	−0.0004	1.839
−0.02	−0.0001	1.869
−0.02	0.0002	1.898
−0.04	−0.0008	1.934
−0.02	−0.0001	1.966
−0.02	0.0009	2.006
−0.01	0.0029	2.043
−0.02	0.0046	2.087
−0.02	0.0063	2.133
−0.02	0.0097	2.184
−0.006	0.0124	2.233
0.02	0.0164	2.283
0.024	0.0249	2.348
0.056	0.0344	2.407
0.094	0.0459	2.469
0.158	0.0655	2.518
0.216	0.0902	2.579
0.288	0.1179	2.633
0.368	0.1524	2.681
0.442	—	2.743
0.530	—	2.789
0.612	—	2.844
0.700	—	2.896
0.784	—	2.959

Titration 6. B = 2.5 mM

Z	η	$-\log h$
−0.04	0.0010	1.800
−0.04	0.0017	1.822
−0.04	0.0020	1.844
0.00	0.0020	1.862
0.00	0.0017	1.883
0.00	0.0024	1.906
0.00	0.0034	1.930
−0.04	0.0044	1.954
−0.04	0.0051	1.977
-0.02_4	0.0064	2.003
−0.004	0.0074	2.026
−0.004	0.0078	2.052
-0.01_2	0.0085	2.080
-0.01_2	0.0091	2.108
−0.004	0.0108	2.136
0.004	0.0112	2.165
0.008	0.0132	2.199
−0.004	0.0142	2.231
0.02_4	0.0159	2.260

Table 2. Continued

0.01_2	0.0186	2.299	0.08	0.0047	1.901
0.02_0	0.0210	2.336	0.04	0.0054	1.925
0.03_2	0.0233	2.375	0.08	0.0057	1.945
0.03_2	0.0270	2.419	0.04	0.0064	1.972
0.060	0.0318	2.459	−0.004	0.0071	2.001
0.068	0.0395	2.508	0.004	0.0085	2.025
0.088	0.0473	2.556	−0.02	0.0091	2.054
0.124	0.0588	2.603	0.01	0.0101	2.077
0.164	0.0744	2.652	−0.02	0.0115	2.109
0.228	0.0953	2.699	−0.02	0.0125	2.138
0.264	0.1170	2.750	−0.01	0.0135	2.167
0.320	0.1487	2.802	−0.004	0.0159	2.196
0.384	0.1792	2.850	0.004	0.0179	2.229
0.460	0.2113	2.897	−0.008	0.0199	2.266
0.528	0.2529	2.951	−0.008	0.0227	2.304
0.616	—	2.988	−0.004	0.0264	2.342
			0.008	0.0294	2.381
			0.02	0.0335	2.422
			0.03	0.0395	2.468
			0.048	0.0507	2.515
			0.080	0.0588	2.559
			0.15	0.0886	2.657
			0.096	0.0669	2.581 *
			0.064	0.0507	2.513 *
			0.036	0.0379	2.452 *
			0.03	0.0318	2.395 *
			0.01	0.0308	2.348 *

Titration 7. B = 2.5 mM

Z	η	−log h
	0.0010	1.737
	0.0017	1.758
	0.0024	1.778
	0.0027	1.798
	0.0027	1.819
	0.0037	1.840
	0.0030	1.862
0.03	0.0044	1.881

* Back titrations

formula, *i. e.* $Me[(OH)_tMe]_n$ where t is a constant and n may be a constant or have several integral values [15,19–22]. If all of the complexes can be described by the "core + links" hypothesis, the curves $Z(\log h)_B$ and $\eta\,(\log h)_B$ must form a family of parallel curves with a constant spacing along the log h axis. The value of t, the number of hydroxyl groups per "link", may be obtained from (5).

$$\left(\frac{\partial \log B}{\partial \log h}\right)_Z = \left(\frac{\partial \log B}{\partial \log h}\right)_\eta = t \qquad (5)$$

It is seen that the data for the hydrolysis of tin(II), given in Figs. 2 and 3, form approximately parallel curves. The spacing between the curves gives the difference quotients

$$\left(\frac{\Delta \log B}{\Delta \log h}\right)_Z = \left(\frac{\Delta \log B}{\Delta \log h}\right)_\eta = 2.0 \qquad (5a)$$

It follows from eqn. (5) that the value of t may be obtained directly from the slope of the curves $\log B\ (\log h)_Z$ and $\log B\ (\log h)_\eta$ given in Figs. 4 and 5. Neglecting the slight deviations at low B, the data form straight lines with slopes of 2.0.

The value of t obtained may be tested by plotting Z and η *versus* $\log B - t \log h$. Since the limitation to "core + links" species requires Z and η

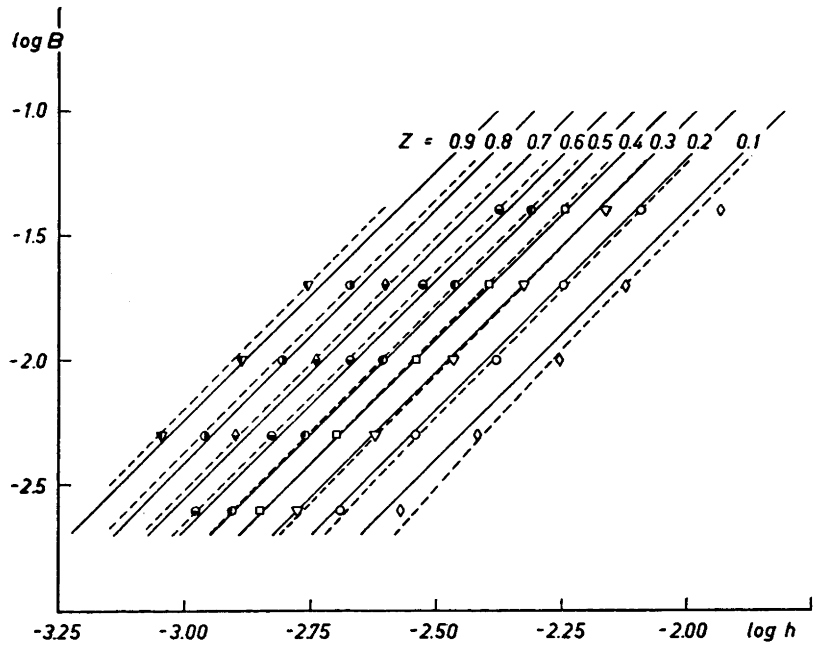

Fig. 4. log B as a function of log h, Z as a parameter. Full curves calculated for $K_{11} = K_{22} = 0$, log $K_{43} = -6.69$. Broken curves calculated for log $K_{11} = -3.92$, log $K_{22} = -4.45$, log $K_{43} = -6.77$.

to be functions of the single variable $u = (bh^{-t})$ and $Bh^{-t} = f(u)$, Z and η are functions of the variable (Bh^{-t}). The data are most conveniently plotted as

$$y = Z/2 \textit{ versus } x = \log (Bh^{-t})$$
$$\eta \textit{ versus } x = \log (Bh^{-t})$$

These data are given in Figs. 6 and 7.

Since all of the experimental points seem to describe the same curve within the range 40 mM $\geqslant B \geqslant$ 5 mM, the "core + links" hypothesis may be considered a good explanation of the data. A significant discrepancy occurs for $B = 2.5$ mM in the plot $\eta(x)$. Deviations in this direction are to be expected if mononuclear species are formed in addition to the "core + links" complexes. Although this deviation appears to be beyond the experimental error, a discussion of the effect will be postponed until the data have been evaluated in the region where the $y(x)$ and also the $\eta(x)$ curves coincide for $t = 2$.

Direct analysis of the curves $y(x)$ and $\eta(x)$

As outlined by Sillén in AB II[8], it is possible to calculate the equilibrium constants for the "core + links" complexes directly from the experimental data $y(x)$ and $\eta(x)$.

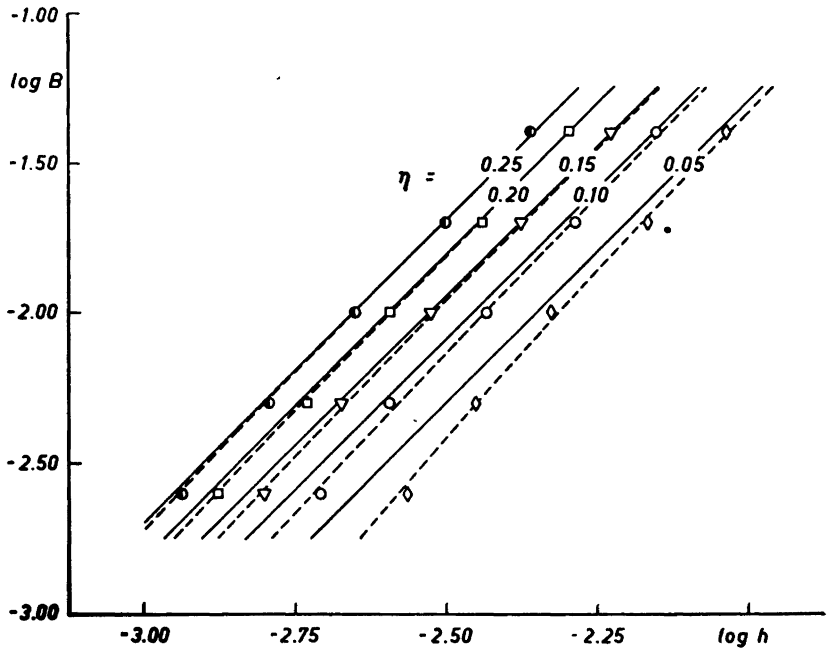

Fig. 5. log B as a function of log h, η as a parameter. Curves calculated for the same sets of constants as in Fig. 4.

If k_n is defined as the equilibrium constant for the reaction

$$(n + 1)\ Sn^{2+} + 2n\ H_2O \rightleftharpoons Sn[(OH)_2Sn]_n^{2+} + 2n\ H^+,$$

then

$$B = b + \sum (n+1)\ [Sn[(OH)_2Sn]_n^{2+}] = b + \sum (n+1)k_n h^{-2n} b^{n+1} \qquad (6)$$

Substituting $u = (h^{-2}b)$ into (6)

$$B = b\ (1 + \sum (n+1)k_n u^n) \qquad (7)$$

if $g = \sum k_n u^n$, $\frac{dg}{du} = g'$, substitution into (7) gives

$$B = b\ \frac{d}{du}\ (u + ug) = b(1 + g + ug') \qquad (8)$$

From (8) it is seen that

$$(1 + g) = u^{-1} \int_0^u Bb^{-1}\ du = u^{-1} \int_0^u 10\eta\ du \qquad (9)$$

It follows directly from the definitions of u, x, and η that

$$\log u = x - \eta. \qquad (10)$$

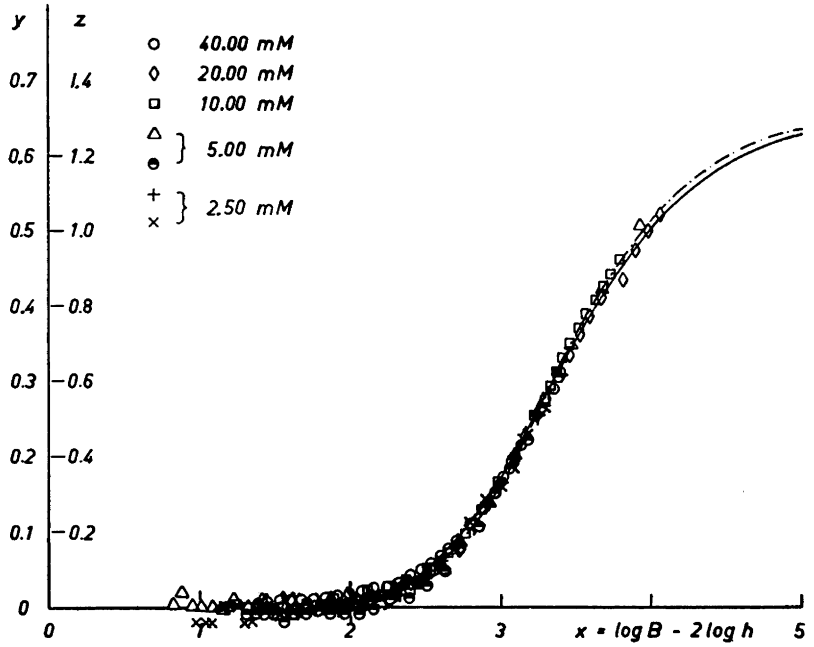

Fig. 6. Z or $y = Z/2$ as a function of $x = \log B - 2 \log h$. All experimental points are shown using the same symbols as in Fig. 2. Full curve calculated for $K_{11} = 0$, $\log K_{23} = -4.43$, $\log K_{43} = -6.74$. Broken curve calculated for $\log K_{43} = -6.69$.

Therefore $g(u)$ may be obtained from the amalgam electrode data $\eta(x)$, using (9) and (10).

One may also calculate the average number of links in the complexes (average degree of polymerization) defined by

$$\bar{n} = \frac{\sum nc_n}{\sum c_n} = \frac{ug'}{g} \tag{11}$$

Substituting from (8)

$$\bar{n} = \frac{Bb^{-1} - g - 1}{g} \tag{12}$$

η can also be obtained as a function of u from the glass electrode data $y(x)$ using the eqn. (15) given by Sillén in AB II [8]. In the present case $y = Z/t = Z/2$.

$$\eta = y \log e + \int_{-\infty}^{x} y dx \qquad \text{together with} \tag{13}$$

$$\log u = x - \eta \tag{10}$$

Although $g(u)$ may then be obtained from (9) as with the amalgam electrode data, it is simpler to apply a relation obtained from eqns. (5a) and (8a) in AB II[8].

$$\log (1 + g) = \eta + \log (1 - y) \tag{14}$$

Equation (14) may be easily derived in the following way. The total number of bound OH groups per liter of solution is given by the following equation (comparing with equations (6) to (8)).

$$BZ = \sum 2n[\mathrm{Sn}[(\mathrm{OH})_2\mathrm{Sn}]_n^{2+}] = 2b\sum nk_nu^n = 2bug' \tag{15}$$

Inserting $Z = 2y$, $Bb^{-1} = (1 + g + ug')$ (8), and $Bb^{-1} = 10^{\eta}$ '(definition) and eliminating Bb^{-1} and ug' gives $(1 + g) = 10^{\eta}(1 - y)$. Upon taking logarithms we obtain (14).

Substituting (14) into (12) we obtain

$$\bar{n} = \frac{y}{1 - y - bB^{-1}} \tag{16}$$

Using (13), (10), and (14), one may obtain $\eta(x)$ and $g(u)$ from the glass electrode data $y(x)$.

In order to calculate $g(u)$ form the amalgam electrode data, a smooth curve was drawn through the data $\eta(x)$ using the lowest values of η where slight deviations occurred at low values of η. η was then read off for a number of values of x. Using eqn. (10), a new curve was constructed for B/b as a function of u. The integration in eqn. (9) was made graphically. The data for g, u, and $\bar{n}$ calculated from eqn. (12) are given in Table 4. Since from eqn. (11) $\bar{n} = u\ g'/g = \mathrm{d}\log g/\mathrm{d}\log u$, $\bar{n}$ may also be obtained from a plot of log g *versus* log u. This is given in Fig. 8. In order to evaluate the polynuclear complexity constants, the function $gu^{-1} = k_1 + k_2u + \ldots$ was plotted *versus* u in Fig. 9.

In a similar fashion, a smooth curve was drawn through the glass electrode data $y(x)$. Again when deviations occurred at low values of y, the lowest values were chosen for each x. The values of B/b, log g, and log u were calculated using

Table 3. Direct analysis of curve $y(x)$.

y	x	$\int_{-\infty}^{x} y\,\mathrm{d}x$	B/b	log u	log g	$\bar{n}$
0.104	2.800	0.0339	1.199	2.7212	−1.1308	1.68
0.135	2.900	0.0458	1.272	2.7953	−1.0000	1.71
0.166	3.000	0.0609	1.358	2.8671	−0.8761	1.69
0.201	3.100	0.0792	1.468	2.9333	−0.762	1.70
0.240	3.200	0.1013	1.605	2.9945	−0.6576	1.75
0.274	3.300	0.1270	1.762	3.0539	−0.5544	1.73
0.319	3.400	0.1566	1.972	3.1052	−0.4647	1.83
0.364	3.500	0.1908	2.233	3.1510	−0.3768	1.94
0.397	3.600	0.2288	2.519	3.1987	−0.2848	1.93
0.427	3.700	0.2704	2.856	3.2442	−0.1965	1.91
0.454	3.800	0.3144	3.248	3.2885	−0.1118	1.91
0.480	3.900	0.3611	3.712	3.3304	−0.0315	1.91
0.506	4.000	0.4104	4.268	3.3698	0.0444	1.95

Table 4. Direct analysis of curve $\eta(x)$.

B/b	u	$\frac{1}{u}\int_0^u B/b\ du$	log u	log g	$\bar{n}$
1.042	200	1.0173	2.3010	−1.7620	1.44
1.073	300	1.0307	2.4771	−1.5129	1.37
1.118	400	1.0469	2.6021	−1.3288	1.51
1.171	500	1.0664	2.6990	−1.1778	1.58
1.236	600	1.0893	2.7782	−1.0491	1.65
1.316	700	1.1159	2.8451	−0.9359	1.72
1.408	800	1.1467	2.9031	−0.8335	1.80
1.505	900	1.1810	2.9542	−0.7423	1.79
1.611	1 000	1.2187	3.0000	−0.6601	1.79
1.719	1 100	1.2592	3.0414	−0.5864	1.77
1.832	1 200	1.3000	3.0792	−0.5229	1.77
1.958	1 300	1.3463	3.1139	−0.4605	1.77
2.068	1 400	1.3939	3.1461	−0.4056	1.71
2.222	1 500	1.4440	3.1761	−0.3526	1.75

eqns. (10) and (14), performing the integration in (13) graphically. These data together with the values of $\bar{n}$ calculated with eqn. (16) are given in Table 3. The data are plotted as log g *versus* log u together with the amalgam electrode data in Fig. 8. The function gu^{-1} is also plotted *versus* u in Fig. 9 together with the amalgam data.

In performing the integration in eqn. (13), it was assumed that the residual integral

$$\delta = \int_{-\infty}^{x=1.7} y\ dx = 0 \qquad (17)$$

It is seen from the data in Tables 3 and 4 and the slope of the curve in Fig. 8 that $\bar{n}$ rises from approximately 1.7 to 2.0, indicating that the trimer $Sn[(OH)_2\ Sn]_2^{2+}$ predominates at high values of y and η. It is seen from the $y(x)$ data that $\bar{n}$ approaches 2.0 as a limit, *i. e.* $d\bar{n}\,/\,du = 0$ at high values of u. This indicates that no complexes higher than the trimer are present in significant amounts.

The data were also used to calculate the number of hydroxyl groups bound per complexed metal atom. This quantity $BZ(B-b)^{-1}$ had an average value 1.30 ± 0.03 for $2.6 \leqslant x \leqslant 3.5$ indicating the complex is primarily $Sn_3(OH)_4^{2+}$.

The values of the equilibrium constants for the dimer and trimer "core + links" complexes may be obtained from the slope and intercept of the curve in Fig. 9. The following values were obtained

$$\log K_{22} = -4.4_3 \pm 0.15$$
$$\log K_{43} = -6.74 \pm 0.04$$

The solid lines in Figs. 6 and 7 were calculated with these constants.

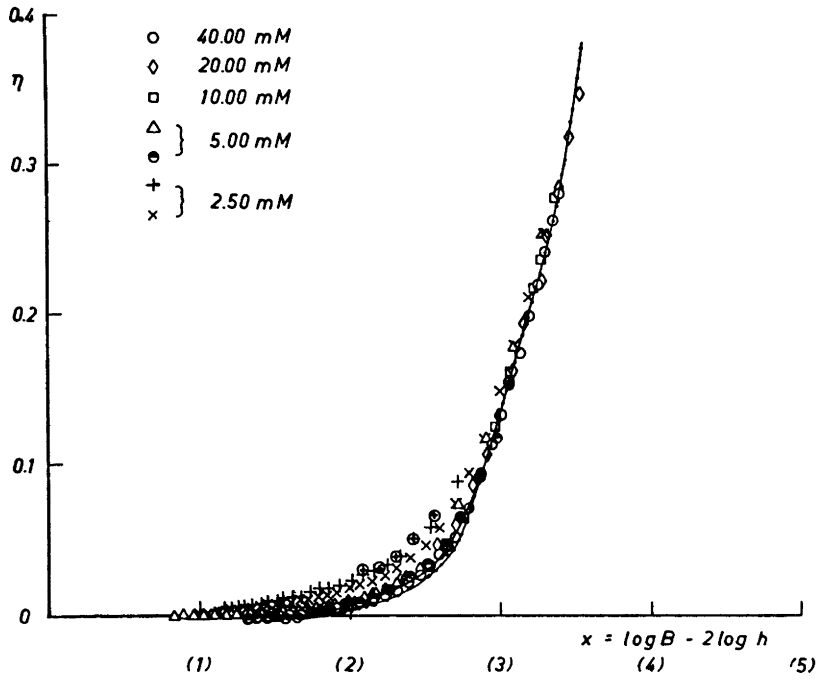

Fig. 7. η as a function of $x = \log B - 2 \log h$. All experimental points are shown using the same symbols as in Fig. 3. Curves calculated for the same sets of constants as in Fig. 6.

Comparison with simple reaction mechanisms

The experimental curves $y(x)$ and $\eta(x)$ were compared with the families of curves $y(X)$ and $\eta(\xi)$ calculated for the simple reaction mechanisms outlined in AB II[8] and part 8[19] of this series.

No agreement was found between the experimental curves and those calculated on the basis of hypothesis I. This hypothesis assumes that no soluble complexes occur and only a precipitate is formed.

Good agreement was obtained between the experimental and theoretical curves calculated for hypothesis II with $N = 2$. This hypothesis assumes the formation of a single soluble complex where n has the single value N. This again indicates that the trimer $Sn[(OH)_2Sn]_2^{2+}$ is the main complex formed by the hydrolysis of solutions of tin(II). The equilibrium constant for the reaction may be obtained in the following way. The constant k is defined by

$$k_n = k^N, \tag{18}$$

when n has the single value N and where k_n is the equilibrium constant for the reaction

$$(n + 1)\ Sn^{2+} + nt\ H_2O \rightleftharpoons Sn[(OH)_tSn]_n^{2+} + nt\ H^+$$

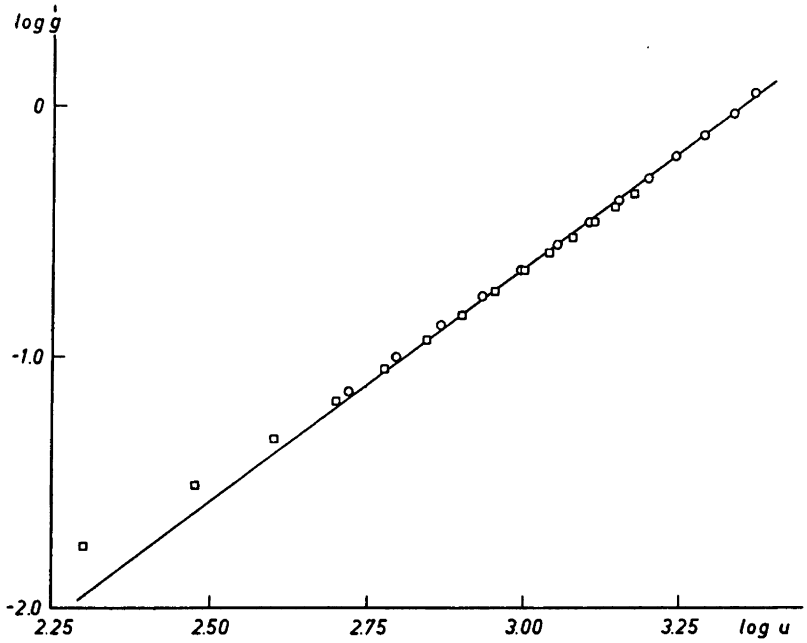

Fig. 8. Direct analysis of the curves $y(x)$ (Fig. 6) O, and $\eta(x)$ (Fig. 7) □: log g as a function of log u, together with the best straight line of slope 1.92.

By moving the calculated curves $y(X)$ and $\eta(\xi)$ across the experimental points, the differences $(X-x)$ and $(\xi-x)$ can be read off at the position of best fit. The value of k is then obtained directly from one of the relations

$$(X-x) = \log 2 - x_{½} = -\log 2 + \log k \text{ [(24), (25) AB II}^{8}\text{]} \quad (19)$$

where $x_{½}$ = value of x at $y = 1/2$, or from

$$(\xi-x) = \log k + \tfrac{1}{2} \log 3 \text{ [(59) AB II}^{8}\text{]} \quad (20)$$

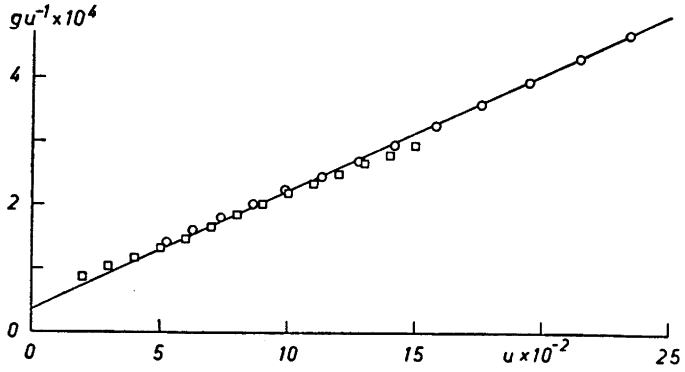

Fig. 9. gu^{-1} as a function of u. $y(x)$ data O, $\eta(x)$ data □. Straight line drawn for log $K_{43} = -6.74$, log $K_{32} = -4.43$.

The best overall fit between the curves $y(X)$ and $y(x)$ gave log $k = -3.36$. If the deviations at low values of y were ignored and the curves matched so the best fit was obtained at high values of y where effects due to complexes lower than the trimer would be small, log $k = -3.37$. The value of the equilibrium constant for the reaction

$$3\ Sn^{2+} + 4\ H_2O = Sn_3(OH)_4^{2+} + 4H^+$$

is related to k by

$$K_{43} = k^N = k^2 \tag{18a}$$

The best overall fit is obtained with log $K_{43} = -6.72$ or for the best fit at high values of y, log $K_{43} = -6.74$.

The curves $\eta(x)$ and $\eta(\xi)$ were compared in the same way. The best overall fit was obtained with log $k = -3.34$, which corresponds to log $K_{43} = -6.68$. From the best fit at high values of η, log $k = -3.37$ which again corresponds to log $K_{43} = -6.74$.

The curves $y(X)$ and $\eta(\xi)$ were also calculated for the repeated mechanisms (AB II[8]), III-a, -b, -c for different values of k_0. A satisfactory agreement could not be obtained between these curves and the experimental data $y(x)$ and $\eta(x)$ using any of these hypotheses. In particular, large deviations occurred for $y > 0.3$, as the theoretical curves all rose too sharply. This is caused by the consideration of polymers higher than the trimer in all of these hypotheses.

Comparison with these simple mechanisms has verified the information obtained from the direct analysis of the experimental data, *i. e.* there seems to be no evidence for the formation of complexes higher than the trimer $Sn_3(OH)_4^{2+}$ during the hydrolysis.

If one views both sets of data $y(x)$ and $\eta(x)$ simultaneously, the best overall fit is with log $K_{43} = -6.69 \pm 0.04$; however, significant deviations occur at both high and low values of y and η. The full lines in Figs. 2, 3, 6, and 7 are calculated for log $K_{43} = -6.69$. The best fit to both sets of data at high values of y and η is obtained with log $K_{43} = -6.74 \pm 0.04$, a value which is identical with that obtained by direct analysis of the data.

Secondary reactions

Although it appears that the main parts of the curves $y(x)$ and $\eta(x)$ are compatible with the formation of a single complex $Sn_3(OH)_4^{2+}$, there are definite deviations at low values of Z,η, and B indicating the presence of small amounts of other complexes.

In an attempt to establish the formulas of the secondary products, an approach similar to that used by Kakihana and Sillén [22] will be used.

It is first assumed that only one other complex besides $Sn_3(OH)_4^{2+}$ is formed. The equilibrium constants for the two species will be written as K_{pq} and K_{43}. Charges will be omitted in the following equations.

$$\begin{aligned} B &= [Sn^{2+}] + q[Sn_q(OH)_p] + 3\ [Sn_3(OH)_4] \\ &= b + qb^q h^{-p} K_{pq} + 3\ b^3 h^{-4} K_{43} \\ BZ &= pb^q h^{-p} K_{pq} + 4\ b^3 h^{-4} K_{43} \\ BZ\ b^{-3} h^4 &- 4K_{43} = pb^{(q-3)} h^{(4-p)} K_{pq} \end{aligned} \tag{21}$$

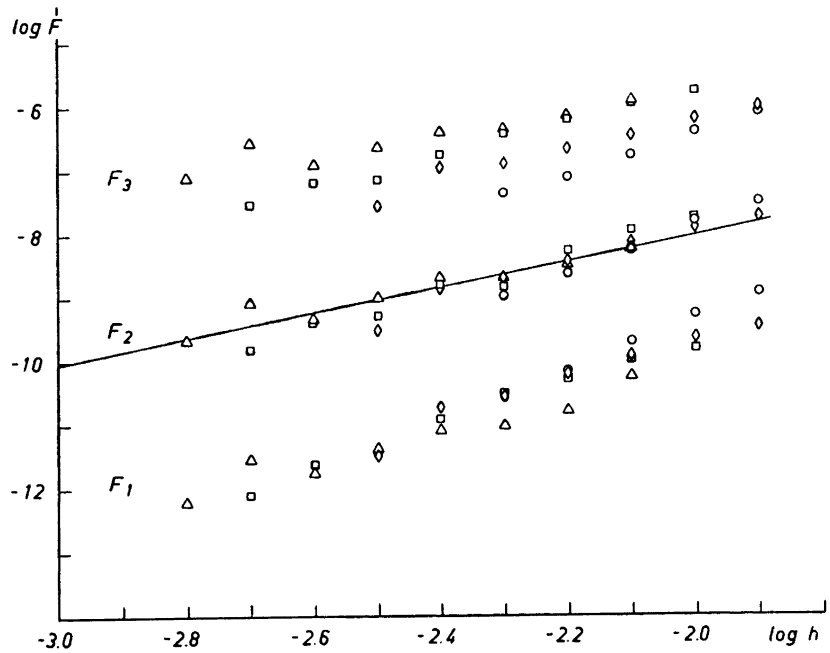

Fig. 10. log F_1, log F_2, and log F_3 (eqn. 22) *versus* log h. Straight line (log F_2) calculated using log $K_{22} = -4.30$. The experimental points are given for 40 mM$>B>$5 mM.

Let
$$(BZ\ b^{-3}h^4 - 4K_{43})b^{(3-q)} = F_q \quad (22)$$
$$\log F_q = \log pK_{pq} + (4\text{-}p) \log h \quad (23)$$

The function F_q was calculated for $q = 1$, 2, and 3, assuming $K_{43} = -6.74$, using the data from the glass and amalgam electrodes for 5 mM $\leq B \leq$ 40 mM, and plotted *versus* log h. If the deviations from the single complex curve can be attributed primarily to one other complex, one should obtain a straight line with slope $(4\text{-}p)$ and intercept log pK_{pq} when the correct value of q has been chosen.

The data are shown in Fig. 10. For $q = 2$ the data form a good approximation to a straight line with a slope of 2. The data for $q = 1$ and 3 both exhibit a greater spread. In agreement with the result of the direct analysis, the hydrolysis data can be well explained for the range 5 mM$\leq B \leq$40 mM by the formation of two polynuclear complexes $Sn_2(OH)_2^{2+}$ and $Sn_3(OH)_4^{2+}$. A value of log $K_{22} = -4.3 \pm 0.2$ is obtained from the position of the best straight line in Fig. 10.

It is still necessary to explain the deviations at the lowest value of B, 2.5 mM. The only reasonable explanation of these deviations is, besides experimental errors, the presence of mononuclear complexes. The method of Hedström [24] was used to obtain values for the mononuclear constants. Using data for both b and h, we may calculate

$$\frac{B\text{-}b}{b} = (K_{11}h^{-1} + K_{21}h^{-2} + K_{31}h^{-3} + \ldots) + 2b\ (K_{12}h^{-1} + K_{22}h^{-2} + K_{32}h^{-3} + \ldots) + 3b^2\ (K_{13}h^{-1} + K_{23}h^{-2} + \ldots) + \ldots \quad (24)$$

Plots were made of (a) $[(B—b)/b]h$ and (b) $[(B—b)/b]h^2$ *versus* b. Because the main complex is a trimer, the functions vary essentially as the square of b. This renders the extrapolation to $b = 0$, required to determine the mononuclear constant, quite inaccurate. If a single complex $SnOH^+$ is formed, the intercept of plot (a) should be K_{11}, while if $Sn(OH)_2$ (aq) is formed the intercept of (b) should be K_{21}. The data appear to be best satisfied by the formation of a mononuclear complex $SnOH^+$ with $K_{11} = 1.2 \times 10^{-4}$. The determination of K_{11} is quite inaccurate, since the extrapolation is governed almost entirely by the set of points for $B = 2.5$ where the experimental errors are greatest.

If the proper mononuclear constant has been chosen, a plot of $\left[\left(\frac{B—b}{b}\right)h—K_{11}\right]h/b$ *versus* b should give a straight line with intercept $2K_{22}$ and $3K_{43}\,h^{-2}$ as slope. Values of $K_{11} = 1.1$, 1.2, and 1.3×10^{-4} were tried, and the best family of straight lines was obtained with $K_{11} = 1.2 \times 10^{-4}$ and gave a value of $\log K_{22} = -4.5 \pm 0.15$. The value of K_{43} obtained in this way is quite inaccurate, $\log K_{43} = -6.7 \pm 0.2$.

Calculation of equilibrium constants with normalized projection maps

Since the effects due to mononuclear and dinuclear complexes are slight, it is best to refine the values of the constants using the method of projection maps.

In the present work, the quantities b, h, B, H are known. The presence of the two polynuclear species may be considered established by the previous discussion; however, there is still some question as to the composition of the mononuclear complex(es).

For this reason projection maps were constructed for the two extreme cases (a) one mononuclear complex $SnOH^+$ (b) one mononuclear complex $Sn(OH)_2$.

In the first case (a)

$$B = b + K_{11}bh^{-1} + 2K_{22}b^2h^{-2} + 3K_{43}b^3h^{-4} \quad (25)$$

$$\eta = \log\ (1 + K_{11}h^{-1} + 2K_{22}bh^{-2} + 3K_{43}b^2h^{-4}) \quad (26)$$

$$BZ = K_{11}bh^{-1} + 2K_{22}b^2h^{-2} + 4K_{43}b^3h^{-4} \quad (27)$$

It is convenient to prepare two different projection maps of the variables

$$\log B = f(\log h)_Z$$
$$\log B = f(\log h)_\eta$$

and to compare these with the calculated, normalized projection maps $\log \boldsymbol{B}\ (\log \alpha)_Z$ and $\log \boldsymbol{B}\ (\log \alpha)_\eta$. The normalized variables β and α are defined by the following equations.

$$\beta = b \cdot 10^{P_2} \qquad \boldsymbol{B} = B \cdot 10^{P_2} \quad (28)$$

$$\alpha = h^{-1}\ 10^{P_1} \quad (29)$$

where P_1 and P_2 are constants.

The two constants P_1 and P_2 may be obtained by the displacement of the curve log $\boldsymbol{B}$ (log a)$_Z$ with respect to log B (log h)$_Z$ and also by the displacement of log $\boldsymbol{B}$ (log a)$_\eta$ with respect to log B (log h)$_\eta$, since

$$P_1 = \log a - \log h$$
$$P_2 = \log \boldsymbol{B} - \log B$$

In order to obtain simple equations for calculation, the constants P_1 and P_2 are chosen so that all equilibrium constants will be eliminated from the equations. This necessitates the assumption of some relation between two of the constants. Since the data at high Z and η are well satisfied by the two constants for $Sn_2(OH)_2^{2+}$ and $Sn_3(OH)_4^{2+}$ (*cf.* Figs. 6, 7), a relation will be chosen between K_{22} and K_{43} which satisfies the values obtained by direct analysis.

$$R = K_{43}K_{22}^{-2} = 10^{2.13}$$

By the proper choice of the constants P_1 and P_2, we may make the following equations, analogous to (25)—(27), valid.

$$\boldsymbol{B} = B \cdot 10^{P_2} = (\beta + \beta\alpha + 2\beta^2\alpha^2 + 3R\beta^3\alpha^4) \quad (30)$$
$$\eta = \log (1 + \alpha + 2\beta\alpha^2 + 3R\beta^2\alpha^4) \quad (31)$$
$$\boldsymbol{B}Z = (\beta\alpha + 2\beta^2\alpha^2 + 4R\beta^3\alpha^4) \quad (32)$$

Inserting (28) and (29) into (30)—(32) and comparing with (25)—(27), gives the necessary condition that

$$\begin{aligned} \log K_{11} &= P_1 \\ \log K_{22} &= 2P_1 + P_2 \\ \log K_{43} &= 2 \log K_{22} + 2.13 \end{aligned} \quad (33)$$

The diagram log $\boldsymbol{B}$ (log a)$_\eta$ was constructed by solution of (31) for β using various values of η and a. The values of β were then substituted into (30). The diagrams log $\boldsymbol{B}$ (log a)$_Z$ were constructed by solution of eqn. (34) for β (eqn. (34) is obtained by eliminating $\boldsymbol{B}$ from (30) and (32))

$$(3Z—4)a^4R\beta^2 + 2a^2(Z—1)\beta + Z(1 + a) — a = 0 \quad (34)$$

This was done for several values of a for each Z giving β. As before, substitution of β into (30) gives $\boldsymbol{B}$.

The construction of the maps for $Sn(OH)_2$ was done in the same manner as for $SnOH^+$. The predominance of an uncharged species cannot be considered unlikely, since the predominating mononuclear complex formed by the hydrolysis of Be^{2+} is apparently [22] $Be(OH)_2$. Also in the hydrolysis of Hg(II)[25], the predominating product is $Hg(OH)_2$ (aq). In this case the equations are

$$B = b + K_{21}bh^{-2} + 2K_{22}b^2h^{-2} + 3K_{43}b^3h^{-4} \quad (35)$$
$$\eta = \log (1 + K_{21}h^{-2} + 2K_{22}bh^{-2} + 3K_{43}b^2h^{-4}) \quad (36)$$
$$BZ = 2K_{21}bh^{-2} + 2K_{22}b^2h^{-2} + 4K_{43}b^3h^{-4} \quad (37)$$

Using the same normalized variables,

$$\boldsymbol{B} = B \cdot 10^{P_2} = \beta + \beta\alpha^2 + 2\beta^2\alpha^2 + 3R\beta^3\alpha^4 \quad (38)$$
$$\eta = \log (1 + \alpha^2 + 2\beta\alpha^2 + 3R\beta^2\alpha^4) \quad (39)$$
$$BZ = 2\beta\alpha^2 + 2\beta^2\alpha^2 + 4R\beta^3\alpha^4 \quad (40)$$

and

$$\log K_{12} = 2 P_1 \qquad \log K_{22} = 2 P_1 + P_2 \qquad (41)$$
$$\log K_{43} = 2 \log K_{22} + 2.13$$

In the position of best fit for the two sets of maps calculated for $SnOH^+$,

$$P_1 = \log \alpha + \log h = -3.925 \qquad (42)$$
$$P_2 = \log B - \log B = 3.40 \pm 0.02.$$

Thus from eqns. (33)

$$\log K_{43} = -6.77 \pm 0.03$$
$$\log K_{22} = -4.4_5 \pm 0.15$$
$$\log K_{11} = -3.9_2 \pm 0.15$$

Comparing the experimental data $\log B\ (\log h)_\eta$ with the curves $\log B\ (\log \alpha)_\eta$ calculated assuming the mononuclear complex $Sn(OH)_2$ a good fit could be obtained for $P_1 = -3.23$ and $P_2 = 2.01$. The agreement between the curves $\log B\ (\log \alpha)_Z$ and the experimental data $\log B\ (\log h)_Z$ was, however, extremely bad for these values of P_1 and P_2, the deviations being far greater than the experimental error. In this case, the advantages of having the complete set of data (B b H h) are apparent, since it allows the rejection of faulty hypotheses which appear to satisfy one of the individual sets (B b h) or (B H h).

Since the projection maps allow the simultaneous determination of the polynuclear and mononuclear constants, the above values will be taken as final.

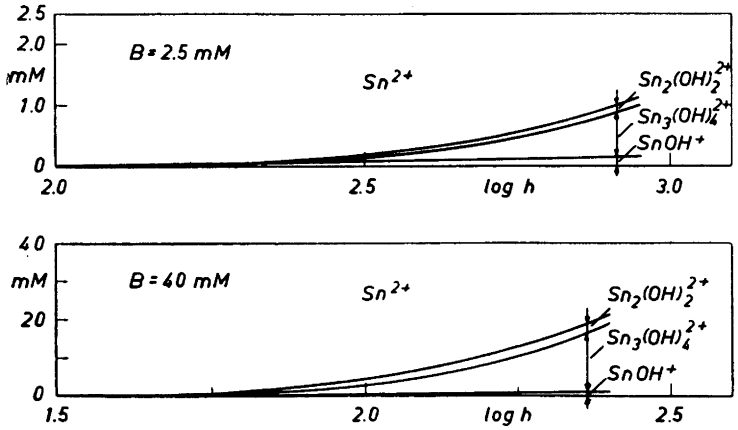

Fig. 11. Distribution of complexes for total tin(II) concentrations B = 2.5, 40 mM as a function of log h, calculated using the constants determined in this work. If a vertical line is drawn for a given value of h, the segment of the line falling in a given area, *e. g.* $Sn_2(OH)_2^{2+}$, represents the concentration of Sn(II) present as this complex in the solution at equilibrium.

The broken lines in Figs. 2 and 3 are calculated with this final set of constants. The projection maps for the final set of constants are given by the broken lines in Figs. 4 and 5.

Fig. 11 shows the distribution of the total tin(II) over the various species as a function of log h and for the total concentrations B = 2.5 mM, 40 mM.

DISCUSSION

Potentiometric measurements giving the set of data (B H b h) for 40 mM $\geq B \geq$ 2.5 mM have shown that the hydrolysis of tin(II) solutions gives the trimer $Sn_3(OH)_4^{2+}$ as the predominating product. In addition, as would be expected, small amounts of the lower complexes $Sn_2(OH)_2^{2+}$ and $SnOH^+$ also are formed. Precipitation occurs shortly above Z = 1.0, and no evidence has been found for the existence of higher polymers than the trimer.

As evidence that the trimer is the primary product, one may cite the good agreement of the values of the equilibrium constant for the reaction

$$3\ Sn^{2+} + 4\ H_2O \rightleftharpoons Sn_3(OH)_4^{2+} + 4\ H^+$$

calculated by different methods.

Direct analysis of $y(x)$ and $\eta(x)$ curves	-6.74 ± 0.04
Curve fitting of data $y(x)$, $y > 0.2$ and $\eta(x)$, $B \geq 5.0$ mM	-6.74 ± 0.04
Projection maps log B (log $h)_Z$ and log B (log $h)_\eta$	-6.77 ± 0.03

The equilibrium constant for the reaction

$$Sn^{2+} + H_2O \rightleftharpoons SnOH^+ + H^+$$

was determined primarily from the data η(log h) for the single value of B=2.5 mM. Unfortunately, K_{11} could not be obtained from data at concentrations lower than 2.5 mM as Z, h, and η could not be measured with sufficient accuracy.

Since the data can be explained by the following equilibria

$$Sn^{2+} + H_2O \rightleftharpoons SnOH^+ + H^+, \quad \log K_{11} = -3.92 \pm 0.15$$
$$2Sn^{2+} + 2H_2O \rightleftharpoons Sn_2(OH)_2^{2+} + 2H^+, \quad \log K_{22} = -4.45 \pm 0.15$$
$$3Sn^{2+} + 4H_2O \rightleftharpoons Sn_3(OH)_4^{2+} + 4H^+, \quad \log K_{43} = -6.77 \pm 0.03$$

it would perhaps be suitable at this time to critically examine the earlier work on the hydrolysis of tin(II) solutions.

As was mentioned earlier, the preparation and handling of solutions of tin(II) presents a rather serious problem, because of the ease with which these solutions become contaminated by small amounts of the much stronger aquo-acid Sn(IV). Milda Prytz, working in N. Bjerrum's laboratory, has the reputation of having been a very careful worker. In her work on tin(II), great care was taken to avoid the oxidation of tin(II), and it is therefore of interest to recalculate these data assuming $Sn_3(OH)_4^{2+}$ to be the hydrolysis product. Because of the nature of the experiments, the values obtained can be considered only roughly approximate. The data, recalculated to give K_{43}, may be summarized as follows.

Mol. conc. $NaClO_4$	B mM	Z	$-\log h$	$\log K_{43}$
0	54.5	0.26	1.85	−5.9
0	43.6	0.29	1.89	−5.7
0	5.45	0.44	2.62	−6.4
0	4.36	0.47	2.68	−6.4
0.5	54.5	0.23	1.91	−6.2

It is seen that the value of K_{43} for the two lowest concentrations of tin(II) and the measurement in 0.5 M $NaClO_4$ agree fairly well with the value calculated above. In this work, the small number of data and their limited accuracy made it impossible to choose the correct reaction.

Gorman [3], also working with perchlorate solutions, obtained a value of $\log K_{11} = -1.70$, corrected to infinite dilution. These data indicate that tin(II) is a much stronger aquo-acid than the work of Prytz does, and if recalculated to give K_{43}, give a constant which is too large by a factor of about 10^2. In this work, the wrong hydrolysis reaction was chosen for the calculations, and a large part of the effect measured was probably caused by tin(IV).

The experiments of Garrett and Heiks [4] were also performed quite carefully to prevent oxidation of tin(II); however, the value of the constant for the reaction

$$SnO(s) + 2H^+ \rightleftharpoons Sn^{2+} + H_2O, \quad K_s = [Sn^{2+}]\,[H^+]^{-2}$$

given in this work is actually the sum of a series of constants $K_s + 2K_s^2K_{22} + 3\,K_s^3K_{43}$, since solubility measurements cannot distinguish between species with the same charge. The hydrolysis constant K_{11} for the monomeric species cannot be obtained with any accuracy when the concentration of the species is very much lower than that of ions with higher charges, as occurs in this case.

In the work of Vanderzee and Rhodes [5], the value of K_{11} was estimated from a term correcting the deviations in the tin(II) halide complexity constants at different hydrogen ion concentrations. Since the effect was quite small, it would be greatly influenced by traces of tin(IV), and the values cannot be considered reliable.

The relatively large value of the constant K_{43} determined in this work and the fact that the data give no indication that species with more than three atoms are formed in any significant concentration makes it unlikely that the complex $Sn_3(OH)_4^{2+}$ has an open chain structure. A ring structure would be more plausible, *e. g.*

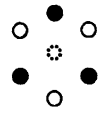

● tin atoms
◌ oxygen atoms below plane of paper
O oxygen atoms above plane of paper

The complex may also contain fewer water molecules such as $Sn_3O(OH)_2^{2+}$, for the equilibrium measurements give no information about the number of solvent molecules bound in the complex. Since equilibrium measurements can give no proof of a structure and there are no crystallographic data available for basic salts of tin(II), no definite conclusions can be drawn.

It may be noted here that a large number of the hydrolysis products of cations may be written in the form $Me[(OH)_2Me]_n$, *i. e.* the "core + links" form with $t = 2$. Among others, Fe(III)[11,19] Cu(II)[26], VO^{2+}[27], Sc^{3+}[28,29], In(III)[15], UO_2^{2+}[21], and Sn(II) appear to exhibit this behavior. When the cation is divalent as in the case of tin(II), the link is uncharged, and the ratio of hydroxide groups to metal ions is the same as in the precipitate.

The author is greatly indebted to Professor Lars Gunnar Sillén for having suggested the problem and for valuable discussions during the course of the work. I would also like to thank Drs. George Biedermann and Åke Olin for help on practical aspects of this research. This work has been made possible by a Post Doctoral Fellowship granted to the author by the *United States National Science Foundation*. It forms part of a program supported by the *Swedish Natural Science Research Council*.

REFERENCES

1. Prytz, M. *Z. anorg. Chem.* **174** (1928) 355.
2. Randall, M. and Murakami, S. *J. Am. Chem. Soc.* **52** (1930) 3967.
3. Gorman, M. *J. Am. Chem. Soc.* **61** (1939) 3342.
4. Garrett, A. B. and Heiks, R. E. *J. Am. Chem. Soc.* **63** (1941) 562.
5. Vanderzee, C. E. and Rhodes, D. E. *J. Am. Chem. Soc.* **74** (1952) 3552.
6. *Ibid.* **74** (1952) 4806.
7. Forsling, W., Hietanen, S. and Sillén, L. G. *Acta Chem. Scand.* **6** (1952) 901 (Part 3).
8. Sillén, L. G. *Acta Chem. Scand.* **8** (1954) 318 (AB II).
9. Biedermann, G. and Sillén, L. G. *Acta Chem. Scand.* **10** (1956) 1011 (AB IV).
10. Sillén, L. G. *Acta Chem. Scand.* **10** (1956) 803.
11. Hedström, B. O. A. *Arkiv Kemi* **6** (1953) 1 (Part 7).
12. Biedermann, G. and Sillén, L. G. *Arkiv Kemi* **5** (1953) 425 (Part 4).
13. Noyes, A. and Toabe, R. *J. Am. Chem. Soc.* **39** (1917) 1537.
14. Lingane, J. J. and Pecsok, R. L. *Anal. Chem.* **20** (1948) 425.
15. Biedermann, G. *Arkiv Kemi* **9** (1955) 277 (Part 14).
16. Haring, M. M. and White, J. C. *J. Electrochem. Soc.* **3** (1938) 211.
17. Brown, A. S. *J. Am. Chem. Soc.* **56** (1934) 646.
18. Sillén, L. G. *Acta Chem. Scand.* **8** (1954) 299 (AB I).
19. Hietanen, S. and Sillén, L. G. *Acta Chem. Scand.* **8** (1954) 1607 (Part 8).
20. Hietanen, S. *Acta Chem. Scand.* **8** (1954) 1626 (Part 9).
21. Ahrland, S., Hietanen, S. and Sillén, L. G. *Acta Chem. Scand.* **8** (1954) 1907 (Part 10).
22. Kakihana, H. and Sillén, L. G. *Acta Chem. Scand.* **10** (1956) 985 (Part 16).
23. Sillén, L. G. *Mimeographed Sheet for Amsterdam Symposium*, April 1955.
24. Hedström, B. O. A. *Acta Chem. Scand.* **9** (1955) 613 (AB III).
25. Hietanen, S. and Sillén, L. G. *Acta Chem. Scand.* **6** (1952) 747 (Part 2).
26. Berecki-Biedermann, C. *Arkiv Kemi* **9** (1956) 175 (Part 13).
27. Rossotti, F. J. C. and Rossotti, H. S. *Acta Chem. Scand.* **9** (1955) 1177 (Part 12).
28. Kilpatrick, M. and Pokras, L. *J. Electrochem. Soc.* **100** (1953) 85.
29. Biedermann, G., Kilpatrick, M., Pokras, L. and Sillén, L. G. *Acta Chem. Scand.* **10** (1956) 1327 (Part 18).

Received October 17, 1957.

ACTA CHEMICA SCANDINAVICA 12 (1958) 224—228

Charakterisierung des Substitutionstyps der Tetracen-Derivative durch ihre Infrarot-Spektren

ARNLJOT NÆRLAND

Forsvarets Forskningsinstitutt, Kjeller pr. Lillestrøm, Norwegen

Bei den einfachen Aromaten von Typ des Benzols bestehen Beziehungen zwischen Frequenz der γ-Schwingung ("out of plane wagging") und Zahl und Stellung der Substituenten, die die Ermittlung des Substitutionstyps von Benzolderivaten erlauben. Es wird in dieser Arbeit bestätigt, dass bei den Derivaten des Tetracens mit vier linear anellierten Benzolringen die gleichen Beziehungen gültig sind.

In den Infrarot-Spektren verschiedener substituierter Benzole treten im Bereich zwischen 11 und 15 μ sehr intensive Banden auf, die für den Substitutionstyp charakteristisch sind. Die intensivsten Banden dieses Gebietes sind Normalschwingungen zuzuordnen, bei welchen die am Benzolring stehenden Wasserstoffatome oder die Kohlenstoffatome senkrecht zur Ringebene schwingen [1]. Bei diesen Deformationsschwingungen von Wasserstoffatomen schwingen alle oder fast alle in Phase [2]. Deformationsschwingungen dieser Art nennt man im deutschen Schriftum »γ-Schwingungen».

Wenn in einem Molekül mehrere Benzolringe von verschiedenen Substitutionstypen durch eine Bindung verknüpft sind, treten im IR-Spektrum die charakteristischen γ-Schwingungsbanden unabhängig von einander auf [3]. Unübersichtlicher liegen die Verhältnisse bei Molekülen, in denen Benzolringe von verschiedenem Substitutionstyp anelliert sind. So treten nach eigenen Untersuchungen die γ-Schwingungen der Naphthalinderivate, wahrscheinlich wegen Zusammenkuppelung der zwei gleichen Benzolringe, nicht in demselben Bereich auf wie bei Benzol. Bei den höheren linear und angular anellierten kondensierten Aromaten scheinen dieselben Gesetzmässigkeiten wie beim Benzol zu gelten. Systematische Untersuchungen, welche dieses bestätigen, sind bei Anthracenen [4], 1,2-Benzanthracenen,[5] und 1,2-*Cyclo*pentenophenanthren durchgeführt worden.[6]

Es wird in dieser Arbeit eine ähnliche Untersuchung für Tetracen-Derivate unternommen. Untersucht wurden Tetracen selbst, acht mono- und di-substituierte und neun tetrasubstituierte Verbindungen. Die Verbindungen wurden im festen Zustand (gepresst in Kaliumbromid) gemessen und, wenn löslich,

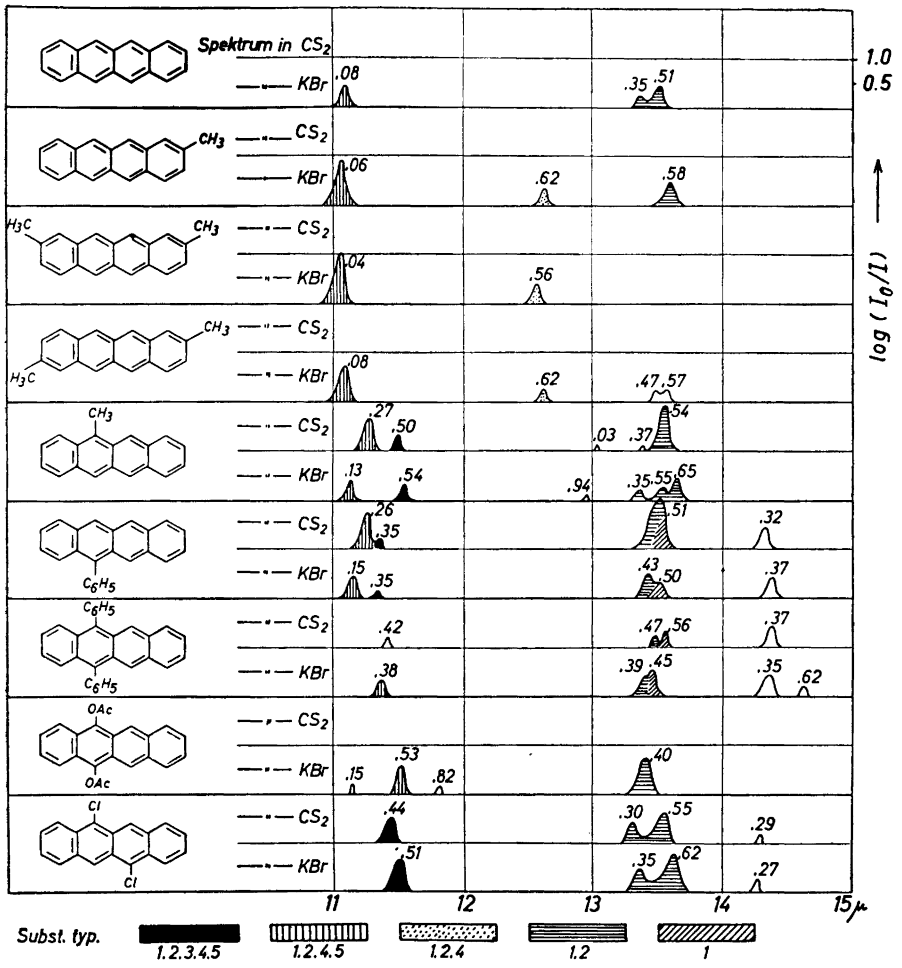

Abb. 1. γ-Schwingungsbanden für Tetracen, sowie mono- und disubstituierte Derivate.

auch in CS_2-Lösung. Die Spektren wurden mit dem Perkin Elmer Modell 21 Infrarot Spectrophotometer aufgenommen. Die γ-Schwingungsbanden für Tetracen, sowie mono- und disubstituierte Tetracene sind in Abb. 1 und für die tetrasubstituierten Tetracene in Abb. 2 angegeben.

Beim Tetracen selbst und Derivaten mit einem Substituenten in den entständigen Ringen liegt die Bande für den 1,2,4,5-Substitutionstyp bei 11,1 μ (Abb. 1, senkrecht schraffiert). Wird der mittelständige Ring substituiert, verschiebt sich die Bande nach rot bis 11,4 μ für Diphenyltetracen und 11,5 μ für Tetracenhydrochinon.

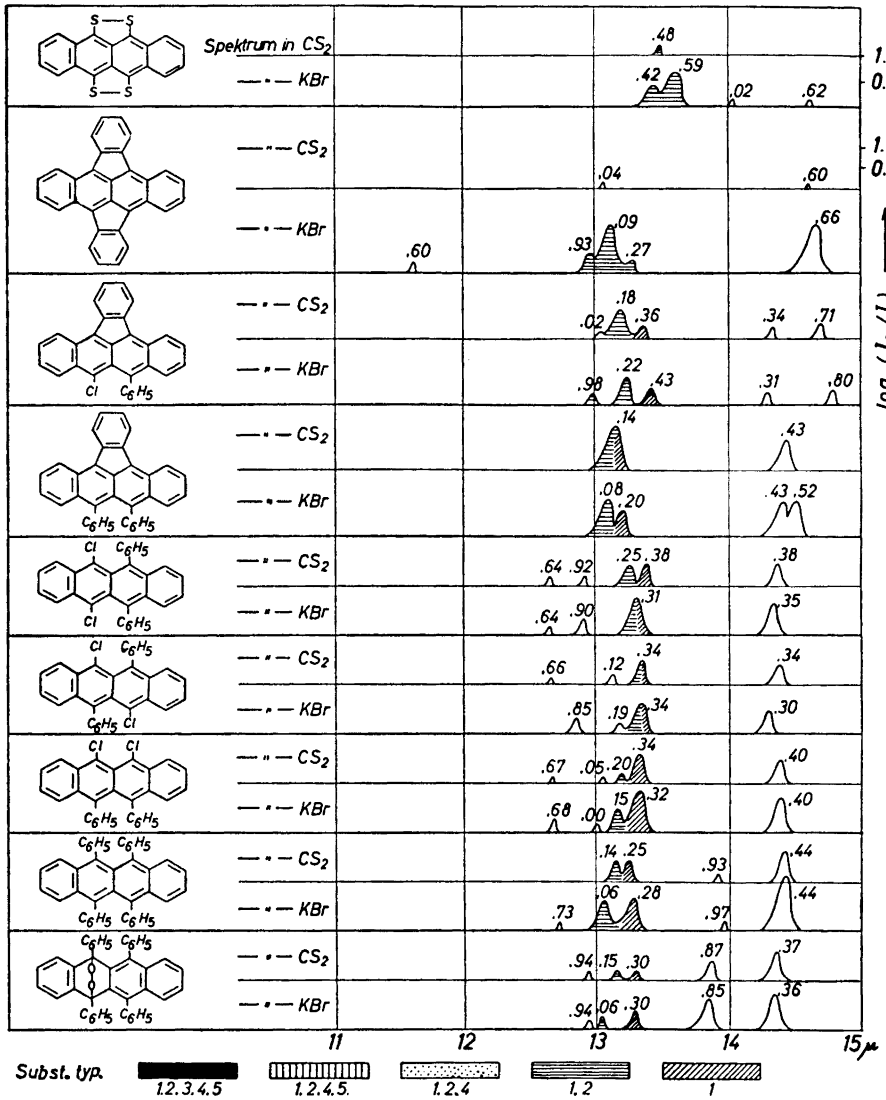

Abb. 2. γ-Schwingungsbanden für tetrasubstituierte Tetracen-Derivate.

Die Bande für die *ortho*-Disubstitution (1,2-Substitutionstyp) liegt in der Gegend zwischen 13,4 und 13,6 μ (Abb. 1, horizontal schraffiert). Sind die beiden mittelständigen Ringe substituiert, verschiebt sich, mit Ausnahme von Tetracentetrasulfid, die Bande nach blau (Abb. 2). So liegt bei Diphenylentetracen eine starke Bande bei 13,1 μ, die von dem *ortho*-Substitutionstyp herrührt. Bei den Verbindungen, in welchen die eine Phenylengruppe durch

Tabelle 1. Lage der γ-Schwingungen bei den Derivaten des Tetracens.

Substitutionstyp		Zahl der Verbind.	*Bereich der γ-Schwingung*	
			Wellenlänge μ	Wellenzahl cm^{-1}
1,2,3,4,5	Lsg.	3	11,35–11,50	881–870
	fest	3	11,35–11,54	881–866
1,2,4,5	Lsg.	3	11,26–11,42	888–876
	fest	8	11,06–11,53	904–867
1,2,4	Lsg.		–	–
	fest	3	12,56–12,62	796–792
1,2	Lsg.	13	13,10–13,55	763–738
	fest	16	13,06–13,65	766–733

Chlor und Phenyl oder durch zwei Phenylgruppen ersetzt sind, kommt, ausser der Bande bei 13,1 μ, längerwellig eine andere Bande vor, die von dem Benzol-monosubstitutionstyp herrührt. Dazu kommt bei allen Phenylsubstituenten eine γ-CC Bande bei 14,4 μ. Bei den drei Dichlor-diphenyl-tetracenen, Rubren und Rubren-photooxyd ist die Wahl zwischen der Bande für die *ortho*-Disubstitution und die Monosubstitution schwieriger zu machen. Beim Vergleich mit Phenylentetracen wird die kurzwelligere Bande dem *ortho*-Disubstitutionstyp zugeordnet.

Die Bande des Pentasubstituierten 5,11-Dichlortetracens liegt bei 11,5 μ (in Abb. 1, schwarz ausgezogen). Bei dem Methyltetracen und dem Phenyltetracen kommt dazu kurzwelliger eine Bande, die von dem 1,2,4,5-Tetrasubstitutionstyp herrühren muss.

Bei den Verbindungen von 1,2,4-Trisubstitutionstyp liegt die Bande ziemlich konstant bei 12,6 μ (in Abb. 1, punktiert).

Wenn man die Spektren in festen Zustand und in CS_2-Lösung vergleicht, sieht man, dass die Banden in festem Zustand im allgemeinen stärker aufgespaltet sind.

Die Bereiche der γ-Schwingungen in Lösung und im festen Zustand sind in Tabelle 1 zusammengestellt. Die Bereiche der γ-Schwingungen der Tetracen-Derivate stimmen mit denen der anderen kondensierten Aromaten gut überein [4].

Die Spektren von Tetracen-5,12-chinon und Tetracen-5,11-chinon wurden ebenfalls aufgenommen. Die bei den Kohlenwasserstoffen gefundene Zuordnung der γ-Schwingungsbanden konnten aber für diese Verbindungen nicht bestätigt werden.

Zum Dank verpflichtet bin ich den Herren Prof. Cook, Glasgow, Dr. E. A. Coulson, Teddington, Prof. Charles Dufraisse, Paris, und Prof. Louis F. Fieser, Cambridge (Mass.) für die Überlassung von Proben. Die übrigen untersuchten Verbindungen wurden im

hiesigen Laboratorium dargestellt. Die Substanzen wurden, sofern sie nicht analysenrein vorlagen, vor Aufnahme des Spektrums durch Chromatographie an Aluminiumoxyd oder durch Umkristallisation gereinigt.

LITERATUR

1. Pitzer, K. S. und Scott, D. W. *J. Am. Chem. Soc.* **65** (1943) 803.
2. Cole, A. R. H. und Thompson, H. W. *Trans. Faraday Soc.* **46** (1950) 103.
3. Cannon, C. G. und Sutherland, G. B. B. M. *Spectrochim. Acta* **4** (1951) 373.
4. Dannenberg, H. und Nærland, A. *Z. Naturforschung* **12b** (1957) 1.
5. Orr, S. F. D. und Thompson, H. W. *J. Chem. Soc.* **1950** 218.
6. Dannenberg, H., Schiedt, U. und Steidle, W. *Z. Naturforschung* **8b** (1953) 269.

Eingegangen am 27. August 1957.

ACTA CHEMICA SCANDINAVICA 12 (1958) 229—232

The Addition of Grignard Reagents to Alkylidenemalonic Esters

GUST.-AD. HOLMBERG

Institutet for organisk kemi, Åbo Akademi, Åbo, Finland

Some aliphatic and aromatic Grignard reagents were allowed to react with ethylidenemalonic and *iso*butylidenemalonic esters. In all cases the corresponding *sec.*-alkylmalonic esters were isolated. The main reaction thus seems to be 1,4-addition to the conjugated system.

For a planned investigation it was necessary to know the way in which ethylidenemalonic ester (I a) and *iso*butylidenemalonic ester (I b) react with Grignard reagents. The literature does not give any information regarding these reactions. However, 1,4-addition has previously been observed in reactions between different Grignard compounds and *iso*propylidenemalonic ester (II).[1,2]

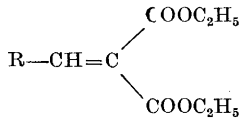

R = (a) CH_3
(b) $CH(CH_3)_2$

I

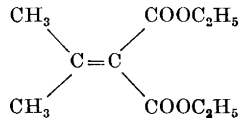

II

As the second methyl group at the β-carbon atom in this ester can hardly alter the course of the reaction with Grignard reagents it was expected that 1,4-addition would also occur with ethylidenemalonic and *iso*butylidenemalonic esters.

This prediction was confirmed when the esters were allowed to react with some aliphatic and aromatic Grignard reagents. The reaction products, *sec.*-alkylmalonic esters, were characterized by conversion into the corresponding barbituric acids. If the latter were not previously known compounds, the malonic esters were also saponified and the corresponding malonic acids iso-

Table 1. Reactions between Grignard reagents and ethyl alkylidenemalonates.

Starting material		Reaction product		
Grignard reagent prepared from	Ethyl alkylidene-malonate	Ethyl malonate	B.p.	Yield %
Methyl iodide	Ethylidene-	*Iso*propyl-	89 — 90°/ 7 mm	82
Ethyl bromide	Ethylidene-	1-Methylpropyl-	107 —108°/10 mm	83
n-Propyl bromide	Ethylidene-	1-Methylbutyl-	117 —118°/10 mm	76
Bromobenzene	Ethylidene-	1-Phenylethyl-	155.5—157°/ 8 mm	76
o-Bromotoluene	Ethylidene-	1-*o*-Tolylethyl-	166.5—168°/10 mm	68
α-Bromonaphthalene	Ethylidene-	1-α-Naphthylethyl-	213 —214°/10 mm	73
Methyl iodide	*Iso*butylidene-	1,2-Dimethylpropyl-	120 —121°/11 mm	81
Bromobenzene	*Iso*butylidene-	1-Phenyl-2-methylpropyl-	167 —169°/ 9 mm	72
o-Bromotoluene	*Iso*butylidene-	1-*o*-Tolyl-2-methylpropyl-	169 —171°/ 9 mm	72

lated. These were then decarboxylated to the corresponding monocarboxylic acids. Both the malonic acids and the monocarboxylic acids were converted into their *p*-nitrobenzyl esters for identification.

The results are collected in Tables 1 and 2.

EXPERIMENTAL

The reactions between the Grignard reagents and the alkylidenemalonic esters were performed in a 250-ml flask fitted with a reflux condenser, a dropping funnel, and a stirrer with precision ground glass bearing. The upper ends of the condenser and the dropping

Table 2. Melting points of substances prepared from the synthesized malonic esters.

Substituent in ethyl malonate R	Barbituric acid 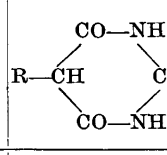	Malonic acid 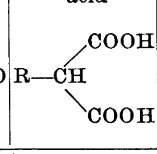	Mono-carboxylic acid $R-CH_2COOH$	*p*-Nitrobenzyl ester of 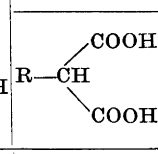	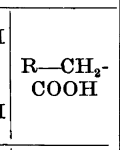
*Iso*propyl-	212 —213°[a]				
1-Methylpropyl-	194 —195°[b]				
1-Methylbutyl-	166 —167°[c]				
1-Phenylethyl-	219 — 220°	142—143°[d]	35 — 36°[e]	111 —112°	60—61°
1-*o*-Tolylethyl-	146 — 147°	118—119°	50 — 51°	129 —130°	42—43°
1-α-Naphthylethyl-	169 — 170°	170—171°	106 —107°[f]	129 —130°	—
1,2-Dimethylpropyl-	222 — 223°	89— 90°	—	63.5 —64.5°	—
1-Phenyl-2-methylpropyl-	200 —201°	136—137°	50 — 51°	112 —113°	41—42°
1-*o*-Tolyl-2-methylpropyl-	181.5—182.5°	152—153°	40.5— 41.5°	96 — 97°	56—57°

The literature gives a) 212—213°, b) 193—194°, c) 167—168°, d) 141—142°, e) 35—36°, f) 108—109°.

Table 3. Analytical data for the new barbituric acids and *p*-nitrobenzyl esters of the prepared malonic and monocarboxylic acids.

R	Barbituric acid 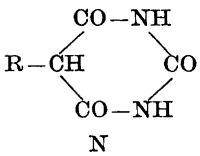 N		*p*-Nitrobenzyl ester of 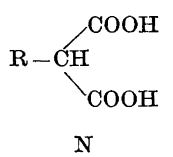 N		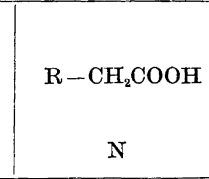 N	
	Found	Calc.	Found	Calc.	Found	Calc.
1-Phenylethyl-	12.26	12.06	5.93	5.86	4.77	4.68
1-*o*-Tolylethyl-	11.52	11.38	5.81	5.69	4.55	4.47
1-*α*-Naphthylethyl-	10.08	9.92	5.50	5.30		
1,2-Dimethylpropyl-	14.25	14.13	6.42	6.30		
1-Phenyl-2-methylpropyl-	10.90	10.76	5.67	5.53	4.36	4.28
1-*o*-Tolyl-2-methylpropyl-	10.32	10.21	5.41	5.38	4.23	4.10

funnel were fitted with calcium chloride tubes. A Grignard reagent was prepared from 0.15 mole of an alkyl or aryl halide, 0.15 mole (3.60 g) of magnesium turnings, and 70 ml of dry ether. After the flask containing the reagent had been cooled in cold water, 0.10 mole of alkylidenemalonic ester was gradually added. After the addition, the stirring was continued for 20 min. The solution was then poured into a mixture consisting of 70 ml of conc. hydrochloric acid, 200 ml of water and about 100 g of ice. After shaking, the organic phase was washed with water and with a dilute potassium carbonate solution. The acid water solution was extracted once with ether, and the ether layer was also washed with water and potassium carbonate before it was combined with the main portion. After drying with anhydrous sodium sulphate, the ether was evaporated and the residue distilled under reduced pressure. The yields and the boiling points are collected in Table 1.

The corresponding barbituric acids were prepared in the following way. A sodium ethoxide solution was prepared from sodium (0.55 g) and absolute ethanol (30 ml). Urea (1.44 g) and malonic ester (0.02 mole) were added. The mixture was boiled for six hours on a boiling water bath. If a precipitate had formed during this time, it was filtered, washed with a small quantity of absolute ethanol, and dissolved in water. The barbituric

Table 4. Analytical data for the new malonic and monocarboxylic acids.

R	$R-CH(COOH)_2$				$R-CH_2COOH$			
	Found		Calc.		Found		Calc.	
	C	H	C	H	C	H	C	H
1-*o*-Tolylethyl-	64.75	6.42	64.85	6.35	74.25	8.01	74.13	7.92
1-*α*-Naphthylethyl-	69.62	5.56	69.75	5.42	78.59	6.71	78.48	6.59
1,2-Dimethylpropyl-	55.02	8.25	55.16	8.10				
1-Phenyl-2-methylpropyl-	66.28	6.70	66.08	6.83	75.18	8.29	74.97	8.29
1-*o*-Tolyl-2-methylpropyl-	67.32	7.18	67.18	7.25	75.54	8.98	75.67	8.80

acid was then precipitated by adding hydrochloric acid. If a precipitate had not formed in the barbituric acid condensation, the alcohol was distilled off under reduced pressure, the residue treated with water and ether, and the barbituric acid in the water phase precipitated by adding hydrochloric acid. The filtered acids were recrystallized from ethanol or aqueous ethanol. The melting points are collected in Table 2 and analytical data for the new barbituric acids in Table 3.

The new malonic esters were converted into the corresponding acids in the following way. The ester (5 g) was boiled for 5 h with a solution of potassium hydroxide (5 g) in water (5 ml) and ethanol (50 ml). In some cases a precipitate of the corresponding potassium salt formed during this time or when the mixture was allowed to cool. The salt was filtered and dissolved in water. The corresponding malonic acid which precipitated on adding hydrochloric acid was filtered. A smaller amount of the same compound could be extracted from the filtrate with ether. A less pure sample was also obtained when the alcoholic filtrate was evaporated, the residue treated with water and ether, and the aqueous phase acidified with hydrochloric acid.

If a precipitate of potassium salt had not formed during the saponification, the alcohol was distilled off and the residue treated with water and ether. The malonic acid was then isolated from the aqueous phase as above.

When 1,2-dimethylpropylmalonic ester (prepared from methylmagnesium bromide and *iso*butylidenemalonic ester) was saponified, no precipitate was formed on adding hydrochloric acid to the aqueous solution. The solution was then extracted three times with ether. After drying and evaporation of the ether, the malonic acid was crystallized by treatment with ligroin and recrystallized from a mixture of benzene and ligroin.

The malonic acids were decarboxylated by heating in a oil bath at 180° until evolution of carbon dioxide ceased. On treatment with ligroin the monocarboxylic acids crystallized. The latter were purified by recrystallization from the same solvent. The yields based on the decrease in weight during the decarboxylation were 97—99 %.

The melting points of the acids are collected in Table 2 and the analytical data for the new compounds in Table 4.

The *p*-nitrobenzyl esters were prepared according to Reid [3].

REFERENCES

1. Wideqvist, S. *Arkiv Kemi, Mineral. Geol.* **23 B** (1946) No. 4.
2. Prout, F. S., Huang, E. P. Y., Hartman, R. J. and Korpics, C. J. *J. Am. Chem. Soc.* **76** (1954) 1911.
3. Reid, E. E. *J. Am. Chem. Soc.* **39** (1917) 124.

Received October 25, 1957.

ACTA CHEMICA SCANDINAVICA 12 (1958) 233—238

Mean Amplitudes of Vibration for the C—H Stretching

S. J. CYVIN

Institutt for Teoretisk Kjemi, Norges Tekniske Høgskole, Trondheim, Norway

Approximate formulae for mean square amplitudes of vibration for the C—H stretching are evaluated. Characteristic numerical values are tabulated.

Calculations of mean amplitudes of vibration from spectroscopic data have proved to be of great interest in molecular structure studies [1]. In the present work the C—H bond distances are studied, and explicit formulae for the mean square amplitudes are given.

When small harmonic vibrations are assumed, the formula to be used is [2]

$$u^2 = \langle r^2 \rangle_{\mathrm{Av}} = \sum_i (hC_i^2/4\pi)\lambda_i^{-\frac{1}{2}} \qquad (1)$$

where $\langle\rangle_{\mathrm{Av}}$ denotes the time average, $\lambda_i = 4\pi^2\nu_i^2$, ν_i being a fundamental frequency, h is Planck's constant, and C_i are the coefficients in

$$r = \sum_i C_i Q_i \qquad (2)$$

where Q_i is a normal coordinate, and r denotes the deviations from the equilibrium C—H distance. The dependence on temperature could be omitted in this case, because the C—H stretching frequencies are comparatively high. The coefficients in eqn. (2) can be computed by means of a normal coordinate analysis. Wilson's GF matrix method [3,4] is very useful for this purpose.

As pointed out by Wilson [4], it is a good approximation to separate the extreme high C—H stretching frequencies in a molecule from the remaining fundamentals. This is very useful in the problem of mean amplitudes of vibration, as explicit formulae for u can be evaluated by applying the method. As a first example, the allene molecule shall be considered, and the formula is going to be worked out in details in the next section.

THE ALLENE MOLECULE

The allene molecule model is of symmetry V_d. If the four C—H distances are taken as a reducible representation of the group, the symmetric structure

$$\Gamma = A_1 + B_2 + E \tag{3}$$

is obtained. Following Wilson's method [3,4], the three symmetry coordinates

$$\begin{aligned} s^{(A_1)} &= (1/2)\ (r_1 + r_2 + r_3 + r_4) \\ s^{(B_2)} &= (1/2)\ (r_1 + r_2 - r_3 - r_4) \\ s^{(E)} &= 2^{-\frac{1}{2}}(r_1 - r_2) \end{aligned} \tag{4}$$

Table 1. Characteristic expressions by calculating mean amplitudes for C—H stretching in certain molecules.

Molecule	Symm. group	Symm. species	F	G	ν/c (cm^{-1})
Acetylene	$D_{\infty h}$	A_{1g}	$k + k''$	$\mu_H + \mu_C$	3 373.7 [5]
		A_{1u}	$k - k''$	$\mu_H + \mu_C$	3 287 [5]
Benzene	D_{6h}	A_{1g}	$K_1 = (k + 2k_p) + (k_m + 2k_o)$	$\mu_H + \mu_C$	3 073 [6]
		B_{1u}	$K_2 = (k + 2k_p) - (k_m + 2k_o)$	$\mu_H + \mu_C$	3 057 [6]
		E_{2g}	$K_3 = (k - k_p) + (k_m - k_o)$	$\mu_H + \mu_C$	3 056 [6]
		E_{1u}	$K_4 = (k - k_p) - (k_m - k_o)$	$\mu_H + \mu_C$	3 064 [6]
Formaldehyde	C_{2v}	A_1	$k + k'$	$\mu_H + 2\mu_C\cos^2\alpha$	2 780 [5]
		B_1	$k - k'$	$\mu_H + 2\mu_C\sin^2\alpha$	2 874 [5]
Ethylene	V_h	A_g	$K_1 = (k + k') + (k'' + k''')$	$\mu_H + 2\mu_C\cos^2\alpha$	3 019.3 [5,7]
		B_{3u}	$K_2 = (k + k') - (k'' + k''')$	$\mu_H + 2\mu_C\cos^2\alpha$	2 989.5 [5,7]
		B_{1g}	$K_3 = (k - k') + (k'' - k''')$	$\mu_H + 2\mu_C\sin^2\alpha$	3 075 [7]
		B_{2u}	$K_4 = (k - k') - (k'' - k''')$	$\mu_H + 2\mu_C\sin^2\alpha$	3 105.5 [5,7]
Allene	V_d	A_1	$K_1 = k + k' + 2k''$	$\mu_H + 2\mu_C\cos^2\alpha$	2 996 [8]
		B_2	$K_2 = k + k' - 2k''$	$\mu_H + 2\mu_C\cos^2\alpha$	3 005 [8]
		E	$K_3 = k - k'$	$\mu_H + 2\mu_C\sin^2\alpha$	3 085 [8]
*Cyclo*propane	D_{3h}	A_1'	$K_1 = (k + k') + 2(k'' + k''')$	$\mu_H + 2\mu_C\cos^2\alpha$	3 029 [5]
		E'	$K_2 = (k + k') - (k'' + k''')$	$\mu_H + 2\mu_C\cos^2\alpha$	3 024.4 [5]
		A_2''	$K_3 = (k - k') + 2(k'' - k''')$	$\mu_H + 2\mu_C\sin^2\alpha$	3 103.0 [5]
		E''	$K_4 = (k - k') - (k'' - k''')$	$\mu_H + 2\mu_C\sin^2\alpha$	3 080 [5]
Chloromethane	C_{3v}	A_1	$k + 2k'$	$\mu_H + \mu_C\,(1 + 2\cos 2\alpha)$	2 966.2 [5]
		E	$k - k'$	$\mu_H + 2\mu_C\sin^2\alpha$	3 041.8 [5]
Ethane (eclipsed)	D_{3h}	A_1'	$K_1 = (k + 2k') + (k'' + 2k''')$	$\mu_H + \mu_C\,(1 + 2\cos 2\alpha)$	2 899.2 [5]
		A_2''	$K_2 = (k + 2k') - (k'' + 2k''')$	$\mu_H + \mu_C\,(1 + 2\cos 2\alpha)$	2 954 [5]
		E'	$K_3 = (k - k') + (k'' - k''')$	$\mu_H + 2\mu_C\sin^2\alpha$	2 994.3 [5]
		E''	$K_4 = (k - k') - (k'' - k''')$	$\mu_H + 2\mu_C\sin^2\alpha$	2 963 [5]
Ethane (staggered)	D_{3d}	A_{1g}	$K_1 = (k + 2k') + (k'' + 2k''')$	$\mu_H + \mu_C\,(1 + 2\cos 2\alpha)$	2 899.2 [5]
		A_{2u}	$K_2 = (k + 2k') - (k'' + 2k''')$	$\mu_H + \mu_C\,(1 + 2\cos 2\alpha)$	2 954 [5]
		E_g	$K_3 = (k - k') + (k'' - k''')$	$\mu_H + 2\mu_C\sin^2\alpha$	2 963 [5]
		E_u	$K_4 = (k - k') - (k'' - k''')$	$\mu_H + 2\mu_C\sin^2\alpha$	2 994.3 [5]
Methane	T_d	A_1	$k + 3k'$	μ_H	2 914.2 [5]
		F_1	$k - k'$	$\mu_H + (4/3)\mu_C$	3 020.3 [5]

are formed. r_1 and r_2 are the deviations from equilibrium C—H distances at the atom C_1, r_3 and r_4 at the atom C_3. The corresponding elements on the principal diagonal of the symmetrized F and G matrix are shown in Table 1. k is the principal force constant for C—H stretching, k' is the interaction force constant between the C—H stretchings at the same carbon atom, and k'' at different carbon atoms. μ_H and μ_C are the inverse masses of H and C atoms, and the equilibriun H—C—H angle is denoted by 2α. From the transformation (4) we obtain

$$r_1 = (1/2)s^{(A_1)} + (1/2)s^{(B_2)} + 2^{-\frac{1}{2}}s^{(E)} \tag{5}$$

Wilson's approximation of separating the extreme high C—H stretching frequencies is equivalent to assuming the symmetry coordinates in eqn. (5) to be proportional with the normal coordinates,

$$\begin{aligned} s^{(A_1)} &= (\mu_H + 2\,\mu_C \cos^2\alpha)^{\frac{1}{2}}\, Q^{(A_1)} \\ s^{(B_2)} &= (\mu_H + 2\,\mu_C \cos^2\alpha)^{\frac{1}{2}}\, Q^{(B_2)} \\ s^{(E)} &= (\mu_H + 2\,\mu_C \sin^2\alpha)^{\frac{1}{2}}\, Q^{(E)} \end{aligned} \tag{6}$$

Then the coefficients C of eqn. (2) can easily be computed, their squares being

$$\begin{aligned} A_1\text{:}\ C^2 &= (1/4)\ (\mu_H + 2\,\mu_C \cos^2\alpha) \\ B_2\text{:}\ C^2 &= (1/4)\ (\mu_H + 2\,\mu_C \cos^2\alpha) \\ E\text{:}\ C^2 &= (1/2)\ (\mu_H + 2\,\mu_C \sin^2\alpha) \end{aligned} \tag{7}$$

Hence eqn. (1) gives the explicit formula for the mean square amplitude of C—H as

$$u^2 = (h/16\pi)\,(K_1^{-\frac{1}{2}} + K_2^{-\frac{1}{2}})\,(\mu_H + \mu_C \cos^2\alpha)^{\frac{1}{2}} + (h/8\pi)\,K_3^{-\frac{1}{2}}\,(\mu_H + 2\mu_C \sin^2\alpha)^{\frac{1}{2}} \tag{8}$$

where the force constants from Table 1 have been introduced according to

$$\begin{aligned} A_1\text{:}\ \lambda_1 &= K_1(\mu_H + 2\mu_C \cos^2\alpha) \\ B_2\text{:}\ \lambda_2 &= K_2(\mu_H + 2\mu_C \cos^2\alpha) \\ E\text{:}\ \lambda_3 &= K_3(\mu_H + 2\mu_C \sin^2\alpha) \end{aligned} \tag{9}$$

The formula (8) is based on following approximations: 1) Small harmonic vibrations are assumed, 2) the temperature dependence is omitted, 3) the high C—H stretching frequencies are separated from the remaining fundamentals. This will be referred to as the first approximation.

FURTHER APPLICATIONS

The method has been applied to several representative molecules containing the C—H bond and are listed in Table 1. The principal diagonal elements of the symmetrized F and G matrices are included in the table, as well as the experimental fundamentals. Troughout the table, the principal force constant for C—H stretching is denoted by k and the interaction constants for pairs of adjacent C—H bonds by k'. The remaining force constants are

Table 2. Mean square amplitude for C—H by the first approximation for certain molecules.

Molecule	First approximation for u^2
Acetylene	$(h/8\pi)[(k+k'')^{-\frac{1}{2}}+(k-k'')^{-\frac{1}{2}}](\mu_H+\mu_C)^{\frac{1}{2}}$
Benzene	$(h/12\pi)[(1/2)K_1^{-\frac{1}{2}}+(1/2)K_2^{-\frac{1}{2}}+K_3^{-\frac{1}{2}}+K_4^{-\frac{1}{2}}](\mu_H+\mu_C)^{\frac{1}{2}}$
Formaldehyde	$(h/8\pi)(k+k')^{-\frac{1}{2}}(\mu_H+2\mu_C\cos^2\alpha)^{-\frac{1}{2}}+(h/8\pi)(k-k')^{-\frac{1}{2}}(\mu_H+2\mu_C\sin^2\alpha)^{\frac{1}{2}}$
Ethylene	$(h/16\pi)(K_1^{-\frac{1}{2}}+K_2^{-\frac{1}{2}})(\mu_H+2\mu_C\cos^2\alpha)^{\frac{1}{2}}+(h/16\pi)(K_3^{-\frac{1}{2}}+K_4^{-\frac{1}{2}})$ $(\mu_H+2\mu_C\sin^2\alpha)^{\frac{1}{2}}$
Allene	$(h/16\pi)(K_1^{-\frac{1}{2}}+K_2^{-\frac{1}{2}})(\mu_H+2\mu_C\cos^2\alpha)^{\frac{1}{2}}+(h/8\pi)K_3^{-\frac{1}{2}}(\mu_H+2\mu_C\sin^2\alpha)^{\frac{1}{2}}$
*Cyclo*propane	$(h/12\pi)[(1/2)K_1^{-\frac{1}{2}}+K_2^{-\frac{1}{2}}](\mu_H+2\mu_C\cos^2\alpha)^{\frac{1}{2}}+(h/12\pi)[(1/2)K_3^{-\frac{1}{2}}+K_4^{-\frac{1}{2}}]$ $(\mu_H+2\mu_C\sin^2\alpha)^{\frac{1}{2}}$
Chloromethane	$(h/12\pi)(k+2k')^{-\frac{1}{2}}[\mu_H+\mu_C(1+2\cos 2\alpha)]^{\frac{1}{2}}+(h/6\pi)(k-k')^{-\frac{1}{2}}$ $(\mu_H+2\mu_C\sin^2\alpha)^{\frac{1}{2}}$
Ethane	$(h/24\pi)(K_1^{-\frac{1}{2}}+K_2^{-\frac{1}{2}})[\mu_H+\mu_C(1+2\cos 2\alpha)]^{\frac{1}{2}}+(h/12\pi)(K_3^{-\frac{1}{2}}+K_4^{-\frac{1}{2}})$ $(\mu_H+2\mu_C\sin^2\alpha)^{\frac{1}{2}}$
Methane	$(h/16\pi)(k+3k')^{-\frac{1}{2}}\mu_H^{\frac{1}{2}}+(3h/16\pi)(k-k')^{-\frac{1}{2}}[\mu_H+(4/3)\mu_C]^{\frac{1}{2}}$

due to interaction between C—H stretchings at different carbon atoms. In the case of benzene, *o*, *m* and *p* refer to *ortho*, *meta* and *para*. The final formulae for the mean square amplitudes for C—H by the first approximation are listed in Table 2.

Table 3. General formulae for the mean square amplitude of C—H.

Type	Second approximation for u^2
≡CH	$(h/4\pi)k^{-\frac{1}{2}}(\mu_H+\mu_C)^{\frac{1}{2}}$
=CH_2	$(h/8\pi)(k+k')^{-\frac{1}{2}}(\mu_H+2\mu_C\cos^2\alpha)^{\frac{1}{2}}+(h/8\pi)(k-k')^{-\frac{1}{2}}(\mu_H+2\mu_C\sin^2\alpha)^{\frac{1}{2}}$
−CH_3	$(h/12\pi)(k+2k')^{-\frac{1}{2}}[\mu_H+\mu_C(1+2\cos 2\alpha)]^{\frac{1}{2}}+(h/6\pi)(k-k')^{-\frac{1}{2}}(\mu_H+2\mu_C\sin^2\alpha)^{\frac{1}{2}}$
CH_4	$(h/16\pi)(k+3k')^{-\frac{1}{2}}\mu_H^{\frac{1}{2}}+(3h/16\pi)(k-k')^{-\frac{1}{2}}[\mu_H+(4/3)\mu_C]^{\frac{1}{2}}$
Type	**Third approximation for u^2**
≡CH	$(h/4\pi)k^{-\frac{1}{2}}(\mu_H+\mu_C)^{\frac{1}{2}}$
=CH_2	$(h/8\pi)k^{-\frac{1}{2}}\{[\mu_H+(1/2)\mu_C]^{\frac{1}{2}}+[\mu_H+(3/2)\mu_C]^{\frac{1}{2}}\}$
−CH_3	$(h/12\pi)k^{-\frac{1}{2}}\{[\mu_H+(1/3)\mu_C]^{\frac{1}{2}}+2[\mu_H+(4/3)\mu_C]^{\frac{1}{2}}\}$
CH_4	$(h/16\pi)k^{-\frac{1}{2}}\{\mu_H^{\frac{1}{2}}+3[\mu_H+(4/3)\mu_C]^{\frac{1}{2}}\}$
Type	**Fourth approximation for u^2**
General	$(h/4\pi)k^{-\frac{1}{2}}(\mu_H+\mu_C)^{\frac{1}{2}}$

Table 4. Calculated mean amplitudes for C—H stretching (Å units).

Molecule	1. appr.	2. appr.	3. appr.	4. appr.
Acetylene	0.07379	0.07378	0.07378	0.07378
Benzene	0.07696	0.07696	0.07696	0.07696
Formaldehyde	0.08007	0.08007	0.08007	0.08007
Ethylene	0.07713	0.07712	0.07712	0.07713
Allene	0.07718	0.07718	0.07718	0.07719
*Cyclo*propane	0.07701	0.07701	0.07700	0.07701
Chloromethane	0.07752	0.07752	0.07751	0.07751
Ethane	0.07824	0.07824	0.07822	0.07822
Methane	0.07781	0.07781	0.07780	0.07781

GENERAL FORMULAE

As a second approximation for u^2, the interactions between bonds attached to different C atoms may be omitted. By doing this, general formulae are obtained for the four types of C—H distances, depending on the number of H atoms attached directly to the C atom. The formulae are listed in Table 3.

The third approximation for u^2 is obtained by putting the interaction constant k' equal to zero in the second approximation formula. Simultaneously, the numerical values 120° and 109°28' have been inserted for the H—C—H angle in the methylene and methyl groups, respectively.

In the third approximation, only the principal C—H stretching force constant, k, is included. By making the corresponding approximation in the G matrix, the proper element on the principal diagonal to be used is $\mu_H + \mu_C$. Hence a general formula for all types of C—H distances is obtained, which is listed in Table 3 as the fourth approximation. This last formula is naturally identical with the second and third approximation for C—H of the ≡CH type.

NUMERICAL CALCULATIONS

All the approximate formulae have been applied for numerical calculations of u values for the molecules here considered. The calculations were based on individual force constants, as obtained from the experimental fundamentals (see Table 1). The results are summarized in Table 4.

Table 5. Characteristic values of mean amplitudes for C—H stretching.

k (10^5dyn cm^{-1})	4.4	4.6	4.8	5.0	5.2
u (Å)	0.0800	0.0791	0.0783	0.0775	0.0767
k (10^5dyn cm^{-1})	5.4	5.6	5.8	6.0	6.2
u (Å)	0.0760	0.0753	0.0746	0.0740	0.0734

CONCLUSION

It may be concluded that the introduced approximations are very good. It is seen from Table 4 that they do not affect the results appreciably. Hence if the C—H stretching force constant is assumed to have a characteristic value in several different molecules, it is possible to give a characteristic value for the root mean square C—H amplitude as well. In Table 5 the proper u values are enumerated in the actual region of force constant values.

REFERENCES

1. Bastiansen, O. and Cyvin, S. J. *Nature* **180** (1957) 980.
2. Morino, Y., Kuchitsu, K. and Shimanouchi, T. *J. Chem. Phys.* **20** (1952) 726.
3. Wilson, E. B. Jr. *J. Chem. Phys.* **7** (1939) 1047.
4. Wilson, E. B. Jr. *J. Chem. Phys.* **9** (1941) 76.
5. Herzberg, G. *Infrared and Raman Spectra of Polyatomic Molecules*, N. Y. 1945.
6. Brodersen, S. and Langseth, A. *Kgl. Danske Videnskab Selskab, Mat. Fys. Skrifter* **1** (1956) 1.
7. Torkington, P. *Proc. Phys. Soc. London* **A 64** (1951) 32.
8. Lord, R. C. and Venkateswarlu, P. *J. Chem. Phys.* **20** (1952) 1237.

Received October 20, 1957.

ACTA CHEMICA SCANDINAVICA 12 (1958) 239—266

Investigation on the Oxidation Mechanism of Titanium

P. KOFSTAD, K. HAUFFE* and H. KJÖLLESDAL

Central Institute for Industrial Research, Blindern, Oslo, Norway

Oxidation of titanium has been studied in the temperature region 300—1 000°C. Four different rate laws have been found in the indicated temperature intervals: logarithmic (< 300°C), cubic (300—600°C), parabolic (600—850°C), and parabolic + linear (> 850°C) rate laws. The indicated temperature regions are only approximate as the rate laws observed are also dependent upon the duration of the oxidation and the amount of oxygen present in the metal before the start of the oxidation. Thus the initial rate laws observed at any temperature eventually changes into the rate law corresponding to the higher temperature interval. For example at 300°C the oxidation follows a logarithmic rate law for the initial 300 min whereupon it gradually changes into a cubic rate law.

The following oxidation mechanisms are proposed: The logarithmic rate law is interpreted as an oxide film formation perhaps governed by a Mott-type mechanism, the cubic rate law is associated with a diffusion of oxygen into the titanium metal, the parabolic rate law is interpreted in terms of the usual Wagner high-temperature mechanism and with the assumption that a diffusion of oxygen ions through the TiO_2 scale is the rate determining step (< 1 000°C), and the linear rate law results from cracks in the oxide scale due to stresses in the oxide and a phase boundary reaction being the rate-determining reaction.

The reaction of oxygen with titanium at different temperatures has been studied by numerous investigators [1–23]. A comparison of the different reports and publications, however, shows large disagreements and discrepancies which include both rate laws and rates of oxidation.

The published data indicate that the processes involved in the reaction are rather complex, and no simple interpretation can be given to the diverse phenomena observed at different temperatures and oxygen pressures. This state of affairs is partly due to the high oxygen solubility in titanium and the possibility of formation of different oxides (TiO, Ti_2O_3, Ti_3O_5, and TiO_2) in the oxide scale. A probable reason for the disagreements between different

---

* Present address: Farbwerke Hoechst, Frankfurt am Main, Germany.

published data is the presence of gaseous impurities (O_2, H_2, N_2) and C in titanium and different pretreatments of titanium used by different investigators. It is well known that titanium dissolves large amounts of oxygen without forming an oxide scale at high temperatures (> 800°C) and low pressures ($p_{O_2} < 10^{-3}$ mm Hg), and dissolved oxygen introduced during pretreatment such as annealing between rolling runs, etc., may change the characteristics of the oxidation reactions.

The mechanism of oxidation of titanium was investigated by studying the rate laws of oxidation and rate of oxidation as a function of temperature and oxygen pressure. As the knowledge of the structure and degree of order of the oxide scale is of primary importance in consideration of oxidation mechanisms, the oxide scale was studied by means of X-ray diffraction, electron microscopy, and metallographic techniques. Furthermore, because of the high solubility of oxygen in titanium and as the kinetics of oxygen penetration into the metal may be of importance for the rate laws observed, the oxygen penetration into titanium during the oxidation was studied by metallographic and microhardness techniques.

EXPERIMENTAL METHODS

Both high-purity van Arkel titanium and commercial Kroll titanium were used in the studies. Spectrographic analysis gave the following results:

	Impurities present		
Type of Ti	0.1 %	0.01 %	traces, 0.001 %
Van Arkel Ti		Fe, Mn, Al, Sn, Mg, Cr	Cu
Kroll Ti	Mg, Fe	Si	Ca, Cu, Fe, Sn, Mn

No analysis was made of gaseous impurities (O_2, N_2, H_2) and C. However, hardness measurements on the titanium gave fair indication as to the impurity level. The hardness, HV_{10}, was measured to 90—100 for the van Arkel titanium and 120—130 for the Kroll titanium annealed in high vacuum at 800°C for 30 min. These results indicate that only small amounts of impurities were present in the titanium.

The titanium was melted in a laboratory type argon arc furnace. The melting was performed with an auxiliary wolfram electrode. A watercooled copper crucible permitted melting of 5 different samples each weighing about 20 g. All samples were remelted.

After melting, the buttons were coldrolled to the desired thickness in a small rolling mill. For specimens of small thickness, it was necessary to anneal in high vacuum at 800°C between rolling runs. The metal sheets were cut in specimens about 3 × 1 cm². The thickness of the specimens varied between 0.05 and 0.003 cm, depending upon the testing temperature. The specimens were furthermore degreased in chloroform and acetone, polished with emerycloth and alumina and finally rinsed in distilled water.

The reaction of oxygen with titanium was measured both by a gravimetric and a volumetric method. The gravimetric method was employed at high temperatures (700—1 000°C), and the experimental setup consisted essentially of a quartz helix hung vertically in a tube. The test specimen was suspended in a platinum wire, and the weight gain was followed by measuring with a cathetometer the vertical displacement of a pointer on the spring. By this method the weight gain was measured with an accuracy of $\pm 5 \times 10^{-5}$ g.

The measuring unit was incorporated in a vacuum system which was made of Pyrex with the exception of the reaction tube, which was made of transparent silica. The system was connected *via* a liquid air trap to a set of oil diffusion and rotary oil pumps.

Before the start of each run, the system was evacuated. After allowing time for temperature stabilization in the furnace surrounding the reaction tube, the run was started by closing the highvacuum line and admitting oxygen to the system. During oxidation at low pressures ($<$ 1 mm Hg) oxygen was continuously pumped through the system and the pressure was regulated with a fine control needle valve.

In the temperature region 300—700°C the weight gain of titanium reacting with oxygen ranged from a few μg per cm^2 at 300°C to a few hundred μg per cm^2 at 700°C after about 5 h of oxidation. The gravimetric apparatus was not sensitive enough for this purpose, and the oxidation rate was therefore studied by measuring the volume of oxygen absorbed by the titanium specimen.

Essentially the apparatus consisted of a reaction chamber (with as small a volume as possible) connected to a large reference volume with a long uniformly graduated capillary. The absorption of oxygen was followed by observing the movement of a small, mobile drop of diethylphthalate indicator from the reference volume to the reaction chamber. In order to increase the mobility and thereby the sensitivity of the indicator drop, the capillary was treated with a water-repellent silicone compound.

With the exception of the reaction tube, which consisted of transparent silica, the apparatus was made entirely of Pyrex. The whole system was connected to an oil diffusion and a rotary oil pump.

The temperature in the furnace was regulated by a transductor regulator in combination with a platinum resistance thermometer within $\pm$ 0.1°C. The rest of the apparatus was enclosed in a chamber, its temperature being kept at 25 $\pm$ 0.1°C.

In order to have a constant temperature gradient from the furnace to the rest of the system, the part of the reaction chamber which was outside the furnace, was equipped with a water jacket, through which water was pumped from a constant temperature bath kept at 25 $\pm$ 0.1°C. A transparent silica rod was placed within the reaction chamber to reduce the volume, and the test specimens were suspended with a short platinum wire connected from a hook at the top of the reaction tube.

Before the start of the run the reaction chamber was evacuated, the furnace was lowered in position and the temperature adjusted to within $\pm$0.1°C. The run began when the highvacuum line was closed off, and the oxygen was admitted to the reaction chamber. Before measuring the movement of the indicator, the pressures in the reaction chamber and the reference volume were equalized *via* a short-cut line for 10 sec. Thus for each run there was an unrecorded period of about 20 sec. Comparison with the gravimetric method at 700—800°C gave excellent agreement.

The X-ray diffraction investigations of the oxide scales were carried out by means of a General Electric XRD-3 recording X-ray diffractometer.

The preparation of metallographic specimens of the oxidized titanium specimens proved rather difficult as the brittle oxide layer became heavily crushed and displaced during grinding and polishing. A number of methods were tried, and the mounting procedure which was finally adopted, was the following: After silver-coating by evaporation of silver *in vacuo* the specimens were heavily electroplated with copper and finally mounted in Wood's metal.

Although this procedure at last was found to be the most satisfactory for this very special type of specimens, it did in no way give the perfect results. Due to the brittle nature of the oxide scale and the outer part of the metal, a trench was usually left between the oxide and the metal.

Only transverse sections of the oxidized specimens were examined. After grinding, polishing with a finegrained diamond paste and final polishing with levigated alumina, the oxide layer was examined. The metal core was best examined after etching for approximately 30 sec. A mixture of 1 part conc. HNO_3 + 1 part $(HF)_n$ in 2 parts of glycerol was found superior to etchants without HNO_3.

The microindentation hardness testing was performed with a Reichert microhardness tester (No. 1109) used in connection with a Reichert universal camera microscope (model MeF). The indenter was a Vickers pyramid.

Variations in microhardness at a single load over transverse sections of the specimens were recorded. A comparatively low load — 17 g — was chosen in order to allow a reason-

able number of indentations to be made. All microhardness indentations were made on specimens which had finally been electropolished and etched. The orientation of the various grains had a clearly visible effect on the shape of the indentation, and sometimes also on the calculated microhardness. Thus passing from one grain into another with a different orientation sometimes resulted in a jump in the hardness curve. Mostly, this effect was not pronounced. It is felt that the reported curves represent a fair average of the microhardness at the various depths below the specimen surface.

The shape of the base of the indentations mostly was not exactly square due to orientation differences of the grains. Near the edges the indentations were mostly very elongated in a direction perpendicular to the metal sheet surface. This is a concequence of the unavoidable rounding of the edges both during the mechanical- and the electropolishing. Normally the surface of the indentation is calculated by using the square of the mean length of the two diagonals of the base of the indentation. In the case of very elongated indentations this leads to an unreasonable large surface. Thus, instead of the square of the mean length, the product of the lengths of the diagonals has been used for d^2 in th formula

$$H_m = 1\,854.4\,\frac{p}{d^2}\ \mathrm{kg/mm^2}$$

when calculating the reported microhardness values.

The hardness values close to the edges are very approximate only for said reason; in addition the brittle metal near the edges often crumbled even under the low load used.

A number of oxidized titanium specimens were studied by electron microscopy (RCA EMU 2D). All specimens were preshadowed and studied by a single stage carbon replica technique. This technique included 1) shadowing of the surface of the test specimen by vacuum evaporation of platinum under a certain angle, 2) direct vacuum evaporation of carbon on the preshadowed surface, 3) pressing the carbon side of the sample against molten polystyrene, 4) dissolving the specimen (TiO_2 layer and Ti) in a mixture of H_2SO_4 and $(HF)_n$ at about 60°C, and after 5) dissolving the polystyrene, the specimens were ready for examination in the electron microscope.

EXPERIMENTAL RESULTS

During the course of the investigations a striking feature of the oxidation of titanium compared to other metals was the difficulty in obtaining satisfactory reproducibility and regularity in the results.

In the opinion of the authors this irregularity may be traced back to different pretreatment of the samples (rolling, high-vacuum preannealing etc.). Unless the pretreatment is performed under very controlled conditions, varying amounts of impurities may be introduced causing irregular oxidation behaviour. It seems of particular importance to achieve a high vacuum ($< 10^{-5}$ mm Hg) during annealing between rolling runs and before the start of the oxidation. As will be seen from the present results, titanium oxidizes equally fast at 10^{-3} mm Hg as at 1 atm. oxygen pressure. Thus, annealing at 10^{-3} mm Hg will cause a partial oxygen saturation of the outer layer of the titanium even without formation of an oxide scale, and this again brings about a different oxidation behaviour. On the basis of microhardness tests on transverse sections of the specimens it was found necessary to anneal the samples (0.30 mm thick) for 24 h at 850°C and $p_{O_2} < 10^{-4}$ mm Hg in order to obtain specimens homogeneous with respect to dissolved oxygen.

In a discussion of the experimental results it is convenient to distinguish between high temperature oxidation (600—1 000°C) and low temperature oxidation (300—600°C).

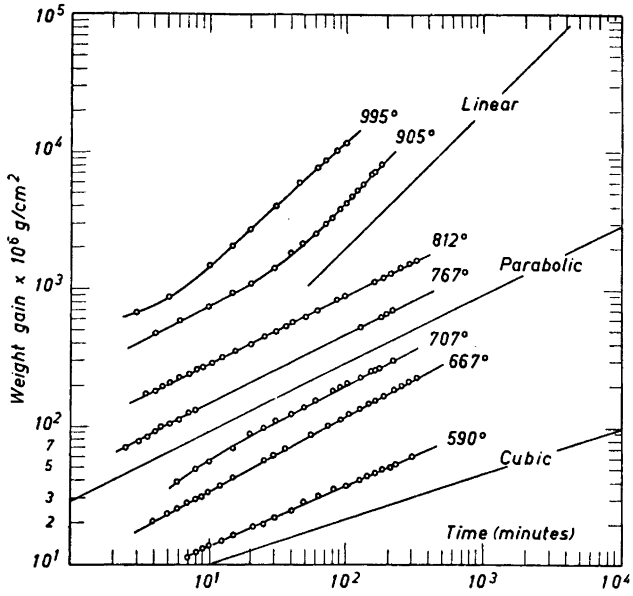

Fig. 1. Oxidation of melted and annealed (30 min at 800°C and $p_{O_2} < 10^{-4}$ mm Hg) van Arkel titanium (600—1 000°C).

High temperature studies. A large number of experiments were carried out on van Arkel titanium, Kroll titanium, and RC-55 titanium. Generally, the length of oxidation lasted for 5 h, while in a few cases the oxidation reaction was followed for 1 week.

Considering the studies as a whole, a striking feature was the irregular oxidation behaviour in the temperature region 900—1 000°C. This irregularity was often associated with sudden increases in the oxidation rates, *e.g.* changes from (approximately) parabolic to (approximately) linear rate laws.

Another feature is the dependence of the oxidation on the type and purity of titanium. The experiments show that the Rem-Cru titanium type RC-55 (containing max. 0.2 % C) was oxidized faster than the relatively pure Kroll titanium (HV_{10} = 120—130) and the van Arkel titanium (HV_{10} = 90—100).

Melted van Arkel titanium. The van Arkel titanium was annealed for 30 min at 800°C at a pressure of 10^{-4} mm Hg. In addition, all specimens were annealed for 10 min in high vacuum at the oxidation temperature, as it took about 10 min to obtain a satisfactory temperature constancy in the furnace before the start of the oxidation run.

The results on melted van Arkel titanium between 600 and 1 000°C are shown in Fig. 1. The oxidation follows a parabolic rate law between approximately 600 and 850°C, while at higher temperatures there seems to be a gradual change from this to an approximately linear one with time. It is interesting to note that the shift from a parabolic rate law region to a generally linear rate law region occurs near to the temperature where titanium changes from

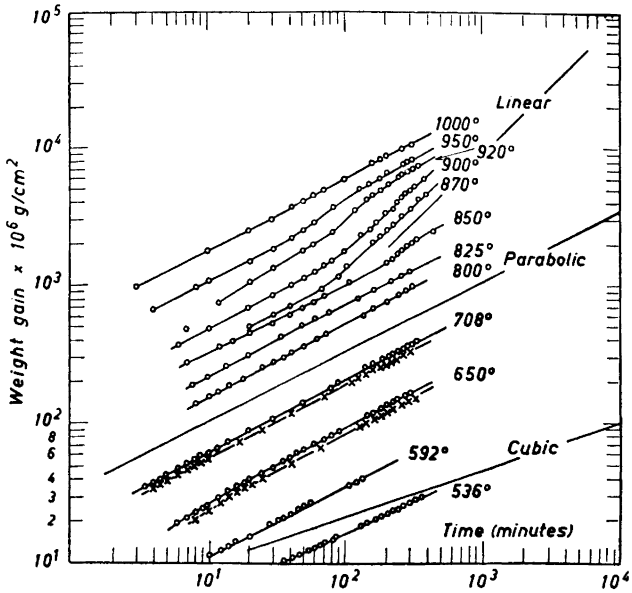

Fig. 2. Oxidation of Kroll titanium 536 and 592°C oxidized in dry air.

the α- to the β-modification. This effect is not unreasonable considering the importance of oxygen solubility in titanium metal during the oxidation reaction, and considering the higher rate of diffusion of oxygen in β- than in α-titanium.

The colour of the oxide scale after 5 h of oxidation in 1 atm. O_2 were as follows: At 1 000°C — light yellow, at 900°C — white, at 800°C — light grey, at 700°C — dark grey, and at 600°C — metallic grey.

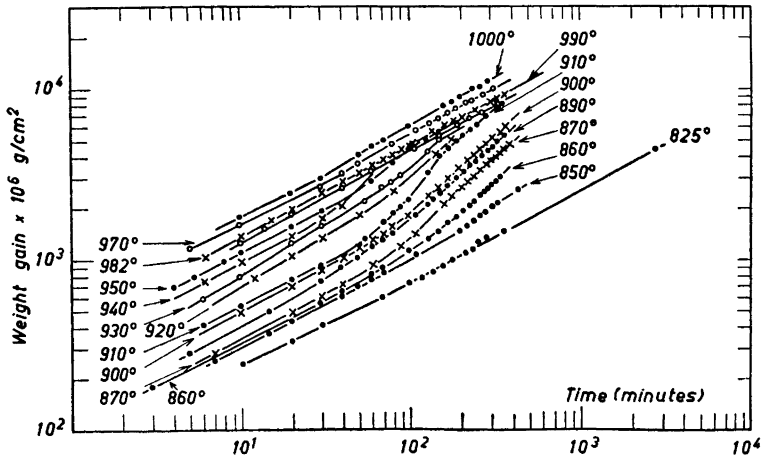

Fig. 3. A detailed study of oxidation of Kroll titanium (800—1 000°C).

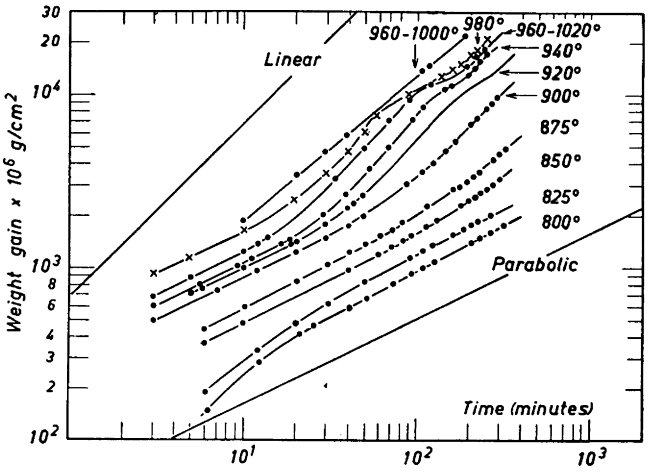

Fig. 4. Oxidation of RC-55 titanium (800—1 020°C).

Kroll titanium. The results on the oxidation of Kroll titanium (cold-rolled and annealed for 10 min in high vacuum of $< 10^{-4}$ mm Hg before the oxidation run) show the same characteristics as for melted van Arkel titanium. As seen in Figs. 2 and 3 the oxidation follows a parabolic rate law between 600 and 800°C, while there are changes from initial parabolic rate laws in the temperature region 850—950°C. It is interesting to note that while van Arkel titanium oxidizes according to an approximately linear rate law at 1 000°C, the oxidation of Kroll titanium again follows an approximately parabolic rate law at this temperature.

The colour of the oxide scales were grey blue, sometimes mottled blue grey white at temperatures above 850°C; at lower temperatures the appearance of the oxide was as for van Arkel titanium.

RC-55. For the sake of comparison it was also of interest to study the oxidation behaviour of a type of commercial titanium. It was also felt that a plate of such titanium would be rather homogeneous both as far as the impurity concentrations and structure of titanium were concerned.

The studies were carried out on RC-55 (max. 0.2 % C) samples (annealed for 10 min at $p_{O_2} = 10^{-4}$ mm Hg at the oxidation temperature) in the temperature region 800—1 000°C. The results are shown in Fig. 4. Compared to the unannealed Kroll titanium the oxidation rates are higher by 50—100 %. Furthermore, one may say that at all temperatures the oxidation initially follows a parabolic rate law which changes into an approximately linear rate law. There seems to be no definite increase in the oxidation rate between 950 and 1 000°C.

The oxidation of RC-55 gave grey oxide scales at 800°C; above 850°C the colour was yellow and mottled brown-yellow.

The effect of the partial pressure of oxygen on the rate of oxidation. Considering studies of oxidation of metals and alloys in general, the effect of the partial

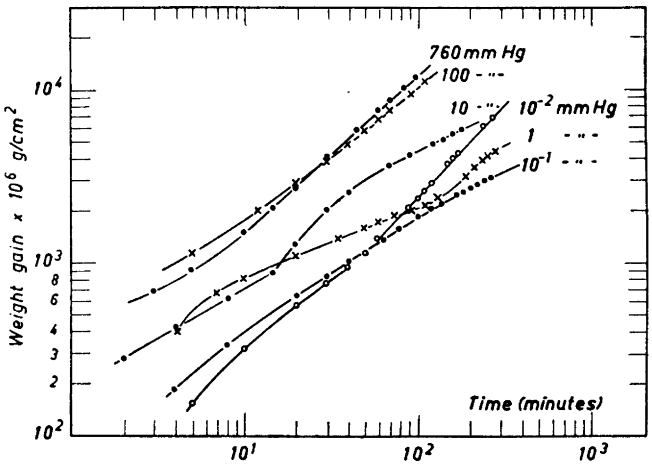

Fig. 5. The effect of oxygen pressure on the oxidation of van Arkel titanium at 1 000°C.

pressure of oxygen on the oxidation rate is of importance in elucidating the mechanism of oxidation. In the case of oxidation of titanium with formation of a compact TiO_2-scale one should on the basis of the general theory of oxidation not expect any effect of the oxygen pressure on the oxidation rate. This should, however, not hold in case of approximately linear rate laws as found for titanium above 900°C. Furthermore, it was of interest to study this effect as the competition between the oxide layer formation and oxygen solution effect probably plays an important role in the oxidation reaction. It is well known that when titanium with TiO_2 films is treated in high vacuum at high

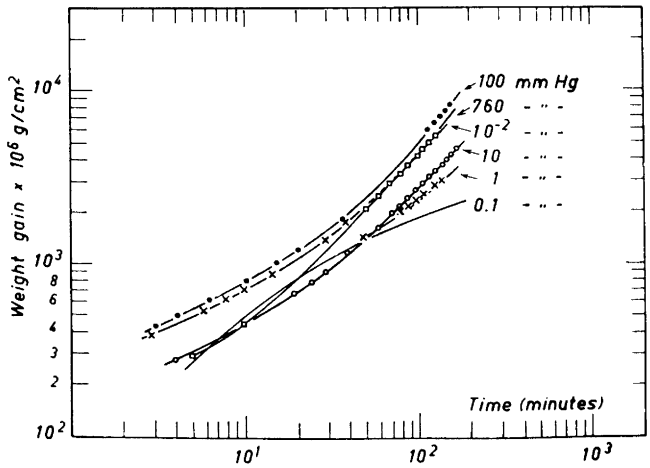

Fig. 6. The effect of oxygen pressure on the oxidation of van Arkel titanium at 900°C.

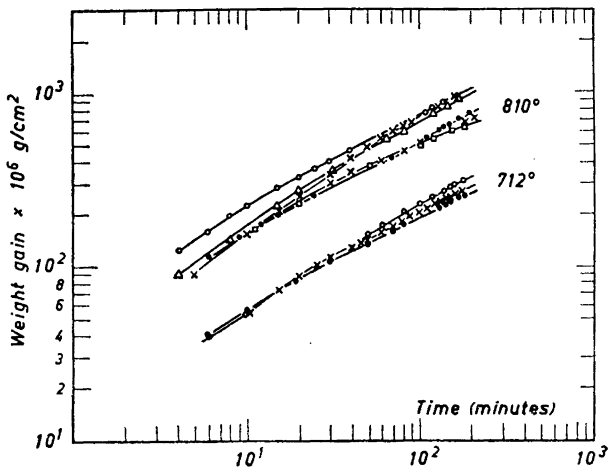

Fig. 7. The effect of oxygen pressure on the oxidation of van Arkel titanium at 810 and 712°C.

810°
△ 760 mm Hg and 1 mm Hg
○ 100 » »
● 10 » »
□ 10^{-1} mm Hg
× 10^{-2} » »
\+ 10^{-3} » »

712°
× 760 mm Hg
● 100 » »
○ 1 » »

temperatures (> 700—800°C), the oxide film dissolves in the titanium, forming a solution of oxygen in titanium. There should consequently exist a temperature dependent critical pressure below which no oxide layer is formed during the initial period of the reaction.

The effect of oxygen pressure was studied at 1 000, 900, 800, and 700°C by oxidizing annealed (30 min at 800°C at $p_{O_2} < 10^{-4}$ mm Hg) van Arkel titanium at oxygen pressures of 760, 100, 10, 1, 10^{-1}, 10^{-2}, and 10^{-3} mm Hg. The results shown in Figs. 5, 6, and 7 were somewhat unexpected, but brought forth new interesting data with regard to the basic processes of the reaction.

Generally one may say that the oxidation is oxygen pressure dependent under conditions of approximately linear rate laws, *e.g.* at 900 and 1 000°C, while the oxidation is oxygen pressure independent under conditions of parabolic rate laws, *e.g.* at 700 and 800°C. At 900 and 1 000°C it is seen that the oxidation behaviour is rather irregular at oxygen pressures below 100 mm Hg. The most interesting conclusions, however, which can be drawn from the curves, is that the oxidation rate does not decrease regularly with decreasing oxygen pressure; rather there exists a certain oxygen pressure ($\sim 10^{-1}$ mm Hg) below which the oxidation rate again increases. The reason for the dependence of the oxidation rate on the oxygen pressure at temperatures above 900°C is probably due to the competition between oxide layer formation and oxygen solution effects.

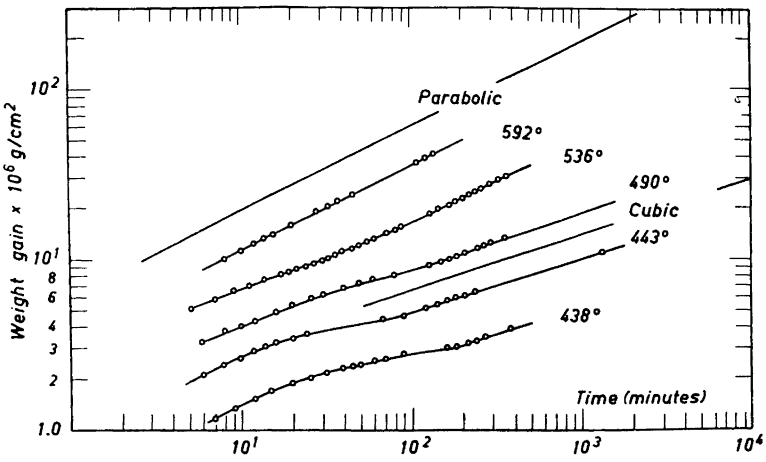

Fig. 8. Oxidation of Kroll titanium in dry air (400—600°C).

It was also interesting to note the effect of oxygen pressure on the appearance and colour of the oxide scale. At 1 000°C the colour changed from light-yellow to white in going from 760 to 0.1 mm Hg. At 10^{-2} and 10^{-3} the colour of the oxide was metallic bluegrey and grey, respectively. At 900°C the colour remained white down to 0.1 mm Hg; below this pressure the colour changed to bluegrey and grey. At 800°C the colour remained light grey in going from 760 to 0.1 mm Hg; at 10^{-2} and 10^{-3} mm Hg the colour was grey white and mottled blue grey, respectively. At 700°C the colour of the surface was dark grey in the pressure range 760 — 1 mm Hg, but the appearance became increasingly metallic with decreasing pressure. At and below 10^{-1} mm Hg the surface was mottled white dark grey.

Low temperature oxidation studies. Low temperature oxidation experiments were made in the temperature region 300—600°C. The characteristic feature of the oxidation reaction in this temperature region is that the oxidation follows non-parabolic rate laws; a logarithmic rate law was found up to about 300°C, while a cubic rate law was obeyed in the temperature region 300—600°C. There are no definite transition temperatures, but rather transition intervals where both rate laws may be found, depending upon the length of oxidation.

The studies were carried out on both cold-rolled, unannealed Kroll titanium and high vacuum annealed (30 min at 800°C) van Arkel titanium. The results are shown in Figs. 8 and 9. The general characteristics of the oxidation reaction are the same for both types of titanium. The logarithmic rate law was found below about 300°C for the length of oxidation of about 5 h, and the cubic rate law was found between 300 and 600°C, while the reaction obeyed a parabolic rate law above approximately 600°C. Furthermore, the duration of the logarithmic rate law period decreased with increasing temperature. Correspondingly the duration of the cubic rate law decreased with

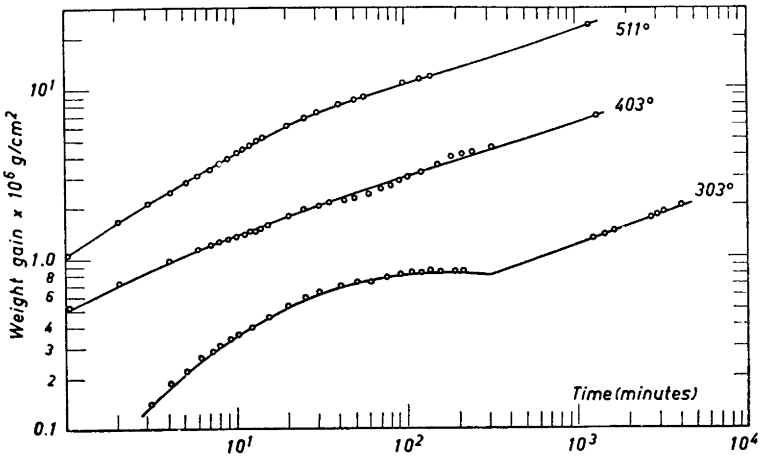

Fig. 9. Oxidation of annealed (30 min at 800°C and $p_{O_2} < 10^{-4}$ mm Hg) van Arkel titanium in dry air (300—500°C.)

increasing temperature at around 500—600°C, until the cubic rate law could no longer be observed and the reaction followed a parabolic rate law at still higher temperatures.

Kofstad and Hauffe [23] have previously proposed that the cubic rate law as found in oxidation of titanium is associated with oxygen solution effects in the titanium metal. With this as a working hypothesis a series of experiments were initiated to investigate the effect of increasing oxygen content on the rate of reaction and the rate law at definite temperatures. According to this hypothesis the duration of the cubic rate law should decrease with increasing oxygen content, and it should eventually disappear for heavy oxygen-saturated titanium. The preliminary studies along these lines substantiated these conclusions.

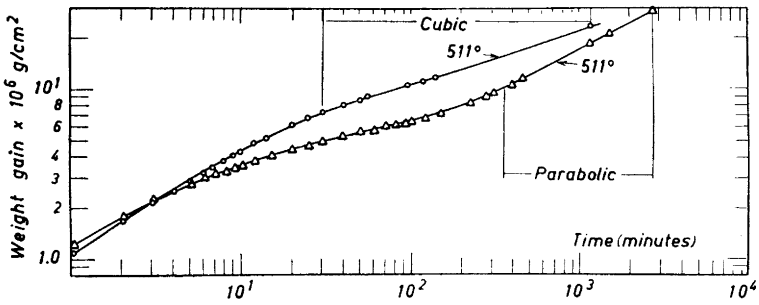

Fig. 10. Oxidation of van Arkel titanium (O) and titanium containing 4 at.% oxygen (△) at 511°C.

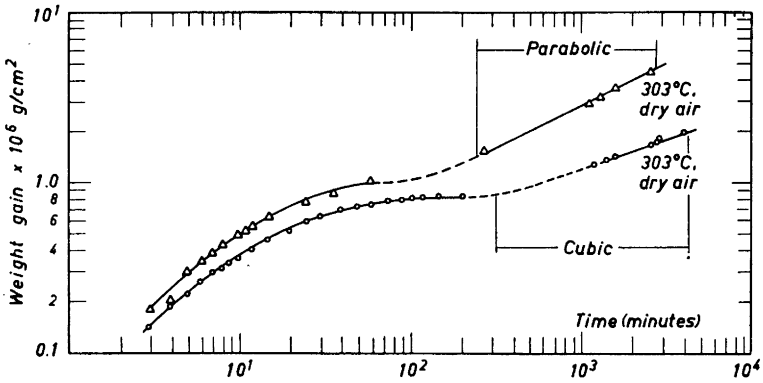

Fig. 11. The effect of oxidation-high vacuum cycles on the oxidation of van Arkel titanium (○) at 303°C. Prior to the oxidation run at 303°C, the oxygen-enriched specimen (△) was oxidized for 4 000 min at 403°C with subsequent annealing for 10 min in high vacuum at 800°C.

In Fig. 10 is shown the difference in oxidation behaviour at 511°C between van Arkel titanium containing 4 at.% oxygen and van Arkel titanium which was made by oxidizing the titanium and treating the specimens in high vacuum ($p_{O_2} = 10^{-5}$ mm Hg) for 24 h. As seen, the van Arkel titanium follows a cubic rate law after about 30 min of oxidation, while the 4 at.% O-Ti alloy oxidizes somewhat slower and follows a parabolic rate law after about 300 min.

Similar experiments at 403 and 303°C gave corresponding results. In these experiments high vacuum annealed van Arkel titanium specimens were oxidized for several days at 403°C, *e.g.* in the cubic rate law region. During these treatments thin films of TiO_2 were formed, but by treating the specimens in high vacuum at 800°C for 10 min the oxide films dissolved in the titanium. The oxidation-high vacuum annealing cycles were continued up to 5 times, and the oxidation was thus measured on titanium samples with increasing oxygen content. It is clear that such short annealing periods in no way distributed the oxygen uniformly through the sample. On the other hand, the outer layer of the titanium metal became more and more saturated after each oxidation-high vacuum cycle. The oxidation experiments consequently gave qualitative results as to the effect of oxygen concentration on the oxidation reaction. Qualitatively the effect of these oxidation-high vacuum annealing cycles in the cubic rate law region was to reduce the duration of the cubic law period. Furthermore, the cubic rate law would also completely disappear for samples which had previously been oxidized for the necessary length of time. Thus the cubic rate law could not be observed for specimens which had previously been oxidized for 2 600 min at 400°C with subsequent annealing for 10 min in high vacuum at 800°C.

Similarly, at 300°C the oxidation of van Arkel titanium followed the logarithmic rate law for the first 300 min, whereupon it changed into a cubic rate law. Oxidizing previously oxidation-high vacuum annealed specimens,

Fig. 12. Oxide surface of Kroll titanium oxidized for 10 min at 890°C and $p_{O_2} = 1$ atm. 3 500 ×.

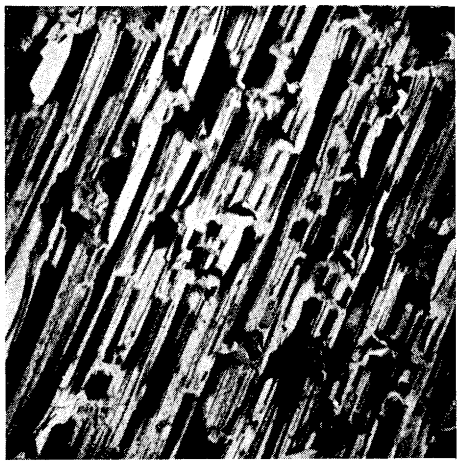

Fig. 13. Oxide surface of Kroll titanium oxidized for 60 min at 890°C and $p_{O_2} = 1$ atm. 8 200 ×.

Fig. 14. Oxide surface of Kroll titanium oxidized for 20 h at 890°C and $p_{O_2} = 1$ atm. 8 200 ×.

Fig. 15. Oxide surface of Kroll titanium oxidized for 10 min at 1 000°C and $p_{O_2} = 1$ atm. 3 500 ×.

the cubic rate law disappeared. After an initial logarithmic period the oxidation followed a parabolic rate law as shown in Fig. 11. The surface of the specimens showed blue or yellow interference colours when oxidized in the cubic and logarithmic rate law regions.

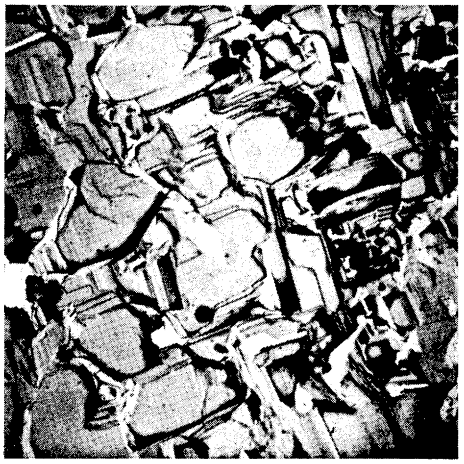

Fig. 16. Oxide surface of Kroll titanium oxidized for 60 min at 1 000°C and p_{O_2} = 1 atm. 3 500 ×.

Fig. 17. Oxide surface of Kroll titanium oxidized for 21 h at 1 000°C and p_{O_2} = 1 atm. 3 500 ×.

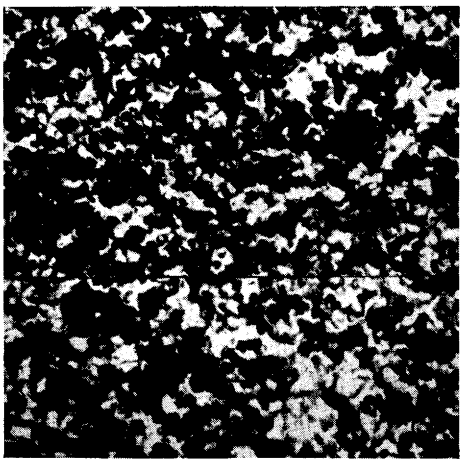

Fig. 18. Back side of detached oxide scale. Kroll titanium oxidized for 20 h at 890°C. 12 500 ×.

Structural investigations. A number of X-ray diffraction diagrams taken of specimens oxidized in pure oxygen indicated only rutile in the oxide scale.*

* Only in one case was the presence of TiO and Ti_2O_3 established with certainty. During a run oxidizing van Arkel titanium at 900°C and low pressures, the oxygen was accidentally saturated with water vapor. The subsequent X-ray diagram showed that the oxide scale, which was black, consisted solely of TiO and Ti_2O_3. This means that any TiO and Ti_2O_3 formed were only present in amounts smaller than a few percent.

Fig. 19. Van Arkel titanium oxidized for 5 h at 700°C. 375 ×.

Fig. 20. Van Arkel titanium oxidized for 5 h at 800°C. 375 ×.

Specimens of Kroll titanium oxidized at 900 and 1 000°C for different length of time were also investigated by electron microscopy techniques. The specimens were cold-rolled and oxidized without high vacuum annealing. This procedure resulted in a preferred orientation in the titanium metal structure, and this again had its effect on the oxide scale. The results are shown in Figs. 12—18.

After 2 min of oxidation the crystals were at both temperatures small and spherical, but in some spots there was a tendency to a preferred orientation. Especially for the specimens oxidized at 900°C the crystals began to take on a lengthened form with normally developed crystal faces. After 10 min of oxidation the 900°C specimens differed from those at 1 000°C in that the rutile crystals were parallel and stretched lengthways, and they showed a decidedly preferred orientation over large parts of the surface. At 1 000°C the crystals were much larger and there was a much smaller tendency to preferred orientation. After one hour of oxidation the specimens at 900°C did not differ appreciable from those oxidized for 10 min, while the specimens oxidized at 1 000°C showed that the tendency to preferred orientation became less pronounced and there was evidence of surface diffusion and crystal growth.

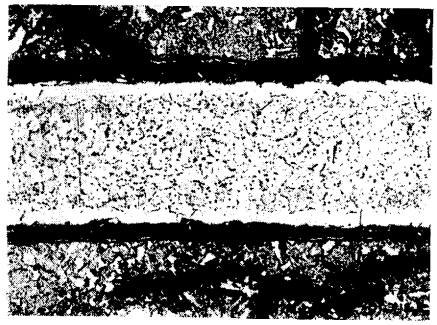

Fig. 21. RC-55 titanium oxidized for 5 h at 825°C. 75 ×.

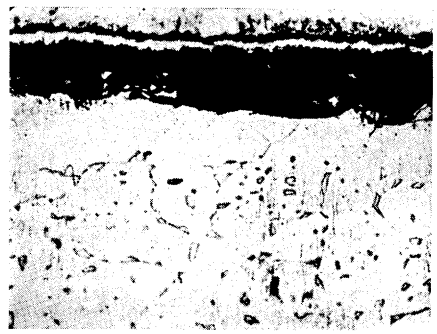

Fig. 22. Fig. 21. at a higher magnification. 325 ×.

Specimens oxidized longer than one hour at 1 000°C showed large crystal growth steps and less preferred orientation. At 900°C the crystals remained relatively small. Even for an oxidation period of 27 h did crystals show a high degree of preferred orientation. At both temperatures the formation of elbow twins was a common phenomenon.

By removing the oxide scale with tape, the back side of the oxide layer was investigated. These investigations showed small, spherically formed crystals without crystal faces for both temperatures and for different lengths of oxidation.

Metallographic examination of a large number of specimens has given the following visual picture of the oxide scale and the metal beneath for oxidation of titanium above 700°C.

The first oxide layer which can be observed, appears to be dense and even, and to be in very close contact with the underlaying metal. Growing in thickness, there can be observed a formation of thin layers parallel to the surface. The density seems to decrease as there appears a large number of elongated holes in the oxide layer which hardly can be a result of polishing alone, although polishing may increase their size and give an exaggerated impression of the amount of total porosity.

When the oxide has reached a rather large thickness, it is comparatively easy to polish and to retain, while at some earlier stage it breaks and is partly removed during polishing.

The oxide layer seems to consist of one phase only; a slightly different tone sometimes observed near the interface oxide/metal is believed only to be an optical effect due to internal reflection. Examination under polarized light (crossed Nicols) shows no sign of the presence of more than one phase.

Already shortly after the first traces of an oxide layer can be observed microscopically, a sort of boundary can be seen to move slowly inwards into the metal core in cold-rolled, unannealed specimens. The area between this boundary and the oxide layer is characterized by a larger grain size, and the grains are more or less columnar with their largest extension perpendicular to the surface. This area is very brittle, and when it reaches a certain thickness, fragments start to break out during polishing. This is shortly before the oxide layer has become thick enough to stand up against the strain of polishing, which means that at any stage of oxidation, there will be hard particles breaking out making the polishing very difficult. Further the holes or grooves formed collect debris and liquids which stain the specimen during drying.

The metal core inside this moving boundary has a much smaller grain-size, and the grains show a more random orientation. It is suggested that this moving boundary represents the delineation between an outer area with a very high oxygen content and an inner core containing only the original or a very low amount of oxygen. Further the boundary is believed at any time to be situated in that part of the metal where the micro-hardness testing shows the very steep change in hardness.

There naturally is a distinct difference in microstructure between the specimens which were oxidized in cold-rolled condition and the specimens which were annealed before oxidation. The last-named shows very much larger grains, very often extending right through the whole cross-section of the specimen. Grain growth during oxidation of such specimens therefore becomes unimportant, and a formation of columnar crystals can hardly be observed.

As most of the photographs show several details, their description has been postponed. In Figs. 19 and 20 are shown the oxide scales formed after oxidation of van Arkel titanium in 1 atm. O_2 for 5 h at 700 and 800°C, respectively. The dark spots near the oxide/metal interface in Fig. 21 are due to holes from the breaking out of hard and brittle particles during polishing.

Fig. 21 (RC-55 titanium oxidized for 300 min at 825°C) shows on both sides of the specimen a comparatively well conserved oxide layer under the plating. Beneath the oxide scale follows a groove where most of the brittle metal has been removed during the polishing. The inner part of this brittle layer stille remains in place, and the boundary between this layer and the rest of the core has revealed a different structure after etching. Fig. 22 shows a detail at higher magnification.

Micro-hardness measurements were made on transverse sections of a series of specimens oxidized for various lengths of time (10 min, 5 h, and 24 h) and at different temperatures. Some of the specimens were oxidized in the cold-rolled condition, others after annealing for 20 min at 1 000°C.

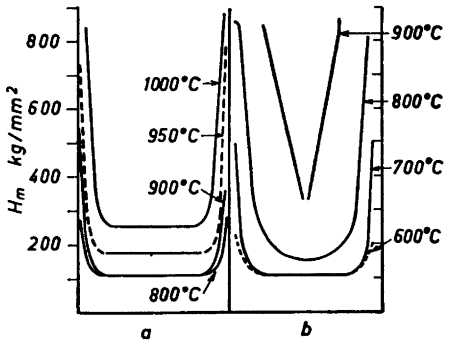

Fig. 23a. The effect of temperature on the oxygen penetration into Kroll titanium after oxidation for 10 min.
Fig.b. The effect of temperature on the oxygen penetration into van Arkel titanium after 5 h of oxidation.

In Fig. 23 a and b are shown the effect of temperature on the oxygen penetration into the titanium metal after oxidation for 10 min and 5 h, respectively. The data shown in Fig. 23 a were obtained by oxidizing Kroll titanium in the cold-rolled condition for 10 min, while Fig. 23 b gives the result of oxidation of van Arkel titanium. All the plates had a thickness of 0.03 cm before the start of oxidation. The results show clearly that oxygen penetration into titanium metal plays an important role in the oxidation reaction.

As seen, the oxygen is concentrated near the metal/oxide interface after oxidation at temperatures below 700°C, while the oxygen penetrates to the core of the specimens by oxidizing at 800°C and above. Especially may be noted the large oxygen penetration above 900°C when the titanium exists in its β-modification. This result is in agreement with the fact that the rate of diffusion of oxygen is much larger in the β- than in the α-phase, even though the solubility of oxygen is higher in the β-modification.

In Fig. 24 is shown the effect of length of oxidation on the oxygen penetration into the van Arkel titanium at 800°C. At this temperature titanium exists in its α-modification with a relatively low rate of oxygen diffusion compared to that of β-titanium, and consequently the inner part is only slowly saturated with oxygen. Most of the oxygen is concentrated at or near the metal/oxide interface, the slope of the oxygen penetration curve is decreasing sharply when going from the metal/oxide interface into the metal.

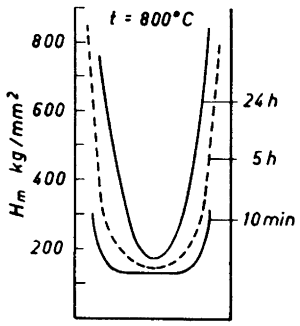

Fig. 24. The effect of length of oxidation on the oxygen penetration into van Arkel titanium after oxidation at 800°C.

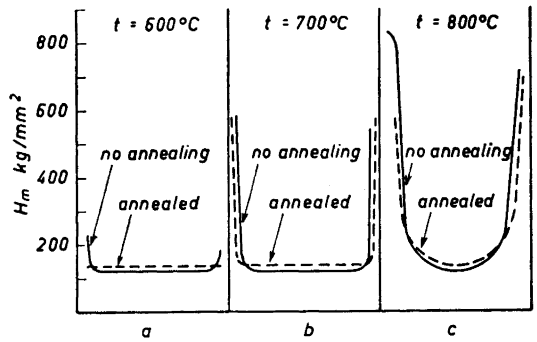

Fig. 25. a, b, c. The effect of annealing (20 mins at 1 000°C and $p_{O_2} < 10^{-4}$ mm Hg) before the oxidation run on the oxygen penetration into van Arkel titanium after 5 h of oxidation at 600, 700, and 800°C, respectively.

Figs. 25 a, b, and c show the effect of the oxygen penetration curves for van Arkel titanium after 5 h oxidation at 600, 700, and 800°C, respectively. All the specimens did have a thin outer zone enriched with oxygen, which was introduced in the metal during annealing between rolling runs. Half of the specimens were oxidized as such, and the other half annealed for 20 min at 1 000°C at $p_{O_2} = 10^{-4}$ mm Hg before the start of the oxidation. The results clearly show the effect of this annealing. Qualitatively one may say that during the annealing the oxygen in the outer zone has diffused into the specimen, and has become distributed throughout the specimen. The hardness throughout the sample is thereby increased as shown by the raising of the oxygen penetration curves in the annealed specimens compared to the unannealed. Correspondingly, the steep parts of the oxygen penetration curves are displaced further into the metal in the case of the unannealed specimens.

It is very reasonable that the effect of annealing has a decisive effect on the oxidation characteristics as the kinetics of the oxygen penetration into the metal very possibly plays an important role in the oxidation reaction. When titanium is oxidized in the cubic rate law region (300—600°C), there is some evidence that the kinetics of oxygen diffusion into the metal is responsible for the cubic rate law. Furthermore, the concentration of oxygen in the outer layer also determines the duration of the cubic rate law period.

DISCUSSION

All the above described results clearly indicate that the mechanism of oxidation of titanium is very complex, and no simple interpretation can be given to the diverse phenomena observed at different temperatures and oxygen pressures. The main reason for this state of affairs is partly due to the high oxygen solubility and the resulting interplay and competition between oxide film formation and oxygen dissolution effects.

Oxidation mechanism

a. Oxide scale. From a thermodynamic reasoning and comparing with iron, one might in the case of oxidation of titanium expect to find a sequence of oxides in the oxide scale with TiO near the metal/oxide phase boundary, Ti_2O_3 in an intermediate region, and TiO_2 at the outer part of the oxide scale. Assuming a compact oxide scale, the amounts of each oxide would on the basis of the Wagner theory of oxidation be dependent upon the rate of formation of the independent oxides, *e.g.* upon their respective defect structures and the rate of ion diffusion through each phase.

Actually, when oxidizing titanium in oxygen, both the X-ray diffraction and metallographic studies show that the oxide scale only consists of one phase, which is rutile. Considering the accuracy of these methods, one may conclude that any TiO and Ti_2O_3 formed are present only in amounts smaller than a few percent.

TiO_2 is a n-type semiconductor and has an oxygen deficient structure [25]. It is generally accepted that this oxygen deficiency results in oxygen ion vacancies rather than interstitial titanium ions in the rutile lattice [26].

b. Diffusion. The oxygen ion vacancies may facilitate a higher rate of diffusion for oxygen than for titanium in TiO_2, and consequently the inward diffusion of oxygen from the outer layer of the oxide might be expected to determine the rate of oxidation of titanium.

Almost all investigators studying the oxidation of titanium below 1 000°C have on the basis of various evidence (marker studies, scratches, and surface markings on the metal specimens) suggested that this mechanism is correct [5,12,21]. Recent marker studies by Kinna and Knorr at 1 000 and 1 200°C indicate that in addition to oxygen ion diffusion, diffusion of titanium ions also plays an important role during the oxidation [22].

There has in this investigation not been made any direct attempts as to establish whether oxygen or titanium ions migrate through the oxide scale. The metallographic and electron microscopy studies do indicate, however, that an overwhelming oxygen diffusion takes place during oxidation below at least 900°C. As the oxide layers grow in thickness, there can in the oxide layer be observed a formation of thin layers parallel to the surface, which indicate that the growth of the oxide layer takes place at the metal/oxide interface. The electron microscope pictures of titanium oxidized for different lengths of time (up to 27 h) at 900°C show a high degree of preferred orientation, which do not change appreciably with the duration of the oxidation. This shows that the crystal growth and corresponding surface diffusion of titanium ions is small at this temperature. Hence titanium ions seem to be relatively immobile at this temperature. This could mean that migration of titanium ions through the oxide scale can hardly be responsible for the oxidation of titanium. At 1 000°C the surface of the oxide scale showed a much smaller tendency to preferred orientation than at 900°C; specimens oxidized longer than one hour at 1 000°C showed large crystal growth steps and few signs of preferred orientation. Thus, at this temperature the surface diffusion of titanium ions seems more pronounced. It is of course to expect that surface diffusion is much faster than volume diffusion, but the observation is at least

in qualitative agreement with the results of Kinna and Knorr, who find that both titanium and oxygen ions migrate through the oxide scale during oxidation at 1 000°C and above.

The relative importance of oxygen ion and titanium ion diffusion through the oxide scale during oxidation of titanium may be described by the following qualitative considerations: Even though the defect structure of rutile favours a predominant oxygen ion diffusion, the titanium ions are of course not frozen in their lattice positions. The question of titanium ion diffusion is also a matter of thermal energy of the ions and potential energy barriers between neighbouring lattice positions. One could perhaps conclude that the activation energy for oxygen ion diffusion is much smaller than the activation energy for titanium ion diffusion in TiO_2. But this situation only implies that the oxygen ion diffusion is the most probable diffusion process in TiO_2 at lower temperatures, but titanium ion diffusion becomes increasingly important with increasing temperature.

For considerations of the oxidation mechanism of the titanium oxidation below 1 000°C, it will be assumed that the oxygen-ion diffusion determines the oxidation reaction.

c. Rate laws. The reported studies on the oxidation rates and the rate laws of oxidation at different temperatures are all in general agreement with data previously reported by other investigators and as reviewed by Kofstad and Hauffe [23]. The rate laws found in this investigation may be represented as follows: The oxidation follows a logarithmic rate equation up to approximately 300°C, a cubic rate law is found in the temperature region 300—600°C, a parabolic rate equation is obeyed between 600 and 850, while no clearcut rate law is found above 850°C. The rate laws observed at high temperatures ($>$ 850°C) may often be described as an initial parabolic rate law followed by a linear rate law, while in other cases the rate law may be interpreted as a mixture of linear and parabolic rate laws.

It should be pointed out that there are no definite temperatures at which the oxidation changes rate law; rather there are temperature intervals where different rate laws may be observed depending upon the duration of the oxidation. At 300°C for example, the logarithmic rate law is conformed with for approximately 300 min whereupon the rate changes into a cubic rate law. With increasing temperature, the duration of the logarithmic rate law period becomes increasingly shorter. Similarly at approximately 550°C the oxidation will for a relatively short period obey the cubic rate law, when after longer periods the oxidation will follow a parabolic rate law. In the parabolic rate law region between 600 and 850°C the oxidation will eventually increase abruptly at very long oxidation periods and change into approximately a linear rate law. The time during which the parabolic rate equation is obeyed, becomes shorter with increasing temperatures until at 900°C the oxidation follows approximately a linear rate law after 10 min of oxidation.

The interpretation of the mechanism of oxidation of titanium is complicated by the high solubility of oxygen in titanium. It is thus not only necessary to consider the formation of an oxide layer and the rate of diffusion of ions through this layer, but also the dissolution of oxygen in titanium, *e.g.* the rate of diffusion of oxygen through oxygen-enriched titanium.

There is no unequivocal interpretation of the logarithmic rate law. It is, however, well known that the oxidation of many metals follows a logarithmic rate equation. This type of relationship is often interpreted in terms of electric field effects across very thin oxide films (up to 50 Å) [27]. After the oxygen is adsorbed on the oxide surface, they combine with electrons and from chemisorbed oxygen ions because of the relatively high electron affinity of oxygen. The chemisorption gives rise to an electric field across the oxide film. According to Hauffe [24] the transfer of electrons across the oxide film is the rate-determining step in the reaction during the logarithmic rate law period.

Another derivation of the logarithmic rate law at low temperatures for oxide films thicker than 50 Å, is due to Evans [28], who makes use of the assumption that the effective area undergoing oxidation is not constant. This situation may be due to disarrayed oxide films, for instance at the junction of grains or the intersection of slip planes. If oxygen at such points can reach the metal, oxidation is likely to penetrate inwards along such paths of disarray, producing localized oxidation and thereby not an uniform film thickening. This situation may also arise in cases where there is a zone mixed with, or consisting of metal and interpenetrating metal and oxide as observed by Vernon, Calman, Clews, and Nurse oxidizing iron below 200°C [29].

Other interpretations of the logarithmic rate law have been proposed by Rideal and Jones [30], Uhlig [31], and Landsberg [32].

At the present time it is difficult to decide as to the correct mechanism in the logarithmic region in the case of titanium oxidation. According to the reported data the logarithmic rate law is obeyed until the weight gain/cm^2 equals about 1×10^{-6} g, which corresponds to a film thickness of approximately 60 Å. On the other hand, the data of Gulbransen and Andrew [23] may be interpreted as obeying a logarithmic rate law up to a weight gain of at least 6×10^{-6} g/cm^2 corresponding to a film thickness of at least 360 Å. Further investigations of this problems are therefore necessary. In this respect it would also be of importance to study the effect of oxygen pressure on the rate of oxidation.

It is reasonable to assume that the logarithmic rate law is associated with an oxide film formation, as it is very unlikely that a diffusion of oxygen into the metal would yield such a rate law. The rate of dissolution and diffusion of oxygen in titanium is consequently very small compared to the rate of film formation during the logarithmic rate law period.

With regard to the cubic rate law in general a few attempts have been made to work out a theoretical treatment. Mott [37] predicted the cubic rate from theoretical studies in connection with the logarithmic equation. A derivation of this rate law has also been made by Hauffe, Engell, and Ilschner in order to interpret the oxidation of nickel at 400°C[33]. The derivations of both Mott and Hauffe presupposes a p-type oxide film, and as TiO_2 is an n-type conductor, these approaches are not applicable in the case of oxidation of titanium.

In view of the fact that the cubic rate law is followed up to about 600°C, where the oxidation is appreciable, it seems that it cannot be interpreted in terms of electric field effects across the oxide layer. These approaches assume a relatively thin oxide film with a maximum thickness of a few hundred Ångströms, a condition which is not well satisfied in the case of titanium

oxidating at 500—600°C. On this basis Kofstad and Hauffe [23] suggested that the cubic rate law was due to another mechanism.

In view of the high solubility of oxygen in titanium it was reasonable to suggest an interpretation of the cubic rate law in terms of diffusion of oxygen through the outer layer of the oxygen-enriched titanium. Using this as a working hypothesis several studies were made, which substantiated this assumption.

In this connection it is interesting to note that the oxidation of zirconium also follows a cubic rate law between 350 and 950°C [34]. As in the case of titanium, it is here also evident that electric field effects cannot explain this high temperature oxidation mechanism. Zirconium and titanium are very much alike in having a very high oxygen solubility, and it is possible that this effect is responsible for the cubic rate law. Furthermore, there is evidence that the rate of diffusion of oxygen in titanium is dependent upon the oxygen concentration in titanium [35].

If the cubic rate law is interpreted in terms of oxygen dissolution in the outer layer of the titanium, one could expect an effect of the oxygen concentration in the titanium on the duration of the cubic rate law period. The length of this period should decrease with increasing oxygen content, and it should eventually disappear for heavily oxygen-saturated titanium.

As seen in Figs. 10 and 11, our preliminary studies along these lines substantiated these assumptions. At 511°C (Fig. 14) the cubic rate law period was shorter for the titanium containing 4 at. % O_2 than for pure titanium. Furthermore, the oxidation changed into a parabolic rate law after about 300 min of oxidation in the case of the oxygen-enriched specimen.

Similar experiments at 403 and 303°C showed corresponding effects. At these temperatures the oxidation was performed on specimens which were highly enriched with oxygen in the outer layer of the titanium by oxidizing the specimens and thereupon treating them in high vacuum at 800°C for 10 min in order to dissolve the oxide film. The intention was to shorten the duration of the cubic rate law period, until the cubic rate law disappeared completely for heavily oxygensaturated specimens. Similarly, at 303°C the oxidation of van Arkel titanium obeyed the logarithmic rate law for the first 300 min and is followed by a cubic rate law, but by oxidizing previously oxidation-high vacuum annealed specimens the cubic rate law disappeared. After an initial logarithmic rate law period the oxidation now followed a parabolic rate law.

On the basis of these studies the following qualitative picture may be given of the oxidation process in the cubic rate law region: The very first part of the reaction involves a chemisorption of oxygen on the titanium, followed by an oxide film formation, the oxide consisting of TiO_2. At the same time the diffusion of oxygen into the titanium metal also takes place: we thus have a competition between oxide film formation and oxygen dissolution in the metal. At low temperatures ($\sim$ 300°C) the diffusion of oxygen into the titanium is so small that the oxide film formation is the predominant feature of the reaction. The oxidation accordingly follows a logarithmic rate law which prevails as long as the rate of oxide film formation is very much faster than the rate of oxygen dissolution. The distinctive stamp of

the logarithmic rate law is of course the rapidly decreasing rate of oxidation with increasing time, and at a certain time (which becomes increasingly longer with decreasing temperatures) the rate of dissolution of oxygen will eventually become the predominant feature of the oxidation reaction. At this time interval, the oxidation changes from a logarithmic to a cubic rate law, as observed when titanium is oxidized at 303°C (Fig. 11).

This same situation does of course exist at higher temperatures. At increasing temperatures, however, the rate of oxygen dissolution plays an increasingly predominant role as compared to the oxide film formation obeying the logarithmic rate law. The logarithmic law period consequently becomes shorter with increasing temperatures. In addition, the oxidation neither follows a logarithmic nor a cubic rate law during the first stages of the oxidation in the temperature region 400—500°C. The observed oxidation may be interpreted as a mixture of a logarithmic and a cubic rate law, as both the rate of oxide film formation and oxygen dissolution is of the same order in this time interval. The rate of oxide film formation rapidly decreases, whereupon the diffusion of oxygen becomes the determining mechanism.

If the proposed interpretation of the data is correct, it would imply that the oxide film has an approximately stationary thickness when the oxidation follows the cubic rate law. The oxygen which dissolves in titanium is taken from the TiO_2 scale; however, a decrease in the thickness of the oxide film would immediately be counteracted by an increase in the electric field across the oxide (assuming the mechanism proposed by Mott). This immediately causes a growth of the oxide film until it reaches the stationary thickness. One way of testing this hypothesis would be to measure the growth of the oxide film in the cubic rate law region.

This may be done by continuously following the oxide film formation by means of X-ray or electron diffraction studies. Of importance in elucidating the mechanism in the logarithmic and cubic rate law regions would also be to study the oxidation as a function of the oxygen pressure.

In the results given in Fig. 11 it is shown that the cubic rate law eventually disappears when the outer region of the titanium becomes heavily enriched with oxygen, and the oxidation eventually follows a parabolic rate law even at 300°C. The following interpretation is proposed to explain this phenomenon: The parabolic rate law, as observed for oxygen enriched specimens even at 300°C, is assumed to represent a growth of the oxide film. However, in order that TiO_2 be formed, the chemical potential of oxygen in the TiO_2 phase, $\mu_{(TiO_2)}$, must be equal to the chemical potential of oxygen dissolved in titanium at the metal/oxide phase boundary, $\mu_{(Ti)}$:

$$\mu_{(TiO_2)} = \mu_{(Ti)}.$$

During the cubic rate law region oxygen dissolves in the titanium, and oxygen consequently continuously migrates away from the region of the titanium in the immediate neighbourhood of the metal/oxide phase boundary. Thus during the cubic rate law period the chemical potential of oxygen in titanium, $\mu_{(Ti)}$, does not reach the value necessary for a further growth of the TiO_2 oxide film. Only when the region of the titanium metal at the metal/oxide interface becomes saturated with oxygen, does the condition exist for a

further growth of the oxide film. When this saturation value is reached, the oxidation does not follow the cubic rate law any longer, rather we get a growth of the oxide scale. The rate determining reaction now becomes the diffusion of oxygen ions through the oxide scale with a corresponding parabolic rate law of oxidation. During the parabolic rate law period the diffusion of oxygen into the titanium metal does of course go on at the same rate, and as the oxygen ion diffusion through the oxide film is the slower process, the oxygen penetrates deeper into the titanium metal core with increasing time, as found by the micro-hardness studies at 800°C (Fig. 24).

The discussion and interpretations presented are of course only qualitative. The interpretations are only given in order to explain the kinetics of the oxidation reaction.

Another interpretation of the parabolic rate law in terms of electric field effects in the oxide film as proposed by Engell and Hauffe [36] for oxidation of zinc at 300°C, may also be considered. It is felt, however, that the interpretations presented may serve as a useful working hypothesis for further studies on the elucidation and understanding of the oxidation mechanism in this temperature region.

Several studies can be proposed for testing the hypothesis. Again it would be of invaluable help to study the growth of the oxide film during oxidation with X-ray or electron diffraction techniques. Furthermore, the oxygen pressure dependence of the oxidation would also provide clues as to the oxidation mechanism. According to this hypothesis all the rate laws (logarithmic, cubic and parabolic) should also be observed during oxidation at one temperature such as 300°C, provided that the oxidation is followed for the necessary length of time. This has not been done at this temperature, as the oxidation as shown in Fig. 11 was only followed for about 3 days. In order to obtain the parabolic rate law at this temperature a length of oxidation of several weeks, perhaps months, will be needed when oxidizing an oxygen free titanium specimen.

The same interpretation of the parabolic rate law for oxygen-enriched specimens at temperatures below 500°C, is proposed to be valid for the parabolic rate law region between 600 and 850°C. When oxidizing oxygen-free specimens at these temperatures, the region of titanium metal at the metal/oxide interface becomes saturated so fast with oxygen, that the cubic rate law is not observed. The parabolic rate law is consequently obeyed after a few minutes of oxidation. The diffusion of oxygen through the oxide is the slower and therefore the rate determining step in the reaction. Simultaneously oxygen diffuses into the titanium metal, and it penetrates deeper into the titanium metal core with increasing length of oxidation as shown by the micro-hardness studies of the oxygen penetration during oxidation at 800°C (Fig. 24).

For long periods of oxidation in this temperature region, the oxidation rate increases abruptly, and the rate law changes into an approximately linear rate law. As pointed out by several investigators [5,12,13] this is a result of the cracking of the oxide scale with subsequent formation of a porous oxide scale. The Pilling-Bedworth ratio is in the case of titanium equal to 1.76, and this

results in stresses in the oxide scale producing cracks and fissures, which causes the linear rate law.

At temperatures of 900°C and above, the oxide scale apparently reaches the critical thickness after a few minutes of oxidation, and the oxidation therefore follows an approximately linear rate law in this temperature region. In addition the effect of the allotropic transformation of titanium at 883°C may have some effect on the oxidation rate in the linear rate law region. Oxygen diffuses faster in β- than in α-titanium, and when there is no protective oxide layer, this increased rate of diffusion in the β-titanium may partially account for the fast oxidation in the linear rate law region. It should be kept in mind, however, that even when oxidizing in the β-region, the outer oxygen-enriched layer of the titanium metal will consist of α-titanium, as dissolved oxygen raises the transition temperature of the α-β transition.

The data on Kroll titanium indicates that the oxidation follows an approximately parabolic rate law at 1 000°C, while the oxidation of van Arkel titanium follows a linear rate law at the same temperature. The reason for this difference is not clear, but one explanation may be that the impurities in the Kroll titanium has a beneficial effect on the mechanical properties of the oxide scale. The reappearance of the parabolic rate law when Kroll titanium is oxidized at 1 000°C, may be interpreted in terms of a sintering effect of the oxide. As pointed out by Jenkins [12,19], rutile has a Tammann temperature of about 1 000°C, and one might consequently expect a relatively high rate of sintering at these temperatures. The difference between Kroll and van Arkel titanium, therefore, may be traced back to the larger amounts of impurities present in Kroll titanium. Impurities of magnesium and iron (present in Kroll titanium) would tend to increase the defect structure of TiO_2, thereby suggesting a higher sintering effect in the case of Kroll titanium. This would decrease the porosity of the oxide scales; furthermore, the growth stresses would be more easily relieved, thereby preventing the formation of cracks in the scale. An investigation of the density of the oxide scale formed would be of help in elucidating this problem.

The electron microscope pictures of the surface of Kroll titanium oxidized at 1 000°C also supports the assumption of a sintering effect at this temperature. The pictures show little preferred orientation of the oxide surface even after 10 min of oxidation, thus indicating that the surface diffusion of ions is relatively fast.

d. Effect of oxygen pressure. The studies of the effect of oxygen pressure on the oxidation rate of van Arkel titanium also brought forth new interesting data with regard to the oxidation mechanism, although further studies are necessary for definite interpretations of the results.

The effect of oxygen pressure was studied at 700, 800, 900, and 1 000°C. Generally one may say that the oxidation is oxygen pressure dependent at 900 and 1 000°, *e.g.* under conditions of approximately linear rate laws, while the oxidation is oxygen pressure independent within the limits of error under conditions of parabolic rate laws at 700 and 800°C. On the basis of the general theory of oxidation, one should in the case of oxidation of titanium with formation of a compact TiO_2-scale, expect no dependence of oxygen pressure on the oxidation rate [21]. This should, however, not be the case under conditions

of linear rate laws as found for van Arkel titanium at 900 and 1 000°C, and in which case the rate determining step probably is a phase boundary reaction at the metal/oxide interface. The present results are therefore generally as would be expected.

As the oxidation of titanium is complicated by oxygen dissolution in titanium, one might at low pressures expect to observe an effect due to the competition between the oxide layer formation and oxygen dissolution. This is particularly so, as it is well known that when titanium with TiO_2 films is treated in high vacuum at high temperatures, (> 700—800°C), the oxide film dissolves in the titanium, forming a solution of oxygen in titanium. There should consequently exist a temperature dependent critical pressure below which no oxide layer is formed during the initial period of the reaction. An oxide layer formation would only occur when the outer layer of the titanium becomes saturated with oxygen thereby raising the chemical potential of oxygen to the value permitting formation of TiO_2.

The oxygen pressure dependence at 900 and 1 000°C may be interpreted in terms of these suggestions. At these temperatures it is seen that the oxidation behaviour is rather irregular below 100 mm Hg. The interesting part is that the oxidation rate does not decrease with decreasing pressure below an oxygen pressure of 10^{-1} mm Hg. Rather the oxidation rate again increases when the oxygen pressure is decreased to 10^{-2} and 10^{-3} mm Hg.

Judging from the results at 1 000°C it is evident that the oxide scale has an increasingly protective effect at 10, 1 and 0.1 mm Hg as compared to 1 atm. and 100 mm Hg. The reason for this is not clear, but it is suggested that the lower oxygen pressures increase the oxygen ion vacancies in the TiO_2. This in turn permits a higher rate of diffusion of ions with a corresponding sintering effect. At pressures below 0.1 mm Hg the competition between oxide film formation and dissolution of oxygen in titanium plays a more dominant role. The tendency to oxide film formation decreases, and at a certain pressure no oxide will be formed. The titanium metal under these conditions is exposed to oxygen atmosphere, and the oxygen migrates directly into the metal. There will be growth of an oxide scale only when the outer layer of the titanium metal is saturated with oxygen.

e. Colour of oxide scales. In this connection it is also interesting to note the change in colour of the oxide scale formed when oxidizing at different pressures. It is well known that rutile may change its colour with changing oxygen content and with small additions of foreign oxides [36–38]. The oxygen deficient structure may with Schottky symboles be expressed as

$$\text{Nil} \rightleftharpoons O_{\square}^{\cdot\cdot} + 2\Theta + \tfrac{1}{2}\, O_2^{(g)}$$

where Nil designates a structure without defects, the squares are ion vacancies, the dots are positive excess charges, and Θ are free electrons. TiO_2 is an n-conductor and with decreasing oxygen content, electrons may be captured according to one or both of the following equations:

$$O_{\square}^{\cdot\cdot} + \Theta \rightleftharpoons O_{\square}^{\cdot} \quad \text{(blue F-center)}$$
$$Ti^{+4} + \Theta \rightleftharpoons Ti^{+3} \quad (Ti^{+3}\text{-ions are blue}).$$

Thus, rutile generally shows an increasingly blue colour with decreasing oxygen content. However, the significance of the observed colour change as a function of oxygen pressure is not clear at the present.

Acknowledgement. This work forms part of a research project sponsored by Air Research and Development Command, Department of the U.S. Air Force.

The authors wish to express their thanks to J. Markali, N. Norman, and E. Bull Simonsen for electron microscopy, X-ray diffraction and metallographic investigations, respectively. Our thanks are also due to S. Leirnes who carried out the oxidation — high vacuum annealing experiments.

REFERENCES

1. Carpenter, L. G. and Reavell, F. R. *Metallurgia* **39** (1948) 63.
2. Gulbransen, E. A. and Andrew, K. F. *J. Metals Trans.* **185** (1949) 741.
3. Hickman, J. W. and Gulbransen, E. A. *J. Anal. Chem.* **20** (1948) 158.
4. Alexander, W. A. and Pidgeon, L. M. *Can. J. Research* (B) **28** (1950) 60.
5. Davies, M. H. and Birchenall, C. E. *J. Metals* **3** (1951) 877.
6. McPherson, D. J. and Fontana, M. G. *Trans. Am. Soc. Metals* **43** (1951) 1098.
7. Pfeiffer, H. and Hauffe, K. *Z. Metallk.* **43** (1952) 364.
8. Morton, P. H. and Baldwin, W. M. *Trans. Am. Soc. Metals* **44** (1952) 1004.
9. Arkharov, V. I. and Lutschkin, G. P. *Doklady Akad. Nauk SSSR* **83** (1954) 837.
10. Waber, J. T. *J. Chem. Phys.* **20** (1952) 734.
11. Waber, J. T., Sturdy, G. E. and Wiise, E. N. *J. Am. Chem. Soc.* **75** (1953) 2269.
12. Jenkins, A. E. *J. Inst. Metals* **82** (1953—54) 213.
13. Spinedi, P. *Alluminio* **23** (1954) 35.
14. Richardson, L. S. and Grant, N. J. *J. Metals* **6** (1954) 69.
15. Wasilevski, R. J. and Kehl, G. L. *J. Inst. Metals* **83** (1954—55) 94.
16. Iitaka, I. and Ohtsuka, R. *Repts of the Sci. Research Inst.* **30** (1954) 265.
17. Simnad, M., Spilners, A. and Katz, O. *J. Metals* **7** (1955) 645.
18. Maynor, Jr. H. W., Barrett, B. R. and Swift, R. E. *WADC Tech. Rept.* 54—109, Contract No. AF 18(600)—60, Project No. 7351, May 1955.
19. Jenkins, A. E. *J. Inst. Metals* **84** (1955—56) 1.
20. Stout, V. L. and Gibbons, M. D. *J. Appl. Phys.* **26** (1955) 1488.
21. Holmes, G. *Doctoral Dissertation Series*, Publ. No 11, 294, University Microfilms, Ann Arbor, Michigan.
22. Kinna, W. and Knorr, W. *Tech. Mitt. Krupp* **14** (1956) 99.
23. Kofstad, P. and Hauffe, K. *Werkstoffe u. Korrosion* **7** (1956) 642.
24. Hauffe, K. *Oxydation von Metallen und Metallegierungen*, Springer Verlag, Berlin 1956.
25. Ehrlich, P. *Z. Elektrochem.* **45** (1939) 362; *Z. anorg. allgem. Chem.* **247** (1941) 53; **259** (1949) 1.
26. Hauffe, K., Grünewald, H. and Tränckler-Greese, R. *Z. Elektrochem.* **56** (1952) 937.
27. Cabrera, N. and Mott, N. F. *Repts. Progr. Phys.* **12** (1949) 163.
28. Evans, U. R. *Rev. Pure and Appl. Chem.* **5** (1955) 1.
29. Vernon, W. H. J., Calman, E. A., Clews, C. J. B. and Nurse, I. H. *Proc. Roy. Soc. London* **A 216** (1953) 375.
30. Rideal, E. and Wansbrough-Jones, O. *Ibid.* **123 A** (1929) 202.
31. Uhlig, H. H. *Acta Met.* **4** (1956) 541.
32. Landsberg, P. T. *J. Chem. Phys.* **23** (1955) 1079.
33. Engell, H. J., Hauffe, K. and Ilschner, B. *Z. Elektrochem.* **58** (1954) 478.
34. Belle, J. and Mallett, M. W. *J. Electrochem. Soc.* **101** (1954) 339.
35. Wasilewski, R. J. and Kehl, G. L. *J. Inst. Metals* **83** (1954—55) 94.
36. Engell, H. J. and Hauffe, K. *Metall* **6** (1952) 285.
37. De Vries, R. C. and Roy, R. *Bull. Ceram.* **33** (1954) 370.
38. Weyl, W. A. and Förland, T. *Ind. Eng. Chem.* **42** (1950) 257.

Received October 25, 1957.

ACTA CHEMICA SCANDINAVICA 12 (1958) 267—273

The Chemistry of the Natural Order Cupressales

XX.* Heartwood Constituents of the Genus *Widdringtonia*

H. ERDTMAN and B. R. THOMAS

Organisk-kemiska Institutionen, Kungl. Tekniska Högskolan, Stockholm, Sweden

The heartwoods of the five recent South African *Widdringtonia* species have been subjected to a comparative chemical investigation. A series of new sesquiterpenoid compounds have been isolated including the hydrocarbon widdrene, the alcohol widdrol, two sesquiterpene alcohols containing two oxygen atoms and a series of acids one of which, widdrenic acid, has also been obtained as an oxidation product of widdrene. Cedrol was usually present in these conifers and eudesmol was isolated from two species.

Superficially the family *Cupressaceae* appears to be a fairly recent, homogeneous group of conifers. However, in contrast to other families it is spread all over the world and there is evidence in favour of the view that the northern and southern genera have long been geographically separated. The family is therefore certainly old — though probably not one of the very oldest — and a comparison of the northern and southern genera is consequently a matter of considerable interest.

Some taxonomists regard the southern genera including *Actinostrobus*, *Callitris*, *Diselma*, *Neocallitropsis (Callitropsis)*, *Widdringtonia*, *Fitzroya*, *Pilgerodendron* and *Libocedrus sensu stricto* as forming a sub-family *Callitroideae*. Of these genera *Callitris* was the subject of the classical studies of Baker and Smith [1] and the monotypic *Neocallitropsis* was investigated by Simonsen [2]. *Diselma* [3], *Pilgerodendron* [4] and *Austrocedrus* [5] (part of *Libocedrus sensu lato*) which are also monotypic have recently been investigated in this laboratory.

Guaiol and (—)-dihydrogeranic acid (callitrol) were found to be characteristic for *Callitris*. Recent unpublished work (Erdtman and Jamieson) showed the presence of eudesmol in *Callitris Roei* (Endl.) F. Muell. and it is quite possible that small amounts of eudesmol occur in other *Callitris* species also. No tropolones were found in any of the *Callitris* species investigated here.

* Part XIX. *Acta Chem. Scand.* **11** (1957) 902.

Pilgerodendron contained sesquiterpenes of the cadinene type but no characteristic constituent was isolated from the heartwood samples of *Diselma Archeri* available. *Austrocedrus* remains the only known tropolone-producing conifer from the southern hemisphere.

The northern monotypic genus *Tetraclinis* (North Africa, southern Spain) has been included in the southern *Callitroideae* but this does not appear entirely justifiable, either geographically, botanically or chemically. The heartwood chemistry indicates on the contrary some affinities with the northern genera.

Of the southern genera, apart from two included in *Libocedrus sensu lato*, only *Callitris* and the African *Widdringtonia* contain more than one or two species and the latter were therefore selected for a comparative study. No chemical relationship to *Tetraclinis* was discovered.

Widdringtonia is a South African genus with five recent species, *W. cupressoides* (L) Endl., *W. dracomontana* Stapf., *W. juniperoides* (L) Endl., *W. Schwarzii* (Marloth) Mast. and *W. Whytei* Rendle. The heartwoods of these species are fragrant and resistant to insects and Docent E. Rennerfelt (private communication) has found that the heartwoods of *W. Whytei* and *W. juniperoides*, the only economically important species, are very resistant to wood decaying fungi *(Coniophora, Lentinus, Poria)*.

We have been able to investigate all five species. The ether soluble part of the acetone extract of the heartwood was an oil possessing a pleasant "cedar wood" odour. There was insufficient of the oil of *W. cupressoides* for a detailed examination but it appeared to resemble that from *W. dracomontana*. Eudesmol was isolated from both of these closely related species. The oils from the latter and from the remaining species were similar although eudesmol was not isolated from the other three. This does not necessarily mean that eudesmol is absent from these other species. The oils appeared to consist mainly of sesquiterpenes with some higher boiling substances. There were only traces of monoterpenes or compounds of similar boiling point range present.

The compounds isolated and a very approximate estimate of the amounts present in the various species are listed in Table 1. The figures are subject to the uncertainties of the estimation and to the wide variations possible in biological material.

The oils were separated into neutral and acid fractions and the former were fractionally distilled. The hydrocarbon fraction consisted of at least two sesquiterpenes of which the lower boiling, $C_{15}H_{24}$, $[\alpha]_D - 107°$, was the principal constituent. This compound, called widdrene*, appears not to have been isolated before but has since been encountered in *Platycladus (Biota) orientalis* [5] and in *Chamaecyparis thyoides* (Enzell, unpublished). Titration with perphthalic acid and the I.R. and U.V. spectra indicated the presence of a trisubstituted double bond. Like cedrene, widdrene must therefore be tricyclic.

Oxidation of widdrene with selenium dioxide gave an aldehyde widdrenal, $C_{15}H_{22}O$, m.p. 75—76°, which is a suitable derivative for the characterisation of widdrene. The compound possessed a strong cedar wood odour espe-

* *Added in proof:* According to Y. Hirose and T. Nakatsuka [*J. Jap. Wood Res. Soc.* **4** (1958) 26], the 'thujopsene' of J. Kawamura [*Bull. Imp. For. Exp. Stn. Japan No.* **30** (1930) 59] from *Thujopsis dolabrata* is essentially identical with widdrene.

Table 1. Constituents of *Widdringtonia* heartwoods.

Species:	*Whytei*	*juniperoides*	*Schwarzii*	*cupressoides*	*dracomontana*
(As a percentage of the air dried wood)					
Total oil (ether soluble acetone extract)	12	15	7.5	0.5	4
Neutral	8	11	5	0.25	3
Alkali soluble	4	4	2.5	0.25	1
(As a percentage of the total oil)					
Neutral	65	65	65	50	80
Low boiling (terpenes etc)	2	0	0		0
Widdrene ($C_{15}H_{24}$)	10	30	30		25
WiddreneII	2	5	3		present
Widdrol ($C_{15}H_{26}O$)	10	10	5	0	3
Cedrol	15	5	5		5
Eudesmol				3	10
Alcohol ($C_{15}H_{26}O_2$) m. p. 154°		1			
Diol ($C_{15}H_{28}O_2$) m. p. 138°					6
Higher boiling neutral material	15	20	10		10
Acids	30	20	10		10
Widdrenic acid ($C_{15}H_{22}O_2$)	3	3	2		present
Acid II ($C_{15}H_{22}O_2$)	3	5	5		present
Acid III, m.p. 160°					
Acid IV, m.p. 140°					
(last two incompletely characterised)					

cially when in a slightly impure or an autoxidised state. The U.V. spectrum shows that it is an $\alpha\beta$-unsaturated aldehyde. Further oxidation with either silver oxide or with alkaline hydrogen peroxide gave the corresponding $\alpha\beta$-unsaturated carboxylic acid, widdrenic acid, $C_{15}H_{22}O_2$, m.p. 169°.

Ozonolysis of widdrene gave a keto acid $C_{15}H_{24}O_3$, m.p. 166—168°, which on oxidation with hypobromite furnished a dicarboxylic acid, widdrene dicarboxylic acid, which readily formed an anhydride. This acid was also obtained from widdrenal by oxidation with alkaline hydrogen peroxide. It was recovered unchanged when treated with hydrogen chloride in chloroform and this, together with the result of the ozonolysis, makes the possibility of the presence of a *cyclo*propane ring or an unreactive double bond unlikely.

These reactions indicate that widdrene like cedrene contains the system C—C=C(CH_3)—C in one of the rings. As in the case of cedrene, dehydrogenation experiments failed to give any characteristic products.

The second slightly higher boiling hydrocarbon provisionally called widdrene II was present only in small amount. It was dextrorotatory and appears to be an isomer of widdrene but it is uncertain whether it is entirely pure.

Further fractional distillation of the neutral oils gave a crude crystalline mixture of sesquiterpene alcohols which were most readily separated by chromatography on alumina. *Widdringtonia Whytei*, *W. juniperoides* and *W. Schwarzii* contained cedrol which is widespread in the Cupressales and a new sesquiterpene alcohol, widdrol. Eudesmol was obtained from *W. dracomontana* together with cedrol and widdrol, while eudesmol only was isolated from the small amount of wood of *W. cupressoides*. No eudesmol was obtained from the first three species although its presence cannot be excluded.

Widdrol melts at 98° and has the composition $C_{15}H_{26}O$, $[\alpha]_D$ + 105°. It could be crystallised only with difficulty but after careful chromatography it could be purified by sublimation along a temperature gradient. The I.R. and U.V. spectra and a perphthalic acid titration indicated the presence of a double bond. It was attacked by ozone and was readily dehydrated by acidic reagents to a mixture of hydrocarbons. Widdrol was acetylated with difficulty and is therefore probably a tertiary bicyclic alcohol. Selenium dehydrogenation gave an oil from which a small amount of 1,7-dimethyl-4-*iso*propylnaphthalene was isolated as the picrate. Since only a small yield of this unusual hydrocarbon was obtained, widdrol may perhaps not contain a preformed naphthalene ring and could be a spirane of the type considered by Ruzicka to constitute intermediates in the biosynthesis of cedrene.

The alkali soluble fraction of the oils contained little or no tropolones or phenols except for *W. cupressoides* which contained some material showing a phenolic type of U.V. spectrum but was insufficient for further investigation. The other four species gave resinous or crystalline acid fractions that all appeared to contain similar mixtures of acids. Four of the acids could be isolated in a crystalline form by crystallisation or by distillation of their methyl esters. One of the acids was identical with widdrenic acid (see above). Acid II, m.p. 190°, like widdrenic acid was $\alpha\beta$-unsaturated. The purity and composition of the acids III and IV are not yet absolutely certain since analyses gave variable results. Judging from the U.V. spectra, acid III appears to be aromatic. On reduction of the ester with $LiAlH_4$ a product was obtained which gave a typical benzenoid spectrum (λ_{max} 263 mμ, ε 900) and the preparations so far available yielded terephthalic acid on oxidation with dilute nitric acid. It was not affected by ozone under normal conditions. Acid IV had a different U.V. spectrum and was readily oxidised by ozone.

This exploratory study indicates that the genus *Widdringtonia* constitutes a rather homogeneous but distinctly separated group of general Cupressales character sharing with some northern genera, widdrene, cedrol and widdrol (the latter has recently been found in *Chamaecyparis thyoides*) and with some southern genera, eudesmol. The isolation of large amounts of sesquiterpene acids from these woods serves to emphasise the necessity of employing the extractive technique in investigations for the purpose of taxonomic comparison.

The co-occurrence of cedrol and eudesmol in at least *W. dracomontana* is interesting in view of the biogenetic schemes suggested by Ruzicka according to which their biosynthesis proceeds along different routes.

EXPERIMENTAL

Rotations were measured in chloroform; U.V. spectra in 95 % ethanol except where otherwise specified. The benzene-alcohol-water azeotrope was usually employed to dry solutions during evaporation. All m.p.s were taken on a hot stage.

Isolation of the oils. The ground, air-dried heartwood of each species was extracted with acetone for two days and the extract concentrated to a small volume. The material was then poured into a large volume of ether. The ether insoluble material which in the case of *W. Whytei* was obtained in large amount was discarded. The ether solution was shaken with water to remove acetone and then with 10 % sodium hydroxide solution to remove the acid fraction which was recovered by extraction with ether after acidification with dilute hydrochloric acid. Removal of the ether gave viscous oils. The neutral fractions from *W. dracomontana* deposited a considerable amount of a white material which was insoluble in light petroleum. The oil was therefore diluted with light petroleum, allowed to stand and further amounts of the material which separated were filtered off. This material was combined with that obtained by chromatography (see below).

All the neutral oils were treated in largely the same way and the separations of the constituents will therefore not be described separately except where they are divergent.

Neutral fractions. These oils after quick preliminary distillation under reduced pressure (about 10 mm) were fractionally distilled through a spinning band column. The hydrocarbons that distilled first (b.p. 115—130°/10 mm) were carefully fractionated and gave, after a small forerun, two fractions only. The material that followed (b.p. 140—150°/10 mm) contained the sesquiterpene alcohols and was distilled as a single fraction until the distillate ceased to crystallise when cold. The next fraction remained a viscous oil on standing; it was readily eluted from alumina by light petroleum and appeared to be the principal component of the higher boiling material. This and the remaining resinous material of still higher boiling point has not yet been investigated.

There was insufficient oil available from *W. cupressoides* for distillation.

Widdrene. The first hydrocarbon fraction was an oil of constant boiling point, b.p. 118—120°/10 mm, $[\alpha]_D$ −107°, n_D^{22} 1.5042. (Found: C 87.91; H 11.80. $C_{15}H_{24}$ requires C 88.16; H 11.84). The U.V. absorption spectrum showed only non-conjugated double bond absorption in the 210 mμ region. Titration with perphthalic acid in ethanol solution was almost complete after 36 h with the consumption of 0.9 mole of perphthalic acid. No attempt was made to isolate widdrene from *W. cupressoides* but widdrene with the same physical constants was isolated from the other four species. Widdrene possesses an odour very similar to that of cedrene, perhaps slightly stronger. The odour increased on standing, probably due to autoxidation.

Widdrenal. Widdrene (1 g) and selenium dioxide (600 mg) were heated in alcohol (20 ml, 95 %) under reflux for 4 h. The reaction solution was cooled, filtered, evaporated to dryness and the product sublimed under reduced pressure on to a cold finger and recrystallised from light petroleum to give *widdrenal*, m. p. 75—76°, $[\alpha]_D$ −27° (*c*, 1.8), λ_{max} 252 mμ, ε 6 000. (Found: C 82.12; H 10.3. $C_{15}H_{22}O$ requires C 82.52; H 10.15).

Widdrenic acid. Widdrenal (100 mg) was added to an aqueous suspension of silver oxide and the mixture heated for one hour on the steam bath. The suspension was acidified and extracted with ether. The ether solution was taken to dryness and the product recrystallised from ethanol and sublimed to give *widdrenic acid* (30 mg), m. p. 169°, $[\alpha]_D$ −86° (*c*, 1.8), λ_{max} 245 mμ, ε 5 000 (*n*-heptane). (Found: C 76.77; H 9.19. $C_{15}H_{22}O_2$ requires C 76.88; H 9.47).

Ozonolysis of widdrene. Ozone was passed through a solution of widdrene (10 g) in a mixture of methanol and ethyl acetate (1:1, 100 ml) at −75° until the solution turned blue. The solution was shaken with zinc dust activated with acetic acid, filtered, washed with water and then evaporated to dryness. The product was crystallised from methanol (5 g) and sublimed *in vacuo* to give a *keto-acid*, m. p. 166—168°, $[\alpha]_D$ −129° (*c*, 2.1). (Found: C 70.91; H 9.59. $C_{15}H_{24}O_3$ requires C 71.40; H 9.59). The keto-acid (200 mg) was treated with excess sodium hypobromite solution for 3 h. The solution was extracted with ether and then sulphur dioxide was bubbled through until the colour was discharged. It was then acidified and extracted with ether and this ether extract was washed with water and taken to dryness to give a resin which was crystallised from methanol to give *widdrene dicarboxylic acid* (130 mg), m. p. 215°, $[\alpha]_D$ −57° (*c*, 2.1). (Found: C 66.06; H 8.72. $C_{14}H_{22}O_4$ requires C 66.10; H 8.73).

The *dimethyl ester* was prepared by methylation with diazomethane and was purified by sublimation under reduced pressure, m. p. 71—73°, $[\alpha]_D$ −59° (*c*, 2.0). (Found: C 68.38; H 9.11. $C_{16}H_{26}O_4$ requires C 68.13; H 9.25).

The acid (100 mg) was refluxed in acetic anhydride (5 ml) for one hour and the reaction mixture was then evaporated to dryness. The resultant resin was sublimed on to a cold finger and crystallised from light petroleum-chloroform to give *widdrene dicarboxylic acid anhydride*, m. p. 113°, $[\alpha]_D$ +39° (*c*, 2.9). (Found: C 70.86; H 8.42. $C_{14}H_{20}O_3$ requires C 71.15; H 8.53).

Widdrene dicarboxylic acid was also obtained by treating widdrenal (300 mg) in methanolic potassium hydroxide solution (20 ml, 5 %) with hydrogen peroxide (2 ml, 30 %) for 3 h at room temperature. The reaction mixture was diluted with water, extracted with ether, acidified and extracted again with ether. This last ether extract was washed with water, evaporated to dryness and the resultant resin crystallised from ethyl acetate, m. p. and mixed m. p. 213—214°.

Widdrene II. The hydrocarbon fraction boiling slightly higher than widdrene was redistilled to give a constant boiling *fraction*, b. p. 128°/10 mm, $[\alpha]_D$ +50° (*c*, 3.0), n_D^{22} 1.5160. (Found: C 87.75; H 11.47. $C_{15}H_{24}$ requires C 88.16; H 11.84). (See forthcoming publication by Enzell and Erdtman on the purification and structure of the main component of this material.)

The sesquiterpene alcohol fractions. After the hydrocarbons had been distilled off, further distillation of the oil gave a large fraction, b. p. 140—150°/10 mm which crystallised on cooling. This material was dissolved in light petroleum and adsorbed on alumina. It was then eluted with benzene. The first fractions gave cedrol which was crystallised from aqueous methanol and then sublimed, m. p. and mixed m. p. 87—89°, $[\alpha]_D$ +10° (*c*, 2.0). Further elution with benzene-ether (1:1) gave a crystalline material which was sublimed, crystallised from cold light petroleum and resublimed along a temperature gradient to give *widdrol*, m. p. 98°, $[\alpha]_D$ +105° (*c*, 2.3), $\varepsilon_{210\,m\mu}$ 1 500. (Found: C 80.98; H 11.71. $C_{15}H_{26}O$ requires C 81.03; H 11.78). It gave a coloration with tetranitromethane.

The alcohol fraction from *W. dracomontana* was treated slightly differently. After removal of the sesquiterpenes the whole of the remaining material was chromatographed on alumina. The cedrol was eluted with benzene and then further elution with benzene-ether (9:1) gave crude crystalline eudesmol which was rechromatographed, recrystallised twice from light petroleum and sublimed, m. p. and mixed m. p. 83—84°, $[\alpha]_D$ +45° (*c*, 1.9). The infrared spectrum of this material was identical with that of an authentic sample of the natural mixture of isomers.

Elution with benzene-ether (1:1) gave widdrol and final elution with benzene-methanol (9:1) gave a product which was crystallised from chloroform-light petroleum to give a white powder which was combined with the material already isolated directly from the crude neutral oil by crystallisation from light petroleum (see above). This was recrystallised several times from chloroform-light petroleum to give a *diol*, m. p. 137—138°, $[\alpha]_D$ −24°. (Found: C 74.81; H 11.54; M (Rast) 239. $C_{15}H_{28}O_2$ requires C 74.93; H 11.75; M 240). An active hydrogen determination gave 0.81 %; two active hydrogens require 0.83 %.

The neutral fraction from *W. cupressoides* was too small for distillation (2.0 g from 700 g of wood) and was therefore chromatographed directly. The benzene-ether (9:10) eluate crystallised partially and on crystallisation from light petroleum and sublimation gave eudesmol, m. p. and mixed m. p. 80—82°, $[\alpha]_D$ +45°.

A sample of the neutral oil from *W. juniperoides* was chromatographed directly after first removing the widdrenes by distillation. In addition to widdrol and cedrol this chromatogram, on elution with ether-methanol (9:1) and recrystallisation of the material in this fraction from light petroleum gave an *alcohol*, m. p. 154°, $[\alpha]_D$ −9°. (Found: C 75.40; H 10.80. $C_{15}H_{26}O_2$ requires C 75.58; H 11.00). An active hydrogen determination gave 0.47 %; one active hydrogen requires 0.42 %. The compound was unattacked by ozone.

Dehydrogenation of widdrol. Widdrol (1 g) and selenium (1 g) were heated at 300° for 24 h in an atmosphere of carbon dioxide. The product was distilled to give an oil (400 mg) with an ultraviolet spectrum corresponding to somewhat less than 50 % of a naphthalenoid hydrocarbon. The picrate of the hydrocarbon was recrystallised five times from methanol to give a small amount of a picrate, m. p. 91—93°, mixed m. p. with the picrate of 1,7-dimethyl-4-*iso*propylnaphthalene, undepressed.

The acid fractions. The sodium hydroxide soluble fractions of the oils were dissolved in a small volume of ether and allowed to stand at 0° for some time. The material that crystallised was separated by crystallisation from a mixture of ether and light petroleum and then from methanol to give *acid I*, m. p. 169—170°, $[\alpha]_D$ −86° (*c*, 1.9), mixed m. p. with widdrenic acid prepared from widdrene (see above) undepressed. The material slightly less soluble in ether gave on recrystallisation from ether-light petroleum and from ethyl acetate, the *acid II*, m. p. 190—191°, $[\alpha]_D$ −76° (*c*, 1.9), $\varepsilon_{220\ m\mu}$ 5 000 (*n*-heptane). (Found: C 76.49; H 9.61; equiv.wt. (titration) 234. $C_{15}H_{22}O_2$ requires C 76.88; H 9.47; equiv.wt. 224).

An attempt was made to separate the two acids by distillation of the methyl esters, prepared by esterification with diazomethane, through a spinning band column. The boiling point curve (85 % b.p. 157—162°/10 mm) showed no obvious separation; the middle fractions contained a mixture that on crystallisation from light petroleum gave *widdrenic acid methyl ester*, m. p. 109—110°, $[\alpha]_D$ −99° (*c*, 2.0). (Found: C 77.69; H 9.85. $C_{16}H_{24}O_2$ requires C 77.39; H 9.73). Saponification of this compound by heating in 10 % methanolic potassium hydroxide solution for 3 h under reflux gave widdrenic acid, m. p. 169—170°. Attempted isomerisation of this ester or of the acid II ester by either acid or alkaline treatment failed.

The end fractions from the distillation through the spinning band column were chromatographed on alumina. Light petroleum eluted an ester which on saponification and recrystallisation from light petroleum gave a crystalline acid material, *acid III*, m. p. 160—161°, $[\alpha]_D$ +63° (*c*, 2.4), λ_{max} 240 mμ, ε 12 000. Benzene-light petroleum eluted an ester which was saponified by refluxing in 10 % aqueous methanolic potassium hydroxide solution for 2 h. Recrystallisation from light petroleum gave an *acid IV*, m. p. 138—140°, λ_{max} 302 mμ, ε 6 000. The acid III, m. p. 160—161°, could also be obtained from a mixture of the two by ozonolysis. These two acid products gave varying analytical results on repeated analysis but were apparently C_{15} compounds with two oxygen atoms.

The acid III (100 mg) was heated with nitric acid (15 ml, 10 %) for 24 h at 170°. The crystalline material that separated from the reaction mixture on cooling was filtered off (20 mg) and methylated with diazomethane. The ester was recrystallised from methanol to give terephthalic acid dimethyl ester, m. p. and mixed m. p. 143—144°.

Acid III (10 mg) was esterified with diazomethane and the reaction mixture was taken to dryness, dissolved in dry ether and refluxed with $LiAlH_4$ for 2 h. The solution was cooled, ethyl acetate was added, then water and acid. This mixture was extracted with ether and taken to dryness. The product showed a U.V. maximum at 263 mμ, ε 900.

Our thanks are due to Mr. J. Beard, the Natal Tanning Extract Company Ltd, Pietermaritzburg, Natal, the Chief Forest Products Officer, Forest Products Institute, Pretoria, and the District Forest Officers, Cathedral Peak, Natal, Stormsrivier and Kingwilliamstown, Cape, for their kind assistance in collecting the wood samples, to Professor F. Šorm, Prague, for a sample of the picrate of 1,7-dimethyl-4-*iso*propylnaphthalene, to Professor Pl. A. Plattner, Basel, for a sample of α-cedrene, and to *Statens Naturvetenskapliga Forskningsråd* for financial support.

REFERENCES

1. Baker, R. T. and Smith, H. G. *A Research on the Pines of Australia.* Sydney 1910, p. 63.
2. Cahn, R. S., Penfold, A. R. and Simonsen, J. L. *J. Chem. Soc.* **1931** 3134.
3. *cf.* Erdtman, H. and Pelchowicz, Z. *Acta Chem. Scand.* **9** (1955) 1728.
4. Erdtman, H., Pelchowicz, Z. and Topliss, J. G. *Acta Chem. Scand.* **10** (1956) 1563.
5. Erdtman, H. and Pelchowicz, Z. *Chem. Ber.* **89** (1956) 341.

Received October 23, 1957.

ACTA CHEMICA SCANDINAVICA 12 (1958) 274—280

1,1-Di-*p*-hydroxyphenyl-2,2-diethyl-ethylene, a New Isomer of Stilbestrol

JEAN FRANÇOIS MIQUEL

The Pharmacological Institute, University of Uppsala, Sweden

Interchanging one of the ethyl groups of diethylstilbestrol with one of the *para*-hydroxyphenyl groups gives a substance, 1,1-di-*p*-hydroxyphenyl-2,2-diethyl-ethylene, which is 50—100 times less estrogenic than diethyl-stilbestrol and is able to interfere with the vaginal estrus reaction if given intravaginally to spayed rats receiving estrogen systemically. The synthesis is made through the *p*-hydroxy-2-ethyl-butyrophenone or directly through the dimethyl ether obtained by an abnormal Friedel-Crafts reaction. The demethylation of the phenolic methoxyl groups must be effected with potassium hydroxide in triethyleneglycol. The demethylated compound decomposes on warming or in acidic media. The U.V. absorption of the new compound has been determined in different solvents.

In connection with work concerning the antagonism between natural or synthetic estrogens and related substances [1], the 2-alkylderivatives of 1,1-di-*p*-hydroxyphenyl-ethylene (I) became of interest. These substances are related to the substituted polyarylethylenes and particularly to TACE (trianisyl-chloroethylene) (II)

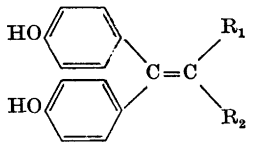

I

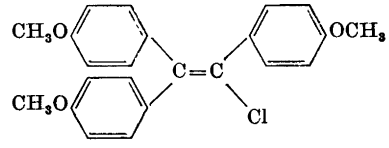

II

No alkyl-derivatives of I are described in the literature except 1,1-di-*p*-hydroxyphenyl-propylene which was prepared by Wessely [2]. He found the diacetate to give 66 % estrus response in 100 μg per rat. Later Lacassagne *et al.*[3] showed that the free compound has a very weak estrogenic activity, giving 66 % response at 15 mg/rat.

We have prepared several of the 2-alkyl and 2,2-dialkyl derivatives but the present report is concerned only with compound III: 1,1-di-*p*-hydroxy-

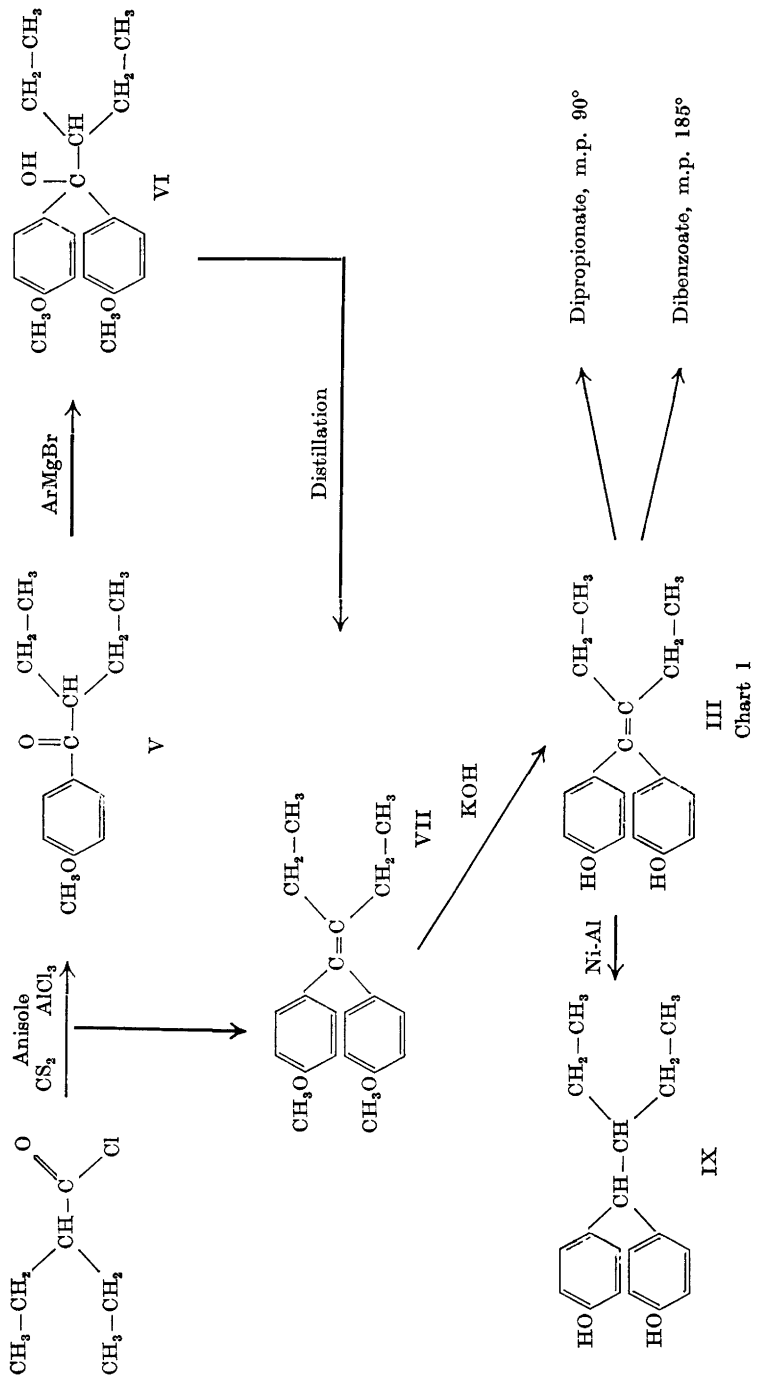
Anisole
CS_2 $AlCl_3$
ArMgBr
Distillation
KOH
Ni-Al
Dipropionate, m.p. 90°
Dibenzoate, m.p. 185°
V
VI
VII
III
IX
Chart 1

phenyl-2,2-diethyl-ethylene (*aa*DE for brevity). This compound is an isomer of diethyl-stilbestrol (IV) the difference being the transposition of an ethyl group and an aromatic group. Hence *aa*DE represents an interesting connection between diethyl-stilbestrol and the triphenyl-ethylene series.

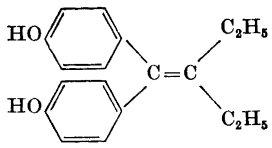

III

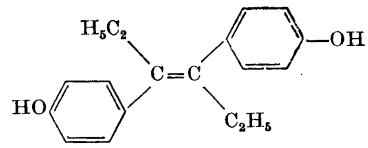

IV

In a similar way Campbell [4] has studied the same transposition in the hexestrol series, where it causes a 50 000 fold drop in activity. In the case of the present compound the transposition has much less effect, the activity of *aa*DE is only 50 to 100 times less than that of diethyl-stilbestrol. Tested according to the technique of Bárány *et al.*[1], it interferes with the vaginal estrus reaction. Under the same conditions diethyl-stilbestrol is inactive. Further biological data will be reported elsewhere.

*aa*DE is prepared by a Grignard reaction of *p*-bromo-anisole with the *p*-methoxy-2-ethyl-butyrophenone (V). The carbinol (VI) so obtained dehydrates spontaneously during the distillation to give 1,1-di-*p*-methoxyphenyl-2,2-diethyl-ethylene (VII) which is then demethylated (Chart I).

The new ketone (V) is prepared with good yields:
a) (74 % from the acid) by methylation of the *p*-hydroxy-2-ethyl-butyrophenone (VIII) obtained by the action of BF_3 on a mixture of diethyl-acetic acid and phenol;
b) (70 % from the acid) by a Friedel-Crafts reaction between diethyl-acetyl chloride and anisole in carbon disulfide.

The hydroxyketone (VIII) is a colourless and microcrystalline substance, the methoxy compound is a pleasantly smelling pale yellow oil which can be demethoxylated easily by pyridine hydrochloride.

Following earlier work on the U.V. absorption of hydroxyarylketones [5] we have now studied the absorption of compounds V and VIII in different solvents. Both show the characteristic band of the *para*-acetophenones. After solution in equal volumes of ethanol and 0.1 N NaOH, the bathochromic effect for the paramethoxy group is weak even for the stronger band, the maximum being 265 mμ in *cyclo*hexane, 273 mμ in ethanol and 277 mμ in the alkaline solution. For the parahydroxyketone the shift is from 280 mμ in ethanol to 328 mμ in alkaline solution and the intensity increase from log $\varepsilon = 4.17$ to log $\varepsilon = 4.41$. The first band shows in this case a shift from 221 mμ to 238 mμ (Fig. 1).

The dimethoxy derivative (VII) can be directly obtained in competition with the methoxyketone (VI) by an interesting modification of the Friedel-Crafts reaction, using more drastic conditions of temperature and the anisole in large excess. This reaction described for the first time by Gattermann [6], who obtained 1,1-di-*p*-methoxyphenyl-propene in addition to *p*-methoxy-propiophenone, has lately been studied by Mentzer and Xuong [7] and extended

Table 1.

	*Cyclo*hexane		Ethanol		50% Ethanol 50% HCl, 0.1 N		50% Ethanol 50% NaOH, 0.1 N	
	λ_{M-m}	log ε	λ_{M-m}	log ε	λ_{M-m}	log ε	λ_{M-m}	log ε
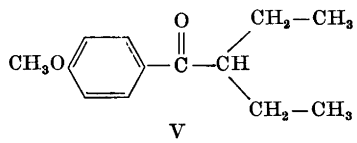 V	—		—		210	3.92	—	
	215	4.19	220	4.10	219	4.04	219	4.08
	230	3.10	235	3.07	236	3.03	236	3.14
	265	4.27	273	4.24	277	4.21	277	4.26
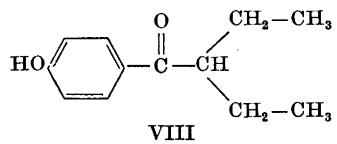 VIII	—		—		210	4.00	223	3.67
	—		221	4.00	220	4.10	238	3.86
	230	3.34	237	2.80	238	3.25	260	3.09
	261	4.19	280	4.17	280	4.23	328	4.46
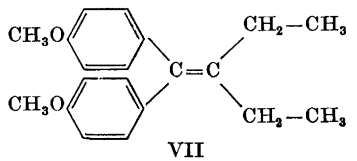 VII			222	4.07				
			241	4.29				
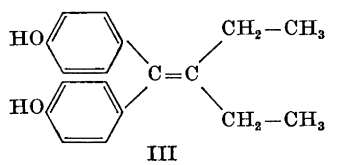 III								
	221	4.12	221	4.31			230	4.16
	237	4.23	239	4.42			256	4.39

to the preparation of the triphenyl-ethylene derivatives by Xuong and Buu-Hoï [8]. We have previously determined the proportions of such 1,1-diaryl-ethylenes in the simultaneous preparation of *ortho*- and *para*-hydroxy-aryl-ketones[9]. Now yields of the ethylene derivative are varying from 12 to 20 % and at the same time 44—55 % of the ketones, calculated from the acid chloride used.

By chromic oxidation of the ethylene derivative (VII) *p,p'*-dimethoxy-benzophenone is formed in good yield. Demethylation of VII cannot be done by hydrobromic acid or other acidic agents which have little activity and produce polymerisation of the hydroxy compound formed. The best demethylation results are obtained with potassium or sodium hydroxide in boiling triethylene glycol.

The compound *αα*DE is a colourless microcrystalline substance. The melting point is 163° (instantaneous m.p.). It is soluble in ethanol, acetone,

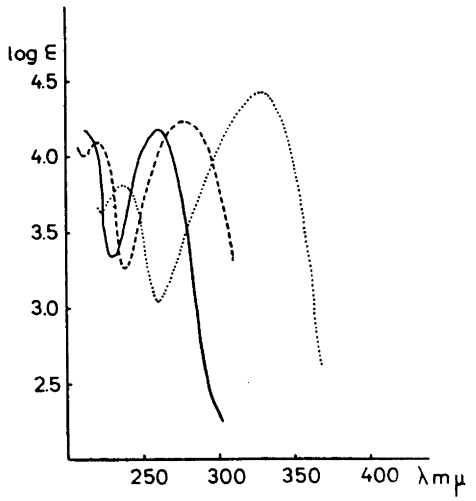

Fig. 1. —— *p*-hydroxy-2-ethyl-butyrophenone (VIII) in *cyclo*hexane. ------ compound VIII in ethanol 50 %, HCl 0.1 N 50 %. ····· compound VIII in ethanol 50 %, NaOH 0.1 N 50 %.

less soluble in benzene. It can be recrystallized from ligroin (100—125°), *cyclo*hexane, or a mixture: methanol 70 %, water 30 %. It is stable under alkaline and neutral conditions but very quickly formes coloured resins in acidic media. It gives a dipropionate, m.p. 89° and a dibenzoate, m.p. 184°. By reduction with nickel-aluminium alloy it forms compound IX which has previously been prepared by Campbell [4] by the action of diethyl-acetaldehyde on phenol.

EXPERIMENTAL

p-Hydroxy-2-ethyl-butyrophenone (VIII)

a) 12.6 g of diethyl-acetic acid and 12 g of phenol were slowly saturated during 2 h with BF_3. The temperature was then slowly elevated to 60—80° and kept there during one hour. The reaction product was poured into water, the ketone distilled easily under pressure 175°/1 mm. The ketone was dissolved at 25° in *cyclo*hexane and then recrystallized in the icebox as shiny soft colourless needles, m. p. 70°, yield 15.75 g (82 %).

b) 5 g of the methoxy derivative was refluxed with 5 g of pyridine hydrochloride for 20 min, then poured into water and extracted with ether. The organic layer was washed with water, dried, the ether distilled off and the ketone distilled. B. p. 175°/1 mm, yield 3.2 g (68 %). (Found: C 75.03; H 8.44. Calc. for $C_{12}H_{16}O_2$ (192.25): C 74.97; H 8.39).

Semicarbazone, colourless needles, m. p. 191° (from diluted ethanol). (Found: N 16.70. Calc. for $C_{13}H_{21}O_2N_3$ (251.32): N 16.72).

p-Methoxy-2-ethyl-butyrophenone (V)

13.5 g (0.1 mole) of diethyl-acetyl chloride [10] was mixed with 12 g anisole (0.1 mole + 10 %) in 80 ml of carbon disulfide, the mixture was cooled to 0° and 15 g of aluminium chloride added, the temperature being kept under 5°. After 24 h the mixture was refluxed one hour and poured into dilute cold hydrochloric acid. The organic layer taken up with ether was washed with 10 % aqueous sodium hydroxide, with water, then dried (Na_2SO_4) and the solvent removed by distillation. The distillation at 16 mm and 150—178° gave a yield of 16 g (78 %). A rectification at 16 mm and 172° afforded nearly colourless oil. n_D^{24} 1.5280 (Found: C 75.55; H 8.72. Calc. for $C_{13}H_{18}O_2$ (206.27) C 75.69; H 8.80).

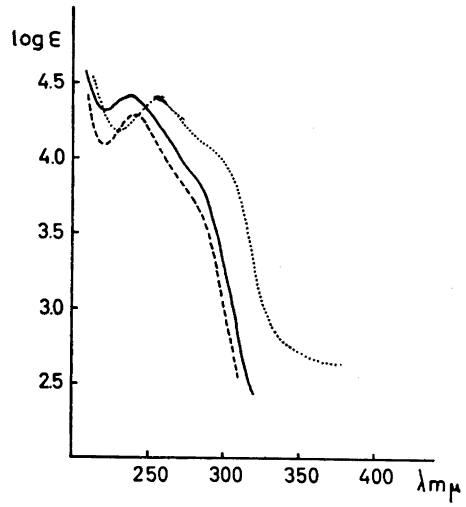

Fig. 2. ——— *aa*DE (III) in ethanol. ------ dimethylether *aa*DE (VII) in ethanol. ..... *aa*DE (III) in ethanol 50 %, NaOH 0.1 N 50 %.

Synthesis of a mixture of ketone (V) and ethylene (VIII)

13.5 (0.1 mole) of diethyl-acetyl chloride, 50 g anisole and 13 g aluminium chloride were mixed with good stirring keeping the temperature between 20 and 30°. After 24 h the mixture was refluxed during one hour and left at room temperature for 72 h. After normal decomposition and treatment, the red oil was distilled. The ketone distilled first under water pump pressure between 170° and 175°. When the temperature rose to 180° the oil pump was used and the ethylene (VIII) distilled at 195—200° under 1 mm Hg. After two recrystallizations from ethanol the ethylene melted at 90—91°.

The proportion of ketone and ethylene seems to depend on the time of contact between the reactants: with a time of 48 h the yield was an average of 61 % ketone and 8 % ethylene, with a time of 96 h the yield came to 42 % ketone and 8 % ethylene. (Found for the ethylene: C 80.93; H 8.12. Calc. for $C_{20}H_{24}O_2$ (296.39) C 81.04; H 8.16).

1,1-Di-*p*-methoxy-phenyl-2,2-diethyl-ethylene by Grignard reaction

11 g of *p*-bromo-anisole were slowly added to 3 g of magnesium-turnings in 80 ml anhydrous ether. After the end of the reaction the mixture was refluxed half an hour, then ice-cooled and 10 g of the ketone (VI), dissolved in 30 ml dried ether, slowly added. After the classical treatment and distillation the orange yellow oil crystallized spontaneously and gave after two recrystallizations in ethanol 10.7 g (72.4 %) of colourless microcrystalline substance. Melting point 90—91°. A mixture of crystals with those obtained by the abnormal Friedel-Crafts reaction gave the same melting point. (Found: C 80.96; H 8.24. Calc. for $C_{20}H_{24}O_2$ (296.39) C 81.04; H 8.16). Péteri[11] who obtained this substance as by-product in a synthesis of diethylstilbestrol gives a melting point of 86-88°.

Oxidation of 1,1-di-*p*-methoxy-phenyl-2,2-diethyl-ethylene

The preceding ethylene (2.5 g) treated with chromic acid (2 g) in acetic acid gave an exothermic reaction: the green solution was then poured into water. The solid precipitate was filtered and recrystallized from ethanol, m. p. 143—144°. The literature [12] gives the same melting point for *p,p'*-dimethoxy-benzophenone. (Found: C 74.28; H 5.76. Calc. for $C_{15}H_{14}O_3$ (242.26) C 74.36; H 5.83).

1,1-Di-*p*-hydroxyphenyl-2,2-diethyl-ethylene (*aa*DE) (III)

5 g of the ethylenic derivative (VIII) was refluxed with 5 g of potassium hydroxide in triethylene glycol with good stirring during 3 h. The mixture was then poured into 60 ml cold water, extracted with ether then acidified to pH 3 under ether. The ether layer was carefully washed with water until pH 6.6, dried with Na_2SO_4 and the ether distilled off. The oily precipitate crystallized on standing; after several recrystallizations from methanol (70 %) and water (30 %) long, colourless, soft needles were obtained, m. p. 163° (instantaneous m. p.), yield 3.2 g (76 %). (Found: C 80.37; H 7.61. Calc. for $C_{18}H_{20}O_2$ (268.34): C 80.56; H 7.51).

The dipropionate was obtained easily by refluxing the crude product with propionic anhydride in pyridine. After 30 min the mixture was poured into water, warmed to decompose the excess of anhydride and slightly acidified with hydrochloric acid, the dipropionate extracted with ether, the ether layer washed with a carbonate solution, with water, and dried (Na_2SO_4). The dipropionate recrystallized from ethanol as a colourless microcrystalline substance, m. p. 89—90°. (Found: C 75.74; H 7.42. Calc. for $C_{24}H_{28}O_4$ (380.46): C 75.76; H 7.42).

The dibenzoate was obtained by action of benzoyl chloride on an alkaline solution of *aa*DE. It recrystallized from ethanol and melted at 183—185°. (Found: C 80.60; H 5.84. Calc. for $C_{32}H_{28}O_4$ (476.54): C 80.64; H 5.92).

1,1-*p*-Hydroxy-phenyl-2,2-diethyl-ethane (IX)

1 g of *aa*DE was dissolved in 30 ml of 10 % NaOH and warmed to 90°. 2.5 g of nickel aluminium alloy was added in small portions with stirring, the mixture was then refluxed during one hour, filtered, the residue washed with hot water and the filtrate poured into hydrochloric acid. The precipitate was extracted with ether which was washed with water, dried and distilled off. The crystals mixed with oil were recrystallized from benzene, m. p. 168°. Campbell [4] who has prepared this compound by condensation of the diethylacetaldehyde with phenol, gives the same melting point.

This work was supported by grants to prof. E. Bárány from the *Swedish Cancer Society.*

REFERENCES

1. Bárány, E., Morsing, P., Müller, W., Ställberg, G. and Stenhagen, E. *Acta Soc. Med. Upsaliensis* **60** (1955) 68.
2. Wessely, F., Kersbaum, E., Kleedorfer, A., Prillinger, F. and Zajic, E. *Monatsh.* **73** (1940) 127.
3. Lacassagne, A., Chamorro, A., Buu-Hoï, N. P. and Dat-Xuong, N. *Compt. rend. soc. biol.* **143** (1954) 419.
4. Campbell, N. R. *Proc. Roy. Soc. London* **129** *B* (1940) 528.
5. Miquel, J. F., Müller, P. and Buu-Hoï, N. P. *Bull. soc. chim.* **1956** 633.
6. Gattermann, L. *Ber.* **22** (1889) 1130.
7. Menzer, C. and Dat-Xuong, N. *Compt. rend.* **222** (1946) 1004.
8. Dat-Xuong, N. and Buu-Hoï, N. P. *J. Chem. Soc.* **1952** 3741.
9. Miquel, J. F., Buu-Hoï, N. P. and Royer, R. *J. Chem. Soc.* **1955** 3417.
10. Freund, M. and Herrman, P. *Ber.* **23** (1890) 189.
11. Péteri, E. *J. Chem. Soc.* **1940** 833.
12. Vorländer, D. *Ber.* **40** (1907) 1415.

Received October 23, 1957.

ACTA CHEMICA SCANDINAVICA 12 (1958) 281—286

On the Crystal Structure of the Rubidium Salt of Hydroxymalonic Dialdehyde

GEORG LUNDGREN and BENGT AURIVILLIUS

Institute of Inorganic and Physical Chemistry, University, Stockholm; Department of Inorganic Chemistry, Royal Institute of Technology, Stockholm 70, Sweden

The crystal structure determination of the rubidium salt of hydroxymalonic dialdehyde (= rubidium "reductonate", $Rb(C_3H_3O_3)H_2O$) is reported. The lattice is monoclinic with $a = 8.3 \pm 0.1$ Å, $b = 18.3 \pm 0.2$ Å, $c = 4.0 \pm 0.1$ Å, $\beta = 93° \pm 1°$. The space group is $P2_1/a$ (No. 14 in the International Tables [1]). The x and y parameters for the atoms have been determined. The z parameters were not calculated since the main features of the structure appeared in its xy projection.

When trying to solve the crystal structure of hydroxymalonic dialdehyde ("reductone") we found that it is probably non-centrosymmetric (space group No. 33 $Pn2_1a$ [1])[2]. The problem of determining the structure should then be very much facilitated if we could get some information concerning its C—O skeleton by investigating some related compounds. The work was thus begun by studying the structures of bromomalonic dialdehyde and rubidium "reductonate" (the rubidium salt of hydroxymalonic dialdehyde). A report concerning the crystal structure of the first compound will be given in *Acta Chem. Scand.*[3] and the second one is dealt with here.

A crystalline preparation of rubidium "reductonate" was kindly supplied by Professor Hans von Euler and Mr H. Hasselquist. It had been prepared by mixing water solutions of rubidium carbonate and hydroxymalonic dialdehyde. By very slow addition of acetone, crystals of rubidium "reductonate" then separated as leaf-like, rather long, yellowish, deliquescent plates. By evidence from the X-ray data, the formula of the compound was later on found to be $Rb(C_3H_3O_3)H_2O$.

By rotation and Weissenberg photographs the symmetry of the crystals was found to be monoclinic with the following cell dimensions:

$$\begin{aligned} a &= 8.3 \pm 0.1 \text{ Å} \\ b &= 18.3 \pm 0.2 \text{ Å} \\ c &= 4.0 \pm 0.1 \text{ Å} \\ \beta &= 93° \pm 1° \\ V &= 607 \text{ Å}^3 \end{aligned}$$

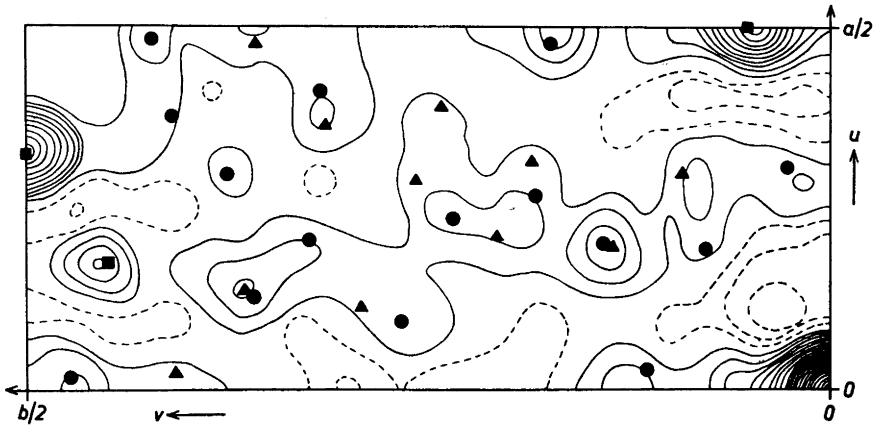

Fig. 1. The Patterson projection $P(uvp)$ for $Rb(C_3H_3O_3)H_2O$. In the figure the final vectors Rb—Rb (■), Rb—O (●), and Rb—C (▲) have been indicated. Dashed lines indicate negative values.

The following reflections were found to be systematically absent:

$$h0l \text{ with } h = \text{odd}$$
$$0k0 \text{ with } k = \text{odd}.$$

This is characteristic of the space group $P2_1/a$, which is another orientation of $P2_1/c$ (No. 14 in the International Tables of X-ray Crystallography [1]).

Because of the deliquescency of the crystals, their density could not be determined. However, by comparing the cell volume (607 Å^3) with that of hydroxymalonic dialdehyde (380 Å^3), we see that there should be 4 or 6 formula units in the unit cell.

POSITIONS OF THE RUBIDIUM ATOMS

The positions of the rubidium atoms were determined from the Patterson projection $P(uvp)$ (Fig. 1) using the estimated intensities corrected for polarization and Lorentz effects. It shows two large maxima: one at $u = 0.324$, $v = \frac{1}{2}$ and one at $u = \frac{1}{2}$, $v = 0.050$, which should certainly correspond to Rb—Rb vectors. They could be explained only if four rubidium atoms are situated in the point position 4(*e*): $\pm(xyz)$; $\pm(\frac{1}{2} + x, \frac{1}{2} - y, z)$ with $x_{Rb} = 0.088$ and $y_{Rb} = 0.225$.

If there are six formula units per unit cell, we should have two additional rubidium atoms in one of the positions 2(*a*)—2(*d*). This would demand a Rb—Rb peak at $u = \frac{1}{2}$, $v = \frac{1}{2}$ in $P(uvp)$. Since there is a negative region at that point, we could safely say that the unit cell contains only four rubidium atoms and consequently only four organic anions.

Since the *c* axis is very short and only a limited number of reflections could be registered in $0kl$, we did not determine the *z* parameters of the atoms. However, this was not necessary since our intention of getting a rough picture of the C—O skeleton could be fulfilled even if the *z* parameters were not known.

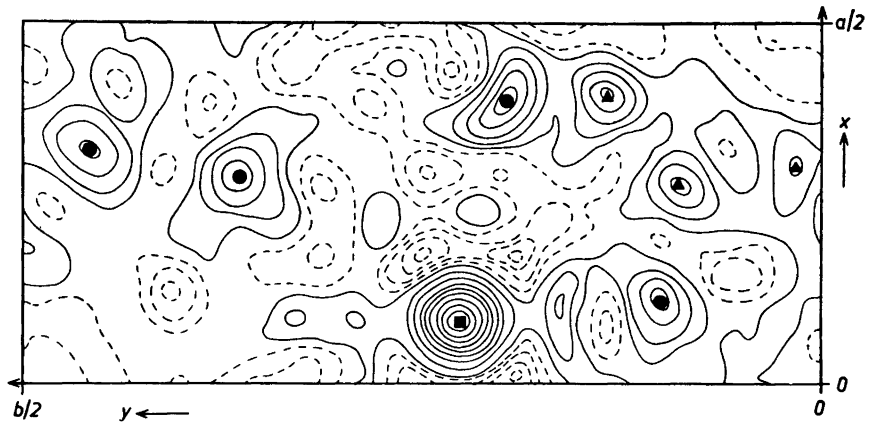

Fig. 2. The final electron density projection $\varrho(xyp)$ of $Rb(C_3H_3O_3)H_2O$. The positions of the Rb (■), C (▲) and O (●) atoms have been indicated. In the rubidium peak only every third contour has been marked. Dashed lines indicate negative values.

POSITIONS OF THE LIGHT ATOMS

To determine the positions of the light atoms the electron density projection $\varrho(xyp)$ was calculated. The signs of the F values were at first determined from the known rubidium contributions to the intensities. Later on, when the x and y parameters of the light atoms were approximately known, $\varrho(xyp)$ was corrected by considering the scattering of the light atoms also. However, only a few changes in the signs of the structure factors were necessary.

As is seen in Fig. 2, $\varrho(xyp)$ shows some low maxima which could be ascribed to oxygen and carbon atoms. Their parameters are:

4 A_1 in	4(e):	$\pm(xyz)$;	$\pm(\frac{1}{2}+x,\frac{1}{2}-y,z)$	with	$x = 0.11_6$, $y = 0.10_1$
4 A_2 »		»	»	»	$x = 0.39_1$, $y = 0.19_8$
4 A_3 »		»	»	»	$x = 0.32_1$, $y = 0.45_8$
4 A_4 »		»	»	»	$x = 0.28_7$, $y = 0.36_5$
4 A_5 »		»	»	»	$x = 0.27_5$, $y = 0.09_0$
4 A_6 »		»	»	»	$x = 0.39_8$, $y = 0.13_4$
4 A_7 »		»	»	»	$x = 0.29_9$, $y = 0.01_7$

In addition there are some very weak maxima close to the large rubidium maximum. They are, however, certainly false peaks caused by diffraction effects from the heavy rubidium atom [4].

Space arguments were used to decide the nature of the atoms A_1 to A_7. It was assumed that oxygen atoms are situated at least 2.60 Å apart. The projection of an O—O distance on the xy plane is thus at least 1.67 Å since the two oxygen atoms could be at most $c/2 = 2.0$ Å apart in the z direction. Now, the xy projections of the shortest distances A_1—A_5, A_2—A_6, A_3—A_7, A_5—A_6, and A_5—A_7 are 1.2_8 Å, 1.1_8 Å, 1.4_7 Å, 1.3_0 Å, and 1.3_5 Å, *i.e.* they

Table 1. Calculated and observed structure factors *hk*0 for $Rb(C_3H_3O_3)H_2O$.

*hk*0	*F* calc	*F* obs	*hk*0	*F* calc	*F* obs	*hk*0	*F* calc	*F* obs
0 2 0	−52	(28)	3 1 0	−10	12	5 10 0	−10	0
0 4 0	34	25	3 2 0	−42	49	5 11 0	16	0
0 6 0	−36	30	3 3 0	1	6	5 12 0	10	0
0 8 0	22	28	3 4 0	44	50	5 13 0	−30	24
0 10 0	7	7	3 5 0	7	9	5 14 0	−10	0
0 12 0	−25	23	3 6 0	−35	30	5 15 0	26	27
0 14 0	19	28	3 7 0	3	0	5 16 0	7	0
0 16 0	−27	33	3 8 0	45	39	5 17 0	−10	0
0 18 0	16	14	3 9 0	0	0	5 18 0	0	0
0 20 0	−17	13	3 10 0	−48	38	5 19 0	0	0
			3 11 0	12	0			
1 1 0	14	14	3 12 0	35	32	6 0 0	−42	59
1 2 0	−23	21	3 13 0	− 3	0	6 1 0	11	0
1 3 0	−16	14	3 14 0	−16	17	6 2 0	42	52
1 4 0	23	15	3 15 0	6	0	6 3 0	7	0
1 5 0	21	18	3 16 0	15	17	6 4 0	−22	20
1 6 0	−26	22	3 17 0	2	0	6 5 0	8	0
1 7 0	−41	34	3 18 0	− 6	0	6 6 0	22	29
1 8 0	47	43	3 19 0	− 2	0	6 7 0	− 8	0
1 9 0	41	34				6 8 0	−11	0
1 10 0	−18	15	4 0 0	−44	53	6 9 0	5	0
1 11 0	−37	40	4 1 0	−48	63	6 10 0	− 7	0
1 12 0	6	0	4 2 0	34	50	6 11 0	3	0
1 13 0	28	35	4 3 0	18	33	6 12 0	7	0
1 14 0	−24	24	4 4 0	−24	26	6 13 0	4	0
1 15 0	−28	37	4 5 0	−33	37	6 14 0	−16	0
1 16 0	5	0	4 6 0	18	21	6 15 0	6	0
1 17 0	12	10	4 7 0	14	8	6 16 0	15	0
1 18 0	− 5	0	4 8 0	− 4	0	6 17 0	− 5	0
1 19 0	0	0	4 9 0	−16	12	6 18 0	−14	0
			4 10 0	− 7	0			
2 0 0	− 1	8	4 11 0	− 7	0	7 1 0	− 2	0
2 1 0	−39	38	4 12 0	10	0	7 2 0	19	22
2 2 0	−48	44	4 13 0	9	0	7 3 0	16	25
2 3 0	50	63	4 14 0	− 7	0	7 4 0	−11	0
2 4 0	26	24	4 15 0	−17	10	7 5 0	−16	20
2 5 0	−36	35	4 16 0	11	0	7 6 0	18	17
2 6 0	−16	20	4 17 0	18	17	7 7 0	15	22
2 7 0	40	38	4 18 0	−12	0	7 8 0	−21	22
2 8 0	0	0	4 19 0	− 4	8	7 9 0	−18	20
2 9 0	3	7				7 10 0	19	17
2 10 0	5	0	5 1 0	0	0	7 11 0	25	22
2 11 0	0	0	5 2 0	− 1	0			
2 12 0	− 3	0	5 3 0	7	8	8 0 0	− 6	0
2 13 0	3	0	5 4 0	9	0	8 1 0	20	28
2 14 0	8	0	5 5 0	−19	24	8 2 0	2	0
2 15 0	−20	14	5 6 0	−20	25	8 3 0	−25	28
2 16 0	− 8	0	5 7 0	35	37	8 4 0	− 8	0
2 17 0	28	28	5 8 0	11	0	8 5 0	22	22
2 18 0	14	17	5 9 0	−39	37			
2 19 0	−24	27						

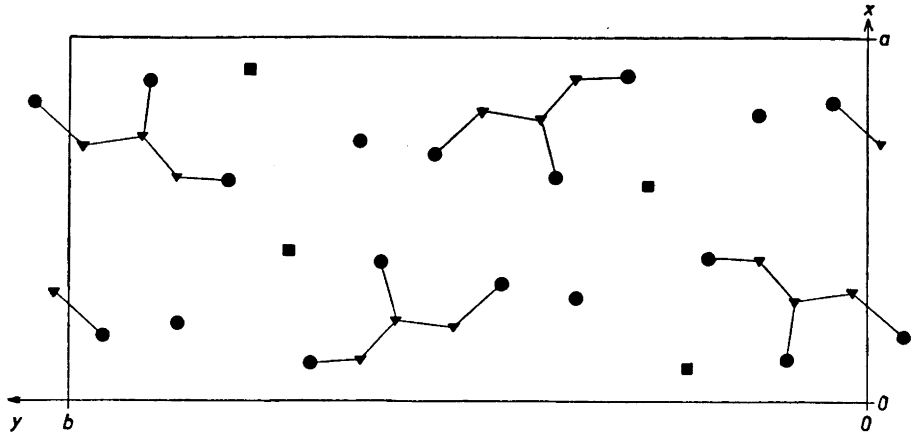

Fig. 3. Schematic picture of the atomic arrangement in the crystals of $Rb(C_3H_3O_3)H_2O$. The positions of the rubidium atoms have been marked with ■, the positions of the carbon atoms with ▲, and the positions of the oxygen atoms with ●.

are all shorter than 1.67 Å. Consequently there must be at least one carbon atom in each of these pairs. In addition to the chemical fact that the carbon atoms must form a chain, this leads to the conclusion that A_1, A_2, and A_3 are oxygen atoms and A_5, A_6, and A_7 carbon atoms. We have thus identified the atoms in the organic anion.

As for the remaining peak, A_4, it must correspond to a molecule of water of crystallization. The presence of such a molecule is also reflected in the relatively large difference in cell volume between the potassium and rubidium salts [2].

STRUCTURE PROPOSED FOR $Rb(C_3H_3O_3)H_2O$

The following x and y parameters are thus proposed for $Rb(C_3H_3O_3)H_2O$: Space group: $P2_1/a$. 4 formula units per unit cell.

4	Rb	in	4(*e*)	with	x	=	0.088	and y = 0.225
4	C_1	»	»	»	x	=	0.27_5	» y = 0.09_0
4	C_2	»	»	»	x	=	0.39_8	» y = 0.13_4
4	C_3	»	»	»	x	=	0.29_9	» y = 0.01_7
4	O_1	»	»	»	x	=	0.11_6	» y = 0.10_1
4	O_2	»	»	»	x	=	0.39_1	» y = 0.19_8
4	O_3	»	»	»	x	=	0.32_1	» y = 0.45_8
4	O_4	(H_2O)		»	x	=	0.28_7	» y = 0.36_5

4(*e*): $\pm(xyz)$; $\pm(\frac{1}{2}+x,\frac{1}{2}-y,z)$

With these parameters the intensities of the *hk*0 reflections were calculated. They were then corrected by an exponential factor of $10^{-0.34\sin^2\Theta}$ obtained with the ordinary procedure for the calculation of temperature factors. As

is seen in Table 1, the agreement between observed and calculated data is satisfactory. The R value according to Booth [5] is 0.17 (absent reflections not included).

DISCUSSION OF THE STRUCTURE

Fig. 3 shows a schematic picture of the xy projection of the structure with the projected interatomic distances indicated. As is seen, the organic anion shows the same configuration as in bromomalonic dialdehyde [2], *i.e.* the oxygen atoms are situated on the same side of the C—C chain.

The coordination Rb—O is rather difficult to determine since the z parameters are not known. However, if we assume that the distances between rubidium and oxygen atoms in contact are about 3.0 Å, we see that the differences in the rubidium and oxygen z parameters should be in the vicinity of $c/2 = 2.0$ Å for Rb (0.088, 0.225)—O_1(0.11_6, 0.10_1), Rb(0.088, 0.225) —O_2 (0.39_1, 0.19_8), and Rb(0.088, 0.225)—O_2(-0.10_9, 0.30_2). Every other z difference gives some Rb—O distances less than 2.8 Å (= the sum of the ionic radii). The rubidium atom is thus in contact with at least 6 oxygen atoms forming a trigonal prism.

The xy projections of the distances between the water molecule O_4 and two rubidium atoms are 3 Å. Thus, if they all three have the same z parameter, the water molecule would be in contact with two rubidium atoms, which seems to be very plausible. We would then have a coordination Rb—8 O in the crystals.

The authors are much indebted to Professor Hans von Euler for his kind, continuous interest in this work. They also wish to thank Professor Lars Gunnar Sillén for valuable discussions.

REFERENCES

1. *International Tables for X-ray Crystallography*, Vol. I, Birmingham 1952.
2. Aurivillius, B. and Lundgren, G. *Acta Chem. Scand.* **9** (1955) 912.
3. Aurivillius, B. and Lundgren, G. *Ibid, to be published.*
4. Doi, K. *Proc. Japan Acad.* **30** (1954) No. 3, p. 180.
5. Booth, A. D. *Fourier Technique in X-ray Organic Structure Analysis*, Cambridge 1948, p. 101.

Received November 8, 1957.

ACTA CHEMICA SCANDINAVICA 12 (1958) 287—297

Synthesis and Reactions of Cinnamyl Phenyl Sulfide

CAMILLA JUSLÉN and TERJE ENKVIST

Chemical Institute of the University of Helsingfors, Finland

Cinnamyl phenyl sulfide was synthesized as part of a study on model compounds for thiolignin. The sulfide was found to be formed from a mixture of cinnamyl alcohol and thiophenol by elimination of water even at room temperature during irradiation with sunlight or ultraviolet light, or alternatively on moderate heating in the presence of aluminium sulfate or sulfuric acid dissolved in glacial acetic acid. The addition of thiophenol to the ethylenic bond also occurred as a side reaction. The ethylenic bond in cinnamyl phenyl sulfide reacted very slowly with, for instance, soda alkaline permanganate solution, bromine, hydrogen peroxide or perbenzoic acid, the two last-named reagents giving mainly cinnamyl phenyl sulfoxide and sulfone. This led to some doubt as to the actual structure of the sulfide. It can however readily be synthesized from cinnamyl bromide and potassium thiophenolate, and its infrared spectrum points to the presence of an ethylenic double bond. Oxidative degradation of the cinnamyl phenyl sulfide with perbenzoic acid or with permanganate solution gave, among other products, sulfuric, benzoic and benzene sulfonic acids. Degradation by hydrogenation with Raney nickel gave benzene and phenyl propane. Thus in fact the cinnamyl phenyl sulfide has a structure corresponding to its name, but its ethylenic bond is peculiarly slow to react.

SYNTHESES

The present work is a continuation of the studies on thiolignin formation with the aid of model compounds by the one of us (E)[1] and later also by Zentner [2] and Lindgren and Mikawa [3]. As it seems probable that thiolignin contains substantial amounts of monosulfidic sulfur [4], it was of special interest to study the formation and properties of lignin model compounds containing such sulfur.

The present paper is an account of the synthesis and reactions of cinnamyl phenyl sulfide. In a later report, corresponding investigations on several other thiolignin models will be described.

Perhaps the most striking observation made during these syntheses was the ease with which sulfides could be formed by splitting off water from cinnamyl or vanillyl alcohol and thiophenol (formula I). The reaction occurred even at room temperature on irradiation with ultraviolet light or sunlight,

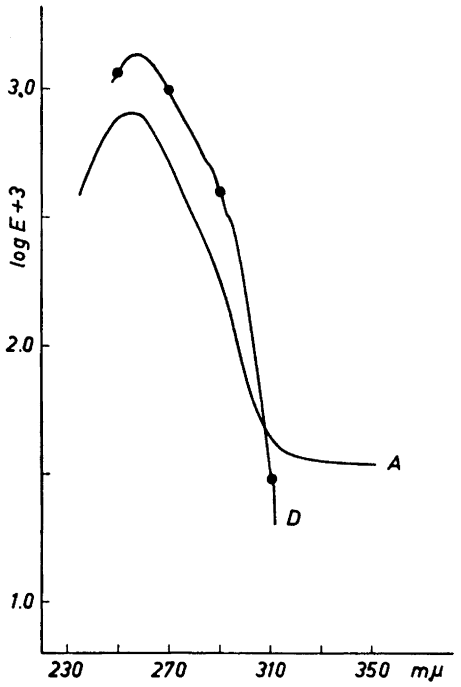

Fig. 1. UV spectrum of cinnamyl phenyl sulfide. D = in dioxan solution. A = in 0.5 N alcoholic sodium hydroxide.

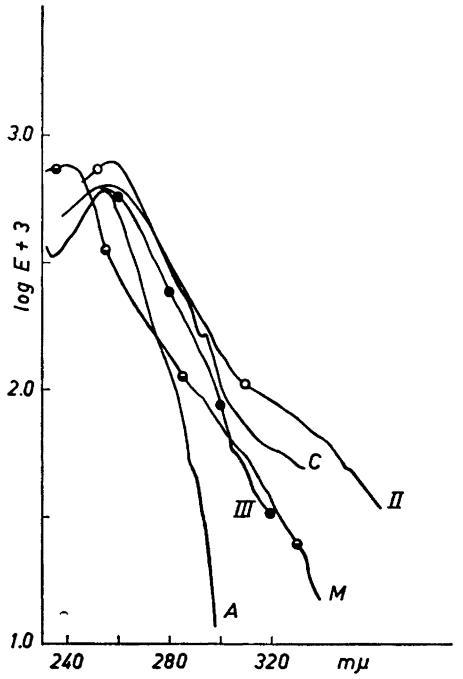

Fig. 2. UV spectra of cinnamyl disulfide (C), of allyl phenyl sulfide (A), of 2-methyl thiocoumarane (M) and of fractions II and III obtained on heating cinnamyl phenyl sulfide.

or alternatively on very moderate heating in the presence of aluminium sulfate or hydrogen ions. Table 1 gives a survey of the syntheses carried out.

The table shows *inter alia* that addition of thiophenol to the ethylenic bond also occurred during the photosynthesis. Attempts to add thiophenol to the ethylenic bond in cinnamyl phenyl sulfide in acetone solution with piperidine as catalyst failed.

I $C_6H_5{\cdot}CH{:}CH{\cdot}CH_2OH + HS{\cdot}C_6H_5 = C_6H_5{\cdot}CH{:}CH{\cdot}CH_2{\cdot}S{\cdot}C_6H_5 + H_2O$
Cinnamyl phenyl sulfide(IV)

THE PROPERTIES OF CINNAMYL PHENYL SULFIDE

Structure. Cinnamyl phenyl sulfoxide has been described in the literature by Barnard[5], who also synthesized cinnamyl phenyl sulfide (private communication), but without publishing anything about it. In June 1956, when the main part of our experimental work was already completed, Briscoe, Challenger and Duckworth [6] published a synthesis of cinnamyl phenyl sulfide and an attempt to determine its structure by reaction with Chloramine T.

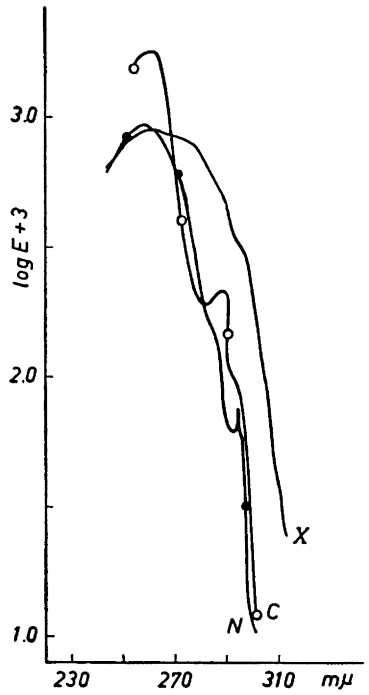

Fig. 3. UV spectra in dioxan of cinnamyl phenyl sulfoxide (X) and sulfone (N) and of cinnamyl alcohol (C).

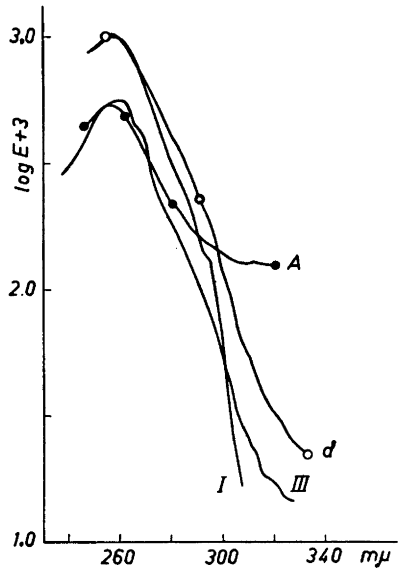

Fig. 4. UV spectra of by-products at syntheses of cinnamyl phenyl sulfide. A = addition product of cinnamyl alcohol and thiophenol (photosyntesis, 1 a). Solvent 0.5 N alcoholic sodium hydroxide. I and III, respectively, first and third chromat.-fraction from synthesis 1 c in dioxan. d = second chromat.fraction from synthesis 1 d in dioxan.

Our work concerning cinnamyl phenyl sulfide started with a photosynthesis of this substance at room temperature from cinnamyl alcohol and thiophenol carried out by Mr Eino Lonkila and one of us (E), in which about 9 mole % of crystalline sulfide was isolated by vacuum sublimation mainly in the fraction 190—230° at 15 mm. Even at this stage it was observed that cinnamyl phenyl sulfide does not react in the usual Baeyer test for unsaturated substances with soda-alkaline permanganate solution at room temperature. This observation led to further investigations concerning the double bond in cinnamyl phenyl sulfide and also raised the question of whether the sulfide possesses the simple structure IV or whether a Claisen rearrangement has occurred during its formation leading ultimately to a thiocoumarane or thiochromane structure (*cf* Ref.[7,8]).

Ultraviolet and infrared spectra. The ultraviolet absorption spectrum of cinnamyl phenyl sulfide (Fig. 1) shows a single maximum at about 255 mμ,

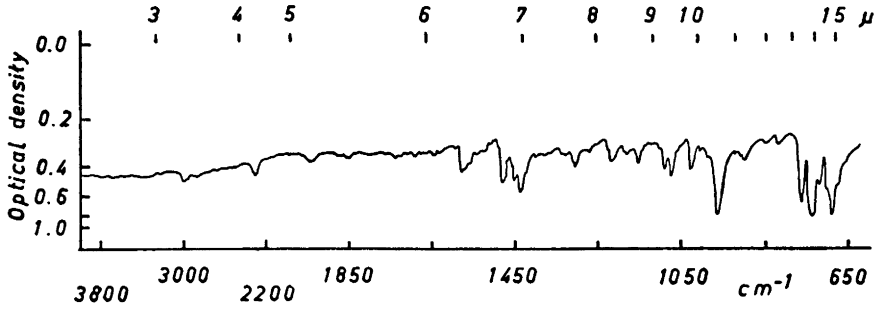

Fig. 5. Infrared spectrum of cinnamyl phenyl sulfide, without solvent.

very much like that of allyl phenyl sulfide and of cinnamyl disulfide, but distinctly different from that of 2-methyl thiocoumarane (Fig. 2). The cinnamyl phenyl sulfoxide and sulfone as well as cinnamyl alcohol have an absorption maximum at a somewhat longer wave length (Fig. 3).

The infrared spectrum of cinnamyl phenyl sulfide (Fig. 5) has an absorption band at 960 cm^{-1}, probably caused by the wagging swings of the :CH·-group. Substances containing a CH_2:C-group show absorption[9] at about 890 cm^{-1}. This band is lacking for cinnamyl phenyl sulfide, showing that rearrangement to vinyl groups during the formation of cinnamyl phenyl sulfide is improbable. Moreover, the absorption band of the hydroxyl groups [9] at 3 380 cm^{-1} is lacking, in contrast to the IR-spectrum of the addition product of cinnamyl alcohol and thiophenol (Fig. 6), where the hydroxyl group could also be demonstrated by acetylation, and which thus very probably contains the substances V or VI or both of them.

V. $C_6H_5CH{\cdot}(SC_6H_5){\cdot}CH_2CH_2OH$ VI. $C_6H_5{\cdot}CH_2{\cdot}CH(SC_6H_5)CH_2OH$

γ-thiophenoxy-γ-phenylpropanol β-thiophenoxy-γ-phenylpropanol

The ethylenic bond in olefines causes absorption at about 1 660 cm^{-1} also, and cinnamic acid absorbs characteristically at 1 590 cm^{-1} and still more strongly [10] at 1 625 cm^{-1}. This latter absorption also occurs in the spectrum

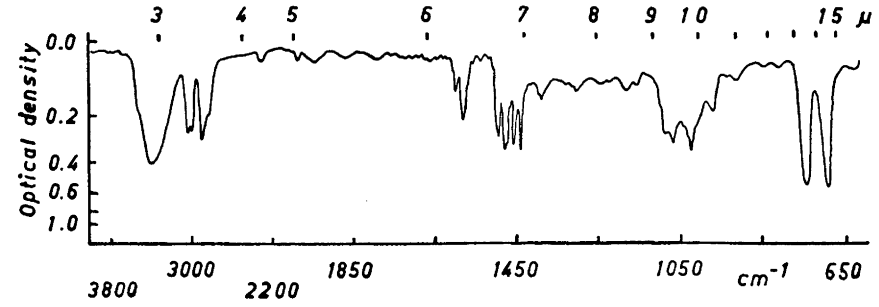

Fig. 6. Infrared spectrum of the addition product of cinnamyl alcohol and thiophenol.

of cinnamyl alcohol and is probably due to the ethylenic bond. In this area of the spectrum of cinnamyl phenyl sulfide, there is an absorption band only at 1 575 cm^{-1}. Probably in this substance, as well as in *trans*-stilbene and indene [11], the absorption band caused in the area in question by the ethylenic bond coincides with the absorption of the double bonds in the benzene nucleus.

OXIDATION REACTIONS

With hydrogen peroxide. Samples of cinnamyl sulfide were oxidized with hydrogen peroxide to the sulfoxide and the sulfone. No glycol derivative, but only the sulfone, could be found among the oxidation products, even after oxidation with 4 moles of 30 % H_2O_2 in acetone solution in UV light for 2 weeks.

The sulfoxide was obtained in 94 mole % yield by using equimolar amounts of hydrogen peroxide and cinnamyl phenyl sulfide at room temperature. The sulfoxide appears in two modifications, one with m.p. 78°, primarily obtained at chromatographic separation on an aluminium oxide column, and another melting at 91.5—92°, formed for instance on recrystallization of the other form from hot petrolether-chloroform solution. The m.p. of Barnards cinnamyl phenyl sulfoxide is recorded as 68°C, but he has privately reported that this figure is a misprint and should be 78°C, and that he likewise has found two modifications of the sulfoxide. A mixed m.p. of our sulfoxide of m.p. 78° and a corresponding sample kindly supplied by Dr Barnard showed that the substances were identical.

With reagents for the ethylenic bond. The sulfide as well as the sulfoxide and the sulfone only very slowly decolorized soda-alkaline permanganate solution at room temperature, after hours of standing, whereas, for instance, cinnamyl alcohol and freshly distilled allyl phenyl sulfide, prepared according to Claisen [12], immediately decolorized the reagent. It was found, however, that cinnamyl phenyl sulfide showed some of the reactions of the ethylenic bond. Thus, when it or the corresponding sulfone are dissolved in pure pyridine, they decolorize potassium permanganate solution.

With tetranitromethane, golden yellow colors were given by cinnamyl phenyl sulfide, the corresponding sulfoxide and sulfone, as well as cinnamyl alcohol, whereas allyl phenyl sulfide gave a red color.

Organic sulfides in general add bromine, and the method of Siggia [13] for determination of sulfidic sulfur makes use of this fact. Cinnamyl phenyl sulfide gave the following bromine numbers: McIlhiney's method [14] (addition only, 3.7 % of the total bromine consumption was found to be due to substitution) 92, Kauffmann's [15] method 89, Siggia's method 117. The theoretical value for cinnamyl phenyl sulfide is 141, supposing that the sulfide sulfur and the ethylenic double bond each of them add two bromine atoms. The actual bromine consumption is thus considerably lower than the theoretical value.

Oxidation with perbenzoic acid.[16] Fig. 7 shows the uptake of oxygen in g.atoms from perbenzoic acid per mole of cinnamyl phenyl sulfide at +3°. It can be seen that 2 atoms of oxygen are added to one molecule of the sulfide within one day, after which the uptake is very slow, in all only 2.72 atoms being consumed after 42 days. According to Stoll and Seebeck [17], in unsatura-

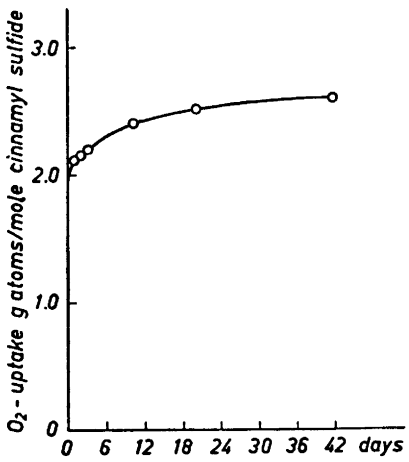

Fig. 7. Oxidation of cinnamyl phenyl sulfide with perbenzoic acid.

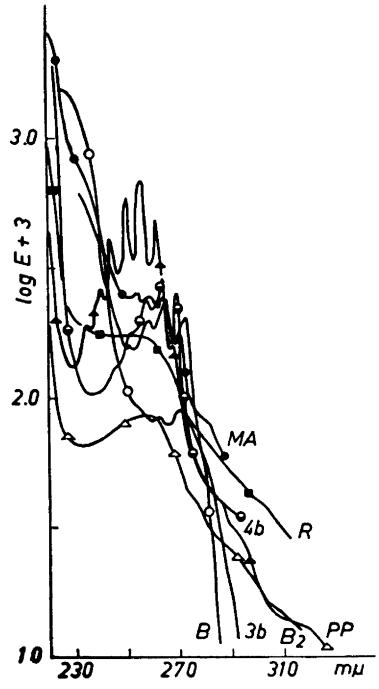

Fig. 8. UV spectra of degradation products of cinnamyl phenyl sulfide. 3 b = crude benzene sulfonic acid from synthesis 3 b. B = benzoic acid from 4 a. MA = mixture of acids (M.A.) from synthesis 4 b. 4 b = purified benzene sulfonic acid from synthesis 4 b. Bz = benzene from synthesis 5. PP = phenyl propane from synthesis 5. R = residue from synthesis 5.

ted sulfides containing an allyl group the sulfur is oxidized faster than the ethylenic bond by perbenzoic acid.

From the neutral fraction of the reaction products, only cinnamyl phenyl sulfone could be isolated. Thus, the fast uptake of the first two oxygen atoms is obviously due to addition to the sulfur, and the later slow uptake of oxygen to the ethylenic bond.

Oxidative degradation. A sample of cinnamyl phenyl sulfone was oxidized with perbenzoic acid, this time at room temperature. Among the acidic oxidation products benzene sulfonic acid could be detected through mixed m.p. of the S-benzyl thiuronium salt.

Cinnamyl phenyl sulfide was oxidized in benzene suspension with soda-alkaline potassium permanganate in aqueous solution for 59 h at room temperature. The reaction products contained cinnamyl phenyl sulfoxide and sulfone, benzoic acid in a yield of 53 mole %, and further benzene sulfonic acid (mixed m.p. of S-benzyl thiuronium derivative) and sulfuric acid.

Table 1. Syntheses of cinnamyl phenyl sulfide.

Reagents	Method [1]	Reaction time	Reaction product	Yield, mole %
Cinnamyl alcohol (II) + thiophenol (III)	Photosynthesis (1 a)	14 days	Cinnamyl phenyl sulfide (IV) + V or VI	9 13
II + III	Press.heating with Al-sulfate (1 b) [2]	16 h	IV	25
II + III	Boiling in acet. acid + H_2SO_4 (1 c)	16 h	IV	85
Cinnamyl bromide + C_6H_5SK	Boiling in acetone (1 d)	8 h	IV	83
»	Boiling in benzene (1 e)	4 h	IV	72

[1] The numbers in parentheses mean paragraphs in the experiment. part.
[2] In a sealed glass tube.

DEGRADATION BY HYDROGENATING TREATMENT WITH RANEY NICKEL

It is well known that treatment with Raney nickel [18] allows the sulfur in thioethers to be replaced by hydrogen. Cinnamyl phenyl sulfide was boiled with a great excess of Raney nickel in alcoholic suspension. Benzene (demonstrated with UV spectrum and from nitration and mixed m.p. determination *m*-dinitrobenzene so formed) and phenylpropane were formed (identified as 2-mono- and 2,4-diacetamino phenylpropane, obtained according to scheme VII).

VII. $C_3H_7{\cdot}C_6H_5 \xrightarrow{HNO_3} C_3H_7{\cdot}C_6H_4{\cdot}NO_2 + C_3H_7{\cdot}C_6H_3(NO_2)_2 \xrightarrow{Sn + HCl}$

$C_3H_7{\cdot}C_6H_4{\cdot}NH_2 + C_3H_7{\cdot}C_6H_3(NH_2)_2 \xrightarrow{\text{acetylation}} C_3H_7{\cdot}C_6H_4{\cdot}NH{\cdot}COCH_3 + C_3H_7{\cdot}C_6H_3(NH{\cdot}COCH_3)_2$

Thus, the hydrogenation with Raney nickel has followed the simple scheme VIII.

VIII. $C_6H_5CH = CH{\cdot}CH_2{\cdot}S{\cdot}C_6H_5 + 6H \rightarrow C_6H_5CH_2CH_2CH_3 + H_2S + C_6H_6$

All these facts thus prove that the cinnamyl phenyl sulfide in fact has the structure IV but that the ethylenic bond reacts very slowly with the usual oxidizing reagents. The same low reactivity seems also to characterize the corresponding sulfoxide and sulfone.

Attempt at obtaining a Claisen rearrangement of cinnamyl phenyl sulfide. As no Claisen rearrangement to *o*-cinnamyl thiophenol or further to a thiocoumarane or thiochromane could be observed during the syntheses of cinnamyl phenyl sulfide, this substance was heated in an atmosphere of nitrogen in order to promote rearrangement or destructive splitting. The sulfide decomposed somewhat below 260°C. From the reaction products

57 % of unchanged starting material could be isolated and further a small amount of thiophenol, which after autoxidation gave phenyl disulfide, proven by mixed m.p. with an authentic sample. Among the neutral products two liquid chromatographic fractions (II and III) showed sulfur contents only a little lower than the starting material and UV spectra not dissimilar to that of 2-methyl thiocoumarane (Fig. 2). The high recovery of starting material indicates, however, that the cinnamyl phenyl sulfide is not easily rearranged or split up.

EXPERIMENTAL PART

1. Syntheses of cinnamyl phenyl sulfide

a) *Photosynthesis.* 1.250 g (0.009 moles) cinnamyl alcohol and 1.000 g (0.009 moles) of thiophenol were allowed to stand 2 weeks in a quartz tube sealed with a rubber stopper 15 cm from a mercury (quartz) lamp. The reaction product was dissolved in ether, washed with 2 N sodium hydroxide and water, dried, and isolated by evaporation of the solvent. The dryings in the present work were generally carried out with sodium sulfate. The residue was recrystallized several times from 99 % ethanol (preparation P) m. p. 78°, undepressed on admixture with a preparation of cinnamyl phenyl sulfide kindly supplied by Dr. Barnard. (Found: C 79.54; H 6.27; S. 14.06 [1]; mol. wt. (Cryosc. Beckmann) 221. Calc. for $C_{15}H_{14}S$: C 79.60; H 6.23; S 14.17, mol.wt. 226). UV-spectrum Fig. 1, IR-spectrum Fig. 5. Yield of crude product with m. p. 74—75° 0.191 g (9 mole %).

By-products: The mother liquor from the crystallization of the cinnamyl phenyl sulfide was evaporated. The residue was washed with cold methanol in order to remove cinnamyl alcohol, and dried in vacuum. The yield was 0.310 g of yellow oil. It was dissolved in 20 ml carbon tetrachloride-petrolether 1:1 and chromatographed in a column containing 20 g of aluminium oxide (Brockmann). By elution with a total of 15 ml of carbon tetrachloride a small first fraction was obtained, which was dark violet in UV light and showed a m.p. 59—60°, undepressed on admixture of *diphenyl disulfide.*

By further elution with ether and alcohol containing carbon tetrachloride a liquid second fraction was obtained, which was lemon yellow in UV light. Yield 0.299 g. It was chromatographed anew with the same solvents. The Baeyer test was positive and the oil gave a red color in tetranitromethane. UV-spectrum Fig. 4. IR spectrum Fig. 6. (Found: C 73.11; H 6.60; S 13.23; mol. wt. (Beckm. cryosc.) 241. Calc. for $C_{15}H_{16}SO$: C 73.73; H 6.59; S 13.12; mol. wt. 244.)

Acetylation: 0.318 g of substance from another, quite similar experiment was heated 4 h on a water bath with 0.76 ml of acetic anhydride and 0.63 ml of pyridine, using a calcium chloride tube to exclude moisture. The reaction product was poured into 10 ml H_2O, was extracted with ether, washed with sodium hydrogen carbonate solution, dried, and, after evaporation, further dried in vacuum over phosphorus pentoxide. (Found: S 11.31; CH_3CO (according to Ref.[20]) 14.61. Calc. for. $C_{17}H_{18}SO_2$: S 11.20; CH_3CO 15.03.) The product is obviously V or VI.

b) *With aluminium sulfate.* 5.954 g (0.044 mole) of cinnamyl alcohol, 4.706 g (0.043 mole) of thiophenol and 0.359 g anhydrous aluminium sulfate were heated in a sealed glass tube 16 h at 127°. Here, as well as in the following syntheses c—e, the neutral reaction product was isolated in the same way as the cinnamyl phenyl sulfide at the photosynthesis. Yield 2.418 g of m.p. 75—76°. Repeated re-crystallization raised the m.p. to 78°, undepressed on admixture of cinnamyl phenyl sulfide from the photosynthesis.

c) *In acetic and sulfuric acid:* 15.342 g (0.114 mole) of cinnamyl alcohol and 12.669 g (0.115 mole) of thiophenol were refluxed 16 h in 100 ml acetic acid containing 10 ml 2 N H_2SO_4. The cinnamyl phenyl sulfide was isolated in the same way as at the photosynthesis. Yield 21.811 g with m.p. 74—76°, undepressed on admixture of sulfide from the photosynthesis. From the mother liquors liquid fractions were obtained by chromatography on aluminium oxide in about the same way as in the photosynthesis, giving the following data: yield 0.115 g, S 3.69, mol. wt. (Childs [21]) 361; 0.098 g, S 5.97; 0.044 g, S 9.65, mol.wt. (Childs) 344; UV spectra Fig. 4.

[1] All sulfur determinations were made titrimetrically according to Grote-Krekeler [19].

d) *From cinnamyl bromide in acetone:* 2.200 g (0.020 mole) thiophenol, 3.940 g (0.020 mole) of cinnamyl bromide, 2.800 g anhydrous potassium carbonate and 6 g acetone were refluxed 6 h. Yield 3.739 g cinnamyl phenyl sulfide of m.p. 74—75°, undepressed on admixture of sulfide from synthesis 1 a. The substance from the mother liquors (0.317 g of yellow oil) was chromatographed on aluminium oxide in carbon tetrachloride-toluene 1:1 and eluted with toluene containing amounts of ethyl ether rising successively from 10 to 50 %. The first fraction was small and showed a m.p. of 61°, undepressed on admixture of diphenyl disulfide. The second fraction was a yellow oil; yield 0.229 g, S 13.22. UV spectrum, Fig. 4, d.

e) *From cinnamyl bromide in benzene.* 7.615 g of cinnamyl bromide (0.0386 mole) and 4.275 g (0.0388 mole) of thiophenol were refluxed 4 h in 16 g benzene containing 5.41 g of anhydrous potassium carbonate. Yield of cinnamyl phenyl sulfide 6.329 g of m.p. 74—76°, after further recrystallization from ethanol 78°, undepressed on admixture of sulfide from 1 a.

2. Investigation of cinnamyl phenyl sulfide. Oxidation with hydrogen peroxide

a) *To sulfoxide.* 0.226 g (0.001 mole) cinnamyl phenyl sulfide were dissolved in 20 ml glacial acetic acid and 0.001 mole 30 % hydrogen peroxide were added with stirring. After the mixture had stood 5 days at room temperature, water was added. The precipitated yellow oil was dissolved in chloroform, washed with sodium hydrogen carbonate solution and dried. After evaporation in vacuum the residue crystallized on cooling to 0°. Yield of crude product 0.227 g (94 mole %); m. p. 90—91° after recrystallization three times from hot petrolether containing 5 % chloroform. (Found: S 13.18. Calc. for $C_{15}H_{14}SO$: S 13.23). UV spectrum, Fig. 3, X. 70 mg of the crude sulfoxide were not purified by recrystallization, but were chromatographed on aluminium oxide (Brockmann) with carbon tetrachloride as solvent and eluting first with carbon tetrachloride containing 5—20 % of ether and then with ether containing 10—20 % of ethanol. The main fraction melted at 76—78°. When a sample of this sulfoxide was recrystallized from hot petrolether containing 5 % chloroform it was transformed into a substance of m. p. 91.5—92°.

b) *To sulfone.* This oxidation was made in the same way as a), but using the double amount (0.002 mole) of 30 % hydrogen peroxide. The reaction product was isolated by the same method as the sulfoxide. Yield 0.236 g (92 mole %); m.p. 111—112° after recrystallization from ligroin; UV spectrum, Fig. 3, N. (Found: C 69.89; H 5.47; S 12.32. Calc. for $C_{15}H_{14}SO_2$: C 69.74; H 5.46; S 12.41.)

c) *Oxidation in UV light.* 0.226 g (0.001 mole) cinnamyl phenyl sulfide was dissolved in 10 ml acetone containing 0.004 mole of 30 % hydrogen peroxide, and was irradiated 10 days in a quartz test tube at 10 cm distance from a mercury lamp. The reaction product was isolated as the sulfone under 2b. M. p. 110—111°, undepressed on admixture of cinnamyl phenyl sulfone from synthesis 2b.

3. Oxidations with perbenzoic acid

a) *Oxidation of cinnamyl phenyl sulfide.* 0.452 g cinnamyl phenyl sulfide were weighed in an Erlenmeyer flask equipped with a ground glass stopper; 50 ml of 0.1249 M solution of perbenzoic acid in chloroform were added and allowed to stand at +3°, in a refrigerator together with a blank perbenzoic acid solution without sulfide. 5 ml samples of the oxidation mixture and the blank solution were titrated with sodium thiosulfate after addition of a potassium iodide solution acidified with acetic acid (Fig. 7). After 41.6 days the neutral reaction products were isolated from the benzoic acid-$CHCl_3$ solution after washing with sodium hydrogen carbonate solution and once with water, drying, evaporating and drying again in vacuum over phosphorus pentoxide. Yield 41 mg of an oil which was dissolved in 20 ml carbon tetrachloride and chromatographed in a column containing aluminium oxide (Brockmann). Only one band could be seen in ultraviolet light. Yield 34 mg, m. p. 109—111°, undepressed on admixture of cinnamyl phenyl sulfone from 2 b.

b) *Oxidation of cinnamyl phenyl sulfone.* 0.190 g cinnamyl phenyl sulfone were oxidized with 0.1429 M perbenzoic acid in $CHCl_3$ at room temperature during 42.6 days.

Thereafter the solution was washed with 5 ml cold water. The water layer was allowed to evaporate at 30° in a glass bowl. The residue, a clear, thickish liquid, was washed with 4 ml ether, and dried 5 h in vacuum over phosphorus pentoxide. Yield 119 mg; UV-spectrum, Fig. 8, 3b. The substance was neutralized with 0.2 N sodium hydroxide and a S-benzyl-thiuronium salt prepared in the usual way [22], m. p. after recrystallization three times from 50 % ethanol 143—145°, undepressed on admixture with S-benzyl thiuronium salt of benzenesulfonic acid of m. p. 147°.

4. Oxidation with permanganate

a) 1.706 g (0.007 mole) of cinnamyl phenyl sulfide were suspended in 60 ml 2 N sodium carbonate solution. 70 ml benzene and thereafter a solution of 4.762 g potassium permanganate in 200 ml water were added with stirring during 59 h. The manganese dioxide precipitate was filtered off and washed first with 2 N soda solution, then with hot water and at last with benzene. The mixed liquids were allowed to separate into a benzene and an alkaline water layer. The benzene layer was dried and evaporated in vacuum, the residue (neutral products) weighing 0.636 g. It was chromatographed on aluminium oxide (Brockmann) as described under 1 a. Three fractions were obtained in yields of 0.101, 0.326 and 0.099 g, m. p. 74—76°, 90—92°, 109—111°, undepressed on admixture of cinnamyl phenyl sulfide, sulfoxide and sulfone, respectively.

The soda alkaline layer was acidified (indicator Congo red) with 2 N sulfuric acid and extracted with ether. Drying and evaporation in vacuum gave a crystalline residue, which was purified by sublimation in vacuum; yield 0.495 g, m. p. 121°, undepressed on admixture of benzoic acid; UV-spectrum, Fig. 8 B.

b) 1.6108 g cinnamyl phenyl sulfide was oxidized with 4.495 g potassium permanganate as under 4 a. The soda-alkaline layer was passed through a cation exchanger Amberlite IR-120, the volume of the liquor so passed being 645 ml and the pH about 1. 150 ml of the solution was evaporated at about 30°, and dried over phosphorus pentoxide. Yield 235 mg; UV-spectrum, Fig. 8 MA. The mixture of acids (MA) thus obtained was chromatographed 16 h at 18° on Whatman paper No. 1 with 50 μg in each spot and *n*-butanol saturated with ammonium carbonate buffer [23] as mobile phase. The spots were developed with 0.1 N silver nitrate solution, or with phenol and 0.5 N sodium hydroxide according to Löffler [24]. Two spots were obtained corresponding to the R_F-values 0 and 0.30, respectively. Since the solution gave a barium salt insoluble in acidic solution, and the substance in the first spot did not give any characteristic UV-spectrum, and a blank chromatography of dilute sulfuric acid also gave $R_F = 0$, the first spot obviously corresponds to sulfuric acid. Parallel tests with benzoic and benzene sulfonic acid showed that both gave $R_F = 0.30$. Therefore an undeveloped spot with $R_F = 0.30$ from a new chromatogram was extracted twice with 5 ml ice-water, a treatment which dissolves benzene sulfonic acid, but leaves the benzoic acid practically undissolved. The UV-spectrum of the cold water eluate (Fig. 8, 4b) is identical with that of autenthic benzene sulfonic acid purified by paper chromatography. A fresh portion of the mixture of acids (MA) described was extracted with ether to remove benzoic acid. The residue (171 mg from 150 ml of acid solution) was converted to an S-benzyl thiuronium salt, m.p. after recrystallization three times from 50 % ethanol 143—145° undepressed on admixture of the corresponding derivative of authentic benzene sulfonic acid.

5. Degradation by hydrogenation

3.722 g cinnamyl phenyl sulfide dissolved in 400 ml aldehyde-free ethanol were refluxed 7 h with about 30 g Raney nickel. The nickel sulfide formed was filtered off and washed with alcohol and ether. Water was added to the filtrate, which was extracted five times with ether. The ether solution was dried with calcium chloride and distilled at 760 mm by means of a Skärblom-Linder column [25]. After the ether had distilled off, the following fractions were obtained: b.p. 79—80°, 0.765 g, UV-spectrum Fig. 8, Bz; b. p. 159—160°, 1.181 g, UV-spectrum Fig. 8, PP, n_D 1.4918 (18.4°C), and residue 0.061 g, UV-spectrum Fig. 8, R. The fraction of b. p. 79—80° was nitrated according to Ref.[26].

The reaction product after recrystallization from 50 % ethanol had m. p. 90°, undepressed on admixture of *m*-dinitrobenzene. The fraction of b. p. 159—160° was redistilled, 0.5 g of the distillate was nitrated and the nitration product reduced to a mixture of amines. This mixture was separated into monoamine and diamine, of which only the former gives an ether soluble salt with tin chloride in presence of hydrochloric acid. Both amines were acetylated, all according to [27]. The acetylated diamine was purified by chromatography on silica gel with chloroform and sublimation in vacuum, m. p. 207—208°. (Found: C 66.63; H 7.72; N 11.88. Calc. for $C_{13}H_{18}N_2O_2$: C 66.64; H 7.74; N 11.96). The acetylated monoamine was purified in a corresponding way, m. p. 97°. The corresponding authentic derivatives were prepared from phenyl propane obtained from benzyl magnesium chloride and diethyl sulfate according to Ref.[28]. No depression on the m. p. occurred on admixture of the two pairs of preparations.

A grant from *Statens naturvetenskapliga kommission* (Helsingfors) to one of us (Enkvist) is gratefully acknowledged.

REFERENCES

1. Enkvist, T. and Moilanen, M. *Svensk Papperstidn.* **52** (1949) 183; **55** (1952) 688.
2. Zentner, T. G. *Diss.* Appleton (1953); *Tappi* **36** (1953) 517.
3. Lindgren, B. and Mikawa, H. *Acta Chem. Scand.* **6** (1954) 954.
4. Enkvist, T. *Svensk Papperstidn.* **51** (1948) 225.
5. Barnard, D. and Hargrave, K. R. *Anal. Chim. Acta* **5** (1951) 544.
6. Briscoe, P. A., Challenger, T. and Duckworth, P. S. *J. Chem. Soc.* **1956** 1755.
7. Claisen, L. and Tietze, E. *Ber.* **58** (1925) 275.
8. Tarbell, D. S. *Chem. Rev.* **27** (1940) 532.
9. Brügel, W. *Einführung in die Ultrarotspektroskopie*, Darmstadt 1954, p. 212, 270.
10. Bellamy, L. J. *The infrared spectra of complex molecules*, London, 1954, p. 36.
11. Barnes, R. B., Gore, R. C., Liddel, U. and Williams, W. Z. *Infrared spectroscopy, Ind. Application*, New York 1954, p. 55, 57.
12. Hurd, C. D. and Greengard, H. J. *J. Am. Chem. Soc.* **52** (1930) 3357.
13. Siggia, S. and Edsberg, R. L. *Anal. Chem.* **20** (1948) 938.
14. Mc Ilhiney, P. C. *J. Am. Chem. Soc.* **16** (1894) 275.
15. Zerbe, C. *Mineralöle und verwandte Produkte*, Berlin 1952, p. 1280.
16. Prileschajew, N. *Ber.* **42** (1910) 4811.
17. Stoll, A. E. and Seebeck, E. *Helv. Chim. Acta* **31** (1948) 199.
18. Mozingo, R., Wolf, D. E., Harris, S. A. and Folkers, K. *J. Am. Chem. Soc.* **65** (1943) 1013.
19. Grote, W. and Krekeler, H. *Angew. Chem.* **46** (1933) 106.
20. Freudenberg, K. and Harder, M. *Ann.* **433** (1923) 230.
21. Childs, C. E. *Anal. Chem.* **26** (1954) 1963.
22. Chambers, E. and Watt, G. W. *J. Org. Chem.* **6** (1941) 376.
23. Fewster, M. and Ball, D. *Nature* **168** (1951) 78.
24. Löffler, J. E. and Reichl, E. R. *Microchim. Acta* **41** (1953) 79.
25. Skärblom, K. J. and Linder, A. *Tek. Tidskr. Kemi* **67** (1937) 12, 25.
26. Huntress, E. H. and Mulliken, S. P. *Identification of org. compounds*, New York 1946; I, 519.
27. Ipatieff, D. N. and Schmerling, L. J. *J. Am. Chem. Soc.* **59** (1937) 1056.
28. Gilman, H. *et al. Org. Synth. Coll. Vol.* **I** (1951) 471.

Received November 8, 1957.

ACTA CHEMICA SCANDINAVICA 12 (1958) 298—302

Infrared Spectral Properties of Hydrogen Bonding Systems Containing Anions

HENNING LUND

Leo Pharmaceutical Products, Copenhagen, Denmark

It is found that hydrogen bonding of the type R—X—H...Y takes place in cases, where Y is an anion, and the spectral properties of a number of such systems are reported. The existence of this kind of hydrogen bonding systems explains the presence of a band about 3 300 cm^{-1} in the spectra of quaternary ammonium halides in a solution of chloroform stabilized with ethanol, but not found in pure chloroform solution.

Several investigations on infrared spectra of hydrogen bonding systems have been made and it is wellknown that hydrogen bonding affects the band about 3 μ attributed to the X-H stretching mode in three ways: The band shows a frequency shift $\Delta\nu$, it has an increased half intensity band width $\Delta\nu_{1/2}$ and the integrated absorption of the band is increased. Investigations of hydrogen bonding systems of the type R—X—H···Y have been made for systems in which X is oxygen, nitrogen or sulfur and Y is oxygen, nitrogen, sulfur or halogen.

No reports, however, seem to have been made on the spectral properties of hydrogen bonding systems in which Y is an anion. Kuhn [1] has shown that addition of dry hydrogen chloride to a solution of a diol in carbon tetrachloride solution weakens the band due to the internally bonding, whereas the free OH band remains unchanged. In the spectrum given (Ref.[1], p. 2497) there is a band about 3 300 cm^{-1} which in view of the results of the present investigation can be attributed to a hydrogen bonding system of the same kind as described here. The investigation of such systems might be of some value in the current discussion on "increased ionic character" [2] or "charge transfer" [3] as a model for explaining the high intensities of the hydrogen bonding stretching mode, and the spectral properties of a number of such systems are reported here.

RESULTS

Unfortunately only an instrument equipped with a sodium chloride prism was available for the investigation and more accurate values would have been obtainable if a lithium fluoride prism could have been used. The frequencies

are believed to have an uncertainty of about 20 cm^{-1} although the reproducibility is somewhat better, and the half intensity band widths are probably correct within 10—15 cm^{-1}. As a measure for the intensities of the bands were chosen the apparent integrated intensity $B = 2.303 \int \varepsilon_\nu \, d\nu$, which by assuming a Lorentzian shape of the band was approximated [4] to $B = (2.303/c \cdot l) \cdot \pi/2 \cdot \Delta\nu_{1/2} \cdot \log_{10} (T_0/T)$, where c is the concentration in mole/liter, l the cell length in cm, $\Delta\nu_{1/2}$ the apparent half intensity band width in wave number units and $\log_{10} T_0/T$ the apparent optical density. The validity of the approximation is open to discussion, but as the experimental conditions due to the poor dispersion of the rock salt prism in the 3 μ region were not the best obtainable a tedious graphical integration of the bands seemed not warranted. The integrated intensities of the bands were reproducible within 5 % and give a satisfactory internal measure for the band intensities.

In Table 1 are compiled the spectral properties of some O—H and N—H compounds (0.10 M) in carbon tetrachloride solution containing 10 mg/ml tetrabutylammonium bromide. In the first column are given the compounds, in the second one the apparent optical density of the band due to the hydrogen bonding system involving the bromide ion and in the third one the frequency in wave number units of the band. The apparent half intensity band width $\Delta\nu_{1/2}$ in wave number units and the apparent integrated absorption B in units of liters · $moles^{-1}$ · cm^{-2} are listed in column four and five, respectively, and in the last one are compiled the frequency shift $\Delta\nu$ between the band due to the monomer X—H stretching mode and the band due to the hydrogen bonded anion-complex.

The effect of varying the Y compound in a series of R—X—H···Y complexes containing the same proton donor was investigated and the spectral

Table 1. Spectral properties of hydrogen bonding systems in carbon tetrachloride containing 10 mg/ml tetrabutylammonium bromide and 0.10 M proton donor. B in liters $moles^{-1}$ cm^{-2}.

Proton donor	$\log_{10}(T_0/T)$	ν cm^{-1}	$\Delta\nu_{1/2}$ cm^{-1}	10^{-4} B	$\Delta\nu$ cm^{-1}
t-Butanol	0.104	3 340	110	1.0	275
*Iso*propanol	0.149	3 345	150	2.0	275
Ethanol	0.204	3 335	155	2.8	285
2,2,2-Trichloroethanol	0.251	3 240	190	4.3	330
Phenol	0.477	3 205	210	9.0	405
p-Cresol	0.497	3 210	200	9.0	402
o-Cresol	0.508	3 210	205	9.4	400
Mesitol	0.166	3 245	240	3.6	365
2,4-Dichlorophenol	0.436	3 100	220	8.7	450
2,4-Dibromophenol	0.470	3 100	215	9.2	420
2,4,6-Trichlorophenol *	0.18	3 050	370	6	535
2,4,6-Tribromophenol *	0.09	3 050	350	3	505
Dibutylamine	0.034	3 355	190	0.6	130
N-Methylaniline	0.080	3 265	100	0.75	170
Diphenylamine 1	0.170	3 225	60	0.90	210
2	0.125	3 195	30	0.35	260
3	0.100	3 105	30	0.3	330
Indole	0.402	3 195	140	5.10	285

* Shoulder on the C—H band.

Table 2. Spectral properties of hydrogen bonding systems in carbon tetrachloride containing 0.10 M *p*-cresol and 0.031 M proton acceptor. B in liters moles^{-1}cm^{-2}.

Anion	$\log_{10}(T_0/T)$	ν cm^{-1}	$\Delta\nu_{1/2}$cm^{-1}	10^{-4} B	$\Delta\nu$ cm^{-1}	Φ
Chloride	0.331	3 165	240	7.2	445	18.0
Bromide	0.312	3 205	205	5.8	405	25.1
Iodide	0.206	3 270	195	3.6	340	36.7
Perchlorate	0.080	3 430	135	1.0	180	44.5
Nitrate	0.230	3 210	260	5.4	400	29.4
Picrate	0.130	3 205	260	3.1	405	

properties of a few of such systems are listed in Table 2. The apparent molar volumes Φ of the anions [5] are included in the table. The spectra of the salts were obtained in chloroform solution containing 0.10 M *p*-cresol and the salt in a concentration corresponding to 10 mg/ml tetrabutylammonium bromide (0.031 M). The cations were in all cases tetrabutylammonium except for the chloride where benzyltributylammonium chloride was used. The spectra were measured in chloroform instead of carbon tetrachloride, as only a few of the salts were sufficiently soluble in carbon tetrachloride.

DISCUSSION

It appears from Table 1 that for the alcohols investigated there is a general trend towards greater $\Delta\nu_{1/2}$, $\Delta\nu$ and B as the acidity of the proton donor increases. The same tendency is found for the phenols as long as the hydroxyl group is not seriously sterically hindered. No simple correlation between $\Delta\nu_{1/2}$, $\Delta\nu$ or B and the acidity constant was, however, found. This is understandable as it may rather be the strength of the proton donor as a Lewis acid than as a Brønsted acid that would enter into such a correlation. It is especially for the sterically hindered phenols that the difference in acid strength as a Lewis acid and a Brønsted acid is noticeable, as the steric hindrance does not affect the proton donor as a Brønsted acid to any appreciable degree, whereas it seriously affects its ability to act as an electron acceptor. $\Delta\nu_{1/2}$ and $\Delta\nu$ increase from phenol through 2,4-dibromophenol to 2,4,6-tribromophenol, whereas the integrated intensity B remains nearly constant from phenol to 2,4-dibromophenol, but decreases significantly when going to the sterically more hindered 2,4,6-tribromophenol.

The lack of the relevant data on the strength of the proton donors as Lewis acids under the experimental conditions makes it difficult to substantiate the expected correlation, but it is a question whether the spectral properties of such systems are not the best accessible measure of the strength of the proton donors as Lewis acids.

In the amine series the most basic amine has the lowest integrated intensity and the least basic amine the highest in accordance with what was found for the alcohols and phenols. Whether the three bands found in the spectrum of diphenylamine are due to well defined polymeric complexes as found for methanol at low temperatures [6] is not known.

From Table 2 it can be seen that complexes containing the same proton donor but different anions have very different spectral properties. No explana-

tion of this difference in behaviour of the anions has been found, although it may be pointed out that for the inorganic ions there apparently is a connection between the apparent molar volumes Φ of the anions and the integrated intensities in such a way that B increases when the apparent molar volume Φ decreases.

The integrated intensities of the band due to the hydrogen bonded anion-complex are somewhat smaller in chloroform than in carbon tetrachloride solution, which might be explained by the greater tendency of chloroform to form molecular interactions similar to hydrogen bonding interactions with electron donors [7]. The competition between chloroform and *p*-cresol about the anions will lower the concentration of the *p*-cresol-anion complex thus diminishing the integrated intensity of the band relatively to its intensity in carbon tetrachloride.

Tsubomura [8] found a smooth curve by plotting $\Delta\nu$ against B for different acceptors and phenol as proton donor. The data from Table 2 do not fit such a correlation, but measurements obtained with better instruments are needed to give unambiguous results. Huggins and Pimentel [9] obtained a linear connection between $\Delta\nu$ and $\Delta\nu_{1/2}$ for a wide variety of hydrogen bonding systems. The spectra of the hydroxyl compounds fit such a relation as long as all sterically hindered compounds are disregarded.

Evidence of complexes of the type R—X—H···Y, where Y is an anion, have previously been found by Bartlett and Dauben [10] in the influence of phenols on the acid strength of hydrogen chloride in dioxane. The addition of a phenol to a solution of hydrogen chloride in dioxane enhanced the acid strength of the hydrogen chloride and this was explained by the assumption of the formation of a complex of the type R—O—H···Cl—H with an acid strength higher than that of hydrogen chloride in dioxane. It was generally found that the acidity of the complex was the higher the stronger the phenol was as an acid in water, but in certain cases as 2,4,6-trichlorophenol where steric hindrance may interfere the enhancement of the acidity obtained on addition of a certain amount of the phenol was not as great as would be expected from the acidity constant of the phenol in water. Alcohols did also increase the acidity of hydrogen chloride in dioxane, but to a lesser degree than did the phenols.

This is in agreement with the results of Swain [11] who measured the rate of the reaction between triphenylmethyl chloride and methanol in a benzene solution containing excess of pyridine. The reaction was found to be first order in triphenylmethyl chloride and second order in methanol. The addition of phenol, which alone reacts relatively slowly with triphenylmethyl chloride, caused one phenol molecule to replace one methanol in the third-order rate equation together with a sevenfold increase in the rate constant. *p*-Nitrophenol caused a greater than twentyfold increase in the rate. This was taken as evidence for the better ability of the phenols compared with methanol to solvate the leaving halogen by hydrogen bonding. It has further been found that it was impossible to dissolve 10 mg/ml tetrabutylammonium iodide in carbon tetrachloride, but the same concentration was readily obtainable when carbon tetrachloride containing 0.10 M *p*-cresol was used as the solvent.

By comparing the integrated intensities B and $\Delta\nu_{1/2}$ from this investigation with the data of Tsubomura [8] and Huggins and Pimentel [9] it appears that the strength of the hydrogen bonding from a hydroxyl compound to a bromide ion is between the strength of the hydrogen bonding from the hydroxyl compound to diethyl ether and to triethyl amine.

The existence of hydrogen bonding systems involving anions explains the presence of a band in the 3 μ region in the spectra of quaternary ammonium halides in a solution of chloroform stabilized with 1 % ethanol, as the ethanol forms hydrogen bonding to the halide ion. In a solution of quaternary ammonium halides in pure chloroform or chloroform stabilized with hexane no band appears in the infrared spectrum about 3 300 cm^{-1}.

EXPERIMENTAL

The spectra were recorded with a Beckman IR-2 single-beam infrared spectrophotometer equipped with a sodium chloride prism. The slit width used throughout the work was 0.095 mm and the cell length 0.40 mm. The spectra were obtained by first recording the spectrum of a solution of the proton donor in carbon tetrachloride and then the spectrum of the same solution containing the salt.

The carbon tetrachloride was Merck's analytical grade. The solution of *p*-cresol in chloroform was made from Riedel de Haën's analytical grade chloroform, which was washed five times with water, dried over calcium chloride and fractionated.

The tetrabutylammonium bromide was prepared by refluxing tributylamine with 10 % excess butylbromide in about 7 times the volume acetonitrile for two days. The solution then remained clear on cooling and the solvent was evaporated *in vacuo*. The residue was crystallized from chloroform-ether, and the resulting crystals, which contained chloroform, were recrystallized from tetrahydrofuran-ether, methanol-ether or benzene-ether. The bromide prepared in this way is transparent to ultraviolet light [12].

The tetrabutylammonium iodide was precipitated from an aqueous solution of the bromide with potassium iodide. The nitrate was prepared by metatesis in acetonitrile between silver nitrate and tetrabutylammonium bromide. The picrate was precipitated from an aqueous solution of the bromide.

The benzyltributylammonium chloride was prepared analogously to the tetrabutylammonium bromide in acetonitrile solution. It melts at 164—65°, solidifies and melts again at 170°. (Found: C 72.98; H 10.88; N 4.39; Cl 11.29. Calc. for $C_{19}H_{34}NCl$: C 73.17; H 10.98; N 4.49; Cl 11.36).

The O—H and N—H compounds were either commercially available or prepared according to wellknown procedures. They were purified by conventional means before use.

REFERENCES

1. Kuhn, L. P. *J. Am. Chem. Soc.* **74** (1952) 2492.
2. Barrow, G. M. *J. Phys. Chem.* **59** (1955) 1129.
3. Tsubomura, H. *J. Chem. Phys.* **23** (1955) 2130.
4. Ramsay, D. A. *J. Am. Chem. Soc.* **74** (1952) 72.
5. Fajans, K. and Johnson, O. *J. Am. Chem. Soc.* **64** (1942) 668.
6. Van Thiel, M., Becker, E. D. and Pimentel, G. C. *J. Chem. Phys.* **27** (1957) 95.
7. Huggins, C. M. and Pimentel, G. C. *J. Chem. Phys.* **23** (1955) 896.
8. Tsubomura, H. *J. Chem. Phys.* **24** (1956) 927.
9. Huggins, C. M. and Pimentel, G. C. *J. Phys. Chem.* **60** (1956) 1615.
10. Bartlett, P. D. and Dauben, H. J. *J. Am. Chem. Soc.* **62** (1940) 1339.
11. Swain, C. G. *J. Am. Chem. Soc.* **70** (1948) 1119.
12. Bergman, I. *Trans. Faraday Soc.* **52** (1956) 690.

Received November 5, 1957.

ACTA CHEMICA SCANDINAVICA 12 (1958) 303—307

Determination of Rate Constants of Hydrolysis by a Distribution Technique and its Application to *iso*Propoxy-methyl-phosphoryl Chloride

LENNART LARSSON

Research Institute of National Defence, Dept. 1, Sundbyberg 4, Sweden

An improved formula [1] for the determination of the distribution constant of a compound reacting with one of the phases according to a first order reaction is given. Based on this formula a method for the study of rapid hydrolyses is described. The application of the method is illustrated by the determination of the rate of the hydrolysis of *iso*propoxy-methyl-phosphoryl chloride, and its relationship to that of the corresponding fluorine derivative (Sarin) is discussed.

In an earlier paper [1] the author has deduced the following formula for the calculation of the distribution constant of a compound which reacts with one of the phases according to a first order or a pseudo-first order reaction:

$$\ln [A]_{aq} = - \frac{k \cdot t}{\frac{v_{org}}{v_{aq}} k_d + 1} + C \qquad (1)$$

where $[A]_{aq}$ = concentration of unhydrolysed compound in the aqueous phase;
C = integration constant;
k = reaction rate constant of A in water;
k_d = distribution constant of A between organic and aqueous phase;
t = time;
v = phase volume.

By plotting log $[A]_{aq}$ against t a straight line is obtained the slope of which, α, is

$$|\alpha| = \frac{0.4343\ k}{\frac{v_{org}}{v_{aq}} k_d + 1} \qquad (2)$$

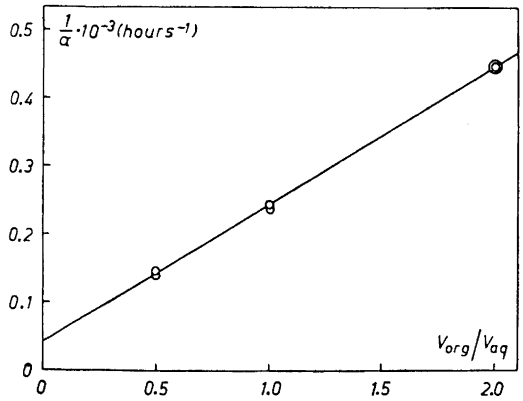

Fig. 1. The reciprocal of the rate of the hydrolysis of 2-methoxy-ethyl nicotinate at various ratios of xylene and water.

The application of the formula was illustrated by the determination of the distribution constant of the ester 2-methoxy-ethyl nicotinate between xylene and water. The rate constant of the hydrolysis was determined in a separate experiment. However, both the rate constant and the distribution constant can be determined simultaneously from a series of experiments where the ratios of the phase volumes are varied. If eqn. (2) is rearranged to

$$\frac{1}{|\alpha|} = \frac{k_d}{0.4343\ k} \cdot \frac{v_{org}}{v_{aq}} + \frac{1}{0.4343\ k} \qquad (3)$$

it appears that a straight line is obtained when $1/|\alpha|$ is plotted against v_{org}/v_{aq}. The rate constant, k, is thus obtained from the intercept of the ordinate and the distribution constant, k_d, from the slope of the line. This is illustrated in Fig. 1 by the example given in the previous paper [1]. As shown in Table 1, k and k_d determined in this way agree well with earlier results.

Table 1. The rate constant of the hydrolysis of 2-methoxy-ethyl nicotinate and its distribution constant between xylene and water.

	According to	
	eqn. (3)	previous paper [1]
k hours^{-1}	5.36×10^{-2}	5.07×10^{-2}
k_d	4.67	4.28

The problem can also be considered as a consecutive reaction *i.e.*:

$$A_{org} \underset{k_{aq}}{\overset{k_{org}}{\rightleftharpoons}} A_{aq} \xrightarrow{k_1} P$$

where P is a hydrolysis product. If this system is treated according to the improved steady-state approximation given by McDaniel and Smoot [2], and $k_{aq}/k_{org} = k_d$, then

$$\ln [A]_{aq} = - \frac{k_1 \cdot t}{\frac{v_{org}}{v_{aq}} \left(k_d + \frac{k_1}{k_{org}} \right) + 1} + C \qquad (4)$$

If $k_{org} >> k_1$ which is the case in slow reactions, eqn. (4) is reduced to eqn. (1). In rapid reactions none of the constants can be neglected and we get, analogously to eqn. (3)

$$\frac{1}{|\alpha|} = \frac{1}{0.4343} \left(\frac{k_d}{k_1} + \frac{1}{k_{org}} \right) \cdot \frac{v_{org}}{v_{aq}} + \frac{1}{0.4343\ k_1} \qquad (5)$$

Obviously from this equation, k_1 can be determined, by plotting $1/|\alpha|$ against v_{org}/v_{aq}; k_d, however, cannot be determined, because it is not possible to estimate k_{org}.

The distribution technique is particularly suitable for studies of rapid hydrolysis. The diminished rate due to the inert phase added permits measurements of reactions which in aqueous solutions run too fast for accurate determinations. The technique was therefore used in the determination of the rate constant of the hydrolysis of *iso*propoxy-methyl-phoshoryl chloride. The study of this hydrolysis forms part of an investigation of the influence of the substituents on the rate of hydrolysis of Sarin analogues [3]. *Iso*propoxy-methyl-phosphoryl chloride is assumed to hydrolyse according to a first-order reaction when the pH is maintained constant, and eqn. (5) is thus valid.

EXPERIMENTAL

Materials: *Iso*propoxy-methyl-phosphoryl chloride was synthesized by reacting methyl-phosphoryl dichloride [4] with *iso*propanol, and was freshly distilled before use. B.p. 51°C/4 mm Hg; n_D^{25} 1.4275; d_4^{25} 1.140.

Chloroform: E. Merck; anal. reagent.

Procedure: The rate of the hydrolysis of *iso*propoxy-methyl-phosphoryl chloride during the distribution between chloroform and a 0.100 M solution of potassium chloride was studied at pH 7.00 and 25.0°C. The pH was maintained constant by means of an automatic recording titrator [5] which was standardized before each run against a 0.05 M solution of potassium hydrogen *o*-phthalate (pH 4.01). A constant temperature, circulating water bath maintained the jacketed reaction vessel at ± 0.1°C or better.

A 0.80 mM stock solution of the compound in dry chloroform was prepared. Experiments were performed with four different ratios of the volumes of chloroform solution to aqueous solution as shown in Table 2. The total volume of each sample was 40 ml.

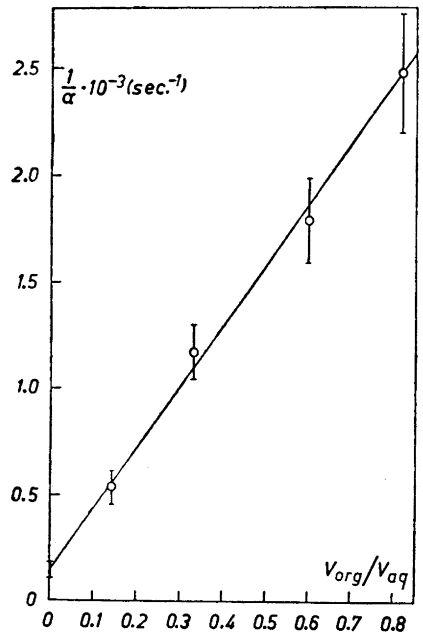

Fig. 2. The reciprocal of the rate of the hydrolysis of *iso*propoxy-methyl-phosphoryl chloride at various ratios of chloroform and water.

Table 2. Ratio of the volumes of chloroform solution to aqueous solution.

v_{org} / v_{aq}	5 : 35	10 : 30	15 : 25	18 : 22

The aqueous solution was in advance adjusted to the desired pH. The addition of pure chloroform to the aqueous solution has no influence upon pH. Each set of experiment was repeated five times. Some difficulties arose in getting a suitable speed of the magnetic stirrer. Too rapid stirring caused great fluctuations of pH during the run owing to chloroform splashing over the electrodes and shielding them. On the other hand slow stirring did not permit equilibrium to be attained. With a few exceptions the variations of pH during the runs were ± 0.1 or less. The products formed in the hydrolysis, hydrochloric acid and *iso*propoxy-methyl-hydroxy-phosphine oxide, are assumed to be completely soluble in the aqueous phase at the actual pH. The curves obtained were treated according to Guggenheim [6]. Straight lines were obtained the slopes of which were calculated. The straight lines indicate that no appreciable association did occur in the chloroform phase [1].

RESULTS AND DISCUSSION

When $1/|\alpha|$ is plotted against v_{org}/v_{aq} for the hydrolysis of *iso*propoxy-methyl-phosphoryl chloride in various ratios of chloroform and water at pH 7.00 a straight line is obtained as shown in Fig. 2. The equation of the line was calculated by the method of least squares with weighted values (9:5:2:1). The intercept of the ordinate of the line was found to be (0.151 ±

0.041) $\times 10^3$ which corresponds to a rate constant of the hydrolysis of $(1.5 \pm 0.4) \times 10^{-2}$ sec.$^{-1}$.

If it is assumed that the rate of the hydrolysis of *iso*propoxy-methyl-phosphoryl chloride is proportional only to the hydroxyl ion concentration as is valid for Sarin [3], the bimolecular rate constant, k_2, would be 1.2×10^5 1 mole^{-1} sec.$^{-1}$, *i.e.* 5×10^3 times greater than that of the fluorine derivative (Sarin). Because of the greater electronegativity of fluorine which makes the phosphours atom more electron deficient and positive, the formation of the P-OH bond is facilitated more in the fluorine than in the chlorine compound. By using Pauling's values of electronegativity of P, Cl and F a rough calculation according to Hannay and Smyth [7] shows that the P—F and P—Cl bonds are 43 and 17 % ionic, respectively. If the difference in the ionic character of the bonds is the rate determining factor, one would expect that the fluorine compound would hydrolyse more rapidly than the chlorine compound. The considerably greater hydrolytic stability of the fluorine derivative may, however, be ascribed principally to the higher bond energy of the P—F bond, 120 kcal/mole, in comparison with that of the P—Cl bond, 80 kcal/mole [8].

The author is indebted to Professor G. Ljunggren, Director of this Institute, for the kind interest he has shown in this work. The author wishes also to express his thanks to Fil.lic. K.-E. Almin, Swedish Forest Products Research Laboratory, for valuable discussions.

REFERENCES

1. Larsson, L. *Acta Chem. Scand.* **10** (1956) 1071.
2. McDaniel, D. H. and Smoot, C. R. *J. Phys. Chem.* **60** (1956) 966.
3. Larsson, L. *Acta Chem. Scand.* **11** (1957) 1131.
4. Kinnear, A. M. and Perren, E. A. *J. Chem. Soc.* **1952** 3437.
5. Larsson, L. and Hansen, B. *Svensk Kem. Tidskr.* **68** (1956) 521.
6. Guggenheim, E. A. *Phil. Mag.* **2** (1926) 538.
7. Hannay, N. B. and Smyth, C. P. *J. Am. Chem. Soc.* **68** (1946) 171.
8. Neale, E., Williams, L. T. D. and Moores, V. T. *J. Chem. Soc.* **1956** 422.

Received October 24, 1957.

ACTA CHEMICA SCANDINAVICA 12 (1958) 308—313

An Investigation of the Me_5Si_3-MeSi Region of the Mn-Fe-Si and some Related Systems

BERTIL ARONSSON

Institute of Chemistry, University of Uppsala, Uppsala, Sweden

From X-ray diffraction data it has been concluded that there is a Me_5Si_3-MeSi two phase region in the Mn—Fe—Si systems at 950°C. The lattice parameters of the MeSi and Me_5Si_3 phases as functions of composition have been determined as well as tie lines in the two phase region. Some observations on the corresponding part of the Cr—Mn—Si, Cr—Fe—Si and Cr—Co—Si systems have been made.

It has been found that the metal with the higher atomic number is enriched in the cubic MeSi phase which is the Si richest phase present in the investigated region of the systems mentioned. The relation of the lattice parameter variations of the Me_5Si_3 phases to the morphotropy of these phases is discussed.

The physical and chemical properties of the borides, carbides and nitrides of the first transition series metals show that the stability of these compounds decreases with increasing atomic number of the metal [1,2,21,22]. In accordance with this decrease in transition metal-non metal "affinity" it has been observed that in Me_1-Me_2-X systems (Me = transition metal from the first transition series, X = nonmetal) the metal with the lower atomic number is concentrated in the X richest phase present [3–6]. This was found to be so in the Me_2B-MeB two phase region of Me_1-Me_2-B systems, in which Hägg and Kiessling [6] determined the distribution of various metal pairs between the two phases mentioned. They found that the larger the difference in atomic number of the metals the more pronounced was the enrichment of the lower atomic number metal in the MeB phase.

In order to see if similar trends were displayed by Me_1-Me_2-Si systems, the Me_5Si_3-MeSi section of some ternary silicide systems has been studied. From older work it is known that Mn_5Si_3 [7] and Fe_5Si_3 [8] as well as MnSi [9] and FeSi [10] are isomorphous. Preliminary experiments indicated that there was a Me_5Si_3-MeSi two phase region in the Mn-Fe-Si systems. The main interest has been devoted to this system as the distribution of the Mn and Fe atoms could be determined in the same way as in the ternary boride systems [6].

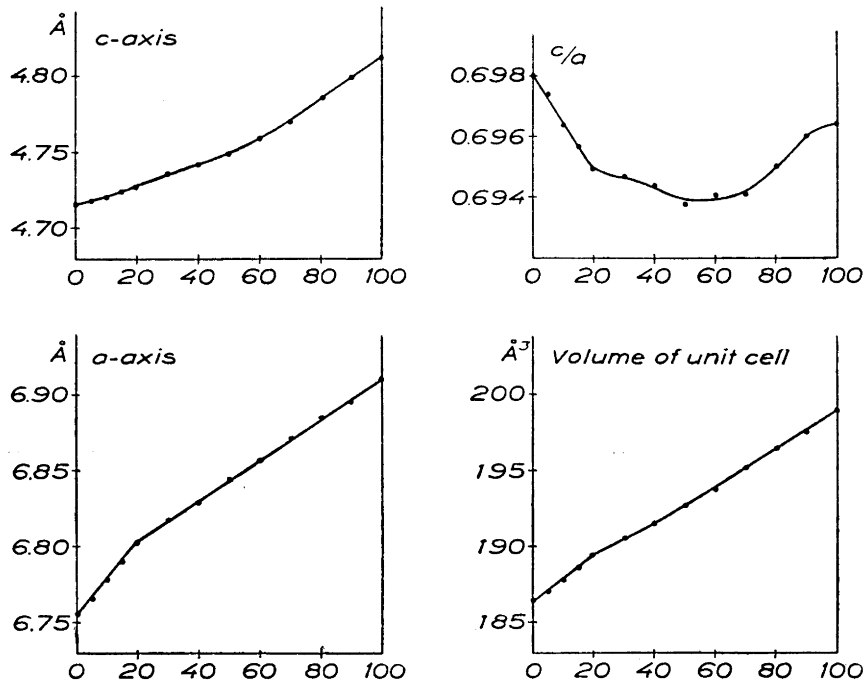

Fig. 1. Unit cell dimension of the Me_5Si_3 phase as function of the atomic ratio Mn/(Mn + Fe) × 100.

In connexion with these investigations information has been collected about the variation of the lattice parameters (l.p.) of the Me_5Si_3 phases with composition. Some relation between these l.p. variations and the morphotropy among the Me_5Si_3 phases has been found and is discussed in the last part of this paper.

EXPERIMENTAL

Weighed amounts of the elements in powder form (claimed purity $\geq$ 99.8 % except for Co which contained 0.45 % Ni) were melted twice in an arc furnace and subsequently annealed in evacuated silica tubes for 8 days at 950°C. As it was found that the compositions obtained from chemical analysis deviated very little from the nominal composition only six alloys were analysed. The analyses added up to 99.2 $\pm$ 0.5 %.

24 alloys were made in the Mn—Fe—Si system, 13 on the Me_5Si_3 line (4 analysed), 4 on the MeSi line (2 analysed) and 7 with compositions $MeSi_{0.75}$ or $MeSi_{0.80}$. Four of the Me_5Si_3 alloys contained traces of a (FeMnSi) and one of (Mn, Fe)Si. For these alloys the Mn/Fe ratio in the Me_5Si_3 phase may be slightly different from that in the alloy. However, this difference was estimated to be too small to affect the l.p. of Me_5Si_3 significantly. In each of the Cr—Me′—Si systems (Me′ = Mn, Fe, Co) four alloys were made with compositions $Cr_{0.2}$ $Me'_{0.8}$ $Si_{0.63}$, $Cr_{0.4}$ $Me'_{0.6}$ $Si_{0.63}$, $Cr_{0.6}$ $Me'_{0.4}$ $Si_{0.63}$ and $Cr_{0.8}$ $Me'_{0.2}$ $Si_{0.63}$.

Powder photographs were taken in a Guinier type focussing camera, using Cr$K\alpha$-radiation. All powder samples were mixed with some CaF_2 before the exposure and the l.p. which are thought to be reliable to about $\pm$ 0.03 % are given assuming the cube edge of CaF_2 to be 5.4630 Å [11] at 21°C.

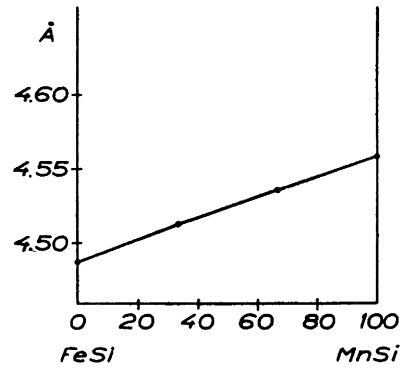

Fig. 2. Cube-edge of the MeSi phase as function of the atomic ratio Mn/(Mn + + Fe) × 100.

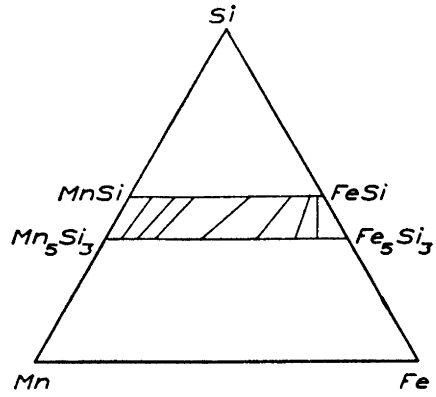

Fig. 3. Some tie lines in the Me_5Si_3-MeSi region of the Mn—Fe—Si system at 950°C.

RESULTS

The Mn-Fe-Si system. All the Me_5Si_3 alloys showed sharp and unsplit powder lines corresponding to the $D8_8$-structure [8]. The variations of the unit cell constants with composition are given in Fig. 1. It was concluded that, at 950°C, the Me_5Si_3 line in the Mn-Fe-Si system is a single phase line (or very nearly so). Similarly it was found that the MeSi line is a single phase line (Fig. 2). For the alloys in the two phase region the l.p. (lattice parameters) of the two phases were determined. From the curves in Fig. 1 and 2 the composition of the two phases in equilibrium with each other was obtained and tie-lines in the Me_5Si_3-MeSi two phase region could be drawn (Fig. 3).

The distribution ratios have been defined and determined as in the paper by Hägg and Kiessling [6]. Let x'_{Mn} be the atomic fraction Mn/(Mn + Fe) and x'_{Fe} the atomic fraction Fe/(Mn + Fe) in the Me_5Si_3-phase. x''_{Mn} and x''_{Fe} are the corresponding fractions in the MeSi phase. In order to be ≤ 1 the distribution ratios are defined as $\alpha_{Mn} = x''_{Mn}/x'_{Mn}$ and $\alpha_{Fe} = x'_{Fe}/x''_{Fe}$. The variations of the distribution ratios as function of $(x'_{Mn} + x''_{Mn})/2$ are given in Fig. 4.

As seen from Fig. 3 and 4, iron is enriched in the MeSi phase. At small Fe concentrations about twice as much iron will be found in this phase as in the Me_5Si_3 phase.

The Cr-Me'-Si systems (Me' = Mn, Fe, Co). Besides the cubic MeSi phase the (Cr, Mn)$Si_{0.63}$ and (Cr, Fe) $Si_{0.63}$ alloys were found to contain Cr_5Si_3 with dissolved Mn or Fe (T 1 (W_5Si_3)-type structure) [12–14] and (or) Mn_5Si_3 (Fe_5Si_3) with dissolved Cr ($D8_8$-type structure [7]). In these systems there are probably a T 1-MeSi two phase region, a T 1-$D8_8$-MeSi three phase region and a $D8_8$-MeSi two phase region. The composition of the MeSi phase could be estimated from its l.p. which was assumed to vary according to Vegard's law from

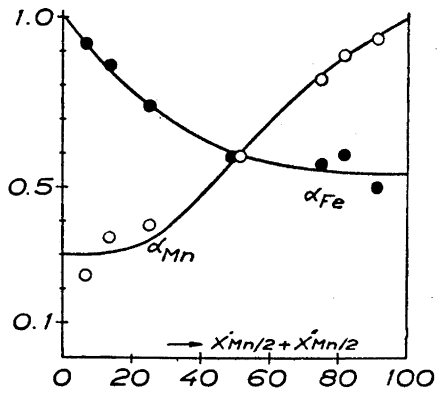

Fig. 4. The distribution ratios α_{Fe} and α_{Mn} as function of $(x'_{Mn} + x''_{Mn})/2$ (See text).

CrSi to MnSi and from CrSi to FeSi. It was found that Mn and Fe, respectively, were enriched in this phase and this enrichment was more marked for Fe.

In all the (Cr, Co)$Si_{0.63}$ alloys the MeSi phase had a cube edge of 4.449 ± 0.004 Å which corresponds closely to that of pure CoSi (4.447 Å) [9]. Therefore, in the Cr-Co-Si system practically pure CoSi is in equilibrium with some Si poorer phase (or phases).

Thus, it has been found that in the investigated part of the Cr-Me'-Si systems the metal with the higher atomic number is concentrated in the MeSi phase.

The l.p. vs composition curves. The unit cell constants of the $D8_8$ phase vary quite irregularly from Mn_5Si_3 to Fe_5Si_3. Especially remarkable is the variation of c/a which goes through a minimum at about $(Fe_{0.5}Mn_{0.5})_5Si_3$. No careful determinations of l.p. variations of the Me_5Si_3 phases in the other systems were made but it was observed that when Cr was dissolved in Mn_5Si_3 or Fe_5Si_3 there was a decrease in c/a for the $D8_8$ phase while the solution of Mn or Fe in Cr_5Si_3, on the contrary, increased the c/a ratio for the latter phase.

DISCUSSION

This study of the Me_5Si_3-MeSi region of some Me_1-Me_2-Si systems (Me = Cr, Mn, Fe, Co) has revealed regular trends in the distribution of the metals: The larger the difference in their atomic number the more pronounced is the enrichment of the *higher* atomic number metal in the MeSi phase. This behaviour is opposite to that found in ternary boride and carbide systems of the same metals: In these systems the *lower* atomic number metal is always concentrated in the nonmetal richest phase. Results of investigations of this type certainly depend on the parts of the ternary systems which are actually studied and no farreaching conclusions can be drawn from the above observations. It seems, however, as if the silicides of Cr, Mn, Fe, Co do not show the same decrease in stability with increasing atomic number of the metal as do the borides, carbides and nitrides.

The l.p. variations of the T 1 and $D8_8$ phases may be worth a few comments. Of the Me_5Si_3 silicides of the first series transition elements Ti_5Si_3 [15], Mn_5Si_3 [7] and Fe_5Si_3 [8] have the $D8_8$ structure while V_5Si_3 [16] and Cr_5Si_3 [13] have the T 1 (W_5Si_3) structure. In the presence of small amounts of carbon, V_5Si_3 (C) [17] and Cr_5Si_3(C) [18] also crystallize in the $D8_8$ structure. The Me_5Si_3 phases belong to a group of phases the structures of which are characterized by straight rows of atoms. In the T 1 and $D8_8$ phases these rows run parallel to the c-axis and the smaller c/a-value these phases have, the shorter are the interatomic distances in the rows ($= c/2$) compared with the average interatomic distances in the structure. Looking at the c/a values of the $D8_8$ phases (V_5Si_3 and Cr_5Si_3 contain some C) we see that the smallest values are found for V and Cr

		Ti	V	Cr	Mn	Fe
$D8_8$	c/a	0.691	0.679	0.676	0.696	0.698
	$c/2$	2.59 Å	2.42 Å	2.36 Å	2.41 Å	2.36 Å
T 1	$c/2$		2.38 Å	2.30 Å		

This gives sense to the fact that c/a for Mn_5Si_3 and Fe_5Si_3 decreases (to about 0.684 and 0.693, respectively) when Cr is dissolved in these phases. It is also compatible with the general observation that rows with the closest contacts between the row atoms are formed by the Va and VIa groups metals (*e.g.* in phases of the β-W and σ-type).

As seen from the table the distances between row atoms ($= c/2$) in the V_5Si_3 and Cr_5Si_3 T 1 phases are still shorter than in the $D8_8$ phases of these metals, which indicates that the atomic arrangement in the T 1 structure is such that the row atoms are closer to each other than they would be in a $D8_8$ structure of the same elements. The Va and VIa group metals being those which form rows with the shortest contact, it is not surprising that the T 1 structure is chosen by V_5Si_3 and Cr_5Si_3 while Ti_5Si_3, Mn_5Si_3 and Fe_5Si_3 crystallize in the $D8_8$ structure.

In a number of investigations it has been shown that several $D8_8$ phases only exist as ternary phases [*e.g.* V_5Si_3 (C) [17] and Cr_5Si_3 (C) [18]] containing small amounts of a third component (B, C, N or O) [19,20]. It is possible that Ti_5Si_3, Mn_5Si_3 and Fe_5Si_3 are in reality ternary phases, too, owing their existence to the presence of small non metals such as C, N or O, but this has not yet been proved.

Acknowledgement. The author wants to thank Professor Hägg who has kindly read the manuscript. I am also indebted to Mr. S. Rundqvist for many stimulating discussions and Dr. Lilly Gustafsson for analytical assistance.

A grant from the *Swedish State Council for Technical Research* is gratefully acknowledged.

REFERENCES

1. Hägg, G. *Z. physik. Chem.* **6 B** (1929) 221.
2. Ehrlich, P. *Z. anorg. Chem.* **259** (1949) 1.
3. Goldschmidt, H. J. *J. Iron Steel Inst. London* **160** (1948) 345.
4. Hultgren, A. and Kuo, K. *Jernkontorets Ann.* **135** (1951) 449.
5. Hägg, G. *Ibid.* **135** (1951) 493 (discussion).

6. Hägg, G. and Kiessling, R. *J. Inst. Metals* **81** (1951–52) 57.
7. Åmark, K., Borén, B. and Westgren, A. *Metallwirtschaft* **15** (1936) 835.
8. Farquhar, C. M., Lipson, H. and Weill, A. R. *J. Iron Steel Inst. London* **152** (1945) 457.
9. Borén, B. *Arkiv Kemi, Mineral. Geol.* **11 A** (1933) No. 10.
10. Phragmén, G. *Jernkontorets Ann.* **107** (1923) 121.
11. Smakula, A. and Kalnajs, J. *Phys. Rev.* **99** (1955) 1737.
12. Parthé, E., Lux, B. and Nowotny, H. *Monatsh.* **86** (1955) 859.
13. Dauben, C. H., Templeton, D. H. and Myers, C. E. *J. Phys. Chem.* **60** (1956) 443.
14. Aronsson, B. *Acta Chem. Scand.* **9** (1955) 1107.
15. Pietrokowsky, P. and Duwez, P. *J. Metals* **3** (1951) 772.
16. Parthé, E., Nowotny, H. and Schmidt, H. *Monatsh.* **86** (1955) 385.
17. Schachner, H., Cerwenka, E. and Nowotny, H. *Monatsh.* **85** (1954) 245.
18. Parthé, E., Schachner, H. and Nowotny, H. *Monatsh.* **86** (1955) 182.
19. Brewer, L. and Krikorian, O. *UCRL*-2544 (1954).
20. Nowotny, H., Lux, B. and Kudielka, H. *Monatsh.* **87** (1956) 447.
21. Kieffer, R. und Schwarzkopf, P. *Hartstoffe und Hartmetalle*, Springer-Verlag, Wien 1953.
22. Kiessling, R. *Fortschr. Chem. Forsch.* **3** (1954) 61.

Received October 28, 1957.

ACTA CHEMICA SCANDINAVICA 12 (1958) 314—323

On the Reaction between Substituted Malonic Esters and Methylene Bromide. I

LENNART EBERSON

Department of Organic Chemistry, Chemical Institute, University of Lund, Sweden

Diethyl methyl-, ethyl-, *n*-propyl-, *iso*propyl-, *n*-butyl-, *iso*butyl-, *n*-amyl-, benzyl-, and acetaminomalonates in the form of their sodium compounds react with methylene bromide in ethanolic solution to form 1,3-disubstituted 1,1,3-tricarbethoxypropanes with the elimination of *one* carbethoxy group as diethyl carbonate, whereas diethyl phenyl- and carbethoxymalonate give 1,3-disubstituted 1,3-dicarbethoxypropanes with the elimination of *two* carbethoxy groups. Diethyl *neo*pentylmalonate yields *α-neo*pentylacrylate, and diethyl *tert.*-butylmalonate and ethyl phenylacetate give no reaction. A reaction scheme is proposed. The preparation of the corresponding glutaric acids from the esters above is described.

The present investigation deals with the reaction between substituted malonic esters and methylene bromide and its use for the preparation of $\alpha\alpha'$-disubstituted glutaric acids. The author has previously found [1] that when the sodium compound of diethyl trimethylsilylmethylmalonate (I, R = $(CH_3)_3SiCH_2$) was allowed to react with methylene bromide in ethanolic solution a triethyl ester was obtained according to formula (1):

$$2\ \underset{\text{I}}{R.CH(COOEt)_2} + CH_2Br_2 + 2\ OEt^- \longrightarrow \underset{\text{II}}{\begin{matrix} R.C(COOEt)_2 \\ | \\ CH_2 \\ | \\ R.CHCOOEt \end{matrix}} + EtOH + (EtO)_2CO + 2\ Br^- \qquad (1)$$

i.e., one carbethoxy group was eliminated. Attempts to prepare the tetraethyl ester by carrying out the synthesis in an inert solvent (toluene or xylene) at a higher temperature resulted in the formation of diethyl bromomethyl-tri-

methylsilylmethylmalonate (III, R = $(CH_3)_3SiCH_2$) which did not react further with a second molecule of I:

$$R.C(Na)(COOEt)_2 + CH_2Br_2 \xrightarrow[140°]{\text{xylene}} R.C(CH_2Br)(COOEt)_2 + NaBr \quad (2)$$

III

An examination of the literature on similar reactions yielded incomplete and with the above result incompatible information, and therefore a more detailed study of the reaction was undertaken. Guthzeit and Dressel [2,3] stated that diethyl malonate and methylene iodide gave 1,1,3,3,-tetracarbethoxypropane in about 80 % yield, diethyl ethylmalonate and methylene iodide a mixture boiling over a large interval [3], and diethyl benzylmalonate and methylene iodide 1,3-dibenzyl-1,1,3,3-tetracarbethoxypropane [3]. Diethyl methylmalonate and methylene iodide gave 1,3-dimethyl-1,1,3,3-tetracarbethoxypropane according to Bischoff [4] and von Auwers [5]. Diethyl acetaminomalonate did not react with methylene iodide [6]. Souther [7] found that diethyl phenylmalonate and methylene iodide reacted according to formula (3):

$$2\ R'.CH(COOEt)_2 + CH_2I_2 + 2\ OEt^- \longrightarrow$$

$$\begin{array}{l} R'.CHCOOEt \\ \quad | \\ \quad CH_2 \\ \quad | \\ R'.CHCOOEt \end{array} + 2\ (EtO)_2CO + 2\ I^- \quad (3)$$

IV ($R' = C_6H_5$ or COOEt)

i.e., two carbethoxy groups were eliminated. However, of the above statements only the first- and last-mentioned were wholly established while the others were not demonstrated satisfactorily.

The following substituted malonic esters were investigated with respect to their reaction with methylene bromide in ethanolic solution: diethyl methyl-, ethyl-, *n*-propyl-, *iso*propyl-, *n*-butyl-, *iso*butyl-, *tert.*-butyl-, *n*-amyl-, *neo*pentyl-, phenyl-, benzyl-, carbethoxy-, and acetaminomalonate. Ethyl phenylacetate was also investigated.

Diethyl methyl-, ethyl-, *n*-propyl-, *iso*propyl-, *n*-butyl-, *iso*butyl-, *n*-amyl-, benzyl-, and acetaminomalonate all reacted according to formula (1) to yield the triesters II. To establish that the inconsistency with the statements from the literature was not due to the nature of the halogenide, methylene iodide was also used in the reaction with diethyl methyl-, ethyl-, and benzylmalonate. However the same result was obtained. Diethyl *tert.*-butylmalonate and ethyl phenylacetate did not give any reaction at all, whereas diethyl *neo*pentylmalonate reacted according to formula (4):

$$(CH_3)_3CCH_2CH(COOEt)_2 + CH_2Br_2 + 2\ OEt^- \longrightarrow$$

$$\begin{array}{l} (CH_3)_3CCH_2C{=}CH_2 \\ \qquad\quad | \\ \qquad\quad COOEt \end{array} + EtOH + (EtO)_2CO + 2\ Br^- \quad (4)$$

The ethyl *α-neo*pentylacrylate was identified by conversion to the corresponding acid, which was known from the work of Hadley *et al.*[8] Diethyl phenylmalonate and tricarbethoxymethane reacted according to formula (3).

A few bromomethyl-alkylmalonates (III, R = CH_3, C_2H_5, *n*-C_5H_{11}, and *neo*-C_5H_{11}) were prepared in toluene solution with excess of methylene bromide. These compounds were thermally stable up to 300°C. III, R = CH_3, reacted with the sodium compound of diethyl methylmalonate to give II, R = CH_3.

The triethyl esters with R = methyl, ethyl, and *iso*propyl were hydrolyzed and decarboxylated directly by boiling with 70—80 % sulphuric acid, while that with R = acetamino was converted into *αα'*-diaminoglutaric acid according to the method of Hellman, Lingens, and Folz[6]. The other compounds were hydrolyzed by boiling with 10 % ethanolic potassium hydroxide (the acid hydrolysis was not used on account of the insolubility of the acids formed in this medium) and the tricarboxylic acids could then easily be decarboxylated by heating to 160—170°. The glutaric acids could be separated into high- and low-melting forms by fractionated crystallization from suitable solvents.

DISCUSSION

The first step in the reaction between a methylene halogenide and a substituted malonic ester in ethanol must be the formation of a bromomethylmalonic ester (III) according to formula (2). The next step is the reaction of an ethoxide ion with III to form the intermediate anion V which then decomposes into an *α*-substituted acrylic ester (VI) with the

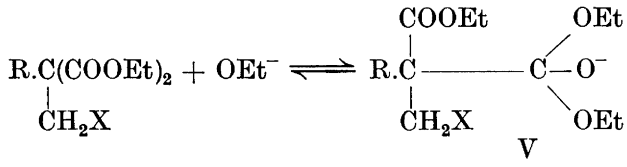

(5)

V

elimination of one molecule of diethyl carbonate and one halide ion:

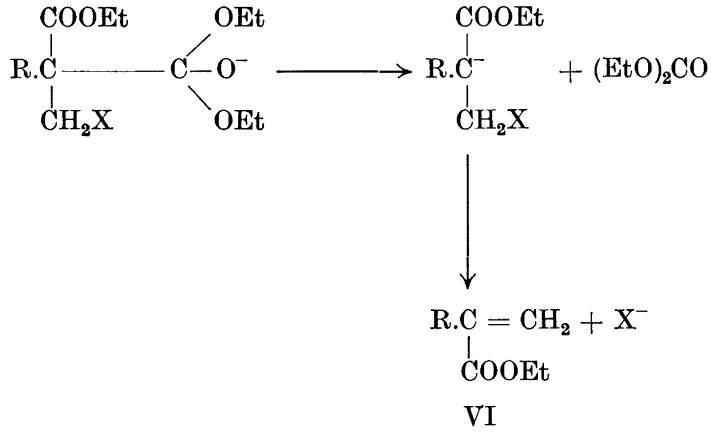

(6)

VI

The last stage consists of a Michael addition of VI to a second molecule of the malonic ester (7):

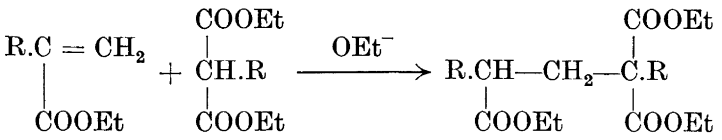

(7)

There is much evidence which favours the above reaction sequence. The formation of the bromomethylmalonic ester III is usually difficult to accomplish in ethanolic solution even with a large excess of methylene halogenide as it immediately reacts further with ethoxide ion. However, when R is a bulky group as trimethylsilylmethyl, the bromo compound can be isolated in good yield [1]. This is not possible with malonic esters containing small R groups (*e.g.* methyl or ethyl). A compound of the type III possesses a *neo*pentyl structure and thus is very unlikely to react according to an S_N2-mechanism with an $R.\bar{C}(COOEt)_2$-ion. Instead the bromomethyl group, being an electronegative substituent, promotes the elimination of a carbethoxy group by ethoxide ion. This cleavage reaction has been found to be enhanced by other electronegative groups such as the phenyl [9–11], nitro [12], vinyl [13], 2,4-dinitrophenyl [14], 2- or 3-indenyl [15], and dichloromethyl group [16]. The behaviour of dichloromethyl-alkylmalonic esters towards ethoxide ion has been studied by Bowman and Rexford [16] and they proposed the following reaction mechanism for the reaction:

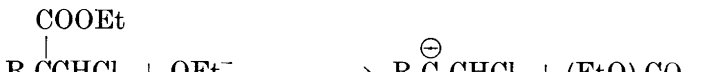

(8)

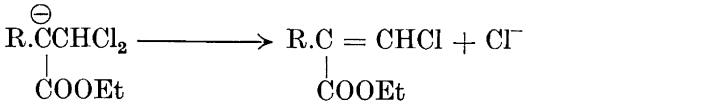

(9)

Reactions (8) and (9) are analogous to (5) and (6).

The elimination of two carbethoxy groups when R is phenyl or carbethoxy, *i.e.*, an electronegative substituent, is readily explained by the reactions (10), (11), and (12):

(10)

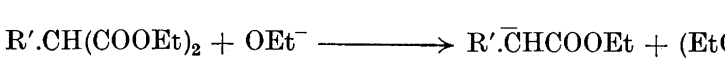

(11)

$$\begin{array}{l} \mathrm{R'.C(=CH_2).COOEt} \\ \mathrm{R'.CH_2COOEt} \end{array} \xrightarrow{\mathrm{OEt^-}} \begin{array}{l} \mathrm{R'.CHCOOEt} \\ \mathrm{CH_2} \\ \mathrm{R'.CHCOOEt} \end{array} \qquad (12)$$

$(\mathrm{R'} = \mathrm{C_6H_5}$ or COOEt)

The alternative route whereby a malonic ester of this type first reacts according to formula (11) and then according to (13)

$$2\ \mathrm{R'CH_2COOEt} + \mathrm{CH_2X_2} + 2\ \mathrm{OEt^-} \longrightarrow \begin{array}{l} \mathrm{R'.CHCOOEt} \\ \mathrm{CH_2} \\ \mathrm{R'.CHCOOEt} \end{array} + 2\ \mathrm{X^-} + 2\ \mathrm{EtOH} \qquad (13)$$

$(\mathrm{R'} = \mathrm{C_6H_5}$ or COOEt)

can be ruled out in the case of R′ = phenyl, as ethyl phenylacetate fails to react with methylene bromide. This is not so in the case of R′ = carbethoxy, however, where both reaction paths are possible.

The isolation of the intermediate α-substituted acrylic ester has been accomplished for R = *neo*pentyl. It is possible that this reaction may be used as a good preparation method for such compounds after certain modifications, but no experiments in this direction have yet been undertaken.

The last step (7) has been demonstrated for R = methyl by von Auwers and Köbner [17], Hoch and Karrer [18], and Ruhl [19].

As a general preparation method for αα′-disubstituted glutaric acids the reaction has several advantages over the existing ones. The starting materials are easily available and the reaction products are easy to isolate and purify. The most serious limitation is the failure of malonic esters containing bulky R groups (such as *tert.*-butyl and *neo*pentyl) to react. The unreactivity of diethyl *tert.*-butylmalonate may in part be due to the considerably reduced acidity of this compound in ethanolic solution as compared with *n*-alkylmalonic esters.

EXPERIMENTAL

All reagents used were carefully dried and fractionated in a glass-helix packed column of about ten theoretical plates. In the malonic ester syntheses precautions were taken to exclude moisture from the reaction vessels. Determinations of the melting points were made with a Kofler micro hot stage. The analyses were carried out at the Department of Analytical Chemistry, Chemical Institute, Lund.

1,3-Dimethyl-1,1,3-tricarbethoxypropane (II, R = CH_3). To a solution of 4.6 g (0.2 mole) of sodium in 80 ml of absolute ethanol 34.8 g (0.2 mole) of diethyl methylmalonate was added, followed by 17.4 g (0.1 mole) of methylene bromide. The reaction mixture was boiled for 20 h after which time it was almost neutral. It was neutralized with a few drops of glacial acetic acid, the ethanol was distilled off through a short column, and water added to dissolve the sodium bromide. The organic layer was taken up in

ether, the ether solution washed with water, and finally dried with anhydrous magnesium sulphate. After distilling off the ether the residue was distilled *in vacuo*. This method yielded 7.5 g (64 %) of diethyl carbonate, b. p. 65—70°/60 mm, and 24.0 g (83 %) of 1,3-dimethyl-1,1,3-tricarbethoxypropane, b. p. 153—154°/11 mm, n_D^{20} 1.4343, d_4^{20} 1.0471, r_D 0.2489. Möller [20] reported b. p. 156—158°/15 mm for the same compound prepared from diethyl methylmalonate and ethyl α-bromo*iso*butyrate, and Ruhl [19] reported b.p. 142—145°/5 mm for a sample prepared from diethyl methylmalonate and ethyl methacrylate.

The reaction was also carried out with methylene iodide instead of the bromide. Diethyl carbonate was obtained in 61 % yield and the triester in 87 % yield.

α,α'-Dimethylglutaric acid. The 1,3-dimethyl-1,1,3-tricarbethoxypropane was hydrolyzed by boiling with 70 % sulphuric acid until the oily layer had disappeared which required about 5 h. The solution was cooled in ice and the solid was filtered and washed with a small amount of ice water. After drying in a vacuum desiccator the yield of the crude acid mixture was 92 %. The separation into diastereoisomers was made according to Möller [20]. A high-melting form was obtained, m. p. 140—141°, in 30 % yield, and a low-melting, m. p. 125—127°, in 37 % yield. Möller reported 139—140° and 127°, respectively [20].

Diethyl bromomethyl-methylmalonate. To a mixture of 23.0 g of 20 % sodium-toluene dispersion and 100 ml of dry toluene there was added 0.2 mole of diethyl methylmalonate at such a rate that the reaction mixture boiled gently. 0.4 mole of methylene bromide was added in one portion and the mixture was boiled with stirring for 3 h. After cooling water was added, the toluene solution separated, washed with water, and dried with anhydrous magnesium sulphate. Distillation yielded 38.0 g of diethyl bromomethyl-methylmalonate (71 %), b. p. 98—100°/3 mm, n_D^{20} 1.4503, d_4^{20} 1.3085. (Found: C 40.7; H 5.8; Br 29.7; r_D 0.2055. Calc. for $C_9H_{15}O_4Br$: C 40.5; H 5.7; Br 29.9; r_D 0.2051.)

Reaction between diethyl bromomethylmethylmalonate and diethyl methylmalonate. 0.2 mole of sodium was dissolved in 70 ml of absolute ethanol, 0.2 mole of diethyl methylmalonate added and finally 0.2 mole of diethyl bromomethyl-methylmalonate dropped into the warm solution during a period of 30 min. The reaction mixture was boiled for 20 h and then worked up in the usual way. A 61 % yield of diethyl carbonate and an 85 % yield of II, R = CH_3, were obtained.

1,3-Diethyl-1,1,3-tricarbethoxypropane (II, R = C_2H_5). This compound was prepared as the methyl derivative from 0.2 mole of sodium in 80 ml of absolute ethanol, 0.2 mole of diethyl ethylmalonate, and 0.1 mole of methylene bromide. The reaction yielded 7.2 g (61 %) of diethyl carbonate and 20.8 g (66 %) of 1,3-diethyl-1,1,3-tricarbethoxypropane, b.p. 144—145°/4 mm, n_D^{20} 1.4395, d_4^{20} 1.0321. (Found: C 60.4; H 9.1; r_D 0.2551. Calc. for $C_{16}H_{28}O_6$: C 60.7; H 8.9; r_D 0.2566.)

When methylene iodide was used in the above reaction, a 46 % yield of diethyl carbonate and a 56 % yield of triester were obtained.

α,α'-Diethylglutaric acid. 1,3-Diethyl-1,1,3-tricarbethoxypropane was hydrolyzed by boiling over night with 75 % sulphuric acid. The yield of crude acid mixture was 90 %, and it was separated into diastereoisomers according to the method of Berner and Landmark [21]. The high-melting acid was obtained in 32 % yield, m. p. 118—121°, and the low-melting one in 25 % yield, m. p. 92—94°. Berner and Landmark reported 119—120° and 93.5—94.5°.

Diethyl bromomethyl-ethylmalonate. This synthesis was carried out in exactly the same way as for diethyl bromomethyl-methylmalonate from 23.0 g of 20 % sodium-toluene dispersion in 100 ml of dry toluene, 0.2 mole of diethyl ethylmalonate and 0.4 mole of methylene bromide. 27.0 g (48 %) of the bromo compound was obtained, b.p. 105—107°/3 mm, n_D^{20} 1.4521, d_4^{20} 1.2753. (Found: C 43.0; H 6.1; Br 28.6; r_D 0.2117. Calc. for $C_{10}H_{17}O_4Br$: C 42.7; H 6.1; Br 28.4; r_D 0.2114.)

Kötz and Zörnig [22] have prepared the corresponding chloromethyl and iodomethyl derivatives.

*1,3-Di-*n*-propyl-1,1,3-tricarbethoxypropane (II, R = n-C_3H_7).* From 0.2 mole of sodium dissolved in 80 ml of absolute ethanol, 0.2 mole of diethyl *n*-propylmalonate, and 0.1 mole of methylene bromide were obtained 6.0 g (51 %) of diethyl carbonate and 23.4 g (68 %) of the triester, b.p. 152—153°/2 mm, n_D^{20} 1.4415, d_4^{20} 1.0091. (Found: C 62.7; H 9.2; r_D 0.2619. Calc. for $C_{18}H_{32}O_6$: C 62.8; H 9.4; r_D 0.2611.)

α,α'-Di-n-*propylglutaric acid.* The triester was hydrolyzed by boiling over night with 10 % ethanolic potassium hydroxide. The ethanol was distilled off and the triacid precipitated in almost quantitative yield upon acidification with concentrated hydrochloric acid. A small amount was recrystallized from ethyl acetate-petroleum ether, m. p. 165—170° (decomp.) (Found: C 55.1; H 7.8. Calc. for $C_{12}H_{20}O_6$: C 55.4; H 7.8.)

The crude triacid was decarboxylated by heating to about 170° until the gas evolution ceased. The resulting product was separated into two forms by fractionated crystallization from a mixture of ethyl acetate and petroleum ether (1:4) giving a 33 % yield of the high-melting form, m. p. 110—112°, and a 19 % yield of the low-melting form, m. p. 81—82°. (Found for the high-melting form: C 61.1; H 9.3; equiv.wt. 107.8. Found for the low-melting form: C 61.0; H 9.3; equiv.wt. 108.6. Calc. for $C_{11}H_{20}O_4$: C 61.1; H 9.3; equiv.wt. 108.1.)

*1,3-Di*iso*propyl-1,1,3-tricarbethoxypropane (II, R = i-C_3H_7).* This compound was prepared as before from 0.2 mole of sodium in 20 ml of absolute ethanol and 100 ml of dry toluene (the toluene was added in order to raise the boiling point), 0.2 mole of diethyl *iso*propylmalonate, and 0.1 mole of methylene bromide. 13.5 g (39 %) of 1,3-di*iso*propyl-1,1,3-tricarbethoxypropane was obtained, b.p. 153—155°/4 mm, n_D^{20} 1.4462, d_4^{20} 1.0219. (Found: C 62.6; H 9.5; r_D 0.2627. Calc. for $C_{18}H_{32}O_6$: C 62.8; H 9.4; r_D 0.2611.) No attempt to isolate the diethyl carbonate formed was made as its boiling point differs too little from that of toluene.

*α,α'-Di*iso*propylglutaric acid.* The triester was hydrolyzed by boiling with 80 % sulphuric acid for 6 h. The yield of crude acid mixture was 94 %. The mixture was dissolved in benzene, treated with decolorizing carbon and allowed to cool. Crystals rich in the high-melting modification separated and were filtered off. From the mother liquor crystals rich in the low-melting form could be isolated. The final purification was performed by two crystallizations from hot water, the melting points of the pure acids being 140—141° and 118—119°, respectively. The yields were 40 and 23 %, respectively. (Found for the high-melting form: C 60.7; H 9.3; equiv.wt. 108.3. Found for the low-melting form: C 60.8; H 9.3; equiv.wt. 107.8. Calc. for $C_{11}H_{20}O_4$: C 61.1; H 9.3; equiv.wt. 108.1.)

1,3-Di-n-*butyl-1,1,3-tricarbethoxypropane (II, R = n-C_4H_9).* From 0.2 mole of sodium dissolved in 80 ml of absolute ethanol, 0.2 mole of diethyl *n*-butylmalonate, and 0.1 mole of methylene bromide were obtained 6.2 g (53 %) of diethyl carbonate and 27.5 g (74 %) of the triester, b.p. 180—182°/7 mm, n_D^{20} 1.4433, d_4^{20} 0.9936. (Found: C 64.3; H 9.6; r_D 0.2670. Calc. for $C_{20}H_{36}O_6$: C 64.5; H 9.7; r_D 0.2679.)

α,α'-Di-n-*butylglutaric acid.* The triester was hydrolyzed by boiling over night with 10 % ethanolic potassium hydroxide. The ethanol was distilled off and the triacid precipitated in quantitative yield upon acidification with concentrated hydrochloric acid. A small amount was recrystallized from ethyl acetate-petroleum ether, m. p. 155—160° (decomp.). (Found: C 58.3; H 8.5. Calc. for $C_{14}H_{24}O_6$: C 58.3; H 8.4.)

The crude triacid was decarboxylated by heating to about 170° until the gas evolution ceased. The product solidified upon standing and the solid was dissolved in petroleum ether. After cooling in an ice-bath the crystals were filtered. They consisted of almost pure high-melting form. Two further fractions of crystals rich in the high-melting form were collected. They were combined and recrystallized once from petroleum ether, giving a 41 % yield of the pure high-melting form, m. p. 92—93°. The mother liquor from the first filtration was evaporated and the residue left in a vacuum desiccator over night, whereby it solidified slowly. It could be recrystallized from petroleum ether if the solution was cooled to −50° and the crystals rapidly filtered, m. p. 53—56°, yield 21 %. Kögl and Erxleben [23] have prepared the *α,α'*-di-*n*-butylglutaric acids by the reaction between disodium 1,1,3,3-tetracarbethoxypropane and *n*-butyl iodide followed by hydrolysis of the tetraester and decarboxylation. They found the m.p.'s 95—96° and 53—56°, respectively.

*1,3-Di*iso*butyl-1,1,3-tricarbethoxypropane (II, R = i-C_4H_9).* From 0.2 mole of sodium dissolved in 80 ml of absolute ethanol, 0.2 mole of diethyl *iso*butylmalonate, and 0.1 mole of methylene bromide were obtained 4.2 g (34 %) of diethyl carbonate and 19.0 g (51 %) of the triester, b.p. 152—4°/1.5 mm, n_D^{20} 1.4428, d_4^{20} 0.9929. (Found: C 64.3; H 10.0; r_D 0.2669. Calc. for $C_{20}H_{36}O_6$: C 64.5; H 9.7; r_D 0.2679.)

*α,α'-Di*iso*butylglutaric acid.* The triester was hydrolyzed by boiling over night with 10 % ethanolic potassium hydroxide. The ethanol was distilled off and the triacid preci-

pitated with concentrated hydrochloric acid in quantitative yield. A small amount was recrystallized from ethyl acetate-petroleum ether, m. p. 165—170° (decomp.). (Found: C 58.3; H 8.4. Calc. for $C_{14}H_{24}O_6$: C 58.3; H 8.4.)

The crude triacid was decarboxylated by heating to about 170° until the gas evolution ceased. The product solidified upon cooling and could be separated into two forms by fractionated crystallization from petroleum ether as in the case of the *n*-butyl derivative. A 28 % yield of the high-melting form, m. p. 85—87°, and a 23 % yield of the low-melting one, m. p. 80—82° were obtained. The high-melting isomer was found to be monotropic and transformed to a stable crystalline modification at about 90°, which then melted at 101—102°. When the liquid was allowed to solidify above 90° the stable form crystallized, whereas solidification at temperatures below this point gave the unstable form with the m. p. 85—87°. (Found for the high-melting form: C 63.8; H 9.9; equiv.wt. 121.6. Found for the low-melting form: C 63.9; H 10.1; equiv.wt. 121.4. Calc. for $C_{13}H_{24}O_4$: C 63.9; H 9.9; equiv.wt. 122.1.)

*1,3-Di-*n*-amyl-1,1,3-tricarbethoxypropane (II, R = n-C_5H_{11}).* From 0.2 mole of sodium dissolved in 80 ml of absolute ethanol, 0.2 mole of diethyl *n*-amylmalonate, and 0.1 mole of methylene bromide were obtained 6.7 g (57 %) of diethyl carbonate and 31.0 g (77 %) of the triester, b.p. 168—171°/2 mm, n_D^{20} 1.4443, d_4^{20} 0.9797. (Found: C 65.7; H 10.0; r_D 0.2713. Calc. for $C_{22}H_{40}O_6$: C 65.9; H 10.1; r_D 0.2724.)

*α,α'-Di-*n*-amylglutaric acid.* The triester was boiled over night with 10 % ethanolic potassium hydroxide. The ethanol was distilled off, and the triacid precipitated in quantitative yield with hydrochloric acid. A small amount was recrystallized from ethyl acetate-petroleum ether, m. p. 140—142°. (Found: C 60.5; H 8.9. Calc. for $C_{16}H_{28}O_6$: C 60.7; H 8.9.)

The crude acid was decarboxylated by heating to 170° until the gas evolution ceased, and the acid mixture was dissolved in petroleum ether, filtered, and allowed to cool. The crystals were filtered, and the mother liquor was evaporated to half its volume. A further fraction of crystals was obtained which was combined with the first one and recrystallized from petroleum ether, m. p. 113—5°. After evaporation of the mother liquor from the second filtration an oil was obtained, which turned to a semisolid mass upon standing. Attempts to isolate the other form from this were not successful, owing to its very poor crystallizing properties and great solubility in the common solvents. The yield of the isomer with m.p. 113—115° was 43 %. (Found for the isomer with m. p. 113—115°: C 66.1; H 10.3; equiv.wt. 136.7. Calc. for $C_{15}H_{28}O_4$: C 66.1; H 10.4; equiv.wt. 136.2.)

*Diethyl bromomethyl-*n*-amylmalonate.* This compound was prepared as above from 23.0 g of 20 % sodium dispersion in 100 ml of dry toluene, 0.2 mole of diethyl *n*-amyl malonate, and 0.4 mole of methylene bromide. 34.0 g (53 %) of the bromo compound was obtained, b. p. 132—133°/3 mm, n_D^{20} 1.4534, d_4^{20} 1.1831. (Found: C 49.0; H 7.5; Br 24.2; r_D 0.2286. Calc. for $C_{13}H_{23}O_4Br$: C 48.3; H 7.2; Br 24.7; r_D 0.2270.)

*Ethyl α-*neo*pentylacrylate.* When 0.2 mole of sodium dissolved in 80 ml of absolute ethanol, 0.2 mole of diethyl *neo*pentylmalonate * and 0.1 mole of methylene bromide was boiled for 24 h and the reaction mixture worked up in the usual manner the only isolable product except recovered starting material was 12.0 g (71 %) of ethyl *α-neo*pentylacrylate, b.p. 68—70°/11 mm, n_D^{20} 1.4273, d_4^{20} 0.8806. (Found: C 69.8; H 10.7; r_D 0.2917. Calc. for $C_{10}H_{18}O_2$: C 70.5; H 10.7; r_D 0.2915.) The ester was hydrolyzed by boiling with 10 % ethanolic potassium hydroxide. The ethanol was evaporated and the acid precipitated by hydrochloric acid. It soon solidified and was filtered and finally recrystallized from dilute acetic acid, m. p. 43—44°. The *p*-bromophenacyl ester had m. p. 53—55°. Hadley *et al.*[8] reported for the acid m. p. 39° and for its *p*-bromophenacyl ester 56°.

An attempt to carry out the reaction at 160° in a steel bomb gave the same result.

*Diethyl bromomethyl-*neo*pentylmalonate.* This compound was prepared as above from 23.0 g of 20 % sodium-toluene dispersion in 100 ml of dry toluene, 0.2 mole of diethyl *neo*pentylmalonate, and 0.4 mole of methylene bromide. 24.0 g (37 %) of the bromo compound was obtained, b.p. 147—150°/13 mm, n_D^{20} 1.4588, d_4^{20} 1.2035. (Found: C 48.5; H 7.1; Br 24.4; r_D 0.2271. Calc. for $C_{13}H_{23}O_4Br$: C 48.3; H 7.2; Br 24.7; r_D 0.2270.)

---

* The author is indebted to docent A. Brändström, *AB Pharmacia*, Uppsala, for this material.

Diethyl α,α'-diphenylglutarate (IV, R' = C_6H_5). This compound was prepared as above from 0.2 mole of sodium dissolved in 80 ml of absolute ethanol, 0.2 mole of diethyl phenylmalonate, and 0.1 mole of methylene bromide. 19.0 g (80 %) of diethyl carbonate and 21.5 g (63 %) of very viscous diethyl αα'-diphenylglutarate, b. p. 183–184°/1 mm, n_D^{20} 1.5274, was obtained. Souther [7] reported b.p. 216–217°/7 mm.

α,α'-Diphenylglutaric acid. The diethyl ester was hydrolyzed by boiling with 10 % ethanolic potassium hydroxide for one hour, and the acid mixture obtained was separated into diastereoisomers by fractionated crystallization from benzene. The melting points and yields of the pure acids were 187–188° (40 %) and 159–160° (22 %), respectively. Souther [7] reported the melting points 185–186.5° and 164.5–165.5°.

1,3-Dibenzyl-1,1,3-tricarbethoxypropane (II, R = $C_6H_5CH_2$). From 0.2 mole of sodium in 80 ml of ethanol, 0.2 mole of diethyl benzylmalonate, and 0.1 mole of methylene bromide were obtained 5.8 g (49 %) of diethyl carbonate and 34.0 g (77 %) of the very viscous triester, b.p. 224–227°/2 mm, n_D^{20} 1.5176. (Found: C 70.7; H 7.4. Calc. for $C_{36}H_{32}O_6$: C 70.9; H 7.3.)

The reaction was also carried out with methylene iodide whereby a 72 % yield of the triester was obtained.

α,α'-Dibenzylglutaric acid. The triester was hydrolyzed by boiling over night with 10 % ethanolic potassium hydroxide. The ethanol was distilled off and the acid precipitated by hydrochloric acid in quantitative yield. A small amount was recrystallized from ethyl acetate-petroleum ether, m. p. 155–160° (decomp.). (Found: C 67.4; H 5.7. Calc. for $C_{20}H_{20}O_6$: C 67.3; H 5.7.)

The crude acid was decarboxylated by heating to 170° until the gas evolution ceased, and the acid mixture was dissolved in benzene, filtered, and allowed to cool. The crystals were filtered off and from the mother liquor one further fraction with about the same melting point was obtained. The combined fractions were recrystallized two times from 80 % acetic acid, m. p. 149–150°. The mother liquor from the second filtration was evaporated. The residue was a crystal mass with m. p. 120–140°. In spite of many recrystallizations from various solvents and solvent pairs no sharply melting isomer could be obtained from this. (Found for the isomer with m. p. 149–150°: C 72.8; H 6.5; equiv.wt. 155.3. Found for the crystals with m. p. 120–140°: C 72.9; H 6.5; equiv.wt. 156.0. Calc. for $C_{19}H_{20}O_4$: C 73.1; H 6.5; equiv.wt. 156.2.)

Reaction between tricarbethoxymethane and methylene bromide. From 0.2 mole of sodium dissolved in 80 ml of absolute ethanol, 0.2 mole of tricarbethoxymethane, and 0.1 mole of methylene bromide 12.2 g (52 %) of diethyl carbonate and 18.3 g (55 %) of 1,1,3,3-tetracarbethoxypropane, b.p. 189–191°/11 mm were obtained.

α,α'-Diaminoglutaric acid. 0.2 mole of sodium was dissolved in 150 ml of absolute ethanol, 0.2 mole of diethyl acetaminomalonate was added followed by 0.1 mole of methylene bromide. The reaction mixture was boiled for 36 h, filtered and the ethanol distilled off on the water-bath through a short column. Then the pressure was lowered to about 60 mm Hg and a small amount, 2.1 g (18 %), of diethyl carbonate was collected. The residue, which was contaminated with unreacted starting material and sodium bromide, was hydrolyzed directly according to the method of Hellman *et al.* The yield of pure α,α'-diaminoglutaric acid was 3.6 g (23 %). It darkens and decomposes at 270–280°.

The author wishes to express his sincere gratitude to Professor Erik Larsson for his kind interest in this work. A grant from the *Kungliga Fysiografiska Sällskapet* is gratefully acknowledged.

REFERENCES

1. Eberson, L. *Acta Chem. Scand.* **9** (1955) 1711.
2. Guthzeit, M. and Dressel, O. *Ber.* **21** (1888) 2233.
3. Guthzeit, M. and Dressel, O. *Ann.* **256** (1890) 171.
4. Bischoff, C. A. *Ber.* **23** (1890) 1464.
5. Auwers, K. and Thorpe, J. F. *Ann.* **285** (1895) 310.
6. Hellman, H., Lingens, F. and Folz, E. *Chem. Ber.* **89** (1956) 2433.
7. Souther, B. L. *J. Am. Chem. Soc.* **46** (1924) 1301.
8. Hadley, D. J., Hall, R. H., Heap, R. and Jacobs, D. I. H. *J. Chem. Soc.* **1954** 1416.
9. Wislicenus, W. and Goldstein, K. *Ber.* **28** (1895) 815.

10. Cope, A. C. and McElvain, S. M. *J. Am. Chem. Soc.* **54** (1932) 4319.
11. Connor, R. *J. Am. Chem. Soc.* **55** (1933) 4597.
12. Boyd, R. N. and Kelly, R. J. *J. Am. Chem. Soc.* **74** (1952) 4600.
13. Cope, A. C. and McElvain, S. M. *J. Am. Chem. Soc.* **54** (1932) 4311.
14. v. Richter, V. *Ber.* **21** (1888) 2470.
15. Ingold, C. K. and Thorpe, J. F. *J. Chem. Soc.* **115** (1919) 143.
16. Bowman, N. S. and Rexford, D. R. *J. Org. Chem.* **19** (1954) 1219.
17. Auwers, K. and Köbner, E. *Ber.* **24** (1891) 1923.
18. Hoch, D. and Karrer, P. *Helv. Chim. Acta* **37** (1954) 397.
19. Ruhl, K. *Z. Naturforsch.* **4 b** (1949) 199.
20. Möller, E. *Kgl. Fysiograf. Sällskap. Lund, Förh.* **30** (1918) Nr 6.
21. Berner, E. and Landmark, L. H. *Acta Chem. Scand.* **7** (1953) 1347.
22. Kötz, A. and Zörnig, W. *J. prakt. Chem.* **74** (1906) 425.
23. Kögl, F., Erxleben, H., Michaelis, R. and Visser, H. S. *Hoppe-Seyler's Z. physiol. Chem.* **235** (1935) 181.

Received November 8, 1957.

ACTA CHEMICA SCANDINAVICA 12 (1958) 324—331

Kinetics of the Hydrolytic Cleavage of Organic Protolytes

BERTIL HANSEN

Research Institute of National Defence, Dept. 1, Sundbyberg 4, Sweden

A method for the investigation of the hydrolytic cleavage of organic protolytes is described. It is based on automatic titrations at constant pH. The mathematical treatment is given. By using a "curve fitting" method the reaction rate constants of the basic and acidic forms of the protolyte and its dissociation constant can be calculated. The method is tested with the hydrobromide of 2-dimethylaminoethyl-thiolopropionate.

The most common method for measuring the alkaline hydrolysis of a compound is to dissolve the compound in excess alkali and then after different long times titrate the alkali not used up in the reaction. In another well-known method the reaction takes place in a buffer solution with the pH remaining almost constant. The reaction can be followed in various ways, *e.g.* by taking optical measurements of the concentration of one of the reaction products as a function of time.

When the compound to be hydrolyzed is a protolyte as, for instance, an ester of an amino acid or a mono ester of a di-basic acid, the composition of the reaction mixture becomes rather complicated. Because of protolysis the compound may exist simultaneously in both acidic and basic forms which react with different rates. For the determination of the corresponding rate constants it is important to know the dissociation constant of the compound. But if the reactions not are so slow that they can be neglected in the buffer zone of the compound, it will be difficult or even impossible to measure the dissociation constant by common methods. This means that we may have three constants which must be regarded as unknowns in all calculations. If the first of the two experimental methods mentioned above is used, the mathematical treatment will be very laborious. When choosing the buffer method the theoretical treatment becomes rather simple, if it is valid to assume that the ions of the solution do not affect the reactions. Unfortunately this is seldom true.[1,2]

This paper describes how the hydrolysis of a protolyte can be investigated according to a method which does not seem to have been used before. It is based on an automatic titration of the reaction mixture so that the pH is

maintained constant.[3] During the reaction the consumption of titrant is recorded, and the curve so obtained is used for the calculation of the reaction velocity. The reaction is carried out at several pH-values, and the resulting rate constants are plotted in a diagram. By comparing this (Fig. 1) with a family of standard curves (Fig. 2) it is possible to find the velocity constants of the hydrolysis of the two forms of the protolyte as well as its dissociation constant. The method is very similar to the buffer method but has the advantage of no complicated effects due to the ions of the solution.

THEORY

A mathematical expression of the alkaline hydrolysis of a protolyte is deduced on the following assumptions.

1) The hydrogen ion activity is constant during the whole reaction.

2) All experiments are carried out at the same temperature.

3) For each of the acidic and basic forms of the compound the reactions with molecules and ions other than the hydroxyl ion can be neglected. That means that there are only two reactions running in parallel, and both are of the second order.

4) The ionic strength is the same in all experiments, and during the reaction it changes only slightly. For that reason the activity factors according to the Debye-Hückel theory can be regarded as constants.

The deduction here is carried out for an ester containing an amino group in its alcohol part, because an ester of this kind was used in the experiments described later in the paper. The result can, however, easily be applied to other classes of compounds.

Symbols

E and EH^+	= ester to be hydrolyzed
HA and A^-	= acid formed in the reaction
B and BH^+	= alcohol formed in the reaction
[E]	= concentration of E
[EHE]	= total concentration of ester
h	= activity of the hydrogen ions
oh	= activity of the hydroxyl ions
k_1 and k_2	= second order reaction constants for the hydrolysis of E and EH^+ resp.
K_E', K_A' and K_B'	= mixed acid dissociation constants of E, HA and B resp. at the actual temperature and ionic strength.
K_w	= thermodynamic ionic product of water.
t	= time
f	= activity factor
C	= integration constant
x and y	= coordinates of the family of standard curves
u and v	= coordinates of the experimental curve
p	= parameter
hydr (as index)	= due to hydrolysis
prot (as index)	= due to protolysis

The protolytic equilibria of the solution are

$$E + H^+ \rightleftharpoons EH^+ \quad (1) \qquad A^- + H^+ \rightleftharpoons HA \quad (2)$$
$$B + H^+ \rightleftharpoons BH^+ \quad (3) \qquad H^+ + OH^- \rightleftharpoons H_2O \quad (4)$$

They are determined by the equations

$$\frac{[E]\cdot h}{[EH^+]} = K'_E \quad (5) \qquad \frac{[A^-]\cdot h}{[HA]} = K'_A \quad (6)$$
$$\frac{[B]\cdot h}{[BH^+]} = K'_B \quad (7) \qquad h \cdot oh = K_w \quad (8)$$

The reactions between the hydroxyl ions and E and EH^+ may be written

$$E + OH^- \xrightarrow{k_1} A^- + B \quad (9)$$
$$EH^+ + OH^- \xrightarrow{k_2} A^- + BH^+ \quad (10)$$

These reactions must be followed by immediate changes in the equilibria (1)—(4).

When differentiating the expression for the total concentration of the ester

$$[EHE] = [E] + [EH^+] \quad (11)$$

we get

$$d[EHE] = d[E] + d[EH^+] \quad (12)$$

The changes of [E] and $[EH^+]$ are due partly to the reactions (9) and (10) and partly to the changes in the equilibrium (1). We may then write

$$d[E] = d[E]_{hydr} + d[E]_{prot} \quad (13)$$
$$d[EH^+] = d[EH^+]_{hydr} + d[EH^+]_{prot} \quad (14)$$

The protolytic change (1) gives

$$d[E]_{prot} = -d[EH^+]_{prot} \quad (15)$$

If we now add up (12)—(15) we see that

$$d[EHE] = d[E]_{hydr} + d[EH^+]_{hydr} \quad (16)$$

The hydrolysis reactions (9) and (10) give us the following differential equations

$$-d[E]_{hydr} = k_1 \cdot [E] \cdot [OH^-] \cdot dt \quad (17)$$
$$-d[EH^+]_{hydr} = k_2 \cdot [EH^+] \cdot [OH^-] \cdot dt \quad (18)$$

According to assumption 1 (p. 325)

$$h = \text{constant} \quad (19)$$

and eqn. (5) written

$$[E] \cdot \frac{h}{K'_E} = [EH^+] \quad (20)$$

then shows that [E] is directly proportional to $[EH^+]$ independently of (9) and (10).

Using (20) when combining (16)—(18) we get

$$-\mathrm{d[EHE]} = (k_1 + k_2 \cdot \frac{h}{K'_E}) \cdot [\mathrm{E}] \cdot [\mathrm{OH^-}] \cdot \mathrm{d}t \tag{21}$$

According to (11) and (20)

$$[\mathrm{E}] = \frac{[\mathrm{EHE}]}{1 + \frac{h}{K'_E}} \tag{22}$$

and consequently

$$-\mathrm{d[EHE]} = \frac{k_1 + k_2 \cdot \frac{h}{K'_E}}{1 + \frac{h}{K'_E}} [\mathrm{EHE}] \cdot [\mathrm{OH^-}] \cdot \mathrm{d}t = k_3 \cdot [\mathrm{EHE}] \cdot [\mathrm{OH^-}] \cdot \mathrm{d}t \tag{23}$$

where

$$k_3 = \frac{k_1 + k_2 \cdot \frac{h}{K'_E}}{1 + \frac{h}{K'_E}} \tag{24}$$

Because of assumption 4 (p. 325) and the eqns. (8) and (19) we have

$$[\mathrm{OH^-}] = \frac{oh}{f_{\mathrm{OH^-}}} = \text{constant} \tag{25}$$

The only variables of (23) are consequently [EHE] and t. The integration of (23) gives

$$\ln[\mathrm{EHE}] = -k_3 \cdot [\mathrm{OH^-}] \cdot t + C \tag{26}$$

We see that the hydrolysis can be treated as a reaction of the first order, and the rate constant $k_3 \cdot [\mathrm{OH^-}]$ contains the three unknowns k_1, k_2 and K'_E.

If k_3 is determined at three different h-values and the obtained sets of values, (h_a,k_{3a}), (h_b,k_{3b}) and (h_c,k_{3c}), are inserted into (24), we get an equation system which has solutions with respect to k_1, k_2 and K'_E. However, the expressions obtained have no practical interest because they consist mainly of a large number of differences, which, as a rule, are small and so give rise to large errors in the calculated constants, *e.g.*

$$k_1 = \frac{h_a h_b k_{3c}(k_{3a}-k_{3b}) + h_b h_c k_{3a}(k_{3b}-k_{3c}) + h_c h_a k_{3b}(k_{3c}-k_{3a})}{h_a h_b\ (k_{3a}-k_{3b}) + h_b h_c\ (k_{3b}-k_{3c}) + h_c h_a\ (k_{3c}-k_{3a})}$$

In his paper on graphical methods Sillén [4] emphasizes the usefulness of "curve fitting methods" for determination of, *e.g.*, equilibrium constants, when the direct calculations give unsatisfactory accuracy. Such a method has for that reason been developed for the determination of k_1, k_2 and K'_E from the sets of values $(h,\ k_3 \cdot [\mathrm{OH^-}])$ obtained from the experiments.

Let us start by looking for a suitable family of standard curves with which an experimental curve can be compared. We shall find that a useful family is obtained from the equation

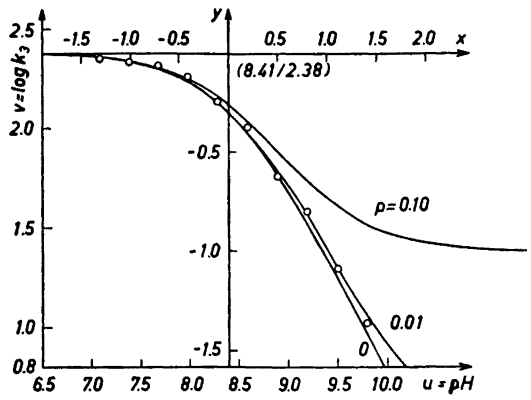

Fig. 1. The experimental values plotted in the family of curves for $u_0 = 8.41$, $v_0 = 2.38$.

$$y = \log \frac{p + 10^{-x}}{1 + 10^{-x}} \tag{28}$$

by plotting the function in an (x,y)-diagram for certain values of p (Fig. 2). After substituting

$$\begin{cases} u = \text{pH} = -\log\ h \\ v = \log\ k_3 \end{cases} \tag{29}$$

into (24) we get

$$v = \log\ k_2 + \log \frac{\frac{k_1}{k_2} + \frac{10^{-u}}{K'_E}}{1 + \frac{10^{-u}}{K'_E}} \tag{30}$$

The family of (u,v)-curves that can be obtained by giving different values to k_1/k_2 in (30) is the same as the family from (28) except that the origins do not coincide.

Let us now use the experimental values of h and k_3 for plotting an (u,v)-diagram (Fig. 1). When comparing the family (28) and the experimental curve (Fig. 1), we see that, for parallel abscissae, the best fit gives a value $p = p_0$. As the shapes of the curves are dependent only on p_0 and k_1/k_2, respectively, these values must be equal

$$p_0 = \frac{k_1}{k_2} \tag{31}$$

The curves are brought to cover each other, and the coordinates (u_0,v_0) of the origin of the (x,y)-system are read off.
As $x = 0$ must correspond to

$$\frac{10^{-u_0}}{K'_E} = 1 \tag{32}$$

in (30), and $y = 0$ to

$$v_0 = \log\ k_2 \tag{33}$$

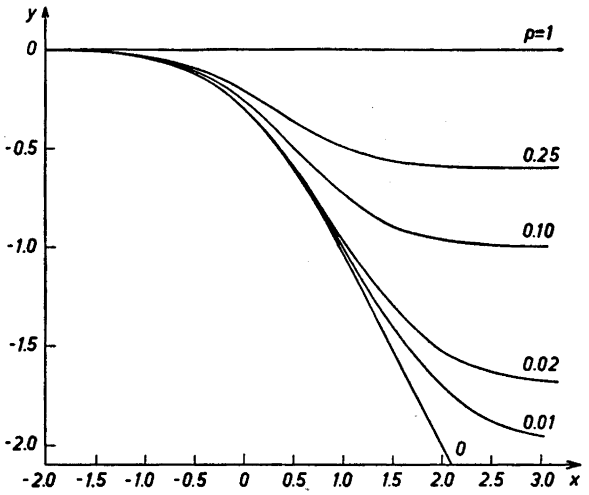

Fig. 2. Some standard curves of the family.

we have obtained three equations (31)—(33) from which k_1, k_2 and K'_E can be calculated.

It is worth mentioning that the family of standard curves can be restricted to values of p in the interval $0 \leqq p \leqq 1$. For $p > 1$ we make the following rearrangement of (28)

$$\begin{cases} x = -x' \\ y = y' - \log\ p' \\ p = 1/p' \end{cases} \tag{34}$$

which gives

$$y' = \log \frac{p' + 10^{-x'}}{1 + 10^{-x'}} \tag{35}$$

We see that (28) and (35) are the same equation, and as $p' = 1/p'$ the family of curves made up for $0 \leqq p \leqq 1$ also can be used for $p > 1$.

This division of the family into two classes requires that, before comparing the curves, we have to find out to which of the classes the experimental curve belongs.

1. If v decreases with increasing u it means that $0 \leqq p \leqq 1$ and we can compare the curves directly and read off the values p_0, u_0 and v_0.

2. If v increases with increasing u we have the case $p > 1$ and must first make the rearrangement of (29)

$$\begin{cases} u = -u' \\ v = v' \end{cases} \tag{36}$$

i.e. we reverse the paper on which the experimental curve is drawn. It is then possible to compare the curves and read off the values p'_0, u'_0 and v'_0. Remembering that (u'_0, v'_0) does not correspond to $x = 0$, $y = 0$ but to $x' = 0$, $y' = 0$, we can calculate k_1, k_2 and K'_E from eqns. (31)—(34) and (36).

EXPERIMENTAL

The hydrolysis experiments have been carried out with the hydrobromide of 2-dimethylaminoethyl-thiolopropionate[5,6] by using the automatic recording titrator described by Larsson and Hansen.[3] The reactions took place in a nitrogen atmosphere at 25° ± 0.1°. From the recorded consumptions of 0.05 M sodium hydroxide the first order rate constants $k_3 \cdot [OH^-]$ were calculated according to Guggenheim.[7]

Assumption 4 (p. 325) was considered fulfilled by performing the reaction in 0.1 M potassium chloride and starting with 0.6 mM concentration of the ester.

The glass electrode used was of the type Radiometer G 202 B and the reference electrode a saturated calomel electrode, Radiometer K 300. The electrodes were standardized against 0.05 M potassium hydrogen *o*-phthalate, pH 4.01. The pH-fluctuations during a single experiment were within ± 0.01 pH-units.

RESULTS

Though many of the experiments were carried out in the pH-range where both the 2-dimethylaminoethyl-thiolopropionate and the reaction product containing the amino group have a good buffering effect the curves plotted for the calculations of $k_3 \cdot [OH^-]$ (eqn. (26)) were straight lines. This shows that the reaction really is first order at constant pH.

As a rule two or more experiments were carried out at each pH. The deviations from the mean values of $k_3 \cdot [OH^-]$ were always less than 5 %, which if they would be due only to the readings of the of the pH-scale corresponds to the acceptable error of 0.02 pH-units or 1 mV.

In Fig. 1 the result was plotted according to (29) with pH on the abscissa and log k_3 on the ordinate. $[OH^-]$, which is required for the calculations of k_3 from $k_3 \cdot [OH^-]$, was obtained from pH assuming [8] $K_w = 10^{-14.00}$ and $f_{OH^-} = 0.76$ (eqn. (25)). As the plotted curve had a negative slope it was immediately comparable with the family of curves (Fig. 2). The comparison showed (Fig. 1) that we had the best fit for a small value of p. The exact p_0-value could not be determined because for practical reasons it was impossible to perform any experiments at pH > 10 and so the curve could not be extended far enough to the right. However, the values $u_0 = 8.41 \pm 0.01$ and $v_0 = 2.38 \pm 0.01$ could be read off. The errors given were estimated from the largest movements of the curves that could be done without getting an unacceptable fit. To the errors must also be added the systematic error 0.02 which was the accuracy of the pH-meter. The calculations of K_E' and k_2 (eqns. (31)—(33)) gave $K_E' = (3.9 \pm 0.3) \times 10^{-9}$ mole/l and $k_2 = (2.4 \pm 0.2) \times 10^2$ l/mole · sec. Regarding k_1 we can only say that $k_1 << k_2$ because it was impossible to find a p_0-value.

Estimating [8] $f_{EH^+} = 0.76$ we can calculate the thermodynamic dissociation constant of the ester $pK_E = 8.29 \pm 0.03$. From pH-measurements of mixtures of aqueous solutions of 2-dimethylaminoethyl-thiolopropionate and its hydrobromide Tammelin [5] found $pK_E = 8.28 \pm 0.03$ which agrees with the value above.

It is very interesting to compare the velocity constant of the alkaline hydrolysis of the acidic form of 2-dimethylaminoethyl-thiolopropionate (I)

and that of the corresponding quaternary compound, propionyl-thiocholine (II), which has been investigated by Heilbronn [9].

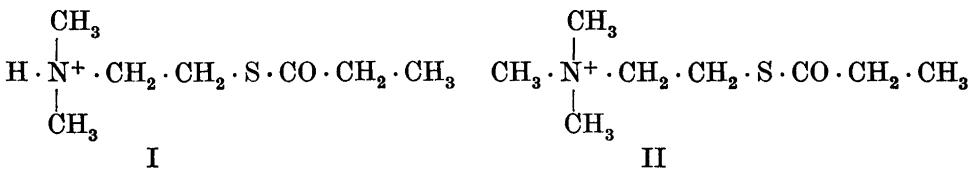

I II

Though both I and II have a positively charged ammonium group the second order rate constant of I is 240 times greater than that of II. The experimental material is, however, insufficient to be used for an explanation of the difference.

To Professor G. Ljunggren, the head of this Institute, I wish to express my gratitude for his interest in this work.

REFERENCES

1. Frost, A. A. and Pearson, R. G. *Kinetics and Mechanism*, John Wiley & Sons, Inc., New York 1956, p. 138.
2. Glasstone, S., Laidler, K. J. and Eyring, H. *The Theory of Rate Processes*, McGraw-Hill Book Company Inc., New York 1941, p. 427.
3. Larsson, L. and Hansen, B. *Svensk Kem. Tidskr.* **68** (1956) 521.
4. Sillén, L. G. *Acta Chem. Scand.* **10** (1956) 186.
5. Tammelin, L.-E. *Acta Chem. Scand.* **11** (1957) 487.
6. Hansen, B. *Acta Chem. Scand.* **11** (1957) 537.
7. Guggenheim, E. A. *Phil.mag.* **2** (1926) 538.
8. Bates, R. G. *Electrometric pH determinations*, John Wiley & Sons, Inc., New York 1952, p. 52.
9. Heilbronn, E. *Personal communication.*

Received November 12, 1957.

ACTA CHEMICA SCANDINAVICA 12 (1958) 332—339

Radiation Induced Tritium Labeling of *p*-Aminosalicylic Acid (PAS)

JAN RYDBERG and ÅKE HANNGREN

Research Institute of National Defence, Dept. 1, Sundbyberg 4, Sweden; Medical Clinic, Serafimer Hospital, and Pharm. Dept., Royal Veterinary College, Stockholm, Sweden

Wilzbach's [1] method of mixing tritium gas with organic substances for labeling them with tritium was used to introduce tritium into *p*-aminosalicylic acid (H—PAS) and its sodium salt (Na—PAS) and the specific activity was studied as a function of time and agitation. Higher activities were obtained with Na—PAS and with agitation than with H—PAS or without agitation. The results are summarized in Fig. 3. Specific activities of the order of 30 mC/g could be obtained in a day.

In the last few years a number of methods have been described for the direct labeling of organic substances by exposing them to radioactive isotopes of high kinetic energy *e.g.* [2-11]. This makes it possible to label substances which previously have been found difficult or impossible to label by other methods as, *e.g.*, chemical synthesis, biosynthesis or isotopic exchange. To this group of substances belongs a great number of complicated organic molecules of biochemical importance. Since the labeling by this direct method is non-specific (a great number of other labeled organic compounds are also formed), the methods for isolating the desired product in pure form are of fundamental importance, and generally constitute the most difficult part of the process. However, very elaborate and selective purification methods are now available as *e.g.* various chromatographic methods.

An important addition to the methods of direct labeling was recently reported by Wilzbach [1] who found that if organic compounds are exposed to tritium gas, some of the hydrogen in the compounds is exchanged for tritium.

This exchange is induced by the β-radiation from the tritium. Some of these reactions may be written

$$T_2 \sim\sim\rightarrow T + T \qquad 1\,a$$
$$RH \sim\sim\rightarrow R + H \qquad 1\,b$$
$$R + T_2 \rightarrow RT + T \qquad 1\,c$$
$$R + T \rightarrow RT \qquad 1\,d$$
$$RH + T \rightarrow RT + H \qquad 1\,e,$$

where RH is the organic compound being irradiated.

The first two reactions indicate how radicals are produced by the β-radiation field. The following reactions show how these radicals may react to form the labeled compound RT; of these reactions, (1d) is least probable. The last reaction can also be regarded as a formation of RT through isotopic exchange. Ions (*e.g.* T^+, T^-, R^-) may be formed in a similar manner, and these ions may also react with each other or with the radicals to form RT. The radiation field is fairly intense and amounts, for 1 Curie of T_2-gas, to about 10^6 rad/min in the volume of the pure gas; the radiation absorbed by solid or liquid samples depends somewhat on the experimental conditions, but may well amount to 10^5 rad/min.

This kind of labeling may not necessarily be induced by the radiation from tritium: It seems quite possible to use radiation from other sources, such as from the decay of other isotopes * or from high-voltage accelerators.

For autoradiographic studies of the pharmacological properties of the tuberculostatic agent *p*-aminosalicylic acid (PAS) [12], tritium labeled PAS was needed. In a previous paper [10], the labeling of PAS with recoil tritons has been reported; however, only low specific activities (~1.5 mC/g) were obtained. In order to obtain higher specific activities, the method of using tritium gas for the labeling of PAS has been investigated. The results are reported in this paper.

EXPERIMENTAL

Apparatus. The apparatus used is shown in Fig. 1. It consists in principle of two vessels, one for the tritium stock (F) and one for the sample to be exposed (A), and a gas-pumping mechanism. The apparatus, which is very compact, is made entirely of glass. It is operated in the following manner:

After the whole system has been evacuated, stop-cock J is connected only to vessel E, and K is closed. The tritium ampoule, F, is then broken by the magnet, and the T_2 gas is allowed to distribute itself through stop-cock D into vessel E. Stop-cock D is then switched over so that A and E are connected through stop-cock B. Air is then let into vessel L *via* stop-cock K, and the mercury level in E is allowed to reach just below stop-cock D, which is then closed. In this manner about 55 % of the T_2 originally present in F is introduced into the reaction vessel A.

If it is desired to remove the reaction vessel from the apparatus, stop-cock B is closed, and the T_2 gas in the volume between B and E is pumped out and transported back to F by repeatedly lowering the mercury level in E when C and E are connected, and raising the level when E and F are connected. This pumping action is effected by turning stop-cock K so that air is either let in or removed from vessel L. Part A—B can then be removed after D has been closed.

When parts A and B are removed from the rest of the apparatus, part C becomes filled with air. This air has to be removed before the tritium gas in volume A—B can be recovered so that the tritium gas will not be diluted with air. This air is therefore removed by the vacuum pump through D—E—J—K; since some T_2 is always left in the hole in stop-cock D, it will be lost during the evacuation process. The amount of this loss is 2—3 % of the total amount T_2 in vessel F. Thus, in about 20 experiments, 50 % of the T_2 has been lost in this way. Corrections (factor f_p) for this successive decrease of the T_2-amount are made in the experiments recorded later.

Labeling experiments. The amount of PAS used in the labeling experiments was varied between 30 and 100 mg. The tritium gas was purchased from AERE, Harwell, and contained 98.8 wt % of T_2, the rest being H_2. The amount of tritium gas in the reaction vessel was at maximum about 2.6 curies at a pressure of about 240 mm Hg, and at minimum about 1.6 curies. All experiments were carried out at room temperature (20 ± 2°C).

* This has recently been shown by Turton, C. N. *Intern. J. of Appl. Radiation and Isotopes* **2** (1957) 182, who used the radiation from ^{85}Kr to improve labeling with ^{14}C in organic compounds.

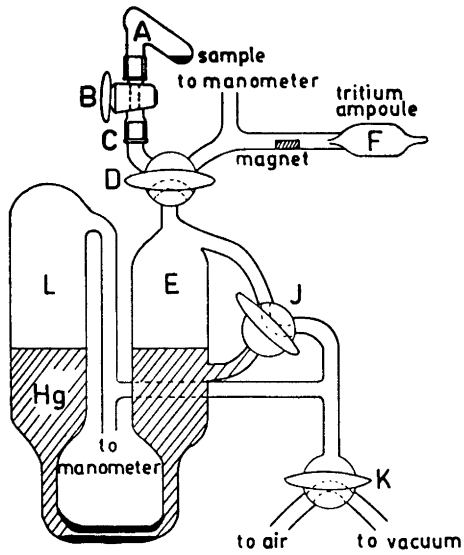

Fig. 1. Apparatus used for the exposure of organic samples to tritium gas.

Chemical procedures. *p*-Aminosalicylic acid (H—PAS, which looks somewhat similar to fineground corn meal) and sodium *p*-aminosalicylate (Na—PAS, which consists of mm-sized crystal needles) of highest commercial purity were used; the products were kindly supplied by AB Ferrosan, Malmö. In order to purify the H—PAS, which has a somewhat greyish color, the same purification procedure was used as described below for the tritiated product. All other chemicals were of analytical grade.

As the primary purification method liquid-liquid extraction was chosen. This method is very suitable for large amounts of samples and the fundamental laws governing the extraction processes are well known, *cf. e.g.* Ref.[13]

The tritiated PAS-sample was dissolved in a mixture of equal volumes of amyl alcohol and 0.1 M $NaHCO_3$ in water (about 10 ml for each 100 mg PAS). Under these circumstances about 95 % of the PAS goes into the aqueous phase. This aqueous phase was then washed 5 times with equal volumes of amyl alcohol. The aqueous phase was then cooled with ice and acidified with HCl to pH ~3; after about one hour PAS—HCl has precipitated and can be filtered off.

This PAS—HCl is put into 1 mM HCl, and the resulting aqueous solution is extracted with an equal volume of amyl alcohol. About 97 % of the PAS now moves over to the organic phase, from which it can be recovered by careful evaporation.

The chemical yields of a great number of such runs have been 50—70 %. The tritium yield, *i. e.* the ratio between non-labile tritium found in the purified PAS product and the total tritium content found in evaporated samples of the crude product dissolved in amyl alcohol, was found to be around 20 %.

The purity of the product was checked by paper chromatography, as described in a previous paper [10], in which the principle of the purification method is more extensively treated.

Tritium measurements. All radioactivity measurements were made on solid samples in a 2 π internal gas-flow proportional counter (Nuclear Measurements Corp., Indianapolis). Corrections for resolving time could be neglected at counting rates $\lesssim$5 000 counts per sec.

The samples were prepared by dissolving a weighed amount of purified, tritiated PAS in a known volume of ethyl alcohol, and carefully evaporating 0.1 ml on flat plates heated to 55°C, *cf.* Ref.[14]

Table 1. Results of tritiating experiments and calculations of specific activity ($f_b = 1.14$ except otherwise stated; f_s is taken from Fig. 2).

Conditions	Sample weight, mg	Reaction time, h	Purified product		f_p	S, mC/g
			μg	cpm		
H–PAS, static runs, symbol ○ in Fig. 3	100	1	12.3	1 740	0.94	0.15
	100	1	10.0	1 080	0.69	0.15
	99	1	11.2	1 905	1.00	0.15
	104	3	13.2	4 350	0.91	0.38
	100	6	12.2	4 270	0.75	0.49
	104	24	12.6	17 600	0.97	1.43 [1]
			10.0	13 700	0.97	1.35 [1]
	100	24	8.7	9 800	0.73	1.39
	100	48	13.5	58 060	1.00	4.1 [2]
	101	165	11.6	121 860	0.77	14
H–PAS, static runs, symbol △ in Fig. 3	31	1	10.4	4 100	0.88	0.45
	36	3	11.5	12 430	0.79	1.05 [3]
	32	24	10.0	34 390	0.82	4.1
	31	45	11.8	71 800	0.85	7.2
H–PAS, agitation runs, symbol □ in Fig. 3	102	1	10.2	9 110	0.65	0.14 [4]
	100	4	11.0	14 200	0.71	1.8 [5]
	100	24	10.0	8 600	0.63	1.34 [4]
	100	26	12.0	9 910	0.61	1.41 [4]
Na–PAS, static runs, symbol ● in Fig. 3	100	1	11.1	2 425	0.79	0.28
	100	6	10.0	5 420	0.77	0.70
	100	19	9.9	21 160	0.85	2.5
	107	95	11.8	102 980	0.88	10.1
Na-PAS, agitation runs, symbol ■ in Fig. 3	95	1	11.6	6 950	0.59	1.09
	96	1	11.2	15 510	1.03	1.36
	98	2.5	11.0	35 710	0.94	3.5
	100	19	11.2	212 610	0.91	21

[1] Double samples from same PAS-product.
[2] $f_b = 1.24$.
[3] $f_b = 1.50$.
[4] Baking from the beginning of the experiment.
[5] Baking starts after about one hour; symbol ◥ used in Fig. 3.

RESULTS AND CALCULATIONS

The labeling runs. Most of the labeling experiments have been »static», *i.e.* the solid sample has been kept with the tritium gas in the reaction vessel for a certain time without any agitation. However, it was believed that agitation would increase the specific activity of the product, so a number of runs were made in which the reaction vessel (parts A and B in Fig. 1) was removed from the apparatus and vigorously shaken in a rocking machine. It was found that with H-PAS the sample stuck to the walls of the vessel, so that in effect the sample did not move at all (called »baking» in Table 1). The introduction of broken glass pieces into the reaction vessel and careful drying of the H-PAS

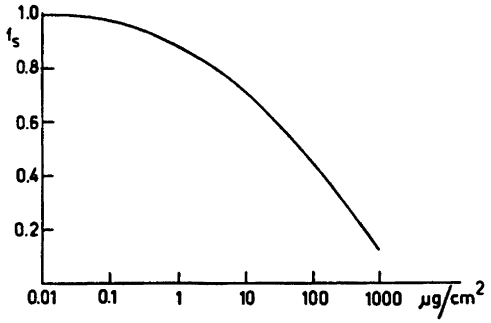

Fig. 2. Correction factor, f_s, for the self-absorption of the tritium beta-radiation in solid PAS samples [14].

did not much increase the agitation of the sample. The results of these runs (see Table 1) also indicated that there was not any great difference between these "agitation" runs and the "static" runs.

This "baking" of the H-PAS samples is believed to be due to electrostatic phenomena. Since H-PAS is amphoteric, while Na-PAS is not, it was hoped that better results would be obtained with the latter. The subsequent experiments showed that no baking at all was obtained with Na-PAS. The only experiments with "true" agitation have therefore been carried out on Na-PAS.

It was thought that the static experiments with H-PAS could be extrapolated to "agitation" by means of the results on agitation of Na-PAS, *i.e.* that labeling would be equally efficient in H-PAS and Na-PAS under identical conditions. In order to check this, static runs with Na-PAS were also made; these are recorded in the fourth part of Table 1.

The results of the various runs are given in Table 1, where also the specific activity has been calculated.

Calculation of specific activity. In order to calculate the true specific activity, S, of non-labile tritium in the PAS product, the following equation [14] was used

$$S = \frac{0.90 \times 10^{-12} \cdot I}{m \cdot f_s \cdot f_p \cdot f_b} \text{ curies/g PAS}$$

where I is the measured activity in counts/min (cpm) in a sample of weight m grams on a plate with a back-scattering factor, f_b, (for the β-radiation from tritium, f_b is 1.14 for aluminium, 1.24 for stainless steel and 1.50 for platinum [14]). The correction factor, f_s, for the self-absorption and self-scattering in the samples is taken from Fig. 2. In order to make all experiments comparable, corrections for the decrease in the amount of tritium gas used in the successive experiments are made through the gas correction factor, f_p, which arbitrarily has been put equal to 1.00 when the reaction vessel contains 2.6 curies of T_2. The factor 0.9×10^{-12} is obtained from $1/2.2 \times 10^{12} \cdot f_g \cdot f_e$, where 1 curie $= 2.2.10^{12}$ dpm, $f_g = 0.50$ is the geometry factor, and $f_e = 1.0$ is the counter efficiency for tritium betas.

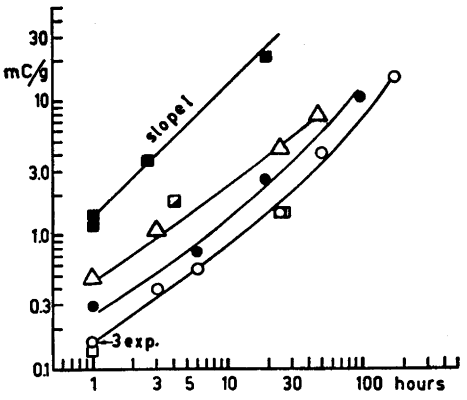

Fig. 3. Specific activity of tritium in non-labile positions in PAS (S mC/g) as a function of time of exposure to tritium gas (t hours). The symbols refer to: ○ 100 mg H—PAS and no agitation, △ 30 mg H—PAS and no agitation, ● 100 mg Na—PAS and no agitation, □ and ◪ 100 mg H—PAS and agitation, ■ 100 mg Na—PAS and agitation.

Reproducibility. The reproducibility of S seems to be surprisingly good. Thus, for static runs with 100 mg samples of H-PAS, $S = 0.15 \pm 0.01$ mC/g has been obtained in three different runs with several months intermission and using two different sources of tritium gas. The poorest reproducibility so far obtained is recorded for 104 mg H-PAS during 24 h, where the deviation between two measurements amounts to about 6 %. However, it is seen from Fig. 3 that some points deviate much more from the average curve drawn through the points of a set of experiments, indicating that the reproducibility sometimes is much worse.

DISCUSSION

The results of the various experiments are shown in Fig. 3, where the specific activity, S mC/g, is plotted as a function of time of exposure to tritium gas (t hours). The general tendency of S to increase with t is obvious, and also expected as long as radiation damage is negligible. When radiation damage becomes important one would expect the curves to level off and then to decrease with a further increase in exposure time t. However, the curves of the "static" experiments marked ○, △ and ● in Fig. 3 tend rather to bend upwards at high irradiation times, which seems quite surprising.

It is thought that mainly the surface layer of the H-PAS sample is labeled. This is supported by the fact that the specific activity of the 30 mg H-PAS samples (marked △), which expose about the same surface area to the tritium gas as the 100 mg samples, are almost exactly 3 times as high as that of the 100 mg H-PAS samples (marked ○).

H-PAS is a fine powder, while Na-PAS is macro-crystalline, thus making samples of the latter more porous. It is therefore believed that the tritium gas diffuses more rapidly into the Na-PAS sample than into the H-PAS sample, causing labeling not only in the surface layer. This assumption may explain why higher specific activities are obtained with Na-PAS (marked ●) then with H-PAS (marked ○) in the "static" runs.

Table 2. Comparison of specific tritium activities obtained in non-labile positions of substances similar to PAS using different labeling methods.

Substance	Met hod	Specific activity	Reference
Benzoic acid	recoil tritons	1 mC/g	Markowitz, Rowland, Wolfgang [15]
» »	tritium exposure	14 »	Wilzbach [1]
» »	accelerated tritons	< 10 »	Wolfgang, Pratt, Rowland [8]
Salicylic acid	recoil tritons	0.1 »	Kaplan [15]
p-Amino salicylic acid	recoil tritons	1.5 »	Hanngren, Rydberg [10]
Na-*p*-aminosalicylate	tritium exposure	~100 * »	this work

* Extrapolated from the upper straight line of Fig. 3 on the assumption that no macro-decomposition of PAS occurs.

The agitation of Na-PAS causes increased labeling owing to the continuous exposure of new surfaces towards the radiation and the tritium gas; the repeated breaking of the Na-PAS crystal needles because of the agitation further increases this effect. As would be expected when the diffusion effect is eliminated through agitation, the specific activity (experiments marked ■) rises almost linearily with exposure time (slope 1 in the log-log scale of Fig. 3).

These experiments show the importance of a very intimate contact between the tritium gas and the sample. Since radiation damage does not seem to interfere for radiation times $\lesssim$ 1 week, very high specific activities should be obtainable; the extrapolated straight line for Na-PAS (marked ■ in Fig. 3) gives, e.g., ~100 mC/g PAS after ~3 days agitation.*

In Table 2, a comparison is made of different methods of labeling organic compounds similar to PAS. The experiments refer to a reaction time of about 3 days, except in the case of accelerated tritons (0.5 h). These experiments are somewhat difficult to compare, even if the recoil tritons in all cases have been produced in a neutron flux of about 10^{12} n/cm^2/sec. If the simplicity of the technique of the tritium exposure method is considered, its superiority over the other methods is obvious, especially when the sample is vigorously agitated in the tritium gas.

As pointed out in the introduction, radiation other than the β-particles from tritium should be useful in producing reactive radicals. If more radicals can be produced, with negligible radiation damage in a shorter time, still higher specific activities may be obtainable.

Acknowledgements. The authors are indebted to the head of FOA 1, Prof. G. Ljunggren, for permission to carry out this work at his institute. They are also grateful to Mrs. B. Olausson and Mr. E. Johansson for experimental assistance.

* *Added in proof:* Later experiments have confirmed this.

REFERENCES

1. Wilzbach, K. E. *J. Am. Chem. Soc.* **79** (1957) 1013.
2. Giacomello, G. *Ricerca sci.* **21** (1951) 1211.
3. Croatto, U., Giacomello, G. and Maddock, A. G. *Ricerca sci.* **21** (1951) 1598.
4. Schrodt, A. G. and Libby, W. F. *J. Am. Chem. Soc.* **76** (1954) 3100.
5. Wolf, A. P. and Andersson, R. C. *J. Am. Chem. Soc.* **77** (1955) 1608.
6. Wolfgang, R., Rowland, F. S. and Turton, C. N. *Science* **121** (1955) 715.
7. Rowland, F. S. and Wolfgang, R. *Nucleonics* **14** No 8 (1956) 58.
8. Wolfgang, R., Pratt, T. and Rowland, F. S. *J. Am. Chem. Soc.* **78** (1956) 5132.
9. Lemmon, R. M., Mazzetti, F., Reynolds, F. L. and Calvin, M. *J. Am. Chem. Soc.* **78** (1956) 6414.
10. Hanngren, Å. and Rydberg, J. *Acta Chem. Scand.* **11** (1957) 202.
11. Muxart, R., Albiero, G., Santoro, V., Belluco, U., Croatto, U., Santoro, V. and Minozzi, G. *Communications at the XVI:th Int. Congr. Pure and Applied Chemistry*, Paris, July 1957.
12. Hanngren, Å. *Acta Tuberc. Scand.* **34** (1957) 200.
13. Rydberg, J. *Svensk Kem. Tidskr.* **67** (1955) 499; *Rec. trav. chim.* **75** (1956) 737.
14. Rydberg, J. *Acta Chem. Scand.* **12** (1958) *In press.*
15. According to Ref.[6]

Received November 18, 1957.

ACTA CHEMICA SCANDINAVICA 12 (1958) 340—342

Alkaline Hydrolysis of Glycosidic Linkages

III. An Investigation of some Methyl α- and β-Glycopyranosides

ELISABETH DRYSELIUS, BENGT LINDBERG and OLOF THEANDER

Träkemiska avdelningen, Svenska Träforskningsinstitutet, and Institutionen för Träkemi, Kungl. Tekniska Högskolan, Stockholm, Sweden

The alkaline hydrolysis of the α- and β-glycopyranosides of glucose, galactose, mannose, xylose and arabinose has been investigated. The glycosides with the aglyconic group and the hydroxyl at $C_{(2)}$ in the *trans* position reacted much faster than the corresponding *cis* anomers, indicating that the former reacts *via* the 1,2-anhydrosugars. Within each group of glycosides, the reactivity increases with the conformational instability of the most stable chair form of the glycoside.

An investigation of the alkaline hydrolysis of cellobiitol and lactitol was described in Part II of this series and it was demonstrated that cleavage of the glycosidic linkage in these substances followed at least two different mechanisms. One of these was assumed to proceed *via* the 1,2-anhydrosugar to the 1,6-anhydrosugar, which was isolated from the reaction products in both cases. The other mechanism, resulting in the formation of 1,4-anhydrosorbitol, was assumed to involve a nucleophilic attack upon the $C_{(4)}$ carbon atom of the sorbitol unit, thus leading to a fission on the other side of the glycosidic oxygen atom.

The present paper describes an investigation of the methyl α- and β-glycopyranosides of D-glucose, D-galactose, D-mannose, D-xylose and L-arabinose. The glycosides were treated with 10 % aqueous sodium hydroxide at 170° for varying times, the solutions were then deionised and the yields of neutral material were determined. The neutral products consisted essentially of unchanged starting material with traces only of other components such as 1,6-anhydroglucopyranose, 1,6-anhydrogalactopyranose and unknown substances. The rate constants for the alkaline hydrolysis were calculated for a first order reaction, assuming that the concentration of alkali, which was present in considerable excess, was constant during the reaction. The values determined in this way are not very accurate, especially for the short reaction times when only a small amount of the material had reacted. Nevertheless they should give an idea of the relative reactivities of the glycosides investigated. The yields and rate constants are summarised in Table 1. It is evident from Table 1 that in all pairs of glycosides, the anomer with methoxyl and

Table 1. Alkaline hydrolysis of methyl glycopyranosides in 10 % sodium hydroxide at 170°.

Sugar	Configuration(1)	Relationship between OCH_3 and $C_{(2)}$-hydroxyl	Neutral residue, %			$k^* \times 10^{-3}$
			6 h	24 h	48 h	
D-Glucose	α	*cis*	99.1	98.5	97.5	0.25
»	β	*trans*	91.1	86.1	77.9	2.5
D-Galactose	α	*cis*	97.1	95.5	88.8	0.97
»	β	*trans*	94.3	72.9	46.5	5.7
D-Mannose	α	*trans*	95.6	85.0	73.8	2.8
»	β	*cis*	98.2	93.9	88.8	1.1
D-Xylose	α	*cis*	98.0	92.4	88.2	1.2
»	β	*trans*	94.6	70.6	54.9	5.8
L-Arabinose	α	*trans*	89.5	56.2	33.6	10
»	β	*cis*	95.6	94.1	90.6	1.0

* Rate constants expressed in Briggs logarithms and in hours.

$C_{(2)}$ hydroxyl group *trans*, react considerably faster than the *cis* anomer. The same is true for the alkaline degradation of the phenyl glycosides (summarised in Ref.[2]) and is explained by the ready formation of the corresponding 1,2-anhydrosugar. The latter is highly reactive and, in the hexose series, when the configuration is favourable, gives the 1,6-anhydrosugar in good yield. As previously demonstrated [1], these 1,6-anhydrosugars are more sensitive to alkaline hydrolysis than the alkyl glycosides and consequently only small amounts accumulate. The presence of 1,6-anhydroglucose and 1,6-anhydrogalactose after alkaline treatment of the methyl β-glucoside and β-galactoside was demonstrated by paper chromatography and further supports the assumption that the reaction *via* the 1,2-anhydride is of major importance for the alkaline hydrolysis of the "*trans*"glycosides.

The relative rates of acid (Ref.[3], p. 209) and alkaline hydrolysis for the "*cis*" and "*trans*" glycosides are given in Tables 2 and 3. For the acid hydrolysis, the relative rates of hydrolysis are explicable by the principles of conformational analysis, as shown by Edward [4] and Huber [5]. A similar analysis of the alkaline hydrolysis, which obviously proceeds by at least two different mechanisms, is not intended. However, some generalisations seem to be

Table 2. Relative rates for acid and alkaline hydrolysis of the *cis* methyl glycopyranosides.

Methyl glycopyranoside	Acid hydrolysis, k_{rel} *	Alkaline hydrolysis, k_{rel} *
α-D-glucoside	1.0	1.0
α-D-galactoside	5.2	3.9
β-D-mannoside	5.7	4.4
α-D-xyloside	4.5	4.8
β-L-arabinoside	9.0	4.0

* $k_{rel} = 1$ for methyl α-D-glucopyranoside.

Table 3. Relative rates for acid and alkaline hydrolysis of the *trans* methyl glycopyranosides.

Methyl glycopyranoside	Acid hydrolysis, k_{rel} *	Alkaline hydrolysis, k_{rel} *
β-D-glucoside	1.9	10
β-D-galactoside	9.3	23
α-D-mannoside	2.4	11
β-D-xyloside	9.0	23
α-L-arabinoside	13.1	40

* $k_{rel} = 1$ for methyl α-D-glucopyranoside.

valid. Firstly, as stated above, the reaction is considerably facilitated by a *trans* arrangement of the aglyconic group and the hydroxyl at $C_{(2)}$, and it is most probable that the hydrolysis of these glycosides involves the intermediate formation of an 1,2-anhydride. Secondly, there is a qualitative agreement between the rates of acid and alkaline hydrolysis within each group. The value for the alkaline hydrolysis of the β-L-arabinoside is somewhat low, but, with that exception, the agreement is remarkably good. This shows that the acid and alkaline hydrolysis are influenced in a similar way by steric factors in the glycosides, and that they both increase with the conformational instability of the most stable chair form of the glycoside (*cf.* Ref.[3], p. 209).

EXPERIMENTAL

The glycosides were prepared by conventional methods and purified until m. p. and specific rotation were in agreement with the accepted values and no impurities could be detected by paper chromatography.

The glycoside (1.000 g) was dissolved in 10 % sodium hydroxide (7 ml, 2.62 N). The solution, in a stainless steel autoclave, was heated at 170° in an oil thermostat for different times. When cold the solution was deionised by filtering through a column, containing a mixed bed of the ion exchange resins Amberlite IR 120 and Dowex 2, in their hydrogen and hydroxyl states, respectively. The column was carefully washed, the solution was concentrated to dryness under reduced pressure in a rotary evaporator and the residue was dried to constant weight over phosphorus pentoxide in a vacuum. The product was usually crystalline. It was investigated by paper chromatography in three different solvent systems. In most cases, only unchanged starting material was detected, but the products from the β-glucoside and β-galactoside also contained small amounts of material, which was chromatographically indistinguishable from the corresponding 1,6-anhydrosugars and traces of unknown components.

Methyl β-mannopyranoside was investigated in the form of its crystalline tetraacetate, in this case using a larger excess of 10 % sodium hydroxide to compensate for the acetic acid liberated.

When a glycoside was dissolved in the alkali and recovered without heating by the procedure above, the recovery was between 99 and 100 %.

REFERENCES

1. Dryselius, E., Lindberg, B. and Theander, O. *Acta Chem. Scand.* **11** (1957) 663.
2. Ballou, C. E. *Advances in Carbohydrate Chem.* **9** (1954) 59.
3. Wolfrom, M. L. and Thompson, A. in Pigman, W. *The Carbohydrates.* New York 1957
4. Edward, J. T. *Chem. & Ind. London* **1955** 1102.
5. Huber, G. *Helv. Chem. Acta* **38** (1955) 1224.

Received November 20, 1957.

ACTA CHEMICA SCANDINAVICA 12 (1958) 343—346

On the Purification of Prorennin with a Note on the Recrystallisation of Rennin

BENT FOLTMANN

Chr. Hansen's Laboratory Ltd., Copenhagen, Denmark

Prorennin was extracted from dried calf-stomachs, using a solution of 2 % $NaHCO_3$. After clarification with $Al_2(SO_4)_3$, neutralisation with Na_2HPO_4 and reprecipitation with NaCl, a purified preparation was obtained. N-Determinations and paperelectrophoresis indicated that at least 50 % of the protein was prorennin. Paperelectrophoresis was carried out with crystalline rennin for purposes of comparison, and it was found that the isoelectric point of prorennin is about 0.3 pH unit higher than that of rennin. Crystallisation and recrystallisation of rennin are described.

Few investigations have been published concerning prorennin, the inactive precursor of the milk-clotting enzyme rennin. Only one attempt has been made to purify the pro-enzyme (Kleiner and Tauber[1]). As the preparation by Kleiner and Tauber actually appears to be rather impure, experiments have been carried out to produce a high-grade prorennin preparation.

METHODS AND RESULTS

Determination of the milk-clotting activity of samples from the preparation was carried out as a relative test, using fresh skim-milk and a sample of liquid rennet as basis for comparison. The activity is expressed in rennin units (RU) according to Berridge [2]. The eluates from the paperelectrophoresis experiments called for a very sensitive test. This determination was carried out with 5 ml skim-milk and 5 ml acetate buffer pH 4.9 (Ege and Menck-Thygesen [3]). In this determination, the activity is expressed directly as the inverse of the time of coagulation. The activity is illustrated in relation to each separate experiment.

Activation. The activation of prorennin was carried out at pH 2 for 15 min for samples of the preparation (*cf.* Ege and Lundsteen [4]). The eluates from the paperelectrophoresis only had a very slight buffer capacity, and as the determination of the milk-clotting activity of these samples was carried out in a milk/acetate mixture, it was most convenient to activate the eluates in acetate buffer pH 4.6 during 20 h before testing (Holwerda [5]).

Table 1. Purification of prorennin.

	ml	RU/ml		mg N/ml	RU per mg N after activation	per cent activity recov.
		preformed activity	after activation			
Raw extract (pH 8.4)	2 000	0	220	2.75	80	100
Addition of 100 ml 1/3 M $Al_2(SO_4)_3$. Precipitate discarded *	1 600	0	208	1.85	112	75
Addition of 80 ml 1/3 M $Al_2(SO_4)_3$ and 80 ml 1 M Na_2HPO_4. Precipitate discarded *	1 500	0	184	1.62	114	63
1 350 ml saturated with NaCl. Left to stand overnight. Precipitate redissolved in phosphate buffer 1/20 M, pH 6.3	220	6.6	690	1.35	510	34
215 ml saturated with NaCl. Left to stand overnight. Precipitate redissolved in 100 ml phosphate buffer 1/20 M, pH 6.3	110	12	1 350			
110 ml dialysed ** during 7 h against 2 × 2 l distilled water	145	9	1 000	1.77	560	33

* During the clarification operation pH fluctuated between 6.1 and 6.9.

** The dialysis was carried out in a rotating bag (Visking Cellulose) at 2°C during 2 h against 2 l of distilled water, and 5 h against a further 2 l of distilled water. (The dialysis was not prolonged in order to prevent activation during the experiment. The final product was not, therefore, free of salt. The N-contents of the freeze-dried preparation was 84 mg N/g.)

Prorennin. After preliminary experiments, the following procedure was adopted: 7 dried calf-stomachs, (taken from a charge proved to have a high prorennin/rennin value), were finely cut, and extracted with 3 000 ml of 2 % $NaHCO_3$ at room temperature whilst stirring continuously. After 2 h, the tissue was separated by means of centrifugation, and the muddy raw extract was purified as described in Table 1. After freeze-drying 135 ml of the purified dialyzate, 2.7 g of powder were obtained. The preformed activity of this powder was 3.6 RU/mg N, the activity after activation 500 RU/mg N.

Crystalline rennin was prepared from rennet after four precipitations with NaCl (Berridge [6], Alais [7]). The fourth precipitate was dissolved in distilled water to give a solution of 2 000 RU per ml. The NaCl enclosed in the wet precipitate produced a concentration in the final solution of approximately 1 N

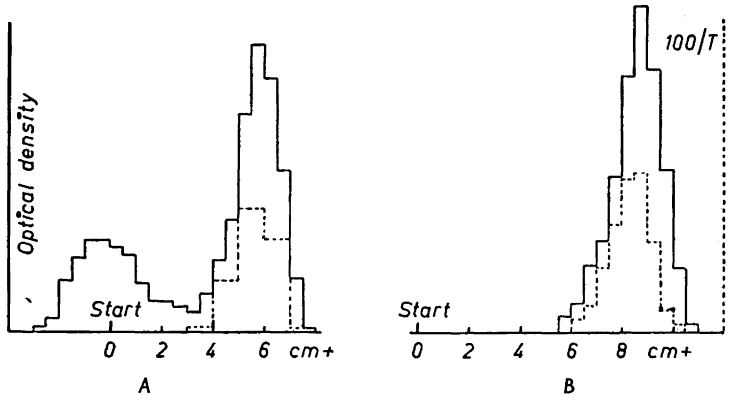

Fig. 1. Paperelectrophoresis of purified prorennin (A) and crystalline rennin (B). The samples are run 7 h in phosphate buffer, pH 6.0, ionic strength 0.1. Field strength 7 V/cm, room temperature. Full line: Colour after staining with bromophenol blue. The density is determined at 595 mμ after elution. Dotted line: The milk-clotting activity of the eluates illustrated as the inverse time of coagulation (in case of prorennin after activation).

NaCl. pH was regulated to 5.4 with 0.5 M phosphate buffer, pH 5.9, (5—10 ml were added per 100 ml solution).

From this solution, 1/2—2/3 of the active material crystallised in rectangular plates after 3—5 weeks in a refrigerator. The crystals were separated by means of centrifugation, and after gently washing with distilled water (2°C) they were dissolved in distilled water to give a solution of 3 000—5 000 RU per ml. Recrystallisation took place after addition of NaCl to a final concentration of 1 N, pH 5.4. When adding NaCl, a precipitate of amorphous rennin was noticed between 0.1—0.3 N NaCl. The precipitate dissolved when the salt concentration was further raised. The yield of the recrystallisation was 90 %. The activity of 10 preparations varied from 880 RU/mg N to 1 000 RU/mg N.

Paperelectrophoresis was carried out according to Kunkel and Tiselius [8]. Experiments were conducted with two spots (0.025 ml) in parallel. One strip was stained with bromophenol blue, and the colour was eluted with 0.1 equimolar hydrocarbonate/carbonate buffer. From the other strip, the enzyme was eluted with buffer, (phosphate buffer 0.05 M, pH 6.3 in the case of rennin, acetate buffer 0.1 M, pH 4.6 in the case of prorennin).

Fig. 1 illustrates two experiments with paperelectrophoresis at pH 6.0 (phosphate buffer, ionic strength 0.1) of purified prorennin and crystalline rennin. The experiment shows a clear difference in mobility of the two proteins. Further electrophoresis experiments at pH's ranging from 5.5 to 7.5 indicate by extrapolation that the isoelectric point of prorennin is about 0.3 pH-unit higher than that of rennin, or approximately 5.0 (Schwander, Zahler and Nitschmann [9], Hankinson [10]).

DISCUSSION

Kleiner and Tauber stated that 1 ml of a solution of 50 mg prorennin preparation in 100 ml of water, after activation, would clot 10 ml reconstituted skim-milk in 11 min at 40°C. As one RU is defined as the rennin activity which clots 10 ml of reconstituted skim-milk in 100 sec at 30°C, it may be surmised that Kleiner and Tauber's preparation, after activation, has had a rennin activity of about 0.3 RU per mg dry substance, (N-contents were not stated). Concerning the rennin activity before activation, a relative rennin activity of less than 5 % would not have been noticed, using the method described by Kleiner and Tauber.

The prorennin preparation resulting from the present work was not fully free of milk-clotting activity, but as experience has shown that purified prorennin easily activates during the process, the milk-clotting activity may be due to rennin formed during the fractionation. Meanwhile, the pre-formed rennin activity is less than 1 % of the total activity.

Assuming that the N-content of prorennin and rennin is of the same order of magnitude, the potential activity of the prorennin preparation corresponds to a prorennin content of approx. 50 %. The milk-clotting activity at the sharp main peak of the paperelectrophoresis indicates that this peak represents the prorennin. The area under this peak, compared with the total area, corresponds fairly well to the above-mentioned 50 %-content of prorennin in the preparation.

As the curve of the milk-clotting activity in the eletrophoresis of crystalline rennin conforms to that of the stained protein, the crystalline rennin should be regarded as electro-homogeneous under the conditions present.

The recrystallisation of rennin described above seems more convenient, and gives a better yield than that previously used by Berridge and Alais. After completion of this work, attention has been drawn to a paper read by Berridge before the International Circle of Research Workers in Dairying (Bern 1957). This paper mentions a recrystallisation similar to that described above.

REFERENCES

1. Kleiner, J. S. and Tauber, H. *J. Biol. Chem.* **96** (1932) 755.
2. Berridge, N. J. *Biochem. J.* **39** (1945) 179.
3. Ege, R. and Menck-Thygesen, P. *Biochem. Z.* **264** (1933) 13.
4. Ege, R. and Lundsteen, E. *Biochem. Z.* **268** (1934) 164.
5. Holwerda, B. J. *Biochem. Z.* **134** (1923) 381.
6. Berridge, N. J. *J. Dairy Research* **20** (1953) 255.
7. Alais, C. *Lait* **36** (1956) 26.
8. Kunkel, H. G. and Tiselius, A. *J. Gen. Physiol.* **35** (1951) 89.
9. Schwander, H., Zahler, P. and Nitschmann, H. *Helv. Chim. Acta* **35** (1952) 553.
10. Hankinson, C. L. *J. Dairy Sci.* **26** (1943) 53.

Received November 26, 1957.

ACTA CHEMICA SCANDINAVICA 12 (1958) 347—368

Short Communications

A Sensitive and Stable Color Reaction for the Quantitative Determination of Vitamin K_1

KURT SCHILLING and HENRIK DAM

Department of Biochemistry and Nutrition, Polytechnic Institute, Copenhagen, Denmark

Various reactions have been proposed for the chemical determination of vitamin K_1. Some of them are based on photometric measurement of a characteristic color obtained with special reagents, others make use of the oxidation-reduction properties of the quinone structure of vitamin K.

Color reactions are preferable in cases where a great number of samples shall be tested.

Among the known color reactions the most promising seems to be that of Irreverre and Sullivan [1]. In this procedure the sample is mixed with an alcoholic solution of sodium diethyldithiocarbamate and treated with sodium ethylate. A transient blue color develops and is measured continuously. The maximum value, which is obtained after about 5 min is used for calculation. Later, the blue color changes to a weak orange yellow.

The disadvantages of this method are the instability of the color and the limited keeping quality of the reagent which makes it necessary to prepare it freshly every day.

It seems likely that the C-N-S grouping in the diethyl-dithiocarbamate is responsible for the development of the color. Therefore, a series of chemical compounds with a similar atomic arrangement have been tested, and attempts made to modify the conditions of the reaction in such a way that stable reagents can be used. A common feature of most of the reactions with these substances was the appearance of a transient violet followed by a yellow to orange color. Various attempts to stabilize the blue or violet color were not successful. The orange end-stage, however, showed in some cases such an intense light absorption that it was adopted for the measurement. Best results were obtained with 5-imino-3-thion-1,2,4-dithiazolidine (xanthane hydride, "perthiocyanic acid") under the conditions described below.

Experimental. Reagents. 1. 80 % saturated xanthane hydride in ethyl alcohol, made by shaking the alcohol with an excess of recrystallized xanthane hydride prepared according to Chattaway and Stevens [2], filtering and addition of 1/4 vol. of alcohol.

2. 1 N KOH in water.

Procedure. 3 ml of the sample dissolved in ethyl alcohol are mixed with 1 ml xanthane hydride solution and 1 ml 1 N KOH. The mixture is placed in a water bath of 50°C for 10 min, and immediately afterwards cooled under the tap. The light absorption is measured at 410 mμ against a reagent blank prepared with 3 ml alcohol instead of the sample. The vitamin content is read from a standard curve prepared in the same way using varying amounts of vitamin K_1.

Results. Standard curves obtained with various concentrations of vitamin K_1 ("Merck", U.S.A.) at three different wavelengths are presented in Fig. 1. Beer's law is followed in the range up to 100 μg/ml. As shown in the figure higher readings may be obtained at shorter wavelengths, but on account of the increasing blank correction, 410 mμ has been chosen for the measurements.

The present method has the following advantages: The reagents are stable for months. The resultant color is stable, the absorption showing a decrease of only

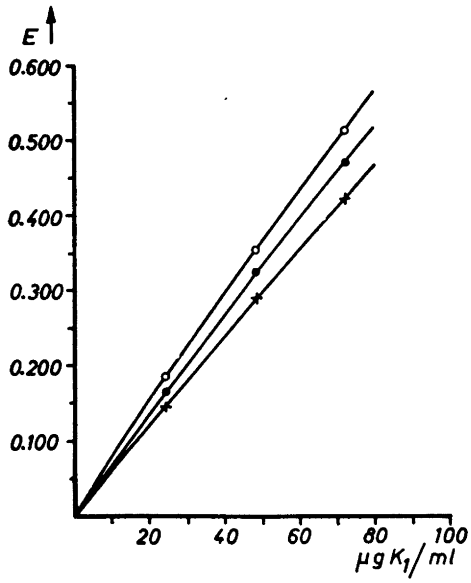

Fig. 1. Absorbancy readings with various amounts of vitamin K_1 at three different wavelengths.

○ 390 mμ. ● 400 mμ. + 410 mμ.

a few per cent after 24 h. The intensity of the light absorption measured at 410 mμ is about twice that obtained with diethyldithiocarbamate according to Irreverre and Sullivan.

When 2-methyl-1,4-naphthoquinone was used instead of vitamin K_1 a reddish color with an absorption maximum about 440 mμ was obtained. Tocopherol-quinone gave only a very slight color, a circumstance which is of importance when the method shall be adapted for the determination of vitamin K in plant material. An analytical procedure for this purpose will be described in a subsequent communication [3].

1. Irreverre, F. and Sullivan, M. X. *Science* **94** (1941) 497.
2. Chattaway, F. D. and Stevens, H. P. *J. Chem. Soc.* **71** (1897) 607.
3. Schilling, K. and Dam, H. *Acta Chem. Scand.* **12** (1958) 348.

Received December 19, 1957.

Colorimetric Estimation of Vitamin K_1 in Plant Material

KURT SCHILLING and HENRIK DAM

Department of Biochemistry and Nutrition, Polytechnic Institute, Copenhagen, Denmark

When vitamin K_1 is to be determined chemically in plant material, the main problem is the separation of the vitamin from interfering substances prior to the measurement.

For this purpose, chromatographic methods in which the vitamin is absorbed on a column have been tried but with little success because absorption of the vitamin usually leads to partial destruction. The best procedure appears to be purification through the hydroquinone form as described by Scudi and Buhs [1], followed by titration with dichlorophenolindophenol. However, this procedure must be carried out in a sealed apparatus without access of air, wherefore it is rather precarious and not very suitable for routine determination.

The difficulties adhering to the usual chromatographic procedures are overcome in the present method in which the extract containing the vitamin is passed through dicalciumphosphate, which absorbs certain accompanying substances but does not retain vitamin K_1. Thereafter the purified extract is submitted to the color reaction with xanthane hydride. The resulting stable coloring matter is soluble in an alkaline water phase, whereby it can be separated from substances with interfering color, especially carotenes.

The principle of the color reaction was described previously [2], but in the present procedure it had to be modified on account of the high lipid content of the extracts.

Experimental. Reagents. 1. Dicalcium phosphate, activated with disodium phosphate according to Moore [3], dried at 110°C and kept in a desiccator over saturated potassium thiocyanate solution as described by Bro-Rasmussen, Hjarde and Porotnikoff [4].

2. 80 % saturated xanthane hydride in ethyl alcohol made by shaking the alcohol with an excess of recrystallized xanthane hydride (5-imino-3-thion-1,2,4-dithiazolidine, "perthiocyanic acid") prepared according to Chattaway and Stevens [5], filtering and adding 1/4 vol. of alcohol.

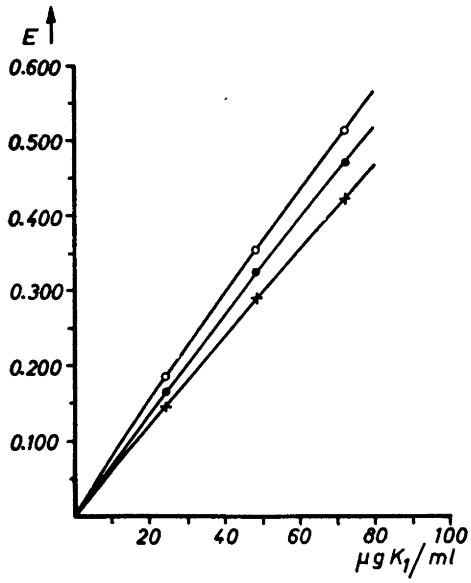

Fig. 1. Absorbancy readings with various amounts of vitamin K_1 at three different wavelengths.

○ 390 mμ. ● 400 mμ. + 410 mμ.

a few per cent after 24 h. The intensity of the light absorption measured at 410 mμ is about twice that obtained with diethyldithiocarbamate according to Irreverre and Sullivan.

When 2-methyl-1,4-naphthoquinone was used instead of vitamin K_1 a reddish color with an absorption maximum about 440 mμ was obtained. Tocopherol-quinone gave only a very slight color, a circumstance which is of importance when the method shall be adapted for the determination of vitamin K in plant material. An analytical procedure for this purpose will be described in a subsequent communication [3].

1. Irreverre, F. and Sullivan, M. X. *Science* **94** (1941) 497.
2. Chattaway, F. D. and Stevens, H. P. *J. Chem. Soc.* **71** (1897) 607.
3. Schilling, K. and Dam, H. *Acta Chem. Scand.* **12** (1958) 348.

Received December 19, 1957.

Colorimetric Estimation of Vitamin K_1 in Plant Material

KURT SCHILLING and HENRIK DAM

Department of Biochemistry and Nutrition, Polytechnic Institute, Copenhagen, Denmark

When vitamin K_1 is to be determined chemically in plant material, the main problem is the separation of the vitamin from interfering substances prior to the measurement.

For this purpose, chromatographic methods in which the vitamin is absorbed on a column have been tried but with little success because absorption of the vitamin usually leads to partial destruction. The best procedure appears to be purification through the hydroquinone form as described by Scudi and Buhs [1], followed by titration with dichlorophenolindophenol. However, this procedure must be carried out in a sealed apparatus without access of air, wherefore it is rather precarious and not very suitable for routine determination.

The difficulties adhering to the usual chromatographic procedures are overcome in the present method in which the extract containing the vitamin is passed through dicalciumphosphate, which absorbs certain accompanying substances but does not retain vitamin K_1. Thereafter the purified extract is submitted to the color reaction with xanthane hydride. The resulting stable coloring matter is soluble in an alkaline water phase, whereby it can be separated from substances with interfering color, especially carotenes.

The principle of the color reaction was described previously [2], but in the present procedure it had to be modified on account of the high lipid content of the extracts.

Experimental. Reagents. 1. Dicalcium phosphate, activated with disodium phosphate according to Moore [3], dried at 110°C and kept in a desiccator over saturated potassium thiocyanate solution as described by Bro-Rasmussen, Hjarde and Porotnikoff [4].

2. 80 % saturated xanthane hydride in ethyl alcohol made by shaking the alcohol with an excess of recrystallized xanthane hydride (5-imino-3-thion-1,2,4-dithiazolidine, "perthiocyanic acid") prepared according to Chattaway and Stevens [5], filtering and adding 1/4 vol. of alcohol.

Table 1. Absorbancy readings on samples of vitamin K_1 and alfalfa extracts.

	E	$E_{average}$	E_{calc}
200 μg K_1 *	0.350		
200 μg K_1 *	0.352	0.339	
200 μg K_1 *	0.319		
200 μg K_1 **	0.335		
10 ml extract	0.081		
10 ml extract	0.089	0.092	
20 ml extract	0.182	(10 ml)	
20 ml extract	0.216		
10 ml extract + 200 μg K_1	0.433		
10 ml extract + 200 μg K_1	0.403	0.423	0.431
20 ml extract + 200 μg K_1	0.501	0.501	0.523

* Measured directly.
** Measured after passage through dicalcium phosphate column and evaporation.

3. 4 N KOH in methanol.

Procedure. A petroleum ether extract of the material to be tested is prepared. The solution is passed through a column of dicalcium phosphate. The chlorophylls and xanthophylls remain in the upper part while the carotenes are distributed along the column. Elution is carried out with petroleum ether, until the β- and α-carotene-bands have passed out. The eluate is evaporated to dryness *in vacuo* at 20°C and redissolved in 3 ml benzene. After addition of 1.5 ml xanthane hydride solution and 0.5 ml methanolic KOH the sample is placed for 5 min in a water bath of 50°C and cooled immediately afterwards under the tap. 10 ml petroleum ether and 2 ml 50 % alcohol are added, and after thorough shaking the upper layer is siphoned off and discarded. The extraction is repeated once with 10 ml petroleum ether, and finally the light absorption of the aqueous layer is measured at 410 mμ against a reagent blank prepared in the same way with 3 ml benzene instead of the extract.

Results. The procedure was standardized with vitamin K_1 ("Merck", U.S.A.) and applied to an extract from dried alfalfa. Representative results are shown in Table 1. When a petroleum ether solution of vitamin K_1 was passed through a dicalcium phosphate column, evaporated to dryness and taken up in benzene, no loss was encountered as compared with samples where chromatography was omitted. Readings on the extract were proportional to the sample size, and when vitamin K_1 was added to extract samples of different size the absorbancy was equal to the sum of absorbancies from separate measurements on extract and vitamin samples.

Tocopherol quinone may be present in extracts from plant material, but as previously reported [2] it gives only a slight color when using the present procedure.

From the absorbancy readings the vitamin K_1 content of the alfalfa meal was calculated to be 28 μg/g, a figure which is in good agreement with previous biological determinations on this material.

1. Scudi, J. V. and Buhs, R. P. *J. Biol. Chem.* **141** (1941) 451.
2. Schilling, K. and Dam, H. *Acta Chem. Scand.* **12** (1958) 347.
3. Moore, L. A. *Ind. Eng. Chem. Anal. Ed.* **14** (1942) 707.
4. Bro-Rasmussen, F., Hjarde, W. and Porotnikoff, O. *Analyst* **80** (1955) 418.
5. Chattaway, F. D. and Stevens, H. P. *J. Chem. Soc.* **71** (1897) 607.

Received December 19, 1957.

Bifunctional Amines and Ammonium Compounds. VII *

Base Strengths of Some *Tert.* Amino Alkyl Ethers

JØRGEN FAKSTORP and GRETHE SPEGGERS

Research Division, Aktieselskabet Pharmacia, Copenhagen — Vanløse, Denmark

It was thought that information concerning the role of charge distribution in the structure-activity relations of a series of biologically active bis-quaternary ammonium salts of aliphatic ethers currently being studied in these laboratories could be had by determining the dissociation constants of the tertiary precursors of these ammonium compounds. The values found are recorded here.

Method. The freshly distilled tertiary amines were estimated by perchloric acid titration. A quantity sufficient to give 100 ml of a 0.0025 M solution was dissolved by addition of the equivalent amount of 0.1 N HCl. This solution was backtitrated according to Marshall [1] (*cf.* also Gero and Markham [2] and Campbell, Fatora and Campbell [3]).

The values for pK obtained with an observed pH > 9 are corrected for contribution of hydroxyl ions present thus:

$$pK = pH - \log \frac{C_B - C_{OH^-}}{C_{BH^+} + C_{OH^-}}$$

The pK values are plotted in Fig. 1 against the number of methyl substituents in the amino groups (lower tracing pK_1, upper tracing pK_2).

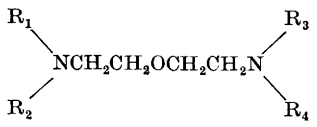

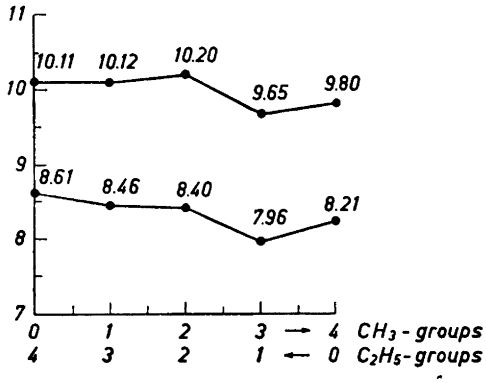

Fig. 1

The ionization constants do not differ very much within the series although both the first and second ionization constant pass through a minimum obtained with the bis-(2-diethyl-amino-2'-ethylmethyl-amino)-ethyl ether.

The interpolation of an ether oxygen between the two nitrogen atoms ought to enhance the inductive mutual hindrance of basic action between them. Thus these amino ethers should be weaker bases than the corresponding polymethylene diamines. No values are recorded for N-alkylsubstituted polymethylene-diamines, but Gero [4] has reported the pK_1 and pK_2 values for the unsubstituted pentamethylene-diamine to be 9.13 and 10.25, respectively.

1. Marshall, P. B. *Brit. J. Pharmacol.* **10** (1955) 270.
2. Gero, A. and Markham, J. J. *J. Org. Chem.* **16** (1951) 1835.
3. Campbell, K. N., Fatora, F. C. jr. and Campbell B. K. *J. Org. Chem.* **17** (1952) 1141.
4. Gero, A. *J. Am. Chem. Soc.* **76** (1954) 5159.

Received December 21, 1957.

* Part. VI *Acta Chem. Scand.* **11** (1957) 1698.

Occurrence in Plaice Myogen of a Low Molecular Weight Protein of Abnormal Amino Acid Composition

J. W. JEBSEN* and G. HAMOIR**

Laboratory of General Biology, Institute Van Beneden, University of Liège, Belgium

The ultracentrifugation of the myogens of frog [1], carp [2] and plaice [3] has shown the presence in these mixtures of a fraction amounting to 40—55 % in the carp and to approximatively 25 % in the plaice sedimenting with a rate of about 1.5 Svedberg units which does not occur in rabbit myogen. A component of this fraction precipitating at neutral pH between 90 and 100 % saturation of ammonium sulphate has been crystallized from carp muscle extracts by Henrotte [4] and further investigated by Hamoir [5]. Its ultraviolet absorption appears to be exclusively due to phenylalanine the amount of which has been evaluated spectrophotometrically to about 15 %. We show here that a similar protein exists in plaice myogen too.

This mixture has been fractionated with neutral ammonium sulphate. The fraction precipitating between 90 and 100 % saturation has been examined by electrophoresis in presence of phosphate buffer of $\mu = 0.05$ and pH = 7.5. A gradient representing about 30 % of the protein content of the fraction and 2 to 3 % of the myogen separates quickly from the slower ones. The corresponding component has been isolated by preparative electrophoresis and examined by ultracentrifugation and spectrophotometry. It sediments as a single peak with a corrected rate of sedimentation of 1.4—1.5 *S*. Its ultraviolet spectrum at pH = 7.5 and 13 is reproduced in Fig. 1. At neutral pH three maxima are observed at 253, 259 and 265 mμ which correspond closely to those of phenylalanine [6,7]. If the absorption at 259 mμ is exclusively ascribed to phenylalanine and if use is made of Fromageot and Schneck's [6] data for the absorption of this amino acid, its content can be evaluated to 16 %. A small absorption of another origin is, however, apparent in both curves at 275—290 mμ. As it varies from one preparation to the other, it is probably due to an impurity containing tyrosine or cystine. The protein isolated from plaice myogen differs in net charge from the crystalline component found by Henrotte [4]. Is electrophoretic mobility at $\mu = 0.05$ and pH = 7.5 on the descending side is of -6.5×10^{-5} cm^2 volt^{-1} sec^{-1} while that of the carp protein at $p = 0.075$ (0.05 in phosphate and 0.025 in NaCl) and pH = 7.3 is of -3.20×10^{-5} cm^1 volt^{-1} sec^{-1}. The content of basic and acid amino acids thus probably varies according to the origin.

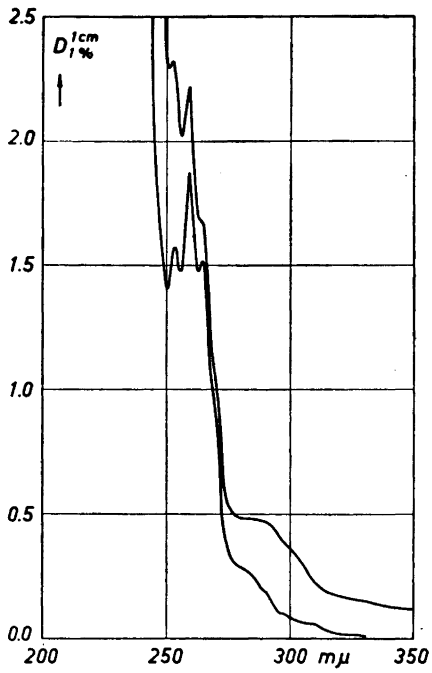

Fig. 1. Ultraviolet spectra at neutral pH (lower curve) and in presence of 0.1 N NaOH (upper curve) of a low molecular weight protein of plaice myogen.

An abnormal type of proteins characterized by a low rate of sedimentation, a very high salting-out range, a high content in phenylalanine and the absence of tyrosine and tryptophane appears therefore to occur generally in fish muscle.

* Norwegian Fisheries Research Institute, Bergen, Norway.

** Associé du F.N.R.S.

This investigation was made possible by a research grant from the *"Fiskeribedriftens Forskningsfond"* of Norway.

1. Deuticke, H. J. *Z. physiol. Chem. Hoppe Seyler* **224** (1934) 216.
2. Hamoir, G. *Arch. intern. physiol. biochem.* **63** (1955) Suppl.
3. Henrotte, J. G. *Unpublished results.*
4. Henrotte, J. G. *Nature* **176** (1955) 1221.
5. Hamoir, G. *Biochem. J.* **66** (1957) 29 P.
6. Fromageot, C. and Schenk, G. *Biochem. et Biophys. Acta* **6** (1950) 113.
7. Beaven, G. H. and Holiday, E. R. *Advances in Protein Chem.* **7** (1952) 319.

Received November 29, 1957.

Corrections to "Equilibrium Studies of Polyanions. II. Polyborates in $NaClO_4$ Medium" *

NILS INGRI, GÖSTA LAGERSTRÖM, MINA FRYDMAN and LARS GUNNAR SILLÉN

Department of Inorganic Chemistry, The Royal Institute of Technology, Stockholm 70, Sweden

P. 1043, Table 2
$v_1 = 7.13$, stands $E = 753.66$, read 753.46

P. 1044, Table 3
$B = 0.02$ M, $Z = 0.513$, stands $-\log h = 9.996$, read 8.996

P. 1045, Table 3
$B = 0.400$ M, $Z = 0.990$, stands $-\log h = 11.583$, read 11.683

P. 1047, Table 4, column 10
"$\Delta(1-R)$" should be lowered half a step so that the figures come in between those of column 11, "R".

* *Acta Chem. Scand.* **11** (1957) 1034.

Received February 1, 1958.

On the Possibility of Periodic Transformations of Enzymes during their Action as Catalysts

J. A. CHRISTIANSEN

Københavns Universitets Fysisk-Kemiske Institut, Copenhagen, Denmark

Against the existence of periodic chemical reactions one may argue that chemical reactions have no inertia, and that for this reason periodic phenomena cannot occur during their advancement. This argument evidently is based on an analogy with mechanical systems like pendulums.

It is, however, not true that inertia is a necessary condition for periodicity in all mechanical systems. *E. g.* an Archimedean screw acting as a motor delivers water periodically and in equally great portions to the lower basin with a well defined frequency. But this frequency is evidently determined by circumstances which have nothing to do with the inertia of the system. Consequently this argument is not valid.

Another argument seems, however, at a first glance to be conclusive. To fix our ideas, let us assume that an irreversible overall reaction (B)

$$B_1 + B_2 + B_3 \rightarrow A_2 + A_3 + A_1 \quad (B)$$

is catalyzed by an enzyme according to the sequence (A)

$$\begin{aligned} B_1 + X_1 &\rightleftharpoons X_2 + A_2 \ (\pm 1) \\ B_2 + X_2 &\rightleftharpoons X_3 + A_3 \ (\pm 2) \\ B_3 + X_3 &\rightleftharpoons X_1 + A_1 \ (\pm 3) \end{aligned} \quad (A)$$

(In preparation for a future paper the A's and B's of Ref.[5] have been interchanged.) The B's and the A's are intended to symbolize the "substrates" while X_1, X_2 and X_3 mean three different forms of the enzyme or complexes of the enzyme with the substrates. The affinity of the overall reaction (B) then compels the enzyme to perform cyclic transformations in the direction 1231. The question now is whether the partition fractions of the enzyme on three forms become steady asymptotically or whether they perform periodic variations around certain mean values. By application of well known ideas one arrives at a system of three linear equations between

the three partition fractions and their first derivatives with respect to time. The solutions of this system are certainly aperiodic and by the way, the two decay constants become so large, that steady state is asymptotically arrived at in minute fractions, *e. g.* 10^{-8}, of a second.

Thus periodic variations should be excluded. However, from nerve physiology it is known with certainty that periodic synchronous phenomena actually occur in certain nerves or rather in their end-organs. As now living organisms have so far as known only chemical reactions as ultimate causes of all observable events which take place in them, we may state with a probability approaching certainty that periodic chemical changes actually occur in nature.

To solve this dilemma one might look for mechanisms of the Volterra [1] type, which allow the appearance of periodic changes. This has been done, *i. a.* by Bonhoeffer [2] and Prigogine [3,4], but such mechanisms must be so artificial that it is hardly possible to believe in their occurrence, *e. g.* in living organisms.

We are therefore turned back on mechanisms of the type described above. Now in solving the corresponding equations we have implicitly assumed, that concentrations and their derivatives with respect to time can be determined simultaneously so accurately as we please. But this may not be true. We can certainly, *e. g.* by means of a "flash" method, determine the concentrations of the forms of the enzyme accurately, at a certain time. But the determination of the derivatives requires a second observation after the lapse of a certain not too short time interval, during which the concentrations may have varied in some unknown way, the more so as the first "flash" to give an observable effect must have changed the state of the enzyme and may have caused some chemical change. Therefore the more accurately we try to determine the concentrations by making the time interval short, the less accurate becomes the determination of the rate of change and *vice versa*.

We thus arrive at the result, that the validity of our system of differential equations can neither be proved nor disproved by direct experiments that is, they are physically unrealistic.

Therefore the occurrence of rhythmic chemical changes in the partition fractions need not surprise us, neither be it surprising that it is actually possible, as shown elsewhere [5], to calculate a frequency of oscillations with time in the values of these fractions.

We have only to remember that the aperiodic and the oscillatory treatment of the kinetic problem mutually exclude each other although separately both are possible.

1. Volterra, V. *Théorie mathématique de la lutte pour la vie.* Gauthier-Villars 1931.
2. Bonhoeffer, K. F. *Naturwiss.* **31** (1943) 270, and later papers.
3. Prigogine, I. and Balescu, R. *Ac. Roy. Belg. Bull. Cl. Sc.* **41** (1955) 917.
4. Prigogine, I. and Balescu, R. *Ac. Roy. Belg. Bull. Cl. Sc.* **43** (1956) 256.
5. Christiansen, J. A. *Acta Chem. Scand.* **11** (1957) 1436.

Received January 3, 1958.

Distillation Head for the Distillation of Small Amounts of Liquids

ARNE B:SON GROTH

Department of Applied Organic Chemistry, Royal Institute of Technology, Stockholm, Sweden

A distillation head suitable for semi-micro distillation columns has been designed and tested. Above all the author has tried to attain the following results:

1. As small a volume of liquid as possible that will adhere to the walls of the distillation head and the condenser.
2. Absence of stopcocks and ground glass joints.
3. Adjustable and continuous outlet.
4. Fitness for use in distillations at atmospheric pressure as well as under vacuum.

One of the difficulties encountered in the distillation of small amounts of liquid in a column provided with an ordinary distillation head, is the fact that a major part of the liquid to be distilled will remain in the condenser and on the walls of the tube connecting the condenser to the receiver. Usually, this tube has an internal diameter of 1.5—2 mm. Part of this remaining liquid will be in a state of

the three partition fractions and their first derivatives with respect to time. The solutions of this system are certainly aperiodic and by the way, the two decay constants become so large, that steady state is asymptotically arrived at in minute fractions, *e. g.* 10^{-8}, of a second.

Thus periodic variations should be excluded. However, from nerve physiology it is known with certainty that periodic synchronous phenomena actually occur in certain nerves or rather in their end-organs. As now living organisms have so far as known only chemical reactions as ultimate causes of all observable events which take place in them, we may state with a probability approaching certainty that periodic chemical changes actually occur in nature.

To solve this dilemma one might look for mechanisms of the Volterra [1] type, which allow the appearance of periodic changes. This has been done, *i. a.* by Bonhoeffer [2] and Prigogine [3,4], but such mechanisms must be so artificial that it is hardly possible to believe in their occurrence, *e. g.* in living organisms.

We are therefore turned back on mechanisms of the type described above. Now in solving the corresponding equations we have implicitly assumed, that concentrations and their derivatives with respect to time can be determined simultaneously so accurately as we please. But this may not be true. We can certainly, *e. g.* by means of a "flash" method, determine the concentrations of the forms of the enzyme accurately, at a certain time. But the determination of the derivatives requires a second observation after the lapse of a certain not too short time interval, during which the concentrations may have varied in some unknown way, the more so as the first "flash" to give an observable effect must have changed the state of the enzyme and may have caused some chemical change. Therefore the more accurately we try to determine the concentrations by making the time interval short, the less accurate becomes the determination of the rate of change and *vice versa*.

We thus arrive at the result, that the validity of our system of differential equations can neither be proved nor disproved by direct experiments that is, they are physically unrealistic.

Therefore the occurrence of rhythmic chemical changes in the partition fractions need not surprise us, neither be it surprising that it is actually possible, as shown elsewhere [5], to calculate a frequency of oscillations with time in the values of these fractions.

We have only to remember that the aperiodic and the oscillatory treatment of the kinetic problem mutually exclude each other although separately both are possible.

1. Volterra, V. *Théorie mathématique de la lutte pour la vie.* Gauthier-Villars 1931.
2. Bonhoeffer, K. F. *Naturwiss.* **31** (1943) 270, and later papers.
3. Prigogine, I. and Balescu, R. *Ac. Roy. Belg. Bull. Cl. Sc.* **41** (1955) 917.
4. Prigogine, I. and Balescu, R. *Ac. Roy. Belg. Bull. Cl. Sc.* **43** (1956) 256.
5. Christiansen, J. A. *Acta Chem. Scand.* **11** (1957) 1436.

Received January 3, 1958.

Distillation Head for the Distillation of Small Amounts of Liquids

ARNE B:SON GROTH

Department of Applied Organic Chemistry, Royal Institute of Technology, Stockholm, Sweden

A distillation head suitable for semi-micro distillation columns has been designed and tested. Above all the author has tried to attain the following results:

1. As small a volume of liquid as possible that will adhere to the walls of the distillation head and the condenser.
2. Absence of stopcocks and ground glass joints.
3. Adjustable and continuous outlet.
4. Fitness for use in distillations at atmospheric pressure as well as under vacuum.

One of the difficulties encountered in the distillation of small amounts of liquid in a column provided with an ordinary distillation head, is the fact that a major part of the liquid to be distilled will remain in the condenser and on the walls of the tube connecting the condenser to the receiver. Usually, this tube has an internal diameter of 1.5—2 mm. Part of this remaining liquid will be in a state of

continual "remixing" with the new condensate, and in this way will contribute to a decrease of the efficiency of separation. The other fraction, which under normal conditions moves slowly through the narrow tube connecting the outlet stopcock to the receiver, will cause a variable difference between the boiling points at the condenser and the receiver ends. Moreover, a stopcock is usually stained with lubricating grease, and this will influence the purity of the distillate in the distillation of small amounts of liquids.

Sager [1], Naragon and Lewis [2], Gould, Holzman and Nieman [3] have designed distillation heads for semi-micro distillation columns.

The author has designed a distillation head in which the distillate is collected through a capillary tube (about 1/10 mm internal diameter). The inlet of this capillary lies on a somewhat lower level than that of the outlet. In order to be able to obtain a continuous and adjustable stream of distillate from the distillation head to the receiver, it is necessary to have an appropriate pressure difference between the distillation head and the receiver. The manner in which this is reached is demonstrated in the flow sheet shown in Fig. 1. According to this figure, the pressure difference between the distillation head and the receiver is adjusted by means of stopcock d, *i.e.* the reflux ratio is regulated. For this purpose, a simple and efficient stopcock may consist of a piece of ordinary vacuum hose which can be squeezed, on a few centimeters of its length, between two metal plates. This effect can be arrived at by using a clamp for rubber tubes and two elongated (rectangular) metal plates. It is recommended that the diameter of the capillary outlet does not exceed 1/10 mm, since otherwise it will not have enough inertia during the short pressure variations due to an uneven boiling.

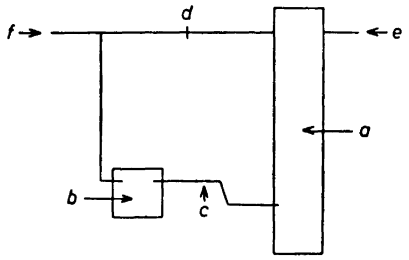

Fig. 1. Flow sheet. a) Distillation head. b) Receiver. c) Capillary tube. d) Adjustable stopcock.
Distillation at atmospheric pressure: e) Introduction of a small gas stream. f) To the surrounding atmosphere.
Distillation under vacuum: e) Introduction of gas through a very fine capillary. f) To vacuum pump.

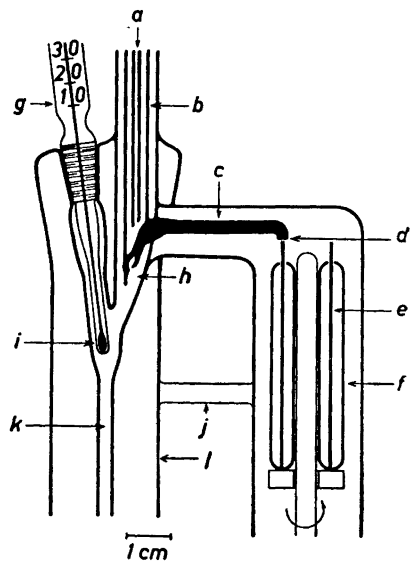

Fig. 2. Description of the distillation head. a) Cooling water. b) Condenser. c) Capillary tube. d) Outlet for distillate. e) Capillary tubes. f) Small test tubes. g) Thermometer. h) Inlet for distillate. i) Thermometer bulb or pocket for a thermocouple (better results are obtained if they are provided with an elongated tip). The distance between the thermometer and the glass walls must be between 1.5 to 2.0 mm. j) Brace. k) Column, 3 mm internal diameter (the packing of the column is not shown in the figure). l) Silvered high-vacuum jacket (the upper part is only halv-silvered).

The distillation head which has been designed by the author is described in Fig. 2. The distillate is sucked from the drop hanging from the tip of the condenser. It is gathered by means of a system similar to that shown by Gould *et al.*[3], *i.e.* through capillaries standing in small test tubes. The capillaries must then be adjusted so as to reach just under the outlet.

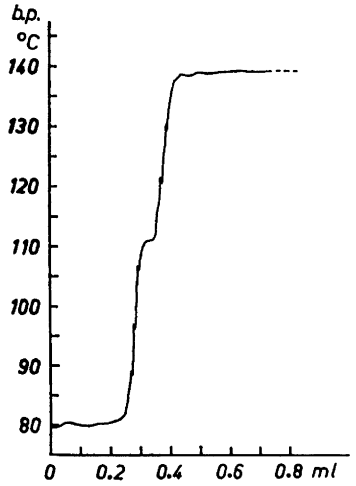

Fig. 3. Distillation curve for a mixture consisting of 0.3 ml benzene, 0.05 ml toluene and 1.0 ml xylene. The temperature was recorded by means of a thermocouple and a recorder.

This will prevent the formation of large drops.

Fig. 3 shows a distillation curve obtained with the apparatus shown in Fig. 2.

It may even be said that this kind of outlet can be applied to larger distillation apparatus. In that case, the system will be designed in such a way that the condensate will drop on the end of the capillary which will have the form of a small cup, with a "dropping tip" at the "outer" bottom.

The construction of the apparatus was executed by the glassblower's firm of Werner Glas (Stockholm).

1. Sager, W. F. in Weissberger, A. *Technique of organic chemistry* Interscience Publishers, Inc. New York 1951, Vol. IV, p. 486.
2. Naragon, E. A. and Lewis, C. J. *Ind. Eng. Chem. Anal. Ed.* **18** (1946) 448.
3. Gould, C. W., Holzman, G. and Nieman, C. *Ind. Eng. Chem. Anal. Ed.* **20** (1948) 361.

Received January 11, 1958.

N-Terminal Amino Acids of Human and Bovine Prothrombin

STAFFAN MAGNUSSON

Chemistry Department II, Karolinska Institutet, Stockholm 60, Sweden

Miller and van Vunakis [1], analyzing bovine prothrombin (~1 500 NIH u/mg), prepared according to Seegers [2], found no N-terminal or C-terminal amino acids, using Sanger's 1-fluoro-2,4-dinitrobenzene method and digestion with carboxypeptidase, respectively.

Recently Miller [3] analyzed bovine prothrombin which he had further purified (~2 000 NIH u/mg) by chromatography on the carboxylic cation exchanger Amberlite IRC 50. He found one mole of N-terminal alanine per mole of prothrombin, again using Sanger's method.

The present author has analyzed bovine and human prothrombin, both prepared according to Seegers [2], using the phenyl-*iso*thiocyanate method of Edman [4] for determination of N-terminal amino acids.

Experimental. Bovine prothrombin was prepared from 20 liter portions of bovine blood. The yield of prothrombin, when freeze-drying the isoelectric precipitate at pH 4.6, after first discarding the precipitate at pH 5.4, was generally 300—400 mg.

Human prothrombin was prepared by the same method from one lot of 3 200 ml pooled plasma from some fifty donors. The yield was 116 mg.

Two methods were used for routine determination of activity.

1. The prothrombin-proconvertin method of Owren and Aas [5], with the modification that barium sulfate adsorbed bovine plasma according to Brodthagen [6] was used as source of fibrinogen and factor V.

2. Activation of prothrombin by dissolving it in 25 % w/w of aqueous trisodium citrate according to Seegers [7]. Clotting activity of the thrombin generated was determined every 15 min, using as substrate bovine fibrinogen (Blombäck and Blombäck [8]) in tris(hydroxymethyl)amino methane buffer of ionic strength 0.15 and pH 7.5.

One of our bovine preparations was compared with a sample of prothrombin (No. 55/02/10) containing 26 000 U/mg tyrosine, obtained from Dr. Seegers and was found to have the same activity as the one of

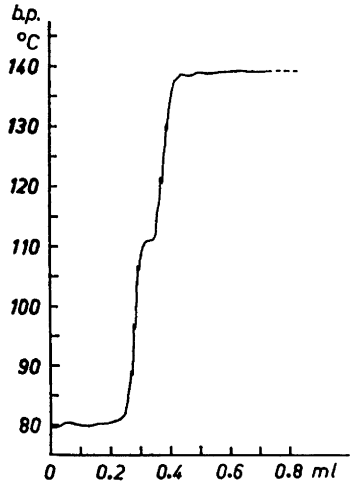

Fig. 3. Distillation curve for a mixture consisting of 0.3 ml benzene, 0.05 ml toluene and 1.0 ml xylene. The temperature was recorded by means of a thermocouple and a recorder.

This will prevent the formation of large drops.

Fig. 3 shows a distillation curve obtained with the apparatus shown in Fig. 2.

It may even be said that this kind of outlet can be applied to larger distillation apparatus. In that case, the system will be designed in such a way that the condensate will drop on the end of the capillary which will have the form of a small cup, with a "dropping tip" at the "outer" bottom.

The construction of the apparatus was executed by the glassblower's firm of Werner Glas (Stockholm).

1. Sager, W. F. in Weissberger, A. *Technique of organic chemistry* Interscience Publishers, Inc. New York 1951, Vol. IV, p. 486.
2. Naragon, E. A. and Lewis, C. J. *Ind. Eng. Chem. Anal. Ed.* **18** (1946) 448.
3. Gould, C. W., Holzman, G. and Nieman, C. *Ind. Eng. Chem. Anal. Ed.* **20** (1948) 361.

Received January 11, 1958.

N-Terminal Amino Acids of Human and Bovine Prothrombin

STAFFAN MAGNUSSON

Chemistry Department II, Karolinska Institutet, Stockholm 60, Sweden

Miller and van Vunakis [1], analyzing bovine prothrombin (~1 500 NIH u/mg), prepared according to Seegers [2], found no N-terminal or C-terminal amino acids, using Sanger's 1-fluoro-2,4-dinitrobenzene method and digestion with carboxypeptidase, respectively.

Recently Miller [3] analyzed bovine prothrombin which he had further purified (~2 000 NIH u/mg) by chromatography on the carboxylic cation exchanger Amberlite IRC 50. He found one mole of N-terminal alanine per mole of prothrombin, again using Sanger's method.

The present author has analyzed bovine and human prothrombin, both prepared according to Seegers [2], using the phenyl-*iso*thiocyanate method of Edman [4] for determination of N-terminal amino acids.

Experimental. Bovine prothrombin was prepared from 20 liter portions of bovine blood. The yield of prothrombin, when freeze-drying the isoelectric precipitate at pH 4.6, after first discarding the precipitate at pH 5.4, was generally 300—400 mg.

Human prothrombin was prepared by the same method from one lot of 3 200 ml pooled plasma from some fifty donors. The yield was 116 mg.

Two methods were used for routine determination of activity.

1. The prothrombin-proconvertin method of Owren and Aas [5], with the modification that barium sulfate adsorbed bovine plasma according to Brodthagen [6] was used as source of fibrinogen and factor V.

2. Activation of prothrombin by dissolving it in 25 % w/w of aqueous trisodium citrate according to Seegers [7]. Clotting activity of the thrombin generated was determined every 15 min, using as substrate bovine fibrinogen (Blombäck and Blombäck [8]) in tris(hydroxymethyl)amino methane buffer of ionic strength 0.15 and pH 7.5.

One of our bovine preparations was compared with a sample of prothrombin (No. 55/02/10) containing 26 000 U/mg tyrosine, obtained from Dr. Seegers and was found to have the same activity as the one of

Seegers, when activated in 25 % sodium citrate. All preparations used in this work had the same or slightly higher activity.

The general procedure for determining N-terminal amino acids was the following. To 0.3 μmoles of prothrombin dissolved in 1 ml of water and 2 ml of pyridine is added 0.1 ml of phenyl*iso*thiocyanate. Coupling is performed at room temperature, keeping the pH at 8.4—9.0 by occasionally adding 0.1 M NaOH. Excess phenyl*iso*thiocyanate is then removed by washing once with benzene and repeatedly with acetone. (In quantitative determinations, where amino acids are added, the acetone washing is replaced by several washings with benzene and freeze-drying.) The vacuum-dried PTC-derivative is then heated in 1 M HCl on a boiling water bath for 60 min. PTH-Amino acids are extracted with ethyl acetate and identified by paper chromatography, using solvents D and E of Edman and Sjöquist [9] and an heptane:formic acid: ethylene chloride solvent (Sjöquist [10]). Spots are visualized by ultraviolet fluorescence on a cadmium borate screen [9] and eluted over night in 95 % ethanol at room temperature. The technique described is mainly in accordance with Blombäck and Yamashina [11].

Results. In qualitative experiments on bovine prothrombin only alanine was identified as N-terminal amino acid in several different preparations. No positive evidence for the occurrence of histidine or arginine in N-terminal position could be obtained.

Assuming the yield of PTH-alanine from N-terminal alanine in prothrombin to be the same as from added free alanine, we found the following amounts (calculated on moisture-free substance and using the value 62 700 for the molecular weight [12]):

Prothrombin, No.	Moles N-term. alanine per 62 700 g prothrombin	Solvent system
33	0.80	D, E[9]
43	0.87	D, E[9]
67	0.85	Sjöquist [10]

With human prothrombin for lack of material only one determination was made. In this case also alanine was found to be the only N-terminal amino acid. Its PTH-derivative was identified by paper chromatography in solvent D and the above mentioned solvent of Sjöquist [10]. Furthermore it had an absorption spectrum in the ultraviolet which is characteristic for PTH-amino acids. Quantitatively 0.7 moles/mole were found, assuming the human and bovine prothrombins to have the same molecular weight.

Preliminary experiments to determine changes in N-terminal amino acids during activation in citrate were performed on bovine prothrombin. At maximum thrombin clotting activity the activation mixture was found to contain alanine, glycine, *iso*leucine (or leucine), phenylalanine, threonine, aspartic and glutamic acids in N-terminal position.

1. Miller, K. and van Vunakis, H. *N. Y. State Dep. Health, Ann. Rep. Div. Labs. and Research* **1955** 60.
2. Seegers, W. H. *Record Chem. Progr. Kresge-Hooker Sci. Lib.* **13** (1952) 143.
3. Miller, K. *Communication to the 12th Conference on Blood Cells and Plasma Proteins, Albany, N.Y.* (1957).
4. Edman, P. *Acta Chem. Scand.* **4** (1950) 283.
5. Owren, P. A. and Aas, K. *Scand. J. Clin. Lab. Invest.* **3** (1951) 201.
6. Brodthagen, H. *Scand. J. Clin. Lab. Invest.* **5** (1953) 376.
7. Seegers, W. H., McClaughry, R. I. and Fahey, J. L. *Blood* **5** (1950) 421.
8. Blombäck, B. and Blombäck, M. *Arkiv Kemi* **10** (1956) 415.
9. Edman, P. and Sjöquist, J. *Acta Chem. Scand.* **10** (1956) 1507.
10. Sjöquist, J. *Personal Communication* (1957).
11. Blombäck, B. and Yamashina, I. *Arkiv Kemi. In print.*
12. Lamy, F. and Waugh, D. F. *J. Biol. Chem.* **203** (1953) 489.

Received February 11, 1958.

Isolation of ^{32}P-labeled Phosphoserine from a Preparation of Intestinal Alkaline Phosphatase Incubated with Radioactive Inorganic Phosphate

LORENTZ ENGSTRÖM and GUNNAR ÅGREN

Department of Medical Chemistry, University of Uppsala, Sweden

In a previous paper it was demonstrated that ^{32}P-labeled phosphoserine could be isolated from a yeast hexokinase preparation incubated with radioactive ATP or glucose 6-phosphate [1]. This was taken as evidence of the formation of an intermediate enzymephosphate in the hexokinase reaction. In the reaction a P—O linkage is opened [2] which means that according to our result a phosphoryl group is transferred to the enzyme. The actual site of the phosphoryl group on the enzyme has so far not been investigated. Stein and Koshland [3] have shown that a P—O linkage also is opened when alkaline phosphatase acts on glycerol phosphate, phenyl phosphate and 3′-adenosine monophosphate. The formation of an intermediate enzymephosphate in the reaction of this enzyme would be of considerable interest.

In our experiments we have used a commercial preparation *. Since the enzyme reaction is reversible it should be possible to use radioactive inorganic phosphate as a substrate. 500 mg of enzyme dissolved in 25 ml of water was incubated with 2 mC ^{32}P. After half a minute the protein was precipitated with trichloroacetic acid. The precipitate was hydrolyzed and radioactive phosphoserine could be isolated as previously described [1]. Alkaline phosphatase activity is completely inhibited by a 0.05 M solution of versene [5]. During these conditions no radioactive phosphoserine could be isolated.

The enzyme was purified by ethanol fractionation at −5°C. In the presence of 0.05 M magnesium acetate 75 % of the phosphatase activity was recovered between 37 and 50 % ethanol. The incorporation of activity in the phosphoserine phosphorus ran parallel with the increase of enzyme activity. To exclude an unspecific reaction between inorganic phosphate and protein-bound serine a number of proteins were incubated with a 2-fold increase of ^{32}P-labeled phosphate but otherwise during the same conditions as in the enzyme experiments. Crystalline serum albumin, egg albumin, pepsin, chymotrypsin, insulin and a γ-globulin preparation were used. No trace of radioactive phosphoserine could be revocered from the hydrolyzed proteins.

In a series of experiments 500 mg samples of enzyme and 2 mC ^{32}P were incubated at different pH for 5 min at room temperature. The total radioactivity of the isolated phosphoserine fractions measured in a L.K.B. Robot Scaler was the following:

pH 5	24 600 cpm (counts per min)	pH 8	13 200 cpm
pH 6	45 000 cpm	pH 9	7 900 cpm
pH 7	34 400 cpm	pH 10	2 200 cpm

At pH 5 the preparation could not be completely dissolved. If the reaction between enzyme and substrate is formulated as follows:

$$\text{Enzyme} + [H_2PO_4^-] \rightleftharpoons \text{Enzymephosphate} + [OH^-]$$

a decrease of hydroxyl ions should drive the reaction to the right. This should be accompanied by an increase of the activity of the phosphoserine isolated from the enzyme-phosphate which was actually found.

The investigation was supported by grants from the *Gustav and Tyra Svensson Memorial Foundation* and the *Swedish Medical Research Council.*

1. Ågren, G. and Engström, L. *Acta Chem. Scand.* **10** (1956) 489.
2. Cohn, M. *Biochim. et Biophys. Acta* **20** (1956) 92.
3. Stein, S. S. and Koshland, D. E. *Arch. Biochem. and Biophys.* **39** (1952) 229.
4. Hofstee, B. H. J. *Arch. Biochem. and Biophys.* **51** (1954) 139.
5. Hofstee, B. H. J. *Arch. Biochem. and Biophys.* **59** (1955) 352.

Received January 23, 1957.

* Worthington intestinal alkaline phosphatase with an activity of 400—500 units [4] per mg of enzyme.

A Note on the Isolation of Solamargine from *Solanum nigrum*

PER M. BOLL

Department of Organic Chemistry, The Royal Danish School of Pharmacy, Copenhagen, Denmark

In the course of an investigation of alkaloids occurring in different species of the plant genus *Solanum* two alkaloidal glycosides were chromatographically detected in *S. nigrum*. The one with the highest R_F-value was subsequently isolated and identified as solamargine, an alkaloidal glycoside first isolated from *S. marginatum* [1].

The isolation procedure reported by Kuhn and Löw [2] was followed. The green, oily residue obtained by this procedure was dissolved in water-saturated 1-butanol and chromatographed on a column of wet-packed alumina (Alcoa). Elution with water-saturated 1-butanol gave a yield of 650 mg alkaloid mixture from 2.93 kg of fresh plant tops.

Using the same developing solvent and technique as Kuhn and Löw [2] for paper chromatography two alkaloid spots with $R_{\alpha\text{-solanine}} = 1.04$ and $R_{\alpha\text{-solanine}} = 1.72$ were obtained (travelling distance of solvent 31.2 cm. The R_F- and $R_{\alpha\text{-solanine}}$-values depend highly upon both experimental conditions and travelling distance of solvent).

When the alkaloid mixture, dissolved in water-saturated 1-butanol, was rechromatographed on a column of wet-packed alumina (Alcoa) and eluted with water-saturated 1-butanol the alkaloid residue consisted mainly of the alkaloid component with the highest R_F-value. Repeated crystallization from ethanol-water (1:1) gave a chromatographically pure compound, m.p. 304–310°C (decomp., corr.), $[\alpha]_D^{23} = -99°$ (methanol, *c* 0.531). (Literature values for solamargine [1]: m. p. 301°C (evacuated tube, decomp.), $[\alpha]_D^{20} = -105°$ (methanol)). Potentiometric titration of the glycoside with 0.02 N perchloric acid in glacial acetic acid gave an equivalent weight of 914 (calc. 868 for anhydrous solamargine).

At this stage of the investigation a review article was published by Schreiber [3]. In his paper a footnote was added in proof stating that two chromatographically detected alkaloids, γ- and δ-solanigrine, from *S. nigrum* [4] were identical with solasonine and solamargine, respectively. No analytical results were submitted.

The aglycone was isolated by acid hydrolysis of the glycoside following the procedure used by Briggs *et al.*[1] The aglycone melted at 199–200°C, $[\alpha]_D^{23} = -98°$ (methanol, *c* 0.481). No melting point depression was observed when mixed with authentic solasodine (Literature values for solasodine [1]: m.p. 197.5–198.5°C, $[\alpha]_D^{20} = -97.1$ (methanol)). The infrared spectrum of the aglycone was identical with the spectrum of solasodine.

The acidic mother liquor remaining after hydrolysis of the glycoside and precipitation of the aglycone was by means of paper chromatography shown to contain D-glucose and L-rhamnose. Aliquots were chromatographed on Whatman No. 1 paper at 23°C. Aniline hydrogen phthalate was used as detecting reagent.

The solvent mixture 1-butanol-ethanol-water (8:1:2) revealed spots with the following R_F-values: 0.44 L-rhamnose, 0.16 D-glucose.

The solvent mixture ethyl acetate-water -pyridine (2:2:1) revealed spots with the following R_F-values: 0.48 L-rhamnose, 0,27 D-glucose.

The results were controlled by parallel runs of pure monosaccharides alone and in mixtures.

The author is indebted to Professor H. Baggesgaard Rasmussen for valuable discussions and to Dr. K. Schreiber, Mühlhausen/Thür. for a specimen of solasodine. The work is part of investigations supported by *Statens almindelige Videnskabsfond (The Danish State Research Foundation)*.

1. Briggs, L. H., Brooker, E. G., Harvey, W. E. and Odell, A. L. *J. Chem. Soc.* **1952** 3587.
2. Kuhn, R. and Löw, I. *Chem. Ber.* **88** (1955) 289.
3. Schreiber, K. Der Züchter **27** (1957) 289.
4. Schreiber, K. *XVI. Congrès International de Chemie Pure et Appliquée, Résumés des Communications*, Tome II, Paris 1957, p. 225.

Received January 29, 1958.

The Sialic Acids of Hog Gastric Mucosa

PAULA ATTERFELT, INGEMAR BLOHMÉ, ANDERS NORRBY and LARS SVENNERHOLM

Department of Medical Biochemistry, University of Gothenburg, Gothenburg, Sweden

The mucoids and the mucopolysaccharides of hog gastric mucosa have been subject to great interest because they contain compounds of physiological importance as, *e. g.*, the intrinsic factor and the bifidus factor. Several carbohydrate components have been isolated from the gastric mucosa, but hitherto not the sialic acids, although Werner and Blix [1] have determined their amount in gastric mucosa to 3—5 %. In previous papers [2-4] it has been shown that the composition of the sialic acids in hog material showed large variations. In the pancreas and the submaxillary gland N-glycolylsialic acid was the main component, but in the serum proteins N-glycolylsialic acid constituted only 10—15 % of the total sialic acids. Therefore, we postulated that in the epithelial mucins N-glycolylsialic acid occurred practically pure but in the glycoproteins of serum type N-acetylsialic acid was the dominating acid.

Experimental. Isolation of sialic acids. Fifty stomachs from hogs were collected immediately after slaughter and washed free from food contaminants and floating mucus. The mucosal linings of the corpus and the canalis were scraped off — yield 2.3 kg — and poured into 10 l of ethanol. The mixture was brought to boiling. The ethanol was filtered off and the residue was treated with ethanol once more. The residue was then treated with weak sulphuric acid and the sialic acids isolated as described for human liver [5]. The yield of lyophilized sialic acids was 580 mg which constituted about 80 % of the calculated value. The sialic acids were crystallized from a methanol-water solution by adding diethyl ether. Yield 534 mg (Fraction A).

As the ethanol solution also gave a positive sialic acid reaction it was concentrated *in vacuo* to about 1 l. It was shaken three times with chloroform in a separatory funnel for removing the lipids. After filtration the lipid-free solution was run through Dowex 50 (H^+) and then on a column with Dowex 1 in hydroxyl-formate (9:1, v/v) form. (Because of the large amount of salt the sialic acids were not attached to the anion exchange resin when it was in acetate or formate form.) The sialic acids were eluted from the resin with 0.3 N formic acid as earlier described [5]. Yield 110 mg. The yield of crystallized material was only 56 mg due to an accident at the crystallization (Fraction B).

Results. Elementary analysis. Fraction A: C 42.37; H 6.22; N 4.42. Calc. for N-acetylsialic acid ($C_{11}H_{19}NO_9$): C 42.72; H 6.19; N 4.53. Calc. for N-glycolylsialic acid ($C_{11}H_{19}NO_{10}$): C 40.61; H 5.89; N 4.31. *Glycolic acid* was determined with the method of Klenk and Uhlenbruck [6] with minor modifications [3]. Fraction A: 4.5 % glycolic acid, corresponding to 19 % N-glycolylsialic acid. Fraction B: 5.8 % glycolic acid, corresponding to 25 % N-glycolylsialic acid. *Optical rotation:* Fraction A: $[\alpha]_D^{20} = -30.8°$.

Paper partition chromatography: As solvent was used *n*-butanol-*n*-propanol-0.1 N hydrochloric acid (1:2:1, v/v). Two spots were indicated with the same position as N-acetylsialic acid and N-glycolylsialic acid. The *X-ray powder diagrams* were of the O-sialic acid (N-acetylsialic acid) type [7]. The *infrared spectrum* was of the same type as that of a mixture of the two sialic acids.

Discussion and summary. The sialic acids from hog gastric mucosa have been isolated and crystallized. They were obtained in a good yield and were shown to be a solid solution of 20 % N-glycolylsialic acid in 80 % N-acetylsialic acid. The ratio N-glycolylsialic acid/N-acetylsialic acid is somewhat greater than in the serum proteins but far from the ratio in the submaxillary mucin. If the hypothesis is valid that the mucoids of the mucous secretions of hog is practically pure N-glycolylsialic acid, the sialic acids in gastric mucosa are mainly derived from proteins of serum type.

The great amount of free sialic acids is remarkable as they have not been found earlier in free form in biological materials. The sialic acids were not liberated during the isolation by the boiling ethanol, as free sialic acids were indicated also at the precipitation of the mucosa with ethanol in the cold. They were probably liberated by the hydrochloric acid in the stomach but no test was made for sialidase. Work is now in progress to analyse the concentration of free sialic acids in the gastric juice from normal and achlorhydric subjects.

Recently it was described that some carbohydrates enhanced the vitamin B_{12} absorption [8]. It is possible that the free sialic acids may be of importance for this transport.

1. Werner, I. and Blix, G. *Bull. soc. chim. Belges* **65** (1956) 202.
2. Mårtensson, E., Raal, A. and Svennerholm, L. *Acta Chem. Scand.* **11** (1957) 1604.
3. Mårtensson, E., Raal, A. and Svennerholm, L. *(In manuscript.)*
4. Pettersson, S-O., Sivertsson, R., Sjögren, S. and Svennerholm, L. *Biochim. et Biophys. Acta. (In press.)*
5. Martinsson, A., Raal, A. and Svennerholm, L. *Biochim. et Biophys. Acta* **23** (1957) 652.
6. Klenk, E. and Uhlenbruck, G. *Hoppe Seyler's Z. physiol. Chem.* **307** (1957) 266.
7. Blix, G., Lindberg, E., Odin, L. and Werner, I. *Acta Soc. Med. Upsaliensis* **61** (1956) 1.
8. Greenberg, S. M., Herndon, J. F., Rice, E. G., Pamelec, E. T., Gulesich, J. J. and van Loon, E. J. *Nature* **180** (1957) 1401.

Received February 8, 1958.

The Losses of Vitamin A during Chromatography

GEORG LAMBERTSEN and OLAF R. BRÆKKAN

Governmental Vitamin Laboratory, Norwegian Fisheries Research Institute, Bergen, Norway

When the irrelevant absorption in the spectrophotometric determination of vitamin A exceeds certain limits, the geometric correction method according to Morton and Stubbs [1] is unreliable, and purification of the vitamin A fraction by chromatography is recommended. Actually chromatography is included in the procedure described in official methods in some countries. The chromatography is most often carried out on alumina columns by some modification of the method described by Gridgeman, Gibson and Savage [2] for the estimation of vitamin A in whale liver oils. A certain activity of the alumina is needed to obtain a sufficient separation of the unsaponifiable substances, but unfortunately a higher activity also means a higher loss of vitamin A in the procedure. In our experience the most potent oils give the highest losses, even up to 10 % for some vitamin A concentrates. Such losses can be counteracted by deactivation of the alumina. Usually a standardized activity is obtained by uniform water addition. To avoid this difficulty the use of a softer adsorbent, *e.g.* calcium phosphate has been introduced [3]. It is, however, of importance to obtain standardized columns in different laboratories, and alumina is the adsorbent preferred as it can be obtained readily in uniform quality everywhere as "Aluminium Oxide Standardized for Adsorption analysis according to Brockman". As mentioned above, a softening of the alumina is necessary to make it useful. Such deactivation will, however, result in a reduced separation of the components in the unsaponifiable matter. A limit thus has to be found where conditions are optimal all factors considered. This means that a certain loss is unavoidable, and must be controlled and taken into consideration by using a standard.

We have been trying to find substances which, added to the vitamin A fraction, would reduce the losses during the chromatography. Gridgeman *et al.*[2a] found it advisable to add cholesterol to make up the weight of the unsaponifiable matter if this amounted to less than 0.35 g. We found cholesterol to be of no effect in preventing the loss of vitamin A. Neither did several other types of substances, *e.g.* fatty alcohols or glyceryl ethers, have any such effect. The unsaponifiable matter of ground nut oil, however, gave a striking reduction in the loss. In one experiment the unsaponifiable matter of 0.5 g of ground nut oil gave a recovery of 98 % of a total of 2 000 I.U. vitamin A compared to 90 % without addition. The effect was found in the fraction of the unsaponifiable matter passing the alumina column with a speed similar to vitamin A. Analysis on paraffinated paper as described by Green, Marcinkiewicz and Watt [4] showed that the effective fraction contained γ-tocopherol. Pure γ-tocopherol (Eastman-Kodak) was then tried, and the effect was obtained with as little as 200 μg added per 1 000 I.U. vitamin A put through the column. α-Tocopherol had no effect, but as other slow moving tocopherols might be effective, the unsaponifiable matter of other vegetable oils were tried. Soy bean oil with its high concentration of γ- and δ-tocopherols (1.000 μg per g compared with 200 μg per g in ground nut oil) protected effectively against losses. Alumina columns of the

Recently it was described that some carbohydrates enhanced the vitamin B_{12} absorption [8]. It is possible that the free sialic acids may be of importance for this transport.

1. Werner, I. and Blix, G. *Bull. soc. chim. Belges* **65** (1956) 202.
2. Mårtensson, E., Raal, A. and Svennerholm, L. *Acta Chem. Scand.* **11** (1957) 1604.
3. Mårtensson, E., Raal, A. and Svennerholm, L. *(In manuscript.)*
4. Pettersson, S-O., Sivertsson, R., Sjögren, S. and Svennerholm, L. *Biochim. et Biophys. Acta. (In press.)*
5. Martinsson, A., Raal, A. and Svennerholm, L. *Biochim. et Biophys. Acta* **23** (1957) 652.
6. Klenk, E. and Uhlenbruck, G. *Hoppe Seyler's Z. physiol. Chem.* **307** (1957) 266.
7. Blix, G., Lindberg, E., Odin, L. and Werner, I. *Acta Soc. Med. Upsaliensis* **61** (1956) 1.
8. Greenberg, S. M., Herndon, J. F., Rice, E. G., Pamelec, E. T., Gulesich, J. J. and van Loon, E. J. *Nature* **180** (1957) 1401.

Received February 8, 1958.

The Losses of Vitamin A during Chromatography

GEORG LAMBERTSEN and OLAF R. BRÆKKAN

Governmental Vitamin Laboratory, Norwegian Fisheries Research Institute, Bergen, Norway

When the irrelevant absorption in the spectrophotometric determination of vitamin A exceeds certain limits, the geometric correction method according to Morton and Stubbs [1] is unreliable, and purification of the vitamin A fraction by chromatography is recommended. Actually chromatography is included in the procedure described in official methods in some countries. The chromatography is most often carried out on alumina columns by some modification of the method described by Gridgeman, Gibson and Savage [2] for the estimation of vitamin A in whale liver oils. A certain activity of the alumina is needed to obtain a sufficient separation of the unsaponifiable substances, but unfortunately a higher activity also means a higher loss of vitamin A in the procedure. In our experience the most potent oils give the highest losses, even up to 10 % for some vitamin A concentrates. Such losses can be counteracted by deactivation of the alumina. Usually a standardized activity is obtained by uniform water addition. To avoid this difficulty the use of a softer adsorbent, *e.g.* calcium phosphate has been introduced [3]. It is, however, of importance to obtain standardized columns in different laboratories, and alumina is the adsorbent preferred as it can be obtained readily in uniform quality everywhere as "Aluminium Oxide Standardized for Adsorption analysis according to Brockman". As mentioned above, a softening of the alumina is necessary to make it useful. Such deactivation will, however, result in a reduced separation of the components in the unsaponifiable matter. A limit thus has to be found where conditions are optimal all factors considered. This means that a certain loss is unavoidable, and must be controlled and taken into consideration by using a standard.

We have been trying to find substances which, added to the vitamin A fraction, would reduce the losses during the chromatography. Gridgeman *et al.*[2a] found it advisable to add cholesterol to make up the weight of the unsaponifiable matter if this amounted to less than 0.35 g. We found cholesterol to be of no effect in preventing the loss of vitamin A. Neither did several other types of substances, *e.g.* fatty alcohols or glyceryl ethers, have any such effect. The unsaponifiable matter of ground nut oil, however, gave a striking reduction in the loss. In one experiment the unsaponifiable matter of 0.5 g of ground nut oil gave a recovery of 98 % of a total of 2 000 I.U. vitamin A compared to 90 % without addition. The effect was found in the fraction of the unsaponifiable matter passing the alumina column with a speed similar to vitamin A. Analysis on paraffinated paper as described by Green, Marcinkiewicz and Watt [4] showed that the effective fraction contained γ-tocopherol. Pure γ-tocopherol (Eastman-Kodak) was then tried, and the effect was obtained with as little as 200 μg added per 1 000 I.U. vitamin A put through the column. α-Tocopherol had no effect, but as other slow moving tocopherols might be effective, the unsaponifiable matter of other vegetable oils were tried. Soy bean oil with its high concentration of γ- and δ-tocopherols (1.000 μg per g compared with 200 μg per g in ground nut oil) protected effectively against losses. Alumina columns of the

type used for vitamin A chromatography will not separate dimethyltocols from momomethyltocols, and the effect of the unsaponifiable matter may be a joint effect of γ- and δ-tocopherols. This is indicated by the fact that soy bean oil containing 5 times as much totally of these tocopherols than ground nut oil, is effective in one-fifth of the concentration.

The effect of these tocopherols is not one of simple displacement, as γ-tocopherol failed to elute further vitamin A from a column where vitamin A had passed through without protection. It may be a pure antioxidant effect protecting against oxidative substances in solvents and adsorbent. A more likely theory is that the tocopherols take the place of vitamin A in irreversible adsorption on the alumina. This is indicated by the recovery of anhydrovitamin A by ethanol elution of a column where vitamin A had passed with a loss.

The last 1—2 % loss of vitamin A during chromatography may arise from the diffusion of the vitamin A-band on the column. It was possible to prove the presence of vitamin A by concentration of the fractions leaving the column before and after the vitamin A-fraction. Carr-Price spot tests or fluorescence test with U.V.-light had given no positive reaction of vitamin A in these fractions.

Tocopherol-fractions useful for the purpose of protection against losses of vitamin A in chromatography can be produced easily from a proper vegetable oil, and be stored in hexane in the freezer for a couple of months. It is recommended to add a suitable aliquot of such a solution to the vitamin A fraction before chromatography of medium and high potent oils.

1. Morton, R. A. and Stubbs, A. L. *Analyst* **71** (1946) 348.
2. Gridgeman, N. T., Gibson, G. P. and Savage, J. P. *Analyst* **73** (1948) 662. 2a. *See discussion.*
3. Hjarde, W. *Acta Chem. Scand.* **4** (1950) 628.
4. Green, J., Marcinkiewicz, S. and Watt, P. R. *J. Sci. Food Agric.* **6** (1955) 274.

Received February 10, 1958.

The Isolation of O-Phosphoethanolamine from the Rest Protein Fraction of *Escherichia coli* B

CARL-HENRIC DE VERDIER and GUNNAR ÅGREN

Institute of Medical Chemistry, University of Uppsala, Sweden

In earlier communications [1,2] it has been shown that acid hydrolysates of the Schneider rest protein fractions from mammalian organs contain O-phosphoserine and O-phosphothreonine. Phosphoserine has also been isolated from the corresponding protein fraction of yeast [3] but in other microorganisms phosphorylated hydroxyamino acids of different composition seem to dominate in the acid hydrolysates [4,5].

It has now been possible to isolate O-phosphoethanolamine in crystalline form from the acid hydrolysate of the rest protein fraction of *E. coli*. Previously published methods for isolation have been followed. The bacteria were harvested at the end of the lag phase. They had been cultivated for about 2 h on a medium containing 1 mC radioactive phosphate per liter [5] to facilitate the identification of phosphorus compounds. Fig. 1 shows the elution curve of the hydrolysed cell walls in the first step of purification through a Dowex-50 column. Of the three main peaks (I, III, V) No. I consists of inorganic phosphate, No. III is a mixture of at least three ninhydrin positive compounds which are not identical with phosphoserine or phosphothreonine. No. V is practically pure phosphoethanolamine. Peak No. II is probably a nucleotide since it gives UV-absorption at 260 mμ and no ninhydrin reaction. A hydrolysate of peak No. IV shows on a paper chromatogram mainly ethanolamine and a few other weaker ninhydrin spots. Sufficient amounts of material for the identification of peak No. V was obtained by mixing radioactive bacteria with large amounts of unlabelled cells. For large scale cultivation the microorganisms were incubated in a 1 000 liter tank on the same medium for about 20 h. The usual yield of fresh bacteria from a single cultivation was about 2.5 kg. Material from two cultivations was used in this study.

type used for vitamin A chromatography will not separate dimethyltocols from momomethyltocols, and the effect of the unsaponifiable matter may be a joint effect of γ- and δ-tocopherols. This is indicated by the fact that soy bean oil containing 5 times as much totally of these tocopherols than ground nut oil, is effective in one-fifth of the concentration.

The effect of these tocopherols is not one of simple displacement, as γ-tocopherol failed to elute further vitamin A from a column where vitamin A had passed through without protection. It may be a pure antioxidant effect protecting against oxidative substances in solvents and adsorbent. A more likely theory is that the tocopherols take the place of vitamin A in irreversible adsorption on the alumina. This is indicated by the recovery of anhydrovitamin A by ethanol elution of a column where vitamin A had passed with a loss.

The last 1—2 % loss of vitamin A during chromatography may arise from the diffusion of the vitamin A-band on the column. It was possible to prove the presence of vitamin A by concentration of the fractions leaving the column before and after the vitamin A-fraction. Carr-Price spot tests or fluorescence test with U.V.-light had given no positive reaction of vitamin A in these fractions.

Tocopherol-fractions useful for the purpose of protection against losses of vitamin A in chromatography can be produced easily from a proper vegetable oil, and be stored in hexane in the freezer for a couple of months. It is recommended to add a suitable aliquot of such a solution to the vitamin A fraction before chromatography of medium and high potent oils.

1. Morton, R. A. and Stubbs, A. L. *Analyst* **71** (1946) 348.
2. Gridgeman, N. T., Gibson, G. P. and Savage, J. P. *Analyst* **73** (1948) 662. 2a. *See discussion.*
3. Hjarde, W. *Acta Chem. Scand.* **4** (1950) 628.
4. Green, J., Marcinkiewicz, S. and Watt, P. R. *J. Sci. Food Agric.* **6** (1955) 274.

Received February 10, 1958.

The Isolation of O-Phosphoethanolamine from the Rest Protein Fraction of *Escherichia coli* B

CARL-HENRIC DE VERDIER and GUNNAR ÅGREN

Institute of Medical Chemistry, University of Uppsala, Sweden

In earlier communications [1,2] it has been shown that acid hydrolysates of the Schneider rest protein fractions from mammalian organs contain O-phosphoserine and O-phosphothreonine. Phosphoserine has also been isolated from the corresponding protein fraction of yeast [3] but in other microorganisms phosphorylated hydroxyamino acids of different composition seem to dominate in the acid hydrolysates [4,5].

It has now been possible to isolate O-phosphoethanolamine in crystalline form from the acid hydrolysate of the rest protein fraction of *E. coli*. Previously published methods for isolation have been followed. The bacteria were harvested at the end of the lag phase. They had been cultivated for about 2 h on a medium containing 1 mC radioactive phosphate per liter [5] to facilitate the identification of phosphorus compounds. Fig. 1 shows the elution curve of the hydrolysed cell walls in the first step of purification through a Dowex-50 column. Of the three main peaks (I, III, V) No. I consists of inorganic phosphate, No. III is a mixture of at least three ninhydrin positive compounds which are not identical with phosphoserine or phosphothreonine. No. V is practically pure phosphoethanolamine. Peak No. II is probably a nucleotide since it gives UV-absorption at 260 mμ and no ninhydrin reaction. A hydrolysate of peak No. IV shows on a paper chromatogram mainly ethanolamine and a few other weaker ninhydrin spots. Sufficient amounts of material for the identification of peak No. V was obtained by mixing radioactive bacteria with large amounts of unlabelled cells. For large scale cultivation the microorganisms were incubated in a 1 000 liter tank on the same medium for about 20 h. The usual yield of fresh bacteria from a single cultivation was about 2.5 kg. Material from two cultivations was used in this study.

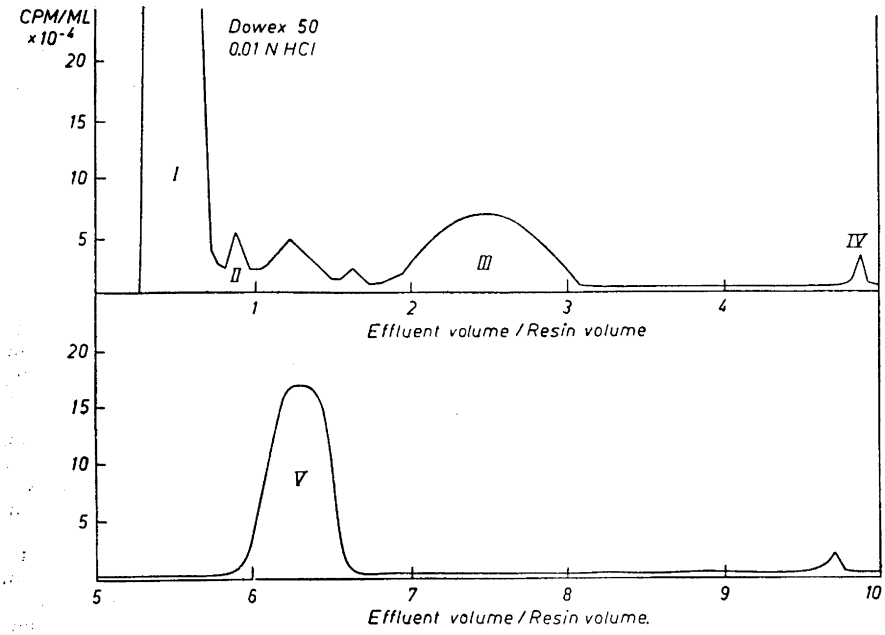

Fig. 1. Radioactivity curve from a hydrolysate of membranes from *E. coli*. incubated for 2½h in a ^{32}P-containing medium. The curve is obtained by plotting the number of impulses per min (cpm) in 1 ml aliquots of each tube.

The identity of peak No. V was verified by elementary analysis (Found: C 17.4; H 5.9; N 9.6; P 23.8. Calc. for $C_2H_8O_4NP$ (141): (C 17.0; H 5.7; N 9.9; P 22.0) and by paper chromatography and ionophoresis. The Debye-Scherrer powder photograph of material from peak No. V was identical with the pattern of a purified commercial preparation of phosphoethanolamine *. The spacings obtained are given in Table 1.

Free phosphoethanolamine has been reported to occur both in normal and neoplastic animal tissues [6]. Ethanolamine has also recently been found in an acid hydrolysate of a peptide-phospholipide-polysaccharide complex from *E. coli* [7]. Recent reports also describe the natural occurrence of phosphatides where the nitrogen moiety consists of a polypeptide [8]. To our knowledge protein-bound phosphoethanolamine has previously not been desribed. We have not found this substance in chromatographic purification of acid hydrolysates from mammalian tissues or in other microcrganisms such as baker's yeast or *L. casei*. The Schneider protein fraction of *E. coli* contained between 0.3—0.5 % of fatty acids. Calculated only as phosphatidylethanolamine the acid hydrolysate of this

Table 1. Values of spacings obtained from phosphoethanolamine.

Intensity	Å
s	5.79
m	4.78
s	4.41
s	4.25
s	3.87
vw	3.77
m	3.57
vw	3.36
w	3.28

vw = very weak, w = weak, m = medium, s = strong.

* Supplied by California Foundation for Biochemical Research.

amount of phospholipid would have yielded less phosphoethanolamine than actually isolated. On the other hand after extraction of lipids in the bacteria the remaining fraction of nucleic acids and protein still contained about 3 % of fatty acids. By the subsequent extraction of nucleic acids with hot 5 % trichloroacetic acid a cephalin-protein compound may have been hydrolyzed giving a part of the phosphoethanolamine bound to the protein part. At present time it is not possible to decide whether the compound is a constituent of a phosphoprotein or represents a link in a lipoprotein complex. In this connection it must be reminded about the fact that *E. coli* as a Gramnegative bacterium contains more phospholipids than a Grampositive microorganism as *L. casei* [9,10]. However, phosphoethanolamine cannot only be isolated from the rest proteins of the walls but also from water soluble fractions of proteins obtained after centrifugation at 105 000 *g* for 30 min at 0°C and precipitation with ethanol or acetone [5].

The investigation was supported by the *Swedish Medical Research Council.*

1. Ågren, G., de Verdier, C.-H. and Glomset, J. *Acta Chem. Scand.* **8** (1954) 1570.
2. Ågren, G., de Verdier, C.-H. and Glomset, J. *Acta Chem. Scand.* **9** (1955) 1041.
3. Engström, L. and Ågren, G. *Acta Chem. Scand.* **10** (1956) 877.
4. Ågren, G., de Verdier, C.-H. and Glomset, J. *Rev. fermentations et inds. aliment.* **11** (1956) 234.
5. Ågren, G. *Acta Chem. Scand.* **10** (1956) 152.
6. Smith, L. C. and Rossi, F. M. *Proc. Soc. Exptl. Biol. Med.* **78** (1954) 643.
7. Ikawa, M., Koepfli, J. B., Madd, S. G. and Niemann, C. *J. Am. Chem. Soc.* **75** (1953) 3439.
8. Baer, E., Marukas, J. and Clarke, D. *J. Biol. Chem.* **228** (1957) 181.
9. Work, E. *Nature* **179** (1957) 841.
10. Mitchell, P. and Moyle, J. *J. Gen. Microbiol.* **10** (1954) 533.

Received February 12, 1958.

Note on the Mutual Solubility of Molybdenum Trioxide and Wolfram Trioxide

SVEN WESTMAN and ARNE MAGNÉLI

Institute of Inorganic and Physical Chemistry, University of Stockholm, Stockholm, Sweden

Previous studies on the molybdenum trioxide-wolfram trioxide system have shown that the mutual solubility of these two substances, if there is any at all, is very low [1] (experiments performed at room temperature using samples prepared at 700°C). Access to a Guinier focusing camera with strictly monochromatized $CuK\alpha_1$ radiation has made possible a quantitative estimation of the limits of solubility.

The samples studied were prepared by prolonged heating of intimate mixtures of the two trioxides (both of reagent grade) in sealed, evacuated silica tubes at 700°C. Precautions as described elsewhere [2] were taken to ensure a constant temperature during the annealing time (two periods, of about one week each with intervenient regrinding of the specimen). The samples were quenched in water from the heating temperature. Potassium chloride (Analar, British Drug Houses, $a = 6.2919$ Å at 20°C [3]) was added to the powder specimens as an internal standard [4].

For wolfram trioxide the following unit cell dimensions were obtained:

$a = 7.306 \pm 0.001$ Å, $b = 7.541 \pm 0.001$ Å,
$c = 3.845 \pm 0.001$ Å, $\beta = 90.85° \pm 0.05°$.

The axial lengths exceed by about 0.3 % those derived previously from photographs taken without an internal standard [5,6]. The axial ratios and monoclinic angles obtained from the two experiments are, however, in fair agreement.

Addition of molybdenum trioxide caused slight, continuous modifications of the wolfram trioxide powder pattern up to the approximate composition $W_{0.96}Mo_{0.04}O_3$, which evidently represents the limit of solubility under the conditions mentioned above. These changes are exclusively attributable to a decrease of the length of the a axis, which for the latter composition was found to reach the limiting value of 7.301 ± 0.001 Å, while the other unit cell dimensions were not perceptibly altered.

amount of phospholipid would have yielded less phosphoethanolamine than actually isolated. On the other hand after extraction of lipids in the bacteria the remaining fraction of nucleic acids and protein still contained about 3 % of fatty acids. By the subsequent extraction of nucleic acids with hot 5 % trichloroacetic acid a cephalin-protein compound may have been hydrolyzed giving a part of the phosphoethanolamine bound to the protein part. At present time it is not possible to decide whether the compound is a constituent of a phosphoprotein or represents a link in a lipoprotein complex. In this connection it must be reminded about the fact that *E. coli* as a Gramnegative bacterium contains more phospholipids than a Grampositive microorganism as *L. casei* [9,10]. However, phosphoethanolamine cannot only be isolated from the rest proteins of the walls but also from water soluble fractions of proteins obtained after centrifugation at 105 000 *g* for 30 min at 0°C and precipitation with ethanol or acetone [5].

The investigation was supported by the *Swedish Medical Research Council.*

1. Ågren, G., de Verdier, C.-H. and Glomset, J. *Acta Chem. Scand.* **8** (1954) 1570.
2. Ågren, G., de Verdier, C.-H. and Glomset, J. *Acta Chem. Scand.* **9** (1955) 1041.
3. Engström, L. and Ågren, G. *Acta Chem. Scand.* **10** (1956) 877.
4. Ågren, G., de Verdier, C.-H. and Glomset, J. *Rev. fermentations et inds. aliment.* **11** (1956) 234.
5. Ågren, G. *Acta Chem. Scand.* **10** (1956) 152.
6. Smith, L. C. and Rossi, F. M. *Proc. Soc. Exptl. Biol. Med.* **78** (1954) 643.
7. Ikawa, M., Koepfli, J. B., Madd, S. G. and Niemann, C. *J. Am. Chem. Soc.* **75** (1953) 3439.
8. Baer, E., Marukas, J. and Clarke, D. *J. Biol. Chem.* **228** (1957) 181.
9. Work, E. *Nature* **179** (1957) 841.
10. Mitchell, P. and Moyle, J. *J. Gen. Microbiol.* **10** (1954) 533.

Received February 12, 1958.

Note on the Mutual Solubility of Molybdenum Trioxide and Wolfram Trioxide

SVEN WESTMAN and ARNE MAGNÉLI

Institute of Inorganic and Physical Chemistry, University of Stockholm, Stockholm, Sweden

Previous studies on the molybdenum trioxide-wolfram trioxide system have shown that the mutual solubility of these two substances, if there is any at all, is very low [1] (experiments performed at room temperature using samples prepared at 700°C). Access to a Guinier focusing camera with strictly monochromatized $CuK\alpha_1$ radiation has made possible a quantitative estimation of the limits of solubility.

The samples studied were prepared by prolonged heating of intimate mixtures of the two trioxides (both of reagent grade) in sealed, evacuated silica tubes at 700°C. Precautions as described elsewhere [2] were taken to ensure a constant temperature during the annealing time (two periods, of about one week each with intervenient regrinding of the specimen). The samples were quenched in water from the heating temperature. Potassium chloride (Analar, British Drug Houses, $a = 6.2919$ Å at 20°C [3]) was added to the powder specimens as an internal standard [4].

For wolfram trioxide the following unit cell dimensions were obtained:

$a = 7.306 \pm 0.001$ Å, $b = 7.541 \pm 0.001$ Å,
$c = 3.845 \pm 0.001$ Å, $\beta = 90.85° \pm 0.05°$.

The axial lengths exceed by about 0.3 % those derived previously from photographs taken without an internal standard [5,6]. The axial ratios and monoclinic angles obtained from the two experiments are, however, in fair agreement.

Addition of molybdenum trioxide caused slight, continuous modifications of the wolfram trioxide powder pattern up to the approximate composition $W_{0.96}Mo_{0.04}O_3$, which evidently represents the limit of solubility under the conditions mentioned above. These changes are exclusively attributable to a decrease of the length of the a axis, which for the latter composition was found to reach the limiting value of 7.301 ± 0.001 Å, while the other unit cell dimensions were not perceptibly altered.

For pure molybdenum trioxide, unit cell dimensions were obtained in fair agreement with previous data [6], *viz.*

$a = 3.9628 \pm 0.0007$ Å $b = 13.855 \pm 0.003$ Å
$c = 3.6964 \pm 0.0006$ Å

The powder patterns of molybdenum trioxide samples containing minor additions of wolfram trioxide gave lattice parameters slightly different from those of pure molybdenum trioxide. Thus the a axis was found to decrease to a limiting value of 3.9590 ± 0.0006 Å at the approximate composition $Mo_{0.96}W_{0.04}O_3$ while the b and c axes reached maximum lengths of 13.862 ± 0.003 Å and 3.6989 ± 0.0007 Å, respectively, at the composition $Mo_{0.98}W_{0.02}O_3$. The results might possibly indicate a considerable deviation from linearity of the parameter changes associated with the substitution of wolfram for molybdenum atoms in the molybdenum trioxide structure. The experimental evidence, however, scarcely allows such a conclusion to be made with any degree of confidence. The limit of solubility may thus only be roughly estimated to be about 3 mole % of wolfram trioxide.

The intermediary range of composition of the system was not studied in any detail. It seems likely, however, that the phase relations in this region [1] are somewhat more complicated than assumed previously.

The low mutual solubility in this system is another instance of the marked difference in crystal-chemical behaviour often shown by molybdenum and wolfram [7]. The variations of the unit cell dimensions associated with the solubility indicate that the metal-oxygen octahedra change towards a more regular shape with inrceasing wolfram content. This is also in accordance with previous observations [2,7].

This investigation was carried out in connection with studies on metal oxides and related compounds financially supported by the *Swedish Natural Science Research Council.*

1. Magnéli, A. *Acta Chem. Scand.* **3** (1949) 88.
2. Magnéli, A., Blomberg-Hansson, B., Kihlborg, L. and Sundkvist, G. *Acta Chem. Scand.* **9** (1955) 1382.
3. Hambling, P. G. *Acta Cryst.* **6** (1953) 98.
4. Westman, S. and Magnéli, A. *Acta Chem. Scand.* **11** (1957) 1587.
5. Andersson, G. *Acta Chem. Scand.* **7** (1953) 154.
6. Magnéli, A., Andersson, G., Blomberg, B. and Kihlborg, L. *Anal. Chem.* **24** (1952) 1998.
7. Magnéli, A. *J. Inorg. & Nuclear Chem.* **2** (1956) 330.

Received February 12, 1958.

A Cytidylic Acid — Peptide Complex from *Polyporus squamosus*

ROLF BERGKVIST

Institute of Biochemistry, University of Lund, Sweden

During the past ten years a variety of ribonucleotides has been isolated and identified from various natural sources. These substances are all nucleoside-5′-mono- or polyphosphates with the exception of triphosphopyridine nucleotide which contains a nucleoside-2′-phosphate moiety and the 2′- and 3′-phosphates obtained by chemical or enzymic hydrolysis of nucleic acids. A recent report has revealed the presence of a new guanosine-3′-phosphate derivative in alcoholic extract of brewer's yeast [1]. In the course of a study of the acid-soluble nucleotides of *Polyporus squamosus* we have isolated one hitherto unknown cytosine nucleotide (CMPX). It is the purpose of this report to present the experimental data about this substance. CMPX appears to be a nucleotide-peptide complex with one phosphate group in the 2′- or 3′-position of the ribose moiety.

The isolation and quantitative analysis of the acid-soluble nucleotides of *P. squamosus* was accomplished using the method described in an earlier paper [2]. The nucleotides were isolated by extraction with cold perchloric acid and, after removal of interfering substances, the solution was applied to a Dowex 1 (formate form) column. The elution of the substances was performed with increasing concentrations of formic acid or a mixture of formic acid and sodium formate. Among the different components eluted from the column, which will be presented in detail later, we obtained the CMPX peak after adenosine-5′-phosphate by elution with 0.1 M formic acid. The quantity of the nucleotide was about 10 μmoles per 1 000 g of

For pure molybdenum trioxide, unit cell dimensions were obtained in fair agreement with previous data [6], *viz.*

$a = 3.9628 \pm 0.0007$ Å $b = 13.855 \pm 0.003$ Å
$c = 3.6964 \pm 0.0006$ Å

The powder patterns of molybdenum trioxide samples containing minor additions of wolfram trioxide gave lattice parameters slightly different from those of pure molybdenum trioxide. Thus the a axis was found to decrease to a limiting value of 3.9590 ± 0.0006 Å at the approximate composition $Mo_{0.96}W_{0.04}O_3$ while the b and c axes reached maximum lengths of 13.862 ± 0.003 Å and 3.6989 ± 0.0007 Å, respectively, at the composition $Mo_{0.98}W_{0.02}O_3$. The results might possibly indicate a considerable deviation from linearity of the parameter changes associated with the substitution of wolfram for molybdenum atoms in the molybdenum trioxide structure. The experimental evidence, however, scarcely allows such a conclusion to be made with any degree of confidence. The limit of solubility may thus only be roughly estimated to be about 3 mole % of wolfram trioxide.

The intermediary range of composition of the system was not studied in any detail. It seems likely, however, that the phase relations in this region [1] are somewhat more complicated than assumed previously.

The low mutual solubility in this system is another instance of the marked difference in crystal-chemical behaviour often shown by molybdenum and wolfram [7]. The variations of the unit cell dimensions associated with the solubility indicate that the metal-oxygen octahedra change towards a more regular shape with inrceasing wolfram content. This is also in accordance with previous observations [2,7].

This investigation was carried out in connection with studies on metal oxides and related compounds financially supported by the *Swedish Natural Science Research Council.*

1. Magnéli, A. *Acta Chem. Scand.* **3** (1949) 88.
2. Magnéli, A., Blomberg-Hansson, B., Kihlborg, L. and Sundkvist, G. *Acta Chem. Scand.* **9** (1955) 1382.
3. Hambling, P. G. *Acta Cryst.* **6** (1953) 98.
4. Westman, S. and Magnéli, A. *Acta Chem. Scand.* **11** (1957) 1587.
5. Andersson, G. *Acta Chem. Scand.* **7** (1953) 154.
6. Magnéli, A., Andersson, G., Blomberg, B. and Kihlborg, L. *Anal. Chem.* **24** (1952) 1998.
7. Magnéli, A. *J. Inorg. & Nuclear Chem.* **2** (1956) 330.

Received February 12, 1958.

A Cytidylic Acid — Peptide Complex from *Polyporus squamosus*

ROLF BERGKVIST

Institute of Biochemistry, University of Lund, Sweden

During the past ten years a variety of ribonucleotides has been isolated and identified from various natural sources. These substances are all nucleoside-5′-mono- or polyphosphates with the exception of triphosphopyridine nucleotide which contains a nucleoside-2′-phosphate moiety and the 2′- and 3′-phosphates obtained by chemical or enzymic hydrolysis of nucleic acids. A recent report has revealed the presence of a new guanosine-3′-phosphate derivative in alcoholic extract of brewer's yeast [1]. In the course of a study of the acid-soluble nucleotides of *Polyporus squamosus* we have isolated one hitherto unknown cytosine nucleotide (CMPX). It is the purpose of this report to present the experimental data about this substance. CMPX appears to be a nucleotide-peptide complex with one phosphate group in the 2′- or 3′-position of the ribose moiety.

The isolation and quantitative analysis of the acid-soluble nucleotides of *P. squamosus* was accomplished using the method described in an earlier paper [2]. The nucleotides were isolated by extraction with cold perchloric acid and, after removal of interfering substances, the solution was applied to a Dowex 1 (formate form) column. The elution of the substances was performed with increasing concentrations of formic acid or a mixture of formic acid and sodium formate. Among the different components eluted from the column, which will be presented in detail later, we obtained the CMPX peak after adenosine-5′-phosphate by elution with 0.1 M formic acid. The quantity of the nucleotide was about 10 μmoles per 1 000 g of

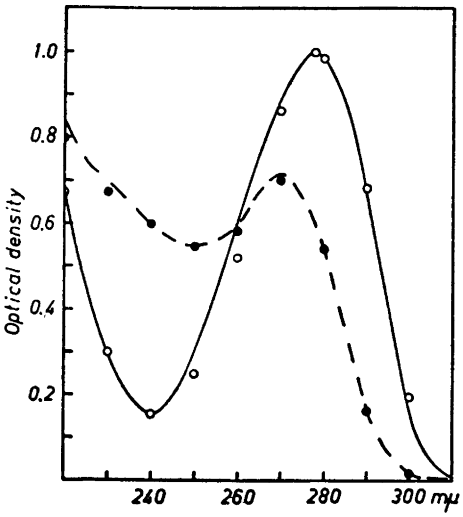

Fig. 1. Ultraviolet absorption curves for CMPX in comparison with 3′-cytidylic acid in acid and in alkali. ———— CMPX in acid and — — — in alkali. O 3′-cytidylic acid in acid and ● in alkali.

material (wet weight) corresponding to 1.3 % of the total nucleotide content in the acid extract. The substance was concentrated and freed from the eluents by adsorption on norite and elution with ammoniacal ethanol. The ultraviolet absorption spectrum of CMPX was very similar to that of cytidylic acid, either in acid or in alkali (Fig. 1). Moreover, cytosine could be identified by paper chromatography in two different solvent systems and its spectrum after hydrolysing CMPX in 70 % perchloric acid for 1 h at 100°C. Analysis showed the presence of one mole of acid-stable phosphorus per mole of base. After hydrolysis of CMPX with 0.05 N hydrochloric acid for 30 min at 100°C the two isomeric cytidine-2′- and 3′-phosphates could be identified as can be seen from Fig. 2, which also shows the chromatographic and ionophoretic behaviour of the unhydrolysed CMPX in comparison with the authentic cytosine nucleotides. The nucleotides were located by contact printing in ultraviolet light. The identities of the nucleotides were confirmed by cutting the appropriate spots out of the paper, eluting the substances, and determining their absorption spectra after the appropriate blank corrections. The hydrolysis mixture contained approximately equal amounts of the 2′- and 3′-phosphates. No consumption of periodate could be shown by CMPX or its hydrolysis products. From the experimental data it is impossible to establish the position of the phosphate group or the eventuality of a cyclic 2′:3′-phosphate.

Although the unhydrolysed nucleotide was ninhydrin-negative, the presence of a short peptide or of amino acids could be revealed by paper chromatography after hydrolysis with 6 N hydrochloric acid at 120°C for 20 h. The hydrolysate was subjected to two-dimensional chromatography using phenol saturated with water in the first direction and *n*-butanol — acetic acid — water (4:1:5) or *n*-propanol — water (7:3) in the second direction. After dipping the paper in an acetone solution of ninhydrin at least 8 ninhydrin-positive spots could be detected. Sufficient material

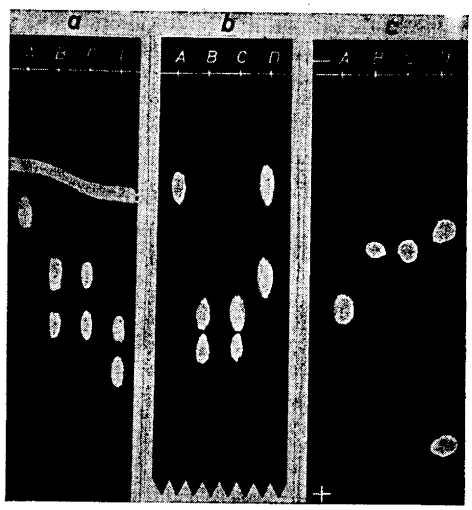

Fig. 2. Paper chromatography and ionophoresis of CMPX and its hydrolysis products in comparison with authentic cytosine nucleotides. (a) Descending chromatogram on long Whatman No. 1 paper (100 cm) in saturated ammonium sulphate solution — *iso*propanol — water (79:2:19) for 35 h. (b) Descending chromatogram in ethanol — 1 M ammonium acetate, pH 7.5 (75:30) for 85 h. (c) Ionophoresis in 0.1 M sodium acetate buffer, pH 4.15; 20 V/cm; 6 h. A) CMPX; B) hydrolysed CMPX; C) 2′- and 3′-cytidylic acid; D) cytidine-5′-mono- and diphosphate.

was not available to permit satisfactory analysis of the spots but the presence of the following amino acids were clearly indicated: leucine, valine, alanine and glycine. Spots corresponding to glutamic acid and aspartic acid were also obtained.

The behaviour of CMPX on acid hydrolysis, together with the ultraviolet absorption spectra suggests that the amino acids or peptide are attached to the ribose moiety and not directly to the pyrimidine ring. Complexes between purine nucleotides and amino acids have been detected in alkaline digests of ribonucleic acids prepared from calf pancreas, rabbit liver and yeast; and these authors proposed a phosphoamide linkage [3]. The amount of CMPX was too small for a more detailed study of the linkage between the two parts of the complex; but in view of the present data the possibility of a phosphoamide linkage is not excluded.

The peaks containing 2′- and 3′-cytidylic acid, which had been eluted with 0.02 M formic acid contained several ninhydrin reacting substances, but we have not found any of them attached to a nucleotide. A substance that shows the same elution position and the same properties as CMPX has been detected in the acid extract of the mycelium of a strain of *Penicillium urticae* [4].

This work has been supported by grants from the *Swedish Natural Science Research Council.*

1. Pontis, H. G. *Biochim. et Biophys. Acta* **25** (1957) 417.
2. Bergkvist, R. *Acta Chem. Scand.* **10** (1956) 1303.
3. Potter, J. L. and Dounce, A. L. *J. Am. Chem. Soc.* **78** (1956) 3078.
4. Persson, K. *Personal communication.*

Received February 18, 1958.

On Different Methyl Derivatives of Hexathia-adamantane

KJELL OLSSON

Chemical Institute, University of Uppsala, Uppsala, Sweden

If thiol acetic acid, formic acid and dried zinc chloride are mixed and left at room temperature, a precipitate is gradually formed. This is usually difficultly soluble in all ordinary solvents and decomposes without melting at approximately 300°. By varying the proportions between the reactants, fractionating the obtained products with the aid of various solvents and recording the infra red spectra of the fractions, five different colourless crystalline compounds were isolated. Two of these were recognized as known compounds, *viz.* hexathia-adamantane (I), recently prepared from formic acid and hydrogen sulphide in strongly acidic media by Fredga and Olsson [1] and its tetramethyl derivative (V), prepared long ago by Bongartz [2] through the action of dried zinc chloride on thiol acetic acid alone. The structure (V) accepted nowadays was proposed much later by Fredga [3].

The analysis and infra red spectra of the remaining three compounds showed these to be mono-, di- and tri-methyl-hexathia-adamantane ((II), (III) and (IV), respectively). The structures (II)—(IV) agree completely with the fact that the properties of the corresponding compounds are intermediate between those of (I) and (V) and vary in a regular manner in the series. Thus the solubility increases rapidly when passing form (I) to (V), but only (IV) and (V) are appreciably soluble in ordinary solvents. The volatility increases in the same direction. All of the compounds can be sublimed *in vacuo*, though (I) requires heating for hours at 225° and 10^{-3} mm Hg. Only (V) melts without decomposition (at 224—225°)[2], whereas (I)—(IV) decompose without melting at higher temperature. Unsymmetrically substituted hexathia-adamantanes like (II)—(IV) have not been prepared before.

As is to be expected the reaction product gets richer in the highly methylated hexathia-adamantanes with increasing excess of thiol acetic acid and *vice versa.* Since certain details of the procedures for the preparation of (II) and (IV) have not been worked out as yet, only the preparation of (III) will be more closely described here. A more detailed account of this investigation, possibly extended to some more thiol acids, will soon be given elsewhere.

Experimental. 3.2 g of dried zinc chloride is added to a mixture of 6.9 g (6.4 ml) of freshly distilled thiol acetic acid (b.p. 91—96°) and 0.98 g (0.80 ml) of absolute formic acid in a hood. In the beginning, the zinc chloride slowly dissolves, hydrogen sulphide is evolved, and gentle heat is generated. A precipitate

was not available to permit satisfactory analysis of the spots but the presence of the following amino acids were clearly indicated: leucine, valine, alanine and glycine. Spots corresponding to glutamic acid and aspartic acid were also obtained.

The behaviour of CMPX on acid hydrolysis, together with the ultraviolet absorption spectra suggests that the amino acids or peptide are attached to the ribose moiety and not directly to the pyrimidine ring. Complexes between purine nucleotides and amino acids have been detected in alkaline digests of ribonucleic acids prepared from calf pancreas, rabbit liver and yeast; and these authors proposed a phosphoamide linkage [3]. The amount of CMPX was too small for a more detailed study of the linkage between the two parts of the complex; but in view of the present data the possibility of a phosphoamide linkage is not excluded.

The peaks containing 2′- and 3′-cytidylic acid, which had been eluted with 0.02 M formic acid contained several ninhydrin reacting substances, but we have not found any of them attached to a nucleotide. A substance that shows the same elution position and the same properties as CMPX has been detected in the acid extract of the mycelium of a strain of *Penicillium urticae* [4].

This work has been supported by grants from the *Swedish Natural Science Research Council.*

1. Pontis, H. G. *Biochim. et Biophys. Acta* **25** (1957) 417.
2. Bergkvist, R. *Acta Chem. Scand.* **10** (1956) 1303.
3. Potter, J. L. and Dounce, A. L. *J. Am. Chem. Soc.* **78** (1956) 3078.
4. Persson, K. *Personal communication.*

Received February 18, 1958.

On Different Methyl Derivatives of Hexathia-adamantane

KJELL OLSSON

Chemical Institute, University of Uppsala, Uppsala, Sweden

If thiol acetic acid, formic acid and dried zinc chloride are mixed and left at room temperature, a precipitate is gradually formed. This is usually difficultly soluble in all ordinary solvents and decomposes without melting at approximately 300°. By varying the proportions between the reactants, fractionating the obtained products with the aid of various solvents and recording the infra red spectra of the fractions, five different colourless crystalline compounds were isolated. Two of these were recognized as known compounds, *viz.* hexathia-adamantane (I), recently prepared from formic acid and hydrogen sulphide in strongly acidic media by Fredga and Olsson [1] and its tetramethyl derivative (V), prepared long ago by Bongartz [2] through the action of dried zinc chloride on thiol acetic acid alone. The structure (V) accepted nowadays was proposed much later by Fredga [3].

The analysis and infra red spectra of the remaining three compounds showed these to be mono-, di- and tri-methyl-hexathia-adamantane ((II), (III) and (IV), respectively). The structures (II)—(IV) agree completely with the fact that the properties of the corresponding compounds are intermediate between those of (I) and (V) and vary in a regular manner in the series. Thus the solubility increases rapidly when passing form (I) to (V), but only (IV) and (V) are appreciably soluble in ordinary solvents. The volatility increases in the same direction. All of the compounds can be sublimed *in vacuo*, though (I) requires heating for hours at 225° and 10^{-3} mm Hg. Only (V) melts without decomposition (at 224—225°)[2], whereas (I)—(IV) decompose without melting at higher temperature. Unsymmetrically substituted hexathia-adamantanes like (II)—(IV) have not been prepared before.

As is to be expected the reaction product gets richer in the highly methylated hexathia-adamantanes with increasing excess of thiol acetic acid and *vice versa.* Since certain details of the procedures for the preparation of (II) and (IV) have not been worked out as yet, only the preparation of (III) will be more closely described here. A more detailed account of this investigation, possibly extended to some more thiol acids, will soon be given elsewhere.

Experimental. 3.2 g of dried zinc chloride is added to a mixture of 6.9 g (6.4 ml) of freshly distilled thiol acetic acid (b.p. 91—96°) and 0.98 g (0.80 ml) of absolute formic acid in a hood. In the beginning, the zinc chloride slowly dissolves, hydrogen sulphide is evolved, and gentle heat is generated. A precipitate

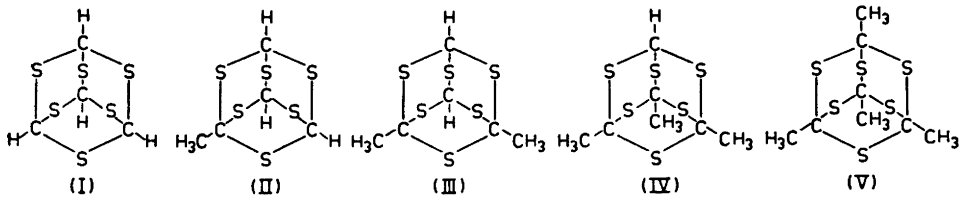

soon starts to form. The mixture is left at room temperature overnight, stirred with 20 ml of conc. hydrochloric acid to dissolve precipitated zinc compounds, and filtered with suction. The precipitate is thoroughly washed with conc. hydrochloric acid, water, methanol and two 25 ml portions of chloroform in that order. The almost colourless product is refluxed for 5 min. with 100 ml of pyridine. The boiling mixture is rapidly filtered through a fluted filter paper. The filtrate is left in the refrigerator overnight. The crystals formed are filtered off, recrystallized from pyridine (95 ml per g of dry substance; a very small amount of insoluble material is removed by rapid filtration of the hot solution) and dried *in vacuo* at 100° for 1 h. Yield about 700 mg of pure dimethyl-hexathia-adamantane (III). (Found: C 26.35; H 2.95; S 70.84. Calc. for $C_6H_8S_6$ (272.5): C 26.44; H 2.96; S 70.60.)

From the chloroform washings, about 200 mg of (IV) is obtained by evaporation to 10 ml, addition of 20 ml of ether, and recrystallization of the precipitate from 5 ml of pyridine. The optimum yield of (IV) (about 600 mg) is obtained, if the amount of formic acid is decreased to 0.35 ml.

From the undissolved residue after the pyridine extraction, about 200 mg of (II) is obtained by recrystallization from 10 ml of dimethyl sulphoxide. The optimum yield of (II) (about 1 g) is obtained, if equal volumes of formic acid and thiol acetic acid are used.

1. Fredga, A. and Olsson, K. *Arkiv Kemi* **9** (1956) 163.
2. Bongartz, J. *Ber.* **19** (1886) 2182.
3. Fredga, A. *Arkiv Kemi, Mineral. Geol.* **25 B** (1947) No. 8.

Received February 22, 1958.

The Strain in the 1,2-Dithiolane Ring

GÖRAN BERGSON and LENNART SCHOTTE*

Chemical Institute, University of Uppsala, Sweden

The 1,2-dithiolane ring (I) has been an important unit in modern sulphur chemistry since its presence in 6-thioctic acid was discovered [1]. The hypothesis advanced by Calvin and co-workers [2] about the role of 6-thuoctic acid in the photosynthesis has caused many efforts to determine the steric strain in the 1,2-dithiolane ring. A necessary condition for Calvin's hypothesis to be true is that the strain is at least 20—25 kcal/mole. The estimates of the steric strain reported in the literature are widely scattered as can be seen from Table 1.

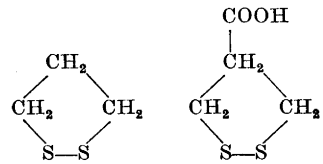

The exact structure of the 1,2-dithiolane ring in 1,2-dithiolane-4-carboxylic acid (II) is now known thanks to an X-ray investigation performed by Professor Olav Foss [3]. On the basis of this investigation, we have calculated the strain energy in a classical manner [4], *i.e.* with the assumptions that the strain is composed of three terms: stretching, bending and torsion. This method gives a strain of 16—30

* Both authors contribute equally.

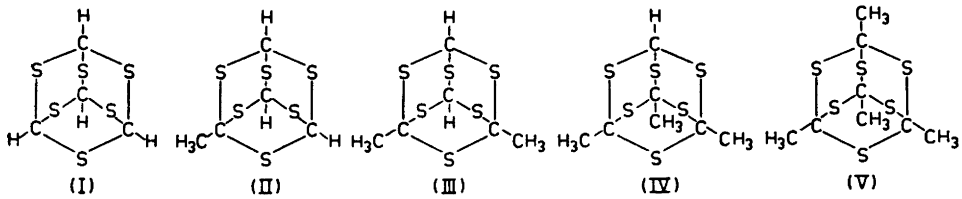

soon starts to form. The mixture is left at room temperature overnight, stirred with 20 ml of conc. hydrochloric acid to dissolve precipitated zinc compounds, and filtered with suction. The precipitate is thoroughly washed with conc. hydrochloric acid, water, methanol and two 25 ml portions of chloroform in that order. The almost colourless product is refluxed for 5 min. with 100 ml of pyridine. The boiling mixture is rapidly filtered through a fluted filter paper. The filtrate is left in the refrigerator overnight. The crystals formed are filtered off, recrystallized from pyridine (95 ml per g of dry substance; a very small amount of insoluble material is removed by rapid filtration of the hot solution) and dried *in vacuo* at 100° for 1 h. Yield about 700 mg of pure dimethyl-hexathia-adamantane (III). (Found: C 26.35; H 2.95; S 70.84. Calc. for $C_6H_8S_6$ (272.5): C 26.44; H 2.96; S 70.60.)

From the chloroform washings, about 200 mg of (IV) is obtained by evaporation to 10 ml, addition of 20 ml of ether, and recrystallization of the precipitate from 5 ml of pyridine. The optimum yield of (IV) (about 600 mg) is obtained, if the amount of formic acid is decreased to 0.35 ml.

From the undissolved residue after the pyridine extraction, about 200 mg of (II) is obtained by recrystallization from 10 ml of dimethyl sulphoxide. The optimum yield of (II) (about 1 g) is obtained, if equal volumes of formic acid and thiol acetic acid are used.

1. Fredga, A. and Olsson, K. *Arkiv Kemi* **9** (1956) 163.
2. Bongartz, J. *Ber.* **19** (1886) 2182.
3. Fredga, A. *Arkiv Kemi, Mineral. Geol.* **25 B** (1947) No. 8.

Received February 22, 1958.

The Strain in the 1,2-Dithiolane Ring

GÖRAN BERGSON and LENNART SCHOTTE*

Chemical Institute, University of Uppsala, Sweden

The 1,2-dithiolane ring (I) has been an important unit in modern sulphur chemistry since its presence in 6-thioctic acid was discovered [1]. The hypothesis advanced by Calvin and co-workers [2] about the role of 6-thuoctic acid in the photosynthesis has caused many efforts to determine the steric strain in the 1,2-dithiolane ring. A necessary condition for Calvin's hypothesis to be true is that the strain is at least 20—25 kcal/mole. The estimates of the steric strain reported in the literature are widely scattered as can be seen from Table 1.

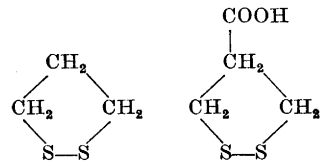

The exact structure of the 1,2-dithiolane ring in 1,2-dithiolane-4-carboxylic acid (II) is now known thanks to an X-ray investigation performed by Professor Olav Foss [3]. On the basis of this investigation, we have calculated the strain energy in a classical manner [4], *i.e.* with the assumptions that the strain is composed of three terms: stretching, bending and torsion. This method gives a strain of 16—30

* Both authors contribute equally.

Table 1.

Strain, kcal/mole	Compound	Reference and method
27	1,2-Dithiolane 6-Thioctic acid	Calvin [2]; UV.
min. 11	1,2-Dithiolane	Calvin [2]; Conformation analysis.
6	1,2-Dithiolane	Calvin [2]; Equilibrium measurements.
4—5	1,2-Dithiolane 6-Thioctic acid	Sunner [5]; Thermochemical measurements.
min. 16	1,2-Dithiolane-4-carboxylic acid	This work; Conformation analysis.

kcal/mole, when uncertainties in structural parameters and assignments of normal valence angles are taken into account. We believe that our smallest value (16 kcal/mole) is too far form the values found in the thermochemical measurements to be explained as due to differences in the structural parameters for 1,2-dithiolane-4-carboxylic acid on the one hand and 6-thioctic acid and the unsubstituted 1,2-dithiolane ring on the other. As far as steric strain is concerned it is therefore our opinion that Calvin's hypothesis about the rôle of 6-thioctic acid in photosynthesis cannot be disregarded.

A detailed report of our calculations will soon be pulished in *Arkiv Kemi*.

1. For a review see the article by Reed, L. J. *Advances in Enzymol.* **18** (1957) 319.
2. Calvin, M. and Barltrop, J. A. *J. Am. Chem. Soc.* **74** (1952) 6153; Barltrop, J. A., Hayes, P. M. and Calvin, M. *Ibid.* **76** (1954) 4348.
3. Foss, O. and Tjomsland, O. *Acta Chem. Scand.* **11** (1957) 1426 and *Private communication.*
4. Newman, M. S. *Steric Effects in Organic Chemistry.* New York 1956, p. 525 ff.
5. Sunner, S. *Nature* **176** (1955) 217.

Received February 26, 1958.

ACTA CHEMICA SCANDINAVICA 12 (1958) 369—376

Composition of Products Formed by Thermal Neutron Fission of ^{235}U

I. Compilation of Nuclear Data of the Fission Products

JAN PRAWITZ and JAN RYDBERG

Research Institute of National Defence, Dept. 1, Sundbyberg 4, Sweden

An extensive compilation is made of the data up to July 1957 for the fission yields, decay schemes, half-lives and thermal neutron cross sections of the ^{235}U fission products.

For the calculation of the beta activity, mole fraction and isotopic composition of the fission elements (Part II[26] and III[27] of this series), an extensive compilation has been made of the fission yields, modes of transformation, half-lives and thermal neutron cross sections of the ^{235}U fission products. Similar compilations have previously been made, *e.g.* by Coryell and Sugerman [1, 2], Steinberg and Glendenin [28], and Lock [17]. These compilations are either less comprehensive or less up to date than the present paper.

In this paper most of the data have been covered up to July 1957. The decay schemes and half-lives are taken mainly from Nuclear Science Abstracts. The thermal neutron capture cross sections are taken from Hughes and Harvey [29]. In the compilation of fission yield values [1–25], mass spectrometric data have generally been preferred; all values have been standardized towards a cumulative fission yield of 6.32 ± 0.24 % for ^{140}Ba [12]. The sum of the fission yields amounts to 202 %.

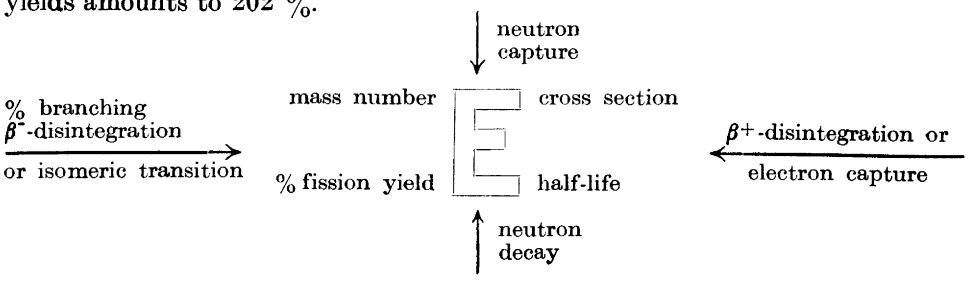

Fig. 1. Key to the presentation of the data; E stands for Element. The figure is more extensively explained in the text.

Table 1. Fission products decay scheme. Legend to the presentation is given in Fig. 1; ----→ stands for a presumptive transformation.

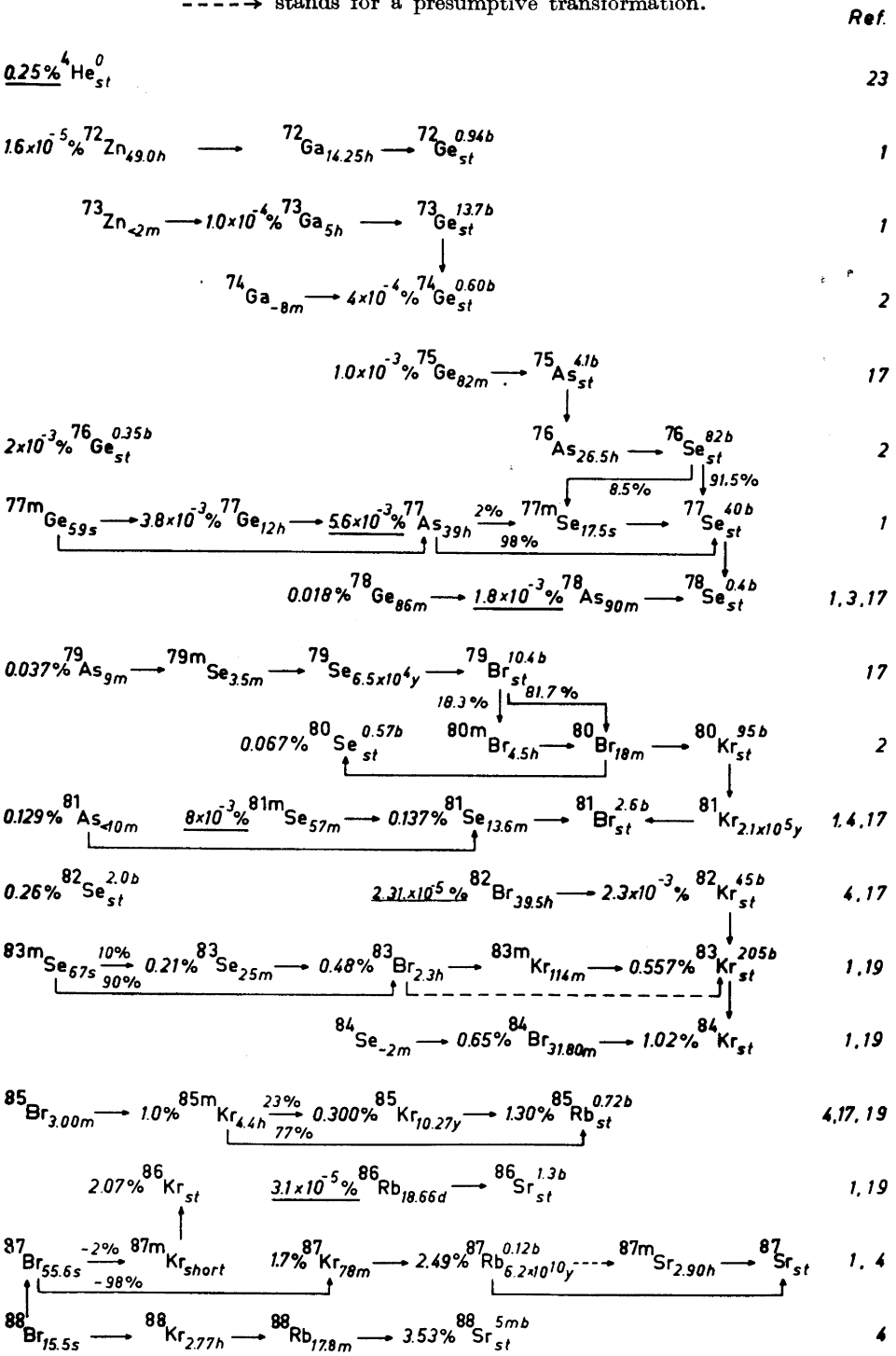

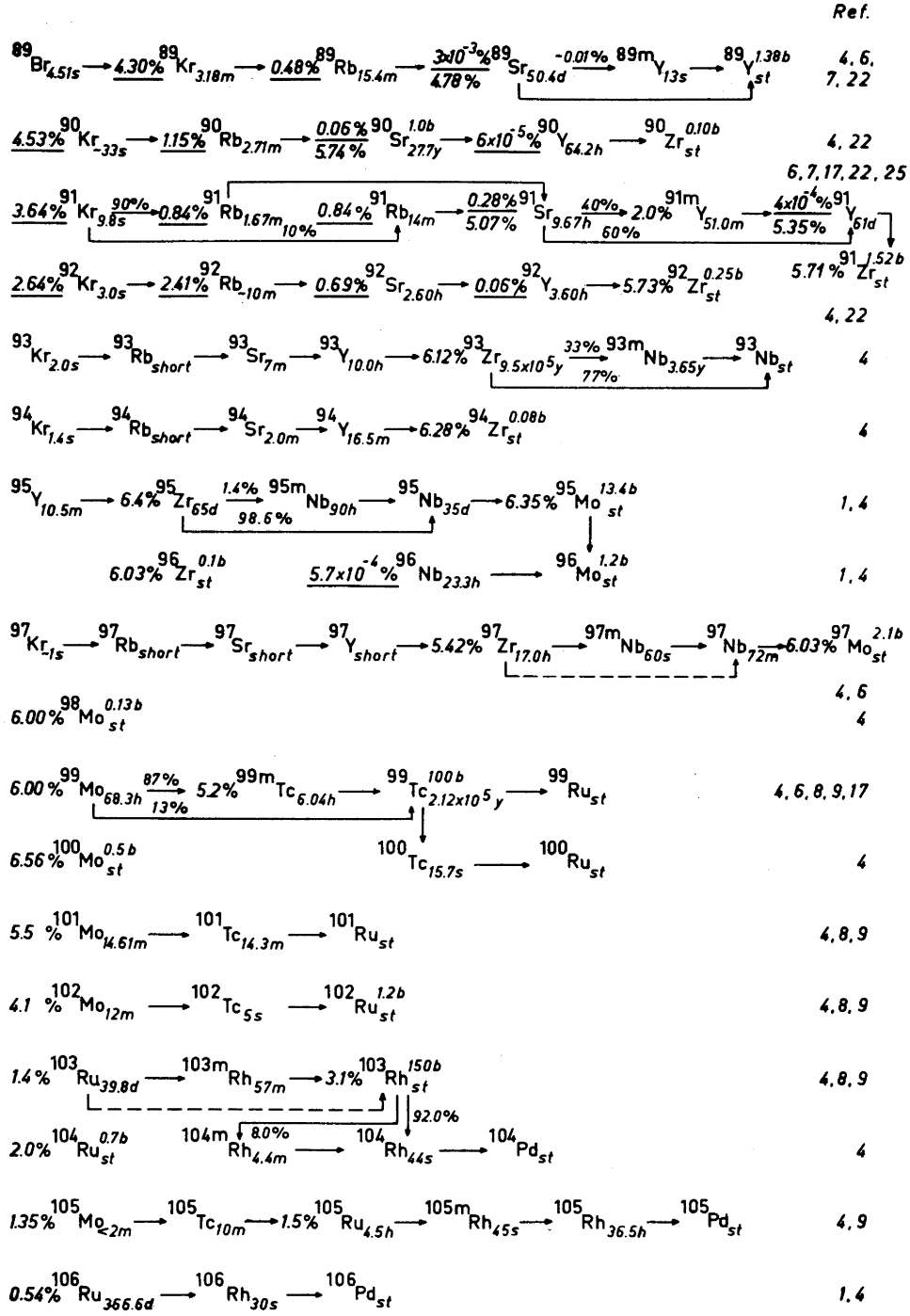
Ref.
89Br4.51s → 4.30% 89Kr3.18m → 0.48% 89Rb15.4m → 3x10-3% / 4.78% 89Sr50.4d -0.01% 89mY13s → 89Yst 1.38b 4, 6, 7, 22
4.53% 90Kr33s → 1.15% 90Rb2.71m → 0.06% / 5.74% 90Sr27.7y 1.0b → 6x10-5% 90Y64.2h → 90Zrst 0.10b 4, 22
6, 7, 17, 22, 25
3.64% 91Kr9.8s 90% → 0.84% 91Rb1.67m 10% → 0.84% 91Rb14m → 0.28% / 5.07% 91Sr9.67h 40% → 2.0% 91mY51.0m → 4x10-4% / 5.35% 91Y61d → 91Zrst 1.52b
5.71%
2.64% 92Kr3.0s → 2.41% 92Rb4.10m → 0.69% 92Sr2.60h → 0.06% 92Y3.60h → 5.73% 92Zrst 0.25b 4, 22
93Kr2.0s → 93Rbshort → 93Sr7m → 93Y10.0h → 6.12% 93Zr9.5x10^5y 33% / 77% → 93mNb3.65y → 93Nbst 4
94Kr1.4s → 94Rbshort → 94Sr2.0m → 94Y16.5m → 6.28% 94Zrst 0.08b 4
95Y10.5m → 6.4% 95Zr65d 1.4% / 98.6% → 95mNb90h → 95Nb35d → 6.35% 95Mo st 13.4b 1, 4
6.03% 96Zrst 0.1b
5.7x10-4% 96Nb23.3h → 96Mo st 1.2b 1, 4
97Kr1s → 97Rbshort → 97Srshort → 97Yshort → 5.42% 97Zr17.0h → 97mNb60s → 97Nb72m → 6.03% 97Mo st 2.1b 4, 6
6.00% 98Mo st 0.13b 4
6.00% 99Mo68.3h 87% / 13% → 5.2% 99mTc6.04h → 99Tc 2.12x10^5y 100b → 99Rust 4, 6, 8, 9, 17
6.56% 100Mo st 0.5b
100Tc15.7s → 100Rust 4
5.5 % 101Mo14.61m → 101Tc14.3m → 101Rust 4, 8, 9
4.1 % 102Mo12m → 102Tc5s → 102Ru st 1.2b 4, 8, 9
1.4 % 103Ru39.8d → 103mRh57m → 3.1% 103Rh st 150b 4, 8, 9
92.0%
2.0% 104Ru st 0.7b
104m Rh4.4m 8.0% → 104Rh44s → 104Pdst 4
1.35% 105Mo<2m → 105Tc10m → 1.5% 105Ru4.5h → 105mRh45s → 105Rh36.5h → 105Pdst 4, 9
0.54% 106Ru366.6d → 106Rh30s → 106Pdst 1, 4

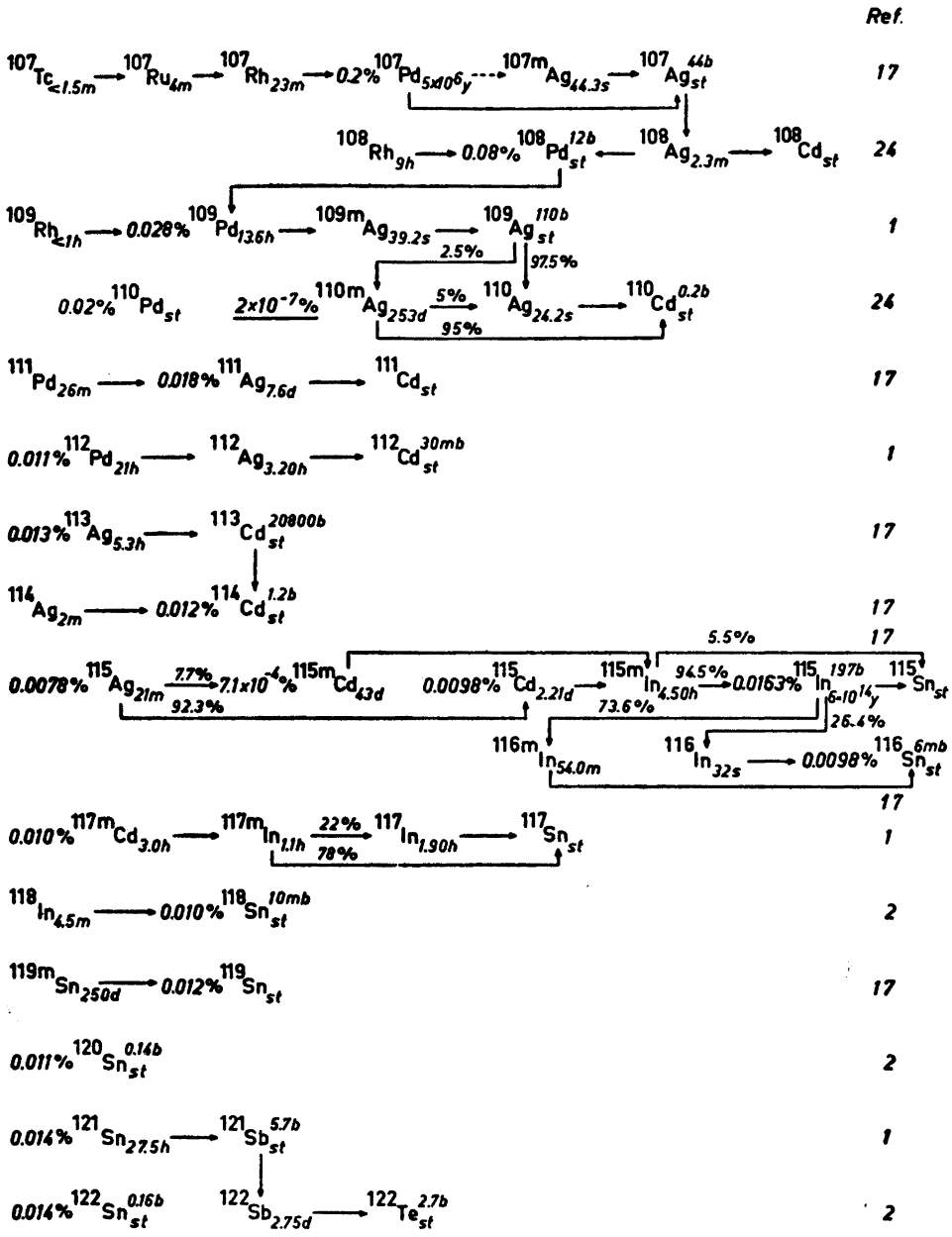
Ref.
107Tc<1.5m → 107Ru4m → 107Rh23m → 0.2% 107Pd5x10^6y ⇢ 107mAg44.3s → 107Ag st 44b
17
108Rh9h → 0.08% 108Pd st 12b ← 108Ag2.3m → 108Cd st
24
109Rh<1h → 0.028% 109Pd13.6h → 109mAg39.2s → 109Ag st 110b
2.5%
97.5%
1
0.02% 110Pd st
2x10^-7% 110mAg253d 5% → 110Ag24.2s → 110Cd st 0.2b
95%
24
111Pd26m → 0.018% 111Ag7.6d → 111Cd st
17
0.011% 112Pd21h → 112Ag3.20h → 112Cd st 30mb
1
0.013% 113Ag5.3h → 113Cd st 20800b
17
114Ag2m → 0.012% 114Cd st 1.2b
17
5.5%
17
0.0078% 115Ag21m 7.7% → 7.1x10^-4% 115mCd43d
92.3%
0.0098% 115Cd2.21d → 115mIn4.50h 94.5% → 0.0163% 115In 197b 6·10^14y → 115Sn st
73.6%
26.4%
116mIn54.0m
116In32s → 0.0098% 116Sn st 6mb
17
0.010% 117mCd3.0h → 117mIn1.1h 22% → 117In1.90h → 117Sn st
78%
1
118In4.5m → 0.010% 118Sn st 10mb
2
119mSn250d → 0.012% 119Sn st
17
0.011% 120Sn st 0.14b
2
0.014% 121Sn27.5h → 121Sb st 5.7b
1
0.014% 122Sn st 0.16b
122Sb2.75d → 122Te st 2.7b
2

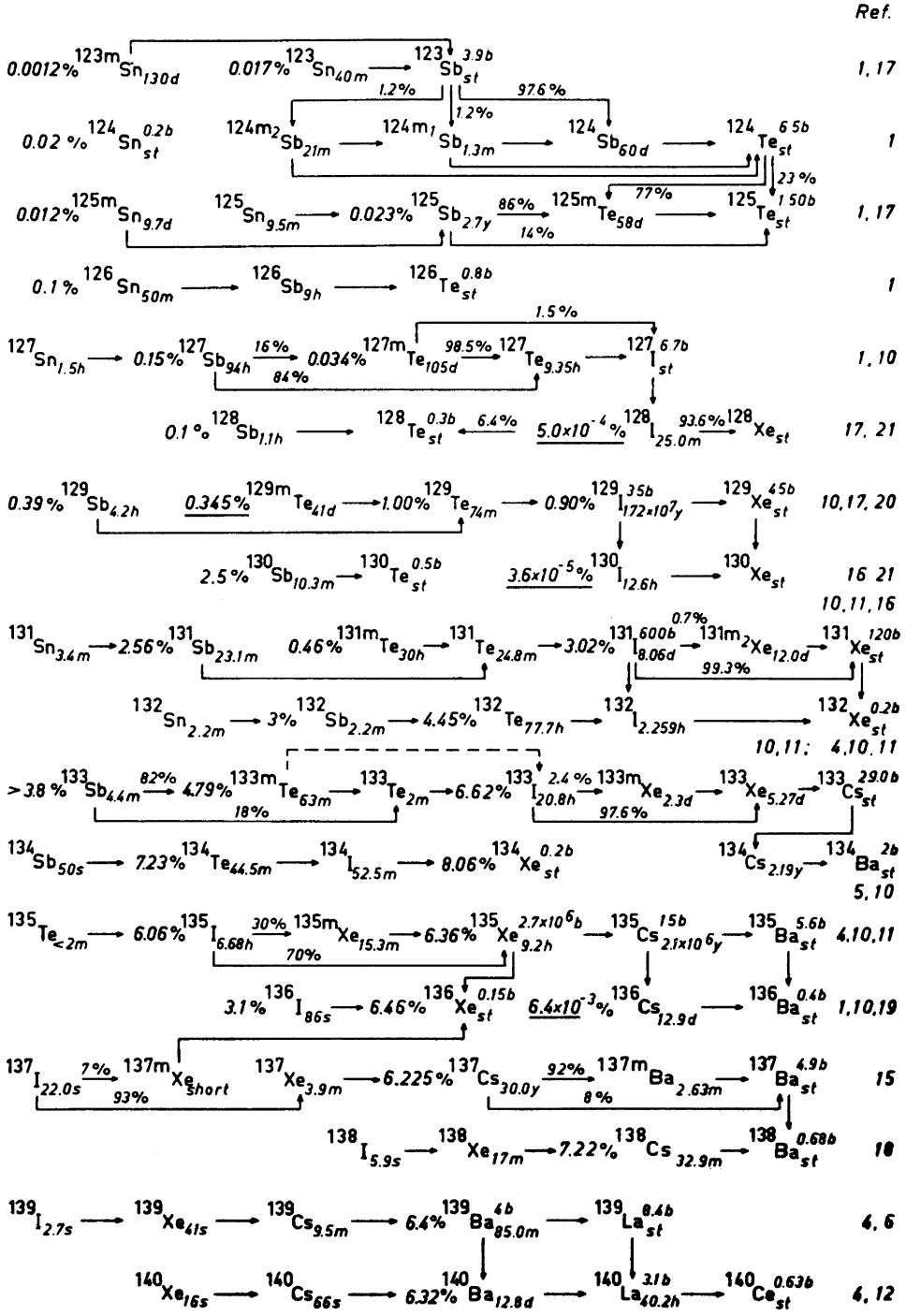
Ref.
0.0012% 123m Sn 130d
0.017% 123 Sn 40m
123 Sb st 3.9b
1.2%
97.6%
1, 17
0.02 % 124 Sn st 0.2b
124m2 Sb 21m
124m1 Sb 1.3m
124 Sb 60d
124 Te st 6.5b
1.2%
23 %
77%
1
0.012% 125m Sn 9.7d
125 Sn 9.5m
0.023% 125 Sb 2.7y
86%
14%
125m Te 58d
125 Te st 1.50b
1, 17
0.1 % 126 Sn 50m
126 Sb 9h
126 Te st 0.8b
1
1.5 %
127 Sn 1.5h
0.15% 127 Sb 94h
16%
84%
0.034% 127m Te 105d
98.5% 127 Te 9.35h
127 I st 6.7b
1, 10
0.1 % 128 Sb 1.1h
128 Te st 0.3b
6.4%
5.0x10-4 % 128 I 25.0m
93.6% 128 Xe st
17, 21
0.39 % 129 Sb 4.2h
0.345% 129m Te 41d
1.00% 129 Te 74m
0.90% 129 I 1.72x10^7y 35b
129 Xe st 45b
10, 17, 20
2.5 % 130 Sb 10.3m
130 Te st 0.5b
3.6x10-5 % 130 I 12.6h
130 Xe st
16 21
10, 11, 16
131 Sn 3.4m
2.56% 131 Sb 23.1m
0.46% 131m Te 30h
131 Te 24.8m
3.02% 131 I 8.06d 600b
0.7%
131m2 Xe 12.0d
99.3%
131 Xe st 120b
132 Sn 2.2m
3% 132 Sb 2.2m
4.45% 132 Te 77.7h
132 I 2.259h
132 Xe st 0.2b
10, 11; 4, 10, 11
> 3.8 % 133 Sb 4.4m
82%
18%
4.79% 133m Te 63m
133 Te 2m
6.62% 133 I 20.8h 2.4 %
133m Xe 2.3d
133 Xe 5.27d
133 Cs st 29.0b
97.6%
134 Sb 50s
7.23% 134 Te 44.5m
134 I 52.5m
8.06% 134 Xe st 0.2b
134 Cs 2.19y
134 Ba st 2b
5, 10
135 Te <2m
6.06% 135 I 6.68h
30%
70%
135m Xe 15.3m
6.36% 135 Xe 9.2h 2.7x10^6b
135 Cs 2.1x10^6y 1.5b
135 Ba st 5.6b
4, 10, 11
3.1% 136 I 86s
6.46% 136 Xe st 0.15b
6.4x10-3 % 136 Cs 12.9d
136 Ba st 0.4b
1, 10, 19
137 I 22.0s
7%
93%
137m Xe short
137 Xe 3.9m
6.225% 137 Cs 30.0y
92%
8%
137m Ba 2.63m
137 Ba st 4.9b
15
138 I 5.9s
138 Xe 17m
7.22% 138 Cs 32.9m
138 Ba st 0.68b
10
139 I 2.7s
139 Xe 41s
139 Cs 9.5m
6.4% 139 Ba 85.0m 4b
139 La st 8.4b
4, 6
140 Xe 16s
140 Cs 66s
6.32% 140 Ba 12.8d
140 La 40.2h 3.1b
140 Ce st 0.63b
4, 12

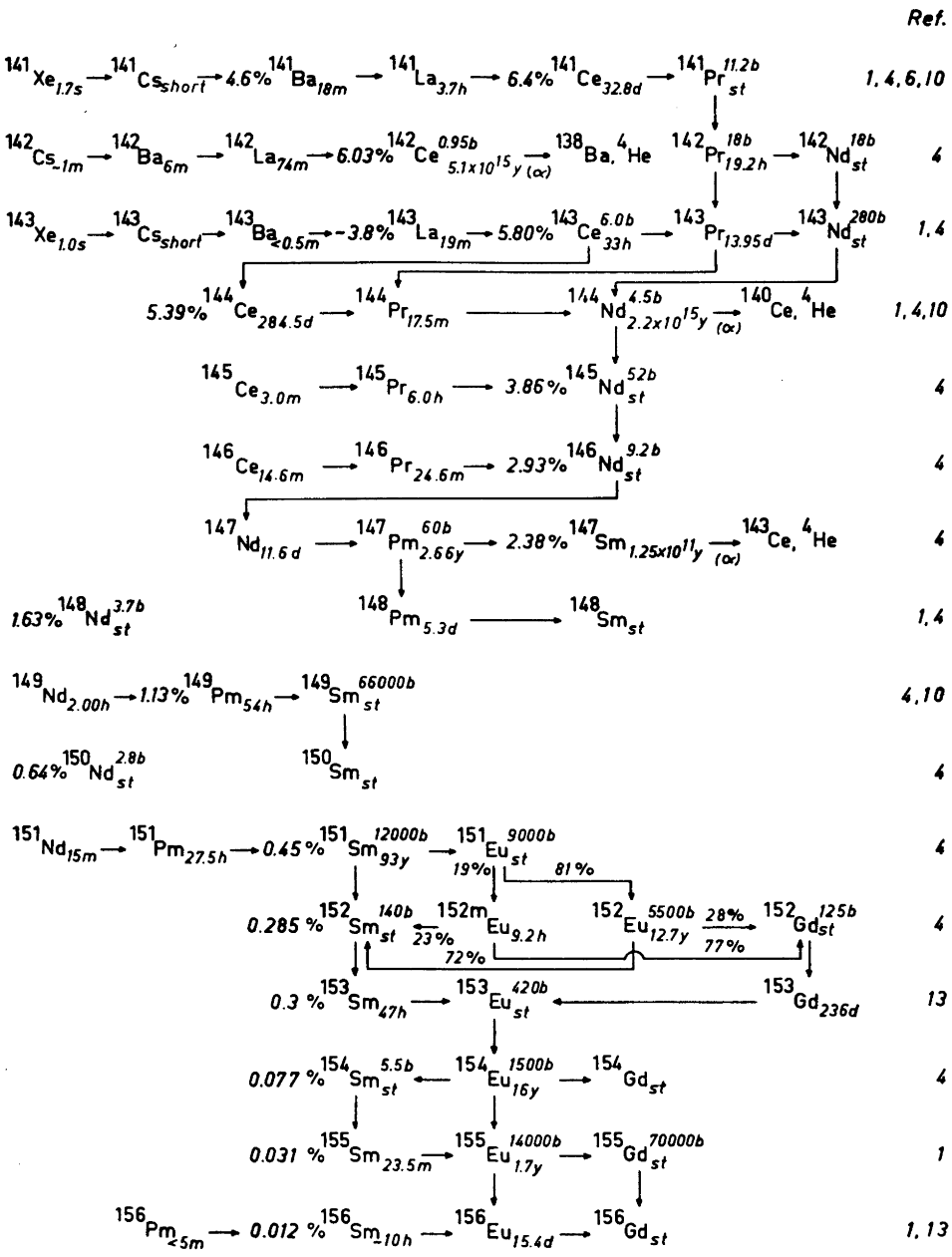
Ref.
141Xe1.7s → 141Cs short → 4.6% 141Ba18m → 141La3.7h → 6.4% 141Ce32.8d → 141Pr st 11.2b
1, 4, 6, 10
142Cs ~1m → 142Ba6m → 142La74m → 6.03% 142Ce 0.95b 5.1x10^15 y (α) → 138Ba, 4He
142Pr 18b 19.2h → 142Nd st 18b
4
143Xe1.0s → 143Cs short → 143Ba <0.5m → ~3.8% 143La19m → 5.80% 143Ce 6.0b 33h → 143Pr13.95d → 143Nd st 280b
1, 4
5.39% 144Ce284.5d → 144Pr17.5m → 144Nd 4.5b 2.2x10^15 y (α) → 140Ce, 4He
1, 4, 10
145Ce3.0m → 145Pr6.0h → 3.86% 145Nd st 52b
4
146Ce14.6m → 146Pr24.6m → 2.93% 146Nd st 9.2b
4
147Nd11.6d → 147Pm 60b 2.66y → 2.38% 147Sm 1.25x10^11 y (α) → 143Ce, 4He
4
1.63% 148Nd st 3.7b
148Pm5.3d → 148Sm st
1, 4
149Nd2.00h → 1.13% 149Pm54h → 149Sm st 66000b
4, 10
0.64% 150Nd st 2.8b
150Sm st
4
151Nd15m → 151Pm27.5h → 0.45% 151Sm 12000b 93y → 151Eu st 9000b
19% 81%
4
0.285% 152Sm st 140b 23% 152mEu9.2h 152Eu 5500b 12.7y 28% 77% 152Gd st 125b
72%
4
0.3% 153Sm47h → 153Eu st 420b ← 153Gd236d
13
0.077% 154Sm st 5.5b ← 154Eu 1500b 16y → 154Gd st
4
0.031% 155Sm23.5m → 155Eu 14000b 1.7y → 155Gd st 70000b
1
156Pm <5m → 0.012% 156Sm10h → 156Eu15.4d → 156Gd st
1, 13

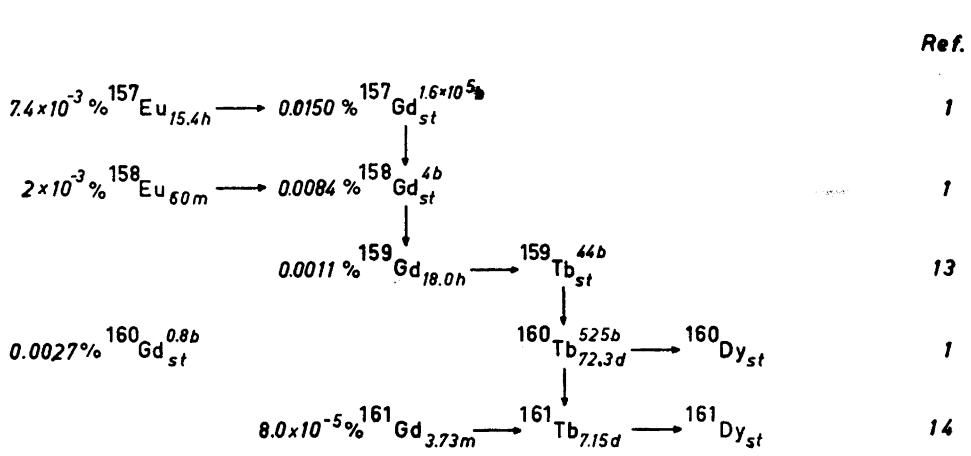

Fig. 1 shows the method of presenting the data, which are given in extenso in Table 1. The arrows indicate the formation process; percentage figures are given when branching ratios are known. The cross sections are given in barns and millibarns (indicated by *b* and *mb*) and half-lives in years (*y*), days (*d*), hours (*h*), minutes (*m*) or seconds (*s*). The percentage value given in front of the element is the cumulative fission yield value, except for underlined values, which refer to primary yields.

The authors wish to thank the head of FOA 1, Professor G. Ljunggren, for his continuous interest in and support of this work.

REFERENCES

1. Coryell, C. D. and Sugerman, N. (Ed.) *Radiochemical Studies. The Fission Products.* Appendix B. McGraw-Hill Book Co, New York 1951.
2. *Ibid*, p. 537.
3. Sugerman, N. *Phys. Rev.* **89** (1953) 570.
4. Petruska, J. A., Thode, H. G. and Tomlinson, R. H. *Can. J. Phys.* **33** (1955) 693.
5. Wannless, R. K. and Thode, H. G. *Can. J. Phys.* **33** (1955) 541.
6. Reed, G. W. and Turkevich, A. *Phys. Rev.* **92** (1953) 1473.
7. Reed, G. W. *Phys. Rev.* **98** (1955) 1327.
8. Wiles, D. R. and Coryell, C. D. *Phys. Rev.* **96** (1954) 696.
9. Wiles, D. R. *Z. Elektrochem.* **58** (1954) 620.
10. Pappas, A. C. *Technical Report No* **63**, *Massachusetts Institute of Technology*, Cambridge, Mass. 1955.
11. Katcoff, S. and Rubinson, W. *Phys. Rev.* **91** (1953) 1458.
12. Yaffe, L., Thode, H. G., Merrit, W. F., Hawkings, R. C., Brown, F. and Bartholomew, R. M. *Can. J. Chem.* **32** (1954) 1017.
13. Petrow, H. G. and Rocco, G. *Phys. Rev.* **96** (1954) 1614.
14. Freiling, E. C., Bunny, L. R. and Ballou, N. E. *Phys. Rev.* **96** (1954) 102.
15. Brown, F. *J. Inorg. & Nuclear Chem.* **1** (1955) 248.
16. Pappas, A. C. and Wiles, D. R. *J. Inorg. & Nuclear Chem.* **2** (1956) 69.
17. Lock, C. J. L. *A. E. R. E. Report C/R* **1715**, Harwell 1955.
18. Bartholomew, R. M. and Baerg, A. P. *Can. J. Chem.* **34** (1956) 201.
19. Blades, A. T., Fleming, W. H. and Thode, H. G. *Can. J. Chem.* **34** (1956) 233.

20. Purkayastha, B. C. and Martin, G. R. *Can. J. Chem.* **34** (1956) 293.
21. Kenett, T. J. and Thode, H. G. *Phys. Rev.* **103** (1956) 323.
22. Herrmann, G. and Strassman, F. *Z. Naturforsch.* **11a** (1956) 946.
23. de Laboulage, H., Tzara, C. and Olkowsky, J. *J. Phys. Radium* **15** (1954) 470.
24. Blomeke, J. O. *O.R.N.L. Report No 1783*, Oak Ridge 1955.
25. Baerg, A. P. and Bartholomew, R. M. *Can. J. Chem.* **35** (1957) 980.
26. Prawitz, J. and Rydberg, J. *Acta Chem. Scand.* **12** (1958) 377, (Part II).
27. Prawitz, J. *Acta Chem. Scand. To be published* (Part III).
28. Steinberg, E. P. and Glendenin, L. E. *Paper P/614, Proc. Int. Conf. Peaceful Uses of Atomic Energy, Geneva 1955*. United Nations, New York 1955.
29. Hughes, D. J. and Harvey, J. A. *Neutron Cross Sections*, McGraw-Hill Book Co, New York 1955.

Received November 28, 1957.

ACTA CHEMICA SCANDINAVICA 12 (1958) 377—398

Composition of Products Formed by Thermal Neutron Fission of ^{235}U

II. Chemical Composition of Stable and Radioactive Fission Products

JAN PRAWITZ and JAN RYDBERG

Research Institute of National Defence, Dept. 1, Sundbyberg 4, Sweden

The chemical composition of stable and radioactive fission products has been calculated for seven different irradiation times between 1 day and 2 years, and for three different neutron fluxes, 10^{12}, 10^{13} and 10^{14} n cm^{-2} sec^{-1}. The results are given in the form of curves showing the β-activity (Figs. 1—7) and mole fraction (Figs. 9—15) of each element as a function of cooling time from 1 day up to about 15 years. The calculations are based on nuclear data published before July 1957 [1].

For the processing of used nuclear fuels, the chemical composition of the fission products has to be known. This composition depends on a number of variables, such as the composition of the fuel "elements", the neutron energy, flux, and irradiation time in the reactor, cooling time outside the reactor, etc. If data for the fission yields, decay schemes, halflives and neutron cross sections of the fission product isotopes are known (see Part I of this series [1]), the chemical composition of the fission products formed in thermal uranium reactors may be calculated as a function of neutron flux (Φ), irradiation time (T) and cooling time (t).

Diagrams and tables of the β-activity of the fission isotopes of ^{235}U have been given by Hunter and Ballou [2], and Björnerstedt *et al.*[3] for instantaneous fission ($T = 0$), and, for various irradiation and cooling times, by Lock [4], and Moteff [5], and as an Appendix to *Progress in Nuclear Chemistry* [6]. The relative elemental activity of the most important fission products is given as a function of cooling time by Coryell *et al.*[7] and Rubinson *et al.*[8] for unpublished flux and irradiation time, and by Keneshea and Saul [10] for $\Phi = 10^{12}$ n cm^{-2} sec^{-1} and T = 1—60 d. Lock [4] gives tables of the elemental composition of the fission products obtained after three irradiation and cooling times at a very high flux (10^{15} n cm^{-2} sec^{-1}). Walton [11] has made a similar, though less comprehensive, calculation.

In this paper the β-activity and mole fraction of each fission element is calculated as a function of cooling time for various irradiation times between 1 day and 2 years and for neutron fluxes between 10^{12} and 10^{14} n cm^{-2} sec^{-1}. The calculations are based on nuclear data which have appeared in the literature up to July 1957 [1].

METHODS OF CALCULATION

A fission product isotope may be formed in several different ways: 1) as a primary fission product, 2) as a decay product in one or several chains, starting with primary fission products, or 3) through neutron capture. All these modes of formation have to be considered separately for each isotope. The elemental composition of the fission products is obtained by adding the corresponding isotopic values.

In the calculations, the following symbols are used:

A_n = activity (in disintegrations/time) of isotope in n:th generation of a primary ($n = 1$) fission product;
X_n = mole fraction (in percent) of an isotope in the n:th generation;
Φ = neutron flux (in neutrons per cm^2 per second);
T = irradiation time;
t = cooling time;
y_n = fission yield (in percent) of an isotope in a decay chain;
λ_n = disintegration constant (in time^{-1}); $\lambda_n = 0$ for stable isotopes;
τ_n = half-life; $\tau_n = \ln 2/\lambda_n$; in the calculations, τ_1 is used in a decay chain for the first isotope which has a half-life of at least one hour;
σ_n = thermal neutron capture cross section (in cm^2)
Λ_n = effective disintegration constant ($= \lambda_n + \sigma_n \cdot \Phi$).

The following equations give the relationships between activity and mole fraction of an isotope and their dependence on neutron flux, irradiation and cooling times.

$$A_n(\Phi, T, t) = R_A \cdot B(\Phi, T, t) \text{ curies per gram (gFP)} \tag{1}$$

where

$$R_A = 8.07 \cdot 10^3 \cdot y_n/T \text{ curies per gram (C/gFP); } T \text{ in days} \tag{2}$$

and

$$X_n(\Phi, T, t) = R_x \cdot B(\Phi, T, t) \text{ mole percent} \tag{3}$$

where

$$R_x = \frac{y_n}{2 \cdot \lambda_n \cdot T} \text{ mole percent} \tag{4}$$

As will be discussed in the paragraph on "burn up", R_A and R_x have this form only so long as the amount of ^{235}U is constant.

In order to convert mole percent for a certain element to weight percent (g of fission element per gram mixed fission products) the relation

$$X \text{ mole percent} = 8.6 \cdot 10^{-3} \cdot X \cdot M \text{ weight percent} \tag{5}$$

should be used, wehre M is the atomic weight of the element.

From eqns. (1—4) one obtains the simple relation

$$X_n \text{ mole percent} = \frac{6.20 \times 10^{-5}}{\lambda_n} A_n \text{ C/gFP; } \lambda_n \text{ in days}^{-1} \quad (6)$$

$B\ (\Phi,\ T,\ t)$ is calculated according to Rubinson [12].

$$\mathrm{B}\ (\Phi,\ T,\ t) = \prod_{i=1}^{n} \lambda_i \sum_{i=1}^{n} [(\prod_{j=1}^{i} \Lambda_j^{-1}) \sum_{j=1}^{i} b_j\ (1 - e^{-\Lambda_j T}) \sum_{k=1}^{n} a_k \cdot e^{-\lambda_k t}] \quad (7)$$

where $b_j = 1$ when $i = 1$,
and when $i > 1$

$$b_i = \prod_{m \neq j} \frac{\Lambda_m}{\Lambda_m - \Lambda_j},\ (m = 1,\ 2,\ \ldots\ldots\ i;\ \Lambda_m \neq \Lambda_j) \quad (7\,a)$$

and $a_k = 1$ when $i = n$,
and when $i < n$,

$$a_k = \prod_{p \neq k} (\lambda_p - \lambda_k)^{-1},\ k = i,\ i + 1,\ \ldots . n;\ \lambda_p \neq \lambda_k) \quad (7\,b)$$

In no practical cases (*i.e.* for $t > 1$ day) has it been necessary to consider $n > 5$. In the rare cases when $\Lambda_m = \Lambda_j$ and $\sigma_m = \sigma_j = 0$, eqn. 7 is no more valid. The following equation can then be used for calculating A_2

$$A_2\ (T,\ t) = R_A\ ((1 + \lambda t)e^{-\lambda t} - [1 + \lambda(T + t)]e^{-\lambda(T+t)}) \quad (8)$$

The complicated eqn. (7) can in most practical cases be considerably simplified. The following equations have been found very useful:

For $n = 1$, one obtains

$$A_1\ (\Phi,\ T,\ t) = R_A \frac{\lambda_1}{\Lambda_1} (1 - e^{-\Lambda_1 T})\ e^{-\lambda_1 t} \quad (9)$$

A similar equation is obtained for $X_1\ (\Phi,\ T,\ t)$.

For all $\sigma_i = 0$, where $i = 1,\ 2,\ \ldots .\ n$, one obtains

$$A_n\ (T,\ t) = R_A \sum_{i=1}^{n} (\prod_{j \neq i} \frac{\lambda_j}{\lambda_j - \lambda_i})\ (1 - e^{-\lambda_i T})\ e^{-\lambda_i t} \quad (10)$$

A similar equation is obtained for $X_n\ (T,\ t)$.

For $\Lambda_2 = 0$ and $\Lambda_1\ T \ll 1$ one obtains

$$X_2\ (\Phi,\ T,\ t) = \frac{y_1 \lambda_1}{2\Lambda_1} \left(\frac{\Lambda_1 T}{2} - \frac{\Lambda_1^2 T^2}{6} + \frac{\Lambda_1^3 T^3}{24} - \ldots . .\right) \quad (11)$$

For all $\sigma_i = 0$ and $\lambda_n = 0$ where i and $n > 1$, one obtains

$$X_n\ (T,\ t) = \frac{y_n}{2} - \sum_{i=1}^{n-1} X_i\ (T,\ t) \quad (12)$$

If $\sigma_1 = \lambda_1 = 0$, eqn. (11) reduces to $X_1\ (T,\ t) = y_1/2$.

For the exact calculation of the mole fractions, the factor 2, used in the denominators in the above eqns. (4), (11) and (12), should rather be 2.0025, because of the formation of ^4He through triple fission (yield 0.25 %).

DISTRIBUTION OF THE β-ACTIVITY OF THE ELEMENTS

The β-activity of the fission elements is given as a function of cooling time at various irradiation times and neutron fluxes in Figs. 1—7. Only nuclear β decays are considered here; the curves therefore do not include any "β-activity" due to internal gamma-beta conversion. In addition, very long-lived activities are summarized in Table 1.

Table 1. Long-lived isotopes with activities practically independent of T and $t < 600$ years.

Isotope	Half-life years	Decay	Activity C/g fiss.prod.
^{79}Se	6.5×10^{4}	β, γ	8.7×10^{-4}
^{87}Rb	6.2×10^{10}	β	6.1×10^{-10}
^{93}Zr	9.5×10^{5}	β	9.8×10^{-5}
^{99}Tc	2.1×10^{5}	β	4.3×10^{-3}
^{107}Pd	5×10^{6}	β	6.1×10^{-7}
^{115}In	6×10^{14}	β	2.6×10^{-16}
^{129}I	1.7×10^{7}	β, γ	6.6×10^{-7}
^{135}Cs	2.1×10^{6}	β	4.1×10^{-5}
^{142}Ce	5.1×10^{15}	α	1.8×10^{-12}
^{144}Nd	2.2×10^{15}	α	3.8×10^{-13}
^{147}Sm	1.3×10^{11}	α	2.8×10^{-10}

In the figures, the solid lines refer to a neutron flux of 10^{13} n cm^{-2} sec^{-1}. If other curves are obtained at lower or higher fluxes, this is indicated by dotted lines for 10^{12} and dashed lines for 10^{14} n cm^{-2} sec^{-1}. The effect of burn up of ^{235}U at high $\Phi \cdot T$ is discussed in a separate paragraph below.

In some cases in Figs. 1—7, only one isotope contributes to the activity of an element (*e.g.* ^{99}Mo, ^{140}Ba, ^{147}Nd), but in most cases the element contains several radioactive isotopes. However, generally only one isotope predominates at a time but, close to inflexion points, two isotopes may contribute about equally. By consulting the data in Part I[1], it is often possible to reveal the isotopic composition of the β-activity of the elements in Figs. 1—7.

Only nine elements are considerably influenced by variation in the neutron flux. They are Tc, Pd, Ag, Xe, Cs, Pm, Sm, Eu and Tb. The various fluxes influence the disintegration curves in two ways: the activity either increases (Pd, Ag, Cs, (Pm), Eu, Tb) or decreases (Eu, Tc, Xe, (Pm), Sm) with increasing neutron flux. In the former case a shorter lived isotope is formed through neutron capture in a longer-lived or stable isotope of the element. In the latter case a shorter-lived isotope captures a neutron forming a longer-lived or stable isotope of the element (*cf.* Part I[1]).

In Fig. 8, the total β-activity of the combined fission elements is given as a function of T and t (1 d $\leq t \leq$ 1 400 years). The curve for $T = 0$ was taken from Björnerstedt *et al.*[3]. If the curve for $T = 0$ is compared with the statistically calculated curve of Way and Wigner [13], one finds that their curve in some parts lies about a factor of 1.5 above the curve given by Björnerstedt

et al. On the other hand, the curve for $T = 0$ in Fig. 8 agrees almost completely with the curve given by Thornton and Houghton [14], who made calculations from known values of individual fission products.

Because the methods of calculation are, in principle, the same, almost complete agreement is obtained with the curves given for various irradiation and cooling times by Koontz and Jarrett [15], and from the summation of the curves for the individual isotopes given in Ref [6].

ELEMENTAL DISTRIBUTION OF FISSION PRODUCTS

The mole fractions of the fission product elements are given in Figs. 9—15 as a function of cooling time for the same irradiation times as given in the previous figures. While the relative activities of the fission elements vary considerably with cooling time, it is immediately seen from Figs. 9—15 that the mole fractions of the elements change very little with cooling times. For some elements, there is practically no change at all; these elements are given at the right margin of the figures. The considerable variation of the curves for Nb, Sb, and Pm is due to the fact that these fission elements consist mainly of relatively short-lived isotopes.

From comparisons of Figs. 1—7 and 9—15 it is seen that many of the elements, which make up a considerable fraction of the mass of the fission products contribute relatively little to the total radioactivity. Thus, about 50 % of the weight of the fission products comes from elements Xe, Nd and Cs, while these elements only make up about 1 % of the total β-activity (*cf.* Figs. 3 and 11 for $T = 1$ month and $t = 2$ months).

ESTIMATED ERRORS

The primary data used in these calculations are impaired by certain errors. One of these errors, *i.e.* unknown modes of branching decay, must here be neglected.

The half-lives are generally fairly accurate, but for long half-lives the standard deviations are assumed to be $\lesssim$ 10 %.

The fission yields and thermal neutron cross sections have often been determined with neutrons obtained from "thermal" uranium reactors, in which also fast neutrons are present. However, since the capture cross sections are higher in the thermal than in the fast neutron energy region, and the cross sections have relatively little influence on A and X except in a few cases, the errors in the cross sections can here be neglected.

The fission yields may be subject to much larger errors because of the presence of fast neutrons. In uranium reactors about 3 % of the fissions may be caused by fast neutrons [16]. This is especially important for the mass numbers in the valley of the fission yield curve, because the fission yields there increase considerably with neutron energy. The standard deviations in the fission yields are assumed to lie between 2 and 10 %.

With the complicated equations used for calculating A and X, it is very difficult to calculate exactly the errors due to uncertainties in the primary

Figs. 1—7. Elemental composition of fission product β-activity (in curies per g fiss. prod.) as a function of cooling time for three different neutron fluxes: ····· 10^{12}, ——— 10^{13} and ------- 10^{14} n cm^{-2} sec^{-1}. T = irradiation time.

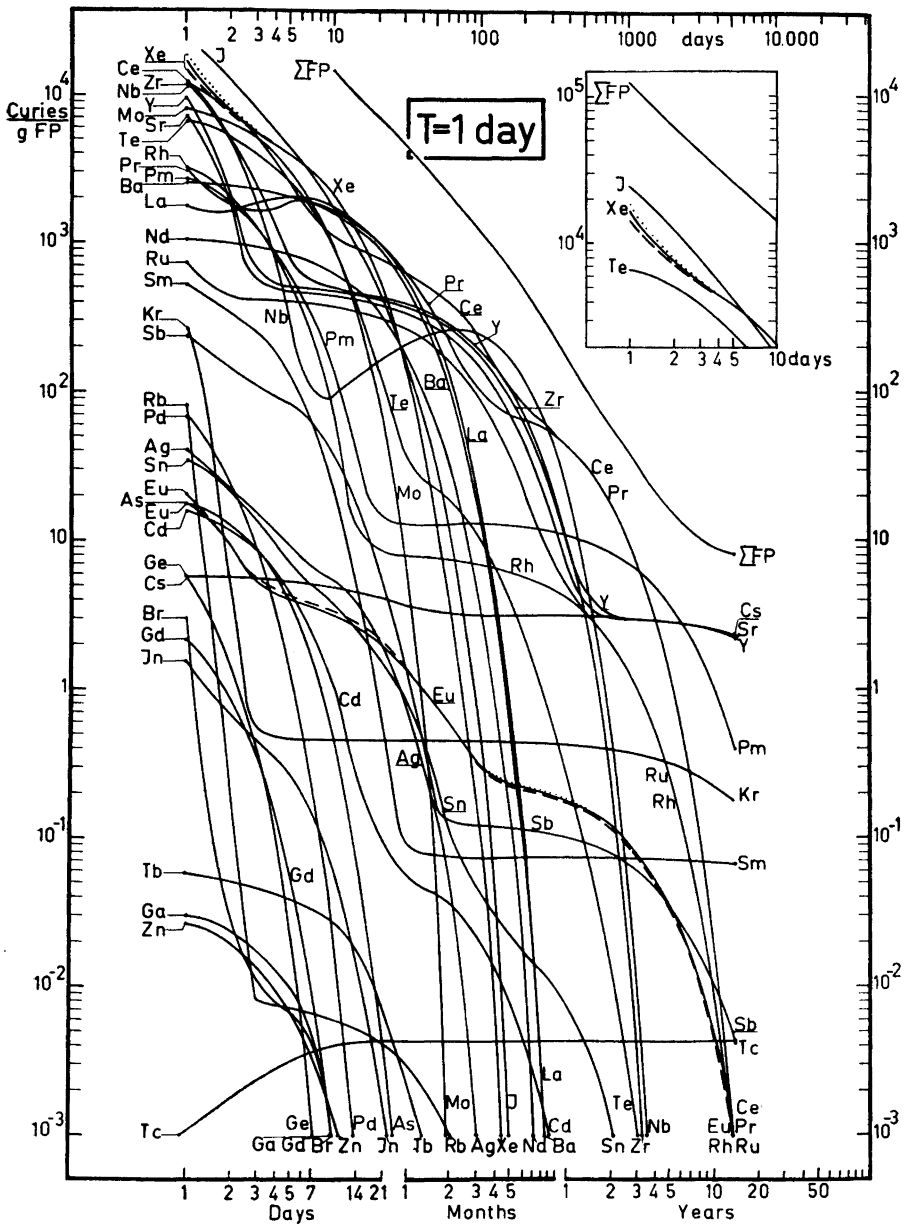

Fig. 1.

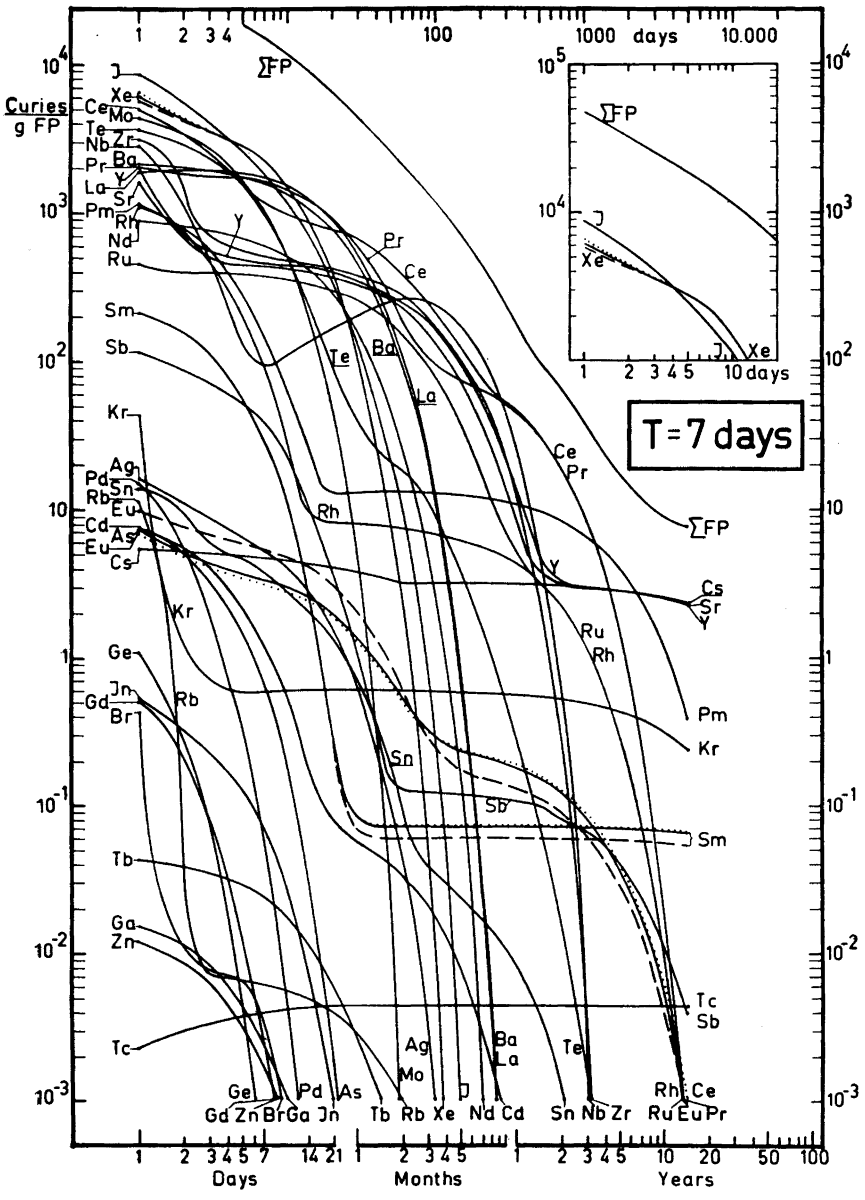
Curies
g FP
1 2 3 4
100
1000 days
10.000
ΣFP
J
Xe
Ce
Mo
Te
Nb
Zr
Pr
Ba
Y
La
Sr
Pm
Rh
Nd
Ru
Sm
Sb
Kr
Ag
Pd
Sn
Rb
Eu
Cd
As
Eu
Cs
Ge
In
Gd
Br
Tb
Ga
Zn
Tc
Pr
Ce
Te
Ba
La
Rh
Y
Ce
Pr
ΣFP
Cs
Sr
Y
Ru
Rh
Pm
Kr
Sn
Sb
Sm
Tc
Sb
Ag
Mo
Ba
La
Te
Rh
Ce
Ge
Gd Zn Br Ga In
Pd
As
Tb Rb Xe Nd Cd
Sn Nb Zr
Ru Eu Pr
Days
Months
Years
T=7 days
10 days

Fig. 2.

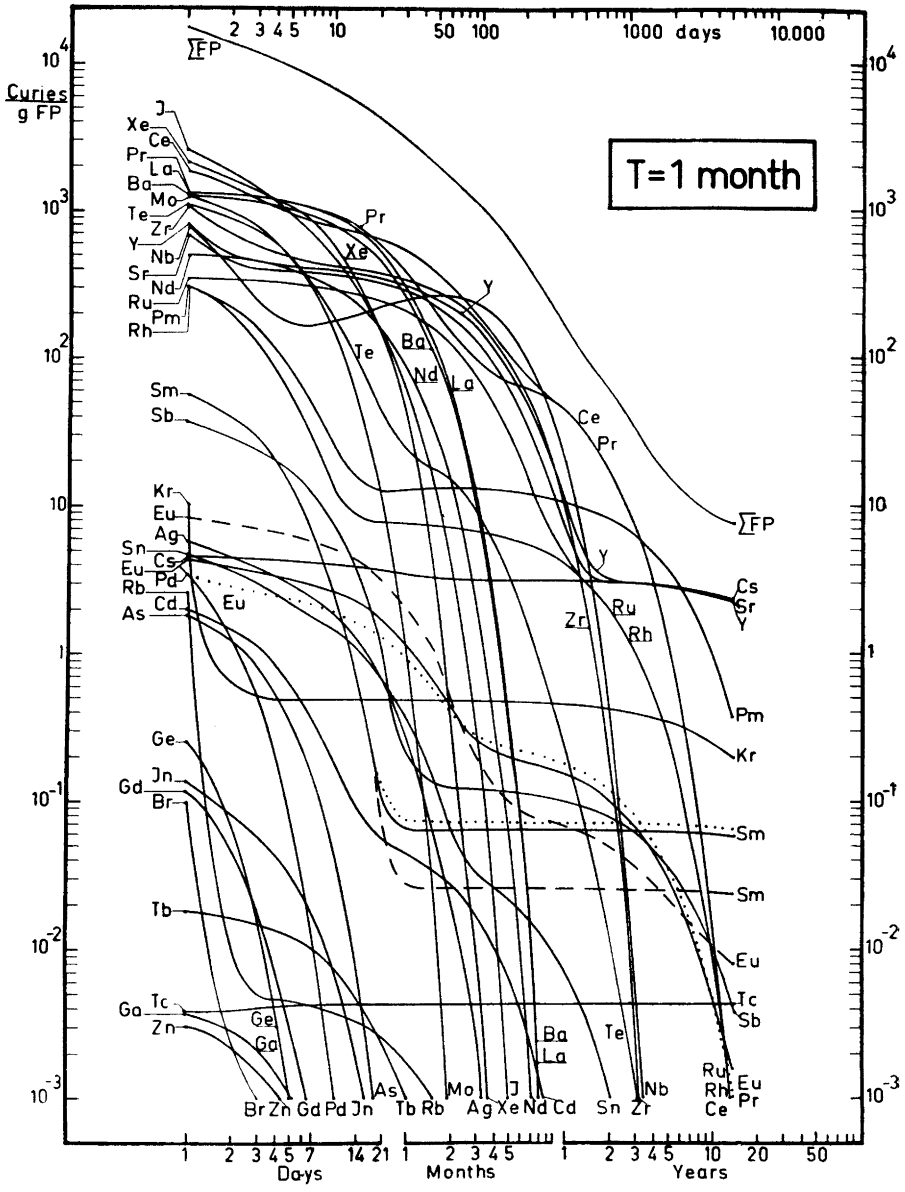
T=1 month
Curies
g FP
2 3 4 5 10 50 100 1000 days 10.000
ΣFP
Days
Months
Years
Br Zn Gd Pd In As Tb Rb Mo Ag Xe Nd Cd Sn Zr Nb Ru Rh Ce Pr Eu

Fig. 3.

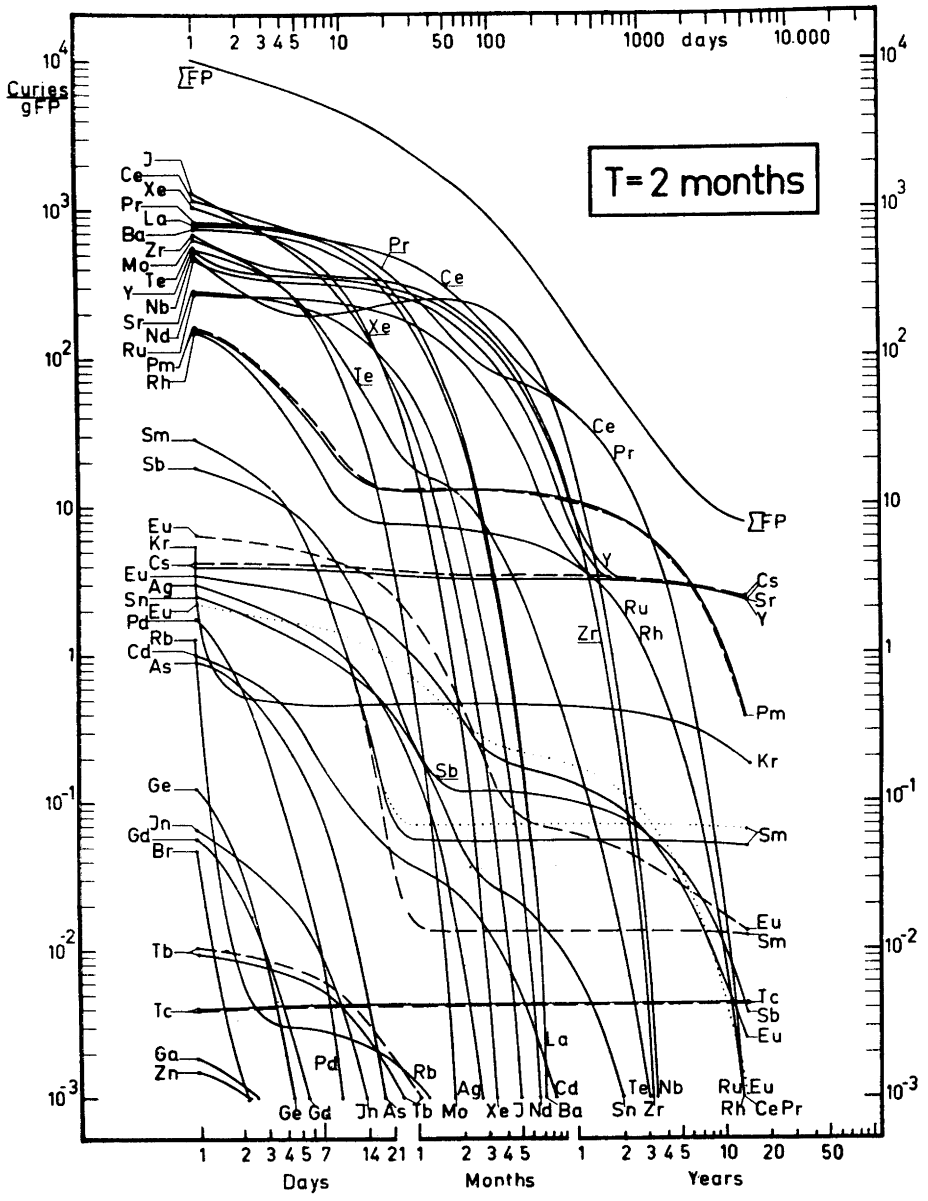
T=2 months
Curies/gFP
1 2 3 4 5 10 50 100 1000 days 10.000
Days
Months
Years
ΣFP
Pr
Ce
Xe
Te
Y
Zr
Ru
Rh
Cs
Sr
Pm
Kr
Sb
Sm
Eu
Tc
La
Pd
Rb
Ag
Cd
Nb
Ba
Nd
Mo
Tb
Ge
Ga
Jn
As
Br
Zn

Fig. 4.

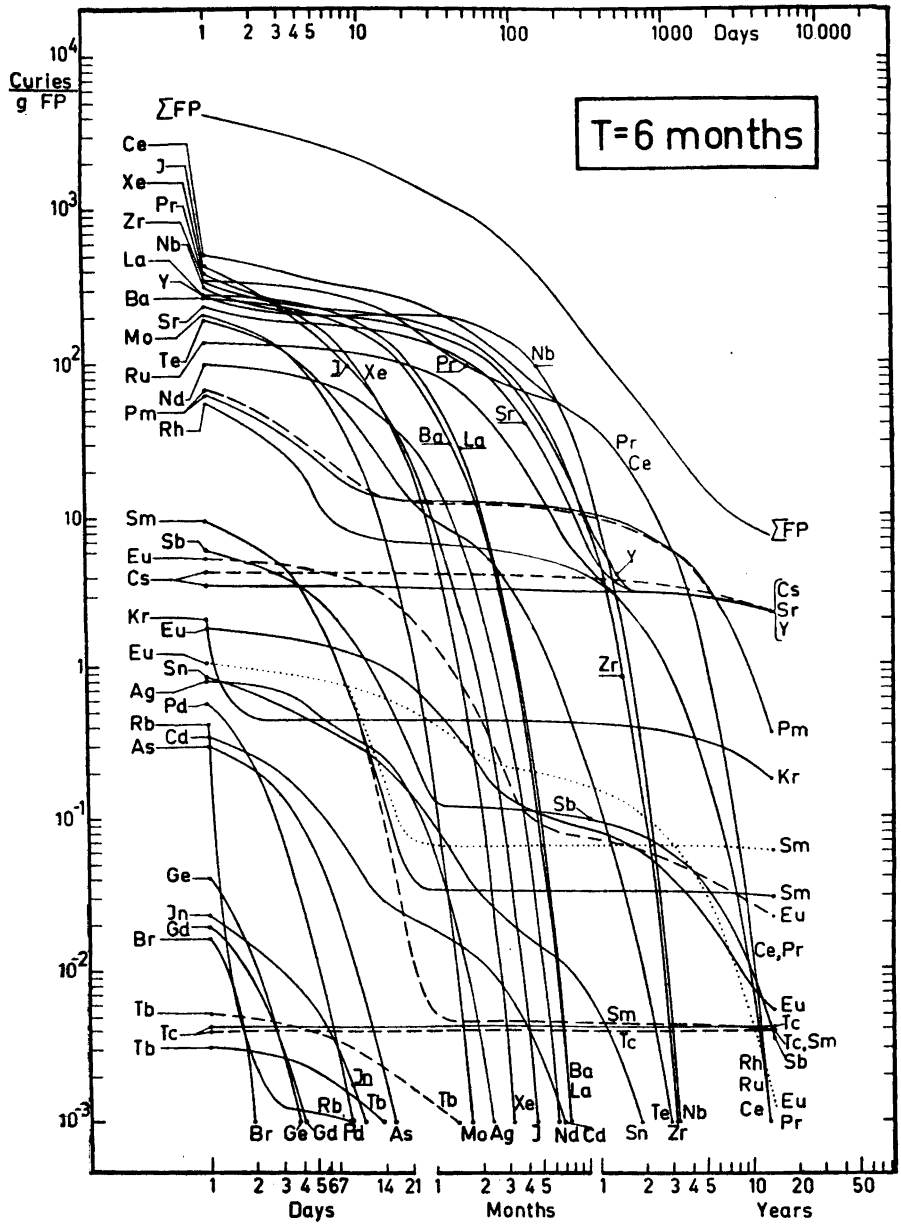
T=6 months
Curies / g FP
Days
Months
Years
ΣFP
Ce
J
Xe
Pr
Zr
Nb
La
Y
Ba
Sr
Mo
Te
Ru
Nd
Pm
Rh
Sm
Sb
Eu
Cs
Kr
Sn
Ag
Pd
Rb
As
Cd
Ge
In
Gd
Br
Tb
Tc
Pm
Sr
Ce,Pr
Sm
Eu
Ru
Mo
Ag
Nd
Cd
Sn
Zr
Tl

Fig. 5.

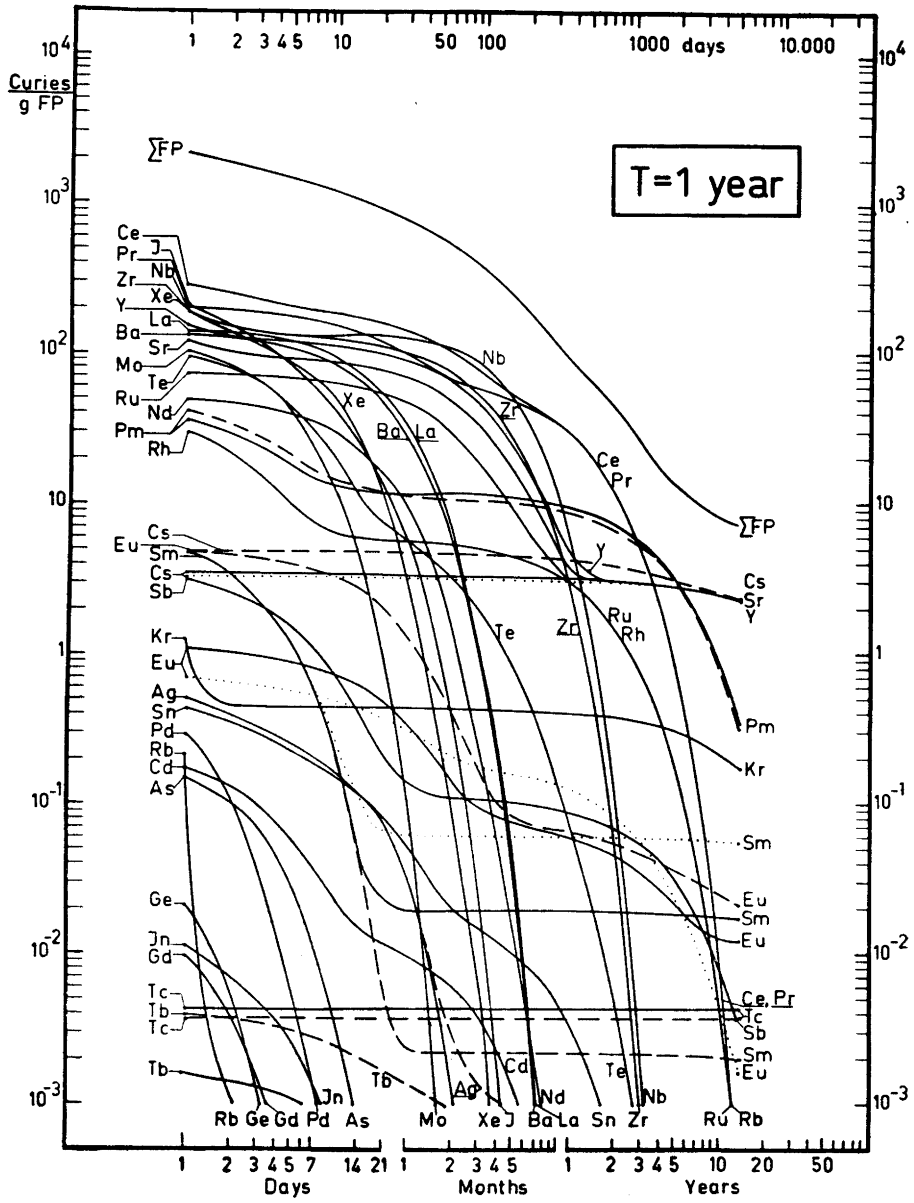
Curies
g FP
1 2 3 4 5 10 50 100 1000 days 10.000
T=1 year
∑FP
Ce
Pr
J
Nb
Zr
Xe
Y
La
Ba
Sr
Mo
Te
Ru
Nd
Pm
Rh
Cs
Eu
Sm
Sb
Kr
Ag
Sn
Pd
Rb
Cd
As
Ge
In
Gd
Tc
Tb
Days
Months
Years

Fig. 6.

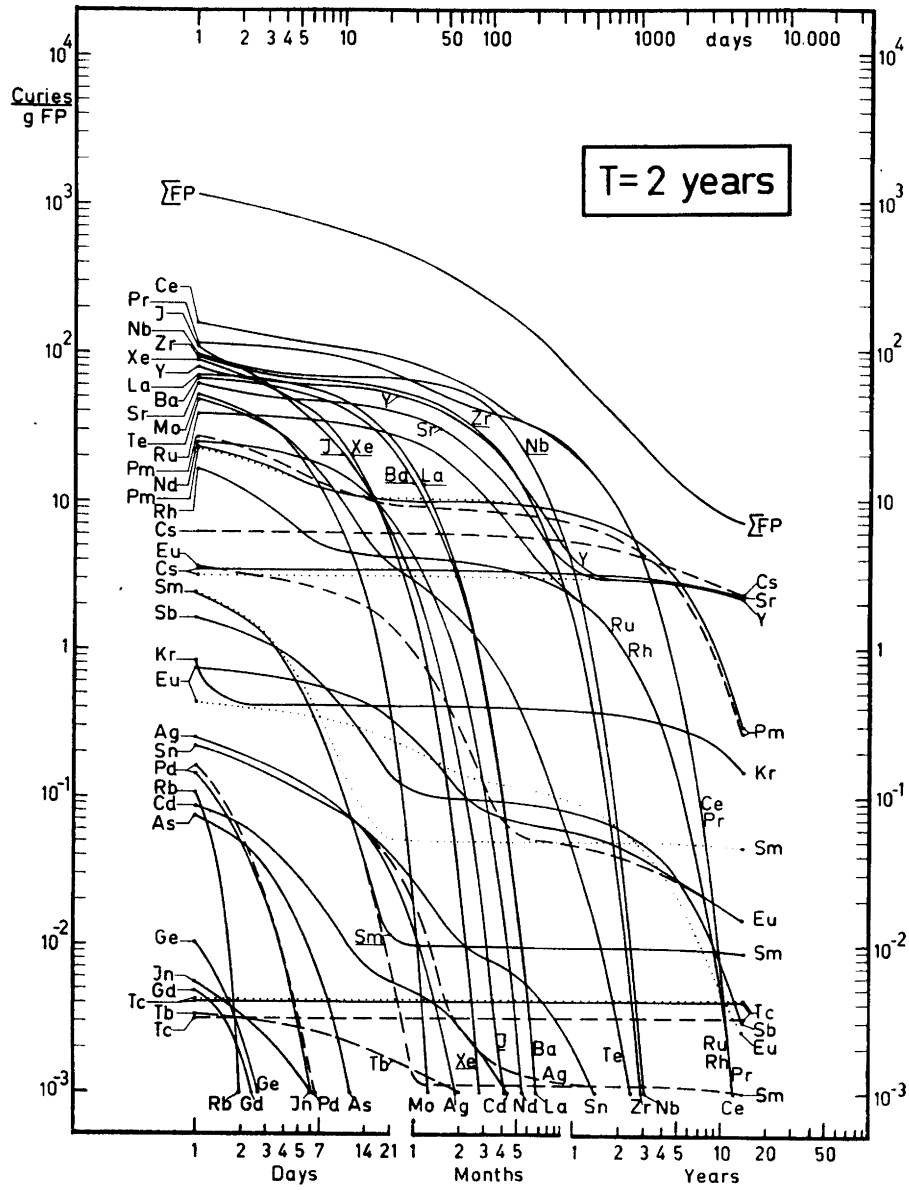
T= 2 years
Curies
g FP
1 2 3 4 5 10 50 100 1000 days 10.000
Days
Months
Years
ΣFP
Ce
Pr
Nb
Zr
Xe
Y
La
Ba
Sr
Mo
Te
Ru
Pm
Nd
Rh
Cs
Eu
Sm
Sb
Kr
Ag
Sn
Pd
Rb
Cd
As
Ge
In
Gd
Tc
Tb
I
Pm
Ce
Pr
Rb Gd In Pd As
Mo Ag Cd Nd La Sn Zr Nb Ce

Fig. 7.

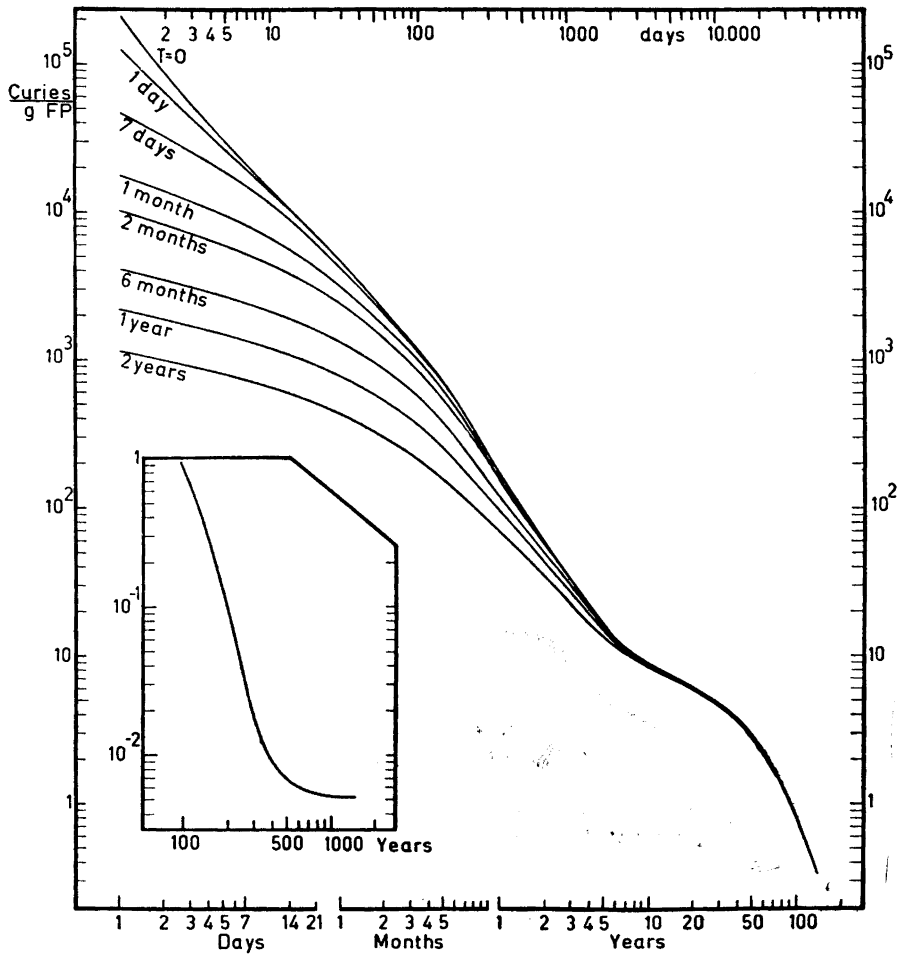

Fig. 8. Total β-activity of the fission products (in curies per g fiss. prod.) as a function of cooling time for irradiation times between 0 and 2 years. The curves are almost independent of neutron fluxes $\leq 10^{14}$ n cm^{-2} sec^{-1}.

Figs. 9—15. Mole percent of fission product elements as a function of cooling time for three different neutron fluxes: ····· 10^{12}, ———— 10^{13} and ------- 10^{14} n $cm^{-2}sec^{-1}$. T = irradiation time.

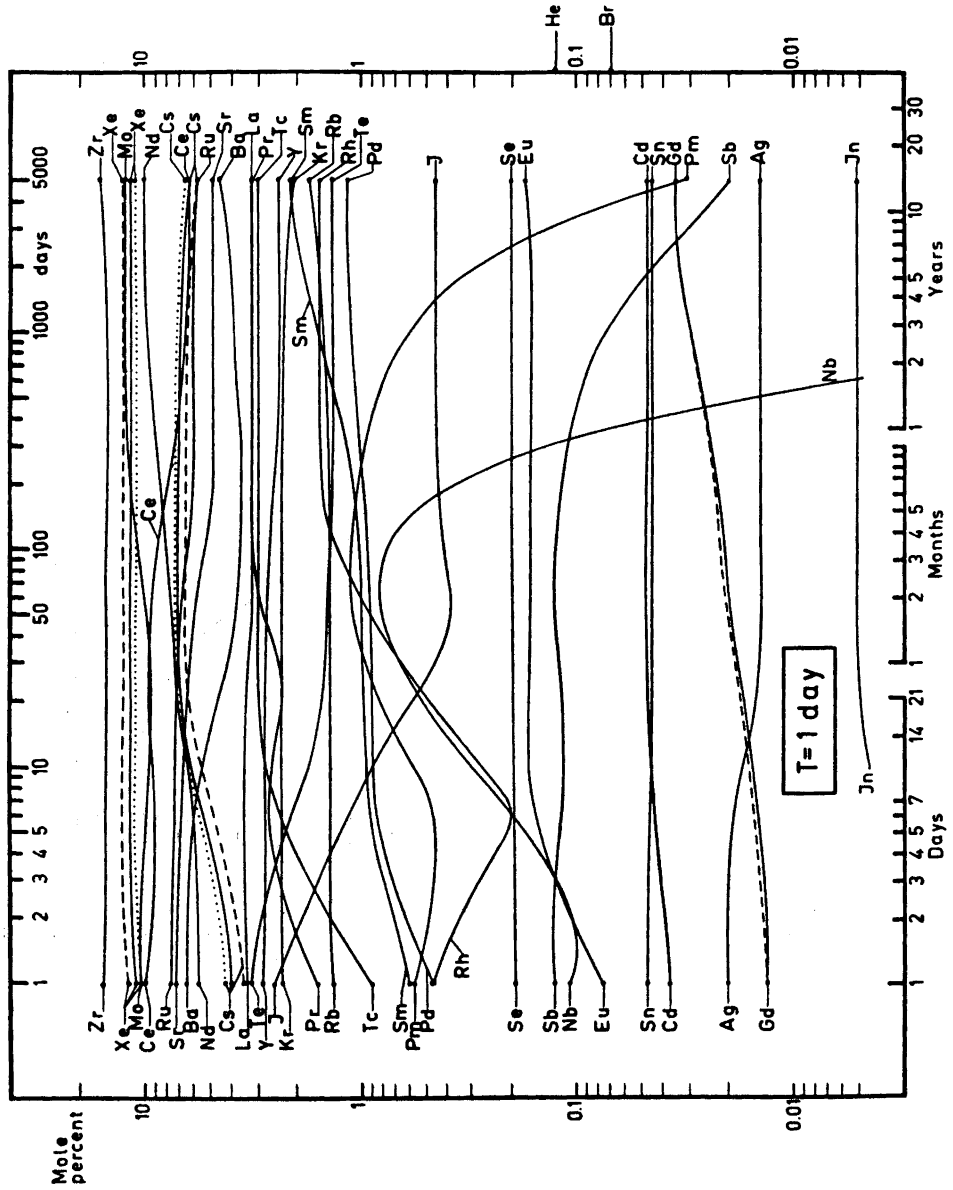

Fig. 9.

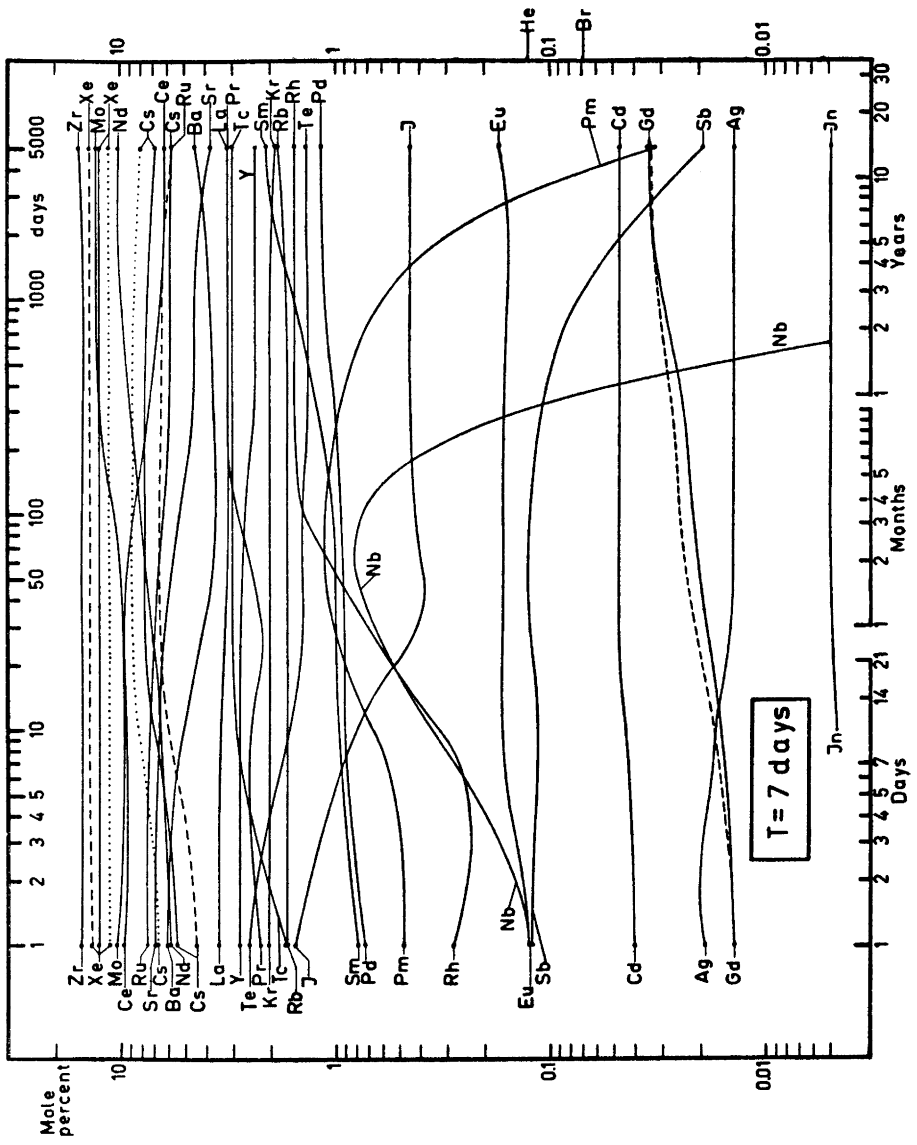
Mole percent
10
1
0.1
0.01
He
Br
0.1
0.01
days
5000
1000
100
50
10
1
Years
30
20
10
5
4
3
2
1
Months
5
4
3
2
1
Days
21
14
7
5
4
3
2
1
T = 7 days
Zr Xe Mo Nd Cs Ce Cs Ba Ru Sr La Pr Tc Y Sm Kr Rb Rh Te Pd
J
Eu
Pm Cd Gd
Sb
Ag
Jn
Nb
Nb
Nb
Zr Xe Mo Ce Ru Sr Cs Ba Nd Cs La Y Te Pr Kr Tc Rb J
Sm Pd Pm Rh Nb Eu Sb Cd Ag Gd
Jn

Fig. 10.

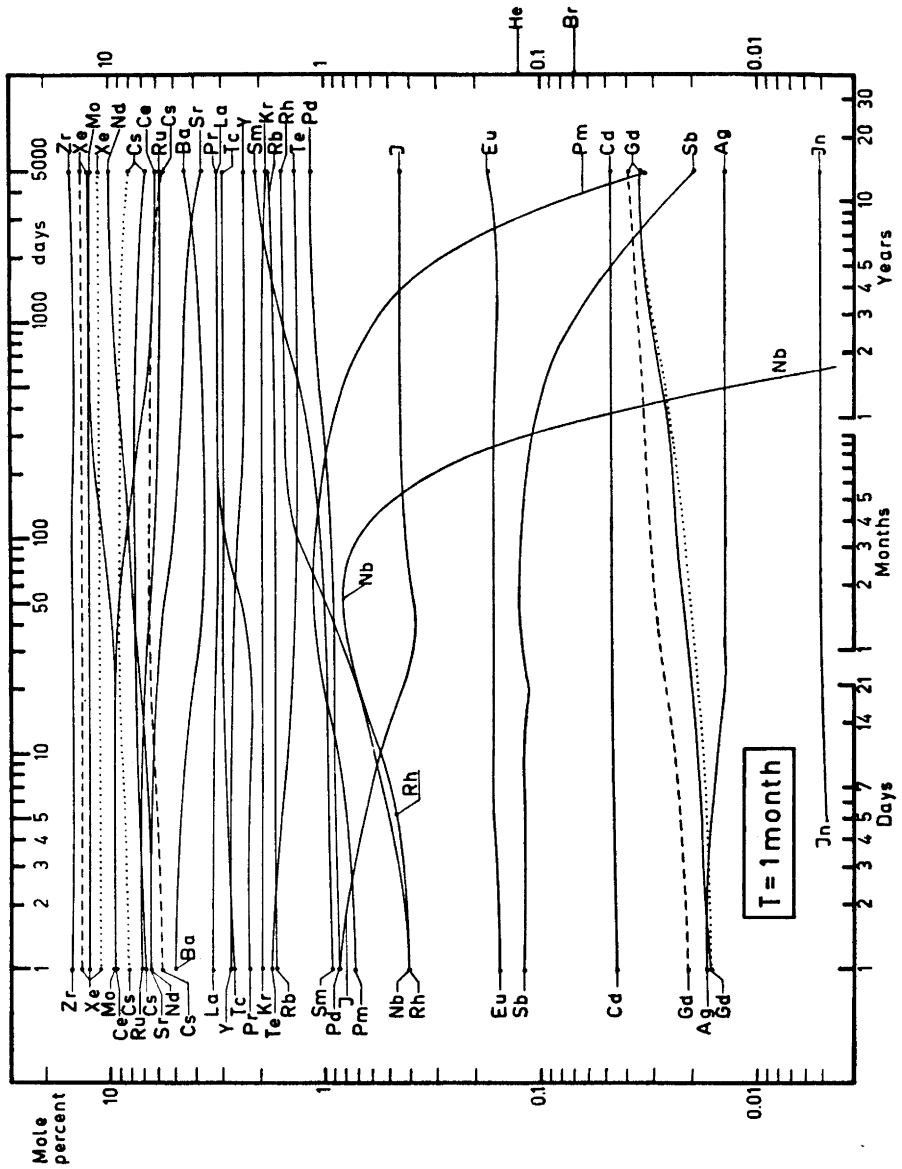
Mole percent
10
1
0.1
0.01
He
Br
days
1000
5000
100
50
10
1
Years
Months
Days
T=1month
Zr
Xe
Mo
Nd
Cs
Ce
Ru
Ba
Sr
Pr
La
Tc
Y
Sm
Kr
Rb
Rh
Te
Pd
J
Eu
Pm
Cd
Gd
Sb
Ag
In
Nb

Fig. 11.

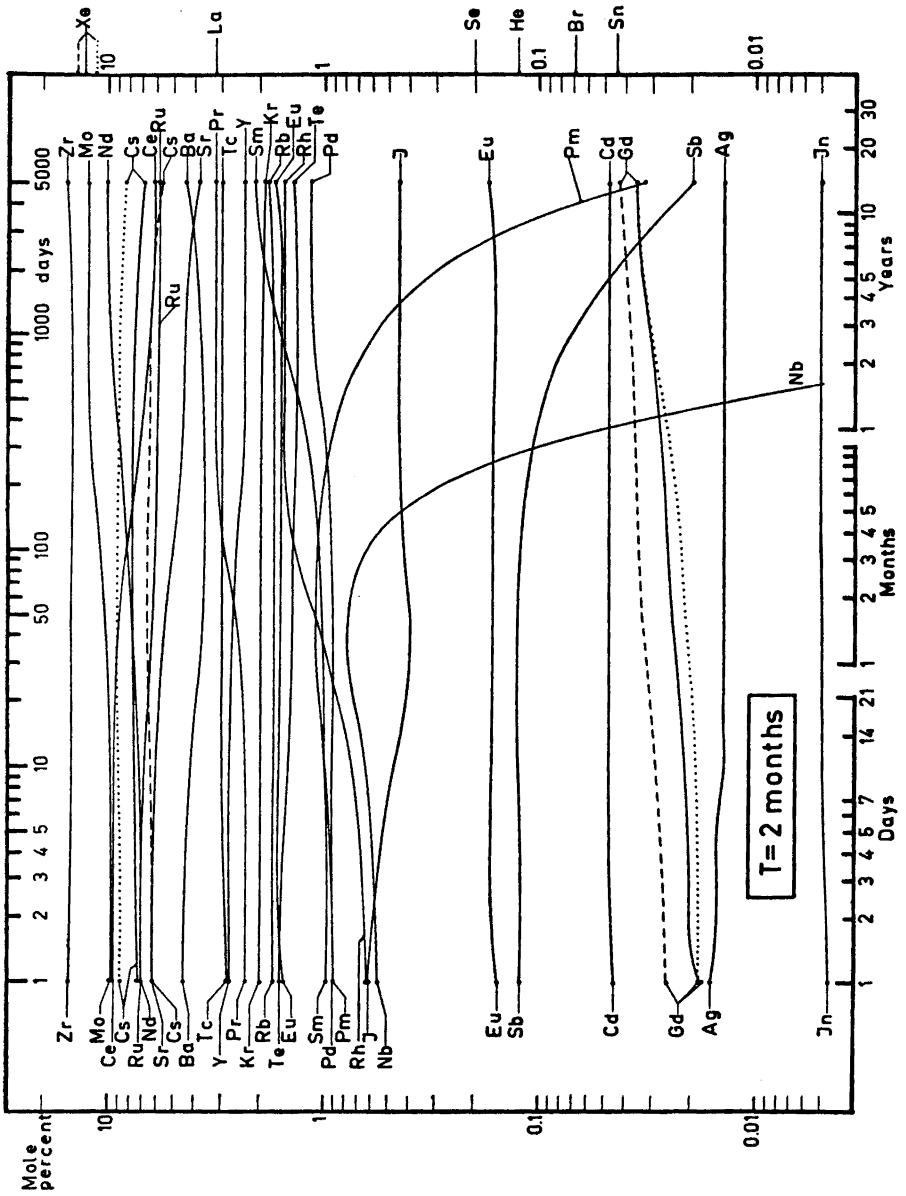
Xe
La
Se
He
Br
Sn
Mole percent
10
1
0.1
0.01
1000 days
5000
100
50
10
Years
Months
Days
T= 2 months
Zr
Mo
Nd
Cs
Ce
Ru
Cs
Ba
Sr
Pr
Tc
Y
Sm
Kr
Rb
Eu
Rh
Te
Pd
J
Eu
Pm
Cd
Gd
Sb
Ag
In
Nb
Ru
Zr
Mo
Ce
Cs
Ru
Nd
Sr
Cs
Ba
Tc
Y
Pr
Kr
Rb
Te
Eu
Sm
Pd
Pm
Rh
J
Nb
Eu
Sb
Cd
Gd
Ag
In

Fig. 12.

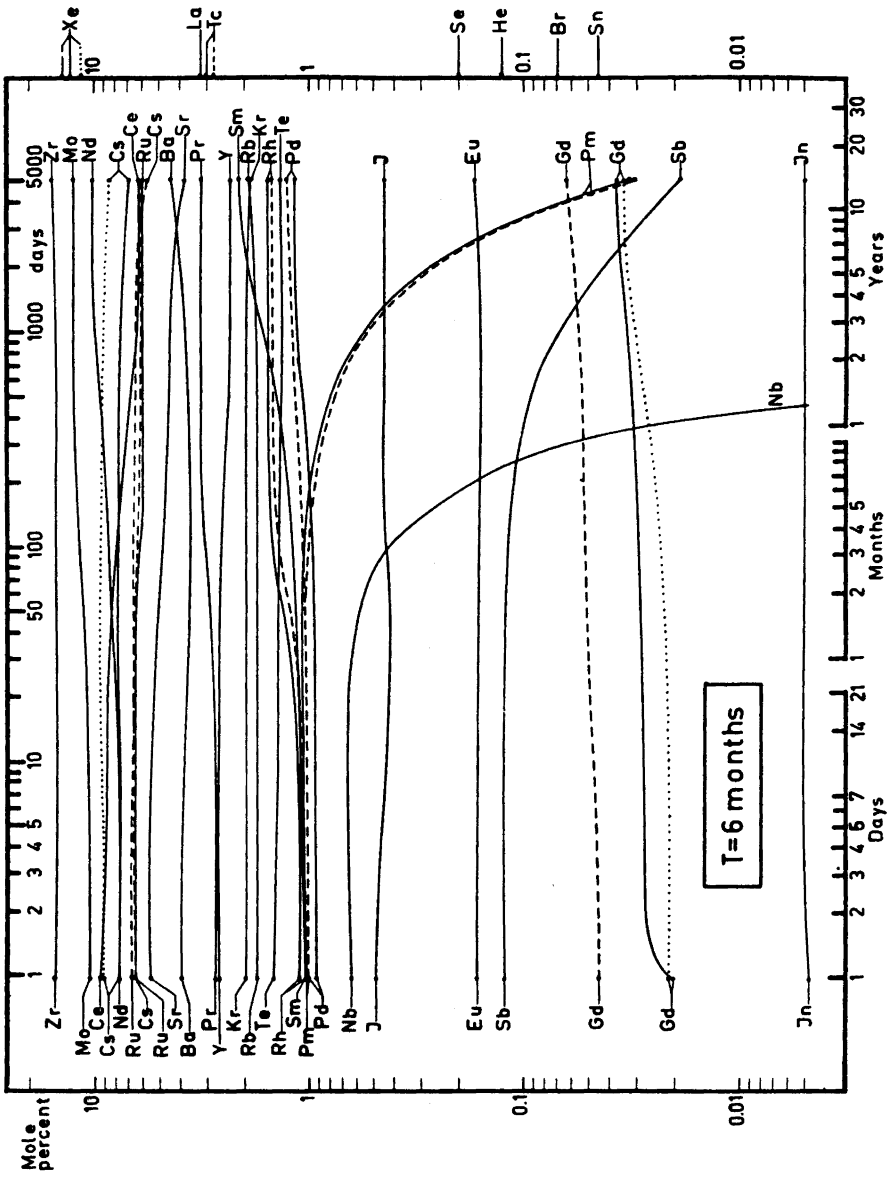
Xe
La
Tc
Se
He
Br
Sn
10
1
0.1
0.01
5000
1000
100
50
10
1
days
Years
Months
Days
Mole percent
T=6 months
Zr
Mo
Nd
Cs
Ce
Ru
Ba
Sr
Pr
Y
Sm
Rb
Kr
Rh
Te
Pd
Nb
J
Eu
Sb
Gd
Pm
In

Fig. 13.

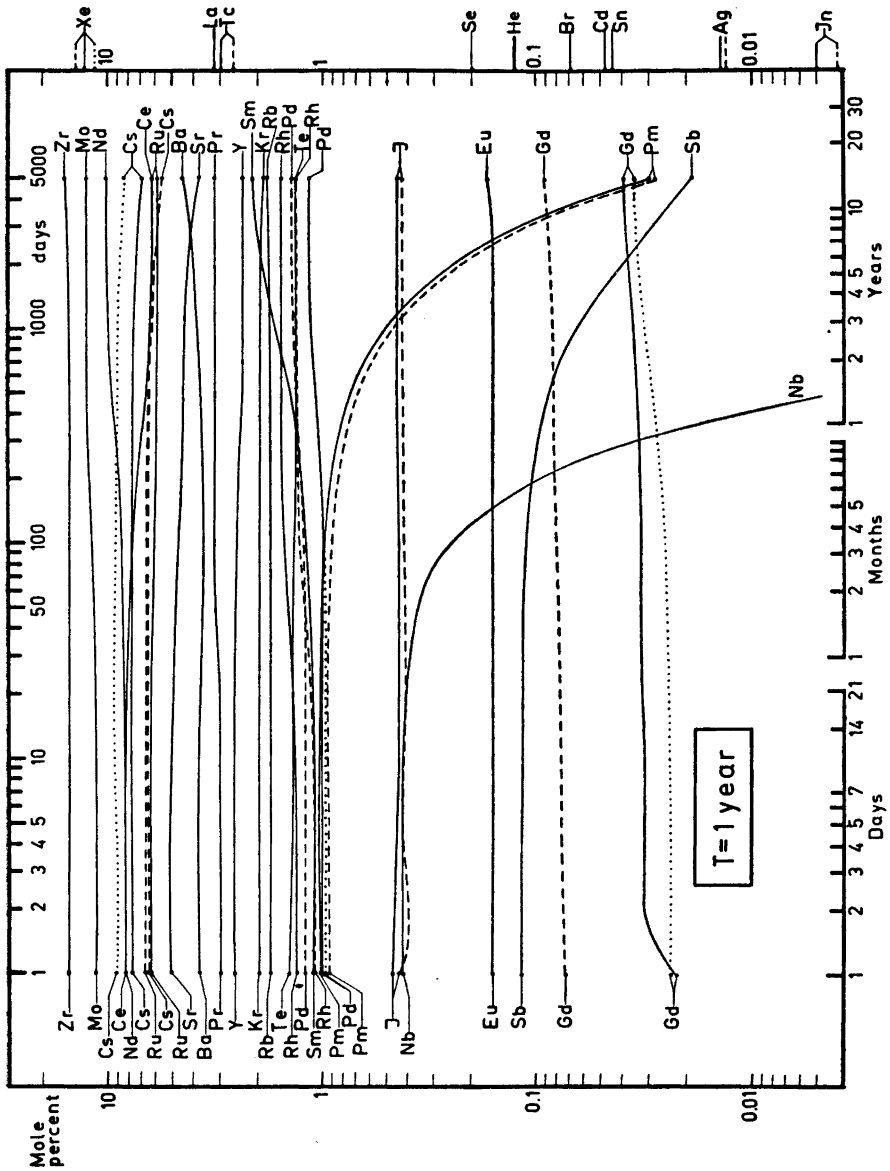
Xe
Ta
Tc
Se
He
Br
Cd
Sn
Ag
In
10
1
0.1
0.01
Zr
Mo
Nd
Cs
Ce
Ru
Ba
Sr
Pr
Y
Sm
Kr
Rb
Rh
Pd
Te
Pm
I
Nb
Eu
Sb
Gd
Gd
Pm
Sb
Nb
T=1 year
Mole percent
10
1
0.1
0.01
1000 days
5000
100
50
10
1
Years
Months
Days
1 2 3 4 5 10 20 30
1 2 3 4 5
1 2 3 4 5 7 14 21

Fig. 14.

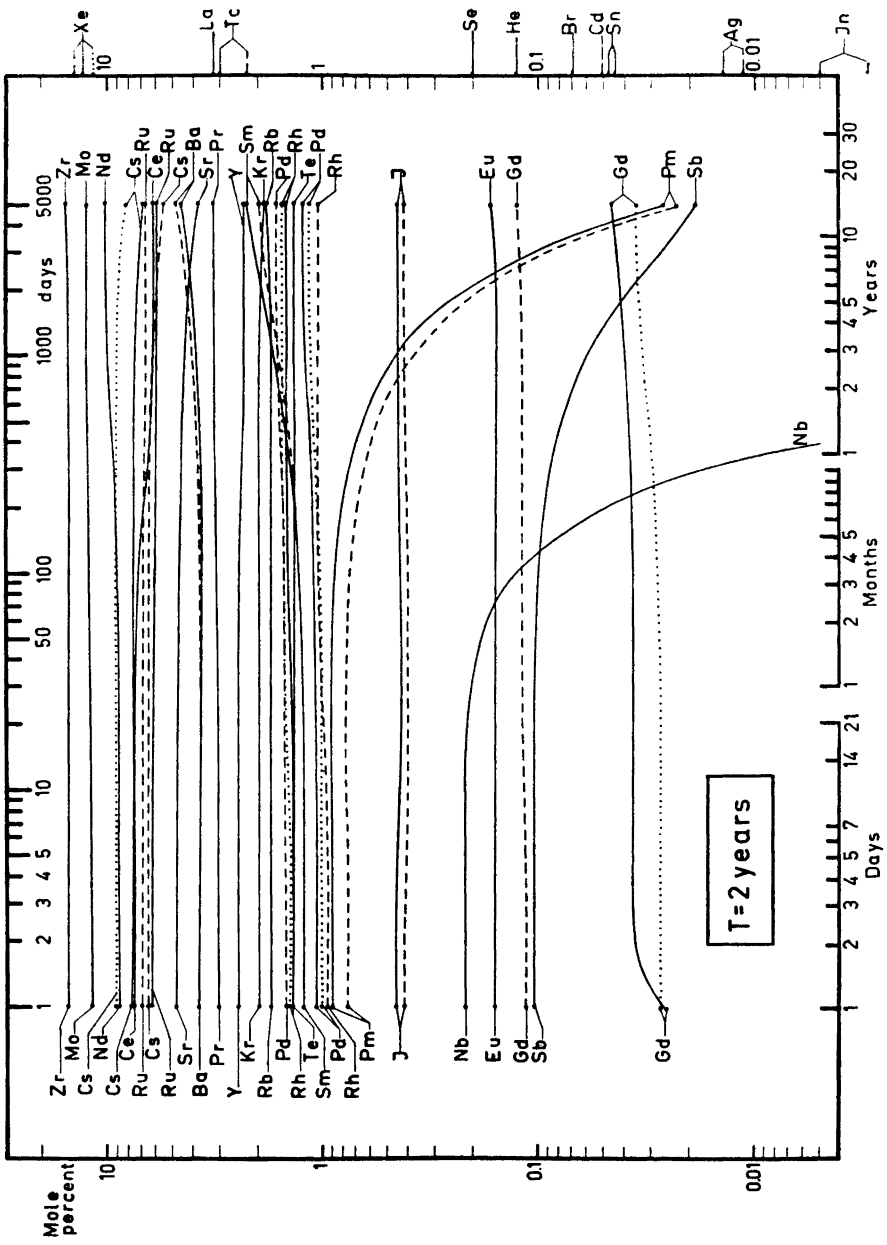
Xe
La
Tc
Se
He
Br
Cd
Sn
Ag
In
10
1
0.1
0.01
Zr
Mo
Nd
Cs
Ce
Ru
Ba
Sr
Pr
Y
Sm
Kr
Rb
Pd
Rh
Te
Tc
I
Eu
Gd
Pm
Sb
Nb
5000
1000
100
50
10
days
Years
Months
Days
T=2 years
Mole percent

Fig. 15.

data. However, an estimation has been made, which shows that for a standard deviation of 3 % in y and 1 % in λ, the deviations in A and X correspond to $\pm$ 0.2 mm in Figs. 1—15. For a standard deviation of 10 % in y and 5 % in λ, the deviations in A and X correspond to $\sim$1 mm for $t \approx \tau$, and to $\sim$2 mm for $t \approx 8\,\tau$. The errors increase for increasing ratio t/τ. However, it can be seen that these errors are of about the same size as the vertical thickness of the lines drawn in the figures.

Another limitation of the diagrams is discussed in the next paragraph.

THE INFLUENCE OF HIGH BURN UP

The calculations resulting in Figs. 1—15 are all based on the fundamental assumption that the amount of ^{235}U is constant during the irradiation time, T, (*i.e.* that the "burn up" of ^{235}U is low). Practically all published calculations of the kind presented in this paper, are based on the same assumption, even if this is not always explicitly stated.

The weight of fission products formed is proportional to $T \cdot \Phi \cdot \sigma_{fiss} \cdot N$, where N is the number of fissile atoms. Since all calculations in this paper refer to a constant weight of fission products (1 g or 1 mole) formed at a constant flux during a constant irradiation time, it follows that N also must be constant. If this is not the case owing to high burn up, either Φ must be increased in order to produce the fixed weight of fission products in the predetermined time T, or the time T must be increased to produce the fission products at a constant flux. In all cases, the conditions of the equations used in the calculations above are violated. The errors due to a burn up of about 10 % of the ^{235}U causes an error of $\lesssim$ 3 % in the activities or mole fractions given in the figures.

A burn up of 10 % is obtained at 1.5×10^{21} n cm^{-2}, *i.e.* at $\Phi = 10^{12}$ n cm^{-2} sec^{-1} after $T \approx 5$ years, at $\Phi = 10^{13}$ after $T \approx 6$ months, and at $\Phi = 10^{14}$ after $T \approx 18$ days. However, all calculations have been continued up to $T = 2$ years for fluxes $\leq 10^{14}$ n cm^{-2} sec^{-1}, even if the practical usefulness of the diagrams for $\Phi \cdot T > 1.5 \times 10^{21}$ n cm^{-2} may be limited to reactors especially designed to keep the ^{235}U amount constant without removing the fission products.

Acknowledgements. The authors wish to thank the head of FOA 1, Prof. G. Ljunggren, for his continuous interest in and support of these studies, Prof. A. Ölander, Mr. I. Österlund and Mr. P. E. Bergner for valuable discussion, and Miss M. Granstrand for drawing the diagrams. The English of this paper has been corrected by Dr. H. S. Dunsmore. Large size copies of the Figures may be obtained on request to the authors.

REFERENCES

1. Prawitz, J. and Rydberg, J. *Acta Chem. Scand.* **12** (1958) 369.
2. Hunter, H. F. and Ballou, N. E. *Nucleonics* **9** No. 5 (1951) C-1.
3. Björnerstedt, R., Löw, K. and Ulvönäs, S. *Swedish Preliminary Report to the United Nations Scientific Committee on Effects of Atomic Radiations*, July 11th 1956; Löw, K. and Björnerstedt, R. *Arkiv Fysik. In press.*
4. Lock, J. C. L. *A.E.R.E. Report C/R 1715*, Harwell 1955.

5. Moteff, J. *General Electric Co Report APEX-134*, USA 1953.
6. Appendix III, *Progress in Nuclear Chemistry, Vol. III. Process Chemistry, Vol. I*, Pergamon Press Ltd, London 1956.
7. Coryell, C. D., Brady, E. L., Ballou, N. E., Burgus, W. H., Campbell, G. W., Engelkemeir, D. W., Glendenin, L. E. and Novey, T. B. *Paper 39* of Ref.[9]
8. Rubinson, W., Metcalf, R. P., Seiler, J. A., Steinberg, E. P. and Winsberg, L. *Paper 40* of Ref.[9]
9. Coryell, C. D. and Sugerman, N. (Ed.) *Radiochemical Studies. The Fission Products*, McGraw-Hill Book Co, New York 1951.
10. Keneshea, Jr., F. J. and Saul, A. M. *Nucleonics* **11** No. 11 (1953) 26.
11. Walton, G. N. *Paper 4, A.E.R.E. Report C/R 1231*, Harwell 1953.
12. Rubinson, W. *J. Chem. Phys.* **17** (1949) 542.
13. Way, K. and Wigner, E. P. *Paper* **43** of Ref.[9]
14. Thornton, J. K. and Houghton, W. J. *J. Appl. Phys.* **24** (1953) 1374.
15. Koontz, R. L. and Jarrett, A. A. *Nucleonics* **12** No. 6 (1954) 26.
16. Tomlinson, R. H. *Private communication.*

Received November 28, 1957.

ACTA CHEMICA SCANDINAVICA 12 (1958) 399—407

Determination of the Absolute Activity of Solid Tritium Samples

JAN RYDBERG

Research Institute of National Defence, Dept. 1, Sundbyberg 4, Sweden

It is shown that the absolute specific beta activity of tritium in solid samples of finite thickness can be accurately determined with 2π internal gas-flow counters. The effects of self-absorption and back-scattering of tritium betas are discussed.

The new simple methods for direct labeling of organic compounds with radioactive hydrogen (for references see Ref.[1]) in combination with the low price of the latter is causing a rapid increase in the use of tritium-tagged organic compunds. This calls for simple methods of measuring tritium activities. The most commonly used seems to be the counting of gaseous samples in various ionization chambers and dissolved samples in liquid scintillation counters (*cf.e.g.* Refs.[2,3]). However, these methods require special or expensive equipment, usually not available in normal radiometric laboratories. Because of the low energy of the β- radiation of ^{3}T (upper energy limit 18 keV), measurements on solid samples present some difficulties, but these can usually be overcome by using internal gas flow counters and a refined sample preparation technique. So far only four papers [4–7] seem to have dealt with this problem in some detail. In none of these papers is the absolute determination of tritium activity discussed, and the results do not seem generally applicable to all kinds of solid tritium samples. In the present paper these problems will therefore be somewhat more extensively treated.

VARIABLES IN ABSOLUTE β-COUNTING

Zumwalt [8] has summarized the different variables which have to be considered in the determination of absolute β-activity of solid samples. Here, only the case of using internal gas-flow counters will be discussed, which limits the number of variables. The correction factors are

f_e, the efficiency of the measuring device to register all β-particles entering the detector;

f_r, the combined resolving time of the detector and the electronic and mechanical components;

f_g, the geometry of the detector viewed from the radiation source;
f_b, the back-scattering of radiation from the backing material into the counter;
f_s, the self-absorption and back-scattering of the β-radiation in the sample.

If the true specific activity is S dpm/g (disintegrations per minute per gram), and the measured activity is I cpm (counts per minute) in a sample of weight m grams, the following relation holds:

$$S = I/m \cdot f_e \cdot f_r \cdot f_g \cdot f_b \cdot f_s \quad \text{dpm/g} \tag{1}$$

When a GM-counter shows a flat plateau (*i.e.* pulse frequency is independent of anode voltage) it is generally assumed that all β-particles entering the detector are registered [9]. This is certainly true if the pulse frequency is so low that no resolution loss is obtained (*i.e.* if $f_r = 1$). The same reasoning should hold when the detector, instead of a GM-tube, is a proportional tube. Experiments made by the author have given identical results for internal gas-flow GM-counters (helium-*iso*butan mixture) and proportional counters (argon-methane mixture). Thus if solid samples are measured in the sensitive volume of these detectors, the factor f_e is very close to 1, when $f_r = 1$ and the tubes are operated at the plateau.

If flat planchettes are used to support the radiation source placed in the sensitive volume of a 2 π internal gas-flow counter, the factor f_g can be put equal to 0.5.

When the radiation source is outside the sensitive volume of the detector, the geometry of the source in relation to the detector has to be calculated (*cf.e.g* Ref.[10]). A more accurate method is to use a calibrated radiation source in the actual geometry, and to determine $f_g \cdot f_e$ in one step; this value of $f_g \cdot f_e$ is only strictly valid for the specific isotope used.

The fraction of β-radiation scattered from the backing material into the detector depends on the β-spectrum, the atomic number and thickness of the backing material. When the thickness of the backing material is $> R_0/3$, where R_0 is the maximum range of the β-particles, maximum ("saturation") back-scattering is obtained. Since accurate predictions of the value of the saturation back-scattering factor, f_b, are difficult to make for low β-energies (*cf.e.g.* Ref.[11]), this factor is most easily determined experimentally.

Fairly simple equations can be given for the dependence of the self-absorption of the mass density of the sample. The derivation and use of these equations have been discussed by several authors (*e.g.*Refs.[12–14]). However, in ordinary experimental work with thick samples it is generally not possible to distinguish between self-absorption and back-scattering in the source [16]. In order to make absolute determination of β-activity in a given sample, experimentally determined values of f_s should be used.

EXPERIMENTAL

Sample preparation

Solid samples. The samples prepared for solid counting were obtained by evaporating solutions of tritiated *p*-aminosalicylic acid (PAS) [1] in 96 % ethyl alcohol. The positions of the tritium atoms in PAS are not definitely known, but they are non-labile in water

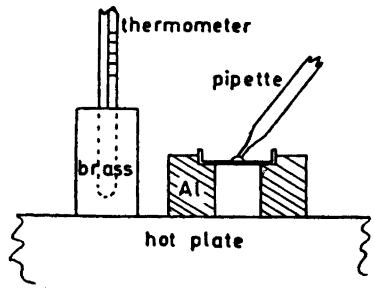

Fig. 1. Arrangement for sample preparation.

of pH 3—7. It is believed that in the alcoholic solutions no exchange of tritium takes place between the PAS and the solvent. 96 % ethyl alcohol was used because no solid residues were left after its evaporation.

Fig. 1 shows the arrangement used to prepare the samples [17]. In order to obtain reproducible samples it is important to keep the hot plate and aluminium ring at the correct temperature (in this case at 55°C), and to put the cold sample-pan on the aluminium ring just before adding the 0.1 ml of the solution through the pipette. The sample-pan should be kept perfectly horizontal and any rapid airflow around it should be avoided. Under these circumstances, there is formed a droplet, which evaporates slowly from its rim. The dry samples obtained had a diameter of 13 ± 1 mm.

The activities measured never exceeded 5 000 cps, which corresponded to a sample thickness of about 100 $\mu g/cm^2$. In order to measure on still thicker samples, inactive PAS was added to the active alcohol solution, and appropriate corrections for the dilution of the active PAS were made.

Gas samples. Gas samples were prepared by converting the tritium in solid tritiated PAS to water. This water was then reduced with magnesium to produce hydrogen for measurements in a GM-counter, according to Melander [18].

Counting arrangements

For the measurements on solid samples an internal gas-flow proportional counter (model PC-3, Nuclear Measurements Corp., Indianapolis) with 90 % A + 10 % CH_4 was used. The resolution loss was around 1 % at 5 000 cps; since higher activities never were measured, corrections for resolution loss could be neglected.

Before the introduction of a sample into the counter, the background was measured. For each sample 5—10 measurements were made to check that the counter worked properly; between each measurement, the counting tube was flushed with the counting gas. In general it was found that in such a sequence of measurements, the activity first rose slightly and then decreased. The rise is believed to be due to insufficient flushing in the beginning, and the decrease due to mechanical loss of sample from the sample-pan because of the flushing. This assumption is supported by the fact that the back-ground count rose steadily with each new sample measured. When the back-ground had reached ~1 000 cpm, the counting chamber was removed and cleaned, after which the background usually dropped to the ordinary value of ~200 cpm (unshielded). The difference between the highest and the lowest activity measured on one sample in this way never amounted to more than 7 % and in general was much less. The average between the two highest values was used.

For comparison with the results obtained on solid samples with the proportional counter, an internal gas-flow GM-counter (Model SC-16, Tracerlab Inc., Boston) using 99 % helium + 1 % *iso*butane was used in a few experiments with samples of low activity. Results completely consistent with those of the proportional counter were obtained when identical samples were used in both counters.

To check the activites obtained by the method described in this paper, a GM-counter especially made for tritium-gas samples [18] was also used (propane-hydrogen mixture at about 100 mm Hg).

Table 1. Measured activity, I, as a function of sample weight, m, for various backing materials; sample area is 1.3 ± 0.2 cm².

Sample weight	Aluminium backing		Stainless steel backing		Platinum backing	
m μg	I cpm $\times 10^{-3}$	I/m $\frac{\text{cpm}}{\mu\text{g}}$	I cpm $\times 10^{-3}$	I/m $\frac{\text{cpm}}{\mu\text{g}}$	I cpm $\times 10^{-3}$	I/m $\frac{\text{cpm}}{\mu\text{g}}$
2 000	712 ± 4	356 ± 2	708 ± 4	354 ± 2	980 ± 5	490 ± 2
1 000	810 ± 2	810 ± 2	880 ± 3	880 ± 3	1 070 ± 3	1 070 ± 3
460	720 ± 1	1 570 ± 3	698 ± 1	1 520 ± 3	837 ± 2	1 820 ± 4
90	245 ± 1	2 720 ± 5	244 ± 1	2 720 ± 5	290 ± 1	3 330 ± 7
9	35.0 ± 0.2	3 780 ± 2	420 ± 0.2	4 670 ± 2	44.5 ± 0.2	4 950 ± 2
0.9	4.2 ± 0.1	4 670 ± 90	4.43 ± 0.1	4 930 ± 90	5.38 ± 0.1	5 990 ± 120
0.09	0.445 ± 0.04	4 950 ± 500	0.537 ± 0.05	5.970 ± 600	0.60 ± 0.06	6.670 ± 670

RESULTS

The experimental data. The results obtained are collected in Table 1. The errors given are only statistical (root mean square), owing to the number of counts measured. The error in the sample weight, which is not considered in the table, is assumed to be less than 10 %. The sample areas are not known more accurately than 1.3 ± 0.2 cm². In Fig. 2, the activity, I (cpm), is plotted against the sample weigth m (μg) on a logarithmic scale. Since the values for the various backing materials lie fairly close to each other, the scale for the three sets of data has been displaced one log unit each along the ordinate. In Fig. 3 the relative activity, I/m, is plotted against log m. The difference between the three backing materials at low sample weights is obvious here. The use of the curves in Figs. 2 and 3 shall be further discussed below.

Calculations. It has been shown (*e.g.* Refs.[12–15]) that the self-absorption of β-radiation can be well described by the equation

$$\frac{A_x}{A_0} = \frac{1 - e^{-\mu x}}{\mu x} \tag{2}$$

where A_x is the activity of a given amount of a radioactive isotope contained in a sample of thickness x mg/cm² (for $x = 0$, the activity is A_0) and μ is the absorption coefficient. If it is assumed that the sample area is constant, this relationship can be rewritten

$$I = \frac{A_0}{\mu}(1 - e^{-\mu m}) \tag{3}$$

where $I = m \cdot A_x$ is the activity from the sample area containing m mg sample (the dimension of μ in eqn. 3 is weight^{-1}). Thus if log I is plotted against log m, a curve should be obtained with the two asymptotes

$$\lim_{m \to 0} \log I = \log A_0 + \log m \tag{4a}$$

$$\lim_{m \to \infty} \log I = \log A_0 - \log \mu \tag{4b}$$

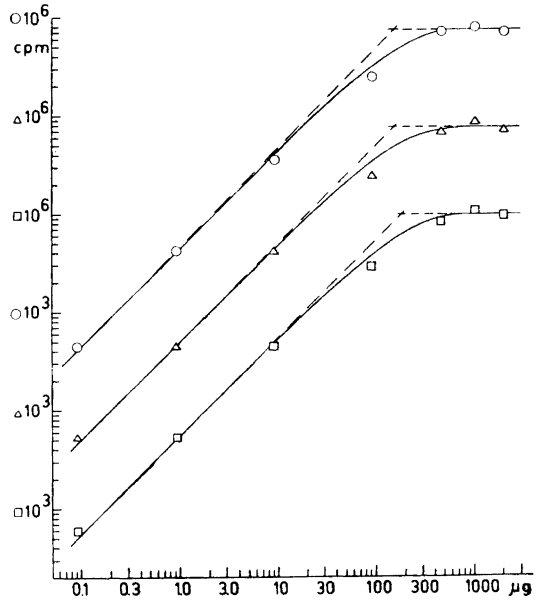

Fig. 2. Measured activity, I cpm, as a function of sample weight, m μg, at constant specific activity. The curves according to eqns. 3 and 4 are displaced one log unit along the ordinate for each backing material (○ aluminium, △ stainless steel, □ platinum backing).

The intercept between these two asymptotes occurs at $\log m = -\log \mu$. This point is easy to determine in a log I *versus* log m plot, since the asymptotes intersect each other at an angle of 135°.

Fig. 2 has been used to determine μ (in μg^{-1}) by this method as well as A_0; the asymptotes are given as dotted lines in the figure. The values obtained are given in Table 2, together with estimated errors. With these values of μ and A_0 introduced into eqn. 3, log I has been calculated as a function of log m, and the result thus obtained is given in the solid curves in Fig. 2.

Table 2. Calculations of μ (in μg^{-1}) and A_0 (in cpm) from Figs. 2 and 3.

Value	according to	Backing material		
		aluminium	stainless steel	platinum
$1/\mu$	Fig. 2	150 ± 30	145 ± 20	180 ± 20
A_0/μ	» 2	(750 ± 50) 10^3	(770 ± 70) 10^3	(1 000 ± 70) 10^3
A_0	» 2	5 000 ± 400	5 300 ± 500	5 600 ± 400
A_0	» 3	5 000 ± 200	5 900 ± 400	6 800 ± 200

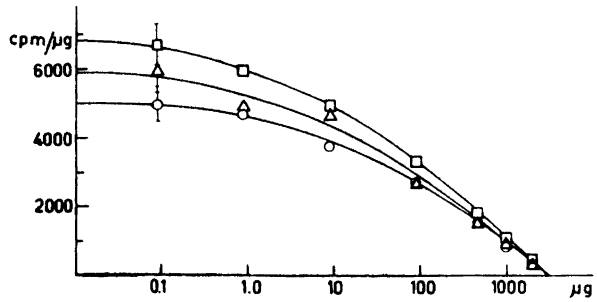

Fig. 3. Apparent specific activity, I/m (cpm/μg), as a function of sample weight, m (μg), for various backing materials (O aluminium, △ stainless steel, □ platinum).

According to eqn. 4a, A_0 can also be obtained from the plot in Fig. 3. The inaccuracy in the A_0-value obtained for $m \to 0$ is rather large; the estimated values are given in Table 2.

The difference between the A_0-values obtained with aluminium, stainless steel and platinum as backing material must be due to the back-scattering of the radiation by these materials. The back-scattering factor, f_b, has been calculated as a function of the atomic number of the backing material in Fig. 4. This has been done by first calculating the relative backscattering factor (f_b') in stainless steel and platinum towards aluminium ($f_b' = 1.00$) and the displacing the curve f_b' *versus* atomic number, Z, so that the extrapolated curve starts with $f_b = 1.00$ at $Z = 0$. In these calculations, the A_0-values obtained from Fig. 3 have been used.

DISCUSSION

The self-absorption factor. As an average of the $1/\mu$-values in Table 2 one obtains 160 ± 25 μg. Since the sample area is 1.3 ± 0.2 cm^2, this corresponds to $1/\mu = 120 \pm 25$ μg/cm^2. From the relationship [13] $d_{½} = 0.693/\mu = 0.139 R_0$, where $d_{½}$ is the half-value thickness of the beta radiation, one thus obtains $d_{½} = 0.08 \pm 0.02$ mg/cm^2 and $R_0 = 0.6 \pm 0.1$ mg/cm^2. These values should be compared with the directly measured values $d_{½} = 0.07$ mg/cm^2 (giving $R_0 = 0.5$ mg/cm^2)[19] and $R_0 = 0.23$ mg/cm^2 (giving $d_{½} = 0.032$ mg/cm^2)[20], and the calculated value $R_0 = 0.7$ mg/cm^2 (giving $d_{½} = 0.10$ mg/cm^2) from the Glendenin [21] energy-range relation. Though the agreement between these three latter values is not remarkably good, two [19,21] of them agree well with the value obtained here.

It is seen from Fig. 2 that the experimental points at intermediate sample weights (~ 100 μg) fall below the theoretical curve given by eqn. 3. The reason for this may be due partly to the fact that eqn. 2 is only strictly valid for collimated radiation, and partly to the interrelation between self-absorption and back-scattering (*cf.* Ref.[16]). As the sample thickness increases, part of the radiation is back-scattered by the sample itself rather than by the backing material and, since the sample material has a lower back-scattering power (lower average atomic number) than the backing material, less radiation will

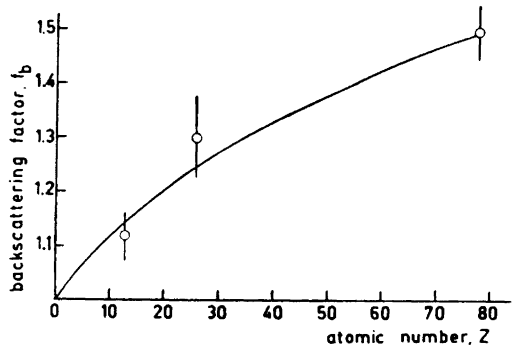

Fig. 4. Saturation back-scattering factor, f_b, as a function of the atomic number Z of the backing materials.

be scattered back into the counter. The back-scattered radiation has a much lower average energy than the unscattered beta-radiation, and is thus more easily absorbed in the sample, which lowers the fraction of back-scattered radiation reaching the sensitive volume of the counter. This is clearly indicated in Fig. 3, which shows that with increasing sample weight, the activity measured becomes more and more independent of the orginal backing material.

Thus the increasing sample weight causes the experimental points to become lower than would have been the case if only self-absorption was operating. The horizontal asymptote should, in such a case, have been situated higher than is shown in Fig. 2, and consequently a higher $1/\mu$-value would also have been obtained. On the other hand, the experimental points at low m-values in Fig. 2 do not fall exactly on the straight line, which indicates that the line of 45° slope should be somewhat displaced to the left (that this is true is seen

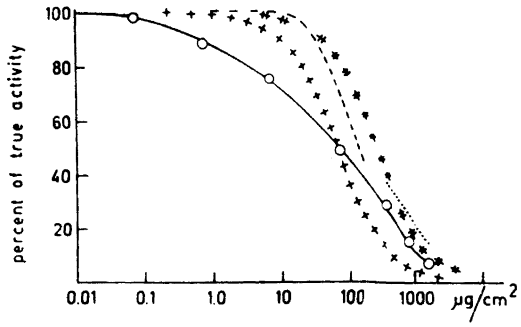

Fig. 5. Percentage of true activity measured from tritium samples of various surface thickness. The experimental results in this work is denoted by --o--o--, curves calculated according to eqn. 2 by + + + + for $R_0 = 0.2$ and by ## ## for $R_0 = 0.8$ mg/cm², while — — — — indicates results by Jackson and Lampe [7], and . . . . by Eidinoff and Knoll [4].

Table 3. Calculations of percent of true activity measured from samples of various thickness (in $\mu g/cm^2$). The A_0:values used are taken from Fig. 3, as given in Table 2.

m μg	m/a $\mu g/cm^2$	100 I A_0^{-1} m^{-1} for various backing materials			
		aluminium	stainless steel	platinum	mean value
2 000	1 540	7 %	6 %	7 %	7 %
1 000	770	16 »	15 »	16 »	16 »
460	350	31 »	26 »	27 »	28 »
90	70	54 »	46 »	49 »	50 »
9	7	76 »	79 »	73 »	75 »
0.9	0.7	94 »	84 »	88 »	89 »
0.09	0.07	99 »	101 »	98 »	99 »
(0.0)	(0.0)	(100) %	(100) %	(100) %	(100) %

from Fig. 3). It is difficult to estimate to what extent these two corrections affects $1/\mu$, but it is believed that the true $d_{½}$-and R_0-values are approximately equal to those obtained from Fig. 2 (*i.e.* $d_{½} = 0.08 \pm 0.02$ mg/cm², $R_0 = 0.6 \pm 0.1$ mg/cm²).

A serious consequence of this is that it points out the difficulties in using eqn. 2 for the determination of the relation between measured and true activity. As has been pointed out by Glendenin and Solomon [15], it is advisable to make self-absorption curves for each particular experimental condition if any accuracy is desired. The self-absorption factor, f_s, is therefore best obtained from curves like those in Fig. 3.

Using these data

$$f_s = \frac{100 \cdot I}{A_0 \cdot m} \% \qquad (5)$$

has been calculated as a function of m/a, (Table 3, and solid line in Fig. 5) where a is the area of the sample.

In Fig. 5, the experimental results obtained by Eidinoff and Knoll [4] (dotted curve) and Jackson and Lampe [7] (dashed curve) are also given. Considering the experimental difficulties, the agreement with the former investigation seems reasonable, but the deviation from the latter investigation is very great. The reason for this deviation may partly be that it is easier to obtain well-defined and even samples with the substances (triglycerides, fatty acids and soaps) investigated by Jackson and Lampe, than with PAS, which tends to form small aggregates of micro crystals. This may also explain why Jackson and Lampe obtained infinitely thin samples at a surface density of $\lesssim 10$ $\mu g/cm^2$, while in our case this was not obtained until $\lesssim 0.1$ $\mu g/cm^2$. However, the steeper rise of the upper part of the curve given by Jackson and Lampe compared with that of the theoretical curve lacks explanation.

The back-scattering factor. The discussion above has indicated that the A_0-values obtained at infinite sample thickness from Fig. 3 are more reliable than those obtained from Fig. 2. If a comparison is made with the results

obtained by Yaffe and Justus [11], the back-scattering factor obtained here seems far too high. However, from Seliger's [22] angle-energy relationship for scattered radiation one is bound to explain this discrepancy as being due to the use of different measuring equipment, *i.e.* in Yaffe's case, the use of low geometry and absorbing materials between the sample and the counter, which removes a considerable fraction of the soft scattered radiation.

Conclusion. Eqn. 1 has been used for the determination of the absolute specific activity, S, of a tritium sample. It has been pointed out that in a 2π internal gasflow proportional counter, the geometry can be assumed to be 50 % (*i.e.*, $f_g = 0.5$) and the efficiency 100 % ($f_e = 1$) when the counter is operated in the plateau at a reasonably low counting rate ($f_r = 1$). Methods for the determination of self-absorption (f_s) and back-scattering (f_b) have been described.

Under these conditions, S was determined for a tritiated solid PAS-sample, giving a result of 790 ± 40 dpm/mmole hydrogen. A fraction of the same sample was then analyzed for tritium as hydrogen gas internally in a GM-counter, giving 860 ± 120 dpm/mmole. Considering the uncertainties caused by all correction factors in eqn. 1, the agreement is very good, indicating the usefulness of the method described in this paper for rapid and absolute determination of tritium activities in solid samples.

Acknowledgement. The author wishes to thank Prof. G. Ljunggren, head of FOA 1, for his support of this work, Dr. L. Melander and Dr. Å. Hanngren, for valuable discussions, Mr. S. Olsson and Mrs. B. Rydberg for experimental aid, and Miss Helen Dunsmore for correcting the English text.

REFERENCES

1. Rydberg, J. and Hanngren, Å. *Acta Chem. Scand.* **12** (1958). 332.
2. Grenan, M. and Vialland, R. *J. Chim. Phys.* **49** (1952) 623.
3. Okita, G. T., Spratt, J. and Leroy, G. V. *Nucleonics* **14** No. 3 (1956) 76.
4. Eidinoff, M. L. and Knoll, J. E. *Science* **112** (1950) 250.
5. Gray, I., Ikeda, S., Benson, A. A. and Kritchevsky, D. *Rev. Sci. Instr.* **21** (1950) 1022.
6. Jenkins, W. A. and Yost, D. M. *J. Chem. Phys.* **20** (1952) 538.
7. Jackson, F. L. and Lampe, H. W. *Anal. Chem.* **28** (1956) 1735.
8. Zumwalt, L. R. *MDDC*-1346 (1947).
9. Frisby, J. H. and Roaf, D. *Proc. Phys. Soc. (London)* **64B** (1951) 169.
10. Gleason, G. I., Taylor, J. D. and Tabern, D. L. *Nucleonics* **8** No. 5 (1951) 12.
11. Yaffe, L. and Justus, K. M. *J. Chem. Soc. Suppl.* **1949** S341.
12. Henriques, F. C., Jr., Kristiakowsky, G. B., Margnetti, C. and Schneider, W G. *Ind. Eng. Chem., Anal. Div.* **18** (1946) 349.
13. Libby, W. F. *Anal. Chem.* **19** (1947) 2.
14. Schweitzer, G. K. and Stein, B. R. *Nucleonics* **7** No. 3 (1950) 65.
15. Glendenin, L. E. and Solomon, A. K. *Science* **112** (1950) 623.
16. Nervik, W. E. and Stevenson, P. C. *Nucleonics* **10** No. 3 (1952) 18.
17. Olausson, B. and Rydberg, J. *FOA Report* 10092–8509, 1954.
18. Melander, L. *Acta Chem. Scand.* **2** (1948) 440.
19. Dorfman, L. M. *Phys. Rev.* **95** (1954) 393.
20. Brown, S. C. *Phys. Rev.* **59** (1941) 954.
21. Glendenin, L. E. *Nucleonics* **2** No. 1 (1948) 12.
22. Seliger, H. H. *Phys. Rev.* **88** (1952) 408.

Received November 4, 1957.

ACTA CHEMICA SCANDINAVICA 12 (1958) 408—414

On Vitamins in Sewage Sludge

VI. The Effect of Cobalt Chloride and Copper Sulphate on Vitamin B_{12} Contents of Microbially Decomposing Sewage Sludge

HALINA Y. NEUJAHR

Division of Food Chemistry, Royal Institute of Technology, Stockholm, Sweden

The effect of the addition of cobalt chloride and copper sulphate to fermenting sewage sludge was studied with respect to *E. coli* activity formed and its distribution between the different vitamin B_{12} factors.

The addition of cobalt chloride was found to stimulate the synthesis of cyanocobalamin and vitamin B_{12}-like factors in aerobically fermenting sewage sludge, whereas under anaerobic conditions its stimulating effect was less pronounced and restricted only to the initial stages of the fermentation.

The addition of copper sulphate had a detrimental effect on the formation of cyanocobalamin and of some vitamin B_{12}-like factors but not of factors Z, the formation of which in the aerobically fermenting sludge was drastically stimulated by the highest additions of copper sulphate used.

Many investigators have observed the growth promoting and vitamin B_{12} sparing effect resulting from the addition of small amounts of antibiotics, arsonic acids, and certain sulfonamides as well as of certain mineral compounds (*i.e.* cobalt, copper and iron salts) to commercial animal rations (*cf. Nutrition Revs 14* (1956) 238). It has been suggested that several of these agents may exert an influence on the intestinal synthesis of vitamin B_{12}, *i.e.* by alteration of the microbial intestinal flora (*cf. Vitamins and Hormones 14* (1956)).

Microbially decomposing sewage sludge is the site of synthesis of different vitamin B_{12} factors[1]. It has been shown in a previous investigation [2] that the addition of small amounts of several antibiotics may exert an influence upon the amounts of the different vitamin B_{12} factors synthesized during the process of microbial decomposition of sludge. A study of a similar effect resulting from the addition of cobalt chloride and copper sulphate is reported in the present paper.

EXPERIMENTAL

Fresh sludge from a settling tank of the Stockholm municipal sewage plant was disintegrated in a "Turmix" blendor, then mixed with ca. 20 % of digested sludge and diluted with water. The material thus obtained had a dry solid content of *ca.* 4 % and pH 5.0—5.5. It was fermented aerobically and anaerobically at 33°C with the addition of graded amounts of $CoCl_2 . 6H_2O$ and $CuSO_4 . 5H_2O$, respectively. The experiments were performed in conical flasks of 300 ml capacity placed in rooms with thermostatically controlled air temperature. In the anaerobic fermentations the flasks were filled with 280 ml of sludge and incubated in the thermostat. In the aerobic fermentations the flasks were placed in a shaking machine and the amount of sludge fermented was 100 ml. All additions were made before the start of the fermentations. Samples were autoclaved in the presence of KCN as described elsewhere [1]. Vitamin B_{12} activity was estimated with the aid of the cup plate, the tube and the bioautographic methods using *Escherichia coli* 113—3. Paper chromatograms were developed for 48 h at 18°C in the following two solvent systems:

Solvent system I: *sec.* butanol: H_2O:HAc (75:24:1) + 0.01 % KCN
Solvent system II: *sec.* butanol: H_2O:NH_3 (75:24:1) + 0.01 % KCN

Two standard solutions were used to identify the spots after chromatographic separation.

Standard solution 1 (S1): cyanocobalamin + factor III + factors (Z2 + Z3) [3].
Standard solution 2 (S2): factor A + factor B.

Each spot corresponded to 1 μl of the solution to be tested. The spot corresponding to that of factor A may represent a mixture of several of the following factors:

A + ψ-B_{12} + III + W + XI + X2 + X3 + X4 in solvent system I, whereas in solvent system II factors III + W can be separated from the other factors. The spot corresponding to factor A is in the following designated as "A". The spot corresponding to factor III may contain also factor W.

The following additions to the sludge were made:

% $CoCl_2 . 6H_2O$	corresp. to *ppm* Co^{++}	% $CuSO_4 . 5H_2O$	corresp. to *ppm* Cu^{++}
0.00	0	0.00	0
0.05	118	0.05	127
0.10	236	0.10	254
0.50	1 118	0.50	1 270
1.00	2 360	1.00	2 540

According to Anderson [4] digested municipal sludges may contain 315—1 980 ppm Cu^{++} (average: 643). No published data about the contents of cobalt in native or digested sludge were available. Total copper in the sludge mixtures used for the fermentation experiments was determined absorptiometrically with diethylammonium diethyldithiocarbamate in the dry ashed sludge according to the method of Abson and Lipscomb [5]. The values obtained were 22—25 μg Cu/ml sludge (determined as Cu^{++}) and showed fair constancy in several investigated batches of the sludge. These values are of a quite different order of magnitude from those reported by Anderson [4] for American digested sludge. The difference probably reflects the influence of industrial products entering sewage purification systems in Stockholm and in the American towns.

The cobalt contents in the sludge mixtures were determined absorptiometrically with 1-nitroso-2-naphthol by the method of Middleton and Stuckey [6]. The determinations were carried out on dry ashed sludge as in the case of copper. The values obtained were 0.5—0.6 μg Co/ml sludge (determined as Co^{++}). This represents an amount about ten times as large as the amount of cobalt bound in the vitamin B_{12} factors.

RESULTS

It can be seen in Fig. 1 that the highest additions of copper sulphate (0.5 — 1.0 %) caused a marked decrease in the pH of the sludge in both the aerobic and the anaerobic fermentation thus indicating that the "normal"

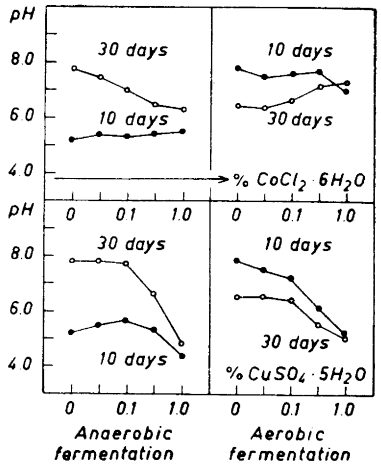

Fig. 1. Effect of addition of cobalt chloride and copper sulphate upon the pH of microbically decomposing sewage sludge.

microbial flora of the decomposing sludge had become modified by the addition. The anaerobic microbial decomposition of the sludge proceeded in two stages; the first stage lasting for at least 10 days was characterized by a lower pH (5.0 — 5.5) and the second stage by a higher pH (7 — 8).

In the aerobic process (continuous shaking) a pH value of 7 — 8 was reached already after 10 days and was followed by a drop to pH 6.5 after 20 more days of microbial decomposition.

Obviously, these differences in pH variations between the aerobic and the anaerobic processes must be taken into account when considering the differences in formation of the different vitamin B_{12} factors during these processes.

Effect of cobalt chloride

a) *Anaerobic fermentation* (Fig. 2a). The addition of 0.1 % $CoCl_2.6H_2O$ corresponding to 236 ppm of Co^{++} slightly stimulated the synthesis of cyanocobalamin and of factor B during the first 10 days of fermentation. The addition of 0.05 — 0.1 % $CoCl_2.6H_2O$, corresponding to 118—236 ppm of Co^{++}, stimulated the synthesis of factors Z in a very pronounced way. With greater amounts of cobalt chloride a detrimental effect on the synthesis of all vitamin B_{12} factors could be observed. After 20 more days of fermentation with 118 ppm Co^{++} a slightly stimulating effect on the synthesis of factors Z and of factors "A" could be noticed whereas the amount of cyanocobalamin remained unaffected by the additions of 118 and 236 ppm and rather diminished by the additions of larger amounts.

b) *Aerobic fermentation* (Fig. 2b). The effect of cobalt chloride was here much more pronounced than under anaerobic conditions. With 118 ppm of Co^{++} a drastic stimulation of the synthesis of cyanocobalamin and of factors Z could be observed after 10 days of fermentation. At the same time the amounts of factors "A" and of factor B decreased with increasing amounts

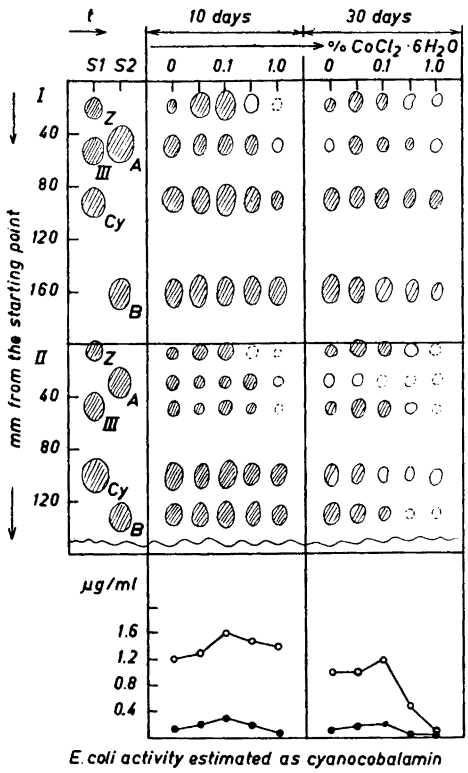

Fig. 2a. Effect of addition of cobalt chloride to fresh sewage sludge, subsequently anaerobically decomposed. Bioautogram.

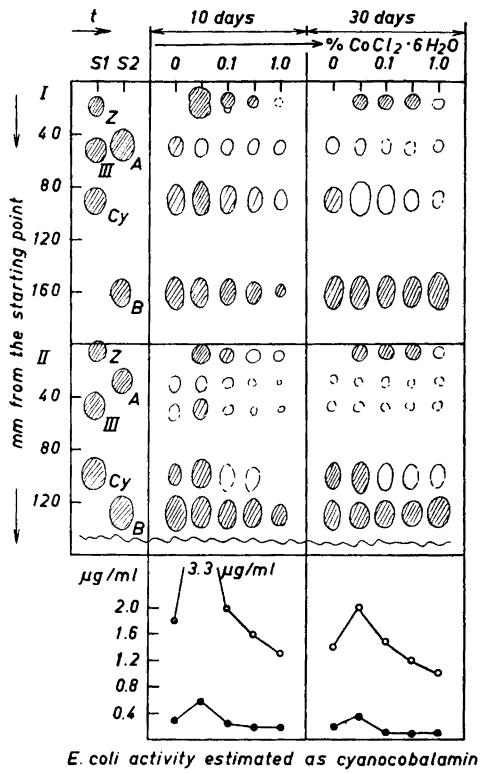

Fig. 2b. Effect of addition of cobalt chloride to fresh sewage sludge, subsequently aerobically decomposed. Bioautogram. ○——○ cup assay; ●——● tube assay.

of Co^{++}. After 20 more days of fermentation the stimulating effect on the synthesis of cyanocobalamin was still very pronounced whereas the effect on the synthesis of factors Z was less pronounced than after 10 days. The addition of 118 — 1 180 ppm of Co^{++} seemed to stimulate the synthesis of the latter factors.

The amount of factor B was greatest in the sludge with the highest addition of Co^{++} (2 360 ppm) which was accompanied by an almost total disappearance of all the other vitamin B_{12} factors.

Effect of copper sulphate

a) *Anaerobic fermentation* (Fig. 3a). The addition of 0.05 % $CuSO_4.5H_2O$ (corresponding to 127 ppm of Cu^{++}) had, after 10 days of fermentation, a slightly stimulating effect on the synthesis of all vitamin B_{12} factors. Higher additions had either no effect or a decreasing one. However, after 20 more

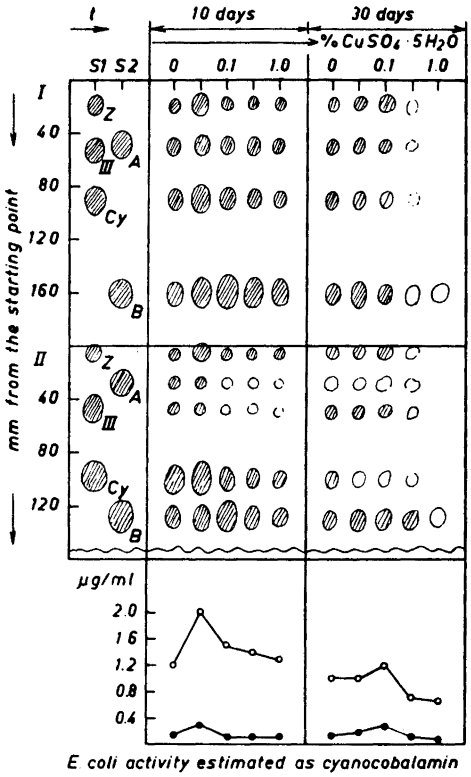

Fig. 3a. Effect of addition of copper sulphate to fresh sewage sludge, subsequently anaerobically decomposed. Bioautogram.

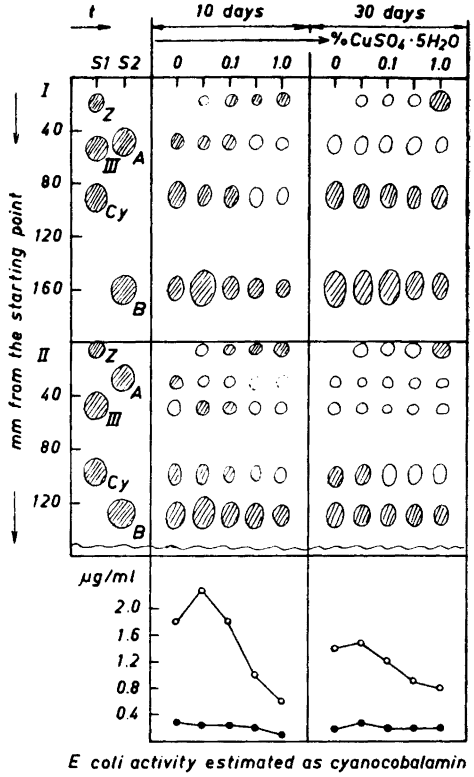

Fig. 3b. Effect of addition of copper sulphate to fresh sewage sludge, subsequently aerobically decomposed. Bioautogram.
○———○ cup assay; ●———● tube assay.

* Abbreviations used in Figs. 1—3.

I — solvent system I
II — solvent system II
t — time of fermentation
S1 — standard solution 1
S2 — standard solution 2
Z — factors Z2 + Z3
III — factor III
Cy — cyanocobalamin
A — factor A
B — factor B

days, the amount of cyanocobalamin decreased in the sludge containing 0.05 % copper sulphate and still more with increasing additions of Cu^{++}, but the synthesis of factors Z and of factor B was slightly stimulated by the additions corresponding to 254 and 127 ppm Cu^{++}, respectively. With higher additions all the vitamin B_{12} factors disappeared.

b) *Aerobic fermentation* (Fig. 3b). Increasing additions of copper sulphate decreased the amount of cyanocobalamin and increased the amount of factors Z. The situation was the same after 10 days as after 20 more days of fermentation. The amount of factor III and of factor B was slightly increased after 10 days in the sludge to which 127 ppm Cu^{++} had been added.

DISCUSSION

It can be concluded from the above that the addition of cobalt chloride to fresh sewage sludge, exerts a stimulating influence on the synthesis of cyanocobalamin and of other vitamin B_{12} factors during the subsequent microbial decomposition. This influence is much more pronounced in aerobic than in anaerobic fermentation. Moreover, under anaerobic conditions the addition of Co^{++} seems to stimulate the synthesis of vitamin B_{12} factors solely during the first stage of the decomposition of the sludge (10 days, pH $\sim$ 5.5) whereas during a latter stage (20 more days, pH $\sim$ 7.5) the amount of cyanocobalamin formed remains unaffected and the synthesis of factors Z and of factors "A" is stimulated only very slightly. In the aerobic fermentation the addition of Co^{++} stimulates the synthesis of cyanocobalamin and of factors Z very markedly both after 10 and after 20 more days of fermentation, which probably may be connected with the faster decomposition rate of the aerobically fermented sludge as reflected by the changes in pH (*cf.* p. 409). In an earlier investigation [1] it has been found that the first stage (pH 5.5) of anaerobic microbial decomposition of sewage sludge is characterized by a disappearance of cyanocobalamin which is probably consumed by some microorganisms active in the sludge at this pH, whereas during the decomposition of the sludge by aerobic organisms cyanocobalamin is synthesized continuously. The present result suggests therefore the possibility that the additon of Co^{++} to sewage sludge with subsequent anaerobic decomposition may exert a stimulating influence on the formation of cyanocobalamin rather by inhibition of the organisms which consume it (or enzymes which destroy it), whereas under aerobic conditions this addition may directly stimulate the synthesis of cyanocobalamin.

The addition of copper sulphate caused a slightly increased formation of cyanocobalamin and of several vitamin B_{12}-like factors during the first stage of microbial anaerobic decomposition of sludge (pH$\sim$5.5), whereas at the later stage (pH$\sim$7.5) the amount of cyanocobalamin was decreased by the addition. In view of the well known antimicrobial properties of copper it is tempting to suggest that its stimulating effect on the synthesis of cyanocobalamin and vitamin B_{12}-like factors during the first stage of anaerobic microbial decomposition of sludge may be due to inhibition of the cyanocobalamin consuming organisms (or enzymes which destroy it) analogously to the mechanism suggested for the effect of cobalt chloride in the first stage of anaerobic fermentation.

The addition of Cu^{++} with subsequent aerobic fermentation of the sludge had a detrimental effect on the formation of cyanocobalamin and of most vitamin B_{12}-like factors but not of factors Z the amounts of which drastically increased with the highest additions of Cu^{++}.

In earlier investigations [1,3] the formation of factors with R_F-values corresponding to those of factors Z was found to accompany very often the formation of cyanocobalamin. Cu^{++} thus seems to have some selective effect on the formation of cyanocobalamin and of these factors.

The amounts of cobalt and copper added to the sludge were chosen with regard to the range of similar additions usually employed in commercial

animal rations (*cf. Nutrition Revs. 14* (1956) 238). With a view, however, to the relatively low natural contents of these elements in sludge (*cf.*p. 409) it would be of interest also to investigate the range 0—100 ppm of both additional copper and cobalt. It is thus too early to draw any conclusions about the optimal amounts of these two elements in fermenting sewage sludge for obtaining largest amounts of vitamin B_{12} factors.

Acknowledgements. The author is grateful to Professor H. Lundin, Head of the Division, for his encouraging interest in and valuable advice on the execution of this work. Thanks are due to Miss R. Wolf for technical assistance. The financial support from *Statens Tekniska Forskningsråd* is gratefully acknowledged.

REFERENCES

1. Neujahr, H. Y. *Acta Chem. Scand.* **9** (1955) 622.
2. Neujahr, H. Y. *Acta Chem. Scand.* **11** (1957) 1191.
3. Neujahr, H. Y. *Acta Chem. Scand.* **10** (1956) 917.
4. Anderson, M. S. *Sewage and Ind. Wastes* **28** (1956) 132.
5. Abson, D. and Lipscomb, A. G. *Analyst* **82** (1957) 152.
6. Middleton, G. and Stuckey, R. E. *Clin. Chim. Acta* **1** (1956) 135.

Received October 22, 1957.

ACTA CHEMICA SCANDINAVICA 12 (1958) 415—437

Servo-controlled Wheatstone Bridge Arrangements for the Simultaneous Recording of Resistance and Capacitance

CARL-OVE ANDERSSON, FREDRIK MÖHL and EINAR STENHAGEN

Department of Medical Biochemistry, Institute of Medical Chemistry, University of Uppsala, and the Institute of Medical Biochemistry, University of Gothenburg, Sweden

The conditions for simultaneous servo-balancing of resistance and capacitance in alternating-current Wheatstone bridges of various types are discussed. A series of experiments are described which confirm the theory, and give information regarding the practical aspects of double-servo-controlled A.C. bridges.

Servo-controlled Wheatstone bridges intended for the continuous recording of resistance in electrolytic systems have been described in the literature. For references see Ref.[1] The arrangements so far described use servo control only for the resistive balance, and the capacitative balance has to be adjusted manually. It was suggested by Andersson, Mellander, and Stenhagen [1] that automatic capacitative correction might be used in the form of a standardization operation, performed in a manner similar to the automatic current standardization in D.C. millivolt recorders of, for example, the "Speedomax" type. A study of the theoretical side of the problem, however, revealed that it should be possible to balance both capacitance and resistance simultaneously by using two independent servo systems, and the results recorded in the experimental part of this communication show that servo-controlled Wheatstone bridge arrangements for the simultaneous recording of resistance and capacitance are capable of practical realization.

THEORY. CONDITIONS FOR OPERATION OF DOUBLE SERVO SYSTEM

I. Normal Wheatstone bridge (Fig. 1)

Consider the Wheatstone bridge arrangement of Fig. 1. It is assumed throughout this communication that the fixed bridge arms AD and DC are identical. The variable impedance to be recorded (for instance that of an electrolytic cell) is connected between points B and C, and considered as a

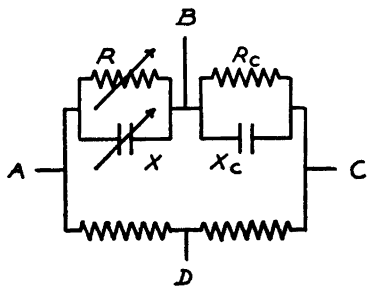

Fig. 1. Normal alternating current bridge. A and C are connected to a source of alternating current; B and D are connected to the detector. Shielding and Wagner earthing arrangements not shown.

resistance and a capacitance in parallel. A source of A.C. current is connected across points A and C. When the bridge is unbalanced, that is, when $R \neq R_C$ and/or $X \neq X_C$, an alternating potential exists across BD. The unbalance is to be automatically corrected through the variable resistance R and reactance X, each controlled by its own servo-motor. The servos are steered by the potential across points B and D, through phase-sensitive detectors. The sign of the D.C. output of a phase sensitive detector depends on the phase difference between the signal and a reference potential of the same frequency (in the present case obtained from the oscillator supplying the bridge current). If the phase difference is $< 90°$, the detector gives a D.C. component in the output current; and if the phase difference is $> 90°$, the D.C. component has the opposite sign. If the phase difference is exactly 90° (or 270°) there will be no D.C. component in the output.

We now connect two phase-sensitive detectors in parallel across BD (in practice they are connected in parallel over the output of the detector amplifier), and the D.C. outputs are fed to the R- and the X-servo, respectively. The reference potentials are termed $V_{R\ ref.}$ and $V_{X\ ref.}$

If the phase of the alternating potential V_{DB} is not exactly 90° out of phase with respect to $V_{X\ ref.}$, the X-servo receives a signal, and will adjust the reactance X until the signal output of the X-detector is zero (or is below the threshold of the servo). The R-servo will operate in a corresponding manner. If the $V_{R\ ref.}$ and $V_{X\ ref.}$ are out of phase with respect to each other,

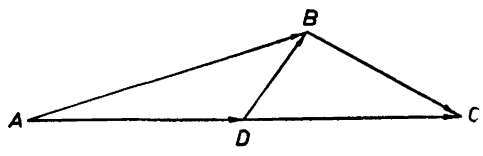

Fig. 2. Vector diagram of the potentials of the bridge shown in Fig. 1 at unbalance.

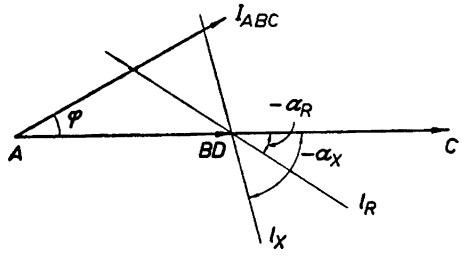

Fig. 3. Current and potential vectors of the bridge shown in Fig. 1 at balance. For the definition of I_X and I_R see text.

it is evident that V_{DB} must be zero in order that neither servo shall operate, which means that the desired balance of the bridge has been attained. The servos may be coupled to recorders that automatically record both the resistance and the reactance of the bridge-arm BC.

In order for the arrangement to function properly, two conditions must be fulfilled: (a) "Coupling" between the servos must be avoided, that is, *if one of the servos receives no signal the other servo should not be able to alter this condition;* and (b) "Parallelism" between a servo and its steering function must be avoided, that is, *if one of the servos receives a signal it must be possible for the servo in question to alter this condition.*

It should be possible to realize condition (a) approximately and condition (b) (which is the more important) exactly, by a suitable choice of phase for the reference signals. Fig. 2 shows in vector form the potentials between the four corners of the bridge at unbalance. The vector representing the potential V_{DB} can form any angle with the vector V_{AC}, but is always small compared with the latter. At balance $V_{DB} = 0$: B coincides with D as shown in Fig. 3. If $R = R_C$, and R, R_C, and X_C are kept constant, and X varies (*cf.* Fig. 1), the point B of the vector V_{DB} of Fig. 3 will move along a curve. If X is kept constant and X_C varies, point B will move along a different curve. In point D these curves have the common tangent l_X, forming an angle α_X with the vector V_{AC}. Analogous relations are valid for R, R_C, and α_R of Figs. 1 and 3. If V_{DB} is kept small we may use the approximation that the point B moves along the tangents l_X and l_R. For the purpose of our discussion we can furthermore assume that the input resistance of the detector amplifier is infinitely high, and that therefore no current flows between points B and D. Any current I_{DB} will cause changes in all potentials, and probably also in α_R and α_X. If $I_{DB} = 0$ it can be shown (see Appendix I) that $\alpha_R = -\varphi$ and $\alpha_X = -(\varphi + 90°)$, where φ is the angle between V_{AC} and I_{ABC}. It follows that if, for example, R_C changes during an experiment, and R (to keep the balance) changes in the same direction, φ and consequently also α_R and α_X will change. In the following discussion, however, we may disregard this change.

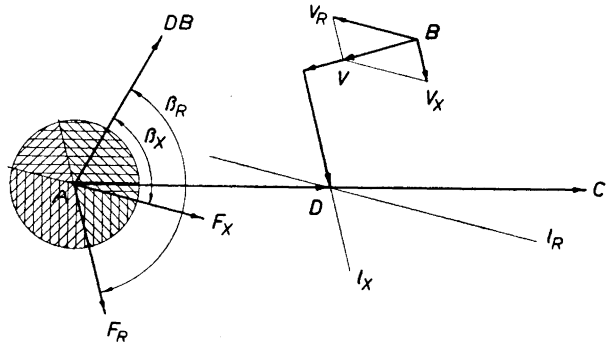

Fig. 4. Diagram illustrating the servo balancing of the bridge shown in Fig. 1.

In order to avoid coupling between the servos, the X-servo must not operate when point B is moving along l_R, and B therefore can be led back to D with the R-servo alone. The X-servo does not operate if the potential vector $V_{X\ ref.}$ is normal to l_R. Analogously, $V_{R\ ref.}$ should be normal to l_X. We then get the conditions shown in Fig. 4. The sign of the output signals from the phase detectors are determined by the angles β_R and β_X between the vector V_{DB} and the vectors F_X and F_R, respectively, which are normals to the corresponding reference potentials. When $\beta_R > 0$ (region \\\\\\) the R-servo will cause point B to move with velocity v_R towards "west-north-west" along a line approximately parallel to l_R. If $\beta_R < 0$ (region //////), v_R will point towards "east-south-east" instead. Similarly, $\beta_X > 0$ (region ≡≡≡) gives v_X pointing towards "south-south-east", approximately parallel to l_X; and $\beta_X < 0$ (region ||||||) gives v_X pointing in the opposite direction ("north-north-west"). In the circumstances illustrated in Fig. 4, both β_R and β_X are > 0 (region ▦), and v_X and v_R add vectorially to v, pointing towards "west-south-west" until point B reaches the line l_X, when the R-servo stops. Only the component v_X of v then remains ($\beta_R = \pm 180°$, but β_X still > 0), and point B moves along l_X until point D is reached. The X-servo then stops, and the bridge is balanced.

A block diagram of the suggested servo-controlled bridge arrangement with independent R- and X-servos is shown in Fig. 5. The adjustment of the phase of the reference signals with the aid of the two phase shifters may be carried out as follows. The electrolytic cell or other impedance to be recorded is connected to the bridge. The phase detectors are disconnected and the bridge balanced manually in the usual manner. The phase detectors are connected to the bridge amplifier and the balance of the bridge slightly altered by altering R only, making point B in the diagram of Fig. 3 move out from D along l_R. This will probably result in output signals from both phase detectors. However, we wish only to get an output signal form the R-detector when R is changed and therefore adjust the phase of the reference signal $V_{X\ ref.}$ of

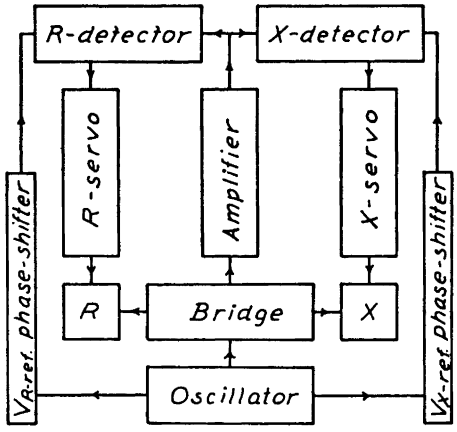

Fig. 5. Block diagram of bridge arrangement with double servo.

the X-detector until no output signal is obtained from this detector. $V_{X\ ref.}$ is then parallel to l_R. The bridge is again balanced manually, and the procedure just described repeated with reactance X and the phase shifter for $V_{R\ ref.}$ The servos are then connected. It may be necessary to shift the polarity of the servo connection if the phase of the corresponding reference signal should happen to be shifted 180°. The apparatus should now be ready for the run. For practical details see the experimental part.

A slight coupling between the servos must be tolerated for the following reasons. (a) The straight lines l_R and l_X are only approximations to the curves along which point B (Fig. 3) moves. (b) As already pointed out, the angles α_R and α_X of Fig. 3 vary with the phase-angle φ between the potential V_{AC} and the current I_{ABC}. This means that the orthogonality between the reference signals and the l-lines will not be exact. The errors can be kept small, however, provided that (a) point B is not allowed to move far away from D, that is, the servos must keep up well, and (b) the phase-angle does not undergo large absolute changes during the run. Difficulties due to phase-angle variation may be overcome by using the series bridge (see III).

II. The "potentiometer" Wheatstone bridge arrangement

The "potentiometer" bridge arrangement is extremely convenient for practical measurements of resistance, as it allows a continuous variation of the recorder range by means of a shunt across the potentiometer. In the apparatus described previously [1], the recorder range could be varied from 2 to 1 800 ohms full scale. The bridge is shown in Fig. 7. The use of a potentiometer in this manner may sometimes lead to errors in the recordings, however. Although the presence of such errors may be checked experimentally, a theoretical analysis is warranted.

As the complicated impedance of the arm BC (Fig. 7) makes theoretical calculations very difficult, the arrangement shown in Fig. 8 is used instead. The "differential" condenser (ganged X_1, X_2) is replaced by two separate condensers connected across A—B_a and C—B_c, respectively. Only X_2 should be

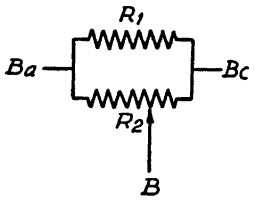

Fig. 6. Diagram showing shunted potentiometer.

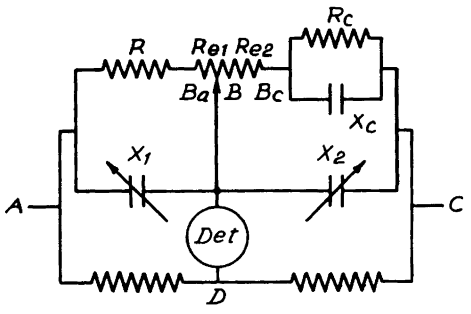

Fig. 7. Potentiometer bridge described in Ref.[1], and used in some of the experiments in Section VI.

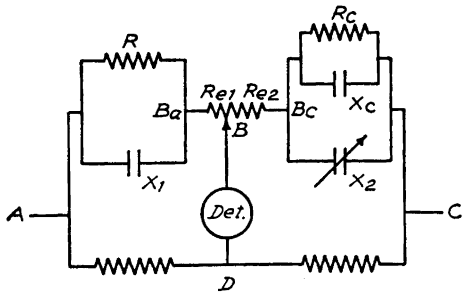

Fig. 8. Bridge arrangements recommended instead of that shown in Fig. 7.

servo-operated, as X_1, not being connected across exactly the same resistance as X_C (R is kept constant but the cell resistance R_C varies during the experiment), does not have the same action as X_C on the circuit. X_1 and X_2 should be as large as possible in order to keep φ small, because, as will be shown, a large φ causes poor linearity and poor servo action.

In order to simplify the calculations the shunted potentiometer (Fig. 6.) is replaced by the equivalent resistance R_e. The potentials B_aB and BB_c depend only on the position of B along R_1 and the total potential B_aB_c and this will be the same if the combination R_1, R_2 is replaced by the equivalent resistance

$$R_e = R_1R_2/(R_1 + R_2).$$

In the bridge arrangement of Fig. 1 it is evident that R is equivalent to R_C, and X to X_C. In the potential vector diagram given in Fig. 3 we therefore have only two "tracks" for the vector arrow point B, *viz.*, l_R and l_X. With the circuit of Fig. 8 this is no longer the case, and from the outset we have to consider four tracks, l_{RC}, l_{XC}, l_{Re}, and l_{X_1}. We need to know the answer to the following questions.

(a) Is it possible to compensate a small change in R_C with R_e only? This is of importance, particularly in the measurement of X_C. If the answer is no, it means that the condenser servo (X_2) responds both to capacitative and resistive changes of the cell, and it may be difficult to derive the capacitative changes from the recordings. This question, which is less important for the measurement of R_C, may also be formulated as follows: Do l_{RC} and l_{Re} coincide?

(b) Do l_{XC} and l_{X_1} coincide? This question is of particular importance in the measurement of R_C.

(c) What are the quantitative relations between R_C and R_e?

(d) What are the quantitative relations between X_C and X_2?

It is evident that question (b) can be answered in the affirmative, because X_C and X_2 are connected in parallel and have the same influence in the circuit. Resistance measurements are thus possible. Calculations, the details of which are given in Appendix II, show that the relation between ΔR_e and ΔR_C is

$$\Delta R_e = \frac{1}{1 - \mathrm{tg}^2\,\varphi} \cdot \tfrac{1}{2}\,\Delta R_C \qquad (14)$$

If R_e is mechanically coupled to a recorder we get a recording of ΔR_C in accordance with eqn. (14). The linearity is good, provided that φ is small and does not vary too much. If $\mathrm{tg}^2\varphi$ is less than 0.003 ($0 < \varphi < 2.75°$) ΔR_e will differ from $\frac{1}{2}\Delta R_C$ by less than 0.3 %. For phase angles smaller than the value just given, the error is thus less than the writing error of precision recorders of the "Speedomax" type. As tg φ increases with increasing frequency, the error due to the shunted potentiometer circuit will be smaller with a lowering of the frequency of the bridge current. On the other hand, the time constants of the filters necessary in the detector circuits have to be increased with a lowering of the frequency, leading to a fall in the speed of response on the part of the servos. The relation between the susceptance, $B_2 = 1/X_2$, of the condenser X_2 and R_C and X_C may be expressed by the following equations (for derivation see Appendix II).

$$\Delta B_2 = -\frac{2 \mathrm{tg}\,\varphi}{R_C^2 (1 - \mathrm{tg}^2\varphi)} \cdot \Delta R_C \tag{13}$$

$$\Delta B_2 = -\Delta \frac{1}{X_C} \tag{15}$$

If we couple a recorder mechanically to the condenser X_2, the recorder will write a curve of the sum of a susceptance curve according to eqn. (15), and a resistance curve according to eqn. (13). From Fig. 9 we obtain the value $90° - 2\varphi_2 \approx 90° - 2\varphi$ for the angle between l_{R_e} and l_X. When $\varphi = 45°$, l_{R_e} and l_X coincide. The action of the potentiometer will then be the same as that of condenser X_2, and it will be impossible to balance the bridge. It may perhaps be possible to allow values of φ as high as 30°, but it must be kept in mind that the permitted variation in φ will become less with increasing φ.

To sum up, the "potentiometer" bridge circuit is unsuitable for the recording of reactance unless tg φ is very close to zero (eqn. 13), but it may be employed for the recording of the resistive component of an impedance that does not vary over large ranges.

III. The series bridge

For the measurement of electrolytic resistance, bridges with parallel combinations of resistances and capacitances are usually employed. However, a

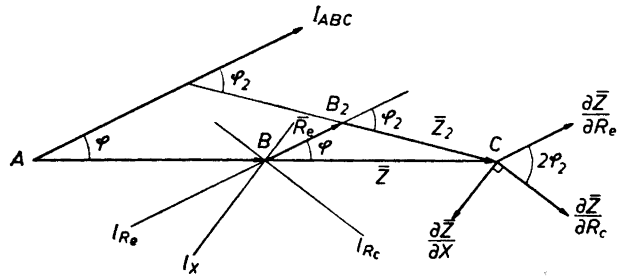

Fig. 9. Vector diagram of the bridge of Fig. 8. For explanation see text.

series bridge arrangement has two very important advantages over the parallel bridge with respect to servo control: (a) It is possible to use a shunted, servo-controlled measuring potentiometer without introducing any theoretical error; and (b) The line l_R of the potential diagram (Fig. 11) is parallel, and the line l_X normal, to I_{ABC}. If the reference potentials of the detectors are based upon the current I_{ABC}, they will retain their theoretically correct value independent of variations in φ; and if the servos follow well, there will never be any coupling between them.

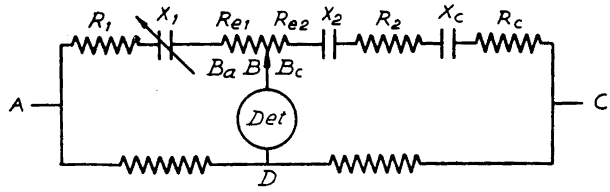

Fig. 10. Series bridge.

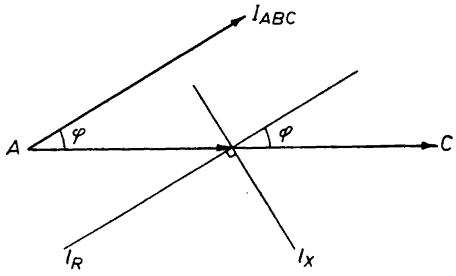

Fig. 11. Vector diagram of the series bridge.

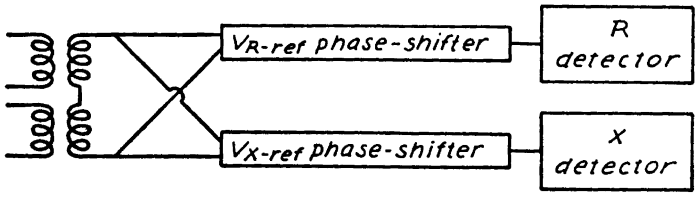

Fig. 12. Suggested detector arrangement for the series bridge.

The bridge may be connected as shown in Fig. 10. The series bridge is particularly useful when measuring impedances with large variations in φ. The reference potentials may be obtained through a suitable transformer with two identical primary windings (Fig. 12) connected in series with X_1 and X_2. An amplifier may have to be used between the transformers and the phase shifters.

In order to measure with the series bridge the parallel components of, say, an electrolytic cell, it is necessary to determine both series components and to calculate the parallel components of the cell using the following expressions

$$R_p = R_s (1 + R_s^2 B_s^2) \text{ and } X_p = \frac{R_s^2 B_s^2 + 1}{R_s B_s^2}.$$

IV. The Easton-Lamson bridge (General Radio Z-Y-bridge)

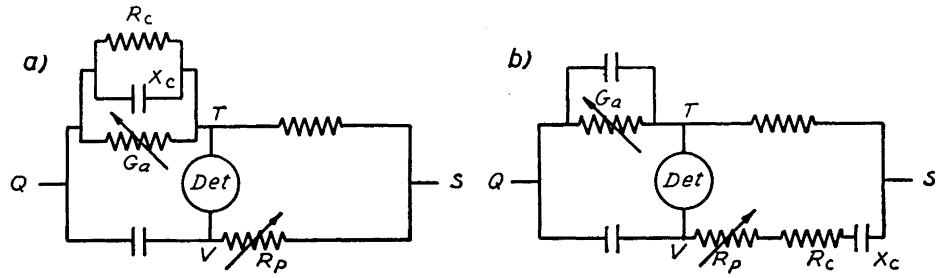

Fig. 13. a) Z—Y bridge with "cell" measured as admittance. b) Z—Y bridge with "cell" measured as impedance.

Easton and Lamson [2] have recently described the bridge arrangement shown in Fig. 13. This bridge has the distinction that it can be balanced for any type of impedance to be measured, and possesses over the normal Wheatstone bridge of Fig. 1 the advantage that both reactance and resistance are balanced with purely resistive components. It is therefore possible to use two similar resistances, one coupled to a recorder and the other to a simple servo, and simply change the connections according to whether the resistance or the reactance is to be recorded.

Fig. 14 shows the potential diagram at unbalance. When the bridge is balanced, points T and V (corresponding to points B and D of the diagram of the normal bridge of Fig. 2) coincide, as in Fig. 15. The resistance G_a moves

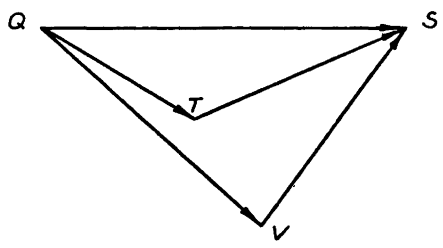

Fig. 14. Vector diagram of Z—Y bridge at unbalance.

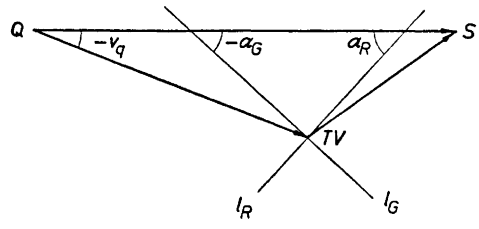

Fig. 15. Vector diagram of Z—Y bridge at balance. For explanation of I_R and I_G see text.

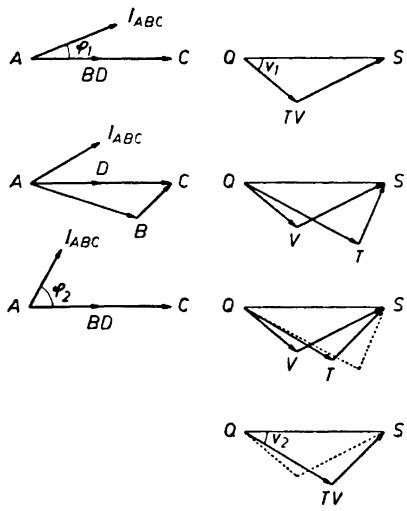

Fig. 16. Vector diagrams showing the balancing of the normal bridge left (1. Bridge balanced. 2. Unbalance introduced. 3. Balance restored with R and X.) and the Z-Y-bridge right (1. Bridge balanced. 2. Unbalance introduced. 3. T moved to balance point by means of G_a. 4. Balance restored by means of R_p.)

the point T along the line l_G, and R_p moves V along l_R. If the "cell" is measured as an "admittance", l_G and l_R correspond to l_R and l_X, respectively, in Fig. 3. The angles α_G and α_R that the lines l_G and l_R form with the impressed voltage QS are derived in appendix III. They are

$$\alpha_G = 2v_q \tag{16}$$

$$\alpha_R = 2v_q + 90° \tag{17}$$

and obviously depend only on the angle v_q between the voltages QS and QT (or QV, which is similar to QT), in the same way as α_R and α_X in Fig. 3 depend on the phase angle φ. And, unfortunately, like α, v_q cannot always be kept constant during the run.

It is clear, however, that in principle it is possible to servo-control the ZY-bridge in the same way as the normal bridge. The series of figures above (Fig. 16) shows what happens when the balance is disturbed and restored in the two cases. The impedance to be measured can be connected to the ZY-bridge in two different ways (Fig. 13). If connected as an "impedance" (Fig. 13 b) it is measured as a resistance and a reactance in series; and if it is connected as an "admittance" (Fig. 13 a) it is measured as a resistance and a reactance in parallel. In the former case the series reactance is not given by G_a directly, because the curve will give the variation of $\Delta\ 1/G_a$ and not $\Delta\ G_a$ if a linear resistance is used. (In the bridge manufactured by the General Radio Co. the measuring resistance is linear in conductance, not in resistance.) This is usually inconvenient, and it is therefore better to connect the unknown impedance according to the second alternative, and measure it as an admittance. If the connected admittance should fall outside the range of the instrument, the parameters of the bridge arms must be changed. When measuring the unknown impedance as admittance, G_a writes a curve giving the parallel resistance, and R_p a curve of the parallel susceptance.

V. Concerning the possibility of using a Wheatstone bridge with servo, without manual or servo-control of the quadrature component

Two cases are at once apparent when a single servo is sufficient, *viz.* when φ is constant and equal to zero, and when φ is constant and equal to 90°. It may be readily assumed that it should also be possible to use a single servo, when, for instance, it is desired to measure changes in resistance in cases where the capacitance remains constant (but $\neq 0$). This is in fact possible if the normal bridge arrangement of Fig. 1 is used, but is in general less satisfactory in case of the "potentiometer" circuit (Figs. 6 and 8), because, as already discussed above, a change in R_C causes both resistive and capacitative unbalance. However, if it is desired to measure only small changes in one of the parallel components, is it then necessary to keep the bridge in balance with respect to both components? A reference to Fig. 4 shows that if φ is constant, and if changes in R always make B move along straight lines parallel to l_R independent of the position of B in the plane, and if corresponding conditions are valid for l_X and X, X may remain in any position and X_C vary at will if R_C is to be measured. The R-servo and the attached recorder ought to record the same curve as when the bridge is kept in complete balance. Instead of remaining at D, the point B would move up and down along l_X, but this would have no influence on the R-servo.

Conditions are of course less perfect in practice, but the smaller the variation in Z, the nearer will be the approach to the ideal. The changes in Z to be recorded are often small compared with Z. It is, however, essential that the phase angle of the reference potential is correctly chosen.

Finally, it must be pointed out that the above reasoning implies that the detector does not lose its sensitivity when a large signal is applied, that is to say, a "logarithmic" detector amplifier cannot be used.

VI. Experimental part

The bridge and associated apparatus were the same as used previously [1], with the addition of a capacitance servo consisting of phase-sensitive detector with built in phase shifter (identical to that used for the recording of resistance) and a "Speedomax" recorder with a writing-speed of 2.5 seconds across the scale. A precision-built air-dielectric condenser * of 500 pF capacitance with linear capacitance variation, contained in a shielded box attached to the back of the recorder housing, was mechanically coupled to the recorder potentiometer shaft via an insulated bushing. A D.C. tachometer generator was attached to the recorder motor as described in the previous paper [1]. In Ref.[1] the bridge was arranged as shown in Fig. 7, but in the first series of experiments to be described below the bridge was set up as in Fig. 1, by joining points B and Bc. The servo-controlled condenser was connected between A and B. The servo was controlled by the detector signal across BD (Fig. 1) *via* the same detector amplifier ** with automatic volume control as the resistance servo, the two phase-sensitive detectors being connected in parallel across the output.

* The condenser used was of an early radio-receiver type manufactured by AB Baltic, Södertälje.

** The time constant of the A.V.C. action is about 0.2 seconds, and not 2 seconds as was erroneously given in Ref.[1]

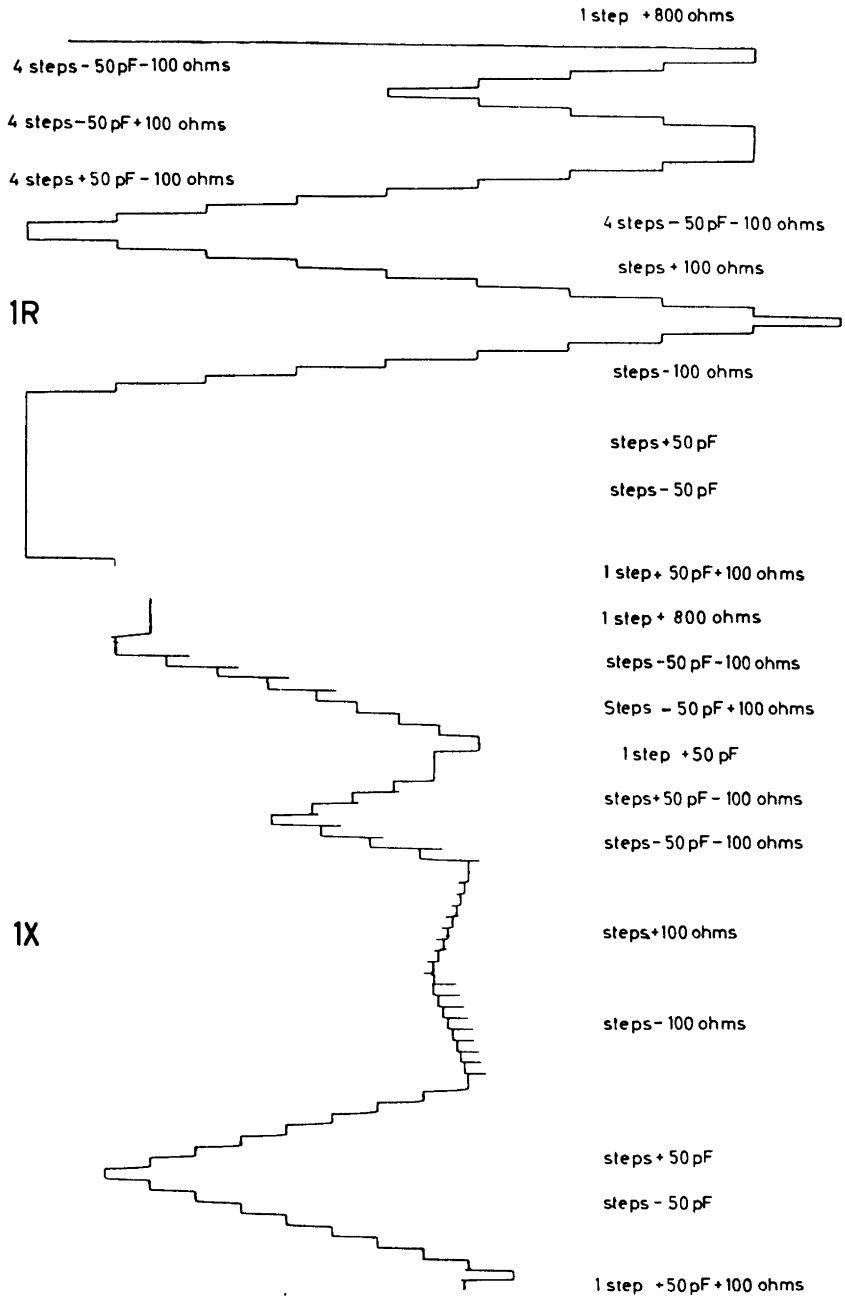

Fig. 17. Double servo-recordings using the bridge shown in Fig. 1. Sinusoidal reference potentials.

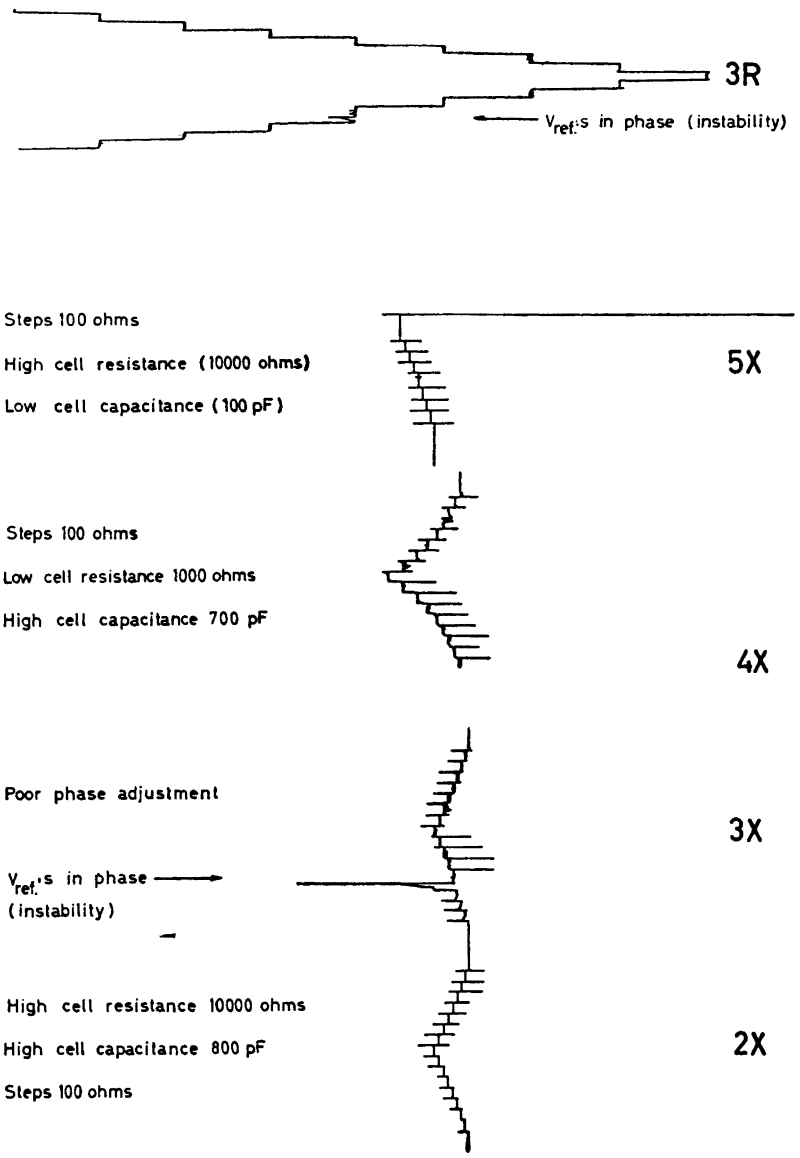

Fig. 18. Double servo-recordings using the bridge shown in Fig. 1. Square wave reference potentials.

The servo-controlled precision resistance was a wire-wound linear resistance of 1 000 ohms (*cf.* Ref.[1]), and as "cell" was used a Leeds & Northrup six-decade resistance (0 to 11 000 ohms in steps of 0.01 ohm) in parallel with a precision-variable-condenser covering the range 100 to 1 000 pF (General Radio Co., type N).

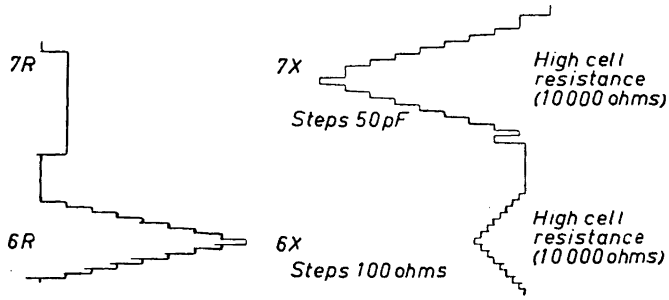

Fig. 19. Double servo-recordings using potentiometer bridge shown in Fig. 7. No shunt used. Square wave reference potentials.

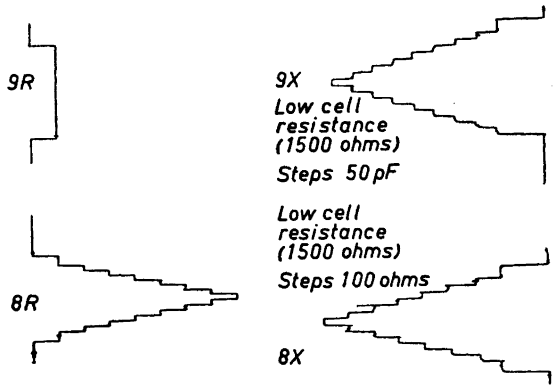

Fig. 20. Double servo-recordings using potentiometer bridge shown in Fig. 7. No shunt used. Square wave reference potentials.

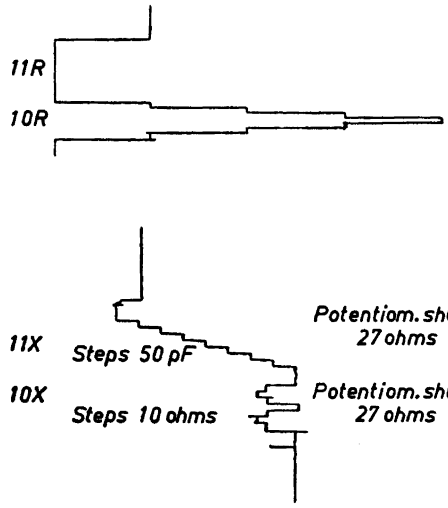

Fig. 21. Double servo-recordings using potentiometer bridge shown in Fig. 7. Recorder range 50 ohms (potentiometer shunted by 27 ohms).

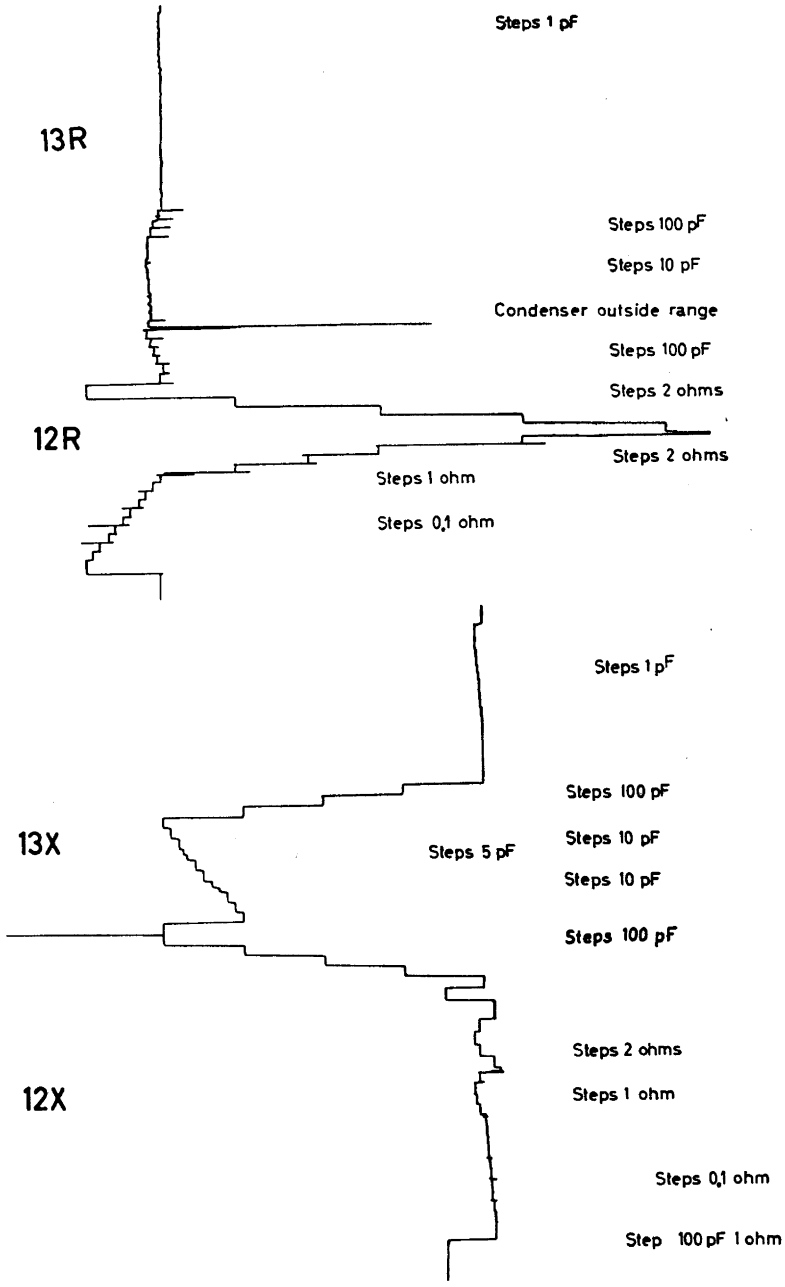

Fig. 22. Double servo-recordings using potentiometer bridge shown in Fig. 7. Recorder range 10 ohms (low resistance shunt).

The adjustment of the reference potential was found difficult, however, because operation of the phase shifter also gave a change in amplitude of the reference signal. As the two mixer-tubes in the homodyne rectifier did not have absolutely identical characteristics, this amplitude change led to an output signal from the detector even in the absence of an input signal from the bridge. Best results were obtained when the phases of the reference potentials were adjusted in such a way that small variations in resistance gave maximum signal to the resistance servo, and small variations in capacitance maximum signal to the capacitance servo. It was found later that perfect phasing could be obtained by allowing the sinusoidal reference potentials to trigger a square-wave generator (Philips type GM 2314) which delivered a square-wave reference potential of constant amplitude (pulse height) to the third grid of the L 7 mixer tubes in the synchronous rectifier. The initial adjustments could then be made as outlined in section I.

The servos were comparatively tolerant with respect to smaller degrees of incorrect phasing of the reference signals, especially at high values for "cell" resistance.

The resistance recorder was completely unaffected by changes in capacitance, but the capacitance recorder was sensitive to resistance changes, probably because the wire-wound, 1 000 ohms measuring resistance in the resistance recorder had a higher residual inductance than the "cell" resistance. The recordings $1R$, $1X$, $2X$, $3R$, $3X$, $4X$, and $5X$ shown in Figs. 17 and 18 were obtained with the bridge connected according to Fig. 1. $1X$ and $1R$ were obtained with sinusoidal reference signals, and show that the system remains stable even when the resistance and capacitance to be measured are changed in a step-wise manner, either one at a time or both simultaneously.

Compared with $2X$, $3X$ shows the influence of poor phasing. $3X$ and $3R$ show that the system becomes unstable when the reference signals are in phase. Compared with $2X$, $4X$ shows how the influence of resistance-changes on the capacitance recorder increases with decreasing total "cell" resistance. This influence did not tend to increase with decreasing total "cell" capacitance, however, as indicated by $5X$ compared with $2X$.

When the bridge was connected according to Fig. 7 with the measuring condenser connected in parallel with X_1 the influence of resistance changes on the capacitance recorder increased, as a comparison between the recordings $6X$ and $8X$ of Figs. 19 and 20, with $2X$ and $4X$, respectively, shows. With the circuit of Fig. 7, change in resistance introduces an extra reactive unbalance over and above that caused by the inductance of the measuring resistance. The resistance recorder is unaffected by capacitance changes, as shown by the recordings $7R$ and $9R$ of Figs. 19 and 20, and the R scale is completely linear from $R = 1\,000$ ohms to $R = 10\,000$ ohms ($6R$ and $8R$).

Shunting of the potentiometer caused a marked change in the influence of resistance changes on the capacitance recordings. At a measuring range of 50 ohms (shunt of 27 ohms), the capacitance recorder changed direction when the mid-point of the potentiometer was passed, as shown by the recordings $10X$ and $12X$ of Figs. 21 and 22, respectively. As shown by the recording $11R$ (Fig. 21) the resistance recorder was still insensitive to capacitance changes; but when the resistance range was decreased to 10 ohms, a certain influence became apparent ($13R$ of Fig. 22), owing to the fact that the measuring condenser across X_1 in Fig. 7 did not have exactly the same influence as X_C in the circuit. This source of error can be eliminated by using the circuit shown in Fig. 8.

CONCLUSIONS

a) It is desirable to use square-wave reference signals of constant amplitude in the homodyne rectifier, and it seems likely that the best type of detector would be a balanced push-pull detector working with square-wave input and reference signals, as discussed by Farren.[3]

b) A completely non-inductive measuring resistance in the resistance servo should be used in order to avoid errors of the capacitance recorder.

c) It is desirable to use the double servo system even in cases where only one component is being recorded, in order to preserve bridge balance. Single servo operation has been discussed in section V.

d) For direct recording of parallel components (resistance and capacitance), the bridge circuit of Fig. 1 is preferable on theoretical grounds. The potentiometer bridge of Fig. 8 may be used when φ is small or resistance only is to be recorded.

APPENDIX I

Calculation of α_R and α_X

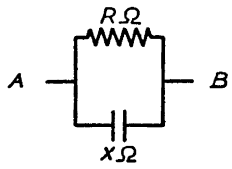

Fig. 23. Resistance and reactance in parallel.

Let us put the total impedance AB of the parallel combination of the resistance R and condenser X of Fig. 23 equal to Z. We then have $\frac{1}{\overline{Z}} = \frac{1}{R} + \frac{1}{\mathrm{j}X}$ *;

$$\overline{Z} = \frac{R\mathrm{j}X}{R + \mathrm{j}X} = \frac{R\mathrm{j}X\,(R - \mathrm{j}X)}{R^2 + X^2} = \frac{RX^2 + R^2\mathrm{j}X}{R^2 + X^2} \tag{1}$$

$$\mathrm{tg}\ \varphi = \frac{R}{X} \tag{2}$$

We want to know how $\overline{Z}$ changes when X is kept constant and R varies, and vice versa. $\overline{Z}$ forms the angle φ with the current vector, and we assume that $\frac{\partial\,\overline{Z}}{\partial\,R}$ and $\frac{\partial\,\overline{Z}}{\partial\,X}$ form the angles γ_R and γ_X, respectively, with the current vector.

$$\frac{\partial\,\overline{Z}}{\partial\,R} = \frac{(R^2 + X^2)\ (X^2 + 2\ R\mathrm{j}X) - 2R(RX^2 + R^2\mathrm{j}X)}{(R^2 + X^2)^2} =$$

$$= (X^2 - R^2 + 2R\mathrm{j}X)\ \frac{X^2}{(R^2 + X^2)^2} \tag{3}$$

$$\mathrm{tg}\ \gamma_R = \frac{2RX}{X^2 - R^2} = \frac{2\,\frac{R}{X}}{1 - \frac{R^2}{X^2}} = \frac{2\ \mathrm{tg}\ \varphi}{1 - \mathrm{tg}^2\varphi} \tag{4}$$

$$\gamma_R = 2\ \varphi \tag{5}$$

$$\frac{\partial\,\overline{Z}}{\partial\,X} = \frac{(R^2 + X^2)\ (RX + \mathrm{j}2R^2) - 2X(RX^2 + R^2\mathrm{j}X}{(R^2 + X^2)} =$$

$$= \left[2RX + \mathrm{j}(R^2 - X^2)\right] \frac{R^2}{(R^2 + X^2)^2} \tag{6}$$

* A good account of symbolic alternating current theory is given by Kemp [4].

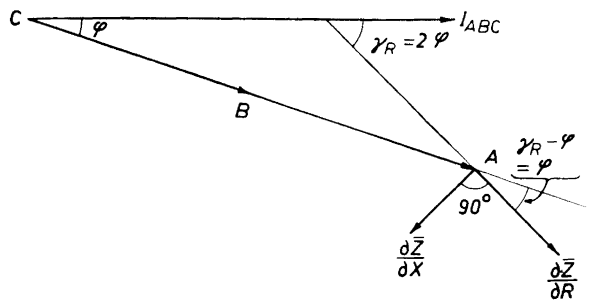

Fig. 24. Diagram showing the directions of certain partial differential quotients related to the bridge shown in Fig. 1. For explanation see text.

$$\operatorname{tg} \gamma_X = \frac{R^2 - X^2}{2\,RX} = \frac{\dfrac{R^2}{X^2} - 1}{2\,\dfrac{R}{X}} = \frac{\operatorname{tg}^2\varphi - 1}{2 \operatorname{tg} \varphi} = -\frac{1}{\operatorname{tg} \gamma_R} \tag{7}$$

$$\gamma_X = \gamma_R + 90° \tag{8}$$

If the current I_{BD} (Fig. 1) through the input circuit of the amplifier can be neglected, the current I_{AB} will be the same as the current $I_{BC} = I_{ABC}$. Fig. 24 shows this current and the impedances AB ($= \bar{Z}$) and BC at balance. If R or X are changed, the point A will move in the direction of $\partial\bar{Z}/\partial R$ or $\partial\bar{Z}/\partial X$ (respectively). If the current I_{ABC} were constant we could let the impedance vectors represent the potential vectors as well, because the latter would have the same length and direction as the impedance vectors relative to the current I_{ABC}. However, I_{ABC} does not remain constant; but the potential V_{CA} is constant provided that the oscillator has a low output resistance. If we let the impedance vectors also represent the potential vectors and change the position of point A in the diagram (*i.e.* alter $\bar{Z}$), we must therefore let the vectors stretch or shrink until the distance CA becomes the same as before, if they are to represent the potentials after the change. In Fig. 25 the point A has moved to A′ in the impedance diagram, owing to an increase of the reactance X. The vectors $\overline{CB}$, $\overline{BA}$, and $\overline{CA}$ represent the impedances and the potentials before the change. The vectors $\overline{CB}$, $\overline{BA'}$, and $\overline{CA'}$ represent the impedances after the change. In order to obtain the potential-vectors after the change, we stretch $\overline{CA'}$ to $\overline{CA'}_1$ which is equal in length to $\overline{CA}$. We then draw the line BA′ and a line parallel to BA′ through A_1'. The latter cuts CA at point B_1. The vectors $\overline{CB}_1$, $\overline{B_1A_1'}$, and $\overline{CA}_1'$ then represent the potentials, because they are related to each other in the same manner as the impedance vectors and furthermore are parallel to the latter, and CA_1' is equal to CA. We now denote the mid-points of CA′ and CA_1' by B′ and B_1'. So far the increase in X has meant that in the potential diagram the point B moves

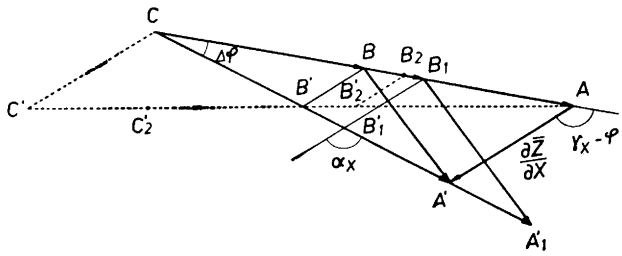

Fig. 25. Geometrical derivation of α_R and α_X of Fig. 3. For explanation see text.

to B_1 and A to A_1'. We may as well consider $\overline{CA_1'}$ to represent the initial potential across AC, however. In this case the change in $\overline{X}$ makes point B move from B_1' to B_1. The triangle $A_1'B_1C$ of Fig. 25 is then similar to the triangle ABC of Fig. 2, and, since only X has been changed, the line $B_1'B_1$ corresponds to l_X. $B_1'B_1$ is parallel to BB' because they occupy the same position in the two similarly positioned triangles A'BC and $A_1'B_1C$. The line BB' is parallel transverse of AA'C, since it cuts the sides AC and A'C at their mid-points. B'B is thus parallel to AA'. If $\Delta\ \varphi$ is small, CA_1' will be parallel to CA, and it follows that $\alpha_X = \gamma_X - \varphi = \varphi + 90°$. Similarly, it may be shown that $\alpha_R = \gamma_R - \varphi = \varphi$.

If instead of increasing X we had decreased X_C (Fig. 1), point C in the diagram of Fig. 25 would have moved to C'. B' would have remained unchanged, but instead of A_1', B_1, and B_1' we would have obtained C_2', B_2, B_2'. B_2B' is parallel to CC' and AA'. When CC' $(= \Delta\ \overline{Z}) \to 0$, $B_2B'_2 \to l_X$ and $\alpha_X \to \gamma_X - \varphi$. The line l_X thus remains the same in both cases.

APPENDIX II

The quantitative relations between the measured and the servo-operated impedance components in the case of the "potentiometer" bridge arrangement

The impedance diagram for the bridge arrangement of Fig. 8 is shown in Fig. 9. The lines l_{R_e}, l_{R_C}, and l_X have been drawn in through point B although strictly they belong to the potential diagram. It can be seen directly that for the circuit of Fig. 8 l_{R_e} is parallel to I_{ABC}, whereas l_{R_C} and l_X form the angles $2\ \varphi_2$ and $2\ \varphi_2 + 90°$ with the current I_{ABC}. In the impedance diagram of Fig. 26 we assume that R_e is small, so that $\overline{Z} = \overline{Z_2}$ and $\varphi = \varphi_2$. If R_C is now changed by $\Delta\ R_C$, the point C will move the distance $\vartheta\ R_C$ to C' towards $\partial\overline{Z}/\partial\overline{R_C}$. The bridge is now to be balanced, and for the purpose of discussion we may assume that the servos operate one at a time (in practice they work simultaneously). The R_e-servo operates first. R_{e1} decreases and R_{e2} increases simultaneously by the same amount, which means that the points A and C' in Fig. 26 move at the same rate and in the same direction, along a path parallel to I_{ABC}. It should be observed that point B retains its position, and will do so in the following because we are working with the impedance diagram

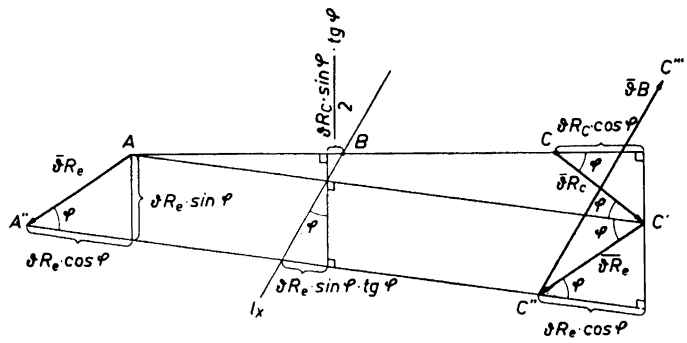

Fig. 26. Vector diagram showing the balancing of the bridge shown in Fig. 8. For explanation see text.

and not with the potential diagram. AC will thus be displaced parallel to itself. The R_e servo will stop when the line DB in the potential diagram (Fig. 2) coincides with l_X. The potential triangle will be conformate to the impedance triangle. The servo thus stops when the mid-point of AC reaches l_X in the impedance diagram. AC then occupies the position A''C''. Now the X-servo starts, and moves point B in the potential triangle (Fig. 2) along l_X to C. In the impedance diagram of Fig. 26 this corresponds to a movement of C'' towards "north-east" along a line parallel to l_X to a point C''' on line A''B prolonged. The result of these operations is, of course, that both in the potential and the impedance diagrams the triangle ABC turns into a straight line with point B at the mid-point.

As we work with condensers that have a linear capacitance variation we introduce the susceptance $B_2 = 1/X_2$ instead of X_2. We shall now investigate how R_{e2} and B_2 have to be changed in order to return the bridge to balance when R_C is changed by ΔR_C. When R_C is changed by the amount ΔR_C, $\overline{Z}$ will be changed by the amount $\partial\overline{Z}/\partial R_C \cdot \Delta R_C = \overline{\vartheta} R_C$. In order to compensate this, R_{e1} is first altered by ΔR_{e1} (and R_{e2} by $\Delta R_{e2} = -\Delta R_{e1}$), whereby $\overline{Z}$ is changed by $\overline{\vartheta} R_{e1}$. Finally, B_2 is changed by ΔB, and $\overline{Z}$ by $\overline{\vartheta} B$. ϑR_e, ϑR_C, and ϑB are indicated in Fig. 26. Bearing in mind that AC is very large compared with the differentials, and that A''C'' is going to be cut at the mid-point by l_X (so that we must add the same amount to both sides of l_X when AC is displaced from AC to A''C'') we obtain (Fig. 21) $\vartheta R_C \cos\varphi + \frac{1}{2}\vartheta R_C \sin\varphi\ tg\ \varphi + \vartheta R_e \sin\varphi\ tg\ \varphi - \vartheta R_e \cos\varphi = \vartheta R_e \cos\varphi - \frac{1}{2}\vartheta R_C \sin\varphi\ tg\ \varphi - \vartheta R_e \sin\varphi\ tg\ \varphi$;

$$\vartheta R_e = \frac{1 + tg^2\,\varphi}{1 - tg^2\,\varphi} \cdot \frac{1}{2}\,\vartheta R_C \tag{9}$$

We now turn to ϑB. The point C is evidently going to be displaced from the point C'' (at a distance of $(\vartheta R_C \sin\varphi + \vartheta R_e \sin\varphi)$ from the line AC) to a point C''' (at a distance of $\vartheta R_e \sin\varphi$ on the other side of AC). The displacement has

to take place in a direction that forms angle φ with the normal to AC. The distance ϑ B will be,

$$\vartheta \text{ B} = \frac{2\,\vartheta\, R_e \sin\varphi + \vartheta\, R_c \sin\varphi}{\cos\varphi} = (2\,\vartheta Re + \vartheta\, R_c)\text{tg}\,\varphi =$$

$$= \vartheta\, R_c \text{tg}\,\varphi\,\left(1 + \frac{1+\text{tg}^2\,\varphi}{1-\text{tg}^2\,\varphi}\right).$$

$$\vartheta \text{ B} = \frac{2\,\text{tg}\,\varphi}{1-\text{tg}^2\,\varphi}\cdot R_c \tag{10}$$

$$\overline{\vartheta\, R_c} = \frac{\overline{\partial\, Z}}{\partial\, R_c}\cdot \Delta\, R_c;\ \vartheta\, R_c = \frac{\partial\, Z}{\partial\, R_c}\cdot \Delta\, R_c$$

$\frac{\partial\, Z}{\partial\, R_c}$ is obtained from $\frac{\overline{\partial\, Z}}{\partial\, R_c}$: which has been calculated previously, eqns. 2 and 3. We obtain $\frac{\partial\, Z}{\partial\, R_c} = \frac{1}{1+\text{tg}^2\,\varphi}$, and

$$\vartheta\, R_c = \frac{1}{1+\text{tg}^2\,\varphi}\cdot \Delta\, R_c \tag{11}$$

$\frac{\partial\, Z}{\partial\, X}$ is obtained from $\frac{\overline{\partial\, Z}}{\partial\, X}$, and is equal to $\frac{\text{tg}^2\,\varphi}{1+\text{tg}^2\,\varphi}$

$$\frac{\partial\, Z}{\partial\, \text{B}} = -\frac{1}{\text{B}^2}\cdot\frac{\partial\, Z}{\partial\, X} = -\frac{R_c}{\text{tg}^2\,\varphi}\cdot\frac{\partial\, Z}{\partial\, X} = -\frac{R_c^2}{1+\text{tg}^2\,\varphi} \tag{12}$$

(Both X_c and X_2 are included in X and B).

$$\Delta\, \text{B} = \frac{\vartheta\, \text{B}}{\overline{\frac{\partial\, Z}{\partial\, \text{B}}}} = \frac{2\,\text{tg}\,\varphi}{1-\text{tg}^2\,\varphi}\cdot\frac{1}{1+\text{tg}^2\,\varphi}\cdot\frac{1+\text{tg}^2\,\varphi}{-R_c^2}\cdot\Delta\, R_c$$

$$\Delta \text{B}_2 = -\frac{2\,\text{tg}\,\varphi}{R_c^2\,(1-\text{tg}^2\,\varphi)}\cdot\Delta\, R_c \tag{13}$$

R_{e2} forms a part of the series component of the impedance Z, and we get

$$\Delta R_e = \vartheta\, R_e = \frac{1+\text{tg}^2\,\varphi}{1-\text{tg}^2\,\varphi}\cdot\frac{1}{2}\cdot\frac{1}{1+\text{tg}^2\,\varphi}\cdot\Delta\, R_c$$

$$\Delta R_e = \frac{1}{1-\text{tg}^2\,\varphi}\cdot\frac{1}{2}\cdot\Delta\, R_c \tag{14}$$

For the sake of completeness we also record how B_2 is related to X_c

$$\Delta \text{B}_2 = -\Delta\frac{1}{X_c} \tag{15}$$

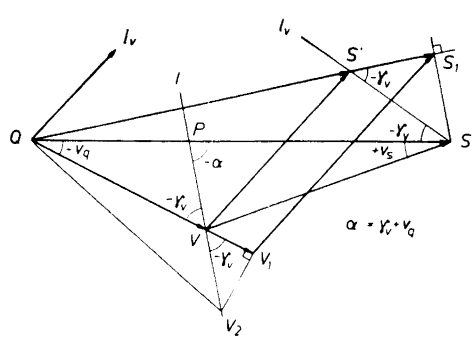

Fig. 27. Geometrical derivation of α_R and α_G of the Z—Y bridge. For explanation see text.

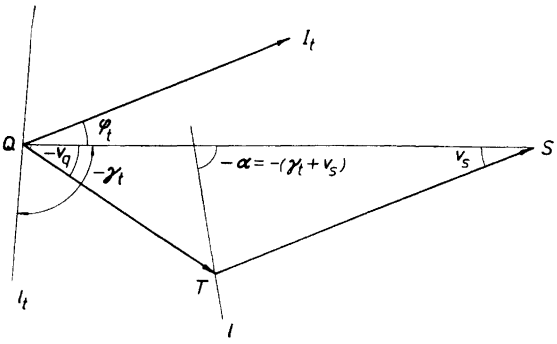

Fig. 28. Geometrical derivation of α_R and α_G of the Z—Y bridge. For explanation see text.

APPENDIX III

Calculations of α_G and α_R of the ZY-bridge

Looking at Fig. 27 we first assume that the bridge is balanced. We let the triangle QSV represent both potentials and impedances. The impedance VS is now altered, causing the point S to move along a line l_v (forming the angle γ_v with QS) to S'. The triangle QS'V represents the impedance after the unbalance has been introduced. In order to get the potential triangle we enlarge the triangle QS'V to QS_1' V_1 (sp that $QS_1' = QS$) and rotate it about Q to position QSV_2. We assume that angle $S_1'QS$ is very small, and that QS_1' is therefore parallel to QS. Triangles $S'S_1'S$ and VV_1V_2 are then conformate (proportional catheti), and the angle V_1VV_2 is equal to $-\gamma_v$. From the triangle QPV we get $\alpha = \gamma_v + v_q$, where α is the angle between line l, along which point V is displaced, and QS. When the change in the impedance VS is purely reactive, l_v will be normal to the current I_v in QVS. The impedance QV is purely reactive, and is therefore also normal to I_v. We therefore obtain $\gamma_v = v_q$ and $\alpha = 2\,v_q$. If the change in VS is purely resistive, l_v, and therefore also l, will be normal to the previous position. Similarly, for the triangle QST (Fig. 28) we get $\alpha = \gamma_t + v_s$, when Q moves along the line l_t in a direction forming angle γ_t with QS.

The impedance QT (Fig. 28) consists of a resistance and a reactance in parallel. When only the resistive component is changed we have previously shown (see Appendix I) that the line of displacement l_t of the point Q forms an angle $2\,\varphi_t$ with the current. φ_t is the angle between the impedance QT and the current vector I_t. This gives $\varphi_t - \gamma_t = 2\,(\varphi_t - v_q)$ or $\varphi_t = 2\,v_q - \gamma_t$. The impedance ST is purely resistive, and is therefore parallel to I_t. Therefore $v_s = \varphi_t = 2\,v_q - \gamma_t$, which gives $\alpha = \gamma_t + v_s = \gamma_t + 2\,v_q - \gamma_t$, or $\alpha = 2\,v_q$. If the reactive component only of the impedance QT is changed we obtain lines l_t and l normal to those in the case just dealt with.

It follows from the discussion above that a change in the reactive component of the impedance SV or in the conductance QT displaces the points V and T, respectively in the potential diagram along the same line l_G, and may therefore be used to compensate each other. Similarly, a change in the resistance of SV or the susceptance of QT will displace V or T along a line l_R normal to l_G. The angles α_G and α_R formed by the lines with the voltage QS are,

$$\alpha_G = 2v_q \tag{16}$$

$$\alpha_R = 2v_q + 90° \tag{17}$$

Acknowledgements. The theory given in this paper has been worked out by F. Möhl. We are indebted to Svenska AB Philips for the loan of square-wave generators, to Seve Radio, Mölnlycke, for the construction of apparatus, and to Professor Olof Mellander for laboratory facilities.

This work was made possible by a grant from the *Swedish Medical Research Council* to one of us (E.S.).

REFERENCES

1. Andersson, C.-O., Stenhagen, E. and Mellander, O. *Acta Chem. Scand.* **10** (1956) 1317.
2. Easton, I. G. and Lamson, H. W. *General Radio Experimenter* **30** (1955) No. 2.
3. Farren, L. I. *The Wireless Engineer* **23** (1946) 330.
4. Kemp, P. *The j operator.* Macmillan and Co., London 1957.

Received November 8, 1957.

ACTA CHEMICA SCANDINAVICA 12 (1958) 438—446

The Interaction of Riboflavin, FMN, and FAD with Various Metal Ions: The Riboflavin Catalyzed Photochemical Reduction of Fe^{III}, and Photooxidation of Fe^{II}

WILLIAM J. RUTTER*

Medicinska Nobelinstitutet, Biokemiska avdelningen, Stockholm, Sweden, and Division of Biochemistry, University of Illinois, Urbana, Illinois, USA

(1) The fluorescence of riboflavin, FMN, and FAD solutions is quenched by certain divalent and trivalent metal ions. Of the ions tested, Hg^{II} and Fe^{II}, Fe^{III}, Co^{III}, and Au^{III} were particularly effective.

(2) Riboflavin, FMN, and FAD solutions catalyze a photooxidation of Fe^{II} ions and a photoreduction of Fe^{III} ions.

(3) The riboflavin catalyzed photoreduction of Fe^{III} is inhibited by oxygen, while the photooxidation of Fe^{II} is strongly dependent on oxygen. Catalase stimulates both of these processes.

(4) The mechanism of the photochemical reactions and their possible relationship to the function of riboflavin in biological systems is discussed.

In certain flavoprotein systems, the fluorescence of the free riboflavin coenzyme is lost on combination with the apoprotein [1,2]. This fact together with recent observations concerning possible interactions of metal ions in certain flavoprotein systems [3,4], prompted a study of the effect of various metal ions on the fluorescence of riboflavin, FMN, and FAD **. It was found that Fe^{III} was a remarkably effective quencher of the fluorescence of these compounds. An inquiry concerning the mechanism of the quenching phenomenon resulted in the discovery of a riboflavin-catalyzed photoreduction of Fe^{III}, as well as a riboflavin-catalyzed photooxidation of Fe^{II}. It is the purpose of this paper to report these observations, and to discuss their significance relative to the functions of riboflavin in biological systems.

MATERIALS AND METHODS

FMN and FAD were purified by ionophoresis and kindly supplied by B. Rolander. A sample of riboflavin procured from Hoffman-LaRoche was recrystallized for use in these experiments.

Crystalline catalase was procured from Worthington Biochemicals, Inc. Activity was measured by the method of Beers and Sizer [5]. One unit is defined as that amount of

* U.S. Public Health Service Fellow, Medicinska Nobelinstitutet, 1954—1955. Present address: Division of Biochemistry, University of Illinois, USA.

** Abbreviations used: FMN — flavin mononucleotide; FAD — flavin adenine dinucleotide; EDTA — ethylene diamine tetraacetate.

enzyme which decomposes 1 mg hydrogen peroxide in 1 min under standard assay conditions.

The concentration of Fe^{II} ions was quantitatively determined with the α,α'-dipyridyl reagent [6], usually from the difference spectra of appropriate experimental samples.

The intensity of fluorescence was measured with the instrument devised and constructed by Theorell and Nygaard [7]. Difference spectra were obtained with the aid of a Cary Recording double beam spectrophotometer.

Photoillumination was accomplished by means of a 250 watt lamp fixed approximately 25 cm from the incubation fluid. The entire system was enclosed in aluminum foil, and partially filled with water so the temperature of the sample remained essentially constant during the photoillumination period.

RESULTS

The fluorescence of riboflavin solutions is quenched by a variety of substances including diphenols, purines, and pyrimidines and electrolytes, particularly [8] I^- and Ag^+. Weber showed that the remarkably strong quenching effect of silver ions is apparently due to the formation of a complex with riboflavin which is non-fluorescent.

The quenching action of electrolytes on riboflavin fluorescence is not a simple function of the ionic strength, but is a function of the particular ionic species present. Theorell and Nygaard [9], for example, have found that halogen ions quench the fluorescence of FMN in the order $I^- > Br^- > Cl^- > F^-$, while $SO_4^=$, $PO_4^=$, and CH_3COO^- ions did not quench at the concentrations tested. $CaCl_2$, KCl, NaCl, and NH_4Cl were equally effective as quenching agents.

Our initial experiments were concerned with the effect of various di- and trivalent metal ions on the fluorescence of riboflavin. Table 1 presents certain of the data obtained. Most divalent ions tested were much less effective quenching agents than silver ions in this regard. Mercury, however, was more effective than Ag^+ in quenching the fluorescence of riboflavin. When $mercury^{II}$ salts were added to aqueous solutions of riboflavin, a light pink color was observed. The color change was similar, but much less pronounced than that produced by silver ions.

Of the trivalent metal ions, Al^{III} was ineffective, but Au^{III}, and especially Co^{III}, and Fe^{III} were remarkably powerful quenching agents. Both Co^{III} and Fe^{III} salts were much more effective than silver salts in quenching riboflavin fluorescence. These results were somewhat unexpected since Albert [10] has shown that divalent metals complex much more strongly with riboflavin than their trivalent counterparts. No binding of Fe^{III} by riboflavin was detected by Albert, for example. The present data nevertheless indicate an Fe^{III}-riboflavin reaction in which either a non-fluorescent complex is involved, or in which the lifetime of the excited state is decreased. A plot of the quenching of fluorescence as a function of Fe^{III} concentration is presented in Fig. 1. The solid points represent experimentally obtained values, whereas the solid curve represents the theoretical curve which would be expected if the reaction involved is simply: (Riboflavin + Fe^{III} → [Riboflavin — Fe^{III}]) and the equilibrium constant

$$K = \frac{[\text{Riboflavin}]\,[Fe^{III}]}{[\text{Riboflavin} - Fe^{III}]} = 4.6 \times 10^{-4}$$

Table 1. Quenching of riboflavin fluorescence by salts. The experimental cuvettes contained 300 mμM riboflavin with ions added as indicated. Volume in all cases 3.0 ml. pH adjusted to 5.5—6.0 with $NaHCO_3$, temperature 30°C. The fluorescence is presented as per cent fluorescence of a control cuvette containing riboflavin alone.

Salt	Concentration (M)	Per cent fluorescence
Monovalent cations		
$NaNO_3$	0.003	87
	0.006	79
	0.01	76
$AgNO_3$	0.003	72
	0.006	58
	0.012	43
	0.018	31
Divalent cations		
$CuSO_4$	0.01	100
	0.10	70 *
$CoSO_4$	0.01	0.77
	0.10	0.29
$FeSO_4$	0.003	0.46
	0.10	0.50
$Hg(CH_3COO)_2$	0.0006	60
$Hg(NO_3)_2$	0.0006	54
$MnSO_4$	0.003	99
	0.01	81
$NiCl_2$	0.01	0.86
$Zn(CH_3COO)_2$	0.003	99
	0.01	90
Trivalent cations		
$AlCl_3$	0.01	100
$AuCl_3$	0.0006	58
$CoNaNO_2$	0.0006	28
$FeCl_3$	0.0001	75
	0.0004	50
	0.0006	28

* visible precipitate.

assuming a non-fluorescent complex [Riboflavin — Fe^{III}] or one in which the lifetime of the excited state is very small compared to that of free riboflavin.

The effectiveness of Fe^{III} as a quenching agent suggested that the quenching observed with Fe^{II} ions (abnormally high for divalent compounds) might in part be due to the formation of Fe^{III} ions. It was observed that with low concentrations (<0.003 M) of Fe^{II}, unlike any of the other divalent ions tested,

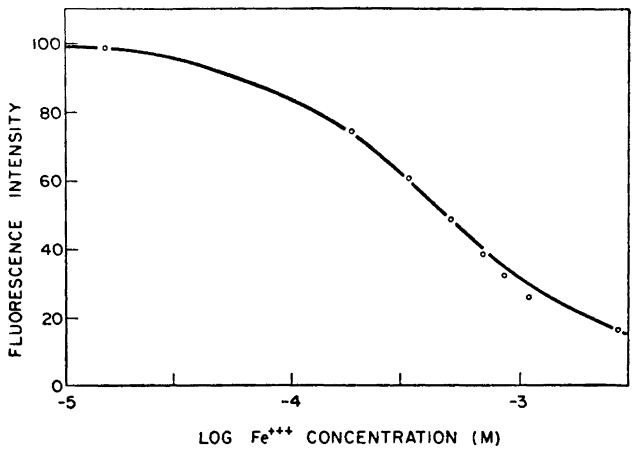

Fig. 1. Quenching of riboflavin fluorescence by Fe^{II} ions. Experimental conditions as described under Table 1.

maximum quenching was obtained only after a considerable time lag (Fig. 2). At higher concentrations of Fe^{II}, the degree of quenching did not change as a function of time; moreover the degree of quenching was approximately the same for 0.003 M and 0.1 M Fe^{II}. Preincubation in the dark did not influence this characteristic behavior. These observations suggest either that Fe^{II} itself is not a particularly effective quenching agent, but that it is converted to Fe^{III} during the course of the measurement of fluorescence, or alternatively that the

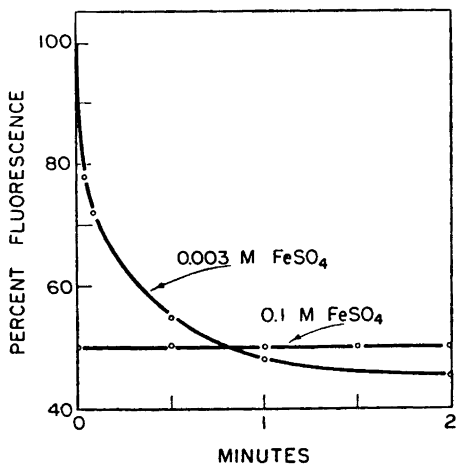

Fig. 2. Quenching of riboflavin fluorescence by Fe^{III} ions. Riboflavin present at a final concentration of 10^{-6} M, $FeCl_3$ added to the concentration indicated, pH adjusted to 5.5 with $NaHCO_3$; temperature 30°C. The per cent of fluorescence of the control riboflavin solution (no $FeCl_3$ added) is plotted as a function of Fe^{III} present.

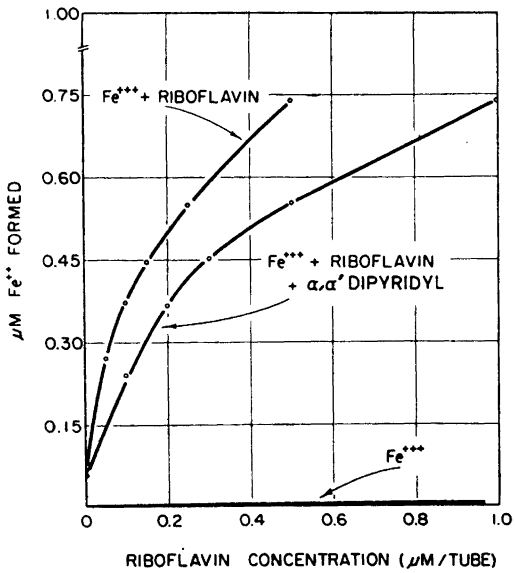

Fig. 3. Riboflavin catalysis of the photoreduction of Fe^{III}. 1 μM $FeCl_3$ was present in all experimental vessels; riboflavin at the concentration indicated; 100 mg α,α'-dipyridyl was added in 0.1 ml ethanol where indicated; pH adjusted to 5.5 in all vessels; period of irradiation, 10 min; temperature 30°C; nitrogen atmosphere. The values for Fe^{II} formation represent increments over Fe^{II} present in similar samples incubated in the dark.

final Fe^{II} riboflavin complex (having about 50 % of the original riboflavin fluorescence) is formed slowly, perhaps through several less stabile Fe^{II} riboflavin complexes.

The other trivalent metal ions which showed inhibition of fluorescence roughly equivalent to Fe^{III}, also showed anomalous quenching behavior. In the experiments with Co^{III} and Au^{III}, the quenching was strongest initially, and decreased with time to a constant level. These observations suggested that a secondary reaction was occurring: one possibility was that these compounds were being partially reduced to the divalent state. Further studies were made with Fe^{III} first, because of the role of Fe in biological systems and secondly, because of the ease of detection of Fe^{II} ions. Appropriate experiments demonstrated that there was indeed a riboflavin-catalyzed photooxidation of Fe^{II}, and a photoreduction of Fe^{III}.

Riboflavin-catalyzed photoreduction of Fe^{III}

After photoillumination of Fe^{III} solutions, an increase in the Fe^{II} concentration was detected in tubes to which riboflavin had been added. As shown in Fig. 3, the rate of formation of Fe^{II} was proportional to the riboflavin present only at comparatively low riboflavin concentrations. The inhibition of Fe^{II} formation by excess α,α'-dipyridyl may be due to complexing with Fe^{III} pre-

Table 2. Effect of oxygen and catalase on riboflavin-catalyzed photoreduction. Experimental cuvettes contained 3 μM $FeCl_3$ and 150 mμM riboflavin and 150 units catalase as indicated; total volume 3.0 ml; pH 5.5; temperature 30°C; illumination period 10 min. The values presented are increments over non-illuminated controls.

Experimental conditions	μM Fe^{II} Formed	
	O_2	N_2
1. a) Fe^{III}	0.04	0.06
b) Fe^{III} + Catalase	0.08	0.085
2. a) Fe^{III} + Riboflavin	0.205	0.500
b) Fe^{III} + Riboflavin + Catalase	0.195	0.595

sent. Fig. 4 shows that the rate of formation of Fe^{II} at a given riboflavin concentration decreases with time. This may be a result either of a conversion of riboflavin to a "less active" form, (*e. g.*, formation of lumiflavin) or perhaps a reflection of approaching the steady state condition.

The data presented in Table 2 illustrate the effect of oxygen and catalase on the photoreduction of Fe^{III} by this reaction. As might be expected, the net formation of Fe^{II} from Fe^{III} is diminished in the presence of oxygen. 10 to

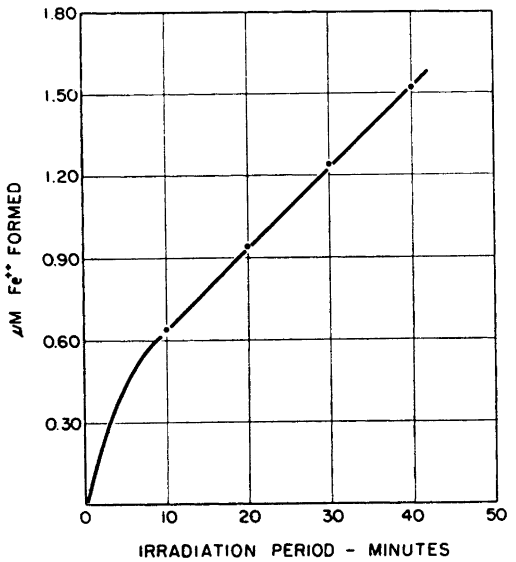

Fig. 4. Riboflavin catalysis of the photoreduction of Fe^{III} as a function of the period of photoillumination. 2 μM $FeCl_3$ and 1 μM riboflavin; 100 mg α,α'-dipyridyl, 0.1 ml 95 % ethanol present in total volume of 3.0 ml; temperature 30.0°C; nitrogen atmosphere. The values of Fe^{II} formed are increments over Fe^{II} present in similar samples incubated in the dark. (Photoillumination of Fe^{III} in the absence of riboflavin for a period of 40 min gives no change over a similar sample incubated in the dark).

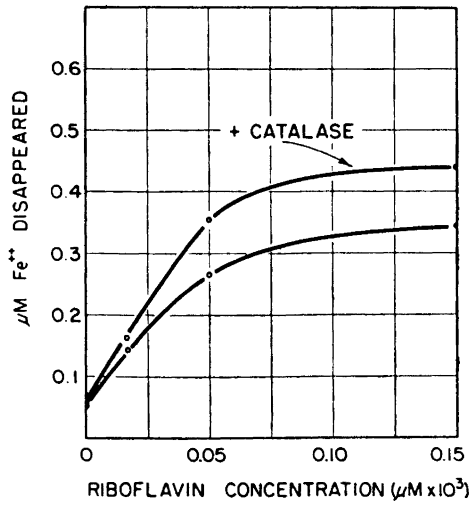

Fig. 5. Effect of catalase on riboflavin catalyzed photooxidation of Fe^{II}. 1 μM $FeSO_4$; riboflavin in the concentration indicated, and sufficient crystalline catalase to decompose 50 mg H_2O_2 per min was added to each sample where indicated; final volume 3.0 ml; pH 5.5; temperature 30°C; oxygen atmosphere; time of photoillumination, 10 min.

20 % increase in Fe^{II} formation were consistently observed in the presence of catalase.

Several attempts to obtain complete conversion of Fe^{III} to Fe^{II} by extended photoillumination periods and by large riboflavin/Fe ratios were unsuccessful. These observations prompted the question of the riboflavin catalysis of the photooxidation of Fe^{II}.

Riboflavin-catalyzed photooxidation of Fe^{II}

The effect of riboflavin on the photooxidation of Fe^{II} salts is shown in Fig. 5. The values represent the difference between illuminated and non-illuminated samples. Catalase consistently stimulated the reaction by 15 to 35 %. The effect of oxygen on the course of the photooxidation is presented in Table 3. It is noteworthy that the absence of oxygen practically eliminates Fe^{II} photooxidation. This observation together with that given in Table 2 for photoreduction of Fe^{III} establishes the conditions under which photoreduction or photooxidation can predominate.

The possibility that riboflavin catalyzed oxidation of Fe^{II} in the dark with oxygen as electron acceptor was tested. Under none of the conditions tested, could any facilitation of this reaction by riboflavin be detected. Even after incubation for 10 h in an oxygen atmosphere there was no difference in the rate of disappearance of Fe^{II} in experimental vessels with riboflavin as compared to controls containing only Fe^{II} ions. Spectral studies of riboflavin in the presence and absence of Fe^{II} ions do not indicate the presence of detectable quantities of reduced riboflavin. During photoillumination there was, of

Table 3. Effect of oxygen on riboflavin-catalyzed photo-oxidation of Fe^{II}. Each experimental cuvette contained 1 μM $FeSO_4$ and 150 mμM riboflavin when present. Total volume 30 ml, pH 5.5, temperature 30°C. The values presented are increments over non-illuminated controls.

Additions	Photoillumination period	Fe^{II} Disappearance (μM)	
		O_2	N_2
1. Fe^{II}	10	0.030	0.045
	30	0.046	0.050
2. Fe^{II} + Riboflavin	10	0.350	0.057
	20	0.437	
	30	0.467	0.067

course, conversion of riboflavin to substances not absorbing in visible region, but this conversion was not markedly influenced by Fe^{II} ions, and bubbling with oxygen did not regenerate the original riboflavin spectra.

FMN and FAD catalyzed photoreduction of Fe^{III} and photooxidation of Fe^{II}

Similar, but not so extensive studies indicate that FMN and FAD also catalyze photooxidation of Fe^{II} and photoreduction of Fe^{III} under similar conditions to those used in the riboflavin experiments.

DISCUSSION

It is known that riboflavin and FMN facilitate photooxidations and photoreductions. Recently Swallow [11] has shown that X-ray irradiation of riboflavin solutions yields a free radical stable in acidic solution, spectrally like the compound produced by chemical reducing agents [12]. Merkel and Nickerson [13] have demonstrated the photochemical reduction of riboflavin salts in aqueous systems containing riboflavin and certain other compounds, *e. g.*, Na_2EDTA, ethylene diamine, cysteine, mercapto succinic, and carboxymethyl succinic acids. Andreae [14] has shown a net formation of Mn^{III} ions upon irradiation of solutions containing Mn^{II}, pyrophosphate, one of a variety of phenols, and riboflavin. Vernon and Ihnen [15] have reported a riboflavin or FMN catalyzed photochemical oxidation of 2,6-dichlorophenol-indophenol and reduced cytochrome c.

The riboflavin catalyzed photochemical oxidation-reduction system reported here is perhaps more easily studied because it is uncomplicated in the sense that a reaction can be observed in aqueous solutions containing only riboflavin and Fe^{II} or Fe^{III}, and because the system is reversible. (This does not necessarily imply that the reduction of Fe^{III} proceeds by a reversal of the same pathway involved in the oxidation of Fe^{II}).

The data obtained are consistent with, but do not prove the postulated series of reactions.

$$R \xrightarrow{h\nu} R^* \quad (1)$$

$$R^* + 2H_2O \xrightarrow{\text{slow}} RH_2 + 2\,{}^{\bullet}OH \quad (2)$$

$$R^* + 2H^+ + 2Fe^{II} \rightarrow RH_2 + 2Fe^{III} \quad (3)$$

$$RH_2 + O_2 \xrightarrow{\text{fast}} R + H_2O_2 \quad (4)$$

$$RH_2 + 2Fe^{III} \xrightarrow{\text{fast}} R + 2Fe^{II} + 2H^+ \quad (5)$$

overall reaction for oxidation of Fe^{II}

$$2H^+ + 2Fe^{II} + O_2 \xrightarrow{h\nu} 2Fe^{III} + H_2O_2 \quad (6)$$

overall reaction for reduction of Fe^{III}

$$2H_2O + 2Fe^{III} \xrightarrow{h\nu} 2Fe^{II} + H_2O_2 + 2H^+ \quad (7)$$

(R = riboflavin; RH_2 = reduced riboflavin; $h\nu$ = photoelectric energy)

The reactions listed should be considered only as one possible formal description of the observations reported.

The interesting observations of Merkel and Nickerson mentioned earlier can perhaps be most easily interpreted in terms of a reaction like (3) above in which the metal chelate acts as an electron donor to riboflavin in the presence of light-energy.

The possible relationship of the present photochemical reactions to the function of riboflavin in biological systems is worthy of consideration. The present observations are most readily explained in terms of a direct electron transference between riboflavin and Fe, and as such, are pertinent to the proposed mechanisms of action of certain of the flavoproteins. The possibility of a role of Fe and riboflavin in photobiologic processes should also not be overlooked.

Acknowledgment. The author wishes to express appreciation to Professor Theorell for his active interest in this work and for the gracious hospitality extended by him and other members of the Biochemical Department.

REFERENCES

1. Theorell, H. in Sumner, J. B. and Myrbäck, K. *The Enzymes*, Vol. II, part I, Academic Press, New York 1951, p. 335.
2. Singer, T. P., and Kearney, E. B. in Neurath, H. and Bailey, K. *The Proteins* Vol. II, part A, Academic Press, New York 1954, p. 124.
3. Mahler, H. *Advances in Enzymol.* **17** (1956) 223.
4. Weber, M. M., Lenhoff, H. M. and Kaplan, N. O. *J. Biol. Chem.* **220** (1956) 93.
5. Beers, R. F., Jr. and Sizer, I. W. *J. Biol. Chem.* **195** (1952) 133.
6. Feigl, F. *Spot Tests*, Elsevier Publishing Co., Amsterdam 1954, p. 154.
7. Theorell, H. and Nygaard, A. P. *Acta Chem. Scand.* **8** (1954) 877.
8. Weber, G. *Biochem. J.* **47** (1950) 114.
9. Theorell, H. and Nygaard, A. P. *Arkiv Kemi* **1** (1954) 205.
10. Albert, A. *Biochem. J.* **54** (1953) 646.
11. Swallow, A. J. *Nature* **176** (1955) 793.
12. Kuhn, R. and Wagner-Jauregg, T. *Ber.* **67** (1934) 361.
13. Merkel, J. R. and Nickerson, W. J. *Biochim. et Biophys. Acta* **14** (1954) 303.
14. Andreae, W. A. *Arch. Biochem. Biophys.* **55** (1955) 584.
15. Vernon, L. P. and Ihnen, E. D. *Biochim. et Biophys. Acta* **24** (1957) 115.

Received December 19, 1957.

ACTA CHEMICA SCANDINAVICA 12 (1958) 447—452

The Lignin-Carbohydrate Linkage

BENGT O. LINDGREN

Wood Chemistry Department, Swedish Forest Products Research Laboratory, Stockholm, Sweden

The lignin materials which Björkman obtained by treatment of thoroughly milled spruce wood with neutral solvents, have been studied by electrophoretic methods. That fraction which he called *LCC* ('lignin-carbohydrate complex') could be separated into two subfractions having different electrophoretic mobilities. The slower subfraction was carbohydrate in nature and the other contained both carbohydrate and lignin materials. This latter fraction on electrophoresis in sodium hydroxide solution moved more slowly than did the lignin material which Björkman called *MWL* ('milled wood lignin'). The results obtained give support to Björkman's hypothesis that the lignin in the *LCC* material is chemically linked to a part of the hemicelluloses.

In spite of much work, the question of whether there is a lignin-hemicellulose linkage in wood is still not settled. The arguments for the existence of such a linkage have been summarized by Merewether [1].

A new approach to the study of this question has been made possible by the recent work of Björkman [2–5]. Wood, which had been milled vigorously under non-swelling conditions, was treated firstly with aqueous dioxane and then either with acetic acid-water or with dimethylformamide. By these means Björkman was able to isolate two lignin fractions.

The first, the *A* fraction (called by Björkman *MWL*), accounted for about 30 % of the wood lignin and contained only small amounts of polysaccharides. The second fraction, the *B* fraction (called by Björkman *LCC*), consisted of about one part of lignin to 3—4 parts of carbohydrates. As Björkman was unable to extract its lignin with those solvents which dissolved the *A* fraction, he concluded that the lignin in the *B* fraction was chemically linked to the hemicellulose components.

After milling a sample of a *B* fraction in toluene Björkman [4,5] extracted from it a material which was soluble in aqueous dioxane and consisted of about 90 % of lignin; such materials will be called *C* preparations. As it is known that chemical bonds can be broken during severe milling, Björkman attributed this chemical modification to a splitting of lignin-carbohydrate linkages. This experiment suggests that during the milling of the wood the *A* lignin may be formed in part, or in its entirety, from material similar to,

or identical to, that found in the *B* fraction. Björkman[4,5] also considered the possibility that new chemical linkages might be formed during the milling, but he concluded that this was unlikely in the present case.

It therefore appeared that the *B* fraction would be a most suitable material on which to study the potential existence of a lignin-carbohydrate linkage. An electrophoretic study of these lignin materials was therefore performed and is described below. The electrophoresis was mostly carried out on glass-fibre sheets. This procedure has been successfully used by Smith[6] to fractionate carbohydrate materials. The study was carried out on lignin and hemicellulose materials from Norway spruce (*Picea Abies* Karst.). The relative electrophoretic mobilities of various fractions are listed in Table 1.

Table 1. Relative electrophoretic mobilities of lignin and hemicellulose materials on glass-fibre electrophoretograms.

Material	Lignins				Hemicelluloses	
	A	*B*		*C*	Xylan [a]	Glucomannan[a]
		B_s	B_f			
Buffer	0.05 N sodium hydroxide					
Rel. mobilities	18–20	2–3	7–18	16–18	10	5
Buffer	Phosphate, pH 6, μ about 0.1					
Rel. mobilities	Insoluble	2–3	6–13	Insoluble	6–10	Insoluble

[a] Obtained from a chlorite holocellulose.

The position of lignin spots on the glass-fibre sheets could be located either by reason of their fluorescense when irradiated with UV-light, or by their reaction with *p*-anisidine-sulphuric acid at room temperature, or by use of the sensitive reaction with 5-nitroso-8-hydroxy-quinoline; this last reagent had been suggested previously by Feigl[7] as a spot test for phenols. The carbohydrates did not interfere with those lignin tests.

The positions of the carbohydrate spots were determined be treating the paper either with α-naphthol and sulphuric acid or with *p*-anisidine and sulphuric acid at 110°C. The lignin material *A* also gave a colour reaction with those reagents but its sensitivity was lower than with the carbohydrates. The possibility cannot be excluded that this coloration could be caused by the small amounts of carbohydrates shown to be present in the *A* preparations[3].

The electrophoretic examination showed that *B* contained two subfractions (Fig. 1) having different mobilities. The slower fraction will be called B_s and the other, B_f. The B_s fraction appeared to consist of carbohydrates uncontaminated by lignin. The B_f fraction, on the other hand, gave positive reactions for lignin. It gave also a colour reaction with the naphthol reagent but as lignin may also react with this reagent, this could not be considered as a specific test for carbohydrates. The B_f fraction, therefore, was isolated from an electrophoretogram and was treated with acid. The hydrolysate contained glucose, mannose and xylose. It was therefore apparent that in the B_f fraction there were present both carbohydrates and lignin.

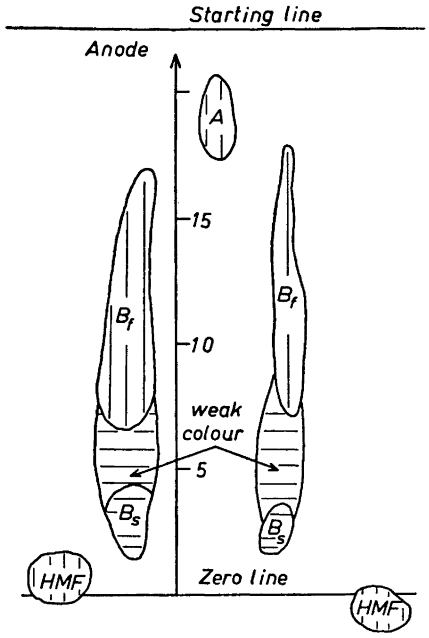

Fig. 1. Sheet electrophoretogram of *A* and *B* materials. Buffer solution, 0.05 N sodium hydroxide. Voltage, 1.8 kV. Time, 3/4 h. Developed with the *p*-anisidine spray. The area marked with vertical lines is that spot which was visible after keeping the sprayed sheet at room temperature. The area marked with horizontal lines is that spot which was visible only after heating the sprayed sheet. HMF is hydroxymethyl-furfural, which was used as reference. Ordinate = distance in cm.

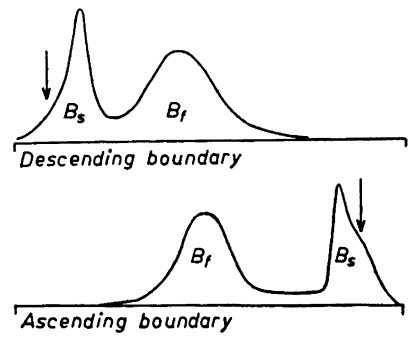

Fig. 2. Zone electrophoretic pattern for *B* material. Buffer, phosphate, pH 7.0. The arrows show the starting points.

The material in the area on the paper between the B_s and the B_f fractions gave a positive reaction for carbohydrates but the reaction was considerably weaker than was that given by the B_s fraction.

B was also fractionated by zone electrophoresis in phosphate buffer at pH 7.0. The refraction pattern (Fig. 2) showed two peaks which were evidently due to the B_s and B_f fractions. From the optical density at 280 mμ it was concluded that essentially all of the lignin was present in the B_f fraction. Assuming as a first approximation that the weights of material in the fractions are directly proportional to the areas of the peaks, the proportion between the lignin and the carbohydrate materials in B_f could be estimated as 1:1.

The fact that the B_f fraction contained both lignin and carbohydrate materials does not, of course, constitute conclusive proof of the existence of a carbohydrate-lignin linkage. It could be that the carbohydrates were free but moved at the same rate as the lignin in the B_f fraction. It was found that a xylan isolated from spruce chlorite holocellulose moved at the same rate as the B_f fraction (Table 1).

The fact that the B_f fraction moved in a neutral solution indicated that it must in some way be associated with groups which were ionised under these conditions. The mobility might be explained if the lignin component of the B_f fraction were chemically linked to a hemicellulose containing uronic acid groups. This cannot be considered as proved, however, as it may be that the ionisable groups are carboxylic groups produced during the severe milling

of the wood. It seems improbable that, during milling, such a large number of these latter groups could be formed to account for the relatively high mobility.

More satisfactory evidence of the existence of a carbohydrate-lignin linkage was obtained by a study of the *A* and *C* lignins which were not associated with carbohydrates. Those lignins moved at about the same rate on glass-fibre electrophoretograms wetted with sodium hydroxide solution (Table 1). This similarity gave further support to the suggestion that the lignin in the *A* fraction is formed during the wood milling from material of the type found in the B_f fraction.

It was also found that the electrophoretic mobility of the *A* and *C* lignin was distinctly higher than that of the B_f fraction (Fig. 1). If the material in the latter fraction is lignin chemically linked to hemicelluloses then its slower movement relative to the other lignins could easily be explained because both glucomannan and xylan move more slowly than do the *A* and *C* lignins (Table 1). It is also possible that the number of ionisable groups was higher in the *A* and *C* lignins than in the lignin in the B_f fraction. This appears to be unlikely as it was found that the proportion of phenolic groups, determined by the spectrophotometric $\Delta\varepsilon$ method [9], was about the same in the *A* lignin as in the lignin in the *B* fraction. As the relative proportion of carboxylic to phenolic groups in the lignins must be low, the former cannot contribute very much to the mobility of the fraction in alkaline solutions. It is, therefore, unlikely that the distinct difference between the lignins was due to a difference in the proportion of carboxylic groups.

In summary, four pieces of evidence may be advanced in support of the theory that a lignin-carbohydrate linkage exists in the B_f fraction *viz.*:

i) The failure to separate the B_f lignin from associated carbohydrates by electrophoresis.

ii) The mobility of the B_f fraction in neutral solution.

iii) The difference in solubility of the *A* and of the *B* fractions.

iv) The higher mobility of the *A* lignin compared to that of the B_f fraction in sodium hydroxide solution.

As mentioned earlier the first two points are not in themselves conclusive evidence proving the existence of a lignin-carbohydrate linkage. The other two points are, however, difficult to explain unless there is such a linkage between the lignin part of the B_f fraction and the hemicelluloses in that fraction.

As Björkman had found it less probable that such linkages are formed during the milling, this study supports the suggestions by Björkman, Pew, Ploetz, Richtzenhain, Traynard and others [1,10] that at least a great part of the wood lignin is linked to hemicelluloses.

EXPERIMENTAL

Lignin materials

A materials. Two samples were isolated and purified according to the normal procedure developed by Björkman [3]. Their methoxyl contents were 15.4 and 15.0 %.

B materials. Two samples were obtained from Björkman. One was isolated by extraction of the dioxane-treated, finely milled wood with acetic acid-water (1:1 v/v)[4],

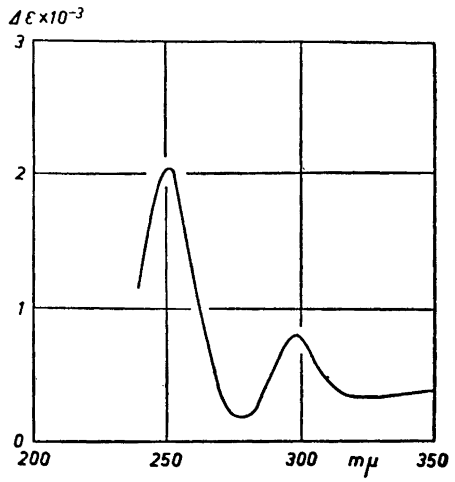

Fig. 3. $\Delta\varepsilon$ curve for *B* material. Solvents: 0.1 N sodium hydroxide and aqueous phosphate buffer, pH 7.

the other, by a corresponding extraction with dimethylformamide [4]. After purification they contained 29.5 and 27.4 % of lignin. No difference was observed in their electrophoretic mobility.

C material. One sample was obtained from Björkman [4,5]. Methoxyl content, 14.3 %.

Solutions of the materials. The lignin materials were dissolved in 0.1 N sodium hydroxide solution. By adding an equal amount of 0.1 M phosphoric acid solution a solution of *B* in a neutral buffer was obtained. By such addition to an alkaline solution of *A* and *C*, the material was precipitated.

The determination of phenolic groups in the B fractions. These determinations were carried out by the $\Delta\varepsilon$ method [9]. The two solvents used were 0.1 N aqueous sodium hydroxide and phosphate buffer (pH 7). The $\Delta\varepsilon$ curve for the *B* fraction extracted from the wood with aqueous acetic acid is shown in the Fig. 3. It shows maxima at 250 mμ, $\Delta\varepsilon$ = 2 100 and at 297 mμ, $\Delta\varepsilon$ = 780. The figures for the $\Delta\varepsilon_{max}$ of the *B* material extracted with dimetylformamide were 1 900 and 690, respectively. Published [3] values for the $\Delta\varepsilon_{max}$ of the *A* fraction are 2 100 and 800, respectively.

Sheet electrophoresis

Glass-fibre sheets. The sheets were made by C. Schleicher & Schüll, Dassel Kr. Einbeck, Germany *(Glasfaserpapier nr. 6)*.

Apparatus. The length of the strips between the electrode vessels was about 50 cm. The strips were pressed between glass plates which were cooled with water.

Procedure. Spots of the solutions (20—40 μl; conc. *ca.* 1 % for the *A* and 2 % for the *B* fractions) were put on the wet strip near the anodic side. It was found that if the solutions were spotted on to dry sheets then the materials were often irreversibly adsorbed. The strips were normally run for 3/4 h at a voltage of 1.8 kV.

The solvent movement caused by the electro-osmotic effect was in all cases stronger than the electrophoretic movement of the materials. Therefore the net effect was a movement against the cathode.

The electro-osmosis was determined by running spots of hydroxy-methyl-furfural together with the samples. This compound does not move in either alkaline or in neutral solutions and is strongly coloured by the anisidine and the naphthol reagents.

Proof of the absence of adsorption. The difference in the electrophoretic mobilities of the materials in the fractions was not due to their having been adsorbed on the glass-fibre sheets as it was shown that they followed the solvent front when they were "chromatographed" on the sheets using 0.05 N sodium hydroxide as developing solvent.

Added in proof. In later experiments when using a new lot of sheets the lignin material *A* moved considerably slower than did the front on the glass-fibre chromatograms; the

hemicelluloses (xylan, glucomannan) on the other hand followed close to the front. The *B* materials gave two spots. One moved slower than did the front and it contained both lignin and polysaccharide materials; the other followed the front and contained only polysaccharides. The lignin materials were therefore to some extent absorbed on these sheets, but if the sheets were first washed with a phosphate buffer solution (pH 6) and then with water no absorption took place.

Zone electrophoresis

Apparatus, Spinco model H. Current: 155 V, 12 mA. Time, 237 min. Buffer, phosphate, pH 7.0, $\mu = 0.1$.

From the front of the descending boundary zone 0.7 ml of the solution containing only the B_s fraction were collected. Similarly, a solution (1.5 ml) containing only the B_f fraction was obtained from the descending boundary. Both solutions gave a normal UV absorption curve for lignin. Log I_0/I were 0.78 and 18.1, respectively and the weight of lignin in those solutions was estimated as 0.01 and 0.57 mg, respectively (log ε was assumed to be 3.50 calculated on the methoxyl basis).

The ratio of the areas under the B_f peak to that under the B_s peak was about 2:1 and the B_f fraction was, therefore, calculated to contain about 2/3 of the material in the *B* fraction. As all of the lignin (1/3 of the *B* material) is present in this fraction it follows that the ratio of the weight of lignin to that of the carbohydrates is *ca.* 1:1.

Spray methods

Sensitivity. 10 µl of 0.1 N sodium hydroxide solution containing different concentrations of the lignin or of the carbohydrate materials were put on a sheet. The percentage figures reported below were the lowest concentrations at which a coloration was clearly observed after spraying.

Method for carbohydrates. Spray solution: α-naphthol (1 g) and concentrated sulphuric acid (5 ml) in *n*-butanol (100 ml). After the spraying the sheets were heated for about 2—5 min at 110°C. The carbohydrates gave blue or purple spots (sensitivity, 0.04 % for spruce xylan). The lignin gave a dark spot (sensitivity, 0.2 % for *A*).

Methods for lignin. 1) Spray solution: 5-nitroso-8-hydroxy-quinoline (1 g) in concentrated sulphuric acid (100 ml). After the spraying the sheets were kept at room temperature for some minutes. Lignin gave dark spots (sensitivity for *A*, 0.01 %). Xylan gave no coloration (the most concentrated solution tested was 1 %).

2) Spray solution: *p*-anisidine (3 g) and concentrated sulphuric acid (8 ml) in ethanol (100 ml). After the spraying the sheets were left at room temperature for 5 min. The lignin gave a yellow spot (sensitivity, 0.04 % for *A*). Xylan gave no colour (the most concentrated solution tested was 1 %). But if the sprayed sheets were heated at 110°C for 30 min the carbohydrate spots were also coloured (sensitivity 0.04 % for xylan).

Acknowledgement. The author wishes to thank Mr. B. Lindquist, Mjölkcentralen, Stockholm, for his kindness in carrying out the zone electrophoresis experiment. He is also grateful to Dr. A. Björkman for his gift of the *B* preparations used in this investigation and to Miss Marit Goliath for skilful assistence.

REFERENCES

1. Merewether, J. W. T. *Holzforschung* **11** (1957) 65.
2. Björkman, A. *Svensk Papperstidn.* **59** (1956) 477.
3. Björkman, A. and Person, B. *Svensk Papperstidn.* **60** (1957) 158.
4. Björkman, A. *Svensk Papperstidn.* **60** (1957) 243.
5. Björkman, A. *Svensk Papperstidn.* **60** (1957) 329.
6. Lewis, Bertha A. and Smith, F. *J. Am. Chem. Soc.* **79** (1957) 3929.
7. Feigl, F. *Qualitative Analysis by Spot Tests*, 3rd English Ed., New York 1947, p. 329.
8. Adler, E., Björkquist, K. J. and Häggroth, S. *Acta Chem. Scand.* **2** (1948) 93.
9. Aulin-Erdtman, G. *Svensk Papperstidn.* **57** (1954) 745.
10. Pew, J. C. *Tappi* **40** (1957) 553.

Received December 9, 1957.

ACTA CHEMICA SCANDINAVICA 12 (1958) 453—458

Studies on Glucomannans from Norwegian Spruce

II. Structural Investigations

INGEMAR CROON and BENGT LINDBERG

Institutionen för Träkemi, Kungl. Tekniska Högskolan och Träkemiska avdelningen, Svenska Träforskningsinstitutet, Stockholm, Sweden

The structures of two glucomannan fractions from *Picea abies* (Norwegian Spruce) have been investigated by methylation and periodate oxidation techniques. It is concluded that both polysaccharides (degree of polymerization, DP_n, 68 and 100, respectively) are composed essentially of α-1,4 linked sugar residues. Both polysaccharides had the same general structure. Each molecule had 3—4 branch points, which were attached to the 3-position of glucose residues. The nonreducing end groups consist principally of mannose residues.

In Part I[1] of this series the isolation of a number of glucomannan fractions from Norwegian Spruce *(Picea abies)* was reported. One fraction was isolated by hot water treatment of the holocellulose (previously swollen with dimethyl sulphoxide [2]). Most of the xylan was then removed from the holocellulose by extraction with 14 % potassium hydroxide. Subsequently, fractions of glucomannan were obtained by treatment of the residual holocellulose with potassium hydroxide-borate solutions by the method of Jones *et al.*[3] This holocellulose after dissolution in cuprammonium solution was regenerated by the addition of acetic acid. From this material another fraction was extracted by treatment with alkali borate. After purification of the fractions by way of their copper complexes they had a nearly constant proportion of glucose to mannose (1:3.5-4). The degree of polymerization of the fractions, determined osmometrically on their nitrates, increased from about 70 for the most easily extractable to 140 for the most difficultly extractable fraction. It appears to be unlikely that the very great differences in the readiness with which the various glucomannan fractions may be extracted can be due only to differences in molecular weight. Variations in the microarrangement of the molecules and in their localisation in the fibre wall could explain the differences as could also variations in their chemical structures, since a highly branched polysaccharide is more soluble than is one which is either less branched or linear.

The present paper reports studies on the structures of the glucomannans in two fractions from *Picea abies*. One was extracted with hot water and the

other with alkali-borate. The glucomannan fractions were investigated by electrophoresis on glass paper, using borate buffer and α-naphthol-sulphuric acid in butanol as spraying reagent. They proved to be electrophoretically homogeneous. No differences in mobilities between the fractions were observed. These fractions were investigated by methylation and periodate oxidation techniques. The properties of the two fractions and the results of the structural studies are given in Table 1.

The methylations were performed in each case by treating the polysaccharide once with methyl sulphate in sodium hydroxide and three times with methyl iodide and silver oxide in dimethylformamide. The latter technique, successfully used by Kuhn *et al.*[4] for the methylation of low molecular weight carbohydrates, has proved also to be very useful for the methylation of polysaccharides such as arabogalactans [5] and glucomannans. The fractionation of the products of the two hydrolyses were performed by carbon column chromatography using the gradient elution technique. In each case the only tetramethyl hexose isolated was 2,3,4,6-tetra-*O*-methyl-D-mannose, identified as its crystalline aniline derivative. On demethylation of the fraction, a trace of glucose was observed in addition to the mannose. One hydrolysate yielded two, the other three, trimethyl-hexoses. Two of those were common to both hydrolysates and were shown to be 2,3,6-tri-*O*-methyl-D-glucose and 2,3,6-tri-*O*-methyl-D-mannose. These substances are very difficult to separate by ordinary paper chromatography but were readily separated on the carbon column. The former crystallised spontaneously when the solvent was removed. The latter, which on demethylation gave mannose only, gave a crystalline aniline derivative in good yield. The fraction containing the 2,3,6-tri-*O*-methyl-D-mannose was converted into its α-acetate and chromatographed on dimethylsulphoxide treated paper using *iso*propyl ether as solvent. The fraction was found to be chromatographically homogeneous. This method was devised by Wickberg [7] and has proved most valuable for the separation of acetylated and methylated sugars. The third trimethyl-hexose (that found in only one hydrolysate) on demethylation yielded glucose. The compound was chromatographically distinguishable from both the 2,3,4- and the 2,3,6-derivatives and may have been present in the other hydrolysate but have escaped detection there due to the larger amount of material added to the carbon column; such a condition would not favour the separation of compounds travelling at nearly the same rate. A number of dimethyl-hexoses was obtained from each hydrolysate as a mixed fraction and they were separated by paper electrophoresis in borate buffer [8]. The principal component was 2,6-di-*O*-methyl-D-glucose, identified by its chromatographic and electrophoretic behaviour. Three di-*O*-methyl-D-hexoses were also observed in each hydrolysate, which were shown by demethylation studies to be mannose derivatives.

The results of the methylation studies indicate that both glucomannans contain chains of 1,4-linked glycopyranosidic glucose and mannose residues. From the value of the optical rotation those residues appear to be linked by β-glycosidic bonds. The presence of a low percentage of other linkages, for example of glucose or of mannose residues linked to the 3-positions of glucose residues, is not excluded. A part of the dimethyl hexoses isolated is certainly derived from incomplete methylation of the polysaccharide. The fairly high

Table 1. Norwegian spruce glucomannan: Properties and results of periodate oxidation and methylation studies.

	Glucomannan A	Glucomannan B
Gal:Gluc:Man:Xyl	(+):21.8:76.9:1.3	(+):19.4:79.9:0.7
DP_n	68	100
$[\alpha]_D^{20}$ ($c = 1$, in 2 N NaOH)	−37°	−39°
Periodate oxidation		
Consumption of periodate (moles per $C_6H_{10}O_5$)	—	0.97
Formic acid released, extrap. to zero time (moles per $C_6H_{10}O_5$)	—	0.09
Molar % methylated hexoses		
2,6-Di-*O*-methyl-D-glucose	6.4	4.4
Di-*O*-methyl-D-mannoses	2.0	0.8
2,3,6-Tri-*O*-methyl-D-mannose	66.6	72.2
2,3,6-Tri-*O*-methyl-D-glucose	17.7	18.6
? -Tri-*O*-methyl-D-glucose	1.4	—
2,3,4,6-Tetra-*O*-methyl-D-mannose	5.8	3.6
% OCH_3 in the methylated polymers	44.0	44.6

yields of 2,6-di-*O*-methyl-D-glucose and of 2,3,4,6-tetra-*O*-methyl-D-mannose, however, strongly indicate that the polysaccharides are slightly branched and that the branches are on the 3-positions of glucose residues. From the analytical figures (Table 1) the number of branches per macromolecule in the glucomannan of DP 68 is calculated as 3—4. As the corresponding calculated value for the glucomannan of DP 100 is the same it must have a relatively lower degree of branching than the other.

Those conclusions are supported by the results of the periodate oxidation studies. The consumption of about 1 mole of periodate per hexose residue accords with such a 1,4-linked structure. The glucomannan of DP 100 on oxidation released 9 moles of formic acid per 100 hexose residues. This value is somewhat higher than that to be expected from a glucomannan having only 3—4 branch-points. The reducing group, unless modified by oxidation during delignification, would yield 2 moles and the non-reducing groups 4—5 moles of formic acid. The total yield then would be 6—7 moles but if the former group were modified it would be less. The oxidised polysaccharide after reduction with borohydride was hydrolysed and the hydrolysate examined chromatographically. Glucose and a trace of mannose were detected as was expected from the methylation studies, since those glucose residues which yield 2,6-di-*O*-methyl-D-glucose should not consume periodate.

These studies do not give any other details of the glucomannan structure. Points remaining undetermined are the distribution of glucose and mannose residues and of branching points and whether the branches are of uniform length or not. The rather small differences observed between the DP_n and

DP_w values, might suggest that the polysaccharide has a main chain with rather short branches (the DP_w was calculated from viscosity measurements making the assumption that the molecules are linear). The polysaccharide is non-crystalline but yields a crystalline product on mild acid hydrolysis [1]. The obvious explanation of this is that it is hydrolysed to shorter and linear fragments which, in contradistinction to the native, branched polysaccharide, have a strong tendency to crystallise. The X-ray diagram of this degraded glucomannan is identical to that given both by ivory nut mannan A and by a hemicellulose fraction from spruce sulphite pulp. During the hydrolysis the ratio of mannose (M) to glucose (G) residues in the polymeric material dropped from 3.6:1 to 2.9:1. This is to be expected as mannosidic linkages are more susceptible to acid hydrolysis than are glucosidic linkages.

The results of this investigation are in good agreement with those reported from the studies of other wood hemicellulose glucomannans. Hamilton *et al.*[9] isolated [from *Tsuga heterophylla* (Western hemlock)] a glucomannan of specific rotation $-38°$ (in 8 % sodium hydroxide) and having M:G = 4:1. Periodate oxidation studies of this material gave results very similar to those obtained in the present investigation. Aspinall *et al.*[10] isolated [from *Picea sitchensis* (Sitka spruce)] a glucomannan having $[\alpha]_D$ $-33°$ (in 10 % sodium hydroxide) and M:G = 2.5:1. The mannose content is quite low, compared to that of other glucomannans from coniferous woods, and it is possible that the material was contaminated by a degraded cellulose of which a fraction was also, separately, isolated. A structural investigation of the glucomannan gave results fairly similar to those reported in the present paper. From aspen wood hemicellulose Jones *et al.*[11] obtained a low yield of a glucomannan fraction having M:G = 2:1. Methylation studies indicated that it had the same general structure. The presence of glucomannans in coniferous wood has also been demonstrated by other investigators [12,13] and it seems fairly certain that glucomannans are amongst the principal hemicellulose components of those woods. The presence of other mannose containing polysaccharides (galactomannans or glucogalactomannans) has also been indicated [14,15] but awaits confirmation.

EXPERIMENTAL

Paper chromatography was carried out on Whatman No. 1 and on 3 MM filter paper. Chromatographic solvents: (a) ethyl acetate-acetic acid-water (3:1:1);
(b) butan-2-one, saturated with water;
(c) *iso*propyl ether (separations on dimethylsulphoxide-impregnated paper).

Paper electrophoresis was carried out on Whatman No. 3 MM filter paper in borate buffer at pH 10.

All concentrations were performed under reduced pressure and at a bath temp. of about 40°C.

Isolation of glucomannan fractions. The procedure was described in a previous paper [1] and further work on one of the fractions (A: DP_n 68) is now described. The other fraction, on which work has been carried out, was removed from a pretreated chlorite holocellulose by 27.6 % potassium hydroxide + 4 % boric acid. The pretreatment involved treating the holocellulose successively with dimethyl sulphoxide, with hot water, with 14 % potassium hydroxide and finally with 5 % potassium hydroxide + 3 % boric acid. The fraction (B) was purified as previously described. From the results of previous studies [1] on similarly derived fractions the DP_n of this fraction was estimated to be about 100.

Methylation of the glucomannans. Material A (2.0 g) was dissolved in 22.5 % sodium hydroxide (50 ml), under nitrogen, and methyl sulphate (10 ml) was added during 1 h with vigorous stirring, the temperature being kept at 20°C by external cooling. After 6 h the solution was neutralised with 6 N sulphuric acid and the polysaccharide recovered by dialysis. Yield 2.13 g (OCH_3, 28.4 %).

The partially methylated product was dissolved in dimethyl formamide (30 ml) and methyl iodide (6 ml) was added in one portion. The solution was kept under nitrogen and silver oxide (3 g) was added during 1 h under vigorous stirring. After 20 h the insoluble material was filtered off and washed with dimethyl formamide (10 ml) and the combined filtrate and washings were poured into water (800 ml) and then concentrated. Most of the dimethyl formamide was removed by repeated co-distillation with water. 200 ml of water and potassium cyanide (2 g) was added and the methylated polysaccharide was then extracted with chloroform (3 × 150 ml). The combined chloroform phases were washed with water (3 × 50 ml) and after drying over anhydrous sodium sulphate were taken to dryness. A further quantity of methylated polysaccharide was recovered from the later aqueous washings which were dialysed against tap water and then lyophilised. The two fractions were combined and were further methylated by two treatments with methyl iodide and silver oxide in dimethyl formamide. The product (0.58 g) had OCH_3, 44.0 %.

The second glucomannan fraction (B) (4.0 g) was methylated in the same way and yielded a product (1.64 g) having OCH_3, 44.6 %.

It is essential for the success of the methylations that all the chemicals are of high purity and perfectly dry. The silver oxide should be freshly prepared. The rather low yields of methylated products are certainly due to incomplete extraction of the aqueous solutions with chloroform and the procedure can probably be considerably improved.

Hydrolysis of the methylated glucomannans. The methylated glucomannans A and B (0.58 g and 1.64 g, respectively) were dissolved in anhydrous formic acid and kept at 100° for 6 h. After concentration of the solutions, the resulting syrup was dissolved in N sulphuric acid and was kept at 100° for 6 h. The solutions were then neutralised by passing them through a column of Amberlite IR-4B and on concentration they yielded syrups (0.44 g and 1.44 g, resp.). Chromatographic examination of the hydrolysates (Solvent a) revealed the presence of di-, tri- and tetra-*O*-methyl hexoses but no glucose, mannose or mono-*O*-methyl hexoses.

Examination of the hydrolysis products from methylated glucomannan A. The hydrolysate from methylated glucomannan A (444 mg) was added to the top of a carbon-Celite column (43 × 3.5 cm) which was then irrigated with the following solvents, using the gradient elution technique.

10 — 30 % aqueous ethanol	5 000 ml
30 — 60 » » »	3 000 »

The eluate was divided into fractions (30 ml) which were examined on paper chromatograms (Solvent a and b) and on paper electrophoretograms. Those fractions which were indistinguishable were combined and taken to dryness.

Fraction 1 (26.3 mg). By paper electrophoresis four components were isolated. The principal component on demethylation yielded glucose only and was chromatographically and electrophoretically indistinguishable from authentic 2,6-di-*O*-methyl-D-glucose. The components were fractionated, in two separate experiments, on paper chromatograms and on paper electrophoretograms and quantitative determinations of the principal component were made by hypoiodite oxidations[6]. The first experiment yielded a value of 82 % but in that case the separation of the components was not as good as when paper electrophoresis was used, then a value of 76 % was obtained. The analysis of mono-*O*-methyl-D-glucoses which had been separated by paper electrophoresis has previously been used[16].

Fraction 2 (219 mg). This fraction on demethylation yielded mannose only. The aniline derivative was prepared from it in a yield of 50 %. It had m. p. 125—127°, alone or in admixture with authentic 2,3,6-tri-*O*-methyl-*N*-phenyl-D-mannosylamine. The fraction was chromatographically homogeneous. Its α-diacetate had an R_F value of 0.26 (Solvent c).

Fraction 3 (58.1 mg). The material crystallised when the solvent was evaporated. One crystallisation from ethyl acetate yielded the pure substance, m. p. 117—119°C, undepressed on admixture with authentic 2,3,6-tri-*O*-methyl-α-D-glucose. The α-diacetate had an R_F value of 0.43 (Solvent c).

Fraction 4 (4.6 mg) on demethylation yielded glucose only. The substance was chromatographically distinguishable from 2,3,4- and 2,3,6-tri-*O*-methyl-D-glucose.

Fraction 5 (20.2 mg) on demethylation yielded mannose and traces of glucose. The aniline derivative had m. p. 142—144°, not depressed on admixture with that of 2,3,4,6-tetra-*O*-methyl-D-mannose.

Examination of hydrolysis products from methylated glucomannan B. The hydrolysate of methylated glucomannan B (1.440 mg) was fractionated as above on the same column. The results are summarised in Table 1.

Periodate oxidation studies. Glucomannan B (252 mg) was kept in water overnight in the refrigerator (2—4°). Then 0.4 M sodium metaperiodate solution (25 ml) was added and the volume was adjusted to 125 ml. The solution was kept in the refrigerator and at intervals samples (5 ml) were withdrawn and analysed for periodate consumption or for formation of acids. The results are summarised in Table 2.

Table 2. Periodate oxidation of glucomannan B.

Time, h	Moles of periodate consumed per $C_6H_{10}O_5$	Acid, equivalents per $C_6H_{10}O_5$
2	0.70	0.049
26	0.89	0.074
74	0.92	0.093
102	0.95	0.096
174	0.96	0.098

The authors are indebted to Miss F. Aeschlimann for her skilful assistance.

REFERENCES

1. Lindberg, B. and Meier, H. *Svensk Papperstidning* **60** (1957) 785.
2. Hägglund, E., Lindberg, B. and Mc Pherson, J. *Acta Chem. Scand.* **10** (1956) 1160.
3. Jones, J. K. W., Wise, L. E. and Jappe, J. P. *Tappi* **39** (1956) 139.
4. Kuhn, R., Trischmann, H. and Löw, I. *Angew. Chem.* **67** (1955) 32.
5. Bouveng, H. *Private communication.*
6. Hough, L., Jones, J. K. N. and Wadman, W. H. *J. Chem. Soc.* **1950** 1702.
7. Wickberg, B. *Private communication.*
8. Foster, A. B. *J. Chem. Soc.* **1953** 982.
9. Hamilton, J. K., Kirchner, H. W. and Thompson, N. S. *J. Am. Chem. Soc.* **78** (1956) 2508
10. Aspinall, G. O., Laidlaw, R. A. and Rashbrook, R. B. *J. Chem. Soc.* **1957** 4444.
11. Jones, J. K. N, Merler, E. and Wise., L. E. *Can. J. Chem.* **35** (1957) 634.
12. Anthis, A. *Tappi* **39** (1956) 401.
13. Timell, T and Tyminski, A. *Tappi* **40** (1957) 519.
14. Ball, D. M., Jones, J. K. N., Nicholson, W. H. and Painter, T. J. *Tappi* **39** (1956) 438.
15. Adams, G. A. *Tappi* **40** (1957) 721.
16. Croon, I. and Lindberg, B. *Svensk Papperstidning* **60** (1957) 843.

Received January 11, 1958.

ACTA CHEMICA SCANDINAVICA 12 (1958) 459—464

On the Purification of Liver Alcohol Dehydrogenase

KEITH DALZIEL*

Nobel Medical Institute, Biochemical Department, Stockholm, Sweden

A modified procedure is described for the preparation of crystalline alcohol dehydrogenase from horse liver, which gives a greater yield of enzyme of apparently higher specific activity than previous methods. The recrystallised product has always contained two components on electrophoresis. The major component has been isolated by chromatography, and its properties determined.

Liver alcohol dehydrogenase has in recent years been the subject of detailed kinetic study [1-4], and its purification and characterisation is therefore a matter of some importance. Following the work of Lutwak-Mann [5], in which partial purification of the enzyme of horse liver was effected by acetone precipitation, heating to remove unwanted protein, and precipitation with ammonium sulphate, Bonnichsen and Wassén [6] crystallised the enzyme after fractionation with ethanol and ammonium sulphate. In a later method [7], which gave a more active product [2], acetone precipitation was omitted, and treatment with ethanol-chloroform mixture was introduced to remove haemoglobin [8].

A further slight modification, which apparently gave a still more active enzyme, was described by Bonnichsen and Brink [9]: the essential steps were (1) heat treatment of the aqueous liver extract, (2) fractionation with ammonium sulphate, (3) ethanol-chloroform treatment, (4) fractionation and crystallisation with ethanol.

The properties of material prepared by this method and repeatedly recrystallised to a constant activity/E_{280} ratio were described recently [10,11]. The specific extinction coefficient at 280 mμ (1 mg/ml, 1 cm) agreed with previous values [7,9], but the specific activity was again increased, by 30 % compared with that reported by Bonnichsen and Brink and by 60 % compared with that of Bonnichsen's earlier preparation [2]. Nevertheless, the protein was not completely homogeneous on electrophoresis.

A further modification of the purification procedure will be described here which has consistently given a crystalline product of this same high

* Rockefeller Fellow, 1955—57. Present address: Department of Clinical Biochemistry, Radcliffe Infirmary, Oxford, England.

activity in twice the yield of previous methods. The product has always contained a small proportion of a second active component on electrophoresis, which can be removed by chromatography. The properties of the electrophoretically homogeneous main component will be described in this and in the following paper [12].

PURIFICATION PROCEDURE

The principal differences from the previous methods [7,9] are that the ethanol-chloroform treatment is carried out first on the liver extract, and after heat treatment and ammonium sulphate fractionation, the crude product is chromatographed on carboxymethyl cellulose; the subsequent crystallisation procedure also differs slightly. The assay of the enzyme has been described previously [10].

(1) *Extraction.* Ground horse liver (5 kg) is extracted with twice the amount of water for 2 h at room temperature, or overnight in the cold, and centrifuged (2 300 r.p.m., 45 min, International Serum Centrifuge, capacity 12 l).

(2) *Removal of haemoglobin.* To the dark brown, slightly turbid extract (10 l) a mixture of ethanol (1 600 ml 95 % ethanol + 800 ml chloroform) is added very slowly with vigorous stirring. After 10 min, with occasional stirring, the denatured haemoglobin is centrifuged off (2 300 r.p.m., 30 min). The green-brown supernatant (10 l) is evaporated under reduced pressure; the minimum amount of octanol is added to reduce foaming, and the flask is immersed in a water bath at 55°. Most of the organic solvents should be removed. The dark green-brown solution (8—9 l), which may contain some precipitate of heat-denatured protein, is thoroughly dialysed at room temperature against phosphate buffer pH 7, $\mu = 0.02$ (2 × 20 l, 18 h).

(3) *Ammonium sulphate fractionation.* The enzyme is precipitated between 0.55 and 0.70 saturation at room temperature. The pH should be kept at 6.0—6.5 by the addition of ammonia. 3.5 kg ammonium sulphate per 10 l solution is added and, after 2 h the brown or green-brown precipitate is removed by centrifuging and discarded (<0.5 g enzyme). To the clear, yellow-green supernatant another 4.7 kg per 10 l is added; after 2 h, the crude enzyme is centrifuged down (2 300 r.p.m., 1 h) as a cream precipitate, and the clear yellow supernatant (<0.1 g enzyme) is discarded. (Difficulty in separating the precipitate indicates that organic solvents have not been completely removed.) The precipitate is washed into dialysis sacs with the minimum volume of phosphate buffer, $\mu = 0.1$, pH 7 (*ca.* 400 ml), and thoroughly dialysed against the same buffer (3 × 4 l) to remove ammonium sulphate, when it dissolves to give a clear yellow-brown solution.

(4) *Heat denaturation.* The dialysed solution is kept at 52° for 15 min, cooled to room temperature and centrifuged. The precipitate is washed with a small volume of buffer, and the combined supernatant and washings, containing 3—4 g enzyme, purity 5—10 %, are dialysed against phosphate buffer, pH 6.0, $\mu = 0.05$.

(5) *Chromatography.* Carboxymethylcellulose, prepared according to Peterson and Sober [13] (except that drying with ethanol is omitted), and equilibrated with phosphate buffer, pH 6.0, $\mu = 0.05$ is packed under 30 cm Hg pressure for a few hours in a column, 3 × 65 cm. The chromatography is carried out at +2°, under the same pressure, with a flow rate of about 60 ml/h. After the enzyme is put onto the column, it is washed with the same buffer until the runnings are colourless. The enzyme is completely retained, together with a yellow pigment. The runnings are first brown, then yellow, and finally colourless. The enzyme, together with the yellow pigment which may be used as an indicator, is rapidly eluted with phosphate buffer, pH 8, $\mu = 0.2$. Over 90 % of the enzyme should be recovered from the column, in a volume of 150 ml: purity 30—40 %.

(6) *Crystallisation.* (a) The enzyme solution is cooled to 0°, and cold 90 % ethanol is added gradually with continuous chilling to a final ethanol concentration of 30 % and a temperature of −12°. The mixture is left at this temperature overnight. The amorphous precipitate containing the whole of the enzyme is separated from the yellow supernatant

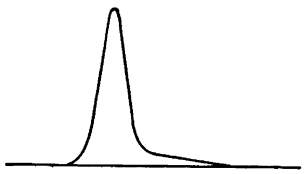

Fig. 1. Electrophoresis of recrystallised enzyme in the 10 ml Tiselius apparatus. $I = 15.5$ mA. Time = 16 h. Sodium phosphate buffer. pH 6.0. $\mu = 0.1$.

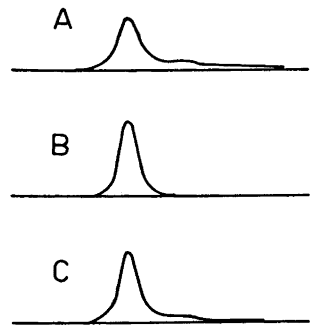

Fig. 2 Electrophoresis in the 10 ml Tiselius apparatus. $I = 15.5$ mA. Sodium phosphate buffer. pH 6.0. $\mu = 0.1$.
A. Recrystallised unresolved enzyme after 21 h.
B. Chromatographic fraction I after 22 h.
C. Mixture of chromatographic fraction I + II after 16 h.

by centrifuging at −12°, washed once with 30 % ethanol in phosphate buffer, and well drained. (b) The remaining steps are carried out at +2°. The precipitate is washed into a dialysis sac with the minimum volume (ca 20 ml per g enzyme) of phosphate buffer, $\mu = 0.1$, pH 7, to which ammonia has been added to raise the pH to 9 and is dialysed against the same buffer until the precipitate largely dissolves to give a pale yellow solution containing some turbidity and precipitate of denatured protein. The solution is then dialysed overnight against phosphate buffer, $\mu = 0.05$, pH 7, and then against the same buffer containing 6 % ethanol for 24 h to crystallise. The crystals are separated by centrifuging, washed once with a little 6 % ethanol dialysate, and dissolved as before in phosphate-ammonia, pH 9. Denatured protein is removed by centrifuging. The very pale yellow solution contains 80 % of the enzyme removed from the column, purity [10] 95 %; the remainder is lost in the 6 % ethanol supernatant and washings. (c) On recrystallisation with 6 % ethanol in the same manner, and removal of denatured protein, the pure [10], colourless crystals are obtained in a yield of 2 g per 5 kg liver.

Electrophoresis and isolation of the main component

The recrystallised product has never been completely homogeneous on electrophoresis. The main component, which is 90 % or more of the total protein in the best preparations, has an isoelectric point of 6.8, phosphate, $\mu = 0.1$. The minor component, which moves behind the main peak at pH 6.0 (Fig. 1) and in advance of it at pH 7.4, was separated in the analytical Tiselius apparatus and found to be active. Because of the small proportion present, and the small difference between the mobilities, it has not been separated in quantity or as a distinct separate peak.

The main component can be obtained in an electrophoretically homogeneous form by chromatography on carboxymethyl cellulose. After the enzyme has been put on the column at pH 6.0, it is developed with phosphate buffer, $\mu = 0.05$, pH 6.8, until about 30 % of the enzyme has been eluted. In accordance with the electrophoretic properties and the chromatographic

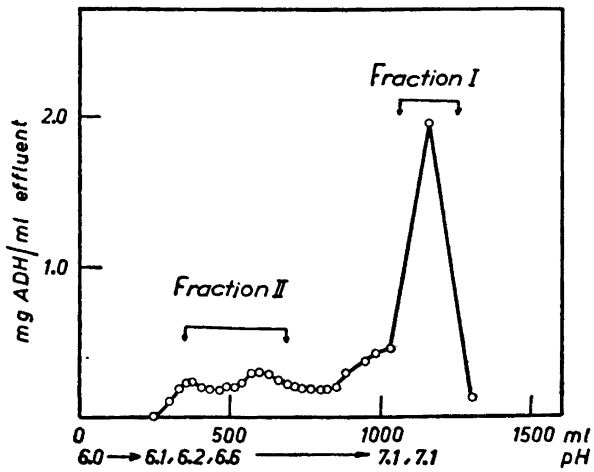

Fig. 3. Elution diagram of recrystallised enzyme on carboxymethylcellulose.

experiments described below, this fraction contains the minor constituent. The remainder of the enzyme is eluted with phosphate buffer, $\mu = 2.0$, pH 8.0, and is electrophoretically homogeneous.

Properties of the main component

The specific extinction coefficient (1 mg/ml, 1 cm) at 280 mμ was 0.42. In the spectrophotometric assay [10] the concentration of the enzyme solution is $\frac{1.13}{t_{0.2} \times v}$ mg/ml, where v is the volume in ml of the enzyme solution used and $t_{0.2}$ is the time in seconds required for the extinction at 340 mμ (1 cm layer) to increase by 0.200. The value of $\frac{1}{E_{280} \times t_{0.2} \times v}$ might be used as a "purity index". Determinations of the molecular weight, sedimentation constant and diffusion constant, and spectrophotometric titration with reduced diphosphopyridine nucleotide, are described in the following paper [12].

Further experiments on inhomogeneous preparations

In preparations in which dialysis after ethanol-chloroform treatment and evaporation was omitted, separation by centrifugation of the crude enzyme precipitated with 0.7 saturated ammonium sulphate was more difficult. The final recrystallised product was apparently pure, as judged by the purity index, but electrophoresis indicated the presence of 20—30 % of the minor component.

The electrophoretic behaviour of such a preparation is illustrated in Fig. 2 and chromatography of the same preparation in Fig. 3. The chromatography was carried out on carboxymethyl cellulose at +2°. 690 mg of recrystallised enzyme, purity index 215, in a concentration of 12 mg/ml was put on the column in phosphate buffer, $\mu = 0.05$, pH 6.0, and eluted first with phosphate buffer, $\mu = 0.05$, pH 6.6, and finally with phosphate buffer, $\mu = 0.1$, pH 7.1. The effluent was collected in 20—30 ml volumes and assayed by activity and E_{280} measurements. There was no significant variation in the purity index during the elution, but the elution diagram indicates the presence of a minor active component, estimated as 15 % of the total, although the separation from the main component is not clear cut. A similar result was obtained with another preparation.

Two fractions of the eluted enzyme, as indicated in Fig. 3, were concentrated and crystallised with alcohol, and dialysed. From fraction I, the main component, 340 mg enzyme, purity index 219, were obtained. The specific extinction at 280 mμ was 0.42, and the preparation was homogeneous on electrophoresis (Fig. 2 B). From fraction II, 40 mg, purity index 226, was obtained. The specific extinction was 0.47. Fractions I and II were mixed in the proportion 80 % I and 20 % II. The electrophoretic behaviour of the mixture (Fig. 2 C) is similar to that of the unresolved enzyme, and confirms the reality and identity of the minor active component observed in electrophoresis and chromatography.

DISCUSSION

In the purification procedures of Bonnichsen [7] and Bonnichsen and Brink [9], ethanol-chloroform treatment after ammonium sulphate fractionation does not remove all the haemoglobin, and the enzyme is crystallised from a deep red solution. By applying the ethanol-chloroform treatment directly to the liver extract, the haemoglobin is completely removed; on general grounds also there is something to be said for introducing this rather drastic treatment at as early a stage as possible. Chromatography prior to crystallisation gives a 6-fold increase fo purity, and is probably mainly responsible for the increased yield; any catalase or haemoglobin which may have escaped earlier steps is also removed here. Finally, a more rational and reproducible crystallisation procedure can be applied to the relatively pure, haemoglobin-free product.

The enzyme readily crystallises together with inactive material, and this seems to have been responsible for the low activity of the orginal crystalline product [6] compared with Bonnichsen's material. The reasons for the subsequent successive gains in activity reported by Bonnischsen and Brink [6], and by Dalziel [10] for a repeatedly recrystallised product of their procedure, are not se clear. These reports are based upon the spectrophotometric assay method of Theorell and Bonnichsen [2,10], in which the rate of reduction of the coenzyme by ethanol at pH 9.6 is measured. A similar gain in activity is indicated by fluorimetric mearurements of the maximum rate of this reaction at pH 7.15:2.5 sec^{-1} for Dalziel's preparation compared with 1.6 sec^{-1} for Bonnichsen's preparation [3], It is possible, of course, that inhibitors were present in the reagents used in the earlier work, perhaps in the less pure coenzyme

then available. There has been no further significant gain in activity by the present method of preparation. It may be mentioned, however, that the purity index of enzyme freshly eluted from carboxymethylcellulose during chromatography of the recrystallised product was usually about 10 % greater than that given above for the pure enzyme, but always decreased to the latter value after recrystallisation and dialysis.

The separation of a recrystallised enzyme into more than one active component by electrophoresis and chromatography recalls similar observations on other enzymes and proteins, especially the lactic acid dehydrogenase of heart muscle [14]. In the present case, the fact that the proportion of the minor component is increased in preparations in which alcohol, chloroform or octyl alcohol may not have been completely removed after the Tsuchihashi treatment suggests that it may be formed during the purification procedure. This question, and the properties of the minor component, require further investigation. It has been shown that the minor component has about the same specific activity as the major one, and in one determination a fraction containing a high proportion of the minor component gave a specific extinction at 280 mμ of 0.47, compared with 0.42 for the major component. This presumably accounts for the specific extinction of 0.45 previously reported [3,10] for the recrystallised enzyme.

The molecular weight of the homogeneous main component is 84 000; [12,15] the sedimentation constant is greater, and the diffusion constant smaller, than the values reported previously [2], which gave a molecular weight of 67 500 [2,11,15]. The difference in the diffusion constant is consistent with inhomogeneity of the earlier preparations. Nevertheless, the earlier finding that 2 molecules of DPNH are bound per molecule of enzyme has been reproduced with the homogeneous material [12].

Acknowledgement. The author is greatly indebted to Mr. Å. Åkeson for generous help and guidance during this work, to Mr. O. Eriksson for expert assistance, and to Professor R. Bonnichsen and Professor H. Theorell for much advice and discussion. The work was carried out during the tenure of a Rockefeller Fellowship in Medicine.

REFERENCES

1. Theorell, H. and Chance, B. *Acta Chem. Scand.* **5** (1951) 1127.
2. Theorell, H. and Bonnichsen, R. *Acta Chem. Scand.* **5** (1951) 1105.
3. Theorell, H., Nygaard, A. P. and Bonnichsen, R. *Acta Chem. Scand.* **9** (1955) 1148.
4. Dalziel, K. and Theorell, H. *Biochem. J.* **66** (1957) 34P.
5. Lutwak-Mann, C. *Biochem. J.* **32** (1938) 1364.
6. Bonnichsen, R. and Wassén, A. M. *Arch. Biochem.* **18** (1948) 361.
7. Bonnichsen, R. *Acta Chem. Scand.* **4** (1950) 715.
8. Tsuchihashi, M. *Biochem. Z.* **140** (1923) 62.
9. Bonnichsen, R. and Brink, N. G. in *Methods in Enzymology*, ed. Colowick, S. P. and Kaplan, N. O., Vol. I, p. 495. Academic Press, New York, 1955.
10. Dalziel, K. *Acta Chem. Scand.* **11** (1957) 397.
11. Ehrenberg, A. and Dalziel, K. *Acta Chem. Scand.* **11** (1957) 398.
12. Ehrenberg, A. and Dalziel, K. *Acta Chem. Scand.* **12** (1958) 465.
13. Peterson, E. A. and Sober, H. A. *J. Am. Chem. Soc.* **78** (1956) 751.
14. Nielands, J. B. *J. Biol. Chem.* **199** (1952) 373.
15. Ehrenberg, A. *Acta Chem. Scand.* **11** (1957) 1257.

Received December 10, 1957.

ACTA CHEMICA SCANDINAVICA 12 (1958) 465—469

The Molecular Weight of Horse Liver Alcohol Dehydrogenase

ANDERS EHRENBERG and KEITH DALZIEL*

Biochemical Department, Nobel Medical Institute, Stockholm, Sweden

The molecular weight of highly purified horse liver alcohol dehydrogenase has been determined to be 83 300. This value is derived from a sedimentation coefficient of 5.11 S at infinite dilution, a diffusion coefficient of 5.96 F at a low protein concentration and a partial specific volume of 0.750. Titration with DPNH confirms that two molecules of coenzyme are bound per molecule of apoprotein.

Crystalline alcohol dehydrogenase (ADH) from horse liver has recently been prepared in an apparently purer and more active form than previously [1,2]. Since the kinetics and mechanism of the reaction catalyzed by this enzyme have been extensively studied, it was of interest to redetermine its molecular weight and its binding capacity for the coenzyme.

MATERIAL AND METHODS

The enzyme was prepared as described by Dalziel in the preceding article [1], including the purification by chromatography. It was precipitated by ethanol, dissolved in the proper buffer and dialyzed against the same buffer overnight immediately before the measurements. The buffer was 0.044 M phosphate of pH 7.0 with 1 % sodium chloride added for the diffusion and sedimentation experiments. The partial specific volume was determined on a sample dissolved in 0.022 M phosphate of pH 7.0. It was not possible to use a more dilute buffer because of the lability of the enzyme at lower ionic strengths. The protein concentration of this sample, determined as the difference between the dry weight of the sample and the buffer, was 9.76 mg/ml. The specific absorbancy of the protein at 280 mμ in a 1 cm layer was determined to be 0.42 for a concentration of 1 mg/ml. This value has been used for the concentration determination of the other samples.

The equipment and technique used for the sedimentation and diffusion studies and for the determination of the partial specific volume have been described elsewhere [2]. The temperature of the rotor in the Spinco ultracentrifuge was kept close to 20°C, while the diffusion experiment was made at 34°C. Both S and D were corrected to 20°C and water as solvent. The pycnometer used for the determination of the partial specific volume was equilibrated at 21.68°C. The absorbancy measurements were made in a Beckman spectrophotometer, model DU.

The DPNH used for the titration was obtained from Sigma chem. Co. The DPNH solution was assayed by measurement of the decrease of extinction at 340 mμ on complete enzymic oxidation to DPN with aldehyde and a catalytic amount of ADH, taking [3] $E_{mM} = 6.25$. The residual extinction after complete oxidation was 5 % of the initial value. The assay showed that the solid sample contained 71 % coenzymically active DPNH.

* Rockefeller fellow 1955—1957. Present address: Department of Clinical Biochemistry, The Radcliffe Infirmary, Oxford, England.

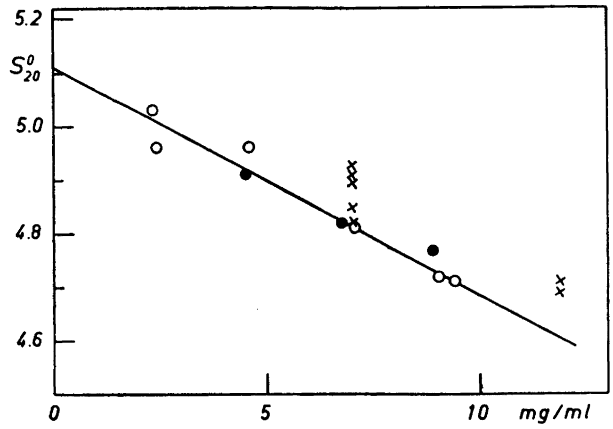

Fig. 1. Concentration dependence of the sedimentation coefficient of ADH. Abscissa: mean protein concentration during observation in the ultracentrifuge. Ordinate: Sedimentation coefficients of pure ADH, O, of a slightly less active material, ●, and the data published in an earlier investigation on salt and pH effects [4], ×.

RESULTS

Sedimentation coefficient. The sedimentation velocity was measured in six experiments at different concentrations. In Fig. 1 the corrected sedimentation coefficients, $S_{20}°$, have been plotted *versus* the mean protein concentration during the experiment. The best fitting line has been calculated by means of the least square method and is drawn in the figure. Its equation is

$$S_{20}° = 5.11 - 0.0425\ a$$

where a is the concentration of ADH in mg/ml and 5.11 is the sedimentation coefficient extrapolated to infinite dilution and measured in Svedberg units.

For comparison three values obtained on another fresh but somewhat less pure preparation (indicated by lower specific activity) have been included in Fig. 1. They do not deviate to any appreciable extent from the calculated line. Earlier data obtained in an investigation on pH and salt effects on the sedimentation [4] are also shown in the figure. This preparation was even less pure, the data are slightly higher than in the present investigation but extrapolate to about the same value at infinite dilution [4].

Diffusion coefficient: Two experiments were performed, one on "100 %" pure ADH and one on "85 %" pure ADH. The purity was judged from activity tests. In both cases the protein concentration was close to 1.54 mg/ml, and the total fringe number was found to be 24.95 and 24.78, respectively. A fringe interval, Δn, of 5 was hence chosen in the calculation of the maximal fringe density, n'_{max}.

When applying the "height-area" method the rate of increase of $\left(\frac{1}{n'_{max}}\right)^2$ with time has to be determined. The corresponding plot of data derived from six exposures on the pure ADH is given in Fig. 2. The equation of the line

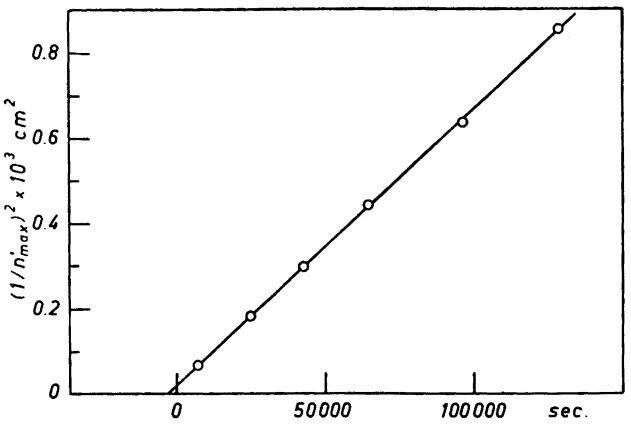

Fig. 2. Graph from which the diffusion coefficient of pure ADH has been calculated according to the "height-area" method. Abscissa: time measured from end of sharpening procedure. Ordinate: inverted square of maximal fringe density.

has been calculated by means of the least square method. The apparent starting time is at —3 100 sec. The diffusion coefficient $D_{1.31} = 3.15\ F$ which after correction becomes $D_{20^\circ} = 5.97\ F$. The fit to the laws of ideal diffusion was investigated by plotting fringe data of the last exposure, taken after 36 h, on a normal distribution graph [2], Fig. 3. The same exposure was also evaluated according to the moment method [2,5], since any small error in the zero time correction in this case can be neglected. A value of 5.93 F was found for D_{20°. $D_{20^\circ} = 5.95\ F$ is obtained as a mean value for the two methods of calculation.

The sample of 85 % active ADH gave for four exposures $D_{20^\circ} = 5.60\ F$ and $t_0 = -7\,300$ sec with the "height-area" method. The moment method applied to the last exposure, taken after 40 h, gave $D_{20^\circ} = 5.86\ F$. The same exposure has been tested on the normal distribution graph, Fig. 3. A close analysis shows that the curve is slightly S-shaped.

The partial specific volume was found to be 0.750 ($\pm$ 0.004) ml/g in a single determination.

DPNH titration. DPNH forms a compound with liver ADH in which the absorption maximum is displaced from 340 mμ to 325 mμ. This spectral shift enabled Theorell and Bonnichsen [6] to demonstrate that at pH 7 one molecule of ADH binds two molecules of DPNH. A similar spectrophotometric titration was made with the enzyme preparation used in the present investigation.

To 3 ml enzyme solution, 5.2 mg/ml in phosphate buffer of pH 7 and μ = 0.1, in a cuvette 5.1 μl portions of 16.1 mM DPNH were added on a stirrer. After each addition the absorbance was measured at 310 and 350 mμ, the wavelengths at which the specific absorptions of free and bound DPNH differ most. The titration was carried out as quickly as possible, but it was necessary to correct the absorbance differences for a slow decline of absorp-

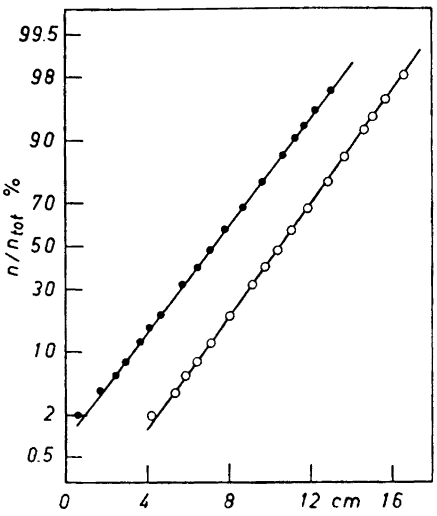

Fig. 3. Normal distribution plots for testing fit of boundary shape to that required by the ideal laws of diffusion. Abscissa: fringe coordinates. Ordinate: relative fringe numbers of exposures on "100 %" pure ADH taken after 36 h, O, and on "85 %" pure ADH taken after 40 h, ●.

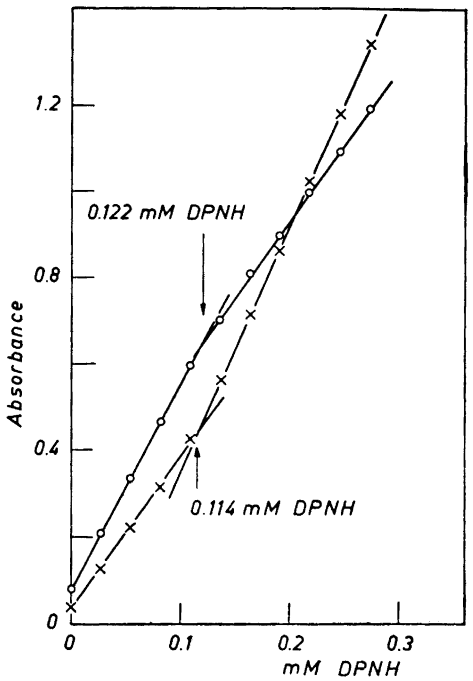

Fig. 4. Titration of ADH, 5.2 mg/ml, with DPNH. Abscissa: concentration of coenzymically active DPNH. Ordinate: Absorbance readings at 310 mμ, O, and 350 mμ, ×. The breaking points of the slopes are indicated.

tion at both wavelengths. The corrected data are plotted in Fig. 4 against the total DPNH concentration.

The equivalence point, indicated by sharp changes of slope, comes at a mean value of 0.118 mM DPNH. The titration indicates hence an equivalent weight of $5.2/118 \times 10^{-6} = 44\,000$ per binding site of the enzyme. The slopes give values of $E_{mM} = 4.8$ and 3.5 for the compound, and $E_{mM} = 3.6$ and 5.9 for free DPNH, at 310 and 350 mμ, respectively, in good agreement with previous values [6].

DISCUSSION

From the values, $S_{20}^{\circ} = 5.11\ S$, $D_{20}^{\circ} = 5.95\ F$ and $V_{sp} = 0.750$ ml/g, a molecular weight of 83 300 is calculated by means of the Svedberg formula. This is in good agreement with the value 84 400 obtained by the Archibald method [7], but deviates considerably from the value 67 500 [6,7] obtained for previous and less active preparations of ADH [8,9]. This discrepancy is due to differences mainly in the sedimentation and diffusion coefficients since the partial specific volume of the present material is 0.750 ml/g, as compared to

the previous value [6] 0.751 ml/g. The sedimentation and diffusion of the previous material was studied by Pedersen [6]. He obtained $S_{20}^{\circ} = 4.9\ S$ on a sample with a protein concentration of about 10 mg/ml when investigated in the oil driven ultracentrifuge. This becomes 4.5 S after correction for a probable error in the measured rotor temperature, as suggested by Pedersen [10]. The present material has a sedimentation coefficient of 4.7 at the same concentration. The main difference in S is thus due to the fact that our data have been extrapolated to infinite dilution. The small remaining difference indicates that the previous material contained some low molecular impurities. This conclusion is supported by the values of the high diffusion coefficient obtained by Pedersen [6], $D_{20}^{\circ} = 6.5\ F$ as calculated by the "height-area" method and $D_{20}^{\circ} = 7.3\ F$ as determined by the moment method.

The main source of error in the present determination of M is the uncertainty in the partial specific volume, which might introduce an error of about $\pm$ 2 % in M. The S and D values are more accurate than that and an error in the molecular weight 83 300 of about $\pm$ 2 000 might be estimated.

The equivalent weight of 44 000 obtained in the DPNH titration confirms [6] that two molecules of DPNH are attached to each molecule of enzyme, for which a molecular weight of 88 000 is indicated. Considering the big errors involved in the experiment this figure is much less reliable than the one given above.

The behaviour of the ADH in the sedimentation velocity experiments, the diffusion experiment and the titration experiment as well as in the molecular weight determination experiment according to Archibald [7] indicates that the present preparation [1] really has a high degree of purity. The best value of the molecular weight of horse liver ADH to be given at the present is 84 000, a mean of the figure reported here and the value obtained by Archibald's method [7].

The less active material exhibited a slightly lower diffusion coefficient, indicating some contamination of larger molecular species. It may be remarked that ADH stored in the buffer solutions for some time lost some activity and often gave higher sedimentation coefficients.

Acknowledgements. The authors wish to thank Mr. B. Lindqvist at Mjölkcentralen, Laboratories, for help in performing the diffusion experiment. Skilled technical assistance has been given by Mr. N. Ekman and Mr. O. Eriksson. Thanks are further due to the *Knut and Alice Wallenberg Foundation* for financial support.

REFERENCES

1. Dalziel, K. *Acta Chem. Scand.* **12** (1958) 459.
2. Ehrenberg, A. and Agner, K. *Acta Chem. Scand.* **12** (1958) 95.
3. Horecker, B. L. and Kornberg, A. *J. Biol. Chem.* **175** (1948) 385.
4. Ehrenberg, A. and Dalziel, K. *Acta Chem. Scand.* **11** (1957) 398.
5. Svensson, H. *Acta Chem. Scand.* **5** (1951) 1410.
6. Theorell, H. and Bonnichsen, R. K. *Acta Chem. Scand.* **5** (1951) 1105.
7. Ehrenberg, A. *Acta Chem. Scand.* **11** (1957) 1257.
8. Bonnichsen, R. K. and Wassén, A. M. *Arch. Biochem.* **18** (1948) 361.
9. Bonnichsen, R. K. *Acta Chem. Scand.* **4** (1950) 715.
10. Pedersen, K. O. in *Les Protéines, Neuvième Conseil de Chimie, Solvay*, Bruxelles 1953, p. 35.

Received December 10, 1957.

ACTA CHEMICA SCANDINAVICA 12 (1958) 470—476

The Catalytic Effect of Peroxidase on the Reaction between Hydrogen Peroxide and Certain Sulfur Compounds

BO SÖRBO and JAN GUSTAF LJUNGGREN

Nobel Medical Institute, Biochemical Department, Stockholm, and Research Institute of National Defence, Dept. 1, Sundbyberg, Sweden

Myeloperoxidase catalyzed the reaction between thiourea and hydrogen peroxide. Some of the reaction products were identified and the formation of an unstable intermediate was demonstrated. Myeloperoxidase also catalyzed the oxidation of thiouracil and thiocyanate, but was inactive with true thiol compounds (cysteine, thioglycolic acid, mercaptoethanol). Horse radish peroxidase was inactive with all the aforementioned sulfur compounds. The results were discussed with respect to the metabolism of the sulfur compounds and to the action of thyreostatic compounds.

In connection with research programs on the oxidation of thiol compounds in biological systems and on the biosynthesis of thyroxine, now in progress in our laboratories, the effect of peroxidase plus hydrogen peroxide on certain sulfur compounds has been investigated. Randall [1] previously reported that thiourea and thiouracil were substrates for horse radish peroxidase, but for different reasons a reinvestigation appeared to be necessary. Thus Randall followed the reaction between hydrogen peroxide and the sulfur compound by a manometric method, which was based on a conversion of remaining hydrogen peroxide to oxygen through the action of catalase. However, the inhibitory effect of the sulfur compounds on catalase [2,3] was apparently not considered. This source of error has been avoided in the present work by following the oxidation of the sulfur compounds by spectrophotometry in the ultraviolet region. The present investigation was also carried out with both animal and plant peroxidase and extended to include true thiol compounds (mercaptans).

EXPERIMENTAL

Materials. Crystalline myeloperoxidase (MPO) was a generous gift from Dr. Kjell Agner. Horse radish peroxidase (PZ-65) was a commercial preparation. Salts of formamidine disulfide [4,5] and formamidine sulfinic acid [6] were prepared according to the indicated references.

Methods. The reactions were followed in phosphate buffer of pH 7.4 at room temperature (20°C) in a Beckman DU spectrophotometer. Paper chromatography of the reaction products from thiourea was carried out on Whatman No. 1 filter paper with water saturated phenol or butanol-acetic acid-water (4:1:1) as developers. The spots were visualized with the iodine-azide reagent or with *p*-dimethylaminobenzaldehyde. Thiourea and formamidine disulfide were not separated from each other in these systems (in fact no solvent system was found, which accomplished this separation), both having the R_F values 0.54 in phenol-water and 0.42 in butanol-acetic acid-water. Formamidine sulfinic acid had R_F 0.44 in phenol-water and 0.21 in butanol-acetic acid-water. The presence of formamidine disulfide in the reaction mixtures could, however, be verified through a cyanolysis reaction. The disulfide reacted rapidly at room temperature with cyanide (0.1 M) to give thiocyanate, which could then be demonstrated in the usual manner with ferric ions. No thiocyanate is obtained from thiourea or formamidine sulfinic acid under these conditions. The formation of sulfate from thiourea and thiocyanate was demonstrated by adding barium ions to the acidified sample. The phosphate buffer in the reaction system was in this case replaced by Tris buffer (in order to avoid precipitation of barium phosphate). The time course of the enzymic reactions was the same in phosphate and Tris buffer. Cyanide was demonstrated with the pyridine-barbituric acid reaction [8] after aeration from the acidified sample into 0.1 M NaOH.

RESULTS

The oxidation of thiourea with hydrogen peroxide with and without MPO was first studied. It is known that the products of this reaction are mainly formamidine disulfide and formamidine sulfinic acid; the first being preferen-

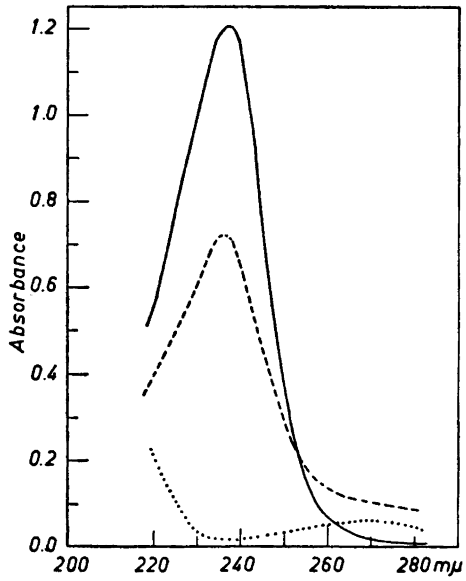

Fig. 1. Ultraviolet absorption curve of thiourea at pH 7.4 ————, formamidine disulfide HCl ------- and formamidine sulfinic acid ····· at 10^{-4}M concentration. (5×10^{-5} M in case of formamidine disulfide calculated as disulfide).

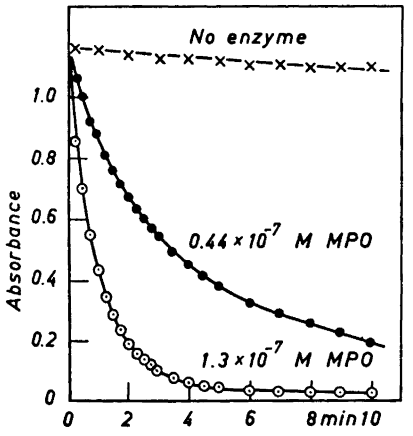

Fig. 2. Reaction of thiourea and hydrogen peroxide followed at 235 mμ. Thiourea 1×10^{-4} M, H_2O_2 2.5×10^{-4} M, phosphate 0.05 M and pH 7.4. Absorbance values corrected for the contribution of MPO.

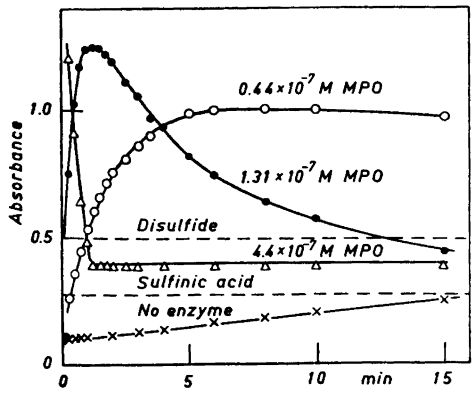

Fig. 3. Thiourea oxidation followed at 270 mμ. Thiourea 5×10^{-4} M, H_2O_2 1.25×10^{-3} M, other conditions as in Fig. 2. Absorbance values corresponding to a complete oxidation of thiourea to formamidine disulfide or sulfinic acid indicated by horisontal lines.

tially formed in acid, the latter in alkaline solution [6]. The spectra of thiourea and the anticipated reaction products * were first compared (Fig. 1) and the reaction was then followed at 235 mμ. A MPO catalyzed reaction was demonstrated (Fig. 2) and the expected decrease in absorbance observed. At 270 mμ, however, the results were different (Fig. 3). With small amounts of enzyme an initial increase in absorbance was obtained, which became more rapid at higher enzyme concentrations. The initial increase in absorbance was then followed by a secondary decrease, and when the enzyme concentration was further increased the initial phase become too rapid to be observed and only the secondary decrease could be followed. As the secondary decrease was faster at higher MPO concentrations, the results indicated that MPO catalyzed not only the formation of a primary reaction product, but also the decomposition of this product. The absorption spectrum of a reaction mixture containing the intermediate showed only a peak at 270 mμ. When the effect of hydrogen peroxide concentration was studied (Fig. 4) it was found that the secondary decrease in absorbance was obtained only with an excess of this compound. Consequently the secondary decomposition of the intermediate must be an oxidation of the latter with hydrogen peroxide. Attempts were now made to identify the reaction products. Paper chromatography (together with the cyanolysis reaction) demonstrated only the presence of formamidine disulfide and formamidine sulfinic acid, but none of these compounds could explain the high absorbance values reached in the enzyme reaction (Fig. 3), and could thus not be the unknown intermediate. Sulfate was also found in the reaction mixtures, but does not absorb light at 270 mμ. The possibility was considered that formamidine sulfonic acid [7], another oxidation product of thiourea, was the intermediate. This sulfonic acid can, however, only be obtained under anhydrous conditions and could also be excluded from being the intermediate by the following experiment. Oxidation of a sulfinic acid with hydrogen peroxide gives the

* Formamidine disulfide is stable only in acid solutions, but at pH 7.4 the spectrum of the compound was essentially unchanged for at least 1 h.

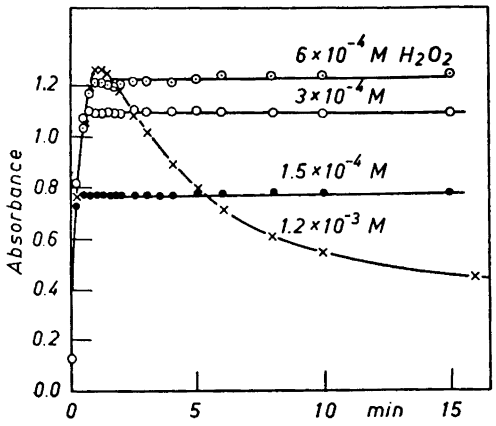

Fig. 4. Effect of hydrogen peroxide concentration on thiourea oxidation. MPO 1.3×10^{-7} M, H_2O_2 as indicated and other conditions as in Fig. 3.

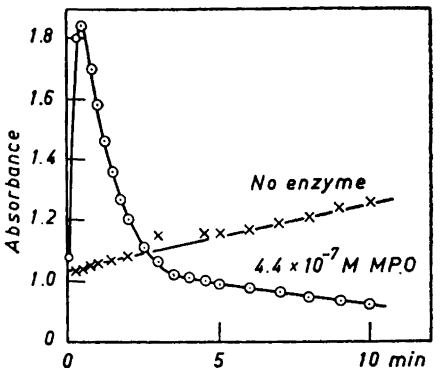

Fig. 5. Oxidation of formamidine disulfide by hydrogen peroxide. Formamidine disulfide 5×10^{-4} M, H_2O_2 2.5×10^{-3} M, phosphate 0.01 M, chloride 2×10^{-3} M and pH 7.4. Followed at 270 mμ.

corresponding sulfonic acid and if formamidine sulfonic acid was the intermediate, strong increase in absorbance should be observed at 270 mμ by treating formamidine sulfinic acid with hydrogen peroxide. This reaction should furthermore be catalyzed by MPO. However, when the experiment was performed only a slow decrease in absorbance was observed and MPO was without effect. On the other hand formamidine disulfide was oxidized by hydrogen peroxide in a MPO catalyzed reaction and an increase and decrease in absorbance, corresponding to the formation and break-down of the intermediate was observed (Fig. 5). Consequently the unknown intermediate must be an oxidation product of the disulfide on an oxidation level between a disulfide and a sulfinic acid. A disulfoxide (R-SO-SO-R) or a sulfenic acid (RSOH) would fulfil these requirements and as both are unstable compounds, which decompose to give a mixture of the corresponding disulfide and sulfinic acid [9], the results obtained by paper chromatography could be explained. As neither a disulfoxide, nor a sulfenic acid has been prepared from thiourea, it was not possible to identify the intermediate further.

Myeloperoxidase was also active with thiouracil (Fig. 6) and with thiocyanate (Fig. 7). The reaction products from thiouracil were not identified, but in the case of thiocyanate the formation of sulfate and cyanide could be demonstrated, and from Fig. 7 the formation of an unstable intermediate is also evident. The catalytic activity of horse radish peroxidase was also studied. Randall [1] had already reported that the plant enzyme catalyzed the oxidation of thiourea and thiouracil, but somewhat unexpectedly we found that the plant enzyme was completely inactive with both these compounds. (The enzyme was tried in concentrations up to 10^{-6} M or about 1 000-fold higher than those used by Randall). It might be added, that a difference in

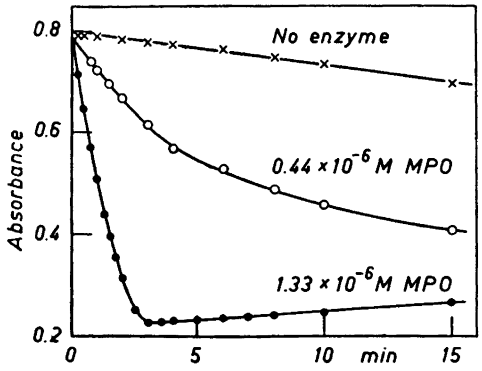

Fig. 6. Oxidation of thiouracil by hydrogen peroxide. Thiouracil 1×10^{-4} M, H_2O_2 2.5×10^{-4} M, reaction followed at 300 mμ. Other conditions as in Fig. 2.

substrate specificity has previously been observed between the animal and plant peroxidase [10,11].

Finally the action of peroxidase-hydrogen peroxide on cysteine, thioglycolic acid and mercaptoethanol was studied. The reactions were followed at pH 7.4 and 220—230 mμ, where both the thiol (0.001 M) and hydrogen peroxide (0.002 M) gave a measurable light absorption. The spontaneous reaction was rather fast in case of cysteine and slower with the other compounds, but in no case could a catalytic activity be demonstrated with peroxidase. Both the animal and plant enzyme was tried at concentrations up to 10^{-6} M. Consequently thiol compounds are not substrates for peroxidase.

DISCUSSION

The present work has demonstrated that thiourea, thiouracil and thiocyanate are substrates for animal peroxidase in contrast to true thiol compounds (cysteine, thioglycolic acid and mercaptoethanol). As thiourea, thiouracil and thiocyanate may exist in two tautomeric forms, one containing a thiol group and the other containing sulfur linked to carbon through a double bond, our results suggest that only the last tautomer (with double bonded sulfur) is the one acted upon by the enzyme. Of interest in this connection is also that thiourea, thiouracil and thiocyanate are well known thyreostatic compounds in contrast to true thiols. Peroxidase-hydrogen peroxide has been implicated with the synthesis of thyroxine [12–14], and it is possible that the antithyroid compounds exert their activity by competing with thyroxine precursors for hydrogen peroxide. It has also been suggested [15] that the thyreostatic compounds owe their activity to their reducing properties on iodine. Iodide must first be oxidized to iodine before being incorporated into the tyrosine residues, and it has been shown that the thyreostatic compounds can prevent this conversion of free iodide to organic bound iodine [16]. However, it seems in this case at first difficult to explain why thiols, such as cysteine or glutathione, which also rapidly react with iodine, do not possess antithyroid properties. But another important biochemical distinc-

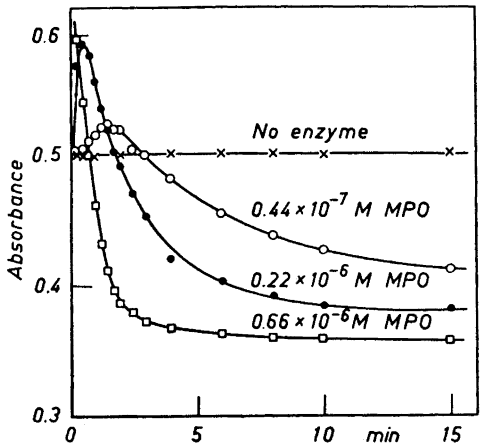

Fig. 7. Oxidation of thiocyanate by hydrogen peroxide. CNS^- 5×10^{-4} M, H_2O_2 1.25×10^{-3} M and other conditions as in Fig. 2 (235 mμ).

tion can be made between the thyreostatic active compounds and the inactive thiols, as the latter are rapidly oxidized through the cytochrome oxidase system [17] in contrast to the thyreostatic compounds. (We have verified that neither thiourea nor thiouracil reduces cytochrome c.) Thus, when thiols are introduced in the body they are probably oxidized before they can reach their presumptive site of action in the thyroid.

Work with ^{35}S-labeled thiourea has shown that the latter is in part oxidized in the body to sulfate, and that the thyroid gland is especially active in this respect [18]. Sulfate was now found to be a reaction product in the peroxidase catalyzed oxidation of thiourea, and as peroxidase is present in the thyroid gland [14] the *in vivo* oxidation of thiourea is probably catalyzed by this enzyme. Of interest in this connection is also that thiocyanate is oxidized *in vivo* to sulfate [19] and to cyanide [20]. The results now obtained strongly suggest that peroxidase is a part also of the "thiocyanate oxidase" [20] system.

When the investigation was started, it was suspected that peroxidase may be responsible for some of the biological effects of ionizing radiations. Hydrogen peroxide is formed when solutions are irradiated and an oxidation of vital thiols or disulfides to sulfinic or sulfonic acids has been suggested as a key reaction in radiation damage [21]. As some well known inhibitors for heme-enzymes, for instance cyanide [22], protect against ionizing radiation, a peroxidase catalyzed destruction of vital thiol or disulfide groups during irradiation was suggested. The results now obtained seem to exclude this possibility.

Acknowledgements. The authors are very grateful to Professor Hugo Theorell for kind advice and criticism, to Dr. Kjell Agner for generous gifts of myeloperoxidase and for valuable discussions, and are indebted to Mrs. Elsa Ekblom for technical assistance.

REFERENCES

1. Randall, L. O. *J. Biol. Chem.* **164** (1946) 521.
2. Dale, W. M. and Davies, J. V. *Radiation Research* **7** (1957) 35.
3. Stern, K. G. *Hoppe-Seyler's Z. physiol. Chem.* **209** (1932) 136.
4. Werner, E. A. *J. Chem. Soc.* **101** (1912) 2168.
5. Hunter, R. F. and Jones, J. W. T. *J. Chem. Soc.* **1930** 2190.
6. Barnett, E. de B. *J. Chem. Soc.* **97** (1910) 63.
7. Böeseken, J. *Rec. trav. chim.* **55** (1936) 1044.
8. Asmus, E. and Garschagen, H. *Z. anal. Chem.* **138** (1953) 414.
9. Connor, R. In Gilman, H. *Organic Chemistry, An advanced Treatise*, John Wiley and Sons, New York 1943, p. 909 and 921.
10. Elliott, K. A. C. *Biochem. J.* **26** (1932) 10.
11. Agner, K. Personal communication.
12. Westerfeld, W. W. and Lowe, C. *J. Biol. Chem.* **145** (1942) 463.
13. Astwood, E. B. *Brookhaven Symposia in Biol.* **7** (1955) 61.
14. Ljunggren, J. G. *Acta Chem. Scand.* **11** (1957) 1072.
15. Miller, W. H., Roblin, R. O. and Astwood, E. B. *J. Am. Chem. Soc.* **67** (1945) 2201.
16. Pitt Rivers, R. *Biochim. et Biophys. Acta* **2** (1948) 311.
17. Keilin, D. *Proc. Roy. Soc. B* **106** (1930) 418.
18. Schulman, J., Jr. *J. Biol. Chem.* **186** (1950) 717.
19. Wood, J. L., Williams, E. F., Jr. and Kingsland, W. *J. Biol. Chem.* **170** (1947) 251.
20. Goldstein, F. and Rieders, F. *Am. J. Physiol.* **173** (1953) 287.
21. Shapiro, B. and Eldjarn, L. *Radiation Research* **3** (1955) 255.
22. Bacq, Z. M., Herve, A., Lecomte, J. and Fischer, P. *Science* **11** (1950) 356.

Received December 13, 1957.

ACTA CHEMICA SCANDINAVICA 12 (1958) 477—484

Solvates of Arsenic Trichloride, Phosphorus Oxychloride and Selenium Oxychloride

MARGARETA AGERMAN, LARS HENRIK ANDERSSON, INGVAR LINDQVIST and MARGARETA ZACKRISSON

Institute of Chemistry, University of Uppsala, Uppsala, Sweden

The liquidus curves have been studied for mixtures between each of the solutes $(CH_3)_4NCl$, $(C_2H_5)_4NCl$, $SnCl_4$, $SbCl_5$ and the solvents $AsCl_3$, $POCl_3$, $SeOCl_2$ and also for mixtures between the solvents. The following new compounds have been found: $(CH_3)_4NCl \cdot 5\ SeOCl_2$, $(CH_3)_4NCl \cdot 3\ SeOCl_2$, $(CH_3)_4NCl \cdot 2\ SeOCl_2$, $(C_2H_5)_4NCl \cdot 5\ SeOCl_2$, $(C_2H_5)_4NCl \cdot 2\ AsCl_3$, $3(C_2H_5)_4NCl \cdot 5AsCl_3$ and $POCl_3 \cdot AsCl_3$. The results are briefly discussed.

The reactions in non-aqueous ionising solvents have attracted much interest during recent years. The chemistry in arsenic trichloride, $AsCl_3$, phosphorus oxychloride, $POCl_3$, and selenium oxychloride, $SeOCl_2$, has recently been reviewed by Gutman [1,2] who mentions the fact that compounds between solute and solvent (solvates) often may be isolated. It has been pointed out by Lindqvist [3] that the knowledge of the structures of the solid solvates is necessary for any detailed discussion of solubility and solvation conditions in these solvents. We have therefore made a survey of the binary systems between some important solutes and the three solvents $AsCl_3$, $POCl_3$ and $SeOCl_2$. This study has partly confirmed earlier results, partly led to isolation of new compounds.

EXPERIMENTAL

Chemicals used. $AsCl_3$ was purified as described earlier [4] with final conductances of $0.9-1.1 \times 10^{-7}$ ohm^{-1} cm^{-1} at room temperature. $POCl_3$ was purified by distillation (boiling point +105°C). $SeOCl_2$ (B.D.H. reagents) with a conductance of 8×10^{-4} ohm^{-1} cm^{-1} at +22°C was not further purified. $SnCl_4$ and $SbCl_5$ were purified according to Dodd and Robinson [5]. $(CH_3)_4NCl$ (Eastman Kodak) was dried for 12 h at 110°C. Crude $(C_2H_5)_4NCl$ was recrystallised from acetone and dried at reduced pressure in a drying pistol at 100°C.

Analytical methods. Cl was determined by potentiometric titrations with 0.1 M $AgNO_3$. N was determined by Kjeldahl distillation. Se was analysed by reduction with sulfurous acid in hydrochloric acid solution [6]. P was determined according to a method given by Scheel [7].

Phase diagrams. The aim of the phase diagram studies has not been to obtain highly accurate data but rather to make a survey of the liquidus curves in the different binary

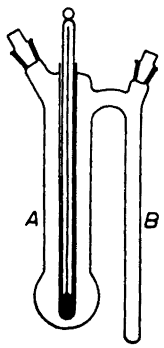

Fig 1

Fig. 1. Vessel for the phase diagram studies.

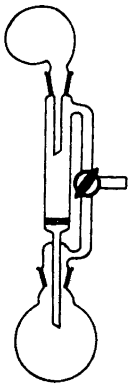

Fig 2

Fig. 2. Apparatus for the analysis.

systems, particularly for large mole fractions of solvent. A rather simple apparatus could therefore be used for these experiments (Fig. 1). With liquid solutes, the solute and solvent are poured or directly distilled into either of the two legs *A* or *B* which have been cooled to −50°C. The amount added to the *A* part has first been weighed and as the *B* tube has been calibrated, the volume of liquid transferred from *B* to *A* during the experiments can be determined (as well as the weight, because the densities are known). Solid solute is added in weighed amounts to the solvent in *A*. The error in the mole fractions obtained in this way is mainly due to adherence of liquid to the glass walls during the transfer from *B* to *A* or to vapor phase reactions, but the accuracy is good enough for our purposes. The thermometer does not dip directly into the liquid (which would have increased the difficulties of working in a closed system) but the thermal contact is improved by a small mercury drop at the bottom of the inner tube. Tests have shown that the reproducibility of the temperature reading is within ±1°. The temperature values may, however, have systematic errors of 2—3° which is of no importance in this type of study (compare also the good agreement with the results of more elaborate measurements). The results are not sensitive to small impurities if the solvates formed have congruent melting points, that is when the reactants completely crystallise as solids.

The analyses were made in an apparatus (Fig. 2) which permitted filtration and washing of the crystals formed. The crystals were then dissolved on the filter in an alkaline water solution and their mole ratios could be determined by analyses. Absolute analyses of weighed amounts of the solvates were also made in some cases but are difficult to carry out because of the extreme sensitivity of these compounds to moisture.

When our investigation was finished, we were informed by Dr. Gutmann, Vienna, of a thesis by Groeneveld, Leyden. Groeneveld has already studied three of our systems: $SnCl_4-POCl_3$, $SbCl_5-POCl_3$ and $SnCl_4-SeOCl_2$ with a more elaborate experimental technique. His phase diagrams, which have never been published, are in very good agreement with ours. The melting points he obtained for the solvates are given together with our results for comparison in the following. The good agreement proves that the very simple and rapid technique used by us was adequate for our purposes.

RESULTS

Tetramethyl ammonium chloride, $(CH_3)_4NCl$

1. $(CH_3)_4NCl \cdot AsCl_3$ and $(CH_3)_4NCl \cdot 3\ AsCl_3$ have been prepared earlier [8,9]. Part of the phase diagram has now been studied (Fig. 3 *a*) and no higher

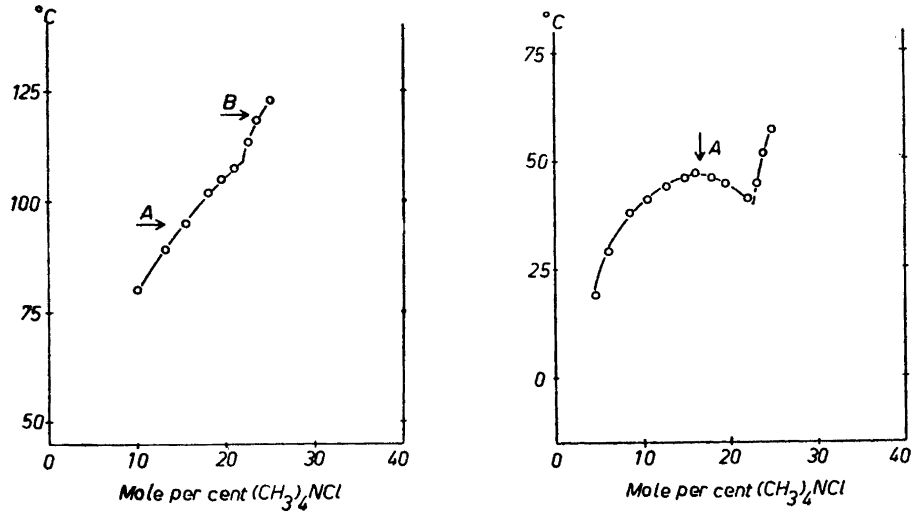

Fig. 3. a. The system $(CH_3)_4NCl-AsCl_3$. Liquidus curves for $A = (CH_3)_4NCl \cdot 3AsCl_3$, $B = (CH_3)_4NCl \cdot AsCl_3$. *b.* The system $(CH_3)_4NCl-SeOCl_2$. Liquidus curve for $A = (CH_3)_4NCl \cdot 5SeOCl_2$.

solvates have been discovered. Mole fractions of $(CH_3)_4NCl$ larger than 0.25 cannot be studied because of the boiling of the solvent.

2. The solubility of $(CH_3)_4NCl$ in $POCl_3$ is very small below + 200°C and does not permit a phase study of this type. (Gutmann [10] found 2 g/l at +20°C corresponding to a mole fraction of 0.0016.)

3. The phase diagram (Fig. 3 *b*) $(CH_3)_4NCl - SeOCl_2$ shows a maximum at the composition $(CH_3)_4NCl \cdot 5\ SeOCl_2$ where the entire liquid phase solidifies. The melting point is +45—47°C. The analysis of this compound is very difficult to carry out accurately, because the crystals lose $SeOCl_2$ when washed with, *e.g.*, ether, and small amounts of liquid adhere to the solid without being washed. The position of the maximum has, however, been studied by direct comparison of the melting points of different accurately weighed mixtures of solute and solvent.

The white residue obtained after washing with a small amount of ether had the composition $(CH_3)_4NCl \cdot 3\ SeOCl_2$. Mole ratio N : Se : Cl calculated 1 : 3 : 7, found 1.00 : 3.04 : 7.01. A thorough washing with ether gave a compound $(CH_3)_4NCl \cdot 2\ SeOCl_2$. Mole ratio N : Se : Cl calculated 1 : 2 : 5, found 1.00 : 2.01 : 5.00. In the latter case an absolute analysis proved that no ether had entered the solid compound. Calculated for N : 3.17 %, found 3.17 %.

The two compounds $(CH_3)_4NCl \cdot 2\ SeOCl_2$ and $(CH_3)_4NCl \cdot 3SeOCl_2$ could not be obtained by cooling of solutions of $(CH_3)_4NCl$ in $SeOCl_2$ because these solutions become very viscous and are always supercooled at mole fractions of $(CH_3)_4NCl$ larger than 0.25.

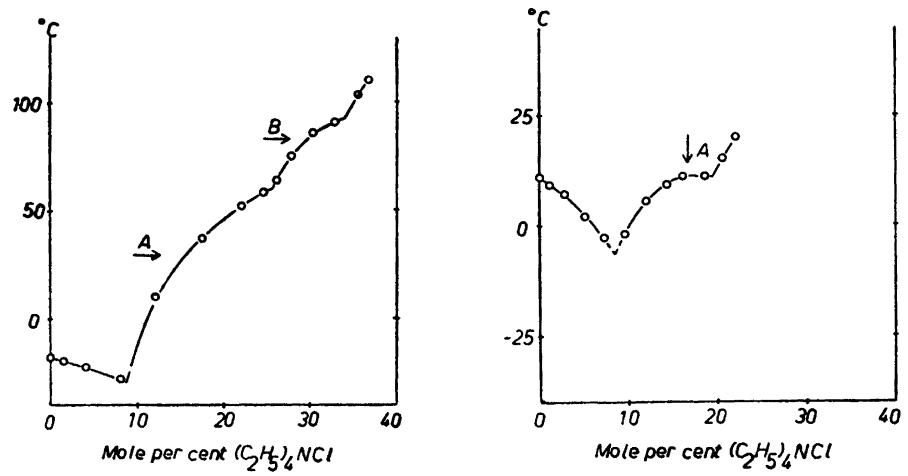

Fig. 4. a. The system $(C_2H_5)_4NCl$-$AsCl_3$. Liquidus curves for $A = (C_2H_5)_4NCl \cdot 2AsCl_3$, $B = 3(C_2H_5)_4NCl \cdot 5AsCl_3$. *b.* The system $(C_2H_5)_4NCl$-$SeOCl_2$. Liquidus curve for $A = (C_2H_5)_4NCl \cdot 5SeOCl_2$.

Tetraethyl ammonium chloride, $(C_2H_5)_4NCl$

1. The phase diagram is shown in Fig. 4 *a*. No congruently melting compounds are obtained in the concentration range studied and the compositions of the phases in equilibrium with the solution have been determined by distillation at reduced pressure at different temperatures. The same method has been used earlier [10] in the study of the compounds between $(CH_3)_4NCl$ and $AsCl_3$. We started with a dilute solution of $(C_2H_5)_4NCl$ in $AsCl_3$ and distilled at 0°C until the weight was constant. The mole ratio $AsCl_3$: $(C_2H_5)_4NCl$ was then 2.06 in agreement with a compound $(C_2H_5)_4NCl \cdot 2AsCl_3$. The temperature of the distillation was then increased to + 22°C when more $AsCl_3$ was lost until the mole ratio became 1.69 in agreement with a compound $3(C_2H_5)_4NCl \cdot 5AsCl_3$. This is no definite proof that these formulae are correct but this system has shown such interesting features that we plan a more detailed study of it.

2. The solubility of $(C_2H_5)_4NCl$ in $POCl_3$ below + 200°C is very low and does not permit a phase study of this type.

3. The phase diagram $(C_2H_5)_4NCl$—$SeOCl_2$ is shown in Fig. 4 *b*. Here the same obstacles to accurate analysis are encountered as in the case of $(CH_3)_4NCl$ but the phase diagram indicates a compound with the composition $(C_2H_5)_4NCl \cdot 5SeOCl_2$. Its melting point is +11—12°C so that the compound cannot be isolated at room temperature and no ether washings have been made.

At mole ratios larger than 0.22 it is impossible to determine the melting points with any accuracy with our methods.

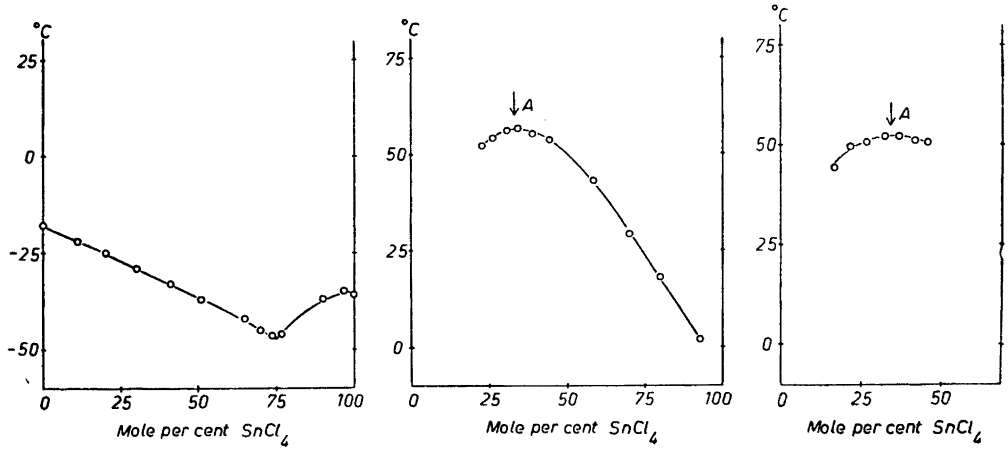

Fig. 5. a. The system $SnCl_4$—$AsCl_3$. *b.* The system $SnCl_4$—$POCl_3$. Liquidus curve for $A = SnCl_4 \cdot 2POCl_3$. *c.* The system $SnCl_4$—$SeOCl_2$. Liquidus curve for $A = SnCl_4 \cdot 2SeOCl_2$.

Tin tetrachloride, $SnCl_4$

1. The phase diagram, given in Fig. 5 *a*, does not indicate any compound formation.

2. The phase diagram $SnCl_4$—$POCl_3$ (Fig. 5 *b*) has only one, well defined maximum corresponding to the compound $SnCl_4 \cdot 2POCl_3$ with a melting point of +55—57°C (Groeneveld 56°C). Three compounds have earlier been described: 2 $SnCl_4 \cdot POCl_3$ by Oddo and Tealdi [11], $SnCl_4 \cdot POCl_3$ and $SnCl_4 \cdot 2\ POCl_3$ by Gutmann [12] who, however, did not definitely prove the existence of a definite compound $SnCl_4 \cdot 2\ POCl_3$. The existence of that solvate was proved by Payne [13] who found a melting point of $+59 \pm 0.5$°C. The compound $SnCl_4 \cdot POCl_3$ was obtained by Gutmann from $SnCl_4 \cdot 2\ POCl_3$ at low pressure. It is evident that it does not exist in the closed system which we have studied, nor does 2 $SnCl_4 \cdot POCl_3$.

3. The phase diagram (Fig. 5 *c*) shows the existence of a compound $SnCl_4 \cdot 2\ SeOCl_2$ with a melting point of +52°—54°C (Groeneveld $\sim$ 52°C). The system could not easily be studied for mole fractions of $SnCl_4$ larger than 0.50 because of the formation of two liquid phases. $SnCl_4 \cdot 2\ SeOCl_2$ has already been reported by Wise [14].

Antimony pentachloride, $SbCl_5$

1. The phase diagram $AsCl_3$—$SbCl_5$ (Fig. 6 *a*) does not show any indication of compound formation. Gutmann [8], however, obtained a small residue of the approximate composition $AsCl_3 \cdot SbCl_5$ by evaporation *in vacuo* at +30—35°C. That compound obviously must be the result of a slow irreversible reaction.

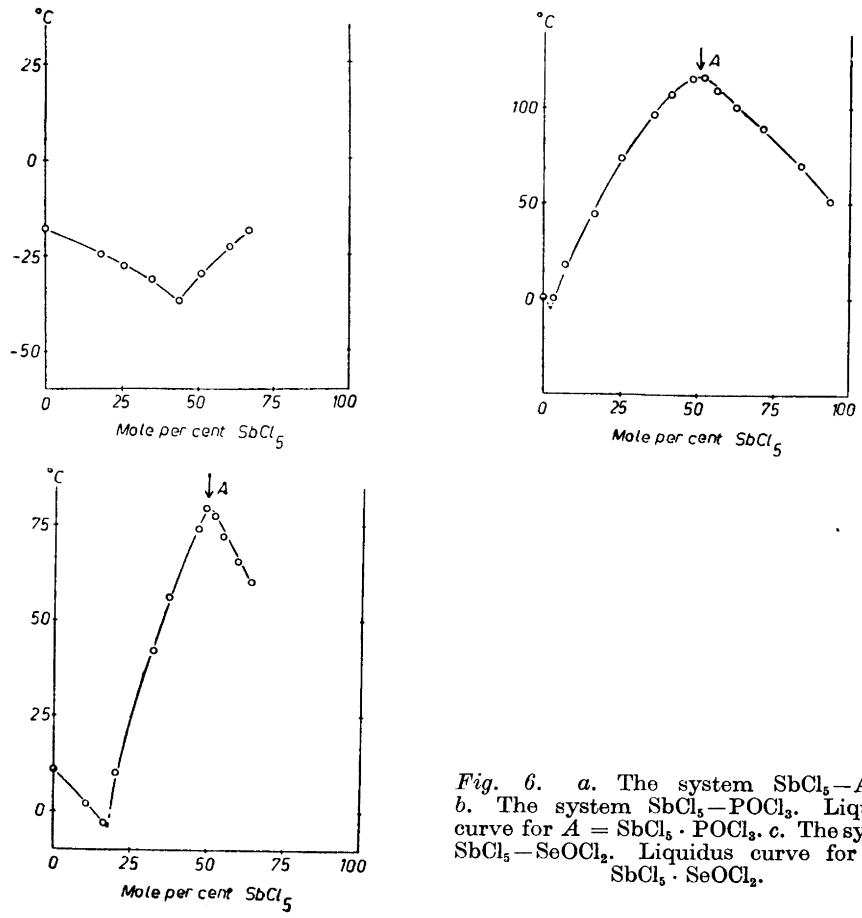

Fig. 6. a. The system $SbCl_5$—$AsCl_3$. *b.* The system $SbCl_5$—$POCl_3$. Liquidus curve for $A = SbCl_5 \cdot POCl_3$. *c.* The system $SbCl_5$—$SeOCl_2$. Liquidus curve for $A = SbCl_5 \cdot SeOCl_2$.

2. The phase diagram $SbCl_5$ — $POCl_3$ (Fig. 6 *b*) confirms the existence of the compound $SbCl_5 \cdot POCl_3$, earlier described by Weber [15] and Gutmann [12]. The melting point is +115—117°C (Groeneveld 117°C). The statement by Gutmann that the compound is not soluble in $SbCl_5$ is not in agreement with our results.

3. The phase diagram $SbCl_5$—$SeOCl_2$ (Fig. 6 *c*) shows the existence of only one compound, $SbCl_5 \cdot SeOCl_2$, with a melting point of +79—80°C. Weber [15] has already described the same solvate but Wise [14] found $SbCl_5 \cdot 2\ SeOCl_2$, the existence of which we have not been able to confirm.

Binary systems between the solvents

1. We have also studied the binary systems between the solvents. Fig. 7 *a* shows the system $POCl_3$—$AsCl_3$. The existence of a compound $AsCl_3 \cdot POCl_3$ with a melting point of —23—25°C has definitely been established.

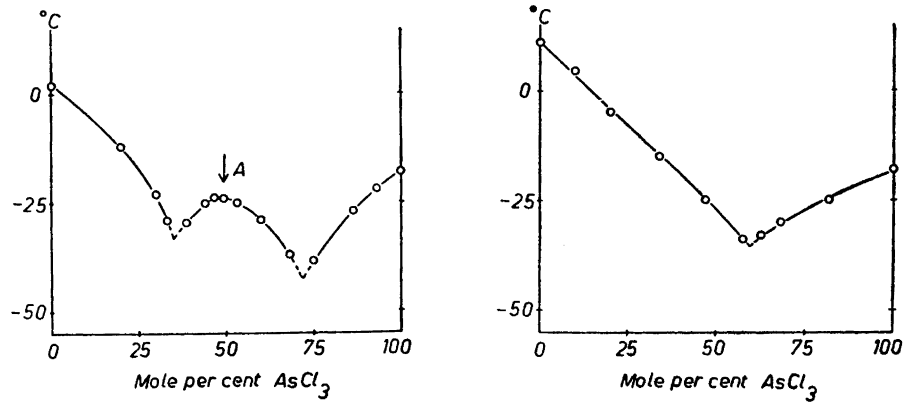

Fig. 7. a. The system $AsCl_3$—$POCl_3$. Liquidus curve for $A = AsCl_3 \cdot POCl_3$. *b.* The system $AsCl_3$—$SeOCl_2$.

2. The system $AsCl_3$—$SeOCl_2$ (Fig. 7 *b*) does not show any indications of compound formation.

3. When $SeOCl_2$ and $POCl_3$ are mixed a yellowish insoluble precipitate is formed after some hours at low mole fractions of $POCl_3$; immediately at mole fractions larger than 0.35—0.45. The composition of this precipitate corresponds to a formula $3\ SeOCl_2 \cdot 2POCl_3$ (calculated mole ratio P: Se: Cl = 2 : 3 : 12, found 2.00 : 3.04 : 11.94). When we tried to determine the melting point, part of the compound formed a red-brown vapour at about + 170°C quite like $SeCl_4$. We could not definitely ascertain whether a compound had formed or not, but we decided that a chemical reaction $3\ SeOCl_2 + 2\ POCl_3 \rightarrow 3\ SeCl_4 + P_2O_5$ had probably taken place. $SeCl_4$ and P_2O_5 are both almost insoluble in $SeOCl_2$ as well as in $POCl_3$. The reaction therefore would always lead to a product of the approximate composition $3\ SeOCl_2 \cdot 2\ POCl_3$ or $3\ SeCl_4 \cdot P_2O_5$.

The stability of solutions of $SbCl_5$ in $SeOCl_2$

The findings in the preceding section open the question of whether solutions in $AsCl_3$, $POCl_3$ and $SeOCl_2$ are stable or only metastable.

We have made one experiment to investigate this problem further. Sb_2O_5 and $SeCl_4$ were mixed in an ampoule, which was sealed (but not evacuated). After one day the mixture looked wet and the colour had become red-brown. When heated to +60°C it partly melted, as would be expected if the reaction $Sb_2O_5 + 5\ SeCl_4 \rightarrow 2\ SbCl_5 + SeOCl_2$ had taken place. This experiment strongly indicates that at least the solution of $SbCl_5$ in $SeOCl_2$ is a stable solution.

DISCUSSION

We do not want to make any far-going theoretical speculations based on this investigation but a few observations in connection with the present study may be summarised:

1. The behaviour of $POCl_3$ is quite different from $AsCl_3$ and $SeOCl_2$ in reactions with $(CH_3)_4NCl$ and $(C_2H_5)_4NCl$. These two salts have a very low solubility in $POCl_3$ (of a different order than in $AsCl_3$ and $SeOCl_2$) and give no solvates. This indicates that the solvation energy of Cl^- is smaller in $POCl_3$ than in $AsCl_3$ and $SeOCl_2$. Using the acid-base concept suggested by Gutmann and Lindqvist [16] this means that $POCl_3$ is a weaker acid than $AsCl_3$ and $SeOCl_2$.

2. $AsCl_3$ reacts with $SnCl_4$ and $SbCl_5$ quite unlike $POCl_3$ and $SeOCl_2$. The latter solvents form congruently melting solvates but $AsCl_3$ gives only eutectic mixtures (the compound $SbCl_5 \cdot AsCl_3$ can be prepared only under special conditions). In a previous paper [17] on the reactions in solutions of $POCl_3$ the reasons for the difference have been discussed.

3. $(CH_3)_4NCl$ is less soluble than $(C_2H_5)_4NCl$ in these solvents. (KCl has a still smaller solubility.) It would be interesting to study quaternary ammonium salts with larger cations to see how far the solubility increases with the cation radius.

This work has been supported by a grant from the *Swedish Natural Science Research Council* which is here gratefully acknowledged. We also wish to thank Professor G. Hägg for all facilities put at our disposal and Mr. N. Larsson for valuable help with the glass blowing.

REFERENCES

1. Gutmann, V. *Svensk Kem. Tidskr.* **68** (1956) 12.
2. Gutmann, V. *Quart. Rev.* **10** (1956) 458.
3. Lindqvist, I. *Acta Chem. Scand.* **9** (1955) 73.
4. Andersson, L. H. and Lindqvist, I. *Acta Chem. Scand.* **9** (1955) 79.
5. Dodd, R. E. and Robinson, P. L. *Experimental Inorganic Chemistry*, Amsterdam 1954, p. 210, 216.
6. Hillebrand, W. F. and Lundell, G. E. *Applied Inorganic Analysis*, New York 1929, p. 264.
7. Scheel, K. C. *Z. anal. Chem.* **105** (1936) 256.
8. Gutmann, V. *Z. anorg. Chem.* **266** (1951) 22.
9. Lindqvist, I. and Andersson, L. H. *Acta Chem. Scand.* **8** (1954) 128.
10. Gutmann, V. *Monatsh.* **83** (1952) 279.
11. Oddo, G. and Tealdi, M. *Gazz. chim. ital.* **33**, II (1903) 427.
12. Gutmann, V. *Z. anorg. Chem.* **269** (1952) 279.
13. Payne, D. S. *Rec. trav. chim.* **75** (1956) 620.
14. Wise, C. R. *J. Am. Chem. Soc.* **45** (1923) 1233.
15. Weber, R. *Pogg. Ann. Physik* **125** (1865) 78; **132** (1867) 452.
16. Gutmann, V. and Lindqvist, I. *Z. physik. Chem.* **203** (1954) 250.
17. Lindqvist, I. *Acta Chem. Scand.* **12** (1958) 135.

Received December 3, 1957.

ACTA CHEMICA SCANDINAVICA 12 (1958) 485—488

Ultra-microsynthesis of 5-Halogeno-derivatives of Uracil

GÖSTA EHRENSVÄRD, JAN LILJEKVIST, KLAUS MOSBACH

Department of Biochemistry, University of Lund, Sweden

and PER FRITZSON

Norsk Hydro's Institute for Cancer Research, The Norwegian Radium Hospital, Oslo, Norway

A method for preparation of 5-iodo-uracil has been worked out in ultra-micro-scale enabling the use of commercial ^{131}I at very high specific activity for the synthesis of 5-^{131}I-uracil in microgram quantities.

The demonstration that 5-bromouracil could be introduced into the deoxyribonucleic acid (DNA) of some microorganisms, especially *Escherichia coli*, replacing up to 50 % of thymine units [1,2], has now been extended to comprise 5-chloro- and 5-iodouracil [3,4]. With regard to relative rate of incorporation of the latter thymine analogues, Zamenhof *et al.*[4] have found that 5-chlorouracil may replace 21 % of thymine units, 5-iodouracil 14 %, whereas no introduction of uracil itself could be demonstrated. These observations are of considerable interest in view of the possibility of introducing 5—^{131}I-uracil into the DNA-structure in order to study the consequences of the subsequent nuclear decay ^{131}I—^{131}Xe *in situ*. This procedure might open up a new way of altering the chemical structure of DNA with the definite possibility of replacing some thymine-units by uracil, resulting from the decay of 5—^{131}I-uracil. More detailed reports with regard to the general chemical aspect of this decay reaction will be published later.

In view of the fact that 1 Curie of ^{131}I corresponds to 7.7 μg of the pure element, the synthesis of substantial amounts of 5—^{131}I-uracil with a minimum of diluting non-radioactive iodine has to be carried out in ultramicroscale. The following procedure has given up to 80 % yields of 5-iodouracil from 5 μg and less of uracil in the presence of an equivalent amount of iodine.

In principle the method is based on iodination of uracil in 0.02 M phosphate buffer at pH 7.5. Iodine is administered to the reaction mixture as a KI-solution, and liberated as iodine by the addition of an equivalent amount of chlorine in an aqueous solution. After completion of the reaction the products formed are separated by paper chromatography in a butanol-water system. In order to check the yield of 5-iodouracil and the amount and distribution of non-iodocompounds formed during the reaction, we have utilized uracil-6-^{14}C of high specific activity as the starting material, integrating the activity distributed of spots along the chromatogram. By this way, amounts down to 0.02 μg could be determined with a fair degree of accuracy. Fig. 1 gives a picture of the distribution of reaction products from a run with uracil-6-^{14}C and non-radioactive iodine as starting material, as compared with non-radioactive uracil and ^{131}I as reaction partners. With regard to the latter combination ^{131}I was

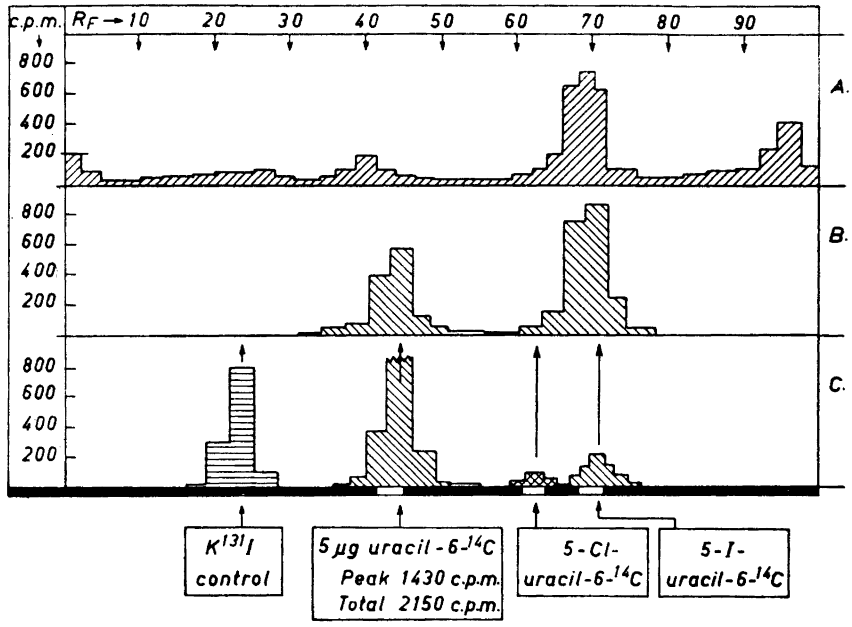

Fig. 1. Diagrammatic representation of the result of iodination of uracil in microgram quantities.

A: Iodination of non-labelled uracil with ^{131}I in tracer amounts followed by chromatographic separation of reaction products on a paper strip in butanol-water. Determination of radioactivity on sections of the paper strip gives a measure of the relative amounts of reaction products. Ordinate: counts per minute; abscissa: R_F-values.

B: Analogue experiment with uracil-6-^{14}C and non-radioactive iodine. The peak of 5-iodouracil corresponds to that of series A.

C: Controls, showing the position of K^{131}I, uracil-6-^{14}C, 5-chlorouracil-6-^{14}C and 5-iodouracil-6-^{14}C. The position of controls in substantial amounts of the three last compounds are shown as white regions in the black base-line, the determination being based on photography in UV-light.

used in tracer amounts during the working out of optimum conditions for the synthesis. The preliminary runs were carried out with uracil-6-^{14}C and non-radioactive iodine.

As seen from Fig. 1 the peak of activity corresponding to 5-I-uracil-6-^{14}C coincides with that of 5-^{131}I-uracil. Both are clearly separated from uracil, as was also verified by parallel controls of substantial amounts of uracil and 5-iodouracil (indicated by photography in UV-light at 254 mμ). With regard to the possible formation of small amounts of 5-chlorouracil a separate control with 5-chlorouracil-6-^{14}C indicates a fair separation from 5-iodouracil-6-^{14}C. In the experiments with ^{131}I we observed, in addition to the peak corresponding to 5-iodouracil, four other peaks of lower activity. Two of them have been found to correspond to KI and iodine, one remains at the starting line of the chromatogram and one follows the locus of uracil. None of the peaks, however, interferes with the locus of 5-iodouracil of $R_F = 0.68 - 0.72$.

EXPERIMENTAL

Uracil-6-^{14}C was prepared according to Fritzson [5]. It gave when chromatographed in 1 μg amounts on paper in butanol-water a total count of 600 cpm per spot. It contained 2 % 5-bromouracil.

^{131}I, as was used in these experiments, was derived from a tellurium source, together with some amounts of shortlived iodine isotopes, mainly ^{132}I. By the ordinary procedure of aeration of the tellurium solution the iodine was driven off and absorbed in a solution of 72.5 μg KI in 2.5 ml of 0.02 M phosphate buffer, pH = 7.5.

As a standard procedure, the following reagents were introduced into a 2 ml test tube, which could be attached to a small condensor by a standard glass joint. First 500 μl of a 0.02 M phosphate buffer solution, pH 7.5, containing 14.5 μg KI was added to the reaction tube, followed by 5—10 μl of a freshly made and standardized solution containing 3.5 μg of chlorine and 5 μg of uracil in 25 μl of water. The condenser was then attached to the tube and the mixture was immediately heated to gentle boiling on a micro-heating stage for 5 min. After cooling to room temperature another addition of chlorine was made, corresponding to 1.7 μg, followed by another 5 min period of heating. After cooling the reaction mixture was evaporated as a small spot on a paper strip, 23 mm wide, about 10 cm from one end. Whatman No. 1 paper was used, and the chromatogram run in a descending system of butanol saturated with water at 22°C for 18 h. Suitable controls of uracil-6-C, 5-I-uracil-6-^{14}C, ^{131}KI were made for the exact localization of the iodouracil from the reaction mixture.

After localization, by radioactivity measurement of controls, of the region containing the iodouracil formed, this region could be quantitatively eluted by 0.01 N HCl and almost quantitatively by water. Controls run in 20 μg scale show the exact UV absorbtion curve of 5-iodouracil, with an E_{max} at 283 mμ and E_{min} at 246 mμ. Table 1 gives the absorption maxima and minima for uracil and some of its halogen—derivatives (solvent: 0.01 N HCl) obtained in this laboratory.

Compound	λ_{max}	λ_{min}
Cl-uracil	273	239
Br-uracil	273	240
I-uracil	283	246
Uracil	260	228

The preparation of 5-bromouracil could be carried out as a simple variation of the procedure outlined above; the yields were about 50 %.

With regard to the preparation of 5-^{131}I-uracil using substantial amounts of ^{131}I in high concentration, adequate shielding should be used; 5 cm of lead give sufficient protection. The above method is suitable for the direct use of commercial solutions of ^{131}I in phosphate buffer for the reaction. Utilizing uracil-6-^{14}C of the highest possible activity together with substantial amounts of ^{131}I, the resulting 5-^{131}I-uracil-6-^{14}C could be used for the study of the nature of non-iodinized derivatives related to uracil, as formed in the course of the decay $^{131}I \rightarrow {}^{131}Xe$.

REFERENCES

1. Weygand, F., Wacker, A. and Dellweg, H. *Z. Naturforsch.* **7 b** (1952) 19.
2. Zamenhof, S. and Griboff, G. *Nature* **174** (1954) 306.
3. Zamenhof, S. *Abstracts Chem. Soc.* 126th meeting.
4. Zamenhof, S., Reiner, B., de Giovanni, R. and Rich, K. *J. Biol. Chem.* **219** (1956) 165.
5. Fritzson, P. *Acta Chem. Scand.* **9** (1955) 1239.

Received December 14, 1957.

ACTA CHEMICA SCANDINAVICA 12 (1958) 489—494

The State of Order in Cellulose as Revealed from X-Ray Diffractograms

JON GJÖNNES, NICOLAI NORMAN and HENRY VIERVOLL

Central Institute for Industrial Research, Oslo, Norway

A comparison has been made between the diffracted X-ray intensity from samples of cellulose and synthetized intensity curves, and it is shown that much more of the X-ray scattering from cellulose can be ascribed to crystalline reflexions than previously done. Thus the recorded intensity from samples of cellulose I (native) to a fair degree of approximation can be explained without introducing the concept of amorphous cellulose. For cellulose II(regenerated) the diffractograms can not be considered built up exclusively of crystalline reflexions, though also here the difference in cellulose qualities more seems to lie in the degree of perfection of the best ordered part of the samples than in different amounts of crystalline and amorphous material.

Several investigations have been carried out in order to determine the degree of order or crystallinity in high polymers by means of X-ray diffraction [1-3]. The methods are based upon a splitting of the coherent intensity in crystalline peaks and a continous background which is ascribed to an amorphous fraction of the sample. The coherently diffracted radiation is consequently interpreted as the sum of intensity scattered from crystalline material and from amorphous material .

The essential point in crystallinity measurements by X-ray methods has been the separation of the intensity into these two components. For substances like polyethylene where the crystalline reflexions are clearly superimposed upon a background due to the scattering from the solidified melt [2], the separation is simple and unambiguous. In the diffraction pattern for cellulose the crystalline reflexions are very broad and partly overlap. Consequently the drawing of a curve separating the two intensities is more difficult. In the procedures used by Hermans [1] and by Ellefsen, Wang Lund, Tönnesen and Öien [3] this curve touches the total intensity curve, implying that the coherent scattering from the crystalline fraction is set equal to zero at the corresponding Bragg angles.

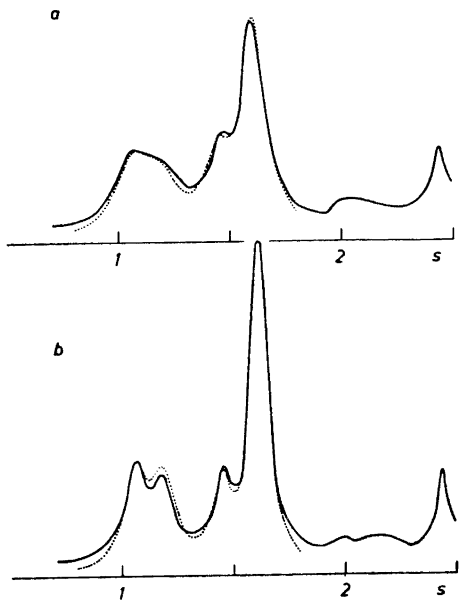

Fig. 1. Experimental (full-line) and synthetized (dotted) intensity curves for cellulose I.
a. Acetate grade wood pulp
b. Sulphuric acid treated surgical cotton

It is well known that small particle size and lattice distortion will cause a broadening of the peaks in the diffractogram, involving a general rise in background due to superposition of the tails of the lines. For cellulose the lines are very broad presumably due to both these factors. It is thus reasonable to believe that the lines may give a considerable contribution to the background in the diffractograms. In order to evaluate how far the description based on crystalline reflexions may fit the experimental data, a comparison has been made between experimental intensity curves and synthetized curves based on a limited number of crystalline reflexions.

THE EXPERIMENTAL AND SYNTHETIZED CURVES

Powder diffractograms of unoriented samples of cellulose were obtained in a Guinier vacuum camera with Cu$K\alpha$-radiation. The intensity curves were corrected for absorption and polarization and normalized to the background of incoherent and structure independent coherent scattering from a glucose unit [4]. After normalization the incoherent scattering was subtracted.

In the calculated intensity curves the crystalline peaks were supposed to have the shape of a Cauchy distribution:

$$I(s) = K \frac{\alpha}{\alpha^2 + (s - s_0)^2}$$

Here $s = 4\,\pi \sin \Theta/\lambda$, s_0 is the peak abscissa, and 2α the half width of the peak. K is a constant that depends on the structure factor of the reflexion. A characteristic feature of the Cauchy distribution is the long tails which was one reason why this function was chosen for cellulose. The Cauchy line profile has been observed for the reflexions of cold worked metals [5], and a study of the diffractograms of cellulose in fact seems to confirm that the well resolved peaks to a fair degree of approximation can be represented by Cauchy distributions.

The position of the lines were determined from the experimental intensity curves, and these curves were further used in the estimation of half widths. Since the structure factors for cellulose are not well known, the values of K also had to be evaluated from the measurements.

In the calculations only the reflexions (1 0 1), (1 0 $\bar{1}$), (0 2 1) and (0 0 2) for cellulose I and (1 0 1), (1 0 $\bar{1}$) and (0 0 2) for cellulose II were considered.

RESULTS

Four different qualities of cellulose I (native) and cellulose II (regenerated) were investigated. The full-line curves in Fig. 1, *a* and *b*, show the corrected intensity from an acetate grade wood pulp and a sulphuric acid treated surgical cotton, respectively. The dotted curves represent the calculated intensity based on the values of s_0, K and 2α in Table 1. In the same way the experimental and calculated intensity curves for the two samples of cellulose II are given by the full-line and dotted curves in Fig. 2. Curve *a* corresponds to an acetate grade wood pulp mercerized in 18 % sodium hydroxide, curve *b* to acetate grade wood pulp treated with 39 % hydrochloric acid. The values of the parameters are found in Table 2.

DISCUSSION

In its broad features the agreement between experimental and calculated intensities in Figs. 1 and 2 up to $s = 1.7$—1.8 is satisfactory. Above this value of s it is easy to obtain a good fit because of the large number of reflexions. There also exist crystalline reflexions below $s = 1.7$ which are not taken into consideration in the calculations and which would add to the theoretical

Table 1. Parameters used in the calculation of intensity curves for cellulose I.

Reflexion	s_0	K	2α	
			Wood pulp	Cotton
1 0 $\bar{1}$	1.06	25	0.20	0.12
1 0 $\bar{1}$	1.18	25	0.21	0.13
0 2 1	1.45	18	0.13	0.09
0 0 2	1.61	66	0.14	0.10

Table 2. Parameters used in the calculation of intensity curves for cellulose II.

Reflexion	s_0	K	2 a	
			Acetate grade wood pulp	
			18 % NaOH	39 % HCl
1 0 1	0.87	15	0.12	0.06
1 0 $\bar{1}$	1.43	61	0.14	0.09
	1.56 *		0.14	
0 0 2		37		
	1.57 **			0.07

* Fig. 2 a, ** Fig. 2 b

intensity distribution and bring out a better fit between experimental and synthetized curves.

Fig. 1 shows a good correspondance between experimental and calculated intensity curves. This seems to indicate that the greater part of the investigated samples of cellulose I very likely consists of aggregates of distorted crystallites, and that only small quantities of highly disordered material are present.

For cellulose II the case is somewhat different. The background, especially in the region between the (1 0 1) and (1 0 $\bar{1}$) lines in Fig. 2, can not be explained

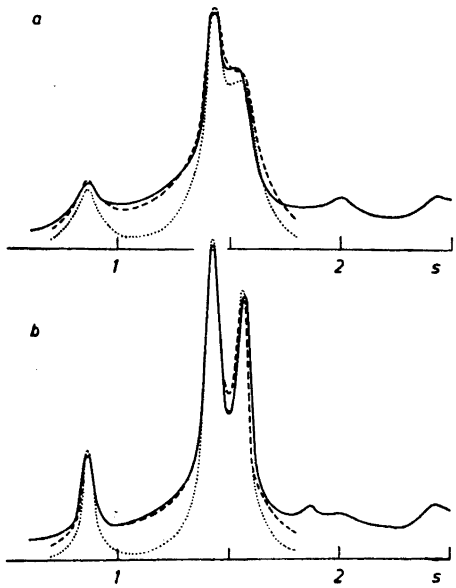

Fig. 2. Experimental (full-line) and synthetized (dotted) intensity curves for cellulose II. The broken curves correspond to synthetized intensities including an amorphous background.

a. Acetate grade wood pulp mercerized in 18 % sodium hydroxide
b. Acetate grade wood pulp treated with 39 % hydrochloric acid.

Table 3. Computed values for the degree of amorphity by the method of Ellefsen, Wang Lund, Tönnesen and Öien [3].

Modification	Sample	Degree of amorphity %
Cellulose I	Acetate grade wood pulp	47
» I	H_2SO_4-treated surgical cotton	38
» II	Acetate grade wood pulp merc. in 18 % NaOH	57
» II	Acetate grade wood pulp treated with 39 % HCl	51

exclusively as due to the outer parts of the crystalline reflexions of the assumed shape, even if the unresolved (0 2 0) peak at $s_0 = 1.22$ is added. It is also seen that the half widths of the peaks are considerably smaller than those obtained for cellulose I. Both these facts suggest that the cellulose II samples to a higher extent than the samples of cellulose I are separable into fractions with widely different states of order. These may well include an amorphous one, corresponding to the dry ground cellulose defined as amorphous cellulose by Ellefsen *et al.*[6]

From the broken curves in Fig. 2 *a* and *b* it is seen that a better correspondance between experimental and calculated intensity curves can be obtained when an amorphous background is added to the theoretical intensity. These curves represent the superposition of scattering curves from dry ground samples of cellulose and the calculated intensities given by the dotted curves of the same figure. The ordinates were reduced to fit the estimated contents of crystalline material. The broken curves in Fig. 2 *a* and *b* both correspond to 40 % amorphous material. For the same samples the method of Ellefsen *et al.*[3] led to the values 57 % and 51 %, respectively (Table 3). It should be mentioned that the adding of an amorphous background also can improve the agreement between experimental and calculated intensity curves for cellulose I, and that a value around 5 % seems to give the best fit for both samples.

CONCLUSION

The present paper shows that it is possible to obtain good correspondance between experimental intensity curves and synthetized curves based on the sum of broad crystalline reflexions and an amorphous background. This superposition of intensities does not necessarily correspond to the true state of order in the sample. However, if a separation of the observed intensity into two components is carried out, it should be kept in mind that a considerable part of the background in the diffractogram is due to the crystalline peaks.

It should be pointed out that for samples of the same modification of cellulose, the difference in state of order seems to lie more in the degree of perfection of the best ordered fraction than in the ratio between this fraction and

the less ordered one. This is clearly illustrated in Fig. 2 where the calculations led to the same amount of amorphous material for the two samples, although the diffractograms show marked differences. These differences are expressed in the half widths used for computing the synthetized curves.

It is thus evident that any description of order or crystallinity in cellulose should take the intrinsic order of the crystallites into consideration. The half widths of the peaks here seem to be suitable parameters. Further experimental and theoretical work along this line is in progress.

This investigation is part of a research program on the structure of cellulose carried out by the Central Institute for Industrial Research and The Norwegian Pulp and Paper Research Institute. Financial support from the *Royal Norwegian Council for Industrial Research* is gratefully acknowledged.

REFERENCES

1. Hermans, P. H. and Weidinger, A. *J. Appl. Phys.* **19** (1948) 491.
2. Krimm, I. and Tobolsky, A. V. *J. Polymer Sci.* **7** (1951) 57.
3. Ellefsen, Ö., Wang Lund, E., Tönnsen, B. A. and Öien, K. *Norsk Skogindustri* **11** (1957) 349. Part II.
4. Norman, N. *Acta Cryst.* **10** (1957) 370.
5. Williamson, G. K. and Smallman, R. E. *Acta Cryst.* **7** (1954) 574.
6. Ellefsen, Ö., Wang Lund, E., Tönnesen, B. A. and Öien, K. *Norsk Skogindustri* **11** (1957) 284. Part I.

Received November 19, 1957.

ACTA CHEMICA SCANDINAVICA 12 (1958) 495—502

Studies in the Determination of Silica

I. Spectrophotometric Determination of Silica as α-Silicomolybdate

LARS HENRIK ANDERSSON

Dept. of Analytical Chemistry, Institute of Chemistry, University of Uppsala, Uppsala, Sweden

A modified silicomolybdate method is described, which is shown to be uninfluenced within wide limits by variables such as pH, molybdate and salt concentrations. The colour produced is stable for long periods of time, and extinction measurements are reproducible with good precision. The reason for these improved properties is that the stable α-silicomolybdate is used instead of the unstable β-compound.

Since the discovery in 1898 by Jolles and Neurath [1] that the reaction between silica and molybdate in water solutions to form yellow silicomolybdic acid could be used for analytical purposes, much work has been devoted to the study of this colorimetric method for silica determination. It was not until the introduction of accurate spectrophotometers, however, that more thorough investigations could be undertaken, and since about 1930 many papers dealing with the subject have been published. Despite this no definite solutions of the problems concerned have been presented, and as recently as 1952 Strickland [2] published a series of papers dealing with the preparation and properties of silicomolybdic acid. Stoll [3] and Lacroix and Labalade [4] had made more restricted experiments. The papers by Mellon [5], Mullin and Riley [6] and Arnfelt *et al.*[7] summarize and give references to the earlier literature as well as to more modern works.

Strickland's [2] most important contribution seems to be his discovery that silicomolybdic acid occurred in two forms, of which the one called β was more or less rapidly converted to the stable α-form under normal temperature and pressure. On the basis of his results he recommended the unstable β-form as suitable for analytical purposes.

Although almost all reactions involved in the formation of the silicomolybdic acids probably are very complicated, the following scheme will give a rough idea of the processes taking place in water solution:

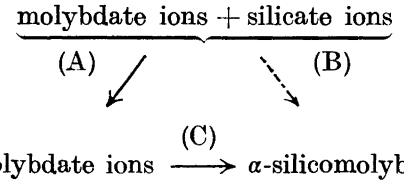

It is not known if reaction (B) actually takes place. The molybdate as well as the silicate ions are to a certain degree polymerised, the degree of polymerisation varying with the composition of the solution. Lindqvist [8] gives the following scheme for the reactions occurring when a molybdate solution is acidified:

$$MoO_4^{2-} \rightarrow Mo_7O_{24}^{6-} \rightarrow Mo_8O_{26}^{4-} \rightarrow \text{larger complexes}$$

An attempt to study the influence of silicate polymerisation was made by Chow and Robinson [9].

In the present paper a few experiments with the earlier silicomolybdate method will be described, which show important drawbacks connected with it. After that a modified method is presented together with an investigation of the influences on that method of some important factors. Interferences from phosphorus, arsenic and germanium as well as from iron and aluminium and fluorine will be dealt with in later papers.

1. EXPERIMENTAL DETAILS

The chemicals used were of analytical grade. Distilled water for the preparation of solutions had not previously been in contact with glass, but was taken from a distillation apparatus with metal parts. All solutions were stored in polythene bottles. Ammonia solutions were prepared by dissolving tank ammonia in distilled water.

Two different preparations of silicic acid were used: one was a commercial chemical (Baker) and the other had been prepared from sodium silicate by a method similar to that used in the ordinary silica separation procedure. Both chemicals were analysed for their water contents by heating samples to constant weight in platinum crucibles, and for their silica contents by treatment with hydrofluoric and sulfuric acid, followed by heating to constant weight; the residues did not exceed 0.2 % of the amount SiO_2 taken.

The dissolution process was accomplished by fusion with Na_2CO_3 in a platinum crucible, and then digesting its contents with water in a platinum dish. In some cases the silicic acid was placed in a platinum dish together with 4 g NaOH and a few ml of water and dissolution carried out by heating on the steambath. However, solutions prepared in this last way always showed low values (by 1—2 %) compared with those prepared in the first way, which were therefore generally preferred.

Blank solutions were prepared in a manner similar to that used for the corresponding silica solutions. They were employed in the preparation of blanks and, when necessary, for diluting the standard silica solutions.

A Beckman model DU spectrophotometer, the cuvette compartment of which was maintained at a constant temperature (20.0°C unless otherwise stated), was used for all extinction measurements. The same set of three numbered cuvettes were used, the first being filled with distilled water, the second with the blank and the third with the coloured solution. A correction for their different optical properties was applied. The instrument was checked with respect to the wavelength scale (using a mercury lamp) and the extinction scale (using a K_2CrO_4 solution as described by Haupt [10]).

pH measurements were carried out with a Beckman model H 2 instrument using a glass electrode and a saturated calomel electrode. 0.05 M KH-phthalate (pH = 4.0) and 0.100 M HCl (pH = 1.1) were employed as reference solutions.

2. EXPERIMENTS WITH EARLIER METHODS

Previous methods have been tested with respect to certain variables and have turned out to be unsatisfactory in different ways. A desription of an experiment designed to furnish the extinction as a function of time at different NaCl concentrations in the solutions used will demonstrate an important property of the silicomolybdic acid system.

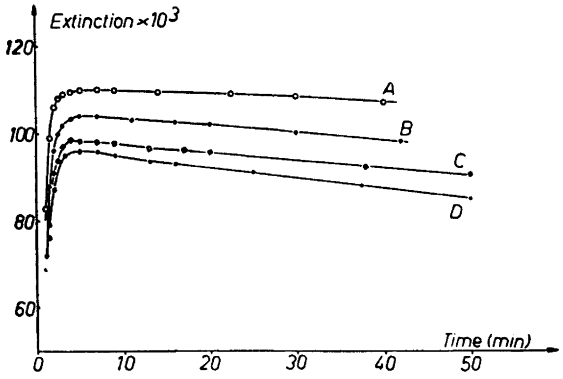

Fig. 1. Extinction-time dependence for earlier method with [NaCl] as a variable. A, [NaCl] = 0; B, [NaCl] = 0.4 M; C, [NaCl] = 0.8 M; D, [NaCl] = 1.2 M.

Of two 100 ml beakers, one was filled with 25 ml of a molybdate solution (0.04 M in Na_2MoO_4, pH = 1.5 with HCl) and the other with 25 ml of silica solution (8 mg Si/l, pH = 1.5 with HCl; appropriate amounts of NaCl added). The two solutions (20.0°C) were quickly mixed and the mixture transferred to a 1 cm cuvette. With the aid of two stopwatches, which were alternately stopped and started just at the instants the moving (the extinction was changing!) meter needle of the DU instrument indicated balance at a preset extinction value, the extinction as a function of time was obtained.

In Fig. 1 curves are given for different NaCl concentrations in the final solutions. It can be seen that the optical properties of the system are strongly influenced by NaCl additions. Actually the effect of salts containing divalent anions such as Na_2SO_4 is still more pronounced.

It follows from this and similar experiments with other salts that pH as well as molybdate concentration influences cannot be treated as independent variables and without reference to the salt content of the solutions. Factors which affect the composition of the final solution to be analysed for silica by this method must be carefully controlled.

3. A MODIFIED METHOD

If the reaction

$$\beta\text{-silicomolybdate} \rightarrow \alpha\text{-silicomolybdate}$$

is allowed to proceed completely to the right a stable yellow colour is obtained. At room temperature the reaction rate is comparatively low but is accelerated by salt additions. When the solution is heated on a steam bath the conversion is practically complete within about 3 h, the actual time being dependent on the composition of the solution in question. On this basis the following general procedure has been worked out which, with appropriate modifications, was used in the following experimental work unless otherwise stated.

The solution to be analysed is mixed with a molybdate solution in a polythene bottle and the bottle is placed on the hot steambath. After the appropriate time interval the bottle with contents is cooled to 20.0°C, transferred to a volumetric flask, made up to volume with water or a suitable solution and mixed. The extinction is measured against a blank which has been treated in an analogous way.

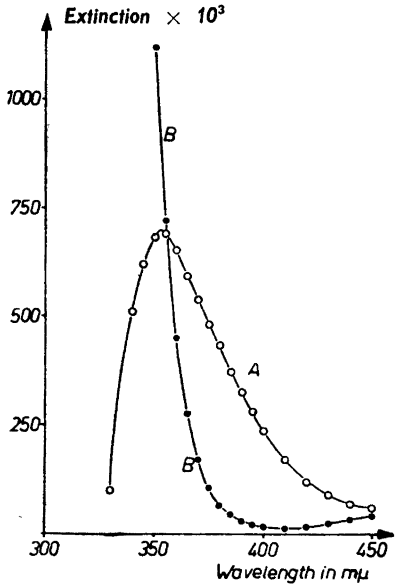

Fig. 2. Extinction as a function of wavelength. Curve A, α-silicomolybdate solution measured against the blank; B, blank measured against water.

Using this procedure the modified method was tested with respect to some important variables. Unless otherwise stated the solutions when heated on the waterbath have a volume of 20 ml, which is later diluted to the final volume, 25 ml.

3. 1. The extinction as a function of wavelength

The measurements were performed with solutions which when heated on the steambath were 0.25×10^{-3} M in Si and 0.05 M in Na_2MoO_4, with a pH of 1.5, adjusted with perchloric acid. The heating time was long enough to ensure a complete conversion to α-silicomolybdate.

In Fig. 2 is plotted the extinction-wavelength curve for α-silicomolybdate (A) and for the blank (B). The yellow complex has an extinction maximum at about 350 mμ, but at this wavelength the blank absorbs strongly. A longer wavelength should be chosen, where the blank absorbs little light compared to the solution containing silica. This is all the more necessary because the light absorption of acidified molybdate solutions depends on their pH, especially at shorter wavelengths [11]. At 400 mμ, a wavelength which has been found suitable for most purposes, the absorption due to the molybdate ion species is small and in practice independent of small pH fluctuations.

It is clear from Fig. 2 that at 400 mμ the rate of change of extinction with wavelength is numerically large. This has two consequences: it is necessary to control the wavelength setting carefully to obtain reproducible extinction values between different series of measurements, and good monochromatic light is necessary for a linear relationship between extinction and silica concentration. The corex filter supplied with the Beckman DU instrument should be used to eliminate scattered radiation.

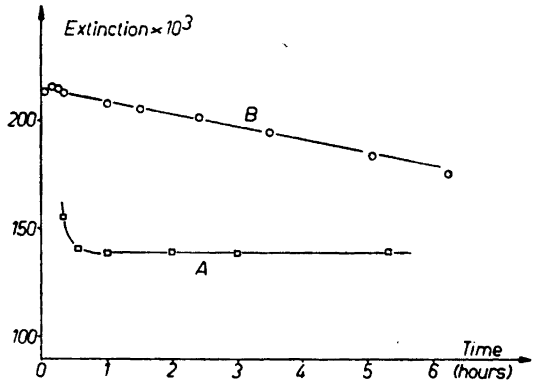

Fig. 3. Extinction-time dependence for solutions treated according to new procedure (curve A) and for solutions which have not been heated.

3.2. Extinction-time dependence

A number of solutions were prepared and put on the water-bath. They were 0.144 × 10^{-3} M in Si, 0.05 M in Na_2MoO_4 and had a pH value of 1.5, adjusted with perchloric acid. From time to time a bottle was withdrawn from the waterbath, its contents prepared according to the directions and the extinction measured. The result is shown in Fig. 3, curve A; curve B represents an identical solution which has not been heated.

The time within which a constant extinction value is obtained is subject to some variations in practice; three hours are usually enough, but solutions containing, *e.g.*, large amounts of silica seem to require a longer heating time, especially if the pH is low.

3.3. Dependence on pH and salt concentration

The solutions were the same as in 3.2, with the exception, that they contained different amounts of perchloric acid or in a few cases sulfuric acid.

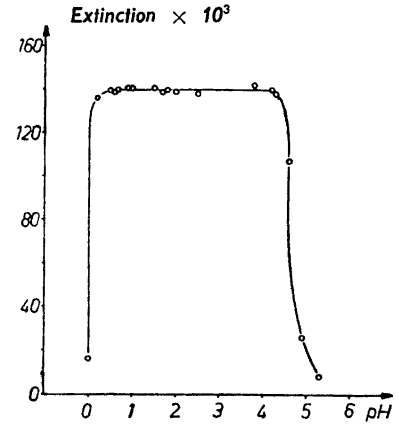

Fig. 4. Extinction as a function of pH.

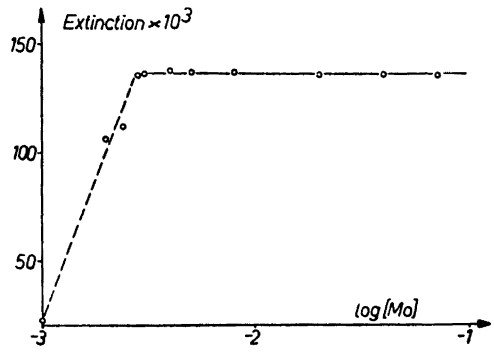

Fig. 5. Influence of the molybdate concentration.

Included in this series of measurements are also some, which have been made on solutions containing up to 0.2 moles of Na_2SO_4 per litre of final solution.

The optical density as a function of pH is plotted in Fig. 4; the horizontal line represents the mean calculated from 16 experiments. From these a maximal deviation of 1.3 % and a standard deviation of a single measurement of 0.8 % is calculated. (pH for these measurements was confined to the interval $0.5 \leqq \text{pH} \leqq 4.3$; the pH values below 1.0 are not very accurate and may well be in error with some tenths of a pH unit.)

3.4. Influence of the molybdate concentration

When treated on the steambath the solutions had the following compositions: 0.144×10^{-3} M in Si, pH in general 2.0 (in a few cases 1.5 and 3.5) adjusted with perchloric or sulfuric acid, the molybdate concentration being variable.

In Fig. 5 is given the extinction as a function of $^{10}\log[\text{Mo}]$. The minimum amount of molybdate required for a full development of the yellow colour is greater than would be calculated for a ratio [Mo] : [Si] = 12, obtained in the crystallized α-silicomolybdate both analytically [2] and from X-ray work [12].

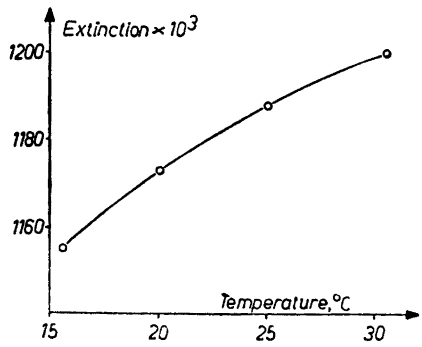

Fig. 6. Extinction as a function of temperature of the solution being measured.

Table 1. Applicability of Beers law to solutions of α-silicomolybdic acid. $k = E/c$; k = extinction coefficient, E = extinction for 1 cm cuvette length, c = molarity of Si.

Number of experiments	$c \times 10^3$	E, mean	$k \times 10^{-3}$		
			mean	max.dev. from the mean, %	Stand.dev. of a single measurement, %
5	1.200	1.461	1.218	0.6	0.4
5	0.900	1.096	1.218	0.5	0.3
5	0.600	0.733	1.222	0.5	0.2
4	0.300	0.366	1.220	0.6	0.5
2	0.120	0.146	1.22		
2	0.060	0.074	1.23		

When solutions which are about 0.2 M in Na_2MoO_4 or higher are heated on a steambath for several hours a white precipitate is often obtained, especially if the polythene bottle used has earlier contained such a precipitate. Solutions which were very concentrated in Na_2MoO_4 and have precipitated large amounts of such a solid phase, have in some cases shown extinction values slightly (about 1—2 %) lower than calculated. However, it has been found perfectly safe to use solutions which when heated are 0.05—0.1 M in Na_2MoO_4 and which may contain so much silica that the resulting extinction is about 1.5, provided no other heteropoly forming ions such as PO_4^{3-}, AsO_4^{3-}, Fe^{3+} and Al^{3+} are present. It might be added that precipitates of the above mentioned type are not easily formed in solutions containing large amounts of sulphate ions.

3.5. Influence of the temperature on the extinction

The solutions used had the following composition when heated on the waterbath: 1.25×10^{-3} M in Si, 0.05 M in Na_2MoO_4, pH = 1.5 with perchloric acid. After complete conversion to α-silicomolybdate the solutions were cooled to 20.0°C and made up to volume with water of the same temperature. Blanks were also prepared quite similarly.

In Fig. 6 the extinction is plotted as a function of the temperature of the solution being measured. No correction for volume changes has been applied. The temperature coefficient is not a constant but a function of temperature; at 20°C the extinction is seen to vary about 0.2—0.3 % per degree C. It may be that with other compositions of the solutions another extinction-temperature dependence can be obtained.

3.6. Applicability of Beers law

The measurements were carried out in the usual manner, great care being taken to ensure that the heating time on the waterbath was long enough.

The results of the measurements are summarized in Table 1. Extinctions for final silica concentrations equal to or greater than 0.3×10^{-3} M have

been measured on solutions subject to slight variations in pH (1.5 and 2.0) and in molybdate concentration (final solutions 0.04 and 0.08 M in Na_2MoO_4); in a few cases Na_2SO_4 was added so that the final solutions were 0.2 M in Na_2SO_4.

I wish to thank Dr. F. Nydahl, Head of the Department of Analytical Chemistry for his interest in this investigation and for the facilities put at my disposal.

REFERENCES

1. Jolles, H. and Neurath, F. *Z. angew. Chem.* **11** (1898) 893.
2. Strickland, J. D. H. *J. Am. Chem. Soc.* **74** (1952) 862, 868, 872.
3. Stoll, K. *Mitt. Naturw. Ver. Vorpomm. in Greifswald* **63** (1936) 1.
4. Lacroix, S. and Labalade, M. *Anal. Chim. Acta* **3** (1949) 383.
5. Mellon, M. G. *Symposium on Structure and Properties of Heteropoly anions*, Am. Chem. Soc., Atlantic City 1956, p. 35.
6. Mullin, J. B. and Riley, J. P. *Anal. Chim. Acta* **12** (1955) 162.
7. Arnfelt, H., Freyschuss, S. and Rönnholm, B. *Jernkontorets ann.* **135** (1951) 75.
8. Lindqvist, I. *Nova Acta Regiae Soc. Sci. Upsaliensis* (4) **15** (1954) No. 1.
9. Chow, D. T. and Robinson, R. J. *Anal. Chem.* **25** (1953) 646.
10. Haupt, G. W. *J. Research Natl. Bur. Standards* **48** (1952) 414.
11. Carpéni, G. *Bull. soc. chim. France* [5] **14** (1947) 484.
12. Keggin, J. F. *Proc. Roy. Soc. A* **144** (1934) 75.

Received December 14, 1957.

ACTA CHEMICA SCANDINAVICA 12 (1958) 503—510

A Peptide Material from Myosin Containing Sulfhydryl Groups

OLLE SNELLMAN

Institute of Biochemistry, University of Uppsala, Uppsala, Sweden

It has been shown that a peptide material is easily split off from myosin when firmly bound bivalent metal ions are removed. The reaction is accompanied by the appearance of a high ultra-violet absorption.

From oxidized myosin the same peptide material has been isolated as two peptides differing only in aspartic acid occurring as N-terminal group in one of them. The sequence in the peptide containing aspartic acid is Asp.CySH.Tyr.Arg.Lys.Val.Gly.Glu. Several pieces of evidence suggest that the peptide material might be part of the ATPase-active centers of the myosin.

In our investigations on myosin, we have observed, that treatments removing all calcium ions from protein cause the stability to be lost. A peptide material is gradually split off and at the same time a strong ultra-violet absorption appears. The latter has generally a maximum between 260—270 mμ but can change with treatments and also with time so that alterations can occur from one day to another. In a large number of different treatments, a release of a peptide material has been observed. This occurs, for example, after such mild treatments as an extensive washing of the rabbit myosin with 0.025 M KCl, or at mere precipitation by dilution of heart myosin. In those cases the ATPase activity will gradually be lost as the peptide material is given off.

It has also been possible [1] to divide myosin into two fractions by treatment with ammonium sulphate at 20°C. One of the fractions is stable and soluble in salt solutions only. This fraction has no phosphatase activity. When the fraction is denaturated by heat, only minute amounts of peptide material will be given off. The other fraction, which is soluble in water, is unstable and gradually gives off a strongly ultra-violet-absorbing material. It does not show any phosphatase activity. In properly designed experiments the fraction can be stabilised by calcium or magnesium hydroxide but not by potassium or sodium hydroxide [2]. This stabilisation must be achieved before the peptide

material is split off. If this is done, the fraction gives an ultra-violet spectrum in which tyrosine and tryptophan are visible, and the phosphatase activity appears again.

In denaturation by heat, certain amounts of the peptide material are given off from this fraction associated with a strong ultra-violet absorption. A peptide material can be isolated which contains the following amino acids: Asp, CySH, Tyr, Arg, Lys, Val, Gly, Glu, and has aspartic acid as its N-terminal group.

On account of certain difficulties in the preparation of the peptide material in a well defined state, other ways, to be reported here, have been tried for this isolation.

MATERIAL AND METHODS

In all experiments myosin from rabbit skeletal muscle was used and prepared according to Mommaerts and Parrish [3]. The myosin obtained was freeze-dried.

Zone electrophoresis was performed in a column according to Porath [4] with stabilizing powder according to Flodin and Kupke [5]. As buffer 0.05 M triethylamine-carbonic acid buffer at pH 7.5 or 0.05 M pyridinium acetate-acetic acid buffer at pH 3.6 was used. The eluate after the electrophoresis was taken up with a fraction collector, generally in 10 ml portions. The concentration in the samples was determined either at 270 mμ in a Beckmann D.U. spectrophotometer or with the ninhydrin reagent according to Moore and Stein [6].

One dimensional paper-chromatographic determinations were performed on the peptide material using either 70 % ethanol, or phenol buffered with citrate, or butanol:acetic acid:water (5:1:4). The last two systems were also used for the two dimensional determination of the amino acids after hydrolysis of the peptides in 5.8 N HCl at 105° for 24 h.

In the experiments with oxidized myosin an ionic exchanger (kindly supplied by Dr. P. Flodin, Pharmacia Ltd, Uppsala) was used. The resin was a special aliphatic polyamine which has a much higher purity than IR4B and did not interfere with the determinations.

TRYPSIN-DIGESTED MYOSIN

In the first experiments a trypsin digestion was directly tried on the myosin.

The myosin was dissolved in a 0.25 M triethylamine-carbonate buffer of pH 8.4 and digested with trypsin (Merck); 2 mg trypsin was used for 100 mg myosin. The digestion was performed during 2 days at 37°C. Dark bottles were used and the solution was saturated with chloroform. After the digestion the solution was evaporated *in vacuo*. The residue was dissolved in 5 ml 0.05 M triethylamine-carbonate buffer and a zone electrophoresis was made on the solution.

A diagram of such a zone electrophoresis is shown in Fig. 1, giving the ultra-violet absorption of the fractions at 270 mμ. Of the components obtained, the

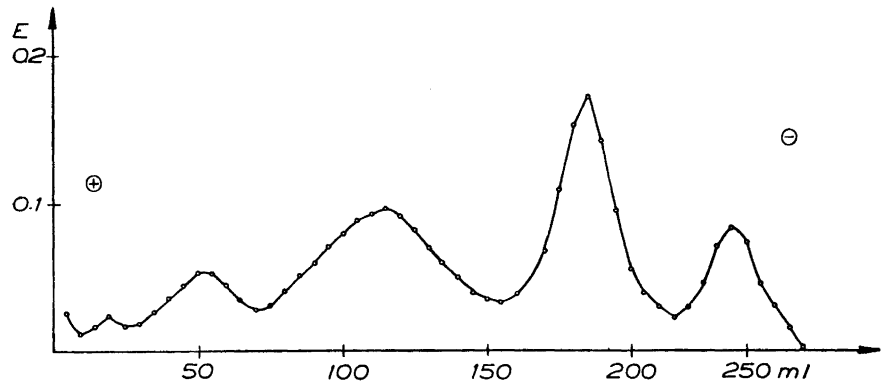

Fig. 1. Electropherogram of trypsin-digested myosin. The run was performed with 40 mA for 11 h in a 3 × 150 cm column in 0.05 M triethylamine carbonate buffer at pH 7.4. Ordinate is the optical density at 270 mμ.

two basic fractions, and sometimes also the neutral one, showed an anomalous ultra-violet absorption (see Fig. 2). The most basic component comprised about 3—4 % of the material and had an ultra-violet absorption at 270 mμ which was about 5—10 times that of any of the other components. In paper-chromatography in different solvents only one spot appeared. The amino acids occurring in this fraction were: CySH, Tyr, Arg, Lys, Val, Gly, Glu.

In the other basic fraction, several components occurred. This fraction comprised 20—25 % of the material while the neutral fraction contained about 50 % of the material.

However, the experiments did not give good reproducibility. In many cases the first component seemed to have disappeared into the second component, and also in the neutral one a strongly ultra-violet absorbing material could occur. In addition other reactions, which partly destroyed the material, appeared several times.

Another preparative method was therefore tried and gave results with a high degree of reproducibility.

PEPTIDES FROM OXIDIZED MYOSIN

The myosin was oxidized according to the method given by Harrington and Schellman [7]. The oxidized myosin was either digested with trypsin as before or treated with 11.6 N HCl at room temperature for 3 days. The solution was dried over sodium hydroxide pellets in a vacuum desiccator. In both cases the same peptide material could be isolated.

The partially broken-down myosin was dissolved in water of pH 4 and put on the ion-exchange column of the polyamine. The greatest part passed through but components containing cysteic acid were adsorbed. The adsorbed

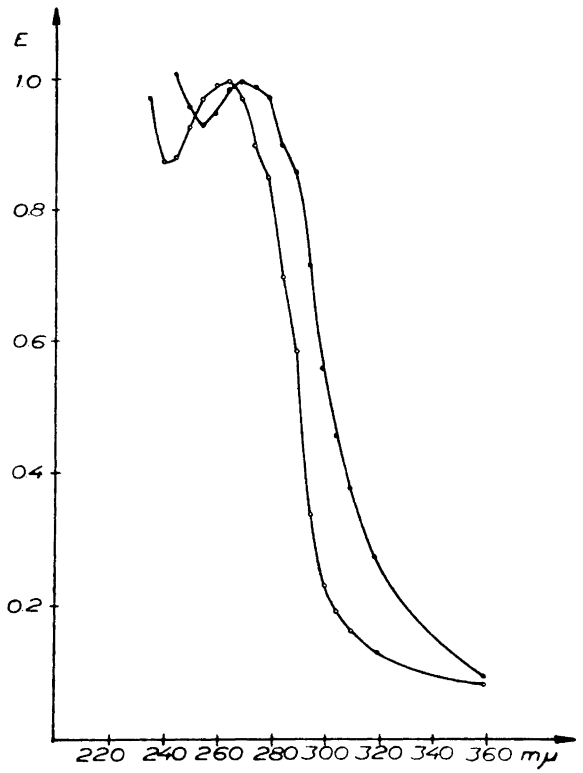

Fig. 2. Ultra-violet absorption spectrum of the most basic component. The extinction at the max. is set equal to 1.

material was eluted with water acidified with formic acid to different pH levels.

Two fractions were obtained, one at pH 2.4 and the other at pH 2.2. The two fractions were of about the same magnitude and comprise together about 8—9 % of the material.

The fraction eluted at pH 2.4 gave in zone electrophoresis one component which moved slowly to the anode. In paper-chromatography only one spot was visible.

The fraction eluted at pH 2.2 gave one component in zone electrophoresis moving a little slower than cysteic acid. In paper-chromatography only one spot was visible.

A qualitative amino acid analysis showed for the fraction at pH 2.4 the following amino acids: $CySO_3H$, Tyr, Arg, Lys, Val, Gly, Glu, and for the fraction at pH 2.2 the same amino acids and aspartic acid.

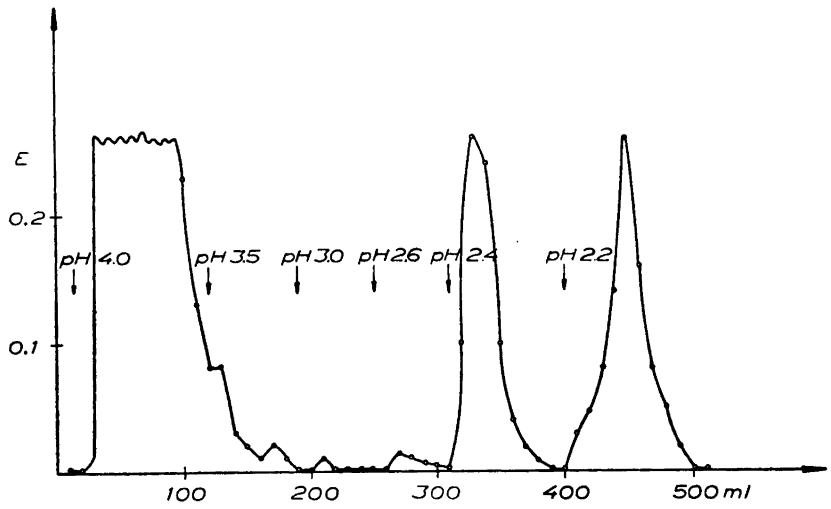

Fig. 3. Elution diagram of oxidized myosin treated with 11.6 N HCl on the polyamine column. The ordinate is the optical density as obtained with the ninhydrin reaction.

As N-terminal groups, determined according to Sanger[8], the component at pH 2.4 gave cysteic acid and the one at pH 2.2 aspartic acid. With carboxypeptidase Gly.Glu appeared in the C-terminal end in both cases.

The peptide obtained at pH 2.2 was digested with a small amount of pepsin at pH 2 for one day. The material was dried *in vacuo* and dissolved in water at pH 4 and then fractionated on the polyamine resin.

Three different main fractions were obtained. One fraction (I) that passed through; a second fraction (II) was eluted at pH 2.4, and a third one (III) in the interval pH 2.2—1.9.

The following amino acids were found in the different fractions.
Fraction I: Tyr, Arg, Lys, Val, Gly, Glu and free Asp
Fraction II: $CySO_3H$, Tyr, Arg, Lys, Val, Gly, Glu
Fraction III: Asp, $CySO_3H$, Tyr, Arg, Lys.

From these observations the sequence Asp.$CySO_3H$ (Tyr, Arg, Lys) Val. Gly.Glu can be deduced.

By zone electrophoresis of fraction III, the following peptides could be isolated

Asp.$CySO_3H$.Tyr.Arg; $CySO_3H$.Tyr.Arg; Asp.CySO/H.Tyr.Arg.Lys.

And from fraction I

Arg.Lys; Tyr.Arg.Lys.Val.Gly; Lys.Val.Gly.Glu; Gly.Glu.

The sequence then ought to be

Asp.$CySO_3H$.Tyr.Arg.Lys.Val.Gly.Glu.

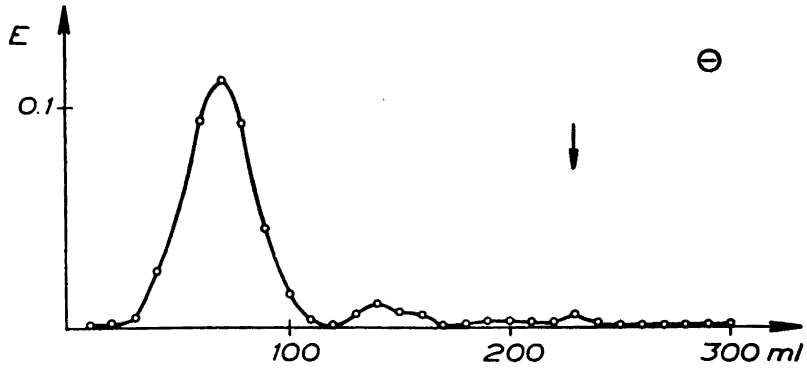

Fig. 4. Electropherogram of the component obtained at pH 2.2 from the polyamine in 0.05 M pyridinium acetate. The ordinate is the optical density as obtained with the ninhydrin reaction.

DISCUSSION

The peptide material so easily split off from myosin when firmly bound calcium is removed consists of two peptides which seem to differ only in one amino acid (aspartic acid) occurring in a N-terminal position in one of the two peptides. Several features indicate that the peptide material ought to belong to the active center of myosin which gives the ATPase activity.

The indirect evidence which support this hypothesis is:

1) Of the two fractions obtained from myosin by treatment with ammonium sulphate at 20°, only the one in which the phosphatase activity can be restored will give off substantial amounts of the peptide material on heat denaturation.

2) Obviously the peptide material is intimately connected with firmly bound calcium and the splitting off of the peptide material occurs only when the calcium is removed. Gelotte [9] has observed that the disappearance of calcium and the appearance of a strong ultra-violet absorption run parallel. The strong ultra-violet absorption is associated with the peptide. Friess [10] and Kielley and Bradley [11] conclude from their investigations on the phosphatase activity in the presence of chelating agents that a bivalent metal ion occurs in the active center. Kielley and Bradley say: "The characteristic properties of EDTA further suggest that the unidentified groups interacting with the SH group is a metal."

3) Singer and Barron [12] demonstrated the inactivation of the ATPase activity by sulfhydryl reagents. Later Kielley and Bradley [11] have studied the inactivation of the SH groups more thoroughly. From their investigation they postulate that at least two SH groups occur in the active center. We have not found any peptide with two SH groups and there does not seem to occur any other SH peptides than those two observed by us. It may therefore be that at least two such peptides occur in one active center.

According to Kielley and Bradley one of the SH groups ought to be active and the other inactive. It is very difficult to say, if there is any real difference between the two peptides obtained in regard to their state in myosin since there is not sufficient information about the mechanism for splitting off the peptides. Some slight indications exist that the difference in aspartic acid content might be real. The two peptides are obtained in the same amounts from myosin and, in an unfinished investigation about the sulfhydryl peptides in L- and H-meromyosin, mostly the peptide without aspartic acid has been found in the phosphatase-inactive L-meromyosin. The question is, however, as yet not settled.

4) Also the tyrosine group might function in the hydrolysis of ATP. Ravikowitch, Syetkina and Lyontyvea [13] have found alterations in the ultraviolet spectrum when actomyosin reacts with ATP. The absorption peak at 277 mμ in actomyosin moves and disappears into the adenine peak. This alteration was only seen in enzymatically active actomyosin, and ADP and AMP did not show this effect. The authors postulate that tyrosine and/or tryptophan takes part in the reaction. Taver and Morales [14] have also observed a similar effect.

5) Laidler and Ethier [15] have interpreted their results on the kinetics of the ATPase activity as indicating a neutralization of charge when the enzyme-substrate complex is formed and a separation of charges when the breakdown occurs. If the two basic groups of the peptide are considered to bind phosphate groups of ATP, this also fits well with the amino acid sequence of the peptide.

Thus there are several indirect pieces of evidence suggesting that the peptides belong to the ATPase-active center.

If that is so, *i. e.* the peptides are parts of the active center, they must be so situated on the myosin that at least one of the two peptides is freely exposed and can form a complex with the substrate in which most of the amino acids residues in the peptide ought to take part. For the activity the bivalent metal ion bound to the peptide is also necessary.

The fact that the treatment with ammonium sulfate can give two different and defined fractions of the myosin might indicate that the active centers, to a large extent, are located near the places where the two parts are connected. In fact, in the water soluble and calcium-hydroxide treated part aspartic acid and cysteine appears as N-terminal groups. However, further studies are necessary to confirm this tentative conclusion.

Acknowledgements. The investigations have been financially supported by grants from the *Swedish Natural Science Research Council* and from *Eli Lilly and Company*, Indianapolis, U.S.A.

REFERENCES

1. Snellman, O. *Biochim. et Biophys. Acta* **21** (1956) 142.
2. Snellman, O. *Acta Chem. Scand.* **10** (1956) 151.
3. Mommaerts, W. F. H. M. and Passish, R. G. *J. Biol. Chem.* **188** (1951) 545.
4. Porath, J. *Acta Chem. Scand.* **8** (1954) 1813.
5. Flodin, P. and Kupke, D. W. *Biochim. et Biophys. Acta* **21** (1956) 368.
6. Moore, S. and Stein, W. H. *J. Biol. Chem.* **211** (1954) 907.

7. Harrington, W. F. and Schellman, J. A. *Compt. Rend. Trav. lab. Carlsberg* **30** (1956) 21.
8. Sanger, F. *Biochem. J.* **39** (1945) 507.
9. Gelotte, B. *Activin, a low molecular-weight substance in the contractile element of muscle* (Thesis), Almqvist and Wiksell, Uppsala 1954.
10. Friess, E. T. *Arch. Biochem. Biophys.* **51** (1954) 18.
11. Kielly, W. W. and Bradley, L. *J. Biol. Chem.* **218** (1956) 653.
12. Singer, T. P. and Barron, E. S. G. *Proc. Soc. Exptl. Biol. Med.* **56** (1944) 120.
13. Ravikowitch, K. M., Syetkina, O. N. and Lyontyeva, K. D. *Doklady Akad. Nauk. SSSR* **40** (1948) 989.
14. Tarver, E. and Morales, M. F. *J. Gen. Physiol.* **37** (1951) 235.
15. Laidler, K. J. and Ethier, M. C. *Arch. Biochem. Biophys.* **44** (1953) 338.

Received December 18, 1957.

ACTA CHEMICA SCANDINAVICA 12 (1958) 511—516

Synthesis of some Model Compounds for Thiolignin

CAMILLA JUSLÉN and TERJE ENKVIST

Chemical Institute of the University of Helsingfors, Finland

A series of model compounds for thiolignin was synthesized. Vanillyl alcohol and thiophenol were found to form vanillyl phenyl sulfide by elimination of water even at room temperature on irradiation with sunlight, or alternatively on moderate heating in the presence of aluminium sulfate or hydrogen ions. Similar reactions were carried out with other substances, including *iso*eugenol and thiophenol, and cinnamyl alcohol and *p*-thiocresol or thioglycolic acid. As a side reaction there also occurred addition of the mercaptan to the ethylenic bond. The ethylenic bond in cinnamyl cresyl sulfide reacted very slowly with soda-alkaline permanganate solution.

The present work is a continuation of our studies on cinnamyl phenyl sulfide as a model substance for thiolignin [1]. Table 1 gives a survey of the syntheses carried out.

Table 1. Syntheses of thiolignin models.

Reagents	Method [a]	time	Reaction product	Yield mole %
Cinnamyl alcohol(I) + *p*-thiocresol(II)	Pressure heating with aluminium sulfate (1)	17.5 h	Cinnamyl-*p*-cresyl-sulfide(III)+IV or V	29
Vanillyl alcohol(VI) + thiophenol(VII)	Photosynthesis (2a)	270 days	Vanillyl phenyl sulfide(VIII [d])	91
—»—	Pressure heating with aluminium sulfate [1] (2b) [b,e]	17 h	—»—	36
I + thioglycolic acid(IX)	Pressure heating with aluminium sulfate (3a) [b]	17 h	S-cinnamylthioglycolic acid(X)	45—51
—»—	Boiling in C_6H_6 with piperidine as catalyst (3b)	36 h	X + XI or XII	15
*Iso*eugenol(XIII) + VII	Pressure heating (4a) [b]	18.3 h	XIV and XV	79
XVI [c] + VII	Pressure heating with aluminium sulfate(4b) [b]	17 h	XIV	59

[a] The numbers in parentheses signify paragraphs in the experim.part. [b] In a sealed glass tube. [c] Kindly supplied by Prof. E. Adler. [d] Is soluble in alkali. The phenyl carbamic acid ester was prepared. [e] Boiling of vanillyl alcohol and thiophenol with HCl as catalyst yielded an amorphous mass containing only 3.5 % S, and molecular weights in 2 chromatographic fractions of 323 and 1069, respectively.

III. $(p)CH_3.C_6H_4.S.CH_2.CH{:}CH.C_6H_5$
IV. $C_6H_5.CH(CH_2.CH_2OH).S.C_6H_4.CH_3(p)$; γ-(*p*-methyl-thiophenoxy)-γ-phenyl-propanol
V. $C_6H_5.CH_2.CH(CH_2OH).S.C_6H_4.CH_3(p)$; β-(*p*-methyl-thiophenoxy)-γ-phenyl-propanol
VIII. $R.CH_2.S.C_6H_5$
X. $C_6H_5.CH{:}CH.CH_2.S.CH_2.COOH$
XI $C_6H_5.CH(CH_2.CH_2OH).S.CH_2.COOH$; S-($\alpha$-phenyl-$\gamma$-hydroxy-propyl)-thioglycolic acid
XII $C_6H_5.CH_2.CH(CH_2OH).S.CH_2.COOH$; S-($\beta$-phenyl-$\beta$'-hydroxy-*iso*propyl)-thioglycolic acid
XIV. $R.CH(S.C_6H_5).CH_2.CH_3$; 1-thiophenoxy-1-(3-methoxy-4-hydroxy-phenyl)-propane
XV. $R.CH_2.CH(S.C_6H_5).CH_3$; 2-thiophenoxy-1-(3-methoxy-4-hydroxy-phenyl)-propane
XVI. $R.CHOH.C_2H_5$; α-(3-methoxy-4-hydroxy-phenyl)-propanol

R in VIII and XIV—XVI = 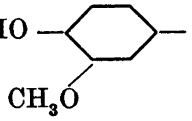

Perhaps the most interesting observation made was the readiness with which vanillyl phenyl sulfide (VIII) was formed in 91 % yield by elimination of water from vanillyl alcohol and thiophenol, even at room temperature, by photosynthesis.

Attempts to add thioglycolic acid to the double bond of S-cinnamyl thioglycolic acid in acetone solution with piperidine as catalyst failed.

Of the pure crystalline substances synthesized III and VIII are, as far as we know, new ones. Of the liquid reaction products, which are possibly mixtures of isomers, IV, V, XI, XII, XIV and XV have also not been reported hitherto. X has been synthesized by Holmberg[2] but by another method than that employed by us. It can be mentioned in this connection that Freudenberg recently has prepared S-vanillyl thioglycolic acid from vanillyl alcohol and thioglycolic acid using boron fluoride as catalyst[3].

Ultraviolet and infrared spectra. The absorption spectrum in ultraviolet of cinnamyl-*p*-cresylsulfide (Fig. 1) shows a single maximum at about 255 mμ, very similar to that of cinnamyl phenyl sulfide[1], S-cinnamylthioglycolic acid (Fig. 2, H, D), allyl phenyl sulfide and cinnamyl disulfide[1], but distinctly different from that of vanillyl phenyl sulfide (Fig. 2, V), 2-methyl thiocoumarane[1] and the addition products of *iso*eugenol and thiophenol (Fig. 3). The addition product (XI or XII) of cinnamyl alcohol and thioglycolic acid shows an UV spectrum (Fig. 4) clearly differing from that of S-cinnamyl thioglycolic acid (Fig. 2). The IR spectrum (Fig. 5) lacks the absorption band of the ethylenic bond at 960 cm.$^{-1}$ The band at 1 710 cm^{-1} is very probably due to the valuence oscillations of the C:O group of the carboxyl grouping. The valence oscillations of the alcoholic hydroxyl group should occur between 2.6 and 3.0 μ. For instance, the addition product of cinnamyl alcohol and thiophenol[1]

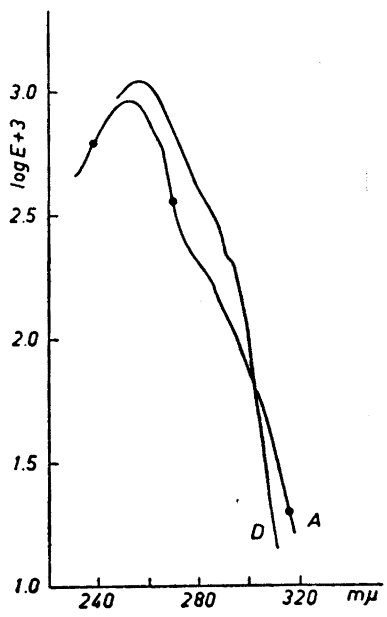

Fig. 1. UV spectrum of cinnamyl-*p*-cresyl sulfide. D = in dioxan. A = in 0.5 N alcoholic sodium hydroxide solution.

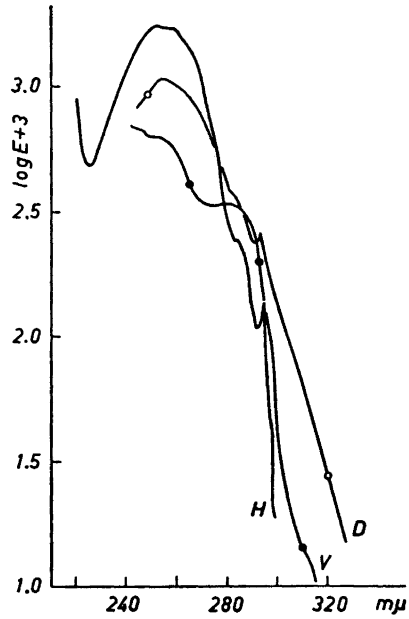

Fig. 2. UV spectrum of vanillyl phenyl sulfide and of S-cinnamyl thioglycolic acid. V = vanillyl phenyl sulfide in dioxan. H = S-cinnamyl thioglycolic acid in hexane, D = the same in dioxan.

absorbs at 2.9 μ. In Fig. 5 this bond is very broad, indicating association or hydrogen bonding [4].

Reactions of the ethylenic bonds. Cinnamyl *p*-cresyl sulfide, like cinnamyl phenyl sulfide [1], decolorized soda-alkaline permanganate solution at room temperature only very slowly, after hours of standing. In contrast, S-cinnamyl thioglycolic acid (X), as well as XI and XII, immediately decolorize the reagent. With tetranitromethane cinnamyl-*p*-cresyl sulfide gave a golden yellow color, whereas the compound XIV gave a red color.

EXPERIMENTAL

1. Cinnamyl-p-cresyl sulfide. The synthesis was almost completely analogous to the synthesis of cinnamyl phenyl sulfide [1], 0.990 g of aluminium oxide being used, however, for 0.044 mole of cinnamyl alcohol and 0.043 mole of *p*-thiocresol. The sulfide obtained was recrystallized from 99 % ethanol, yield 3.001 g, m. p. 67—68°C. (Found: C 80.20; H 7.01; S 13.14. Calc. for $C_{16}H_{16}S$: C 79.95; H 6.71; S 13.34). UV spectrum Fig. 1. From the mother liquors a main fraction was isolated by chromatography in about the same way as in the synthesis of cinnamyl phenyl sulfide [1]. (Found: S 12.09. Calc. for $C_{16}H_{18}SO$: S 12.41).

2. *Vanillyl phenyl sulfide.* a) *Photosynthesis.* Vanillyl alcohol was prepared by catalytic hydrogenation of vanillin according to Ref.[5] Yield 72 mole %.

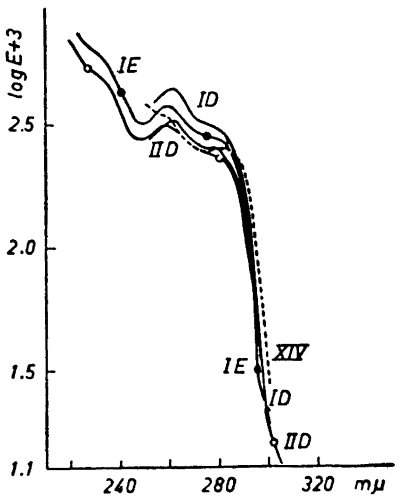

Fig. 3. UV spectrum of addition product (XIV or XV) of *iso*eugenol and thiophenol (4a). I D = first chromatographic fraction in dioxan, I E = the same in ethanol. II D = second chromatographic fraction in dioxan, II E = the same in ethanol. XIV = XIV in dioxan.

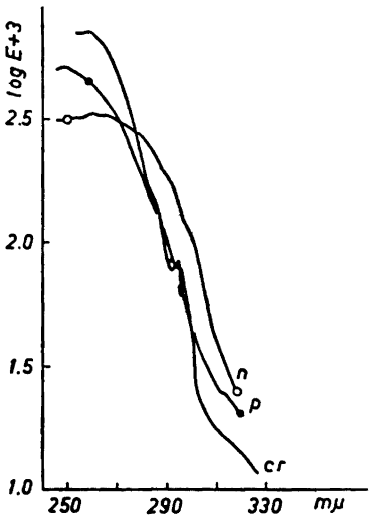

Fig. 4. UV spectra of addition products XI and XII of cinnamyl alcohol and thioglycolic acid. cr = crude, p = chromatographically purified acids. n = neutral product from 3 b.

1.54 g (0.010 mole) vanillyl alcohol and 1.100 g (0.010 mole) thiophenol were mixed in a glass test tube sealed with a rubber stopper. The tube was allowed to stand in a sunny window from December to the end of August. The reaction product was recrystallized from 99 % ethanol. Yield 2.239 g with m.p. 87—90.5°. Part of the material was chromatographed on aluminium oxide (Brockmann) previously washed with 2 N hydrochloric acid and with water, and dried 24 h at 150°, in about the same way as in the synthesis of cinnamyl phenyl sulfide [1], benzene being used instead of carbon tetrachloride, however. The sulfide thus purified melted at 91.5—92°. (Found: C 68.23; H 5.76; S 12.92; mol.weight (Beckmann, cryosc.) 239. Calc. for $C_{14}H_{14}SO_2$: C 68.26; H 5.73; S 13.02; mol.weight 246). UV spectrum Fig. 2, V.

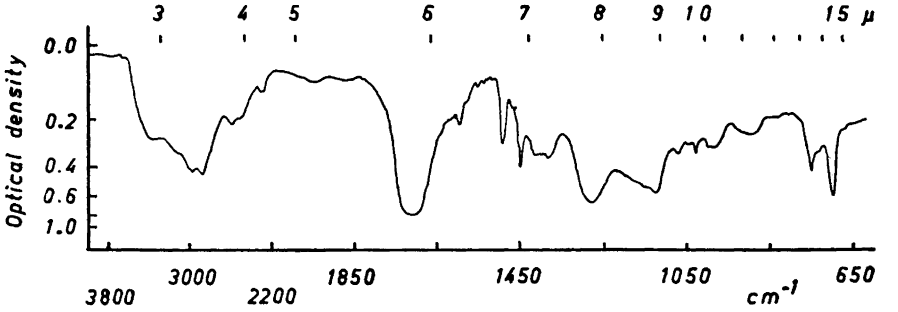

Fig. 5. IR spectrum of addition product of cinnamyl alcohol and thioglycolic acid (3 b).

120.1 mg of vanillyl phenyl sulfide were heated 5 h at 140—145° with 60.1 mg of phenyl *iso*cyanate, moisture being excluded by means of a calcium chloride tube. The phenyl carbamic acid ester formed was recrystallized three times from hot ligroin and then once more from carbon tetrachloride containing 10 % of petrol ether. Yield 86 mg; m. p. 137—138°. (Found: C 68.95; H 5.48; N 3.66; S 8.69. Calc. for $C_{21}H_{19}NSO_3$: C 69.02; H 5.24; N 3.83; S 8.77).

b) *With aluminium sulfate.* The synthesis was analogous to that used in Ref.[1], using 5.932 g of vanillyl alcohol, 4.298 g of thiophenol and 0.350 g of aluminium sulfate. The reaction product was dissolved in ether, washed three times with a sodium hydrogen carbonate solution, which dissolves the bulk of the thiophenol, and finally with water. The isolated neutral substance was recrystallized first from ligroin containing 5 % of chloroform and then from 50 % alcohol. Yield 3.406 g, m. p. 89—91°. 100 mg of the substance was chromatographed on aluminium oxide treated with hydrochloric acid, after which it showed a m. p. of 91.5—92°.

3. *S-Cinnamyl thioglycolic acid.* a) With aluminium sulfate. 3.807 g (0.0413 mole) of thioglycolic acid and 5.545 g (0.0413 mole) of cinnamyl alcohol were heated with 0.343 g anh. aluminium sulfate 17 h at 127°. The reaction product was dissolved in benzene and extracted from the benzene by repeated shaking with 2 N sodium hydroxide. The alkaline layer was acidified with 2 N sulfuric acid and extracted five times with benzene. The final benzene solution was washed with water, dried and evaporated at room temperature. The residue was dried in vacuum over phosphorus pentoxide. The yield varied in the various experiments between 45—51 mole % calculated as S-cinnamyl thioglycolic acid. By recrystallization from ligroin containing 5 % chloroform a crystalline substance with m. p. 78—79° was isolated. UV spectrum Fig. 2. (Found: C 63.46; H 5.88; S 15.35. Calc. for $C_{11}H_{12}SO_2$: C 63.43; H 5.81; S 15.40).

b) With piperidine catalyst, substances XI and XII. 2.530 g (0.0275 mole) of thioglycolic acid, 3.2210 g (0.24 mole) of cinnamyl alcohol and 0.2 ml of piperidine were dissolved in 10 ml of benzene and refluxed 36 h. The acidic reaction products were separated from the neutral ones as described under 3 a. Yield 1.593 g of yellow oil giving a positive Baeyer test, S 14.53 %, UV spectrum Fig. 4, cr. Paper chromatography was carried out on Whatman paper No. 1 with toluene-methanol-water (10:5:5), developing with 0.1 N silver nitrate solution and heating[6] 15 min at 110°, with 0.5 N permanganate solution in the dark, or with starch solution and iodine-azide solution according to Feigl[7]. Three spots corresponding to R_F 0.92, 0.88 and 0.00 were found. Of these R_F 0.92 was found by a parallel run to correspond to cinnamyl thioglycolic acid.

On chromatography on a Whatman cellulose column (32 × 2.5 cm) washed with 350 ml of the toluene-methanol-water-mixture described, 0.288 g of the substance was applied, dissolved in 4 ml chloroform, and the chromatogram was developed with the solvent mixture. The substance separated into one fraction which could be eluted with the toluene mixture, and another, which was eluted with ether-ethanol 1:1. The first fraction was a partially crystallized oil, from which S-cinnamyl thioglycolic acid with m.p. 74—76° (undepressed on admixture of acid from synthesis 3 a) could be prepared through crystallization from ligroin. The second fraction was a yellow oil, which was dried 3 days in vacuum over P_2O_5; yield 0.148 g, UV spectrum Fig. 4 p. R_F-value 0.00 with the toluene mixture. (Found: C 57.50; H 5.59; S 13.67; mol.weight (Childs) 294. Calc. for $C_{11}H_{14}SO_3$: C 58.38; H 6.24; S 14.17; mol.weight 226). IR spectrum Fig. 5. The product gave a S-benzyl thiuronium salt with m. p. 150—152°.

A sample of the neutral product was purified by chromatography on aluminium oxide in benzene solution and elution with benzene containing increasing amounts (5—50 %) of ethanol. S 9.65 %. UV spectrum Fig. 4, n.

4. *Synthesis of XIV and XV.* a) From *iso*eugenol. 4.785 g (0.0291 mole) of thiophenol were heated in a sealed glass tube 18.3 h at 127°. The yield of reaction products soluble in 2 N sodium hydroxide was 6.623 g. 4.025 g were dissolved in 15 ml of carbon tetrachloride and separated into two fractions by chromatography on 21.7 g of aluminium oxide treated with hydrochloric acid by elution with carbon tetrachloride containing 0.10 and finally 25 % ethanol. Both fractions gave a red colour with tetranitromethan. The first fraction, a light yellow oil, was obtained mainly with pure carbon tetrachloride. Yield 2.008 g, UV spectrum Fig. 3, ID and IE. (Found: C 69.56; H 6.86; S 11.52; mol.weight (Beckmann, cryosc.) 265. Calc. for $C_{16}H_{18}SO_2$: C 70.04; H 6.61; S 11.69; mol.weight 274).

Acetylation according to Ref.[1] (synthesis 1 a): reaction product a yellow oil. (Found: CH_3CO 13.23 %. Calc. for $C_{16}H_{17}SO_2 \cdot COCH_3$: CH_3CO 13.60). Phenyl carbamic ester was prepared by heating 85 mg of the fraction with a 20 mole % excess of phenyl *iso*-cyanate. The excess of reagent was removed by digestion with ligroin. The liquid reaction product was dissolved in hot ligroin containing 5 % chloroform and cooled. Only a few mg were obtained of a crystalline product, melting after recrystallization at 95—98°, the greater part remaining liquid.

The second fraction was also a light yellow oil. Yield 1.843 g, UV spectra Fig. 3, II D and II E. (Found: C 69.76; H 6.50; S 11.74; mol.weight 276. Calc. for $C_{16}H_{18}SO_2$: see above!)

The following derivatives were prepared in a manner corresponding to the first fraction: 315.3 mg were acetylated, giving a light yellow oil. (Found: CH_3CO 13.11.) Phenyl carbamic ester, m. p. 94—96°, undepressed on admixture of the corresponding derivative from the first fraction.

b) From XVI. 0.605 g (0.0033 mole) of α-(3-methoxy-4-hydroxy-phenyl)- propanol (XVI), 1.795 g thiophenol and some anhydrous aluminium sulfate were heated 17 h at 127° in a sealed glass tube. A liquid reaction product, obviously 1-thiophenoxy-1-(3-methoxy-4-hydroxy-phenyl)-propane (XIII) was isolated chromatographically as described under 4 a. Yield 0.539 g; UV spectrum Fig. 3, XIV. (Found: S 11.43. Calc. for $C_{16}H_{18}SO_2$: S 11.69.)

REFERENCES

1. Juslén, C. and Enkvist, T. *Acta Chem. Scand.* **12** (1958) 287.
2. Holmberg, B. *J. prakt. Chem.* [2] **141** (1934) 93.
3. Freudenberg, K. *Angew. Chem.* **68** (1956) 508.
4. Brügel, W. *Einführung in die Ultrarotspektroskopie*, Darmstadt **1954**, p. 277.
5. Carothers, W. H. and Adams, R. J. *J. Am. Chem. Soc.* **46** (1929) 1675.
6. Löffler, J. E. and Reichl, E. R. *Mikrochim. Acta* **41** (1953) 79.
7. Chargaff, E. *J. Biol. Chem.* **175** (1948) 67.

Received November 26, 1957.

ACTA CHEMICA SCANDINAVICA 12 (1958) 517—527

Some Aspects of the Nutrition of *Lactobacillus fermenti* 36 in the Tube Assay of Thiamine

Z. G. BÁNHIDI

The Wenner-Gren Institute for Experimental Biology, University of Stockholm, Sweden

Reinvestigating the nutritional requirement of *L. fermenti* 36 on different media, it was found that:

a. the alkali treated peptone is a dispensable supplement if the basal medium is completed with tryptophane, since tryptophane was shown to be an essential nutrient for *L. fermenti.*

b. by using weak inoculum, it was found that whole yeast extract and panthetine are both stimulatory for growth of *L. fermenti.*

c. charcoal treated yeast extract appeared to be inhibitory under similar conditions.

d. the inhibition with the latter and the stimulation with pantethine can be compensated by reducing the medium with cysteine and/or ascorbic acid.

e. with tryptophane and increased level of casein hydrolysate as sources for amino acids, as well as with cysteine and ascorbic acid, a semisynthetic medium can be prepared, which allows good growth and reliable uniform response toward thiamine.

f. the size of the inoculum is a crucial factor in the *L. fermenti* test and should be carefully adjusted turbidimetrically for each run.

The assay of thiamine seems to be still in its developing stage, and it is difficult to find a reliable technique when designing a program of investigation of the occurrence of thiamine and its derivatives in extracts of complex biological materials. Chemical methods can hardly be considered for such a task except for analysis of relatively pure solutions of this vitamin. While many different microbiological methods have been described for the analysis of the total vitamin B_1 content of food stuffs and other natural products, *Lactobacillus fermenti 36* was favored in most of the procedures [1-8] and this organism is still considered as a potential tool with the least failure when thiamine is analyzed [9]. Nevertheless, owing to inconsistencies in the results, several nutritional trials were performed in different laboratories in order to minimize the anomalies in the behavior of *Lactobacillus fermenti* 36 in the thiamine test [3, 7, 10, 8]. In every work referred to, the original basal medium of Sarett and Cheldelin [1] was accepted as a nutritional basis for *L. fermenti.* This medium is already supplemented with a natural extract *viz.* alkali treated

or photolysed peptone. This complex natural complement obscured the results in the usual nutritional experiments, which are rather informative if performed with pure synthetic (amino acid mixture) or semisynthetic (casein hydrolysate) media.

The present work deals with the establishment of some nutritional requirements of *L. fermenti*, the fulfillment of which renders this organism useful for the tube assay of thiamine in small amounts of tissue and organ extracts on a semisynthetic basal medium.

METHODS

Stock cultures of *Lactobacillus fermenti 36* (ATCC 9833) were kept on Bacto Micro Assay Culture Agar, stored at 6—8°C after growth for 24 h at 35°C. The stock cultures were "renewed" in every four to six weeks by transferring to a fortified litmus-skim milk medium [11]*. Several agar subcultures were prepared from a milk tube after each "renewing", and used for the preparation of inocula or for stock cultures. The fortification of the agar medium with 10 μg per liter thiamine [3,5] was found to be unnecessary in our work, probably because of the more complete composition of the Micro Assay Culture Agar compared with the original yeast extract — dextrose agar, recommended in other methods [1, 12, 13].

Inoculum was prepared by transfer from an agar subculture to Bacto Micro Inoculum Broth fortified with 10 % tomato juice filtrate[6]. After 18 h at 35°C this was found to give abundant growth compared to unsupplemented broth (see Table 1) or that with other different supplements.

The time of incubation for the inoculum was originally set at 24 h by Sarett and Cheldelin [1], but this period was decreased by others [12,5]. In this way the interference of bacteria already adapted to the breakdown products of thiamine could be avoided in the test, since the adaption was stated to occur only when cultures passed the limit of 18 h [1,5].

The cell suspension was washed twice in saline, as usual, and was used for inoculation within one hour. The density of inocula was adjusted turbidimetrically in every experiment and two or three uniformly administered drops of inoculum, respectively, were used for tubes with 7 or 10 ml of final volume. Two main type of inocula were used in our experiments, the "weak inoculum" adjusted to 90 % transmission and the "medium

Table 1. Growth of *Lactobacillus fermenti* 36 on Bacto Micro Inoculum Broth with and without addition of tomato juice filtrate. Turbidimetric readings after 18 h of incubation expressed in per cent of transmission (% T) values representing means of triplicates.

Broth / Blanks	Uncompleted	Reinforced with tomato juice	
		1 % v/v	10 % v/v
Readings against blanks as 100	33	28	13.5
Readings against inoculated uncompleted broth as 100	100	79	37.5

* Bacto Yeast Extract 5 g; Bacto Liver 1.5 g (or Parke-Davis Liver Concentrate 0.5 ml); tomato juice filtrate (canned, unseasoned) 100 ml; glucose 2 g; agar 1 g; Tween 80 1 ml; litmus 1 g dissolved in 10 ml 0.1 N sodium hydroxide and filtered; skim milk to 1 000 ml; pH should be adjusted carefully to 6.4 with 0.1 N hydrochloric acid.

strength inoculum" with 40 % T. Heavier inoculum was found to be unsatisfactory because of high blanks (*cf.* Sarett and Cheldelin [1]).

Techniques. Calibrated pyrex tubes of 18 mm diameter were used for the test with 7 or 10 ml final volume.

Media combined with standard or test solutions were autoclaved for 15 min at 1 atm. overpressure in small autoclaves, where the total time needed for heating and cooling does not exceed 45 min. While only steaming was recommended by Sarett and Cheldelin [1] in their original method, Fitzgerald and Hughes [5] found no destruction of thiamine in assay tubes when autoclaved for 10 min at 10 lb. We found serious loss of thiamine activity if the vitamin was autoclaved in pure solutions or in buffer solutions at pH 6.4—6.6. However, rather good protection could be observed if thiamine was autoclaved together with the basal media, and a comparative test with steril-filtered standards showed no special advantage in the rutine test.

Incubation was made in a water bath at 35°C for 17—18 h except when noted otherwise.

Measurement of cell growth through turbidity was achieved by readings of per cent light transmission at 6 000 Å in a Coleman Universal Spectrophotometer.

Preparations. Bacto-Peptone and Bacto-Yeast Extract were used both in the untreated form as whole extracts or in form of preparations in which the thiamine content was minimized by chemical destruction or absorption, *viz.*:

alkali treated peptone [14],
photolyzed peptone [15,12],
Norit A (charcoal) treated yeast extract [16],
sulphite treated yeast extract [17],

which were prepared according to the original prescriptions quoted.

Basal media of several different compositions were used in this work, as noted below. The composition of a semisynthetic basal medium is given in Table 2. This medium represents the recommended final medium for the thiamine test and the results of our nutritional experiments were considered for its composition. Although incorporation of further supplements was found not to improve the turbidimetric method, in case of an acidimetric semimicro assay, a completed semisynthetic basal medium was used. According to the terminology used in the description of our experiments, the medium presented herewith is a "high amino acid reduced semisynthetic medium".

In the course of the nutritional studies the following main types of media were substituted for the final basal medium, except when noted otherwise:

"Low amino acid medium" as in Table 2 with only 5 g per liter casein hydrolysate, without cysteine, ascorbic acid and pantethine.

"High amino acid medium" as above with 12 g casein hydrolysate.

"Reduced low amino acid medium" similar to the low amino acid medium but with 1 g of cysteine and 400 mg of ascorbic acid.

"Reduced high amino acid medium" as above with 12 g casein hydrolysate.

Bacto Thiamine Assay Medium was used in the present experiments in place of the Sarett and Cheldelin medium despite small differences in the composition of the two media, such as the incorporation of photolysed peptone in the former, instead of alkali treated peptone as described for the original method. Actually the Bacto medium represents the standard medium used for present analytical methods [12,5].

EXPERIMENTS AND RESULTS

Tryptophane requirement of *Lactobacillus fermenti* 36

In the original basal medium of Sarett and Cheldelin [1] tryptophane is not incorporated, despite the fact that tryptophane is usually essential for Lactobacilli [18] and is practically missing from acid hydrolyzed casein. It is to be mentioned that the same authors found tryptophane to be superfluous, similar

Table 2. Semisynthetic Basal Medium.

Bacto Vitamin Free Casamino Acids	12	g
(» » » » » in the "low amino acids" media	5	g)
Glucose	40	g
* Maltose	10	g
* Sodium acetate, anhydrous	20	g
L-Cystine	200	mg
* L-Cysteine	1	g
* Ascorbic acid	400	mg
DL-Tryptophane	400	mg
Adenine sulfate	20	mg
Guanine hydrochloride	20	mg
Uracil	20	mg
Riboflavin	200	μg
p-Aminobenzoic acid	200	μg
Nicotinic acid	200	μg
Pyridoxine hydrochloride	200	μg
Calcium-D-pantothenate	200	μg
* Panthetine	10	μg
Biotin	0.8	μg
Folic acid	0.5	μg
Tween 80	2	ml
K_2HPO_4	1	g
KH_2PO_4	1	g
$MgSO_4 \cdot 7\ H_2O$	0.4	g
NaCl	0.01	g
$FeSO_4 \cdot 7\ H_2O$	0.01	g
$MnSO_4 \cdot H_2O$	0.025	g

Distilled water to 1 000 ml for the double strength medium. The pH of the medium should be adjusted to 6.5 with aqueous sodium hydroxide.

* Variable components.

to several other metabolites if tested in their medium which was already supplemented with alkali treated peptone. We repeated the experiment of Sarett and Cheldelin with asparagine, tryptophane, inositol and choline with the same basal medium except for omission of the alkali treated (or photolyzed) peptone supplement, and with the addition of high levels of thiamine. Whole yeast extract and norit treated yeast extract complements served for comparison. As seen on Table 3, there was no growth of *L. fermenti* with thiamine on the peptone-free basal medium lacking tryptophane. On the other hand, the addition of DL-tryptophane to the medium gave full growth which cannot be further increased with norit treated yeast extract. Repetition of the experiment with 0.1 % Tween 80 included in the medium does not alter the results. Photolyzed peptone used as supplement at similar levels gave results in agreement with those obtained with yeast extract.

Thus tryptophane must be considered as an essential nutrient for *L. fermenti*, and the addition of different thiamine-free natural extracts as supplements to the basal medium are mainly justified as sources for tryptophane. Since alkali treatment of natural extracts not only destroys thiamine, but in the mean time decreases the original tryptophane content (*cf.* Ref.[19]), the incorporation of pure tryptophane in the basal media for *L. fermenti* is preferable.

Table 3. Tryptophane as an essential nutrient for *Lactobacillus fermenti* 36. Turbidimetric readings of growth expressed in per cent transmission (% T). Blanks were adjusted 100 % T.
Basal medium according to Sarett and Cheldelin [1] with omission of the alkali-treated peptone component was used with medium size inoculum. Each value represents the mean of triplicate readings.

Media / Test solutions added	Without tryptophane	With 4 mg DL-tryptophane per 10 ml	With tryptophane plus 10 % Norit treated Yeast Extract
Thiamine 0.25 μg per 10 ml	99.5	40.5	49
Bacto-Yeast Extract 4 mg per ml	49	39	47
	as above but with 0.2 % Tween 80 in each tube		
Thiamine 0.25 μg per 10 ml	99	42.5	45
Bacto-Yeast Extract 4 mg per 10 ml	48	39	47.5

Experiments performed with faint inoculum

Inoculum size was found by several workers [3,5] to be one of the crucial points in the thiamine assay with *L. fermenti*. We found it desirable to adjust the density of the inoculum turbidimetrically in each run in order to ensure standard conditions, instead of the simple dilution of the washed inoculum 10 to 25 times. In contrast to the recommended "medium strength inoculum" (40 % T) a rather weak one was used in most of the present nutritional tests. Thus there were better possibilities for the detection of small changes in the growth of this organism due to stimulatory or inhibitory action of different supplements, which usually affect the initial growth.

Effect of yeast extract. When initial growth with thiamine standards was measured after 12 h of incubation on different supplemented media, a marked early growth stimulation was found with whole yeast extract as seen in Fig. 1. Since the stimulation was clearly correlated to different thiamine concentrations, it cannot be accounted for by the presence of excess thiamine in the yeast extract. Norit treatment removes the stimulating factor from the yeast extract. This points to the possibility that the factor in question might be one of the B-vitamin type of growth stimulants. (It will be shown in a later chapter that the stimulatory effect can probably be due to Lactobacillus Bulgaricus Factor.)

Similar early growth stimulation would be disturbing in the case of routine assay procedure if complex natural extracts must be tested. However, the effect was eliminated by using a medium strength inoculum.

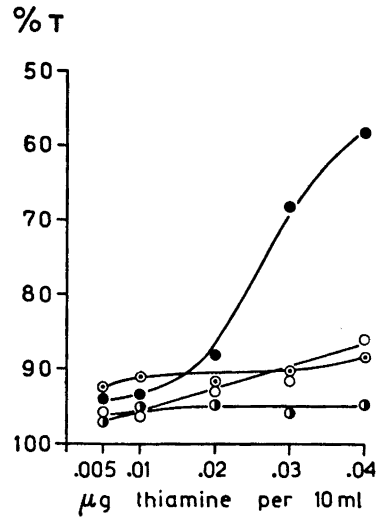

Fig. 1. Initial growth of *L. fermenti* 36 with thiamine standards using weak inoculum on different media: ○ Bacto Thiamine Assay Medium fortified with 0.1 % Tween 80; ⊙ the same with 10 % Norit treated yeast extract added; ◑ reduced low amino acid medium plus 10 % Norit treated yeast extract; ● reduced low amino acid medium with 2 mg per tube Bacto-Yeast-Extract added.

The effect of depleted yeast autolysates on the growth was considered for investigation because similar preparations were often recommended for use as supplement in assay media serving for sources of minute amounts of unidentified growth factors as well as of amino acids. Actually, thiamine-free yeast supplement was used in early work as a source of folic acid in the thiamine test [1,12], and sulphite treated yeast extract was found by Bacharach and Cuthbertson [4] to improve the visibility and diminish the "drift" when added to the Sarett and Cheldelin medium in the cup plate test. This contradicted the findings of Sarett and Cheldelin, who mention the trial with sulphite and Fuller's earth-treated yeast and liver extracts as a test for the lack of improvement in the assay of which was considered as proof for the completeness of their medium. Charcoal (Norit A) adsorption of yeast autolyzate solution originally introduced by Strong *et al.*[16] was designed as a valuable supplement in the pantothenate test with *Lactobacillus casei*, a rather exacting organism. This preparation was tested by us with success in several microbiological assay media and is believed to be preferable to sulphite or alkali treated yeast extracts because these rather harsh treatments necessarily destroy many growth factors besides thiamine, leaving behind several split products and artefacts.

Contrary to the expectations the experiment with incorporation of Norit-treated yeast extract in the basal media does not result in any improvement of the assay, but in marked inhibition of the growth of *L. fermenti* on both low and high amino acid unreduced media as seen in Fig. 2. Such inhibitory effect of a natural extract is evidently disturbing from the analytical viewpoint. Nevertheless, the inhibitory effect of the unknown substance(s) in the Norit-treated yeast extract can be compensated by using reducing agents in the media, as seen in Fig. 3.

The effect of reducing agents, especially that of cysteine [10] and of ascorbic acid [7,10], on *L. fermenti* was studied thoroughly in the last years mainly be-

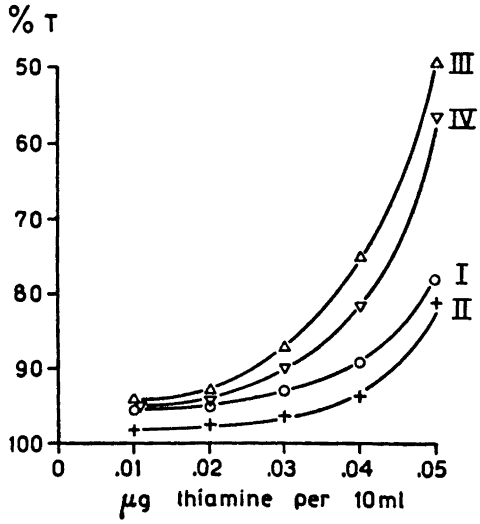

Fig. 2. Retardation of growth response of *L. fermenti* 36 toward thiamine by charcoal treated yeast extract with a weak inoculum. Curves I and II were obtained with low amino acid media, while III and IV with high amino acid media. Media in runs II and IV were supplemented with 10 % Norit A treated Bacto-Yeast-Extract. Each value show the mean of readings in duplicates after 17 h incubation.

cause of expected improvement in the response of this organism toward thiamine. Reducing agents were found to enhance the growth especially in case of light inoculum and by using fructose or maltose instead of glucose. Ascorbic acid was claimed to act not only as a reducing agent, but also as a growth factor able to replace thiamine [13]. These findings were based again on the Sarett and Cheldelin basal medium with photolyzed peptone in it.

Testing the different semisynthetic media we found some stimulations with reducing agents in case of faint inoculum (*cf.* Figs. 3 and 4) which were equali-

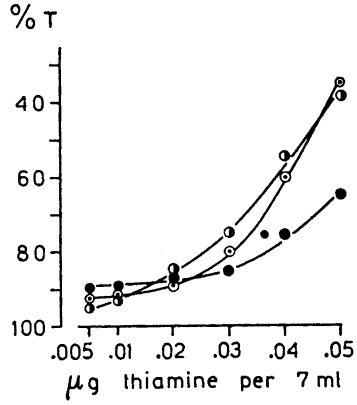

Fig. 3. Compensation of the inhibitory effect of charcoal absorbed yeast extract supplement on the growth of *L. fermenti* 36 in the thiamine tube test by reducing agents. Weak inoculum was used and readings of duplicates were made after 16 h of incubation on low amino acid media with: ⊙ no supplement; ● 10 % Norit A treated Bacto-Yeast Extract supplement; ◑ the same as the latter supplemented with additional cysteine (1 g/l) and ascorbic acid (400 mg/l).

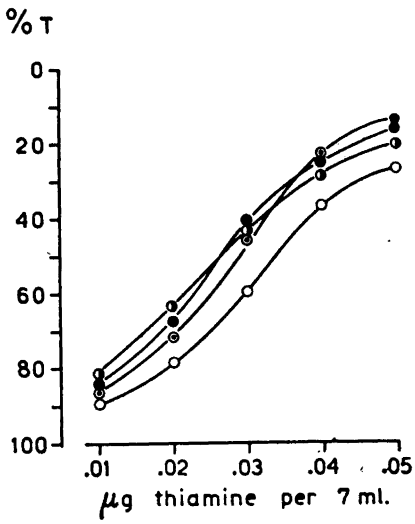

Fig. 4. Growth stimulation of *L. fermenti* 36 with pantethine. Experimental conditions similar to those for Fig. 3. Media: ○ high amino acid medium; ◑ the same with 25 μg pantethine per liter final volume; ⊙ reduced high amino acid medium; ● the latter with pantethine as above.

zed by choosing suitable medium size inoculum (*cf.* Fig. 5). It was not possible to find any significant difference between the action of cysteine or ascorbic acid supposing that cystine was present in the semisynthetic media when testing ascorbic acid. Neither could we find a concentration-dependent thiamine-replacing effect of ascorbic acid on these media.

As seen in Fig. 3 the effect of reducing agents is rather marked when overcomming the inhibitory action of charcoal treated yeast extract. The beneficial effect of reducing agents is shown also in Fig. 4, where comparison of curves ⊙ and ● gives a typical picture of growth stimulation by either cysteine or ascorbic acid or the combination, when *L. fermenti* was tested with thiamine on high amino acid medium, and the inoculum was weak.

Growth stimulation with Lactobacillus Bulgaricus Factor (LBF). As was already pointed out in connection with the interpretation of the experiment presented in Fig. 1, whole yeast extract contains some stimulatory factor(s) effective for early growth of weak inoculum. Because this type of growth stimulant might under certain conditions affect the thiamine assay, extended work seemed to be desirable at that point. Since the earlier nutritional studies with *L. fermenti* [1, 13, 10], several new growth factors and stimulatory substances — mainly B vitamins — were detected partly with the aid of exacting Lactobacilli [20]. For this reason Vitamin B_{12}, Citrovorum Factor (Folinic acid), Thioctic acid (Protogen) and Lactobacillus Bulgaricus Factor (Pantethine) were tested by us. None of these factors showed additional growth stimulation with weak inocula on the media used in our work, except pantethine which is known to be a rather typical early growth stimulant for many lactic organisms, and with wide-spread occurrence.

As seen in Fig. 4 pantethine was found to be stimulatory for *L. fermenti* in a small but significant degree on a high amino acid medium with cystine. However, this stimulation was eliminated by incorporation of reducing agents in

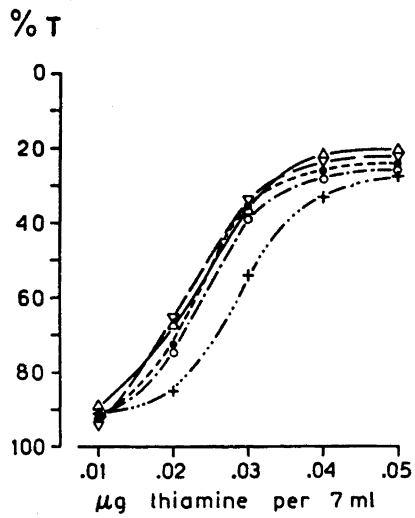

Fig. 5. Assay of thiamine standards with *L. fermenti* 36 on different media. Inoculum: 3 drops of 40 % T suspension per 10 ml media. Each value represents the mean of duplicate readings after 17 h of growth. Media 1—4, reduced high amino acid media with alkali treated peptone (20 g per l) in I (△————△); Norit A treated Bacto- Yeast Extract (10 %) in 2 (▽——▽); Pantethine (10 µg per l) in 3 (●- - -●); without supplement in 4 (○——○). For comparison in 5 (+·····+) a reduced low amino acid medium was used.

the medium. No such enhancing effect of pantethine was found to take place with more dense inocula. However, the incorporation of pantethine in a basal medium for analytical work with *L. fermenti* is still recommended.

The above results seem to be at first sight in contradiction with those of Craig and Snell [21], who found an activity coefficient of less than 0.05 with pantethine for *L. fermenti* compared with pantothenic acid as unit. Still this result cannot be compared directly with ours, since the medium used by these authors was different from that of ours (*e. g.* calcium-D-pantothenate was not incorporated in the Craig and Snell medium) and the conditions of the inocula were not specified.

Thiamine assay with medium size of inoculum

Considering the important role of the inoculum for the assay of thiamine with *L. fermenti*, a final comparison was made with inocula of 40 % transmission (2 drops per 7 ml) in different media. As seen in Fig. 5 the addition of different supplements does not influence the assay when the amount of acid-hydrolyzed vitamin-free casein is increased to a level common for vitamin assay media (12 g instead of 5 g per liter final volume). The low amount of casein hydrolysate recommended by Sarett and Cheldelin [1] was evidently calculated to be compensated by the incorporation of the peptone preparation (another source of amino acids). While the right size of the inoculum seems to be a limiting factor for reliable thiamine assay method for this organism on a semisynthetic medium, the composition of the medium is of great importance too. As a conclusion of the results presented herewith, a medium described in Table 2 is recommended for use. The addition of further supplements, though not essential, could be allowed except that the osmotic pressure of the final medium should not be too high to disturb the growth of *L. fermenti*.

Table 4. The effect of the pyrimidine and thiazole moieties of thiamine on the growth of *L. fermenti* 36 in semisynthetic media. Turbidimetric readings, 24 h of growth.

Media / Breakdown products of thiamine	Low amino acid medium with 10 % Norit A treated Bacto-Yeast Extract	High amino acid media with 0.1 % Tween 80			
		Tween 80 omitted	—	with 10 mg per liter Leucovorine	with 10 % Norit A treated Bacto-Yeast
2-Methyl-4-amino-methyl pyrimidine-hydrochloride	95	98.5	98	97	96
0.03 μg per 7 ml	*43*	98	*31.5*	94.5	98
4-Methyl-5(-oxyethyl)-thiazole	*30*	99	17.5	93.5	94.5
0.03 μg per 7 ml	94.5	99	93	92.5	94.5

The growth of *L. fermenti* with the pyrimidine and thiazole moieties of the thiamine molecule in absence of thiamine is one of the nutritional aspects which also needed to be controlled in case of introduction of a new medium. These moieties often interfere with microbiological procedures since different organisms can use one or both of these substances as precursors for the synthesis of thiamine. *L. fermenti* was reported to be unable to utilize either the pyrimidine or the thiazole parts under the first 20 to 24 h of growth, but seems to be stimulated by them during prolonged incubation [1,5]. Owing to this fact, the measurement of the growth of *L. fermenti* must take place before 18 h of incubation, which necessitates the use of turbidimetric readings instead of acidimetry. We tested both halves of thiamine on different media and found no growth after 20 h of incubation, while readings at 24 h showed occasional irregular randomly distributed growth, which points to the possibility of an adaptational mechanism (see Table 4) instead of direct utilization as is commonly believed.

Addendum: After the preparation of the present paper, the work of MaciasR[22] was considered, in which a new thiamine test method with *L. fermenti* was presented. This method is based on a medium containing 5 to 400 times higher concentrations of the different B vitamin components than the conventional levels. MaciasR's investigations were focused mainly on the carbohydrate requirements of *L. fermenti*, in variance with our present work. However, the experiments of MaciasR were conducted on the complete Sarett and Cheldelin medium, the disadvantages of which were discussed by us. Efforts to reproduce the work of MaciasR gave no satisfactory results in our laboratory.

The valuable assistance of Miss E. Börje and the financial support of the *Swedish Natural Science Research Council* is acknowledged.

REFERENCES

1. Sarett, H. P. and Cheldelin, V. H. *J. Biol. Chem.* **155** (1944) 153.
2. Barton-Wright, E. C. *Analyst* **70** (1945) 283.
3. Cheldelin, V. H., Bennett, M. J. and Kornberg, H. A. *J. Biol. Chem.* **166** (1946) 779.

4. Bacharach, A. L. and Cuthbertson, W. F. J. *Analyst* **73** (1948) 334.
5. Fitzgerald, E. E. and Hughes, E. B. *Analyst* **74** (1949) 340.
6. Camien, N.N., Dunn, N.S. and Salle, A. J. *J. Biol. Chem.* **168** (1947) 33.
7. Fang, S. C. and Butts, J. S. *Proc. Soc. Exptl. Biol. Med.* **78** (1951) 463.
8. Dellweg, H. and Bernhauer, K. *Biochem. Z.* **328** (1956) 264.
9. Analytical Methods Committee, *Analyst* **79** (1954) 118.
10. Snell, N. and Lewis, J. C. *J. Bacteriol.* **65** (1953) 671.
11. Bánhidi, Z. G., Sjöström, A. G. M., Grömmer, S. and Lundin, H. *Arkiv Kemi* **5** (1953) 393.
12. Barton-Wright, E. C. *The Microbiological Assay of the Vitamin B-Complex and Amino Acids*, London 1952.
13. Fang, S. C. and Butts, J. S. *Proc. Soc. Exptl. Biol. Med.* **82** (1953) 617.
14. Pennington, D., Snell, E. E. and Williams, R. J. *J. Biol. Chem.* **135** (1940) 213.
15. Snell, E. E. and Strong, F. M. *Ind. Eng. Chem. Anal. Ed.* **14** (1939) 346.
16. Strong, F. M., Geeney, R. E. and Earle, A. *Ind. Eng. Chem. Anal. Ed.* **13** (1941) 566.
17. Schultz, A. S., Atkin, L. and Frey, C. N. *Ind. Eng. Chem. Anal. Ed.* **14** (1942) 35.
18. Prescott, J. M., Schweigert, B. S., Lyman, C. M. and Kuiken, K. A. *J. Biol. Chem.* **178** (1949) 727.
19. Wooley, J. G. and Sebrell, W. H. *J. Biol. Chem.* **157** (1945) 141.
20. Kitay, E. and Snell, E. E. *J. Bact.* **60** (1950) 49.
21. Craig, J. A. and Snell, E. E. *J. Bact.* **61** (1951) 283.
22. MaciasR, F.M. *Appl. Microbiol.* **5** (1957) 249.

Received December 20, 1957.

ACTA CHEMICA SCANDINAVICA 12 (1958) 528—536

Stability Constants of Metal Complexes with Mononucleotides

EVA WALAAS

Institute of Medical Biochemistry and Physiology, Department of Medical Biochemistry, University of Oslo, Norway

The formation constants of mononucleotide complexes with Ca(II), Mg(II) Co(II) and Mn(II) are determined. It has been shown that the formation constants of these metal complexes mainly depend upon the nature of the metal and the length of the phosphate chain in the nucleotide. With a few exceptions the stability of the complexes are characterized by the sequence Ca<Mg<Co<Mn. With increased length of the phosphate chain in the nucleotide the stability increases in the order * AMP(UMP)<ADP (UDP)<ATP(UTP). The influence of the heterocyclic base of nucleotides in metal complex formation is studied with several purines and pyrimidine riboside phosphates and with flavin nucleotides.

Enzymatic transphosphorylation reactions involving mononucleotides as the phosphate donor or acceptor depend upon metal activation. It has therefore been suggested that the metals chelate with ligand groups in the nucleotide and in the enzyme apoprotein. Information of the structure and function of such complexes may be obtained by investigations on model systems. In the present work data on the stability constants of metals with purine-, pyrimidine- and flavinnucleotides will be presented.

In recent years several investigators have determined the stability constants of adenine nucleotides with metals, particularly Mg and Ca [1-5]. The stability constants of Sr-complexes with adenosine-3′-monophosphate and cytidine-3′-monophosphate have been reported by Schubert [6], and an approximate value of the stability constant of manganese with ATP has been given by Cohn and Townsend [8]. Investigations on the weakly associated complexes of sodium and potassium with adeninenucleotides have been carried out by Melchior [7].

* Throughout the paper the following abbreviations will be used: ATP: adenosinetriphosphate, ITP: inosinetriphosphate, GTP: guanosinetriphosphate, CTP: cytidinetriphosphate, UTP: uridinetriphosphate, ADP: adenosinediphosphate, UDP: uridinediphosphate, AMP: adenosine-5′-monophosphate, UMP: uridine-5′-monophosphate, FMN: flavin mononucleotide, FAD: flavin adenine dinucleotide.

In the present work complex formation of metals with nucleotides have been studied by means of the ion exchange resin method according to Schubert [9]. The significance of three main factors for the formation constants has been considered. This involves the nature of the metal ion, and the structure of the nucleotide, particularly the length of the phosphate chain and the configuration of the heterocyclic base. Four metals most commonly required by phosphorylation reactions involving nucleotides have been investigated, which include two alkaline earth metals: Ca(II) and Mg(II), and two metals of the first transition series: Mn(II) and Co(II).

EXPERIMENTAL

Method. The ion exchange method described by Schubert [9,11] has been used for the determination of the formation constants. In the experiments solutions of nucleotides with and without addition of metals were equilibrated with an anion exchange resin. The distribution of nucleotides between the resin and the solution was determined by ultraviolet absorption measurements.

Materials

Resin. The syntetic organic anion exchanger Dowex-1, 200—400 mesh, in the chloride form was used. The resin was put through several alternate Cl^- and OH^- cycles with 5 % solutions of NaCl and NaOH. Subsequently the resin was equilibrated with 0.1 M NaCl. The supernatant solution in contact with the resin was adjusted to pH 8.0—8.2 with dilute NaOH solution. The mixture was stirred for an hour, pH of the solution tested again and readjusted until no change of pH took place after stirring. The resin was filtered, washed rapidly with distilled water and air dried. Analyses showed a moisture content of 11.6 %. All experiments were conducted with the air dried resin.

Reagents. The solutions of sodium chloride and the solutions of the chlorides of Mg, Ca, Co and Mn were prepared from Merck products, analytical grade. All nucleotides used were derived from "Sigma" Chemical Company, Saint Louis, Mo. The purity of these compounds was investigated by the chromatographic procedure of Hurlberth *et al.*[10] on Dowex-1 resin by the gradient elution technique with a formic acid system. If ultraviolet absorbing impurities were detected, pure fractions of the nucleotide to be tested were collected and lyophilized before use.

Procedure

Ten 25 ml flasks were used in each experiment. To eight of these flasks (two were used as blanks) were added a weighed amount of the prepared Dowex-1 resin and subsequently solutions of buffer, nucleotide, metal chloride and 0.1 M NaCl. The 0.01 M tris (hydroxymethyl)-aminomethane buffer used, pH 8.2, was prepared in 0.1 M NaCl. Solutions of nucleotides were prepared in 0.1 M NaCl, adjusted to pH 8.2 and added (freshly made) to the flasks. The final volume and ionic strength in the flasks were 20 ml and 0.1, respectively.

In preliminary experiments the appropriate amount of resin at the concentration of nucleotide chosen was determined (*i. e.* approximately 75 % of the nucleotide bound to the resin). The affinity of the purine-nucleotides for the resin was greater than that of the pyrimidine-nucleotides. In experiments with adenosine-, guanosine- and inosinetriphosphate, 25 mg of resin at concentrations of 0.6×10^{-4} M of nucleotide was used. In experiments with cytidine- and uridinetriphosphates 50 mg resin was used at a similar range of nucleotide concentration. With ADP and UDP 100 mg and 200 mg, respectively, were necessary to obtain 70 % binding of nucleotide to the resin. With AMP and UMP the absorption of nucleotides was somewhat lower, even when the amount of resin was in-

creased (AMP 500 mg, UMP 1 000 mg). In experiments with flavinnucleotides appropriate absorption was obtained with 200 mg (FAD) or 300 mg (FMN).

The upper limit of the nucleotide concentration to give a constant and reproducible distribution coefficient with 25 mg resin was found experimentally to be 1×10^{-4} M. No deviation in the distribution coefficient (K_d^0) was found for the concentration range employed, ($0.5-0.625 \times 10^{-4}$ M).

Solutions of divalent metals as chlorides, dissolved in 0.1 M NaCl were added to the flasks at different levels of concentration. The concentration range chosen depended upon the affinity of the metal for the nucleotide. Usually three concentrations were employed in each experiment. Because of the high affinity for the nucleosidetriphosphates, low concentrations of metals could be used in these experiments ($0.625-3.75 \times 10^{-4}$ M). With nucleosidediphosphates a range of concentration of $0.125-1.5 \times 10^{-3}$ M was used. A higher concentration was required when the affinity for the nucleotide was low. In the case of AMP, UMP, FMN and FAD $0.75-7.5 \times 10^{-3}$ M had to be used. The same formation constants were found at low and high metal concentrations. Thus, the small variations of the ionic strength in different experiments did not influence the results, since the supporting electrolyte had the much higher ionic strength of 0.1. Theoretically, the effect on K_d of increasing ionic strength in experiments with nucleosidetri- and diphosphates was negligible, when calculated according to Schubert [6]. In experiments with nucleosidemonophosphate a maximal deviation of 6 % of K_d was calculated when 7.5×10^{-3} M metal solution was used.

The general procedure in a typical experiment was as follows: Two flasks contained nucleotide without metal ion added. These flasks were used to determine the nucleotide equilibrium between the resin and the solution. Two other flasks containing nucleotide but no resin were used as blanks. In the remaining 6 flasks metal solutions at different concentrations were added together with nucleotide. The glass-stoppered flasks were placed on a mechanical shaking apparatus and shaken vigorously for 3 h, which was sufficient to obtain equilibrium. The shaking was carried out at 23°C in a constant temperature room. Thereupon the resin was spun down by slight centrifugation, and the nucleotide concentration was measured by ultraviolet absorption at 260 mμ or other appropriate wavelengths in a Beckman Spectrophotometer Model DU in an aliquot of the supernatant. In the experiments with FAD the manganese complex formation was determined by U.V. absorption measurements. The other metal complex formation constants were investigated by determining the fluorescence in a Farrand Spectrofluorometer, using excitation maximum of FAD at 360 mμ and fluorescence maximum at 520 mμ.

The method is based upon the assumption that metal nucleotide complexes exert the same U.V. absorption spectrum as the free nucleotide. This was confirmed as no shift in absorption maximum wavelength nor any change in degree of absorption was observed by addition of metal solutions to nucleotides. This is in accordance with observations made by Nanninga [4] and by Blum [12]. No effect by the metals on the fluorescence of FAD was observed either.

Calculations

The formation constant is defined by

$$K_f = \frac{(MA)}{(M)\ (A)} \tag{1}$$

where M represents the metal and A represents the complexing anion. The formation constant is regarded as an equilibrium constant for the successive reactions between the metal ion and the ligand groups giving the complex [13]. In the present work performed at pH 8.2, the phosphate chain of the nucleotides does not take up protons, and the intermediate and terminal phosphate groups are negatively charged. In a buffered solution the anions are taken up by the resin until equilibrium. The addition of Me^{2+} reduces the concentration of free nucleotide in solution and thus decreases the uptake of negatively charged nucleotide by the anion exchanger.

It is convenient to employ a simple distribution coefficient K_d, as suggested by Schubert [9] for determining the formation constants.

$$K_d = \frac{\% \text{ in exchanger}}{\% \text{ in solution}} \times \frac{\text{volum of solution}}{\text{mass of resin}} \quad (2)$$

The term K_d^0 is taken as the value of distribution coefficient in the absence of a specific complexer, such as the complexing metal cation. Therefore the value of K_f can simply be formulated:

$$K_f = \frac{(K_d^0 / K_d) - 1}{(Me^{2+})^n}$$

where (Me^{2+}) represents the molar concentration of the complexing divalent metal, K_d the measured distribution coefficient for a given concentration of the metal and n the number of ions of Me^{2+} relative to nucleotide in the complex. K_d^0 and K_d are determined by measuring the fraction of nucleotide present in the solution at equilibrium.

Eqn. (3) can be written:

$$1/K_d = 1/K_d^0 + (Me^{2+})^n \cdot K_f/K_d^0 \quad (4)$$

A plot of $1/K_d$ *versus* (Me^{2+}) for proper values of n gives a linear correlation. By extrapolating to $(Me^{2+}) = 0$, the value of $1/K_d^0$ is obtained.

By the present application of the anion exchange resin method an accuracy of $\pm$ 5 % (standard error of mean) was obtained.

RESULTS

The type of complex formation of metals with mononucleotides is illustrated in Fig. 1. By plotting $1/K_d$ (the reciprocal distribution coefficient) against metal concentration (eqn. 4) a linear correlation is obtained. This type of curve was found without exception in all experiments. Thus, in these complexes one mole of the nucleotide combines with one mole of the metal. This is in accordance with experiments performed by Martell and Schwarzenbach [3] who demonstrated monometallic complex formation with inorganic triphosphates as well as with the adenosine phosphates AMP, ADP and ATP. In the

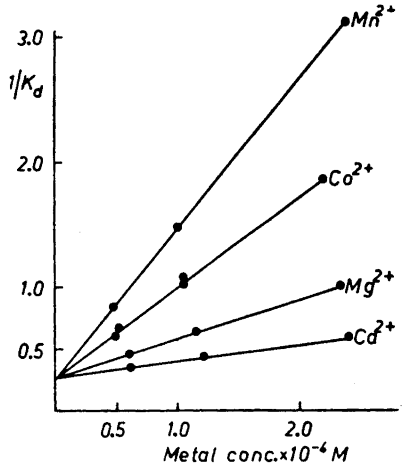

Fig. 1. Complex formation (1:1) of ATP with divalent metals. Determination by anion exchange resin method. See text for experimental conditions.

Table 1. Apparent stability constants (log K_f) of metal complexes at $\mu = 0.1$, pH: 8.2 and 23°C in 0.1 M NaCl.

Metal	ATP	ADP	GTP	ITP	UTP	UDP	CTP
Ca^{2+}	3.77	2.82	3.58	3.76	3.71		3.81
Mg^{2+}	4.04	3.15	4.02	4.04	4.02	3.17	4.01
Mn^{2+}	4.75	3.94	4.73	4.57	4.78		4.78
Co^{2+}	4.62	3.68	4.63	4.74	4.55		4.48

present work this type of metal complex formation has been demonstrated with pyrimidine and purine riboside phosphates as well as with FMN and FAD. Apparently monometallic complexes are characteristic for these group of biologically important substances.

In Table 1 the stability constants of metals with nucleoside triphosphates ATP, GTP, ITP, UTP, CTP and two of the corresponding diphosphates, ADP and UDP, are reported. The formation constants of the different metals with these compounds increase in the order Ca<Mg<Co<Mn. Thus, the lowest formation constants are obtained with Ca(II) and somewhat higher with Mg(II). This is in accordance with earlier observations on adenine nucleotides [3,5,4], and corresponds to the sequence of stability of the alkaline earth metal complexes in general as pointed out by Williams [14].

With metals of the first transition series the formation constants are considerably higher, perhaps due to the higher ability of these metals to form covalent bonds. It is of interest to note that the stability of Mn(II)-complexes with nucleoside triphosphates and nucleoside diphosphates as ligands are greater than with Co(II). Thus, the nucleotide molecule gives preference for the atomic structure of manganese with half filled 3*d*-shell. In this respect these complexes differ from the usual sequence of stability of metals with many other ligands reported by Irving and Williams [13]. This preference for manganese must be due to the molecular geometry of these nucleotides and is consistent with the high affinity of manganese for ligands of the oxygen type [15]. Thus the importance of bonding to oxygen atoms in the polyphosphate chain of the nucleotides is indicated. Table 1 shows a striking conformity of the formation constants, these being dependent upon the metal ion and the number of phosphate groups and independent of the rest of the nucleotide molecule. There is one exception to this rule, ITP forms a more stable complex with Co than with Mn, an observation which at present cannot be explained in terms of the structure of the ligand. ITP thus follows the ordinary sequence of stability: Mn<Co (Irving and Williams [13]).

Complex formation of the metals with nucleotide ligands containing one phosphate group (AMP, UMP, FMN) or with two "intermediate" phosphate groups (FAD) is of a somewhat different character (Table 2). Complexes of the 1:1 type are formed, but they are weakly associated and the order of

Table 2. Apparent stability constants (log K_f) of metal complexes at $\mu = 0.1$, pH: 8.2 and 23°C in 0.1 M NaCl.

Metal	AMP	UMP	FMN	FAD
Ca^{2+}	1.76		2.06	2.02
Mg^{2+}	1.95	2.25	2.03	2.02
Mn^{2+}	2.31		2.17	2.39
Co^{2+}	2.58		2.41	2.36

stability with different metals is not as characteristic as with the nucleoside triphosphate- and diphosphate groups. This is clearly seen from Table 3 where the relative stabilities of metal complexes with the different ligands are calculated. Particularly it should be pointed out that the great stability of manganese-complexes with nucleosidetriphosphates is not observed with nucleosidemonophosphates or with FAD which contains two phosphate groups in "intermediate" position. The stabilities of Mn(II) and Co(II) complexes with the last mentioned ligands are but slighthly higher than the stability of the Ca(II) and Mg(II) complexes, and the order of stability is not as typical as that obtained with nucleosidetri- and diphosphate compounds.

The significance of the length of the terminal phosphate chain on the formation constant is illustrated by experiments with ATP, ADP and AMP.

Table 3. Relative stability of metal nucleotide complexes (calculated ratio of K_f).

Complexing agent	Ca	Mg	Mn	Co
ATP	1	1.8	9.6	7.1
ITP	1	1.9	8.2	11.3
GTP	1	2.9	14.1	11.1
CTP	1	1.6	9.3	4.6
UTP	1	2.1	11.8	6.9
ADP	1	2.1	13.3	7.3
AMP	1	1.5	3.5	6.5
FMN	1	0.9	1.3	2.2
FAD	1	0.5	2.3	2.2

Table 4. Relative stability of metal complexes with nucleoside mono-, di- and triphosphates (calculated ratio of K_f).

Metal	AMP	ADP	ATP	UMP	UDP	UTP
Ca^{2+}	1	11.4	110			
Mg^{2+}	1	15.7	121	1	8.4	61
Mn^{2+}	1	43.2	268			
Co^{2+}	1	12.8	112			

The relative stabilities of the metal complexes with adenosinemono-, di- and triphosphates are shown in Table 4. At pH 8.2 used in the experiments these nucleotides contain, respectively, 2, 3 and 4 negatively charged oxygen atoms in the phosphate chain. In complexes with Ca(II), Mg(II) and Co(II) addition of one intermediate phosphate group in the molecule (ADP) increases the formation constant by a factor of approximately 10. Two intermediate phosphate groups (ATP) increase the stability of the complex with a factor of approximately 100. Similar results have been reported by Martell and Schwarzenbach [3] in experiments with Ca(II) and Mg(II) complexes of adenosine phosphates. This definitely, indicates the formation of chelating structures of metals with poly-phosphates in purine nucleotides. Similar observations have been made with metal complexes of condensed polyphosphates [16,3]. Experiments performed with Mg-complexes of uridine phosphates (Table 4) show that this is valid also for pyrimidine nucleotides.

The unique properties of manganese to form chelate structures with adenosine polyphosphates is indicated from Table 4. Thus, the stability constants of manganese with AMP, ADP and ATP increase by a ratio of 1:43:268. However, such a preference for manganese is not present in complexes with FAD where the two phosphate groups are in intermediate position.

DISCUSSION

In recent years considerable attention has been given to the molecular structure of metal complexes of adeninenucleotides. Thus, it has been suggested by Calvin [17] that a metal chelate structure between the metal and the phosphate residue of the ADP or ATP molecule is formed. On the other hand Szent-Györgyi [18] has proposed a structure where the 6-NH_2-group and the N_7 in the adenine as well as the phosphate residue contribute ligand groups to the metal.

In several investigations the problem has been studied by determination of stability constants of metals with adeninenucleotides. Investigations based upon titration measurements have been reported [2,3,5]. Further the problem has been studied by cation exchange method [1,6], by anion exchange method [4] and paramagnetic resonance absorption [7]. As far as the results are concerned

great discrepancies exist depending upon the method used and the experimental conditions, as discussed by Smith and Alberty [5].

The anion exchange method adopted in the present work has earlier been used by Nanninga [4]. However, the formation constants of Mg and Ca complexes with adeninenucleotides reported by him differ considerable from the results obtained in the present work. On the other hand our results completely agree with the stability of Mg and Ca adeninenucleotide complexes determined by Martell and Schwarzenbach [3] by very accurate titration measurements.

It may therefore be of some interest to point out the limitations and accuracy of the ion exchange method. Several important factors as discussed thoroughly by Schubert [11], must be taken into consideration. By the present application of the anion exchange resin method the equilibrium of nucleotide between the resin and the solution, *i. e.* K_d must be independent of the amount of nucleotides bound by the complexing metal. As mentioned in the experimental part this point was investigated by measuring K_d^0 in a system usually containing 25 mg resin at several concentrations of ATP. Above 10^{-4} M ATP, deviation in K_d^0 occurred in accordance with theoretical calculations [11]. Therefore in all experiments the nucleotide concentration was kept below the critical level. The lower formation constants reported by Nanninga can possibly be explained by the different experimental conditions with regard to the concentration of nucleotide and the amount of resin. Further it has been observed that deviation of K_d^0 occurred when more than 85 % was bound to the resin. Therefore, in each experiment, an amount of resin was chosen which permitted the determination of K_d^0 where 60—70 % of the nucleotide was absorbed. The formation constants were calculated on the assumption that the buffer ions did not form complexes with the reactants. The fact that constant values of formation constants were obtained at different metal concentrations indicated that a single complex was formed. Experimental support for this assumption was further obtained as Tris buffer at different concentrations in the range 0.05—0.005 M had no effect on the formation constant. A weak complexing action of the Na ions in the solution must be expected [8]. Finally it should be mentioned that the conformity of the extrapolated and experimental determinal K_d^0 excludes some of the disturbing factors described by Feldman *et al.*[19]

From the present work the conclusion can be drawn that two main factors determine the formation constants of metalnucleotide complexes, namely the nature of the metal and the length of the phosphate chain. The high stability of metals with di- and triphosphate ligand groups, depends upon terminal localization of the phosphate residue, such as in purine- and pyrimidine nucleotides. On the other hand the stability of metal complexes of FAD containing two intermediate phosphates groups is not increased compared with FMN or AMP.

At the pH employed no particular indication has been obtained of any significance of the heterocyclic base. This is in accordance with the findings of Martell and Schwarzenbach [3] who did not find any complex formation of metals with adenine. In the present work the stability constants of the different purine- and pyrimidinenucleosidetriphosphates were of the same order of magnitude. Further the sequences of stability were always the same, Ca<Mg<Co<Mn. The only exception is ITP characterized by the order Mn<Co.

The more stabile complexes with transition metals than with the group II A must be expected due to the more favourable acceptor factors in the former. However, the different acceptor abilities of cobalt and manganese also influence complex formation with nucleotides. The extent of increased stability characterized by the sequence AMP<ADP<ATP is much more pronounced with Mn(II) than with Co(II).

In the literature some information on the significance of metal nucleotide complexes in activation of enzymes involving phosphorylations has been given. Most commonly a requirement for Mg exists, but activation with Mn, Ca and Co has also been observed [20]. Indications that metal complexes are the actual substrates of the enzymes have been presented. Thus, with fructokinase at high ionic strength [21] and with muscle ATPase activity [22], maximal enzyme activity was obtained at a metal/ATP ratio of 1. At present scanty information is available on the structure of metal nucleotide complexes with the apoprotein part of phosphorylating enzymes [23]. This problem will be more fully discussed in a forthcoming paper. A biochemical significance of the highly stable complexes of Mn with ADP and ATP must be considered, as it is known that manganese can restore respiration and phosphorylations in Ca-inactivated mitochondrial preparations [23].

Acknowledgement. The work has been supported by grants from *Eli Lilly and Company*, and from *Det Videnskapelige forskningsfond av 1919*. A working grant has been received from the *Norwegian Council for Research and Humanities*. Thanks are due to Mrs. Reidun Midthjell for valuable technical assistance.

REFERENCES

1. DiStefano, V. and Neuman, W. F. *J. Biol. Chem.* **200** (1953) 759.
2. Burton, K. and Krebs, H. A. *Biochem. J.* **55** (1953) 94.
3. Martell, A. E. and Schwarzenbach, G. *Helv. Chim. Acta* **76** (1956) 653.
4. Nanninga, L. *Federation Proc.* **15** (1956) 319.
5. Smith, R. M. and Alberty, R. A. *J. Am. Chem. Soc.* **78** (1956) 2376.
6. Schubert, J. *J. Am. Chem. Soc.* **76** (1954) 3442.
7. Cohn, M. and Townsend, J. *Nature* **163** (1954) 1090.
8. Melchior, N. C. *J. Biol. Chem.* **208** (1954) 613.
9. Schubert, J. *J. Phys. Chem.* **56** (1952) 113.
10. Hurlberth, R. B. Schmitz, H., Brumm, A. F. and Potter, V. R. *J. Biol. Chem.* **209** (1954) 23.
11. Schubert, J. *in Methods of Biochemical Analysis* **3** (1956) 247.
12. Blum, J. J. *Arch. Biochem. and Biophys.* **55** (1955) 486.
13. Irving, H. and Williams, R. J. P. *J. Chem. Soc.* **1953** 3192.
14. Williams, R. J. P. *J. Chem. Soc.* **1952** 3770.
15. Irving, H. and Williams, R. J. P. *Analyst* **77** (1952) 813.
16. Wazer, J. R. van and Campanella, D. A. *J. Am. Chem. Soc.* **72** (1950) 655.
17. Calvin, M. *in* McElroy, D. and Glass, B. *A Symposium of the Mechanism of Enzyme Action*, 1954, p. 221.
18. Szent-Györgyi, A. *The International Enzyme Symposium, Ford Foundation*, 1955.
19. Feldman, I., Toribara, T. Y., Havill, J. R. and Neuman, W. F. *J. Am. Chem. Soc.* **77** (1955) 878.
20. Lardy, H. A. *in* McElroy, D. and Glass, D. *Phosphorus Metabolism I* (1951) 477.
21. Hers, H. G. *Biochim. et Biophys. Acta* **8** (1952) 424.
22. Brigham, E., Brinch-Johnsen, T. and Walaas, O. *Acta Physiol. Scand.* **37** (1956) 48.
23. Lindberg, O. and Ernster, L. *Nature* **173** (1954) 1038.

Received December 6, 1957.

ACTA CHEMICA SCANDINAVICA 12 (1958) 537—546

Synthesis of Compounds Related to Muscarufin

III.* The Ullmann Reaction with *o*-Chloro-iodobenzene

MARTIN NILSSON

Organisk-kemiska Institutionen, Kungl. Tekniska Högskolan, Stockholm, Sweden

Reaction of *o*-chloro-iodobenzene with copper gave 2,2′-dichlorodiphenyl in relatively poor yield. Chlorobenzene and, surprisingly, *o*-dichlorobenzene were the major by-products but several others were also isolated.

m-Chloro- and *p*-chloro-iodobenzene gave fair yields of the symmetrical dichlorodiphenyls. No dichlorobenzenes were detected in the reaction products.

The results are discussed in relation to the mechanism of the Ullmann reaction.

Attempts to convert 2,3,5-triacetoxy-1,4-bis-(2-carbomethoxyphenyl)-benzene into 3-hydroxy-2,5-bis-(2-carboxyphenyl)-*p*-benzoquinone were not successful. This has been due mainly to the ready formation of dilactones (*cf.* Part I [1]) and to the instability to alkali of any monohydroxyquinone which might have been formed.

Some analogues without carboxyl groups were therefore prepared. The simplest, 3-hydroxy-2,5-diphenyl-*p*-benzoquinone, was obtained from 2,5-diphenyl-*p*-benzoquinone by Thiele acetylation, acid methanolysis and oxidation with nitrous acid. It dissolved readily in dilute aqueous alkali giving a violet solution, which turned brown in a few minutes. No hydroxyquinone could be recovered from this solution.

An analogue with chlorine atoms in place of the carboxyl groups was prepared with the intention of replacing them at a later stage by carboxyl groups. The Ullmann coupling of *o*-chloro-iodobenzene and 2,5-di-iodohydroquinone dimethylether gave a mixture, which was more heterogeneous than those obtained from similar couplings. On careful fractionation it gave 2,2′-dichlorodiphenyl (I), 2,5-dimethoxy-1,4-bis-(2-chlorophenyl)-benzene (II, 8 % yield based on the di-iodo compound) and a product A.

Compound II on oxidation with nitric acid gave 2,5-bis-(2-chlorophenyl)-*p*-benzoquinone. This compound, which has previously been obtained in small

* Part II. *Acta Chem. Scand.* **10** (1956) 1377.

quantities from *o*-chlorobenzenediazonium chloride and *p*-benzoquinone [2] was converted into 3-hydroxy-2,5-bis-(2-chlorophenyl)-*p*-benzoquinone by the route described above.

The product A, $C_{14}H_{12}Cl_2O_2$, m. p. 106° (yield 11 %), on treatment with nitric acid gave a quinone, $C_{12}H_6Cl_2O_2$, and was therefore presumed to be 2',4--dichloro-2,5-dimethoxydiphenyl (III).

An independent synthesis was made by a mixed Ullmann coupling of *o*-chloro-iodobenzene and 2-chloro-5-iodohydroquinone dimethylether, which gave a mixture from which 2,2'-dichlorodiphenyl, 2',4-dichloro-2,5-dimethoxydiphenyl (III) and 4,4'-dichloro-2,2',5,5'-tetramethoxydiphenyl (IV) were isolated by distillation. An unexpected by-product, 2,5-dichlorohydroquinone dimethylether (V), was also encountered in this reaction. Compound III proved to be identical with A and oxidation with nitric acid gave 5-chloro-2--(2-chlorophenyl)-*p*-benzoquinone identical with that obtained from A.

As there appeared to be a side-reaction involving a transfer of chlorine atoms in the mixed Ullmann couplings with *o*-chloro-iodobenzene it was of interest to study the reaction of *o*-chloro-iodobenzene with copper in greater detail. This reaction has previously been used for the synthesis of 2,2'-dichlorodiphenyl by Bretscher [3] (20 % yield) and by van Alphen [4]. The reaction was run under the same conditions as before, except that the reaction time was prolonged to avoid traces of unchanged starting material which might complicate the isolation procedure. No special precautions were taken to exclude air and commercial copper bronze was used without purification or activation.

Careful fractionation of the reaction product by distillation and chromatography on alumina gave: chlorobenzene (VI, 8 %), *o*-dichlorobenzene (VII, 5 %), 2,2'-dichlorodiphenyl (I, 39 %), dibenzofuran (VIII, 3 %), triphenylene (IX, 0.5 %) and two unidentified products.

Coupling of *m*-chloro-iodobenzene under the same conditions gave chlorobenzene (6 %) and 3,3'-dichlorodiphenyl (55 %) while *p*-chloro-iodobenzene gave chlorobenzene (11 %) and 4,4'-dichlorodiphenyl (63 %). No dichlorobenzene was detected in either case and the high boiling material was therefore not investigated. These results are in agreement with those of Ullmann [5] and van Alphen [6].

The copper bronze used in these experiments contained small amounts of fatty acids (*ca.* 0.4 %), partly as copper salts. According to previous experience in this laboratory it is a superior reagent for Ullmann couplings; it gives reproducible yields and usually no unchanged iodo-compounds can be recovered from reactions carried out above 220°. The isolation of dibenzofuran and small quantities of aliphatic ketones indicated, however, some uncontrolled reaction with atmospheric oxygen and with impurities in the copper. The reaction was therefore repeated under anaerobic conditions with purified copper.

The fatty acids and their copper salts were removed by ether extraction and the copper was then heated to 360° *in vacuo*. The coupling reaction was carried out under oxygen-free nitrogen using the same conditions of time and temperature as in the previous experiment. The reaction product was fractionated in a spinning band column and the distillation residue was chromatographed on alumina. Somewhat surprisingly a large amount of starting material was recovered (48 %). Chlorobenzene (VI, 8 %), *o*-dichlorobenzene

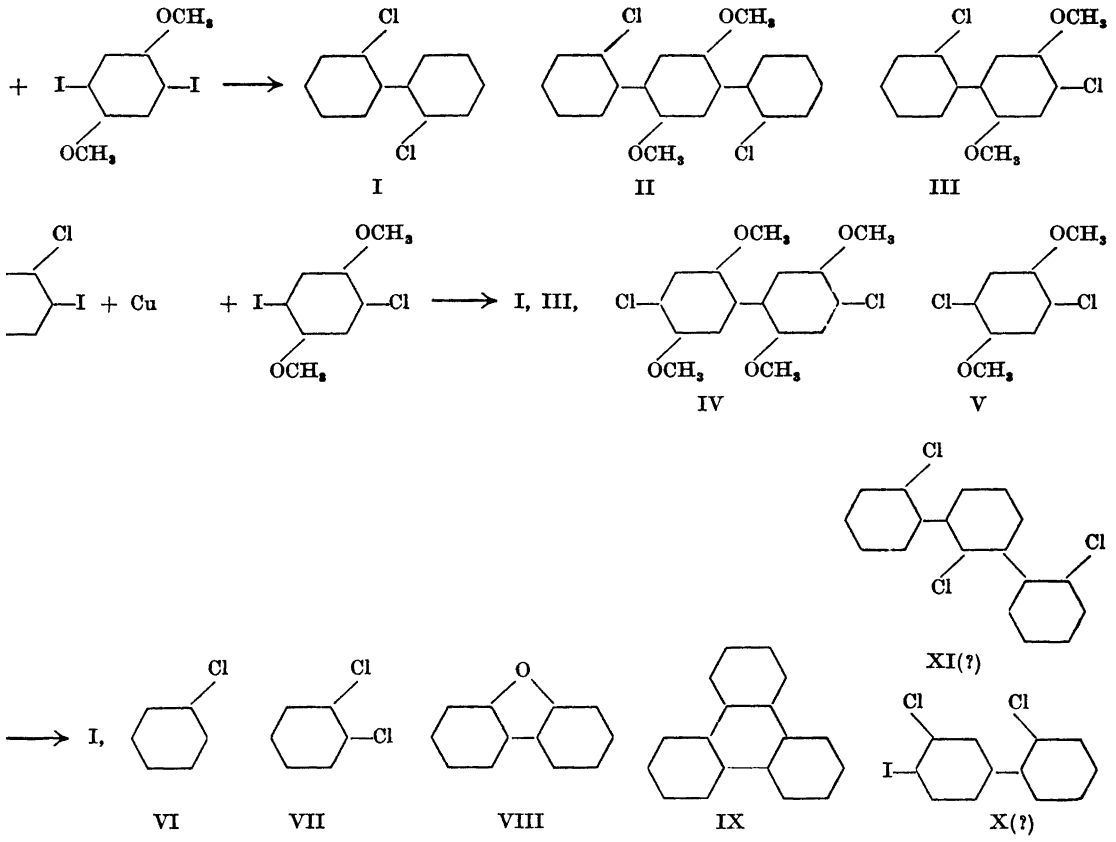

Fig. 1. Products isolated from Ullmann couplings with *o*-chloro-iodobenzene.

(VII, 3 %) and 2,2′-dichlorodiphenyl (I, 31 %) were isolated as before (yields based on starting material consumed). In addition, two new crystalline by-products were obtained. One of them, m. p. 85°, proved to be a dichloro--iododiphenyl (yield 3 %) and spectral studies indicate it to be either 2,3′--dichloro-4′-iodo- or 2,4′-dichloro-3′-iododiphenyl (X). The other one, m. p. 124°, contained carbon, hydrogen and chlorine only. UV, IR and mass spectral data showed that it was probably 2-chloro-1,3-bis-(2-chlorophenyl)-benzene (XI, yield 4 %). No triphenylene, diphenylene or dibenzofuran were detected in the mother liquors and non-crystalline fractions (UV).

The possible role of copper(I) chloride in the halogen exchange reaction was investigated briefly. 2,5-Di-iodohydroquinone dimethylether was treated with an excess of copper(I) chloride alone (250°, 15 h) and also in boiling N,N-dimethylformamide to give 2,5-dichlorohydroquinone dimethylether (*ca.* 70 % yield).

DISCUSSION

The Ullmann reaction with *o*-chloro-iodobenzene and copper gives *o*-dichlorobenzene as a by-product. Mixed Ullmann couplings with *o*-chloro-iodobenzene give other products in which aromatic iodine has been replaced by chlorine.

Somewhat similar halogen exchange reactions can be brought about by heating an iodo-arene with copper(I) chloride either alone or in a basic solvent. An analogous reaction for the conversion of bromo-arenes into the chloro-analogues has recently been patented [7]. These reactions appear to be a new example of copper-catalysed S_N reactions [8].

However, in the reaction of *o*-chloro-iodobenzene with copper no copper(I) chloride is present initially and it appears therefore as if copper(I) chloride or its equivalent is formed during the reaction and then reacts with an iodo-arene to give the halogen exchange product. This is somewhat surprising as aromatic chlorine is not attacked by copper unless it is activated, *e. g.* by a nitro or carbonyl group in the *ortho* position.

The mechanism of the Ullmann reaction is not known but has been the subject of much discussion, and free radicals, "crypto-radicals", copper organic compounds and carbanions have been proposed as intermediates. It has been suggested that the intermediate either dimerises or reacts with a second molecule of iodo-compound (*cf.* review by Fanta [9]); in the latter case the reaction may be related to the copper-catalysed substitution reactions [8].

The mobility of chlorine in the reaction with *o*-chloro-iodobenzene may be related to an intermediate or to the main reaction product, 2,2′-dichlorodiphenyl. The latter appears unlikely and it thus seems possible that chlorine can be eliminated from the intermediate from *o*-chloro-iodobenzene though not from the intermediates from *m*-chloro- and *p*-chloro-iodobenzene.

This recalls the lability of *o*-halogenophenyllithium and *o*-halogenophenylmagnesium halides, which split off metal halide giving dehydrobenzene (benzyne), which undergoes addition reactions, reacts with dienes and polymerises to diphenylene, triphenylene *etc.*[10] The isolation of small amounts of triphenylene in the present case is a slight indication of the formation of dehydrobenzene.

On this analogy the reactive intermediate in the Ullmann reaction is likely to be an arylcopper. Phenylcopper is reported to react with certain carbonyl groups and also with allyl bromide, acyl halides *etc.*[11] and it is thus possible that *o*-chlorophenylcopper can eliminate copper(I) chloride to give dehydrobenzene.

Further work is, however, necessary to establish this and to clarify the relation to the main reaction and to the dehalogenation process, which is a major side reaction in Ullmann couplings.

In the present investigations chlorobenzene was obtained as the normal dehalogenation product; some of the corresponding "dehydrogenation" products, a dichloro-iododiphenyl and a trichloroterphenyl were also isolated and together account for one third of the dehalogenation. These findings are analogous to those of Rapson and Shuttleworth [12], who obtained 2-carbethoxy- and 4-carbethoxydiphenyl from the reaction of iodobenzene with copper in the presence of ethyl benzoate.

No satisfactory explanation can as yet be given for the formation of dibenzofuran.

EXPERIMENTAL

The melting points were determined on a Kofler block. The ultraviolet spectra were measured in ethanol (99.5 %) with a Beckman DU instrument. The infrared spectra were recorded on a Perkin Elmer No. 21 instrument with a sodium chloride prism. Light petroleum refers to the fraction b.p. 40—60°. The copper used was a lithographic bronze containing *ca.* 0.2—0.5 % fatty acids, mainly stearic, palmitic and oleic acids, partly as the copper salts.

3-Hydroxy-2,5-diphenyl-p-*benzoquinone.* Perchloric acid (15 ml, *d* 1.67) was added with stirring to 2,5-diphenyl-*p*-benzoquinone [13] (20 g) suspended in acetic anhydride (300 ml). The temperature was kept below 35°. Stirring was continued for 24 h and the mixture was then poured onto crushed ice. After standing overnight the product was collected (21 g) and a portion recrystallised from ethanol (charcoal), prisms, m. p. 195—198°. Kvalnes [14] reported m. p. 191°. (Found: C 70.9; H 5.3. Calc. for $C_{24}H_{20}O_3$: C 71.3; H 5.0.)

The crude triacetate (20 g) was heated under reflux with absolute methanol (200 ml) and concentrated sulphuric acid (10 ml) for 1 h. Most of the solvent was distilled off and after cooling the hydroxyhydroquinone was collected, washed with methanol and dried. It was very sensitive to air and was therefore not purified but was suspended in acetic acid (200 ml) and oxidised with sodium nitrite (8 g) in water (40 ml) at room temperature. After a few minutes the red product was filtered off and was then recrystallised from acetic acid giving 3-hydroxy-2,5-diphenyl-*p*-benzoquinone as dark red plates, m. p. 235—238° (slight decomp.). Overall yield 50 %. (Found: C 78.2; H 4.7. Calc. for $C_{18}H_{12}O_3$: C 78.3; H 4.4.) It was further characterised as the acetate (acetic anhydride, perchloric acid, room temperature), yellow needles from acetic anhydride, m. p. 174—175°. (Found: C 75.3; H 4.6. Calc. for $C_{20}H_{14}O_4$: C 75.5; H 4.4.)

2,5-Dimethoxy-1,4-bis-(2-chlorophenyl)-benzene (II). 2,5-Di-iodohydroquinone dimethylether (40 g, 0.1 mole), 2-chloro-iodobenzene (95 g, 0.4 mole) and copper bronze (300 g) were mixed and heated in a salt bath. The reaction started at 210° and the temperature rose to 270°. After cooling, the mass was extracted exhaustively with chloroform (Soxhlet) and after removal of the solvent the extract was distilled at 0.5—1 mm. Fraction 1: b. p. below 110°, 27 g; 2: 110—130°, 2.7 g; 3: 130—160°, 5.8 g; 4: 160—230°, 15.2 g; 5: 230—290°, 8.8 g.

Fraction 1 was discarded; fraction 2 solidified and was found to be 2,2′-dichlorodiphenyl, m. p. 45—54°. Fraction 3 on trituration with *cyclo*hexane gave a product A (1.6 g) m. p. *ca.* 100° and fraction 4 on trituration with benzene-*cyclo*hexane mixtures gave a compound B (2.6 g), m. p. *ca.* 200°. Fraction 5 gave only small amounts of high melting material, which was not further investigated.

The non-crystalline parts of fractions 3—5 were combined and redistilled through a 5 cm Vigreux column and further quantities of A (1.5 g) and B (0.3 g) were obtained by trituration of the distillate.

The investigation of A is described later, B proved to be the desired terphenyl derivative II. It was recrystallised from benzene giving prisms containing *ca.* 1 mole of benzene of crystallisation. The dried product melted at 214—216°. (Found: 15 % loss of weight on drying at 100°, 1 mm. Calc. for $C_{20}H_{16}Cl_2O_2 \cdot C_6H_6$: 18 %. Found: C 66.9; H 4.6; Cl 19.5. Calc.: C 66.9; H 4.5; Cl 19.7.)

2,5-Bis-(2-chlorophenyl)-p-*benzoquinone.* Finely powdered 2,5-dimethoxy-1,4-bis-(2-chlorophenyl)-benzene (1.2 g) was suspended in nitric acid (25 ml, *d* 1.42) and the mixture was shaken for 10 min. Water (100 ml) was then added and after a few hours the precipitate was collected and recrystallised from ethyl acetate to give yellow plates or prisms, m. p. 200—202° (0.7 g). (Found: C 65.8; H 3.1; Cl 21.2. Calc. for $C_{18}H_{10}Cl_2O_2$: C 65.7; H 3.1; Cl 21.5.)

3-Hydroxy-2,5-bis-(2-chlorophenyl)-p-*benzoquinone.* The quinone (1.1 g) in acetic anhydride (20 ml) was shaken with perchloric acid (2 ml, *d* 1.67) for 15 h. The dark solution was poured onto ice and the product was collected and recrystallised from methanol (charcoal) giving *2,3,5-triacetoxy-1,4-bis-(2-chlorophenyl)-benzene*, prisms, m. p. 154—158° (0.65 g). (Found: C 61.3; H 3.7; Cl 15.1. Calc. for $C_{24}H_{18}Cl_2O_6$: C 60.9; H 3.8; Cl 15.0.)

The triacetate (0.33 g) was heated under reflux with absolute methanol (25 ml) and concentrated sulphuric acid (1 ml) for 1 h. On addition of water (50 ml) the hydroxy-

hydroquinone precipitated as a colourless solid (0.22 g). A small portion was recrystallised from methanol and sublimed giving prisms, m. p. 206—209°. (Found: C 61.6; H 3.3. Calc. for $C_{18}H_{12}Cl_2O_3$: C 62.3; H 3.5.) The main portion (0.19 g) was dissolved in acetic acid (5 ml) and oxidised with sodium nitrite (0.2 g) in water (1 ml). After 0.5 h the mixture was diluted with water (20 ml) and the orange product was collected (0.18 g). Sublimation gave 3-hydroxy-2,5-bis-(2-chlorophenyl)-*p*-benzoquinone as yellow prisms, m. p. 187—190°. (Found: C 62.2; H 2.7; Cl 20.3. Calc. for $C_{18}H_{10}Cl_2O_3$: C 62.6; H 2.9; Cl 20.5.)

Investigation of A. The crude product was recrystallised from *cyclo*hexane and from methanol giving needles, m. p. 105—106°. Qualitative tests indicated the presence of chlorine and the absence of iodine. (Found: C 59.5; H 4.3; Cl 25.2. Calc. for $C_{14}H_{12}Cl_2O_2$: C 59.4; H 4.3; Cl 25.1.) Ultraviolet absorption spectrum: λ_{max} 303 mμ, (ε 6 700), λ_{min} 270 mμ (ε 1 200), shoulder at *ca.* 255 mμ.

For oxidation, A (0.5 g) was shaken for a few minutes with nitric acid (10 ml, *d* 1.42). Water (50 ml) was then added and the product collected (0.4 g). Sublimation and recrystallisation from methanol gave needles, m. p. 111—112°, resolidifying and finally melting at 117—118°. The analytical sample was resublimed. (Found: C 56.7; H 2.2; Cl 26.1. Calc. for $C_{12}H_6Cl_2O_2$: C 56.9; H 2.4; Cl 28.0.)

Synthesis of 2',4-dichloro-2,5-dimethoxydiphenyl (III). Chlorohydroquinone dimethylether (17.2 g, 0.10 mole) in acetic acid (25 ml) was treated with iodine monochloride (19.4 g, 0.12 mole) in acetic acid (10 ml). When the initial reaction had subsided the mixture was heated overnight on the water bath. The cooled solution was treated with sulphur dioxide and some water, the colourless precipitate was collected and recrystallised from ethanol giving pure 2-chloro-5-iodohydroquinone dimethylether, m. p. 114—116°, in 56 % yield. Posternak *et al.*[15] report m. p. 114—115°.

o-Chloro-iodobenzene (12 g, 0.05 mole), 2-chloro-5-iodohydroquinone dimethylether (7.5 g, 0.025 mole) and copper bronze (48 g) were mixed and heated in a salt bath. At 210° the reaction raised the temperature to 245°. The mixture was kept at this temperature for 20 min, then cooled and extracted with chloroform (Soxhlet). Evaporation of the solvent gave an oil, which was distilled through a 5 cm Vigreux column at *ca.* 0.5 mm. Fraction 1: b. p. 75—80°, 1.1 g; 2: 90—98°, 0.9 g; 3: 98—118°, 1.4 g; 4: 140—150°, 2.6 g; 5: 180—190°, 1.9 g.

The first two fractions deposited crystalline material, which was filtered off and washed with *cyclo*hexane. The product (0.3 g) was freed from oily contaminants by sublimation and was finally purified by recrystallisation from methanol, prisms m. p. 132—133°. A second form, needles m. p. 125—127°, was occasionally observed. Mixed melting point with 2,5-dichlorohydroquinone dimethylether gave no depression. Fraction 3 solidified on standing, recrystallisation from methanol gave 2,2'-dichlorodiphenyl, m. p. 49—54°. Fraction 4 on trituration with methanol gave a product, m. p. 102—105° (1.8 g); recrystallisation from methanol and from *cyclo*hexane raised the m. p. to 105—106° alone or in admixture with A. It was further oxidised to 5-chloro-2-(2-chlorophenyl)-*p*-benzoquinone as described for A; the same dimorphism was encountered and the mixed m. p. gave no depression.

Fraction 5 solidified and was recrystallised from ethanol to give needles (0.6 g, m. p. 143—150°). Further recrystallisation from acetic acid gave plates, m. p. 154—156°, undepressed by 4,4'-dichloro-2,2',5,5'-tetramethoxydiphenyl obtained from the reaction of 2-chloro-5-iodohydroquinone dimethylether with copper. Posternak *et al.*[15] report m. p. 151°. (Found: C 56.0; H 4.7; Cl 21.0. Calc. for $C_{16}H_{16}Cl_2O_4$: C 56.0; H 4.7; Cl 20.7.)

Ullmann coupling of o-chloro-iodobenzene. *o*-Chloro-iodobenzene (95 g, 0.4 mole) and copper bronze (256 g) were intimately mixed in a flask fitted with a reflux condenser and a thermometer and placed in a salt bath (180°). The temperature was raised and at *ca.* 190° the reaction raised the temperature to 230°. When the reaction had subsided the temperature was raised further and kept at 250—260° for 2 h. The reflux condenser was replaced by a still head and some volatile material distilled off at atmospheric pressure directly from the reaction vessel. Fraction 1: b. p. 130—140°, 3.5 g; 2: 150—180°, 2.8 g. The residue was extracted with chloroform yielding on evaporation of the solvent a brown oil (*ca.* 40 g) which was distilled through a 5 cm Vigreux column at *ca.* 10 mm to give fractions 3: 45—60°, 0.15 g; 4: 60—150°, 0.91 g; 5: 140—145°, 8.95 g, and then at *ca.* 1.5 mm giving: 6: 105—125°, 13.8 g; 7: 125—140°, 2.2 g; 8: 140—175°, 1.5 g; 9: 175—185°, 2.3 g; 10: 185—210°, 1.2 g. The distillation was interrupted and the residue extracted with chloroform to give fraction 11: 3.1 g, a brown oil.

Fraction 1 from b. p. and IR data was found to be fairly pure *chlorobenzene*. Nitration gave *2,4-dinitrochlorobenzene*, m. p. 49—52°, undepressed by an authentic sample.

Fraction 2 was similarly found to be mainly o-*dichlorobenzene*. Treatment with chlorosulphonic acid gave *bis-(3,4-dichlorophenyl)-sulphone*, m. p. 175—177°, undepressed by an authentic specimen. Fraction 3 contained largely *o*-dichlorobenzene (IR), and fraction 4 appeared to be heterogeneous (IR, UV).

Fractions 5—7 largely solidified on standing and on recrystallisation afforded crude *2,2'-dichlorodiphenyl*, m. p. 55—60° (16.3 g).

Fraction 8 was triturated with ethanol to give *product C*, m. p. 156—170° (0.12 g).

The mother liquors from fractions 5—8 were combined and chromatographed on alumina (1 kg). Elution with light petroleum (1.7 l) gave an oil (4.7 g), which solidified on standing. Recrystallisation from methanol gave *2,2'-dichlorodiphenyl*, m. p. 57—60°, (3.9 g). Further elution with the same solvent (12.1) gave a semi-solid product (3.2 g) which was recrystallised from methanol to give *substance D*, m. p. 78—83° (*ca.* 2 g). Further elution with light petroleum gave crude *C* (0.5 g).

Fractions 9 and 10, which were strongly fluorescent yellow oils were combined and chromatographed on alumina (200 g). Elution with *cyclo*hexane (450 ml) gave an oil (2.9 g), which on trituration with ethanol gave *C* (0.7 g). Further elution gave fractions (0.2 g) which were triturated with ethanol to give a *product E*, m. p. 95—105° (0.04 g). Elution with *cyclo*hexane-benzene (9:1) gave a crystalline *material F*, m. p. *ca.* 190° (0.2 g).

Fraction 13 was chromatographed on alumina. The light petroleum eluate gave crude *C* (0.5 g) and *E* (0.1 g). Light petroleum-benzene (9:1) gave crude *F* (0.3 g) and a waxy product *G* (0.2 g) m. p. around 80°. Elution with benzene stripped the column giving a brownish yellow resin *H* (0.6 g).

Product C (total *ca.* 1 g) was recrystallised from ethanol and sublimed to give prisms, m. p. 179—181°. Qualitative tests indicated the presence of chlorine and absence of iodine.

C dissolved in concentrated sulphuric acid to give a blue solution. No satisfactory analysis has so far been obtained.

Product D (total *ca.* 2 g). Recrystallisation from methanol gave plates, m. p. 83—85°. The picrate was crystallised from ethanol, yellow needles, m. p. 98—101°. The UV-spectrum agreed with that of dibenzofuran and mixed m. p.s with authentic dibenzofuran and its picrate gave no depression.

Product E (total *ca.* 0.1 g) was not obtained in a state of purity. It melted around 100° and gave a picrate, m. p. *ca.* 150°.

Product F (total *ca.* 0.2 g) was recrystallised from ethanol and sublimed to give needles, m. p. 197—199°. The picrate was prepared in acetone and was recrystallised from ethanol; needles, m. p. 222—225°. The UV and IR-spectra agreed with those given for triphenylene and the mixed m. p.s with a commercial sample and the picrate prepared from it gave no depression.

Product G (total *ca.* 0.3 g). The IR spectrum of this waxy material contained bands characteristic for aliphatic ketones but no aromatic bands. This product must be a mixture of aliphatic ketones originating from the fatty acids in the copper bronze.

Product H was a brown resin with an extremely strong yellow fluorescence. The IR indicated that it was contaminated with aliphatic and ketonic material and it was not further investigated.

Ullmann coupling of m-*chloro-iodobenzene*. *m*-Chloro-iodobenzene (0.4 mole) was allowed to react with copper under the conditions described above. Direct distillation from the reaction mixture gave fraction 1: b. p. 130—135°, 3.8 g. The chloroform extract on distillation gave fraction 2: b. p. below 50°/15 mm, 0.1 g; 3: 123—130°/1.5, 21.1 g; 4: 130—140°, 8.0 g; 5: 140—160°, 3.5 g.

Fraction 1 was fairly pure *chlorobenzene* (b. p., IR) and was characterised as the 2,4-dinitro-derivative. Fraction 2 contained largely chlorobenzene. No evidence for the presence of *m*-dichlorobenzene was obtained from the IR spectrum.

The IR spectra of fractions 3 and 4 were identical but fraction 5 was contaminated by aliphatic and ketonic material. All these fractions however solidified in the refrigerator and on recrystallisation from methanol gave *3,3'-dichlorodiphenyl*, m. p. 28—29.5°, in 55 % yield. The mother liquors and the distillation residue were not investigated.

Ullmann coupling of p-*chloro-iodobenzene*. *p*-Chloro-iodobenzene (m. p. 54—57°) treated in the same way gave a distillate, b. p. 130—135°, 6.7 g, indentified as chloro-

benzene by IR and by nitration. The extract could not be conveniently distilled because of the tendency of the product to sublime. It was therefore sublimed on to a cold finger (160—170°, 2 mm) and the sublimate was recrystallised from methanol giving 4,4'-dichlorodiphenyl, m. p. 144—148°, in 63 % yield. No evidence was obtained for the presence of a dichlorobenzene and the sublimation residue was not investigated.

Coupling of o-chloro-iodobenzene under modified conditions. Copper bronze (260 g) was exhaustively extracted with ether in a Soxhlet apparatus (extract: 1.0 g of a green wax), transferred while moist to a 250 ml three-necked flask fitted with thermometer, reflux condenser and a nitrogen inlet tube, and dried by heating *in vacuo*, finally at 360°/3 mm for 2 h. After cooling the flask was filled with oxygen-free nitrogen and *o*-chloro-iodobenzene (0.4 mole), which had been freshly distilled through a 30-plate column (b. p. 136.5—137.5°/50 mm), was then added with a slow current of nitrogen passing through the apparatus, the flask was placed in a salt bath (180°) and the temperature was raised to 250° (0.5 h) and kept at this level for 2 h. There was no marked evolution of heat and in contrast to previous experiments the inner temperature was all the time somewhat below that of the bath. The reflux condenser was then replaced by a still head and some volatile material formed was distilled off in a current of nitrogen. The distillate (2.8 g, b. p. 150—210°) was shown by IR spectra to contain chlorobenzene and *o*-dichlorobenzene.

After cooling, the contents of the flask were extracted with chloroform (Soxhlet), most of the solvent was removed and the oil obtained was combined with the previous distillate and distilled through a spinning band column. The following fractions were collected: 1: b. p. 126—135°/760 mm, 1.8 g; 2: 156—175°/760, 0.9 g; 3: 100—103°/9, 46.9 g; 4: 139—149°/9, 0.5 g; 5: 149—156°/9, 8.2 g; 6: 171—181°/9, 1.0 g; 7: 189—191°/7, 2.1 g.

Fraction 1. *Chlorobenzene* as shown by b. p., IR and conversion to *2,4-dinitrochlorobenzene.*

Fraction 2. *o-Dichlorobenzene* as shown by b. p., IR and conversion to *bis-(3,4-dichlorophenyl)-sulphone.*

Fraction 3 on standing acquired a reddish colour. B. p. and IR indicated *o-chloro-iodobenzene.*

Fraction 4. UV and IR spectra indicated a mixture of *o*-chloro-iodobenzene and 2,2'-dichlorodiphenyl. No dibenzofuran or diphenylene peaks were detected in the spectra.

Fraction 5 solidified and was recrystallised from methanol to give *2,2'-dichlorodiphenyl* (7.3 g, m. p. 55—61°).

Fraction 6 was a brown oil. The UV-spectrum was of the 2,2'-dichlorodiphenyl type.

Fraction 7 on standing became reddish and partly solidified. Recrystallisation from methanol gave a *product K* (0.3 g, m. p. 67—68°).

The distillation residue on extraction with chloroform gave a reddish brown solution evaporated to give a brown oil (6.3 g), which was chromatographed on alumina (1 kg). The first and the last fractions of the light petroleum eluate (5 l) solidified giving an additional quantity of *K* (0.7 g) and a *product L* (1 g, m. p. *ca.* 120°). The intermediate fractions were colourless oils. Light petroleum-benzene (9:1, 4 l) gave colourless resins, with a blue fluorescence under a quartz lamp. The UV-spectra gave no indication of the presence of triphenylene. Benzene (2 l) stripped the column giving brownish resins with intense yellow fluorescense.

Substance K (total 1 g). Recrystallisation from methanol gave needles, m. p. 85—87° (strongly depressed by dibenzofuran). Qualitative tests indicated the presence of chlorine and iodine. (Found: C 41.3; H 1.9; Cl 20.3; I 36.2. Calc. for $C_{12}H_7Cl_2I$: C 41.3; H 2.0; Cl 20.3; I 36.4.) UV-spectrum: λ_{max} 252 mμ (ε 15 000), λ_{min} 233 mμ (ε 10 000). IR-spectrum (KBr-disc): 3 090 w, 1 640 w, 1 577 w, 1 545 m, 1 492 w, 1 460 s, 1 440 m, 1 375 s, 1 303 w, 1 275 w, 1 248 w, 1 125 w, 1 112 m, 1 080 m, 1 042 m, 1 012 s, 950 w, 890 m, 865 w, 820 m, 755 s, 730 m, 705 m, 675 m.

The C—H out-of-plane region thus indicates 1, 2 and 4 adjacent hydrogen atoms. The UV-spectrum rules out 2,2'-substitution and makes a 2-iododiphenyl improbable [16]. Substance K therefore is probably *2,4'-dichloro-3'-iodo- or 2,3'-dichloro-4'-iodo-diphenyl* (X).

Substance L (total 1 g) was recrystallised from methanol and sublimed (0.05 mm) giving needles, m. p. 122—124°. It contained chlorine but no iodine. The analysis was consistent with a dichlorodiphenyl or a trichloroterphenyl. (Found: C 64.9; H 3.4;

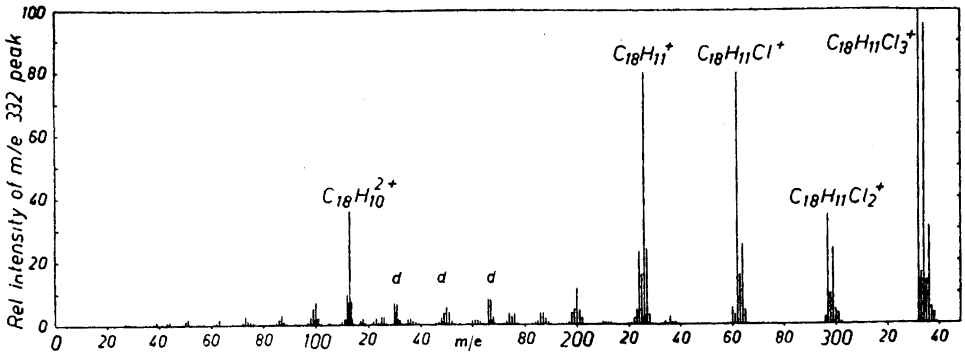

Fig. 2. Mass spectrum of compound *L* (*d* denotes doubly-charged ion).

Cl 32.0. Calc. for $C_{18}H_{11}Cl_3$: C 64.8; H 3.3; Cl 31.9.) Molecular weight determination according to Rast gave results, which were inconsistent with the low volatility of the substance.

The mass spectrum was kindly recorded by Ing. R. Ryhage, Laboratory for Mass Spectrometry, Karolinska Institutet, Stockholm, using an instrument with an all-glass heated inlet system [17]. The mass numbers were checked by recording the mass spectrum of a mixture of compound *L* and methyl *n*-eicosanate [18] obtained from Prof. E. Stenhagen. In the mass spectrum (Fig. 2) groups of peaks near m/e = 332, 297, 262 and 226 (!) indicate the successive loss of three chlorine atoms from a parent molecule $C_{18}H_{11}Cl_3$ (m/e = 332, 334, 336, 338) and compound *L* can therefore be assigned the empirical formula $C_{18}H_{11}Cl_3$.

The ultraviolet spectrum had no maxima and was very similar to that given for 2,2'--dichlorodiphenyl [19].

Infrared spectrum (KBr-disc): 3 090 m, 1 975 w, 1 950 w, 1 900 w, 1 818 w, 1 715 w, 1 635 w, 1 605 w, 1 590 w, 1 575 m, 1 493 s, 1 458 s, 1 440 s, 1 410 s, 1 260 w, 1 189 w, 1 160 w, 1 140 m, 1 080 w, 1 052 s, 1 039 s, 978 w, 956 w, 820 w, 803 s, 755 vs, 735 s, 728 m, 703 m, 690 s. The C—H out-of-plane region is thus consistent with 4 and 3 neighboring hydrogens and substance *L* is therefore probably *2-chloro-1,3-bis-(2-chlorophenyl)-benzene* (XI).

Acknowledgements. Thanks are due to Ing. R. Ryhage for the determination of the mass spectrum and to *Statens Tekniska Forskningsråd* for a fellowship.

REFERENCES

1. Erdtman, H. and Nilsson, M. *Acta Chem. Scand.* **10** (1956) 735.
2. Schimmelschmidt, K. *Ann.* **566** (1950) 184.
3. Bretscher, E. *Helv. Phys. Acta* **2** (1929) 257.
4. van Alphen, J. *Rec. trav. chim.* **51** (1932) 453.
5. Ullmann, F. *Ann.* **332** (1904) 38.
6. van Alphen, J. *Rec. trav. chim.* **51** (1932) 361.
7. Hardy, W. B. and Fortenbaugh, R. B. **U.S.2,769,818** (1956). *Cf. Idem. J. Am. Chem. Soc.* **80** (1958) 1716.
8. Bunnet, J. F. and Zahler, R. E. *Chem. Rev.* **49** (1951) 273.
9. Fanta, P. E. *Chem. Rev.* **38** (1946) 139.
10. Wittig, G. *Angew. Chem.* **69** (1957) 245.
11. Gilman, H. and Straley, J. M. *Rec. trav. chim.* **55** (1936) 821.
12. Rapson, W. S. and Shuttleworth, R. G. *Nature* **147** (1941) 675.

13. Schildneck, P. R. and Adams, R. *J. Am. Chem. Soc.* **53** (1931) 2373.
14. Kvalnes, D. E. *J. Am. Chem. Soc.* **56** (1934) 2478.
15. Posternak, T., Alcalay, W., Luzzati, R. and Tardent, A. *Helv. Chim. Acta* **31** (1948) 525.
16. Dunn, T. M. and Iredale, T. *J. Chem. Soc.* **1952** 1592.
17. Ryhage, R. *To be published.*
18. Asselineau, J., Ryhage, R. and Stenhagen, E. *Acta Chem. Scand.* **11** (1957) **196.**
19. Friedel, R. A. and Orchin, M. *Ultraviolet Spectra of Aromatic Compounds,* Wiley and Sons, Inc., New York 1951, No 182.

Received December 31, 1957.

ACTA CHEMICA SCANDINAVICA 12 (1958) 547—554

Quantitative Estimation of Sialic Acids

III. An Anion Exchange Resin Method

L. SVENNERHOLM

Department of Medical Biochemistry, University of Gothenburg, Gothenburg, Sweden

The increasing interest in the distribution of sialic acids in biological materials made it desirable to have a simple method for their analysis. As the colour reactions of the sialic acids are unspecific and influenced by a lot of naturally occurring substances, mainly carbohydrates, a direct analysis of sialic acid is inconvenient for many materials.

In the procedure elaborated the sialic acids are liberated with weak sulphuric acid and retained by a column with Dowex-2 in acetate form. Most of the contaminants are eluted with distilled water and then the sialic acids are displaced with an acetate buffer of pH 4.6. The concentration of sialic acid in the eluates is analysed with the resorcinol method. The optimum conditions for the liberation of the sialic acids are studied in particular.

The method has been satisfactorily applied to the analysis of sialic acids in body fluids and tissues (brain, kidney, liver, pancreas and submaxillary gland).

The concentrations of sialic acids have until now only been determined in biological fluids or isolated watersoluble compounds [1]. For these purposes some colour reactions have been applied to the unhydrolysed material and the colour developed has been determined by photometrical reading. The reactions are not specific but to a greater or lesser extent other biological compounds, mainly carbohydrates, give colours when using the reagents [2–5]. As sialic acids exist together with other carbohydrate components in biological materials, the quantitative figures for sialic acids obtained by direct colorimetry become too high. The positive error given by the other sugars has been corrected by dichromatic readings [3,4] but if the ratio total carbohydrates to sialic acids is great, it is only possible to make an approximate correction. It is also necessary to know the nature of the other sugars and their relative amount which restricts the general application of the procedure of dichromatic readings. There is also an uncertainty as to which degree the colour development of the sialic acids is influenced by substances other than carbohydrates in biological materials. Another disadvantage of direct colorimetric

analyses is that the colour development of bound sialic acids [3] is slower than that of free sialic acids. A prolonged reaction time is, however, unsuitable as the interference from the other carbohydrates then increases considerably [3,4]. It has also become an increasing need for a simple procedure at the analysis of sialic acids in tissues. In the latter case it is in general necessary to split off the sialic acids before they can be assayed with the colour reactions.

For these reasons a quantitative method was elaborated in which the sialic acids were liberated by acid hydrolysis and most of interfering substances removed on columns with an anion exchange resin.

METHODS

Preparation of the ion exchange columns

Dowex 2-X 8, 200—400 mesh, wetscreened through 150 mesh, was heated on the steam bath with three times the volume of 2 N hydrochloric acid. After the resin had settled for 30 min, the supernatant was decanted to remove the fines. After undergoing this treatment four times the resin was stirred up in water and poured into a large tube fitted with a glass filter. The resin was converted to acetate form by passing 2 N sodium acetate through the column until the effluent gave a negative test for chloride. The resin was then slurred up in 1 N acetic acid, transferred to a Büchner funnel and excessive moisture was removed by suction.

For the preparation of the columns about 3 g of the moist resin was suspended in about two volumes of distilled water and poured into a chromatographic tube (inner dimensions 0.7 × 20.0 cm), fitted with a glass filter plate (G 2) at the bottom and widened at the top (2 × 3 cm). The resin was allowed to settle to a height of 6.0 cm and excess resin then poured off. A small filter paper was placed over the resin and above it sand to a height of 0.5 cm. After washing the resin with 10 ml of 0.1 N acetic acid the column was ready for use.

Dowex 50-X 8, 100—200 mesh, was washed slowly several times on a Büchner funnel with 2 N sodium hydroxide, 2 N hydrochloric acid and distilled water in that order. A suspension of the resin in water was poured into a tube of the same dimensions as used for Dowex 2. The height of the column used was about 5 cm.

Regeneration of the columns. Having completed elution the columns were regenerated in the following order. 10 ml of each solution was used.

Dowex 2: 2 N sodium hydroxide, distilled water, 2 N sodium acetate and 0.1 N acetic acid.

Dowex 50: 2 N sodium hydroxide, distilled water, 2 N hydrochloric acid and distilled water.

Hydrolysis of the samples

Samples, containing 25—200 μg of sialic acid, were hydrolysed in small tubes having glass stoppers in 5 ml of 0.1 N sulphuric acid at 80°C and in 5 ml of 0.05 N sulphuric acid at 90°C for one hour. (When lipid extracts were investigated the lipids were dissolved in 0.5—1.0 ml of methanol by heating and the sulphuric acid was added initially in drops to give a fine emulsion.) Having been heated, the tubes were cooled to room temperature and the hydrolysates filtered into the column with Dowex 2. If the sample contained more than 0.1 mequiv. of inorganic cations, the hydrolysate was filtered into the tube with Dowex 50 which was placed immediately above the column with Dowex 2, so that the effluent from the first tube dropped into the Dowex 2 column. After filtration the hydrolysis tubes and the columns were washed twice with 5 ml of water.

Standards of 0, 100 and 200 μg N-acetylsialic acid were treated under the same conditions as the samples in each experiment.

Elution of sialic acids

The sialic acids were eluted from the Dowex 2 columns with 8 ml of 1 M acetic acid-sodium acetate buffer (pH 4.6). The effluent was collected in a 10 ml cylinder. Distilled water was added to the 10 ml mark.

Analysis of sialic acids

Resorcinol method. — Reagent. 0.2 g of resorcinol A.R. was dissolved in 10 ml distilled water. 80 ml conc. hydrochloric acid and 0.25 ml 0.1 M copper sulphate were added, and the volume was made up to 100 ml with distilled water.

Procedure: 2 ml of effluent in duplicates was pipetted into a centrifuge tube (16 × 120 mm) and 2 ml of resorcinol reagent added. The tubes were heated for 15 min in a bath of boiling water. After cooling in tap water, 5 ml of *iso*amyl alcohol was added and the tubes were vigorously shaken and chilled for 10 min in a bath of ice water. After centrifuging the amyl alcohol phase was transferred to 50 mm microcells and read in a Beckman Spectrophotometer model B at 450 and 580 mμ. In the eluates of hydrolysed tissues also ribose esters occurred. Their influence on the absorbancy values at 580 mμ was calculated from the reading at 450 mμ.

RESULTS

Stability of sialic acids in acid milieu. For the quantitative estimation of sialic acids only acid hydrolysis is applicable, as alkaline hydrolysis transforms part of the sialic acids to 2-carboxypyrrole [6,7]. The sialic acids are easily split off in acid milieu but the problem is to achieve such mild conditions that the destruction of sialic acids is negligible. The stability of the sialic acids was tested by heating N-acetylsialic acid under varying conditions and afterwards analysing the hydrolysates with the resorcinol method:

After heating N-acetylsialic acid, dissolved in distilled water, for one hour in a bath of boiling water, the absorbancy diminished by 1—2 %. When the substance was dissolved in 0.05 N and 0.1 N sulphuric acid the absorbancy diminished by 3 and 5 %, respectively. In these tests the concentration of N-acetylsialic acid was 20—40 μg/ml; if the concentration was 10-fold the destruction increased to about twice this value. Therefore, in all the following tests the low concentration of sialic acid was used. When the heating was performed at a lower temperature, 80—90°C, the destruction of N-acetylsialic acid was less. After heating for one hour with distilled water the absorbancy

Table 1. The recovery of N-acetylsialic acid (Ac. sial.) and N-glycolylsialic acid (Glyc. sial.) from Dowex 2 columns after heating with sulphuric acid under varying conditions.

Material	Sulphuric acid N	Temp. C°	Time of heating, h	No. of expts	Recovery, % M. ± S.E.M.
Ac.sial.	0.05	90	1	10	94.5 ± 0.6
Glyc.sial.	0.05	90	1	10	94.2 ± 0.6
Ac.sial.	0.05	90	2	4	89
Ac.sial.	0.10	80	1	10	95.0 ± 0.5
Glyc.sial.	0.10	80	1	10	94.3 ± 0.7
Ac.sial.	0.10	80	2	4	90
Ac.sial.	0.20	80	1	4	93

was unchanged. When heated for one hour with sulphuric acid no measurable decrease in absorbancy was found for a concentration of sulphuric acid $\leq$ 0.05 N at 90°C, $\leq$ 0.2 N at 80°C and $\leq$ 0.4 N at 70°C. The stability of N-acetylsialic acid was somewhat lower in hydrochloric acid than in sulphuric acid of the same strength. Trichloroacetic acid (10 %) and formic acid (1 N) did not destroy the sialic acid at 80 or 90°C, but the concentrations necessary for the quantitative release of bound sialic acid from, *e. g.*, serum proteins were too high for the capacity of the ion exchange resin. It was thus found that sulphuric acid was the most convenient acid for the hydrolysis. Addition of sodium chloride in a concentration of up to 10 mequiv/l did not give any measurable increased destruction of N-acetylsialic acid.

Recovery of sialic acids after the resin procedure. N-acetylsialic acid and N-glycolylsialic acid were hydrolysed with 0.05 N sulphuric acid at 90°C and with 0.1 N and 0.2 N sulphuric acid at 80°C for 1 and 2 h. The hydrolysates were then poured on the anion exchange resin columns, and after washing with water the sialic acids were eluted with 8 ml of acetate buffer as described. The recovery of the sialic acids is shown in Table 1. There was thus a difference in the recoveries of sialic acids between direct colorimetry and colorimetry after previous resin purification. Analysis of sialic acids in the effluents of the hydrolysate and the wash water were negative. Nor were any sialic acids eluted after a further addition of 10 ml of acetate buffer. This may be explained by a partial destruction of the sialic acids during the heating resulting in products still reacting with the colour reagents. However, they may be so strongly adsorbed to the resin that it is impossible to eluate them with the buffer used. At the isolation of N-acetylsialic acid with the resin technique [8], small fractions of Bial-positive substances were eluted after the main fraction. In paper partition chromatography the R_F-values for all these sialic acids were the same as those of N-acetylsialic acid. Odin and Berggård [9] found, however, when samples of sialic acids were heated with acids, that Bial-positive substances were formed which run faster than N-acetylsialic acid. Therefore it seems likely that the latter compounds will be attached so firmly to the anion resin, that they are not eluted.

It should also be pointed out that special precautions must be taken when isolating the sialic acids, which should be used as standard substances. When the sialic acids were prepared with the anion exchange method [8] and the eluates concentrated to a small volume on the water bath before lyophilization, 2–5 % of the sialic acids were changed and could no longer be attached to the resin. By eluting the sialic acid with acetate buffer, removing the sodium ions with a cation exchange resin in hydrogen form, extracting the acetic acid with diethyl ether, and lyophilizing more dilute solutions, the change of the sialic acids was negligible. For routine work it is however more simple to calculate the concentration of authentic sialic acid in a standard substance by estimating its amount. Unhydrolysed samples of the standard substances were analysed with the resin method and the yield of sialic acid determined. As the recovery of the sialic acids obtained with the described isolation procedure was 100 % after resin treatment the difference in absorbancy for the common standard substances with direct colorimetry and after resin treatment may be attributed to the change of the sialic acids during the isolation.

The destruction of the sialic acids during the liberation were also evaluated by heating biological samples for varying times. With serum and brain tissue

Table 2. Liberation of sialic acids from serum with sulphuric acid. 0.2 ml of serum was hydrolysed with 5 ml of sulphuric acid under varying conditions. The hydrolysates were treated according to the standard procedure.

Temp.	Sulphuric acid	Absorbancy			
		Heating time			
	N	1/2 h	1 h	2 h	3 h
80°C	0.05	0.906	0.904	0.894	0.875
	0.10	0.907	*0.924*	0.882	0.835
	0.20	0.888	0.890	0.850	—
90°C	0.05	0.922	*0.935*	0.881	0.817
	0.10	0.886	0.899	0.819	—

the yield of sialic acid decreased with about 5 % per hour when heated under standard conditions.

Liberation of sialic acids. Serum and brain tissue were hydrolysed with varying concentrations of sulphuric acid at 70°C, 80°C and 90°C for 1—3 h. The optimum conditions were tested by analysing the sialic acid content in the eluates from the anion exchange resin columns. The largest concentration of sialic acid was found in the materials by heating with 0.1 N sulphuric acid at 80°C for one hour or with 0.05 N acid at 90°C for one hour. In Table 2 the figures found for serum are given. At 70°C only 80—90 % of the optimum concentrations of sialic acid were achieved.

In the experiment listed the largest absorbancy was found after heating at 90°C but in most experiments maximum absorbancy was achieved after heating at 80°C. When lipid extract was hydrolysed the higher temperature often gave the largest value, while the lower temperature was optimal for tissues with a low concentration of sialic acids. It is therefore preferable to hydrolyse the samples both with 0.1 N sulphuric acid at 80°C and with 0.05 N acid at 90°C.

In recovery experiments pure N-acetylsialic acid was added to the samples before hydrolysis. The recovery of N-acetylsialic acid added to serum was 95.5 % $\pm$ 0.7. The recovery of N-acetylsialic acid added to different tissues was from 90 to 98 %. The lower the concentration of sialic acid, the lower was the recovery. It is therefore preferable to add the standard of sialic acid to each new material which is investigated if exact figures are wanted.

Anion exchange resin column. Dowex 2 X-8, 200—400 mesh, was used throughout. The resin was in the preliminary experiments used both in formate and acetate form. The capacity of the resin in retaining sialic acid was somewhat larger when it was in acetate form. Up to 5 ml of 0.4 N sulphuric acid could be added to the column without any sialic acid occurring in the effluent. If the material, however, contained more than 0.2 mequiv of inorganic cations the capacity of the resin to retain sialic acids was measurably lower. Therefore, the hydrolysed sample was first run through a Dowex-50 resin (H^+-form) when the concentration of inorganic cations was more than 0.1 mequiv.

Table 3. Elution of N-acetylsialic acid from Dowex 2 columns. 225 μg of N-acetylsialic acid was hydrolysed with 5 ml of 0.1 N sulphuric acid at 80°C for 1 h and quantitatively transferred to the resin column. Elution was performed under varying conditions. The effluent was analysed with the resorcinol method, and the total absorbancy determined.

	Acetate buffer pH 4.6			
Volume	Molarity			
(ml)	0.2	0.5	0.8	1.0
	Absorbancy			
4	—	1.25	4.60	5.45
6	—	5.50	5.85	6.10
8	0.600	6.00	6.20	6.25
10	—	—	6.20	6.15
20	—	—	6.15	6.10

Elution of sialic acid. An acetate buffer of pH 4.6 was used for the quantitative elution of sialic acid. At pH 4.6 the stability of the sialic acids is optimal, as judged from the reading of the samples in ultraviolet light [9]. The sialic acids were quantitatively eluted with 8 ml of 1 M acetate buffer (Table 3). The yield of sialic acid was neither enlarged by increasing the volume and the strength of acetate nor by changing the pH of the buffer. With a lower concentration of the acetate buffer or with a smaller volume the elution was not quite quantitative.

Sialic acid determination. Of the colorimetric methods applied for the determination of sialic acids the resorcinol method is the most sensitive one and give the lowest standard error. Therefore, it was used as the standard method. The colour development with the reagent was not influenced by an acetate concentration of up to 2 M in the samples. At the determination of sialic acid in body fluids as serum, lymph, milk, synovial fluids and transudates no other carbohydrate was eluted together with the sialic acids. However, when tissues were hydrolysed also nucleic acids were released and the phosphate esters of ribose were retained by the columns and eluted together with the sialic acids. The ribose esters were displaced somewhat slower than the sialic acids but it was impossible to eluate sialic acid quantitatively without a large part of the ribose also being eluted. A rather accurate calculation of the interference from ribose could be made by dichromatic readings, but it would be preferable to analyse the samples with another method, too. Several methods have been applied but none has been quite satisfactory. With the diphenylamine reagents [11,12] ribose had a low absorbancy, but some unknown substances in the tissues gave a false absorbancy of sialic acid. The direct Ehrlich reaction [2] was rather specific but it was insensitive with a very large standard error. A good reproducibility was also obtained with the orcinol method [3] but the absorbancy of ribose was high. The reactions mentioned will be discussed further in a forthcoming paper on the determination of sialic acid in nervous tissue [10].

Table 4. The concentration of sialic acid in different biological materials. All values are expressed as N-acetylsialic acid ($C_{11}H_{19}NO_9$).

Samples	Number of analyses	N-acetylsialic acid mg per 100 g wet weight	dry weight
Serum, human	25	63.0	
» rabbit	2	64.1	
» sheep (pooled)	2	63.6	
Joint fluid, human	2	80.8	
Milk, human	20	118.8	
» cow (pooled)	2	12.2	
» cow's colostrum	2	180.7	
Semen, human	4	105.5	
Brain, calf (total)	3	82.0	465
» pig (total)	3	84.9	446
» » (grey matter)	3	95.8	630
» sheep (total)	3	87.1	417
Kidney, human	4	35.5	291
» bovine	2	29.9	254
» calf	2	48.7	243
» horse	2	24.9	128
» pig	2	33.5	234
Liver, human	2	16.0	114
Pancreas, sheep	3	41.5	159
Parotis gland, horse	2	29.2	104
Submaxillary gland, elk	2	138.5	591
» » horse	3	111.5	482
» » pig	3	659	2 732

Accuracy. The standard error of the whole procedure was calculated from duplicate determinations of 20 sera. 0.2 ml of serum was hydrolysed with 5 ml of 0.1 N sulphuric acid at 80°C for one hour. The standard deviation was $\pm$ 1.4 %. In parallel determinations the sialic acid concentration was also determined by a direct analysis of alcohol-precipitated sera and the absorbancy of the hexoses was corrected by dichromatic readings. The standard deviation with the latter procedure was considerably larger, $\pm$ 3.6 %. Normal as well as pathological sera were analysed. The agreement between the two procedures was good. The standard error was also calculated on the analyses of sialic acid in fresh brain tissue of human fetuses. The standard deviation was there $\pm$ 1.6 %.

APPLICATION OF THE METHOD

The resin separation method has been applied to hydrolysates of several biological materials. The hydrolysis was performed with 5 ml of 0.1 N sulphuric acid at 80°C and 5 ml of 0.05 N sulphuric acid at 90°C for one hour. In

general there was a good agreement between the two procedures but for some tissues with a rather low concentration of sialic acid (e.g. kidney and liver) the value found with 0.05 N sulphuric acid was 5—10 % lower. In these cases only the figures found with the stronger sulphuric acid were used for the calculations of the sialic acid content.

All the figures are calculated as N-acetylsialic acid. In the physiological state the sialic acids often contain at least one O-acetyl groups as well. Besides, instead of the N-acetyl group the sialic acids may partly be substituted by an N-glycolyl group. In fact only in human sources the N-glycolylsialic occurs in negligible amounts. In all the other species investigated (beef, horse, pig and sheep) the N-glycolylsialic acid constitutes from 10—90 % of the total amount of sialic acids [10]. The molar absorbancy index of N-glycolylsialic acid is 15—20 % greater * than that of N-acetylsialic or N,O-diacetylsialic acid in the common colorimetric methods for sialic acids [3-5]. Therefore the figures for sialic acid in many cases are too high especially in beef tissues and pig submaxillary gland where N-glycolylsialic acid constitutes at least 50 %.

All the figures are calculated from the values of the hydrolysed and resin-treated standard samples of N-acetylsialic acid. In this procedure about 5 % of the standard substance was destroyed but in some tissues (liver and kidney) the destruction of sialic acid was probably larger. However, no correction was made for this excess destruction.

Acknowledgement. The skilful assistance of Mrs. Inga Björklund and Mrs. Aino Raal is gratefully acknowledged. The investigation was supported by grants from *Statens Medicinska Forskningsråd.*

REFERENCES

1. Böhm, P., Dauber, St. and Baumeister, L. *Klin. Wschr.* **23** (1954) 289; Böhm, P. and Baumeister, L. *Hoppe-Seyler's Z. physiol. Chem.* **305** (1956) 42.
2. Werner, I. and Odin, L. *Acta Soc. Med. Upsaliensis* **57** (1952) 230.
3. Svennerholm, L. *Arkiv Kemi* **10** (1957) 577.
4. Svennerholm, L. *Biochim. et Biophys. Acta* **24** (1957) 604.
5. Svennerholm, L. *Biochem. J.* **64** (1956) 11P.
6. Gottschalk, A. *Nature* **177** (1955) 881.
7. Klenk, E. and Faillard, H. *Hoppe-Seyler's Z. physiol. Chem.* **298** (1954) 230.
8. Svennerholm, L. *Acta Soc. Med. Upsaliensis* **61** (1956) 75.
9. Berggård, I. and Odin, L. *Personal communication.*
10. Svennerholm, L. and associates, *Unpublished results.*
11. Dische, Z. *Mikrochemie* **7** (1929) 33.
12. Dische, Z. *Mikrochemie* **8** (1930) 4.

Received January 7, 1958.

* *Added in proof:* With a recently prepared sample of N-glycolylsialic acid the molar absorbancy index was 30 % greater than that of N-acetylsialic acid.

ACTA CHEMICA SCANDINAVICA 12 (1958) 555—560

The Separation of Nucleotides by Continuous Ionophoresis

ROLF BERGKVIST

Institute of Biochemistry, University of Lund, Sweden

The separation of the adenine, guanine, cytosine and uracil 5′-ribonucleotides by continuous ionophoresis is described. The method is used for a quantitative separation and estimation of a complex nucleotide mixture.

The results obtained in a previous investigation [1] have demonstrated the value of paper ionophoresis for the separation and estimation of nucleotides. An apparatus was described which allows the ionophoretic separation of substances with very small differences in mobility. By a combination of paper chromatography and ionophoresis a complete separation of the 5′-mono-, di- and triphosphates of adenosine, guanosine, cytidine and uridine together with uridine diphosphate glucose, uridine diphosphate acetylglucosamine, diphospho- and triphosphopyridine nucleotides was obtained. The method to be described differs from the other one in that the mixture to be separated is continuously fed into the apparatus and the separated components can be continuously removed, so that it can be used for preparative purposes.

The method is based on the principle of passing a background electrolyte down a filter paper sheet by gravity. The mixture to be separated is applied at a prescribed intermediate position and passes along with the electrolyte as a narrow band. An electrical potential is applied across the filter paper curtain at right angles to the direction of flow and the various substances are deflected toward the anode or the cathode in accordance with their mobility behaviour in the electrical field.

The first successful apparatus using filter paper as a supporting medium for continuous ionophoresis was described by Grassmann and Hannig [2]. We have used a commercial model of their apparatus, which is available from the firm Bender and Hobein (Munich, Germany) under the name of "Elphor Va". This instrument has a free hanging curtain and is without cooling. A uniform field of potential is achieved by attaching the platinum wire electrodes to the vertical edges of the paper. In order to prevent diffusion of electrolysis products from the electrodes to the main body of the curtain, the electrodes are continually bathed with fresh buffer solution and are separated from the paper by a cellophan membrane. The rate of flow of the electrolyte down the paper and its composition must be kept constant. For this reason a supply of fresh

electrolyte is provided by allowing the paper to dip into a trough supplied with a device that maintains the electrolyte at a constant level. After passing through the paper the liquid is collected from 42 tongues cut in the paper along the lower edge. In this way the effluent is equally distributed over a number of fractions, each containing substances with mobilities within a certain small range. The mixture to be separated is injected by a mechanically operated syringe.

The degree of separation is determined by the electrophoretic mobility of the different components, the composition of the electrolyte, the voltage across the paper and the length of time that the substances are subjected to the field, which in turn depends on the grade of filter paper used. For a given flow rate, an increase in field intensity produces an improved resolution. When the current is too high, however, the water from the electrolyte may evaporate so rapidly that the downward flow is not sufficient to wash the paper, and in extreme cases electrolyte solids may be deposited, thus disrupting the steady state. A high flow rate enables larger amounts of material to be separated, but the separation of the different components increases the longer they remain on the paper. The final choice in the selection of experimental condition must be a compromise of the factors mentioned above.

The best separation of the nucleotides was obtained using an acetate buffer of pH 4.15, as has been shown earlier [1]. Since electrolytes of low ionic strength permit higher field intensities to be applied with relatively low current, it was found suitable to use a buffer of ionic strength 0.033. Many different types of filter paper with various degrees of porosity and thickness were tested and the best separation was obtained with Whatman No. 1 paper sheets, which were well washed with hydrochloric acid before use.

The maximum usable potential was found to be 320 volts. This voltage was applied across the platinum electrodes, and after about 6 h a steady state had been established. With this voltage a current of 17 mA was observed to flow constantly. The mechanically operated syringe was charged with the nucleotide mixture to be separated and fixed into position at a point in the upper part of the paper near the cathode and the synchronous motor was started. In order to obtain a quantitative recovery, it was necessary to collect fractions for about 20 h after all the sample had been applied to the paper.

Much useful information about the efficiency of the separation and to the location of the individual substances in the collecting tubes could be obtained from a study of the paper curtain itself. For this purpose the paper was carefully dried and then the different bands were located by making a contact print of the curtain in monochromatic ultraviolet light of 254 mμ.

The separation of mixtures of authentic adenine, guanine, cytosine and uracil nucleotides can be seen in Fig. 1, which shows the contact prints of the paper curtains from the separations. All the nucleotides tested could be separated with the exception of UDPG * and UDPAG, which were obtained as one fraction UDPX.

* Abbreviations used: A, adenosine; G, guanosine; C, cytidine; U, uridine; MP, monophosphate; DP, diphosphate; TP, triphosphate; UDPG, uridine diphosphate glucose; UDPAG, uridine diphosphate acetylglucosamine; DPN, diphosphopyridine nucleotide; TPN, triphosphopyridine nucleotide.

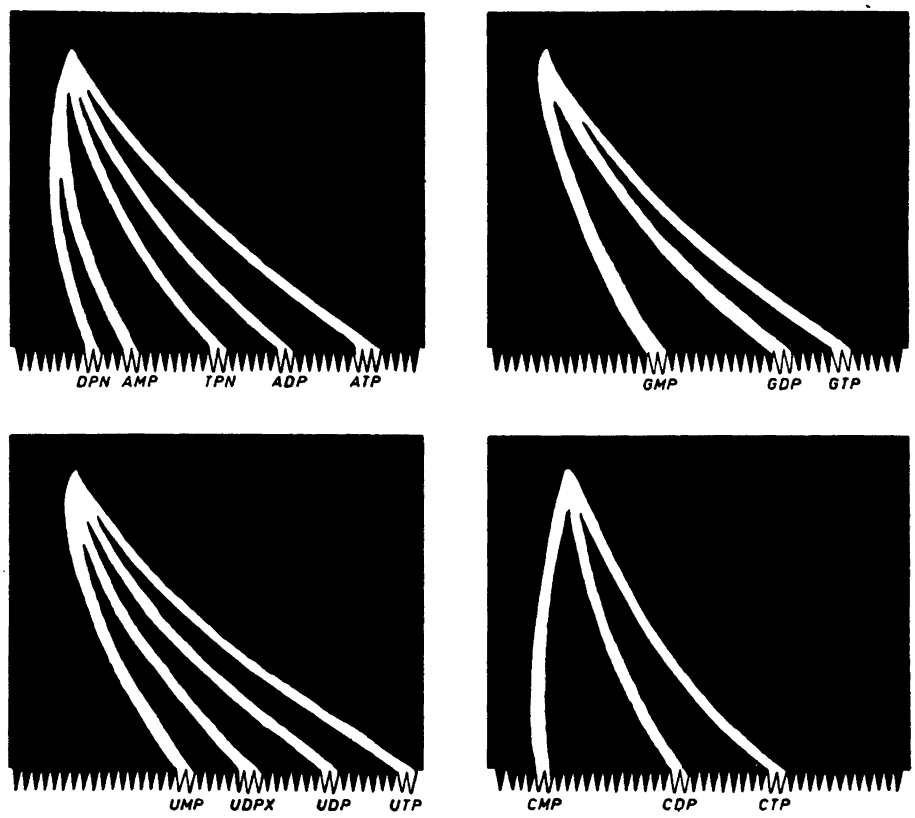

Fig. 1. Contact prints of the paper curtains from separations of groups of nucleotides by continuous ionophoresis. Conditions employed: Whatman No. 1 filter paper; sodium acetate buffer of ionic strength 0.033 and of pH 4.15; 320 V. The cathode was attached to the left edge of the paper curtain and the anode to the right one.

All the actual purine and pyrimidine nucleotides could be quantitatively separated after first fractionating the original mixture by means of paper chromatography [1] into the following groups: (1) AMP, ADP, ATP and DPN; (2) TPN and GMP; (3) GDP and GTP; and (4) CMP, CDP, CTP, UMP, UDP, UTP, UDPG and UDPAG. The different groups were eluted from the paper and concentrated sufficiently for further analysis by adsorption on norite and subsequent elution by ethanol-ammonia.

The concentrated solutions thus obtained could be separated into the different components by continuous ionophoresis. The separation of the different nucleotides was studied measuring the optical densities of the fractions collected from the individual tongues at 250, 260 and 270 mμ with the buffer as the blank. The fraction number and the absorbancy ratios E_{250}/E_{260} and E_{270}/E_{260} could be used for identification of the various nucleotides.

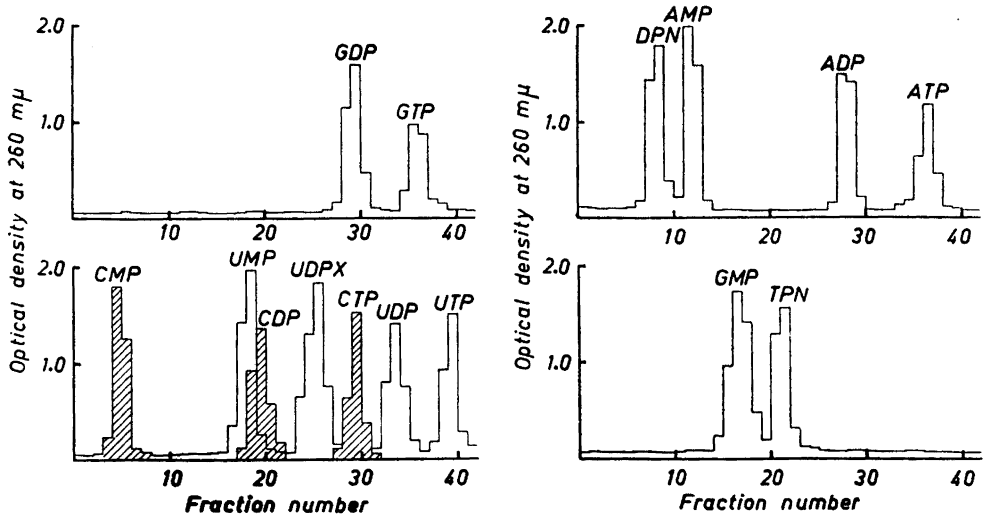

Fig. 2. Separations by continuous ionophoresis of the groups of nucleotides obtained after paper chromatographic fractionation. The same experimental conditions were used as described for Fig. 1. The fraction volumes were adjusted to 3.0 ml with buffer.

To obtain some quantitative measure of the separation efficiency test mixtures of known compositions were analysed by the combination of paper chromatography and continuous ionophoresis. Fig. 2 shows the diagrams obtained by the ionophoretic separation of the groups of nucleotides obtained after paper chromatographic fractionation.

The only components, which were not sufficiently separated, in addition to the uridine diphosphate sugar compounds, were UMP and CDP, but these

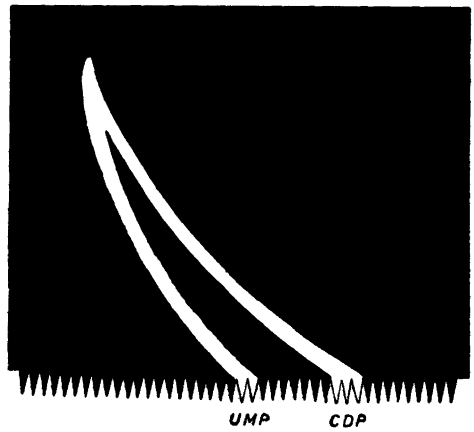

Fig. 3. Contact print of the paper curtain from the separation of UMP and CDP. The same experimental conditions as described for Fig. 1 were used besides that the buffer had a pH of 5.0 and the potential was 340 V.

Table 1. Analysis of a mixture of authentic nucleotides. The concentrations were calculated using the molecular extinction coefficients previously reported [3].

Compound	μmoles of nucleotide		Recovery %
	Calculated	Found	
AMP	3.16	3.13	99
ADP	2.80	2.58	92
ATP	2.32	2.16	93
DPN	2.56	2.25	88
TPN	2.36	2.17	92
GMP	5.48	5.15	94
GDP	3.92	3.80	97
GTP	2.72	2.45	90
CMP	6.52	6.25	96
CDP	6.04	5.75	95
CTP	5.20	4.95	95
UMP	4.96	5.00	101
UDP	4.00	3.84	96
UTP	3.68	3.24	88
UDPG	3.36	2.89	86
UDPAG	2.36	2.19	93

substances could easily be separated by paper chromatography or continuous ionophoresis with a buffer of other pH. Fig. 3 shows the separation of these substances with an acetate buffer of pH 5.0 and ionic strength 0.033.

Recoveries of 85—95 % were obtained, as can be seen from Table 1. Because of the number of components which are to be separated and the number end nature of the operations in these analyses, higher recoveries can hardly be expected. Yields of 95—100 % could be obtained for mixtures of nucleotides which could be separated directly on a single paper curtain. DPN was slightly decomposed during the separation but none of the other substances were found to be destroyed.

The earlier described apparatus [1] for one-dimensional ionophoresis with long travelling distances gives a sharper and more rapid separation of nucleotides than is obtainable by continuous ionophoresis. The presently described method is, however, more suitable for separations of larger amounts of material where the capacity of the other apparatus would be exceeded.

EXPERIMENTAL

Continuous ionophoresis. The apparatus consists of a framework holding a trough and the vertical electrode chambers. This frame is placed in a cemented glass case. The dimensions of the paper sheet are 47 × 47 cm, excluding the tongues. A 4 cm portion at the top dips into the trough and the vertical edges are pressed against the electrode chambers, but separated from them by a cellophan membrane. The washing of the electrodes and the constant level control of the solution in the trough is regulated by three Mariotte flasks.

Ionophoresis was carried out on Whatman No. 1 papers purified by washing three times with N hydrochloric acid and finally with water until the pH of the paper was about 7. An acetate buffer of ionic strength 0.033 and of pH 4.15 was used both as background electrolyte and to wash the electrodes. For the separation of UMP and CDP the buffer had a pH of 5.0.

The substance is applied by the insertion of the plunger of a glass syringe by means of a synchronous motor. This apparatus can give 0.020—0.900 ml per hour with different transmissions and syringes. The syringe is fitted with a glass tip joined to the syringe by polyvinyl chloride tubing of 0.6 mm bore. The point of application of the material is 8 cm below the lip of the trough and 9 cm from the cathode. The amount of each component applied per hour varied from 0.03 to 0.50 μmoles. At higher concentrations the zones became a little wider.

The different nucleotides could be identified and their concentrations determined from the optical densities of the fractions using the absorbancy ratios and molar absorbancies reported earlier [3]. The concentrations of the overlapping cytosine and uracil nucleotides could be approximately calculated from the absorbancy ratios.

When using exactly the same experimental conditions substances appeared in the same tubes for different analyses. With care the same paper curtain could be used for many separations.

Paper chromatography. The group separation of the nucleotides was performed as described earlier [1] on large sheets of Whatman No. 1 papers (50 × 110 cm) with the following solvent system: saturated ammonium sulphate-water-*iso*propanol (79:19:2).

The separation of the uridine diphosphate sugar compounds could be attained by paper chromatography in a solvent composed of 7.5 volumes of 95 % ethanol and 3 volumes of 1 M ammonium acetate solution of pH 7.5. UMP and CDP could also be separated in this as well as in many other solvent systems.

Materials. The nucleotides used were obtained from the Sigma Chemical Company. The mixtures to be analysed were obtained by mixing measured volumes of stock solutions of known composition.

The author wishes to express his gratitude to *Sigma Chemical Company* for gifts of many of the nucleotides.

This work has been supported by grants from the *Swedish Natural Science Research Council.*

REFERENCES

1. Bergkvist, R. *Acta Chem. Scand.* **11** (1957) 1465.
2. Grassmann, W. and Hannig, K. *Naturwiss.* **37** (1950) 397.
3. Bergkvist, R. *Acta Chem. Scand.* **10** (1956) 1303.

Received January 14, 1958.

ACTA CHEMICA SCANDINAVICA 12 (1958) 561—567

Synthesis of Phosphopeptides

I. Peptides of DL-Serine and Glycine

GEORG FÖLSCH

Department of Medical Biochemistry, University of Gothenburg, Sweden

The synthesis of unphosphorylated, O-phosphorylated and O-monophenylphosphorylated DL-serylglycine, glycyl-DL-serine and glycyl-DL-serylglycine is described. Infrared absorption spectra of O-phosphorylated peptides are shown.

In 1933 Schmidt [1] as well as Levene and Hill [2] isolated a phosphorus-containing peptide from hydrolysed casein. Posternak and Pollaczek [3] proved that the structure of this peptide was O-phosphoryl-L-seryl-L-glutamic acid. Later, this and other phosphopeptides have been obtained *, particularly in recent years in connection with structural studies on phosphorus-containing proteins [4–11]. Phosphorylated peptides containing glycine have mainly been isolated from hydrolysates of phosphorylated α-chymotrypsin [5–8], but also from an enzymatically synthesized polypeptide [4]. O-Phosphorylserylglycine (Fig. 1., compound Ia) was the phosphopeptide from α-chymotrypsin first described and Shaeffer showed that this peptide was partly converted to glycyl-O-phosphorylserine (Fig. 1., compound IIa) during acid hydrolysis [7]. These two peptides, containing only glycine beside one serine residue are well adepted for model compounds in synthetic studies. As only one asymmetric centrum is present, DL-serine can be used in studies of this kind without the formation of diastereoisomers, a complication that occurs, when other amino acids than glycine are used.

We have prepared synthetic phosphorylated peptides in two different ways **. The most successful route so far has been to synthesize an N-carbobenzoxypeptide benzyl ester first, then introduce a suitable phosphoryl group and finally remove all protecting groups by catalytic hydrogenolysis [13].

* A review of earlier work is given by Perlmann, G. E. *Advances in Protein Chem.* **10** (1955) 1.

** In some cases, mixed anhydrides from N-acylamino acids [12] have been used for N-acylation of O-phosphorylserine. Such N-acylations of phosphorylated serine derivatives, including O-diphenylphosphorylserine [13] and the corresponding benzyl ester [14] will be further investigated.

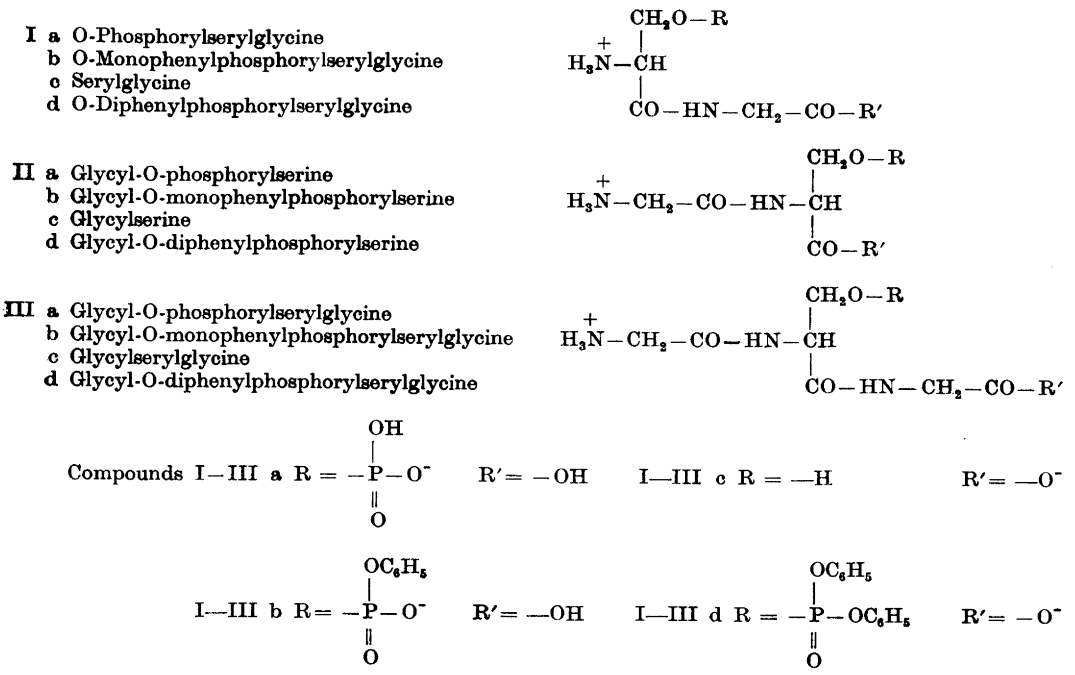

Fig. 1. Structure of serine and glycine peptides.

In the synthesis of N-carbobenzoxypeptide benzyl esters used in this work, the procedure of Sheehan [15] has given equal or better over all yields than with the azide route [16] or with the mixed anhydride technique [12]. The phosphorylation and hydrogenolysis have been performed in this work as described in the synthesis of O-phosphorylserine *, and in the case of peptides it was also possible to isolate diphenylphosphorylated and monophenylphosphorylated intermediates during the hydrogenolysis **. The structure of the compounds is shown in Fig. 1.

Infrared absorption spectra have been recorded and some of them are shown in Fig. 2. The paper chromatographic behaviour of the compounds has been studied, and R_F values are given in Table 1. As in the case of other peptides containing N-terminal glycine, also all the synthesised O-phosphorylated, mono-and diphenylphosphorylated peptides having N-terminal glycine

* For an reaction scheme, see this synthesis (Ref.[13]). Riley *et al.*[14] have recently described the synthesis of O-phosphorylated derivatives of hydroxyamino acids and peptides, for the investigation of which alkaline hydrolysis was used as an alternative for the elimination of phenylic ester groups.

** Bevan *et al.*[17] recently isolated this type of O-monophenylphosphorylated derivatives by hydrogenolytic cleavage of diphenylphosphates.

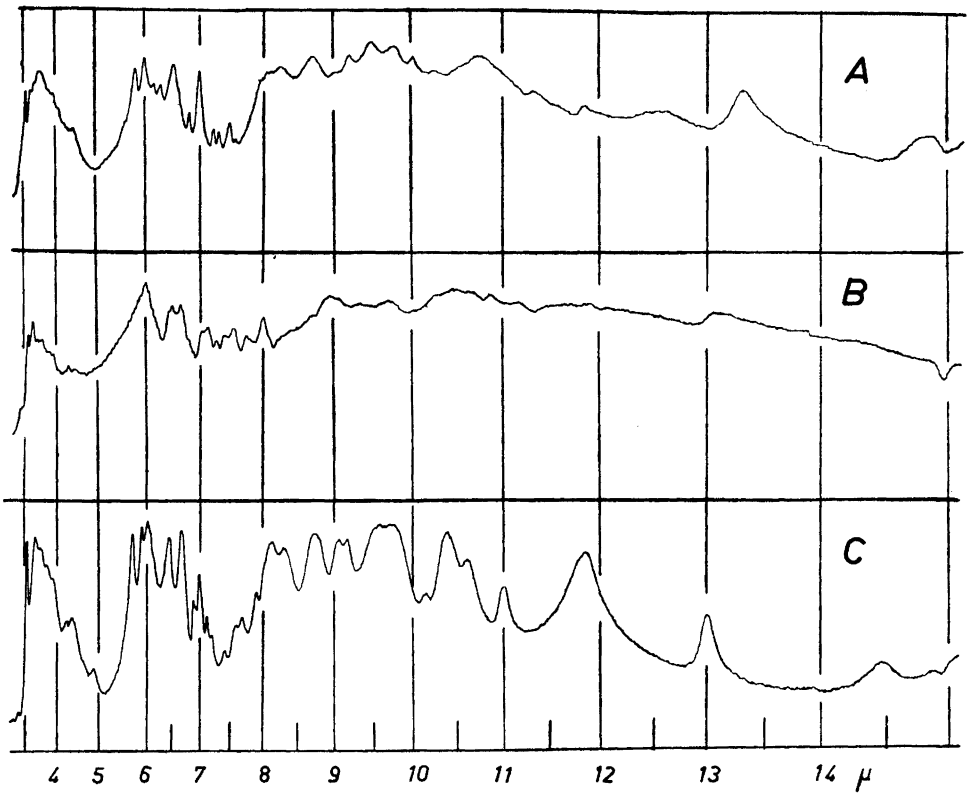

Fig. 2. Infrared absorption spectra of O-phosphoryl-DL-serylglycine (A), glycyl-O-phosphoryl-DL-serine (B) and glycyl-O-phosphoryl-DL-seryl-glycine (C). Compounds (1.4 mg) in potassium bromide (300 mg) pellets.

give an initial yellow colour with ninhydrin spray reagent. After some time (about half an hour) the colour changes slowly to the normal brown-violet tones.

EXPERIMENTAL

Melting or decomposition points, elementary analyses and infrared spectra were all determined as described previously [13]. Solvents in the paper chromatography were also as before: (I) Phenol-water (80/20 v/v), ascending, about 6 h, (II) *n*-Butanol-acetic acid-water (40/10/50 v/v), descending, about 18 h.

N-Carbobenzoxy-DL-serylglycine benzyl ester

a) By the azide route [16]: A vigorously stirred mixture containing 15.6 g (0.1 mole) of DL-serine methyl ester hydrochloride, 5.2 g (0.13 moles) of magnesium oxide, 75 ml of water and 180 ml of chloroform was cooled in an ice-salt mixture, and 23 g of carbobenzoxy chloride [18] was added dropwise within 1/2 h. After continued stirring for 1/2 h,

Table 1. DL-Serine and glycine peptides.

Compounds *	Molecular formula	Decomp. p.** °C	R_F values *** in solvent I	R_F values *** in solvent II	Analysis Found C	Found H	Found N	Found P	Calc. C	Calc. H	Calc. N	Calc. P
					O-phosphorylated peptides							
I a H.SerP-Gly.OH ****	$C_5H_{11}O_7N_2P$	(242.1) 189—192	0.12	0.11	25.0	4.6	11.5	11.7	24.8	4.6	11.6	12.8
II a H.Gly-SerP.OH	$C_5H_{11}O_7N_2P$	(242.1) 201—204	0.09	0.08	25.3	4.6	11.4	12.4	24.8	4.6	11.6	12·8
III a H.Gly-SerP-Gly.OH	$C_7H_{14}O_8N_3P$	(299.2) 220—223	0.13	0.08	28.2	4.7	13.9	10.3	28.1	4.7	14.0	10.4
					O-monophenylphosphorylated peptides							
I b H.SerφP-Gly.OH	$C_{11}H_{15}O_7N_2P$	(318.2) 207—209	0.42	0.37	41.6	4.8	8.6	9.7	41.5	4.8	8.8	9.7
II b H.Gly-SerφP.OH	$C_{11}H_{15}O_7N_2P$	(318.2) 176—178	0.38	0.30	38.4	4.8	8.5	9.3	41.5	4.8	8.8	9.7
III b H.Gly-SerφP-Gly.OH	$C_{13}H_{18}O_8N_3P$	(375.3) 198—202	0.40	0.34	40.8	4.7	10.9	8.4	41.6	4.8	11.2	8.3
					Corresponding peptides							
I c H.Ser-Gly.OH	$C_5H_{10}O_4N_2$	(162.1) 203—205	0.40	0.18	35.2	5.6	16.5		37.0	6.2	17.3	
II c H.Gly-Ser.OH	$C_5H_{10}O_4N_2$	(162.1) 197—199	0.35	0.16	36.1	5.8	16.7		37.0	6.2	17.3	
III c H.Gly-Ser-Gly.OH	$C_7H_{13}O_5N_3$	(219.2) 208—210	0.40	0.16	37.7	6.2	18.7		38.4	6.0	19.2	

* For abbreviations and symbols, see Sachs, H. and Brand, E. *J. Am. Chem. Soc.* **75** (1953) 4608. The symbol SerP is here used for an O-phosphorylserine residue, $HN \cdot CH[CH_2OPO(OH)_2]CO$, SerφP for an O-monophenylphosphorylserine residue, $HN \cdot CH[CH_2OPO(OH)OC_6H_5]CO$. Compounds numbered according to Fig. 1.

** See Ref.[13], p. 1237, foot note three.

*** The R_F values are calculated from several one-dimensional chromatograms, on which serine had R_F 0.36 in solvent I and 0.18 in solvent II. The three phosphorylated peptides are well separated on two-dimensional chromatograms in solvent I and II.

**** This compound has also been obtained in a low yield by the use of dibenzylphosphoryl chloride as phosphorylating reagent [22]. Riley *et al.*[14] report a m.p. of 150—154° (decomp.) for the compound obtained by alkaline hydrolysis.

5 ml of pyridine was added and the mixture acidified with cold 5 N hydrochloric acid (Congo red). The N-carbobenzoxy-DL-serine methyl ester was taken up in chloroform. The solution was washed with hydrochloric acid, bicarbonate and water, and was finally dried over sodium sulphate. The chloroform was distilled off *in vacuo*, the residue evaporated three times with ethanol and finally dissolved in 100 ml of absolute ethanol. Seven ml of hydrazin hydrate (b.p. 120—121°) was added and the solution left over night. N-carbobenzoxy-DL-seryl hydrazide, 17.2 g (66 %), thus crystallised. M. p. 158—160° (Reported [14] 162—163°). To a solution of 13.2 g (0.05 moles) of the hydrazide in 60 ml of acetic acid, 25 ml of 5 N hydrochloric acid and 250 ml of water was added at −5° a concentrated solution of 3.3 g (0.053 moles) of sodium nitrite. The azide formed, was taken up in 300 ml of cold ether, and the solution was washed and dried in the cold. A cold dry etheral solution of free glycine benzyl ester, freshly prepared from 15.2 g (0.075 moles) of the hydrochloride [19] was added to this solution. The mixture was left for 24 h, whereby a large part of the peptide derivative crystallised out from the solution. The crystals were filtered off, washed with ether, the combined ether solutions were washed with acid, bicarbonate, and water and after drying over sodium sulphate, evaporated to dryness. The residue was crystallised from ethyl acetate and light petroleum (b.p. 20—40°). The total yield of crystalline N-carbobenzoxy-DL-serylglycine benzyl ester was 13.2 g (68 %). M. p. 100—101°. (Found: C 62.7; H 5.8; N 7.3. Calc. for $C_{20}H_{22}O_6N_2$ (386.2): C 62.1; H 5.7; N 7.3).

b) By the mixed anhydride route [12]: 1.95 ml (20 mmoles) of ethyl chlorocarbonate was added to a solution of 4.8 g (20 mmoles) of N-carbobenzoxy-DL-serine [20] and 2.8 ml, (20 mmoles) of triethylamine in 25 ml of anhydrous dimethylformamide at a temperature of 0—5°. Ten minutes later a solution of 4.0 g (20 mmoles) of glycine benzylester hydrochloride [19] and 2.8 ml of triethylamine in 25 ml of dimethylformamide was added, causing a vigorous evolution of carbon dioxide. Next day the mixture was evaporated to dryness *in vacuo* and the residue was extracted in ethyl acetate. The solution was washed and worked up as above, yielding 3.8 g (50 %) crystals from ethyl acetate and light petroleum, m. p. 100—101°.

c) By the carbodiimide procedure [15]: To a solution of 2.4 g (10 mmoles) of N-carbobenzoxy-DL-serine in 25 ml of dimethylformamide was added 1.8 g (15 mmoles) of free glycine benzyl ester [19] and 2.1 g (10 mmoles) of N,N′-di*cyclo*hexylcarbodiimide. The reaction mixture was filtered after 5 h, yielding 2.0 g of N,N′-di*cyclo*hexylurea (m.p. 237—240° decomp.). The solution was evaporated to dryness *in vacuo*, and the residue was dissolved in 75 ml of ethyl acetate. This solution was worked up as above, yielding 2.8 g (72 %) of N-carbobenzoxy-DL-serylglycine benzyl ester m.p. 100—101°.

Carbobenzoxyglycyl-DL-serine benzyl ester

a) By the mixed anhydride route: To the mixed anhydride, prepared as above from 8.4 g (40 mmoles) of carbobenzoxyglycine, 5.6 ml of triethylamine and 3.84 ml of ethyl chlorocarbonate in 40 ml anhydrous dimethylformamide was added a cold mixture of 10.2 g (44 mmoles) of DL-serine benzyl ester hydrochloride [21], 6.2 ml of triethylamine and 40 ml of dimethylformamide. After 5 h at room temperature, the reaction mixture was filtered and evaporated to dryness, and the residue shaken with 100 ml of ethyl acetate and 50 ml of water. The ethyl acetate solution was worked up as in the case of the aforegoing compound, yielding 11.2 g (72 %) of carbobenzoxyglycyl-DL-serine benzyl ester, m. p. 141—142° (from ethanol-ether). (Found: C 62.1; H 5.8; N 7.3. Calc. for $C_{20}H_{22}O_6N_2$ (386.2) C 62.1; H 5.7; N 7.3).

b) By the carbodiimide procedure: From 8.4 g (40 mmoles) of carbobenzoxyglycine, 10.2 g (44 mmoles) of DL-serine benzyl ester hydrochloride, 5.6 ml of triethylamine and 8.4 g of N,N′-dicyclohexylcarbodiimide, a yield of 10.7 g (69 %) m. p. 141—142° was obtained by the same procedure as already described.

Carbobenzoxy glycyl-DL-seryl glycine benzyl ester

To the mixed anhydride prepared as above from 8.4 g of carbobenzoxyglycine, was added a cold solution of 4.4 g (40 mmoles) of DL-serine in 20 ml of 2 N sodium hydroxide. Carbon dioxide was vigorously evolved. After 6 h at room temperature the mixture

was evaporated to dryness *in vacuo*, the residue dissolved in 50 ml of water, washed with ether, and acidified with cold 5 N hydrochloric acid. The oil which separated was taken up with three 50 ml portions of ethyl acetate, the ethyl acetate distilled off at reduced pressure and the residue treated with ether and scratched, resulting in crystals of carbobenzoxyglycyl-DL-serine, 10.5 g (88 %) separating. M. p. 153—154° (recryst. from ethanol-ether). (Found C 52.6; H 5.6; N 9.3. Calc. for $C_{13}H_{16}O_6N_2$ (296.3): C 52.7; H 5.4; N 9.5). To a solution of 5.9 g (20 mmoles) of this compound in 25 ml of dimethylformamide was added 4.4 g (20 mmoles) of glycin benzyl ester hydrochloride, 2.8 ml (20 mmoles) of triethylamine, followed by 4.2 g (20 mmoles) of N,N'-di*cyclo*hexylcarbodiimide. After 6 h, the precipitate of di*cyclo*hexylurea (4.0 g) was filtered off and the solution was evaporated ty dryness *in vacuo*. The remaining oil was brought to crystallisation by shaking and scratching in water and ether. After recrystallisation from ethanol, carbobenzoxyglycyl-DL-serylglycine benzyl ester, 5.8 g (65 %) was obtained. M. p. 169—170°. (Found: C 59.9; H 5.7; N 9.7. Calc. for $C_{22}H_{25}O_7N_3$ (443.4): C 59.6; H 5.7; N 9.5).

Phosphorylation

The procedure previously described [13] was used throughout. To 20 mmoles of carbobenzoxypeptide benzyl ester in 10 to 15 ml of anhydrous pyridine was added 6.4 g (24 mmoles) of diphenylphosphoryl chloride with shaking and moderate cooling. After 4 h 1 ml of water was added, 1/2 h later the reaction mixture was poured into 150 ml of water and 100 ml of chloroform *. The chloroform solution was washed with cold 4 N sulphuric acid, water, 20 % bicarbonate solution, and again with water. After drying over sodium sulphate, the solvent was evaporated *in vacuo*, the residue being the expected diphenylphosphate ester in about 90 % yield. This procedure resulted in O-diphenylphosphoryl-N-carbobenzoxy-DL-serylglycine benzyl ester, colourless oil, $n_D^{21°}$ 1.5642. (Found: N 4.7. Calc. for $C_{32}H_{31}O_9N_3P$ (618.6): N 4.5), O-diphenylphosphoryl-N-(carbobenzoxyglycyl)-DL-serine benzyl ester, colourless oil, $n_D^{20°}$ 1.5620, (Found: N 4.8. Calc. for $C_{32}H_{31}O_9N_3P$ (618.6): N 4.5) and O-diphenylphosphoryl-N-(carbobenzoxyglycyl)-DL-serylglycine benzyl ester, colourless crystals, m. p. 85—86° (from ethanol-light petroleum). (Found: C 60.3; H 5.1; N 6.2; P 4.5. Calc. for $C_{34}H_{34}O_{10}N_3P$ (675.6): C 60.4; H 5.1; N 6.2; P 4.6).

Hydrogenolysis

When monophosphate esters (free phosphorylated peptides) were wanted, the hydrogenation was performed in glacial acetic acid with platinum oxide as catalyst. Water was added after some time to dissolve precipitated material. The time required for complete hydrogenolysis varied between 8 h and 15 h. Paper chromatography was useful for checking the amount of partly hydrogenated derivatives [13]. The residue obtained after filtration and evaporation of the solvent was treated in water solution with Amberlite IR 120 cation exchange resin (H^+ form) to eliminate metal cations, the filtered solutions was evaporated again and the phosphopeptide crystallised from hot water — ethanol.

Diphenylphosphoryl derivatives of the peptides were easily obtained when the hydrogenolysis was performed in ethanol solution with palladium oxide catalyst. Monophenylphosphoryl derivatives were obtained when hydrogenolysis in glacial acetic acid with platinum oxide catalyst was discontinued after a short time. The yields varied with the solubility of the diester **.

The carbobenzoxy peptide benzyl esters and carbobenzoxyglycyl-DL-serine were also hydrogenolysed with palladium catalyst to the free peptides. Analytical data, decomposition points and R_F values of the peptides are shown in Table 1.

* The glycylserine and glycylserylglycine derivatives are only sparingly soluble in ether.

** In a synthesis of O-phosphorylserylleucine (to be published) it vas difficult to isolate the monophenylphosphoryl derivative by hydrogenolysis in acetic acid. This compound, however, crystallised out when an acetic acid-ethanol (1:2) mixture was used.

Acknowledgements. The author wishes to express his sincere thanks to Professor Olof Mellander for his support in this work. He is also much indebted to Mrs. Karin Nilsson, Uppsala, for the infrared absorption spectra, to Miss Ulla-Britt Dahlberg, Uppsala, for the elementary analyses and to Mrs. Birgit Boman for technical assistance.

The work was supported by grants from *Swedish Medical Research Council* to Professor Olof Mellander.

REFERENCES

1. Schmidt, G. *Z. physiol. Chem. Hoppe-Seyler* **223** (1934) 86.
2. Levene, P. A. and Hill, D. W. *J. Biol. Chem.* **101** (1933) 711.
3. Posternak, T. and Pollaczek, H. *Helv. Chim. Acta* **24** (1941) 921.
4. Thoai, N.-V. and Pin, P. *Compt. rend.* **238** (1954) 737.
5. Turba, F. and Gundlach, G. *Biochem. Z.* **327** (1955) 186.
6. Oosterbaan, R. A., Kunst, P. and Cohen, J. A. *Biochim. et Biophys. Acta* **16** (1955) 299.
7. Schaffer, N. K., Harshman, S. and Engle, R. R. *J. Biol. Chem.* **214** (1955) 799.
8. Schaffer, N. K., Simet, L., Harshman, S., Engle, R. R. and Drisko, R. W. *J. Biol. Chem.* **225** (1957) 197.
9. Sampath Kumar, K. S. V., Sundararajan, T. A. and Sarma, P. S. *Biochim. et Biophys. Acta* **24** (1957) 218.
10. Anderson, L. and Jollés, G. R. *Arch. Biochem. Biophys.* **70** (1957) 121.
11. Hipp, N. J., Groves, M. L. and McMeekin, T. L. *J. Am. Chem. Soc.* **79** (1957) 2559.
12. Boissonas, R. A. *Helv. Chim. Acta* **34** (1951) 874.
13. Fölsch, G. and Mellander, O. *Acta Chem. Scand.* **11** (1957) 1232.
14. Riley, G., Turnbull, J. A. and Wilson, W. *J. Chem. Soc.* **1957** 1373.
15. Sheehan, J. C., Goodman, M. and Hess, G. P. *J. Am. Chem. Soc.* **78** (1956) 1367.
16. Fruton, J. S. *J. Biol. Chem.* **146** (1942) 463.
17. Bevan, T. H., Malkin, T. and Tiplady, J. M. *J. Chem. Soc.* **1957** 3086.
18. Bergmann, M. and Zervas, L. *Ber.* **65** (1932) 1192.
19. Miller, H. K. and Waelsch, H. *J. Am. Chem. Soc.* **74** (1952) 1092.
20. Baer, E. and Maurukas, J. *J. Biol. Chem.* **212** (1955) 25.
21. Li, S.-O. and Eakin, R. E. *J. Am. Chem. Soc.* **77** (1955) 1866.
22. Fölsch, G. *Acta Chem. Scand.* **9** (1955) 1039.

Received December 24, 1957.

ACTA CHEMICA SCANDINAVICA 12 (1958) 568—573

Distribution of Compounds in Polysaccharide Syntheses Using Dextransucrase

BENGT WEIBULL*

Tekniska Forskningscentralen, Svenska Sockerfabriks Aktiebolaget, Arlöv, Sweden

Quantitative results for the synthesis of methyl α-*iso*maltoside and its homologues from methyl α-D-glucoside and sucrose using dextransucrase were recently reported. The distribution of the saccharides can be accounted for if it is assumed that the synthesis proceeds by means of a stepwise transfer of glucosyl groups from sucrose to the primary hydroxyl group of the growing polymer. The rate of the first step is lower than that of the following ones, which seem to be kinetically identical. The reaction thus formally is analogous to the polyaddition of ethylene oxide to water and alcohols. The consequences of these results for the synthesis of dextran are discussed.

Some years ago Hehre [1] put forward the hypothesis that there exists a formal analogy between enzymic polysaccharide syntheses and the formation of polyethylene glycol by polyaddition of ethylene oxide to ethylene glycol. Reactions of the latter type have been studied extensively. The reaction proceeds by means of a stepwise addition of ethylene oxide, the reacting hydroxyl group being regenerated at each step. The distribution of compounds formed was recently studied theoretically and experimentally by Weibull and Nycander [2], and by Weibull [3]. The reaction steps were found to be kinetically identical with the exception of the first one, which generally proceeds at a rate different from the following ones. This accords with the fact that the reacting hydroxyl group is identically bound at every step except the first one. Formulae were derived for the molecular distribution of the polymer product. The following scheme illustrates the reaction:

$$ROH + \underset{\diagdown\,O\,\diagup}{CH_2CH_2} \rightarrow ROCH_2CH_2OH$$

$$ROCH_2CH_2OH + \underset{\diagdown\,O\,\diagup}{CH_2CH_2} \rightarrow ROCH_2CH_2OCH_2CH_2OH \; \textit{etc.}$$

* Present address: Mo och Domsjö AB, Örnsköldsvik, Sweden.

According to Hehre [1] the corresponding scheme for the synthesis of dextran from sucrose should be (Gl = glucose or anhydroglucose, Fr = fructose or anhydrofructose):

$$(\text{Gl-})_n + \text{Gl-Fr} \rightarrow (\text{Gl-})_{n+1} + \text{Fr}$$
dextran sucrose dextran fructose

Unfortunately the initial steps are not known, so it is not possible to apply the distribution formulae derived for the ethylene oxide reactions. A great many other enzymic polysaccharide syntheses have been investigated and also corresponding syntheses of oligosaccharides [4], but practically none of the results published lend themselves to a theoretical interpretation on these lines*. However, results were recently published concerning the synthesis of methyl *α-iso*-maltoside and its homologues from methyl α-D-glucoside and sucrose by means of dextransucrase [5]. The compounds formed were quantitatively separated by means of chromatographic methods as far as the oligosaccharide containing five glucose residues. The data given are well suited to test Hehre's hypothesis and, more specifically, the distribution formulae derived for ethylene oxide reactions. The role of the enzyme will not be considered — it is assumed to act as an ideal catalyst.

THEORETICAL

The derivation of the distribution formulae will not be repeated here. For convenience the final result is reproduced. The following notation accords with that previously used [2].

N_i molecule with i added monomer units (in this case glucose units)
m number of moles of monomer donor (in this case sucrose)
n_{00} » » » » acceptor or starting material (in this case methyl glucoside)
n_i » » » » N_i in the reaction product
c distribution constant = ratio of the equal velocity constants of the higher steps to that of the first step
$v = m/n_{00}$ average degree of polymerisation

The distribution formulae are:

$$v = c \ln \frac{n_{00}}{n_0} - (c - 1)\left(1 - \frac{n_0}{n_{00}}\right) \quad (1)$$

$$\frac{n_i}{n_{00}} = \frac{c^{i-1}}{(c-1)^i}\left\{\frac{n_0}{n_{00}} - \left(\frac{n_0}{n_{00}}\right)^c \sum_{j=0}^{i-1} \frac{1}{j!}\left[(c-1)\ln\frac{n_{00}}{n_0}\right]^j\right\} \quad (2)$$

Calculations

The present calculations are based on the data given in Table II of the paper mentioned [5]. For the sake of convenience this material is reproduced in Table 1 using the notation given above. Further, v_0 is the molar ratio of sucrose

* *Added in proof:* W. J. Whelan and J. M. Bailey (*Biochem. J.* 58 (1954) 560) investigated the molecular distribution of amylose synthesised with potato phosphorylase. They found agreement with the distribution calculated for a stepwise polyaddition.

to methyl glucoside at the beginning of the reaction, N_F, N_G, and N_L represent fructose, glucose and leucrose (5-*O*-α-D-glucopyranosyl-α-D-fructopyranose). Experiments 1, 2, 3, and 5 were carried out on a small scale and the analyses made by quantitative paper chromatography while experiment 4 was made on a preparative scale and the reaction product separated on a carbon-celite column. In experiment 4, 98 % of the total carbohydrate was soluble in 50 % methanol. About 2 % of these solubles contained more than five glucose residues and were not quantitatively determined. The insolubles were more highly polymerised material, presumably dextran.

Table 1. Composition of 50 % methanol-soluble fraction of the glycoside mixture, as glucose in % of total.

Expt. No.	v_0	N_0	N_1	N_2	N_3	N_4	$N_F + N_G$	N_L
1	3.0	11.8	4.6	8.8	10.8	7.2	51.5	5.2
2	1.5	15.5	10.6	11.4	11.4	7.8	40.8	2.4
3	0.75	27.5	12.9	13.5	10.5	5.1	29.9	0.6
4	0.75	26.0	12.7	13.9	10.9	5.1	30.2	1.2
5	0.3	51.0	17.3	10.1	3.5	0.5	17.5	—

Since the data in Table 1 refer to only a part of the reaction product, there is no direct connection between them and the amounts of sucrose and methyl α-glucoside at the beginning of the reaction. These amounts must therefore be indirectly calculated from the material balances. The following set of equations is self-explanatory (n_F, n_G, n_S, and n_L are the number of moles of fructose, glucose, sucrose and leucrose):

$$n_{00} = \sum n_i \quad \text{material balance for the methyl groups} \tag{3}$$

$$m = \sum i n_i \quad \text{» » » » glucose units added to methyl glucoside} \tag{4}$$

$$n_S = n_F + n_L \quad \text{» » » » fructose units} \tag{5}$$

$$n_S = n_{00} v_0 \quad \text{» » » » sucrose} \tag{6}$$

$$v = m/n_{00} \quad \text{definition of } v \tag{7}$$

Eqns. (5) and (6) give:

$$n_F = n_{00} v_0 - n_L \tag{8}$$

In the material balances the amounts of the higher homologues (N_5 *etc.*) could generally not be disregarded. Since they were not experimentally determined, they have been estimated by extrapolation from the amounts of the lower homologues. This was not possible for experiment 1 since the amounts in this case seem to be rather large. Table 2 contains recalculated figures from Table 1 together with extrapolated data (within parentheses) and figures calculated by means of formulae (3), (4), (7), and (8). For simplicity the figures are based on the amounts of N_0 given in Table 1.

The data in Table 2 were used to calculate the molar ratios n_i/n_{00}. Using the values for v and n_0/n_{00}, the distribution constant c' was calculated by means of formula (1). An independent value, c'', was calculated by means

Table 2. Composition of the glycoside mixture, molar proportions.

Expt. No.	v_0	n_0	n_1	n_2	n_3	n_4	n_5	n_6	n_7	n_F+n_G	n_L	n_{00}	m	v	n_F
1	3.0	11.8	2.3	2.9	2.7	1.4				51.5	2.6	21.2	22.0	1.0	60.9
2	1.5	15.5	5.3	3.8	2.9	1.6	(0.8)	(0.3)	(0.1)	40.8	1.2	30.3	34.4	1.138	44.2
3	0.75	27.5	6.5	4.5	2.6	1.0	(0.3)	(0.04)	—	29.9	0.3	42.4	29.1	0.685	31.5
4	0.75	26.0	6.4	4.6	2.7	1.0	(0.3)	(0.04)	—	30.2	0.6	41.0	29.5	0.719	30.2
5	0.3	51.0	8.7	3.4	0.9	0.1	—	—	—	17.5	—	64.0	18.4	0.288	19.2

of formula (2) using the values for n_0/n_{00} and n_1/n_{00}. These figures are given in Table 3. The mean value, $c = 3.80$, was used together with the values for v to calculate theoretical distributions by means of formulae (1) and (2). The results are given in Fig. 1. The experimental figures are indicated as points.

Table 3. Distribution constants for the synthesis of methyl *α-iso*maltoside and its homologues from methyl α-D-glucoside and sucrose using dextransucrase.

Expt. No.	2	3	4	5
c′	3.59	4.07	3.91	3.55
c″	3.29	4.22	4.10	3.69

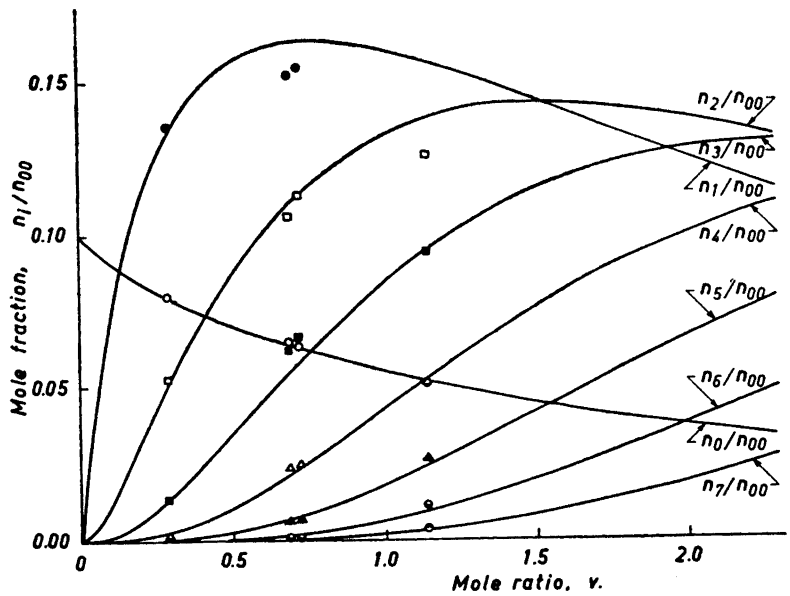

Fig. 1. Distribution of saccharides of the methyl *α-iso*maltoside series, synthesised using dextransucrase; n_i/n_{00} = mole fraction of saccharide with i added glucosyl groups; v = mole ratio of reactants, sucrose to methyl α-glucoside. For convenience, the scale for n_0/n_{00} is ten times smaller than that for the other mole fractions.

DISCUSSION

If all sucrose was used up for the formation of methyl saccharides, the proportion of sucrose to methyl glucoside at the beginning of the experiments, v_0, should equal the corresponding proportion, v, calculated from the analysis of the reaction product. As is seen in Table 2 this is approximately the case in experiments 3, 4, and 5. With the larger amounts of sucrose in experiments 2 and 1, only part of the glucose from the sucrose is bound in the methyl saccharides. Part of the remainder is accounted for as leucrose, but most of it should be bound in the dextran.

The fructose figures in Table 2 reveal a discrepancy in the experimental material. The amounts of fructose calculated from the material balances generally are higher than the experimentally determined sum of fructose and glucose. The discrepancy increases with increasing proportion of sucrose. Since practically all sucrose reacted, there is a loss of fructose which is not accounted for.

Inspection of Table 3 shows that the calculated distribution constants, c' and c'', are rather similar in each experiment. The differences between the constants of the various experiments are also rather small. It thus seems warranted to use a mean value of these figures to calculate the distribution of all the methyl saccharides. As is seen, this calculation gives a rather good picture of the experimental distribution. Of course the experimental material is rather small. It is regrettable that the figures from experiment 1 do not permit an interpretation. However, it seems permissible to state that the reactivity of the primary hydroxyl group of methyl α-D-glucoside is smaller than that of the corresponding groups of at least the next higher homologues, these latter appearing to be of equal reactivity. This conclusion is only a formal one since the details of the enzyme action are not considered.

Unfortunately these conclusions cannot be directly applied to the formation of dextran from sucrose using dextransucrase, in which the initial steps are not known. However, it would be very strange if this reaction was not essentially analogous, *i.e.* a stepwise addition of glucose units to a growing polymer. It seems most simple and natural to assume that sucrose itself is the primary acceptor. The main difficulty is that no intermediates in the form of oligosaccharides have been identified since high molecular dextran is almost the only product even at low degrees of conversion of sucrose [6]. One is then forced to conclude that the enzyme has a very low affinity to sucrose as an acceptor and favours very much the transfer of glucosyl groups to higher saccharides. The significance of branching should not be overlooked in this connection. All natural dextrans are branched but the exact nature of the branching is not settled. However, if a significant part of the branch end groups can function as glucosyl acceptors, the dextran molecule will grow like an avalanche.

Several recent results are in accord with the view that sucrose is the primary acceptor. Hehre [7] has shown one type of natural dextran with a low molecular weight to contain a sucrose unit as end group. Bailey, Barker, Bourne, Stacey, and Theander [8] have synthesised the glucosylsucrose corresponding to the first step of this hypothetical scheme and shown it to be an

excellent acceptor for glucosyl groups transferred from sucrose by dextransucrase. In most experiments described in the literature, crude preparations of dextransucrase were used. In particular, the enzyme was not freed from small amounts of dextran which may act as an acceptor. Recently Bailey, Barker, Bourne, and Stacey [9] have shown that an enzyme preparation with only traces of dextran has a low activity towards sucrose, which can however be increased many times if a suitable acceptor is added. Recent work with the analogous sucrose — levansucrase — levan system is also in accord with the view that sucrose is the primary acceptor in the building up of the polysaccharide.[10-12]

It should be pointed out that formulae (1) and (2) apply only if the amount of acceptor is constant throughout the polymerisation. If the acceptor and monomer donor are identical, as is assumed in the dextran system, very much more complicated formulae are obtained. The occurrence of branching complicates the situation still further. Without more experimental material it seems, however, not worth while to speculate on these problems.

The author would like to thank Svenska Sockerfabriks Aktiebolaget for permission to publish this paper.

REFERENCES

1. Hehre, E. J. *Advances in Enzymol.* **11** (1951) 297.
2. Weibull, B. and Nycander, B. *Acta Chem. Scand.* **8** (1954) 847.
3. Weibull, B. *Congress Handbook. XIVth International Congress of Pure and Applied Chemistry*, Zürich 1955, Abstract No. 113.
4. Edelman, J. *Advances in Enzymol.* **17** (1956) 189.
5. Jones, R. W., Jeanes, A., Stringer, C. S. and Tsuchiya, H. M. *J. Am. Chem. Soc.* **78** (1956) 2499.
6. Tsuchiya, H. M., Hellman, N. N., Koepsell, H. J., Corman, J., Stringer, C. S., Rogovin, S. P., Bogard, M. O., Bryant, G., Feger, V. H., Hoffman, C. A., Senti, F. R. and Jackson, R. W. *J. Am. Chem. Soc.* **77** (1955) 2412.
7. Hehre, E. J. *J. Biol. Chem.* **222** (1956) 739.
8. Bailey, R. W., Barker, S. A., Bourne, E. J., Stacey, M. and Theander, O. *Nature* **179** (1957) 310.
9. Bailey, R. W., Barker, S. A., Bourne, E. J. and Stacey, M. *J. Chem. Soc.* **1957** 3536.
10. Hestrin, S., Feingold, D. S. and Avigad, G. *Biochem. J.* **64** (1956) 340.
11. Feingold, D. S., Avigad, G. and Hestrin, S. *Biochem. J.* **64** (1956) 351.
12. Péaud-Lenoël, C. *Bull. soc. chim. biol.* **39** (1957) 757.

Received December 7, 1957.

ACTA CHEMICA SCANDINAVICA 12 (1958) 574—594

Short Communications

Action of Thrombin on Plasmin Digested Fibrinogen

PER WALLÉN and KURT BERGSTRÖM

Kemiska Institutionen II, Karolinska Institutet, Stockholm, Sweden

During the last years convincing evidence has been presented indicating that the effect of thrombin on fibrinogen is a proteolytic reaction [1]. At this proteolysis glycine appears as a new N-terminal residue. The reports concerning the amount of glycine residues, released from one mole fibrinogen, have varied. Recently published investigations [2] carried out by means of Edman's phenyl*iso*thiocyanate method have indicated that 4 moles of glycine appear at the proteolysis of one mole of fibrinogen with thrombin. From the supernatant after clotting Bettelheim and Bailey isolated two peptides, A and B, by electrophoresis [3]. The A peptide contained glutamic acid in N-terminal position and its isoelectric point was lower than that of the B peptide in which no N-terminal amino acid could be demonstrated. Recently Blombäck and Vestermark [4] have been able to isolate the A and B peptides by means of chromatography on 2 % crosslinked Dowex-50.

The purpose of this work was to study the effect of thrombin on the split products from the digestion of fibrinogen by plasmin. One way of doing this is to determine if addition of thrombin to a sample of digested fibrinogen causes any difference in the N-terminal amino-acid composition as compared with a similar sample to which no thrombin had been added. In an earlier work [5] it was shown that Edman's phenyl-*iso*thiocyanate method is very well suited for the study of the fibrinogenolysis.

The fibrinogen used was bovine fraction I-4 of Blombäck and Blombäck [6]. This highly purified fibrinogen contains traces of plasminogen which on activation gives rise to enough plasmin to make the fibrinogen unclottable within a relatively short time. As activator urokinase was used. It was prepared from human urine according to a method described by us earlier [5]. The thrombin used was citrate-activated prothrombin, prepared according to the method of Seegers [7,8]. It contained about 800 NIH units per mg.

The digestion mixture consisted of 1 g of bovine fibrinogen and 15 mg urokinase dissolved in 100 ml 0.02 M phosphate buffer, pH 7.2, containing NaCl to a concentration of 0.15 M. This mixture was incubated at 37°C. Clots obtained by adding 10 NIH units of thrombin to one ml of the reaction mixture dissolved in about 15 min at 37°C. At different times two 10 ml portions were removed from the digestion mixture. To one of them was added 1 ml of a thrombin solution containing 200 NIH units. Both aliquots were incubated for 15 min at 37°C. The enzyme activity was interrupted by adding 10 ml of pyridine containing 0.75 ml phenyl*iso*thiocyanate. The coupling with phenyl*iso*thiocyanate and the conversion of the PTC-amino acids to the corresponding PTH derivates were performed as described by Blombäck and Yamashina [2] and by us in an earlier communication [5]. The PTH-amino acids were identified and quantitatively estimated by the method of Edman and Sjöqvist [9]. The solvents used for the chromatography were those of Edman and Sjöqvist [9] and Sjöqvist [10].

During the fibrinogenolysis quantitative estimations of the following N-terminal amino acids were made: aspartic acid, glutamic acid, glycine, alanine, valine, threonine, tyrosine and lysine. Probably there are some additional N-terminal amino acids, which have not been studied. At least 150 bonds seem to be split by plasmin at maximal digestion.

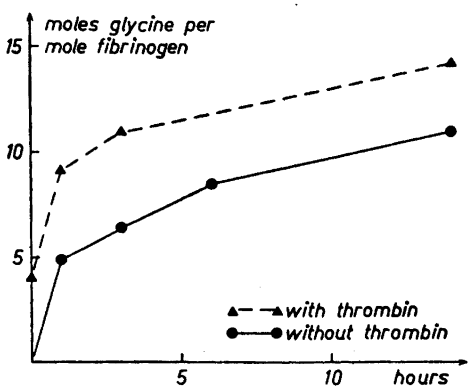

Fig. 1. Increase of N-terminal glycine in a fibrinogenolytic mixture at the addition of thrombin. (The values are corrected for a yield of 80 %.)

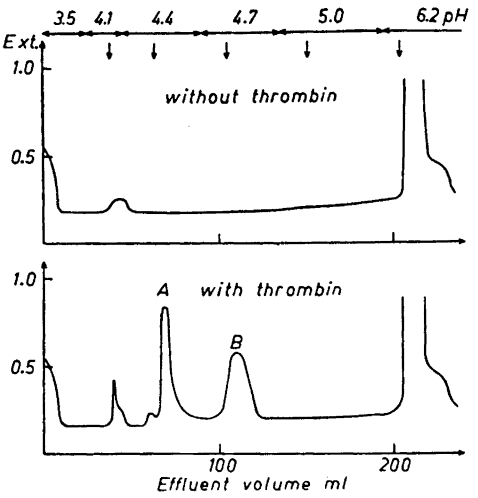

Fig. 2. Release of fibrinopeptides at the addition of thrombin to a fibrinogenolytic mixture. The extinction was read at 700 mμ. The following buffers were used: Na-formate at pH 3.5, Na-acetate at pH 4.1 to 5.0 and Na-phosphate at pH 6.2. The ionic strength of all buffers was 0.1. The vertical arrows indicate the points at which the same pH, as that of the eluting buffer, was obtained.

In the tests to which thrombin was added to the digestion mixture there was an immediate increase in N-terminally bound glycine as compared to the samples taken at the same time but to which no thrombin had been added. This increase in glycine corresponded to nearly 4 moles per mole fibrinogen in the original mixture. This was true even after a digestion time of 14 h when nearly 50 peptide bonds were split (Fig. 1). After still longer digestion times, however, the increase of glycine after the addition of thrombin gradually decreased but seemed to reach the level of about 2 additional moles of glycine at maximal digestion.

In order to determine whether the bonds split by thrombin are the same in the digested as in the intact fibrinogen, an attempt was made to isolate the peptides liberated by the action of thrombin on the digestion mixture described above. The method used was that described by Blombäck and Vestermark [4]. After a digestion time of 5 h two 20 ml samples were removed from the digestion mixture. To one of them 400 NIH units thrombin dissolved in 2 ml were added. Both samples were incubated for 15 min at 37°C. The enzyme action was interrupted by adjusting the pH of the samples to 2 with formic acid. After being kept over night at —20°C they were thawed and the pH adjusted to 4.5. A heavy precipitate formed and was removed by centrifugation. After adjusting the pH of the supernatants to 3.1 they were put on Dowex-50 × 2 columns, 0.9 × 40 cm, previously equilibrated with sodium formate buffer, pH 3.1, of ionic strength 0.1. The columns were eluted with sodium buffers of ionic strength 0.1 with varying pH as seen from Fig. 2. The flow rate of the columns was about 1.5 ml/h. Hourly fractions were collected in a fraction collector. The peptide contents in the fractions were estimated with the colour reaction of Lowry *et al.*[11]

In the chromatograms of peptides from plasmin-digested fibrinogen eluted at pH 4.4 to pH 5.0, *i. e.* in the region where the fibrinopeptides A and B should appear [4], no peptides were found. However, when thrombin was added to the digestion mixture there appeared one peptide at pH 4.4 (A) and another peptide at pH 4.7 (B). With these exceptions the two chromatograms showed an identical pattern. Further it was shown that the first of these peptides (A) contained glutamic acid in N-terminal position, whereas no N-terminal residue could be detected in the second one (B). It is most probable that the peptides A and B, which are released through the action of throm-

bin on the fibrinogenolytic mixture, are identical to the peptides in the supernatant after clotting.

Our results indicate that through the action of thrombin the same peptide bonds are split in fibrinogen irrespective of whether its molecule is intact or has been digested with plasmin. Recently Niewarowski and Kowalski [12] have reported that at the digestion of pure fibrin and fibrinogen by plasmin there appears antithrombin activity in the digestion mixture. It is possible that the protein fragments which are formed during fibrinogenolysis and which are substrates for thrombin can act as competitive inhibitors in the reaction between thrombin and fibrinogen and thus contribute to the antithrombin activity. Work is in progress to study the conditions at maximal plasmin digestion and to isolate the protein fragments, that can be proteolysed by thrombin. A more detailed paper on this subject is to be published in *Arkiv för Kemi*.

1. Bailey, K., Bettelheim, F. R., Lorand, L. and Middlebrook, W. R. *Nature* **167** (1951) 233.
2. Blombäck, B. and Yamashina, I. *Arkiv Kemi* **12** (1958) 299.
3. Bettelheim, F. R. and Bailey, K. *Biochim. et Biophys. Acta* **9** (1952) 578.
4. Blombäck, B. and Vestermark, A. *Arkiv Kemi* **12** (1958) 173.
5. Wallén, P. and Bergström, K. *Acta Chem. Scand.* **11** (1957) 754.
6. Blombäck, B. and Blombäck, M. *Arkiv Kemi* **10** (1956) 415.
7. Seegers, W. H., Mc Claughry, R. I. and Fahey, J. L. *Blood* **5** (1950) 421.
8. Seegers, W. H. *Record Chem. Progr. Kresge-Hooker Sci. Lib.* **13** (1952) 143.
9. Edman, P. and Sjöquist, J. *Acta Chem. Scand.* **10** (1956) 1507.
10. Sjöquist, J. *Personal communication.*
11. Lowry, O. H., Rosebrough, N. J., Farr, A. L. and Randall, R. J. *J. Biol. Chem.* **193** (1951) 265.
12. Niewarowski, S. and Kowalski, E. *VIe Congrès de la Societé Europeenne d'Hematologie*, Copenhagen, 1957.

Received March 4, 1958.

Chromic Acid Esters
A Correction

ULRIK KLÄNING

Laboratoriet for Fotokemi, Fotografi og Reproduktionsteknik, Polyteknisk Læreanstalt, Copenhagen, Denmark

In a recent paper evidence for the existence of 1:1 complexes of alcohols or acetaldehyde with acid chromate ion was presented. The equilibrium was written $X + HCrO_4^- = X \cdot HCrO_4^-$, where X stands for methanol, ethanol, propanol, 2-propanol, 2-butanol or acetaldehyde. But the equilibrium constants became incorrect as no allowance was made for the change of the total number of moles per liter with the alcohol or acetaldehyde concentration.

According to Westheimer *et al.*[2,3] the complexes formed in the alcoholic solutions are esters.

$$ROH + HCrO_4^- = ROCrO_3^- + H_2O$$

In solutions containing acetaldehyde the complex formed may be pictured as chromic acid ester of ethylideneglycol.

The equilibrium constant is

$$K_e = \frac{c_e \cdot \gamma_e \cdot c_w \cdot \gamma_w}{c_l \cdot \gamma_l \cdot c_a \cdot \gamma_a} \qquad (1)$$

c_e, c_w, c_l and c_a being molar concentrations of the ester, water, acid chromate and the alcohol, respectively. γ_e, γ_w, γ_l and γ_a are acticity coefficients. For some of the above-mentioned alcohols γ_w and γ_a are known [4,5], but since we do not know γ_e and γ_l we assume that $\gamma_l = \gamma_a \cdot \gamma_l$ and neglect variations in γ_w. This enables us to calculate values of K_e from the reported measurements of $\Delta\varepsilon$[1]. $\Delta\varepsilon$ is the difference between the extinctions at 375 mμ of two solutions both containing 10^{-4} M acid chromate and 10^{-3} M perchloric acid, and one of them also an alcohol or acetaldehyde in varying concentration. Assuming that the extinction coefficients are independent of alcohol or acetaldehyde concentration, we have $\Delta\varepsilon = \Delta\varepsilon_{KI} \cdot l \cdot c_e$, where l is the length of the optical path in cm and $\Delta\varepsilon_{KI}$ the difference between the extinction coefficient of the ester and that of the acid chromate ion at 375 mμ. On introduction of $\Delta\varepsilon$ and the total chromate concentra-

bin on the fibrinogenolytic mixture, are identical to the peptides in the supernatant after clotting.

Our results indicate that through the action of thrombin the same peptide bonds are split in fibrinogen irrespective of whether its molecule is intact or has been digested with plasmin. Recently Niewarowski and Kowalski [12] have reported that at the digestion of pure fibrin and fibrinogen by plasmin there appears antithrombin activity in the digestion mixture. It is possible that the protein fragments which are formed during fibrinogenolysis and which are substrates for thrombin can act as competitive inhibitors in the reaction between thrombin and fibrinogen and thus contribute to the antithrombin activity. Work is in progress to study the conditions at maximal plasmin digestion and to isolate the protein fragments, that can be proteolysed by thrombin. A more detailed paper on this subject is to be published in *Arkiv för Kemi*.

1. Bailey, K., Bettelheim, F. R., Lorand, L. and Middlebrook, W. R. *Nature* **167** (1951) 233.
2. Blombäck, B. and Yamashina, I. *Arkiv Kemi* **12** (1958) 299.
3. Bettelheim, F. R. and Bailey, K. *Biochim. et Biophys. Acta* **9** (1952) 578.
4. Blombäck, B. and Vestermark, A. *Arkiv Kemi* **12** (1958) 173.
5. Wallén, P. and Bergström, K. *Acta Chem. Scand.* **11** (1957) 754.
6. Blombäck, B. and Blombäck, M. *Arkiv Kemi* **10** (1956) 415.
7. Seegers, W. H., Mc Claughry, R. I. and Fahey, J. L. *Blood* **5** (1950) 421.
8. Seegers, W. H. *Record Chem. Progr. Kresge-Hooker Sci. Lib.* **13** (1952) 143.
9. Edman, P. and Sjöquist, J. *Acta Chem. Scand.* **10** (1956) 1507.
10. Sjöquist, J. *Personal communication.*
11. Lowry, O. H., Rosebrough, N. J., Farr, A. L. and Randall, R. J. *J. Biol. Chem.* **193** (1951) 265.
12. Niewarowski, S. and Kowalski, E. *VIe Congrès de la Societé Europeenne d'Hematologie*, Copenhagen, 1957.

Received March 4, 1958.

Chromic Acid Esters
A Correction

ULRIK KLÄNING

Laboratoriet for Fotokemi, Fotografi og Reproduktionsteknik, Polyteknisk Læreanstalt, Copenhagen, Denmark

In a recent paper evidence for the existence of 1:1 complexes of alcohols or acetaldehyde with acid chromate ion was presented. The equilibrium was written $X + HCrO_4^- = X \cdot HCrO_4^-$, where X stands for methanol, ethanol, propanol, 2-propanol, 2-butanol or acetaldehyde. But the equilibrium constants became incorrect as no allowance was made for the change of the total number of moles per liter with the alcohol or acetaldehyde concentration.

According to Westheimer *et al.*[2,3] the complexes formed in the alcoholic solutions are esters.

$$ROH + HCrO_4^- = ROCrO_3^- + H_2O$$

In solutions containing acetaldehyde the complex formed may be pictured as chromic acid ester of ethylideneglycol.

The equilibrium constant is

$$K_e = \frac{c_e \cdot \gamma_e \cdot c_w \cdot \gamma_w}{c_l \cdot \gamma_l \cdot c_a \cdot \gamma_a} \qquad (1)$$

c_e, c_w, c_l and c_a being molar concentrations of the ester, water, acid chromate and the alcohol, respectively. γ_e, γ_w, γ_l and γ_a are acticity coefficients. For some of the above-mentioned alcohols γ_w and γ_a are known [4,5], but since we do not know γ_e and γ_l we assume that $\gamma_l = \gamma_a \cdot \gamma_l$ and neglect variations in γ_w. This enables us to calculate values of K_e from the reported measurements of $\Delta\varepsilon$[1]. $\Delta\varepsilon$ is the difference between the extinctions at 375 mμ of two solutions both containing 10^{-4} M acid chromate and 10^{-3} M perchloric acid, and one of them also an alcohol or acetaldehyde in varying concentration. Assuming that the extinction coefficients are independent of alcohol or acetaldehyde concentration, we have $\Delta\varepsilon = \Delta\varepsilon_{KI} \cdot l \cdot c_e$, where l is the length of the optical path in cm and $\Delta\varepsilon_{KI}$ the difference between the extinction coefficient of the ester and that of the acid chromate ion at 375 mμ. On introduction of $\Delta\varepsilon$ and the total chromate concentra-

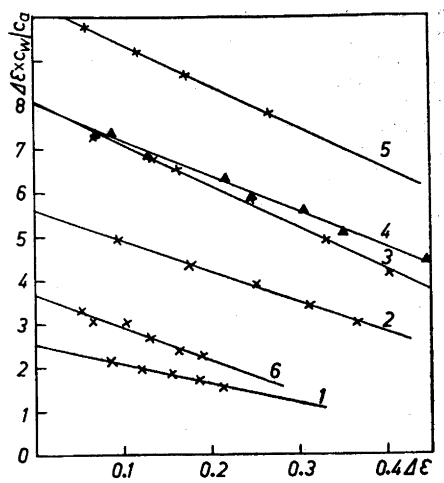

Fig. 1. $\Delta\varepsilon \cdot c_w/c_a$ *versus* $\Delta\varepsilon$ for acid chromate solutions containing 1) methanol, 2) ethanol, 3) *n*-propanol, 4) 2-propanol, 5) 2-butanol and 6) ethylideneglycol.

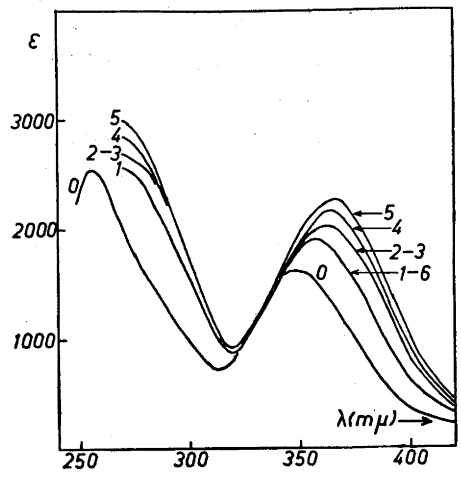

Fig. 2. The absorption spectrum of the acid chromate ion 0), and the absorption spectra of the esters of acid chromate with 1) methanol, 2) ethanol, 3) *n*-propanol, 4) 2-propanol, 5) 2-butanol and 6) ethylideneglycol.

tion c_0 in (1) we obtain the following expression.

$$\frac{\Delta\varepsilon \cdot c_w}{c_a} = \Delta\varepsilon_{KI} \cdot K_e \cdot l \cdot c_0 - K_e \cdot \Delta\varepsilon \quad (2)$$

c_w has been calculated from the densities of the solutions [6]. The concentration of ethylideneglycol has been calculated from the value of the equilibrium constant for formation of ethylideneglycol in dilute aqueous acetaldehyde solutions [7]. Fig. 1. shows $\Delta\varepsilon c_w/c_a$ plotted against $\Delta\varepsilon$. From the slope of the straight lines K_e was calculated. Table 1 shows the values of K_e and the values of the equilibrium constants K, reported in Ref.[1] for the equilibrium $X + HCrO^- = X.HCrO_4^-$. From the measurements of $\Delta\varepsilon$ at varying wavelength the absorption spectra of the esters in the near ultraviolet has been calculated (Fig. 2).

Table 1. K_e and the equilibrium constants K reported in Ref.[1] (25°C).

	$10^2 \times K$ litre/mole	K_e pure numbers
Methanol	4.3	4.7
Ethanol	7.7	6.9
n-Propanol	10.9	9.7
2-Propanol	7.8	8.3
2-Butanol	8.2	9.5
Ethylideneglycol		7.2
Acetaldehyde	3.4	

1. Kläning, U. *Acta Chem. Scand.* **11** (1957) 1313.
2. Holloway, F., Cohen, M. and Westheimer, F. H. *J. Am. Chem. Soc.* **75** (1951) 65.
3. Westheimer, F. H. *Chem. Revs.* **45** (1949) 419. Errata June 1950.
4. Galler, H. and Wicke, E. *Angew. Chem. B* **19** (1947) 117.
5. *Landolt-Börnstein Phys. Chem. Tab.* **Eg III c** (1936) 2158.
6. *International Chritical Tables Vol. III* (1928) 111.
7. Bell, R. P. and Clunie, J. C. *Trans. Faraday Soc.* **48** (1952) 439.

Received March 21, 1958.

Paramagnetism of Na_2NO_2

Studies in Magnetochemistry 22 *

R. W. ASMUSSEN

The Chemical Laboratory B, Technical University of Denmark, Copenhagen, Denmark

When a solution of sodium nitrite in liquid ammonia is treated with a solution of sodium in liquid ammonia the blue colour of the solution disappears and a yellow compound of the composition Na_2NO_2 is deposited. This substance was first obtained by Maxted [1] and later prepared by Zintl and Kohn [2], who also studied the chemical properties of the salt. The present author investigated the magnetic properties of Na_2NO_2 in 1940 and published in 1941 the qualitative results of the measurements and discussed their chemical significance in the paper [3] "Magnetochemical Studies on Free Radicals" (in Danish). Parts of this article, also that which concerns Na_2NO_2, has been quoted by Selwood [4]. In the present note the quantitative results are reported. Klemm and Pauli [5] published in 1951 a paper on the magnetic properties of the same compound.

The preparation of Na_2NO_2 was carried out according to the method given by Zintl and Kohn [2] using an apparatus and a technique similar to those applied by these authors. The samples were extracted with liquid ammonia in order to remove $NaNO_2$ with which the preparations were contaminated. Seven independent specimens were prepared but the magnetic measurements are given for four only. Two preparations (Nos. 1 and 2) possessed very small paramagnetic susceptibilities. The analyses proved that 1 and 2 were rather impure. One preparation (No. 5) exploded in the magnetic measuring tube.

In trying to prepare $LiNaNO_2$ we did not succeed in getting sufficiently pure substances.

The determination of the magnetic susceptibilities were performed by the Gouy-method as described by Christiansen and Asmussen [6]. The substances were transferred to the magnetic measuring tubes protected by an atmosphere of dry nitrogen. The results of the magnetic measurements and the chemical analyses are given in Table 1. The molar susceptibilities (column 5) were corrected for the diamagnetic contribution of the electron system of the ions Na^+ and O^{-2}. The gram ionic susceptibilities used for these ions are -3.7×10^{-6} and -11.3×10^{-6}, respectively. The total diamagnetic correction is then -30×10^{-6} neglecting the correction for N^{+2}, which doubtless is very small since the value for N^{+5} is about -0.1×10^{-6}.

Na_2NO_2 is formed in a reaction similar to that of the metal ketyls and may be considered as an inorganic ketyl. If the crystal contains Na^+ and NO_2^{-2} ions only, the molar magnetic susceptibility should be $1\,271 \times 10^{-6}$ (spin only; at 20°C). The observed small susceptibility values may be interpreted as being due to a certain dissociation in the crystal of the dimer $Na_4N_2O_4$, the sodium salt of a hypothetical tetraoxyhydrazine:

$$\underset{\mu = 0}{Na_4N_2O_4} \rightleftharpoons \underset{\mu = 1.73\ \mu_B}{2Na_2NO_2}$$

* No. 21 appeared in *Acta Chem. Scand.* **12** (1958) 24.

Table 1. Analyses, paramagnetic susceptibilities and degrees of dissociation for four independent preparations of Na_2NO_2.

Prep. No.	% Na Calc.	% Na Found	Temp. °K	$\chi_g \times 10^6$	$\chi_M \times 10^6$ for Na_2NO_2	$\chi_M \times 10^6$ for Na_2NO_2 Corr.	$\chi_M \times 10^6$ for $Na_4N_2O_4$ Corr.	$\chi_M \times 10^6$ for 100 % dis. $Na_4N_2O_4$	Degree of dissociation
3	49.98	49.4	294	2.0	184	214	428	2 524	0.17
4	49.98	49.8	292	2.4	221	251	502	2 542	0.20
6	49.98	49.7	292	2.1	193	223	446	2 542	0.18
7	49.98	49.2	293	1.9	175	205	410	2 534	0.16

The degrees of dissociation at room temperature calculated by means of the data in columns Nos. 7 and 8 are in column 9. The mean value is 0.18. Klemm and Pauli [5] report 0.23 at 20°C. Their susceptibility values at two lower temperatures may be interpreted as indicating a decrease in the degree of dissociation with decreasing temperature.

1. Maxted, E. B. *J. Chem. Soc. London* **111** (1917) 1016.
2. Zintl, E. and Kohn, O. *Ber.* **61** (1928) 189.
3. Asmussen, R. W. *Kemisk Maanedsblad* **1941** 81.
4. Selwood, P. W. *Magnetochemistry* (1956) 255.
5. Klemm, W. and Pauli, R. *Z. anorg. allgem. Chem.* **266** (1951) 30.
6. Christiansen, J. A. and Asmussen, R. W. *Kgl. Danske Videnskab. Selskab Mat.-Fys. Medd.* **12** (1934) No. 10.

Received March 3, 1958.

Isolation of an Anti-*Sclerotinia* Factor, 7-Hydroxy-4′-methoxy-*iso*flavone from Red Clover

ARTTURI I. VIRTANEN and PENTTI K. HIETALA

Laboratory of the Foundation for Chemical Research, Biochemical Institute, Helsinki, Finland

When investigating the antifungal substances in red clover, we isolated a new compound (A 1) the characteristics of which we have earlier reported [1,2]. The structure elucidation of this compound is still in progress. When isolating this compound, we also came to isolate an other substance (A 2) which is found in comparatively large amounts in the leaves and the stems of red clover. From fresh clover plants the isolation and separation of the two substances in pure form was difficult, since on paper chromatograms both substances behaved in much the same way in different solvent systems. The separation succeeded, however, using O'Keeffe fractionation. 2.69 g (m.p. 217°C) of A 1 was obtained in crystalline form from 10.75 kg of fresh red clover and 4.6 g (m.p. 262°C) of A 2, likewise in crystalline form. A large amount of the latter remained in the motherliquor, however. The total amount of A 2 was calculated on the basis of paper chromatography from the fluorescence of the spots to about 10 g per 10 kg fresh clover harvested 26.7. Since A 1 disappears on drying of the clover, the isolation of A 2 from dried clover is easy (ether extraction, extraction of the ether residue by petroleum ether and sublimation of the undissolved residue *in vacuo* at 260 to 280°C).

The structure of A 2. Elementary analysis: C 71.89; H 4.66; Calc. for $C_{16}H_{12}O_4$: C 71.63; H 4.51. The substance contained one hydroxy and one methoxy group. The content of the methoxy group in the substance was 11.1 %, determined by the method of Vieböck and Brecher, calculated for the compound $(C_{15}H_9O_3)$-OCH_3 11.57 %.

Using Rossman's method the substance in 30 min took up an amount of bromine corresponding to one double bond. In the alkali melt (131 mg of A 2, 2.74 g of solid KOH, 230–250°C, 2 h) 2,4-dihydroxybenzoic acid and *p*-hydroxybenzoic acid were formed. When heated in $BaOH_2$ solution anisic acid was formed. The structure of the A 2 compound accordingly is I or II.

On heating 400 mg of the substance in NaOH solution on a water bath for 20 min a substance was obtained after neutralisation with hydrochloric acid, acidification with acidic sodium phosphate and extraction by ether. This substance crystallized in flaky crystals and melted at 164°C. The yield was 285 mg. The elementary analysis of the substance was C 69.36; H 5.61; O 24.62. If the compound formed had been a chalcone $(C_{16}H_{12}O_4 + H_2O)$ corresponding to A 2, the calculated values

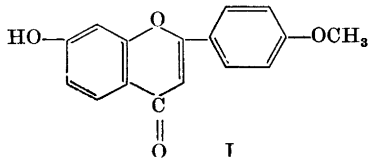

I

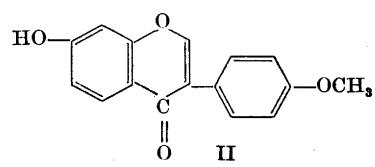

II

The degrees of dissociation at room temperature calculated by means of the data in columns Nos. 7 and 8 are in column 9. The mean value is 0.18. Klemm and Pauli [5] report 0.23 at 20°C. Their susceptibility values at two lower temperatures may be interpreted as indicating a decrease in the degree of dissociation with decreasing temperature.

1. Maxted, E. B. *J. Chem. Soc. London* **111** (1917) 1016.
2. Zintl, E. and Kohn, O. *Ber.* **61** (1928) 189.
3. Asmussen, R. W. *Kemisk Maanedsblad* **1941** 81.
4. Selwood, P. W. *Magnetochemistry* (1956) 255.
5. Klemm, W. and Pauli, R. *Z. anorg. allgem. Chem.* **266** (1951) 30.
6. Christiansen, J. A. and Asmussen, R. W. *Kgl. Danske Videnskab. Selskab Mat.-Fys. Medd.* **12** (1934) No. 10.

Received March 3, 1958.

Isolation of an Anti-*Sclerotinia* Factor, 7-Hydroxy-4′-methoxy-*iso*flavone from Red Clover

ARTTURI I. VIRTANEN and PENTTI K. HIETALA

Laboratory of the Foundation for Chemical Research, Biochemical Institute, Helsinki, Finland

When investigating the antifungal substances in red clover, we isolated a new compound (A 1) the characteristics of which we have earlier reported [1,2]. The structure elucidation of this compound is still in progress. When isolating this compound, we also came to isolate an other substance (A 2) which is found in comparatively large amounts in the leaves and the stems of red clover. From fresh clover plants the isolation and separation of the two substances in pure form was difficult, since on paper chromatograms both substances behaved in much the same way in different solvent systems. The separation succeeded, however, using O'Keeffe fractionation. 2.69 g (m.p. 217°C) of A 1 was obtained in crystalline form from 10.75 kg of fresh red clover and 4.6 g (m.p. 262°C) of A 2, likewise in crystalline form. A large amount of the latter remained in the motherliquor, however. The total amount of A 2 was calculated on the basis of paper chromatography from the fluorescence of the spots to about 10 g per 10 kg fresh clover harvested 26.7. Since A 1 disappears on drying of the clover, the isolation of A 2 from dried clover is easy (ether extraction, extraction of the ether residue by petroleum ether and sublimation of the undissolved residue *in vacuo* at 260 to 280°C).

The structure of A 2. Elementary analysis: C 71.89; H 4.66; Calc. for $C_{16}H_{12}O_4$: C 71.63; H 4.51. The substance contained one hydroxy and one methoxy group. The content of the methoxy group in the substance was 11.1 %, determined by the method of Vieböck and Brecher, calculated for the compound $(C_{15}H_9O_3)$-OCH_3 11.57 %.

Using Rossman's method the substance in 30 min took up an amount of bromine corresponding to one double bond. In the alkali melt (131 mg of A 2, 2.74 g of solid KOH, 230–250°C, 2 h) 2,4-dihydroxybenzoic acid and *p*-hydroxybenzoic acid were formed. When heated in $BaOH_2$ solution anisic acid was formed. The structure of the A 2 compound accordingly is I or II.

On heating 400 mg of the substance in NaOH solution on a water bath for 20 min a substance was obtained after neutralisation with hydrochloric acid, acidification with acidic sodium phosphate and extraction by ether. This substance crystallized in flaky crystals and melted at 164°C. The yield was 285 mg. The elementary analysis of the substance was C 69.36; H 5.61; O 24.62. If the compound formed had been a chalcone $(C_{16}H_{12}O_4 + H_2O)$ corresponding to A 2, the calculated values

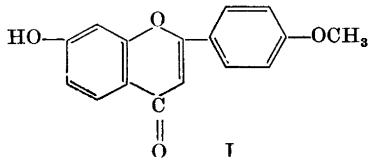

I

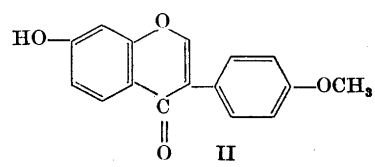

II

had been: C 67.11; H 4.95; O 27.94. The values found do not agree with the calculated ones. The CO group had thus apparently split off as formic acid on the alkali treatment, why the composition of the compound was $C_{15}H_{14}O_4$, for which the calculated values are: C 69.77; H 5.44; O 24.79. The determination of the methoxy group gave a value corresponding to this. (Found: 11.71 %-OCH_3; calc. for ($C_{14}H_{11}O_3$)-OCH_3: 12.02 %.)

The compound reacted with 2,4-dinitrophenylhydrazine. The structure of the compound is, on the basis of the results obtained, the following (III)

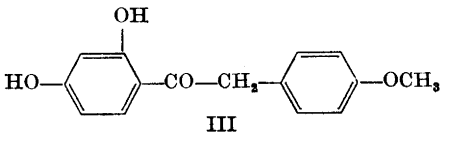

III

This can be formed only if compound A 2 has an *iso*flavone structure (*i.e.* structure II). The substance isolated by us is thus 7-hydroxy-4'-methoxy*iso*flavone.

By methylation a methoxy compound is obtained from the ketone III. The m.p. of this compund is 102—104°C. The methoxy determination gave values which correspond to the formula ($C_{14}H_{10}O_2$)·(-OCH_3)$_2$ (Found: 22.6 % -OCH_3; calc. 22.8 %).

In an investigation by Power and Salway [3] a compound $C_{16}H_{12}O_4$, m.p. 253°C, was isolated from flowers of red clover. This substance, called pratol, is clearly identical with the substance isolated by us. Structure I has been proposed for it, *i.e.* a flavone structure. On the basis of our investigations this concept has to be corrected. By the method of Robinson and Venkatamaran [4] we synthesized 7-hydroxy-4'-methoxyflavone and found that it differs from the A 2 substance isolated from clover, both with regard to the melting point and to the UV-spectrum.

The isolated antifungal substances A 1 and A 2 are active against *Sclerotinia trifoliorum* and *Fusarium nivale*. A 1 has a higher activity against *Fusarium* than *Sclerotinia*, A 2 again is much more active against the latter.

This is a preliminary report of our results and further details will be published in a more comprehensive article.

Added in proof: F. Wessely (*Monatshefte Chem.* **57** (1931) 395) has synthesized an *iso*flavone, formononetin, which has the same structure as our substance isolated from red clover. Professor Wessely (Vienna) was kind enough to send us a sample of his substance and we could identify it with our substance.

In literature we have found a paper by Cheng *et al.* (*Science* **120** (1954) 575) where determinations of the estrogenic effect of some synthetic *iso*flavones are presented. Formononetin has also been found to have such an effect.

Mr. P. O. Karvonen has actively taken part in this work, among other things in the determination of the methoxy groups.

The support given by the *Rockefeller Foundation* is gratefully acknowledged.

1. Virtanen, A. I. and Hietala, P. K. *Suomen Kemistilehti A* **29** (1956) 280; *B* **30** (1957) 99.
2. Virtanen, A. I., Hietala, P. K. and Wahlroos, Ö. *Arch. Biochem. Biophys.* **69** (1957) 486.
3. Power, F. B. and Salway, A. H. *J. Chem. Soc.* **97** (1910) 231.
4. Robinson, R. and Venkatamaran, K. *J. Chem. Soc.* **1926** 2344.

Received March 3, 1958.

The Transfer of L-5-Vinyl-2-thiooxazolidone (oxazolidinethione) to Milk

ARTTURI I. VIRTANEN, MATTI KREULA and MARTTI KIESVAARA

Laboratory of Valio, Biochemical Institute, Helsinki, Finland

From the seeds of *Brassica* plants Astwood *et al.*[1] have isolated a strongly antithyroid substance which they established as L-5-vinyl-2-thiooxazolidone. In the edible portions of *Brassica* vegetables, such as cabbage, kale, cauliflower, broccoli, mustardgreens, and horseradish root, they did not find this substance. In this laboratory Kreula and Kiesvaara [2] developed a chromatographic-spectrophotometric method by which vinyl-thiooxazolidone can be determined in green plants in a concentration of 1 μg/g fresh plants and 5 μg/litre milk. Contrary to the findings by Astwood *et al.* the present authors found

had been: C 67.11; H 4.95; O 27.94. The values found do not agree with the calculated ones. The CO group had thus apparently split off as formic acid on the alkali treatment, why the composition of the compound was $C_{15}H_{14}O_4$, for which the calculated values are: C 69.77; H 5.44; O 24.79. The determination of the methoxy group gave a value corresponding to this. (Found: 11.71 %-OCH_3; calc. for ($C_{14}H_{11}O_3$)-OCH_3: 12.02 %.)

The compound reacted with 2,4-dinitrophenylhydrazine. The structure of the compound is, on the basis of the results obtained, the following (III)

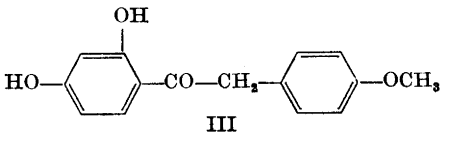

III

This can be formed only if compound A 2 has an *iso*flavone structure (*i.e.* structure II). The substance isolated by us is thus 7-hydroxy-4'-methoxy*iso*flavone.

By methylation a methoxy compound is obtained from the ketone III. The m.p. of this compund is 102—104°C. The methoxy determination gave values which correspond to the formula ($C_{14}H_{10}O_2$)·(-OCH_3)$_2$ (Found: 22.6 % -OCH_3; calc. 22.8 %).

In an investigation by Power and Salway [3] a compound $C_{16}H_{12}O_4$, m.p. 253°C, was isolated from flowers of red clover. This substance, called pratol, is clearly identical with the substance isolated by us. Structure I has been proposed for it, *i.e.* a flavone structure. On the basis of our investigations this concept has to be corrected. By the method of Robinson and Venkatamaran [4] we synthesized 7-hydroxy-4'-methoxyflavone and found that it differs from the A 2 substance isolated from clover, both with regard to the melting point and to the UV-spectrum.

The isolated antifungal substances A 1 and A 2 are active against *Sclerotinia trifoliorum* and *Fusarium nivale*. A 1 has a higher activity against *Fusarium* than *Sclerotinia*, A 2 again is much more active against the latter.

This is a preliminary report of our results and further details will be published in a more comprehensive article.

Added in proof: F. Wessely (*Monatshefte Chem.* **57** (1931) 395) has synthesized an *iso*flavone, formononetin, which has the same structure as our substance isolated from red clover. Professor Wessely (Vienna) was kind enough to send us a sample of his substance and we could identify it with our substance.

In literature we have found a paper by Cheng *et al.* (*Science* **120** (1954) 575) where determinations of the estrogenic effect of some synthetic *iso*flavones are presented. Formononetin has also been found to have such an effect.

Mr. P. O. Karvonen has actively taken part in this work, among other things in the determination of the methoxy groups.

The support given by the *Rockefeller Foundation* is gratefully acknowledged.

1. Virtanen, A. I. and Hietala, P. K. *Suomen Kemistilehti A* **29** (1956) 280; *B* **30** (1957) 99.
2. Virtanen, A. I., Hietala, P. K. and Wahlroos, Ö. *Arch. Biochem. Biophys.* **69** (1957) 486.
3. Power, F. B. and Salway, A. H. *J. Chem. Soc.* **97** (1910) 231.
4. Robinson, R. and Venkatamaran, K. *J. Chem. Soc.* **1926** 2344.

Received March 3, 1958.

The Transfer of L-5-Vinyl-2-thiooxazolidone (oxazolidinethione) to Milk

ARTTURI I. VIRTANEN, MATTI KREULA and MARTTI KIESVAARA

Laboratory of Valio, Biochemical Institute, Helsinki, Finland

From the seeds of *Brassica* plants Astwood *et al.*[1] have isolated a strongly antithyroid substance which they established as L-5-vinyl-2-thiooxazolidone. In the edible portions of *Brassica* vegetables, such as cabbage, kale, cauliflower, broccoli, mustardgreens, and horseradish root, they did not find this substance. In this laboratory Kreula and Kiesvaara [2] developed a chromatographic-spectrophotometric method by which vinyl-thiooxazolidone can be determined in green plants in a concentration of 1 μg/g fresh plants and 5 μg/litre milk. Contrary to the findings by Astwood *et al.* the present authors found

considerable amounts of vinyl-thiooxazolidone in cabbage, kale, rape, *etc.*, in cabbage for instance 5-40 μg/g fresh weight.

In the literature there has lately occurred information about the antithyroid effect of milk when cruciferous plants are used as fodder [3]. In order to find out to what extent vinyl-thiooxazolidone is possibly transferred to milk, a feeding experiment was performed with a cow, the daily production of which was 8.2 kg of milk. At 7 o'clock p.m. on the 3rd of March the cow was fed with 0.5 kg of finely ground moistened rape seeds which according to analysis contained 4.5 g of vinyl-thiooxazolidone. The active substance is formed from a glycoside found in the seeds by enzymatic action. In the moistened seeds the liberation takes place rapidly, and this presumably happens in the rumen too. A milk sample was taken before feeding, 12 h after feeding, and then every 12 h for 6 days.

Not even a trace of vinyl-thiooxazolidone, which has a strong absorption maximum at 240 mμ, was found in any milk sample. On the other hand, a small amount of a substance with a strong absorption maximum at 255 mμ was found in the milk 12 h after feeding (after 24 h the amount was already very small). After 48 h there were only traces of it in the milk (Fig. 1).

Since strong reductive processes take place in the rumen — among other things unsaturated fatty acids are largely reduced to saturated ones — it is possible that vinyl-thiooxazolidone is reduced to the corresponding 5-ethyl-2-thiooxazolidone in the rumen. The substance excreted into milk could thus be this compound. According to Astwood *et al.* the spectra of 5,5-dimethyl-2-thiooxazolidone and 2-thiooxazolidone are nearly identical with the spectrum of 5-vinyl-2-thiooxazolidone. On the basis of this, the side chain would have no greater influence on the spectrum of compounds of this type, and the substance found in milk would accordingly not be ethyl-thiooxazolidone. The amount of the substance excreted into milk was minimal, about 0.1 % of the vinyl-thiooxazolidone given to the cow, provided that the specific absorption of the substances at 240 and 255 mμ, respectively, is approximately the same. The investigations concerning the substance found in milk continue.

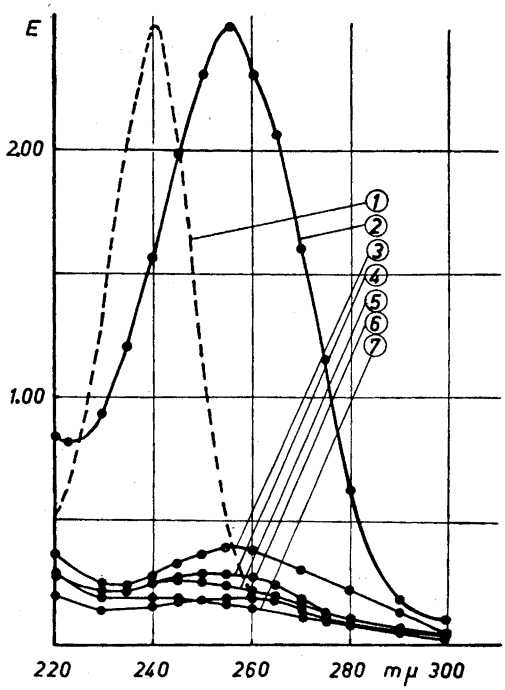

Fig. 1. UV-spectra of the compound which appears in cow's milk after feeding of 0.5 kg of finely ground moistened rape seeds containing 4.5 g of L-5-vinyl-2-thiooxazolidone (2—7). The curves show the relative values after 12 h (2), 30 h (3), 54 h (4), 78 h (5), 102 h (6), and 126 h (7). The dashed curve (1) shows the spectrum of L-5-vinyl-2-thiooxazolidone.

1. Astwood, E. B., Greer, M. A. and Ettlinger, M. G. *J. Biol. Chem.* **181** (1949) 121.
2. Kreula, M. and Kiesvaara, M. (To be published in *Acta Chem. Scand.*).
3. Clements, F. W. and Wishart, J. W. *Metabolism Clin. and Exptl.* **5** (1956) 623.

Received March 25, 1958.

A new Synthesis of 6-Selenoctic Acid and a Related Compound

GÖRAN BERGSON

Chemical Institute, University of Uppsala, Sweden

Recently the author described the synthesis of 6-selenoctic acid (I) in this journal [1]. As this substance had not been characterized before and since operations with cyclic selenium compounds are not easy, the author then applied a method of synthesis analogous to one used in the preparation of 6-thioctic acid [2]. The method involved the synthesis of 6,8-dibenzylselenoloctanoic acid from ethyl 6,8-dichlorooctanoate followed by reductive cleavage with sodium in liquid ammonia and oxidation with air. In this way 6-selenoctic acid was obtained in fair yield, and some of its properties could be determined. It now seemed advisable to look for other synthetic methods.

The simplest of all methods for preparing organic diselenides is the alkylation of alkali diselenides. As pointed out by Fredga [3], however, this method fails to give the six-membered cyclic diselenide 1,2-diselenane-3,6-dicarboxylic acid (II) when α,α'-dibromoadipic acid is treated with potassium diselenide. In this case the reaction leads to the five-membered cyclic monoselenide tetrahydroselenophene-2,5-dicarboxylic acid (III) and elementary selenium. When ethyl 6,8-dichlorooctanoate (IV) is treated with sodium diselenide, however, only a small amount of elementary selenium remains after the reaction, and ring closure takes place to form 6-selenoctic acid. In a similar way reaction between 2,2-(bisiodomethyl)-propanediol-1,3 and sodium diselenide gives the cyclic compound 4,4-(bishydroxymethyl)-1,2-diselenolane (V).

From the point of view of steric strain in the cyclic diselenides it seems difficult to explain why the fivemembered rings seem to form more easily than the six-membered. The presence of the carboxylic groups in the vicinity of the bromine atoms in dibromoadipic acid possibly complicates the reaction. A preliminary experiment with dibromoglutaric acid and sodium diselenide points in this direction. It must be borne in mind that α-halogen substituted carboxylic acids (contrary to other halogen compounds) completely oxidize sodium ditelluride to elementary tellurium, the acid being reduced to the unsubstituted fatty acid [4]. In view of the possible oxidative action of the halogen compounds towards the alkali diselenide it seems advisable to use chlorine compounds whenever possible. It must be pointed out that 6-selenoctic acid is obtained in better yield than 4,4-(bishydroxymethyl)-1,2-diselenolane, which may be due to the fact that a chlorine compound was used in the preparation of the former and an iodine compound for the latter. Backer and Winter also got only a low yield of 4-phenyl-4-methyl-1,2-diselenolane when phenyl methyldibromopropane was treated with potassium diselenide. The chief products were elementary selenium and a hydrocarbon.[5] When complications of these kinds occur the second method worked out by

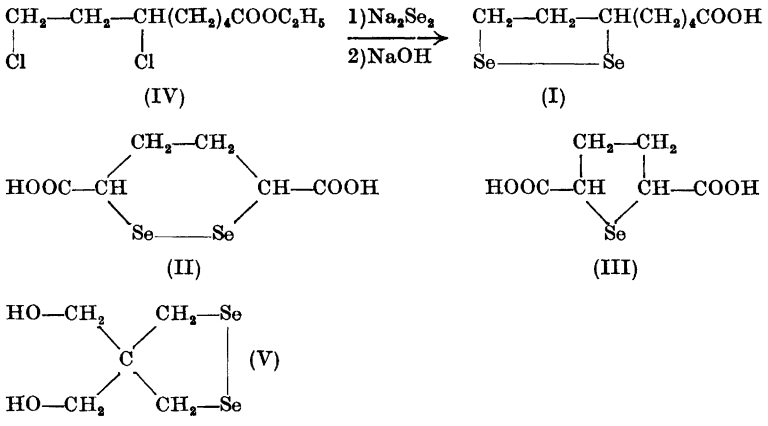

Fredga, *viz.* hydrolysis of selenocyanates must be recommended [3]. In this way, Fredga obtained 1,2-diselenane-3,6-dicarboxylic acid, and Backer and Winter 4-phenyl-4-methyl-1,2-diselenolane and 4,4-dimethyl-1,2-diselenolane [5].

6-Selenoctic acid has its characteristic UV-peak at 442 mμ as can be seen from Fig. 1, curve 1. The spectrum of 4,4-(bishydroxymethyl)-1,2-diselenolane is closely related as well as that of 1,2-diselenolane itself [6]. Non-cyclic diselenides absorb at about 310 mμ [7]. Whether the shoulder at about 300 mμ in the spectra of the five-membered ring compounds is due to the presence of a small amount of polymer in the solution or to a hitherto unrecognized band cannot be answered at present. After standing over night the spectrum of the solution of 6-selenoctic acid did not change significantly. When 6-selenoctic acid was treated with $NaBH_4$, the absorption band at 442 mμ disappeared, indicating complete reduction to the selenol (Fig. 1 curve 2). 1,2-Dithiolane derivatives are said not to be reduced by sodium borohydride [8]. When the reduced solution was allowed to stand in the air for about one hour, oxidation to 6-selenoctic acid occurred, as seen from Fig. 1 curve 3. A complete report of the UV and IR spectra of diselenides is to be published in *Arkiv Kemi*. Preparation of optically active 6-selenoctic acid is planned.

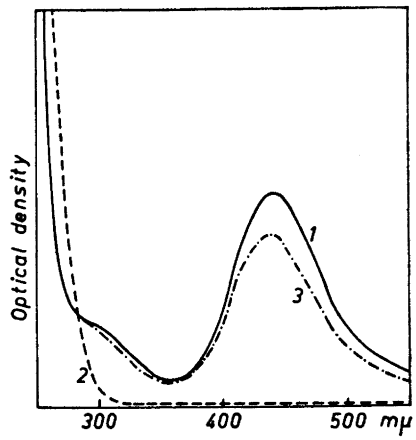

Fig. 1. Light absorption of 1) 6-selenoctic acid in ethanol, 2) 6-selenoctic acid reduced with $NaBH_4$, 3) the reduced solution after 1 h exposure to air.

Experimental: 6-Selenoctic acid. Sodium diselenide solution was prepared by dissolving 2.17 g of sodium formaldehydesulphoxylate (Rongalite C), 1.47 g of sodium hydroxide and 2.91 g of selenium in 30 ml of water in a nitrogen atmosphere. 4.43 g of ethyl 6,8-dichlorooctanoate dissolved in 30 ml of ethanol was added dropwise and the reaction mixture stirred for 90 min, the temperature being kept at 60—70°. 1.47 g of sodium hydroxide in 25 ml of water was added and stirring and warming continued for 5 h. After standing over night the mixture was acidified with 6 N hydrochloric acid. The product was taken up in 50 ml of chloroform. This extract was dried with sodium sulphate and the solvent removed in vacuum. The residue was extracted with boiling *n*-hexane, and when this solution cooled, the crude 6-selenoctic acid separated (m. p. 86—89°). The yield was about 25 % but it seems possible to increase it. After recrystallization from *n*-hexane, the product melted at 89—90.5°.

4,4 - (Bishydroxymethyl) - 1,2 - diselenolane. The sodium diselenide solution was prepared as above, and the calculated quantity of 2,2-(bisiodomethyl)-propanediol-1,3 dissolved in ethanol was added. After 5 h reflux, the mixture was extracted with 3 × 50 ml of ether. The extract was dried with sodium sulphate and the ether evaporated. The residue was boiled with some petroleum ether to remove impurities and then recrystallized twice from benzene. The product crystallized in long dark red needles m. p. 133—135°. (Found: Se 59.8. Calc. 60.6.) Yield 8 %.

I wish to express my gratitude to Professor Arne Fredga for much helpful advice. I am also indebted to Dr. Lennart Schotte for his interest in this work. A grant from the *Swedish Natural Science Research Council* is gratefully acknowledged.

1. Bergson, G. *Acta Chem. Scand.* **11** (1957) 1607.
2. Reed, L. J. and Ching-I Niu. *J. Am. Chem. Soc.* **77** (1955) 416.
3. Fredga, A. *Uppsala Universitets Årsskrift* **1935** 5.
4. Bergson, G. *Acta Chem. Scand.* **11** (1957) 571.
5. Backer, H. J. and Winter, H. J. *Rec. trav. chim.* **56** (1937) 691.
6. Bergson, G. and Claeson, G. *Acta Chem. Scand.* **11** (1957) 911.
7. Bergson, G. *Arkiv Kemi* **9** (1956) 121.
8. Barltrop, J. A., Hayes, P. M. and Calvin, M. *J. Am. Chem. Soc.* **76** (1954) 4364.

Received March 18, 1958.

Studies of the Hydrogen Bond

IV. Theoretical Determination of Electronic Polarization Energies

INGA FISCHER-HJALMARS
and RAGNAR GRAHN

Institute of Theoretical Physics, University of Stockholm, Stockholm, Sweden

The problem why some molecules associate by aid of hydrogen bonds (H bonds) while others seem to have no disposition for the formation of such bonds has been thoroughly discussed for many years but has not yet been solved in a completely satisfactory way. The main factors, which cooperate in the formation of an H bond, are supposed to be: 1) electrostatic interaction, 2) covalent binding, 3) polarization. In many investigations of the H bond only the two first factors have been taken into consideration. The factor 3) seems, however, to be of the same importance as the other two. It has been discussed previously by, *e.g.*, Bauer and Magat [1] and by Ehrenberg and Fischer [2-4] (Studies of the Hydrogen Bond I, II, III). Bauer and Magat [1] have calculated the energy of an H bond between water molecules with due consideration to polarization effects. This calculation was carried out in a classical way by use of the experimental value of the polarizability of the whole molecule. Ehrenberg and Fischer [2,3] have pointed out that certain organic compounds with a less polarizable hetero-atom are less soluble in water than others with a more polarizable hetero-atom. They proposed quantum mechanical calculations to clarify the rôle of polarization for H bond formation, and a very rough calculation of this kind was carried out [4].

The influence from the above-mentioned three factors upon an H bond cannot be strictly separated. It would therefore have been desirable to make a complete, quantum mechanical calculation of the total energy of H-bonded systems. Because of the complexity of such systems we have chosen to investigate primarily the electronic polarization effects and less rigorously the other two factors. Even this simplified programme must be further reduced to make the computational work tolerable.

Hitherto we have studied the association of H_2O, where there is a strong H bond, and of H_2S, where there is no H bond. Calculations on the association of HF and of HCl are going on but will not be reported here. They will be published later by one of us (R.G.) together with a more detailed description of the calculations on H_2O and H_2S.

In the study of the H bond between H_2O molecules we have considered the following system: 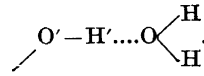 We have used the intermolecular distances given by the ice-structure, proposed by Bernal and Fowler [5]. For the description of the electron distribution of a free H_2O molecule we have used the molecular orbitals (MO's), calculated by Ellison and Shull [6]. Our investigation includes a study of i) the strengthening of the H bond, caused by the electronic polarization of the whole H_2O in the field from the net positive charge on H′ and ii) the strengthening of the H bond, caused by the polarization of H′ in the field from the adjacent H_2O.

The energy gain from the effect i) has been obtained from a computation of the change of the original MO's of H_2O, caused by the potential from H′. Now, the O atom of the free H_2O has two filled lone-pair MO's. When expressing the electron distribution by aid of equivalent orbitals, it is seen that already in the free H_2O these MO's are almost completely localized at the "back" of the O atom. Thus, the computed electron density at the back of the O atom cannot increase as a result of the H′ potential, unless excited atomic orbitals (AO's) are included in the changed MO's. However, for computational reasons, we have assumed the changed MO's to be linear combinations of the same AO's as the original MO's. Consequently, our calculation can only take into account that part of the effect from H′, which consists in moving the electrons of the O—H bonds closer towards the O atom. The energy gain from this movement is found to be comparatively small, only 0.2 kcal/mole. However, the sign of this energy change indicates that the effect i) would give a much larger energy gain, if excited AO's of the O atom were included.

The effect ii) has been computed by replacing the 1s AO of H′ by a hybrid of the three AO's 1s, $2p\sigma$ and $2p\pi$. The coefficients of this hybrid have been determined by a variation method. The energy

gain from this polarization of H′ has been found to be about 1.5 kcal/mole.

Summing up, the total computed energy gain from polarization effects is 0.2 + 1.5 = 1.7 kcal/mole. This value is, however, not very definite. There are several factors, which could modify it in one direction or the other. One factor, which would increase it, is the fact that 0.2 and 1.5 kcal/mole should be considered as lower limits of the effects i) and ii). Another, which would diminish it, is the fact that the effect ii) should cause a slight weakening of the O′—H′ bond. Although the value 1.7 kcal/mole is rather approximate, it is interesting to compare it with the purely electrostatic interaction energy. Using the point charge model, discussed by Bauer and Magat [1], this energy is computed to 5.1 kcal/mole. Thus, it is seen that the polarization energy is not a negligible part of the total H bond energy.

For comparison with H_2O we have also studied the association of H_2S, which has an electronic structure similar to that of H_2O. H_2S solidifies at −82.9°C, but it does not seem to have a definite crystalline form. We have studied the interaction of two H_2S molecules, $S'-H'....S\begin{matrix}H\\H\end{matrix}$, assuming the atoms S′H′S to be on a straight line. In the case of H_2S we have only computed the above-mentioned polarization effect ii). We have found a small energy gain, about 0.05 kcal/mole. Since the effect ii) is giving the main contribution to the polarization energy in the H_2O case, it is reasonable to assume the total polarization energy in the association of H_2S to be of the order of magnitude of 0.05 kcal/mole. The purely electrostatic interaction energy is in this case computed to be 0.25 kcal/mole, when a point charge model is used.

The numerical results of the present investigation are collected in Table 1.

Table 1. Effects contributing to H bond formation. Energies in kcal/mole.

Molecule	Polarization energy			Electrostatic energy	Exptl. H bond energy
	i)	ii)	total		
H_2O	0.2	1.5	1.7	5.1	5.8
H_2S	—	0.05	~0.05	0.25	—

From Table 1 it is seen that the polarization effects are important for the H bond formation in the H_2O case, whereas they cannot have any influence in the H_2S case.

1. Bauer, E. and Magat, M. *J. phys. radium* [7] **9** (1938) 319.
2. Ehrenberg, L. and Fischer, I. *Acta Chem. Scand.* **2** (1948) 657.
3. Fischer, I. and Ehrenberg, L. *Acta Chem. Scand.* **2** (1948) 669.
4. Fischer, I. *Arkiv Fysik* **1** (1949) 495.
5. Bernal, J. D. and Fowler, R. *J. Chem. Phys.* **1** (1933) 515.
6. Ellison, F. O. and Shull, H. *J. Chem. Phys.* **21** (1953) 1420.

Received March 26, 1958.

Some Advantages of Using a Mercury Cathode in the Kolbe Electro-synthesis

NGUYEN DINH-NGUYEN

Department of Medical Biochemistry, University of Gothenburg, Sweden

When the anodic reaction $2\ -\overset{|}{\underset{|}{C}}-COO^- \xrightarrow{-2e} -\overset{|}{\underset{|}{C}}-\overset{|}{\underset{|}{C}}- + 2\ CO_2$, named after Hermann Kolbe [1], is used for the preparation of alkali-sensitive substances such as esters, present practice usually avoids hydrolysis by electrolysing free carboxylic acids in the presence of only a few per cent of their sodium salts, the reaction being stopped when the electrolyte turns neutral. The solvent is generally methanol and the electrodes smooth platinum sheets.

In an attempt to prepare dimethyl adipate from methyl hydrogen succinate using this technique, a yield of only 38 % was obtained, in contrast to the 70 % reported by Bouveault [2]. He electrolysed equivalent amounts of succinic anhydride and sodium in methanol, using a water-cooled platinum-tube anode and a mercury cathode. New runs were therefore made with mercury as cathode at the bottom of a beaker, and a platinum-sheet anode

gain from this polarization of H′ has been found to be about 1.5 kcal/mole.

Summing up, the total computed energy gain from polarization effects is 0.2 + 1.5 = 1.7 kcal/mole. This value is, however, not very definite. There are several factors, which could modify it in one direction or the other. One factor, which would increase it, is the fact that 0.2 and 1.5 kcal/mole should be considered as lower limits of the effects i) and ii). Another, which would diminish it, is the fact that the effect ii) should cause a slight weakening of the O′—H′ bond. Although the value 1.7 kcal/mole is rather approximate, it is interesting to compare it with the purely electrostatic interaction energy. Using the point charge model, discussed by Bauer and Magat [1], this energy is computed to 5.1 kcal/mole. Thus, it is seen that the polarization energy is not a negligible part of the total H bond energy.

For comparison with H_2O we have also studied the association of H_2S, which has an electronic structure similar to that of H_2O. H_2S solidifies at −82.9°C, but it does not seem to have a definite crystalline form. We have studied the interaction of two H_2S molecules, $S'-H'....S\begin{matrix}H\\H\end{matrix}$, assuming the atoms S′H′S to be on a straight line. In the case of H_2S we have only computed the above-mentioned polarization effect ii). We have found a small energy gain, about 0.05 kcal/mole. Since the effect ii) is giving the main contribution to the polarization energy in the H_2O case, it is reasonable to assume the total polarization energy in the association of H_2S to be of the order of magnitude of 0.05 kcal/mole. The purely electrostatic interaction energy is in this case computed to be 0.25 kcal/mole, when a point charge model is used.

The numerical results of the present investigation are collected in Table 1.

Table 1. Effects contributing to H bond formation. Energies in kcal/mole.

Molecule	Polarization energy			Electrostatic energy	Exptl. H bond energy
	i)	ii)	total		
H_2O	0.2	1.5	1.7	5.1	5.8
H_2S	—	0.05	~0.05	0.25	—

From Table 1 it is seen that the polarization effects are important for the H bond formation in the H_2O case, whereas they cannot have any influence in the H_2S case.

1. Bauer, E. and Magat, M. *J. phys. radium* [7] **9** (1938) 319.
2. Ehrenberg, L. and Fischer, I. *Acta Chem. Scand.* **2** (1948) 657.
3. Fischer, I. and Ehrenberg, L. *Acta Chem. Scand.* **2** (1948) 669.
4. Fischer, I. *Arkiv Fysik* **1** (1949) 495.
5. Bernal, J. D. and Fowler, R. *J. Chem. Phys.* **1** (1933) 515.
6. Ellison, F. O. and Shull, H. *J. Chem. Phys.* **21** (1953) 1420.

Received March 26, 1958.

Some Advantages of Using a Mercury Cathode in the Kolbe Electro-synthesis

NGUYEN DINH-NGUYEN

Department of Medical Biochemistry, University of Gothenburg, Sweden

When the anodic reaction $2\ -\overset{|}{\underset{|}{C}}-COO^- \xrightarrow{-2e} -\overset{|}{\underset{|}{C}}-\overset{|}{\underset{|}{C}}- + 2\ CO_2$, named after Hermann Kolbe [1], is used for the preparation of alkali-sensitive substances such as esters, present practice usually avoids hydrolysis by electrolysing free carboxylic acids in the presence of only a few per cent of their sodium salts, the reaction being stopped when the electrolyte turns neutral. The solvent is generally methanol and the electrodes smooth platinum sheets.

In an attempt to prepare dimethyl adipate from methyl hydrogen succinate using this technique, a yield of only 38 % was obtained, in contrast to the 70 % reported by Bouveault [2]. He electrolysed equivalent amounts of succinic anhydride and sodium in methanol, using a water-cooled platinum-tube anode and a mercury cathode. New runs were therefore made with mercury as cathode at the bottom of a beaker, and a platinum-sheet anode

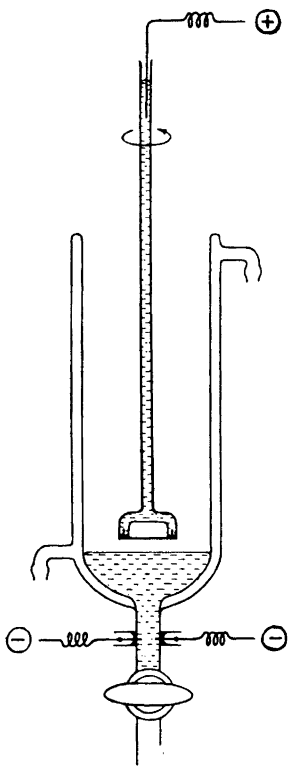

Fig. 1. Apparatus for Kolbe electro-synthesis with mercury as cathode.

was mounted horizontally 1 cm above the surface of the mercury. 50 to 100 % of the half-ester in methanol was neutralized with sodium, and the beaker was cooled in running water as before. In this way the yield of dimethyl adipate rose to 55 %, and finally reached 68 % when the anode was rotated at a speed high enough to bring about efficient stirring.

Apart from the improved yield in this particular case, the use of a mercury cathode has several other advantages. The mercury amalgamates the excess of discharged sodium ions, and the electrolyte does not turn alkaline as long as the voltage is applied. As much sodium as is practical may therefore be added, with the advantage of increased current density and consequently reduced reaction time. The current drops during the electrolysis, and the necessity of watching the pH is eliminated, as the ammeter indicates when the reaction should be interrupted. The electrolysis may probably be run for any length of time without harm, however, and is thus easily fitted into other work going on.

To facilitate separation of the electrolyte from the mercury without first stopping the electrolysis, the simple apparatus shown in Fig. 1 was devised. It is a beaker with double walls for water cooling, and with an outlet at the bottom. The outlet stem has a stopcock, and between this and the bottom of the beaker are two platinum threads melted through the stem wall, to connect the mercury with the negative pole. The platinum-sheet anode has short platinum threads melted into the stirrer tube, which is filled with mercury connected with the positive pole through the open upper end of the tube.

This work was made possible by grants from *Statens naturvetenskapliga forskningsråd* to S. Ställberg-Stenhagen. The hospitality of *Hässle-Tika AB* is gratefully acknowledged.

1. For reviews on the Kolbe electro-synthesis see:
Knobel, M. and Brockman, C. J. *Bibliography of Electro-organic Chemistry*, National Research Council, Washington 1926;
Swann, S. Jr. *Bibliography of Electro-organic Chemistry. Part I, University of Illinois Engineering Experiment Station Circular Series No. 50, University of Illinois Bulletin* **45** (1948) No. 69;
Weedon, B. C. L., *Quart. Rev. London* **4** (1952) 380;
Wladislaw, B. *Selecta Chimica* **14** (1955) 77;
Swann, S. Jr. *Electrolytic Reactions* in Weissberger, A. *Technique of Organic Chemistry*, Interscience Publishers, New York and London 1956, vol. 2, p. 385.
2. Bouveault, L. *Bull. soc. chim. France* **29** (1903) 1038, 1043.

Received April 3, 1958.

Infra-red Spectroscopic Evidence on the Structure of Isomerized Dimethylaminoethoxy-methyl-phosphoryl Fluoride

LENNART LARSSON

Research Institute of National Defence, Dept. 1, Sundbyberg 4, Sweden

It was found by Tammelin [1] that, when dimethylaminoethoxy-methyl-phosphoryl fluoride is stored at room temperature, the liquid is transformed in a few days into a solid compound with the same per cent composition as the initial liquid. In contrast to the liquid isomer, the solid one is not easily hydrolyzed in alkaline solutions but is in acid solutions and apparently yields the same products of hydrolysis as the liquid compound. Moreover, the solid isomer gives no Schönemann reaction whereas the liquid one does. On the basis of these results Tammelin has postulated the following rearrangement for dimethylaminoethoxy-methyl-phosphoryl fluoride (I).

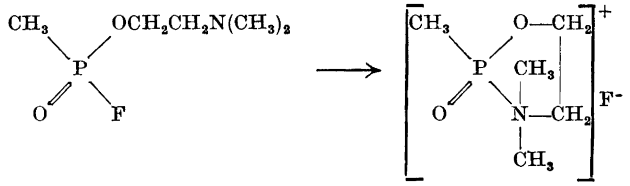

I

When *iso*propoxy-methyl-phosphoryl fluoride (Sarin) was mixed with triethylamine in mole ratio 1:1, no reaction seemed to occur. This observation is not consistent with the rearrangement proposed above.

Another conceivable rearrangement analogous to that described by Fukuto and Stafford [2] for the isomerization of diethoxy-diethylaminoethoxy-thionophosphate to the thiolo-isomer is that the liquid is transformed to an ethylene-immonium salt (II) or to the more stable piperazinium salt (III).

It was thus of interest to make an infra-red spectroscopic study of the rearranged product to elucidate its structure. As appears from Fig. 1, the infra-red spectrum of the solid isomer (1) shows mainly the same pattern as that of the quaternized derivative of the liquid compound, methyl-fluoro-phosphorylcholine iodide (2), with two fundamental exceptions: in the spectra of the solid isomer the strong absorption band at 11.79 μ (848 cm^{-1}), assigned to the vibration of the P—F bond [3], is absent and at 13.52 μ (740 cm^{-1}) a band appears which can probably be attributed to the vibration of a P—N bond [3]. The spectrum of the solid isomer adheres closely also to that of ethoxy-methyl-phosphorylcholine iodide (3) with the exception of the absorption band at 13.52 μ mentioned above. The absorption bands at about 3 μ and 6 μ in all the

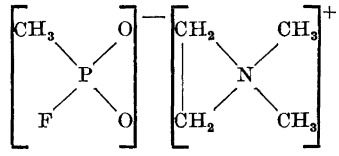

II

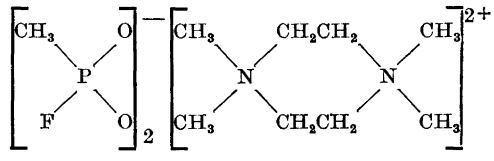

III

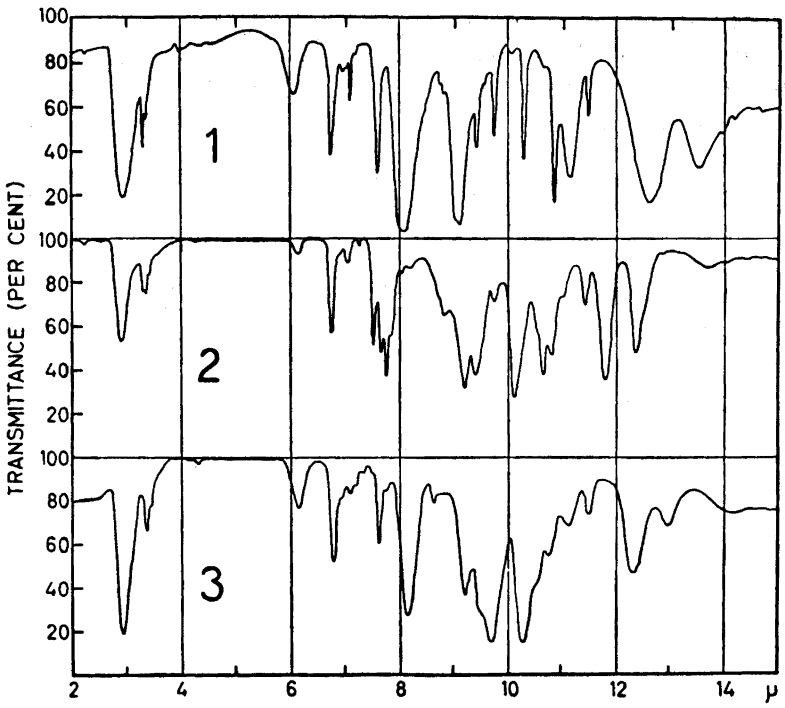

Fig. 1. The infra-red spectra of the solid isomer of dimethyl-aminoethoxy-methyl-phosphoryl fluoride (1) and the iodides of methyl-fluoro-phosphorylcholine (2) and of ethoxy-methyl-phosphorylcholine (3).

spectra are probably caused by moisture, picked up during the preparation of the potassium bromide disks. The remaining absorption bands agree well with those usually obtained in the infra-red spectra of organic phosphorus compounds. The results obtained from the infra-red measurements are thus entirely in accordance with the structure that Tammelin has suggested for the solid isomer of dimethyl-aminoethoxy-methyl-phosphoryl fluoride, and they exclude structures like II and III.

It has been shown that thiosulphate ion reacts with ethylene-immonium ion [5]. From a study, performed in the same manner as described by Fukuto and Stafford [2], it has been found that the solid isomer does not react with thiosulphate ion indicating that there is no immonium ion present in the solid isomer. This result is a further argument against structure II.

Experimental. The compounds studied were synthesized by Tammelin [1,4] at this institute. The infra-red spectra were recorded by means of a Perkin-Elmer spectrometer, Model 21, equipped with a rock salt prism, and the following settings were used: Resolution 927; response 2:1170; gain 6; suppression 3; speed about 1 μ/min; scale 5 cm/μ. The potassium bromide disk technique was employed, and 1 mg of sample was mechanically ground together with 300 mg of potassium bromide.

My sincere thanks are due to Professor G. Ljunggren, Director of this Institute, for the kind interest he has shown in this work.

1. Tammelin, L.-E. *Acta Chem. Scand.* **11** (1957) 859.
2. Fukuto, T. R. and Stafford, E. M. *J. Am. Chem. Soc.* **79** (1957) 6083.
3. Larsson, L. *Acta Chem. Scand.* **6** (1952) 1470.
4. Tammelin, L.-E. *Acta Chem. Scand.* **11** (1957) 1340.
5. Bartlett, P. D., Ross, S. D. and Swain, C. G. *J. Am. Chem. Soc.* **69** (1947) 2971.

Received March 25, 1958.

The Effect of Nitrous Oxide on Biological Nitrogen Fixation and the Uptake of Combined Nitrogen

SINIKKA LUNDBOM

Laboratory of the Foundation for Chemical Research, Biochemical Institute, Helsinki, Finland

Some years ago it was found in this laboratory [1] in long time growth experiments with *Azotobacter vinelandii* that N_2O inhibits not only the fixation of molecular nitrogen but also the utilization of nitrate nitrogen. The utilization of ammonium nitrogen was not inhibited. Later Mozen *et al.*[2] observed in short time experiments with the same strain of *A. vinelandii*, using nitrate labelled with ^{15}N, that the utilization of nitrate nitrogen was not inhibited by N_2O. In the last mentioned experiments the cells were harvested 3—24 h after inoculation. The reason for this difference between long time and short time experiments is unexplained. I have controlled the previous results from long time growth experiments with *A. vinelandii* harvesting the cells 48 and 144 h after inoculation. The results of the experiments are presented in this paper. The experiments were performed with the same strain

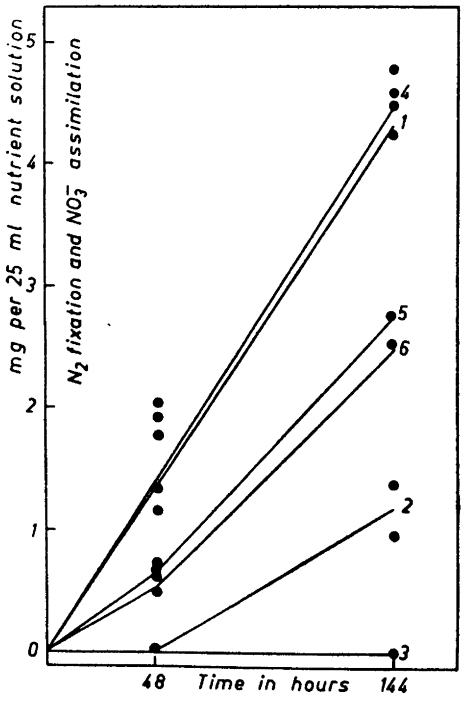

Fig. 1. The effect of N_2O on N_2 fixation and NO_3^- assimilation by *Azotobacter*.

Curve	Gas-mixture			N source
	N_2	O_2	N_2O	
1	0.2	0.2	—	N_2
2	0.2	0.2	0.6	N_2
3	—	0.2	0.8	—
4	0.2	0.2	—	NO_3^-
5	0.2	0.2	0.6	NO_3^-
6	—	0.2	0.8	NO_3^-

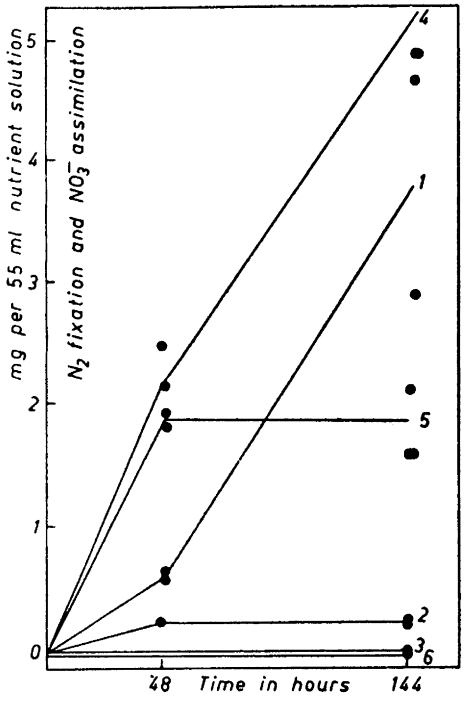

Fig. 2. The effect of N_2O on N_2 fixation and NO_3^- assimilation by *Clostridium*.

Curve	Gas-mixture		N source
	N_2	N_2O	
1	1.0	—	N_2
2	0.4	0.6	N_2
3	—	1.0	—
4	1.0	—	NO_3^-
5	0.4	0.6	NO_3^-
6	—	1.0	NO_3^-

Table 1. The effect of N_2O on N_2 fixation by *Azotobacter vinelandii* K.

N_2 fixation mg N/25 ml nutrient solution

Gas-mixtures	0.2 atm. N_2 0.2 atm. O_2		0.2 atm. N_2 0.2 atm. O_2 0.6 atm. N_2O		0.2 atm. O_2 0.8 atm. N_2O	
Inoculum + nutrient	Tot. N in cells	Increase of N	Tot. N in cells	Increase of N	Tot. N in cells	Increase of N
	0.130		0.130		0.130	
48 hours	1.317	1.187	0.195	0.065	0.100	—
	1.934	1.804	0.154	0.024	0.160	0.030
144 hours	4.251	4.121	1.512	1.382	0.131	—
	4.799	4.669	1.080	0.950	—	—

of *A. vinelandii* as earlier. Similar experiments were also performed with *Clostridium pasteurianum.*

Azotobacter was incubated at 30°C in Burk's medium containing 10 p.p.m. Mo, and *Clostridium* was incubated at 37°C in synthetic nutrient solution containing the essential vitamins [3].

The inocula for *Azotobacter* were grown for 24 h, aerating the culture very heavily. The inocula for nitrate culture were adapted thrice in the basal nutrient solution containing 500 p.p.m. nitrate nitrogen as KNO_3.

The inocula for *Clostridium* were grown for 36 h and the culture was enriched with nitrogen, bubbling a nitrogen-stream continually through the culture. The nitrate inocula were adapted in a similar way as by *Azotobacter.*

The experiments were carried out in six vacuum desiccators each of 8 l. Each desiccator contained 4 bottles of 100 ml each containing 25 ml nutrient solution. Gas-mixtures: *Azotobacter:* 0.2 atm. N_2 and 0.2 atm. O_2, 0.2 atm. N_2, 0.2 atm. O_2 and 0.6 atm. N_2O, and 0.2 atm. O_2 and 0.8 atm. N_2O. *Clostridium:* 1.0 atm. N_2, 0.4 atm. N_2 and 0.6 atm. N_2O, and 1.0 atm. N_2O.

In order to get the gas-mixtures into the desiccators the treatment of *Azotobacter* desiccators was: vacuum, flushing with air, filling with the required gas-mixture; and of *Clostridium* desiccators: vacuum, flushing with nitrogen twice, filling with required gas-mixtures.

48 and 144 h after inoculation two bottles from each desiccator were taken for analyses. The samples were immediately put on ice, centrifuged and the supernatant was used for nitrate analysis (bottles with nitrate). The

Table 2. The effect of N_2O on NO_3^- assimilation by *Azotobacter vinelandii* K.

Utilization of NO_3^- mg/25 ml nutrient solution

Gas-mixtures	0.2 atm. N_2 0.2 atm. O_2				0.2 atm. N_2 0.2 atm. O_2 0.6 atm. N_2O				0.2 atm. O_2 0.8 atm. N_2O			
Inoculum + nutrient	Tot. N in cells	Increase of N	NO_3-N in sol.	NO_3-N used	Tot. N in cells	Increase of N	NO_3-N in sol.	NO_3-N used	Tot. N in cells	Increase of N	NO_3-N in sol.	NO_3-N used
	0.397		18.90		0.397		18.90		0.397		18.90	
48 hours	1.771	1.374	17.42	1.48	1.060	0.663	18.23	0.66	1.096	0.699	18.17	0.73
	2.488	2.091	16.75	2.15	1.080	0.683			0.990	0.593	18.37	0.51
	2.360	1.963			1.139	0.742	18.10	0.79				
144 hours	4.776	4.379	14.57	4.33	3.14	2.743	16.12	2.78	2.782	2.385		
	4.847	4.450	14.50	4.40			16.20	2.71	2.963	2.566	16.40	2.51

Table 3. The effect of N_2O on N_2 fixation by *Clostridium pasteurianum* W 5.

N_2 fixation mg/55 ml nutrient solution

Gas-mixtures	1.00 atm. N_2		0.4 atm. N_2 0.6 atm. N_2O		1.00 atm. N_2O	
Inoculum + nutrient	Tot. N in cells	Increase of N	Tot. N in cells	Increase of N	Tot. N in cells	Increase of N
	0.526		0.526		0.526	
48 hours	1.136	0.610	0.775	0.249	0.504	—
	1.050	0.524	0.429	—	0.492	—
144 hours	5.137	4.611	0.715	0.189	0.512	—
	3.388	2.864	0.698	0.172	0.461	

cells were washed once with distilled water and a Kjeldahl-analysis was made from the washed cells. The increase of nitrogen in the cell mass and the decrease of nitrate in the solution correspond well with each other in the *Azotobacter* experiments, wherefore analytical errors have not influenced the results essentially. In *Clostridium* experiments the increase of nitrogen in the cells is somewhat larger than the decrease of nitrate in the solution, and hence a slight N_2 fixation might have occurred even when nitrate formed the source of nitrogen.

Tables 1 and 2 and Fig. 1 present nitrogen fixation and the utilization of nitrate nitrogen by *Azotobacter*. During 48 h practically no N_2 fixation could be found in *Azotobacter* cultures with 0.6 atm. N_2O. After 144 h some N_2 fixation was, strangely enough, found under these conditions (Fig. 1, curves 1, and 2). The inhibition of the utilization of nitrate nitrogen is clear already 48 h after inoculation and especially after 144 h at both N_2O concentrations (Fig. 1, curves 4, 5, and 6).

The results with *Clostridium* are presented in Tables 3 and 4, and in Fig. 2. In *Clostridium* cultures 1.0 atm. N_2O totally prevented nitrate utilization after 48 h. 48 h after inoculation the utilization of NO_3-N was about 1 mg/55 ml nutrient solution (Tables 3 and 4). The inhibiting effect of nitrous oxide on the utilization of nitrate in long time growth experiments is difficult to explain. Since it is not met with in short time experiments, as is the case with molecular nitrogen fixation, in long time growth experiments we probably have to do with some secondary influence which is not known more closely.

The experimental part of the work was performed in the autumn of 1954.

Table 4. The effect of N_2O on NO^- assimilation by *Clostridium pasteurianum* W 5.

Utilization of NO_3^- mg/55 ml nutrient solution

Gas-mixtures	1.00 atm. N_2				0.4 atm. N_2 0.6 atm. N_2O				1.00 atm. N_2O			
Inoculum + nutrient	Tot. N in cells	Increase of N	NO_3-N in sol.	NO_3-N used	Tot. N in cells	Increase of N	NO_3-N in sol.	NO_3-N used	Tot. N in cells	Increase of N	NO_3-N in sol.	NO_3-N used
	0.759		10.94		0.759		10.94		0.759		10.94	
48 hours	2.94	2.181	9.16	1.78	2.56	1.801	9.95	0.99	0.720	—	10.85	—
	3.25	2.491	8.95	1.99	2.70	1.941	9.90	1.04	0.735	—	10.99	—
144 hours	5.61	4.851	7.96	3.98	2.32	1.561	10.07	0.87	0.691	—	10.47	—
	6.09	5.331	6.77	4.17	2.34	1.581	9.99	0.95	0.701	—	10.05	—
	5.61	4.851			2.95	2.191						

1. Virtanen, A. I. and Lundbom, S. *Acta Chem. Scand.* **7** (1953) 1223.
2. Mozen, M. M., Burris, R. H., Lundbom, S. and Virtanen, A. I. *Acta Chem. Scand.* **9** (1955) 1232.
3. Virtanen, A. I. and Lundbom, S. *Acta Chem. Scand.* **8** (1954) 870.

Received January 7, 1958.

On the Rearrangement Products of Humulone

L.-O. SPETSIG

Forskningslaboratoriet LKB, Äppelviken, Sweden

The main bitter substances of beer are the *iso*humulones formed by rearrangement of the humulone, cohumulone and adhumulone of hops during the wort boiling. They have been isolated from trimethylpentane extracts of beer by countercurrent distribution [1]. According to Windisch *et al*, however, two products were formed from humulone when rearranged in a buffer solution, as the preformed *iso*humulone (Harzkörper A) was in part degraded to a second compound of similar properties (Harzkörper B)[2]. The latter compound and its analogues have not been observed in beer. When treated with boiling alkaline ethanol humulone is stated to give *iso*humulone only[3].

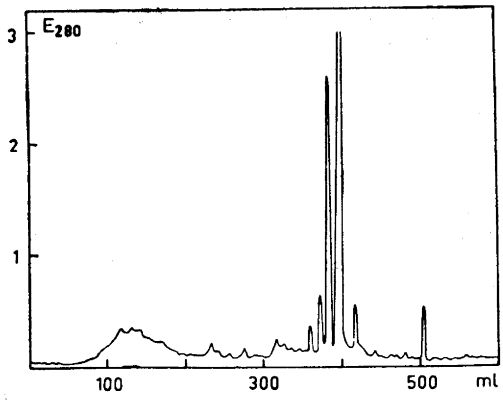

Fig. 1. Distribution diagram for rearrangement products of humulone in an acetate buffer of pH 5.1. The last peak is unreacted humulone.

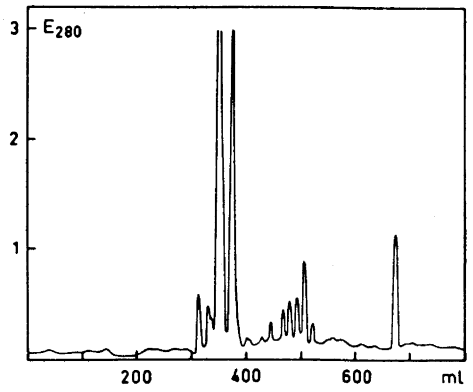

Fig. 2. Chromatographic pattern of the rearrangement products of humulone from alkaline ethanol.

We have now tried to study humulone rearrangement products of different origins by reversed-phase partition chromatography. The separations were performed on 800 × 8 mm columns of hydrophobic Hyflo Super Cel with chloroform as the stationary solvent. Gradient elution was accomplished with a buffer solution containing 25% methanol, the pH-value of which was steadily increased. The optical density of the elute was measured continuously by a spectrophotometer connected to a recorder [4].

When humulone was rearranged at 100°C in a number of buffer solutions of medium pH-value two principal components were always found, which were eluted at pH 5.8—6.0 (Fig. 1). Their ultraviolet absorption spectra were similar to that of the *iso*humulones of beer and to that of humulinic acid. It has been shown earlier [4] that the chromatographic pattern of the bitter substances of beer was predominated by a five (or six) peaks appearing at pH 5.6—6.2. It seemed probable that the group consisted of six components, two from each of the three humulones.

These results have led us to assume that the two same principal compounds are formed from humulone in beer and in buffer solutions of medium pH-value. A detailed study of the humulone rearrangements in buffer solutions thus is to be desired.

1. Virtanen, A. I. and Lundbom, S. *Acta Chem. Scand.* **7** (1953) 1223.
2. Mozen, M. M., Burris, R. H., Lundbom, S. and Virtanen, A. I. *Acta Chem. Scand.* **9** (1955) 1232.
3. Virtanen, A. I. and Lundbom, S. *Acta Chem. Scand.* **8** (1954) 870.

Received January 7, 1958.

On the Rearrangement Products of Humulone

L.-O. SPETSIG

Forskningslaboratoriet LKB, Äppelviken, Sweden

The main bitter substances of beer are the *iso*humulones formed by rearrangement of the humulone, cohumulone and adhumulone of hops during the wort boiling. They have been isolated from trimethylpentane extracts of beer by countercurrent distribution [1]. According to Windisch *et al*, however, two products were formed from humulone when rearranged in a buffer solution, as the preformed *iso*humulone (Harzkörper A) was in part degraded to a second compound of similar properties (Harzkörper B)[2]. The latter compound and its analogues have not been observed in beer. When treated with boiling alkaline ethanol humulone is stated to give *iso*humulone only[3].

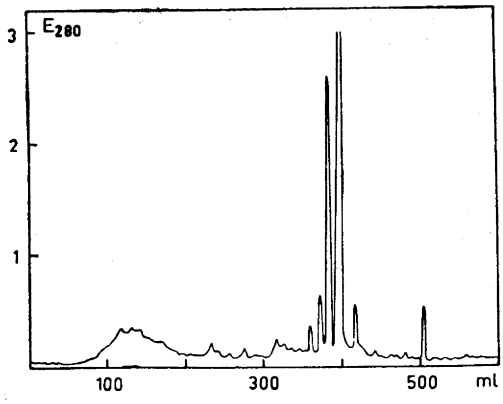

Fig. 1. Distribution diagram for rearrangement products of humulone in an acetate buffer of pH 5.1. The last peak is unreacted humulone.

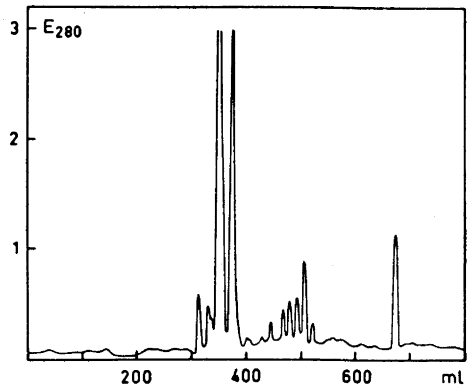

Fig. 2. Chromatographic pattern of the rearrangement products of humulone from alkaline ethanol.

We have now tried to study humulone rearrangement products of different origins by reversed-phase partition chromatography. The separations were performed on 800 × 8 mm columns of hydrophobic Hyflo Super Cel with chloroform as the stationary solvent. Gradient elution was accomplished with a buffer solution containing 25% methanol, the pH-value of which was steadily increased. The optical density of the elute was measured continuously by a spectrophotometer connected to a recorder [4].

When humulone was rearranged at 100°C in a number of buffer solutions of medium pH-value two principal components were always found, which were eluted at pH 5.8—6.0 (Fig. 1). Their ultraviolet absorption spectra were similar to that of the *iso*humulones of beer and to that of humulinic acid. It has been shown earlier [4] that the chromatographic pattern of the bitter substances of beer was predominated by a five (or six) peaks appearing at pH 5.6—6.2. It seemed probable that the group consisted of six components, two from each of the three humulones.

These results have led us to assume that the two same principal compounds are formed from humulone in beer and in buffer solutions of medium pH-value. A detailed study of the humulone rearrangements in buffer solutions thus is to be desired.

An attempt was also made to prepare *iso*humulone by treating humulone with boiling alcoholic alkali [3]. However, a rather complex reaction mixture resulted, as was also found by Carson [5] and by Howard [6] (Fig. 2). Moreover, none of the main compounds could be identical with the *iso*humulone of beer, though they had ressembling ultraviolet absorption curves, as they were eluted already at pH 4.5 and 4.7, respectively. Some minor components only appeared at pH ~ 6 where the *iso*-humulones of beer are normally found. The last peak in the chromatogram was formed by unreacted humulone.

1. Rigby, F. L. and Bethune, J. L. *Am. Soc. Brewing Chemists, Proc.* **1952** 98.
2. Windisch, W., Kolbach, P. and Schleicher, R. *Wochschr. Brauerei* **44** (1927) 453, 473, 485, 497.
3. Verzele, M. and Govaert, F. *Intern. Congr. Fermentation Inds. Lectures and Communs. Ghent 1947*, p. 297.
4. Spetsig, L. O., Steninger, M. and Brohult, S. *European Brewery Conv. Proc. Congr. Copenhagen 1957*, p. 22.
5. Carsson, J. F. *J. Am. Chem. Soc.* **74** (1952) 4615.
6. Howard, G. A., Slater, C. A. and Tatchell, A. R. *J. Inst. Brewing* **63** (1957) 237.

Received April 10, 1958.

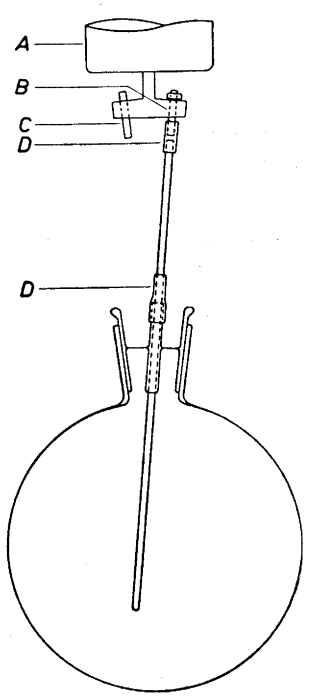

Fig. 1. Stirrer for flasks totally enclosed. A motor, B bearing eccentric to the motor axle, C counter weight, D rubber bushings.

A Stirrer for Flasks Totally Enclosed

OLOV E. ÖHRN

Institute of Physical Chemistry, University of Uppsala, Uppsala, Sweden

In connection with some fractionation work[1] a stirrer for flasks totally enclosed has been constructed. The design is based on the principle that if one end of a rod, the middle of which is connected to a ball joint, is driven in a circle the other end will also describe a circle, whereas the middle remains fixed. The middle can of course be connected to a flexible membrane instead of a ball joint. In this way it is possible to get a perfect seal. The stirrer is shown in Fig. 1.

It is designed to be used in flasks with joints of Standard Taper 29. The stopper, made of teflon, has been machined so that we have a relatively thin-walled cylinder, closed in the center with a plate only 0.5 mm thick, through the middle of which runs a tube that fits tightly around the stirring rod. To obtain a better seal the teflon tube may be pressed against the rod with a thick rubber bushing and in this way we also avoid a slow rotation of the stirrer in the direction opposite to that of the motor. The connection of the motor to the rod, *via* a bearing eccentric to the motor axle, will be clear from the figure. A length of 30 cm for the rod with a maximum amplitude of 2 cm is adequate.

The simple shape of the rod has proved most satisfactory for fractionate work since very little precipitate becomes attached to the stirrer.

1. Öhrn, O. E. *Arkiv Kemi* **12** (1958) 397.

Received April 3, 1958.

An attempt was also made to prepare *iso*humulone by treating humulone with boiling alcoholic alkali [3]. However, a rather complex reaction mixture resulted, as was also found by Carson [5] and by Howard [6] (Fig. 2). Moreover, none of the main compounds could be identical with the *iso*humulone of beer, though they had ressembling ultraviolet absorption curves, as they were eluted already at pH 4.5 and 4.7, respectively. Some minor components only appeared at pH ~ 6 where the *iso*-humulones of beer are normally found. The last peak in the chromatogram was formed by unreacted humulone.

1. Rigby, F. L. and Bethune, J. L. *Am. Soc. Brewing Chemists, Proc.* **1952** 98.
2. Windisch, W., Kolbach, P. and Schleicher, R. *Wochschr. Brauerei* **44** (1927) 453, 473, 485, 497.
3. Verzele, M. and Govaert, F. *Intern. Congr. Fermentation Inds. Lectures and Communs. Ghent 1947*, p. 297.
4. Spetsig, L. O., Steninger, M. and Brohult, S. *European Brewery Conv. Proc. Congr. Copenhagen 1957*, p. 22.
5. Carsson, J. F. *J. Am. Chem. Soc.* **74** (1952) 4615.
6. Howard, G. A., Slater, C. A. and Tatchell, A. R. *J. Inst. Brewing* **63** (1957) 237.

Received April 10, 1958.

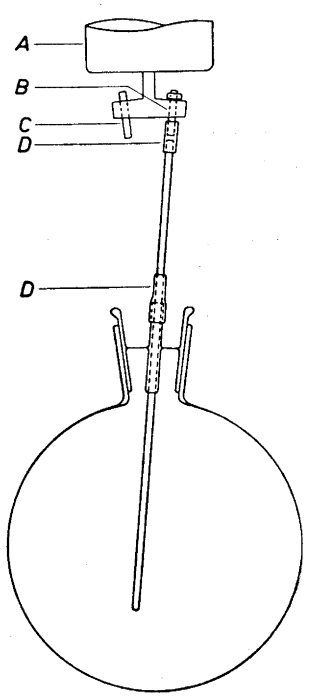

Fig. 1. Stirrer for flasks totally enclosed. A motor, B bearing eccentric to the motor axle, C counter weight, D rubber bushings.

A Stirrer for Flasks Totally Enclosed

OLOV E. ÖHRN

Institute of Physical Chemistry, University of Uppsala, Uppsala, Sweden

In connection with some fractionation work[1] a stirrer for flasks totally enclosed has been constructed. The design is based on the principle that if one end of a rod, the middle of which is connected to a ball joint, is driven in a circle the other end will also describe a circle, whereas the middle remains fixed. The middle can of course be connected to a flexible membrane instead of a ball joint. In this way it is possible to get a perfect seal. The stirrer is shown in Fig. 1.

It is designed to be used in flasks with joints of Standard Taper 29. The stopper, made of teflon, has been machined so that we have a relatively thin-walled cylinder, closed in the center with a plate only 0.5 mm thick, through the middle of which runs a tube that fits tightly around the stirring rod. To obtain a better seal the teflon tube may be pressed against the rod with a thick rubber bushing and in this way we also avoid a slow rotation of the stirrer in the direction opposite to that of the motor. The connection of the motor to the rod, *via* a bearing eccentric to the motor axle, will be clear from the figure. A length of 30 cm for the rod with a maximum amplitude of 2 cm is adequate.

The simple shape of the rod has proved most satisfactory for fractionate work since very little precipitate becomes attached to the stirrer.

1. Öhrn, O. E. *Arkiv Kemi* **12** (1958) 397.

Received April 3, 1958.

Mean Amplitudes of Vibration in Certain Four-Atomic Molecules

J. BAKKEN

Institutt for teoretisk kjemi, Norges tekniske høgskole, Trondheim, Norway

Mean amplitudes of vibration (u) for the interatomic distances in certain four-atomic molecules have been calculated from spectroscopic data (Table 1). When the instantaneous interatomic distance is denoted by R and R_e is the equilibrium distance, then u is defined by

$$u = [\overline{(R - R_e)^2}]^{\frac{1}{2}}$$

The average is taken over the molecules in the gaseous state by thermodynamic equilibrium at a given temperature T. The calculations are based on the assumption of small harmonic vibrations, the method being described by Morino *et al.*[1]

Informations concerning u-values from spectroscopic data are of great interest for electron diffraction investigations. As to studies of mean amplitudes both from electron diffraction data and spectroscopic calculations, references are made to Karle and Karle [2], Kimura *et al.*[3] and Bastiansen *et al.*[4-6]. Electron diffraction investigations of the molecules studied in this work would contribute appreciably to our knowledge of mean amplitudes and are under consideration.

Table 1. Calculated mean amplitudes of vibration (u).

Molecule	Interatomic distance	u (Å) $T = 0$	298°K
P_4	P—P	0.0478	0.0533
BF_3	B—F	0.0433	0.0437
	F—F	0.0408	0.0442
BCl_3	B—Cl	0.0485	0.0508
	Cl—Cl	0.0442	0.0569
BBr_3	B—Br	0.0494	0.0545
	Br—Br	0.0402	0.0585
PH_3	P—H	0.0862	0.0862
	H—H	0.1516	0.1521
AsH_3	As—H	0.0894	0.0894
	H—H	0.1586	0.1597
SbH_3	Sb—H	0.0944	0.0944
	H—H	0.1712	0.1736
PF_3	P—F	0.0410	0.0418
	F—F	0.0700	0.0788
PCl_3	P—Cl	0.0467	0.0526
	Cl—Cl	0.0770	0.1033
NF_3	N—F	0.0515	0.0535
	F—F	0.0751	0.0786
CH_2O	C—H	0.0801	0.0801
	C—O	0.0372	0.0372
	H—H	0.1170	0.1170
	O—H	0.0911	0.0912
CD_2O	C—D	0.0682	0.0682
	C—O	0.0365	0.0366
	D—D	0.0823	0.0824
	O—D	0.0727	0.0730
C_2H_2	C—C	0.0357	
	C—H	0.0743	
	C—C—H	0.0784	
	H—H	0.1049	
C_2D_2	C—C	0.0362	
	C—D	0.0637	
	C—C—D	0.0717	
	D—D	0.0951	
C_2HD	C—C	0.0358	
	C—H	0.0743	
	C—D	0.0634	
	C—C—H	0.0795	
	C—C—D	0.0687	
	H—D	0.0988	

1. Morino, Y., Kuchitsu, K. and Shimanouchi, T. *J. Chem. Phys.* **20** (1952) 726.
2. Karle, I. L. and Karle, J. *J. Chem. Phys.* **17** (1949) 1052.
3. Kimura, M., Kimura, K. and Shibata, S. *J. Chem. Phys.* **24** (1956) 622.
4. Almenningen, A., Bastiansen, O. and Munthe-Kaas, T. *Acta Chem. Scand.* **10** (1956) 261.
5. Bastiansen, O. and Cyvin, S. J. *Acta Chem. Scand.* **11** (1957) 1789.
6. Bastiansen, O. and Cyvin, S. J. *Nature* **180** (1957) 980.

Received February 26, 1958.

ACTA CHEMICA SCANDINAVICA 12 (1958) 595—602

Proceedings of the Swedish Biochemical Society

Papers read at the meeting in Stockholm, March 8, 1958

Soluble Diaphorase in Animal Tissues

Lars Ernster and Franco Navazio*

Wenner-Gren Institute, University of Stockholm, Stockholm, Sweden

The soluble fraction obtained upon centrifugation of rat liver homogenates made in 0.25 M sucrose-3 % polyvinylpyrrolidone at 105 000 *g* for 60 min exhibits a high diaphorase activity as revealed by measuring the rate of reduction of 2,6-dichlorophenolindophenol by reduced di- or triphosphopyridine nucleotide (DPNH of TPNH). As emerges from the typical data shown in Table 1, this activity is, in contrast to those found in mitochondria and microsomes, virtually equally high with DPNH and TPNH, and it exceeds, in terms of total protein content, the diaphorase activities of the particulate fractions more than twice in the case of DPNH and about twenty times in the case of TPNH. The soluble diaphorase resembles the particulate one in that it reacts with methylene blue at about half the rate obtained with 2,6-dichlorophenolindophenol, but differs from the latter in being inactive towards cytochrome c or ferricyanide; treatment of the enzyme with ferric chloride according to Mahler and Elowe [1] did not alter this state of affairs. The following findings indicate that the soluble DPNH- and TPNH-diaphorase reactions are catalyzed by one common enzyme: 1) the two activities are not additive; 2) they are equally sensitive to various inhibitors such as *p*-chloromercuribenzoate, atebrine, or flavin adenine dinucleotide (flavin mononucleotide is not inhibitory); 3) they show no tendency to separate upon ammonium sulphate fractionation of the soluble fraction. Preliminary data indicate that this type of soluble diaphorase is ubiquitous as to its occurrence among animal tissues, although the highest activity hitherto found is that present in rat liver.

Table 1. Cytoplasmic distribution of diaphorase activities in rat liver.

Homogenates of rat liver were made in 0.25 M sucrose solution containing 3 % polyvinylpyrrolidone (pH adjusted to 7). 100 ml homogenate, containing 10 g wet weight liver, was centrifuged *a*) at 1 600 *g* for 10 min, *b*) at 4 100 *g* for 15 min, and *c*) at 105 000 *g* for 60 min. The denotions, mitochondrial, microsomal and soluble fractions, refer to the pellets obtained in *b* and *c*, and the supernatant obtained in *c*, respectively. The mitochondrial pellet was washed, and the microsomal pellet rinsed, twice with 0.25 M sucrose, and both pellets were suspended in 0.25 M sucrose. The test system contained 0.5 ml 0.3 M tris buffer (pH 7.5), 2.3 ml 0.25 M sucrose (containing, in the case of the soluble fraction, 3 % polyvinylpyrrolidone, pH adjusted to 7), 0.1 ml 3 mM DPNH or TPNH, 0.1 ml 1.7 mM 2,6-dichlorophenolindophenol, and 0.1 ml of the fraction to be tested, containing 5 mg wet weight liver equivalent in the case of mitochondria or microsomes, and 0.5 mg in the case of the soluble fraction. The decolorization of the dye was recorded in a Beckman DK2 spectrophotometer at 600 mμ, using glass cuvettes of 1 cm light path. The reaction was started by the addition of the reduced pyridine nucleotides, and followed for 4—6 min at room temperature. The values are expressed in terms of 1 g wet weight liver equivalent.

Fraction	Total protein content, mg	Diaphorase activity (μmoles dye reduced per min) DPNH	TPNH
Mitochondrial	23.3	4.3	1.0
Microsomal	31.1	13.1	1.9
Soluble	29.2	39.0	35.0

1. Mahler, H. R. and Elowe, D. G. *J. Biol. Chem.* **210** (1954) 165.

* On leave of absence from the Dept. of Biochemistry, Istituto Superiore di Sanità, Rome, Italy.

On the Relation of Mitochondrial ATPase to Diaphorase Flavin

Hans Löw

Wenner-Gren Institute, University of Stockholm, Stockholm, Sweden

Recent studies [1,2] of the relationship between oxidative phosphorylation and 2,4-dinitrophenol (DNP) stimulated adenosinetriphosphatase (ATPase) have indicated that the mitochondrial enzyme sequence which can be stimulated by DNP to break down ATP includes one link which is a part of the electron transport chain, *viz.* the diaphorase flavoenzyme. Further support for this conclusion could be obtained by showing that atebrin, a drug known to interfere with flavins probably in a competetive manner [3], stimulates the DNP-activated ATPase by about 40 % in low concentrations, while in higher concentrations it almost completely inhibits this reaction. Typical data are shown in Table 1. Due to a certain structural

Table 1. The effect of atebrin and promazines on DNP-ATPase

Compounds	Concentration, mM	Relative activity %
None	—	100
Atebrin	1.5	149
Atebrin	8.0	11
Promazine	0.1	135
Promazine	0.5	11
Chloropromazine	0.05	142
Chloropromazine	0.2	15
Acetylpromazine	0.2	134
Acetylpromazine	1.0	6

Each incubation tube contained the following: 5 mM ATP, 5 mM tris buffer pH 7.5, 0.1 mM DNP and 0.25 M sucrose. Final volume 2.0 ml. The tubes were incubated at 30° C for 20 min.

relationship between atebrin and promazine derivatives and to the fact that these are known to influence oxidative phosphorylation in isolated mitochondria [4] the effect of a series of promazine compounds was also tested. As is shown in Table 1 these gave an effect similar to that of atebrin.

The significance of these findings will be discussed.

1. Siekevitz, P., Löw, H., Ernster, L. and Lindberg, O. *Biochim. et Biophys. Acta (In press.)*
2. Löw, H., Siekevitz, P., Ernster, L. and Lindberg, O. *Biochem. et Biophys. Acta (In press.)*
3. Haas, E. *J. Biol. Chem.* **155** (1944) 321.
4. Berger, M., Strecker, H. J. and Waelsch, H. *Nature* **177** (1956) 1234.

The Potency of the Microsomal Material to Metabolize and Bind Carcinogens during Liver Regeneration

Tore Hultin and Alexandra von der Decken

Wenner-Gren Institute, University of Stockholm, Stockholm, Sweden

As a result of partial hepatectomy pronounced modifications are induced in the microsomal material of liver cytoplasm [1]. After a lag period of about 12—14 h there is a fairly rapid increase of the RNA/protein ratio. About simultaneously the activity of the microsomes in amino acid incorporating systems shows a rapid increase. The culmination generally occurs about 30 h after the operation.

Concurrently with this activation other components of the microsomal material decrease. The activity of glucose-6-phosphatase, measured per mg microsomal protein, is reduced by approximately 15 %. The concentration of DPNH-cytochrome c reductase is reduced to approximately the same degree. Liver microsomes are capable of demethylating the carcinogenic azo dye methylaminoazobenzene in the presence of TPNH under aerobic conditions [2]. The capacity of the microsomal material for carrying out this oxygen transfer, is reduced during regeneration, usually by about 20 %. Under the same conditions of oxygen transfer, reactive metabolites of the azo dye are produced. When ^{14}C-labeled azo compounds are used in the system, the isotope becomes bound to the microsomal proteins. Microsomes from regenerating liver have a considerably reduced capacity for producing reactive metabolites from ^{14}C-labeled azo dyes. This effect is most easily demonstrated by adding soluble proteins to the microsomal systems metabolizing ^{14}C-labeled carcinogenic azo compounds. Reactive metabolites are secondarily emitted from the microsomes, and became trapped by the soluble proteins. Subsequently the specific activities of the soluble proteins may be determined. Similar experiments have been carried out with 2-aminofluorene-9-^{14}C. In the regenerating livers, finally, the concentration of cytochrome b_5

(determined on deoxycholate extracts by dithionite reduction) is diminished by about 30%.

It is generally considered that the endoplasmic reticulum of the cytoplasm is the main origin of the microsomal material. Since RNA is concentrated to the nucleoprotein granules, which are attached to the delicate membranes of this network, while the enzymes and cytochrome b_5 apparently are associated with the membranes, the experiments suggest a richer attachment of nucleoprotein granules to the membranes during liver regeneration. Apparently, however, the composition of the membranes may become modified at the same time.

1. von der Decken, A. and Hultin, T. *Exptl. Cell Research* **14** (1958) 88.
2. Hultin, T. *Exptl. Cell Research* **13** (1957) 47.

On Submitochondrial Particles with High DPNH-oxidase * and Low Succinic Oxidase Activity

Herrick Baltscheffsky**

Wenner-Gren Institute, University of Stockholm, Stockholm, Sweden

A new method for obtaining submitochondrial particles capable of respiration and oxidative phosphorylation has been briefly reported [1]. After grinding liver mitochondria from rat or guinea pig with Al_2O_3 and centrifuging the ground material at 25 000 × *g* for 10 min, in order to get down the alumina and heavier mitochondrial structural fragments the particles are in the supernatant. After centrifugation for 1 h at 100 000 × *g* practically all the DPNH-oxidase activity of this supernatant is in the sediment, which is then suspended in a suitable medium.

Two slightly different methods of preparation (I and II) have been used. In I the medium for the last centrifugation before grinding and for the subsequent operations is 30 mM phosphate buffer of pH 7.0, in II 0.25 M sucrose. Significant differences between the preparations so obtained are: II gives a several fold higher final yield and the stimulation of its DPNH-oxidase by added cytochrome c is lower (usually less than 50 %, compared to more than 200 % for I). In II the supernatant after the 25 000 × *g* centrifugation consists of two separate layers, the bottom one being small in volume and red-colored.

2 mM amytal inhibits practically all the DPNH-oxidase activity in the absence of added cytochrome c, which eliminates the possibility that a significant part of this respiration is due to microsomal contamination.

The submitochondrial particles have a high DPNH-oxidase activity compared to their succinic oxidase activity [1]. Also, the DPNH-cytochrome c reductase activity is much higher than the succinate-cytochrome c reductase activity. The ratio for five different preparations varied between 7.7 and 17, mean value 10 (I gave somewhat higher ratios than II). In the heavier structural fragments the ratio is much lower. The almost complete separation obtained, of the system responsible for the oxidation of DPNH from that responsible for the oxidation of succinate is thus possibly due to a tighter binding of the latter to these fragments.

The rate of oxidation of DPNH is stimulated by $Na_4P_2O_7$, EDTA and ATP, active where ADP and AMP are not. ITP also stimulates this respiration, but only in higher concentration and to a lesser degree than ATP. These stimulations are inhibited by amytal.

The TPNH-oxidase and the TPNH-cytochrome c reductase activities of the particles are low compared to the corresponding DPNH-activities, but are several fold increased by addition of DPN.

The particles have ATP-ase activity. It is increased up to 100-fold by added Mg^{++} whereas 2,4-dinitrophenol only has a slight (about 2-fold) stimulating effect.

1. Baltscheffsky, H. *Exptl. Cell Research* **13** (1957) 630.

* Abbreviations: DPN, diphosphopyridine nucleotide; DPNH, reduced diphosphopyridine nucleotide; TPNH, reduced triphosphopyridine nucleotide; ATP, adenosine triphosphate; ADP, adenosine diphosphate; AMP, adenosine monophosphate; ITP, inosine triphosphate; EDTA, ethylenediaminetetraacetate; M, moles per liter.

** Supported by a grant from *Ella och Georg Ehrnrooths stiftelse.*

Activity of Amino Acid Activating Enzyme Systems during Liver Regeneration

Alexandra von der Decken and Tore Hultin

Wenner-Gren Institute, University of Stockholm, Stockholm, Sweden

In order to attain an incorporation of labeled amino acids into proteins by cell-free liver preparations, microsomal material and certain

On the Relation of Mitochondrial ATPase to Diaphorase Flavin

Hans Löw

Wenner-Gren Institute, University of Stockholm, Stockholm, Sweden

Recent studies [1,2] of the relationship between oxidative phosphorylation and 2,4-dinitrophenol (DNP) stimulated adenosinetriphosphatase (ATPase) have indicated that the mitochondrial enzyme sequence which can be stimulated by DNP to break down ATP includes one link which is a part of the electron transport chain, *viz.* the diaphorase flavoenzyme. Further support for this conclusion could be obtained by showing that atebrin, a drug known to interfere with flavins probably in a competetive manner [3], stimulates the DNP-activated ATPase by about 40 % in low concentrations, while in higher concentrations it almost completely inhibits this reaction. Typical data are shown in Table 1. Due to a certain structural

Table 1. The effect of atebrin and promazines on DNP-ATPase

Compounds	Concentration, mM	Relative activity %
None	—	100
Atebrin	1.5	149
Atebrin	8.0	11
Promazine	0.1	135
Promazine	0.5	11
Chloropromazine	0.05	142
Chloropromazine	0.2	15
Acetylpromazine	0.2	134
Acetylpromazine	1.0	6

Each incubation tube contained the following: 5 mM ATP, 5 mM tris buffer pH 7.5, 0.1 mM DNP and 0.25 M sucrose. Final volume 2.0 ml. The tubes were incubated at 30° C for 20 min.

relationship between atebrin and promazine derivatives and to the fact that these are known to influence oxidative phosphorylation in isolated mitochondria [4] the effect of a series of promazine compounds was also tested. As is shown in Table 1 these gave an effect similar to that of atebrin.

The significance of these findings will be discussed.

1. Siekevitz, P., Löw, H., Ernster, L. and Lindberg, O. *Biochim. et Biophys. Acta (In press.)*
2. Löw, H., Siekevitz, P., Ernster, L. and Lindberg, O. *Biochem. et Biophys. Acta (In press.)*
3. Haas, E. *J. Biol. Chem.* **155** (1944) 321.
4. Berger, M., Strecker, H. J. and Waelsch, H. *Nature* **177** (1956) 1234.

The Potency of the Microsomal Material to Metabolize and Bind Carcinogens during Liver Regeneration

Tore Hultin and Alexandra von der Decken

Wenner-Gren Institute, University of Stockholm, Stockholm, Sweden

As a result of partial hepatectomy pronounced modifications are induced in the microsomal material of liver cytoplasm [1]. After a lag period of about 12—14 h there is a fairly rapid increase of the RNA/protein ratio. About simultaneously the activity of the microsomes in amino acid incorporating systems shows a rapid increase. The culmination generally occurs about 30 h after the operation.

Concurrently with this activation other components of the microsomal material decrease. The activity of glucose-6-phosphatase, measured per mg microsomal protein, is reduced by approximately 15 %. The concentration of DPNH-cytochrome c reductase is reduced to approximately the same degree. Liver microsomes are capable of demethylating the carcinogenic azo dye methylaminoazobenzene in the presence of TPNH under aerobic conditions [2]. The capacity of the microsomal material for carrying out this oxygen transfer, is reduced during regeneration, usually by about 20 %. Under the same conditions of oxygen transfer, reactive metabolites of the azo dye are produced. When ^{14}C-labeled azo compounds are used in the system, the isotope becomes bound to the microsomal proteins. Microsomes from regenerating liver have a considerably reduced capacity for producing reactive metabolites from ^{14}C-labeled azo dyes. This effect is most easily demonstrated by adding soluble proteins to the microsomal systems metabolizing ^{14}C-labeled carcinogenic azo compounds. Reactive metabolites are secondarily emitted from the microsomes, and became trapped by the soluble proteins. Subsequently the specific activities of the soluble proteins may be determined. Similar experiments have been carried out with 2-aminofluorene-9-^{14}C. In the regenerating livers, finally, the concentration of cytochrome b_5

(determined on deoxycholate extracts by dithionite reduction) is diminished by about 30%.

It is generally considered that the endoplasmic reticulum of the cytoplasm is the main origin of the microsomal material. Since RNA is concentrated to the nucleoprotein granules, which are attached to the delicate membranes of this network, while the enzymes and cytochrome b_5 apparently are associated with the membranes, the experiments suggest a richer attachment of nucleoprotein granules to the membranes during liver regeneration. Apparently, however, the composition of the membranes may become modified at the same time.

1. von der Decken, A. and Hultin, T. *Exptl. Cell Research* **14** (1958) 88.
2. Hultin, T. *Exptl. Cell Research* **13** (1957) 47.

On Submitochondrial Particles with High DPNH-oxidase * and Low Succinic Oxidase Activity

Herrick Baltscheffsky**

Wenner-Gren Institute, University of Stockholm, Stockholm, Sweden

A new method for obtaining submitochondrial particles capable of respiration and oxidative phosphorylation has been briefly reported [1]. After grinding liver mitochondria from rat or guinea pig with Al_2O_3 and centrifuging the ground material at 25 000 × *g* for 10 min, in order to get down the alumina and heavier mitochondrial structural fragments the particles are in the supernatant. After centrifugation for 1 h at 100 000 × *g* practically all the DPNH-oxidase activity of this supernatant is in the sediment, which is then suspended in a suitable medium.

Two slightly different methods of preparation (I and II) have been used. In I the medium for the last centrifugation before grinding and for the subsequent operations is 30 mM phosphate buffer of pH 7.0, in II 0.25 M sucrose. Significant differences between the preparations so obtained are: II gives a several fold higher final yield and the stimulation of its DPNH-oxidase by added cytochrome c is lower (usually less than 50 %, compared to more than 200 % for I). In II the supernatant after the 25 000 × *g* centrifugation consists of two separate layers, the bottom one being small in volume and red-colored.

2 mM amytal inhibits practically all the DPNH-oxidase activity in the absence of added cytochrome c, which eliminates the possibility that a significant part of this respiration is due to microsomal contamination.

The submitochondrial particles have a high DPNH-oxidase activity compared to their succinic oxidase activity [1]. Also, the DPNH-cytochrome c reductase activity is much higher than the succinate-cytochrome c reductase activity. The ratio for five different preparations varied between 7.7 and 17, mean value 10 (I gave somewhat higher ratios than II). In the heavier structural fragments the ratio is much lower. The almost complete separation obtained, of the system responsible for the oxidation of DPNH from that responsible for the oxidation of succinate is thus possibly due to a tighter binding of the latter to these fragments.

The rate of oxidation of DPNH is stimulated by $Na_4P_2O_7$, EDTA and ATP, active where ADP and AMP are not. ITP also stimulates this respiration, but only in higher concentration and to a lesser degree than ATP. These stimulations are inhibited by amytal.

The TPNH-oxidase and the TPNH-cytochrome c reductase activities of the particles are low compared to the corresponding DPNH-activities, but are several fold increased by addition of DPN.

The particles have ATP-ase activity. It is increased up to 100-fold by added Mg^{++} whereas 2,4-dinitrophenol only has a slight (about 2-fold) stimulating effect.

1. Baltscheffsky, H. *Exptl. Cell Research* **13** (1957) 630.

* Abbreviations: DPN, diphosphopyridine nucleotide; DPNH, reduced diphosphopyridine nucleotide; TPNH, reduced triphosphopyridine nucleotide; ATP, adenosine triphosphate; ADP, adenosine diphosphate; AMP, adenosine monophosphate; ITP, inosine triphosphate; EDTA, ethylenediaminetetraacetate; M, moles per liter.

** Supported by a grant from *Ella och Georg Ehrnrooths stiftelse.*

Activity of Amino Acid Activating Enzyme Systems during Liver Regeneration

Alexandra von der Decken and Tore Hultin

Wenner-Gren Institute, University of Stockholm, Stockholm, Sweden

In order to attain an incorporation of labeled amino acids into proteins by cell-free liver preparations, microsomal material and certain

soluble cytoplasmic components have to be included in the system [1]. It has been shown previously that microsomes, isolated from regenerating rat liver, work more effectively in incorporation systems of this kind than normal microsomes [2,3]. The present report is concerned with the effects of regenerative growth induction on the soluble components of the incorporation system. As is well known, these components are required for the initial activation of the labeled amino acids at the expense of high-energy phosphates [4]. The complete soluble system used in these experiments contained the following essential components: (1) a mechanism for ATP-generation (in the present experiments composed of phosphoenolpyruvate, pyruvate kinase and adenylate kinase), (2) guanosine triphosphate [5], (3) amino acid activating enzymes, associated in an hitherto unknown way with soluble RNA.

With standard amounts of liver microsomes as acceptor for activated amino acids, cell fluid from regenerating livers effected, per mg protein, a more rapid incorporation of ^{14}C-L-leucine into protein than cell fluid from normal liver. The increase was preceded by a lag period of 12—14 h and culminated about 30 h after hepatectomy. As a rule, the activity then was 60—80 % higher in the case of regenerating livers.

In order to elucidate which of the components of the activation chain were affected by the regeneration, some of these components were studied separately. The higher efficiency of the cell fluid from regenerating liver was not due to increased contents of phosphoenolpyruvate, ATP or guanosine triphosphate, since these compounds were added separately to the incorporation system in adequate amounts. The concentrations of pyruvate kinase and adenylate kinase were not significantly higher in the preparations from regenerating liver. In several experiments, moreover, these enzymes (prepared from rabbit muscle) were added in excess to the incubation samples without influencing the regeneration effects. The amounts of amino acid activating enzymes were determined in dialyzed cell fluid from normal and regenerating livers by measuring the rate of ^{32}P-exchange between ^{32}P-pyrophosphate and ATP in the presence of L-leucine or an amino acid mixture. An increase of nearly 40 % was observed in the regenerating livers. The RNA-content showed a slight increase at the same time.

It is concluded, therefore, that the higher efficiency of the amino acid activating system, observed in regenerating liver, was primarily due to a higher activity of the amino acid activating enzymes proper.

1. Zamecnik, P. C. and Keller, E. B. *J. Biol. Chem.* **209** (1954) 337.
2. Hultin, T. and von der Decken, A. *Exptl. Cell Research* **13** (1957) 83.
3. von der Decken, A. and Hultin, T. *Exptl. Cell Research* **14** (1958) 88.
4. Hoagland, M. B., Keller, E. B. and Zamecnik, P. C. *J. Biol. Chem.* **218** (1956) 345.
5. Zamecnik, P. C., Keller, E. B., Littlefield, J. W., Hoagland, M. B. and Loftfield, R. B. *J. Cellular Comp. Physiol.* **47** (1956) 81.

The Initial Reactions Involved in Respiratory Chain Phosphorylations

O. Lindberg, B. Grabe, H. Löw, P. Siekevitz* and L. Ernster

Wenner-Gren Institute and Institute of Theoretical Physics, University of Stockholm, Stockholm, Sweden

Recent studies have indicated that the mitochondrial PO_4-ATP ** exchange and DNP-activated ATPase reactions involve a reversible electron transport through the diaphorase-FAD of the respiratory chain [1,2]. On the basis of these conclusions and of certain quantum-chemical considerations [3,4] pointing to a possible participation of phosphorylated quinoid structures as intermediates in respiratory chain phosphorylations the following reaction sequence appears to be a satisfactory formulation of the mechanism of the first of the three phosphorylations occurring along the mitochondrial oxidation of DPNH by oxygen:

1) DPNH is oxidized by the diaphorase-FAD with the simultaneous cleavage of one of the P—O bonds of a molecule of inorganic phosphate and the attachment of the phosphoryl radical to the 2-keto group of the *iso*-alloxazine ring:

---

* On leave of absence from The Rockefeller Institute for Medical Research and the recipient of a travel grant from the National Research Council, U.S.A.

** Abbreviations: PO_4, inorganic phosphate; ATP, adenosine triphosphate; ADP, adenosine diphosphate; DPNH, reduced diphosphopyridine nucleotide; FAD, flavin adenine dinucleotide; DNP, 2,4-dinitrophenol.

(determined on deoxycholate extracts by dithionite reduction) is diminished by about 30%.

It is generally considered that the endoplasmic reticulum of the cytoplasm is the main origin of the microsomal material. Since RNA is concentrated to the nucleoprotein granules, which are attached to the delicate membranes of this network, while the enzymes and cytochrome b_5 apparently are associated with the membranes, the experiments suggest a richer attachment of nucleoprotein granules to the membranes during liver regeneration. Apparently, however, the composition of the membranes may become modified at the same time.

1. von der Decken, A. and Hultin, T. *Exptl. Cell Research* **14** (1958) 88.
2. Hultin, T. *Exptl. Cell Research* **13** (1957) 47.

On Submitochondrial Particles with High DPNH-oxidase * and Low Succinic Oxidase Activity

Herrick Baltscheffsky**

Wenner-Gren Institute, University of Stockholm, Stockholm, Sweden

A new method for obtaining submitochondrial particles capable of respiration and oxidative phosphorylation has been briefly reported [1]. After grinding liver mitochondria from rat or guinea pig with Al_2O_3 and centrifuging the ground material at 25 000 × *g* for 10 min, in order to get down the alumina and heavier mitochondrial structural fragments the particles are in the supernatant. After centrifugation for 1 h at 100 000 × *g* practically all the DPNH-oxidase activity of this supernatant is in the sediment, which is then suspended in a suitable medium.

Two slightly different methods of preparation (I and II) have been used. In I the medium for the last centrifugation before grinding and for the subsequent operations is 30 mM phosphate buffer of pH 7.0, in II 0.25 M sucrose. Significant differences between the preparations so obtained are: II gives a several fold higher final yield and the stimulation of its DPNH-oxidase by added cytochrome c is lower (usually less than 50 %, compared to more than 200 % for I). In II the supernatant after the 25 000 × *g* centrifugation consists of two separate layers, the bottom one being small in volume and red-colored.

2 mM amytal inhibits practically all the DPNH-oxidase activity in the absence of added cytochrome c, which eliminates the possibility that a significant part of this respiration is due to microsomal contamination.

The submitochondrial particles have a high DPNH-oxidase activity compared to their succinic oxidase activity [1]. Also, the DPNH-cytochrome c reductase activity is much higher than the succinate-cytochrome c reductase activity. The ratio for five different preparations varied between 7.7 and 17, mean value 10 (I gave somewhat higher ratios than II). In the heavier structural fragments the ratio is much lower. The almost complete separation obtained, of the system responsible for the oxidation of DPNH from that responsible for the oxidation of succinate is thus possibly due to a tighter binding of the latter to these fragments.

The rate of oxidation of DPNH is stimulated by $Na_4P_2O_7$, EDTA and ATP, active where ADP and AMP are not. ITP also stimulates this respiration, but only in higher concentration and to a lesser degree than ATP. These stimulations are inhibited by amytal.

The TPNH-oxidase and the TPNH-cytochrome c reductase activities of the particles are low compared to the corresponding DPNH-activities, but are several fold increased by addition of DPN.

The particles have ATP-ase activity. It is increased up to 100-fold by added Mg^{++} whereas 2,4-dinitrophenol only has a slight (about 2-fold) stimulating effect.

1. Baltscheffsky, H. *Exptl. Cell Research* **13** (1957) 630.

* Abbreviations: DPN, diphosphopyridine nucleotide; DPNH, reduced diphosphopyridine nucleotide; TPNH, reduced triphosphopyridine nucleotide; ATP, adenosine triphosphate; ADP, adenosine diphosphate; AMP, adenosine monophosphate; ITP, inosine triphosphate; EDTA, ethylenediaminetetraacetate; M, moles per liter.

** Supported by a grant from *Ella och Georg Ehrnrooths stiftelse.*

Activity of Amino Acid Activating Enzyme Systems during Liver Regeneration

Alexandra von der Decken and Tore Hultin

Wenner-Gren Institute, University of Stockholm, Stockholm, Sweden

In order to attain an incorporation of labeled amino acids into proteins by cell-free liver preparations, microsomal material and certain

soluble cytoplasmic components have to be included in the system [1]. It has been shown previously that microsomes, isolated from regenerating rat liver, work more effectively in incorporation systems of this kind than normal microsomes [2,3]. The present report is concerned with the effects of regenerative growth induction on the soluble components of the incorporation system. As is well known, these components are required for the initial activation of the labeled amino acids at the expense of high-energy phosphates [4]. The complete soluble system used in these experiments contained the following essential components: (1) a mechanism for ATP-generation (in the present experiments composed of phosphoenolpyruvate, pyruvate kinase and adenylate kinase), (2) guanosine triphosphate [5], (3) amino acid activating enzymes, associated in an hitherto unknown way with soluble RNA.

With standard amounts of liver microsomes as acceptor for activated amino acids, cell fluid from regenerating livers effected, per mg protein, a more rapid incorporation of ^{14}C-L-leucine into protein than cell fluid from normal liver. The increase was preceded by a lag period of 12—14 h and culminated about 30 h after hepatectomy. As a rule, the activity then was 60—80 % higher in the case of regenerating livers.

In order to elucidate which of the components of the activation chain were affected by the regeneration, some of these components were studied separately. The higher efficiency of the cell fluid from regenerating liver was not due to increased contents of phosphoenolpyruvate, ATP or guanosine triphosphate, since these compounds were added separately to the incorporation system in adequate amounts. The concentrations of pyruvate kinase and adenylate kinase were not significantly higher in the preparations from regenerating liver. In several experiments, moreover, these enzymes (prepared from rabbit muscle) were added in excess to the incubation samples without influencing the regeneration effects. The amounts of amino acid activating enzymes were determined in dialyzed cell fluid from normal and regenerating livers by measuring the rate of ^{32}P-exchange between ^{32}P-pyrophosphate and ATP in the presence of L-leucine or an amino acid mixture. An increase of nearly 40 % was observed in the regenerating livers. The RNA-content showed a slight increase at the same time.

It is concluded, therefore, that the higher efficiency of the amino acid activating system, observed in regenerating liver, was primarily due to a higher activity of the amino acid activating enzymes proper.

1. Zamecnik, P. C. and Keller, E. B. *J. Biol. Chem.* **209** (1954) 337.
2. Hultin, T. and von der Decken, A. *Exptl. Cell Research* **13** (1957) 83.
3. von der Decken, A. and Hultin, T. *Exptl. Cell Research* **14** (1958) 88.
4. Hoagland, M. B., Keller, E. B. and Zamecnik, P. C. *J. Biol. Chem.* **218** (1956) 345.
5. Zamecnik, P. C., Keller, E. B., Littlefield, J. W., Hoagland, M. B. and Loftfield, R. B. *J. Cellular Comp. Physiol.* **47** (1956) 81.

The Initial Reactions Involved in Respiratory Chain Phosphorylations

O. Lindberg, B. Grabe, H. Löw, P. Siekevitz* and L. Ernster

Wenner-Gren Institute and Institute of Theoretical Physics, University of Stockholm, Stockholm, Sweden

Recent studies have indicated that the mitochondrial PO_4-ATP ** exchange and DNP-activated ATPase reactions involve a reversible electron transport through the diaphorase-FAD of the respiratory chain [1,2]. On the basis of these conclusions and of certain quantum-chemical considerations [3,4] pointing to a possible participation of phosphorylated quinoid structures as intermediates in respiratory chain phosphorylations the following reaction sequence appears to be a satisfactory formulation of the mechanism of the first of the three phosphorylations occurring along the mitochondrial oxidation of DPNH by oxygen:

1) DPNH is oxidized by the diaphorase-FAD with the simultaneous cleavage of one of the P—O bonds of a molecule of inorganic phosphate and the attachment of the phosphoryl radical to the 2-keto group of the *iso*-alloxazine ring:

---

* On leave of absence from The Rockefeller Institute for Medical Research and the recipient of a travel grant from the National Research Council, U.S.A.

** Abbreviations: PO_4, inorganic phosphate; ATP, adenosine triphosphate; ADP, adenosine diphosphate; DPNH, reduced diphosphopyridine nucleotide; FAD, flavin adenine dinucleotide; DNP, 2,4-dinitrophenol.

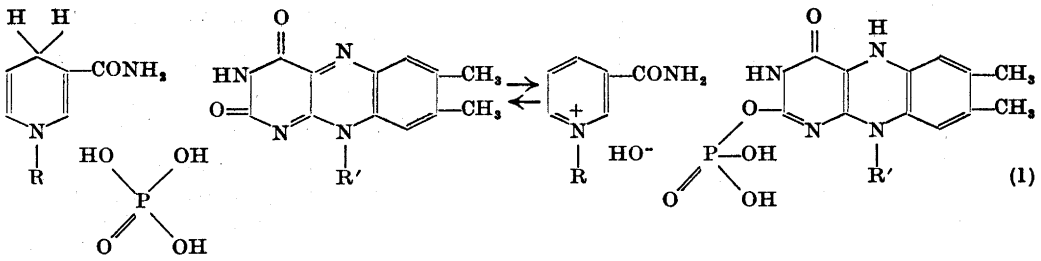

(1)

2) The reduced phosphoryl-FAD is reoxidized by the subsequent carrier along the respiratory chain, with the simultaneous transfer of the phosphoryl group to ADP:

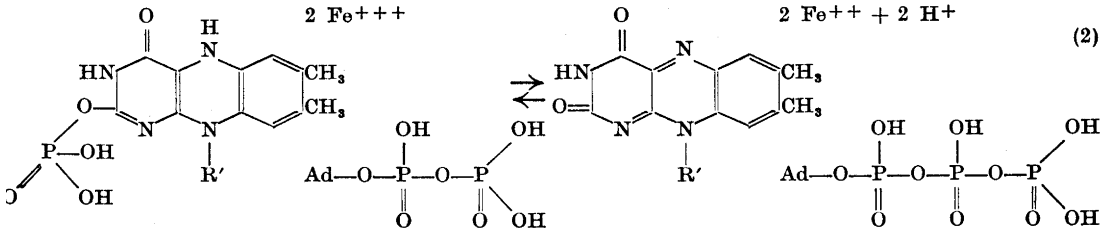

(2)

Reaction (1) is dependent on the spatial arrangement of the reactants. It requires that the pyridine ring of DPNH and the *iso*alloxazine ring of FAD be oriented in two parallel planes close enough to be bridged over by a phosphate ion, the latter being an obligatory component of the reaction; one of the OH-groups of the phosphate may be attracted by the amide group of DPNH.

Reaction (1) is thought to be sensitive to amytal *, which blocks both electron trans fer and the concomitant attachment of phosphate, and to DNP, which interferes with the attachment of phosphate in the left-to-right reaction, thus rendering the electron transfer uncoupled from, and independent of, the activation of inorganic phosphate.

By assuming that Reaction (1) is more rapid than Reaction (2) in the intact mitochondria the proposed mechanism can be visualized to account for the known [5] discrepancy between the rates of H_2O—$P^{18}O_4$ and $^{32}PO_4$—ATP exchange during oxidative phosphorylation.

The possibility to generalize the present type of mechanism to be valid also for the two other instances of respiratory chain phosphorylation will be discussed.

1. Siekevitz, P., Löw, H., Ernster, L. and Lindberg, O. *Biochim. et Biophys. Acta. In press.*
2. Löw, H., Siekevitz, P., Ernster, L. and Lindberg, O. *Biochim. et Biophys. Acta. In press.*
3. Grabe, B. *Exptl. Cell Research* **13** (1957) 588.
4. Grabe, B. *Exptl. Cell Research. In press.*
5. Boyer, P. D., Falcone, A. B. and Harrison, W. H. *Nature* **174** (1954) 401.

* 5-Ethyl-5-*iso*amylbarbituric acid.

Toxic Liver Injury: Some Biochemical Changes in the Liver caused by Dimethylnitrosamine

P. N. Magee **

Wenner-Gren Institute, University of Stockholm, Stockholm, Sweden

Dimethylnitrosamine (N-nitrosodimethylamine) is used industrially as a solvent and as an intermediate in synthetic processes. It has been shown to cause acute haemorrhagic centrilobular necrosis of the liver in the rat and other laboratory animals when administered in doses of the order of 25 mg pr kg body weight [1]. The acute liver lesions may be accompanied by bleeding into the gut and haemorrhagic peritoneal effusion, but there is little evidence of damage to other tissues and organs.

** On leave of absence from Medical Research Council Toxicology Research Unit, Carshalton, England.

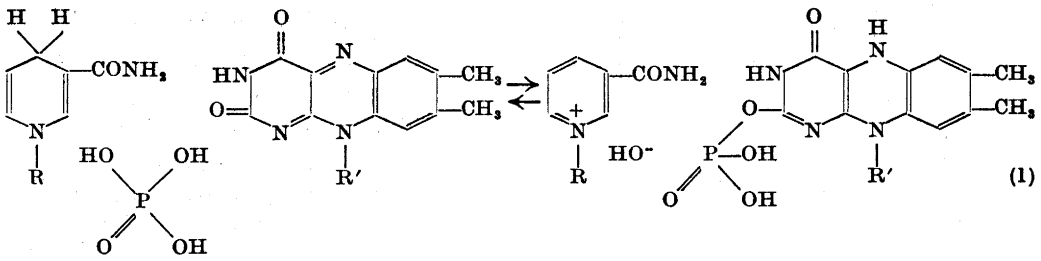

(1)

2) The reduced phosphoryl-FAD is reoxidized by the subsequent carrier along the respiratory chain, with the simultaneous transfer of the phosphoryl group to ADP:

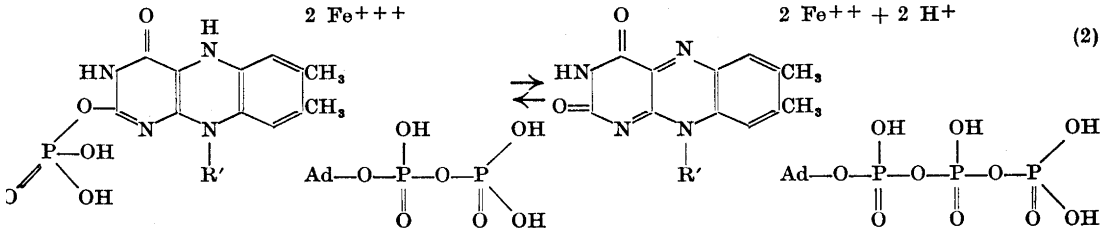

(2)

Reaction (1) is dependent on the spatial arrangement of the reactants. It requires that the pyridine ring of DPNH and the *iso*alloxazine ring of FAD be oriented in two parallel planes close enough to be bridged over by a phosphate ion, the latter being an obligatory component of the reaction; one of the OH-groups of the phosphate may be attracted by the amide group of DPNH.

Reaction (1) is thought to be sensitive to amytal *, which blocks both electron trans fer and the concomitant attachment of phosphate, and to DNP, which interferes with the attachment of phosphate in the left-to-right reaction, thus rendering the electron transfer uncoupled from, and independent of, the activation of inorganic phosphate.

By assuming that Reaction (1) is more rapid than Reaction (2) in the intact mitochondria the proposed mechanism can be visualized to account for the known [5] discrepancy between the rates of H_2O—$P^{18}O_4$ and $^{32}PO_4$—ATP exchange during oxidative phosphorylation.

The possibility to generalize the present type of mechanism to be valid also for the two other instances of respiratory chain phosphorylation will be discussed.

1. Siekevitz, P., Löw, H., Ernster, L. and Lindberg, O. *Biochim. et Biophys. Acta. In press.*
2. Löw, H., Siekevitz, P., Ernster, L. and Lindberg, O. *Biochim. et Biophys. Acta. In press.*
3. Grabe, B. *Exptl. Cell Research* **13** (1957) 588.
4. Grabe, B. *Exptl. Cell Research. In press.*
5. Boyer, P. D., Falcone, A. B. and Harrison, W. H. *Nature* **174** (1954) 401.

* 5-Ethyl-5-*iso*amylbarbituric acid.

Toxic Liver Injury: Some Biochemical Changes in the Liver caused by Dimethylnitrosamine

P. N. Magee **

Wenner-Gren Institute, University of Stockholm, Stockholm, Sweden

Dimethylnitrosamine (N-nitrosodimethylamine) is used industrially as a solvent and as an intermediate in synthetic processes. It has been shown to cause acute haemorrhagic centrilobular necrosis of the liver in the rat and other laboratory animals when administered in doses of the order of 25 mg pr kg body weight [1]. The acute liver lesions may be accompanied by bleeding into the gut and haemorrhagic peritoneal effusion, but there is little evidence of damage to other tissues and organs.

** On leave of absence from Medical Research Council Toxicology Research Unit, Carshalton, England.

When dimethylnitrosamine was added to the normal diet of rats at a level of 50 parts per million a high incidence of malignant tumours of the liver was found between the 26th and 40th weeks [2]. Dimethylnitrosamine is a useful agent for the experimental study of toxic liver injury because its acute effects are regular and reproducible and also it can be readily estimated in tissues and body fluids by the polarographic method of Heath and Jarvis [3]. The compound is rapidly metabolised *in vivo*, mainly, and perhaps exclusively by the liver [4,5]. It is distributed almost uniformly in the different tissues and organs with no preferential accumulation in the liver, and there is evidence that it becomes uniformly distributed in the body water soon after administration [5]. Metabolism occurs *in vitro* by liver slices and broken-cell preparations, but not to a significant extent with other tissues with the possible exception of kidney. There is a strong requirement for oxygen and complete inhibition by anaerobiosis. Metabolic activity of broken-cell preparations can be removed by dialysis and partially restored by the addition of TPN and to a less extent DPN. All the activity occurs in the microsome+cell sap fraction of the liver with negligible metabolism by the nuclear+mitochondrial fraction [6].

Incorporation of labelled amino acids into rat liver protein *in vivo* is markedly reduced 3 h after the animal has received a necrotising dose of dimethylnitrosamine but incorporation into kidney and spleen protein is not altered significantly nor is the labelling of the free amino acids in the liver. Incorporation of ^{32}P into acid-soluble, lipid and residual phosphorus fractions of the liver is not significantly changed 6 h after the same dose of dimethylnitrosamine, but incorporation into a partially purified RNA fraction is reduced at this time [7].

Some histochemical and biochemical changes found in the liver during the development of the necrosis will be described, also some recent work on the metabolism of ^{14}C-dimethylnitrosamine and on the effect of the compound on rat liver slices *in vitro*.

1. Barnes, J. M. and Magee, P. N. *Brit. J. Ind. Med.* **11** (1954) 167.
2. Magee, P. N. and Barnes, J. M. *Brit. J. Cancer* **10** (1956) 114.
3. Heath, D. F. and Jarvis, J. A. E. *Analyst.* **80** (1955) 613.
4. Dutton, A. H. and Heath, D. F. *Nature* **178** (1956) 644.
5. Magee, P. N. *Biochem. J.* **64** (1956) 676.
6. Magee, P. N. and Vandekar, M. *Biochem. J. (In the press.)*
7. Magee, P. N. *Biochem. J. (In the press.)*

Structural Factors Involved in the Diaphorase and Cytochrome c-Reductase Activities of Mitochondria and Microsomes

Lars Ernster

Wenner-Gren Institute, University of Stockholm, Stockholm, Sweden

As indicated by previous studies [1,2], the low activity at which TPNH * is oxidized by way of the cytochrome system may constitute a limiting factor for the function of TPN-dependent oxidations in liver tissue. The great discrepancy in activity, known to prevail between the liver TPNH- and DPNH-cytochrome c reductase systems [3], and recent evidence reported in the literature [4,5] that the former may be selectively regulated by metabolic control mechanisms, prompted a comparative study of the two systems with respect to their catalytic components. Interest was in the first place focused on the diaphorase components, since these are believed to constitute the first catalytic links of the cytochrome c-reductase systems with the reduced pyridine nucleotides.

While the TPNH- and DPNH-cytochrome c reductases are located exclusively in the particulate elements of the cytoplasm [3,6,7], recent studies [8] revealed the occurrence of a considerable diaphorase activity in the soluble cytoplasm. This activity was found to be equally high with DPNH and TPNH, in contrast to those present in mitochondria and microsomes, which are 3—7 times higher with DPNH than with TPNH. Since there are indications that the TPNH- and DPNH-diaphorase activities of the soluble cytoplasm are catalyzed by one common enzyme [8] it appeared to be of interest to investigate whether the same could be valid for the particulate DPNH- and TPNH diaphorases, their discrepancy in activity being due to secondary factors, connected with the organized nature of the structures in which they are located. The data collected in Tables 1 and 2 seem to support this concept.

As emerges from Table 1, precipitation of a suspension of mitochondria or microsomes with acetone resulted in a selective stimulation of the TPNH-diaphorase activity, with a shift of the TPNH/DPNH activity ratio towards unity. A similar effect ensued if mitochondria or microsomes were exposed to a hypotonic

* The symbols, DPNH and TPNH, stand for the reduced forms of di- and triphosphopyridine nucleotide, respectively.

When dimethylnitrosamine was added to the normal diet of rats at a level of 50 parts per million a high incidence of malignant tumours of the liver was found between the 26th and 40th weeks [2]. Dimethylnitrosamine is a useful agent for the experimental study of toxic liver injury because its acute effects are regular and reproducible and also it can be readily estimated in tissues and body fluids by the polarographic method of Heath and Jarvis [3]. The compound is rapidly metabolised *in vivo*, mainly, and perhaps exclusively by the liver [4,5]. It is distributed almost uniformly in the different tissues and organs with no preferential accumulation in the liver, and there is evidence that it becomes uniformly distributed in the body water soon after administration [5]. Metabolism occurs *in vitro* by liver slices and broken-cell preparations, but not to a significant extent with other tissues with the possible exception of kidney. There is a strong requirement for oxygen and complete inhibition by anaerobiosis. Metabolic activity of broken-cell preparations can be removed by dialysis and partially restored by the addition of TPN and to a less extent DPN. All the activity occurs in the microsome+cell sap fraction of the liver with negligible metabolism by the nuclear+mitochondrial fraction [6].

Incorporation of labelled amino acids into rat liver protein *in vivo* is markedly reduced 3 h after the animal has received a necrotising dose of dimethylnitrosamine but incorporation into kidney and spleen protein is not altered significantly nor is the labelling of the free amino acids in the liver. Incorporation of ^{32}P into acid-soluble, lipid and residual phosphorus fractions of the liver is not significantly changed 6 h after the same dose of dimethylnitrosamine, but incorporation into a partially purified RNA fraction is reduced at this time [7].

Some histochemical and biochemical changes found in the liver during the development of the necrosis will be described, also some recent work on the metabolism of ^{14}C-dimethylnitrosamine and on the effect of the compound on rat liver slices *in vitro*.

1. Barnes, J. M. and Magee, P. N. *Brit. J. Ind. Med.* **11** (1954) 167.
2. Magee, P. N. and Barnes, J. M. *Brit. J. Cancer* **10** (1956) 114.
3. Heath, D. F. and Jarvis, J. A. E. *Analyst.* **80** (1955) 613.
4. Dutton, A. H. and Heath, D. F. *Nature* **178** (1956) 644.
5. Magee, P. N. *Biochem. J.* **64** (1956) 676.
6. Magee, P. N. and Vandekar, M. *Biochem. J. (In the press.)*
7. Magee, P. N. *Biochem. J. (In the press.)*

Structural Factors Involved in the Diaphorase and Cytochrome c-Reductase Activities of Mitochondria and Microsomes

Lars Ernster

Wenner-Gren Institute, University of Stockholm, Stockholm, Sweden

As indicated by previous studies [1,2], the low activity at which TPNH * is oxidized by way of the cytochrome system may constitute a limiting factor for the function of TPN-dependent oxidations in liver tissue. The great discrepancy in activity, known to prevail between the liver TPNH- and DPNH-cytochrome c reductase systems [3], and recent evidence reported in the literature [4,5] that the former may be selectively regulated by metabolic control mechanisms, prompted a comparative study of the two systems with respect to their catalytic components. Interest was in the first place focused on the diaphorase components, since these are believed to constitute the first catalytic links of the cytochrome c-reductase systems with the reduced pyridine nucleotides.

While the TPNH- and DPNH-cytochrome c reductases are located exclusively in the particulate elements of the cytoplasm [3,6,7], recent studies [8] revealed the occurrence of a considerable diaphorase activity in the soluble cytoplasm. This activity was found to be equally high with DPNH and TPNH, in contrast to those present in mitochondria and microsomes, which are 3—7 times higher with DPNH than with TPNH. Since there are indications that the TPNH- and DPNH-diaphorase activities of the soluble cytoplasm are catalyzed by one common enzyme [8] it appeared to be of interest to investigate whether the same could be valid for the particulate DPNH- and TPNH diaphorases, their discrepancy in activity being due to secondary factors, connected with the organized nature of the structures in which they are located. The data collected in Tables 1 and 2 seem to support this concept.

As emerges from Table 1, precipitation of a suspension of mitochondria or microsomes with acetone resulted in a selective stimulation of the TPNH-diaphorase activity, with a shift of the TPNH/DPNH activity ratio towards unity. A similar effect ensued if mitochondria or microsomes were exposed to a hypotonic

* The symbols, DPNH and TPNH, stand for the reduced forms of di- and triphosphopyridine nucleotide, respectively.

Table 1. Effects of acetone treatment and hypotonicity on the activities of particulate liver diaphorases.

Homogenates of rat liver were made in 0.25 M sucrose solution. 100 ml homogenate, containing 10 g wet weight liver, was centrifuged *a*) at 1 600 *g* for 10 min, *b*) at 4 100 *g* for 15 min, and *c*) at 105 000 *g* for 60 min. The denotions, mitochondria and microsomes, refer to the pellets obtained in *b* and *c*, respectively. The mitochondrial pellet was washed, and the microsomal pellet rinsed, twice with 0.25 M sucrose, and both pellets were suspended in 10 ml 0.25 M sucrose. 4 ml aliquots of both suspensions were added to 36 ml cold (—12°C) acetone, the precipitates separated by centrifugation at 0°C, and dried in a desiccator. The dry precipitates were suspended in 4 ml 0.25 M sucrose. Another aliquot of the mitochondrial and microsomal suspensions was diluted with 9 volumes of distilled water and allowed to stand at 0°C for 30 min before test. The test system contained 0.5 ml 0.3 M tris buffer (pH 7.5), 2.3 ml 0.25 M sucrose, 0.1 ml 3 mM DPNH or TPNH, 0.1 ml 1.7 mM 2,6-dichlorophenolindophenol, and 10 mg wet weight liver equivalent mitochondria or 5 mg equivalent microsomes in a volume of 0.1 ml 0.25 M sucrose. When indicated, ATP was added in a final concentration of 3 mM and Mn++ in a final concentration of 0.3 mM. The decolorization of the dye was recorded in a Beckman DK2 spectrophotometer at 600 mμ, using glass cuvettes of 1 cm light path. The reaction was started by the addition of the reduced pyridine nucleotides, and followed for 4—6 min at room temperature. The values are expressed in terms of 1 g wet weight liver equivalent.

Treatment	*Mitochondria*			*Microsomes*		
	Diaphorase activities (μmoles dye reduced/min)					
	TPNH	DPNH	$\frac{\text{TPNH}}{\text{DPNH}}$	TPNH	DPNH	$\frac{\text{TPNH}}{\text{DPNH}}$
None	1.0	4.3	0.23	1.9	10.2	0.15
Acetone	1.9	3.0	0.65	3.5	3.4	1.03
Hypotonicity	2.8	4.5	0.61	2.9	10.8	0.27
» + ATP	1.5	4.3	0.34			
» + ATP + Mn++	0.9	4.3	0.21			

medium (0.05 M sucrose) at 0°C for 30 min; in this case the effect on the mitochondria could be counteracted by ATP and Mn++, which are known protectors of the mitochondrial structure [9].

Since deoxycholate has previously proved to be a useful tool in studying the biochemical organization of mitochondria [10-12] and microsomes [13] the effect of this agent was investigated in greater detail. Table 2 illustrates the effects of increasing concentrations of deoxycholate on the mitochondrial and microsomal diaphorase and cytochrome c reductase activities. Again, the structural destruction was accompanied by an increase of the TPNH/DPNH activity ratio in both instances and with both types of activities measured. However, whereas in the case of mitochondria this increase was mainly due to an absolute increase of the TPNH-diaphorase and cytochrome c-reductase activities, in the case of microsomes these activities remained virtually constant and the increase of the activity ratios could entirely be accounted for by a decrease of the DPNH-linked activities; yet, the mitochondrial DPNH-cytochrome c-reductase was also strongly inhibited by deoxycholate. Whether the different behaviors of the mitochondrial and microsomal TPNH-diaphorase and cytochrome c-reductase activities towards deoxycholate are related to the known difference existing between the actions of deoxycholate on the mitochondrial [10,11] and microsomal [13] membranes is the subject of continued studies. The data as yet available point to the possibility that the great difference prevailing between the cellular activities of the TPNH- and DPNH-cytochrome c-reductase systems is primarily due to different locations within, or relations to, the cytoplasmic structures rather than to different catalytic compositions.

1. Ernster, L. and Navazio, F. *Biochim. et Biophys. Acta* **26** (1957) 408.

Table 2. Effects of varying concentrations of deoxycholate on the diaphorase and cytochrome c-reductase activities of rat liver mitochondria and microsomes.

Diaphorase activities were tested as described in Table 1. The test system used for the determination of the cytochrome c-reductase activity contained the following: 0.5 ml 0.3 M tris buffer (pH 7.5), 2.2 ml 0.25 M sucrose, 0.1 ml 10 mM KCN, 0.1 ml 3 mM DPNH or TPNH, and 0.1 ml 1.5 mM cytochrome c. The reaction was started by the addition of the reduced pyridine nucleotides, and followed by recording the increase in optical density at 550 mμ, due to the reduction of cytochrome c. The amounts of enzyme used in the different tests, expressed in mg wet weight liver equivalents, were as follows: *Mitochondria:* TPNH- or DPNH-diaphorase, 10; TPNH-cytochrome c-reductase, 33; DPNH-cytochrome c-reductase, 3.3. *Microsomes:* TPNH- or DPNH-diaphorase, 3.3; TPNH-cytochrome c-reductase, 17; DPNH-cytochrome c-reductase, 1.7. Deoxycholate was included in the test systems in concentrations as indicated. The values below are expressed in relative terms, giving the value 100 to the activity obtained with DPNH as substrate in the absence of deoxycholate within each individual type of test.

Deoxycholate, %	*Mitochondria*			*Microsomes*		
	TPNH	DPNH	TPNH/DPNH	TPNH	DPNH	TPNH/DPNH
	Relative Diaphorase Activity					
0	15	100	0.15	20	100	0.20
0.005	21	92	0.23	20	106	0.19
0.01	21	97	0.22	17	109	0.16
0.02	39	108	0.36	17	91	0.19
0.035	82	126	0.65	13	93	0.14
0.05	97	131	0.74	20	57	0.35
0.075	87	116	0.75	20	48	0.42
0.1	90	116	0.78	22	48	0.46
	Relative Cytochrome c-Reductase Activity					
0	1.3	100	0.01	5.0	100	0.05
0.005	2.1	87	0.02	4.6	104	0.04
0.01	2.9	74	0.04	4.6	100	0.05
0.02	1.8	74	0.02	5.0	104	0.05
0.035	4.5	65	0.07	5.4	113	0.05
0.05	12.5	45	0.28	5.8	83	0.07
0.075	8.8	16	0.55	5.8	8	0.73
0.1	10.1	6	1.69	5.8	4	1.45

2. Navazio, F., Ernster, B. B. and Ernster, L. *Biochim. et Biophys. Acta* **26** (1957) 416.
3. de Duve, C., Pressman, B. C., Gianetto, R., Wattiaux, R. and Appelmans, F. *Biochem. J.* **60** (1955) 604.
4. Phillips, A. H. and Langdon, R. G. *Biochim. et Biophys. Acta* **19** (1956) 380.
5. Vignais, P. V. *Exptl. Cell Research* **13** (1957) 414.
6. Hogeboom, G. H. *J. Biol. Chem.* **177** (1949) 847.
7. Hogeboom, G. H. and Schneider, W. C. *J. Biol. Chem.* **186** (1950) 417.
8. Ernster, L. and Navazio, F. *Acta Chem. Scand. In the press.*
9. Beyer, R. E., Ernster, L., Löw, H. and Beyer, T. *Exptl. Cell Research* **8** (1955) 586.
10. Watson, M. and Siekevitz, P. *J. Biophys. Biochem. Cytol.* **2** (1956) 639.
11. Siekevitz, P. and Watson, M. *J. Biophys. Biochem. Cytol.* **2** (1956) 653.
12. Siekevitz, P., Löw, H., Ernster, L. and Lindberg, O. *In the press.*
13. Palade, G. E. and Siekevitz, P. *J. Biophys. Cytol.* **2** (1956) 171.

ACTA CHEMICA SCANDINAVICA 12 (1958) 603—610

Fungus Pigments

VIII *. The Structure of Cinnabarin and Cinnabarinic Acid

JARL GRIPENBERG

Department of Chemistry, Finland Institute of Technology Helsingfors, Finland

Hydrolysis of cinnabarin with alkali gives cinnaquinone, $C_7H_5NO_5$, which upon further hydrolysis gives 2,5-dihydroxybenzoquinone. The formation of these compounds and the results of reductive acetylation of cinnabarin and its derivatives has led to the conclusion that cinnabarin is 2-amino-9-hydroxymethylphenoxazin-3-one-1-carboxylic acid (IX). Cinnabarinic acid is formulated as 2-aminophenoxazin-3-one-1,9-dicarboxylic acid (XV), and it is identical with a compound obtained earlier by oxidation of 3-hydroxyanthranilic acid.

Since cinnabarin was first isolated, it has been known that alkaline hydrolysis gives one molecule of ammonia, but no other definite product could be isolated from this reaction [1-3]. It has now been found that on hydrolysis with a small volume of 2 N sodium hydroxide at room temperature for a short time a sparingly soluble sodium salt is precipitated. Acidification yields an orange-red crystalline compound, $C_7H_5NO_5$, which we have called cinnaquinone. Further hydrolysis of cinnaquinone gives 2,5-dihydroxybenzoquinone, ammonia and carbon dioxide [5].

In view of the mild conditions for this further hydrolysis and the similarity of the U.V.-spectra of cinnaquinone and of 2,5-dihydroxybenzoquinone (Fig. 1) it is assumed that the reaction is not accompanied by any deepseated changes in structure. The structures I—VI therefore represent the theoretical possibilities for the structure of cinnaquinone.

Of these, I can be dismissed at once because cinnaquinone has peaks at 1 683 and 1 613 cm^{-1} in the carbonyl region, whereas I should have a peak at $\sim$ 1 725 cm^{-1} typical of carbamates [4]. It is more difficult to decide between the other possible structures. VI, incorporating the carboxamide group suspected in cinnabarin [3,6] is the structure most likely to have been formed under the conditions used, and was considered the most probable alternative [5].

* The paper in *Proc. Chem. Soc.* **1957** 233 is regarded as Part VII of this series. Part VI *Suomen Kemistilehti B* **30** (1957) 134.

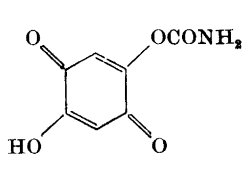

I

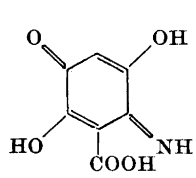

II

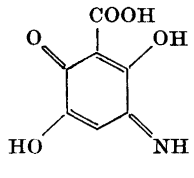

III

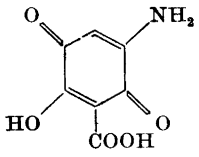

IV

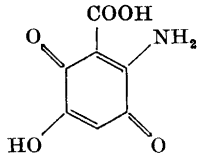

V

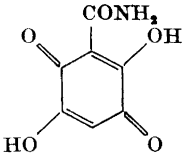

VI

The formation of a hydroxybenzoquinone derivative on alkaline hydrolysis of cinnabarin is in complete accordance with its formulation as a phenoxazin-3-one derivative [7,8] because phenoxazin-3-ones are known to give hydroxybenzoquinones, although more drastic conditions have usually been employed [9,10]. Cinnabarin was accordingly formulated [5] as VII or VIII

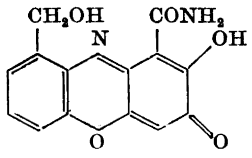

VII

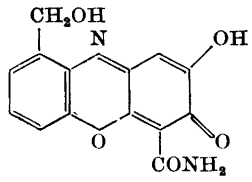

VIII

Both these formulae, however, suffer from the disadvantage that they do not permit any rational formulation of the products of reductive acetylation of cinnabarin and its derivatives.

The first paper in this series [1] described the formation of two substances by reductive acetylation of cinnabarin. They were designated as cinnabarin leucoacetate A and cinnabarin leucoacetate B, respectively. The former was given the composition $C_{16}H_{16}N_2O_6$ and the latter $C_{18}H_{16}N_2O_6$ and it was shown that leucoacetate A upon further acetylation gives leucoacetate B. Cavill *et al.*[3] also prepared leucoacetate B, but assigned it the composition $C_{20}H_{16}N_2O_7$. More recent analytical evidence is also more consistent with this formula, and we therefore regard it as correct. Cinnabarin leucoacetate B is thus triacetylanhydrodihydrocinnabarin. Cavill *et al*[3] also prepared a triacetyl-O-methyldihydrocinnabarin. Since no anhydro compound was formed in this case they drew the natural conclusion that the hydroxylgroup, which is methylated is that involved in the formation of the anhydro compound.

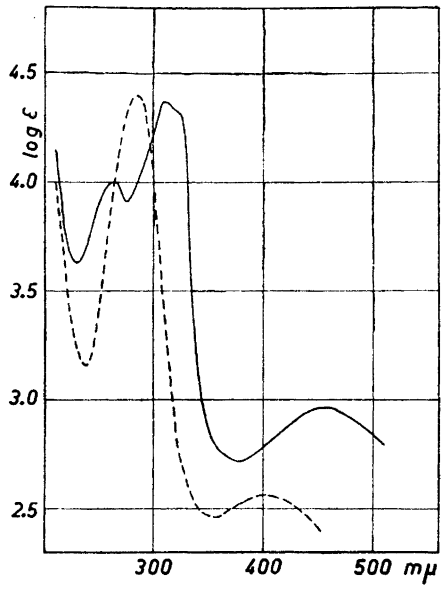

Fig. 1. Absorption curves for cinnaquinone (———). and 2,5-dihydroxybenzoquinone (– – – –). Both in alcohol.

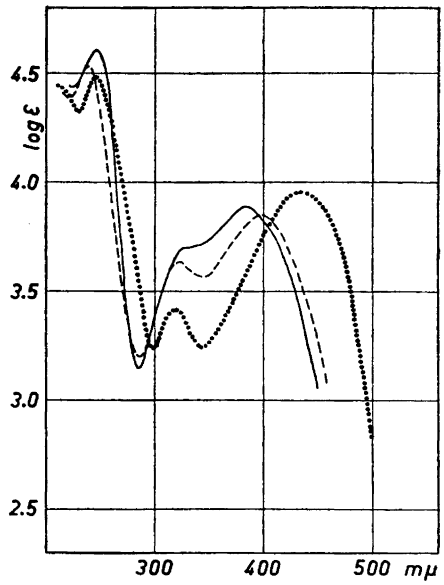

Fig. 2. Absorption curves for triacetyldihydrocinnabarin (XI) (————), triacetyldihydrocinnabarin methyl ester (XII) (– – – –) and triacetylanhydrodihydrocinnabarin (XIII) (·····). All in alcohol.

A comparison of the U.V.-spectra of cinnabarin leucoacetate A and triacetyl-O-methyldihydrocinnabarin indicated a close relationship between them (Fig. 2). This was also established by methylation of leucoacetate A with diazomethane, which gave triacetyl-O-methyldihydrocinnabarin. In our hands this substance had m.p. 173.5—174.5°, whether prepared by methylation of cinnabarin leucoacetate A or by reductive acetylation of O-methyl cinnabarin, whereas Cavill *et al.*[3] report 156°. This difference is probably due to dimorphism. Cinnabarin leucoacetate A must thus be triacetyldihydrocinnabarin with a composition $C_{20}H_{18}N_2O_8$, although the nitrogen value (8.42 %) is much higher than that required by the above formula (6.76 %). The carbon and hydrogen values (C 57.63; H 4.93) fit this formula reasonably well (Calc. C 57.97; H 4.38).

All attempts to repeat the preparation of leucoacetate A have given only very minute amounts of material insufficient for further analysis.

The results of reductive acetylation show that the hydroxyl group in triacetyldihydrocinnabarin, which is responsible for the acidity [1], is also present in cinnabarin, and is that which is methylated in the formation of O-methylcinnabarin. This hydroxyl group also takes part in the reaction leading to the formation of triacetylanhydrodihydrocinnabarin.

Formulae VII or VIII for cinnabarin do not give a satisfactory explanation of the behaviour of cinnabarin.

If, however, cinnabarin has the structure IX these reactions can be formulated as shown below,

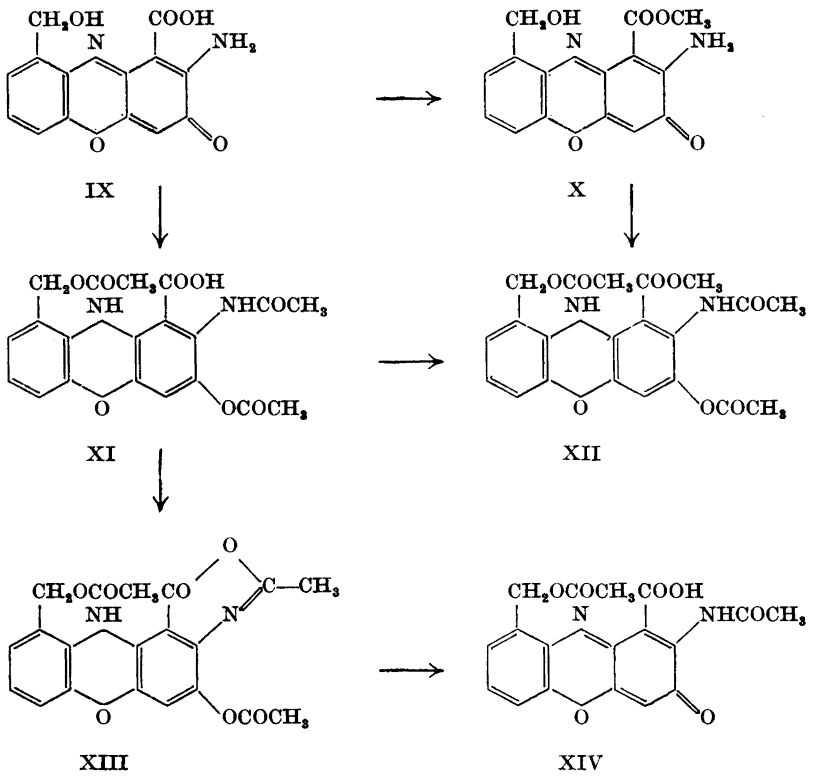

O-Methylcinnabarin (X) is, on this basis, more properly named cinnabarin methyl ester. Triacetyldihydrocinnabarin (leucoacetate A) is XI, triacetyldihydrocinnabarin methyl ester (triacetyl-O-methyldihydrocinnabarin) is XII and triacetylanhydrodihydrocinnabarin (leucoacetate B) is XIII. The conversion of XI into XIII is a well known reaction [11]. That the NH-group of the phenoxazine ring cannot be acetylated can be ascribed to steric hindrance.

These structures are also supported by the I.R.-spectra (Our I.R.-spectra differ in some respects from these reported by Cavill *et al.*[3], but these differences are probably due to the difference in technique employed [12], and in the case of triacetyldihydrocinnabarin methyl ester also to different crystalline forms.) The bands at 1 672 and 1 653 cm^{-1} in the spectrum of cinnabarin, which were originally assigned to the carboxamide group [3], can equally well be due to strongly chelated carboxyl and the carbonyl of the phenoxazin-3-one [13]. Cinnabarin methyl ester has a single much stronger band at 1 657 cm^{-1} in this region [3]. The strong, partly resolved absorption just below 1 600 cm^{-1} is typical of phenoxazin-3-ones [13] and disappears on reductive acetylation. Instead there are a number of bands above 1 650 cm^{-1}. In the spectrum

of XI the bands at 1 770 and 1 740 cm^{-1} can be assigned to the aromatic acetate and the aliphatic acetate, and those at 1 690 and 1 677 cm^{-1} to the carboxyl and the N-acetyl-group, or *vice versa*. In XII the corresponding bands occurs at 1 760, 1 740, 1 682 and 1 657 cm^{-1}. XIII has, as expected, a third band above 1 700 cm^{-1}, due to the carbonyl group of the oxazinone ring [11]. The band at 1 775 cm^{-1} can be assigned to the aromatic acetate and the band at 1 750 cm^{-1} to the oxazinone carbonyl or vice versa and the one at 1 732 cm^{-1} to the aliphatic acetate. The band at 1 655 cm^{-1} is probably due to the C = N-bond in the oxazinone ring [11].

One objection that could be raised against these formulations for the leucoderivatives of cinnabarin is, that the transformation of XI into XIII causes a large bathochromic shift in the spectrum (see Fig. 2) while the change from N-acetylanthranilic acid into 2-methylbenzoxazin-4-one is accompanied by a slight hypsochromic shift [11]. It is, however, doubtful whether any significant conclusion can be put on a comparison of systems that are as different as these.

These leucoderivatives of cinnabarin are quite stable, unlike the leucoacetate of actinomycin, which according to Brockmann and Franck [14] can be readily partially hydrolysed and reoxidised to N-acetylactinomycin. Such a hydrolysis appears to take place with triacetylanhydrodihydrocinnabarin (XIII) only in the presence of an oxidant, *e.g.* nitrous acid. Cavill *et al.*[15] who discovered this reaction called their product diacetyl*iso*polystictin (in our nomenclature diacetyl*iso*cinnabarin) but it might just as well be diacetylcinnabarin (XIV). Their assumption that this product should be identical with our leucoacetate A is incorrect, as shown by the completely different U.V.- and I.R.-spectra for the two compounds and by the strong mixed m.p. depression.

The formulation of cinnabarin as IX and not as VII or VIII finds further support in a colour reaction. Brockmann and Franck [16] have observed that actinomycin, which has an amino-group in the 2-position of the phenoxazin-3-one ring gives a yellow colour with stannous chloride, while desaminoactinomycin, with a hydroxyl group in the 2-position gives a green colour. This difference between 2-amino- and 2-hydroxyphenoxazin-3-ones is even more pronounced in the parent compounds; 2-aminophenoxazin-3-one gives with stannous chloride a colourless solution and 2-hydroxyphenoxazin-3-one a blue colour [9]. Cinnabarin gives in accordance with its formulation as a 2-aminoderivative only a yellow colour.

If cinnabarin is IX it means that cinnaquinone must be V. Its properties agree equally well with this structure, although it is somewhat surprising that such a compound is stable under alkaline conditions. The formation of oxamic acid on oxidation of cinnabarin under slightly alkaline conditions [6] can of course also be explained on the basis of structure IX for cinnabarin.

In a previous paper [6] we described the isolation of cinnabarinic acid, which accompanies cinnabarin. The assumed close similarity of cinnabarinic acid and cinnabarin, which was inferred from their almost identical U.V.-absorption in pyridine solution has now found further support in that both show the same characteristic shift of absorption maximum in strongly acidic solution (see below) and both give the same yellow colour reaction with stannous chloride.

Cinnabarinic acid has the composition $C_{14}H_8N_2O_6$, having two hydrogen atoms less and one oxygen atom more than cinnabarin. It was therefore very tempting to speculate that cinnabarinic acid differs from cinnabarin in having a carboxyl group instead of the primary hydroxyl group. The presence of a second carboxyl group in cinnabarinic acid, which finds strong support in a band at 1 727 cm^{-1} also explains the greater acidity of cinnabarinic acid [6]. If cinnabarin has structure IX, cinnabarinic acid should be XV.

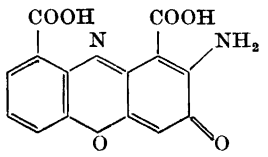

XV

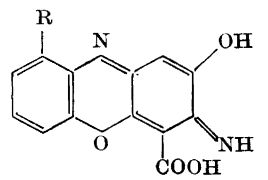

XVI R = COOH
XVII R = CH_2OH

XV has been proposed by Butenandt *et al.*[10] as an alternative structure for the product obtained by oxidation of 3-hydroxyanthranilic acid, the other being XVI. Through the kindness of Professor Butenandt we received a sample of his »Farbstoff IV». Although the I.R.-spectrum of »Farbstoff IV» is not quite as sharp as that of cinnabarinic acid, there can be no doubt that the two substances are identical (Fig. 3). The identity of the U.V.-spectra both in neutral and strongly acidic solution [10] confirms this identity further.

One remarkable difference between cinnabarin and cinnabarinic acid is in their behaviour towards alkali. Cinnabarin, as has been shown above, splits off cinnaquinone, while cinnabarinic acid is converted into 2-hydroxyphenoxazin-3-one-9-carboxylic acid [10]. Attempts to obtain cinnaquinone from cinnabarinic acid gave only a minute amount of a substance, which showed the characteristic U.V. spectrum of cinnaquinone but the amount available was not sufficient for further purification.

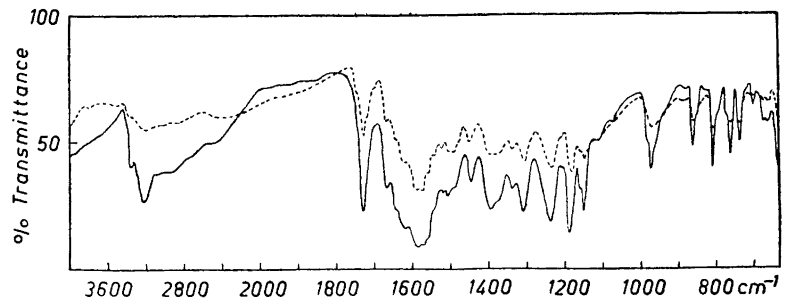

Fig. 3. Infrared absorption curves for natural cinnabarinic acid (————) and synthetic cinnabarinic acid (— — — — —). In KBr-discs.

In spite of this difference, which can be accounted for by the influence of the 9-carboxylic group on the rate of hydrolysis of the C = N-bond, it is considered that cinnabarin and cinnabarinic acid have analogous structures. This definitely excludes structures VII and VIII for cinnabarin. The possibility that cinnabarinic acid has structure XVI and cinnabarin XVII is highly improbable because XVII ought to form a dimethyl derivative. The formation of phenoxazin-3-one (or more probably 9-methylphenoxazin-3-one) on zinc dust distillation [6,7] and oxamic acid on oxidation of cinnabarin [6] is also difficult to reconcile with structure XVII.

IX and XV thus appear to be the most probable structures for cinnabarin and cinnabarinic acid, respectively.

After this paper had been written a paper by Cavill, Clezy and Tetaz [17] appeared, in which the structure IX is also suggested for cinnabarin.

EXPERIMENTAL

(The analyses are by Dr. A. Bernhardt, Mühlheim, and the I.R.-spectra by Mr. B. C. Fogelberg, Ab Centrallaboratorium, Helsingfors.)

Cinnaquinone. Cinnabarin (400 mg) was added to 2 N sodium hydroxide (2 ml) and the mixture was stirred with a glass rod. The cinnabarin dissolved in a few minutes and a brown crystalline precipitate soon formed. This was at once filtered off. A second crop of crystals forming in the filtrate was also filtered off and usually a third crop of crystals could also be obtained. The combined precipitates were dissolved in the minimum amount of water and the solution was acidified. Brown-yellow crystals of cinnaquinone, mixed with some dark-brown amorphous material were obtained. The precipitate was filtered off and treated with ethyl acetate which leaves the amorphous material undissolved. The filtrate which still contained a considerable amount of cinnaquinone was extracted with ethyl acetate. The combined ethyl acetate extracts were evaporated under reduced pressure and the crystalline residue recrystallised from dioxan giving orange-brown needles (70 mg), decomp. above 200° without melting. (Found: C 45.78; H 2.95; N 7.39; $C_7H_5NO_5$ requires C 45.91; H 2.75; N 7.65). I.R. maxima (KBr): 3 375 (m), 3 230 (m), 1 683 (m), 1 613 (m), 1 580 (s), 1 490 (m), 1 422 (m), 1 395 (s), 1 332 (s), 1 302 (m), 1 247 (m), 1 212 (w), 1 167 (m), 955 (w), 882 (w), 865 (w), 820 (w), 763 (w), 742 (w) cm^{-1}.

2,5-Dihydroxybenzoquinone. Cinnaquinone (10 mg) was added to 20 % sodium hydroxide (0.5 ml) and warmed slightly. In a few minutes a red precipitate was formed and was filtered off, treated with acid and extracted with ethyl acetate. The residue from the ethyl acetate extract was sublimed at 90°/0.005 mm. The red sublimate had an I.R.-spectrum indistinguishable from that of 2,5-dihydroxybenzoquinone prepared according to Jones and Shonle [18].

Triacetyldihydrocinnabarin methyl ester. a) Cinnabarin methyl ester [3] (30 mg) was suspended in acetic anhydride (2 ml). A few drops of pyridine and zinc dust were added and the mixture was warmed giving a yellow solution. This was filtered hot to remove unreacted zinc and then poured into water. The yellow precipitate was filtered off and recrystallised from benzene, small yellow needles m. p. 173.5—174.5° (Found: C 59.49; H 4.64; $C_{21}H_{20}N_2O_8$ requires C 58.87; H 4.71). I.R. maxima (KBr): 3 330 (w), 3 250 (w), 1 760 (s), 1 740 (s), 1 682 (s), 1 657 (s), 1 612 (w), 1 582 (w), 1 513 (s), 1 475 (s), 1 437 (m), 1 375 (m), 1 349 (w), 1 312 (m), 1 290 (s), 1 254 (s), 1 240 (s), 1 207 (s), 1 116 (m), 1 020 (m), 965 (w), 912 (w), 875 (w), 847 (w), 789 (w), 771 (m), 720 (w) cm^{-1}.

b) Triacetyldihydrocinnabarin [1] (10 mg) was suspended in ether and an ethereal solution of diazomethane was added. The clear solution which formed after some time was evaporated leaving fine yellow needles, m. p. 173—174°. No depression of m. p. when mixed with material prepared according to a).

Triacetylanhydrodihydrocinnabarin was prepared as described before [1]. (Found: C 60.24; H 4.39; N 7.03; O 28.29; $C_{20}H_{16}N_2O_7$ requires C 60.60; H 4.07; N 7.07; O 28.26). I.R. maxima (KBr): 3 340 (m), 1 775 (s), 1 750 (s), 1 732 (s), 1 655 (s), 1 619 (w), 1 589

(w), 1 519 (s), 1 481 (s), 1 465 (s), 1 432 (m), 1 405 (m), 1 375 (s), 1 351 (m), 1 317 (s), 1 292 (s), 1 260 (m), 1 230 (s), 1 198 (s), 1 163 (m), 1 131 (s), 1 063 (s), 1 027 (m), 1 009 (m), 999 (m), 970 (m), 914 (m), 883 (m), 790 (m), 780 (s), 716 (w), 685 (m) cm^{-1}.

Triacetyldihydrocinnabarin [1] has I.R. maxima (KBr): 3 380 (m), 1 770 (s), 1 740 (m), 1 690 (s), 1 677 (s), 1 630 (m), 1 587 (m), 1 508 (s), 1 480 (s), 1 435 (m), 1 381 (m), 1 295 (s), 1 260 (s), 1 237 (s), 1 198 (s), 1 120 (w), 1 022 (m), 993 (w), 955 (w), 938 (w), 920 (w), 878 (m), 847 (w), 796 (w), 779 (m), 768 (w), 745 (w), 730 (m), 715 (w), 695 (w) cm^{-1}.

Cinnabarinic acid [6] was purified further by extractive crystallisation, first from dioxan and then from acetone. I.R. maxima (KBr); 3 370 (m), 3 240 (s), 1 727 (s), 1 662 (m), 1 615 (s), 1 587 (s), 1 570 (s), 1 516 (m), 1 507 (m), 1 448 (m), 1 395 (s), 1 338 (m), 1 310 (s), 1 237 (s), 1 184 (s), 1 150 (s), 973 (m), 860 (m), 807 (m), 761 (m), 736 (m), 701 (w), 670 (w), 663 (w), 633 (m) cm^{-1}.

This investigation has been supported by a grant from *Statens Naturvetenskapliga Kommission*, which is gratefully acknowledged. The author also wishes to thank Professor A. Butenandt, München, for kindly providing a reference sample.

REFERENCES

1. Gripenberg, J. *Acta Chem. Scand.* **5** (1951) 590.
2. Lemberg, R. *Austral. J. Exp. Biol. Med. Sci.* **30** (1952) 271.
3. Cavill, G. W. K., Ralph, B. J., Tetaz, J. R. and Werner, R. L. *J. Chem. Soc.* **1953** 525.
4. Pinchas, S. and Ben-Ishai, D. *J. Am. Chem. Soc.* **79** (1957) 4099.
5. Gripenberg, J. *Proc. Chem. Soc.* **1957** 233.
6. Gripenberg, J., Honkanen, E. and Patoharju, O. *Acta Chem. Scand.* **11** (1957) 1485.
7. Cavill, G. W. K. and Tetaz, J. R. *Chem. & Ind. London* **1956** 986.
8. Gripenberg, J., Honkanen, E. and Patoharju, O. *Chem. & Ind. London* **1956** 1505.
9. Diepolder, E. *Ber.* **35** (1902) 2816.
10. Butenandt, A., Keck, J. and Neubert, G. *Ann.* **602** (1957) 61.
11. Zentmyer, D. T. and Wagner, E. C. *J. Org. Chem.* **14** (1949) 967.
12. Baker, A. W. *J. Phys. Chem.* **61** (1957) 450.
13. Musso, H. and Matties, H-G. *Chem. Ber.* **90** (1957) 1814.
14. Brockmann, H. and Franck, B. *Angew. Chem.* **68** (1956) 68.
15. Cavill, G. W. K., Clezy, P. S. and Tetaz, J. R. *J. Chem. Soc.* **1957** 2646.
16. Brockmann, H. and Franck, B. *Chem. Ber.* **87** (1954) 1767.
17. Cavill, G. W. K., Clezy, P. S. and Tetaz, J. R. *Proc. Chem. Soc.* **1957** 346.
18. Jones, R. G. and Shonle, H. A. *J. Am. Chem. Soc.* **67** (1945) 1034.

Received January 15, 1958.

ACTA CHEMICA SCANDINAVICA 12 (1958) 611—614

The Solubility of Argon and Ethane in Perfluoro-*n*-Heptane and Carbon Disulfide

J. CHR. GJALDBÆK and H. NIEMANN

Department of Inorganic Chemistry, The Royal Danish School of Pharmacy, Copenhagen Denmark

Solubility experiments carried out at 25°C resulted in the following values expressed as Bunsen coefficients: Argon in perfluoro-*n*-heptane 0.528, argon in carbon disulfide 0.180; ethane in perfluoro-*n*-heptane 2.03, ethane in carbon disulfide 3.94. From these values together with existing data in other solvents the solubility parameters for argon and ethane have been calculated to 5.43 and 7.55, respectively.

For a subsequent investigation of the solubility of gases in alcohols and water we needed values for the solubility parameters of argon and ethane. Concerning the concept "solubility parameter" the reader is referred to Hildebrand and Scott's monograph [1, p. 129].

Preliminary values for these parameters (argon 5.4 and ethane 6.45) have been published in an earlier paper [2, p. 56]. These values were considered to be rather inaccurate since the calculation was based on only two solvents for each gas. For the new experiments we have chosen a solvent with a very low and one with a very high solubility parameter, *viz.* perfluoro-*n*-heptane (5.85) and carbon disulfide (10.0).

EXPERIMENTAL AND RESULTS

The solubility determinations of argon were carried out in an apparatus and by a procedure described in an earlier paper [3]. The solubility determinations of ethane were carried out in an analogous apparatus having a 20 ml container for both the solvent and the gas.

Argon (from "L'air liquide") was identified by its emission spectrum. A sample of the gas was filled in a Geissler tube and the wave lengths of about fifty lines in the red and the blue spectrum were measured and found to be in accordance with values given in the literature. The gas was dried over phosphorus pentoxide and proved to contain less than 0.05 % water.

Ethane (Research Grade from Phillips Petroleum-Company) was analyzed in a gas-chromatograph; 25 ml of the gas (measured at 20°C and 1 atm) was adsorbed on a column of silica gel. The length of the column was 25 cm and the cross section about 0.8 cm^2.

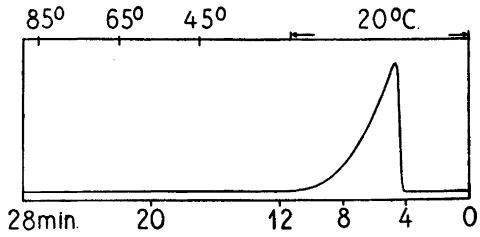

Fig. 1.

The speed of the supporting gas, hydrogen, was about 50 ml per minute. The detector was a thermal conductivity cell. The resulting curve is reproduced in Fig. 1, where the abscissa is the time in minutes. The first part of the analysis was carried out at 20°C. The sharp front after about 4 min shows that the gas contains no methane. 11 min after the beginning of the experimert the temperature was gradually increased to 85°C as shown in Fig. 1. Butane and higher hydrocarbons must be absent, since the curve shows only one peak.

To prove that lower hydrocarbons were absent the gas was analyzed in a Beckman spectrograph; the length of the cuvette was 10 cm and the pressure about 530 mm; the wave length was varied from 15 to 3 μ corresponding to wave numbers from 670 to 3 300 cm^{-1}.

The curve showed three characteristic bands for ethane at about 820, 1 450 and 2 934 cm^{-1}. A weak band at 949 cm^{-1} was interpreted as originating from ethene, the content of which was estimated to be less than 0.5 and possibly as low as 0.1 %. A very weak band at about 1 250 cm^{-1} was not identified.

By combustion analysis in an apparatus, as described by Christiansen and Wulff [4], we found results between 99.6 and 100.4 % ethane.

Perfluoro-n-heptane was fractionated in a 35-plate column (boiling point from 82.44 to 82.53°C at 760 mm). The fractions were analyzed in a Beckman spectrophotometer DU and showed a strong absorption in ultraviolet with maximum at about 216 mμ. Using the purification method of Glew and Reeves [5] we passed the fluoroheptane through a column of dry silica gel. After this purification we found the extinction coefficient to be about 0.02 at 216 mμ. The boiling point was now 82.55−82.56° ± 0.02 at 760 mm.

Carbon disulfide (analytical reagent) was fractionated in the distillation column and showed a boiling point of 46.03°C (760 mm).

The experimental results are given in Table 1 and expressed as Bunsen coefficients. The calculated means are considered to be reliable to within one per cent. The experiments were finished in June 1956. Since then Reeves and Hildebrand [6] have published a value for the solubility of argon in carbon disulfide; their value differs less than 1 % from our value.

CALULCATION OF THE SOLUBILITY PARAMETERS FOR ARGON AND ETHANE

The solubilities of argon and ethane are given in Tables 2 and 3 together with existing values for the solubilities in other solvents; the values are given in mole fractions ($x_2 \times 10^4$).

The solubility parameter (δ_2) for argon has been calculated from the equation

$$-\log x_2 = -\log x_2^i + 0.4343 \frac{\overline{V}_2}{RT}(\delta_1 - \delta_2)^2 + \log \frac{\overline{V}_2}{V_1} + 0.4343\left(1 - \frac{\overline{V}_2}{V_1}\right) \quad (1)$$

Table 1. Solubilities of argon and ethane expressed in Bunsen coefficients at 25°C.

	Argon		Ethane	
	singel determi-nations	mean	singel determi-nations	mean
CS_2	0.1815 0.179 0.1796	0.180	3.927 3.944	3.94
n-C_7F_{16}	0.5286 0.5275	0.528	(1.922) * 2.032 2.027	2.03

* this result is regarded to be too low.

in such a way that the equation reproduces the experimental values as closely as possible. With regard to the derivation of eqn. (1) reference should be made to Hildebrand and Scott [1, p. 131]. The ideal solubility, x_2^i, of argon has been calculated from

$$-\log x_2^i = -\frac{\Delta H \cdot 0.4343}{R}\left(\frac{1}{T} - \frac{1}{T_b}\right)$$

using $\Delta H = 1\,500$ cal/mole (*Int. Crit. Tables* V, p. 135) at the boiling point for argon $T_b = 87°K$. The result is $x_2^i = 21.6 \times 10^{-4}$ at $T = 298.1°K$. Since the partial molal volume ($\bar{V}_2$) of argon is not determined we have used the value for oxygen ($\bar{V}_2 = 46$ ml), see *Gjaldbœk* [2, p. 57].

From eqn. (1) we have calculated $\delta_2 = 5.43$. The accuracy with which this value represents the experimental data appears from Table 2.

The ideal solubility of ethane has been calculated from

$$x_2^i = \frac{1}{41.37} = 0.0242$$

where 41.37 atm is the vapour pressure of ethane at 25°C, confer Beattie et al.[9]

The density 0.338 of liquid ethane at 25°C has been interpolated using densities given in *Int. Crit. Tables* (III, p. 230); from this density we calculated the molal volume of liquid ethane to be 88 ml.

The accuracy with which the empirical value $\delta_2 = 7.55$ represents the experimental data appears in Table 3.

McDaniel [11] has measured the solubilities of ethane in n-hexane and n-heptane. If we recalculate his values into mole fractions we get 0.0177 and 0.0266, respectively. From equation (1) we calculate 0.026 and 0.0268.

Acknowledgements. The analyses of ethane were carried out in the Chemical Laboratory of the University, Copenhagen. We wish to express our gratitude to civil engineer Daniel Christensen and mag.scient. Flemming Andersen for their kind help with the analyses and interpretation of the results. We also thank Professor Carl Faurholt, director of the laboratory, for his kind interest in the investigations. The financial support from *Statens almindelige Videnskabsfond* is gratefully acknowledged.

Table 2. Solubilities of argon in non-polar solvents at 25°C. Comparison of experimental and calculated values.

$x_2^i = 21.6 \times 10^{-4}$ $\quad \bar{V}_2 = 46$ ml $\quad \delta_2 = 5.43$

	V_1	δ_1	$x_2 \times 10^4$	$-\log x_2$ exp.	$-\log x_2$ calc.	Δ
n-C_7F_{16}	226	5.85	53.0	2.276	2.326	+ 0.05
c-C_7F_{14}	195	6.0	46.0 a)	2.337	2.381	+ 0.04
i-C_8H_{18}	166	6.85	29.1 b)	2.536	2.490	− 0.05
n-C_6H_{14}	132	7.3	25.3 b)	2.597	2.609	+ 0.01
n-C_7H_{16}	147	7.45	25.0 b)	2.602	2.597	− 0.01
c-C_7H_{14}	128	7.85	18.55 a)	2.732	2.697	− 0.04
c-C_6H_{12}	109	8.2	14.8 c)	2.830	2.801	− 0.03
CCl_4	97.1	8.6	13.44 a)	2.872	2.909	+ 0.04
C_6H_6	89.3	9.15	8.85 c)	3.053	3.055	0.00
CS_2	60.6	10.0	4.87	3.313	3.355	+ 0.04

a) Reeves and Hildebrand [6], b) Clever *et al.*[7], c) Lannung [8].

Table 3. Solubilities of ethane in non-polar solvents at 25°C. Comparison of experimental and calculated values.

$x_2^i = 242 \times 10^{-4}$ $\quad V_2 = 88$ ml $\quad \delta_2 = 7.55$

	V_1	δ_1	$x_2 \times 10^4$	$-\log x_2$ exp.	$-\log x_2$ calc.	Δ
n-C_7F_{16}	226	5.85	203	1.693	1.658	− 0.04
CCl_4	97.1	8.6	213 a)	1.672	1.685	+ 0.01
C_6H_6	89.3	9.15	151 a)	1.821	1.781	− 0.04
CS_2	60.6	10.0	107	1.971	1.969	0.00

a) Horiuti [10].

REFERENCES

1. Hildebrand, J. H. and Scott, R. L. *Solubility of Non-electrolytes*, Reinhold Publ. Co., New York 1950.
2. Gjaldbæk, J. Chr. *Thesis*, Copenhagen 1954.
3. Gjaldbæk, J. Chr. *Acta Chem. Scand.* **6** (1952) 623.
4. Christiansen, J. A. and Wulff, I. *Kgl. Danske Videnskab. Selskab, Mat.-fys. Medd.* **22** (1945) No. 4.
5. Glew, D. N. and Reeves, L. W. *J. Phys. Chem.* **60** (1956) 615.
6. Reeves, L. W. and Hildebrand, J. H. *J. Am. Chem. Soc.* **79** (1957) 1313.
7. Clever, H. L., Battino, R., Saylor, J. H. and Gross, P. M. *J. Phys. Chem.* **61** (1957) 1078.
8. Lannung, A. *J. Am. Chem. Soc.* **52** (1930) 68.
9. Beattie, I. A., Hadlock, C. and Poffenberger, N. *J. Chem. Phys.* **3** (1935) 93.
10. Horiuti, J. *Sci. Papers, Inst. Phys. Chem. Research (Tokyo)* **17** (1931) 182.
11. McDaniel, A. S. *J. Phys. Chem.* **15** (1911) 587.

Received February 4, 1958.

ACTA CHEMICA SCANDINAVICA 12 (1958) 615—623

Separation of Acetylated Sugars and Related Compounds by Paper Chromatography in Organic Two-phase Solvent Systems

BÖRJE WICKBERG

Organisk-kemiska Institutionen, Kungl. Tekniska Högskolan, Stockholm, Sweden

The paper chromatography of acetates of sugars, sugar alcohols, cyclitols and glycosides using two-phase organic solvent systems has been investigated. Dimethyl sulphoxide, formamide and dimethyl formamide have been used as polar solvents but though all of them gave about the same resolution, dimethyl sulphoxide was preferred for practical reasons. The mobilities were found to be very dependent on the structure of the compounds but were little influenced by the molecular weight. Exceptionally great differences in mobilities were observed with the sugar alcohol derivatives. Of the fully acetylated sugars and glycosides of the D-series which were investigated, all α-anomers travelled faster than the corresponding β-anomers. The 2,3,6-tri-*O*-methyl derivatives of D-glucose and D-mannose which are difficult to distinguish by ordinary paper chromatography and by electrophoresis were easily separated as their acetates. This method should be of general value for the separation and characterisation of *O*-methyl sugars.

In the paper chromatography of carbohydrates the relative R_F values in the aqueous solvent systems commonly used generally vary little with the solvent composition. This is a serious limitation of the method as there is usually little hope of radically improving a poor resolution by changing solvents and further, the characterisation of carbohydrate compounds by paper chromatography only may be misleading. Sometimes these difficulties are overcome in indirect ways as is the case with the sugar alcohols. These may be converted into anhydrides which are then characterised by R_F values and colour reactions [1] but the method is time-consuming and leaves the problem of isolating the original alcohols unsolved.

In connection with work on the carbohydrate constituents of some lichens and algae which contain complicated mixtures of sugar alcohols, cyclitols and glycosides, some attempts were made to find a complementary method for the paper chromatographic separation and characterisation of such compounds.

As further search for suitable aqueous mixtures seemed unprofitable recourse was made to two-phase organic solvent systems, such as have been

Table 1. Relative mobilities (R_{GA})[a] of some sugars and sugar alcohol acetates in various solvents.

Solvents:	Light petroleum			*Iso*propyl ether			Ethyl ether		Benzene	
	FA	DMF[c]	DMS	FA	DMF[cd]	DMS	FA	DMS	FA	DMS[de]
Compound[b]:										
1,2,3,4-*O*-Ac *α*-D-xylose	2.0	3.0	1.9	1.2	1.3	1.2	1.1	1.1	1.0	1.0
1,2,3,4,5,6-*O*-Ac D-sorbitol	1.1	0.8	1.2	1.1	0.9	1.0	1.0	1.0	1.1	1.0
1,2,3,4,5,6-*O*-Ac D-mannitol	3,8	2.5	4.0	1.6	1.3	1.4	1.2	1.2	1.1	1.0
1,2,3,6, 2′,3′,4′,6′-*O*-Ac *β*-maltose	0.1	—	0.1	0.4	—	0.6	0.9	0.8	1.1	1.0
1,2,3,4-*O*-Ac *α*-D-glucose	0.0	—	0.0	0.1	—	0.1	0.3	0.4	0.1	0.9
2,3,4,6-*O*-Ac *α,β*-D-glucose	0.0	—	0.0	0.4 0.1	—	0.2 0.1	0.5 0.2	0.5 0.3	0.1	0.9
R_F-values of 1,2,3,4,6-*O*-Ac *α*-D-glucose	0.05	0.01	0.07	0.4	0.4	0.45	0.7	0.6	0.85	0.6

[a] $R_{GA} = \frac{\text{Movement of compound}}{\text{Movement of 1,2,3,4,6-penta-}O\text{-acetyl }\alpha\text{-D-glucose}}$

[b] 1,2,3,4-*O*-Ac *α*-D-xylose stands for 1,2,3,4-tetra-*O*-acetyl *α*-D-xylose *etc.*

[c] Elongated spots

[d] Diffuse solvent front

[e] 5% v/v of DMS added to the benzene

successfully employed for the separation of various lipophilic compounds, *e.g.*[2–6]. In addition to formamide (FA) and dimethyl formamide (DMF) which have been used earlier, dimethyl sulphoxide (DMS) also was tried as the polar stationary phase. Attempts were first made to separate some hexoses using 25 % v/v solutions of FA or DMS in ethyl acetate as solvents but as the relative R_F values were about the same as in the usual aqueous solvents and the spots produced in the case of DMS rather trailing, the experiments were continued with acetylated sugars.

A method for the separation of sugar acetates by reversed phase chromatography on acetylated paper has been described by Micheel and Schweppe [7] but though monosaccharide acetates were well separated from disaccharide acetates the resolution within each of these groups was generally rather poor.

Preliminary experiments were made using FA, DMF and DMS as stationary solvents and light petroleum, *iso*propyl ether, ethyl ether and benzene as mobile solvents (Table 1). No precautions were taken against atmospheric moisture in the chromatogram tanks.

It is evident that despite significant differences in some cases the stationary phases give on the whole about the same resolution. FA has the advantage of being sparingly soluble in all the mobile solvents and is thus strongly retained by the paper but on the other hand the silver nitrate spray (see Experimental part) cannot be used in this case for detection of the spots. DMF and DMS do not interfere with any of the spray reagents but they are less firmly held by the paper. DMS gives distinct spots in combination with light petroleum, *iso*propyl ether and slightly moist ethyl ether but elongated spots and very diffuse solvent fronts with sodium-dried ethyl ether and with benzene. DMF gave trailing spots with both light petroleum and *iso*propyl ether and was partly washed off the paper by the latter solvent.

As spraying with silver nitrate — sodium hydroxide is the most convenient way of detecting the spots, DMS is the most satisfactory of the stationary solvents tried. It is cheap and sufficiently stable when stored in glass bottles and as far as is known to the author toxic effects have not been observed. However, it should be handled with some care as when inhaled or absorbed through the skin it may produce a somewhat annoying sensation of taste.

In the following the discussion of the chromatographic technique is based mainly upon experience from work with DMS, but the same conclusions will most probably be valid for other solvents of the same type.

Before use it was necessary to impregnate the papers with the stationary solvent by dipping in a solution of the latter, blotting and drying. In order to minimise the effect of accidental irregularities in the process two such treatments with a dilute solution were preferred to one treatment with a more concentrated.

It was found that a suitable loading with DMS was obtained by using a ca 25 % v/v solution in toluene. If the concentration was below 20 % the spots became elongated or trailed and if it was above 30 % the paper had a wet and spotted appearance and the solvent front tended to be uneven. When drying the papers after impregnation DMS tended to evaporate faster along the edges, causing a faster flow through these parts during development. The drying time should therefore not be prolonged unduly.

In view of the hygroscopicity of the stationary solvents it is necessary to take precautions against atmospheric moisture when handling the impregnated chromatograms as otherwise the R_F values and resolution will vary with the weather. As is to be expected the R_F values increase with the moisture content of the solvents and with the polarity of the mobile phase. With rising R_F values the resolution generally decreases and maximum selectivity was therefore obtained by running the chromatograms in light petroleum in the presence of silica gel as a desiccant.

Because of the low solubility of DMS and its strong affinity to the paper, light petroleum and *iso*propyl ether were used as developing agents without being saturated with the stationary phase. With moist ethyl ether, 2 % v/v of DMS was added if the chromatograms were to be developed for several hours with this solvent. The resulting impoverishment of the stationary phase in the upper parts of the paper will of course affect the migration of the spots but this occurs only to a small extent. When α- and β-glucose pentaacetates were run on chromatograms in DMS — light petroleum the average R_{GA} values

Table 2. R_F and R_{GA} values of fully acetylated polyols. Stationary phase: DMS.

Mobile phase:	Light petroleum R_{GA} values	*Iso*propyl ether R_F values
Parent compound:		
Glycerol	5.6	0.43
Erythritol	4.2	0.42
Adonitol	3.0	0.39
D-Arabitol	3.1	0.37
Xylitol	1.1	0.23
Dulcitol	2.6	0.37
L-Iditol	0.44	0.16
D-Mannitol	3.7	0.42
D-Sorbitol	1.2	0.26
Volemitol	2.0	0.35
D-Inositol	1.3	0.31
myo-Inositol	0.19	0.12
Laminitol	0.75	0.26
Mytilitol	0.47	0.19
Pinitol	1.6	0.31

(*cf.* Table 1, note *a*) for the β-acetate were 0.43, 0.47 and 0.49 when the α-acetate had travelled 3, 5 and 11 cm, respectively. Using the method described above the reproducibility was tolerably good. However, when chromatograms were run for several hours it was often found that the distance travelled by a compound might vary considerably across the paper even if the solvent front not had been perceptibly oblique before leaving the paper. This error can be detected and corrected for by adding a reference compound at short intervals along the starting line. If this compound has a slightly higher R_F value than the components of the samples it may be spotted on the paper at the same points as the samples to keep down the size of paper needed. The resolution is checked by running two reference compounds, the relative movements of which should be constant. Tables 2 and 3 list the R_F or R_{GA} values of a number of acetylated sugar derivatives run in light petroleum or *iso*propyl ether on DMS treated paper.

As is apparent especially from the behaviour of the sugar alcohol acetates the mobilities of isomeric compounds show differences which could not be obtained previously in the paper chromatography of carbohydrates while the influence of the molecular weight is of secondary importance. This makes the new method a useful complement to the standard methods for paper chromatography in aqueous solvents where the opposite usually applies. The pyranosidic acetates and acetylated glycosides investigated should all have a C 1 conformation, and it is interesting to note that in all cases the derivatives carrying an axial substituent on carbon atom 1 have much higher R_{GA} values than their respective anomers. This effect is more pronounced for the anomeric glycoside acetates of galactose than for the corresponding pentaacetyl deriva-

Table 3. R_F and R_{GA} values of fully acetylated monosaccharides and glycosides. Stationary phase: DMS

Mobile phase:	Light petroleum R_{GA} values		*Iso*propyl ether R_F values	
Anomer:	α	β	α	β
Parent compound:				
D-Glucopyranose	(R_F = 0.024)	0.48	0.25	0.15
D-Galactopyranose	1.2	0.33	0.30	0.14
D-Mannopyranose	0.69	0.25	0.23	0.12
L-Arabinopyranose	0.63	1.6	0.17	0.31
D-Xylopyranose	2.2	1.2	0.33	0.23
D-Fructopyranose		0.40		0.15
Methyl D-glucopyranoside	2.3		0.29	
Ethyl D-glucopyranoside		1.8		0.28
Methyl D-galactopyranoside	3.0	0.6	0.35	0.18
Ethyl D-galactopyranoside	6.4	1.3	0.49	0.26
Ethyl D-galactofuranoside		4.3		0.41
o-Cresyl D-galactopyranoside	5.9	0.7	0.52	0.23
1-D-Glycerol D-galactopyranoside	0.45	0.08	0.20	0.08
1-L-Glycerol D-galactopyranoside	0.45	0.07	0.20	0.06

tives and the difference also seems to increase with the bulk of the aglycon group. Although axial substitution in the 2- or 4-position usually seems to reduce the rate of migration, some α-D-galactopyranose derivatives investigated do not obey this rule and so far the experimental material is too small for definite conclusions to be drawn.

Disadvantages of the method are that in some cases the procedures for detection of the spots are rather complicated and sometimes insensitive and also that the samples may have to be acetylated before chromatography. However, the difficulty of detecting a compound is often compensated by the fairly large quantities of material which can be run as a single spot. The acetylation is easily carried out on a micro scale and the low viscosity of the mobile solvents in combination with the high power of resolution usually allows the development to be completed within a few hours.

An important case where the standard method fails is in the separation of arabitol and adonitol as their acetates, since the relative rates of the spots are 1 : 0.96, respectively, in the system DMS — light petroleum. Substitution of FA or even better, a mixture of FA and DMF for the DMS gave complete resolution of the acetates, the relative rates of the components now being 1 : 0.86—0.88.

Treatment of sugar alcohols with formic acid and phosphorous pentoxide gives the corresponding fully formylated esters in fair yield [10], and these may be run on paper chromatograms using DMS and ethyl or *iso*propyl ether as solvents. The mobilities are rather low, adonitol pentaformate travels about 1 cm/h in *iso*propyl ether, and the relative rates for the adonitol, arabitol, xylitol and sorbitol derivatives were found to be 1.00 : 0.74 : 0.40 :

Table 4. R_F and R_{GA} values of 1,4-di-*O*-acetyl-2,3,6-tri-*O*-methyl derivatives of D-glucose and D-mannose. Stationary phase: DMS.

Mobile phase:	Light petroleum R_{GA} values	*Iso*propyl ether R_F values
Parent compound:		
α-D-Glucose	6.1	0.45
β-D-Glucose	4.9	0.42
α-D-Mannose	1.8	0.25
β-D-Mannose	0.57	0.12

0.28 in the same solvent. Unfortunately the formates are not easily prepared on a micro scale, they are not very stable and some of them, *e.g.* those of mannitol, dulcitol and erythritol are unsuitable for paper chromatography because of their very low solubility.

Detailed experiments on the separation of methylated sugars in these solvents have not been carried out, but there are indications that DMS and ethyl or *iso*propyl ether may be used for chromatography of hexose tetramethyl ethers. Dr. I. Croon, Svenska Träforskningsinstitutet, has found that 2,3,6-tri-*O*-methyl D-glucose and 2,3,6-tri-*O*-methyl D-mannose can be separated on DMS treated paper by developing with an ethyl ether — DMS (19 : 1) mixture. This separation is not easily accomplished with the usual aqueous solvent systems. However, while the mannose derivative gave mainly one spot (rate: 5.4 cm/6 h) the glucose derivative gave two (rates: 6.2 and 8.0 cm/6 h), the relative intensities of which changed on storing the sample solution. Probably the mutarotation in this case was slow enough to allow the separation of the α- and β-anomers. A similar phenomenon was observed for 2,3,4,6-tetra-*O*-acetyl D-glucose (see Table 1). To avoid this complication and to obtain derivatives with higher mobilities, milligram samples of the trimethyl ethers were acetylated with pyridine, sulphuric acid or sodium acetate as catalyst. The resulting products were subjected to paper chromatography using DMS as the stationary phase (Table 4). The spots were detected by spraying with anisidine hydrochloride (see Experimental part). Since the acetyl derivatives are somewhat volatile the chromatograms were not dried before spraying with hexamethylene diamine solution. The structures were assigned on the assumption that the catalysts directed the formation of α- and β-acetates in the usual way. In the presence of sulphuric acid or pyridine the mannose derivative yielded the α-acetate almost exclusively and even with sodium acetate as catalyst the same anomer was still the major product. In the case of the glucose trimethyl ether the β-acetate was the more favoured anomer.

The very different R_{GA} values found for the glucose and mannose derivatives (Table 4) shows that paper chromatography of acetylated sugar methyl ethers may be a useful method for both identification and isolation.

Separation on a preparative scale of closely related compounds may occasionally be effected by a simple counter-current extraction technique as is illustrated by the preparation of *o*-cresyl α- and β-D-galactopyranoside tetraacetate. From the mixture of acetylated galactosides which is formed on heating

penta-*O*-acetyl β-D-galactopyranose with *o*-cresol in the presence of zinc chloride Helferich *et al.*[11] isolated the pyranosidic α- and β-derivatives by fractional crystallisation, but this separation was now found to be very unpredictable. As calculated from the R_F values of the α- and β-compounds using DMS and moist ethyl ether as solvents (R_F *ca.* 0.9 and 0.8, resp.) the corresponding partition coefficients (C_{ether}/C_{DMS}) were in the approximate ratio 2.3 : 1. Separation of the mixture by counter-current extraction was therefore attempted using ethyl ether and DMS containing 5 % v/v of water as solvents. The process was followed on paper chromatograms and by a suitable withdrawal of enriched fractions only six separating funnels were required. The pure components could finally be isolated in a good yield.

EXPERIMENTAL

Paper. Whatman No. 1 filter paper was used throughout.

Solvents. All solvents were of reagent grade. Formamide (FA), dimethyl formamide (DMF) and dimethyl sulphoxide (DMS)* were distilled under reduced pressure; other solvents were used without purification. The light petroleum had b.p. 60—71° (Skellysolve B).

Impregnation with the stationary phase. In the standard procedure for impregnation with DMS the chromatogram papers were passed at an even rate through a 25 % v/v solution of DMS in toluene, uniformly blotted between layers of filter paper and then dried at 60° for 1 min to remove the toluene. This process was repeated once and after the second drying the papers were immediately placed between glass plates leaving only the starting line and paper above it uncovered. After application of the spots the papers were transferred to the chromatogram tank in such a manner that absorption of atmospheric moisture was avoided.

When the reproducibility is of secondary importance the above procedure may be simplified, *e. g.* by blowing off the toluene from the papers with hot air. If the papers are to be handled without protection from moisture it is advisable to impregnate with a more dilute DMS solution, *e. g.* 20 %.

In the preliminary experiments on acetylated compounds (Table 1) the following impregnating solutions were used: 20 % v/v FA in ethyl acetate; 20 % v/v DMF in benzene; 20 % v/v DMS in benzene. Each paper was dipped in the impregnating solution, blotted and dried at 60° for 30 sec. After a second impregnation in the same manner the papers were dried at 60° for 1 min and then covered with glass slides while the samples were applied.

For separation of the pentaacetates of arabitol and adonitol using FA as the stationary phase the papers were impregnated twice with a 20 % v/v solution of FA in ethyl acetate analogous to the DMS treatment described above. To obtain a mixed FA—DMF phase the second impregnation was made with a 20 % v/v solution of DMF in benzene.

Application of samples. The samples were usually applied as 2 % solutions in ethyl ether or chloroform but provided that no crystallisation occurred upon drying the concentration could be raised to 5 or even 10 %.

Development. All chromatograms were run by the descending technique. In view of the fire hazard and for general convenience, small glass tanks were used for development with benzene, *iso*propyl ether or ethyl ether, the papers being ca 23 cm long with the starting line 5 cm from the upper end. Where not otherwise stated, separations in light petroleum were made on papers ca 46 cm long with the starting line 7 cm from the upper end and with silica gel present as a desiccant in the chromatogram tank. The solvent reached the lower end in 25—35 min for the short papers and 60—90 min for the long ones.

Detection of spots. a) *Silver nitrate — sodium hydroxide spray* [8]. After drying for 5—10 min at 120° the chromatograms were sprayed with aqueous silver nitrate (saturated aqueous solution — water 1:100 v/v) and dried in a current of hot air, excessive heating

* Purchased from Nitroglycerin AB, Gyttorp, Sweden.

being avoided. (While the paper was still wet some compounds appeared as greasy spots.) The chromatograms were then sprayed on both sides with an alcoholic sodium hydroxide solution prepared from 1 part of an aqueous solution (40 g NaOH in 100 ml water) and 9 parts of ethanol. Some compounds, *e. g.* acetates of reducing sugars reacted quickly while others like acetylated alkyl glycosides gave spots very slowly. In the latter case it was found favourable to keep the wet chromatograms after spraying with alkali between glass slides to prevent evaporation of ethanol. As soon as possible and before the background had become too dark the papers were washed successively with dilute ammonia and water and finally treated with aqueous hydrogen sulphide. (Prolonged treatment with ammonia or hydrogen sulphide has a bleaching action.) This method could not be used for chromatograms impregnated with FA.

b) *Hexamethylene diamine.* Commercial 70 % aqueous hexamethylenediamine solution was distilled under reduced pressure and the distillate was diluted with 4 parts of ethanol. When chromatograms were sprayed with this reagent and then heated at 120° over a period of 5—10 min the acetates of reducing sugars showed up as faint yellowish spots which were strongly fluorescent in ultraviolet light. Usually the chromatograms were dried for 5—10 min at 120° before spraying, but in the case of DMS this was found to be unnecessary.

c) p-*Anisidine hydrochloride.* After treatment as in b) to remove the acetate groups the chromatograms were sprayed with a solution of *p*-anisidine (2.3 g) in a mixture of concentrated hydrochloric acid (5 ml), ethanol (30 ml) and butanol (60 ml). After a few minutes heating at 120° the chromatograms were inspected by visible and ultraviolet light. The acetates of the 2,3,6-trimethyl ethers of glucose and mannose showed up as bright red-violet spots and glucose pentaacetates as light brown spots. The chromatograms were then rinsed with water.

d) *Sodium periodate*[9]. After treatment as in b) the chromatograms were dipped in 90 % aqueous acetone containing 10 % phthalic acid, dried and then sprayed with 0.2 % aqueous sodium metaperiodate. After ca 5 min they were sprayed with a reagent prepared by mixing equal parts of 5 % aqueous manganese sulphate and 5 % 4,4-methylenebis (N,N-dimethyl aniline) in 2 N aqueous formic acid. On drying in a current of hot air, white spots appeared against a blue-green background. The spots were unstable to prolonged heating and disappeared after a few days at room temperature. Insufficient acidification with phthalic acid was found to give rise to an uneven background, the colour partly appearing before the chromatograms were dried. Acetates of sugar alcohols and their glycosides were easily detected but in the case of acetylated alkyl glycosides and cyclitols the sensitivity was less satisfactory.

Acetylation of O-methyl sugars. a) *Acetic anhydride — pyridine.* A sample (1—2 mg) of the sugar was dissolved in acetic anhydride (30 μl) and pyridine (30 μl) in a capillary tube and the solution was heated to 100—105° for 5 min. After decomposition of unreacted acetic anhydride with a few drops of water the product was extracted with chloroform (0.2 ml) and the extract successively washed with dilute sulphuric acid, aqueous sodium bicarbonate and water and finally dried with magnesium sulphate. When applied to paper chromatograms 5—10 μl of this solution were put on the same spot.

b) *Acetic anhydride — sulphuric acid.* The sample (1—2 mg) dissolved in acetic anhydride (40 μl) containing 1 % v/v of sulphuric acid was heated to 100° for 1 min. The solution especially in the case of 2,3,6-tri-*O*-methyl D-mannose turned very dark. After cooling and adding 2 drops of pyridine the mixture was worked up as under a).

c) *Acetic anhydride — sodium acetate.* A mixture of the sample (1—2 mg), acetic anhydride (40 μl) and a few crystals of anhydrous sodium acetate was heated to 110° for 1 h. Pyridine (2 drops) was added after cooling and the product isolated as above.

Separation of anomeric o-cresyl D-galactopyranoside tetraacetates by counter-current extraction. β-pentaacetyl D-galactose (93 g) was added with stirring to a mixture of *o*-cresol (85 g) and anhydrous zinc chloride (5 g) kept at 120°. The temperature was then raised to 135—140° for 40 mins. After cooling the reaction mixture was dissolved in benzene and the solution was washed with 2 N aqueous sodium hydroxide and water, dried with sodium sulphate and concentrated to dryness. The residue, dissolved in dilute ethanol gave a crude crystalline mixture of the anomeric *o*-cresyl D-galactopyranoside tetraacetates.

The above acetate mixture was added to No. 1 of a series of six separating funnels each of which contained ethyl ether (300 ml) saturated with DMS containing 5 % v/v

of water. Successive 75 ml portions of DMS, containing 5 % of water and saturated with ether, were used for the extraction. At the stage at which DMS portion No. 1 had reached funnel No. 6, funnel No. 1 contained DMS portion No. 6, *etc.* The separation was followed by chromatograms of the ether phase. The chromatograms were run for about 5 mins in DMS-*iso*propyl ether. When ether phase No. 1 was sufficiently free from the β-anomer (after seven extractions) it was withdrawn and the funnel after being refilled with fresh ether phase placed as No. 7 in the series of funnels and the extraction continued. When possible the number of funnels was reduced one by one. When only one remained the contents of this were discarded. Altogether 18 portions of ether and 35 of DMS were required. The combined ether solutions were freed from DMS by washing with water, concentrated and the residue was recrystallised yielding crude *o*-cresyl α-D-galactopyranoside tetraacetate (43 g), m. p.* 80–90°, $[\alpha]_D$ +160° (chloroform, $c = 2$). By paper chromatography it was shown to contain traces of the β-anomer. The pure compound with m. p. 90–92° and $[\alpha]_D$ +176° was obtained by treating the crude product with 2 N aqueous sodium hydroxide (1 400 ml) at 100° for 16 h and reacetylating the hydrolysed material (yield 31 g).

The combined DMS solutions were diluted with water and extracted with ether. The ether solution was concentrated and the residue recrystallised giving pure *o*-cresyl β-D-galactopyranoside tetraacetate (22 g), m. p. 114–116°, $[\alpha]_D$ ±0.

Acknowledgement. The author is indebted to *Statens Naturvetenskapliga Forskningsråd* for financial support, to Ing. Gurli Hammarberg for her skilful assistance and to Dr. B. Thomas for checking the English.

* All melting points are corrected.

REFERENCES

1. Baddiley, J., Buchanan, J. G. and Carss, B. *J. Chem. Soc.* **1957** 4138.
2. Zaffaroni, A., Burton, R. B. and Keutmann, E. H. *Science* **111** (1950) 6.
3. Schindler, O. and Reichstein, T. *Helv. Chim. Acta* **34** (1951) 108.
4. Jörgensen, C. and Kofod, H. *Acta Chem. Scand.* **8** (1954) 941.
5. Kaiser, F. *Chem. Ber.* **88** (1955) 556.
6. Mitchell, L. C. *J. Assoc. Offic. Agr. Chemists* **37** (1954) 216; from *Chem. Abstr.* **48** (1954) 14088 e.
7. Micheel, F. and Schweppe, H. *Mikrochim. Acta* **1954** 53.
8. Trevelyan, W. E., Procter, D. P. and Harrison, J. S. *Nature* **166** (1950) 444.
9. Yoda, A. *J. Chem. Soc. Japan Pure Chem. Sect.* **73** (1952) 18; from *Chem. Abstr.* **47** (1953) 3185 c.
10. Wickberg, B. *Acta Chem. Scand.* **12** (1958) 624.
11. Helferich, B., Scheiber, H. E., Streeck, R. and Vorsatz, F. *Ann.* **518** (1935) 211.

Received February 14, 1958.

ACTA CHEMICA SCANDINAVICA 12 (1958) 624—629

The Preparation of Formate Esters of Polyols

LARS SELLEBY and BÖRJE WICKBERG

Organisk-kemiska Institutionen, Kungl. Tekniska Högskolan, Stockholm, Sweden

Treatment of polyols with formic acid and phosphorus pentoxide has been found to yield the fully formylated esters in a good yield. These formates show a strong tendency to crystallise, and should be suitable as derivatives. The formylation of D-glucose by the same method has been investigated by chromatographic methods.

A previous communication [1] on the paper chromatography of sugar acetates and related compounds, also described the separation of some fully formylated polyols. These compounds have not been reported earlier in the literature and as they crystallised with great ease and should be of potential value as derivatives, their synthesis was investigated more thoroughly. Their preparation is complicated by the fact that formic acid does not form a stable anhydride or stable halides except the fluoride.

The method first used for the formylation of polyols was simply a repeated treatment of the alcohols with anhydrous formic acid, and ethylene glycol diformate [2], glycerol triformate [3] and erythritol tetraformate [4] have been prepared in this way. Formic acid forms a fairly stable mixed anhydride with acetic acid [5] and from the reaction of this anhydride with erythritol Freudenberg and Jacob [6] obtained the corresponding tetraformate in 60 % yield. However, no definite products could be isolated when D-mannitol and D-glucitol were subjected to the same treatment.

Wolf *et al.*[7] found that a mean maximum of 2.3 hydroxyl groups per glucose unit were esterified when starch was treated with formic acid at room temperature. Attempts to remove water from the reaction mixture by distilling with benzene or by adding anhydrous calcium sulphate had almost no effect.

The reaction between D-glucose and formic acid has been investigated by Tarkow and Stamm [8] who found that formylation took place preferentially at the primary hydroxyl group, though the hydroxyl group in the 4-position would react also. Richtzenhain and Lidman [9] have shown that β- but not α-acetates of pyranosidic D-sugars react with formic acid at room temperature. The reaction products were not investigated further.

Experiments with some pentitols and hexitols showed that fully formylated products could be isolated in 20-30 % yield if the alcohols were repeatedly treated with anhydrous formic acid at 100°. Formyl fluoride [10] and the mixed anhydride from formic and acetic acid were tried as formylating agents but unfortunately both compounds decomposed in the presence of catalysts like sulphuric acid or pyridine. Preliminary attempts to formylate D-glucitol or D-glucose with formyl fluoride in dimethyl formamide solution failed and when D-glucose was allowed to react with the mixed anhydride, paper chromatograms indicated that the formates formed initially (17 h reaction time) reacted further, probably with the introduction of acetyl groups. As some experiments with transesterification reactions also were unsuccessful, the possibility of continuously removing the water formed in the reaction between formic acid and the alcohol component was considered.

Aqueous formic acid may be concentrated by azeotropic distillation with propyl formate [11] or various amines, [12,13] but attempts to use propyl formate in an esterification reaction gave negative results. According to Jones [14] a 99.5 % formic acid is obtained from dilute acid by adding phosphorus pentoxide with efficient cooling and subsequently distilling the mixture. A similar procedure is described by Schlesinger and Martin [15] who use boron trioxide as drying agent. Because of complex formation between boric acid and polyols, boron trioxide is probably less suitable for the preparation of formates; this was confirmed by experiments with D-mannitol. On the other hand addition of phosphorus pentoxide to a mixture of 99 % formic acid and D-mannitol was found to raise the yield of mannitol hexaformate considerably, and experiments were now made with D-mannitol, D-glucitol and galactitol to find the best conditions for the reaction (see Table 1). The formates of the pentitols and of *myo*-inositol were prepared under the conditions giving the highest yields of the hexitol derivatives.

All the polyol formates crystallised with unusual ease, even the xylitol derivative. Both xylitol and most of its previously known derivatives are notoriously difficult to obtain in a crystalline state. At room temperature the D-mannitol and galactitol derivatives were almost insoluble in common solvents and only slightly soluble (0.1-0.2 %) in dimethyl formamide or dimethyl sulphoxide. They were recrystallised from large volumes of boiling pyridine or acetonitrile. The low-melting formates are unfortunately rather unstable and after exposure for a few days to atmospheric moisture at room temperature they often gave a smell of formic acid. The analytical values for carbon and hydrogen were not entirely satisfactory and a more suitable method of analysis was found to be alkaline hydrolysis and titration. Paper chromatographic data for the compounds are given in a previous paper [1].

The formylation of D-glucose by the same method was investigated qualitatively by a chromatographic technique. To obtain mild reaction conditions a pyrophosphoric acid mixture with the average composition $H_3PO_4.2P_2O_5$ was substituted for the phosphorus pentoxide. On chromatograms run in a benzene - dimethyl sulphoxide system, the reaction product gave mainly 3 fairly fast spots. In addition to these there were also a few weak and very slow spots. When a sample was deformylated with ethanol containing catalytic amounts of sodium ethoxide, the product gave a spot only for glucose on paper

Table 1 *. Esterification of some hexitols with formic acid in the presence of phosphorus pentoxide.

Hexitol	HCOOH ml	P_2O_5 g	Time h	Yield of hexaformate %
D-Mannitol	5.0	1.0	20	68
»	5.0	1.5	20	79
»	5.0	1.75	20	85
»	5.0	2.0	20	87
»	5.0	2.2	20	85
»	10.0	2.0	20	90
»	10.0	2.5	20	89
»	10.0	2.2	2	67
»	10.0	2.2	4	81
»	10.0	2.2	6	85
Galactitol	5.0	2.0	20	80
»	10.0	2.2	20	90
»	10.0	2.5	20	91
D-Glucitol	10.0	2.2	1	17
»	10.0	2.2	2	37
»	10.0	2.2	3.5	51
»	10.0	2.2	20	71

* All yields refer to crude crystalline products. The phosphorus pentoxide was added over a period of 10 min to a solution of the hexitol (1.00 g) in 99 % formic acid with cooling in ice-water. The reaction was then allowed to proceed at room temperature.

chromatograms run in an ethyl acetate - acetic acid - water system. The formate mixture was then separated on a cellulose column using a light petroleum - benzene - dimethyl sulphoxide mixture as solvent. The fastest component (Fraction 1) was obtained in a chromatographically pure state but did not crystallise. No separation was observed with the following two components (Fraction 2), but this behaviour could be expected if they were an anomeric pair with a moderately slow interconversion.

Fraction 1 was acetylated with acetic anhydride and pyridine, but the product showed the same R_F value as the starting material. This indicated that Fraction 1 was penta-*O*-formyl D-glucose, either as a single compound or as an inseparable mixture. Acetylation of Fraction 2 in the same way gave a product which gave two spots both of which were much faster than those observed before acetylation. When sodium acetate was substituted for pyridine in the acetylation of Fraction 2 only the faster of the acetate spots was observed on paper chromatograms. This result indicates that Fraction 2 was most probably an anomeric mixture of D-glucose tetraformates with a free hydroxyl group on carbon atom 1. The β-acetate, assuming that this is as usual the anomer formed preferentially with sodium acetate as a catalyst, has, contrary to earlier experience [1], a higher R_F value than the α-anomer. Attempts to obtain the acetylated formates in a crystalline state after separation on a cellulose column were unsuccessful.

EXPERIMENTAL*

Formylation of polyols. The polyol (1 g) was dissolved in commercial *ca.* 99 % formic acid (10 ml), if necessary with slight warming and phosphorus pentoxide (2.2 g) was added gradually with shaking and efficient cooling in ice-water. At the beginning, the addition of phosphorus pentoxide caused a rather vigorous evolution of gas but the reaction soon subsided. After 10 min the cooling bath was removed and the reaction was allowed to proceed at room temperature for 20 h. If the formate crystallised during the reaction (this occurred with the D-mannitol, D-glucitol, galactitol, D-arabitol and erythritol derivatives) the mixture was stirred mechanically with crushed ice and water (10 ml) and the crystals were then filtered off as quickly as possible. If the formate was more soluble the formic acid solution was diluted with ice and water (15 ml), extracted with ethyl acetate and the extract washed with cold aqueous sodium bicarbonate and water. The ethyl acetate solution was dried over ignited magnesium sulphate and concentrated under reduced pressure yielding the crude formate. Because of the low stability of the formates the last procedure was later modified by adding pyridine (20 ml) to the formic acid solution before dilution with ice-water.

D-*Mannitol hexaformate* was obtained in 90 % yield. Recrystallisation from large volumes of boiling pyridine gave a product with m. p. 208—210° (decomp.). When it was recrystallised from acetonitrile the melting point fell, even when a small quantity of pyridine was added to the solvent. $[\alpha]_D^{22}$ +60° (dimethyl sulphoxide, c = 0.1). (Found: C 40.9; H 4.37; HCO_2 76.0. Calc. for $C_{12}H_{14}O_{12}$: C 41.2; H 4.03; HCO_2 77.2.)

Galactitol hexaformate was obtained in 90 % yield. It was slightly more soluble than the mannitol derivative and after recrystallisation from boiling pyridine it had m. p. 200—202° (decomp.). (Found: C 42.2; H 4.27; HCO_2 77.7. Calc. for $C_{12}H_{14}O_{12}$: C 41.2; H 4.03; HCO_2 77.2.)

D-*Glucitol hexaformate* was obtained in 76 % yield and was recrystallised from acetone. M. p. 164—166.5°, $[\alpha]_D^{22}$ +19° (dimethyl formamide, c = 2.0). (Found: C 41.0; H 4.03; HCO_2 78.7. Calc. for $C_{12}H_{14}O_{12}$: C 41.2; H 4.03; HCO_2 77.2.)

D-*Arabitol pentaformate* was obtained in 76 % yield. It was recrystallised from aqueous acetone. M. p. 142.5—143.5°, $[\alpha]_D^{22}$ +48° (dimethyl formamide, c = 2.0). (Found: HCO_2 76.8. Calc. for $C_{10}H_{12}O_{10}$: HCO_2 77.0.)

Ribitol pentaformate was isolated by diluting the reaction mixture with pyridine (20 ml) and ice-water (15 ml) and extracting with ethyl acetate as described above. The crude product crystallised from chloroform — ethyl ether in 68 % yield. It was recrystallised from aqueous acetone, m. p. 63—64°. (Found: HCO_2 75.7. Calc. for $C_{10}H_{12}O_{10}$: HCO_2 77.0.)

Xylitol pentaformate. Part of the formate (0.48 g) crystallised when the reaction mixture was diluted with ice-water (15 ml). Immediately after filtration the mother liquors were combined with the aqueous washings and extracted with ethyl acetate. The extract phase was washed, dried and concentrated. The residue (0.47 g) was crystallised from aqueous methanol giving a further quantity of formate (0.15 g). The total yield of the crude product was thus only 35 % of theory. The m. p., after recrystallising from water, was 88—90.5°. (Found: HCO_2 76.2. Calc. for $C_{10}H_{12}O_{10}$: HCO_2 77.0.)

Erythritol tetraformate was obtained in 93 % yield and was recrystallised from acetone. M. p. 155.5—158°. (Found: HCO_2 76.7. Calc. for $C_8H_{10}O_8$: HCO_2 76.9.)

(From a solution of erythritol (1 g) in formic acid (10 ml) the tetraformate slowly crystallised in 44 % yield.)

myo-*Inositol hexaformate* was isolated as described for adonitol pentaformate. The syrup remaining after concentration of the ethyl acetate extract was dissolved in acetone and the solution was saturated with ethyl ether. The crude formate crystallised overnight. Yield 41 %. After recrystallisation from aqueous acetone it had m. p. 183—185°. (Found: HCO_2 77.5. Calc. for $C_{12}H_{12}O_{12}$: HCO_2 77.6.)

Determination of ester groups by saponification. The sample (ca 100 mg) was dissolved in 0.25 N ethanolic potassium hydroxide solution (10 ml). After 24 h an excess of 0.25 M hydrochloric acid was added, and after a few hours the acid was back-titrated with 0.1 M sodium hydroxide using phenolphthalein as indicator. A blank was run simultaneously.

* All melting points are corrected.

Formylation of D-*glucose.* The pyrophosphoric acid used in the formylation of glucose had the average composition $H_3PO_4 . 2P_2O_5$ and was prepared by dropping 85 % phosphoric acid onto phosphorus pentoxide with vigorous shaking. It formed granules 2 – 4 mm in diameter.

Pyrophosphoric acid (2.5 g) was added to a solution of D-glucose (1 g) in 99 % formic acid (10 ml) with cooling in ice-water and mechanical stirring. After all the granules had dissolved the mixture was left at room temperature overnight. A slight evolution of gas was observed. The solution was then stirred into ice-water and the mixture was extracted with ethyl acetate (3 × 25 ml). The extract was washed with aqueous sodium bicarbonate and water, dried over magnesium sulphate and concentrated at 15 mm pressure and 35 – 40° bath temperature. The yield of syrup was 0.55 g (31 % of the theoretical yield of pentaformate).

The product was chromatographed on paper using the technique previously described[1]. Before adding the sample the chromatogram was impregnated with a 25 % v/v solution of dimethyl sulphoxide in toluene, blotted and dried for 2 min at 60°. After a second impregnation the toluene was allowed to evaporate at room temperature and the sample was put on the paper as a 3 % solution in chloroform. Benzene containing 4 % v/v of dimethyl sulphoxide and 1 % v/v of water (Solvent 1) or benzene – light petroleum (3:1, v/v) with 4 % v/v of dimethyl sulphoxide and 1 % v/v of water added (Solvent 2) were used as developing solutions. The spots were detected by spraying the chromatograms with aqueous silver nitrate and ethanolic sodium hydroxide. The main spots had R_F 0.45, 0.25 and 0.16 (Solvent 1) and R_F 0.13, 0.05 and 0.00 (Solvent 2).

The main part of the syrup (500 mg) was dissolved in a 4:1, v/v benzene – light petroleum mixture (25 ml) by adding the minimum quantity of dimethyl sulphoxide. The solution was added to the top of a cellulose column (36 × 2.2 cm) which had been prewashed with benzene – light petroleum (4:1, v/v) containing 5 % v/v of dimethyl sulphoxide. The column was then irrigated with the same solvent. The first part of the eluate gave a spot for the fastest component only. It was concentrated and the residue was dissolved in ethyl acetate. The solution was washed repeatedly with water, dried and concentrated yielding Fraction 1 as a syrup (110 mg). After a small empty fraction the next two compounds appeared simultaneously in the eluate. The mixture was isolated as before yielding Fraction 2 (140 mg).

Samples of Fraction 1 and 2 were acetylated by heating to 100° for 5 min with acetic anhydride and pyridine, and the products were run on paper chromatograms. According to these Fraction 1 had been recovered unchanged, but Fraction 2 had been acetylated to give two spots with R_F 0.77 and 0.65 in Solvent 1 and R_F 0.47 and 0.28 in Solvent 2. Fraction 2 when heated with acetic anhydride and sodium acetate at 100° for 1 h gave a product which showed mainly a single spot with R_F 0.77 in Solvent 1 and R_F 0.47 in Solvent 2.

A second lot of D-glucose (1.5 g) was formylated as before using formic acid (15 ml) and pyrophosphoric acid (3.8 g). After standing overnight the reaction mixture was stirred into pyridine (50 ml), ethyl acetate was added and the upper phase was washed repeatedly with water and aqueous sodium bicarbonate. It was dried and concentrated under reduced pressure to give a syrup (2.6 g) which still contained traces of pyridine. The product was shown by paper chromatography to be similar to that obtained in the first formylation, but the fastest spot was a little fainter. Treatment with acetic anhydride and sodium acetate (1 h at 100°) yielded a syrup which gave spots with R_F 0.77, 0.65 and 0.45 (Solvent 1) and R_F 0.47, 0.28 and 0.13 (Solvent 2).

Part of the acetylated formate mixture (480 mg) was separated on a cellulose column as before, using Solvent 2 as eluant. The two fastest components were obtained in separate fractions which were worked up in the usual way. However, these preparations did not crystallise. As only a part (160 mg) of the material added to the column was recovered in this way, the column was afterwards stripped with ethyl acetate. The washings were extracted with water to remove dimethyl sulphoxide, dried and concentrated. The residue (270 mg), which gave rather faint spots with R_F 0.65 and 0.45 on chromatograms run in Solvent 1, was deformylated in cold absolute ethanol containing catalytic amounts of sodium ethoxide. To prevent the hydrolysis of any orthoesters, the mixture was afterwards diluted with a small quantity of water and neutralised by saturation with carbon dioxide. On chromatograms run in ethyl acetate – acetic acid – water (3:1:1) the deformylated product gave a single spot, indistinguishable from that of D-glucose. This was also the only product detected on paper chromatograms after deformylation in the same way of a freshly prepared D-glucose formate mixture.

Acknowledgement. The authors are indebted to *Statens Naturvetenskapliga Forskningsråd* for financial support, to Ing. Gurli Hammarberg for her skilful assistance and to Dr B. Thomas for checking the English.

REFERENCES

1. Wickberg, B. *Acta Chem. Scand.* **12** (1958) 615.
2. Henninger, A. *Ber.* **7** (1874) 263.
3. van Romburgh, P. *Z. physik. Chem.* **70** (1910) 459.
4. Henninger, A. *Ann. chim. phys.* [6] **7** (1886) 227.
5. Behal, A. *Ger.* 113, 165 (1899).
6. Freudenberg, K. and Jacob, W. *Chem. Ber.* **80** (1947) 325.
7. Wolff, J. A., Olds, D. W. and Hilbert, G. E. *J. Am. Chem. Soc.* **79** (1957) 3860.
8. Tarkow, H. and Stamm, A. J. *J. Phys. Chem.* **56** (1952) 262.
9. Richtzenhain, H. and Lidman, S. *Chem. Ber.* **86** (1953) 947.
10. Nesmejanow, A. N. and Kahn, E. J. *Ber.* **67** (1934) 370.
11. British Celanese Ltd. *Brit.* 597.078 (1948).
12. Léveque, J. *U. S.* 2.357.412 (1944).
13. Engel, K. H. *U. S.* 2.511.198 (1950).
14. Jones, D. C. *J. Soc. Chem. Ind. London* **38** (1919) 362 T.
15. Schlesinger, H. I. and Martin, A. W. *J. Am. Chem. Soc.* **36** (1914) 1589.

Received March 4, 1958.

ACTA CHEMICA SCANDINAVICA 12 (1958) 630—634

The Heats of Hydrolysis of Some Alkyl Acetates

INGEMAR WADSÖ

Thermochemistry Laboratory, University of Lund, Sweden

The heats of hydrolysis of some alkyl acetates have been determined at 25°C. For the idealized, isothermal hydrolysis reactions

$$ROAc(l) + H_2O(l) \rightarrow ROH(l) + HOAc(l)$$

the enthalpy changes were found as follows:
0.89 ± 0.04 kcal/mole for R = Et; 0.80 ± 0.05 kcal/mole for R = *n*-Bu; 0.54 ± 0.05 kcal/mole for R = *i*-Pr. These data have been compared with the corresponding values for the hydrolysis of thiolesters.

In previous papers the heats of hydrolysis of thiolacetic acid [1] and of some alkyl thiol acetates [2] have been reported. In continuing the study of the thermochemistry of acyl derivatives and transacylation processes of biochemical interest it was felt important to determine heats of hydrolysis for some simple alkyl acetates.

EXPERIMENTAL

Materials. The esters were commercially available preparations. They were purified by distillation through a 10-plate column. Purities were found to be 99.9 % or better as judged by measurements of equivalent weights. These were determined after alkaline hydrolysis by titration of acetic acid. The hydrolysis was carried out in alcohol—water solution containing 2 moles of NaOH per mole of ester. After 12 h the sample was titrated potentiometrically with 0.1 N HCl.

Table 1. Equivalent weight, density and refractive index for the esters ROAc.

R	Equivalent weight		d_4^{25}	n_D^{25}
	Found	Theoretical		
Et	88.15	88.10	0.8950	1.3707
n-Bu	116.16	116.16	0.8758	1.3928
i-Pr	102.20	102.13	0.8709	1.3757

Auxiliary substances. Alcohols used for heats of solution measurements were thoroughly dried and distilled. Acetic acid was purified by freezing out 4 times. Its purity was found to be 100.0 % (potentiometric titration with NaOH).

Apparatus. The reactions were carried out in an isothermal calorimeter, which will be described in detail elsewhere [3]. The calorimeter consisted of a steel reaction vessel with stirrer, heating element, and a thermistor (Stantel U 236120) for measuring the temperature changes.

Calibration. The heat capacity of the calorimeter was determined electrically by passing a known current for a given time (240—315 sec) through the heating element. The calibrations were carried out on the system after the hydrolysis. In the runs, corrections were made for the small differences in heat capacity of the ampoule and its content.

Heat of reaction measurements. The calorimeter was charged with 90 ml of 0.8 N sodium hydroxide solution in water-ethanol (2:3). The sealed glass ampoule contained about 3 mmoles of ester (alcohol, acetic acid or water). The reaction was completed within 5 min, the duration of the reaction period was 8 min *. The initial and final thermistor resistance (R_i and R_f, respectively) could therefore be obtained graphically without introducing significant errors.

Corrections to standard states. The ideal isothermal hydrolysis reaction V is obtained from eqns. I to IV, corresponding to the reactions taking place under actual experimental conditions.

I	$ROAc(l) + H_2O(soln) \rightarrow ROH(soln) + HOAc(soln)$	ΔH_1
II	$ROH(l) \rightarrow ROH(soln)$	ΔH_2
III	$HOAc(l) \rightarrow HOAc(soln)$	ΔH_3
IV	$H_2O(l) \rightarrow H_2O(soln)$	ΔH_4
V	$ROAc(l) + H_2O(l) \rightarrow ROH(l) + HOAc(l)$	$\Delta H°$
	$\Delta H° = \Delta H_1 - \Delta H_2 - \Delta H_3 + \Delta H_4$	

Units of measurement. The results of the calorimetry experiments are expressed in terms of the defined calorie equal to 4.1840 abs. joules and refer to the isothermal process at 25° and to the true mass.

The molecular weights were computed from the 1951 table of international atomic weights [4].

RESULTS

The experimental results are summarised in Tables 2 to 5. Table 2 gives the results of a series of calibration experiments. The following symbols have been used:

q input of electrical energy

$\log R_i/R_f$ the expression proportional to the temperature change; R_i and R_f are the thermistor resistance values at the start and the end, respectively, of the main period

ε the heat capacity of the calorimetric system in calories per unit of $\log R_i/R_f$

Table 2. Calibration experiments.

q, cal	$10^4 \times \log R_i/R_f$	$\varepsilon \times 10^{-2}$
37.28	64.42	57.87
37.25	64.34	57.90
48.85	84.63	57.72
41.89	72.45	57.82
		57.83 ± 0.04 **

* Attempts to determine the heat of hydrolysis of *t*-BuOAc with this apparatus failed due to the slowness of the hydrolysis.

** All the uncertainties are given as the standard deviation of the mean.

In Table 3, the first column identifies R in ROAc, the second gives the amount of ester hydrolyzed, the fourth gives the amount of heat evolved during the experiment, and the last column gives the enthalpy change.

Table 3. Determination of heats of hydrolysis of some alkyl esters, ROAc.

R	mmole	$10^4 \times \log R_i/R_f$	q cal		$-\Delta H$ kcal/mole
Et	3.551	64.87	37.51		10.56
	3.019	55.24	31.95		10.58
	3.015	55.31	31.99		10.61
	2.934	53.61	31.00		10.57
				Mean	10.58 ± 0.02
n-Bu	3.105	52.34	30.27		9.75
	2.940	49.70	28.74		9.78
	3.220	53.73	31.07		9.65
	3.201	53.71	31.06		9.70
				Mean	9.72 ± 0.02
i-Pr	3.214	58.49	33.82		10.52
	3.232	59.45	34.38		10.64
	2.967	53.98	31.22		10.52
	3.108	57.04	32.99		10.61
				Mean	10.57 ± 0.02

Table 4. Heats of solution measurements.

Substance	mmole	$10^4 \times \log R_i/R_f$	q (cal)		$-\Delta H$ kcal/mole
EtOH	3.333	0.27	0.16		0.05
	3.339	0.20	0.12		0.04
	3.215	0.30	0.17		0.05
				Mean	0.05 ± 0.01
n-BuOH	3.117	−4.59	−2.65		−0.85
	3.141	−5.04	−2.91		−0.93
	3.452	−5.47	−3.16		−0.92
				Mean	−0.90 ± 0.03
i-PrOH	3.288	−1.97	−1.14		−0.35
	2.992	−1.55	−0.90		−0.30
	3.732	−1.86	−1.07		−0.29
				Mean	−0.31 ± 0.03
HOAc	3.340	66.72	38.54		11.54
	3.384	68.26	39.43		11.65
	3.466	69.78	40.30		11.63
	3.291	66.20	38.24		11.62
				Mean	11.61 ± 0.03
H_2O	2.982	0.98	0.57		0.19
	4.009	1.29	0.74		0.18
				Mean	0.19 ± 0.01

Table 5 contains a summary of the obtained data and the heat of hydrolysis of the idealized reaction V, $\Delta H°$.

Table 5.

R	$-\Delta H_1$	$-\Delta H_2$	$-\Delta H_3$	$-\Delta H_4$	$-\Delta H°$
Et	10.58	0.05	11.61	0.19	−0.89 ± 0.04
n-Bu	9.72	−0.90	11.61	0.19	−0.80 ± 0.05
i-Pr	10.57	−0.31	11.61	0.19	−0.54 ± 0.05

DISCUSSION

Previously the heat of hydrolysis of EtOAc has been determined by Berenger-Calvet [5]. The value obtained by her is in resonably good agreement with that obtained in the present work. No other calorimetric determination of heats of hydrolysis of alkyl acetates has been found in the literature.

Unfortunately, there is an appreciable uncertainty in the heat of formation value for acetic acid [1]. Therefore, heat of hydrolysis values derived from heat of formation data cannot be calculated with the desired accuracy at the present time.

Table 6. Comparison between values of heats of hydrolysis of ROAc and RSAc in the liquid state.

R	$\Delta H°$, kcal/mole		Difference
	ROAc	RSAc	
Et	0.89	−0.95	1.84
n-Bu	0.80	−1.09	1.89
i-Pr	0.54	−1.39	1.93

As has been stated before [2], there is only a small difference between the standard heats of hydrolysis for alkyl thiolesters and alkyl O-esters in the liquid state. Table 6 shows that this difference for Et, *n*-Bu and *i*-Pr amounts to less than 2 kcal/mole. However, if the reactions are compared in the gaseous state (Table 7) there is a much greater difference, depending on the high heats of vaporisation of alcohols compared with those of the corresponding thiols. The heats of vaporisation of esters, alcohols and thiols were calculated from the equations given by Klages [6]. The heat of vaporisation of acetic acid [7] (monomeric vapor) and water [8] were taken to 12.5 and 10.5 kcal/mole, respectively.

Table 7. Comparison between heats of hydrolysis of ROAc and RSAc in the gaseous state.

R	$\Delta H°$, kcal/mole		Difference
	ROAc	RSAc	
Et	5.0	−1.7	6.7
n-Bu	5.0	−1.5	6.5
i-Pr	4.4	−2.0	6.4

REFERENCES

1. Sunner, S. and Wadsö, I. *Trans. Faraday Soc.* **53** (1957) 455.
2. Wadsö, I. *Acta Chem. Scand.* **11** (1957) 1745.
3. Sunner, S. and Wadsö, I. *Acta Chem. Scand. To be published.*
4. Wichers, E. *J. Am. Chem. Soc.* **74** (1952) 2447.
5. Berenger-Calvet, Mme *J. Chim. Phys.* **24** (1927) 325.
6. Klages, E. *Chem. Ber.* **82** (1949) 358.
7. Parks, G. S. and Huffman, H. M. *The Free Energies of Some Organic Compounds.* Catalog Company Inc. 1932.
8. *Selected Values of Chemical Thermodynamic Properties (SVCTP), Natl. Bur. Standards Circ. 500,* Washington 1950.

Received January 24, 1958.

ACTA CHEMICA SCANDINAVICA 12 (1958) 635—640

The Heats of Aminolysis of *n*-Butyl Thiolacetate and Acetic Anhydride

INGEMAR WADSÖ

Thermochemistry Laboratory, University of Lund, Sweden

The heat of aminolysis of *n*-butyl thiolacetate by *n*-butylamine was determined at 25°C. For the idealized, isothermal aminolysis reaction

n-BuSAc (l) + *n*-$BuNH_2$ (l) → *n*-BuSH (l) + *n*-BuNHAc (l)

the enthalpy change was found to be -13.7 ± 0.2 kcal/mole. The heat of aminolysis of acetic anhydride was also determined and from the obtained value and known values of the heats of hydrolysis of acetic anhydride and *n*-butyl thiolacetate a value of -13.80 ± 0.15 kcal/mole was derived for the heat of aminolysis of *n*-butyl thiolacetate.

The heat of hydrolysis of *n*-butyl acetamide was calculated to be 12.69 ± 0.10 kcal/mole.

Recently much interest has been directed towards S-acyl compounds as acetylating agents in biochemical systems. It is known that a thiolester of an aminoacid easily forms a peptide by aminolysis [1]. In connection with previous work [2] on energy relationships of S-acylated compounds it seemed of interest to determine the enthalpy change of the reaction

$$RCOSR' + R''NH_2 \longrightarrow R'SH + RCONHR''$$

The reaction can be looked upon as an model for peptide formation, where RCOSR' corresponds to a S-acyl activated amino acid and $R''NH_2$ to an amino acid.

In the simplified system investigated here, R was methyl and R', R'' were *n*-butyl. Thus the thiol ester was *n*-BuSAc and the amine was *n*-$BuNH_2$. However, the value obtained might be significantly in error. It was therefore checked by an indirect determination, by measuring the heat of aminolysis of acetic anhydride and combining this with known values for the heats of hydrolysis of Ac_2O and *n*-BuSAc, from which the heat of aminolysis of *n*-BuSAc could then be calculated.

PART I. AMINOLYSIS OF *n*-BUTYL THIOLACETATE

Experimental

Materials. *n*-BuSAc was prepared and purified according to Ref.[2] The equivalent weight was determined by iodometric titration of the thiol formed by alkaline hydrolysis [2].

The equivalent weight indicated 100.0 % purity. $n^{25}_D = 1.4584$ $d_4^{25} = 0.9385$. n-$BuNH_2$ (purum grade) was dried by refluxing with NaOH-pellets. The amine was distilled through an efficient column and a fraction boiling at 76.2°C (760 mm Hg) was collected. Potentiometric titration gave an equivalent weight corresponding to 99.6 % purity.

Auxiliary substances. n-BuSH was freshly distilled and its purity as checked by iodometric titration was found to be 100.0 %. n-BuNHAc was prepared from n-BuSAc and n-$BuNH_2$. The synthesis and physical data of the substance are described below.

Chemistry of the process. In order to secure a rapid reaction and to avoid side reactions the aminolysis was carried out in butyl amine. However, the thiol formed was extremely rapidly oxidised by air in the alkaline medium. The rate of oxidation was studied by exposing to air solutions of n-BuSH in n-$BuNH_2$. After a given time the solution (5 ml of a 3 % solution in a 100 ml conical flask) was cooled with dry ice, acidified with glacial acetic acid and titrated with iodine. The experiments showed that *ca.* 10 % of the thiol was oxidised within 30 min.

In order to check that the reaction products of the aminolysis reaction were as expected, the following synthesis was carried out. 20.0 g of n-BuSAc were added rapidly to 150 ml of n-$BuNH_2$. After 30 min at room temperature the excess of amine and the thiol formed were driven off by distillation at atmospheric pressure. The presence of thiol in the distillate was confirmed by the nitroprusside reaction. The remaining product was distilled at reduced pressure. n-BuNHAc was collected at 140–141°C and 21 mm Hg. Yield 16.6 g or 95 %. After further distillation the physical data of the substance were in good agreement with those given in the literature [3]. B. p. 230°C at 760 mm Hg, $n_D^{25} = 1.4391$, $d_4^{25} = 0.8951$.

Apparatus. The reactions were carried out in an isothermal calorimeter which will be described in a forthcoming paper [4].

Calibration. The heat capacity of the system was determined electrically by passing a known current for a known time (20 min) through the heating element. Thermal leakage was calculated by the Regnault-Pfaundler's method. The calibration experiments was carried out after the aminolysis experiments. In the runs, corrections were made for the small differences in heat capacity of the ampoule and its content.

Procedure. As stated above, it was not possible to avoid air oxidation of the thiol formed during an experiment. In order to suppress the influence of this exothermic reaction a small amount of butanethiol was added to the solution prior to the reaction. The heat of oxidation increased much less than expected from the increase in thiol concentration due to aminolysis. However, a significant error was introduced, which could be seen from the values of the thermal leakage constant, K. If thiol was added prior to the reaction the value of K was only 10 % lower than in calibration experiments whereas the value of K was found to be negative when butanethiol was not added.

The calorimeter was charged with 90 ml of n-$BuNH_2$ to which 9 mmoles of n-BuSH were added. The sealed glass ampoule contained *ca.* 3 mmoles of n-BuSAc. After equilibration the reaction was started by breaking the ampoule. The duration of the reaction period was 45 min, so that the thermal leakage had to be calculated by the Regnault-Pfaundler method. As the K-values obtained from the runs were abnormally low, the mean of those from the calibration experiments was used in the calculations. The small systematic error introduced by the oxidation of the thiol formed during the aminolysis cancels out to a great extent by the error in the heat of solution experiment of butanethiol — the only difference between the two series of experiments being the slow appearance of thiol in the aminolysis and the momentary mixing of thiol and solvent in the solution experiment.

Heat of solution measurements. n-BuSH: In order to obtain a close similarity between the solution measurements and the aminolysis experiments, the reactino period was kept at 45 min. n-BuNHAc: The reaction period was 5 min and R_i and R_f were obtained graphically.

Corrections to standard state. The idealised aminolysis reaction IV is obtained from reactions I to III, which correspond to the actual experiments.

I	n-$BuNH_2$ (l) + n-BuSAc (l) → n-BuSH (soln) + n-BuNHAc (soln)	ΔH_1
II	n-BuSH (l) → n-BuSH (soln)	ΔH_2
III	n-BuNHAc (l) → n-BuNHAc (soln)	ΔH_3
IV	n-$BuNH_2$ (l) + n-BuSAc (l) → n-BuSH (l) + n-BuNHAc (l)	$\Delta H°_4$

$$\Delta H°_4 = \Delta H_1 - \Delta H_2 - \Delta H_3 \quad (1)$$

Units of measurement. The results of the calorimetric experiments are expressed in terms of the defined calorie equal to 4.1840 abs. joules and refer to the isothermal process at 25°C and to the true mass. The molecular weights were computed from the 1951 Table of international atomic weights [5].

Results

The experimental results are summarised in Tables 1 to 3. In Table 1 the results from the calibration experiments are given. The first column shows the input of electrical energy, the second the expression proportional to the temperature increase and the third the value of the heat capacity in calories per unit of log (R_i/R_f). Uncertainties are given as the standard deviation of the mean.

Table 1. Calibration experiments.

q, cal	$10^4 \times \log (R_i/R_f)$		$10^{-2} \times \varepsilon$
36.34	103.69		35.05
36.43	104.09		35.00
36.66	104.35		35.13
36.56	104.39		35.02
		Mean	35.05 ± 0.03

Tables 2 and 3 give the results of the aminolysis experiments. The first column gives the amount of substance, the third the amount of heat evolved, and the last gives the enthalpy change in kcal/mole.

Table 2. Determination of the heat of aminolysis of *n*-butyl thiolacetate by *n*-butylamine.

mmole	$10^4 \times \log (R_i/R_f)$	q, cal		$-\Delta H$, kcal/mole
3.034	131.20	45.99		15.16
2.823	121.01	42.41		15.02
2.864	122.72	43.01		15.02
3.080	133.27	46.71		15.17
2.919	126.61	44.38		15.20
			Mean	15.11 ± 0.04

Table 3. Heat of solution measurements.

Substance	mmole	$10^4 \times \log (R_i/R_f)$	q, cal		$-\Delta H$, kcal/mole
n-BuSH	2.915	1.02	0.36		0.12
	2.778	−1.77	−0.62		−0.22
	3.112	0.11	0.04		0.01
	3.429	−0.56	−0.20		−0.06
				Mean	−0.04 ± 0.07
n-BuNHAc	3.077	12.12	4.25		1.38
	3.105	13.05	4.57		1.47
				Mean	1.42 ± 0.04

From eqn. (1) ΔH_4^0 is calculated to be 13.73 ± 0.09 kcal/mole. However, uncertainty in the K-value used is estimated to be 2 %. This will cause an uncertainty in ΔH_1 amounting to 0.1 kcal/mole. Therefore, the best value that can be obtained from these experiments is believed to be

$$\Delta H_4^0 = -13.7 \pm 0.2 \text{ kcal/mole.}$$

PART II. AMINOLYSIS OF ACETIC ANHYDRIDE

Materials. Ac_2O was freshly distilled immediately before the experiments. Its equivalent weight (determined by potentiometric titration of the acetic acid formed by hydrolysis) indicated 99.9 % purity. n-$BuNH_2$ was treated as given in part I.

Auxiliary substances. HOAc was purified by freezing out 4 times. The equivalent weight corresponded to 100.0 % purity. n-BuNHAc was prepared from Ac_2O and n-$BuNH_2$. Details of the method of synthesis and physical data of the substance are given below. Benzene, free from thiophene was dried with KOH-pellets and distilled.

Chemistry of the process. Ac_2O reacts vigorously with pure n-$BuNH_2$. In the calorimetric experiments the reaction rate was moderated by performing the aminolysis in benzene solution. The reaction products were soluble in this medium at the concentrations used. To confirm that n-BuNHAc was obtained in the reaction, the following experiment was carried out.

0.3 mole of Ac_2O was added rapidly to a solution of 1.2 moles of n-$BuNH_2$ in 150 ml benzene. The temperature of the mixture was kept below 30°C by cooling with ice water. After *ca.* 10 min the benzene and the excess of amine was distilled off. To the residue, 50 ml of water were added and the solution was extracted three times with ether. The product was dried with anhydrous $CaCl_2$ and the ether distilled off. The residue was distilled under reduced pressure through an efficient column. 28.6 g (83 %) n-BuNHAc was collected at 92.5°C (1 mm Hg). The physical data of the substance were in good agreement with those given in the literature [3]. B.p. 230°C at 760 mm Hg, $n_D^{25} = 1.4393$, $d_4^{25} = 0.8950$.

Apparatus. See Part I.

Calibration experiments. The calorimeter was calibrated as in Part I, except that the heat was supplied for 4 min only. The main period lasted for 7 min and R_i and R_f were obtained graphically.

Correction to standard state. The idealized aminolysis reaction IX is obtained from reactions V to VIII which correspond to the reactions taken place under actual experimental conditions.

V	Ac_2O (l) + n-$BuNH_2$ (soln) → n-BuNHAc (soln) + HOAc (soln)	ΔH_5
VI	HOAc (l) → HOAc (soln)	ΔH_6
VII	n-BuNHAc (l) → n-BuNHAc (soln)	ΔH_7
VIII	n-$BuNH_2$ (l) → n-$BuNH_2$ (soln)	ΔH_8
IX	Ac_2O (l) + n-$BuNH_2$ (l) → n-BuNHAc (l) + HOAc (l)	ΔH_9^0

$$\Delta H_9^0 = \Delta H_5 - \Delta H_6 - \Delta H_7 + \Delta H_8 \quad (2)$$

The experimental results are summarized in Tables 4 to 6.

Table 4. Calibration experiments.

q cal	$10^4 \times \log (R_i/R_f)$	$10^{-2} \times \varepsilon$
35.62	123.35	28.88
35.49	121.02	29.32
35.10	120.94	29.02
35.58	123.42	28.83
35.43	121.71	29.11
32.62	112.64	28.96
	Mean	29.02 ± 0.08

Table 5. Heat of aminolysis of acetic anhydride by *n*-butylamine.

mmole	$10^4 \times \log (R_i/R_f)$	q cal	$-\Delta H$, kcal/mole
1.073	144.13	41.83	38.98
0.983	132.57	38.47	39.14
1.102	148.43	43.07	39.08
1.038	140.18	40.68	39.19
1.207	163.38	47.41	39.28
		Mean	39.13 ± 0.06

Table 6. Heat of solution measurements.

Substance	mmole	$10^4 \times \log (R_f/R_i)$	q, cal	$-\Delta H$, kcal/mole
HOAc	1.389	64.77	18.79	13.53
	1.376	64.11	18.60	13.52
	1.041	48.25	14.00	13.45
			Mean	13.50 ± 0.02
n-BuNHAc	1.202	−6.40	−1.86	−1.55
	1.115	−5.82	−1.69	−1.52
	1.027	−5.62	−1.63	−1.59
			Mean	−1.55 ± 0.04
n-$BuNH_2$	0.827	−1.46	−0.42	−0.51
	0.710	−1.21	−0.35	−0.49
	1.073	−2.13	−0.62	−0.58
			Mean	−0.53 ±0.03

From eqn. (2) is obtained $\Delta H_9^0 = -26.65 \pm 0.08$ kcal/mole.

Calculation of the heat of aminolysis of *n*-BuSAc

The heat of aminolysis of *n*-BuSAc (reaction IV) can be obtained from ΔH_9^0 and the known heats of hydrolysis of *n*-BuSAc[2] and Ac_2O[6], $\Delta H°$ equals −1.09 ± 0.06 kcal/mole and −13.92 ± 0.05 * kcal/mole, respectively.

IX Ac_2O (l) + *n*-$BuNH_2$ (l) → *n*-BuNHAc (l) + HOAc (l) ΔH_9^0

X *n*-BuSAc (l) + H_2O (l) → *n*-BuSH (l) + HOAc (l) ΔH_{10}^0

XI Ac_2O (l) + H_2O (l) → 2 HOAc (l) ΔH_{11}^0

IV *n*-BuSAc (l) + *n*-$BuNH_2$ (l) → *n*-BuNHAc (l) + *n*-BuSH (l) ΔH_4^0

$$\Delta H_4^0 = \Delta H_9^0 + \Delta H_{10}^0 - \Delta H_{11}^0 \quad (3)$$

Thus we find ΔH_4^0 to be −13.82 ± 0.11 kcal/mole. This value is in good agreement with the value given in Part I. Taken into consideration the more favourable experimental conditions of the indirect determination $\Delta H_4^0 =$ −13.80 ± 0.15 kcal/mole seems at present to be the best value that can be given.

Calculation of the heat of hydrolysis of *n*-BuNHAc

It is well known that N-alkyl acetamides do not easily hydrolyze at room temperature. It is therefore difficult to obtain a good value for the heat of hydrolysis from direct measurements. However, by subtracting reaction IX from reaction XI we get the idealized hydrolysis reaction XII

XII $\quad n\text{-BuNHAc(l)} + H_2O(l) \rightarrow n\text{-BuNH}_2(l) + HOAc(l) \qquad \Delta H_{12}^0$

$$\Delta H_{12}^0 = \Delta H_{11}^0 - \Delta H_9^0 \qquad (4)$$

Thus the heat of hydrolysis of *n*-BuNHAc is calculated to be 12.73 ± 0.10 kcal/mole.

REFERENCES

1. Wieland, Th. and Bokelmann, E. *Ann.* **576** (1952) 20. Schwyzer, R. *Helv. Chim. Acta* **36** (1953) 414; Wieland, Th. and Heinke, B. *Angew. Chem.* **69** (1957) 362.
2. Wadsö, I. *Acta Chem. Scand.* **11** (1957) 1745.
3. Hawkins, P. J. and Tarbell, D. S. *J. Am. Chem. Soc.* **75** (1953) 2982.
4. Sunner, S. and Wadsö, I. *Acta Chem. Scand. To be published.*
5. Wichers, E. *J. Am. Chem. Soc.* **74** (1952) 2447.
6. Conn, J. B., Kistiakowsky, G. B., Roberts, R. M. and Smith, E. A. *J. Am. Chem. Soc.* **64** (1942) 1747.

* The value has been recalculated to 25°C. The uncertainty is an estimate.

Received January 24, 1958.

ACTA CHEMICA SCANDINAVICA 12 (1958) 641—645

The Fractionation of Rat Liver Supernatant by Salt Gradient Elution from Triethylaminoethyl Cellulose Columns

JOHN GLOMSET

Institute of Medical Chemistry, University of Uppsala, Uppsala, Sweden

Gradient elution from triethylaminoethyl cellulose columns has been employed for the separation of fractions from rat liver containing proteins and nucleotides. The method has proved to be useful for the chromatographic separation of each of these types of compound.

The experiments of Sober and Peterson and others [1-3] successfully employing acidic and basic cellulose derivatives for the chromatographic separation of proteins have aroused a great deal of interest. Many papers describing the utilization of various types of cellulose ion exchange columns have appeared in the literature. Not infrequently columns of DEAE * cellulose prepared according to Peterson and Sober [4] have been employed. Recently Porath [5] has described the preparation of triethylaminoethyl cellulose, and reports of the successful use of this material have appeared [6,7]. In an earlier paper [8] the present author described some experiments utilizing stepwise elution chromatography with columns of TEAE cellulose. The main object of these experiments was to separate and purify phosphoproteins present in the supernatant fraction of rat liver as obtained by centrifugation according to Schneider and Hogeboom [9]. In the present paper the use of a simple saline gradient at constant pH for the fractionation of the same starting material will be described. To further characterize the salt gradient system employed here as a preliminary to later experiments nucleotide extracts have also been chromatographed.

EXPERIMENTAL

Rat liver supernatant was prepared as before [8] except that 0.01 M sodium EDTA, pH 7.4 was included in the initial perfusion saline and omitted from the sucrose. In experiments in which the whole supernatant fraction was to be chromatographed the material was applied to the column immediately after the final centrifugation. When the

* The following abbreviations will be used: DEAE cellulose, diethylaminoethyl cellulose; TEAE cellulose, triethylaminoethyl cellulose; EDTA, ethylenediaminetetraacetic acid; Tris, Tris (hydroxymethyl)-aminomethane; TCA, trichloroacetic acid; ATP, adenosine triphosphate; ADP, adenosinediphosphate.

acetone precipitated proteins of the supernatant were to be chromatographed the pH of the supernatant was first adjusted to 6.5 with 0.1 N acetic acid. Analytical grade acetone which had been pre-cooled to −14°C was then added dropwise with continuous stirring in an alcohol-dry ice bath at −14°C. Precipitates were collected by centrifugation in refrigerated centrifuges at −14°C after addition of acetone to concentrations of 50 and 70 % by volume. The precipitates were washed twice, dissolved in 0.01 N Tris-HCl, pH 7.4, combined, and immediately applied to the ion exchange column.

In one type of experiment a mixture of radioactive mitochondrial nucleotides was prepared in the course of the preparation of the supernatant fraction. The method described by Beyer *et al.*[10] was used except that the sucrose did not contain EDTA and the radioactive phosphate was added to a sucrose suspension of the washed mitochondria. The reaction was stopped after 10 min. at 0°C by the addition of TCA.

TEAE was prepared from DEAE according to Porath [5]. It contained 24.3 mg N per g dry powder. It was used in the chloride form after equilibration with 0.01 N Tris-Cl buffer, pH 7.4. All chromatographic separations were performed at +4°C. The gradient system comprised two steps. The first extended from 0 to 0.2 N NaCl. The second extended from 0.2 to 1.0 N NaCl. The entire system was buffered throughout with 0.01 N Tris-HCl, pH 7.4. The gradients were established as described by Boman [11]. A beaker was used as the mixing flask, and an Erlenmeyer flask of the same volume as the reservoir flask. All that was required in addition was a magnetic stirrer and some plastic tubing. In the different experiments two flask sizes were used, 500 ml or 1 000 ml, depending on whether the column contained 15 or 35 g of the ion exchanger, respectively.

The effluent from the columns was collected in 3−5 ml portions. The chromatographic separation was followed by spectrophotometric readings in the Beckman model DU apparatus, employing cuvettes of 1 cm light path at 260 and 280 mμ. Radioactivity determinations were made on aliquots which had been dried on glass planchets. The chloride content of the effluent was followed by a modification of the method of Bergman and Senik [12] worked out by the Analytical laboratory of AB Pharmacia, Uppsala.

RESULTS AND DISCUSSION

Three different types of experiment were performed. In the first the fresh supernatant, obtained directly after centrifugation of the liver homogenate, was immediately filtered into a column containing 35 g of TEAE, previously equilibrated with 0.01 N Tris-HCl, pH 7.4. After washing the column with the same buffer elution was carried out as described in the Experimental section. Fig. 1 shows the type of chromatogram obtained with this procedure. The first peak consists of compounds not adsorbed to the ion exchanger under these conditions. The succeeding peaks comprise both proteins and nucleotides as will be seen by comparing the relative absorption at 260 and 280 mμ in Fig. 1 with that of Fig. 3. The last peak in Fig. 1 contains most of the RNA of the supernatant. As noted previously [8], however, a significant percentage of the RNA of the supernatant (about 20 %) cannot be eluted from the column under these conditions nor by increasing the salt concentration or reducing the pH. It can be removed, however, using 1 % NaOH. With these reservations this method should be a convenient way to prepare soluble RNA from rat liver homogenates. A cardinal advantage of the method is that no preliminary precipitation steps or lengthy dialysis are needed.

In order to obtain a clearer conception of the behaviour of nucleotide material when chromatographed by salt gradient elution using columns of TEAE cellulose a second type of experiment was performed. Here, various types of nucleotide extracts were chromatographed. Fig. 2 shows a chromatogram of a TCA extract of rat liver mitochondria.

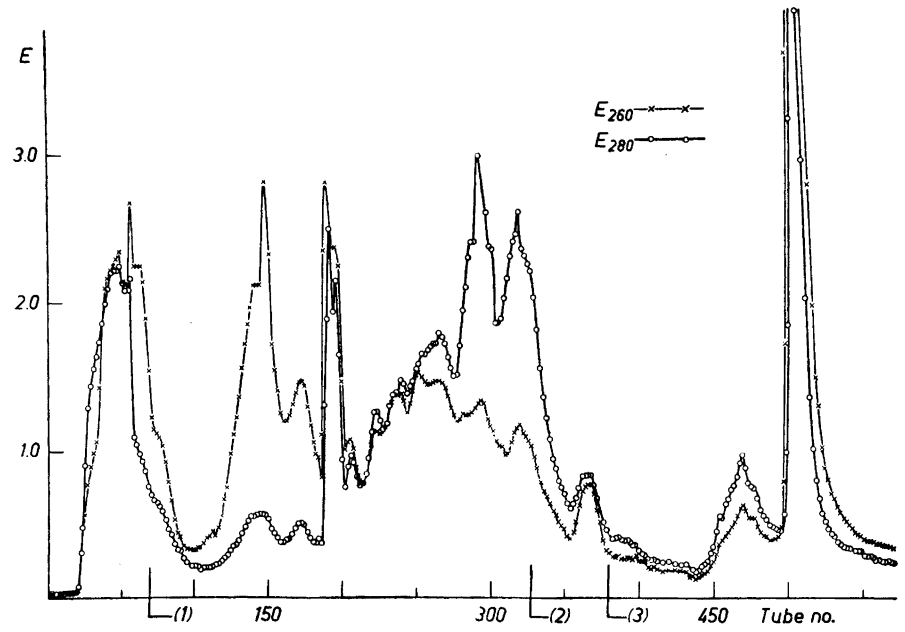

Fig. 1. Chromatogram of whole rat liver supernatant on TEAE cellulose. 4 livers used. The column contained 35 g TEAE cellulose. 1 000 ml vessels used to obtain the gradient. The first marker on the abscissa indicates the beginning of the first step of the gradient. From the second to the third marker, 0.2 N NaCl in 0.01 N Tris-HCl, pH 7.4 was filtered through the column. The third marker indicates the beginning of the second step of the gradient.

It will be seen that a satisfactory fractionation has been obtained, comparable with that obtained earlier [10] using a formic acid gradient system on Dowex 1. It was of primary interest for subsequent experiments (to be published) to determine the positions of inorganic phosphate, ADP, and ATP on the chromatogram. These are peaks IV, VIII, and IX, respectivly, and are the only radioactive peaks obtained under the conditions of the experiment. The successful use of TEAE cellulose for nucleotide chromatography would appear to be of value as a complement to those ion exchange methods already available, especially with compounds containing labile groups which might otherwise be destroyed by the lower pHs generally used in conventional nucleotide chromatography.

The third type of experiment was performed with acetone-precipitated liver supernatant protein. The precipitation was performed as quickly as possible to reduce the risk of denaturation. The combined precipitates were dissolved in buffer and chromatographed in the same way as in Fig. 1 without, however, having attempted to remove the small amount of residual acetone present. This explains the absorption properties of the first peak in Fig. 3, a typical chromatogram from this type of experiment.

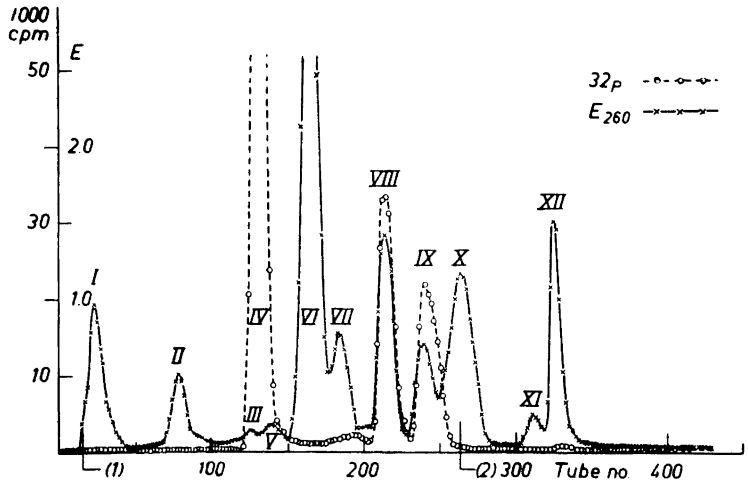

Fig. 2. Chromatogram of radioactive TCA extract of rat liver mitochondria on TEAE cellulose. Mitochondria from 4 rat livers used. 15 g of TEAE cellulose. 500 ml gradient vessels. The first and second markers on the abscissa indicate the beginning of steps 1 and 2 of the gradient, respectively.

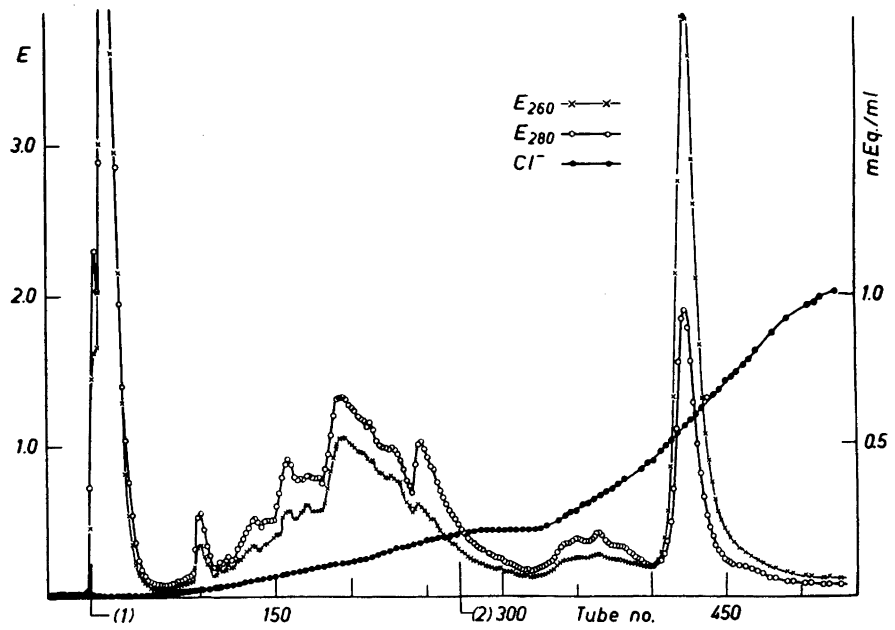

Fig. 3. Chromatogram of acetone-precipitated protein of rat liver supernatant on TEAE cellulose. 4 livers. 35 g of TEAE cellulose. 1 000 ml gradient vessels. The first and second markers on the abscissa indicate the beginning of steps 1 and 2 of the gradient, respectively. The chloride concentration in the effluent in mequiv. per ml may be determined from the ordinate at the right.

In this experiment the chloride concentration of the effluent was followed in order to indicate the nature of the gradient obtained. It will be seen that the nucleotide material present in the experiment reproduced in Fig. 1 has been removed and that the only two peaks with a high relative absorption at 260 mμ are the first and last, respectively. The first owes its absorption properties to the acetone present, while the last peak, as in Fig. 1, contains RNA. Although the chromatogram shown in Fig. 3 is of interest in that it gives a picture of the normal pattern of soluble rat liver proteins (and as such may profitably be compared with the electropherograms of soluble liver protein fractions obtained previously [8]) the identity of the remaining peaks has not been investigated further at this time. The object of the present experiments has been to study the chromatographic behaviour of nucleotide extracts and the soluble proteins of rat liver on gradient elution from columns of TEAE cellulose. The use of this method for the separation of the phosphoproteins of rat liver supernatant will be described in a subsequent paper.

Acknowledgments. This investigation was supported by a grant from the *Medical Faculty of the University of Uppsala.* The author is indebted to Dr. J. Porath for a generous gift of DEAE cellulose. He is also grateful to Dr. W. Kirsten for making available the chloride determination method.

REFERENCES

1. Sober, H. A., Gutter, F. J., Wyckoff, M. M. and Peterson, E. A. *J. Am. Chem. Soc.* **78** (1956) 756.
2. Boman, H. G. and Kaletta, U. *Biochim. et Biophys. Acta* **24** (1957) 619.
3. Sober, H. A. and Peterson, E. A. *J. Am. Chem. Soc.* **76** (1954) 1711.
4. Peterson, E. A. and Sober, H. A. *J. Am. Chem. Soc.* **78** (1956) 751.
5. Porath, J. *Arkiv kemi* **11** (1957) 97.
6. Boman, H. G. and Westlund, L. E. *Arch. Biochem. Biophys.* **70** (1957) 572.
7. Porath, J. *Arkiv kemi* **11** (1957) 259.
8. Glomset, J. *Acta Chem. Scand.* **11** (1957) 512.
9. Schneider, W. C. and Hogeboom, C. H. *J. Biol. Chem.* **183** (1950) 123.
10. Beyer, R. E., Glomset, J. and Beyer, T. *Biochim. et Biophys. Acta* **18** (1955).
11. Boman, H. G. *Biochim. et Biophys. Acta* **16** (1955) 245.
12. Bergmann, J. G. and Sanik, J. *Anal. Chem.* **29** (1957) 241.

Received February 13, 1958.

ACTA CHEMICA SCANDINAVICA 12 (1958) 646—649

Formation of Trehalose during Dissimilation of Glucose by *Propionibacterium* *

RUNE STJERNHOLM**

Department of Biochemistry, Western Reserve University, School of Medicine, Cleveland 6, Ohio, USA

A non-reducing carbohydrate has been isolated and purified from media and cells of three species of *Propionibacterium* fermenting glucose. This sugar was identified as trehalose after crystallization and preparation of its octaacetate derivative. Further criteria used were mixed melting points, paper chromatography and optical rotation.

A non-reducing carbohydrate has been observed in the media from fermentations of glucose by three species of *Propionibacterium* [1,2]. With proliferating cells 9 % of the fermented glucose was converted to a non-reducing sugar [1], and with resting cells [2] as much as 30 %. After the glucose had been utilized there was a subsequent conversion of the non-reducing carbohydrate to CO_2 and propionic, acetic and succinic acids [1]. The present report deals with the isolation and identification of this non-reducing sugar.

METHODS AND EXPERIMENTAL

The three species of *Propionibacterium* used in this investigation were *P. arabinosum* strain 34W, *P. shermanii* strain 52W and *P. pentosaceum* strain 49W. All fermentations were carried out anaerobically with washed cell suspensions. The bacteria had previously been carried through three transfers, grown for 4 to 5 days each, on the following medium which contained, per liter, glucose (5.0 g), yeast extract (5.0 g), K-phosphate buffer (0.5 M, pH 6.8), and 1 mg of each of the following vitamins: calcium-pantothenate, thiamine-HCl and biotine. The cells from the last transfer were collected by centrifugation and washed twice by resuspension in distilled water followed by centrifugation.

In a typical experiment 120 ml of a reaction mixture containing glucose (0.05 M), K-phosphate buffer (0.15 M, pH 7.2), and washed cells (2.5 % w/v) in a 300 ml round bottom flask was shaken and continuously gassed with nitrogen. After a variable period of time (6 to 22 h) the fermentation was stopped by the addition of sulfuric acid to pH 1, and the cells were then removed by centrifugation and washed twice with distilled water. The combined supernatant solutions (about 140 ml) were extracted with ether for 48 h

* This investigation was supported in part by a grant from the U.S. Public Health Service, No. E-1003 (C-2).

** DuPont Fellow, 1956—1958.

and the aqueous residue was then deionized by successive passage through a column containing Dowex-50 H^+ ($\times 12$, 200 mesh) and Duolite A4. The deionized solution was concentrated to 5 ml at 80° under an air jet, and placed on a celite-charcoal column [3] (30 mm × 500 mm if the total amount of carbohydrate did not exceed 300 mg). Water with an increasing concentration of ethanol was used for development of and elution from the column. The total carbohydrate in each fraction of eluate was determined by the anthrone method [4].

Table 1. Chromatography of fermentation residue on celite-charcoal.

Fraction	Eluant	Volume	Compound eluted
1	Water	100 ml	nil
2	1 % EtOH	100 »	»
3	2 » »	100 »	hexoses
4	3 » »	100 »	»
5	4 » »	100 »	nil
6	5 » »	100 »	»
7	6 » »	100 »	non-red. sugar
8	7 » »	100 »	» » »
9	8 » »	100 »	nil
10	9 » »	100 »	»
11	95 » »	500 »	»

A non-reducing sugar appeared in the fraction eluted with 6 and 7 % ethanol (Table 1). This elution behavior is typical of disaccharides [3], and when this substance was hydrolyzed with H_2SO_4 (1 M, 30 min, 100°) in a sealed tube glucose was the sole product. These preliminary data suggested that the non-reducing sugar might be trehalose [1-(α-D-glucopyranosido)-α-D-glucopyranoside].

Paper chromatography of the non-reducing material in four different solvent systems (Table 2) showed in each case a single spot, which could be detected when sprayed with reagents such as $AgNO_3$—NaOH [5] and HIO_4—KI-starch that react with non-reducing compounds [6]. The spot could not be detected when sprayed with aniline-phthalate [7] or *p*-anisidine-HCl [8] reagents which are specific for aldoses and reducing sugar in general. The R_F values of the non-reducing material were identical with that of known trehalose in the four solvent systems (Table 2).

Table 2. Paper chromatography of non-reducing compound and trehalose.

Solvent-system	R_F of non-red. compound	R_F of trehalose
Phenol-water	0.26	0.26
Collidine-water	0.28	0.28
n-BuOH-water	0.04	0.04
Ethylacetate-pyridine-water	0.09	0.09

When the non-reducing compound and known trehalose were mixed and chromatographed in each solvent system no separation took place.

Crystallization of the eluted non-reducing material from 80 % ethanol gave colorless rhombic crystals [m. p. 98°, $[\alpha]_D^{25}$ +179 (*c* 2, H_2O)]. The mixed melting point with a recrystallized commercial preparation of α,α′-trehalose-dihydrate [m. p. 98°, $[\alpha]_D^{20}$ +178 (*c* 2, H_2O)] showed no depression.

An acetate of the isolated material was prepared by reaction with excess acetic anhydride in pyridine [9] (12 h, 25°). Crystallization from 60 % ethanol gave colorless

needles [m. p. 100—102°, $[\alpha]_D^{25}$ +164.5 (*c.* 1.16, $CHCl_3$)]. The mixed melting point with a known sample of trehalose octa-acetate [9] (m. p. 100—102°, $[\alpha]_D^{20}$ +162.5, $CHCl_3$) showed no depression.

That trehalose is the only non-reducing sugar in the media was revealed from balance studies of several fermentations (Table 3). However, intracellularly a glycogen-like substance has been found in addition to trehalose.

Table 3. Balance studies on the aqueous residue after ether extraction of fermentation media.

Fermentation 1		
Total carbohydrate (anthrone method) [4]		141 mg *
Reducing sugar (Somogyi analysis) [10]		105 mg
Non-reducing sugar (calc.)		36 mg
Individual fractions from charcoal-celite column (anthrone method)	hexoses	118 mg
	trehalose	29 mg
Fermentation 2		
Total carbohydrate (anthrone method)		190 mg
Individual fractions from charcoal-celite column (anthrone method)	hexoses	129 mg
	trehalose	70 mg

* All values calculated as glucose.

Three species of *Propionibacterium* were analyzed for their cellular content of trehalose (Table 4). Cells of 34W, 52W and 49W, grown for two days on the above described glucose, yeast extract, phosphate and vitamin medium, were centrifuged, washed twice with water, lyophilized, and then treated according to the method given by Myrbäck [11] and Stewart *et al.*[12] for the isolation of trehalose from baker's yeast. By paper chromatographic assay (*cf.* Table 2), these preparations were found to contain trehalose and no other carbohydrates. Anthrone analysis of these fractions gave the trehalose content of the three species as shown in Table 4.

Table 4. Anthrone analysis of the trehalose content in the cells of *Propionibacterium*.

34W	5.3 %	trehalose (as glucose) *
52W	1.9 %	trehalose (as glucose) *
49W	0.7 %	trehalose (as glucose) *

* Calculated on dry weight of cells.

DISCUSSION

The findings of trehalose inside the cells of three species of *Propionibacterium*, and the production of the disaccharide in their media, may indicate that the presence of this sugar is characteristic of the entire genus.

Trehalose has earlier been identified or isolated from human tubercle bacilli [13], *Mycobacterium phlei* [14], mushrooms [15], brewer's yeast [16], lichens [17], algae [18] and insects [19]. The enzymatic synthesis of trehalose has been postulated to proceed *via* trehalose-6-phosphate, formed from UDPG and glucose-6-phosphate [20].

Trehalose samples, obtained from fermentation of glucose-1-^{14}C, -2-^{14}C, 3,4-^{14}C and -6-^{14}C by *P. arabinosum* and *P. shermanii*, after hydrolysis to glucose have been degraded by the method of Bernstein *et al.*[21], to determine the

isotopic distribution of the individual carbon atoms in order to study the mechanism of trehalose formation in these organisms. The results of these investigations will be published elsewhere.

Acknowledgement. The author wishes to express his sincere appreciation to Dr. H. G. Wood for suggesting this problem, and for helpful discussion during the progress of the work and the preparation of the manuscript.

REFERENCES

1. Wood, H. G. and Werkman, C. H. *J. Biol. Chem.* **105** (1934) 63.
2. Wood, H. G. and Werkman, C. H. *Biochem. J.* **34** (1940) 129.
3. Whistler, R. L. and Durso, D. F. *J. Am. Chem. Soc.* **72** (1950) 677.
4. Koehler, L. M. *Anal. Chem.* **24** (1952) 1576.
5. Trevelyan, W. E., Proctor, D. P. and Harrison, J. S. *Nature* **166** (1950) 444.
6. Metzenberg, R. L. and Mitchell, H. K. *J. Am. Chem. Soc.* **76** (1954) 4187.
7. Partridge, S. M. *Biochem. J.* **42** (1948) 238.
8. Hough, L., Jones, J. K. N. and Wadman, W. H. *J. Chem. Soc.* (1950) 1702.
9. Pangborn, M. C. and Anderson, R. J. *J. Am. Chem. Soc.* **58** (1936) 105.
10. Somogyi, M. *J. Biol. Chem.* **160** (1945) 61; Nelson, N. *Ibid.* **153** (1944) 375.
11. Myrbäck, K. *Ergeb. Enzymforsch.* **10** (1949) 68.
12. Stewart, L. C., Richtmyer, N. K. and Hudson, C. S. *J. Am. Chem. Soc.* **71** (1949) 2277.
13. Pangborn, M. C. and Anderson, R. J. *J. Biol. Chem.* **101** (1933) 105.
14. Anderson, R. J. and Newman, M. S. *Ibid.* **101** (1933) 499.
15. Inagaki, S. and Toki, M. *J. Pharm. Soc. Japan* **64** (1944) 132.
16. Elander, M. and Myrbäck, K. *Arch. Biochem.* **21** (1949) 249.
17. Lindberg, B. and Wickberg, B. *Acta Chem. Scand.* **7** (1953) 140.
18. Payen, J. *Compt. rend.* **236** (1953) 1811.
19. Wyatt, G. R. and Kalf, G. F. *J. Gen. Physiol.* **40** (1957) 833.
20. Leloir, L. F. and Cabib, E. *J. Am. Chem. Soc.* **75** (1953) 5445.
21. Bernstein, I. A., Lentz, K., Malm, M., Schambye, P. and Wood, H. G. *J. Biol. Chem.* **215** (1955) 137.

Received January 13, 1958.

ACTA CHEMICA SCANDINAVICA 12 (1958) 650—657

Phenolic Compounds in Brown Algae
I. The Presence of Reducing Compounds in *Ascophyllum nodosum* (L.) Le Jol.

ARNE HAUG and BJØRN LARSEN

Norwegian Institute of Seaweed Research, N.T.H., Trondheim, Norway

The brown alga *Ascophyllum nodosum* contains amounts of reducing compounds varying from 0.4 to 2.25 mequiv. per g dry matter depending on place of growth. Evidence is presented which indicates that the reducing compounds show reactions characteristic of phenols, and that they are identical with the compounds giving the color reaction of the physodes ("fucosan").

It has been known for more than sixty years that the cells of brown algae often contain a large number of highly refractive, colorless vesicles which are usually termed physodes. In 1893 Crato [1] showed that the physodes could reduce silver nitrate, and that they could be stained by vanillin hydrochloric acid. From this and other evidence he concluded that the physodes contained phenols, and that these phenols consisted partly, at least, of phloroglucinol. His results were later confirmed by several authors, among them Kylin [2,3] who described the contents of the physodes as compounds related to tannins. He noticed that these tannin-like compounds were rapidly oxidised to brown colored substances under alkaline conditions. In a note from this laboratory [4] it was shown that a diazo reagent could be used to distinguish between *Laminaria hyperborea* (Gunn.) Foslie and *Laminaria digitata* (Huds.) Lamour., and later, unpublished work showed that the diazo reagent colored specifically the physodes.

In 1943 Rönnerstrand [5] reported that brown algae contained a compound that interfered in the titration of vitamin C with dichlorophenol-indophenol, and he assumed that this reducing component ("fucosan") was contained in the physodes. He also attempted a quantitative estimation of the "fucosan" content by titration with dichlorophenol-indophenol in dilute metaphosphoric acid after vitamin C was destroyed by means of ascorbinase. In *Ascophyllum nodosum* he found a "fucosan" content corresponding to 18—32 mg ascorbic acid per 100 g fresh algae.

In 1957, Esping [6] reported that the enzyme inhibitory effect of extracts from *Fucus vesiculosus* L. probably was due to a polyphenol.

It was observed in this laboratory that the acid extracts of d r i e d *Ascophyllum nodosum* contained considerable amounts of reducing compounds, while the reducing power of similar extracts of d r i e d *Laminaria* species was insignificant. It was shown that it was possible in this way to distinguish between meal produced from Fucaceae and Laminariaceae species. Extracts of f r e s h *Laminaria* species, on the other hand, showed a considerable reducing power. The difference is thus due to a loss of reducing power during drying of *Laminaria* species, and will be subject to further investigation.

The present investigation is confined to the reducing compounds of *Ascophyllum nodosum*.

EXPERIMENTAL

Extraction. Extracts of fresh material were prepared in the following way: 40 g fresh algae was disintegrated with 200 ml 0.2 N sulfuric acid in a Waring blendor. Solid particles were removed by centrifuging.

When dry material was used, 1 g ground algae was extracted with 50 ml 0.2 N sulfuric acid overnight, and the extract was filtered.

Potentiometric titration. 10 ml extract was neutralised with approximately 1 ml 2 N sodium hydroxide. After addition of 10 ml 0.5 N sodium hydroxide, the extract was titrated by batchwise addition of 0.01 N potassium ferricyanide solution in 0.25 N sodium hydroxide. The solution was stirred vigorously throughout the titration. Near the endpoint of the titration, the reaction proceeds slowly, and the solution must be allowed to stand for about 5 min before the equilibrium potential is reached. The potential was measured against a saturated calomel electrode.

The relation between the potential and pH was determined in the following way: 10 ml extract was made alkaline with 2 ml 2 N sodium hydroxide. A 0.05 N solution of potassium ferricyanide in water was added in a quantity sufficient to oxidise half the amount of reducing components present. After 5 min 1 ml 2 N hydrochloric acid and 10 ml buffer solution of the desired pH were added and the potential was measured.

Color reactions. The vanillin reagent was prepared by dissolving 5 g vanillin in a mixture of 20 ml conc. sulfuric acid and 10 ml water. 1 ml extract and 5 ml reagent were thoroughly mixed and after about half an hour the red color was measured in a Beckman DU spectrophotometer at 515 mμ. Extracts with a high content of phenolic compounds formed a colored precipitate with the reagent, and such extracts were therefore diluted before the reagent was added.

The diazo reagent was prepared by dissolving 100 mg diazosulfanilic acid in 20 ml 3 % sodium carbonate solution. 2 ml reagent was then mixed with 2 ml extract diluted with sufficient 3 % (w/v) sodium carbonate solution to give a color intensity which could be measured directly. The optical density at 470 mμ was then determined. As a blank was used 2 ml reagent mixed with 2 ml 3 % sodium carbonate solution. The reagent is unstable and the measurements must be carried out as fast as possible.

The brown color in alkaline solution was obtained by mixing 1 ml extract with 4 ml 3 % sodium carbonate solution and heating the mixture for 15 min at 120°C. The color was measured at 420 mμ.

Determinations with hide powder. 20 g dried seaweed sample was extracted with 1 000 ml 40 % (v/v) aqueous acetone overnight. The acetone was removed *in vacuo*, and water was added to give 1 000 ml. 50 ml of this extract was used for determination of dry matter and ash. To 200 ml extract acidified with 5 drops conc. hydrochloric acid was added 100 g hide powder *. After 24 h 50 ml of the filtered solution was used for determination of ash and dry matter. The amount of "tannins" is taken as the organic dry matter removed by the hide powder treatment.

* Hide Powder p.a. Merck 4332.

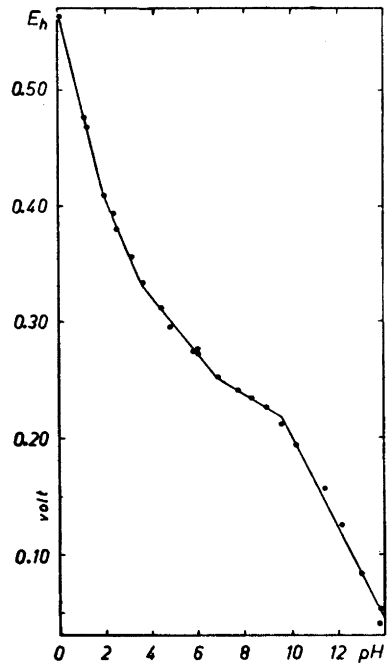

Fig. 1. pH dependence of the potential of extracts from *Ascophyllum nodosum.*

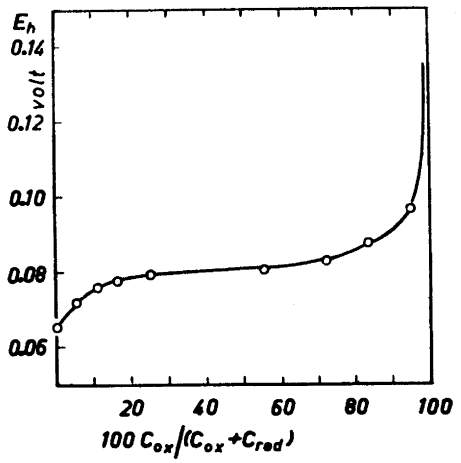

Fig. 2. Titration curve for *Ascophyllum* extracts.

RESULTS

Paper chromatography. Extracts from fresh and dried *Ascophyllum* were subjected to paper chromatography (S & S 2043 b). The solvent system used was butanol:pyridine:saturated sodium chloride solution, 1:1:2 [7]. Bisdiazotised benzidine was used as spray reagent. The extracts from both fresh and dried weed showed two major spots with R_F values of approximately 0.18 and 0.95. In addition a weak spot with an R_F value of 0.70 and traces of other components were observed. The major spots observed using the diazo reagent could also be demonstrated by spraying with ammoniacal silver nitrate.

Potentiometric titration. In Fig. 1 the potential (E_h) of an extract of fresh *Ascophyllum* is plotted as a function of pH. It will be seen that the reducing power increases with increasing pH. The curve is of a complex shape, indicating a number of dissociation steps.

Experiments have been carried out with several oxidising agents, such as potassium ferricyanide, Fremy's salt, ceric ammonium sulfate, sodium nitroprusside and dichlorophenol-indophenol. Potassium ferricyanide in alkaline solution was found to be the most convenient oxidising agent and has been

Table 1. Reducing power, mequiv. per g dry matter.

Locality	Fresh	Dried
1. Tarva	2.25	2.20
2. Garten	1.56	1.70
3. Hysnes	2.25	2.20
4. Munkaunet	0.94	0.86
5. Korsvika	0.40	0.31
6. Leangen	0.67	0.73
7. Være	1.11	1.00
8. Midtsannan	1.27	1.46
9. Muruvik	0.63	0.67

used throughout this work. Satisfactory results were also obtained with Fremy's salt, while ceric ammonium sulfate, sodium nitroprusside and dichlorophenol-indophenol gave no satisfactory endpoint.

Fig. 2 shows a titration curve of an *Ascophyllum* extract. The index potential is low, indicating that a considerable number of electrons are involved in the reaction [8].

Ascophyllum nodosum was collected at nine different localities in the Trondheimsfjord area in the first week of July 1957. The reducing power of fresh and dried material was determined. The results (Table 1) are given as milliequiv. per g dry matter.

It will be seen that there is no systematic difference between the reducing power of fresh and dried weed. The differences observed are probably due to incomplete extraction. Dried samples showed no loss of reducing power after three months of storage.

According to Rönnerstrand the vitamin C content of *Ascophyllum* corresponds to less than 0.02 mequiv. per g dry matter. Vitamin C makes therefore only a very small contribution to the reducing power of the extracts.

The reducing power of the *Ascophyllum* extracts varied from 0.4 to 2.25 mequiv. per g dry alga between the different localities. Localities Nos. 1, 2 and 3 are outside or in the outer parts of the Trondheimsfjord, localities Nos. 4, 5 and 6 are in the immediate neighbourhood of Trondheim, and localities Nos. 7, 8 and 9 are east of Trondheim, towards the inner parts of the fjord. Low reducing power was observed at localities where the salinity was lowered due to contamination with fresh water from river outlets. A more detailed study of these variations with place of growth will be published later.

Color reactions. In order to determine if the reducing compounds were identical with the substances responsible for the color reactions of the physodes, the nine *Ascophyllum* samples were extracted with dilute acid and the extracts subjected to color tests. As we wanted to include in the series an extract with a very low reducing power, a tenth sample was prepared in the following way: Water was added to the ground and dried material from locality No. 1 to reduce the dry matter content to 60 %. The sample was then heated to 120°C for 30 min. After this treatment the reducing power of the sample had decreased to 0.05 mequiv. per g dry matter. A detailed study of the

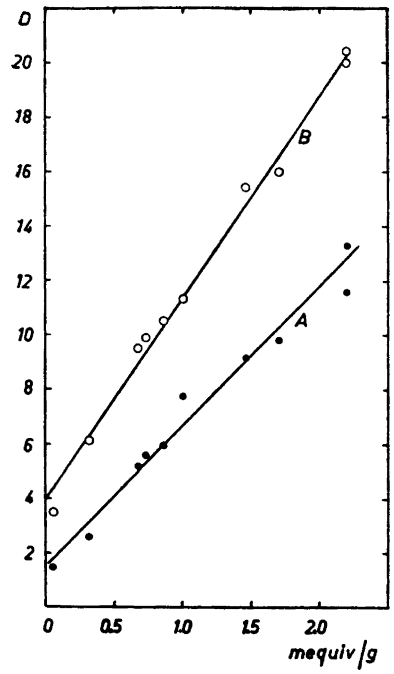

Fig. 3. Correlation between reducing power (mequiv. per g) and color with vanillin sulfuric acid (A) and diazosulfanilic acid (B) (optical density corrected for dilution).

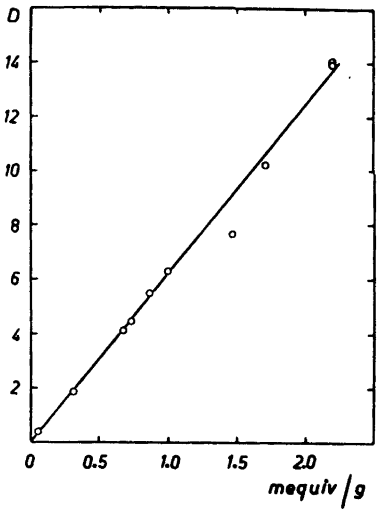

Fig. 4. Correlation between reducing power (mequiv. per g) and color of extracts after heating for 15 min at 120°C in alkali (optical density corrected for dilution).

effect of heat on the reducing power of the extracts will be published later.

In Fig. 3, curve A, the intensity of the red color of the extracts after addition of vanillin sulfuric acid is plotted as a function of the reducing power. The distinct correlation between the amount of reducing compounds and the red color given with vanillin sulfuric acid indicates that the substance in the physodes responsible for this reaction is identical with the reducing compounds.

Curve B in Fig. 3 shows the relation between the reducing power of the extracts and the color produced by diazotised sulfanilic acid in alkaline solution. Also in this case the correlation is pronounced and indicates that the reducing compounds and the compounds colored by diazo reagent are identical.

Fig. 4 shows the relation between the reducing power and the color obtained by heating the extracts for 15 min at 120°C after addition of alkali. The curve indicates that the reducing compounds are responsible for the formation of brown-colored substances in alkaline seaweed extracts.

It will be seen that the curve in Fig. 4 passes through the origin, while the curves in Fig. 3 pass through a point on the ordinate axis. This may be explained by assuming that the seaweed extracts contained a small amount

of a non-reducing substance that gave color reactions with diazotised sulfanilic acid and vanillin sulfuric acid, but which did not form brown colored substances when heated in alkaline solution.

The reaction of formaldehyde, gelatin and hide powder on the reducing compounds. When fresh *Ascophyllum* is treated with formaldehyde, the physodes become resistant to drying, freezing and boiling, while such treatment otherwise completely destroys the structureof the physodes. If an *Ascophyllum* sample treated with formaldehyde was extracted in the usual manner after careful removal of the formaldehyde *in vacuo*, the extract showed no reducing was not colored by the addition of diazo reagents or vanillin sulfuric acid power, was and furthermore no brown color was formed when the extract heated after addition of alkali.

It is known that tannins are precipitated by gelatin. When a solution of gelatin was added to an *Ascophyllum* extract adjusted to pH 3, a precipitate was formed. When the precipitate was removed by centrifugation, the supernatant became only slightly colored on adding vanillin sulfuric acid or diazo reagent, or when the extract was heated with alkali. It could also be shown that only traces of reducing compounds were present.

Similar results were obtained when we used hide powder instead of gelatin as the protein component of the reaction. It was then possible to carry out the reaction quantitatively by determining the amount of dry matter removed from the extracts by the hide powder treatment [9]. For practical reasons, the extraction was in this case carried out with 40 % (v/v) aqueous acetone solution. It was shown that this solvent extracted approximately the same amount of reducing compounds as the dilute acid used in the other determinations. The results are presented in Fig. 5 as a function of the reducing power of the acetone extracts. The curve can be extrapolated to a point on the ordinate axis corresponding to 4 g "tannins" per 100 g dry alga, indicating that the hide powder also reacted with non-reducing compounds in the extracts.

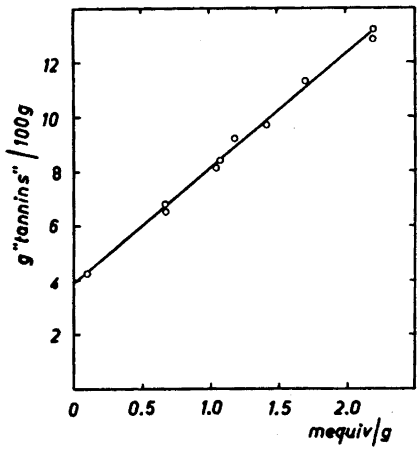

Fig. 5. Correlation between reducing power (mequiv. per g) and organic matter removed by hide powder treatment (g per 100 g dry matter).

The nature of these compounds is not known. If we assume that the content of interfering, non-reducing compounds is approximately the same in all samples, independent of the place of growth, the samples with the highest reducing power contain approximately 9 g reducing compounds per 100 g dry matter, which is in agreement with the result obtained when an equivalent weight of 40 is postulated.

DISCUSSION AND CONCLUSIONS

Extracts of *Ascophyllum nodosum* contain compounds which show a reducing potential measured against a saturated calomel electrode at pH values above 7. The relative amounts of these compounds can be estimated by potentiometric titration with potassium ferricyanide in alkaline solution. Plants from the outer parts of the Trondheimsfjord were found to contain about six times as much reducing compounds as a sample from a locality in the neighbourhood of Trondheim. Even the lowest reducing power observed corresponds to about ten times the "fucosan" content reported by Rönnerstrand. This is probably due to the fact that Rönnerstrand carried out his titrations in an acid medium, where the difference in potential between the seaweed extracts and the oxidising agent is small and a clear endpoint could not be obtained.

The pronounced correlation between the reducing power and the color reactions characteristic of the physodes strongly indicates that the reducing compounds are located in the physodes. This assumption is also supported by the fact that formaldehyde leads to a structural change in the physodes with the result that extracts of material treated with formaldehyde show no reducing power. Unpublished work by E. Baardseth of this institute indicated that the number of physodes per g fresh alga is positively correlated to the amount of reducing compounds in the plants.

The reactions of the reducing compounds with formaldehyde, gelatin, hide powder and color reagents are reactions characteristic of phenols. It is therefore probable that the physodes of *Ascophyllum* contain reducing, phenolic compounds. The results from the potentiometric titration and the analyses with hide powder showed that the reducing compounds occurred in considerable quantities, amounting to about 9 g per 100 g dry matter in the samples from the outer parts of the Trondheimsfjord.

So far the exact chemical nature of these compounds is not known. The results of this investigation indicate that the equivalent weight of the compound is low, that a number of electrons are involved in the reduction (Fig. 2) and furthermore that dissociation of the reducing groups occurs in several steps as the pH is increased.

REFERENCES

1. Crato, E. *Bot. Zeit.* **51** (1893) 157.
2. Kylin, H. *Hoppe-Seylers Z. physiol. Chem.* **83** (1913) 171.
3. Kylin, H. *Kungl. Fysiograf. Sällskap. Lund., Förh.* **8** [20] (1938) 1.
4. Jensen, A. og Haug, A. *Tidskr. Kjemi, Bergvesen Met.* **8** (1952) 138.

5. Rönnerstrand, S. *Untersuchungen über Oxydase, Peroxydase und Ascorbinsäure in einigen Meeresalgen.* C. W. Lindström, Lund 1943.
6. Esping, U. *Arkiv Kemi* **11** (1957) 107.
7. Evans, R. A., Evans, W. C. and Parr, W. H. *Nature* **164** (1949) 674.
8. Jørgensen, H. *Redox-Maalinger.* Jul. Gjellerup, København 1945.
9. Friedrich, H. *Pharmazie* **9** (1954) 138.

Received February 7, 1958.

ACTA CHEMICA SCANDINAVICA 12 (1958) 658—662

Crystal Structure of Ni_3B and Co_3B

STIG RUNDQVIST

Institute of Chemistry, University of Uppsala, Uppsala, Sweden

Ni_3B and Co_3B are isostructural with cementite (Fe_3C). A single-crystal structure determination of Ni_3B has been made. Some properties of the cementite structure are discussed.

X-Ray investigations of the Co-B and Ni-B systems have revealed the existence of two isomorphous borides Co_3B and Ni_3B. Co_3B has not been reported in earlier work on the Co-B system [1-3]. Ni_3B has previously been found by Andersson and Kiessling [4] but no X-ray data were published. The powder diffraction lines of Co_3B and Ni_3B, which could be indexed with orthorhombic unit cells (Table 1), showed close resemblance to the cementite (Fe_3C) powder pattern [5].

The first X-ray investigation of cementite was carried out by Westgren and Phragmén [6,7], who determined the orthorhombic unit cell using powder and single-crystal methods. From Westgren's and Phragmén's data Hendricks [8] deduced the space group ($P\,b\,n\,m$) and the iron positions. Different positions of the carbon atoms were proposed by Hendricks and by Westgren [9]. Westgren's structure proposal was later confirmed by Lipson and Petch [10] who settled the carbon positions with threedimensional Fourier methods using accurate intensity measurements from powder photographs. However, Lipson's and Petch's intensity material was rather limited (26 independent reflexions, in four cases with overlaps) and since no actual single-crystal determination of the cementite structure has been made, it seemed desirable to determine the structure of Co_3B or Ni_3B with the single-crystal technique.

EXPERIMENTAL

The borides were prepared from elementary boron (97.5 %), nickel powder (99.8 %) and cobalt powder (99.2 %, containing 0.45 % nickel) either by arcmelting or by sintering at 900°—1 000°C in evacuated and sealed silica tubes. X-Ray powder photographs were taken in Guinier-type focusing cameras with Cr-$K\alpha$ or Cu-$K\alpha$ radiation, using CaF_2 as standard. Ni_3B was chosen for the single-crystal work, and small crystal fragments were picked from crushed melts. The zero-layer line around the b-axis and the layer-lines 0—8 around the c-axis were recorded with Mo-K radiation in a multiple-film Weissenberg camera with thin iron foils between successive films. About 250 nonequivalent intensities were visually estimated by comparison with a standard intensity scale. Relative $|F|^2$.

values were calculated with the aid of Lu's curves [11]. An empirical correction for thermal movement and Θ-dependent absorption was obtained by plotting log F_o/F_c against $\sin^2\Theta$. Fourier summations were made on the Hägg-Laurent machine [12].

DETERMINATION OF THE STRUCTURE

All reflexions were consistent with space group $P\,b\,n\,m$. Starting with the assumption that the signs of the corresponding structure factors in Fe_3C and Ni_3B were the same, correct signs of all Ni_3B reflexions were determined by successive refinements of the electron density projections $\varrho\,(xz)$ and $\varrho\,(xy)$. The nickel positions obtained from the projections were further refined with electron density maps in the $(x\ y\ 1/4)$ plane using the entire intensity material. By difference synthesis in the same plane the positions of the boron atoms were found. After the last refinement, the reliability index was 0.11.

The result of the structure determination is collected in Table 2. Interatomic distances are listed in Table 3.

DESCRIPTION OF THE STRUCTURE AND DISCUSSION

The cementite structure has been discussed by several authors [8-10,13,14]. The packing of the metal atoms is rather complicated and attempts have been made to interpret the structure in terms of deformed austenite or martensite structures. In view of the result of the Ni_3B structure determination, a comparison of the cementite structure with boride structures might also be justified.

As pointed out by Lipson and Petch, the cementite structure is built up of successive metal atom layers parallel with {103}. The layers are composed of a slightly corrugated array of interconnected squares and triangles with

Table 1. Unit cell dimensions of Co_3B and Ni_3B in Å. (Estimated accuracy ± 0.05 %).

	Co_3B	Ni_3B
a	4.408	4.389
b	5.225	5.211
c	6.629	6.619

Table 2. Atomic parameters in Ni_3B (space group $P\,b\,n\,m$). (Estimated accuracy of the Ni parameters ± 0.002).

	x	y	z
Ni_I in 8 d	0.347	0.178	0.061
Ni_{II} in 4 c	−0.136	0.028	—
B in 4 c	0.43_3	0.11_0	—

Table 3. Interatomic distances in Ni_3B in Å.

Ni_I −11 Ni	2.43, 2.46 (2), 2.50 (2), 2.55, 2.57, 2.58, 2.71, 2.74 (2).
Ni_{II}−12 Ni	2.50 (2), 2.55 (2), 2.57 (2), 2.58 (2), 2.71 (2), 2.79 (2).
B − 9 Ni	1.99 (2), 2.02, 2.07 (2), 2.09, 2.30 (2), 2.59.

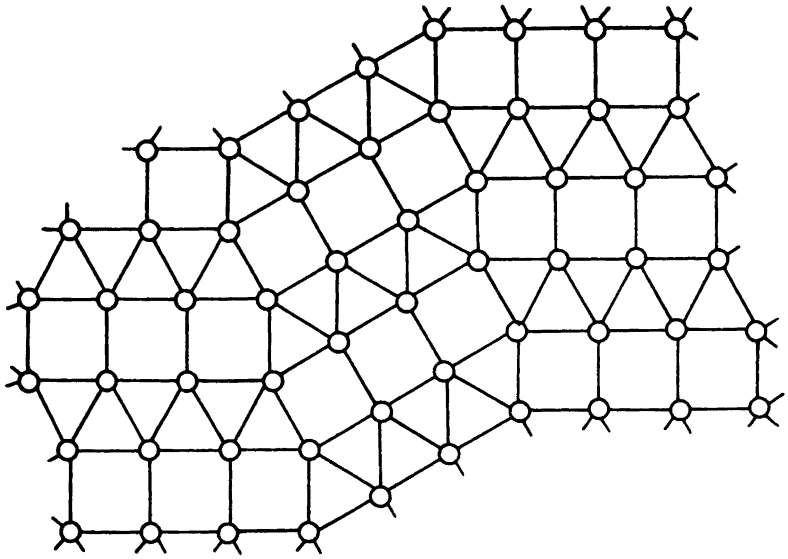

Fig. 1. Nickel atom layers parallel with {103} in Ni_3B.

metal atoms in the corners (Fig. 1). It is seen From Figs. 1, 2 and 3, that these layers may be regarded as an intermediate between the slightly corrugated atom layers parallel with $\{10\bar{1}1\}$ in hexagonal close-packed structures and the metal atom layers parallel with {001} in Ni_2B and Co_2B. These borides both have the $CuAl_2$ structure, which has been discussed by Black [15].

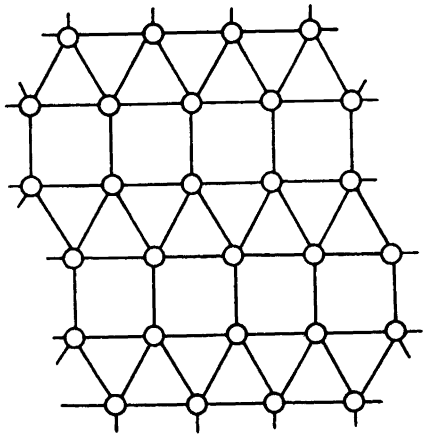

Fig. 2. Atom layers parallel with $\{10\bar{1}1\}$ in hexagonal close-packed structures.

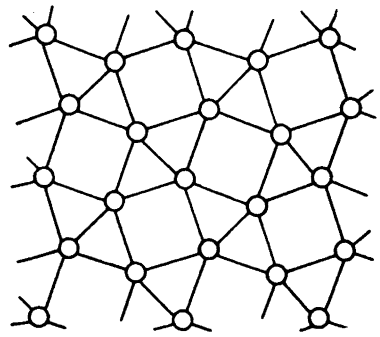

Fig. 3. Metal atom layers parallel with {001} in Me_2B-borides with the $CuAl_2$ structure.

The resemblance to other boride structures becomes more evident when the environment of the boron atoms in Ni_3B is considered. As seen from Table 3, the boron atoms are surrounded by nine nickel atoms. The six closest neighbours are situated in the corners of a triangular prism, the remaining three are situated at larger distances outside the rectangular sides of the prism. The triangular prismatic coordination around the boron atoms has been found in several types of transition metal borides [16]. The mean distance between the boron atoms and the six closest nickel atoms is 2.04 Å. Assuming the nickel radius to be 1.25 Å, the boron atom radius is only 0.79 Å, approaching the value 0.77 Å of the carbon atom radius in cementite. According to Kiessling [16] the normal boron radius is 0.86 Å.

Besides Fe_3C, very few compounds with the cementite structure have hitherto been reported. Meyer and Kohlhaas [17,18] claimed the existence of cobalt cementite and nickel cementite, but Jacobson and Westgren [19] could not confirm the cementite structure of Ni_3C. Kuo and Persson [20] have prepared manganese cementite (Mn_3C).

The possibility of substituting some other element for carbon in Fe_3C while retaining the structure was discussed by Petch [13] from size-factor considerations. Since the atomic radii of B, C and N are, respectively, 0.86, 0.76 and 0.71 Å it might be expected that nitrogen should replace carbon easily whereas boron should experience difficulties. Analogously, carbon should replace boron in Co_3B and Ni_3B. In fact, it has been found that Co_3B dissolves carbon to a limited extent, probably less than 20 % at 1 000° as found from measurements of the contraction of the Co_3B unit cell in ternary Co-B-C alloys. The solubility of carbon in Ni_3B is probably very small, since no significant contraction of the Ni_3B unit cell in ternary Ni-B-C alloys has been detected.

However, in Fe_3C, no solubility of nitrogen has been found [21] whereas an extended solubility of boron exists [22,23]. The boron solubility limit in Fe_3C has been determined by Nicholson [23] who found it possible to replace up to 80 % of the carbon by boron at 1 000°C. Recently, Aronsson (private communication) has prepared a ternary phase $Fe_3(B, Si)$ with cementite structure.

From the foregoing it is evident that simple size-factor considerations cannot be used to predict the existence of new compounds with the cementite structure. An attempt to explain the stability of boron-substituted Fe_3C has been made by Massalski [24] and Nicholson. They assume that the cementite structure is critically adjusted to the electronic environment produced by carbon atoms in interstitial positions. When boron is substituting for carbon in these positions, a similar electronic environment can be maintained if one electron is donated from the 3d shell of iron. This theory is supported by the results of magnetic measurements made by Nicholson.

Acknowledgements. The author wishes to thank professor G. Hägg for his kind interest. Thanks are also due to Dr. B. Aronsson for many valuable suggestions. The work has been supported with a scholarship from the *Statens Tekniska Forskningsråd* which is gratefully acknowledged.

REFERENCES

1. Bjurström, T. *Arkiv Kemi, Mineral. Geol.* **11** *A* (1933) 5.
2. Köster, W. and Mulfinger, W. *Z. Metallkunde* **30** (1938) 348.

3. Chizhevskiy, N. P. and Schmelev, B. A. *Trudy Moskov. Inst. Staliim. I. V. Stalina* **17** (1940) 3.
4. Andersson, L.-H. and Kiessling, R. *Acta Chem. Scand.* **4** (1950) 160.
5. Rundqvist, S. *Nature* **181** (1958) 259.
6. Westgren, A. and Phragmén, G. *J. Iron Steel Inst.* **105** (1922) 241.
7. Westgren, A. and Phragmén, G. *Ibid.* **109** (1924) 159.
8. Hendricks, S. B. *Z. Krist.* **74** (1930) 534.
9. Westgren, A. *Jernkontorets Ann.* **87** (1932) 457.
10. Lipson, H. and Petch, N. J. *J. Iron Steel. Inst.* **142** (1940) 95.
11. Lu, Chia-Si *Rev. Sci. Instr.* **14** (1943) 331.
12. Hägg, G. and Laurent, T. J. *J. Sci. Instr.* **23** (1946) 155.
13. Petch, N. J. *J. Iron Steel Inst.* **149** (1944) 143.
14. Hume-Rothery, W., Raynor, G. V. and Little, A. T. *Ibid.* **145** (1942) 143.
15. Black, P. J. *Acta Met.* **4** (1956) 172.
16. Kiessling, R. *Acta Chem. Scand.* **4** (1950) 209.
17. Meyer, W. Fr. *Metallwirtsch.* **17** (1938) 413.
18. Kohlhaas, R. and Meyer, W. Fr. *Ibid.* **17** (1938) 786.
19. Jacobson, B. and Westgren, A. *Z. physik. Chem.* **20** *B* (1933) 361.
20. Kuo, K. and Persson, L. E. *J. Iron Steel Inst.* **178** (1954) 39.
21. Jack, K. H. *Proc. Roy. Soc. London* **195** *A* (1948) 34.
22. Vogel, R. and Tamman, G. *Z. anorg. Chem.* **123** (1922) 225.
23. Nicholson, M. E. *J. Metals* **9** (1957) 1.
24. Massalski, T. B. *Theory of Alloy Phases* (1956) 97—98 (Am. Soc. for Metals, Cleveland, Ohio).

Received February 4, 1958.

ACTA CHEMICA SCANDINAVICA 12 (1958) 663—667

Cocarboxylase Activity of Thiamine Triphosphate in Yeast Transketolase

KARL-HEINZ KIESSLING

Institute of Zoophysiology, University of Uppsala, Sweden

The ability of thiamine tri- and monophosphate to replace thiamine diphosphate (cocarboxylase) in transketolase isolated from baker's yeast has been studied.

Neither the tri- nor the monophosphate showed any remarkable cocarboxylase activity in this system. Only when thiamine triphosphate was transformed into thiamine diphosphate by means of phosphatases cocarboxylase activity was obtained.

Thiamine triphosphate * has been found in rat liver [1] and in baker's yeast [2,3]. Isolated from yeast this compound was shown to be identical with synthetic thiamine triphosphate with regard to the arrangement of the phosphate groups [3].

Very little is known about the action of TTP and its localization. On the basis of the observed action of TTP on the frog's heart Plotka *et al.* [4] put forward the hypothesis that TTP plays a role in the special metabolism related to nerve impulse transmission.

The ability of synthetic TTP to replace TDP in an isolated carboxylase from baker's yeast has been studied by de la Fuente and Diaz-Cadavieco [5], Kiessling [3], and Rossi-Fanelli *et al.*[6] In this system TTP was found to be inactive. This was also the case with TTP isolated from yeast [3]. Cocarboxylase activity was obtained from TTP only after pre-incubation with a potato apyrase at 0°C, when γ-P is split off [3].

An entirely different explanation of the above negative results has been put forward by Bartos [7] who suggests the existence in yeast of two distinct apoenzymes, one combining with TDP, the other with TTP. Thus only the former should have been isolated in the experiments referred to above [5,3,6].

The turnover rate of the different phosphate groups of TTP in baker's yeast has been studied with glucose as a substrate and in the presence of

* Abbreviations: TTP, thiamine triphosphate; TDP, thiamine diphosphate (cocarboxylase); TMP, thiamine monophosphate; EDTA, ethylenediaminetetraacetate (Versene); DPNH, reduced diphosphopyridine nucleotide; AMP, adenosine-5-phosphate.

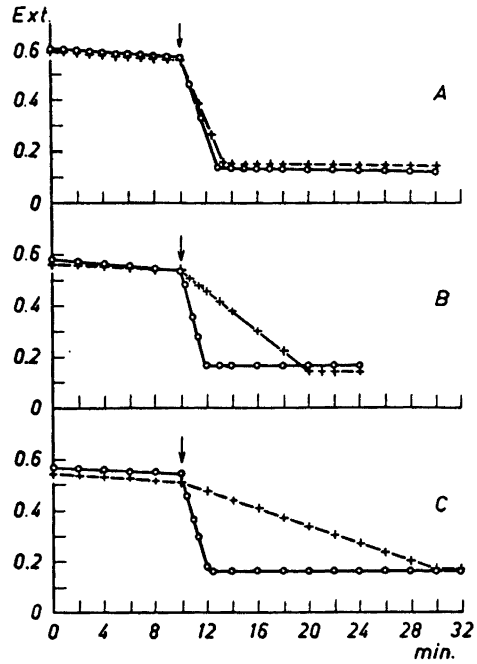

Fig. 1. The necessity of TDP by transketolase after dialysis.
The isolation of the enzyme was performed according to de la Haba *et al.*[12], and carried on to the protamine step.
The arrows indicate the addition of transketolase. For remaining additions, see "Composition of samples".
A, no dialysis; B, 23 h; and C, 43 h dialysis.

+———+ no synthetic TDP present
O———O 0.05 ml 0.1 % TDP present

radioactive inorganic phosphate [8]. The terminal phosphate group became radioactive more rapidly than the β- and α-P. Synthetic TTP added to rat liver mitochondria did, however, not exchange its phosphate groups [9].

In homogenates and in protein fractions from rat liver, however, Greiling and Kiesow [10] found, in the absence of ATP, an enzymatic transfer of phosphate from TTP to glucose.

From yeast an enzyme, named transketolase, has been crystallized [11,12] which transforms ribose-5-phosphate and ribulose-5-phosphate into a mixture of heptulose-7-phosphate and glyceraldehyde-3-phosphate:

Ribose-5-phosphate + ribulose-5-phosphate $\rightleftharpoons$
$\rightleftharpoons$ heptulose-7-phosphate + glyceraldehyde-3-phosphate

This reaction has been shown to be conditioned by TDP and magnesium [11]. As TTP occurs in yeast and the concentration can be considerably increased by suitable pre-incubation of the yeast [2,3], the ability of TTP to replace TDP in a transketolase isolated from baker's yeast has been investigated in this paper.

EXPERIMENTAL

Transketolase. The transketolase has been isolated from baker's yeast * according to de la Haba *et al.*[12] The isolation was carried on to the protamine treatment. At this stage transketolase is stable for weeks if kept at 5°C. The enzyme shows no need of TDP and magnesium (Fig. 1 A). Only after prolonged dialysis against a solution [11] of 0.6 % EDTA-0.9 % KCl, pH 7.4, reduction and eventual loss of transketolase activity was obtained. This was, however, restored by the addition of magnesium and TDP (Figs. 1 B and 1 C).

Ribose-5-phosphate was prepared by boiling adenosine-5-phosphate for ten minutes in 1 N HCl, removal of insoluble barium salts, and precipitation of the barium salt of ribose-5-phosphate with four volumes of ethyl alcohol [13].

Isomerase, free of transketolase, was isolated from baker's yeast as described by de la Haba *et al.*[12]

Isomerase product. The equilibrium mixture of ribose-5-phosphate and ribulose-5-phosphate (isomerase product) was prepared from ribose-5-phosphate by incubation for 3 h with dialyzed isomerase [12]. The resulting product was kept in the form of the barium salt at 2°C, and transformed into the ammonium salt before use [12].

α-Glycerophosphate dehydrogenase from rabbit muscle was prepared according to Racker [13].

TTP, TDP, TMP. A mixture of thiamine phosphates was prepared according to Viscontini *et al.*[14], and TTP, TDP and TMP were isolated according to Kiessling [15]. As, however, the samples obtained in this way were poisonous when added to the transketolase, the solvent impurities were removed by re-chromatography of the isolated compounds in a second non-poisonous solvent (*n*-propanol-H_2O-1 M acetate buffer pH 5, 70:20:10) described by Siliprandi and Siliprandi [16].

DPNH and crystalline *AMP*, both from yeast, were obtained from Sigma Chemical Company. The extinction was measured in a Beckman spectrophotometer at 340 mμ.

Composition of samples. The incubation was performed mainly according to de la Haba *et al.*[12] Into a quartz cell (holding 4 ml) were pipetted: 0.05 ml of 0.5 M glycylglycine buffer, pH 7.6, 0.05 ml of 0.002 M DPNH, 0.05 ml of crude glycerophosphate dehydrogenase, 0.05 ml of the ammonium salt of isomerase product solution, 0.05 ml of 0.06 M $MgCl_2$, 0.1 ml of a transketolase solution containing about 1 000 units per ml **, samples of TTP, TDP or TMP (see below), and water to make 4 ml.

RESULTS

Dialysis of the transketolase preparation for 48 h gives an enzyme which, without addition of TDP, is inactive (Fig. 2A). Addition of TDP rapidly gives rise to an oxidation of DPNH. The same amount of TTP is less active (Fig. 2A). That TTP is active at all may be explained in different ways. Either TTP, to a certain degree, can replace TDP, or it is decomposed to TDP by phosphatases. The possibility that the added TTP is initially contaminated with TDP is excluded by the paper chromatographic controls. In order to find out if TDP is formed from TTP by phosphatases, samples were taken after different incubation intervals, and analyzed by paper chromatography according to Kiessling[15]. The chromatograms showed that TTP was rapidly transformed into TDP and TMP. After 15 min only about 30 % remained as TTP.

When, on the other hand, TTP and TDP are added later during the incubation (Fig. 2B), the oxidation of DPNH in the TTP incubation is considerably retarded, whereas in the TDP incubation the oxidation starts almost immedia-

* The baker's yeast was from Uppsala Ångkvarn Ltd., Sweden.

** A unit of enzyme is defined according to de la Haba *et al.*[12] as the amount of enzyme which gives an extinction change of 0.001 per min under the conditions of the assay.

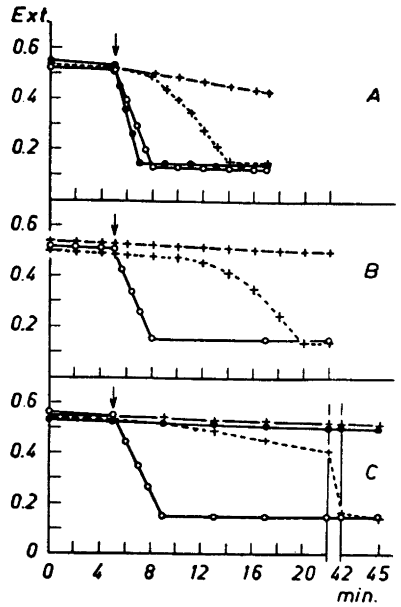

Fig. 2A. Effect of TDP and TTP on transketolase dialyzed for 48 h. The arrow indicates the addition of transketolase. TDP and TTP have been purified by paper chromatography as described in "Experimental".

+————+ no thiamine phosphate added
+– – – –+ 0.36 ml TTP (100 μg)
○————○ 0.11 ml TDP (100 μg)
●————● 0.36 ml TDP (327 μg)

B. Effect of the later addition of TTP and TDP. Transketolase is present from the beginning. The arrow indicates the point, when the thiamine phosphates are added. The designations of the curves are the same as in Fig. 2 A.

C. Effect of TTP, TDP and TMP on transketolase in the presence of thiamine. The arrow indicates the addition of the thiamine phosphates. 300 μg thiamine were added to each sample at the beginning of the incubation.

+————+ no thiamine phosphate added
+– – – –+ 0.36 ml TTP (100 μg)
●————● 0.30 ml TMP (100 μg)
○————○ 0.11 ml TDP (100 μg)

tely after the addition of TDP. This result gives further evidence for TTP being inactive as coenzyme in transketolase, and becoming active only after phosphatases have transformed it into TDP.

Westenbrink and van Dorp [17] have shown that yeast phosphatases acting on thiamine phosphates are strongly inhibited by thiamine. Thus addition of thiamine to the incubation mixture might prevent the decomposition of TTP to TDP. The results from an experiment are shown in Fig. 2C. It is seen that the complete oxidation of DPNH is effected at a much slower rate in

the presence of thiamine than in its absence when phosphatase activity is not inhibited. The oxidation rate in the presence of TDP is not noticeably affected by thiamine.

Fig. 2C also shows that TMP has no ability to replace TDP in this system.

Acknowledgements. I am indebted to Mrs. Margot Persson for skilful technical assistance in preparing the enzymes and performing the incubations. This work is part of investigations made possible by grants from the *Swedish Natural Science Research Council.*

REFERENCE

1. Rossi-Fanelli, A., Siliprandi, N. and Fasella, P. *Science* **116** (1952) 711.
2. Kiessling, K.-H. *Nature* **172** (1953) 1187.
3. Kiessling, K.-H. *Biochim. et Biophys. Acta* **20** (1956) 293.
4. Plotka, C., Peterfalvi, M., Jequier, R. and Velluz, L. *Am. J. Physiol.* **158** (1949) 279.
5. de la Fuente, G. and Diaz-Cadavieco, R. *Nature* **174** (1954) 1014.
6. Rossi-Fanelli, A., Siliprandi, N., Siliprandi, D. and Ciccarone, P. *Arch. Biochem. Biophys.* **58** (1955) 237.
7. Bartos, J. *Bull. soc. chim. biol.* **38** (1956) 429.
8. Kiessling, K.-H. *Acta Chem. Scand.* **10** (1956) 831.
9. Kiessling, K.-H. *Acta Chem. Scand.* **11** (1957) 917.
10. Greiling, H. and Kiesow, L. Z. *Naturforsch.* **11 b** (1956) 491.
11. Racker, E., de la Haba, G. and Leder, I. G. *J. Am. Chem. Soc.* **75** (1953) 1010.
12. de la Haba, G., Leder, I. G. and Racker, E. *J. Biol. Chem.* **214** (1955) 409.
13. Racker, E. *J. Biol. Chem.* **196** (1952) 347.
14. Viscontini, M., Bonetti, G. and Karrer, P. *Helv. Chim. Acta* **32** (1949) 1478.
15. Kiessling, K.-H. *Acta Chem. Scand.* **10** (1956) 1356.
16. Siliprandi, D. and Siliprandi, N. *Biochim. et Biophys. Acta* **14** (1954) 52.
17. Westenbrink, H. G. K. and van Dorp, D. A. *Enzymologia* **10** (1941/42) 212.

Received January 15, 1958.

ACTA CHEMICA SCANDINAVICA 12 (1958) 668—677

The Crystal Structure of Piperazinium Di-dichloroiodide

CHRISTIAN RØMMING

Universitetets Kjemiske Institutt, Blindern-Oslo, Norway

The crystal structure of piperazinium di-dichloroiodide, $C_4H_{10}N_2 \cdot 2(HCl \cdot ICl)$, has been determined by X-ray methods. The ICl_2^- ion, being linear but not symmetrical, has the configuration $Cl^- — I — Cl$ with the $Cl^- — I$ distance 2.69 Å and the $I — Cl$ distance 2.47 Å. The Cl^- is coordinated to three positive groups and one iodine atom in a distorted tetrahedral arrangement, the three $N^+ — Cl^-$ distances being 3.23 Å.

It has been known for a long time that addition compounds between an amine and one halogen molecule form compounds with one molecule hydrogen halide. In the course of an investigation carried out in this department of the former type of addition compounds [1] it was thought to be of interest to examine one of the hydrogen halide compounds. The choice of the present compound, piperazine with two molecules ICl and two molecules HCl added to it, was made because of its centrosymmetrical configuration.

Earlier structure determinations of this type of compounds include $NH_4 \cdot I_3$ [2], $NH_4 \cdot ClIBr$ [3] and $(CH_3)_4N \cdot ICl_2$ [4]. The structure of the trihalide ions is discussed by Hach and Rundle [5].

EXPERIMENTAL

Piperazinium di-dichloroiodide was prepared by adding a solution of iodine monochloride in hydrochloric acid to a hot solution of piperazine in water. After slow cooling to room temperature small yellow needle-formed crystals of the compound separated from the solution. Oscillation and Weissenberg photographs about two crystallographic axes were taken in order to determine the unit cell dimensions. The (0*kl*)-intensities were estimated visually from a set of Weissenberg films while the (*hk*0)-intensities were measured microphotometrically from photographs taken with a Wiebenga integrating Weissenberg camera. The crystals used had a cross-section of 0.10 × 0.10 mm. Copper $K\alpha$ radiation was employed (λ = 1.542 Å). 103 (0*kl*)-reflections out of 114 obtainable with this radiation and 113 (*hk*0)-reflections out of 131 possible were recorded. Absorbtion corrections were not applied.

CRYSTAL DATA

The crystals were found to be triclinic with the unit cell dimensions:

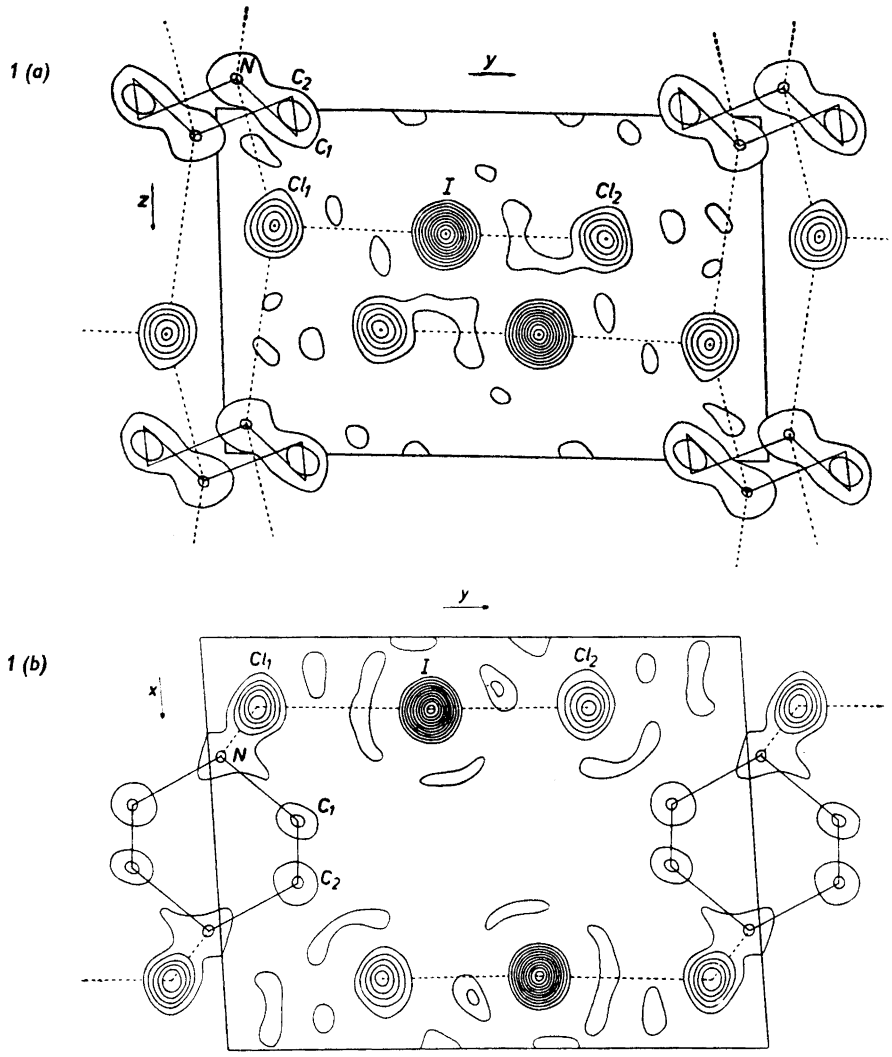

Fig. 1. Electron density projection along the *a*-axis (a) and c-axis (b). Contours at intervals of 5 e·Å^{-2}. Every second contour in the iodine peak is omitted.

a = 7.55 Å	b = 8.45 Å	c = 6.25 Å
α = 87.6°	β = 121.8°	γ = 84.4°

The figures given are believed to be accurate to within 0.5 % for the axial lengths and 0.5° for the angles.

The density was determined from flotation experiments and was found equal to 2.33 g/cm^3. With one molecule in the unit cell the calculated density is 2.38 g/cm^3.

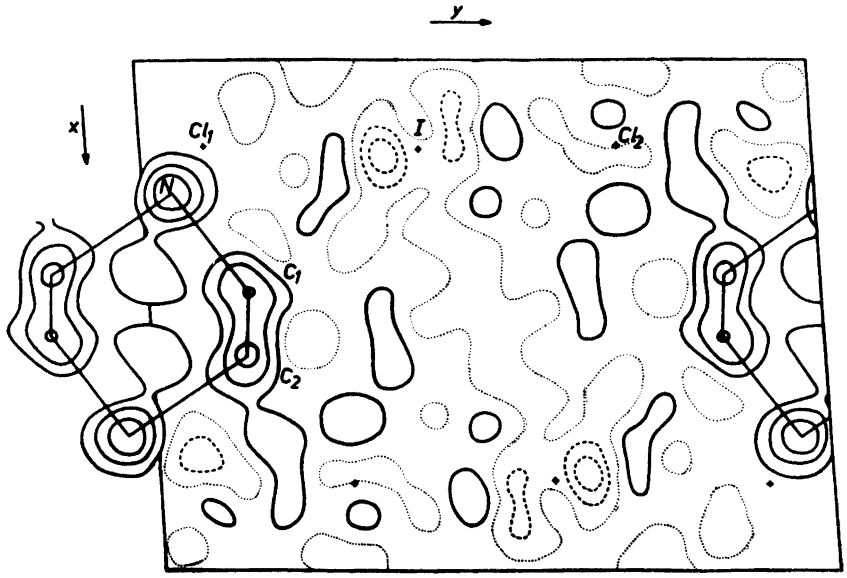

Fig. 2. ($F_o - F_{hal}$) projection along the *c*-axis. Contours at intervals of 2 e.Å^{-2}. Negative contours are broken and zero contour dotted. The halogen positions are indicated by crosses.

The space group P$\bar{1}$ was assumed to be the correct one as a centre of symmetry has previously been observed to exist in the piperazine ring, suggesting a symmetrical distribution of the (HCl.ICl) groups with respect to the two nitrogen atoms.

THE STRUCTURE DETERMINATION

Projection along the c-axis. Approximate x and y parameters for the iodine atom were determined by inspection of the (h00)- and (0k0)-reflections, and the signs for the structure factors based on these parameters were evaluated. A preliminary Fourier synthesis resulted in an electron density map showing well separated peaks for the iodine and the two chlorine atoms in the asymmetric unit. The position of the piperazine ring around the symmetry centre in (0,0) was also roughly indicated. After two refinements the electron density map of Fig. 1(a) was obtained, showing the halogen and nitrogen positions, whereas the two carbon atoms are too close together to be resolved as separate peaks.

Projection along the a-axis. The determination of this projection was carried out independently, using the same methods. The Fourier map obtained after three refinements is given in Fig. 1(b), showing all the atoms as separate peaks. The termination of series error introduces positive areas around the heavy atoms, and this effect is seen to have some influence on the position of the nitrogen peak. In order to find more precise parameters for this atom

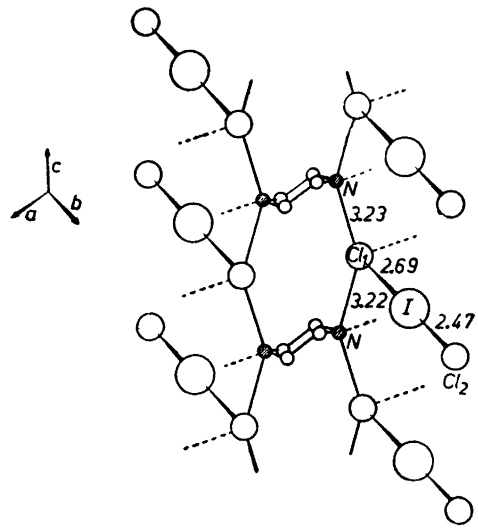

Fig. 3. Structure of piperazinium di-dichloroiodide. The figure shows a few of the units in a chain of piperazinium ions and ICl_2^- ions along the *c*-axis. The broken lines indicate the bonds between neighbouring chains. Bond lengths are in Å units.

a (F_0—F_{hal}) synthesis [6] was carried out, F_0 is the observed structure factor and F_{hal} is the contribution to the calculated structure factor from the halogen atoms alone. The difference map is given in Fig. 2. The nitrogen atom is now closer to the Cl_1 atom, but the positions of the carbon atoms remain nearly the same as before. The gradients at the halogen positions are too small to indicate any adjustments of the parameters.

The *y* parameters found for the halogen atoms in the two projections agree to within 0.001 of the axial length. For the nitrogen atom the difference is 0.006. The *z* parameters for the carbon atoms were calculated using *x* and *y* parameters found in the (F_0—F_{hal}) synthesis and assuming the carbon-carbon distance across the ring through the symmetry centre to be 1.90 Å. The atomic coordinates are given in Table 1.

Table 1. Atomic coordinates as fractions of the cell edges.

Atom	*x*	*y*	*z*
I	0.177	0.416	0.362
Cl_1	0.169	0.099	0.341
Cl_2	0.168	0.709	0.366
N	0.277	0.040	−0.086
C_1	0.455	0.148 *	0.082 *
C_2	0.582	0.140 *	−0.036 *

* The mean value of the *y* and calculated *z* parameters are 0.144 and 0.023, respectively, whereas the common maximum in the *a*-projection has the parameters 0.140 and 0.017.

Table 2. Bond lengths in trihalide ions.

Compound	Bond type	Bond length	Sum of covalent radii	Reference
NH_4ClIBr	I—Cl	2.38 Å	2.32 Å	3
	I—Br	2.50 Å	2.47 Å	3
$(CH_3)_4NICl_2$	$I—Cl_1$	2.34 Å	2.32 Å	4
	$I—Cl_2$	2.34 Å	2.32 Å	4
$PICl_6$	$I—Cl_1$	2.36 Å	2.32 Å	10
	$I—Cl_2$	2.36 Å	2.32 Å	10
NH_4I_3	$I_1—I_2$	3.10 Å	2.66 Å	2
	$I_2—I_3$	2.82 Å	2.66 Å	2
CsI_3	$I_1—I_2$	3.04 Å	2.66 Å	11
	$I_2—I_3$	2.86 Å	2.66 Å	11
$C_4H_{12}N_2 \cdot 2ICl_2$	$I—Cl_1$	2.69 Å	2.32 Å	Present examination
	$I—Cl_2$	2.47 Å	2.32 Å	

Observed and calculated structure factors are listed in Table 3. For the 12 largest (marked with an asterisk) the observed values are seen to be considerably lower than the calculated ones. This effect is thought to be mainly due to extinction, and these reflections are therefore disregarded in the calculation of the reliability index and the (F_0—F_{hal}) synthesis. They are, however, included in the estimations of the standard deviations.

For the different atoms the following B values in the temperature factor exp ($-B \sin^2\Theta / \lambda^2$) were used:

($0kl$)- reflections: $B_I = 2{\cdot}0$ Å^2; $B_{Cl} = 2.5$ Å^2; $B_{N \text{ and } C} = 3.0$ Å^2
($hk0$)-reflections: $B_I = 1{\cdot}5$ Å^2; $B_{Cl} = 2.0$ Å^2; $B_{N \text{ and } C} = 2.5$ Å^2

The atomic scattering factors given in *Internationale Tabellen* [7] were used in the calculations. The reliability index R is 0.11 for the ($0kl$)-reflections and 0.12 for the ($hk0$)-reflections.

Estimates of the standard deviations [8] for the halogen positions were as follows:

I: $\sigma(x) = 0.002$ Å; $\sigma(y) = 0.003$ Å; $\sigma(z) = 0.003$ Å
Cl: $\sigma(x) = 0.008$ Å; $\sigma(y) = 0.012$ Å; $\sigma(z) = 0.010$ Å

The standard deviation for the nitrogen coordinates is 0.06 Å.

DESCRIPTION AND DISCUSSION OF THE STRUCTURE

The crystal may be regarded as being built up of chains running parallel to the c-axis, as shown in Fig. 3. In every chain piperazinium ions alternate with ICl_2^- ions. In such a chain a chlorine atom like Cl_1 is coordinated to *two* equivalent nitrogens. The nitrogen and Cl_1 atoms in one chain are coordinated to Cl_1, respectively nitrogen atoms in a neighbouring chain to form a net paral-

Table 3. Observed and calculated structure factors. The given values are one half of the absolute values. F_0's suffering from extinction are marked with an asterisk.

hkl	F_0	F_c	*hkl*	F_0	F_c
100	29.1	26.6	031	37.0 *	−44.9
200	31.5 *	−38.8	032	37.5	47.9 *
300	39.0	−53.8 *	033	14.8	−16.4
400	13.3	−13.0	034	15.4	−15.4
500	23.2	25.0	035	19.4	22.0
600	24.1	26.5	036	14.8	−14.3
700	8.3	6.0			
800	13.3	−16.5	03$\bar{1}$	28.0 *	36.0
			03$\bar{2}$	28.6 *	−47.7
010	13.7	−22.5	03$\bar{3}$	15.4	17.1
020	14.8	18.1	03$\bar{4}$	6.8	7.0
030	2.9	2.5	03$\bar{5}$	20.5	−19.4
040	23.4	−23.0	03$\bar{6}$	12.0	12.9
050	11.4	11.8			
060	30.2	−29.1	041	31.4	35.2
070	26.2	26.4	042	23.4	−22.5
080	12.5	− 8.8	043	< 3.4	1.1
090	< 3.4	− 1.3	044	13.7	14.4
0.10.0	12.0	9.7	045	12.5	−14.0
			046	3.4	5.9
001	23.0 *	−35.3			
002	5.1	− 6.3	04$\bar{1}$	14.8	−14.5
003	40.9	42.3	04$\bar{2}$	26.8	27.6
004	30.8	−32.9	04$\bar{3}$	27.4	28.1
005	7.4	6.2	04$\bar{4}$	< 3.4	2.6
006	9.7	9.2	04$\bar{5}$	8.6	10.5
			04$\bar{6}$	13.7	13.7
011	16.5	16.8			
012	19.4	21.6	051	17.1	−16.0
013	20.5	−22.4	052	13.7	12.6
014	10.8	12.4	053	3.4	4.2
015	< 3.4	− 0.7	054	9.7	−10.1
016	8.6	− 7.4	055	8.0	9.6
			056	2.9	− 3.1
01$\bar{1}$	30.2 *	46.7			
01$\bar{2}$	6.8	− 8.4	05$\bar{1}$	2.9	− 0.1
01$\bar{3}$	12.5	−13.2	05$\bar{2}$	16.0	−13.4
01$\bar{4}$	24.5	21.6	05$\bar{3}$	10.3	9.4
01$\bar{5}$	15.4	−15.6	05$\bar{4}$	5.7	− 6.4
01$\bar{6}$	< 2.8	− 0.9	05$\bar{5}$	4.6	− 1.9
021	6.3	8.2	061	19.4	19.3
022	19.4	−20.3	062	12.0	11.3
023	16.5	20.1	063	20.5	−21.5
024	6.3	− 5.6	064	17.1	18.7
025	8.5	− 7.9	065	< 2.8	− 3.1
026	9.1	11.1			
			06$\bar{1}$	23.9	21.3
02$\bar{1}$	20.0	−21.6	06$\bar{2}$	< 3.3	1.9
02$\bar{2}$	12.0	15.6	06$\bar{3}$	18.2	−17.7
02$\bar{3}$	< 2.8	− 1.3	06$\bar{4}$	14.8	15.0
02$\bar{4}$	12.5	−10.0	06$\bar{5}$	4.0	− 5.5
02$\bar{5}$	8.6	8.9			
02$\bar{6}$	3.4	− 6.5			

hkl	F_o	F_c
071	< 3.4	1.6
072	17.7	−15.7
073	21.1	20.7
074	6.8	− 8.3
075	4.0	− 3.3
07$\bar{1}$	32.5	−25.1
07$\bar{2}$	14.3	12.4
07$\bar{3}$	8.6	8.0
07$\bar{4}$	17.1	−17.2
07$\bar{5}$	10.3	12.3
081	3.4	1.0
082	9.1	9.3
083	10.8	−10.1
084	6.8	5.8
08$\bar{1}$	16.5	12.2
08$\bar{2}$	5.1	− 5.9
08$\bar{3}$	< 2.8	− 1.6
08$\bar{4}$	7.4	6.6
091	11.4	11.1
092	14.8	−13.9
093	5.7	5.7
094	3.4	5.5
09$\bar{1}$	13.7	−11.2
09$\bar{2}$	12.5	11.0
09$\bar{3}$	4.0	− 5.2
0.10.1	17.7	−16.5
0.10.2	7.4	7.9
0.10.$\bar{1}$	< 2.2	0.2
0.10.$\bar{2}$	13.1	−13.1
110	24.1 *	−38.6
210	< 4.2	4.0
310	24.9	31.1
410	19.9	18.6
510	10.0	− 9.6
610	17.4	−17.6
710	8.3	− 6.5
$\bar{1}$10	5.8	− 2.8
$\bar{2}$10	22.4	30.8
$\bar{3}$10	19.1	21.2
$\bar{4}$10	9.1	− 5.4
$\bar{5}$10	17.4	−19.5
$\bar{6}$10	11.6	−11.3
$\bar{7}$10	8.3	8.7
120	21.6	24.5
220	< 3.3	1.0
320	13.3	−14.1
420	15.8	−16.7
520	< 5.8	− 2.1
620	14.9	16.7
720	9.1	8.4
$\bar{1}$20	8.3	−10.3
$\bar{2}$20	21.6	−26.8
$\bar{3}$20	7.5	− 6.6
$\bar{4}$20	11.6	15.1
$\bar{5}$20	15.8	13.2
$\bar{6}$20	< 6.6	− 1.2
$\bar{7}$20	6.6	− 7.9
130	31.5 *	−47.9
230	36.5 *	−50.7
330	9.1	7.3
430	34.0	36.0
530	21.6	22.6
630	< 6.6	− 4.4
730	19.9	−21.0
$\bar{1}$30	39.8 *	58.7
$\bar{2}$30	25.7	33.7
$\bar{3}$30	11.6	− 9.6
$\bar{4}$30	25.7	−35.0
$\bar{5}$30	19.1	−20.6
$\bar{6}$30	7.5	8.7
$\bar{7}$30	19.1	19.8
140	18.3	20.8
240	27.4	34.2
340	15.8	15.6
440	18.3	−19.1
540	26.6	−24.5
640	< 5.8	− 3.2
740	13.3	13.3
$\bar{1}$40	28.2	−32.3
$\bar{2}$40	15.8	−16.1
$\bar{3}$40	17.4	20.3
$\bar{4}$40	23.2	25.9
$\bar{5}$40	< 6.6	3.0
$\bar{6}$40	11.6	−13.7
$\bar{7}$40	12.5	−13.8
150	11.6	− 9.1
250	15.8	−18.2
350	5.6	− 6.5
450	9.1	9.1
550	13.3	12.8
650	< 5.8	4.3
750	5.8	− 7.0
$\bar{1}$50	19.9	19.2
$\bar{2}$50	< 5.8	− 0.7
$\bar{3}$50	14.1	−12.5
$\bar{4}$50	9.1	− 7.7
$\bar{5}$50	5.8	2.7
$\bar{6}$50	8.3	8.4

hkl	F_o	F_c	*hkl*	F_o	F_c
160	23.2	−21.6	180	17.4	−14.4
260	18.3	18.0	280	< 6.6	1.4
360	26.6	28.5	380	14.9	12.5
460	10.0	8.5	480	10.0	9.6
560	15.8	−14.1	580	< 5.0	− 2.3
660	18.3	−18.2			
			$\bar{1}80$	< 6.6	5.2
$\bar{1}60$	11.6	−10.8	$\bar{2}80$	14.1	12.4
$\bar{2}60$	20.8	19.9	$\bar{3}80$	8.3	4.8
$\bar{3}60$	24.9	24.2	$\bar{4}80$	5.8	− 5.4
$\bar{4}60$	8.3	5.0			
$\bar{5}60$	14.1	−14.8	190	15.8	14.8
$\bar{6}60$	16.6	−15.3	290	15.8	14.6
			390	< 5.0	− 1.9
170	26.6	25.6	490	15.8	−13.9
270	< 6.6	2.3	590	8.3	− 8.9
370	22.4	−22.6			
470	20.8	−20.2	$\bar{1}90$	15.8	−18.8
570	< 5.8	2.3	$\bar{2}90$	11.6	−12.0
670	14.1	16.5	$\bar{3}90$	< 4.1	4.1
$\bar{1}70$	9.1	− 6.1	1.10.0	< 5.0	− 5.2
$\bar{2}70$	26.6	−25.3	2.10.0	21.6	−18.9
$\bar{3}70$	19.9	−17.5	3.10.0	11.6	− 9.5
$\bar{4}70$	6.6	7.7			
$\bar{5}70$	20.8	19.2	$\bar{1}.10.0$	21.6	19.1

lel to the *a*-*c* plane. The bonds between the chains are indicated in Fig. 3 by broken lines. The ICl_2^- ions are linear and their direction approximately normal to the net. In Fig. 4 is shown a projection of the structure along the chain axis (*c*-axis), the broken lines here too indicating the bonds between the chains.

Cl_1 is surrounded by three nitrogens and one iodine atom in a distorted tetrahedral arrangement. The distance to the nitrogen atoms are 3.22 Å, 3.23 Å and 3.25 Å, respectively, as indicated in the figures. The angles N-Cl_1-N are 152°, 122° and 122° and the angles N-Cl_1-I are 102°, 95° and 120°. The Cl_1-N distances are somewhat shorter than the distance found in ammonium chloride (3.35 Å), but are equal to the shortest Cl-N distance observed in ammonium chlorobromoiodide [3].

As may be seen from Fig. 4 the distance between the Cl_2 atom in one net and the Cl_1 atom in the next one is only 3.29 Å and the shortest I—I separation is 4.06 Å while the sum of the van der Waals radii as given by Pauling [9] are 3.60 Å and 4.30 Å, respectively. These short intermolecular distances indicate a comparatively strong interaction between the nets, and the forces here are probably mainly responsible for the packing of the nets along the *b*-axis into the three dimensional lattice. All other intermolecular distances are found to be larger than the sums of the van der Waals radii.

The N—N′ distance across the piperazine ring as calculated from the coordinates given above is 2.94 Å which is close to the expected value.

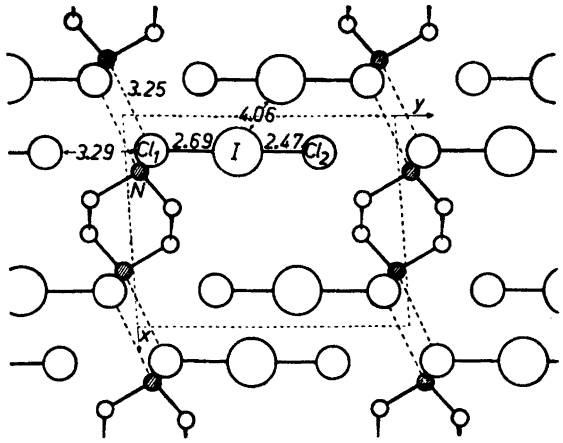

Fig. 4. The structure as seen along the chain axis. The broken lines denote the connection between the chains as in Fig. 3. Distances are in Å units.

The three halogen atoms form a linear $(Cl—I—Cl)^-$ ion which, however, is unsymmetrical, the Cl_1-I distance being 2.69 Å and the I-Cl_2 distance 2.47 Å. Since the standard deviation for the Cl-I distance is only 0.012 Å the difference between the two distances is certainly significant. Both of the I-Cl distances are substantially larger than the sum of the covalent radii [9] (2.32 Å), and also larger than the distances found in earlier examinations of the ICl_2^- ion. The halogen-halogen distances so far determined in X-ray examinations of trihalides are listed in Table 2.

Since the Cl_1 atom is surrounded closely by the positive ammonium groups while the distance from Cl_2 to the nearest nitrogen is 4.30 Å it seems very probable that Cl_1 carries a negative charge. The present ion is more analogous to the I_3^- ion than to the earlier examined ICl_2^- and $ClIBr^-$ ions as may be seen from Table 2.

It appears natural to describe the present ion as an addition complex between an electron donor (Cl^-) and an electron acceptor (ICl) and to suggest that the bond is of the same type as in the addition compounds between amines and halogens [1]. The I-Cl distance in pyridine · ICl is thus very nearly the same as in the present Cl^--I-Cl ion, and it may also be mentioned that the I-I distance found in the addition compound between benzyl sulphide and I_2 [1] corresponds closely to the shorter one in the I_3^- ion.

The author wishes to express his sincere thanks to professor Odd Hassel for his help and very kind interest in this work. The investigation has been supported by *The Rockefeller Foundation.*

REFERENCES

1. Hassel, O. *Proc. Chem. Soc.* **1957** 250.
2. Mooney, R. C. L. *Z. Krist.* **90** (1935) 143.
3. Mooney, R. C. L. *Z. Krist.* **98** (1938) 324.

4. Mooney, R. C. L. *Z. Krist.* **100** (1939) 514.
5. Hach, R. J. and Rundle, R. E. *J. Am. Chem. Soc.* **73** (1951) 4321.
6. Cochran, W. *Acta Cryst.* **4** (1951) 81.
7. *Internationale Tabellen zur Bestimmung von Kristallstrukturen*, Gebrüder Borntraeger, Berlin 1935.
8. Cruickshank, D. W. J. *Acta Cryst.* **2** (1949) 65.
9. Pauling, L. *The Nature of the Chemical Bond*, Cornell University Press, New York 1948.
10. Zelezny, W. F. and Baenziger, N. C. *J. Am. Chem. Soc.* **74** (1952) 6151.
11. Tasman, H. A. and Boswijk, K. H. *Acta Cryst.* **8** (1955) 59.

Received January 4, 1958.

ACTA CHEMICA SCANDINAVICA 12 (1958) 678—683

On the Photo-transformation of Ergot Alkaloids
II. Lumilysergic Acids

HANS HELLBERG

Chemical Department, State Pharmaceutical Laboratory, Stockholm, Sweden

The preparation of the four theoretically possible lumilysergic acids is here reported together with a description of the physical properties of these substances such as the appearance of crystals, optical rotation, light absorption, pK_a-values. A scheme for the identification of the acids by paper chromatography has been elaborated. Finally the stereochemical connections between the lumiacids on one hand and the lumialkaloids and the dihydroalkaloids on the other have been discussed and established with rather great probability.

Several series of lumiergot alkaloids are known today and there are good reasons for assuming that all their members derive from the four theoretically possible lumilysergic acids, which differ stereochemically at the atoms C_8 and C_{10} [1,2]. Stoll and Schlientz [1] have described the preparation of lumilysergic acid I, and — as preliminarily reported [3] — we have now succeeded in preparing all four acids.

Paper chromatography was used for the identification of the lumilysergic acids. The first method was taken over from our previous work on the lumiergometrins [2]. It works with an acetic acidic aqueous phase and is here called "the acidic method". The main feature of the second method is the ammoniacal water phase, and it is therefore referred to as "the ammoniacal method".

Already in experiments on a micro scale, the products being identified only by paper chromatography, did we find four lumilysergic acids (Table 1). For a logical discussion we may provisionally denote them as A, B, C and D. In the acidic method the acids B and C do not differ in R_F-values, and in the ammoniacal method the difference between the R_F-values for A and D is too small to be of use for the purpose of identification. But used in combination the two methods give a fairly reliable identification of the lumilysergic acids.

The preparation of the lumiacids took place both by irradiation of lysergic and *iso*lysergic acids in acidic solution, and by alkaline hydrolysis of lumialkaloids. The products were separated by partition chromatography on kieselguhr (celite) with the solvents from the methods on paper but in somewhat changed proportions. Details are given in the experimental part, but the results may be summarized as follows: —

Irradiation (acidic solution)

Lysergic acid → A + C (traces)
*Iso*lysergic acid → B + A (small quantity) + C (small quantity) + D (traces).

Hydrolysis (KOH in 50 % ethanol, boiling 1 $^1/_2$ h)

Lumiergocristine I → A + B
Lumiergocristinine II → C + D

Thus the irradiation of lysergic acid gave an almost pure lumiacid in conformity with the behaviour of the alkaloids derived from lysergic acid. However, also *iso*lysergic acid gave one strongly dominating product, unlike its alkaloidal derivatives, which on irradiation give the two possible C_{10}-alternatives in measurable yields. The appearance here of the acids A + C in small quantities may at least partly be attributed to a transformation of *iso*lysergic acid into lysergic acid in the strongly acidic solution which was irradiated.

At the alkaline hydrolysis of both lumiergocristine I and lumiergocristinine II two acids were obtained in yields of comparable magnitude. However, the treatment of pure lumiacids with ethanolic KOH under the conditions of hydrolysis used did not cause any transformation detectable even by paper chromatography, and so the transformation occurring during the hydrolysis of the lumialkaloids must be coupled with the hydrolytic cleavage. Very probably it is an epimerization at C_8. According to Stoll *et al.*[4] the same treatment of the analogous dihydroalkaloids leads to only one acid in each case. In the main this could be confirmed by us on paper chromatograms for dihydroergotamine I and dihydroergocristine I. Thus there seems to be a distinct difference between lumialkaloids and dihydroalkaloids in their ability to epimerize at C_8 on alkaline hydrolysis.

The stereochemical connections of the lumilysergic acids to lumialkaloids and dihydroalkaloids can, to begin with, be discussed on the basis of the preparative experiments made. If we postulate that the hydrolytic decomposition leads to an epimerization at C_8, the lumiacids A and B must be denoted as I while C and D must be assigned the figure II. From the results of the irradiation of lysergic acid it may be concluded that A is lumilysergic acid I. Then B must be lumi*iso*lysergic acid I, which is not contrary to the results of the irradiation of *iso*lysergic acid. The appearance of C and D, respectively, at the irradiation of lysergic and *iso*lysergic acid, respectively, indicates that C is lumilysergic acid II and D lumi*iso*lysergic acid II.

The connections thus made probable are corroborated by a comparison of the R_F-values obtained by the acidic methods for lumialkaloids in the first paper of this series [2] and for lumiacids in this paper (Table 1). Using the same provisional nomenclature as in Ref.[2] * the scheme given there may be extended as follows:

* α denotes the slower and β the faster component of a pair of substances, probably having the same steric configuration at C_8.

Table 1. Paper chromatography of lumilysergic acids (see experimental part).

	R_F	
	Acidic method	Ammoniacal method
Lumilysergic acid I (= substance A)	0.39	0.16
Lumi*iso*lysergic acid I (= substance B)	0.32	0.41
Lumilysergic acid II (= substance C)	0.32	0.06
Lumi*iso*lysergic acid II (= substance D)	0.48	0.18

α-lumi-ine = lumi-ine II ; lumilys.acid II = α-lumilys.acid.
β-lumi-ine = lumi-ine I ; lumilys.acid I = β-lumilys.acid.
α-lumi-inine = lumi-inine I ; lumi*iso*lys.acid I = α-lumi*iso*lys.acid
β-lumi-inine = lumi-inine II; lumi*iso*lys.acid II = β-lumi*iso*lys.acid

Also a glance at those lumialkaloid and lumiacid pairs which are supposed here to be sterically similar at C_{10} reveals a corresponding regularity, possibly with one weak point, *viz.* the lumiergometrine I and the lumiergometrinine I, which show approximately identical R_F-values.

Finally reference may be made to the tentative discussion of the same sterical connections which appeared in the former paper of this series [2], where from an argument entirely different from those of this paper the same allotment of configurations was obtained.

EXPERIMENTAL

A. Paper chromatography

The acetic acid method has been described in the first paper of this series [2].

The ammoniacal method was performed in a very similar way, the main difference being that the acetic acid was exchanged for ammonia. The solvent mixture had the following definite composition: Benzene, butanol, 2 M ammonia (1:3:4).

In Table 1 there are collected the average R_F-values of the lumilysergic acids, obtained with both methods.

B. Preparation of the lumilysergic acids

Irradiation of lysergic acid. A solution of 0.75 g of crystallized lysergic acid ($[\alpha]_D^{20}$ = +43°; c = 1 in pyridine) in 30 ml of 0.2 M HCl, kept air-free by a stream of N_2, was irradiated in a quartz flask until transformation ceased. (Time: ca. 3 h with a Hanovia S-4 U.V.-lamp). The dark blue solution was made alkaline with 3 ml of 5 M ammonia and saturated with a stream of CO_2. Gradually a crystalline substance, corresponding paper-chromatographically to lumilysergic acid I (substance A) was precipitated. The crystallization was completed over-night in the refrigerator. The precipitate was redissolved in 50 ml of 0.2 M ammonia and precipitated again with CO_2. Yield: 0.25 g of a light grey substance. Before the determination of physical constants (Tables 1, 2 and 3)

Table 2. Summary of appearance and some physical properties of the lumilysergic acids (constants corrected to dry basis).

	Appearance	Heating on Kofler block	Optical rotation $[\alpha]_D^{20}$ $c = 0.5$ in 0.5 M HCl	Light Absorption E (1 %, 1 cm) in 0.1 M HCl
Lumilysergic acid I (substance A)	From water: Short pillars From methanol: Long needles, breaking up to short rods	Decomposition at 240°C	+ 38°	224 at 283 mμ (max.)
Lumi*iso*lysergic acid I (substance B)	From water: Conglomerate of thin plates	Melting and decomp. 185°–190°C	+ 47°	230 at 283 mμ (max.)
Lumilysergic acid II (substance C)	From water: Rectangular plates	Melting and decomp. ca. 190°C	+ 10°	228 at 284 mμ (max.)
Lumi*iso*lysergic acid II (substance D)	From methanol: Conglomerate of small apparently irregular crystals	Decomposition at 210°C	− 13°	205 at 281 mμ (max.)

and elementary composition the lumilysergic acid I was recrystallized from a great quantity of methanol. (Substance dried in a high vacuum at 140°C. Found: C 65.85; H 6.44; N 9.54; O 16.88. Calc. for $C_{16}H_{18}O_3N_2$ (286.34): C 67.12; H 6.34; N 9.78; O 16.76).

In the mother liquor of the first crystallization lumilysergic acid II (substance C) was identified by paper chromatography.

Irradiation of iso*lysergic acid.* 0.5 g of crystallized isolysergic acid ($[\alpha]_D^{20}$ between +260° and +270°; $c = 1$ in pyridine) dissolved in 7.5 ml of acetic acid and 20 ml of water was treated as the solution of lysergic acid. The irradiated solution was neutralized to pH 7 with ammonia and evaporated to dryness in a CO_2-atmosphere under reduced pres-

Table 3. Estimated pK_a-values for lysergic and lumilysergic acids. Water Solution. 22°C. (See experimental part.)

	pK_1	pK_2
Lysergic acid *	3.22	7.93
*Iso*lysergic acid *	3.12	8.57
Lumilysergic acid I	3.38	9.00
Lumi*iso*lysergic acid I	3.94	9.17
Lumilysergic acid II	3.42	8.33
Lumi*iso*lysergic acid II	3.38	9.20

* Ref.[5] reports the following figures (24°C): Lysergic acid $pK_1 = 3.19$. 3.44; $pK_2 = 7.96$, 7.68. *Iso*lysergic acid $pK_1 = 3.21$, 3.44; $pK_2 = 8.31$, 8.61.

sure. The residue, freed from the ammonium salts by sublimation at 60°C in a high vacuum, was subjected to partition chromatography. Column: 38 × 3.4 cm; 120 g of celite. Solvent mixture at the start: benzene, butanol, 2 M ammonia (1:1:2). The dominating fraction, lumi*iso*lysergic acid I (substance B) came out as the second peak. After changing the elutrient to the organic phase of the mixture benzene, butanol, 2 M ammonia (1:3:4) there were obtained two more small fractions. From the first of these ca. 20 mg of lumilysergic acid I (substance A) and from the second a few mg of lumilysergic acid II (substance C) were isolated. Lumi*iso*lysergic acid II (substance D) was identified paper-chromatographically in the liquid fraction containing lumilysergic acid I.

The main fraction, containing lumi*iso*lysergic acid I was evaporated in a vacuum (N_2-atmosphere). The residue, dissolved in 20 ml of 0.4 M ammonia, was filtered, neutralized with CO_2 and evaporated in a CO_2-atmosphere to a volume of ca. 2 ml. The lumi*iso*lysergic acid crystallized from the solution. The yield, 120 mg, was recrystallized once from water. Physical properties in Tables 1, 2 and 3. (Substance dried in a high vacuum at 80°C. Found: C; 67.00 H 6.44; N 9.83; O 16.52. Calc. for $C_{16}H_{18}O_3N_2$ (286.34): C 67.12; H 6.34; N 9.78; O 16.76).

Hydrolysis of lumiergocristine I. A solution of 1 g of crystallized lumiergocristine I ($[\alpha]_D^{20} = +17°$; $c = 1$ in pyridine) in 16 ml of M KOH in 50 % ethanol was boiled under reflux in an N_2-atmosphere for 1 1/2 h. After cooling most of the ethanol was evaporated in an N_2-atmosphere, and then the solution was saturated with CO_2 and evaporated to dryness in a CO_2-atmosphere, both distillations being made under reduced pressure. The residue was chromatographed as described in the former section, the elutrient being changed after lumi*iso*lysergic acid I *(v. supra)*. The second and the third fractions were dominating and contained lumi*iso*lysergic acid I (substance B) and lumilysergic acid I (substance A), respectively. After the removal of the solvent the residues were treated as described under the headlines "irradiation of isolysergic acid" and "irradiation of lysergic acid". The yields of crude crystalline material were 50 mg of lumi*iso*lysergic acid I and 95 mg of lumilysergic acid I. The recrystallized products were identified through the physical properties given in Tables 1, 2 and 3. They were not submitted to elementary analysis.

Hydrolysis of lumiergocristinine II. 0.45 g of lumiergocristinine II (pure according to the criteria given in Part I of this series; Ref.[2]) was hydrolyzed as described for lumiergocristine I. The reaction mixture was neutralized with CO_2 and evaporated under reduced pressure in a CO_2-atmosphere. The residue was extracted with 100 + 50 + 50 ml of absolute ethanol, the filtered extracts evaporated to dryness in an N_2-atmosphere under reduced pressure and submitted to partition chromatography. Column: 40 × 3.4 cm; 140 g of celite. Solvent mixture at the start: benzene, butanol and 20 % acetic acid (1:1:2). Two main fractions were obtained, the first one containing lumi*iso*lysergic acid II (substance D) and the second lumilysergic acid II (substance C). The fractions were evaporated to dryness.

The residue containing lumilysergic acid II was dissolved in 20 ml of 0.4 M ammonia. The solution was filtered, neutralized with CO_2 and evaporated in a CO_2-atmosphere to ca. 2 ml. The substance crystallized from this solution in a yield of 45 mg, and after recrystallization from water the material had the physical properties given in Tables 1, 2 and 3. (Substance dried in a high vacuum at 100°C. Found: C 67.20; H 6.36; N 9.51; O 16.56. Calc. for $C_{16}H_{18}O_3N_2$ (286.34): C 67.12; H 6.34; N 9.78; O 16.76).

The residue containing lumi*iso*lysergic acid II having been dissolved in a few ml of methanol, the substance crystallized. The yield was 55 mg. After recrystallization from methanol lumi*iso*lysergic acid II showed the physical properties given in Tables 1, 2 and 3. (Substance dried in a high vacum at 80°C. Found: C 66.63; H 6.59; N 9.90; O 16.90. Calc. for $C_{16}H_{18}O_3N_2$ (286.34): C 67.12; H 6.34; N 9.78; O 16.76).

C. Determination of protolytic constants

About 6 mg of the substance, dissolved in ca. 5 ml of CO_2-free water by the addition of ca. 0.25 ml of 0.1 N hydrochloric or methanesulphonic acid, were titrated potentiometrically with 0.02 N CO_2-free sodium hydroxide. The measuring system used (glass-electrode, calomel electrode, Radiometer PHM 3) was constantly and carefully calibrated by means

of pH-standards (M/20 potassium hydrogen phthalate and M/20 sodium borate). The temperature was 22°C. The first equivalence point of the acids could be fixed by a sufficient pH-change. From this value the volumes for half-neutralization in either direction were calculated, using the weight of substance taken, the molecular weight of the acids and the normality of the sodium hydroxide. Then the pK_a-values were read from the titration curve without further correction. The individual results obtained did not as a rule differ more than ± 0.05 pH-units from the averages given in Table 3. pK_a-values for the lysergic acids in aqueous solution have been determined by Craig *et al.*[5] Their figures, which do not seem to be very accurate, are not inconsistent with ours.

Acknowledgements. The elementary analyses were performed by Dr. Alfred Bernhardt, Max-Planck-Institut für Kohlenforschung, Mühlheim (Ruhr), which is gratefully acknowledged. My thanks are also due to *Statens Medicinska Forskningsråd* for financial support, and to Mrs M. Spilsbury, who revised the English.

REFERENCES

1. Stoll, A. and Schlientz, W. *Helv. Chim. Acta* **38** (1955) 585.
2. Hellberg, H. *Acta Chem. Scand.* **11** (1957) 219.
3. Hellberg, H. *Pharm. Weekblad* **93** (1958) 1.
4. Stoll, A., Hoffmann, A. and Petrzilka, Th. *Helv. Chim. Acta.* **29** (1946) 635.
5. Craig, L. C., Shedlovsky, Th., Gould, R. G. and Jacobs, W. A. *J. Biol. Chem.* **125** (1938) 289.

Received February 10, 1958.

ACTA CHEMICA SCANDINAVICA 12 (1958) 684—700

Interferometric Studies of Boundary Formation and Deviations from Ideality in Diffusion Experiments

OLOF BRYNGDAHL

Institute of Optical Reseach, The Royal Institute of Technology, Stockholm 70, Sweden

Various types of diffusion cells have been studied by means of the birefringence interference method especially with regard to the methods used for producing a sharp interface. This method, which is very sensitive to small concentration differences, was found to give valuable information concerning the beginning of the diffusion process. Thus, the boundary formation has been compared for different types of cells. The small influence of convection, in spite of the small concentration differences used, was quite remarkable. The various factors influencing ideality in diffusion experiments using the birefringence interference method on very dilute solutions have been discussed in some detail.

STUDIES ON BOUNDARY FORMATION IN DIFFUSION CELLS

Optical methods are of great value in the study of liquid diffusion because of their precision and the great amount of information which they yield. One of the main problems in arranging diffusion experiments is the formation of an initially sharp interface.

This problem has been solved in many different ways. Diffusion cells belonging to the types mentioned below have been designed specially for registration by optical methods.

The diffusion equation is usually solved using the initial condition that the solution and solvent are separated by a sharp interface in an infinitely long tube at $t = 0$. Turbulence and other disturbing phenomena arising from the boundary formation process must therefore be suppressed. Thus, the way in which the boundary is formed has proved to be of great importance, since this is decisive for the magnitude of the zero-time correction and the lapse of time after which the first measurements can be taken.

The magnitude of the concentration difference influences the ideality of the initial gradient. With decreasing concentration difference, the density gradient decreases and the disturbances arising from the formation process disappear more slowly. On working with very dilute solutions it is consequently important that the disturbing phenomena be minimized. It will be shown below that sharp interfaces can be formed using the boundary-sharpening technique [1] even with very small concentration differences.

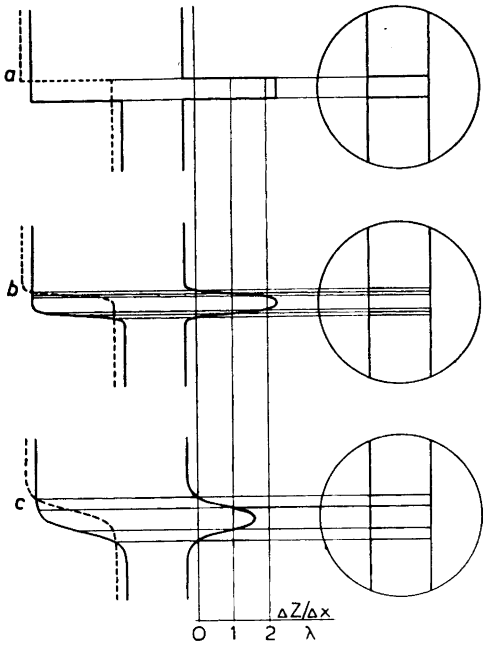

Fig. 1. (Left) The refractive index as a function of x for the concentration gradient. (Middle) The corresponding difference graph for the path differences between the two wave fronts produced by the Savart plate. (Right) The appearance of destructive interference in the object plane.

a) An ideal initial boundary gives rise to a concentration step which in this method is represented by a fringe pair.

b) At the beginning of the diffusion run, a record of the refractive index instead of its gradient is obtained because of the steepness of the concentration gradient.

c) As a rule, however, the photograph gives the derivative dn/dx directly due to the doubling of the wave front and no correction is necessary.

I. OPTICAL METHOD

The shearing interferometer utilizing birefringence interferences [2-4] and giving an image of the whole diffusion column is very sensitive to small concentration differences and is also suitable for the registration of rapid processes. Studies of the beginning of the diffusion process have been performed with this recording interferometric method, the optical arrangement of which has been described in an earlier paper [4].

By placing a birefringent double crystal plate (Savart plate) in parallel light behind the cell in the optical arrangement, a doubling of the wave front (representing the concentration curve) is effected (Fig. 1). If the crossed polarizers have their oscillation planes at 45° with respect to the principal planes of the Savart plate, the light is extinguished at those points where the optical path difference between the wave fronts is a whole number of wave lengths [4]. From Fig. 1a it is evident that an ideal boundary formation is represented

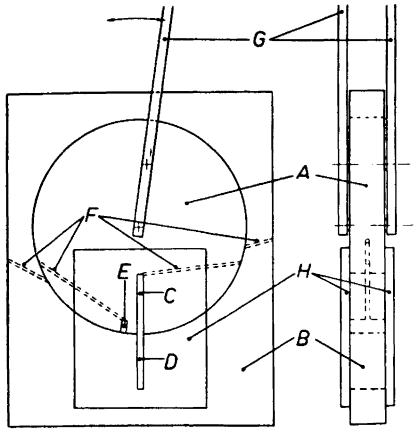

Fig. 2. Diffusion cell. By means of a lever *G* it is possible to turn the inner disk *A* until the two halves of the diffusion column *C* and *D* coincide. In this way the boundary will be formed and the diffusion started. The cell is tightened with silica lubricant at the glass plates *H* forming the walls of the diffusion cell.

by one horizontal fringe pair with a distance between the fringes equal to the displacement between the wavefronts. In Fig. 1 it is seen that at first the optical method gives a doubling of the integral curve and that later, when the refractive index gradient becomes broader, the method gives a record of the derivative dn/dx. Actually, the measurements give $\Delta n/\Delta x$ but the correction for obtaining the derivative can be easily calculated [2-4]. The correction is as a rule very small and can be neglected [2]. Only at the start of the diffusion has one to pay attention to the correction term. Hence, if no measurements are made at the beginning, the method becomes quite convenient.

II. DIFFUSION CELLS

In optical methods the following demands are made upon the diffusion cells:

a) plane parallel, transparent, homogeneous walls in the light direction,

b) a rectangular cross section to eliminate optical distortions,

c) uniformly thick diffusion column forming no wedge.

Thanks to Prof. O. Lamm and Dr. H. Svensson who kindly put diffusion cells at our disposal, a fairly complete examination could be performed and the different ways of producing boundary layers compared.

The types of cells commonly used and examined here can be classified in three groups according to the technique of boundary formation:

I "Draw-slide cell" — usually referred to as the Lamm cell. A slide separating solution and solvent is drawn out — two cells of this type [5] with thicknesses of 1 cm (*Ia*) and 5 cm (*Ib*) were studied.

II "Flowing-junction cell". The boundary is formed by allowing solution and solvent to flow out together through a narrow horizontal exit slit in the side wall of the cell [6-9]. The cell [6] examined here was 5 cm thick.

III "Sliding-solvent cell". In this cell the interface is formed by sliding the solvent over the solution [10-12].

After some unsuccessful experiments with cells of type *III* built according to descriptions found in the literature, the author decided to design a new cell of this type (Fig. 2). The material used was perspex, 1.2 cm thick. A circular disk *A* (diameter = 10 cm) was fitted into a corresponding hole in a plate *B*. Narrow slits *C* and *D* (3 mm) were cut and used as a diffusion column. A slit *E* was also cut for pouring in the bottom solution. Small channels *F* are bored to permit filling by means of a syringe. The boundary layer is formed by turning the disk until the slits *C* and *D* coincide.

III. REGISTRATION

In order to get a complete mapping of the phenomena arising from the boundary formation process, two different photographic registration methods have been used.

1. A registration of the whole of the cell plane was performed at equal time intervals. The time of exposure was about 1 sec.

2. A continuous registration of the interference pattern gives much information about the symmetry and various disturbing phenomena and their influence. A narrow vertical strip of the image plane was reproduced on a film attached to a continuously moving drum. A film speed of 3 cm/min was employed.

Ilford HPS film was used to attain a minimum of exposure.

IV. EXPERIMENTS

Monochromatic light (5 461 Å) was used in all experiments. The solutions, always with distilled water as solvent, were carefully thermostated at a temperature of about 21°C.

The following experiments were carried out:

Run	Solution diffusing against water	g/100 ml	Cell thickness in cm	Zero-time correction in sec	
Ia, 1 *	glycine	0.0942	1.0	29	Draw-slide cell
Ib, 1	sucrose	0.0503	5.0	22	
Ib, 2	sucrose	0.0503	5.0	18 (20)	
II, 1	sucrose	0.0500	5.0	4	Flowing-junction cell
II, 2	sucrose	0.0500	5.0	3	
III, 1	sucrose	0.2508	1.2	20	Sliding-solvent cell

V. RESULTS

In all cases the concentration was chosen so as to give rise to 3—5 fringe pairs at the beginning of the run.

* The first figure refers to the cell types described in Section II, and the last figure to the registration methods listed in Section III.

Run I a, 1

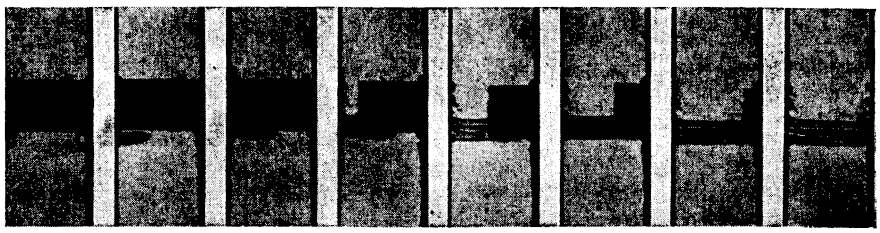

I. "Draw-slide cell"

Ia, 1. The registrations were performed at 6 sec intervals. From the recordings it is seen how a region of mixing is developed below the slide. If the dividing wall is withdrawn at a uniform speed, a sucking effect acts upon the liquid so that a sharp boundary is formed. It should be added that the zero-time point (starting point of the diffusion run) will generally occur in the period between when the slide starts to leave the cell wall and when it is completely removed from the diffusion column. The slide was 2 mm thick.

Ib, 1. The slide thickness here was 1 mm. A turbulent motion under the slide is also visible in this run. However, another phenomenon occurs - at the instant the slide leaves the cell wall a narrow beam of solution is forced up into the solvent layer. It spreads out at a definite height but sinks and disappears with time (*cf. Ib, 2*).

The influence of the slide velocity on the boundary formed has been examined. In the case of the 2 mm slide (*Ia*), only slow speeds (less than 0.2 mm/sec) are possible since turbulence sets in at higher speeds. A speed of 0.1 mm/sec gave a smooth symmetrical gradient and was found to be the

I b, 1

Run I b, 2

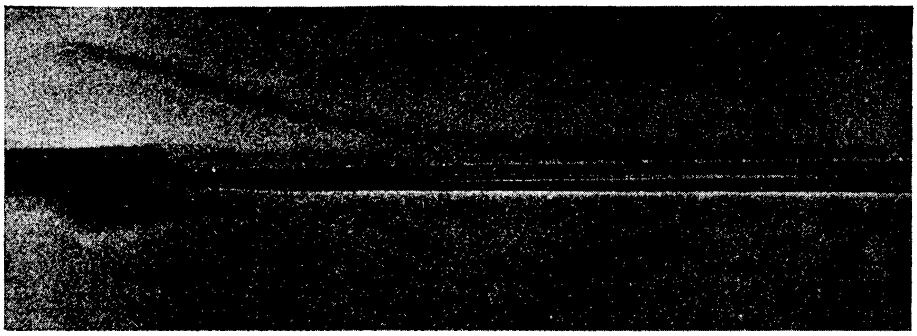

Run I b, 2

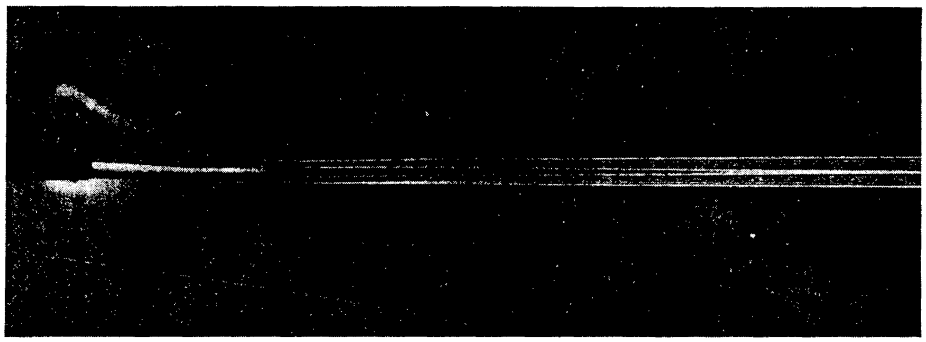

most suitable value. The cell with the 1 mm slide (*Ib*) gave a sharp boundary with a slide speed of 1 mm/sec. However, at this speed disturbing vibrations of the boundary occurred. The most satisfactory results were obtained with a value of about 0.2 mm/sec. The slide speed must not be too slow in order to avoid lateral skewness of the gradient.

Ib, 2. Two records showing the change in the interference pattern with time. Here the vanishing of the disturbing processes in clearly seen. The sharpness of the gradient is also apparent.

Run II, 1

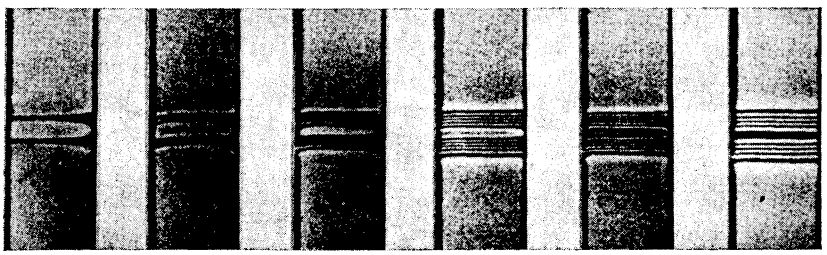

Run II, 2

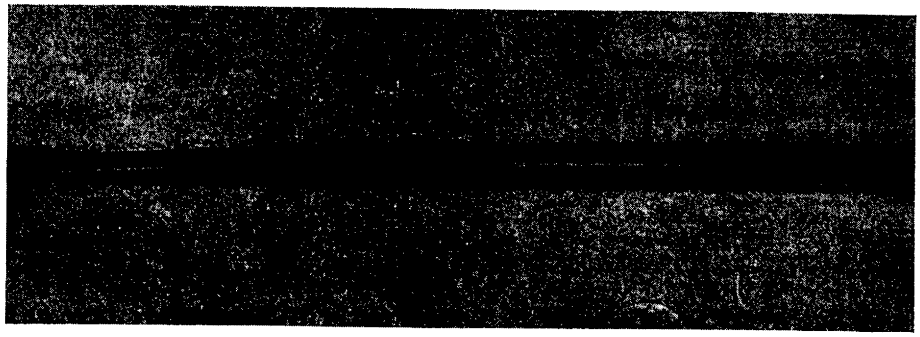

II. "Flowing-junction cell"

II, 1. The sharp gradient is obtained as a state of equilibrium. As is seen from the photographs, the boundary is sharper near the exit slit. The outflow rate considerably influences the symmetry of the gradient. The outflow was about one drop every two seconds. However, a continuous flow was obtained by placing the capillary outlet in a beaker of water. Different concentrations required different sized capillaries.

II, 2. No disturbances can be observed in this photograph. This cell gave the most ideal boundary obtained in this work. However, there is asymmetry due to incorrect focusing. This skewness of the gradient disappears if the camera is focused on a plane 1/3 of the cell thickness from the front wall [13].

III. "Sliding-solvent cell"

III, 1. This cell resembles cell type *I* but here the displacement of the upper column of liquid has been eliminated. The liquid column was moved with a speed of 0.3 mm/sec which was found to be the best one for this cell. Only small asymmetries along the gradient have been observed. Sharp boundaries were also obtained for very dilute solutions.

Run III, 1

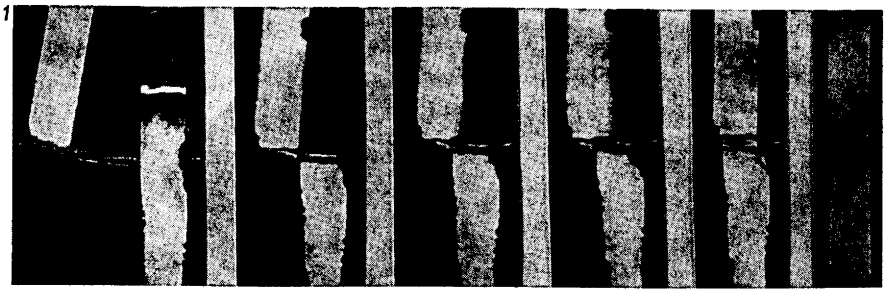

These experiments confirm the possibility of forming sharp interfaces between solutions with very small density differences. The boundary-sharpening technique works well without leaving any disturbing convections and no superimposed thermal gradient is necessary to increase the density gradient. As is seen from the photographs of the formation of the interfaces, *all* the cells examined work very well and can be used for precise measurements at the smallest concentration differences.

It would perhaps be worth while investigating the possibility of improving the boundary-sharpening technique further by equipping the cell with two outflow slits opposite each other. By varying the outflows through the two slits, the optimum conditions could be obtained (*i.e.* the outflows need not necessarely be equal).

DIGRESSION ON DEVIATIONS FROM IDEALITY IN DIFFUSION EXPERIMENTS

VI. THE EFFECT OF THE MAGNITUDE OF THE DENSITY DIFFERENCE ON THE FORMATION OF IDEAL GRADIENTS

It is possible to sharpen the boundary using a transient, superimposed thermal gradient. This procedure cannot be used when working with very dilute solutions since the time for the disappearance of the thermal gradient is comparable to the length of the run.

The values of the parameters, *e.g.* slide speed, outflow rate and pressure difference, have proved to be very critical when working with small concentration differences. The adjustment of the different parameters is easiest with the flowing-junction cell. Initially sharp boundary layers have been observed with the flowing-junction cell down to a concentration difference (sucrose solution) corresponding to an optical path decrement of about 1 000 Å.

One may ask how great a concentration difference is necessary to form a sharp interface. Convection caused by transient temperature gradients, which cannot be totally eliminated by good thermostating, must be prevented by a sufficiently large concentration gradient.

An estimate of the amount of convection produced can be obtained from Grashof's number * (Gr_1) and another dimensionless number (Gr_2) specifying the convection caused by a density gradient.

$$Gr_1 = \frac{l^3 g \gamma \Theta}{\nu^2}$$

$$Gr_2 = \frac{l^3 g \frac{1}{V}\left(\frac{\partial V}{\partial c}\right) \Delta c}{\nu^2 d}$$

The influence of the various parameters (l — characteristic length, Θ — temperature difference, Δc — concentration difference, ν — kinematic viscosity) on the convection can be obtained using these numbers.

* See, *e. g.*, *Lexikon der Physik*, H. Franke, Stuttgart 1950, p. 593.

The following notations are used: g — gravity, γ — thermal expansion coefficient, V — volume, c — concentration, ϱ — density of the solution.

$Gr_1 = Gr_2$ gives the concentration gradient necessary to counteract a transient thermal gradient (Θ).

$$\frac{\Theta}{\Delta c} = \frac{\partial V/\partial c}{V\gamma} = \frac{1}{\gamma}\frac{\partial \ln V}{\partial c} = -\frac{1}{\gamma}\frac{\partial \ln \varrho}{\partial c} \tag{1}$$

A rather trivial fact also apparent from Grashof's number is that the cell should be as narrow as possible if the convection is to be a minimum.

VII. ADVANTAGES OF PERFORMING DIFFUSION EXPERIMENTS WITH SMALL CONCENTRATION DIFFERENCES

Working with small concentration differences diminishes most of the problems pertaining to the non-linear relation between refractive index and concentration as well as to the concentration dependance of the diffusion coefficient.

The time necessary for performing a diffusion run by the birefringence interference method is greatly dependant upon the concentration difference. Small concentration differences make possible a saving of time and the use of smaller amounts of materials which may be difficult to obtain or purify.

With systems having a density maximum or minimum at a certain concentration, it is necessary to work in a range where the density-concentration curve is monotonic and this can always be achieved by working with very small concentration differences.

VIII. FACTORS DECISIVE FOR THE LENGTH OF TIME BEFORE MEASUREMENTS CAN BE PERFORMED

No measurements can be performed before the lapse of a sufficient period of time to allow:

1) disturbing processes arising from the shearing procedure to die out (see Section X, a),

2) the aberrations to decrease to 1/50 of a light wavelength (the critical time of diffusion of Svensson) [14].

However, even working with such low concentration differences as those here, the critical time is surprisingly small, about a few seconds, and can be left out of consideration. What sets a limit to measurements at the beginning of the diffusion process are consequently the disturbances arising from the formation of the boundary. It is difficult to give a strict mathematical treatment of this.

An intuitive conception may be conveyed by the following picture:

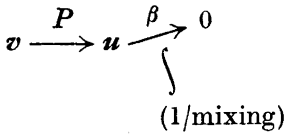

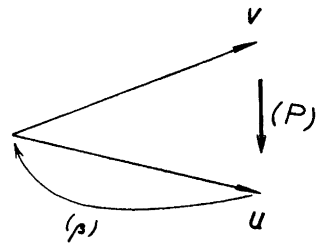

Fig. 3. Velocity field representation in *Hilbert space* l^2 (projected in two dimensions).

where v represents the velocity field of the liquid during the formation process, u the velocity field after closing the outflow or removing the slide and β = damping factor of the liquid. The extent of mixing is inversely proportional to β. P indicates a transformation (operator) of the velocity field in function space and β is related to the decay of the vector field u *. A "projection" of function space (Hilbert space) on the twodimensional subspace represented by the plane of the paper (Fig. 3) shows that the question — "How long will the decay of the turbulent field take?" — is answered as soon as the operator P and β can be formulated. A more detailed study of this question would be of great value in suggesting new ways for the further improvement of the cell construction.

* Let us denote the velocity of flow at a single point by v. v, which is a vector function of the position vector, can be expanded in an infinite series of mutually orthogonal vector functions $\bar{\varphi}_i$, satisfying the same boundary conditions as v:

$$v = \sum_{i=1}^{\infty} a_i \bar{\varphi}_i$$

Now, the functions v and $\bar{\varphi}_i$ can be regarded as elements of a so called Hilbert space. The infinite sequence

$$v = \{a_i\}_1^{\infty} \ (= \{a_1, a_2, a_3, \ldots, a_i, \ldots\}),$$

where the a_i are the same as above, is an element of another Hilbert space (l^2 called). It can be shown that there is a one to one correspondence between the two Hilbert spaces mentioned. In this way the whole of the velocity field v can be represented by a single point in Hilbert space. With the use of these concepts the kinetical energy of the streaming liquid may be regarded as a so called functional of points in Hilbert space:

$$\Phi = \Phi(v)$$

If on closing the outflow the velocity field v goes over into another velocity field, u, with the same energy,

then

$$\Phi(u) = \Phi(v),$$

and the transformation from v to u may be thought of as effected by an *operator*, P:

$$u = P\,v.$$

Thus, by an operator, a point of one Hilbert space is assigned to each point of another Hilbert space in a one to one fashion in exactly the same manner as an ordinary function $y = f(x)$ assigns a point on the y-axis to each point of the x-axis.

IX. ZERO-TIME CORRECTION

From the registrations it is evident that the smallest zero-time correction is obtained with the flowing-junction cell. Two principles for determining the zero-time correction are possible, namely

1) insertion of the real initial condition into Fick's law, and

2) extrapolation to zero time from the points obtained.

Our findings prove that the second method is the most reliable since all cell types show deviations from the ideal process during the first part of the run. Methods for obtaining the zero-time correction in these experiments are found in Ref.[4]

X. THE INFLUENCE OF DEVIATIONS FROM IDEALITY ON THE MEASUREMENTS

When studying free diffusion by measuring the refractive index gradient in the diffusion cell as a function of time, one has to take the following factors into consideration in order to obtain accurate measurements:

1) occasional skewness arising from the boundary formation process,

2) the Wiener skewness (an optical effect),

3) deviations from the linear relation between refractive index and solute concentration,

4) the concentration dependance of the diffusion coefficient,

5) deviations from ideality due to polydispersity or impure preparations.

a. Solution of Fick's equation with an asymmetrical initial condition. A skew gradient caused by the mechanical boundary formation process (occasional skewness) leads to the problem of solving Fick's second equation with an asymmetrical initial condition, *e.g.* of the form $c(\xi,0) = c_0(1-e^{-\xi/a})$ for $\xi>0$ and $c(\xi,0) = 0$ for $\xi<0$, where ξ is the coordinate in the diffusion direction and a is a parameter proportional to the amount of asymmetry.

The influence of the skewness on the measurements can be estimated by the solution of the diffusion equation with an unsymmetrical initial condition. The solution has the following form [15]

$$c(x,t) = \int_{-\infty}^{+\infty} \frac{1}{2\sqrt{\pi Dt}}\, e^{-\frac{(x-\xi)^2}{4Dt}}\, c(\xi,0)\, d\xi \qquad (2)$$

With $c(\xi,0) = c_0(1-e^{-\xi/a})\ U(\xi)$, where U is the "unit step function"

$$U(\xi) = \begin{cases} 1 \text{ for } \xi > 0 \\ 1/2 \text{ for } \xi = 0 \\ 0 \text{ for } \xi < 0 \end{cases}$$

we get

$$c(x,t) = \int_{0}^{\infty} \frac{c_0}{2\sqrt{\pi Dt}}\, e^{-\frac{(x-\xi)^2}{4Dt}}\, (1-e^{-\xi/a})\, d\xi \qquad (3)$$

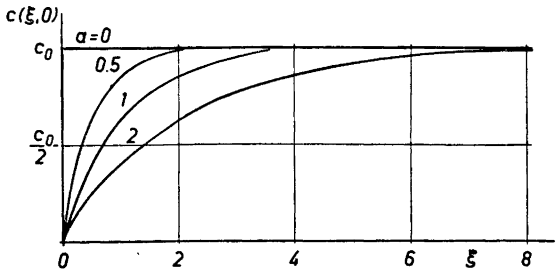

Fig. 4. Initially skew concentration distribution with the asymmetry parameter $a = 0$ (ideal distribution), 0.5, 1, and 2, respectively.

The solution can be written in the form

$$c(x,t) = \frac{c_0}{2}\left\{1 + \operatorname{erf}\left(\frac{x}{\sqrt{4Dt}}\right)\right\} - \frac{c_0}{2}\exp\left(\frac{Dt}{a^2} - \frac{x}{a}\right)\left\{1 - \operatorname{erf}\left(\frac{\sqrt{Dt}}{a} - \frac{x}{\sqrt{4Dt}}\right)\right\} \quad (4)$$

where the first term is the ordinary solution (for $c(\xi,0) = U(\xi)$) and the second term is the correction due to the skewness.

An asymptotic expansion of the expression for the correction term in (4) shows that the correction will approach zero for large values of t.

A quantitative estimation of the influence of an occasional skewness on the diffusion coefficient determined by the present method can be obtained as follows.

Derivation of (4) gives

$$\frac{\partial c(x,t)}{\partial x} = \frac{c_0}{2a}\exp\left(\frac{Dt}{a^2} - \frac{x}{a}\right)\left\{1 - \operatorname{erf}\left(\frac{\sqrt{Dt}}{a} - \frac{x}{\sqrt{4Dt}}\right)\right\} \quad (5)$$

In Fig. 4 the initial concentration distributions are shown for some values of the asymmetry parameter a. Fig. 5 shows the derivative curve for the same values of a.

In the method of evaluation described in Ref. [4] an unsymmetrical gradient will cause a small error in the measured value of $2x$ and accordingly in the diffusion coefficient *. Now a theoretical explanation of the appearance of the experimental curves in Figs. 8 and 11 of Ref.[4] is possible. In the neighbourhood of the inflexion point (see Fig. 5) an asymmetrical gradient will give too small a value of $2x$ while, on the other hand, measurements on the outermost fringe pairs correspond to the lower part of the Gaussian curve. Fig. 8 refers to measurements near the inflexion points and it is seen that the curves break down for small values of $(2x)^2$. In Fig. 11 too high a value for the

* The distances $2x$ between corresponding fringes in the interference pattern are measured. Following a definite fringe pair with time, we may plot $(2x)^2$ *vs.* t and the diffusion coefficient is then obtained from a value of $(2x)^2$ and its corresponding times t_1 and t_2 by the equation

$$D = \frac{(2x)^2(1/t_1 - 1/t_2)}{8 \ln t_2/t_1}$$

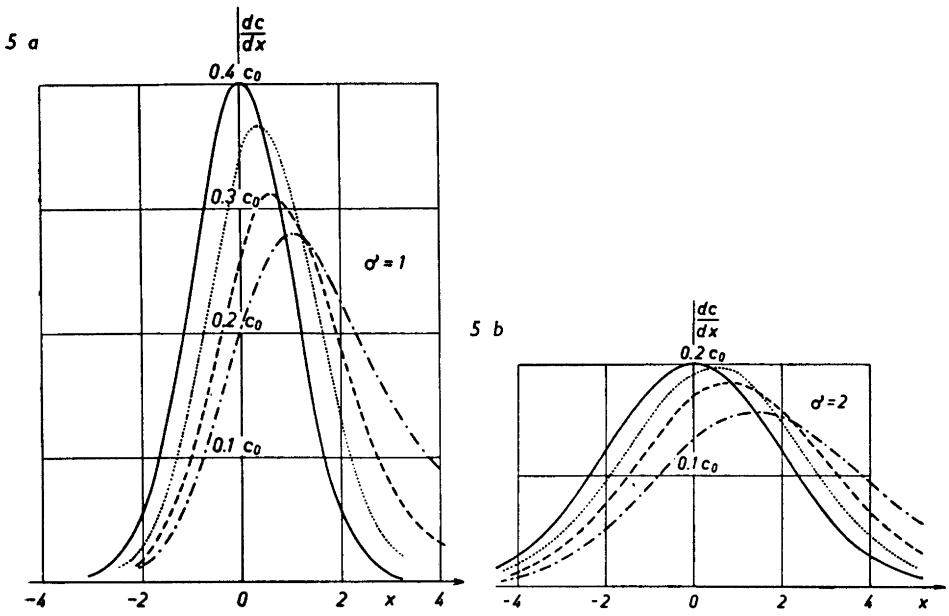

Fig. 5. dn/dx curves corresponding to the curves of Fig. 4 plotted for $\sigma = 1$ and 2, respectively ($\sigma = \sqrt{2Dt}$). —.—.— $a = 2$; — — — $a = 1$; . . . . . $a = 0.5$; ——— $a = 0$.

diffusion coefficient is obtained; here however, the corrections are not so large owing to a more ideal boundary formation, (*i.e.* a smaller zero-time correction).

Generally, measurements are performed in the neighbourhood of the inflexion points of the Gaussian curve, where $x = \sigma = \sqrt{2Dt}$. Knowing the slope at the inflexion points it is possible to estimate the error in the determination of $2x$, and from this an estimation of the error in D can be made, *viz.* $\Delta D/D = 2\Delta(2x)/2x$.

From Fig. 6 it is possible to obtain a convenient expression for the displacement (δ_+) of the fringes from the ideal curve.

With the notation of Fig. 6 we conclude

$$f(x_a) = f_0(x_i) \approx f(x_i) + (x_a - x_i)\ f'_0(x_i)$$

$$\text{and hence} \quad \delta_+ = x_a - x_i \approx \frac{f_0(x_i) - f(x_i)}{f'_0(x_i)} \tag{6}$$

for positive x-values and correspondingly for negative values of x.

$$\Delta(2x) = \delta_+ - \delta_- \text{ and hence} \qquad \frac{\Delta D}{D} = \frac{\delta_+ - \delta_-}{x}$$

From Fig. 7 $\Delta D/D$ can be read as a function of a and σ.

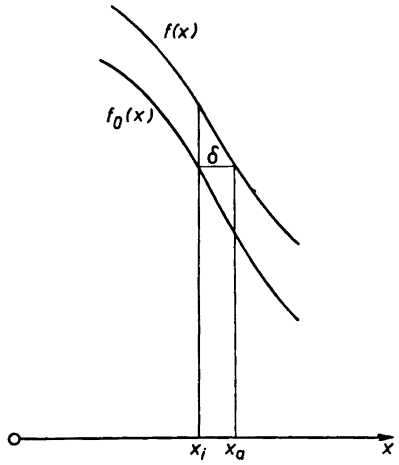

Fig. 6. Illustration of the method used for calculating δ in the neighbourhood of an inflexion point of the ideal curve (f_0 (x)) and the actual curve (f (x)).

From the character of the curves in Fig. 7 it is seen, following a horizontal line, how fast the corrections due to an asymmetrical initial condition die out. The great amount of asymmetry which can be tolerated is surprising.

It is obvious, however, when working with very dilute solutions and thus rapid diffusion experiments, that the initial skewness must be minimized if satisfactory results are to be obtained. In fact the demands on the symmetry are nearly inversely proportional to the time of experiment.

From Fig. 7 the impossibility of using the beginning of a diffusion run for extrapolation to zero-time is apparent. For a run with an occasional skewness (fixed a in Fig. 7), an estimation of the correction as a function of time can be obtained. Since this function is non-linear for small time values, the extrapolation to zero-time fails, as can be seen from the appearance of the curve (increasing correction on going to smaller time values). In practice this must be taken into account, especially when working with very dilute solutions.

b. Elimination of the Wiener skewness. Svensson [13,16] has shown that the aberration causing the Wiener skewness disappears if the camera is focused on a plane 1/3 of the cell thickness from the front wall.

c. The influence of the concentration dependance of the diffusion coefficient. In order to obtain a better interpretation of the data from optical interferometers, attempts have been made to solve the second equation of Fick in the case of a concentration dependant diffusion coefficient using a series expansion method [17]. For sucrose, *e.g.*, there is a variation of 2 % in D between 1.5 % solution and infinite dilution [18].

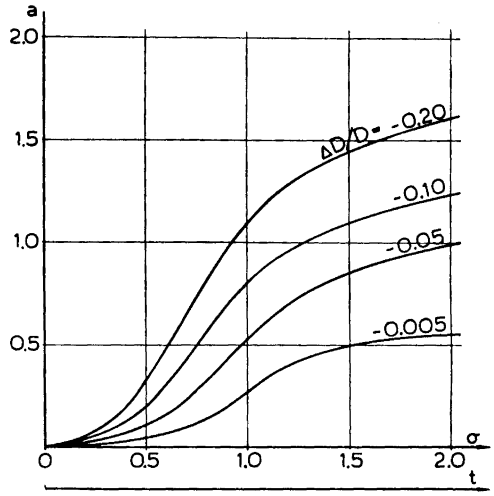

Fig. 7. Illustration of the influence of an asymmetrical initial condition on the diffusion coefficient measured.

In order to examine the influence of a concentration-dependant diffusion coefficient on the appearance of the interference pattern in *this method*, the solution of Fick's equation for the case of an exponential variation of the diffusion coefficient with concentration was studied.
If we put

$$D(c) = D_0 \, e^{\alpha c} \tag{7}$$

for the diffusion coefficient, then the Fick equation takes on the following form

$$\frac{\partial c}{\partial t} = \frac{\partial}{\partial x}(D_0 \, e^{\alpha c} \frac{\partial c}{\partial x}) \tag{8}$$

An approximate solution of this equation has been derived by Clarke [19]. Of interest here is the solution for small concentration differences

$$\left(\frac{\partial c}{\partial x}\right)_{\Delta c \text{ small}} \approx \frac{\Delta c}{2\sqrt{\pi D_0 t}} e^{-\frac{x^2}{4D_0 t}} \left\{1 - \alpha \bar{c}\left(\frac{1}{2} - \frac{x^2}{4D_0 t}\right) + \right.$$
$$\left. + \frac{\alpha^2 \bar{c}^2}{8}\left[7 - 8\frac{x^2}{4D_0 t} + 4\left(\frac{x^2}{4D_0 t}\right)^2\right]\right\} \tag{9}$$

where $\bar{c} = \frac{c_I + c_{II}}{2}$ (the arithmetic mean of the concentrations of the upper and the lower solution).

It should be noted that according to this expression, the position of the maximum point is the same as for the ideal case with a constant diffusion coefficient.

In the neighbourhood of the inflexion points ($x = \sigma = \sqrt{2Dt}$) we have

$$\frac{\partial c}{\partial x} = \frac{\Delta c}{\sigma\sqrt{2\pi}} e^{-\frac{1}{2}} \left\{1 + \frac{\alpha^2\bar{c}^2}{2}\right\} \tag{10}$$

Using (6) we obtain the following expression for the error in $(2x)$

$$\Delta(2x) = 2\delta = \frac{\sigma\alpha^2\bar{c}^2}{2} \tag{11}$$

and consequently

$$\frac{\Delta D}{D} = 2\frac{\Delta(2x)}{2x} = \frac{\alpha^2\bar{c}^2}{2} \tag{12}$$

In Ref.[4] diffusion runs with sucrose are described with concentration differences from 0.01 to 0.1 % sucrose. From eqn. (12) we conclude the corresponding values of $(\Delta D/D)$ to be from 0.0001 to 0.01 %, which can be left out of consideration.

A number of mathematical methods has been devised to compensate for effects 3 and 4 which cause rather large deviations if the experiments are performed with large concentration differences. Effects 3 and 4 give rise to a skew deviation of the refractive index gradient curve from the ideal Gaussian curve. These two sources of skewness may occasionally cancel [17] but there are also systems in which these effects act in the same direction and in such cases the resulting effect cannot be neglected.

The possibility of using quite small concentration differences in experiments with the birefringence interference method [4] reduces the magnitude of these errors substantially. The corrections necessary are much smaller and the mathematical difficulties correspondingly less.

XI. REMARKS ON SOME TECHNICAL DETAILS

A very great advantage of the flowing-junction cell over the other cell types is that no moving mechanical parts are situated in the optical field. Thus, the optical field is clear and the tightening problems are simplified. The flowing-junction cell is very convenient for volatile organic solutions since it can easily be tightened with teflon packings [9] (there are indeed sparingly soluble lubricants but no ideal ones).

Another advantage of the flowing-junction cell is that one is in control of the formation of the boundary and can study the interface before starting the diffusion run. On the other hand, the flowing-junction cell is more sensitive to impurities in the liquids, but by inserting sintered glass filters in the input tubes to remove grease and other impurities, this disadvantage can probably be eliminated.

A disadvantage of the draw-slide cell is the trace of lubricant which is always left on the glass walls at the position where the slide is drawn out. The same criticism applies to the sliding-solvent cell.

The adsorption danger must be taken into account in diffusion experiments. In Ref.[4] the difficulty of performing diffusion runs with glycine in

cell *Ia* (a stainless steel cell) was pointed out. Lamm [5] describes an apparent downward drift of the diffusion coefficient of pentaerythrite during a run which he ascribes to the adsorption of pentaerythrite on the elastolite side walls of the cell used.

XII. RECOMMENDATION FOR FUTURE INVESTIGATIONS

In addition to the present method there are numerous others, the most important of which are the scale- and schlieren methods of Lamm, the Gouy-interferometer, the Rayleigh-Calvet-Philpot interferometer, the Jamin interferometer and a modified schlieren method utilizing a Wolter phase plate [20] instead of a slit or an edge. All these methods are used side by side and so far no really satisfactory attempt has been made to compare the accuracy attainable by various methods. There is, however, indication that the present method should be superior to at least some of the earlier ones. There are two reasons for this. Firstly the method employs interferences with only a few wave-length differences. The advantage of this has been pointed out elsewhere [2]. Secondly it is caracterised by what Wolter calls "Minimistrahlkennzeichnung" [21] which is advantageous from a measuring point of view. (Wolter ascribes the advantage of the "Minimistrahlkennzeichnung" to the so called wave uncertainty principle, the application of which is questionable).

It seems to the author that a satisfactory theory, which permits a quantitative calculation of the accuracy attainable by various methods would be highly desirable.

REFERENCES

1. Kahn, D. S. and Polson, A. *J. Phys. & Colloid Chem.* **51** (1947) 816.
2. Ingelstam, E. *Arkiv Fysik* **9** (1955) 197.
3. Ingelstam, E. *J. Opt. Soc. Am.* **47** (1957) 536.
4. Bryngdahl, O. *Acta Chem. Scand.* **11** (1957) 1017.
5. Lamm, O. *Nova Acta Regiae Soc. Sci. Upsaliensis* **10** (1937) No. 6.
6. Svensson, H. *Acta Chem. Scand.* **3** (1949) 1170.
7. Coulson, C. A., Cox, J. T., Ogston, A. G., and Philpot, J. St L. *Proc. Roy. Soc. London* **192** (1948) 382.
8. Longsworth, L. G. *Rev. Sci. Instr.* **21** (1950) 72.
9. Caldwell, C. S., Hall, J. R., and Babb, A. L. *Rev. Sci. Instr.* **28** (1957) 816.
10. Neurath, H. *Science* **93** (1941) 431.
11. Loughborough, D. L. and Stamm, A. J. *J. Phys. Chem.* **40** (1936) 1113.
12. Claesson, S. *Nature* **158** (1946) 834.
13. Svensson, H. *Optica Acta* **1** (1954) 25.
14. Svensson, H. *Optica Acta* **3** (1956) 164.
15. Margenau, H. and Murphy, G. M. *The Mathematics of Physics and Chemistry*, D. van Nostrand, New York 1943, p. 233–4.
16. Forsberg, R. and Svensson, H. *Optica Acta* **2** (1954) 90.
17. Gosting, L. J. and Fujita, H. *J. Am. Chem. Soc.* **79** (1957) 1359.
18. Gosting, L. J. and Morris, M. S. *J. Am. Chem. Soc.* **71** (1949) 1998.
19. Clarke, D. M. *J. Chem. Phys.* **27** (1957) 29.
20. Trautman, R. and Burns, V. W. *The Wolter Phaseplate in Ultracentifugation and Electrophoresis*, University of California, UCRL–2453 (1954).
21. *Handbuch der Physik*, Bd XXIV, p. 577–88, Springer Verlag, Berlin 1956.

Received January 10, 1958.

ACTA CHEMICA SCANDINAVICA 12 (1958) 701—707

Oxidation of Metals: Determination of Activation Energies

PER KOFSTAD

Central Institute for Industrial Research, Blindern, Oslo, Norway

A new method is proposed for the determination of energies of activation of oxidation of metals and alloys. Metals are oxidized under conditions of linearly increasing temperature, and the activation energy may be determined from one single oxidation run. In addition the method also gives the approximate temperature regions in which different rate laws of oxidation are found.

The described method has been applied to high-temperature oxidation of nickel, zirconium, copper, and titanium.

In the study of oxidation of metals and alloys the activation energies are of fundamental importance in the consideration of oxidation mechanisms. Hitherto, however, the reported values often show large mutual disagreements for the same metal. A good example is the oxidation of copper, where activation energies ranging from 29.4 to 42 kcal have been reported in the temperature region 500—1 000°C by different investigators.[1–6]

An accurate determination of activation energies involves a large number of isothermal runs at different temperatures. In this communication a faster method is proposed for the determination of activation energies. The metals are oxidized under conditions of linearly increasing temperature, and the method gives the activation energy of oxidation from one single oxidation run, and in addition gives the approximate temperature regions in which different rate laws are found. Although the proposal of oxidizing metals under such conditions is not new,[7] it is believed that the present treatment of the results provides a new approach for a simple and rapid method for studies of oxidation of metals and alloys.

OXIDATION OF METALS

The oxidation of metals follows different rate laws depending upon the metal, the nature and semi-conducting properties of the oxide formed, and the temperature. At high temperatures (generally greater than 200—300°C) we usually have 1) linear, 2) parabolic, or 3) cubic rate laws, which may be expressed as,

$$\frac{d(m/A)}{dt} = k_1 \qquad \text{(Linear)} \qquad (1)$$

$$m/A \frac{d(m/A)}{dt} = k_2 \qquad \text{(Parabolic)} \qquad (2)$$

$$(m/A)^2 \frac{d(m/A)}{dt} = k_3 \qquad \text{(Cubic)} \qquad (3)$$

In these equations m/A represent gain in weight per unit area at time t, and k_1, k_2, and k_3 are the oxidation rate constants for the linear, parabolic, and cubic rate laws, respectively.

The temperature dependence of oxidation reactions may be expressed by the empirical Arrhenius equation

$$k = B \exp(-Q/RT) \qquad (4)$$

where k is the rate constant for the oxidation at temperature T, B is a parameter whose dimensions depend on units for k, and Q is the activation energy.

In order to provide a more complete interpretation of B, Gulbransen [8] applied the absolute reaction rate theory to oxidation reactions obeying parabolic rate laws. The rate constant was accordingly expressed in terms of the entropy and heat of activation and with a preexponential factor proportional to T.

In as much as oxidation processes obey the Arrhenius equation and as also non-parabolic rate laws are included in this treatment, the following approach will be confined to the use of eqn. 4.

Eqns. 1, 2, and 3 may be written as

$$(m/A)^n \frac{d(m/A)}{dt} = k \qquad (5)$$

where n is a constant having values of 0, 1, and 2 for the linear, parabolic, and cubic rate laws, respectively.

Oxidizing under conditions with linear increase of temperature, we have

$$T = at + b \text{ or } dT = adt \qquad (6)$$

Substituting (4) and (6) in eqn. 5, we get

$$(m/A)^n \frac{d(m/A)}{dT} = (B/a) \exp(-Q/RT) \qquad (7)$$

Taking the logarithm and rearranging, eqn. 7 may be written

$$(n + 1)\ln(m/A) + \ln \frac{d\ln(m/A)}{dT} = \ln B/a - Q/RT \qquad (8)$$

According to eqn. 8 a plot of $(n + 1) \ln (m/A) + \ln \frac{d\ln(m/A)}{dT}$ *versus* $1/T$ should yield a straight line whose slope is equal to $(-Q/R)$ and which permits calculation of the activation energy, Q. The value of the parameter B in eqn. 4 may also be determined by introducing corresponding experimental values of (m/A), T, and a.

The use of eqn. 8 necessitates the evaluation of $\frac{\mathrm{d}\ln(m/A)}{\mathrm{d}T}$, and the approximate values for this differential quotient were calculated as

$$\left(\frac{\mathrm{d}\ln(m/A)}{\mathrm{d}T}\right)_{T=T_j} = \frac{\ln(m/A)_{j+1} - \ln(m/A)_{j-1}}{T_{+1} - T_{j-1}} \qquad \text{(a)}$$

Temperature intervals of 25°K were found suitable in the described runs, and a table of the following type was used for each oxidation run:

T°C	$1/T$	$x = m/A$	$\ln x$	$(n+1)\,2\ln x$	$\frac{\Delta \ln x}{\Delta T}$	$\ln \frac{\Delta \ln x}{\Delta T}$
Intervals of 25°K		x_1	$\ln x_1$			
		x_2	$\ln x_2$	z_2	y_2	$\ln y_2$
		x_3	$\ln x_3$	z_3	y_3	$\ln y_3$
		x_4	$\ln x_4$	z_4	y_4	$\ln y_4$

where $z_j = \ln x_{j+1} - \ln x_{j-1}$
and $y_j = z_j/50$

In applying this approach to metals oxidizing according to linear rate laws, it is necessary to plot $\ln(m/A) + \ln \frac{\ln(m/A)}{T}$ *versus* $1/T$, in the case of parabolic rate laws $2\ln(m/A) + \ln \frac{\ln(m/A)}{T}$ *versus* $1/T$, and cubic rate laws $3\ln(m/A) + \ln \frac{\ln(m/A)}{T}$ *versus* 1/T. This treatment of the data should yield straight lines for the particular rate laws in the corresponding temperature regions. If the oxidation of a metal follows different rate laws in different temperature regions, one should also obtain distinct breaks in the curves at the temperature regions where the oxidation changes rate laws. For example if the oxidation of a metal follows the cubic, parabolic, and linear rate laws successively with increasing temperature, the plotted curve will be a straight line only in the temperature regions where the assumed rate law is valid, while the plotted curve should show a curvature in the temperature regions where the other rate laws are valid. Thus in addition to the activation energy, such a treatment would also give approximate values as to the temperature regions in which the different rate laws may be found.

It should be emphasized that eqn. 8 is valid only under conditions of cubic, parabolic, and linear rate laws. The described approach is thus not applicable for oxidation of metals at low temperatures or at the very beginning of the oxidation at higher temperatures, at which conditions logarithmic and reciprocal logarithmic rate laws are generally obeyed. These latter rate laws may, however, also be treated in the same manner as described above.

EXPERIMENTAL RESULTS

The described method was tried on Ni, Zr, Cu, and Ti, and the experimental results gave activation energies in satisfactory agreement with previously published values obtained from isothermal runs.

The metals were oxidized under conditions with linearly increasing temperature from 400°C to 1 100°C with a temperature increase of either 3.86 or 2.22°C/min. Owing to the small weight gain before 600—700°C during these runs, activation energies could only be determined for temperature regions 700—1 100°C.

The oxidation of titanium has previously been found to obey the cubic (400—600°), the parabolic (600—900°C), an linear rate law (900—1 000°C) in the indicated temperature regions.[9] With the above mentioned experimental conditions one should consequently obtain a break in the curve corresponding to a transition from the parabolic to the linear rate law region.

In Fig. 1 are shown the data for unannealed van Arkel titanium oxidized under linear temperature increase of 3.86°C/min plotted under the assumption of linear and parabolic rate laws. As seen the parabolic rate law plot yields a straight line between 700°C and 900°C, while the linear rate law plot gives a straight line above 900°C, thus confirming the results obtained from isotherm-

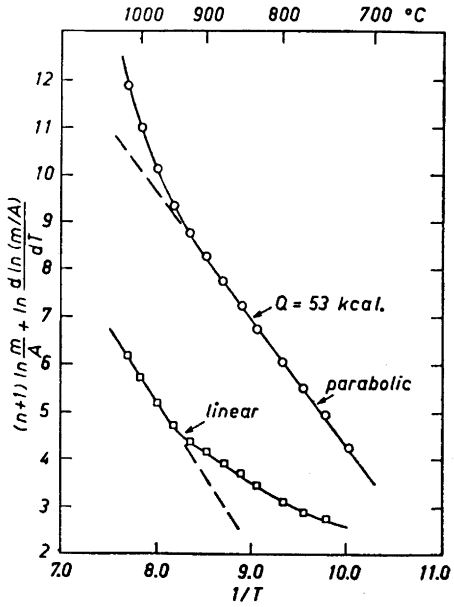

Fig. 1. Oxidation of van Arkel titanium with temperature increase of 3.86°C/min. Data plotted under assumption of linear and parabolic rate laws.

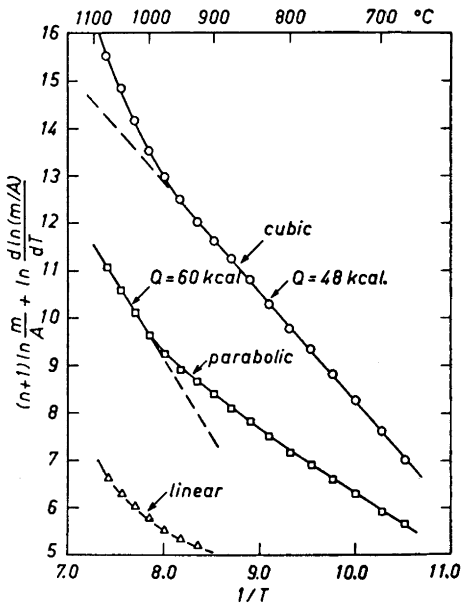

Fig. 2. Oxidation of zirconium (2.22°C/min). Data plotted under assumption of linear, parabolic, and cubic rate laws.

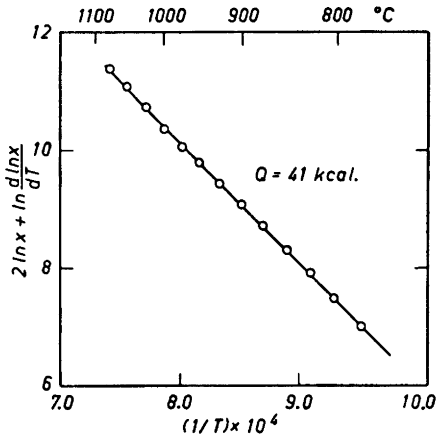

Fig. 3. Oxidation of nickel (2.22°C/min).

al runs. Furthermore, the activation energy in the parabolic rate law region amounts to 53 kcal, which is in excellent agreement with the value of 52 ± 2 kcal, which was obtained by isothermal oxidation of the same metal in this laboratory.

Fig. 2 shows the results on oxidation of zirconium (2.22°C/min) plotted under the assumption of linear, parabolic, and cubic rate laws. As seen the cubic rate law plot yields a straight line between 650 and 950°C giving an activation energy of 48 kcal in agreement with the results of Belle and Mallett,[10] who found that the oxidation of zirconium conformed with a cubic rate law between 400 and 1 000°C and with an activation energy of 47.2 kcal. Furthermore, the plots in Fig. 2 also indicate that the cubic rate law is not conformed with between 950 and 1 100°C, but in this region the parabolic rate law plot yields a straight line and an activation energy of approximately 60 kcal, and thus indicating conformity with the parabolic rate law in this temperature region. Two runs with a temperature increase of 3.86°C/min showed conformity with the cubic rate law between 700 and 1 050°C, and with an activation energy of 46 kcal.

Isothermal oxidation of zirconium by both Cubicciotti [11] and Gulbransen [12] has previously been found to obey a parabolic rate law, and the disagreement between these data and those of Belle and Mallett cannot be explained at present. A tentative explanation may be that the amount and type of impurities may have a decisive effect on the rate law observed, as Mallett and Albrecht [13] showed that 1.5 and 2.5 wt. % Zn—Zr alloys oxidize according to cubic and parabolic rate laws, respectively.

Isothermal oxidation of nickel has previously been found to follow a parabolic rate law at high temperatures, and in accordance with this a parabolic rate law plot yields a straight line between 750 and 1 050°C, as shown in Fig. 3. The activation energy was found to be 41 kcal. As a comparison previously published values range from 34 to 51 kcal [14–17].

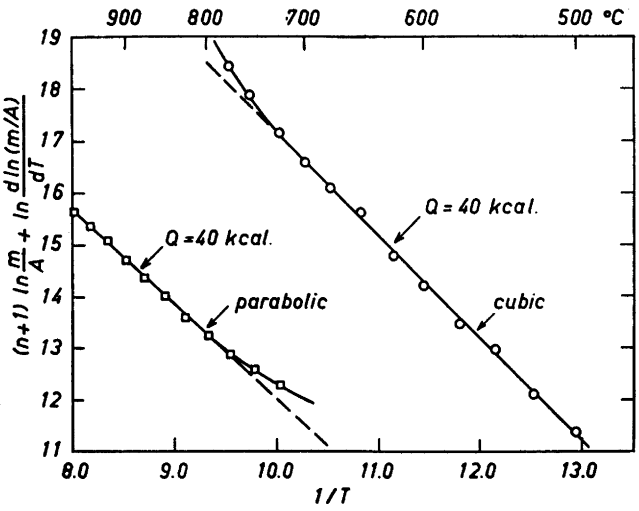

Fig. 4. Oxidation of copper (2.22°C/min). Data plotted assuming parabolic and cubic rate laws.

The results for oxidation of copper for a temperature increase of 2.22°C/min are given in Fig. 4. According to the plots the assumption of a parabolic rate law is only valid in the temperature region 750—1 000°C, while it may be inferred that the oxidation obeys a cubic rate law between 500 and 750°C. The activation energies for the parabolic and the cubic rate law regions was found to be 35 and 40 kcal, respectively. As a comparison previously published values for the parabolic rate law region range from 29.2 to 42.0 kcal [1–6].

DISCUSSION

The described results indicate that activation energies determined under conditions of linearly increasing temperature are in agreement with corresponding values determined from isothermal runs. Furthermore, the method also gives approximate temperature regions in which different rate laws are found.

While the activation energy found should be independent of the heating rate, it is to be expected that the appearance of different rate law regions are somewhat dependent on the rate of temperature increase, which is also apparent from the present results. The rate law observed in isothermal runs may be dependent upon the thickness of the oxide scale, and a certain rate law may thus be found to extend to higher temperatures for a fast than for a slow rate of temperature increase. This is indicated by the results on zirconium, in which case the cubic rate law was conformed with up to 1 050°C for a temperature increase of 3.86°C/min, but only up to 950°C for a temperature increase

of 2.22°C/min. In the case of oxidation of copper it might seem surprising, when comparing to the isothermal studies, that the cubic rate law is valid up to a temperature of about 700°C. However, in addition to the effect of the relationship between rate of temperature increase, film thickness, and rate law observed, this may be due to the fact that the oxide formed consists both of CuO and Cu_2O, and that their relative amounts changes with temperature. At 500°C the oxide scale consists mainly of CuO, and the relative amounts of CuO decreases with increasing temperature until it at 900°C only accounts for 10 % of the oxide scale [6]. The oxidation of Cu_2O to CuO has previously been [18] found to obey a cubic rate law between 600 and 1 000°C, and it does not therefore seem unreasonable that the cubic rate law is obeyed up to 700°C under the described experimental conditions.

REFERENCES

1. Pilling, N. B. and Bedworth, R. E. *J. Inst. Metals* **29** (1923) 523.
2. Feitknecht, W. *Z. Elektrochem.* **35** (1929) 142, 500.
3. Krupowski, A. and Jasczurowski, J. *Rev. Mét.* **33** (1936) 646.
4. Castellan, C. W. and Moore, J. W. *J. Chem. Phys.* **17** (1939) 41.
5. Valensi, G. *Pittsburgh International Conf. on Surface Reactions* (Proc.) **1948** 156.
6. Tylecote, R. F. *J. Inst. Metals* **78** (1950) 327.
7. Baur, J. P., Bridges, D. W. and Fassel jr., W. M. *J. Elektrochem. Soc.* **102** (1955) 490.
8. Gulbransen, E. A. *Trans Electrochem. Soc.* **83** (1943) 301.
9. Kofstad, P., Kjöllesdal, H. and Hauffe, K. *Acta Chem. Scand.* **12** (1958) 239.
10. Belle, J. and Mallett, M. W. *J. Electrochem. Soc.* **101** (1954) 339.
11. Cubicciotti, D. *J. Am. Chem. Soc.* **72** (1950) 4138.
12. Gulbransen, E. A. and Andrew, K. F. *J. Metals* **9** (1957) 394.
13. Mallett, M. W. and Albrecht, M. W. *J. Electrochem. Soc.* **102** (1955) 407.
14. Kubaschewski, O. and von Goldbeck, O. *Z. Metallk.* **39** (1948) 158.
15. Moore, W. J. and Lee, J. K. *J. Chem. Phys.* **19** (1951) 255.
16. Gulbransen, E. A. and Andrew, K. F. *J. Electrochem. Soc.* **101** (1954) 128.
17. Frederick, S. F. and Cornet, I. *Ibid.* **102** (1955) 285.
18. Hauffe, K. and Kofstad, P. *Z. Elektrochem.* **59** (1955) 399.

Received February 7, 1958.

ACTA CHEMICA SCANDINAVICA 12 (1958) 708—722

Studies on Cobaltammines

II. Association of Ammonia with the Hexammine Cobalt(III) Ion in Aqueous Solution

RAGNAR LARSSON

Department of Inorganic and Physical Chemistry, Chemical Institute, University of Lund, Lund, Sweden

The solubilities of $Co(NH_3)_6(ClO_4)_3$ and $Ba(IO_3)_2$ in 1 M NH_4ClO_4 are reported for mixed solvents, the non-aqueous component being ammonia, methanol, ethanol, acetone, glycerol and dioxane. Using these measurements, a method is devised for the calculation of the association constants when ammonia is associated with the $Co(NH_3)_6^{3+}$ ion. The first constant is reported. Evidence for an association of acetone with the $Co(NH_3)_6^{3+}$ ion is discussed. A spectrophotometric method is used which confirms the results from the solubility measurements.

From a solution containing some ammonium nitrate a solid phase has been isolated, having the composition $(Co(NH_3)_6 . NH_3)(ClO_4)_2NO_3$.

The hexammine cobalt(III) ion, a complex seemingly saturated with respect to further coordination, has been the subject of several investigations on ion association. For example, the association of sulphate or thiosulphate ions has been investigated conductometrically [1] and spectrophotometrically [2,3], by measurements of solubility [4,5] and dialysis [6] as well as by a polarographic method [7]. Association of halide and pseudohalide ions has been studied both conductometrically [8] and spectrophotometrically [9–11], whereas oxalate ion association has been studied by measurements of conductivity [12] and dialysis [6].

It must be noted, however, that some of the interpretations of these experimental data are not generally accepted.

It seemed to be of interest to investigate the association of an uncharged, polar molecule with the $Co(NH_3)_6^{3+}$ ion. No such measurements have apparently been made though several authors [13,14] have pointed out the importance of such an association in determining the velocity of inner-sphere substitutions.

In the first part [15] of this series it was reported that there is an increase in the solubility of $Co(NH_3)_6(ClO_4)_3$ in 1 M NH_4ClO_4 as the concentration of ammonia is increased. This fact was then explained as the result of an outer-

sphere ammine formation. In this work those solubility measurements have been extended in an effort to make possible the calculation of association constants.

As a check of the results obtained, an extinctiometric method has also been used.

THEORY OF THE SOLUBILITY MEASUREMENTS

The notations will be those of the preceding paper [15] except when otherwise stated.

The reactions under investigation may be written in the general form:

$$MA_6 \cdot mH_2O + n\ A \rightleftharpoons (MA_6)A_n \cdot (m\text{-}n)H_2O + n\ H_2O \quad (1)$$

Excluding the solvating water, the conrresponding association constant is defined by

$$\beta_n = \frac{[(MA_6)A_n] f_{(MA_6)A_n} \cdot a_{aq}{}^n}{[MA_6] \cdot f_{MA_6} \cdot [A]^n \cdot f_A{}^n} \quad (2)$$

where brackets mean free concentrations and f the activity coefficients of the species in question. a_{aq} is the activity of water. Now, $f_{(MA_6)A_n}$ and f_{MA_6} may be considered as almost equal, as they are related to ions of the same charge and almost nearly the same size. Thus eqn. (2) may be rewritten as

$$\beta_n = \frac{[(MA_6)A_n] a_{aq}{}^n}{[MA_6] \cdot a_A{}^n} \quad (3)$$

where $a_A = [A] \cdot f_A$

We define $X = \sum_{n=1}^{N} \beta_n \cdot a_A^n / a_{aq}^n$ (4)

Thus $C_M = [MA_6]\ (1 + X)$ (5)

In a solution saturated with $MA_6(ClO_4)_3$, we have

$$[MA_6]\ [ClO_4]^3 = L \quad (6)$$

and in the case when $C_A = 0$, *i.e.*, $C_M = [MA_6]_0$, we have

$$[MA_6]_0\ [ClO_4]_0^3 = L_0 \quad (7)$$

If, as is the case in the present investigation, only the concentration of ammonia is changed, the salt medium being constantly kept 1 M NH_4ClO_4, and if C_M is low, we can put

$$[ClO_4] = [ClO_4]_0 \quad (8)$$

Combining eqns. (6)—(8) we get

$$[MA_6]/[MA_6]_0 = L/L_0 \quad (9)$$

Inserting eqn. [9] into eqn. [5] we get

$$1 + X = \frac{C_M}{[MA_6]_0} \cdot \frac{L_0}{L} \quad (10)$$

Knowledge of L/L_0 as a function of [A] would enable us to calculate X.

The evaluation of L/L_0

With this purpose in mind we will consider the effects on the solubility of a sparingly soluble salt in an aqueous solution of high ionic strength when a part of the water is exchanged for another solvent, *e.g.*, ammonia. This other solvent will be called here, for the sake of brevity, an "aquo-substitute".

The following items may be considered important:

1. The aquo-substitute may form complexes with the cation — or the anion — of the sparingly soluble salt.

2. A change in solvation conditions may result in a change in the "distance of closest approach" and thus cause activity changes of the ions in question.

3. The change in the dielectric constant of the solvent will cause a change in the activity coefficients of the ions. According to Owen [16], two effects are operating: the primary and the secondary medium effects. The first one, arising from changes in ion-solvent interaction, is more or less correctly described by the theoretical equation of Born [17] or by the empirical equation of Davies and Ricci [18]. However, it must be emphasized that none of those equations is generally valid. (*Cf.* Mayper, Clever and Verhoek [19].) The secondary effect, connected with ion-ion interactions, is dependent on the ionic strength and is implied in the Debye-Hückel-Gronwall-LaMer equation.

One way to estimate the quotient L/L_0 for $Co(NH_3)_6(ClO_4)_3$ in aqueous ammonia would be to use an ion of reference that does not form ammine complexes and is solvated as the $Co(NH_3)_6^{3+}$ ion. It should preferably be of the same size and have the same charge as this ion.

An ion fulfilling these demands is not easy to find, as most tervalent positive ions are hydrolyzed in aqueous ammonia, even at a high ammonium ion concentration.

As a reference ion Ba^{2+} has therefore been chosen. The measurements of Bjerrum [20, p. 145] indicate that this ion has a very low tendency of ammine formation.

However, the change of the solubilities of $MA_6(ClO_4)_3$ and a barium salt are not directly comparable for obvious reasons.

To overcome this difficulty, we might try to find another aquo-substitute, call it B, that does not form complexes with either $Co(NH_3)_6^{3+}$ or Ba^{2+} ions. Through a comparison of the solubility decrease of a barium salt in solutions of ammonia and in solutions of the aquo-substitute B, information might be obtained on the function $(L/L_0)_{MA_6}$. We now make the following definitions:

The formal solubility product * of $Co(NH_3)_6(ClO_4)_3$ is given by $l_{MA_6} = C_{MA_6} \cdot C^3_{ClO_4}$. The formal solubility product of the barium salt to be used (BaX_2) is given by $l_{Ba} = C_{Ba} \cdot C_x^2$.

What we set out to measure is then the relative change of these formal quantities, l/l_0, where l_0 $(= L_0)$ means l in solutions having C_B $(C_A) = 0$.

The reasoning will proceed as follows: If no MA_6-B nor any Ba^{2+}-A or Ba^{2+}-B complexes are formed and if the solvation effects can be ignored, the quotients $(l/l_0)_{MA_6}$ and $(l/l_0)_{Ba}$ in the different solvents will depend only

* Note the difference between the usage of the symbol l in this paper and in the preceding one [15].

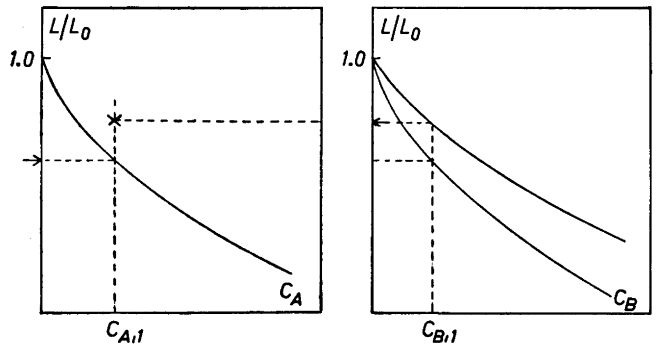

Fig. 1. Expected appearance of $(L/L_0)_{Ba}$ plotted against C_A (left figure) and $(L/L_0)_{MA_4}$ (right figure, upper curve) and $(L/L_0)_{Ba}$ (right figure, lower curve) plotted against C_B

on the dielectric constant of the solvent, as pointed out in item 3 previously mentioned. If now the quotients l/l_0, which in these special cases turn into L/L_0, are plotted against C_B — or C_A in the relevant case — we may expect curves of the form indicated in Fig. 1. For a certain value of L/L_0, indicated by an arrow in the left diagram, we find the concentrations C_{A_1} and C_{B_1} for which the solubility product of the barium salt is decreased to the same amount. According to the assumptions made, these solutions must then have the same dielectric constant. At $C_B = C_{B_1}$ we can read the value of L/L_0 of $Co(NH_3)_6(ClO_4)_3$ from the upper curve in the right diagram, indicated there by an arrow. This value of L/L_0, however, must be that of $Co(NH_3)_6(ClO_4)_3$ at the concentration C_{A_1}; this point is indicated by a cross in the left diagram.

Thus we may construct a set of points and from these draw a curve, describing the change of the solubility product of $Co(NH_3)_6(ClO_4)_3$ in ammonia solution. This curve represents the function L/L_0 of eqn. (10) and insertion in this equation thus gives X, from which function the complexity constants may be obtained according to eqn. (4).

Calculation of f_A/a_{aq}

The standard state of the ammonia activity has been chosen so that $f_{NH_3} = 1$ in 1 M NH_4ClO_4, $C_A = 0$. The activity of water is put = 1 in that same solution.

Following Bjerrum (Ref. [20], p. 143) we assume that f_A as a function of C_A when $C_{NH_4ClO_4} = 1$ M will run approximately parallel to f_A when $C_{NH_4ClO_4} = 0$.

Thus the vapour pressure data of Perman [21] at zero ionic strength and 20°C can be used. From these it is found, if $C_A < 5$ M,

$$f_A = 1 + 0.066_3 C_A + 0.00106\ C_A^2 \qquad (11\,a)$$

$$a_{aq} = 1 - 0.0244\ C_A \qquad (11\,b)$$

EXPERIMENTAL

As the sparingly soluble barium salt *$Ba(IO_3)_2$ was chosen.* In order to make the best possible choice of the aquo-substitute B, the formal solubility products, l, for $Co(NH_3)_6(ClO_4)_3$ and $Ba(IO_3)_2$ were determined in 1 M NH_4ClO_4 at 20°C in aqueous solutions containing varying amounts of the following solvents: Methanol, ethanol, glycerol, acetone and dioxane.

For all these solvent mixtures the dielectric constant is known from the measurements of Åkerlöf [22].

Chemicals used. The radioactive preparation of $Co(NH_3)_6(ClO_4)_3$ was the same as in Part I [15].

The *barium iodate* was prepared from solutions of reagent quality barium chloride and potassium iodate.

The *ammonium perchlorate* and *ammonia* solutions were prepared as in Part I [15]. The solutions of *methanol, ethanol, glycerol* and *acetone* were made from weighed amounts of absolute, acetone-free methanol, absolute ethanol, glycerol, p.a., heated to 180°C to expel water, and acetone, p.a., respectively. The *dioxane*, Eastman 2144, was purified according to Eigenberger [23], and distilled at the constant boiling point 101.2°C. The melting point was found to be 11.5°C. The small amounts of impurities present certainly do not seriously affect the general features of the solubility curves.

Procedure. Solutions of 1 M NH_4ClO_4, C_B M B (or C_A M A) were shaken with $Co^*(NH_3)_6(ClO_4)_3$ or $Ba(IO_3)_2$ in 100 ml flasks at 20°C in a thermostatically controlled room for two days to ensure saturation. The method of separation and measuring of the cobalt solutions was the same as in Part I [15]. The saturated solution of barium iodate was withdrawn with a 10 ml pipette provided with a filter-stick. The iodate content was determined iodometrically. The solubility product, l_{Ba}, was then easily calculated. As acetone and dioxane interfere in iodometric titrations, the solutions containing these solvents were freed from them before titration of the iodate content. The acetone solutions were made alkaline and boiled until all traces of ammonia were gone; it was then considered to be free from acetone also. The dioxane solutions were evaporated to dryness on the steambath. The quotient l/l_0 could be determined within ±1 % for $Ba(IO_3)_2$ and ±2 % for $Co(NH_3)_6(ClO_4)_3$.

RESULTS

The quotients l/l_0 found are reported in Tables 1 and 2. Along with these are given values, $(D)_{I=0}$, of the dielectric constants of the solvent mixtures that should be valid if the ionic strength, I, was zero. They are arrived at from density determinations of the stock solutions employed and linear interpolation from the data of Åkerlöf [22]. As the curves given by Åkerlöf describing D as a function of the concentration of aquo-substitute (given as weight-percent) are not exactly linear, the values of Tables 1 and 2 are not quite accurate, but they will serve well enough to give a rough picture of the dependency of l/l_0 on D. It must also be remembered that these values of D are certainly not those of the actual solutions having an ionic strength I = 1 M. $(D)_{I=1}$ may be some 10 % lower than $(D)_{I=0}$, (*cf.* Hasted, Ritson and Collie [24]). However, the quotient $(D_0/D)_{I=0} - D_0$ being the dielectric constant for $C_B = 0$ — will perhaps be more directly comparable to $(D_0/D)_{I=1}$ and has been used in Figs. 2 and 3.

It is seen that the curves of solubility of $Ba(IO_3)_2$ show the same relative positions as reported by Monk [25] at zero ionic strength.

Now, if the curves l/l_0 *versus* $(D_0/D)_{I=0}$ for different aquo-substitutes coincide, it might be inferred that the assumptions made on the exclusive dependency of l/l_0 on D are fulfilled. For $MA_6(ClO_4)_3$ this is the case in the

Table 1. Corresponding values of C_B, l/l_0 and $(D)_{I=0}$ · $Co(NH_3)_6(ClO_4)_3$.

Ammonia *		Methanol			Ethanol		
C_A M	l/l_0	C_B M	l/l_0	$(D)_{I=0}$	C_B M	l/l_0	$(D)_{I=0}$
0	1.00	0	1.00	80.4	0	1.00	80.4
0.250	1.02	0.339	0.94	79.8	0.223	0.87	79.7
0.500	1.05	0.508	0.88	79.6	0.557	0.78	78.8
1.000	1.13	0.846	0.82	79.0	1.114	0.64	77.1
1.500	1.23	1.354	0.74	78.2	1.560	0.55	75.8
2.500	1.47	2.030	0.64	77.2	1.782	0.50	75.2
3.50	1.88	3.38	0.49	75.0	2.228	0.43	73.9

Glycerol			Acetone			Dioxane		
C_B M	l/l_0	$(D)_{I=0}$	C_B M	l/l_0	$(D)_{I=0}$	C_B M	l/l_0	$(D)_{I=0}$
0	1.00	80.4	0	1.00	80.4	0	1.00	80.4
0.237	0.95	79.8	0.223	0.99	79.6	0.128	1.00	79.2
0.711	0.88	78.5	0.488	1.03	78.6	0.383	1.04	77.2
1.185	0.84	77.3	0.863	1.10	77.3	0.511	1.05	76.2
1.421	0.79	76.6	1.343	1.23	75.5	0.766	1.11	74.1
1.895	0.75	75.4	1.678	1.31	74.2	1.021	1.15	72.0
2.369	0.71	74.1	2.158	1.53	72.3	1.532	1.26	67.7

* These values are obtained by graphical interpolation from the values reported in Table 1 of Part I [15].

Table 2. Corresponding values of C_B, l/l_0 and $(D)_{I=0}$. $Ba(IO_3)_2$.

Ammonia		Methanol			Ethanol		
C_A M	l/l_0	C_B M	l/l_0	$(D)_{I=0}$	C_B M	l/l_0	$(D)_{I=0}$
0	1.00	0	1.00	80.4	0	1.00	80.4
0.376	0.88	0.379	0.80	79.8	0.250	0.78	79.6
0.872	0.71	0.569	0.71	79.5	0.624	0.52	78.6
1.500	0.53	0.948	0.58	78.9	1.248	0.273	76.8
2.013	0.41	1.516	0.40	78.0	1.747	0.172	75.3
2.550	0.33	2.274	0.267	76.7	1.996	0.134	74.6
3.62	0.209	3.79	0.111	74.3	2.495	0.083	73.1

Glycerol			Acetone			Dioxane		
C_B M	l/l_0	$(D)_{I=0}$	C_B M	l/l_0	$(D)_{I=0}$	C_B M	l/l_0	$(D)_{I=0}$
0	1.00	80.4	0	1.00	80.4	0	1.00	80.4
0.796	0.93	78.3	0.223	0.80	79.6	0.286	0.71	78.0
1.327	0.90	76.9	0.558	0.55	78.4	0.572	0.54	75.7
1.592	0.89	76.2	0.893	0.37	77.2	0.715	0.47	74.5
2.122	0.87	74.8	1.339	0.231	75.5	1.144	0.268	70.9
2.653	0.85	73.4	1.678	0.162	74.2	1.430	0.231	68.5
			2.174	0.088	72.2	1.907	0.129	64.6

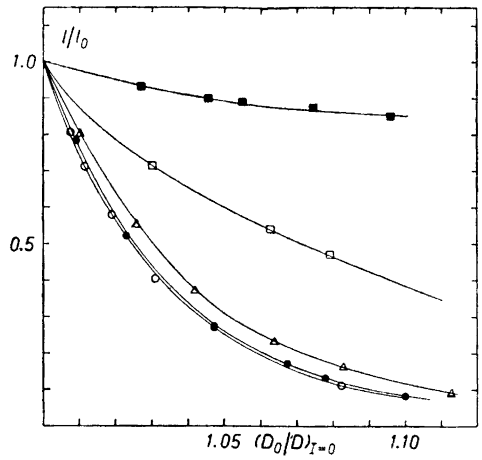

Fig. 2. The $Ba(IO_3)_2$ solubility curves; l/l_0 plotted against $(D_0/D)_{I=0}$. The symbols refer to the following aquo-substitutes: methanol (○); ethanol (●); acetone (△); dioxane (□); glycerol (■).

ethanol and methanol systems; for $Ba(IO_3)_2$ the ethanol, methanol and acetone curves lie rather close.

For these systems l/l_0 thus equals or nearly equals L/L_0 and the procedure indicated in Fig. 1 may be applied.

The measurements of Monk [25], also including the propanols, show that as the aquo-substitute molecule is made smaller, the solubility curves seem to converge to a common limit.

Thus, as ammonia, for which aquo-substitute we seek an analoque, is a small molecule, and as methanol is the smallest molecule of the reference aquo-substitutes investigated and also fulfills the demands stated, methanol will be chosen as the aquo-substitute to be used in the following calculations.

Discussion of anomalies

The l/l_0-curves in dioxane and glycerol media do not coincide with the curves of the primary alcohol media (Figs. 2 and 3). Thus the change of the formal solubility products of the salts in question is not exclusively dependent on the dielectric constant of these solvents. Other factors must operate, such as an incorporation of the aquo-substitute in the solvation sheath of the ions (item 2 in the foregoing) or a complex formation (item 1). If a pure electrostatic attraction is operating, we should expect this effect to be greater for the Ba^{2+} ion than for the larger $Co(NH_3)_6^{3+}$ ion. The different courses of the curves of glycerol and dioxane media indicate that several factors are of importance, such as, *e.g.*, the degree of selective solvation and the dimensions of the aquo-substitute molecules. This latter effect may perhaps be accounted for by assuming the operation of London dispersion forces as discussed by Bockris, Bowler-Reed and Kitchener [26].

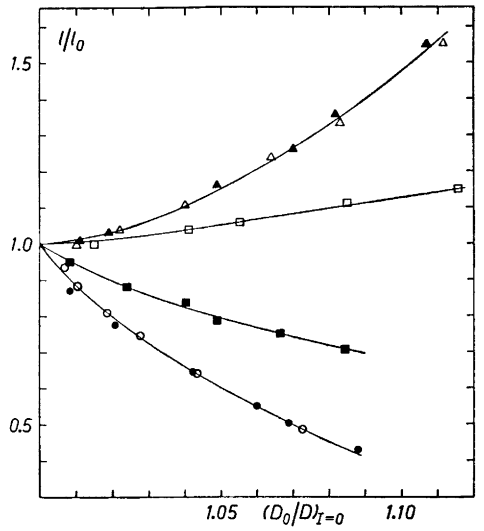

Fig. 3. The $MA_6(ClO_4)_3$ solubility curves; l/l_0 plotted against $(D_0/D)_{I=0}$. The symbols refer to the following aquo-substitutes: methanol (○); ethanol (●); glycerol (■); dioxane (□); acetone, when a small amount of chloride ions is present in the solutions (△); acetone, when perchlorate ions are the only anions in the solutions (▲).

Of course a distinction between a strongly selective solvation and complex formation is very difficult to make. In this connection reference [27] may be made to the well-known glycerol compounds of the alkaline earth metals.

The solubility curves in the acetone medium, however, exhibit a different picture. The $Ba(IO_3)_2$-curve lies quite close to those of the primary alcohol media. The $Co(NH_3)_6(ClO_4)_3$-curve, on the other hand, indicates an increase of solubility. If we attribute the solubility increase of $Co(NH_3)_6(ClO_4)_3$ in ammonia solutions to an ammonia complex formation, we must for the sake of consequence infer a complex formation between acetone and the $Co(NH_3)_6^{3+}$ ion. This is not entirely inconceivable as examples of ketonic complexes are known, *e.g.*, from the chemistry of the actinides (*cf.* Rydberg [28] and references quoted there).

In a recent review Katzin [29] has advanced the opinion that the increase in solubility found for salts in acetone-water solutions originates solely from an increased complex formation between the metal ion and the anions of the salt in question; this should be related to the small affinity of acetone for hydrogen ions and thus — according to Katzin — its small ability to compete with the anions for coordination sites when the water activity is diminished. However, it must be remembered that the parallel between complex formation and base strength, underlying that reasoning, holds true only for ligands of similar structure yielding pure σ-bonds; other factors would invalidate that parallelism.

Now, for practical reasons, the cobalt stock solution of the present work holds a certain amount of chloride ions, which are introduced in the solutions considered in concentrations of about 5 mM. Are these chloride ions responsible for the observed increase in solubility? The decisive experiment is, of course, to determine the solubility in solutions containing only perchlorate ions as anions — tacitly assuming that perchlorate ions do

Table 3. Corresponding values of C_A and C_B (B = methanol) yielding corresponding values of $(L/L_0)_{MA_6}$ and $(L/L_0)_{Ba}$. Calculation of $1 + X$.

C_A M	$(L/L_0)_{Ba}$ The ammonia system	C_B M	$(L/L_0)_{MA_6}$ The methanol system	$(C_M/C_{M_0})_{MA_6}$ The ammonia system	$1 + X$	$\frac{a_A}{a_{aq}}$
0.100	0.964	0.057	0.986	1.007	1.021	0.101
0.250	0.912	0.158	0.963	1.02	1.06	0.256
0.500	0.827	0.328	0.927	1.05	1.13	0.523
0.750	0.747	0.505	0.890	1.09	1.22	0.803
1.000	0.668	0.703	0.851	1.13	1.33	1.094
1.250	0.594	0.902	0.814	1.18	1.45	1.400
1.500	0.526	1.103	0.781	1.23	1.57	1.716
2.000	0.411	1.503	0.720	1.34	1.85	2.392
2.500	0.328	1.915	0.658	1.47	2.24	3.12
3.00	0.267	2.275	0.610	1.65	2.71	3.92
3.50	0.213	2.633	0.565	1.88	3.32	4.77

not form any complexes. Such measurements are reported in Fig. 2. The increase of solubility is not less than for the solutions containing chloride ions. Thus, in this case, an explanation as that proposed by Katzin [29] must be ruled out.

Calculations

In the first two columns of Table 3 are given some values of C_A and the corresponding relative decrease of the solubility product of $Ba(IO_3)_2$ in ammonia solution, obtained by graphical interpolation from the data of Table 2. The third column contains the methanol concentrations that give the same relative decrease of L_{Ba}, also obtained by graphical interpolation form Table 2. The relative decrease of L_{MA_6}, as obtained from the values of Table 1, for these values of C_B is given in column 4 of Table 3. This column thus gives L/L_0 of $MA_6(ClO_4)_3$ for the values of C_A in column 1 (*Cf.* Fig. 1). From the values of $(L/L_0)_{MA_6}$ thus obtained and the corresponding values of C_M/C_{M_0} given in column 5, $1 + X_A$ has been calculated from eqn. (10).

In the definition of β_n (eqn. (2)) we have used the free ligand concentration [A]. However, as C_A is large, C_M very small and the complexity very weak, the approximation $[A] = C_A$ is not an improper one and will be used in the following.

In the last column of Table 3 a_A/a_{aq} is calculated from eqn. (11). In Fig. 4 $X \cdot (a_{aq}/a_A)$ is plotted against a_A/a_{aq}. It is seen that there exists a linear relation between these two quantities.

If we take only the first two terms of eqn. (4) into consideration, it may be transformed to

$$\frac{a_{aq}}{a_A} X = \beta_1 + \beta_2 \cdot \frac{a_A}{a_{aq}} \qquad (12)$$

Thus, from the above-mentioned linear relation the first two complexity constants may be obtained.

$$\beta_1 = 0.24 \pm 0.05 \text{ M}^{-1}; \ \beta_2 \approx 0.05 \text{ M}^{-2}$$

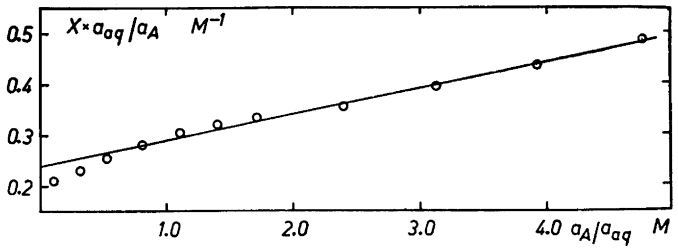

Fig. 4. $X \cdot \frac{a_{aq}}{a_A}$ as a function of a_A/a_{aq}.

However, if we assume the existence of the first complex only but take into consideration the increase of the complexity constant as the dielectric constant of the solvent diminishes (*cf.* Ref.[30]), we also obtain a linear relation between $\frac{a_{aq}}{a_A} X$ and $\frac{a_A}{a_{aq}}$:

Making the simplifying assumptions of linear dependency of D on C_A and of β_1 on D_0/D, valid at not too large values of D_0/D, we may write

$$D = D_0 - k\,C_A \tag{13 a}$$

which equation becomes

$$D_0/D = 1 + k'C_A \tag{13 b}$$

and

$$\beta_1 = (\beta_1)_0\ (1 + k''D_0/D) \tag{14}$$

where k, k' and k'' are constants. Combining eqns. (13 b) and (14) we obtain the linear relation

$$\beta_1 = (\beta_1)_0\ (1 + k'' + k'k''C_A) \tag{15}$$

Thus

$$\frac{a_{aq}}{a_A} X = \beta_1 = (\beta_1)_0(1 + k'') + k'k''(\beta_1)_0C_A \tag{16}$$

Or, as C_A is approximately proportional to a_A/a_{aq} (*cf.* eqns. (11)), $\frac{a_{aq}}{a_A} X$ will be a linear function of a_A/a_{aq}, as in Fig. 4.

It is difficult to see how to distinguish between the effects of eqns. (12) and (16). At least we can say that a value of β_2 calculated from eqn. (12) must be a maximum value.

FORMATION OF THE SOLID PHASE $[Co(NH_3)_5NH_3](ClO_4)_2NO_3$

Some solubility measurements have also been carried out in a salt medium consisting of 0.150 M NH_4NO_3 and 0.850 M NH_4ClO_4.

The solubility curve then obtained is presented in Fig. 5. It is seen that at a certain value of the ammonia concentration the curve exhibits a distinct break, indicating that a new solid phase is formed. As the appearance of this

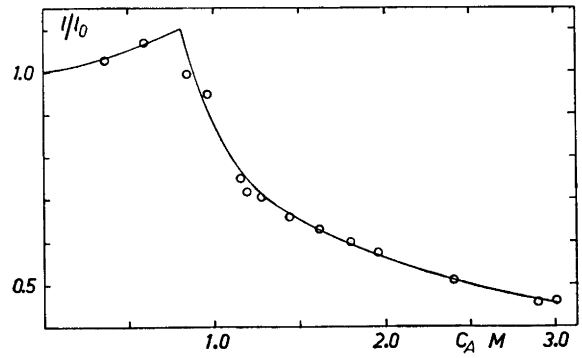

Fig. 5. $(I/I_0)_{MA_6}$ as a function of C_A in a salt medium of the composition 0.850 M NH_4ClO_4, 0.150 M NH_4NO_3.

new phase is obviously dependent on the presence of both nitrate ions and ammonia, we may expect it to be of the general composition $(Co(NH_3)_6)(NH_3)_x(ClO_4)_{3-y}(NO_3)_y$

Analysis of the solid phase. Some $Co(NH_3)_6(ClO_4)_3$ — unlabelled — was shaken with 100 ml of a solution of the following composition: 2.4 M NH_3, 0.15 M NH_4NO_3 and 0.85 M NH_4ClO_4. After a day the solid phase was separated and washed with alcohol until no ammonia could be detected, then washed with ether and air-dried. The substance thus obtained lost ammonia slowly on storage in open vessels at room temperature and rapidly at 100°C. The dried substance was analyzed for nitrate content according to Lindo [31] and for cobalt by a colorimetric determination of the $Co(NH_3)_6^{3+}$ ion at 472 mμ. (NO_3^-: Calc. for $Co(NH_3)_6(ClO_4)_2NO_3$ 14.7 %; Found 14.8 %, Co: Calc. 13.97 %; Found 13.96 %.)

If the ether-dried substance was rapidly weighed and thereafter dried at 100°C, it lost 3.7 % of its weight. (Calc. for $[Co(NH_3)_6NH_3](ClO_4)_2NO_3$ 3.9 %.) This result is in agreement with solid phase studies of Ephraim [32] and of Spacu and Voishescu [33], which indicate that $[Co(NH_3)_6NH_3]Cl_3$, though not stable, may be isolated at room temperature.

Thus we may conclude that the new solid phase is $[Co(NH_3)_6NH_3](ClO_4)_2NO_3$. However, as the composition of the solid phase gives no direct information on the composition of the ionic species in solution, no further investigation was made.

THE LIGHT ABSORPTION MEASUREMENTS

The absorption spectrum of the $Co(NH_3)_6^{3+}$ ion in ammonia solutions has been investigated once by Nakatsuka [34] who, however, reports no perceptible change with increasing ammonia concentration.

The low solubility of $Co(NH_3)_6(ClO_4)_3$ and the weak complexity under consideration render a complete extinctiometric investigation impossible. However, an approximate method has been attempted, under the assumption that only the first complex is present in appreciable amounts. (For a complete theory see, *e.g.*, Ahrland [35].) In order to reach higher values of C_M, the measurements have been performed at ionic strength 0.1 M.

The following notations are used:

ε_0 = extinction coefficient of the MA_6^{3+} ion
ε_1 = » » » » $(MA_6)A^{3+}$ ion
E = measured optical density
d = cell thickness (cm)

The quantity ε_M is defined by

$$E = d\varepsilon_M C_M \tag{17}$$

Hence,

$$\varepsilon_M C_M = \varepsilon_0[MA_6] + \varepsilon_1[(MA_6)A] \tag{18}$$

Introducing the complexity constant β_1 from eqn. (3) we can rewrite eqn. (18)

$$\varepsilon_M - \varepsilon_0 = \frac{(\varepsilon_1 - \varepsilon_0)\beta_1 \cdot [A] \cdot f_A/a_{aq}}{1 + \beta_1 \cdot [A] \cdot f_A/a_{aq}} \tag{19}$$

If $q = \dfrac{\varepsilon'_M - \varepsilon_0}{\varepsilon''_M - \varepsilon_0}$ where ε'_M and ε''_M are measured at $C_A = C_A'$ and C_A'' respectively, and if we put $C_A' = [A]'$ and $C_A'' = [A]''$ we obtain from eqn. (19)

$$\beta_1 = \frac{qC_A''f_A''/a''_{aq} - C_A'f_A'/a'_{aq}}{C_A'f_A'/a'_{aq} \cdot C_A''f_A''/a''_{aq}(1-q)} \tag{20}$$

Here f'_A and a'_{aq} denote the activity coefficient of A and water activity at $C_A = C'_A$, etc.

These quantities are calculated from eqns. (11 a) and (11 b) under the same assumption as before, *i.e.*, that f_A and a_{aq} are functions dependent only on C_A. This means that f_A and a_{aq} are now determined by the condition that $f_A = 1$ and $a_{aq} = 1$ in solutions 0.1 M NH_4ClO_4, $C_A = 0$.

From the paper [35] referred to it follows that if other complexes than the first one also exist, the value of β_1 will be too small.

On the other hand, if only the first complex exists, as assumed here, but the determination is performed at a rather high ammonia concentration, the value of β_1 thus found will be greater than that valid at zero ammonia concentration, as follows from eqn. (15).

From these measurements we can thus expect only an indication of the order of magnitude of β_1.

Experimental. The measurements were performed in the ultraviolet wave length region, where outer-sphere association has previously been found to cause the greatest change in the absorption spectrum of the cobalt hexammine ion (Refs. [2,3,9-11]). The apparatus used was a Beckman Quartz Spectrophotometer (Model DU), changed as described by Adell [36].

The solutions were all 5.00 mM with respect to $Co(NH_3)_6(ClO_4)_3$. The ionic strength was kept 0.1 M by adding NH_4ClO_4. Four sets of measurements were made, with $C_A = 0$, 0.320, 0.640 and 0.960 M. The reference cell contained ammonia at the same concentration and so much of NH_4ClO_4 that the perchlorate concentration was equal to that in the other cell.

For $E > 0.1$ the reproducibility was ± 2 %, which may be accepted in view of the great systematic errors of the method.

Table 4. Calculation of the quotient q and β_1 from the experimental values of ε_M and ε_0.

$C'_A = 0.320$ M; $q_1 = \frac{\varepsilon'_M - \varepsilon_0}{\varepsilon'''_M - \varepsilon_0}$		$C''_A = 0.640$ M;		$C'''_A = 0.960$ M $q_2 = \frac{\varepsilon''_M - \varepsilon_0}{\varepsilon'''_M - \varepsilon_0}$		
mμ	$\log \varepsilon_0$	$\log \varepsilon'_M$	$\log \varepsilon''_M$	$\log \varepsilon'''_M$	q_1	q_2
255	0.765	0.925	1.00	1.075	0.43	0.69
250	1.105	1.235	1.305	1.37	0.42	0.70
248	1.27	1.38	1.445	1.505	0.40	0.69
246	1.455	1.55	1.605	1.66	0.41	0.69
244	1.645	1.72	1.765	1.815	0.39	0.67
242	1.85	1.91	1.95	1.99	0.39	0.68
240	2.06	2.105	2.135	2.17	0.38	0.65
238	2.265	2.30	2.33	2.355	0.37	0.71
236	2.465	2.495	2.515	2.535	0.41	0.69
234	2.66	2.68	2.70	2.715	0.36	0.71
233	2.75	2.77	2.785	2.805	0.35	0.63
232	2.84	2.865	2.88	2.895	0.44	0.72
231	2.93	2.95	2.965	2.98	0.38	0.69
				Mean	0.39	0.69
					β_1 M^{-1}	
					0.38	0.20
					0.3 ± 0.2	

If we attribute the second-order term in a_A/a_{aq}, that was found from the solubility measurements, exclusively to the change in the dielectric constant we can introduce in eqn. (19) the correction:

$$\beta_1 = (\beta_1)_0 + 0.05\ a_A/a_{aq}$$

This gives us a second-order equation in $(\beta_1)_0$ which renders $(\beta_1)_0 = 0.44$ and 0.32, valid at $C_A = 0$ and $I = 0.1$ M and corresponding to the two values of q of Table 4.
This correction thus reduces the relative spreading appreciably.

Results. In Table 4 the calculations are shown for those wave lengths where the shift of the extinction coefficients is large enough to permit calculations of some degree of accuracy.

COMPARISON BETWEEN THE SOLUBILITY AND THE LIGHT ABSORPTION METHODS

As different standard states have been used for f_A in the solubility measurements and in the light absorption measurements, the constants obtained are not directly comparable.

However, from theoretical considerations Bjerrum (Ref.[20], p. 129) presents the formula,

$$\log \beta = \log \beta_0 + 0.03\ C_{NH_4^+} \qquad (21)$$

where β denotes the association constant for the association of one ammonia to a metal ion. Experimentally he finds very different values of the coefficient, both positive and negative ones, and especially for the reaction

$$MA_5H_2O + A \rightleftharpoons MA_6 + H_2O$$

he finds (Ref.[20], p. 281) for the equilibrium constant β

$$\log \beta = \log \beta_0 + 0.18\ C_{NH_4^+} \qquad (22)$$

If this surprisingly great coefficient is assumed to apply also for the very similar reaction considered here,

$$MA_6 + A \rightleftharpoons (MA_6)A$$

we must conclude that β_1 at ionic strength 1 M should be about 40 % greater than at ionic strength 0.1 M.

Thus for ionic strength 1 M we have:

$\beta_1 = 0.24 \pm 0.05\ M^{-1}$ (solubility method)
$\beta_1 = 0.4 \pm 0.3\ M^{-1}$ (light abs. method)

If we prefer to make the "salt effect" correction with the help of eqn. (21), we obtain a smaller value $\beta_1 = 0.3 \pm 0.2\ M^{-1}$ (light abs. method).

Furthermore, if there exists a slight barium-ammonia complexity, which we have assumed not to be the case, the value of β_1 calculated from the solubility measurements should be somewhat greater. (The curve in the left diagram of Fig. 1 should be steeper and for a given value of C_A we should obtain a greater X than that reported.)

To sum up, we can state that the results of the two methods are not inconsistent.

The author is indebted to Prof. S. Bodforss, Dr. B. Adell, Dr. S. Ahrland and Dr. S. Fronæus for their kind interest that has promoted this work.

REFERENCES

1. Posey, F. A. and Taube, H. *J. Am. Chem. Soc.* **78** (1956) 15.
2. Bale, W. D., Davies, E. W. and Monk, C. B. *Trans. Faraday Soc.* **52** (1956) 816.
3. Grimblett, F. G. R. and Monk, C. B. *Trans. Faraday Soc.* **51** (1955) 793.
4. Davies, C. W. *J. Chem. Soc.* **1930** 2421.
5. Denney, T. O. and Monk, C. B. *Trans. Faraday Soc.* **47** (1951) 992.
6. Brintzinger, H. and Osswald, H. *Z. anorg. u. allgem. Chem.* **223** (1935) 253.
7. Laitinen, H. A., Frank, A. J. and Kivalo, P. *J. Am. Chem. Soc.* **75** (1953) 2865.
8. Jenkins, I. L. and Monk, C. B. *J. Chem. Soc.* **1951** 68.
9. Linhard, M. *Z. Elektrochem.* **50** (1944) 224.
10. Evans, M. G. and Nancollas, G. H. *Trans. Faraday Soc.* **49** (1953) 363.
11. Kubota, T. *J. Chem. Soc. Japan* **75** (1954) 552.
12. Percock, J. M. and James, J. C. *J. Chem. Soc.* **1951** 2233.
13. Adamson, A. W. and Basolo, F. *Acta Chem. Scand.* **9** (1955) 1261.
14. Ašperger, S. and Ingold, C. K. *J. Chem. Soc.* **1956** 2862.
15. Larsson, R. *Acta Chem. Scand.* **11** (1957) 1405.
16. Owen, B. B. *J. Am. Chem. Soc.* **54** (1932) 1758.
17. Born, M. *Z. Physik* **1** (1920) 45.
18. Davies, T. W. and Ricci, J. E. *J. Am. Chem. Soc.* **61** (1939) 3274.

19. Mayper, S. A., Clever, H. L. and Verhoek, F. H. *J. Phys. Chem.* **58** (1954) 90.
20. Bjerrum, J. *Metal Ammine Formation in Aqueous Solution*, (Diss.) University, Copenhagen 1941.
21. Perman, E. P. *J. Chem. Soc.* **83** (1903) 1168.
22. Åkerlöf, G. *J. Am. Chem. Soc.* **54** (1932) 4125; **58** (1936) 1241.
23. Eigenberger, E. *J. prakt. Chem.* **130** (2) (1931) 75.
24. Hasted, J. B., Ritson, D. M. and Collie, C. H. *J. Chem. Phys.* **16** (1948) 1.
25. Monk, C. B. *J. Chem. Soc.* **1951** 2723.
26. Bockris, J. O'M., Bowler-Reed, J. and Kitchener, J. A. *Trans. Faraday Soc.* **47** (1951) 184.
27. Grün, A. and Husmann, J. *Chem. Ber.* **43** (1910) 1291.
28. Rydberg, J. *Arkiv Kemi* **8** (1956) 113.
29. Katzin, L. I. *J. Inorg. & Nuclear Chem.* **4** (1957) 187.
30. Kratohvil, J. and Težak, B. *Rec. trav. chim.* **75** (1956) 775.
31. Lindo, D. *Chem. News* **58** (1888) 176.
32. Ephraim, F. *Z. anorg. u. allgem. Chem.* **147** (1925) 24.
33. Spacu, G. and Voichescu, P. *Z. anorg. u. allgem. Chem.* **243** (1940) 288.
34. Nakatsuka, Y. *Bull. Chem. Soc. Japan* **11** (1936) 629.
35. Ahrland, S. *Acta Chem. Scand.* **5** (1951) 1271.
36. Adell, B. *Acta Chem. Scand.* **4** (1950) 1.

Received February 22, 1958.

ACTA CHEMICA SCANDINAVICA 12 (1958) 723—730

A Kinetic Study of the Reaction of *iso*Propoxy-methyl-phosphoryl Fluoride (Sarin) with Hydrogen Peroxide

LENNART LARSSON

Research Institute of National Defence, Dept. 1, Sundbyberg 4, Sweden

The reaction of *iso*propoxy-methyl-phosphoryl fluoride (Sarin) and hydrogen peroxide has been investigated and the bimolecular rate constant and energy and entropy of activation of the formation of *iso*propoxy-methyl-perhydroxy-phosphine oxide have been calculated. It has been suggested that the reaction involves a nucleophilic attack of the perhydroxyl ion on the phosphorus atom, and that the transition state is stabilized by the formation of a hydrogen bond between the perhydroxyl ion and the oxygen atom of the phosphoryl group. It has been shown that the decomposition of the peroxy acid proceeds by two competitive reactions, the rate constants of which have been calculated.

The reaction of organic phosphorus compounds with hydrogen peroxide plays an important role in the Schönemann reaction. The principle of this reaction is the oxidation of amines, such as benzidine, to coloured products by hydrogen peroxide in the presence of various phosphorus compounds [1]. The reaction has been made the basis of a sensitive method for the quantitative determination of nerve gases [2,3].

In this connection it was of interest to study the reaction between Sarin and alkaline solutions of hydrogen peroxide in the absence of an oxidizable amine. Gehauf *et al.*[2] have discussed the mechanism of this reaction and have postulated the following scheme for the formation and decomposition of *iso*propoxy-methyl-perhydroxy-phosphine oxide. In the same scheme the alkaline hydrolysis of Sarin (I) is also given.

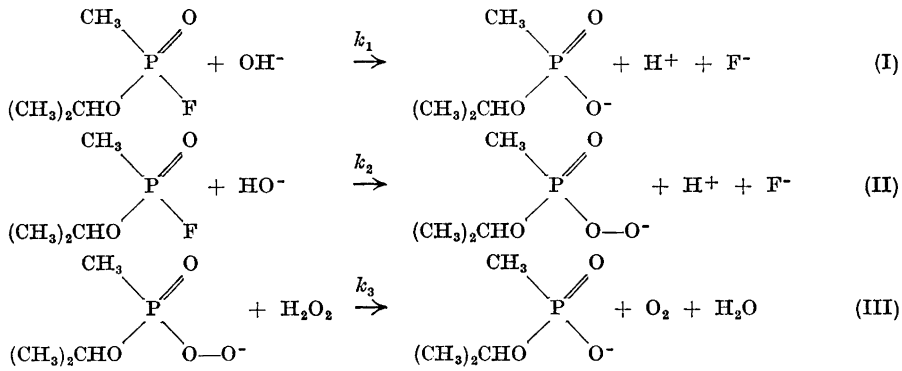

The same mechanism has also been proposed by Epstein *et al.*[4] in the study of the reaction between diethyl *p*-nitrophenyl phosphate (Paraoxon) and hydrogen peroxide. The present report is an attempt to make a detailed investigation of the reaction of Sarin with hydrogen peroxide at various pH-values and temperatures.

EXPERIMENTAL

Materials. Sarin was synthesized in this institute and freshly distilled before use[5]. A stock solution of Sarin in dioxane, E. Merck c.p. purified from peroxides and redistilled over sodium, was prepared. The concentration of Sarin in this solution was 8.0 mM.

Hydrogen peroxide (about 30 %), E. Merck anal. reagent. The exact concentration was determined by titration with 0.1 N solution of potassium permanganate.

Paper chromatographic technique. The final products of the reaction were analyzed by means of paper chromatographic technique. A solution containing 0.5 % Sarin and 0.5 % hydrogen peroxide in 0.1 M ammonium hydroxide was prepared. At this pH the reaction is almost instantaneously completed. By means of a micropipette 5 μl of this solution were placed on a filter paper, Whatman No. 1, and the spot was dried in hot air. Ascending technique was used, and the chromatogram was run at 25°C. An acid solvent with the following composition was used: *n*-butanol:ethanol:acetic acid:water (8:2:1:3)[6]. After the drying, phosphorus was developed by spraying the paper with an acid solution of ammonium molybdate and treating the dried paper with hydrogen sulfide[7].

Kinetic measurements. The kinetics of the reaction were studied in a manner similar to that described for the hydrolysis of Sarin and its analogues by means of an automatic recording titrator[5]. Two types of experiments were performed.

Procedure I. In the first series of experiments the reaction rate constant, k_2 (Reaction II), was determined by excess of hydrogen peroxide at 25°C at the pH-values 7.70, 8.00 and 8.50, and at 35°C at the pH-values 7.70 and 8.00. A solution containing 38.00 ml of 0.10 M potassium chloride and 1.00 ml of appropriately diluted hydrogen peroxide was adjusted by the titrator to a preselected pH-value, after which 1.00 ml of the stock solution of Sarin was added. The initial concentration of Sarin was 0.20 mM in every run and the initial concentration of hydrogen peroxide varied between 2.50 and 10.00 mM. The reaction was allowed to terminate, and the concentrations of Sarin at different times were calculated from the recorded amount of alkali consumed in the reaction. Such a calculation presupposes that the *iso*propoxy-methyl-hydroxy-phosphine oxide as well as the *iso*propoxy-methyl-perhydroxy-phosphine oxide formed in the reaction is totally ionized in the prevailing pH range.

Procedure II. In a second series of experiments which were performed at 25°C and pH 8.50, the initial concentration of Sarin was the same as mentioned above but that of the hydrogen peroxide was 0.50 mM. The initial and final concentrations of hydrogen peroxide were determined colorimetrically with titanium sulphate[8]. In other respects the same experimental technique was used as described under I. The spontaneous decomposition of hydrogen peroxide was checked during 2 h in a separate run and was found to be insignificant.

In two runs 1.00 ml of sample was withdrawn from the reaction vessel at intervals and added to 2.00 ml of a 1.25 % solution of *o*-tolidine in acetone and 2.00 ml of water. The optical density of the mixture was determined after 2 min in a 5 cm absorption cell at 4 250 Å with a Beckmann spectrophotometer, Type B. From these measurements it was possible to determine at which time during the reaction the concentration of the "peroxyphosphorus acid" attained its maximum value. A determination of the actual concentration of the peroxy acid, however, would be very difficult, because the rate of the colour reaction is unknown.

Determination of dissociation constants. The mixed dissociation constant, K_a', of *iso*propoxy-methyl-hydroxy-phosphine oxide was determined by potentiometric titration of a 5 mM hydrolysate of *iso*propoxy-methyl-phosphoryl chloride in 0.10 M potassium chloride solution with 0.1 M sodium hydroxide. The details of the procedure and the calculations are described in an earlier paper[9]. Two runs at 25°C gave $pK_a' = 2.10 \pm 0.05$.

Owing to the instability of the "peroxyphosphorus acid" formed it has not been possible to determine its dissociation constant. However, presuming that the relationship

between the dissociation constants of the "phosphorus acid" and the peroxy acid is the same as that between those of a carboxylic acid and the corresponding peroxy acid [10], pK'_a of the "peroxyphosphorus acid" may be estimated at 5—6.

RESULTS AND DISCUSSION

Formation of *iso*propoxy-methyl-perhydroxy-phosphine oxide

The formation of a "peroxyphosphorus acid" as an intermediate in the reaction of Sarin with hydrogen peroxide has been supported by the fact that the reaction mixture oxidizes thiosulphate ion to sulphate ion [2]. According to Feigl this anomalous oxidation of thiosulphate has been attributed to peroxy acids [11]. Also the oxidation of certain amines by hydrogen peroxide in the presence of organic phosphorus compounds indicates the formation of this intermediate. Furthermore the fluorine atom is split off more rapidly than the oxygen molecule is formed [2].

In the reaction two equivalents of acid were formed. On the basis of the estimated value of the dissociation constant of the "peroxyphosphorus acid", this acid was considered as totally ionized in the pH range in question. The subsequent decomposition of the peroxy acid according to Reaction III will then not cause any further consumption of alkali. The concentration of Sarin at different times was therefore calculated from the amount of alkali consumed. When hydrogen peroxide is in excess, the reaction can be treated as a pseudo first-order reaction. When the logarithm of the concentration of Sarin (c_{PF}) was plotted against the time a straight line was obtained as appears in Fig. 1. It is also shown in the figure that at low concentrations of hydrogen peroxide the curve deviates from the straight line at the end of the reaction, indicating that the decrease of the hydrogen peroxide concentration can only be neglected in the first part of the reaction.

From the curves obtained the observed rate constants, k_{obs}, were calculated. It is obvious from Table 1 that, at the lower pH-values, where sponta-

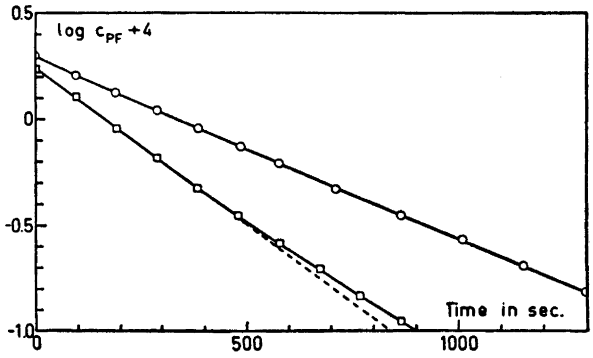

Fig. 1. First order plots for the reaction of Sarin with hydrogen peroxide when initial concentrations of hydrogen peroxide are 10.0 mM (○) and 2.5 mM (□) at pH 7.70 and 8.50, respectively, at 25°C.

Table 1. The rate constants for the reaction of Sarin with hydrogen peroxide at various temperatures and pH-values. The initial concentration of Sarin was 0.20 mM.

t°C	pH	$c_{H_2O_2}$ mM	$k_{obs} \times 10^3$ sec^{-1}	$k_1 \times 10^3$ sec^{-1}	$k_2 \times 10^{-3}$ l mole^{-1} sec^{-1}
25.0	7.70	5.00	1.04	0.017	1.40
	7.70	5.00	1.04	0.017	1.40
	7.70	10.00	2.00	0.017	1.36
	7.70	10.00	1.93	0.017	1.31
	8.00	5.00	1.96	0.034	1.32
	8.00	5.00	1.96	0.034	1.32
	8.00	10.00	3.70	0.034	1.26
	8.00	10.00	3.98	0.034	1.35
	8.50	2.50	3.39	0.106	1.42
	8.50	2.50	2.98	0.106	1.24
35.0	7.70	5.00	2.60	0.058	2.18
	7.70	5.00	2.40	0.058	2.01
	7.70	5.00	2.37	0.058	1.98
	8.00	2.50	2.42	0.116	1.97
	8.00	2.50	2.40	0.116	1.96
	8.00	2.50	2.59	0.116	2.12

neous hydrolysis is negligible, k_{obs}, at constant pH, is proportional to the concentration of hydrogen peroxide, which indicates a bimolecular reaction mechanism. The variation of rate with pH shows that the perhydroxyl ion is the active component in the reaction.

The true second-order rate constant, k_2, was calculated from the expression:

$$k_2 = \frac{k_{obs} - k_1}{c_{HO_2^-}} \tag{1}$$

where the observed rate constant is corrected for the rate constant of the spontaneous hydrolysis, k_1, found from earlier experiments [5]. According to the law of mass action the perhydroxyl ion concentration is:

$$c_{HO_2^-} = \frac{K'_{H_2O_2} \cdot c^\circ_{H_2O_2}}{a_{H+} + K'_{H_2O_2}} \tag{2}$$

where $c^\circ_{H_2O_2}$ is the total concentration of hydrogen peroxide and $K'_{H_2O_2}$, the mixed dissociation constant. The values of $K'_{H_2O_2}$ at 25°C and 35°C in 0.10 M potassium chloride solution were estimated at 2.92×10^{-12} and 4.66×10^{-12}, respectively, from the thermodynamic constants given by Evans and Uri [12]. When $a_{H+} \gg K'_{H_2O_2}$ which is valid in the present pH range, eqn. (2) is reduced to:

$$c_{HO_2^-} = \frac{K'_{H_2O_2} \cdot c^\circ_{H_2O_2}}{a_{H+}} \tag{3}$$

The values of k_2 at 25°C and 35°C are given in Table 1 and their mean values were found to be $k_2^{25} = (1.34 \pm 0.06) \times 10^3$ l mole^{-1} sec^{-1} and $k_2^{35} = (2.04 \pm 0.09) \times 10^3$ l mole^{-1} sec^{-1}. From these rate constants the energy of activation

was calculated as 7.7 ± 1.6 kcal mole^{-1} and the entropy of activation as -20 ± 5 E.U.

The facts that straight line plots are obtained from the experiments and that k_2 is independent of pH, support the hypothesis that *iso*propoxy-methyl-perhydroxy-phosphine oxide is totally ionized in the present pH range.

The mechanism of the reaction of Sarin with perhydroxyl ions may be considered to be analogous to that of the alkaline hydrolysis of Sarin, *i.e.* it involves a nucleophilic attack of the perhydroxyl ion on the phosphorus atom. The rate of this reaction has been shown to be about 50 times greater than that of the alkaline hydrolysis. This difference may be due to perhydroxyl ion being more nucleophilic than hydroxyl ion in spite of the greater basicity of the latter. Another reason for the greater rate of reaction is that perhydroxyl ion will contribute to the stabilization of the transition state by the formation of a hydrogen bond such as

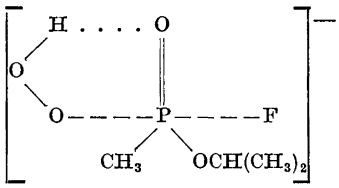

The formation of a hydrogen bond in the association of phenol with Sarin has been demonstrated in an infra-red spectroscopic study [13]. It has also been shown in this study that the absorption band of the P=O group shifts to lower frequency corresponding to a bond weakening, and that of the P—F group shifts to higher frequency corresponding to a bond strengthening. These results indicate that a hydrogen bond to the oxygen atom in the P=O group is formed. Thus it seems very probable that such a hydrogen bond also will be formed between the perhydroxyl ion and the oxygen atom in the P=O group in the transition state as suggested above.

Decomposition of *iso*propoxy-methyl-perhydroxy-phosphine oxide

The decomposition of the "peroxyphosphorus acid" shown in Reaction III has been supported by the consumption of two moles of hydrogen peroxide and the evolution of one mole of oxygen per mole of Sarin [2] when excess of hydrogen peroxide was used. By means of paper chromatography only a single final product containing phosphorus was found, and this was identified from its R_F value as *iso*propoxy-methyl-hydroxy-phosphine oxide, *i.e.* the same product as was formed in the spontaneous hydrolysis [5].

For the detailed kinetic study of the decomposition only a slight excess of hydrogen peroxide was used. In this case the spontaneous hydrolysis of Sarin was obvious, and it was necessary to take it into consideration in the calculations. To get a conception of the magnitude of the rate constant k_3, two separate calculations of the constant k_2 were made. In one case it was assumed that $k_3 \gg k_2$ and in the other that $k_3 \ll k_2$. The differential equations obtained

were evaluated by means of graphical integration analogously to the method described by Wideqvist [14]. The constant k_2 for the two cases was calculated after various times of reaction. For a value of k_3 between these extreme values, k_2 might increase with time when the calculations are based on the first assumption, and decrease when the calculations are based on the second one. It was, however, found that in both alternatives k_2 was increasing which indicates that Sarin reacts in an additional way to the one which was postulated before. A supplementary reaction such as the following is probable:

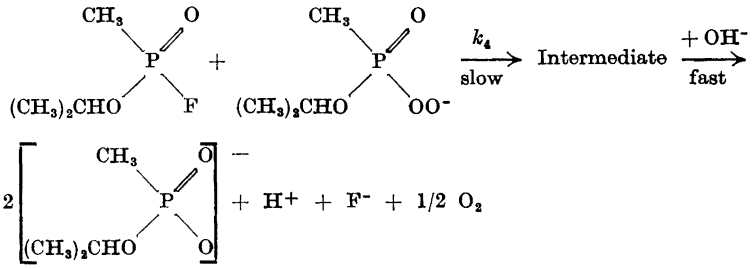

(IV)

For the Reactions I—IV the following differential equations can be set up:

$$\frac{dc_{PF}}{dt} = -k_1 c_{PF} - k_2 c_{PF} c_{HO_2^-} - k_4 c_{PF} c_{POO^-} \tag{4}$$

$$\frac{dc_{H_2O_2}}{dt} = -k_2 c_{PF} c_{HO_2^-} - k_3 c_{POO^-} c_{H_2O_2} \tag{5}$$

$$\frac{dc_{POO^-}}{dt} = k_2 c_{PF} c_{HO_2^-} - k_3 c_{POO^-} c_{H_2O_2} - k_4 c_{PF} c_{POO^-} \tag{6}$$

The differential equations were treated by means of a recording electronic computer (Precision Analog Computing Equipment, Electronic Associates, Inc.). The known values of c°_{PF}, $c^\circ_{H_2O_2}$, $c^\circ_{POO^-}$, k_1 and k_2 were put into the equations and k_3 and k_4 were varied until the recorded curve of the function c_{PF} against t coincided with the experimental one. The best agreement was obtained when $k_3 = 3.0$ l mole^{-1} sec^{-1} and $k_4 = 3.5$ l mole^{-1} sec^{-1} as appears from Fig. 2. For comparison the curves obtained from some other values of the constants k_3 and k_4 are given in the same figure.

In Fig. 3 the functions c_{PF}, c_{POO^-} and $c_{H_2O_2}$ against t are given with the values of k_3 and k_4 found above. From the c_{POO^-} curve it is shown that the maximum concentration of "peroxyphosphorus acid" is reached after 900 sec. From the colorimetric determination the maximum concentration was found to be between 800 and 900 sec which agrees fairly well with the calculated value. From the $c_{H_2O_2}$ curve the amount of hydrogen peroxide consumed in the reaction after 7 000 sec was estimated as 1.30 moles per mole of Sarin. The corresponding value from the determinations of the concentrations of hydrogen peroxide at the start and at the end of the reaction (after 4 h) was found to be 1.42. It is possible that the discrepancy between the found

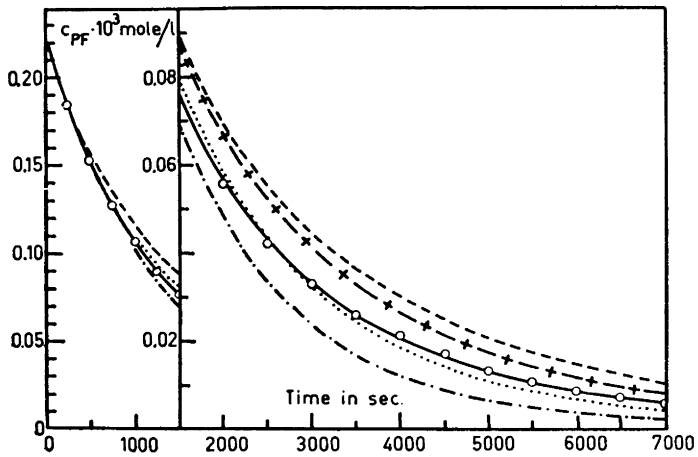

Fig. 2. The computed curves for the function c_{PF} against t at pH 8.50 and 25°C at various values of k_3 and k_4.
$k_1 = 0.106 \times 10^{-3}$ sec^{-1}; $k_2 = 1.34 \times 10^3$ l mole^{-1} sec^{-1}

k_3 l mole^{-1} sec^{-1}	k_4 l mole^{-1} sec^{-1}	Designation
3.0	3.5	————
5.0	1.0	— — — —
0.50	1.0	. . . . .
0.50	3.0	— . — . —
1.0	0.10	— + — +

The experimental values are designed O.

and calculated consumption of hydrogen peroxide depends upon the spontaneous decomposition of hydrogen peroxide which has been neglected in the calculations.

In the determination of the rate constant, k_2, the influence of Reaction IV is practically negligible, because in those experiments the concentration of hydrogen peroxide was so high that Reaction III predominated over Reaction IV.

From the experimental data obtained no conclusions concerning the mechanisms of Reaction III can be drawn. Reaction IV probably proceeds over a peroxypyrophosphate formed by a nucleophilic attack of the peroxy acid on the phosphorus atom of the Sarin molecule. The hydrolysis of the intermediate is certainly very fast. There is a possibility that the intermediate is hydrolysed to one molecule "peroxyhosphorus acid" and one molecule "phosphorus acid" in contrast to what is stated in Reaction IV. However, the good agreement obtained between the experimental and calculated curves argues against the latter hypothesis and favours the process given in Reaction IV.

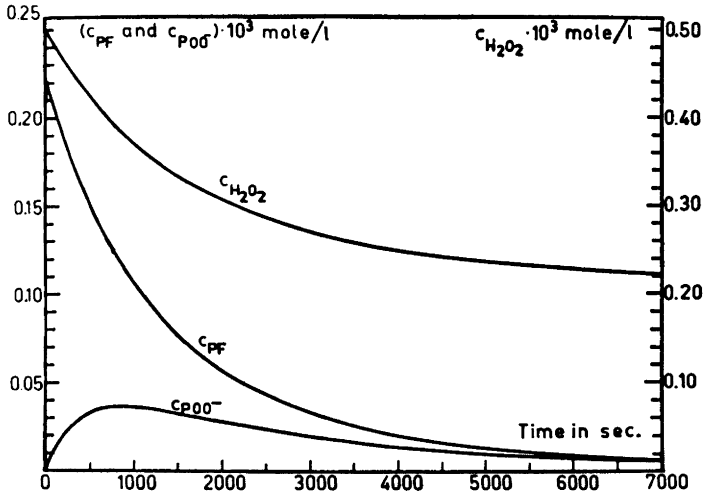

Fig. 3. The computed curves for the functions c_{PF}, c_{POO^-} and $c_{H_2O_2}$ against t at pH 8.50 and 25°C. $k_1 = 0.106 \times 10^{-3}$ sec^{-1}, $k_2 = 1.34 \times 10^3$ l mole^{-1} sec^{-1}, $k_3 = 3.0$ l mole^{-1} sec^{-1} and $k_4 = 3.5$ l mole^{-1} sec^{-1}.

My sincere thanks are due to Professor G. Ljunggren, Director of this Institute, for the kind interest he has shown in this work. The author wishes also to express his sincere thanks to Docent L. Melander, Nobel Institute of Chemistry, for stimulating criticism and discussions, and to Fil.kand. J. Prawitz for his kind assistance in programming the computor.

REFERENCES

1. Wheeler, C. L. (translator). *A new reaction for the detection for the metalloid (non-metal) labile halogen linkage*, **PB 119887** U.S. Department of Commerce, August 1944.
2. Gehauf, B., Epstein, J., Wilson, G. B., Witten, B., Sass, S., Bauer, V. E. and Rueggeberg, W. H. C. *Anal. Chem.* **29** (1957) 278.
3. Marsh, D. J. and Neale, E. *Chem. & Ind. London* **1956** 494.
4. Epstein, J., Demek, M. M. and Rosenblatt, D. H. *J. Org. Chem.* **21** (1956) 796.
5. Larsson, L. *Acta Chem. Scand.* **11** (1957) 1131.
6. Augustinsson, K.-B. and Grahn, M. *Acta Chem. Scand.* **7** (1953) 906.
7. Hanes, C. S. and Isherwood, F. A. *Nature* **164** (1949) 1107.
8. Eisenberg, G. M. *Ind. Eng. Chem. Anal. Ed.* **15** (1943) 327.
9. Larsson, L. and Hansen, B. *Svensk Kem. Tidskr.* **68** (1956) 521.
10. Everett, A. J. and Minkoff, G. J. *Trans. Faraday Soc.* **49** (1953) 410.
11. Feigl, F. *Specific and special reactions.* Elsevier Publishing Co, Inc., New York 1940, pp. 127–128.
12. Evans, M. G. and Uri, N. *Trans. Faraday Soc.* **45** (1949) 224.
13. Larsson, L. *Arkiv Kemi* **13** (1958) *(In press)*.
14. Wideqvist, S. *Acta Chem. Scand.* **4** (1950) 1216.

Received February 19, 1958.

ACTA CHEMICA SCANDINAVICA 12 (1958) 731—736

On the Reaction between Substituted Malonic Esters and Methylene Bromide. II

LENNART EBERSON

Department of Organic Chemistry, Chemical Institute, University of Lund, Sweden

$\alpha,\alpha,\omega,\omega$-Tetracarbethoxyalkanes of the type III with n = 0, 2, 3, in the form of their disodium compounds, react with methylene bromide in ethanolic solution with the formation of the tetraesters IV, n = 0, 2, 3. With III, n = 1, the reaction takes another course and mainly pentaethyl 1,1,3,3,5-pentacarboxylate (VI) is formed.

The reaction between the sodium compound of a monosubstituted malonic ester and methylene bromide in ethanolic solution has been found to proceed according to the formula [1,2]:

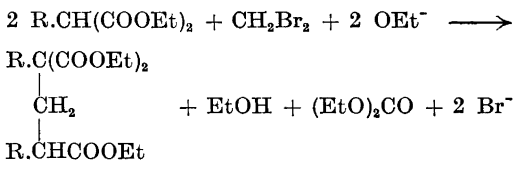

I

for R = methyl, ethyl, *n*-propyl, *iso*propyl, *n*-butyl, *iso*butyl-, *n*-amyl, benzyl, trimethylsilylmethyl, and acetamino, *i.e.*, one carbethoxy group is eliminated and a tricarboxylic ester (I) is formed. When R is an electronegative group, such as phenyl or carbethoxy, an $\alpha\alpha'$-disubstituted glutaric ester (II) is formed directly with the elimination of two carbethoxy groups.

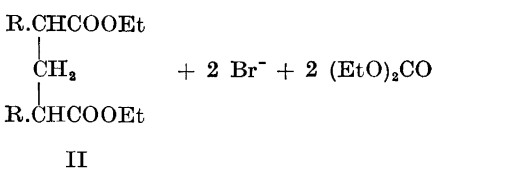

II

The investigation now has been extended to the study of the reaction between an $\alpha,\alpha,\omega,\omega$,-tetracarbethoxyalkane (III, n = 0—3) and methylene bromide.

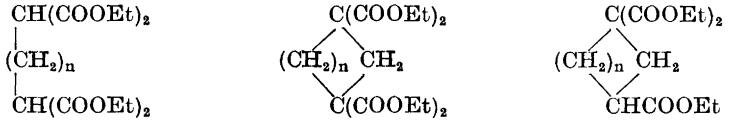

III IV V

Various examples of this reaction leading to cyclic compounds of the type IV are found in the literature. Kötz and Stalmann [3] investigated the reaction between the disodium compound of 1,1,2,2,-tetracarbethoxyethane and methylene iodide at 130° in absolute ethanol. They claimed that one solid (m. p. 43°) and one liquid form of tetraethyl *cyclo*propane-1,1,2,2-tetracarboxylate (IV, n = 0) were formed. They also stated that no reaction took place at temperatures below 130° and that the exchange of methylene iodide for the corresponding chloride led to very poor yields.

Guthzeit and Dressel [4] claimed that the main product from the reaction between 1,1,3,3-tetracarbethoxypropane (III, n = 1) and methylene iodide was tetraethyl *cyclo*butane-1,1,3,3-tetracarboxylate (IV, n = 1). However no proof of structure was given. Furthermore the same reaction with 1,1,4,4-tetracarbethoxybutane (III, n = 2) [5–8] and 1,1,5,5-tetracarbethoxypentane (III, n = 3) [9] has been shown to yield IV, n = 2 and 3, respectively.

In view of the above results for alkylmalonic esters it seemed worth while to reinvestigate the cited reactions to establish whether a similar elimination of a carbethoxy group with the formation of V occurs parallel to the formation of IV.

1. The reaction between 1,1,2,2-tetracarbethoxyethane and methylene bromide (iodide). This reaction took place in boiling ethanolic solution both with the bromide and the iodide, contrary to the statement of Kötz and Stalmann [3] that temperatures above 130° were required to obtain reasonable yields. The product was distillable and consisted exclusively of tetraethyl *cyclo*propane-1,1,2,2-tetracarboxylate with m. p. 41—43°. No trace of diethyl carbonate, which would have resulted if a carbethoxy group had been eliminated, could be detected.

2. The reaction between 1,1,3,3-tetracarbethoxypropane and methylene bromide (iodide). If this reaction was carried out in boiling ethanolic solution (about 80°) with methylene bromide or iodide a very viscous oil was obtained. When distilled *in vacuo* it decomposed and the decomposition products smelt very strongly of diethyl methylenemalonate. Apparently the crude reaction product consisted of polymeric diethyl methylenemalonate to a great extent. On alkaline or acid hydrolysis only tarry products were obtained. However, if the reaction temperature was raised to 100°, the product was distillable and a main fraction boiling at 210—215°/4 mm was obtained. On acid hydrolysis it yielded an acid with m.p. 212—215°, which was identified as *cyclo*hexane-1,3,5-tricarboxylic acid. On alkaline hydrolysis an acid with m.p. 180—184° (decomp.) was obtained, which lost carbon dioxide upon boiling with dilute

hydrochloric acid and gave *cyclo*hexane-1,3,5-tricarboxylic acid. The analyses indicated that the original ester was pentaethyl *cyclo*hexane-1,1,3,3,5-pentacarboxylate (VI) and that the acid with m. p. 180—184° was *cyclo*hexane-1,1,3,3,5-pentacarboxylic acid.

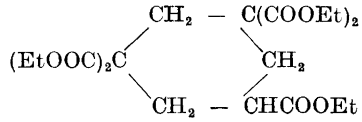

VI

A small amount of diethyl carbonate was isolated. No compound belonging to the *cyclo*butane series could be found.

3. The reaction between 1,1,4,4-tetracarbethoxybutane and methylene bromide. The investigation of this reaction confirmed the results of Pospischill [5], Thole and Thorpe [6], Perkin and Scarborough [7], and Guha and Ranganathan [8]. The yield of IV, n = 2, was poor and considerable amounts of tarry by-products were obtained as the above authors also have found. A small amount of diethyl carbonate, which probably resulted from the reaction between 1,1,4,4-tetracarbethoxybutane and ethoxide ion [10], was isolated. IV, n = 2, has been found to be stable under the reaction conditions employed [6].

4. The reaction between 1,1,5,5-tetracarbethoxypentane and methylene bromide. Perkin's [9] results were fully confirmed and only IV, n = 3, could be isolated. No diethyl carbonate was found.

DISCUSSION

At first the reaction between 1,1,3,3-tetracarbethoxypropane and a methylene halide will be considered, as it deviates from the normal behaviour. Meerwein and Schürmann [11] have shown that 1,1,3,3-carbomethoxypropane reacts with sodium methylate in methanol in a complex manner with the formation of a bi*cyclo*nonane derivative. They were also able to demonstrate the intermediate steps of the reaction and that the same products were obtained irrespective of whether the starting materials were sodium methoxide and 1,1,3,3-tetracarbomethoxypropane, sodium methoxide, 1,1,3,3-tetracarbomethoxypropane, and dimethyl methylenemalonate or sodium methoxide, methylene iodide, and dimethyl malonate.

The formation of pentaethyl *cyclo*hexane-1,1,3,3,5-pentacarboxylate can be easily explained on the basis of Meerwein and Schürmann's investigations in the following way: In an alkaline medium 1,1,3,3-tetracarbethoxypropane is in equilibrium with a mixture of diethyl methylenemalonate and diethyl malonate.

$$(EtOOC)_2CHCH_2CH(COOEt)_2 \rightleftharpoons CH_2 = C(COOEt)_2 + CH_2(COOEt)_2$$

Diethyl methylenemalonate then reacts with 1,1,3,3-tetracarbethoxypropane (a Michael addition) according to the formula:

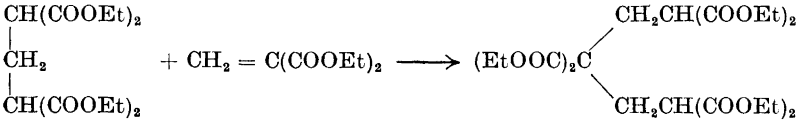

1,1,3,3,5,5-hexacarbethoxypentane is formed as has been proved by Meerwein and Schürmann in the case of the methyl derivative and is cyclized with the excess of methylene halide with the formation of VI and the elimination of one carbethoxy group as diethyl carbonate.

In the previous paper dealing with this subject [2], a reaction scheme for the reaction between a monosubstituted malonic ester and a methylene halide was proposed. It can be summarized in the following way:

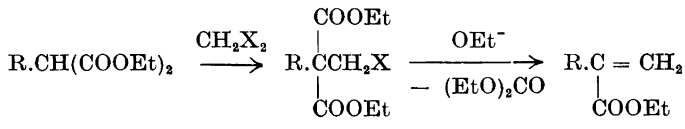

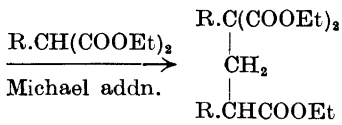

Apparently this mechanism is not always valid when the two malonic ester residues are situated within the same molecule. However, the first step must be the formation of a bromomethyl-substituted compound VII.

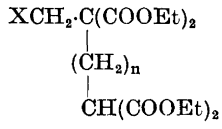

VII

The second step may take place either according to the above mechanism *via* an unsaturated compound (elimination of one carbethoxy group to form V) or the halogen atom may be displaced directly by reaction with the second anionic center. Actually both situations have been observed (formation of compound VI and compound IV, n = 0, 2, 3), but it is difficult to draw any conclusions from the above data regarding the structural features which determine the course of the reaction. The second mechanism is rather remarkable as it involves displacement of a halogen atom under normal conditions in a structure analogous to the *neo*pentyl halides [12]. Probably this is a manifestation of the well known but not entirely understood effect, that accommodation of substituents at the ends of a closing carbon chain facilitates ring formation.

EXPERIMENTAL

Tetraethyl cyclo*propane-1,1,2,2-tetracarboxylate.* Sodium, 9.2 g (0.4 mole), was dissolved in 150 ml of absolute ethanol, and 63.6 g (0.2 mole) of 1,1,2,2-tetracarbethoxyethane were added whereby a stiff porridge of its disodium compound was obtained. Methylene bromide, 34.8 g (0.2 mole), was added and the mixture was held at reflux temperature for 20 h. After this time the mixture was thinly fluid and almost neutral. It was neutralized with a few drops of glacial acetic acid and the ethanol was distilled off

through a short column. Water was added and the semi-solid mass was taken up in ether, the ether solution dried with anhydrous magnesium sulphate, and finally the ether distilled off. Distillation of the residue yielded 48.5 g (71 %) of tetraethyl *cyclo*propane-1,1,2,2-tetracarboxylate, which soon solidified. It could eventually be recrystallized from a mixture of absolute ether and petroleum ether and then melted at 41–43° *. No diethyl carbonate could be detected in the fore-runs.

When the same procedure was repeated with methylene iodide instead of the bromide the reaction mixture became entirely clear after refluxing over night. After neutralization with a few drops of glacial acetic acid, the ethanol was distilled off and water was added. In this case the reaction product solidified completely and could be filtered off. After drying in a vacuum-desiccator it was recrystallized from a mixture of absolute ether and petroleum ether, m. p. 41–43°. The yield was 72 %. (Found: C 54.2; H 6.7. Calc. for $C_{15}H_{22}O_8$: C 54.5; H 6.7). Kötz and Stalmann [3] reported m. p. 43°. Guthzeit and Dressel [4] also reported m. p. 43° for a specimen prepared from 1,1,3,3-tetracarbethoxypropane and bromine.

The tetraethyl ester was hydrolyzed by boiling with 10 % ethanolic potassium hydroxide over night. The ethanol was evaporated on the water-bath and the residue treated with dilute hydrochloric acid. The resulting solution was evaporated to dryness on the water-bath (the tetraacid is sufficiently stable to permit this operation) and the residue repeatedly extracted with boiling acetone. The combined acetone extracts were concentrated to a small volume and left to crystallize. An 81 % yield of rather pure tetraacid was obtained. After recrystallization from acetone it melted at 205–210° (decomp.). (Found: C 38.7; H 2.8. Calc. for $C_7H_6O_8$: C 38.5; H 2.8). Guthzeit and Dressel [4] reported m. p. 200° (decomp.).

Pentaethyl cyclo*hexane-1,1,3,3,5-pentacarboxylate.* Sodium, 11.5 g (0.5 mole), was dissolved in 180 ml of absolute ethanol and the solution poured into a soda-water bottle together with 83.0 g (0.25 mole) of 1,1,3,3-tetracarbethoxypropane and 67.0 g (0.25 mole) of methylene iodide. When the first reaction had subsided (after about 5 min) the bottle was sealed and heated in a water-bath at 100° for 30 h. The reaction mixture, which was almost neutral was worked up as in the foregoing experiment. Distillation *in vacuo* yielded one fraction (2.8 g) boiling at 50–60°/50 mm, which consisted of diethyl carbonate, one fraction boiling up to 210°/4 mm, and one main fraction at 210–215°/4 mm. The second fraction, which weighed 19.5 g, boiled inconstantly through the whole interval and gave on acid hydrolysis a small amount of a substance with m. p. 235–240°. It was readily oxidized with alkaline potassium permanganate but was not further investigated. No other definite compounds were found among the hydrolysis products.

The third fraction (33.8 g) consisted of pentaethyl *cyclo*hexane-1,1,3,3,5-pentacarboxylate, as indicated by the analysis and its behaviour upon hydrolysis. (Found: C 56.4; H 7.3. Calc. for $C_{21}H_{32}O_{10}$: C 56.7; H 7.3.)

The pentaethyl ester, 20.0 g, was hydrolyzed by boiling over night with 10 % ethanolic potassium hydroxide. The ethanol was removed on the water-bath and the residue was treated with dilute hydrochloric acid. The solution was then continuously extracted with ether for two days. The ether solution, which gradually deposited large amounts of crystals, was filtered and the mother liquor was evaporated to dryness, whereby a second crop of crystals was obtained. The total yield of crude product was 12.1 g (88 %). The crystals were somewhat sticky. A pure product was obtained after recrystallization from hot (80°) glacial acetic acid, though with considerable loss of substance. The m. p. was 180–184° (decomp.). The substance had to be dried at 110° for 2 h before analysis. (Found: C 43.6; H 4.2. Calc. for $C_{11}H_{12}O_{10}$: C 43.4; H 4.0.) When boiled with dilute hydrochloric acid for some hours, carbon dioxide was evolved and the pentacarboxylic acid converted to *cyclo*hexane-1,3,5-tricarboxylic acid, m. p. 208–213° (see below).

The pentaethyl ester, 5.0 g, was boiled over night with concentrated hydrochloric acid. The solution was evaporated to dryness on a water-bath and an almost quantitative yield of crude *cyclo*hexane-1,3,5-tricarboxylic acid was obtained, m. p. 205–210°. It was recrystallized twice from a mixture of benzene and acetone and then melted at 212–215°. Before analysis it had to be dried at 110° for 2 h in order to remove traces of solvent, which was held firmly by the crystals. (Found: C 49.9; H 5.7; equiv. wt. 73.0. Calc. for $C_9H_{12}O_6$: C 50.0; H 5.6; equiv. wt. 72.1.) The acid was converted into its triamide accord-

* The melting points were determined with a Kofler apparatus.

ing to Newman and Lowrie [13], m. p. 286–289° (decomp.) after recrystallization from water, and to its trimethyl ester by esterification with methanol, m. p. 43–45° after recrystallization from petroleum ether. Newman and Lowrie reported for the acid m. p. 216–218°, the amide 287.5–288.5° (decomp.), and the methyl ester 48–49°.

If methylene bromide was used instead of the iodide and the reaction carried out at 100° for 30 h, the same products were obtained.

Tetraethyl cyclo*pentane-1,1,3,3-tetracarboxylate.* Sodium, 4.6 g (0.2 mole), was dissolved in 70 ml of absolute ethanol and 34.6 g (0.1 mole) of 1,1,4,4-tetracarbethoxybutane together with 17.4 g (0.1 mole) of methylene bromide were added during a few minutes. The mixture was boiled under reflux for 20 h, after which time it was almost neutral. It was worked up as usual. The crude product was not distillable even at low pressures without extensive decomposition, and therefore it was hydrolyzed directly. However a small amount (1.2 g) of diethyl carbonate was distilled off, b. p. 50–60°/ca. 50 mm.

The crude ester (30.2 g) was boiled with 10 % ethanolic potassium hydroxide over night. The ethanol was distilled off and dilute hydrochloric acid was added. The solution was continuously extracted with ether for 36 h. The ether solution gradually deposited crystals which were filtered and dried, m. p. 185–190° (decomp.). The substance (4.3 g) was *cyclo*pentane-1,1,3,3-tetracarboxylic acid as indicated by analysis. (Found: C 44.0; H 4.2. Calc. for $C_9H_{10}O_8$: C 43.9; H 4.1). Pospischill [5] reported m. p. 186–188° (decomp.). From the mother liquor of the above filtration a dark viscous oil was obtained. No definite compounds could be isolated from this oil.

Tetraethyl cyclo*hexane-1,1,3,3-tetracarboxylate.* Sodium, 9.2 g (0.4 mole), was dissolved in 150 ml of absolute ethanol. To the solution were added 72.0 g (0.2 mole) of 1,1,5,5-tetracarbethoxypentane and then dropwise 34.8 g (0.2 mole) of methylene bromide. A vigorous reaction soon set in and when it had subsided the mixture was boiled under reflux for 20 h. The mixture then was almost neutral and was worked up in the usual manner. The crude product (68.3 g) which did not contain any detectable amounts of diethyl carbonate, could not be distilled without decomposition, even at low pressures. It was therefore directly hydrolyzed with 10 % potassium hydroxide over night and the tetraacid was isolated by means of continuous ether-extraction as above. A yield of 16.4 g of a rather pure product was obtained. It was recrystallized from hot (80°) water and then melted at 210–220° (decomp.). (Found: C 46.3; H 4.7. Calc. for $C_{10}H_{12}O_8$: C 46.2; H 4.7.) Perkin [9] reported m. p. 218–220°. The mother liquors were examined for other compounds but without success.

The author wishes to express his sincere gratitude to Professor Erik Larsson for his kind interest in this work. A grant from *Kungliga Fysiografiska Sällskapet* is gratefully acknowledged.

REFERENCES

1. Eberson, L. *Acta Chem. Scand.* **9** (1956) 1711.
2. Eberson, L. *Acta Chem. Scand.* **12** (1958) 314.
3. Kötz, A. and Stalmann, G. *J. prakt. Chem.* **68** (1903) 156.
4. Guthzeit, M. and Dressel, O. *Ann.* **256** (1890) 171.
5. Pospischill, K. T. *Ber.* **31** (1898) 1950.
6. Thole, F. B. and Thorpe, J. F. *J. Chem. Soc.* **99** (1911) 2183.
7. Perkin, W. H. and Scarborough, H. A. *J. Chem. Soc.* **119** (1921) 1400.
8. Guha, P. C. and Ranganathan, S. K. *Ber.* **69** (1936) 1199.
9. Perkin, W. H. *J. Chem. Soc.* **59** (1881) 798.
10. Lean, B. A. *J. Chem. Soc.* **65** (1894) 995.
11. Meerwein, H. and Schürmann, W. *Ann.* **398** (1913) 196.
12. Newman, M. S. *Steric Effects in Organic Chemistry*, Wiley & Sons, Inc., New York 1956, p. 76 ff.
13. Newman, M. S. and Lowrie, H. S. *J. Am. Chem. Soc.* **76** (1954) 4598.

Received February 22, 1958.

ACTA CHEMICA SCANDINAVICA 12 (1958) 737—751

Studies of Allergens from Alder Pollen (*Alnus Glutinosa*)

STIG HERBERTSON and JERKER PORATH

Institute of Biochemistry, University of Uppsala, Sweden

and

HELGE COLLDAHL

Medical Clinic II, Allergy Department, S:t Göran's Hospital, Stockholm, Sweden

An alder-pollen (*Alnus glutinosa*) extract has been fractionated and examined for allergenic activity by skin tests.

The activity was found in a non dialysable fraction. No decrease in activity was observed when this fraction was heated to 100°C for 1 hour. Treatment with pepsin, trypsin and chymotrypsin did not cause any significant inactivation.

Further fractionation by zone electrophoresis and chromatography on cellulose ion exchangers yielded a peptide-like fraction, 300 times as potent as the crude extract. This fraction contained at least 11 different amino acids.

The chemical and immunological properties of pollen allergens have been studied for about fifty years. Although much work has been done to isolate and to characterize active components in pollen, a chemically pure allergen has not yet been isolated. The activity appears, at least in some pollen species, to be shared by several substances. This circumstance, together with the lack of accurate test methods and methods for quantitative studies, has often led to contradictory reports. In spite of these facts, it can be concluded that allergens from different pollen have some characteristics in common. Chiefly ragweed and grass pollen have been studied. It is therefore appropriate to mention something about the methods that have been used for the fractionation of extracts of these pollen species and to point to some conclusions that have been drawn about the nature of the allergens.

The allergens of ragweed and grass pollen are generally found to be non-dialysable when ordinary dialysis membranes are used.[1,2] Weakly active components sometimes found in the dialysate have been referred to as break-down products formed during the procedures [16].

Abramson *et al.*[3] employed Tiselius' moving boundary electrophoresis technique for the separation of components in crude extracts of ragweed

pollen. An active colourless fraction contained subtances with molecular weights of about 5 000, as determined by ultracentrifugation.

Fractionations by chromatography on ion exchange resins have been preliminary described by Bookman and Wax [4]. Using crude water extracts of ragweed pollen, they found that the best results were obtained when a sulfonic acid resin (Dowex-50) was used. However, only a small part of the initial activity was recovered.

From results obtained by using different precipitating agents, such as ammonium sulfate [5–8, 9–11], alcohols [12–15], acetone [16], lead acetate [17], acids [18–20], and bases [8,13] for fractionations of extracts, it has been suggested that the active substances in ragweed pollen are carbohydrate-protein complexes, proteins or carbohydrates.

Augustin has published preliminary reports on fractionations of grass pollen [21–23]. Salt fractionations of the extracts yielded a number of active proteins associated with carbohydrate-pigment complexes which could not be removed from the protein moiety by prolonged dialysis. Diffusion and ultracentrifuge studies on the active fraction indicated a molecular weight of 14 000.

Critical summaries of chemical and immunological studies in pollen allergy have recently been written by Augustin [23,24].

The present study is an attempt to apply modern fractionation techniques to the isolation of allergens and to quantitate the procedures involved. Zone electrophoresis and chromatography on cellulose ion exchangers are methods that would be suitable for problems of this kind. Alder pollen (*Alnus glutinosa*) are used in this work because large samples of this species were available. The general chemical composition of alder pollen *(Alnus glutinosa, Alnus incana)* has been studied by Nielsen *et al.*[25], but no reports on the purification of alder pollen allergens are found in the literature.

MATERIALS AND METHODS

Pollen. The pollen used in this investigation have been collected from the alder tree, *Alnus glutinosa,* in 1954 by A.B. Cernelle, Vegeholm, Sweden. Immediately after collection, the pollen samples were dried to a moisture content of 5—6 % and were kept cool and dry. The quantity of other pollen species amounted only to about 0.1 % [25].

Proteolytic enzymes. Pepsin was obtained from Parke, Davis and Co., London; *Trypsin* was obtained from Worthington Biochemical Corp., Freehold, New Jersey; *Chymotrypsin* was obtained from the Armour laboratories, Armour and Co., Chicago, Ill.

Ion exchangers. Triethylaminoethylcellulose anion exchange powder (TEAE-cellulose) was prepared as described by Porath [27]. The nitrogen content of the preparation was 5.1 mg per g of dry powder.

Sulfoethylcellulose ion exchange powder (SE-cellulose) was prepared as described by Porath [27]. The SE-cellulose contained 0.45 mequiv. sulfur per gram dry powder.

Zone electrophoresis. Zone electrophoresis was performed in externally cooled columns, using the technique described by Porath [31]. In one experiment ethanolised cellulose was used as supporting medium. In two other experiments a gel B 196* was used instead of cellulose.

Biological test. The biological activity was measured by intradermal tests on alder-sensitive patients.

A standard test solution is made up by dissolving material from 1 g pollen in 10 ml of a 0.5 % phenol solution (1:10). Before the testing there are made tenfold serial dilutions

* Obtained from AB Pharmacia, Uppsala.

of the standard test solution up to 1: 10^6 (*i. e.* 1: 10^2, 1: 10^3, ... 1: 10^6). Physiologic salt solution containing 0.5 % phenol is used for the dilution.

A control is made by injection salt-phenol solution in the skin of the patient. With the same syringe the different antigen containing dilutions are injected. The highest dilution is first injected, and this is followed by the next lower until a dilution is found which just gives a positive skin reaction. More or less strong responses are indicated by ‡ resp. ±. If a reaction is found only for the dilution 1: 10^2, this response can not with certainty be regarded as positive because nonspecific factors will interfere with the reaction at such a low dilution. This effect is more pronounced for crude extracts.

EXPERIMENTAL

Flow sheet

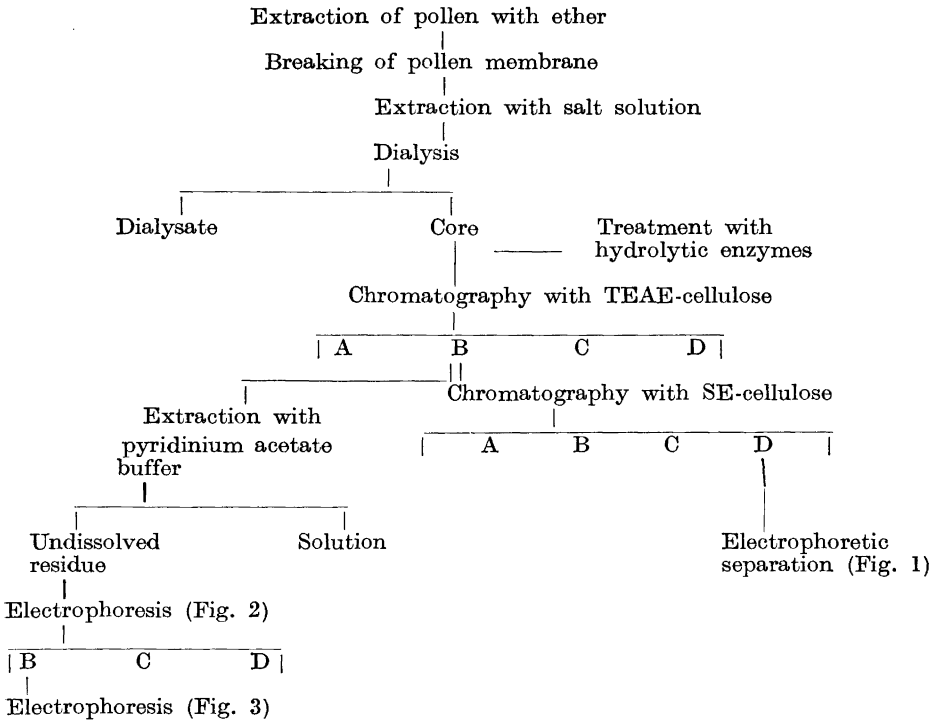

Sampling for activity assays

If a fractionation had been made in an experiment and a certain fraction was to be tested, there was taken the portion of 1 g pollen that was recovered in the fraction (*i. e.* if say 500 g of pollen have been fractionated, one should take 1/500 of the material in the fraction to be tested). This portion was made up to standard condition by being dissolved in 10 ml of 0.5 % phenol solution and then prepared for testing. The dilution (1: 10 ×) which gave a positive skin reaction was marked as the activity. Consequently the activity value of this solution will never exceed that of the standard test solution from crude extract.

A. Pretreatment of pollen

1. *Ether extraction.* The pollen grains were defatted by extraction with ether in the following way. A sample of pollen (500 g) was suspended in peroxide free diethylether (1 l) and transferred to a glass tube of the type used for chromatography. Fresh ether was slowly percolated through the column. After 24 h when no more material went into the solution the extracted pollen sample was poured out and the residual ether was removed in vacuum.

13 % of the original pollen weight was thus removed by the extraction.

2. *Breaking of the pollen membranes.* In order to facilitate a subsequent extraction of active material the pollen membranes were ruptured as follows. A sample of pollen (100 g) was suspended in a small amount (200 ml) of extracting fluid (see below). The suspension was frozen to −70°C and was then thawed. The procedure was repeated three times or till nearly all of the pollen grains were ruptured (checked by observation in a microscope).

B. Extraction of active material

1. *Extraction with salt solution.* The active material was extracted from the ruptured pollen by using the same procedure as for the ether extraction, but the extracting fluid was composed of 0.9 % sodium chloride and 0.5 % phenol dissolved in boiled distilled water. A sample corresponding to 1 000 g of fresh pollen was extracted during 36 h at 4°C with 3 600 ml of fluid. Extract exceeding 3 600 ml was collected separately in one experiment, but was not used for preparations because the activity in this fraction was only about one hundredth of that in the first collected fraction.

Each gram pollen yielded 251 mg of dry material and 18.2 mg of nitrogen (Kjeldahl). The activity of the extract was determined to ‡ 1: 10^4 ± 1: 10^5 (Patient L.F.).

2. *Extraction with sulfuric acid.* For comparison an extraction was made under condition where proteolytic activity in the extract is supposed to be prevented. A small scale extraction of 10 g pollen was made with 0.25 N sulfuric acid in the same way as indicated above. 50 ml of extract was collected during 24 h. 10 ml of the extract was dialysed in a cellophane sac for 1 h against water. The dialysed residue was neutralized to pH 7 with sodium bicarbonate (sample E). Another 10 ml of the initial extract was dialysed against 0.25 N sulfuric acid for 20 h. The residue (sample R) and the dialysate (sample D) were neutralized to pH 7. Results of the testing in Table 1.

Table 1.

Sample	Activity Patient L.F.
E	‡ 1: 10^4
R	+ 1: 10^4
D	+ 1: 10^2

Reference: Extract (NaCl) (‡ 1: 10^4 ± 1: 10^5)

The sulfuric acid extract was not used for the subsequent fractionations.

C. Dialysis of the salt extract obtained as described under B 1

The phenol-sodium chloride extract was dialysed in Visking cellophane sacs of 4 cm diameter. The extract inside the sacs was stirred with a rotating glass rod. During the first 24 h the extract was dialysed twice against 0.5 % phenol in water. The dialysis was continued for another 24 h but the residue in the sacs was now dialysed twice against boiled water. The whole procedure was performed in a cold room at 4°C. The liquid inside the sacs was centrifuged in order to remove a precipitate formed during the dialysis.

The precipitate which was dissolved in sodium chloride solution was inactive. The centrifuged liquid (referred to as "Core" in Table 2) had the same activity as the extract. The pooled outside liquids (dialysate) had no activity.

Table 2.

Sample	Nitrogen, mg per g pollen	Weight, mg per g pollen	Activity Patients L.F.	J.U.
Core	2.1	35	$+1:10^4$	$\pm 1:10^5$
Dialysate	10.2		$+1:10^2$	
Precipitate	3.0	18	$+1:10^2$	
Extract	18.2	251	$+1:10^4$	$\pm 1:10^5$

The active material did not pass the dialysis membrane. The extract was purified sevenfold by weight.

D. Properties of preparation "Core".

1. *Stability to heating.* 35 mg of preparation "Core" (Table 2) was dissolved in distilled water and heated in a closed glass tube at 100°C during 1 h. Results from testing in Table 3.

Table 3.

Sample	Activity (Patient L.F.)
Core	$+1:10^5$
Heated Core	$+1:10^5$

2. *Treatment with proteolytic enzymes.* The procedures used in the following experiments are similar to those described by Li *et al.*[26]

Pepsin. 35 mg of preparation "Core" (Table 2) and 25 mg of cryst. pepsin (1:3 000 U.S.P.) were dissolved in 45 ml of 0.01 N hydrochloric acid solution. A standard was prepared by dissolving 35 mg of preparation "Core" in 45 ml of hydrochloric acid. For comparison a solution was prepared by dissolving 25 mg pepsin in 0.01 N hydrochloric acid solution (sample "pepsin"). To all solutions were added a few drops of toluene. When all the solutions had been kept at 37°C for 4 h they were placed in a boiling water-bath for 2 min to terminate the enzymatic activity. The results from the testing are given in Table 4.

Table 4.

Sample	Activity Patient L.F.		Patient J.U.		Patient A.N.
Core	$+1:10^4$	$\pm 1:10^5$	$+1:10^4$	$\pm 1:10^5$	$+1:10^3$
Digest	$+1:10^4$	$\pm 1:10^5$	$+1:10^4$	$\pm 1:10^5$	neg.
Pepsin	$+1:10^2$	$\pm 1:10^3$	$+1:10^2$		neg.

Trypsin. 35 mg of preparation "Core" (Table 2) and 10 mg of cryst. trypsin were dissolved in 50 ml of water. pH was adjusted to 9.3 by dropwise addition of 2 % ammonia solution. A standard was prepared by dissolving 35 mg of preparation "Core" in ammonia solution. For comparison a solution was prepared by dissolving 10 mg trypsin in 50 ml ammonia solution. After the mixtures had been kept at 37°C for 6 h the enzymatic activity was terminated by heating to 100°C for 2 min. The results from the testing are compiled in Table 5.

Table 5.

Sample	Activity Patient L.F.		Patient J.U.		Patient A.N.
Core	$+1:10^4$	$\pm 1:10^5$	$+1:10^4$	$\pm 1:10^5$	$+1:10^3$
Digest	$+1:10^5$		$+1:10^4$		$\pm 1:10^3$
Trypsin	neg.		neg.		neg.

Chymotrypsin. 35 mg of preparation "Core" (Table 2) and 10 mg chymotrypsin were dissolved in 0.2 N ammonium acetate buffer of pH 8.2. A standard solution was prepared by dissolving 35 mg of preparation "Core" in ammonium acetate buffer. For comparison a solution was prepared by dissolving 10 mg chymotrypsin in the buffer. The mixtures were kept at 38°C for 5 h and then the enzymatic activity was terminated at 100°C for two min. The results from the testing are shown in Table 6.

Table 6.

Sample	Activity Patient L.F.		Patient J.U.		Patient A.B.
Core	$+1:10^4$	$\pm 1:10^5$	$+1:10^4$	$\pm 1:10^5$	$+1:10^3$
Digest	$+1:10^4$		$+1:10^4$		$+1:10^3$
Chymotrypsin	$+1:10^3$		$\pm 1:10^2$		$\pm 1:10^2$

E. Fractionation of preparation "Core" by chromatography on triethylaminoethyl cellulose.

100 g of TEAE-cellulose ion exchanger containing 5.1 mg nitrogen per g was prepared as free base. The TEAE-cellulose was suspended in distilled water and packed in a Büchner funnel (19 cm in diameter) which was placed on a vacuum flask. 2 000 ml of preparation "Core" (Table 2) (corresponding to 435 g of pollen) were gently sucked through the ion exchanger during 1 h. Unadsorbed material was washed out with 1 l of water. The adsorbed material was displaced with three different solutions in the following order:

1) 2 l of 0.1 N pyridinium acetate (PyAc) buffer of pH 5.0.
2) 1 l of 1.0 N pyridinium acetate buffer of pH 5.0.
3) 0.5 l of 1 N acetic acid (HAc).

The collected fractions were freed from buffer and acid by vacuum distillation and finally lyophilized. The results obtained in one experiment is found in Table 7.

Table 7.

Sample	Fraction	Weight (mg)	Nitrogen (mg)	Activity Patient L.F. (2 measurements)	
TEAE–A	Eluate	6.6		$+1:10^2$	$+1:10^3$
TEAE–B	0.1 N PyAc	4.6	441	$+1:10^4$	$+1:10^5$
TEAE–C	1 N PyAc	3.2		$+1:10^2$ $\pm 1:10^3$	-------
TEAE–D	1 N HAc	0.1		neg	-------
	Total	14.6			
Core		15.2	929	$+1:10^4$	$+1:10^5$

The total loss of material amounted to 4 %, provided that material from the ion exchanger itself was not eluted during the process. The activity in preparation TEAE—B was the same as in preparation "Core". Preparation "Core" was purified threefold by weight and twofold by nitrogen. The experiment was easily reproduced. The ion exchange powder was packed in a wide funnel. If a column with a small diameter is used the elution easily stops because of the strong accumulation of material at the top of the column.

F. Fractionation of preparation TEAE-B on sulfoethyl cellulose

SE-cellulose, which contained 0.45 mequiv. sulfur per g dry powder was worked up as free acid. The powder was suspended in dist. water and was packed in a glass tube under pressure. Preparation TEAE-B (Table 7) was dissolved in distilled water and was applied to the column. The chromatogram was developed first with dist. water followed by a three step displacement with different solvents in the following order:

1) 0.1 N triethylammonium acetate buffer of pH 5.0
2) 1.0 N triethylammonium acetate buffer of pH 5.0
3) 0.1 N triethylamine.

Fig. 1 shows an experiment where 374 mg of preparation TEAE-B has been chromatographed on 25 g of SE-cellulose which was packed to a column of 2 cm diameter. Fractions of 7 ml were collected every 10 min.

Aliquots of 0.25 ml were taken from each fraction in the fraction range 1—85 and aliquots of 0.1 ml from each fraction in the fraction range 86—170 and were then analysed with ninhydrin [28]. Aliquots of 0.5 ml were taken for orcinol analysis [29]. 0.1 ml samples were used for turbidimetric determination of proteins with trichloroacetic acid [30]. No turbidity was observed. The distribution of yellow pigments is indicated in Fig. 1 (visually observed).

Fractions were pooled as indicated in Table 8 and were freed from buffer. After lyophilization the activity was determined.

Table 8.

Sample	Fraction range in Fig. 1	Weight (mg)	Activity Patient	Activity M.C.
SE—A	0— 15	0.1	$\pm 1:10^2$	$\pm 1:10^3$
SE—B	16— 85	67.4	$+ 1:10^3$	$\pm 1:10^4$
SE—C	86—100	238.4	$+ 1:10^2$	
SE—D	101—170	68.2	$\ddagger 1:10^4$	$\pm 1:10^5$
	Total	374.1		
TEAE—B		374.0	$\ddagger 1:10^4$	$\pm 1:10^5$

By the fractionation Preparation TEAE—B was purified fivefold by weight.

G. Electrophoretic separation of preparation SE-D.

In order to study the heterogeneity of preparation SE—D (Table 8) this fraction was investigated by zone electrophoresis using the technique described by Porath [31]. The column which had a length of 150 cm and a diameter of 3 cm was washed with 0.1 N triethylammonium acetate buffer of pH 5.0.

60.2 mg of preparation SE—D was dissolved in 3.0 ml of 0.1 N triethylammonium acetate buffer of pH 5.0. Undissolved material (sample SE—P) was removed by centrifugation. The brownish yellow solution, containing 47.0 mg of dissolved material, was

placed on the top of the column and was slowly forced into it by gravity to a position 10 cm from the top. 1 200—1 300 V were applied giving a current of 85 mA. After 52 h the electrophoresis was stopped and the liquid in the column was displaced at a rate of 60 ml per h. 6.7 ml fractions were collected.

From every second fraction 0.5 ml was taken for ninhydrin analysis. The ultraviolet absorption at 280 mμ was also measured on undiluted fractions. 0.5 ml samples from every other fraction were hydrolysed in 4.5 N hydrochloric acid at 110°C for 15 h and then subjected to ninhydrin analysis [32]. The values from the measurements are recorded in Fig. 2. Fractions were pooled according to Table 9 and freed from buffer, lyophilized and tested. A correction is made in the weight values because samples had been withdrawn for analysis.

Table 9.

Sample	Fraction range in Fig. 2	Weight (mg)	Activity Patient	Activity L.F.
E—1A	0— 55	1.0	$\pm 1:10^2$	
E—1B	56— 75	7.2	$+1:10^2$	$\pm 1:10^3$
E—1C	76—100	10.1	$+1:10^2$	
E—1D	101—120	7.1	$+1:10^2$	
E—1E	121—170	10.8	$+1:10^2$	
	Total	36.2		
SE—P		13.2	$\pm 1:10^2$	
SE—D		47.2	$\ddagger 1:10^4$	$\pm 1:10^5$

H. Extraction of preparation TEAE-B with buffer

A considerable purification of the active material was achieved by extraction of preparation TEAE—B (Table 7) with buffer as described below. The procedure was not always reproducible. However, the following experiment gave data about the allergen(s).

500 mg of preparation TEAE—B (Table 7) was thoroughly mixed with 2 ml of 0.1 N pyridinium acetate buffer of pH 5.0. Undissolved material was treated again with 1 ml of buffer. Still undissolved material (sample TEAE—BP) was separated by centrifugation. The solutions were pooled (TEAE—BP). Preparation TEAE—BP was freed from buffer and lyophilized. The test results are shown in Table 10.

Table 10.

Sample	Weight (mg)	Activity Patient L.F.	Activity Patient J.U.	
TEAE—B	500	$\ddagger 1:10^4$	$+1:10^4$	
TEAE—BP	70	$+1:10^4$	$+1:10^3$	$\pm 1:10^4$
TEAE—BS		$+1:10^2$	neg	

By the extraction preparation TEAE—B was purified about sevenfold.

I. Electrophoresis of preparation TEAE-BP

The electrophoresis was performed in an externally cooled column 90 cm long and with a diameter of 1.6 cm. Gel B 196 was used as supporting medium. 0.05 N triethylammonium carbonate buffer of pH 8.6 was used [33].

69 mg of preparation TEAE—BP (Table 10) was dissolved in 4 ml of triethylammonium carbonate buffer of pH 8.6. The brownish yellow solution was applied on the column

and by gravity forced 26 cm down into the column. 600 V were applied yielding a current of 15 mA. After 15 h the electrophoresis was stopped and the liquid in the column was displaced at a rate of 40 ml per h. 3 ml fractions were collected.

From every second fraction 0.1 ml was taken for ninhydrin analysis. The measured values are recorded in Fig. 3. The fractions were pooled according to Table 11, freed from buffer, lyophilized and tested. The brownish yellow colour was concentrated in fraction E−2B.

Table 11.

Sample	Fraction range	Weight (mg)	Activity Patient U.B.		Patient G.J.M.		Patient Y.N.	
E−2A	0−11	1.1						
E−2B	12−18	33.6	‡1: 10^2	±1: 10^3	‡1: 10^2	±1: 10^3	+1: 10^3	±1: 10^4
E−2C	19−29	21.9	neg		±1: 10^2		±1: 10^3	
E−2D	30−50	7.6	±1: 10^2		±1: 10^2		±1: 10^3	
TEAE−BP			+1: 10^3		±1: 10^3		±1: 10^4	

Preparation TEAE−BP was purified about twofold by the procedure, and had now about 300 times as high specific activity as the initial extract. The nitrogen value of preparation E−2B was 1.19 mg.

A too big amount of material from preparation E−2B is required for detection on paper. Therefore a new zone electrophoresis experiment was made instead of using paper electrophoresis.

Electrophoresis. The same column (90 × 1.6) was used but the buffer was now 0.05 N triethylammonium carbonate buffer of pH 9.0.

30 mg of preparation E−2B (Table 11) was dissolved in 2 ml of buffer and was forced 25 cm into the column. The electrophoresis was run for 39 h using 700 V and a current of 25 mA. To make it possible to run the electrophoresis during 39 h and still keep the substances in the column, the liquid in the column was slowly forced in the opposite direction to that in which the substances migrated. This was arranged by keeping the buffer in the two electrode vessels at different levels.

The liquid in the column was displaced at a rate of 40 ml per h. 2.5 ml fractions were collected.

0.1 ml samples from every second fraction were used for ninhydrin analysis.

0.05 ml samples were hydrolysed in 4.5 N hydrochloric acid at 110°C during 15 h and the ninhydrin values determined. Absorption at 275 mμ was measured. The measured values are shown in Fig. 4. The highest ninhydrin value and the strongest colour (yellow) was found in the same tube. 25 mg of material was found in the fraction range 26−120.

The material in the fraction range 28−43 was preliminarily examined. One sample was hydrolysed with 6 N hydrochloric acid at 110°C for 15 h. The hydrolysate was studied by means of paper electrophoresis and paper chromatography. Both acid, basic and neutral amino acids were present (at least 11 different spots). The same amount of unhydrolysed material did not give any colour with ninhydrin on paper. When enough of unhydrolysed material had been chromatographed on paper, using 80 % phenol in borate buffer of pH 9.3 as solvent system, the yellow pigment stayed at the starting point and a 'ninhydrin spot' was found with an R_F-value of about 0.5.

DISCUSSION

From the results of the semi-quantitative skin test method used in this study it is not always possible to conclude whether one of several active components has lost its activity during the fractionation procedure. This is the main reason why methods as mild as possible have been applied. The tests were performed with the same patient (Patient L.F.) except in the experi-

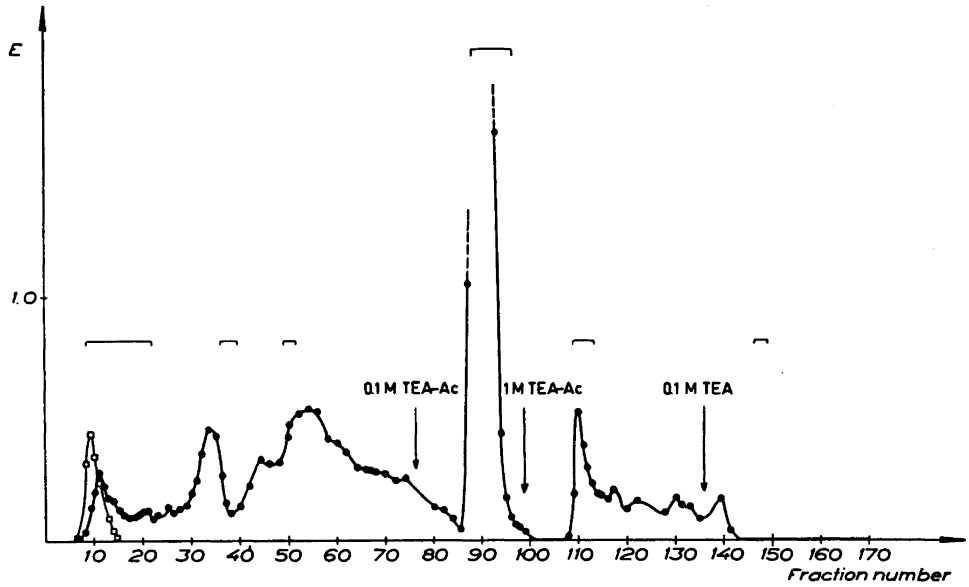

Fig. 1. Chromatographic separation of 374 mg of preparation TEAE—B on 25 g of SM-cellulose (column diameter: 2 cm). Fractions of 7 ml were collected.

——·——·—— Ninhydrin curve obtained from 0.25 ml samples in the fraction range 1—85 and 0.1 ml samples in the fraction range 86—170.
—□—□— Orcinol curve obtained from 0.5 ml samples.
|————| Visually observed yellow pigments.

ment described in passages F and I. Patient M.C. (passage F) and Patient L.F. gave about equal response to preparation TEAE-B.

It has been questioned whether allergens from pollen are broken down by hydrolytic enzymes in the extract during preparations. Loveless *et al.*[1] found appreciable losses of nitrogen and carbohydrates from ragweed extract during extensive dialysis through cellophane. Frankel *et al.*[16] examined the same pollen species and they believe that a number of weakly active peptide carbohydrate complexes in the dialysate have arisen by fragmentation of the undialysable residue, which represented the main activity.

Either inactive or still active components could be formed by an enzymatic cleavage. In the case of alder pollen (Table 2) no loss of activity was found after dialysis. Even if a limited hydrolysis of allergens could have taken place, it is of interest to purify and study an active fragment. The small scale extraction with sulphuric acid was made in order to study the activity yield under conditions where proteolytic cleavage is supposed to be prevented[34]. The activity in this extract, however, was not higher than in the phenol-sodium chloride extract used for the fractionations. The activity of the sulphuric acid extract was lowered only a little when it was kept at 4°C during 20 h.

The active material did not pass the dialysis membrane used in the initial step of the fractionation. This does not exclude the possibillity that a pene-

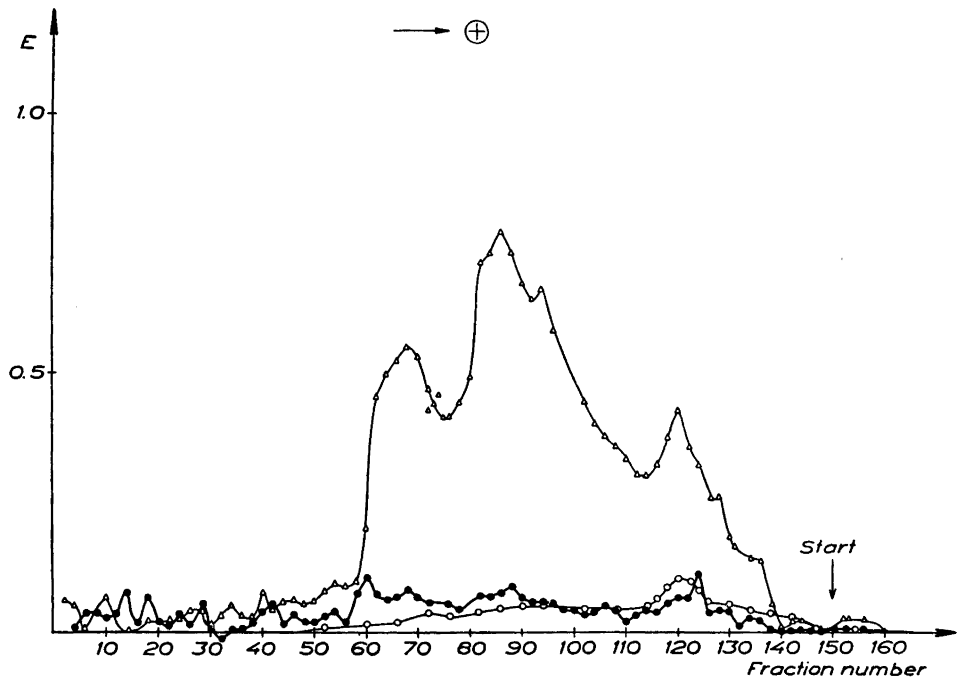

Fig. 2. Electropherogram of 47 mg of preparation SE—D obtained after 52 h electrophoresis at 85 mA in a 150 × 3 cm column using 0.1 N triethylammonium acetate buffer of pH 5.0. Fractions of 6.7 ml were collected. The direction of the current is indicated by the sign →O

——•——•—— Ninhydrin curve obtained from 0.5 ml samples.
—△—△— Ninhydrin curve obtained from hydrolysed 0.5 ml samples.
—O—O— Ultraviolet absorption at 260 mμ

tration could take place in a later stage, when originally present weak complexes could have been split. Consequently no definite conclusions can be drawn from this experiment about the molecular size of the allergens.

The experiments reveal that fraction "Core" was remarkably stable to heating. The heat stability of pollen allergens is of considerable interest, because already differences in this property may give hints to differences in their chemical nature. It is therefore important to emphasize that in the case of alder pollen here investigated, no inactivation was observed even after one hour's heating at 100°C. It is interesting to compare this result with similar studies made by Augustin [23] on grass pollen. She found that only 10 % of the activity remained after 15 min at 100°C, and that already after one minute's heating all precipitating power for the rabbit antibody was lost and that precipitates were no longer formed in gel diffusion tests.

As seen from the experiments no loss of activity was found after treatment of fraction "Core" with trypsin or chymotrypsin. The same result was found

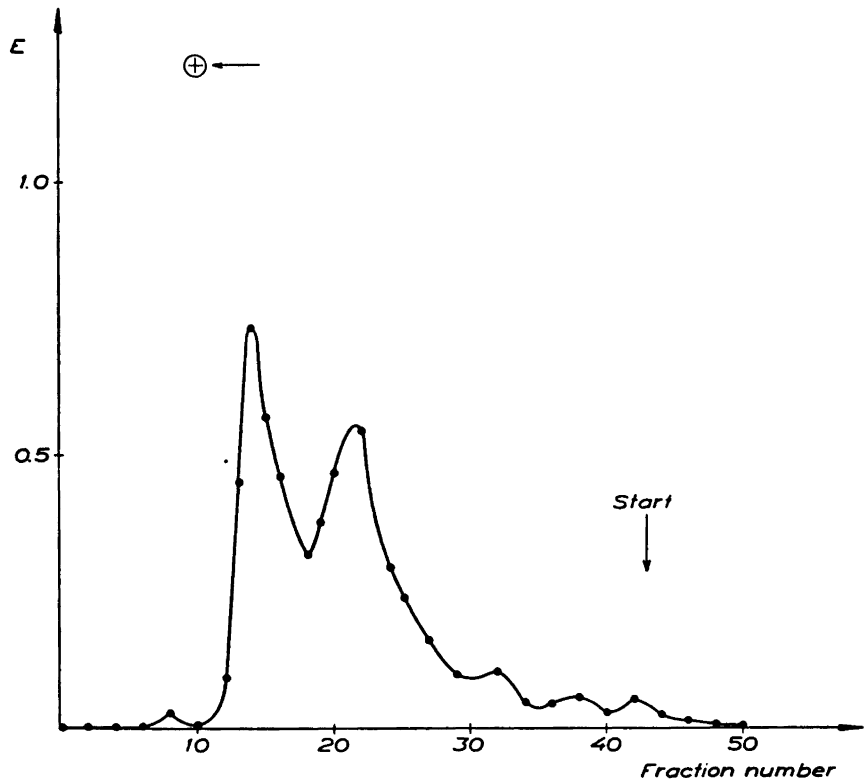

Fig. 3. Electropherogram of 69 mg of preparation TEAE—BP obtained after 15 h electrophoresis at 15 mA in a 90 × 1.6 cm column using 0.05 N triethylammonium carbonate buffer of pH 8.6. Fractions of 3 ml were collected.

—·—·— Ninhydrin curve obtained from 0.1 ml samples from every other tube.

with pepsin in the tests made on two of the patients. A third patient gave a negative response to the pepsin digest, but the initial activity value was in this case rather low, and therefore no definite conslusions can be drawn. There might be several allergens and some of these do not exhibit resistance towards pepsin. Augustin has preliminarly described similar studies on grass pollen extracts [23]. In those cases the treatment with pepsin and trypsin destroyed all activity within one hour, whether the digestion was carried out on the crude extract or on the purified protein solution.

Allergens from pollen are often referred to as pigmented carbohydrate-rich compounds. On the other hand, it is preliminarily reported that one of the allergens from grass pollen contains only 2 % of carbohydrates [23]. Referring to the experiments on alder pollen, it is seen from Fig. 1 that the orcinol curve does not indicate the presence of any carbohydrates in the active fractions displaced from the SE-cellulose. On the other hand, it cannot be excluded

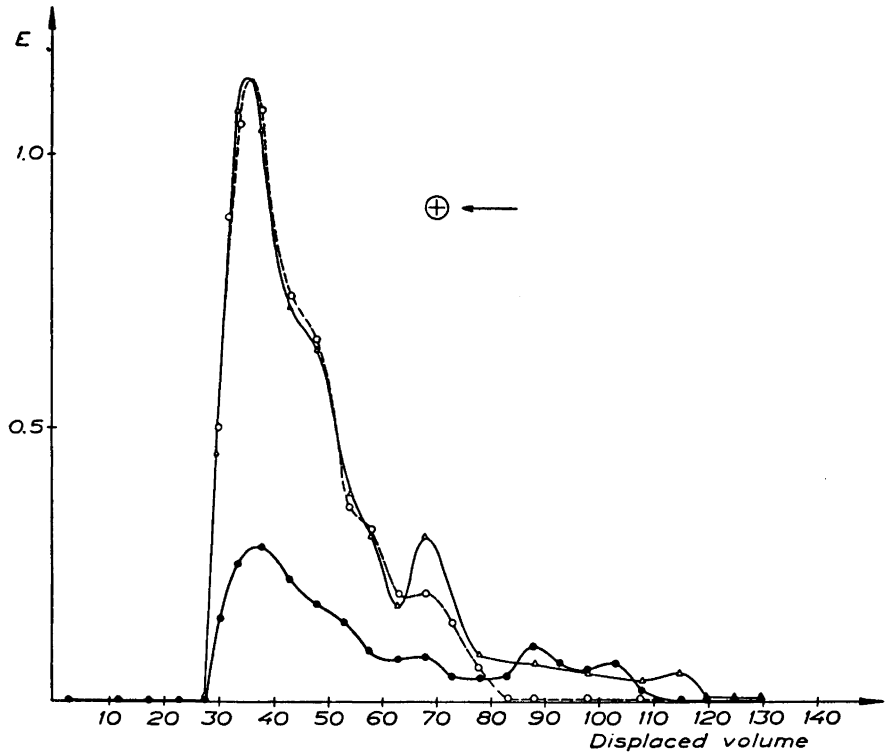

Fig. 4. Electropherogram of 30 mg of preparation E—2B obtained after 39 h electrophoresis at 25 mA in a 90 × 1.6 cm column using 0.05 N triethylammonium carbonate buffer of pH 9.0. Fractions of 2.5 ml were collected.

—•—•— Ninhydrin curve obtained from 0.1 ml samples from every other tube.
—△—△— Ninhydrin curve obtained from 0.05 ml hydrolysed samples from every other tube.
—O—O— Ultraviolet absorption at 275 mμ.

that there are components present containing small amounts of carbohydrates, which are not revealed by the reagent. It is possible that the cellulose ion-exchangers used in the purification may give off small amounts of cellulose, and this would interfere in an accurate carbohydrate determination. Consequently a final fractionation has to be made in order to get rid of ion-exchange material.

No experiments have been made in order to determine whether the activity in fraction SE-B (Table 8) is caused by an overloading of the column, or if the material in this fraction is different from that in fraction SE-D (Table 8). In the fully active fraction SE-D no proteins were found, and there were probably no free amino acids. A sample of this kind would presumably be suitable for fractionation with zone electrophoresis. The unfortunate reduction of activity during the electrophoresis (Fig. 2) can perhaps be explained by

the fact that too small amounts of material have been used. Under these conditions oxidation, bacterial growth and adsorption have a pronounced effect on the activity yield.

When the extract is stored and during evaporations of solutions the solubility of the components is often changed. Especially the pigments tend to crystallize. Consequently there are risks of coprecipitations. Precipitates are often difficult to get into solution without drastic treatments. It was possible to make use of this fact in order to obtain information about the allergens. As seen from the experiment (passage H) a highly pure fraction (sample TEAE-BP) was obtained. The electrophoretic patterns are shown in Figs. 3 and 4. The active peak contains bound amino acids together with a yellow pigment. No experiments have been made in order to reveal if the activity is caused by the bound amino acids or by the pigment or by a possible complex between them. Stevens *et al.*[35,23] have met with a similar problem in the course of studies of an amorphous glucoside precipitate that was formed in the extract of giant ragweed pollen. They found that biologic activity remained as long as nitrogen was associated with the glucoside (*iso*quercetin), while the pure glucoside was inactive.

The stability towards drastic treatments such as heating, evaporation and proteolysis suggests that the bulk of the activity in the dialysed extract is not due to proteins. The adsorption of the active material on the cellulose ion-exchangers strongly indicates the presence of acid and basic groups in the active molecule(s). The electrophoretic behavior (Fig. 2) of a fraction, with about 300 times as high specific activity as the initial extract, reveals that the allergen(s) is (are) negatively charged at pH 8.6. The bound amino acids found in the active peak are probably parts of the allergen(s).

The data that are presented point to the conclusion that the allergen(s) is (are) of peptide nature.

Acknowledgements. We wish to express our thanks to Professor A. Tiselius for kind advice and helpful discussions. This work has been financially supported by grants from *The Swedish Natural Science Research Council, The Rockefeller Foundation and King Gustaf's V. 80 Year Fund.*

REFERENCES

1. Lovess, M. H., Wright, M. A. and Ryan, A. *J. Allergy* **22** (1951) 120.
2. Augustin, R. *Biochem. J.* **54** (1953) x.
3. Abramson, H. A., Moore, D. H. and Gettner, H. H. *J. Phys. Chem.* **46** (1942) 192.
4. Bookman, R. and Wax, H. *J. Allergy* **25** (1954) 12.
5. Stull, A. *J. Allergy* **8** (1936) 85.
6. Stull, A., Chobot, R. and Cooke, R. A. *J. Allergy* **1** (1930) 470.
7. Stull, A., Sherman, W. B. and Hampton, S. F. *J. Allergy* **12** (1940–41) 117.
8. Stull, A., Sherman, W. B. and Wing, M. *J. Allergy* **13** (1941–42) 537.
9. Rappaport, B. Z. and Johnson, C. A. *Proc. Soc. Exptl. Biol. Med.* **26** (1929) 771.
10. Cohen, M. B. and Friedman, H. J. *J. Allergy* **14** (1943) 368.
11. Harley, D. Brit. J. Exptl. Pathol. **18** (1937) 469.
12. Heyl, F. W. *J. Am. Chem. Soc.* **41** (1919) 1285.
13. Moore, M. B., Cromwell, H. W. and Moore, E. E. *J. Allergy* **2** (1930–31) 85.
14. Black, J. H. *J. Allergy* **2** (1931) 161.
15. Baldwin, H. S., Mayer, A. W. and Dagara, P. F. *J. Allergy* **18** (1947) 296.
16. Frankel, S., Johnson, M., Schiele, A., Bukantz, S. and Alexander, H. *J. Allergy* **26** (1955) 33.

17. Caufeild, A. H. W., Brown, M. H. and Waters, E. T. *J. Allergy* **7** (1936–37) 1.
18. Hecht, R., Rappaport, B. Z. and Welkers, W. H. *Proc. Soc. Exptl. Biol. Med.* **39** (1938) 588.
19. Mosko, M., Hecht, R. and Weil, H. *J. Allergy* **13** (1941–42) 149.
20. Stone, G. C., Harkavy, J. and Brooks, G. *Ann. Allergy* **5** (1947) 546.
21. Augustin, R. *Biochem. J.* **54** (1953) x.
22. Augustin, R. *Biochem. J.* **64** (1956) 28P.
23. Augustin, R. *Quart. Rev. Allergy Appl. Immunol.* **9** (1955) 504.
24. Augustin-Friedman, R. *Quart. Rev. Allergy Appl. Immunol.* **6** (1952) 290.
25. Nielsen, N., Grömmer, J. and Lundén, R. *Acta Chem. Scand.* **9** (1955) 1100.
26. Li, C. H., Geschwind, I. I., Cole, D., Raacke, D., Harris, J. I. and Dixon, J. S. *Nature* **176** (1955) 687.
27. Porath, J. *Arkiv Kemi* **11** (1957) 97.
28. Moore, S. and Stein, W. H. *J. Biol. Chem.* **211** (1954) 907.
29. Fisher, H., Hansen, R. G. and Norton, H. W. *Anal. Chem.* **27** (1955) 907.
30. Stadtman, E. R., Novelli, G. D. and Lipman, F. *J. Biol. Chem.* **191** (1951) 365.
31. Porath, J. *Biochem. et Biophys. Acta* **22** (1956) 151.
32. v. Hofsten, B. *Acta Chem. Scand.* **10** (1956) 1432.
33. Porath, J. *Nature* **175** (1955) 478.
34. Kunitz, M. *Science* **90** (1939) 112.
35. Stevens, F. A., Moore, D. and Baer, H. *J. Allergy* **22** (1951) 165.

Received February 5, 1958.

ACTA CHEMICA SCANDINAVICA 12 (1958) 752—755

The Separation of Nucleotides by Ionophoresis and Chromatography on Paper

ROLF BERGKVIST

Institute of Biochemistry, University of Lund, Sweden

The separation of a complex mixture of 5′-ribonucleotides by a combination of ionophoresis and chromatography on paper is described.

The development of ionophoresis on paper has greatly facilitated separations of substances which would be impossible by paper chromatography and time consuming by ion exchange methods. The combination of paper ionophoresis with chromatography, either carried out simultaneously or separately, sometimes permits separations to be effected that can not be carried out by either technique alone. Numerous workers have used this method for the separation of different substances but most of the methods concerned with the separation of nucleotides have been found to give satisfactory separations of only a few nucleotides. In the course of studies of the nucleotide content of various plant materials, a method has been developed for the separation of all the main components to be found in these materials [1]. The nucleotides are fractionated into groups by paper chromatography and then completely separated by ionophoresis. The present paper describes a two-dimensional fractionation of these substances on a single sheet of filter paper.

The mixture of nucleotides to be separated was applied as a narrow band about 15 mm in length and 6 cm from the edge of a large sheet of Whatman No. 1 filter paper (Fig. 1). The resolution in the first direction was obtained by ionophoresis using the long-paper apparatus described earlier [1]. The paper was impregnated with an acetate buffer of pH 4.15 and of ionic strength 0.1 by dipping as previously described. Then the paper was folded along the line CD and placed on a glass frame. The frame and paper were then immersed in a carbon tetrachloride vessel so that the ends FG and HI dipped into the electrode vessels. The frame was constructed as a three piece unit in order to facilitate placing the paper on it as illustrated in Fig. 2. The ionophoresis was carried out at 1 000 V for 10 h, at which time the nucleotides were distributed over the interval BE. The paper was then dried at room temperature and, after cutting away the tabs BCGF and EDHI, the separation in the second

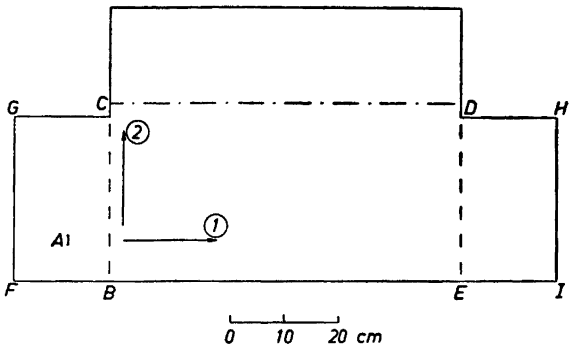

Fig. 1. The dimensions and shape of the filter paper sheet. The substances are applied at point A. The paper is folded along the line CD and the tabs FG and HI dip into the electrode vessels. The substances are fractionated by ionophoresis in direction 1 and then by paper chromatography in direction 2.

direction was achieved by chromatography. The previously described solvent system consisting of saturated ammonium sulphate solution — *iso*propanol — water (79:2:19) could be used for obtaining a complete separation of all the components, but better separation of the pyrimidine nucleotides was achieved using *n*-butanol instead of *iso*propanol. The paper sheet was impregnated with buffer salts from the ionophoretic development; but, when using the butanol mixture, these salts did not interfere with the separation of the various substances. The spots obtained by this method are as compact as those which result from other two-dimensional systems. All the 5′-mono-, di- and triphosphates of adenosine (AMP, ADP and ATP), guanosine (GMP, GDP and GTP), cytidine (CMP, CDP and CTP) und uridine (UMP, UDP and UTP) together with diphospho- and triphosphopyridine nucleotides (DPN and TPN) are separated as shown in Fig. 3. Uridine diphosphate glucose (UDPG) and

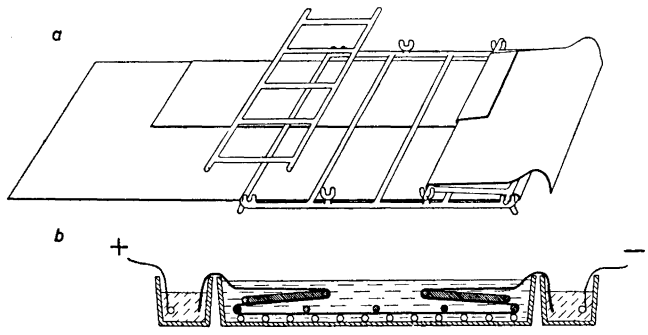

Fig. 2. a) The fitting of the paper to the glass frame. b) Cross section showing the paper and frame in place in the ionophoresis apparatus.

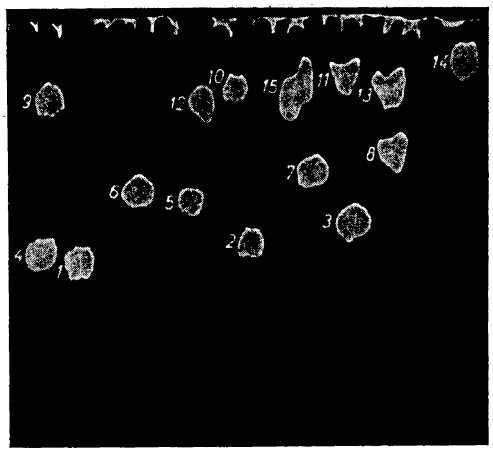

Fig. 3. The ultraviolet photograph of the two-dimensional ionophoretic — chromatographic separation of nucleotides.

1) AMP; 2) ADP; 3) ATP; 4) DPN; 5) TPN; 6) GMP; 7) GDP; 8) GTP; 9) CMP; 10) CDP; 11) CTP; 12) UMP; 13) UDP; 14) UTP; 15) UDPG and UDPAG.

uridine diphosphate acetylglucosamine (UDPAG) are not completely separated from each other, but are clearly separated from the other nucleotides.

The method described gives a rapid separation of the nucleotides. It is usable for preliminary analyses of mixtures and especially when only small amounts of material are available. An approximate estimation of the amounts of the different substances can be obtained by eluting the ultraviolet absorbing spots with 0.1 N hydrochloric acid and estimating the ultraviolet absorption of these eluents.

EXPERIMENTAL

The ionophoretic fractionation was performed using the apparatus and technique previously described [1]. The two-dimensional separation was carried out on Whatman No. 1 paper purified by washing with 1 N hydrochloric acid and water. The mixture to be separated was applied as a line to the dry paper and then the paper was impregnated with sodium acetate buffer of pH 4.15 and of ionic strength 0.1. The nucleotides were distributed over a maximum usable interval after the paper had been exposed to a voltage of 1 000 V for 10 h. The paper was dried at room temperature and then the initial fractionation of the mixture was observed by photographic printing in ultraviolet light of 254 mμ.

The chromatographic separation in the second direction was made after cutting away the unnecessary parts of the paper sheet. The best separations were obtained by the descending technique with a solvent system of saturated ammonium sulphate solution — *n*-butanol — water (79:0.5:19). The chromatogram was run for 10 h at 20—22°C. The resulting separations of the nucleotides were established by making a contact print in ultraviolet light of the whole sheet.

Materials. The nucleotides used as standard substances were obtained from the Sigma Chemical Company.

This work has been supported by grants from the *Swedish Natural Science Research Council.*

REFERENCES

1. Bergkvist, R. *Acta Chem. Scand.* **11** (1957) 1465.

Received February 18, 1958.

ACTA CHEMICA SCANDINAVICA 12 (1958) 756—764

Studies Related to Naturally Occurring Acetylene Compounds. XXII * Correctional Studies on the Constitution of the Polyacetylenes of some Annual *Coreopsis* Species

JÖRGINE STENE SÖRENSEN and NILS ANDREAS SÖRENSEN

Institutt for Organisk Kjemi, Norges Tekniske Högskole, Trondheim, Norway

One of the polyacetylenes previously isolated from some annual *Coreopsis*-species and supposed to be *1*-phenyl-undeca-1:3:5-triyne-7:9-diene (IV) is shown to be a mixture of trideca-1:3:11-triene-5:7:9-triyne (V, R = H), probably with *cis* configuration at the 3:4 double bond, and *trans*-1-phenyl-hepta-1:3-diyn-5-ene (I, R = H).

In the XVII[th] Communication of this series J. Stene Sörensen and N. A. Sörensen [1] described the isolation of 4 new acetylenic compounds from some annual garden varieties of the genus *Coreopsis, viz. C. tinctoria Nutt., C. Drummondii* Torr. & Gray and *C. cardaminifolia* (D.C.) Torr & Gray. The 4 new acetylenic compounds were given the following constitutional formulas I, R = $OCOCH_3$, II, III, R = H, and IV.

—C≡C—C≡C—CH=CH—CH_2—R I

RH_2C—CH=CH—C≡C—C≡C—CH=CH—CH=CH—CH=CH_2 II

RHC=CH—C≡C—C≡C—C≡C—C≡C—CH=CH_2 III

—C≡C—C≡C—C≡C—CH=CH—CH=CH—CH_3 IV

The correctness of I, R = $OCOCH_3$ was proved by Bruun, Skatteböl and Sörensen [2] by the total synthesis, revealing that the configuration of the double bond is *trans*.II was shortly afterwards synthesised by Bohlmann [3]; this synthesis confirmed the supposition of Sörensen and Sörensen [1] that the configuration was all-*trans*.

* XXI Communication, *cf.* Festschrift Arthur Stoll, Basel 1957.

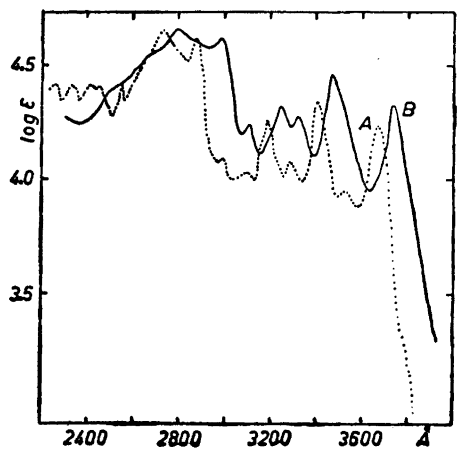

Fig. 1. Ultraviolet absorption of
A: "3650" Hydrocarbon supposed to be IV according to Sörensen *et al.*[1]
B: *trans* IV, redrawn from Bohlmann *et al.*[3]

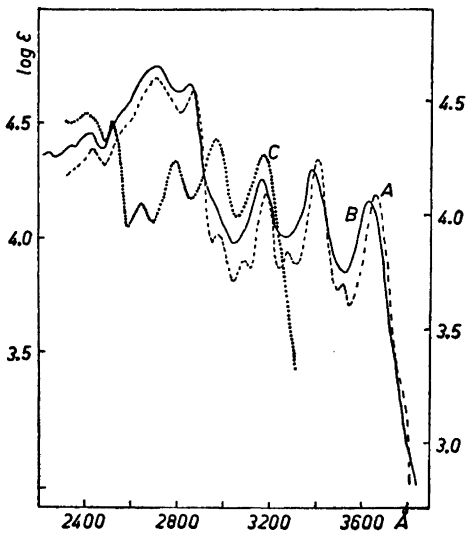

Fig. 2. Ultraviolet absorption in hexane of:
A. *cis* trideca-1:3:11-triene-5:7:9-triyne — — — — — —
B. *trans* trideca-1:3:11-triene-5:7:9-triyne ————
C. *trans* 1-phenyl-hepta-1:3-diyn-5-ene (scale right side) .....

The hydrocarbon III, R = H was synthesised by Jones, Thompson and Whiting [4] and turned out to be very similar but not identical with the so-called 3910-hydrocarbon from *Coreopsis* oils; Skatteböl [5] synthesised both the *trans* and the *cis* isomers of the homologue III, $R = CH_3$. The *trans* compound turned out to be identical with the 3910-hydrocarbon, m.p. 43°C, which has a rather wide occurrence inside some tribes of the family *Compositae*. This brilliant synthetic work further established that the *cis* compound III, $R = CH_3$, undoubtedly also occurred in some chromatographic fractions from *Coreopsis* species measured by Sörensen and Sörensen [1] in the infrared.

Bohlmann [6] described the synthesis of the *trans* isomer of IV. Although there was some similarity in the ultraviolet spectra, synthetic *trans* IV was undoubtedly different from the compound occurring in the flowering parts of the investigated annual *Coreopsis* species, *cf.* Fig. 1. Bohlmann put forward the hypothesis that the naturally occurring compound might be one of the possible *cis* isomers. This, however, was unlikely since the synthetic *trans* isomer has the ultraviolet absorption maxima about 65 Å at longer wave-lengths than the natural compound, whereas *cis* polyen-ynic isomers mostly absorb at longer wave-lengths than their corresponding *trans* isomers [7].

I—III were solids which could be purified by recrystallisation; IV, however, was a liquid the homogeneity of which was difficult to guarantee. Sörensen and Sörensen [1] recorded some difficulties in their experimental work; thus

the perhydrogenation product, which should be 1-phenyl-*n*-undecane could not be brought to correct melting point, — 5°C, although the melting point obtained, —8 to —6.5°C, came very close to that of the best synthetic preparation of 1-phenyl-*n*-undecane which Sörensen and Sörensen were able to synthesise and no clear-cut m.p. depression could be observed.

That in reality the constitution of the perhydrogenation product was completely misinterpreted became clear when Dr. A. J. P. Martin most kindly investigated a melting point sample of the perhydrogenation product in his vapour fractometer. According to a personal report from Dr. Martin the perhydrogenation product contained at least two products one of which might possibly be *n*-tridecane. Thus the constitution of the compound supposed to be IV had to be reinvestigated.

The characteristic double maxima in the longwaved band group of this compound, *cf.* Fig. 1, were taken by Sörensen and Sörensen as an indication of the occurrence of a mixture of compounds. However, all chromatographic fractions from the different garden varieties showed the same relative intensity of the main and subsidiary maxima, a very improbable happening with a mixture of compounds.

By the reinvestigations these double maxima in ultraviolet were again taken as the analytical mark, but every effort to obtain an alteration in the relative intensities by taking narrower cuts in the chromatographic fractions were again without success.

The picture remained unchanged when the chromatographic cuts were made still narrower; elution with 2—4 % benzene in petroleum ether taking 5—20 fractions at each concentration. When, however, these fractions with conform long-wave band group in the ultraviolet region simultaneously were investigated in the infrared region characteristic definite differences emerged. The characteristic phenyl-peaks at 1 494, 753 and 686 cm^{-1} changed in intensity relative to the acetylenic one at 2 200 cm^{-1} and a characteristic peak at 775 cm^{-1}.

Reinspection of the ultraviolet spectra then revealed that the fractions with the most intensive phenyl peaks in the infrared had some extra ultraviolet bands at 3 180 and 2 970 ÅU. With these experimental facts well established repeated chromatography on deactivated alumina finally led to a separation of this part of the flower oil into two components of constant properties. Both could be crystallised. Recrystallisation seemed rather unsuccessful however, as a method of separation, possibly because of mixed crystals. Both components were very readily soluble in most solvents which of course hampered purification of small amounts of substance by recrystallisation.

Fig. 2. gives the ultraviolet spectra of the 2 compounds. As will be seen the main component still has the characteristic double maxima in the long-wave band group. Fig. 3, which gives the infrared spectra, reveals that the most long-wave chromophore belongs to a compound containing no phenyl group, whereas the minor component with first maximum in ultraviolet at 3 180 Å obviously is a phenyl compound.

With the tedious separation of the two components achieved constitutional work could again be started.

Table 1. Ultraviolet absorption maxima of ene-triynes and phenyl-triynes (Å).

$H_3C-(C\equiv C-)_3-CH=CH-CH_2-CH_2-C(=O)-CH_2-CH_3$ [9]	3 286	3 081	2 890	2 725	2 577	2 425	2 310
$H_3C-CH=CH-(C\equiv C-)_3-CH_2-CH_2-C(=O)-CH_2-CH_3$ [8]	3 300	3 085	2 895	2 730	2 580	2 422	2 305
$H_3C-(C\equiv C-)_3-CH=CH-CH_2OC_2H_5$ [10]	3 295	3 080	2 890	2 725	2 578	2 410	2 300
$H_3C-(C\equiv C-)_3-CH=CH-CH_2-COOH$ [10]	3 300	3 090	2 900	2 730	2 570	2 435	2 335
$H_5C_6-(C\equiv C-)_3-CH_3$ [11]	3 309	3 097	2 908	2 735	2 590	2 504	2 380
$H_5C_6-(C\equiv C-)_3-C_2H_5$ [2]	3 315	3 100	2 905	2 735	2 595	2 510	2 387
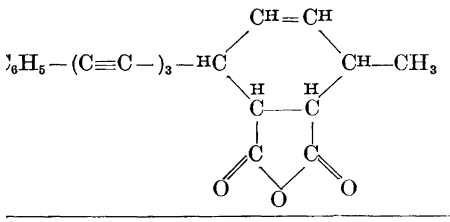	3 335	3 125	2 935	2 767	—	2 545	2408*

* in ether

The hydrocarbon with the first maximum at 3 670 Å could be crystallised from petroleum ether and showed m.p. 50.5—56°C. By the catalytical hydrogenation 8.25 moles of hydrogen were taken up. The perhydrocompound crystallised readily in the refrigerator m.p. —7°. *n*-Tridecane has m.p. —6.5 to —6°, a 1:1 mixture showed no depression. The infrared spectrum was in every detail identical with that of *n*-tridecane. Although normal paraffins higher than *n*-decane show nearly identical infrared spectra the identity of the perhydrogenation product and *n*-tridecane should be well established.

Sörensen and Sörensen [1] obtained in very small yield an adduct with maleic anhydride from what they supposed to be 1-phenyl-undeca-1:3:5-triyne-7:9-diene IV. The yield was to small for elementary analysis, the m.p. was given as 146°C and the adduct was characterised by a U.V.spectrum which came very close to that of *1*-phenyl-octa-1:3:5-triyne.

It turned out that this adduct belongs to the aliphatic hydrocarbon with the characteristic double maxima. From the pure hydrocarbon the yield was appreciably higher, but still low.

The fact which was overlooked by Sörensen and Sörensen was that the spectra of phenyl-triynes and ene-triynes are very similar, especially in the long-wave band group. The main differense is a small displacement of the first sharp maximum of the short-wave band group. As will be seen from Table 1 where some characteristic examples are collected, the phenyl triynes have this maximum some 90 Å at longer wave-lengths.

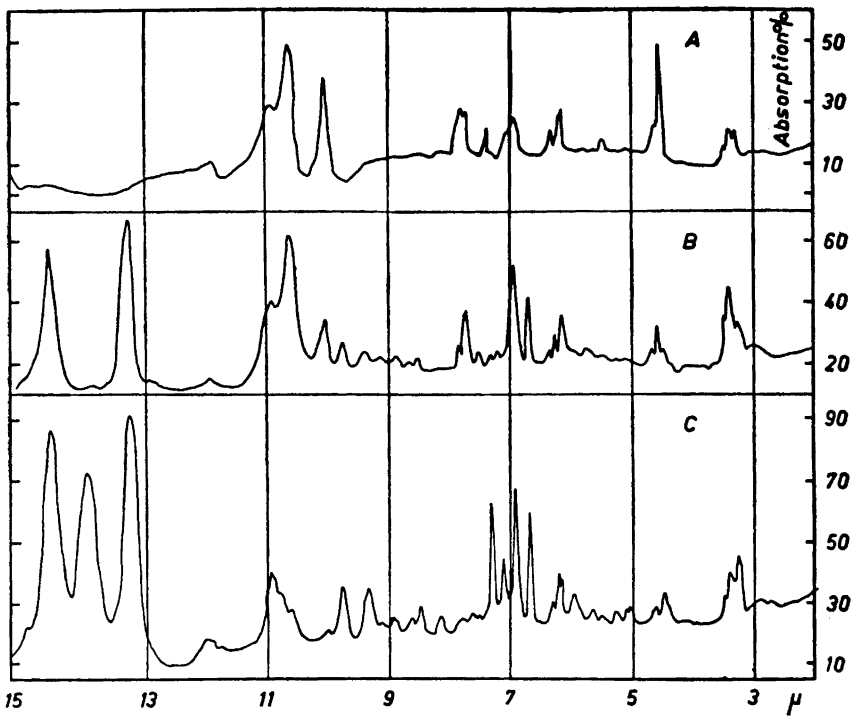

Fig. 3. Infrared absorption of:

A. trideca-1:3:11-triene-5:7:9-triyne in $CHCl_3$, c = 10.6 %, l = 0.05 mm.
B. *trans* 1-phenyl-hepta-1:3-diyne-5-ene liq.
C. *cis* 1-phenyl-hepta-1:3-diyne-5-ene liq.

The maleic anhydride adduct isolated by Sörensen and Sörensen from the "3 650"-hydrocarbon has the strongest band at 2 450 Å and so Bohlmann [6] was correct in his suggestion that the adduct had originated from an other poly-yne-diene present in the fraction. As Table 1 demonstrates the adduct belongs to the ene-triyne class.

The hydrogenation experiments and the properties of the dien-adducts reveal that the hydrocarbon is a *n*-trideca-triene-triyne. So it is the missing link between the *n*-trideca-tetrayne-diene (II, R = CH_3) isolated from the root part of the annual *Coreopsis* species and the *n*-trideca-diyne-tetraene II (R = H) isolated from their leaves.

The infrared spectrum, *cf.* Fig. 3, gives clear indication (1 840 cm^{-1}) of a vinyl group in the triene-triyne.

The ultraviolet spectrum of the maleic anhydride adduct further gives the information that the acetylenic bonds are conjugated; it remains then only 2 possible formulas for a *n*-trideca-triene-triyne, *viz* V, R = H, and VI.

$$R-H_2C-CH=CH-C\equiv C-C\equiv C-C\equiv C-CH=CH-CH=CH_2 \qquad V$$
$$H_3C-C\equiv C-C\equiv C-C\equiv C-CH=CH-CH=CH-CH=CH_2 \qquad VI$$

Of these possibilities V, R = H, should be the correct one for the following reasons. From *Carlina vulgaris* Sörensen and Sörensen [12] isolated an acetate for which they deduced formula V, R = $OCOCH_3$. Bohlmann [13] has synthesised the *trans* isomer of this 1-acetoxy-*n*-trideca-2:10:12-triene-4:6:8:triyne which differed from the *Carlina* acetate but gave the same anhydride adduct. Bohlmann concluded that the Carlina acetate differs in having *cis* configuration at C_{10-11}.

These *cis* and *trans* 1-acetoxy-trideca-triene-triynes (V, R = $OCOCH_3$) show ultraviolet spectra conform with our triene-triyne-hydrocarbon which definitely points to V, R = H, as the correct formula. V, R = H is just the 9:10-dihydro-compound of III, R = CH_3 and the 5:6-dehydro-compound of II, R = H. Finally the choice between V, R = H and VI has been supported by synthetic work, which, because of some interesting side-reactions, will be described in a separate communication.

As to the configuration of the *n*-deca-triene-triyne from *Coreopsis* species an accidental observation gave valuable hints. A chromatographic fraction of nearly pure triene-triyne was so small that both ultraviolet and infrared spectra had to be taken on the same sample. Accidentally the infrared spectrum was recorded first. Surprisingly the subsequent ultraviolet spectrum demonstrated remarkable changes. As Fig. 2 demonstrates, the long-wave group has lost the characteristic double maxima, at the same time the main maxima have moved about 40 Å towards shorter wave-lengths.

This spectral difference relative to the nearest fractions indicated that a *cis-trans* isomerisation had taken place during the infrared measurement. It was not further investigated if the transformation was due to heat alone or to traces of HCl in the solvent chloroform. Instead the *cis-trans* isomerisation was achieved in the usual way through action of light in the presence of traces of iodine in spectral hexane.

As mentioned above [7] it is usual in polyenynes that the *cis* isomers absorb at somewhat longer wave-lenghts than the *trans* isomers; in the known pair of spectra of *cis-trans* isomers the spectra have, however, been very nearly conform. Therefore the characteristic double maxima in the naturally occurring *cis* isomer of V, R = H, might be due to special constitutional details. We find it reasonable to suppose that the *cis-trans* isomerism occurs at least at the C_{3-4} double bond. Assuming that a conjugated molecule tends to exist in a planar conformation, if at all possible, inspection of models, *cf.* Fig. 4, revealed that the 3-*cis*-*n*-trideca-1:3:11-triene-5:7:9-triyne may exist in two planar conformations of rather different molecular shape. Synthetically it should be possible to provide spectra of model compounds which might elucidate whether the double maxima are due to a coexistence of these two rotational isomers.

The second, phenyl-containing component was difficult to purify because of low crystallising power and high solubility in all solvents. The purest fraction obtained had m.p. 25—27°.

The ultraviolet spectrum of this fraction showed great similarity with the 1-phenylhepta-1:3-diyn-5-en-7-ol acetate isolated from all parts of the investigated annual *Coreopsis* species. For this reason we guessed on the structure 1-phenylhepta-1:3-diyn-5-ene (I, R = H) and tested this hypothesis by

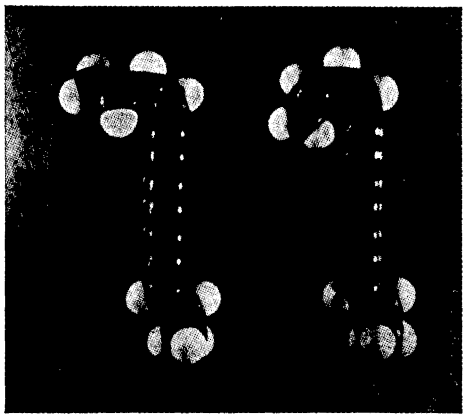

Fig. 4. The two planar conformations of 3-*cis* 1:3:11-triene-5:7:9-triyne (V, R = H).

the synthesis of the *cis* and *trans* isomers of this hydrocarbon by oxidative coupling of phenyl-acetylene with *cis* and *trans* pent-3-en-1-yne, respectively. The synthesis is described in the experimental part. Comparison with the synthetic isomer proved that the phenyl compound from *Coreopsis* leaves was 1-phenyl-1:3-diyn-5-*trans*-ene (I, R = H).

This correctional work revealed some interesting facts. First that the 5 acetylenic compounds so far isolated from annual *Coreopsis* species are all C_{13}-compounds.

The two new polyacetylenes described in this paper I, R = H, and V, R = H are isomeric $C_{13}H_{10}$-compounds differing only in the curling up of the dien-yne-tail of V, R = H, to the phenylresidue of I, R = H.

The same type of isomerism was demonstrated in our XIXth communication to exist between the *Carlina* acetate, V, R = $OCOCH_3$, and the 1-phenyl-hepta-1:3-diyn-5-en-7-ol acetate, I, R = $OCOCH_3$, from *Coreopsis*. Thus it seems possible that some *Compositae* are able to synthesise the phenyl residue in this direct way, not passing oxygenated 6-ring precursors.

EXPERIMENTAL

1. *Separation of the "3650"-hydrocarbon into components.* The starting material was a sample of 5 g of the essential oil of the flowering part of *Coreopsis cardaminifolis* harvested late in the autumn (Sept. 23rd). The main separational procedure was chromatography on the slightly deactivated alumina of Mancera *et al.*[14] Washings with petroleum ether eluted only saturated paraffins and nonchromophoric hydrocarbons. Then followed elution with increasing concentrations of benzene, *viz.* 1.5 %, 2 %, 4 %, 10 % *etc.*

The first polyacetylenic substance to be eluted was the diene-tetrayne (III, R = CH_3) mixed with the "3650"-hydrocarbon. When reaching 10 % benzene in petroleum ether there appeared mixtures exhibiting the "3650"-chromophore spectrum with the indistinct spectrum of the tetraene-diyne (II). II crystallised readily from these fractions in a pure state. All the fractions eluted between the polyenynes II and III showed ultraviolet spectra very similar to that originally given for the "3650"-hydrocarbon. When these fractions were inspected in infrared (mostly 12–20 fractions were taken between 2 % and 10 % benzene in petroleum ether) it turned out that the intensity of the peaks be-

longing to a monosubstituted phenyl-residue (1 493, 752 and 686 cm^{-1}) increased relative to the other infrared bands with increasing concentration of benzene. Chromatography alone only lead to a slight displacement of the concentrations. By fractional distillation at $10^{-3}-10^{-4}$ mm Hg the phenyl-containing component was slightly more volatile than the aliphatic component. Redistillation, therefore, on the one hand was suitable to get rid of solvents and decomposition products, on the other hand some enrichment of the phenyl-compound took place in the most volatile part.

All fractions solidified at -40 to $-70°$; also from petroleum ether crystals will mostly be deposited at $-70°$. The crystallisates were more or less greasy and mostly the solutions had the same composition as the whole fraction. However, when chromatography, distillation and rechromatography had brought the separation above a certain concentration, crystallisation at $-70°$ sometimes gave the components nearly spectroscopically pure.

2. n-*Trideca-1:3:11-triene-5:7:9-triyne, (V, R = H)*. The purest fraction obtained showed a rather unsharp m.p. at 51—56°, vacuum; the U.V.spectrum is given in Fig. 2, the infrared spectrum in Fig. 3.

Catalytical hydrogenation: 30.8 mg V, R = H, were hydrogenated in absolute alcohol with 20 mg palladium on barium sulphate as catalyst. At 764 mm, t = 20°C, 37.3 ml of hydrogen (8.25 ⌶) were taken up, calculated for 9 ⌶ 40.8 ml. The solution was worked up in the usual way. After distillation at 8 mm the distilled product melted at -7.5 to $-6.8°$. *n*-Tridecane [1] melted at -6.5 to $-5.5°$, mixed m. p. -7.3 to -6.3°C. The infrared spectrum agreed in every detail with that given for *n*-tridecane [1].

3. trans-*1-phenylhepta-1:3-diyn-5-ene from* Coreopsis. The purest fraction obtained melted at 22—24°. The U.V.-spectrum is given in Fig. 2, the infrared spectrum in Fig. 3.

Synthesis of cis *and* trans *hepta-1:3-diyn-5-ene*. The synthesis was achieved by oxidative coupling of phenylacetylene with *cis* and *trans*-pentenyne. The pentenyne isomers were prepared according to Eglinton and Whiting [15], the fractionation being controlled by infrared measurements. Both oxidative couplings were carried out under the same experimental conditions, as exemplified for the *cis* compound:

2 ml of *cis*-pentenyne and 4 ml of phenylacetylene were dissolved in 200 ml of a 1:1 mixture of methanol and acetone at -20°C; to this mixture was slowly added a solution of 15 g of cuprous chloride, 40 g of ammonium chloride, 2 g of iron(III) chloride and 1 ml of conc.hydrochloric acid in 125 ml of water with a vivid stream of oxygen bubbling through the solution. The flask containing the mixture was kept in a bath of acetone-carbon dioxide maintained at $-20°$ for 18 h. The reaction mixture was extracted with ether; the ether solution on evaporation left a crystalline mass. Some of the diphenyldiacetylene remained undissolved by washing with ether. This ether solution again was evaporated and the residue dissolved in petroleum ether and chromatographed on alumina with 2 % benzene in petroleum ether.

The first fractions were oily at room temperature, these fractions were distilled at 0.0001 mm. At room temperature deca-diene-2:8-diyne-4:6 went off, at 50° (bath temperature) 0.15 g of a colourless liquid distilled off. This fraction remained as a liquid at -20°C.

Ultraviolet absorption of *cis*-1-phenylhepta-1:3-diyn-5-ene in hexane:

ε_{max}	20 400	24 000	17 800	10 800	32 400	33 900	
λ_{max}	3 190	2 990	2 800	2 650	2 520	2 410	Å

The maxima differ neither in position nor in intensity from the naturally occurring and the synthetic *trans* isomer within the limits of experimental errors (*cf.* below). The synthetic *trans* isomer melted at 23—24°C.

Ultraviolet absorption of *trans*-1-phenylhepta-1:3-diyn-5-ene in hexane:

ε_{max}	19 300	22 650	18 200	11 750	26 900	29 200	
λ_{max}	3 180	2 975	2 795	2 645	2 525	2 410	Å

As will be seen from Fig. 3 the *cis* and *trans* isomers differ appreciably in the infrared and just in the positions expected. The infrared spectra confirm the conclusion from the melting point that the *Coreopsis* Compound is the *trans* isomer. At the same time small

additional peaks in the infrared spectrum of the phenylheptadiynene from *Coreopsis* species just agree with the strongest peaks in the *n*-decatrienetriyne, and clearly indicate that the separation was not completely successfull, although the contamination is so small that it does not disturb the identification.

Acknowledgements. Grants from *Norges Almenvitenskapelige Forskningsråd*, which have enabled these investigations to be carried out, are gratefully acknowledged.

REFERENCES

1. Sörensen, J. Stene and Sörensen, N. A. *Acta Chem. Scand.* **8** (1954) 1743.
2. Bruun, T., Skatteböl, L. and Sörensen, N. A. *Acta Chem. Scand.* **8** (1954) 1757.
3. Bohlmann, F. and Mannhardt, H.-J. *Chem. Ber.* **88** (1955) 1330.
4. Jones, E. R. H., Thompson, J. M. and Whiting, M. C. *Acta Chem. Scand.* **8** (1954) 1944.
5. Skatteböl, L. *Studies in the field of highly unsaturated systems, Thesis*, Manchester 1956.
6. Bohlmann, F. *Chem. Ber.* **88** (1955) 1755.
7. Bruun, T., Haug, C. M. and Sörensen, N. A. *Acta Chem. Scand.* **4** (1950) 850; Sörensen, J. Stene, Bruun, T., Holme, D. and Sörensen, N. A. *Acta Chem. Scand.* **8** (1954) 26.
8. Bohlmann, F., Mannhardt, H.-J. and Viehe, H. G. *Chem. Ber.* **88** (1955) 361.
9. Stavholt, K. and Sörensen, N. A. *Acta Chem. Scand.* **4** (1950) 1567.
10. Bohlmann, F. and Viehe, H. G. *Chem. Ber.* **87** (1954) 712.
11. Sörensen, J. Stene, and Sörensen, N. A. *Acta Chem. Scand.* **12** (1958) 765.
12. Sörensen, J. Stene, and Sörensen, N. A. *Acta Chem. Scand.* **8** (1954) 1763.
13. Bohlmann, F. and Inhoffen, E. *Chem. Ber.* **89** (1956) 21.
14. Mancera, O., Barton, D. R. H., Rosenkranz, G. and Djerassi, C. *J. Chem. Soc.* **1925** 1025.
15. Eglinton, G. and Whiting, M. C. *J. Chem. Soc.* **1950** 3653.

Received February 14, 1958.

ACTA CHEMICA SCANDINAVICA 12 (1958) 765—770

Studies Related to Naturally Occurring Acetylene Compounds XXIII. 1-Phenylhepta-1:3:5-triyne from *Coreopsis grandiflora*, Hogg ex Sweet

JÖRGINE STENE SÖRENSEN and NILS ANDREAS SÖRENSEN

Institutt for Organisk Kjemi, Norges Tekniske Högskole, Trondheim, Norway

A preliminary investigation of some perennial species belonging to the genus *Coreopsis* revealed the occurrence of 1-phenylhepta-1:3:5-triyne (VII) in Nature. The constitution of this new polyacetylene has been confirmed by synthesis.

In the XVII[th] communication of this series Sörensen and Sörensen [1] described the isolation of 4 new polyacetylenic compounds from some annual garden varieties of the genus *Coreopsis* L., family *Compositae*. As shown in the preceding communication [2] one of these compounds turned out to be a mixture of two previously unknown polyacetylenes raising the number of acetylenic compounds with established structure in annual *Coreopsis* species to the 5 compounds (I)—(V).

(I) $CH_3-CH=CH-C\equiv C-C\equiv C-C\equiv C-C\equiv C-CH=CH_2$

(II) $CH_3-CH=CH-C\equiv C-C\equiv C-C\equiv C-CH=CH-CH=CH_2$

(III) $CH_3-CH=CH-C\equiv C-C\equiv C-CH=CH-CH=CH-CH=CH_2$

$-C\equiv C-C\equiv C-CH=CH-CH_2-R$, (IV) R=H, (V) R=OCOCH$_3$

(VI) $CH_3-C\equiv C-C\equiv C-C\equiv C-C\equiv C-C\equiv C-CH=CH_2$

(VII)

$-C\equiv C-C\equiv C-C\equiv C-CH_3$

In that preliminary work only one single perennial *Coreopsis* species was investigated, *viz. C. verticillata* L. The tetrayne (I) was present in the roots, but otherwise *C. verticillata* differed remarkably from the other *Coreopsis* species through a high content of 2:6-dimethyloctatetraene = Cosmene, first isolated

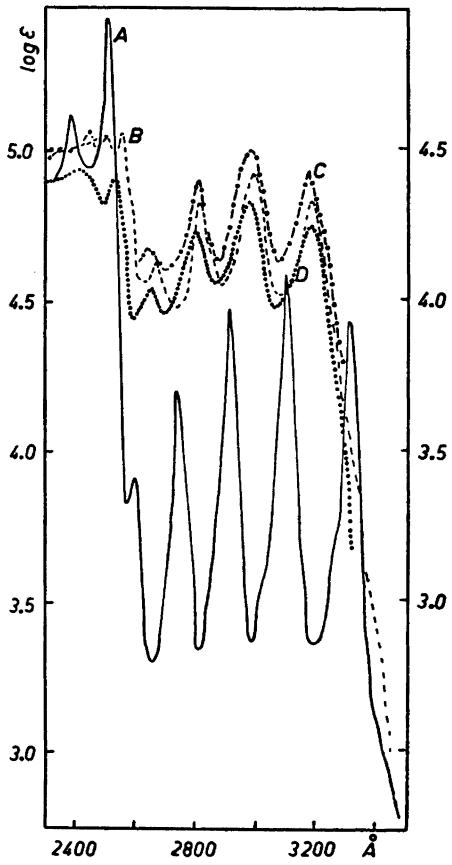

Fig. 1. Ultraviolet absorption in hexane of

A.	1-Phenyl-hepta-triyne-1:3:5 (VII) ————	(scale left side)
B.	6(?)-chloro-1-phenyl-hepta-1:3-diyn-5-ene — — — — — — —	» » »
C.	1-Phenyl-hepta-1:3-diyn-5-en-ol-7-acetate (V) —.—.—.	» » »
D.	1-Phenyl-hepta-1:3-diyn-5-ene (IV)	» » »

from *Cosmos bipinnatus*, but so far only found in traces in one annual *Coreopsis*, *viz. C. Drummondii* [3].

The next perennial *Coreopsis* which incidentally was investigated was *C. grandiflora*, Hogg ex Sweet. Although the tetrayne (I) was readily recognisable in the long-wave part of the spectrum of the primary acetone exctracts from the root part, the U.V.-spectra of all parts of *C. grandiflora* were dominated by a fine structure spectrum, *cf.* Fig. 1, curve A, so far not found in the investigated annual members of the genus. By chromatography on alumina the new chromophore followed immediately after small fractions containing the characteristic absorption bands of the tetra-acetylene (I) and the penta-acetylene (VI). The occurrence of (VI) seems to be characteristic of tribus *Inuleae* but

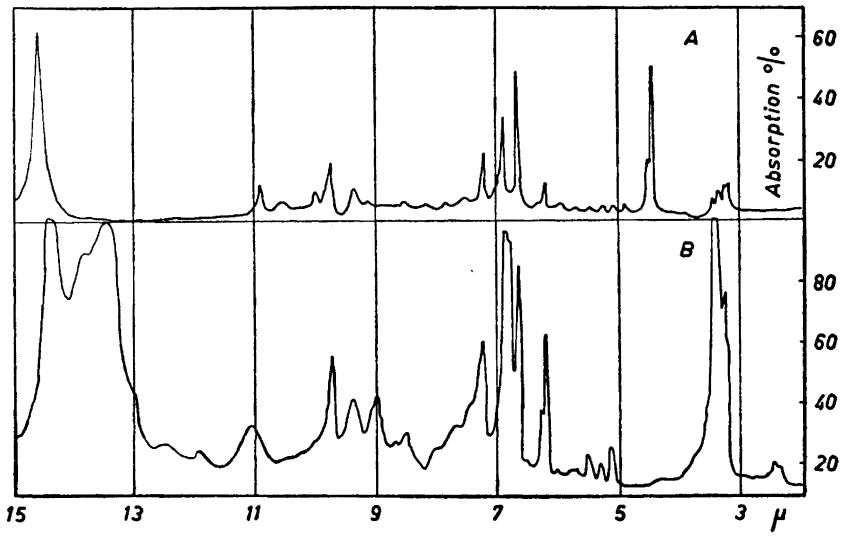

Fig. 2. Infra red absorption of
A. 1-Phenyl-hepta-1:3:5-triyne in $CHCl_3$, c = 11 %, l = 0.05 mm
B. 1-Phenyl-*n*-heptane, liq. l = 0.025 mm.

has not so far been found in the genus *Coreopsis* itself; it has already been found in other members of tribus *Heliantheae* including representatives of sub-tribus *Coreopsidinae*. A number of chromatographic fractions eluted with 10 % benzene in petroleum ether immediately delivered the new chromophore in crystalline condition. Recrystallisation from petroleum ether gave colourless prisms m.p. 55—56°C.

The ultraviolet spectrum was much sharper in fine structure than that of the 1-phenyloeta-1:3:5-triyne synthesised by Bruun, Skatteböl and Sörensen [4] but identical in position of the maxima within the limits of the experimental errors:

$C_6H_5-(C\equiv C)_3-CH_2-CH_3$	λ_{max} :	3 315	3 100	2 905	2 735	2 595	2 510	2 387 Å
C. grandiflora, m. p. 55—56°	λ_{max} :	3 309	3 097	2 908	2 735	2 590	2 504	2 380 Å

That the new compound did contain the phenyl group was obvious from strong peaks in the infrared at 1 495 and 686 cm^{-1}, *cf.* Fig. 2, curve A.

Catalytical hydrogenation gave a liquid hexahydrocompound with a consumption of 5.9 mole hydrogen (calc. as $C_{13}H_8$). The infrared spectrum of this hexahydrocompound agreed almost completely with that of 1-phenyl-*n*-octane. These few facts strongly indicated the structure 1-phenylhepta-1:3:5-triyne (VII). This compound was synthesised along the same route which was used for the homologue [4], *viz.* reaction of phenylpropargylaldehyde with the di-Grignard derivative of but-1-yn-3-ol to give 1-phenylhepta-1:4-diyne-3:6-diol. Through the dichloride this glycol was converted into 1-phenylheptatriyne.

The intermediate glycol could not be obtained crystalline and although the synthesis was successful and the synthetic 1-phenylheptatriyne was identical with the new hydrocarbon from *C. grandiflora* a number of side reactions were met with. Some of these are described in the experimental part.

1-Phenylheptatriyne is a rather stable compound. It is volatile with steam and so it may also be isolated from essential oils. Due to the characteristic U.V.-spectrum it is easily recognised also when present in small quantities. For this reason we do not think it is a general component of the essential oil of all members of the genus *Coreopsis*. Rather it seems more abundant in the perennial members than in the annual. Of *C. tripteris* L. only a few plants were available and (VI) was present only in traces.

In *C. lanceolata* L. and *C. saxicola* Alex., of which the first is botanically closely related to *C. grandiflora*, the oils were in part so enriched in (VII) that it crystallised out when stored in a refrigerator.

That (VII) is not restricted to some section of the genus *Coreopsis* was established by a preliminary investigation of some members of the genus *Bidens*, some of which turned out to be very rich in VII. These investigations will be described in later communications of this series.

The botanists long ago have placed the 3 genera: *Bidens*, *Coreopsis* and *Cosmos* close together and many of their species have synonymous names in all three genera. A close relation *Bidens-Coreopsis* has been confirmed by the investigations of their acetylenes; so far, however, the few members of *Cosmos* which have been investigated have not shown any of those extensive variations in polyacetylenes which make *Bidens* and *Coreopsis* a promising field of further studies.

EXPERIMENTAL

Coreopsis grandiflora, Hogg ex Sweet, flowers. The flowering heads collected medio June 1954 were extracted with acetone and the lipids transferred to petroleum ether. The crude extract (0.75 ‰ of the fresh flowers), which was still deep orange from flower pigments, was chromatographed on alumina from petroleum ether solution. Washing with petroleum ether removed rather large amounts of colourless hydrocarbons (28 %). No chromophore appeared until the content of benzene in the eluting mixture was raised to about 10 %. In the first fraction the U.V.-maxima of the tetra-yne (I) which were just traceable in the spectrum of the crude oil, came out very clearly, however, with faint extra maxima belonging to the penta-yne (VI). This penta-yne, with the characteristic first maximum at 4 100 has been found in a lot of tribes of the *Compositae*, but so far not in the genus *Coreopsis*. As the calculated amounts of (I) and (VI) were far below 1 mg no attempt was made to isolate them in the crystalline state.

The subsequent washings with 10 % benzene in petroleum ether contained the new hydrocarbon, which on evaporation crystallised immediately. Recrystallisation of the residues from petroleum ether gave long, colourless prisms, m. p. 55° – 56°, unchanged on further recrystallisation.

U.V.-Spectrum, Fig. 1, curve A, infrared Fig. 2, curve A. Catalytical hydrogenation: 222.9 mg were hydrogenated with $Pd/BaSO_4$ catalyst; consumed 232 ml calculated for $C_{13}H_8$, 6 = 237 ml (759 mm, 21.5°C). The hexahydro compound was isolated in the usual way and the oil distilled. U.V.-Spectrum typical toluene type, λ_{max} 2 683 Å, log ε_{max} = 2.315. Infrared, Fig. 2, curve B.

Another batch of flowers of *C. grandiflora* was distilled in steam, yield 0.75 ‰. The essential oil (1.5 g) was stored in a refrigerator at −18°; phenyl-triyne (VII) after some time crystallised directly from the crude oil. Further amounts could be obtained in pure condition by chromatography as above. Total amount 0.22 g or close to 15 % of the essential oil.

Synthesis of 1-phenylhepta-1:3:5-triyne. But-1-yn-3-ol was prepared according to Campbell *et al.*[5] Phenylpropargyl aldehyde was prepared from α-bromo-cinnamic aldehyde (*Org. Syntheses 25*, 92) via the ethylene glycol acetal [6]. The dehydrobromination of this acetal was effected by boiling 113 g of the acetal with a solution of 50 g of potassium hydroxide in 500 ml of ethanol for 75 min. The phenylpropargyl aldehyde ethylene acetal was extracted with chloroform, dried and distilled, yield 96 %. The hydrolysis was carried out as for the diethyl acetal.

1-Phenylhepta-1:4-diyne-3:6-diol. 23 g of ethyl bromide was grignardised with Mg in 40 ml of dry ether. 7 g of but-1-yn-3-ol was added slowly during 1 h with external cooling. Dry tetrahydrofurane, 3 × 50 ml, was added to keep the Grignard compound in solution. To this solution 13 g of phenyl-propargyl aldehyde were added slowly, the temperature not being allowed to raise above 5°C. The reaction mixture was left for 12 h at room temperature, then decomposed with ammonium chloride and extracted with ether. The product was a viscous oil which could not be brought to crystallisation. In preliminary experiments purification by chromatography and high vaccum distillation was attempted, but with no success.

The crude diol was dissolved in 200 ml of dry ether, 10 ml of dry pyridine was added, and the temperature was brought down to −35°. As addition of thionyl chloride still gave vigorous reaction and dark tars, the thionyl chloride was diluted with 5 parts of dry ether and the reaction continued at −50 to −70°. The solvent was evaporated at 0° by suction. The oily residue was slowly added to a solution of 8 g of potassium in 140 ml of absolute alcohol at −30° and the reaction mixture stirred for half an hour during which the temperature rose to −20°. Pure nitrogen was led through the solution which was allowed slowly to reach 12° (1.5 h). It was decomposed with water and extracted with ether in the usual way.

The U.V.-spectrum of the crude reaction product was disappointingly unsharp, the unusual sharp peaks of the *C. grandiflora* substance being just noticeable. Chromatography on alumina removed all discolouring impurities but the fraction eluted with 10 % benzene in petroleum ether still had a very complex spectrum. Rechromatography and redistillation at first furnished 2 crystalline substances. The final chromatographic washings with 10 % benzene afforded fractions with U.V.-spectra identical with the *C. grandiflora* substance. These fractions gave a crude crystallisate, m. range 38−45°, after one recrystallisation from petroleum ether m. p. 52−53°, recrystallisation m. p. 55−55.5°, mixed m. p. 1:1 mixture 55 to 55.8° sharp. Infrared and U.V.-spectra identical within the errors of observation.

Whereas the main chromatographic fractions still gave very complex spectra, the first fractions with 10 % benzene gave oils devoid of the phenyl-triyne-chromophor. These could be induced to crystallise from petroleum ether in the low temperature refrigerator. The crystals did not show a sharp m. p., range 45−49°, but could be recrystallised to a rather sharp m. p. 61−62°. (Found: C 79.8; H 5.05. Infrared gave no indication of hydroxylic or carbonyl oxygen. The Beilstein test revealed halogen. Calc. for $C_{13}H_8Cl$: C 77.8; H 4.52.) As evident from the U.V.-spectrum, *cf.* Fig. 1, curve B, the substance must contain a phenyldiyn-ene chromophore, $C_6H_5-C\equiv C-C\equiv C-\underset{|}{C}=\underset{|}{C}-R$. In Fig. 1, curve C, *trans* 1-phenylhept-5-ene-1:3-diyn-7-ol acetate [1] and *trans* 1-phenylhept-5-ene-1:3-diyne [2] are given for comparison, both previously isolated from annual *Coreopsis* species and the constitution proved by total synthesis. It thus seems very probable that the crystalline side product, m. p. 61°, is 6-chloro-1-phenylhept-5-ene-1:3-diyne.

The liquid fractions were measured in the infrared. A band at 1 960 cm^{-1} indicated the presence of allenes; the nearest possibility should be 1-phenylhepta-5:6-diene-1:3-diyne. However, this liquid fraction did not give further amounts of 1-phenyl-hepta-triyne by treatment with potassium hydroxide.

Coreopsis grandiflora; leaves. The leaves and stems were distilled in steam; the essential oil amounted to 1.2 ‰. The U.V.-spectrum of the essential oil was nearly conformed with that of phenylheptatriyne (VII), calculated content 6.3 %. Chromatography as above furnished 440 mg of pure (VII).

Coreopsis grandiflora, root. The roots were extracted with acetone and the lipids transferred to petroleum ether. Yield 1.3 %. The U.V.-spectrum of the crude extract was dominated by the characteristic bands of (VII), but those of both (I) and (VI) could be recognised. Chromatography as above afforded 215 mg = 2.5 % of pure (VII). The components of some of the minor fractions will be treated in a following communication.

Coreopsis saxicola, leaves. The plants were cultivated at N.T.H., Trondheim, on open ground and harvested on September 16th 1955. Only very few flowers had appeared, altogether weighing 16 g from which 12 mg of essential oil was prepared. The U.V.-absorption of this small amount of essential oil from the flowers came very close to that of the leaves and so no further investigation of the flower oil was carried out.

5.2 kg of fresh leaves gave 0.7 ‰ of essential oil. The crude essential oil gave a sharp U.V.-absorption spectrum dominated by phenylhepta-triyne, calc. concentration of (VII) = 25 %. Incidentally this oil was stored for a long time in a refrigerator (−15°C) and then had deposited a layer of crystals, which after one recrystallisation from petroleum ether, melted at 54°. Mixed m. p. with authentic phenyl-heptatriyne (VII) 53−54°; ultraviolet and infrared spectra identical.

The mother liquor was chromatographed on deactivated alumina. The eluates with 8−10 % benzene in petroleum ether gave U.V.-spectra of pure (VII), all crystallised, giving altogether 1 g of pure (VII).

Coreopsis lanceolata, leaves. The plants were cultivated at N.T.H., Trondheim, on open ground and harvested during September 1955. Yield of essential oil 0.25 ‰. The oil was chromatographed on deactivated alumina and eluted with mixtures of petroleum ether and benzene. The eluates with less than 8 % benzene were devoid of absorption in the ultraviolet. All fractions eluted with petroleum ether with 8 % benzene gave the U.V.-spectrum of pure (VII) and all of them crystallised directly on evaporation, giving altogether some 100 mg of pure (VII) m. p. 55°, undepressed by authentic phenylhepta-triyne.

Acknowledgements. Grants from *Norges Almenvitenskapelige Forskningsråd,* which have enabled these investigations to be carried out, are gratefully acknowledged.

REFERENCE

1. Sörensen, J. S. and Sörensen, N. A. *Acta Chem. Scand.* **8** (1954) 1741.
2. Sörensen, J. S. and Sörensen, N. A. *Acta Chem. Scand.* **12** (1958) 756.
3. Sörensen, J. S. and Sörensen, N. A. *Acta Chem. Scand.* **8** (1954) 284.
4. Bruun, T., Skatteböl, L. and Sörensen, N. A. *Acta Chem. Scand.* **8** (1954) 1757.
5. Campbell, K. N., Campbell, B. K. and Eby, L. T. *J. Am. Chem. Soc.* **60** (1938) 2883.
6. Dauben, Hypp, J., Löken, B. and Ringold, H. J. *J. Am. Chem. Soc.* **76** (1954) 1359.

Received February 14, 1958.

ACTA CHEMICA SCANDINAVICA 12 (1958) 771—776

Studies Related to Naturally Occurring Acetylene Compounds XXIV. 2-Phenyl-5(α-propynyl)-thiophene from the essential oils of *Coreopsis grandiflora*, Hogg ex Sweet

JÖRGINE STENE SÖRENSEN and NILS ANDREAS SÖRENSEN

Institutt for Organisk Kjemi, Norges Tekniske Högskole, Trondheim, Norway

A crystalline compound, m. p. 43°, isolated from the flowers and leaves of *Coreopsis grandiflora*, Hogg ex Sweet, has been shown to be 2-phenyl-5-(α-propynyl)-thiophene (III) by synthesis of the tetrahydro compound 2-phenyl-5-*n*-propyl-thiophene. The relation of (III) and other naturally occurring thiophenes to polyacetylenic compounds is discussed.

The preceding (XXIII[rd]) communication of this series described the isolation of 1-phenylheptatriyne (I) from some perennial members of the genus *Coreopsis*[1]. (I) was the dominating chromophore of all parts of these oils and in some cases (I) crystallised directly from the crude oils. The oils from all parts of the plants were, however, fractionated by chromatography on slightly deactivated alumina in the usual way. (I) then appeared with the eluates with 10 % benzene in petroleum ether. Since *Coreopsis* species mostly have been characterised by a mixture of polyenynic hydrocarbons, the eluates with 10 % benzene in petroleum were arbitrarily divided into a number of fractions. After evaporation of these solutions in vacuum pure (I) crystallised immediately.

(I) 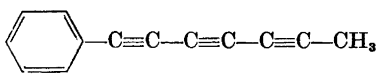

(II) 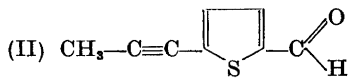

(III) 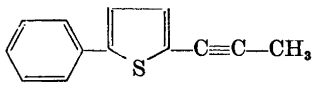

When this standard procedure was applied to the extract from *Coreopsis grandiflora*, Hogg ex Sweet, five nice looking crystallisates were obtained, to the naked eye apparently very similar. The three first fractions melted sharply

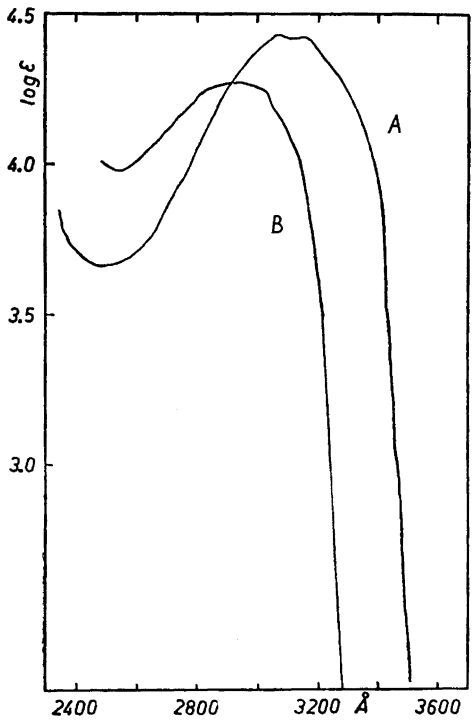

Fig. 1. Ultraviolet absorption in hexane of
A. 2-Phenyl-5-(α-propynyl)-thiophene.
B. 2-Phenyl-5-(*n*-propyl)-thiophene.

around 54°C, the two later also rather sharply, but around 40°C. Recrystallisation brought the m.p. of the later to 43°.

The U.V.-Spectrum, Fig. 1, curve A, with the broad single maximum at 3 100 Å did not indicate any relationship to phenylheptatriyne-1. The infrared spectrum, Fig. 2, curve A, with the sharp peak at 2 240 cm^{-1} revealed that the new compound was a disubstituted acetylene, further the characteristic peaks at 688 and 753 cm^{-1} indicated a monosubstituted phenyl residue.

Catalytical hydrogenation gave a liquid hydrocompound with a consumption of hydrogen so small that on a reasonable molecular weight obviously only the acetylenic bond had been hydrogenated. This was confirmed by the infrared spectrum of the tetrahydrocompound where the acetylenic band had disappeared, Fig. 2, curve B. The U.V.-spectrum of the tetrahydro compound, Fig. 1, curve B, demonstrated on one hand by the movement of the maximum about 200 Å towards shorter wavelengths relative to the starting material that the acetylenic bond was conjugated with the main chromophore, on the other hand that the tetrahydro compound must contain another chromophore resistant towards hydrogenation and conjugated with the phenyl group. Since carbonyl groups were absent, this result was somewhat surprising. Just at this stage of the investigations, however, appeared the communication of Birkinshaw and Chaplen [1] about one of the volatile components, "Junipal", of *Daedelia juniperina*, for which they proved the constitution 6-(α-propynyl)-

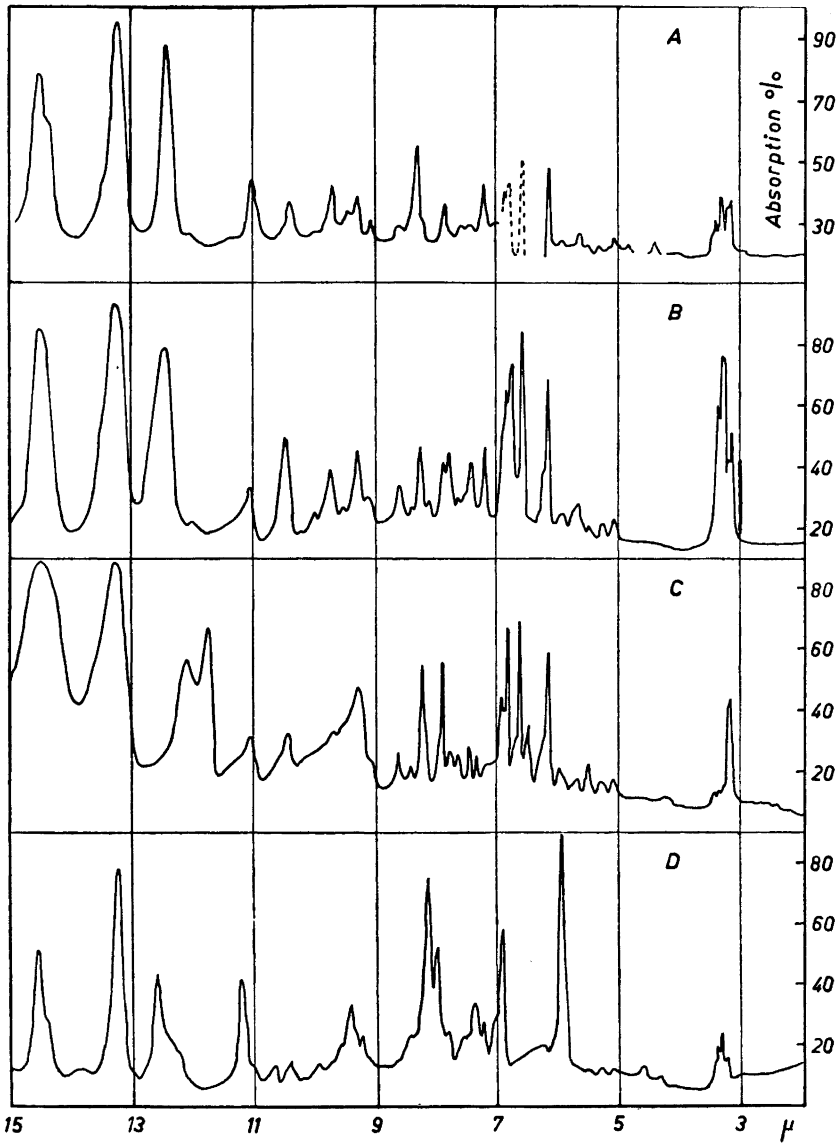

Fig. 2. Infrared absorption of

A. 2-phenyl-5-(α-propynyl)-thiophene (III) in CS_2; c = 24 %; l = 0.05 mm; dotted curve in CCl_4.
B. 2-phenyl-5-*n*-propyl thiophene liq.
C. 2-phenyl-thiophene liq. l = 0.0125 mm.
D. 2-phenyl-5-propionyl-thiophene in CS_2, c = 9.6 %; l = 0.05 mm.

2-formyl-thiophene (II). As there were some similarities in the infrared spectra the new compound, m.p 43°, was analysed on sulphur and gave 16.0 % S, calc. for $C_{13}H_{10}S$: S 16.3.

A compilation of the known infrared spectra of thiophenes, surveyed in the following communication [3], revealed that 2.5-disubstituted thiophenes are characterised by a single, strong peak at about 12.5 μ whereas all the other types of substituted thiophenes have two or more bands in other positions in the 11—15 μ area.

As will be seen from Fig. 2 the new compound fits well into the 2:5-disubstituted class and the observations cited then definitely pointed to the constitution as 2-phenyl-5-(α-propynyl)-thiophene (III).

The easiest way to prove this conclusion was by synthesis of the tetrahydro compound, 2-phenyl-5-*n*-propylthiophene, which followed the route 2-phenylthiophene → 2-phenyl-5-propionylthiophene → 2-phenyl-5-*n*-propylthiophene which, as expected, turned out to be identical in the U.V. and infrared with the tetrahydro compound.

The new compound, m.p. 43, so definitely was proved to be 2-phenyl-5-(α-propynyl)-thiophene. Only 2 thiophene derivatives so far have been considered as naturally occurring thiophenes. The origin of the very numerous thiophene derivatives isolated from petroleum or shale oils is still quite uncertain. The first to be found was terthienyl (IV) isolated by Zechmeister and Sease [4] from the petals of the so-called "African" variety of *Tagetes erecta* L., belonging to the family of the *Compositae, Tribus Helenieae*. The second was the above metioned "Junipal" (II) from *Daedelia juniperina*, a bassidiomycete. Challenger and Holmes [5] suggested a connection between the occurrence of terthienyl and various polyacetylenes in the *Compositae*. Such a connection could be a very close one between 1-phenylheptatriyne (I) and 2-phenyl-5-(α-propynyl)-thiophene (III), as only an addition of hydrogen sulphide to a di-acetylenic group would transform (I) into (III) — chemically not at all an unlikely reaction. Terthienyl, which recently has been found in another *Compositae* plant, *Echinops sphaereocephalus*, would, however, by such a process demand the acetylenic precursor hexa-acetylene V

(V) $H-C\equiv C-C\equiv C-C\equiv C-C\equiv C-C\equiv C-C\equiv CH$

(VI) $HOOC-\underset{\underset{O}{\|}}{C}-CH_2-CH_2-\underset{\underset{O}{\|}}{C}-\underset{\underset{O}{\|}}{C}-CH_2-CH_2-\underset{\underset{O}{\|}}{C}-\underset{\underset{O}{\|}}{C}-CH_2-CH_2-\underset{\underset{O}{\|}}{C}-COOH$

As is well known the stability of unsubstituted acetylenes decreases very rapidly with chain-length. Diacetylene may be distilled, b.p. 9.5—10° [7], triacetylene decomposes already at −50° [8]; efforts to synthesise higher free polyacetylenes have only led to carbonaceous material [9]. Thus even in dilute solution in plant cells in the presence of possible stabilisers the occurrence of hexa-acetylene itself sounds very unlikely. We think it is more probable that some poly-keto precursors analogous to the poly-β-keto-precursors originally proposed by Collie [10] and revived in recent years by Robinson [11], Birch [12], Lipmann [13] and Woodward [14], may be the common precursors to both polyacetylenes and naturally occurring thiophenes. A direct formation of the

thiophene nucleus demands 1:4-diketo groupings, for example VI. It may be, however, that the ordinary β-keto-scheme is at work, that however, dehydration and thiophene formation follow stepwise:

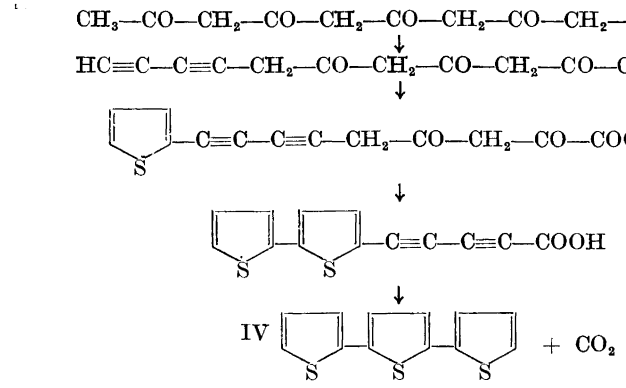

We hope to bring further information on this interesting problem as preliminary investigations have revealed that about a dozen new compounds from members of the *Compositae* are really thiophene derivatives, in part acetylenic thiophenes.

The above mentioned *Echinops sphaereocephalus* is a very interesting case since it contains both terthienyl (IV) and some new polyacetylenes. The content of acetylenic compounds is low which makes progress rather difficult.

That the connection formally is in some cases as close as between phenylheptatriyne (I) and 2-phenyl-5-(α-propynyl) thiophene (III) has been demonstrated by a new compound isolated by E. Guddal from *Chrysanthemum vulgare* and for which he so far has been able to restrict the constitutional possibilities to (VII) and (VIII) which, however, formally are generated from the dehydromatricaria ester (IX) — found in closely related species — by addition of H_2S.

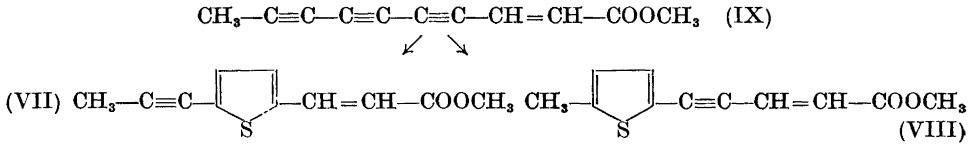

EXPERIMENTAL

The *Coreopsis grandiflora* oils used in this investigation are the same as in the preceding communication. III was not found in the extract from the root; the behaviour of the essential oils from the leaves and the flowers was so similar that only one of them is reported. *Ca.* 4 g of essential oil from the leaves (no accurate weight is given as the evaporation of the solvent (petroleum ether) intentionally was somewhat incomplete) was chromatographed on deactivated alumina. The material in the fractions containing 4—8 % benzene in petroleum ether crystallised immediately, all gave the correct m. p. 54—55° and had the characteristic ultraviolet spectrum of phenyl-heptatriyne (I). The succeeding eluates containing 8—15 % benzene in petroleum ether also crystallised very

well on evaporation to give prismatic needles resembling those of (I) very much, the m. p., however, was in the 40° range. Admixture with (I) gave a liquid at room temperature. Recrystallisation gave a sharp m. p. 42—43°. (Found (Zimmermann): S 15.4 and 16.0. Calc. for $C_{13}H_{10}S$: S 16.3). Ultraviolet spectrum in hexane, Fig. 1, curve A; log $\varepsilon_{max} = 4.43$; $\lambda_{max} = 3\,100$ Å; infrared spectrum, Fig. 2, curve A.

Catalytical hydrogenation. 27.7 mg (III) was hydrogenated with a Pd—$BaSO_4$ catalyst in alcohol. Consumed 6.9 ml hydrogen, $t = 18.5°C$, $p = 758$, calculated for $C_{13}H_{10}S$, 1 = 6.95 ml. The tetrahydro compound was isolated in the usual way and distilled, b. p. 45° (air bath) at 0.001 mm Hg. Ultraviolet spectrum of the tetrahydro compound in hexane, Fig. 1, curve B; log $\varepsilon_{max} = 4.30$: $\lambda_{max} = 2\,900$ Å. Infrared spectrum of the tetrahydro compound, Fig. 2, curve B.

*Synthesis of 2-phenyl-5-*n*-propylthiopene.* 2-Phenyl-thiophene was synthesised from β-benzoylpropionic acid according to Chrzasz-Czewska [15]. The m. p. of 2-phenylthiophene could not be raised above 32—33°C; reported [15] 42—43°. (Found: S 19.8 and 19.5. Calc. for $C_{10}H_8S$: S 20.0). Infrared spectrum Fig. 2, curve C.

650 mg of 2-phenylthiophene was condensed with 1 g of propionyl chloride according to Hartough and Kosak [16]. The reaction mixture was diluted with ether and then washed with water, potassium hydroxyde, water and the solvent was evaporated. The residue was distilled in high vacuum giving 360 mg of distillate which partly crystallised. Recrystallisation from petroleum ether gave slightly coloured plates, m. p. 87—88°. (Found: S 14.8. Calc. for $C_{13}H_{12}SO$: S 14.75). Infrared spectrum of 2-phenyl-5-propionylthiophene, Fig. 2, curve D. A Clemmensen reduction of 2-phenyl-5-propionylthiophene was first attempted in water at room temperature according to Fieser and Kenelly [17]. About one half of the unchanged ketone was recovered, the rest was lost. Then 100 mg of 2-phenyl-5-propionylthiophene was reduced with 2 g of amalgamated zink in alcoholic solution (6 ml of ethanol, 4 ml of hydrogen chloride (1:1)). The solution became turbid but turned clear with stirring and slight warming, reaction time 2 h.

The crude reaction product was devoid of carbonyl bands in the infrared. The oil was distilled, b.range 60—65°, air bath, 0.001 mm Hg. Ultraviolet and infrared spectra of the distillate were identical with those of the tetrahydro compound, which thus is 2-phenyl-5-*n*-propylthiophene.

Acknowledgements. Grants from *Norges Almenvitenskapelige Forskningsråd,* which have enabled these investigations to be carried out, are gratefully acknowledged.

REFERENCES

1. Sörensen, J. S. and Sörensen, N. A. *Acta Chem. Scand.* **12** (1958) 765.
2. Birkinshaw, J. H. and Chaplen, P. *Biochem. J.* **60** (1955) 255.
3. Sörensen, N. A. *Acta Chem. Scand. To be published.*
4. Zechmeister, L. and Sease, J. W. *J. Am. Chem. Soc.* **69** (1947) 273.
5. Challenger, F. and Holmes, J. L. *J. Chem. Soc.* **1953** 1837.
6. Jensen, S., Liaaen and Sörensen, N. A. *Acta Chem. Scand. To be published.*
7. Straus, F. and Kollek, L. *Ber.* **59** (1926) 1664.
8. Armitage, J. B., Cook, C. L., Jones, E. R. H. and Whiting, M. C. *J. Chem. Soc.* **1952** 2011.
9. Bohlmann, F. *Ber.* **84** (1951) 789.
10. Collie, J. N. *J. Chem. Soc.* **63** (1893) 329; **91** (1907) 1506.
11. Robinson, R. *J. Chem. Soc.* **111** (1917) 876, and *The structural Relations of Natural Products,* Oxford 1955, p. 4—7 and 55—56.
12. Birch, A. J. and Donovan, F. W. *Austral. J. Chem.* **6** (1953) 360, 373.
13. Lipmann, F. *Science* **120** (1954) 855.
14. Woodward, R. B. *Angew. Chem.* **68** (1956) 13.
15. Chrzasz-Czewska, *Chem. Zentr.* **1926** II 2905.
16. Hartough, H. D. and Kosak, A. J. *J. Am. Chem. Soc.* **69** (1947) 3095.
17. Fieser, L. F. and Kenelly, R. G. *J. Am. Chem. Soc.* **57** (1935) 1615.

Received February 14, 1958.

ACTA CHEMICA SCANDINAVICA 12 (1958) 777—792

Short Communications

The Crystal Structure of (—)-2-Methyl-2-Ethyleicosanoic Acid

ERIK von SYDOW

Institute of Chemistry, University of Uppsala, Uppsala, Sweden

In connection with crystal structure investigations of normal and branched chain fatty acids [1-3], the molecular packing of (—) - 2 - methyl - 2 - ethyleicosanoic acid ($C_{23}H_{46}O_2$) has been determined. Only one X-ray investigation of a fatty acid substituted with a larger group than a methyl group is published: the unit cell dimensions of 14-DL-ethylhexadecanoic acid by Clark and Chu [4].

Ställberg-Stenhagen [5] points out that (—)-2-methyl-2-ethyleicosanoic acid crystallizes from light petroleum (b.p. 40—60°C) in a very beautiful way. The crystals are extremely long (5 cm) and lath-shaped, and they have a lustrous appearance. The racemic form of the acid does not crystallize so easily. No polymorphism is reported or observed.

The shape and the optical properties of the crystals indicated an orthorhombic space group, which was confirmed by the single crystal X-ray investigation, from which the following data was obtained:

$a = 8.150$, $b = 9.214$, $c = 31.50$ Å (± 0.2 %)
$d_{calc.} = 0.996$ gcm^{-3}, $d_{meas.} = 0.991$ gcm^{-3},
4 molecules per unit cell.

Absent reflexions: ($h00$) when h odd, ($0k0$) when k odd.
Space group: D_2^3—$P\,2_12_12$ (No. 18).

Sharpened Patterson projections along the three axes were calculated. From these and from the reciprocal lattice the subcell, *i. e.* the cell which describes the repetition in and of the hydrocarbon chains, was evaluated (Fig. 1). Its dimensions are $a_s = a = 8.150$, $b_s = b = 9.214$ and $c_s = 2.551$ Å (± 0.2 %), 8 CH_2-groups per subcell and space group D_2^3—$P\,2_12_12$ with $x_1 = 0.315$, $y_1 = 0.205$, $z_1 = 0$ and $x_2 = 0.315$, $y_2 = 0.295$, $z_2 = 0.500$. The chains are parallel and run parallel with c_s and c, and all the chain planes are also parallel with each other and with the $_sc_s$-plane (bc-plane). This subcell has never been found before.

Knowing the subcell structure and the main cell symmetry, the positional parameters of the atoms in the hydrocarbon chains could be directly determined. From spatial considerations the rest of the atoms were placed in the main cell and cycles of structure factor calculations and electron density projections along the shortest axes were performed. The molecular packing is shown schematically in Fig. 2. The structure will be refined in three dimensions.

There are two particularly interesting things in this structure: the new subcell and the hydrogen bond system. This subcell will be called O ∥ as compared with O ⊥ for the common orthorhombic chain pack-

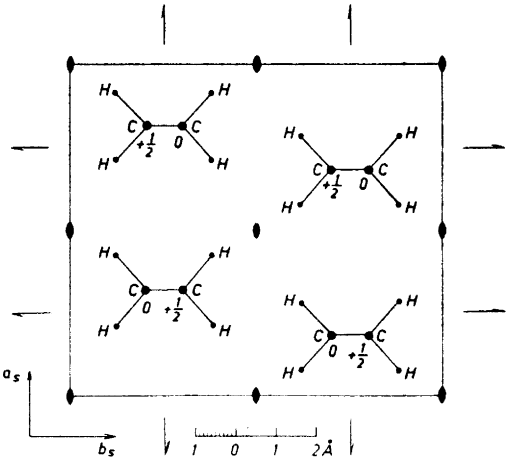

Fig. 1. The new orthorhombic subcell O ∥.

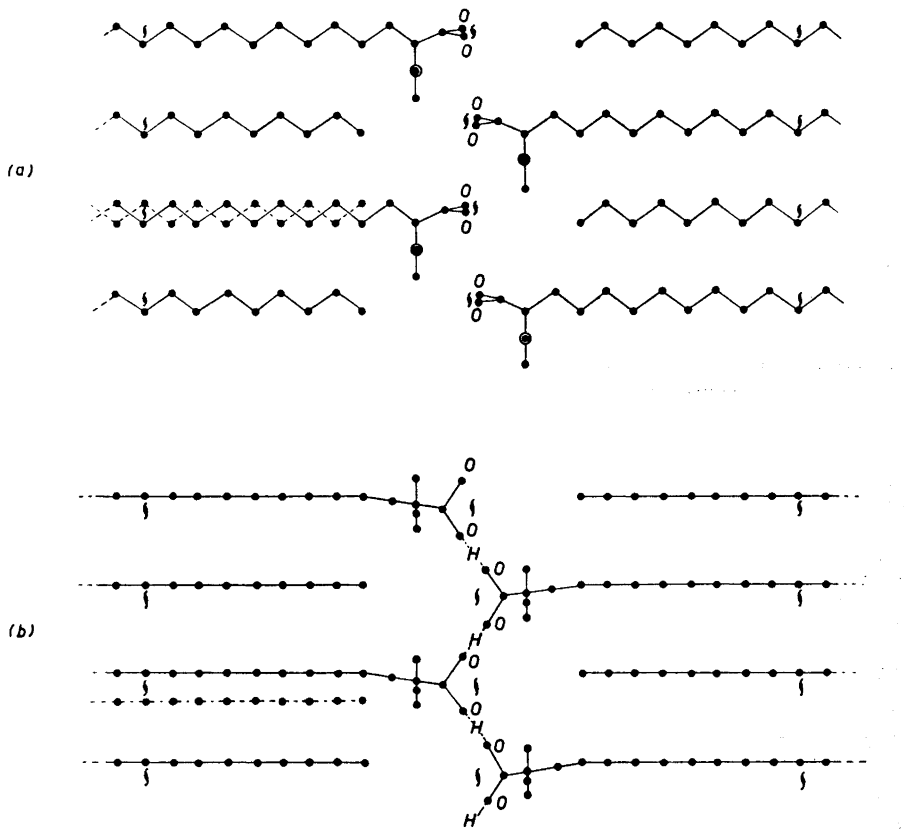

Fig. 2. (a) Schematic view along the *a*-axis and (b) along the *b*-axis of (—)-2-methyl-2-ethyleicosanoic acid.

ing [1], in which every second chain plane is approximately perpendicular to the others, and with T ∥ for the triclinic chain packing [1], in which all chain planes are parallel. Following a suggestion by Vand [6], the crystal structure of (—)-2-methyl-2-ethyleicosanoic acid should be classified as O ∥ (001), where (001) are the indices in the subcell of the *ab*-plane of the main cell.

A detailed comparison with the X-ray photographs given by Buerger [7] for *a*-sodium stearate hemihydrate reveals that that compound has the same hydrocarbon chain packing as (—)-2-methyl-2-ethyleicosanoic acid, *i. e.* O ∥.

The volume per CH_2-group in O ∥ is 23.95 Å^3, which is significantly larger than the corresponding volume in O | with comparable chain length [1] (23.3 Å^3). This means that the van der Waals interaction between chains of this length is larger in O ⊥ than in O ∥. In the case of (—)-2-methyl-2-ethyl-eicosanoic acid, however, this is compensated by the fact that, seen along the chains, the space occupied by two chains (Figs. 1 and 2) in O ∥ is the same as the space occupied by the branching groups and the carboxyl group of one molecule. The resulting hydrogen bond system (Fig. 2 b) is interesting in that one molecule is not bound to one other molecule (dimerization), as is usually the case with fatty acids [1-3], but to two other molecules, giving an one dimensional hydrogen bond helix parallel with the *a*-axis. Thus it is not surprising to find that

the *a*-direction is the same as the very much pronounced lath-direction of the crystals, mentioned above. The cleavage is also consistent with this arrangement. A somewhat similar hydrogen bond system has been found for formic acid [8], but never before for a long chain carboxylic acid.

Thanks are due to Professor S. Ställberg-Stenhagen for the crystals and to Professor E. Stenhagen for the measured density and his constant interest in this work. The expenses involved have been defrayed by grants from the *Swedish Natural Science Research Council.*

Full details of this work will be published later.

1. von Sydow, E. *Arkiv Kemi* **9** (1956) 231.
2. Abrahamsson, S. *Acta Cryst.* **9** (1956) 663
3. Abrahamsson, S. *Acta Cryst.* **11** (1958) *In press.*
4. Clark, G. L. and Chu, C.-C. *Acta Cryst.* **4** (1951) 470.
5. Ställberg-Stenhagen, S. *Arkiv Kemi* **3** (1951) 273.
6. Vand, V. *Acta Cryst.* **7** (1954) 697.
7. Buerger, M. J. *Amer. Mineral.* **30** (1945) 551.
8. Holtzberg, F., Post, B. and Fankuchen, I. *Acta Cryst.* **6** (1953) 127.

Received March 26, 1958.

The Fractionation of Spruce Wood

J. A. McPHERSON

Institutt for Treforedlingskjemi, Norges tekniske högskole, Trondheim, Norway

During the investigations on milled spruce wood, Björkman [1] was able to isolate material containing both lignin and carbohydrates and which was designated lignin-carbohydrate complexes (LCC).

It is proposed to report the preliminary results of further investigations on the extraction of wood with dimethyl sulphoxide (DMSO), of which brief mention has already been made [2].

The fractionation of milled spruce wood has been carried out by the successive extraction with dioxane, dimethyl formamide (DMF), DMSO and water, following which the cellulosic residues were recovered in yields of 41—43 %. These residues contained small amounts of lignin and hemicelluloses.

The extracts were fractionated at first by precipitation with selective solvents, but in an effort to avoid coprecipitation, later work involved distribution on columns of alumina, sand, or metallic oxides. However, when these were found to degrade the lignin, Celite columns were used instead. But in each case it was possible to isolate a series of lignin-carbohydrate complexes, together with relatively pure lignin and hemicellulose fractions. Except in one case where a small amount of a fraction containing glucose and mannose only (1:1.24) together with small amounts of lignin, was isolated from an alumina column, the LCC even where the lignin content was very small, still contained carbohydrates in the same approximate ratio as in the original hemicelluloses.

In one series of fractionations of milled spruce wood, the total amount extracted (31 %) was recovered almost entirely in the dioxane (9 %), DMF (7 %), DMSO (11.2 %) and the aqueous extracts (2 %). The difference is to be found in the DMSO mother liquors which were not further investigated in this series. The dioxane extract yielded a series of lignin fractions (CH_3O, 13—15 %) containing small amounts of carbohydrates, while the DMF extract gave a series of LCC (CH_3O, 5—12 % and lignin 10—90 %). Both the DMSO and the aqueous extracts could be largely precipitated by ethanol, yielding LCC material with 4 % CH_3O and about 22 % lignin. Whether the DMSO extract was precipitated by dioxane, ethanol or benzene, the complexes obtained still had methoxyl contents of about 3.5—4 % and lignin of about 22 %. Refractionations of these LCC gave a number of widely different fractions, with respect to their lignin content. Such fractionations were usually carried out on Celite columns with a combination of various solvent systems, *e. g.* ethyl acetate-acetic acid-water, butanol-pyridine-water or DMF-dinitromethane-water *etc.*

Intermediate lignin fractions, soluble in benzene and sometimes ether, were obtained in the first fractions from the Celite columns.

Since the relative proportion of the lignin to hemicellulose in the LCC modifies the solubility of the complex it was not surprising that LCC were isolated from clear solutions of benzene, dioxane, ethanol, water etc. Perhaps better methods for their isolation may be based on electrophoretic techniques.

the *a*-direction is the same as the very much pronounced lath-direction of the crystals, mentioned above. The cleavage is also consistent with this arrangement. A somewhat similar hydrogen bond system has been found for formic acid [8], but never before for a long chain carboxylic acid.

Thanks are due to Professor S. Ställberg-Stenhagen for the crystals and to Professor E. Stenhagen for the measured density and his constant interest in this work. The expenses involved have been defrayed by grants from the *Swedish Natural Science Research Council.*

Full details of this work will be published later.

1. von Sydow, E. *Arkiv Kemi* **9** (1956) 231.
2. Abrahamsson, S. *Acta Cryst.* **9** (1956) 663
3. Abrahamsson, S. *Acta Cryst.* **11** (1958) *In press.*
4. Clark, G. L. and Chu, C.-C. *Acta Cryst.* **4** (1951) 470.
5. Ställberg-Stenhagen, S. *Arkiv Kemi* **3** (1951) 273.
6. Vand, V. *Acta Cryst.* **7** (1954) 697.
7. Buerger, M. J. *Amer. Mineral.* **30** (1945) 551.
8. Holtzberg, F., Post, B. and Fankuchen, I. *Acta Cryst.* **6** (1953) 127.

Received March 26, 1958.

The Fractionation of Spruce Wood

J. A. McPHERSON

Institutt for Treforedlingskjemi, Norges tekniske högskole, Trondheim, Norway

During the investigations on milled spruce wood, Björkman [1] was able to isolate material containing both lignin and carbohydrates and which was designated lignin-carbohydrate complexes (LCC).

It is proposed to report the preliminary results of further investigations on the extraction of wood with dimethyl sulphoxide (DMSO), of which brief mention has already been made [2].

The fractionation of milled spruce wood has been carried out by the successive extraction with dioxane, dimethyl formamide (DMF), DMSO and water, following which the cellulosic residues were recovered in yields of 41—43 %. These residues contained small amounts of lignin and hemicelluloses.

The extracts were fractionated at first by precipitation with selective solvents, but in an effort to avoid coprecipitation, later work involved distribution on columns of alumina, sand, or metallic oxides. However, when these were found to degrade the lignin, Celite columns were used instead. But in each case it was possible to isolate a series of lignin-carbohydrate complexes, together with relatively pure lignin and hemicellulose fractions. Except in one case where a small amount of a fraction containing glucose and mannose only (1:1.24) together with small amounts of lignin, was isolated from an alumina column, the LCC even where the lignin content was very small, still contained carbohydrates in the same approximate ratio as in the original hemicelluloses.

In one series of fractionations of milled spruce wood, the total amount extracted (31 %) was recovered almost entirely in the dioxane (9 %), DMF (7 %), DMSO (11.2 %) and the aqueous extracts (2 %). The difference is to be found in the DMSO mother liquors which were not further investigated in this series. The dioxane extract yielded a series of lignin fractions (CH_3O, 13—15 %) containing small amounts of carbohydrates, while the DMF extract gave a series of LCC (CH_3O, 5—12 % and lignin 10—90 %). Both the DMSO and the aqueous extracts could be largely precipitated by ethanol, yielding LCC material with 4 % CH_3O and about 22 % lignin. Whether the DMSO extract was precipitated by dioxane, ethanol or benzene, the complexes obtained still had methoxyl contents of about 3.5—4 % and lignin of about 22 %. Refractionations of these LCC gave a number of widely different fractions, with respect to their lignin content. Such fractionations were usually carried out on Celite columns with a combination of various solvent systems, *e. g.* ethyl acetate-acetic acid-water, butanol-pyridine-water or DMF-dinitromethane-water *etc.*

Intermediate lignin fractions, soluble in benzene and sometimes ether, were obtained in the first fractions from the Celite columns.

Since the relative proportion of the lignin to hemicellulose in the LCC modifies the solubility of the complex it was not surprising that LCC were isolated from clear solutions of benzene, dioxane, ethanol, water etc. Perhaps better methods for their isolation may be based on electrophoretic techniques.

Spruce wood chlorite holocellulose was also milled under the same conditions as for the wood, where it was found that extraction with DMF yielded about 10 % of a brown film, containing both modified lignin and hemicelluloses, while extraction with water gave about 22 % of a very white powder, which contained only hemicelluloses. The cellulosic residue was obtained in a yield of 43 %.

1. Björkman, A. *Svensk Papperstidn.* **60** (1957) 243.
2. Giertz, H. W. and McPherson, J. A. *Norsk Skogsindustri* **10** (1956) 348.

Received April 9, 1958.

Experiments with Methyl-fluoro-phosphorylcholine-inhibited Cholinesterase

INGER ENANDER

Research Institute of National Defence, Dept. 1, Sundbyberg 4, Sweden

Organophosphorus cholinesterase inhibitors are considered to phosphorylate an esteratic site of the enzyme [1]. It has been demonstrated that phosphorylated cholinesterase can be reactivated through dephosphorylation by hydroxylamine derivatives [2].

Methyl-fluoro-phosphorylcholines have been shown to be potent cholinesterase inhibitors and cholinergic drugs [3,4]. It seemed thus to be of interest to investigate the possibilities of reactivating methyl-fluoro-phosphorylcholine-inhibited human erythrocyte acetylcholinesterase.

The inhibitors investigated were:

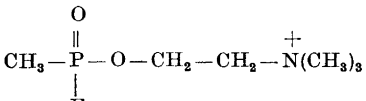

Methyl-fluoro-phosphorylcholine

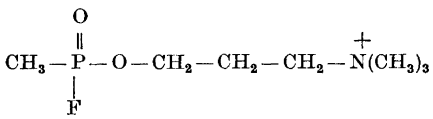

Methyl-fluoro-phosphorylhomocholine

The reactivators investigated were: Pyridine-2-aldoxime methiodide (PAM)[5]; Nicotinhydroxamic acid methiodide (NAM)[6]; Di*iso*nitrosoacetone (DINA)[6]; Diacetylmonoxime (DAM, Hopkin and Williams Ltd. Chadwell Heath Essex, Engl.)

The reactivators were solved in Michel's veronal buffer (pH = 8) [7], the concentrations being 4×10^{-3} and 5×10^{-4} M. The experiments were carried out according to Davies and Green [6].

Washed erythrocytes, diluted to blood volume with saline, were treated with an aqueous inhibitor solution (10^{-6} M) for 10 min at 25°C. The inhibited cell-suspension was centrifuged, the erytrocytes washed and diluted to the same volume as before. Equal volumes of this cell-suspension and the reactivator-buffer solution were mixed and stored at 25°C. At intervals between 10 and 60 min after incubation, samples were taken for enzyme activity determinations, which were carried out by means of an electrometric method [7].

None of the reactivators reactivated the enzyme preparations, inhibited with any of the three methyl-fluoro-phosphorylcholines. However, as could be expected, Sarin-inhibited enzyme was reactivated by PAM[8] in parallel runs.

The prevented reactivation is interesting because it may throw some further light on the nature of the inhibitor-enzyme reaction. An ionic bond in the inhibited enzyme, analogous to that postulated in the substrate enzyme complex [9], and a shielding (Fig. 1) of the ionic site from the reactivator seem to explain the obstructed reactivation. The ionic bond increases the attraction of the organophosphoryl residue to the enzyme, which alone may be a sufficient explanation in case of DINA and DAM. In case of PAM and NAM

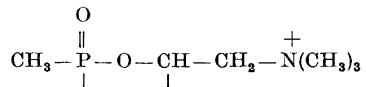

Methyl-fluoro-phosphoryl-β-methylcholine

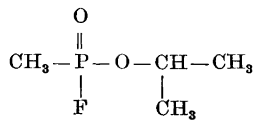

Methyl-*iso*propoxy-phosphoryl fluoride, Sarin

Spruce wood chlorite holocellulose was also milled under the same conditions as for the wood, where it was found that extraction with DMF yielded about 10 % of a brown film, containing both modified lignin and hemicelluloses, while extraction with water gave about 22 % of a very white powder, which contained only hemicelluloses. The cellulosic residue was obtained in a yield of 43 %.

1. Björkman, A. *Svensk Papperstidn.* **60** (1957) 243.
2. Giertz, H. W. and McPherson, J. A. *Norsk Skogsindustri* **10** (1956) 348.

Received April 9, 1958.

Experiments with Methyl-fluoro-phosphorylcholine-inhibited Cholinesterase

INGER ENANDER

Research Institute of National Defence, Dept. 1, Sundbyberg 4, Sweden

Organophosphorus cholinesterase inhibitors are considered to phosphorylate an esteratic site of the enzyme [1]. It has been demonstrated that phosphorylated cholinesterase can be reactivated through dephosphorylation by hydroxylamine derivatives [2].

Methyl-fluoro-phosphorylcholines have been shown to be potent cholinesterase inhibitors and cholinergic drugs [3,4]. It seemed thus to be of interest to investigate the possibilities of reactivating methyl-fluoro-phosphorylcholine-inhibited human erythrocyte acetylcholinesterase.

The inhibitors investigated were:

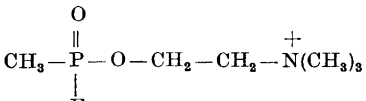

Methyl-fluoro-phosphorylcholine

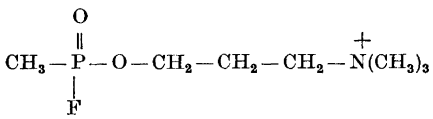

Methyl-fluoro-phosphorylhomocholine

The reactivators investigated were: Pyridine-2-aldoxime methiodide (PAM)[5]; Nicotinhydroxamic acid methiodide (NAM)[6]; Di*iso*nitrosoacetone (DINA)[6]; Diacetylmonoxime (DAM, Hopkin and Williams Ltd. Chadwell Heath Essex, Engl.)

The reactivators were solved in Michel's veronal buffer (pH = 8) [7], the concentrations being 4×10^{-3} and 5×10^{-4} M. The experiments were carried out according to Davies and Green [6].

Washed erythrocytes, diluted to blood volume with saline, were treated with an aqueous inhibitor solution (10^{-6} M) for 10 min at 25°C. The inhibited cell-suspension was centrifuged, the erytrocytes washed and diluted to the same volume as before. Equal volumes of this cell-suspension and the reactivator-buffer solution were mixed and stored at 25°C. At intervals between 10 and 60 min after incubation, samples were taken for enzyme activity determinations, which were carried out by means of an electrometric method [7].

None of the reactivators reactivated the enzyme preparations, inhibited with any of the three methyl-fluoro-phosphorylcholines. However, as could be expected, Sarin-inhibited enzyme was reactivated by PAM[8] in parallel runs.

The prevented reactivation is interesting because it may throw some further light on the nature of the inhibitor-enzyme reaction. An ionic bond in the inhibited enzyme, analogous to that postulated in the substrate enzyme complex [9], and a shielding (Fig. 1) of the ionic site from the reactivator seem to explain the obstructed reactivation. The ionic bond increases the attraction of the organophosphoryl residue to the enzyme, which alone may be a sufficient explanation in case of DINA and DAM. In case of PAM and NAM

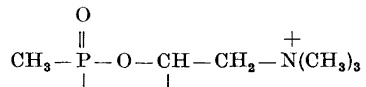

Methyl-fluoro-phosphoryl-β-methylcholine

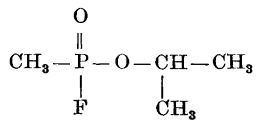

Methyl-*iso*propoxy-phosphoryl fluoride, Sarin

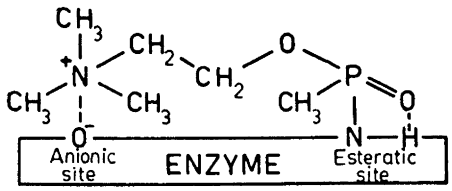

Fig. 1. Hypothetical model of methyl-fluorophosphorylcholine inhibited cholinesterase.

which contain a positively charged ion, the shielding of the anionic site is likely to contribute.

My thanks are due to the Head of this Institute Professor G. Ljunggren for his kind interest in this work.

1. Aldridge, W. N. and Davison, A. N. *Biochem. J.* **55** (1953) 763.
2. Wilson, I. B. and Meislich, E. K. *J. Am. Chem. Soc.* **75** (1953) 4628.
3. Tammelin, L.-E. *Acta Chem. Scand.* **11** (1957) 859.
4. Fredriksson, T. *Arch. intern. pharmacodynamie* **113** (1954) 101.
5. Wilson, I. B. *Biochim. et Biophys. Acta* **18** (1955) 168.
6. Davies, D. R. and Green, A. L. *Biochem. J.* **63** (1956) 529.
7. Tammelin, L.-E. *Scand. J. Clin. & Lab. Invest.* **5** (1953) 267.
8. Green, A. L. and Smith, H. J. *Biochem. J.* **68** (1958) 32.
9. Wilson, I. B., Bergmann, F. and Nachmansohn, D. *J. Biol. Chem.* **188** (1950) 693.

Received April 11, 1958.

Antitryptic Effect of Some Seromucoids

HANS BENNICH and JOHN GOA

Department of Medical Biochemistry, University of Gothenburg, Gothenburg, Sweden

It has since long been established that human plasma exerts an antitryptic effect, and many attempts have been made to isolate the active inhibitor from plasma. These experiments have been reviewed by Laskowski and Laskowski [1]. Thus Landsteiner [2] found the inhibitory activity within the albumin fraction, whereas Fujimoto [3] found inhibitory activity in both the albumin and globulin fractions. By means of paper electrophoresis Jacobsson [4] was able to confirm the suggestion that there are at least two different trypsin inhibitors in human serum, one moving with the α_1- and one with the α_2-globulin fraction.

It is also known that orosomucoid is resistent to tryptic digestion as shown by Yamashina [5] and by Popenoe and Drew [6]. In an earlier investigation [7] crude seromucoid was prepared by perchloric acid precipitation of human serum, and from the crude preparation seven subfractions were obtained by means of chromatography and preparative electrophoresis. The subfractions were called A-1, A-2, B-1, B-2, C-1, C-2 and C-3. Fraction B-1 was identical with the well known orosomucoid. With this fraction the earlier experiments showing its stability against tryptic hydrolysis were confirmed. Fraction B-1 or orosomucoid was also tested for antitryptic action. No inhibitory effect could be found when a pure preparation was used, whereas the crude seromucoid fraction inhibited tryptic hydrolysis of casein.

In the present investigation the inhibiting action against trypsin of all the subfractions of seromucoid have been studied. The experiments were performed at a constant pH with automatic registration of the amount of sodium hydroxide consumed as a function of time and with casein as substrate.

Experimental. The equipment used for the experiments consisted of a titrator, type TTT 1 a, Radiometer, Copenhagen. The amount of reagent consumed was registered by a mechanical recorder (constructed by Ole Dich, Copenhagen). The recorder also drives a microsyringe (0.5 ml) (Agla). The pH-stat is in detail described by Jacobsen *et al.*[8] The reaction vessel used was a three-necked beaker of pyrex glass so dimensioned that volumes down to 2 ml may be used without inconvenience. The electrodes and stirrer were affixed to a cover of perspex. The type of glass electrode used was a G 202 BT, Radiometer. Sodium hydroxide and nitrogen gas were instilled through the two smaller necks. The reaction vessel was kept at 25 ± 0.01°C in a water bath. Changes in room temperature during the experiments did not exceed more

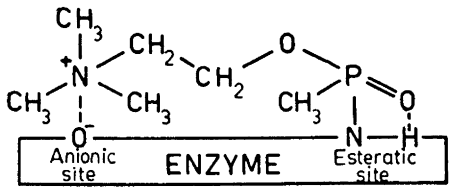

Fig. 1. Hypothetical model of methyl-fluorophosphorylcholine inhibited cholinesterase.

which contain a positively charged ion, the shielding of the anionic site is likely to contribute.

My thanks are due to the Head of this Institute Professor G. Ljunggren for his kind interest in this work.

1. Aldridge, W. N. and Davison, A. N. *Biochem. J.* **55** (1953) 763.
2. Wilson, I. B. and Meislich, E. K. *J. Am. Chem. Soc.* **75** (1953) 4628.
3. Tammelin, L.-E. *Acta Chem. Scand.* **11** (1957) 859.
4. Fredriksson, T. *Arch. intern. pharmacodynamie* **113** (1954) 101.
5. Wilson, I. B. *Biochim. et Biophys. Acta* **18** (1955) 168.
6. Davies, D. R. and Green, A. L. *Biochem. J.* **63** (1956) 529.
7. Tammelin, L.-E. *Scand. J. Clin. & Lab. Invest.* **5** (1953) 267.
8. Green, A. L. and Smith, H. J. *Biochem. J.* **68** (1958) 32.
9. Wilson, I. B., Bergmann, F. and Nachmansohn, D. *J. Biol. Chem.* **188** (1950) 693.

Received April 11, 1958.

Antitryptic Effect of Some Seromucoids

HANS BENNICH and JOHN GOA

Department of Medical Biochemistry, University of Gothenburg, Gothenburg, Sweden

It has since long been established that human plasma exerts an antitryptic effect, and many attempts have been made to isolate the active inhibitor from plasma. These experiments have been reviewed by Laskowski and Laskowski [1]. Thus Landsteiner [2] found the inhibitory activity within the albumin fraction, whereas Fujimoto [3] found inhibitory activity in both the albumin and globulin fractions. By means of paper electrophoresis Jacobsson [4] was able to confirm the suggestion that there are at least two different trypsin inhibitors in human serum, one moving with the α_1- and one with the α_2-globulin fraction.

It is also known that orosomucoid is resistent to tryptic digestion as shown by Yamashina [5] and by Popenoe and Drew [6]. In an earlier investigation [7] crude seromucoid was prepared by perchloric acid precipitation of human serum, and from the crude preparation seven subfractions were obtained by means of chromatography and preparative electrophoresis. The subfractions were called A-1, A-2, B-1, B-2, C-1, C-2 and C-3. Fraction B-1 was identical with the well known orosomucoid. With this fraction the earlier experiments showing its stability against tryptic hydrolysis were confirmed. Fraction B-1 or orosomucoid was also tested for antitryptic action. No inhibitory effect could be found when a pure preparation was used, whereas the crude seromucoid fraction inhibited tryptic hydrolysis of casein.

In the present investigation the inhibiting action against trypsin of all the subfractions of seromucoid have been studied. The experiments were performed at a constant pH with automatic registration of the amount of sodium hydroxide consumed as a function of time and with casein as substrate.

Experimental. The equipment used for the experiments consisted of a titrator, type TTT 1 a, Radiometer, Copenhagen. The amount of reagent consumed was registered by a mechanical recorder (constructed by Ole Dich, Copenhagen). The recorder also drives a microsyringe (0.5 ml) (Agla). The pH-stat is in detail described by Jacobsen *et al.*[8] The reaction vessel used was a three-necked beaker of pyrex glass so dimensioned that volumes down to 2 ml may be used without inconvenience. The electrodes and stirrer were affixed to a cover of perspex. The type of glass electrode used was a G 202 BT, Radiometer. Sodium hydroxide and nitrogen gas were instilled through the two smaller necks. The reaction vessel was kept at 25 ± 0.01°C in a water bath. Changes in room temperature during the experiments did not exceed more

than ± 1.0°C from the temperature of the water bath.

In all experiments a 2.7 % solution of casein was used as substrate. The substrate was prepared as follows: 5—6 g casein were mixed with 80 ml 0.1 M KCl and the pH adjusted to 6—7 by addition of 0.1 N NaOH (55 ml). The mixture was boiled until all casein was dissolved (about 15 min). After boiling, the solution was cooled to room temperature and filtered. The protein concentration of the filtrate was determined by the micro Kjeldahl method, whereupon the solution was diluted with 0.1 M KCl to a final concentration of 2.7 %. The enzymes used were crystalline preparations of trypsin (containing 50 % $MgSO_4$; Mann) and chymotrypsin (containing 50 % $(NH_4)_2SO_4$; Armour). In each experiment 4 ml of substrate was incubated for 10 min in a water bath (25°C) and pH was adjusted to 8.2 with 0.1 N NaOH in the pH-stat. The enzyme dissolved in distilled water was added to the casein solution to give a 0.001 % solution. Three groups of experiments were performed. In each group the same preparation of enzyme and substrate solutions was used. Before and after each group of experiments a reference experiment was performed — enzyme + substrate — in order to test the activity of the enzyme.

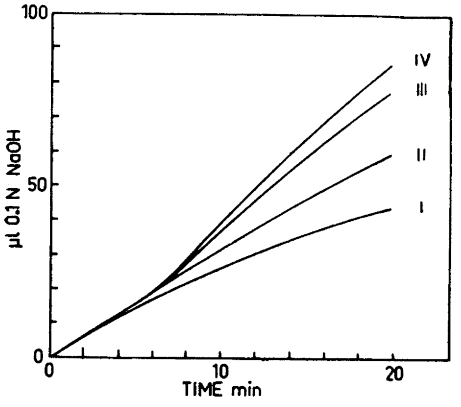

Fig. 1. Trypsin-inhibiting effect of crude seromucoid. In I, 4.3 mg of seromucoid was mixed with the substrate after which the enzyme was added. II is a reference experiment in which the standard amount of substrate was digested with the standard amount of enzyme. In III, a standard amount of enzyme digested a standard amount of substrate for 6 min, after which another standard amount of enzyme mixed with 0.3 mg seromucoid was added. In IV, a standard amount of substrate and enzyme reacted for 6 min and then an additional standard amount of trypsin was added.

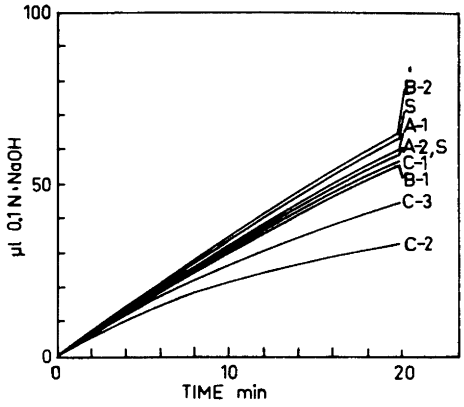

Fig. 2. Experiments with the subfractions of seromucoid. S means the reference experiments with standard amount of substrate and enzyme only. In each of the other experiments 5 mg of one of the different subfractions were incubated with substrate before addition of enzyme.

Results. Fig. 1 illustrates the experiments performed with crude seromucoid. The results indicate some trypsin-inhibiting effect of the crude fraction, this effect was obtained whether the seromucoid was incubated with the substrate or with enzyme as shown in the figure.

The next step was to test the effect on trypsin of each of the different subfractions prepared from the crude seromucoid as mentioned above. In each experiment 5 mg of each of the subfractions was dissolved in 4 ml substrate, incubated in a water bath and adjusted to pH 8.2 as described above.

From Fig. 2 it will be seen that mixing the substrate with either of the fractions C-2 or C-3 gave decreased hydrolysis as compared to that found in the reference experiments, thus indicating an inhibitory action of these fractions. This is in agreement with the observations of Jacobsson [4], as fraction C-2 electrophoretically is an α_1-globulin and fraction C-3 and α_2-globulin [7], as well as with the findings of Grob [8], that Cohn fractions IV-1 and IV-4 of human serum have protease-inhibitory

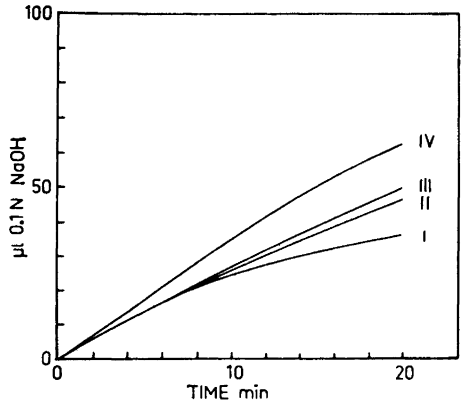

Fig. 3. In experiments I and IV, trypsin is used as enzyme. In I 5 mg of fraction C-2 is added, in IV no inhibitor. In experiments II and III chymotrypsin is used as enzyme, II with addition of 5 mg of fraction C-2, III without inhibitor.

activity. It will also be seen that fraction C-2 apparently has a stronger effect than fraction C-3. No inhibitory effect could be found when mixing the other subfractions of crude seromucoid with the substrate; the deviations from the reference experiments found were within the range of the experimental error (±5 %).

Finally the effect of fraction C-2 on hydrolysing casein with chymotrypsin was studied. Fig. 3 illustrates these experiments including a control experiment with trypsin. From the figure it will be seen that fraction C-2 showed no inhibitory effect on chymotrypsin.

1. Laskowski, M. and Laskowski, M. Jr., *Advances in Protein Chem.* **9** (1954) 203.
2. Landsteiner, K. *Zentr. Bakteriol.* **27** (1900) 357.
3. Fujimoto, B. *J. Immunol.* **3** (1918) 51.
4. Jacobsson, K. *Scand. J. Clin. & Lab. Invest.* **5** (1953) 97.
5. Yamashina, I. *Acta Chem. Scand.* **10** (1956) 1666.
6. Popenoe, E. A. and Drew, R. M. *J. Biol. Chem.* **228** (1957) 673.
7. Goa, J. *To be published.*
8. Jacobsen, C. F., Léonis, J., Linderström-Lang, K. and Ottesen, M. *Methods of Biochemical Analysis*, **4** (1957) 171.
9. Grob, D. *J. Gen. Physiol.* **33** (1949) 103.

Received May 16, 1958.

The Alkaline Hydrolysis of Two Sarin Analogues and of Tabun

LENNART LARSSON

Research Institute of National Defence, Dept. 1, Sundbyberg 4, Sweden

In an earlier report the alkaline hydrolysis of *iso*propoxy-methyl-phosphoryl fluoride (Sarin) has been studied, and the influence of substituents in the alkoxy and alkyl groups have been discussed [1]. In this paper the rate of the alkaline hydrolysis of two analogous compounds, dimethylamido-methyl-phosphoryl fluoride and ethylthio-methyl-phosphoryl fluoride, has been determined. Further it was of interest to study the alkaline hydrolysis of dimethyl-amido-ethoxy-phosphoryl cyanide (Tabun), the acid hydrolysis of which has earlier been examined [2].

The hydrolysis of the compounds was studied at various temperatures and pH-values in a 0.1 M solution of potassium chloride by means of an automatic recording titrator [3] by which the pH of the solution was maintained constant during the reaction. When the hydrolysis curves obtained from the recorder were treated according to the method given by Guggenheim, straight lines were obtained indicating first-order reactions.

In the hydrolysis of the two Sarin analogues two equivalents of acid were formed. In the hydrolysis of the dimethylamino derivative the P—N bond is assumed to be quite stable at the pH-values in question [4], and only the P—F bond can be considered to be broken. The hydrolysis products of the ethylthio derivative were analyzed by paper chromatography and only one spot indicating a phosphorus compound was obtained. When the paper was developed for sulphur one spot appeared which had the same R_F-value, 0.41, as the spot developed with the phosphorus reagent. These results indicate that only the P—F bond is split in the hydrolysis of the thio-compound also.

The first-order rate constants, k_1, for the hydrolysis of the two Sarin analogues are given in Table 1. The second-order rate constants, k_2, were calculated from

$$k_1 = k_2 \cdot c_{OH^-} = k_2 \cdot \frac{a_{OH^-}}{f_{OH^-}} = k_2 \cdot \frac{K_w}{f_{OH^-} \cdot a_{H+}}$$

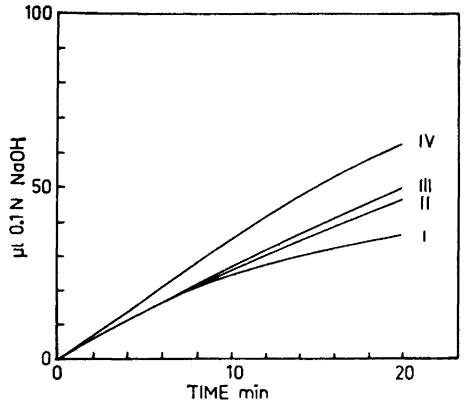

Fig. 3. In experiments I and IV, trypsin is used as enzyme. In I 5 mg of fraction C-2 is added, in IV no inhibitor. In experiments II and III chymotrypsin is used as enzyme, II with addition of 5 mg of fraction C-2, III without inhibitor.

activity. It will also be seen that fraction C-2 apparently has a stronger effect than fraction C-3. No inhibitory effect could be found when mixing the other subfractions of crude seromucoid with the substrate; the deviations from the reference experiments found were within the range of the experimental error (±5 %).

Finally the effect of fraction C-2 on hydrolysing casein with chymotrypsin was studied. Fig. 3 illustrates these experiments including a control experiment with trypsin. From the figure it will be seen that fraction C-2 showed no inhibitory effect on chymotrypsin.

1. Laskowski, M. and Laskowski, M. Jr., *Advances in Protein Chem.* **9** (1954) 203.
2. Landsteiner, K. *Zentr. Bakteriol.* **27** (1900) 357.
3. Fujimoto, B. *J. Immunol.* **3** (1918) 51.
4. Jacobsson, K. *Scand. J. Clin. & Lab. Invest.* **5** (1953) 97.
5. Yamashina, I. *Acta Chem. Scand.* **10** (1956) 1666.
6. Popenoe, E. A. and Drew, R. M. *J. Biol. Chem.* **228** (1957) 673.
7. Goa, J. *To be published.*
8. Jacobsen, C. F., Léonis, J., Linderström-Lang, K. and Ottesen, M. *Methods of Biochemical Analysis*, **4** (1957) 171.
9. Grob, D. *J. Gen. Physiol.* **33** (1949) 103.

Received May 16, 1958.

The Alkaline Hydrolysis of Two Sarin Analogues and of Tabun

LENNART LARSSON

Research Institute of National Defence, Dept. 1, Sundbyberg 4, Sweden

In an earlier report the alkaline hydrolysis of *iso*propoxy-methyl-phosphoryl fluoride (Sarin) has been studied, and the influence of substituents in the alkoxy and alkyl groups have been discussed [1]. In this paper the rate of the alkaline hydrolysis of two analogous compounds, dimethylamido-methyl-phosphoryl fluoride and ethylthio-methyl-phosphoryl fluoride, has been determined. Further it was of interest to study the alkaline hydrolysis of dimethyl-amido-ethoxy-phosphoryl cyanide (Tabun), the acid hydrolysis of which has earlier been examined [2].

The hydrolysis of the compounds was studied at various temperatures and pH-values in a 0.1 M solution of potassium chloride by means of an automatic recording titrator [3] by which the pH of the solution was maintained constant during the reaction. When the hydrolysis curves obtained from the recorder were treated according to the method given by Guggenheim, straight lines were obtained indicating first-order reactions.

In the hydrolysis of the two Sarin analogues two equivalents of acid were formed. In the hydrolysis of the dimethylamino derivative the P—N bond is assumed to be quite stable at the pH-values in question [4], and only the P—F bond can be considered to be broken. The hydrolysis products of the ethylthio derivative were analyzed by paper chromatography and only one spot indicating a phosphorus compound was obtained. When the paper was developed for sulphur one spot appeared which had the same R_F-value, 0.41, as the spot developed with the phosphorus reagent. These results indicate that only the P—F bond is split in the hydrolysis of the thio-compound also.

The first-order rate constants, k_1, for the hydrolysis of the two Sarin analogues are given in Table 1. The second-order rate constants, k_2, were calculated from

$$k_1 = k_2 \cdot c_{OH^-} = k_2 \cdot \frac{a_{OH^-}}{f_{OH^-}} = k_2 \cdot \frac{K_w}{f_{OH^-} \cdot a_{H+}}$$

Table 1. The first-order rate constants for the hydrolysis of dimethylamido-methyl-phosphoryl fluoride and ethylthio-methyl-phosphoryl fluoride at various temperatures and pH-values.

Dimethylamido-methyl-phosphoryl fluoride			Ethylthio-methyl-phosphoryl fluoride		
t°C	pH	$k_1 \times 10^4$ sec^{-1}	t°C	pH	$k_1 \times 10^3$ sec^{-1}
25.0	9.50	0.422	15.0	7.00	0.813
	9.50	0.428		7.00	0.770
	10.00	1.42		7.00	0.825
	10.00	1.42		7.50	2.49
	10.50	4.14		7.50	2.32
	10.50	4.29		7.50	2.53
35.0	9.42	1.42	25.0	7.00	2.60
	9.42	1.44		7.00	2.48
				7.00	2.56

The values of the activity coefficient, f_{OH^-}, and of the ionic product of water, K_w, were those reported in an earlier paper [1]. The values of k_2 and the energies and entropies of activation are given in Table 3.

The low rate of hydrolysis of the dimethylamino derivative can be attributed to the mesomeric effect of the nitrogen atom. Owing to the lower electronegativity of sulphur in comparison with that of oxygen it would be expected that the rate of hydrolysis of the ethylthio derivative should be lower than that of Sarin. However, the great hydrolytic instability of the thio-compound may probably be ascribed to the ready polarisability of sulphur [5] which also has been postulated by Heath for some related thio-compounds [6].

It has been shown that in the acid hydrolysis of Tabun the cyano group as well as the dimethylamino group are split off [2]. To check if the latter reaction occurred at pH 8.50 also, the reaction mixture was analyzed colorimetrically [7] for dimethylamine when the reaction had terminated (after about 20 h). It was found that about 4 % of dimethylamine had been formed. At higher pH-values the formation of dimethylamine was still less. This reaction could thus be neglected in the calculation of the rate constant for the split off of the cyano group. In the hydrolysis of Tabun less than two equivalents of alkali were consumed owing to the low dissociation constant of hydrocyanic acid. The observed rate constant, k_{obs}, was not found to be directly proportional to the hydroxyl ion concentration as appears from Table 2. Experiments with a 0.05 M solution of potassium chloride showed that the rate of hydrolysis was independent of the concentration of this salt. From these results one could conclude that a reaction between Tabun and water molecules also takes place and the following expression was found to be valid for the hydrolysis of Tabun:

$$k_{obs} = k_{H_2O} + k_2 \cdot c_{OH^-} = k_{H_2O} + k_2 \cdot \frac{K_w}{f_{OH^-} \cdot a_{H+}}$$

By plotting k_{obs} *versus* c_{OH^-} a straight line was obtained, and k_{H_2O} was found to be

Table 2. The observed rate constants for the hydrolysis of dimethylamido-ethoxy-phosphoryl cyanide (Tabun) at various temperatures and pH values.

t°C	pH	$k_{obs} \times 10^4$ sec^{-1}
25.0	8.50	0.726
	8.50	0.736
	8.75	0.887
	8.75	0.921
	9.00	1.40
	9.00	1.37
	9.50	3.48
	9.50	3.50
35.0	9.00	4.01
	9.00	4.00
	9.50	11.8
	9.50	11.6

Table 3. Second-order rate constants and energies and entropies of activation of the three organic phosphorus compounds.

Compound	k_2^{15} 1 mole^{-1} sec^{-1}	k_2^{25} 1 mole^{-1} sec^{-1}	k_2^{35} 1 mole^{-1} sec^{-1}	E_a kcal. mole^{-1}	$\Delta S^{\neq}$ E.U.
Dimethylamido-methyl-phosphoryl fluoride	—	1.04 ± 0.04	1.99 ± 0.02	11.9 ± 0.9	−21 ± 3
Ethylthio-methyl-phosphoryl fluoride	$(1.36 \pm 0.06) \times 10^{4}$	$(1.95 \pm 0.05) \times 10^{4}$	—	6.2 ± 1.2	−22 ± 4
Dimethylamido-ethoxy-phosphoryl cyanide	—	7.49 ± 0.08	13.0 ± 0.18	10.1 ± 0.4	−23 ± 1

$(0.40 \pm 0.02) \times 10^{-4}$ sec^{-1} at 25°C and $(0.44 \pm 0.11) \times 10^{-4}$ sec^{-1} at 35°C. The values of k_2 and the energies and entropies of activation for the alkaline hydrolysis of Tabun are given in Table 3.

Experimental. The syntheses of the two Sarin analogues have recently been published [8] and Tabun was synthesized according to Holmstedt [9]. In the kinetic experiments performed with the automatic titrator [3] the concentrations of the dimethylamino derivative and of Tabun were 0.40 mM and of the ethylthio derivative 0.20 mM. The first one was titrated with 0.1 M sodium hydroxide and the latter two with 0.05 mM sodium hydroxide. In other respects the procedure closely adhered to that described for the determination of the alkaline hydrolysis of Sarin [1]. In the paper chromatography ascending technique was used and 50 µl in portions of 5 µl of a 1 % aqueous solution of the ethylthio derivative were placed on a filter paper (Whatman No. 1). *Solvent: Tert.*-butanol: *iso*propanol: 2 M ammonium hydroxide (2:2:1). *Reagents:* Ammonium molybdate + hydrogen sulphide for the development of phosphorus [10] and N-ethyl-maleinimide for sulphur [11].

My sincere thanks are due to Professor G. Ljunggren, Director of this Institute, for the kind interest he has shown in this work.

1. Larsson, L. *Acta Chem. Scand.* **11** (1957) 1131.
2. Larsson, L. *Acta Chem. Scand.* **7** (1953) 306.
3. Larsson, L. and Hansen, B. *Svensk Kem. Tidskr.* **68** (1956) 521.
4. Heath, D. F. and Casapieri, P. *Trans. Faraday Soc.* **47** (1951) 1093.
5. Branch, G. E. K. and Calvin, M. *The Theory of Organic Chemistry.* Prentice-Hall, Inc., New York 1945, p. 422.
6. Heath, D. F. *J. Chem. Soc.* **1956** 3796.
7. Dowden, H. C. *Biochem. J.* **32** (1938) 455.
8. Larsson, L. *Arkiv Kemi. In press.*
9. Holmstedt, B. *Acta Physiol. Scand.* **25** (1951) suppl. 90.
10. Hanes, C. S. and Isherwood, F. A. *Nature* **164** (1949) 1107.
11. Benesch, R., Benesch, R. E., Gutcho, M. and Laufer, L. *Science* **123** (1956) 981.

Received June 2, 1958.

The Influence of Anharmonicity upon the Vibrational Probability Densities and Mean Amplitudes in Molecules. The General Case of a Polyatomic Molecule with Non-Degenerate Normal Vibrations

ARNE REITAN

Institutt for teoretisk kjemi, NTH, Trondheim, Norway

The vibrational probability density for a general polyatomic molecule with non-degenerate normal vibrations and without accidental degeneracies has been calculated to terms of second order, making use of the Hamiltonian introduced by Darling and

Table 3. Second-order rate constants and energies and entropies of activation of the three organic phosphorus compounds.

Compound	k_2^{15} 1 mole^{-1} sec^{-1}	k_2^{25} 1 mole^{-1} sec^{-1}	k_2^{35} 1 mole^{-1} sec^{-1}	E_a kcal. mole^{-1}	$\Delta S^{\neq}$ E.U.
Dimethylamido-methyl-phosphoryl fluoride	—	1.04 ± 0.04	1.99 ± 0.02	11.9 ± 0.9	−21 ± 3
Ethylthio-methyl-phosphoryl fluoride	$(1.36 \pm 0.06) \times 10^{4}$	$(1.95 \pm 0.05) \times 10^{4}$	—	6.2 ± 1.2	−22 ± 4
Dimethylamido-ethoxy-phosphoryl cyanide	—	7.49 ± 0.08	13.0 ± 0.18	10.1 ± 0.4	−23 ± 1

$(0.40 \pm 0.02) \times 10^{-4}$ sec^{-1} at 25°C and $(0.44 \pm 0.11) \times 10^{-4}$ sec^{-1} at 35°C. The values of k_2 and the energies and entropies of activation for the alkaline hydrolysis of Tabun are given in Table 3.

Experimental. The syntheses of the two Sarin analogues have recently been published [8] and Tabun was synthesized according to Holmstedt [9]. In the kinetic experiments performed with the automatic titrator [3] the concentrations of the dimethylamino derivative and of Tabun were 0.40 mM and of the ethylthio derivative 0.20 mM. The first one was titrated with 0.1 M sodium hydroxide and the latter two with 0.05 mM sodium hydroxide. In other respects the procedure closely adhered to that described for the determination of the alkaline hydrolysis of Sarin [1]. In the paper chromatography ascending technique was used and 50 µl in portions of 5 µl of a 1 % aqueous solution of the ethylthio derivative were placed on a filter paper (Whatman No. 1). *Solvent: Tert.*-butanol: *iso*propanol: 2 M ammonium hydroxide (2:2:1). *Reagents:* Ammonium molybdate + hydrogen sulphide for the development of phosphorus [10] and N-ethyl-maleinimide for sulphur [11].

My sincere thanks are due to Professor G. Ljunggren, Director of this Institute, for the kind interest he has shown in this work.

1. Larsson, L. *Acta Chem. Scand.* **11** (1957) 1131.
2. Larsson, L. *Acta Chem. Scand.* **7** (1953) 306.
3. Larsson, L. and Hansen, B. *Svensk Kem. Tidskr.* **68** (1956) 521.
4. Heath, D. F. and Casapieri, P. *Trans. Faraday Soc.* **47** (1951) 1093.
5. Branch, G. E. K. and Calvin, M. *The Theory of Organic Chemistry.* Prentice-Hall, Inc., New York 1945, p. 422.
6. Heath, D. F. *J. Chem. Soc.* **1956** 3796.
7. Dowden, H. C. *Biochem. J.* **32** (1938) 455.
8. Larsson, L. *Arkiv Kemi. In press.*
9. Holmstedt, B. *Acta Physiol. Scand.* **25** (1951) suppl. 90.
10. Hanes, C. S. and Isherwood, F. A. *Nature* **164** (1949) 1107.
11. Benesch, R., Benesch, R. E., Gutcho, M. and Laufer, L. *Science* **123** (1956) 981.

Received June 2, 1958.

The Influence of Anharmonicity upon the Vibrational Probability Densities and Mean Amplitudes in Molecules. The General Case of a Polyatomic Molecule with Non-Degenerate Normal Vibrations

ARNE REITAN

Institutt for teoretisk kjemi, NTH, Trondheim, Norway

The vibrational probability density for a general polyatomic molecule with non-degenerate normal vibrations and without accidental degeneracies has been calculated to terms of second order, making use of the Hamiltonian introduced by Darling and

Dennison [1], Herzberg [2], and Wilson, Decius and Cross [3]. The eigenvalues and eigenfunctions have been calculated by a standard second order perturbation calculation, and the summations over the different states have been performed by methods similar to those employed in the authors papers [4,5], the resulting probability density being

$$w(q_1,q_2,\ldots,q_f) = w^0\,(1 + a_0 + \sum_r a_r q_r + \sum_{r\leqslant s}\sum_s a_{rs}q_rq_s + \sum_{r\leqslant s}\sum_{s\leqslant t}\sum_t a_{rst}q_rq_sq_t + \sum_{r\leqslant s}\sum_{s\leqslant t}\sum_{t\leqslant u}\sum_u a_{rstu}q_rq_sq_tq_u + \sum_{r\leqslant s}\sum_{s\leqslant t}\sum_{t\leqslant u}\sum_{u\leqslant v}\sum_{v\leqslant x}\sum_x a_{rstuvx}q_rq_sq_tq_uq_vq_x)$$

where

$$w^0\,(q_1,q_2,\ldots,q_f) = \pi^{-f/2}\prod_{k=1}^{f}[\tanh(hc\omega_k/2kT)]^{1/2}\exp[-\tanh(hc\omega_k/2kT)\,q_k^2]$$

We have here introduced the convenient dimensionless coordinates

$$q_k = 2\pi(c\omega_k/h)^{1/2}\,Q_k$$

where ω_k is the wave-number corresponding to the normal coordinate Q_k, c is the velocity of light, and h is Planck's constant. The first order coefficients a_r and a_{rst}, as well as the second order coefficients a_0, a_{rs}, a_{rstu}, and a_{rstuvx} have been calculated in terms of the potential constants of the Hamiltonian, the wavenumbers ω_k, and the absolute temperature T, the obtained results being somewhat complex.

The results have been applied to the cases of non-linear and linear symmetrical XY_2 molecules (in the latter case the degeneracy of one of the normal vibrations has to be taken appropriately into account), and numerical calculations have been performed for the molecules H_2O and CO_2. The force constants have been obtained from Darling and Dennison [1] and Dennison [6]. The mean amplitudes

$$u_e^{AB} = [\overline{(R_{AB} - R_{AB}^{(e)})^2}]^{1/2}$$
$$u_a^{AB} = [\overline{(R_{AB} - \overline{R_{AB}})^2}]^{1/2}$$
$$u_m^{AB} = [\overline{(R_{AB} - R_{AB,m})^2}]^{1/2}$$

as well as the mean values $\overline{r_{AB}}$ and the most probable values $r_{AB,m}$ of the deviations $r_{AB} = R_{AB} - R_{AB}^{(e)}$, have been calculated. R_{AB} is here the distance between the nuclei A and B, $R_{AB}^{(e)}$, $\overline{R_{AB}}$, and $R_{AB,m}$ are the equilibrium value, the mean value, and the most probable value of R_{AB}, respectively. The results are listed in Tables 1 and 2.

Table 1. Mean amplitudes etc. for H_2O in Å units at $T = 300°K$.

O—H	Harmonic	Anharmonic	H—H	Harmonic	Anharmonic
$\overline{r_{OH}}$	0	0.0175	$\overline{r_{HH}}$	0	0.0277
$r_{OH,m}$	0	0.0121	$r_{HH,m}$	0	0.0274
u_e^{OH}	0.0655	0.0707	u_e^{HH}	0.1088	0.1166
u_a^{OH}	0.0655	0.0687	u_a^{HH}	0.1088	0.1135
u_m^{OH}	0.0655	0.0689	u_m^{HH}	0.1088	0.1135

Table 2. Mean amplitudes etc. for CO_2 in Å units at $T = 300°K$.

C—O	Harmonic	Anharmonic	O—O	Harmonic	Anharmonic
$\overline{r_{CO}}$	0	0.0045	$\overline{r_{OO}}$	0	0.0041
$r_{CO,m}$	0	0.0033	$r_{OO,m}$	0	0.0035
u_e^{CO}	0.0346	0.0351	u_e^{OO}	0.0395	0.0399
u_a^{CO}	0.0346	0.0348	u_a^{OO}	0.0395	0.0396
u_m^{CO}	0.0346	0.0349	u_m^{OO}	0.0395	0.0397

By electron diffraction Karle and Karle [7] have obtained

$$u^{CO} = (0.034 \pm 0.003)\ Å$$
$$u^{OO} = (0.040 \pm 0.007)\ Å$$

1. Darling, B. T. and Dennison, D. M. *Phys. Rev.* **57** (1940) 128.
2. Herzberg, G. *Molecular Spectra and Molecular Structure*, Vol. II. *Infrared and Raman Spectra of Polyatomic Molecules*, Nostrand, New York 1945.
3. Wilson, E. B. Jr., Decius, J. C. and Cross, P. C. *Molecular Vibrations*, McGraw-Hill, New York 1955.
4. Reitan, A. *The Influence of Anharmonicity upon the Vibrational Probability Densities and Mean Amplitudes in Molecules.* I. *Diatomic Molecules, Kgl. Norske Videnskabs Selskabs Skrifter* (1958). *In press.*
5. Reitan, A. *Acta Chem. Scand.* **12** (1958) 131.
6. Dennison, D. M. *Revs. Modern Phys.* **12** (1940) 175.
7. Karle, I. L. and Karle, J. *J. Chem. Phys.* **17** (1949) 1052.

Received May 31, 1958.

A New γ-Glutamyltripeptide in *Juncus* Species

ARTTURI I. VIRTANEN and TERTTU ETTALA

Laboratory of the Foundation for Chemical Research, Biochemical Institute, Helsinki, Finland

Some years ago an acidic peptide was found in this laboratory in the ethanol extract of *Juncus conglomeratus* (Fig. 1). On a two-dimensional paper chromatogram the acid gave a violet spot on spraying with ninhydrin. After strong hydrolysis (6 N HCl, 20 h, 108°C), as well as after a mild one (0.5 N HCl, 10 h, 100° C), the spot was not detected on the chromatogram any longer, and hence it was apparently an easily decomposed peptide. The peptide was isolated in fairly pure form and was found to contain an easily split off glutamic acid molecule [1]. This peptide has now been isolated in completely pure form and its structure has been established.

For the isolation of the peptide 5 kg of *Juncus conglomeratus* was extracted in 70 % ethanol. The ethanol extract was run through an Amberlite IR-120 column. Amino acids were eluted by 1 N NH_4OH. When ammonia had been distilled off *in vacuo*, the residue was dissolved into 100 ml of water. The insoluble substance was filtered off and the filtrate was run through an Amberlite IR-45 column in acetate form. Neutral and basic amino acids were removed by water and the acidic ones by 0.5 N acetic acid. The unknown peptide (I) remained in the fraction with acidic amino acids, being accordingly acidic. After acetic acid had been distilled off there also was a substance (II) in the fraction of acidic amino acids which at first turned yellow on spraying with ninhydrin and then violet. This substance had apparently been formed through the partial decomposition of the original peptide. This peptide (I) was separated from the acidic amino acids on a cellulose powder column using butanol-acetic acid-water (630—100—270) as solvent. 160 fractions of 10 ml were taken and fractions 130—158 contained only the peptide without any free amino acids. These fractions were combined and the solvent was distilled off. The residue obtained was brown, however.

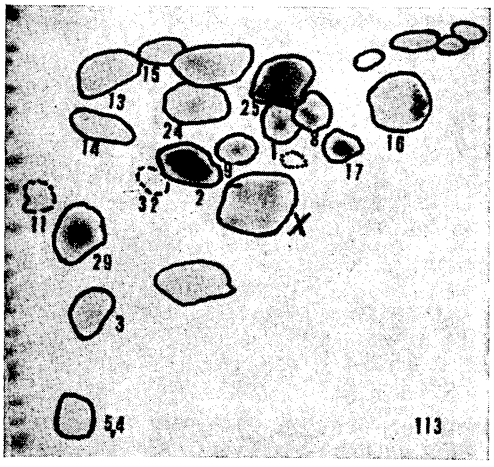

Fig. 1. Paper chromatogram of free amino acids (and some lowmolecular peptides) in *Juncus conglomeratus*. Solvents in text. × = unknown acidic peptide, 1 = gly, 2 = ala, 3 = val, 9 = threo, 16 = asp, 17 = glu, 29 = γ-amino-butyric acid.

As another method Dowex 1 resin (200—400 mesh, in acetate form) was used for the separation. About 100 mg of amino acids, eluted by 1 N NH_4OH from the Amberlite IR-120 column, were dissolved into 2 ml of 0.5 N acetic acid, and the solution was run through the Dowex 1 column (0.9 × 30 cm). The elution was performed by 0.5 N acetic acid and 1 ml fractions were taken. Also by this method the unknown peptide could be isolated, but the residue obtained after acetic acid had been distilled off was still brown.

After this both preparations were combined and once again run through the cellulose powder column, using water-saturated butanol as solvent. Now the brown impurity emerged from the column before the peptide, and the peptide-containing fractions were uncoloured. When the solvent was distilled off, the residue was white. The yield of peptide I was 160 mg.

When fractionating the original peptide from the cellulose powder column, the substance II was also collected. Since also this fraction was slightly coloured it was once again run through the cellulose powder column with water-saturated butanol. The yield obtained was 45 mg.

When hydrolysing the original peptide with 0.5 N HCl for 20 h at 100°C, glutamic acid was formed, as well as the substance

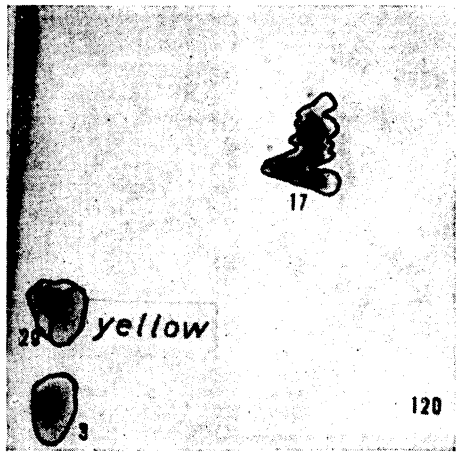

Fig. 2. Paper chromatogram of the unknown peptide after hydrolysis with 0.5 N HCl for 20 h at 100°C. 17 = glu, yellow = dipeptide formed on hydrolysis, 29 = added γ-amino-butyric acid, 3 = added val.

II which turned yellow on spraying with ninhydrin, and later on violet (Fig. 2). On hydrolysis of this substance in strong acid (6 N HCl, 20 h, 108°C) glutamic acid and valine were formed, and hence this substance also is a peptide. The same amino acids were also formed when hydrolysing the original peptide in strong acid.

The amounts of amino acids formed on hydrolysis were determined quantitatively using the copper salt method [2]. It was then found that on hydrolysis in dilute acid one molecule of glutamic acid was split off from the original peptide, and from the substance II one molecule glutamic acid and one molecule valine on hydrolysis in strong acid. The latter hydrolysis was not quite complete.

Tripeptide (I) (mild hydrolysis)	49	μg	glutamic	acid,	calc.	value*	50 μg
	45	»	»	»	»	»	50 »
Dipeptide (II) (strong hydrolysis)	25	»	»	»	»	»	39 »
	23	»	valine		»	»	31 »

The *molecular weight* of the original peptide, determined according to the method of Childs [3], was 341 (calc. value for a tripeptide containing two glutamic acid molecules and one valine molecule is 375). Glycyl-L-tyrosine, mol. wt. 238, was used as reference substance. The value obtained can be considered satisfactory when the low molecular weight of the known substance is taken into consideration.

The *nitrogen content* of the original peptide was determined by Kjeldahl according to Beet [4]; found 10.9 % N, calc. value for a tripeptide containing two glutamic acid molecules and one valine molecule ($C_{15}H_{25}O_8N_3$) 11.2 %.

The nitrogen content of the dipeptide formed on hydrolysis of the tripeptide in dilute acid was 10.81 %, calc. value for a dipeptide containing glutamic acid and valine ($C_{10}H_{18}O_5N_2$) 11.38 %.

R_F-values:	BuOH—AcOH—H_2O	Phenol
Tripeptide	0.31	0.49
Dipeptide	0.38	0.84

The position of glutamic acid and valine in the dipeptide was determined according to the method of Sanger [5]. It was found that the amino group in valine is free. Accordingly, the dipeptide is valyl-glutamic acid. Since the first glutamic acid molecule is split off from the tripeptide already on hydrolysis in dilute acid, it has to be linked to the dipeptide by its γ-carboxyl group, and the structure of the tripeptide is thus γ-glutamyl-valyl-glutamic acid HOOC · $CH(NH_2)$ · CH_2 · CH_2 · CO · NH · $CH(C_3H_7)$ · CO · NH · $CH(C_3H_5O_2)$ · COOH [6].

The tripeptide has been found by paper chromatography also in *Juncus effusus* and *Juncus filiformis*. There is about 100 mg/1 kg fresh plants of the tripeptide in *Juncus conglomeratus*.

Thanks are due to Miss Pirkko Kovakoski for her assistance in the isolation of the peptide and in the closer investigation of it in the first stage of the work in 1955.

* In the calculated values the original peptide has been supposed to be a tripeptide containing two glutamic acid molecules and one valine molecule.

1. *The annual report of the Foundation for Chemical Research* **1956**, p. 8.
2. Fischer, F. G. *Biochem. Z.* **324** (1953) 544.
3. Childs, C. E. *Anal. Chem.* **26** (1954) 1963.

4. Beet, A. E. *Nature* **175** (1954) 513.
5. Sanger, F. and Thompson, E. O. P. *Biochem. J.* **53** (1953) 353.
6. Virtanen, A. I. and Ettala, T. *Suomen Kemistilehti B* **31** (1958). *In press.*

Received June 2, 1958.

Mass Spectrometric Evidence Regarding the Structural Relations between Dextropimaric, *Iso*dextropimaric, and Cryptopimaric Acids *

HENRIK H. BRUUN

Institute for Wood Chemistry, Åbo Akademi, Åbo, Finland,

RAGNAR RYHAGE

Laboratory for Mass Spectrometry, Kemiska Institutionen I, Karolinska Institutet, Stockholm, Sweden, and

EINAR STENHAGEN

Department of Medical Biochemistry, Institute of Medical Chemistry, University of Uppsala, Sweden

A study of the mass spectra of the methyl esters of rosin acids, performed with a high-mass, high-resolution mass spectrometer with heated inlet system [1], has provided new evidence regarding the structural relations between dextropimaric acid, *iso*dextropimaric acid, and cryptopimaric acid [2].

The mass spectrum of the methyl ester of cryptopimaric acid (Fig. 1a) is strikingly similar to that of the methyl ester of dextropimaric acid (Fig. 1b). The base peak of the spectra is at *m/e* 121, and strong peaks occur at *m/e* 316 (molecular peak), 180, 181, 241, 257, and 301. The methyl ester of *iso*dextropimaric acid gives a quite different mass spectrum (Fig. 1c) that has the base peak at *m/e* 241 and strong peaks at *m/e* 316 (molecular peak), 256, 257, 287, and 301.

We interpret these results as showing that dextropimaric acid and cryptopimaric acid can be structurally different only with regard to the orientation of the methyl and vinyl groups attached to C7, and that dextropimaric acid and *iso*dextropimaric acid must be different with regard to the geometry of the ring system. The opinion of Wenkert [3] that the two last mentioned acids differ in the configuration at C13 is thus supported by the present evidence: As the proposed stereochemical difference at C7 [4] has recently been confirmed [5] it follows that the acids are stereochemically different both at C7 and C13.

The above conclusions seem to tally with monolayer [6] and infrared absorption [7-9] data.

Experimental. The cryptopimaric acid used had $[\alpha]_D^{12} - 21.7°$ and m.p. 160—162°.** Because of the small amount of material, the optical rotation was not checked by us. Keimatsu *et al.*[2] give m.p. 159—161° and $[\alpha]_D^{17.5} - 18.99°$ (in ethanol). The sample of dextropimaric acid had m.p. 207—208°, $[\alpha]_D^{25} + 70° \pm 3°$ ** (ethanol, micro tube), and the *iso*dextropimaric acid m.p. 160°, $[\alpha]_D^{25} \pm 0.00°$ ** in ethanol. The acids were converted into methyl esters by means of fresh diazomethane in ether solution. The mass spectra were run on 0.5 mg samples with the inlet system kept at a temperature of 200°.

Acknowledgements. We are indebted to Prof. H. Inamura, Government Forest Experiment Station, Meguro, Tokyo, for a sample of cryptopimaric acid, to Dr. R. V. Lawrence, Naval Stores Research Station, United States Department of Agriculture, Olustee, Florida, for dextro- and *iso*dextropimaric acids, and to Dr. O. Jeger, Institute of Organic Chemistry, Eidg. Technische Hochschule, Zürich, for dextropimaric acid. The two samples of dextropimaric acid gave identical infrared absorption spectra.

1. Ryhage, R. *To be published shortly.*
2. Keimatsu, S., Ishiguro, T., and Fukuri, G. *J. Pharm. Soc. Japan* **57** (1937) 69.

* This work was reported at the meeting of the Swedish Biochemical Society at Uppsala, June 6—7, 1958.

** Determined by us.

4. Beet, A. E. *Nature* **175** (1954) 513.
5. Sanger, F. and Thompson, E. O. P. *Biochem. J.* **53** (1953) 353.
6. Virtanen, A. I. and Ettala, T. *Suomen Kemistilehti B* **31** (1958). *In press.*

Received June 2, 1958.

Mass Spectrometric Evidence Regarding the Structural Relations between Dextropimaric, *Iso*dextropimaric, and Cryptopimaric Acids *

HENRIK H. BRUUN

Institute for Wood Chemistry, Åbo Akademi, Åbo, Finland,

RAGNAR RYHAGE

Laboratory for Mass Spectrometry, Kemiska Institutionen I, Karolinska Institutet, Stockholm, Sweden, and

EINAR STENHAGEN

Department of Medical Biochemistry, Institute of Medical Chemistry, University of Uppsala, Sweden

A study of the mass spectra of the methyl esters of rosin acids, performed with a high-mass, high-resolution mass spectrometer with heated inlet system [1], has provided new evidence regarding the structural relations between dextropimaric acid, *iso*dextropimaric acid, and cryptopimaric acid [2].

The mass spectrum of the methyl ester of cryptopimaric acid (Fig. 1a) is strikingly similar to that of the methyl ester of dextropimaric acid (Fig. 1b). The base peak of the spectra is at *m/e* 121, and strong peaks occur at *m/e* 316 (molecular peak), 180, 181, 241, 257, and 301. The methyl ester of *iso*dextropimaric acid gives a quite different mass spectrum (Fig. 1c) that has the base peak at *m/e* 241 and strong peaks at *m/e* 316 (molecular peak), 256, 257, 287, and 301.

We interpret these results as showing that dextropimaric acid and cryptopimaric acid can be structurally different only with regard to the orientation of the methyl and vinyl groups attached to C7, and that dextropimaric acid and *iso*dextropimaric acid must be different with regard to the geometry of the ring system. The opinion of Wenkert [3] that the two last mentioned acids differ in the configuration at C13 is thus supported by the present evidence: As the proposed stereochemical difference at C7 [4] has recently been confirmed [5] it follows that the acids are stereochemically different both at C7 and C13.

The above conclusions seem to tally with monolayer [6] and infrared absorption [7-9] data.

Experimental. The cryptopimaric acid used had $[\alpha]_D^{12} - 21.7°$ and m.p. 160—162°.** Because of the small amount of material, the optical rotation was not checked by us. Keimatsu *et al.*[2] give m.p. 159—161° and $[\alpha]_D^{17.5} - 18.99°$ (in ethanol). The sample of dextropimaric acid had m.p. 207—208°, $[\alpha]_D^{25} + 70° \pm 3°$ ** (ethanol, micro tube), and the *iso*dextropimaric acid m.p. 160°, $[\alpha]_D^{25} \pm 0.00°$ ** in ethanol. The acids were converted into methyl esters by means of fresh diazomethane in ether solution. The mass spectra were run on 0.5 mg samples with the inlet system kept at a temperature of 200°.

Acknowledgements. We are indebted to Prof. H. Inamura, Government Forest Experiment Station, Meguro, Tokyo, for a sample of cryptopimaric acid, to Dr. R. V. Lawrence, Naval Stores Research Station, United States Department of Agriculture, Olustee, Florida, for dextro- and *iso*dextropimaric acids, and to Dr. O. Jeger, Institute of Organic Chemistry, Eidg. Technische Hochschule, Zürich, for dextropimaric acid. The two samples of dextropimaric acid gave identical infrared absorption spectra.

1. Ryhage, R. *To be published shortly.*
2. Keimatsu, S., Ishiguro, T., and Fukuri, G. *J. Pharm. Soc. Japan* **57** (1937) 69.

* This work was reported at the meeting of the Swedish Biochemical Society at Uppsala, June 6—7, 1958.

** Determined by us.

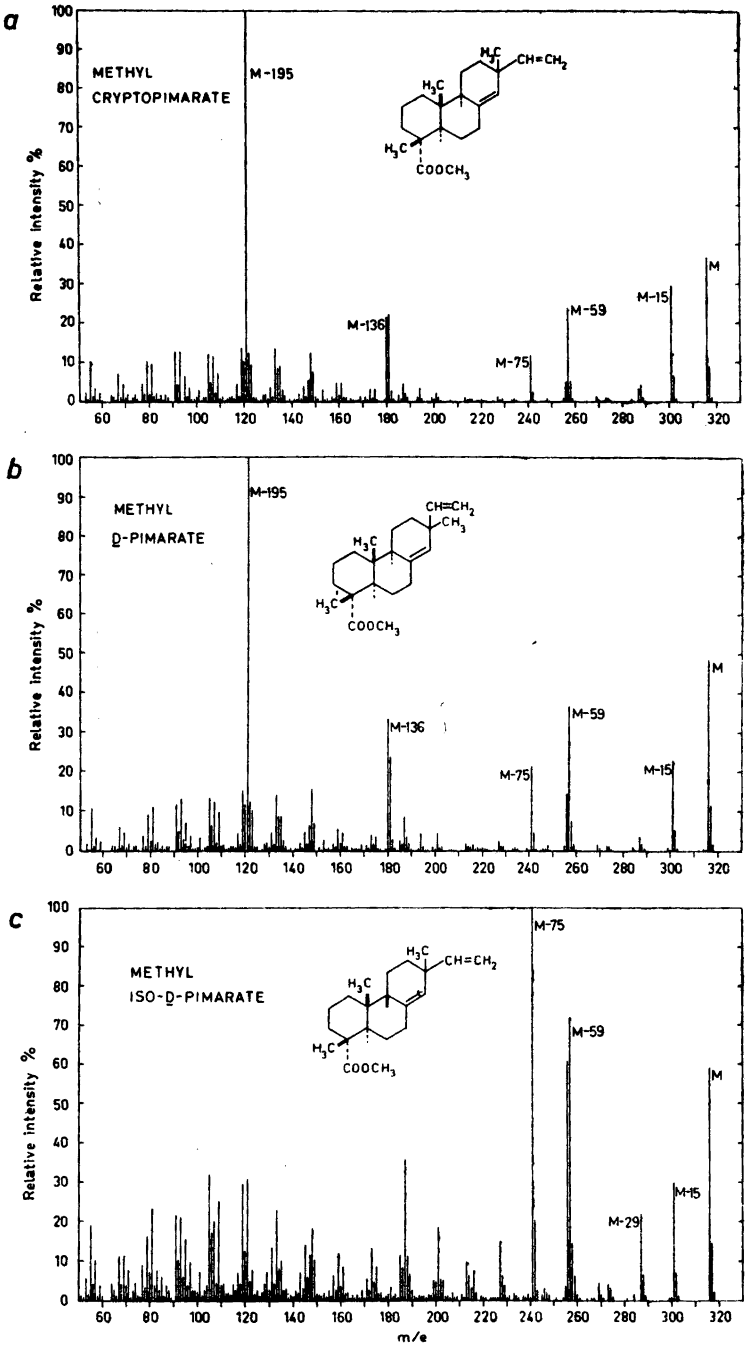
a
METHYL
CRYPTOPIMARATE
M-195
M-136
M-75
M-59
M-15
M
b
METHYL
D-PIMARATE
M-195
M-136
M-75
M-59
M-15
M
c
METHYL
ISO-D-PIMARATE
M-75
M-59
M-29
M-15
M
Relative intensity %
m/e

Fig. 1

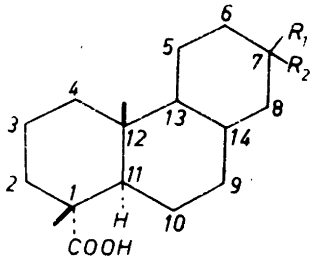

Fig. 2. Ring system numbering of rosin acids. Stereochemical configuration at carbon atoms 1, 11, and 12 indicated.

3. Wenkert, E., *Chem. & Ind. London* **1955** 282.
4. Harris, G. C., and Sanderson, T. F. *J. Am. Chem.Soc.* **70** (1948) 2079, 2081.
5. Edwards, O. E. and Howe, R. *Chem. & Ind. London* **1958** 629.
6. Bruun, H. H. *Surface Balance Studies of Rosin Acid Monolayers* (Thesis) *Acta Acad. Åboensis, Math. et Phys.* **19** (1954).
7. Bruun, H. H. *Paper and Timber (Finland)* **38** (1956) 577.
8. Bruun, H. H. *Paper and Timber (Finland)* **39** (1957) 221.
9. Brossi, A. and Jeger, O. *Helv. Chim. Acta* **33** (1950) 722.

Received June 12, 1958.

Reactions between Quinones and Carbonyl Compounds Catalysed by Aluminium Oxide

RUNE MAGNUSSON

Institutionen för organisk kemi, Chalmers tekniska högskola, Göteborg, Sweden

In the course of studies on the oxidation of 2,6-dimethoxyphenol with sodium periodate [1], an attempt was made to separate, by chromatography on a column of aluminium oxide, a benzene solution of the previously unknown 3,8-dimethoxy-1,2-naphthoquinone (I) and 2,6-dimethoxy-*p*-benzoquinone (III). By irrigation with benzene, compound III was eluted while a red compound, assumed to be the naphthoquinone I, remained strongly adsorbed on the upper part of the column. This latter material was eluted with acetone and from the eluate two crystalline products were obtained. One of those was the expected naphthoquinone I; the other was a yellow substance. This indicated that an unexpected transformation of I had taken place either during the adsorption or during the elution step. To clarify this question, the following investigations were carried out.

When an acetone solution of the pure naphthoquinone I (m. p. 196°) was boiled for a few minutes in the presence of aluminium oxide the red solution became yellow, and from it yellow crystals (m. p. 142°) were obtained in a yield of 90 %. (In the absence of aluminium oxide a reaction did not occur and acetone was then a very suitable recrystallization solvent for I.) Analysis of the substance indicated that it might be an addition product formed from equimolar amounts of acetone and compound I. Ultra-violet and infrared absorption data, and the fact that on reduction the substance was converted into a compound having the properties of an α-naphthol with a free *p*-position, all suggested that the addition product might be the *o*-naphthoquinol of structure II.

2,6-Dimethoxy-*p*-benzoquinone (III) when heated in acetone solution in the presence of aluminium oxide also yielded an apparently similar type of addition product having m. p. 154°. Spectrographic examination of this compound, and its reduction to a phenol, to which the structure of 3,5-dimethoxy-4-acetonylphenol could be ascribed, indicated that the acetone addition compound of III was a *p*-quinol of structure IV.

Since the formation of the quinols II and IV involves a reaction of the aldol condensation type, it appeared possible that it might have been catalysed by traces of alkali present in the commercial aluminium oxide. This is improbable, however, as the catalytic effect of the aluminium oxide preparation was retained even after its thorough treatment with dilute hydrochloric acid (followed by washing with water). Thus, neutral aluminium oxide would appear to act as a catalyst of the reactions described.

Other ketones, for example methyl ethyl ketone, were also found to add to the quinones I and II in the presence of aluminium oxide.

Addition of acetone and of other ketones to tetrachloro-*o*-quinone has been reported by Schenck *et al.*[2] to be catalysed by dry

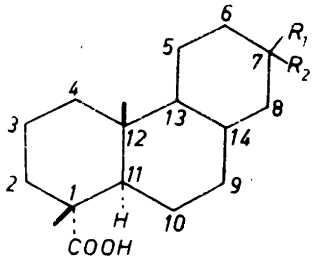

Fig. 2. Ring system numbering of rosin acids. Stereochemical configuration at carbon atoms 1, 11, and 12 indicated.

3. Wenkert, E., *Chem. & Ind. London* **1955** 282.
4. Harris, G. C., and Sanderson, T. F. *J. Am. Chem.Soc.* **70** (1948) 2079, 2081.
5. Edwards, O. E. and Howe, R. *Chem. & Ind. London* **1958** 629.
6. Bruun, H. H. *Surface Balance Studies of Rosin Acid Monolayers* (Thesis) *Acta Acad. Åboensis, Math. et Phys.* **19** (1954).
7. Bruun, H. H. *Paper and Timber (Finland)* **38** (1956) 577.
8. Bruun, H. H. *Paper and Timber (Finland)* **39** (1957) 221.
9. Brossi, A. and Jeger, O. *Helv. Chim. Acta* **33** (1950) 722.

Received June 12, 1958.

Reactions between Quinones and Carbonyl Compounds Catalysed by Aluminium Oxide

RUNE MAGNUSSON

Institutionen för organisk kemi, Chalmers tekniska högskola, Göteborg, Sweden

In the course of studies on the oxidation of 2,6-dimethoxyphenol with sodium periodate [1], an attempt was made to separate, by chromatography on a column of aluminium oxide, a benzene solution of the previously unknown 3,8-dimethoxy-1,2-naphthoquinone (I) and 2,6-dimethoxy-*p*-benzoquinone (III). By irrigation with benzene, compound III was eluted while a red compound, assumed to be the naphthoquinone I, remained strongly adsorbed on the upper part of the column. This latter material was eluted with acetone and from the eluate two crystalline products were obtained. One of those was the expected naphthoquinone I; the other was a yellow substance. This indicated that an unexpected transformation of I had taken place either during the adsorption or during the elution step. To clarify this question, the following investigations were carried out.

When an acetone solution of the pure naphthoquinone I (m. p. 196°) was boiled for a few minutes in the presence of aluminium oxide the red solution became yellow, and from it yellow crystals (m. p. 142°) were obtained in a yield of 90 %. (In the absence of aluminium oxide a reaction did not occur and acetone was then a very suitable recrystallization solvent for I.) Analysis of the substance indicated that it might be an addition product formed from equimolar amounts of acetone and compound I. Ultra-violet and infrared absorption data, and the fact that on reduction the substance was converted into a compound having the properties of an α-naphthol with a free *p*-position, all suggested that the addition product might be the *o*-naphthoquinol of structure II.

2,6-Dimethoxy-*p*-benzoquinone (III) when heated in acetone solution in the presence of aluminium oxide also yielded an apparently similar type of addition product having m. p. 154°. Spectrographic examination of this compound, and its reduction to a phenol, to which the structure of 3,5-dimethoxy-4-acetonylphenol could be ascribed, indicated that the acetone addition compound of III was a *p*-quinol of structure IV.

Since the formation of the quinols II and IV involves a reaction of the aldol condensation type, it appeared possible that it might have been catalysed by traces of alkali present in the commercial aluminium oxide. This is improbable, however, as the catalytic effect of the aluminium oxide preparation was retained even after its thorough treatment with dilute hydrochloric acid (followed by washing with water). Thus, neutral aluminium oxide would appear to act as a catalyst of the reactions described.

Other ketones, for example methyl ethyl ketone, were also found to add to the quinones I and II in the presence of aluminium oxide.

Addition of acetone and of other ketones to tetrachloro-*o*-quinone has been reported by Schenck *et al.*[2] to be catalysed by dry

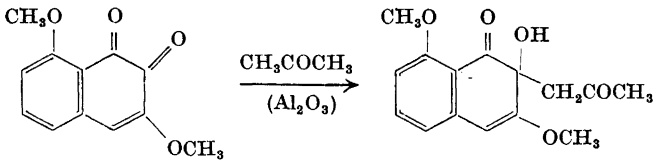

I II

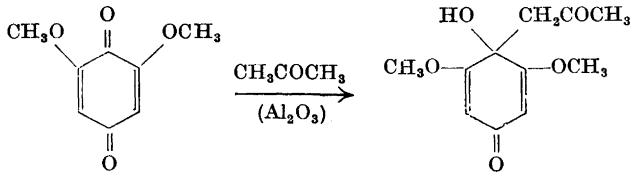

III IV

hydrogen chloride and probably resulted in the formation of the corresponding *o*-quinols. No other observations on the addition of ketones to quinones appear to have been published.

The quinols II and IV are stable in ethanol and in other neutral solvents. However, if an ethanolic solution of IV is heated in the presence of aluminium oxide, the quinone III is regenerated. It is possible, therefore, to reverse the reaction under those modified conditions.

This work is being continued and a detailed report will be published later.

The author is indebted to *Statens Tekniska Forskningsråd* for financial support.

1. Adler, E. and Magnusson R. *To be published.*
2. Schenck, G. O., Brähler, B. and Cziesla, M. *Angew. Chem.* **68** (1956) 247.

Received June 6, 1958.

ACTA CHEMICA SCANDINAVICA 12 (1958) 793—796

Chlorination of *o*-Cresoxyacetic Acid

A Peculiar Side Reaction

HAKON LUND

Chemical Institute, Aarhus University, Denmark

When *o*-cresoxyacetic acid is chlorinated in an organic solvent 4-chloro-2-methyl-phenoxyacetic acid is the main product, but a small amount of material which is insoluble in aqueous alkali is simultaneously formed. A compound, $C_9H_9O_3Cl_3$, has been isolated and is shown to be a cyclic ester-acetal of glycolic acid and 2-methyl-4,5,6-trichloro-*cyclo*hex-2-en-1-one.

The "weed-killer" 2-methyl-4-chloro-phenoxyacetic acid is industrially prepared by chlorination of *o*-cresoxyacetic acid in an organic solvent [1]. The acid is extracted by means of aqueous alkali. In the organic solvent remains, however, a small quantity of material which is not directly soluble in aqueous alkali. After removal of the solvent *in vacuo* a rather viscous oil is obtained which, on cooling, partially crystallizes. Filtration is almost impossible; but when the hot oil is diluted with alcohol a well-defined compound A, m.p. 137°, is easily isolated. From the dark mother liquor a mixture of compounds can be obtained by distillation at 0.5—1 mm pressure. The percentage composition of this material is the same as that of compound A and corresponds to the formula $C_9H_9O_3Cl_3$. Apparently the material is a mixture of isomers of A.

Compound A can be isolated in an amount of about 30 % of the total product. The constitution of A seems to be

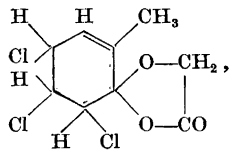

A thus being an ester-acetal of 2-methyl-4,5,6-trichloro*cyclo*hex-2-en-1-one and glycolic acid.

The formation of such a compound is rather surprising. Apparently 4 atoms of chlorine are *added* to the benzene ring and one molecule of hydrogen chloride split off with formation of the dioxolone ring:

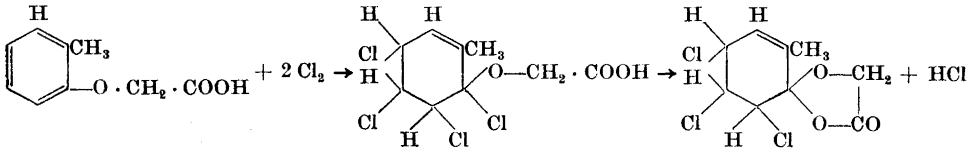

Considering the very high rate of the *para* substitution reaction it is quite unexpected that an addition to the *unsubstituted* molecule takes place to a measurable extent. It is well-known [2] that aromatic amines and phenols can, on prolonged chlorination, *after* completed substitution add chlorine with the formation of highly chlorinated *cyclo*hexenones. If, however, *para* or *ortho* substitution had preceded addition of chlorine in the present case the non-aromatic molecule arising from *o*-cresoxyacetic acid by treatment with chlorine, and containing the dioxolone ring, should contain an even number of chlorine atoms, and if a dichloro cresoxy acetic acid had been formed before addition a $>CCl_2$-group should be present in the non-aromatic molecule. The infrared spectrum of the compound seems to exclude this possibility.

The constitution of A given above is based on the following evidence:

1. Quantitative analysis has established the formula $C_9H_9O_3Cl_3$.

2. The ultraviolet absorption spectrum exhibits no bands above 250 mμ, whereas phenol derivatives have high absorption around 275 mμ.

3. In alcoholic solution the compound reacts vigorously with potassium hydroxide with quantitative formation of 4,6-dichloro-2-methyl-phenol. 2 molecules of potassium hydroxide are consumed in the reaction.

4. Metallic zinc removes all chlorine from the compound in boiling alcoholic solution and *o*-cresoxyacetic acid is formed.

5. Anhydrous diethyl amine removes 1 molecule of hydrogen chloride with the formation of a dichloro cresoxyacetic acid, presumably the 5,6-derivative. The compound is different from both the 4,6- and 4,5-dichloro acid.

6. An aqueous-alcoholic solution of A liberates iodine from potassium iodide with formation of, *i.a.*, 6-chloro-2-methylphenoxyacetic acid. Besides, an oil is formed which is insoluble in aqueous potassium carbonate and thus probably consists of compounds in which the dioxolone ring is intact.

All these reactions are well explained by the constitution proposed above:

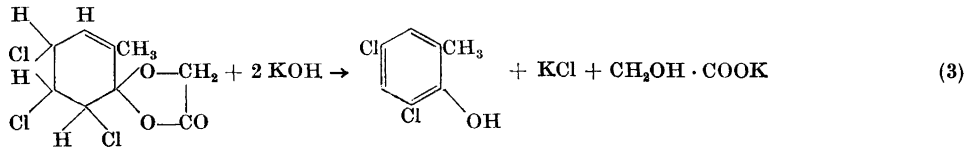

(3)

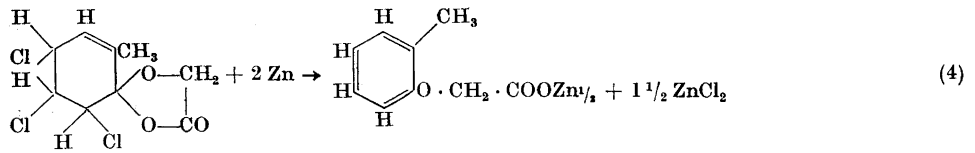

(4)

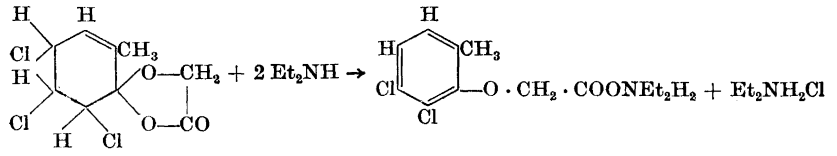

(5)

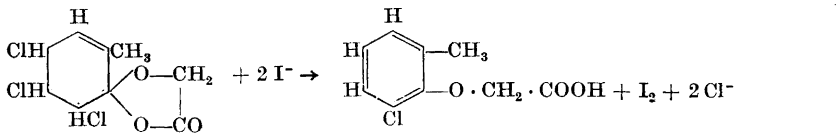

(6)

In the infrared spectrum * an unusually strong absorption band with two peaks at 5.49 and 5.58 μ indicates the presence of a somewhat anomalous carbonyl group. In order to test the absorption band of a carbonyl group in a dioxolone ring the compound 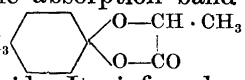 was synthesized from *p*-methyl*cyclo*hexanone and lactic acid. Its infrared spectrum contained a similarly intensive band with a peak at 5.59 μ. The similarity in intensity and position supports the dioxolone structure in compound A.

The formula contains 4 asymmetric carbon atoms in the homocyclic ring and explains the existence of a large number of isomers formed in the addition reaction.

On prolonged boiling in an alcoholic solution of hydrogen chloride compound A, as well as the mixture of isomers, is decomposed with formation of 4,6-dichloro-*o*-cresol.

EXPERIMENTAL

1. *Isolation of compound A.* The crude material is heated on a steam bath until completely liquid. 500 g is poured into 500 ml alcohol and cooled to 10°. The crystals are filtered off, yield about 170 g. They are dissolved in 1 200 ml of boiling alcohol and filtered hot from a small amount of inorganic material (sodium chloride) and on cooling to 0° about 150 g of pure material, mp. 137°, is obtained. Found: C 39.8; 39.6; H 3.35; 3.28; Cl 39.1; 39.0 %. $C_9H_9O_3Cl_3$ requires: C 39.76; H 3.34; Cl 39.2 %. Equiv.wt. by quantitative saponification with alcoholic potassium hydroxide, indicator methyl red (in order to avoid interference of the cresol): 135.0; 135.5; calc. 135.7).

2. *Reaction with potassium hydroxide.* To a hot solution of A (10 g) in alcohol (75 ml) was added slowly through the condenser 20 % aqueous potassium hydroxide (30 ml). The mixture boiled vigorously without external heating during the addition. Boiling was continued for 15 min. Water was added (50 ml) and the alcohol distilled off. On acidification and cooling 4,6-dichloro-*o*-cresol separated, yield 6.4 g (98 % of theory) and was identified by melting point (55°) and by preparation of the corresponding dichloro cresoxyacetic acid (mp. 184—85°).

3. *Reaction with metallic zinc.* To a solution of A (10 g) in boiling alcohol (75 ml) was added zinc wool (7 g). The reduction proceeded rapidly and from the resulting solution 5.0 g of *o*-cresoxyacetic acid was isolated, m. p. 155°, equiv.wt. by titration 165.5 (calc. 166).

4. *Reaction with diethyl amine.* To 10 g of A was added diethyl amine (20 ml) and the solution was boiled for 15 min. The excess of diethyl amine was distilled off and the

* Thanks are due to professor Børge Bak, Copenhagen, who has taken the infrared spectrograms.

residue dissolved in water and acidified. Yield of crystals 7.5 g, mp. 128°. (Found: C 45.7; 45.8; H 3.33; 3.36; Cl 30.3; 30.4 %; equiv.wt 234. Calc. for $C_9H_8O_3Cl_2$: C 45.9; H 3.43; Cl 30.2 %; equiv.wt. 235).

4,5-Dichloro-2-methyl-phenoxyacetic acid was prepared from 4,5-dichloro-2-methyl phenol [3] by condensation with monochloroacetic acid in alkaline solution, mp. 165—66°, thus evidently different from the acid obtained above, which, therefore, is assigned the 5,6-dichloro structure.

5. *Reaction with potassium iodide.* To a boiling solution of A (10 g) in alcohol (100 ml) was added an aqueous solution of potassium iodide (10 g). Iodine was slowly liberated and time after time reduced with sodium thiosulfate. After 3 hours' boiling no more iodine was formed. The alcohol was distilled off at diminished pressure and the remaining milky liquid was extracted with ether. The ethereal solution was extracted with aqueous sodium carbonate, from which 6-chloro-2-methyl-phenoxyacetic acid was obtained (mp. 110° after recrystallization from benzene, equiv.wt. by titration 199.5, calc. 200.5).

The ethereal solution on evaporation left an uncrystallizable oil which was not examined further.

6. *Catalytic hydrogenation of A was attempted (catalyst PtO_2).* The reaction proceeded rapidly at first, but stopped when 2—3 moles of hydrogen had been absorbed. The product, however, still contained chlorine and was obviously a complicated mixture of compounds distilling *in vacuo* over a very wide range of temperature; further examination was abandoned.

7. *Decomposition of A with alcoholic hydrogen chloride.* A solution of 15 g of A in 10 % alcoholic hydrogen chloride (60 ml) was boiled for 3 h. The alcohol was distilled off at diminished pressure. The oily residue was dissolved in ether and washed with aqueous sodium carbonate, dried, and the ether distilled off. The remaining oil solidified when cooled to 0°. The crystals were identified as 4,6-dichloro-*o*-cresol.

A similar process was carried out with an amount of the vacuum-distilled mother liquid from the crude product, giving similar results.

REFERENCES

1. Dan. Pat. 78535 (1946).
2. Zincke, Th. and Schaum, C. *Ber.* **27** (1894) 537.
3. Zincke, Th. *Ann.* **417** (1918) 207.

Received November 5, 1957.

ACTA CHEMICA SCANDINAVICA 12 (1958) 797—801

Studies on Monoalkyl Carbonates

XIV. The Monoalkyl Carbonates of Tetrahydrofurfuryl Alcohol and Furfuryl Alcohol

MARIANNE BOEG HANSEN and CARL FAURHOLT

The Royal Danish School of Pharmacy, Copenhagen, Denmark

The velocity constants of the reaction 'alcohol + OH^- + CO_2 = alkyl · CO_3^- + H_2O' and the equilibrium constants for the equilibrium 'alkyl · CO_3^- + H_2O = HCO_3^- + alcohol' have been determined for tetrahydrofurfuryl alcohol and furfuryl alcohol. The velocity of the decomposition of the monoalkyl carbonates in strongly basic medium is investigated and may be explained by assuming that the decomposition is a two-stage reaction, *viz.* 1) monoalkyl carbonate = alkoholate + CO_2; 2) CO_2 + OH^- = HCO_3^-.

1. The present investigation deals with the equilibrium conditions and the reaction mechanism for the formation and decomposition of the monoalkyl carbonates of tetrahydrofurfuryl alcohol and furfuryl alcohol in aqueous medium.

2. Tetrahydrofurfuryl alcohol was purified by distillation through a wiregauze column with 49 sets of platinum plates. The obtained tetrahydrofurfuryl alcohol boiled at 178.2—178.3°C/773 mm Hg (177.6—177.7°C/760 mm Hg), $n_D^{20.0°} = 1.4518$.

Furfuryl alcohol was purified first by simple distillation in vacuum and then by distillation through a wiregauze column with 49 sets of platinum plates at 100 mm Hg. The furfuryl alcohol thus obtained boiled at 171.5—172.3°C/764 mm Hg, $n_D^{20.0°} = 1.4872$.

As furfuryl alcohol is unstable under ordinary conditions and discolours, it is used immediately after the distillation.

3. No solid monoalkyl carbonate was prepared. Solutions were made by dissolving carbon dioxide in basic solutions of the alcohols.

4. As to the method of analysis we refer to previous investigations [1]. The data presented are corrected with regard to blank values unless otherwise stated. "Uncorr." values are not corrected at all and "corr." values are corrected not only with regard to blank values but also with regard to the decomposi-

tion mentioned in the next section. The blank values may amount to about 3 units of the percentage of monoalkyl carbonate in some of the experiments.

5. The experiments were carried out at 0°C. Velocity constants are expressed on the basis of the Briggs' logaritms and the minute.

On the formation of the monoalkyl carbonate from carbon dioxide and alcohol in basic solution and on the reaction

$$\text{alcoholate} + CO_2 = \text{monoalkyl carbonate}$$

The experiments were carried out in a 2 litre flask by vigorously shaking 1 100 ml of a basic solution of the alcohols with atmospheric air of which 550 ml were substituted by carbon dioxide. The strong basic solution of furfuryl alcohol was light yellow and became slight opalescent by standing at 0°C. The solutions were immediately analysed to determine the percentage of monoalkyl carbonate. Due to the rapid decomposition of the monoalkyl carbonates, we had to correct the results by means of the velocity constant which we also have determined, see later.

By introduction of the adjusted results in the expression:

$$k' = \frac{\%\ \text{monoalkyl carbonate} \cdot k_{CO_2OH^-}}{\%\ \text{carbonate} \cdot c_{\text{alcohol}}}$$

the k' values presented in Table 1 are calculated. k' is the velocity constant of the overall reaction:

$$CO_2 + \text{alcohol} + OH^- = \text{alkyl} \cdot CO_3^- + H_2O$$

For the value of $k_{\text{alkyl}\cdot CO_3^-}$ we get 0.0074 for tetrahydrofurfuryl alcohol and 0.054 for furfuryl alcohol when the values of K_{Eq} found in Table 2 are employed.

The equilibrium of the reactions

$$\text{alkyl} \cdot CO_3^- + H_2O = HCO_3^- + \text{alcohol}$$

The above equilibrium was established in aqueous solutions of alcohol, potassium bicarbonate and sodium carbonate.

Table 1. Carbon dioxide in tetrahydrofurfuryl alcohol + NaOH and in furfuryl alcohol + NaOH. 0°C.

	c_{NaOH}	$c_{alcohol}$	Absorb. CO_2 $\frac{\text{mole}}{\text{litre}}$	% Alkyl-carbonate	% Alkyl-carbonate corr.	k'	Mean of k'
Tetrahydro-furfuryl alcohol	0.10	1.00	0.0215	51.3	57.5	$10^{4.52}$	$10^{4.51}$
	0.10	0.50	0.0198	36.5	38.3	$10^{4.49}$	
Furfuryl alcohol	0.10	1.00	0.0214	68.2	81.9	$10^{5.09}$	$10^{5.08}$
	0.10	0.50	0.0212	61.2	70.2	$10^{5.07}$	

Table 2. The solutions of carbonate-monoalkyl carbonate in equilibrium. 0°C.

	Initial solution			% Alkylcarbonate		K_{Eq}	Mean of K_{Eq}
	$c_{alcohol}$	c_{KHCO_3}	$c_{Na_2CO_3}$	uncorr.	corr.		
Tetrahydro-furfuryl alcohol	1.00	0.10	0.05	2.99	2.43 [1]	$10^{1.61}$	$10^{1.64}$
	1.00	0.20	0.10	2.39	2.16 [2]	$10^{1.65}$	
	0.50	0.10	0.05	1.77	1.24 [3]	$10^{1.60}$	
	0.50	0.20	0.10	1.25	1.00 [4]	$10^{1.69}$	
Furfuryl alcohol	1.00	0.20	0.10	1.59	1.15 [5]	$10^{1.93}$	

1 mean of 3 determinations 2.41, 2.56, 2.35
2 » » 3 » 2.30, 2.07, 2.11
3 » » 3 » 1.22, 1.22, 1.27
4 » » 3 » 0.99, 1.01, 0.99
5 » » 3 » 1.17, 1.13, 1.15

The contents of monoalkyl carbonate have been calculated as a percentage of HCO_3^- initially present; thus no attention was paid to carbonate.

In Table 2 are presented not only the '% monoalkyl carbonate' corrected for blank values and the decomposition taking place until the precipitate has been separated from the supernate, but the uncorrected as well. This has been done in order to illustrate the accuracy that may be attached to the values found. From the experimental results the equilibrium constant of the reaction

$$K_{Eq} = \frac{c_{alcohol} \cdot c_{HCO_3^-} \cdot f}{c_{alkyl \cdot CO_3^-} \cdot f}$$

may be calculated, the activity constants neutralizing each other.

On the velocity of the reactions

$$alkyl \cdot CO_3^- + H_2O = HCO_3^- + alcohol$$

Determinations have been made from the monoalkyl carbonate side only and in strongly basic medium, the alkyl carbonate thus being practically completely converted into carbonate.

The monoalkyl carbonate has been made by shaking the basic solutions with CO_2 as stated in the introduction. The solutions, therefore, contain ordinary carbonate, which, however, is of no importance in the present investigations.

In Table 3 are listed the experimental results of the decomposition of the alkyl carbonates. k_{mono} is the value of $\frac{1}{t} \log \frac{a}{a-x}$

The experiments are interpreted in a similar way to the one applied to the monoalkyl carbonates previously investigated. The decomposition takes place through the reactions:

1. $alkyl \cdot CO_3^- = alkylate^- + CO_2$
2. $CO_2 + OH^- = HCO_3^-$

Table 3. Monoalkyl carbonate in NaOH + alcohol. 0°C.

	$c_{monoalkyl-carbonate}$	c_{NaOH}	$c_{alcohol}$	Min	% Monoalkyl-carbonate left	k_{mono}
Tetrahydro-furfuryl alcohol	0.012	0.10	1.00	0	100	—
				9	90.0	(0.00510)
				21	84.2	0.00356
				30	75.5	0.00407
				50	60.8	0.00432
				88	46.6	0.00376
				147	27.6	0.00381
				204	16.7	0.00381
				259	11.4	0.00364
					Mean	0.0039
	0.007	0.10	0.50	0	100	—
				7	91.5	0.00553
				16	83.9	0.00478
				35	63.8	0.00559
				53	51.5	0.00544
				85	33.4	0.00560
				120	21.6	0.00554
				151	15.2	0.00542
				186	13.2	0.00474
					Mean	0.0053
Furfuryl alcohol	0.017	0.10	1.00	0	100	—
				5	86.7	(0.0124)
				12	74.9	0.0105
				18	66.7	0.0098
				22	57.9	0.0108
				28	52.0	0.0101
				39	44.1	0.0091
				58	25.9	0.0101
				107	10.2	0.0093
					Mean	0.010
	0.013	0.10	0.50	0	100	—
				6	75.3	0.0205
				12	56.6	0.0206
				17	45.8	0.0200
				28	31.9	0.0177
				37	23.5	0.0170
				51	10.1	0.0195
				80	5.25	0.0160
					Mean	0.019

k_{mono} may be calculated at $pa_H > 10$ by means of the following expression

$$k_{mono} = \frac{k' \cdot K_{Eq} \frac{K_{H_2O}}{K_{CO_2}}}{1 + k' \cdot \frac{c_{alcohol}}{k_{CO_2} \cdot OH^-}}$$

the values of K_{H_2O} and K_{CO_2} being $10^{-14.93}$ and $10^{-6.65}$, respectively.

Upon introduction of the constants the equation for tetrahydrofurfuryl alcohol is:

$$k_{mono} = \frac{0.0074}{1 + 1.3 \cdot c_{alcohol}}$$

and k_{mono} in 1 M and 0.5 M solutions of alcohol, $pa_H > 10$, will then be calculated to 0.0032 and 0.0045, respectively.

For furfuryl alcohol is:

$$k_{mono} = \frac{0.054}{1 + 4.9 \cdot c_{alcohol}}$$

and k_{mono} in 1 M and 0.5 M solution of alcohol, $pa_H > 10$, will be calculated to 0.0092 and 0.016, respectively.

The experimental and calculated values agree rather well.

REFERENCE

1. Jensen, A., Jørgensen, E. and Faurholt, C. *Acta Chem. Scand.* **6** (1952) 1036.

Received January 14, 1958.

ACTA CHEMICA SCANDINAVICA 12 (1958) 802—806

Soladulcamarine, the Alkaloidal Glycoside of *Solanum dulcamara*

H. BAGGESGAARD RASMUSSEN and PER M. BOLL

Department of Organic Chemistry, The Royal Danish School of Pharmacy, Copenhagen, Denmark

Extraction of the fresh leaves and stems of *Solanum dulcamara* led to the iolation of an alkaloidal glycoside m. p. 193—197°C (decomp.), which on hydrolysis yielded 1 mole of D-glucose, 1 mole of L-arabinose, 2 moles of L-rhamnose and an unsaturated alkaloidal aglycone m. p. 220—222°C. The names soladulcamarine and soladulcamaridine are suggested for the glycoside and its aglycone, respectively. Soladulcamaridine is tentatively assigned a solanidane structure.

Recently J. Tuzson [1], P. Tuzson and Kiss [2], and McKee [3] by paper chromatography have shown that the alkaloids in *Solanum dulcamara* and *Solanum turberosum* are not identical. P. Tuzson and Kiss[2] isolated from the latter plant, after acid hydrolysis, a steroidal saturated alkaloidal aglycone. They proposed the name soladulcidine for the aglycone, a name already in use to identify a bitter principle occurring in the same plant [4].

Schreiber [4] by paper chromatography found three alkaloidal glycosides and has shown all three glycosides to have soladulcidine as aglycone. Schreiber gives the empirical formula as $C_{27}H_{43}O_2N$ (m.p. 206.5° and $[\alpha]_D = -52.6°$ ($CHCl_3$)). Soladulcidine was found to be identical with 5α-solasodanol-(3β).

Our investigation has by paper chromatography indicated two alkaloidal glycosides to be present in *S. dulcamara*. The one of them is considered as the main alkaloid and has been isolated. It is neither solanine nor another known alkaloid, but a new alkaloidal glycoside for which we suggest the name *soladulcamarine*. The aglycone, also a new compound, has been designated *soladulcamaridine*.

The plant material used in this investigation consisted of naturally occurring plants. Only the tops were used. After crushing, the tops were extracted with 5 % acetic acid and the alkaloid together with inorganic salts were precipitated with ammonia-water. The yield was 0.3 g of crude alkaloid per kg of fresh material.

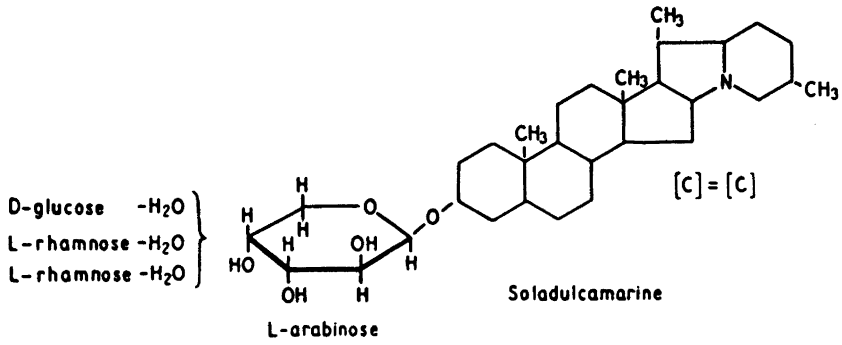

The alkaloid mixture was to some extent purified by column chromatography. Unfortunately, recrystallization of the alkaloid from various solvents was not possible as the alkaloid separated out as a gel in every attempt, but a chromatographically pure semi-crystalline alkaloidal glycoside was obtained through fractional crystallization.

By acid hydrolysis the glycoside was found to consist of an aglycone portion, soladulcamaridine, and a tetrasaccharide moiety composed of D-glucose, L-arabinose and two D-rhamnose units. The isolation from the plant genus *Solanum* of an alkaloidal glycoside containing L-arabinose has not been reported before. Soladulcamarine does not reduce Fehling's solution or react with phenylhydrazin. These results indicate that no free aldehyde groups are present and that the monosaccharides are united through their potential aldehyde groups. Oxidation of soladulcamarine with periodic acid revealed after hydrolysis and paper chromatography only L-arabinose. Since periodic acid oxidizes vicinal hydroxyl groups and the L-arabinose after oxidation still is attached to the alkaloidal aglycone, it can be concluded that the glycoside besides being an arabinoside has the hydroxyl groups of arabinose linked through glycosidic linkages to the monosaccharides in such a manner that arabinose has no vicinal hydroxyl groups. Soladulcamarine is not hydrolyzed when treated with 0.01 N hydrochloric acid for 10 h as shown by the lack of reducing power towards Fehling's solution. From this it is assumed that all the sugars are pyranose [5]. All *Solanum* alkaloids so far isolated have been shown to have the hydroxyl group of the aglycone connected to the sugar unit through a β-linkage. From biogenetic reasons it is assumed that an identical linkage also is present in soladulcamarine. The glycoside was found to have the empirical formula $C_{50}H_{81}O_{18}N$, 5 H_2O (M 1 074) and the equivalent weight was determined to 1 087 (titration in glacial acetic acid with perchloric acid) and 1 165 (acid/base titration). The aglycone has the empirical formula $C_{27}H_{43}ON$, 1 1/2 H_2O (M 425) and the equivalent weight was determined to 438.

The basicity of soladulcamarine and soladulcamaridine was determined in term of their pK_b-values and found to be 5.57 and 5.78, respectively. Bloom and Briggs [6] have determined the basicity of solanidine and solasodine and their derivatives. They found that the pK_b of solasodine and solasonine were

6.30 and 6.26, respectively, and of solanidine 5.38. They concluded that the weak basicity of solasodine was due to the inductive effect of the ether-oxygen atom attached to the same carbon atom as the nitrogen atom, *i.e.*

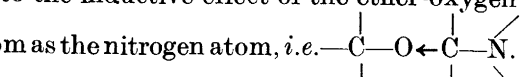

The pK_b values for soladulcamarine and soladulcamaridine seem to be closer to the values for solanidine.

All alkaloids isolated from the plant genus *Solanum* have either been solanidane or solasodane derivatives. The results discussed above indicate that soladulcamaridine probably is a solanidane derivative. The aglycone gave positive Alberti and Liebermann-Burchard [8] reactions for a steroid-double bond, but a negative reaction for conjugated double bonds or α,β-unsaturated alcohols [9]. The aglycone gave no precipitate with digitonin and can, therefore, not have a 3β-hydroxyl group. The colour reactions given by the aglycone were not similar to the colours given by solanidine, but closer to the colours given by solasodine.

It was not possible to prepare a picrate of the aglycone, which is in accordance with the difficulty often met in preparing picrates of tertiary amines.

Stipes dulcamara which is an old drug and consists of the stems of *Solanum dulcamara* was examined for alkaloids. The stems gave an extremely small yield of an alkaloidal glycoside. By paper chromatography it was found identical with soladulcamarine. The small yield is in conformity with the fact that the stems mostly consist of xylem and very little green bark.

EXPERIMENTAL

The melting points are corrected and have been determined with the hot stage microscope essentially according to Kofler.

Isolation of the glycoside. The plant material was collected at Lyngby Aamose near Copenhagen. 7 kg of the fresh tops were crushed in a mill and immediately extracted with 5 % acetic acid using the isolation procedure described by Kuhn and Löw [10]. The yield of crude alkaloidal glycoside was 2.2 g. Paper chromatography with following developing solvents: The upper phase of ethyl acetate — glacial acetic acid — water (3:1:3) to which is added 15 ml of 85 % ethanol per 160 ml of upper phase [10], and ethanol — N hydrochloric acid — water (50:2:48) [11] revealed two alkaloids when the spots were developed with Dragendorff reagent. The alkaloid with highest R_F-value was only present to a small extent.

The glycoside mixture formed a gel when attempted to dissolve it in water-saturated 1-butanol. Therefore, a solution in methanol was chromatographed on neutral aluminium oxide (Alcoa) and eluted with the same solvent. In this manner a certain degree of purification was obtained.

It was not possible to recrystallize the glycoside from various solvents due to formation of a gel. The solvents used both as pure solvents and in aqueous solution to attempt recrystallization were: 1-butanol, 1-propanol, ethanol, dioxan, acetone and ethyl ether.

Fractional recrystallization, on the other hand, was more successful. Addition of acetone to a concentrated methanol solution of the glycoside mixture produced an amorphous precipitate which adsorbed the green coloured impurities. In this manner 1.55 g of material was obtained. Addition of petroleum ether to the mother liquor gave 115 mg of faint yellow coloured material. This latter material was redissolved in a small volume of methanol and gave by repeated fractional recrystallization 20 mg of semi-crystalline glycoside. Repeated fractionation of crude glycoside gave some more semi-crystalline glycoside. M. p. 193—197°C (decomp.) (Found: C 55.80, 55.95; H 8.52, 8.79; H_2O 8.73. Calc. for $C_{50}H_{81}O_{18}N$, 5 H_2O: C 55.91; H 8.54; H_2O 8.40).

1 kg of commercially available *Stipes dulcamara* was extracted in the same manner as above. About 2 mg of crude glycoside mixture was obtained. By paper chromatography it was found to be identical with soladulcamarine.

The equivalent weight of the pure glycoside was determined by potentiometric titration of the glycoside dissolved in glacial acetic acid with 0.02 N perchloric acid (Found 1 101, 1 087. Calc. 1 074). The equivalent weight determined by dissolving the glycoside in a known excess of 0.01 N hydrochloric acid and back-titrating with 0.01 N sodium hydroxide was found to be 1 165 and 1 180. The glycoside gave a positive α-naphthol reaction for carbohydrates and a positive orcinol test (Bial reaction) for pentoses [7].

Isolation of the aglycone, soladulcamaridine. 0.5 g of soladulcamarine was refluxed with 25 ml N hydrochloric acid for 2 h. During the hydrolysis the hydrochloride of the aglycone began to precipitate. The hydrochloride was collected by filtration, dissolved in 80 % methanol and concentrated ammonia-water was added to precipitate the free alkaloid. 255 mg alkaloid was obtained. For further purification the alkaloid was dissolved in a small volume of benzene and chromatographed on a column of neutral aluminium oxide (13 × 1.6 cm). Benzene-methanol (9:1) was used as eluant and 30 ml fractions were collected. Fraction III contained the alkaloid and none of the other fractions gave any residue after evaporation of the solvent. The alkaloid was recrystallized from acetone and gave needle-shaped crystals melting at 220–222°C, $[\alpha]_D^{23}$ −78.4°, $[\alpha]_{Hg}^{23}$ −111° (methanol, c = 0.428). Before analysis the compound was dried at 105°C for 8 h. (Found: C 76.19, 76.24; H 10.34, 10.12. Calc. for $C_{27}H_{43}ON$, 1 1/2 H_2O: C 76.36; H 10.92.)

The equivalent weight was determined to 438 and 442 by dissolving the aglycone in a known excess of 0.01 N hydrochloric acid and backtitrating with 0.01 N sodium hydroxide. Soladulcamaridine dissolved in methanol does not give a precipitate with an ethanolic solution of digitonin. The compound gives positive Alberti [7] and Liebermann-Burchard reactions[9] for steroid double bonds, but no Rosenheim reaction [8] for conjugated double bonds or α,β-unsaturated alcohols.

Identification of the carbohydrates. The acidic mother-liquor remaining after precipitation of the aglycone from the hydrolysate as described above was treated with Amberlite IR-4B. Aliquots were chromatographed on Whatman No. 1 paper at 23°C. Aniline hydrogen phthalate was used as colour-developing reagent.

The solvent 1-butanol — ethanol — water (8:1:2) revealed spots with the following R_F-values: 0.43 L-rhamnose, 0.21 L-arabinose, 0.15 D-glucose.

The solvent 2,6-lutidine — water (65:35) revealed spots with R_F-values: 0.68 L-rhamnose, 0.54 L-arabinose, 0.51 D-glucose.

The results were controlled by chromatographing pure monosaccharides alone and in mixtures alongside the unknown monosaccharides.

Quantitative determination of the carbohydrates. Furthermore, the amounts of individual monosaccharides were determined quantitatively utilizing the ability of the sugars to reduce 2,3,5-triphenyltetrazolium chloride to red formazan. 2.4 mg of glycoside was refluxed in 0.5 ml N hydrochloric acid for 2 h (sealed tube).* Aliquots containing 98 μg hydrolysed glycoside were chromatographed and the amount of monosaccharide in each spot determined by the method of Fischer and Dörfel [12].

The results are given in Table 1.

Table 1. Quantitative determination of monosaccharides in 98 μg aliquots of hydrolysed soladulcamarine.

	μg	mole × 10^8	μg	mole × 10^8
L-Glucose	16	8.9	15.5	8.6
D-Rhamnose	28	17	30.5	19
L-Arabinose	12	8.0	9.0	6.0

* It was found unnecessary to neutralise the hydrolysate with Amberlite IR-4B before chromatographing. If the paper was well dried at room temparature after application of the solution to the paper no change in the R_F-values was observed.

The optical rotation of the carbohydrate mixture. 0.32 g of soladulcamarine was hydrolysed by refluxing with 20 ml N sulfuric acid for 2 h. The hydrolyzate was neutralized with barium carbonate and allowed to stand overnight. The precipitate was removed by filtration and carefully washed with water. The filtrate was concentrated to 10.0 ml *in vacuo*. The rotation found was $[\alpha]_D^{23}$ + 41.8° on the assumption that 1 074 g of glycoside gave 654 g of carbohydrate. For a mixture of 1 mole of D-glucose, 1 mole of L-arabinose and 2 moles of L-rhamnose the optical rotation can be calculated to $[\alpha]_{Hg}^{25}$ +43.4. The carbohydrate content of the hydrolysate was determined after the method of Rupp and Lehmann [13]. 585 g of carbohydrate was found, calculated as glucose per mole of glycoside. The theoretical value is 654 g of "glucose".

Periodate-oxidation of the glycoside (Kuhn and Löw [10]). 20 mg of soladulcamarine was allowed to stand for three days at room temperature with 4 ml 0.05 N acetic acid and 2 ml 0.25 N potassium periodate. After addition of 1 ml ethylene glycol the solution was heated shortly, made alkaline with solid sodium carbonate and then heated again to 50—60°C. The precipitate was collected by centrifugation, washed with water and then boiled with 2 ml N sulfuric acid. The sulfuric acid was neutralized with barium carbonate and the sugar solution separated from barium sulfate by filtration. After evaporation of the water the residue was chromatographed. Only L-arabinose was detected.

Colour reactions of soladulcamaridine [14]. 2—3 mg of soladulcamaridine and 2—3 mg of the following aldehydes were dissolved in about 1 ml of acetic acid to which 1 ml of conc. sulphuric acid was then carefully added. By mixing and heating following colour changes did develop:

p-*hydroxybenzaldehyde:* red/violet dichroic-purple-blue-violet/brown dichroic.
anisaldehyde: red/green dichroic — violet/green dichroic — blueviolet.
vanillin: green — blue — violet.
resorcinol: yellow — brown — olive — blue — violet — red/violet dichroic — fuchsin — cherry red — cherry red / chocolate fluorescent.

Elementary analysis are by Mr. P. Hansen, Universitetets kemiske laboratorium, Copenhagen. This work is part of investigations supported by *Statens almindelige Videnskabsfond (The Danish State Research Foundation)*.

REFERENCES

1. Tuzson, J. *Naturwiss.* **43** (1956) 198.
2. Tuzson, P. and Kiss, Z. *Acta Chim. Acad. Sci. Hung.* **12** (1957) 31.
3. McKee, R. K. *Nature* **179** (1957) 313.
4. Schreiber, K. *Personal communication.*
5. Haworth, W. N. *Ber.* **65** (1932) 50.
6. Bloom, H. and Briggs, L. H. *J. Chem. Soc.* **1952** 3591.
7. Schreiber, K. *Die Pharmazie* **10** (1955) 379.
8. Fieser, L. F. *Experiments in Organic Chemistry*, Heath & Co, Boston 1955, p. 69.
9. Rosenheim, O. *Biochem. J.* **25** (1931) 74.
10. Kuhn, R. and Löw, I. *Ber.* **88** (1955) 289.
11. Boll, P. M. *Isolation, Identification, and Chemistry of the Antibacterial alkaloid Solanocapsine*, Thesis, Michigan State, 1957, p. 58.
12. Fischer, F. G. and Dörfel, H. *Z. physiol. Chem. Hoppe-Seyler* **297** (1954) 164.
13. Rupp, E. and Lehmann, F. *Arch. Pharm.* **247** (1909) 516.
14. Briggs, L. H., Newhold, R. P. and Stace, N. E. *J. Chem. Soc.* **1942** 3.

Received January 24, 1958.

ACTA CHEMICA SCANDINAVICA 12 (1958) 807—813

The Photoinduced Oxidation of 2-Propanol by Acid Chromate

ULRIK KLÄNING

Laboratoriet for Fotokemi, Fotografi og Reproduktionsteknik, Polyteknisk Læreanstalt, Copenhagen, Denmark

The quantum yield of the photoinduced oxidation of 2-propanol by acid chromate depends on the concentration of 2-propanol, the acidity, the intensity and wave length of light and the concentration of acid chromate. At low intensity of light and high acidities the quantum yield approaches a value twice that obtained at high intensities of light and low acidities. The experimental results fit a mechanism in which chromium compounds in the oxidation states +6, +5, +4, +3 and +2 are involved. The photochemically active compound is shown to be an ester of acid chromate with 2-propanol. Furthermore the influence of the solvent on the quantum yield is discussed.

In slightly acid aqueous solutions the oxidation of aliphatic alcohols by chromic acid proceeds at negligible rate. When irradiated by ultraviolet light the oxidation takes place. Bowen *et al.*[1] have investigated these photoinduced oxidations. Their results may be summarized as follows. With the alcohols in excess the reactions are stoichiometrically pure. The quantum yields are small, not exceeding two in the pure alcohol. The oxidation therefore does not seem to be a chain process. Further Bowen and Chatwin [1] have shown, that of the two ions present in a dilute aqueous solution, $HCrO_4^-$ and $Cr_2O_7^{--}$, only $HCrO_4^-$ is photochemically active. Comparisons between the quantum yields obtained by oxidation of different alcohols, led to the conclusion, that only "alcoholated" forms of the acid chromate ions are photochemically active. From the relationship between quantum yield and acidity Bowen and Chatwin proposed the mechanism:

$$X \cdot HCrO_4^- + h\nu \rightarrow \text{aldehyde or ketone} + Cr^{IV}$$

$$Cr^{IV} + Cr^{IV} \rightarrow Cr^{V} + Cr^{III}$$

$$Cr^{IV} + Cr^{VI} \xrightarrow{H^+} 2Cr^{V}$$

$$Cr^{V} + \text{alcohol} \rightarrow \text{aldehyde or ketone} + Cr^{III}$$

where X stands for an alcohol and Cr^{VI}, Cr^{V}, Cr^{IV} and Cr^{III} represent chromium compounds in the oxidation states +6, +5, +4 and +3, respectively. Preliminary experiments made by the present author have shown that oxygen interferes with the photoinduced oxidation of 2-propanol by acid chromate. As Bowen and Chatwin have not taken the precaution to remove oxygen a reinvestigation has been undertaken.

Westheimer *et al.*[2,3] have investigated the kinetics of the oxidation of 2-propanol to acetone by acid chromate ions in aqueous solution, and have shown that the reaction proceeds by the way of the chromic acid ester, $(CH_3)_2CHOCrO_3H$.

The photochemical experiments reported here were made at low acidities ($<2 \times 10^{-2}$ M), at which the dark process proceeds at negligible rate. It may therefore be concluded that at low acidities the above mentioned ester is completely ionized to $(CH_3)_2CHOCrO_3^-$, the stability constant and spectrum of which have been determined by the present author [4,5] (in Ref.[4] no assumption concerning the nature of the complex of 2-propanol with acid chromate has been made and the formula has been written $CH_3CHOHCH_3 \cdot HCrO_4^-$). Our experiments show that the ester $(CH_3)_2CHOCrO_3^-$ is the only photochemically active ion as suggested by Bowen and Chatwin, but it has not proved possible to verify the mechanism proposed by these authors. The experimental data agreed with the following mechanism:

a) $CH_3CHOHCH_3 + HCrO_4^- = (CH_3)_2CHOCrO_3^- + H_2O$ equil.const.[5] $K = 8.3$

b) $(CH_3)_2CHOCrO_3^- + h\nu \rightarrow (CH_3)_2CHO\overset{*}{C}rO_3^-$ absorption

c) $(CH_3)_2CHO\overset{*}{C}rO_3^- + \text{solvent} \rightarrow (CH_3)_2CHOCrO_3^-$ deactivation

d) $(CH_3)_2CHO\overset{*}{C}rO_3^- \rightarrow Cr^{IV} + CH_3COCH_3$

1) $CH_3CHOHCH_3 + Cr^{IV} \rightarrow CH_3COCH_3 + Cr^{II}$ k_1

2) $Cr^{II} + Cr^{IV} \rightarrow 2Cr^{III}$ k_2

3) $HCrO_4^- + H^+ = H_2CrO_4$ equil.const. K_3

4) $Cr^{II} + H_2CrO_4 \rightarrow Cr^{V} + Cr^{III}$ k_4

5) $(CH_3)_2CHOCrO_3^- + H^+ = (CH_3)_2CHOCrO_3H$ equil.const. K_5

6) $\left.\begin{array}{l} Cr^{II} + (CH_3)_2CHOCrO_3H \rightarrow Cr^{V} + Cr^{III} + CH_3CHOHCH_3 \\ Cr^{II} + (CH_3)_2CHOCrO_3H \rightarrow 2Cr^{III} + CH_3COCH_3 \end{array}\right\} k_6$

7) $Cr^{V} + CH_3CHOHCH_3 \rightarrow Cr^{III} + CH_3COCH_3$.

In all experiments the total concentration of chromic acid was kept small enough to permit the neglection of the concentration of dichromate, and so small that stirring secured a uniform concentration of intermediates throughout the irradiated solutions. Denoting the quantum yield for formation of Cr^{IV} by Φ° we may therefore derive the following expression for the total quantum yield Φ, assuming a steady state concentration of the intermediates:

$$\Phi = \frac{1}{I_0}\left(-\frac{dc_1}{dt}\right) = \Phi^\circ - \left(\tfrac{1}{2}\Phi^\circ + c_a \cdot c_1 \cdot c_{H^+} \cdot \frac{1}{I_0} \cdot \frac{k_1 k^*}{2k_2}\right) \quad (8)$$

$$+\left(\tfrac{1}{2}\Phi^\circ + c_a \cdot c_1 \cdot c_{H^+} \cdot \frac{1}{I_0} \cdot \frac{k_1 k^*}{2k_2}\right)\left[1 + \frac{c_a \cdot \Phi^\circ \cdot c_1 \cdot c_{H^+} \cdot \frac{1}{I_0} \cdot \frac{k_1 k^*}{k_2}}{\left(\tfrac{1}{2}\Phi^\circ + \frac{k_1 k^*}{2k_2} \cdot c_a \cdot c_1 \cdot c_{H^+} \cdot \frac{1}{I_0}\right)^2}\right]^{\frac{1}{2}}$$

where c_a and c_1 are the alcohol concentration and the total concentration of acid chromate. I_0 is the intensity of the absorbed light. k^* is given by

$$k^* = K_3 k_4 + \frac{(K_5 k_6 - K_3 k_4) K \cdot c_a}{c_w + K \cdot c_a} \quad (9)$$

where c_w is the concentration of water.

The equation (8) gives that $\Phi^\circ < \Phi < 2\Phi^\circ$, and we note that Φ approaches $2\Phi^\circ$ at high values of $c_{H^+} \cdot c_a \cdot c_1/I_0$.

At 25°C Φ was measured at 366 mμ and at various light intensities, acidities, and alcohol concentrations. From (8), written in the form

$$\frac{k_1 k^*}{k_2} = \frac{\Phi^2 - \Phi \cdot \Phi^\circ}{(2\Phi^\circ - \Phi) \cdot c_1 \cdot c_{H^+} \cdot c_a \cdot \frac{1}{I_0}} \quad (10)$$

$k_1 k^*/k_2$ and Φ° were found by trial and error at each alcohol concentration. Tables 1, 2, and 3 show the measurements at $c_a = 1$ M, 2 M, and 3 M. The accuracy of the determination of $k_1 k^*/k_2$ is low as a change of 25 % in $c_{H^+} \cdot c_a \cdot c_1/I_0$ give a change of not more than 4—5 % in Φ, which is the experimental error in determining Φ. The reaction, therefore, was followed to a degree of advancement of 0.3, and the values of I_0, c_{H^+}, c_1, and c_a used in formula (10) to calculate Φ° and $k_1 k^*/k_2$ are the values at a degree of advancement of 0.15. From the three values of $k_1 k^*/k_2$ found at $c_a = 1$ M, 2 M, and 3 M $K_3 k_4 k_1/k_2$ and $K_5 k_6 k_1/k_2$ were found to be 13 litre^2/mole^2 · min and 55 litre^2/mole^2 · min, respectively (Fig. 1).

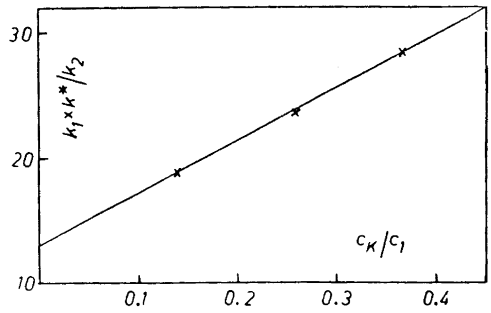

Fig. 1. $k_1 k^*/k_2 = K_3 k_4 k_1/k_2 + (K_5 k_6 k_1/k_2 - K_3 k_4 k_1/k_2) K \cdot c_a/c_w + K \cdot c_a$ (eqn. 9) plotted against the relative concentration of the complex: $c_K/c_1 = K \cdot c_a/c_w + K \cdot c_a$.

Table 1. Measured and calculated values of Φ_{366}.

$\left(\frac{k^*k_1}{k_2}\right)$ mean $= 18.8 \frac{\text{(litre)}^2}{\text{(mole)}^2 \text{ min.}}$, $c_a = 1.00$ M, $c_1 = 4.25 \times 10^{-5}$ M, $I_0 = 1.23 \times 10^{-5} \frac{\text{Einstein}}{\text{litre. min,}}$, $\Phi^\circ = 0.0385 \frac{\text{mole}}{\text{Einstein}}$

c_{H^+} mole/litre	$\frac{k^*k_1}{k_2}$ (litre)²/(mole)² min.	Φ found mole/Einstein.	Φ calc. mole/Einstein
3.15×10^{-4}	16.0	0.0480	0.0497
6.6×10^{-4}	22.0	0.0567	0.0553
1.35×10^{-3}	16.3	0.0600	0.0612
3.42×10^{-3}	21.9	0.0689	0.0679
6.9×10^{-3}	17.6	0.0714	0.0715
1.38×10^{-2}	—	0.0751	0.0741

Tables 1, 2, and 3 show that k_1k^*/k_2 at constant concentration of alcohol does not vary systematically with acidity and with light intensity, thus indicating the correctness of the proposed mechanism. The variation of k_1k^*/k_2 with the alcohol concentration is interpreted as being due to the reactions 5) and 6). Introduction of 5) and 6) in the reaction scheme is very natural, remembering that the concentration of the ester is rather high (at $c_a = 3$ M equal to 36 % of total concentration of acid chromate). The two equilibria 3) and 5) have been introduced as the oxidation agent in acid solution in the dark process seems to be the undissociated chromic acid [6]. The rates of 4) and 6) are proportional to c_{H^+} as both the acid chromate ion and the ester are very weak bases [4, 7].

Table 2. Measured and calculated values of Φ_{366}.

$\left(\frac{k^*k_1}{k_2}\right)$ mean $= 23.5 \frac{\text{(litre)}^2}{\text{(mole)}^2 \cdot \text{min.}}$, $c_a = 2.00$ M, $c_1 = 4.25 \times 10^{-5}$ M, $\Phi^\circ = 0.106 \frac{\text{mole}}{\text{Einstein}}$, $I_0 = 1.25 \times 10^{-5} \frac{\text{Einstein}}{\text{litre. min.}}$

c_{H^+} mole/litre	$\frac{k^*k_1}{k_2}$ (litre)²/(mole)² min.	Φ found mole/Einstein	Φ calc. mole/Einstein
3.15×10^{-4}	23.7	0.135	0.134
6.6×10^{-4}	21.7	0.148	0.149
1.35×10^{-3}	24.2	0.166	0.165
3.42×10^{-3}	23.8	0.185	0.185
6.9×10^{-3}	24.0	0.196	0.195
1.38×10^{-2}	—	0.206	0.203

Table 3. Measured and calculated values of Φ_{366}.

$\left(\frac{k_1 k^*}{k_2}\right)_{\text{mean}} = 28.5 \frac{(\text{litre})^2}{(\text{mole})^2\,\text{min.}}$, $c_a = 3.00$ M, $c_1 = 4.25 \times 10^{-5}$ M, $\Phi^\circ = 0.207$

I_0 Einstein / litre min.	c_{H^+} mole / litre	$\frac{k^* k_1}{k_2}$ (litre)² / (mole)² min.	Φ found mole / Einstein	Φ calc. mole / Einstein
1.29×10^{-5}	1.08×10^{-4}	29.2	0.232	0.231
1.29×10^{-5}	6.6×10^{-4}	26.5	0.285	0.288
1.29×10^{-5}	2.04×10^{-3}	28.3	0.337	0.337
1.29×10^{-5}	3.42×10^{-3}	27.1	0.356	0.358
1.29×10^{-5}	6.9×10^{-3}	30.6	0.382	0.380
1.29×10^{-5}	1.38×10^{-2}	—	0.388	0.394
4.38×10^{-6}	1.08×10^{-4}	22.7	0.253	0.260
2.37×10^{-6}	1.08×10^{-4}	33.9	0.290	0.284
5.25×10^{-7}	1.08×10^{-4}	27.0	0.346	0.349
* 1.96×10^{-7}	1.26×10^{-4}	31.2	0.389	0.388

* $c_1 = 4.70 \times 10^{-5}$ M.

The fraction of the absorbed light I_0, which is absorbed by the ester is

$$\varphi = \frac{\varepsilon_k \cdot c_a \cdot K}{\varepsilon_k \cdot c_a \cdot K + \varepsilon_1 \cdot c_w} \tag{11}$$

where ε_k and ε_1 are the extinction coefficients of the ester and of the acid chromate ion, respectively. If the ester is the only photochemically active component we may expect that the following relation for the ratio between $\Phi^\circ(\lambda_1)$ and $\Phi^\circ(\lambda_2)$ at the two wave lengths λ_1 and λ_2 will be valid at constant alcohol concentration:

Table 4. Values of $\Phi^\circ(\lambda)$ and $\varphi(\lambda)$ at the wave lengths 313 mμ, 334 mμ, and 366 mμ.

λ mμ	c_a mole / litre	I_0 Einstein / litre.min	c_{H^+} mole / litre	Φ mole / Einstein	Φ° mole / Einstein	φ
313	2.00	2.06×10^{-6}	3.42×10^{-3}	0.175	0.080	0.323
	3.00	2.06×10^{-6}	3.42×10^{-3}	0.337	0.175	0.438
334	2.00	2.19×10^{-6}	1.42×10^{-3}	0.145	0.076	0.249
	3.00	2.19×10^{-6}	1.35×10^{-3}	0.276	0.145	0.352
366	2.00	1.27×10^{-5}	6.9×10^{-3}	0.195	0.106	0.368
	3.00	1.29×10^{-5}	6.9×10^{-3}	0.380	0.207	0.490

Table 5. φ_{366} and Φ°_{366} at varying concentration c_a of 2-propanol, $c_1 = 4.25 \times 10^{-5}$ M, $c_{H+} = 6.9 \times 10^{-3}$ M.

c_a mole/litre	I_0 Einstein/litre.min	φ_{366}	Φ_{366} mole/Einstein	Φ°_{366} mole/Einstein
0.25	1.19×10^{-5}	0.060	0.0123	0.0065
0.50	1.20×10^{-5}	0.116	0.0311	0.0167
1.00	1.22×10^{-5}	0.214	0.0715	0.0385
1.50	1.245×10^{-5}	0.298	0.135	0.073
2.00	1.27×10^{-5}	0.368	0.195	0.106
2.50	1.285×10^{-5}	0.434	0.282	0.153
3.00	1.29×10^{-5}	0.490	0.380	0.207

$$\frac{\Phi^{\circ}(\lambda_1)}{\Phi^{\circ}(\lambda_2)} = \frac{\varphi(\lambda_1)}{\varphi(\lambda_2)} \tag{12}$$

$\varphi(\lambda)$ may be calculated as K and the absorption spectra of the ester and of the acid chromate ion are known [5]. Table 4 shows φ_{313}, φ_{334}, φ_{366}, Φ°_{313}, Φ°_{334}, and Φ°_{366} at the alcohol concentrations 2 M and 3 M. It may be noted that the agreement between $\frac{\varphi(\lambda_1)}{\varphi(\lambda_2)}$ and $\frac{\Phi^{\circ}(\lambda_1)}{\Phi^{\circ}(\lambda_2)}$ is rather good, proving that the ester is the only photochemically active ion in the solutions.

Table 5 shows Φ°_{366} at various concentrations. It may be noted that Φ°_{366} is not directly proportional to φ_{366}, but $\Phi^{\circ}_{366}/\varphi_{366}$ increases linear with the alcohol concentration indicating that the probability for the excited ester to decompose to Cr^{IV} and acetone increases if one of the nearest neighbours to the excited ester is an alcohol molecule (Fig. 2). To get a complete picture

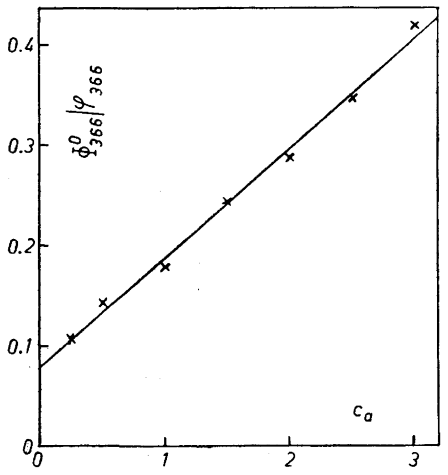

Fig. 2. $\Phi^{\circ}_{366}/\varphi_{366}$ plotted against c_a.

of the mechanism of deactivation the photoinduced oxidation of several alcohols would have to be investigated in a larger concentration interval.

EXPERIMENTAL

The light source was a mercury lamp (Osram HQA 1000, the outer bulb removed, operated on d—c with an adjustable ballast resistance). The light was made parallel with quartz lenses. The optical path of the quartz cell was 10 cm. The cell was furnished with a magnetic stirrer and was immersed in a 25°C thermostated water bath provided with windows of Uviol glass. The solutions to be irradiated were freed from oxygen by the bubbling through of nitrogen, deoxygenated over copper wire at 500°C. The light intensity was determined by means of the uranyl oxalate actinometer [8]. The actinometer solution was irradiated in the same cell as used in all experiments. The mercury lines 365—366 mμ, 334 mμ, and 312.6—313 mμ were isolated by means of filters described by Kasha [9]. The reaction was followed by measuring the change in optical density by means of a Baldwin Photometer M.N.D. The water was redistilled in Pyrex from alkaline permanganate, 2-propanol (Shell chemically pure) was distilled in a Glinsky still (b.p. 780 mm Hg 81.5—81.7°C (uncorr)) and controlled for acetone content by measuring the optical density at 280 mμ. Perchloric acid and potassium dichromate were Mercks pro analysi.

The author's thanks are due to professor Max Møller for information and help in the work.

REFERENCES

1. Bowen, E. J. and Chatwin, J. E. *J. Chem. Soc.* **1932** 2081.
2. Holloway, F., Cohen, M. and Westheimer, F. H. *J. Am. Chem. Soc.* **75** (1951) 65.
3. Westheimer, F. H. *Chem. Revs.* **45** (1949) 419. Errata June 1950.
4. Kläning, U. *Acta Chem. Scand.* **11** (1957). 1313.
5. Kläning, U. *Acta Chem. Scand. To be published.*
6. Edwards, J. O. *Chem. Revs.* **50** (1952) 455.
7. Tong, J. Y. and King, E. U. *J. Am. Chem. Soc.* **75** (1953) 6180.
8. Noyes, W. A. and Leighton, P. A. *The Photochemistry of Gases*, Reinhold Publishing Co. New York 1941, p. 82.
9. Kasha, M. *J. Opt. Soc. Am.* **38** (1948) 929.

Received September 12, 1957.

ACTA CHEMICA SCANDINAVICA 12 (1958) 814—822

Gas-Liquid Chromatographic Determination of the Fatty Acid Composition in Oil from Seeds of *Ulmus*

IB SØRENSEN and P. SØLTOFT

Laboratoriet for almen teknisk Kemi, Danmarks tekniske Højskole, Copenhagen, Denmark

By means of low-pressure chromatography methyl esters of the fatty acids in seeds from various species and varieties of the genus *Ulmus* have been determined. The statements in the literature according to which elm seed oil has a surprisingly high content of C_{10} fatty acids has been confirmed.

Gas-liquid chromatography was introduced in 1952 by James and Martin [1] and used for instance for the separation of volatile fatty acids with up to 11 carbon atoms on a column with Celite impregnated with silicon fluid in which 10 % stearic acid has been dissolved and using nitrogen as carrier gas. Later James and Martin [2] extended the applicability of the method to fatty acids with up to 18 carbon atoms, separating the methyl esters on a Celite column impregnated with Apiezon vacuum stopcock grease at 197°C. Cropper and Heywood [3] state that they are able to separate fatty acids with up to 22 carbon atoms as methyl esters at 230°C and a pressure of 20 mm Hg at the column outlet. Their column was packed with Celite impregnated with Dow Corning silicone grease and the carrier gas used was nitrogen. However, the pressure drop along a Celite column is great, and Cropper and Heywood [4] have therefore proposed the use of sodium chloride crystals to obtain a reduction of the pressure drop to one twentieth of that of the Celite column.

Since February 1955 work on gas-liquid chromatography has been in progress in »Laboratoriet for almen teknisk Kemi» with a view to the development of methods for quantitative analysis of mixtures of methyl esters of fatty acids. In the present article an account will be given of the experience gained with regard to suitable equipment, and the method is illustrated through an examination of oil from seeds of the genus *Ulmus*.

EQUIPMENT

Column. The chromatographic column (Fig. 1) is made up of four stainless steel tubes, each 1 meter long and secured by brazing to a top and a bottom flange. The bore of the tubes is 8 mm. The bottom flange is closed by means of a plate and a lead gasket by

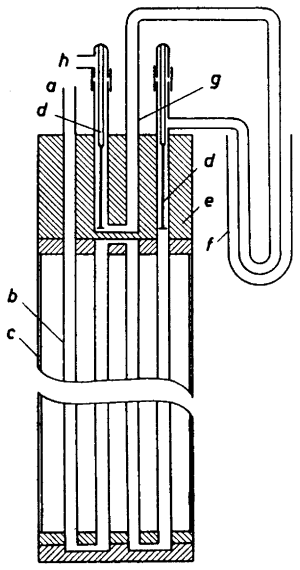

Fig. 1. Chromatographic column. a. Nitrogen inlet tube, in which the ampoule breaker is placed. b. Column tube. c. Furnace tube for heating of the column. d. Catharometer wire support. e. Catharometer block. f. Cold trap. g. Reheating tube. h. Nitrogen outlet.

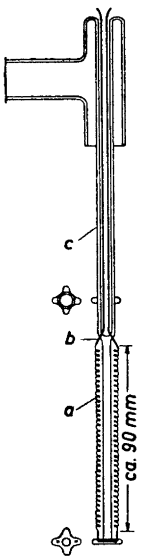

Fig. 2. Sensitive element of the catharometer. a. Platinum filament. b. Platinum wire. c. Glass support.

means of which it is possible to connect all four tubes in series to form one column (4 m long) or to connect two tubes only to form a 2 m column. The detector is secured to the top flange by means of bolts and a lead gasket.

The detector. The detector used is a catharometer prepared from a brass block with four borings lined with stainless steel tubes of the same type as those used for the column. Two of the tubes (d) in the block are used for measurements of the thermal conductivity of the gas flow from the column, both directly and after removal by condensation of entrained material in a U-tube cooled in a mixture of solid carbon dioxide and acetone. In Fig. 1 this cooling-tube is shown attached to the column. The third tube (g) in the catharometer block is used for reheating the gas flow after the cooling process. The thermal conductivity is measured by means of two electrically heated platinum filaments which form a Wheatstone bridge together with two permanent resistances. The bridge is supplied with current from a storage battery which is charged continuously during the experiment. A 5 mV recording potentiometer is connected across the Wheatstone bridge. The platinum filaments are finely coiled and attached to platinum wires sealed into a glass support (Fig. 2). The sensitivity of the catharometer has been found by calculation to be 5/16 μg/ml N_2 at 20 mm Hg and 8 ml N_2/minute both for C_8 and C_{12} methyl esters.

Ampoule breaker. The fourth tube (a) in the catharometer block is used for the admission of nitrogen to the column. It also contains an ampoule breaker in which the small spherical glass ampoule with the weighed sample of methyl esters is placed at the beginning of the run. When the appropriate temperature and nitrogen flow conditions are attained the ampoule is broken admitting the sample to the column without interruption of the nitrogen stream.

The column with its detector is surrounded by an electrically heated furnace tube, in which the temperature is kept constant by means of a regulating transformer.

The pressure at the column outlet is kept constant by means of a manostat consisting of a 1 litre reference flask placed in a water bath and connected to one side of a regulating (electric contact) pressure gauge, the other side of which is connected to the system. The pressure gauge, which contains diethylene glycol, controls a magnetic air inlet valve through an electronic relay.

The rate of flow of nitrogen, which is used as carrier gas, is controlled by a needle valve at the column inlet.

Column packing. Acetate-washed silicone grease [4] was used as the static phase in all the experiments.

As inert carrier of the static phase either (1) sodium chloride crystals, or (2) Dixon rings of stainless steel gauze [5] were used. Preparation of the column packing took place according to either of the following methods:

(1) Stir 10 g acetate-washed silicone grease with 30 ml ethyl acetate and add 200 g sodium chloride, according to Dan. Pharm., which has passed through sieve No. 30, but which is retained on sieve No. 40. Mix thoroughly, but gently, so as not to crush the crystals. Stirring frequently heat in drying cabinet at 50°C until ethyl acetate has evaporated off.

(2) Wash 126 g Dixon rings, 1/16″ × 1/16″, Griffin & George Ltd., Cat. No. B 24—420, thoroughly with ethyl acetate. Add 18 g acetate-washed silicone grease to the gauze rings which must be thoroughly moistened with ethyl acetate, and distribute the grease uniformly by protracted, but gentle, stirring. Remove ethyl acetate by heating in drying cabinet at 100°C. After this procedure the grease will form a film filling the meshes of the gauze, but leaving the interior of the rings free.

COLUMN EFFICIENCY

The efficiency of a gas-liquid chromatograph may be expressed in terms of the number of theoretical plates, TP, calculated from the expression:

$$TP = 16(x/y)^2$$

where x is the distance from the starting point of the chromatogram to the centre of the elution peak, and where y is the distance between the points of intersection between the flex tangents of the elution peak and the base line.

Table 1 and 2 list the TP values obtained in a number of experiments made partly with the NaCl-column and partly with the Dixon ring-column at different temperatures and pressures. In all the experiments the rate of flow of nitrogen was 8.0 ml/min measured at atmospheric pressure and temperature.

Direct comparison between sodium chloride columns and Dixon ring columns shows the difference between the efficiencies of the two column

Table 1.

Length of column		2 m Dx	4 m Dx	4 m Dx	2 m NaCl
Temperature, °C		200	200	240	200
Outlet pressure, mm Hg		20	20	20	20
Pressure drop, mm Hg		4.5	8	10	52
Inlet pressure, mm Hg		24.5	28	30	72
TP	Methyl laurate	48	106	41	55
	Methyl myristate	89	183	112	102
	Methyl palmitate	137	374	121	200
	Methyl stearate	205	—	226	296

Table 2.

Length of column		2 m Dx	2 m Dx	2 m Dx
Temperature, °C		200	200	180
Outlet pressure, mm Hg		20	50	20
Pressure drop, mm Hg		4.5	4	4
Inlet pressure, mm Hg		24.5	54	24
TP	Methyl caprylate	16	30	21
	Methyl caprate	23	54	35
	Methyl laurate	36	90	64

types to be small. A comparison based on identical outlet pressures shows the Dixon rings to be only slightly inferior, while, in case it was possible to base the comparison on identical inlet pressures, the result of the comparison would change considerably in favour of the Dixon rings, since the pressure drop in this case is so low as to enable a considerable increase in the outlet pressure. It will be seen that the number of theoretical plates increases with increasing pressure and column length and with decreasing temperature.

CALIBRATION OF APPARATUS

The apparatus has been standardized against pure methyl esters of fatty acids. The methyl esters used were purified by repeated fractional distillations on a spinning band column, and the purity was ascertained by gas-liquid chromatographic analysis of large quantities of the compounds.

The following procedure was used: temperature, pressure, rate of flow of nitrogen and detector potential were adjusted at specified values. It is essential to perform this adjustment accurately to obtain reproducible values of the areas of elution peaks without using an "internal standard". The areas found are plotted against quantities according to a double-logarithmic scale, resulting in a family of rectilinear curves, one curve for each methyl ester. The equation

$$\log A = n \cdot \log M + \log k,$$

where A is the area, M the quantity of material, while n and k are constants, applies, and the conversion factors may be found from the curves. By means of these factors the quantity of material corresponding to the measured area in the analysis of an unknown mixture can readily be calculated.

In the calibration a temperature of 180°C, a pressure of 20 mm Hg, and a rate of flow of nitrogen of 8.0 ml/min were used for methyl esters of C_8, C_{10}, and C_{12} fatty acids. The following equations were found:

$$\begin{aligned} &\text{for } C_8 && \log A = 0.944 \log M + \log 9.0 \\ &\text{" } C_{10} && \log A = 1.045 \log M + \log 10.15 \\ &\text{" } C_{12} && \log A = 1.002 \log M + \log 12.35 \end{aligned}$$

For methyl esters of C_{14}, C_{16}, and C_{18} fatty acids a temperature of 200°C, a pressure of 20 mm Hg, and a rate of flow of nitrogen of 8.0 ml/min were used. The points determined are all on the same straight line, *viz*:

$$\log A = 1.041 \log M + \log 11.6$$

It was hoped that methyl esters of saturated and unsaturated fatty acids of the same chain length would prove to have identical calibration curves, since fatty acids of these types are not clearly separated under the usual experimental conditions, but occur in the same maxima. Unfortunately, experiments seem to indicate that this is not the case, since the equation for methyl oleate is

$$\log A = 1.115 \log M + \log 9.15$$

This circumstance complicates the conversion of areas into quantities by weight, since an accurate conversion cannot be made without knowledge of the ratio in which the quantities of stearic acid and unsaturated C_{18} acids are present in the methyl ester mixture to be analyzed. The problem may be circumvented by complete hydrogenation prior to the chromatography, a method which is necessary when very accurate analyses are required.

In the present work a calculation of the content of C_{18} acids in the elm seed oils based on the methyl oleate calibration has been considered to represent a sufficiently accurate compromise.

COMPOSITION OF ELM SEED OILS

The applicability of gas-liquid chromatography to fatty acid analysis has been demonstrated by the determinations of the fatty acid composition of oil from seeds of various types of elm trees. In an earlier examination [6] of a few types of elm seed oils C_{10} acids have been found to be present in quantities ranging from 50 to 60 %, which is very remarkable since no other plants outside the tropical zones are known to contain considerable quantities of lower fatty acids. It would therefore be interesting to find out whether oil from Danish elm types could be shown to have the same peculiar composition.

The investigation has included determinations of water and fat in the seeds. In addition refractive indices, iodine values and saponification values were determined (Table 3). The seeds were obtained from The Botanical Garden of the University of Copenhagen and from the gardens of The Royal Agricultural and Veterinary College *. The seeds were dried and the wings removed by gentle crushing and air separation.

The oil was obtained by extraction with petroleum ether. Fairly large quantities of seeds were used for the extraction because it served the double purpose of providing a determination of the fat content and material for subsequent experiments.

On the whole the examined seeds had a remarkably high oil content, considerably higher than the values given in the literature. Incidentally, the magnitude of the oil content does not, apparently, bear any relationship to the type or variety concerned, variations being presumably due to variations in growth condition.

* The authors wish to acknowledge their indebtedness to the staff of these two institutions for their kind assistance in supplying the seeds.

Table 3.

	Moisture %	Oil content %	$n_D^{25°}$	Saponification value determined	Saponification value calculated	Iodine value
Ulmus glabra (Huds.), Botanical Garden	7.0	36.4	1.4542	281	—	18
U. glabra (Huds.), Vet. College	3.5	46.9	1.4523	283	287	15
U. glabra (Huds.), var. *cornuta* (Rehd.)	5.5	30.6	1.4565	—	267	24
U. glabra (Huds.), var. *pendula*	—	42.1	1.4533	284	280	16
U. carpinifolia (Gled.), var. *cornubiensis*	6.0	31.5	1.4553	—	282	24
U. carpinifolia (Gled.), var. *propendens*	6.4	17.7	1.4585	—	258	—
U. procera (Salisb.), var. *purpurea*	5.8	47.8	1.4536	278	279	18
U. laevis (Pall.)	—	34.4	1.4548	—	272	—
U. fulva (Michx.)	5.7	39.1	1.4537	276	275	19
U. pumila (L.)	6.2	30.8	1.4552	—	276	22
U. campestris [6]				277.3		32.3
U. americana [6]		25.6	1.4535—1.4574	273—275		24—25
U. manshurica [7]		27	1.4552	251.4		22.5

Iodine value was determined according to AOCS, Cd 1—25, but using only 60 % of the stated quantities of material and reagents. A graphical representation of the relationship between iodine value and refractive index is given in Fig. 3. On the basis of this graph it is possible to arrive at an estimated iodine value in cases where no determination of this value has been made because the quantity of oil available was too small.

Saponification value was determined according to AOCS, Cd 3—25, likewise with reduced quantities of material and reagents.

To enable the gas-liquid chromatographic determination of the fatty acid composition, the fatty acids were converted into their methyl esters by the following method which takes into account the high solubility in water of the lower methyl esters:

About 1 g oil was dissolved in 20 ml hot methanol and a solution of 20 mg sodium methoxide in 2 ml methanol was added. The resulting solution was

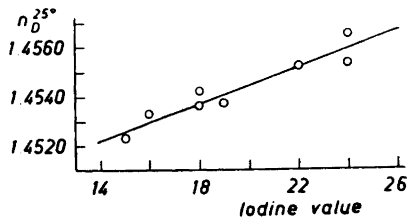

Fig. 3. The relation between iodine value and refractive index.

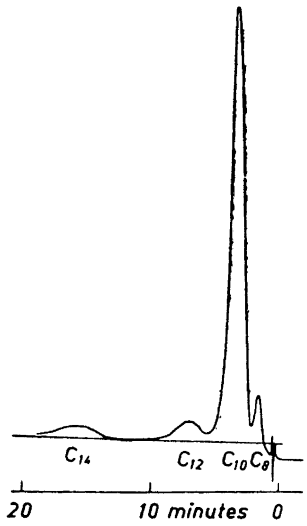

Fig. 4. Chromatogram of methyl esters from oil *U. glabra*, 180°C.

refluxed for a few hours and allowed to stand overnight. Now 20 ml ethyl ether was added and subsequently small portions of distilled water until the solution separated into two phases. The two phases were separated, and the aqueous phase was again extracted with ether. The ether extracts were combined and an equal volume of petroleum ether was added, resulting in the separation of a considerable quantity of water. The ether mixture was now dried with anhydrous sodium sulphate, and the solvents were removed by evaporation on a steam bath. Finally the methyl ester was kept at 60°C and 15 mm Hg for about one hour.

A column temperature of 180°C in the gas-liquid chromatograph was required to obtain good separation of C_8—C_{10}—C_{12} esters. Fig. 4 shows a characteristic chromatogram. The column efficiency is just sufficient to enable a fairly accurate determination. But the chromatogram further suggests that a determination of C_{14}—C_{16}—C_{18} esters will be difficult on account of their flattish maxima at this low column temperature. Fig. 5 shows a chromatogram run at 200°C and with a larger quantity of material. On the basis of this chromatogram a very accurate determination of C_{14}—C_{16}—C_{18} esters can be made, while C_8—C_{10}—C_{12} esters are only just separated.

It was thus necessary to run two chromatograms for each seed sample, *viz.* at 180 °C with about 1.8 mg for the determination of C_8—C_{10}—C_{12}, and at 200°C with 10—20 mg material for the determination of C_{14}—C_{16}—C_{18}. Altogether about 30 chromatograms have been run.

It is not possible by calculation to arrive at any numerical evaluation of the errors incident to the measurements made. Deviations of about 3 % have bee observed in most duplicate runs, although deviations right up to 10—20 % also occur. Presumably the error in connection with the determination of C_8 and C_{12} esters is 5—10 %, while with regard to determinations of C_{10}, C_{14} and C_{16} the error is 2—5 %. For the reason referred to in the section

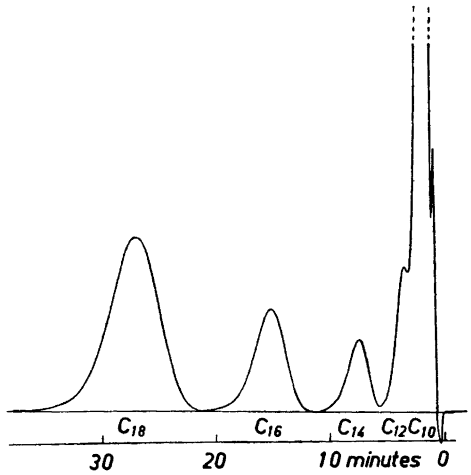

Fig. 5. Chromatogram of the same sample as in Fig. 4, 200°C.

on calibration the error in connection with the determination of C_{18} is considerably greater, perhaps 10—20 %. In the case of analytical samples with a more even distribution of saturated fatty acids the error may reasonably be assumed to be 1—2 %, which is greatly superior to the accuracy of other known analytical methods for similar determinations.

The gas-liquid chromatogram provides information as to the composition of the methyl ester mixture. The fatty acid composition may be obtained by calculation from the analytical results, since

$$S = \frac{E \cdot \frac{M}{14 + M}}{\Sigma E \cdot \frac{M}{14 + M}} \cdot 100$$

where S is the quantity of fatty acid and E the quantity of ester, both in per cent by weight, while M is the molecular weight of the fatty acid in question.

Table 4 lists the fatty acid composition for the species and varieties of elm examined. The table moreover includes a mean value which has been calculated for the purpose of enabling comparison with values given in the literature.

On the basis of the fatty acid composition found the saponification value of the corresponding elm seed oil has been calculated, the result has been included in Table 3. In the four cases where comparison has been possible, the agreement is satisfactory.

Table 4.

	Fatty acid composition, %					
	C_8	C_{10}	C_{12}	C_{14}	C_{16}	C_{18}
Ulmus glabra, Vet. College	6.2	72.4	5.3	3.3	5.0	7.8
U. glabra, var. *cornuta*	3.2	58.2	4.4	3.5	7.6	23.1
U. glabra, var. *pendula*	5.0	68.9	4.0	3.0	5.2	13.9
U. carpinifolia, var. *cornubiensis*	5.5	68.5	5.1	3.2	5.4	12.3
U. carpinifolia, var. *propendens*	1.8	54.4	3.3	3.0	6.6	30.9
U. procera, var. *purpurea*	3.2	68.1	5.3	4.0	7.0	12.4
U. laevis	0.8	66.2	5.1	2.8	5.5	19.6
U. fulva	3.7	64.2	6.4	4.1	7.0	14.6
U. pumila	3.0	65.6	3.5	3.9	8.1	15.9
Mean value	3.6	65.2	4.7	3.4	6.4	16.7
U. americana [6]	5.3	61.3	5.9	4.6	2.9	20.0
U. manshurica [7]	2—11	55—59	2—8	1—3	12—21	5—8

The statements in the literature with regard to a high content of C_{10} acid as being particularly characteristic of elm seed oil have been fully confirmed.

REFERENCES

1. James, A. T. and Martin, A. J. P. *Biochem. J.* **50** (1952) 679.
2. James, A. T. and Martin, A. J. P. *Endeavour* **15** (1956) No. 58, 73.
3. Cropper, F. R. and Heywood, A. *Nature* **172** (1953) **1101.**
4. Cropper, F. R. and Heywood, A. *Nature* **174** (1954) 1063.
5. Sørensen, Ib and Søltoft, P. *Acta Chem. Scand.* **10** (1956) 1673.
6. Eckey, E. W. *Vegetable Fats and Oils*, Reinhold Publishing Co., New York 1954, p. 386—387.
7. *J. Chem. Soc. Japan. Pure Chem. Sect.* **70** (1949); *cf. Chem. Abstracts* **45** (1951) 2690.

Received December 4, 1957.

ACTA CHEMICA SCANDINAVICA 12 (1958) 823—832

The Quenching of the Long-lived Fluorescence of Biacetyl in Solution

HANS L. J. BÄCKSTRÖM and KJELL SANDROS

Institutionen för fysikalisk kemi, Chalmers Tekniska Högskola, Göteborg, Sweden

The quenching effect of different types of compounds on the long-lived fluorescence of biacetyl has been studied in solution at 20°C by measuring fluorescence decay rates. The results are in accord with the conclusion of Lewis and Kasha that the emitting state of biacetyl is a triplet or biradical state. Photochemical reactions of carbonyl compounds indicate that the structure of the biradical may be written as

$CH_3C(=O)-\dot{C}(-\dot{O})CH_3$ and that, due to the odd electron on oxygen, it has

the power of abstracting H-atoms from colliding molecules.

Two different classes of quenchers are distinguished. The first class comprises substances having a loosely bound hydrogen atom, such as primary and secondary amines, phenols, aldehydes, and alcohols. In this case the quenching mechanism is assumed to consist in a photochemical reaction of the kind indicated. The second class of quenchers comprises unsaturated and aromatic compounds, the strongest quenchers of this type being polynuclear hydrocarbons. Here the quenching mechanism is assumed to be an energy transfer, causing a triplet → singlet transition in the biacetyl molecule and the reverse transition in the quencher. This assumption is in accord with known values of triplet state energies, and is further supported by the results of preliminary photochemical experiments, showing that irradiation of a benzene solution of biacetyl and anthracene gives rise to a photosensitized formation of dianthracene. The quantum efficiency under the conditions employed is of the order of 1 %, increasing with increasing light intensity.

When solid solutions of unsaturated compounds are irradiated with ultraviolet light at liquid air temperatures, two kinds of photo-luminescence may be observed: normal fluorescence, and a more long-lived luminescence with an entirely different spectrum, displaced toward longer wavelengths. Under suitable experimental conditions the latter emission may be observed as phosphorescence. According to Lewis and Kasha [1], the phosphorescent state may be identified with the triplet or biradical state of the molecule. In accord-

ance with the selection rule prohibiting intercombinations between levels of different multiplicity, the radiative return from the triplet to the ground (singlet) level is a slow process.

In the case of most substances, warming the solution leads to a gradual disappearance of the long-lived emission as the fluidity of the solvent increases. A few exceptions are known, however, where it may be observed at ordinary temperatures [2]. In these cases the triplet state of the molecule must possess exceptional stability toward collisional deactivation. The most notable of these cases is that of biacetyl. The so-called "delayed fluorescense" of biacetyl has been studied extensively in the vapour state and to some extent also in water solution [3]. Its quenching by O_2 has been studied quantitatively in the vapour state [3]. The same phenomenon has been observed in water solution but no quantitative data have been reported.

The present study of the quenching effect of different types of compounds on the long-lived fluorescence of biacetyl in solution [4] was undertaken with the aim of obtaining information on the chemistry of the triplet state, about which very little is known [5].

The paper also gives some preliminary results of photochemical experiments on solutions of biacetyl and anthracene.

EXPERIMENTAL

In some preliminary experiments, quenching was studied by measuring the intensity of fluorescence under constant conditions of illumination. The final experiments, however, were made by studying the effect of quenchers on the rate of decay of fluorescence.

Apparatus

The experimental arrangement for measuring fluorescence decay rates is shown schematically in Fig. 1. Light from a single condenser discharge through the flash tube *a* passed through filter combination *c* before entering the solution through one of the end

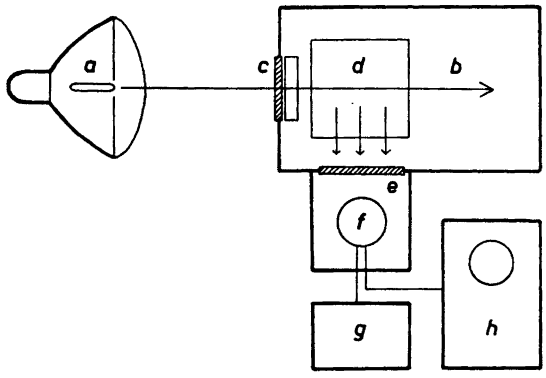

Fig. 1. Schematic diagram of apparatus for measuring fluorescence decay rates. (a) Flash tube. (b) Light-tight box. (c) Filter combination, consisting of 4 mm Chance glass OB1 + 1 cm 0.5 M sodium nitrite solution. (d) Cylindrical fluorescence cell. (e) Light filter (Chance OY3, 4 mm). (f) Photomultiplier tube. (g) Stabilized adjustable voltage supply. (h) Oscilloscope.

plates of the cylindrical fluorescence cell *d*. This filter combination confined the exciting light to the wavelength region 3 800—5 000 Å. The cell had a diameter of 4 cm and a length of 4 cm. Fluorescence radiation, perpendicular to the exciting light, passed through filter *e* to remove scattered incident light before inpinging on the photomultiplier tube *f*. Filter *e* removed all wavelengths below 5 000 Å. The long-wave fluorescence of biacetyl lies mainly in the region 5 000—6 000 Å. The voltage applied to the photomultiplier tube (RCA 931A) was varied between 600 and 900 V. About 700 V was generally found suitable. The output of the multiplier tube was fed into a resistance of 20 000 ohms and the voltage developed across the resistance applied to the vertical deflection terminals of a Tektronix Type 514D oscilloscope. The latter was equipped with a blue-fluorescing screen (Type P7) permitting photographic registration of the trace even at high sweep speeds. The multiplier tube was furnished with a cathode follower which reduced its response time to < 1 μsec. The sweep speeds of the oscillograph were checked using a Tektronix Time-Mark Generator, Type 180. Errors exceeding 1 % were not observed, and no corrections were applied. The oscilloscope was used with signal triggering, the photomultiplier signal automatically starting the sweep.

Our first measurements were made with flashes from a Philips stroboscope GM 5 500*. As only single flashes of moderate intensity were required, the stroboscope was later replaced by a simple electronic device built according to a description by de Bruin [6], using the same kind of argon-filled flash tube (Type 57 900 P/06) and the same relay valve (thyratron PL5) as in the Philips stroboscope. The condenser had a capacity of 4 μF and was charged to 700 V. Care was taken to use short and suitably designed leads to reduce the time of the flash. By direct observation of the flash by means of the multiplier-oscilloscope combination (using suitable light filters for preventing damage to the multiplier tube) it was found that the peak in light intensity occurred 4 μsec after flash initiation and that after 12 μsec the decrease in intensity followed an exponential curve with a half-time of 2.6 μsec. These data represent a marked improvement compared to the flash used previously and considerably extended the range of fluorescence decay rates that could be measured.

The procedure used in photographing a decay curve was as follows. With the fluorescence cell brought to the desired temperature and placed in position, the voltage of the photomultiplier tube, the sweep speed, and the intensity of the cathode ray were adjusted by the aid of trial flashes so as to give a satisfactory trace. The electron beam was displaced a sufficient distance for registration to begin at least 12 μsec after flash initiation. The camera was then placed in position, the shutter opened, and another flash produced. The photograph was enlarged by projection and analyzed. The decay curves were found to be strictly exponential. Usually four decay curves were registered for each solution. The mean life values calculated from these curves usually did not differ by more than 1 %, and there was no trend in the values, showing that the solutions were not changed by the exciting flashes **.

Because of the very strong quenching action of oxygen, all fluorescence measurements had to be made in the absence of air and on solutions that had been carefully freed from dissolved oxygen. The fluorescence cell with arrangements for degassing the solution is shown in Fig. 2. The cell itself (*a*) was a cylindrical flow-through absorptiometer cell from The Tintometer Ltd., Salisbury, made of glass with negligible fluorescence. For degassing a solution, the apparatus, in an inclined position and with the solution in bulb *b*, was connected to a vacuum system by means of ground-glass joint *f*. The volume of the bulb was about 110 ml, that of the cell 40 ml. The pump used for evacuation was a two-stage rotary oil pump, capable of giving a vacuum of 10^{-4} mm. Pressure readings were made on a McLeod gauge. After cooling the bulb with carbon dioxide ice and alcohol the stop-cock was opened and the air removed by pumping. With the stop-cock closed, the solution was then warmed to 20°C to liberate dissolved air. By repeating these operations four times, the air pressure in the vessel was reduced to < 0.01 mm. After bringing the solution to 20°C, it was transferred to the fluorescence cell by tilting the apparatus, and the fluorescence decay rate was measured as described.

* Kindly placed at our disposal by Professor S. Lundberg of the Department of Mechanical Engineering.

** Prolonged irradiation may lead to measurable changes in the composition of the solution. *Cf.* p. 830.

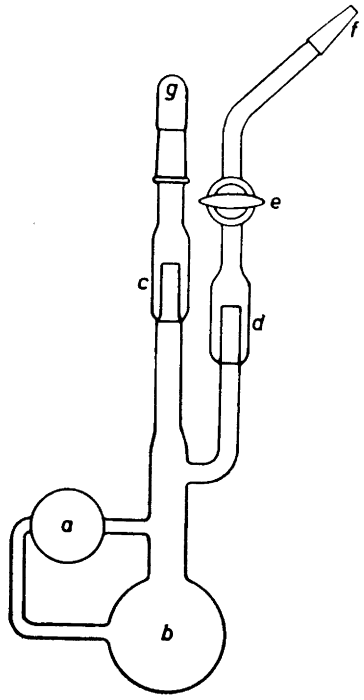

Fig. 2. Fluorescence cell with arrangements for degassing the solution. (a) Cylindrical fluorescence cell. (b) Spherical glass bulb. (c) and (d) Pockets for trapping stop-cock grease. (e) Stop-cock. (f) Ground glass joint. (g) Cap with ground glass joint.

When studying the quenching action of oxygen, known small quantities of air were admitted into the apparatus above the frozen and degassed biacetyl solution. For this purpose a special gas burette was used, made of 2 mm manometer tubing, where volumes were measured under reduced pressure. As little as 10^{-6} mole of oxygen could be measured with an accuracy of 1 %. After adjusting the temperature to 20°C, the solution was shaken to attain equilibrium. Knowing the volume of the apparatus (188.5 ml), the volume of the solution (44.0 ml), and the solubility coefficient, the concentration of oxygen in the solution could be calculated.

Materials

The chemicals used were of the highest purity obtainable commercially and were further purified as indicated below.

Biacetyl was fractionally distilled in a nitrogen atmosphere under reduced pressure (100 mm), using a column corresponding to 15 theoretical plates. The same column was used for all other distillations. The purified biacetyl was stored in the dark. Its fluorescence properties remained unchanged for months.

Benzyl alcohol, *aniline*, and *nitrobenzene* were distilled at 9—12 mm, the following at NP: *benzene*, *carbon tetrachloride*, *perchloroethylene*, cyclo*hexene*, *methanol*, and iso*propanol*, the latter in a nitrogen atmosphere. *Stilbene* and *1,3,5-trinitrobenzene* were recrystallized from ethanol, p-*chlorobenzaldehyde* from a water-ethanol mixture, and *resorcinol* from benzene. *Triphenylamine* in benzene solution was repeatedly shaken with 5 M sulfuric acid to remove diphenylamine. It was then recrystallized from an ethanol-water mixture. *Naphthalene*, *phenanthrene*, *pyrene*, and *chrysene* were freed from anthracene by treatment with maleic anhydride in benzene or toluene solution [7,8]. The first three were then recrystallized from ethanol. Chrysene was refluxed with carbon tetrachloride containing benzoyl peroxide [7] and recrystallized once from acetone and twice from benzene.

Phenol, *hydroquinone*, *diphenylamine*, m-*dinitrobenzene*, *anthracene*, *benzpyrene*, and *1,2-benzanthracene* were used without further purification.

RESULTS AND DISCUSSION

The solvent found most suitable for our purpose was benzene. Dilute solutions of biacetyl in high quality benzene from different sources gave strongly varying values of fluorescence mean life (τ). However, by fractional distillation of the benzene we generally succeeded in raising the value of τ to about 0.98×10^{-3} sec at 20°C. The highest value observed was 1.03×10^{-3} sec. For biacetyl vapour at 25°C a value of 1.80×10^{-3} sec has been reported [9], as against 2.25×10^{-3} sec for a solid solution at 77°K[10].

Solutions of biacetyl showed the phenomenon of self-quenching, the value of τ decreasing with increasing biacetyl concentration. However, the effect was slight and variable, indicating that it was due to remaining traces of impurities in the biacetyl. It was found to obey the Stern-Volmer quenching formula [11], in that τ could be represented as a function of biacetyl concentration (C) by the equation:

$$\frac{1}{\tau_0} = \frac{1}{\tau} + kC \qquad (1)$$

The lowest value observed for k was 460 l mole^{-1} sec^{-1}. In studying quenching by foreign substances, the biacetyl concentration was kept so low that self-quenching was negligible.

Other liquids tried as solvents gave the following values of τ in μsec: carbon tetrachloride 784, chlorobenzene 447, anisole 307, methyl benzoate 278, water 229.

Stronger quenchers were studied in benzene solution. The results were found to obey the Stern-Volmer formula (1). In all cases the decay rate was measured at six different concentrations of the quencher such that τ varied between τ_0 and $\tau_0/10$. For anthracene a determination giving $\tau = \tau_0/40$ also gave good agreement with eqn. (1). The straight line relation between $1/\tau$ and C had a standard error in regression coefficients of 1—2 %. Table 1 gives the calculated values of k in l mole^{-1} sec^{-1}. The oxygen concentration in benzene solution was calculated using the solubility value given by Horiuti [12].

A closer study of the table leads to the conclusion, that substances with pronounced quenching action may be divided into two classes:

1. In the first class, comprising *i.a.* phenols, amines, and alcohols, quenching power is connected with the presence in the molecule of a loosely bound hydrogen atom. This is indicated by the almost complete loss of quenching power in going from phenol to anisol and from diphenylamine to triphenylamine. Also the general parallelism between quenching power and inhibitory action in autoxidation reactions, which is apparent, points in the same direction. It is interesting to note in this connection that the only aldehyde investigated, *p*-chlorobenzaldehyde, is a stronger quencher than the alcohols, that act as weak inhibitors (sometimes called retarders) of aldehyde oxidation. On the other hand, strong oxidation inhibitors like phenols and primary and secondary amines have quenching constants that exceed the value for the aldehyde by several powers of ten.

There can be little doubt that the quenching mechanism indicated by these results may be identified with a type of chemical reaction which is well-known

Table 1. Quenching constants (l mole^{-1} sec^{-1}) in benzene solution at 20°C.

Methanol	2.6×10^2
*Iso*propanol	2.7×10^3
Benzyl alcohol	6.9×10^3
p-Chlorobenzaldehyde	2.4×10^4
Phenol	8.9×10^7
Resorcinol	2.7×10^8
Hydroquinone	5.3×10^9
Aniline	1.8×10^9
Diphenylamine	6.8×10^9
Triphenylamine	3.9×10^4
Perchloroethylene	3.5×10^4
*Cyclo*hexene	1.0×10^5
Nitrobenzene	4.4×10^4
m-Dinitrobenzene	3.6×10^5
1,3,5-Trinitrobenzene	1.1×10^6
Stilbene	4.4×10^9
Naphthalene	3.8×10^3
Phenanthrene	2.3×10^3
Anthracene	8.1×10^9
Chrysene	2.4×10^8
Pyrene	7.5×10^9
Benzpyrene	8.2×10^9
1,2-Benzanthracene	3.8×10^9
Oxygen	5.1×10^9

from the photochemistry of carbonyl compounds. In the words of Plotnikow [13]: "Die Verbindungen, die die CO-Gruppe enthalten, besitzen die Eigenschaft, im Licht anderen organischen Körpern den Wasserstoff zu entziehen (sie zu dehydrieren) und ihn an diese CO-Gruppe anzulagern: $-C=O+H \rightarrow -C(OH)-$. Die Doppelbindung wird somit aufgehoben und eine Bindung frei gemacht. Dadurch wird der Verbindung die Möglichkeit gegeben, sich entweder zu kondensieren oder andere Moleküle anzugliedern." An example is the formation of benzopinacol, $(C_6H_5)_2C(OH)C(OH)(C_6H_5)_2$, and acetone when solutions of benzophenone in *iso*propanol are irradiated with ultraviolet light. It was suggested long ago [14,15] that an intermediate in this reaction is a biradical $(C_6H_5)_2\dot{C}-O\cdot$, formed from benzophenone as a result of light absorption, which due to its unpaired electron on the oxygen atom has the power of abstracting a loosely bound hydrogen atom from a neighbouring molecule. This biradical may be identified with the triplet state responsible for the phosphorescence of benzophenone in solid solution at low temperatures *.

Similarly biacetyl, when irradiated in ethanol solution [16], gives acetaldehyde and 3,4-dimethyl-hexanediol-(3,4)-dione-(2,5) (I).

I 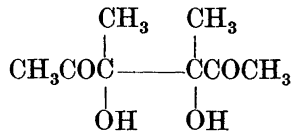

II 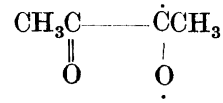

* For a discussion of this point, see Bäckström, H. L. J., Steneryr, A. and Perlmann, P. *This Journal* **12** (1958) 8.

Thus the biradical of biacetyl reacts as if it had the structure II. Obviously, however, the true state of this biradical must be largely determined by the exceptional possibilities for resonance. Probably the resulting resonance stabilization is the cause of its remarkable stability.

2. The second class of quenchers consists of unsaturated and aromatic compounds. In view of the biradical nature of the triplet state it is of interest that these compounds are known to undergo addition reactions with free radicals. This is particularly the case with the polynuclear hydrocarbons, and a general parallelism between the quenching constants and the "relative methyl affinities" of Szwarc [17] seems to exist where comparison can be made. In the series of aromatic nitro compounds, increase in quenching constant parallels the tendency to undergo radical addition reactions.

Probably, however, we are here dealing with a quenching mechanism which is physical rather than chemical in nature. Terenin and Ermolaev [18] have shown that sensitized phosphorescence may take place in solid solutions at low temperatures. For instance, when a solution of naphthalene in ethanol at −195°C is excited by filtered radiation of wavelength 3 660 Å no luminescence is observed, since the onset of the absorption spectrum of naphthalene lies at 3 270 Å. However, when the solution contains, in addition, a suitable sensitizer like benzophenone, which absorbs at 3 660 Å, a bright phosphorescent emission of the triplet spectrum of naphthalene in the visible appears. By measuring intensities and decay times of the emission spectra as a function of the concentrations the authors were able to prove that the process taking place is a transfer of excitation energy, causing a triplet → singlet transition in the sensitizer and the reverse transition in the acceptor. The necessary condition is that the energy level of the triplet state of the sensitizer must lie above that of the acceptor.

The same process of energy transfer may be expected to take place in liquid solutions at ordinary temperatures. The approximate triplet state energy (E_T) of biacetyl as determined from its phosphorescence spectrum [1] is 56 kcal/mole, taking the energy of the ground state as zero. Table 2 gives the corresponding values for quenchers of class 2 where such data are available *. It will be seen that E_T-values below 56 kcal/mole correspond to high values of the quenching constant, those well above 56 kcal/mole to low values. Chrysene with $E_T = 57$ kcal/mole occupies an intermediate position.

In liquid solution at ordinary temperature, excitation of the acceptor to the triplet state will not normally result in sensitized phosphorescence. Molecules in this state will be deactivated by collisions before they have time to radiate. The only visible effect in the present case will therefore be the quenching of biacetyl fluorescence. The possibility exists, however, that the triplet excited quencher molecules may undergo some sufficiently rapid chemical reaction. This is how we interpret the sensitized formation of dianthracene described on p. 830.

Oxygen as a quencher represents a case by itself. It has long been known that oxygen reacts with biacetyl under the influence of light [20] but nothing

* According to Kasha and McGlynn[5], the value for stilbene given by Lewis and Kasha [1] is now known to be wrong.

Table 2. The relation between quenching constant and triplet state energy for some quenchers of class 2.

	log k	E_T kcal/mole	Ref.
Phenanthrene	3.4	62	19
Naphthalene	3.6	61	1
Nitrobenzene	4.6	60	1
Chrysene	8.4	57	19
Pyrene	9.9	48	19
1,2-Benzanthracene	9.6	47	19
Anthracene	9.9	42	1

is known about the reaction products. Since one of the carbon atoms of the biradical has an unpaired electron, the primary act is probably the addition of an oxygen molecule to this carbon atom.

In cases where the rate of a bimolecular reaction in solution is determined entirely by the rate of diffusion of the reactants towards each other, the value of the rate constant may be estimated by a formula given by Debye [21]. For benzene solutions at 20°C the calculated value is 1.0×10^{10} l mole^{-1} sec^{-1}. It will be seen that the values of k for the strongest quenchers closely approach this value, showing that in these cases the quenching process is so rapid as to be essentially diffusion controlled [22].

As regards the weaker quenchers in Table 1, special methods of purification were employed for removing as far as possible traces of chemically related substances with strong quenching action. As always, the purification process was followed by measuring the quenching constant. For instance, the k-value found for unpurified phenanthrene was 2.5×10^6. Two purifications by the method described above (p.826) reduced the value to 7×10^3, and four to the value given in the table (2.3×10^3). Presumably this is not far from the true value but provisionally it must be regarded as a maximum. The same applies to the k-values for other weak quenchers.

PRELIMINARY RESULTS OF PHOTOCHEMICAL EXPERIMENTS WITH ANTHRACENE

A degassed solution of 0.41 g of biacetyl and 0.42 g of anthracene in 50 ml of purified benzene, contained in an evacuated and sealed glass bulb, was exposed to daylight near a south window. In order to exclude wavelengths absorbed by anthracene, the bulb was immersed in a beaker with 1 M sodium nitrite solution. After about 2 weeks colourless crystals began to appear. After 9 months the bulb was opened and the crystals formed were washed with alcohol and dried. A microanalysis gave: C 93.97; H 5.71. Calc. for dianthracene: C 94.34; H 5.66.

The absorption spectrum in ethanol solution showed substantial agreement with that of dianthracene [23] but indicated that the product contained about 5 mole % of anthracene.

Confirmatory evidence for the photosensitized formation of dianthracene was obtained from similar experiments using light from a mercury arc, filtered to remove wavelengths absorbed by anthracene. The initial concentration of anthracene was lower (10^{-4} — 10^{-5} mole/l) and its rate of disappearance from the solution was followed by observation of biacetyl fluorescene and by measuring its decay rate when the anthracene concentration had decreased sufficiently for such measurements to the possible. The τ-values finally reached on prolonged irradiation were close to τ_0, showing that the reaction product had no noticeable quenching action. In order to prove that the disappearance of the anthracene was not, in spite of all precautions, caused by light absorbed by that substance, a degassed solution containing the same amount of anthracene but no biacetyl was irradiated twice the time used in the foregoing experiment. After opening the bulb, adding biacetyl, and degassing the solution, it was found that the fluorescence of biacetyl was completely quenched by the anthracene still present.

In the experiments described, the quantum efficiency of the photosensitized reaction of anthracene was determined using the potassium ferrioxalate actinometer of Parker [24]. The values obtained ranged from 0.1 to 1.9 %. They increased with increasing light intensity, but apparently also other factors such as the concentration of biacetyl are of importance.

The reaction product formed slowly decomposes again at room temperature. This is shown by the fact that when the solution is kept in the dark, τ again decreases. From the rate of decrease in τ, the rate of decomposition of dianthracene could be calculated. It corresponded to a half-life of about 1 400 days.

REFERENCES

1. Lewis, G. N. and Kasha, M. *J. Am. Chem. Soc.* **66** (1944) 2100; Lewis, G. N., Lipkin, D. and Magel, Th. T. *Ibid.* **63** (1941) 3005; *cf.* also: Terenin, A. N. *Acta Physicochim. U.R.S.S.* **18** (1943) 210.
2. Lewis, G. N. and Kasha, M. *J. Am. Chem. Soc.* **67** (1945) 994.
3. A very complete list of references is to be found in Sheats, G. F. and Noyes, Jr., W. A. *Ibid.* **77** (1955) 1421.
4. Preliminary communication: Bäckström, H. L. J. and Sandros, K. *J. Chem. Phys.* **23** (1955) 2197.
5. Reid, C. *Excited States in Chemistry and Biology*, Butterworths Scientific Publications, London, 1957; Kasha, M. and McGlynn, S. P. *Ann. Rev. of Phys. Chem.* **7** (1956) 403.
6. de Bruin, S. L. *Philips Tech. Rev.* **8** (1946) 25.
7. Kooyman, E. C. and Fahrenhorst, E. *Trans. Faraday Soc.* **49** (1953) 58.
8. Marvel, C. S. and Anderson, W. S. *J. Am. Chem. Soc.* **76** (1954) 5435.
9. Kaskan, W. E. and Duncan, A. B. F. *J. Chem. Phys.* **18** (1950) 427.
10. McClure, D. S. *J. Chem. Phys.* **17** (1949) 905.
11. Förster, Th. *Fluoreszenz organischer Verbindungen*, Vandenhoeck & Ruprecht, Göttingen, 1951, p. 209.
12. Horiuti, J. *Sci. Papers, Inst. Phys. Chem. Research (Tokio)* **17** (1931) No. 341, 214.
13. Plotnikow, J. *Allgemeine Photochemie*, Vereinigung Wiss. Verleger, Berlin, 1920, p. 607.
14. Bäckström, H. L. J. *Z. physik. Chem.* **B25** (1934) 99.
15. Hirschberg, Y. and Farkas, L. *J. Am. Chem. Soc.* **59** (1937) 2453.
16. Cohen, W. D. *Chem. Weekblad* **13** (1916) 590.

17. Levy, M. and Szwarc, M. *J. Am. Chem. Soc.* **77** (1955) 1949.
18. Terenin, A. N. and Ermolaev, V. L. *Trans. Faraday Soc.* **52** (1956) 1042.
19. McClure, D. S. *J. Chem. Phys.* **17** (1949) 905.
20. Almy, G. M., Fuller, H. Q. and Kinzer, G. D. *Phys. Rev.* **55** (1939) 238.
21. Debye, P. *Trans. Electrochem. Soc.* **82** (1942) 265.
22. *Cf.* Christiansen, J. A. *J. Colloid Sci.* **6** (1951) 213.
23. Coulson, C. A., Orgel, L. E., Taylor, W. and Weiss, J. *J. Chem. Soc.* **1955** 2961.
24. Parker, C. A. *Proc. Roy. Soc. London* **A220** (1953) 104; Hatchard, C. G. and Parker, C. A. *Ibid.* **A235** (1956) 518.

Received February 19, 1958.

ACTA CHEMICA SCANDINAVICA 12 (1958) 833—838

*iso*Thiocyanates XXX *. Glucohirsutin, a New Naturally Occurring Glucoside Furnishing (—)-8-Methylsulphinyloctyl *iso*Thiocyanate on Enzymic Hydrolysis

ANDERS KJÆR** and BO CHRISTENSEN

Chemical Laboratory of the University of Copenhagen, Denmark

A survey is presented of the straight-chain, *levo*rotatory ω-methylsulphinylalkyl *iso*thiocyanates (I) formerly recognized as enzymic hydrolysis products of glucosidic progenitors present in various plant species belonging to the family *Cruciferae*. Besides sulphoraphene (II), these mustard oils comprise the compounds I with n = 3, 4, 5, 9 and 10.

The present paper reports the identification of an additional glucoside, *glucohirsutin*, of this general type, present in seeds of *Arabis hirsuta* (L.) Scop. and affording *hirsutin*, the *levo*rotatory 8-methylsulphinyloctyl *iso*thiocyanate (I, n = 8), upon enzymic hydrolysis. The structure of the latter is proved by degradation.

On acid hydrolysis glucohirsutin furnishes hydroxylamine whereas its enzymic cleavage proceeds with liberation of glucose and sulphate in addition to hirsutin. These results establish (VII) as the correct expression for glucohirsutin.

In the course of a systematic search in this laboratory for mustard oil glucosides in seed material of various crucifers, several compounds have been encountered which possess in common the property of furnishing *levo*rotatory *iso*thiocyanates of the general structure (I) on enzymic hydrolysis.

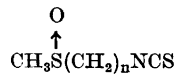

I ***

n = 3: Iberin
n = 4: Sulphoraphane
n = 5: Alyssin

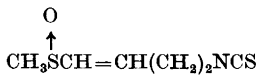

II

n = 8: Hirsutin
n = 9: Arabin
n = 10: Camelinin

* Part XXIX of this series: *Acta Chem. Scand.* **11** (1957) 1423.

** Senior author. Present address: Organic Chemical Laboratory, Royal Veterinary and Agricultural College, Copenhagen V., Denmark.

*** Experimental work is in progress to establish the absolute configuration around the asymmetric sulphur atom. Comparable rotatory data for the homologous *iso*thiocyanates (I), as well as several series of the corresponding thiourea-derivatives, renders it almost certain that all of the parent glucosides, containing a sulphoxide-grouping in the side chain, belong to the same configurational series.

The first recorded compound of this type was sulphoraphene (II), isolated by Schmid and Karrer [1] subsequent to enzymic hydrolysis of a glucoside in seeds of radish (*Raphanus sativus* L. var. *alba*). A few years later, Schultz and Gmelin [2] isolated the crystalline glucoside glucoiberin from seeds of *Iberis amara* L. On enzymic hydrolysis it furnished a mustard oil (iberin) for which the structure (I, n = 3) was advanced, a formulation which has since been unequivocally established in this laboratory [3]. The homologous sulphoxide *iso*thiocyanate, (−)-sulphoraphane (I, n = 4), was synthesized by Schmid and Karrer [4] and has recently been recognized in this laboratory as an enzymic hydrolysis product of a glucoside of rather wide-spread natural occurrence [5]. A previous communication of this series [3] announced the discovery of a new glucoside, glucoalyssin, present in seeds of *Alyssum argenteum* Vitm. and several other *Alyssum* species (*cf.* also Ref.[6]). It was enzymically hydrolyzed to the mustardoil alyssin, identified as (−)-5-methylsulphinylpentyl *iso*thiocyanate (I, n = 5). Seed material of *Arabis alpina* L. served as the source of a formally similar glucoside (glucoarabin), the structure of which appeared from the fact that enzymic hydrolysis resulted in the formation of arabin, unambiguously identified as (−)-9-methylsulphinylnonyl *iso*thiocyanate (I, n = 9) [7,8]. Again, studies of seed extracts of *Camelina sativa* (L.) Crantz resulted in the discovery of glucocamelinin, undergoing enzymic fission to give camelinin which proved to be the next higher homologue, *viz.* (−)-10-methylsulphinyldecyl *iso*thiocyanate (I, n = 10) [9]. In the present paper we wish to extend this class of natural compounds by an additional glucoside, present in seed extracts of *Arabis hirsuta* (L.) Scop. and affording (−)-8-methylsulphinyloctyl *iso*thiocyanate (I, n = 8) upon enzymic hydrolysis.

Paperchromatographic analysis of a methanolic seed extract of *Arabis hirsuta* (L.) Scop. revealed its contents of two major glucosides, travelling in *n*-butanol: ethanol: water (4:1:4) as a single spot with an R_B-value [10] of 0.95 but distinguishable in the solvent system *n*-butanol: pyridine: water (6:4:3) as two spots possessing R_B-values of 0.90 and 0.75. The former glucoside is being further studied at the present, whereas the compound being strongly depressed in the basic solvent system has been identified as a glucoside different from all heretofore recorded species [11]. In accord with general usage in this field we propose the designation *glucohirsutin* for the new constituent which may be identical with an unidentified glucoside, paperchromatographically observed by Schultz and Wagner [10,12] in fresh parts of *Arabis hirsuta* and other *Arabis* species as a spot possessing R_B-values of 0.94 and 0.86 in *n*-butanol:acetic acid:water (4:1:3) and the above pyridine system, respectively.

When the residue from a seed extract of *A. hirsuta* (93 g of seeds) * was subjected to enzymic hydrolysis with a myrosinase preparation in a dilute phosphate buffer at pH 6.7, a chloroform-extractable, non-volatile mustard oil was liberated, derivable from glucohirsutin. The chloroform solution was washed with dilute alkali and water, dried and evaporated to yield the *levo*-rotatory mustard oil (hirsutin). Without further purification this was allowed

* An ample supply of seed material was procured by large-scale cultivation of the plant during the summer of 1957 in the *Botanical Garden of the University of Copenhagen*. We are greatly indebted for the generous assistance of the garden and wish to acknowledge also the good offices of Professor T. Böcher who supplied authentic seed material for sowing.

to react with aniline in chloroform solution to furnish the crystalline *phenylthiourea* (220 mg), $C_{16}H_{26}ON_2S_2$ (III). This *levo*rotatory derivative displayed a strong and characteristic sulphoxide band in the infra-red spectrum. Treatment of the phenylthiourea in aqueous ethanol with silver nitrate, a procedure successfully employed by us in similar cases [3,7,9], resulted in formation of the corresponding *levo*rotatory *phenylurea*, $C_{16}H_{26}O_2N_2S$ (IV), still possessing the sulphoxide-grouping as apparent from its infra-red spectrum. Reduction of the latter compound with zinc dust in acid solution was accompanied by disappearance of the optical rotation as well as the sulphoxide-band in the infra-red spectrum and resulted in production of the crystalline *phenylurea*, $C_{16}H_{26}ON_2S$ (V). This was identified as 1-(8-methylthiooctyl)-3-phenylurea upon critical comparison with an authentic, synthetic specimen produced by reaction of 8-methylthiooctylamine (VI), recently synthesized in this laboratory [8], with phenyl *iso*cyanate. Mixed melting point determination and coinciding infra-red spectra served to establish the identity of the two preparations.

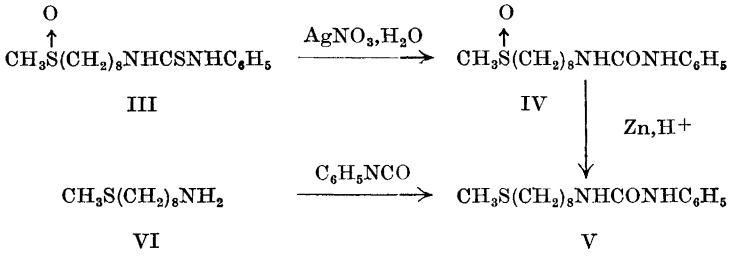

The above sequence of reactions establishes beyond doubt the structure of hirsutin as (−)-8-methylsulphinyloctyl *iso*thiocyanate (I, n = 8).

For further characterization, a separate hirsutin preparation was transformed into the corresponding, *levo*rotatory *8-methylsulphinyloctylthiourea* upon treatment with methanolic ammonia.

Thus far, no attempts have been made to isolate glucohirsutin in pure form, but the following evidence has been adduced to indicate that the glucoside is of the ordinary type. Acid hydrolysis of a paperchromatographically purified specimen of glucohirsutin, conducted according to the directions of Ettlinger and Lundeen [13], resulted in the production of hydroxylamine. The enzymic hydrolysis of a similarly purified glucoside preparation to give hirsutin proceeded with concomitant liberation of glucose and sulphate, a characteristic behaviour of the common mustard oil glucosides. Hence, there can be little doubt that the glucohirsutinate ion, the parent constituent of the employed seed material, possesses the structure (VII), depicted in accord with the recently established general formula for the mustard oil glucosides [13]. In addition to the absolute configuration of the sulphoxide-grouping the stereochemistry around the oxime double bond of (VII) still remains to be clarified.

EXPERIMENTAL

All melting points are uncorrected and determined in capillary tubes in a slowly heated bath. Rotations are measured in a 1 dm tube.

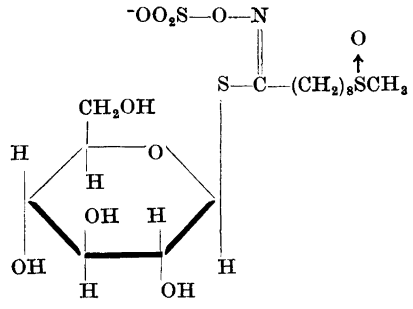

VII

Isolation of hirsutin phenylthiourea (III). A seed sample (93 g) of *Arabis hirsuta* (L.) Scop., produced by cultivation of plants derivable from seed material of wild plants collected near Beograd in Yugoslavia, was finely ground and extracted with one portion (300 ml) of 80 % methanol and two (each of 300 ml) of 70 % methanol. The combined extracts were taken to dryness *in vacuo* and the residue was dissolved in water (200 ml). To the filtered solution were added 1/15 M Na_2HPO_4-(20 ml) and 1/15 M KH_2PO_4-solution (20 ml), together with a cell-free myrosinase preparation (20 ml), and the mixture was set aside at room temperature for 18 h. Next day, it was extracted with three 100 ml-portions of chloroform and the organic layer was washed with 0.2 N NaOH (50 ml) and water. Centrifugation helped to overcome the troublesome emulsion formation at this stage. After being dried over anhydrous Na_2SO_4 the *levo*rotatory solution was concentrated *in vacuo* to a volume of 10 ml whereupon redistilled aniline (1 ml) was added. Next day, the solvent was removed and the residue triturated with ethyl acetate (10 ml) to give the crude, crystalline phenylthiourea derivative. This was dissolved in hot ethyl acetate (100 ml), treated with a little charcoal and the filtered solution concentrated to a volume of 25 ml. On cooling, colourless needles crystallized (117 mg, m. p. 137.5–138.5°). They were combined with additional material (103 mg) of the same m. p., separating from the mother liquor on standing. A specimen for analysis was prepared by two additional crystallizations from the same solvent, m. p. 139° (Found: C 58.90; H 8.18; N 8.65; S 19.81. Calc. for $C_{16}H_{26}ON_2S_2$: C 58.86; H 8.03; N 8.58; S 19.64), $[\alpha]_D^{24}$ −45.0° ± 1.5° ($CHCl_3$, c = 0.8). The infra-red spectrum (in KBr) displayed strong sulphoxide group absorption, apparent as a double band at 986 cm^{-1} and 1 003 cm^{-1}, the former peak being of highest extinction. This split peak character of the sulphoxide band has been frequently observed in this laboratory in spectra of similar compounds in the solid phase and may be attributable to strong hydrogen bonding or even chelation with the substituted thiourea-grouping. The split peak character of the S–O stretching mode around 1 000 cm^{-1} has been observed also by Susi *et al.*[14] in spectra of acids of the general type $RSO(CH_2)_{10}COOH$ in the solid state.

(−)-1-(8-Methylsulphinyloctyl)-3-phenylurea (IV). The above phenylthiourea (191 mg), dissolved in a mixture of ethanol (25 ml) and water (3.5 ml), was treated with a solution of $AgNO_3$ (199 mg) in ethanol, containing a slight amount of water, and the mixture was heated on the steam-bath for about 15 min. During this treatment a total of 1.17 ml of 1 N NaOH was gradually added to maintain neutral reaction. After cooling, precipitated Ag_2S (150 mg) (theoretical amount: 144 mg) was removed by filtration and the filtrate was evaporated to dryness. The residue crystallized in contact with a few ml of water and a pure specimen of the phenylurea was obtained as colourless, rhombic platelets after two recrystallizations from ethyl acetate, m. p. 121°, $[\alpha]_D^{23}$ − 59.7° ± 1.5° (96 % ethanol, c = 1.32) (Found: C 61.87; H 8.32; N 9.05. Calc. for $C_{16}H_{26}O_2N_2S$: C 61.91; H 8.44; N 9.03). The infra-red spectrum (in KBr) was indicative of the presence of a sulphoxide grouping exerting a strong absorption band at 1 005 cm^{-1} with an inflexion near 1 015 cm^{-1}.

Reduction of (IV) to (V). A solution of the sulphoxide-phenylurea (IV) (84 mg) in ethanol (10 ml), containing conc. HCl (0.4 ml), possessed the initial rotation −0.46°. Acid-activated zinc dust (54 mg) was added and the mixture was heated to reflux for 15 min, when the rotation had changed to zero. After filtration, the solution was taken to dryness *in vacuo;* the oily residue crystallized in contact with water to give the crude sulphide-phenylurea (V) (73 mg). Recrystallizations, first from 70 % ethanol and then from ethyl acetate:hexane afforded a pure specimen with m. p. 69°, alone or in admixture with the synthetic sample described below. The two specimens furnished infra-red spectra which were identical throughout the spectral region examined (650−4 000 cm^{-1} cm).

Authentic 1-(8-methylthiooctyl)-3-phenylurea (V). A solution of 8-methylthiooctylamine [8] (268 mg) and phenyl *iso*cyanate (182 mg) in anhydrous xylene (5 ml) was refluxed for 10 min and the solvent then removed *in vacuo*. The crude reaction product (340 mg) was recrystallized from 70 % ethanol and twice from ethyl acetate : hexane to give an analytically pure specimen (175 mg) of the phenylurea, m. p. 70° (Found: C 65.15; H 8.86; N 9.49. Calc. for $C_{16}H_{26}ON_2S$: C 65.29; H 8.90; N 9.52).

(−)-8-Methylsulphinyloctylthiourea. An alkali-washed mustard oil fraction, prepared from 65 g of *Arabis hirsuta* seeds as described above, was treated overnight at room temperature with methanol (25 ml), saturated at 0° with ammonia. Next day, the solution was treated with charcoal and the solvent removed to give an oily residue, which was repeatedly extracted with hot ethyl acetate from which the crystalline thiourea (145 mg) separated on cooling. Two additional recrystallizations from the same solvent afforded an analytically pure specimen of hirsutin-thiourea as colourless prisms, m. p. 88° (Found: C 47.95; H 8.87; N 11.17. Calc. for $C_{10}H_{22}ON_2S_2$: C 47.97; H 8.86; N 11.19), $[\alpha]_D^{23}$ −76° (96 % ethanol, c = 1.0). The IR-spectrum (in KBr) exhibited strong bands at 3 400, 3 280, 3 200, 3 120, 2 930, 2 845, 1 624, 1 575, 1 460, 1 422, 1 342, 1 302, 1 258, 1 230, 1 193, 1 162, 1 070, 1 000 (S−O), 942 and 730 cm^{-1}. On paper chromatography in water-saturated chloroform the thiourea migrated at a rate corresponding to an R_{Ph}-value [15] of 0.84.

Identification of hydrolysis products of glucohirsutin. A band chromatogram of the crude glucoside mixture from seeds of *Arabis hirsuta* was produced by using the upper layer of the solvent system: *n*-butanol:pyridine:water (6:4:3) as the mobile phase. The glucohirsutin-band (R_B-value 0.75), located by spraying two edge-cuts with $AgNO_3$, was eluted with water.

The dry residue was subjected to hydrolysis with conc. HCl for 18 h at room temperature and the concentrated solution chromatographed on paper for hydroxylamine by the method of Bremner [16] with methanol:6 N HCl (7:3) as the solvent system. Spraying with ethanolic picryl chloride revealed a spot of hydroxylamine indistinguishable from that given by an authentic sample of hydroxylamine hydrochloride on the same chromatogram.

Separate band eluates, prepared in the same manner, were subjected to enzymic hydrolysis in unbuffered solution with a sulphate-free myrosinase preparation. Sulphate liberation was revealed by precipitation of $BaSO_4$, and glucose established as a hydrolytic fragment by paper chromatography in *n*-butanol:ethanol:water (4:1:4) followed by spraying with aniline phthalate. Appropriate blanks were checked in all determinations.

The authors are indebted to Dr. R. Gmelin for valuable assistance in the preliminary phases of the present work. Microanalyses were performed in this laboratory by Mr. P. Hansen.

The work is part of investigations supported by *Statens Almindelige Videnskabsfond (The Danish State Research Foundation)* and *Carlsbergfondet (The Carlsberg Foundation)*. A special grant from *Kai Hansens Fond* is gratefully acknowledged.

REFERENCES

1. Schmid, H. and Karrer, P. *Helv. Chim. Acta* **31** (1948) 1017.
2. Schultz, O.-E. and Gmelin, R. *Arch. Pharm.* **287/59** (1954) 404.
3. Kjær, A. and Gmelin, R. *Acta Chem. Scand.* **10** (1956) 1100.
4. Schmid, H. and Karrer, P. *Helv. Chim. Acta* **31** (1948) 1497.

5. Kjær *et al. To be published.*
6. Schultz, O.-E. and Wagner, W. *Z. Naturforsch.* **11b** (1956) 417.
7. Kjær, A. and Gmelin, R. *Acta Chem. Scand.* **10** (1956) 1358.
8. Kjær, A. and Christensen, B. *Acta Chem. Scand.* **11** (1957) 1298.
9. Kjær, A., Gmelin, R. and Boe Jensen, R. *Acta Chem. Scand.* **10** (1956) 1614.
10. Schultz, O.-E. and Wagner, W. *Z. Naturforsch.* **11b** (1956) 73.
11. Kjær, A. *Encyclopedia of Plant Physiology*, Springer-Verlag, Berlin-Göttingen-Heidelberg, 1958, Vol. IX, p. 71.
12. Wagner, W. *Papierchromatographische Analyse der Senfölglucoside, präparative Darstellung ihrer Acetylderivate und ein Beitrag zu ihrer allgemeinen Struktur* (Diss.) University, Tübingen 1956, p. 18.
13. Ettlinger, M. G. and Lundeen, A. J. *J. Am. Chem. Soc.* **78** (1956) 4172.
14. Susi, H., Koenig, N. H., Parker, W. E. and Swern, D. *Anal. Chem.* **30** (1958) 443.
15. Kjær, A. and Rubinstein, K. *Acta Chem. Scand.* **7** (1953) 528.
16. Bremner, J. M. *Analyst* **79** (1954) 198.

Received February 15, 1958.

ACTA CHEMICA SCANDINAVICA 12 (1958) 839—850

Studies on Yeast Invertase

III. Inhibition by Ag^+. Model Experiments with Egg Albumin *

KARL MYRBÄCK

Institute of Organic Chemistry and Biochemistry, University of Stockholm, Sweden

Yeast invertase is strongly inactivated by Ag+ and certain other metal ions. Several reasons, *i. a.* the fact that iodine-treated invertase is rather insensitive to Ag+, support the assumption that Ag+ is bound to HS-groups of the protein. Since the Ag-inhibition of the enzyme is strongly dependent on pH in the range 4—7 it is concluded that certain groups, probably imidazole groups, of the enzyme interfere with the HS-groups, rendering them unavailable to Ag+ in acid solution where the imidazole groups are protonated. For a comparison the Ag-binding capacity of egg albumin has been determined, directly as well as indirectly, using invertase for the Ag determination. The experiments support the view that Ag+ is bound to egg albumin principally if not exclusively to HS-groups. The binding of Ag+ by egg albumin is practically independent of pH in the pH-range mentioned, *i. e.* the HS-groups of egg albumin are, in contrast to those of invertase, freely available to Ag+ in this range. In agreement with earlier investigations the number of HS-groups in an egg albumin molecule (M = 44 000) is found to be 5.

In earlier investigations from this laboratory it was found [1,2] that, to explain the inhibition of yeast invertase by various mercury compounds, the assumption of a reaction of Hg with sulfhydryl groups of the enzyme appears to be consistent with all known facts. The enzyme is also strongly inhibited by Ag^+ (and several other heavy metal ions) and *a priori* one would be inclined to regard HS-groups as responsible also for these inhibitions. However, the inhibition by Ag^+ and certain other metal ions show a dependence on the acidity of the medium which seems to indicate a reaction of the metal ions with groups of the enzyme [3–9] having pK-values around 7. Several reasons, among others the fact that the complexing of Ag^+ by histidine [8] shows the same dependence on pH as the inhibition of the enzyme, suggest a participation of imidazole groups in the reaction of the enzyme with Ag^+. However, the affinity of histidine, not to speak of histamine [2] or imidazole [6], for Ag^+

* Part II, *cf.* Ref.[2]

is very weak compared to that of the enzyme, and if the assumption is correct that the Hg-inhibition of the enzyme is mediated by HS-groups it seems impossible to believe that Ag^+ with its very high affinity for sulfhydryl groups [6] should react preferentially with imidazole groups of invertase.

Investigations on iodine-treated invertase [2] appear to furnish an explanation of the somewhat conflicting experimental evidence. Treatment of yeast invertase with moderate amounts of iodine for a short time results in the formation of a modified enzyme "I-invertase", having an activity about 55 % of that of the native enzyme. Although iodine may conceivably act in several different ways on a protein, the simplest explanation is an oxidation of HS-groups. In the case of yeast invertase this assumption is strongly supported by the fact that I-invertase is much less sensitive to Ag-, Hg- and other inhibiting metal ions than the native enzyme [2]. In fact, the affinity of I-invertase for Ag^+ is so low that the Ag-inhibition of this modified enzyme may well be explained as a reaction of the metal ion with imidazole groups of the protein.

The experiments on the metal ion inhibition of invertase and I-invertase appear to show conclusively that HS-groups are in the first place responsible for the high affinity of the native enzyme for Hg, Ag and certain other metal ions. However, it remains to explain the pH-dependence of the Ag-inhibition of the enzyme. A tentative explanation has been given [2], involving the assumption of some sort of interaction, in the native enzyme, of the HS-groups with adjacent imidazole groups, possibly hydrogen bonding. Under all circumstances we have to conclude that in acid solution (pH $<$ *ca.* 5) the HS-groups of native invertase are unavailable ("masked") to the Ag ion. However, with pK $\sim$ 6.7 the native enzyme is converted reversibly to a structurally different form in which the HS-groups are available to Ag^+. If the groups with pK $\sim$ 6.7 are imidazole groups, which seems probable, it must be concluded that in the active enzyme these groups are protonated, but that loss of the proton is followed by a more or less radical change of protein structure, accompanied by reversible inactivation of the enzyme and by unmasking of the HS-groups. The reactivity of the HS-groups toward Ag and certain other metal ions will be determined by the presence or absence of the proton on the imidazole groups. Thus, in the interaction with Ag^+ (Cu^{++} etc.) the HS-groups of native invertase will have an apparent pK value of ca. 6.7. This is in accord with the assumption [3] that the Ag-binding groups of invertase are identical with the "acidic" group with pK $\sim$ 6.7, assumed by Michaelis [10] to explain the alkaline branch of the activity-pH-curve of invertase.

In order to compare the binding of Ag^+ by invertase and by a well-known, "ordinary" protein, experiments have been carried out with egg albumin which is known to contain more or less reactive HS-groups. Since this protein is easily available and can be obtained in a high degree of purity, it has been the object of a large number of investigations. The molecular weight has been determined by several authors; the values differ somewhat but a value of M = 44 000 should not be far from correct [11,12]. This value has been used in the following.

The number of HS-groups in an egg albumin molecule (or its cysteine content, respectively) has been determined by means of many different methods. Mirsky and Anson [13] and Anson [14] compared the action of several HS-

reagents; oxidation with ferricyanide under specified condition was considered to give reliable values. Native egg albumin was found to be inert to this reagent, but the denatured protein reduced ferricyanide: 10 mg protein corresponded to 0.001 mmole of the oxidant, *i.e.* one molecule of egg albumin was found to contain ca. 4.4 HS-groups. Iodine and iodoacetamide were found to react with the native protein, other HS-reagents generally only after denaturation. Egg albumin, treated with iodine, iodoacetamide or formaldehyde did not reduce ferricyanide. The authors conclude that native egg albumin has "free and accessible but relatively unreactive HS-groups which can react with iodine and acetamide despite the fact that they do not react with ferricyanide, porphyrindin or nitroprusside". Greenstein [15] and Brand and Kassell [16] likewise state that native egg albumin does not react with porphyrindin; in the denatured protein the HS-groups are oxidized. Values quoted by Greenstein and Jenrette [17] tend to show that at least 4, probably 5 HS-groups are present in an egg albumin molecule. Hellerman *et al.*[18], using iodosobenzoate, also give the number of HS-groups in egg albumin as 5. MacDonnell, Silva and Feeney [19] applied *p*-chloromercuribenzoate to egg albumin. They found, contrary to Anson's results, that 3 HS groups are reactive already in the *native* protein and 4 after denaturation. With a spectrometric method Boyer [20] found that 4.0 moles *p*-chloromercuribenzoate are bound at pH 4.6 by one egg albumin molecule, whereas Benesh, Lardy and Benesh [21] using an amperometric titration method with silver found 5 HS-groups per protein molecule.

Anson [14] found that iodine destroys the HS-groups of egg albumin. It seems to be generally assumed that the oxidation of protein HS-groups results in the formation of disulphide linkages. It should be noted, however, that according to Fraenkel-Conrat [22] the HS-groups of tobacco mosaic virus protein on treatment with iodine give stable sulphenyl iodide groups. "Overoxidation" of thiol groups to levels higher than the disulphide must also be considered. It should be emphasized that formation of disulphide linkages on treatment of proteins with iodine requires a sterically favourable position of the thiol groups, especially if intramolecular disulphide linkages are formed (*cf.* Ingram [23]).

EXPERIMENTAL

Materials

Invertase. The enzyme preparations used in the experiments were partly purified from autolysates of baker's yeast. The solutions were thoroughly dialyzed before use.

I-Invertase was prepared as described earlier [2]. The solutions were dialyzed with particular care to remove all iodide ions.

Buffer. Acetate-acetic acid buffers were used in all experiments. The buffer concentration was kept so low that complexing av Ag^+ by the acetate ion did not cause any serious decrease of the calculated Ag-ion concentration [5]. In the assay mixtures used for determination of enzymatic activity the concentration of the acetate ion was 0.01 N and in the solutions used for electrometric Ag-determination 0.05 N.

pH was determined by means of the glass electrode in all assay mixtures.

Egg albumin. Crystallized egg albumin was prepared according to the method of Sørensen and Høyrup [24] with minor modifications: *Albumin I* was recrystallized once, *Albumin II* three times. All albumin solutions were dialyzed thoroughly before use. The two albumin preparations behaved identically in all experiments; consequently the observed effects can be ascribed to egg albumin itself. *Albumin III* was a commercial pre-

paration; dialyzed solutions were used for a comparison in some experiments without further purification. Qualitatively it behaved as the crystalline preparations but its Ag-binding capacity was somewhat lower.

Methods

Invertase activity was determined polarimetrically as described earlier [4]. The relative activity (RA) refers to the activity of the same amount of enzyme without inhibitor at pH 4.5. The RA-values are means of 4—5 polarimetric determinations at different reaction times. All enzymatic determinations were carried out in 100 ml volume, containing 4.75 g saccharose. Temperature 30°C.

Electrometric determination of the Ag+ ion was carried out according to the simple method originally described by v. Euler and Svanberg [25]. These authors determined the Ag-binding capacity of various substances in order to find out the chemical nature of the Ag-binding groups of enzymes. They found, among other things, that egg albumin binds Ag+ very strongly. In the present investigation the electrometric determinations were carried out at several different pH-values; this is necessary since the Ag-binding capacity of invertase varies strongly with pH.

RESULTS

Binding of Ag^+ by egg albumin, determined electrometrically

The electrode vessels contained 5×10^{-5} M silver nitrate, acetate buffer (0.05 N Ac^-); to one of the vessels egg albumin solution was added. Total volume 20 ml, temperature 20°C. The constancy of the potential differences between the silver electrodes was checked by repeated measurements during at least 30 min. The Ag^+ concentrations were calculated in the conventional way (Table 1).

Table 1. Binding of Ag+ by crystalline egg albumin. $[Ag_{tot}] = 5 \times 10^{-5}$.

mg Albumin II in 20 ml	$[Ag^+] \times 10^5$		
	pH 4.5	pH 5.3	pH 5.95
0	5.00	5.00	5.00
2.82	3.55	3.25	2.74
5.64	1.94	1.33	1.12
8.46	0.44		

Fig. 1 shows the number of Ag^+ ions bound per molecule of egg albumin at different pH-values. For a comparison Fig. 2 shows corresponding results [8] for histidine. The Ag-binding capacity of histidine varies very strongly with pH in the range 4.5—6; the explanation is that H^+ competes with Ag^+ for the imidazole ($pK \sim 6.1$). In contrast, the Ag-binding of egg albumin is nearly independent of pH in the same range, showing that the groups essentially responsible for the binding of Ag^+ to the protein do not change their charge appreciably in the pH-range mentioned. This is obviously in accord with the assumption, that the binding of silver to egg albumin is mediated principally by HS-groups of the protein. The weak dependence of the silver-

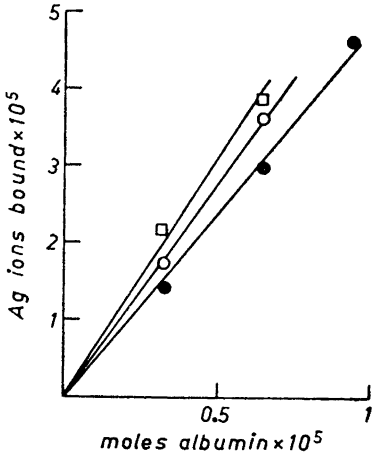

Fig. 1. Number of Ag ions (volume 1 000 ml) bound by egg albumin at pH 4.5 (●) pH 5.3 (○), and pH 5.95 (□).

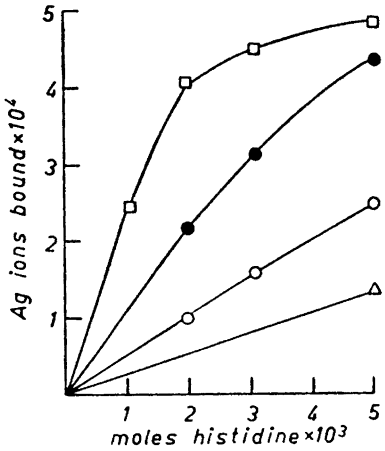

Fig. 2. Number of Ag ions (volume 1 000 ml) bound by histidine at pH 4.5 (△), pH 4.8 (○), pH 5.3 (●), and pH 5.95 (□).

binding of egg albumin upon pH may intimate that other groups than HS-groups are, to some small degree, responsible for the binding of silver ions, and that these groups have pK-values in the range 4—8.

In Fig. 1 the molar concentration of albumin has been calculated, assuming the molecular weight to be 44 000. The practically straight lines of the figure show that the affinity of egg albumin for Ag^+ is very high and the number of Ag^+ ions bound by one molecule of egg albumin can be calculated fairly accurately. One albumin molecule binds:

at pH 4.5	4.8 Ag^+ ions
at pH 5.3	5.5 » »
at pH 5.95	6.2 » »

Similar experiments were also carried out at the 10-fold Ag^+ concentration, 5×10^{-4} M. These experiments were less well reproducible; sometimes a precipitate was formed when protein and silver solutions were mixed. Nevertheless, as seen from Table 2, the results are in good agreement with those

Table 2. Binding of Ag+ by crystalline egg albumin. $[Ag_{tot}] = 5 \times 10^{-4}$.

mg Albumin II in 20 ml	$[Ag^+] \times 10^4$	
	pH 4.5	pH 5.3
0	5.00	5.00
14.1	—	3.68
28.2	2.89	2.58
42.3	1.72	1.64
56.4	0.84	0.65

Table 3. Binding of Ag+ by commercial egg albumin. $[Ag_{tot}] = 5 \times 10^{-5}$.

mg Albumin III in 20 ml	[Ag+] × 10^5			
	pH 4.5	pH 5.3	pH 5.7	pH 5.95
0	5.00	5.00	5.00	5.00
2.35	3.57	3.72	3.31	3.57
4.70	—	2.87	2.47	2.27
7.05	1.94	1.77	1.40	1.20
11.75	0.72	—	—	—
23.50	—	0.24	—	—

obtained in more diluted solutions: The metal ion is bound very strongly and the amounts bound at pH 5.3 are only slightly larger than those bound at pH 4.5. About 6 Ag ions are bound per molecule of albumin. This value is somewhat higher than that found in the experiments in more diluted solution. The explanation may be that at higher concentrations more Ag^+ ion is bound by non-HS-groups of the albumin.

Corresponding determinations were also carried out with the albumin preparation III. The lower Ag^+ concentration was used. Table 3 shows that the Ag-binding capacity of albumin III is slightly lower than that of albumins I and II; otherwise the results with all three preparations are very similar.

Binding of Ag^+ to egg albumin, determined by inhibition experiments with invertase

The Ag-binding capacity of egg albumin (or any other Ag-binding substance, not interfering with invertase) may be determined by studying the inhibition of invertase by Ag^+ in the presence of the substance in question. These deter-

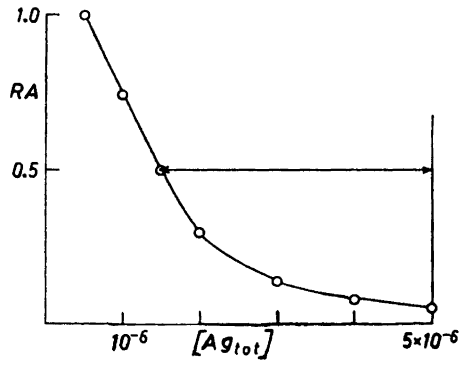

Fig. 3. Relative activity (RA) of invertase at various concentrations, $[Ag_{tot}]$, of silver ions; pH 5.3.

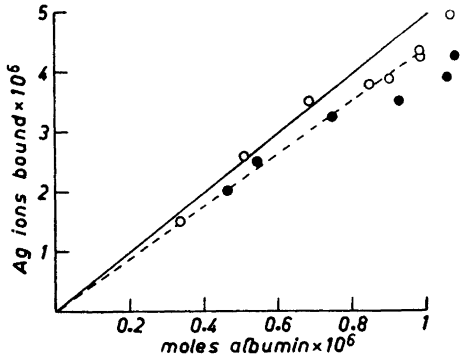

Fig. 4. Number of Ag ions in 1 000 ml bound by egg albumin at pH 5.3 as calculated from inhibition of invertase. Crystalline egg albumin (○), commercial preparation of albumin (●).

minations may be carried out at considerably lower Ag^+ concentrations than the electrometrical determination described above.

The invertase used for experiments of this kind need not be of any extremely high purity. The relative activity of a certain amount of enzyme is determined at constant pH and various Ag^+ concentrations. In one series of experiments the curve shown in Fig. 3 was obtained. A certain RA-value corresponds to a certain concentration of free Ag^+ ions, $[Ag_{free}]$, in equilibrium with $[Ag_{bound}]$, *i. e.* the concentration of Ag bound to invertase and, usually, to impurities in the invertase solution. For instance, RA = 0.06 corresponds to $[Ag_{tot}] = [Ag_{free}] + [Ag_{bound}] = 5 \times 10^{-6}$. If an experiment is carried out at this total Ag-concentration in the presence of, *e.g.* 3 mg of egg albumin, part of the silver will be bound to the albumin and a higher RA-value will be obtained, *e.g.* RA = 0.5. It is seen from Fig. 3 that this RA-value corresponds to a sum of free Ag-ion and Ag bound to substances in the enzyme solution $= 1.5 \times 10^{-6}$. Since the volume of the solution is 100 ml, we find that 3.5×10^{-7} g-ions Ag^+ have been bound by 3 mg egg albumine or 0.68×10^{-7} albumin molecules, *i.e.* one albumin molecule has bound 5 silver ions.

It should be added that experiments of this kind can give clearcut results only if *a*) the inhibition of the enzyme by Ag+ is independent or practically independent of the time of incubation of enzyme and inhibitor, and *b*) the binding of Ag^+ by the tested substance (egg albumin) is (practically) independent of any incubation time. If these requirements are not fulfilled the determination of the RA-values will be impossible or precarious. In the case of yeast invertase and Ag+ and of egg albumin and Ag+ the binding of the metal ion occurs with unmeasurably high velocity, and incubation of the proteins with Ag+ for reasonable times does not increase materially the uptake of the metal ion.

Using the method outlined above a series of experiments was carried out at pH 5.3 and $[Ag_{tot}] = 5 \times 10^{-6}$ in the presence of various amounts of recrystallized egg albumin (Table 4). The concentration of Ag bound by the albumin was estimated by means of the curve shown in Fig. 3. Fig. 4 shows the number of bound Ag-ions *vs* the number of albumin molecules. The curve is a practi-

Table 4. Relative activity (RA) of invertase at pH 5.3 and $[Ag_{tot}] = 5 \times 10^{-6}$ in the presence of crystalline egg albumin.

Albumin I mg/100 ml	RA	$[Ag_{tot}] \times 10^6$ corresponding to RA	$[Ag] \times 10^6$ bound by albumin
0	0.064	5.0	0
1.48	0.114	3.5	1.5
2.22	0.214	2.4	2.6
2.96	0.479	1.5	3.5
2.96 *	0.479	1.5	3.5
3.70	0.647	1.2	3.8
4.00	0.721	1.1	3.9
4.28	0.875	0.75	4.25
4.28 *	0.923	0.65	4.35
4.73	1.00	0	5.00

* Albumin incubated with Ag+ during 30 min before determination of RA.

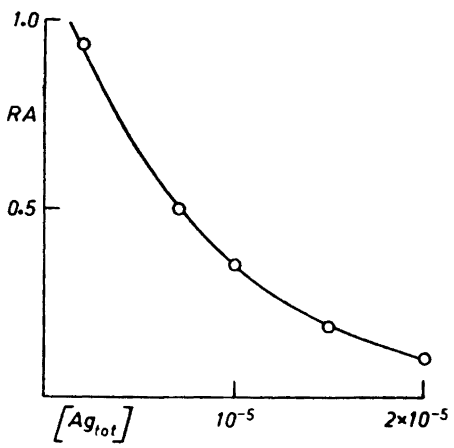

Fig. 5. Relative activity (RA) of invertase at various concentrations, [Ag_{tot}], of silver ions; pH 4.5.

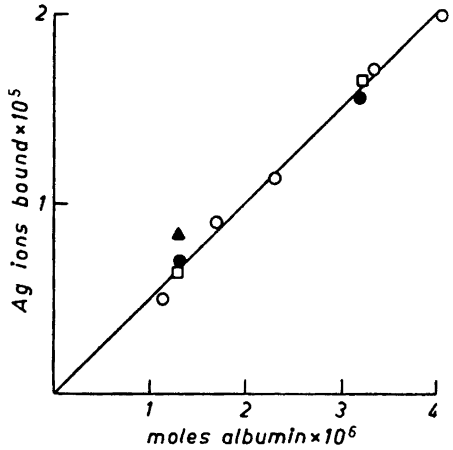

Fig. 6. Number of Ag ions in 1 000 ml bound by egg albumin at pH 4.5 as calculated from inhibition of invertase. Crystalline egg albumin I (○), crystalline egg albumin II (□), crystalline egg albumin II, treated with N NaOH (▲), crystalline egg albumin, treated with pepsin (●).

cally straight line, showing that Ag is bound very strongly by the albumin. One molecule of egg albumin binds 5.0 Ag ions; this number is in reasonably good agreement with that obtained (5.5) by electrometrical Ag-determination at the same pH.

In Fig. 4 have also been plotted corresponding values obtained with the commercial egg albumin preparation III. The results are qualitatively the same as with the crystalline albumin preparation but, as in the electrometric determinations, the values are somewhat lower with the commercial preparation.

Similar experiments with crystalline egg albumin were carried out at pH 4.5. The same invertase preparation was used and the RA-values in absence of egg albumin are plotted in Fig. 5 *vs.* [Ag_{tot}]; a comparison with the corresponding curve for pH 5.3 (Fig. 3) shows the much weaker inhibition by Ag^+ in the more acid solution: 50 % inhibition at pH 5.3 is caused by [Ag_{tot}] = 1.5×10^{-6} N Ag^+, at pH 4.5 by [Ag_{tot}] = 7×10^{-6} N.

The experiments in presence of egg albumin were carried out at [Ag_{tot}] = 2×10^{-5} and the amounts of Ag bound were calculated as above (Table 5). The native albumin preparations I and II were used as well as albumin II treated with alkali (N sodium hydroxide, 120 h, 20°). A peptic hydrolysate of egg albumin was also tested: Heat-coagulated albumin was treated with a small amount of pepsin at pH 1.6 (sulphuric acid). The coagulum was dissolved after *ca.* 5 h. The Ag-binding capacity of the hydrolysate was determined after 24 and 72 h, respectively. In Fig. 6 the number of bound Ag-ions have been plotted *vs.* the number of albumin molecules. The figure shows that all albumin preparations have the same Ag-binding capacity.

Table 5. Relative activity (RA) of invertase at pH 4.5 and $[Ag_{tot}]$ 2×10^{-5} in the presence of various albumin preparations.

Albumin preparation	mg Albumin in 100 ml	RA	$[Ag_{tot}] \times 10^5$ corresponding to RA	$[Ag] \times 10^5$ bound by albumin
—	0	0.100	2.00	0
Albumin I	4.44	0.168	1.50	0.50
	7.40	0.294	1.10	0.90
	10.36	0.420	0.86	1.14
	14.80	0.846	0.30	1.70
Albumin II	5.64	0.206	1.35	0.65
	14.10	0.804	0.33	1.67
Albumin II stored in N NaOH	5.65	0.287	1.15	0.85
	28.2	1.00	0	2.00
Albumin treated with papain	5.64	0.234	1.30	0.70
	14.1	0.700	0.44	1.56

The straight line of the figure demonstrates that at pH 4.5, just as in the experiments at pH 5.3, Ag^+ is bound by egg albumin very strongly. The number of Ag-ions bound per molecule of egg albumin is 5.0, *i.e.* the same number as was found at pH 5.3. Thus these experiments, in agreement with the electrometrical determinations, show that the Ag-binding capacity of egg albumin, in contrast to that of invertase, does not vary appreciably with pH in the range mentioned. The experiments are in accord with the view that Ag is bound to egg albumin by means of the HS-groups.

Ag-binding capacity of iodine-treated egg albumin

Iodine-treated invertase (I-invertase) is very much less sensitive toward Ag-ions than is the native enzyme [2]. This strongly supports the assumption that the high Ag-binding capacity of native invertase is due chiefly to HS-groups of the enzyme which, on treatment with iodine, are oxidized to yield groups (disulfides or possibly higher oxidation products) that have no or only a weak affinity for the Ag-ion.

If the binding of Ag by egg albumin, established in the experiments described in the foregoing, is mediated chiefly by HS-groups of the protein, then it should be expected that treatment of the egg albumin with iodine would markedly decrease its Ag-binding capacity. As mentioned, Anson [14] found that the HS-groups of native egg albumin are available to iodine; iodine-treated egg albumin does not reduce ferricyanide.

A diluted solution of crystalline egg albumin was treated with iodine approximately in the same manner as that used for the oxidation of invertase. The transformation of invertase to I-invertase occurs practically instan-

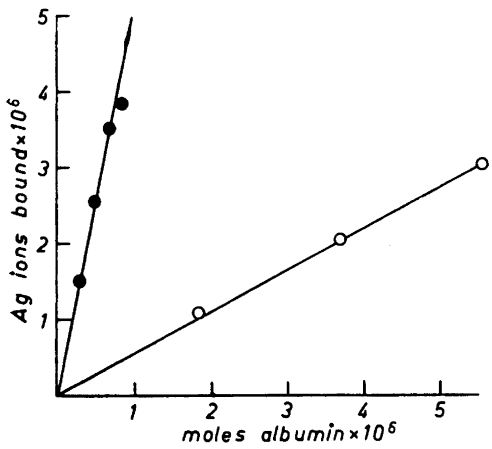

Fig. 7. Number of Ag ions in 1 000 ml bound at pH 5.3 by crystalline egg albumin (●), and by the same albumin oxidized with iodine (O).

taneously if a sufficient amount of iodine is added to the enzyme solution (pH about 5). To a certain volume of albumin solution was added a few drops of starch solution and then, dropwise, 0.01 N iodine solution until the blue colour persisted for about 30 sec. The same amount of iodine solution was then added to another albumin solution without starch. The oxidized albumin solution was freed from iodide ions by dialysis, the dry weight of the dialyzed solution was determined and suitable portions were used for the determination of the Ag-binding capacity at pH 5.3. The results are shown in Fig. 7 together with corresponding results for native egg albumin. It appears that the Ag-binding capacity of native egg albumin (5 Ag-ions per albumin molecule) has been strongly reduced by the treatment with iodine. The oxidized albumin binds less than 1 silver ion per molecule of M = 44 000. This supports the assumption that the combination of Ag with native egg albumin is mediated principally if not exclusively by the HS-groups.

DISCUSSION

A comparison of the binding of Ag^+ by yeast invertase and by egg albumin reveals several interesting facts. Both proteins bind Ag^+ very strongly, the egg albumin even more so than the enzyme; compare the straight lines of Figs. 1, 4 and 6 with the "dissociations curves" of Figs. 3 and 5. Whereas the invertase-Ag complex appears to have a dissociation constant[3,7] about 10^{-8}, the dissociation constant of the albumin-Ag compound seems to be considerably lower.

The number of Ag-ions bound by one molecule of egg albumin (M = 44 000), as determined by means of two independent methods, is 5.0—5.5. The slight deviation of the curves of Fig. 5 from the straight line may implicate that a small portion of the bound Ag is bound more loosely than the bulk which is bound very strongly. It seems probable that per molecule of egg albumin 5 Ag ions are bound by HS-groups and a further small number loosely bound by other groups, possibly imidazole groups. The weak dependence of the

silver-binding capacity of egg albumin on pH (Fig. 1) is also in accord with this view. The number of groups in egg albumin, strongly binding the silver ion, agrees with the number of HS-groups generally assumed to be present in the protein molecule. The fact that treatment of very diluted solutions of egg albumin with small amounts of iodine reduces the Ag-binding capacity to a very low value seems to show conclusively that Ag is bound to egg albumin chiefly by means of the HS-groups.

As mentioned before, previous investigations have shown the HS-groups of native egg albumin to be inaccessible to several HS-reagents, but accessible ("unmasked") after denaturation, *i.e.* an "unfolding" of the protein structure. It seems, however, that the HS-groups of the native protein react freely with silver ions, and practically no dependence of the silver-binding capacity on pH in the range investigated can be observed.

The reaction of invertase with iodine is probably accompanied by rather extensive changes in the superstructure of the protein. Such changes may explain why the activity of native invertase is not restored on treatment of I-invertase with cysteine or other reducing agents [2]. The binding of Ag^+ by invertase is not, or at least not immediately, followed by irreversible changes of the protein structure, since the inactivation of the enzyme by Ag^+ is freely reversible by H_2S, mercaptans etc., provided that the enzyme has not been incubated with the metal salt for a long time. From the behaviour of invertase in this respect no conclusion can of course be drawn regarding the behaviour of egg albumin; however, since the binding of Ag^+ by egg albumin is instantaneous and does not increase at incubation of protein and silver salt for a moderate time, it seems safe to assume that the reaction of Ag^+ with the HS-groups of egg albumin is not (rapidly) followed by destruction of the native protein structure. Thus it appears probable, that the HS-groups in native egg albumin are freely available to the silver ions without previous or simultaneous change of the protein structure.

The binding of Ag^+ by the HS-groups of egg albumin is not or only weakly dependent on pH in the range investigated. This means, that the phenomenon of a pH-dependent "masking" of the HS-groups, typical of yeast invertase, is not observed with egg albumin.

The experimental part of this investigation has been carried out by Mrs. Ebba Willstaedt whose assistance is gratefully acknowledged.

REFERENCES

1. Myrbäck, K. *Arkiv Kemi* **11** (1957) 471.
2. Myrbäck, K. and Willstaedt, E. *Arkiv Kemi* **12** (1958) 203.
3. Myrbäck, K. *Z. physiol. Chem. Hoppe-Seyler* **158** (1926) 160.
4. Myrbäck, K. and Willstaedt, E. *Arkiv Kemi* **8** (1954) 53.
5. Myrbäck, K. *Arkiv Kemi* **8** (1955) 393.
6. Myrbäck, K. *Arkiv Kemi* **11** (1957) 47.
7. Myrbäck, K. and Willstaedt, E. *Arkiv Kemi* **11** (1957) 275.
8. Myrbäck, K. *Stoll-Festschrift*, Birkhäuser, Basel 1957.
9. Myrbäck, K. *Arch. Biochem. and Biophys.* **69** (1957) 138.
10. Michaelis, L. und Davidsohn, H. *Biochem. Z.* **35** (1911) 386; Michaelis, L. und Rothstein, M. *Ibid.* **110** (1920) 217.
11. Rothen, A. *Ann. N. Y. Acad. Sci.* **43** (1942/43) 229.

12. Fevold, H. L. *Advances in Protein Chem.* **6** (1951) 188.
13. Mirsky, A. E. and Anson, M. L. *J. Gen. Physiol.* **18** (1934/35) 307; **19** (1935/36) 451.
14. Anson, M. L. *Science* **90** (1939) 142; *J. Gen. Physiol.* **23** (1939/40) 247, 321; *J. Biol. Chem.* **135** (1940) 797.
15. Greenstein, M. *J. Biol. Chem.* **125** (1938) 501; **128** (1939) 233; **130** (1939) 519; **136** (1940) 795.
16. Brand, E. and Kassell, B. *J. Biol. Chem.* **133** (1940) 437.
17. Greenstein, M. and Jenrette, W. V. *J. Biol. Chem.* **142** (1942) 175.
18. Hellerman, L., Chinard, F. P. and Ramsdell, P. A. *J. Am. Chem. Soc.* **63** (1941) 2551; Hellerman, L., Chinard, F. P. and Deitz, V. R. *J. Biol. Chem.* **147** (1943) 443.
19. MacDonnell, L. R., Silva, R. B. and Feeney, R. E. *Arch. Biochem. and Biophys.* **32** (1951) 288.
20. Boyer, P. D. *J. Am. Chem. Soc.* **76** (1954) 4331.
21. Benesh, R. E., Lardy, H. A. and Benesh, R. *J. Biol. Chem.* **216** (1955) 663.
22. Fraenkel-Conrat, H. *J. Biol. Chem.* **217** (1955) 373.
23. Ingram, V. M. *Biochem. J.* **59** (1955) 613.
24. Sørensen, S. P. L. and Høyrup, M. *Medd. Carlsberg Lab.* **12** (1915–1917) 12.
25. v. Euler, H. and Svanberg, O. *Fermentforsch.* **4** (1921) 142.

Received January 31, 1958.

ACTA CHEMICA SCANDINAVICA 12 (1958) 851—854

Distribution of D- and L-Amino Acids along the Chain of Poly-DL-Alanine

K. LINDERSTRØM-LANG

Carlsberg Laboratory, Copenhagen, Denmark

The question concerning the distribution of D- and L-forms along the peptide poly-DL-alanine has been investigated by digestion with carboxypeptidase and aminopolypeptidase which preferably attack bonds between two L-amino acids. The analysis of the digestion curves makes it likely that the distribution of D- and L-forms is very nearly random in the particular preparation under investigation.

In two previous papers [1,2] Arieh Berger and the author have explained the relatively high stability of the helix of poly-DL-alanine (PDLA) in aqueous solution by assuming that a certain number of pairs of D- and L-methyl groups form internal hydrophobic bonds from one turn of the helix to the next. Provided that the distribution of D- and L-forms is entirely random one fourth of all methyl groups would be able to form such bonds. Fig. 1 shows a model of the helix in question. It is built up by 30 alanine residues [1] and is right-handed. The pitch is 1.5 Å and there are 15 residues in four turns (see *e.g.* Refs.[3-5]). The D- and L-forms have been distributed by throwing a coin and it is therefore by chance that 7 out of 30 methyl groups are able to form hydrophobic bonds of the type assumed. Fig. 2 shows some of the characteristic distances in the model. The most important of these are:

1. Distance $C\beta\ L_5 \rightarrow C\beta\ D_8$, the closest approach of two methyl groups, one belonging to an L-alanine residue (8) and one to a D-alanine residue (5) (see Fig. 1). This distance is 3.74 Å.

2. Distance $C\beta\ D_8 \rightarrow O_8$ from a D-methyl group in a given residue to the carbonyl oxygen of the same residue. This distance is 2.70 Å.

The X-ray diffraction pattern of DL-alanine crystals [6,7] indicate that the corresponding minimum distances in the crystals are 3.64 and 2.52 Å, respectively. Hence from this comparison it may be concluded that there is no particular strain in our helical model.

However, other possible helical models have not been investigated and in view of reported strains in right-handed helical structures containing D-residues [8,9] an attempt was made to determine the distribution of D- and L-forms in the particular preparation of PDLA, the stability of which has

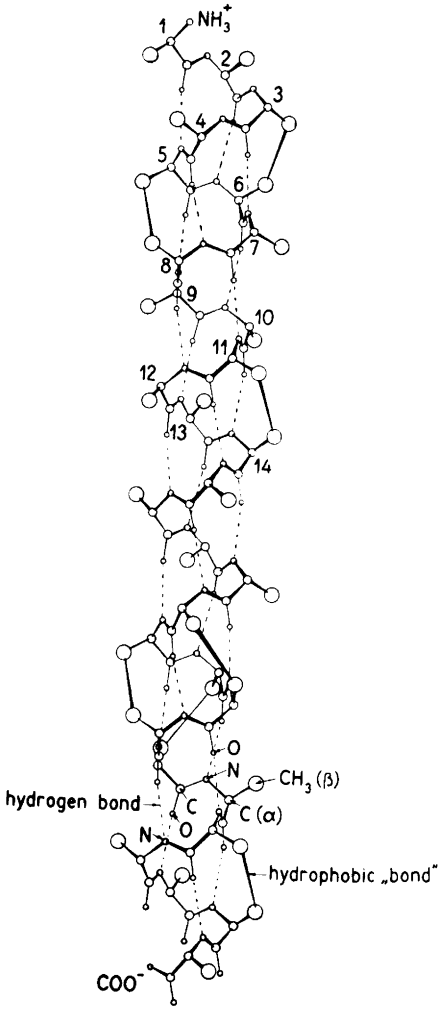

Fig. 1. Right-handed α-helix with 30 residues.

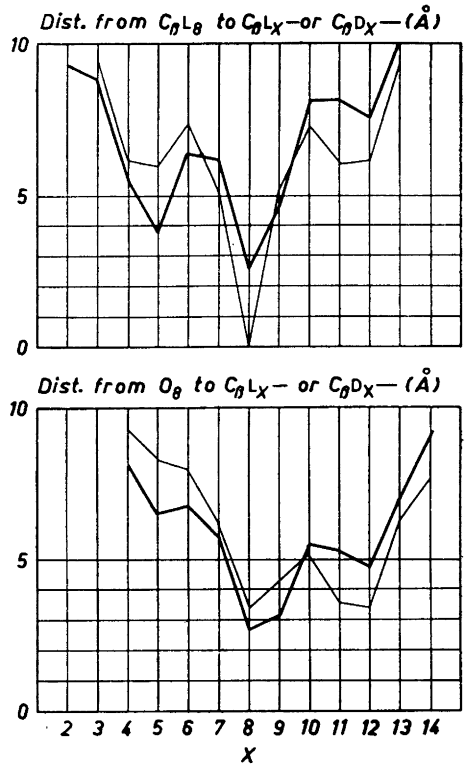

Fig. 2. Distances from atoms in residue 8 (see Fig. 1) to other atoms, numbered X. The distance $C\beta L_8 - C\beta D_8$ is between two β-carbon atoms (two methyl groups) on one α-carbon atom. Many of the other distances are calculated for arbitrary distributions of D- and L-forms and are not found in Fig. 1.

been studied [1,2]. In theory an optically inactive PDLA may consist of equal parts of right-handed helices with L-amino acid residues only and left-handed helices with D-amino acid residues only. Both these forms are generally acknowledged as being without strain. If now our preparation were constituted in this way, the above mentioned explanation of the stability as being due to internal hydrophobic bonds would fail, since the distance between the L-methyl groups in our right-handed model is too large to give effective hydrophobic bonds from one helical turn to another. The same is true for a left-handed helix with D-residues. In order to decide this important ques-

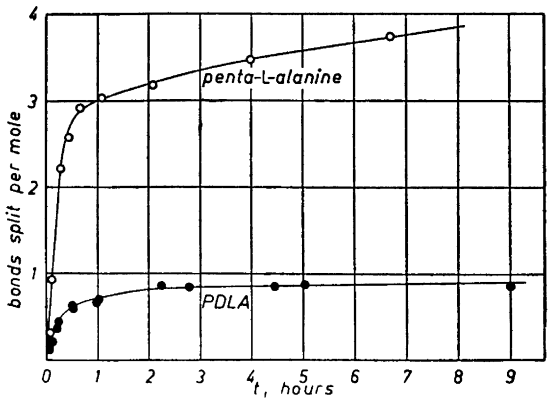

Fig. 3. Splitting of penta-L-alanine and PDLA by carboxypeptidase.

tion our PDLA preparation was digested with carboxypeptidase *, an enzyme which splits polypeptides from the carboxyl end provided the terminal amino acid residues have the L-configuration. Thus in penta-L-alanine ** 3 bonds were broken very fast while the last — in the remaining alanylalanine — was slowly split due to the proximity of the amino end group (Fig. 3). If now half of our PDLA preparation consisted of poly-L-alanine, we should expect a splitting of 14—15 bonds per mole of preparation, the remaining 14—15 bonds being situated in poly-D-alanine which is not attacked by the enzyme. As shown in Fig. 3 only 1/2—1 bond is actually split, indicating that D-amino acid residues are situated close to the carboxyl end in the majority of the molecules. It is easy to show that for random distribution of D- and L-residues the number of bonds, n, split per mole is given by

$$n = \frac{1 - (\frac{1}{2})^{q-1}}{2}$$

where q is the number of residues in the polypeptide, provided the action of carboxypeptidase is restricted to bonds between two L-amino acid residues, and

$$n = 1 - \tfrac{1}{2}^{q-1}$$

if bonds between L- and D-amino acid residues

$$\text{---}\ \text{---}\ \text{---}\ \text{D} \underset{\uparrow}{-} \text{L}$$

are attacked as well. For q equal to 30 it is therefore compatible with a random distribution of D- and L-residues that a fast reaction involving 1/2 bond per mole is observed. The further reaction leading to a splitting of another 1/2 bond may be due to a slow attack of the enzyme on the L—D-bonds, but it may also be the result of the action of a slight proteinase impurity in the

* The enzyme used was kindly placed at our disposal by Professor H. Neurath.
** This preparation was kindly given us by Professor Hans T. Clarke.

carboxypeptidase (see below). Such an impurity might open a bond in the middle of the chains thus exposing new C-terminal L—L-sequences to the carboxypeptidase. Finally the results might indicate a slight deviation from randomness of the distribution of D- and L-amino acid residues.

Similar experiments with aminopolypeptidase * gave essentially the same, though slightly lower results which might be explained by a low content of substituted terminal amino groups in PDLA [1]. We feel therefore justified in assuming random — or nearly random — distribution of D- and L-alanine residues along the chain of PDLA.

In the case of PDLA the carboxypeptidase experiments were carried out as follows: To 500 μl 1.57×10^{-2} M PDLA solution were added 500 μl 0.2 M veronal buffer pH 8.61 and 5 μl of a 1.8×10^{-4} M carboxypeptidase solution which was pre-treated with di*iso*propylfluorophosphate to knock out proteinase contaminations. The digestion mixture was prepared at 39.7°C and samples of 100 μl were taken out at intervals and mixed with 85 μl N/10 alcoholic HCl whereby the enzymatic reaction stopped. For determination of the splitting 2 ml acetone were added and the solution titrated with N/10 HCl in alcohol, using naphthylred as an indicator.

Substrate concentration	7.3×10^{-3} M
Enzyme »	8.6×10^{-7} M
Temperature	39.7°C

In the penta-alanine experiments the procedure was the same.

Substrate concentration	6.7×10^{-3} M
Enzyme »	8.6×10^{-7} M
Temperature	39.7°C

The author is indebted to Mrs. K. Mikkelsen for technical assistance.

REFERENCES

1. Berger, Arieh and Linderstrøm-Lang, K. *Arch. Biochem. and Biophys.* **30** (1957) 106.
2. Linderstrøm-Lang, K. *Symposium on Protein Chemistry*, Paris 1957 (*In press*).
3. Pauling, L., Corey, R. B. and Branson, H. R. *Proc. Natl. Acad. Sci. U. S.* **37** (1951) 205.
4. Pauling, L. *Record of Chemical Progress, Fall Issue, 1951*, p. 155.
5. Low, B. W. and Grenville-Wells, H. J. *Proc. Natl. Acad. Sci. U. S.* **39** (1953) 785.
6. Levy, H. A. and Corey, R. B. *J. Am. Chem. Soc.* **63** (1941) 2095.
7. Donohue, J. *J. Am. Chem. Soc.* **72** (1950) 949.
8. Yang, J. T. and Doty, P. *J. Am. Chem. Soc.* **79** (1957) 749, 761.
9. Elliott, A., Hanby, W. E. and Malcolm, B. R. *Nature* **178** (1956) 1170.

Received March 4, 1958.

* The preparation was kindly sent to us by Dr. Emil L. Smith.

ACTA CHEMICA SCANDINAVICA 12 (1958) 855—860

Investigations on the Osmotic Pressure of Aqueous Solutions of Dextran Glycerol Glycoside and of Potassium Hyaluronate

C. E. JENSEN and K. MARCKER

Københavns Universitets Fysisk-Kemiske Institut, Copenhagen, Denmark

A preparation of dextran giving a constant colloid osmotic pressure and having a molecular weight of 1.2×10^5 is prepared. It is shown that the ratio between the weight concentration (c) and the osmotic pressure (p) is fairly constant in the case of dilute solutions of the electrically neutral dextran; in case of dilute solutions of the electrically charged hyaluronate the value of this ratio decreases with increasing concentration. In respect to hyaluronate it is found that the relation between pressure and concentration can be given by the following expression: $c/p = A(1-Bc)$, where the constant B is independent of the molecular weight.

Although blood plasma substitutes, artificial "plasma expanders", were tried during the first world war, it was only during the second world war that their use developed. It seems to be a fact that dextrans surpass all plasma substitutes used so far, as they afford the most marked and most prolonged increase in circulating blood volume. Dextran which is a polymer of glucose joined chiefly through α-1,6-glycosidic linkages, is derived from the fermentation of sucrose by various strains of *Leuconostoc mesenterioides*. The native dextran has a molecular weight of several millions, and has a harmful effect when injected into the animal organism. When this so-called crude dextran is degraded, *e.g.* by acid hydrolysis, to a molecular size corresponding approximately to plasma proteins it becomes usable as "clinical dextran". If the partial depolymerization is carried out in glycerol solution (Hultin and Nordström [1]) the biologically active free aldehyde groups, often giving rise to allergic manifestations, are inactivated. By this process dextran glycerol glycoside is formed. Such a preparation is commercially available as "Infudex" or "Plasmodex *". The results of some osmotic investigations on such a preparation are reported in the present paper.

* This commercial preparation was kindly placed at our disposal by Roskilde Medical Company, Roskilde, Denmark.

EXPERIMENTS ON DEXTRAN

The colloid osmotic pressures were measured by means of the inverted microosmometer described by Christiansen and Jensen [2]. The solution of collodion used for the preparation of semipermeable membranes was made in the following way: 4 g of completely dry pyroxylin (Parlodion "Mallinckrodt") was dissolved in a mixture of 75 ml of absolute alcohol and 25 ml of anhydrous ether; to this mixture were added 5 ml of ethylene glycol freshly distilled *in vacuo*.

The first measurements were performed on an 1 % solution of "Plasmodex", the osmotic pressure of which was estimated at about 5.4 cm water pressure. It was observed, however, that the pressure was decreasing with time indicating that this preparation of dextran contained low molecular components capable of permeating the membrane employed. After 15 h the "equilibrium length" of the first mentioned solution had fallen to 4.5 cm; the result of this measurement is in Table 1.

In order to determine the proportion of low molecular components contained in this preparation of dextran the aqueous solution of the preparation was dialyzed for 24 h against running tap water in a tube of cellophane at room temperature. Then the dialyzed solution was distilled *in vacuo*, the temperature of the water being 40—45°C, and freeze-dried. The yield was 96 % of the starting material. Osmotic pressure measurements performed on this preparation showed, that a fraction of the dextran molecules was still permeating the collodion membrane and that the osmotic pressure was slightly lower than that of the nondialyzed preparation of dextran at the same concentration.

Then the dextran was dialyzed in a test-tube shaped membrane of collodion prepared in exactly the same way as the membranes used for the osmotic pressure measurements. The dialysis lasted for 6 days, the outer solution (distilled water) being replaced twice every 24 h, whereafter the solution was distilled *in vacuo* and freeze-dried. Yield: 40 % of the starting material. The osmotic pressure of a 0.6 % solution of this preparation was found to be about 2.6 cm water column. But even now some dextran molecules were permeating,

Table 1. Osmotic pressure of an 1 % solution of dextran. h = height of air column. V = rate of movement of the upper meniscus of the air column in micrometer divisions in 10 min. For details *cf.* Christiansen and Jensen [2].

h in cm	V in 10 min.
4.89	+0.18
3.80	−0.30
5.29	+0.38
6.27	+1.20
4.10	−0.18
5.73	+0.55

Equilibrium length: 4.5 cm

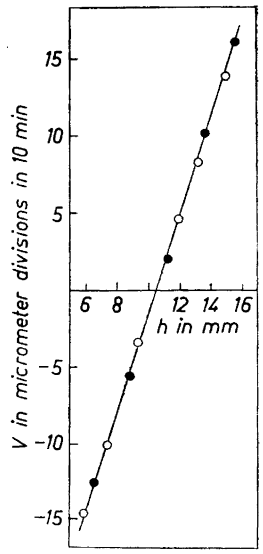

Fig. 1. Osmotic pressure of an aqueous solution of dextran. The graph shows the relation between height of the air column (abscissae), and the rate of movement of the upper meniscus of the air column (ordinates) in micrometer divisions in 10 min. Concentration of dextran: 5.20 mg in 1 ml of water. Equilibrium length: 10.5 mm water column. The measurements represented by the black spots are performed 24 h after the measurements represented by the circles.

although to a smaller degree than in the preceding experiment. Therefore another attempt was made to get rid of the low-molecular components by means of precipitation with acetone. 60 ml of acetone were added to 100 ml of a 10 % aqueous solution of dextran, which resulted in the appearance of a two-phase system. The lower layer was yellow and consisted predominantly of water and dextran, while the upper layer was white and consisted predominantly of acetone and little dextran. The upper layer was decanted, whereafter the lower layer was treated with acetone; by doing so the dextran was precipitated. The filtrate was washed several times with acetone and dried for 24 h in a vacuum desiccator containing phosphorus pentoxide. After dialysis in a collodion tube this preparation showed a constant osmotic pressure. The pressure of a 0.52 % aqueous solution was measured at 1.05 cm water column corresponding to a molecular weight of this preparation of 1.2×10^5. The result of these measurements are given in Fig. 1, the black spots corresponding to measurements performed 24 h after the measurements indicated by circles.

In order to investigate the validity of the well known limiting law of van't Hoff: $\lim_{c=0} (p/c) = RT$, where p is the difference in hydrostatic pressure between the inner and outer solutions at equilibrium, and c is the concentration of the solute in moles per liter of solution, we determined the osmotic pressure of dextran solutions at different concentrations of dextran. The results of these measurements are in Table 2. Evidently van't Hoff's law is valid at the lower concentrations, while at concentrations from about 2 g/100 ml a slight decrease of the ratio c/p is observed. Our results agree closely with those obtained by Mariani *et al.*[3] Further our results are in fair agreement with those obtained by Autio [4] who determined the osmotic pressure of solutions of dextran ("Macrodex") by means of the Holm-Jensen osmometer.

Table 2. The relation between concentration (c) and colloid osmotic pressure (p) of aqueous solutions of dextran.

c mg/ml	p cm	c/p
5.19	1.05	4.94
19.40	2.07	5.31
31.51	6.45	4.89
40.00	8.80	4.55

EXPERIMENTS ON POTASSIUM HYALURONATE

Using osmotic meaurements, Christiansen and Jensen [2,5] estimated the molecular weight of potassium hyaluronate isolated from human umbilical cords and from vitreous bodies of cattle at 5×10^5 and 2.7×10^5, respectively. These determinations were performed on solutions which contained about 10 mg of hyaluronate per 1 ml of solution.

Molecular weight calculations from osmotic pressure data were made by means of the equation: $\frac{246.8 \times 10^5 \times c}{p}$ where c = concentration of dry substance in g per 1 ml of solution and p = osmotic pressure in cm water pressure. All measurements were performed at 20°C.

It has long been known, however, that this equation is not valid for electrically charged thread-shaped molecules at concentrations where experiments could be performed. The ratio p/c, the so-called reduced osmotic pressure, usually increases with the concentration so that its limiting value must be determined by some sort of extrapolation. To perform this extrapolation we plotted p/c against c, but this yielded a curve with a distinct bend upwards. When, however, we plotted c/p against c we got curves which were very nearly straight lines with a downward slope.

Four preparations of different molecular weight were used, three of them having relatively small and one a relatively high molecular weight. The measurements of the colloid osmotic pressure were determined at four or five different concentrations of hyaluronate. The molecular weights calculated from the pressures obtained from extrapolation to zero concentration (the so-called reduced molecular weight) appeared to be about one and a half as big as the uncorrected values obtained from measurements performed on solutions containing about 10 mg of hyaluronate in 1 ml of solution.

Attempts at finding an adequate relation between the colloid osmotic pressure of the solution (or the molecular weight) and the concentration of the solute resulted in the following empirical expression: $c/p = A(1-Bc)$. Here c is the weight concentration (mg/ml); p is the colloid osmotic pressure in cm water pressure; A is a quantity which is constant for a given preparation, but proportional to the molecular weight; B is a constant for all the employed preparations (independent of the molecular weight). The values of A and AB were obtained graphically by plotting c/p against c. The results of the

Table 3. The osmotic pressure of some preparations of potassium hyaluronate and some calculated quantities showing that the ratio between concentration and pressure is equal to A(1−Bc) where A and B are constants (For details see the text).

Prep.	c Conc. in mg/ml	p Osmotic pressure in cm	c/p expt.	A From graph	AB From graph	$\frac{AB}{A} = B$	$A(1-B_{Av}c) = (c/p)_{calc.}$	$(c/p)_{expt.} - (c/p)_{calc.}$
I	16.00	7.9	2.03	5.1	0.190	0.0372	2.02	+0.01
	13.00	4.9	2.65				2.60	+0.05
	11.00	3.7	2.97				2.98	−0.01
	7.00	1.85	3.78				3.75	+0.03
	5.00	1.29	3.87				4.14	−0.27
II	16.00	6.5	2.46	5.8	0.215	0.0371	2.30	+0.16
	13.00	4.2	3.10				2.96	+0.14
	11.18	3.2	3.49				3.36	+0.13
	5.00	1.00	4.72				4.70	+0.02
III	7.51	1.85	4.06	6.0	0.219	0.0365	4.30	−0.24
	5.10	1.10	4.64				4.85	−0.21
	3.53	0.71	4.97				5.26	−0.29
	2.56	0.49	5.22				5.42	−0.20
IV	19.99	3.49	5.72	38.5	1.595	0.0401	9.47	−3.75
	16.00	1.20	13.33				15.28	−1.95
	13.78	0.85	16.21				14.48	−2.27
	10.21	0.45	22.69				23.68	−0.99
	7.48	0.28	26.71				27.64	−0.93

$B_{AV} = 0.0377$

measurements and the values of A, AB and B $\left(B = \frac{AB}{A}\right)$ are in Table 3. It is seen that the agreement between the measured values of c/p and $A(1 - B_{Av}c)$ is reasonably good. The most pronounced deviation is found in series IV at the highest concentration of hyaluronate, at which the measurements are difficult on account of the high viscosity of the solution. It is to be noted that the value used for B in the calculations is the average value of the individual B's of the four experiments. If we, in series IV, make use of the method of least squares giving equal weight to the individual experimental points we find the corrected values of A and AB to be 39.4 and 1.675, respectively. Using these values the differences between $(c/p)_{expt}$ and $(c/p)_{calc}$ are: − 0.24; 0.58; − 0.14; 0.34 and − 0.18, respectively.

From the results obtained from the experiments performed on dextran and on hyaluronate the difference in osmotic behaviour between solutions of electrically neutral and electrically charged substances is obvious from the fact that the values of c/p do not vary with the concentration of solute in the case of dextran, but do vary in the case of hyaluronate.

We are gratefully indebted to Professor J. A. Christiansen, head of the University Institute of Physical Chemistry, Copenhagen, for his inspiring guidance and valuable suggestions. One of us (C.E.J.) wishes to thank *Købmand i Odense Johann and Hanne Weimann, né Seedorf's Foundation*, and the *University of Copenhagen* for financial support.

REFERENCES

1. Hultin, E. and Nordström, L. *Acta Chem. Scand.* **8** (1954) 1296.
2. Christiansen, J. A. and Jensen, C. E. *Acta Chem. Scand.* **7** (1953) 1247.
3. Mariani, E., Ciferri, A. and Maraghini, M. *Ann. Chim.* **45** (1955) 1091.
4. Autio, L. *Studies on the Determination of Colloid Osmotic Pressure.* Mercatorin Kirjapaino. Helsinki 1955.
5. Christiansen, J. A. and Jensen, C. E. *Acta Chem. Scand.* **9** (1955) 1405.
6. Jensen, C. E. *Acta Chem. Scand.* **7** (1953) 603.

Received February 18, 1958.

ACTA CHEMICA SCANDINAVICA 12 (1958) 861—867

The Accelerating Capacity of Organic Polythionates and Polysulphides

N. HOFMAN-BANG and H. LETH PEDERSEN

Chemistry Department A, Technical University of Denmark, and Chemical Research Laboratory, Northern Cable and Wire Works Ltd, Copenhagen, Denmark

In natural rubber bis-*p*-tolylsulphonyl sulphide, disulphide and trisulphide (the socalled organic polythionates), di-benzoyl trisulphide and tetrasulphide provoke a fair vulcanisation at 162°C preferably in combination with 2 PHR (parts per hundred rubber) sulphur. The coefficients of vulcanisation are determined by means of ^{35}S. The physical state of China Clay containing vulcanisates are intermediate and the ageing stability equals that of similar DPG-vulcanisates, the benzoyl tetrasulphide being the best.

The formal analogy of the sulphur bond in thiurams and polysulphides —S — S— suggests a possibility of vulcanisation with polythionates. X-Ray investigations by Dawson *et al.*[1] of bis-*p*-tolylsulphonyl sulphide and trisulphide indicated a zig zag sulphur chain. Orientating measurements comprising bis-*p*-tolylsulphonyl sulphide and disulphide (abbrev. tol-tri, tol-tetra) and di-benzoyl trisulphide and tetrasulphide (abbrev. benz-tri, benz-tetra) revealed practically no cure in absence of sulphur, the ability to vulcanising was, however, distinct upon addition of 1 PHR of sulphur. For instance the sulphurfree tol-tetra in a clay-whiting compound showed a tensile of 55 kg/cm^2 and a halving time for the tensile at 70°C in air of 17 days.

The following experiments were carried out with 2 PHR of sulphur in combination with 2 PHR of accelerator. Rates of vulcanisation were indicated as moduli at 110 % elongation, measured with a 32 oz strain gage (Statham Laboratories [2]), operated at a strain rate of 750 mm/min. Sensitivity is about 2 g in stress.

The sulphur reaction was determined after introduction [3] of ^{35}S on a micro mill (10—20 g rubber) and vulcanisation of discs, 65 mm diam., 0.75 mm thick.

From these samples discs of 25 mm (4.91 cm^2) were cut for measurement of activity using a Geiger-Müller-tube and a Frieseke-Höpfner scaler counting 10 000 counts. The sulphur had an activity of about 60 μC and 2 parts gave with the 4.91 cm^2 sample about 1 500 counts per min. Afterwards the samples were wrapped in gauze and acetone-extracted for 18 h either in the bottom of an ordinary Soxhlet filled with silica Raschig rings in order to reduce the volume or in a ASTM micro extractor [4]. The samples were then airdried and the activity measured. The ratio of activities of unextracted to extracted specimens duly corrected for decay is used as a very convenient measure of gross bound sulphur. Ten or more samples are measured in a few hours and the determination of the coefficients of vulcanisation completed in 24 h.

Ageing tests were performed at 70°C ($\pm$ 0.5°) in air with dumbbell specimen[5] tested with a Zwick Z.125 tensile machine at an elongation rate of 800 mm/min at 25°C.

RATE OF VULCANISATION

The basic composition of the mixes was

Smoked sheets	100	
Zinc oxide	10	
Stearic acid	1	
Whiting (Kragelund)	53	batch
China clay (Erbslöh P)	51	216.5 parts
Nonox CI	1.5	
Accelerator	2	
Sulphur	2	

The compounds were made from the batch using 108.25 g (= 50.0 g smoked sheets) and S and the accelerator was added on a micro mill (150 × 90 Φ mm rollers) thermostated by water circulation at 50°C. The radioactive sulphur compounds were made on the same mill using 21.65 g batch and 0.200 g ^{35}S. The micro mill was equipped with a hood and an absorber containing active carbon (Carboraffin). A vacuum cleaner performed the suction.

The state of vulcanisation was determined as modulus at 110 % elongation 15 sec after application of the load (rate 750 mm/sec) and is shown in Table 1.

Table 1. A. Sulphurfree compounds.

Mix No.	Accelerator	Modules 110 % (kg/cm^2) 15′/162°C	75′/162°C
57.295, 58.06	tol-tri	1.08 [a]	0.89 $\pm$ 0.19
58.04	tol-tetra	2.42	1.81
58.05	tol-penta	3.60	2.43
57.296, 58.07	benz-tri	1.35	1.05 $\pm$ 0.07
57.297, 58.08	benz-tetra	2.65	1.23 $\pm$ 0.05

a) The vulcanisate tends to porosity.

B. 2 sulphur (2 accelerator compounds).

Mix No.	57.274	57.273	57.276		57.371	57.282		57.304	
acc.	nil	tol-tetra	tol-tri		tol-penta	benz-tri		benz-tetra	
min. 162°C			a	b		a	b	a	b
1								3.34	
2					3.97	5.70	4.17	6.82	5.50
3						7.35	5.58	9.17	7.12
4					7.15	8.31			
5		7.90	6.29	4.35		9.46		10.26	
8					10.48		8.08	10.53	8.82
10	4.00	10.98	10.30	8.97		9.82			
12								10.03	8.22
15	5.76	12.31	12.15	9.54	13.27	7.95			
20	6.05			12.40					
30	7.29			12.35	14.71				

a) Sulphur rubber grade. b) ^{35}S passed 100 mesh.

Table 1 A. Bound sulphur at 162°C. 2 parts ^{35}S added.

57.274 A: nil acc.

min./162°C	U[a]	E[b]	S_b[c]
	cpm		
15	1 429	525	0.361
60	1 453	1 490	0.027
120	1 446	1 473	1.015
180	1 409	1 449	0.999

57.305 : tol-tri

min./162°C	U	E	S_b
	cpm		
5	1 559	345	0.221
10	1 511	671	0.443
20	1 522	1 113	0.731
	1 496	1 097	0.733
30	1 552	1 378	0.889

57.311 : benz-tri

min./162°C	U	E	S_b
	cpm		
2	1 223	466	0.381
3	1 418	575	0.406
8	1 447	776	0.536
15	1 334	803	0.602

57.317 : benz-tetra

min./162°C	U	E	S_b
	cpm		
1.5	1 365	338	0.248
2	1 372	388	0.282
3	1 517	542	0.357
8	1 367	664	0.486
12	1 455	755	0.519

58.02 : tol-penta[d]

min./162°C	U	E	S_b
	cpm		
1,5	706	59	0.084
2	704	72	0.102
4	690	131	0.189
8	766	256	0.334
16	673	423	0.628
32	707	682	0.964
64	710	692	0.975

a, untreated sample
b, extracted with acetone 18 h (ASTM)
c, $S_b = E/U$, bound $S = 2 \times S_b$ PHR
d, bis-*p*-tolylsulphonyl trisulphide
cpm, counts per minute

The data are illustrated in Fig. 1.

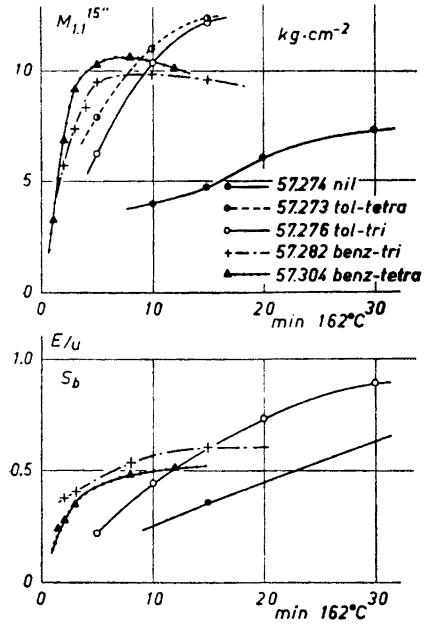

Fig. 1. Rate of vulcanisation: Modulus 110 % elongation and percent bound sulphur *vs.* time of vulcanisation at 162°C.

RATES OF OXIDATION

The rates of oxidation were measured at 1 mm thick slabs as described elsewhere [6].

In pure oxygen at 95°C the following rates were found, *cf.* Table 2. Initial rate was determined after 1 h oxidation at a starting pressure about 150 mm Hg below atmospheric pressure.

Table 2.

Mix No.	Accelerator	Rate[a] initial[b]	final[b]
57.274	nil	674^{697}	
57.312	nil 0.01 Cu	553^{639}	469^{359}
57.325 [a]	TMT	$2\,230^{701}$	1 420
57.273	tol-tetra	$2\,500^{631}$	$1\,800^{538}$
57.302	tol-tri	$3\,390^{559}$	$1\,451^{359}$
57.303	benz-tri	592^{689}	558^{459}
57.304	benz-tetra	897^{661}	881^{411}
57.371	tol-penta	$2\,590^{649}$	$1\,460^{569}$

a, moles oxygen per h and g Smoked sheets ($\times 10^8$).
b, exp., mm Hg.
TMT, tetramethyl-thiuramdisulphide.

The graphs (height of mercury *versus* time) are collected in Fig. 2.

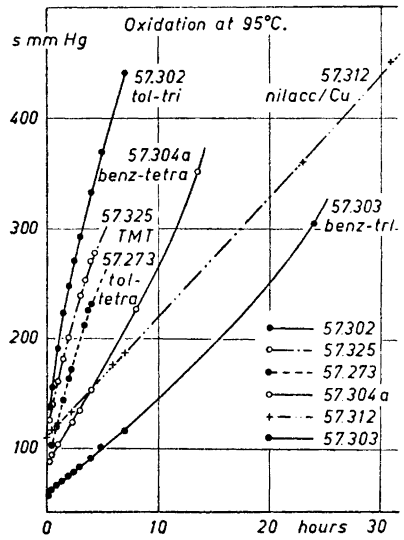

Fig. 2. Rate of oxidation at 95°C measured as height of mercury in the capillary of the absorber *vs.* time.

RATE OF AGEING

Ageing data are recorded in Table 3 and shown in Fig. 3.

Table 3.

Mix No.	Accelerator	TB°	$t_{\frac{1}{2}}$	σ	Ageing at 70°C μ	ε	δ
57.274	nil	83	58	0.63	−0.35	4.0	$+8^{48}$
57.325 [a]	TMT	114	1.90r	30_0	-5^1	90^1	$+2^1$
57.276	tol-tri	131	21.1r	3_{12}	0.25	5.4	$+1^{24}$
57.273	tol-tetra	126	31.2	1_{86}	0.17	2.8	$+3^{36}$
57.282	benz-tri	108	43(r)	1_{25}	0.0	3.7	$+1^{36}$
57.304 [a]	benz-tetra	137	34r	2_{00}	0.0	4.0	$+2^{35}$
57.371	tol-penta	126	15_2r	3_{95}	−0.15	13.5	$+5^{20}$

TB°, tensile at break before ageing.
$t_{\frac{1}{2}}$, days for half value of TB°.
σ, rate of decrease of tensile in kg/cm² per day.
μ, same for modulus at 300 % elongation.
ε, same for elongation at rupture in percent per day.
δ, marginal change of Shore A hardness.
r, straight line
exponents, period in days.

The ageing was only controlled until half value of the tensile was reached, at which point the samples in all cases were in fair condition. No tackiness or serious hardening was observed whereas generally a strong discoloration (brown) was noticed.

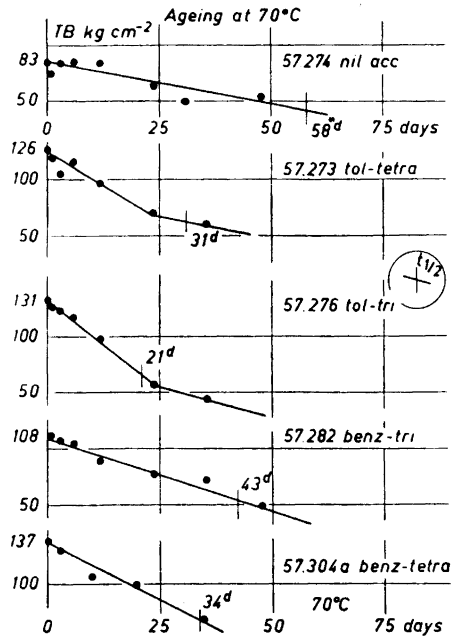

Fig. 3. Rate of ageing: Tensile strength at break *vs.* days at 70°C.

PREPARATIONS

Bis-*p*-tolylsulphonyl sulphide $(C_7H_7SO_2)_2S$, was prepared according to Otto and Troeger [7] by oxidation with iodine of equimolar mixture of potassium *p*-tolylthiosulphonate and *p*-tolylsulphinate. Crystallization from glacial acetic acid gave a product with m. p. 137°C corr. (Otto and Troeger [7] found 133—134°C, Dawson, Mathieson and Robertson [1] 138°C). (Found: S 28.5. Calc. for $C_{14}H_{14}O_4S_3$: S 28.1).

Bis-*p*-tolylsulphonyl disulphide $(C_7H_7SO_2)S_2$, was prepared according to Troeger and Hornung [8] by interaction of sodium *p*-tolylsulphinate with disulphur dichloride in carbon tetrachloride. We have slightly modified the preparation so as to get a higher yield (ca. 60 %). The raw product of bis-*p*-tolylsulphonyl disulphide is formed as a suspension in carbon tetrachloride, which according to Troeger and Hornung is distilled off on a water bath. However, the solubility of the said compound in cold carbon tetrachloride is rather small, so we just filtered off and discarded the filtrate. The raw product was then dried, washed with water, dried, washed with carbon disulphide, again dried, and then crystallized from glacial acetic acid. M. p. 113—114°C corr. (Christiansen [9] found 114°C). (Found: S 34.0. Calc. for $C_{14}H_{14}O_4S_4$: S 34.2).

Bis-*p*-tolylsulphonyl trisulphide $(C_7H_7SO_2)_2S_3$, was prepared according to Troeger and Hornung [8] by interaction of sodium *p*-tolylthiosulphonate and sulphur dichloride in carbon tetrachloride. Also in this case (*cf.* bis-*p*-tolylsulphonyl disulphide) we discarded the carbon tetrachloride solution. Crystallization from glacial acetic acid gave a product with m. p. 179.5—180°C corr. Christiansen [9] found 183°C just as Troeger and Hornung [8]; Dawson, Mathieson and Robertson [1] found 180°C). (Found: C 41.3; H 3.53; S 39.5. Calc. for $C_{14}H_{14}O_4S_5$: C 41.4; H 3.44 S 39.4).

Di-benzoyl trisulphide; $(C_6H_5CO)_2S_3$, and dibenzoyl tetrasulphide $(C_6H_5CO)_2S_4$, were prepared according to Bloch and Bergmann [10] by interaction of potassium thiobenzoate and sulphur dichloride in the former case and disulphur dichloride in the latter. M. p. of the trisulphide was 160°C corr., while Bloch and Bergmann [10] found 165—167°C. (Found: S 31.3. Calc. for $C_{14}H_{10}O_2S_3$: S 31.4 %). M. p. of the tetrasulphide was 68—69°C corr. while Bloch and Bergmann [10] found 83—84°C. (Found: S 39.3. Calc. for $C_{14}H_{10}O_2S_4$: S 37.8).

DISCUSSION

The accelerating power is moderate but definite. As shown the tensiles are about 120 as compared with about 180 obtainable with conventional accelerators. In their behaviour the accelerators show only slight analogy to thiurams. The ability to vulcanising in absence of sulphur is not very pronounced, and the oxidation and ageing characteristics are quite different. It is interesting to note that the S-addition curves show very varying amounts of bound S corresponding to optimum moduli, *e.g.* the benzoyl sulphides show rapid cure and a low percent of chemically bound sulphur, whereas the thionates vulcanise slowly but ending at about total binding of sulphur. Benz-tetra gives the fastest cure and maximum tensile. The sulphur determination and melting point of this compound showed a small content of free sulphur. This explains the high tensile and the reduced ageing stability of benzoyl tetrasulphide as compared with the trisulphide.

The oxidation curves show some interesting features, *e.g.* the thionates have about linear curves whereas the benzoyl sulphides have obvious autocatalytic curves resembling those of peroxide-vulcanisates. This might be explained as an analogy between S and O in the —X — X— group. The rates are in agreement with the $t_{\frac{1}{2}}$ values from the ageing tests. Thus the manometric method gives a fair screening here.

Finally the ageing resembles that of diphenylguanidine vulcanisates more than that of thiuram vulcanisates both in the decreasing moduli and the magnitude of $t_{\frac{1}{2}}$ *(70°C)*.

REFERENCES

1. Dawson, I. M., Mathieson, A. McL. and Robertson, J. M. *J. Chem. Soc.* **1948** 322.
2. Statham Laboratories Inc., 12401, W. Olympic Boulevard, Los Angeles 64, Calif. *cf. Bulletin No. 10*, Dec. 1955.
3. Radiochemical Centre, Amersham, Bucks.
4. *A. S. T. M. Standard on Rubber Products* **1957** 125.
5. Leth Pedersen, H. *J. Pol. Sci.* **10** (1953) 451.
6. Leth Pedersen, H. *Acta Chem. Scand.* **4** (1950) 487.
7. Otto, R. and Troeger, J. *Ber.* **24** (1891) 1130.
8. Troeger, J. and Hornung, V. *J. prakt. Chem.* **60** (1899) 113.
9. Christiansen, J. A. *Z. Elektrochem.* **34** (1928) 638.
10. Bloch, I. and Bergmann, M. *Ber.* **53** (1920) 961.

Received January 29, 1958.

ACTA CHEMICA SCANDINAVICA 12 (1958) 868—872

Some Solution Equilibria Involving Calcium Sulfite and Carbonate

I. Simple Solubility Equilibria of CO_2, SO_2, $CaCO_3$, and $CaSO_4$

GERHARD NILSSON, TORSTEN RENGEMO and LARS GUNNAR SILLÉN

Department of Inorganic Chemistry, Royal Institute of Technology, Stockholm 70, Sweden

Equilibrium constants for the reactions: 1) $CaSO_4(H_2O)_2(s) \rightleftharpoons Ca^{2+} + SO_4^{2-} + 2H_2O$ 2) $SO_2(g) + H_2O \rightleftharpoons H_2SO_3$ 3) $CaSO_3(H_2O)_{\frac{1}{2}}(s) + SO_2(g) + \frac{1}{2}H_2O \rightleftharpoons Ca^{2+} + 2\ HSO_3^-$ 4) $CO_2(g) + H_2O \rightleftharpoons H_2CO_3$ 5) $CaCO_3(s) + CO_2(g) + H_2O \rightleftharpoons Ca^{2+} + 2\ HCO_3^-$ were determined at 25, 35, and 75°C, using 1 m and 3.5 m $NaClO_4$ as ionic medium. The log K values (m scale) are given in Table 1.

The impetus to the work to be described below was a process once proposed for sulfur recovery in sulfite pulp mills. The principle is as follows:

(1) The sulfite waste liquor is burned and the SO_2 of the flue gases is absorbed in an ammonium sulfite solution; (2) or (2a) from this solution, calcium sulfite is precipitated by the addition of calcium carbonate.

$$SO_3^{2-} + SO_2(g) + H_2O \rightarrow 2\ HSO_3^- \quad (1)$$
$$2\ HSO_3^- + CaCO_3(s) \rightarrow CaSO_3(s) + CO_2(g) + H_2O + SO_3^{2-} \quad (2)$$
$$HSO_3^- + CaCO_3(s) \rightarrow CaSO_3(s) + HCO_3^- \quad (2a)$$

The calcium sulfite would then be separated and used for making fresh liquor; the remaining solution would be sent back to the absorber, to take up new SO_2, according to (1) or

$$HCO_3^- + SO_2(g) \rightarrow HSO_3^- + CO_2(g) \quad (1a)$$

The process might be advantageous in such mills where the excess steam available does not suffice for stripping the ammonium sulfite solution in the traditional way.

To study the feasibility of this process, a number of equilibria were studied involving solid $CaSO_3$ or $CaCO_3$ and a solution containing SO_3^{2-} ions. Since some oxidation to sulfate is unavoidable, the behavior of $CaSO_4$ and its hydrates in the solutions was also studied.

The main results of these equilibrium studies will now be published since the equilibrium constants may have an interest independent of the special process described. Even if the accuracy might have been better, it is thought that these data will give more precise information than was possible on the basis of previously published data, which were often conflicting.

Choice of experimental conditions

Three *temperatures* were studied, namely 25°C, 35°C, and 75°C. The first, 25°C, was chosen because it is a standard temperature for physicochemical measurements, and so makes our data directly comparable with a large amount of data compiled by other workers. It was kept constant by keeping the reaction vessel in a water thermostat of 25.0 ± better than 0.1°C. The experiments were moreover carried out in a thermostat room with 25.0 ± 0.5°C. The temperature 75°C was maintained by keeping the apparatus in an air thermostat of 75°C ± 1°; in the aqueous solutions the fluctuations were smoothed out so that the variations were considerably less.

As an intermediate temperature, one might have proposed 50°C; however, 35°C was chosen since it allows working with water thermostats without too much trouble from condensation of water vapor.

The *ionic medium* was kept constant, as far as possible, by making the solutions always contain either 1 m Na^+ or 3.5 m Na^+ (m = mole per 1 000 g of H_2O). The concentrations were given on a weight rather than a volume basis because the reactions would be considered at several temperatures. At 25°C, 3.5 m $NaClO_4$ is practically the same as 3.0 M $NaClO_4$. As anions the solutions contained sulfite, sulfate, and carbonate ions, depending upon which equilibria were to be studied; the balance was ClO_4^-.

As inert positive ion, Na^+ was chosen rather than NH_4^+, to avoid the necessity of making small corrections for the formation of NH_3, which would complicate the calculations unnecessarily without being essential for the process.

In the usual absorption process [1], combined with steam stripping, high concentration is an advantage, and the ionic concentrations are usually chosen above 10 m. However, in the precipitation processes to be studied, it would be preferable to work with a lower concentration, since this makes it easier to separate a pure precipitate. This was our reason for choosing 1 m and 3.5 m.

EXPERIMENTAL

Substances

Sulfur dioxide and *carbon dioxide* were taken from gas cylinders, and then washed first with water and then with a $NaClO_4$ solution of the desired concentration and temperature, to get the right water vapor pressure. Sodium carbonate, sodium sulfite, sodium sulfate, perchloric acid 70–72 %, calcium chloride, calcium sulfate dihydrate, and calcium carbonate were all of p. a. purity of Baker's, Kahlbaum's, or Merck's make.

Sodium perchlorate was prepared from sodium carbonate and perchloric acid. *Calcium sulfite* was precipitated from calcium chloride and sodium sulfite solutions, washed and sucked dry, all in a nitrogen atmosphere.

Ammonia was taken from a cylinder and purified only by being washed with distilled water.

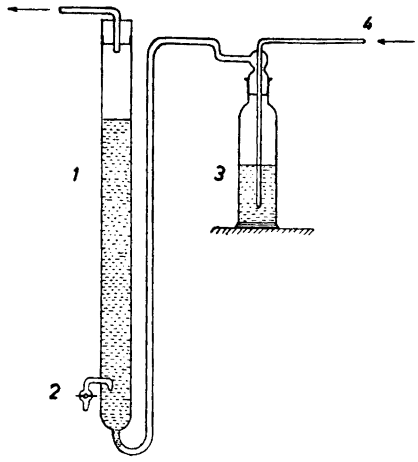

Fig. 1. Sketch of apparatus for equilibrating gas and solution (suspension). 1: glass tube, diameter 3 cm. 2: stop-cock for taking samples. 3: washing-bottle for preliminary equilibration with water vapor. 4: inlet for purified gas.

To avoid the oxidation of sulfite to sulfate by the oxygen of the air, all equilibrium experiments were carried out in an atmosphere of nitrogen from which oxygen had been removed by Meyer and Ronge's method [2], if a CO_2 or SO_2 atmosphere was not used. Moreover, the solutions contained 0.3 ml of benzyl alcohol per liter; this is an efficient chain inhibitor for the oxidation of SO_3^{2-} as found by Bäckström [3].

Apparatus

The central, thermostated, part of the apparatus is indicated in Fig. 1. The glass tube is about 60 cm long with an inner diameter of 3 cm. Like the washing bottle, it contains $NaClO_4$ solution, 1 m or 3.5 m. In some experiments, the tube also contained a solid in excess, $CaCO_3$(s) or $CaSO_3(H_2O)_{\frac{1}{2}}$(s).

The gas to be studied, CO_2 or SO_2, was first bubbled through the wash bottle, to become approximately saturated with water vapor, and then through the long tube. The solid phases were added only after the stream of gas had been started.

When no solid phase was present, samples were taken from the stop-cock at the lower part of the tube. Otherwise, samples were sucked very cautiously with an inverted bicycle pump (to avoid excessive under-pressure) through a pipette provided with a sintered-glass filter-stick.

In our 35°C thermostat, there was not enough room for this apparatus. Instead, a 500 ml bottle, provided with a stirrer, inlet and outlet tubes for the gas was used. Samples were taken by sucking, if necessary through a filter-stick.

The solubility of calcium sulfate, really $CaSO_4(H_2O)_2$, was determined simply by shaking 1 m or 3.5 m $NaClO_4$ solution with excess calcium sulfate dihydrate in bottles.

Analysis

Calcium was precipitated as oxalate, which was dissolved in sulfuric acid and titrated with $KMnO_4$.

To analyse for *sulfite*, excess of 0.05 M I_2 solution was added, the solution was acidified (if necessary), and excess iodine was titrated with thiosulfate.

Table 1. Summary of results (averages of two or more measurements).

	1 m $NaClO_4$			3.5 m $NaClO_4$		
	25°C	35°C	75°C	25°C	35°C	75°C
1. $CaSO_4$ (s) ⇌ Ca^{2+} + SO_4^{2-}						
mmole/kg solution	30.8	31.3	29.9	18.5	19.9	15.0
mmole/kg H_2O	34.7	35.3	33.7	26.4	28.4	21.4
log K	−2.92	−2.91	−2.94	−3.16	−3.09	−3.34
2. SO_2(g) + H_2O ⇌ H_2SO_3						
mmole/kg solution	1 040	727	209	825	594	170
mmole/kg H_2O	1 256	860	238	1 234	883	245
log K	0.03	−0.13	−0.53	0.06	−0.09	−0.50
3. $CaSO_3$(s) + SO_2(g) + H_2O ⇌ Ca^{2+} + 2 HSO_3^-						
mmole Ca/kg solution	497	395	168	260	198	87.7
mmole Ca/kg H_2O	667	507	198	417	308	129
log K	0.09	−0.26	−1.30	−0.52	−0.91	−1.89
4. CO_2(g) + H_2O ⇌ H_2CO_3						
mmole/kg	26.5	21.7	9.25	19.2	16.0	7.75
mmole/kg H_2O	29.8	24.4	10.4	27.4	22.9	11.1
log K	− 1.51	− 1.59	− 1.78	− 1.55	− 1.62	− 1.78
5. $CaCO_3$(s) + CO_2(g) + H_2O ⇌ Ca^{2+} + 2 HCO_3^-						
mmole Ca/kg solution	12.8	10.9	6.72	6.42	5.05	2.64
mmole Ca/kg H_2O	14.4	12.3	7.55	9.18	7.22	3.77
log K	− 4.91	− 5.10	− 5.56	− 5.50	− 5.80	− 6.49

The *total carbonate* of the solution was precipitated by excess of barium hydroxide, the precipitate was washed in a centrifuge, and dissolved in excess of 0.1 M HCl. This solution was boiled and then the excess HCl was determined by titration with 0.1 M NaOH.

Sulfate was determined gravimetrically as $BaSO_4$.

RESULTS

The results of this part of our work are summarized in Table 1.

In the second reaction formula for brevity, H_2SO_3 means the uncharged molecular species present in the aqueous solution, whether it be H_2SO_3, SO_2, or $SO_2(H_2O)_n$. The same holds for H_2CO_3 in the fourth reaction. The formulas $CaCO_3$, $CaSO_3$, and $CaSO_4$ stand for the solid phase present at equilibrium, under our conditions they were $CaCO_3$ (calcite), $CaSO_3(H_2O)_{\frac{1}{2}}$ (see part II), and $CaSO_4(H_2O)_2$ (gypsum).

For each reaction, the first line gives the average of the data primarily obtained. Since the samples were weighed before analysis, the unit is mmole/kg solution. Each value is the average of two or more separate experiments; the difference was less than 1 % for the experiments involving SO_2, and less than 1.5 % for the others. The figures are the uncorrected analytical data: total solubility for the gases, and total Ca in the experiments with solid phases.

The second line of figures, for each equilibrium, gives the primary data corrected to the unit mmole/kg H_2O.

To obtain the figures in the third line, log K of the reaction, one must consider that the partial pressures of SO_2 and CO_2 were 1.00 atm minus the equilib-

rium pressure of water vapor, 0.031 atm at 25°C, 0.055 atm at 35°C, and 0.380 atm at 75°C, for pure water, which should be multiplied by the activity of water, which we calculated from Jones' osmotic coefficients [4] as 0.96_8 in 1 m $NaClO_4$ and 0.88_4 in 3.5 m $NaClO_4$.

Moreover, in the second equilibrium, the solubility of SO_2 in water, one should correct for the dissociation of H_2SO_3, which is a fairly strong acid. For 25°C, according to part III, log K_a is —1.37 in 1 m and —1.72 in 3.5 m $NaClO_4$. Assuming the same temperature dependence of log K as at zero ionic strength [6], we estimate —1.46 and —1.81 for 35°C, and —1.83 and —2.18 at 75°C. The corresponding correction can be neglected for H_2CO_3.

The spread of the experimental data corresponds to an uncertainty of about 0.01 in the first, third and fourth log K_a and $\pm$ 0.02 in the fifth. The systematic error in the constant for SO_2 solubility, because of the uncertainty of the K_a, may be of the same order of magnitude for 25°C, and larger for the other temperatures. The solubility of $CaSO_3$ is so large that the ionic medium is considerably changed, introducing an unknown error in the activity factors.

Comparison with literature data

There is an abundant literature on the solubility of gypsum in water and aqueous solutions [5]. Although there are no data that can be directly compared with ours, the general trend, with a solubility maximum around 40—50°C, agrees with our data. The value for the activity-solubility product at 25°C, according to Latimer *et al.*[8], is log $K_s = -4.625$ which, with our values, would give reasonable activity coefficients.

The solubilities of CO_2 and SO_2 agree well with previous determinations [6,7], with due regard to the salting-out effect.

The equilibrium $CaCO_3(s) + H_2O + CO_2(g) \rightleftharpoons Ca^{2+} + 2\ HCO_3^-$ has been studied carefully by Frear and Johnston [9]. Their value for log K at 25°C is —5.83, using activities.

The equilibrium $CaSO_3\ (H_2O)\frac{1}{2}(s) + \frac{1}{2}H_2O + SO_2(g) \rightleftharpoons Ca^{2+} + 2\ HSO_3^-$ has been studied by Conrad and Beuschlein [10] who, however, did not try to calculate the equilibrium constants. Their ionic strengths varied, and were too high for extrapolation to zero. Their lowest concentrations, 0.142 M $Ca(HSO_3)_2$ and $p_{SO_2} = 16.2$ torr at 25°C would give log $K = -0.27$ (M, atm units), which compares reasonably well with our value.

REFERENCES

1. Johstone, H. F. *Pulp & Paper Mag. Can.* **53** (1952) No 4, 105.
2. Meyer, F. R. and Ronge, G. *Angew. Chem.* **52** (1939) 637.
3. Bäckström, H. L. J. *J. Am. Chem. Soc.* **49** (1927) 1460.
4. Jones, J. H. *J. Phys. & Colloid Chem.* **51** (1947) 516.
5. Seidell, A. *Solubilities of inorganic and metal organic compounds*, Vol. I (1940) p. 328; supplement (1952) p. 136.
6. Johnstone, H. F. and Leppla, P. W. *J. Am. Chem. Soc.* **56** (1934) 2233.
7. Harned, H. S. and Davis, R. Jr *J. Am. Chem. Soc.* **65** (1943) 2030.
8. Latimer, W. M., Hicks, J. F. G. Jr. and Schutz, P. W. *J. Chem. Phys.* **1** (1933) 620.
9. Frear, G. L. and Johnston, J. *J. Am. Chem. Soc.* **51** (1929) 2082.
10. Conrad, F. H. and Beuschlein, W. L. *J. Am. Chem. Soc.* **56** (1934) 2554.

Received January 25, 1958.

ACTA CHEMICA SCANDINAVICA 12 (1958) 873—877

Some Solution Equilibria Involving Calcium Sulfite and Carbonate

II. The Equilibrium between Calcium Sulfate and Calcium Sulfite in Aqueous Solutions [1]

TORSTEN RENGEMO, URSULA BRUNE and LARS GUNNAR SILLÉN

Department of Inorganic Chemistry, Royal Institute of Technology, Stockholm 70, Sweden

The equilibrium constant for the reaction $CaSO_4(H_2O)_2(s) + SO_3^{2-} \rightleftharpoons CaSO_3(H_2O)_{\frac{1}{2}}(s) + SO_4^{2-} + 1.5\ H_2O$ has been determined at 25°C, 35°C, and 75°C, with Na+ concentrations 1 m and 3.5 m, and ClO_4^- as neutral anion. The average values for log K are, for both Na+ concentrations; at 25°C 1.88; at 35°C 1.96; and at 75°C 2.23; thus $K = [SO_4^{2-}]\,[SO_3^{2-}]^{-1} = 76$, 91, and 170 at the three temperatures.

The measurements suggest log $K_s = -6.5 \pm 0.2$ for the activity solubility product of $CaSO_3(H_2O)_{\frac{1}{2}}$ at 25°C.

The present paper will describe studies of the equilibrium

$$CaSO_4(s) + SO_3^{2-} = CaSO_3(s) + SO_4^{2-};\ K = [SO_4^{2-}] / [SO_3^{2-}] \qquad (1)$$

The available literature data that could be used for estimating K are in very bad agreement, giving values of K ranging from about 1 to several hundreds.

ESTIMATION OF K FROM LITERATURE DATA

The equilibrium constant K in (1) is the ratio of the concentrations of two binegative ions of practically the same size. The activity factors of these ions can be expected to be approximately equal although their values will, of course, vary very much with the ionic medium. If this is so, the apparent K in any aqueous solution will not be far from the real activity constant, and K will be fairly independent of ionic strength.

We made an attempt to estimate K from the relevant literature data, summarized in Table 1. The solubility of $CaSO_4(H_2O)_2$ in water at temperatures below 100°C has been very accurately measured by several workers, whose results agree well. The last column in Tab. 1 gives the concentration of the saturated aqueous solutions [2] in mM.

Table 1. Literature data on the solubilities of $CaSO_3(H_2O)_{\frac{1}{2}}$ in water and in saturated $CaSO_4(H_2O)_2$, expressed in mg $CaSO_3$ per 1 000 g solution.

Temp. °C	$CaSO_3$ in pure water R	L	W+S	$CaSO_3$ in saturated $CaSO_4$ solutions L	W+S	$CaSO_4$ in water mM
10						14.177
15	1 670					
18						14.817
20			99.5	29.0		
25						15.295
30		49.2 (64)		23.8 (31)		15.361
40		48.5 (63)	92.7	22.3 (29)	32.8	15.413
45						15.310
50	1 710	43.9 (57)		19.2 (25)		
55						14.765
60		46.9 (61)	83.1	14.6 (19)	36.6	
65.3						14.20
70		34.6 (45)		9.2 (12)		
75						13.575
80		23.8 (31)	59.0	6.9 (9)	43.0	
90		20.8 (27)		6.2 (8)		
100	1 590	8.5 (11)		4.6 (6)		11.900

R = Robart 1913.
L = van der Linden 1916 (The values in parentheses are the original data, expressed as mg of "$CaSO_3(H_2O)_2$" per 1 000 g solution).
W+S = Wurz and Swoboda 1948.

On the other hand, the data on $CaSO_3$ (really $CaSO_3(H_2O)_{\frac{1}{2}}$) are scarce and contradictory as seen from Table 1 where the data of Robart [3], van der Linden [4] and Wurz and Swoboda [5] are compared. The constant K could be estimated from them in two ways.

From the solubilities of $CaSO_3$ and $CaSO_4$ in pure water, we calculated the solubility products, making reasonable assumptions regarding the activity factors; K was then obtained as the ratio of the solubility products of $CaSO_4$ and $CaSO_3$. For both salts we used the activity factors for $ZnSO_4$ as given by Harned and Owen [6] on the basis of data of Cowperthwaite and LaMer [7] and Bray [8]; the activity factors for all metal(II) sulfates seem to vary with concentration in practically the same way [6].

In this way we obtained the following very approximate values for K:

from Robart's data	1.2(15°C) to	0.8(100°C)
from van der Linden's data	200(30°C) to	6 000(100°C)
from Wurz and Swoboda's data	70(20°C) to	140(80°C)

If, instead, one uses Kielland's activity factor tables [9], the constants in the two latter cases will be multiplied with a factor of about 1.5, and thus become 300 to 9 000, and 100 to 200; however, the $ZnSO_4$ values seem preferable.

We may also use the solubility of $CaSO_3$ in saturated calcium sulfate solutions. In these experiments one may expect $[SO_4^{2-}]$ to be practically the same

as in a saturated solution of $CaSO_4(H_2O)_2$ in pure water; since the two binegative ions are in the same solution no activity factor correction is needed, and the constant K is obtained as the ratio SO_4^{2-}/SO_3^{2-} in the solution. The values so obtained are approximately

from van der Linden's data	80(30°C) to 300(100°C)
from Wurz and Swoboda's data	65(20°C) to 40(80°C)

Not only do van der Linden's and Wurz-Swoboda's values disagree with each other; in each paper the two sets of data seem to lead to disagreeing results.

Robart's solubility values are so much higher than those given in the two other papers that one may suspect they are misquoted; since, however, Latimer and Hildebrand [10] had selected Robart's data we felt we should not discard them without making experiments of our own.

EXPERIMENTAL

The equilibrium (1) was studied in solutions with 1 m Na+ at 25°C, 35°C, and 75°C, and with 3.5 m Na+ at 25°C and 35°C (with one stray experiment at 75°C).

At the two lower temperatures, the solutions were shaken to equilibrium in 100 ml glass bottles in a water thermostat. At 75°C the solution was kept in an Erlenmeyer flask with a magnetic stirrer; the flask was kept in an air thermostat at 75°C.

The solutions were generally made up by adding to a sodium sulfite solution an excess of $CaSO_4(H_2O)_2$. In one case, the equilibrium was approached from the other direction, solid $CaSO_3(H_2O)$ being added to a sodium sulfate solution. As in part I [1] the solutions contained perchlorate ions as balance.

Especially at the lower temperatures, the time of contact was very long, 5—38 days, to assure that equilibrium was obtained. — At the end of an experiment, the stirring was stopped but the flask was still left in the thermostat. After a few hours, the solids had settled, and samples of the solution were sucked out through a glass filter-stick. The samples were weighed and analysed for sulfate and sulfite ions.

Sulfite was determined iodometrically (part I). Since the sulfite concentration in our solutions was low, the accuracy was only about 5 % at the lowest concentrations.

For determining *sulfate* the standard gravimetric method could not be used here because of the fear of the coprecipitation of sodium owing to the high Na+ concentration in the solutions. Instead, a volumetric method with the following principle [11] was used. The sulfite ions are first bound as a formalin complex and then sulfate precipitated with barium chloride at room temperature after adding acetic acid. The precipitate of $BaSO_4$ is washed, centrifuged, and then converted to $BaCO_3$ by means of a strong sodium carbonate solution. This reaction takes about 1 h at 100°C. The barium carbonate precipitate is washed till the reaction is neutral, and then the carbonate content determined by dissolving in a known excess of hydrochloric acid, and back-titrating with sodium hydroxide. The accuracy of the sulfate determination is better than 1 %, which is satisfactory considering the much larger uncertainty in the sulfite determination.

The solid phases. In order to make sure in what form calcium sulfite and sulfate were present, X-ray powder photographs were taken of the powder mixture in a number of the equilibrium solutions at 25°C and 75°C and compared with photographs of synthetic specimens. Calcium sulfate proved to be present in the form of the dihydrate $CaSO_4(H_2O)_2$, gypsum. Calcium sulfite was present in one and the same form at 25°C and 75°C; this phase was also prepared synthetically. The diffraction lines of this phase agreed very well with the data of Matthews and McIntosh [12]; these authors state that the composition of the phase is $CaSO_3(H_2O)_{\frac{1}{2}}$.

Table 2. Experiments on the equilibrium

$$CaSO_4(s) + SO_3^{2-} \rightleftharpoons CaSO_3(s) + SO_4^{2-}$$

Temp. °C	Na+ mole/kg H_2O	Time days	SO_4^{2-} mmole/kg	SO_3^{2-} solution	K	log K
25	1.0	19	455	6.28	72.4	1.86
25	1.0	23	455	6.28	72.4	1.86
25	3.5	5	349	5.05	69.1	1.84
25	3.5	9	354	4.73	74.8	1.87
25	3.5	24	354	3.61	98	1.99
35	1.0	28	461	5.25	87.8	1.94
35	1.0	35	466	5.17	90.1	1.95
35 *	1.0	10	500	5.46	91.6	1.96
35	3.5	28	355	3.57	99.4	2.00
35	3.5	38	357	3.94	90.7	1.96
75	1.0	0.1	456	3.16	144	2.16
75	1.0	0.3	453	2.73	166	2.22
75	1.0	1.0	459	2.76	166	2.22
75	1.0	4.0	464	2.25	206	2.31
75	3.5	0.1	743	4.31	172	2.24

RESULTS

Our results are given in Table 2. Since the equilibrium constant K of the reaction studied is a pure number, it is immaterial whether we express the concentrations in m, in M, or in mole/kg of solution. It is the latter unit we have chosen in the table, since it gives the easiest calculations, and thus the smallest chance of computation errors.

The columns of Table 2 are: temperature °C; concentration of Na^+, in mole/kg of water; time of equilibration, days; final concentration of SO_4^{2-}; final concentration of SO_3^{2-}; equilibrium constant K, and log K.

The single experiment where the equilibrium was approached starting with calcium sulfite is marked with an asterisk.

The correction for the hydrolysis of the sulfite ion according to

$$SO_3^{2-} + H_2O \rightleftharpoons HSO_3^- + OH^-$$

can be shown to be negligible in comparison with the other experimental errors; it is less than 1 %.

The equilibrium constant K is found to increase with temperature. There may be a slight increase with increasing ionic strength, though the accuracy of the data does not allow a certain conclusion. We prefer to give an average K for both ionic strengths:

$$\begin{array}{lll} 25°C & \log K = 1.88 & K = 76 \\ 35°C & \log K = 1.96 & K = 91 \\ 75°C & \log K = 2.23 & K = 170 \end{array}$$

If we compare these values with the literature data given above, our data are found to be in complete disagreement with Robart's. The best agreement

is with the K values from Wurz and Swoboda's solubilities in pure water, and with those from van der Linden's solubilities in calcium sulfate solutions.

The accuracy of our values for log K is, we hope, better than $\pm$ 0.10.

If we assume that the log K so obtained represents the true activity equilibrium constant, we can find the true activity solubility product for $CaSO_3$ by combination with the activity solubility product [13] $[Ca^{2+}]\,[SO_4^{2-}] = 10^{-4.63}$ at 25°C

$$[Ca^{2+}]\,[SO_3^{2-}] = K_s = 10^{-6.51}$$

The uncertainty in log K_s is estimated as $\pm$ 0.2.

From this value of K_s we may calculate the solubility of $CaSO_3(H_2O)_{\frac{1}{2}}$ at 25°C in pure water to be around 0.76 mM or 91 mg $CaSO_3$/l.

REFERENCES

1. Part I. Nilsson, G., Rengemo, T. and Sillén, L. G. *Acta Chem. Scand.* **12** (1958) **868.**
2. Hulett, G. A. and Allen, L. E. *J. Am. Chem. Soc.* **24** (1902) 667.
3. Robart, J. *Bull. assoc. chimistes sucr. dist.* **31** (1913) 108, quoted by Landolt-Börnstein, Hw I (1923), p. 644.
4. van der Linden, T. *Arch. Suikerind. Ned-Indië* **24** (1916) 1113.
5. Wurz, O. and Swoboda, O. *Textil-Rundschau* **3** (1948) 201.
6. Harned, H. S. and Owen, B. B. *The physical chemistry of electrolytic solutions,* 2 ed, New York 1950, p. 426.
7. Cowperthwaite, I. A. and La Mer, V. K. *J. Am. Chem. Soc.* **53** (1931) 4333.
8. Bray, U. B. *J. Am. Chem. Soc.* **49** (1927) 2372.
9. Kielland, J. *J. Am. Chem. Soc.* **59** (1937) 1675.
10. Latimer, W. M. and Hildebrand, J. H. *Reference book of inorganic chemistry,* New York 1951, p. 581.
11. Ekedahl, E. and Sillén, L. G. *Svensk Kem. Tidskr.* **58** (1946) 177.
12. Matthews, F. W. and McIntosh, A. O. *Can. J. Research* **26B** (1948) 747.
13. Latimer, W. M., Hicks, J. F. G. Jr. and Schutz, P. W. *J. Chem. Phys.* **1** (1933) 620.

Received January 25, 1958.

ACTA CHEMICA SCANDINAVICA 12 (1958) 878—884

Some Solution Equilibria Involving Calcium Sulfite and Carbonate

III. The Acidity Constants of H_2CO_3 and H_2SO_3, and $CaCO_3$ + $CaSO_3$ Equilibria in $NaClO_4$ Medium at 25° C

MINA FRYDMAN, GERHARD NILSSON, TORSTEN RENGEMO and LARS GUNNAR SILLÉN

Department of Inorganic Chemistry, Royal Institute of Technology, Stockholm 70, Sweden

A number of equilibrium constants have been determined, involving aqueous solutions, solid $CaSO_4(H_2O)_2$, $CaCO_3$ and $CaSO_3(H_2O)_{\frac{1}{2}}$ and gaseous CO_2 and SO_2. The equilibria have been studied at Na^+ concentrations 1 m and 3.5 m and at the temperatures 25, 35 and 75°C. The results are summarized in Table 1; applications to practical cases are given in the diagrams, Fig. 1 and Fig. 2.

In connection with the work in parts I and II, the acidity constants of H_2CO_3 and H_2SO_3 were determined for the ionic media studied, 1 m and 3.5 m Na^+, with ClO_4^- as neutral anion. Although some preliminary experiments were made at higher temperatures, only those at 25°C had an accuracy that made them worth publishing.

The experiments were carried out as potentiometric titrations, using a glass electrode for measuring $[H^+] = h$, and a silver-silver ion electrode as reference electrode:

— glass electrode/I m $NaClO_4$/0.01 m $AgClO_4$, (I—0.01) m $NaClO_4$/Ag +

$$E = E_o + E_j - 59.15 \log h$$

E_o and the liquid junction potential E_j were determined by comparison with solutions of the same ionic strength $I = 1$ or 3.5, but with some Na^+ replaced by H^+. These solutions either occurred naturally at one end of the titration, or were specially prepared and inserted in the cell before or after a titration. The procedure has been described in several papers from this laboratory, *e.g.* Refs.[1,2].

THE SECOND ACIDITY CONSTANT OF CARBONIC ACID

For convenience in the titrations, all concentrations were expressed in M units for the calculations (although, of course, the Na^+ concentration was always 1 m or 3.5 m).

The main experiments were made as titrations of 200 mM Na_2CO_3 or 100 mM Na_2CO_3 (balance $NaClO_4$) with $HClO_4$, with careful addition and mechanical stirring, to prevent loss of CO_2. For each point one could calculate, from the analytical data, $Z = [HCO_3^-]/([HCO_3^-] + [CO_3^{2-}])$, the number of protons bound per CO_3 group, and plot it as a function of log h. The experimental curve $Z(\log h)$ was fitted to a calculated normalized curve, $Z = v(1 + v)^{-1}$ *versus* $v(= \log h - \log K)$, and from the position of best agreement, log K was obtained [3].

For each of the two ionic media used, two titrations were carried out with 200 mM CO_3^{2-}, and one with 100 mM CO_3^{2-}. The curves $Z(\log h)$ coincided, as one might expect for a mononuclear process. The best values found were, at 25°C:

for $[Na^+] = 1\,000$ mm $\sim$ 950 mM: $K_{a2} = 10^{-9.59}$ M $= 10^{-9.57}$ m
for $[Na^+] = 3\,500$ mm $\sim 3\,000$ mM: $K_{a2} = 10^{-9.63}$ M $= 10^{-9.56}$ m

with an uncertainty of less than ± 0.02 in log K.

In a few preliminary experiments, we were thoughtless enough to start with an $NaHCO_3$ solution and stir with a stream of nitrogen. This led to losses of CO_2 with the gas stream, amounting to about 10 % of the whole carbonate content. When the curve-fitting [3] was applied, this error was immediately discovered because the apparent Z curve was shifted (*cf.* Fig. 2 d in Ref[3]); a correction could then easily be applied.

Titrations of $NaHCO_3$ with NaOH, applying mechanical stirring, gave somewhat smaller corrections, but we preferred the titrations of Na_2CO_3 with $HClO_4$, since they gave immediately Z curves of the right shape and, moreover, could be easily extended to an acid-base titration giving E_o and E_j.

FIRST ACIDITY CONSTANT OF CARBONIC ACID

In titrations of HCO_3^-—H_2CO_3 buffers, it is always hard to avoid the escape of some CO_2. It was decided to titrate instead $NaHCO_3$ with H^+, keeping $[H_2CO_3]$ constant by equilibrating with CO_2(g) at 1 atm. The constant obtained will be the following:

$$CO_2(g) + H_2O \rightleftharpoons HCO_3^- + H^+; \quad K_pK_{a1} = [H^+][HCO_3^-]p_{CO_2}^{-1}$$

In each point of the titration, one knows $[H^+] = h$ from the emf measurement, and $[HCO_3^-]$ from the original amount of HCO_3^- and from the amount of H^+ added.

The experiments were carried out in the same way as for K_{a2}, adding H^+ to a known amount of HCO_3^-, and bubbling CO_2 through the solution. The points after the equivalence point, when all the HCO_3^- had been consumed, could be used for determining E_o and E_j.

After correction to $p_{CO_2} = 1$ atm, the following results were obtained from two experiments with each ionic strength, starting with 200 mM HCO_3^-:

$[Na^+] = 1\,000$ mm $\sim$ 950 mM; $K_pK_{a1} = 10^{-7.59}$ M^2 atm^{-1} $= 10^{-7.55}$ m^2 atm^{-1}
$[Na^+] = 3\,500$ mm $\sim 3\,000$ mM; $K_pK_{a1} = 10^{-8.02}$ M^2 atm^{-1} $= 10^{-7.88}$ m^2 atm^{-1}

These values may be combined with the values for K_p found in part I, —1.51 for 1 m Na^+ and —1.55 for 3.5 m Na^+, to give

$$-\log K_{a1} = -6.04 \text{ for 1 m } Na^+, \; -6.33 \text{ for 3.5 m } Na^+$$

The accuracy is estimated to be ± 0.02. Literature values for 25°C and at infinite dilution are log K_{a1} = —6.366 (Shedlovsky and MacInnes [4]), —6.352 (Harned and Davis [6]), and —6.51 (Kauko and Carlberg [5]); log K_{a2} = —10.25 (MacInnes and Belcher [7]) and —10.24 (Kauko and Airola [8])

THE ACIDITY CONSTANTS OF H_2SO_3

After a number of preliminary experiments, we chose to start the titrations with initial [OH^-] from 20 to 100 mM, and to titrate with a solution of SO_2, from 0.16 to 1.2 M, and of the desired sodium concentration. By this procedure, losses of SO_2 were avoided.

The average values were:

for 1 m Na^+: $K_{a1} = 10^{-1.39}$ M $= 10^{-1.37}$ m: $K_{a2} = 10^{-6.36}$ M $= 10^{-6.34}$ m
for 3.5 m Na^+: $K_{a1} = 10^{-1.79}$ M $= 10^{-1.72}$ m: $K_{a2} = 10^{-6.43}$ M $= 10^{-6.36}$ m

The limits of error of these figures are somewhat higher, about ± 0.05 for log K_{a2} and ± 0.10 for log K_{a1}. Literature values for 25°C and infinite dilution are log K_{a1} = from —1.89 (Johnstone and Leppla[9]) to —1.76 (Tartar and Garretson [10]), and log K_{a2} = —7.20 (Tartar and Garretson [10])

CHECK OF CONSTANTS

Table 1 gives a summary of the log K values determined in the present work. At 25°C, it is possible to make a check on the constants, since the equilibrium constant of the reaction

$$SO_3^{2-} + H_2SO_3 \rightleftharpoons 2\ HSO_3^-$$

Table 1. Logarithms of measured and derived equilibrium constants.

No.	Reaction	1 m 25°C	1 m 35°C	1 m 75°C	3.5 m 25°C	3.5 m 35°C	3.5 m 75°C
1	$CaSO_4 \rightleftharpoons Ca^{2+} + SO_4^{2-}$	−2.92	−2.91	−2.94	−3.16	−3.09	−3.34
2	$SO_2 + H_2O \rightleftharpoons H_2SO_3$	0.03	−0.13	−0.53	0.06	−0.09	−0.50
3	$CaSO_3 + SO_2 + H_2O \rightleftharpoons Ca^{2+} + 2\ HSO_3^-$	0.09	−0.26	−1.30	−0.52	−0.91	−1.89
4	$CO_2 + H_2O \rightleftharpoons H_2CO_3$	−1.51	−1.59	−1.78	−1.55	−1.62	−1.78
5	$CaCO_3 + CO_2 + H_2O \rightleftharpoons Ca^{2+} + 2\ HCO_3^-$	−4.91	−5.10	−5.56	−5.50	−5.80	−6.49
6	$CaSO_4 + SO_3^{2-} \rightleftharpoons CaSO_3 + SO_4^{2-}$	1.88	1.96	2.23	1.88	1.96	2.23
7	$CO_2 + H_2O \rightleftharpoons H^+ + HCO_3^-$	−7.55			−7.88		
8	$HCO_3^- \rightleftharpoons H^+ + CO_3^{2-}$	−9.57			−9.56		
9	$H_2SO_3 \rightleftharpoons H^+ + HSO_3^-$	−1.37			−1.72		
10	$HSO_3^- \rightleftharpoons H^+ + SO_3^{2-}$	−6.34			−6.36		
1−6	$CaSO_3 \rightleftharpoons Ca^{2+} + SO_3^{2-}$	−4.80	−4.87	−5.17	−5.04	−5.05	−5.57
3−2	$CaSO_3 + H_2SO_3 \rightleftharpoons Ca^{2+} + 2HSO_3^-$	0.06	−0.13	−0.77	−0.58	−0.82	−1.39
(3−2)−(1−6)	$SO_3^{2-} + H_2SO_3 \rightleftharpoons 2\ HSO_3^-$	4.86	4.74	4.40	4.46	4.23	4.18
9−10	$SO_3^{2-} + H_2SO_3 \rightleftharpoons 2\ HSO_3^-$	4.97			4.64		
7−4	$H_2CO_3 \rightleftharpoons H^+ + HCO_3^-$	−6.04			−6.33		

Note: CO_2 and SO_2 are gaseous (pressure in atm), H_2CO_3 and H_2SO_3 are in aqueous solution. "$CaSO_4$" = $CaSO_4(H_2O)_2$, "$CaSO_3$" = $CaSO_3(H_2O)_{\frac{1}{2}}$, $CaCO_3$ = calcite.

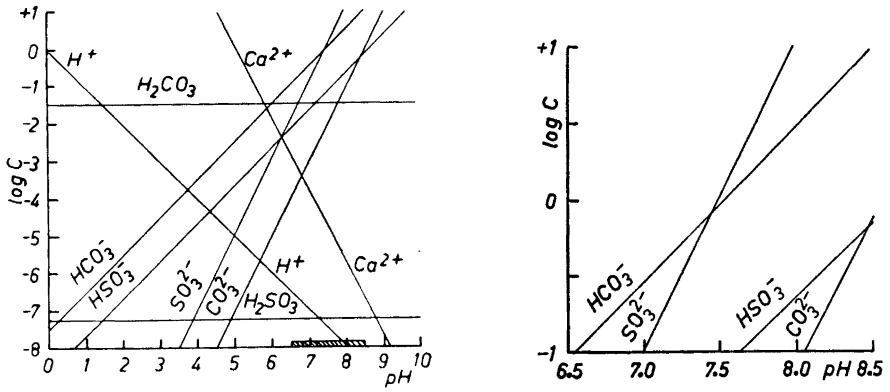

Fig. 1. Logarithmic diagram for aqueous solution (25°C, 1 m $NaClO_4$) in equilibrium with solid $CaCO_3$ and $CaSO_3$, and CO_2 of 1 atm. Horizontal axis: pH (= $-\log [H^+]$). Vertical axis: log of concentration of species in question. The approximate pH range of practical interest is marked out on the pH scale.

can be calculated in two independent ways, namely by combining the reactions 3 + 6 — 2 — 1 or 9 — 10 (Table 1). For 1 m Na^+ the results of the two calculations are 4.86 and 4.97; for 3.5 m Na^+ they are 4.46 and 4.64. The difference is 0.11 (0.18) in the logarithm, which is not too bad, considering the spread in the individual determinations, and the fact that for reactions 2 and 3 the ionic medium in the equilibrium solution differs substantially from the original one.

LOGARITHMIC EQUILIBRIUM DIAGRAMS

We shall now construct logarithmic diagrams, using the equilibrium constants we have found for 25°C and 1 m Na^+. First let us study the conditions imposed on the concentrations, if the solution is in equilibrium with CO_2 of 1 atm, solid $CaCO_3$, and solid $CaSO_3$. This is the state one may obtain by adding excess of calcium carbonate to a sulfite solution which has already absorbed some SO_2. We shall use the equilibrium constants for 4, 7, 8, 5, (1—6), 10 and 9. We use (1 minus 6), rather than (3 minus 2), which are slightly more uncertain. We find the following equilibrium conditions (Fig. 1):

1 atm CO_2: $\log [H_2CO_3] = -1.51$
$\log (HCO_3^-] = \text{pH} - 7.55$
$\log [CO_3^{2-}] = \log [HCO_3^-] + \text{pH} - 9.57 = 2\ \text{pH} - 17.12$
$CaCO_3$(s): $\log [Ca^{2+}] = -4.91 - 2 \log [HCO_3^-] = 10.19 - 2\ \text{pH}$
$CaSO_3$(s): $\log [SO_3^{2-}] = -4.80 - \log [Ca^{2+}] = 2\ \text{pH} - 14.99$
$\log [HSO_3^-] = \log [SO_3^{2-}] - \text{pH} + 6.34 = \text{pH} - 8.65$
$\log [H_2SO_3] = \log [HSO_3^-] - \text{pH} + 1.37 = -7.28$

From equilibrium 2 we see that $\log p_{SO_2}$ is less than — 7.
Provided that we have started with a pure sodium sulfite solution before

absorbing SO_2, we find the following condition on the concentrations (the charge, or electroneutrality condition):

$$2\,[Ca^{2+}] + [Na^+] + [H^+] = [HCO_3^-] + 2\,[CO_3^{2-}] + [HSO_3^-] + 2\,[SO_3^{2-}]\,(+\,[OH^-])$$

It will be immediately seen from the diagram that if $[Na^+]$ is 0.5 m or higher, $[Ca^{2+}]$ can certainly be neglected. The two predominant anionic species will be HCO_3^- and SO_3^{2-}; since the ratios $[HSO_3^-]/[HCO_3^-] = 10^{-1.10} = 0.079$ and $[CO_3^{2-}]/[SO_3^{2-}] = 10^{-2.13} = 0.0074$, the charge condition will be:

$$[Na^+] = 1.079\,[HCO_3^-] + 1.007\,[SO_3^{2-}] \approx [HCO_3^-] + [SO_3^{2-}]$$

We may thus expect the processes suggested in part I to be favored by equilibrium: if SO_2 is sorbed in a Na_2SO_3 solution, and excess $CaCO_3$ added, so much $CaSO_3$ will precipitate that the solution will finally contain a considerable amount of HCO_3^-.

Kinetic experiments on the reaction of $CaCO_3$ with $SO_3^{2-} + HSO_3^-$ solutions have confirmed that the reaction goes quickly to an equilibrium state corresponding to a mixture $HCO_3^- + SO_3^{2-}$. In the temperature interval studied, the times for establishment of equilibrium were of the order of minutes or tens of minutes.

CHECK ON $CaCO_3$ + $CaSO_3$ EQUILIBRIUM

Fist a series of experiments were made, where solid $CaCO_3$ and $CaSO_3$ were shaken with various $SO_3^{2-} + CO_3^{2-}$ solutions in order to study the equilibrium $CaCO_3(s) + SO_3^{2-} \rightleftharpoons CaSO_3(s) + CO_3^{2-}$. However, in these alkaline solutions, the reactions proved to be very slow, and even after several weeks had not reached equilibrium. The analytical ratios CO_3^{2-}/SO_3^{2-} kept changing and differed from each other and from any constant that could be calculated from the constants in Table 1. One reason may have been that the dissolution of $CaCO_3$ was inhibited, as may sometimes occur especially in the presence of traces of heavy metal ions (Erga and Terjesen [11]).

Attempts were made instead to study equilibria such as those described in Fig. 1, in the presence of $CaSO_3$, $CaCO_3$ and $CO_2(g)$ of 1 atm pressure. In

Table 2. Equilibrium with $CO_2(g)$, solid $CaCO_3$ + $CaSO_3(H_2O)_{\frac{1}{2}}$ at 25°C.

[Na+]	*a*	*b*	pH	log $[HCO_3^-]$	log $[HSO_3^-]$		log *K*	
					(a),	*(b)*,	*(a)*,	*(b)*
1.0	0.1064	0.0140	6.52	−1.08	−2.22	−2.24	1.14	1.16
1.0	0.1334	0.0168	6.61	−0.99	−2.17	−2.22	1.18	1.23
3.5	0.1326	0.0193	6.99	−1.04	−2.30	−2.38	1.26	1.34
3.5	0.1333	0.0262	6.95	−1.08	−2.18	−2.22	1.10	1.14
3.5	0.0928	0.0228	6.81	−1.22	−2.25	−2.17	1.03	0.97

Note: Concentrations on M scale, exept [Na+], which is 1.0 or 3.5 m.

$a = [HSO_3^-] + 2\,[SO_3^{2-}] + [HCO_3^-]$
$b = [HSO_3^-] + [SO_3^{2-}]$
$pH = -\log [H+]$

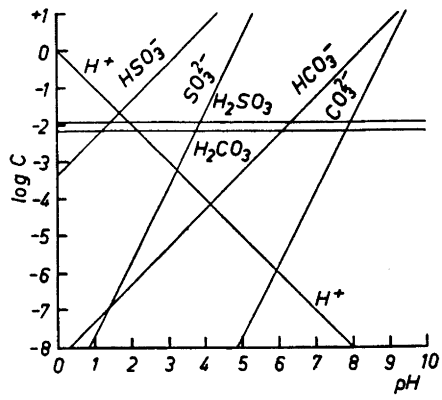

Fig. 2. Logarithmic diagram for aqueous solution in equilibrium with CO_2 of partial pressure 0.20 atm, and SO_2 of partial pressure 0.01 atm. Horizontal scale: pH, range of practical interest is between 2.5 and 4. Vertical axis: log of concentration of the various species.

this case, the equilibrium was established quite rapidly. From the original composition of the solution (a M $NaHSO_3$ or 2 a M Na_2SO_3) one knows

$$a = [HSO_3^-] + 2[SO_3^{2-}] + [HCO_3^-]$$

One may neglect $[CO_3^{2-}]$.

The solutions were analysed for Ca^{2+} (which was negligible) and total sulfite

$$b = [HSO_3^-] + [SO_3^{2-}]$$

as described in Part I. For the calculations it was necessary to know the "pH" (as above, —log h) which was measured for a sample of the equilibrium solution, still keeping it in 1 atm CO_2 atmosphere. Our experimental data are given in Table 2.

One could then calculate, using M units and the log K values 7.59 and 6.36 for 1 m Na^+ (for 3.5 m Na^+ 8.02 and 6.43):

$$[HCO_3^-] = p_{CO_2} \cdot 10^{pH-7.59}$$

$$[HSO_3^-] = \frac{a - [HCO_3^-]}{1 + 2.10^{pH-6.36}} \text{ or } [HSO_3^-] = \frac{b}{1 + 10^{pH-6.36}}$$

Table 2 gives the values of log K for

$$CaCO_3(s) + HSO_3^- \rightleftharpoons CaSO_3(s) + HCO_3^- \quad K = [HCO_3^-]/[HSO_3^-]$$

calculated with $[HSO_3^-]$ obtained in the two ways above, from a or from b. The average values are 1.18 ± 0.05 (1 m Na^+) and 1.15 ± 0.20 (3.5 m Na^+). We may also calculate this constant by means of two combinations:

(5—7) + (10 + 6 — 1) gives log K = 1.10 (1 m Na^+) and 1.06 (3.5 m Na^+)
(5—7 + (2 + 9 — 3) gives log K = 1.21 (1 m Na^+) and 1.24 (3.5 m Na^+)

The agreement with the direct equilibrium data is as good as might be expected.

SORPTION EQUILIBRIUM

We shall finally look at the equilibria in the sorption process. Let us suppose that the solution is brought to equilibrium with a flue gas with the partial pressures 0.01 atm for SO_2 and 0.20 atm for CO_2. By applying the equilibrium constants 2, 9, 10, 4, 7, and 8 for 25°C and 1 m Na^+ in Table 1 we find

$$\log [H_2SO_3] = -1.97$$
$$\log [HSO_3^-] = \log [H_2SO_3] + pH - 1.37 = pH - 3.34$$
$$\log [SO_3^{2-}] = \log [HSO_3^-] + pH - 6.34 = 2\ pH - 9.68$$
$$\log [H_2CO_3] = -1.51 - 0.70 = -2.21$$
$$\log [HCO_3^-] = -7.55 - 0.70 + pH = pH - 8.25$$
$$\log [CO_3^{2-}] = \log [HCO_3^-] + pH - 9.57 = 2\ pH - 17.82$$

The corresponding logarithmic diagram is given in Fig. 2. The charge condition will be:

$$[H^+] + [Na^+] + 2\ [Ca^{2+}] = [HSO_3^-] + 2\ [SO_3^{2-}] + [HCO_3^-] + 2\ [CO_3^{2-}]\ (+ [OH^-])$$

It is easily seen from Fig. 2 that under these conditions any ions of carbonic acid will be very thoroughly removed from the solution and replaced by HSO_3^- ions.

Acknowledgment. The work in these papers has been made possible by the generous support of Mo och Domsjö AB. We are especially indebted to Sixten Ulfsparre, Vice President in charge of production and development, and to Dr. Axel Scholander for valuable discussions and assistance in many ways. In the practical work, many members of the staff of the Department of Inorganic Chemistry have given valuable aid. Especially Mr. Erik Ekedahl and Dr. George Biedermann have been very helpful in discussing analytical problems, and Mr. Frans Ericson has given valuable practical aid. Some of the analyses were carried out by Mr. Bo Mueller and Mrs. Margareta Millén.

REFERENCES

1. Hietanen, S. and Sillén, L. G. *Acta Chem. Scand.* **6** (1952) 747.
2. Biedermann, G. *Arkiv Kemi* **9** (1955) 277.
3. Sillén, L. G. *Acta Chem. Scand.* **10** (1956) 186.
4. Shedlovsky, T. and MacInnes, D. A. *J. Am. Chem. Soc.* **57** (1935) 1705.
5. Kauko, Y. and Carlberg, J. *Z. physik. Chem. A* **173** (1935) 141.
6. Harned, H. S. and Davis, R. Jr. *J. Am. Chem. Soc.* **65** (1943) 2030.
7. MacInnes, D. A. and Belcher, D. *J. Am. Chem. Soc.* **55** (1933) 2630.
8. Kauko, Y. and Airola, A. *Z. physik. Chem. A* **179** (1937) 307.
9. Johnstone, H. F. and Leppla, P. W. *J. Am. Chem. Soc.* **56** (1934) 2233.
10. Tartar, H. V. and Garretson, H. H. *J. Am. Chem. Soc.* **63** (1941) 808.
11. Erga, O. and Terjesen, S. G. *Acta Chem. Scand.* **10** (1956) 872.

Received January 25, 1958.

ACTA CHEMICA SCANDINAVICA 12 (1958) 885—890

On the Characterization of 2-Nitromorphine

H. BAGGESGAARD RASMUSSEN and PER M. BOLL

Department of Organic Chemistry, Royal Danish School of Pharmacy, Copenhagen, Denmark

2-Nitromorphine, which has been stated to be either a nitroso or a nitro derivative, is found to be, in fact, 2-nitromorphine. The elementary analyses and the titanometric titration were in agreement with a nitro derivative. Four moles of hydrogen were used for reduction. If the compound had been a nitroso derivative the uptake of 4 moles of hydrogen could only have been explained through a reductive splitting of the oxygen bridge in the molecule. That was not the case as it was possible to isolate dihydromorphine after diazotization of the reduced compound and replacement of the diazo group with hydrogen. Furthermore, the infrared spectrum supports the concept that a nitro group is present *ortho* to the phenolic hydroxyl group.

In 1918 Wieland and Kappelmeier [1] prepared a derivative of morphine, called 2-nitrosomorphine, by reacting an aqueous suspension of morphine hydrochloride with nitrous fumes at —2°C to —3°C. This compound has in alkaline solution a distinct red colour and has been used in colourimetric methods for determination of morphine in the presence of other alkaloids.

Baggesgaard Rasmussen *et al.*[2] have developed a method for determination of morphine based on the polarographic determination of 2-nitrosomorphine. The elementary analyses given in this paper for the latter compound were in agreement with a nitroso derivative.

However, two Japanese workers, Ochiai and Nakamura [3], have shown that the compound formed by the procedure of Wieland and Kappelmeier is not 2-nitrosomorphine but 2-nitromorphine. None of the numerous papers published on the determination of morphine by means of "2-nitrosomorphine" seem to have taken notice of the Japanese publication, as all papers mention the "2-nitrosomorphine method".

The purpose of this publication is to confirm the results obtained by Ochiai and Nakamura.

The 2-nitromorphine was prepared following the procedure given by Wieland and Kappelmeier. In the course of the investigation several batches of the compound were prepared and each time the experimental conditions mentioned by the latter authors were followed as closely as possible. The compound was extremely difficult to purify by recrystallization just as it

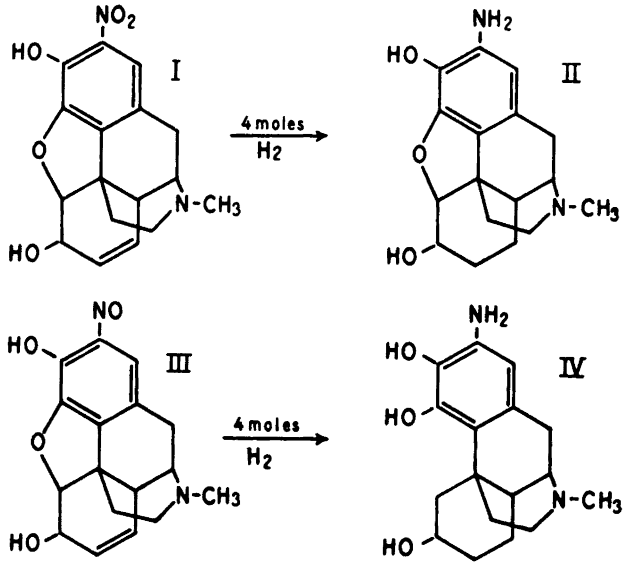

was difficult to reproduce the elementary analyses, especially the Dumas nitrogen determinations. This is apparently due to the fact that the compound is difficultly combustible. Column chromatography on alumina gave a pure compound and left a fairly large amount of side products adsorbed on the alumina. This is in agreement with the findings of Wieland and Kappelmeier that the reaction of nitrous acid with morphine affords different products and is highly dependent on temperature and time of reaction.

The resulting chromatographically pure 2-nitromorphine hydrochloride was titrated with titanium trichloride and gave an equivalent weight of 67. If the compound had been a nitroso derivative it would have required 4 equivalents of titanium trichloride for reduction and would have given a molecular weight of 268, whereas a nitro derivative requires 6 equivalents of titanium trichloride. The equivalent weight multiplied by 6 gives a molecular weight of 402, a value which is in agreement with the calculated value for 2-nitromorphine hydrochloride with 2 1/2 moles water of crystallization. The elementary analyses found and the analyses given by Ochiai and Nakamura are also in agreement with a hydrate of this composition.

By catalytic reduction of 2-nitromorphine the uptake of hydrogen was 4 moles. If the compound had been a nitroso derivative(III) this fact could only have been explained by an additional reductive splitting of the oxygen bridge. The reaction product would then be a monoaminotrihydroxy derivative(IV). This did not seem to be the case as it was possible to convert the reduced amino compound(II) to dihydromorphine by means of diazotization and a following replacement of the diazo group with hydrogen.

The absorption curves for 2-nitromorphine hydrochloride and the potassium salt 2-nitromorphine recorded for the ultraviolet part of the spectrum

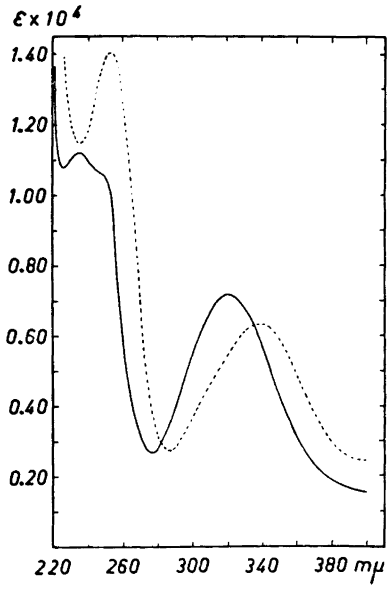

Fig. 1. The ultraviolet absorption spectra of 2-nitromorphine hydrochloride (full line) and the potassium salt of 2-nitromorphine (broken line).

are given in Fig. 1 and are similar to curves given earlier for "2-nitrosomorphine hydrochloride" and the potassium salt of "2-nitrosomorphine" [2].

Ochiai and Nakamura [3] observed that the compound did not give Liebermann's nitroso reaction or liberate iodine of an acidified potassium iodide solution. This was confirmed by this investigation just as the compound was found not to reduce Fehling's or Tollens' reagents. These negative results are, of course, in agreement with the concept that the compound is a nitro compound. On the other hand, we have tried the same reactions on 1-nitroso-2-naphtol and even in this case found them negative.

In the infrared part of the spectrum a nitroso compound (N↔O) is characterized by only one absorption band whereas a nitro compound due to both symmetrical stretching $\left(-\mathrm{N}\begin{smallmatrix}\swarrow\mathrm{O}\\ \rightarrow\\ \nwarrow\mathrm{O}\end{smallmatrix}\right)$ and unsymmetrical stretching $\left(-\mathrm{N}\begin{smallmatrix}\nearrow\mathrm{O}\\ \rightarrow\\ \nwarrow\mathrm{O}\end{smallmatrix}\right)$ is characterized by two absorption bands. All these bands have to be strong. The spectrum of the compound considered to be 2-nitromorphine hydrochloride has indeed such two bands at 1 525 and 1 350 cm^{-1}. These frequencies correspond closely to the frequencies expected for a nitro compound. A nitroso compound, on the other hand, should have given only one band at 1 525 cm^{-1}.

It has been shown by Amstuts *et al.*[4] that the fundamental band of hydroxyl absorption in the infrared part of the spectrum is lacking for 1-nitroso-2-naphtol, whereas 1-nitro-2-naphtol exhibits a definite, although weak band at approximately 3 250 cm^{-1}. This has been confirmed by one of us[5], who also

Table 1. Fundamental bands of hydroxyl and amine absorption in the infrared part of the spectrum.

Compound	Hydroxyl and amine band (cm^{-1})				Interpretation
	solid (KBr)		in $CHCl_3$		
2-Nitromorphine hydrochloride	3 450	(NH)	3 620	(NH)	intermolecular H-bond
	3 360	(OH)	3 540	(OH)	intermolecular H-bond
	3 220	(OH)	3 220	(OH)	intramolecular H-bond
Morphine hydrochloride	3 450	(NH)	3 620	(NH)	intermolecular H-bond
	3 360	(OH)	3 540	(OH)	intermolecular H-bond

showed that 4-nitrosoresorcinol did not give the fundamental band of hydroxyl absorption contrary to 4-nitroresorcinol *, which gave a distinct band.

2-Nitromorphine hydrochloride exhibits the same type of band as 1-nitro-2-naphtol and 4-nitroresorcinol at approximately 3 220 cm^{-1} and the bond is not shifted to a higher frequency by dissolving the compound indicating an intramolecular type of bonding. This observation that an intramolecular hydrogen bond is present, even in solution, appears to give further evidence for the compound being a nitro derivative. The presence of this intramolecular type of hydrogen bonding seems also to support the concept that the nitro group is *ortho* to the phenolic hydroxyl group.

EXPERIMENTAL

The melting points are corrected and have been determined with the hot stage microscope essentially according to Kofler.

Potassium salt of 2-nitromorphine. The compound was prepared according to Wieland and Kappelmeier [1] and purified by column chromatography in the following manner:

3.5 g of the crude potassium salt of 2-nitromorphine dissolved in 100 ml of methanol was poured onto a column of wet-packed alumina (Alcoa) and eluted with 90 % methanol. After collection of a 200 ml fraction, the eluant was changed to 70 % methanol and 120 ml had to be collected before the strongly red-coloured salt appeared in the eluate.On the alumina remained a very dark red-coloured band which only could be eluted with dilute hydrochloric acid.

Table 2. Fractionation of the potassium salt of 2-nitromorphine by column chromatography on alumina.

Fraction	Eluant	Volume (ml)	Colour	Weight of residue
I	effluent	100	colourless	0.004 g
II	90 % CH_3OH	200	weak yellow	0.012 g
III	70 % CH_3OH	120	weak yellow	0.037 g
IV	70 % CH_3OH	375	red	2.71 g

* It has to be mentioned that the hydroxyl group placed in the *para*-position to the nitro or nitroso group in 4-nitroresorcinol and 4-nitrosoresorcinol, respectively, showed intermolecular type of hydrogen bonding.

The salt which appeared as the residue after evaporation of fraction IV to dryness was recrystallized twice from 96 % ethanol. The needle-shaped, dark red crystals were dried in the air. When tested by paper chromatography the crystals gave only one spot. The crystals were chromatographed by descending chromatography at 25°C on Whatman No. 1 paper using water-saturated 1-butanol as developing reagent. The compound was visible as a red spot with an R_F-value = 0.42. In ultraviolet light no other spots could be detected. (Found: C 47.15; H 6.00; H_2O 13.40. Calc. for $C_{17}H_{18}O_3N(NO_2)K \cdot 3\ 1/2\ H_2O$ (mol.wt. 432.5): C 47.33; H 5.84; H_2O 14.61).

2-Nitromorphine hydrochloride. To a suspension of 2 g potassium salt in 10 ml of water was at one time and under stirring added 4 ml of 4 N hydrochloric acid. The salt dissolved and the yellow hydrochloride precipitated shortly after. After standing the hydrochloride was collected by filtration and washed with N hydrochloric acid. The yellow crystals were recrystallized from N hydrochloric acid and air-dried. (Found: C 49.40; H 5.77; H_2O 10.05. Calc. for $C_{17}H_{18}O_3N(NO_2) \cdot HCl \cdot 2\ ½\ H_2O$ (mol.wt. 411.8): C 49.59; H 5.87; H_2O 10.94.)

The uptake of hydrogen was determined quantitatively by means of the microhydrogenation apparatus described by Clauson-Kaas and Limborg [6]. Uptake: 4.03 moles of H_2 (Calc. for $C_{17}H_{18}O_3N(NO_2) \cdot HCl \cdot 2\ ½\ H_2O$: 4.00 moles of H_2).

After drying 2-nitromorphine hydrochloride *in vacuo* over phosphorus pentoxide the values were as follows: Found: C 53.25; H 5.57. Calc. for $C_{17}H_{18}O_3N(NO_2) \cdot HCl \cdot H_2O$: C 63.08; H 5.50.

Silver salt of 2-nitromorphine. The salt was prepared according to the procedure given by Wieland and Kappelmeier [1]. The salt precipitated as an insoluble voluminous red compound, which after drying changed to a nearly black powder. (Found: Ag 24.80. Calc. for $C_{17}H_{18}O_3N(NO_2)Ag$: Ag 24.61.)

2-Aminodihydromorphine hydrochloride. 3 g of the potassium salt of 2-nitromorphine was dissolved in 70 ml of water, 2 equivalents of hydrochloric acid were added and the compound was catalytically reduced using palladium carbon (5 %). After reduction the catalyst was removed by filtration and the filtrate evaporated under reduced pressure. The oily residue was dissolved in a little methanol and evaporated again. Addition of ethanol to the residue gave sandy crystals which after recrystallization from ethanol-methanol melted at 320—325°C (Lit.value[3] 325°C).

Transformation of 2-aminodihydromorphine to dihydromorphine. The aminomorphine was diazotized following the procedure of Wieland and Kappelmeier [1]. To 1.5 g of the hydrochloride suspended in 30 ml absolute ethanol was added under cooling 2.25 g of ethyl nitrite (prepared after Wallach and Otto [7]) and finally 3 ml of 19.5 % ethanolic hydrochloric acid.

The diazo compound was precipitated by addition of ethyl ether, removed by filtration, washed with more ethyl ether and immediately dissolved in 5 ml of absolute ethanol. Now 0.5 g of copper powder was added and the suspension was carefully heated to beginning nitrogen evolution. After cooling the suspension was filtered and the filtrate evaporated to dryness and then extracted with ethyl ether. The residue was now dissolved in a little water and sodium carbonate was added to precipitate the alkaloid. An amorphous and dark-coloured compound precipitated. Recrystallization from ethanol-water gave no purification. Therefore, it was purified on Amberlite IR-120. 100 mg of the crude product dissolved in 10 ml of methanol was chromatographed on the resin (H+ form, 9 cm × 1.6 cm), washed with 30 ml methanol and eluted with 0.5 N methanolic ammonia water. Only a few mg of product was obtained after evaporation of solvent. After recrystallization from methanol the crystals melted at 154—156°C (Lit. value [8] 155—157°C) and mixed with authentic dihydromorphine the melting point did not show any depression. Furthermore, the infrared spectrum of the isolated compound was identical with the spectrum of dihydromorphine.

Titanometric titration of the potassium salt and the hydrochloride. To a weighed sample (about 50 mg) in 10 ml glacial acetic acid was added 30 ml 2 N sodium acetate solution. During the titration carbon dioxide was led through the solution. After 5 min of carbon dioxide flow, a measured excess of titanium trichloride solution kept in a carbon dioxide atmosphere was added. After another 5 min, 20 ml of concentrated hydrochloric acid was added and the excess of titanium trichloride was titrated with 0.06 N ammonium thiocyanate using ferric ammonium sulphate as an indicator. The actual amount of titanium trichloride used for reduction was determined by titration of a blank (Table 3).

Table 3. Titanometric titration of two nitromorphine derivatives.

Compound	Equiv. wt. found	Mol. wt. of nitroso cpd.	Mol. wt. of nitro cpd.
Potassium salt of 2-nitromorphine	68 68.5	272 274	408 411
2-Nitromorphine hydrochloride	67 67	268 268	402 402

The infrared spectra of 2-nitromorphine hydrochloride, morphine hydrochloride and dihydromorphine were obtained on a Perkin-Elmer Spectrophotometer Model 21. Besides recording the spectra of the compounds in pressed potassium bromide discs, the spectra of the two first compounds were recorded as saturated solutions in chloroform.

Elementary analyses are by Mr. P. Hansen, Universitetets kemiske laboratorium, Copenhagen and the microhydrogenation determination by Mr. W. Egger, Novo Terapeutisk Laboratorium, Copenhagen. The authors are indebted to Professor Børge Bak, University of Copenhagen, for a discussion of the infrared spectrum of 2-nitromorphine hydrochloride.

REFERENCES

1. Wieland, H. and Kappelmeier, P. *Ann.* **382** (1911) 306.
2. Baggesgaard Rasmussen, H., Hahn, C. and Ilver, K. *Dansk Tidskr. Farm.* **19** (1945) 41.
3. Ochiai, E. and Nakamura, T. *Proc. Imp. Acad. Tokyo* **15** (1938) 134.
4. Amstutz, E. D., Hunsberger, I. M. and Chessich, J. J. *J. Am. Chem. Soc.* **73** (1951) 1220.
5. Boll, P. M. *In press.*
6. Clausen-Kaas, N. and Limborg, F. *Acta Chem. Scand.* **1** (1947) 884.
7. Wallach, O. and Otto, A. *Ann.* **253** (1889) 249.
8. Oldenberg, L. Ber. **44** (1911) 1829.

Received April 20, 1958.

ACTA CHEMICA SCANDINAVICA 12 (1958) 891—895

On the Products Obtained from Ketones with Ammonium Polysulphide

ARNE FREDGA

Chemical Institute, University of Uppsala, Uppsala, Sweden

Two compounds obtained from *cyclo*hexanone and *cyclo*heptanone with ammonium polysulphide at room temperature are described (II, IV). The former contains a 1,2,4,5-tetrathiane ring in spirocyclic combination. The latter has a seven-membered ring with two carbon and five sulphur atoms (1,2,3,5,6-pentathiepane ring).

In 1887 Willgerodt published his first investigations on the reaction between ketones and ammonium polysulphide [1]. At higher temperatures, the ketone is transformed to an amide; this rather peculiar reaction has been studied by several authors and is now generally known as Willgerodt's reaction [2].

If a solution of polysulphide was left to stand with acetone at room temperature, however, Willgerodt obtained a crystalline compound answering to the formula $(CH_3)_2CS_2$. He assumed it to be dimeric and called it "duplodithioacetone". The structure was not discussed, but of course the formula I with a 1,2,4,5-tetrathiane ring is near at hand. In the "Ring Index" this structure is also postulated [3]. In connection with work in progress on the

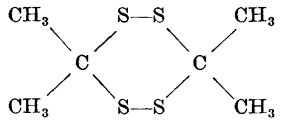

I

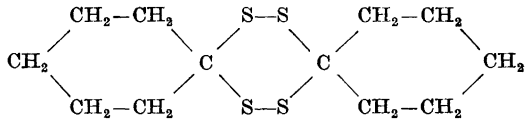

II

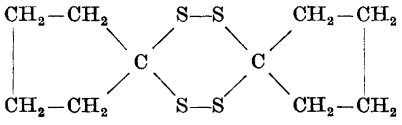

III

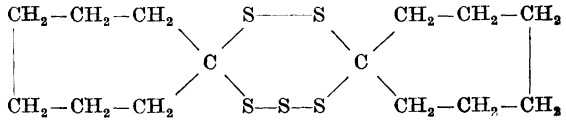

IV

disulphide group, an investigation on compounds of this type has been started in collaboration with Mr. B. Magnusson.

The acetone derivative is easily obtained according to Willgerodt's directions, but the preparation of higher homologues and derivatives from aromatic ketones met with difficulties, which have not been overcome as yet. Camphor did not react at all, even on standing for a long time. More promising results were obtained, however, with simple cyclic ketones. *Cyclo*hexanone yields a readily crystallising compound (m.p. 130.5—131.5°), which must be ascribed the spirocyclic structure II. *Cyclo*pentanone gives mostly dark-coloured, smeary products, but Mr. Magnusson could isolate the compound III (m.p. 151.5—153°) in low yield [4].

The results obtained with *cyclo*heptanone were rather unexpected. The compound isolated (m.p. 127—128°) has the formula $C_{14}H_{24}S_5$, thus containing five sulphur atoms instead of four. According to modern investigations [5,6], the occurrence of branched sulphur chains in organic compounds is very unlikely and the compound obtained from *cyclo*heptanone must thus be ascribed the formula IV. To the author's knowledge, a ring containing two carbon and five sulphur atoms (1,2,3,5,6-pentathiepane) has not been described previously.

An explanation of the different behaviours of *cyclo*hexanone and *cyclo*heptanone cannot be given at present. Preliminary experiments with the two ketones and preparations of ammonium polysulphide with various amounts of sulphur (from $(NH_4)_2S_2$ to $(NH_4)_2S_4$) gave only the compounds II and IV, respectively, in some cases contaminated with free sulphur. It is possible that the crude reaction mixture represents a dynamic equilibrium of substances with different sulphur-containing rings (perhaps also open chain polymers), and that the most readily crystallising compound ultimately separates.

The question of the conformation of the sulphur-containing rings is of a certain interest. For the six-membered ring, the rigid chair form (Fig. 1 A) is of course possible. The corresponding boat form is pliable and permits a series of arrangements; two extreme forms are represented by Figs. 1 B and C. Owing to the rather bulky groups attached to the carbon atoms, formula B must be excluded, but the boat form C seems quite reasonable and must be taken into consideration. The formulas A and B are symmetrical (the former has also a center of symmetry) and the sulphur atoms lie in one plane. Formula C has no plane or center of symmetry and the sulphur atoms are not situated in the same plane.

A crystallographic investigation has been started by Dr. I. Lindqvist in collaboration with Mr. R. Rosenstein, who have kindly submitted some preliminary results. As stated already by Willgerodt, the acetone derivative (I)

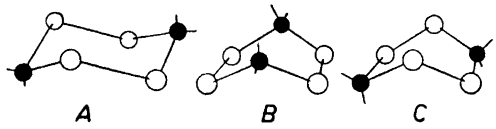

Fig. 1. Conformations of the tetrathiane ring.

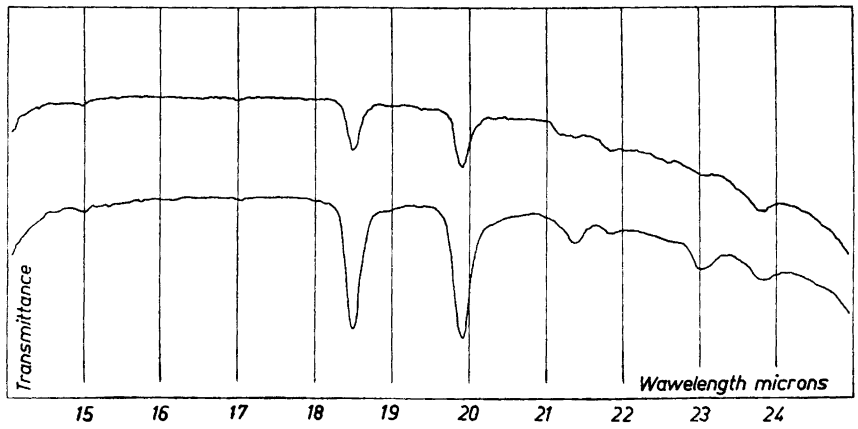

Fig. 2. IR absorption curve of the *cyclo*hexanone derivative.

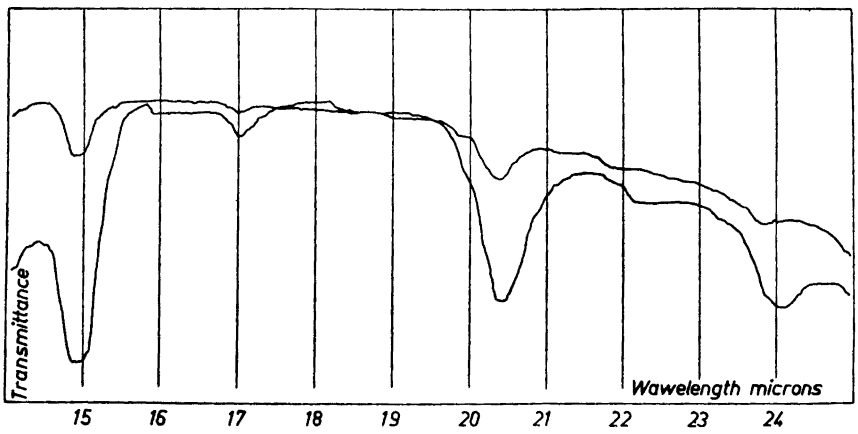

Fig. 3. IR absorption curve of the *cyclo*heptanone derivative.

is tetragonal and it seems that the molecules in the crystal have the conformation C (Fig. 1). The *cyclo*pentanone derivative (III) might possibly represent the conformation A. Both structures are comparatively simple.

The structure of the *cyclo*hexanone derivative (II) is more complicated and the results obtained as yet do not permit any conclusions as to the conformation.

For the seven-membered sulphur-containing ring in the *cyclo*heptanone derivative (IV) several conformations are possible. The preliminary data indicate that the structure is very complicated with a rather large unit cell.

Figs. 2 and 3 show the IR-spectra for the compounds II and IV in the region 14—25 μ, where the C—S and S—S bond frequencies should be located.

In the spectrum of the *cyclo*hexanone derivative (Fig. 2), the band at 19.9 μ might possibly be attributed to the S—S linkage; it should be said, however, that in our experience the S—S bands are in most cases broader and less distinct. Curiously enough there is no indication for a C—S band in the region 14—16 μ; the distinct band at 18.5 μ must have another origin and might be due to structural vibrations. The non-appearance of the C—S frequency might perhaps be due to special symmetry conditions in the molecule.

In the spectrum of the *cyclo*heptanone derivative, which is less symmetrical (Fig. 3), we find the C—S band at 14.9 μ and the S—S band at 20.4 μ. It is obvious that the sulphur-containing ring system is not the same in the two compounds. On the other side, there is no indication for the occurrence of a branched chain containing a coordinative or double sulphur-sulphur bond.

Preliminary IR-studies on the compounds I and III indicate that the acetone derivative (I) shows the normal C—S and S—S bonds, whereas they are missing in the spectrum of the *cyclo*pentanone derivative (III). This is in agreement with the crystallographic results, according to which only the latter compound should have a ring conformation with a center of symmetry.

A more detailed discussion of the spectra should be postponed until the conformation of the rings is established by crystallographic methods.

EXPERIMENTAL

Cyclo*hexanone derivative (Bis-3,3,6,6-pentamethylene-1,2,4,5-tetrathiane)*. *Cyclo*hexanone (0.1 mole) is left to stand with a concentrated solution of ammonium disulphide (0.25 mole) in a closed vessel with occasional shaking. Gradually the ketone layer sinks to the bottom and changes to a yellow mixture of smears and crystals. When no further change can be observed (after 4—5 days), the product is separated, washed with water and triturated with ethanol or methanol, which dissolves the smeary by-products leaving dry, pale yellow crystals. Repeated recrystallisations from ligroin and propanol, if necessary with charcoal, give a colourless product. Short-prismatic crystals with m. p. 130.5 —131.5°. The compound is easily soluble in benzene, chloroform and carbon disulphide. (Found: C 48.9; H 6.87; S 44.07; mol.weight 293, 299, 286. Calc. for $C_{12}H_{20}S_4$: C 49.25; H 6.89; S 43.83; mol.weight 292.5).

Cyclo*heptanone derivative (Bis-4,4,7,7-hexamethylene-1,2,3,5,6-pentathiepane)*. *Cyclo*heptanone (0.1 mole) was added to a solution of ammonium disulphide (0.25 mole) as described above. In this case the reaction proceeds more slowly and it is appropriate to shake the mixture on a machine for the first 10 h. After standing for about one week, the mixture is worked up as described above and the product recrystallised from propanol and ligroin. Colourless, thin needles with m. p. 127—128°, easily soluble in benzene, chloroform, and carbon disulphide. (Found: C 47.85; H 6.90; S 45.39; mol.weight 363, 340, 336. Calc. for $C_{14}H_{24}S_5$: C 47.68; H 6.86; S 45.46; mol.weight 352.6).

The *molecular weights* were determined by the boiling point method in benzene solution. Some experiments with the Rast method gave consistent results. The *IR-spectra* were recorded with a Perkin-Elmer model 21 double-beam spectrophotometer with a potassium bromide prism. The substances were studied in Nujol emulsions of two different concentrations.

The author is indebted to Dr. I. Lindqvist for preliminary reports on the crystallographic investigation and to Mr. B. Magnusson for private communications and part of the analyses. Thanks are also due to Dr. A. Rosenberg and Mr. S. Bergwall for expert advice and technical assistance in the IR-work.

REFERENCES

1. Willgerodt, C. *Ber.* **20** (1887) 2467.
2. Carmack, M. *Organic Reactions 3*, New York 1946, p. 83.
3. Patterson, A. M. and Capell, L. T. *The Ring Index*, New York 1940, p. 47.
4. Magnusson, B. *To be published.*
5. Foss, O. *Acta Chem. Scand.* **4** (1950) 404.
6. Schotte, L. *Arkiv Kemi* **9** (1956) 361.

Received January 28, 1958.

ACTA CHEMICA SCANDINAVICA 12 (1958) 896—902

On the Effect of Small Amounts of some Organic Compounds on the Ferric Ion Catalyzed Hydrogen Peroxide Decomposition

V. STEN ANDERSEN and H. NIEMANN

Department of Inorganic Chemistry, The Royal Danish School of Pharmacy, Copenhagen, Denmark

The authors have investigated the influence of benzene, phenol, phenacetin, and hydroquinone on the rate of the ferric-ion catalyzed hydrogen peroxide decomposition.

The experiments show that benzene, phenol, and phenacetin cause an induction period, the length of which depends on the amount of compound added; after the induction period the rate of reaction is greater than that of the pure ferric-catalyzed reaction. Hydroquinone does not retard the reaction but acts as a promotor from the very start of the reaction.

These findings seem to indicate that a reaction mechanism based on a chain reaction catalyzed by ferrous ions, similar to that proposed by Koefoed [1], is to prefer to the one put forward by Christiansen and Andersen [2], which is based on an open sequence reaction.

The experiments were carried out in a Brønsted shaking apparatus [3] modified in such a manner that the pressure of the oxygen evolved could be measured at constant volume, although the manometer was made of fairly wide glass tubing, in order to suppress the capillary forces.

In 1950 Christiansen and Andersen [2] proposed a reaction mechanism for the Fe(III)-catalyzed hydrogen peroxide decomposition which was based on an open sequence:

$$\begin{aligned} FeOOH^{++} &\rightleftharpoons Fe^{+++} + H\overset{*}{O}_2^- \\ H\overset{*}{O}_2^- + H_2O_2 &\rightarrow O_2 + OH^- + H_2O \end{aligned} \qquad \text{I}$$

($H\overset{*}{O}_2^-$ represents an activated hydrogen peroxide ion).

This scheme, although it fits very closely to the experimental results, has been met with some scepticism because it does not explain the fact that the

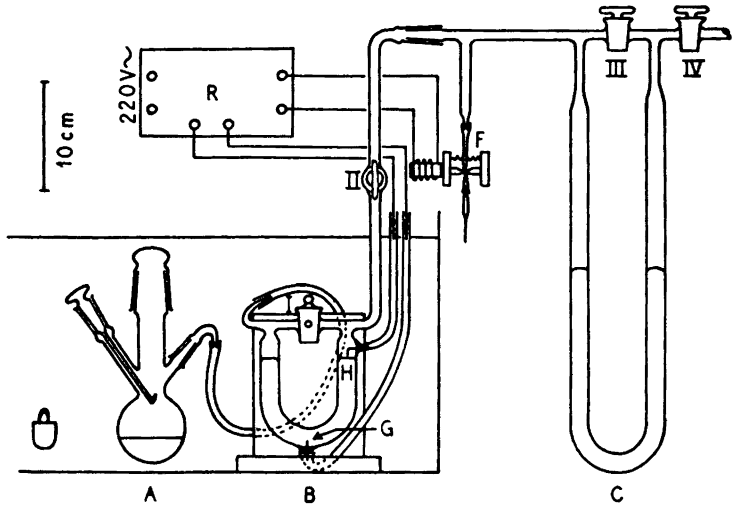

Fig. 1. A modified Brønsted shaking apparatus used for the experiments.

reaction is strongly retarded by small amounts of organic compounds (Bray and Peterson [4]) or the finding of Kuhn and Wassermann [5] who have demonstrated that ferrous ions can be detected in the reaction mixture. These features indicate a chain reaction and a valence shift of the iron ions. Koefoed [1] and Christiansen [6] have discussed such a reaction pattern, proposed by the former and based on a closed sequence.

In the present paper we have given an account of some new kinetic experiments on the influence of some benzene derivatives: benzene, phenol, phenacetin, and hydroquinone on the reaction in question and we have from a qualitative point of view discussed the experimental results in connection with the reaction schemes mentioned above.

EXPERIMENTAL

The kinetic experiments were carried out in a modified Brønsted shaking apparatus [3] by measuring the pressure of the oxygen evolved. The apparatus (Fig. 1) was constructed in such a manner that it was possible to measure the gas pressure at constant volume even though the manometer was made of glass tubing with an inner diameter of 14 mm. The reaction vessel A (volume about 165 ml) was mounted in an ordinary shaking apparatus. It was furnished with a side arm closed by a glass stopper onto which was sealed a glass rod; the end of this rod was formed as a small hook upon which a small plastic vessel (volume about 2 ml) could be hung.

The reaction vessel was connected to one side of a differential-tensiometer B by a piece of flexible plastic tubing. The tensiometer was again connected to a mercury manometer C, which was connected to a vacuum line on the other side. F is a piece of soft plastic tubing which served as a valve. This valve could be closed by means of two metal jaws pressed together by an ajustable spring. To prevent the walls sticking together they were lubricated with silicone oil ('formslip').

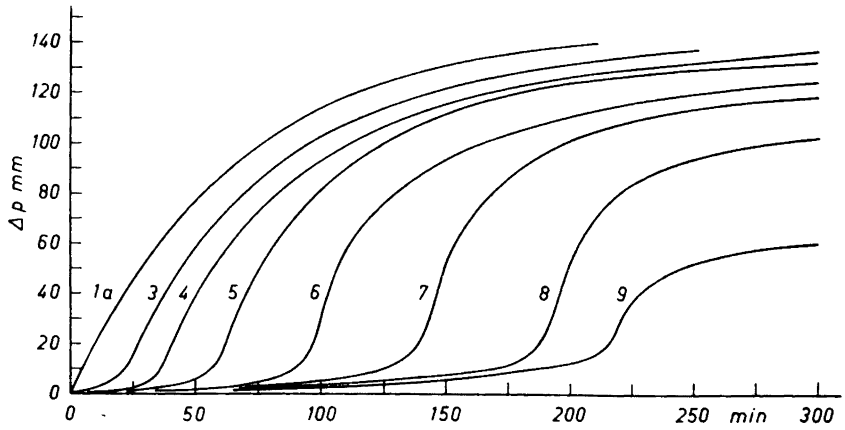

Fig. 2. Reaction curves from the experiments with phenacetin as an inhibitor. The pressure of the oxygen evolved is plotted against time. The reacting mixtures were all 0.003 M as to ferric perchlorate, 0.01 M as to perchloric acid and 0.046 M as to hydrogen peroxide. Temp. 25°C.

The molar concentrations of phenacetin were:

Concentration of phenacetin × 10^5:	0.0	3.03	6.06	12.1	24.2	45.5	91.0	227
Curve No:	1 a	3	4	5	6	7	8	9

The differential-tensiometer was furnished with two wolfram electrodes, G and H, and it was filled with enough mercury to enable the mercury level to touch the electrode H, when tap I was open. To avoid vibrations the tensiometer was mounted on a stand attached to a heavy lead base. The electrodes were used as a pick-up for a thyratron relay R, which was able to open the valve F by the electromagnet M when the mercury in the tensiometer touched the electrode H.

In this manner it is possible, on the wide manometer C, to measure at constant volume an increasing pressure which is smaller than the atmospheric pressure, in the reaction vessel A; of course the relay can easily be rearranged so that it works at decreasing pressure.

The modified Brønsted apparatus has the following advantages in preference to the original one:

1) It is possible to measure the pressure at constant volume.

2) The pressure can be measured with a greater accuracy in the wide manometer because the capillary effect is much smaller than in a narrow one *.

3) The resistance in the plastic tubing is much smaller than in the flexible glass tubing used by Brønsted because it is made much shorter and wider; in addition to this it is not breakable and therefore easier to handle.

The experiments were carried out as follows:

40.00 ml of an aqueous solution of ferric perchlorate acidified with perchloric acid was pipetted into the flask A; a known amount (about 1 ml) of a hydrogen peroxide stock-solution was placed in the plastic vessel which then was hung on the turnable hook. The flask was closed, the taps I, II, III and IV were opened, the relay switched off to close valve F and the whole system was evacuated for about 5 min. Subsequently the tap I was closed and the system (minus the reaction vessel) was evacuated to a pressure not

* See for instance: Ostwald-Luther, *Hand- und Hilfsbuch zur Ausführung physiko-chemischer Messungen.* Academische Verlagsges. Leipzig 1931, p. 197.

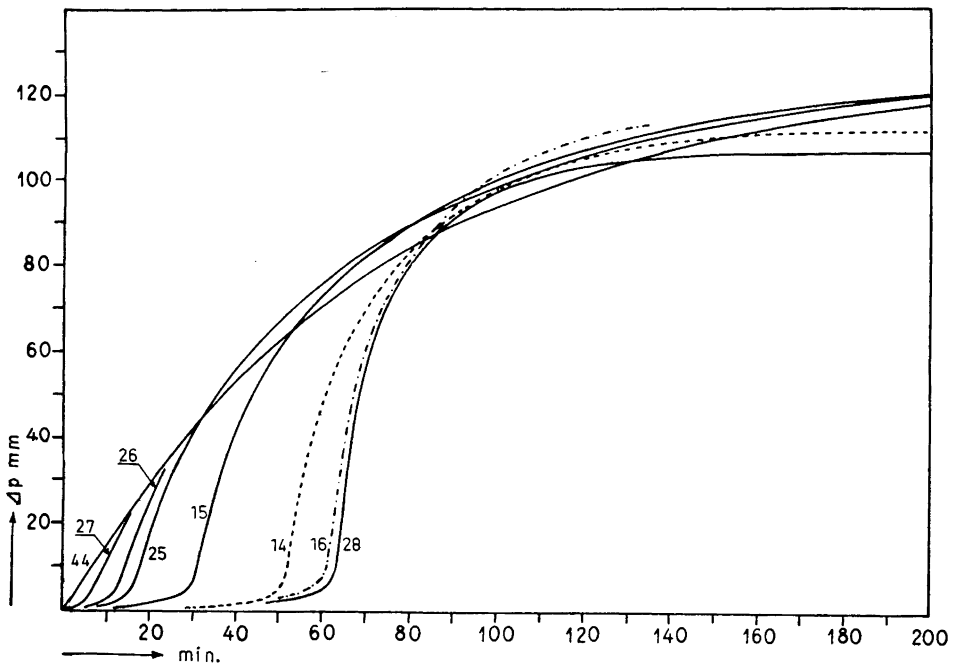

Fig. 3. Reaction curves from the experiments with phenol as inhibitor. The experimental conditions were all the same as those given in the subscript to Fig. 2.

The concentrations of phenol were:								
Concentration of phenol × 10^3:	0.0	0.010	0.030	0.052	0.102	0.260	0.517	1.03
Curve No:	44	27	26	25	15	14	16	28

exceeding 0.01 mm and the taps III and IV were closed. During this phase of the evacuation the water vapour in the reaction flask had moved the mercury in the tensiometer so much that the electrode H was submerged in the mercury. Therefore, when the relay then was switched on, it began to work and opened the valve F which let in air until the mercury no longer touched the electrode H; simultaneously the mercury in the manometer moved, so that when equilibrium was obtained, the pressure in the reaction vessel could be read on the manometer, by means of a reading microscope.

The reaction was started by dropping the plastic vessel with hydrogen peroxide into the solution in the reaction flask, and switching on the shaking apparatus; the rate of reaction was measured by reading the gas pressure as described above.

Four series of experiments were carried out: One with phenacetin, one with benzene, one with phenol, and finally one with hydroquinone.

The experimental results, together with the experimental conditions, are given in the Figs. 2, 3 and 4. We have not given the results from the experiments with benzene as inhibitor because they were not reproducible; due to the volatility of the benzene it was not possible to prevent its disappearance from the reaction mixture during evacuation of the apparatus.

It appears from Figs. 2 and 3 that phenacetin and phenol on the whole act in the same way; both interfere very strongly with the pure Fe(III)-catalyzed reaction: They cause an induction period during which no oxygen or only a small amount of oxygen is evolved.

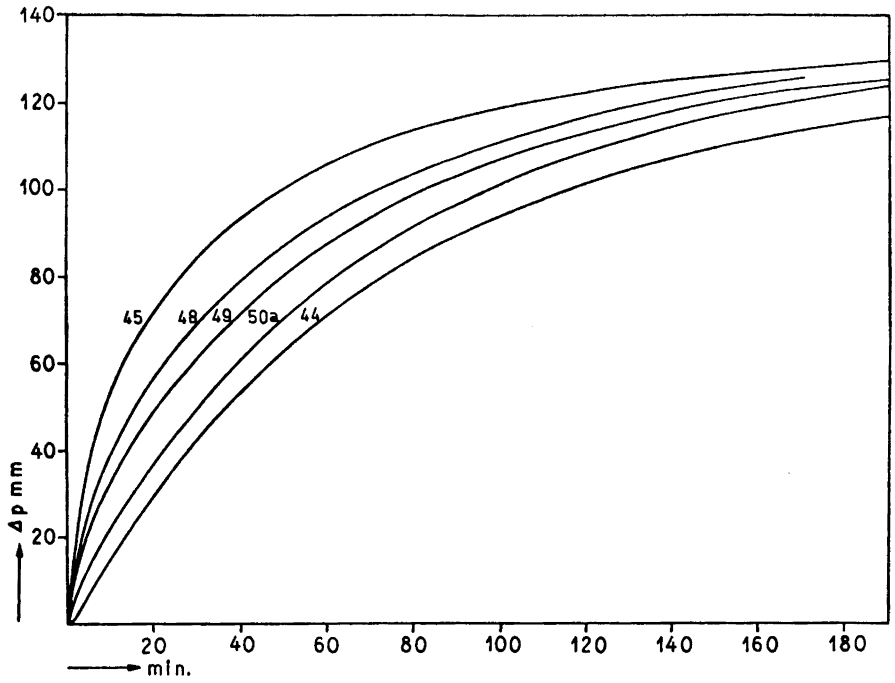

Fig. 4. Reaction curves for the experiments with hydroquinone. The experimental conditions were the same as those given in the subscript to Fig. 2.

The concentrations of hydroquinone were:

Concentration of hydroquinone × 10^4:	0.0	0.09	0.46	0.90	2.29
Curve No:	44	50 a	49	48	45

After this period, the hydrogen peroxide starts to decompose with a rate which is greater than that of the pure Fe(III)-catalyzed reaction. The experiments with greater amounts of inhibitor (see Fig. 2) show that a portion of the hydrogen peroxide is not decomposed into oxygen; obviously it is used for oxidizing the organic compound added. It should be mentioned that the experiments with benzene showed the same features as those just described. The reaction mixtures all turned more or less brown during the induction period.

The reaction curves in Fig. 4 show that hydroquinone, contrary to the compounds dealt with above, does not cause any induction period, but that it acts as a promotor from the very start of the reaction — or in other words it speeds up the Fe(III)-catalysis.

DISCUSSION

It seems difficult, if not impossible, to explain the experimental results by means of a reaction mechanism containing an open sequence similar to that proposed by Christiansen and Andersen [2] (scheme No. I on page 896). As pointed out by Bray and Peterson [4] and recently by Koefoed [1] the retarding

effect described above is much better explained by a reaction pattern containing a closed sequence. Koefoed has proposed the following chain reaction:

$$\begin{aligned} &Fe^{++} + FeO_2H^{++} \rightleftharpoons Fe \cdot FeO_2H^{++++} && 12 \\ &Fe \cdot FeO_2H^{++++} \rightleftharpoons OFeOH^{+} + Fe^{+++} && 23 \qquad \text{II} \\ &OFeOH^{+} + H_2O_2 \rightarrow Fe^{++} + O_2 + OH^{-} + H_2O && 31 \end{aligned}$$

(Concerning details of this scheme the reader is referred to Koefoed's paper).

If we, as Koefoed did, consider the $OFeOH^{+}$-ion as the most reactive intermediate the action of the inhibitor must be the removal of that intermediate (with benzene as an example):

$$OFeOH^{+} + C_6H_6 = Fe^{++} + C_6H_5OH + OH^{-} \qquad \overline{31}$$

that is to say that the inhibitor itself as illustrated in Fig. 5 is oxidized by a chain reaction.

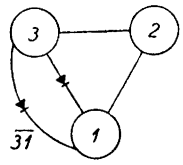

Fig. 5. Flow sheet of Koefoed's reaction cycle supplemented by reaction $\overline{31}$.

It does not seem unreasonable to assume that the phenol formed by reaction $\overline{31}$ again is oxidized to hydroquinone by a reaction similar to $\overline{31}$, because we know from the experiments that phenol also acts as an inhibitor.

In Koefoed's scheme the ferrous ion is presumed to act as a catalyst. Therefore, if we are able to increase the ferrous ion concentration in the reaction mixture, that should involve an increase of the rate of reaction. That is presumably what happens in the reacting mixtures containing benzene, phenol, or phenacetin when the rate of reaction suddenly increases, because, when hydroquinone is formed, it will react with ferric ions forming ferrous ions. At the same time the hydroquinone will be oxidized to quinhydrone in accordance with the brown colouring of the reaction mixture mentioned above.

From the above it follows that hydroquinone is to be expected to act, not as an inhibitor, but as a promotor for the reaction, which is in accordance with the experimental results given in Fig. 4.

CONCLUSION

Kinetic experiments on the influence of phenacetin, benzene, phenol, and hydroquinone under well defined conditions seem to indicate qualitatively that a reaction scheme for the Fe(III)-catalyzed hydrogen peroxide decomposition must be based on a closed sequence. Furthermore, they seem to confirm Koefoed's [1] assumption that ferrous ions act as a catalyst.

It appears from the experiments referred to in this paper and from earlier experiments [7] that benzene acting as an inhibitor successively is oxidized to phenol, hydroquinone, and finally to oxalic acid and carbon dioxide. Phenacetin, which is used as a stabilizer of medical hydrogen peroxide, obviously acts in the same way.

We wish to thank *Statens Almindelige Videnskabsfond* for financial support.

REFERENCES

1. Koefoed, J. *Acta Chem. Scand.* **9** (1955) 283.
2. Christiansen, J. A. and Andersen, V. S. *Acta Chem. Scand.* **4** (1950) 1538.
3. Brønsted, J. N. *J. Am. Chem. Soc.* **53** (1931) 2478.
4. Bray, W. C. and Peterson, S. *J. Am. Chem. Soc.* **72** (1950) 1401.
5. Kuhn, R. and Wassermann, A. *Ann.* **503** (1933) 203.
6. Christiansen, J. A. *Acta Chem. Scand.* **9** (1955) 272.
7. Andersen, V. S. *Acta Chem. Scand.* **4** (1950) 207.

Received January 18, 1958.

ACTA CHEMICA SCANDINAVICA 12 (1958) 903—918

The Interelectronic Repulsion Integrals and the Purity of Molecular Orbital Configurations, as Derived from the Absorption Spectra of Transition Group Complexes

CHR. KLIXBÜLL JØRGENSEN

Chemistry Department A, Technical University of Denmark, Copenhagen, Denmark

The ligand field theory has made several steps of increasing generality regarding the partly filled shell in transition group complexes. The electrostatic model, where the radial function is not varied, is disproven by the nephelauxetic series (see eqn. 8), where the term distances are decreased, relative to the gaseous ions. It is here shown that the two possibilities: expanded radial functions of a *d*-shell, with appropriate angular dependence, or a molecular orbital theory with an integral number of γ_3 and γ_5 electrons, but without the assumption of $l = 2$, give nearly identical results of the interelectronic repulsion integrals, separating the levels of a given sub-shell configuration. Tanabe and Sugano's theory and the role of configuration intermixing in complexes and gaseous ions is discussed, and it is concluded that the number of electrons in the partly filled shell of a monomeric complex is very well defined.

Slater, Condon, and Shortley [1] demonstrated that it is a rather good approximation to the wavefunction of gaseous atoms and ions to assume well-defined electron configurations, *i.e.* an integral number between 0 and $4l + 2$ electrons in each *nl*-shell, by writing the wavefunction as the anti-symmetrized product of one-electron functions

$$\psi = \frac{1}{r} \cdot R_{nl}(r) \cdot A_l(\varphi,\vartheta) \qquad (1)$$

where the angular part A_l is a linear combination of the angular functions known from the theory of the hydrogen atom, while the radial part R_{nl} is not at all hydrogen-like, but must be determined, *e.g.* by Hartree's methods, for each atomic number Z and ionic charge $Z_0 - 1$. If the electron configuration contains at least one partly filled shell (with l at least 1), it corresponds to several energy levels, which in Russell-Saunders coupling can be assem-

bled in multiplet terms, characterized by definite values of the quantum numbers L and the total spin S. The fine structure of the multiplet terms, giving energy levels with different J, is caused by electrodynamic (*i.e.* magnetic) and relativistic effects and is proportional to the Landé factors ζ_{nl}. The energy differences between the LS-terms are caused by the electrostatic repulsion between the electrons in the partly filled shell. This repulsion depends even for identical R_{nl} and thus identical attraction by the nucleus on the angular distribution A. In the case of one partly filled l-shell, the relative energy differences are expressed [1] as linear combinations of the integrals F^2, F^4, . . . , F^{2l}, which are approximately [2] inversely proportional to the average distance from the nucleus. The much larger contribution $\frac{1}{2}q(q-1)F^\circ$ is identical for all terms of a given configuration and can be considered as the spherical symmetrical average of the electrostatic repulsion between the q electrons in the partly filled shell, just as the central field from the electrons in closed shells, which determines the radial function R_{nl}.

In systems with several nuclei, *i.e.* in molecules and complex ions, the nl-shells are substituted by molecular orbitals γ_n, and the LS-terms are substituted by energy levels, characterized by Γ_n and S. The quantum numbers γ_n and Γ_n are found by group theoretical methods and depend on the symmetry of the complex. Thus, in the symmetry O_h (that of cubes and regular octahedrons [3]) the wavefunctions must obey certain conditions when performing the transformations of the group (such as rotations of the system of coordinates around the axes of the complex *etc.*). In this way, the wavefunctions always fall in one of the ten classes γ_n (electrons) or Γ_n (whole systems), where $n =$ 1, 2, 3, 4, or 5, and the parity is odd or even. However, in molecules, the approximation of molecular orbital configurations is not as generally valid as in the gaseous ions placed in the high symmetry of empty space. The principal purpose of this paper is to study whether this approximation seems to be valid in octahedral complexes of the three transition groups, where the absorption spectra recently have been interpreted by ligand field theory [4–11].

Even though the intermixing of molecular orbital configurations presents much difficulty, *e.g.* in the aromatic hydrocarbons [12,13], its extent has not generally been recognized in chemical textbooks. For large internuclear distances in H_2 or O_2, the configurations are highly intermixed and do not correspond much to the equilibrium groundstate [14]. Since the covalent bonding in d^n-complexes does not depend alone on the behaviour of the partly filled shell, similar conditions might prevail there. Another feature of particular importance for d^n-complexes is the electrostatic repulsion between the d-electrons, producing the same correlation effects as those mentioned above in the gaseous ions. Actually, the relevant multiples of F^2 and F^4 have the same order or magnitude as the ligand field parameter Δ (also called (E_1-E_2) or 10 Dq) which is the energy difference between the γ_3- and the γ_5-subshell. Therefore, it is not always valid to assume the groundstate to have the maximum number of γ_5-electrons possible, even though γ_5 has lower orbital energy than γ_3. In the case of d^4, d^5, d^6, and d^7, this would produce states with lower values of S, *i.e.* magnetically anomalous complexes, than has the gaseous ion. How-

ever, this is only possible, when the spin-pairing energy [6,8,15], *i.e.* an appropriate linear combination of F^2 and F^4, is smaller than Δ.

Theoretically, the electrostatic repulsion energies can be found in molecular orbital theory as sums of four-electron integrals

$$(\mathrm{a\ b}\ g\ \mathrm{c\ d}) = \int\int \Psi_\mathrm{a}^*(\tau_1)\Psi_\mathrm{b}^*(\tau_2)\ \frac{e^2}{r_{12}}\ \Psi_\mathrm{c}(\tau_1)\Psi_\mathrm{d}(\tau_2)\ \mathrm{d}\tau_1\mathrm{d}\tau_2 \qquad (2)$$

which has the physical significance of the electrostatic interaction between two extended charge distributions $\Psi_\mathrm{a}^*\Psi_\mathrm{c}$ and $\Psi_\mathrm{b}^*\Psi_\mathrm{d}$. If the diagonal element of g for a given configuration is wanted, it is only necessary to use two types of two-electron integrals:

$$\mathrm{J(ab)} = (\mathrm{ab}\ g\ \mathrm{ab}) \text{ and } \mathrm{K(ab)} = (\mathrm{ab}\ g\ \mathrm{ba}) \qquad (3)$$

where a summation is performed over all pairs ab in the configurations, and with negative sign of the K-integrals, when they do not vanish. Since (2) vanishes *, if a and c do not have the same spin component m_s, or if b and d do not have the same m_s, the results will be for each pair

$$\begin{array}{llll} \mathrm{a^+b^+} : \mathrm{J(ab)} - \mathrm{K(ab)} & & \mathrm{a^+a^-} : \mathrm{J(aa)} & \\ \mathrm{a^+b^-} : \mathrm{J(ab)} & & \mathrm{b^+b^-} : \mathrm{J(bb)} & \\ \mathrm{a^-b^+} : \mathrm{J(ab)} & & & \\ \mathrm{a^-b^-} : \mathrm{J(ab)} - \mathrm{K(ab)} & & & \end{array} \qquad (4)$$

Since the wavefunctions usually do not need to be chosen as complex functions, the asterisks in (2) denoting complex conjugation will generally be superfluous, and in this case, the following relation will be valid:

$$(\mathrm{aa}\ g\ \mathrm{bb}) = (\mathrm{ab}\ g\ \mathrm{ba}) = \mathrm{K(ab)} \qquad (5)$$

representing the interaction of the charge distribution ab with itself, while J(ab) still is the classical interaction between the actual electron densities $\mathrm{a^2}$ and $\mathrm{b^2}$. It may be remembered that the integral of ab over the total space is zero and of $\mathrm{a^2}$ equal to one, being the orthogonalization and normalization conditions, respectively.

The electrostatic energies can now be found as the eigenvalues of determinants having as diagonal elements the molecular orbital configurations with given spin directions m_s (+ and − in eqn. 4) and identical values of M_s. The problem of an electronic configuration with two electrons with $l = 0$ and a higher value, as treated by Heisenberg in case of the excited

* Further, it is a group-theoretical requirement for (2) not to vanish that abcd contains the representation Γ_1, since g is a totally symmetric operator. This is equivalent to the condition that ac and bd have the same Γ_n in their products as applied p. 911.

states 1s *nl* of a helium atom *, and by Houston as a general problem with intermediate coupling in heavy atoms, corresponds to a determinant for $M_s = 0$ with two equal diagonal elements J(ab) of eqn. 4 and the non-diagonal element K(ab), having as eigenvalues the triplet energy J(ab)—K(ab) and the singlet energy J(ab) + K(ab). Below, the similar problem with three identical diagonal elements J and three non-diagonal elements $\pm$ K is of interest. If an odd number of the non-diagonal elements is + K, the eigenvalues will be J + 2K, J — K, and J — K, while if an even number has the positive sign of K, the eigenvalues will be J — 2K, J + K, and J + K. Generally, a determinant with q equal diagonal elements = J and all the $\frac{q}{2}(q-1)$ non-diagonal elements = K will have the eigen-value J + (q — 1)K and (q — 1)-fold the eigen-value J—K.

The determinant with a given value of M_s can be divided in subdeterminants, each being diagonal in a group-theoretical quantum number Γ_n appropriate to the symmetry, where all the orbitals a and b have different γ_n. Unfortunately, this is not possible in O_h, where the three degenerate γ_5-orbitals do not necessarily have the same electrostatic interaction with the two γ_3-orbitals. This difficulty can be removed by considering lower symmetries, such as tetragonal or rhombic, without altering the energies of the orbitals belonging to the same cubic γ_n. Mr. Schäffer has kindly informed me that there exist essentially different forms of rhombic symmetry, while the difference between the two tetragonal symmetries I and II (Ref.[16], p. 6) has no physical significance. The rhombic symmetry I is a case of C_{2v} with the two-fold axis and the two two-fold mirror axes in the direction of the ligands (being placed on the x,y,z-axes) while II is another C_{2v} with the z-axis still as the two-fold axis, but the two two-fold mirror axes along the lines x + y and x — y in the xy-plane. The behaviour of the five orbitals is then:

	tetragonal	rhombic I	rhombic II
cubic 3	1 + 3	1 + 1	1 + 3
cubic 5	4 + 5	2 + 3 + 4	1 + 2 + 4

* The following Table indicates the ratio T in per cent between the triplet-singlet distance, *viz.* 2K(ab) = 2 G_1 in Slater integrals[1] and the energy of the triplet-singlet midpoint, *viz.* the orbital *nl*-energy, for a set of series of He, Li^+, and Be. Further, T is shown to be approximately inversely proportional to the principal quantum number *n*:

	n =	2	3	4	5	6	7	8
He 1s *ns*	T =	18.22	11.42	8.35	6.59	5.44	4.63	4.04
	*n*T	36.44	34.25	33.39	32.93	32.64	32.42	32.32
He 1s *np*	T =	7.26	5.22	3.96	3.19	2.66	2.29	2.00
	*n*T	14.52	15.65	15.84	15.96	15.98	16.03	15.98
Li^+1s *ns*	T =	10.80	7.54	5.49	4.35	3.55	3.06	—
	*n*T =	21.59	22.61	21.96	21.74	21.30	21.39	—
Li^+1s *np*	T =	6.45	4.55	3.37	2.82	—	—	—
	*n*T =	12.89	13.63	13.49	14.08	—	—	—
Be $1s^2$2s *nd*	T =	—	19.94	12.26	9.02	7.23	5.85	5.25
	*n*T =	—	59.82	49.06	45.08	43.36	40.99	41.96

Since the orbital energies are inversely proportional to $(n+\delta)^2$, where δ is the Rydberg correction, the exchange integrals K(ab) are shown to vary nearly as n^{-3}, as mentioned by Van Vleck[30].

These group-theoretical results are very useful for the following arguments, when it is no longer supposed that the molecular orbital can be written as eqn. 1, *i.e.* that l is no longer well-defined. In most cases, it will be a linear combination of different radial and different angular functions, such that a separability into a product R·A will not be possible. In this case, the expansion of the electrostatic energy in a series of F^k-contributions (k = 0, 2, 4, ...) will no longer terminate, but contain members with very high k.

The ligand field theory has applied more or less refined approximations in the description of d^n-complexes, of which a fair selection would be:

1. First-order perturbation energy on A is considered, but only the diagonal elements of weak field (assuming well-defined L) or strong field (assuming well-defined sub-shell configuration $\gamma_5^a\gamma_3^b$) determinants are considered.

2. The same as 1, but the restriction of sharply defined L or $\gamma_5^a\gamma_3^b$ removed, such that the energy levels are eigenvalues of determinants of q'th degree, if q levels present the same combination of S and Γ_n. The theory has thus one parameter Δ, assuming fixed atomic term distances, and can be expressed as in the Orgel-diagram [6].

3. Besides the first-order perturbation energy on A, there subsist second-order perturbations on R, changing the central field and thus the radial function R. But there is still assumed hydrogen-like A, *i.e.* $l = 2$. The theory has two types of parameters, Δ and the relative decrease of F^k- integrals in complexes, relative to those of the gaseous ion and can be expressed in the Tanabe-Sugano-diagram [5], where the independent variable is $\Delta : B$. The ratio between $B = 1/49\ F^2 - 5/441\ F^4$ and $C = 5/63\ F^4$ is assumed to be constant $\sim 1/4$.

4. The molecular orbitals γ_3 and γ_5 are not assumed to have the same radial function, but still the set of A corresponding to $l = 2$. Thus, the parameters B and C change in each sub-shell configuration $\gamma_5^a\gamma_3^b$.

5. The molecular orbitals are even not assumed to have hydrogen-like angular dependence, but their configurations are assumed to be rather well-defined. In this case, the different J- and K-integrals are applied, as outlined above, in the place of B and C.

6. The complete molecular orbital theory is presumed with large intermixing of configurations.

Of these approximations, 1 is obsolete, as are also the discussions of whether a given complex could be said to have strong or weak ligand field (incidentally, the best agreement is obtained in nearly all complexes with the former type of diagonal elements). It was often overseen that also the strong field diagonal elements contain multiples of F^k besides the multiples of Δ, and some misleading remarks were made about the complete "quenching" of the interelectronic repulsion for $\Delta \to \infty$.

Approximation 2 concentrated the interest on Tsuchida's spectrochemical series, *i.e.* the variation of Δ as a function of the ligands for a given metal ion:

$$Br^- < Cl^- < F^- < \text{urea} < ox^{--} \lesssim H_2O < SCN^- < NH_3 < en \ll CN^- \qquad (6)$$

while the series as function of the central ion for the same ligand is:

$$Mn(II) < Ni(II) < V(II) < Fe(III) < Cr(III) < Co(III) < Mo(III) < Rh(III) < Ir(III) < Pt(IV) \qquad (7)$$

The most characteristic property of the "electrostatic model" of ligand fields is that the radial function is not made subject to a variation. However, the series (6) was nearly incredible as a result of a purely electrostatic effect of the ligands, and it was soon proposed [6,9] to re-investigate Van Vleck's old remark [17] that the intermixing of orbitals with the same γ_n and parity from the central ion and the ligands, *i.e.* partly covalent bonding in the L.C.A.O. description, might as well explain * the magnitude of Δ, which was a successful empirical parameter rather than an absolute result of the electrostatic model (where the hydrogen-like radial functions and point dipoles necessarily must imply wrong results [8]). Thus, the low values of Δ in halide complexes was now ascribed to π-bonding effects, which increase the energy of the anti-bonding γ_5-orbital, while σ-bonding and electrostatic effects tended to increase Δ.

The first reliable method of estimating the relative extent of the partly covalent bonding from the absorption spectra appeared, when it was realized that the approximation 3 very nearly describes the observed energy levels. It has, however, been a general error by most investigators (including the present author) of d^n-complexes, to draw the opposite conclusion that no other explanation could reasonably be valid, if a given model worked quite well. It is actually possible to arrange the complexes in a two-dimensional system, according to Δ and to $\beta = B_{\text{complex}} : B_{\text{gaseous ion}}$. Schäffer and the present author [18] have studied the nephelauxetic ** series, *i.e.* the tendency to decrease β below 1 as a function of the central ion (giving nearly the same series as (7) except that Mo(III) is placed before and Fe(III) after Cr(III)) and of the ligands:

$$F^- > H_2O > \text{urea} > NH_3 > \text{en} \gtrsim ox^{--} > SCN^- > Cl^- \gtrsim CN^- > Br^- \qquad (8)$$

which is quite different from (6). The nephelauxetic series corresponds to the general opinion about the relative tendency towards covalent bonding, and it corresponds nearly to the hyperchromic series [19,20] of increasing inten-

* The absolute magnitude of Δ can also be estimated from the intermixing of molecular orbitals (from the ligands and the central ion) with the same γ_n and parity, assuming known diagonal elements of energy, and non-diagonal elements proportional to known overlap integrals multiplied by the average of the two diagonal elements. There is no doubt that reasonable agreement can be obtained by this form of approximation No. 5 choosing among an infinite set of assumed diagonal energies and overlap integrals (which in most papers refer to the un-realistic hydrogen-like radial functions). However, the three interesting attempts [34-36] to explain the absorption spectra without making any allusion to the electrostatic model No. 2 have all neglected the interelectronic repulsion integrals, separating the levels of the same molecular orbital configuration. Especially, the recent treatment [36] of $Co(NH_3)_5Cl^{++}$ and $Co(NH_3)_4Cl_2^+$ have ascribed the distance, occurring in $Co(NH_3)_6^{+++}$ between $^1\Gamma_4$ and $^1\Gamma_5$, to the energy difference between the σ-anti-bonding orbitals γ_{t_3} and γ_{t_1}. An erroneous extension of this thought [36] has necessitated the identification of the two first bands of trans-$Co(NH_3)_4Cl_2^+$ as transitions to $^1\Gamma_{t_5}$ and $^1\Gamma_{t_4}$, *i.e.* implying $^1\Gamma_5$ in O_h, as originally supported by the electrostatic model of ligand fields[16]. The molecular orbital theory for D_{4h} explains the actual behaviour[23] assuming π-bonding from the halide ligands. There is no doubt that a very fine description could be obtained by taking also the interelectronic repulsion integrals into account, if the first-order perturbations on the diagonal elements could be reasonably estimated. *Cf.* the recent treatment of cobalt(III) complexes by Yamatera [37].

** The word »nephelauxetic» (= cloud-expanding) has been kindly proposed by Professor Kaj Barr, University of Copenhagen.

sities of the Laporte-forbidden d^n-transitions and to decreasing oxidation potential of the ligands, *i.e.* decreasing energy for the removal of an electron.* All these three properties are undoubtedly connected; the intensities are roughly inversely proportional to the square of the distance in wavenumbers between the ligand field bands and the "redox" electron transfer bands, and the covalent bonding is enhanced by the easy transfer of electrons from the ligands to the central ion. Schäffer [21] investigated a series of chromium(III) complexes with oxygen atoms in the first co-ordination sphere and found a wide distribution in the nephelauxetic series: sulfate has even higher β than water, while most anion complexes and the red ruby fall in middle of the series, and green Cr_2O_3 has even smaller β than $Cr(CN)_6^{-3}$. For all these complexes, Δ does not vary more than between 14 640 and 18 520 K (= cm^{-1}).

Since γ_3-electrons have more repulsive effects on the ligands than γ_5-electrons have, as can be implied from the differences in ionic radii and from the bandwidths, it is obvious to introduce the fourth approximation, p. 907. However, a new difficulty arises: the spin-forbidden bands deliver a linear combination of B and C, while the states with maximum value of S are separated by multiples of B only. Thus, it is not easily decided, whether β_3 is smaller in the γ_3 sub-shell. This problem is discussed in Refs.[22,23]. For the following discussion, it might be useful to classify the experimental evidence, which is used for the determination of Δ and B in the complexes:

Only the Jahn-Teller regular systems are considered, because the determination of β is so sensitive for small irregularities in the wavenumbers. Perhaps, d^2- and d^7-systems might also be studied, while the tetragonal distortions are too large in d^4 and d^8 ($S = 0$). Among the regular systems, Δ can be directly found as the wavenumber ** of the first spin allowed band (when corrected for possible intermixing with spin-forbidden bands) in d^3- and d^8 ($S = 1$) systems. In d^5 ($S = 5/2$) and d^6 ($S = 0$), it is necessary to correct the distances $^4\Gamma_4(G)-{}^4\Gamma_{1,3}(G)$ and $^1\Gamma_1-{}^1\Gamma_4$, respectively, for a contribution of F^k- type

* However, Bailey [38] has recently determined the electron affinity of gaseous fluorine atoms to be between that of chlorine and that of bromine atoms. Thus, the nephelauxetic series and the chemical intuition must be connected with polarizabilities rather than ionization potentials.

** This is only valid until approximation No. 3. As seen from eqns. 14 and 16, the energy difference between $^4\Gamma_5$ and $^4\Gamma_2$ of d^3 is $\Delta + 2\Theta$, where $\Theta = J(3.5) - K(3.5) - J(4.5) + K(4.5)$ (*cf.* eqn. 12). Similarly, the energy difference in d^2 between $\frac{3}{4}\,(^3\Gamma_5) + \frac{1}{4}\,(^3\Gamma_4\gamma_5\gamma_3) - (^3\Gamma_4\gamma_5^2)$ is $\Delta + \Theta$ (*cf.* eqns. 13 and 15). The quantity Θ is zero in the electrostatic model, but will probably tend to have a negative value in the molecular orbital theory. The most important contributions to Θ comes from the J-integrals (eqn. 10) which contain the Racah parameter A and thus F^0. It will probably be a rather good approximation to assume that the interaction between a γ_3- and a γ_5-electron is decreased ϑ and between two γ_3-electrons decreased $2\,\vartheta$, relative to the interaction between two γ_5-electrons, which are in average concentrated in a smaller volume. If the latter approximation is valid, the value of Δ will always be decreased $(n-1)\,\vartheta$ in a d^n-system. Thus, in this case the same apparent value of Δ will always be implied from one and two-electron transitions. Since F^0 is a large but unknown quantity$\sim$100 000 K, (=cm^{-1}) ϑ will have an important effect on Δ, even if it amounts only to some per cent of F^0. However, the physical significance of F^0 is of analogous nature to the whole self-consistent field influence, which determines the not very accessible orbital energies. Systems as d^8 can profitably be treated as d^{10}-systems, where two positively charged holes occur. The interaction between the ten electrons $\gamma_5^6\gamma_3^4$ is 6 J(1.3) + 2K(1.3) + 12J(1.4) − 6K(1.4) + 12J(3.4) − 6K(3.4) + 12J (4.5) + 3J(4.4) — 6K(4.5) which gives a mathematically complicated contribution to the energy of, *e.g.*, a zinc(II) complex.

(*viz.* C), and for effects of sub-shell configuration intermixing, for obtaining Δ. The value of β can be obtained with reasonable accuracy from six classes of energy differences:

$^4\Gamma_2 - ^2\Gamma_3$, $^2\Gamma_4$, $^2\Gamma_5$, all of γ_5^3 in d^3. They are the sharp "ruby" lines of Cr(III), Mo(III), and Re(IV) which are nearly independent of Δ. The suppression, due to interaction with other sub-shell configurations is largest for $^2\Gamma_5$, while it is smaller for $^2\Gamma_3$ and negligible for $^2\Gamma_4$. However, $^2\Gamma_3$ is distinctly the sharpest transition.

$^4\Gamma_5(F) - ^4\Gamma_4(F)$ (and $^4\Gamma_4(P)$) of d^3. The two first of the three broad bands yield a value of B directly from the second-degree determinant for $^4\Gamma_4$. Schäffer has demonstrated that the third band of Cr(III), when known, often deviates from the prediction contrary to the analogous d^8-case. This effect is perhaps caused by interactions with electron transfer states.

$^6\Gamma_1(S) - ^4\Gamma_1(G)$, $^4\Gamma_3(G)$ (and also $^4\Gamma_5(D)$, $^4\Gamma_5(D)$, and $^4\Gamma_2(F)$) of $\gamma_5^3\gamma_3^2$ in d^5. The two first quartet levels * are degenerate for $l = 2$ and produce the sharp band[39] of Mn(II) and Fe(III). They are independent of Δ to a high approximation* and indicate $10B + 5C$.

$^1\Gamma_4 - ^1\Gamma_5$ of $\gamma_5^5\gamma_3$ in d^6. This distance between the two first spin-allowed bands of diamagnetic Co(III), Rh(III), and Ir(III) complexes is $16B$ for $\Delta \rightarrow \infty$, but shall be corrected for the influence of other sub-shell configurations, which is larger for $^1\Gamma_5$ than for $^1\Gamma_4$ with resulting decrease of the distance in the Tanabe-Sugano diagram.

$^3\Gamma_2 - ^1\Gamma_3$ of $\gamma_5^6\gamma_3^2$ in d^8. The excited level of the first spin-forbidden band of Ni(II) is intermixed with the triplet levels by intermediate coupling[7,22]. The value of $8B + 2C$ is very little influenced by the other $^1\Gamma_3$ from $\gamma_5^4\gamma_3^4$.

$^3\Gamma_5(F) - ^3\Gamma_4(F)$ and $^3\Gamma_4(P)$ of d^8. Contrary to the case of Cr(III), all three excited quartet levels can be observed of most Ni(II) complexes, and 15 B thus found form the diagonal sum rule. Further, it has been demonstrated [7,22] that the individual positions of the two $^3\Gamma_4$ agree with the theory within some 200 K, (= cm^{-1}) if the deviations from cubic symmetry are not too large.

---

* When the determinants of d^5 are calculated by use of the rules Ref. [1], p. 173, it is found that most of the non-diagonal elements contain multiples of K-integrals only. The absolute number of J-integrals in each diagonal element is always $n(n-1)/2$ in a d^n-system (because it contains the F^0-integral in the electrostatic case). Thus, the groundstate $^6\Gamma_1$ has the energy J(1.3) − K(1.3) + 3J(1.4) − 3K(1.4) + 3J(3.4) − 3K(3.4) + 3J(4.5) − 3K(4.5), while the other states of $\gamma_5^3\gamma_3^2$ have excitation energies such as $^5/_2$ K(1.4) + $^5/_2$ K(3.4) for $^4\Gamma_1(G)$, while the energies of $^4\Gamma_3(G)$ and $^4\Gamma_3(D)$ are a complicated square-root expression in J- and K-integrals, analogous to configurations in gaseous ions, where several multiplet terms present the same *LS*. The two $^4\Gamma_3$ have different parent terms, $(^4\Gamma_2 . {}^1\Gamma_3)$ and $(^2\Gamma_3 . {}^3\Gamma_2)$, having as diagonal elements of excitation energy 2K(1.3) + $^3/_2$K(1.4) + $^3/_2$K(3.4) and K(1.4) + K(3.4) + 3K(4.5), respectively, but also a non-diagonal element $\sqrt{3}$ (K(1.4) — K(3.4))/2. The other quartet terms of $\gamma_5^3\gamma_3^2$ have excitation energies, relative to $^6\Gamma_1$, which are the sum of the excitation energies of the parent terms within γ_5^3 (eqn. 14) and γ_3^2 plus a contribution S'(K(1.4) + K(3.4)), where $S' = {}^3/_2$ for the quartet-singlet and $S' = 1$ for the doublet-triplet parent terms. It is thus possible to describe the excitation energy within a sub-shell configuration in terms of spin-pairing energy (which can either be a number of K-integrals, or, by the formation of doubly occupied orbitals, differences between J(aa) and J(ab)) and energy due to decreased seniority number v (v = 0 for $^1\Gamma_1$ of γ_5^2 and γ_3^2, v = 1 for $^2\Gamma_5$ of γ_5^3).

If the assumption No. 5 on p. 907 of well-defined molecular orbital configurations $\gamma_5^a\gamma_3^b$, but not necessarily with $l = 2$, is applied to this material, the initial treatment, given by Tanabe and Sugano [5], must be followed. For d-electrons in the octahedral symmetry, a particular theorem is valid:

$$J(aa) = J(ab) + 2\ K(ab) \tag{9}$$

for two different orbitals a and b, which both belong to one of the classes γ_3 or γ_5. Tanabe and Sugano [5] proved that (9) is valid for γ_3, even when it is no d-electron, while (9) is not generally valid for γ_5. Schäffer and the present author have demonstrated from the group-theoretical result, p. 906 that one sufficient condition for (9) is that $J(aa) = J(bb) = J(cc)$ for a, b, c being the irreducible representations in rhombicII. However, this cannot be expected to be valid for all possible γ_5-electrons. The physical significance is the following: if we write the angular function $A = x^a y^b z^c/rl$ (with $a + b + c = l$ and $x^2 + y^2 + z^2 = r^2$) as homogeneous polynomiae in the Cartesian coordinates, the three γ_5-orbitals with $l = 2$ have the three functions xy, xz, and yz. If these functions are rotated 45° in the xy-plane, new linea rcombinations $\sqrt{1/2}$ (xz + yz), and $\sqrt{1/2}$ (xz − yz) are formed with the same physical shape. Analogously, among the p-electrons with $A = x, y, z$, the linear combination $\sqrt{1/2}$ (x + y) is simply a new p-orbital, only rotated in space. However, for any new such combination $c = \sqrt{1/2}$ (a + b), where $J(aa) = J(bb)$ and ab having another Γ_n than Γ_1 of a^2 and b^2 (*cf.* the foot-note p. 905), it will be valid

$$J(cc) = \tfrac{1}{4}\{J(aa) + J(bb) + 2J(ab) + 4K(ab)\} \tag{10}$$

giving (9) if $J(cc) = J(aa)$. This will obviously be the case, if c has the same physical shape as a, only rotated in space. Therefore, Slater's rules mentioned below will be valid for γ_4(p-) and γ_5(d-) electrons, but not for any set of such three equivalent orbitals. Further, by rotation of the xy-orbital, belonging to γ_5, the $(x^2 - y^2)$ orbital of γ_3-symmetry can be obtained. Since $(z^2 - \frac{1}{2}x^2 - \frac{1}{2}y^2)$ can be shown to be equivalent with $(x^2 - y^2)$ also in this respect, the J-integrals between two electrons in the same of the five d-orbitals are always identical. In the cases, where (9) is valid, it follows that ${}^1\Gamma_3$ and ${}^1\Gamma_5$ of γ_5^2 have the same energy, and that ${}^2\Gamma_3$ and ${}^2\Gamma_4$ of γ_5^3 also are systematically degenerate.

It is not easy to compare the molecular orbital theory with experiments, since the interelectronic repulsion energies in the pure sub-shell configurations are described by nine rather than two parameters (the coefficients to the constant $A = F^0 - F^4$, and to B and C in approximation No. 3 are indicated below), *viz*:

$J\ (1.3) \sim A - 4B + C$	$K\ (1.3) \sim 4B + C$
$J\ (4.5) \sim A - 2B + C$	$K\ (4.5) \sim 3B + C$
$J\ (1.4) \sim A - 4B + C$	$K\ (1.4) \sim 4B + C$
$J\ (3.4) \sim A + 4B + C$	$K\ (3.4) \sim C$
$J\ (4.4) \sim A + 4B + 3C$	

(11)

since J (1.1) = J (3.3) can be found from eqn. 9, and J (4.4) = J (5, same 5). The numbers denote the tetragonal quantum numbers [3,16]. An interesting theorem is that

$$\begin{aligned}
\mathrm{J}\ (1.5) &= \frac{1}{4}\ \mathrm{J}\ (1.4) + \frac{3}{4}\ \mathrm{J}\ (3.4) \sim \mathrm{A} + 2\mathrm{B} + \mathrm{C} \\
\mathrm{J}\ (3.5) &= \frac{3}{4}\ \mathrm{J}\ (1.4) + \frac{1}{4}\ \mathrm{J}\ (3.4) \sim \mathrm{A} - 2\mathrm{B} + \mathrm{C} \\
\mathrm{K}\ (1.5) &= \frac{1}{4}\ \mathrm{K}\ (1.4) + \frac{3}{4}\ \mathrm{K}\ (3.4) \sim \mathrm{B} + \mathrm{C} \\
\mathrm{K}\ (3.5) &= \frac{3}{4}\ \mathrm{K}\ (1.4) + \frac{1}{4}\ \mathrm{K}\ (3.4) \sim 3\mathrm{B} + \mathrm{C}
\end{aligned} \tag{12}$$

where 5 denotes one of the two γ_{t5}-orbitals. Thus, the interaction of a filled γ_5^6-shell containing four t5 and two t4-electrons is identical with a t1- or a t3-orbital.

The eigenvalues in the sub-shell configuration γ_5^2

$$\begin{aligned}
&^3\Gamma_4: && \mathrm{J}\ (4.5) - \mathrm{K}\ (4.5) \\
&^1\Gamma_5: && \mathrm{J}\ (4.5) + \mathrm{K}\ (4.5) \\
&^1\Gamma_3: && \mathrm{J}\ (4.4) - \mathrm{K}\ (4.5) \\
&^1\Gamma_1: && \mathrm{J}\ (4.4) + 2\mathrm{K}\ (4.5)
\end{aligned} \tag{13}$$

can be found from the determinants with identical M_s and a given rhombic Γ_n, giving, *e.g.*, the result that $^1\Gamma_1$ the two states of $^1\Gamma_3$ are members of a Heisenberg-determinant (p. 905) with the eigen-values J (4.4) + 2 K (4.4) and J (4.4) − K (4.4) twice. With a similar application of one of the two sets of rhombic quantum numbers, the eigen-values in γ_5^3 are:

$$\begin{aligned}
&^4\Gamma_2: && 3\ \mathrm{J}\ (4.5) - 3\ \mathrm{K}\ (4.5) \\
&^2\Gamma_3: && 3\ \mathrm{J}\ (4.5) \\
&^2\Gamma_4: && 2\ \mathrm{J}\ (4.5) + \mathrm{J}\ (4.4) - 2\ \mathrm{K}\ (4.5) \\
&^2\Gamma_5: && 2\ \mathrm{J}\ (4.5) + \mathrm{J}\ (4.4)
\end{aligned} \tag{14}$$

proving the degeneracy of $^2\Gamma_3$ and $^2\Gamma_4$ and the ratio 3:5 between the wave-numbers of the first and the third ruby line for γ_5-orbitals satisfying eqn. 9. In the mixed configuration $\gamma_5\gamma_3$, the four energy levels are:

$$\begin{aligned}
&^3\Gamma_5: && \mathrm{J}\ (1.4) - \mathrm{K}\ (1.4) \\
&^3\Gamma_4: && \mathrm{J}\ (3.4) - \mathrm{K}\ (3.4) \\
&^1\Gamma_5: && \mathrm{J}\ (1.4) + \mathrm{K}\ (1.4) \\
&^1\Gamma_4: && \mathrm{J}\ (3.4) + \mathrm{K}\ (3.4)
\end{aligned} \tag{15}$$

while the quartet levels of $\gamma_5^2\gamma_3$ and $\gamma_5\gamma_3^2$ have the energies of interelectronic repulsion:

$^4\Gamma_5(\gamma_5^2\gamma_3)$: 3/2 J (1.4) − 3/2 K (1.4) + 1/2 J (3.4) − 1/2 K (3.4) + J (4.5) − K (4.5) (16)

$^4\Gamma_4(\gamma_5^2\gamma_3)$: 1/2 J (1.4) − 1/2 K (1.4) + 3/2 J (3.4) − 3/2 K (3.4) + J (4.5) − K (4.5)

$^4\Gamma_4(\gamma_5\gamma_3^2)$: J (1.3) − K (1.3) + J (1.4) − K (1.4) + J (3.4) − K (3.4)

Schäffer and the present author [23] shall discuss, why the structure of all the sub-shell configurations, containing a Γ_4 and a Γ_5 level with maximum value of S, is similar to that of (15) and (16). Thus, the distance between the two spin-allowed bands in d^2-, d^3-, d^7-, and d^8-systems with the symmetry O_h, which is 12 B under assumption of $l = 2$ and an arbitrary radial function, will be:

$$\text{J (3.4)} - \text{K (3.4)} - \text{J (1.4)} + \text{K (1.4)} \tag{17}$$

In the special case of diamagnetic d^6-complexes the energy difference (= 16 B for $l = 2$) between $^1\Gamma_4$ and $^1\Gamma_5$ of $\gamma_5^5\gamma_3$ is not given by (17) but by

$$\text{J (3.4)} - 2\ \text{K (3.4)} - \text{J (1.4)} + 2\ \text{K (1.4)} \tag{18}$$

and the energy difference between the analogous triplet terms $^3\Gamma_4$ and $^3\Gamma_4$ is only J (3.4) − J (1.4). This can be explained by the interaction with the γ_{t5}^4 core in the five pure tetragonal sub-shell configurations:

t5	t4	t3	t1			
4	2	0	0	$^1\Gamma_1$(t1)	12 J (4.5) + 3 J (4.4) − 6 K (4.5)	(19)
4	1	1	0	$^3\Gamma_4$(t2)	8 J (4.5) + 2 J (4.4) − 4 K (4.5) + 3 J (1.4) + 2 J (3.4) − 3/2 K (1.4) − 3/2 K (3.4)	
4	1	1	0	$^1\Gamma_4$(t2)	8 J (4.5) + 2 J (4.4) − 4 K (4.5) + 3 J (1.4) + 2 J (3.4) − 3/2 K (1.4) + 1/2 K (3.4)	
4	1	0	1	$^3\Gamma_5$(t4)	8 J (4.5) + 2 J (4.4) − 4 K (4.5) + 2 J (1.4) + 3 J (3.4) − 3/2 K (1.4) − 3/2 K (3.4)	
4	1	0	1	$^1\Gamma_5$(t4)	8 J (4.5) + 2 J (4.4) − 4 K (4.5) + 2 J (1.4) + 3 J (3.4) + 1/2 K (1.4) − 3/2 K (3.4)	

The two tetragonal sub-shell configurations (3 2 1 0) and (3 2 0 1) do not correspond to pure cubic quantum numbers, Γ_n but have energies, which are

$$\frac{1}{4}(\Gamma_4) + \frac{3}{4}(\Gamma_4) \text{ and } \frac{3}{4}(\Gamma_4) + \frac{1}{4}(\Gamma_5) \tag{20}$$

according to eqn. 11. This behaviour of the two levels Γ_{t5} is a general feature for all the sub-shell configurations discussed by Schäffer and the present author [23].

In nickel(II) complexes, the spin-forbidden transitions from $^3\Gamma_2$ to $^1\Gamma_3$ and $^1\Gamma_1$ of the ground configuration $\gamma_5^6\gamma_3^2$ should have the ratio 1:2 between the wavenumbers, because the excitation energies are those calculated [5] for γ_3^2, *viz.* 2 K (1.3) and 4 K (1.3). It is interesting that the promotion energy forming a planar, diamagnetic complex with the pure tetragonal configuration having an empty γ_{t_2}-orbital is 3 K (1.3) because in this case, the level $^1\Gamma_{t_1}$ is not intermixed with other tetragonal sub-shell configurations. Thus, the promotion energy [16] indicated as $\frac{4}{7}$ (^{1}D) + $\frac{3}{7}$ (^{1}G), *viz.* 8 B + 2 C or 2 K (1.3), is too low. In Ni^{++}, however, the state ^{1}S does not seem to have as high an energy as predicted by Slater's theory (22 B + 7 C above ^{3}F) with the result that $^1\Gamma_1$ has probably lower energy [22] and that the promotion energy for formation of planar complexes is smaller than 3/2 times the first spin-forbidden transition of the corresponding octahedral complex.

Of course, eqns. 12—19 allow a wider range of variability in the energy differences, where 12 B and 16 B now is explained as a sum of two positive and two negative quantities, and the wavenumbers of the spin-forbidden bands are multiples of K-integrals. It is not easily determined, whether the freedom of molecular orbitals without defined l actually is demanded by experimental evidence. The most surprising fact is that even this theory would predict the same type of ratios between the interelectronic repulsion energies as would the electrostatic model. This has two different aspects: on the one hand, it is very promising for the ligand field theory that nearly any assumption about the wavefunctions would lead to the same distribution of the energy levels of the partly filled shell (agreeing to a high accuracy with observations); on the other hand, unfortunately, it is not easy to draw any conclusions about the wavefunctions from the absorption spectra, except that the electrostatic model is disproven by the nephelauxetic series. One type of evidence about the question how good an approximation is $l = 2$, might be delivered by the temperature-independent paramagnetism, which is proportional to matrix elements of L without regard to the spatial extension of the wavefunctions. Ballhausen and Asmussen [24] have found so enormous residual diamagnetisms by application of Van Vleck's high-frequency formula (which rather was expected to yield too small paramagnetism, due to the neglect of other excited levels) that, disregarding the scattering of the calculated material, the agreement would be much better by taking only 40 % of Van Vleck's correction. This may be explained by a similar break-down of $l = 2$ as the change of the radial functions in approximation No. 3, expressed by the decrease of β. Griffith and Orgel [25] have treated the same problem, but though they applied different experimental values they concluded with the "possible quenching of L", suggesting a similar necessity of molecular orbitals, which are not d-electrons to a very large extent.

However, the success of the ligand field theory seems indirectly to prove that the last of the six approximations, p. 907, the strong intermixing of molecular orbital configurations, is at least not needed for explaining the energy levels. The calculations of this intermixing would be extremely complicated, but of course, it cannot be excluded that the final results would still resemble

the observed energy levels. The problem is here common to atomic spectroscopy of gaseous ions: it is not easily proven that the configurations are very pure. However, the magnitude of the correction $\alpha L(L+1)$ with $\alpha \sim 100$ K, which Trees [26] and Racah [27] introduced to the Slater theory [1] seems to indicate that the configurations usually are ~ 99 % pure in the squares of the wave-function. It is clearly proven, *e.g.* by Furlani's calculation [28] for Fe^{++}, that the correction due to configuration interaction is monotonically increasing with L. However, the present author has the impression that the terms of the lowest configurations rather are suppressed by a quantity, proportional to $1/(2L+1)$ or $1/(L+1)$, as also supported by the calculations of Ufford [29], where the non-diagonal elements between LS-terms of d^3 and d^2s are increasing in the series ^2G, ^2F, and ^2P. If such a proportionality with the constant $\sim 10\,000$ K can be applied, it would explain, why nearly all terms with $L = 0$ seem anomalously much depressed.

However, the agreement of atomic spectroscopy with Slater's theory [1] and of ligand field transitions with Tanabe and Sugano's theory [1] seems to indicate that the electron configurations in gaseous ions and the molecular orbital configurations in octahedral complexes have a purity of the same order of magnitude, *viz.* between 90 and 99 % in most cases.* This may be connected with the fact that the octahedral complexes (more so than, *e.g.*, the square-planar) are so near to having spherical symmetry that most of the electrostatic repulsion between the electrons in the partly filled shell is a common contribution of central field type to all the energy levels, which are not electron transfer states. The latter concept must now be defined as states, where the population of other orbitals than the partly filled γ_3 and γ_5 is changed, relative to the ground-state, since also the d^n-transitions from the old electrostatic model now must be assumed to involve change of the electron density in the ligands. It is a special case of the relatively high purity of molecular orbital configurations in complexes that the number a + b of electrons in the partly filled sub-shells $\gamma_5^a\gamma_3^b$ still is very good for classification of the complexes according to the oxidation state of the central ion, as implied from the primitive idea of a + b electrons in the d-shell. The classification after d^n may be expected to break down in strongly coloured polymeric complexes of the molybdenum(V,VI) blue or ferro-ferricyanide type, where the partly filled orbitals may be highly de-localized.

It is generally believed that the properties of atoms and molecules are functions of integers (especially the number of electrons) and that these functions are characterized by shell structure, *i.e.* the properties change suddenly by passing certain stabilized numbers. The periodical system of elements is

---

* We must here distinguish between the validity of pure configurations in the weak or in the strong sense. In the former, the observed energy differences can be brought in agreement with Slater's theory [1], assuming reasonable values of the parameters of interelectronic repulsion, while the parameters are directly calculated from the radial functions, assuming eqn. 1, in the latter case. Dr. Per Olov Löwdin and Dr. Klaus Appel, Kvantkemiska Gruppen, Uppsala University, have kindly informed me that the interelectronic repulsion invariably is calculated 10—40 % too large in gaseous d^n-ions, showing a rather large deviation from the "strong sense" theory. Thus, we must expect the configuration interaction, introduced by the electronic correlation, to have a similar extent in the transition group complexes [39].

strongly dominated by the stability of 2, 10, 18, 36, 54, 86, . . .electrons, while the nuclei with 2, 6, 8, 14, 20, 28, 40, 50, 82, 126, . . .neutrons or protons are especially stable, as explained by the action of Pauli's exclusion principle on another set of quantum numbers than those of the electrons. It must be realized that these shell structures are entirely dependent on the occurrence of quite pure configurations. In the nuclei, the central field seems strongly apt to deviations from spherical symmetry, and the configurations seem rather intermixed [31,32].

In complexes, it could not be assumed *a priori* that any electron configuration was a good approximation to the wavefunction. Since the time of Sidgwick, it has often been stated that since $S = 0$ of the groundstate of $Co(NH_3)_6^{+++}$, its configuration is to a certain approximation $[A]3d^{10}4s^24p^6$, *i.e.* [Kr], rather than [A] 3 d^6, which would give $S = 2$ and thus a paramagnetic complex. Pauling refined this idea in his hybridization theory, which is actually a molecular orbital theory with assumption of equal radial functions for the d-, s-, and p-part of d^2sp^3. Pauling [33] recognizes that the actual groundstate of most complexes is a resonance structure, *i.e.* an intermixing, of ionic and covalent formulae, and that the magnetic criterion cannot be used for an absolute distinction. However, just the assumption of identical radial functions makes a consistent refinement of this theory very difficult. It was not realized by many authors, that even though the configuration $[A]3d^{10}4s^24p^6$ might be a good description,* i.e. corresponding to the hydrogen-like angular functions for given l, the radial functions may vary from one complex to another, just as they do in the gaseous ions. When the excited states attracted more interest, it was necessary to abandon the valency-bond method for the more general molecular orbital theory. Here, other authors do not recognize that the bonding γ_3- and γ_5-orbitals always are filled, whatever the degree of partly covalent bonding may be, while the total number of electrons in the partly filled shell, represented by the anti-bonding γ_3- and γ_5-orbitals, is constant to a very high approximation. The evolution of partly covalent bonding, as expressed by the nephelauxetic series, corresponds to these anti-bonding orbitals smoothly varying from the d-shell of the gaseous ion to more expanded wavefunctions also present in the ligands. During this development, they may or may not retain $l = 2$ (approximation Nos. 3 and 4) with expanded radial functions, and they do not seem to reach the Pauling value with 50 % participation from the central ion and the ligands, since β still is above 0.3.

The conclusion of this paper is that the assumption (No. 5, p. 907) of negligible intermixing between the configurations $\gamma_5^a\gamma_3^b$ and other molecular orbital configurations seems to be consistent with all facts known about the energy levels and the corresponding wavefunctions. However, the electrostatic model has given a rather fine description, except of the absolute value of Δ (but it must now be rejected due to the nephelauxetic effect) so it cannot easily be concluded conversely that satisfactory agreement has proven the

* However, corresponding to spherical symmetry of the electron cloud. Only after having formed the covalent bonds, the hybridized configurations have any directional character, as not always recognized.

validity of the approximation of pure molecular orbital configurations of the partly filled shell, which is rather near to being a d-shell.

Acknowledgements. I am much indebted to my colleague, Mr. Claus E. Schäffer and to Professor Asger Nielsen, Physics Department of the Technical University of Denmark, for many interesting discussions about the subject of the present paper. Finally, I thank Dr. Robert Feltham, University of California, for several interesting comments, and Dr. John S. Griffith, Department of Theoretical Chemistry, University of Cambridge, for a very valuable remark about the independence of J(4.4) and J (4.5).

REFERENCES

1. Condon, E. U. and Shortley, G. H. *Theory of Atomic Spectra.* Cambridge 1953.
2. Jørgensen, C. Klixbüll *Energy Levels of Complexes and Gaseous Ions.* Gjellerups Forlag, Copenhagen 1957.
3. Bethe, H. *Ann. Physik* [5] **3** (1929) 133.
4. Hartmann, H. and Schläfer, H. L. *Z. Naturforsch.* **6a** (1951) 754.
5. Tanabe, Y. and Sugano, S. *J. Phys. Soc. Japan* **9** (1954) 753, 766.
6. Orgel, L. E. *J. Chem. Phys.* **23** (1955) 1004, 1819, 1824, 1958.
7. Jørgensen, C. Klixbüll *Acta Chem. Scand.* **9** (1955) 116, 1362; **10** (1956) 500, 518, 887; **11** (1957) 53, 73, 151, 166.
8. Jørgensen, C. Klixbüll *Quelques Problèmes de Chimie Minérale, Dixième Conseil de Chimie Solvay,* R. Stoops, Bruxelles, 1956, p. 355.
9. Owen, J. *Proc. Roy. Soc. London* **A 227** (1955) 183.
10. Moffitt, W. and Ballhausen, C. J. *Ann. Rev. Phys. Chem.* **7** (1956) 107.
11. Holmes, O. G. and McClure, D. S. *J. Chem. Phys.* **26** (1957) 1686.
12. Coulson, C. A., Craig, D. P. and Jacobs, J. *Proc. Roy. Soc. London* **A 206** (1951) 297.
13. Pariser, R. *J. Chem. Phys.* **24** (1956) 250.
14. Slater, J. C. *Electronic States of Atoms and Molecules. Technical Report No. 3, Solid-State and Molecular Theory Group.* Massachusetts Institute of Technology 1953.
15. Jørgensen, C. Klixbüll *Acta Chem. Scand.* **10** (1956) 1505.
16. Ballhausen, C. J. and Jørgensen, C. Klixbüll *Kgl. Danske Videnskab. Selskab, Mat.-fys. Medd.* **29** (1955) No. 14.
17. Van Vleck, J. H. *J. Chem. Phys.* **3** (1935) 803, 807.
18. Schäffer, C. E. and Jørgensen, C. Klixbüll, *Symposium on Co-Ordination Compounds.* Rome, September 1957. (*Suppl. La Ricerca Scientifica,* **28** 143).
19. Yamada, S. and Tsuchida, R. *Bull. Chem. Soc. Japan* **26** (1953) 15.
20. Jørgensen, C. Klixbüll, *Acta Chem. Scand.* **9** (1955) 405.
21. Schäffer, C. E. *Symposium on Co-Ordination Compounds.* Rome, September 1957. (*Suppl. La Ricerca Scientifica* **28** 149).
22. Bostrup, O. and Jørgensen, C. Klixbüll, *Acta Chem. Scand.* **11** (1957) 1223.
23. Schäffer, C. E. and Jørgensen, C. Klixbüll, *Acta Chem. Scand. To be published.*
24. Ballhausen, C. J. and Asmussen, R. W. *Acta Chem. Scand.* **11** (1957) 479.
25. Griffith, J. S. and Orgel, L. E. *Trans. Faraday Soc.* **53** (1957) 601.
26. Trees, R. E. *Phys. Rev. 83* (1951) 756; **84** (1951) 1089.
27. Racah, G. *Proceedings of the Rydberg Centennial Conference on Atomic Spectroscopy,* p. 31, in *Lunds Universitets Årsskrift, 2. avd.* **50** (1954) No. 21.
28. Furlani, C. and Sartori, G. *Gazz. chim. ital.* **87** (1957) 371, 380. (*Suppl. La Ricerca Scientifica,* **28** 149).
29. Ufford, C. W. *Phys. Rev.* **44** (1933) 732.
30. Van Vleck, J. H. and Whitelaw, N. G. *Phys. Rev.* **44** (1933) 551.
31. Alder, K., Bohr, Å., Huus, T., Mottelson, B. R., and Winther, Å. *Revs. Modern Phys.* **28** (1956) 432.

32. Jensen, J. H. D. *Revs. Modern Phys.* **29** (1957) 182.
33. Pauling, L. *J. Chem. Soc.* **1948** 1461.
34. Yamatera, H. *Journal Inst. Polytechn. Osaka City Univ. Series C.* **5** (1956) 163.
35. Ito, K. and Kuroda, Y. *J. Chem. Soc. Japan* **76** (1955) 542, 762, 766, 934.
36. Nakamoto, K., Fujita, J., Kobayashi, M., and Tsuchida, R. *J. Chem. Phys.* **27** (1957) 439.
37. Yamatera, H. *Bull Chem. Soc. Japan* **31** (1958) 95.
38. Bailey, T. L. *J. Chem. Phys.* **28** (1958) 792.
39. Jørgensen, C. Klixbüll, *Discus. Faraday Soc.* No. 26 (1958).

Received January 7, 1958.

ACTA CHEMICA SCANDINAVICA 12 (1958) 919—933

The Rate of Decarboxylation and the Dissociation Constants of Acetosuccinic Acid

KAI JULIUS PEDERSEN

Chemical Laboratory, Royal Veterinary and Agricultural College, Copenhagen, Denmark

Solutions of acetosuccinic acid were prepared from the diethyl ester which was first hydrolysed in alkaline solution. In order to find the time required for practically complete hydrolysis, a few experiments on the rate of hydrolysis were carried out, but, owing to the complicated nature of the reaction, a complete kinetic analysis of the data was not attempted.

As a contribution to the study of the spontaneous decarboxylation of β-keto carboxylic acids in aqueous solution, a kinetic investigation was made of the decomposition of acetosuccinic acid into levulinic acid and carbon dioxide at the temperatures 25.0 and 37.0°C in solutions containing an excess of barium hydroxide (by titration), and in solutions of hydrochloric acid and in acetate buffer solutions (manometrically). By analysis of the data, separate rate constants were evaluated for each of the three simultaneous reactions: decarboxylation of undissociated acetosuccinic acid, of its univalent and divalent ion. It was found that acetate ions catalyse the decomposition of the undissociated acid. It was shown that cupric ions have only a small catalytic effect in the decarboxylation of acetosuccinic acid. In this respect the acid differs from other dibasic β-keto carboxylic acids, such as oxaloacetic acid, dihydroxytartaric acid, and acetonedicarboxylic acid, where cupric ions have a powerful catalytic effect.

The two dissociation constants of acetosuccinic acid at 25.0°C were determined by glass-electrode measurements on acetosuccinate buffer solutions containing various concentrations of sodium chloride. From the rate of change of the e.m.f. with time it was possible to compute rate constants for the decarboxylation which are in reasonable agreement with those obtained by manometry and by titration.

ALKALINE HYDROLYSIS OF DIETHYL ACETOSUCCINATE

The solutions of acetosuccinic acid examined in this paper were prepared from diethyl acetosuccinate which was hydrolysed in alkaline solution at room temperature or at 25°C shortly before the experiment was started. The ester was prepared as described in *Organic Syntheses* [1] and was distilled twice under reduced pressure through a Widmer stillhead in an all-glass apparatus. The purified preparation distilled within a temperature interval of 0.3°C.

Table 1. Hydrolysis of diethyl acetosuccinate at 25.0°C. Initial concentrations: x_0 M ester, u_0 M sodium hydroxide.

$x_0 = 0.03932$ $u_0 = 0.0899$			$x_0 = 0.03947$ $u_0 = 0.1198$			$x_0 = 0.04015$ $u_0 = 0.2099$		
t min	u	k^* 10^2	t min	u	k^* 10^2	t min	u	k^* 10^2
3.1	0.0808	1.72	4.0	0.1071	1.91	3.85	0.1941	2.52
7.9	0.0694	1.66	8.25	0.0961	1.88	7.9	0.1807	2.52
12.65	0.0601	1.64	12.2	0.0874	1.88	11.85	0.1700	2.54
17.45	0.0520	1.64	16.9	0.0788	1.89	16.1	0.1609	2.56
23.9	0.0436	1.62	22.5	0.0705	1.89	20.2	0.1541	2.56
30.0	0.0373	1.60	30.0	0.0619	1.92	25.1	0.1478	2.58
38.05	0.0310	1.58	40.0	0.0543	1.93	32.05	0.1411	2.64
48.1	0.0254	1.55	52.0	0.0485	1.95	39.5	0.1365	2.70
60.05	0.0208	1.52	65.0	0.0449	1.99	48.0	0.1332	2.81
			80.0	0.0426	2.08	60.05	0.1310	2.93

In order to get an idea of the time required for practically complete hydrolysis of the ester, a few rate-experiments were carried out at 25.0°C. The results are shown in Table 1 where the initial concentrations, x_0 M ester (Et_2X), u_0 M sodium hydroxide, are given at the top. At various times, t min after the ester was dissolved, samples were pipetted into a small excess of 0.05 M tartaric acid, and the mixture was quickly titrated back with sodium hydroxide. The concentrations of titratable base (u normal) found in the samples are given in the table. The reaction is kinetically rather complicated since it consists of two consecutive second- or first-order reactions, and, at large values of t, the slow decarboxylation of the acetosuccinate ion may affect the result. A complete kinetic analysis was therefore not attempted. Instead, $x = [Et_2X] + \frac{1}{2}[EtX^-]$ was computed by means of the equation $2x = u - (u_0 - 2x_0)$, and the equation for a first-order reaction, $k^*\ t = \log(x_0/x)$, was formally applied. Table 1 shows that k^*, within each of the three experiments, is roughly constant. In the first experiment k^* decreases a little, in the second it is almost constant until 90 %, in the third until 75 % of the ester is hydrolysed, after which it increases slowly. When the solutions examined in the following parts of this paper were prepared, the initial concentration of ester was in general about 0.04 M, and the concentration of base was about 0.12 N or more. It follows from Table 1 that the time of half life will here be less than 20 min at 25°C. In order to obtain practically complete hydrolysis, the solutions were therefore left for at least 4 h at 25°C or for at least 8 h at room temperature.

RATE OF DECARBOXYLATION IN BARIUM HYDROXIDE SOLUTIONS

When diethyl acetosuccinate is dissolved in an excess of strong base, the hydrolysis of the ester will be followed by a slow spontaneous decarboxylation of the divalent acetosuccinate ion

$$CH_3COCH(COO^-)CH_2COO^- + HO^- \rightarrow CH_3COCH_2CH_2COO^- + CO_3^{--}$$

Table 2. Rate of decarboxylation of the divalent acetosuccinate ion by titration. Initial concentrations: x_0 M ester, u_0 N barium hydroxide.

Temperature 25.0°C $x_0 = 0.03903$, $u_0 = 0.1096$ $k = 0.191 \times 10^{-5}$ sec^{-1}				Temperature 37.0°C $x_0 = 0.03886$, $u_0 = 0.1093$ $k = 0.876 \times 10^{-5}$ sec^{-1}			
t hours	u	x	x_0e^{-kt}	t hours	u	x	x_0e^{-kt}
23.8	0.0255	0.0330	0.0331	4.50	0.0262	0.0335	0.0335
30.3	0.0241	0.0316	0.0314	6.33	0.0244	0.0317	0.0316
48.6	0.0205	0.0280	0.0280	8.00	0.0227	0.0300	0.0300
71.9	0.0163	0.0238	0.0238	12.33	0.0189	0.0262	0.0262
97.8	0.0127	0.0202	0.0200	24.50	0.0105	0.0178	0.0178
121.7	0.0095	0.0170	0.0169	28.50	0.0085	0.0158	0.0157
144.3	0.0071	0.0146	0.0145	31.25	0.0071	0.0144	0.0144
167.5	0.0049	0.0124	0.0124	48.83	0.0010	0.0083	0.0083
196.9	0.0025	0.0100	0.0101	48.92	0.0009	0.0082	0.0082
221.7	0.0006	0.0081	0.0086				

When the strong base is barium hydroxide, the carbonate ion will be precipitated as barium carbonate, and the rate of decarboxylation may be followed by taking samples of the solution, adding phenolphthalein, and titrating them with hydrochloric acid. Data for two experiments, at 25.0 and 37.0°C, respectively, are shown in Table 2. The initial concentrations, x_0 M ester and u_0 N barium hydroxide, are given at the top of the table. The concentration of acetosuccinate ion (x M) at the time t hours after the ester was dissolved, was calculated from the concentration of titratable base (u N) by means of the equation $x = 3x_0 - u_0 + u$. The reaction was found to obey the first-order law with the values of the rate constant k given at the top of the table. When k is expressed in reciprocal hours, and x_0e^{-kt} is computed, the values given in the last column of the two halves of the table are obtained. Comparison with the observed values of x shows that the agreement with the first-order formula is good. Table 3 gives a summary of all the experiments on the decomposition in barium hydroxide solution. It is seen that k decreases a little when salt is

Table 3. Rate of decarboxylation of the divalent acetosuccinate ion by titration.

Temperature °C	Initial concentrations in mole / liter				$k \times 10^5$ sec^{-1}
	Ester	$Ba(OH)_2$	$BaCl_2$	KCl	
25.0	0.03903	0.0548	0	0	0.191
25.0	0.03876	0.0732	0	0	0.192
25.0	0.03902	0.1100	0	0	0.202
25.0	0.04067	0.0549	0.200	0	0.165
25.0	0.04082	0.0549	0	0.400	0.182
37.0	0.03886	0.0546	0	0	0.876
37.0	0.03917	0.1096	0	0	0.960

added. The decrease is larger for barium chloride than for potassium chloride. On the other hand, k increases with increasing hydroxyl ion concentration. This increase may possibly be due to an error caused by a simultaneous reaction

$$CH_3COCH(COO^-)CH_2COO^- + HO^- \rightarrow CH_3COO^- + (CH_2COO^-)_2$$

It is however known that this type of reaction, the so called acid decomposition of β-keto carboxylate ions, is predominant only in concentrated alkali. As the most probable values of the rate constant k_2 for the spontaneous decarboxylation of the divalent acetosuccinate ion we therefore adopt

at 25.0°C: $k_2 = 0.191 \times 10^{-5}$ sec^{-1}

at 37.0°C: $k_2 = 0.876 \times 10^{-5}$ sec^{-1}

When the Arrhenius equation is applied, the following expression is obtained

$$k_2 = 2.39 \times 10^{11} \, e^{-23\,300/RT} \text{ sec}^{-1}$$

DECOMPOSITION IN SOLUTIONS OF HYDROGEN CHLORIDE

Rate experiments were carried out at 25.0 and 37.0°C on solutions of hydrogen chloride and sodium chloride, the total chloride ion concentration being 0.300 M. The reaction was followed by observing the pressure above the solution in an apparatus described in an earlier paper [2]. The difference P between the final pressure reading and the reading at the time t, is proportional to the total concentration (x M) of acetosuccinic acid at the time t: $P = \varphi x$, where φ is a constant. When α_0, α_1, and α_2 denote the fractions of the acid present in the form of undissociated acid (H_2X), univalent ion (HX^-), and divalent ion (X^{--}), respectively, the rate of decarboxylation may be written as follows

$$-\frac{dx}{dt} = (k_0\alpha_0 + k_1\alpha_1, + k_2\alpha_2)\, x \qquad (1)$$

where k_0, k_1, and k_2 are rate constants for the spontaneous decomposition of the molecules H_2X, HX^-, and X^{--}, respectively. The expression in parenthesis will vary more or less during the reaction. At the end it will approach the value

$$k = k_0\,\alpha_{0\,\infty} + k_1\,\alpha_{1\,\infty} + k_2\,\alpha_{2\,\infty} \qquad (2)$$

where the subscript ∞ denotes final values of the variables, corresponding to a hydrogen ion concentration equal to the concentration of hydrogen chloride (h M).

In order to interpret the experiments, it was necessary to know the dissociation constants of acetosuccinic acid and levulinic acid. Those for acetosuccinic acid were determined in a later section of this paper where $K_1 = 1.56 \times 10^{-3}$ and $K_2 = 3.64 \times 10^{-5}$ were found for 0.300 M sodium chloride at 25°C. Owing to the instability of the acid, it was not possible to measure the constants at 37°. The values found for 25° were therefore applied also at 37°. Accascina [3] has found the value 2.32×10^{-5} for the activity dissociation con-

stant of levulinic acid at 25°C. On the assumption that it increases with addition of sodium chloride in the same proportion as the dissociation constant of pyruvic acid [4], the value 4.57×10^{-5} is estimated for the solvent 0.300 M sodium chloride.

We shall now deduce a formula by means of which we shall compute k for the decomposition in solutions containing hydrogen chloride. We may here neglect the second dissociation of acetosuccinic acid and the dissociation of levulinic acid. We therefore obtain from eqns. 1 and 2 and the expression for the first dissociation constant of acetosuccinic acid

$$-\frac{dx}{dt} = k_0 x - (k_0 - k_1)\ \alpha_1 x \tag{3}$$

$$k = k_0 - (k_0 - k_1)\ \alpha_{1\infty} \tag{4}$$

$$\frac{\alpha_1\ (h + \alpha_1 x)}{1 - \alpha_1} = \frac{\alpha_{1\infty}\ h}{1 - \alpha_{1\infty}} \tag{5}$$

By means of eqn. 5, x may be written as a function of $\alpha_1 x$

$$x = \frac{1}{\alpha_{1\infty}}\ (\alpha_1 x) + \frac{1 - \alpha_{1\infty}}{\alpha_{1\infty}\ h}\ (\alpha_1 x)^2 \tag{6}$$

When first eqn. 6 and then eqn. 4 are introduced into eqn. 3, is obtained

$$-\frac{1}{\alpha_{1\infty}}\ \frac{d(\alpha_1 x)}{dt} - \frac{2\ (1-\alpha_{1\infty})}{\alpha_{1\infty}\ h}\ (\alpha_1 x)\ \frac{d(\alpha_1 x)}{dt} = \frac{k}{\alpha_{1\infty}}\ (\alpha_1 x) + \frac{k_0\ (1-\alpha_{1\infty})}{\alpha_{1\infty} h}\ (\alpha_1 x)^2$$

from which we get

$$-k\ dt = \frac{h\ d(\alpha_1 x) + 2\ (1 - \alpha_{1\infty})\ (\alpha_1 x)\ d(\alpha_1 x)}{h\ (\alpha_1 x) + \frac{k_0}{k}\ (1 - \alpha_{1\infty})\ (\alpha_1 x)^2}$$

which on integration gives

$$-kt + \text{const.} = \ln\ (\alpha_1 x) + \left(\frac{2k}{k_0} - 1\right) \ln\left[h + \frac{k_0}{k}\ (1-\alpha_{1\infty})\ (\alpha_1 x)\right] \tag{7}$$

When eqn. 6 is solved with respect to $\alpha_1 x$ and the abbreviation

$$\lambda = 4\ \alpha_{1\infty}\ (1 - \alpha_{1\infty})/h \tag{8}$$

is used, we obtain

$$\alpha_1 x = \frac{h}{2\ (1-\alpha_{1\infty})}\ (\sqrt{1 + \lambda x} - 1) = \frac{h\ \lambda\ x}{2\ (1 - \alpha_{1\infty})\ (1 + \sqrt{1 + \lambda x})} \tag{9}$$

If we further use the abbreviation

$$\varepsilon = 2\ (k_0 - k)/k_0 \tag{10}$$

and introduce eqn. 9 into eqn. 7, we get the formula

$$-kt + \text{const.} = \ln x - \ln (1 + \sqrt{1 + \lambda x}) + (1-\varepsilon) \ln (1-\varepsilon + \sqrt{1 + \lambda x}) \quad (11)$$

which may also be written in the form

$$-kt + \text{const.} = \ln x - \ln \left(1 + \frac{\sqrt{1 + \lambda x}-1}{2}\right) + (1-\varepsilon) \ln \left(1 + \frac{\sqrt{1 + \lambda x}-1}{2-\varepsilon}\right) \quad (12)$$

If we introduce $P = \varphi x$, write λ' instead of λ/φ, and transform to decadic logarithms, we get

$$-0.4343\ kt + \text{const.} = \log P - \log \left(1 + \frac{\sqrt{1 + \lambda' P}-1}{2}\right) + (1-\varepsilon) \log \left(1 + \frac{\sqrt{1 + \lambda' P}-1}{2-\varepsilon}\right) \quad (13)$$

When the hydrogen ion concentration is sufficiently large, λ will be so small that formula 13 may be simplified (using $\ln(1 + \delta) \simeq \delta$, and $\sqrt{1 + \delta} - 1 \simeq \delta/2$) to

$$-0.4343\ kt + \text{const.} = \log P - \frac{0.4343\ \varepsilon\lambda'}{4\ (2-\varepsilon)}\ P \quad (14)$$

If further $k_1\alpha_{1\,\infty} \ll k_0\ (1-\alpha_{1\,\infty})$ we find by means of eqns. 4 and 10 that $\varepsilon \simeq 2\alpha_{1\,\infty}$ which on introduction into eqn. 14 gives the following approximate formula in which k does not appear on the right side of the equation

$$-0.4343\ kt + \text{const.} = \log P - \frac{0.4343\ \alpha_{1\,\infty}^2}{\varphi\ h}\ P \quad (15)$$

The composition of the solutions examined and the results obtained are given in Table 4. The initial concentrations of acetosuccinic acid (x_0 M), given in the third column, have been calculated on the assumption that the ester has been completely hydrolysed while none of the acetosuccinic acid has been decarboxylated. Actually, up to 20 % of the acid had been decomposed when readings began, partly in alkaline solution and partly after the addition of hydrochloric acid, but this, of course, does not affect the kinetic result. The ethanol ($2x_0$ M) present in the solutions was produced by the hydrolysis. The degrees of dissociation $\alpha_{1\,\infty}$ and $\alpha_{2\,\infty}$ were calculated by means of the dissociation constants given before. In computing the rate constants k, it was for most of the solutions accurate enough to apply formula 15. For the other solutions, the approximate value of k found by means of this formula was used for the calculation of ε by means of eqn. 10 after which the exact formula 13 was applied. When the values of the expression on the right side of the equation were plotted against t, the points fell always very close to a straight line from the slope of which the final value of k was determined.

The reaction is, in the solutions examined here, predominantly a spontaneous decarboxylation of the undissociated acid. The data were therefore used for calculating k_0 by means of eqn. 2. It follows from the values of k_2

Table 4. Decarboxylation of acetosuccinic acid (initially x_0 M) in the solvent: h M hydrogen chloride, c M cupric nitrate, $(0.300-h-3c)$ M sodium chloride, $2x_0$ M ethanol.

h	c	x_0	$a_{1\infty}$	$a_{2\infty}$	$k \times 10^5$ sec^{-1}	$k_0 \times 10^5$ sec^{-1}
Temperature 25.0°C:						
0.2700	0	0.0100	0.0057	0.0000	17.18	17.26
0.2400	0	0.0196	0.0065	0.0000	17.19	17.28
0.0900	0	0.0207	0.0170	0.0000	17.08	17.32
0.0900	0.00400	0.0208	0.0170	0.0000	17.02	17.26
0.0400	0	0.0194	0.0375	0.0000	16.71	17.24
0.0200	0	0.0199	0.0723	0.0001	16.11	17.13
0.01494	0	0.0103	0.0948	0.0002	15.86	17.20
0.01200	0	0.0197	0.1150	0.0004	15.64	17.28
0.01200	0.00400	0.0200	0.1150	0.0004	15.57	17.20
0.00591	0	0.0101	0.2086	0.0013	14.15	17.10
0.00293	0	0.0106	0.3460	0.0042	12.30	17.30
Temperature 37.0°C:						
0.2400	0	0.0200	0.0065	0.0000	73.8	74.1
0.0900	0	0.0201	0.0170	0.0000	72.8	73.8
0.0400	0	0.0205	0.0375	0.0000	71.7	73.9
0.01980	0	0.0200	0.0730	0.0002	70.4	74.7
0.01946	0	0.0198	0.0741	0.0002	70.5	75.0
0.01190	0	0.0206	0.1159	0.0004	68.3	75.1

found in the preceding part of the paper that the last term of the equation may be neglected. When k_1 found in experiments on acetate buffers in the next part of the paper is applied, k_0 given in the last column of Table 4 is computed The average values at the two temperatures are

$$\text{at } 25.0°\text{C:} \qquad k_0 = 17.23 \times 10^{-5} \text{ sec}^{-1}$$

$$\text{at } 37.0°\text{C:} \qquad k_0 = 74.3 \times 10^{-5} \text{ sec}^{-1}$$

When the Arrhenius equation is applied, the following expression is obtained

$$k_0 = 4.38 \times 10^{12} \, e^{-22\,400/RT} \text{ sec}^{-1}$$

Two of the solutions in Table 4 contained cupric nitrate while the total ionic strength was the same as in the other solutions. The results show that cupric ions have no catalytic effect.

DECOMPOSITION IN ACETATE BUFFER SOLUTIONS

The rate of decarboxylation was studied by the manometric method at 25.0 and 37.0°C in solutions containing acetic acid, sodium acetate, and, in some cases, sodium chloride, the total ionic strength being always close to 0.300. The composition of the solutions examined is shown in Table 5.

In applying eqn. 1 to the experimental data, it must be taken into account that a_0, a_1, and a_2 change a little as the reaction progresses, from their initial values $a_{0\,0}$, a_{10}, and a_{20} (corresponding to the presence of x_0 M acetosuccinic

acid) to their final values $\alpha_{0\,\infty}$, $\alpha_{1\,\infty}$, and $\alpha_{2\,\infty}$ (when practically all acetosuccinic acid has been transformed into levulinic acid and carbon dioxide). In order to correct for this change, it was as an approximation assumed that α_0, α_1, and α_2 vary linearly with x. Eqn. 1 may then be written as

$$-\frac{dx}{dt} = (k + \beta x)x \tag{16}$$

where we have used the abbreviation

$$\beta = [k_0\ (\alpha_{0\,0} - \alpha_{0\,\infty}) + k_1\ (\alpha_{10} - \alpha_{1\,\infty}) + k_2\ (\alpha_{20} - \alpha_{2\,\infty})] / x_0 \tag{17}$$

By integration of eqn. 16, transformation to decadic logarithms, and insertion of $P = \varphi x$ and $\beta' = \beta/\varphi$, is obtained

$$-0.4343\ kt + \text{const.} = \log P - \log\ (1 + \beta' P) \tag{18}$$

The initial and final values of α_0, α_1, and α_2 were computed for all the solutions examined. In this computation were used the values of the dissociation constants of acetosuccinic acid and levulinic acid given in the preceding section of the paper. For the dissociation constant of acetic acid was, both at 25 and 37°C, used the value 3.20×10^{-5} estimated for the solvent 0.3 M sodium chloride on the basis of measurements by Harned and Hickey [5] and by Kilpatrick and Eanes [6]. The slight dissociation of carbonic acid was neglected. In Table 5 are, to save space, given only $\alpha_{0\,\infty}$ and $\alpha_{1\,\infty}$ together with the final acetate ion concentration $[Ac^-]_\infty$.

Table 5. Decarboxylation of acetosuccinic acid (initially x_0 M) in the solvent: a M acetic acid, b M sodium acetate, $(0.300 - b)$ M sodium chloride, $2x_0$ M ethanol.

a	b	x_0	$[Ac^-]_\infty$	$\alpha_{0\infty}$	$\alpha_{1\infty}$	$k \times 10^5$ sec^{-1}	$k \times 10^5$ sec^{-1} calc.
Temperature 25.0°C:							
0.4923	0.3000	0.01146	0.2948	0.0203	0.587	2.503	2.504
0.3182	0.3001	0.01156	0.2936	0.0111	0.490	1.936	1.938
0.1797	0.3000	0.01147	0.2921	0.0048	0.361	1.369	1.374
0.1091	0.3000	0.01157	0.2910	0.0022	0.264	1.011	1.015
0.4923	0.1500	0.01169	0.1466	0.0494	0.713	3.423	3.418
0.3182	0.1501	0.01146	0.1456	0.0292	0.644	2.736	2.734
0.1797	0.1500	0.01145	0.1441	0.0139	0.526	2.033	2.029
0.1091	0.1501	0.01167	0.1427	0.0070	0.417	1.559	1.552
Temperature 37.0°C:							
0.4920	0.3000	0.01095	0.2950	0.0203	0.587	12.48	12.45
0.2836	0.3000	0.01118	0.2933	0.0094	0.463	9.14	9.20
0.1786	0.3000	0.01112	0.2924	0.0047	0.359	7.05	7.02
0.1088	0.3000	0.01140	0.2911	0.0022	0.263	5.25	5.22
0.4920	0.1500	0.01134	0.1468	0.0493	0.712	16.81	16.74
0.3876	0.1501	0.01137	0.1462	0.0372	0.677	15.00	15.01
0.2832	0.1501	0.01127	0.1454	0.0252	0.621	12.92	12.95
0.1786	0.1500	0.01125	0.1445	0.0137	0.523	10.13	10.32
0.1088	0.1500	0.01123	0.1429	0.0069	0.415	8.06	7.98

When k was computed from the observed data by means of eqn. 18, a method of successive approximations had to be used, since β' was unknown at the start. In the final step, when β' was calculated from eqn. 17 by means of the constants in the expressions for k given below (eqns. 19 and 20), the values of k shown in the next to the last column of Table 5 were obtained. When eqn. 2 was applied, it was found that k_0 could not have the value found previously for solutions of hydrogen chloride. Agreement could, however, be obtained when it was assumed that k_0 increases linearly with the acetate ion concentration, that is, acetate ions catalyse the decarboxylation of undissociated acetosuccinic acid. On this basis the following expressions for the rate constants were obtained

$$25.0°: \quad k \times 10^5 = (17.23 + 47.8\ [Ac^-])a_{0\infty} + 3.054\ a_{1\infty} + 0.191\ a_{2\infty} \qquad (19)$$

$$37.0°: \quad k \times 10^5 = (74.3 + 166\ [Ac^-])a_{0\infty} + 16.37\ a_{1\infty} + 0.876\ a_{2\infty} \qquad (20)$$

Each of the expressions contains two new constants, k_1 and the catalytic coefficient of the acetate ion (k_{Ac^-}), which have been computed so as to obtain the best agreement with the observed values of k. The last column of Table 5 shows k calculated by means of eqns. 19 and 20. When the Arrhenius equation is applied, the following expressions are obtained

$$k_1 = 2.10 \times 10^{14}\ e^{-25\,700/RT}\ sec^{-1}$$

and

$$k_{Ac^-} = 4.54 \times 10^{10}\ e^{-19\,100/RT}\ liter\ mole^{-1}\ sec^{-1}$$

Cupric ion catalysis. In Table 6 are given the results of rate measurements on acetate buffer solutions containing 0.00480 M cupric nitrate, the total ionic

Table 6. Decarboxylation of acetosuccinic acid (initially x_0 M) in the solvent: a M acetic acid, b M sodium acetate, 0.00480 M cupric nitrate, (0.286 − b) M sodium chloride, $2x_0$ M ethanol.

a	b	x_0	$[Ac^-]_\infty$	$[Cu^{++}]_\infty \times 10^3$	$a_{0\infty}$	$a_{1\infty}$	$k \times 10^5$ sec^{-1}	$k \times 10^5$ sec^{-1} calc.
Temperature 25.0°C:								
0.3029	0.2856	0.01101	0.2719	0.151	0.0116	0.496	2.026	1.960
0.1711	0.2856	0.01101	0.2705	0.152	0.0050	0.367	1.481	1.392
0.1039	0.2856	0.01102	0.2695	0.153	0.0023	0.269	1.140	1.031
0.4687	0.1428	0.01113	0.1334	0.429	0.0522	0.719	3.513	3.471
0.3029	0.1428	0.01091	0.1324	0.433	0.0310	0.652	2.824	2.782
0.1711	0.1428	0.01090	0.1309	0.440	0.0149	0.537	2.173	2.075
0.1039	0.1428	0.01111	0.1296	0.445	0.0075	0.428	1.729	1.591
Temperature 37.0°C:								
0.4684	0.2855	0.01084	0.2731	0.150	0.0211	0.593	12.87	12.57
0.2700	0.2855	0.01074	0.2718	0.151	0.0098	0.469	9.64	9.31
0.1700	0.2856	0.01095	0.2705	0.153	0.0049	0.366	7.64	7.13
0.1036	0.2856	0.01068	0.2697	0.153	0.0023	0.268	6.03	5.30
0.1700	0.1429	0.01070	0.1311	0.439	0.0147	0.535	10.94	10.57
0.1036	0.1429	0.01099	0.1297	0.445	0.0075	0.427	8.93	8.21

strength being 0.300. It was here necessary to take into account the complex formation between cupric and acetate ions while that between cupric and chloride ions was neglected. The initial and final values of the acetate, cupric, and hydrogen ion concentrations, and of α_0, α_1, and α_2, were computed by means of the dissociation constants of the acids given before and the following values of the complexity constants [7], corresponding to the ionic strength 0.300

$$[CuAc^+] / [Cu^{++}]\ [Ac^-] = 41.2$$

$$[CuAc_2] / [Cu^{++}]\ [Ac^-]^2 = 264$$

Only the final values of the acetate and cupric ion concentrations, and of α_0 and α_1, are given in Table 6. Rate constants k, computed from the observed data by the same procedure as for solutions without cupric nitrate, are given in the next to the last column. They are from 1 to 14 % higher than those shown in the last column which were computed by means of eqns. 19 and 20 on the assumption that cupric ions do not catalyse. The difference indicates that cupric ions have a small catalytic effect in the decarboxylation of acetosuccinic acid. The data are not accurate enough to establish a mechanism for the catalytic reaction, but they agree best with the assumption that the rate is proportional to the product $[CuAc^+]\alpha_2$.

It has been found earlier that certain metal ions, especially cupric ions, have a powerful catalytic effect in the decarboxylation of other dibasic β-keto carboxylic acids, such as oxaloacetic acid [8,9], dimethyloxaloacetic acid [10], acetonedicarboxylic acid [11], and dihydroxytartaric acid [12]. This catalysis was explained as being the result of a rapid decarboxylation of a complex of the chelate type between the metal ion and the divalent β-keto carboxylate ion. In this complex, the metal ion is bound to a keto and a carboxylate group. It is essential that a carboxylate group having a keto group in β-position is free, since a metal ion seems to stabilise the carboxylate group to which it is bound. Thus, the metal ion complexes of the nitroacetate ion do not split off carbon dioxide [13]. The chelates which decompose rapidly would therefore in oxaloacetic acid have the five-membered ring structure I, and in acetonedicarboxylic acid the six-membered ring structure II. In acetosuccinic acid two chelates are conceivable, the six-membered ring structure III and the seven-membered ring structure IV. The former would not be expected to split off carbon dioxide, and the latter may possibly be formed less readily since it has a seven-membered ring.

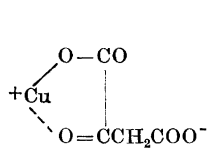

I

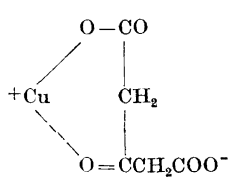

II

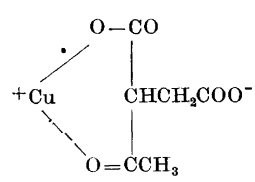

III

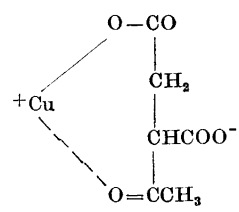

IV

THE DISSOCIATION CONSTANTS OF ACETOSUCCINIC ACID

The first and second dissociation constant of acetosuccinic acid were determined by glass-electrode measurements at 25.0°C on acetosuccinate buffer solutions containing various concentrations of sodium chloride. The measurements were carried out, and the hydrogen ion concentrations computed, by the procedure followed by the author in earlier papers [4,14]. By the measurements was determined what is actually the e.m.f. (E volts) of cells of the composition

$$H_2;\ X;\ 3.5\ M\ KCl;\ 0.00999\ M\ HCl,\ 0.0900\ M\ NaCl;\ H_2$$

where X is the acetosuccinate buffer under investigation.

The buffer solutions were prepared in the following way. Diethyl acetosuccinate was weighed out and dissolved in a solution of sodium hydroxide and sodium chloride (concentrations shown in Table 10). The mixture was placed in a thermostat at 25.0°C. According to measurements in the first part of this paper, the ester was completely hydrolysed within 4 h. The buffer solutions to be measured were prepared by adding appropriate volumes of hydrochloric acid and water to samples taken from the alkaline solution after complete hydrolysis. If no decarboxylation had taken place, the solutions would have the composition shown in Tables 7 and 8 (x_0 M acetosuccinic acid, b M sodium hydroxide, s M sodium chloride, $2x_0$ M ethanol). Actually, more or less of the acetosuccinic acid had been transformed into levulinic acid and carbon dioxide when the measurement took place, partly by a slow reaction in alkaline solution, and partly by a more rapid reaction after acidification. In order to find the hydrogen ion concentration of solutions where no decarboxylation had taken place, two extrapolations were made, one to correct for decarboxylation in acid solution and another to correct for decarboxylation in the alkaline solution from which the buffer was made. In order to make the first extrapolation, E was measured with an interval of one minute in the time from 4 or 5 to 25 or 30 min after the acidification. When E was plotted against the time (t minutes after acidification of the solution), the points fell close to a straight line by means of which E corresponding to $t = 0$ was found. Three or four such series of measurements were carried out on buffer solutions of the same composition except that they were made up from the alkaline solution at different times (τ hours after its preparation). E corresponding to $t = 0$ for each series was plotted against τ, and E_0 was found by extrapolation to $\tau = 0$. In evaluating τ, a small correction was subtracted (estimated to be 0.4 h) in order to allow for the space of time in which the ester was not completely hydrolysed. Values of $-\log[H^+]_0$, pertaining to solutions where no decarboxylation had taken place, were calculated from E_0. They are given in Tables 7 and 8 together with, respectively, $-\log K_1$ and $-\log K_2$ computed from them in the usual way. In the tables are also shown the ionic strengths I of the solutions. When Debye-Hückel's limiting law is applied, it is found that the results may be expressed by the formulae

$$-\log K_1 = 3.048 - 1.013\ \sqrt{I}/(1 + 2.38\ \sqrt{I}) \qquad (21)$$

$$-\log K_2 = 4.952 - 2.026\ \sqrt{I}/(1 + 2.12\ \sqrt{I}) \qquad (22)$$

Table 7. First dissociation constant (K_1) of acetosuccinic acid at 25.0°C.

	$x_0 \times 10^3$	$b \times 10^3$	s	I	$-\log [H^+]_0$	$-\log K_1$	$-\log K_1$ calc.
A1	9.99	3.90	0.2959	0.3014	2.836	2.805	2.807
A2	10.00	4.92	0.2948	0.3010	2.493	2.802	2.807
A3	10.03	5.78	0.2939	0.3009	3.047	2.814	2.807
A4	10.03	3.89	0.1959	0.2013	2.853	2.835	2.828
A5	10.02	4.92	0.1949	0.2011	2.956	2.820	2.828
A6	10.04	5.80	0.1941	0.2010	3.065	2.831	2.828
A7	10.02	3.90	0.0960	0.1013	2.876	2.865	2.865
A8	10.01	4.92	0.0949	0.1010	2.994	2.870	2.865
A9	10.02	5.78	0.0941	0.1009	3.089	2.857	2.865

When $-\log K_1$ and $-\log K_2$ are calculated by means of these expressions, the values given in the last column of Tables 7 and 8 are obtained. If it is permissible to extrapolate to $I = 0$ by means of eqns. 21 and 22, the two activity dissociation constants are $K_1 = 8.95 \times 10^{-4}$ and $K_2 = 1.12 \times 10^{-5}$.

For the buffer solutions examined in the first three lines of Table 7 (A 1—3) and the first three lines of Table 8 (B 1—3) are in Table 9 given the values of E and $-\log[H^+]$ found by extrapolation of the observed data to the time ($t = 0$) when the solution was acidified. In order to show how rapidly E changes, values of E and $-\log [H^+]$ corresponding to either $t = 10$ or $t = 20$ min are also given for most of the solutions. All the solutions of Table 9 were prepared from alkaline solutions of the same initial composition (given in the first line of Table 10).

Rate of decarboxylation from e.m.f. measurements. In order to estimate the rate of decarboxylation both in the alkaline solutions and in the buffer solutions, the concentrations of undecomposed acetosuccinic acid (x molar) were calculated from the hydrogen ion concentrations by means of the following formula (expressing the principle of electroneutrality)

$$(\alpha_1 + 2\alpha_2)\ x + (\alpha' + \alpha'')\ (x_0 - x) = b + [H^+] \qquad (23)$$

Table 8. Second dissociation constant (K_2) of acetosuccinic acid at 25.0°C.

	$x_0 \times 10^3$	$b \times 10^3$	s	I	$-\log [H^+]_0$	$-\log K_2$	$-\log K_2$ calc.
B1	9.99	13.89	0.2858	0.3039	4.299	4.436	4.437
B2	10.00	14.91	0.2848	0.3048	4.460	4.441	4.437
B3	10.03	15.89	0.2838	0.3057	4.603	4.433	4.436
B4	10.03	13.88	0.1859	0.2039	4.337	4.489	4.484
B5	10.02	14.90	0.1848	0.2048	4.502	4.491	4.484
B6	10.04	15.90	0.1840	0.2059	4.638	4.468	4.483
B7	10.02	13.89	0.0860	0.1040	4.419	4.574	4.564
B8	10.01	14.90	0.0849	0.1048	4.577	4.566	4.563
B9	10.02	15.89	0.0840	0.1058	4.719	4.550	4.562

Table 9. Glass-electrode measurements at 25.0°C on acetosuccinate buffer solutions.

	τ hours	t min	E	−log [H+]	$x \times 10^3$	$k_2 \times 10^5$ sec^{-1}	$k \times 10^5$ sec^{-1}	$k \times 10^5$ sec^{-1} calc.
A1	5.3	0	0.0498	2.854	9.67	0.171		
		10	0.0516	2.884	9.14		9.4	9.5
	24.4	0	0.05345	2.915	8.65	0.164		
		10	0.0553	2.946	8.19		9.1	9.0
	30.6	0	0.0547	2.938	8.31	0.167		
		10	0.0565	2.969	7.88		8.7	8.8
A2	4.7	0	0.0563	2.963	9.73	0.162		
		10	0.0583	2.997	9.25		8.4	8.6
	22.9	0	0.06095	3.042	8.65	0.176		
		10	0.06295	3.076	8.25		7.9	7.9
	48.0	0	0.06725	3.149	7.48	0.168		
		10	0.06925	3.183	7.16		7.3	7.1
A3	5.2	0	0.0629	3.074	9.63	0.217		
		10	0.06495	3.109	9.20		7.6	7.7
	10.2	0	0.0645	3.101	9.30	0.206		
		10	0.0666	3.137	8.89		7.4	7.5
	28.5	0	0.0694	3.184	8.40	0.173		
		10	0.0715	3.220	8.06		6.9	6.8
B1	5.8	0	0.13795	4.343	9.68	0.151		
		20	0.1401	4.379	9.42		2.3	2.0
	23.7	0	0.1461	4.481	8.70	0.162		
		20	0.1477	4.508	8.52		1.7	1.7
	29.9	0	0.14835	4.519	8.44	0.157		
		20	0.1502	4.550	8.23		2.1	1.6
	48.9	0	0.1563	4.653	7.54	0.160		
		20	0.1578	4.678	7.38		1.8	1.3
B2	5.2	0	0.14735	4.502	9.68	0.173		
	23.4	0	0.1559	4.647	8.70	0.166		
	29.1	0	0.15865	4.693	8.41	0.165		
	48.8	0	0.1673	4.839	7.53	0.161		
B3	5.8	0	0.1564	4.653	9.72	0.150		
	10.7	0	0.1591	4.698	9.44	0.157		
	25.5	0	0.16655	4.824	8.69	0.156		
	28.9	0	0.16845	4.856	8.50	0.159		

Table 10. Rate of decarboxylation in alkaline solution at 25.0°C from glass-electrode measurements.

Solutions	Ester mole/liter	NaOH mole/liter	NaCl mole/liter	$k_2 \times 10^5$ sec^{-1} (A)	$k_2 \times 10^5$ sec^{-1} (B)
A 1—3, B 1—3	0.0400	0.0995	1.100	0.173	0.160
A 4—6, B 4—6	0.0400	0.0995	0.700	0.177	0.166
A 7—9, B 7—9	0.0400	0.0995	0.300	0.188	0.174

While α_1 and α_2 have the same meaning as earlier in this paper, α' is the fraction of levulinic acid present as ion, and α'' is the fraction of carbon dioxide present as univalent ion (may be neglected for the solutions A 1—9). The values of α_0, α_1, and α_2 were computed from $[H^+]$ by means of the dissociation constants calculated from eqns. 21 and 22. In the computation of α' were used the following values of the dissociation constant of levulinic acid: 3.95×10^{-5}, 4.42×10^{-5}, and 4.57×10^{-5}, at the ionic strengths 0.1, 0.2, and 0.3, respectively (estimated from the measurements of Accascina [3] as explained earlier). The values of the dissociation constant of carbonic acid used in calculating α'', 7.8×10^{-7}, 9.0×10^{-7}, and 9.8×10^{-7}, at the ionic strengths 0.1, 0.2, and 0.3, respectively, were taken from a paper by Näsänen [15].

Values of x calculated by means of eqn. 23 are given in the sixth column of Table 9. In the next column are given the rate constants k_2 for the decarboxylation in alkaline solution computed by means of the formula for a first-order reaction from the values of x corresponding to $t = 0$ and x_0 given in Tables 7 and 8. The average value of k_2 for the series A 1—3 is 0.173×10^{-5} sec^{-1}, while for the series B 1—3 it is a little lower, 0.160×10^{-5} sec^{-1}. The results of similar calculations for the other solutions examined are summarised in Table 10. It is seen that the B-series always give a lower value than the A-series. A comparison with the values of k in Table 3 will show that there is a reasonable agreement between the values obtained by the titration method and those found by means of glass-electrode measurements.

The rate constants k for the decarboxylation in the buffer solutions given in the next to the last column of Table 9 were computed by means of the first-order formula from the two values of x shown in the table for each solution. Since the fractions α_0, α_1, and α_2 change a little in the interval examined, the reaction will not follow the first-order law strictly, but the values of k obtained should hold approximately for a solution in which α_0, α_1, and α_2 are constant and equal to the average of their values at the beginning and end of the interval. If k is calculated from the average values by means of formula 19 ($[Ac^-] = 0$), the values shown in the last column of Table 9 are obtained. They are in reasonable agreement with those found from the electrometric measurements.

REFERENCES

1. *Org. Syntheses*, Coll. Vol. **2** (1943) 262.
2. Pedersen, K. J. *J. Am. Chem. Soc.* **53** (1931) 18.
3. Accascina, F. *Ricerca sci.* **24** (1954) 314.
4. Pedersen, K. J. *Acta Chem. Scand.* **6** (1952) 243.
5. Harned, H. S. and Hickey, F. C. *J. Am. Chem. Soc.* **59** (1937) 1284.
6. Kilpatrick, M. and Eanes, R. D. *J. Am. Chem. Soc.* **75** (1953) 586.
7. Pedersen, K. J. *Kgl. Danske Videnskab. Selskab, Mat.-fys. Medd.* **22** (1945) No. 12.
8. Pedersen, K. J. *Acta Chem. Scand.* **6** (1952) 285.
9. Pedersen, K. J. *Acta Chem. Scand.* **8** (1954) 710.
10. Steinberger, R. and Westheimer, F. H. *J. Am. Chem. Soc.* **71** (1949) 4158; **73** (1951) 429.
11. Prue, J. E. *J. Chem. Soc.* **1952** 2331.
12. Pedersen, K. J. *Acta Chem. Scand.* **9** (1955) 1640.
13. Pedersen, K. J. *Acta Chem. Scand.* **3** (1949) 676.
14. Pedersen, K. J. *Acta Chem. Scand.* **9** (1955) 1634.
15. Näsänen, R. *Acta Chem. Scand.* **1** (1947) 204.

Received October 25, 1957.

ACTA CHEMICA SCANDINAVICA 12 (1958) 934—938

A Study of the Pyrazoles formed by Reaction between *p*-Carboxyphenylhydrazine and some β-Diketones

STIG VEIBEL, BENT JUHL NIELSEN and SUSANNE REFN

Department of Organic Chemistry, University of Technology, Copenhagen, Denmark

It has been stated previously that pyrazole derivatives, crystallising with 1 mole of water, and not *p*-carboxyphenylhydrazones, are formed when reacting β-diketones with *p*-carboxyphenylhydrazine. This statement has been corroborated by investigating the UV- and the IR-absorption of the derivatives as well as their titration curves when titrated as acids and as bases.

Some 10 years ago it was proposed to use *p*-carboxyphenylhydrazine as a reagent for the identification of carbonyl compounds, the *p*-carboxyphenylhydrazones formed by the condensation reaction being titratable as acids and thus of value in determining the equivalent weight of the carbonyl compound investigated [1].

It is well known that β-diketones, when reacting with hydrazine derivatives, do not form mono- or bis-hydrazones but, by ring closure of the initial monohydrazones, pyrazole derivatives. This means that when calculating the molecular weight of the carbonyl compound from that of the *p*-carboxyphenylhydrazine-derivative one has to use the formula $E = E_{p\text{-Carb.}}—116.1$ instead of the formula $E = E_{p\text{-Carb.}}—134.1$ ordinarily used, as two molecules of water have been eliminated during the condensation reaction.

If was found, on the other hand, that when isolated and purified as usually (recrystallised from ethanol or aqueous ethanol) acetylacetone, benzoylacetone and dibenzoylmethane gave derivatives which titrated as the ordinary *p*-carboxyphenylhydrazones, not as the corresponding pyrazoles. When, however, these derivaties were dried *in vacuo* over phosphorus pentoxide at 56° or at atmospheric pressure at 130°, they titrated as pyrazoles. Recrystallised from ethanol they once more titrated as *p*-carboxyphenylhydrazones. It was, without further proof, stated that the pyrazoles crystallise with 1 mole of water of crystallisation which is removed by drying and taken up again by recrystallisation [1], thus ignoring the possibility that ring closure might take place when drying the substances, ring opening during their recrystallisation.

In order to settle this question finally we decided to compare the UV- and the IR-absorption of the dried and the recrystallised preparations with the UV- and the IR-absorption of a genuine *p*-carboxyphenylhydrazone of a monoketone with a CH_2-group instead of one of the carbonyl groups in the β-diketones.

Besides, we determined the titration curves of these substances when titrated as acids with sodium hydroxide and as bases with perchloric acid in glacial acetic acid, this last mentioned method making an estimation of the pK_B-values possible [2].

The result of this investigation is a corroboration of the previous statement. The absorption curves of the dried and of the dried and recrystallised preparations are within the limit of the experiment identical and different from the absorption curves of *p*-carboxyphenylhydrazones. The titration curves, too, indicate the identity of the dried and the dried and recrystallised preparations and their difference from a *p*-carboxyphenylhydrazone structure.

EXPERIMENTAL PART

All substances were prepared as described [1] and showed the m.p.'s indicated there.

Drying of the derivatives of acetylacetone (I), benzoylacetone (II) and dibenzoylmethane (III). Samples were dried at 56° *in vacuo* over phosphorus pentoxide. Loss of weight was: I, 8.37 %, II, 6.56 %, III, 6.54 %, calculated for 1 mole of water, I, 7.69 %, II, 6.08 %, III, 5.03 %.

Titration of the derivatives as acids. 1 mmole of the substances, once before drying, then after drying and finally after recrystallisation of the dried sample, was dissolved in 50 ml of ethanol and titrated with 0.1 N sodium hydroxide. At the same time the *p*-carboxyphenylhydrazones of methyl propyl ketone (IV) and of propiophenone (V) were titrated. Table 1 gives the equivalent weights found.

Table 1. Titration of the derivatives with NaOH.

	I			II		
	Undried	Dried	Recryst.	Undried	Dried	Recryst.
E found	235.9	214.7	234.3	295.6	278.6	297.4
E calc.	234.3	216.3	234.3	296.3	278.3	296.3
	III				IV	V
E found	362.6	342.9	362.4		218.1	265.5
E calc.	358.4	340.4	358.4		220.3	268.3

Ultraviolet absorption of I—V. Fig. 1 shows that the absorption curves of I, II and III are of the same type, especially in the region 2 700 Å—3 000 Å, and in this region quite different from the absorption of IV and V. No significant difference between the dried and the recrystallised preparations can be observed.

Infrared absorption of I—V. The absorption in the region from 3 700 cm^{-1} to 670 cm^{-1} was determined, using a Beckman IR 2 spectrophotometer and applying the potassium bromide disk technique.

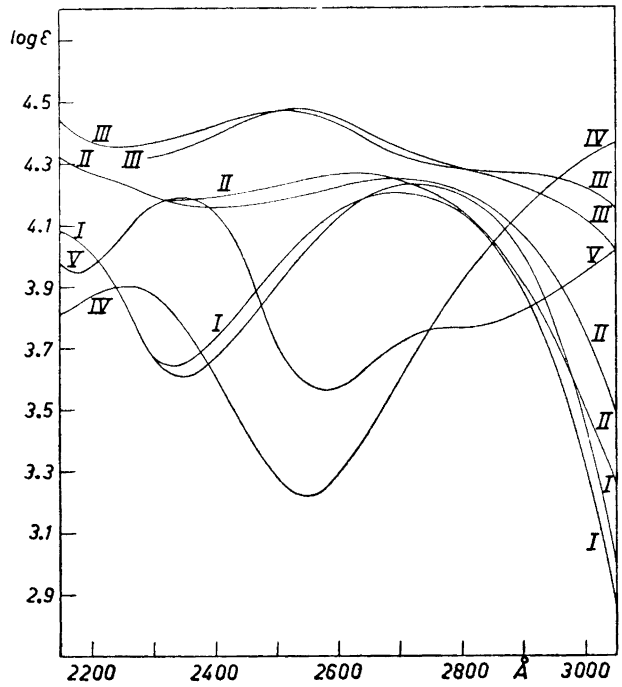

Fig. 1. UV-absorption curves of the substances investigated.
I. Acetylacetone-derivative. II. Benzoylacetone-derivative. III. Dibenzoylmethane-derivative. IV. Methyl propyl ketone-*p*-carboxyphenylhydrazone. V. Propiophenone-*p*-carboxyphenylhydrazone.

Neither the genuine *p*-carboxyphenylhydrazones (IV—V) nor the genuine pyrazoles (I—III dried *in vacuo*) possess absorption bands sufficiently characteristic to decide from such bands alone whether or not ring closure has taken place.

The spectra of the undried and of the dried and recrystallised specimens are identical for each of the substances I, II and III respectively. Of the dried specimens, II shows a spectrum identical with that of the other specimens of II, whereas in I insignificant changes in the relative intensities of adjacent bands at 870 cm^{-1}, 1 130 cm^{-1} and 1 260 cm^{1}, and in III similar insignificant changes at 765 cm^{-1}, 810 cm^{-1} and 1 430 cm^{-1} could be observed.

The spectra of the 3 specimens of I, II and III were, however, for each substance so closely identical that the identity of structure of the 3 specimens is unambiguous, the slight differences observed being possibly caused by the presence of water of crystallisation in the two specimens, whereas the third is anhydrous.

Titration of the derivatives as bases. 1 mmole of I, II, IV and V was dissolved in 50 ml of glacial acetic acid and titrated with 0.0985 N perchloric acid in glacial acetic acid, using a glass electrode and a calomel electrode as reference electrode. III is so sparingly soluble in glacial acetic acid that its titration under comparable conditions could not be carried through.

Table 2 shows that here, too, the dried and the recrystallised preparations are identical, the jump of potential being somewhat greater for the anhydrous preparations than for those with water of crystallisation, in accordance with the fact that water always will decrease the jump of potential in these titrations.

Table 2. Titration of *p*-carboxyphenylhydrazine-derivatives with perchloric acid.

ml $HClO_4$	MV					
	I		II		IV *	V
	Dried	Recryst.	Dried	Recryst.		
0	385	370	360	343	355	365
1	454	450	502	485	424	543
2	468	465	520	514	446	565
3	477	474	530	527	458	582
4	485	481	539	536	468	591
5	492	490	545	545	479	600
6	500	497	554	554	490	609
7	508	506	562	562	505	619
8	519	517	574	574	530	627
9	531	535	590	584	628	640
10	559	580	620	601	663	655
11	673	652	658	640	675	667
12	687	668	675	660	680	678

* Only 0.85 millimole

Table 3 gives the half-neutralisation potentials and the pK_B-values (taken from fig. 2, giving the slope of the line indicating the dependency between half-neutralisation potentials and pK_B for the particular glass electrode and potentiometer used [2]). It is seen

Table 3. Half-neutralisation potentials and pK_B-values.

	II		I		IV	V
	Dried	Recryst.	Dried	Recryst.		
Half-neutralisation potential	493	491	546	546	470	601
$pK_{B(H_2O)}$	12.4	12.3	13.1	13.1	12.1	13.7

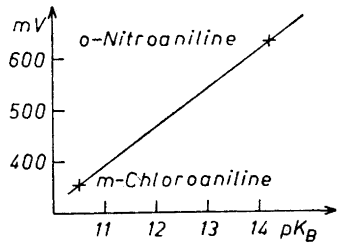

Fig. 2. Dependency of half-neutralisation potentials and $pK_{B(H_2O)}$.

that there is no great difference in basic properties of the pyrazoles and the *p*-carboxyphenylhydrazones, the influence of the substituents being, however, somewhat greater in the latter than in the former group of derivatives.

The financial support of *Statens almindelige Videnskabsfond* and of *Otto Mønsteds Fond* is gratefully acknowledged.

REFERENCES

1. Veibel, S. *Acta Chem. Scand.* **1** (1947) 54.
2. Veibel, S., Eggersen, K. and Linholt, S. C. *Acta Chem. Scand.* **6** (1952) 1066.

Received February 24, 1958.

ACTA CHEMICA SCANDINAVICA 12 (1958) 939—944

The Magnetic Properties of the Thermochromic Compounds Cu_2HgI_4, Ag_2HgI_4 and Tl_2HgI_4

Studies in Magnetochemistry 23 *

R. W. ASMUSSEN and PALLE ANDERSEN

The Chemical Laboratory B, Technical University of Denmark, Copenhagen, Denmark

The magnetic susceptibilities of Cu_2HgI_4, Ag_2HgI_4 and Tl_2HgI_4 have been measured at varying temperatures: 90—403 °K, 88—335 °K and 84—403 °K, respectively. The compounds are diamagnetic at all temperatures in the intervals stated. The χ_g, T curves are nearly parallel to the T-axis. After correction for the diamagnetism of the electron systems of the ions it is shown that the corrected χ_M values represent a weak paramagnetism nearly independent of the temperature. No discontinuity is observed in any of the susceptibility curves at the colour transition temperatures. A colourimetric method for the determination of the colour transition temperatures has been worked out. The transition temperatures for Cu_2HgI_4, Ag_2HgI_4 and Tl_2HgI_4 are determined to be 69.5, 50.5 and 116.5 °C, respectively, for our preparations.

Silver(I)iodomercurate and copper(I)iodomercurate were prepared by Caventou and Willm [1], Mensel [2], Wegelius and Kilpi [3] and Popow [4]. Gallais [5] prepared the compounds mentioned and also the thallium(I)iodomercurate. The compounds are thermochromic having a low and a high temperature form of different colour. The two phases are usually designed β and α, respectively. Ketelaar [6,7] studied the crystal structures of the β and α forms of the silver and copper compound. The β forms are reported to be of pseudocubic tetragonal symmetry and the α phases cubic. Recently Hahn, Frank and Klingler [8] determined the structure of β-Cu_2HgI_4 and β-Ag_2HgI_4 with results differing from those of Ketelaar (compare also Suchow and Keck [9], Olsen and Harris [10] and Frevel and North [11]). Hoshino's [12] structure determination on α-Ag_2HgI_4 also differs from that of Ketelaar.

Furthermore, Ketelaar [13-15] measured the electric conductivity and the specific heat capacity of the different forms of the silver compound at varying

* No. 22 appeared in *Acta Chem. Scand.* 12 (1958) 578.

temperatures. Ag_2HgI_4 has ionic conductivity [13,15], which inreases rapidly just below the colour transition temperature. In the case of the copper compound an electronic conductivity is superimposed upon the ionic conductivity. Ketelaar has interpreted his experimental results in terms of an order-disorder mechanism. Suchow and Keck [9] investigated the system Cu_2HgI_4-Ag_2HgI_4 and report also Munsell colour specifications and reflectance measurements. Suchow and Pond [16] studied the temperature dependence of the electrical conductivity of the copper and the silver compound and their eutectoid.

Magnetic properties. Gallais [5] measured the magnetic susceptibilities of Cu_2HgI_4, Ag_2HgI_4 and Tl_2HgI_4 at room temperature. We considered it of value to study the magnetic properties of these compounds in a larger temperature interval covering the transition temperatures and the temperatures at which the electrical conductivities increase rapidly. The results of our measurements are given in the lower part of Fig. 1, where the diamagnetic gram susceptibilities measured are plotted against the absolute temperature. It is seen that the straight lines are nearly parallel to the temperature axis. If we correct the molar susceptibilities for the diamagnetism of the electron systems of Cu^+, Ag^+, Tl^+, Hg^{+2} and I^- (see experimental part) we obtain the small but paramagnetic susceptibilities, which are plotted against the absolute temperature in the upper part of Fig. 1. The vertical arrows indicate the position of the colour transition temperatures. The straight lines like those for χ_g are of course nearly parallel to the temperature axis.

The correction for diamagnetism has been performed under the assumption that the diamagnetic susceptibility of an ion is the same in the crystal as in the free state. The obvious and direct result of the calculation is that the total calculated molar diamagnetic susceptibility is numerically greater than the observed numerical value. The reason for the difference between the observed and the calculated diamagnetism may be that the ions are deformed in the crystal. The true diamagnetic susceptibility of the ions in the crystal may be numerically smaller than that in the free state because the mean square radii of the electrons in the ions are decreased. However, we must point out that the weak paramagnetism plotted in Fig. 1 may be a physical reality as a temperature independent paramagnetism, the general existence of which has been predicted by Van Vleck [17]. The presence of this paramagnetism has been verified experimentally in many deeply coloured substances (compare for instance Ballhausen and Asmussen [18]).

The magnetic measurements prove that no discontinuity in the magnetic properties occurs at the colour transition temperatures. This is so far in accordance with Ketelaar's order-disorder mechanism, since this does not involve a change in the electron configuration of the ions but a motion of metal ions to other positions during the continuous transformation process.

Colour transition temperatures. The colour transition temperatures were determined by means of reflectance measurements as described in the experimental part. In Fig. 2 the reflectances F are plotted against the temperature in °C. The black points represent measurements carried out during cooling of the preparation. Hysteresis phenomena were only observed when not quite pure preparations were used. The observations on Tl_2HgI_4 are of particular interest indicating that thermochromi is also a property of this substance.

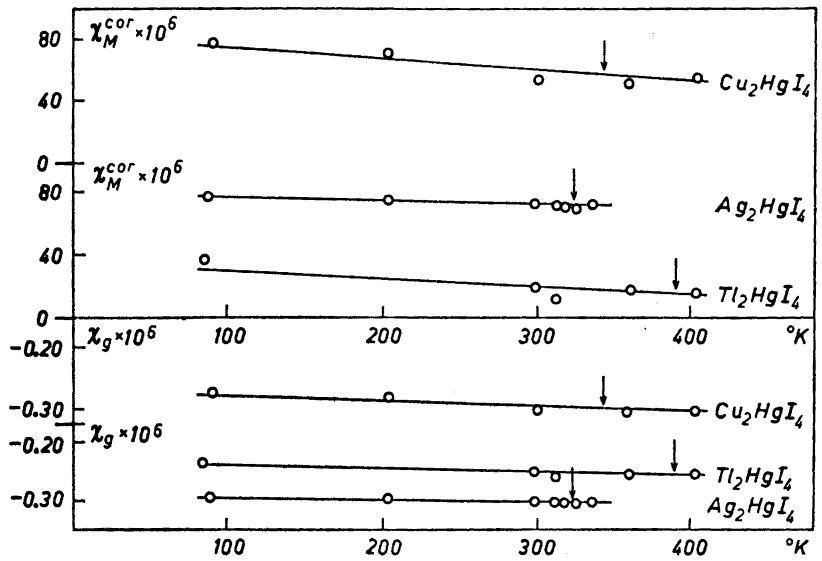

Fig. 1. Gram susceptibility and corrected molar susceptibility of Cu_2HgI_4, Ag_2HgI_4 and Tl_2HgI_4 plotted against the abs. temperature. The vertical arrows indicate the colour transition temperature.

The curves give the values 69.5, 50.5 and 116.5°C for the transition temperatures of Cu_2HgI_4, Ag_2HgI_4 and Tl_2HgI_4, respectively. In Table 1 is given a comparison between these observations and those of other authors.

Table 1. Colour transition temperatures.

Substance	Colour		Colour transition temperature, °C		
	β	α	Ketelaar [7]	Suchow and Pond [16]	Present paper
Cu_2HgI_4	ruby	darkbrown	70	66.6	69.5
Ag_2HgI_4	yellow	redorange	50.7	50.0	50.5
Tl_2HgI_4	orange	red			116.5

In Fig. 3 we report reflectance measurements on HgI_2. The red tetragonal crystal is transformed into a yellow rhombic form at 127 °C. The reflectance measurements show that the colour change occurs abruptly near 127 °C in contrast to the picture given in Fig. 2 of the colour change during the disordering process.

EXPERIMENTAL

Preparation and analysis of the compounds

Cu_2HgI_4 can be precipitated from a solution of K_2HgI_4 containing the equivalent amount of $CuSO_4$ (referred to the formula Cu_2HgI_4), by bubbling SO_2 through the solution.

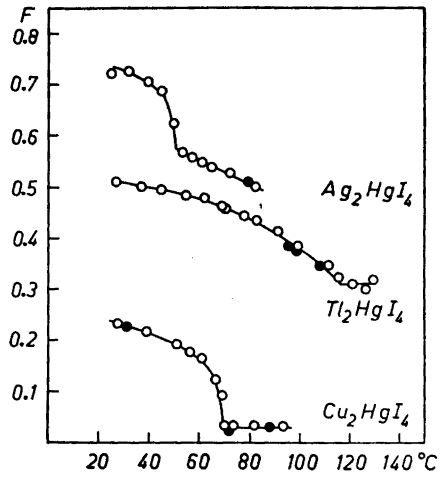

Fig. 2. Reflectance F of the compounds Cu_2HgI_4, Ag_2HgI_4 and Tl_2HgI_4 plotted against the Celsius temperature. The "black" points represent F-values measured at decreasing temperatures.

However, our experiences have shown that better developed and purer crystals can be obtained by a diffusion method. The preparations used for the magnetic and optical measurements were obtained as follows:

Two crystallizing dishes *A* and *B* of 7 cm diameter and 4.5 cm height were placed in a 21 × 11 × 11 cm glass vessel. The distance between *A* and *B* was 12 cm. *A* contained a 0.1 M aqueous solution of K_2HgI_4. *B* contained a saturated solution of CuCl in 20 % hydrochloric acid and a few pieces of copper turnings. *A* and *B* were completely filled with solutions. The junction liquid was 20 % hydrochloric acid saturated with SO_2. The glass vessel had an airtight glass lid. The first crystals were formed after 24 h. After 24 days the junction liquid was siphoned off and the crop of ruby crystals formed (mainly in *A*) was isolated, washed with water, and dried on filterpaper. A few larger crystal needles were also obtained. The yield was 50 %.

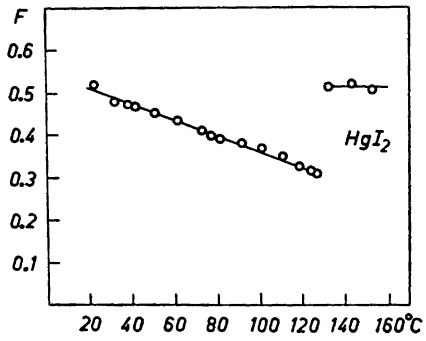

Fig. 3. Reflectance F of HgI_2 plotted against the Celsius temperature.

The amount of crystal needles could be increased by replacing *A* and *B* by two smaller dishes having a lesser diameter at the top part than at the bottom. The two dishes were covered with a piece of circular filterpaper. After 30 days a small crop of crystals was formed on the filterpaper upon *A*. The length of the needles was nearly 4 mm.

The quantitative analysis was carried out as follows: The sample was treated with conc. nitric acid in order to remove iodine and to convert Cu^{+1} to Cu^{+2}. The solution was evaporated (nearly to dryness). Nitrogen oxides were removed by boiling with dil. hydrochloric acid. Hg was determined by weighing as HgS, and Cu iodometrically. Iodine was determined by the iodate-method, the metals being eliminated by means of zinc.

Found: Cu 14.91 %; calc. 15.22 %
Found: Hg 23.95 %; calc. 24.01 %
Found: I 60.71 %; calc. 60.77 %

The copper determination gives values for per cent Cu, which are 2 % (relatively) lower than the theoretical value, when the analysis is carried out as described.

Ag_2HgI_4. Experiments were carried out in order to prepare this compound according to the diffusion method described above. The dish *B* contained a silver sulphate solution and the junction liquid was dil. sulphuric acid. We have, however, not succeeded in obtaining crystals of a purity sufficient for our purpose. The samples used for the physical measurements were prepared by precipitation as described by Henderson and Fernelius [19].

The quantitative analysis was confined to a determination of iodine by the iodate method after conversion of the metal ions to the metallic state (zinc-reductor).

Found: I 54.63 %; calc. 54.94 %

Tl_2HgI_4. The diffusion method gives crystal mixtures containing yellow, red, and black crystals. No well defined preparation could be obtained. The samples used for the measurements were prepared according to Gallais [5]. X-Ray powder-photos prove that the substance is a well defined compound. The crystals are of orange colour. The compound is decomposed above 130°C.

Magnetic measurements

The magnetic susceptibilities were measured by means of the Gouy method similar to that of Asmussen and Soling [20]. The observed diamagnetic gram susceptibilities are plotted against the temperature in °K in the lower part of Fig. 1. In the upper part of Fig. 1 the corrected molar susceptibilities are plotted against T°K. It should be noticed that the ordinates for each curve are measured from a zero-point, the position of which is fixed for each curve. The corrections applied for the diamagnetism of the electron systems of the ions Hg^{+2}, Cu^{+}, Ag^{+}, Tl^{+}, and I^{-} are, respectively: 47.6×10^{-6}, -19.3×10^{-6}, -42.1×10^{-6}, -17.0×10^{-6}, and -55.3×10^{-6}.

Gallais [5] has measured the magnetic susceptibilities of Cu_2HgI_4, Ag_2HgI_4, and Tl_2HgI_4 at room temperature only and gives the following diamagnetic gram susceptibilities: -0.26×10^{-6}, -0.19×10^{-6}, and -0.24×10^{-6}, respectively. Gallais' value for Ag_2HgI_4 is 37 % lesser than our room temperature susceptibility.

Determination of the colour transition temperatures

The colour transition temperature is usually measured by immersing small glass tubes containing the substance in a water-bath. The temperature of the water-bath is slowly increased and the colour change is observed visually.

We considered it of value to carry out objective measurements of the colour change for the $\beta \rightarrow \alpha$ transitions by means of the photoelectric tricolourimeter constructed by Buchmann-Olsen [21]. We have determined one coefficient only applying the filter OY 12, the transmission curves of which are given in the paper of Buchmann-Olsen [21] (page 82). This filter allows a recording of the reflections in a wavelength interval corresponding to that of visible light. In order to measure the reflectance at different temperatures a heating block of nickel plated brass (60 mm diameter and 85 mm height) was used. In the lower end of the block was a chamber, in which an incandescent lamp was mounted.

Regulation of the electric current through the filament allows to fix the temperature of the block. In the upper end of the block was a small chamber for the specimen powder (35 mm diameter and 0.5 mm deep). The block was thermally isolated from the surroundings by a brass tube covered with asbestos. A copper-constantan thermocouple was mounted in the specimen chamber through a drill sloping upwards so that the bead of the thermocouple was situated in the center of the bottom of the chamber. The temperature measured may be considered as a mean temperature of the surface of the specimen powder; the bead of the thermocouple being just covered with powder.

The photo-cell used in the tricolourimeter was a selenium photo-cell from Ewans Electro-selenium Ltd. The photo-current was measured with a Cambridge light spot galvanometer. The reflectance was measured as the ratio F of the readings on the galvanometer when light is reflected from the specimen powder and from a white standard. Each of the F values plotted in Figs. 2 and 3 are mean values of 3 measurements of F. The time necessary for these measurements was about 8 min. In this time interval the observed temperature did not vary more than 0.25 degrees. The F values were found to be reproducible within 1 %.

REFERENCES

1. Caventou, E. and Willm, E. *Bull. soc. chim. France II* **13** (1870) 194.
2. Mensel, E. *Ber.* **3** (1870) 123.
3. Wegelius, H. and Kilpi, S. *Z. anorg. allgem. Chem.* **61** (1909) 413.
4. Popow, P. G. *Ukraine Chem. J.* **11** (1936) 11; *Chem. Zentr.* **1936** II 448.
5. Gallais, F. *Ann. Chim. 11*, **10** (1938) 117.
6. Ketelaar, J. A. A. *Z. Krist. A* **80** (1931) 190.
7. Ketelaar, J. A. A. *Z. Krist. A* **87** (1934) 436.
8. Hahn, H., Frank, G. and Klingler, W. *Z. anorg. allgem. Chem.* **279** (1955) 271.
9. Suchow, L. and Keck, P. H. *J. Am. Chem. Soc.* **75** (1953) 518.
10. Olsen, C. E. and Harris, P. M. *Phys. Rev.* **286** (1952) 651.
11. Frevel, L. K. and North, P. P. *J. Appl. Phys.* **21** (1950) 1038.
12. Hoshino, S. *J. Phys. Soc. Japan* **10** (1955) 197.
13. Ketelaar, J. A. A. *Z. physik. Chem. B* **26** (1934) 327.
14. Ketelaar, J. A. A. *Z. physik. Chem. B* **30** (1935) 53.
15. Ketelaar, J. A. A. *Trans. Faraday Soc.* **34** (1938) 874.
16. Suchow, L. and Pond, G. R. *J. Am. Chem. Soc.* **75** (1953) 5242.
17. Van Vleck, J. H. *The Theory of Electric and Magnetic Susceptibilities.* Oxford University Press, Oxford, 1932.
18. Ballhausen, C. J. and Asmussen, R. W. *Acta Chem. Scand.* **11** (1957) 479.
19. Henderson, W. E. and Fernelius, W. C. *Inorganic Preparations* (1935) 149.
20. Asmussen, R. W. and Soling, H. *Acta Chem. Scand.* **8** (1954) 558, 563.
21. Buchmann-Olsen, B. *Trans. Danish Acad. Tech. Sci.* **1950** No. 4.

Received March 3, 1958.

ACTA CHEMICA SCANDINAVICA 12 (1958) 945—950

The Electrical Contact Potential and the Individual Activity of Single Ions

NIELS BJERRUM

Chemical Laboratory, The Royal Veterinary and Agricultural College, Copenhagen, Denmark

The difficulties met with in determinations of the site and the value of the electrical contact potential between different phases are described. They have as yet made it impossible to determine these contact potentials.

The relationship between these contact potentials and the activities and the partition coefficients of single ions is mentioned. As it has been impossible to determine contact potentials, it has also been impossible to determine the activities and the partition coefficients for single ions. This impossibility creates difficulties for an exact definition of Sørensen's pH-values and of Brönsted's concept of acidity, and these difficulties are discussed.

It is shown that by transfers of particles with electric charges from one phase to another not only the total work of transfer, but also the *electrical* part of it must depend on the nature of the particle considered. The electrical contact potential between two different phases therefore is not a single valued function of the nature of the two phases, but it also depends on the nature of the electric particle (ion or electron) to be transferred.

This fact explains the elusive character of the concept of a definite electrical contact potential between two different phases.

Since the discovery of the electrical contact potentials between different substances it has been difficult to ascribe definite values to these potentials. Volta constructed the first galvanic cell, consisting of plates of two different metals, separated by a moist plate. He assumed in the beginning that the electricity was created at the surfaces, where the metals were in contact with the moist plate, but experiments with a condenser made him think that the production of electricity took place mainly at the surface between the two metals [1].

The condenser experiment of Volta as modified by William Thomson (Lord Kelvin) [2] uses a condenser with plates of the two metals whose contact potential is to be measured. One of the plates is connected to a sensitive electrometer, and in the connection between the two plates is introduced a variable electromotive force. The value of that electromotive force which makes

possible the separation of the two condenser plates (after removal of the connection between them) without change in the electrometer is considered as the measure of the contact potential.

Millikan [3] later used a thermionic valve for determining the contact potential. In the valve two pieces of different metals could alternately be used as the anode, and Millikan assumed that the contact potential between them is equal to the displacement of the current-voltage curve along the voltage axis, observed when the one anode was replaced by the other.

These two methods have been found to give similar values for the contact potential. The accuracy obtained is not great, but the potential values found are similar in size to the electromotive force of the corresponding galvanic cell. This seems to support the conclusion of Volta that the site of the electromotive force is at the surface between the two metals, but this is erroneous. The quantity determined by the two methods is not the desired contact potential. It is determined by the force field in the air (or vacuum) between the two plates, and thus it is not the potential between two points within the two connected pieces of metal, but the potential between two points just outside the surfaces of the metals. Consequently the potential is in reality equal to the sum of three contact potentials: one between the two metals and two others between the metals and the surrounding air (or vacuum).

The first idea of Volta, that the site of the electromotive force in his galvanic cell was at the surface, where the metals are in contact with the moist plate, later got many adherents. De la Rive, Lodge, W. Ostwald, and most of the physical chemists of Ostwald's and van't Hoff's school, were of this opinion. The source of the electrical energy, given off by the element, must be the chemical processes at these surfaces, and it was also soon found that the electromotive force of a galvanic cell depended on the nature of the solution between the two metal, and that impurities on the surfaces of the two metals and the nature of the gas between the metal plates in the condenser experiments strongly influenced the value obtained for the contact potential.

Much work was done on the determination of the contact potentials at these surfaces, especially by the study of capillary phenomena at the surface of a mercury electrode. This method is based on the hypothesis that the surface tension should have its maximum value, when the contact potential is zero, because then there would not be an electrical double layer at the surface. But after much work had been done, it was found that this hypothesis did not lead to reliable results.

Attempts to determine the contact potential using the Peltier effect (the heat effect at the surface of contact of two metals, when an electric current is passed across it) also failed.

A theoretical calculation of the contact potential between two aqueous solutions of electrolytes was given by Nernst in 1888. The work of Nernst seemed to make it possible, for the first time, to calculate the value of a contact potential between two different phases. Nernst once told me about the enthusiasm of the old v. Helmholtz, when he told him about this result. For nearly a hundred years research on the contact potentials had been going on and now, at last Helmholtz saw the possibility of gaining an understanding of these mysterious and important phenomena.

Later developments, however, have shown that Nernst's solution of the problem is exact only in the limit, when the two aqueous solutions are very dilute, *i. e.* when in reality we have to do with a potential difference between points in the same phase.

In the nineteen-twenties a new interest in the contact potential, especially that between electrolytic solutions, arose. From several sides it was pointed out that the determination of activity or partition coefficients of *individual* ions was connected with the determination of contact potentials between electrolytic solutions (Bjerrum [4], Taylor [5], Guggenheim [6], Brönsted [7], Schottky [8]). An especially clear and exact description of the problem is found in Guggenheim's papers.

If we cannot determine the electrical potential difference between two electrolytic solutions in connection with each other, we cannot determine the activities of the individual ion species, and conversely, if we do not know the ratio of the activities in the two solutions of at least one individual ion species, we cannot determine the contact potential between them. It is possible, however, to determine the product of the activities of a group of ionic species with a total electric charge of zero (*e.g.* of $K^+ + Cl^-$ or of $K^+ - Na^+$) as the transfer of such a group of ions from one phase to another will result in no net transfer of electricity at all.

As both Guggenheim and Brönsted have pointed out, however, all equilibria and isothermal changes towards equilibria of the individual ions are describable in terms of a new thermodynamic function which they call the electrochemical potential of an ion. This function can be considered as the sum of the chemical potential of the ion, and the electrical potential at the position of the ion. But when an ionic species is present in two different media, this resolution of its electrochemical potential into a chemical term and an electrical term is quite arbitrary and without physical significance, unless the contact potential between the two media is known.

The reason for the failure of the classical definition of the electrical potential difference, when we have to do with points in different media, is that, as we now know, the electricity has an atomistic structure. We cannot determine nor speak of the work necessary for transferring an infinitely small amount of electricity from one medium to another, since we can only transfer the electricity in the form of electrons or ions.

As early as 1899 Gibbs [9] wrote in a letter: "Again, the consideration of the electrical potential in the electrolyte, and especially the consideration of the difference of potential in electrolyte and electrode, involves the consideration of quantities of which we have no apparent means of physical measurement, while the difference of potential in pieces of metal of the same kind attached to the electrodes is exactly one of the things which we can and do measure".

And in 1929 Guggenheim wrote: "It has previously been realized that only these" (*i.e.* the electrochemical potentials of individual ions) "and not the u_i" (*i.e.* the chemical potentials of the individual ions) "have any *thermodynamic* importance, but we maintain that only they have any *physical* significance, for only they are definable in terms of physical realities".

This result has consequences for many concepts used by chemists, *e.g.* Sørensen's pH-value and Brönsted's definition of acidity.

The pH-value of Sørensen was defined by him as the negative logarithm of the molar concentration of the hydrogen ion, but on account of later views on electrolytes it was necessary to change from the concentration of the hydrogen ions to the activity of these ions, defined in such a way that in aqueous solutions at the limit of infinite dilution the activity was equal to the molar concentration.

According to our present view on the impossibility of determining the activity of individual ions the pH-values defined in this way cannot be determined by electrometric measurements. The pA_H-values determined by Bjerrum and Unmack in a paper in 1929 [4] by use of a 3.5 molar KCl solution to diminish the contact potential between two electrolytic solutions and calculating the remaining potential by means of Henderson's formula are, as indicated by the authors, not exactly equal to the negative logarithms of the hydrogen ion activities. Their pA_H-values must also depend to a certain degree on the activities of the other ions present, since the transfer of hydrogen ions from one solution to another must be accompanied by the transfer of other ions (in this case, especially K^+ and Cl^-) whose charge can compensate the charge transferred on the hydrogen ions. In spite of this, by using their pA_H values in calculations of thermodynamically definable quantities, one always arrives at the right values, and the pA_H values will generally lead to individual ions activity coefficients which, at increasing dilution, converge to a well defined limit.

Brönsted wished to extend his conception of the acidity of acids to non-aqueous solutions. In order to obtain in non-aqueous solutions a numerical measure of this acidity, as defined by the activity of the hydrogen ions, it was necessary to have a definition of the electrical potential difference between solutions in which the solvents were different. As a conventional definition he made the proposal that the electrical potential in an isolated, homogeneous phase be considered as zero when the phase is electrically neutral, *i.e.* when it contains equal amounts of positive and negative electricity. Guggenheim [6] admits that Brönsted's definition leads to an electrical potential between different phases which is a potential in the mathematical sense. But he finds that it does not lead to a potential in the strict dynamic sense, *i.e.* it does not meaure the work done in any real process.

Brönsted writes [7] (p. 310—311): "Unsere Betrachtungen haben uns somit dazu geführt, dass auch für Ionen thermodynamische Funktionen definiert werden können, die durch die chemische Beschaffenheit der Lösungen, die die Ionen enthalten, und unabhängig von elektrischen Ladungspotentialen gegeben sind. Es sind derartige Funktionen, die zur Darstellung der chemischen Eigenschaften von Ionenlösungen geeignet sind, und von welchen wir z. B. für unsere Aciditätsdefinition hier Gebrauch machen wollen".

Brönsted further writes that his ion functions defined above cannot be determined by the common electrometric methods, but finally concludes: "Dass die Ionenfunktionen für ungleiche Medien durch die direkten thermodynamischen Methoden nicht messbar sind, besagt, dass sie auch thermodynamisch nur von untergeordneter Bedeutung sein können. Man darf daraus

jedoch nicht schliessen, dass sie überhaupt bedeutungslos sind. Speziell für den Begriff der Acidität, wie er oben definiert worden ist, müssen wir z. B. annehmen, dass er eine grosse kinetische Bedeutung besitzt, wenn es auch mit Schwierigkeiten verbunden wäre, den Aciditätseinfluss von der allgemeinen Wirkung des Mediums zu trennen". This idea of Brönsted that the acidity, determined according to his instructions, has a great kinetic significance does not seem to have been shown by him to be probable much less to have been proved, and it does not agree with the statement of Guggenheim according to which the chemical potentials of individual ions do not have any physical significance.

Brönsted has not given a laboratory method by the use of which we can determine the acidity by means of his definitions. So far I can see, Brönsted's proposal leads to an electrical potential difference between two phases which is determined by the electric field outside the two phases and thus to an electrical potential difference between them, equal to the work done by transferring an unit of electricity from a point just outside the surface of one phase to a point just outside the surface of the other phase. This is the electrical potential difference between two points outside the two phases, and not between two points inside the two phases.

Brönsted's definition can perhaps be used in the following way for the experimental determination of the difference in acidity of two phases. In each of the two phases is placed a hydrogen electrode and in the connection between the two hydrogen electrodes is introduced a variable electromotive force. The two phases are also used as plates in a condenser and these parts of the phases are each in direct connection with the part of the same phase, containing a hydrogen electrode. Finally one of the phases is connected with a sensitive electrometer. The value of the variable electromotive force, by which the condenser plates can be separated without change in the electrometer, will then be a measure of the sought for acidity difference. A practical difficulty arises when the two phases are both liquids. If the two plates in the condenser are placed horizontally the bottom plate can of course be a liquid, but the top plate can not. In that case it will therefore be necessary to use two condensers with the two liquid phases as bottom plates and as top plates two plates of same metal. The sought for acidity difference will then be measured by the value of the variable electromotive force by which it is possible to separate the plates in both condensers without change in the sensitive electrometer connected with the condensers.

Such a determination will certainly be very difficult to perform and will scarcely lead to an experimentally well defined value of the acidity difference, and as the result will be only the determination of a conventionally defined acidity difference of no great interest, I think that it will not pay to try it.

The concept of an electrical contact potential between two different phases is as elusive in character as the concept of absolute velocity in space. Not only is this potential difficult to determine experimentally, and apparently without physical interest, but also, from an atomistic point of view, it is not a single-valued potential which can be used in calculations of the electric work of transfer of all the different species of electrically charged particles from one phase to another. This can be seen in the following way. If we knew

exactly the positions of all the electrons and nuclei in two insulated and homogeneous pieces of two different phases in contact with each other, we could calculate in principle by means of Coulomb's law, the electric force in all points in and around the two pieces (except in the interior of the electrons and the nuclei), and we could therefore also calculate the classical electrical potential at all these points. But in order to obtain a phenomenological value for the electrical potential difference between the two different phases we would further have to determine the mean value in time and space of the electrical potential in the interior of the two phases. The space, however, over which we have to take the mean value is not given in a definite way. *E.g.*, how near should we go to the electrons and to the nuclei? It depends on the particle considered. And what weight should we assign to the potentials at the different points inside the two phases in the determination of the mean value? It is not sufficient to assume that an amount of electricity transferred to a phase is infinitely divisible and spread over the available space according to Boltzmann's distribution law. If we wish to use the mean value in calculations of the work of transfer of an electron or of a particular ion the mean value must be determined corresponding to the properties of this particular electrically charged particle. We thus arrive at the conclusion that a general and single-valued mean for the electrical contact potential which can be used in calculations of the electrical work of transfer of all species of particles with electric charge, does not exist.

There is also the other difficulty that according to the rules of quantum mechanics (Heisenberg's uncertainty relations) we cannot know exactly the positions and the velocities of the particles at a definite time. This uncertainty, however, does not seem to preclude the existence of a well defined and single-valued electric contact potential.

If we wish to use the concept of a definite electrical contact potential, we have to introduce a conventional definition for it, and when using such a conventionally defined potential we must always remember that it is not a physical reality, but only a mathematical device. It can be used in intermediate calculations, but must not appear in final expressions.

REFERENCES

1. *Cf.* Ostwald, W. *Elektrochemie*, Veit and Co., Leipzig 1896, p. 57.
2. *Cf.* Mönch, G. *Z. Physik* **65** (1930) 233.
3. Millikan, R. A. *Phys. Rev.* **7** (1916) 18, 362; **18** (1921) 236. *Cf.* also Mönch, G. *Z. Physik* **65** (1930) 233 and Heinze, W. *Z. Physik* **109** (1938) 459.
4. Bjerrum, N. *Nordic Chemist Meeting* 1926. English translation in *Niels Bjerrum, Selected Papers*, Munksgaard, Copenhagen 1949, p. 120; Bjerrum, N. and Larsson, E. *Z. physik. Chem.* **127** (1927) 358, p. 381; Bjerrum, N. and Unmack, A. *Kgl. Danske Videnskab. Selskab, Mat.fys. Medd.* **9** No. 1 (1929) 7.
5. Taylor, P. B. *J. Phys. Chem.* **31** (1927) 1478.
6. Guggenheim, E. A. *J. Phys. Chem.* **33** (1929) 842; **34** (1930) 1540.
7. Brönsted, J. N. *Z. physik. Chem.* **A 143** (1929) 301.
8. Schottky, W. *Thermodynamik*, Springer, Berlin 1929, p. 117–156.
9. *The Collected Works of J. W. Gibbs*, Longmans, Green and Co., New York, London, Toronto 1928, *I*, p. 429.

Received January 29, 1958.

ACTA CHEMICA SCANDINAVICA 12 (1958) 951—958

The Kinetics of Crystal Growth in Barium Sulfate Precipitation

ARNE E. NIELSEN

Universitetets fysisk-kemiske institut, Copenhagen, Denmark

The kinetics of barium sulfate precipitation is followed turbidimetrically and conductometrically. It is found that when the concentration of Ba^{++} and SO_4^{--} are larger than about 0.4 mM the kinetics may be expressed by

$$k_D t = \int_0^\alpha \alpha^{-1/3} (1 - \alpha)^{-1} \, d\alpha$$

where t is the time and α the degree of reaction (precipitation). When the said concentrations are smaller than 0.4 mM, approximately, the kinetics observed agrees with

$$k_R t = \int_0^\alpha \alpha^{-2/3} (1 - \alpha)^{-4} \, d\alpha$$

These findings agree with the assumption that below 0.4 mM the rate determining step in the crystal growth process is a fourth order reaction at the crystal-solution interface and, above 0.4 mM, the diffusional transport of matter from the bulk of the liquid to the surface of the growing crystals.

In a previous work on the kinetics of electrolyte precipitation [1] it was concluded that the rate of growth of barium sulfate crystals is controlled by some sort of chemical reaction with the rate determining step

$$2\ Ba^{++}\ (soln.) + 2\ SO_4^{--}\ (soln.) \rightarrow 2\ BaSO_4(crystal)$$

or, perhaps

$$2\ BaSO_4\ (soln.) \rightarrow 2\ BaSO_4(crystal)$$

taking place in the surface of the growing particles. This was found to be in agreement with experiments where the concentration of barium sulfate was less than 0.2 mM. In this work the experimental range is extended to much higher concentrations and it is observed that the above mentioned mechanism ceases to be rate determining at higher concentrations. According to the fourth order low the rate of crystal growth increases with the fourth power of concentration. Above 0.4 mM the rate becomes too high for the matter to diffuse

sufficiently fast to the surface of the crystals and therefore diffusion becomes the bottle-neck of the growth process. Nernst [2] and Brunner [3] found the dissolution process for several salts to be diffusion controlled, but the kinetics of the reverse process turned out [4] to be more difficult to explain.

It has been shown [1] that when the growth of a constant number of small particles of the same size is diffusion controlled, the degree of reaction α depends on time according to

$$k_D t = \int_0^\alpha \alpha^{-1/3}(1 - \alpha)^{-1} d\alpha = I_D$$

and when the rate is controlled by a fourth order reaction in the surface

$$k_R t = \int_0^\alpha \alpha^{-2/3}(1 - \alpha)^{-4} d\alpha = I_4$$

From this follows that if I_D is plotted against time a straight-line plot is obtained if the rate is determined by diffusion. In the following we shall prefer to plot log I_D against log t. This should give parallel straight lines 45° to the axis.

EXPERIMENTAL

The reacting systems were supersaturated solutions of $BaSO_4$ prepared by mixing equal volumes of solutions of the same molarity ($2c_0$) of $BaCl_2$ and Na_2SO_4. In three experiments NaCl was added in order to get the required ionic strength.

The advancement of the reaction was measured in two different ways: in the fastest experiments ($c_0 \geqq 1$ mM) the electric conductivity was measured with Radiometer's direct reading AC(70 – 3 000 c/s) conductivity meter. The degree of reaction α was found from the conductivity by means of a chart based on measurements of the conductivities of mixtures of solutions of $BaCl_2$, Na_2SO_4 and NaCl. The slower experiments were followed photometrically by means of an apparatus especially designed by Dr. J. Koefoed (of this institute) for measuring small optical densities. The voltages from the measuring selenium photocell and a similar reference cell both illuminated from the same lamp were compensated one against the other, giving the light intensity ratio I_0/I as the ratio of the resistors of the compensating bridge. From I_0/I α was found by taking $(\log(I_0/I))^{3/2}$ proportional to α. In order to find the proportionality factor the electric conductivity was measured at the end of each experiment. The advantage of not following the whole experiment conductometrically consists in that it is not necessary, then, to remove the layer of barium sulfate formed on the walls of the conductivity cell.

It is well known [5] that under these conditions the barium sulfate precipitation is a rather irreproducible process. The reason for this is probably that the number of particles formed per unit of volume comes out very differently even if one tries to make several identical experiments consecutively [6]. But during a precipitation experiment the number is constant and from microscopy it seems that the shape of the particles does not change much during growth. Therefore it is reasonable to put the volume proportional to the three halves power of the surface of the precipitate and this, again, proportional to the logarithm of the light intensity ratio I_0/I. Table 1 shows how the calculations were made.

In experiments with added salt (for ionic strenght) it would be a rather inexact method to find α from electric conductivity. Instead of this α was found by putting it equal to $1/7 = 0.143$ (as is required by the formula for I_4) at the point of inflexion on the curve of $(\log(I_0/I))^{3/2}$ against t. Since the point of inflexion in case of I_D is at $\alpha = 1/4 = 0.25$ this method can only be applied when it is known that the experiments follow I_4. This assumption is confirmed through the rectilinear arrangement of the points (squares and triangles) on Fig. 3.

The temperature was always between 22 and 23°C. All conductivities were corrected to 22.0°C by means of the empirically determined temperature coefficient $d\varkappa/dt = 0.022\,\varkappa$.

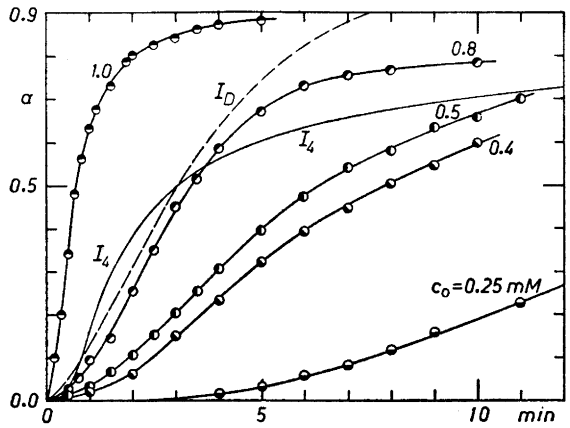

Fig. 1. The fraction α of the $BaSO_4$ present having deposited on the crystals at time t. I_D and I_4 are theoretical curves (in arbitrary time units) corresponding to diffusional and fourth-order-surface-reaction rate control, respectively. The experimental curves resemble I_D at small t (high concentration) and I_4 at large t (low concentration) as required by theory.

RESULTS

In Fig. 1 are some of the experimental values of α plotted against the time. For comparison I_D and I_4 — from numerical integration — are also shown, in arbitrary time units. It is seen that the experimental curves, except those of the lowest c_0, have the shape of I_D at small times (high concentrations) and become more like I_4 in the later parts of the experiments.

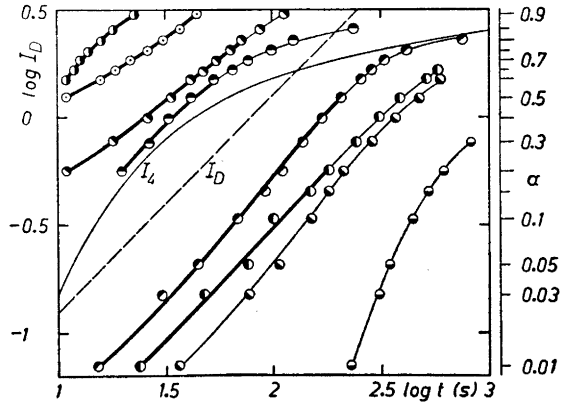

Fig. 2. A transformation of Fig. 1. which yields straight lines in case of diffusional rate control. The heavy (parts of the) lines correspond to $(BaSO_4) > 0.4$ mM.

Table 1. 50 ml 1.6 mM $BaCl_2$ + 50 ml 1.6 mM Na_2SO_4; c_0 = 0.8 mM.

t min	I_0/I	a	l μ	Δl μ	$\Delta l/\Delta t$ μ/min	mμ/s	c mM
0.5	1.013	0.025	1.67				
1.0	1.032	0.094	2.60	1.33	1.33	21.2	0.725
1.5	1.045	0.144	3.00				
2.0	1.063	0.253	3.60	1.02	1.02	17.0	0.598
2.5	1.079	0.350	4.02				
3.0	1.094	0.450	4.38	0.56	0.56	9.3	0.440
3.5	1.103	0.514	4.58				
4.0	1.112	0.582	4.76	0.62	0.31	5.2	0.334
5.0	1.124	0.670	5.00	0.38	0.19	3.15	0.264
6.0	1.132	0.730	5.14	0.20	0.10	1.67	0.216
7.0	1.135	0.755	5.20	0.09	0.045	0.75	0.196
8.0	1.137	0.768	5.23				
10.0	(1.139)	(0.785)	5.26				

Comments on Table 1. Immediately after the measurements at t = 10 min the solution was stirred and a drop transferred to a blood cell counting chamber of volume 0.9 mm³, and 202 particles were counted; N = 202/0.9 = 224 mm^{-3}. From this number and c_0 = 800 μM l_∞ was found by means of

$$l\infty = \sqrt[3]{800 \times 52/224} = 5.71 \ \mu$$

The value of I_0/I at t = 10 min (1.139) is extrapolated, since at this moment the electric conductivity was measured: $\varkappa = 224 \times 10^{-6}$ ohm^{-1} cm^{-1} (uncorrected) at 22.3°C. This corresponds to $\varkappa = 222.5 \times 10^{-6}$ ohm^{-1} cm^{-1} at 22.0°C. Applying a chart based on empirical values of $\varkappa$, a was found to be 0.785 at t = 10 min. The other values of a were calculated by means of

$$a = 0.785 \ [\log(I_0/I)/\log \ 1.139]^{3/2}$$

and l was obtained from

$$l = l_\infty a^{1/3}$$

In this and similar experiments $\Delta l/\Delta t$ was found directly from the measured values using intervals symmetric about the experimental t-values. This gives a reasonable degree of smoothing and reduces the calculating work. (In the fastest experiments all a-values were found conductometrically and had to be smoothed graphically before the differentiation).

Finally c was found as $(1-a)c_0$.

In Fig. 2 log I_D is shown as a function of log t. The part of the curves where ($BaSO_4$) < 0.4 mM is drawn in a heavier line than the rest of the curves. The high-concentration-parts of the curves are more straight than the low-concentration-parts.

Fig. 3 displays the dependence of the linear growth rate dl/dt on time; l is the length of the edge in a cube of the same volume as the single crystals. The growth rate was obtained from the measurements in the following way. The value of l at "infinite time" l_∞ was calculated from the molar volume of barium sulfate, 52 cm³/mole, the concentration c_0 of barium sulfate at t = 0 in the unit μM and the number N of particles per mm³, by means of

$$l_\infty = (52c_0/N)^{1/3} \qquad \text{(microns)}$$

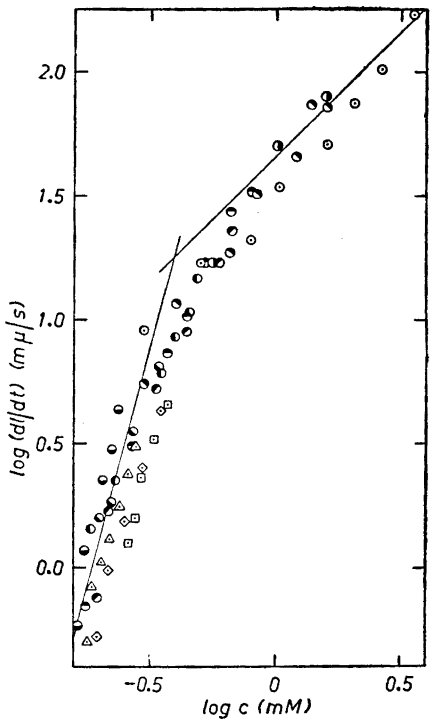

Fig. 3. The linear rate of crystal growth as function of ($BaSO_4$) in a logarithmic diagram. Below 0.4 mM (log $c = -0.4$) the rate increases proportional to the fourth power of concentration, above 0.4 mM the rate is directly proportional to the concentration of the supersaturated barium sulfate solution. The asymptotes are drawn without regard to the triangular and square "points".

l was found by multiplying l_∞ with $\alpha^{1/3}$. Then $\mathrm{d}l/\mathrm{d}t$ could be obtained through numerical differentiation. In a few cases (of very high c_0) the α-values had to be smoothed by means of a graph like Fig. 1.

The straight lines drawn in Fig. 3 are the apparent asymptotes to the curve determined by the points. Their inclinations are 4 and 1 respectively, and from the figure their equations are seen to be, respectively

$$\log(\mathrm{d}l/\mathrm{d}t) = 4 \log c + 2.80 \qquad (c < 0.3 \text{ mM})$$
$$\log(\mathrm{d}l/\mathrm{d}t) = \log c + 1.65 \qquad (c > 0.6 \text{ mM})$$

which is equivalent to

$$\mathrm{d}l/\mathrm{d}t = 630\ c^4 \qquad (c < 0.3 \text{ mM})$$
$$\mathrm{d}l/\mathrm{d}t = 45\ c \qquad (c > 0.6 \text{ mM})$$

when $\mathrm{d}l/\mathrm{d}t$ is measured in mμ/s and c in mM.
Similar points, even in different figures, refer to the same run of a kinetic experiment.

Salt effect

A reaction between two Ba^{++}- and two SO_4^{--}-ions must be subject to a large negative kinetic salt effect, decreasing the growth rate at higher ionic strengths, although it would probably be misleading to try to calculate it

from the Debye-Hückel limiting law or similar generalized expressions for the activity coefficients. Since this salt effect will reduce the rate most at high concentrations just as diffusion, it is important to know its magnitude. At the highest concentrations investigated ($c_0 = 5$ mM, circular "points" with a dot in the centre) the ionic strength was 0.030 M. In the experiments shown by square and triangular "points" with a dot in the centre the ionic strength was therefore adjusted to 0.030 M by means of NaCl. In this way all points with a dot in the centre correspond to experiments with approximately the same ionic strength. As expected there is a negative salt effect, since the "dotted" points mostly lie about 0.3 decadic units below the other points, showing that the addition of salt has halved the rate of crystal growth. This effect is, however, by far too small to explain the deviation from the fourth-power-law.

The rate of diffusion

On the other hand we may calculate from the diffusion coefficient of barium sulfate the greatest possible rate of transport of matter from the bulk of the solution to the surface of the growing particles. The geometry of the diffusional area looks rather different in case of a large and a small particle. For large particles Nernst [2] pointed out that the phenomenon may be described by means of a diffusion layer of thickness 10—100 μ, depending, among other things, on the stirring rate. But for particles of radius r comparable with or smaller than the thickness of such a diffusion layer Smoluchowski [7] showed by means of Fick's diffusion laws, that after a very short time (a fraction of a second) the concentration around such a "spherical sink" follows

$$(\mathrm{d}c/\mathrm{d}x)_{x=r} = (c - c_r)/r$$

where x is the distance from the center of the sink. In the present case we may neglect c_r in $c - c_r$. In the experiments on barium sulfate reported here c_r is about $c/100$. We then have, by Fick's first law, for the amount of matter deposited in unit time

$$\mathrm{d}n/\mathrm{d}t = 4\pi r^2 D(\mathrm{d}c/\mathrm{d}x) = 4\pi r c D$$

If this is multiplied by the molar volume of $BaSO_4$ one gets the rate by which the volume increases

$$v \times 4\pi r c D = v\mathrm{d}n/\mathrm{d}t = \mathrm{d}(\tfrac{4}{3}\pi r^3)/\mathrm{d}t = 4\pi r^2 \mathrm{d}r/\mathrm{d}t$$

or

$$\mathrm{d}r/\mathrm{d}t = vDc/r$$

Now we may use this in an estimate even though the actual particles are not spherical. In the following it will be convenient to express the volume of the crystals by means of the length l of the edge in a cube of the same volume, and we may substitute

$$l^3 = \tfrac{4}{3}\pi r^3 = 4.19r^3;\ l = 1.61r;\ l^2 = 2.60r^2$$

so that $dl/dt = 2.60vDc/l$. The diffusion coefficient of $BaSO_4$ may be calculated from the electric mobilities according to Nernst [8]

$$D = 2D_+D_-/(D_+ + D_-)$$

where

$$D_+ = kTl_+/q_+$$

$$D_- = kTl_-/q_-$$

Here l_+ and l_- are the electric mobilities of the Ba^{++} and SO_4^{--} ions, respectively, and $q_+ = q_- = q$ the electric charges of the ions, that is twice the proton charge. When we insert [9] $l_+ = 6.59 \times 10^{-4}$, $l_- = 8.27 \times 10^{-4}$ cm²/s·V and $2kT/q = 0.02569$V we find the diffusion coefficient of barium sulfate

$$D = (2kT/q)l_+l_-/(l_+ + l_-) = 9.42 \times 10^{-6} \text{ cm}^2/\text{s (at 25°C)}$$

Since the molar volume is $M/d = 233.4/4.499 = 51.9$ cm³/mole (at 15°C) we have

$$dl/dt = 2.60vDc/l = 1.27 \times 10^{-3}c/l$$

where dl/dt is measured in cm/s, c in mole/cm³ and l in cm; if we change to mμ/s, mM and μ, respectively, we get

$$dl/dt = 127c/l$$

From Fig. 3 we have from the upper asymptote

$$dl/dt = 45c$$

Now these two formulae cannot be compared directly since l is a parameter in only one of them. But we may substitute for l the mean value of all the experimental points, (half-black—half-white) closest to the upper line in Fig. 3. We have from the experiments the following values of l: 2.67, 3.39, 3.93, 4.34, 3.00, 4.96, 1.62 and 1.93 μ. The arithmetic mean value is 3.23 μ. This gives

$$dl/dt = 127c/3.23 = 39c$$

The experimental value of the coefficient (45) and the value calculated from the diffusion theory (39) agree within the accuracy of the measurements.

In Fig. 3 the two asymptotes intercept at $\log c = -0.4$, that is $c = 0.4$ mM. We may therefore say that the rate determining mechanism of crystal growth of barium sulfate changes from a fourth order surface reaction into diffusion around $c = 0.4$ mM. Further evidence of this is obtained by microscopy. The precipitate formed when $c_0 < 0.5$ mM consist of small prisms, which in the microscope look like rectangles with the longer side approximately twice as long as the shorter one. With initial concentrations between 0.5 and 1.5 mM the particles are more or less distorted prisms, the corners having grown more than the middle of the faces. And at $c_0 > 1.5$ mM the corners have grown far more than the other parts of the crystals, giving them the appearance of "stars"; see Figs. 2 and 3 in the previous work [6]. This appearance is to be expected in case of diffusional control of the growth rate, since the concentration then is greatest at the corners. The rectangular (orthorhombic)

shape is obtained when the concentration is approximately the same all over the surface, and it cannot be so when the consumption of matter is fast compared with the diffusion.

REFERENCES

1. Nielsen, A. E. *J. Colloid Sci.* **10** (1955) 576.
2. Nernst, W. *Z. physik. Chem.* **47** (1904) 52.
3. Brunner, E. *Z. physik. Chem.* **47** (1904) 56.
4. Marc, R. *Z. physik. Chem.* **79** (1912) 71.
5. Wells, P. V. *Chem. Rev.* **3** (1927) 331.
6. Nielsen, A. E. *Acta Chem. Scand.* **11** (1957) 1512.
7. Smoluchowski, M. v. *Z. physik. Chem.* **92** (1918) 129.
8. Nernst, W. *Z. physik. Chem.* **2** (1888) 613.
9. Moore, W. J. *Physical Chemistry*, Longmans, London 1956, p. 446.

Received February 18, 1958.

ACTA CHEMICA SCANDINAVICA 12 (1958) 959—966

Remarks on the Reactivities of the Penta- and Hexathionate Ions

OLAV FOSS

Chemical Institute, University of Bergen, Bergen, Norway

The reactions of higher polythionates with nucleophilic reagents are discussed on the basis of existing possibilities of heterolytic cleavage of the sulphur-sulphur bonds. In addition to the principal reaction type involving a release of thiosulphate from the penta- and hexathionate ions, other modes of cleavage may lead to the release of sulphite, and of thiosulphate and sulphur.

The presence of unbranched and non-planar sulphur chains in the tetra- and pentathionate ions has recently been demonstrated through crystal structure determinations of barium tetrathionate dihydrate [1], orthorhombic and triclinic barium pentathionate dihydrate [2,3], and a solvate of barium pentathionate with acetone [4]. The structure analyses, which were made by two-dimensional Fourier methods by use of the heavy atom technique, were based on X-ray data alone, without recourse to assumptions of chemical nature.

The tetra- and pentathionate chains contain two and three divalent sulphur atoms, respectively, and terminal sulphur atoms to each of which are attached three oxygen atoms. The sulphonate groups, together with the adjacent divalent sulphur atoms, constitute thiosulphate groups, which have the shape of distorted tetrahedrons. The tetrathionate ion is thus built of two thiosulphate groups, linked together through their divalent sulphur atoms, and the pentathionate ion consists of a divalent sulphur atom to which are attached, through sulphur-sulphur, bonds, two thiosulphate groups. The structures, assigned to the ions on chemical grounds [5,6], are confirmed through the X-ray studies.

No structure determination of a salt of hexathionic acid has so far been reported. However, in view of chemical evidence, which speaks in favour of unbranched chains [5,6], and the fact that branching of sulphur chains has never been demonstrated to occur, it appears reasonably safe to conclude that the sulphur chain of hexathionate is unbranched, like that of pentathionate and tetrathionate.

The following brief review of some features of polythionate chemistry may be pertinent to the succeeding discussion of reaction schemes.

The polythionates are chemically characterized by the ease with which they undergo heterolytic cleavage in reactions with nucleophilic reagents. This behaviour is, presumably, due to a pronounced electrophilic character of the divalent sulphur atoms of the chains. Nucleophilic attacks have been found to take place at either one of the two equivalent, divalent sulphur atoms of the tetrathionate ion, at the middle sulphur atom of the pentathionate ion, and at the middle disulphur group of the hexathionate ion. The principal reactions of the polythionates with nucleophilic reagents may be summarized as follows [5-11].

Pentathionate and hexathionate behave as sulphur thiosulphates, $S(S_2O_3)_2^{--}$ and $S_2(S_2O_3)_2^{--}$. In some reactions with nucleophilic reagents, both thiosulphate groups are displaced by the reagent; in other reactions, only one.

Tetrathionate behaves as a sulphur sulphite-thiosulphate, with displacement of the sulphite and the thiosulphate group by a nucleophilic reagent, or of only one of the groups. A thiosulphate group is displaced more readily than a sulphite group.

Trithionate acts as a sulphur disulphite, $S(SO_3)_2^{--}$, with displacement of both sulphite groups, or of only one. Trithionate may also act as a thiosulphato-sulphonate, the nucleophilic attack in this case occurring at one of the sulphonate sulphur atoms.

The reactions, as far as their kinetics have been established, are bimolecular, and thus of the S_N2 type. This applies to the following reactions involving nucleophilic displacements on divalent sulphur: Those of tetra- and pentathionate with sulphite [12], hydrogensulphite [13] and cyanide [14-16] ions, of tetrathionate with azide ion [17,18] and of pentathionate with hydroxyl ion [19], of tri- and tetrathionate with thiosulphate ion [20,21] and of trithionate with sulphite ion [22]. Likewise, nucleophilic displacements on the divalent sulphur of sulphenyl sulphites [23] (thiosulphate esters) and disulphides [24] are of the S_N2 type, as is also the reaction of triphenylphosphine with elemental sulphur [25].

The electrophilic species in S_N2 reactions have no independent existence, and electropositive ions of divalent sulphur, even short-lived ones, do therefore not occur in the reactions.

The recognition of polythionates as derivatives of divalent electropositive sulphur, and their reactions as nucleophilic displacements, removes older arguments, on chemical basis, against the unbranched chain structures [6].

The occurrence of various displacement reactions, predicted on the basis of the reactivity principles outlined above, have been confirmed through experiments with sulphite and thiosulphate labelled with radioactive sulphur. Thus, the reactions of hexa-, penta- and tetrathionate with sulphite ion, to give the next lower polythionate, and thiosulphate, were formulated [5] as nucleophilic displacements of thiosulphate by sulphite:

$$^-O_3S-S-S-S-S-SO_3^- + S^*O_3^{--} = {}^-OS_3-S-S-S-S^*O_3^{--} + S_2O_3^{--} \quad (1)$$

$$^-O_3S-S-S-S-SO_3^- + S^*O_3^{--} = {}^-O_3S-S-S-S^*O_3^- + S_2O_3^{--} \quad (2)$$

$$^-O_3S-S-S-SO_3^- + S^*O_3^{--} = {}^-O_3S-S-S^*O_3^- + S_2O_3^{--} \quad (3)$$

The validity of this view, at any rate as far as tetra- and pentathionate are concerned, has been demonstrated by Christiansen and Drost-Hansen [26,27]. The reverse reactions, of tri- and tetrathionate with thiosulphate to give sulphite and the next higher polythionate, are also nucleophilic displacements [10,20,21].

In a study of exchange reactions of polythionates with thiosulphate, Fava [28] has shown that the displacement equilibria [5,10,29]:

$$^-O_3S_2-S-S-S_2O_3^- + S_2^*O_3^{--} = {}^-O_3S_2-S-S-S_2^*O_3^- + S_2O_3^{--} \quad (4)$$

$$^-O_3S_2-S-S_2O_3^- + S_2^*O_3^{--} = {}^-O_3S_2-S-S_2^*O_3^- + S_2O_3^{--} \quad (5)$$

$$^-O_3S_2-S_2O_3^- + S_2^*O_3^{--} = {}^-O_3S_2-S_2^*O_3^- + S_2O_3^{--} \quad (6)$$

are established very rapidly at ordinary temperatures. The mechanism of the thiosulphate-catalyzed rearrangement of tetrathionate into tri- and pentathionate, formulated [10] as subsequent displacements of sulphite by thiosulphate and of thiosulphate by sulphite, has been confirmed by Fava and Bresadola [21]. Likewise, Fava and Pajaro [22] have found that trithionate exchanges with sulphite ion, although rather slowly.

Thus, recent studies on polythionates have established the unbranched chain structure, and the characteristic sensitivity towards basic reagents as due to nucleophilic attacks on the divalent sulphur chains. The reactivity principles recognize the electrophilic character of the middle sulphur atom of pentathionate and of the two equivalent, middle sulphur atoms of hexathionate. Nucleophilic attacks on these atoms, in directions so as to displace thiosulphate, are responsible for the principal reactions of the ions. There are, however, indications that nucleophilic attacks may occur also at other of the divalent sulphur atoms of the penta- and hexathionate ions, and in different directions.

SCHEMES FOR THE REACTIONS OF HIGHER POLYTHIONATES WITH NUCLEOPHILIC REAGENTS

The various possibilities of nucleophilic attack on the divalent sulphur atoms of the tetra-, penta- and hexathionate ions are depicted through arrows in schemes 1 to 4 below. In each case there are two equivalent possibilities, corresponding to the two halves of the ions. The arrows are drawn so as to indicate a linear transition state, as in displacements on carbon; there is, however, as yet no definite information available concerning the configuration of the transition state.

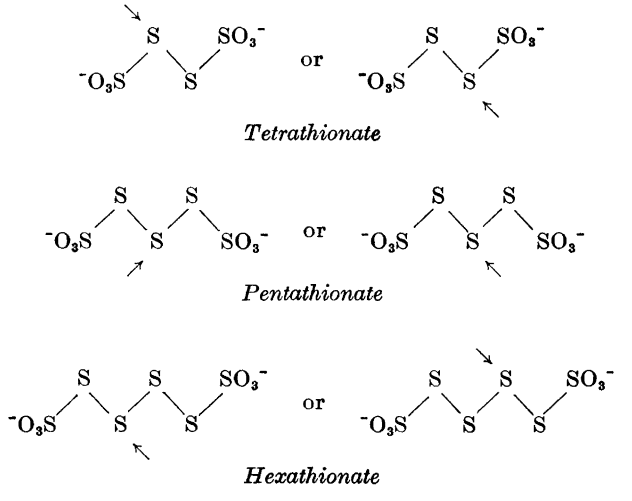

Scheme 1. Principal directions of nucleophilic attack on the tetra-, penta- and hexathionate ions: Displacement of thiosulphate.

Schemes 1 and 2 lead to the displacement of thiosulphate and sulphite, respectively. The tetra-, penta- and hexathionate ions, on the action of the appropriate nucleophilic agent, eliminate thiosulphate more readily than sulphite; displacement of thiosulphate does, indeed, occur in the majority of the reactions of the ions, *e.g.*, in the reactions (1)—(6) above. Other examples include the reactions with piperidine, hydroxide, thiocarbonyl ions, and cyanide and sulphide ions.

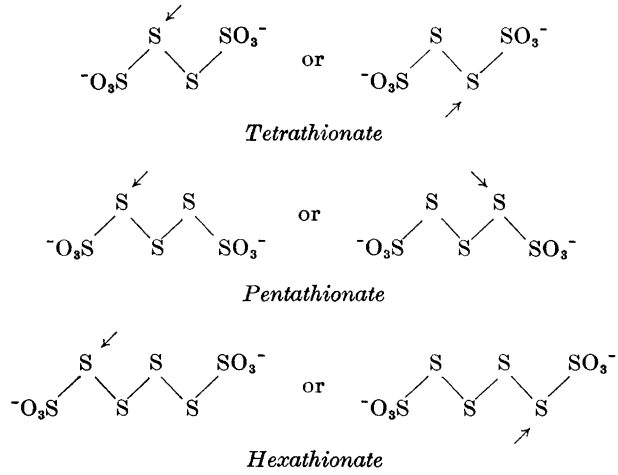

Scheme 2. Alternative (less predominant) directions of nucleophilic attack on the tetra-, penta- and hexathionate ions: Displacement of sulphite.

Displacement of sulphite according to scheme 2 was first found to occur in the case of tetrathionate. In the reactions of tetrathionate with piperidine [5,8] and hydroxide [5,30,31], displacements of thiosulphate *and* sulphite take place, to like extents but probably in two steps of which a primary displacement of thiosulphate is more predominant than a primary displacement of sulphite. With thiosulphate as the nucleophilic reagent [10,21], the process is the reverse of the reaction of pentathionate with sulphite (Eqn. (2)) and takes place markedly slower than the displacement of a thiosulphate group of tetrathionate by the same reagent, as represented by Eqn. (6). Displacement of sulphite by sulphide also occurs [32,33], though to a small extent compared with the simultaneous predominant reaction, which is the displacement of thiosulphate.

For penta- and hexathionate, the probability, or ease, of reacting according to scheme 2 should be about the same as for tetrathionate. The attacks are on the divalent sulphur atoms situated next to the sulphite groups, so as to displace these, and the length of the sulphur chain on the other side of the electrophilic centre (one, two or three divalent sulphur atoms) should have relatively little influence. With thiosulphate as the nucleophilic reagent, the relevant reactions are, again, the reverse of the reactions of the next higher polythionates with sulphite.

The reversal of the reactions of tetra- and pentathionate with sulphite takes place in acid solutions [34,35], since under such conditions sulphite is partly removed from the equilibria, as hydrogensulphite. Corresponding reactions of the still higher polythionates were held possible by Kurtenacker and Czernotzky [36], but Stamm, Seipold and Goehring [34,35] found no evidence for the formation of hexathionate and hydrogensulphite from pentathionate and thiosulphate in acid solutions. Nevertheless, it has been repeatedly maintained [21,29,37] that the reaction of hexathionate with sulphite is reversible, like those of pentathionate and tetrathionate. Preliminary experiments by the author indicate that pentathionate does react with thiosulphate, to give hexathionate and sulphite, if formaldehyde is used as a sulphite acceptor.

Like thiosulphate, other reagents with comparable or greater nucleophilicity towards divalent sulphur, *e.g.*, sulphide, cyanide or thiocarbonyl ions, should be able to displace sulphite from penta- and hexathionate, though in such cases the simultaneous, always predominant displacement of thiosulphate leads to the rapid formation of different species which do not eliminate sulphite. Thiosulphate is unique as a reagent for demonstrations of the less predominant schemes, because its participation in the preferential scheme 1 displacements leaves the polythionate unaltered, except in tracer experiments.

ADDITIONAL SCHEMES

In the case of tetrathionate, schemes 1 and 2 involve attacks at the same electrophilic centre, although in different directions. This is because the two divalent sulphur atoms of tetrathionate are equivalent. In penta- and hexathionate, the two types of attack occur at different centres, corresponding to the presence of two non-equivalent divalent sulphur atoms in these ions. However, attacks on any divalent sulphur atom of the polythionate chains, also of penta- and hexathionate, may in principle occur in two directions, to displace either one of the two groups bonded to the divalent atom.

Accordingly, scheme 3 for penta- and hexathionate involves nucleophilic attacks on the same sulphur atoms as in scheme 2, but in different directions, so as to lead, not to a displacement of sulphite, but of the species $(S{-}S_2O_3)^{--}$ and $(S{-}S{-}S_2O_3)^{--}$, which are unstable and will decompose into thiosulphate and sulphur.

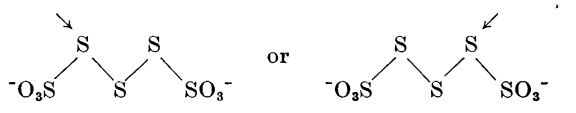

Pentathionate

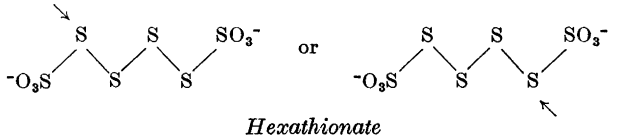

Hexathionate

Scheme 3. Possible directions of nucleophilic attack on the penta- and hexathionate ions, leading to the release of thiosulphate and one or two sulphur atoms, respectively.

Similarly, scheme 4, which applies to hexathionate only, involves attacks on the same sulphur atoms as in the displacement of thiosulphate according to scheme 1, but in the other one of the two possible directions.

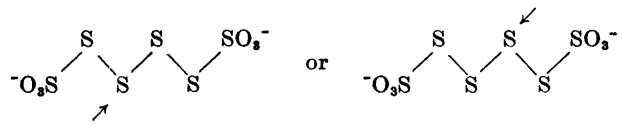

Hexathionate

Scheme 4. Possible directions of nucleophilic attack on the hexathionate ion, leading to the release of thiosulphate and one sulphur atom.

Concerning these last possibilities, the following points may be made. Scheme 3 requires a heterolysis of the same sulphur-sulphur bond as in scheme 1. The latter represents a predominant type of reaction of the penta- and hexathionate ions, and has been interpreted [4,5] as due to a certain amount of ionic character, or polarity of the σ bond, in the direction of heterolysis. In scheme 3 the heterolysis is required to take place in the opposite direction of that in scheme 1 and thus in the opposite direction of the presumed polarity. Likewise, the electrophilic characters of the bond partners, *i.e.*, of the centres of nucleophilic attack in the two schemes, are probably different, so as, once more, to favour scheme 1. In view of the known tendency of sulphur-sulphur bonds to undergo heterolysis, it does not appear warranted, however, to exclude the possibility that penta- and hexathionate may react according to scheme 3, if acted upon by an appropriate nucleophilic agent. The displacements, even if occurring to a slight extent only, with small equilibrium concentrations of the primary products, $(S{-}S_2O_3)^{--}$ and $(S{-}S{-}S_2O_3)^{--}$, will lead to continuous changes because of the instability and subsequent decomposition of these species, into thiosulphate and sulphur. Thus, with thiosulphate as the nucleophilic reagent, the reactions:

$$^-O_3S_2{-}S{-}S_2O_3^- + S_2^*O_3^{--} = {}^-O_3S_2{-}S_2^*O_3^- + (S{-}S_2O_3)^{--} \quad (7)$$

$$^-O_3S_2{-}S{-}S{-}S_2O_3^{--} + S_2^*O_3^{--} = {}^-O_3S_2{-}S_2^*O_3^- + (S{-}S{-}S_2O_3)^{--} \quad (8)$$

with release of sulphur from the displaced groups, will proceed continuously to the right, and cause a break-down of the penta- and hexathionate ions into tetrathionate.

For hexathionate, the possibility of reacting according to scheme 4 should be greater than for penta- and hexathionate according to scheme 3. The nucleophilic attacks are at the same electrophilic centres as in scheme 1, and the sulphur-sulphur bond required to undergo heterolysis is the middle one, and is thus non-polar, *i.e.*, there is no opposing polarity as probable in scheme 3. In presence of thiosulphate, the process:

$$^-O_3S_2{-}S{-}S{-}S_2O_3^- + S_2^*O_3^{--} = O_3S_2{-}S{-}S_2^*O_3 + (S{-}S_2O_3)^{--} \quad (9)$$

should therefore occur more readily than the corresponding reaction (8) of hexathionate and (7) of pentathionate, although slower than the scheme 1 displacement of thiosulphate.

Scheme 4 bears resemblance to scheme 1 for tetrathionate, which also involves heterolysis of the middle sulphur-sulphur bond, and to the heterolytic cleavage of organic disulphides.

It is known that hexathionate, under the catalytic influence of thiosulphate ions, decomposes into pentathionate and sulphur [29,35,38]. Pentathionate, more slowly, decomposes into tetrathionate and sulphur. Whether hexathionate to some extent can decompose directly into tetrathionate, is not clear, since the analytical methods give the average sulphur content only, of hexa-, penta- and tetrathionate mixtures. It appears that the thiosulphate-catalyzed decompositions may be due to primary displacements according to schemes 3 and 4; in particular, the displacements represented by Eqns. (7) and (9). The greater lability of hexathionate as compared with pentathionate would be in accordance with the additional availability of the more probable scheme 4 for hexathionate.

The possibility of scheme 3 displacements as the cause of the catalytic decompositions was pointed out by the author [29] in 1949, but rejected in favour of a mechanism connected with displacements of thiosulphate according to scheme 1. Such displacements "proceed through a transition state, the energy of which is higher than that of the molecules in the initial state. The molecules are labile even in the initial state, and the increase in energy associated with the passing of the transition state serves to decrease the thermodynamic stability and accelerate the decompositions" [29]. The transition state complex, ordinarily unstable along one reaction coordinate only, was in this case thought to be unstable in two directions, *viz.*, in the one leading to displacements, as represented by Eqns. (4) and (5) of the present paper, and in the one leading to the release of sulphur.

Fava [28] in 1953 described the thiosulphate-catalyzed decompositions as due to nucleophilic attacks corresponding to schemes 3 and 4. There appears to be no way in which to decide experimentally between the possibilities. In the related case of iodide and acetate ion catalysis on the decomposition of telluropentathionate, an attack on tellurium, there substituted for the middle sulphur atom of pentathionate, is indicated [29]. However, the different catalysts do not necessarily act by the same mechanism, and in lack of definite information, the fact that thiosulphate does exert a catalytic influence on the decompositions serves as an indication that displacements according to schemes 3 and 4 may be possible.

In concluding, it appears that, as far as the available evidence goes, the more rapid displacement of thiosulphate according to scheme 1 will take place simultaneously with any other displacement, and in most cases dominate the reaction picture. A fuller understanding of the relative importance of the various schemes must await a knowledge of, *e.g.*, the nature of the transition state in nucleophilic displacements on divalent sulphur.

REFERENCES

1. Foss, O., Furberg, S. and Zachariasen, H. *Acta Chem. Scand.* **8** (1954) 459.
2. Foss, O. and Zachariasen, H. *Acta Chem. Scand.* **8** (1954) 473.
3. Foss, O. and Tjomsland, O. *Acta Chem. Scand.* **10** (1956) 288.
4. Foss, O. and Tjomsland, O. *Acta Chem. Scand.* **12** (1958) 44.
5. Foss, O. *Kgl. Norske Videnskab. Selskabs Skrifter* **1945** No. 2.
6. Foss, O. *Acta Chem. Scand.* **4** (1950) 404.
7. Foss, O. *Kgl. Norske Videnskab. Selskabs Forh.* **15** (1942) No. 31.
8. Foss, O. *Kgl. Norske Videnskab. Selskabs Forh.* **16** (1943) No. 20.
9. Foss, O. *Tidsskr. Kjem. Bergv. Met.* **10** (1950) 28.

10. Foss, O. *Acta Chem. Scand.* **4** (1950) 866.
11. Foss, O. *Sjunde nordiska kemistmötet* (1951) Helsingfors, p. 117.
12. Foerster, F. and Centner, K. *Z. anorg. u. allgem. Chem.* **157** (1926) 45.
13. Turner, G. B. *The Thermal Decomposition of Aqueous Solutions of Sulphur Dioxide* (Diss.) University, London 1954.
14. Ishikawa, F. *Z. physik. Chem.* **130** (1927) 73.
15. Ishikawa, F., Murooka, T. and Hagisawa, H. *Sci. Rep. Tohoku Imp. Univ.* [1] **21** (1932) 511 (from *Chem. Zentr.* **1933** I 2036).
16. Foresti, B. *Z. anorg. u. allgem. Chem.* **217** (1934) 33.
17. Hofman-Bang, N. *Acta Chem. Scand.* **5** (1951) 1375.
18. Hofman-Bang, N. *The Iodine-Azide Reaction* (Diss.) University, Copenhagen 1952.
19. Christiansen, J. A., Drost-Hansen, W. and Nielsen, A. E. *Acta Chem. Scand.* **6** (1952) 333.
20. Fava, A. and Pajaro, G. *J. chim. phys.* **51** (1954) 594.
21. Fava, A. and Bresadola, S. *J. Am. Chem. Soc.* **77** (1955) 5792.
22. Fava, A. and Pajaro, G. *Ann. chim. (Rome)* **44** (1954) 545.
23. Fava, A. and Pajaro, G. *J. Am. Chem. Soc.* **78** (1956) 5203.
24. Fava, A., Iliceto, A. and Camera, E. *J. Am. Chem. Soc.* **79** (1957) 833.
25. Bartlett, P. D. and Meguerian, G. *J. Am. Chem. Soc.* **78** (1956) 3710.
26. Christiansen, J. A. and Drost-Hansen, W. *Nature* **164** (1949) 759.
27. Fava, A. and Divo, D. *Gazz. chim. ital.* **82** (1952) 558. Footnote p. 560.
28. Fava, A. *Gazz. chim. ital.* **83** (1953) 87.
29. Foss, O. *Acta Chem. Scand.* **3** (1949) 1385.
30. Fava, A. and Divo, D. *Gazz. chim. ital.* **82** (1952) 564.
31. Fava, A. and Divo, D. *Gazz. chim. ital.* **83** (1953) 98.
32. van der Heijde, H. B. *Rec. trav. chim.* **72** (1953) 510.
33. van der Heijde, H. B. *Contribution to the Chemistry of the Inorganic Acids of Sulphur* (Diss.) University, Amsterdam 1955.
34. Stamm, H., Seipold, O. and Goehring, M. *Z. anorg. u. allgem. Chem.* **247** (1941) 277.
35. Goehring, M. *Fortschr. chem. Forsch.* **2** (1952) 444.
36. Kurtenacker, A. and Czernotzky, A. *Z. anorg. u. allgem. Chem.* **174** (1928) 179.
37. Goehring, M., Helbing, W. and Appel, I. *Z. anorg. u. allgem. Chem.* **254** (1947) 185.
38. Kurtenacker, A., Mutschin, A. and Stastny, F. *Z. anorg. u. allgem. Chem.* **224** (1935) 399.

Received February 5, 1958.

ACTA CHEMICA SCANDINAVICA 12 (1958) 967—970

Conjugate Additions of Grignard Reagents to alpha, beta-Unsaturated Esters

II. The Preparation of 3-Methyl- and 2,3-Dimethylalkanoic Acids

JON MUNCH-PETERSEN

Organisk-kemisk Laboratorium, Polyteknisk Læreanstalt, Copenhagen, Denmark

A previously published method for the preparation of 3-methyl-alkanoic acids from *sec*-butyl crotonate and Grignard reagents has been revised, improved and simplified. It has further been extended to *sec*-butyl tiglate, from which fair yields of 2,3-dimethylalkanoic acids are obtained.

In a recent publication [1] the addition of Grignard reagents to the double bond of *sec*-butyl crotonate as a way of preparing in high yields 3-methyl-substituted fatty acids was described. Certain other α,β-unsaturated esters were investigated, but only with cinnamic ester were reasonable yields obtained, whereas the reaction with tiglic and methacrylic esters failed. Of these, the reaction with tiglic esters would be of particular interest, on one hand since this ester is rather easily accessible, and on the other hand because of the difficulties reported [2] in obtaining 2,3-dimethyl-substituted fatty acids by other routes:

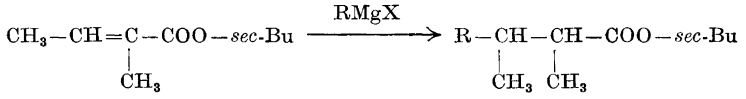

Since the publication of the first paper there have been difficulties in obtaining the high yield stated for the preparation of *sec*-butyl 3-methylheptanoate from *sec*-butyl crotonate and *n*-butylmagnesium bromide. This has prompted a reinvestigation of the reaction and of most of the work reported in the first paper. Although no explanation for the discrepancy has been found so far, a new procedure has been worked out, which gives almost as good a yield, and which is considerably simpler. Furthermore, by this procedure tiglic ester gives good to fair yields of *sec*-butyl esters of 2,3-dimethylalkanoic acids (Table 1).

In the first paper it was reported that the presence of cuprous chloride was essential to the success of the addition reaction, since it had been found that, under the conditions there described, the absence of this catalyst resulted in the formation of a high-boiling condensation-addition product. It has not been possible to verify this remarkable catalytic effect of cuprous chloride in promoting the simple 1,4-addition to the conjugated carbon-carbon double bound in competition with the condensation-addition process. On the contrary, carrying out the addition as described resulted in varying, but rather low yields (30—50 %), and with the formation of larger amounts of the high-boiling condensation compound. In numerous experiments with *sec*-butyl

Table 1.

sec-Butyl ester	Grignard reagent RMgBr	Product: *sec*-butyl ester	Yield %	Yield Ref. [1] %	Data
Crotonate	n-C_4H_9	3-methylheptanoic	67—80	84—86	Ref. [1]
»	CH_3	*iso*valeric	0	45	Ref. [1]
»	C_2H_5	3-methylvaleric	78	56	Ref. [1]
»	i-C_3H_7	3,4-dimethylvaleric	57	39	Ref. [1]
»	t-C_4H_9 [a]	3,4,4-trimethylvaleric	14	14	Ref. [1]
»	n-C_8H_{17}	3-methylhendecanoic	—	75	Ref. [1]
»	n-$C_{14}H_{29}$	3-methylheptadecanoic	—	86	Ref. [1]
»	C_6H_5	3-phenylbutyric	72	67	Ref. [1]
Tiglate	n-C_4H_9	2,3-dimethylheptanoic [b]	71	0	b. p. 109°/13 n_D^{25} 1.4257
»	i-C_3H_7	2,3,4-trimethylvaleric [c]	68 [d]	—	b. p. 90°/12 mm n_D^{20} 1.4262
»	n-C_5H_{11}	2,3-dimethyloctanoic [e]	47 [d]	—	b. p. 87°/1.5 mm n_D^{20} 1.4307
»	n-C_8H_{17}	2,3-dimethylhendecanoic	(55) [d,f]	—	b. p. 109—110°/1 mm
»	C_6H_5	2-methyl-3-phenyl-butyric [g]	53 [d]	—	b. p. 94—95°/1 mm n_D^{20} 1.4838
Methacrylate	n-C_4H_9	—	0	0	
Acrylate	n-C_4H_9	—	0	—	
β,β-Dimethyl-acrylate	n-C_4H_9	—	0	—	
Cinnamate	n-C_4H_9	3-phenylheptanoic	52	46	Ref. [1]

[a]) *tert*-Butylmagnesium chloride used. [b]) Calcd. for $C_{13}H_{26}O_2$ (214.34): C 72.84; H 12.23 Found: C 72.80; H 12.27. [c]) Calcd. for $C_{12}H_{24}O_2$ (200.31): C 71.95; H 12.08. Found: C 71.90 H 12.07. [d]) Reaction carried out in 0.1 mole scale. [e]) Calcd. for $C_{14}H_{28}O_2$ (228.36): C 73.63; H 12.36. Found: C 73.75; H 12.45. f) This product is not pure, probably contaminated with n-hexadecane; over-all yield of 2,3-dimethylhendecanoic acid, obtained by saponification (see experimental part), is 40 %. [g]) Calcd. for $C_{15}H_{22}O_2$ (234.33): C 76.88; H 9.46. Found: C 76.85; H 9.53.

crotonate and *n*-butylmagnesium bromide the conditions have been varied systematically (including the testing of different qualities of cuprous chloride and magnesium, and changes in the addition temperature, the addition time and the dilution of the ester), apparently without effect on the yield.

Eventually the use of a greater excess of Grignard reagent (at least 0.5 mole with 0.2 mole of ester) was found to result in an increase in the yield, and at the same time the use of cuprous chloride appeared to be of little effect. The procedure now worked out and described below gives about a 75 % yield for the reaction of crotonic ester with *n*-butylmagnesium bromide.

Using the new procedure, those other additions, which had previously been found to give low or no yields of simple 1,4-addition product, were repeated. These results, as well as those of some new addition reactions, are given in Table 1, which for comparison also includes the results previously reported using the cuprous chloride procedure.

The yields for crotonic ester with ethyl- and *iso*propylmagnesium bromides have increased, but methylmagnesium bromide — in contrast to the earlier findings with cuprous chloride — now gives an unseparable mixture of compounds. Similar results of reactions of methylmagnesium halides with α,β-unsaturated systems have been reported previously [3,1]. The yields with tiglic ester from *n*-butyl- and *iso*propylmagnesium bromides are quite good, whereas those from *n*-amyl-, *n*-octyl-, and phenylmagnesium bromides are somewhat lower. Methacrylic and acrylic esters give mostly polymerisation products, β,β-dimethylacrylic ester gives a mixture of unreacted ester and some unidentified low-boiling compound as well as some polymerisation product.

The high-boiling compounds obtained as by-products from the reactions with crotonic and tiglic esters were identified previously [1] and were not further investigated during the course of this work. They are considered to be di-*sec*-butyl α-(2-alkyl)-β-methylglutarates and di-*sec*-butyl α-(2-alkyl)-α, β, γ-trimethylglutarates, respectively, (2-alkyl = $R-\underset{\displaystyle CH_3}{\underset{|}{CH}}-CH_3$), produced by addition of the Grignard reagents to the α,β-unsaturated dimerisation products, which are again formed by a Michael-type self-condensation of the original esters.

Further investigations of the reaction are in progress.

EXPERIMENTAL

Analyses are by Mr. Preben Hansen, Microanalytical Division, The Chemical Laboratory, The University of Copenhagen. Fractional distillations were through a simple 45 cm × 8 mm Podbielniak-type column with a tantalum wire spiral, heated jacket and a partial reflux head.

sec-Butyl esters were obtained by esterification of the corresponding acids in 75—85 % yield, according to the general procedure previously described [1] for crotonic, tiglic, methacrylic, and cinnamic esters. The yield for *sec*-butyl tiglate, b. p. 75°/16 mm, n_D^{25} 1.4339, has been raised to 75 % (Ref.[1] b. p. 86—87°/30 mm, n_D^{25} 1.4335, yield 60 %). New esters are: *sec*-butyl acrylate, b. p. 29°/18 mm, n_D^{20} 1.4268, and *sec*-butyl β,β-dimethylacrylate, b. p. 68—70°/13 mm, n_D^{20} 1.4379.

The corresponding acids were commercial products (Fluka AG., Buchs/SG, Switzerland), except for methacrylic [4] and tiglic [5] acids, which were prepared through the corresponding ketone cyanohydrins as described in the literature. It should be pointed out that it has been found essential for the success of the tiglic acid synthesis [5] that the temperature-controlled hydrolysis and elimination process between methyl ethyl ketone cyanohydrin and 100 % sulfuric acid be carried out under extremely vigorous stirring, since otherwise foaming and tar-formation takes place, resulting in low yields.

Additions of Grignard reagents to α,β-unsaturated esters. The solution of Grignard reagent was prepared (without use of iodine or other catalyst) in an 1 liter three-necked flask, provided with effective stirrer, from 12.5 g (0.52 g-atom) of magnesium turnings and 0.65 mole of halide dissolved in 150—200 ml of ether. The reaction is completed by boiling for 10—15 min, after which the Grignard solution is cooled for 15—20 min in an ice-water bath. Under effective stirring in the ice-bath, 0.20 mole of ester, dissolved in 200 ml of ether is now added dropwise from a graduated dropping funnel during a period of at least 1.5 h. When the addition is completed, stirring is continued in the ice-bath for additional 15 min, and for 1 h at room temperature. The reaction mixture is then worked up in the conventional way, as previously described [1].

The higher halides (octyl *etc.*) are dissolved in a somewhat greater quantity of ether in order to prevent crystallisation of the Grignard reagent during the cooling. Working up after reactions with phenylmagnesium bromide should include a washing of the ether extract with sodium hydroxide solution in order to remove phenol, which will otherwise make distillation troublesome and contaminate the product.

Saponification of sec-butyl esters may be carried out with ethanolic potassium hydroxide as previously described [1]. In this way (on a 0.05 mole scale) *2,3-dimethylheptanoic acid*, b. p. 89°/1 mm, n_D^{20} 1.4356, was obtained in 80 % yield; neutr.equiv. calcd. for $C_9H_{18}O_2$ 158.2, found 157. *2,3-Dimethylhendecanoic acid*, b. p. 131°/1 mm, n_D^{20} 1.4461, yield 73 % (*cf.* Table 1); calcd. for $C_{13}H_{26}O_2$ (214.34): C 72.84; H 12.23. Found C 72.85; H 12.20; neutr. equiv. 213.

REFERENCES

1. Munch-Petersen, J. *J. Org. Chem.* **22** (1957) 170.
2. Cason, J., Wolfhagen, H. J., Tarpey, W. and Adams, R. E. *J. Org. Chem.* **14** (1949) 147; Cason, J., Sumrell, G. and Mitchell, R. S. *J. Org. Chem.* **15** (1950) 850; Cason, J. and Fessenden, R. J. *J. Org. Chem.* **22** (1957) 1328.
3. Gilbert, G. and Aycock, B. F. *J. Org. Chem.* **22** (1957) 1013.
4. Larsson, E. *Svensk Kem. Tidskr.* **55** (1943) 169; *Chem. Abstr.* **38** (1944) 5798 [3]; Heyboer, J. and Staverman, A. J. *Rec. trav. chim.* **69** (1950) 790.
5. Buckles, R. E. and Mock, G. V. *J. Org. Chem.* **15** (1950) 680.

Received February 3, 1958.

ACTA CHEMICA SCANDINAVICA 12 (1958) 971—982

A Study of the Vanadium Tellurides

FREDRIK GRØNVOLD, OLAF HAGBERG and HAAKON HARALDSEN

Kjemisk institutt A, Universitetet i Oslo, Blindern, Norway

The existence of two intermediate phases, β and γ, has been established in the system vanadium tellurium. None of these phases have a simple stoichiometric composition, corresponding to the mono- or ditelluride.

The β-phase has a composition close to V_5Te_4 and no appreciable homogeneity range. The structure is monoclinic with the lattice constants:

$$a = 13.48 \text{ Å}, b = 3.91_3 \text{ Å}, c = 13.82 \text{ Å}, \beta = 93.5_8°$$

when quenched from 1 000°C.

The *γ-phase* has a homogeneity range between about 53 and 62 atomic per cent tellurium in samples quenched from 1 000°C, and between 55.6 and 64.9 atomic per cent tellurium in samples quenched from 750°C. For slowly cooled samples the vanadium rich limit of the γ-phase is at about 56.5 atomic per cent tellurium. Within the γ-phase region four structurally related phases are recognized:

1. The γ_1-phase with a hexagonal NiAs-like structure and composition around 53 atomic per cent tellurium in samples quenched from 1 000°C only. The lattice constants of the hexagonal structure as determined from the two-phase preparation with 52.38 atomic per cent tellurium are:

$$a = 3.942 \text{ Å}, \quad c = 6.126 \text{ Å}, \quad c/a = 1.55_3$$

2. The γ_2-phase with a related monoclinic structure and composition between 55.5 and 63.0 atomic per cent tellurium in samples quenched from 750°C. In this range the lattice constants vary continuously between the limits:

$$a = 6.763 \text{ Å}, \quad b = 3.807 \text{ Å}, \quad c = 2\times 6.225 \text{ Å}, \quad \beta = 91.52°$$

at 55.56 atomic per cent tellurium, and

$$a = 6.460 \text{ Å}, \quad b = 3.685 \text{ Å}, \quad c = 2\times 6.335 \text{ Å}, \quad \beta = 90.3°$$

at 62.96 atomic per cent tellurium.

For samples quenched from 1 000°C the tellurium-rich limit of the γ_2-phase is close to 62 atomic per cent tellurium.

3. The γ_3-phase with a hexagonal NiAs-$Cd(OH)_2$-like structure and a narrow composition range in samples quenched from 750°C. The lattice constants for this structure at the composition 63.96 atomic per cent tellurium are:

$$a = 3.689 \text{ Å}, \quad c = 6.405 \text{ Å}, \quad c/a = 1.736$$

This phase was neither observed in samples quenched from 1 000°C nor in slowly cooled.

4. The γ_4-phase with an orthorhombic $Cd(OH)_2$-like structure and composition between 64.3 and 64.9 atomic per cent tellurium. For a sample with 64.91 atomic per cent tellurium, quenched from 750°C, the lattice constants are:

$$a = 6.333 \text{ Å}, \quad b = 3.618 \text{ Å}, \quad c = 2 \times 6.427 \text{ Å}$$

Density measurements show that the solid solution within the γ-phase takes place by subtraction of vanadium atoms as the tellurium content increases.

Only a few references to vanadium tellurides are present in the literature and the earliest work seems to be by Hoschek and Klemm [1]. The tellurides prepared by these authors by the reaction between vanadium (III) oxide or chloride with hydrogen telluride generally had a composition close to the ratio V:Te = 1. Hoschek and Klemm were not able to establish the composition or structure of any of the tellurides formed in their experiments and the tellurium was reported to be relatively weakly bonded. Montignie [2] was not successful in preparing vanadium tellurides by heating vanadium (V) oxide and tellurium under hydrogen.

The first description of a well defined vanadium telluride is due to Ehrlich [3], who obtained the monotelluride by heating the elements in evacuated, sealed silica tubes at 800 to 1 000°C. The compound was found to have a structure of the NiAs-type with unit cell dimensions * $a = 3.81_3$ Å, $c = 6.13_2$ Å and $c/a = 1.60_8$. The X-ray powder photograph of the compound contained, however, some weak reflections which could not be explained on basis of a simple NiAs-like structure. Whether these additional reflections were due to a superstructure or to other phases could not be decided by Ehrlich.

Gal'perin and Perekalina [4] found that the structure of vanadium monotelluride was not of the NiAs-type, but were unable to interpret it.

Ehrlich [5] has indicated the existence of a compound with structure of the $Cd(OH_2)$-type in the system vanadium tellurium, without giving any experimental evidence for the existence of such a phase.

EXPERIMENTAL

The alloys used in this study were synthesized by heating the elements in the desired ratio in evacuated and sealed silica tubes. In a few cases preparations were made also by adding tellurium to previously prepared alloys containing less tellurium.

The metallic *vanadium* was supplied by the Vanadium Corporation of America and reported to contain 99.6—99.8 % vanadium. The impurities were specified as follows: iron 0.05 %, silicon 0.05 %, aluminium less than 0.05 %, nitrogen less than 0.001 %, and oxygen balance.

The *tellurium* was from the British Drug Houses Ltd. and purified further by distillation *in vacuo*. A spectrographic analysis, which was kindly carried out by siv.ing. S. Rutlin at the Central Institute for Industrial Research, Norway, showed that the puri-

* The lattice constant values given by Ehrlich, presumably expressed in kX units, have been changed into Å by multiplication by the factor 1.00202.

fied tellurium contained less than 0.01 % iron and only traces of aluminium, magnesium and lead.

During the first preparations of the alloys it was observed that samples with more than 45.5 atomic per cent vanadium heavily attacked the silica tubes by reducing the silicon dioxide and forming trivanadium monosilicide, V_3Si. In order to avoid this detrimental reaction, alloys with more than 45.5 atomic per cent vanadium were prepared in small crucibles of pure alumina ("Degussit" from Degussa) placed inside the silica tubes. Alloys with less than 45.5 atomic per cent vanadium could be prepared without this precaution.

A number of alloys with compositions varying from 24.81 to 71.43 atomic per cent tellurium were synthesized. The mixture of vanadium and tellurium was first heated for 2 days at 1 000°C. By this heating a sintered reaction product was obtained which could easily be changed into a powder by shaking the silica tube. The heating was continued at 1 000°C for 2 more days in the same tube. It was then quenched in ice water and small portions of each sample taken out for X-ray investigation. The rest of the sample was heated further for 20 days at 750°C and quenched from that temperature.

In this way it was only possible to obtain alloys with less than 62 atomic per cent tellurium. In alloys with higher tellurium content some tellurium was left unreacted after quenching from 1 000°C. In order to make the reaction complete above 62 atomic per cent tellurium it was necessary to cool the samples slowly down from 1 000 to 750°C. In this way alloys with up to 71.43 atomic per cent tellurium could be prepared. They were also annealed for 20 days at 750°C and quenched.

In addition to these two series of samples, one quenched from 1 000°C and the other from 750°C, small parts of some of the samples were heated further for 30 days at 550°C and cooled slowly to room temperature during 5 days. In one case a sample was also cooled slowly from 750°C. The purpose of these heat treatments was to check if the lower annealing temperature and the slower cooling rate might cause any changes of the phases and structures observed in the quenched samples. The samples slowly cooled from 550°C contained 52.38, 54.55, 64.29 and 66.67 atomic per cent tellurium and that from 750°C 63.64 atomic per cent tellurium.

The samples were all easily crushed in an agate mortar into dark gray powders. They were then subjected to an X-ray examination by the powder method.

The X-ray photographs were taken in 11.48 cm diameter cameras with asymmetric film mounting. Vanadium filtered chromium radiation was used in most cases. In a few cases nickel filtered copper radiation was also used. The lattice constants are expressed in Ångström units on the basis of $\lambda CrK\alpha_1 = 2.2896$ Å and $\lambda CuK\alpha_1 = 1.5405$ Å. The mean error in the lattice constants in judged to be less than 0.1 %.

PHASE ANALYSIS

1. Samples quenched from 1 000 °C

The most vanadium-rich sample that was prepared contained 24.81 atomic per cent tellurium, corresponding to the composition $VTe_{0.33}$. By X-ray examination this sample was found to consist of two phases: metallic vanadium — the *α-phase* — and an intermediate phase — the *β-phase*. Samples with 41.18 and 44.44 atomic per cent tellurium ($VTe_{0.70}$ and $VTe_{0.80}$, respectively) gave only reflections from the β-phase, whereas another phase — the *γ_1-phase* — was observed together with the β-phase at 47.37 atomic per cent tellurium ($VTe_{0.90}$). Accordingly, it is concluded that the β-phase contains about 44 atomic per cent tellurium ($VTe_{0.8}$) and thus has a composition which is markedly different from that of a monotelluride. As no displacement of the X-ray reflections on photographs of samples containing the β-phase is observed, the phase probably has a rather narrow homogeneity range.

The β-phase is observed together with the γ_1-phase in preparations with 50.00 and 52.38 atomic per cent tellurium ($VTe_{1.00}$ and $VTe_{1.10}$, respectively).

At the latter composition the reflections from the β-phase are few and weak. The remaining reflections can all be explained in terms of the hexagonal, NiAs-like structure which Ehrlich [3] attributed to vanadium monotelluride. However, all the samples with 50 atomic per cent tellurium studied here turned out to be two-phase preparations, containing both the β-phase and the γ_1-phase. Thus, a vanadium monotelluride with the exact stoichiometric composition VTe does apparently not exist. The additional reflections which Ehrlich observed on the photograph of the sample with composition corresponding to the monotelluride, were probably due to the β-phase.

The X-ray photographs of samples with compositions in the concentration range 52.38 to 62.26 atomic per cent tellurium ($VTe_{1.10}$ to $VTe_{1.65}$, respectively) are all very similar. Some characteristic features should, however, be emphasized. First of all, no reflections from the β-phase are present for samples with 54.55 atomic per cent tellurium ($VTe_{1.20}$). Furthermore, a splitting of many of the hexagonal reflections is observed at the same composition. Finally, a marked shift in the positions of the reflections is observed as the tellurium content of the samples increases in the whole concentration range up to 60.00 atomic per cent tellurium.

These observations show that the γ_1-phase with a hexagonal, NiAs-like structure has only a narrow existence range between 52.38 and 54.55 atomic per cent tellurium ($VTe_{1.10}$ and $VTe_{1.20}$, respectively). With increasing tellurium concentration the hexagonal structure changes into one with a lower, probably monoclinic, symmetry as has earlier been found for many of the chalcogen systems of the 3*d* transition elements (see for instance Haraldsen [6]). The corresponding phase — the *γ_2-phase* — has a homogeneity range between about 54.55 and 62.26 atomic per cent tellurium, the latter composition being the highest one in tellurium which could be attained for samples quenched from 1 000°C without the tellurium phase being present.

The designations γ_1 and γ_2 are chosen to indicate that the phase γ_1 with hexagonal structure and γ_2 with monoclinic structure might constitute only one phase — the *γ-phase* — in analogy with what has been found for many related systems[6]. This further means that the hexagonal structure, present at the vanadium-rich limit of the homogeneity range, continuously changes into the monoclinic structure as the tellurium content increases.

2. Samples quenched from 750°C

In the series quenched from 750°C, a phase with a hexagonal structure, corresponding to that of the γ_1-phase in the series quenched from 1 000°C, could not at all be observed. Instead, large amounts of the β-phase were present in the sample with 52.38 atomic per cent tellurium, and also the γ_2-phase with its splitted reflections. A considerable change in the positions of these reflections was observed in the range from 55.56 to 62.96 atomic per cent tellurium ($VTe_{1.25}$ to $VTe_{1.70}$.).

The X-ray powder photographs of the preparation with 63.64 atomic per cent tellurium ($VTe_{1.75}$) could, however, be indexed hexagonal. Consequently, the system vanadium tellurium shows the same characteristic features as has

been found in many other chalcogen systems of the 3*d* transition elements [6]. Depending upon the temperature to which the statement refers, there exists in the range between 50 and 66.7 atomic per cent chalcogen one or more phases which at concentrations low in chalcogen possess a hexagonal NiAs-like structure, at intermediate concentrations a monoclinic structure and at concentrations high in chalcogen again a hexagonal $Cd(OH)_2$-like structure, derived from the NiAs-like structure by subtraction of metal atoms. In the present case it could not be decided whether the hexagonal structures and the monoclinic structure constitute a single phase or three different phases, γ_1, γ_2 and γ_3, separated-by two-phase regions.

The hexagonal $Cd(OH)_2$-like structure was found to exist also at the composition 63.96 atomic per cent tellurium ($VTe_{1.775}$), but not at 64.29 atomic per cent tellurium ($VTe_{1.80}$), where a splitting of the X-ray reflections was again noted. The hexagonal γ_3-phase has thus only a narrow existence range, just as the hexagonal γ_1-phase which was observed in the series quenched from 1 000°C.

In samples with 64.29 to 64.91 atomic per cent tellurium probably another phase — the *γ_4-phase* — exists. The corresponding X-ray powder photograph was tentatively indexed as orthorhombic (see Table 5). The photographs of the samples with 65.52, 66.67 and 71.43 atomic per cent tellurium ($VTe_{1.90}$, $VTe_{2.00}$, and $VTe_{2.50}$ respectively) contained also a few weak reflections which might be caused by elemental tellurium, in addition to the reflections from the γ_4-phase. No shift in the positions of the reflections from the γ_4-phase is observed on the photographs of the samples with 64.91 to 71.43 atomic per cent tellurium, and the γ_4-phase should therefore not contain more than 64.91 atomic per cent tellurium ($VTe_{1.85}$). The change from hexagonal to orthorhombic structure takes place within a narrow composition range, 63.96 to 64.29 atomic per cent tellurium, and it is very slight. It seems reasonable to suppose that the transition from the monoclinic γ_2-phase, *via* the hexagonal γ_3-phase, into the orthorhombic γ_4-phase is continuous at high temperatures and that the γ-phase has a homogeneity range between about 55.56 and 64.91 atomic per cent tellurium ($VTe_{1.25}$ and $VTe_{1.85}$) at 750°C, as far as it can be judged from the quenched samples.

3. Slowly cooled samples

The most striking feature of the slowly cooled preparations is the absence of the hexagonal structure both at low and at high tellurium concentrations. Consequently, neither the γ_1-phase, nor the γ_3-phase exists at low temperatures.

The preparation with 52.38 atomic per cent tellurium ($VTe_{1.10}$) consists also in this case of two phases, β and γ_2, whereas at 54.55 atomic per cent tellurium ($VTe_{1.30}$) only the γ_2-phase remains. With regard to the position of the X-ray reflections the photographs of these two samples are practically identical with that of $VTe_{1.30}$ quenched from 750°C, which indicates that the γ_2-phase does not contain less than 56.52 atomic per cent tellurium at room temperature. Similarly, the photograph of the slowly cooled sample with 63.64 atomic per cent tellurium indicates that the tellurium-rich limit of the γ_2-phase is close to 61.54 atomic per cent, as it is very similar to that of $VTe_{1.60}$ quenched from 750°C. The γ_4-phase was found free from other phases at 64.29 atomic

per cent tellurium ($VTe_{1.80}$) and mixed with free tellurium at 66.67 atomic per cent tellurium ($VTe_{2.00}$).

It follows from the results obtained here that a vanadium ditelluride with the exact stoichiometric composition VTe_2 does not exist, no more than a stoichiometric monotelluride VTe, at least not under the described experimental conditions. The most tellurium-rich phase obtained, the γ_4-phase, has a composition which differs markedly from the formula VTe_2, and changes in the heat-treatment apparently makes no difference as to the non-existence of the stoichiometric mono- and ditelluride.

LATTICE CONSTANT VALUES

1. The β-phase

Single crystals of the β-phase were found in the preparation with 44.44 per cent tellurium, quenched from 1 000°C. Weissenberg photographs showed that the crystals were monoclinic, and also gave approximate values for the unit cell dimensions. The powder photographs of the β-phase could then be

Table 1. Powder photograph data of the β-phase, quenched from 1 000°C, Cu$K\alpha$ radiation.

I_{obs}	$\sin^2\Theta \times 10^4$	hkl	I_{obs}	$\sin^2\Theta \times 10^4$	hkl
m	451	$11\bar{1}$, 111	vw	1 786	604
m	499	004	vw	1 870	$51\bar{5}$
m	525	400	vw	1 918	$11\bar{7}$
m	595	$20\bar{4}$	w	1 979	117
m	615	$40\bar{2}$	st	2 054	711
m	665	204	st	2 153	$80\bar{2}$, $60\bar{6}$ / $22\bar{4}$
vst	687	402, $11\bar{3}$			
vst	727	311	vw	2 211	208, 224
m	924	$31\bar{3}$	vw	2 298	802
m	1 001	313	vw	2 458	$80\bar{4}$
st	1 201	$20\bar{6}$	vw	2 584	$51\bar{7}$
m	1 217	$51\bar{1}$	w	2 662	408
m	1 361	602	m	2 746	$22\bar{6}$
vst	1 424	$51\bar{3}$	m	2 906	622
st	1 530	315	w	3 006	$80\bar{6}$
st	1 552	020			

indexed as shown in Table 1. The lattice constants, as determined for samples of the three series, are listed in Table 2 and they are practically the same.

Missing reflections on the photographs are of the type:

$$hkl \text{ when } h + k = 2n + 1,\ k + l = 2n + 1,\ (l + h = 2n + 1)$$

$$h0l \text{ when } l = 2n + 1,\ (h = 2n + 1)$$

$$0k0 \text{ when } (k = 2n + 1)$$

Table 2. Lattice constants of the β-phase.

Annealing temperature °C	a in Å	b in Å	c in Å	β	Volume of the unit cell in Å^3
1 000	13.48	3.91_3	13.82	93.5_8°	727.1
750	13.47	3.92_7	13.86	93.66°	731.6
550	13.47	3.92_0	13.85	93.6°	729.9

They are characteristic of the space groups C_s^4 and C_{2h}^6. The observed density, 6.73_7 g cm^{-3}, corresponds to 19.3 vanadium and 15.4 tellurium atoms in the unit cell. The true content is probably 20 vanadium and 16 tellurium atoms, which corresponds to the formula V_5Te_4 or $VTe_{0.80}$. The determination of the structure is under way.

2. The γ-phase

The lattice constants of the γ-phase determined for the three series of samples at different compositions are given in Table 3. Weak additional lines on the photographs of the monoclinic samples, both when quenched from 750°C and when slowly cooled, require for their explanation a doubling of the c-axis, and this is indicated in the table.

The values determined for the hexagonal γ_1-phase at the composition 52.38 atomic per cent tellurium and 1 000°C agree fairly well with the values found by Ehrlich [3] as far as the c-axis is concerned ($a = 3.81_3$ Å, $c = 6.13_2$ Å). The a-axis is, however, considerably larger.

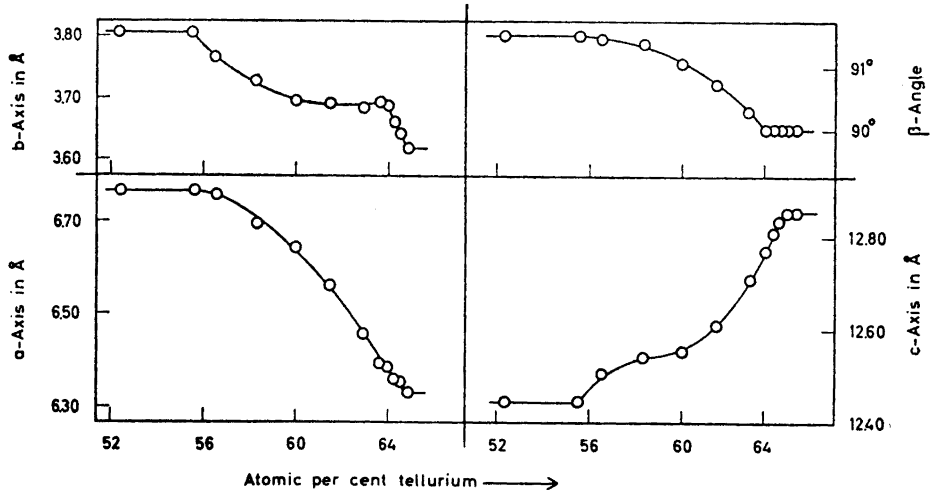

Fig. 1. Lattice constants of the γ-phase after quenching from 750°C.

Table 3. Lattice constants of the γ-phase.

Atomic per cent tellurium	Annealing Temperatur °C	a ($b\sqrt{3}$) in Å	b in Å	c in Å	β	Volume of the unit cell in Å^3
	1 000	(6.828)	3.942	6.126	(90°)	82.44
52.38	750	6.763	3.807	2 × 6.225	91.52°	4 × 80.10
	550 *	6.760	3.770	2 × 6.25	91.5°	4 × 79.62
	1 000	6.788	3.828	6.221	91.15°	2 × 80.81
54.55	750	6.763	3.807	2 × 6.225	91.52°	4 × 80.10
	550 *	6.759	3.767	2 × 6.254	91.46°	4 × 79.59
55.56	750	6.763	3.807	2 × 6.225	91.52°	4 × 80.10
56.52	1 000	6.761	3.767	2 × 6.240	91.58°	4 × 79.43
	750	6.759	3.767	2 × 6.254	91.46°	4 × 79.59
58.33	750	6.692	3.728	2 × 6.273	91.40°	4 × 78.23
60.00	1 000	6.637	3.693	2 × 6.276	91.00°	4 × 76.90
	750	6.642	3.696	2 × 6.279	91.07°	4 × 77.06
61.17	1 000	6.598	3.680	2 × 6.26	90.9°	4 × 76.0
61.54	750	6.563	3.693	2 × 6.306	90.72°	4 × 76.41
62.26	1 000	6.541	3.677	2 × 6.255	90.73°	4 × 75.25
62.96	750	6.460	3.685	2 × 6.355	90.3°	4 × 75.64
63.64	750	(6.398)	3.695	6.385	(90°)	75.50
	750 *	6.550	3.664	2 × 6.295	90.67°	4 × 75.53
63.96	750	(6.390)	3.689	6.405	(90°)	75.49
64.29	750	6.362	3.661	2 × 6.412	(90°)	4 × 74.66
64.60	750	6.356	3.642	2 × 6.427	(90°)	4 × 74.39
64.91	1 000	6.541	3.677	2 × 6.255	90.73°	4 × 75.25
	750	6.333	3.618	2 × 6.427	(90°)	4 × 73.62

* slowly cooled.

The variations in lattice constants with composition are seen from Fig. 1, where the lattice constants of the γ-phase for the 750°C series are plotted against the composition. The a-axis decreases smoothly with increasing tellurium content in the whole concentration range, while the b-axis shows an abrupt decrease at about 64 atomic per cent tellurium as the structure changes

Table 4. Powder photograph data of the γ_4-phase, $VTe_{1,85}$ quenched from 750°C, Cu$K\alpha$ radiation.

I_{obs}	$\sin^2\Theta \times 10^4$ obs.	hkl	$\sin^2\Theta \times 10^4$ calc.	I_{obs}	$\sin^2\Theta \times 10^4$ obs.	hkl	$\sin^2\Theta \times 10^4$ calc.
w	143	002	144	vw	1 520	—	—
vw	448	010	453	vw	1 657	—	—
vw	466	—	—	m	1 780	310	1 785
m	575	004	575	w	1 813	020	1 813
w	594	200	592	st	1 894	116	1 894
w	604	110	601	w	2 001	—	—
m	730	202	735	vw	2 068	—	—
vst	751	112	745	m	2 303	008	2 298
vw	845	—	—	w	2 336	314	2 359
vw	870	—	—	w	2 399	024	2 388
vw	967	—	—	w	2 504	402	2 510
vw	1 120	—	—	m	2 545	222	2 548
st	1 176	204	1 166	w	2 906	118	2 900
		114	1 176	m	2 982	224	2 980
vw	1 255	—	—	m	3 697	226	3 698
vw	1 296	006	1 293				
vw	1 452	103	1 441				

from hexagonal to orthorhombic. Even though the c-axis increases, the volume of the unit cell decreases as well, see Table 3.

It is furthermore apparent from Fig. 1 that the vanadium rich limit of the homogeneity range of the γ-phase for the 750°C series is at about 55.5 atomic per cent tellurium. This is somewhat higher than found on basis of the 1 000°C series, where the limit lies between 52.38 and 54.55 atomic per cent tellurium if the hexagonal range is included.

The lattice constant values for the hexagonal structures fall nicely on the curves drawn through the values for the monoclinic structure. This is also the case with the hexagonal lattice constants of the 1 000°C series (not shown in the figure). This might indicate that the transition from one structure into the other is continuous under the experimental conditions used here. The observations are, however, too few for deciding this question with certainty.

As already stated, the X-ray powder photograph of the γ_4-phase was indexed orthorhombic. This gave a satisfactory agreement between observed and calculated $\sin^2\Theta$-values for most of the reflections, as can be seen from Table 4 where the values are listed. There remain, however, a few, very weak reflections which cannot be accounted for in this way. They might be due to a superstructure, indicating that the true unit cell is larger.*

The lattice constants calculated for the orthorhombic unit cell are:

$$a = 6.333 \text{ Å}, \; b = 3.618 \text{ Å}, \; c = 2 \times 6.427 \text{ Å}$$

at 64.91 atomic per cent tellurium.

* Note added in proof: Weissenberg photographs of a crystal of $VTe_{1.85}$ has confirmed the correctness of the orthorhombic interpretation and shown that she b-axis must be tripled.

Table 5. Interatomic distances in the hexagonal γ_1 and γ_3 structures.

Atomic per cent tellurium	V—Te	V—V	Te—Te within the layers	Te—Te between the layers
52.38	2.74 Å	3.06 Å	3.94 Å	3.82 Å
63.64	2.67 Å	3.20 Å	3.69 Å	3.85 Å

The structure bears a close relationship to that of the hexagonal γ_3-phase, but it has so far no parallel among the other sulfides, selenides and tellurides of the 3*d* transition elements. It is especially worth mentioning that the structure is not of the marcasite type as one might have thought on basis of its orthorhombic structure and its composition.

In the hexagonal γ-phase, each vanadium atom is surrounded by six tellurium atoms at the corners of a deformed octahedron (trigonal antiprism) and two vanadium atoms at the distance $c/2$. The tellurium atoms form an approximately hexagonal closepacking. The distances vanadium-tellurium, vanadium-vanadium and tellurium-tellurium found in the two preparations with 52.38 and 63.96 atomic per cent tellurium are listed in Table 5.

The distances vanadium-tellurium are distinctly shorter than the sum of the ionic radii: 0.74 Å + 2.11 Å = 2.85 Å. They agree, however, very well with the sum of the metallic radii as given by Pauling [7]. With an average coordination number of 7.6 for vanadium and 5.5 for tellurium in the vanadium rich preparation and 6.4 for vanadium and 3.5 for tellurium in the tellurium rich preparation, the sum of the metallic radii is:
1.27 Å + 1.50 Å = 2.77 Å and 1.26 Å + 1.44 Å = 2.70 Å, respectively, *i.e.* only 0.03 Å higher than the experimental values.

The distance tellurium-tellurium between the layers remains almost unchanged from 52.38 to 63.96 atomic per cent tellurium, whereas the distance within

Table 6. The distance metal-tellurium in tellurides with NiAs-like, respectively $Cd(OH)_2$-like structure.

Composition $MeTe_n$	Distance Me-Te in Å	Sum of ionic radii r(Me) + r(Te) in Å	Sum of metallic radii r(Me) + r(Te) in Å
TiTe	2.736		1.41 + 1.51 = 2.92
$TiTe_2$	2.717	0.64 + 2.11 = 2.75	1.38 + 1.42 = 2.80
$VTe_{1.1}$	2.74	0.74 + 2.11 = 2.85	1.27 + 1.50 = 2.77
$VTe_{1.7}$	2.67		1.26 + 1.44 = 2.70
$CrTe_{1.5}$	2.726	0.65 + 2.11 = 2.76	1.28 + 1.46 = 2.74
MnTe	2.923	0.91 + 2.11 = 3.02	1.21 + 1.51 = 2.72
$FeTe_{1.5}$	2.62	0.67 + 2.11 = 2.78	1.18 + 1.46 = 2.64
$CoTe_{1.2}$	2.62	0.82 + 2.11 = 2.93	1.19 + 1.49 = 2.68
$CoTe_{1.8}$	2.58		1.17 + 1.43 = 2.60
$NiTe_{1.1}$	2.654	0.78 + 2.11 = 2.89	1.18 + 1.50 = 2.68
$NiTe_2$	2.584		1.15 + 1.42 = 2.57

Table 7. Pycnometric densities of vanadium-tellurium preparations.

Atomic per cent tellurium	Density in g cm^{-3}	Atomic per cent tellurium	Density in g cm^{-3}
41.18	6.682	60.00	6.876
44.44	6.737	61.54	6.855
47.37	6.775	62.96	6.844
50.00	6.770	63.64	6.840
54.54	6.830	64.29	6.850
55.56	6.850	65.52	6.854
56.52	6.860	66.67	6.841
58.33	6.869		

the layers changes from 3.94 Å to 3.69 Å. This great change brings about that the distance within the layers, which is the larger one at 52.38 atomic per cent tellurium, is the smaller one at the tellurium rich composition.

The system vanadium-tellurium was the only tellurium system of the 3*d* transition elements from titanium to nickel for which data about the distance metal-tellurium still lacked. A compilation of the values found for this distance in the phases with NiAs-like, respectively $Cd(OH)_2$-like structure, is presented in Table 6 and compared with distances calculated on the basis of the ionic radii of Goldschmidt, and the metallic radii of Pauling. The metallic radi have been corrected for the coordination number valid for the compositions given in the table.

It can be seen from Table 6 that the observed distance metal-tellurium for the titanium tellurides TiTe and $TiTe_2$ and for manganese monotelluride MnTe is best in accordance with the sum of the ionic radii, whereas the metallic radii lead to the most satisfactory agreement for the vanadium, iron, cobalt and nickel tellurides. The chromium telluride $CrTe_{1.5}$ represents an intermediate case in so far as the distance chromium-tellurium agrees equally well with the sum of the ionic radii as that of the metallic radii.

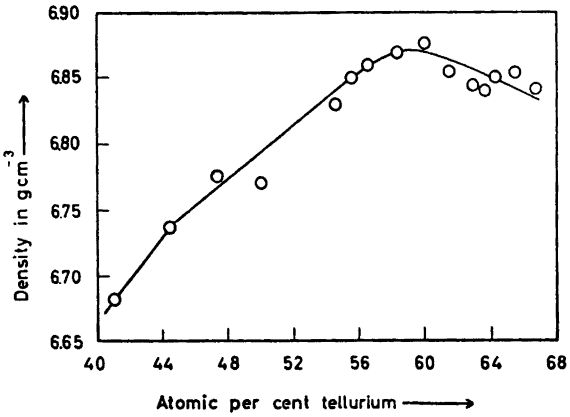

Fig. 2. Densities of the vanadium tellurides.

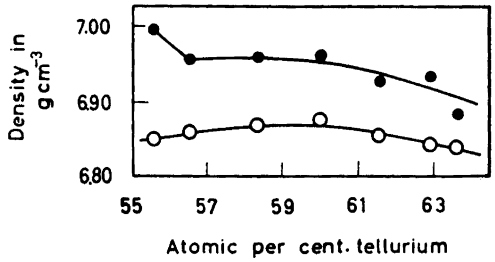

Fig. 3. Observed density o and calculated density ● of the γ-phase.

DENSITY MEASUREMENTS

Density measurements of the 750°C series were carried out at 25°C by the vacuum pycnometric method and with kerosene as displacement liquid. The results are listed in Table 7, and plotted against the composition of the samples in Fig. 2. There is a break in the curve at about 44.4 atomic per cent tellurium, coinciding with the composition of the β-phase, and a maximum at about 60 atomic per cent tellurium, *i.e.* within the homogeneity range of the γ-phase.

The densities which are found within the homogeneity range of the γ-phase confirm, furthermore, that the solid solubility in this concentration range is due to a subtraction of vanadium atoms. This appears from Fig. 3 where the densities, calculated on the basis of this hypothesis, are compared with the observed values. The agreement between the calculated and observed values in the concentration range 56.5 to about 64 atomic per cent tellurium leaves no doubt that a subtraction of vanadium atoms occurs in this region. An addition of tellurium atoms to the lattice or substitution of vanadium atoms by tellurium atoms would lead to an increase in the values of the calculated densities, and is not at all consistent with the observations. The subtraction of the vanadium atoms does, however, not go so far that a complete transition into a structure of the $Cd(OH)_2$-type is reached. The subtraction comes to an end at the tellurium rich limit of the γ_4-phase, *i.e.* at about 64 atomic per cent tellurium.

Certain changes which are observed in the relative intensities of the X-ray reflections, are also in favour of the hypothesis that the solid solution is of the subtractive type. The reflection (001) for example, which is forbidden in a structure of the NiAs-type, is distinctly seen on the photograph of the preparation with 62.96 atomic per cent tellurium.

REFERENCES

1. Hoschek, E. and Klemm, W. *Z. anorg. u. allgem. Chem.* **242** (1939) 59.
2. Montignie, E. *Bull. soc. chim. France* **1946**, 176; *Ann. pharm. franc.* **4** (1946) 253.
3. Ehrlich, P. *Z. anorg. Chem.* **260** (1949) 13.
4. Gal'perin, F. M. and Perekalina, T. M. *Doklady Akad. Nauk.* S.S.S.R. **69** (1949) 19; cited from *Chem. Abstr.* **44** (1950) 994d.
5. Ehrlich, P. *Z. anorg. Chem.* **260** (1949) 30.
6. Haraldsen, H. Experientia Supplementum VII, *XVI*th *International Congress of Pure and Applied Chemistry*, Paris 1957, p. 165; *9. Nordiske Kemikermøde*, Aarhus 1956, p. 83.
7. Pauling, L. *J. Am. Chem. Soc.* **69** (1947) 542.

Received February 1, 1958.

ACTA CHEMICA SCANDINAVICA 12 (1958) 983—994

Determination of Specific Gravity with Divers and Hydrometers with Loose Stem

SØREN BERG and J. J. V. LUNDBERG

The Laboratory of Porcelænsfabriken "Danmark" Ltd., Lyngby-Copenhagen, Denmark

A new method has been developed for determining the specific gravity of liquids, with divers or floats which may be loaded with metal weights to attain the floating equilibrium. The diver may also be provided with a loose stem of metal wire so that the instrument may function as a hydrometer.

Generally, only two divers are required for the measurements, *viz.* one of density 0.75 and another of density 0.95. Both divers are so dimensioned that their weights and volumes approximately satisfy an equation indicated in the article. Under these conditions, the specific gravity of the liquid may be calculated with sufficient accuracy from the results of the measurements by the diver method as well as from the results of measurements by the hydrometer method, using only a slide rule.

The random error of the diver method is about 0.9×10^{-5}. The random error of the hydrometer method is greater, and further a systematic error is introduced, *e. g.* because of adhesion between the fluid and the stem. The order of magnitude of this systematic error may be determined by comparative measurements according to the diver method and the hydrometer method.

Many investigators have tried to measure the specific gravity of fluids by applying bodies of known specific gravity, so-called divers, which during the measurements are completely submerged. The floating equilibrium of the diver is attained by addition of platinum weights to the diver, by alteration of the temperature of the fluid, by diluting the fluid, *etc.*

Divers have particularly been used for determining the specific gravity of sea water [1-4] and heavy water *etc.*[5-11] and in the fineness analysis [12-17] to determine the specific gravity in sedimenting suspensions, where the application of divers is advantageous for two reasons. First, in a heterodisperse, sedimenting suspension the specific gravity increases from the surface downwards, and there will therefore always be a level at which a diver with lower specific gravity than the homogeneous suspension, but with higher specific gravity than the suspending medium, may attain the floating equlibrium. Such special arrangements to attain the floating equilibrium may therefore be omitted, when a series of divers of different specific gravities are available.

Second, a consideration of the sedimentation process shows that a diver, which is in equilibrium in a sedimenting suspension, will move downwards with the same velocity as the largest particles present at the level of its geometric centre of gravity. *I.e.* it moves downwards faster than the sedimenting velocity of every particle present above this level. As a hydrometer, therefore, it will not be overtaken by sedimenting particles and systematic errors caused by deposition of particles onto the diver will be very small.

Finally, it may be mentioned that Nansen [3] has proposed to provide the diver with a loose stem, which, when the diver is in equilibrium, protrudes through the surface of the fluid so that the instrument is altered to a hydrometer (with loose stem).

With the exception of the examination of the specific gravity in sedimenting suspensions by the fineness analysis, it seems as if the method is not widely used for the determination of the specific gravity of fluids in spite of its very great precision and the quickness of the measurements. This is probably due to the fact that hitherto it has been necessary to calculate the specific gravity from a non-logarithmic expression by the application of logarithms with at least five figures.

It may, however, be shown that by applying two divers, the weights and volumes of which both satisfy a later indicated equation, one may calculate the specific gravity of the fluid with sufficient accuracy without other calculating facilities than a slide rule. By this method the specific gravity is determined with a random error of $\pm 0.9 \times 10^{-5}$ and the method is therefore more precise than the hydrometer method and Westphal's balance. It is further possible to make the method still more accurate, but this will require a very precise thermostat and the application of more than two divers, if the calculations are still to be simply made.

By providing the diver with a loose stem of platinum wire, for instance, one can, with moderate decrease in preciseness, make the measurements according to the hydrometer method. To obtain a satisfactory preciseness in this case, it is necessary to carry out comparative measurements according to the diver method and the hydrometer method for each new fluid which may be examined in order to determine the systematic error of the hydrometer method and to be able to correct for it. These errors are particularly due to adhesion between the fluid and the stem, to changes in the condition of the surface of the stem, and to fluid attached to the protruding part of the stem.

In the following:

a	indicates the weight of the diver (*in vacuo*),
x	" " " " " load (" "),
$\varrho_{20,20}$	the specific gravity of the unloaded diver at 20°C
$\varrho_{20,4}$	compared to water at 20° and 4°C, respectively,
$\alpha_{20,20}$	the increase in specific gravity of the diver at 20°C
$\alpha_{20,4}$	compared to water at 20°C and 4°C, due to the load,
$p_{20,20}$	the specific gravity of the load at 20°C compared
$p_{20,4}$	to water at 20°C and 4°C, respectively,
$z_{20,20}$	an arbitrary specific gravity at 20°C compared
$z_{20,4}$	to water at 20°C and 4°C, respectively.

When a diver is in floating equilibrium in a medium with the load x one has:

$$\frac{a+x}{\frac{a}{\varrho_{20,4}}+\frac{x}{p_{20,4}}} = \varrho_{20,4} + \alpha_{20,4} \tag{1}$$

and since

$$z_{20,4} = z_{20,20} \times 0.99823$$

one gets

$$\frac{a+x}{\frac{a}{\varrho_{20,20}}+\frac{x}{p_{20,20}}} = \varrho_{20,20} + \alpha_{20,20}$$

from which may be deduced

$$\frac{a+x}{\frac{a\,p_{20,20}}{\varrho_{20,20}}+x} = \frac{\varrho_{20,20}+\alpha_{20,20}}{p_{20,20}}$$

and

$$\frac{a+x}{a\left(\frac{p_{20,20}}{\varrho_{20,20}}-1\right)} = \frac{\varrho_{20,20}+\alpha_{20,20}}{p_{20,20}-\varrho_{20,20}-\alpha_{20,20}} = \frac{1+\frac{\alpha_{20,20}}{\varrho_{20,20}}}{\frac{p_{20,20}}{\varrho_{20,20}}-\frac{\alpha_{20,20}}{\varrho_{20,20}}-1}$$

Multiplying by $\left(\frac{p_{20,20}}{\varrho_{20,20}}-1\right)$ one gets

$$\frac{a+x}{a} = \frac{\frac{p_{20,20}}{\varrho_{20,20}}+\frac{p_{20,20}\cdot\alpha_{20,20}}{\varrho_{20,20}^2}-\frac{\alpha_{20,20}}{\varrho_{20,20}}-1}{\frac{p_{20,20}}{\varrho_{20,20}}-\frac{\alpha_{20,20}}{\varrho_{20,20}}-1}$$

and

$$1+\frac{x}{a} = 1+\frac{\frac{p_{20,20}\cdot\alpha_{20,20}}{\varrho_{20,20}^2}}{\frac{p_{20,20}}{\varrho_{20,20}}-\frac{\alpha_{20,20}}{\varrho_{20,20}}-1}$$

from which may be derived

$$x = \frac{a\cdot\alpha_{20,20}}{\frac{\varrho_{20,20}^2}{p_{20,20}}\left(\frac{p_{20,20}}{\varrho_{20,20}}-\frac{\alpha_{20,20}}{\varrho_{20,20}}-1\right)}$$

and we have

$$x = \frac{a\cdot\alpha_{20,20}}{\varrho_{20,20}\left(1-\frac{\varrho_{20,20}-\alpha_{20,20}}{p_{20,20}}\right)} \tag{2}$$

from which may be derived

$$a_{20,20} = \frac{x \cdot \varrho_{20,20}\left(1 - \frac{\varrho_{20,20}}{p_{20,20}}\right)}{a\left(1 + \frac{\varrho_{20,20} \cdot x}{a \cdot p_{20,20}}\right)} \tag{3}$$

(3) is the non-logarithmic expression by which the difference between the specific gravity of the loaded and the unloaded diver may be calculated.

x being the load which corresponds to the floating equilibrium in water at 20°C, we have

$$\varrho_{20,20} + a_{20,20} = 1 \tag{4}$$

By substituting (4) into (2) it may be shown that

$$a_{20,20} = \frac{1}{1 + \frac{a \cdot p_{20,20}}{x\,(p_{20,20}-1)}} \tag{5}$$

Using (4) and (5), the specific gravity of the unloaded diver may be determined by floating experiments in water since only divers with lower specific gravity than water are used.

Eqn. (3) may be written

$$a_{20,20} = \frac{x \cdot \varrho_{20,20}\,(p_{20,20} - \varrho_{20,20})}{a \cdot p_{20,20}\left(1 + \frac{\varrho_{20,20} \cdot (p_{20,20} - \varrho_{20,20}) \cdot x}{a \cdot p_{20,20}\,(p_{20,20} - \varrho_{20,20})}\right)}$$

Simplifying, we introduce

$$\frac{a \cdot p_{20,20}}{\varrho_{20,20}\,(p_{20,20} - \varrho_{20,20})} = C \tag{6}$$

which gives

$$a_{20,20} = \frac{x}{C} \frac{1}{1 + \frac{x}{C(p_{20,20} - \varrho_{20,20})}} \tag{7}$$

As

$$\frac{1}{1+\beta} = 1 - \frac{\beta}{1+\beta}$$

where β is an arbitrary number, eqn. (7) may be written:

$$a_{20,20} = \frac{x}{C}\left(1 - \frac{\frac{x}{C(p_{20,20} - \varrho_{20,20})}}{1 + \frac{x}{C(p_{20,20} - \varrho_{20,20})}}\right)$$

and

$$a_{20,20} = \frac{x}{C}\left(1 - \frac{1}{1 + \frac{C}{x}\,(p_{20,20} - \varrho_{20,20})}\right)$$

and we further have:

$$\alpha_{20,20} = \frac{x}{C} - \frac{\left(\frac{x}{C}\right)^2}{\frac{x}{C} + p_{20,20} - \varrho_{20,20}} \tag{8}$$

When the weight and specific gravity of the diver are so chosen that C is a whole number, for instance 10, 20 or 50, x/C may conveniently be calculated by mental calculation and as the second term is smaller than 0.00350 except in special cases, it may be calculated with sufficient preciseness by a slide rule.

It may further be shown that when $\frac{x}{C} < 0.1$ and $p_{20,20} - \varrho_{20,20} > 20$ or $\frac{x}{C} < 0.08$ and $p_{20,20} - \varrho_{20,20} > 15$ the following approximate equation may be used

$$\alpha_{20,20} = \frac{x}{C} - \frac{\left(\frac{x}{C}\right)^2}{p_{20,20} - \varrho_{20,20}} \tag{9}$$

When C is not exactly a whole number

$$C = N\ (1 + \varepsilon)$$

where ε is a small number and N is a whole number.

When $\varepsilon < 0.001$ x/C may be computed by mental calculation by the following approximate equation

$$\frac{x}{C} = \frac{x(1 - \varepsilon)}{N} \tag{10}$$

The diver is made preferably from thermometer glass (Jena 16 III) to minimize the thermal after-effect, or from quartz, and the upper tip of the diver is drawn out into a short glass stem. The instrument is shown on Fig. 1 without and with the metal stem. Q is a ballast of mercury. M is a horizontal plate of soft iron, supported by a rod S fixed by shellac to the inside of the diver's lower tip. The diver may therefore be manipulated from the outside with a magnet when it is in floating equilibrium.

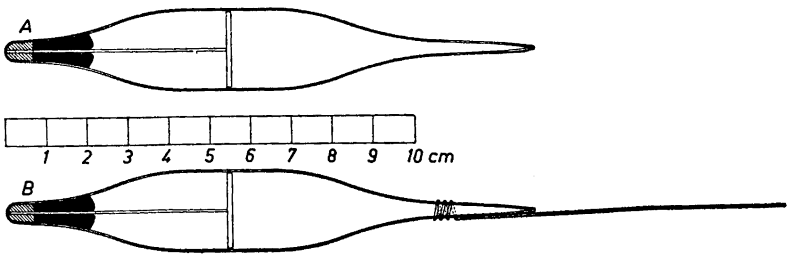

Fig. 1. A: Diver. B: Hydrometer with loose stem.

To secure that C and $\varrho_{20,20}$ do not differ more than 1 ‰ from N and the desired specific gravities, 0.75 and 0.95, respectively, the following course of procedure may be applied: From (6) we have

$$\frac{a}{\varrho_{20,20}} = C\,\frac{p_{20,20} - \varrho_{20,20}}{p_{20,20}} = Y \tag{11}$$

where Y is the weight of the water displaced by the diver at 20°C.
As

$$\varrho_{20,20} = \frac{\varrho_{20,4}}{0.99823}$$

where 0.99823 is the density of water at 20°C, we further have

$$\frac{a}{0.99823\,\varrho_{20,20}} = \frac{a}{\varrho_{20,4}} = \frac{C(p_{20,20} - \varrho_{20,20})}{0.99823\,p_{20,20}} = V \tag{12}$$

where V is the volume of the diver. From (11) and (12) it is seen, that Y and V are determined when C and $\varrho_{20,20}$ are chosen.

Before the stem of the diver is cut off to the desired length, the diver is put down in a graduated glass filled to a mark with mercury and the approximate volume of the diver is read from the rising of the mercury. The stem is then cut off to such a length that the volume of the diver is somewhat greater than the volume calculated by (11). Enough mercury is now introduced into the diver so that the latter may float submerged in water at 20°C with the stem closed by a small rubber hood. The stem is then sealed with a flame and by loading the diver with weights of platinum it is brought to floating equilibrium in water at 20°C.

From the load and the weight of the diver its specific gravity and volume may be calculated by (3), (4) and (12). By etching with hydrofluoric acid and by new floating experiments, the volume of the diver may now be decreased to approximately the calculated volume.

The tip of the stem is then cut off and sufficient mercury is removed from the diver to bring its specific gravity approximately to the desired one. The stem is now once more sealed in a flame. By new floating experiments and repeated etching, it is now possible to adjust both the C-value and the specific gravity of the diver to the desired values within a tolerance of less than 1 ‰. This is sufficient, but it is of course necessary afterwards to determine both values with a tolerance of less than about 0.5×10^{-5} by loading experiments in water by 20°C. These determinations may conveniently be repeated up to 10 times in order to give a good average.

For the measurements, one diver with a specific gravity of about 0.75 and another with a specific gravity of about 0.95 are applied and $\alpha_{20,20}$ is computed by (8) or (9) and (10).

For the most part, ringshaped weights of platinum are used which may be conveniently placed around the glass stem of the diver. Weights smaller than 10 mg should be made from stainless steel or titanium, preferably, (densities 7.85 and 4.5, respectively) provided that these materials are not corroded by the liquid to be investigated. The reason is that such small platinum weights (density 21.5), 5 mg and less, are rather difficult to handle.

As stainless steel and titanium have almost the same appearance as platinum, it is also advantageous to make 10, 20, and 50 mg weights of gold (density 19.3).

The weights of stainless steel, titanium and gold are made sufficiently more heavy than the corresponding weights of platinum so that the buoyancy of the weights in water is the same. All these weights being small, their relative accuracy may be rather limited, and thus in many cases it is not necessary to correct for the difference in buoyancy when the medium has a specific gravity different from 1.

For weights of stainless steel of specific gravity 7.85 and weight R the correction ΔR is calculated from the following formula, when the specific gravity of the medium is $\sigma_{20,20}$:

$$\Delta R = 0.1\ (1 - \sigma_{20,20})R \tag{13}$$

For weights of gold of specific gravity 19.3 and weight G the corresponding formula is

$$\Delta G = 0.005\ (1 - \sigma_{20,20})G \tag{14}$$

Big weights may be made of tantalum (density 16.6) instead of platinum as tantalum is very wear-resistant and almost as resistant against corrosion as gold and platinum.

To estimate loads smaller than the smallest weights applied, one may interpolate from the ascending and sinking velocities of the diver near the floating equilibrium. The velocity varies approximately directly with the load.

The medium which is to be examined is filled into a glass container which is placed in a water thermostat regulated at 20°C. Before the determinations, the diver with load must be freed from air bubbles by brushing it with a brush with soft hairs. To avoid a greater random error than $\pm 0.5 \times 10^{-5}$ the thermostat must regulate with a tolerance of $\pm$ 0.02°C.

In the examination of mixtures it is necessary to take precautions against alteration of the composition by evaporation of one of the components.

To save time it is advantageous to provide the diver with a loose stem, ordinarily of platinum wire, with a winding at one of its ends, so that it may be fixed around the glass stem of the diver. In computing the load which the stem represents, it must be taken into consideration that the buoyancy is acting only on that part of the stem which is situated under the surface of the fluid. Since the volume of that part of the stem which is above the surface of the fluid is ordinarily small, it is very often possible to estimate the weight of the corresponding volume of fluid with sufficient accuracy without knowing the accurate density of the fluid. When this weight is added to the weight of the stem, we get the weight of loads submerged in the fluid which corresponds to the actual weight of the stem, provided the stem and the loads are of the same material. The calculation of $\sigma_{20,20}$ may then be carried out as by the diver method.

Before the stem is placed on the diver, the latter must be loaded with such a weight that it will come into floating equilibrium when part of the stem is above the surface of the fluid. With some practice this may be estimated by observing how large a part of the glass stem is protruding from the surface of the fluid before the platinum stem is placed on the diver.

The surface tension of water being about 70 dyn/cm, the influence of the surface tension of a fluid of the same surface tension as water on a stem of diameter 0.5 mm may under certain conditions amount to

$$0.05\ \pi \cdot 70 = 11 \text{ dyn } (ca.\ 11 \text{ mg})$$

It is therefore necessary to determine the systematic error of the hydrometer method for every new fluid by comparative measurements with the apparatus according to the diver method and the hydrometer method.

EXPERIMENTAL

The diver method. To determine the specific gravity of the divers used and the random error of the diver method, the load was determined by floating equilibrium in water at 20 ± 0.02°C, ten times with a diver of density about 0.75 and ten times with a diver of density about 0.95.

From the average loads of the two divers their specific gravities are calculated from (4) and (5) and their C-values from (6).

To determine the random error of the diver method the specific gravity of the water examined has been calculated from (8) and (4) as well as the deviations λ of the single measurements from the average (1.000000). These deviations are numerically the same as the deviations from the average one would find when calculating from (8) and (4) as well as the specific gravity of the diver $\varrho_{20,20}$, the increase in specific gravity of the diver $a_{20,20}$ corresponding to the single measurement. From the λ-values it is therefore possible to calculate the random error $\mu_{d,m}$ of the specific gravity of the diver (taken as an average of ten measurements)

$$\mu_{d,m} = \sqrt{\frac{\sum_1^n \lambda^2}{n(n-1)}} \tag{15}$$

in which n is 10.

Further it is possible to calculate the random error μ of a single determination of the specific gravity of the water from the formula

$$\mu = \sqrt{\frac{\sum_1^n \lambda^2}{n\,(n-1)} + \frac{\sum_1^n \lambda^2}{n-1}} = \sqrt{\frac{(n+1)\sum_1^n \lambda^2}{n(n-1)}} \tag{16}$$

in which n = 10

The results of the experiments are given in Tables 1 and 2.

The hydrometer method. To determine the systematic as well as the random error of the hydrometer method the specific gravity of distilled water at 20 ± 0.02°C has been determined according to the hydrometer method with the two divers, the specific gravity of which were determined by ten floating experiments according to the diver method.

Three platinum stems with the diameters 0.5, 0.3 and 0.2 mm were used and ten experiments were carried out with each stem in combination with each diver. The total load on the diver was calculated as the weight in g of the load + the weight in g of the stem + the volume of the protruding stem in cm³. From the total load, the specific gravity of the water is calculated from (8) and (4) disregarding the systematic error of the hydrometer method.

The quantity K defined by the equation

$$K = 1 - \varrho_{20,20} - a_{20,20} \tag{17}$$

Table 1. Diver method, diver No. 8, weight of diver *in vacuo* 14.4679 g.

Load	$\varrho_{20,20}$ of diver	$\varrho_{20,20}$ of water	$\lambda \times 10^6$
5.07045	0.749528	1.000006	+ 6
5.07036	0.749533	1.000001	+ 1
5.07064	0.749519	1.000015	+15
5.07045	0.749528	1.000006	+ 6
5.07033	0.749534	1.000000	0
5.07010	0.749546	0.999988	−12
5.07039	0.749531	1.000003	+ 3
5.07007	0.749547	0.999987	−13
5.07025	0.749538	0.999996	− 4
5.07029	0.749540	0.999998	− 2
5.070333	0.749534	1.000000	

$a_{20,20} = 0.250466$, $\varrho_{20,20} = 0.749534$
$C = 19.9994$
$\mu_{d,m} = 2.7 \times 10^{-6}$
$\mu = 9 \times 10^{-6}$

Table 2. Diver method, diver No. 37, weight of diver *in vacuo* 18.1646 g.

Load	$\varrho_{20,20}$ of diver	$\varrho_{20,20}$ of water	$\lambda \times 10^6$
0.99937	0.950155	1.000001	+ 1
0.99933	0.950157	0.999999	− 1
0.99919	0.950164	0.999992	− 8
0.99945	0.950151	1.000005	+ 5
0.99933	0.950157	0.999999	− 1
0.99942	0.950153	1.000003	+ 3
0.99929	0.950159	0.999997	− 3
0.99937	0.950155	1.000001	+ 1
0.99931	0.950158	0.999998	− 2
0.99948	0.950150	1.000006	+ 6
0.999354	0.950156	1.000000	

$a_{20,20} = 0.049844$; $\varrho_{20,20} = 0.950156$
$C = 20.0010$
$\mu_{d,m} = 1.3 \times 10^{-6}$
$\mu = 4.3 \times 10^{-6}$

is then tabulated and the average K_m of the K-values is calculated.

A corrected value $\varrho_{f,20,20}$ of the specific gravity of the water is determined from the equation

$$\varrho_{f,20,20} = \varrho_{m,20,20} + K_m + a_{20,20} \quad (18)$$

Here $\varrho_{m,20,20}$ is the specific gravity of the diver determined by the diver method as an average of 10 determinations.

The differences λ between the corrected specific gravities of the water and 1.000000 are tabulated.

These differences are numerically the same as the differences one would get by subtracting K_m from the individual K-values and by subtracting the average of the $a_{20,20}$-values from the individual $a_{20,20}$-values.

The random error μ_{K_m} of the quantity K_m, which is approximately the systematic error of the hydrometer method, may therefore be calculated from the formula

Table 3. Hydrometer method, diver No. 8, diameter of stem 0.5 mm, $\varrho_{20,20} = 0.749534$, $C = 19.9994$; weight of stem 0.500 g.

Load g	Protruding cm³ × 10⁴	Total g	$\varrho_{20,20}$ with syst.error	$K \times 10^5$	$\varrho_{20,20}$ corrected for syst.error	$\lambda \times 10^5$
4.564	32	5.0672	0.99985	15	0.99997	−3
4.563	30	5.0660	0.99979	21	0.99991	−9
4.563	66	5.0696	0.99997	3	1.00009	+9
4.564	30	5.0670	0.99984	16	0.99996	−4
4.563	60	5.0690	0.99994	6	1.00006	+6
4.562	64	5.0684	0.99991	9	1.00003	+3
4.564	32	5.0672	0.99985	15	0.99997	−3
4.565	44	5.0694	0.99996	4	1.00008	+8
4.563	34	5.0664	0.99981	19	0.99993	−7
4.563	46	5.0676	0.99987	13	0.99999	−1
		50.6778		121		
$\mu_{Km} = 20 \times 10^{-6}$		5.06778	0.999876	12		
$\mu_{\varrho f,20,20} = 66 \times 10^{-6}$						

Table 4. Hydrometer method, diver No. 8, diameter of stem 0.3 mm, $\varrho_{20,20} = 0.749532$, $C = 19.9994$; weight of stem 0.200 g.

Load	Protruding cm³ × 10⁴	Total	$\varrho_{20,20}$ with syst.error	$K \times 10^5$	$\varrho_{20,20}$ corrected for syst.error	$\lambda \times 10^5$
4.864	49	5.0689	0.99993	7	1.00004	+4
4.864	37	5.0677	0.99987	13	0.99998	−2
4.864	31	5.0671	0.99984	16	0.99995	−5
4.865	35	5.0685	0.99991	9	1.00002	+2
4.864	32	5.0672	0.99985	15	0.99996	−4
4.864	50	5.0690	0.99994	6	1.00005	+5
4.865	29	5.0679	0.99988	12	0.99999	−1
4.865	31	5.0681	0.99989	11	1.00000	0
4.865	38	5.0688	0.99993	7	1.00004	+4
4.864	34	5.0674	0.99986	14	0.99997	−3
		50.6806		110		
$\mu_{K,m} = 12 \times 10^{-6}$		5.06806	0.999889	11		
$\mu_{\varrho f,20,20} = 38 \times 10^{-6}$						

Table 5. Hydrometer method, diver No. 8, diameter of stem 0.2 mm, $\varrho_{20,20} = 0.749534$, $C = 19.9994$; weight of stem 0.100 g.

Load g	Protruding cm³ × 10⁴	Total g	$\varrho_{20,20}$ with syst.error	$K \times 10^5$	$\varrho_{20,20}$ corrected for syst.error	$\lambda \times 10^5$
4.965	29	5.0679	0.99988	12	0.99998	−2
4.967	10	5.0680	0.99989	11	0.99999	−1
4.966	23	5.0683	0.99990	10	1.00000	0
4.965	23	5.0673	0.99985	15	0.99995	−5
4.966	23	5.0683	0.99990	10	1.00000	0
4.967	15	5.0685	0.99991	9	1.00001	+1
4.968	14	5.0694	0.99996	4	1.00006	+6
4.966	17	5.0677	0.99987	13	0.99997	−3
4.967	16	5.0686	0.99992	8	1.00002	+2
4.966	19	5.0679	0.99988	12	0.99998	−2
		50.6819		104		
$\mu_{K,m} = 10 \times 10^{-6}$		5.06819	0.999896	10		
$\mu_{\varrho f,20,20} = 33 \times 10^{-6}$						

Table 6. Hydrometer method, diver No. 37, diameter of stem 0.5 mm, $\varrho_{20,20} = 0.950156$, $C = 20.0010$; weight of stem 0.500 g.

Load g	Protruding $cm^3 \times 10^4$	Total g	$\varrho_{20,20}$ with syst.error	$K \times 10^5$	$\varrho_{20,20}$ corrected for syst.error	$\lambda \times 10^5$
0.494	40	0.9980	0.99993	7	1.00003	+3
0.495	20	0.9970	0.99988	12	0.99998	−2
0.494	52	0.9992	0.99999	1	1.00009	+9
0.495	26	0.9976	0.99991	9	1.00001	+1
0.496	8	0.9968	0.99987	13	0.99997	−3
0.494	38	0.9978	0.99992	8	1.00002	+2
0.493	62	0.9992	0.99999	1	1.00009	+9
0.495	16	0.9966	0.99986	14	0.99996	−4
0.494	12	0.9952	0.99979	21	0.99989	−11
0.494	32	0.9972	0.99989	11	0.99999	−1
		9.9746		97		
$\mu_{K\mathrm{m}} = 19 \times 10^{-6}$		0.99746	0.999906	10		
$\mu_{\varrho_{f,20,20}} = 63 \times 10^{-6}$						

Table 7. Hydrometer method, diver No. 37, diameter of stem 0.3 mm, $\varrho_{20,20} = 0.950156$, $C = 20.0010$; weight of stem 0.200 g.

Load g	Protruding $cm^3 \times 10^4$	Total g	$\varrho_{20,20}$ with syst.error	$K \times 10^5$	$\varrho_{20,20}$ corrected for syst.error	$\lambda \times 10^5$
0.796	22	0.9982	0.99994	6	1.00002	+2
0.797	9	0.9979	0.99993	7	1.00001	+1
0.798	3	0.9983	0.99995	5	1.00003	+3
0.796	16	0.9976	0.99991	9	0.99999	−1
0.795	19	0.9969	0.99988	12	0.99996	−4
0.796	17	0.9977	0.99992	8	1.00000	0
0.797	11	0.9981	0.99994	6	1.00002	+2
0.796	19	0.9979	0.99993	7	1.00001	+1
0.795	22	0.9972	0.99989	11	0.99997	−3
0.796	13	0.9973	0.99990	10	0.99998	−2
		9.9771		81		
$\mu_{K,\mathrm{m}} = 7.5 \times 10^{-6}$		0.99771	0.999919	8		
$\mu_{\varrho_{f,20,20}} = 25 \times 10^{-6}$						

Table 8. Hydrometer method, diver No. 37, diameter of stem: 0.2 mm, $\varrho_{20,20} = 0.950156$, $C = 20.0010$; weight of stem 0.100 g.

Load g	Protruding $cm^3 \times 10^4$	Total g	$\varrho_{20,20}$ with syst.error	$K \times 10^5$	$\varrho_{20,20}$ corrected for syst.error	$\lambda \times 10^5$
0.895	17	0.9967	0.99987	13	0.99998	−2
0.897	4	0.9974	0.99990	10	1.00001	+1
0.896	14	0.9974	0.99990	10	1.00001	+1
0.895	16	0.9966	0.99986	14	0.99997	−3
0.897	7	0.9977	0.99992	8	1.00003	+3
0.896	14	0.9974	0.99990	10	1.00001	+1
0.896	8	0.9968	0.99987	13	0.99998	−2
0.896	12	0.9972	0.99989	11	1.00000	0
0.897	12	0.9982	0.99994	6	1.00005	+5
0.895	17	0.9967	0.99987	13	0.99998	−2
		9.9721		108		
$\mu_{K,\mathrm{m}} = 8.1 \times 10^{-6}$		0.99721	0.999894	11		
$\mu_{\varrho_{f,20,20}} = 27 \times 10^{-6}$						

$$\mu_{K_m} = \sqrt{\mu_{dm}^2 + \frac{\sum_1^n \lambda^2}{n(n-1)}} \tag{19}$$

where n = 10 (and μ_{dm} is the random error of the determination of the specific gravity of the diver by 10 experiments).

Further the random error of a single determination $\mu_{f,20,20}$ of the specific gravity $\varrho_{f,20,20}$ of water determined by the hydrometer method may be expressed by the equation

$$\mu_{\varrho f,20,20} = \sqrt{\mu_{dm}^2 + \mu_{Km}^2 + \frac{\sum_1^n \lambda^2}{n-1}} = \sqrt{2\mu_{dm}^2 + \frac{(n+1)\sum_1^n \lambda^2}{n(n-1)}} \tag{20}$$

where n = 10.

The results of the experiments are given in Tables 3 – 8.

The author gratefully acknowledges financial support from the *Foundation for Applied Chemistry of the Technical University of Denmark.*

REFERENCES

1. Marsigli, J. *Histoire physique de la mer*, Amsterdam 1725.
2. Pisati, G. and Reggiani N. *Rend. accad. naz. Lincei* **6** (1890) 99.
3. Nansen, F. *The Norwegian North Polar Expedition, Scientific Results*, Christiania and London 1902, Vol. III, p. 78.
4. Thoulet, J. *Bull. Inst. Océanograph.* (1910) No. 181.
5. Warrington, A. W. *Phil. Mag.* **48** (1899) 498.
6. Richards, T. W. and Shipley, J. W. *J. Am. Chem. Soc.* **34** (1912) 599.
7. Richards, T. W. and Shipley, J. W. *J. Am. Chem. Soc.* **36** (1914) 1.
8. Richards, T. W. and Harris, G. W. *J. Am. Chem. Soc.* **38** (1916) 1000.
9. Lamb, A. B. and Lee, R. E. *J. Am. Chem. Soc.* **35** (1913) 1666.
10. Emeleus, H. J., James, F. W., King, A., Pearson, T. G., Purcell, R. H. and Briscoe, H. V. A. *J. Chem. Soc.* **1934** 1207.
11. Anderson, J. S., Purcell, R. H., Pearson, T. G., King, A., James, F. W., Emeleus, H. J. and Briscoe, H. V. A. *J. Chem. Soc.* **1937** 1492.
12. Berg, S. *Studies on Particle-Size Distribution* (Diss.) The Technical University of Denmark. G. E. C. Gad, Copenhagen 1940.
13. Berg, S. *Untersuchungen über Korngrössenverteilung* (Diss.) *Kolloid-Beih.* **53** (1941) 149.
14. Berg, S. *Ber. deut. keram. Ges.* **23** (1942) 271.
15. Berg, S. *Transact. Intern. Ceram. Congr.*, Maestricht 1948.
16. Berg, S. *Atti IV Congr. Intern. Ceram.*, Firenze 1954.
17. Berg, S. *Ber. deut. keram. Ges.* **33** (1956) 229.

Received February 2°, 1958.

ACTA CHEMICA SCANDINAVICA 12 (1958) 995—998

Syntheses of Pyridine-2-^{13}C and Pyridine-3-^{13}C

BØRGE BAK

Københavns Universitets kemiske Laboratorium, Copenhagen, Denmark and

NIELS CLAUSON-KAAS

Centrallaboratoriet, Sadolin & Holmblad A/S, Copenhagen, Denmark

For the exact determination of interatomic distances in pyridine pyridine-2-^{13}C and pyridine-3-^{13}C have been prepared.

For the exact determination of interatomic distances in pyridine mixtures of isotopic pyridines containing pyridine-2-^{13}C and pyridine-3-^{13}C have been prepared by the series of reactions shown in Fig. 1. Potassium cyanide containing about 20 % of potassium cyanide-^{13}C was used as starting material. It is evident from the syntheses that the mixture containing pyridine and pyridine-2-^{13}C also must contain a minor amount af pyridine-2,6-$^{13}C_2$.

The constitution and the purity of the two pyridines follows from the syntheses, the infrared and microwave spectra and measurements of their vapor pressure. A report on the infrared spectra of all ^{13}C-compounds prepared here and on the microwave spectra of the pyridines will be published later.

EXPERIMENTAL

Diethyl malonate-1-^{13}C. Potassium cyanide [35.0 g (0.538 mole) of a product containing 21.6 % of potassium cyanide-^{13}C] and chloroacetic acid (44.0 g, 0.465 mole) were transformed into 52.5 g (0.328 mole, 61 %) of diethyl malonate after the directions of Vogel [1].

1,3-Dibromopropane-1-^{13}C, cf. Ref.[2] Diethyl malonate-1-^{13}C (52.5 g, 0.328 mole) in ether (500 ml) was added to a stirred mixture of lithium aluminium hydride (21.8 g, 0.575 mole) and ether (700 ml) during 20 min. The reaction mixture was heated under reflux (1 h). Acetic anhydride (700 ml) was added and about 1 100 ml of solvent distilled. Acetic anhydride (150 ml) and acetic acid (50 ml) were added to the residue and the mixture kept in an oil-bath of 125° (4 h). After cooling, ether (1 250 ml) was added and the precipitate of salts removed by filtration (G 3) and washed with ether (200 ml). The

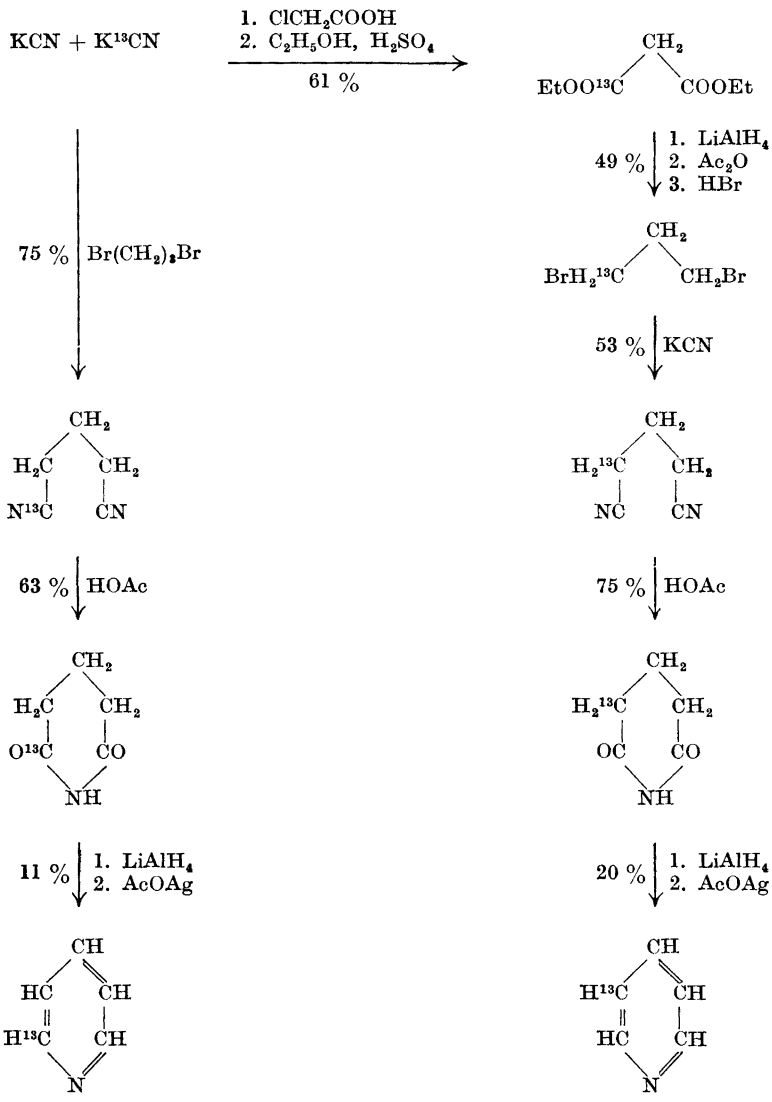

Fig. 1. Routes to pyridine-2-^{13}C and pyridine-3-^{13}C.

solvent was distilled through a small packed column. Ether (100 ml) was added to the semisolid residue and another crop of salts removed by filtration and washed with ether (50 ml). The solution was distilled through the above column, first under atmospheric pressure, then under 15 mm. The fraction boiling at 86—108° (35.0 g) and consisting mainly of 1,3-propanediol diacetate was collected and heated under reflux (7 h) with hydrobromic acid (48 %, 300 ml). About 100 ml of liquid containing dibromopropane was distilled. The dibromopropane layer was separated and washed with the same volume of

water, concentrated hydrochloric acid, water, potassium hydrogen carbonate (20 %) and water. Ether was added and the etheral solution dried with magnesium sulfate and distilled. The yield was 32.3 g (0.160 mole, 49 %) of dibromopropane (b.p.$_{760}$ 164—170°).

Glutaronitrile-2-^{13}C. 1,3-Dibromopropane-1-^{13}C (32.3 g, 0.160 mole) and potassium cyanide (25.0 g, 0.384 mole) were transformed into 8.00 g (0.0849 mole, 53 %) of glutaronitrile following the directions of Vogel [3]. The reaction mixture was heated under reflux for 48 h instead of the recommended 35 h and chloroform was used instead of ethyl acetate for extraction of the inorganic salts. An infrared spectrum of the final product showed it to contain certain impurities, but not less than 95 % of glutaronitrile.

Glutarimide-3-^{13}C cf. Ref.[4] Glutaronitrile-2-^{13}C (8.00 g, 0.0849 mole) was dissolved in glacial acetic acid (65 ml) and the solution heated in a sealed tube (210°, 15 h). The solvent was distilled under 15 mm from a water-bath (85°) and the semisolid residue crystallized from ethanol (30 ml). The crystals were washed with ethanol (10 ml) and dried. The yield was 7.19 g (0.0636 mole, 75 %) of glutarimide.

Pyridine-3-^{13}C. Glutarimide-2-^{13}C (7.19 g, 0.0635 mole) was suspended in dry ether (300 ml). Lithium aluminium hydride (8.4 g, 0.22 mole) was added in one portion and the mixture heated with stirring under reflux (8 h). Water (25 ml), followed by a solution of sodium hydroxide (50 g) in water (275 ml), was added dropwise with stirring. The mixture was distilled, first from a water-bath and then by heating with a free flame until the residue solidified. Water (100 ml) was added to the residue and distilled. Acetic acid (30 ml) was added to the combined distillates consisting of ether, water and piperidine. The mixture was distilled from a water-bath (80°), finally under 15 mm. 6.5 g of an oil consisting mainly of piperidine acetate remained.

The oil was dissolved in water (130 ml) and the solution stirred to a paste with silver acetate (130 g), *cf.* Ref.[5] The paste was heated in a glass-lined autoclave under 100 atmospheres of nitrogen (210°, 18 h). The reaction mixture was washed into a 250 ml flask with water (15 ml). A solution of sodium hydroxide (66 g) in water (60 ml) was added together with a large portion of boiling chips, and the mixture distilled by heating with a free flame. After 100 ml of distillate had been collected, water (40 ml) was added to the distillate and another 40 ml distilled. Concentrated hydrochloric acid (14 ml) was added to the combined distillates and the solution evaporated under 20 mm to dryness from a water-bath (70°). The residue was kept in the bath for 3 min under 0.5 mm. The remaining crystals containing pyridine hydrochloride were dissolved in water (20 ml) and a warm solution of mercury chloride (20 g) in water (100 ml) added, *cf.* Ref.[6] The mixture was left standing (1 h) at 0° and the crystals removed by filtration and dried under 0.1 mm. The dry crystals were cooled in liquid air and sodium hydroxide powder (12 g) added rapidly. The solids were mixed thoroughly by shaking with cooling. The mixture was heated slowly under 0.1 mm in an oil-bath to 220°. At 180—200° pyridine and water was evolved rather suddenly and condensed in a receiver containing pulverized sodium hydroxide (2.0 g). The reaction was complete after 20—30 min. The distillate of aqueous pyridine was dried by successive distillations from sodium hydroxide as described previously [7]. The yield was 1.02 g (0.0129 mole, 20 %). The infrared and microwave spectra and the vapor pressure showed the product to be a mixture of pyridine and pyridine-3-^{13}C.

Glutaronitrile-1-^{13}C. 1,3-Dibromopropane (15.5 g, 0.0772 mole) and potassium cyanide [10.0 g (0.154 mole) of a product containing 21.6 % of potassium cyanide-^{13}C] were transformed into 5.45 g (0.0579 mole, 75 %) of glutaronitrile as described above.

Glutarimide-2-^{13}C. Glutaronitrile-1-^{13}C (5.41 g, 0.0574 mole) was transformed into 3.88 g (0.0343 mole, 63 %) of glutarimide as described above.

Pyridine-2-^{13}C. Glutarimide-2-^{13}C (3.88 g, 0.0343 mole) was transformed into 0.30 g (0.038 mole, 11 %) of pyridine as described above. The infrared and microwave spectra and the vapor pressure showed the product to be a pyridine-mixture containing pyridine and pyridine-2-^{13}C. Pyridine-2,6-$^{13}C_2$, which also must be present in the mixture, was not identified.

REFERENCES

1. Vogel, A. J. *Practical Organic Chemistry*, Longmans, Green and Co., London 1956, 3rd. Ed., p. 484.
2. Elming, N. and Clauson-Kaas, N. *Acta Chem. Scand.* **9** (1955) 23.
3. Vogel, A. J. Ref.[1], p. 409.
4. Seldner, R. *Am. Chem. J.* **17** (1895) 532.
5. Tafel, J. *Ber.* **25** (1893) 1619.
6. Ladenburg, A. *Ann.* **247** (1888) 1.
7. Bak, B. *J. Chem. Phys.* **22** (1954) 2013.

Received February 21, 1958.

ACTA CHEMICA SCANDINAVICA 12 (1958) 999—1004

A Note on Oscillating Reactions

THOR A. BAK

Universitetets Fysisk-Kemiske Institut, Copenhagen, Denmark

The equations originally set up by Volterra to describe the interaction between two biological species are interpreted as a set of chemical reactions and discussed from a thermodynamic point of view. The equations are solved by the methods of Kryloff and Bogoliuboff, and it is shown that the frequency is lower the farther the system is from the stationary state, decreasing proportional to the square of the average distance from the stationary state.

1. In recent years the possible existence of oscillating chemical reactions and their use in explaining certain biological phenomena have attracted considerable attention [1–5]. Burton [1] discussed it from a biological point of view in connection with "overshoot phenomena", and Christiansen [2] has recently suggested it as an explanation of "spike potentials". Moore [3] has studied a specific model closely related to the one we shall discuss here, where the periodicity is caused by autocatalytic steps. Hearon [4] has considered the possibility of oscillations for several simple reaction mechanisms and concludes that, under certain general conditions, periodicities are not possible for them. Finally Bierman [5] has discussed more complicated mechanisms and shown how autocatalytic steps or reactions at the wall (where the absorption is assumed to be governed by a Langmuir isotherm) can lead to oscillatory behaviour. This paper also contains a discussion of the biological implications of these mechanisms. It must be remarked that in no cases have the differential equations set up by Bierman actually been solved.

By far the simplest example of an oscillating system, however, is that proposed by Volterra [6,7] as a model of interacting biological species. A similar model was discussed by Lotka [8] who gave an interpretation in terms of chemical reactions. Prigogine and Balescu [9] have used the Volterra equations, similarly interpreted, as an example in a discussion of the thermodynamics of irreversible processes.

Although these interpretations in principle are correct, it is exceedingly doubtful whether the Volterra equations represent a set of chemical reactions which actually occur in nature. Even as a model for the study of population dynamics [10] it probably is too simplified. On the other hand it is as realistic

as any other model proposed so far, and therefore, because of its simplicity, the one that should be studied first. The interpretation in terms of chemical reactions is convenient, because it easily leads to an expression for the entropy-production.

It is the purpose of this note to show how the Volterra equations can be solved using the methods of Kryloff and Bogoliuboff. We start by giving the equations and deriving expressions for the relevant thermodynamic quantities.

2. It was assumed by Volterra that the interaction between two biological species, 1 and 2, of which 2 feeds on 1, can be described by the equations

$$\dot{A}_1 = w_1 A_1 - w_2 A_1 A_2$$

$$\dot{A}_2 = w_3 A_1 A_2 - w_4 A_2$$

n which A_1 and A_2 are concentrations and w_i (i = 1, 2, 3, 4) are constants. Below we give and interpretation of these equations in four partial reactions. J_i (i = 1, 2, 3, 4) are the corresponding flows and X_i (i = 1, 2, 3, 4) are the thermodynamic forces defined so that $\sigma = \Sigma X_i J_i$ is the entropy production in units of the gas-constant R per second.

Reaction	Flow	Force
$A_1 \rightarrow 2A_1$	$J_1 = k_1 A_1$	$X_1 = \ln \frac{k_1}{k_{-1} A_1}$
$A_1 + A_2 \rightarrow A_2$	$J_2 = k_2 A_1 A_2$	$X_2 = \ln \frac{k_2 A_1}{k_{-2}}$
$A_1 + A_2 \rightarrow 2A_2$	$J_3 = k_3 A_1 A_2$	$X_3 = \ln \frac{k_3 A_1}{k_{-3} A_2}$
$A_2 \rightarrow M$	$J_4 = k_4 A_2$	$X_4 = \ln \frac{k_4 A_2}{k_{-4}}$

(M is an inert substance)

The four reactions correspond biologically to growth of species 1, species 2 feeding on 1, species 2 propagating the faster the more food there is, species 2 dying.

If the four reactions are considered as chemical reactions it is evident that they do not conserve matter, *i.e.*, other substances, whose concentrations are kept constant, must be involved.

We see that with $k_1 = w_1$, $k_2 + k_3 = w_2$, $k_3 = w_3$, and $k_4 = w_4$ we have $\dot{A}_1 = J_1 - J_2 - J_3$ and $\dot{A}_2 = J_3 - J_4$. We must now eliminate k_{-1}, k_{-2}, k_{-3}, k_{-4} from the expressions for the forces. To do so we observe that the original equations have a stable stationary point $(A_1^s, A_2^s) = (w_4/w_3, w_1/w_2)$. It is known form the investigations of Volterra [6] that the representative point in the A_1, A_2-plane moves in closed curves counter-clockwise around this stationary point. This suggests introducing relative forces $\Delta X_i = X_i - X_i^s$ in which X_i^s is the force at the stationary point.

We find:

$$\Delta X_1 + \Delta X_3 + \Delta X_4 = 0 = \Delta X_1 + \Delta X_2$$

so that

$$\sigma - \sigma^s = \Sigma \Delta X_i J_i = (J_1 - J_2 - J_3)\ \Delta X_1 + (J_3 - J_4)\ (\Delta X_1 + \Delta X_3) = \Sigma j_i x_i$$

with

$$x_1 = \Delta X_1 = \ln \frac{w_4}{w_4 + w_3 a_1} \sim - \frac{w_3}{w_4} a_1$$

$$x_2 = \Delta X_1 + \Delta X_3 = \ln \frac{w_1}{w_1 + w_2 a_2} \sim - \frac{w_2}{w_1} a_2$$

In these equations j_i is the time derivative of A_i (or a_i) and $a_i = A_i - A_i^s$. The approximate values given are valid for $a_i \sim 0$. In terms of the a_i's the original equations read

$$\dot{a}_1 = - \frac{w_2 w_4}{w_3} a_2 - w_2 a_1 a_2$$

$$\dot{a}_2 = \frac{w_1 w_3}{w_2} a_1 + w_3 a_1 a_2$$

and we see that when $a_1 a_2$ can be neglected compared with a_1 or a_2, *i.e.*, when we linearize the equations, the representative point describes an ellipse around the stationary point (0,0) in the a_1, a_2-plane.

We see that near the stationary point $\dot{a}$ and a as well as x and j are connected by matrices with constant coefficients and no diagonal elements. They are, however, not simply antisymmetric matrices as in the simpler case discussed by Prigogine and Balescu [9]. To ensure oscillations the 2×2 matrix must have purely imaginary eigenvalues. The conditions for this is that the determinant is positive and the trace vanishes. These conditions are satisfied.

The system so far described has no tendency to approach the stationary state, and this state is therefore, thermodynamically speaking, not a stable state. If $w_1 A_1$ is replaced by a constant as suggested by Lotka [8] or if terms containing A_1^2 and A_2^2 are included in the equations [6], the representative point in the A_1, A_2-plane will spiral in towards the stationary state. This is seen by linearizing the equations. Arbitrarily close to the stationary state there will, however, exist states with $\sigma - \sigma^s < 0$ and therefore the approach to the statinary state does not minimize σ. Nor does it seems possible to construct a physically meaningful function which is minimized. We have, therefore, here a thermodynamically stable state which seemingly is not governed by a minimum principle related to the principle of minimum entropy production.

Finally we should mention the differential form

$$\Sigma j_i dx_i = w_2 a_2 \mathrm{d}a_1 - w_3 a_1 \mathrm{d}a_2$$

which has been shown by Glansdorff and Prigogine [12] to be always negative. Since the rotation is counter-clockwise this is immediately verified, and the theorem of Glansdorff and Prigogine can be said to fix the sense of rotation as pointed out by Prigogine and Balescu [9]. This differential form will not in general possess an integrating multiplier [13] although in this case, with only two independent variables, it does (*i.e.*, $(\alpha_1\alpha_2)^{-1}$).

3. If one tries to solve the non-linear equations of Volterra by usual iteration-methods starting from the solution of the linearized equation one immediately gets terms which diverge strongly as $t \to \infty$. We must therefore use an iterative procedure where, at each step, the occurrence of such terms is prevented. Such a method has been devised by Kryloff and Bogoliuboff [11], and we refer to their book for details.

It is convenient to introduce new variables y_1 and y_2 by $\alpha_1 = w_2\sqrt{w_4}y_1$ and $\alpha_2 = w_3a\sqrt{w_1}y_2$. We then have

$$\dot{y}_1 = -\nu y_2 - a y_1 y_2$$

$$\dot{y}_1 = \nu y_1 + b y_1 y_2$$

with $\nu = \sqrt{w_1 w_4}$; $a = w_2 w_3 \sqrt{w_1}$; $b = w_2 w_3 \sqrt{w_4}$ or:

$$\ddot{y}_1 + \nu^2 y_1 = b y_1 \dot{y}_1 - a\nu y_1^2 + \frac{a\dot{y}_1^2}{\nu + a y_1}$$

and an analogous equation for y_2.

In the first approximation the representative point in y_1y_2 space now moves on a circle around (0,0). We see that the right-hand side of the last equation contains terms which, when expanded in power series near (0,0), are smaller than the terms on the left-hand side by increasing orders of magnitude. Expanding the fraction on the right-hand side we rewrite the equation as:

$$\ddot{y}_1 + \nu^2 y_1 = \varepsilon(b y_1 \dot{y}_1 - a\nu y_1^2 + \frac{a}{\nu}\dot{y}_1^2) - \varepsilon^2(\frac{a}{\nu})^2 \dot{y}_1^2 y_1 + \ldots$$

$$= -\varepsilon f_1(y_1, \dot{y}_1) - \varepsilon^2 f_2(y_1, \dot{y}_1) - \ldots$$

where the factor ε indicates the smallness of the perturbation. This separation of the right-hand side into terms of increasing order of smallness appears to be necessary for the successful application of the Kryloff-Bogoliuboff method. In the final solution we shall of course put $\varepsilon = 1$.

We want to find a solution of the form $y_1 = z(\tau)$, with $\tau = \omega t + \varphi$, where $z(\tau)$ is a function with period 2π. Substitutiong we get

$$\omega^2 z'' + \nu^2 z = -\varepsilon f_1(z, \omega z') - \varepsilon^2 f_2(z, \omega z') - \ldots$$

and we now assume

$$z = z_0(\tau) + \varepsilon z_1(\tau) + \varepsilon^2 z_2(\tau) + \ldots$$

$$\omega = \omega_0 + \varepsilon\omega_1 + \varepsilon^2\omega_2 + \ldots$$

Using the above assumption and collecting powers of a we have the recursive system:

1. $\omega_0^2 z_0'' + \nu^2 z_0 = 0$

2. $\omega_0^2 z_1'' + \nu^2 z_1 = -f_1(z_0,\ \omega_0 z_0') - 2\omega_0\omega_1 z_0''$

3. $\omega_0^2 z_2'' + \nu^2 z_2 = -f_1'(z_0,\ \omega_0 z_0') - f_2(z_0,\ \omega_0 z_0') - (\omega_1^2 + 2\omega_0\omega_2) z_0'' - 2\omega_0\omega_1 z_1$

etc.

These linear differential equations are solved, and at each step in the iterative procedure we adjust ω so that secular terms do not develop, *i.e.*, we adjust ω so that the Fourier-expansion of the right-hand side does not contain terms with sin ωt or cos ωt. We obtain:

1. $y_1 = r\ \cos(\nu t + \varphi) \quad \nu = \sqrt{w_1 w_4}$
   $y_2 = r\ \sin(\nu t + \varphi)$

2. $y_1 = r\ \cos(\nu t + \varphi) + \frac{a}{3\nu} r^2 \cos 2(\nu t + \varphi) + \frac{b}{6\nu} r^2 \sin 2(\nu t + \varphi)$

   $y_2 = r \sin(\nu t + \varphi) - \frac{b}{3\nu} r^2 \cos 2(\nu t + \varphi) + \frac{a}{6\nu} r^2 \sin 2(\nu t + \varphi)$

   $\omega_1 = 0$, *i. e.*, the frequency is as in the first approximation

3. $\omega_2 = -\frac{r^2}{12}(a^2 + b^2)$, *i. e.*, the frequency is

   $\nu - \frac{r^2}{12}(a^2 + b^2) = \sqrt{w_1 w_4} - \frac{w_2^2 w_3^2 r^2}{12}(w_1 + w_4)$

It is hardly worth while to go on to higher approximations for y_1 and y_2, since the most important result certainly is the expression for the frequency. Experimentally the frequency will be easily accessible even for very fast reactions, and if the chemical reactions leading to the Volterra equations could be realized, it would be easy to check this expression, since at least one rate-constant can be changed at will simply by adding the substance which must serve as "food" for A_1 to conserve matter. It is of course intuitively clear that the frequency will decrease when r increases, since the path length increases towards infinity and at the same time the path approaches the other stationary point (which is unstable). Although the frequency goes down, the actual velocity of the system in its path in a_1, a_2 space increases — in the first approximation proportional to r.

The method we have applied here can be used on most second order non-linear differential equations leading to oscillations and should therefore make it possible to discuss more closely the models for oscillatory behaviour which are found in the literature.

The author is indebted to professor J. A. Christiansen for having drawn his attention to this problem as well as for numerous discussions.

REFERENCES

1. Burton, A. C. *Cellular Comp. Physiol.* **14** (1939) 327.
2. Christiansen, J. A. *Acta Chem. Scand.* **11** (1957) 1436.
3. Moore, M. J. *Trans. Faraday Soc.* **45** (1949) 1098.
4. Hearon, J. Z. *Bull. Math. Biophys.* **15** (1953) 121.
5. Bierman, A. *Bull. Math. Biophys.* **16** (1954) 203.
6. Volterra, V. *Théorie Mathematique de la lutte pour la vie*, Paris 1931.
7. Volterra, V. *Acta Biotheoretica* **3** (1937) 1.
8. Lotka, A. J. *J. Phys. Chem.* **14** (1910) 271.
9. Prigogine, I. and Balescu, R. *Bull. classe Sci. Acad. roy. Belg.* **42** (1956) 256.
10. Kerner, E. H. *Bull. Math. Biophys.* **19** (1957) 121.
11. Kryloff, N. and Bogoliuboff, N. *Introduction to Non-Linear Mechanics*, Princeton 1947.
12. Glansdorff, P. and Prigogine, I. *Physica* **20** (1954) 773.
13. Bak, T. A. *J. Phys. Chem.* **60** (1956) 1611.

Received January 29, 1958.

ACTA CHEMICA SCANDINAVICA 12 (1958) 1005—1014

Determination of Magnetic Susceptibilities between 81 and 295°K by Means of a Modified Sucksmith Balance

Studies in Magnetochemistry 24 *

H. SOLING

The Chemical Laboratory B, Technical University of Denmark, Copenhagen, Denmark

A detailed description is given of the construction and use of a Sucksmith ring balance, which is operated according to a compensation principle: The current exiting the electromagnet is regulated until the magnetic force exerted upon the sample exactly compensates the removal of a known weight from the elastic phosphor bronze ring, which constitutes the sensitive part of the balance. By introduction of the compensation principle errors due to changes in the elasticity of the ring have been eliminated. An electromagnetically operated weight manipulator, which may be charged with three ring-formed weights at a time, allows 13 different loads to be applied to the phosphor bronze ring. A set of six interchangeable ring weights cover the scale from less than 1 mg to about 80 mg. A cryostat arrangement is also described. The sample is surrounded by a double walled glass tube, which is immersed in liquid air. When the space between the walls of the glass tube has been suitably evacuated, the sample may be given any temperature between 81 and 295°K by heating the inner wall of the tube electrically. Examples of the reliability of the apparatus during actual measurements both at room temperature and at lower temperatures are given.

Several methods of measuring the magnetic gram susceptibility, χ_g, rest upon the relation

$$K = \chi_g \, m \, H \frac{\delta H}{\delta z} \tag{1}$$

where K is the force exerted upon a sample of mass m, which is suspended in an inhomogeneous magnetic field H with the gradient $\delta H/\delta z$ perpendicular to the magnetic lines of force. Accurate determinations of $\delta H/\delta z$ are rather difficult, measurements of the gram susceptibility are therefore often relative. That is, the magnetic force exerted upon the sample under investigation is

* No. 23 appeared in *Acta Chem. Scand.* **12** (1958) 939.

compared with that exerted upon some standard substance placed in the same position in the magnetic field. The measuring problem is thus essentially reduced to that of measuring the force K.

A very convenient apparatus for measurements of magnetic susceptibilities over a wide range of temperatures is the ring balance originally designed by Sucksmith [1,2] and later modified by Jackson [3], v. Oort [4], and others [5,6]. The essential features of the ring balance are as follows (*cf.* Fig. 1): An elastic ring made of phosphor bronze is clamped at the top, while a quarts capillary carrying the sample is attached to the diametrically opposite point. Two small mirrors facing each other are fixed to the ring. The light from a distant lamp passing a lens is reflected from the mirrors and focused on a vertical scale. When the magnetic field is switched on, the force acting on the sample deforms the ring and so causes a displacement of the light spot upon the scale, which may be calibrated in terms of the force acting on the sample.

When the balance is used in this manner, it needs rather frequent recalibration, probably due to small changes in the elasticity of the ring. This difficulty is circumvented if the ring balance, as mentioned by Cooke and Duffus [5], is used as a pure zero instrument. The current exiting the electromagnet is regulated until the effect of removing a known load from the ring is exactly compensated. By this means all the facilities connected with a compensation method are introduced. In order to obtain the necessary flexibility in the choice of loads to be compensated, a weight manipulator has been constructed. In the following sections the constructional details of the balance and its accessories together with a description of the operating procedure and the calibration are given.

THE APPARATUS

In Fig. 1 the main features of the apparatus are shown. The ring A, which is made from a strip of phosphor bronze 0.1 mm thick and 3 mm wide, is clamped at the top in vertical position. The diameter of the ring is 60 mm.

The perfectly straight quarts capillary B, which carries the sample C is attached to the lowest point of the ring by means of an aluminium clamp D. The external diameter of the capillary is 1 mm.

Two flat spiral springs pasted to the quarts capillary with a drop of shellac at E_1 and E_2 effectively prevent lateral movements of the sample. In a special experiment it was demonstrated that the spirals reduce the lateral movements of a strongly paramagnetic sample to less than 0.1 mm under the influence of the strongest field obtainable with the magnet. In the absence of the spirals the sample suddenly adhered to the pole pieces even when moderate fields were applied. The spirals are cut from a sheet of phosphor bronze of 0.05 mm's thickness.* They only diminish the sensitivity of the balance 1—2 %.

The quadratic mirrors F_1 and F_2 ** of 10 mm edge and 1 mm thickness are made from optically plane glass and coated on the front side with a reflecting layer of aluminium. They are pasted with shellac to small pieces of phosphor

* The author is thanks due to Mr. O. Gram Jeppesen for the design of the spirals.

** The mirrors were obtained from Messrs. I. G. Müller GmbH Wedel, Holsten, who guarantee a planarity of at least 600 m.

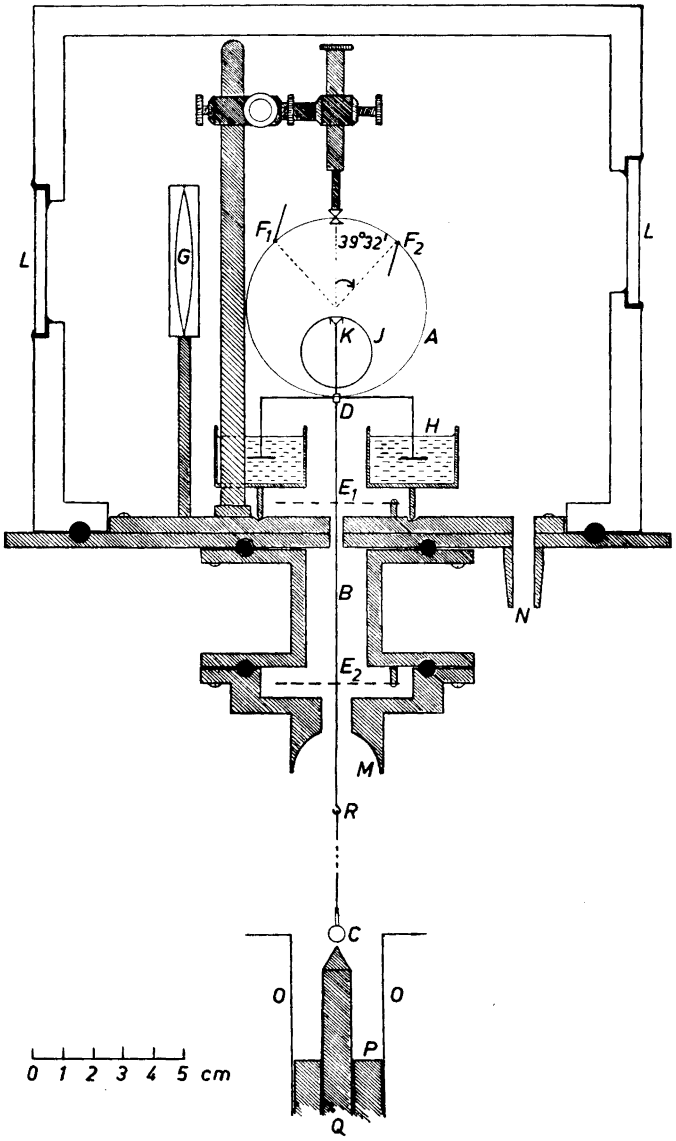

Fig. 1. General view of the apparatus.

bronze and bolted to the ring at the points, where the angular deflection is calculated to be a maximum [1,7].

A mated glass plate illuminated from behind serves as a source of light. A transparent glass plate with an engraved fine cross is pressed against the

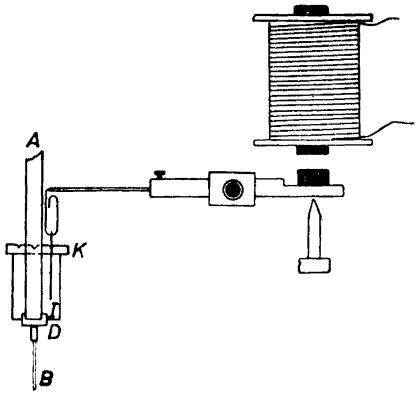

Fig. 2. Side view of a single unit of the weight manipulator.

mated plate. When the light has passed the lens G and has been reflected from the mirrors, the sharp shadow of the cross is easily observed by a low power microscope. The microscope is provided with a cross hair in the ocular. For a given load on the ring the exact position of the reflected light beam is indicated by setting the microscope so that the centers of the shadow cross and the ocular cross coincide. This zero-position is very stable and reproducible. The ring may be loaded and unloaded several times before slight readjustment is necessary.

The elastic ring is extremely sensitive to vibrations, which completely blur out the shadow cross and render the setting of the zero-position impossible. The balance is therefore placed on a large cement block in the basement of the laboratory building, and supported adequately by thickwalled rubber tubes. However, occasional heavy traffic in the building still causes severe blurring. An aluminium damping vane H immersed in Apiezon oil reduces these disturbances to a tolerable level.

The balance is loaded by placing ring formed weights J on the beam K (*cf.* also Fig. 2). Six carefully calibrated ring weights ranging from 4 to 40 mg have been prepared from platinum wires.

The loading an unloading of the balance is performed by means of a weight manipulator, which can be operated electromagnetically from the observers table. For the sake of simplicity the weight manipulator, which can be charged with three ring loads at a time, is not shown on Fig. 1. A single of the three identical units of the manipulator is shown, slightly schematically on Fig. 2. The capital letters on the latter figure have the same meaning as those on the former.

From the six platinum weights available 20 sets of three weights can be selected. Each set may be combined to 13 different loads, *viz.* 7 sums and 6 differences. The differences may be utilized in the following way: A given load is placed on the rider beam and the zero-position is adjusted. The load is then exchanged with another ligther one. The magnetic force necessary to reestablish the zero-position is equal to the difference between the two loads. The 260 possible combinations give 116 different loads, which cover a scale from less than 1 mg to about 80 mg.

The balance is enclosed in a cubic box of plexiglas provided with plane glass windows L. During the measurements the sample is surrounded by a glass tube (not shown) connected to the balance compartment by a spherically ground joint M. The temperature is measured by a calibrated copper-constantan thermocouple placed immediately below the sample. When measurements at lower temperatures are performed, the glass tube is replaced by the cryostat tube described below. The balance compartment may be evacuated through N and refilled with a suitable gas.

The electromagnet is mounted on a turning table provided with three levelling screws by means of which the magnet can be moved vertically. Plane cylindrical pole pieces O of 10 cm diameter ensure a sufficiently large volume, where $H\delta H/\delta z$ may be considered constant. The width of the pole gap is always kept at exactly the same value, 27 mm, by a brass block P inserted between the pole pieces. With an exiting current of about 10 A, a maximum value of $H\delta H/\delta z$ of about 1.2×10^7 Gauss^2/cm is obtained. The electric current is taken from the 220 volts main lines and regulated by a system of rheostats. The current is read on a Siemens & Halske precision ammeter.

OPERATING PROCEDURE

Only finely powdered substances are measured. The powder is packed in the spherical part of the pyrex phial shown in Fig. 3 a. After thoroughly cleansing of the capillary the phial is evacuated and the bulb is sealed off and pasted to a quarts capillary by a minimum of wax (Fig. 3 b and c.). The quarts capillary is then in turn cemented rigidly to the balance system at R (Fig. 1.). The bulbs usually contain 100—200 mg of powder.

It is very essential that all samples are placed accurately in the rather narrow region of the magnetic field where $H\delta H/\delta z$ has a rather flat maximum. That is, where the current necessary to compensate the removal of a given load is a minimum. This position must be found by trial for each particular sample under investigation. During this procedure the vertical position of the sample is controlled by the brass rod Q, which defines the vertical axis of the magnetic field. A brass cylinder (not shown) with a drill, which fits to Q controls the horizontal position of the sample by means of a horizontally

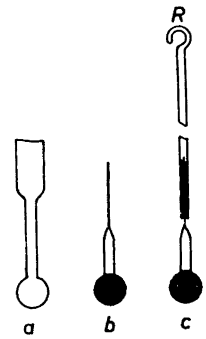

Fig. 3. Preparation of the sample.

a) The empty phial.
b) The filled, evacuated and sealed-off bulb.
c) The bulb pasted to the quarts capillary.

moving fine screw. The presence of this device in the pole gap has no detectable influence upon the field characteristics. Five independent settings of the same sample gave the following compensation currents in amperes: 8.36, 8.37, 8.36, 8.38, 8.37. It has been verified that the position of the maximum of $H\delta H/\delta z$ is independent of the field strength.

The final measurements are carried out in the following manner. A suitable weight is placed on the rider beam, and the zero-position is adjusted. After removal of the weight the magnetic field is switched on and three readings of the compensation current are taken. The zero-position is checked at once. Changes are rarely observed. The mean value of the three readings is taken as the result of a single measurement. This procedure is repeated twice and the mean value of the three mean values constitutes the final result of the measurements at that particular field strength. The spread of the ammeter readings is illustrated by two typical examples from the measuring book.

$Fe(NH_4)_2(SO_4)_2 \cdot 6H_2O$	No. VI
Mass of substance	134.6 mg
Force in dynes	39.20
Compensation current, A:	
Direct readings:	Mean:
8.13 −14 −13	8.13
8.14 −14 −13	8.14
8.16 −14 −14	8.15
Mean of mean:	8.15

8.15 A ~ 8.993 × 10^6 Gauss²/cm

$$\chi g \times 10^6 = \frac{39.20}{8.993 \times 0.1346} = 32.38$$

Temperature 20.0°C

$Ni(NH_4)_2(SO_4)_2 \cdot 6H_2O$	No. II
Mass of substance	209.3 mg
Force in dynes	23.20
Compensation current, A:	
Direct readings:	Mean:
9.01 −02 8.99	9.01
8.98 −97 −98	8.98
8.99 9.00 −01	9.00
Mean of mean:	9.00

9.00 A ~ 10.54 × 10^6 Gauss²/cm

$$\chi g \times 10^6 = \frac{23.20}{10.54 \times 0.2093} = 10.52$$

Temperature 19.0°C

METHOD OF CALIBRATION

By a series of measurements on samples of $Fe(NH_4)_2(SO_4)_2 \cdot 6H_2O$, Mohr's salt, the relation between the compensation current and $H\delta H/\delta z$ was established. Three different samples from a preparation of Mohr's salt, which has served as a magnetic standard in this laboratory for several years, were measured at as many values of $H\delta H/\delta z$ as were permitted by the possible load combinations. The gram susceptibility of the standard was put equal to $9\,500 \times 10^{-6}/(T+1)$, ($T$ = abs. temperature) [8,9]. $H\delta H/\delta z$ was then calculated from eqn. (1) and plotted against the observed compensation currents. The plot comprehended 80 points, through which a smooth curve could be drawn. The calibration has been checked several times through more than a year, but no change has been observed. These latter measurements then reflect the reproducibility of independent measurements on the same substance. The standard deviation from the calculated value was 0.3 %.

Since the measurements are made on powdered substances, appropriate corrections must be applied for the force exerted upon the glass container. For this purpose eqn. (1) is rewritten

$$K = H\frac{\delta H}{\delta z}(\mathrm{m}\,\chi_g + m^{\mathrm{glass}}\chi_g^{\mathrm{glass}}) \qquad (2)$$

The gram susceptibility of the glass sort used for the bulbs has been determined separately with a Gouy balance to -0.285×10^{-6}. The mass of the bulb is about 0.03 g. The correction for the diamagnetism of the container is thus small. In the two examples mentioned above the corrected values for the gram susceptibilities are 32.45×10^{-6} and 10.56×10^{-6}, respectively.

With the purpose of tracing possible systematic errors either in the calibration of the apparatus or in the measuring method, the susceptibilities of some simple substances were measured. The substances selected for this test represent a rather wide scale of susceptibilities. The results of the measurements are collected in Table 1 together with some relevant results taken from the literature. The value of a comparison of results obtained in different laboratories is severely limited by the difficulty of obtaining materials of high magnetic purity. Nevertheless the general accordance between the susceptibilities found and those qouted from the literature can scarcely be accidental, so it is concluded that systematic errors are scarcely present.

Table 1. Magnetic gram susceptibilities of various substances at 22.0°C.

Substance	$\chi_g \times 10^6$ found	$\chi_g \times 10^6$ literature	
$FeSO_4 \cdot 7H_2O$	41.80	40.70[8]	42.04[10]
$Mn(NH_4)_2(SO_4)_2 \cdot 6H_2O$	37.05	37.11[11]	
$Fe(NH_4)_2(SO_4)_2 \cdot 6H_2O$	32.14	32.09[8]	
$NiSO_4$	26.12	26.27[8]	
$NiSO_4 \cdot 7H_2O$ I	15.35	15.24[12]	
$NiSO_4 \cdot 7H_2O$ II	15.56	15.85[8]	15.53[8]
$Ni(NH_4)_2(SO_4)_2 \cdot 6H_2O$	10.45	10.38[8]	
$CuSO_4 \cdot 5H_2O$	5.89	5.76[13]	5.85[14]

The susceptibilities have been adjusted to 22.0°C by means of the temperature dependence given in the literature.

Concerning the materials used for the test is stated: $NiSO_4$ was prepared by quantitative conversion of a very pure Ni-bis-acetylacetonate into the sulphate. The hydrated sulphates were the finest c.p. chemicals available, which were recrystallized to constant susceptibility. The double sulphates were prepared from the above mentioned recrystallized simple sulphates and $(NH_4)_2SO_4$ c.p. The preparate of Mohr's salt used for the test was thus independent of that used for the calibration.

Each susceptibility listed in Table 1 is the mean value of measurements at several different values of $H\delta H/\delta z$. Field strength dependence of the susceptibility was not traced in any case. In Table 2 are shown two arbitrarily selected examples of the values of χ_g found at different $H\delta H/\delta z$ values. The standard deviation only measures the precision of the physical method.

Table 2. Magnetic gram susceptibilities at different values of $H\delta H/\delta z$.

$NiSO_4$ at 22.0°C		$FeSO_4 \cdot 7H_2O$ at 21.5°C	
$H\delta H/\delta z \times 10^{-6}$ Gauss²/cm	$\chi_g \times 10^6$	$H\delta H/\delta z \times 10^{-6}$ Gauss²/cm	$\chi_g \times 10^6$
4.730	26.06	5.166	42.05
5.331	26.10	5.579	41.83
6.860	26.01	5.647	41.80
8.323	26.17	5.987	41.72
8.560	26.06	8.213	41.80
10.02	26.19	8.597	41.84
11.51	26.22	11.19	41.96
Mean	26.12	Mean	41.86
Stand. dev.	0.08	Stand. dev.	0.11

MEASUREMENTS AT LOW TEMPERATURES

The value of a magnetochemical investigation is considerably enhanced if it is extended over a range of temperatures. In the following section a fairly simple device, which allows measurements at any temperature in the range 81 to 295°K, is described.

The cryostat arrangement shown on Fig. 4 consists of a silvered Dewar vessel A and a cryostat tube B. The latter is connected to the balance com-

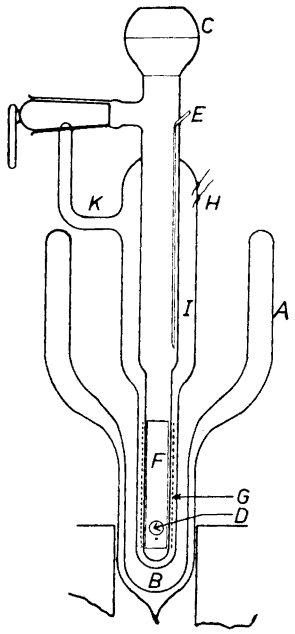

Fig. 4. General view of the cryostat arrangement.

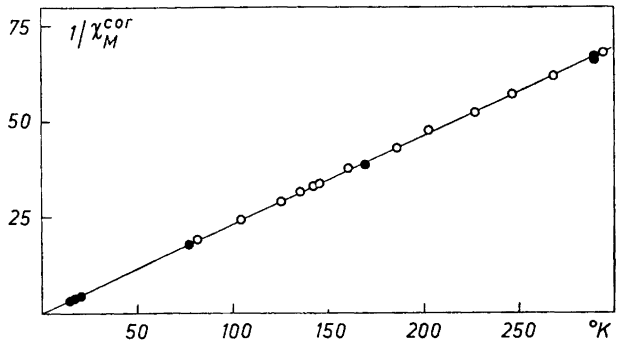

Fig. 5. Reciprocal, corrected molar susceptibility of $Mn(NH_4)_2(SO_4)_2 . 6H_2O$. O Present author. ● Jackson and Kamerlingh Onnes [11]

partment by the spherically ground joint C. The position of the sample inside the inner tube is indicated by a circle D. The point immediately below the circle indicates the position of the measuring junction of the copper-constantan thermocouple. The thermocouple is introduced through the narrow tube E and kept in a fixed position by a sheet of phosphor bronze F. The tube E is sealed with Apiezon wax. A coil G of 0.1 mm Ø constantan wire is wound around the inner tube and connected to a variable transformer by means of the sealed-in wires H. When the space I is evacuated and liquid air is poured into the Dewar vessel, any temperature between 81 and 295°K may be established by application of a suitable heating current in the coil. Only slight regulation of the heating current is necessary to keep the temperature constant within half a degree.

In actual laboratory work two cryostat tubes are used. One, which has been evacuated to a few mm and sealed off at K, covers the temperature scale from 81 to 145°K by application of a maximum heating effect of 1.1 W in the coil. The temperatures from 140 to 295°K are established by means of a second cryostat tube, which must be evacuated to less than 10^{-4} mm the day before use. A permanently evacuated tube like the first one would indeed have been more convenient. The insulated wire of the heating coil, however, cannot be effectively outgassed, so that the necessary high vacuum cannot be maintained for more than a couple of days at a time. The maximum heating effect used in this cryostat tube is 0.8 W.

The thermocouples have been compared *in situ* with a thermocouple, which in turn has been compared with a standard resistance thermometer at 80.5, 195.5 and 293.0°K. The EMF's of the thermocouples are determined by compensation. The detailed EMF/temperature relation for the cryostat thermocouples has been established magnetically by means of the relation

$$(T - \Theta)\ \chi_g = C. \qquad (3)$$

Mohr's salt again served as a reference substance ($\Theta = -1$). The temperatures determined magnetically nicely supplement the above mentioned fix point values to a temperature scale which is considered reliable within at least one degree.

The effectivity of the entire apparatus was finally checked by a series of measurements on $Mn(NH_4)_2(SO_4)_2 \cdot 6H_2O$, which has been investigated magnetically by Jackson and Kamerlingh Onnes [11]. The result of these measurements is shown in Fig. 5, where the reciprocal corrected molar susceptibilities are plotted against the absolute temperature (open circles). For comparison the measurements of Jackson and Kamerlingh Onnes are also shown, appropriately corrected for the diamagnetism (full circles). The accordance is considered very satisfactory.

In conclusion just a few remarks concerning the details of the operating procedure should be given. During all measurements at low temperatures the apparatus is filled with hydrogen. Measurements are taken at both falling and raising temperatures during the same investigation, and the results are carefully inspected for signs of temperature hysteresis. Measurements at a single temperature usually take one hour. In the course of 10 min the temperature in question is etablished. 20 min later the first series of measurements is taken. After another 20 min interval the measurements are repeated. In a special experiment it was found that the sample came to thermal equilibrium with the surroundings within less than 10 min. All later experiences during actual measurements confirm this.

It should be mentioned that even 295°K may be established by means of the cryostats set-up, that is with liquid air in the Dewar vessel and a suitable heating of the coil. Results obtained under these conditions are in wholly accordance with those obtained in a more straightforward manner.

Acknowledgment. The author is very much indebted to the head of the laboratory professor R. W. Asmussen for having suggested this work and for valuable criticism.

REFERENCES

1. Sucksmith, W. *Phil. Mag. VII* **8** (1929) 158.
2. Sucksmith, W. and Pierce, R. R. *Proc. Roy. Soc. London* **167A** (1938) 189.
3. Jackson, L. C. *Proc. Roy. Soc. London* **140A** (1933) 695.
4. v. Oort, W. P. *J. Sci. Instr.* **28** (1951) 279.
5. Cooke, A. H. and Duffus, H. J. *Proc. Phys. Soc. London* **67A** (1954) 525.
6. Bates, L. F. and Hughes, D. *Proc. Phys. Soc. London* **67B** (1954) 28.
7. Swindlehurst, E. *Proc. Leeds Phil. Lit. Soc.* **5** (1947—50) 225.
8. Jackson, L. C. *Phil. Trans. Roy. Soc. London* **224A** (1923) 1.
9. Selwood, P. W. *Magnetochemistry*, 2nd Ed. Interscience Publ. New York 1956, p. 26.
10. Ishiwara, T. *Tohoku Sci. Rep.* **3** (1914) 303.
11. Jackson, L. C. and Kamerlingh Onnes, H. *Proc. Roy. Soc. London* **104A** (1923) 671.
12. Gorter, C. J., De Haas, W. J. and v. den Handel, J. *Commun. Phys. Lab. Univ. Leiden* **218b** (1931).
13. Reekie, J. *Proc. Roy. Soc. London* **173A** (1939) 367.
14. De Haas, W. J. and Gorter, C. J. *Commun, Phys. Lab. Univ. Leiden* **210b** (1930).

Received March 3, 1958.

ACTA CHEMICA SCANDINAVICA 12 (1958) 1015—1023

The Solubility of Nitrogen, Argon and Ethane in Alcohols and Water

J. CHR. GJALDBÆK and H. NIEMANN

Department of Inorganic Chemistry, The Royal Danish School of Pharmacy, Copenhagen, Denmark

The solubility of nitrogen expressed as the Bunsen absorption coefficient is determined at 25°C in the following solvents: *n*-propanol 0.121, *n*-pentanol 0.102, *c*-hexanol 0.0562 and ethylene glycol 0.0140. For argon the following solubilities were determined at 25°C: *n*-propanol 0.231, *n*-butanol 0.220, *n*-pentanol 0.205 and ethylene glycol 0.0317. For ethane at 25°C: methanol 2.14, ethanol 2.52, *n*-propanol 2.60, *n*-butanol 2.61, *n*-pentanol 2.53, *c*-hexanol 1.75, and ethylene glycol 0.215.

Several of the experiments were also carried out at 35°C. A semi-empirical explanation of the magnitude of the gas solubilities in the solvents is given using solubility parameters and dielectric constants for the solvents and solubility parameters and polarizabilities for the gases. Solubilities of helium, hydrogen, carbon monoxide, and nitrous oxide have been included in the investigation.

The solubilities of non-polar gases in non-polar liquids can be calculated from the equation

$$-\log x_2 = -\log x_2^i + 0.4343\frac{\overline{V}_2}{RT}(\delta_1-\delta_2)^2 + \log\frac{\overline{V}_2}{V_1} + 0.4343\left(1-\frac{\overline{V}_2}{V_1}\right) \qquad (1)$$

In this equation, x_2 denotes the solubility in mole fraction, x_2^i the "ideal" solubility, $\overline{V}_2$ the partial molal volume of the dissolved gas, V_1 the molal volume of the solvent, δ_1 and δ_2 solubility parameters of solvent and gas, respectively, R the gas constant and T absolute temperature. With regard to the derivation of eqn. (1) reference should be made to Hildebrand and Scott [1].

In a recent paper [2] it was shown that eqn. (1) predicts too small solubilities of gases in polar non-associated solvents. It was, moreover, shown that for oxygen, carbon monoxide, nitrogen, and carbon dioxide the ratios between experimental values and values calculated from eqn. (1) are approximately proportional to the dipole moments of the solvents.

The purpose of the present paper is to examine the solubilities in the associated solvents: water and alcohols. In these solvents, all of which have nearly the same dipole moment (μ about 1.8 Debye), the solubilities vary

considerably. The solubilities of nitrogen, argon, and ethane increase in the following order of the solvents: water, ethylene glycol, methanol, ethanol, *n*-propanol, *n*-butanol, *n*-pentanol, see Table 5. The solubility of ethane is about 360 times higher in *n*-pentanol than in water. It will be shown how it is possible to account fairly accurately for the solubilities in methanol, ethanol, *n*-propanol, *n*-butanol, *n*-pentanol, and *c*-hexanol and even obtain a rough estimate for the solubilities in ethylene glycol and water.

MATERIALS AND PROCEDURE

The solubility determinations were carried out by a procedure described in an earlier paper [3].

Nitrogen from "Dansk Ilt- og Brintfabrik" was shown to contain less than 0.13 % oxygen by absorption analysis in an apparatus as described by Christiansen and Wulff [4]. *Argon* and *ethane* were of the same purity as described in a previous paper [5].

Methanol, ethanol, and n-*propanol* were dried by means of magnesium using iodine as a catalyst according to Lund and Bjerrum [6]; these three alcohols were fractionated in a wire gauze column which had about 35 theoretical plates. The fractions used showed the following constants: methanol b. p. 64.60 – 64.63°C and n_D (20°) 1.3285; ethanol b.p. 78.49°C and n_D (20°) 1.3614; *n*-propanol b.p. 97.1 – 97.4°C and n_D (20°) 1.3856. n-*Butanol* was fractionated in the same column and showed a b.p. of 117.75 – 117.83°C and n_D (20°) 1.3995. n-*Pentanol* was fractionated twice in the column at about 115 mm pressure and showed a b.p. of 137.83 – 137.90°C (760 mm) and n_D (20°) 1.412.

c-*Hexanol* was dried by boiling with quicklime and then fractionated in the column at about 115 mm pressure. The bottles containing those fractions which were solid at room temperature were placed upside down in a thermostat; the temperature of the thermostat was slowly increased from 20° to 24°C; slight amounts of liquid impure c-*hexanol*, which were collected in the neck of the bottles, were rejected. By this procedure we obtained samples which were completely solid at 24°C. The melting point reported in the literature [7] is 25.15°C, corresponding to a content of 0.05 % water in our fractions.

Ethylene glycol was fractionated in the column at about 53 mm pressure; the fractions used showed a b.p. of 197.30 – 197.42°C (760 mm) and n_D (20°) 1.4320.

All the boiling points mentioned were determined by distillation of 30 ml liquid in a boiling point apparatus as described by Baggesgaard Rasmussen and Reimers [8]. At least 90 % of each of the samples distilled in the temperature intervals stated. All the temperatures were recalculated to a pressure of 760 mm, but no thermometer corrections were used. The temperature intervals mentioned are a criterion for the purity of the liquids.

EXPERIMENTAL RESULTS

The results of the solubility determinations are given in Tables 1, 2, and 3. The experiments were carried out at 25°C, and in addition some were carried out at 35°C.

It appears from Table 4 that our values for the solubility of ethane in methanol and ethanol are slightly higher than values given by McDaniel [10]. Our value for the solubility of ethane in *c*-hexanol is about three times as high as the value given by Cauquil[11]. Cauquil found that one liter of *c*-hexanol dissolved 711.5 ml ethane at 26°C and 755 mm corresponding to the Bunsen absorption coefficient $\alpha = 0.64$ at 26°C. If we use the same temperature coefficient for the solubility of ethane in *n*-propanol and in *c*-hexanol our value

Table 1. The solubility of nitrogen. Experimental values expressed in Bunsen absorption coefficients.

Solvent	t°C	α	Mean of α at 25°
n-Propanol	24.91 24.91	0.1209 0.1208	0.121
n-Pentanol	24.91 25.00	0.1021 0.1013	0.102
c-Hexanol	24.91 25.00	(0.0549) 0.0562	0.0562
Ethylene glycol	25.02 25.01	0.01428 0.01374	0.0140

Table 2. The solubility of argon. Experimental values expressed in Bunsen absorption coefficients.

Solvent	t°C	α	Mean of α 25°.0	35°.0
n-Propanol	24.98 25.00 25.01	(0.2284) 0.2315 0.2310	0.231	
	35.06 34.98 35.00	0.2231 0.2249 0.2248		0.224
n-Butanol	24.99 25.00	0.2206 0.2198	0.220	
	34.98 35.00	0.2156 0.2146		0.215
n-Pentanol	24.97 25.00	0.2055 0.2049	0.205	
	35.03 35.01	0.2025 0.1993		0.201
Ethylene glycol	24.99 24.99	0.0320 0.0314	0.0317	
	35.00 35.00	0.0325 0.0315		0.0320

Table 3. The solubility of ethane. Experimental values expressed in Bunsen absorption coefficients.

Solvent	t°C	α	Mean of α 25°.0	35°.0
Methanol	25.00	2.124	2.14	
	25.01	2.161		
	25.00	2.075		
Ethanol	25.00	2.523	2.52	
	25.00	2.519		
n-Propanol	25.00	2.599	2.60	
	25.01	2.593		
	35.00	2.235		2.24
	35.00	2.239		
n-Butanol	25.00	2.623	2.61	
	25.01	2.597		
n-Pentanol	25.01	2.520	2.53	
	25.00	2.565		
	25.00	2.498		
	35.00	2.190		2.18
	34.99	2.176		
c-Hexanol	25.00	1.750	1.75	
	25.01	1.747		
Ethylene glycol	25.01	(0.2141)	0.215	
	25.01	0.2159		
	25.01	0.2150		
	34.99	0.1949		0.195
	34.99	0.1945		

Table 4. Solubilities of nitrogen and ethane expressed in Bunsen absorption coefficients (α) at 25°C. Comparison with older measurements.

	Solvent	Author	α	α present invest.
Nitrogen	*n*-pentanol	Just [9]	0.112	0.102
Ethane	methanol (99 %)	McDaniel [10]	1.81	2.16
	ethanol (99.8 %)	McDaniel [10]	2.10	2.52
	c-hexanol	Cauquil [11]	0.64 *	1.75

* 26°C

Table 5. Solubilities of nitrogen, argon and ethane expressed in mole fractions, $x_2 \times 10^4$ at 25°C.

	δ_1	V_1	ε_1*	N_2	A	C_2H_6
H_2O	23.4	18.1	78	0.120 [a]	0.254 [c]	0.339
$(CH_2OH)_2$	17.1	55.9	37.7	0.349	0.792	5.42
CH_3OH	14.35	40.7	32.8	2.75 [b]	4.46 [c]	39.2
C_2H_5OH	12.80	58.7	24.3	3.56 [b]	6.21 [c]	66.3
n-C_3H_7OH	11.95	75.2	21.1	4.06	7.75	87.5
n-C_4H_9OH	11.2	92.0	17.8	4.60 [b]	9.04	107
n-$C_5H_{11}OH$	10.9	109	15.2	4.95	9.95	123
c-$C_6H_{11}OH$	11.7	106	15.0	2.66	5.30 [c]	83.0

* Values from *Int. Crit. Tables* except for ethanol, for which the value is from *Le Fèvre* (1938).
a) Orcutt and Seevers, *J. Biol. Chem.* **117** (1936) 501.
b) Kretschmer, C. B. *et al. Ind. Eng. Chem.* 38 (1946) 506.
c) Lannung [14].

at 26°C is $\alpha = 1.72$. To prove that our ethane was pure it was analyzed by means of gaschromatography, and the absorption spectrum in infrared was determined, see a previous paper [5]. As a further criterion for the purity of ethane we determined the solubility in water. The result was $\alpha = 0.0416$ at 25°C. Winkler [12] found $\alpha = 0.0410$ and Morrison and Billett [13] $\alpha = 0.0391$. It can be mentioned that Cauquil's value for the solubility of argon in c-hexanol ($\alpha = 0.157$ at 26°C) is somewhat higher than the value given by Lannung [14] ($\alpha = 0.112$ at 25°C).

A survey of the solubilities expressed as mole fractions ($x_2 \times 10^4$) at 25°C is given in Table 5 together with some values from the literature.

CORRELATION WITH THEORY

It will be shown in the following how it is possible to account for the solubilities using solubility parameters, molal volumes, and dielectric constants for the solvents together with solubility parameters and polarizabilities for the gases. The solubility parameters of the solvents are calculated from heats of vaporization, which will now be discussed.

The heat of vaporization (ΔH) for *methanol* equal to 9 034 ± 30 cal/mole at 25°C was calculated from vapour pressure measurements by Young [15]; a 1.8 % deviation from ideality of the methanol vapours was used. The value $\Delta H = 9\,000 \pm 140$ at 25°C was estimated by graphical interpolation using calorimetric measurements between 20° and 110°C by Fioch et al.[16] and Bartoszewiczowna [17]. From values given in *Int. Crit. Tables* (V, p. 138) we interpolated $\Delta H = 8\,930$ at 25°C. The value $\Delta H = 9\,000$ cal/mole will be used in the present paper.

ΔH for *ethanol* equal to 10 170 at 25°C was calculated from vapour pressure measurements given by Merriman [18]. A 0.3 % deviation from ideality of the ethanol vapours was used. From calorimetric measurements by Fioch et al.[16] and Bartoszewiczowna [17] we interpolated $\Delta H = 10\,200$ at 25°C; an identical value was found by interpolation of values given in *Int. Crit. Tables* (V, p. 138). We will use the value 10 170 cal/mole, which presumably is valid within an accuracy of about 2 %.

ΔH for n-*propanol* equal to 11 330 at 25°C was calculated from vapour pressure measurements by Young [15]. Bartoszewiczowna [17] gives the calorimetric value 180 cal/g at 20°C corresponding to about 10 740 cal/mole at 25°C. The vapour pressures of propanol and of the alcohols mentioned below are so small, that the vapours can be regarded as ideal for our purpose. The value 11 300 cal/mole will be used in the following.

ΔH for n-*butanol* equal to 13 050 at 25°C was calculated from vapour pressure measurements by Kahlbaum [19]. Heats of vaporization were also calculated from vapour pressure measurements by Dreisbach and Schrader [20]; extrapolation to 25°C resulted in the value 12 100. Bartoszewiczowna [17] gives the calorimetric value 149.5 cal/g at 20°C corresponding to about 11 000 cal/mole at 25°C. We will use the value 12 100 cal/mole, which is estimated to be reliable within 8 %.

For ΔH for n-*pentanol* we use the estimated value 13 500 cal/mole at 25°C. This estimate is based on the approximate linear dependence between heats of vaporization of methanol, ethanol, *n*-propanol, and *n*-butanol and the molecular weights of these alcohols. From vapour pressure measurements given in *Int. Crit. Tables* (III, p. 220) we calculated the value 12 200; this result is considered to be rather erroneous due to the low and inaccurate vapour pressure data.

McKinley-McKee and Moelwyn-Hughes [21] have given the formula

$$\Delta H \text{ (cal/mole)} = 24\,357 - 12.48 \cdot RT$$

which is a result of vapour pressure measurements for *ethylene glycol* between 86° and 198°C. If we use this formula at 25°C we get about 17 000 cal/mole.

From vapour pressure data of cyclo*hexanol* given by Nitta [22] we have calculated $\Delta H = 14\,900$ between 28° and 37°C and $\Delta H = 14\,400$ between 40° and 60°C; from these values we get $\Delta H = 15\,000$ cal/mole at 25°C. The vapour pressures vary from only 0.906 mm at 27.9°C to 9.202 mm at 60.0°C, and therefore the calculated value of the heat of vaporization is regarded as being rather inaccurate.

ΔH for *water* equal to 2 436 joule/g at 25°C (*Int. Crit. Tables* V, p. 138) corresponds to $\Delta H = 10\,490$ cal/mole.

The solubility parameters of the solvents are calculated from

$$\delta_1 = \sqrt{\frac{\Delta H - RT}{V_1}} \tag{2}$$

where ΔH is the heat of vaporization. The results of the calculations at 25°C are given in Table 5 together with values for the molal volumes (V_1) and the dielectric constants (ε) of the solvents.

Table 6. Values of ideal solubilities, solubility parameters, molal volumes and polarizabilities for nitrogen, argon, and ethane at 25°C.

	N_2	A	C_2H_6
$x_2^i \times 10^4$	16.0	21.6	242
δ_2	5.2	5.43	7.55
$\overline{V}_2$	53	46	88
$\alpha \times 10^{25}$	17.6	16.4	44.7

If we calculate the solubilities of the gases in the alcohols, using eqns. (1) and (2) together with the constants x_2^i, δ_2 and $\overline{V}_2$ from Table 6, we get values which are too low. If we use

$$-\log x_2 = -\log x_2^i + 0.4343 \frac{\overline{V}_2}{RT}(\delta_1^* - \delta_2)^2 + \log \frac{\overline{V}_2}{V_1} + 0.4343\left(1 - \frac{\overline{V}_2}{V_1}\right) \quad (3)$$

where

$$\delta_1^* = \delta_1 - (\varepsilon - 1)\,(0.165 - 0.00143\,\alpha \times 10^{25}) \quad (4)$$

we can account for the experiments with an accuracy which appears from Table 8. The values of

$$\Delta = (-\log x_2)_{\text{calc.}} - (-\log x_2)_{\text{exp.}} = \log \frac{x_{2(\text{exp.})}}{x_{2(\text{calc.})}}$$

are given in Table 8. The antilogarithm of Δ shows how many times the experimental value of the mole fraction is greater than the calculated value.

We have evaluated eqn. (4) in the following manner. By means of eqn. (1) and the experimental values for the solubilities of argon we calculated values δ'_1 for each alcohol and for water. It is shown in Fig. 1 that there is an approximate linear dependence between the difference $\delta_1 - \delta'_1$ and the

Table 7. Polarizabilities for some gases.

Gas	Slope S (see the text)	$\alpha \times 10^{25}$
He	0.163	2.2
H_2	0.150	7.9
N_2	0.144	17.6
A	0.138	16.4
CO	0.136	19.5
N_2O	0.123	30
C_2H_6	0.101	44.7

Table 8. Deviations between calculated and experimental values of the solubilities expressed as $\Delta = (-\log x_2)_{\text{calc.}} - (-\log x_2)_{\text{exp.}}$.

Solvent	N_2	A	C_2H_6
Methanol	0.08	−0.02	−0.12
Ethanol	0.07	0.00	−0.07
n-Propanol	−0.02	−0.04	−0.09
n-Butanol	−0.08	−0.08	−0.11
n-Pentanol	−0.07	−0.06	−0.07
c-Hexanol	−0.07	−0.11	0.00
Ethylene glycol	0.14	−0.01	0.52
Water	−0.35	−0.51	0.35

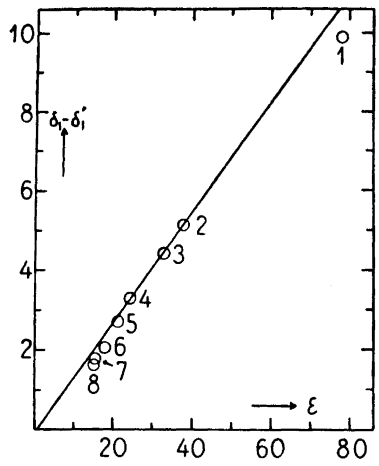

Fig. 1. ($\delta_1-\delta_1'$)-values for *argon* in water (1), ethylene glycol (2), methanol (3), ethanol (4), *n*-propanol (5), *n*-butanol (6), *n*-pentanol (7), and *cyclo*hexanol (8). ε is the dielectric constant of the solvent.

dielectric constant ε. The straight line is drawn through the abscissa value ε—1. The same linear dependence was found for nitrogen, ethane, helium, hydrogen, carbon monoxide, and nitrous oxide. The slopes of the lines are given in Table 7 together with polarizabilities of the gases ($\alpha \times 10^{25}$). The approximate linear dependence between the slopes (S) of these lines and the polarizabilities of the gases is shown in Fig. 2. By means of the slope of the straight line in Fig. 2 (0.00143) and the intersection on the ordinate axis (0.165) we get eqn. (4).

It appears from Table 8, that the calculations of the solubilities of the three gases in water and of ethane in ethylene glycol are very inaccurate. The largest deviation is found for the solubility of argon in water for which the calculated and experimental values are $x_2 = 0.82 \times 10^{-4}$ and 0.25×10^{-4}, respectively. It should be emphasized that the differences Δ in Table 8 are very sensitive to small variations in the δ_1 values. If we use $\delta_1 = 10.64$ for *n*-butanol instead of $\delta_1 = 10.2$ we get $\Delta = 0.04$, $\Delta = 0.03$ and $\Delta = 0.01$

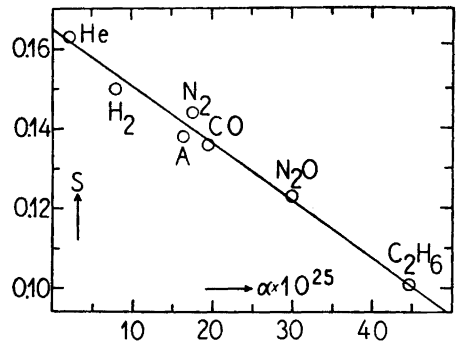

Fig. 2. S (see the text) for different gases. $\alpha \times 10^{25}$ is the polarizability of the gas.

for nitrogen, argon, and ethane, respectively. $\delta_1 = 10.64$ corresponds to the heat of vaporization 13 050 cal/mole (see p. 1020).

Acknowledgements. We wish to express our gratitude to Professor Carl Faurholt, director of the laboratory, for his kind interest in the investigations. Our thanks are also due to lecturer Georg Kilde for many valuable discussions. The financial support from *Statens almindelige Videnskabsfond* is gratefully acknowledged.

REFERENCES

1. Hildebrand, J. H. and Scott, R. L. *Solubility of Non-electrolytes, 3rd Ed., Reinhold Publishing Co., New York* 1950.
2. Gjaldbæk, J. Chr. and Krogh Andersen, E. *Acta Chem. Scand.* **8** (1954) 1398.
3. Gjaldbæk, J. Chr. *Acta Chem. Scand.* **6** (1952) 623.
4. Christiansen, J. A. and Wulff, I. *Kgl. Danske Videnskab. Selskab, Mat.-fys. Medd.* **22** (1945) No. 4.
5. Gjaldbæk, J. Chr. and Niemann, H. *Acta Chem. Scand.* **12** (1958) 611.
6. Lund, H. und Bjerrum, J. *Ber.* **64** (1931) 210.
7. Trav. Bur. Int. Et. Phys.-Chim. *J. chim. phys.* **34** (1937) 693.
8. Baggesgaard Rasmussen, H. og Reimers, F. *Dansk Tidsskrift for Farmaci* **16** (1942) 161.
9. Just, G. *Z. physik. Chem.* **37** (1901) 342.
10. McDaniel, A. S. *J. Phys. Chem.* **15** (1931) 587.
11. Cauquil, G. *J. chim. phys.* **24** (1927) 53.
12. Winkler, L. W. *Ber.* **34** (1901) 1409.
13. Morrison, T. and Billett, F. *J. Chem. Soc.* **1952** 3819.
14. Lannung, A. *J. Am. Chem. Soc.* **52** (1930) 68.
15. Young, S. *Sci. Proc. Dublin N.S.* **12** (1910) 374.
16. Fioch, E. F., Ginnings, D. C. and Holton, W. B. *Nat. Bur. Standards* **6** (1931) 881.
17. Bartoszewiczowna, E. *Roczniki Chem.* **11** (1931) 90.
18. Merriman, R. W. *J. Chem. Soc.* **103** (1913) 628.
19. Kahlbaum, G. W. A. *Z. physik. Chem.* **26** (1898) 577.
20. Dreisbach, R. R. and Schrader, S. A. *Ind. Eng. Chem.* **41** (1949) 2879.
21. McKinley-McKee, J. S. and Moelwyn-Hughes, E. A. *J. Chem. Soc.* **1952** 838.
22. Nitta, I. *J. Chem. Soc. Japan, Pure Chem. Sect.* **69** (1948) 141.

Received February 4, 1958.

ACTA CHEMICA SCANDINAVICA 12 (1958) 1024—1029

Capillary Height in Inclined Tubes

H. HØJGAARD JENSEN

Physics department, Technical University, Copenhagen, Denmark

The surface form and the length of the liquid column in a cylindrical capillary tube inclined against the vertical direction are studied by a method of successive approximations. The results are obtained as expansions in powers of $\lambda = \varrho G a^2/2C$, where a is the radius of the tube, G the acceleration of gravity, ϱ the density and C the surface tension of the liquid. The length of the liquid column is given to third order in λ.

Expressions for the form and height of the surface of a liquid in a vertical, cylindrical capillary tube are known from the literature [1]. They are, *e.g.*, used in precision measurements of surface tension by the method of capillary rise.

Recently Koefoed and Villadsen [2] have improved this method by using capillary tubes which are not vertical. For this reason we have found it worthwhile to derive expressions analogous to those in Ref.[1], but valid also for tubes inclined against the vertical direction.

We have only treated the case in which the angle of contact between the liquid and the tube is 180°, this being the most important from the metrological point of view.

This note describes the principles and results of the calculations. The detailed and somewhat lengthy derivations are largely omitted, since they do not present any novel features.

NOMENCLATURE AND METHOD

We consider a free surface in a capillary tube, the radius of which is a. We want to treat both cases shown in Fig. 1 in one calculation. We therefore introduce a cylindrical system of coordinates (r, φ, z) according to the following rules (*cf.* Fig. 1):

The origin is at the level of the undisturbed surface of the liquid outside the tube. The z-axis is the axis of the tube, oriented *from liquid to gas*. The angle from the z-axis to the upward vertical is denoted by α.

The height and form of the surface will adjust itself in such a way that the free energy F of the system is a minimum. The variable part of F has

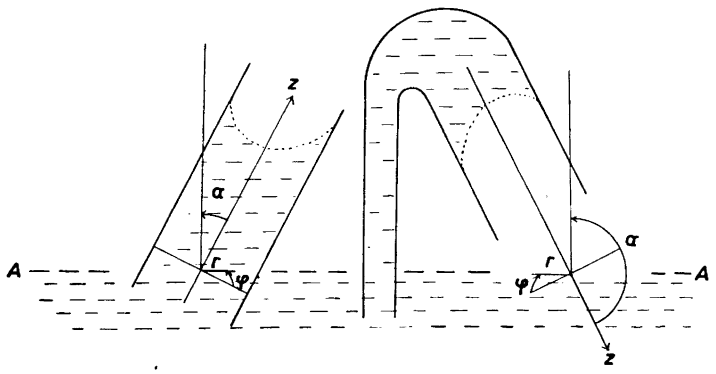

Fig. 1. Cylindrical coordinate systems used for surfaces turned upward and downward, respectively. A—A is the level of the undisturbed surface.

three components, the gravitational energy F_G, the energy of the free surface in the tube F_S, and the energy due to the interface between the liquid and the wall of the tube, F_T. Let $z = z(r, \varphi)$ be the equation of the surface. The three contributions to F can then be written in the following forms valid for all values of α. (The arbitrary additive constants are chosen so as to give simple expressions):

$$F_G = \varrho G \int_0^{2\pi} d\varphi \int_0^a r dr (\tfrac{1}{2} z^2 \cos \alpha - zr \cos \varphi \sin \alpha) \tag{1}$$

$$F_S = C \cdot S = C \int_0^{2\pi} d\varphi \int_0^a r dr \sqrt{1 + (z'_r)^2 + (z'_\varphi)^2/r^2} \tag{2}$$

$$F_T = -C \int_0^{2\pi} d\varphi \cdot a z(a, \varphi) \tag{3}$$

Here G is the acceleration of gravity, C the surface tension and ϱ the density of the liquid. (Strictly speaking ϱ should be the difference between the densities of the liquid and the medium outside the surface.) S is the area of the free surface in the tube. z'_r and z'_φ mean $\partial z/\partial n$ and $\partial z/\partial \varphi$, respectively. The integral in (3) is the area of the interface between liquid and tube.

The function $z(r,\varphi)$ is now a solution of the variational equation

$$\delta F \overset{def}{=} \delta(F_G + F_S + F_T) = 0 \tag{4}$$

where $z(r,\varphi)$ is to be varied subject to the boundary condition that the angle of contact shall be constant and equal to 180°, *i.e.* z'_r must go to plus infinity when r goes to a. Furthermore we assume that $z(r,\varphi)$ is at least twice differentiable.

By varying the height, but not the form, of the surface, *i.e.* by letting $\delta z = \text{const.}$, we are able to derive one exact equation from eqn. (4). In this case only F_G and F_T contribute to δF, and we get

$$\frac{1}{\pi a^2}\int_0^{2\pi} d\varphi \int_0^a r\, dr \cdot z \overset{def}{=\!=} \bar{z} = \frac{h}{\cos\, \alpha} \tag{5}$$

where $\bar{z}$ is written for the mean value of z over the surface, and where

$$h \overset{def}{=\!=} \frac{2C}{\varrho G a} \tag{6}$$

is the expression valid for the capillary height in a very narrow, vertical tube. Eqn. (5) may also be derived from an elementary consideration of the equilibrium between the forces from the walls of the tube and those due to gravity.

It is not possible to give the solution to eqn. (4) in closed form by means of tabulated functions. We therefore try to solve it by successive approximations, $z(r, \varphi)$ being written as an expansion in a suitable dimensionless perturbation parameter. As such we shall choose

$$\lambda \overset{def}{=\!=} \frac{a}{h} = \frac{\varrho G a^2}{2C} \tag{7}$$

When λ is very small the surface will be a hemisphere of radius a. It has the parametric representation (with Θ as a parameter defined by eqn. (8)):

$$r = a\, \sin\Theta \tag{8}$$

$$z = A - a\, \cos\Theta \tag{9}$$

The single adjustable constant A is most easily found by inserting eqns. (8) and (9) in eqn. (5). The result is

$$A = h/\cos\, \alpha + \tfrac{2}{3}\, a \tag{10}$$

This, then, has led to the terms in z/h proportional to λ^0 and λ^1, respectively, *i.e.* to the wellknown first and second order approximations.

In order to improve the result two ways are possible. First, one may choose for $z(r, \varphi)$ a suitable trial function with a number of adjustable constants to be determined from eqn. (4). The simplest trial function, which takes into account both the departure from spherical form and from axial symmetry, is an inclined ellipsoid: $z = k_1 - k_2 \cos\varphi + k_3 \cos\varphi \sin\Theta$, where Θ is still defined by eqn. (8). The use of this function leads to a result which is sufficiently accurate for many purposes. The other method is a consistent perturbation calculation. We put

$$\frac{z}{h} = \frac{1}{\cos\alpha} + \lambda(\tfrac{2}{3} - \cos\Theta) + \lambda^2 f_1(\Theta,\varphi) + \lambda^3 f_2(\Theta,\varphi) + \cdots \tag{11}$$

and by means of eqn. (4), where F is also expanded in powers of λ, we derive differential equations for the unknown functions f_1, f_2. The first few of these equations turn out to be exactly soluble. We therefore prefer this way of attack and shall not give the results of the first method mentioned.

THE THIRD AND FOURTH ORDER APPROXIMATIONS

Eqns. (11), (1), (2) and (3) lead to an expansion of F in powers of λ. The first term, which depends on the unknown functions in eqn. (11), is the following:

$$F_4 = \frac{2C^2\lambda^3}{\varrho G} \cdot \int_0^{2\pi} \mathrm{d}\varphi \int_0^{\pi/2} L_1 \, \mathrm{d}\Theta \tag{12}$$

where $L_1 = \sin\Theta \cos\Theta \, [(^4/_3 \cdot \cos\alpha - 2\cos\alpha \cos\Theta - 2\sin\alpha \cos\varphi \sin\Theta) \cdot f_1$

$$+ \tfrac{1}{2} \cos\Theta (f'_{1,\Theta})^2 + \tfrac{1}{2} \frac{\cos\Theta}{\sin^2\Theta} (f'_{1,\varphi})^2] \tag{13}$$

The first step in the perturbation calculus now consists in determining f_1 so that F_4 is a minimum. On varying f_1 (and later f_2) we keep the boundary values $f_1\left(\frac{\pi}{2}, \varphi\right)$ (and $f_2\left(\frac{\pi}{2}, \varphi\right)$)fixed, but on the other hand we require, in agreement with eqn. (5), that $\overline{f_1} = 0$ (and $\overline{f_2} = 0$). This fixes an otherwise arbitrary constant in f_1 (and f_2). The variational problem is of standard form and leads to the Euler-Lagrange differential equation

$$\frac{\partial}{\partial\Theta} \frac{\partial L_1}{\partial f'_{1,\Theta}} + \frac{\partial}{\partial\varphi} \frac{\partial L_1}{\partial f'_{1,\varphi}} = \frac{\partial L_1}{\partial f_1} \tag{14}$$

From the differential equation or directly from the variational problem and the way in which φ appears in L_1, it follows that f_1 must be of the form

$$f_1 (\Theta,\varphi) = g_1 (\Theta) + g_2 (\Theta) \cos \varphi \tag{15}$$

Eqn. (14) thus separates into two equations, one for g_1 and one for g_2.

The differential equation determining g_1 becomes

$$\frac{\mathrm{d}}{\mathrm{d}\Theta}\left(\sin\Theta \cos^2\Theta \frac{\mathrm{d}g_1}{\mathrm{d}\Theta}\right) = \tfrac{4}{3} \cos\alpha \sin\Theta \cos\Theta - 2\cos\alpha \cos^2\Theta \sin\Theta \tag{16}$$

The integration is elementary. The first constant of integration follows from the requirement that $\mathrm{d}g_1/\mathrm{d}\Theta$ must be finite for $\Theta = 0$. The second is determined from the condition $\overline{f_2} = 0$. The result is

$$g_1 = \tfrac{1}{3} \cos \alpha \, (2 \ln (1 + \cos\Theta) - 1) \tag{17}$$

The equation determining g_2 is

$$\frac{\mathrm{d}}{\mathrm{d}\Theta}\left(\sin\Theta \cos^2\Theta \frac{\mathrm{d}g_2}{\mathrm{d}\Theta}\right) = \frac{\cos^2\Theta}{\sin\Theta} g_2 - 2\sin\alpha \sin^2\Theta \cos\Theta \tag{18}$$

The condition that g_2 must be finite at both ends of the interval $0 \leq \Theta \leq \frac{\pi}{2}$ determines both constants in the complete integral to this equation.

We find

$$g_2 = \tfrac{2}{3} \sin\alpha \sin\Theta \left(\frac{\ln (1 + \cos\Theta)}{\cos\Theta} + \frac{1}{1 + \cos\Theta}\right) \tag{19}$$

For $r \to a$, the partial derivative $f'_{1,r}$ must not go so rapidly to negative infinity that the boundary condition for the complete function $z(r, \varphi)$ can not be fulfilled. This puts a limit on the magnitude of λ, but it is found from eqns. (15), (17) and (19) that the condition ($\lambda \lessapprox 1$, dependent on α) is fulfilled for all values of λ which lead to a useful perturbation expansion.

We are now able to carry the perturbation calculus one step further. The known function f_1 is introduced into the free energy and the first term in the expansion which depends on f_2 is minimized. This leads to an equation like (14), from which it is seen that f_2 is of the form

$$f_2(\Theta,\varphi) = G_1(\Theta) + G_2(\Theta)\cos\varphi + G_3(\Theta)\cos 2\varphi \qquad (20)$$

We have only determined $G_1(\Theta)$. The reason is that G_2 and G_3 vanish (like Θ and Θ^2, respectively) for $\Theta \to 0$; their contributions to the height of the meniscus will therefore be of higher order in λ than the contribution form G_1.

G_1 is found in the same way as g_1. We omit the details in the calculations. The result is

$$G_1(\Theta) = \tfrac{2}{3}\cos^2\alpha\left[\frac{\ln(1+u)}{u} - 2\ln(1+u) + u\right]$$
$$+ \tfrac{1}{9}\sin^2\alpha\left[(\ln(1+u))^2\left(\frac{1}{u}+\frac{1}{u^3}\right) + 2\ln(1+u)\left(\frac{5}{u}-\frac{1}{u^2}\right) + \frac{4}{1+u} + \frac{1}{u} - 3u\right]$$
$$- \tfrac{8}{3}\ln 2 + \tfrac{14}{9} - \tfrac{2}{3}\sin^2\alpha, \qquad (21)$$

where, for brevity, $\cos\Theta$ has been denoted by u.

THE CAPILLARY HEIGHT

From eqn. (11) we now find the parameters of that point of the surface where the tangential plane is perpendicular to the axis of the tube ($z'_\Theta = 0$). The value of z/h for this point is denoted by z_m/h and is found on inserting the said parameters in eqn. (11). z_m/h is written as an expansion in λ:

$$\frac{z_m}{h} = \frac{1}{\cos\alpha} - \tfrac{1}{3}\lambda + \tfrac{1}{3}\cos\alpha\,[2\ln 2 - 1]\cdot\lambda^2 - [\cos^2\alpha(\tfrac{10}{3}\ln 2 - \tfrac{20}{9}) + \sin^2\alpha(2\ln 2 - \tfrac{5}{6})]\cdot\lambda^3 + \cdots$$
$$= \frac{1}{\cos\alpha} - \tfrac{1}{3}\lambda + 0.129\cos\alpha\cdot\lambda^2 - [0.088\cos^2\alpha + 0.553\sin^2\alpha]\cdot\lambda^{3'}_{,} + \ldots \qquad (22)$$

For $\alpha = 0$ the first three terms in this expansion have been found by Poisson and Volkmann [1]. On considering the way in which the acceleration of gravity enters into h and λ, one sees that the first three terms in (22) are obtained from Poissons expression on replacing G by $G\cos\alpha$, *i.e.* by the component of the acceleration of gravity along the negative z-axis. However, it is also seen that the term in (22) proportional to λ^3 is affected by the asymmetry of the surface and consequently it depends also on the component of G perpendicular to the axis of the tube.

The results obtained are valid for both positive and negative values of $\cos\alpha$. However, it must be remembered that the z-axis is oriented downwards

for cosα negative (hanging surface). In the method of Koefoed and Villadsen [2], the distance is measured between two surfaces in tubes of different radii (a_1 and a_2) and with different values of α ($\alpha_1 = \alpha$; $\alpha_2 = \pi + \alpha$). This distance l will be

$$l = z_1 - |z_2| = z_1 + z_2$$
$$= \frac{h_1 - h_2}{\cos\alpha} - \tfrac{1}{3}(a_1 + a_2) + 0.129 \cos\alpha \left(\frac{a_1^2}{h_1} - \frac{a_2^2}{h_2}\right) -$$
$$- (0.088 \cos^2\alpha + 0.553 \sin^2\alpha)\left(\frac{a_1^3}{h_1^2} + \frac{a_2^3}{h_2^2}\right) + \ldots \qquad (23)$$

where $h_1 = 2C/\varrho G a_1$, and $h_2 = 2C/\varrho G a_2$.

For the purpose of measuring surface tension, the formula (23) is most easily utilized when inverted so as to give $2C/\varrho G$ as an expansion in powers of, *e.g.*, a_2/l.

We conclude with a few words about the practical convergence of the expansion found. The last term in eqn. (22) becomes equal to 0.1 % of the first term at a value of λ approximately equal to 1/5, but somewhat dependent on α. For water this corresponds to a tube diameter of $2a \approx 3.5$ mm. When $\sin^2\alpha$ is small, an accuracy of about 0.1 % may be expected even for values of λ as large as 1/3 ($2a \approx 4.5$ mm for water). However, for larger values of $\sin^2\alpha$ this is presumably not the case, because the fourth term in eqn. (22) becomes larger than the third term, a fact that points to a slow convergence of the expansion.

REFERENCES

1. Poisson, S.D. *Nouvelle théorie de l'action capillaire*, also quoted in *Hdb.d. Exp.Phys.* **6** (1928) 93; Volkmann, P. *Wied.ann.* **11** (1880) 177.
2. Koefoed, J. and Villadsen, J. *Acta Chem. Scand.* **12** (1958) 1124.

ACTA CHEMICA SCANDINAVICA 12 (1958) 1030—1041

Determination of the Solidus Curve by a Tracer Technique. The System $CaCl_2$—NaCl

A. SELTVEIT and H. FLOOD

Royal Norwegian Council for Scientific and Industrial Research, Institute of Silicate Science, Norwegian Institute of Technology, Trondheim, Norway

Based on a modification of the high-temperature filtration previously described [1], a new technique for the determination of the solidus curve of a phase diagram is described. A small amount is added of a third, radioactive component which is soluble in the liquid, but insoluble in the solid phase in question.

The method is applied to the system calcium chloride — sodium chloride. The data of the composition of the solid phase are in favour of the existence of an incongruently melting compound Na_4CaCl_6. The solubility of calcium chloride in solid sodium chloride reaches a maximum of 15 mole percent. A discussion of the data indicates the occurrence of $CaCl_4^{--}$ ions in the liquid phase.

METHOD

In phase diagrams involving solid solutions, the extent of this solid solution, described by the solidus line, is often difficult to establish. This is particularly true for high-temperature systems. Thermal analysis will in general give only very approximate results for the solidus curve. Quenching techniques, with microscopic and/or X-ray examination of the quenched sample, have given a considerable amount of information, particularly in silicate systems where the phase transformations appear sufficiently slowly for the quenching to be effective. High-temperature X-ray techniques have also been used, but this method is rather elaborate and, notably at higher temperatures, difficult.

A knowledge of the solidus curve, however, is of decisive importance for a discussion of the thermodynamic and structural properties of the liquid (as well as the solid) solution, based on the phase diagram. Such discussion has yielded information of considerable interest for a number of systems, but so far the work has been limited to the consideration of systems without solid solution, since the solidus curves for other systems are in general not known with sufficient accuracy. Hence it became desirable to devise a method

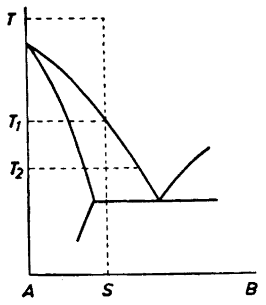

Fig. 1. Binary phase diagram where component A forms solid solutions with component B (schematic).

for reliable determination of the solidus curve in high-temperature systems. Such a method, employing the addition of a radiactive tracer, will be described.

The procedure is in principle as follows. To the components of the system (mixed in known amounts) is added a small amount of a third, radioactive component, which is so chosen that it cannot enter into the solid phase in question. The procedure may be illustrated by considering the binary system A—B (Fig. 1). The components A and B are mixed to give the chosen composition *s*, a small amount of radioactive tracer (order of magnitude 0.05 %) is added, and the mixture is brought to the temperature T where only liquid is present. A sample is withdrawn from this liquid and its radioactivity per gram is determined. (Eventually the composition of the melt may also be checked by chemical analysis of the same sample.) Next, the system is cooled. The system is then brought to equilibrium at the temperature T_2 (which for practical reasons must be so chosen that the ratio of liquid to solid phases is roughly within the limits 1.5 and 0.5). At this temperature, another sample is withdrawn from the liquid phase, and its radioactivity is determined. The radioactivity per gram of this second sample must necessarily be higher than that of the first, since the total amounts of liquid phase in the system has diminished while all of the radioactive tracer is present in that phase only. The ratio between these two specific activities gives directly the fraction of the total system present in the liquid state at temperature T_2.

The composition of the second sample, *i.e.* the liquid phase, is determined by chemical analysis. This analysis may be checked against the liquidus curve obtained from thermal analysis, or otherwise, one might rely upon the thermal analysis and omit the chemical analyses altogether.

Now, the gross composition is known from the outset, the relative amounts of liquid and solid has been determined from measurements of the radioactivity, and the composition of the liquid is known. By combination of this information, the composition of the solid phase may easily be calculated.

ON THE SYSTEM SODIUM CHLORIDE — CALCIUM CHLORIDE

As the first system to be investigated by the method outlined above was chosen the system sodium chloride — calcium chloride. At least five earlier investigations of this system are to be found in the literature. Lamplough [2] concluded from his work in 1911 that probably neither solid solution nor any compound between the components exist in this system. Menge [3] on the other hand, found in the same year a compound to which he attributes the formula $4\,NaCl \cdot CaCl_2$, and he also found that solid solutions are formed on the sodium chloride side. He indicates a maximum solid solubility of about 10 weight-%. His conclusions are based on thermal analysis in combination with microscopy.

In 1920, Scholich [4] re-investigated the system, and concluded that neither solid solution nor any compound is present. According to this author, Menge's results may probably be explained by assuming the presence of hydrated calcium chloride in his samples.

The presence of solid solutions is again maintained by Sato and Amano in 1935 [5] who find a maximum solid solubility of 4 to 5 % calcium chloride in sodium chloride, but no compound formation. These results are again supported by Miyake and Suzuki in 1954 [6] on basis of their X-ray investigations which were, however, carried out on slowly cooled samples.

EXPERIMENTAL

In the tracer method, the first question concerns the choice of a suitable tracer. In the case at hand, some radioactive ion which cannot enter into the solid sodium chloride lattice had to be used. As such, cobalt (^{60}Co) was used, and later on cesium (^{134}Cs), both in the form of the chlorides. Cobalt ion has about 18 % lower ionic radius than sodium ion, in addition to its double charge, and there are also reasons to believe that Co will be present in the NaCl-melt as $CoCl_4^{-2}$ complexes. Cesium ion has an ionic radius about 65 % higher than that of sodium ion. The fact that points obtained with the two different tracers agree may be taken as an indication that neither of them have entered the solid phase to any measurable extent.

Sodium chloride and calcium chloride (both *fusum pro analysi* from E. Merck A.G., Darmstadt) were weighed into a platinum crucible to a total of about 40 g for each run, with about 20 mg of radioactive cobalt chloride or cesium chloride added.

The furnace is shown in Fig. 2. It consists essentially of a Pythagoras tube wound with Kanthal resistance wire, the windings being closer spaced towards the ends to compensate for the extra heat loss at the ends. The furnace shell was water-cooled to do away with the influence of changes in ambient temperature. The temperature was controlled by a Kent Multelec potentiometric controller in connection with a platinum-platinumrhodium thermocouple located closely outside the heater windings. The temperature in the melt was followed with another thermocouple with the bare wires of the hot junction dipping directly into the melt. This thermocouple was connected to a Tinsley thermoelectric-free potentiometer in combination with a recording galvanometer (Multiflex galvanometer with Nachlaufschreiber from Dr. B. Lange, Berlin). This equipment will record, *e. g.*, a coolingcurve with an accuracy of about 0.07° per mm. The thermocouple was checked against the melting points of pure sodium chloride (800.6°) and sodium sulphate (885.0°). The furnace was equipped with a rotating stirrer which was lowered into the crucible after the salts had melted, to insure thorough mixing as well as even temperature. The stirrer shaft and thermocouple were running through packing glands in the top lid. A third packing gland was provided for the sample takers, an open scoop for sampling the homogeneous liquid and a platinum filter for sampling the heterogeneous system.

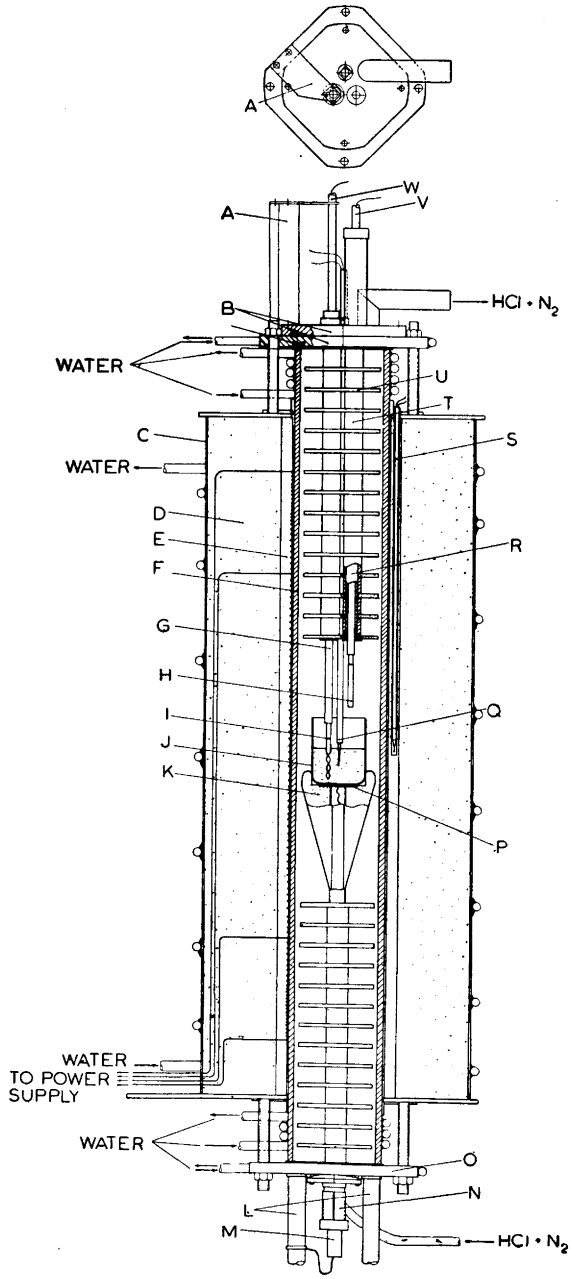

Fig. 2. High-temperature filtration furnace.

H = filtration tube
I = Pt stirrer on ceramic shaft
J = crucible with the equilibrium mixture
K = supporter
Q = thermocouple
U = radiation shields

The cobalt and calcium chlorides were protected from hydrolysis and oxidation by using an atmosphere of nitrogen plus hydrogen chloride in the furnace. In order to withstand this atmosphere, the top and bottom lids were made of pure nickel, with rubber gaskets.

A typical run was as follows. The platinum crucible with contents was placed in the furnace, which was then closed and a slow stream of the protective gas mixture was conducted through the furnace while it was heated. When a temperature was reached at which all of the charge would be molten, the stirrer and thermocouple was lowered into the melt. After 10—15 min of stirring, a sample (varying from about 0.2 to 0.5 g) was taken from the homogeneous melt, and the sample taker removed from the furnace and replaced by the platinum filter tube (see below). The furnace was then allowed to cool at a rate of about 1° per min, while the temperature of the melt was followed by the recording galvanometer described above.

After the break had been recorded (corresponding to temperature T_1 of Fig. 1) the cooling was continued to the chosen temperature (T_2), and the melt was held constant at this temperature sufficiently long for the equilibrium to be established. Experiments showed that 2 h was sufficient, but for practical reasons the constant temperature was usually held overnight. (Some particular run in which equilibrium was difficult to establish will be discussed under "Results".)

After equilibrium was supposedly established, the platinum filter assembly was lowered into the crucible. This consisted essentially of a platinum tube about 40 mm long, closed at the lower end by a platinum bottom with fine needle holes. The platinum tube was joined moderately gas-tight to a fused-quartz tube running through the packing gland at the top of the furnace. An electrical lead to the crucible and another to the filter, in combination with a low-voltage source and a pilot light, showed when the filter was in contact with the melt. The filter was then lowered some 5 mm more, and a sample sucked into the filter by application of a syringe at the top of the quartz tube. The filter assembly was then removed and replaced by a sample taker.

The temperature was then raised again until all of the charge had melted, stirred for a while, and another sample taken from this homogeneous liquid. This last sample served to check the total radioactivity present, *i. e.*, that nothing had disappeared from the crucible except for the samples.

Analysis for composition and radioactivity.

Each of the samples was dissolved in water and diluted to a known volume. In one part of the solution, the calcium content was determined by titration with ethylenediamine-tetraacetic acid, disodium salt ("Titriplex III", E. Merck A. G., Darmstadt) with "Eriochrome black T" as indicator. The sodium chloride content was determined as difference.

In another part of the solution, the radioactivity was measured with a scintillation counter for liquids (Scintillation Counter for Ultrasensitive Measurements, Type N 550, in connection with a Decatron Scaler N 530 A, both from E. K. Cole, Ltd., London). Only the ratios between the radioactivities (per gram) of the three different samples from the same run were of interest.

RESULTS

A part of the experimental data are given in Table 1, and the phase diagram is shown in Fig. 3. The eutectic lies at 500 $\pm$ 2°C and 48 mole percent NaCl. At 600°C the solubility of $CaCl_2$ in solid NaCl is about 15 mole percent (24 weight percent), hence is appreciably higher than estimated by earlier investigators. In the solid $CaCl_2$, on the other hand, no solubility of NaCl was detected.

The observations regarding the composition of the solid phase on the NaCl side of the diagram are not entirely unambiguous, and two different interpretations seem possible:

Table 1. Data of thermal analysis and high temperature filtrations of the system $NaCl-CaCl_2$.

Mole % NaCl	Cooling curve T_1 (°C)	Filtration T_2 (°C)	Mole % $CaCl_2$		Tracer
			liq.	sol.	
NaCl Side					
100	800.6				
96.0	789.5				
91.0		748.8	13.9	2.7	^{60}Co
92.5		721.5	18.7	4.4	^{134}Cs
82.3	729.6	689.4	25.4	7.4	^{60}Co
77.3	703.8	649.3	30.8	11.3	^{60}Co
74.0	686.6				
70.0		571.8	41.9	13.5	^{60}Co
70.0		594.3	38.6	13.5	^{60}Co
69.6	659	594.4	37.9	15.3	^{60}Co
66.7		550.7	45.2	19.8	^{134}Cs
65.7	632	605.9	37.8	15.0	^{60}Co
62.0	602.5	569.3	43.1	14.4	^{60}Co
61.0	590.8	554.6	44.0	9.2	^{60}Co
60.0		525.0	47.8	20.1	^{134}Cs
60.0		578.2	40.3	12.3	^{134}Cs
58.2	572.0	515.4	50.1	18.8	^{60}Co
58.2		515.7	49.2	19.0	^{134}Cs
58.2		529.9	47.6	18.8	^{134}Cs
56.1	560.4				
$CaCl_2$ Side					
0	771.6				
6	748.0				
17.4	695.8	631.8	69.78		
38.7	566.5	525.0	54.85	100.0	^{134}Cs

Column 1: Total composition solid + liquid.
» 2: Temp. of the first crystallization.
» 3: Filtration temperature.
» 4 and 5: Calculated composition of liquid and solid solutions.
» 6: Tracer.

1. As assumed by Menge, there exists a compound of the composition $CaCl_2 \cdot 4$ NaCl, which melts incongruently at 594°C (*cf.* the full lines in the diagram, Fig. 3).

2. No compound exists, but the content of $CaCl_2$ in the solid NaCl increases with decreasing temperature, reaching the maximum value of 20 mole percent at the eutectic temperature (*cf.* the broken line in Fig. 3). In favour of this latter alternative is that we have not yet succeeded in obtaining any X-ray evidence for the existence of a compound. Melts with about 58 mole percent NaCl were slowly cooled, or quenched, in both cases powder patterns showed strong lines of NaCl.

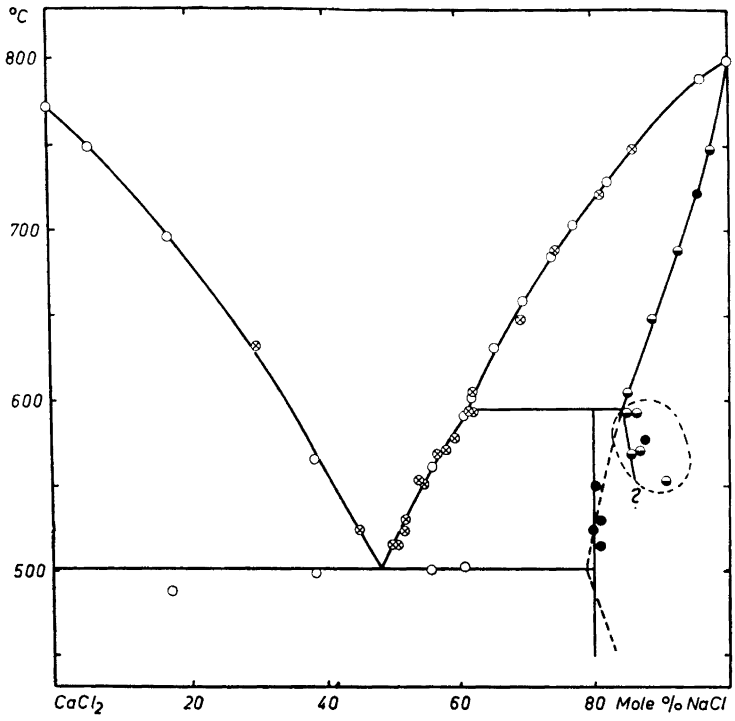

Fig. 3. The system NaCl—$CaCl_2$.

Open circles: Liquidus line determined by thermal analysis.
Crossed » » » » » high-temperature filtration.
Half filled circles: Solidus line determinations with ^{60}Co-tracer.
Filled circles: » » » » ^{134}Cs-tracer.

The data in the composition of the solid phase in the temperature range 500 to 550°C are not incompatible with this interpretation, but they fit better with the assumption of a compound $CaCl_2 \cdot 4\ NaCl$. Two other arguments also favour the existence of this compound. First, the liquidus curve has a weak but definite discontinuity at 594°C (as also observed by Menge). The second argument is the group of obviously erratic points for the solid phase composition in the temperature range 550 to 600°C (inside the circled area in the diagram Fig. 3). These points have been obtained using both CsCl and $CoCl_2$ tracers, and they seem to indicate that in this area it is difficult to attain true equilibrium between solid and liquid. This would be difficult to explain if a continuous range of solid solutions exists down to the eutectic temperature. If on the other hand the compound exists below 594°C, the following explanation seems reasonable. Our filtration technique demands that the system is cooled at least some 50° below the temperature of the first crystallization in order to get an appropriate ratio between the amounts of liquid and solid

compositions. In the range 550 to 600°C it is therefore necessary to start with melts containing more than 62 mole % NaCl, resulting in primary cyrstallization above 594°C. When next the melt is cooled below this temperature, a certain amount or $NaCl-CaCl_2$ solid solution will have to react with the liquid to form the compound before equilibrium is established. This reaction may very well be a slow process. Difficulties of this kind should be absent when the compound is the primary product of crystallization, and this is just what is observed. Starting with mixtures with less than 62 mole percent NaCl, the results for the solid phase composition show very little scattering.

If the existence of the compound is accepted, one will have to explain why it does not appear in the X-ray powder patterns. One reason might be that it is unstable at room temperature. It is evident that the solid solubility decreases strongly with decreasing temperature, (compare Sato and Amano [5]), furthermore the weakness of the break in the liquidus line at the peritectic temperature may indicate that the stability of the compound does not greatly exceed that of the undercooled solid solution. The final answer in this case should be given by high-temperature X-ray examination.

Another possibility is that the compound is stable down to room temperature, but has a crystal lattice very similar to that of NaCl. The solid solution in all probability has a NaCl lattice in which part of the Na^+ ions are replaced by Ca^{++} ions and cation vacancies (eventually forming pairs), distributed at random over the cation sites. The compound might have a similar structure, but with 1/5 of the Na^+ ions replaced by 1/10 Ca^{++} ions and 1/10 cation vacancies in an *ordered* distribution over the cation sites. In this case, X-ray examination at elevated temperatures would not be expected to furnish further evidence.

The question cannot be considered to be finally settled. When we have discussed it in some detail here, one reason is that if the compound formation is real (as we believe) the observations indicate a difficulty in the present method of determining the solidus line which may be expected to occur also in other systems.

STRUCTURAL INTERPRETATIONS

Considerable evidence favours the view that molten salt mixtures can in many cases be considered as ideal or regular mixtures of simple ionic components over certain ranges of composition. The study of phase diagrams may give valuable information about the validity of any chosen model for the structure of the melt, compare the alkali chloride — magnesium chloride systems, where the formation of $MgCl_4^{--}$ complex ions in the molten mixtures is strongly indicated [7]. In the following the system $NaCl-CaCl_2$ is examined from similar points of view.

In a system of coexisting solid and liquid phases, the equilibrium condition for the major component can be expressed by the well-known equation

$$\ln a_{(l)} - \ln a_{(s)} = \frac{\Delta H_m}{R}\left(\frac{1}{T} - \frac{1}{T_m}\right)$$

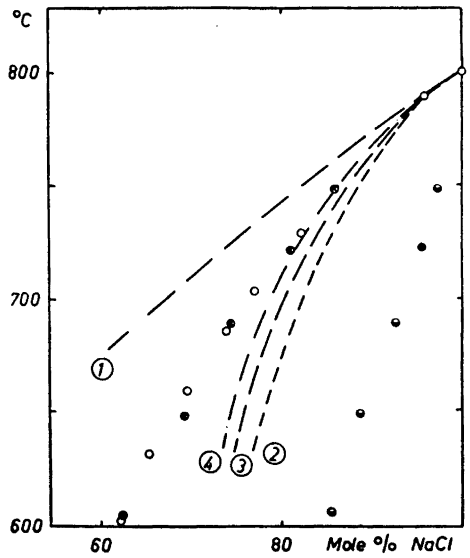

Fig. 4. The NaCl side of the diagram. Experimental data compared with calculated curves.

Here $a_{(l)}$ and $a_{(s)}$ are the activities of the component in the two phases, referring to its pure liquid and its pure solid respectively as standard states, and ΔH_m is the molar heat of melting of the component, considered to be independent of the temperature over the range studied.

a) *The NaCl side.* The molar heat of melting of NaCl is determined calorimetrically by Lyashenko [8] to 6.8 kcal, and by Roth and Berthrand [9] to 7.4 kcal. Careful investigations of the systems NaCl—Na_2SO_4 (Flood, Förland and Leirnes [10]) and NaCl—NaF (Grjotheim [11]), however, are in agreement with 7.1 kcal; this value will be adopted in the following.

We will first examine the possibility that the melt behaves as an ideal Temkin mixture of Na^+, Ca^{++} and C^- lions. This would give

$$a_{NaCl} = N_{Na+} \cdot N_{Cl} = \frac{n_{Na}}{n_{Na} + n_{Ca}} \cdot 1 = \frac{n_{NaCl}}{n_{NaCl} + n_{NaCl_2}} \qquad (1)$$

If, as a first approximation, the correction for the solid solubility is neglected, a calculation according to this model gives curve 1 in Fig. 4. It is evident that the real melt shows strong negative deviations from ideality according to this model, or in other words, the components seem to be more strongly bonded in the melt than corresponding to the ideal Temkin mixture of simple ions.

The second model to be tried is the same as proved valuable in the corresponding magnesium system [6], *viz.*, that tetrachloro complexes are formed in the melt according to the reaction

$$2\ Cl^- + CaCl_2 = CaCl_4^{--}$$

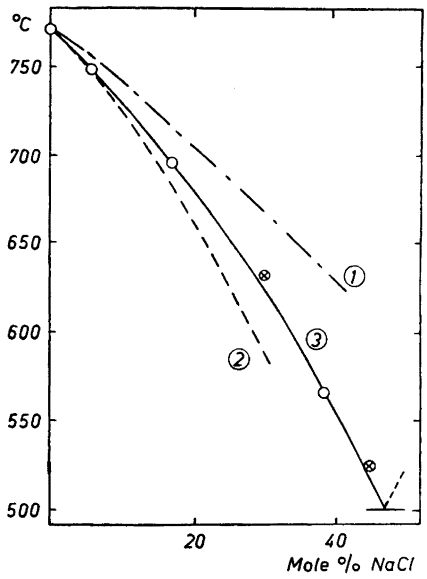

Fig. 5. The $CaCl_2$ side of the diagram. Experimental data compared with calculated curves.

Again assuming ideal Temkin ionic mixture:

$$a_{NaCl} = N_{Na^+} \cdot N_{Cl^-} = \frac{n_{Cl^-}}{n_{Cl^-} + n_{CaCl_4^{--}}} = \frac{n_{NaCl} - 2\, n_{NaCl_2}}{n_{CaCl_2} - n_{CaCl_2}}$$

Neglecting the solid solubility correction, the curve 2 in Fig. 4 is calculated. This curve shows a better agreement with the experimental data, remembering that the correction for the solid solubility will tend to lift the curve and thus bring it closer to the experimental points.

The calculation of the solid solubility correction depends upon the chosen model for the solid solution. Assuming a Temkin ideal solution for the solid (and no complex ions), the calculation gives curve 3 of Fig. 4. The second (more probable) model for the solid is the "equivalent fraction" model, which gives

$$a_{NaCl} = \frac{n_{NaCl}}{n_{NaCl} + 2\, n_{CaCl_2}}$$

The calculation based on this model for the solid and tetrachloro complexes for the liquid is shown as curve 4 in Fig. 4. This curve shows excellent agreement with the observations up to about 20 mole percent $CaCl_2$. The introduction of the "equivalent fraction" is in accordance with present ideas regarding solid solutions, when $CaCl_2$ is introduced in a NaCl lattice it is assumed that two Na^+ ions are exchanged with one Ca^{++} ion and one cation vacancy.

The deviations that occur between calculation and experiment at higher $CaCl_2$ concentrations may be explained either as a negative deviation from ideality in the solid solution or positive deviation in the liquid solution. Since the solid solubility is limited, negative deviations in the solid is improbable. Positive deviations in the liquid, on the other hand, could be explained simply as due to incomplete complex formation at the higher $CaCl_2$ concentrations.

b) *The $CaCl_2$ side.* The curve 1 in Fig. 5 has been calculated on the assumption of a simple Temkin mixture, and shows that this model disagrees with experiment also on the $CaCl_2$ side of the diagram. A formation of tetrachloro complexes could take place according to the following scheme

$$CaCl_2 + 2\ NaCl = CaCl_4^{2-} + 2\ Na^+$$

The corresponding expression for the (ideal) activity of $CaCl_2$ is:

$$a_{CaCl_2} = \left[\frac{n_{Na}}{n_{Ca} + n_{Na}}\right]\left[\frac{n_{Cl}}{n_{Cl} + n_{CaCl_4}}\right]^2 =$$

$$\left[\frac{n_{CaCl_2} - 1/2\, n_{CaCl}}{n_{CaCl_4} + 1/2\, n_{CaCl}}\right]\left[\frac{2\, n_{CaCl_2} - n_{NaCl}}{2\, n_{CaCl_2} - 1/2\, n_{NaCl}}\right]$$

and the result of the calculation is given as curve 2 in Fig. 5. Although this curve is in somewhat better agreement with the experiments than curve 1, the deviations are still considerable at NaCl concentrations above 5 mole percent. It should be noted that this latter model results in a mixture composed of two different anions (Cl^- and $CaCl_4^{2-}$). Theoretical considerations [12] have shown that such mixtures with both mixed cations and mixed anions in general would be expected to show considerably larger deviations from ideality than mixtures with one common ion.

According to the theory, the expression for the activity of $CaCl_2$ should be corrected by an activity coefficient

$$\gamma_{CaCl_2} = \exp\ (N'_{Na} N'_{CaCl_4}\ \Delta G/RT)$$

where the N's are equivalent fractions and ΔG is the free enthalpy change for the reaction

$$CaCl_2 + Na_2(CaCl_4) \rightleftharpoons Ca(CaCl_4) + 2\ NaCl$$

But a calculation along these lines would need support from other evidence before it could be considered to be of more than formal interest. The possibility of a treatment based on an entirely different type of model should be kept in mind, and will be considered in connection with a more extensive study now in progress regarding systems of this type.

It should finally be mentioned that surprisingly good agreement between calculation ad experiment can be obtained over the whole range by assuming the formation of $CaCl_6^{4-}$ complex ions in the melt, see curve 3 of Fig. 5. But it seems difficult to believe in the existence of discrete $CaCl_6^{4-}$ units in such a melt.

Our investigations have been carried out with aid of grants from *Statsminister Gunnar Knudsen og hustru Sophie f. Cappelen Familjelegat (Borgestad Legat IV)*, for which we wish to express our sincere gratitude.

The authors also wish to thank Mrs. G. Hägh for assisting at the experimental work and instituttingeniör K. Motzfeldt for valuable discussions and also help in preparing the English manuscript.

REFERENCES

1. Flood, H., Förland, T. and Nesland, A. *Acta Chem. Scand.* **5** (1951) 1193.
2. Lamplough, F. E. *Proc. Cambridge Phil. Soc.* **16** (1911) 194.
3. Menge, O. *Z. anorg. u. allgem. Chem.* **72** (1911) 162.
4. Scholich, K. *Neues Jahrb. Mineral. Geol.* **43** (1920) 251.
5. Sato, T. and Amano, T. *Metal Research (Japan)* **11** (1934) 305.
6. Miyake, S. and Suzuki, K. *J. Phil. Soc. Japan* **9** (1954) 702.
7. Flood, H. and Urnes, S. *Z. Elektrochem.* **51** (1955) 364.
8. Roth, W. A. and Berthand, W. W. *Z. Elektrochem.* **35** (1929) 297.
9. Lyashenko, V. S. *Metallurg.* **10** (1955) 85.
10. Flood, H., Förland, T. and Leirnes, S. *Unpublished.*
11. Grjotheim, K. *Unpublished.*
12. Flood, H., Förland, T. and Grjotheim, K. *Z. anorg. Chem.* **276** (1954) 289.

Received January 28, 1958.

ACTA CHEMICA SCANDINAVICA 12 (1958) 1042—1046

Ein Vergleich zwischen Pyridin, Äthylalkohol und Azeton als Löslichkeitsvermittler

GUSTAF HOLST

Försvarsväsendets kemiska anstalt, Sundbyberg 4, Schweden

In Zusammenhang mit Untersuchungen über die Hydrolyse von $\beta\beta'$-Dichlordiäthylsulfid sind die Homogenitätsgebiete einiger Lösungsmittelgemische bestimmt worden.

Bei der Durchführung chemischer Reaktionen zwischen wasserunlöslichen organischen Flüssigkeiten und wässrigen Lösungen anorganischer Verbindungen ist es für eine möglichst schnelle und vollständige Umsetzung vielfach wünschenswert, dass die reagierenden Stoffe in einer einzigen Phase vorhanden sind. In solchen Fällen bietet der Zusatz eines mit Wasser einerseits und mit der organischen Flüssigkeit andererseits in allen Verhältnissen mischbaren (chemisch indifferenten) Lösungsmittels die fast einzige Möglichkeit, ein homogenes System zu erreichen.

Die vorliegende Arbeit entstand in Zusammenhang mit einer kinetischen Untersuchung über die oxydative Zerstörung von $\beta\beta'$-Dichlordiäthylsulfid durch wässrige Hypochloritlösungen, worüber an anderer Stelle kurz berichtet wurde [1]. Sie enthält einige vergleichende Messungen über die Mischungsverhältnisse in einigen flüssigen Dreistoffsystemen mit Wasser als eine Komponente.

Die folgenden vier organischen Flüssigkeiten ziemlich weit verschiedener Konstitution wurden dabei jeweils als die "wasserunlösliche" Komponente gewählt: Benzol, Tetrachlorkohlenstoff, Schwefelkohlenstoff und $\beta\beta'$-Dichlordiäthylsulfid. Die Löslichkeit dieser Verbindungen in Wasser ist sehr klein. Sie beträgt z.B. in 100 Vol. H_2O bei 22° für CS_2, 0,17 Vol. und für C_6H_6 0,08 Vol. Ebenso löst sich [2] in 100 Vol. CS_2 bzw. C_6H_6 nur 0,96 bzw. 0,22 Vol. H_2O.

Als Vertreter der dritten Komponente (Löslichkeitsvermittler) kamen Pyridin, Äthylalkohol und Azeton zur Verwendung, so dass insgesamt zwölf verschiedene Kombinationen untersucht wurden.

Der Einfluss einer *dritten* Komponente auf die gegenseitige Löslichkeit zweier Flüssigkeiten ist vielfach ausserordentlich gross, was sich in einer erheblichen *Verschiebung der kritischen Entmischungstemperatur* des binären Systems wiederspiegelt. Grundlegende Untersuchungen auf diesem Gebiete verdanken wir u.a. Timmermans [3].

Als Beispiel der Löslichkeitsverhältnisse sei ferner erwähnt, dass sich Dichlordiäthylsulfid in jedem Verhältnis in absolutem Äthylalkohol oberhalb 15,6° löst, dagegen erst oberhalb 38,6° in 92,5 %-igem Äthylalkohol [4].

VERSUCHE

Die verwendete Versuchsmethodik war sehr einfach. In ein kleines Reagenzglas wurde mit einer Mikropipette je 0,50 ml der organischen Flüssigkeit (F) und des Löslichkeitsvermittlers (L) eingeführt, wobei ein homogenes Gemisch erhalten wurde. Danach wurde aus einer in 0,01 ml geteilten Mikrobürette mit feiner Spitze Wasser (W) tropfenweise zugesetzt, bis eine momentane Trübung beobachtet wurde, wobei zwei Phasen entstanden, die beim Schütteln bestehen blieben. Das zugesetzte Wasservolumen wurde abgelesen. Dann wurde noch 0,50 ml (L) und aus der Bürette (W) zugeführt, bis eine Entmischung wieder beobachtet werden konnte usw. Die aus den zugesetzten Volumen (ml) berechneten Molprozente (N) gehen aus den folgenden Dreieck-Diagrammen hervor (Fig. 1—4). Alle Bestimmungen wurden bei Zimmertemperatur (etwa 20°) ausgeführt.

Es sei hier nebenbei bemerkt, dass diese einfache sog. "Trübungstitration" für das Studium der Lösung hochmolekularer Polymerisationsverbindungen eine wichtige Verwendung gefunden hat.

In dem folgenden Ausdruck bedeutet n die Anzahl Millimole der jeweils vorhandenen Komponenten (W, F und L). Die Grösse N bedeutet der Molprozent, z.B.

$$N_F = 100 \cdot \frac{n_F}{n_F + n_W + n_L}$$

und 0,50 ml Flüssigkeit (F) entspricht den folgenden Werten von n_F

F	C_6H_6	CCl_4	CS_2	$S(CH_2 \cdot CH_2Cl)_2$
n_F	5,65	5,19	8,32	4,08

In den Dreieckdiagrammen (Fig. 1—4) bedeuten:
Kurve I C_5H_5N — Mischungen
Kurve II C_2H_5OH — "
Kurve III $(CH_3)_2CO$ — "

Wenn wir die gegenseitige Lage der drei Entmischungskurven in den vier Dreiecken mit einander vergleichen, so erkennen wir zunächst, dass von

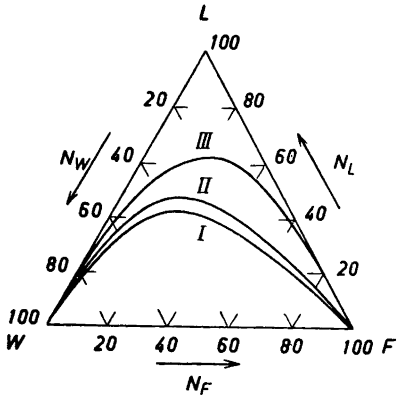

Fig. 1.

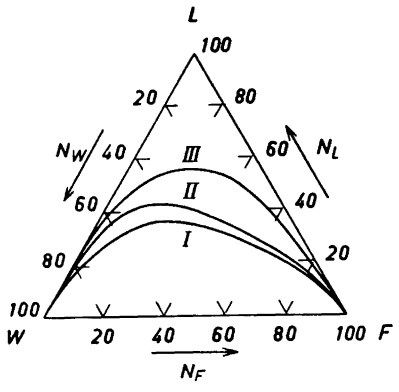

Fig. 2.

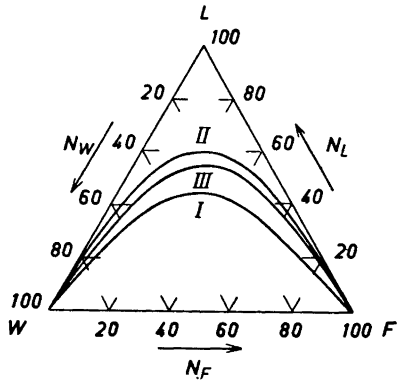

Fig. 3.

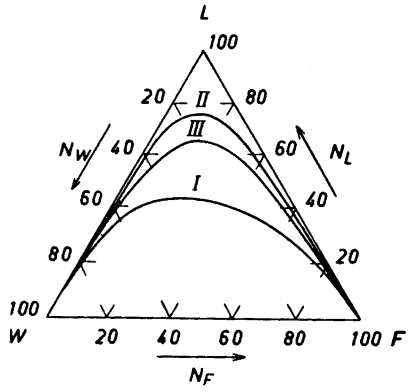

Fig. 4.

Pyridin (Kurve I) in sämtlichen Fällen ein kleinerer Molprozent (N) erforderlich ist um eine vollständige Mischung zu erreichen und dass diese Kurve sehr flach ist. Dabei ist allerdings zu bedenken, dass Pyridin ein höheres Molgewicht (79) besitzt als die anderen wasserlöslichen Verbindungen, Alkohol (46) und Azeton (58).

Zwischen den letzten Flüssigkeiten bestehen charakteristische Unterschiede. Wenn wir z.B. die zwei Substanzpaare: C_6H_6—CS_2 in Fig. 1 und 3, bzw. CCl_4—$S(CH_2{\cdot}CH_2Cl)_2$ in Fig. 2 und 4 mit einander vergleichen, wobei die Molgewichte von C_6H_6 (78) und CS_2 (76), bzw. CCl_4 (154) und $S(CH_2.CH_2Cl)$ (159) je etwa dieselben Grössen besitzen, so erkennen wir, dass für die *Schwefelverbindungen* die Alkohol-Kurve höher liegt als die Azeton-Kurve, während für die *anderen Verbindungen* die Verhältnisse umgekehrt liegen.

Aus den Diagrammen 1 und 2 geht mit aller Deutlichkeit hervor, dass Äthylalkohol für C_6H_6 und CCl_4 ein wesentlich besserer Löslichkeitsvermittler ist als Azeton. Ebenso zeigen die Kurven II der Diagramme 2 und 4, dass ein erheblich kleinerer Zusatz von Alkohol nötig ist, um für das binäre System CCl_4-Wasser eine vollständige Mischung zu erreichen, als für das System $S(CH_2CH_2Cl)_2$-Wasser. Dasselbe gilt, obwohl etwas weinger scharf ausgeprägt, für die binäre Mischung C_6H_6—H_2O im Vergleich mit CS_2—H_2O (Kurven II, Fig. 1 und 3).

ANHANG

Hydrolyseversuch mit ββ'-Dichlordiäthylsulfid in alkalischer Äthylalkohol-Wasserlösung

Die Hydrolyse dieser Verbindung wurde in *homogenem System* untersucht, worüber hier kurz berichtet wird. Die wässrige Hydrolyse und deren Abhängigkeit von dem Verteilungszustand des Sulfids war schon früher von Wilson und Mitarbeitern [5] untersucht worden. Nach den Ergebnissen Wilsons ist die Hydrolyse der Dihalogenverbindung ausschliesslich an den in der wässrigen Phase gelöst vorhandenen Molekeln geknüpft, und die Grösse der Phasengrenzfläche bestimmt nur die Lösungsgeschwindigkeit des Sulfids in Wasser. Es wurde ferner eine merkliche Beschleunigung in Anwesenheit sulfonierter pflanzlicher und tierischer Öle festgestellt. Diese Stoffe, z.B. "Türkischrotöl" besitzen nämlich die Eigenschaft, den Dispersionsgrad des Sulfids zu erhöhen. Die *Auflösung* des Sulfids ist also der langsamste Vorgang und für die Gesamtreaktion *in heterogenem System massgebend.*

Die von mir gewählten Versuchsbedingungen gehen aus dem folgenden Beispiel hervor.

Eine benzolische Lösung von 1,000 g Dichlordiäthylsulfid in 50 ml Volumen wurde bereitet und im Thermostaten bei 50° aufbewahrt. 5 ml von dieser Lösung wurde zu einer ebenfalls bei 50° temperierten Mischung von 75 ml Äthylalkohol und 25 ml 0,1 N NaOH-Wasserlösung gesetzt und diese Reaktionslösung wurde während der ganzen Versuchszeit bei 50° gehalten. 10 ml Proben der Lösung wurden zu bestimmten Zeiten auspipettiert, und die Reaktion durch Titration mit 0,05 N HCl gegen Methylrot verfolgt. Ausgangskonzentrationen: NaOH = 0,024 N; Sulfid = 0,006 M

Zeit, Min.	5	10	15	20	30	45	60	100
Hydrolyse, %	17,3	32,1	43,0	56,8	71,6	85,3	92,4	99,3

Die Umsetzung ist also schon nach 20 Minuten zu mehr als 50 % fortgeschritten und nach 2 Stunden praktisch beendet.

Diese Untersuchung wurde im Jahre 1941 in der Forschungsabteilung von *Försvarsväsendets Kemiska Anstalt*, Ulriksdal bei Stockholm, durchgeführt, jedoch zufolge verschiedenen Umständen bisher nicht veröffentlicht.

Der Verfasser dankt seinem damaligen Chef, Herrn Prof. Dr. G. Ljunggren, für sein Interesse, sowie Herrn Dr. L. Melander für seine Mithilfe in der experimentellen Arbeit.

LITERATUR

1. Holst, G. *Svensk Kem. Tidskr.* **53** (1941) 319.
2. Walker, J. *Introduction to Physical Chemistry*, 10th Ed., MacMillan & Co. London and New York 1927, p. 48.
3. Timmermans, J. *Recherches expérimentales sur les phénomèns de démixtion des mélanges liquides*, Bruxelles 1911.
4. Thompson, T. G., Blach, J. H. and Sohl, G. T. *J. Am. Chem. Soc.* **43** (1921) 877.
5. Wilson, R. E., Fuller, E. W. and Schur, M. O. *J. Am. Chem. Soc.* **44** (1922) 2762, 2867.

Eingegangen am 13 December 1957.

ACTA CHEMICA SCANDINAVICA 12 (1958) 1047—1061

Kinetics of Complex Formation

IV. Rates of Decomposition and Transformation Mechanisms of Chromium(III) Ammines in Aqueous Solution

ERIK JØRGENSEN and JANNIK BJERRUM

Chemistry Department A, Technical University of Denmark and The Royal Danish School of Pharmacy, Copenhagen, Denmark

The aquation of the hexammine, pentammine and tetrammine chromium(III) ions in acidic as well as in basic solution was studied by chromatographic analysis of the reaction mixtures. Further, the aquation of tetraquodiammine ion was followed by a pH-titration method, and the existence of a relatively stable monammine ion was proved. The monammine which completes the series of chromium(III) ammines from hexammine to hexaquo ion was isolated as a cesium alum.

In a previous paper [1] of this series one of the authors has found that the aquation of the hexammine chromium(III) ion in nitric acid solution is independent of the hydrogen ion concentration, and the following expression was found for the pseudo-unimolecular velocity constant (in sec^{-1})

$$k_{-6} = 10^{12.3} \exp \frac{-26\,000}{RT} .$$

This study has now been extended to the pentammine, tetrammine and diammine chromium complexes both in acidic and alkaline solution (*cf.* Ref.[2]).

The aquation is most simple in acidic solution because the equilibria between aquo- and hydroxo complexes can be stoichiometrically neglected and are also without importance to the reaction rates which are independent of the hydrogen ion concentration contrary to what is found for most acido complexes, *e.g.* for the aquation of the chloro chromium complexes [3]. This is in agreement with the fact that the reaction rates, at least for the higher ammines, are of the same order of magnitude in a basic solution as in an acidic solution. Hydroxo-pentammine decomposes even more slowly than aquopentammine. It is also an advantage that an acid reaction mixture remains homogeneous and that the formation of polynuclear compounds is suppressed.

The aquation of the luteo ion in acidic solution may then be supposed to consist of 20 consecutive and simultaneous exchanges of ammonia with water and *cis-trans* isomerizations:

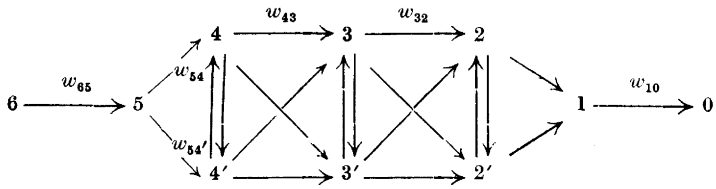

The figures give n in $Cr(NH_3)_n(H_2O)_{6-n}^{+++}$: 2,3,4 stand for the *cis*, and 2',3',4' for the *trans* complexes. w_{65} is the probability per unit time [4] of the hexammine reacting to form the pentammine. The other w's are analogously defined.

In basic solution a similar scheme can be established for the hydroxylation of hexammine down to trihydroxotriammine — more or less complicated by the formation of polynuclear compounds (*cf.* Figs. 1 and 2).

The complete solution for every intermediate is rather complex but may be readily calculated by matrix algebra as indicated in the appendix by one of the authors (E.J.).

Such calculations show that the relative amounts, a_j, of reaction product j can be expressed as the following function of t:

$$a_j = \sum_i Q_{ji} \exp(-\lambda_i t)$$

with 10 possible values of λ, which can be identified with the conventional gross velocity constants k_{-6}, k_{-5}, k_{-4}, $k_{-4'}$, . . . , k_{-1} plus a zero for the components present at equilibria, in this case hexaquo chromium ions only. Q_{ji} is a constant, usually a fraction containing the reaction probabilities, see appendix.

For k_{-6}, k_{-5} and k_{-1} we have the simple expressions:

$$k_{-6} = \frac{-\mathrm{d}\ \ln[Cr(NH_3)_6]}{\mathrm{d}t} = w_{65},\quad k_{-5} = w_{54} + w_{-54'},\quad k_{-1} = w_{10},$$

while the other gross constants are complicated functions of the w's. Of course, k_{-4} and $k_{-4'}$ and similarly k_{-3}, $k_{-3'}$ and k_{-2}, $k_{-2'}$ will only have their intuitive meaning when the *cis-trans* isomerization is very slow compared to the liberation of ammonia. Otherwise it is impossible to attach a definite one of the k's to a definite one of the tetrammines. Their bearing on the reaction probabilities are such that k_{-4} and $k_{-4'}$, are roots of

$$R^2 - (w_{44'} + w_{43} + w_{43'} + w_{4'4} + w_{4'3} + w_{4'3'}) \cdot R + (w_{44'} + w_{43} + w_{43'}) \cdot (w_{4'4} + w_{4'3} + w_{4'2'}) - w_{44'} \cdot w_{4'4} = 0,$$

and similar expressions exist for k_{-3}, $k_{-3'}$, and k_{-2}, $k_{-2'}$.

The rate experiments were all carried out in darkness at 40°C.

The concentration of the complexes most rich in ammonia in the reaction mixtures were determined by chromatography on alumina as developed by

Bjerrum, Jensen and Woldbye [5]. A separation of some lower ammines by chromatographic analysis on alumina was also attempted, but without success due to their low robustness in alkaline solution.

A representative selection of experiments in nitric acid solution ($c_{HNO_3} + c_{KNO_3} = 0.4$ M) is given in Tables 1—4, and similarly in alkaline solution ($c_{NaOH} + c_{KNO_3} = 0.4$ M) in Tables 5—7.

When the ammine complexes split off ammonia, an equivalent amount of acid is neutralized, and in a number of experiments also the amount of free acid has been determined in order to calculate the average number of ammonia bound per chromium atom in the reaction products. It was done by a pH titration and the equivalence point was estimated from the appearance of the titration curve. This procedure was used in the experiments with hexammine, pentammine and tetrammine chromium(III) salts. Some more accurate titrations of this kind were carried out in order to follow the aquation of the tetraquodiammine chromium(III) ion since in this case we were unable to analyze the mixture of ammines by chromatography. Most of these results are given in Table 8.

EXPERIMENTAL

Preparation of salts. The complex salts used were the following: $Cr(NH_3)_6(NO_3)_3$. *Anal.* Calc.: Cr 15.29; NH_3 30.02. Found: Cr 15.23; NH_3 29.76. $Cr(NH_3)_5(H_2O)(NO_3)_3$. *Anal.* Calc.: Cr 15.24. Found: Cr 15.10.

trans(?)-$[Cr(NH_3)_2(H_2O)_2(OH)_2]Cl,H_2O$ *Anal.* Calc.: Cr 24.81; NH_3 16.25; OH 16.23; Cl 16.91. Found: Cr 24.69; NH_3 16.30; OH 16.22; Cl 17.15.

cis-$[Cr(NH_3)_4(H_2O)OH]SO_4$ and *cis*-$[Cr(NH_3)_4(H_2O)OH]S_2O_6$.

With minor modifications the complex salts were prepared according to methods described in the literature. The *cis*-hydroxoaquotetrammine chromium(III) sulphate was kindly supplied by C. E. Schäffer, who also suggested making the dichlorodiaquodiammine chromium(III) chloride which was used in preparing the dihydroxodiaquodiammine chloride by oxidizing the Reinecke salt with hydrogen peroxide: The hydrogen peroxide (30 %) was added dropwise to the solid Reinecke salt moistened with concentrated hydrochloric acid. The vigorous reaction was slowed down by cooling in ice. The dark red solution was frequently decanted off and the joined fractions were saturated with hydrogen chloride in the cold. The solution was placed at room temperature till the next day. The precipitate formed was used for the next preparation after a single reprecipitation with hydrochloric acid.

Reinecke salt has been shown to be the *trans*-diammine compound [6], and we have assumed that the tetraquodiammine ion also has *trans*-configuration.

Chromatography. 2—5 ml were brought to the approximate composition of the eluating liquid by adding the necessary electrolytes [5]. The dimension of the column was usually 11 × 200 mm. For the separation of hexammine and pentammine solutions were used of the following composition: 0.1 M KOH, 0.2 M KCl, 0.8 M $(C_2H_5)_4NBr$ followed by 0.1 M KOH, 1.0 M KCl. Pentammine passes first. Hexammine is recovered practically quantitatively by addition of the latter solution. A shorter column was used for the separation of pentammine and tetrammine. Pentammine is displaced quickly with a solution of the composition 1.0 M NH_3, 0.1 M NH_4Cl, 1.0 M $NaNO_3$ with a loss of about 10 %, after which the tetrammine is displaced with 0.1 M NaOH, 1.0 M LiCl. Separation of tetrammine from the lower ammines was performed with solutions of the composition 0.1 M NaOH, 1.0 M $NaNO_3$, giving a loss of approximately 30 % due to the relatively low robustness of the tetrammine. The lower ammines were completely decomposed by this treatment.

The concentration in the eluate was in a few cases determined from the optical density, but in the majority of cases the acidified solutions were boiled until there was complete transformation to hexaquo ions. The chromium(III) ions were oxidized by

persulphate, using silver ions as catalyst. The chromate formed was then titrated with ferrous ions [7].

pH-titrations. A pH Meter 22 (Radiometer) was used. In order to increase its sensibility in the more accurate titrations (Table 8) it was supplied with an external meter covering the pH range 6—8. Between the calomel electrode and the input was inserted a pH-standard (PHN 2a, Radiometer). It was then possible to change the input voltage in jumps which correspond to one half unit in pH.

The procedure for the experiments given in Table 8 was the following: A sample of 10 ml of the reaction mixture was taken out and cooled. The extinction at 570, 540, 520, 480 and 385 mμ was measured in a Beckman DU spectrophotometer. Then it was transferred into the titration vessel together with 15 ml 0.5 M $NaNO_3$, and the titration curve was determined at ca. 20°C. with 0.5018 M NaOH as titrant.

The equivalence point is not a sharp point of inflection, and the various complexes have different values for the first acid dissociation exponent, pK_{a1}. It was, therefore, necessary to determine both equivalence point and a mean value of pK_{a1} for every titration. The interdependence of these quantities is, under the conditions of the experiments in Table 8 (0.473 mmole chromium complex contained in 25 ml liquid), expressed by

$$pH_{titr} = 0.5\left\{ pK_{a1} - \log\left(\frac{10^{-pH_0+1.372}}{x(25+x)} - 10^{-pH_{titr}}\right)\right\}$$

where

x: ml 0.5018 M NaOH used until the equivalence point

pH_{titr}: pH at the equivalence point

pH_0: pH of the initial solution before the titration

pK_{a1}: calculated from the data when the first aquo group in the complex is 50 % neutralized.

The true values for x, pH_{titr} and pK_{a1} are then found by iteration.

Table 1. 0.0478 M $Cr(NH_3)_6^{+++}$ in 0.4 M HNO_3 at 40°C.

Time (hours)	Hexammine found	Hexammine k_{-6} : 0.0051	Aquopentammine found	Aquopentammine k_{-6} : 0.0051 k_{-5} : 0.085	NH_3/Cr in products
0	—	0.0478	—	—	—
5	0.0468	466	0.0008	0.0009	2.9
18	420	437	17	21	2.9
50	364	370	19	23	2.2
74	313	328	21	21	1.7
122	234	257	10	16	1.7
167	199	204	10	13	1.6
218	152	157	7	10	1.2
289	108	109	—	7	0.9
384	66	67	—	4	0.7
501	32	37	—	2	0.5
670	19	16	—	1	0.3

Table 2. 0.0569 M $Cr(NH_3)_5(H_2O)^{+++}$ in 0.4 M HNO_3 at 40°C.

Hours	found	k_{-5} : 0.085	NH_3/Cr in products
0	0.0538	0.0569	—
1	504	522	3.0
2	475	480	2.6
3	431	441	2.8
5	355	372	2.6
8	280	288	2.7
25	58	68	2.2

Table 3. 0.0597 M $Cr(NH_3)_5(H_2O)^{+++}$ in 0.2 M HNO_3, 0.2 M KNO_3 at 40°C.

Hours	Aquopentammine found	k_{-5} : 0.088	Diaquotetrammine found	k_{-4} : 0.10	$k_{-4'}$: 1.0
0	0.0521	0.0597	—	—	—
0.5	520	570	0.0028	0.0026	0.0020
1	486	546	26	49	32
2	473	500	21	88	41
3.5	386	438	36	132	41
5	333	385	41	163	37
7	302	322	35	189	31

Table 4. *cis*-$Cr(NH_3)_4(H_2O)_2^{+++}$ in 0.4 M HNO_3 at 40°C.

Hours	found	k_{-4} : 0.10
0	0.0187	0.0211
4	132	141
9.5	72	82

Hours	found	k_{-4} : 0.12	NH_3/Cr in products
0	0.0220	0.0323	—
2	181	254	2.6
5	134	177	2.6
10	70	97	2.5
20	20	29	2.4

Table 5. 0.0534 M $Cr(NH_3)_6^{+++}$ in 0.1 M NaOH, 0.3 M KNO_3 at 40°C.

Hours	Hexammine found	k_{-6} : 0.0100	Hydroxopentammine found	k_{-6} : 0.0100 k_{-5} : 0.035
1	0.0505	0.0529	0.0010	0.0006
3	484	518	19	17
6	457	503	36	31
24	400	420	54	82
35	345	376	65	98
46	322	337	76	103
55	298	308	72	103
75	228	252	63	95
101	188	194	51	80

Table 6. 0.0530 M $Cr(NH_3)_5OH^{++}$ in 0.1 M NaOH 0.3 M KNO_3 at 40°C.

Hours	found	k_{-5} : 0.035
0.0	0.0485	0.0530
0.5	442	521
1.0	437	512
2.0	420	494
3.0	405	477
4.0	388	461
8.0	320	401
12.0	304	348
19.8	227	265
28.5	176	196
36.0	134	150

Table 7. 0.0309 M *cis*-$Cr(NH_3)_4(OH)_2^+$ in 0.1 M NaOH, 0.3 M KNO_3 at 40°C.

Hours	found	k_{-4} : 3
0.0	0.0165	0.0309
0.1	132	239
0.2	76	177
0.3	50	131
0.4	48	97

Table 8. 0.0473 M $Cr(NH_3)_2(H_2O)_4^{+++}$ in 0.2046 M HNO_3, 0.2 M KNO_3 at 40°C.
a. pH-titration data, and measured molar extinction coefficients.

Hours	x ml NaOH 0.5018 M	$-\Delta[H^+]$	ε_{570}	ε_{540}	ε_{520}	ε_{480}	ε_{385}
0.35	4.058	0.0005	12.2	19.5	21.2	12.2	24.4
0.60	4.044	0.0012	12.4	19.8	21.4	12.4	24.7
2	4.020	0.0024	12.7	19.5	20.9	11.9	24.1
4	3.954	0.0057	13.2	19.7	20.9	11.8	24.1
8	3.844	0.0112	13.5	19.4	20.0	10.8	22.7
12	3.745	0.0161	13.9	19.5	19.5	10.4	22.2
22	3.542	0.0263	14.7	19.2	18.6	9.43	20.7
34	3.336	0.0366	15.1	18.6	17.1	8.12	18.7
52	3.123	0.0472	15.9	18.2	15.9	7.15	17.5
76	2.974	0.0546	15.8	16.9	14.3	6.16	16.2
142	2.686	0.0690	15.2	14.7	11.4	4.67	14.4
225	2.477	0.0794	14.3	12.5	9.23	3.87	12.9
338	2.355	0.0855	14.2	11.4	8.08	3.81	12.7
506	2.281	0.0892	13.6	10.4	7.11	3.45	12.0
646	2.246	0.0910	13.4	10.2	6.95	3.33	11.8
∞	2.173	0.0946	13.6	10.1	6.90	3.44	11.9

b. pK_{a1} and calculated distribution of chromium on the various complexes. $n = 2$, $pK_{a1} = 4.11$, $pK_{a2} = 6.59$, $pK_{a3} = 9.17$.

Hours	pK_{a1}	$\bar{n}_{exp}$	$\alpha_2 + \alpha_{2'}$	α_1	α_0	$\bar{n}_{calc}$	α_2
0.35	4.11	1.989	0.988	0.012	0.000	1.988	0.002
0.6	4.11	1.975	0.979	0.021	0.000	1.978	0.003
2	4.12	1.949	0.932	0.068	0.000	1.932	0.011
4	4.15	1.880	0.870	0.128	0.002	1.867	0.021
8	4.19	1.764	0.759	0.232	0.009	1.750	0.038
12	4.22	1.659	0.666	0.315	0.019	1.646	0.052
22	4.23	1.445	0.487	0.458	0.055	1.431	0.079
34	4.28	1.227	0.349	0.540	0.111	1.238	0.098
52	4.30	1.003	0.233	0.563	0.204	1.028	0.110
76	4.36	0.845	0.162	0.514	0.324	0.838	0.114
142	4.33	0.541	0.108	0.316	0.576	0.532	0.102
225	4.26	0.321	0.086	0.162	0.752	0.333	0.083
338	4.24	0.192	0.064	0.071	0.865	0.200	0.062
506	4.22	0.114	0.042	0.026	0.932	0.111	0.041
646	4.26	0.077	0.030	0.015	0.955	0.075	0.029
∞	4.26	0	0	0	1	0	0

RESULTS AND DISCUSSION

The rate constants which head the third column of Tables 1—7 are evaluated graphically from the slope of the straight line obtained by plotting the logarithm of the experimental complex concentrations (given in the second column) against the time measured in hours. The concentrations in the third column are calculated from the rate constant and the initial complex concentration. When the figures of these two columns are compared, it is easily seen that the agreement is satisfactory only when due regard is paid to the loss of chromium on the column during the chromatographic analysis. This is certainly the case with the tetrammine chromium ions and particularly with the figures of Table 7. The value of k_{-4} is in this case given only as a size of order guess. As a whole, however, the numerical values of the rate constants are considered reliable. The value of k_{-6} given in the previous publication [1] from an altogether different way of analysis is 1.34×10^{-6} sec^{-1} = 0.0048 h^{-1}.

In Tables 1 and 5 are also given the concentrations of aquopentammine and hydroxopentammine found during the aquation and hydroxylation, respectively, of the hexammine, and they are seen to agree with the concentrations which can be calculated from the expression for the intermediate in two consecutive unimolecular reactions, see for example the second example in the appendix. Similarly, in Table 3 the concentration of tetrammine accumulated during the aquation of pentammine is given but does not at all correspond to the rate constant found for *cis*-diaquotetrammine (Table 4). It must then be concluded that the aquopentammine aquates mainly through the *trans*-diaquotetrammine. A column in Table 3 shows the concentrations of tetrammine to be expected if the pentammine was aquated through the *trans*-diaquotetrammine exclusively and if this complex disappeared at a rate ten times faster. It will be seen that this assumption gives a rather good agreement. It should be mentioned that *cis-trans* isomerization has been completely neglected.

The last column in Tables 1, 2 and 4 indicates the average number of ammonia per chromium atom in the aquated reaction products exclusive of the initial complex. The figures give immediately the impression that di- and monammine are just as robust as hexammine and that triammine roughly is as robust as pentammine.

The interpretation of the experimental results concerning the aquation of tetraquodiammine given in Table 8 requires a somewhat different practice. Already a look at the experimental values of pK_{a1} in Table 8b shows qualitatively that there must exist an intermediate of comparatively high stability with a higher value of pK_{a1} than that of the diammine and hexaquo ion. To the quantitative treatment we have the following relationships: The decrease in the hydrogen ion concentration $-\Delta[H^+]$ according to the appendix can be described by

$$\frac{-\Delta[H^+]}{C_{Cr}} = 2 - a_1\exp(-k_{-2'}t) - a_2\exp(-k_{-2}t) - a_3\exp(-k_{-1}t)$$

or

$$\bar{n} = a_1\exp(-k_{-2'}t) + a_2\exp(-k_{-2}t) + a_3\exp(-k_{-1}t)$$

where C_{Cr} is the total chromium concentration, and $\bar{n}$ is the average number of ammonia molecules bound per chromium atom in the reaction mixture.

The experimental values for $\bar{n}$ which are given in the third column of Table 8b are now fitted to these expressions by trial and error. A particularly systematic "least square method" has not been used because of the overwhelming number of numerical calculations necessary. Due regard is paid to the fact that the 6 parameters are not independent. From the appendix it will be seen that a_1, a_2, a_3 can be expressed by 4 independent parameters: k_{-1}, k_{-2}, $k_{-2'}$ and $w_{2'1}$. In addition there are 3 different possibilities for choosing k_{-1}, but for the remaining two the indices are exchangeable. For the eighteen esperimental results, most of them given in Table 8, the following parameters were chosen:

a_1: 0.60	a_2: 0.36	a_3: 1.04
$k_{-2'}$: 0.041	k_{-2}: 0.0025	k_{-1}: 0.0093

The seventh column contains $\bar{n}$ calculated from these parameters.

w_{10} is identical with $k_{-1} = 0.0093$ and $w_{2'1}$ can be directly calculated as the sum $a_1k_{-2'}$, $+ a_2k_{-2} + a_3k_{-1} = 0.035$.

It is now possible to calculate the relative amounts of *cis* and *trans* diammine ($a_2 + a_{2'}$), monammine a_1 and hexaquo chromium ion a_0 as a function of time, since the previously mentioned Q_{j_i}'s contain $k_{-2'}$, k_{-2}, k_{-1} and $w_{2'1}$ only. They are listed in Table 8b and show quantitatively that the monammine is the predominant complex for the period of 30—80 h after the start of the reaction.

If we denote the measured properties of the reacting solution (pK_{a1} and the molar extinction coefficients at various wavelenths) by U, the corresponding property of the monammine is obtained as the slope of the straight line in a plot of $\frac{U - a_0u_0}{a_{2'} + a_2}$ *versus* $\frac{a_1}{a_{2'} + a_2}$. This relationship should only be a straight line when the properties of *cis* and *trans* diammine are only slightly different, and this seems to be the case with a possible exception for ε_{480}, in which case the plot indicates a higher extinction for the *cis* than for the *trans* isomer.

The estimated properties for the monammine are given in Table 9 compared with the corresponding properties for the diammine and the hexaquo chromium ion. The molar extinctions of the monammine are also represented as crosses in Fig. 3.

Table 9. Estimated properties for the pentaquomonammine chromium(III) ion at ~20°C.

	pK_{a1}	ε_{570}	ε_{540}	ε_{520}	ε_{480}	ε_{385}
$Cr(NH_3)_2(H_2O)_4^{+++}$	4.11	12.1	19.2	21.0	12.1	24.2
$Cr(NH_3)(H_2O)_5^{+++}$	4.4	18	20	17	5.5	16
$Cr(H_2O)_6^{+++}$	4.26	13.6	10.1	6.9	3.44	11.9

The remaining reaction probabilities are related by

$$k_{-2}k_{-2'} = w_{2'2}w_{21} + w_{22'}w_{2'1} + w_{2'1}w_{21}$$
$$k_{-2} + k_{-2'} = w_{2'2} + w_{2'1} + w_{22'} + w_{21}$$

giving

$$w_{2'2} \cong 0.0056 \qquad w_{21} + w_{22'} \cong 0.0027$$

The distribution of the diammine chromium ion between the *cis* and *trans* isomer throughout the reaction can also be approximated, and it is seen from the last column of Table 8b that the maximum amount of the *cis* isomer is more than 11 %. However, it is necessary to make serious reservations regarding this figure as well as regarding the estimates of $w_{2'2}$ and $w_{21} + w_{22'}$, because the rate equation is not critically influenced by these quantities.

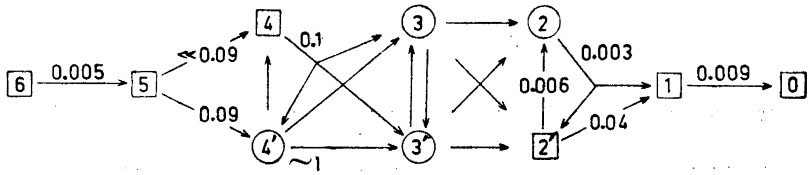

Fig. 1. Velocity constants (hour^{-1}) in > 0.1 M HNO_3 at 40°C.

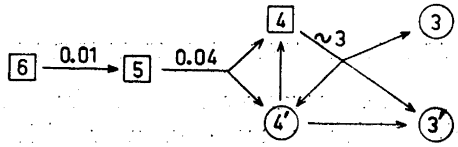

Fig. 2. Velocity constants (hour^{-1}) in ~ 0.1 M NaOH at 40°C.

The reaction probabilities found in acidic and basic solution are summarized in Figs. 1 and 2. As a whole, the hydroxo-ammine complexes are less robust than the corresponding aquo complexes. It is therefore remarkable that hydroxopentammine is seen to decompose more slowly than the aquopentammine chromium ion. Triaquotriammine chromium(III) salts have been prepared by Werner [8] but have not been utilized in this study. The squares in Figs. 1 and 2 indicate the components which have been used in our experiments. The spectra of these complexes in acidic solution are recorded in Fig. 3, which also gives the spectrum of the monammine. This compound was obtained in crystalline form in a preliminary attempt to prepare it from the reaction mixture. The data which were calculated from the mixed spectra are seen to be represented by the curve fairly well.

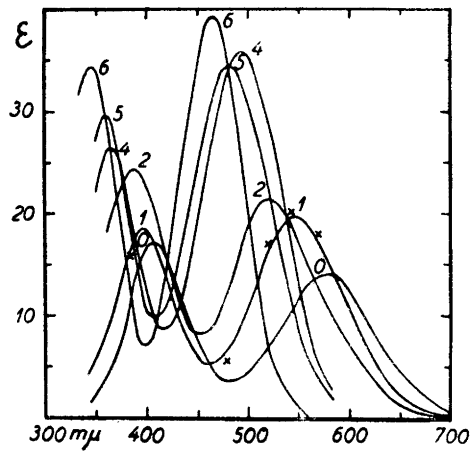

Fig. 3. Some absorption spectra of aquoammine chromium(III) ions in 0.5 M nitric acid at room temperature.

Curve 6: hexammine, 5: aquopentammine, 4: *cis*-diaquotetrammine, 2: *trans*(?)-tetraquodiammine, 1: pentaquomonammine (0.1 M HNO_3) and 0: hexaquo ions (1 M HNO_3). ×-points for the monammine are calculated from the data given for the mixed spectra in the reaction mixtures of Table 8.

PREPARATION OF THE MONAMMINE AS CONSTITUENT OF A CESIUM ALUM

The monammine, which completes, apart from isomers, the series $Cr(NH_3)_6^{+++}$ . . . $Cr(H_2O)_6^{+++}$, was prepared in the following way. 0.440 g $[Cr(NH_3)_2(H_2O)_2(OH)_2]Cl$ was dissolved in 40 ml 0.55 M HNO_3 and placed at 40°C for 48 h. After this time the reaction mixture contained the maximum amount of monammine, *cf.* Table 8. It was now intended to precipitate the hexaquo ions as the cesium alum, which according to N. Bjerrum and Faurholt [9] is shown to be a very complete precipitation under the following conditions: To the cold solution 1 ml 2 M H_2SO_4 and 2 g cesium sulphate were added, followed by 20 ml 96 % alcohol after 1 h. It was remarkable that the precipitate did not have the greyish violet colour of the hexaquo ion but had a distinct purple colour probably due to the presence of monammine. The supernatant was placed for some hours at 0°C and a slight precipitate was formed which consisted of cyclamen coloured octaeders. An examination under the polarization microscope showed them to be isotropic. The crystals were not isolated but dissolved in 4—5 ml 0.1 M HNO_3 after rinsing with alcohol. After the spectrum had been taken, the concentrations of chromium and ammonia were found to be 0.0252 M and 0.0259 M, respectively. It is thus shown to be a monammine, and the octaederform of the crystals suggests it to be an alum, $CsCr(SO_4)_2,NH_3,11\ H_2O$.

In order to confirm the presence of monammine in the main precipitate it was dissolved in 40 ml of water and 1/4 ml H_2SO_4, and 2 g cesium sulphate

was added. The precipitate was still somewhat more reddish than the hexaquo chromium ion. The concentrations of chromium and ammonia in the supernatant were 0.00815 M and 0.00842 M, respectively.

THE ACID-BASE CONSTANTS OF THE TETRAQUODIAMMINE CHROMIUM(III) ION

From the data for the titration of the tetraquodiammine solution the second and third dissociation exponents, pK_{a2} and pK_{a3}, were estimated in addition to pK_{a1}. The following values (also mentioned in Table 8b) were determined in $\sim$ 0.5 M nitrate solution at $\sim$ 20°C:

$$pK_{a1} = 4.11, \quad pK_{a2} = 6.59, \quad pK_{a3} = 9.17.$$

A slow drift towards larger values of pH took place when more than 2 mole NaOH per chromium atom was added, showing that $[Cr(NH_3)_2(OH)_3H_2O]$ splits off its ammonia rather quickly at room temperature. This drift was accounted for by the estimate of pK_{a3}. A drift in the opposite direction was observed in the 22 hours' reaction mixture after an addition of 1.33 base equivalents, and after the lapse of a longer time even after addition of little more than one base equivalent per chromium atom due to the formation of polynuclears from the increasing amount of $Cr(H_2O)_4(OH)_2^+$.

Our thanks are due to Mr. C. E. Schäffer for valuable help in the preparing of salts.

APPENDIX

(by *Erik Jørgensen*)

The reactions dealt with in this paper belong to a rather common class. The partial reactions can be expressed by

$$X_i + (A) \rightarrow X_j + (X_k)$$

X_i is the i'th of the time dependent components and A is a component in great excess (or a component the concentration of which for some other reason can be kept constant during the reaction), it may be the solvent molecules. A and X_k are bracketed as they need not necessarily enter the scheme.

The calculations necessary to obtain the integrated rate expression can be systematized and simplified by introducing matrix methods. In the following it will be aimed at bringing this class of reactions within the framework of matrix algebra as, for example, it is formulated by Margenau and Murphy [10] whose widespread book is referred to concerning definitions and symbolism.

Let the initial component be X_1 and the reaction products $X_2, X_3, X_4, \ldots, X_n$ in a convenient numerical order, X_n being one of the components present at equilibrium.

Setting c_{Xi} equal to x_i, we will define the *concentration vector* $\boldsymbol{x}$ as the column vector $\{x_1, x_2, x_3, \ldots, x_n\}$. The mass action law determines a matrix $\boldsymbol{A}$ which transfers $\boldsymbol{x}$ to $-\mathrm{d}\boldsymbol{x}/\mathrm{d}t$.

$$-\mathrm{d}\boldsymbol{x}/\mathrm{d}t = \boldsymbol{A}\boldsymbol{x} \qquad (1)$$

A contains only constants at the conditions given. These constants are the "microscopic velocity constants" in question, which we according to Christiansen [4] may call "reaction probabilities per unit time" and represent by $w_{i,j(k)}$ for the above-mentioned partial reaction.

The characteristic matrix of A is $K = (\lambda E - A)$. The eigenvalues will be called λ_i — one of them, let it be λ_n, always being zero. If all the eigenvalues are different, which is practically no qualification, A can be reduced to true diagonal form.

Two orthogonal matrices, P and Q, may be constructed for this purpose in the following way:

$$P_{ij} = \frac{K^{jn}(\lambda_i)}{K^{1n}(\lambda_i)} \qquad Q_{ij} = \frac{P^{ji}}{|P|} \tag{2}$$

Now
$$PAQ = \{\lambda_i \delta_{ij}\} \tag{3}$$

Forming another *concentration vector*

$$y = Px \tag{4}$$

i.e. $x = Qy$, we get from (1)

$$-Q\mathrm{d}y/\mathrm{d}t = AQy$$

which multiplied by P gives

$$\mathrm{d}y/\mathrm{d}t = -\{\lambda_i \delta_{ij}\}y$$

with the solution

$$y = \{c_1 \cdot \exp(-\lambda_1 \cdot t), c_2 \cdot \exp(-\lambda_2 \cdot t), \ldots, c_n \cdot \exp(-\lambda_n \cdot t)\}$$

Setting the initial concentration of x_1 equal to x_1^0, we have at $t = 0$ from (4)

$$y = x_1^0\{P_{11}, P_{21}, P_{31}, \ldots, P_{n1}\}$$

From (2) it is seen that $P_{i1} = 1$, meaning that the c's are all equal to x_1^0. Then the complete solution including the boundary condition is

$$y = x_1^0\{\exp(-\lambda_1 \cdot t), \exp(-\lambda_2 \cdot t), \ldots, \exp(-\lambda_n \cdot t)\}$$

or

$$x = x_1^0 Q\{\exp(-\lambda_1 \cdot t), \exp(-\lambda_2 \cdot t), \ldots, \exp(-\lambda_n \cdot t)\} \tag{5}$$

P and Q may also be valuable tools for additive molar properties of the n components — conductivity, optical density, etc. If $u = \{u_1, u_2, \ldots, u_n\}$ is the vector containing these properties, the total property, $U = \tilde{u}x$, can be described as a function of time by $\tilde{u}_\lambda\{\exp(-\lambda_1 \cdot t), \exp(-\lambda_2 \cdot t), \ldots, \exp(-\lambda_n \cdot t)\}$.

Now the following relations hold between the *property vector* u and the *coefficient vector* u_λ:

$$u_\lambda = x_1^0 \tilde{Q} u \tag{6}$$

$$u = (x_1^0)^{-1} \tilde{P} u_\lambda \tag{7}$$

Differentiation of U with respect to t and setting t equal to zero leads to another useful formula:

$$\tilde{u}\{A_{11}, A_{21}, \ldots, A_{n1}\}\, x_1^0 = \tilde{u}_\lambda\{\lambda_1, \lambda_2, \ldots, \lambda_n\} \tag{8}$$

How the matrix algebra is to be applied should be evident from the following rather simple examples.

The first example is that of isomerism between 2 components. In this case

$$X_1 \rightleftharpoons X_2$$

$$A = \begin{bmatrix} w_{12} & -w_{21} \\ -w_{12} & w_{21} \end{bmatrix} \qquad K = \begin{bmatrix} \lambda - w_{12} & w_{21} \\ w_{12} & \lambda - w_{21} \end{bmatrix}$$

$$\lambda_1 = w_{12} + w_{21} \qquad \lambda_2 = 0$$

$$K^{12} = -w_{12} \qquad K^{22} = \lambda - w_{12}$$

$$P = \begin{bmatrix} 1 & -\dfrac{w_{21}}{w_{12}} \\ 1 & 1 \end{bmatrix} \qquad Q = \begin{bmatrix} \dfrac{w_{12}}{w_{12}+w_{21}} & \dfrac{w_{21}}{w_{12}+w_{21}} \\ -\dfrac{w_{12}}{w_{12}+w_{21}} & \dfrac{w_{12}}{w_{12}+w_{21}} \end{bmatrix}$$

The second example is the wellknown one of two consecutive reactions:

$$X_1 \rightarrow X_2$$
$$X_2 \rightarrow X_3$$

$$A = \begin{bmatrix} w_{12} & 0 & 0 \\ -w_{12} & w_{23} & 0 \\ 0 & -w_{23} & 0 \end{bmatrix} \qquad K = \begin{bmatrix} \lambda - w_{12} & 0 & 0 \\ w_{12} & \lambda - w_{23} & 0 \\ 0 & w_{23} & \lambda \end{bmatrix}$$

$$\lambda_1 = w_{12} \quad \lambda_2 = w_{23} \quad \lambda_3 = 0$$

$$K^{13} = w_{12}w_{23} \quad K^{23} = -w_{23}(\lambda - w_{12}) \quad K^{33} = (\lambda - w_{12})(\lambda - w_{23})$$

$$P = \begin{bmatrix} 1 & 0 & 0 \\ 1 & \dfrac{w_{12} - w_{23}}{w_{12}} & 0 \\ 1 & 1 & 1 \end{bmatrix} \qquad Q = \begin{bmatrix} 1 & 0 & 0 \\ -\dfrac{w_{12}}{w_{12} - w_{23}} & \dfrac{w_{12}}{w_{12} - w_{23}} & 0 \\ \dfrac{w_{23}}{w_{12} - w_{23}} & \dfrac{-w_{12}}{w_{12} - w_{23}} & 1 \end{bmatrix}$$

The third example is the reaction scheme which has been necessary to describe the aquation of the *trans*-tetraquodiammine chromium(III) ion in the present paper. Therefore, the indices have been changed to conform with those of the main text (2′∼1, 2∼2, 1∼3, 0∼4).

$$\begin{array}{lcl} X_{2'} & \rightleftharpoons & X_2 \\ X_{2'} & \rightarrow & X_1 \\ X_2 & \rightarrow & X_1 \\ X_1 & \rightarrow & X_0 \end{array}$$

$$A = \begin{bmatrix} w_{2'2} + w_{2'1} & - w_{2'2} & 0 & 0 \\ - w_{2'2} & w_{22'} + w_{21} & 0 & 0 \\ - w_{2'1} & - w_{21} & w_{10} & 0 \\ 0 & 0 & - w_{10} & 0 \end{bmatrix}$$

$$\lambda_1 \cdot \lambda_2 = k_{-2'} \cdot k_{-2} = w_{2'2}w_{21} + w_{22'}w_{2'1} + w_{2'1}w_{21}$$

$$\lambda_1 + \lambda_2 = k_{-2'} + k_{-2} = w_{2'2} + w_{2'1} + w_{22'} + w_{21}$$

$$\lambda_3 = k_{-1} = w_{10} \qquad \lambda_4 = 0$$

$$K^{14} = - k_{-1}(k_{-2'}k_{-2} - w_{2'1}\lambda) \qquad K^{24} = - k_{-1}(k_{-2'}k_{-2} - w_{21}\lambda)$$

$$K^{34} = - k_{-1}(\lambda - k_{-2})(\lambda - k_{-2'}) \qquad K^{44} = (\lambda - k_{-1})(\lambda - k_{-2})(\lambda - k_{-2'})$$

$$P = \begin{bmatrix} 1 & \dfrac{k_{-2}-w_{21}}{k_{-2}-w_{2'1}} & 0 & 0 \\ 1 & \dfrac{k_{-2'}-w_{21}}{k_{-2'}-w_{2'1}} & 0 & 0 \\ 1 & \dfrac{k_{-2'}k_{-2}-w_{21}k_{-1}}{k_{-2'}k_{-2}-w_{2'1}k_{-1}} & \dfrac{(k_{-1}-k_{-2})(k_{-1}-k_{-2'})}{k_{-2'}k_{-2}-w_{2'1}k_{-1}} & 0 \\ 1 & 1 & 1 & 1 \end{bmatrix}$$

$$Q = \begin{bmatrix} \dfrac{(k_{-2}-w_{2'1})(k_{-2'}-w_{21})}{(k_{-2'}-k_{-2})(w_{21}-w_{2'1})} & - \dfrac{(k_{-2}-w_{21})(k_{-2'}-w_{2'1})}{(k_{-2'}-k_{-2})(w_{21}-w_{2'1})} & 0 & 0 \\ - \dfrac{(k_{-2}-w_{2'1})(k_{-2'}-w_{2'1})}{(k_{-2'}-k_{-2})(w_{21}-w_{2'1})} & \dfrac{(k_{-2}-w_{2'1})(k_{-2'}-w_{2'1})}{(k_{-2'}-k_{-2})(w_{21}-w_{2'1})} & 0 & 0 \\ - \dfrac{k_{-2'}(k_{-2}-w_{2'1})}{(k_{-2'}-k_{-2})(k_{-1}-k_{-2'})} & \dfrac{k_{-2}(k_{-2'}-w_{2'1})}{(k_{-2'}-k_{-2})(k_{-1}-k_{-2})} & \dfrac{k_{-2'}k_{-2}-w_{2'1}k_{-1}}{(k_{-1}-k_{-2'})(k_{-1}-k_{-2})} & 0 \\ \dfrac{k_{-1}(k_{-2}-w_{2'1})}{(k_{-2'}-k_{-2})(k_{-1}-k_{-2'})} & - \dfrac{k_{-1}(k_{-2'}-w_{2'1})}{(k_{-2'}-k_{-2})(k_{-1}-k_{-2})} & - \dfrac{k_{-2'}k_{-2}-w_{2'1}k_{-1}}{(k_{-1}-k_{-2'})(k_{-1}-k_{-2})} & 1 \end{bmatrix}$$

The property measured was the decrease of the hydrogen ion concentration during the reaction. Accordingly, the *property vector* and *coefficient vector* are the following:

$$\boldsymbol{u} = \begin{bmatrix} 0 \\ 0 \\ 1 \\ 2 \end{bmatrix} \quad \boldsymbol{u}_\lambda = x_1^0 \widetilde{\boldsymbol{Q}} \boldsymbol{u} = x_1^0 \begin{bmatrix} \dfrac{(2k_{-1}-k_{-2'})(k_{-2}-w_{2'1})}{(k_{-2'}-k_{-2})(k_{-1}-k_{-2'})} \\ -\dfrac{(2k_{-1}-k_{-2})(k_{-2'}-w_{2'1})}{(k_{-2'}-k_{-2})(k_{-1}-k_{-2})} \\ -\dfrac{k_{-2'}-k_{-2}-w_{2'1}k_{-1}}{(k_{-1}-k_{-2'})(k_{-1}-k_{-2})} \\ 2 \end{bmatrix} = x_1^0 \begin{bmatrix} -a_1 \\ -a_2 \\ -a_3 \\ 2 \end{bmatrix}$$

Eqn. (8) gives

$$w_{2'1} = -(x_1^0)^{-1} \widetilde{\boldsymbol{u}}_\lambda \{\lambda_1, \lambda_2, \lambda_3, \lambda_4\} = a_1 k_{-2'} + a_2 k_{-2} + a_3 k_{-1}$$

which of course can also be seen by direct calculation.

The experimental results in one way or other written as a sum of exponential functions are seen directly to give w_{10} and $w_{2'1}$. $k_{-2'}$ and k_{-2} contain the remaining three reaction probabilities, and at least one further independent determination is necessary to calculate all of them.

REFERENCES

1. Bjerrum, J. and Lamm, C. G. *Acta Chem. Scand.* **9** (1955) 216.
2. Bjerrum, J. and Jørgensen, E. *Proceedings of the Symposium on Coordination Chemistry*, Roma 1957.
3. Bjerrum, N. *Z. physik. Chem.* **59** (1907) 336.
4. Christiansen, J. A. in Schwab, G.-M. *Handbuch der Katalyse* I, Springer-Verlag, Wien 1941, p. 257.
5. Bjerrum, J., Jensen, A. and Woldbye, F. *Communications, XVth International Congress of Pure and Applied Chemistry*, Lisboa 1956.
6. Takéuchi, Y. and Saito, Y. *Bull. Chem. Soc. Japan* **30** (1957) 319.
7. Kolthoff, I. M. and Sandell, E. B. *Textbook of Quantitative Inorganic Analysis*, New York 1943, p. 608.
8. Werner, A. *Ber.* **39** (1906) 2656.
9. Bjerrum, N. and Faurholt, C. *Z. physik. Chem.* **130** (1927) 584.
10. Margenau, H. and Murphy, G. M. *The Mathematics of Physics and Chemistry*, Van Nostrand, New York 1956, p. 301.

Received February 15, 1958.

ACTA CHEMICA SCANDINAVICA 12 (1958) 1062—1078

On the Isomerism of Hydroxyurea

X. Kinetics of the Isomerization

HELMER KOFOD

Royal Danish School of Pharmacy, Dept. of Organic Chemistry, Copenhagen, Denmark

The kinetics of the conversion of the lower melting isomeride in alkaline buffers, pH 9.2—12.3, have been examined, using a polarographic method of analysis.

At 25°C and pH 12 the reaction conformed to the empirical expression $Bt = \log(c_0/c) + A(c^{-1} - c_0^{-1})$. The constant A did not vary significantly with concentration in the range 1 to 8 mM but appeared to decrease with increasing pH, the overall reaction thus approximating to first-order kinetics in strongly alkaline solution.

At elevated temperatures and pH 12 the isomerization appears to be complicated by partial decomposition of the reactant into hydroxylamine and cyanate, in close analogy to the established chemical reversibility of the classical Wöhler synthesis of urea.

In the course of a general investigation on the polarographic behaviour of the lower melting isomeride (OU_{72}) it was previously observed (Ref. [1], Fig. 1) that on remeasurement of alkaline aqueous solutions, stored at 25°C, the characteristic cathodic wave rapidly vanished. In slightly alkaline and neutral buffers the process was found to be much slower, and in acidic buffers no diminution of the wave was noticed within a period of 72 h, (Ref [1], Table 1).

It is fortunate that the pH-region, ca. 9—13, in which the isomerization proceeds at a convenient velocity also happens to be the most favourable one for polarographic analysis (Ref.[1], Fig 2). It was feasible, therefore, if desired to follow the advancement of the isomerization in the polarographic cell itself. The OU_{72}-wave is well developed in this pH-region, and the isomerization product, OU_{140}, does not produce any interfering wave. Previously published paper-chromatographic work of a qualitative nature [2] suggested that in alkaline solution the conversion process might be sufficiently simple to justify a closer kinetic examination.

THE pH-DEPENDENCY OF THE ISOMERIZATION $OU_{72} \rightarrow OU_{140}$ AT 25°C

In the first series two experiments were carried out with 0.1 M potassium borate buffers at pH 10.5 and 12.3, respectively. The composition of the buffers and general technique are described p. 1077. The initial concentration of OU_{72} was 5.0 mM in both experiments.

5 ml of potassium borate buffer at pH 10.5 containing 0.1 % methylcellulose as a maximum suppressor was deaerated in the polarographic cell and the absence of dissolved oxygen was secured polarographically at high sensitivity. 1.90 mg of OU_{72} was weighed out and quickly dissolved in the cell contents (zero time). Polarographic recordings were run at time intervals. The results are listed in Table 1; t is the time in minutes from the dissolution of the solid until the maximum wave-height was attained during the recording of the polarogram. This point on the wave was reached 3 min after the recording had been started, the scanning speed being 1/3 V per min.

Table 1. Isomerization of OU_{72} at pH 10.5 and 25°C; initial concentration $c_0 = 5.0$ mM; capillary No. 1.

t	i	$10^3 \log (c_0/c)$	$10^4 k_1$
0	$(i_0) = 39.3$	0	
6	39.3	0	
10	39.3	0	
14	39.3	0	
18	39.3	0	
23	39.3	0	
33	38.7	6	4.2
63	38.0	14	5.1
123	36.7	29	5.4
251	33.5	69	6.3
303	32.5	82	6.3
440	29.5	124	6.5
513	27.0	163	7.3
590	26.0	179	7.0
657	24.7	201	7.0
1 307	17.7	346	6.1
1 547	14.1	445	6.0

In the next column i represents the diffusion current in μA, calculated from from the wave-height. The data are plotted in Fig 1, upper curve. The experimental points fit a straight line; although this suggests a zero-order reaction, it should be remembered that the degree of advancement in this experiment amounts to about 30 % only.

The reaction was accelerated in the next experiment by raising the pH to 12.3, other conditions remaining as above. The data are listed in Table 2, columns 1—2, and graphically represented in Fig 1, lower curve. The degree of advancement in this experiment is 98 %. The remaining data in Table 2 will be discussed under the heading "Order of reaction", p. 1073.

Table 2. Isomerization of OU_{72} at pH 12.3 and 25°C; capillary No. 1; initial concentration $c_o = 5.0$ mM; $f(c) = \log (c_o/c) + 0.20 (c^{-1} - c_o^{-1})$.

t	i	$10^3 \log(c_o/c)$	$10^3 k_1$	$10^3 f(c)$	$t_{calc.}$
0	40.0	0		0	0
5	36.7	37		41	0
8	35.3	54		59	5
13	33.3	80		88	12
18	32.0	97	12.4	107	17
23	30.7	115		127	22
28	29.3	135		150	27
33	28.0	155	10.8	172	33
43	26.0	187		268	42
53	24.0	222		249	52
63	22.0	260		293	63
73	20.5	290	9.2	328	71
83	19.0	323		367	82
93	17.3	364		417	94
103	16.3	390		448	102
113	15.0	426	8.7	493	114
128	13.3	478		558	129
148	11.7	534		631	148
163	10.3	589	8.4	704	166
183	9.3	633		766	182
198	8.5	673		821	195
213	7.6	721	7.9	892	213
233	6.8	769		964	231
253	6.1	817		1 041	250
273	5.5	862	7.3	1 113	268
293	4.9	912		1 198	290
318	4.4	959		1 282	310
343	3.6	1 036	7.1	1 441	350
363	3.3	1 083		1 528	372
393	3.1	1 111		1 586	387
428	2.5	1 204		1 804	441
468	2.3	1 240	6.1	1 896	464
520	1.4	1 456		2 560	630
1 169	0.8	1 699	3.4	3 651	901
1 423	0.7	1 757			

In another series of experiments, Tables 3—6, the initial concentration was fixed at $c_o = 2.0$ mM, and measurements were carried out in phosphate buffers at pH 12.3 and 11.5, a carbonate buffer at 10.7 and a borate buffer at 9.2. A 20.0 mM stock-solution of OU_{72} in redistilled water was freshly prepared, and 5.4 ml of the appropriate buffer solution was measured into the thermostated polarographic cell and deaerated; 0.6 ml of the stock solution was added (zero time). Immediate mixing was secured by passing the nitrogen stream through the cell for another minute, and polarograms were recorded at suitable time-intervals. The experiment at pH 12.3 (Table 3) was carried out separately, whereas the solutions at pH 11.5, 10.7 and 9.2 (Tables 4—6) were measured intermittantly in one and the same experiment. The cells were stored, well stoppered, in the thermostat at 25.0°C and removed for polarographic recording, according to a minute rota. The experimental data

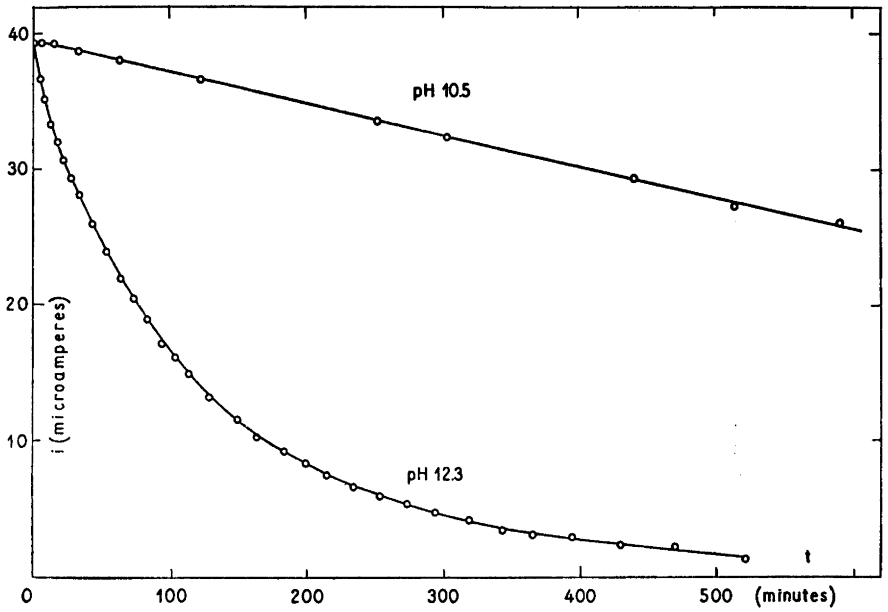

Fig. 1. Isomerization of OU_{72} at 25°C. Polarographic wave-height against time. Initial concentration c_0 = 5.0 mM. Data in Tables 1 and 2.

in Tables 3—6 are graphically represented in Fig 2. As above t represents the time in minutes from the mixing of the stock solution with the appropriate buffer until the maximum wave-height was attained during the recording of the individual polarogram.

CONCENTRATION DEPENDENCY OF THE ISOMERIZATION AT pH 12.0 AND 25°C

On the basis of the preceding experiments the potassium phosphate buffer at pH ≈ 12 was selected for the investigation of concentration influences upon the rate of isomerization.

In planning the experiment in detail the following had to be taken into account: (1) In order to keep the autoisomerization of the unbuffered stock solution at a negligible level the experiment should be carried out within a single day; (2) Recording of the requisite part of the polarogram from −0.8 to 1.8 V *vs.* SCE required 3 min. Rinsing and wiping off the electrodes and changing from one cell to another took a further 2 min; (3) The concentrated solutions should be measured every 5 min at the outset and every 10 and 20 min at later stages. The dilute solutions should be measured every 20 min from the outset; (4) The zero time for the respective solutions should be arranged so as to avoid too frequent alterations in the set sensitivity of the polarographic instrument.

These requirements were met by the rota indicated in Tables 7a and 7b.

Table 3. Isomerization of OU_{72} at pH 12.3 and 25°C; capillary No. 2; initial concentration $c_0 = 2.0$ mM; $f(c) = \log (c_0/c) + 0.20\ (c^{-1} - c_0^{-1})$.

t	i	$10^3 \log(c_0/c)$	$10^3\ k_1$	$10^3\ f(c)$
0	16.6	0		0
4	16.3	8		10
7	16.1	13	4.27	16
12	15.6	27		34
18	15.1	41	5.25	51
23	14.9	47		59
30	14.4	62	4.76	77
36	14.0	74		93
44	13.5	90		113
55	12.6	120	5.03	152
63	12.1	141		178
73	11.6	155		198
82	11.2	175		223
99	10.5	199	4.63	257
106	10.2	211		274
115	9.8	229		299
127	9.3	251		330
140	9.0	266	4.38	351
1b5	8.5	291		386
181	7.8	328		441
207	7.2	363		494
228	6.5	407		563
252	6.0	442		619
278	5.5	480	3.98	682
304	5.0	521		753
333	4.7	548	3.80	802

Table 4. Isomerization of OU_{72} at pH 11.5 and 25°C; capillary No. 2; initial concentration $c_0 = 2.0$; $f(c) = \log (c_0/c) + 0.20\ (c^{-1} - c_0^{-1})$.

t	i	$10^3 \log (c_0/c)$	$10^3\ k_1$	$10^3\ f(c)$
0	16.6	0		0
5	16.6	0		0
9	16.6	0		0
36	15.4	32	2.0	40
60	14.9	47	1.8	58
90	14.0	74	1.9	93
120	13.5	90	1.7	112
150	13.1	113	1.7	140
180	12.4	127	1.6	161
210	11.7	152	1.7	194
240	11.4	163	1.6	209
270	10.7	191	1.6	246
301	10.5	199	1.5	257
361	9.6	238	1.5	311
427	8.6	285	1.5	378
480	7.9	322	1.6	432
1 465	1.7	990	1.6	1 865

Table 5. Isomerization of OU_{72} at pH 10.7 and 25°C; c_o = 2.0 mM; capillary No. 2.

t	i	$10^3 \log (c_o/c)$
0	16.6	0
5	16.6	0
35	16.6	0
60	16.3	8
90	16.1	13
120	15.9	21
150	15.6	27
180	15.4	32
210	15.4	32
270	15.1	41
331	14.9	47
391	14.7	53
451	14.5	59
1 435	8.2	306

Table 6. Isomerization of OU_{72} at pH 9.2 and 25°C; c_o = 2.0 mM; capillary No. 2.

t	i	$10^3 \log (c_o/c)$	$10^3 k_1$
0	16.6	0	
5	16.6	0	
30	16.6	0	
60	16.3	8	3.1
91	16.1	13	3.3
120	16.1	13	2.5
150	15.9	19	2.9
210	15.4	32	3.5
271	15.4	32	2.7
331	15.4	32	2.2
1 317	11.0	178	3.1

An aqueous stock solution containing 10.0 mmoles/l of OU_{72} was freshly prepared, deaerated and stored in a well-stoppered flask. Solution No. 1 was prepared by mixing stock solution and buffer in appropriate proportions to give an initial concentration of 8.0 mM. The zero time was 10 o'clock (Table 7a) and polarographic recordings were run according to Table 7b. When this reaction had slowed down solution No. 2 was started *etc.* The

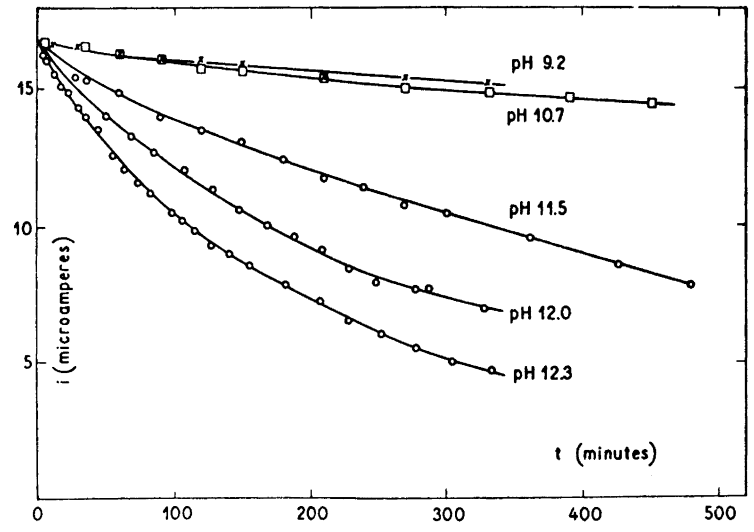

Fig. 2. Isomerization of OU_{72} at 25°C; pH dependency. Polarographic wave-height against time. Initial concentration c_o = 2.0 mM. Data in Tables 3—6 and 11.

Table 7 a.

Solution	c_o	Zero time
1	8.0	10h0 min
2	6.0	11h5 min
3	4.0	12h5 min
4	2.0	13h0 min
5	1.0	15h15 min

Table 7 b. Time for commencement of polarographic recordings in Tables 8—12.

h / min.	10	11	12	13	14	15	16	17	18	19	20
2				4	4	4	4	4		4	4
7	1	2	3	3	3	3	3	3		3	
12	1	2	2	2	2	2	1	2	1		5
17	1	1	1	1	1	5	5	5	5	5	
22	1	2		4	4	4	4	4	4		
27	1		3	3	3	3	3		3		
32		2	2	2	2	1	2	1	2	4	
39	1	1	1	1	1	5	5	5			
42		2		4	4	4	4	4			
47	1		3	3	3	3	3	3		3	
52		2	2	2	2	2	1	2			
57	1	1	1	1	1	5	5	5	5	5	

solutions were prepared in separate polarographic cells. They were stored in a thermostat at 25.0°C and removed periodically for recording.

The experimental data are collected in Tables 8—12; t represents the time in minutes from zero time, defined as above, until the maximum wave-height was attained during the recording.

Table 8. Isomerization of OU_{72} at pH 12.0 and 25°C; c_o = 8.0 mM; capillary No. 2; $f(c) = \log (c_o/c) + 0.8\ (c^{-1} - c_o^{-1})$.

t	i	$10^3 \log (c_o/c)$	10^3 f(c)
0	66.4	0	0
11	66.0	2	3
16	65.0	9	11
23	62.0	30	37
30	60.0	44	55
35	59.0	51	63
43	56.0	74	92
54	53.0	98	123
63	51.0	114	144
84	48.0	141	179
103	44.0	179	229
123	40.0	220	285
143	38.0	242	316
163	35.0	278	367
183	32.0	318	427
203	30.5	338	455
223	28.0	375	511
243	26.5	399	549
264	24.5	433	603
283	23.0	460	648
303	21.5	490	697
338	19.5	532	771
378	17.3	584	866
418	15.4	636	965
458	14.0	676	1 047
498	12.7	718	1 137

Table 9. Isomerization of OU_{72} at pH 12.0 and 25°C; c_o = 6.0 mM; capillary No. 2; f(c) as in Table 8.

t	i	10^3 log (c_o/c)	10^3 f(c)
0	49.8	0	0
8	49.0	7	9
14	48.0	16	21
23	47.0	25	34
33	45.0	44	58
43	42.0	74	100
53	40.0	95	127
73	37.3	129	173
93	34.0	165	226
113	31.3	201	279
133	28.5	242	341
153	26.5	274	390
173	24.5	308	444
193	22.7	341	499
213	21.0	375	553
233	19.7	403	605
253	18.0	442	676
293	15.9	496	778
333	14.2	545	884
373	12.6	597	988
413	11.3	644	1 094
453	10.3	684	1 192

Table 10. Isomerization of OU_{72} at pH 12.0 and 25°C; c_o = 4.0 mM; capillary No. 2; f(c) as in Table 8.

t	i	$10^3 \log(c_o/c)$	f(c)
0	33.2	0	0
8	32.0	16	24
28	30.0	44	65
48	27.3	85	128
68	24.5	132	203
88	23.1	157	246
108	21.5	189	297
128	19.3	235	378
148	18.3	258	420
168	17.3	283	466
188	16.0	317	531
208	14.7	354	604
228	13.5	391	681
248	12.8	414	731
268	12.1	438	784
288	11.4	464	844
308	10.5	500	930
348	9.5	543	1 039
388	8.7	581	1 141
428	7.8	629	1 276
468	7.3	658	1 363

Table 11. Isomerization of OU_{72} at pH 12.0 and 25°C; c_o = 2.0 mM; capillary No. 2.

t	i	$10^3 \log(c_o/c)$
0	16.6	0
8	16.5	2
28	15.5	30
49	14.0	74
68	13.3	96
85	12.7	116
108	12.0	141
128	11.3	167
148	10.5	199
168	10.0	220
188	9.6	238
208	9.1	261
228	8.4	296
248	7.9	321
278	7.7	333
288	7.7	333
328	7.0	375
369	6.8	387
398	6.7	394
438	6.5	407

Table 12. Isomerization of OU_{72} at pH 12.0 and 25°C; c_o = 1.0 mM; capillary No. 2.

t	i	$10^3 \log(c_o/c)$
0	8.3	0
8	7.3	56
28	7.2	62
48	7.0	74
68	6.3	121
89	6.1	134
108	5.8	156
128	5.4	187
148	5.5	179
168	5.3	195
188	5.3	195
230	5.0	220
248	5.0	220
288	5.0	220
303	4.8	238

Table 13 (*cf.* Fig. 3).

Stoichiometric		Extrapolated (timelag assumed)	Inflection point
c_o, mM	i_o *, μA	i_o, μA	min.
8.0	66.4 ± 0.5	67.0 ± 1.0	18 ± 3
6.0	49.8	50.0 ± 1.0	25 ± 10
4.0	33.2	32.5 ± 1.0	30 ± 15
2.0	16.6	16.5 ± 1.0	35 ± 15
1.0	8.3	8.0 ± 1.0	40 ± 15

* calculated by means of the relation $i = 8.3\,c$.

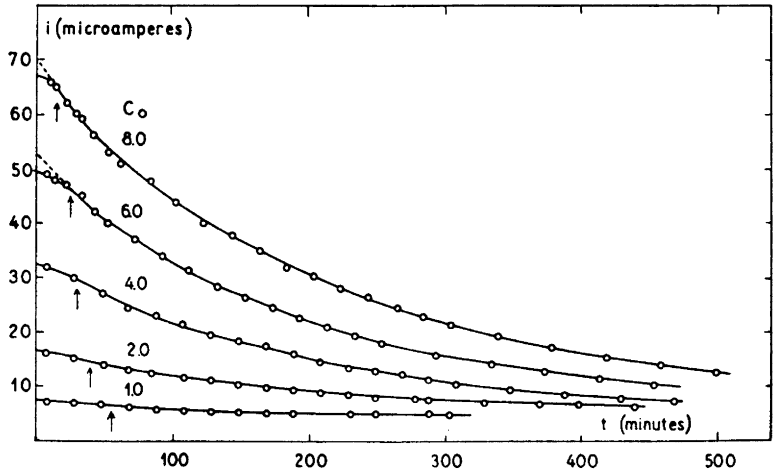

Fig. 3. Isomerization of OU_{72} at 25°C and pH 12.0. Influence of initial concentration c_o. Polarographic wave-height against time. Data in Tables 8—12.

The results are graphically represented in Fig. 3. The polarographic wave height i in μA has been plotted against time and the experimental points were visually fitted with the best curve. The initial values of i ($t = 0$) were calculated from the stoichiometric concentration c_o of OU_{72} by means of the relation $i = 8.3\ c$ (Table 13)

On the graphs, Fig. 3, there appears to be a time-lag at the outset of the reaction. Although the irregularities are close to the experimental error, there is a definite trend in all the graphs, and furthermore the time-lag has to be assumed in order to get a reasonable accordance, *cf.* Table 13, between the stoichiometric value for the initial wave-height i_o and the extrapolated one. Extrapolation from the main part of the graph ($t > 50$ min) is seen to give too high initial values.

The pH of the solutions were checked at the end of the experiment. They all had pH 12.0 ± 0.1.

ISOMERIZATION AT 35°C AND pH 12

In a provisional experiment the isomerization was studied in a phosphate buffer at pH 12 and at 35°C, the initial concentration was 6 mmoles/l. The reaction was quenched by reducing the pH to approximately 7; this was done by diluting withdrawn samples in the proportion 1:10 with the appropriate buffer; polarographic recordings of the dilutions were run immediately. The reaction was, however, found to be inconveniently rapid under these conditions and in a subsequent experiment it was slowed down by reducing the pH to 9.2, the temperature being maintained at 35°C.

CONVERSION PROCESSES AT 35°C AND pH 9.2

The initial concentration was 5.0 mmoles/l and the reaction was quenched in withdrawn samples simply by rapidly reducing the temperature to 25°C. Immediately upon temperature equilibration in the polarographic cell, recordings were run directly on the undiluted samples at pH 9.2. The current-voltage curves are reproduced in Fig. 4 Nos. 2—10. They display a characteristic

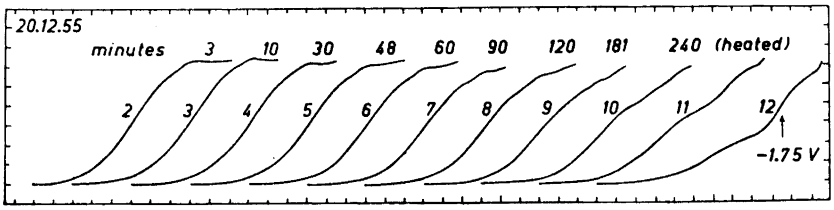

Fig. 4. Conversion of OU_{72} at 35°C and pH 9.2. Cathodic polarographic waves recorded at 25°C. Initial concentration $c_o = 5.0$ mM. All waves begin at -0.8 V *versus* the saturated calomel electrode (SCE). One unit on the abscissa represents 0.1 V. One unit on the ordinate represents 6.66 μA. Drop-time of mercury electrode 3.6 sec; rate of mercury outflow 2.46 mg sec^{-1}.

feature, which was not noticed at 25°C, namely the appearance of a new wave with a half-wave potential of approximately −1.75 V. In order to corroborate this observation a withdrawn sample from the reaction vessel was briefly heated to 80°C, cooled to 25° and polarographed (No. 11). The cell contents were heated once more to 80°C for 2 min and now produced curve No. 12, in which the new wave is clearly distinguishable.

A blank test with the supporting buffer alone proved that the new wave did not originate from the buffer or the vessel upon heating. Neither was it due to the isomerization product OU_{140}, since this has been shown to be polarographically inactive in the voltage region covered by these experiments.

A solution of 5 mg of OU_{140} in 5 ml borate buffer pH 9.2 was heated to 80°C for a short time and subsequently polarographed at 25°C. The current-voltage curve was identical with that of the buffer itself, even at a sensitivity increased by a factor 10. The isomeric hydroxyurea OU_{140} does not, therefore, appear to produce the wave at −1.75 V, observed in the experiment with OU_{72} under similar conditions.

It appears reasonable to regard the wave as being due to hydroxylamine. The estimated half-wave potential −1.75 *vs.* S.C.E. is in accordance with the value previously determined for hydroxylamine (Ref.[1] p. 463, Fig. 6), and the formation of hydroxylamine in alkaline solution at elevated temperatures by reversion of the formation process

$$HONH_3^+ + {}^-OCN \rightleftharpoons OU_{72} \qquad (1)$$

has a close analogy in the well-established reversibility — in the chemical sense — of the urea formation from ammonium cyanate

$$NH_4^+ + {}^-OCH \rightleftharpoons U \qquad (2)$$

Walker and Hambley [3] in 1895 first called attention to the reversibility of Wöhler's classical synthesis, and since then several authors have studied the kinetics of the reaction [4]. Although they all agree that ammonium cyanate is an intermediate in the decomposition, the numerical values of the rate constants differ and so do the proposed mechanisms. Lately the decomposition of urea in aqueous solution has been subjected to a careful investigation by Shaw and Bordeaux [4]. The reaction was studied at urea concentrations ranging from 6 to 1 200 mmoles/l at six different temperatures in the presence and absence of acid. The reaction is reported to be first-order with respect to urea and — contrary to the findings of other authors — uncatalyzed by acid. Within the experimental uncertainties the rate constants were the same in water and in acid, though with a slight trend towards higher rate constants in acid. This was explained by assuming that in water alone recombination of the ions to form urea occurs to a small degree. In acid this reaction is prohibited, because the cyanate ion formed by the decomposition (the reverse of reaction 2) is rapidly and quantitatively converted into ammonium ion[4,5].

$$HOCN + H_3O^+ \rightarrow CO_2 + NH_4^+ \qquad (3)$$

or

$$^-OCN + 2H^+ + 2H_2O \rightarrow NH_4^+ + H_2CO_3 \qquad (4)$$

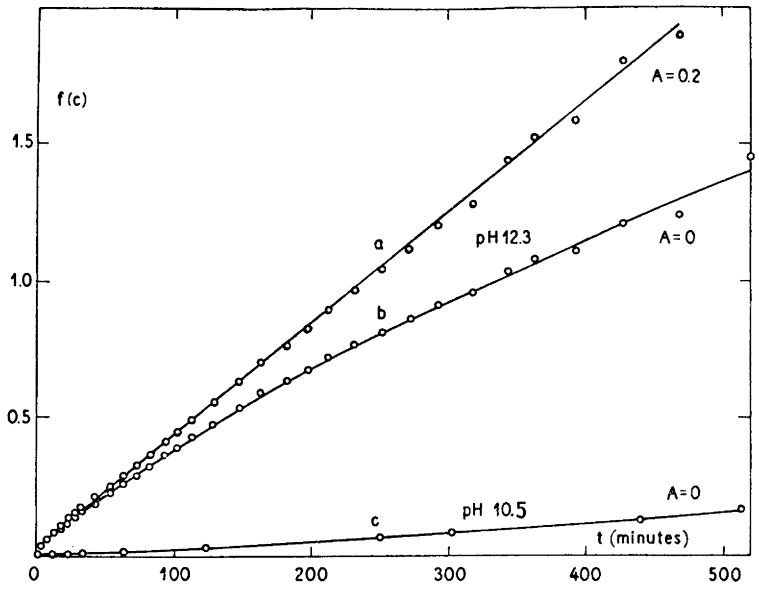

Fig. 5. Plot of the empirical function $f(c) = \log_{10}(c_0/c) + A(c^{-1} - c_0^{-1})$ against time; $c_0 = 5.0$ mM. Data in Tables 1 and 2.

Certain anomalies at high acid concentrations were explained as a result of the equilibrium $U + H^+ \rightleftharpoons UH^+$ (U standing for urea) assuming that the uronium ion UH^+ cannot be directly decomposed into ammonium cyanate. This has previously been postulated by several authors. The stability of OU_{72} in acid solution at room temperature [6] (Ref.[1], Table 1), may be understood on similar grounds; this substance has even more pronounced basic properties than urea (Ref. [6], p. 498). OU_{140} on the other hand is a weak acid. The existence of a stabilized anion in alkaline solution may account for the fact that this substance does not decompose readily into hydroxylamine as shown above by polarographic tests.

ORDER OF REACTION

Since the isomerization at higher temperatures was found to be complicated by competing decomposition reactions, the discussion of the order of reaction will be based entirely on the data obtained at 25°C. The data on Table 2 obtained at pH 12.3 will first be considered on the basic assumption that they correspond to a simple isomerization mechanism, either a single reaction or a set of consecutive reactions.

The data were tested in the integrated first-order equation

$$k_1 t = 2.303 \log_{10}(c_0/c) \qquad (5)$$

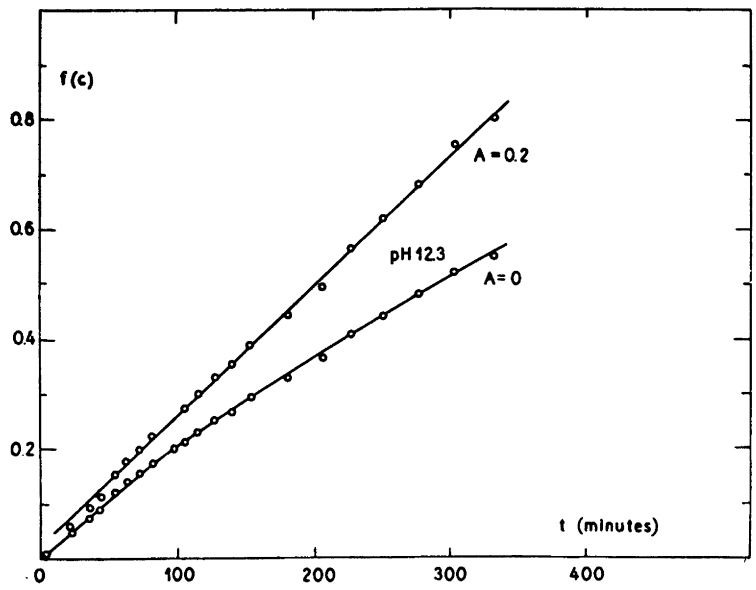

Fig. 6. Plot of the empirical function $f(c) = \log_{10} (c_o/c) + A(c^{-1} - c_o^{-1})$ against time $c_o = 2.0$ mM. Data in Table 3.

c_o being the initial concentration of OU_{72} and c the concentration at any time t. Since a linear relationship between concentration and polarographic wave-height i has been experimentally demonstrated, c_o/c may be replaced by i_o/i

$$k_1 t = 2.303 \log_{10} (i_o/i) \tag{6}$$

Calculated representative values for the first-order rate "constant" k_1 are given in Table 2, col. 4. The systematic drift of the "constant" indicates the invalidity of the assumption of first-order or pseudo-first-order kinetics. The same is obvious from the decided curvature of the graph Fig. 5 b, which in fact is a plot of log (c_o/c) *versus* t and hence should be linear. Salt effects have been neglected, but they are not apt to alter the order of reaction under the present conditions. Though the same reaction mixture was polarographed repeatedly, the consumption of OU_{72} due to the electrode process cannot be made responsible for the deviation. On the first hand it is of a negligible magnitude, and on the other hand it would give rise to an error in the opposite direction.

The data were then tested in the second-order equation

$$k_2 t = c^{-1} - c_o^{-1}$$

or

$$k'_2 t = i^{-1} - i_o^{-1} \tag{7}$$

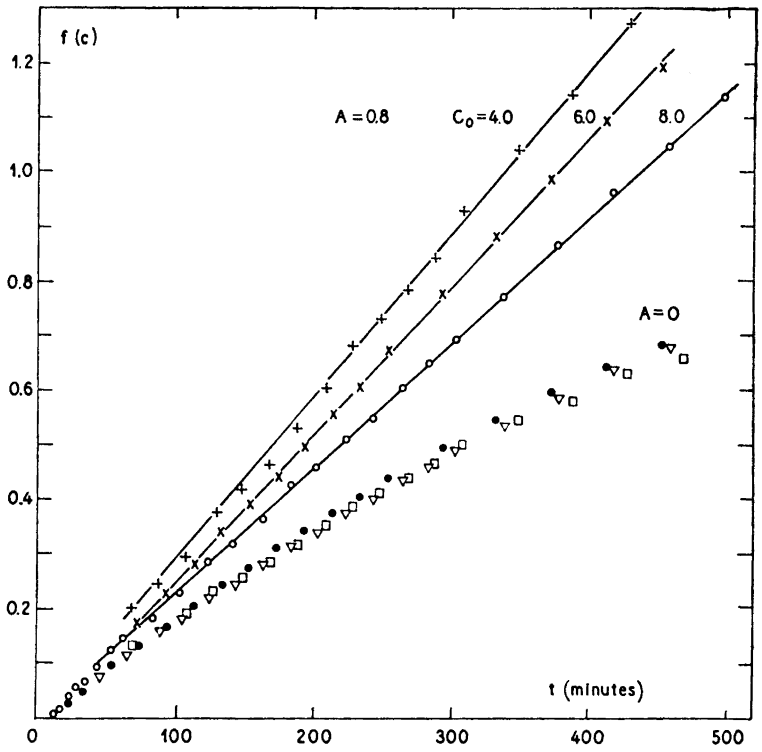

Fig. 7. Plot of the empirical function $f(c) = \log_{10}(c_o/c) + A(c^{-1} - c_o^{-1})$ against time. Data in Tables 8—10.

Non-linearity of the plot of i^{-1} *versus* t indicated that the reaction does not conform to second-order kinetics with respect to OU_{72}.

When general chemical observations are scarce, or present a complicated picture, it is customary to attempt by the method of trial and error to construct a combined function fitting the experimental data with reasonable accuracy. The procedure of Christiansen [7] for a linear sequence of reactions was adopted.

In the equation

$$t = B_1 \cdot I_1 + B_2 \cdot I_2 + \ldots . \qquad (8)$$

t stands for time in minutes, B_1, B_2 . . . are constants and I_1, I_2 . . . are the common integrated kinetic expressions c, $\log(c_o/c)$, $(c^{-1} - c_o^{-1})$, $(c^{-2} - c_o^{-2})$ *etc.* As above c_o is the initial concentration and c the concentration remaining at any time t.

By selecting first- and second-order expressions, respectively, for I_1 and I_2 the modified function (9) was obtained.

$$Bt = \underbrace{\log_{10}(c_o/c)}_{f(c)} + A(c^{-1} - c_o^{-1}) \qquad (9)$$

By the method of hit and miss a value of the constant A was found, which upon insertion of the experimental sets of data c,t (Table 2) rendered the right-hand side of (9) a linear function of t (Fig. 5a). The value $A = 0.2$ is seen to give a statisfactory linearity, except for a short interval at the outset of the reaction (*cf.* p. 1073). The slope of the line is $B = 0.004$. Towards the end of the reaction the scattering is somewhat large, owing to experimental errors, but there is no systematic deviation from linearity up to 95 % advancement. The line does not pass exactly through the origin, but there is a small positive intercept on the ordinate axis. It is uncertain whether this is kinetically significant, but the empirical expression fitting the data in Table 2 is

$$0.004\ t + 0.004 = \log_{10}(c_o/c) + 0.20(c^{-1} - c_o^{-1}) \qquad (10)$$

For the sake of control values of t have been calculated from eqn. 10 They are included in Table 2, col. 6, and show a fair agreement with the experi mental values.

The data in Table 3 were similarly tested in the empirical eqn. 9. In this experiment the pH was unaltered and equal to 12.3 within the accuracy of measurement, ± 0.1, but the initial concentration of OU_{72} was $c_o = 0.2$ mmoles/l. Fig. 6 ($A = 0$) shows the plot of log c_o/c *versus* t. It is decidedly curved, again indicating the invalidity of first-order kinetics. The upper graph represents the mixed function f(c). The selected value of A, which rendered the plot linear, is the same (0.2) as previously found, but it should be pointed out that a reasonable linearity may be achieved for values of A between the limits 0.15 and 0.25 so that the accordance may be incidental rather than significant.

The crucial test of the validity of the empirical expression (9) is the independency of the constants A and B of concentration. The data in Tables 8—12 (*cf.* Fig. 3) were intended for this test. This series of experiments is not directly comparable with the previous ones, since the pH was somewhat lower (12.0). It appears from Fig. 7 that for the three highest concentrations a linear plot of f(c) *versus* t is obtained when 0.8 is selected for the constant A. For the lower concentrations the experimental error gives rise to a considerable scattering of the calculated values of f(c) and it is not possible to select a reasonably well-defined value of A to give linearity. There is no direct indication, however, that A varies with concentration, but this actually needs confirmation by experiments carried out at still higher concentrations. For such measurements, however, the polarographic method is unsuitable.

Table 14. Values of constants A and B (eqn. 9) at 25°C.

pH	12.3 b	12.3 p	12.0 p	12.0 p	12.0 p
c_o	5.0	2.0	8.0	6.0	4.0
A	0.2 ± 0.1	0.20 ± 0.05	0.80 ± 0.05	0.8 ± 0.1	0.8 ± 0.2
$10^3\ B$	4.0 ± 0.5	2.3 ± 0.2	2.3 ± 0.1	2.7 ± 0.2	2.9 ± 0.5
Table	2	3	8	9	10
Fig.	5	6	7	7	7

* b borate buffer p phosphate buffer

The selected values of A and the graphically determined slopes B are summarized in Table 14, with the estimated errors.

The value of A seems to decrease rapidly with increasing pH. The overall process, therefore, seems to approximate to simple first-order kinetics in strongly alkaline solution, probably because a rapid, base-catalyzed, pseudo-first-order isomerization is predominating. In weakly alkaline or neutral solution the overall process seems to proceed by a more complicated sequence of reactions or alternatively by a mechanism of concurrent reactions. The possibility of decomposition into hydroxylamine and cyanate obviously should be taken into account, *cf.* p. 1072.

A discussion of reaction mechanisms in terms of the actual molecular structures will be presented elsewhere in a larger context.

MATERIALS AND GENERAL TECHNIQUE

The preparation and characterisation of the isomeric oxyureas have been reported in a previous publication [8]. Freshly prepared samples were used.

All chemicals used for preparing the supporting buffer-solutions were analytical grade products. The solvent was water, carefully redistilled in Pyrex apparatus.

The compositions of the buffer stock solutions are indicated in Table 15.

Table 15. Composition of buffer stock solutions.

A. 1 M boric acid, 1 M potassium dihydrogen borate
B. 1 M potassium monohydrogen phosphate
C. 1 M potassium hydrogen carbonate
D. 1 M potassium hydroxide

The set of stock solutions used in the various experiments are given in Table 16. Unless otherwise stated appropriate volumes were mixed and diluted to the tenfold volume with water containing 0.02 % methylcellulose as a maximum suppressor.

The instrument for measurement of the pH as well as the polarographic equipment and technique have been described in a previous paper (Ref[1]., p. 468–469).

Table 16.

Experiment Table	Fig.	pH	Stock solutions (c_o. Table 15)		Buffer type
1	1	10.5	A	D	borate
2	1	12.3	A	D	borate
3	2	12.3	B	D	phosphate
4	2	11.5	B	D	phosphate
5	2	10.7	C	D	carbonate
6	2	9.2	A		borate
8–12	3	12.0	B	D	phosphate

Two different capillaries were used for the dropping mercury electrode in the present experiments. The characteristic data for No. 1, employed in the experiments, Tables 1 and 2, were as follows; height of mercury column 45 cm, drop time 3.3 sec, rate of mercury outflow into water 2.7 mg sec^{-1}. The experimental relationship between wave-height i

(diffusion current in μA) and concentration c of OU_{72} was $i/c = 8.0$; (*cf.* Ref.[1], Fig. 4.) Capillary No. 2, employed for the rest of the experiments (Tables 3—6 and 8—12) had the following characteristics; heights of mercury column 23 cm, drop time 3.0 sec, rate of mercury outflow into water 3.0 mg sec^{-1}. The relation between wave-height and concentration for this capillary was $i/c = 8.3$. The conversion factor cannot be determined directly at pH 12 and 25°C with any great accuracy, owing to the rapid isomerization of the substance. It has been established for the employed capillary by measurements of a series of concentrations at pH 9.2, and it is assumed that the same conversion constant is valid at pH 12.2. The assumption is justified by previous experiments (Ref.[1], Fig. 2) showing that the wave-height for a given concentration does not vary significantly with pH in the region 6.3—12.3.

REFERENCES

1. Kofod, H. *Acta Chem. Scand.* **9** (1955) 455, p. 456, Fig. 1.
2. Kofod, H. *Acta Chem. Scand.* **9** (1955) 1575, diagram p. 1584—85.
3. Walker, J. and Hambley, F. J. *J. Chem. Soc.* **67** (1895) 746.
4. Shaw, W. H. R. and Bordeaux, J. J. *Am. Chem. Soc.* **77** (1955) 4729 with further references.
5. Lister, M. W. *Can. J. Chem.* **33** (1955) 426.
6. Kofod, H. and Huang Tso-Yueh. *Acta Chem. Scand.* **8** (1954) 494, p. 496.
7. Christiansen, J. A. *Advances in Catalysis* **5** (1953) 344.
8. Kofod, H. *Acta Chem. Scand.* **7** (1953) 938.

Received February 5, 1958.

ACTA CHEMICA SCANDINAVICA 12 (1958) 1079—1094

Acid-base, *cis-trans* and Complex Equilibria in the Chromium(III) Ethylenediamine System

FLEMMING WOLDBYE

Chemistry Department A, Technical University of Denmark, Copenhagen, Denmark

The three *cis-trans* equilibrium constants and the four acid dissociation constants related to the ions $Cren_2(H_2O)_2^{+++}$, $Cren_2(OH)(H_2O)^{++}$ and $Cren_2(OH)_2^{+}$ have been determined by spectrophotometric and glass electrode measurements, respectively. The absorption spectra of these six ions and of the $Cren_3^{+++}$ ion have been recorded. In an attempt to determine the stability constant of this last ion its hydrolysis in ethylenediamine buffers at pH $\geq$ 9.5 has been followed spectrophotometrically. The product of this hydrolysis which proceeds until almost completion except in very concentrated buffers is the *cis-trans* equilibrium mixture of dihydroxobisethylenediaminechromium(III) ions. Only an estimate of the upper limit of the stability constant could be given.

An error in the calculation of the stability constant for the $Coen_3^{+++}$ ion in Ref.[1] has been corrected (p. 1093).

In the present investigation the acid-base and *cis-trans* equilibria of the following system:

$$\begin{array}{ccccccc} cis\text{-}Cren_2(H_2O)_2^{+++} & \rightleftharpoons & cis\text{-}Cren_2(H_2O)(OH)^{++} + H^+ & \rightleftharpoons & cis\text{-}Cren_2(OH)_2^{+} + 2H^+ \\ \updownarrow & & \updownarrow & & \updownarrow \\ tr.\text{-}Cren_2(H_2O)_2^{+++} & \rightleftharpoons & tr.\text{-}Cren_2(H_2O)(OH)^{++} + H^+ & \rightleftharpoons & tr.\text{-}Cren_2(OH)_2^{+} + 2H^+ \end{array}$$

have been determined and the hydrolysis of $Cren_3^{+++}$ in acid and alkaline solution has been studied with the intention to determine the complexity constants

$$k_3 = \frac{[Cren_3^{+++}]}{[Cren_2(H_2O)_2^{+++}]\,[en]}$$

for the *cis-* and *trans* ions, respectively.

Further, the spectra between 650 and 325 mμ of all the species mentioned have been recorded.

The measurements have been carried out at 25.0±0.1°C, and in order to eliminate salt effects a comparatively strong constant salt medium of 1 M

$NaNO_3$ has been used. This also renders the quantities calculated directly comparable with those obtained by Bjerrum and Rasmussen [1] for the corresponding Co(III) system.

Following the notation in Ref.[1] * the constants pertaining to the acid-base equilibria are defined as follows:

$$*k_{s,1}(cis) = \frac{[H^+]\ [cis\text{-}Cren_2(H_2O)(OH)^{++}]}{[cis\text{-}Cren_2(H_2O)_2{}^{+++}]}$$

$$*k_{s,2}(cis) = \frac{[H^+][cis\text{-}Cren_2(OH)_2{}^+]}{[cis\text{-}Cren_2(H_2O)(OH)^{++}]}$$

(and the analogous $k_{s,1}(tr.)$ and $k_{s,2}(tr.)$ for the *trans* system), and the *cis-trans* equilibrium constants are defined as follows:

$$q_0 = \frac{[cis\text{-}Cren_2(H_2O)_2{}^{+++}]}{[tr.\text{-}Cren_2(H_2O)_2{}^{+++}]} \qquad q_1 = \frac{[cis\text{-}Cren_2(H_2O)(OH)^{++}]}{[tr.\text{-}Cren_2(H_2O)(OH)^{++}]} \qquad q_2 = \frac{[cis\text{-}Cren_2(OH)_2{}^+]}{[tr.\text{-}Cren_2(OH)_2{}^+]}$$

Between these seven constants there are two independent relations, so when five of them are determined experimentally, the remaining two can be calculated.

Preliminary spectrophotometric experiments showed that in acid solution ($1 < pH < 2$) the tris-ethylenediamine ion will hydrolyze to form the *cis*-diaquo ion **, which will in turn hydrolyze forming blue, violet and finally green solutions, while the *trans*-diaquo ion apparently partly will isomerize to form the *cis*-diaquo ion at a rate somewhat higher than that of the hydrolysis.

In alkaline solution, however, it has been possible to establish the *cis-trans* equilibrium and so to determine q_2.

The values of the constants obtained at 25°C and in 1 M $NaNO_3$ are:

$*k_{s,1}(cis) = 10^{-4.80}$ mole/l (Co $10^{-6.06}$) $*k_{s,2}(cis) = 10^{-7.17}$ mole/l (Co $10^{-8.19}$)

$*k_{s,1}(tr.) = 10^{-4.08}$ mole/l (Co $10^{-4.45}$) $*k_{s,4}(tr.) = 10^{-7.49}$ mole/l (Co $10^{-7.94}$)

$q_0 = 12.8$ (Co 58) $q_1 = 2.44$ (Co 1.42) $*q_2 = 5.1$ (Co 0.80)

the quantities marked by an asterisk being calculated directly from measurements upon solutions in which the corresponding equilibria were established.

On comparison with the cobalt system (values from Ref.[1] given in parenthesis) it is seen that the chromium compounds are stronger acids than the corresponding cobalt compounds.

As might be expected empirically [1,3], the *trans*-diaquo ion is a stronger acid than the *cis*-diaquo ion with respect to the dissociation of the first proton, but this difference is smaller than that between the corresponding cobaltic ions. The ratio of the first and second acid dissociation constants is

for the *cis*-diaquo ions $10^{2.37}$ (Co $10^{2.13}$)

" " *trans* " " $10^{3.41}$ (Co $10^{3.39}$)

* C_A and [A] designate initial and actual concentration of A in mole/liter.

** This is in accordance with the findings of Schläfer and Kling[2], who have made a kinetic investigation of this reaction.

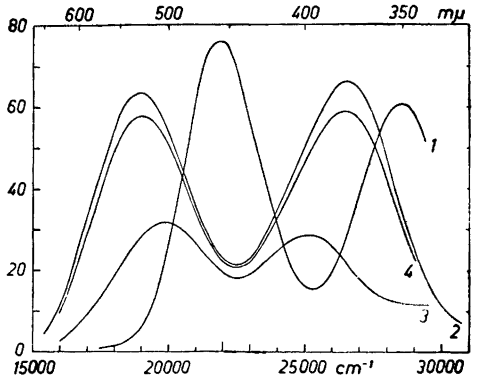

Fig. 1. Spectra in 1 M $NaNO_3$ at 25°C of the ions $Cren_3^{+++}$ (1), *cis*-$Cren_2(OH)_2^+$(2) *trans*-$Cren_2(OH)_2^+$(3) and of the *cis-trans* equilibrium mixture of the $Cren_2(OH)_2^+$ ions(4). The equilibrium spectrum has been calculated from the spectra of the pure isomers using the *cis-trans* equilibrium constant $q_2 = 5.1$ (see Table 5).
Abscissa: Wave numbers in cm^{-1} and wavelength in mμ.
Ordinate: The molar decadic extinction coefficient.

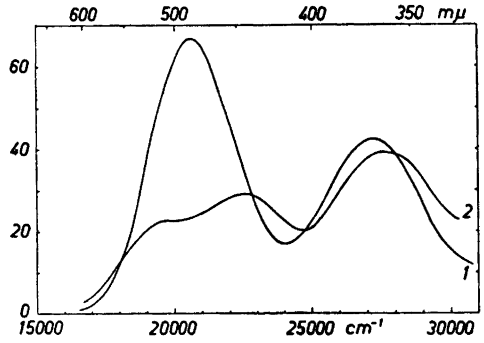

Fig. 2. Spectra in 1 M $NaNO_3$ at 25°C of the ions *cis*-$Cren_2(H_2O)_2^{+++}$ (1) and *trans*-$Cren_2(H_2O)_2^{+++}$(2).
Abscissa: Wave numbers in cm^{-1} and wavelength in mμ.
Ordinate: The molar decadic extinction coefficient.

Figs. 1, 2 and 3 show the spectra of the species concerned in this investigation recorded in 1 M $NaNO_3$ solution in the region of 650 mμ—325 mμ, and in Table 1 are given the data of the maxima in the spectra.

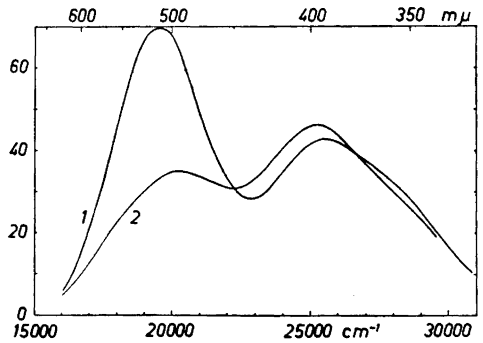

Fig. 3. Spectra in 1 M $NaNO_3$ at 25°C of the ions *cis*-$Cren_2(OH)(H_2O)^{++}$(1) and *trans*-$Cren_2(OH)(H_2O)^{++}$(2). These spectra are the averages of those calculated from the solutions in Table 2 which differed 2—3 % with respect to the extinction coefficients.
Abscissa: Wave numbers in cm^{-1} and wavelength in mμ.
Ordinate: The molar decadic extinction coefficient.

Table 1. Data of maxima in the spectra shown in Figs. 1, 2 and 3; 25°C, 1 M $NaNO_3$.

Ion	1. maximum		2. maximum		3. maximum	
	cm^{-1}	ε	cm^{-1}	ε	cm^{-1}	ε
$Cren_3^{+++}$	21 880	76.5	28 500	60.7		
cis-$Cren_2(H_2O)_2^{+++}$	20 650	67.0	27 250	42.5		
tr.-$Cren_2(H_2O)_2^{+++}$	19 700	22.5	22 600	29.3	27 700	39.2
cis-$Cren_2(OH)(H_2O)^{++}$	19 550	69.3	25 550	43.0		
tr.-$Cren_2(OH)(H_2O)^{++}$	20 200	35.0	25 250	46.0		
cis-$Cren_2(OH)_2^{+}$	19 000	63.6	26 550	66.0		
tr.-$Cren_2(OH)_2^{+}$	19 900	31.8	25 250	28.9		

The absorption curves have been measured at 25° ± 1°C by means of a Cary Recording Spectrophotometer.

The $Cren_3^{+++}$ ion is sufficiently robust for a direct recording of its spectrum in acid, neutral and alkaline solutions. As expected the spectra thus obtained are identical and in fair agreement with spectra published earlier [2,4].

The *cis*- and *trans*-$Cren_2(H_2O)_2^{+++}$ and $Cren_2(OH)_2^{+}$ ions, however, are so labile that small changes in the absorption of their solutions can be registered within a few minutes after preparation of the solutions. Therefore the following procedure was used in recording their spectra: The solvent was prepared at 25°C, the solute added and dissolved at time 0 and the solution made up to the mark and the first absorption curve recorded at time 3 min. During the next 15 min another 3 absorption curves were recorded on the same sheet, and the absorption curve of the pure substance was then obtained by extrapolation to time 0. In all cases the differences between the curve obtained after 3 min and the extrapolated curve were very small, namely from 1 to 3 times the experimental uncertainty. In each case the pH of the solution was measured immediately after preparation.

The spectra of the *cis*- and *trans*-aquohydroxo ions have been calculated from the absorption curves of solutions, the pH of which has been adjusted so that they would contain a relatively large concentration of the ion in question, a smaller concentration of either the corresponding diaquo or dihydroxo ion and a negligible amount of the remaining of these three ions. The data of these solutions are given in Table 2.

A calculation of the spectrum of the *cis*-$Cren_2(OH)(H_2O)^{++}$ from the two first solutions by subtracting the absorption of the $Cren_2(H_2O)_2^{+++}$ and the $Cren_2(OH)_2^{+}$, respectively, from the total absorption of the solutions yielded

Table 2. Composition of the solutions from which the spectra of the *cis*- and *trans*-$Cren_2(OH)(H_2O)^{++}$ have been calculated. C_{Cr} indicates total complex concentration. Concentrations are in mole/l. 25°C, 1 M $NaNO_3$.

C_{Cr}	pH	$[Cren_2(OH)(H_2O)^{++}]$	$[Cren_2(OH)_2^{+}]$	$[Cren_2(H_2O)_2^{+++}]$
0.02875 *cis*	5.033	0.0181	0.0002	0.0105
0.02879 *cis*	6.517	0.0235	0.0052	0.0001
0.01268 *tr.*	5.876	0.0122	0.0003	0.0002
0.00973 *tr.*	4.159	0.00532	negligible	0.00441

two curves which were in complete agreement with respect to the wavelengths of their maxima and differed less than 2 % with respect to the extinction coefficients. Similar results were obtained for the *trans*-$Cren_2(OH)(H_2O)^{++}$ except that the difference between the extinction coefficients at some wavelengths amounted to as much as 3 %. This agreement furnishes a good cross-check of the values of the acid dissociation constants.

An interesting feature of these two spectra is the "shoulder" near 29 000 cm^{-1} which at least in the *cis*-spectrum seems far beyond the experimental uncertainty.

EXPERIMENTAL

Preparations. *$Cren_3Cl_3,3\frac{1}{2}H_2O$* was prepared from $CrCl_3$ and anhydrous ethylenediamine according to the method of Linhard and Weigel [5] except that the precipitation was effected by means of ethanol instead of NH_4Cl. (It was found by analysis that precipitates produced by NH_4Cl contained NH_4Cl which was difficult to remove by recrystallization.) The salt was reprecipitated and the spectrum was shown not to be influenced by further reprecipitations or recrystallizations.

cis- and trans-$Cren_2(H_2O)_2Br_3$ were prepared according to the following scheme:

$$Cren_3(ClO_4)_3 \xrightarrow[70°]{HCl} \left[\begin{array}{l} cis\text{-}Cren_2Cl_2ClO_4 \rightarrow cis\text{-}Cren_2(OH)(H_2O)S_2O_6 \rightarrow cis\text{-}Cren_2(H_2O)_2Br_3,2H_2O \\ \qquad\qquad \downarrow \; HgBr_2 \;\Big|\; HBr \\ tr.\text{-}(Cren_2Br_2)Br,HgBr_2 \rightarrow tr.\text{-}Cren_2(OH)(H_2O)Br_2 \rightarrow tr\text{-}Cren_2(H_2O)_2Br_3,2H_2O \end{array}\right.$$

cis-$Cren_2Cl_2ClO_4$ was prepared according to Ref.[5], p. 119. To prepare *cis*-$Cren_2(H_2O)_2Br_3$, 6 g *cis*-$Cren_2Cl_2ClO_4$ was dissolved in *ca.* 50 ml warm water and the solution heated until colour change from violet to orange. 10 ml pyridine and excess of $Na_2S_2O_6$ were added and the solution cooled in ice for 1 h whereby the *cis*-aquohydroxo dithionate was precipitated. Treament of this with HBr yielded *ca.* 3 g *cis*-$Cren_2(H_2O)_2Br_3$, $2H_2O$.

To prepare the corresponding *trans*-compound 8.5 g *cis*-$Cren_2Cl_2ClO_4$ was dissolved in 30 ml water at 50°C and 16 g $HgBr_2$ and 16 ml const. boil. HBr were added. The solution was evaporated to dryness on the steam bath and the residue washed with water containing HBr until colourless filtrate, leaving bright green, slightly soluble crystals of *trans*-$(Cren_2Br_2)Br,HgBr_2$ in a yield of 13.5 g. A suspension of 19 g of this salt in 20 ml water was saturated with H_2S and the HgS removed by centrifuging. Spectra of the solution recorded at regular intervals indicated that a maximum of *trans*-$Cren_2(H_2O)_2^{+++}$ was present after 24—36 h at *ca.* 22°C. The solution was then saturated with KBr and 20 ml pyridine was added. The pink precipitate formed after cooling in ice for 1 h was washed several times with 50 % ethanol to remove most of a considerable content of KBr, leaving 2.5 g *trans*-$Cren_2(H_2O)(OH)Br_2$. Treatment of this salt with the equivalent amount of const. boil. HBr yielded 2.2 g *trans*-$Cren_2(H_2O)_2Br_3,H_2O$.

The diaquobisethylenediamine salts were originally prepared by Pfeiffer [6] along the path outlined here

$$CrCl_2(H_2O)_4Cl,2H_2O \xrightarrow{py} Crpy_2(OH)_2(H_2O)_2Cl \xrightarrow{en} (Cren_2(H_2O)Br)Br_2$$

$$(Cren_2(H_2O)Br)Br_2 \rightarrow cis\text{-}Cren_2(OH)(H_2O)Br_2 \rightarrow cis\text{-}Cren_2(H_2O)_2Br_3,2H_2O$$

$$\downarrow \; HgBr_2 \;\Big|\; HBr$$

$$tr.\text{-}(Cren_2Br_2)Br,HgBr_2 \rightarrow tr.\text{-}Cren_2(OH)(H_2O)Br_2 \rightarrow tr.\text{-}Cren_2(H_2O)_2Br_3,H_2O$$

Considering that $Cren_3Cl_3$ is now so easily accessible, the procedure outlined above seems more convenient.

Analysis. The salts prepared have been analyzed as follows. *Chromium* has been determined on a semimicro scale either by decomposition with sulfuric acid, heating in

Table 3. Analysis.

Formula and formula weight	Equiv. weight based on Cr	Equiv. weight based on halogen	Equiv. weight based on N	Equiv. weight as an acid
$Cren_3Cl_3,3\frac{1}{2}H_2O$ 401.8	calc. 401.8 found 400.0 (titr.)	calc. 133.9 found 132.6	calc. 66.97 found 67.30	
cis-$Cren_2(H_2O)_2Br_3,2H_2O$ 484.1	calc. 484.1 found 481.3 (titr.)	calc. 161.4 found 161.3		calc. 242.0 found 242.3
tr.-$Cren_2(H_2O)_2Br_3,H_2O$ 466.0	calc. 466.0 found 464.4 (Cr_2O_3)	calc. 155.3 found 155.6		calc. 233.0 found 233.8

hydrogen atmosphere and weighing as Cr_2O_3, or by a complexometric method, boiling the salt with a known amount of ethylenediaminetetraacetic acid in a buffer solution at pH about 4.6 and back titrating the excess of ENTA with zinc sulfate, using eriochromschwartz as an indicator [2].

Halogen has been determined by weighing as silver halide and *nitrogen* by the Kjeldahl method.

The diaquo salts have been titrated potentiometrically as dibasic acids.

The results of these analyses are given in Table 3.

ACID DISSOCIATION CONSTANTS OF THE DIAQUO- AND THE AQUOHYDROXO-IONS

The acid dissociation constants of the *cis*- and *trans*-diaquobisethylenediamine ions at 25°C were calculated from glass electrode measurements of hydrogen ion concentrations in solutions of the complex salts partly neutralized with sodium hydroxide.

The measurements were made with a selected glass-electrode the performance of which had been tested [7] and a PHM 3 pH-meter from "Radiometer", Copenhagen.

Readings of the EMF of the cell glass-electrode calomel electrode are designated E.

As a standard was used dilute nitric acid in which $C_{HNO_3} = 0.005005$; $C_{NaNO_3} = 1.000$. Readings in this solution are designated E_{st}.

As a consequence of the isomerization of the *cis*- and *trans*-ions and the difference in acid strength of the corresponding *cis*- and *trans*-acids, the hydrogen ion concentration in a (freshly prepared) solution of a pure *cis*- or *trans*-salt will vary with time.

By a rapid preparation of the solutions it was possible to make the first measurement 30 sec after the solid had dissolved * (when finely powdered, the salts dissolve very rapidly). The measurements were then continued for

* The glass-electrode requires some time for its adjustment, so meaningful measurements can hardly be made faster.

some time and E was recorded as a function of time. The E data of Table 4 are the results of an extrapolation of these functions to time zero. The rate of change of E was in no case higher than 1.5 mV/min. E_{st} was recorded before and after each set of measurements, and the results never varied more than 0.3 mV.

The acid dissociation constants have been calculated by means of formulae of the type derived by J. Bjerrum [1,8].

The average number of protons produced by the diaquo ion may be calculated from the experimental quantities as

$$\bar{\nu} = \frac{C_{NaOH} + [H^+] - [OH^-]}{C_{Cr}}$$

and expressed in terms of $k_{s,1}$ and $k_{s,2}$ as

$$\bar{\nu} = \frac{k_{s,1}[H^+] + 2k_{s,2}\cdot k_{s,2}}{[H^+]^2 + k_{s,1}[H^+] + k_{s,1}\cdot k_{s,2}}$$

Combining these expressions and rearranging, one obtains for $\nu < 1$

$$-\log k_{s,1} = -\log[H^+] + \log\frac{1-\bar{\nu}}{\bar{\nu}} + \log\left(1 + \frac{(2-\bar{\nu})k_{s,2}}{(1-\bar{\nu})\ [H^+]}\right)$$

for $\bar{\nu} > 1$

$$-\log k_{s,2} = -\log\ [H^+] + \log\frac{2-\bar{\nu}}{1-\bar{\nu}} - \log\left(1 + \frac{\bar{\nu}[H^+]}{(\bar{\nu}-1)k_{s,1}}\right)$$

In the experiments recorded in Table 4 $\bar{\nu}$ has been kept close to 0.5 and 1.5, respectively, in order to ensure the smallest possible uncertainty in the calculated constants (*i.e.* in the terms $\frac{1-\bar{\nu}}{\bar{\nu}}$ and $\frac{2-\bar{\nu}}{\bar{\nu}-1}$, respectively).

THE *cis-trans* EQUILIBRIUM CONSTANTS

Spectrophotometric experiments have shown that in acid solution the *trans*-$Cren_2(H_2O)_2^{+++}$ isomerizes to form the corresponding *cis*-ion (roughly estimated the conversion is almost completed within 24 h at 25°C in 1 M $NaNO_3$, $[H^+] \sim 0.02$). But the rate of hydrolysis of the *cis*- and the *trans*-ions can not be neglected in comparison to the rate of isomerization. Thus the spectrum of a 24 h old solution of the *cis*-salt cannot be very accurately represented by a linear combination of the spectra of the *cis*- and *trans*-ions. Because of this hydrolysis and because of the fact that the equilibrium mixture of the two ions according to a rough calculation would contain less than 10 % of the *trans*-ion, no attempt has been made to determine the *cis-trans* equilibrium constant in acid solution.

In an ethylenediamine buffer solution at about pH = 10 the *cis*- and *trans*-$Cren_2(OH)_2^+$ are sufficiently stable to allow the *cis-trans* equilibrium to be established. Such equilibrium mixtures have been analyzed spectrophotometrically and chromatographically.

Table 4. The acid dissociation constants of the diaquobisethylenediaminechromium(III) ions in 1 M sodium nitrate at 25°C.

$C_{NaNO_3} = 1.000$ $\quad -\log[H^+]_{st} = 2.3006$

The first dissociation constant $\quad \Delta = \dfrac{(2-\bar{\nu})k_{s,2}}{(1-\bar{\nu})[H^+]}$

No.	$C_{Cr}(cis)$	C_{NaOH}	$\bar{\nu}$	$E_{st}-E$	$-\log[H^+]$	$\log\frac{1-\bar{\nu}}{\bar{\nu}}$	$\log(1+\Delta)$	$-\log k_{s,1}$
1	0.009841	0.005094	0.5191	0.1505	4.8471	−0.0331	0.0055	4.820
2	0.01058	0.005106	0.4843	0.1454	4.7608	0.02731	0.0045	4.793
3	0.01606	0.005094	0.3194	0.1273	4.4546	0.3286	0.0019	4.785
						Av. $-\log k_{s,1}$ (*cis*):		4.80
	$C_{Cr}(tr.)$							
4	0.01726	0.01562	0.9054	0.1624	5.0485	−0.9811	0.0183	4.086
5	0.01046	0.005106	0.4965	0.1039	4.0586	0.0061	0.0005	4.065
6	0.01068	0.005106	0.4865	0.1035	4.0519	0.0234	0.0005	4.076
						Av. $-\log k_{s,1}$ (*tr.*):		4.08

The second dissociation constant $\quad \Delta = \dfrac{\bar{\nu}[H^+]}{(\bar{\nu}-1)k_{s,1}}$

No.	$C_{Cr}(cis)$	C_{NaOH}	$\bar{\nu}$	$E_{st}-E$	$-\log[H^+]$	$\log\frac{2-\bar{\nu}}{\bar{\nu}-1}$	$-\log(1+\Delta)$	$-\log k_{s,2}$
7	0.01057	0.01566	1.4815	0.2862	7.1432	0.0321	0.0059	7.169
8	0.01016	0.01562	1.5372	0.2914	7.2312	−0.0647	0.0045	7.162
9	0.008397	0.01566	1.8645	0.3355	7.9774	−0.8049	0.0006	7.172
						Av. $-\log k_{s,2}$ (*cis*):		7.17
	C_{Cr}(tr.)							
10	0.01145	0.01566	1.3675	0.2926	7.2515	0.2357	−0.0011	7.485
11	0.009407	0.01562	1.6603	0.3231	7.7676	−0.2886	−0.0002	7.479
12	0.009065	0.01566	1.7272	0.3331	7.9368	−0.4259	−0.0001	7.511
						Av. $-\log k_{s,2}$ (*tr.*):		7.49

For the spectrophotometric determination of the *cis-trans* constant a weighed amount of *cis-* (or *trans-*) $Cren_2(H_2O)_2Br_3,2H_2O$ was dissolved in a suitable ethylene diamine buffer solution prepared from standard ethylene diamine solution, standard nitric acid and 5 M $NaNO_3$ in such a way that in the final solution pH would be close to 10 and $[NO_3^-] = 1$.

The solution was prepared and kept at 25°C in a dark bottle, and the spectrum of the solution was recorded immediately after preparation and at intervals until no further change could be observed. The *cis-* as well as the *trans*-solutions finally exhibited the equilibrium spectrum shown in Fig. 1 corresponding to 83.6 % *cis-* and 16.4 % *trans*-$Cren_2(OH)_2^+$.

Table 5 shows the data from four experiments of this type from which q_2 may be calculated. ε_{cis} and $\varepsilon_{tr.}$ designate the extinction coefficients of *cis-* and *trans*-$Cren_2(OH)_2^+$, respectively. The quantities $\varepsilon_{cis} - \varepsilon_t$ and $\varepsilon_t - \varepsilon_{tr.}$ have been calculated from the spectra using the formula $\dfrac{|D^\circ - D^t|}{l \times C_{Cr}}$ where

$|D^0—D^t|$ is the difference in the optical density of the solution at time 0 and at time t read directly from the curves recorded by the Cary, and l is the cell length. The degree of reaction, α, α has been calculated from $\alpha = \frac{\varepsilon_{cis} - \varepsilon_t}{\varepsilon_{cis} - \varepsilon_{tr.}}$ and $\alpha = \frac{\varepsilon_t - \varepsilon_{tr.}}{\varepsilon_{cis} - \varepsilon_{tr.}}$ and q_2 from $q_2 = \frac{1-\alpha}{\alpha}$, and $q_2 = \frac{\alpha}{1-\alpha}$, respectively.

In order to check these values further, an aliquot of each of the equilibrium solutions was acidified by means of nitric acid, the volume was doubled after addition of sufficient $NaNO_3$ to keep $[NO_3^-] = 1$, and the spectrum was recorded immediately after. When working fast, one may assume that the ratio of the *cis*- and *trans*-ions will remain almost unchanged during this procedure, so q_2 may likewise be calculated from these spectra. The results of these experiments are also given in Table 5. Here ε_{cis} and $\varepsilon_{tr.}$ designate the extinction coefficients of *cis*- and *trans*- $Cren_2(H_2O)_2^{+++}$, respectively.

For the chromatographic determination of the *cis-trans* constant was used a two years old solution prepared by dissolving $Cren_3Cl_3$ in an ethylenediamine buffer of a composition similar to that mentioned above *. As will be seen from the following, the $Cren_3^{+++}$ in such a solution will be converted into an equilibrium mixture of *cis*- and *trans*-$Cren_2(OH)_2^+$ whereupon a very slow process of unknown character takes place. Due to practical difficulties the solution could not be kept at 25 + 0.1°C for two years but prior to the following experiment it was kept at 25°C for some days in order to establish the equilibrium between possible contents of *cis*- and *trans*-$Cren_2(OH)_2^+$ corresponding to this temperature.

By a technique similar to that described in Ref.[9] an aliquot of the solution was then chromatographed on a column of Al_2O_3. The eluate obtained using 0.1 M KOH, 1 M KCl as an eluent, contained two red fractions which were collected separately in nitric acid at 0° and examined spectrophotometrically. The shape of the spectra (*i.e.* number and position of bands and the relative heights of these bands) was identical with the shape of the spectra of *trans*- and *cis*-$Cren_2(H_2O)_2^{+++}$, respectively, the first of the fractions exhibiting the *trans* spectrum.

Experiments showed that when a freshly prepared solution of *cis*- and *trans*-$Cren_2(OH)_2^+$ is run through the column, the two ions get separated and may be collected at a loss of only a few per cent of each. In accordance with a rule that seems rather general the *trans* ion shows the weaker adsorption on the column.

This strongly indicates that the two red fractions from the equilibrium solution actually represent its content of *trans*- and *cis*-$Cren_2(OH)_2^+$.

Since the eluate from the column was too dilute to permit an accurate spectrophotometric determination of the content of *cis*- and *trans*-$Cren_2(H_2O)_2^{+++}$, the chromium content in the two fractions was instead determined titrimetrically. (Decomposition by evaporating to dryness, heating the residue with H_2SO_4, dissolving and oxidizing chromium(III) to chromium(VI) by means of $K_2S_2O_8$ in the presence of Ag^+, and finally titrating with Fe^{++} using barium diphenylaminesulfonate as an indicator [10].)

* solution No. 2 in Table 7.

*Table 5. cis-trans*Equilibrium of the dihydroxobisethylenediaminechromium(III) ions in *ca.* 1 M $NaNO_3$ at 25°C.

Initial composition of solutions.

No.	Cr salt	$C_{Cr}(cis)$	C_{en}	C_{HNO_3}	C_{NaNO_3}	$-\log[H^+]$
1	*cis*-$Cren_2(H_2O)_2Br_3$, $2H_2O$	0.00920	0.0978	0.0463	0.900	9.90
2	—»—	0.00884	0.1413	0.0463	0.900	10.30
		$C_{Cr}(tr.)$				
3	*tr.*-$Cren_2(H_2O)_2Br_3$, H_2O	0.00810	0.0978	0.0463	0.900	9.95
4	—»—	0.01148	0.1413	0.0463	0.900	10.30

Extinction coefficients measured in alkaline solution.

	λ	t h	375	400	500	525 mμ	Av.
	ε_{cis}		65.7	50.1	54.2	63.4	
	$\varepsilon_{tr.}$		20.3	28.7	31.6	28.5	
	$\varepsilon_{cis}-\varepsilon_{tr.}$		45.4	21.4	22.6	24.9	
1	$\varepsilon_{cis}-\varepsilon_t$	216 (const. for 3 months)	9.2	4.5	4.2	6.3	
	α		20.3 %	21.0 %	18.6 %	18.0 %	19.5 %
	q_2						4.13
2	$\varepsilon_{cis}-\varepsilon_t$	168 (const. for 2 months)	6.2	2.8	3.0	4.5	
	α		13.7 %	13.1 %	13.3 %	12.9 %	13.3 %
	q_2						6.52
3	$\varepsilon_t-\varepsilon_{tr.}$	21	21.0	9.9	9.9	16.7	
	α		46.3 %	46.4 %	43.8 %	47.8 %	46.1 %
	$\varepsilon_t-\varepsilon_{tr.}$	70 (const. for 2 months)	37.2	17.6	18.1	28.3	
	α		81.4 %	82.2 %	80.1 %	81.1 %	81.2 %
	q_2						4.32
4	$\varepsilon_t-\varepsilon_{tr.}$	27 h	20.7	10.1	9.6	15.0	
	α	27 h	45.6 %	47.2 %	42.5 %	43.0 %	44.6 %
	$\varepsilon_t-\varepsilon_{tr.}$	72 (const. for 2 weeks)	38.4	18.0	19.4	28.3	
	α		84.5 %	84.0 %	85.8 %	81.1 %	83.9 %
	q_2						5.21
			Average of q_2 for soln. No. 1—4:				5.1

Extinction coefficients measured immediately after acidifying.

	λ	t days	487.5	500 mμ	Av.	Av.
	ε_{cis}		66.3	61.0		
	$\varepsilon_{tr.}$		22.9	22.5		
	$\varepsilon_{cis}-\varepsilon_{tr.}$		43.4	38.5		
1	$\varepsilon_{cis}-\varepsilon_t$	99	9.6	6.7		
	α		22.1 %	17.4 %	19.8 %	
	q_2					4.05
2	$\varepsilon_{cis}-\varepsilon_t$	14	6.3	5.5		
	α		14.7 %	14.3 %	14.5 %	
	q_2					5.90
3	$\varepsilon_t-\varepsilon_{tr.}$	65	35.1	31.8		
	α		80.9 %	82.6 %	81.7 %	
	q_2					4.46
4	$\varepsilon_t-\varepsilon_{tr.}$	14	37.2	32.8		
	α		85.6 %	85.2 %	85.4 %	
	q_2					5.84
			Average of q_2 for soln. No. 1—4:			5.1

The eluate from a chromatogram of 20 ml equilibrium solution was found to contain: in the *trans* fraction 0.029 mmole and in the *cis* fraction 0.133 mmole chromium. (This corresponds to about 60 % of the original chromium content of the solution. The rest of the chromium was so strongly adsorbed on the column that it could not be displaced.) Thus $q_2 = 4.6$ with an estimated uncertainty of $\pm$ 10 %.

However, the spectrophotometric determinations of q_2 given in Table 5 must be considered the more accurate, and the average of these $q_2 = 5.1$ combined with $k_{s,1}(cis)$, $k_{s,2}(cis)$, $k_{s,1}(tr.)$ and $k_{s,2}(tr.)$ yields $q_1 = 2.44$ and $q_0 = 12.8$.

THE HYDROLYSIS OF THE TRISETHYLENEDIAMINECHROMIUM(III) ION IN ALKALINE SOLUTION

In order to determine the complexity constants

$$k_3 = \frac{[\mathrm{Cren_3}]}{[\mathrm{Cren_2(H_2O)_2}^{+++}][\mathrm{en}]}$$

(for the *cis*- and *trans*-ions, respectively) it was attempted to establish the equilibrium

$$\mathrm{Cren_3}^{+++} + 2\ \mathrm{OH}^- \rightleftharpoons \mathrm{Cren_2(OH)_2}^{+} + \mathrm{en}$$

at 25°C in a 1 M salt medium. Preliminary spectrophotometric experiments have shown that in a strongly alkaline (as well as in acid) solution the hydrolysis will proceed further than this first step. On the other hand, test tube experiments have shown that a solution of $\mathrm{Cren_3Cl_3}$ in the following medium: 2 g en,2HCl + 2 g 75 % en + 3 ml $\mathrm{H_2O}$ ($\mathrm{enH}^+/\mathrm{en} \sim 3$) will stay yellow at room temperature as well as at 100°C. And a solution of $\mathrm{Cren_2(H_2O)_2Br_3}$ in this medium slowly turns yellow. Therefore it was hoped that the above equilibrium could be established in an ethylenediamine buffer at about pH = 10 ($\mathrm{p}k_{\mathrm{enH}^+} = 10.2$, Ref. [11]).

In such solutions it would be possible to follow the hydrolysis and to calculate $[\mathrm{Cren_3}^{+++}]$ and $[\mathrm{Cren_2(OH)_2}^{+}]$ in an eventual equilibrium solution spectrophotometrically, and [en] could be determined by means of glass-electrode measurements. Provided that the above hydrolysis is the only reaction taking place, the degree of conversion of $\mathrm{Cren_3}^{+++}$ into $\mathrm{Cren_2(OH)_2}^{+}$, α, in a solution in which the initial concentration of $\mathrm{Cren_3}^{+++}$ is C_{Cr}, may be calculated from

$$\alpha = \frac{D_0 - D_\alpha}{l \times C_{\mathrm{Cr}}(\varepsilon_{\mathrm{Cren_3}^{+++}} - \varepsilon_{\mathrm{Cren_2(OH)_2}^{+}})} \qquad (1)$$

where D_0 and D_α are the optical densities at the wavelength λ of the solution before and after the conversion has taken place, while ε is the extinction coefficient at the wavelength λ of the species in the subscript, and l is the cell length.

Table 6. Data of isosbestic points. The uncertainties refer to the reproducibility of the isosbestic points.

Composition of solution	$Cren_3^{+++}$ *cis*-$Cren_2(OH)_2^+$	$Cren_3^{+++}$ *cis-trans* equilibrium mixture of $Cren_2(OH)_2^+$	No. 1 Table 7	No. 2 Table 7
Isosbestic points	Calculated from spectra in Fig. 1		Observed	
mμ	360.7	362.3	362.2 ± 1.0	362.5 ± 0.5
	418.3	417.5	417.0 ± 0.5	417.0 ± 0.5
	487.8	489.0	488.5 ± 0.5	488.8 ± 0.5
ε	53.9	50.2	49.7 ± 0.5	50.5 ± 0.5
	33.3	32.3	32.0 ± 0.5	33.3 ± 0.5
	44.5	43.0	44.0 ± 0.5	42.8 ± 0.5

Calculating α in an equilibrium solution, one should obviously insert for $\varepsilon_{Cren_2(OH)_2^+}$ the extinction coefficient of the *cis-trans* equilibrium mixture of the dihydroxo ions *. When calculating α in a solution not yet in equilibrium, one is presented with the question of which value to insert for $\varepsilon_{Cren_2(OH)_2^+}$. It seems reasonable to assume that the first hydrolysis product would be the *cis*-dihydroxo ion which would then isomerize to form the *cis-trans* equilibrium mixture:

$$Cren_3^{+++} \rightarrow \textit{cis}\text{-}Cren_2(OH)_2^+ \rightleftharpoons \textit{tr.}\text{-}Cren_2(OH)_2^+$$

Qualitatively it may be seen that if the isomerization were fast compared to the hydrolysis, it would be permissible to consider the ratio

$$\frac{[\textit{tr.}\text{-}Cren_2(OH)_2^+]}{[\textit{cis}\text{-}Cren_2(OH)_2^+]}$$

as a constant (and equal to the equilibrium ratio) during the reaction; otherwise this ratio would be a function of time increasing from zero to the equilibrium ratio.

This problem might be circumvented by choosing values of λ within a range where there is very little difference between the extinction of the *cis* ions and the extinction of the *cis-trans* equilibrium mixture (*vide* Fig. 1).

But fortunately the question may be settled spectrophotometrically by consideration of the isosbestic points which are likewise useful in deciding whether $Cren_3^{+++}$ and *cis*- and *trans*-$Cren_2(OH)_2^+$ are the only species present in the solutions.

* provided concentrations of *cis*- and *trans*-$Cren_2(OH)(H_2O)^{++}$ may be neglected. For the purpose of the following discussion this approximation is certainly sufficient for pH > 9.5. Due to the similarity between the spectra of the ions in question the correction that would have to be made for the content of $Cren_2(OH)(H_2O)^{++}$ does not exceed the experimental uncertainty until this content exceeds 5 % of $[Cren_2(OH)_2^+]$.

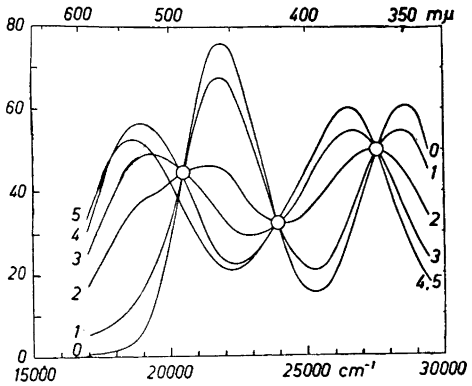

Fig. 4. Spectra in 1 M $NaNO_3$ at 25°C of solution No. 1 in Table 7 at time 0 (0), 69 h (1), 334 h (2), 624 h (3), 1 800 h (4) and 5 900 h (5).
Abscissa: Wave numbers in cm^{-1} and wavelength in mμ.
Ordinate: The molar decadic extinction coefficient.

A number of solutions of $Cren_3Cl_3$ in ethylenediamine buffers at pH $\geqq$ 9 containing the buffer system in various concentrations has been prepared and followed spectrophotometrically and by glass electrode measurements. In no cases, however, it was possible to establish an equilibrium containing analyzable amounts of $Cren_3^{+++}$.

To illustrate the results of these experiments the data of two representative solutions are given in Table 7 and the spectra of No. 1 of these are recorded in Fig. 4. It is seen that all of the consecutive spectra (except that at $t=5$ 900 h) have three common points of intersection. In Table 6 the wavelengths at which these points occur are compared to those which may be predicted from the spectra in Fig. 1 assuming that the components of the mixture are either $Cren_3^{+++}$ and *cis*-$Cren_2(OH)_2^+$ or $Cren_3^{+++}$ and the *cis-trans* equilibrium mixture of the dihydroxo ions. Further the isosbestic extinction coefficients observed ($\varepsilon = D/C_{Cr} \times$ cell length) are compared to those calculated under the two assumptions. A fairly good agreement is found with the assumption that the *cis-* and *trans*-dihydroxo ions are present in their equilibrium ratio. But the points of intersection in the spectra of the reaction mixtures can of course not be determined very accurately until the shape of the spectrum is considerably different from the initial shape. The validity of the above arguments is therefore limited to solutions in which $\alpha >$ *ca.* 40 %, although there is no experimental evidence against their validity at lower values of α*.

* This agreement is, therefore, not at variance with the assumption that the *cis*-dihydroxo ion is the first hydrolysis product. If one solves the differential equations pertaining to the mechanism

$$A \xrightarrow{k_1} B \underset{k_3}{\overset{k_2}{\rightleftharpoons}} C$$

and calculates the ratio [B]/[C] as a function of time in a system which at time zero contains only A inserting $k_3 = 5k_2 = 10k_1$ (which is not very far from correct for the solutions considered here, vide Tables 5 and 7), one finds that when 50 % of A has disappeared [B]/[C] is only 12 % greater than the equilibrium value.

Table 7. The hydrolysis of the trisethylenediaminechromium(III) ion in ethylenediamine buffers at pH ~10 in *ca.* 1 M nitrate at 25°C.

Data of initial solutions. $-\log[H^+]_{st} = 2.3006$

No.	Cr salt	C_{Cr}	C_{en}	C_{HNO_3}	C_{NaNO_3}	$E_{st}-E$	$-\log[H^+]$
1	$Cren_3Cl_3$, $3\frac{1}{2}H_2O$	0.01235	0.09806	0.06545	0.9000	0.4436	9.807
2	—»—	0.01371	0.4903	0.3200	0.6700	0.4523	9.954

Spectrophotometric measurements.

	λ		340	350	390	460	525	550 mμ	
	$\varepsilon_{Cren_3}{}^{+++}$		51.3	60.7	16.0	75.6	6.2	1.6	
	$\varepsilon_{Cren_2(OH)_2}{}^{+}$		16.0	30.3	54.0	24.6	57.6	51.8	
	$\varepsilon_{Cren_3}{}^{+++}-\varepsilon_{Cren_2(OH)_2}{}^{+}$		35.3	30.4	−38.0	51.0	−51.4	−50.2	
		t h							Av.
1	$\varepsilon_o-\varepsilon_t$	239	18.0	16.2	−18.8	23.9	−26.9	−24.7	
	α	239	0.510	0.533	0.495	0.469	0.523	0.492	0.50
	$\varepsilon_o-\varepsilon_t$	334	21.0	18.8	−24.1	30.4	−32.8	−30.6	
	α	334	0.595	0.618	0.634	0.596	0.638	0.609	0.62
	$\varepsilon_o-\varepsilon_t$	624	27.9	24.7	−33.8	40.9	−43.9	−42.1	
	α	624	0.790	0.812	0.889	0.802	0.854	0.838	0.83
	$\varepsilon_o-\varepsilon_t$	1 727	33.4	28.1	−39.9	50.2	−49.8	−49.2	
	α	272	0.946	0.924	1.05	0.984	0.969	0.980	0.98
	$\varepsilon_o-\varepsilon_t$	1 800	34.2	29.4	−40.8	51.0	−51.2	−51.0	
	α	1 800	0.969	0.966	1.07	1.00	0.996	1.03	1.01
2	$\varepsilon_o-\varepsilon_t$	1 147	32.6	27.3	−39.3	48.3	−48.6	−47.6	
	α	1 147	0.924	0.898	(1.03)	0.946	0.945	0.948	0.93
	$\varepsilon_o-\varepsilon_t$	5 220			−39.2	50.6	−51.4	−50.9	
	α	5 220			1.03	0.992	1.01	1.00	1.01
	$\varepsilon_o-\varepsilon_t$	11 500			−39.2	53.6	−51.0	−50.8	
	α	11 500			1.03	1.05	1.00	1.01	1.02

The results of calculating α from (1) at suitable wavelengths inserting the *cis-trans* equilibrium values of $\varepsilon_{Cren_2(OH)_2}{}^{+}$ are given in Table 7. Here, the quantity $\frac{D_o-D_\alpha}{l \times C_{Cr}}$ has been designated $\varepsilon_o-\varepsilon_t$. From the data concerning solution No. 1 it may be concluded that the primary reaction is an almost complete conversion of $Cren_3{}^{+++}$ into $Cren_2(OH)_2{}^{+}$. But the solution thus formed is not a true equilibrium solution, as its spectrum continues to change very slowly so that the absorption in the ultraviolet increases while the band at 19 000 cm^{-1} moves towards longer wavelengths and decreases slightly. This behaviour is typical of most of the solutions investigated.

In solution No. 2 the buffer concentration has been increased. Also in this medium $Cren_3{}^{+++}$ is almost completely converted into $Cren_2(OH)_2{}^{+}$, but the following changes in the spectrum are extremely slow (the spectrum was practically unchanged for a year except for a slight increase in the ultraviolet). It may therefore be assumed that the desired equilibrium has very nearly been established in this solution. The accuracy of the spectrophotometric measurements, however, does not permit a determination of $[Cren_3{}^{+++}]$.

An attempt was therefore made to determine this concentration chromatographically. It was shown that when a mixture of the trisethylenediamine and the *trans*- and *cis*-dihydroxo ions was chromatographed on a column of Al_2O_3 using 0.1 M KOH, 1 M KCl as an eluent, the three ions were clearly separated and eluated in the said order. 20 ml of solution No. 2 were chromatographed this way and all of the apparently colourless effluent (*ca.* 30 ml) leaving the column in front of the *trans* band was collected. The optical density of this effluent in an absorption cell with a 10 cm light path was recorded by the Cary whereby it should be possible to ascertain the presence of $Cren_3^{+++}$ in concentrations down to about 7×10^{-5} mole/l which would give rise to the optical density 0.05 at the maximum of the highest absorption band. However, the optical density observed was smaller than this, and it would hardly be safe to draw any other conslusion from the experiment than that $[Cren_3^{+++}]$ in the effluent was below 5×10^{-5} mole/l and in solution No. 2 therefore below 7.5×10^{-5} mole/l corresponding to $\alpha \sim 99.5$ %.

Although it is impossible to determine the stability constant k_3 from the present experiments, it is still of some interest to estimate its maximum value. Using the data of solution No. 2 in Table 7 at $t = 5\,220$ h: $-\log[H^+] = 9.85$, $[en] = 0.16$ (calculated under the assumption that one molecule en has been split off by the $Cren_3^{+++}$), $[OH^-] = 1.07 \times 10^{-4}$ (calculated using for the ionic concentration product of water, $k_{H_2O} = 10^{-13.82}$, the value given by Bjerrum and Unmack [12] for 1 M KCl at 25°C) and $\alpha \geqq 99.5$ %, this may be done as follows. Let us define a hydrolysis constant for $Cren_3^{+++}$

$$k_{h,1} = \frac{[Cren_2(OH)_2^+]\,[en]}{[Cren_3^{+++}]\,[OH^-]^2} = \frac{\alpha\,[en]}{(1-\alpha)\,[OH^-]^2}$$

Inserting the above values, we obtain $k_{h,1} \geqq 3 \times 10^5$ (Co 1.76). The corresponding constants $k_{h,1}(cis)$ and $k_{h,1}(tr.)$ are connected through

$$k_{h,1}(cis) + k_{h,1}(tr.) = k_{h,1} \text{ and } \frac{k_{h,1}(cis)}{k_{h,1}(tr.)} = q_2$$

Thus $k_{h,1}\ (cis) \geqq 2.5 \times 10^5$ (Co 0.78) and $k_{h,1}\ (tr.) \geqq 5 \times 10^4$ (Co 0.98). k_3 is related to these quantities through

$$k_3 = \frac{k_{s,1} \cdot k_{s,2}}{k_{h,1} \cdot k_{H_2O}^2}$$

In Ref.[1] k_3 for the cobalt(III) ethylenediamine system has erroneously been calculated from

$$k_3 = \frac{k_{h,1} \cdot k_{s,1} \cdot k_{s,2}}{k_{H_2O}^2}$$

Due to the fact that in the cobalt system $k_{h,1}$ is not very far from unity (when measured in liter/mole) the errors thus introduced are fortunately relatively small. The corrected values are given in parenthesis below.*

* As a consequence of these corrections the quantities calculated for the cobalt (III) ethylenediamine system at ionic strength, $\mu = 1$ and 30°C (Table 1 of Ref. 1) should be changed as follows:

$\log k_1 = 19.2$ $\log k_2 = 16.2$ $\log k_3 = 13.31$ $\beta_1 = 1986$ $\beta_2 = 137$

Inserting the appropriate constants, we arrive at

$$k_3(cis) \leqq 10^{10.2}\ (\mathrm{Co}\ 10^{13.50})\ k_3(tr.) \leqq 10^{11.3}\ (\mathrm{Co}\ 10^{15.26})$$

and defining $k_3(gr.)$ as k_3 for a system in *cis-trans* equilibrium so that

$$\frac{1}{k_3(cis)} + \frac{1}{k_3(tr.)} = \frac{1}{k_3(gr.)}$$

we obtain

$$k_3(gr.) \leqq 10^{10.2}\ \text{liter/mole}\ (\mathrm{Co}\ 10^{13.49}).$$

Acknowledgement. I wish to thank the head of this laboratory, Professor Jannik Bjerrum for having suggested this investigation, for valuable advice and encouragement and for his never failing interest in this work. My thanks are further due to Civilingeniør C. W. Kallenbach Pedersen, for his valuable experimental assistance.

REFERENCES

1. Bjerrum, J. and Rasmussen, S. E. *Acta Chem. Scand.* **6** (1952) 1265.
2. Schläfer, H. L. and Kling, O. *Z. anorg. Chem.* **287** (1956) 296; Kling, O. Diss. Frankfurt a.M. 1957.
3. Jensen, K. A. *Z. anorg. Chem.* **242** (1939) 87.
4. Linhard, M. *Z. Elektrochem.* **50** (1944) 224.
5. Linhard, M. and Weigel, M. *Z. anorg. Chem.* **271** (1953) 118.
6. Pfeiffer, P. *Z. anorg. Chem.* **56** (1908) 286; **58** (1908) 242, 253; *Ber.* **37** (1904) 4275; **40** (1907) 3832, 3834, 3836.
7. Bjerrum, J. *Metal Ammine Formation in Aqueous Solution.* Haase and Son, Copenhagen 1941 and 1957, p. 119.
8. Bjerrum, J. and Andersen, P. *Kgl. Danske Videnskab. Selskab, Mat.-fys. Medd.* **22** (1945) No. 7, p. 13.
9. Bjerrum, J., Jensen, A. and Woldbye, F. *Om adskillelsen af robuste komplexer ved sejlechromatografi.* 9. Nordiske Kemikermøde, 1956.
10. Kolthoff, I. M. and Belcher, R. *Volumetric Analysis III.* New York 1957, p. 180.
11. Bjerrum, J., Schwarzenbach, G. and Sillén, L. G. *Stability Constants I.* The Chemical Society of London 1957, p. 5.
12. Bjerrum, N. and Unmack, A. *Kgl. Danske Videnskab. Selskab, Mat.-fys. Medd.* **9** (1929) no. 1.

Received March 29, 1958.

ACTA CHEMICA SCANDINAVICA 12 (1958) 1095—1110

Remarks on Evaluating Kinetic Data for Technical Purposes

OTTO STELLING and OTTO von KRUSENSTIERNA

Division of Applied Inorganic Chemistry, Royal Institute of Technology, Stockholm, Sweden

The chemical engineer studying the kinetics of catalyzed reactions is often unaware of the limitations of his experimental method and uses hidden parameters which diminish the value of his data. The Langmuir-Hinshelwood method, the Hougen-Watson method and the exponential equations of Temkin are critically discussed. The conclusion is that, independant of the choice of adsorption isotherm, the same rate equation can be derived. The backward rate expression cannot be derived exactly from the forward rate expression but some restrictions on the form of the backward rate expression can be obtained with the help of Horiuti's "stoichiometric numbers". Some often occurring weak points in kinetic investigations are summarized and a standard procedure for kinetic investigations is outlined and illustrated with an experimental investigation of the watergas-shift reaction.

The processing techniques of the chemical industry show now a very marked tendency to change from the classical discontinuous processes as those of the dye industry to modern continuous processes exemplified by the petrochemical industry. These modern processes are often based on heterogeneous catalysis and the desired product is obtained by the use of the highest possible accuracy in the process control. This change in the industry has been made possible by a better general knowledge of the processes and especially by a more detailed understanding of all the kinetic problems involved. These problems have to be solved before a calculation of the engineering equipment of a process can start. If kinetics is defined as including both the chemical processes and the physical processes of mass- and heat-transfer one is bound to state that the branch of kinetics has a dominating position in modern chemical engineering research.

The chemical engineer and the research-chemist approach the problems of heterogeneous kinetics from two different sides. The chemical engineer is usually satisfied if he can find a rate equation reliable enough to permit reactor calculations and process control in the practical working range of pressures and temperatures. The research-chemist on the other hand wants to find the reaction mechanism itself with the help of experimental kinetic data and

tries to determine the simple primary reaction steps from which the complicated total reaction is built up. The distance between these two outlooks has been lessening during the last decades in as much as the interest of the chemical engineer is changing into a more exact knowledge of the mechanism of a reaction and its bearings on process possibilities and catalyst characteristics. The exact determination of the reaction mechanism in detail to its primary steps is, however, still very difficult and even such simple classical reactions as the oxidation of hydrogen and of carbon monoxide are still debated.

The main difficulty in mechanism determinations is often the experimental accuracy which is too limited to determine the often very small differences between different reaction mechanisms. This means that it usually pays back to invest work in increasing the experimental accuracy and to use an experimental approach that gives crucial data rather than general ones which are used for calculations based on more or less plausible mechanisms. On the other hand, as Christiansen [1] recently has pointed out, an *underestimation* of the accuracy can lead to serious consequences when data are used to fit a chosen mechanism.

Many different experimental methods and methods of data evaluation have been used in the study of kinetics and it is easy to understand that sometimes kineticists have been unaware of the limitations in their experimental method. Very often hidden parameters make the general treatment of valuable experimental data impossible. An often occurring case is the laboratory chemist who neglects the importance of diffusion processes and produces data which have only a limited value outside the laboratory. The chemical engineer on the other side often makes too far reaching conclusions about the nature of the plausible reaction mechanism which fits his data.

With these views in mind we have thought it to be of some value to discuss critically some of the methods which usually have been used for the kinetic investigations of heterogeneous processes of technical interest. In connection with this discussion we propose a standard procedure to be followed in investigations of this kind and which perhaps could help to diminish the confusion which one encounters in the current literature. As an example of this procedure we finally give some data from a kinetic investigation of the watergas-shift reaction.

THE LANGMUIR-HINSHELWOOD METHOD

The classical Langmuir-Hinshelwood method has in many cases given a good qualitative and sometimes also a quantitative explanation of experimental data by an assumed reaction mechanism. A reaction of the type

$$A + B = R + S$$

is studied by measuring the conversion at different partial pressures p_A while the other partial pressures are kept constant. If a low conversion is chosen the consumed and produced amounts of A, B, R and S are so small that the initial pressures p_A, p_B, p_R and p_S need to be only very slightly corrected. When reversible reactions are studied it is usually convenient to chose pressure conditions so that the backward reaction can be neglected.

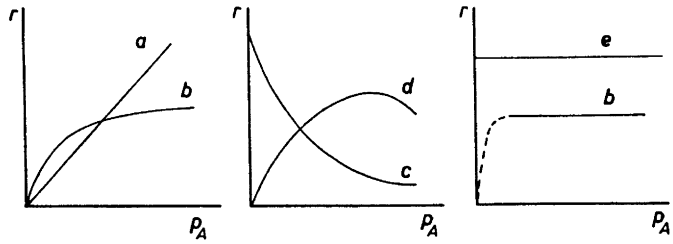

Fig. 1. The rate of reaction, r, as a function of the partial pressure p_A when p_B, p_R and p_S are constant. Each curve a—e corresponds to a Langmuir-Hinshelwood mechanism (Eqns. 1a—1e).

If for instance the rate of the forward reaction r_f and its variation with p_A is investigated, the experimental data often can be correlated with one of the following equations graphically represented in Fig. 1 (curves a—e).

$$r_f = kp_A \quad (1a); \qquad r_f = kp_A/(b + K_A p_A) \quad (1b); \qquad r_f = k/(c + K_A p_A) \quad (1c);$$
$$r_f = kp_A/(d + K_A p_A)^2 \quad (1d); \qquad r_f = k \quad (1e);$$

The following mechanisms can be derived from these different cases with the Langmuir-Hinshelwood method: Eqn. (1a) shows that the rate is proportional to the number of collisions of A with the active catalyst surface. Eqn. (1b) shows that the rate is proportional to that part of the active surface which is covered with adsorbed A. Eqn. (1c) shows that the rate is dependant on the part of the surface that is not covered with A and that A acts as an inhibitor. Eqn. (1d) shows that the rate is proportional to the product of two adsorbed substances one of which is A. Finally eqn. (1e) shows that the rate is independant of A. This can be interpreted as an mechanism in which A is not involved or that A is so strongly adsorbed — eqn. (1b) — that $K_A p_A \gg b$.

The same measurements are performed with the other gascomponents and finally the rate can be expressed as a function of all the involved reactants and products, *i.e.*

$$r_f = f[(p_A), (p_B), (p_R), (p_S)]$$

This function can then, after closer inspection of the involved constant pressures, be written in the form of a rate equation.

Assume for instance that the experimental data have resulted in $r_f = f[(p_A), (p_B/(b+K_B p_B)), (1/(c+K_R p_R), (p_S)^\circ]$
and that closer examination of the constants b and c has revealed the connections $q = 1 + K_R p_R$ and $c = 1 + K_B p_B$. The rate equation can then be formulated

$$r_f = k\, p_A p_B/(1 + K_B p_B + K_R p_R)$$

This equation should describe the reaction rate for the experimental conditions as well as the rate of the forward reaction when the reactants are converted simultaneously in the technical process. The equivalent mechanism is the collision of A, from the gas phase, with adsorbed B as the slowest and rate determining step and with the product R partly covering the active surface and therefore diminishing the rate.

Technical investigations often only determine the rate of the forward reaction but for some reversible reactions as the NH_3-synthesis, the SO_2-

oxidation etc., the total rate must be determined. The backward rate r_b is then evaluated in the same manner as r_f and the total (net) rate becomes

$$r = r_f - r_b$$

The experimental apparatus used in connection with the Langmuir-Hinshelwood method have been both of the static and of the flow-system type. In modern investigations, however, the flow system is preferred as it gives defined diffusion conditions and very often a higher accuracy of analysis.

An excellent example of the Langmuir-Hinshelwood method applied to a technical process is the investigation of Gadsby, Hinshelwood and Sykes [2] and the following investigations [3-5] of the complicated system steam-carbon with four different simultaneous reactions.

THE HOUGEN-WATSON METHOD

An extension of the Langmuir-Hinshelwood approach has been developed by Hougen and Watson [6] and Hougen and Yang [7] and this method has often been used during the last decade mostly in the U.S.A. for the kinetic investigation of technical processes.

The Hougen-Watson method uses an elegant formal way of expressing the chemisorption of a gas on the active catalyst surface and together with other simplifications is it possible to derive the rate equation for every possible reaction mechanism with a minimum of calculations.

The Hougen-Watson method can, for instance, be used to derive the rate equation for the mechanism of the before mentioned example. The first reaction step is assumed to be the collision of A from the gas-phase with B adsorbed on the surface. The products formed are adsorbed R and S in the gas-phase. If the adsorptions of B and R are fast in comparison with the first step, they can be treated as adsorption equilibria and the first step becomes rate determining. The rate of the reversed reaction is then the collision of S with adsorbed R.

The concentrations of the adsorbed particles are represented by c_B and c_R, the concentration of free active centers by c_l and the total concentration of active centers by L. The chemisorption can then be written as a chemical reaction between a gas particle and an active center l. In this case

$$B + l = Bl \qquad R + l = Rl \qquad A + Bl = Rl + S$$

where the last expression constitutes the rate determining step. The rate, the adsorption equilibria and the surface-concentrations can now be written

$$r = k_1 p_A c_B - k_2 p_S c_R$$

$$K_R = c_R/p_R c_l \qquad K_B = c_B/p_B c_l$$

$$L = c_l + c_B + c_R$$

The elimination of the unknown surface-concentrations gives the rate equation expressed in the measurable partial pressures

$$r = \frac{k_1 K_B (p_A p_B - (1/K) p_R p_S)}{1 + K_B p_B + K_R p_R}$$

where K is the equilibrium constant for the reaction. For the forward reaction this

expression is identical with the one in the foregoing example. However, this rate equation could have been written directly with the help of formula tables which have been constructed by Hougen and Yang [7] *.

The formal ease with which the different rate equations can be derived has often influenced the experimental approach when the Hougen-Watson method is used.

The reaction rates are measured with an isothermal flow-reactor for which the general equation holds

$$F\ \mathrm{d}x = r\ \mathrm{d}W$$

where F = feed (mole) / (min), $\mathrm{d}x$ = conversion (mole) / (mole F), $\mathrm{d}W$ = mass catalyst (g) and r = rate (mole) / (g catalyst) (min). Other units, dimensionally consistent, could of course be used. If diffusion is not a limiting factor a differential reactor (small catalyst bed, low conversion) or an integral reactor (large catalyst bed, high conversion) can be used and the rates would be, respectively

$$r_{\mathrm{diff}} = (\Delta x/\Delta W)\ F \qquad\qquad r_{\mathrm{int}} = \mathrm{d}x/(\mathrm{d}W/F)$$

For the integral-reactor the rate is the tangent to the experimentally determined function $x = \mathrm{f}(W/F)$ and can be calculated by graphical derivation. By variation of the partial pressures, usually in a restricted range, as compared to the Langmuir-Hinshelwood-method, a number of r-values are produced.

The next step is to derive all the theoretical possible rate mechanisms and their equivalent rate equations. In this way as much as 75—100 equations can be set up [8] but this number can often be reduced to 10—20 by an inspection of initial-rate data. Hougen and Yang [7] have demonstrated useful relations between the initial rate, the pressure and the mole fractions for different rate equations which are similar to the curves in Fig. 1.

After this test the constants of the remaining equations are determined graphically or by the method of least-squares. Equations with negative constants are eliminated as being physically unsound and the last 3—4 equations usually show a good fit to the experimental data. The last decision is often difficult but a comparison of the integrated equation with data from an integral-reactor can usually be helpful. An unnormal variation of the constants with temperature can also be used for the elimination of equations.

Apart from the mentioned original articles [6,7] the Hougen-Watson method has been presented in some textbooks [9,10] and the calculations involved have been discussed in detail by Corrigan [11].

THE VALIDITY OF THE LANGMUIR-HINSHELWOOD AND THE HOUGEN-WATSON METHODS

Recently the LH- and the HW-methods have been critically discussed by Weller [12] and Boudart [13] and the use of the HW-method in technical investigations has been questioned. Weller points out that the Langmuir adsorption isotherm, which is the base of both methods, has been derived with the assumption of a constant heat of adsorption independant of the surface coverage. However, experiments always show a decreasing heat of adsorption with increasing coverage. This interaction of adsorbed molecules or atoms has also been observed when several gases are adsorbed simultaneously. The

* For the example treated here a misprint in the original work, Table 4, has led to a misleading discussion of initial-rate effects for this case, p. 154 and Table 5.

adsorption of one gas can sometimes increase the adsorption of another gas. If the adsorption of A increases when B also is adsorbed the amount of adsorbed A, c_A, can according to Weller be expressed in the following form:

$$c_A = kp_A/(1 + K_Ap_A - K_Bp_B)$$

This expression has a negative adsorption-constant which in the Hougen-Watson-method was a characteristic mark of physically unsound rate equations which therefore were ruled out.

According to Weller the Langmuir-Hinshelwood method should be used with care and only for qualitative considerations. The Hougen-Watson method should be used as a purely empirical method for data-fitting and as a method by which a mechanism can be determined "which the unwary investigator is often led to believe that he has uniquely deduced".

Instead the use is recommended of exponential expressions of the form $r = k\,(p_A)^m(p_B)^n(p_R)^q \ldots\ldots$ where the exponents have integral or half-integral values or zero. Weller demonstrates on several investigations described in the literature how a simple exponential expression with only one constant gives the same data fitting as complicated Hougen-Watson expressions with up to 4 constants. Rate equations of the simple exponential form can therefore with advantage be used for technical calculations.

The real difference between Wellers exponential expressions and the Langmuir-Hinshelwood and Hougen-Watson expressions is, however, not so large. It is a matter of choice of the adsorption isotherm. Weller uses indirectly the Freundlich isotherm and the other expressions are based on Langmuir.

Boudart [13] shows in a following article that the use of Langmuir's isotherm for non-ideal surfaces, "the paradox of surface catalysis", can be explained by the broad energy distribution of the active centers and also by the possible mathematical approximation

$$\Theta_F = k\ p^n \approx \Theta_L = bp/(1 + bp)$$

This means that the pure empirical Freundlich isotherm, Θ_F with an exponential distribution of the heat of adsorption always can be approximated by an expression Θ_L of the same mathematical form as the Langmuir isotherm. This is of course the reason why Weller can fit his simple one-constant expressions with about the same deviations as those found with the Hougen-Watson method.

Some rate equations which are believed to be uniquely expressed in the exponential form must with the same argument be derivable from the Langmuir isotherm and Boudart shows how this can be done for the well-known Temkin-Pyzhev rate equation for the ammonia synthesis.

To sum up it can be said that the Langmuir isotherm, exactly valid only for ideal surfaces, can be used with advantage for the derivation of rate equations. It must be observed, however, that the involved constants are not real adsorption constants but rather a kind of average constants for the different "surfaces" of which a heterogeneous surface is made up. This is independant

of the real nature of the variation in the heat of adsorption, it may be due to surface heterogeneity, interaction between adsorbed particles or to some form of electron effects of the bulk of the catalyst.

Deviations from the normal adsorption mechanisms occur. As shown above Weller pointed out that mixed chemisorption sometimes can give effects which can be interpreted by negative adsorption constants. These cases of mixed chemisorption, so important for the understanding of heterogeneous catalytic processes, are still not very much investigated [14–16]. Most likely the observed effects are due to a kind of surface compounds ("adducts") and by this assumption it will be shown here how adsorption isotherms can be derived without the use of negative adsorption coefficients. Assume that the adsorption of CO is increased with increasing pressures of H_2 and that the surface compound CO-H_2-1 is produced. With the formal writing of the Hougen-Watson method:

$$\begin{aligned} H_2 + 1 &= H_2\text{-}1 & K_1 &= c_{H_2}/(p_{H_2}c_1) \\ CO + 1 &= CO\text{-}1 & K_2 &= c_{CO}/(p_{CO}c_1) \\ H_2\text{—}1 + CO &= CO\text{—}H_2\text{—}1 & K_3 &= c_{CO\text{-}H_2}/(p_{CO}p_{H_2}) \end{aligned}$$

$$L = c_1 + c_{H_2} + c_{CO} + c_{CO\text{-}H_2}$$

If the total amount of adsorbed CO is $C_{CO} = c_{CO} + c_{CO\text{-}H_2}$

then

$$C_{CO} = \frac{L\,K_2 p_{CO}}{\left(\dfrac{1 + K_1 p_{H_2}}{1 + \dfrac{K_3}{K_2} K_1 p_{H_2}}\right) + K_2 p_{CO}} \approx k \left(\frac{1 + \dfrac{K_3}{K_2} K_1 pH_2}{1 + K_1\, pH_2}\right)^m \left(K_2 p_{CO}\right)^m$$

If $K_3 > K_2$ the adsorbed amount of CO is increasing with increasing pressure p_{H_2} as observed and if $(K_3K_1/K_2)p_{H_2} \gg 1$ the isotherm can be written $C_{CO} = k(p_{CO})^m(p_{H_2})^{am}$; $(0 < a,\ m < 1)$.
With the mechanism $H_2 + CO\text{—}1 = H_2\text{—}CO\text{—}1$, a similar simpler expression can be derived, $C_{CO} = k(p_{CO})^n(1 + K_2 p_{H_2})^n$; $(0 < n < 1)$.

Other forms that deviate from the normal Langmuir isotherm are derived from switch-mechanisms like

$$AB + 1 = B\text{—}1 + A \qquad \text{or} \qquad A + B\text{—}1 = A\text{—}1 + B$$

For instance the amount of adsorbed N_2 in Temkins mechanism for the ammonia synthesis, C_{N_2}, is obtained from the step:

$$2\ NH_3 + 2\ 1 = 2\ N\text{-}1 + 3\ H_2$$

$$C_{N_2} = k\ p_{NH_3} / \left(p_{H_2}^{1.5} + K^{0.5}\ p_{NH_3}\right)^2$$

The large number of possible mechanisms makes an *a priori* derivation of every plausible mechanism impossible. In spite of this, technical investigations show a tendency to overestimate the calculating possibilities. It is not unusual

that some simple experimental series solve the problems faster and more reliable than tideous and unsure calculations of data fitting. A "most plausible" mechanism is often overvalued. As an example the work of Barkley, Corrigan, Wainwright and Sands [17] on the catalytic reversed shift reaction will be discussed.

They investigated the rate of the reaction $CO_2 + H_2 = H_2O + CO$ and found on the basis of a least-square treatment of plausible equations

$$r = k\frac{(p_{CO_2}p_{H_2} - p_{CO}p_{H_2O}/K)}{1 + K_A p_{CO_2} + K_R p_{CO}}$$

As the products CO and H_2O are produced in equivalent amounts and only CO_2 and H_2 are shown to have been experimentally varied in the feed, the experimental data could as well have been expressed by a rate equation with a denominator of the form $(1 + K_A p_{CO_2} + K_S p_{H_2O})$. This equation is founded on a mechanism which was not selected as plausible but seems to be more in accordance with other investigations [18,19].

THE TEMKIN METHOD

In their derivation in 1940 of the well-known rate equation for the ammonia synthesis, Temkin and Pyzhev [20] started with a non-ideal adsorption isotherm with a linear decrease of the heat of adsorption with coverage. The assumed mechanism was

$$N_2 \rightleftharpoons N_2\text{-ads} \qquad \text{(a)}$$

$$3\ H_2 + N_2\text{-ads} = 2\ NH_3 \qquad \text{(b)}$$

The adsorption of nitrogen (a) is rate determining and reaction (b) is assumed to be in equilibrium. The rate of the slow reaction is now the difference between the rates of adsorption and desorption or

$$r = k_a p_{N_2} e^{-g\Theta} - k_d e^{h\Theta}$$

The adsorption isotherm has the form

$$\Theta = \frac{1}{g + h} \ln a_0 p_{N_2}$$

The equilibrium (b) gives

$$P^*_{N_2} = (N_2\text{-ads}) = K_N \frac{(p_{NH_3})^2}{(p_{H_2})^3}$$

where $P^*_{N_2}$ is the fictitious pressure that gives the equivalent N_2-adsorption. If this "pressure" or fugacity is put into the adsorption isotherm and then Θ is eliminated from the rate equation the final equation becomes

$$r = k_1 p_{N_2}\left[\frac{(p_{H_2})^3}{(p_{NH_3})^2}\right]^{\alpha} - k_2\left[\frac{(p_{NH_3})^2}{(p_{H_2})^3}\right]^{1-\alpha}$$

Later Temkin [21] showed that the same expression could be derived with the Freundlich isotherm which has an exponential decrease of the heat of adsorption with coverage and Boudart has demonstrated, as mentioned, that the Temkin equation could be derived with a pure Langmuir-Hinshelwood reasoning.

With the formal Hougen-Watson writing this derivation is simply done and if the slow step is assumed to be $N_2 + 2l = 2$ N-l the rate equations becomes

$$r = \frac{k_1 L^2 [p_{N_2}(p_{H_2})^3 - (p_{NH_3})^2/K]}{((p_{H_2})^{1.5} + K_N{}^{0.5} p_{NH_3})^2}$$

With the approximation $kx/(1 + kx) \approx ax^{1-a}$ and with $x = K_N{}^{0.5}(p_{NH_3})/(p_{H_2})^{1.5}$ the equation above is transformed into the Temkin equation.

The different ways of deriving the Temkin rate equation have shown that rate equations seem to be quite insensible to the choice of adsorption isotherm. The exponential form of the rate equations may be easier to fit to the experimental data but the Langmuir form has the advantage of covering the whole pressure range. The Langmuir expression above shows for instance the limiting rates for high p_{H_2} and low p_{NH_3} and the reverse, to be $r = k\ p_{N_2}$ and $-r = k$, which has been experimentally observed.

In Table 1 some experimentally determined rate equations have been grouped together with their equivalent Langmuir or Temkin expressions. A star marks out the form in which the equation was presented in the literature. The equations in the table all show, when properly rewritten, how the factor $1/(P_1^a + K_1 P_2^b)$ in the Langmuir expressions is equivalent to $1/[(P_1^a)^n (P_2^b)^{1-n}]$. This last expression is similar in form to the "inhomogeneity factor" $F = [\Theta^n (1\text{-}\Theta)^{1-n}]$ which de Bruijn [20,24] derived from the Temkin ammonia-equation, assuming an arbitrary distribution of active centers. In fact, $1/F$ is exactly the factor which transforms, without mathematical approximations, a Langmuir expression ("ideal surface") to an exponent expression of the Temkin type ("inhomogeneous surface").

THE RELATION BETWEEN THE FORWARD AND BACKWARD REACTION RATES

The rate of a reaction can be written as the difference between the forward rate r_f and the backward rate r_b

$$r = r_f - r_b = k_f F_f - k_b F_b$$

where k_f and k_b are rate constants and F_f and F_b are algebraic expressions of the reactants and products A,B, . . . and R,S, . . . At equilibrium $r = 0$ and

$$\frac{F_b}{F_f} = \frac{k_f}{k_b} = f(T)$$

where k_f/k_b is a constant only determined by temperature. Usually this constant is put equal to the equilibrium constant of the reaction

Table 1. Comparison of rate equations.

r_T = exponential Temkin-form r_L = Langmuir-form

1. Reaction: $3\ H_2 + N_2 = 2\ NH_3$

* $$r_T = k_1 P_{N_2}\left(\frac{P_{H_2}^3}{P_{NH_3}^2}\right)^n - k_2\left(\frac{P_{NH_3}^2}{P_{H_2}^3}\right)^{1-n} \qquad n = \tfrac{1}{2} \qquad (20)$$

$$r_T = \left[\frac{1}{(P_{H2}^3)^{1-n}\,(P_{NH_3}^2)^n}\right] k\ (P_{N_2}\ P_{H2}^3 - P_{NH_3}^2/K)$$

$$r_L = \left[\frac{1}{P_{H2}^3 + K_N\ P_{NH_3}^2}\right] k\ (P_{N_2}\ P_{H2}^3 - P_{NH_3}^2/K);\ N_2 \text{ not dissociated}$$

$$r_L = \left[\frac{1}{(P_{H_2}^{1.5} + K_N^{0.5} P_{NH_3})^2}\right] k\ (P_{N_2}\ P_{H2}^3 - P_{NH_3}^2/K);\ N_2 \text{ dissociated}$$

2. Reaction: $2\ SO_2 + O_2 = 2\ SO_3$

* $$r_T = k_1\ P_{O2}\left(\frac{P_{SO2}}{P_{SO3}}\right)^{2n} - k_2\left(\frac{P_{SO3}}{P_{SO2}}\right)^{2(1-n)} \qquad \begin{matrix} V_2O_5\text{–cat: } n = \tfrac{1}{4} \\ Fe_2O_3\text{–cat: } n = \tfrac{3}{4} \end{matrix} \qquad \begin{matrix} (22) \\ (23) \end{matrix}$$

$$r_T = \left[\frac{1}{(P_{SO_2}^2)^{1-n}\ (P_{SO_3}^2)^n}\right] k\ (P_{O2}\ P_{SO_2}^2 - P_{SO_3}^2/K)$$

$$r_L = \left[\frac{1}{P_{SO_2}^2 + K_O\ P_{SO_3}^2}\right] k\ (P_{O2}\ P_{SO_2}^2 - P_{SO_3}^2/K);\ O_2 \text{ not dissociated}$$

$$r_L = \left[\frac{1}{(P_{SO_2} + K_O^{0.5}\ P_{SO_3})^2}\right] k\ (P_{O2}\ P_{SO_2}^2 - P_{SO_3}^2/K);\ O_2 \text{ dissociated}$$

* $$r_T = k_1\ P_{SO_2}\left(\frac{P_{O_2}^{0.5}}{P_{SO_2}}\right)^n - k_2\left(\frac{P_{SO3}}{P_{O_2}^{0.5}}\right)^{1-n} \qquad \text{Pt–cat: } n = 1/2 \qquad (23)$$

$$r_T = \left[\frac{1}{(P_{O_2}^{0.5})^{1-n}\ (P_{SO_2})^n}\right] k\ (P_{SO_2}\ P_{O_2}^{0.5} - P_{SO_3}/K)$$

$$r_L = \left[\frac{1}{P_{O_2}^{0.5} + K_S\ P_{SO_3}}\right] k\ (P_{SO_2}\ P_{O_2}^{0.5} - P_{SO_3}/K)$$

3. Reaction: $CO + H_2O = CO_2 + H_2$

* $$r_T = k_1 P_{CO}\left(\frac{P_{H2O}}{P_{H_2}}\right)^n - k_2\ P_{CO_2}\left(\frac{P_{H_2}}{P_{H2O}}\right)^{1-n} \qquad (18)$$

$$r_T = \left[\frac{1}{(P_{H_2})^n\ (P_{H2O})^{1-n}}\right] k\ (P_{CO}\ P_{H2O} - P_{CO_2}\ P_{H_2}/K)$$

$$r_L = \left[\frac{1}{P_{H_2} + K_O\ P_{H2O}}\right] k\ (P_{CO}\ P_{H2O} - P_{CO_2}\ P_{H_2}/K)$$

* $$r_L = \left[\frac{1}{P_{CO_2} + K_{CO}\ P_{H2O}}\right] k\ (P_{CO}\ P_{H2O} - P_{CO_2}\ P_{H_2}/K) \qquad (19)$$

$$r_T = \left[\frac{1}{(P_{CO_2})^n\ (P_{H2O})^{1-n}}\right] k\ (P_{CO}\ P_{H2O} - P_{CO_2}\ P_{H_2}/K)$$

$K_c = (R)^r(S)^s/(A)^a(B)^b$. Manes, Hofer and Weller [25] and Denbigh and Prince [26] have shown that this is not a necessary condition but that all thermodynamic conditions are fulfilled if only

$$\frac{k_f}{k_b} = f(T) = (K_c)^z \quad \text{and} \quad z > 0$$

Very often $z = 1$, which gives the classical relation $k_f/k_b = K_c$. Horiuti developed in 1939 the "stoichiometric number" which is defined as the coefficient with which the stoichiometric formula of every reaction step has to be multiplied to give the wanted coefficients in the stoichiometric formula of the total reaction. The stoichiometric number ν_r of the slowest, rate determining step has been shown by Horiuti [27,28] to be identical with $1/z$, and therefore

$$\frac{k_f}{k_b} = (K_c)^{1/\nu_r}$$

The relation between the algebraic expressions for the forward and the backward reaction rate can now be written

$$\frac{F_b}{F_f} = \frac{k_f}{k_b} = (K_c)^{1/\nu_r} = \left[\frac{(R)^r(S)^s}{(A)^a(B)^b}\right]^{1/\nu_r}$$

or

$$F_b = F_f\left[\frac{(R)^r(S)^s}{(A)^a(B)^b}\right]^{1/\nu_r}$$

The value of ν_r, the stoichiometric number of the rate determining step, is however not known. A reaction step must be assumed to be a reaction between whole particles — molecules or atoms — and therefore ν_r or $1/\nu_r$ must be an integral number. If different values of ν_r are inserted in the last equation above, different expressions for the backward rate will be obtained. Denbigh and Prince [26] found for instance in an experimental investigation $z = 1/\nu_r = 1/4$ in contrast to the expected classical $z = 1/\nu_r = 1$. The value of z is restricted as total reactions with high stoichiometric coefficients are seldom which is due to the fact that primary reactions between more than three particles are highly inprobable. The stoichiometric number is therefore assumed to vary between 1/4 and 4.

It may be that some more restrictions on the stoichiometric number ν_r can be deduced in each investigated case and that reasoning in line with Christiansens [1] theory of sequences could be applied. The final determination must however, be made experimentally. If both F_f and F_b are determined it should be possible to calculate ν_r and from that obtain information useful for the determination of the rate determining step. Finally it can be mentioned that a relation exists, near equilibrium, between the free energy of the total reaction, the forward rate, the total rate and the stoichiometric number

$$\nu_r = (r_f/r)\ \Delta G/RT$$

which in special cases can be used for the determination of ν_r.

THE EXPERIMENTAL DESIGN OF KINETIC INVESTIGATIONS

It was pointed out in the introduction that even relatively modern kinetic investigations have a tendency of using hidden parameters and it is astonishing how limited the value often is of even large experimental series described in the literature on kinetics of reactions based on heterogeneous catalysis.

Some of the most often occurring factors which diminish the value of experimental data are

1. Too many variables such as contact-time, partial pressure and temperature have been varied at the same time so that only a few data points are unambigously showing the influence of one single variable.
2. The partial pressures have been varied only in narrow ranges of technical interest. A recalculation of the used pressures to mole-fractions will show this very clearly.
3. The contact-time has not been defined clearly.
4. The experiment has been designed so that too many temperatures have been investigated with too few data points for every temperature.
5. The absolute accuracy of analysis has been low.
6. Diffusion effects have been neglected or measured at low temperatures where the reaction rate has not its maximum value. Sometimes diffusion calculations are based on unsafe assumptions.
7. Different catalysts and different particle dimensions have been used without measuring the pore-diffusion effects.
8. The temperature distribution in the catalyst bed has not been measured during the reaction.
9. The catalyst has not been described in detail, has been undefined and chemical changes, ageing, and weight losses have been neglected.
10. The possibility of exchanging experimental data with calculated data has been overvalued.

The pronounced technical character of many investigations is naturally an explanation of the occurrence of some of these factors. A more careful experimental design would, however, without any marked increase in the amount of work, give experimental data of a much more general value. If a kind of standard procedure could be accepted for technical investigations some of the confusion in the literature would be eliminated and comparison of the literature data would be simpler.

With these views in mind a standard experimental design will be roughly outlined.

Apparatus

On the assumption that the analysis is accurate enough to permit the detection of small conversions a differential reactor should be used. For preliminary measurements integral-reactor measurements should also be possible. The constancy of the temperature must be better than $\pm$ 5°C at 500°C and it must be possible to measure the temperature all along the catalyst bed. The flow-meters — one for each gascomponent and one for the inert dilution gas — should have an absolute accuracy of better than 1 %. This can practically be obtained with the general calibration method for capillary flow-meters described by Ergun [29]; *cf.* also Benton [30]. If the total pressure of the system is held constant by means of a valve in the exhaust line, the flow measurements are further simplified.

Nomenclature

The reaction rate r should always be expressed as mass of converted material per unit mass of catalyst and unit time, *e.g.* (mole)/(g catalyst)(min). The mass of catalyst W should be expressed in (g). The area of the catalyst is often expressed in square-meters per g by the B.E.T. standard method. The gas feed F is expressed in mass per unit time, *e.g.* (mole)/(min). The contact-time W/F is then independant of the temperature of the reactor and is exactly defined as for instance (g catalyst)(min)/(mole F). The conversion x is expressed as converted mass of initial feed F_o, *e.g.* (mole converted F_O)/(mole F_O). When integral-reactor data are represented by the function $x = f(W/F)$, the conversion x must always be calculated on the same feed F with which the contact-time is calculated. If for instance F is the total feed of gas then x must be calculated on the total feed F, etc.

Program for experimental runs

1. Diffusion effects. The effect of the external diffusion is determined at the highest temperature used in the investigation (highest rate) by the relation between the conversion x and the feed F at constant W/F. Above a certain limiting gas velocity F_D the conversion x is constant. A simple approximation formula is given by Wheeler [31].

The internal diffusion (pore-diffusion) is determined by measuring x at constant W/F and varying the diameter of the catalyst particles d. Under a certain diameter d_D the conversion x is constant. Calculating formulas are given by Wheeler [31] and recently a general formula by Weisz [32].

2. Preliminary data. Integral-reactor data with $F \geq F_D$ and $d \leq d_D$ are taken for different contact-times W/F and the function $x = f(W/F)$ is obtained. This function can be considered as a graphical form of the rate equation and can be used for preliminary calculations. The initial feed-gas-mixture should be varied widely for instance in the proportions 1:4, 1:1 and 4:1.

3. Initial-rate data with variation of one partial pressure. Initial-rate data are produced in the following way: The total pressure and all partial pressures except one (and the inert gas) are kept constant. One partial pressure is varied from very low to very high values while the whole gas-mixture always is kept far away from equilibrium values to avoid the influence of the reverse reaction. As the conversion x is kept low the reaction rate is $r = x(F/W)$ where $x \leqq 5$ % of the equilibrium conversion. All reactants and products are studied in this way and the experimental data are graphically represented. Inspection of the curves with the help of the Langmuir-Hinshelwood reasoning gives hints to possible mechanisms and these can be further investigated by experiments with pressures chosen in a crucial way. For instance the mole-fraction method of Hougen and Yang [7].

4. Tests with the established rate equation. A final rate equation with its mechanism — for derivations the Hougen-Watson formalism can be used with advantage — is established and the expressions for the formal and backward reaction are examined from a thermodynamic point of view by means of Horiuti's theorem for stoichiometric numbers. A fit to the integral-reactor curves is made and constants are evaluated by graphical methods.

5. Influence of temperature. After the establishment of the rate equation measurements at two relatively different temperatures are started. Only a limited number of runs are necessary as the rate equation is known. Activation energies are calculated from the temperature variation of the constants. Bends in the Arrhenius lines have been discussed by Christiansen[1]. A bend concave upward or downward shows that two parallell or two series reactions are involved.

6. Investigations of other catalysts. If the purpose of the investigation was not only the establishment of the rate equation but also information about the catalyst, the change in mechanism when promotors are added etc., the investigation can with advantage be carried on with the initial-rate method. Determination of the activation energy can give informations concerning the influence of additives and of different methods of treatment. A detailed program on catalyst-testing has recently been given by Dowden and Bridger [33].

Finally experiments in static systems can sometimes complement the outlined course of the investigations, as for instance adsorption measurements of the different gas-components. Reference is again made to the work of Gadsby, Hinshelwood and Sykes [2] and subsequent works [3–5].

The watergas-shift reaction

As an example of how the proposed experimental procedure can be applied some results will be presented here of an investigation of the watergas-shift reaction [34].

The rate of the reaction

$$CO + H_2O = CO_2 + H_2$$

was studied in the presence of an iron-oxide catalyst. The diffusion- and pore-diffusion effects were measured and the allowed minimum gas velocity and maximum particle size was determined. With an integral reactor preliminary data were produced but partly due to the ageing of the catalyst a Hougen-Watson treatment to determine the rate equation was not successful.

Then the initial-rate method was applied and the difficulties of ageing gave no trouble as now the general form of the curves, rather than their exact slope, is the important factor for the evaluation. The experimental rate expressions for the different varied partial pressures were then united in one rate equation. A comparison with the integral-reactor data was made and constants were determined. Some of the measurements are presented in Fig. 2 which shows the variation of the forward rate when different gas-components are varied in pressure. From Fig. 2 c it can be seen that even very small amounts of CO_2 have a strong inhibiting effect. If the experimental curve I in Fig. 2 a is corrected for the small CO_2-amount produced at the low conversion used, the corrected curve II shows that the rate is directly proportional to p_{CO}.

The other curves indicate that H_2O and CO_2 are strongly adsorbed and that H_2 does not take part in the reaction. The experimental rates can be grouped together to the form

$$r_f = f\left[(p_{CO}), \left(\frac{p_{H_2O}}{b + K_1 p_{H_2O}}\right), \left(\frac{1}{c + K_2 p_{CO_2}}\right), (p_{H_2})^0 \right]$$

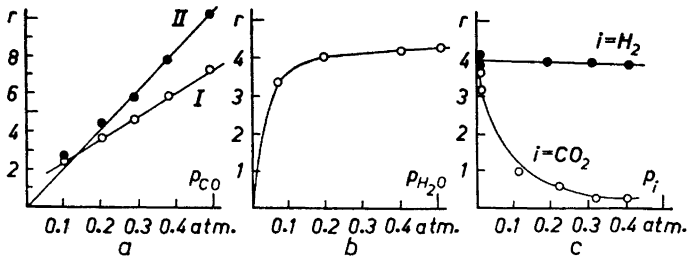

Fig. 2. The variation of the forward rate of the watergas-shift reaction when partial pressures of only one reactant or product are varied. Iron-oxide catalyst. Temperature 390°C. Pressures in atm. Rates in (10^{-4} mole) / (g catalyst) (min). In Fig. 2 a the curve II represents the values of curve I, corrected for CO_2-inhibition.

By closer inspection of the data this is transformed into the rate equation for the forward reaction

$$r_f = k \frac{p_{CO} p_{H_2O}}{p_{CO_2} + K_B p_{H_2O}} \approx k\, p_{CO} \left[\frac{p_{H_2O}}{p_{CO_2}}\right]^n$$

In this rate equation the influence of each gas-component has been unambigously determined and the experimental approach has eliminated such parameters as diffusion, particle size and temperature variations. Variables as partial pressures and contact-times have been used directly for the rate determination and are not parameters.

REFERENCES

1. Christiansen, J. A. *Advances in Catalysis* **5** (1933) 311.
2. Gadsby, J., Hinshelwood, C. N. and Sykes, K. W. *Proc. Roy. Soc. A* **187** (1946) 129.
3. Gadsby, J., Long, F. J., Sleightholm, P. and Sykes, K. W. *Proc. Roy. Soc. A* **193** (1948) 357.
4. Long, F. J. and Sykes, K. W. *Proc. Roy. Soc. A* **193** (1948) 377.
5. Long, F. J. and Sykes, K. W. *J. chim. phys.* **47** (1950) 361.
6. Hougen, O. A. and Watson, K. M. *Ind. Eng. Chem.* **35** (1943) 529.
7. Yang, K. H. and Hougen, O. A. *Chem. Eng. Progr.* **46** (1950) 146.
8. Kircher, O. and Hougen, O. A. *A. I. Ch. E. Journal* **3** (1957) 331.
9. Hougen, O. A. and Watson, K. M. *Chemical Process Principles*, J. Wiley & Sons, N. Y. 1947, Vol. III.
10. Smith, J. M. *Chemical Engineering Kinetics*, McGraw-Hill Book Co, N.Y. 1956.
11. Corrigan, T. E. *Chem. Eng.* **1954** Nov. 236. — **1955** July 227.
12. Weller, S. *A. I. Ch. E. Journal* **2** (1956) 59.
13. Boudart, M. *A. I. Ch. E. Journal* **2** (1956) 62.
14. Ghosh, J. C., Sastri, M. V. C. and Kini, K. A. *Ind. Eng. Chem.* **44** (1952) 2463.
15. Brunauer, S. and Emmet, P. H. *J. Am. Chem. Soc.* **62** (1940) 1732.
16. Krebs, M. *Zum Reaktionsmekanismus der Fischer-Tropsch-Synthese* (Diss. D 83) Techn. University, Berlin 1956.
17. Barkley, L. W., Corrigan, T. E., Wainwright, H. W. and Sands, A. E. *Ind. Eng. Chem.* **44** (1952) 1066.
18. Kulkova, N. V. and Temkin, M. I. *J. Phys. Chem. (USSR)* **23** (1949) 695. *Chem. Abstracts* **43** (1949) 7308.

19. Kodama, S., Fukui, K., Tame, T. and Kinoshita, M. *Shokubai* **8** (1952) 50. *Chem. Abstracts* **47** (1953) 11920.
20. Emmet, P. H. *Catalysis*, Reinhold Publ. Co, N.Y. 1955, Vol. III, p. 318, 338.
21. Temkin, M. I. *Problems in Kinetics and Catalysis*, Moscow 1949.
22. Eklund, R. B. *The rate of oxidation of sulfur dioxide with a commercial vanadium catalyst* (Diss.) Roy. Inst. Technology, Stockholm 1956.
23. Boreskov, G. K. *J. Phys. Chem. (USSR)* **19** (1945) 535. *C. A.* **40** (1946) 2943.
24. de Bruijn, H. *Discussions Faraday Soc.* **8** (1950) 69.
25. Manes, M., Hofer, L. J. E. and Weller, S. *J. Chem. Phys.***18** (1950) 1355.
26. Denbigh, K. G. and Prince, A. J. *J. Chem. Soc.* **1947** 790.
27. Horiuti, J. *J. Res. Inst. Catalysis, Hokkaido Univ.* **5** (1957) 1.
28. Horiuti, J. and Nakamura, T. *Z. physik. Chem. (Neue Folge)* **11** (1957) 358.
29. Ergun, S. *Anal. Chem.* **25** (1953) 791.
30. Benton, A. F. *Ind. Eng. Chem.* **11** (1919) 623.
31. Emmet, P. H. *Catalysis*, Reinhold Publ. Co. N.Y. 1955, Vol. II, p. 150.
32. Weisz, P. B. *Z. physik. Chem. (Neue Folge)* **11** (1957) 1.
33. Dowden, D. A. and Bridger, G. W. *Advances in Catalysis* **9** (1957) 669.
34. von Krusenstierna, O. To be published elsewhere.

Received March 17, 1958.

ACTA CHEMICA SCANDINAVICA 12 (1958) 1111—1116

A Frequency Rule for Non-Isotopic Molecules

SVEND BRODERSEN and A. LANGSETH

Chemical Laboratory of the University of Copenhagen, Denmark

Recently the present authors have pointed out that there exists a simple relation between the vibrational frequencies of certain isotopic molecules. A complete isotopic rule was formulated which allows the calculation of all vibrational frequencies of one isotopic molecule from those of two others.

In the present paper it is shown that this rule may even be applied to chemically different (non-isotopic) molecules with reasonable success. For a few molecules, taken as examples, all the vibrational frequencies are calculated, in each case from the known frequencies of two related molecules. In spite of the apparently rough approximations, introduced when the isotopic rule is applied to non-isotopic molecules, the results obtained are sufficiently accurate to be a valuable help in the interpretation of complex vibrational spectra.

One of the objectives of molecular spectroscopy is — through measurement and interpretation of the spectra — to determine the potential function of the molecule under investigation. As the potential function may be regarded as a quantitative representation of the valence forces within the molecule, it is of evident chemical interest and of fundamental importance for the further development of the quantum-mechanical valence theory.

The interpretation of the observed bands in a spectrum in terms of fundamentals, combination frequencies, and overtones is often a rather difficult task. Except for di-atomic and certain high-symmetrical tri-atomic molecules it will always be necessary to include an investigation of certain istopic molecules as well, in order to make an unambiguous interpretation of the spectrum possible, and — at the same time — to get sufficient experimental data for the evaluation of the potential constants.

As the potential function is unaltered by isotopic substitution there exist certain relations between the fundamental frequencies of isotopic molecules. Such relations (so-called "isotopic rules") represent one or more single relations between the vibrational frequencies and the geometrical parameters of the isotopic molecules, but the potential constants ("force constants") do not occur. Therefore, the fulfilment of the requirements of these isotopic rules is a very useful check on the correctness of a given interpretation.

Recently the present authors have reported on a new isotopic rule [1]. This rule we have called "the complete isotopic rule" because it allows the calculation of all the vibrational frequencies of certain molecules from the frequencies of other definite isotopic molecules.

The proof of this rule is based on the assumption of a harmonic (quadratic) potential function. The agreement between observed and calculated frequencies achieved by use of the complete isotopic rule is, however, much better than that obtained by the ordinary calculation of vibrational frequencies based on a definite harmonic potential function. This is due to the fact that the application of the complete rule actually amounts to a sort of interpolation between the frequencies of two "extreme" molecules to give the frequencies of the "intermediate" molecule in question. This means that we need not assume one definite harmonic potential function — which would be an approximation, the real potential function always being more or less anharmonic — but implicitely uses three slightly different harmonic functions for the three isotopic molecules involved in the calculation. If these functions are "linearly" related a significantly better approximation to the real anharmonic potential function of the "intermediate" molecule is to be expected. This has been verified in an extensive study and calculation of the fundamental frequencies of all the different deuterated species of benzene [2].

This situation suggests that the complete isotopic rule may even be applied to chemically different molecules with tolerable success. Derivatives of a definite compound formed by substitution of one or more atoms for equivalent atoms of other elements will have materially different potential functions

Table 1. Vibrational frequencies (in cm^{-1}) of CO_2, OCS, and CS_2.

	Sym. Class	Obs.	Calc.	Calc. — Obs.
CO_2	Σ_g^+	1 337 [a]		
	Σ_u^+	2 349		
	Π_u	667		
OCS	Σ^+	858	880	+ 22
		2 062	2 068	+6
	Π	522	549	+27
CS_2	Σ_g^+	660 [a]		
	Σ_u^+	1 536		
	Π_u	397		

[a] Assumed unperturbed value.

even if the geometry of these derivatives is approximately the same. It may, however, be expected that the potential function of an "intermediate" derivative with a fair approximation can be obtained by "linear" interpolation between the potential functions of two "extreme" molecules, as for instance that of O=C=S from those of O=C=O and S=C=S. If this is the case the complete frequency rule may be applied with reasonable success.

As discussed in detail in our previous paper [1] the complete isotopic rule is strictly valid for all fundamental frequencies of linear molecules and for the out-of-plane fundamentals of plane molecules (as for instance ethylene and aromatic hydrocarbons). As examples for the application of the complete frequency rule to non-isotopic molecules we have therefore chosen O=C=S and some fluoro and chloro derivatives of ethylene: CF_2=CFCl, CF_2=CCl_2, *trans*-CFCl=CFCl, and CFCl=CCl_2. The fundamentals of O=C=S are cal-

Table 2. Out-of-plane frequencies (in cm^{-1}) of ethylene derivatives.

	Sym. Class	Obs.[3]	Calc. This Invest.	Calc. Mann *et al.*[3]	Calc. − Obs. This Invest.	Calc. − Obs. Mann *et al.*[3]
$F_2C=CF_2$	A_{1u}	190				
	B_{1u}	406				
	B_{2g}	508				
$F_2C=CFCl$	A″	166	171	169	+5	+3
		369	382	377	+13	+8
		538	509	516	−29	−22
trans-FClC=CFCl	A_u	ca. 140	139	140	ca. −1	ca. 0
		333	359	358	+26	+25
	B_g	529	510	514	−19	−15
$F_2C=CCl_2$	A_2	ca. 167	155	157	ca. −12	ca. −10
	B_2	323	353	337	+30	+14
		564	509	523	−53	−41
$FClC=CCl_2$	A″	ca. 130	129	129	ca. −1	ca. −1
		313	324	318	+11	+5
		537	511	517	−26	−20
$Cl_2C=CCl_2$	A_{1u}	110				
	B_{1u}	288				
	B_{2g}	512				

Table 3. In-plane frequencies (in cm^{-1}) of ethylene derivatives.

	Sym. Class	Obs.[3]	Calc. This Invest.	Calc. Mann *et al.*[3]	Calc. − Obs. This Invest.	Calc. − Obs. Mann *et al.*[3]
$F_2C=CF_2$	A_{1g}	394				
		778				
		1 872				
	B_{1g}	551				
		1 340				
	B_{2u}	218				
		1 337				
	B_{3u}	558				
		1 186				
trans-$FClC=CFCl$	A_g	288	299	302	+11	+14
		425	420	414	−5	−11
		632	648	645	+16	+13
		1 186	1 157	1 207	−29	+21
		1 707	1 755	1 734	+48	+27
	B_u	175	184	186	+9	+11
		426	467	437	+41	+11
		892	818	880	−74	−12
		1 190	1 278	1 234	+88	+44
$F_2C=CCl_2$	A_1	258	271	260	+13	+2
		434	420	433	−14	−1
		622	622	611	0	−11
		1 032	1 003	1 065	−29	+33
		1 749	1 749	1 731	0	−18
	B_1	192	189	192	−3	0
		459	453	443	−6	−16
		993	960	957	−33	−36
		1 327	1 339	1 327	+12	0
$Cl_2C=CCl_2$	A_{1g}	235				
		447				
		1 517				
	B_{1g}	347				
		1 000				
	B_{2u}	176				
		908				
	$B_{3\,1}$	310				
		777				

culated from those of CO_2 and CS_2, and all the out-of-plane fundamentals of the ethylene derivatives from those of $CF_2=CF_2$ and $CCl_2=CCl_2$. The procedure used in the calculations is exactly the same as that described for isotopic molecules [1]. The results are given in Tables 1 and 2 together with the observed frequencies. The agreement obtained is quite satisfactory in consideration of the material differences between the potential functions of the various molecules. An accuracy like that obtained in these examples will in most cases be sufficient for assignment purposes.

Recently Mann *et al.*[3] have calculated the vibrational frequencies of the fluoro and chloro derivatives of ethylene using a method of calculation which in principle has much in common with the one proposed here. According to these authors the frequencies are calculated from a definite potential function for each molecule. Every separate one of these functions has been derived from those of $CF_2=CF_2$ and $CCl_2=CCl_2$ by interpolation for each potential constant separately. The results obtained by Mann *et al.* are for the sake of comparison included in Table 2. It is seen that they are slightly better than ours.

As we have shown in our previous papers [1,2] the field of application of the complete isotopic rule may be extended considerably for hydrocarbons by introducing a splitting of the rule into separate rules comprising either the low frequencies or the high hydrogen (or deuterium) stretching frequencies. Because of the great difference in frequency the interaction between these groups of fundamentals is small enough to make the separation permissible. This approximation extends the applicability of the complete isotopic rule also to the planar vibrational frequencies of a great number of plane molecules.

For the halogen derivatives, which we are considering here, a corresponding separation should from a theoretical point of wiew not be permissible because the C—F and the C—Cl stretching frequencies are much lower, being actually of the same order of magnitude as several of the other fundamental frequencies. On the basis of this consideration one should therefore not expect the frequency rule to hold to a sufficient aproximation when applied to the planar frequencies of the substituted ethylenes. If we, nevertheless, use the frequency rule as if the separation were permissible we get the results shown in Table 3. It is seen that the results are almost as good as those obtained from the "valid" rule given in Tables 1 and 2. The results of Mann *et al.*, included in Table 3, are again slightly, but not essentially, better than ours. However, considering the enormous simplification of the calculations achieved by use of the frequency rule rather than the extremely elaborate procedure used by Mann *et al.*, the small gain in quality of the results seems insignificant.

The unexpected success of applying the complete isotopic rule to these cases seems to indicate that the potential functions to a fairly good approximation allow the separation of stretching frequencies from other vibrational frequencies even if they all are of the same order of magnitude. A definite establishment of this interesting feature will, however, require a much larger material than that presented here. If it actually can be shown that the separation is generally permissible the frequency rule will be a most valuable instrument for the interpretation of a great many vibrational spectra. We hope to be able to give a more detailed discussion of this problem in a later paper.

REFERENCES

1. Brodersen, S. and Langseth, A. *Kgl. Danske Videnskab. Selskab. Mat. fys. Skr.* **1** (1958) No. 5
2. Brodersen, S. and Langseth, A. *Kgl. Danske Videnskab. Selskab. Mat. fys. Skr.* **1** (1958) *(In press)*.
3. Mann, D. E., Fano, L., Meal, J. H. and Shimanouchi, T. *J. Chem. Phys.* **27** (1957) 51.

Received February 21, 1958.

ACTA CHEMICA SCANDINAVICA 12 (1958) 1117—1123

Simple Proof of the Ergodic Theorem

HARALD WERGELAND

Fysisk Institutt, Norges Tekniske Högskole, Trondheim, Norway

An attempt is made to prove the equivalence of time and space averages in statistical mechanics, without invoking the theory of sets. Apology is therefore due because of the lack in rigor, but there appear to be possibilities to show how the argument could be sharpened to mathematical precision*.

Ergodic theory is now a province of pure mathematices, but its origin is in the mechanical theory of heat. Specifically it is the assumptions made by Boltzmann and Maxwell to justify the substitution of the time average of mechanical quantities by an average over the phase space. By ergodic theorem we shall presently just mean the statement (when true), that *time average equals phase average*, and not the original hypotheses upon which this conclusion has been based. It is well known, that the latter — though sufficient to prove the theorem — did not stand the test of mathematical critique.

The first encounter with this situation will usually arouse the curiosity of the student of statistical mechanics. Now, the immediate answer to him is of course that the ergodic theorem in the sense defined above, was indeed proved by Birkhoff, Neumann and others [1] in 1932. But I think that those who look up the original papers may be a little overwhelmed by their abstractness and mathematical subtlety.

It is therefore desirable to have a proof in plainer language even if not rigorous. This is the aim of the present paper. In this spirit we shall employ only the ordinary calculus and in particular no more general concept of measure than the Riemann integral. Thus point sets of Lebesgue measure zero, which play a great role in the more mathematical formulations, will be bypassed in silence.

1. STATEMENT OF THE PROBLEM

The mechanical state of a system is determined by a point,

$$\mathbf{P} = \{q_1 q_2 \ldots q_f p_1 \ldots p_f\} \tag{1}$$

or eventually delimited by the cartesian volume element,

$$\mathrm{d}\Omega = \mathrm{d}q_1 \mathrm{d}q_2, \ldots \mathrm{d}p_f \tag{2}$$

* Private communication from Professor Kac.

in the $2f$-dimensional phase space. The system will be restricted by external conditions to a finite part Ω of the phase space, for example the energy shell,

$$E \leq H(\mathbf{P}) \leq E + \mathrm{d}E \tag{3}$$

A thermodynamical variable must primarily be identified with the time average

$$f^* = \lim_{t \to \infty} \frac{1}{t} \int_0^t f(\mathbf{P}(t))\ \mathrm{d}t \tag{4}$$

of some phase function $f(\mathbf{P})$. Now, for mathematical reasons we are only able to compute phase averages

$$\overline{f} = \frac{1}{\Omega} \int_{\Omega} f(\mathbf{P})\ \mathrm{d}\Omega \tag{5}$$

But the ergodic theorem asserts that these two kinds of average are equivalent:

$$\boxed{f^* = \overline{f}} \tag{6}$$

which is the proposition to be proved.

2. TRANSITIVITY

The decisive progress in the ergodic problem was Birkhoffs idea of transitivity. In order to explain this concept it will be convenient to survey briefly also some other notions of general dynamics:

a) A region Ω of phase space is said to be *invariant* if for any point $\mathbf{P}$ in Ω also the total orbit through $\mathbf{P}$ belongs to Ω.
b) Such a region is said to be *indecomposable* if it cannot be divided into parts $\Omega' + \Omega''$ which are separately invariant.
c) If the orbit from any point $\mathbf{P}$ in Ω will come arbitrarily close to any other point $\mathbf{P}'$ in Ω, then the motion is said to be *transitive*. Indecomposability and transitivity are equivalent. It is evidently a property of the Hamiltonian.

In the ergodic problem we consider closed systems, and hence the energy as constant. Certainly one might instead conceive a thermodynamical system as an open one with a stochastically time dependent Hamiltonian. Such an interpretation has actually been worked out by Delbrück and Molière [2]. There are, however, two drawbacks in this point of view: Firstly it deprives us of the justification of statistical mechanics for a closed system. Secondly, although ergodicity could no doubt be ensured that way, it would be — as Rosenfeld has once put it — so to speak *a fortiori*. Therefore we shall assume the Hamiltonian to be independent of time and consider the energy shell as the region to be inspected for transitivity.

A little further insight into the meaning of transitivity can be obtained from a general classification of the integrals of the motion. By the elementary theory of linear partial differential equations [3] the $2f-1$ time independent integrals of the Hamiltonian system can be taken to be of the form:

$$g_i(\mathbf{P}) = c_i \quad (i = 1,2 \ldots 2f-1) \tag{7}$$

Here a characteristic alternative shows up: S u c h a n i n t e g r a l m a y o r m a y n o t d e f i n e a s u r f a c e i n Ω. In the former case eqn. (7), considered as an equation for any one single variable p_k or q_k, has only isolated solutions. The alternative is infinitely many roots in a finite interval. The integrals defining surfaces are denoted as *univalued.*

The existence of a univalued integral will lower the dimensionality of Ω by one. In the extreme case that there are $2f-1$ of them, Ω will be reduced to the one-dimensional continuum of the orbit, which now appears as a section between surfaces c_i, $c_1 \ldots c_{2f-1}$. Probably this means a closed orbit, or in other words, exact periodicity.

When the number of univalued integrals is less than $2f-1$, a phase space Ω of more than one dimension remains, and fixing the non unique integrals will not further reduce the dimensionality. It is of course still true that specification of all the constants of integration, c_i, $(i = 1 \ldots 2f-1)$, will determine the orbit completely, but it is only the constants fixing univalued integrals which affect the long time averages. Whatever values we choose for the others, — because of the infinite multivaluedness of any variable — the orbit must interweave the remaining phase Ω space densely. We could also say the univalued integrals decompose the phase space into invariant parts $g_1(\mathbf{P}) = c_1, \ldots g_m(\mathbf{P}) = c_m$. The intersection of these, which is of dimension $2f-1-m\ldots$, is indecomposable.

A simple illustration is afforded by any completely separable many body problem *e.g.* the Conditionally Periodic Systems of the old quantum theory. For these, the action variables constitute a complete set of f univalued integrals. If the frequencies are incommensurable, a remaining f-dimensional space of the coordinates is indecomposable. A two dimensional projection of the orbit will then have the character of a Lissajou figure. It should be remembered, however, that separable systems are not ergodic in the sense of statistical thermodynamics; since they have no transfer of energy between the different degrees of freedom and therefore cannot approach thermodynamical equilibrium.

The question is how many univalued integrals are in general to be expected. At any rate the energy $E(\mathbf{P}) = E$ will always be one. It is perhaps a reasonable guess that in large systems there are essentially * no others. This would leave the widest possible region, namely the energy shell indecomposable.

Apart from the hypothesis of transitivity — which is possibly a strong one — only well established theorems of dynamics are needed in the proof, *viz.* Liouvilles theorem: that the motion of the elements of phase space is an incompressible flow, and Poincaré's theorem: that any state, $\mathbf{P}$ in $\Delta\Omega$, will recur. These three premises will be used repeatedly in the following.

* Strictly speaking, also the total linear momentum and the total angular momentum are always univalued integrals, but they can be disregarded for special reasons.

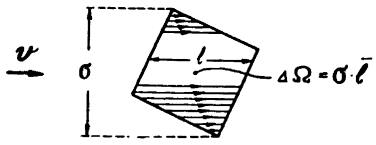

Fig. 1.

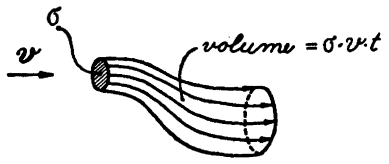

Fig. 2.

3. TWO LEMMAS

In order to avoid digression in the main proof, it will be useful to derive two auxiliary formulae beforehand.

3.1 The life time of a state: {P in $\Delta\Omega_i$}

When the representative point **P** traverses a particular cell $\Delta\Omega_i$ in phase space the duration of the passage depends strongly upon how it hits the cell, whether centrally or grazingly, see Fig. 1.
The mean duration or "life time" τ_i must be equal to the mean segment $\bar{l}$ of the orbit inside $\Delta\Omega_i$ — divided by the velocity v:

$$\tau_i = \frac{\bar{l}}{v(\mathbf{P}_i)} \tag{8}$$

where

$$v = [\dot{q}_1^2 + \dot{q}_2^2 + \ldots . \dot{p}_f^2]^{1/2}$$

In the course of long times the orbit will intersect $\Delta\Omega$ with a dense array of parallel chords. Introducing now by an obvious geometrical analogy the "projection" σ of $\Delta\Omega$ along v (see Fig. 1) we have for the mean chord

$$\bar{l} = \frac{\Delta\Omega}{\sigma} \tag{9}$$

and consequently:

$$\tau = \frac{\Delta\Omega}{\sigma v} \tag{10}$$

3.2. The recurrence time T of **P** in $\Delta\Omega$.

Consider now an area σ orthogonal to the velocity field v in phase space. In a time t a phase volume $\sigma \cdot v \cdot t$ will have passed the cross section σ. At latest after a time $\Omega/\sigma v$, recurrences must have taken place.
Some points may be delayed, but others will be advanced and it is a natural guess that the mean recurrence time is just

$$T = \frac{\Omega}{\sigma \cdot v} \tag{11}$$

We shall substantiate this a little: Denote the number of phase points which have passed σ once by n_0, twice by n_1 and so forth. The total number of recurrences in a time t will then be:

$$N(t) = 1 \cdot n_1 + 2 \cdot n_2 + \ldots . \tag{12}$$

while the total flow points is

$$\sigma \varrho v t = n_0 + 1 \cdot n_1 + 2 \cdot n_2 + \ldots . \tag{13}$$

where ϱ is a constant density to be fixed later. Hence the mean interval between two recurrences is

$$\frac{t}{N} = \frac{t}{\sigma \varrho v t - n_0} \tag{14}$$

Now again by Poincaré's theorem the class of points n_0 cannot increase *i.e.* all orbits crossing σ once must sooner or later cross it again. Therefore in the course of long time

$$\frac{t}{N} = \frac{\lambda}{\sigma \varrho v} \tag{15}$$

We must now speak more definitely about the density ϱ. It may be looked upon as representing an ensemble of $\mathcal{N} = \varrho \cdot \Omega$ systems, uniformly distributed in phase. We might therefore also write

$$\frac{t}{N} = \frac{\Omega}{\sigma v} \cdot \frac{1}{\mathcal{N}} \tag{16}$$

Now since the number of recurrences as well as the number of points crossing σ in unit time is proportional to $\mathcal{N}$, the conclusion seems certain that $\mathcal{N} = 1$ or a density $\varrho = 1/\Omega$ gives the appropriate average count of recurrences in one single system. This leads then to the formula (21).

4. THE PROOF

In the integral (4) we shall understand the representation point **P** to move according to a definite Hamiltonian, transitive in Ω, so that we have incompressibility, recurrence and indecomposability. The first step is to replace the time integral by its Riemann sum:

$$\int_0^t f(t)\ \mathrm{d}t = \lim \sum_n f(t_n)\ \Delta t_n \tag{17}$$

Here the subdivision of the time interval is arbitrary as long as

$$t = \Sigma \Delta t_n = \text{constant} \tag{18}$$

We may in particular choose the time differences Δt in (18) equal to the transit times of **P** through the cells $\Delta\Omega_i$ of a fixed subdivision of Ω. Now by Poincaré's theorem every cell will be traversed many times. Let Δt_{ir} be the time spent by the representation point inside $\Delta\Omega_i$ during the r'th passage. And let $N_i(t)$ be the number of recurrences in the time interval $(0, t)$. We have then

$$\sum_n f(t_n)\,\Delta t_n = \sum_{i=0}^{\Omega/\Delta\Omega} \sum_{r=0}^{N_i} f(\mathbf{P}_i)\cdot \Delta t_{ir} \tag{19}$$

In the second sum we may write

$$\sum_{r=0}^{N_i} f(\mathbf{P}_i)\Delta t_{ir} = f(\mathbf{P}_i)\cdot N_i\,\overline{\Delta t_i} \tag{20}$$

where $\overline{\Delta t_i}$ is the average transit time over N_i recurrences.

After these preparations we can rewrite the time average of a phase function $f(\mathbf{P})$:

$$\frac{1}{t}\int_0^t f(\mathbf{P}(t))\,\mathrm{d}t = \lim_{\Delta\Omega\to 0} \sum_{i=0}^{\Omega/\Delta\Omega} f(\mathbf{P}_i)\cdot\frac{\overline{\Delta t_i}}{t/N_i} \tag{21}$$

According to the proposition (6) we have still to consider the limit $t\to\infty$ and this must be carried out before making the cells $\Delta\Omega$ infinitesimal.

Now $\overline{\Delta t_i}$ and t/N_i must obviously approach definite limits for $t\to\infty$:

$\lim \overline{\Delta t_i} = \tau_i =$ mean life time of the state: {**P** in $\Delta\Omega_i$}
$\lim t/N_i = T_i =$ » recurrence time » » » » » »

Thus we have for the time average of f over an infinite period:

$$f^* = \lim_{\Delta\Omega\to 0} \sum f(\mathbf{P}_i)\,\frac{\tau_i}{T_i} \tag{22}$$

But according to the formulae (10) and (11), the ratio of the life time to the recurrence time of the state: **P** in $\Delta\Omega_i$ is

$$\frac{\tau_i}{T_i} = \frac{\Delta\Omega_i}{\Omega} \tag{23}$$

Therefore we have

$$\sum_i f(\mathbf{P}_i)\,\frac{\tau_i}{T_i} = \sum_i f(\mathbf{P}_i)\,\frac{\Delta\Omega_i}{\Omega}$$

and passing to the limit in eqn. (22)

$$\lim_{i\to\infty}\frac{1}{t}\int_0^i f(\mathbf{P}(t))\,\mathrm{d}t = \frac{1}{\Omega}\int_\Omega f(\mathbf{P})\,\mathrm{d}\Omega$$

as was to be proved.

REFERENCES

1. See, ter Haar, D. *Rev. Mod. Phys.* **27** (1955) 289, for full references.
2. Delbrück, M. and Molière, G. *Preuss. Akad. d. Wissensch. Phys. Math. Klasse* **1936**, No. 1.
3. For example, Forsythe, R. *Differential Equations*, 6. Ed. London 1933, p. 394.

Received February 20, 1958.

ACTA CHEMICA SCANDINAVICA 12 (1958) 1124—1135

Surface Tension of Liquid Mixtures

A Micro-Method Applied to the Systems: Chloroform-Carbon-tetrachloride, Benzene-Diphenylmethane and Heptane-Hexadecane

JØRGEN KOEFOED and JOHN V. VILLADSEN

Universitetets Fysisk-Kemiske Institut, Copenhagen, Denmark

An apparatus is described which measures surface tension of small samples (10—30 μl) with an accuracy better than one in thousand. A glass capillary of 2 mm diameter in the lower end and 0.25 mm in the upper end was inclined to bring the liquid in equilibrium each time at the same position in the capillary.

Experimental results are reported for 10 pure liquids and for three sets of mixtures of varying mole fraction. The applicability of recent theories of the surface tension of regular mixtures is discussed and a new treatment is proposed.

THE APPARATUS

The apparatus was designed for measuring surface tension of some biological fluids which were available in very small quantities only. These measurements will be described elsewhere. For the measurements described in this paper the extreme economy in volume was not particularly advantageous, but did no harm either, even in the work with mixtures because evaporation could be kept correspondingly low.

For adaptation to micro-scale, the capillary rise method is obviously the most suitable. Surfaces of intermediate dimensions ($50 > d > 2$ mm) have a complicated shape and involve awkward correction terms. Usually the reference surface is kept above this interval and treated as a plane surface, but another possibility is to keep both surfaces so small that they can be treated as perfectly spherical. An unfortunate circumstance in this arrangement is that only one of the surfaces can approach the equilibrium position in receding motion. It has, however, been possible to make very accurate measurements.

The laborious search for a capillary of sufficiently constant diameter was saved by measuring to the same narrow region of an ordinary first class capillary. To be able to have both surfaces at prescribed positions in the capillary, gravitational force on the liquid was varied by inclination of the capillary.

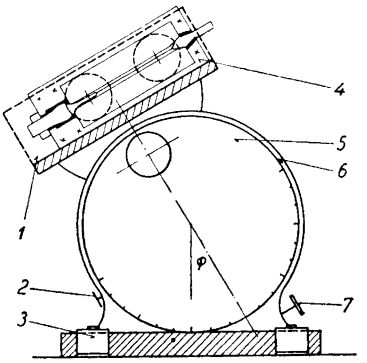

Fig. 1. Sketch of the apparatus. The optical measuring table is solidly clamped to the desk. On the movable table is fixed a U steel, 1, carrying the two microscopes and the Perspex chamber, 4. The fine adjustment screw 7 is engaged or disengaged by turning 2.

The measuring capillary (made to order by F. C. Jacob, Copenhagen) is shown on Fig. 1 together with the Perspex chamber,4, in which it is inserted. Two pieces of Portex tubing (soft PVC) on the two bulbs provide the packing material, the lower one being expanded when the screw is tightened on a thin brass runner. Water is circulated through the chamber from a thermostat. The chamber is fixed to the one side of a length of U-shaped steel,1, (37 × 50 mm) and two microscopes (Hensoldt Metami, 20 ×) are fitted into holes in the other side, focussing on the capillary around its two etched markings which are 50 mm apart. The plane bottom of the U-steel rests against the plane table of an "Optischer Winkel-Mess-Tisch" (Miller, Innsbruck) commercially available from precision-tool dealers. The scale has divisions for every 5′ permitting easy interpolation to 1′.

The horizontal position, read as 0°, is carefully adjusted as the position in which a small mercury drop does not move in the narrow capillary (± 2′).

Although mounting and dismounting of the capillary is very easy, the rinsing and filling is usually made *in situ*. For the filling, the table is moved to bring the tube in an upside down position (—70°), the narrow end is closed with a finger and the liquid is applied as a drop in the wide end of the capillary from a 25 μl capillary pipette. The finger is released until the drop is caught by the narrow part of the capillary and the table is tilted back to a small positive angle (+ 10 — + 15°). The upper surface will now be in the conical part of the tube above the narrow capillary and can be "vacuum-cleaned" for surface impurities through a thin polythene tube.

The capillary is brought to vertical position (+ 90°) and tilted backwards and forwards until the upper surface is at the desired place. The position of both surfaces l_1 and l_2 are read on the ocular scales of the microscopes (0.05 mm divisions). The angle φ is read and the surface tension can be worked out from the following expression, the meniscus to meniscus distance in mm being $50 + l_1 - l_2$:

$$\begin{aligned} \gamma &= Kd(1 + (l_1 - l_2)/50) \sin\varphi \\ K &= g(50 + (r_1 + r_2)/3) / (2/r_1 - 2/r_2) \\ d &= d_{\text{liq}} - d_{\text{air}} \end{aligned} \qquad (1)$$

Actually, the constant K was determined by standardization on pure benzene and checked on several other substances. The questions of the correction term $(r_1 + r_2)/3$ and of the neglected terms of higher order in r_1 and r_2 have been treated by Højgaard Jensen.[1]

SURFACE TENSION OF SOME PURE LIQUIDS

Ten readings were taken for each liquid. The largest discrepancy was usually within 2 parts in thousand and the accuracy of the mean value should therefore be about 7/10 000. The results are given in Table 1 together with the best values, found in the literature.

The agreement between our measurements and others is very satisfactory. Only diphenylmethane appears not to have been measured before. The measurements on *n*-paraffins by JKG are made in vacuum and seem very accurate, but it is surprising that they report surface tensions of higher paraffins far below the melting point of any reasonably pure sample. Their method gives no proper check on systematic errors in their apparatus and the impressive consistency in their results may depend on their use of the same apparatus throughout. The paraffins used by Vogel appear to have been of moderate purity.

In measuring ethyl ether a small correction (0.23 %) was made for the weight of the air stem in the tube on both sides of the liquid, because the saturation with ether made the air heavier. For the other liquids a similar correction would be smaller than 0.05 % and was neglected.

Table 1. Surface tensions of pure compounds.

	t°C	d g/ml	γ dyn/cm	γ (literature)			
Benzene	25.0	0.8736	[28.24]	28.24	(RC)		
	30.0	0.8683	27.59	27.54	27.61		(T)
Carbontetrachloride	25.0	1.5845	26.14	26.16	26.06		(T)
Chloroform	25.0	1.4799	26.56	26.5	26.67		(T)
n-Heptane	20.0	(0.6836)	20.32	20.28	(JKG)	20.30	(T)
	30.0	(0.6753)	19.30	19.27	(JKG)	19.29	(T)
n-Dodecane	20.0	(0.7492)	25.42	25.48	(JKG)	25.45	(V)
	30.0	(0.7425)	24.52	24.60	(JKG)	24.44	(V)
n-Hexadecane	20.0	(0.7736)	27.42	27.64	(JKG)	27.58	(V)
	30.0	(0.7667)	26.62	26.79	(JKG)	26.87	(V)
Diphenylmethane	30.0	0.9995	38.09				
Methanol	25.0	(0.7566)	22.28	22.18	(T)		
Ethanol	25.0	(0.7077)	21.97	21.85	21.90	(T)	
Ethylether	25.0	(0.7851)	16.50	16.50	(T)		

Density d is $d_{liq} - d_{air}$. Values in brackets are taken from the literature.

References: RC: Richards, T. V. and Carver, E. K. *J. Am. Chem. Soc.* **43** (1921) 829.
T: Timmermans, J. *Physico-Chemical Constants of Pure Organic Compounds*, Elsevier 1950.
JKG: Jasper, J. S., Kerr, E. R. and Gregorich, F. *J. Am. Chem. Soc.* **75** (1953) 5253.
V: Interpolated values from Vogel, A. I. *J. Chem. Soc.* **1946** 133.

MATERIALS

Benzene and *carbon tetrachloride.* Merck p.a., dried with silica gel and distilled.

Chloroform. Merck p.a., 1 % alcohol added. Alcohol removed by washing twice with water. Separated. Dried with silica gel and distilled. All samples containing chloroform were stored in dark bottles and measured within a few days from their preparation.

n-*Heptane.* Phillips Petroleum Comp. "more than 99 % pure" (presented by the makers to the late prof. J. N. Brønsted in 1947).

n-*Dodecane* and n-*hexadecane.* Synthetic samples of high purity, as used for the measurements by Brønsted and Koefoed [2].

Diphenylmethane. Fluka, highest purity. 6 times recrystallized, each time discarding about 1/5 as liquid phase, m. p. 26.8°C.

Methanol. Merck p. a.

Ethanol. Alcohol absolutus 99.9 %. Ph. Dan., De Danske Spritfabrikker.

Ethyl ether. Struers, Copenhagen. Best commercial quality, distilled from sodium metal.

SURFACE TENSION OF SOME MIXTURES

Chloroform-Carbontetrachloride. The surface tensions of these mixtures have been measured many years ago by Whatmough [3] and our results agree qualitatively with his. Densities and vapour pressures are known from the work of McGlashan and Prue [4] who showed that the mixtures are regular with the parameter $W = 930$ joule/mole.

Our determinations of densities agree well with those of McGlashan and Prue[4] which are certainly more accurate than ours whereas the values tabulated in *International Critical Tables* appear incorrect. We must have had some losses of chloroform in the making up of the mixtures and we obtained the most consistent results if we based our x-values on the density measurements and not on the weighings.

The experimental results are tabulated in Table 2 and plotted in Fig. 2. In the same figure are plotted values calculated from Guggenheim's equation [5] (2) and from Hoar and Melfords equation [6] (3) for regular solutions:

$$\begin{aligned}\gamma &= \gamma_1 + \frac{RT}{\sigma_1}\ln\frac{x_1'}{x_1} + \frac{W}{\sigma_1}\left(\frac{x_2'^2}{2} - \frac{3x_2^2}{4}\right)\\ &= \gamma_2 + \frac{RT}{\sigma_2}\ln\frac{x_2'}{x_2} + \frac{W}{\sigma_2}\left(\frac{x_1'^2}{2} - \frac{3x_1^2}{4}\right)\end{aligned} \qquad (2)$$

$$\begin{aligned}\gamma &= \gamma_1 + \frac{RT}{\sigma_1}\ln\frac{x_1'}{x_1} + \frac{W}{\sigma_1}\left(\frac{x_2'^2}{2} - x_2^2\right)\\ &= \gamma_2 + \frac{RT}{\sigma_2}\ln\frac{x_2'}{x_2} + \frac{W}{\sigma_2}\left(\frac{x_1'^2}{2} - x_1^2\right)\end{aligned} \qquad (3)$$

Eqn. (2) corresponds to Guggenheims derivation but σ_1 and σ_2 are not put equal to one another.

The calculations were carried through in the following way: For $x_1 \leqq 0.5$ was inserted: $x_1'/x_1 = 1 + \delta$; $\ln x_1'/x_1 = \delta$; $\ln x'_2/x_2 = -x_1\delta/(1-x_1)$; $(x_1'/x_1)^2 = 1 + 2\delta$ and $(x_2'/x_2)^2 = 1 - 2x_1\delta/(1-x_1)$. An explicit expression for δ was developed from each of eqns. (2) and (3). For each of them δ was calculated and inserted in both equations for γ. If the two values of γ agreed, this was taken as evidence for a satisfactory approximation. If not, small corrections were made by iteration until agreement was obtained. After-

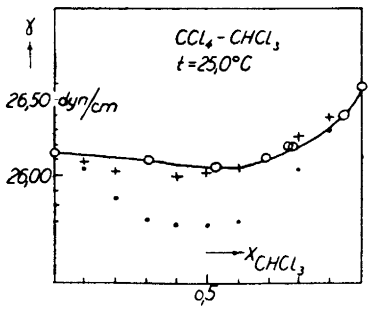

Fig. 2. Surface tension of CCl_4—$CHCl_3$ mixtures
o experimental values
+ calc. from Guggenheims eqn. (2)
● calc. from Hoar and Melfords eqn. (3)

wards the other halves of the curves, $x_1 > 0.5$, were found by similar sets of equations with x_1 and x_2 interchanged so that $x_2'/x_2 = 1 + \delta'$ *etc.* The reason for using two different expressions is that the terms $x/(1—x)$ get large as x approaches 1 and threaten the successfulness of the approximations.

It is evident from Fig. 2 that Guggenheim's expression gives a much better agreement with the experimental values than Hoar and Melfords. A discussion of the two models is found in the last part of this paper.

Benzene-Diphenylmethane. No measurements of density or surface tension of these mixtures have been published. Everett [7] has mentioned the existence of unpublished density measurements by Duff. From the work of Everett [8] we know the vapour pressures, which follow the rules of "athermal" mixtures.

Our measurements are tabulated in Table 3 and the surface tensions are plotted against mole fraction in Fig. 3. The curve is on the positive side of the right line and plotted against volume fraction it comes out on the negative side. The density measurements show that mixing is accompanied by an appreciable contraction (2.9 % at $x = 0.5$).

In measuring the surface tensions we had to take precautions to prevent evaporation from the surface. The two ends of the tube were connected to a T-tube and the air in the tubes was kept at about the right benzene pressure by evaporation from moistened bits of cotton wool. The solutions rich in diphenylmethane were very viscous and by standing unprotected over night the surface tension approached that of pure diphenylmethane, but a subsequent mixing of the 20 μl lot showed that it was only the surface which had lost an appreciable amount of benzene.

Table 2. Carbontetrachloride-chloroform (25.0°C).

	d g/ml	x (weight)	x (density)	γ dyn/cm
CCl_4	1.5845	0		26.14
Mixture 1	1.5535	0.304	0.310	26.10
2	1.5284	0.526	0.548	26.06
3	1.5092	0.685	0.735	26.12
4	1.5054	0.745	0.766	26.19
5	1.5045	0.760	0.775	26.18
6	1.4854	0.940	0.950	26.40
$CHCl_3$	1.4799	1		26.56

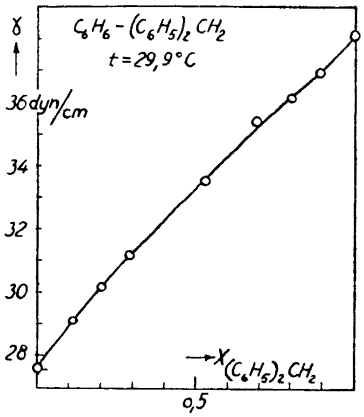

Fig. 3. Surface tension of benzene-diphenylmethane mixtures.

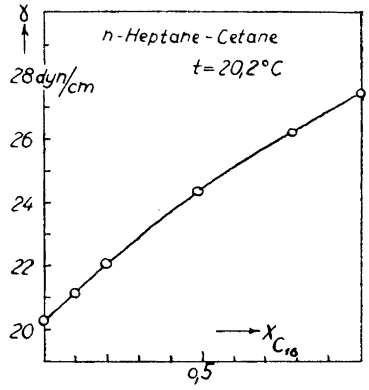

Fig. 4. Surface tension of *n*-heptane-*n*-hexadecane mixtures.

n-*Heptane* — n-*Hexadecane*. Surface tension of paraffin mixtures are not reported in the literature. From earlier, unpublished measurements in this laboratory of densities and volumes of mixing, we know that *n*-paraffins mix under contraction and that the densities correspond as closely to the principle of congruence as it has been possible to ascertain it. The vapour

Table 3. Benzene-diphenylmethane (29.9°C).

	x	d g/ml	γ dyn/cm
Benzene	0	0.86833	27.60
Mixture 1	0.1125	0.89490	29.07
2	0.2038	0.91253	30.15
3	0.2883	0.92683	31.11
4	0.5226	0.95811	33.54
5	0.6864	0.97512	35.38
6	0.8006	0.98479	36.07
7	0.8927	0.99174	36.90
Diphenylmethane	1	0.99954	38.10

Table 4. Heptane-hexadecane.

	x	$x_{vol.}$	γ (20.2°C)	γ (29.9°C)
Heptane	0	0	20.30	19.31
Mixture 1	0.097	0.177	21.15	20.16
2	0.195	0.326	22.05	21.05
3	0.492	0.660	24.35	23.46
4	0.785	0.879	26.23	25.48
Hexadecane	1	1	27.40	26.63

pressure of n-paraffins have been studied extensively in this laboratory [2] and elsewhere and heats of mixing are known from the work of van der Waals [9]. His results are in moderate agreement with unpublished measurements by Brønsted and Halvard in this laboratory.

The surface tensions were measured at two temperatures and the results are tabulated in Table 4. In Fig. 4 the values at 20°C are plotted against mole fraction. The results at 30°C give exactly the same appearance. The curves are positive and exactly as in the system benzene-diphenylmethane we find on plotting against volume fraction a negative deviation from linear behaviour. For vapour pressures, inversely, the curves are negative when plotted against mole fraction and positive when plotted against volume fraction.

Both of the last two systems are known to deviate rather little from ideality. But starting from Guggenheim's equation for an ideal surface we find that very large deviations from ideal surface behaviour have to be introduced to account for the fact that the curve is much nearer to the straight line than a Guggenheim-ideal surface tension would be. We take this as evidence for the soundness of accepting the straight line relationship as representing ideal behaviour as discussed below.

THE THERMODYNAMICS OF SURFACES

"In the thermodynamics of surfaces there is no theorem more important than that known as Gibbs' adsorption theorem, which determines how the surface tension of a solution varies when the composition is varied at constant temperature. Its derivation by Gibbs has all the logical conviction and elegance characteristic of Gibbs" (Guggenheim[10]).

The situation with regard to this theorem is unsatisfactory in two respects. The existing proofs of the theorem are not irreproachable and the theories of surface tension of binary mixtures lead to disagreement with the theorem as soon as such terms are included in the partition function which take account of the interaction with the bulk phase. Guggenheim's equation, (2), thus is not consistent with Gibbs' theorem. We first thought that the answer to these questions was that Gibbs' theorem was not correct. However elegant Gibbs' proof may be, it involves the use of chemical potentials of molecules in the surface layer with no proper analysis of whatever this may mean. The proof given by Guggenheim [10] involves a hypothetical experiment which is treated as if it were reversible although it most obviously cannot be reversed. It was pointed out to us, however, by H. Højgaard Jensen that it is possible to give a proof which involves nothing more than the second law and the conservation of mass.

A careful analysis of the energetic conditions of molecules in the surface and what could be meant by the chemical potentials of these brought out, then, that it was possible to give a treatment which is inherently consistent with Gibbs' theorem and which leads to a different concept of ideal behaviour with regard to surface tension.

How this result was originally derived from Brønsted's energetic theory and how it relates to other "transport complex" treatments will be discussed elsewhere. We will give here only a short account of its derivation along the lines of Guggenheims *Thermodynamics* [11].

The actual difficulty is in the definition of a chemical potential when other energetic variables are involved than the classical: S, V, N, T, P, μ. The same problem is involved in electrochemistry and in a gravitational field. In surface problems it is the field of the cohesive forces which interferes as a *partly* external force.

If we decide to specify the potential energy of the i'th component with respect to cohesive forces in a gas and in a liquid we can introduce a parameter χ_i. We can split up our ordinary chemical potential accordingly:

$$\mu_i = \mu_i^l + \chi_i^l = \mu_i^g + \chi_i^g \tag{7}$$

and in analogy with the nomenclature for electrochemical and gravitational systems we would refer to μ_i^l and μ_i^g as the "purely chemical potentials" and to our ordinary μ_i as the "cohesion-chemical potential". It will be the latter which determines the equilibrium between two phases in the same way as the electro-chemical and the gravitation-chemical potentials within their fields.

In the bulk phases χ_i is constant but in a surface layer the molecules will move in a field from the cohesive forces. Within a very short distance the potential energy of the van der Waals attraction rises from a large negative value, χ_i^l, in the bulk liquid phase to a value $\chi_i^g \simeq 0$ in the gas. In the same way as in a gravitational field, therefore, the equilibrium conditions are *not* homogeneity in P and the μ_i's but P,μ_i and χ_i are all functions of the position in the surface layer described through a parameter, t, measured along an axis normal to the surface, here supposed to be plane. The condition for equilibrium of a single component, i, is the same as in a mixture in a gravitational field (Guggenheim [11], eqn. 11.07.2):

$$\mathrm{D}\mu_i^t + V_i^t \mathrm{d}P^t + \mathrm{d}\chi_i^t = 0 \tag{8}$$

where $\mathrm{D}\mu_i = \Sigma_s(\partial\mu_i/\partial x_s)\mathrm{d}x_s$ accounts for the variations with composition of the bulk phase (*cf.* Guggenheim [11]). This condition shall be fulfilled for any value of t and therefore also in the bulk phases, whence we have at changing compositions of the bulk phases and hydrostatic pressure P:

$$\mathrm{D}\mu_i^t + V_i^t \mathrm{d}P^t + \mathrm{d}\chi_i^t = \mathrm{D}\mu_i^l + V_i \mathrm{d}P + \mathrm{d}\chi_i^l \tag{9}$$

We have no possibility neither in practise nor in principle to define the functions $\mu_i(t)$, $V_i(t)$, $P(t)$ or $x_i(t)$ in a thermodynamic way. The splitting up of the electrochemical potential in an electric part and a chemical part implies non-thermodynamic and to a certain degree arbitrary assumptions, and the same applies here.

The only entity which is physically measurable is the surface tension:

$$\gamma = \int_l^g (P - P^t)\mathrm{d}t \tag{10}$$

The integral extending from a point $t = l$ which is with certainty in the potential-homogeneous interior of the liquid to a point $t = g$ which is similarly situated in the gas. At both ends therefore $P^t = P$, making the exact positions of l and g immaterial.

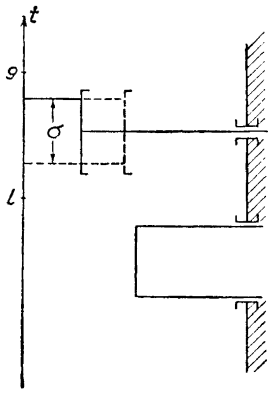

Fig. 5. "Surface piston."

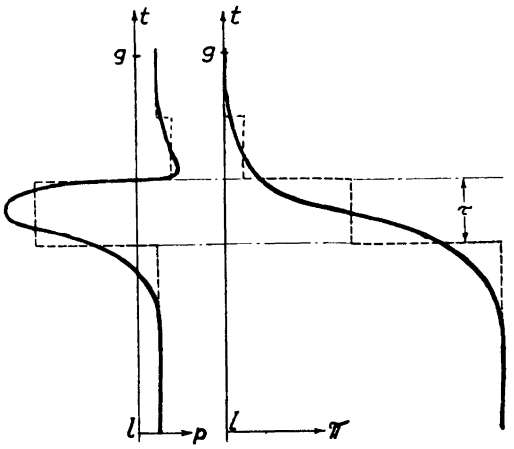

Fig. 6. Hypothetical shape of curves showing changes in pressure, p, and internal pressure, π, in passing from a point in the liquid, l, through the surface to a point in the gas, g.

γ can be measured by a surface piston arrangement (Fig. 5), but any attempt to measure P^t by sliding in pistons with an edge in the zone of potential-inhomogeneity, σ, will imply the creation of new boundary layers and yield no useful information on P^t.

To be able to give our functions definite values we must therefore assume some potential function, χ_i^t, and some equation of state $\Phi_i = \Phi_i(V_i, P, \chi_i) = 0$, and we can imagine that we could get a pressure curve like that of Fig. 6 with a narrow zone of expanded liquid under a large negative pressure and a zone of adsorbed, slightly compressed gas, but such assumptions are obviously outside the domain of thermodynamics, and a further treatment along such a line would fall under the theory of the liquid state and would remind of the classical works of van der Waals and Bakker [12].

To develop thermodynamic equations which are useful for the kind of problems we are dealing with here, we will choose another approach: the monolayer model. We neglect the adsorbed gas-layer and assume that what is different from the bulk phases can be thought of as concentrated in one homogeneous liquid layer of thickness τ. This represents a way of averaging the deviations from bulk phase behaviour by substituting continuous curves as those in Fig. 6 with "square wave" functions. Average values in the monolayer we designate by index s and obtain:

$$\gamma = (P - P^s)\ \tau \qquad\qquad \sigma_i = V_i^s/\tau$$

The equilibrium condition (9) takes the form

$$D\mu_i^s + V_i^s dP^s + d\chi_i^s = D\mu_i^l + V_i dP + d\chi_i^l \qquad (11)$$

Neglecting compressibility we can put $V_i^s = V_i$ and imagine a transfer from l to s in a continuous way which allows the integration:

$$\mu_i^s + V_i P^s + \chi_i^s = \mu_i^l + V_i P + \chi_i^l \quad (12)$$

or after insertion of γ and σ_i:

$$\mu_i^s + \chi_i^s - \gamma\sigma_i = \mu_i^l + \chi_i^l \quad (13)$$

Reverting to usual chemical potentials, or cohesion-chemical potentials, we put:

$$\mu_i^s + \chi_i^s = \mu_i' \qquad \text{and} \qquad \mu_i^l + \chi_i^l = \mu_i$$

and derive:

$$\mu_i' - \gamma\sigma_i = \mu_i \quad (14)$$

Our μ_i' is a cohesion-chemical potential and if we want a chemical potential which is the same both in surface and in bulk phases in equilibrium we must interpret the last equation as *defining* a special surface-cohesion-chemical potential, the surface part of which is zero in the bulk phases. Whichever view we take of this equation we can derive the same relations if we work in a consistent way. Equation (14) corresponds to similar relations derived by Defay and Prigogine[14], and the difference from their treatment appears only in the application, when we take into account that μ_i' itself depends on γ, because $\partial\mu_i'/\partial\gamma = -\sigma_i$ corresponding to the usual relation $\partial\mu_i/\partial P = V_i$ as in the surface layer $V_i = \tau\sigma_i$ and $\tau \mathrm{d}P^s = -\mathrm{d}\gamma$.

The thermodynamic difference between μ_i and μ_i' is:

$$\mu_i' = (\partial F'/\partial n_i')_{T,\gamma,\mathrm{nj}'} \neq \mu_i = (\partial F'/\partial n_i')_{T,A,\mathrm{nj}'}$$

Before we turn to the application of (14) to special cases, we should make its scope and its limitations clear. The introduction of a σ_i- or of a n_i'-parameter will always involve some arbitrary choice which relates closely to the arbitrariness involved for instance in the splitting up of the electro-chemical potential in a chemical and an electrical term. The derivation above indicates clearly that the possibility of introducing a characteristic partial molar surface area σ_i for a component rests on the neglection of the gaseous part of the surface layer. This neglection can be justified only at moderate pressures and far from critical point conditions. To investigate the influence of gas pressure on surface tension or the behaviour of surface tension near the critical point we would have to choose some other approach.

It will be of interest to see what order of magnitude the negative pressure in the surface layer will get. Taking CCl_4 at 25°C, 1 atm. as an example, we derive for close-packed lattice dimensions: $V = 97.07$ ml/mole; $\sigma = 19.5 \times 10^8$ cm²/mole; $\tau = 5.0$ Å; $P^s = 1 - \gamma/\tau = -500$ atm.

We can also compare the internal pressures $\pi = (\partial E/\partial V)_T$ in liquid and in monolayer, relating the latter to the surface energy $E' = (\partial E/\partial A)_T$. We have the two thermodynamic equations of state:

$$P + \pi = T(\partial P/\partial T)_V \quad (15)$$

$$-\gamma + E' = -T(\partial\gamma/\partial T)_A \quad (16)$$

The latter we can interpret as:

$$(P - P^s)\tau + (\pi - \pi^s)\tau = T\ (\partial(P - P^s)/\partial T)_V \tau \quad (17)$$

In CCl_4: $\pi = 3\,310$ atm (Hildebrand and Carter[16]) and $E' = 65.6$ dyn/cm giving $\pi - \pi^s = 1\,300$ atm and $\pi^s = 2\,010$ atm.

[MONO-LAYER SURFACES OF IDEAL AND REGULAR MIXTURES

Having derived the condition $\mu_i' - \gamma\sigma_i = \mu_i$ we can directly write down the expressions for μ' and μ corresponding to the model of regular solutions or we can construct partition functions and derive the μ's from these. We will differ from previous treatments in two respects: by letting the potential of the forces from the bulk phase, χ_i^b, contain not only a quadratic term but also a linear term in the mole fraction of the bulk phase and by appreciating that μ'_i depend on the surface tension. With a constant term $2\gamma_1\sigma_1$ in χ_1^b adjusted to fit in the limit $x_2 = 0$ we get for component 1:

$$\mu_1 - \mu_1^\circ = RT\ln x_1 + Wx_2^2 \tag{18}$$

$$\mu_1' - \mu_1^\circ = RT\ln x_1' + W'x_2'^2 + \chi_1^b - \sigma_1\gamma \tag{19}$$

$$\chi_1^b = 2\sigma_1\gamma_1 + \alpha_1 x_2 + W''x_2^2 \tag{20}$$

These expressions and the analogous for component 2 are in agreement with Gibbs' theorem which incidentally is identical with the Gibbs-Duhem condition applied to the mono-layer phase:

$$\begin{aligned} 0 &= x_1'\mathrm{d}\mu_1' + x_2'\mathrm{d}\mu_2' \\ &= x_1'\mathrm{d}\mu_1 + x_2'\mathrm{d}\mu_2 + (x_1'\sigma_1 + x_2'\sigma_2)\mathrm{d}\gamma \\ &= \left\{RT\left(\frac{x'_1}{x_1} - \frac{x'_2}{x_2}\right) - 2W(x_1' - x_1)\right\}\mathrm{d}x_1 + (x_1'\sigma_1 - x_2'\sigma_2)\mathrm{d}\gamma \\ &= 0\mathrm{d}x_1' + \{\alpha_2 x_2' - \alpha_1 x_1' - 2W''(x_1' - x_1)\}\,\mathrm{d}x_1 - (x_1'\sigma_1 + x_2'\sigma_2)\mathrm{d}\gamma \end{aligned} \tag{21}$$

The general relation between the surface tension of the mixture, γ, and those of the pure components, γ_1 and γ_2 is then:

$$\begin{aligned} \gamma &= \gamma_1 + \frac{1}{2\sigma_1}\left\{\alpha_1 x_2 + RT\ln\frac{x_1'}{x_1} + W'x'^2_2 - (W - W'')x_2^2\right\} \\ &= \gamma_2 + \frac{1}{2\sigma_2}\left\{\alpha_2 x_1 + RT\ln\frac{x_2'}{x_2} + W'x'^2_1 - (W - W'')x_1^2\right\} \end{aligned} \tag{22}$$

To derive Guggenheim's equation for regular mixtures we put $\alpha_1 = \alpha_2 = 0$, $\sigma_1 = \sigma_2 = A/2$ and $W = 2W' = 4W''$. Guggenheim's ideality requires further $W = 0$. Similarly Hoar and Melford's eqn. (18) appears if $\alpha_1 = \alpha_2 = 0$, $W = 2W'$ and $W'' = 0$. It is only in a formal way that (22) is brought to agree with these other expressions by doubling the surface area.

Since μ' contains a χ-term, there is no reason why α_1 and α_2 should be zero. Hence a more natural choice of what to define as an ideal or perfect surface will be:

$$\alpha_1/\sigma_1 = -\alpha_2/\sigma_2 = \gamma_2 - \gamma_1 \tag{23}$$

$$W = W' = W'' = 0 \tag{24}$$

which implies the relations:

$$x_1'/x_1 = \exp(\sigma_1(\gamma - \gamma_1)/RT) \tag{25}$$

$$\gamma_{id} = x_1\gamma_1 + x_2\gamma_2 \tag{26}$$

which give exactly the same distribution between bulk phase and monolayer as previous treatments. The difference is the rectilinear dependence of surface tension on mole fraction.

The same concept of ideal surface behaviour has been advanced before. Defay and Prigogine [13,14] use it, but only as an approximation which may be reasonable when γ_1 and γ_2 are not too different from each other.

Passing to regular solutions it is reasonable to maintain the α-values (23) and introduce values for W,W' and W'' corresponding to Guggenheim's model. This leads to the same distribution of the components as Guggenheim's own expressions, eqn. (2) above. The surface tension, however, comes out as the mean between the ideal value, γ_{id}, from eqn. (26) and the γ as calculated from Guggenheim's equation (2). This improves the agreement with our experiments in the region of low chloroform concentrations, but makes it worse in the other end.

The reason why our results for chloroform-carbontetrachloride mixtures corresponded quite well to Guggenheim's regularity is probably that the two components not only form regular mixtures but also have about the same surface tensions.

More experimental data are needed, particularly on regular mixtures of components with widely different surface tension.

The thermodynamic derivations in this paper draw heavily on ten years old discussions with Dr. Th. Rosenberg, now at the Danish Atomic Energy Research Station, Risø, and on recent discussions with professor H. Højgaard Jensen. The experimental work was carried out in collaboration with Dr. T. A. Bak and K. Andersen, who measured the viscosities of the same mixtures (to be published later).

REFERENCES

1. Jensen, H. Højgaard *Acta Chem. Scand.* **12** (1958) 1024.
2. Brønsted, J. N. and Koefoed, J. *Kgl. Danske Videnskab. Selskab, Mat. fys. Medd.* **22** (1946) No. 17.
3. Whatmough, W. H. *Z. physik. Chem.* **39** (1901) 157.
4. Mc Glashan, M. L., Prue, J. E. and Sainsbury, E. J. *Trans. Faraday Soc.* **50** (1954) 1284.
5. Guggenheim, E. A. *Trans. Faraday Soc.* **41** (1945) 150 or *Mixtures*, Oxford U.P. 1952.
6. Hoar, T. P. and Melford, D. A. *Trans. Faraday Soc.* **53** (1957) 318.
7. Everett, D. H. *Discussions Faraday Soc.* **15** (1953) 258.
8. Everett, D. H. and Penney, M. F. *Proc. Roy. Soc.* **A212** (1952) 164.
9. van der Waals, J. H. *Diss.* Amsterdam 1950.
10. Guggenheim, E. A. *J. Chem. Phys.* **4** (1936) 689.
11. Guggenheim, E. A. *Thermodynamics*, North Holland Publ. 1949.
12. *Handbuch der Experimentalphysik.* Bd 6.
13. Defay, R. and Prigogine, I. *Bull. soc. chim. Belges* **53** (1944) 115.
14. Defay, R. and Prigogine, I. *Tension superficielle.* Dunod 1957.
15. Prigogine, I. *et al. J. chim. phys.* **47** (1950) 33, 807; *J. Colloid Sci.* **7** (1952) 122 etc.
16. Hildebrand, J. H. and Carter, J. M. *J. Am. Chem. Soc.* **54** (1932) 3592.

Received February 26, 1958.

ACTA CHEMICA SCANDINAVICA 12 (1958) 1136—1142

On the Mathematical Iteration Principle and its Application to Chemical Equilibrium Calculations

A. E. LANSNER

Universitetets Fysisk-Kemiske Institut, Copenhagen, Denmark

The practical application of the method of iteration for the numerical calculation of roots in equations which cannot be solved is discussed.

It is shown that the theoretical condition of iteration convergence is to be substituted with a practical condition which makes the method appropriate for actual calculation. The method is demonstrated on chemical equilibrium calculations.

The importance of a particular "sensitive" variable is stressed.

In his work with chemical equilibrium expressions the chemist very often has to determine a root in an equation which cannot be solved or which can be solved only with difficulty. In the following the method of successive approximation (iteration) will briefly be mentioned. This method seems to be very useful for determination of approximate root values.

Suppose the given equation is $F(x) = 0$, and that r is the unknown root of interest. If it is possible to rewrite the equation $F(x) = 0$ in the form:

$$x = f(x)$$

where $f(x)$ is differentiable and $|f'(x)| \leq c < 1$ in the interval to be considered containing the root r, then the series

$$x_0,\ x_1 = f(x_0),\ x_2 = f(x_1), \ldots,\ x_n = f(x_{n-1}), \ldots$$

where x_0 is an estimated value for the root r, will be convergent with the limit

$$r = f(r)$$

This follows by repeated application of the meanvalue theorem:

$$\begin{aligned} |x_n - r| &= |f(x_{n-1}) - f(r)| \\ &= |f'(u)|\ |x_{n-1} - r| \\ &\leq c\ |x_{n-1} - r| = c\ |f(x_{n-2}) - f(r)| \\ &= c\ |f'(v)|\ |x_{n-2} - r| \\ &\leq c^2\ |x_{n-2} - r| = \ldots \\ &\leq c^n\ |x_0 - r| \rightarrow 0 \end{aligned}$$

when $n \rightarrow \infty$, *q.e.d.*

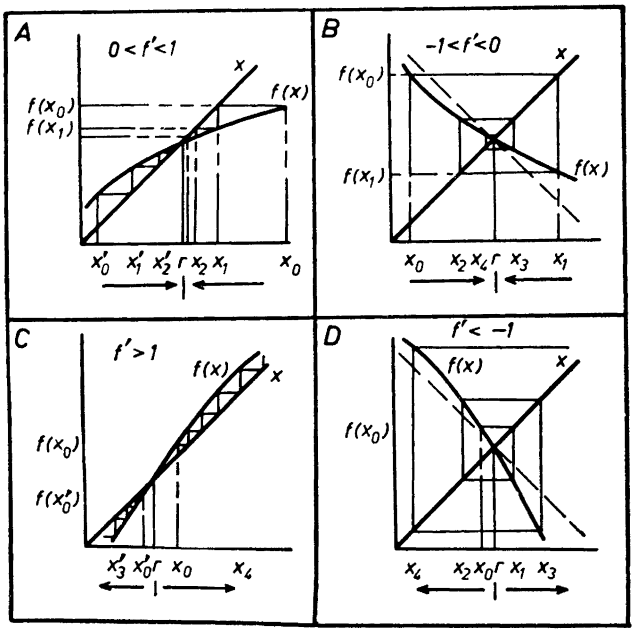

Fig. 1. A and B: condition of iteration is fulfilled, *i. e.* convergence.
C and D: condition of iteration is not fulfilled, *i. e.* divergence.
A and C: $f' > 0$, *i. e.* steady motion.
B and D: $f' < 0$, *i. e.* oscillating motion.

Further and analogous considerations in the case: $|f'(x)| \geq c \geq 1$ make clear, that the *condition of iteration convergence*

$$|f'(x)| < 1$$

in the neighbourhood of r, in theoretical respect is necessary and sufficient for the series convergence, but it must be emphazised that this condition is *not* sufficient for practical purposes, as will be seen in the following example: If $1 \simeq |f'(x)| < 1$, then n must be large if $x_n \simeq r$. This is tantamount to the necessity of calculation of many $f(x)$-values, which follows from: $|x_n - r| \leq c^n |x_0 - r|$ where $1 \simeq c < 1$. It is also evident from A, B-type diagrams (see Fig. 1).
Consequently the *practical condition of iteration convergence* must be:

$$|f'(x)| < c,$$

where c is essentially less than 1. Or otherwise expressed: The nearer $f(x)$ is by constancy in the interval containing the root, the faster the iteration process will progress (consider A,B-type diagrams for $f'(x) \simeq$ or $= 0$).

In many cases it is possible and appropriate first to rewrite the $F(x)$ given, so that the $F(x)$ function is mainly (and preferably strongly) depending on a

certain, single $x = x_s$ (the most "*sensitive*" x) in the $F(x)$ expression. Then this x_s is to be isolated in the equation given, *i.e.* $F(x) = 0$ is rewritten as $x_s = f(x)$. This $f(x)$ will fulfill the practical condition of iteration.

The principle of this successive approximation method is shown graphically in four characteristic cases where the condition of iteration: $|f'(x)| < 1$ partly is and partly is not fulfilled (diagrams A and B, and C and D, respectively).

Mathematical example

Suppose that calculations on a mass action expression has given the equation:

$$F(x) = x^4 + 10^{-2}x^3 - 10^{-4} = 0$$

where x is the degree of reaction. Consequently $0 < r < 1$. It is evident that the equation $F(x) = 0$ can be rewritten in many other forms. On account of the practical condition of iteration, it is appropriate to select an $f(x)$ function which depends only slightly on x ($f'(x)$ near 0).
Hence $F(x) = 0$ is rewritten in the form:

$$(x + 10^{-2})x^3 = 10^{-4} = 0$$

The greater x-exponent difference in this equation causes one of the two $f(x)$ functions, $(f_B(x))$, which is the most natural to select here, to be only slightly dependent on x, while the other, $(f_D(x))$, contrary to the condition of iteration, varies strongly with x. Obviously the most "sensitive" $x(= x_s)$ is contained in the factor x^3. Consequently

$$x_s = f_B(x) = \left(\frac{10^{-4}}{x + 10^{-2}}\right)^{1/3}$$

$$(x = f_D(x) = \frac{10^{-4}}{x_s^3} - 10^{-2}),$$

where $f'_B(x)$ and $f'_D(x)$ is < 0, and subscripts B and D refer to diagrams B and D. Notice that it is neither convenient nor necessary in general to calculate $f'(x)$. As $f(x)$, $f_B(x)$ is chosen because it is only a slightly varying function.

Now it only remains to choose a suitable x_0 (preferably in the neighbourhood of the root r). The general method for selection of x_0 is that the equation given is first solved qualitatively, with more or less good approximation. In most cases one can be helped through chemical considerations (pH-diagrams etc; see also "chemical example"). But in this and other cases one must try to estimate the root directly from the equation given. Thus it is often convenient to try the insertion of probable powers of ten for x_0. From $F(x) = 0$ rewritten in the form:

$$g(x) = (x + 10^{-2})x^3 = 10^{-4}$$

is estimated, that $r = 10^{-1}$, which gives:

$$g(10^{-1}) = 1.1 \times 10^{-4} \simeq 10^{-4}$$

i.e., 10^{-1} is an applicable value for x_0.

Consequently the convergence series is:

			error (%)
$x_0 = 10^{-1} =$		0.10000	2.4
$x_1 = f_a(x_0) = \left(\frac{10^{-4}}{10^{-1} + 10^{-2}}\right)^{1/3} =$		0.09688	0.7
$x_2 = f_a(x_1) =$		0.09781	0.2
$x_3 = f_a(x_2) =$		0.09752	0.07
$x_4 = f_a(x_3) =$		0.09761	0.02
$x_5 = f_a(x_4) =$		0.09759	0.01
$x_6 = f_a(x_5) =$		0.09759	0.01
—			
—			

Notice that even $x_1 = f(x_0)$ is a good approximation to $r = 0.09759\ldots$ Hence continuation of the iteration process for $n > 2$ generally will be superfluous in cases like the present.

Chemical example 1

Given is a gaseous mixture having the following composition

SO_2	7.8 vol %
O_2	10.8 vol %
N_2	81.4 vol %
	100.0 vol %

This gaseous mixture is passed into a converter where in the presence of a catalyst the SO_2 is oxidized to SO_3. The temperature in the converter is maintained at 500°C and the pressure at 1 atm, which is corresponding to $K_c = 177\ 800$ l/st* for the equilibrium:

$$2SO_2 + O_2 = 2SO_3$$

Calculate the composition of the gases leaving the converter, assuming that equilibrium conditions are reached. It may be assumed that the fugacity coefficients are equal to unity.

Qualitative solution. Notice that $K_c \gg 1$ and the amount of O_2 equivalent to the 7.8 vol % SO_2 (in the gas mixture given) is $1/2 \times 7.8 = 3.9 < 10.8$ vol % (= vol % O_2 in the mixture). Consequently the composition of the equilibrium mixture must approximately be:

SO_2	0 vol %	SO_3	8 vol %
O_2	7 "	N_2	85 "

Quantitative solution

$$2SO_2 + O_2 = 2SO_3$$

$n_{total} = n_{SO_2} + n_{O_2} + n_{SO_3} + n_{N_2}$	moles of equilibrium mixture
$n_{total} = (a - 2x) + (b - x) + (0 + 2x) + c$	" " "
$n_{total} = a + b + c - x$	" " "

* st is by definition the number of moles equal to the stoichiometrical coefficients in the given scheme of reaction.

where a, b, 0 and c is the initial number of moles of SO_2, O_2. SO_3 and N_2, and x is the equilibrium conversion of SO_2.
Suppose $a + b + c = 100$ moles; then we get $n_{total} = 10 - x$ moles.
If by definition

$$K_n = \Pi n_i^{\nu_i} = \frac{(n_{SO_3})^2}{(n_{SO_2})^2\,(n_{O_2})}$$

where ν_i is the stoichiometrical coefficient of the i-th component, then:

$$K_c = K_n v^{-\Sigma\nu_i} = K_n v \text{ (for } -\Sigma\nu_i = -(2-2-1) = 1.$$

If the ideal gas laws are valid

$$v = n_{total} RT/p = (100-x)RT/p$$

i.e.,

$$K_c = \frac{(2x)^2(100-x)\;RT}{(a-2x)^2(b-x)\;p}, \text{ or}$$

$$\frac{x^2(100-x)}{(a/2-x)^2\,(b-x)} = \frac{pK_c}{RT}$$

Now

a	$= 7.8$ mole	p	$= 1$ atm
b	$= 10.8$ "	R	$= 0.08205$ l.atm/K.mole
K_c	$= 177\,800$ l.atm/K.mole	T	$= 773.2$ K

Hence the equation $F(x) = 0$ is

$$\frac{x^2\,(100-x)}{(3.9-x)^2\;(10.8-x)} - 2802.6 = 0$$

From the qualitative solution we have:
$n_{SO_3} = a - 2x \simeq 0$ (almost complete reaction), *i.e.*

$$x \simeq \frac{a}{2} = 3.9.$$

Consequently 3.9 must be suitable as the initial value x_0. The qualitative result, $x \simeq 3.9$, also makes clear that it is the x $(= x_s)$ in the group $3.9-x$ which is the most "sensitive". Hence we rewrite $F(x) = 0$ in the form

$$x_s = 3.9 - \frac{x}{53}\sqrt{\frac{100-x}{10.8-x}}$$

We now use the iteration principle

$$x_{n+1} = 3.9 - \frac{x_n}{53}\sqrt{\frac{100-x_n}{10.8-x_n}}$$

and get the following convergence series

x_0	$=$	3.900
x_1	$= 2.9 - \frac{3.9}{53}\sqrt{\frac{100-3.9}{10.8-3.9}} =$	3.63
x_2	$=$	3.649
x_3	$=$	3.647
—		
—		

i.e.

$$x = r \simeq 3.647 \simeq 3.65.$$

Consequently

n_{SO_3}	$= 2x$	$= 2 \times 3.65$	$=$	7.30	mole or	7.58	vol %
n_{O_2}	$= b\text{-}x$	$= 10.8 - 3.65$	$=$	7.15	" "	7.42	"
n_{SO_2}	$= a\text{-}2x$	$= 7.8 - 7.30$	$=$	0.50	" "	0.52	"
n_{N_2}	$=$			81.40	" "	84.47	"
				96.35	mole or	100.00	vol %

which is in agreement with the qualitative solution.

Simultaneous equations

In the general case, with simultaneous equations in several unknowns, the method of iteration is given by the following two-equation example:

Suppose the given equations are

$$F(x,y) = 0 \text{ and } G(x,y) = 0.$$

In general the two independent variables are asymmetrical in the equations, and this is to be utilized for a fast working iteration process.

Assume that a certain $x = x_s$ in $F(x,y)$ is the relatively most "sensitive" of all the x's *and* y's in the two (eventually rewritten) functions given, and that y_s is the most "sensitive" of the y's only in the other function $G(x,y)$. Then isolate x_s in $F(x,y) = 0$ and y_s in $G(x,y) = 0$:

$$x_s = f(x,y) \text{ and } y_s = g(xy).$$

Now the two iteration principles are

$$x_{n+1} = f(x_n,y_n)$$

and

$$y_{n+1} = g(x_{n+1}, y_n)$$

i.e.

$$y_{n+1} = u(x_n, y_n) = g(f(x_n, y_n), y_n).$$

The initial values x_0 and y_0 are also in this case to be selected by qualitative solution of the problem considered.

Chemical example 2

Calculate c_{H+} and c_{H_2Ox} in a 0.1 M solution of potassium hydrogen oxalate in water. Assume that the activity coefficients are equal to unity, and that

$$K_1 = 10^{-1.19} \text{ and } K_2 = 10^{-4.21}$$

The schemes of significant reactions are

		degree of reaction
HOx^-	$= H^+ + Ox^{--}$	x
$2HOx^-$	$= H_2Ox + Ox^{--}$	y

Qualitative solution

$pH = 1/2(pK_1 + pK_2) = 2.7$, *i.e.* $C_{H+} = x = 0.002$ and $y = 0.003$

Quantitative solution

$$\begin{array}{llll} H^+ & = x & Ox^{--} & = x + y \\ H_2Ox & = y & HOx^- & = 0.1 - x - 2y \end{array}$$

Hence

$$K_1 = 10^{-1.19} = \frac{x}{y}(0.1 - x - 2y)$$

$$K_2 = 10^{-4.21} = \frac{x(x+y)}{0.1 - x - 2y}$$

rewritten as

$$F(x,y) = x^2\left(1 + \frac{10^{-1.19}}{0.1 - x - 2y}\right) = 10^{-5.40} = 0$$

$$G(x,y) = x\frac{0.1 - x - 2y}{y} - 10^{-1.19} = 0$$

It is to be seen that "x_s" is contained in the group x^2 in the F function. Hence

$$x_{n+1} = f(x_n, y_n) = \left(\frac{10^{-5.40}}{1 + \dfrac{10^{-1.19}}{0.1 - x_n - 2y_n}}\right)^{1/2}$$

and analogously

$$y_{n+1} = g(x_{n+1}, y_n) = x_{n+1}\frac{0.1 - x_{n+1} - 2y_n}{10^{-1.19}}$$

From the qualitative solution we choose $x_0 = y_0 = 0$. Consequently the two convergence series are derived as follows:

$$\begin{array}{llll} x_0 & = 0 & y_0 & = 0 \\ x_1 & = f(x_0,y_0) & y_1 & = g(x_1, y_0) \\ & = 1.556.10^{-3} & & = 2.371.10^{-3} \\ x_2 & = f(x_1, y_1) & y_2 & = g(x_2, y_1) \\ & = 1.535.10^{-3} & & = 2.229.10^{-3} \\ x_3 & = f(x_2, y_2) & y_3 & = g(x_3, y_2) \\ & = 1.536.10^{-3} & & = 2.237.10^{-3} \\ - & & y_4 & = g(x_3, y_3) \\ - & & & = 2.236.10^{-3} \end{array}$$

i.e.

$$x = 1.54.10^{-3} \text{ and } y = 2.24.10^{-3} \text{ (mole/l)}$$

It is a matter of course that the practical condition of iteration convergence is also well applicable to the approximative solution of transcendental equations as, for instance, $F(x) = 2\,\mathrm{tg}x - x = 0$.

Finally it is noticed that the iteration process can easily be accelerated, if by the calculation of say x^{n+1}, it is possible, from the foregoing series values to estimate a better value x'_n than the x_n, and then insert this x'_n instead of x_n.

Received February 21, 1958.

ACTA CHEMICA SCANDINAVICA 12 (1958) 1143—1152

Short Communications

Mass Transfer by Laminar Free Convection at Vertical Electrodes

GÖSTA WRANGLÉN

Division of Applied Electrochemistry, Royal Institute of Technology, Stockholm 70, Sweden

The following notion is used:

x = distance along electrode surface from lower edge of cathode or upper edge of anode
y = distance from electrode surface
h = electrode height
$\delta_{d\,0.99}$ = thickness of diffusion boundary layer or electrode film, defined so that $|c-c_e| = 0.99\,\Delta c$
δ_h = thickness of hydrodynamic boundary layer
δ_N = thickness of the Nernst diffusion layer or effective film thickness
$\delta_=$ = distance from electrode at which diffusion = convection
u = vertical flow velocity in boundary layer
c, c_b, c_e and c_s = concentrations in diffusion layer, of bulk electrolyte, on electrode surface and at saturation, respectively
$\Delta c = |c_e - c_b|$
ϱ = density in diffusion layer
$a = \frac{\delta \ln \varrho}{\delta c}$ = specific densification coefficient
ν = kinematic viscosity
D = diffusion coefficient
g = acceleration of gravity
i = current density
$j = \frac{i(1-t)}{zF}$ = diffusion current density
t = transference number of reacting ion
z = valency of electrode reaction
F = Faraday's constant
i_{lim} = local limiting current density
Nu_x = $jx/D\Delta c$ and Nu_{av} local and average Nusselt numbers, respectively
$Sc = \frac{\nu}{D}$ = Schmidt number
Gr_x = local Grashof number

In earlier work on mass transfer under free convection conditions, in which the analogy with heat transfer was used, δ_d and δ_h have usually been assumed identical [1,2]. While this is often justified in heat transfer, available numerical solutions of the boundary layer equations [3,4] show that with high Schmidt numbers ($Sc \simeq 1\,000$), as in mass transfer in liquids, δ_h is 10—15 times larger than δ_d. Generally [5], $\delta_h/\delta_d \simeq Sc^{1/3}$. Furthermore, u_{max} is reached at a distance of about 2/3 δ_d from the electrode.

As to boundary conditions, two important cases have to be distinguished, *viz.* I) constant concentration or potential on the electrode surface, and II) constant concentration gradient or current density on the electrode surface. Case I is probably realized only under limiting current conditions [6].

Considering the numerical solutions referred to [3,4], the following approximations are applied for the concentration profile in the boundary layer

$$|c - c_b| = \Delta c \left(1 - \frac{y}{\delta_d}\right)^2 \qquad \text{(case I)}$$

$$|c - c_b| = \frac{j\delta_d}{2D}\left(1 - \frac{y}{\delta_d}\right)^2 \qquad \text{(case II)}$$

and for the velocity profile in both cases

$$u = 3.375\, u_{max} \frac{y}{\delta_d}\left(1 - \frac{y}{2\delta_d}\right)^2 \text{ for } 0 \leq y \leq \frac{2}{3}\delta_d$$

and

$$u = 0.07\, u_{max}\, Sc^{1/3}\left(1.5\, Sc^{1/3} - \frac{y}{\delta_d}\right) \text{for } \frac{2}{3}\,\delta_d \leq y \leq 1.5\, Sc^{1/3}\delta_d$$

With these expressions, the boundary layer equations can be integrated according to von Kármán to give approximate analytical solutions. The numerical coefficients are then obtained by comparison with the numerical solutions of the analogous heat transfer problems, corresponding to case I (3) and case II (4). The following results are obtained. They refer to cathodic deposition and anodic dissolution of metals. Details of the calculations will be published elsewhere.

Case I (limiting current density)

$$i_{\lim} = 0.499 \frac{zF}{1-t} D \Delta c \left(\frac{g a \Delta c}{D \nu x}\right)^{1/4}$$

$$\delta_{d\,0.99} = 3.54 \left(\frac{D \nu x}{g a \Delta c}\right)^{1/4}$$

$$\delta_N = 0.57\ \delta_{d\,0.99}, \quad \delta_{\infty} = 0.55\ \delta_{d\,0.99}$$

$$u_{\max} = 1.0 \left(\frac{D g a \Delta c x}{\nu}\right)^{\frac{1}{2}}$$

$$Nu_x = 0.499\ (ScGr_x)^{1/4}$$

$$Nu_{\mathrm{av}} = \frac{4}{3} Nu_h = 0.665\ (ScGr_h)^{1/4}$$

At the cathode $c_e = 0$, at the anode $c_e = c_s$ under limiting current condition. $i_{\lim}$ is then the passivating c.d. at the anode.

Case II (normal electrolysis)

$$\Delta c = 1.59\ j \left(\frac{\nu x}{D^2 g a j}\right)^{1/5}$$

$$\delta_{d\,0.99} = 3.09 \left(\frac{D^2 \nu x}{g a j}\right)^{1/5}$$

$$\delta_N = 0.51\ \delta_{d\,0.99}$$

$$u_{\max} = 1.1 \left(\frac{g a j}{\nu}\right)^{2/5} D^{1/5} x^{3/5}$$

$$Nu_x = 0.558\ (ScGr_x)^{1/4}$$

$$Nu_{\mathrm{av}} = \frac{6}{5} Nu_h = 0.670\ (ScGr_h)^{1/4}$$

In the presence of a conducting inert electrolyte, a correction term appears in a. The correction derived by Wilke and coworkers [2] for case I is applicable also in case II.

1. Wagner, C. *Trans. Electrochem. Soc.* **95** (1949) 161.
2. Wilke, C. R., Tobias, C. W. and Eisenberg, M. *J. Electrochem. Soc.* **100** (1953) 513; *Chem. Eng. Progr.* **49** (1953) 663.
3. Ostrach, S. *NACA Report* **1111** (1953).
4. Sparrow, E. M. and Gregg, J. L. *Trans. ASME* **78** (1956) 435.
5. Levich, B. *Acta Physiochim. URSS* **17** (1942) 257; **19** (1944) 117.
6. Wagner, C. *J. Electrochem. Soc.* **104** (1957) 129.

Received April 16, 1958.

Detection of Small Amounts of Δ^3-Carene in α-Pinene

ERKKI PULKKINEN, EERO SILTANEN and VEIKKO PIRILÄ

Institute of Chemistry, University of Helsinki and Institute of Occupational Health, Helsinki, Finland

In connection with investigations on the sensitization of the skin to oil of turpentine [1-3] it was necessary to detect small amounts of Δ^3-carene in α-pinene. Widmark [4] has investigated the purity of various terpenes with the microsorption method according to Blohm [5]. With this method he was able to show the index inhomogeneity of α-pinene into which 0.2 % or more Δ^3-carene had been added [6]. When investigating the purity of various terpenes we have used the infrared spectrophotometry which has the advantage of being specific. As a criterion for purity we have used the spectra of the series of American Petroleum Institute Research Project 44 *.

In order to purify different terpenes, fractional distillation with Podbielniak-column and displacement chromatography were used. The latter method was more practicable giving equal or better results in shorter time. The displacement was performed on a macro scale by jointing together some columns with different diameters [7,8], in order to gain sharp fronts. The fractions were analyzed with infrared spectrophotometry [8,9]. For detection of Δ^3-carene in α-pinene the absorption peak of wave number 714 cm^{-1} appeared to be most suitable and made it possible to show 0.39 % Δ^3-carene (Fig. 1) with a liquid

* Serial No. 566 for α-pinene, 567 for β-pinene, 1 469 for Δ^3-carene and 462 for *d*-limonene.

With these expressions, the boundary layer equations can be integrated according to von Kármán to give approximate analytical solutions. The numerical coefficients are then obtained by comparison with the numerical solutions of the analogous heat transfer problems, corresponding to case I (3) and case II (4). The following results are obtained. They refer to cathodic deposition and anodic dissolution of metals. Details of the calculations will be published elsewhere.

Case I (limiting current density)

$$i_{\lim} = 0.499 \frac{zF}{1-t} D \Delta c \left(\frac{g a \Delta c}{D \nu x}\right)^{1/4}$$

$$\delta_{d\,0.99} = 3.54 \left(\frac{D \nu x}{g a \Delta c}\right)^{1/4}$$

$$\delta_N = 0.57\ \delta_{d\,0.99}, \quad \delta_{\infty} = 0.55\ \delta_{d\,0.99}$$

$$u_{\max} = 1.0 \left(\frac{D g a \Delta c x}{\nu}\right)^{\frac{1}{2}}$$

$$Nu_x = 0.499\ (ScGr_x)^{1/4}$$

$$Nu_{\mathrm{av}} = \frac{4}{3} Nu_h = 0.665\ (ScGr_h)^{1/4}$$

At the cathode $c_e = 0$, at the anode $c_e = c_s$ under limiting current condition. $i_{\lim}$ is then the passivating c.d. at the anode.

Case II (normal electrolysis)

$$\Delta c = 1.59\ j \left(\frac{\nu x}{D^2 g a j}\right)^{1/5}$$

$$\delta_{d\,0.99} = 3.09 \left(\frac{D^2 \nu x}{g a j}\right)^{1/5}$$

$$\delta_N = 0.51\ \delta_{d\,0.99}$$

$$u_{\max} = 1.1 \left(\frac{g a j}{\nu}\right)^{2/5} D^{1/5} x^{3/5}$$

$$Nu_x = 0.558\ (ScGr_x)^{1/4}$$

$$Nu_{\mathrm{av}} = \frac{6}{5} Nu_h = 0.670\ (ScGr_h)^{1/4}$$

In the presence of a conducting inert electrolyte, a correction term appears in a. The correction derived by Wilke and coworkers [2] for case I is applicable also in case II.

1. Wagner, C. *Trans. Electrochem. Soc.* **95** (1949) 161.
2. Wilke, C. R., Tobias, C. W. and Eisenberg, M. *J. Electrochem. Soc.* **100** (1953) 513; *Chem. Eng. Progr.* **49** (1953) 663.
3. Ostrach, S. *NACA Report* **1111** (1953).
4. Sparrow, E. M. and Gregg, J. L. *Trans. ASME* **78** (1956) 435.
5. Levich, B. *Acta Physiochim. URSS* **17** (1942) 257; **19** (1944) 117.
6. Wagner, C. *J. Electrochem. Soc.* **104** (1957) 129.

Received April 16, 1958.

Detection of Small Amounts of Δ^3-Carene in α-Pinene

ERKKI PULKKINEN, EERO SILTANEN and VEIKKO PIRILÄ

Institute of Chemistry, University of Helsinki and Institute of Occupational Health, Helsinki, Finland

In connection with investigations on the sensitization of the skin to oil of turpentine [1-3] it was necessary to detect small amounts of Δ^3-carene in α-pinene. Widmark [4] has investigated the purity of various terpenes with the microsorption method according to Blohm [5]. With this method he was able to show the index inhomogeneity of α-pinene into which 0.2 % or more Δ^3-carene had been added [6]. When investigating the purity of various terpenes we have used the infrared spectrophotometry which has the advantage of being specific. As a criterion for purity we have used the spectra of the series of American Petroleum Institute Research Project 44 *.

In order to purify different terpenes, fractional distillation with Podbielniak-column and displacement chromatography were used. The latter method was more practicable giving equal or better results in shorter time. The displacement was performed on a macro scale by jointing together some columns with different diameters [7,8], in order to gain sharp fronts. The fractions were analyzed with infrared spectrophotometry [8,9]. For detection of Δ^3-carene in α-pinene the absorption peak of wave number 714 cm^{-1} appeared to be most suitable and made it possible to show 0.39 % Δ^3-carene (Fig. 1) with a liquid

* Serial No. 566 for α-pinene, 567 for β-pinene, 1 469 for Δ^3-carene and 462 for *d*-limonene.

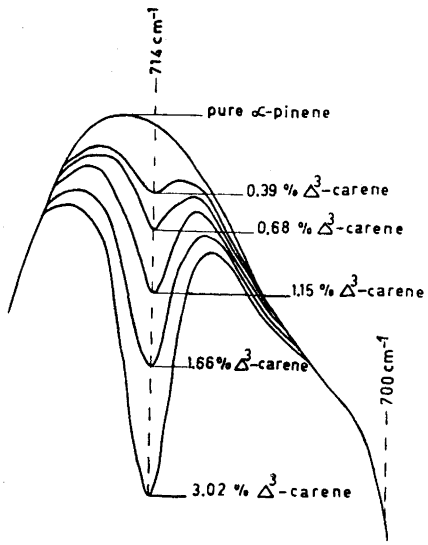

Fig. 1. A part of the infrared spectrum of Δ^3-carene in α-pinene with the peak at 714 cm^{-1} (1.0 mm cell).

layer of 1.0 mm thickness. After enrichment by displacement chromatography 0.1 % of Δ^3-carene could be detected in some experiments. Silica gel and aluminium oxide were used as adsorbents. With both these adsorbents *d*-α-pinene and Δ^3-carene could be separated sharply from their mixtures. According to our observations, however, when using silica gel it must be taken into consideration, that the adsorbent, if too activated, tends to cause rearrangement of α-pinene.

Experimental part. Purification of α-pinene by chromatography.

20 ml of *d*-α-pinene (Variochem VVB Schimmel, Miltitz, Bz Leipzig, $[\alpha]_D$ +38.42°, distilled over sodium, infrared spectrophotometrically impure) was displaced by ethyl alcohol with alumina (E. Merck, Darmstadt, standardised according to Brockmann) as adsorbent using a series of three columns (41 300π + 11 000π + 4 500π mm^3). Judging from the infrared spectra of the collected fractions, about 70 % of the input was free of impurities.

Purification of Δ^3-carene by chromatography. The raw product of Δ^3-carene (from Enso-Gutzeit Oy, Finland) was rectified with Podbielniak-Skärblom-Linder-column [10] and a fraction, boiling range 170—171°C, was purified by displacement with ethyl alcohol using silica gel (Davison, 1 # Grade 922 Mesh Size T. 200, Davison Code No. 922—08-4X-1926) as adsorbent. Filters: 2 200π + 1 000π mm^3. The infrared spectra of the collected fractions showed that about 50 % of the input had at least 95 % purity, comparing with the spectrum of Δ^3-carene of the American Petroleum Institute.

Detection of small amounts of Δ^3-carene in α-pinene. 20 ml of the mixture, which contained 0.1 % Δ^3-carene in *d*-α-pinene was submitted to displacement using, as above, ethyl alcohol as the displacing agent and silica gel (Davison, 922-08-4X-1926) as the adsorbent. Filters: 41 000π+11 500π + 4 250π mm^3. After 18.2 ml of the effluent had been collected, the next 0.4 ml (fraction 18.2—18.6 ml) gave the peak of Δ^3-carene at 714 cm^{-1} in the infrared spectrum. It could be calculated that about 18 % of the amount of Δ^3-carene added to α-pinene was found in this fraction. Similar results were obtained using alumina as the adsorbent.

All infrared spectra were measured with a Perkin-Elmer Spectrometer Model 12-C equipped with a rock salt prism.

1. Pirilä, V. and Siltanen, E. *Duodecim* **72** (1956) 43.
2. Pirilä, V. and Siltanen, E. *Dermatologica* **113** (1956) 1.
3. Pirilä, V. and Siltanen, E. *Dermatologica* **115** (1958) *In press.*
4. Widmark, G. *Svensk Kem. Tidskr.* **69** (1957) 175.
5. Blohm, S.-G. *Arkiv Kemi* **6** (1954) 317.
6. Widmark, G. and Blohm, S.-G. *Acta Chem. Scand.* **9** (1955) 1296.
7. Claesson, S. *Arkiv Kemi, Mineral. Geol. A* **24** (1947) No. 16.
8. Pulkkinen, E. *Suomen Kemistilehti B* **31** (1958) 125.
9. Pulkkinen, E. J. *Ann. Acad. Sci. Fennicae, Ser. A* **74** (1956).
10. Skärblom, K.-I. and Linder, Å. *Tek. Tidskr.* **67** Kemi (1937) 25.

Received May 12, 1958.

Structure of the Crystalline Compound Benzene-Bromine (1 : 1)

O. HASSEL and KNUT O. STRØMME

Universitetets kjemiske institutt, Blindern-Oslo, Norway

Several models have been suggested for the complexes between benzene and halogen molecules known to exist in solutions, one of which, the "axial" model, has the halogen atoms situated on the six-fold axis of the benzene molecule, the symmetry being C_{6v}.

In order to gain some direct experience regarding the structure of complexes containing aromatic hydrocarbons and halogens we have tried to prepare solid compounds and to investigate the crystals by X-rays. In the case of benzene we obtained single crystals of a 1:1 compound with bromine (m.p. −14°C) which were studied at temperatures between −40° and −50°C. Crystals having one of their chief crystallographic axes approximately parallel to the capillary tube in which they were grown were chosen for exposure in a Weissenberg camera. The (monoclinic) axes are $a = 7.75$; $b = 8.83$; $c = 5.94$; $\beta = 99.3°$. From observed extinctions all space groups but $C2/m$, $C2$ and Cm could be excluded. Assuming a reasonable value of the density it follows that *two* molecules of either kind are contained in the unit cell. Suggesting the most symmetrical group $C2/m$ to be the correct one, the parameters of the bromine atoms were worked out from Patterson projections and trial and error computations.

A very satisfactory agreement between observed and calculated intensities was thus obtained. From the coordinates of the bromine atoms alone Fourier maps giving projections of the structure along the a and c axes were computed. Although all structure factor signs were computed neglecting the lighter atoms, the resultant charts turned out to contain, besides the heavy peaks corresponding to the bromine atoms, lower peaks allowing the localisation of the carbon atoms also with some degree of accuracy. The final maps are reproduced in Fig. 1 (*a*) and (*c*). No spurios peaks are observed and termination of series effects are small due to strong thermal vibrations resulting in an unusually marked fall in intensities for larger ϑ values.

The bromine-bromine distance found is 2.28 Å and appears therefore to be very nearly the same as observed in the free molecule. The line joining the two bromine atoms is parallel to [101] and passes through the symmetry centre of the benzene ring. The angle between this direction and the benzene plane is at least very nearly 90°. The distance from each bromine atom to the adjacent benzene plane is 3.36 Å. It is interesting to note that the π electrons of all six C−C bonds must be equally involved in formation of the electron transfer bond. This is not necessarily so, of course, in the case of the 1:1 complex present in solutions. Here a somewhat stronger binding may possibly result if the axis of the bromine molecule is parallel to the benzene plane. The symmetrical chains of alternating benzene and bromine molecules and the fact that both atoms of a bromine molecule take part in bond formation provide an interesting analogy to the structure of the dioxan-bromine compound.

The very marked drop in X-ray intensities for increasing reflexion angles, in fact more marked than in any addition compound so far examined, indicates the weakness of the binding forces between the two components. The amplitudes of vibration appear to be particularly large in directions perpendicular to the direction of the molecule chains — [101]. This may indicate either that the potential energy of the bromine atom has only one very flat minimum for a position on the chief axis of the benzene ring or perhaps six minima outside this axis.

The computed "reliability factor" R (taking into account the anisotropic vibrations) is found equal to 0.12 for both projections reproduced in Fig. 1 (*a*) and (*c*). We think that the structure derived from our present material is certainly essentially correct, but hope to be able to supplement the investigation with material obtained at lower temperatures. Such investigations might contribute towards clearing up the question (mentioned above) regarding the potential energy curve of the bromine atom.

Received May 6, 1958.

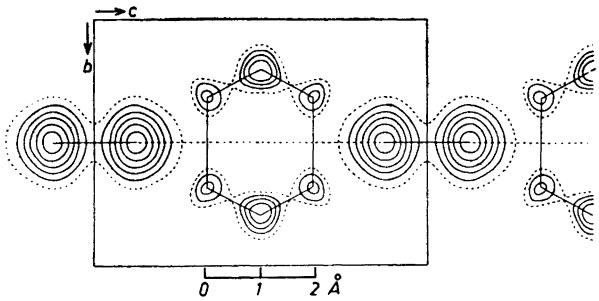

Fig. 1. (a).

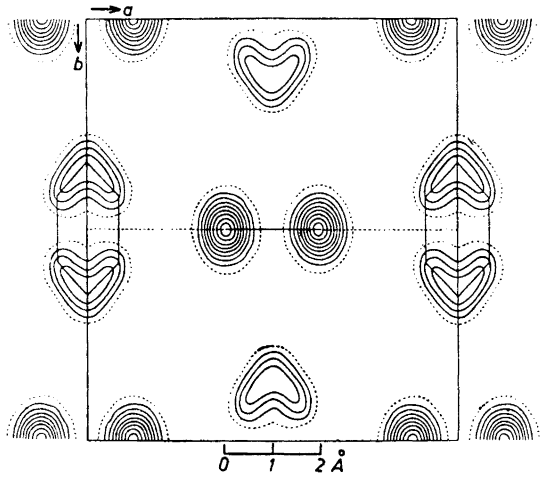

Fig 1. (c).

Preparation of Deuterated Vinyl Fluorides

BØRGE BAK and DANIEL H. CHRISTENSEN

Chemical Laboratory of the University of Copenhagen, Denmark

Recent attempts to analyze the infrared spectrum of *vinyl fluoride* [1] and to determine the structure of the molecule by microwave measurements [2] necessitated the preparation of all the deuterated derivatives. Since the combination of processes used and the yields obtained may be of value for future work on vinyl fluoride in the above-mentioned or quite different directions (such as reaction kinetics) it seemed justified to give a brief account of our results. Vinyl fluoride (I) and its seven deuterated derivatives have been prepared, three as pure compounds, CH_2CDF (II), CD_2CHF (V), and CD_3CDF (VI), and four as *cis-trans* mixtures, *cis-trans* CHDCHF (III), and *cis-trans* CHDCDF (IV).

Experimental. All the preparations described here are combinations of 4 or 6 of the following 7 processes (A—G), for sake of brevity illustrated below with 'light' ethylene bromide, vinyl bromide *etc.*

A: $\begin{matrix}CH_2Br\\|\\CH_2Br\end{matrix} \xrightarrow[KOH]{} \begin{matrix}CH_2\\\|\\CHBr\end{matrix}$ Ref.[3]

B: $\begin{matrix}CH_2\\\|\\CHBr\end{matrix} \xrightarrow[Br_2]{} \begin{matrix}CH_2Br\\|\\CHBr_2\end{matrix}$ Ref.[3]

C: $\begin{matrix}CH_2Br\\|\\CHBr_2\end{matrix} \xrightarrow[SbF_3]{} \begin{matrix}CH_2Br\\|\\CHBrF\end{matrix} + \begin{matrix}CH_2Br\\|\\CHF_2\end{matrix}$ =mixture M Ref.[3,4]

D: M $\xrightarrow[Zn]{}$ $\begin{matrix}CH_2\\\|\\CHF\end{matrix}$ Ref.[3]

E: $\begin{matrix}CH_2Br\\|\\CHBr_2\end{matrix} \xrightarrow[EtONa]{} \begin{matrix}CH_2\\\|\\CBr_2\end{matrix}$ Ref.[5]

F: $\begin{matrix}CH_2\\\|\\CBr_2\end{matrix} \xrightarrow[HBr]{} \begin{matrix}CH_2Br\\|\\CHBr_2\end{matrix}$ Ref.[6,7]

G: $\begin{matrix}CH_2\\\|\\CBr_2\end{matrix} \xrightarrow[DBr]{} \begin{matrix}CH_2Br\\|\\CDBr_2\end{matrix}$ Ref.[6,7]

The directions given in the literature [3-6] were modified with respect to the fact that much smaller quantities than usual were prepared. For example, procedure *C* was carried out in a sealed-off glass tube (24 h at 100°C) instead of in the platinum apparatus prescribed by Swarts, without serious decrease in the yield. In the *E* process, 2.5 ml $CH_2BrCHBr_2$ (or $CD_2BrCDBr_2$ a.s.o.) were converted to CH_2CBr_2 in a nitrogen atmosphere. Vinylidene bromide was removed from the small reaction container by a syringe and rapidly transferred to a nitrogen-filled test tube, from which it was distilled *in vacuo* at 20°C ($p \sim 60$ mm) after drying over $CaCl_2$ for a couple of hours. — SbF_3 and DBr were prepared according to prescriptions in Ref.[8] resp. Ref.[7]

The purity of all intermediates was controlled by infrared spectra. In all cases except one, the intermediates were 95—100 % pure. The reaction product from *C* is a mixture ('M') which was not separated into its components, since both yield the product desired. The addition of HBr, resp. DBr to the double bond (processes *F* and *G*) occurred very smoothly at room temperature under irradiation by mercury light in containers of ordinary Pyrex glass. Addition of a trace of pure oxygen had a pronounced catalytical effect. No exchange reactions took place.

The isotopic vinyl fluorides were liberated as gases (b.p. —51°C) from the mixture of 'M', Zn-dust, and ethyl alcohol. They were condensed in a trap cooled by liquid air and afterwards distilled, the trap being immersed in a —80°C bath. Only fractions of approximately correct pressure were taken. The final purification occurred on dry silica-gel in a gas chromatograph at 43°C (inside diameter of tube $\sim$ 10 mm, length of column 11 cm). In this way, the last non-isotopic impurities were removed as demonstrated by the infrared spectra taken. Also, since a complete collection of deuterated species was prepared, a useful check on the *isotopic* purity of the samples was obtained from the spectra.

Prior to the present investigation we thought that the *stability* of vinyl fluoride, kept in glass containers at room temperature and in daylight would be a problem. Infrared spectra of samples kept for months under the conditions mentioned showed the samples to be stable.

Our results are given in condensed form in Tables 1 and 2.

Table 1. Procedures applied (A—G), per cent yields obtained, and amount of final product (in ml at t°C = 25, p = 760 mm) at the preparation of vinyl fluoride (I), CH_2CDF (II), CD_2CHF (V), CD_2CDF (VI), the *cis-trans* mixture CHDCHF (III), and *cis-trans* mixture CHDCDF (IV). The general formula of the starting material is taken as CXYBrCXYBr, Z grams of this material being applied.

Table 1 continued.

X Y Z	Processes	Respective yields	Final product
H H 16.5	A B C D	72 80 ~40 ~50	CH_2CHF (240 ml)
H H 19.5	A B E G C D	65 90 77 73 ~47 ~23	CH_2CDF (90 —)
D D 13.7	A B C D	69 97 ~44 ~35	CD_2CDF (180 —)
D D 9.9	A B E F C D	69 97 74 75 ~52 ~42	CD_2CHF (102 —)
H D 29.5	A B E F C D	65 82 76 75 ~38 ~30	CHDCHF* (175 —)
H D 19.0	A B E G C D	69 89 72 72 ~50 ~9	CHDCDF* (35 —)
	Average yields	68 89 75 74 45 23	

* *cis-trans* mixture

CHDBrCHDBr was prepared from acetylene and DBr [7].

Table 2. Per cent isotopic contaminations in the deuterated vinyl fluoride samples prepared. Amounts estimated from infrared gas spectra.

Sample **	Per cent contaminant (I—VI)					
	I	II	III	IV	V	VI
I	—	0	0	0	0	0
II	0	—	0	0	0	0
III*	5—10	0	—	0	0	0
IV*	0	0	3—5	—	0	0
V	0	0	3—5	0	—	0
VI	0	0	0	3—5	3—5	—

* *cis-trans* mixture.

V and VI were prepared from CD_2BrCD_2Br with an indicated isotopic purity of 95 %. The sample was kindly given to us by dr. Leitch, N.R.C., Ottawa.

** Designation as in Table 1, consistent with Ref.[1].

1. Bak, B. and Christensen, D. *Spectrochim. Acta (In the press).*
2. Bak, B., Christensen, D., Hansen-Nygaard, L. and Rastrup-Andersen, J. *Spectrochim. Acta (In the press).*
3. Swarts, F. *Bull. Classe sci. Acad. roy. Belg.* **1901** 383.
4. Swarts, F. *Bull. Classe sci. Acad. roy. Belg.* **1909** 728.
5. Gray, T. *J. Chem. Soc.* **1897** 1023.
6. Jungers, I. C. and Verhulst, J. *Acad. roy. Belg. Classe sci. Mém. 2-ser.* **23** (1949) 44.
7. Leitch, L. C. and Morse, A. T. *Can. J. Chem.* **30** (1952) 924.
8. Andersen, F. A., Bak, B. and Hillebert, A. *Acta Chem. Scand.* **7** (1953) 236.

Received May 20, 1958.

Determination of Barbituric Acid Derivatives as Mercury Complexes

C. O. BJÖRLING, A. BERGGREN and B. WILLMAN-JOHNSON

Research Laboratories, Pharmacia Ltd., Uppsala

A. GRÖNVALL and B. ZAAR

Department of Clinical Chemistry, University Hospital, Uppsala, Sweden

Barbituric acid derivatives give precipitates with mercuric ions and this characteristic has since long been used for their detection and determination [1-3]. The precipitates are, however, soluble in certain organic solvents and this fact has been the base for the present method, the principles of which are as follows.

To a solution of 50—250 μg of a barbituric acid in 10 ml of water add 1 ml of 0.3 % mercuric nitrate solution and buffer solution to pH 8.0. Extract with 3 or 4 × 10 ml of a suitable organic solvent. Filter the organic phase through glass-wool moistened with the solvent, carefully avoiding any entrainment. To the combined extracts add an exactly measured volume of a 0.0015 % dithizone solution in chloroform and dilute to 100 ml with chloroform. Make a blank by mixing an equal amount of the dithizone solution with the same volume of the extraction solvent as above and making up to 100 ml with chloroform. Measure the extinction difference at 605 mμ. Calculate the amount of the barbituric acid from a standard curve prepared by applying the method to known quantities of barbiturate. It is, however, more convenient to use mercuric chloride when constructing a standard curve which can be used for all barbituric acids. 1 mole of mercury corresponds to 2 moles of the N-substituted barbiturates and to 1 mole of all the others.

Smaller amounts of barbituric acid can easily be determined by reducing the volumes. Thus, 2 μg of amylobarbitone (amytal) in a final volume of 5 ml gives an extinction difference of 0.130 in 1 cm cuvette, which corresponds to a sensitivity 5 times greater than that obtained by the ultraviolet methods now in use [4].

CHDBrCHDBr was prepared from acetylene and DBr [7].

Table 2. Per cent isotopic contaminations in the deuterated vinyl fluoride samples prepared. Amounts estimated from infrared gas spectra.

Sample **	Per cent contaminant (I—VI)					
	I	II	III	IV	V	VI
I	—	0	0	0	0	0
II	0	—	0	0	0	0
III*	5—10	0	—	0	0	0
IV*	0	0	3—5	—	0	0
V	0	0	3—5	0	—	0
VI	0	0	0	3—5	3—5	—

* *cis-trans* mixture.

V and VI were prepared from CD_2BrCD_2Br with an indicated isotopic purity of 95 %. The sample was kindly given to us by dr. Leitch, N.R.C., Ottawa.

** Designation as in Table 1, consistent with Ref.[1].

1. Bak, B. and Christensen, D. *Spectrochim. Acta (In the press).*
2. Bak, B., Christensen, D., Hansen-Nygaard, L. and Rastrup-Andersen, J. *Spectrochim. Acta (In the press).*
3. Swarts, F. *Bull. Classe sci. Acad. roy. Belg.* **1901** 383.
4. Swarts, F. *Bull. Classe sci. Acad. roy. Belg.* **1909** 728.
5. Gray, T. *J. Chem. Soc.* **1897** 1023.
6. Jungers, I. C. and Verhulst, J. *Acad. roy. Belg. Classe sci. Mém. 2-ser.* **23** (1949) 44.
7. Leitch, L. C. and Morse, A. T. *Can. J. Chem.* **30** (1952) 924.
8. Andersen, F. A., Bak, B. and Hillebert, A. *Acta Chem. Scand.* **7** (1953) 236.

Received May 20, 1958.

Determination of Barbituric Acid Derivatives as Mercury Complexes

C. O. BJÖRLING, A. BERGGREN and B. WILLMAN-JOHNSON

Research Laboratories, Pharmacia Ltd., Uppsala

A. GRÖNVALL and B. ZAAR

Department of Clinical Chemistry, University Hospital, Uppsala, Sweden

Barbituric acid derivatives give precipitates with mercuric ions and this characteristic has since long been used for their detection and determination [1-3]. The precipitates are, however, soluble in certain organic solvents and this fact has been the base for the present method, the principles of which are as follows.

To a solution of 50—250 μg of a barbituric acid in 10 ml of water add 1 ml of 0.3 % mercuric nitrate solution and buffer solution to pH 8.0. Extract with 3 or 4 × 10 ml of a suitable organic solvent. Filter the organic phase through glass-wool moistened with the solvent, carefully avoiding any entrainment. To the combined extracts add an exactly measured volume of a 0.0015 % dithizone solution in chloroform and dilute to 100 ml with chloroform. Make a blank by mixing an equal amount of the dithizone solution with the same volume of the extraction solvent as above and making up to 100 ml with chloroform. Measure the extinction difference at 605 mμ. Calculate the amount of the barbituric acid from a standard curve prepared by applying the method to known quantities of barbiturate. It is, however, more convenient to use mercuric chloride when constructing a standard curve which can be used for all barbituric acids. 1 mole of mercury corresponds to 2 moles of the N-substituted barbiturates and to 1 mole of all the others.

Smaller amounts of barbituric acid can easily be determined by reducing the volumes. Thus, 2 μg of amylobarbitone (amytal) in a final volume of 5 ml gives an extinction difference of 0.130 in 1 cm cuvette, which corresponds to a sensitivity 5 times greater than that obtained by the ultraviolet methods now in use [4].

The optimum pH range of the extraction varies for different barbiturates, but a pH of 8.0 is suitable for most of the compounds.

Chloroform can be used for the extraction of the N-substituted compounds and of 5-*iso*amyl-5-ethyl- and 5-allyl-5-phenyl-barbituric acids. Chloroform with 20 % dioxane is suitable for 5-ethyl-5-phenyl-barbituric acid. Chloroform with 20 % of benzyl alcohol extracts 5,5-diallyl-, 5,5-diethyl-, 5-allyl-5-*iso*propyl-, and 5-ethyl-5-*cyclo*hexenyl-barbituric acids.

The infrared spectra of some barbituric acids and their compounds with sodium, barium, and mercuric ions indicate that the mercury forms complexes rather than salts with the barbituric acids.

Of compounds containing nitrogen and having a structure similar to barbituric acid certain hydantoins and cyclic imides of dicarboxylic acids will be extracted and interfere.

The method has been applied to the determination of barbituric acids in blood. A full report will be published elsewhere.

1. Heyndrick, A. *J. pharm. belg.* **9** (1954) 132.
2. Pedley, E. *J. Pharm. and Pharmacol.* **2** (1950) 39.
3. Pfeil, E. and Goldbach, H.-J. *Z. physiol. Chem. Hoppe-Seyler's* **302** (1955) 263.
4. Richterich, R. *Clin. Chim. Acta* **3** (1958) 183.

Received June 7, 1958.

A New Type of Cholinesterase in Sow's Milk

KLAS-BERTIL AUGUSTINSSON

Institute of Organic Chemistry and Biochemistry, University, Stockholm, Sweden

Choline esters are generally not hydrolysed by milk. In two instances, however, milk was shown to exhibit high or moderate cholinesterase activity (acetylcholine used as substrate), *i.e.*, the colostrum of dog [1] and the colostrum and milk of swine [2]. These two sources of cholinesterases are interesting species differences in biochemical behaviour for which no biological explanation is known so far.

Table 1. Enzymic hydrolysis of various choline esters and phenyl esters by the milk of sow and cow. Substrate concentration, 0.01 M. Activity expressed in b_{30} per 0.1 ml of milk.

Acyl radical	Choline esters		Phenyl esters	
	Sow	Cow	Sow	Cow
Acetyl	290	0	465	1
Propionyl	280	1	255	1.5
Butyryl	500	1	205	0
Benzoyl	65	1	—	—
Succinyl	55	0	—	—

The properties of cholinesterase present in sow's colostrum and milk were investigated in connection with studies on the variation of esterase activities of milk and plasma of swine during the course of lactation and suckling [3]. The most characteristic feature of this esterase (Table 1) is the rapid hydrolysis of choline esters and phenyl esters; in the first group of esters butyrylcholine is hydrolysed at the highest rate, in the second group the acetate is hydrolysed more rapidly than both the propionate and butyrate. The specificity pattern with choline esters as substrates differs from those of all other cholinesterases known, except that of swine plasma cholinesterase which contains the same enzyme in 20—25 times lower concentration; the exceptional substrate specificity of the plasma enzyme as far as choline esters are concerned was reported previously [4,5]. Both acetylcholine and propionylcholine are hydrolysed more slowly than butyrylcholine, and acetylcholine more rapidly than propionylcholine. Benzoylcholine and succinylcholine are also split by the milk esterase; the hydrolysis of the latter ester is exceptional since no other animal tissue so far studied hydrolyses this ester at such a relatively high rate.

It was demonstrated in summation experiments, as well as in inhibition experiments with selective esterase inhibitors, that a single enzyme in sow's milk is responsible for the hydrolysis of both the choline and aromatic esters tested. It is characteristic of this esterase that butyrylcholine and phenyl acetate are hydrolysed at about the same high rate when tested at the same substrate concentration ($[S] > 5 \times 10^{-3}$ M); in this concentration range K_S is the same for the two reactions (2.8×10^{-3}). Triglycerides are also

The optimum pH range of the extraction varies for different barbiturates, but a pH of 8.0 is suitable for most of the compounds.

Chloroform can be used for the extraction of the N-substituted compounds and of 5-*iso*amyl-5-ethyl- and 5-allyl-5-phenyl-barbituric acids. Chloroform with 20 % dioxane is suitable for 5-ethyl-5-phenyl-barbituric acid. Chloroform with 20 % of benzyl alcohol extracts 5,5-diallyl-, 5,5-diethyl-, 5-allyl-5-*iso*propyl-, and 5-ethyl-5-*cyclo*hexenyl-barbituric acids.

The infrared spectra of some barbituric acids and their compounds with sodium, barium, and mercuric ions indicate that the mercury forms complexes rather than salts with the barbituric acids.

Of compounds containing nitrogen and having a structure similar to barbituric acid certain hydantoins and cyclic imides of dicarboxylic acids will be extracted and interfere.

The method has been applied to the determination of barbituric acids in blood. A full report will be published elsewhere.

1. Heyndrick, A. *J. pharm. belg.* **9** (1954) 132.
2. Pedley, E. *J. Pharm. and Pharmacol.* **2** (1950) 39.
3. Pfeil, E. and Goldbach, H.-J. *Z. physiol. Chem. Hoppe-Seyler's* **302** (1955) 263.
4. Richterich, R. *Clin. Chim. Acta* **3** (1958) 183.

Received June 7, 1958.

A New Type of Cholinesterase in Sow's Milk

KLAS-BERTIL AUGUSTINSSON

Institute of Organic Chemistry and Biochemistry, University, Stockholm, Sweden

Choline esters are generally not hydrolysed by milk. In two instances, however, milk was shown to exhibit high or moderate cholinesterase activity (acetylcholine used as substrate), *i.e.*, the colostrum of dog [1] and the colostrum and milk of swine [2]. These two sources of cholinesterases are interesting species differences in biochemical behaviour for which no biological explanation is known so far.

Table 1. Enzymic hydrolysis of various choline esters and phenyl esters by the milk of sow and cow. Substrate concentration, 0.01 M. Activity expressed in b_{30} per 0.1 ml of milk.

Acyl radical	Choline esters		Phenyl esters	
	Sow	Cow	Sow	Cow
Acetyl	290	0	465	1
Propionyl	280	1	255	1.5
Butyryl	500	1	205	0
Benzoyl	65	1	—	—
Succinyl	55	0	—	—

The properties of cholinesterase present in sow's colostrum and milk were investigated in connection with studies on the variation of esterase activities of milk and plasma of swine during the course of lactation and suckling [3]. The most characteristic feature of this esterase (Table 1) is the rapid hydrolysis of choline esters and phenyl esters; in the first group of esters butyrylcholine is hydrolysed at the highest rate, in the second group the acetate is hydrolysed more rapidly than both the propionate and butyrate. The specificity pattern with choline esters as substrates differs from those of all other cholinesterases known, except that of swine plasma cholinesterase which contains the same enzyme in 20—25 times lower concentration; the exceptional substrate specificity of the plasma enzyme as far as choline esters are concerned was reported previously [4,5]. Both acetylcholine and propionylcholine are hydrolysed more slowly than butyrylcholine, and acetylcholine more rapidly than propionylcholine. Benzoylcholine and succinylcholine are also split by the milk esterase; the hydrolysis of the latter ester is exceptional since no other animal tissue so far studied hydrolyses this ester at such a relatively high rate.

It was demonstrated in summation experiments, as well as in inhibition experiments with selective esterase inhibitors, that a single enzyme in sow's milk is responsible for the hydrolysis of both the choline and aromatic esters tested. It is characteristic of this esterase that butyrylcholine and phenyl acetate are hydrolysed at about the same high rate when tested at the same substrate concentration ($[S] > 5 \times 10^{-3}$ M); in this concentration range K_S is the same for the two reactions (2.8×10^{-3}). Triglycerides are also

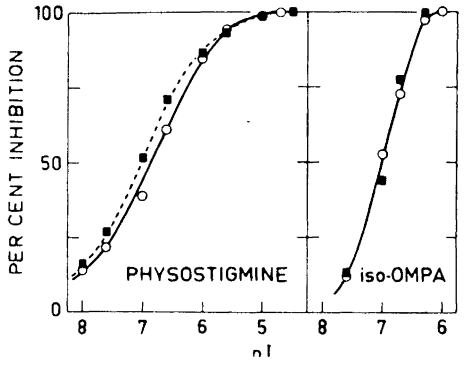

Fig. 1. Inhibition of sow's milk esterase by physostigmine salicylate and tetra-*iso*propyl-pyrophosphoramide (iso-OMPA). Substrates (0.01 M): butyrylcholine iodide (■) and phenyl acetate (○). pI = — log molar inhibitor concentration in the reaction mixture. Enzyme incubated 50 min with the inhibitor prior to addition of substrate.

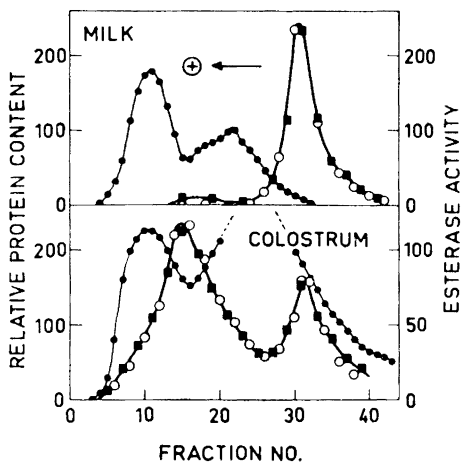

Fig. 2. Electropherograms of sow's milk and colostrum obtained with 3.0 ml material in cellulose columns (1.5 cm. × 40 cm.; veronal buffer, pH 8.4, $I = 0.1$). Displacement from the column in 1.5 ml fractions. Thin line (●): relative protein contents (optical density of the Folin colour). Heavy line: esterase activity (b_{30}/0.4 ml fractions); ■, butyrylcholine; ○, phenyl acetate.

hydrolysed by this enzyme, but the hydrolysis rate is only 1—3 % of those obtained with butyrylcholine and phenyl acetate.

The esterase is a cholinesterase, because it is sensitive to both physostigmine and organophosphorus compounds ($pI_{50} > 5$). Phenothiazine derivatives (*e.g.*, 10-[-diethylamine-propionyl] phenothiazine hydrochloride) are comparatively strong inhibitors, indicating that the enzyme is classified as a Group II cholinesterase [6], to which the butyrylcholinesterases of other sources belong. The sensitivity to 62C47 (1,5-bis[4-trimethyl-ammoniumphenyl] pentane-3-one diiodide) is in favour of this suggestion. Fig. 1 shows the inhibition curves obtained with butyrylcholine and phenyl acetate as substrates and physostigmine and iso-OMPA (tetra-*iso*propylpyrophosphoramide) as inhibitors; these results are indicative evidence that the same enzyme hydrolyses the two substrates. The inihibition by physostigmine differs from that of other cholinesterases by not being of the true competitive type.

Additional proof for the existence of one esterase in sow's milk was performed by electrophoresis analysis in cellulose columns [7]. Typical electrophoresis patterns of sow's milk and colostrum are illustrated in Fig. 2. The milk electropherogram is characteristic by a sharp esterase peak, being due to the highly active butyrylcholinesterase, which moves slower than all major milk protein components. In contrast to mature milk, colostrum gives an electropherogram in which a second, faster-moving peak is much more prominent, and the slow-moving peak correspondingly reduced. The two esterase fractions of colostrum have identical properties, as far as enzyme specificity and sensitivity to inhibitors are concerned. The mobility of the faster-moving cholinesterase fraction of colostrum is identical with the cholinesterase fraction of swine plasma, and the substrate specificity and other properties are also the same for the two fractions. It is therefore suggested that the faster-moving esterase component of sow's colostrum and swine plasma cholinesterase are identical, and that the electrophoretic mobility of the esterase present in colostrum is previously lowered during the course of lactation.

Evidence has been presented recently that esterases are localized mainly in the microsomes of animal tissues. Milk con-

tains microsomes [8] which are derived from mammary tissue and might serve as a vehicle for its butyrylcholinesterase. It may therefore well be that the slow-moving component represents microsomal esterase and the fast-moving one, free enzyme.

A full account of this work including studies on the esterases present in swine plasma will be published in *Biochem. J.*

This investigation was supported by a grant from the *Swedish Natural Science Research Council*. I am grateful to Dr. Bertil Olsson (Royal Veterinary College, Stockholm) for the milk samples.

1. McCance, R. A., Hutchinson, A. O., Dean, R. F. A. and Jones, R. E. H. *Biochem. J.* **45** (1949) 493.
2. Hines, B. E. and McCance, R. A. *J. Physiol.* **122** (1953) 188.
3. Augustinsson, K.-B. and Olsson, B. *Biochem. J. In press.*
4. Levine, M. G. and Suran, A. A. *Nature* **166** (1950) 698; *Enzymologia* **15** (1951) 17.
5. Myers, D. K. *Biochem. J.* **55** (1953) 67.
6. Augustinsson, K.-B. *Methods Biochem. Anal.* **5** (1957) 1.
7. Augustinsson, K.-B. *Nature* **181**(1958) 1786.
8. Bailie, M. J. and Morton, R. K. *Biochem. J.* **69** (1958) 35.

Received June 14, 1958.

ACTA CHEMICA SCANDINAVICA 12 (1958) 1153—1166

On Vitamins in Sewage Sludge

VII. Production of Vitamin B_{12} by an Enrichment Culture of *Methanobacterium omelianskii*

HALINA Y. NEUJAHR and DANLEY A. CALLIERI

Royal Institute of Technology, Division of Food Chemistry, Stockholm 70, Sweden

An enrichment culture of *Methanobacterium omelianskii* was grown in the synthetic medium of Barker with and without the addition of various compounds. The ability of the culture to produce vitamin B_{12} factors was investigated.

The culture was shown to produce one single vitamin B_{12} factor when grown in the simple Barker medium. This factor has an R_c-value = 0.7 (R_F-value relative to that of cyanocobalamin) and could not be identified with any other factor. It is called factor Met. In the presence of Co^{2+}, factors B and Z were produced simultaneously with factor Met. It is suggested that both these latter factors are precursors of factor Met and cyanocobalamin. When supplied with 5,6-dimethyl benziminazole and Co^{2+}, the culture produced only cyanocobalamin, the yield of which was 80 mμg/ml. The addition of Bacto Peptone stimulated the formation of vitamin B_{12} activity, mainly due to the formation of factor Met. Cyanocobalamin was formed only when 5,6-dimethyl benziminazole was supplied and its yield was not increased by Bacto Peptone. It is suggested that the enrichment culture has a limited synthetic ability with respect to 5,6-dimethyl benziminazole but can produce all the other parts of the vitamin B_{12} molecule and join them together. Unlike 5,6-dimethyl benziminazole, adenine could not be used by the culture to produce $\psi-B_{12}$. The ability of sterilized sewage and sewage sludge to maintain the growth and vitamin B_{12} production of the enrichment culture was also investigated.

The culture did not produce any vitamins of the folic and folinic acid groups. Cu++ was found to have an inhibiting effect upon the growth and vitamin B_{12} production of the culture.

The anaerobic bacterium *Methanobacterium omelianskii* was isolated in pure culture by Barker in 1939[1]. This organism appears to be one of the most abundant bacteria active in the anaerobic digestion of sewage sludge[2]. It has been shown in previous reports from this laboratory[3] that the anaerobic digestion of sewage sludge is accompanied by a considerable production of vitamin B_{12} factors. It was therefore interesting to investigate the ability

of *Methanobacterium omelianskii* to produce vitamin B_{12} factors. A pure strain of *Methanobacterium omelianskii* was received through the courtesy of Professor Barker. However, this strain proved to be very difficult to handle and, in fact, we were not able to obtain an active, quickly fermenting culture from it.

Barker's method was used to isolate a strain of *Methanobacterium omelianskii* from digesting sewage sludge but required, of course, a considerable amount of time. The ability of this strain to produce vitamin B_{12} will be investigated in the near future. In the present work, the authors used enrichment cultures of *Methanobacterium omelianskii* prepared from digesting sludge by successive reinoculations into the medium of Barker [1]. Microscopic examinations of such cultures revealed that they consisted mostly of *Methanobacterium omelianskii*. They proved to be very convenient for large experimental series since, with the chosen, carefully standardized conditions, the gas production started relatively soon after the inoculation and it was found that the agreement between the parallel series was very good. The determination of the gas production is of special importance when culturing methane bacteria since these bacteria tend to form bulky precipitates and occur mostly in the sediment thus making accurate turbidity measurements impossible. The quantity of gas evolved is a good measure of the amount of growth.

Using such an enrichment culture of *Methanobacterium omelianskii*, the authors investigated its ability to produce vitamin B_{12} factors, partly in the simple medium elaborated by Barker [1], which contains ethanol as the only organic compound, and partly in the Barker medium with various additions, *e.g.* organic nutrient extracts, Co^{2+}, Cu^{2+}, 5,6-dimethyl benziminazole, adenine. The ability of the culture to ferment sterilized sewage and sewage sludge was also investigated.

EXPERIMENTAL

The enrichment culture of *Methanobacterium omelianskii* was prepared by successively reinoculating a raw culture obtained from digesting sludge using the medium given by Barker [1]: K_2HPO_4 0.6 %; KH_2PO_4 0.9 %; $(NH_4)_2SO_4$ 0.03 %; $MgSO_4 \cdot 7\ H_2O$ 0.01 %; $FeSO_4 \cdot 7\ H_2O$ 0.001 %; saturated $CaSO_4$ solution 1 %; C_2H_5OH 2 % and tap water. An additional component (2 ml of 1 % $Na_2S \cdot 9\ H_2O$ solution +8 ml of 5 % $Na_2CO_3 \cdot 10\ H_2O$ solution) was sterilized separately and added to every 100 ml of the medium.

A few milliliters of digesting sludge were put into 300 ml substrate in a conical flask and incubated at 37°C. When the gas evolution became considerable, a reinoculation was done in the same way, followed by a second reinoculation and so on. After 10—15 reinoculations the culture was almost totally free from the initial sludge solids.

The inocula for the experimental series were prepared from the enrichment culture by reinoculating into the same medium in conical flasks of 100—300 ml capacity and incubating until a considerable gas evolution was established (usually 2—10 days). During the earlier part of the work, longer periods, 7—10 days, were usually required to obtain an active inoculum whereas, in the later series, an active inoculum could be obtained even after 2—3 days.

The experimental series were performed in test tubes of 15 ml capacity. Each series consisted of several identical tubes which were removed one by one during the course of the experiment, their contents being analyzed for vitamin B_{12} activity. Each tube contained a small gas tube and was filled with 5 ml of the medium. After sterilization, 0.5 ml of the separately sterilized component was put into each tube and thereafter, at an appropriate temperature, 5 drops of the inoculum were released from a pipet.

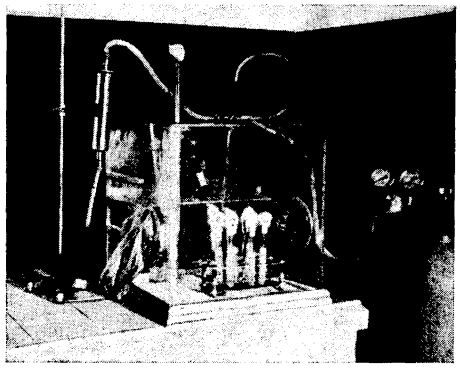

Fig. 1. Carbon dioxide chamber for inoculating methane bacteria. For description see text.

To *ensure anaerobic conditions* all manipulations, *e. g.* necessary additions to the medium, inoculations and reinoculations, were performed in a specially constructed chamber (Fig. 1). The chamber consisted of a box (40 × 40 × 40 cm) five sides of which consisted of plexiglas plates firmly attached to each other whereas the sixth consisted of a wooden base plate provided with tightening arrangements along its edges. The upper (plexiglas) part could be easily removed from the bottom plate so that the various vessels could be put inside. The two parts of the box fitted tightly together. The chamber was provided with gas inlets and outlets, a few openings for the insertion of pipets and two openings with plastic sleeves for the hands. Compressed carbon dioxide or nitrogen could be passed into the chamber at its bottom and removed at the top. Both gases passed a microbiological filter before entering the chamber. The substrate-containing vessels were put into the chamber while still hot after the sterilization in the autoclave, nitrogen being blown through the chamber at 0.5 kg/cm². The extra component was then added to the substrate. When the temperature of the substrate had reached 40 – 30°C, carbon dioxide instead of nitrogen was blown * through (0.5 kg/cm²) and the reinoculations were performed.

All the cultures were incubated at 37°C.

To *maintain the anaerobic conditions after the inoculation* the liquid surfaces in the tubes as well as in the conical flasks were covered with a 0.5 – 1 cm thick layer of sterilized paraffin oil. During the first of these investigations, the test tubes and flasks were also plugged with cotton wool impregnated with an alkaline pyrogallol solution (containing equal parts of 20 % pyrogallol solution and 20 % K_2CO_3 solution). This additional security was found superfluous in later work and the tubes were plugged with ordinary cotton wool.

Sampling was achieved by removing a tube from each series at appropriate time intervals. The samples were autoclaved with cyanide (100 μg KCN/ml sample) and kept at −20°C. Their activity for *E. coli* 113 – 3 and, in a few cases, also for *S. faecalis* and *Leuconostoc citrovorum*, was determined in the cup plate assay. The presence of different vitamin B_{12} factors [4] was revealed by bioautography on *E. coli* plates using chromatography in two solvent systems as described elsewhere [5] and by ionophoresis according to Holdsworth [6]. The R_F-values of the chromatographic spots are always given relative to that of cyanocobalamin and are called R_c. Two groups of experiments were performed. In the first group (expts 1 – 4) an inoculum was used which had been obtained by ten successive reinoculations of the raw culture into the medium of Barker [1]. The second group of experiments was performed several months later and the inoculum was obtained

* Carbon dioxide was not introduced from beginning in order to avoid pH-changes in the substrate.

by twenty five successive reinoculations. The details of the different experiments were as follows:

Experiment 1. Influence of different nutrients. Preliminary investigation. The following additions to Barker's medium were made: Co^{2+} 2 500 mμg/ml; Bacto Vitamin-free Casamino Acids (Difco) 0.25 %; Bacto Yeast Extract Dehydrated (Difco) 0.25 %; Bacto Peptone (Difco) 0.25 %; biotin 0.002 ppm. Samples were taken 3, 10, 17 and 30 days after the beginning of gas evolution. The results are given in Table 1.

Experiment 2. Influence of 5,6-dimethyl benziminazole and adenine. The two bases were added to the medium at the following levels: 100; 1 000 and 10 000 mμg/ml. The simple Barker medium was used both without any addition (a) and also with the addition of 0.25 % Bacto Peptone (b). Samples were taken 3, 10, 17 and 30 days after the beginning of gas evolution. The results can be seen in Table 2 and Fig. 2.

Experiment 3. Influence of Co^{2+}. The following additions of Co^{2+} were used: 0; 1 000; 2 000; 5 000; 10 000 and 25 000 mμg/ml*. The Co^{2+} was added to the medium as $CoCl_2 \cdot 6H_2O$. Barker's medium without (a) and with 0.25 % Bacto Peptone (b) was used. Samples were taken after 3, 10, 17 and 30 days. The results are given in Table 3.

Experiment 4. Influence of Cu^{2+}. The following additions of Cu^{2+} were used: 0; 1 000; 2 000; 5 000; 10 000 mμg/ml. The Cu^{2+} was added to the medium as $CuSO_4 \cdot 5 H_2O$. Barker's medium without (a) and with 0.25 % Bacto Peptone (b) was used. Samples were taken after 3, 10, 17 and 30 days. The results can be seen in Table 4.

Experiment 5. Influence of Co^{2+} and of 5,6-dimethyl benziminazole in the simple medium. Three parallel series were performed with (I) the medium of Barker (a), (II) (a) with added 3 000 mμg Co^{2+}/ml, (III) (a) with added 3 000 mμg Co^{2+}/ml and 1 000 mμg 5,6-dimethyl benziminazole/ml. Samples were taken every day. The results are given in Figs. 2a, 2b and 2c.

Experiment 6. Influence of Co^{2+} and 5,6-dimethyl benziminazole in the presence of Bacto Peptone. This experiment was performed in exactly the same way as expt. 5, except that the Barker medium was supplemented with 0.25 % Bacto Peptone. The results can be seen in Figs. 3a, 3b and 3c.

Experiment 7. In this experiment the ability of five "natural" substrates to maintain the growth of the enrichment culture was investigated. The substrates were taken from a sewage plant where the sewage is sedimented and where the sedimented solids (fresh sludge) undergo digestion in digestion tanks. Liquid separated during the digestion process is withdrawn and is called "digested sludge water". The effluent from the sedimentation tanks is not further treated.

The following five substrates were used in the experiment: incoming sewage, I; effluent, E; digested sludge water, W; fresh sludge, F; digested sludge diluted 100 times, D. The substrates were sterilized by tyndallization. F was diluted 10 times and D 10 times (called Dl). A part of D was alkali treated (called D2). I, E, and W were not diluted. The substrates were buffered with phosphate (total concentration 1.5 %) to pH 7.7.

The final substrates thus obtained had the following dry solid contents and *E. coli* activities:

Substrate	Dry solids mg/ml	*E. coli* activity calc. as cyanocobalamin mμg/ml
I	0.7	0.5
E	0.6	0.5
W	1.9	1.5
F	3.0	0.5
D	0.9	2.5
Dl	0.09	2.0
D2	0.9	—

Conical flasks of 100 ml capacity were filled with the different media, sterilized and inoculated with the enrichment culture. The results are given in Table 5.

* Due to the presence of S^{2-} the actual concentration of Co^{2+} in the fermentation liquor was probably lower than indicated by the additions.

RESULTS AND DISCUSSION

Experiment 1. Yeast extract, peptone and casamino acids stimulated considerably the growth of the culture as deemed by the gas evolution. Yeast extract was most effective in this respect — the gas started to evolve after only 60 h of incubation as compared with about 100 h for the cultures containing the other two organic nutrients. The addition of Co^{2+} (2.5 μg/ml) in the absence of organic nutrients seemed to retard the growth of the culture — the gas evolution starting after ~ 200 h of incubation. This phenomenon, however, could not be observed in later experiments in which a more purified enrichment culture was used. Biotin was without effect upon the growth.

The effect of the nutrient additions upon the formation of vitamin B_{12} factors can be seen in Table 1. The total *E. coli* activity is markedly stimulated by the different additions, except biotin. The stimulating effect depends

Table 1. Influence of different nutrients on vitamin B_{12} production by an enrichment culture of *Methanobacterium omelianskii;* medium according to Barker; underlined factors occur in the largest amounts and the factors within brackets in the smallest amounts.

Met designates a factor — not yet identified — which is specifically produced by the culture. It has a R_c-value = 0.7 in solvent system I[5].

Additions	*E. coli* activity in samples taken			
	after 3 days of fermentation		after 10 days of fermentation	
	mμg/ml *	factors	mμg/ml *	factors
No addition	30	Met; B; (Cy); (Z)	40	Met
Co^{2+} 2 500 mμg/ml	200	B; (Met); (Z)	120	B; (Met); (Z)
Casaminoacids 0.25 %	50	Met; B; Z (III)	80	Met
Casaminoacids 0.25 % + Co^{2+} 2 500 mμg/ml	60	Met; Z; B	110	Met
Yeast extract 0.25 %	80	Met; III; (Z) (B)	80	Met
Yeast extract 0.25 % + Co^{2+} 2 500 mμg/ml	120	Met; Z; (B)	100	Met
Bactopeptone 0.25 %	90	Met; III; Z; (Cy)	150	Met
Bactopeptone 0.25 % + Co^{2+} 2 500 mμg/ml	90	Met; III; Z; (Cy)	90	Met
Casaminoacids 0.25 % + biotin 2 mμg/ml	30	Z; (B)	70	Met
Casaminoacids 0.25 % + biotin 2 mμg/ml + Co^{2+} 2 500 mμg/ml	70	Z; (B)	90	Met
Biotin 2 mμg/ml	20	Met; (Cy); (B)	50	Met
Biotin 2 mμg/ml + Co^{2+} 2 500 mμg/ml	300	B; (Z); (Cy)		B; (Z)

* Calculated as cyanocobalamin, cup plate assay.

probably upon the better growth of the culture obtained with the active nutrients. It can be seen in Table 1 that, at the beginning of the fermentation, the culture produced, in most cases, smaller amounts of several factors together with a greater amount of one single factor whereas after 10 days of fermentation only this latter factor was produced. It is a striking fact that cyanocobalamin was not produced at all. The very small amounts of cyanocobalamin produced in the beginning of the fermentation could not be found in later investigations with a more purified enrichment culture. The addition of Co^{2+} alone, or together with biotin, markedly stimulated the formation of factor B. It is easily seen in Table 1 that biotin does not contribute to this effect. Since factor B has been shown to be the fundamental part of all B_{12} vitamins [7] so far characterized, the phenomenon observed suggests that the enrichment culture has a limited synthetic ability with respect to the other parts of the vitamin B_{12} molecule. From Table 1, it seems evident that the enrichment culture of *Methanobacterium omelianskii*, grown in the simple Barker medium, produces specifically one single vitamin B_{12} factor, albeit in limited amounts. This has also been proved by all later experiments. So far we have not succeeded in identifying this factor with any other vitamin B_{12} factor hitherto described (*cf.* p. 1165). It is provisionally called factor Met. The culture produces greater amounts of this factor when supplied with some organic nutrient (see Table 3). It cannot, however, be concluded whether these additions stimulate the formation of factor Met *per se* or if the effect depends merely upon the enhanced growth of the culture.

Table 2. Influence of 5,6-dimethylbenziminazole and adenine on vitamin B_{12} production by an enrichment culture of *Methanobacterium omelianskii;* a — medium according to Barker; b — medium according to Barker + 0.25 % Bactopeptone; DMB — 5,6-dimethyl benziminazole; Ad — adenine.

Medium	Additions mμg/ml medium	Largest *E. coli* activity obtained (usually in samples taken after 20—30 days of fermentation)	
		mμg/ml *	factors present
a	No	15	Met
b	No	30	Met
a	DMB 100	25	cyanocobalamin
a	Ad 100	20	Met
b	DMB 100	20	cyanocobalamin
b	Ad 100	45	Met
a	DMB 1 000	30	cyanocobalamin
a	Ad 1 000	40	Met
b	DMB 1 000	40	cyanocobalamin
b	Ad 1 000	40	Met
a	DMB 10 000	10	cyanocobalamin
a	Ad 10 000	40	Met
b	DMB 10 000	15	cyanocobalamin
b	Ad 10 000	60	Met

* Calculated as cyanocobalamin.

Since Bacto Peptone evidently had the greatest stimulating effect upon the formation of factor Met, we chose this nutrient as a standard addition to the medium in several further experiments.

Experiment 2. This experiment was performed in order to elucidate whether the formation of factor Met by the enrichment culture is to be considered as an individual biochemical feature of the culture or whether it was merely caused by absence of precursors for other vitamin B_{12} factors when the culture was grown in the simple Barker medium [1] or in this medium modified as in expt. 1.

It can be seen in Table 2 that the culture produces cyanocobalamin when supplied with the specific base of this factor — 5,6-dimethyl benziminazole. Adenine, however, which is the specific base of ψ-B_{12}, cannot be utilized by the culture to produce the corresponding factor. Instead of ψ-B_{12}, factor Met is produced as in the case without the addition of adenine. These results suggest that the organism is unable to synthesize 5,6-dimethyl benziminazole but can synthesize all the other parts of the cyanocobalamin molecule and couple them together. Such a suggestion cannot of course be conclusive since only an enrichment culture, and not a pure strain, was used in this experiment. It would be interesting to see if some compounds of adenine, *e.g.* the appropriate nucleoside and nucleotide, can be utilized in a better way by the culture. Such compounds, however, were not available in this preliminary study.

For subsequent experiments, 1 000 mμg/ml of 5,6-dimethyl benziminazole was chosen as a standard addition.

Experiment 3. The highest total *E. coli* activity was obtained with 2 000 —5 000 mμg Co^{2+}/ml of medium a (*cf.* Table 3). The activity values reached,

Table 3. Influence of Co^{2+} on vitamin B_{12} production by an enrichment culture of *Methanobacterium omelianskii;* a — medium according to Barker [1]; b — medium according to Barker +0.25 % Bactopeptone.

Medium	Amount of Co^{2+} in the medium mμg/ml	*E. coli* activity in samples taken after 10 days of fermentation **	
		mμg/ml *	factors present
a	0	10	Met
b	0	30	Met
a	1 000	480	Met (B)
b	1 000	140	Met; B; Cy; (Z)
a	2 000	550	Met; (B); (Cy)
b	2 000	150	Met; (B); (Cy)
a	5 000	640	Met; B; (Cy); (Z)
b	5 000	160	Met; B; Cy; Z
a	10 000	470	Met; B
b	10 000	110	Met; B
a	25 000	490	Met; (B); (Z)
b	25 000	310	Met; (B); (Z)

* Calculated as cyanocobalamin.

** These samples contained the highest activity obtained in the series.

Table 4. Influence of Cu^{2+} on vitamin B_{12} production by an enrichment culture of *Methanobacterium omelianskii;* a — medium according to Barker [1]; b — medium according to Barker + 0.25 % Bactopeptone.

Medium	Amount of Cu^{2+} in the medium mμg/ml	*E. coli* activity in samples taken after 20 days of fermentation **	
		mμg/ml *	factors present
a	0	20	Met
b	0	100	Met
a	1 000	20	Met
b	1 000	30	Met
a	2 000	10	Met
b	2 000	30	Met
a	5 000	9	Met
b	5 000	30	Met
a	10 000	7	Met
b	10 000	30	Met

* Calculated as cyanocobalamin.
** These samples contained the highest activity obtained in the series.

640 mμg/ml (calculated as cyanocobalamin), are much higher than the corresponding values obtained in expt. 1. The latter values were also confirmed in later experiments. The main factor produced was factor Met. With 5 000—10 000 mμg Co^{2+}/ml, considerable amounts of factor B were

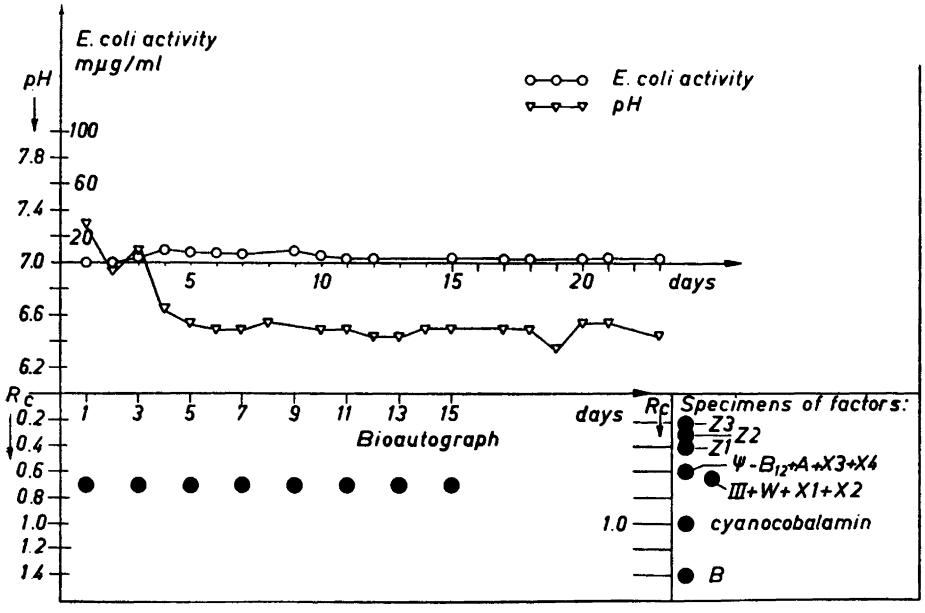

a.

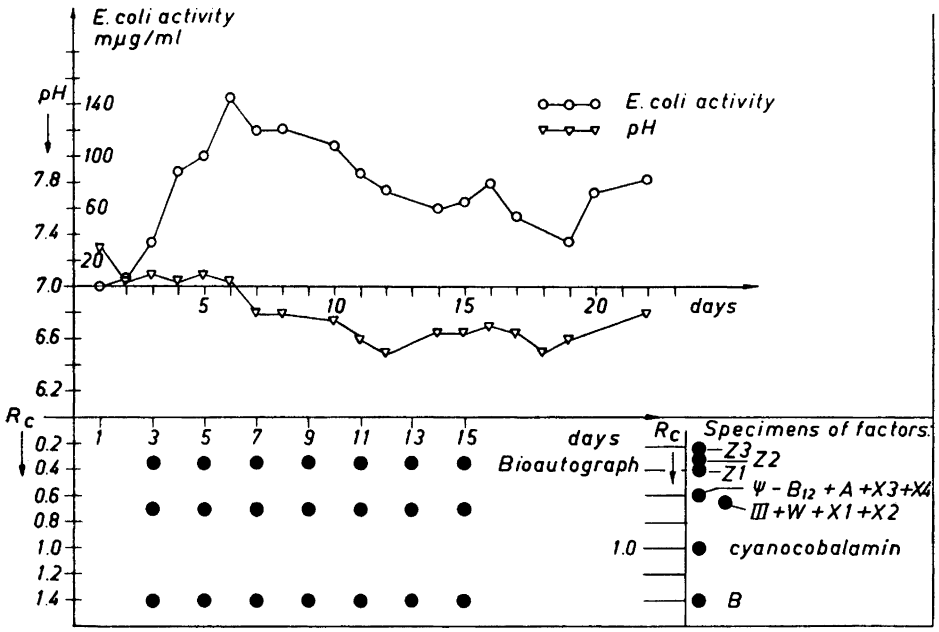

b.

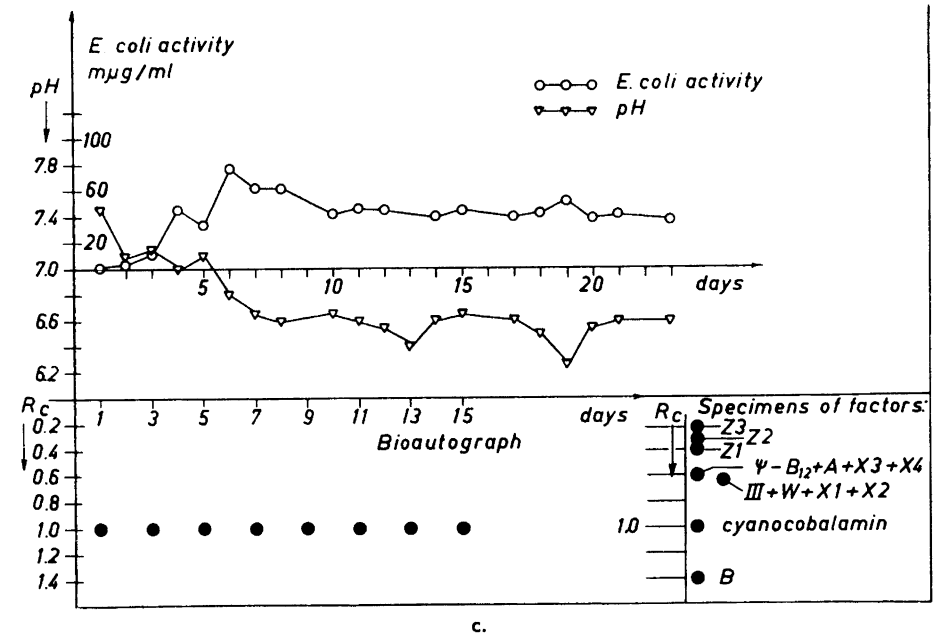

c.

Fig. 2. Fermentation and vitamin B_{12} production by an enrichment culture of *Methanobacterium omelianskii* grown in the medium of Barker:

a. not supplemented;
b. supplemented with Co^{2+} (3 000 mμg/ml);
c. supplemented with Co^{2+} (3 000 mμg/ml) and 5,6-dimethyl benziminazole (1 000 mμg/ml).

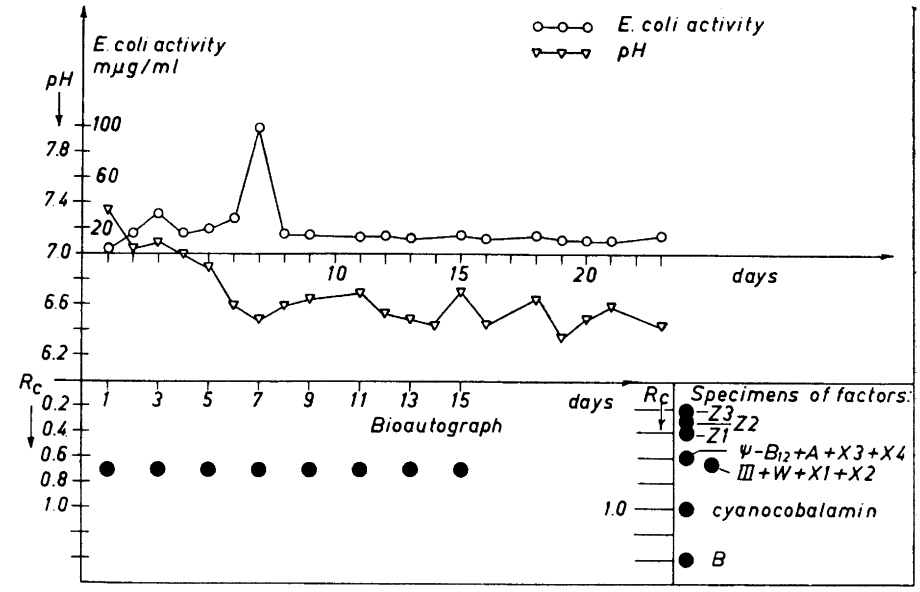
E. coli activity
pH
E. coli activity
mμg/ml
pH
100
60
20
7.8
7.4
7.0
6.6
6.2
10
15
20
days
Rc
0.2
0.4
0.6
0.8
1.0
1
3
5
7
9
11
13
15
days
Bioautograph
Rc
Specimens of factors:
Z3
Z2
Z1
Ψ-B12+A+X3+X4
III+W+X1+X2
1.0
cyanocobalamin
B

a.

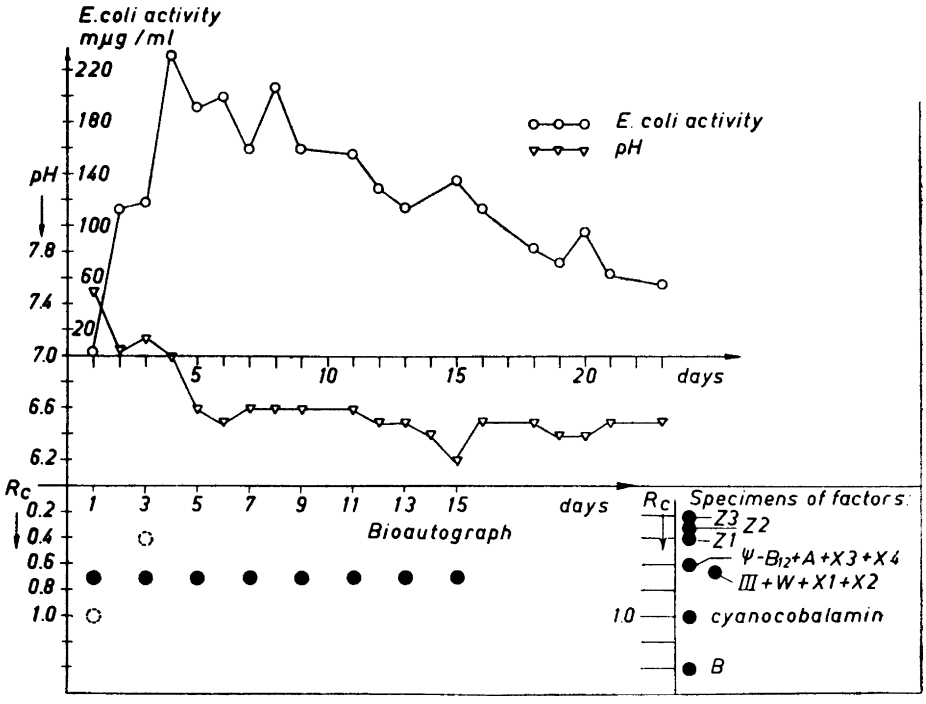
E.coli activity
mμg /ml
220
180
140
100
60
20
pH
7.8
7.4
7.0
6.6
6.2
E. coli activity
pH
5
10
15
20
days
Rc
0.2
0.4
0.6
0.8
1.0
1
3
5
7
9
11
13
15
days
Bioautograph
Rc
Specimens of factors:
Z3
Z2
Z1
Ψ-B12+A+X3+X4
III+W+X1+X2
1.0
cyanocobalamin
B

b.

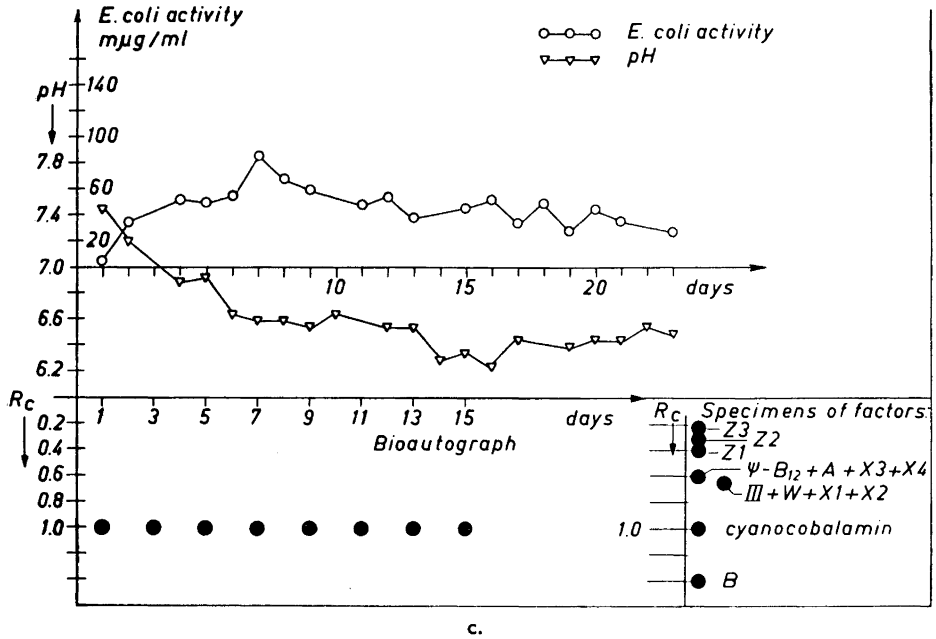

Fig. 3. Fermentation and vitamin B_{12} production by an enrichment culture of *Methanobacterium omelianskii* grown in the medium of Barker modified by the addition of 0.25 % Bacto Peptone:

a. not supplemented;
b. supplemented with Co^{2+} (3 000 mμg/ml);
c. supplemented with Co^{2+} (3 000 mμg/ml) and 5,6-dimethyl benziminazole (1 000 mμg/ml).

also formed. For subsequent experiments, 3 000 mμg/ml of Co^{2+} was chosen as standard addition.

Experiment 4. 1 000—2 000 mμg Cu^{2+}/ml had a retarding effect upon the growth and vitamin B_{12} production of the enrichment culture. 5 000—10 000 mμg Cu^{2+}/ml markedly inhibited both growth and vitamin B_{12} production (*cf.* Table 4).

Experiment 5. The results of this experiment which has been performed more thoroughly and with a more purified enrichment culture than expts. 1—4 confirm the preliminary findings of these early experiments. An examination of Fig. 2a, 2b and 2c leads to the following conclusions:

1) When grown in the simple Barker medium, the enrichment culture of *Methanobacterium omelianskii* produces one single factor Met (with $R_c = 0.7$) as shown by chromatography and ionophoresis (*cf.* p. 1165). The yield of factor Met is rather low and corresponds to at most 10 mμg/ml calculated as cyanocobalamin (*cf.* Fig. 2a).

2) When supplied with Co^{2+} (3 000 mμg/ml), the culture produces factors B and Z together with factor Met suggesting that both the two former factors

are precursors of factor Met and cyanocobalamin. The total *E. coli* activity is at most 140 mμg/ml calculated as cyanocobalamin (*cf.* Fig. 2b).

3) With Co^{2+} (3 000 mμg/ml) and 5,6-dimethyl benziminazole (1 000 mμg/ml), the culture produces only cyanocobalamin, the yield of which is at most 80 mμg/ml (*cf.* Fig. 2c).

Experiment 6. It can be seen from Fig. 4a that the addition of Bacto Peptone to the simple Barker [1] medium stimulates the formation of *E. coli* activity (*cf.* Fig. 3a) but does not influence the kind of factors formed since, as before, factor Met is exclusively produced. With Co^{2+} (3 000 mμg/ml) in the modified medium, only factor Met is again formed (see Fig. 3b) except in the beginning of the fermentation when small amounts of cyanocobalamin and of one of the factors Z are formed. The fermentation in the presence of Bacto Peptone differs in this respect markedly from that without this nutrient (*cf.* Fig. 2b). The total *E. coli* activity in the presence of Bacto Peptone is much higher than in experiment 5 and reaches at most 240 mμg/ml. With additions of Co^{2+} and 5,6-dimethyl benziminazole (see Fig. 3c), cyanocobalamin is formed exclusively as in the corresponding experiment without Bacto Peptone (*cf.* Fig. 2c). The yield of cyanocobalamin is likewise of the same order of magnitude, *viz.* 85 mμg/ml.

Experiment 7. It can be seen in Table 5 that the sterilized and buffered effluent E and digested sludge, diluted 100 times, D, and 1 000 times, D1, could not be fermented by the enrichment culture. However, sterilized and buffered incoming sewage, I, digested sludge water, W, alkali treated diluted digested sludge, D2, and fresh sludge, F, could maintain the growth of the culture. The total *E. coli* activity/ml substrate was largest with fresh sludge (70 mμg/ml) and lowest with incoming sewage and alkali treated digested sludge (~15 mμg/ml. However, calculated on the basis of initial dry solid content, the yields obtained with fresh sludge and incoming sewage were

Table 5. The ability of sterilized sewage to maintain the growth and vitamin B_{12} production of an enrichment culture of *Methanobacterium omelianskii.*

Medium *	Initial pH	Begin. of gas evol. days	pH and *E. coli* activity in samples taken after 7 days of fermentation			15 days of fermentation		
			pH	*E. coli* activity ** mμg/ml	*E. coli* activity ** mμg per g initial solids	pH	*E. coli* activity ** mμg/ml	*E. coli* activity ** mμg per g initial solids
I	7.7	7	6.8	15	21 000	6.7	15	21 000
E	7.7	No evol.						
W	7.6	6	6.5	30	16 000	6.3	20	11 000
F	7.5	3	6.7	70	23 000	6.6	70	23 000
D	7.6	No evol.						
D1	7.7	No evol.						
D2	7.7	6	6.8	15	17 000	6.7	10	11 000

* For the characteristics of the different media, *cf.* p. 1156.
** Calculated as cyanocobalamin.

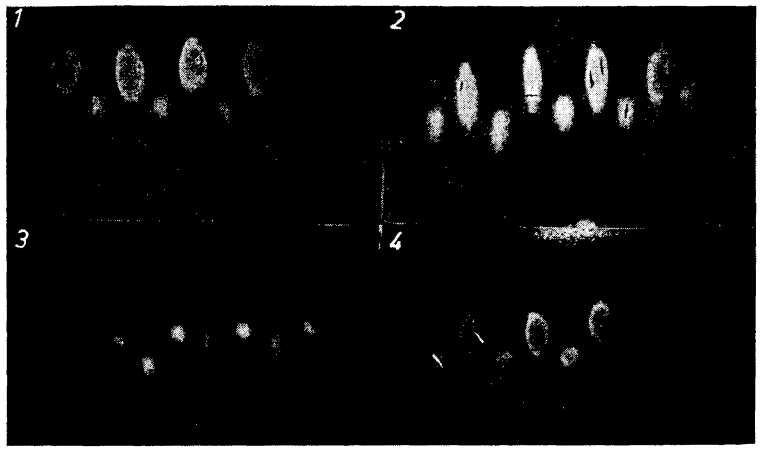

Fig. 4. Experiments to identify factor Met by paper chromatography. Bioautographs on *E. coli* 113—3 plates.
1. Factor A (upper spots) and factor Met (lower spots). 2. Factor X4 (upper spots) and factor Met (lower spots). 3. Factor W (upper spots) and factor Met (lower spots). 4. Factor III (upper spots) and factor Met (lower spots).

comparable ($\sim$ 20 000 mμg/g) and comparable with that of spontaneously digested sewage sludge. These yields are considerably higher than the yield obtained with the other substrates. Paper chromatography revealed two spots, one due to cyanocobalamin, the other due to some factor or factors with R_c in the range 0.6—0.7. As reported above, the factor produced by *Methanobacterium omelianskii* in synthetic substrates, factor Met, has a R_c-value = 0.7 and it might be that this factor is also produced when the enrichment culture is grown in sterilized sewage. This, however, has not yet been more closely investigated.

Experiments to identify factor Met. When chromatographed in solvent system I [5], factor Met moved distinctly quicker than all the other factors with R_c-values in the range 0.6—0.7. Some of the experiments are shown in Fig. 4, which contains bioautographs of some of the factors together with factor Met. Spots of factor Met were put on each chromatogram alternately with spots of the respective factors. The uncertainty due to uneven wandering of the solvent front was thus eliminated.

However, upon ionophoresis in 2 M HAc in the presence of KCN, the mobility of factor Met was found to be almost identical with that of factor W, factor III, cyanocobalamin and of the slower fraction of factor X4.

The latter factor, though found a homogeneous three years ago, has now been found to separate into two electrophoretic fractions, one with a mobility about that of factor B (or A?) (quick-moving) and the other with a mobility about that of factor Met (*cf.* Fig. 2). The solution of factor X4 was kept at —20°C but had been thawed on several occasions.

As has been noticed many times before, the identification of vitamin B_{12} factors on the basis of their chromatographic and ionophoretic mobilities very often seems to give misleading results.

Vitamins of the folic and folinic acid groups. Fermentations, performed with the enrichment culture of *Methanobacterium omelianskii* in the simple Barker medium with and without the addition of various compounds, were tested for *S. faecalis* and *Leuconostoc citrovorum* activity. No such activity could, however, be detected.

Acknowledgements. The authors are grateful to Professor H. Lundin, Head of the Division, for his encouraging interest in and valuable advice on the execution of this work.

REFERENCES

1. Barker, H. A. *Antonie van Leeuwenhoek* **6** (1939/40) 201.
2. Heukelekian, H. and Heinemann, B. *Sewage Works J.* **11** (1939) 426, 436, 571.
3. Neujahr, H. Y. *Acta Chem. Scand.* **9** (1955) 622.
4. Neujahr, H. Y. *Acta Chem. Scand.* **10** (1956) 917.
5. Neujahr, H. Y. *Acta Chem. Scand.* **11** (1957) 1191.
6. Holdsworth, E. S. *Nature* **171** (1953) 148.
7. *Biochemical Society Symposia No 13. The Biochemistry of Vitamin* B_{12}, Cambridge University Press 1955, p. 24.

Received March 29, 1958.

ACTA CHEMICA SCANDINAVICA 12 (1958) 1167—1175

On Vitamins in Sewage Sludge

VIII. Utilization of Some Vitamin B_{12} Factors by an Enrichment Culture of *Methanobacterium omelianskii*

HALINA Y. NEUJAHR and DANLEY A. CALLIERI

Royal Institute of Technology, Division of Food Chemistry, Stockholm 70, Sweden

An enrichment culture of *Methanobacterium omelianskii* was grown in the synthetic medium of Barker [3], with and without the addition of 1 000 mμg/ml of 5,6-dimethyl benziminazole and some vitamin B_{12} factors previously isolated from sewage sludge.

In the absence of 5,6-dimethyl benziminazole, most factors were converted to factor Met [1].

In the presence of 5,6-dimethyl benzimianzole, the incomplete factors B, Z1, Z2, Z3 and a greater part of the factor X4 preparation could easily be converted to cyanocobalamin by the culture.

The complete, nucleotide-containing factor W may also to a certain extent be converted to cyanocobalamin.

In a preceding paper [1], a series of experiments performed in order to investigate the ability of an enrichment culture of *Methanobacterium omelianskii* to produce vitamin B_{12} factors was reported. Using the same enrichment culture and an identical experimental technique, the authors have now investigated the ability of the culture to utilize some vitamin B_{12} factors previously isolated from sewage sludge [2]. The culture was grown in the synthetic medium of Barker [3] containing 2 % ethanol as the only organic compound. The different factors were added to the medium at levels of approximately 1 000 mμg/ml. Two series of experiments were made. Series I was a preliminary investigation and was carried out with a less purified enrichment culture. The inoculum had been prepared by ten successive reinoculations of the raw culture into Barker's medium. In series II, an inoculum was used which had been obtained by 25 successive reinoculations of the raw culture.

RESULTS AND DISCUSSION

Series I

From the results of the preliminary investigation which are shown in Table 1, it seems as though the different factors are converted by the enrichment culture into factor Met. The effectivity of the conversion seems be higher in the simple medium than in the presence of Bacto Peptone. However, when Bacto Peptone was present, cyanocobalamin was formed together with factor Met and this fact may account for the lower activity values obtained in the presence of Bacto Peptone. In plate assay with *E. coli*, several vitamin B_{12} factors are known to cause greater growth zones than cyanocobalamin and this may also apply to factor Met.

When adenine was added together with factor B or factor X4, small amounts of factor B were detected in the fermentation liquor together with factor Met but no ψ-B_{12} was found. Thus, adenine in the presence of factor B is not utilized for the production of ψ-B_{12}. This is in agreement with an earlier observation [1] that the enrichment culture of *Methanobacterium omelianskii* cannot use adenine to produce ψ-B_{12}. It is interesting to observe that the microbiologically inactive factor Z1 was converted in medium a to the microbiologically active factor Met. That a conversion really took place can be

Table 1. Utilization of Vitamin B_{12} factors by an enrichment culture of *Methanobacterium omelianskii;* a — medium according to Barker [3]; b — medium according to Barker + 0.25 % Bacto Peptone; Cy — cyanocobalamin, R_c = 1.0. Brackets mean that the factor in question is present only in small amounts.

Medium	Factor added	*E. coli* activity immediately after the addition mμg/ml *	Beginning of gas evolution h	*E. coli* activity in samples taken after 20 days of fermentation	
				mμg/ml *	Factors present **
a	no	0	40	20	Met
b	no	+	30	80	Met
a	factor B	170	40	130	Met
b	factor B +adenine	170	40	130	Met; (B)
b	factor B	1 000	30	70	Met
a	factor Z1	+	60	130	Met
b	factor Z1	+	30	15	Met; Cy
a	factor Z2	370	60	100	Met
b	factor Z2	1 000	30	70	Met; Cy
a	factor Z3	110	50	70	Met
b	factor Z3	600	30	80	Met; Cy
a	factor X4	60	60	90	Met (and X4?)
b	factor X4 +adenine	60	60	250	Met (and X4?); (B)
b	factor X4	140	30	180	Met (and X4?); (B)

* Calculated as cyanocobalamin in plate assay.
** Identified by chromatography and ionophoresis. Factor Met has R_c-value = 0.7.

seen from *E. coli* activity values: 20 mμg/ml when the fermentation was carried out without factor Z1 and 130 mμg/ml in the presence of it. The corresponding values for medium b cannot be so readily explained.

The conversion of factor B as well as factor X4 to factor Met (in medium a) seems to be more effective than the conversion of the other factors investigated.

The question of whether the enrichment culture of *Methanobacterium omelianskii* can utilize the different factors as precursors for the cyanocobalamin molecule has been more thoroughly investigated in Series II.

Series II

The fermentations of this series were carried out in the simple medium of Barker[3] supplemented with 1 000 mμg/ml of 5,6-dimethyl benziminazole. The different factors were added at levels of approximately 1 000 mμg/ml. A series of 24 tubes was prepared for every factor. Twenty of these were inoculated, the reamaining four serving as non-inoculated controls. A control

Table 2. Utilization of factor B by an enrichment culture of *Methanobacterium omelianskii*, grown in Barker's medium supplemented with 5,6-dimethyl benziminazole (1 000 mμg/ml); Cy = cyanocobalamin.

Time of fermentation (days)	pH	*E. coli* activity		Non-inoculated controls		
		mμg/ml*	factors present **	pH	*E. coli* activity	
					mμg/ml*	factors present **
0		1 130	B		1 130	B
0.5	7.2	1 130	B			
2	7.2	1 130	B			
3	6.6	750	B; (Cy)			
4	6.1	380	B; Cy	7.3	720	B
5	6.1					
6	6.1	90	Cy			
7	6.2	100	Cy			
9	6.3	110	Cy	7.7	690	B
10	6.3	70	Cy			
11	6.2	100	Cy			
12	6.2	100	Cy			
13	6.2	80	Cy			
14	6.3	60	Cy	7.7	320	B
16	6.2	70	Cy			
17	6.2	90	Cy			
18	6.2	60	Cy			
19	6.2	70	Cy			
20	6.3	70	Cy			
21	6.2	50	Cy			
27	6.1	60	Cy	8.3	410	B

* Calculated as cyanocobalamin in plate assay.
** Identified by paper chromatography in solvent system I[4].

Table 3. Utilization of factor Z1 by an enrichment culture of *Methanobacterium omelianskii*, grown in Barker's medium supplemented with 5,6-dimethyl benziminazole (1 000 mμg/ml); Cy = cyanocobalamin; Z = factor(s) Z.

Time of fermentation (days)	pH	*E. coli* activity		Non-inoculated controls		
		mμg/ml *	factors present **	pH	*E. coli* activity mμg/ml *	*E. coli* activity factors present **
0		5	Z1		5	Z1
0.5	7.2	5	Z; B; (Cy)			
2	7.1	30	Cy			
3	6.9	60	Cy			
4	6.2	60	Cy	7.4	4	B
5	6.3					
6	6.2	40	Cy			
7	6.4	70	Cy			
9	6.4	50	Cy	7.6	3	B
10	6.3	40	Cy			
11	6.3	50	Cy			
12	6.3	50	Cy			
13	6.3	30	Cy			
14	6.4	30	Cy	7.9	<3	not identified
16	6.1	40	Cy			
17	6.1	30	Cy			
18	6.1	<3	not identified			
19	6.1	<3	» »			
20	6.3	<3	» »			
21	6.2	<3	» »			
27				8.2	<3	not identified

* Calculated as cyanocobalamin in plate assay.
** Identified by paper chromatography in solvent system I[4].

series to which dimethyl benziminazole but no vitamin B_{12} factor had been added was fermented simultaneously with the other series. Samples were taken almost every day by removing a tube from each series. Samples from the non-inoculated controls were taken at 5 day intervals. The results of these experiments are given in Table 2—8.

Factor B. An examination of Tables 2 and 8 leads to the conclusion that factor B in the presence of dimethyl benzimidazole can be converted into cyanocobalamin by the enrichment culture. Taking into consideration the decrease of *E. coli* activity in the non-inoculated controls, a conversion of at least 20 % can be estimated as follows. After fermentation for 7—12 days, the *E. coli* activity had decreased from about 1 000 to about 100 mμg/ml. This would suggest a conversion of factor B to cyanocobalamin of about 10 %. In the non-inoculated controls there was a decrease to about half of the original *E. coli* activity. This means that the conversion of factor B to cyanocobalamin in the fermented series was at least 20 %.

Table 4. Utilization of factor Z2 by an enrichment culture of *Methanobacterium omelianskii*, grown in Barker's medium supplemented with 5,6-dimethyl benziminazole (1 000 mμg/ml); Cy = cyanocobalamin; Z = factor(s) Z.

Time of fermentation (days)	pH	*E. coli* activity		Non-inoculated controls		
		mμg/ml*	factors present **	pH	*E. coli* activity	
					mμg/ml*	factors present **
0		1 800	Z		1 800	Z
0.5	7.3	1 800	Z			
2	7.1	1 050	Z			
3	6.5	700	Z; Cy			
4	6.2	280	Z; Cy	7.5	410	Z
5	6.2					
6	6.2	80	Cy; (Z)			
7	6.3	60	Cy			
9	6.3	70	Cy	7.7	420	Z
10	6.3	70	Cy			
11	6.3	80	Cy			
12	6.3	70	Cy			
13	6.4	70	Cy			
14	6.4	80	Cy	7.7	370	Z
16	6.1	60	Cy			
17	6.1	70	Cy			
18	6.3	60	Cy			
19	6.3	60	Cy			
20	6.2	60	Cy			
21	6.3	50	Cy			
27	6.2	60	Cy	8.4	360	Z

* Calculated as cyanocobalamin in plate assay.
** Identified by paper chromatography in solvent system I[4].

In reality the yield might be much higher since factor B is known to give much greater growth zones than cyanocobalamin when assayed with *E. coli* in the plate assay. The considerable stability of factor B and of cyanocobalamin upon incubation at 37°C for several days is rather surprising. The reducing character of Barker's medium might be favourable for this stability. The maximum yield of cyanocobalamin was about 100 mμg/ml.

Factor Z1. It can be seen in Table 3 (*cf.* also Table 8) that the microbiologically almost inactive factor Z1 is converted by the enrichment culture into cyanocobalamin. In this fermentation, cyanocobalamin seems to be less stable than in the fermentation with factor B. The maximum yield of cyanocobalamin was 50—70 mμg/ml. Factor Z1 seems to be unstable upon incubation at 37°C and is spontaneously converted into factor B in the reducing medium of Barker (*cf.* values for non-inoculated controls). A partial spontaneous conversion of the factors Z into factor B was observed during their isolation [2].

The conversion of factor Z1 to cyanocobalamin seems to take place more rapidly than that of factor B (*cf.* Table 2).

Table 5. Utilization of factor Z3 by an enrichment culture of *Methanobacterium omelianskii*, grown in Barker's medium supplemented with 5,6-dimethyl benziminazole (1 000 mμg/ml). Brackets mean that the factor in question is present only in small amounts; Cy = cyanocobalamin; Z = factor(s) Z.

Time of fermentation (days)	pH	*E. coli* activity		Non-inoculated controls		
		mμg/ml *	factors present **	pH	*E. coli* activity	
					mμg/ml *	factors present **
0		400	Z		400	Z
0.5	7.1	400	Z			
2	7.2	350	Z			
3	7.1	190	Z			
4	6.5	90	Cy	7.4	110	Z; (B)
5	6.3					
6	6.3	70	Cy			
7	6.2	50	Cy			
9	6.1	50	Cy	7.6	90	Z; (B)
10	6.4	80	Cy			
11	6.3	60	Cy			
13	6.2	70	Cy			
13	6.1	50	Cy			
14	6.1	50	Cy	7.8	80	Z
16	6.1	70	Cy			
17	6.3	50	Cy			
18	6.2	50	Cy			
19	6.2	60	Cy			
20	6.2	40	Cy			
21	6.1	60	Cy			
27	6.1	60	Cy	8.0	70	Z

* Calculated as cyanocobalamin in plate assay.
** Identified by paper chromatography in solvent system I [4].

Factor Z2. Unlike factor Z1, factor Z2 is fairly stable on incubation at 37°C (see Table 4 and *cf.* Table 8). This factor is also converted into cyanocobalamin by the enrichment culture. The maximum yield of cyanocobalamin was about 80 mμg/ml. The rate and possibly also the extent of conversion of factor Z2 was comparable with that of factor B (Table 2).

Factor Z3. This factor seems to be less stable than factor Z2, but more stable than factor Z1. Upon incubation at 37°C, a small part of it is spontaneously converted into factor B (see Table 5, *cf.* also Tables 4 and 8). The enrichment culture converts it to cyanocobalamin, the maximum yield reaching 90 mμg/ml.

Factor X4 (see Table 6 and *cf.* Table 8). This factor seems to be surprisingly stable during incubation at 37°C. The enrichment culture converts a part of it (~half of the amount) into cyanocobalamin, but the other part remains unconverted or is converted to a factor which is indistinguishable from factor X4 by paper chromatography in solvent system I. The conversion or other-

Table 6. Utilization of factor X4 by an enrichment culture of *Methanobacterium omelianskii*, grown in Barker's medium supplemented with 5,6-dimethyl benziminazole (1 000 mμg/ml); Cy = cyanocobalamin.

Time of fermentation (days)	pH	*E. coli* activity		Non-inoculated controls		
		mμg/ml*	factors present **	pH	*E. coli* activity	
					mμg/ml*	factors present **
0		1 000	X4		1 000	X4
0.5	7.1	990	X4			
2	7.2	1 040	X4			
3	7.3	870	X4			
4	6.7	990	X4; (Cy)	7.4	1 350	X4
5	6.4					
6	6.4	360	X4; Cy			
7	6.2	240	X4; Cy			
9	6.2	360	X4; Cy	7.5	930	X4
10	6.4	230	X4; Cy			
11	6.3	250	X4; Cy			
12	6.3	210	X4; Cy			
13	6.3	240	X4; Cy			
14	6.3	290	X4; Cy	7.7	1 380	X4
16	6.2	250	X4; Cy			
17	6.2	280	X4; Cy			
18	6.3	350	X4; Cy			
19	6.3	220	X4; Cy			
20	6.2	230	X4; Cy			
21	6.3	340	X4; Cy			
27	6.4	150	X4; Cy	8.0	1 290	X4

* Calculated as cyanocobalamin in plate assay.
** Identified by paper chromatography in solvent system I[4].

wise of this latter part was not further investigated. That conversion of a part of factor X4 really took place (*i.e.*, that the cyanocobalamin produced was not due merely to an independent synthesis in the presence of 5,6-dimethyl benziminazole) was indicated by the decrease in *E. coli* activity values in the fermentation liquor as compared with the practically unchanged values in the non-inoculated controls.

The yield of cyanocobalamin obtained from this factor cannot be estimated since factor X4 is also present in the fermentation liquor and contributes to the *E. coli* activity.

Factor W (see Table 7 and *cf.* Table 8). This factor was not very stable on incubation at 37°C. After only 3—4 days, the *E. coli* activity had decreased to almost one third. In the medium fermented for 3—4 days by the enrichment culture, the activity of the factor was almost unchanged. A pronounced decrease took place only after 6—7 days. However, with a longer fermentation time (> 7 days), the *E. coli* activity values for the fermented medium were always lower than those for the non-inoculated controls, which may suggest some conversion at least.

Table 7. Utilization of factor W by an enrichment culture of *Methanobacterium omelianskii*, grown in Barker's medium supplemented with 5,6-dimethyl benziminazole (1 000 mμg/ml); Cy = cyanocobalamin.

Time of fermentation (days)	*E. coli* activity			Non-inoculated controls		
	pH	mμg/ml*	factors present **	pH	*E. coli* activity	
					mμg/ml*	factors present **
0		250	W		250	W
0.5	7.2	250	W			
2	7.2	260	W			
3	7.0	240	W			
4	6.5	220	W; (Cy)	7.3	90	W
5	6.3					
6	6.2	120	W; Cy			
7	6.3	90	W; Cy			
9	6.3	40	W; Cy	7.6	80	W
10	6.3	40	W; Cy			
11	6.3	40	W; Cy			
12	6.3	40	W; Cy			
13	6.3	40	W; Cy			
14	6.3	40	W; Cy	7.8	70	W
16	6.3	40	W; Cy			
17	6.1	40	W; Cy			
18	6.2	30	W; Cy			
19	6.3	30	W; Cy			
20	6.1	30	W; Cy			
21	6.2	30	W; Cy			
27	6.2	30	W; Cy	8.1	70	W

* Calculated as cyanocobalamin in plate assay.
** Identified by paper chromatography in solvent system I [4].

CONCLUSIONS

As already reported [4], factor W behaves as a complete, nucleotide-containing factor whereas the other factors used here behave like incomplete nucleotide-lacking factors. In agreement with this, factors B, Z1, Z2, Z3 can easily be converted into cyanocobalamin by the enrichment culture if 5,6-dimethyl benziminazole is present in the medium. Factor X4, which has also been characterized as an incomplete factor, is converted only partially to cyanocobalamin. This may be explained by the fact that the preparation has now, after 3 years, been shown to separate into two electrophoretic fractions [1]. This investigation suggests that even factor W — being a complete nucleotide-containing factor — may to a certain extent be converted to cyanocobalamin when 5,6-dimethyl benziminazole is present in the medium.

Table 8. Production of vitamin B_{12} factors by an enrichment culture of *Methanobacterium omelianskii*, grown in Barker's medium supplemented with 5,6-dimethyl benziminazole (1 000 mμg/ml), Control series. To be compared with Tables 2—7.
Cy = cyanocobalamin.

Time of fermentation (days)	pH	*E. coli* activity		Non-inoculated controls	
		mμg/ml *	factors present **	pH	*E. coli* activity mμg/ml
0.5	7.3	+			
2	7.1	3	Cy		
3	7.1	3	Cy		
4	6.7	3	Cy	7.4	+
5	6.4				
6	6.3	3	Cy		
7	6.5	3	Cy		
9	6.4	3	Cy	7.6	+
10	6.5	3	Cy		
11	6.4	3	Cy		
12	6.4	3	Cy		
13	6.3	3	Cy		
14	6.5	3	Cy	7.8	+
16	6.5	3	Cy		
17	6.3	3	Cy		
18	6.4	3	Cy		
19	6.4	3	Cy		
20	6.3	3	Cy		
21	6.4	3	Cy		
27	6.5	3	Cy	7.6	—

* Calculated as cyanocobalamin in plate assay.
** Identified by paper chromatography in solvent system I[4].

Acknowledgements. The authors are grateful to Professor H. Lundin, Head of the Division, for his encouraging interest in and valuable advice on the execution of this work.

REFERENCES

1. Neujahr, H. Y. and Callieri, D. A. *Acta Chem. Scand.* **12** (1958) 1153.
2. Neujahr, H. Y. *Acta Chem. Scand.* **10** (1956) 917.
3. Barker, H. A. *Antonie van Leeuwenhoek* **6** (1939/40) 201.
4. Neujahr, H. Y. *Acta Chem. Scand.* **11** (1957) 1191.

Received March 29, 1958.

ACTA CHEMICA SCANDINAVICA 12 (1958) 1176—1182

An X-Ray Investigation of the Binary System Stearic Acid—Palmitic Acid

GUNNAR DEGERMAN and ERIK von SYDOW

Institute of Chemistry, University of Uppsala, Uppsala, Sweden

The molecular arrangement for the 1:1 compound between stearic (S) and palmitic (P) acid has been determined. The structure is built up of S—P pairs. Its unit cell is very like those of the components, but the symmetry is lower: $P\ 2_1$ instead of $P\ 2_1/a$. To get disordered 1:1 phases, which are of technical importance, the number of solid $\rightleftharpoons$ liquid transitions should be limited, the lowest possible temperatures should be used and solidification accomplished as rapidly as possible.

Long chain alifatic materials of biological and technical importance are generally complicated mixtures of several related compounds, *e.g.* homologous members of series such as fatty acids, glycerides and sodium soaps. Although the number of components is very often larger than two, binary systems are the only ones which have been fairly well investigated.

PHASE DIAGRAMS

Smith [1] summarizes the phase diagrams of binary systems of homologues of long chain alifatic compounds, classifying them into three different types: continuous series of solid solutions (with no maximum or minimum or with minimum), eutectic mixtures, and compound formation (with congruently or incongruently melting compounds). To the last category belong the binary systems of homologues of normal chain acids, methylesters, iodides, amides, anilides [1] and triglycerides [2]. The pure components of these systems all form double molecular sheets in the solid state. Compound formation has also been observed under certain conditions between normal fatty acids and *anteiso*- and *iso*-acids[3,4] and between normal amides and *anteiso*-amides [3]. Varying the polar groups or the position of the polar group often seems to give simple eutectic mixtures [1], *e.g.* 11-bromohendecanoic acid and 10-bromohendecanoic acid [5]. This is not unexpected, of course, considering steric variations as well as the variation in chemical bonding between the different polar groups.

Of the binary systems between homologues showing compound formation, the stearic acid — palmitic acid system (here called the S—P system) has been the most extensively investigated. In 1898 de Visser [6] published the first phase diagram of the S—P system using very pure components (setting point 69.32°C and 62.62°C, respectively). It indicates an incongruently melting compound at 50 % (s.p. 56.4°C) with an eutectic point at 54.8°C and 27.5 % S. This phase diagram has later been confirmed by Francis *et al.*[7], Schuette and Vogel [8] and Rawitsch and Volnova [2]. The last two investigators succeeded also in getting an eutectic point (55.9°C, 59 % S) on the S side of the compound by extremely slow cooling of the melts, thus having better equilibrium conditions. Similar phase diagrams for systems of other even-numbered fatty acids have also been found [8–13]. There seems to be no ambiguities or uncertainties about the phase diagram and its interpretation for the S—P system, and we have accepted it as correct.

The fact that there is a 1:1 compound formed in the solid state between stearic and palmitic acid has been said by some authors to imply necessarily the existence of S—P pairs instead of S—S pairs and P—P pairs in the compound structure. This is, however, not theoretically necessary, as the lattice in principle can be equally well built up with, *e.g.*, one S—S pair and one P—P pair in each unit cell instead of two S—P pairs.

Sarkadi and de Boer [14] find from infrared absorption measurements that the association degree for fatty acids in the liquid state, *e.g.* 0.953 at 123°C for stearic acid, is almost independent of chain length. If this is assumed to be exactly true, there will be equally many S—P pairs in the 1:1 melt as there are S—S and P—P pairs together, so whatever pairs the crystal structure contains, considerable time is required at the solidification point for the completion of the reaction 2 S—P $\rightleftharpoons$ S—S + P—P. As has been pointed out already, the best phase diagrams are obtained by extremely slow cooling [2,9].

LONG SPACING INVESTIGATIONS

The long spacing, which is frequently given for long chain compounds, is the perpendicular distance between planes containing the end groups of the molecules. Such measurements with X-rays on the S—P system have been performed by Slagle and Ott [15], Francis *et al.*[7] and by the authors. The result for specimens crystallized from melt is summarized in Fig. 1, where our own values are included. The pure acids give only one long spacing value (the C-form) when crystallized form melt. On rapid cooling of specimens of intermediate compositions, only one long spacing value is found as well [7,15] (Fig. 1), but on slower cooling two spacings may appear at compositions separated from 0, 50, and 100 %. The values group themselves around three spacings: 39.9 Å (the C-form of S), 36 Å (35.5 Å for the C-form of P) and 38.6 Å suggested by Francis *et al.*[7] to be the long spacing of the 1:1 compound.

Francis *et al.*[7] have also investigated S—P specimens crystallized from solvent, but the result of that investigation falls outside the scope of this paper.

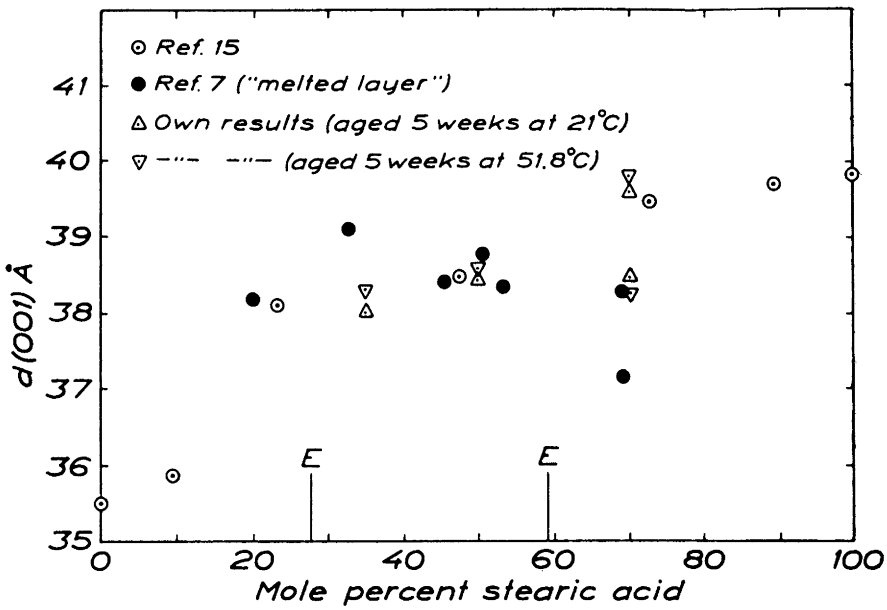

Fig. 1. Long-spacing as a function of composition for S—P specimens crystallized from melt. E = Eutectic composition.

In this work we are mostly dealing with the 1:1 compound, which has been investigated with X-ray powder and single crystal methods. The result is correlated with the structural behaviour of the components, which has been described by von Sydow [16] and Abrahamsson and von Sydow [17] and with the known crystal structures of homologues of the components: lauric acid determined by Vand *et al.*[18] and *n*-hendecanoic acid determined by von Sydow [19]. These structures have the orthorhombic chainpacking with every second chain plane perpendicular to the others [16]. The structures can be classified as O⊥ (021), if *a* is the shortest axis, following a suggestion by Vand [20] complemented by von Sydow [21].

MATERIAL USED

The very pure acids used were kindly put at our disposal by Prof. E. Stenhagen. The stearic acid has m. p. 69.4—69.7°C, and the palmitic acid has m. p. 62.6—62.9°C, as compared with 69.6 and 62.9°C, respectively, given by Francis and Piper [22]. Mixtures of the acids with 35.1, 50.1 and 70.1 mole % stearic acid, respectively, were melted together in an oil bath and kept at 100°C for 15 min, in order to attain equilibrium. The temperature was then lowered below the solidification point at 0.75°C/min. Parts of the specimens were annealed at 51.8°C for 5 weeks.

X-Ray powder photographs were taken at 20°C in a Guinier camera using Cu $K\alpha$ radiation. KCl was mixed into the samples as a calibrating substance (a = 6.292 Å).

Single crystals from the 1:1 specimen of a fairly large size were investigated optically and in a Weissenberg camera. Two out of ten gave good diffraction pictures; they were mounted along the *a*- and *b*-axes, respectively. Rotation and Weissenberg photographs were taken, using very long exposure times.

THE 1:1 COMPOUND

The X-ray powder photographs of the 1:1 specimens compared with those of the pure components (C-form) immediately revealed a striking resemblance between the structure of the compound and components. The powder photograph of the compound was indexed with use of the single crystal data obtained and the cell dimensions were accurately determined. They are given in Table 1 together with the cell dimensions for the components *, taken from the work by Abrahamsson and von Sydow [17]. A suggestion by Kofler [23] that the 1:1 specimen is a "stabilisierte Zwischenphase" is thus not adequate. The short spacings given by Fieldes and Hartman [24] for two reflexions, which can be identified as (110) and (200), are roughly in agreement with our cell dimensions.

Table 1. Cell dimensions and calculated densities at +20°C and space groups for stearic acid (C-form), palmitic acid (C-form) and the 1:1 compound between the two.

	a Å	b Å	c Å	β	Long spacing $d(001)$ Å	Calculated density gcm^{-3}	Space group
Stearic acid C-form	9.357 ±0.020	4.956 ±0.004	50.76 ±0.08	128° 14′ ±6′	39.87 ±0.04	1.022 ±0.002	$P\ 2_1/a$
1:1 Compound of stearic and palmitic acid	9.46 ±0.04	4.96 ±0.01	49.13 ±0.20	128° 14′ ±8′	38.59 ±0.08	0.992 ±0.005	$P\ 2_1$
Palmitic acid C-form	9.42 ±0.02	4.96 ±0.01	45.73 ±0.08	128° 40′ ±6′	35.72 ±0.04	1.020 ±0.002	$P\ 2_1/a$

The fact that the unit cell of the 1:1 compound is approximately an "average" between the cells of the components, leads to a rather limited number of possible molecular arrangements. They are shown in Fig. 2 as deduced from the works by Vand *et al.*[18] and von Sydow [19]. The first one ($P\ 2_1/a$), which is also representative of either of the components, represents a completely disordered phase with 1:1 composition containing S—P pairs or S—S and P—P pairs or all three. This is, however, not a very probable solution for a phase diagram showing compound formation, but rather for a system with a continuous series of solid solutions, *e.g.* for hydrocarbons or ethyl esters [1].

The following arrangements in Fig. 2 are ordered phases. The two middle ones are built up with S—P pairs and have the space groups $P\ 2_1$ and Pa, which also are monoclinic but with a lower symmetry than $P\ 2_1/a$. The last one is built up with S—S and P—P pairs and has the triclinic symmetry $P\ \bar{1}$ with a *pseudo*-monoclinic unit cell. As can be seen from Fig. 2 it is a rather

* There seems to be a slight increase in the differences for the c-dimension and the long spacing with increasing chain length. Thus the error limits given for the coefficients P and p in the linear equations for c and d (001) should be doubled.

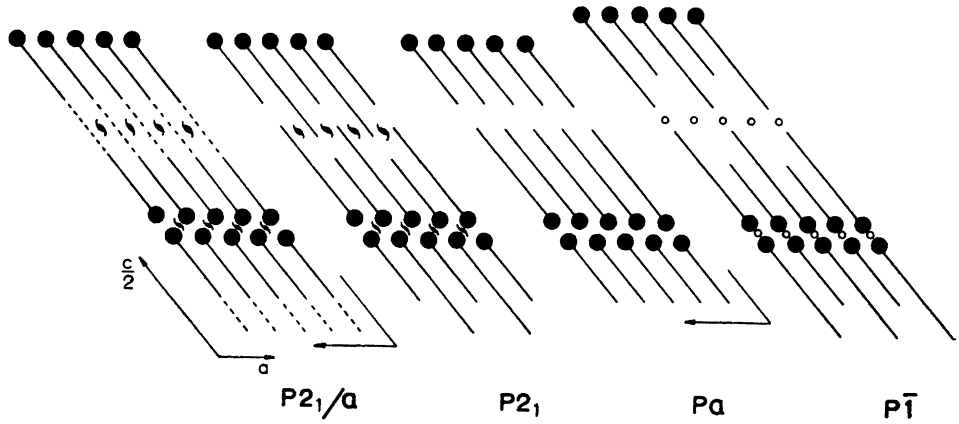

Fig. 2. Hypothetical molecular arrangements for the 1:1 compound between stearic and palmitic acid. $P\ 2_1$ is the correct one.

bulky structure with large holes in it and thus very improbable. A more close-packed arrangement of S—S and P—P pairs than the one to the right in Fig. 2 ($P\ \bar{1}$) will lead to a higher long spacing value (approximately twice the ones for the structures shown to the left in Fig. 2), which in one case (alternating S—S and P—P sheets through the crystal) should be easily measurable. In four cases (A- or B-centering of the $P\ \bar{1}$-type in Fig. 2) there will be systematic absences among the $00l$-reflexions for l odd, so the large real long spacing value will be halved. These four cases, which will be found inconsistent with the result from the single crystal measurements (see below), can, however, be ruled out at once from structural reasons, in that they will lead to the result that the chain planes of either two hydrogen bonded molecules or two molecules with close-packed end groups (CH_3-) are perpendicular. This has never been found to be the case for any crystal form of the normal fatty acids [16].

Each of the space groups of the four possibilities in Fig. 2 has different conditions for systematic absences, which are given in Table 2. Any possible deviation from $P\ 2_1/a$ will, however, be very weak, as all cases are *pseudo*-$P\ 2_1/a$, and the contribution will be from only two extra methylene groups on every second molecule. In order to secure the correct choice, very long

Table 2. Space group and absent reflexions for the four hypothetical molecular arrangements of the 1:1 compound (Fig. 2).

Space group	Conditions for systematic absences
$P\ 2_1/a$	$h0l$, when h odd and $0k0$ when k odd
$P\ 2_1$	$0k0$, when k odd
$P\ a$	$h0l$, when h odd
$P\ \bar{1}$	no

exposure times were used for the Weissenberg photographs. There was absolutely no trace of any $0k0$-reflextions with k odd, but $h0l$-reflexions with h odd appeared (Table 3). This definitely confirms the space group $P2_1$ and the molecular arrangement (marked $P\ 2_1$ in Fig. 2) for the 1:1 compound between stearic and palmitic acid. (The space group $P\ 2_1/m$, which has the same extinction conditions as $P\ 2_1$ has a mirror plane (m), which is inconsistent with the chain-packing [16].)

A comparison between the structure of the compound and the components (Table 1 and Fig. 2) reveals that the acid molecules are packed side by side in a slightly different way. This is caused by the puckered end group planes (Fig. 2), which when they are packed together, arrange themselves so they fit into the chain packing of the opposite sheet. This makes the c-dimension and long spacing higher than the arithmetic mean between those of the components. This is probably somewhat compensated by increased possibilities in van der Waals interaction over the methyl group gap [16] (Fig. 2). The result is, however, a less effective molecular packing for the compound than for the pure components, as revealed by the density 0.992 gcm^{-3} for the compound compared with 1.022 and 1.020 gcm^{-3}, respectively, for the components (Table 1). This is also consistent with the melting temperatures for the compound and the components given above.

It is now easy to understand the conditions for the formation of ordered and disordered phases of the 1:1 compound. If the melt contains few S—P-pairs, *i.e.* many S—S and P—P pairs, (by rapid melting together of the pure components at lowest possible temperature) and one wants an ordered phase, an extremely low rate of cooling must be used in the solidification, so that the reaction S—S + P—P → 2 S—P will take place completely. A repeated procedure of melting and solidification of the compound within a very small temperature interval should give the best ordered compound phase.

In technical processes of this kind there is generally a desire for obtaining disordered phases, however, as they are smoother and less grainy. To get such phases one should therefore limit the number of solid ⇌ liquid transitions, work at lowest possible temperatures and solidify as rapidly as possible.

Table 3. Observed reflexions $h0l$, which definitely establish the correct space group $P\ 2_1$ and the molecular arrangement for the 1:1 compound (Fig. 2). Visibility limit = 0.

I	hkl	I	hkl	I	hkl	I	hkl
0	$10\bar{9}$	0	$3,0,\bar{3}\bar{7}$	1	$30\bar{1}$	0	308
	*	0	$3,0,\bar{3}0$	1	300	0	3,0,23
0	101	0	$3,0,\bar{2}7$?	1	301		
		½	$30\bar{3}$	½	302	½	$5,0,\bar{2}\bar{3}$

* $10\bar{6}-100$ obscured by the beam stop.

TWO-PHASE MIXTURES

Several specimens from melt with compositions differing from 0, 50 and 100 mole % S were investigated with X-rays by Slagle and Ott [15] and Francis *et al.*[7] (Fig. 1). Their long-spacing values found are in excellent agreement with the phase diagram (except 37.1 Å for a composition of 69 % S[7]) considering the rapid cooling used.

These values have been complemented by investigating unannealed and annealed specimens with 35.1 % and 70.1 % S prepared under slow cooling. The first ones, which are between the P-eutectic point and the compound, show one diffuse long-spacing (Fig. 1) slightly lower than that for the 1:1 compound. The last ones, which are between the S-eutectic point and pure stearic acid, show two spacings (Fig. 1) corresponding to those of pure stearic acid and compound. This is in line with an observation by Francis *et al.*[7], that the palmitic rich phases have a more variable long-spacing than the ones rich in stearic acid. This is reasonable, as it must be easier to replace S-molecules with P-molecules in pure stearic acid than to replace P-molecules with S-molecules in pure palmitic acid. This is, of course, also the reason for the unsymmetrical phase diagram for the S—P system and for the difficulties in obtaining the S-eutectic point in comparison with the P-eutectic point, as it must be easier to make the compound richer in P than in S (Fig. 2).

We are indebted to Professors G. Hägg and E. Stenhagen for their interest in this work and for the facilities put at our disposal. The expenses involved have been defrayed by a grant from the *Swedish Natural Science Research Council.*

REFERENCES

1. Smith, J. C. *Ann. Reports* **35** (1938) 251.
2. Rawitsch, G. B. and Volnova, V. A. *Acta Physicochim. U.R.S.S.* **17** (1942) 323; *cf. Chem. Abstr.* **38** (1944) 677 and **37** (1943) 5263.
3. Weitkamp, A. W. *J. Am. Chem. Soc.* **67** (1945) 447.
4. von Sydow, E. *Acta Chem. Scand.* **8** (1954) 1513.
5. Harris, P. L. and Smith, J. C. *J. Chem. Soc.* **1935** 1108.
6. de Visser, L. E. O. *Rec. trav. chim.* **17** (1898) 182.
7. Francis, F., Collins, F. J. E. and Piper, S. H. *Proc. Roy. Soc. London* **A 158** (1937) 691.
8. Schuette, H. A. and Vogel, H. A. *Oil & Soap* **17** (1940) 155.
9. Jantzen, E. *Z. angew. Chem.* **44** (1931) 482.
10. Piper, S. H., Chibnall, A. C. and Williams, E. F. *Biochem. J.* **28** (1934) 2175.
11. Kulka, M. and Sandin, R. B. *J. Am. Chem. Soc.* **59** (1937) 1347.
12. Schuette, H. A. and Vogel, H. A. *Oil & Soap* **16** (1939) 209.
13. Grondal, B. J. and Rogers, D. A. *Oil & Soap* **21** (1944) 303.
14. Sarkadi, D. S. and de Boer, J. H. *Rec. trav. chim.* **76** (1957) 628.
15. Slagle, F. B. and Ott, E. *J. Chem. Soc.* **55** (1933) 4404.
16. von Sydow, E. *Arkiv Kemi* **9** (1956) 231.
17. Abrahamsson, S. and von Sydow, E. *Acta Cryst.* **7** (1954) 591.
18. Vand, V., Morley, W. M. and Lomer, T. R. *Acta Cryst.* **4** (1951) 324.
19. von Sydow, E. *Acta Cryst.* **8** (1955) 810.
20. Vand, V. *Acta Cryst.* **7** (1954) 697.
21. von Sydow, E. *Acta Chem. Scand.* **12** (1958) 777.
22. Francis, F. and Piper, S. H. *J. Am. Chem. Soc.* **61** (1939) 577.
23. Kofler, A. *Mikrochim. Acta* **1954**, 444.
24. Fieldes, M. and Hartman, L. *Proc. Roy. Soc. London* **A 233** (1955) 195.

Received April 16, 1958.

ACTA CHEMICA SCANDINAVICA 12 (1958) 1183—1186

Structure of a Glyceritol Glycoside from *Polysiphonia fastigiata* and *Corallina officinalis*

BÖRJE WICKBERG

Organisk-kemiska Institutionen, Kungl. Tekniska Högskolan, Stockholm, Sweden

The O-α-D-galactopyranosyl-(1→6)-O-β-D-galactopyranosyl-(1→1)-glyceritol previously isolated from wheat flour lipids, has been found in the red algae *Polysiphonia fastigiata* and *Corallina officinalis*. The glyceritol residue has been shown to have the D-configuration.

Investigation of the red alga *Polysiphonia fastigiata*[1] gave a glycoside (A), m. p. 196—198°, $[\alpha]_D^{23}$ +88°, which after acid hydrolysis gave spots indistinguishable from those given by D-galactose and glyceritol on paper chromatograms. The same glycoside has now been obtained in small quantities from another red alga, *Corallina officinalis, Florideae*, order *Cryptonemiales*, which was previously found to contain floridoside [2]. The structure of glycoside A has now been investigated in greater detail.

A quantitative determination of the products of hydrolysis, which were assumed to be galactose and glyceritol, analysis for carbon and hydrogen and the results of periodate oxidation, including periodate consumption and formic acid and formaldehyde liberated, indicated that A could be assigned the general structure O-galactopyranosyl-(1 → 6)-O-galactopyranosyl-(1 → 1)-glyceritol. Provided the galactose belongs to the D-series the moderately high optical rotation of A is consistent with the presence of one α- and one β-linkage in the molecule.

Glycoside A was strikingly similar to a glycoside (B), O-α-D-galactopyranosyl-(1 → 6)-O-β-D-galactopyranosyl-(1 → 1)-glyceritol, m. p. 182—184°, $[\alpha]_D$ + 86.4°, which had recently been isolated from wheat flour lipids by Carter *et al.* [3] A second glycoside (C), O-β-D-galactopyranosyl-(1 → 1)-glyceritol, m. p. 139—140°, $[\alpha]_D$ + 3.77° was also isolated from the same source. The anomeric configurations of B and C were evident from enzymatic degradations; B, though unaffected by β-galactosidase from *E. coli*, was split by α-galactosidase in a yeast hexokinase preparation to yield D-galactose and glycoside C. The latter compound was hydrolysed by β-galactosidase to give D-galactose and glyceritol.

As glycosides A and B might have differed in the position of the α- and β-linkages, A was incubated with α- and β-galactosidase preparations from sweet almonds, and the reaction was followed qualitatively on paper chromatograms. It was found that A was attacked very slowly by a β-galactosidase with low α-activity, which rapidly hydrolysed a synthetic specimen of O-β-D-galactopyranosyl-(1 → 1)-D, L-glyceritol. An enzyme preparation with about equal α- and β-galactosidase activity liberated galactose and later also glyceritol. The identity of A with B indicated by these experiments, was later confirmed by direct comparison with a sample of glycoside B *. The corrected melting point of B determined with the same apparatus used for A was 195—197°, the mixed melting point showed no depression and the infrared spectra of the two samples were identical.

The question of the configuration of the glyceritol residue, which is optically active due to substitution in the 1-position, has been solved by synthesis of O-β-D-galactopyranosyl-(1 → 1)-D- and -L-glyceritol [4]. The D-glyceritol galactoside was found to be identical with a sample of glycoside C* and therefore the glyceritol residue in A also has D-configuration.

EXPERIMENTAL **

The isolation of glycoside A from *Polysiphonia fastigiata* was described in a previous paper [1]. It was purified by chromatography on Whatman 3 MM thick filter paper and recrystallised from aqueous ethanol, m. p. 196—198°, $[\alpha]_D^{23}$ + 88° (water, c = 1.8). (Found: C 43.5; H 6.68. Calc. for $C_{18}H_{28}O_{18}$: C 43.3; H 6.78).

A sample of *Corallina officinalis* (575 g) was extracted with ether and methanol and the methanol extract was worked up as described earlier [1] yielding a syrup (6.1 g). This was separated on a carbon — Celite column in the usual way [1]. Paper chromatograms of the eluate indicated the presence of floridoside and a number of other carbohydrates. One fraction gave a spot with about the same R_F value as glycoside A. This fraction was concentrated, the residue (100 mg) was dissolved in aqueous ethanol and the solution was seeded with a trace of glycoside A. The crystals separating (41 mg), after recrystallisation had m. p. 194—196.5° and $[\alpha]_D^{20}$ +90° (water, c = 1.8). The melting point was undepressed on admixture with glycoside A or B, and the infrared spectra of the three preparations were identical.

Molar ratio of D-*galactose and glyceritol in glycoside A.* The glycoside (*ca.* 5 mg) was hydrolysed in 0.2 N hydrochloric acid (0.15 ml) at 105° for 17 h. The hydrolysate was passed through a small column of Amberlite IR 4B and was then put on a strip of Whatman 3 MM filter paper which had been prewashed with water and then dried. The chromatogram was developed with ethyl acetate — acetic acid — water (3:1:1) and the appropriate areas were then cut out and extracted with water; adjoining empty areas of the paper were treated in the same way and these extracts were used as blanks. Suitable amounts of the extracts were oxidised with sodium metaperiodate overnight and the excess of periodate was determined essentially as described in a previous paper [5]. The glyceritol and galactose content of the hydrolysate was calculated empirically by comparison with synthetic mixtures of glyceritol and D-galactose which were separated and oxidised in the same way. The amounts of glyceritol and galactose thus obtained were 98 and 97 %, respectively, of the theoretical calculated for a glyceritol digalactoside.

Periodate oxidations. a) The consumption of periodate, determined as described earlier [5], was *ca.* 4.9 moles/mole of glycoside A after 3 h and 5.0 moles/mole after 21 h.

* A sample was kindly supplied by Dr. Carter.
** All melting points are corrected.

b) The formaldehyde was determined as its dimedone compound, essentially by the method of Reeves [6]. Aqueous sodium metaperiodate (0.2 M, 0.5 ml) was added to a solution of glycoside A (7.08 mg) in water (4 ml) and after 4.5 h the oxidant was reduced by the addition of 0.8 M aqueous disodium arsenite (0.5 ml), 0.8 N hydrochloric acid (0.5 ml) and 1 N aqueous sodium acetate (0.5 ml). After the addition of a 5 % ethanolic solution of dimedone (0.5 ml) the mixture was heated at 100° for 10 min and left in a cool place for 1 h. The sticky precipitate (10 mg) was collected on a filter stick, washed with water and after drying sublimed at *ca.* 0.01 mm pressure. Yield 3.75 mg corresponding to 0.75 mole of formaldehyde/mole of glycoside A; m. p. 186—193°. Recrystallisation from aqueous ethanol gave a product with m. p. 191—194°, alone or mixed with an authentic sample.

c) A sample of glycoside A (6.95 mg) was oxidised in 0.2 M sodium metaperiodate solution (1 ml) overnight, ethylene glycol (2 drops) was added and the formic acid produced was titrated with 0.01 N sodium hydroxide solution using phenol red as an indicator. Found: 1.93 moles of formic acid/mole of glycoside A.

Enzymatic degradation. a) Enzyme activity. The activity of the enzyme preparations was determined approximately by incubation with 5 % solutions of melibiose or lactose in 0.1 M sodium acetate buffer (pH 4.6) at 25°: the hydrolysis was followed polarimetrically over periods of 15—170 h. The activities were calculated as mg of disaccharide hydrolysed in 1 h by 1 ml of enzyme solution. Alternatively a mixture of enzyme solution (13.3 μl) and a 2 % solution (1 ml) of *o*-cresyl α- or β-D-galactopyranoside [7,8] in 0.1 M acetate buffer of pH 4.6 was kept at 25° for 5 min (β-galactoside) or 1 h (α-galactoside). The hydrolysis was stopped by the addition of 0.5 M sodium carbonate buffer of pH 10.6 (2 ml), 0.05 N iodine solution (1.00 ml) was added and after 20 min the mixture was acidified with acetic acid (2 ml) and the excess of iodine was titrated with 0.01 N sodium thiosulphate solution. A blank was run in a similar way but the carbonate buffer was added before the enzyme solution and oxidation with iodine was done immediately. The activities were calculated as mg of cresyl galactoside hydrolysed by 1 ml of enzyme solution in 1 h.

b) α-Galactosidase. Emulsin was extracted from de-fatted sweet almond meal essentially according to the procedure described by Sumner and Somers [9]. The meal (10 g), which had been stored in a refrigerator for about a year, was stirred with 1/2-saturated aqueous ammonium sulphate (100 ml) for 5 min. After filtration the filter cake was extracted with 1/4-saturated aqueous ammonium sulphate (100 ml), ammonium sulphate (2 g/10 ml of filtrate) was added to the extract which was centrifuged and the precipitate was dialysed against distilled water. The dialysed solution was centrifuged and the supernatant solution concentrated to a small volume (0.75 ml). Acetone (0.25 ml) was added in the cold, the solution was clarified by centrifuging, a further quantity of acetone (0.5 ml) added and after 1 h the precipitated emulsin was isolated by centrifuging. It was dissolved in water (1 ml). α-Galactosidase activity: 2.1 mg of melibiose/ml/h; 11 $\pm$ 2 mg of *o*-cresyl α-D-galactopyranoside/ml/h. β-Galactosidase activity: 2.2 mg of lactose/ml/h; 90 $\pm$ 20 mg of *o*-cresyl β-D-galactopyranoside/ml/h.

c) β-Galactosidase was prepared by the method of Edman and Jorpes [10], omitting the final steps of purification. Sweet almonds (1 000 g), with the cuticle, were ground and de-fatted, the meal was extracted with dilute aqueous ammonia, impurities were precipitated from the extract by adding dilute acetic acid, the emulsin fraction was precipitated by adding ammonium sulphate and the precipitate after centrifuging dialysed against distilled water and clarified. The final solution (100 ml) contained 52 mg of dry material/ml. α-Galactosidase activity: 0.1 mg of melibiose/ml/h; 2 $\pm$ 2 mg of *o*-cresyl α-D-galactopyranoside/ml/h. β-Galactosidase activity: 18 mg of lactose/ml/h; 940 $\pm$ 20 mg of *o*-cresyl β-D-galactopyranoside/ml/h.

d) Enzymatic hydrolysis. A mixture of the substrate (2 mg) in 0.1 M sodium acetate buffer (pH 4.6, 0.1 ml) and enzyme solution (13.3 μl) was kept at 25°. At intervals samples were withdrawn and run on paper chromatograms in ethyl acetate — acetic acid — water (3:1:1). The spots were detected by spraying with periodate — benzidine [11], silver nitrate — sodium hydroxide [12] or anisidine hydrochloride reagents. The β-galactosidase preparation gave almost complete hydrolysis of O-β-D-galactopyranosyl-(1 → 6)-D-galactose in 24 h, and after 16 h synthetic O-β-D-galactopyranosyl-(1 → 1)-D,L-glyceritol gave strong spots for D-galactose and glyceritol. However, after 21 h a sample of glycoside A, which had been incubated with the β-galactosidase, gave only a faint spot for D-galactose with the silver nitrate and anisidine reagents, and even after 36 h no hydrolysis products were

detected with the periodate spray. With the α-galactosidase preparation glycoside A gave spots for D-galactose with all spray reagents after 4.5 h, and after 12 h the periodate spray revealed a faint spot from glyceritol. With the same spray the galactose spot acquired a yellowish tinge which has been observed with 1-glyceritol galactopyranosides in general. These compounds would not separate from D-galactose on the chromatograms. The experiments strongly indicate that glycoside A is first attacked by α-galactosidase to yield D-galactose and a glyceritol β-D-galactopyranoside, which is later split by the β-galactosidase present to give D-galactose and glyceritol.

Identification of glycoside C with O-β-D-galactopyranosyl-(1 → 1)-D-glyceritol. The synthesis of O-β-D-galactopyranosyl-(1 → 1)-D-glyceritol, m. p. 140.5—141.5°, $[\alpha]_D^{20}$ −7° (water, c = 2.0), and the corresponding L-glyceritol derivative, m. p. 104—107°, $[\alpha]_D^{20}$ +2° (water, c = 2.1) is described in a later paper [4]. The compounds are isomorphous and both of them can be induced to crystallise from an ethanolic solution upon seeding with glycoside C. Though the specific rotation reported [3] for glycoside C agrees best with that of the L-glyceritol derivative, the corrected m. p. of C, 139.5—142°, and the infrared spectra [4] prove its identity with the D-glyceritol derivative.

Infrared spectra were recorded with a *Perkin-Elmer* double-beam spectrometer Model 21 with a rock-salt prism, using the potassium bromide disc technique.

Acknowledgements. The author is indebted to Dr. H. E. Carter, University of Illinois, for a generous gift of samples, to *Statens Naturvetenskapliga Forskningsråd* for financial support and to Ing. Gurli Hammarberg for her skilful assistance. The alga was kindly supplied by *Norsk Institutt for Tang- och Tare-forskning, Trondheim.*

REFERENCES

1. Wickberg, B. *Acta Chem. Scand.* **11** (1957) 506.
2. Haas, P. and Hill, T. G. *Biochem. J.* **27** (1933) 1801.
3. Carter, H. E., Mc Cluer, R. H. and Slifer, E. D. *J. Am. Chem. Soc.* **78** (1956) 3735.
4. Wickberg, B. *Acta Chem. Scand.* **12** (1958) 1187.
5. Wickberg, B. *Acta Chem. Scand.* **10** (1956) 1097.
6. Reeves, R. E. *J. Am. Chem. Soc.* **63** (1941) 1476.
7. Helferich, B., Scheiber, H. E., Streeck, R. and Vorsatz, F. *Ann* **518** (1935) 211.
8. Wickberg, B. *Acta Chem. Scand.* **12** (1958) 615.
9. Sumner, B. and Somers, F. *Laboratory Experiments in Biological Chemistry.* Academic Press, New York 1944, p. 146.
10. Edman, P. and Jorpes, E. *Acta Physiol. Scand.* **2** (1941) 41.
11. Cifonelli, J. A. and Smith, F. *Anal. Chem.* **26** (1954) 1132.
12. Trevelyan, W. E., Procter, D. P. and Harrison, J. S. *Nature* **166** (1950) 444.

Received March 29, 1958.

ACTA CHEMICA SCANDINAVICA 12 (1958) 1187—1201

Synthesis of 1-Glyceritol D-Galactopyranosides

BÖRJE WICKBERG

Organisk-kemiska Institutionen, Kungl. Tekniska Högskolan, Stockholm, Sweden

The so called *iso*floridoside, which has been isolated from *Porphyra umbilicalis* and shown to be an O-α-D-galactopyranosyl-(1 → 1)-glyceritol, has now been reinvestigated. It has been found to be an isomorphous mixture of the diastereoisomeric D- and L-glyceritol derivatives of the structure given above. These compounds and the corresponding β-D-galactopyranosides have been synthesised from glyceritol derivatives of known configuration; the α-glycosides were also isomorphous. The reaction between 2,3-O-*iso*propylidene-D-glyceritol and tetra-O-acetyl-α-D-galactopyranosyl bromide in the presence of silver oxide unexpectedly gave a mixture of D- and L-glyceritol derivatives. In one case a Koenigs-Knorr synthesis using silver oxide gave an unusually high yield of the α-anomer. The infrared spectra of the 1-glyceritol D-galactopyranosides are recorded.

A glyceritol glycoside (glycoside A) found in the red algae *Polysiphonia fastigiata*[1] and *Corallina officinalis*[2] was shown in a preceding paper[2] to be an O-α-D-galactopyranosyl-(1 → 6)-O-β-D-galactopyranosyl-(1 → 1)-glyceritol. This compound was first found in wheat flour lipids by Carter *et al.*[3] who showed it to have the above structure. The occurrence of this glycoside in plant materials of such widely different origin gives greater interest to the possible biochemical role of the glyceritol glycosides in red algae. Those previously found are: O-α-D-galactopyranosyl-(1 → 2)-glyceritol (floridoside)[4–7] O-α-D-mannopyranosyl-(1 → 3)-O-α-D-galactopyranosyl-(1 → 2)-glyceritol [8] and O-α-D-galactopyranosyl-(1 → 1)-glyceritol (*iso*floridoside) [9]. In *iso*floridoside and glycoside A the glyceritol is asymmetrically substituted, and as a possible relationship between the two compounds might have been revealed by the configuration of the glyceritol residues, the synthesis of the four possible 1-glyceritol D-galactopyranosides * was undertaken to provide material for comparison with the natural compounds. As a result of this work the glyceritol residue of glycoside A has been shown to have the D-configuration [2]; the investigation of *iso*floridoside and the synthetic work will be described below.

In an attempt to prepare 1-D-glyceritol β-galactoside, 2,3-O-*iso*propylidene-D-glyceritol (I), which is easily available from 1,2:5,6-di-O-*iso*propylidene-

* For convenience, O-α-D-galactopyranosyl-(1 → 1)-D-glyceritol will be referred to in the following as 1-D-glyceritol α-galactoside *etc.*

D-mannitol[10–12], was allowed to react with tetra-O-acetyl-α-D-galactopyranosyl bromide following Reynolds' and Evans' modification [13] of the Koenigs-Knorr method, but neither the intermediate products nor the expected 1-D-glyceritol β-galactoside crystallised spontaneously. It was thought that the α-anomer of this glycoside might be identical with *iso*floridoside; the hexaacetate of the presumed 1-D-glyceritol β-galactoside was therefore treated with titanium tetrachloride in chloroform [14] to effect anomerisation. Residual β-galactoside in the product after deacetylation was hydrolysed with a β-galactosidase preparation and the carbohydrate mixture obtained was separated on a carbon column. One fraction was chromatographically similar to *iso*floridoside * and crystallised upon seeding with it, but the melting point **, 121—127°, raised to 125—127° after repeated recrystallisations, was much lower than that previously reported for *iso*floridoside [9] (134—135° uncorr.) and the mixed melting point showed a wide range but no depression. However, the melting point of analytically pure *iso*floridoside, as redetermined on a Kofler hot stage, was 132—141°, and a reasonable explanation compatible with the experimental data was thus that both samples were isomorphous mixtures of 1-D- and 1-L-glyceritol α-galactosides. This assumption was confirmed by resolving the mixtures on a carbon column which had previously been found to give very sharp separations. Both *iso*floridoside and the synthetic sample gave the same two components, m. p. *ca* 131—133° and 149—151.5° (*cf.* Table 1); no melting point depression was observed with mechanically mixed samples of these compounds but the mixed fusion technique gave a melting point minimum of 120°.

Table 1. 1-Glyceritol galactopyranosides.

	M. p.	$[\alpha]_D^{20}$	Analysis			
			Per-iodate[a]	Formic acid[b]	C	H
Calculated for $C_9H_{18}O_8$:			3.00	1.00	42.5	7.14
Compound:						
O-α-D-Galactopyranosyl-(1→1)-D-glyceritol	150 —152°	+155°	2.91	0.93	42.8	7.37
O-α-D-Galactopyranosyl-(1→1)-L-glyceritol	131.5—133°	+159°	2.90	0.95	42.9	7.45
O-β-D-Galactopyranosyl-(1→1)-D-glyceritol	140.5—141.5°	−7°	2.89	0.97		
O-β-D-Galactopyranosyl-(1→1)-L-glyceritol[c]	104—107°	+2°	2.89	0.97	42.4	7.45

[a] Moles of sodium metaperiodate consumed overnight by 1 mole of glycoside [27].
[b] Moles of formic acid formed from 1 mole of glycoside on periodate oxidation overnight.
[c] The central parts of crystals in a solidified sample melted at 108—110°.

* Kindly supplied by Dr. B. Lindberg.
** Melting points are corrected unless stated otherwise.

The 1-glyceritol β-galactoside preparation obtained above crystallised when seeded with 1-D-glyceritol β-galactoside * from wheat flour lipids [2,3], m. p. 139.5—142°, but the product had m. p. 124—128°, and this value was not appreciably raised by recrystallisation. The low specific rotation, $[\alpha]_D^{20}$ -3°, excludes the presence of α-D-galactopyranosides, and as no melting point depression was observed on admixture with the high-melting glycoside used for seeding, the synthetic preparation was assumed to be an isomorphous mixture of 1-D- and 1-L-glyceritol β-galactosides.

The results show, either that the 2,3-O-*iso*propylidene-D-glyceritol used as starting material in the Koenigs-Knorr reaction was extensively racemised before the reaction or that racemisation took place during the reaction. The first alternative seems very improbable as two different preparations of 2,3-O-*iso*propylidene-D-glyceritol had $[\alpha]_D^{23}$ +14.0° and 14.1°. On the other hand the racemisation could be due to traces of acid liberated in the Koenigs-Knorr reaction and the experiment was therefore repeated using a large excess of silver oxide. However, after alkaline and mild acid hydrolysis and subsequent fractionation of the product on a small carbon column, crystalline preparations were obtained which melted over the ranges 97—116° and 124—129°, indicating that extensive racemisation still took place. This phenomenon remains to be explained.

The synthesis of the 1-D-glyceritol α- and β-galactosides was finally accomplished in the following way. 2,2'-O-Methylene-bis-(3-O-benzoyl-D-glycerose)[15], obtained by oxidising II with lead tetraacetate, was reduced catalytically to the crystalline glyceritol derivative (IV) and this was allowed to react with tetra-O-acetyl-α-D-galactopyranosyl bromide under Reynolds' and Evans'

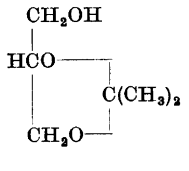

I

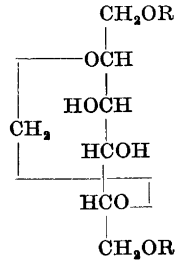

II R = C_6H_5CO
III R = Tetra-O-acetyl-α,β-D-galactopyranosyl

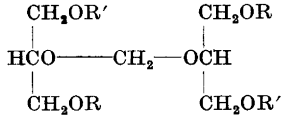

IV R = C_6H_5CO; R' = H
V R = C_6H_5CO; R' = Tetra-O-acetyl-α,β-D-galactopyranosyl
VI R = H; R' = $(C_6H_5)_3C$
VII R = Tetra-O-acetyl-α,β-D-galactopyranosyl; R' = H

* Kindly supplied by Dr. Carter.

conditions, giving V. After acetolysis and alkaline alcoholysis the product was separated on a carbon column and then gave 17 % of the α- and 36 % of the β-galactoside. As this yield of α-anomer is unexpectedly high the experiment was repeated adding the halide much more rapidly to see whether this would influence the yields. These were now *ca.* 3 % and 28 % for the α- and β-anomer, respectively. The yield of α-galactoside was thus still fairly high.

Mixed fusion confirmed the identity of 1-D-glyceritol α-galactoside and the high-melting component of *iso*floridoside.

The anomalous course of the above reaction is probably not due to simple steric hindrance in the aglycone, as a much more hindered molecule, 2,2'-O-methylene-bis-(3-O-trityl-L-glyceritol) (VI), under similar conditions gave 21 % of the theoretical yield of 1-L-glyceritol β-galactoside only; no α-anomer was isolated. VI was prepared from IV by tritylation and debenzoylation.

1-L-Glyceritol β-galactoside was more readily prepared starting from 2,3-O-*iso*propylidene-D-glyceritol (I). Benzylation of I and acid hydrolysis of the benzyl ether gave VIII [16,17] witch was tritylated and the trityl ether (IX) was benzylated to give crystalline 1-O-trityl-2,3-di-O-benzyl-L-glyceritol (X). This was detritylated by heating with aqueous acetic acid and the crude amorphous 2,3-di-O-benzyl-L-glyceritol (XI) obtained was used directly in the Koenigs-Knorr reaction without distillation. The product from this reaction (XII) was deacetylated, the benzyl groups were removed by catalytic hydrogenolysis and the glycoside mixture was separated by recrystallisation and fractionation on a carbon column, giving 1 % and 59 %, respectively,

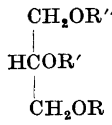

VIII R,R′ = H; R″ = $C_6H_5CH_2$
IX R = $(C_6H_5)_3C$; R′ = H; R″ = $C_6H_5CH_2$
X R = $(C_6H_5)_3C$; R′, R″ = $C_6H_5CH_2$
XI R = H; R′, R″ = $C_6H_5CH_2$
XII R = Tetra-O-acetyl-α,β-D-galactopyranosyl; R′, R″ = $C_6H_5CH_2$

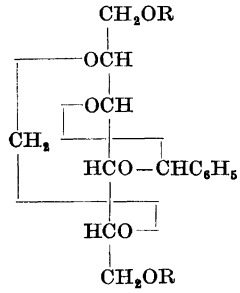

XIII R = H
XIV R = C_6H_5CO
XV R = Tetra-O-acetyl-α,β-D-galactopyranosyl

of 1-L-glyceritol α- and β-galactosides. The α-anomer had a lower melting point (127—129°) than the low-melting component of *iso*floridoside (m. p. 131.5—133°), but the two samples were shown to be identical by mixed fusion. If the synthetic sample had contained considerable amounts of the isomorphous 1-D-glyceritol α-galactoside a melting point minimum would have been observed, but the presence of a small quantity of this diastereoisomer could not be excluded. This would imply that the 1-L-glyceritol β-galactoside was contaminated with some of the corresponding D-glyceritol derivative, and the rather broad range of the melting point (*ca.* 101—107°) lent some support to this idea. However, chromatography on an efficient carbon column showed that this was most probably not the case. The material was slightly hygroscopic, and a pure sample after intensive drying had m. p. 104—107°. On mixed fusion with 1-D-glyceritol β-galactoside (m. p. 140.5—141.5°) it gave a melting point minimum of 98—99°.

Another possible route to the 1-L-glyceritol galactosides was also considered. 2,5-O-methylene-3,4-O-benzylidene-D-mannitol (XIII), prepared from its easily available dibenzoate (XIV)[15], was allowed to react with tetra-O-acetyl-α-D-galactopyranosyl bromide. This would be expected to give the digalacto-

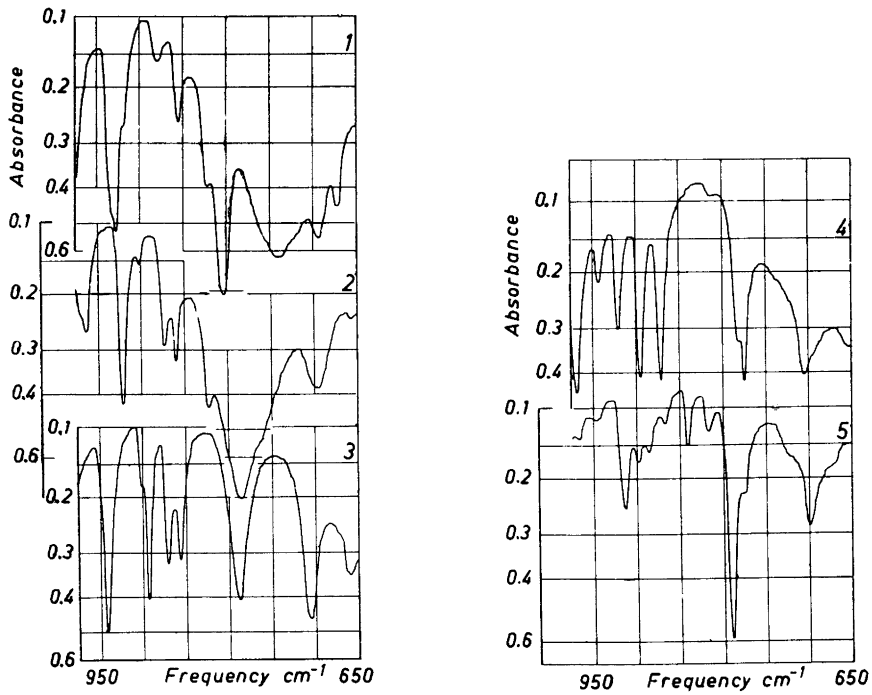

Fig. 1. Infrared absorption curves of 1) O-α-D-Galactopyranosyl-(1 → 1)-D-glyceritol; 2) O-α-D-Galactopyranosyl-(1→1)-L-glyceritol; 3) O-β-D-Galactopyranosyl-(1→1)-D-glyceritol; 4) O-β-D-Galactopyranosyl-(1→1)-L-glyceritol; 5) O-α-D-Galactopyranosyl-(1→6)-O-β-D-galactopyranosyl-(1→1)-D-glyceritol.

side octaacetates (XV) which by catalytic hydrogenolysis to III, lead tetraacetate oxidation and catalytic hydrogenation to VII and subsequent hydrolysis would ultimately give the desired 1-L-glyceritol galactosides. However, while XIII rapidly consumed the theoretical volume of hydrogen in the presence of palladium on charcoal, the product that should have contained XV was not susceptible to hydrogenolysis under similar conditions. Raney nickel catalyst gave some reaction as was evident from the change in optical rotation, but the product finally obtained by following the scheme above was a rather complex mixture. Chromatography on a carbon column gave fractions with the chromatographic properties of a glyceritol galactoside but could not be induced to crystallise. It is possible that some ketal migration analogous to that observed with the 2,3-O-*iso*propylidene-D-glyceritol above takes place in this Koenigs-Knorr reaction.

Infrared spectra of glycoside A and of the 1-glyceritol galactosides were recorded with a Perkin-Elmer double beam spectrometer Model 21 with a sodium chloride prism, using the potassium bromide disc technique. Previous studies of the infrared spectra of carbohydrates have been confined to the frequency range 730—960 cm^{-1} (Ref.[18]); the corresponding sections of the spectra recorded here are shown in Fig. 1. The frequencies of the absorption bands in this region are given in Table 2. Barker *et al.*[19] made the following assignments for some of the characteristic infrared bands of D-galactopyranose derivatives (Nujol mull): Type 2 a, 825 ± 11 cm^{-1}, deformation mode of equatorial hydrogen at the anomeric carbon atom of α-anomers; type 2 b, 895 ± 9 cm^{-1}, deformation mode of axial hydrogen at the anomeric carbon atom of β-anomers; type 2 c, 871 ± 7 cm, deformation mode of equatorial hydrogen at carbon atom 4. The spectra now recorded agree with these interpretations. It is known that with compounds which take up water of crystallisation, the spectra may gradually change as the potassium bromide discs are stored [20]. However, no hydrates of the 1-glyceritol glycosides have been found, and no spectral changes were observed.

Table 2. Infrared bands of 1-glyceritol glycosides in the region 730—960 cm^{-1}. Frequencies * in cm^{-1}.

Frequencies assigned[18]:			Type 2a 825 ± 11		Type 2c 871 ± 7		Type 2b 895 ± 9			
Compound:										
O-α-D-Galactopyranosyl-(1→1)-D-glyceritol	740	802	821	854	879			(918)	927	(932)
O-α-D-Galactopyranosyl-(1→1)-L-glyceritol		783	821	863	871			900	920	
O-β-D-Galactopyranosyl-(1→1)-D-glyceritol		786		855	869		892	(900)	940	
O-β-D-Galactopyranosyl-(1→1)-L-glyceritol	775	(781)	(815)		871		895	921	944	
O-α-D-Galactopyranosyl-(1→6)-O-β-D-Galactopyranosyl-1→1)-D-glyceritol	(775)	789	815	840	866	884	896	914	945	

* Points of inflexion are given in brackets.

EXPERIMENTAL

*2,3-O-*Iso*propylidene-*D*-glyceritol (I).* 2,3-O-*Iso*propylidene-D-glycerose, b. p.$_{20}$ 55°, was prepared from D-mannitol by the method of Baer and Fischer [10,11]. The aldehyde (23 g), which had polymerised to some extent, was dissolved in ethanol and this solution was added with shaking to potassium borohydride (7 g) in 0.2 M disodium phosphate solution (150 ml). After standing overnight the mixture was acidified to pH *ca.* 6 by adding acetic acid and when the evolution of hydrogen had stopped the solution was made alkaline with sodium hydroxide and extracted repeatedly with chloroform. The extract was dried over potassium carbonate and concentrated. The residual oil was distilled through a short Vigreux column. Yield 18.9 g (81 %), b. p.$_{14}$ 82—83°, $[\alpha]_D^{23}$ +14.1° (pure oil), Baer and Kates report [12] $[\alpha]_D^{20}$ +14.0°.

Attempted preparation of 1-D-*glyceritol β-galactoside from I.* 2,3-O-*Iso*propylidene-D-glyceritol (I) (9.1 g), Drierite (100 g), freshly prepared silver oxide (25 g) and dry chloroform (100 ml) were stirred together in the dark for 1 h. A solution of acetobromogalactose (31 g) and iodine (4 g) in chloroform (120 ml) was gradually added with stirring during the next 2 h, and the mixture was then kept with stirring overnight. After filtration the chloroform solution was washed with water, dried over magnesium sulphate and concentrated under reduced pressure to a syrup (*ca.* 36 g). Paper chromatograms run in ethyl ether—dimethyl sulphoxide [21] showed one spot with R_F *ca.* 0.8 which appeared slowly with the silver nitrate—sodium hydroxide reagent and two spots with R_F *ca.* 0.2 and 0.4 which appeared quickly with this reagent. By countercurrent extraction between ethyl ether and dimethyl sulphoxide containing 10 % of water using 5 separating funnels [21], the fastest component was obtained in a chromatographically pure state (14.2 g from 27 g of the crude product). It did not crystallise and was obviously a mixture of diastereoisomers, consisting of 2,3-O-*iso*propylidene-D-glyceritol β-galactoside tetraacetate and the corresponding L-glyceritol derivative. Later a sample was deacetylated with sodium ethoxide in ethanol and hydrolysed (0.02 N sulphuric acid, 20°, 17 h) to give a syrup which crystallised from methanol—ethanol only when seeded with 1-D-glyceritol β-galactoside; m. p. 124—128°, undepressed on admixture with the material used for seeding, $[\alpha]_D^{20}$ −3° (water, c = 2.0). *Cf.* Table 1.

Part of the crude acetate (9 g) from the Koenigs-Knorr reaction was deacetylated with sodium ethoxide in ethanol, a small quantity of water was added and the solution was saturated with carbon dioxide, filtered and concentrated. On paper chromatograms run in ethyl acetate—acetic acid—water (3:1:1) * and then sprayed with periodate—benzidine [22], the deacetylated material gave a rather strong and somewhat trailing spot with R_F *ca.* 0.7. Some much slower spots were also observed. The deacetylated material was dissolved in water and added to a carbon—Celite mixture (100 g + 100 g) contained in a Büchner funnel. On batch-wise elution with aqueous ethanol (1, 2, 4, 6, 8, 10, 15, 25, 35 and 50 %, 500 ml of each) a fraction (2.8 g of dry material) was obtained which on paper chromatograms gave one main spot with R_F 0.7. It did not crystallise, but was assumed to be a mixture of *2,3-O-*iso*propylidene-*D*-glyceritol β-galactoside* and the corresponding L-glyceritol derivative, as mild hydrolysis (0.02 N sulphuric acid at 20° overnight) gave a homogeneous product (paper chromatographically) which when seeded with 1-D-glyceritol β-galactoside (from wheat flour lipids) gave crystals from methanol—ethanol having m. p. 120—124° and $[\alpha]_D^{18}$ −3° (water, c = 2.3). *Cf.* values for pure 1-D- and 1-L-glyceritol-galactosides, Table 1. On paper chromatograms run in ethyl acetate—acetic acid—water the 1-glyceritol β-galactosides travel with the same rate and slightly faster than galactose.

In a second run a mixture of I (0.72 g), silver oxide (4 g), Drierite (10 g) and chloroform (10 ml) was stirred for 1 h and then a solution of acetobromogalactose (2.5 g) and iodine (0.3 g) in chloroform (12 ml) was added with stirring over a period of 3 h. After stirring overnight the chloroform solution was washed with water, dried over magnesium sulphate and concentrated. The residue was deacetylated with sodium ethoxide in ethanol, and then hydrolysed for 30 min at 50° in 0.1 N hydrochloric acid. After treatment with Amberlite resin IR 4B and concentrating, the aqueous solution was added to a

* This solvent system was used throughout unless stated otherwise.

carbon—Celite column (1:1, 24 × 3 cm). On gradient elution with aqueous ethanol (2 000 ml), the concentration of which was raised linearly from 1 to 30 %, material with low optical rotation and with the paper chromatographic properties of a 1-glyceritol β-galactoside was obtained as an apparently homogeneous fraction. The first and last halves of this were collected and worked up separately. The first gave material (0.5 g) which crystallised from methanol—ethanol when seeded with 1-D-glyceritol β-galactoside. Yield 0.39 g; m. p. 124—129°, $[\alpha]_D^{18}$ −4° (water, c = 2.4). The second half (0.4 g) similarly gave 0.20 g, m. p. 110—116°, $[\alpha]_D^{18}$ −3° (water, c = 2.1). It is thus evident that some separation of the 1-D- and 1-L-glyceritol β-galactosides was achieved.

Anomerisation of D,L-glyceritol β-galactoside [14]. Purified 2,3-O-*iso*propylidene-D,L-glyceritol β-galactoside tetraacetate (4.0 g) from the preparation described above was refluxed for 20 min with 2 N sulphuric acid (2 ml) in 60 % aqueous ethanol (100 ml) to remove the *iso*propylidene group. The solution was treated with Amberlite resin IR 4B and concentrated to dryness under reduced pressure. The residue so obtained was acetylated with acetic anhydride and pyridine to give 1-D,L-glyceritol β-galactoside hexaacetate (3.9 g). This was dissolved in dry chloroform (100 ml), titanium tetrachloride (1.2 ml) was slowly added and the mixture was refluxed for 20 h with the exclusion of moisture. Pyridine (4 ml) and an excess of water were then added, the mixture was filtered with Celite and the chloroform phase was washed with sodium carbonate and water, dried over magnesium sulphate and concentrated under reduced pressure. To deacetylate the residual syrup (3.8 g) it was dissolved in absolute ethanol (100 ml) to which sodium (0.2 g) had previously been added and was then left at room temperature overnight. The solution obtained on dilution with water (100 ml), was filtered through Amberlite resins IR 120 H and IR 4B, concentrated under reduced pressure to a small volume, treated with decolorising carbon, filtered and concentrated to give the mixed α- and β-galactosides as a syrup (1.75 g).

To hydrolyse the remaining β-galactoside the syrup was incubated at 30° with a β-galactosidase solution [2,23] (5 ml) in 0.1 N sodium acetate buffer (pH 4.6, 100 ml). When the optical rotation of the solution had reached a constant value (after 60 h) acetone (120 ml) was added and after centrifugation the solution was further purified by precipitation with aqueous lead acetate, filtration with Celite, saturation with hydrogen sulphide and filtration. The solution obtained was concentrated under reduced pressure to a small volume (30 ml) and was then added to a carbon—Celite column (1:1, 24 × 3 cm). Gradient elution with aqueous ethanol (1—30 %, 2 000 ml) gave three separate fractions which were shown by paper chromatography to contain glyceritol, galactose and 1-glyceritol galactosides, respectively. The glycoside fraction crystallised from a methanol—ethanol mixture on seeding with *iso*floridoside (m. p. 132—141°, $[\alpha]_D^{21}$ +157°). Yield 0.51 g; m. p. 121—127°, $[\alpha]_D^{21}$ +157° (water, c = 2.0). After three further recrystallisations the product (*ca.* 0.2 g) had m. p. 125—137°, undepressed on admixture with *iso*floridoside.

The synthetic glycoside mixture and its concentrated mother liquors were combined (0.6 g in total), dissolved in water (10 ml) and the solution was added to the top of an efficient carbon—Celite column (1:1, 43 × 3.5 cm). Aqueous ethanol (4 000 ml), the concentration of which was raised linearly from 3 % to 6 %, was used as eluant. The optical rotation of the eluate showed two strong peaks which were only partly separated. The optically active part of the eluate was cut into 3 fractions. Fraction 1, corresponding to the first peak and fraction 2, corresponding to the second peak, were separated at the point of minimum rotation; the "tail" of the slowest component was collected separately to give fraction 3. As some overlapping could be expected, fraction 2 was run through the column again in the same way. However, there were no indications of the presence of any material from fraction 1 in the eluate.

Fraction 1 was concentrated to dryness and the residue (0.24 g) was recrystallised from methanol—ethanol. Yield 0.21 g; m. p. 131.5—133°, $[\alpha]_D^{20}$ +159° (water, c = 1.9). The properties did not change on further recrystallisation (analysis: see Table 1).

Fraction 2 similarly gave crystalline material (0.15 g), m. p. 149—151.5°, $[\alpha]_D^{20}$ +152° (water, c = 2.0).

Fraction 3 (35 mg) gave a small crop of crystals with m. p. 143—149°.

Fractionation of iso*floridoside on carbon.* A sample of *iso*floridoside [9] (0.25 g), m. p. 132—141°, $[\alpha]_D$ +157° from which the low-melting component had been partially removed by extensive recrystallisation, was fractionated in the same way as the synthetic α-galactosides and then gave fraction 1′ (0.06 g), m. p. 130.5—132°, $[\alpha]_D^{18}$ +155° (water, c = 1.9) and fraction 2′ (0.12 g), m. p. 149.5—151.5°, $[\alpha]_D^{18}$ +156° (water, c = 1.7).

As the melting point of mechanically mixed samples of the high- and low-melting glycoside showed no depression, but a very wide range (*ca.* 130—150°), further comparisons were made by the mixed fusion technique [24] using a Kofler hot stage. The samples to be compared were placed on each side of and close to a *ca.* 1 mm wide splinter of a cover glass which was placed on the glass slide of the hot stage. Heating was applied gradually until the molten material spreading from each side under the cover glass had met, if possible so that a few crystals of the most high-melting component were left. If necessary a seed crystal was added. The temperature was then adjusted so that the crystals grew at a maximum rate and the process was followed by polarised light. When all had solidified the new melting points were determined.

On mixed fusion of fraction 1′ and 2′ the crystallisation of the latter was found to be fairly fast up to the boundary between the samples. The zone of mixing was passed only very slowly, but then the rate of the crystal growth increased again and when all had solidified the crystals appeared perfectly homogeneous. On renewed heating a narrow channel indicating the zone of mixing formed at *ca.* 120°; fraction 1′ melted at 129—132° and fraction 2′ at 149—151°. When compared in the same way, 1-L-glyceritol α-galactoside (m. p. 127—129°; from 2,3-di-O-benzyl-L-glyceritol, XI) and fraction 1 and 1′ behaved as one compound, though the melting points of the solidified samples were slightly different, 126—129°, 131—134° and 129—132°, respectively. 1-D-Glyceritol α-galactoside (m. p. 150—152°; from 2,2′-O-methylene-bis-(3-O-benzoyl-D-glyceritol), (IV) was in the same way found to be identical with fraction 2 and 2′; the melting points of the solidified samples were 150—152°, 149—151° and 149—151°, respectively.

*2,2′-O-Methylene-bis-(3-O-benzoyl-*D*-glyceritol) (IV).* 1,6-Di-O-benzoyl-2,5-O-methylene-D-mannitol (II) was prepared from D-mannitol by the procedure of Ness *et al.*[15] As the synthesis was carried out on about 25 times the scale used by these authors, special care was taken to avoid overheating; the overall yield of a crude product, m. p. 117—121°, was 69 %. A sample was recrystallised from methanol, m. p. 119.5—121°, $[\alpha]_D^{22}$ −66° (chloroform, c = 2.0).

Finely powdered lead tetraacetate (44 g) was added slowly with stirring to a solution of II (40 g) in dry ethyl acetate (300 ml) and after standing for an hour the precipitated lead salts were filtered off. The filtrate was washed successively with water, aqueous sodium bicarbonate and water, and was then dried for a short time over sodium sulphate, filtered and concentrated to a smaller volume (*ca.* 100 ml). Carefully washed Raney nickel W-2 catalyst [25] (*ca.* 10 ml) was added and the mixture was hydrogenated at 70° and 130 atm pressure for 3 h. When the cooled hydrogenation vessel was opened the product had partly crystallised. It was brought into solution by gentle heating, the solution was filtered and an equal volume of light petroleum (b. p. 45—65°) was added to the combined filtrate and washings. After the mixture had been kept cold for a while the crystals (28 g, m. p. 104.5—106°) were filtered off, the mother liquors were concentrated under reduced pressure and the residue was recrystallised from carbon tetrachloride, giving a second crop (4 g, m. p. 101—105°). The combined material was recrystallised from chloroform—carbon tetrachloride. Yield 30 g (75 %), m. p. 105—106.5° $[\alpha]_D^{20}$ −58° (chloroform, c = 2.0). After recrystallisation from aqueous ethanol a sample had m. p. 106.5—108° and $[\alpha]_D^{18}$ −60° (chloroform, c = 2.3). (Found: C 61.9; H 6.00. Calc. for $C_{21}H_{24}O_8$: C 62.4; H 5.98.)

In order to test the stability of IV to silver oxide, a sample (m. p. 105—107°; 80 mg) was shaken with freshly prepared silver oxide (200 mg) in chloroform (4 ml) for 120 h at room temperature. The specific rotation of the samples remained unchanged and afterwards the filtered chloroform solution, when concentrated, gave a crystalline residue with m. p. 103—106° without further purification. Thus no significant racemisation took place.

*1-*D*-Glyceritol α- and β-galactosides.* A mixture of 2,2′-O-methylene-bis-(3-O-benzoyl-D-glyceritol) (IV) (10 g), freshly prepared silver oxide (17 g), Drierite (75 g) and dry chloro-

form (150 ml) was stirred for 1 h and then a solution of acetobromogalactose (22.5 g) and iodine (3 g) in chloroform (100 ml) was added dropwise with stirring during 2 h. Care was taken to protect the reaction mixture from light. After 2 days in a dark place, inorganic material was removed by filtration, the filtrate was washed with water, dried over magnesium sulphate and concentrated under reduced pressure. To split the methylenedioxy-bridge of V, the residual syrup was dissolved in a mixture of acetic anhydride (70 ml), acetic acid (30 ml) and sulphuric acid (1 ml). After 1 h at room temperature anhydrous sodium acetate (4 g) and water (100 ml) were added and when the anhydride had decomposed, the mixture was diluted with more water and extracted with chloroform. The chloroform solution was washed with aqueous sodium carbonate and water, dried over magnesium sulphate and concentrated. The residue was treated with a solution of sodium (4 g) in absolute ethanol (600 ml) at room temperature overnight. Water (600 ml) was then added, the solution was filtered through Amberlite resins IR 120 H and IR 4B and the filtrate was concentrated under reduced pressure. When dissolved in methanol (10 ml), the residue crystallised spontaneously but the product (7.3 g) had m. p. 121—136° and $[\alpha]_D^{21}$ +38° (water, c = 2.0) and was probably a mixture of the α- and β-galactosides. Recrystallisation from methanol gave 1-D-glyceritol β-galactoside (2.1 g) m. p. 138—140°, $[\alpha]_D^{21}$ ±0 (water, c = 2.0), and 1-D-glyceritol-α-galactoside (0.2 g), m. p. 150—152°, $[\alpha]_D^{18}$ +155° (water, c = 1.8), (analysis: See Table 1.)

The combined mother liquors were concentrated, the residue was dissolved in water and the solution was added to the top of a carbon—Celite column (1:1, 50 × 5 cm). Gradient elution with aqueous ethanol (2—8 %) gave two fractions containing material with the R_F value of a 1-glyceritol galactoside. The fractions were not completely separated, as judged by spot tests, but the first of them was easily distinguished by its high positive optical rotation. On concentration and recrystallisation of the residue from methanol—ethanol this fraction gave 1-D-glyceritol α-galactoside (1.9 g), m. p. 150—151.5°. The next fraction similarly gave 1-D-glyceritol β-galactoside (2.4 g), m. p. 138.5—140.5°. A sample was recrystallised from methanol and then had m. p. 140.5—141.5°, $[\alpha]_D^{20}$ −7° (water, c = 2.0), (analysis: See Table 1.)

The total yield of the α- and β-anomer was thus 2.1 g and 4.5 g or 17 % and 36 % calculated on IV, respectively.

The synthesis was repeated on half the scale described above; one quarter of the acetobromogalactose solution was added at once and the rest during *ca.* 40 min. The yield of α-anomer (m. p. 150—152°) and β-anomer (m. p. 137—140°) was now only 3 % and 28 % of the theoretical, respectively.

2,2'-O-Methylene-bis-(3-O-trityl-L-glyceritol) (VI). A solution of 2,2'-O-methylene-bis-(3-O-benzoyl-D-glyceritol) (IV) (8.1 g) and trityl chloride (13 g) in dry pyridine (60 ml) was kept at 100° for 4 h and was then poured into ice-water. The mixture was extracted with ether and the ether phase was washed successively with water, sodium bicarbonate and water and was then dried over sodium sulphate. After filtration the ether solution was concentrated and the remaining amorphous *2,2'-O-methylene-bis-(1-O-trityl-3-O-benzoyl-D-glyceritol)* was dissolved in ethanol (50 ml) containing potassium hydroxide (6 g). After heating on a water bath for 1 h the mixture was diluted with water and extracted with chloroform. The chloroform extract was washed with water, dried over sodium sulphate and concentrated under reduced pressure and the residue was recrystallised from carbon tetrachloride. Yield 11.3 g (83 %); m. p. 142—146°. A pure sample obtained by recrystallisation from an ethanol—ethyl acetate mixture had m. p. 146—147.5° and $[\alpha]_D^{18}$ +58° (chloroform, c = 2.0). (Found: C 79.0; H 6.39. Calc. for $C_{45}H_{44}O_6$: C 79.4; H 6.51.)

1-L-Glyceritol β-galactoside from VI. A mixture of 2,2'-O-methylene-bis-(3-O-trityl-L-glyceritol) (VI) m. p. 142—146°; 5.0 g), freshly prepared silver oxide (7.4 g), Drierite (29 g) and dry chloroform (40 ml) was stirred for 1 h and then a solution of acetobromogalactose (6.7 g) and iodine (0.9 g) in chloroform (30 ml) was added with stirring during 3 hours. The mixture was kept with stirring in a dark place until a sample of the chloroform solution no longer gave a positive bromide test with silver nitrate in ethanol (12 days).

The reaction product was isolated and subjected to acetolysis and deacetylation, essentially as described above for V in the preparation of the 1-D-glyceritol galactosides. Most of the tritanol which was liberated in the acetolysis, could be filtered off after the excess of acetic anhydride had been destroyed by the addition of water.

The deacetylated material gave strong spots for galactose and glyceritol on paper chromatograms. It was separated on a carbon—Celite column (1:1, 50 × 5 cm) by the gradient elution technique. Aqueous ethanol (1—8 %, 8 000 ml) was used as eluant and the eluate was investigated polarimetrically and by paper chromatography. One fraction (1.0 g) had the chromatographic properties of a 1-glyceritol galactoside and crystallised from a methanol—ethanol mixture when seeded with 1-D-glyceritol β-galactoside. Yield 0.78 g, (21 % calc. on VI), m. p. 97—100°. After recrystallisation from the same solvent it still had m. p. 97—100° and $[\alpha]_D^{18}$ +1° (water, c = 2.5). These values are somewhat lower than those observed with the same compound prepared from 2,3-di-O-benzyl-L-glyceritol (see Table I).

1-L-Glyceritol α-galactoside travels a little faster than the corresponding β-galactoside on carbon columns, but when the part of the eluate which would contain the α-galactoside was concentrated, the residue (0.16 g) had a low specific rotation ($[\alpha]_D$ +16°) and could not be induced to crystallise.

3-O-Benzyl-L-glyceritol (VIII) has previously been prepared by treating the sodium salt of 2,3-O-*iso*propylidene-D-glyceritol (I) with benzyl bromide and then removing the *iso*propylidene group by mild hydrolysis [16,17]. The benzylation procedure of Zemplén *et al.*[26] was used in the present investigation and seems to give a higher yield.

A mixture of 2,3-O-*iso*propylidene-D-glyceritol (18.9 g), finely powdered potassium hydroxide (115 g) and dioxane (250 ml) was placed in a three-necked flask equipped with a mechanical stirrer, a reflux condenser and a dropping funnel. The flask was immersed in an oil bath which was kept at 80° and freshly distilled benzyl chloride (100 ml) was added through the funnel over a period of 45 min with vigorous stirring. The reaction mixture was kept at 80—90° with stirring overnight. After cooling it was filtered, the filter cake was dissolved in water and the solution was extracted with benzene. The dioxane solution and the benzene extract were combined, dried over magnesium sulphate, filtered and concentrated under reduced pressure (to *ca.* 100 ml). This residue was distilled *in vacuo*, giving a fore-run (54 g) of unreacted benzyl chloride, b. $p._{13}$ 65—66° and then a fraction (43 g), b. $p._{0.3}$ 90—96° and α_D^{21} +13.7° (1 dm, pure oil), containing *1-O-benzyl-2,3-O-*iso*propylidene-D-glyceritol.* In a pure state this compound has b. $p._{0.3}$ 95—97° and α_D +17.8° (1 dm, pure oil) [16]; the theoretical yield should be only 31.8 g. The crude product was probably contaminated with dibenzyl ether, but it was used in the next step without further purification.

The crude benzyl ether obtained above (43 g) was dissolved in methanol (300 ml). Water (100 ml) and 2 N sulphuric acid (20 ml) were added and the mixture was heated to the boiling point and then left at room temperature overnight. The methanolic solution was extracted with five 50 ml portions of light petroleum (b. p. 45—65°) to remove any dibenzyl ether; the light petroleum extracts were washed successively with two 50 ml portions of 80 % aqueous methanol to retain any VIII carried away. The combined methanolic solutions were concentrated under reduced pressure to remove most of the methanol and the residual aqueous solution (*ca.* 150 ml) was extracted with chloroform. The chloroform extract was washed with aqueous sodium carbonate and water, dried over sodium sulphate, filtered and concentrated under reduced pressure and the residual syrup (25.4 g) was distilled *in vacuo* through a Vigreux column. A small fore-run (1.7 g) b. $p._{0.15}$ 123°, n_D^{21} 1.5450, was discarded; VIII then distilled at 128—133° and ca 0.05 mm pressure. Yield 23.1 g (88 % calc. on I; n_D^{21} 1.5322, α_D^{21} +6.6° (1 dm, pure oil). Sowden and Fischer [16] give b. $p._{0.3}$ 138—139°, n_D^{16} 1.5342, α_D +6.1° (1 dm, pure oil).

1-O-Trityl-2,3-di-O-benzyl-L-glyceritol (X). A solution of 3-O-benzyl-L-glyceritol (VIII) (23.1 g), and trityl chloride (35.4 g) in dry pyridine (150 ml) was kept at room temperature for 2 days and then heated at 60° for 4 h. It was then stirred into ice-water and the aqueous mixture was extracted with ether. The ether phase was washed several times with water, then as quickly as possible with cold 0.5 N sulphuric acid and finally with aqueous sodium carbonate and water. After drying over sodium sulphate the ether-

eal solution was filtered and concentrated under reduced pressure to give crude *1-O-trityl-3-O-benzyl-*L*-glyceritol* (IX) as a syrup which, however, did not crystallise.

Freshly distilled benzyl chloride (60 ml) was added gradually with vigorous stirring to a mixture of the crude trityl compound and finely powdered potassium hydroxide (50 g) in dioxane (150 ml), while the temperature was kept at 80°. Stirring was continued overnight at this temperature. The insoluble material was then filtered off, the filter cake was dissolved in water and the aqueous suspension obtained was extracted with benzene and the benzene extract was added to the residue remaining after the dioxane filtrate had been concentrated under reduced pressure. The benzene solution was washed with sodium bicarbonate and water, dried over sodium sulphate, filtered, concentrated and finally taken to dryness at *ca.* 0.3 mm pressure and 150° (bath temperature). The residue crystallised when stirred with light petroleum. The crude product was ground to a paste with light petroleum—*iso*propyl ether (1:1, 50 ml), filtered and then recrystallised from benzene—ethanol. After recovering a few grams from the mother liquors, the yield of pure X was 52 g (80 % calc. on VIII); m. p. 84.5—86°, $[\alpha]_D^{18}$ −9° (chloroform, c = 2.5). (Found: C 83.6; H 6.69. Calc. for $C_{36}H_{34}O_3$: C 84.0; H 6.66.)

*2,3-Di-O-benzyl-*L*-glyceritol (XI).* A solution of 1-O-trityl-2,3-di-O-benzyl-L-glyceritol (X) (48,8 g) in acetic acid (340 ml) was heated under reflux and water (240 ml) was added at a moderate rate so that no oil separated. The mixture was refluxed for a further hour and then kept in a refrigerator overnight. Tritanol (23.5 g or 95 %) was filtered off and the mother liquors were concentrated under reduced pressure to give crude XI as a colourless oil (26.7 g). After drying azeotropically with benzene, it was used in the next step without further purification. A sample was distilled *in vacuo*. It had b.p.$_{0.05}$ *ca.* 150°, n_D^{25} 1.5490, d_4^{23} 1.106 and $[\alpha]_D^{23}$ +3.8° (pure oil).

*1-*L*-Glyceritol α- and β-galactosides from XI.* A mixture of crude, dry 2,3-di-O-benzyl-L-glyceritol XI (11 g), freshly prepared silver oxide (19 g), Drierite (50 g) and dry chloroform (100 ml) was stirred for 1 h and then a solution of acetobromogalactose (18 g) and iodine (2.4 g) in dry chloroform (100 ml) was added during 3 h. The reaction mixture was shielded from light. After stirring for a further 20 h a sample of the chloroform solution gave no reaction with ethanolic silver nitrate solution. Insoluble material was then filtered off, the filtrate was washed with water, dried over sodium sulphate and concentrated under reduced pressure. The residue was treated overnight with absolute ethanol (500 ml) to which sodium (0.75 g) had been added, the alkali was neutralised by adding 2 N sulphuric acid (16 ml) and after filtration the ethanolic solution was concentrated to a small volume. 2 N sodium carbonate solution (5 ml) was added to the residue and the di-O-benzylglyceritol galactosides were extracted with three 200 ml portions of ethyl acetate. The extracts were filtered successively through a cellulose column (10 × 3.5 cm), pre-equilibrated with water-saturated ethyl acetate, and then concentrated under reduced pressure. The amorphous residue (16 g) was free from reducing sugars. It was dissolved in methanol (200 ml) and hydrogenolysed in the presence of palladium on charcoal catalyst (2 g) containing 10 % of Pd. The uptake of hydrogen was 2 000 ml in 4 h; theory requires 1 940 ml. After filtration the methanolic solution was concentrated under reduced pressure and the residue was dissolved in a small quantity of water. Some crystalline material (0.2 g, m. p. 80—94°), probably triphenylmethane, was filtered off and the filtrate was concentrated under reduced pressure. The residual syrup was dissolved in methanol—ethanol and seeded with 1-D-glyceritol β-galactoside, giving crystalline 1-L-glyceritol β-galactoside (5.0 g), m. p. 101—103°, $[\alpha]_D^{20}$ +2° (water, c = 3.0).

The residue (3.0 g) obtained on concentration of the mother liquors was separated on a carbon—Celite column (50 × 5 cm) as described previously, using aqueous ethanol (2—8 %, 8 000 ml) as the eluant. Glyceritol was present in the first part of the eluate as indicated on paper chromatograms. After a large empty fraction there followed a fraction with a low positive optical activity and immediately after this another which gave a spot for a 1-glyceritol galactoside on paper chromatograms but was optically inactive.

The optically active fraction was concentrated under reduced pressure giving a residue (0.12 g) which crystallised from methanol—ethanol. Recrystallisation from the same solvent gave 1-L-glyceritol α-galactoside (70 mg), m. p. 127—129°, $[\alpha]_D^{18}$ +156° (water, c = 1.8). As described above, this compound was shown by mixed fusion to be identical with the low-melting component of *iso*floridoside.

The residue (1.5 g) from the next fraction gave 1-L-glyceritol β-galactoside (1.0 g), m. p. 102—107°, $[\alpha]_D^{20}$ +2° (water, c = 2.0). The total yield of this compound was thus 6.0 g (59 %). The melting points of various preparations were somewhat irregular and a sample (400 mg) was therefore added to an efficient carbon—Celite column (1:1, 43 × 3.5 cm) and then eluted with aqueous ethanol (3.5—6.5 %, 4 000 ml). 0.5 ml aliquots of the eluate were oxidised with sodium metaperiodate and the excess of oxidant was determined iodometrically [27] after 4 h. The periodate consumption showed only one peak; the two successive halves of the corresponding part of the eluate were worked up separately giving two crystalline preparations which both had m. p. 102.5—105°. They were combined and recrystallised but the melting point was unchanged except that a few crystals remained up to 107°. However, when a sample was dried intensively and then immediately transferred to the hot stage so that contact with atmospheric moisture was avoided, the m. p. was raised to 104—107°; $[\alpha]_D^{18}$ +2° (water, c = 2.0), (analysis: See Table 1.) Mixed fusion with 1-D-glyceritol β-galactoside gave a melting point minimum of 98—99°, the solidified D- and L-glyceritol derivatives melted at 140—141.5° and 105—110°, respectively. About two days were required for the melt to crystallise at 85°; the crystals appeared homogeneous.

1,6-Di-O-benzoyl-2,5-O-methylene-3,4-O-benzylidene-D-mannitol (XIV). Ness *et al.*[15] prepared XIV in 83 % yield by treating 1,6-di-O-benzoyl-2,5-O-methylene-D-mannitol (II) with 5 parts of benzaldehyde in the presence of 1 part of fused zinc chloride at room temperature. This procedure was somewhat modified to facilitate the preparation of XIV on a larger scale.

Powdered anhydrous zinc chloride (110 g) was added with stirring to freshly distilled benzaldehyde (1 100 ml). When all had dissolved the solution was cooled to room temperature and diluted with dry *iso*propyl ether (1 100 ml). 1,6-Di-O-benzoyl-2,5-O-methylene-D-mannitol (225 g) was added with stirring and when completely dissolved the mixture was allowed to stand at room temperature overnight. The benzylidene compound soon started to crystallise. After keeping in a refrigerator for a day the mixture was filtered and the filter cake was carefully washed with water, aqueous sodium bicarbonate and water and was then dried. Yield 180 g; m. p. 153—156°. A further quantity (60 g), m. p. 153—156° was obtained from the mother liquors by washing with water and aqueous sodium bicarbonate, drying over sodium sulphate, concentrating under reduced pressure and recrystallising the residue from ethyl acetate—methanol (1:3). The total yield of XIV was thus 88 %; $[\alpha]_D^{20}$ +59° (chloroform, c = 2.0). Ness *et al.*[15] record m. p. 151—152° and $[\alpha]_D^{20}$ +61.2°.

2,5-O-Methylene-3,4-O-benzylidene-D-mannitol (XIII) was prepared by refluxing its dibenzoate (XIV) (240 g) with a solution of sodium hydroxide (45 g) in ethanol (1 200 ml) and water (500 ml) for 90 min. Most of the ethanol was distilled off under reduced pressure, water (500 ml) was added and after cooling the crystals were filtered off and recrystallised from water. Yield 108 g (82 %); m. p. 129.5—132°. After concentration under reduced pressure the mother liquors gave a second crop of crystals. A sample was recrystallised from ethyl acetate, m. p. 130—132°, $[\alpha]_D^{18}$ +28° (chloroform, c = 2.3). (Found: C 59.7; H 6.49. Calc. for $C_{14}H_{18}O_6$: C 59.6; 6.43.) On treatment of XIII with benzoyl chloride in pyridine the expected dibenzoate (XIV) was regenerated.

Attempted preparation of 1-L-glyceritol β-galactoside from XIII. A mixture of 2,5-O-methylene-3,4-O-benzylidene-D-mannitol (XIII) (1.0 g), freshly prepared silver oxide (2.7 g), Drierite (10 g) and dry chloroform (10 ml) was stirred for 1 h and then a solution of acetobromogalactose (3.4 g) and iodine (0.4 g) in dry chloroform (15 ml) was added during the next 2 h. After the mixture had been stirred overnight the chloroform solution was free from reactive bromide. Insoluble material was filtered off and the filtrate was washed, dried and concentrated in the usual way giving a syrup (3.7 g), presumed to be XV, which was only moderately soluble in ethanol. A very small quantity of crystals, m. p. 235—237°, which separated from an ethanolic solution, gave a positive formaldehyde test with chromotropic acid.

Part of the syrup (1.8 g) was dissolved in ethanol (40 ml) and hydrogenated at room temperature for 87 h in the presence of palladium on charcoal catalyst (0.5 g) containing 10 % of Pd. However, the hydrogen uptake was of the order 2 ml/h and could be attri-

buted to losses by diffusion. The theoretical volume of hydrogen required for removal of a benzylidene group from XV is *ca.* 80 ml. The hydrogenolysis of a comparable amount (0.54 g, 2 mmoles) of XIII using the same catalyst (0.5 g) was complete in 1 h, giving 2,5-O-methylene-D-mannitol [15], m. p. 176—177.5°, $[\alpha]_D^{20}$ −50° (water, c = 2.0). The presence of catalyst poisons seems to be excluded by the fact that subsequent addition of XIII to the hydrogenation mixture containing the product from the Koenigs-Knorr reaction, resulted in a rapid hydrogen uptake. Either the hydrogenolysis of XV is sterically hindered or XIII rearranges before the Koenigs-Knorr reaction takes place, to give a less reactive molecule.

As an experiment showed that XIII could be hydrogenolysed using Raney nickel as the catalyst, the product (3.4 g, from 3.4 mmoles of XIII) from a Koenigs-Knorr reaction, carried out as described above, was dissolved in ethyl acetate (20 ml) and then Raney nickel catalyst W-2[26] (3 ml) was added. Treating the mixture with hydrogen at 95° and 150 atm, the optical rotation of the solution read in a 1 dm tube was +0.76° at the start and then reached a constant value of −0.78° in 24 h. The catalyst was filtered off and lead tetraacetate was gradually added to the filtrate. *Ca.* 1.0 g of oxidant was rapidly consumed; calculated on the amount of XIII used as starting material the theoretical consumption should be 1.5 g. The excess oxidant was destroyed by adding ethylene glycol, the mixture was filtered and the filtrate was washed with water and aqueous sodium bicarbonate, dried over magnesium sulphate and concentrated under reduced pressure. The residue was hydrogenated for 15 h at 75° and 140 atm in the presence of Raney nickel catalyst (1 ml) in ethyl acetate (15 ml). The hydrogenated product (*cf.* VII) was acetylated and deacetylated as described for V in the preparation of 1-D-glyceritol galactosides. The final product (0.66 g) on paper chromatograms gave an elongated spot with about the R_F value of galactose as well as two slow fairly strong spots and traces of faster spots (periodate—benzidine spray [22]). The mixture was separated on a small carbon column in the usual way giving two adjoining fractions (75 mg and 180 mg) which had the chromatographic properties of 1-glyceritol galactosides but could not be induced to crystallise.

Acetylation of pure samples of the 1-glyceritol galactosides described above, using acetic anhydride in pyridine, gave amorphous products. The paper chromatography of the acetates in dimethyl sulphoxide solvent systems has been described in a previous paper [21].

Acknowledgements. The author is indebted to *Statens Naturvetenskapliga Forskningsråd* for financial support, to Ing. Gurli Hammarberg for her skilful assistance and to Dr. B. Thomas for checking the English.

REFERENCES

1. Wickberg, B. *Acta Chem. Scand.* **11** (1957) 506.
2. Wickberg, B. *Acta Chem. Scand.* **12** (1958) 1183.
3. Carter, H. E., McCluer, R. H. and Slifer, E. D. *J. Am. Chem. Soc.* **78** (1956) 3735.
4. Colin, H. and Gueguen, E. *Compt. rend.* **191** (1930) 163.
5. Augier, J. and du Mérac, M.-L. *Compt. rend.* **238** (1954) 387.
6. Putman, E. W. and Hassid, W. Z. *J. Am. Chem. Soc.* **76** (1954) 2221.
7. Lindberg, B. *Second International Seaweed Symposium.* Pergamon Press, London 1956, p. 33.
8. Lindberg, B. *Acta Chem. Scand.* **9** (1955) 1093.
9. Lindberg, B. *Acta Chem. Scand.* **9** (1955) 1097.
10. Baer, E. *J. Am. Chem. Soc.* **67** (1945) 338.
11. Baer, E. and Fischer, H. O. L. *J. Biol. Chem.* **128** (1939) 463.
12. Baer, E. and Kates, M. *J. Am. Chem. Soc.* **70** (1948) 1394.
13. Reynolds, D. D. and Evans, W. L. *J. Am. Chem. Soc.* **60** (1938) 2559.
14. Pacsu, E. *Ber.* **61** (1928) 1508.
15. Ness, A. T., Hann, R. M. and Hudson, C. S. *J. Am. Chem. Soc.* **65** (1943) 2215.
16. Sowden, J. C. and Fischer, H. O. L. *J. Am. Chem. Soc.* **63** (1941) 3244.

17. Baer, E. and Kates, M. *J. Am. Chem. Soc.* **72** (1950) 942.
18. Neely, W. B. *Advances in Carbohydrate Chem.* **12** (1957) 13.
19. Barker, S. A., Bourne, E. J., Stephens, R. and Whiffen, D. H. *J. Chem. Soc.* **1954** 3468.
20. Barker, S. A., Bourne, E. J., Weigl, H. and Whiffen, D. H. *Chem. & Ind. London* **1956** 318.
21. Wickberg, B. *Acta Chem. Scand.* **12** (1958) 615.
22. Cifonelli, J. A. and Smith, F. *Anal. Chem.* **26** (1954) 1132.
23. Edman, P. and Jorpes, E. *Acta Physiol. Scand.* **2** (1941) 41.
24. Cheronis, N. D. and Entrikin, J. B. *Semimicro Qualitative Organic Analysis.* Interscience Publishers, New York 1957, p. 166.
25. *Org. Synthesis* Coll. Vol. **3** (1955) 181.
26. Zemplén, G., Csürös, Z. and Angyal, S. *Ber.* **70** (1937) 1848.
27. Wickberg, B. *Acta Chem. Scand.* **10** (1956) 1097.

Received March 29, 1958.

ACTA CHEMICA SCANDINAVICA 12 (1958) 1202—1210

On the Separation of Cobalt(III) and Chromium(III) Ammines by Column Chromatography

ARNE JENSEN*, JANNIK BJERRUM and FLEMMING WOLDBYE

Chemistry Department A, Technical University of Denmark, Copenhagen, Denmark

A method is developed for the separation of cobalt(III) and other robust coordination complexes on columns of activated alumina with the aid of aqueous salt solutions of proper composition as eluents. The scope and applicability of the method are illustrated by a variety of separations which have been achieved. Some of the factors influencing and producing the separations are considered.

A problem of increasing importance in modern coordination chemistry is the separation and analysis of reaction mixtures of robust complexes, for example of Co(III) and Cr(III), a task which can be accomplished by classical and spectrophotometric methods only in special cases. It seems therefore desirable to attack problems of this kind from different angles, for example by adsorption methods. Ion exchange technique may be used for separations of this kind with good results, as shown *e.g.* by Gustavson[1] and King and coworkers [2]. Lederer [3] has made some experiments on the separation of cobalt(III) nitroammines in non-aqueous solutions by means of paper chromatography, and Maki [4] has separated robust complexes, *e.g.* the chloroaquochromium(III) complexes in aqueous buffer solutions by means of electrochromatography on filter paper. In preliminary communications [5] we have described how robust complexes can be separated on columns of activated alumina using aqueous salt solutions as eluents. Sacconi [6] has obtained some qualitative results with pure aqueous solutions of cobalt(III) ammines, and Hein [7] has used columns of alumina for separating aqueous mixtures of phenylchromium compounds in a way which in principle is similar to the method used by us.

Chromatography on activated alumina is a very complex phenomenon as especially shown by Umland [8]. However, under specific conditions (proper composition and controlled pH of the solutions) we have developed this

* Guest from: Dept. of Inorganic Chemistry, The Royal Danish School of Pharmacy, Copenhagen.

technique to a useful method for analyzing aqueous mixtures of robust complexes. Cation complexes are separated in basic solution, the anions on the other hand in weakly acidic buffers. As displacing agents were used relatively concentrated solutions of various colourless electrolytes with which the columns were also treated in advance. The separations are highly dependent on the salt applied, being in some cases limited to special kinds of electrolytes. Thus $Co(NH_3)_6^{+++}$ could be separated quantitatively from $Cr(NH_3)_6^{+++}$ with 0.01 M KOH, 1 M KCl as a displacing agent, with much better results than with basic solutions of NaCl or $N(C_2H_5)_4Cl$. On the other hand, alkaline $N(C_2H_5)_4Cl$ was necessary for separating mixtures of Co en_3^{+++} and Cr en_3^{+++} (see Table 2).

According to Tiselius [9] one can distinguish between displacement analysis and elution analysis. In the separations considered here the displacing electrolyte penetrates and separates the coloured zones of the complexes. The case seems, therefore, to correspond closely to what Tiselius and coworkers [10] denote as non-ideal displacement. Accordingly, our guiding principle was to look for salts whose cations or anions, respectively, were supposed to have an adsorption tendency comparable with that of the complex cations and anions. Added in a sufficiently high concentration the proper salts were found to separate completely very similar complexes such as the luteo ions mentioned. The displacing power of the various cations decreases with increasing ionic radius, *i.e.* in the sequence Li^+, Na^+, K^+, $N(C_2H_5)_4^+$ and $C_{16}H_{33}N(CH_3)_3^+$. It was found that Tl^+ enters this series before Na^+. On the other hand, very little difference was found between the displacing power of anions, such as Cl^-, Br^- and NO_3^-.

EXPERIMENTAL

The columns were prepared from Merck's alumina standardized according to Brockmann. The apparatus was constructed to permit continuous addition of solutions and eluating agents.

Technique. The adsorption tubes were made of Pyrex glass. Their normal dimensions were 11 by 250 mm, but larger columns with an internal diameter of 15 mm and a length of up to 500 mm were also used in special cases. The tubes were provided with a ground-glass joint which contained a removable sintered glass disc. The tubes and the ground-glass joints were held together with wire spirals.

The columns were made by quickly pouring a thick aqueous slurry of the alumina [11] into the tubes. Especially with the normal size tubes columns made in this way lead to a uniform development of the zones. The tubes were usually filled to about three fourth of the volume, leaving the upper part of the volume for the addition of solutions. In order to save time the solutions were pressed through the columns by means of the pressure produced and regulated with the aid of two movable mercury reservoirs. The columns were equipped with a construction according to Sannie [12] which permits the introduction of eluating agents without releasing the pressure.

Procedure. Before an analysis the column was treated with the eluating solution to be used. Then 2–5 ml of the mixture of complexes were added to the column. The complex salts were sometimes but not necessarily dissolved in the eluating solvent. The eluating solution was added just at the moment when the complex mixture had passed into the column, but so quickly that the top of the column was not sucked dry. When an extra pressure of 0.5–1 atm. was applied, an experiment could usually be finished within 15–30 min. If no air bubbles happened to be evolved when the pressure was released, the same column could be used for other experiments.

The coloured effluents were collected in individual flasks, and in most cases the complexes could be separated and eluated completely. This could be done either with a

single eluent, or occasionally by the successive use of two eluents of increasing displacing power so that — in the ideal case — each component of the mixture was eluated by a specific eluent leaving the others for the following eluent.

For quantitative studies the collected samples of a given component were diluted to a known volume in a measuring flask, and the absorption curve of the solution measured with a recording Cary spectrophotometer. The absorption curve of the initial solution of the pure component diluted to the same extent was measured with the same instrument, and in this way information about the quality of the separations was obtained.

Various reagents were used to test the intermediate fractions. Sodium sulphide was an especially good reagent for testing traces of Co(III) complexes in mixtures of Co(III) and Cr(III) complexes.

Materials. The complex salts used were prepared according to prescriptions in the literature, or were from the laboratory collection of complex salts prepared by S. M. Jörgensen.

Basic alkali metal and quaternary ammonium salt solutions were used as eluating agents. Tetraethylammonium bromide and cetyltrimethylammonium bromide (technical pure) from Milton Industrial Chemicals (London) Ltd. gave colourless solutions and were sufficiently pure for the experiments. The bromides were converted to the corresponding hydroxides by means of an anion exchanger (Amberlite Resin IRA-400); in other cases we have applied mixed solutions of the quaternary ammonium salts and potassium hydroxide. The cetylammonium salt separated out on standing, but was easily dissolved before use by gentle heating.

In a few cases, *e. g.* for the separation of anion complexes, acidic solutions were used as eluents. To escape turbidity (due to colloidal dissolution of the alumina) acid-treated alumina was used. The alumina (Brockmann) was treated with 0.5 M HCl for a few minutes, washed with water and dried at 120°C.

RESULTS AND DISCUSSION

We have experimented with a single complex on the column in order to decide to what extent it can be recovered by displacement. Some examples are given in Table 1. 2 ml of a luteo salt solution were added to the columns and eluated with the basic salt solution mentioned in the table. The forerun was usually 10—15 ml, and the fraction containing the luteo salt had about the same volume. It was diluted to 25 ml in a measuring flask and the absorption curve compared with that of the initial solution diluted to the same extent. The losses (given in per cent) were somewhat variable especially in the case of $Co(NH_3)_6Cl_3$, which is bound so strongly to the alumina that the colour of the absorbed complex is distinctly more reddish than that of the solid salt. Here as for the chromium(III) ammines the loss is probably to some extent caused by decomposition of some of the luteo salt (not necessarily caused

Table 1. Experiments on the recovery of luteo salts. Loss in per cent.

Displacing sol. / Luteo salt sol.	0.1 M NaOH 1 M LiCl	0.1 M NaOH 5 M LiCl	0.1 M NaOH 1 M NaCl	0.01 M NaOH 1 M LiCl	1 M NH_3 1M NH_4Cl
0.03 M $[Co(NH_3)_6]Cl_3$	av. 4.1				2.4
0.03 M $[Co\ en_3]Cl_3$	av. 3.6	3.5		0.5	
0.1 M $[Co\ en_3]Cl_3$	0.5				
0.03 M $[Cr(NH_3)_6]Cl_3$	2.7				
0.03 M $[Cr\ en_3]Cl_3$		3.0	3.0		

by the column). Thus a column which had been used for 10—15 determinations gave a cobalt reaction only near the top when developed with Na_2S.

To decrease decomposition the hydroxyl ion concentration of the eluents should be as low as possible. Furthermore, it seems to be of some importance not to have too low a concentration of the salts to be displaced (*cf.* the experiments with Co en_3Cl_3).

Separation of luteo complexes

In Table 2 the results of some experiments on the separation of mixtures of luteo complexes are compared. About 0.03 M solutions of the luteo salts dissolved in the displacing solvent were mixed in equivalent amounts, and 2 (or 3) ml of the solution were analyzed. The coloured fractions of the two (or three) components diluted to 25 ml, were measured in 5 cm cells, and the absorption curve compared with that of the pure luteo salt solution at the same dilution.

Table 2. Separation of luteo complexes. Conc. (mole/l) in solution to be analyzed.

Salts separated	According to prep.	Chromatogr. found	Displacing solutions
Cr en_3Cl_3	0.0162	0.0155	0.1 M KOH, 1 M $(C_2H_5)_4NBr$
Co en_3Cl_3	0.0142	0.0139	
Co en_3Cl_3	0.0136	0.0136	0.1 M KOH, 1 M $(C_2H_5)_4NBr$
$Cr(NH_3)_6Cl_3$	0.0135	0.0135	0.1 M KOH, 1 M KCl
$Co(NH_3)_6Cl_3$	0.0138	0.0130	
Co en_3Cl_3	0.0158	0.0139	0.1 M KOH, 1 M $(C_2H_5)_4NBr$
$Cr(NH_3)_6Cl_3$	0.0160	0.0152	0.01 M KOH, 1 M KCl
Cr en_3Cl_3	0.0150	0.0147	0.01 M KOH, 1 M KCl
$Co(NH_3)_6Cl_3$	0.0150	0.0146	
$Cr(NH_3)_6Cl_3$	0.0160	0.0140	0.01 M KOH, 1 M KCl
$Co(NH_3)_6Cl_3$	0.0144	0.0132	

It will be seen that the tendency to adsorption increases in the series: Cr en_3^{+++}<Co en_3^{+++}<$Cr(NH_3)_6^{+++}$<$Co(NH_3)_6^{+++}$. Quaternary ammonium salts were necessary in order to accomplish the separation of the two ethylenediamine complexes. The use of 0.1 M KOH, 1 M $(C_2H_5)_4NBr$ as a displacing agent gave a clear separation into two yellow fractions the first of which gave only a very weak reaction for cobalt with Na_2S. But already substitution of the quaternary ammonium salt with KCl gave no separation. Separation could also be performed with alkaline cetyltrimethylammonium salt solutions, but the eluates became more diluted, and the quasicrystalline character of the solvent also gave other difficulties in this case. In the table is given an example of the separation of a mixed solution of three of the luteo salts. Co en_3^{+++} was first displaced with 0.1 M KOH, 1 M $(C_2H_5)_4NBr$ after which

$Cr(NH_3)_6^{+++}$ and $Co(NH_3)_6^{+++}$ were separated and displaced with 0.1 M KOH, 1 M KCl. The three luteo fractions alternated with colourless runs, and the intermediate Cr(III)-fraction gave no reaction for cobalt.

Hexammine, pentammine and tetrammine complexes

We have also used the method in the analysis of other kinds of mixtures of cobalt(III) and chromium(III) ammines. J. Bjerrum [13] has shown that if hexammine cobalt(III) nitrate is shaken with activated carbon in an ammoniacal ammonium salt solution, an equilibrium mixture of hexammine, hydroxopentammine and dihydroxotetrammine is formed. Of the three complexes, dihydroxotetrammine is fixed very strongly to the column, while on the other hand hexammine is bound more strongly than hydroxopentammine. A mixture of pentammine and hexammine can be separated practically quantitatively using 0.01 M KOH, 1 M KCl as displacing agent (see Fig. 1). We have found that the separation is poor when K^+ is replaced by Na^+, but that a good separation is still obtained when Cl^- is replaced by F^-. Hexammine as well as hydroxopentammine can be displaced, but not separated with a less basic solution of the composition: 0.1 M NH_4Cl, 1 M NH_3, 1 M KCl. Dihydroxotetrammine has a much shorter lifetime than the two other complexes in alkaline solution, but is stable as a diaquo ion in acidic solution. These considerations lead to the procedure described in Table 2. The mixture of all three ions is introduced into column I, which preferably should be a short column, and the pentammine and hexammine are displaced from

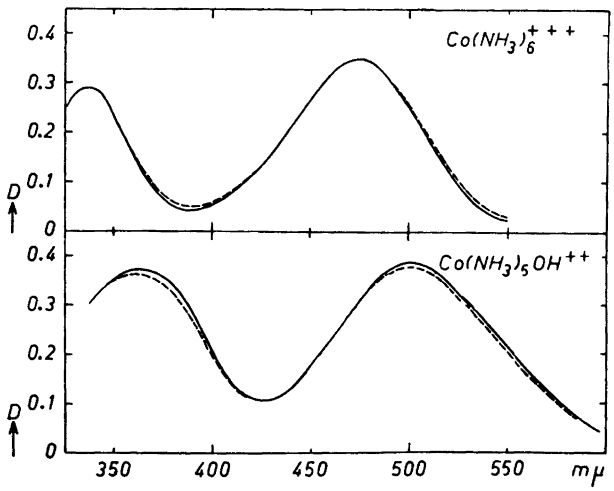

Fig. 1. Analysis of a mixture of $Co(NH_3)_6^{+++}$ and $Co(NH_3)_5OH^{++}$. 1 ml 0.030 M hexammine chloride and 1 ml 0.029 M pentammine nitrate were mixed, separated and displaced with 0.01 M KOH, 1 M KCl, and the fractions containing each component diluted to 25 ml. The optical density D was measured in 5 cm cells. Original mixture after dilution (0.0012 M $Co(NH_3)_6^{+++}$ and 0.00115 M $Co(NH_3)_5OH^{++}$): fulldrawn curves. Fractions after separation: dotted curves.

Table 3. Analysis of mixtures of: $Co(NH_3)_6^{+++}$, $Co(NH_3)_5OH^{++}$, $Co(NH_3)_4(OH)_2^{+}$. Equilibrium established with activated carbon as a catalyst.

$$Co(NH_3)_6^{+++} + H_2O \rightleftharpoons Co(NH_3)_5OH^{++} + NH_4^{+} \quad (1)$$
$$Co(NH_3)_5OH^{++} + H_2O \rightleftharpoons Co(NH_3)_4(OH)_2^{+} + NH_4^{+} \quad (2)$$

	Column I Separation	Column I Displacement	Column II Separation
Pentammine Luteo Tetrammine	0.1 M NH_4Cl, 1 M NH_3 + 1 M KCl	1 M HNO_3	0.01 M KOH + 1 M KCl

Sol. 1. Initial: 0.040 M $[Co(NH_3)_6](NO_3)_3$, 1.00 M NH_3

	$C_{Lut.}$	$C_{Pent.}$	$C_{Tetr.}$	$[NH_4^+]$	K(1)	K(2)
Chromatogr.	0.0081	0.0264	0.0018	0.036	0.117	0.0025
Classical methods	0.0097	0.0258	0.0023	0.034	0.091	0.0031

Sol. 2. Initial: 0.040 M $[Co(NH_3)_4(H_2O)_2](NO_3)_3$, 1.00 M NH_3, 0.1 NaOH

	$C_{Lut.}$	$C_{Pent.}$	$C_{Tetr.}$	$[NH_4^+]$	K(1)	K(2)
Chromatogr.	0.0028	0.0234	0.0062	0.0096	0.080	0.0025

the column with 0.1 M NH_4Cl, 1 M NH_3, 1 M KCl. Then the tetrammine is displaced as quickly as possible with 1 M HNO_3. The pentammine and hexammine are then separated on column II (of normal length, about 25 cm) by means of 0.01 M KOH, 1 M KCl.

The tetrammine could also be displaced with 0.1 M NaOH, 5 M LiCl and collected in dilute nitric acid, but due to fast decomposition in alkaline solution there is a considerably lower yield than when displaced with nitric acid. The use of nitric acid requires preliminary treatment of the alumina with acid as already described in the experimental section.

In Table 3 is given the result of an analysis of two equilibrium solutions of different composition. The ammonium ion concentration in the equilibrium solutions was determined by glass electrode measurements against a standard solution with known concentrations of ammonia and ammonium ion. It will be seen that the estimated hydrolysis constants corresponding to eqns. (1) and (2) agree satisfactorily for the two solutions, and that there is also a fair agreement with the data previously obtained by J. Bjerrum [13] for one of the solutions. In the case of solution 1 J. Bjerrum determined the hexammine gravimetrically as luteo oxalate, the pentammine as chloropentammine, and the tetrammine indirectly by titration of the amount of cobalt which was reduced to Co(II) when boiled with 20 % HCl. Mixtures of only hexammine and pentammine were analyzed spectrophotometrically [13], but the contents of these ions can also be estimated polarographically in 0.1 M H_2SO_4 as found by R. A. Vasadeva Murthy *. As a rule, however, polarography is not a good method for analyzing mixtures of related complexes with the same central ion.

* Visitor from The Indian Institute of Science, Bangalore, India.

In a study on the decomposition of chromium(III) ammines Jørgensen and Bjerrum [14] have used a procedure for separating hexammine, hydroxopentammine and dihydroxotetrammine, which in principle is similar to that described here for the corresponding cobalt(III) complexes. Hexammine and pentammine are first displaced leaving the tetrammine on the column, and then separated on another column.

Separation of *cis* and *trans* complexes

The chromatographic method is also suitable for the separation of *cis* and *trans* complexes. Thus we have analyzed an alkaline equilibrium mixture of the *cis* and *trans* dihydroxobis(ethylenediamine)cobalt(III) ion prepared from a solution of the composition: 0.02 M *cis*-[Co $en_2(H_2O)_2](NO_3)_3$,0.1 M NaOH, 1 M $NaNO_3$. At room temperature equilibrium is reached in about a week [15]. We used a column of the larger type. The *trans*-compound was first displaced by means of 0.1 M NaOH, 1 M NaCl, and the *cis*-compound afterwards by means of the stronger displacing agent 0.1 M NaOH, 1 M LiCl. In this way it was found that $C_{cis}/C_{trans} = 0.57$. When calculating this ratio from the absorption spectrum of the mixture we found $C_{cis}/C_{trans} = 0.65$ in fairly good agreement. It should be mentioned that Woldbye[16] similarly has determined the *cis-trans* equilibrium constant for the dihydroxobis(ethylenediamine)chromium(III) ions, using 0.1 M KOH, 1 M KCl as eluating agent.

The hydroxyl group is a strongly polar group, and there is much evidence that the complex with the two strongest polar groups in *cis* position is more strongly bound than the corresponding *trans* compound. This rule was also confirmed in case of the dinitrotetrammines.

Separation of nitroammines

Systematically we have examined the wellknown series of nitroammines of the type $Co(NH_3)_{6-x}(NO_2)_x^{3-x}$ for x = 0, 1, 2, 3 and 4, and we have established conditions under which they can be separated in the case that two or three of the complexes are present simultaneously. *Tr.*-$Co(NH_3)_4(NO_2)_2^+$ and $Co(NH_3)_2(NO_2)_4^-$ form a slightly soluble salt, but otherwise all combinations are possible. The results are summarized in Table 4. Some of the complexes, especially Erdmann's salt $Co(NH_3)_3(NO_3)_3$ are considerably decomposed in alkaline solution, and for this reason the recovery of the complexes was not complete. It will be seen that the adsorption tendency in basic solution decreases in the series: $Co(NH_3)_6^{+++} > Co(NH_3)_5NO_2^{++} >$ *cis*-$Co(NH_3)_4(NO_2)_2^+ > Co(NH_3)_3(NO_2)_3 >$ *tr.*-$Co(NH_3)_4(NO_2)_2^+$, and inversely in acidic solution the anion complex $Co(NH_3)_2(NO_2)_4^-$ is more strongly adsorbed than $Co(NH_3)_3(NO_2)_3$ and the cation complexes. In the example given *cis*-$Co(NH_3)_4(NO_2)_2^+$ and $Co(NH_3)_3(NO_2)_3$ are displaced from $Co(NH_3)_2(NO_2)_4^-$ with a weak acetic acid buffer while a 1 M LiCl-acetic acid buffer is necessary to eluate the anion complex from the column. The *cis* and *trans* complexes $Co(NH_3)_4(NO_2)_2^+$ have previously been separated by King and Walters [2] by the ion exchange method. Table 4 shows that the separation of these two isomers can be accomplished just as well, and more conveniently, by the chromatographic method. On the other

Table 4. Separation of mixtures of $Co(NH_3)_{6-x}(NO_2)_x^{3-x}$ for x = 0, 1, 2, 3, 4. Conc. (mole/l) in solution to be analyzed.

Salts separated	According to prep.	Chromatogr. found	Displacing solutions (R = $C_{16}H_{33}(CH_3)_3N$)
cis-$[Co(NH_3)_4(NO_2)_2]NO_3$	0.0062	0.0060	0.1 M KOH, 1 M $(C_2H_5)_4NBr$
$[Co(NH_3)_5(NO_2)](NO_3)_2$	0.0065	0.0062	0.1 M KOH, 1 M KCl
$[Co(NH_3)_6](NO_3)_3$	0.0067	0.0064	0.1 M NaOH, 1 M LiCl
tr-$[Co(NH_3)_4(NO_2)_2]NO_3$	0.0075	0.0067	0.01 M ROH, 0.02 M RBr
cis-$[Co(NH_3)_4(NO_2)_2]NO_3$	0.0105	0.0105	0.01 M KOH, 1 M KCl
tr-$[Co(NH_3)_4(NO_2)_2]NO_3$	0.0050	0.0048	0.01 M ROH, 0.02 M RBr
$[Co(NH_3)_3(NO_2)_3]$	0.0056	0.0031	
$[Co(NH_3)_3(NO_2)_3]$	0.0071	0.0062	0.01 M ROH, 0.02 M RBr
cis-$[Co(NH_3)_4(NO_2)_2]NO_3$	0.0051	0.0051	0.01 M ROH, 0.02 M RBr, 0.8 M KCl
$[Co(NH_3)_3(NO_2)_3]$	0.0046	0.0023	0.01 M HAc, 0.001 M NaAc }
cis-$[Co(NH_3)_4(NO_2)_2]NO_3$	0.0054	0.0043	further sep., see above }
$Rb[Co(NH_3)_2(NO_2)_4]$	0.0049	0.0049	0.09 M HAc, 0.01 M NaAc, 1 M LiCl

hand, the corresponding ethylenediamine complexes are more difficult to separate chromatographically, and we have obtained only partial separation of *cis* and *trans* $[Co\ en_2(NO_2)_2]NO_3$ using our longest column (55 cm) and 0.01 M $C_{16}H_{33}N(CH_3)_3OH$, 0.02 M $C_{16}H_{33}N(CH_3)_3Br$ as displacing solvent. Experiments with mixed solvents of water, dioxan or *tert.*-butanol gave no better results. The complexes were fixed more strongly to the column and were more difficult to displace, but the separations were not improved.

In general cations are easily eluated and poorly separated in acidic solution. Inversely anions are easily eluated and poorly separated in basic solution. However, we have established the following adsorption tendency in solutions buffered with $NaHCO_3$: $Co(CO_3)_3^{---} > Co\ enta^- > Fe(CN)_6^{----} > Fe(CN)_6^{---}$. In acidic solution the highest charged anions are relatively much more strongly adsorbed. Thus in acetic acid buffers $Fe(CN)_6^{---}$ is more strongly adsorbed than the ethylenediaminetetraacetatocobalt(III) ion, and $Co(NH_3)_2NO_2)_4^-$ much more weakly than $Co(NO_2)_6^{---}$. This last ion can be removed from the column with 0.09 M HAc, 0.01 M HAc, 1 M LiCl, but more easily when 1 M LiCl is replaced by 1 M Na_2SO_4.

In conclusion it may be said that the chromatographic method developed here for separation of robust complexes seems to have a considerable range of application and offers several advantages over the ion exchange method. Thus, contrary to what is the case for ion exchange resins, even trivalent complexes can easily be removed from the column, and the coloured zones of the complexes are much more easily seen on the white alumina than on the resins.

Our thanks are due to Mr. Erik Jørgensen, who has performed some of the measurements.

REFERENCES

1. Gustavson, K. H. *Svensk Kem. Tidskr.* **56** (1944) 14.
2. King, E. L. and Walters, R. B. *J. Am. Chem. Soc.* **74** (1952) 4471.
3. Lederer, M. *Anal. Chim. Acta* **13** (1955) 350.
4. Maki, M. *Japan Analyst* **4** (1956) 512.
5. Bjerrum, J., Jensen, A. and Woldbye, F. *9. Nordiske Kemikermøde*, Aarhus, 1956; *XVth International Congress of Pure and Applied Chemistry*, Lisboa, September 1956.
6. Sacconi, L. *Gazz. chim. Ital.* **79** (1949) 152.
7. Hein, Fr. and Fischer, K. W. *Z. anorg. Chem.* **288** (1956) 279.
8. Umland, F. *Z. Elektrochem.* **60** (1956) 689, 701, 711.
9. Tiselius, A. *Kolloid Z.* **105** (1943) 101.
10. Hagdahl, L., Williams, R. J. P. and Tiselius, A. *Arkiv Kemi* **4** (1952) 193.
11. Schwab, G. M. and Jockers, K. *Angew. Chem.* **50** (1937) 546.
12. Zechmeister, L. and Cholnoky, L. *Principles and Practice of Chromatography*. English edition, p. 72.
13. Bjerrum, J. *Metal ammine formation in aqueous solution*. Thesis 1941, p. 254 ff. Reprinted 1957, P. Haase and Son, Copenhagen.
14. Jørgensen, E. and Bjerrum, J. *Acta Chem. Scand.* **12** (1958) 1047.
15. Bjerrum, J. and Rasmussen, S. E. *Acta Chem. Scand.* **6** (1952) 1265.
16. Woldbye, F. *Acta Chem. Scand.* **12** (1958) 1079.

Received April 8, 1958.

ACTA CHEMICA SCANDINAVICA 12 (1958) 1211—1214

Incorporation of Labelled Acetate in Emodin in *Penicillium islandicum*

STEN GATENBECK

Department of Biochemistry, University of Lund, Sweden

The distribution of the isotopic content in emodin obtained from *Penicillium islandicum* when grown on $CH_3-{}^{14}COOH$ has been studied. The results clearly indicate that the biosynthesis of emodin involves a head to tail condensation of acetate.

The field of aromatic biosynthesis has been extended in recent years with the demonstration by Birch of a head to tail condensation of acetate as the source of the aromatic rings in various phenolic products [1,2]. Birch and others have employed the acetate theory as a working hypothesis for the determination of the then unknown structures of complex ring systems [3]. Since there are many natural polyhydroxyanthraquinones which fit such a theory of origin, it was decided to attempt to confirm the direct incorporation of acetate into emodin.

If the biosynthesis of emodin involves head to tail condensations of acetic acid units it is reasonable to suppose that the methyl group of emodin is an unchanged methyl group from acetic acid. Starting with that methyl group, the acetic acid residues must be orientated as indicated in Fig. 1. The methyl groups from acetic acid will then be found in the positions m, 1, 3, 6, 8, 9, 11 and 14 as indicated in Fig. 2.

Emodin is produced in very small amounts in organisms suitable for growth experiments with labelled compounds. Skyrin [4], a dimer of emodin,

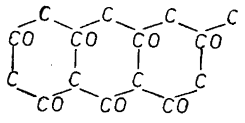

Fig. 1.

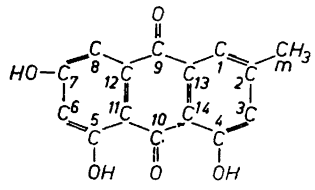

Fig. 2.

occurs in large amounts in the mycelium of *Penicillium islandicum* when supplied with glucose as a carbon source. Skyrin is easily transformed into emodin by reductive cleavage with sodium dithionite. As it is highly probable that skyrin is formed by a condensation of emodin, or a common precursor, skyrin has been used as a source of emodin. Free emodin is produced by *P. islandicum* in amounts that are scarcely detectable by paper chromatographic techniques.

P. islandicum Sopp N.R.R.L. 1175 was supplied with $CH_3{}^{14}COONa$ and the emodin was isolated from the skyrin fraction of the mycelium. The radioactive emodin was diluted with inactive emodin obtained from chrysarobin [5]. The emodin was totally oxidized to carbon dioxide collected as barium carbonate, and the radioactivity was measured. Acetic acid was obtained from the carbons m and 2 after a Kuhn-Roth oxidation. The degradation of the acetic acid, according to Phares [6], gave the radioactivity of each of these carbon atoms. Nitration of emodin to 1,3,6,8-tetranitroemodin and hypobromite cleavage of the nitrocompound gave the carbons 1, 3, 6 and 8 as bromopicrin which was converted to carbon dioxide and the radioactivity measured as above.

EXPERIMENTAL

Culture conditions. Penicillium islandicum Sopp, N.R.R.L. 1175 was grown under the conditions described by Howard and Raistrick. 4 flasks, each containing 500 ml of medium, were grown for 12 days, at this time a solution containing about 0.3 mC of carboxyl labelled sodium acetate was added to each flask. Growth was continued for another 10 days.

Isolation of emodin. The mycelium, from each flask, was removed by filtration, washed with distilled water, and air dried. The dried mycelium was extracted with petroleum ether (b.p. 40—60°) for 1.5 h in a Soxhlet apparatus. The extraction was continued with acetone until nearly all of the pigment had been extracted. The acetone solution was then evaporated to dryness on a steam bath. The dry weight of the acetone extract was 3.32 g. It was dissolved in 750 ml of 1 N Na_2CO_3. The solution was heated on a steam bath and 700 ml of water containing 100 g of $Na_2S_2O_4$ was added during a 10—15 min period with stirring. The solution was stirred continuously for another 20 min and then cooled to room temperature under running water, and neutralized with concentrated HCl. The neutralized solution was then extracted several times with ether. The ether phase was next washed with 1 N Na_2CO_3. The sodium carbonate phase was separated, acidified with concentrated HCl, and again extracted with ether. The ether solution was dried over anhydrous Na_2SO_4 and then evaporated to dryness. The residue was run through a silica column with a mixture of chloroform-acetone (4—1) as solvent. The fraction with a yellow-green fluorescence in UV-light was collected, evaporated to dryness and washed with petroleum ether. The weight of the dried residue was 72.4 mg with m. p. 254—255°. This substance gave all the color reactions of emodin and the melting point was not depressed on admixture of authentic emodin.

The radioactive emodin was diluted about 5-fold with inactive emodin and recrystallized from chloroform yielding 282 mg, m. p. 256—257°.

Radioactive assay. Radioactivity measurements were made with a Tracerlab Autoscaler Type SC-51 in conjunction with a Tracerlab TGC-2 Geiger tube. All the determinations of radioactivity were made after converting the material to barium carbonate. Only self-absorption corrections were made, since all other variables were kept constant.

Combustion. Emodin and bromopicrin were oxidized by the van Slyke-Folch method [7]. The evolved carbon dioxide was trapped in a carbonate free barium hydroxide solution.

Kuhn-Roth oxidation of emodin: The Kuhn-Roth oxidation of emodin (75 mg) gave acetic acid that was isolated by steam distillation. The carbon dioxide formed during the reaction was trapped in barium hydroxide solution. The Kuhn-Roth reaction was quantitative, both for the acetic acid and the carbon dioxide. The acetic acid was degra

Table 1. Determined and calculated isotopic content of emodin.

Material	Carbon atoms isolated	Numbers of theoretical COOH and CH_3 groups	Specific activity *			
			Found			Calculated
			Experiment I	Experiment II	Average	
(1)	(2)	(3)	(4)	(5)	(6)	(7)
Total combustion	all	COOH 7; CH_3 8	32.7	—	32.7	32.1
K—R ox:carbon dioxide	1, 3, 4, 5, 6, 7, 8, 9, 10, 11,12,13,14	COOH 6; CH_3 7	32.4	32.4	32.4	31.8
K—R ox:carboxyl group of acetic acid	2	COOH 1	61.0	64.0	62.5	62.5
K—R ox:methyl group of acetic acid	m	CH_3 1	5.2	5.3	5.3	5.3
Bromopicrin	1, 3, 6, 8	CH_3 4	9.9	6.6	8.3	5.3
Hypobromite degradation: carbon dioxide	4,5,7,9,10, 11,12,13,14	COOH 6; CH_3 3	44.5	39.8	42.2	43.4

* Specific activity in counts/min/mg $BaCO_3$ corrected for selfabsorption.

ded by a Schmidt reaction and the carboxyl group isolated as barium carbonate. The methylamine produced by the Schmidt reaction was oxidized with alkaline permanganate to carbon dioxide, which, after acidification, was trapped as barium carbonate.

1,3,6,8-Tetranitroemodin. Emodin (90.3 mg) was dissolved in sulfuric acid (2.0 ml, *d* 1.84) and nitric acid (0.33 ml, *d* 1.52) was added dropwise. The mixture was heated on a steam bath for 45 min and then cooled with ice and diluted with ice-water. The yellow crystalline product was filtered and washed with distilled water. The air dried substance was recrystallized from glacial acetic acid, yielding tetranitroemodin (61.4 mg) m. p. 301—302° (decomp.). Tetranitroemodin was prepared in the same way about ten times from non-labelled material. The nitrogen content in these experiments varied between 11.4 and 12.5 %, the theoretical value being 12.4 %.

Hypobromite degradation of 1,3,6,8-tetranitroemodin. Tetranitroemodin (60.0 mg) was suspended in 5 ml aqueous, carbonate-free, saturated barium hydroxide. 40 ml of cold (0°), carbonate-free, aqueous barium hypobromite was added to the nitroemodin suspension. The barium hypobromite solution was prepared from barium hydroxide (2.5 g) and bromine (0.3 ml) in 40 ml of water. The reaction mixture was kept at 0° for 24 h with occasionally shaking. The bromopicrin formed by this process, was isolated by steam distillation. The distillate was trapped in a conical centrifuge tube cooled with ice-water. The bromopicrin was washed with distilled water by centrifugation, and oxidized to carbon dioxide according to van Slyke-Folch. The barium carbonate that was formed during the hypobromite reaction was filtered off and washed with distilled water. The carbon dioxide was regenerated by acidification with perchloric acid and again trapped in aqueous barium hydroxide. Tests with unlabelled nitroemodin showed that the yield of the bromopicrin and carbon dioxide was about 80 %, indicating that all the nitrogen atoms in tetranitroemodin were represented in the bromopicrin and that the central ring in the anthraquinone molecule was oxidized to carbon dioxide.

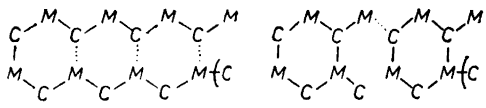

Fig. 3.

RESULTS AND DISCUSSION

The data of the various radioactivity measurements are given in Table 1 in counts/min/mg $BaCO_3$. All radioactive measurements were counted for a sufficient time to give a probable error of less than 1 %. The data in columns 4 and 5 are obtained from two different experiments. In column 3 are found the numbers of carboxyl and methyl groups from acetic acid which the emodin molecule will contain if the acetate theory is valid. Since the radioactivity of the carboxyl group and the methyl group of the acetate obtained in the Kuhn-Roth oxidation are measured directly, these values have been taken as a basis of calculating the theoretical activities of the samples measured which are listed in column 7. These theoretical values show a very good agreement to the experimentally determined. The results support entirely the acetate theory of the biosynthesis of emodin, but do not distinguish between various possible intermediary compounds between acetic acid and emodin. The work by Birch on 2-hydroxy-6-methylbenzoic acid indicates that the formation of emodin by intermolecular condensation of a polyketoacid or a condensation of two phenol carboxylic acids will give the same labelling of emodin from acetic acid, Fig. 3.

The author thanks Professor G. Ehrensvärd for advice and encouragement.

REFERENCES

1. Birch, A. J., Massy-Westropp, R. A. and Moye, C. J. *Austral. J. Chem.* **8** (1955) 539.
2. Birch, A. J., Massy-Westropp, R. A., Rickards, R. W. and Smith, H. *J. Chem. Soc.* **1958** 360.
3. Birch, A. J. and Massy-Westropp, R. A. *J. Chem. Soc.* **1957** 2215.
4. Howard, B. H. and Raistrick, H. *Biochem. J.* **56** (1954) 56.
5. Gardner, J. H. *J. Am. Pharm. Assoc.* **28** (1939) 143.
6. Phares, E. F. *Arch. Biochem. Biophys.* **33** (1951) 173.
7. *Cf.* Calvin, Heidelberger, Reid, Tolbert and Yankwich *Isotopic carbon* Wiley, New York 1949, p. 92.

Received April 12, 1958.

ACTA CHEMICA SCANDINAVICA 12 (1958) 1215—1220

Electron Diffraction Studies of Hexaphenylbenzene Vapour

A. ALMENNINGEN, O. BASTIANSEN and P. N. SKANCKE

Universitetets Kjemiske Institutt, Blindern-Oslo, Norway;
Institutt for teoretisk kjemi, Norges Tekniske Høgskole, Trondheim, Norway

Electron diffraction studies of hexaphenylbenzene in vapour have been carried out. The peripherical rings are found to be nearly orthogonal to the central ring. The model is, however, not found to be rigid and it is concluded that the outer rings of the molecule oscillate with no appreciable restriction in a rather limited angle interval of approcimately $\pm 10°$ from the orthogonal form.

The arrangement of aromatic ring systems connected with single bonds have been studied in a series of papers [1–5]. In this connection we found it of interest to include hexaphenylbenzene.

A sample of the compound was kindly placed at our disposal by Professor E. R. H. Jones, Oxford. The diagrams were taken at a temperature of approximately 340°C using a modified s^3-sector. The intensity data were read off from the photometer curves and the various corrections were carried out [6]. In Fig. 1 is presented the final intensity curve after subtraction of the background. The theoretical background gave as a whole a fairly good agreement with the experimental curve, but corrections had to be carried out particularly for the innermost and the outermost part of the intensity curve.

Radial distribution curves were calculated using the damping factor $\exp(-ks^2)$.

The results for $k = 0.0009$ and 0.0036 are reproduced in Fig. 2. An analysis of the position of the maxima of these curves gives the following bond distances: C—C in the rings 1.40 Å, C—C bridge distance 1.52 Å and C—H 1.08 Å. The error of the first C—C distance and of the C—H distance is less than 0.005 Å. The situation is less favourable for the bridge C—C distance as this is determined indirectly by larger internuclear distances between two different rings. Error estimates suggest that the error is probably less than 0.01 Å.

By applying the observed bond distances and the assumption of 120° valence angles all through the molecule, the internuclear distances of the whole molecule have been calculated. There is a large group of distances which depend upon the angle of twist around the C—C bridges, but there are also altogether 23 CC distances which are independent of the angle of twist. In

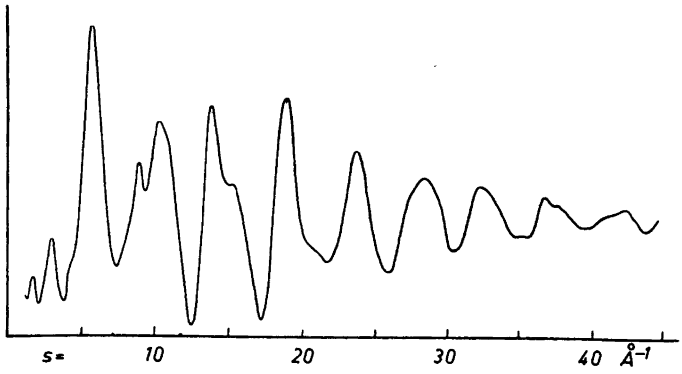

Fig. 1. Intensity curve of hexaphenylbenzene.

addition there is a whole series of CH distances. In Fig. 2 all the invariable CC distances for the calculated radial distribution curve are represented by vertical lines. The length of each line is proportional to the weight of the corresponding distance. The CH distances are omitted with the exception of the two shorter ones. The line diagram of the invariable distances explains essential features of the radial distribution curve. For r values less than 7 Å there are, however, three easily detectable irregularities. The first one is a well resolved peak at 3.39 Å, the second one is a maximum at 4.63 Å, and the third is an extra contribution to the peak at approximately 6 Å. The position of this latter peak is at higher r-values than expected from the invari-

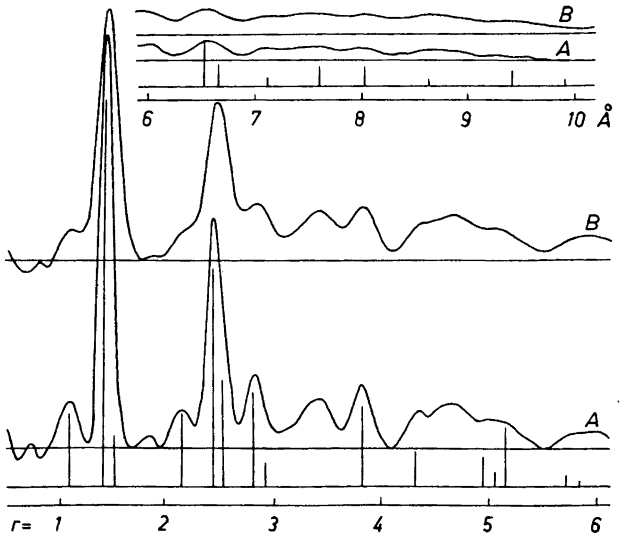

Fig. 2. Radial distribution curves of hexaphenylbenzene. A, $k = 0.0009$; B, $k = 0.0036$.

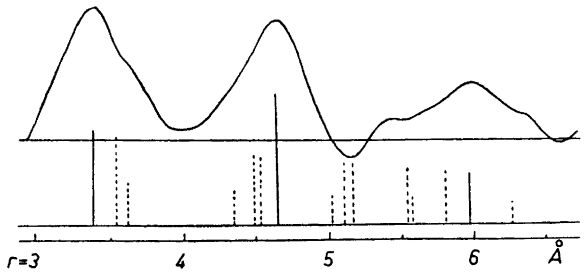

Fig. 3. Difference radial distribution curve when the contribution of invariable distances have been subtracted.

able distances only. The subtraction of the contribution of the invariable distances gives at these three points peaks with maxima 3.39 Å, 4.63 Å and 5.97 Å, respectively. The result of such a subtraction of the invariable distances is demonstrated in Fig. 3 ($k = 0.0036$). The variable distances which would first of all be expected to contribute to this radial distrubution curve are the following: C_2C_8, C_2C_{12}, C_2C_9, C_2C_{11}, C_3C_9, and C_3C_{11}. (For the numbering of the atoms see Fig. 4). In the case of an angle of 90° the six indicated distances will be reduced to three, as pairs like C_2C_8 and C_2C_{12} will be equal. The three main peaks of the curve in Fig. 3 correspond to an angle of 90° between the central ring and the outer rings, as the theoretical distances in an orthogonal

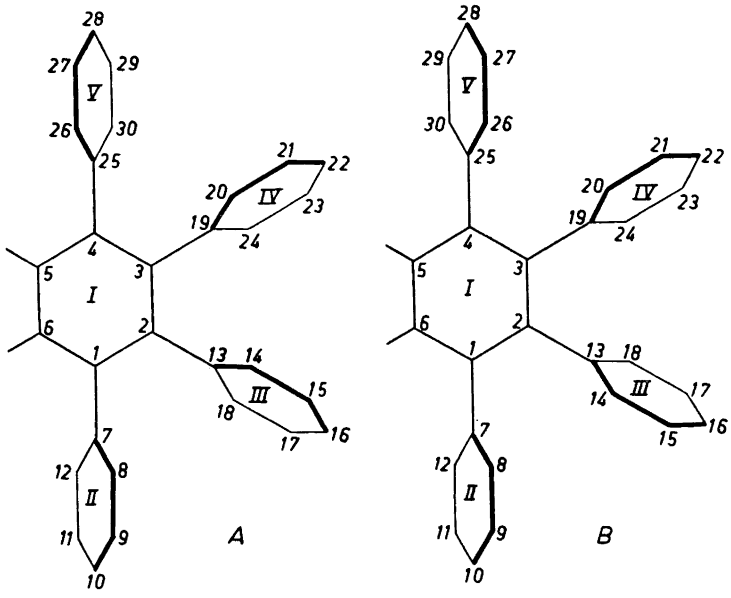

Fig. 4. Structure models of hexaphenylbenzene. A "propeller" and B "antipropeller" model.

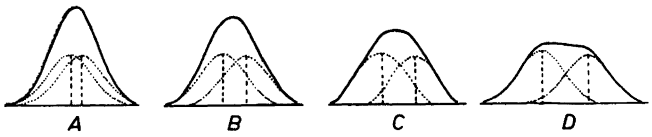

Fig. 5. Radial distribution peak for the C_2C_8 and C_2C_{12} distances corresponding to various angle deviations from orthogonality. A, 5°; B, 10°; C, 15°; and D, 20°.

case are 3.39 Å, 4.65 Å, and 5.97 Å, respectively. The positions and the weights of the three distances in question are given as solid vertical lines under the peaks of Fig. 3. The conclusion one would be tempted to draw from this is that all the peripherical rings are orthogonal to the central ring. On the other hand, it can easily be shown that a limited deviation from orthogonality will not appreciably change the maximum position of the three peaks under consideration. In case of a rotation from the orthogonal position each of the three distances will split up in two distances, one of which is smaller and one larger, leaving the average very nearly the same. As a demonstration of this the theoretical form of the 3.39 Å peak is given in Fig. 5 for four various angles of twist from the orthogonal position. The half width of the Gaussian-normal curve used for this construction is obtained from the corresponding resolved peak in the radial distribution curve of biphenyl [5]. A comparison of the peaks in Fig. 5 with the corresponding experimental one in Fig. 3 shows that the split, if any, cannot be larger than 15°. On the other hand, the comparison also indicates that a rigid model is less probable. An angle of 10° seems to be the right order of magnitude. It is of course impossible from the study of the three peaks in Fig. 3 to decide between a rigid model with a deviation of say 10° from orthogonality and a model with some oscillation around an orthogonal conformation. In fact the latter assumption would from usual structural experience be the more probable one.

For further information on this point a study of the internuclear distances between the peripherical rings would obviously be necessary. The line diagram of broken lines under the difference radial distrubution curve of Fig. 3 gives the positions and weights of all variable internuclear CC distances in the presented interval between peripherical rings, in a rigid and orthogonal model. A study of this diagram leads to the rejection of the entirely rigid orthogonal model. To obtain information about the possibility of other rigid models than the orthogonal one a whole series of various models was considered. None of them lead to a decisive conclusion. As an example both the experimental and two theoretical radial distrubution curves are presented in Fig. 6 for the interval 3 to 6.5 Å. The two calculated models are a "propeller" and an "antipropeller" model described in Fig. 4 with an angle of twist from orthogonality of 10°. The correspondence between experimental and calculated curves in Fig. 6 is not satisfactory and do not give possibilities for a choice, though the "antipropeller" model seems to be somewhat more favourable. Further considerations along this line lead to abandoning rigid models. A natural conclusion should then be that the outer rings of the molecule oscillate with

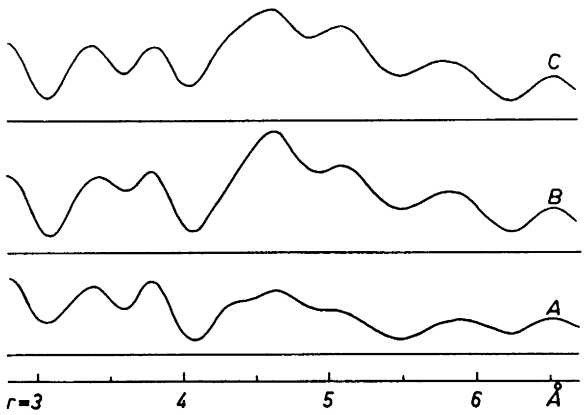

Fig. 6. Radial distribution curves. A, experimental curve; B, "propeller" model; C, "antipropeller" model. (10° deviation from orthogonality.)

no appreciable restriction in a rather limited angle interval of approximately $\pm 10°$ from the orthogonal form.

So far the discussion is based upon the radial distribution curve interval up to approximately 7 Å. The outer part of the curve is also of considerable interest in this connection. Studying the theoretical contribution to this part of the curve it is easily seen that the total weight of the variable distances should be considerably larger than the total weight of the invariable distances. On the other hand, a comparison of the line diagram of the invariable distances with the radial distribution curve shows that the curve can to a great extent be explained by the invariable distances alone (Fig. 2). The contribution of all the variable distances seems to have been evened out. The fact that practically all peaks in the interval 7—10 Å are interpretable is a strong argument for the correctness of the curve. The variable distances in this interval are of the type going between ring II and IV and between II and V. The fact that these distances are smoothed is in agreement with the general idea presented above and serves as a demonstration of the nonrigidity of the hexaphenylbenzene molecule. The variable distances, of course, contribute to the diffraction patterns, but they do not lead to detectable peaks and are therefore to a great extent lost when drawing the envelope [6].

It is no doubt of interest to study if our general sturucture picture can be brought into accordance with steric considerations. The effect of p orbital is no doubt insignificant for the bridge C—C bond so far away from the planar form. If two neighbouring peripherical rings are rotated towards each other the hydrogen atoms of the type H_8 and H_{14} will be the first pair of atoms to be brought into contact. If a packing distance of 2.4 Å is applied corresponding to the Pauling van der Waals radius for hydrogen [7] of 1.2 Å, contact will be reached at an angle of 10.5° from orthogonality. If a "propeller" model is assumed, steric conflicts will not lead to serious difficulties until a rotation

of approximately 40° is performed. In order to realize such a form it is necessary to rotate all the peripherical rings in the same direction. If only one ring is out of order the rest would have to assume an arrangement near the orthogonal conformation. The probability of the symmetrical 40° "propeller" should, therefore, be rather small for pure statistical reasons. On the other hand, this symmetrical form might well be present in the crystalline state. X-Ray crystallographic studies are in progress in the Institute of Theoretical Chemistry, Trondheim.

Acknowledgement. The authors wish to thank Professor E. R. H. Jones, Oxford, for having placed a sample of hexaphenylbenzene at their disposal.

REFERENCES

1. Bastiansen, O. *Acta Chem. Scand.* **3** (1949) 408.
2. Bastiansen, O. *Acta Chem. Scand.* **4** (1950) 926.
3. Bastiansen, O. *Acta Chem. Scand.* **6** (1952) 205.
4. Bastiansen, O. and Smedvik, L. *Acta Chem. Scand.* **8** (1954) 1593.
5. Almenningen, A. and Bastiansen, O. *Kgl. Norske Videnskabs Selskabs Skrifter* (1958). *In press.*
6. Almenningen, A. and Bastiansen, O. *Acta Chem. Scand.* **9** (1955) 815.
7. Pauling, L. *The Nature of the Chemical Bond*, Ithaca 1945.

Received March 26, 1958.

ACTA CHEMICA SCANDINAVICA 12 (1958) 1221—1225

An Electron Diffraction Reinvestigation of the Molecular Structure of 1,3-Butadiene

A. ALMENNINGEN, O. BASTIANSEN and M. TRÆTTEBERG

Universitetets Kjemiske Institutt, Blindern — Oslo;
Institutt for teoretisk kjemi, Norges Tekniske Høgskole, Trondheim, Norway

The electron diffraction sector method was used for a reinvestigation of the structure of 1,3-butadiene vapour. It was shown that the planar *trans* form is predominating, and no signs of other conformations were observed. The observed molecular parameters are the following: C—H: 1.082 Å, C—C: 1.483 Å, C=C: 1.337 Å, ∠ C = C—C: 122.4°, and ∠ C = C—H: 119.8°. The probable error of C = C is less than 0.005 Å. For the C—H and C—C distances the error is somewhat larger, about 0.01 Å.

The present work is a part of our endeavour to collect more precise informations of C-C bond lengths, particularly in conjugated systems. 1,3-butadiene was already studied in 1939 by Schomaker and Pauling [1], using the visual electron diffraction method. Their parameter determinations were in good agreement with the present knowledge of this type of distance.

The justification of the present work is the narrower error limits that can be obtained by the modern electron diffraction technique rather than any doubt of the values obtained earlier. The fact that the earlier work was not able to determine unambiguously the general shape of the molecule also made a reinvestigation desireable.

Electron diffraction diagrams were taken at various distances between the diffraction point and the photographic plate, using a somewhat modified s^3-sector. Photometer records of the plates were read off at intervals of $\Delta s = 1/4$ Å^{-1}. The necessary corrections were made to transfer the photometer curves into intensity values. At this stage a theoretical background was fitted in. The overall correspondence between intensity curve and background was good except for the inner s range ($s < 5$). The background was fitted in by a least square procedure asking for the position of the intensity zero line and the intensity scale [2]. After the sector correction had been carried out, minor refinements of the background were made and the corrected background subtracted from the intensity curve. The first radial distribution curves were calculated using a damping factor exp $(-0.0009\, s^2)$. The best molecular

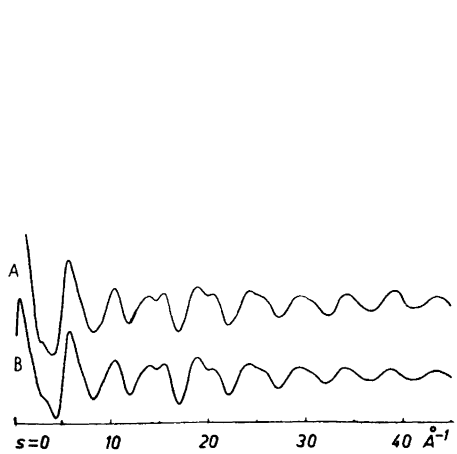

Fig. 1. Experimental (A) and theoretical (B) intensity curves for 1,3-butadiene.

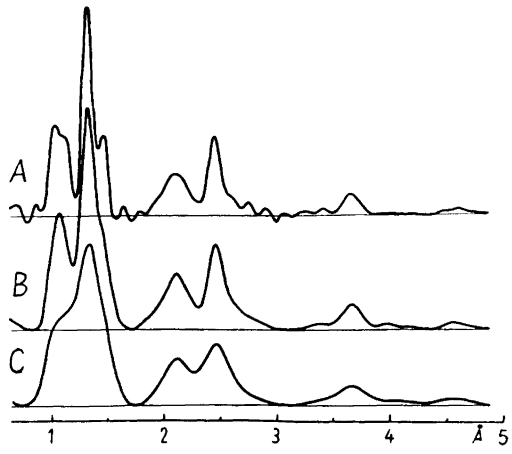

Fig. 2. Radial distribution curves of 1,3-butadiene. (A: $k = 0$, B: $k = 0.0009$, and C: $k = 0.0036$).

model obtained from these curves was used as a basis for theoretical intensity-curve calculations. The correspondence between experimental and theoretical intensity curves is very good (Fig. 1), except for some disagreement at the inner s-range indicating the necessity of a further background correction for $s < 5$. In fact a correction of this type has been necessary in a series of investigations, indicating a measurable deviation between calculated and observed backgrounds for small s values. After subtraction of the final background a series of radial distribution curves was calculated using three different k-values (0, 0.0009, and 0.0036) and Δs values of 1/4 and 1/2. As a matter of

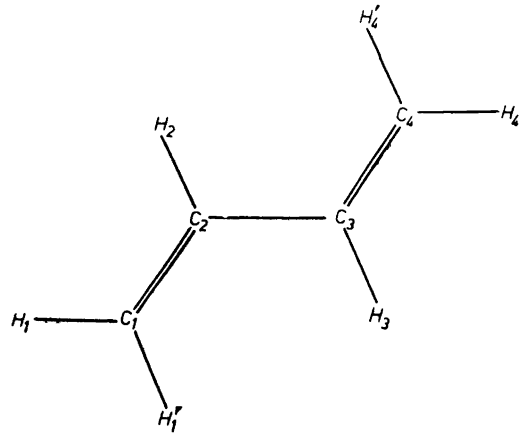

Fig. 3. Numbering of the atoms in the 1,3-butadiene molecule.

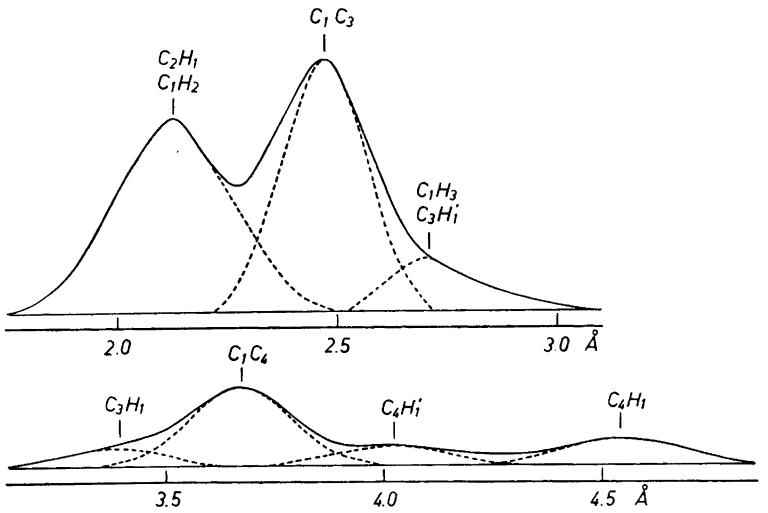

Fig. 4. An example of the resolution of parts of a radial distribution curve in Gaussian-like peaks ($k = 0.0036$).

fact two complete sets of diagrams were taken and each set treated independently by two persons. As a whole the correspondence between the results of the two investigations was very good, and the preliminary results as to structure data were almost identical. Therefore, in the final refinements it was preferred to use curves obtained as an average of the two sets.

In Fig. 2 three radial distribution curves are given with damping constants $k = 0$, 0.0009, and 0.0036, respectively.

From an analysis of the radial distribution curves a set of internuclear distances was obtained. These distances are listed in Table 1, second column. The numbering of the atoms in the first column of Table 1 is demonstrated in Fig. 3. For the shorter distances (bond distances) the values obtained from the radial distribution curve of $k = 0$ gave the best consistency. For the longer distances the radial distribution curves of higher k values were preferred. As a matter of fact the longest C—H distances are hardly recognizable on a radial distribution curve from an undamped intensity curve. On the other hand the radial distribution curves of $k = 0.0036$ have easily separable peaks corresponding to the larger C—H distances. The internuclear distances mentioned were obtained by resolving the radial distribution curves into Gaussian peaks including the use of the least square method. In Fig. 4, as an example, there is shown the outer parts of a radial distribution curve ($k = 0.0036$) resolved in Gaussian shaped peaks corresponding to the various distances.

The observed distance values settle beyond doubt the overall structure of the molecule. The molecular structure is a planar *trans* form without observable contribution from other conformations.

Table 1. Internuclear distances in the 1,3-butadiene molecule.

Distances and angles	Observed values	2nd order approximation values
C—H	1.083 Å	1.082 Å
C=C	1.341 Å	1.337 Å*
C—C	1.484 Å	1.483 Å
∠C=C—C		122.40°
∠C=C—H		119.78°
C_2H_1 } C_1H_2 }	2.125 Å	2.124 Å
C_1C_3	2.477 Å	2.472 Å
C_1H_3 } C_3H_1' }	2.721 Å	2.699 Å
C_3H_1	3.402 Å	3.453 Å
C_1C_4	3.680 Å	3.688 Å
C_4H_1'	4.031 Å	4.019 Å
C_4H_1	4.568 Å	4.567 Å

As is seen from Table 1 there are altogether 10 observed internuclear distances. If a planar *trans* molecule is assumed, the carbon structure is described by three parameters. If the hydrogen atoms are included, two additional parameters have to be considered, even with the assumption of the same C—H bond distances and the same C=C—H angles throughout the molecule. There should then be 10 equations for the determination of 5 parameters. The parameters were now determined by a least square procedure, using proper weight factors on the various observed distances. Except for minor changes in the fourth decimal place, the parameters and the deduced internuclear distances of the 1st approximation were preserved in the 2nd approximation. The results are given in third column of Table 1.

Because of the unavoidable overlap of the C=C and C—C bond peaks, the accuracy of these bond distances is somewhat lower than in the cases of well-resolved peaks. The C=C double bond distance is determined with an error less than 0.005 Å, but for the C—C single bond distance the situation is less favourable. The rather large C—C distance of 1.483 Å is obtained even if the zero order approximation value in the least square procedure is as low as 1.473 Å. Though the analysis of the inner part of the radial distribution curve of $k = 0$ strongly indicates this large distance, it has to be admitted that a least square analysis of the carbon-carbon bond complex in a radial distribution curve with $k = 0.0009$ leads to a value of 1.473 Å for the single bond. If the observed value of 1.484 Å is substituted by 1.473 Å in the list of second column of Table 1, the final C—C bond distance from the least square calculations is as large as 1.478 Å, while the other parameters are practically uninfluenced. This demonstrates that the longer internuclear distances are

* *Added in proof:* After this article was submitted for publication a study of the infrared spectra of ethylene has been published (Allen, H. C. and Plyler, E. K., *J. Am. Chem. Soc.* **80** (1958) 2763). The C=C distance is found to be **1.337** Å in good agreement with the result of this work and with the electron diffraction study of ethylene (Bartell, L. S. and Bonham, R. A., *J. Chem. Phys.* **27** (1957) 1414).

Table 2. Theoretical and experimental values for areas under the peaks in the radial distribution curves.

Distances	Theoretical	Experimental
C—H	41.7	38
C=C	53.5	55
C—C	24.7	22
C_1H_2; C_2H_1; C_3H_2	28.2	23
C_1C_3	29.0	24
C_1H_3; $C_3H'_1$	10.8	9
C_3H_1	4.3	3
C_1C_4	9.8	12
$C_4H'_1$	3.7	4
C_4H_1	3.3	4

in better accordance with the large C—C bond distance. It is very difficult to give a definite statement concerning the error limits of the single bond, but it is unlikely that the error is more than 0.01 Å. However, the analysis indicates an unsymmetrical error distribution, making an error of + 0.01 Å less probable than an error of — 0.01 Å.

In order to look for a possible contribution of a *cis* form, the areas under the resolved peaks of the radial distribution curves have been studied. Again the less damped curves were used for the inner peaks and the more damped curves for the outer peaks. These areas were compared with the theoretical calculated values obtained by the formula $n \cdot Z_i Z_j / r_{ij}$, where n is the number of times the distance in question occurs in the molecule and r_{ij} is the distance itself. Z is 6 for carbon and 1.25 for hydrogen. The theoretical and measured areas are listed in Table 2, normalized on the same arbitrary scale. The correspondence is satisfactory and gives no indication of any misinterpretation of the peaks. In fact the experimental area for the C_1C_4 peak is somewhat larger than anticipated from theory. If any other conformations than the *trans* form were present, this peak should have a smaller area than that calculated for a rigid *trans* molecule. The deviation in the area of the C_1C_4 distance is probably merely due to errors caused by difficulties in determining the exact form of the envelope.[3]

Acknowledgement. The authors wish to thank Dr. Boris Stoicheff, Ottawa, for valuable discussions. Thanks are also due to *Fridtjof Nansens Fond* for financial support.

REFERENCES

1. Schomaker, V. and Pauling, L. *J. Am. Chem. Soc.* **61** (1939) 1769.
2. Almenningen, A., Bastiansen, O. and Fernholt, L. *Kgl. Norske Videnskabs Selskabs Skrifter* (1957). *In press.*
3. Almenningen, A. and Bastiansen, O. *Acta Chem. Scand.* **9** (1955) 815.

Received March 1, 1958.

ACTA CHEMICA SCANDINAVICA 12 (1958) 1226—1230

The Catalytic Effect of CrO_4^{2-}, MoO_4^{2-} and WO_4^{2-} on the Hydrolysis of *iso*Propoxy-methyl-phosphoryl Fluoride (Sarin)

LENNART LARSSON

Research Institute of National Defence, Dept. 1, Sundbyberg 4, Sweden

The catalytic effect of eighteen anions on the hydrolysis of Sarin has been examined. Based on these results a detailed study of the effect of chromate, molybdate and tungstate ions has been performed. The catalytic constants of these ions, as well as their energies and entropies of activation, have been given. The catalytic effect of the ions has been ascribed mainly to complex formation of the ions with the Sarin molecule.

In the study of the pH-dependence of the hydrolysis of *iso*propoxy-methyl-phosphoryl fluoride (Sarin) in different buffer solutions it was evident that, in addition to the catalytic effect of the hydroxyl ions, the ions included in the buffer solutions also influenced the rate of hydrolysis. For that reason the hydroxyl ion catalyzed hydrolysis of Sarin was studied by means of an automatic titrator which maintained the pH constant at a preselected value in the absence of disturbing ions [1]. The influence of some ions on the hydrolysis of di*iso*propoxy-phosphoryl fluoride (DFP) has earlier been reported by Kilpatrick [2]. Wagner-Jauregg *et al.* have shown that the hydrolysis of DFP is accelerated by some metal salts and complexes, in particular copper(II) chelates of dipyridyl and histidine [3]. It was also shown that sodium molybdate markedly catalyzed the hydrolysis.

It was thus of interest to study the catalytic effect of a lot of common anions on the rate of hydrolysis of Sarin. The effect of chromate, molybdate and tungstate ions was of special interest and was the object of a more detailed study.

A similar study of the effect of different anions on spontaneous and enzymatically catalyzed hydrolysis of dimethylamido-ethoxy-phosphoryl cyanide (Tabun) has been performed by Augustinsson [4].

EXPERIMENTAL

Materials. Sarin was synthesized in this institute and a stock solution of Sarin in dioxane (E. Merck c.p. purified from peroxides and redistilled over sodium) was prepared[1].

The salts used were of anal. reagent grade except sodium persulphate which was chemically pure, and sodium hypochlorite which was supplied as a solution, the exact concentration of which was determined iodometrically.

Kinetic measurements. Procedure I. Introductory experiments were performed by a Warburg manometric method, and the technique closely adheres to that described by Augustinsson [5]. The reaction took place at 25°C in a sodium bicarbonate buffer at pH 7.6. The amount of CO_2 evolved during the reaction was read at intervals during 60 min and from these data the rate of the reaction was determined. The initial concentration of Sarin was 5.0 mM, and that of the catalyst was 1.0 mM.

Procedure II. The detailed study of the catalytic effect of chromate, molybdate and tungstate ions was performed by means of an automatic recording titrator [6] at 15°C, 25°C and 35°C at pH 8.50, and at 25°C also at pH 9.00. A solution containing 38.00 ml of 0.10 M potassium chloride and 1.00 ml of appropriately diluted solution of the catalyst was adjusted by the titrator to the desired pH-value, after which 1.00 ml of the stock solution of Sarin was added. In other respects the procedure adheres to that described in an earlier paper [1]. The initial concentrations of Sarin and the catalysts in the different runs appear in Table 1.

RESULTS

Introductory experiments

From the introductory experiments performed by the manometric Warburg method the following results were obtained:

1) Potassium sulphate, ammonium chloride and sodium chlorate, perchlorate, sulphite, azide, hypophosphite, formate and salicylate showed no, or slight, catalytic effect.

2) Potassium persulphate and sodium nitrite and phosphate showed a small catalytic effect.

3) Sodium molybdate (Na_2MoO_4) and ammonium molybdate ($[NH_4]_6Mo_7O_{24}$) showed a marked, catalytic effect.

4) A considerable acceleration of the hydrolysis was obtained with sodium hypochlorite and perborate (the effect of the latter can probably be attributed to the formation of perhydroxyl ions).

The hydrolysis of Sarin catalyzed by hypochlorite ions has been described by Epstein *et al.*[7], and the reaction of perhydroxyl ions with Sarin has recently been published [8,9].

Catalytic effect of chromate, molybdate and tungstate ions

When the recorded curves from the automatic titrator were treated according to Guggenheim, straight lines were obtained indicating that the catalyzed hydrolyses proceed as first-order reactions. This fact shows that the chromate, molybdate and tungstate ions are not consumed in the reactions but function as true catalysts. From the slopes of the straight lines the observed rate constants, k_{obs}, were determined, and the catalytic constants, k_c, were calculated from the expression:

$$k_c = \frac{k_{obs} - k_s}{c_c}$$

Table 1. Rate constants for the hydrolysis of Sarin catalyzed by chromate, molybdate and tungstate ions at various concentrations, pH-values and temperatures.

t°C	pH	c_s mM	c_c mM	$k_{obs} \times 10^4$ sec^{-1}			$k_s \times 10^4$ sec^{-1}	$k_c \times 10^2$ 1 mole^{-1} sec^{-1}		
				CrO_4^{2-}	MoO_4^{2-}	WO_4^{2-}		CrO_4^{2-}	MoO_4^{2-}	WO_4^{2-}
15.0	8.85	0.300	2.50	1.59	2.35	2.62	0.62	3.86	6.90	7.96
		0.300	2.50	1.62	2.28	2.47		4.00	6.63	7.40
25.0	8.50	0.420	1.00	2.01	2.35	2.54	1.06	9.39	12.8	14.7
		0.420	1.00	2.03	2.47	2.59		9.65	14.0	15.2
		0.420	2.50	3.45	4.31	4.61		9.55	13.0	14.2
		0.300	2.50	3.34	4.36	4.66		9.50	13.2	14.4
	9.00	0.300	1.00	4.32	4.63	4.83	3.37	9.49	12.6	14.6
		0.300	1.00	4.20	4.63	4.77		8.29	12.6	14.0
35.0	8.18	0.300	2.50	6.42	8.50	8.92	1.76	18.6	27.0	28.6
		0.300	2.50	6.73	8.59	8.66		19.9	27.3	27.6

where k_s is the rate constant of the spontaneous hydrolysis [1] and c_c is the concentration of the catalyst.

The constants are given in Table 1, where it is shown that the catalytic constants are independent of pH above 8.50. The catalytic ions are probably present in the monomeric form, *i.e.* CrO_4^{2-}, MoO_4^{2-} and WO_4^{2-}. In the preliminary experiments at pH 7.6 $(NH_4)_6Mo_7O_{24}$ was found to be 6—7 times more effective a catalyst than Na_2MoO_4, which supports this hypothesis. The mean values of the catalytic constants given in Table 2 are calculated from the values obtained only at pH 8.50, because the difference between k_{obs} and k_s at pH 9.00 is so small that it markedly influences upon the accuracy of k_c.

By plotting $1/T$ against k_c straight lines were obtained. From the slopes of the lines, calculated by the method of least squares, the energies of activation were obtained. The entropies of activation were calculated from the equation of absolute reaction rates. The values of the entropies and energies of activation are given in Table 2.

Table 2. Catalytic constants, and energies and entropies of activation for the hydrolysis of Sarin catalyzed by chromate, molybdate and tungstate ions.

Catalyst	$k_c \times 10^2$ 1 mole^{-1} sec^{-1}			E_a	$\Delta S^{\neq}$
	15.0°C	25.0°C	35.0°C	kcal.mole^{-1}	E.U.
CrO_4^{2-}	3.93 ± 0.07	9.52 ± 0.13	19.3 ± 0.7	14.0 ± 0.4	-18 ± 1
MoO_4^{2-}	6.77 ± 0.14	13.3 ± 0.7	27.2 ± 0.2	12.3 ± 0.4	-23 ± 1
WO_4^{2-}	7.68 ± 0.28	14.6 ± 0.6	28.2 ± 0.5	11.5 ± 0.3	-26 ± 1

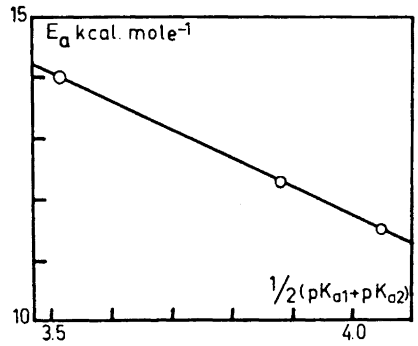

Fig. 1. Relationship between 1/2 (pK_{a1} + pK_{a2}) and E_a in the hydrolysis of Sarin catalyzed by chromate, molybdate and tungstate ions.

DISCUSSION

For reactions involving nucleophilic displacements in general Edwards [10] has pointed out that the character of a nucleophilic reagent is related to its electrode potential as well as to its basicity. It has, however, been reported that the thiosulphate ion which has a high electrode potential but low basicity, has no effect upon the hydrolysis of either Tabun [4] or Sarin [7]. On the other hand it has been shown from a study of the reaction of Sarin with catechols that the rate of the reactions is related to the basicity of the catechols [11]. This favours the theory that the basicity of the reagent is the decisive factor in nucleophilic attacks on the phosphorus atom.

As appears from Fig. 1, the activation energies of the hydrolysis of Sarin catalyzed by chromate, molybdate and tungstate ions are found to be inversely proportional to the negative logarithms of the mean dissociation constants of the acids given by Schwarzenbach [12], indicating the relationship between the catalytic effect and the basicity of the catalysts. The slight catalytic effects obtained in the preliminary experiments with other ions of about the same basicity as chromate, molybdate and tungstate ions indicate, however, that the catalytic effects of the latter ions cannot be attributed only to the basicity of the ions. Moreover, a lower energy of activation of the alkaline hydrolysis of Sarin [1] would be expected if such a relationship were valid. In the main the catalytic effect of the ions can probably be ascribed to complex formation of the ions with the Sarin molecule which facilitates the cleavage of the P—F bond. The decreasing entropy of activation, when going from chromate to tungstate ions, is consistent with an increasing stability of the activated complex. The tendency of chromate, molybdate and tungstate ions to form complex with phosphorus compounds is also wellknown from their insoluble complex with phosphate ions.

My sincere thanks are due to the Director of the Research Institute of National Defence, Dept. 1, Professor G. Ljunggren, for the kind interest he has shown in this work.

REFERENCES

1. Larsson, L. *Acta Chem. Scand.* **11** (1957) 1131.
2. Kilpatrick, M. and Kilpatrick, M. L. *J. Phys. & Colloid Chem.* **53** (1949) 1371.
3. Wagner-Jauregg, T., Hackley, B. E., Lies, T. A., Owens, O. O. and Proper, R. *J. Am. Chem. Soc.* **77** (1955) 922.
4. Augustinsson, K.-B. *Acta Chem. Scand.* **12** (1958) 1286.
5. Augustinsson, K.-B. and Heimbürger, G. *Acta Chem. Scand.* **8** (1954) 753.
6. Larsson, L. and Hansen, B. *Svensk Kem. Tidskr.* **68** (1956) 521.
7. Epstein, J., Bauer, V. E., Saxe, M. and Demek, M. M. *J. Am. Chem. Soc.* **78** (1956) 4068.
8. Gehauf, B., Epstein, J., Wilson, G. B., Witten, B., Sass, S., Bauer, V. E. and Rueggeberg, W. H. C. *Anal. Chem.* **29** (1957) 278.
9. Larsson, L. *Acta Chem. Scand.* **12** (1958) 723.
10. Edwards, J. O. *J. Am. Chem. Soc.* **76** (1954) 1540.
11. Epstein, J., Rosenblatt, D. H. and Demek, M. M. *J. Am. Chem. Soc.* **78** (1956) 341.
12. Schwarzenbach, G. *4th Symposium on the Chemistry of the Coordination Compounds*, Rome 1957.

Received March 12, 1958.

ACTA CHEMICA SCANDINAVICA 12 (1958) 1231—1235

Synthesis of Adrenochrome Alkyl Ethers *

JAAKKO HUKKI and NIILO SEPPÄLÄINEN

Lääketehdas Orion Oy, Helsinki, Finland

From adrenaline, its alkyl ethers (methyl, ethyl and *iso*propyl) were prepared through a common intermediate, methylaminomethyl-3,4-dihydroxyphenylchloromethane. On oxidation with silver oxide, these ethers were converted into those of adrenochrome and isolated as their monosemicarbazones.

Adrenochrome (III a), the quinoid oxidation product of adrenaline, is a well-known hemostatic agent. But, being an *ortho*-quinone, it readily deteriorates in aqueous solution. Several stable derivatives have been prepared from it, one of which, the monosemicarbazone (IV a), is commercially available under the name of adrenoxyl. Some homologs of adrenochrome, noradrenochrome [1], N-*iso*propylnoradrenochrome [2] and 2-ethylnoradrenochrome [2] have been reported. Two halogen substitution products, 2-iodo- [3] and 2-bromoadrenochrome [3], are described in the literature. Recently N-[β-hydroxyethyl]-noradrenochrome [4] has been synthesized. Most of the above compounds have been prepared as their monosemicarbazones.

The present paper is concerned with the synthesis of adrenochrome ethers. Owing to the instability of the adrenochrome molecule, direct etherification was not attempted. Instead, a circuitous route, starting from the corresponding adrenaline ethers, was chosen.

A methyl and an ethyl ether of adrenaline (II b and II c) have previously been prepared by Funk and Freedman [5] by passing dry hydrogen chloride into a boiling solution of adrenaline in the appropriate alcohol. The present method made use of an intermediate, methylaminomethyl-3,4-dihydroxyphenylchloromethane hydrochloride (I), which is readily formed from adrenaline with excess of thionyl chloride. It proved to be a crystalline compound, only stable if kept in the refrigerator and protected from light and moisture. It could not be recrystallized for analysis. The correctness of the above formula is shown by the formation of the following reaction products. It readily formed adrenaline hydrochloride with water. Heating with methanol or ethanol at 60° led to the formation of ethers identical with the corresponding ones pre-

* From the thesis for the M. A. degree of Niilo Seppäläinen, University of Helsinki, 1955.

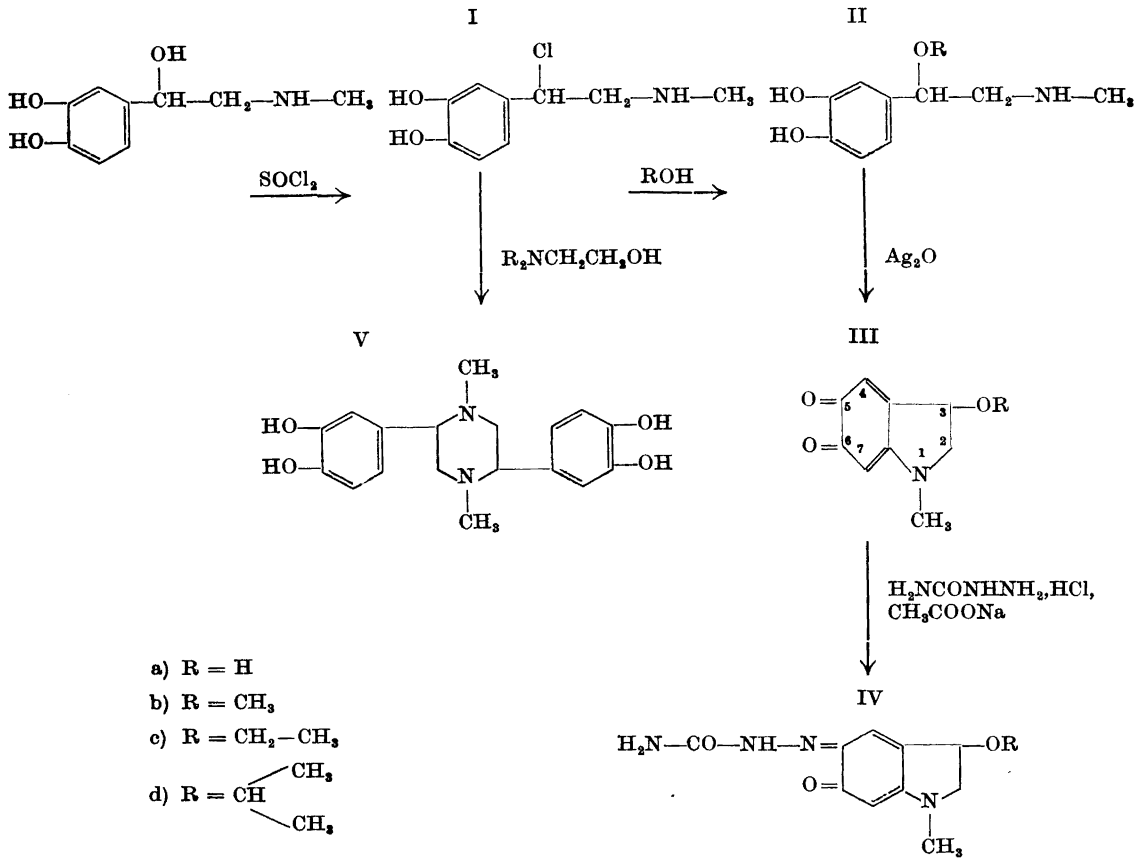

pared by the method of Funk and Freedman [5]. The former etherification method was used throughout in this work. An *iso*propyl ether of adrenaline was also synthesized. Some data on the adrenaline ethers, which were all obtained as hydrochlorides, are presented in Table 1.

When the synthesis of amino alkyl ethers of adrenaline was attempted by the above method, complications arose. A high-melting compound was formed in all cases, irrespective of the amino alcohol used. By analysis and melting point determination it was shown to be identical with the dimolecular ring condensation product obtained by Bretschneider [6] from methylaminomethyl-3,4-diacetoxyphenylchloromethane hydrochloride with diethylamine. Obviously the ring condensation reaction predominates under the strongly alkaline conditions produced by the amino alcohols. A structural formula of 2,5-bis(3,4-dihydroxyphenyl)-1,4-dimethylpiperazine (V) was suggested for this compound by Bretschneider.

The oxidation methods used for converting the adrenaline ethers into the corresponding adrenochrome ethers were essentially analogous with the famil-

Table 1. Adrenaline ethers.

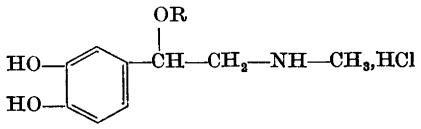

R	Formula	Yield %	M. P., °C	
			Found	In literature [5]
Methyl	$C_{10}H_{15}NO_3$, HCl	70	175	175
Ethyl	$C_{11}H_{17}NO_3$, HCl	82	169	169
*Iso*propyl	$C_{12}H_{19}NO_3$, HCl	35	177–8	—

iar ones employed in the synthesis of adrenochrome from adrenaline. Oxidation with silver oxide in methanol acidified with formic acid proved the best. The resultant adrenochrome ethers were isolated as the monosemicarbazones. All these were dark red, glistening, crystalline compounds. They were crystallized from aqueous pyridine, from which they were obtained without water of crystallization. The data for the ethers are presented in Table 2. For further characterization of these new compounds ultraviolet absorption spectra were made both of these and of the unetherified adrenochrome monosemicarbazone (adrenoxyl). The curves obtained are presented in Fig. 1. As can be seen, the general shape of the curves of the three ethers and the position of their maxima and inflection points are fully coincident with those of the curve of adrenoxyl.

As would be expected, the solubility of the monosemicarbazones of adrenochrome ethers in water is even poorer than that of adrenoxyl. In order to improve the solubility of adrenoxyl, its ability to form salts was studied. A bright yellow crystalline hydrochloride of adrenoxyl could readily be ob-

Table 2. Adrenochrome ethers (as monosemicarbazones).*

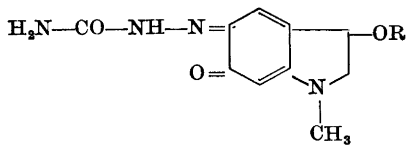

R	Formula	Yield %	M.P. °C	Analyses					
				Calc.			Found		
				C	H	N	C	H	N
Methyl	$C_{11}H_{14}N_4O_3$	56	217–18	52.79	5.64	22.39	52.71	5.44	22.43
Ethyl	$C_{12}H_{16}N_4O_3$	71	214–15	54.55	6.10	21.10	55.15	6.30	21.46
*Iso*propyl	$C_{13}H_{18}N_4O_3$	57	206– 7	56.10	6.52	20.13	55.52	6.51	20.03

* New features disclosed in this paper are covered by pending Finnish patent application.

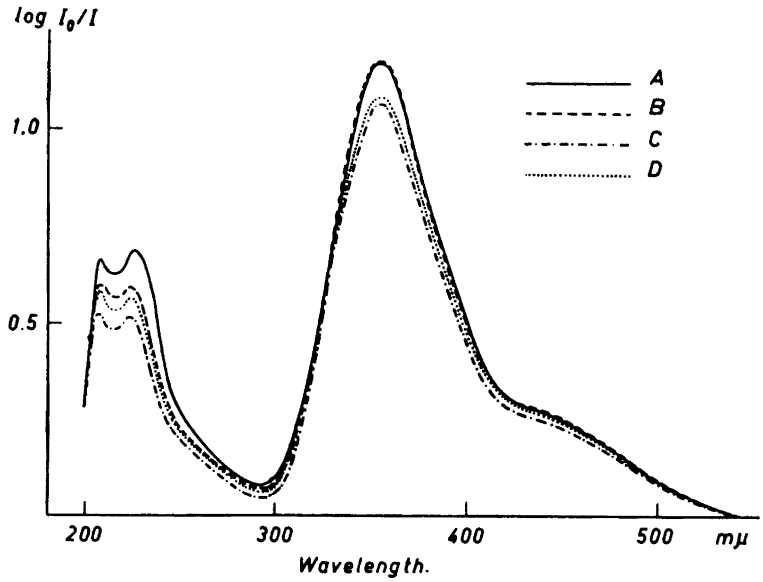

Fig. 1. Ultraviolet absorption spectra of the monosemicarbazones of A) adrenochrome, B) adrenochrome methyl ether, C) adrenochrome ethyl ether and D) adrenochrome *iso*propyl ether.

tained with a nearly quantitative yield. This was shown by analysis to be a monohydrochloride containing one molecule of water of crystallization. The salt is distinctly more soluble in water than adrenoxyl, but unfortunately it readily decomposes in solution, especially in the light. That the compound really was a salt of adrenoxyl was proved by liberating the base with pyridine. The base was shown to be identical with the starting adrenoxyl by melting point determination and ultraviolet absorptium spectrum. Whether the salt-forming ability of adrenoxyl is to be ascribed to the tertiary ring-nitrogen atom or to the semicarbazone side chain, was not investigated. The former possibility was taken into account by Ramirez and Ostwalden[7] when they studied the structure of adrenoxyl in the light of ultraviolet absorption spectra.

EXPERIMENTAL

All melting points are uncorrected. Microanalyses were performed by the Microanalytisches Laboratorium im Max-Planck-Institut für Kohlenforschung, Mülheim, Germany. Ultraviolet data, from the Analytical Laboratory of Lääketehdas Orion Oy, are for solutions in absolute methanol (concentration 0.01 g per liter).

Starting materials. The adrenaline used was an Uclaf product, m. p. 207—208.5°. The adrenoxyl was from Labaz, for parenteral use, m. p. 206—207°.

Methylaminomethyl-3,4-dihydroxyphenylchloromethane hydrochloride (I). To 70 g of thionyl chloride in an Erlenmeyer flask of 500 ml capacity was added 10 g of adrenaline after removal of the air with nitrogen. In about one minute a vigorous reaction set in, resulting in the formation of a clear solution. The gaseous reaction products were swept

off by passing in a continual stream of nitrogen. After about half an hour crystals began to separate from the liquid. When crystallization was complete, the product was filtered off and washed, first with benzene, then with ether. The yield of the colorless material was 13 g (99 %), m. p. 90—100° (decomp.). It could not be recrystallized, owing either to its insolubility in or to its reactivity with the usual solvents. It darkened rapidly in daylight but could be kept for some days in the refrigerator when protected from light and moisture.

Adrenaline ethers (II). A mixture of 2 g of methylaminomethyl-3,4-dihydroxyphenylchloromethane hydrochloride in 20 ml of the appropriate alcohol was refluxed for 1 h, the temperature of the boiling reaction mixture being kept at 60° by means of ether added through the condenser. The resulting solution was evaporated *in vacuo* almost to dryness. After addition of 25 ml of acetone the mixture was allowed to stand in the refrigerator overnight. The crystals deposited were filtered off, washed with acetone and dried in a desiccator. The ethers so obtained were sufficiently pure for oxidation to adrenochromes. For purification of an ether it was dissolved in hot absolute ethanol and as much acetone was added as possible without causing turbidity. The mixture was allowed to stand in the refrigerator overnight to ensure complete crystallization. No analysis of the ethers was made. Their constitution was confirmed by analyzing the corresponding adrenochrome ether monosemicarbazones prepared from them.

2,5-Bis(3,4-dihydroxyphenyl)-1,4-dimethylpiperazine hydrochloride (V). When dimethylaminoethanol was used as the alcohol component in the above etherification reaction, a high-melting (m. p. 303°) compound was the only product that could be isolated. The same compound was also obtained by allowing methylaminomethyl-3,4-dihydroxyphenylchloromethane hydrochloride to react with conc. aqueous ammonia. (Found: C 53.39; H 6.16; N 6.78. Calc. for $C_{18}H_{22}N_2O_4$, 2HCl: C 53.59; H 6.00; N 6.94.)

Adrenochrome ether monosemicarbazones (IV). The appropriate adrenaline ether hydrochloride (0.027 mole) was dissolved in a mixture of 2 ml of formic acid (99—100 %) and 100 ml of dry methanol. Freshly precipitated dry silver oxide (0.108 mole) was added. The mixture was shaken vigorously for 2—4 min at about 40° and filtered by suction into a solution previously prepared by dissolving semicarbazide hydrochloride (0.027 mole) and sodium acetate (0.073 mole) in 40 ml of distilled water. After washing with 10 ml of dry methanol the combined dark red filtrates were allowed to stand for 10 min at room temperature and then overnight at 0°. The dark red, glistening crystals were filtered, washed with water and dried in a desiccator.

Adrenoxyl hydrochloride. 3 g of adrenoxyl was placed in an Erlenmeyer flask, from which the air had been displaced with nitrogen and 120 ml of 2 % hydrochloric acid was added. The stoppered flask was shaken at room temperature until all the adrenoxyl had dissolved. Almost immediately a bright yellow crystalline compound began to separate. After separation had been completed in the refrigerator, the crystals were filtered off, washed with acetone and dried in a desiccator (without vacuum). The yield of the hydrochloride was almost quantitative. Upon crystallization from 2 % hydrochloric acid it melted at about 150° (decomp.). (Found: C 41.41; H 5.40; N 19.04; Cl 12.09. Calc. for $C_{10}H_{12}N_4O_3$, HCl, H_2O: C 41.31; H 5.20; N 19.27; Cl 12.20.)

REFERENCES

1. Marquardt, P. and Carl, E. *Naturwiss.* **39** (1952) 210.
2. Beaudet, C. *Experientia* **7** (1951) 291.
3. Sobotka, H. and Austin, J. *J. Am. Chem. Soc.* **73** (1951) 3077.
4. Iwao, J. and Tomio, K. *Chem. Abstracts* **51** (1957) 1177.
5. Funk, C. and Freedman, L. *J. Am. Chem. Soc.* **45** (1923) 1792.
6. Bretschneider, H. *Monatsh.* **78** (1948) 101.
7. Ramirez, F. and v. Ostwalden, P. *J. Org. Chem.* **20** (1955) 1676.

Received March 3, 1958.

ACTA CHEMICA SCANDINAVICA 12 (1958) 1236—1240

Rearrangement of 4-Phenylazo-5-hydroxy-1,2,3-triazoles to Amides of 2-Phenyl-5-carboxytetrazole

CHRISTIAN PEDERSEN

Department of Organic Chemistry, University of Technology, Copenhagen, Denmark

4-Phenylazo-5-hydroxy-1,2,3-triazoles (II), unsubstituted or substituted with methyl-, phenyl-, and benzyl- in position 1, have been prepared. It has been shown that II, when heated in glacial acetic acid, rearrange to amides of 2-phenyl-5-carboxytetrazole (IV). The rearrangement is believed to take place through an intermediate, aliphatic diazocompound (III).

Dimroth [1] and Curtius [2] have shown that 5-hydroxy-1,2,3-triazoles (I) couple with diazonium salts in alkaline solution with formation of 4-arylazo-5-hydroxy-1,2,3-triazoles (II).

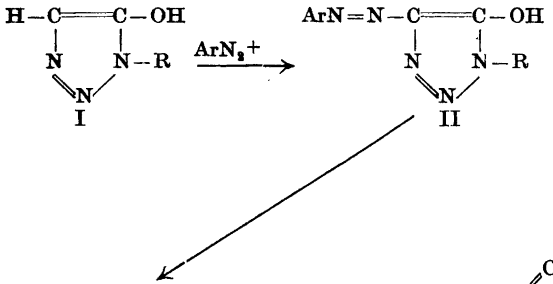

	R—	Ar—
a	C_6H_5—	C_6H_5—
b	H—	C_6H_5—
c	CH_3—	C_6H_5—
d	$C_6H_5CH_2$—	C_6H_5—
e	—CH_2CONH_2	*p*-$CH_3C_6H_4$—

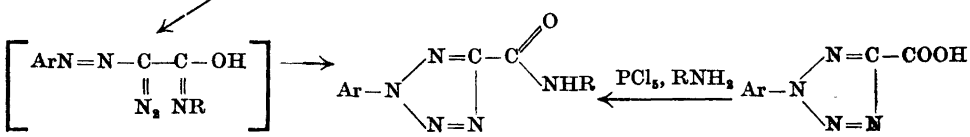

III IV VII

It was reported by Dimroth [1] that the orange-coloured 1-phenyl-4-phenylazo-5-hydroxy-1,2,3-triazole (IIa), on recrystallization from glacial acetic acid, rearranged to an isomeric, colourless compound which, as opposed to IIa,

had no acidic properties *. In the same way Curtius and Thomson [2] obtained a colourless isomer of IIe. No attempt has been made to find the structures of the two colourless compounds.

A number of esters of 4-carboxy-5-hydroxy-1,2,3-triazoles (V) were prepared by Dimroth and he showed that these compounds can isomerize to amides of diazomalonic ester (VI) when heated, alone or dissolved in water or organic solvents [3a-d]. When 1-*p*-nitrophenyl-4-ethoxycarbonyl-5-hydroxy-1,2,3-triazole was recrystallized from glacial acetic acid it gave the corresponding diazocompound (VI, R = *p*-nitrophenyl-) in quantitative yield [3c]. The mechanism of this reaction has been reinvestigated in more recent papers [4,5].

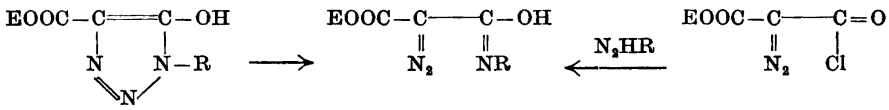

V VI VIII

In view of this it would be reasonable to assume that compounds of type II can also isomerize to aliphatic diazocompounds with the structure III. Compounds of type III will probably undergo a spontaneous ring closure with formation of amides of 2-aryl-5-carboxytetrazole (IV), in analogy with the preparation of 2,5-disubstituted tetrazoles by reaction of amidrazones with nitrous acid where intermediates with structure similar to III are likely to be formed [6,7]. This means that Dimroth's colourless isomer, formed by rearrangement of IIa, should be 2-phenyltetrazole 5-carboxanilide (IVa).

To prove this IVa was prepared by an unambiguous method, starting with the known 2-phenyl-5-carboxytetrazole (VII), which was made according to Bladin [6]. The acid (VII), *via* the chloride, gave the anilide (IVa) which had the same melting point and infrared spectrum as the rearrangement product from II and thus proving the structure of the latter.

To test the generality of this rearrangement it was tried in three other cases, starting with 5-hydroxy-1,2,3-triazoles, unsubstituted or substituted with methyl- and benzyl- in position 1. The coupling with phenyldiazonium chloride was done in 2 N sodium hydroxide and gave the 4-phenylazo-5-hydroxy-1,2,3-triazoles (Table 1). The latter, when boiled in glacial acetic acid solution for a few minutes, gave the corresponding tetrazoles (IV) in good yields (Table 2). The authentic tetrazoles, prepared from 2-phenyl--carboxytetrazole, all had melting points and infrared spectra completely identical with the tetrazoles prepared by rearrangement.

The 4-hydroxy-1,2,3-triazole (Ib) was prepared from ethyl diazomalonate monochloride (VIII) which with ammonia gives the monoamide (VI, R = H) [8]. VI was rearranged to 4-ethoxycarbonyl-5-hydroxy-1,2,3-triazole (V, R = H) with ethanolic potassium hydroxide. Saponification and decarboxylation of V

* Dimroth[1] thought that he obtained the coloured isomer (IIa)by coupling in 20 % sodium carbonate and the colourless isomer in weak basic solution, but according to our experience the coloured isomer is formed in both cases and the rearrangement takes place on recrystallization from acetic acid.

yielded 4-hydroxy-1,2,3-triazole [3c]. The 1-methyl-5-hydroxy-1,2,3-triazole was prepared in the same way.

The colourless isomer which Curtius and Thomsen [2] obtained from 1-carboxamidomethyl-4-*p*-tolylazo-5-hydroxy-1,2,3-triazole (IIe) on recrystallization from glacial acetic acid has not been included in the present investigation, but there can hardly be any doubt that it is also a tetrazole derivative and has the structure IVe.

Dimroth [1,3] showed that the rearrangement of V to VI takes place in a number of different solvents. Whether the rearrangement of II to IV can be effected in solvents other than glacial acetic acid has not been tried extensively, but prolonged heating of compounds of type II in ethanolic solution gave oily decomposition products with a strong smell of *iso*cyanides. Boiling in acetonitrile or dimethyl formamide also caused decomposition.

Table 1. 1-Substituted-4-phenylazo-5-hydroxy-1,2,3-triazoles (II).

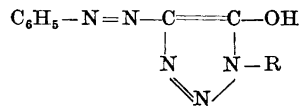

R—	Yields %	M. p.°	Formula	Analyses					
				Carbon		Hydrogen		Nitrogen	
				Found	Calc.	Found	Calc.	Found	Calc.
H—	93	155—156	$C_8H_7N_5O$	50.65	50.80	3.72	3.76	37.20	37.00
CH_3—	59	156—157	$C_9H_9N_5O$	53.70	53.30	4.61	4.47	34.68	34.50
C_6H_5—	83	142—143*	$C_{14}H_{11}N_5O$	63.60	63.50	4.22	4.18	26.66	26.42
$C_6H_5CH_2$—	68	150—151	$C_{15}H_{13}N_5O$	64.65	64.60	4.51	4.69	25.23	25.05

* Dimroth[1] reported m.p. 131—132°.

Table 2. 2-Phenyl-5-carboxamidotetrazoles.

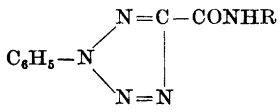

R—	Yields %	M. p.	Formula	Analyses					
				Carbon		Hydrogen		Nitrogen	
				Found	Calc.	Found	Calc.	Found	Calc.
H—	79(76)[a]	167—168*	$C_8H_7N_5O$	50.70	50.80	3.97	3.76	36.84	37.00
CH_3—	77(40)[b]	141—142	$C_9H_9N_5O$	53.20	53.30	4.35	4.47	34.30	34.50
C_6H_5—	78(83)[c]	160—161	$C_{14}H_{11}N_5O$	63.30	63.50	4.14	4.18	26.58	26.42
$C_6H_5CH_2$	63(50)[a]	108—109	$C_{15}H_{13}N_5O$	64.75	64.60	4.81	4.69	25.05	25.05

* Reported m.p. 167.7—168.5[6].

Solvents used for recrystallization: a) ethanol, b) light petrol (b.p. 100/140°), c) glacial acetic acid. Yields given in brackets refer to preparation of authentic tetrazoles.

EXPERIMENTAL

Melting points are uncorrected.

5(4)-Hydroxy-1,2,3-triazoles

4-Hydroxy-1,2,3-triazole. Ethyl diazomalonate monochloride [8] (8.5 g) was added during 5 min to 30 ml of ice-cold, stirred, 25 % ammonia. Stirring and cooling was continued for 30 min. The cream-coloured ethyl diazomalonate monoamide was filtered off and washed with water. Yield 6.2 g (81 %), m. p. 142—143° (reported [3c,8] m. p. 142° and 143°.)

The monoamide (4.15 g) was dissolved in 40 ml of hot absolute ethanol and the solution added to 4.45 g (3 moles) of KOH in 50 ml of hot ethanol. The potassium salt of 4-ethoxycarbonyl-5-hydroxy-1,2,3-triazole precipitated immediately, causing the mixture to solidify. After 10 min the ethanol was removed *in vacuo*, 25 ml of water was added and the resulting solution refluxed for 1 h. The solution was then acidified with conc. HCl (pH should be 3—4; excess of acid decomposes the 4-hydroxytriazole and a product results which is very difficult to purify) and boiled for 1—2 min to complete the decarboxylation. The mixture was evaporated to dryness *in vacuo* and the residue extracted with boiling absolute ethanol (3 × 15 ml). The ethanolic solution was evaporated to dryness and the residue extracted 7—8 times with 25 ml portions of boiling ether; the ether solution was concentrated to ca 50 ml and the 4-hydroxytriazole precipitated with light petrol. Yield 1.60 g (70 %), m. p. 126—128°. A sample was recrystallized twice from ethyl acetate and finally sublimed *in vacuo* (0.1 mm) at 110°. M. p. 130—132° (reported [3c,2] m. p. 130° and 135°). (Found: C 28.15; H 3.63; N 49.29. Calc. for $C_2H_3N_3O$: C 28.20; H 3.55; N 49.40.)

1-Methyl-5-hydroxy-1,2,3-triazole. Ethyl diazomalonate monochloride in ether was treated with dry methylamine; the methylamine hydrochloride was filtered off and the ether removed *in vacuo* leaving ethyl diazomalonate monomethylamide as a yellow oil, which could not be induced to crystallize. The crude oil was treated in the same way as above and gave 1-methyl-5-hydroxy-1,2,3-triazole in 65 % yield. The product was recrystallized from ethanol, m. p. 168—170°. (Found: C 36.45; H 5.00; N 42.48; Calc. for $C_3H_5N_3O$: C 36.30; H 5.08; N 42.40.)

1-Phenyl-5-hydroxy-1,2,3-triazole was prepared according to Dimroth [1].

1-Benzyl-5-hydroxy-1,2,3-triazole. 1-Benzyl-4-ethoxycarbonyl-5-hydroxy-1,2,3-triazole [9] was saponified and decarboxylated in the same way which Gompper [10] used for the methylester. Yield 85 %, m. p. 157—158°.

4-Phenylazo-5-hydroxy-1,2,3-triazoles

4-Phenylazo-5-hydroxy-1,2,3-triazole. A phenyldiazonium chloride solution, prepared from 0.54 ml of aniline in 15 ml N HCl and 0.41 g (1 mole) of sodium nitrite, was added during ca 5 min with stirring and ice cooling, to a solution of 4-hydroxy-1,2,3-triazole (0.5 g, 1 mole) in 15 ml 2N NaOH. The orange solution was kept for 1 h at 0°. Acidification with conc. HCl gave 4-phenylazo-5-hydroxy-1,2,3-triazole as a yellow precipitate which was filtered off and washed with water. Yield 1.03 g (93 %), m. p. 151—153°. After two recrystallizations from ethanol the substance was pure, forming yellow needles.

The same product was obtained when 4-carboxamido-5-hydroxy-1,2,3-triazole was used, the carboxamido group being split off during the reaction. With the same conditions as above the yield of azocompound was 96 %.

1-Methyl- and *1-benzyl-4-phenylazo-5-hydroxy-1,2,3-triazole* were prepared in the same way from 1-methyl- and 1-benzyl-5-hydroxy-1,2,3-triazole, respectively. They were both recrystallized from ethanol. Properties are given in Table 1.

1-Phenyl-4-phenylazo-5-hydroxy-1,2,3-triazole was prepared according to Dimroth [1] by coupling in 20 % Na_2CO_3. When 2N NaOH was used the product was very impure. The product was recrystallized from methanol; prolonged heating should be avoided during the recrystallization to avoid decomposition.

Rearrangement of 4-phenylazo-5-hydroxy-1,2,3-triazoles

2-Phenyltetrazole-5-carboxanilide. 1-Phenyl-4-phenylazo-5-hydroxy-1,2,3-triazole (1.2 g) was dissolved in 10 ml of boiling glacial acetic acid and the solution was boiled for 5 min. The orange colour of the azocompound disappeared almost immediately. On cooling the tetrazole crystallized; it was filtered off and washed with ether. Yield 0.75 g, m. p. 159–161°.

In the other three cases the rearrangement was done in the same way. If the product did not crystallize on cooling of the acetic acid solution it was precipitated with ether or light petrol. Their properties are given in Table 2.

Preparation of authentic tetrazoles

2-Phenyltetrazole-5-carboxanilide. Dried 2-phenyl-5-carboxytetrazole [6] (0.5 g) and phosphorus pentachloride (0.6 g, 1.1 mole) were mixed and heated for a few minutes until the vigorous reaction had ceased. Phosphorus oxychloride and excess of phosphorus pentachloride were then removed *in vacuo* at 100°. The crude chloride, which formed a solid, was cooled in ice and treated with excess aniline dissolved in ether. The mixture was stirred and the lumps were broken with a glass rod to complete the reaction. The solid was then collected by filtration and washed with diluted HCl and water.

The three other tetrazoles were prepared in the same way, IVb and IVc with 25 % aqueous ammonia and methylamine, respectively, and IVd with benzylamine in ether. Yields are given in brackets in Table 2. They were all analysed but the values are not given here; the analyses in Table 2 are those of the rearrangement products.

The infrared spectra were taken on a Beckman I.R.2 in strument using the KBr-disk technique.

The author is indebted to Civilingeniør S. Refn for the infrared spectra. Microanalyses were made by Mr. P. Hansen.

REFERENCES

1. Dimroth, O. *Ann.* **335** (1904) 1.
2. Curtius, Th. and Thomsen, J. *Ber.* **39** (1906) 4143.
3a. Dimroth, O. *Ann.* **338** (1904) 143.
b. Dimroth, O. *Ann.* **364** (1909) 183.
c. Dimroth, O. *Ann.* **373** (1910) 336.
d. Dimroth, O. *Ann.* **399** (1913) 91.
4. Brown, B. R. and Hammich, D. L. *J. Chem. Soc.* **1947** 1384.
5. Leffler, J. E. and Shih-Kung Lu *J. Am. Chem. Soc.* **78** (1956) 1949.
6. Bladin, J. A. *Ber.* **18** (1885) 2908.
7. Pinner, A. *Ber.* **27** (1894) 995; *Ann.* **297** (1897) 229.
8. Staudinger, H., Becker, J. and Hirzel, H. *Ber.* **49** (1916) 1978.
9. Hoover, J. R. E. and Day, A. R. *J. Am. Chem. Soc.* **78** (1956) 5832.
10. Gompper, R. *Ber.* **90** (1957) 382.

Received February 1, 1958.

ACTA CHEMICA SCANDINAVICA 12 (1958) 1241—1246

On the Reaction between Polyacrylonitrile and Hydrazine

SVEN SÖNNERSKOG

A-B Svenskt Konstsilke, Borås, Sweden

Polyacrylonitrile reacts with hydrazine or hydrazine hydrate. The new polymer is insoluble in all known solvents for polyacrylonitrile even at low extents of reaction. Insolubilization is caused by intermolecular reactions. The interlinking unit is 4-*N*-amino-1,2,4-triazole.

Solutions of polyacrylonitrile in dimethylformamide slowly react with hydrazine or hydrazine hydrate at room temperature. A gel gradually separates, insoluble in all known solvents for unmodified polymer. Ammonia and dimethyl amine are simultaneously formed and easily identified in the vapor phase of a closed system. At elevated temperature — 80°C — gelation is complete within 50—65 min. The reaction seems to be specific for hydrazine in the meaning that ammonia, amines and even aliphatic diamines only cause a discoloration of polymer solutions but no observable change of solubility characteristics. What is said above refers to 2 % solutions of polyacrylonitrile (red.ox.grade, aver.-visc.mol.wt. about 8×10^4), dissolved in a mixture of three parts (by wt) of dimethylformamide and one part of hydrazine (technical grade, content of hydrazine 95—97 %). The polymer dissolves in this mixture above 40°C and is stable at room temperature for several hours until the action of hydrazine is noticeable. Even at 80°C the system remains fluid until incipient gelation takes place within the last few minutes, when the gel expands to a viscous foam. The escaping gas contains ammonia, dimethyl amine and hydrazine vapor, which are partly separable in a series of cooling traps.

Identical effects have been observed for other stoichiometric ratios between reacting species and it is well established that the gel formation is not limited to the special working conditions mentioned above. Insolubilization takes place in other solvents, such as dimethylsulfoxide. The action of hydrazine hydrate is equivalent to that of hydrazine. Even solid polymer, suspended in aqueous solutions of hydrazine, is gradually converted into a reddish-orange modification, definitely insoluble in customary solvents for linear polymer. Of course this does not mean that the *extent* of reaction is the same in all these cases, yet high enough to cause insolubility even of the primary polymer particle.

The primary gel is rubbery in character. During purification by repeated soaking in hot water and methanol (absence of air) it is gradually converted into a brittle, distinctly yellow powder. The color turns into orange on drying in air at room temperature. Contrary to standard homopolymer this final modification is resistent to alkaline hydrolysis. It evolves only a minor amount of ammonia on boiling in 10—20 % sodium hydroxide solution. The degree of swelling is low compared with the primary gel volume. Such a drastic change of physical properties might be caused by

1) a reduction of the number of solvogenic groups,

2) a decrease of the number of independent kinetic units,

or by both cases in combination. In other words both inter- and intramolecular type reactions between polyacrylonitrile and hydrazine must be considered. However, it is equally important to pay attention to competing side reactions between solvent and hydrazine, including the contribution from water and ammonia always present in technical grades of said chemicals. The following list is given as a summary:

A. Interchange reactions between dimethylformamide and hydrazine:

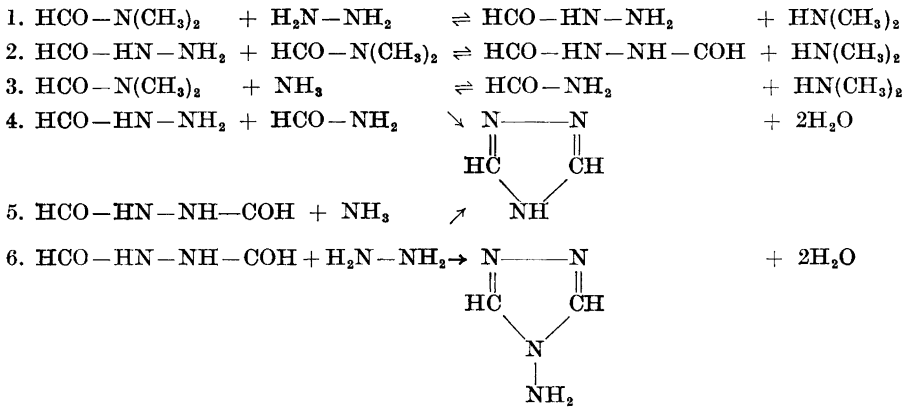

B. Reactions between polymer, hydrazine, coreactants:

1. Hydrazidine formation, accompanied by hydrolysis and amide interchange:

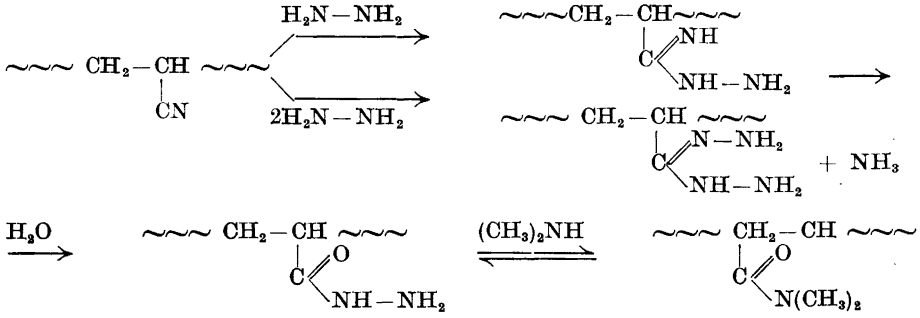

2. Intramolecular cyclization at isotactic sequences [1,2]:

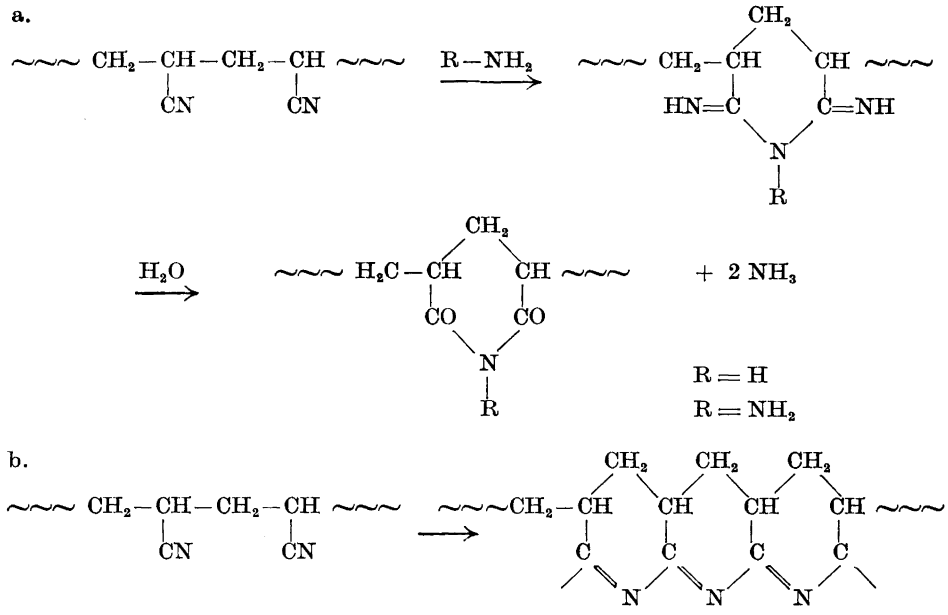

3. Intermolecular reaction at random between hydrazide or hydrazidine groupings (compare case A: 4,6). The interlinking unit formed in this way is 4-*N*-amino-1,2,4- triazole:

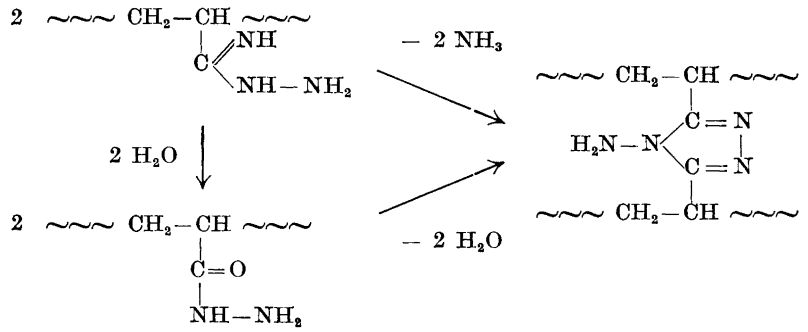

As is seen from this survey of type reactions the formation of water is initiated by ammonia as well as of hydrazine. Water is consumed by hydrolysis of imino groups in the reacting polymer but regenerated when hydrazide groups are converted into heterocyclic units by intermolecular condensation.

The ammonia, liberated according to B:1 -3, is recycled in secondary reactions and represents a potential source of new water molecules. This explains why the rate of gelation is fairly constant even at a large change of water

content in the initial reaction mixture (*e.g.* when hydrazine hydrate is used instead of hydrazine).

The final structure of the polymer can evidently be realized in so many ways that it is hardly permitted to speak of a single, reproducible composition. This does not imply that the gelation effect is caused by all reactions between polymer and active reagents. The extent of *intra*molecular cyclization cannot be made responsible for insolubilization, as this would contradict all previous [1,2] experience on color formation in polyacrylonitrile, caused by the action of ammonia and aliphatic amines. These chemicals do not decrease solubility of the polymer in dimethylformamide. It is much more probable that the gel effect is caused by intermolecular reactions. Insolubilization would then take place, regardless of the intramolecular balance between nitrile, hydrazidine, hydrazide and naphtyridine groupings, when the amount of interlinking units has reached, on an average, the critical value of incipient gelation. As the reaction also has been observed in the system hydrazine—solid polymer it seems permitted to anticipate its existense also in the gel phase. This only emphasizes the difficulty of obtaining a good reproducibility, as the termination of the reaction is depending on the following schedule of purification.

A crosslinked polymer, formed in this way, would act as an anion exchanger due to the presence of primary amino groups in the interlinking units. This has been confirmed by saturation with hydrochloric acid, followed by regeneration with sodium hydroxide solution and titration of liberated chloride ions. The exchange capacity amounts to 0.2—0.3 mequiv./g dry polymer in a series of six specimens. This property remains after heating the polymer at 80—100°C in strong sodium hydroxide solution. The degree of swelling increases at this saponification step, as stated above, but no dissolution of polymer has been detected.

The triazole nucleus is known to be very stable to the hydrolytic action of mineral acids. The present polymer is not dissolved by hot concentrated hydrochloric acid or by 70 % sulphuric acid. The latter is known to be a good solvent for the parent polymer. Strong nitric acid also shows good solvent properties for polyacrylonitrile and polyacrylic acid, but is incapable of dissolving the actual polymer at moderate temperatures. However, dissolution takes place rapidly in strong (60—80 %) acid at 110—115°C, apparently connected with an oxidative degradation of the sample. On dilution with water after cooling a voluminous precipitate is obtained, easily soluble in dimethylformamide. Viscosity measurements indicate a very low molecular weight. Similar effects have been obtained on samples previously reacted with nitrous acid.

Infra-red spectra of the polymers, prepared in homogeneous or heterogeneous system, show essentially the same features. Fig. 1 is a juxtaposition of relevant regions of infrared absorption for I:primary polymer, II:reacted polymer, obtained by the action of 10 % hydrazine hydrate solution in a suspension of primary polymer, III: "gel polymer", obtained from reaction in homogeneous system, followed by immediate washing and drying after insolubilization. A most striking difference is the low extent of reaction in case II and the very high one in case III, as indicated by the band at 2 260 cm^{-1}, measuring the amount of unreacted nitrile groups. The lower level,

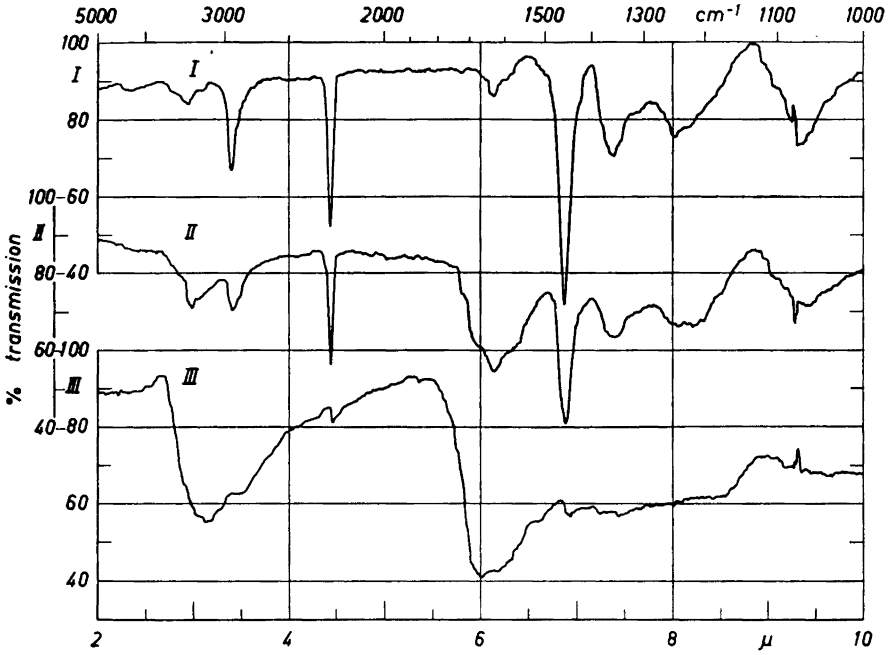

Fig. 1. Infra-red spectra of I: pure polyacrylonitrile II: polymer powder heated in 10 % hydrazine hydrate solution, III: polymer dissolved in dimethyl formamide-hydrazine, soaked after reaction in water and methanol, dried at room temperature in air.

however, is sufficient for complete insolubilization. New, broad bands arise in two regions with absorption maxima approximately at 3 and 6 μ. Their intensities are apparently related to the extent of reaction (disappearence of nitrile groups) likewise the exact location of the absorption maxima. In the case of completely reacted polymer (III) the latter band covers a variety of conceivable groupings (amides, amines, hydrazides) usually found at 1 600—1 700 cm^{-1}. The absorption maximum at 1 625 cm^{-1} is earlier [1] offered as evidence for the formation of C = N linkages in similar systems. The other (3 350 cm^{-1}) band, fairly distinct at a low extent of reaction (II), is located in the region where amino and imino groups show their stretching frequences. The list above of type reactions would thus fit at least qualitatively into the picture obtained from the infra-red spectra. A more detailed analysis requires a variety of model substances for exact frequency determinations.

Analytical. The presence of oxygen in the final polymer (III) was confirmed by elementary analysis (Unterzaucher-Zimmermann *). The oxygen content is 13.7 %. Nitrogen determination, according to Kjeldahl, was carried out on six specimens, showing a considerable scattering (12.3—13.4 %). The limiting nitrogen content after saponi-

* Carried out by Dr. A. Bernhardt, Mülheim, Ruhr.

fication at 100°C in 30 % sodium hydroxide solution is 5.1—5.5 %. Work is continued on model substances, obtained by reaction between polyacrylonitrile and hydrazine in an inert solvent (dimethylsulfoxide). This facilitates separation of the different reaction steps, ending in insolubilization, as the influence of water can be excluded. The single volatile byproduct is ammonia.

Acknowledgement. The author is greatly indebted to professor Erich Adler for good advice and valuable criticism, and to his coworker Mr. Bo Gustafsson for recording of the infra-red spectra shown in Fig. 1.

REFERENCES

1. La Combe, E. M. *J. Polymer Sci.* **24** (1957) 152.
2. Mc Cartney, J. R. in *Polymer Degradation Mechanisms, Natl. Bur. Standards,* Circular 525, Washington 1953, p. 123.

Received March 25, 1958.

ACTA CHEMICA SCANDINAVICA 12 (1958) 1247—1258

Acid Compounds of Hemins and Hemoproteins (B–Compounds) *

A. C. MAEHLY

E. R. Johnson Foundation for Medical Physics, University of Pennsylvania, Philadelphia, and Nobel Medical Institute, Biochemical Department, Stockholm, Sweden **

Acid compounds of several hemoproteins and free hemins are studied and described, notably in respect to their spectra, equilibrium constants and their reaction with halogen ions. Fluorescent measurements are used to study the possible dissociation of the central iron atom from the porphyrin molecule in acid solutions.

The possible reactions involved are briefly discussed. A detailed discussion will be found in the second communication of these series.

The properties of hemins and hemoproteins in strongly acid aqueous solutions have been relatively little studied. Many hemoproteins, like hemoglobin, myoglobin, and to some extent catalase, are denatured below pH 4. So far only horseradish peroxidase [1,2] and cytochrome c [3–5] have been investigated in strongly acid solutions which did not denature the protein irreversibly.

Iron-porphyrins in their free state have very low solubilities in aqueous systems in the acid range, and it is therefore difficult to study them. In 1929, Hicks and Holden [6] measured the absorption of hemoglobin and of protohemin in the Soret region (*ca.* 350—450 mμ) at low pH, and in 1947 Erdman and Corwin [7] published a very interesting paper on the acid spectra of mesohemin-dimethylester in pyridine and dioxane.

The present investigation was begun in order to study the nature of compounds observed by Theorell and Paul [8], by B. Chance [9] and by this author [1] on acidifying solutions of horseradish peroxidase (HRP) with acid. At least two such compounds were identified and this author proposed to call them compounds A and B, respectively. Acidification of HRP by H_2SO_4, HNO_3, or $HClO_4$ yields the acid compound B, where the protein moiety is denatured. With HCl, a hydrochloride, HRP-HCl or compound A is formed, which on further acidification reversibly splits into hemin and undenatured protein.

* Part of the results published here have been reported at a meeting of the Swedish Biochemical Society in Uppsala in December 1953.

** Present address: Statens rättskemiska laboratorium, Stockholm, Sweden.

Compound B is only present in small concentrations. HBr, HF, and HCN have effects similar to HCl. B-Compounds can be defined as compounds formed from hemin-containing substances at low pH in the absence of halogen or cyanide ions and are characterized by a high sharp absorption band, somewhere between 380 and 398 mμ [1].

METHODS AND MATERIALS

The hemins were prepared by known methods as described in an earlier paper [10] and were crystallized once from acetic acid saturated with sodium chloride. A sample of crystalline horseradish peroxidase (HRP) mentioned in previous work [2] was used. Its ratio of optical densities at 403 mμ and 275 mμ (RZ,*) was 2.68. Hemoglobin (Hb) was prepared from washed human erythrocytes and the dialyzed solution was used without further treatment. Sheep myoglobin (ShMb) was kindly donated by Dr. M. Beznák and had the properties described in her paper [11]. A sample of human serum albumin was kindly given us by Dr. M. Surgenor (Boston) in the form of fraction V.

Two types of recording spectrophotometers were used in addition to a standard Beckman DU instrument: an apparatus designed by B. Chance [12] recording changes of transmission with respect to time, and a spectrophotometer built by Yang and Legallais [13] recording absorption spectra (optical density *versus* wavelength). Cuvettes with 1 cm lightpath were used and the temperature was adjusted by circulating thermostated water through »thermospacers». As a rule, measurements of pH were made inside the optical cuvettes using micro-electrodes (Beckman »baby stomach» electrodes) and pH meters of the same firm. The reproducibility of this setup was better than ± 0.1 pH units, wich was sufficient for this type of work. The accuracy was considerably higher for the duration of a given experiment.

RESULTS

Spectral data on the acid compounds of HRP. Virtually complete transformation of HRP into HRP—B was accomplished by the addition of sulfuric acid to an aqueous solution of the peroxidase to give a pH of 0.6. The spectrum of the relatively unstable compound B was measured at +5° with the recorder of Yang and Legallais and checked at critical wavelengths with Chance's double-beam spectrophotometer. The formation of B from HRP is most easily observed in the Soret region [1]. In 1944, Theorell and Paul [8] found that the addition of HCl to HRP leads to spectral changes, notably a pronounced increase in optical density at 615 mμ and a smaller decrease at 655 mμ. They attributed these to pH changes and found, by titrating HRP with HCl, two pK values: 4.0 (measured at 655 mμ) and 5.0 (measured at 615 mμ).

Chance [9] showed that the negative logarithm of the dissociation constant of the HCl compound of HRP is $pK_{FeH^+Cl^-} = 5.5$, but in terms of H^+ ion concentration the pK appears [9] to lie at 3.4. Sulfuric acid, in contrast to hydrochloric acid, does not influence the spectrum of HRP above pH 3.5 and the pK of compound B by spectrophotometric titration with H_2SO_4 at 397 mμ was found [1] to be 2.30. Chance and Maehly working at 615 mμ (*cf.* Ref.[9]) confirmed this value.

* For a definition of this unit see Maehly, A. C. in *Methods in Enzymology*, Vol. II, S. P. Colowick and N. O. Kaplan, eds., Academic Press, New York 1955, p. 801.

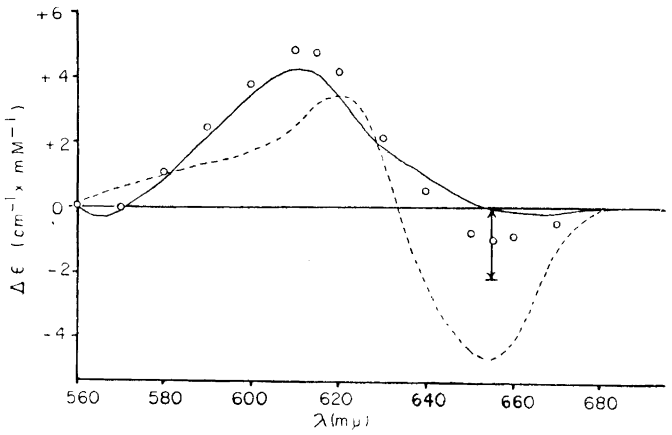

Fig. 1. The spectra of the difference "HRP-B minus HRP" as well as "Theorell and Paul's data" [8] and "compound A minus HRP".

- - - - - - - - HRP-B at pH 0.6 minus neutral HRP (concentration 7.5×10^{-6} M).

O O O O Theorell and Paul's measurements of acidified HRP (extrapolated to pH 2.7) minus neutral HRP (concentration 4.7×10^{-4} M).

———— Theorell and Paul's data, corrected for the calculated contribution of HRP-B at pH 2.7. A continuous curve is drawn to fit the calculated points and the resulting spectrum is assumed to represent the difference spectrum of HRP compound A (cf (1)) minus neutral HRP.

The arrow indicates the maximal decrease of the extinction coefficient obtained by Theorell and Paul by addition of HCl to HRP in a separate experiment (pH5.4).

Addition of HCl to HRP has two separate effects, namely (i) the formation of compound A (HRP · HCl) with absorption bands at 407 and 615 mμ, and (ii) the partial formation of compound B (acid compound) with bands at 397, 500, and 635 mμ. Fig. 1 shows the difference spectrum obtained by subtracting the spectrum of neutral HRP from that of compound B (obtained by addition of H_2SO_4). It also shows some data of Theorell and Paul[8]. These values were arrived at by subtracting the extinction values of neutral HRP from those measured after the addition of HCl. If the "dip" of these data at 655 mμ is attributed to partial B formation, then the values can be corrected for the contribution of compound B and the difference spectrum of compound A minus neutral HRP obtained (solid line). It shows a peak at 611 mμ. Some implications of these findings have been discussed by Chance [9].

Acid compounds of other hemoproteins. The formation of acid compounds (B compounds) from HRP and from horseblood catalase (HBC) by sulfuric, perchloric, or nitric acids have been described previously [1]. It has since been found that Hb and ShMb also give B compounds under these conditions. Fig. 2 shows the original recordings of their spectra obtained with the recorder of

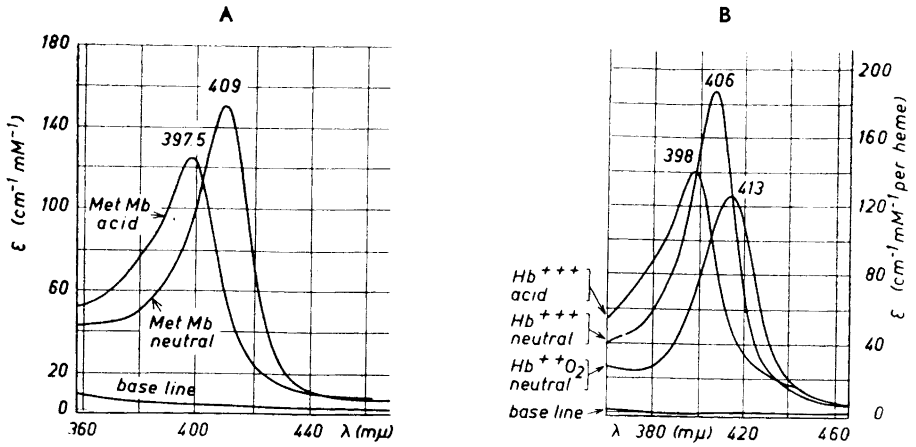

Fig. 2. Original recordings on the apparatus of Yang and Legallais [13]. A: The spectra of sheep metmyoglobin at pH 7.0 (phosphate buffer) and of ShMb-B (H_2SO_4, pH ~ 1). The concentration of ShMb was 3.8 μM. B: The spectra of HbO_2, MetHb (both at pH 7, 0.01 M phosphate buffer) and of Hb-B, formed by the addition of H_2SO_4 to give pH 1. The concentration of hemoglobin was 3.8 μM.

Yang and Legallais. The peak of the Soret band of B lies at 397 mμ. A typical titration curve for Hb-B is presented in Fig. 3.

Human serum albumin is known to bind hemins, but the resulting "hemalbumins" have not been shown to exhibit any biological activity. Protohemalbumin, studied in some detail by Rosenfeld and Surgenor [14] and others, shows a spectrum that is very similar to that of HRP. When H_2SO_4

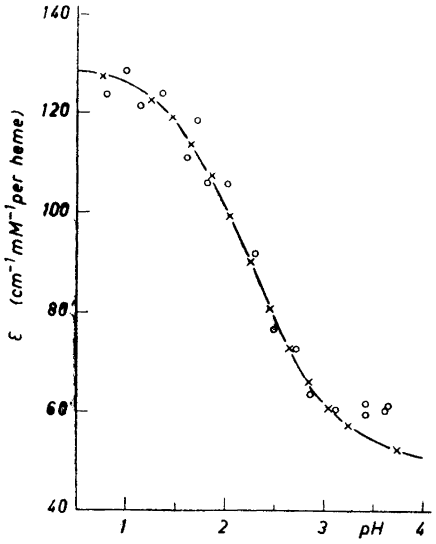

Fig. 3. The titration of hemoglobin with H_2SO_4. — Each point represents the results of a separate experiment: addition of H_2SO_4 to neutral 2.4 μM HbO_2 solution and determination of the maximal optical density at 397 mμ reached during the reaction, as well as of the pH.

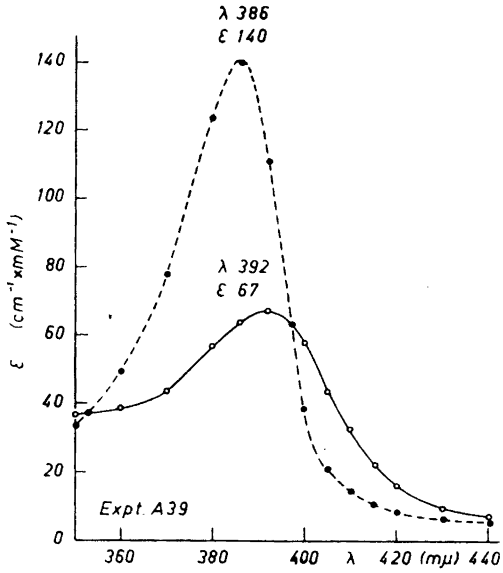

Fig. 4. The Soret spectra of deuterohemalbumin and its B compound.

O—O—O deuterohemalbumin, obtained by adding 2.9 μM deuterohemin to 5.8 μM human serum albumin in 0.02 M phosphate buffer, pH 6.8.

●-----● deuterohemalbumin-B, formed by the addition of 0.3 N. H_2SO_4 to the solution described above.

is added, the B compound is formed with a peak at 397 mμ and $\varepsilon = 130$ $cm^{-1}mM^{-1}$, quite comparable to the compounds of HRP, HBC, ShMb, and Hb. If deuterohemin is added to albumin solutions at pH 6.8 (0.02 M phosphate), deuterohemalbumin is formed. This compound has not been previously reported and its Soret spectrum is therefore rendered in Fig. 4*. When the pH is lowered to about 1 by adding H_2SO_4, the corresponding B compound is readily formed with a peak at 387 mμ and $\varepsilon = 140$ $cm^{-1}mM^{-1}$.

Acid compounds of some free hemins. Protohemin is soluble in water only at alkaline pH. Sodium carbonate, or better 0.1 N NaOH, is required to dissolve the compound completely. However, considerable polymerization takes place. This polymerization increases when the pH is lowered, as Shack and Clark [15] have found by experiments involving diffusion, dialysis, and ultracentrifugation. Further acidification leads to a change in spectrum, and the addition of more acid precipitates the hemin from all but the most dilute solutions. At very low pH a further change takes place: compound B is formed, as indicated by the spectrum in the Soret region (Fig. 5). This acid compound

* Compounds formed by a combination of mesohemin with human serum albumin and other proteins have been described by Rosenberg, L. L. and Clark, W. M. *J. Biol. Chem. 205* (1953) 617.

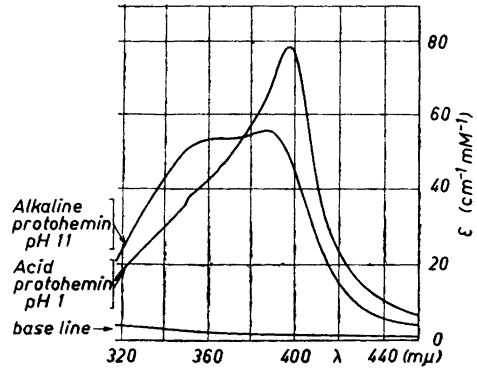

Fig. 5. The Soret spectra of protohemin and protohemin-B. This original recording shows the spectra of protohemin in dilute NaOH (pH 11) and of the B compound obtained from it by adding H_2SO_4 to a final pH of 1.

is also only slightly water-soluble and undergoes further, irreversible changes on standing.

Deutero- and mesohemin lack the two vinyl groups of protohemin and are therefore chemically simpler model compounds. Mesohemin gives a B compound with a Soret band at 380 mμ, deuterohemin forms a similar compound with a peak at 388 mμ. Titration data show that deuterohemin (having no sidechains in 2- and 4-positions) is most readily transformed into its B-form (p*K* 3.0—3.1). Mesohemin (2 ethyl groups as sidechains) requires more acid

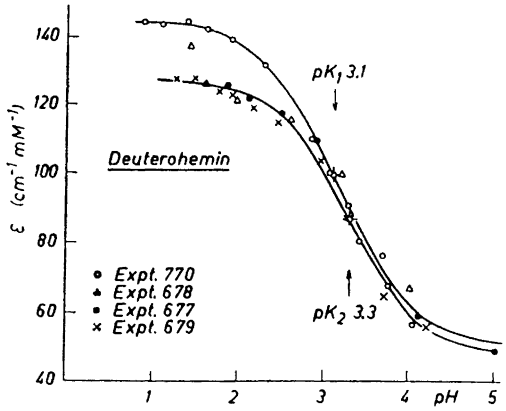

Fig. 6. The reversibility of the formation of the B compound obtained from deuterohemin. A solution of deuterohemin was acidified with H_2SO_4, acid potassium tartrate was added, and the pH as well as the optical density at 388 mμ were measured after addition of increasing amounts of NaOH to the sample (Expts. 677—679). The "normal" titration curve from Fig. 8A is represented forcomparison (Exp. 779). The concentration of deuterohemin was 5.8 μM when going from high to low pH, and 2.1—2.4 μM when the pH was raised.

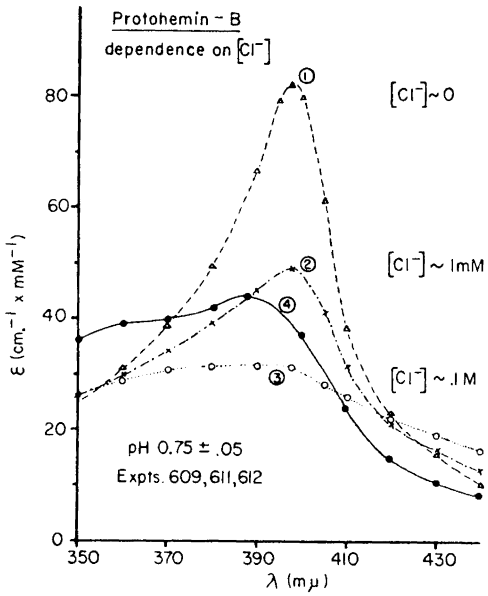

Fig. 7. The influence of the Cl′ ion concentration on the Soret band of protohemin-B (PHB). Protohemin was acidified with H_2SO_4 (pH .75) and its spectrum recorded. The recording was repeated with identical solutions, except for the presence of increasing concentrations of KCl.

(1) △-------△ PHB, no KCl

(2) x·····x PHB, ~ 1 mM KCl

(3) O.....O PHB, ~.1 M KCl

(4) ●——● protohemin at pH 7 (0.01 M phosphate buffer) shown for comparison.

The protohemin concentration varied between 7 and 11 μM.

(pK 2.25), and protohemin (2 vinyl groups) still more (pK 1.5). Deuterohemin-B appears to be best suited for further studies on the nature of B compounds since it can be obtained under relatively mild conditions. The instability of protohemin in aqueous solutions and its tendency to polymerize make it the least suitable of these hemins for such studies.

The relatively high stability of deuterohemin-B allowed a measurement of the reversibility of B formation. The technique for obtaining titration data for hemoproteins as well as hemins consisted of adding a definite and increasing amount of acid to each of as many aliquots of the solution of a neutral sample of the compound as there were values needed (*cf.* Ref.[1]). The instability of B made a simple reversal of this technique impractical. Some tartrate and increasing amounts of NaOH were added to only one sample of acidified deuterohemin (compound B), and the pH as well as the optical density were rapidly

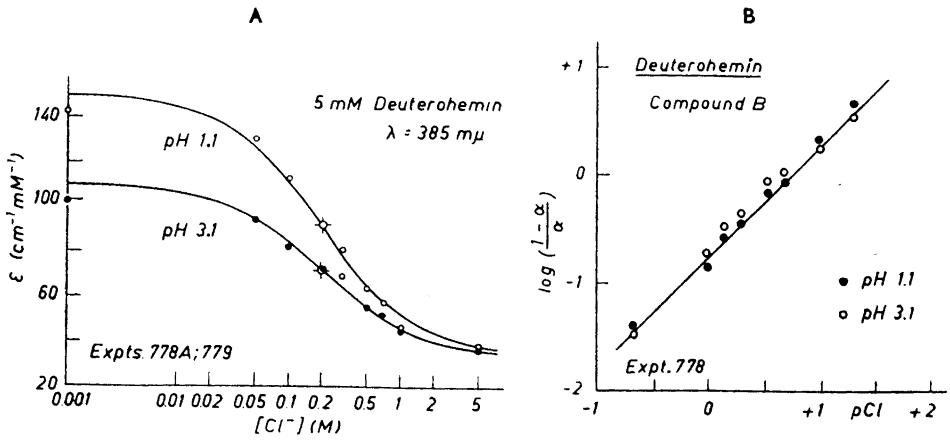

Fig. 8A. The "titration" of deuterohemin-B (DHB) with chloride. Aliquots of a neutral deuterohemin solution were added to solutions of increasing concentrations of KCl, all of them acidified with H_2SO_4 to give either pH 1.1 or 3.1. The optical density of each sample was measured near the peak of the Soret band (385 mμ). The final DHB concentration was 4.4—5.2 μM.

Fig. 8B. A straight line plot of the data represented in Fig. 8A. A logarithmic expression of the law of mass action is used:

$$K = \frac{[DHB]\,[Cl']^n}{[DHB\,(Cl')_n]} \quad (1); \qquad a = \frac{[DHB]}{[\text{Total deuterohemin}]} \quad (2)$$

$$\frac{1}{K} = \left(\frac{1-a}{a}\right)\frac{1}{[Cl']^n} \quad (3) \qquad \log\left(\frac{1-a}{a}\right) = n \log [Cl'] - \log K \quad (4)$$

Abscissa: the negative logarithm of the Cl′ ion concentration

Ordinate: $\log\left(\frac{1-a}{a}\right)$

The data lie on a line with the slope n = 1 and a pK_{Cl} = 0.7.

measured after each addition. The data are plotted in Fig. 6 and show that the titration is essentially reversible. The diminished extinction values are believed to be due to the slow decomposition of B, the shift of the pK from 3.1 to 3.3 may be caused by the presence of high concentrations of tartrate.

The reaction of B compounds with chloride ions was investigated next. In the case of HRP, the addition of chloride at neutral pH has no observable influence. When the solution is acidified, the HCl compound of HRP is formed. If the pH is lowered even more, splitting of the enzyme is brought about and the rate of splitting is accelerated by the presence of chloride [1]. In the case of free hemins, increasing concentrations of Cl^- depress the height of the Soret band at 397 mμ upon acidification of the solutions, indicating the formation of a compound of hemin with either Cl^- or with both Cl^- and H^+. Fig. 7 shows the Soret spectra of protohemin B at concentrations of $<10^{-5}$, 10^{-3}, and 10^{-1} M Cl^-. A complete "titration" of deuterohemin-B with chloride at two different pH values is shown in Fig. 8. At pH 3.1 only half of the

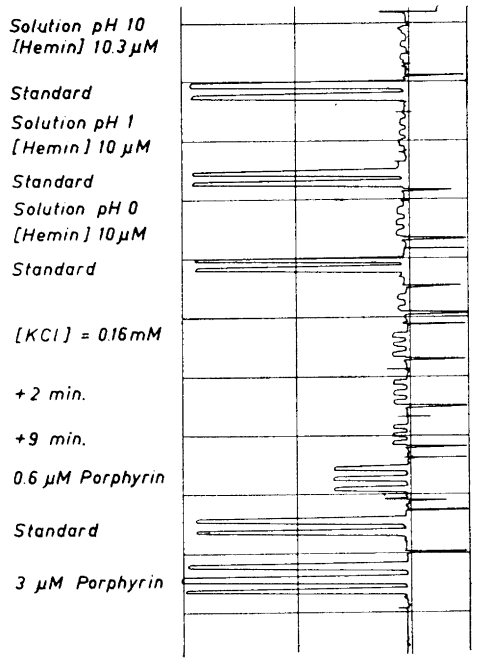

Fig. 9. Original recording of fluorescence measurements on protohemin-B. The apparatus described by Theorell and Nygaard [17] was used to investigate the possible fluorescence of protohemin-B. The experimental procedure is described in the text.

Ordinate: amount of fluorescence.

Abscissa: time sequence. The recorder was started for short time intervals after each addition of reactants. The record should be read from top to bottom.

Standard: A piece of fluorescent plastic was inserted into the apparatus as a reference standard.

hemin is present as B compound, so that the extinction coefficient at 385 mμ reaches only a value of about 108 $cm^{-1}mM^{-1}$ at infinitely low Cl^- concentration. At pH 1.1, compound B is almost fully formed at low [Cl^-]. The inflection point, however, lies at 0.2 M Cl^- in both cases ($pK_{Cl'} = 0.7$).

Fluorescence measurements. It is well known that hemins lose their iron under strongly acid conditions, notably if the iron is kept in the reduced state. The resulting porphyrins have well-defined spectra and show sharp bands in the Soret region not far from 400 mμ. Lemberg and Legge [16] cite from the literature the following Soret bands of porphyrins in strong HCl: Protoporphyrin: 408 mμ; deuteroporphyrin: 404 mμ; mesoporphyrin: 401 mμ. Since these wavelengths are close to the peaks of the B compounds, it was important to check whether a complete or partial removal of iron could take place on B formation. Professor H. Theorell kindly allowed the author to use his recording fluorescence meter [17].

Free porphyrins fluoresce strongly, whereas hemins do not. The apparatus was therefore used for detecting the possible formation of porphyrin from protohemin by strong acid at room temperature. A 10 μM solution of protohemin was prepared and its fluorescence measured, as shown in Fig. 9. The pH was lowered to 0 by the addition of sulfuric acid and the fluorescence remeasured. Addition of 1.6×10^{-4}M KCl did not change the result, even after 9 min waiting: the fluorescence remained insignificant, indicating the virtual absence of protoporphyrin. As a check, first 0.6 μM, then 3.0 μM protoporphyrindimethylester were now added and gave the expected large deflections.

DISCUSSION

The formation in aqueous solutions of well defined acid compounds is common to hemoproteins and to free hemins as far as they were investigated. These compounds, called B compounds, all show characteristic sharply defined Soret bands with peaks between 380 and 398 mμ and ε between 81 and 163 $cm^{-1}mM^{-1}$. Their visible spectra are far less conspicuous, showing relatively flat and low bands. HRP—B has such bands at around 500 mμ (ε = 6.4 $cm^{-1}mM^{-1}$) and at about 632 mμ (ε = 2.3 $cm^{-1}mM^{-1}$). The titration of hemin solutions with sulfuric acid yields sigmoid titration curves with n = 1 and pK values of between 1.5 and 3.1. Table 1 gives a summary of the spectrophotometric and titrimetric data on B compounds. It is seen that the height and position of the 397 mμ band is the same for all five protohemin-containing proteins investigated ($\varepsilon = 131 \pm 1$ $cm^{-1}mM^{-1}$ per hemin). Free protohemin-B, while showing the same position of the peak, has a much lower extinction coefficient. The low extinction coefficient of protein-free protohemin-B might well be due to polymerization, which is known to occur in aqueous solutions of this hemin. The addition of protein to protohemin-B increases the Soret band. Alcohols seem to act in a similar way as will be further discussed in the following paper [18]. Deuterohemin-B and mesohemin-B do not show abnormally low bands in the Soret region and apparently undergo less polymerization than protohemin *. If this assumption is correct one should not expect any marked intensification of the Soret band of these hemins by the presence of protein, which was indeed observed with the B compound of deuterohemalbumin.

A comparison of the data of Table 1 with the scant values from the literature shows some similarities, even though the experimental conditions were different. Erdman and Corwin's spectrum of acid mesohemindimethylester in dioxane [7] has a Soret peak at 390 mμ (ε = 175 $cm^{-1}mM^{-1}$), compared to 380 mμ and ε = 163 for mesohemin-B in water at pH 1 reported here. Hicks and Holden [6] acidified protohemin with HCl and obtained a peak between 374 and 386 mμ (emission lines of the iron spark source of their spectrograph) and a minimal extinction coefficient of 45.6 $cm^{-1}mM^{-1}$. Comparison with Fig. 7 indicates that the pH must have been about 2, corresponding to a Cl^- concentration of 0.01 M.

* Shack and Clark [15] observed that mesohemin has a much smaller particle weight than protohemin in aqueous solution.

Table 1. Soret bands and pK values of some B compounds.

Starting material / Magnitudes measured		"pK" [a]	$cm^{-1}mM^{-1}$ per hemin [b]	max [c] mμ
Peroxidase	HRP	2.30	132	397
Hemoglobin	Hb	2.25	130	397
Catalase	HBC	2.00	132	397
Myoglobin	ShMb	2.05	131	397
Protohemalbumin	PHA	?	130	397
Protohemin	PH	1.50	81	397
Mesohemin	MH	2.25	163	380
Deuterohemin	DH	3.05	144	388
Deuterohemalbumin	DHA	?	140	387

a) accuracy ± 0.05 pH units. For the meaning of »pK» *cf.* text.
b) accuracy ± 1 %
c) accuracy ± 1 mμ

The "pK" values of Table 1 do not all simply refer to true dissociation constants of the reaction

$$\text{Hemin} + H^+ \rightleftharpoons \text{compound B}$$

In the case of deuterohemin, the reversibility of B formation with a dissociation constant of about 10^{-3} has been demonstrated. The "pK" values of hemoproteins, on the other hand, represent merely the pH at which half of the B compound has been formed, since the breaking of bonds between protein and hemin is also reflected in the data and is thought to be responsible for the variations in "pK" between 2.00 and 2.30 for several protohemin-containing hemoproteins. The abnormally low "pK" of free protohemin suggests that an additional chemical reaction may be required for forming the B compound. This may very well be a partial depolymerization of the hemin.

The results of the fluorescence experiments show that at the most 1 % of the hemin could possibly have been converted to protoporphyrin under the conditions of B formation and also when chloride was added to the solution.

The data presented here make it seem probable that the formation of B compounds involves the configuration around the iron atom of the hemin molecule: The vinyl groups can be excluded as participants, since deutero- and mesohemin also give B compounds. At pH 1.5 (the "pK" of protohemin B) one should expect the propionyl groups to be present in their undissociated and uncharged form, even though their pK has never been determined directly. A further discussion of the possible structure and the reactions of the B compounds is included in the following paper [18].

Acknowledgments. The author wishes to thank Prof. B. Chance for his interest and encouragement, and Prof. H. Theorell for the permission to use the fluorescence recorder and his hospitality at the Nobel Medical Institute in Stockholm.

Many thanks are due to the organisations which made this work possible, *i. e.* the *U. S. Public Health Service, Divisions of Research Grants and Fellowships*, the *Swedish Medical Research Council*, and the *Swiss Academy of Medical Sciences.*

REFERENCES

1. Maehly, A. C. *Biochim. et Biophys. Acta* **8** (1952) 1.
2. Maehly, A. C. *Arch. Biochem. Biophys.* **44** (1953) 430.
3. Theorell, H. and Åkeson, Å. *J. Am. Chem. Soc.* **63** (1941) 1812.
4. Boeri, E., Ehrenberg, A., Paul, K. G. and Theorell, H. *Biochim. et Biophys. Acta* **12** (1953) 273.
5. Paul, K. G. *Acta Chem. Scand.* **2** (1948) 430.
6. Hicks, C. S. and Holden, H. F. *Austral. J. Exptl. Biol. Med. Sci.* **6** (1929) 175.
7. Erdman, J. G. and Corwin, A. H. *J. Am. Chem. Soc.* **69** (1947) 750.
8. Theorell, H. and Paul, K. G. *Arkiv Kemi, Mineral. Geol.* **18A** (1944) No. 12.
9. Chance, B. *Arch. Biochem. Biophys.* **40** (1952) 153.
10. Theorell, H. and Maehly, A. C. *Acta Chem. Scand.* **4** (1950) 422.
11. Beznák, M. *Acta Chem. Scand.* **2** (1948) 333.
12. Chance, B. *Rev. Sci. Instr.* **22** (1951) 619.
13. Yang, C. C. and Legallais, V. *Rev. Sci. Instr.* **25** (1954) 801; Yang, C. C. *Ibid.* **25** (1954) 807.
14. Rosenfeld, M. and Surgenor, D. M. *J. Biol. Chem.* **183** (1950) 663.
15. Shack, J. and Clark, W. M. *J. Biol. Chem.* **171** (1947) 143.
16. Lemberg, R. and Legge, J. W. *Hematin Compounds and Bile Pigments* Interscience, New York and London 1949.
17. Theorell, H. and Nygaard, A. P. *Acta Chem. Scand.* **8** (1954) 877.
18. Maehly, A. C. and Åkeson, Å. *Acta Chem. Scand.* **12** (1958) 1259.

Received April 10, 1958.

ACTA CHEMICA SCANDINAVICA 12 (1958) 1259—1273

Stabilization of Aqueous Hemin Solutions *

A. C. MAEHLY** and Å. ÅKESON

E. R. Johnson Foundation for Medical Physics, University of Pennsylvania, Philadelphia, Pa., U.S.A. and Nobel Medical Institute, Biochemical Department, Stockholm, Sweden

The deterioration of aqueous hemin solutions upon standing in light and air is studied and ways of stabilizing such solutions are described. Alcohols are found to be efficient stabilizing agents, apparently due to the formation of hemin-alcohol compounds. The paper describes spectra, titration data and magnetic properties of these hemin compounds. Their possible structures are included in the discussion which also covers data of the preceding publication.

The properties of aqueous solutions of protohemin change quite rapidly on standing. This is apparently due to several processes closely related to each other. Polymerization is one of these processes and has been studied by Zeile, Haurowitz, Gralén, and especially by Shack and Clark [1] in 1947 who also cite earlier literature. The particle size depends on the pH, the kind of buffer and time, and the apparent molecular weight varies between about 3 000 and 100 000 [1].

The spectral changes of hemin solutions as a function of time have also been measured by Shack and Clark [1] from 400 mμ to 700 mμ. They find that, under their experimental conditions, the spectrum of a freshly prepared solution undergoes a change for several days when a new spectrum is formed which then remains stable for more than 60 days. Similar results were obtained more recently by Blyumenfeldt [2] who studied the spectrum in the Soret region.

At least one method for preventing or slowing down the reactions responsible for the instability of protohemin in water will be described here.

EXPERIMENTAL

The hemins and hemoproteins used in these studies are described in the preceding paper [3]. The horse myoglobin (HMb) mentioned here was prepared as described by Theorell and Åkeson [4]. The spectra and the pH were measured with the same apparatus mentioned in *Ref.*[3]. The magnetic measurements were performed by A. Ehrenberg (Nobel Medical Institute, Stockholm) using a highly sensitive apparatus designed by Theorell and Ehrenberg [5].

* A preliminary report of some of the data presented here was made by one of us (A. C. M.) at the 128th Meeting of the Am. Chem. Soc. in Minneapolis (1955), p. 68 C.

** Present address: Statens rättskemiska laboratorium, Stockholm, Sweden.

RESULTS

Spontaneous changes of aqueous hemin solutions

Blyumenfeldt's results with protohemin [2] were, on the whole, confirmed. It was found that the Soret band changes its appearance and that this change follows the kinetics of a first order reaction which is half complete after one to twenty hours after preparing a fresh solution, the half-time depending on the conditions of the experiment. The initial and final spectra from 230 to 490 mμ, the latter extrapolated to infinite time and from a series of experiments, are plotted in Fig. 1.

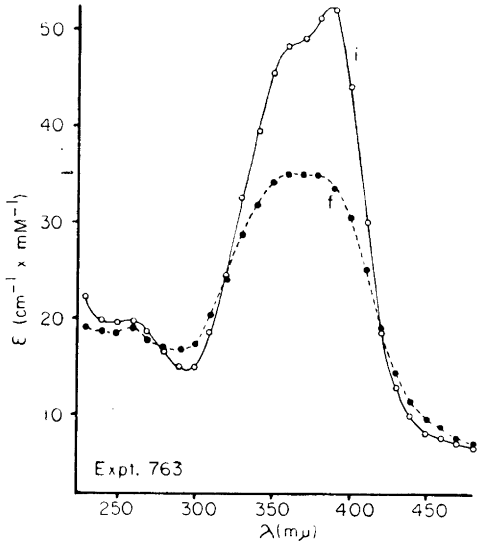

Fig. 1. The spectra of a fresh and an aged solution of protohemin at pH 10.4. Protohemin was dissolved in 0.1 N NaOH and diluted to 1.46×10^{-5} μM with 0.01 M phosphate buffer. The resulting pH was 10.4. The spectrum of the solution was measured within a few minutes and the measurements repeated at appropriate intervals for several hours. Extrapolation of the values to infinite time gave the spectrum of the final product. The reaction is of first order, as shown in Fig. 3.

i—O—O— initial spectrum of a fresh solution (2—20 min after dissolving the protohemin).
f- -●- -●- - final spectrum of the aged solution at infinite time.

Shack and Clark [1] had reported that the changes of the visible spectrum were the same, whether the hemin solution was kept under hydrogen or in the air. Joan Keilin [6], on the other hand, found that hemin solutions in Na_2CO_3 would change several of their properties (formation of a caffeine-CO compound, solubility in ether-acetic acid, crystallizability from acetic acid and NaCl) when standing in air, but not under strictly anaerobic conditions.

We found that the hemin spectrum remained unchanged for more than a week if the solutions were kept and measured in an anaerobic cuvette [7], which

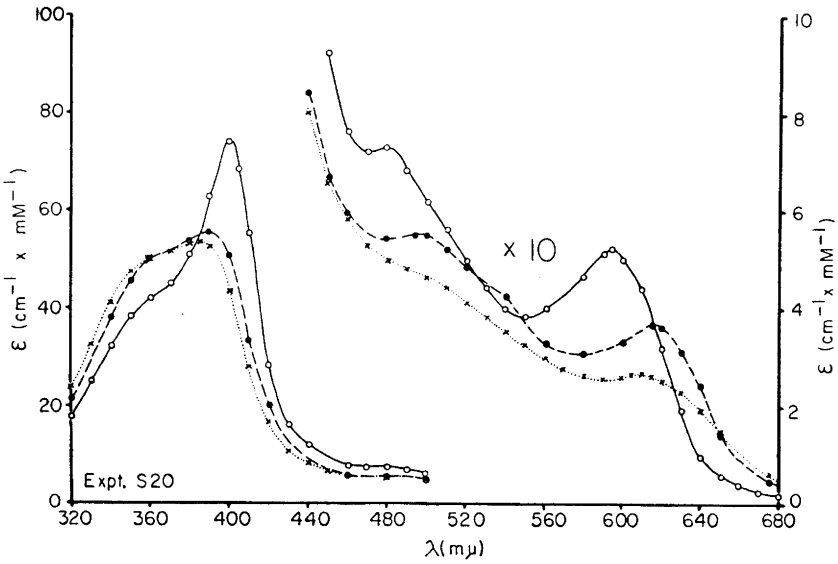

Fig. 2. The spectra of protohemin in water, 50 % ethanol and 30 % sucrose. Phosphate buffer of pH 7.0 was added to give a final concentration of 0.01 M.

X·····X solvent: water
O———O solvent: 50 % ethanol
●-----● solvent: 30 % sucrose or 30 % glycerol
The final concentration of protohemin was of the order of 10^{-5} M in each case.

was evacuated after some wet $Na_2S_2O_4$ had been placed in one of its sidearms, a procedure recommended by Keilin [6]. The reaction was also slowed down considerably, even in air, if light was excluded. It was further found that the Soret spectrum of aqueous mesohemin and deuterohemin solutions exposed to light and air did not change within three days.

Alcohol has been used by several workers for solubilizing hemin solutions[8–10]. Davies [11] suspected the formation of an alcohol compound of hemin from spectroscopic observations. Around 1930, Hamsik [12] crystallized "active hematin" or α-hematin from aqueous acetone or alcohol. He reported spectroscopic differences between hemin dissolved in these solvents and dissolved in water. He found further that the ability of protohemin to couple with free globin from hemoglobin is lost on standing for some time ("nach einiger Zeit") if the hemin is dissolved in aqueous buffer, but is maintained longer if aqueous acetone or alcohol are used as solvents.

Ethanol, glycerol, and sucrose were tried as stabilizing agents in the present studies. Fig. 2 shows the spectra of freshly prepared hemin solutions in phosphate buffer at pH 7 without addition and in the presence of these solvents. It is readily seen that only ethanol has a strong influence on the spectrum, both in the visible and in the Soret regions. The bands at 385, (495) and 610 mμ of aqueous hemin are sharpened and shifted to 400, 482, and 597 mμ, respectively.

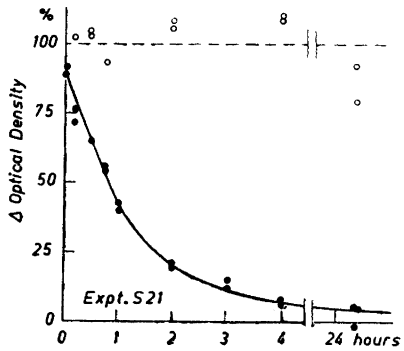

Fig. 3. The change in the Soret spectrum of aqueous and of alcoholic protohemin solutions. The optical density of the Soret band at 385 mμ of aqueous protohemin (0.01 M phosphate buffer of pH 7.0) was determined as a measure of the spontaneous reaction of protohemin described in the text. The optical density of 50 % alcoholic protohemin (in the presence of the same phosphate buffer as above) at 400 mμ was also determined. The measurements were repeated as often as practical and the data plotted in percent of the corresponding values at zerotime at the ordinate, and time in hours at the abscissa, including one final value after 24 h.

O— — —O optical density at 400 mμ of 50 % alcoholic protohemin
O———O optical density at 385 mμ of aqueous protohemin. The curve is a theoretical first order reaction curve.

The stability of the hemin solutions was tested in two different ways. One was the change of the Soret spectrum, the other the velocity of the coupling reaction of hemin with apomyoglobin (the protein part of myoglobin after removing the hemin by HCl in acetone) to yield active myoglobin. The completely reversible splitting of myoglobin was first described by Theorell and Åkeson [4] and some detailed aspects of the coupling reaction will be published later. In Fig. 3, the decrease in the height of the Soret band is plotted *versus* time. Other experiments show that an addition of ethanol preserved these properties of the hemin best whereas glycerol is less satisfactory and sucrose is practically useless for this purpose. The velocity of the coupling reaction with apomyoglobin of aqueous protohemin solutions decreases markedly after some hours whereas 50 % alcoholic solutions of protohemin retain their coupling speed for at least 24 h.

Alcohol compounds of protohemin

The spectral changes of freshly prepared aqueous hemin solutions of pH 7 (0.01 M phosphate buffer) upon the addition of ethanol were measured quantitatively at 400 mμ and yielded a titration curve with a slope n = 2 and pK = −0.75 (the concentration of ethanol bringing about one half of the change is 5.6 M). The extinction coefficient of the ethanol compound was computed to be 81 cm^{-1} mM^{-1} (using the fact that 100 % EtOH is 17.2 M) as compared to ε_{385} = 53 cm^{-1} mM^{-1} for aqueous hemin. The results of such experiments are

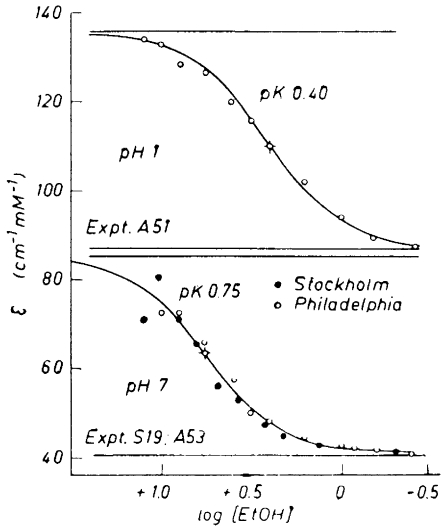

Fig. 4. Spectrophotometric titration of protohemin with ethanol at pH 1 and pH 7. Solutions of 0.1 N H_2SO_4 and 0.02 M phosphate buffer respectively, containing increasing amounts of ethanol were made up. An equal small amount of a concentrated solution of protohemin was added to each sample and the optical density at the maximum of the Soret band (398 mμ at pH 1, and 400 mμ at pH 7) was measured. The hemin concentration was 8—11 μM. The millimolar extinction coefficient is plotted versus the logarithm of the ethanol concentration.

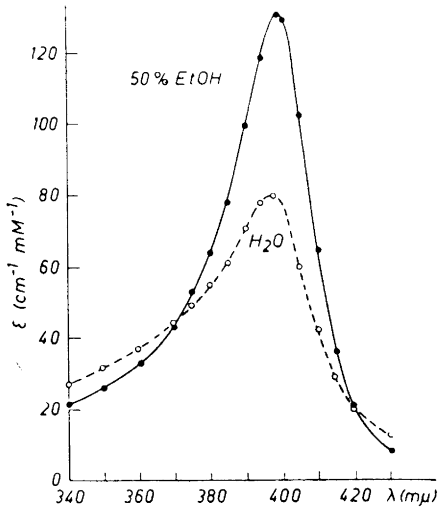

Fig. 5. The Soret spectra of protohemin in water and alcohol at low pH. Protohemin was dissolved in 0.01 N NaOH and added to 0.1 N H_2SO_4 in water and in 50 % ethanol respectively. Final concentration, 5—8 μM hemin.

O- - - - - - -O aqueous protohemin solution
●————● alcoholic protohemin solution

presented in Fig. 4. The very high dissociation constants obtained from these plots suggested the possibility that an impurity in the alcohol might be the true reactant. In order to exclude this possibility, three experiments were made. First, especially purified double distilled ethyl alcohol was used. The results obtained with the "ordinary" alcohol were duplicated within the experimental error. Second, Swedish ethanol, and ethanol obtained in Philadelphia gave identical results. Finally, aqueous protohemin solutions were titrated with methanol (absolute, redistilled). This alcohol also forms a hemin compound with a Soret band at 396 mμ (= 81 cm^{-1} mM^{-1} by extrapolation to 100 % or 24.7 M MeOH). The slope of the titration curve was also found to be n = 2 (at pH 7, 0.01 M phosphate buffer) and the dissociation constant 10.7 M (pK −1.03), higher than in the case of ethanol.

These results indicate the formation of true alcohol compounds of hemin, with a high tendency to dissociate. Dilution of such alcohol-hemin solutions with aqueous buffer yields the spectrum normally observed with hemin solutions in water, proving the reversibility of the reaction. The readings of optical density at 400 mμ in the above mentioned titration experiment with ethanol were repeated after 24 h to test the stability of the alcoholic solutions. At alcohol concentrations above 5 M, no spectral change was noted. Since this corresponds to 23 % (w/v) or 29 % (v/v) ethanol, a 0.01 M phosphate buffer containing 30 % (v/v) ethanol is sufficient to insure the stability of protohemin solutions for at least one day. At this alcohol concentration, each hemin binds on the average, about 1 molecule of ethanol.

At low pH, a different alcohol compound of protohemin is formed. The spectra of protohemin B (*cf.* Ref.[3]) and of this acid ethanol compound at 50 % or 8.6 M EtOH are represented in Fig. 5. The Soret peak lies in this case at 398 mμ. Spectrophotometric titration gave the values represented in Fig. 4. The data lie on a theoretical dissociation curve with a pK of −0.40, somewhat different from that at pH 7.0. The slope of the curve, here also, is n = 2. Extrapolation to 100 % ethanol gives $\varepsilon = 134$ cm^{-1} mM^{-1} *.

There is an intermediate pH range where the titration values lie on curves with very high n values. At pH 4, n was found to be >4. This is the pH region where the alcoholic hemin precipitates even at low concentrations.

Reduction of the alcohol compound at pH 6.8 by sodium dithionite did not change the Soret spectrum but gave a very featureless spectrum in the visible region. The characteristic double bands of hemochromogens were completely absent.

Protohemin in 50 % EtOH showed only the two spectra reproduced above: an acid type (Fig. 5) and an alkaline type (Fig. 2). The pH of conversion lies between 4 and 6 (pH of the buffers before adding the alcohol) but attempts to measure the pK more accurately failed: spectrophotometric titration gave data which were scattered about a straight line instead of the expected sigmoid curve, and potentiometric titration was made impossible by the low solubility of protohemin between pH 4 and 6 (though the solubility seems to be higher than in the absence of alcohol).

* Sulfuric acid was exclusively used in order to avoid effects of halogen ions wich are so dramatically reflected in the Soret spectrum of aqueous acid hemin solutions (*cf.* Ref. [3]).

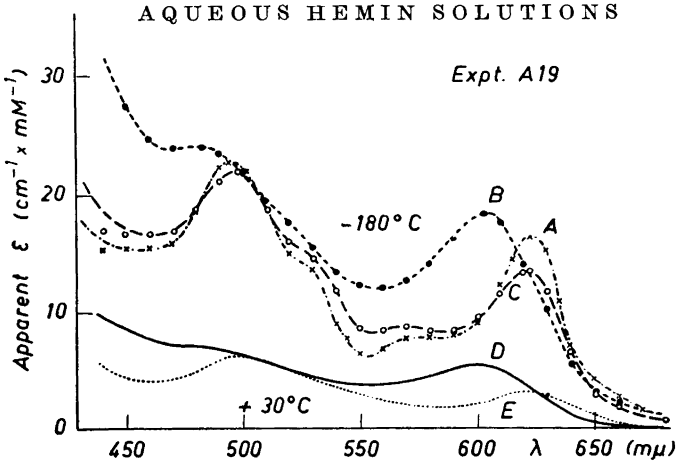

Fig. 6. The effect of temperature upon the absorption spectrum of protohemin. Three solutions were prepared, each containing 50 % ethanol. Solution A had 50 % 0.1 N H_2SO_4, solution B 0.1 N NaOH, and solution C 0.02 M phosphate buffer of pH 6.8. Small identical amounts of protohemin in 50 % alcoholic 0.05 N NaOH were added and the spectrum was measured using lucite cuvettes of 1 mm lightpath. D is the spectrum of alkaline protohemin-ethanol, and E that of acid protohemin-alcohol at room temperature. The "neutral" compound (in phosphate buffer) also showed spectrum D. The cuvettes were now chilled in liquid air, warmed up to about −55° and chilled again, as described by Estabrook and Mackler [13]. The resulting hemin spectra in solutions A, B, and C are plotted and marked in this order.

The influence of low temperatures on the spectra of protohemin-alcohol compounds was studied in co-operation with Dr. R. W. Estabrook of the Johnson Foundation *. Lucite cuvettes were filled with the hemin-ethanol solutions (50 % EtOH) and the spectrum recorded on the Yang and Legallais apparatus [3]. The cuvettes were then cooled in liquid air and the spectra recorded again, at about −180°. The details of this procedure are described elsewhere [13]. Low temperature treatment had two separate effects. One was a 3-fold intensification of the visible bands, without any significant shifts of the peaks as shown in Fig. 6. The other effect was a conversion of the alkaline type of spectrum to the acid type within a certain pH range. At pH 6.8 (0.01 M phosphate) and room temperature, the spectrum of the alkaline protohemin-EtOH compound was found. At the temperature of liquid air, the same solution showed an almost complete spectral conversion into the acid form (curve C in Fig. 6). An investigation of these phenomena (changes of K_w, hydratation etc. with temperature) lies outside the scope of these experiments.

Interaction of ethanol, hydroxyl ions, and cyanide ions with protohemin

In alkaline aqueous solutions, one hydroxyl group per iron atom is bound to protohemin, and the resulting compound is known as hematin. Hogness

* Measurements of spectra of biological material at low temperatures have been undertaken by Sinsheimer, Scott, and Loofbourow[14] and, for hemin compouns, by Keilin and Hartree[15] who used visual spectroscopy.

and coworkers [16] showed in 1937 that hematin in aqueous solutions forms dimers * and that cyanide ions are able to dissociate them according to eqn. (1):

$$Fe_2(OH')_2 + 4CN' \rightleftharpoons 2Fe\ (CN')_2 + 2OH' \qquad (1)$$

If ethanol is bound to the central iron atom, the former would be expected to interact with both CN′ and OH′ ions. Experiments were designed to study such interactions.

The spectrum of an aqueous solution of hemindicyanide in 25 mM borate buffer (pH 9.2) containing 2.5 μM of protohemin and 20 mM of KCN was measured in the presence and in the absence of ethanol. The effect of 50 % ethanol on the spectrum was very small, resulting in a shift of the Soret band from 425 to 427 mμ, whereas the position of the bands at 355 and 542 mμ ** remained unchanged. The bands increased in intensity, but this increase was at the most 13 %.

A protohemin solution in 50 % ethanol and 25 mM borate (pH 9.2) was titrated with KCN and the values obtained were found to lie on a theoretical dissociation curve with a dissociation constant of 1.6×10^{-3} and n = 2, when calculated for the reacting species, namely CN′. When the dissociation constant for hemin cyanide in aqueous solution is computed from the data of Hogness *et al.*[16] for this particular pH, a value of $K = 0.21 \times 10^{-3}$ is found. The dissociation constant is therefore about 8 times greater for alcoholic hemin cyanide than for hemin cyanide in water.

The extinction coefficient of alcoholic hemin solutions (50 % EtOH) was found to be independent of the protohemin concentration from 0.5 to 5.0 μM hemin at pH 1.0, and from 0.32 to 6.40 μM hemin at pH 7.0: Beer's law is valid within these limits. At pH 13 (0.1 M NaOH) it was found, on the other hand, that the extinction coefficient decreases with the concentration of protohemin, all other experimental conditions being held constant. The possibility was therefore considered that ethanol may depolymerize the hemin dimer molecules in a similar manner as cyanide does. The equilibrium of this reaction is then (*cf.* eqn. (1) and Ref.[16]):

$$K = \frac{[Fe_2(OH)_2]\ [EtOH]^4}{[Fe(EtOH)_2]^2[OH']^2} \qquad (2)$$

If the pH and the ethanol concentration are kept constant, we obtain:

$$K^* = \frac{[Fe_2(OH)_2]}{[Fe(EtOH)_2]^2}\ ;\ \text{equivalent to}$$

$$\log\ [Fe(EtOH)_2] = \log\ [Fe_2(OH)_2]^{\frac{1}{2}} - \tfrac{1}{2}\ \log\ K^* \qquad (3)$$

A plot of log $[Fe(EtOH)_2]$ *versus* log $[Fe_2(OH)_2]^{\frac{1}{2}}$ should thus give a straight line with a slope of 1 and an intercept of $-\frac{1}{2}$ log K.* Fig. 7 shows that the experimental data do lie on such a line.

---

* The assumption of dimeric hemin molecules is, however, not generally accepted, as will be discussed below.

** Hogness *et al.*[16] report the bands of aqueous hemin cyanide to lie at 365, 422.5, and 545 mμ, respectively.

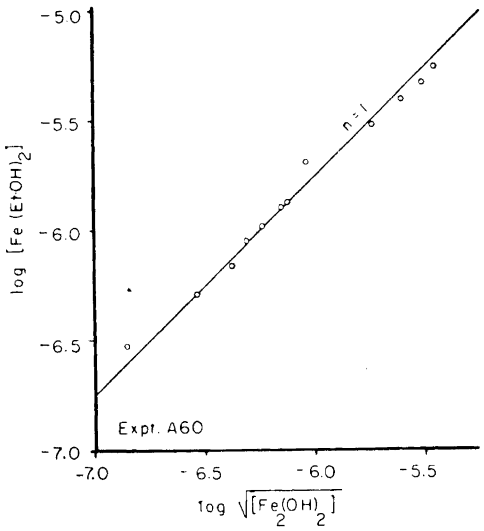

Fig. 7. A plot of the relationship of eqn. (3). While keeping the concentrations of ethanol and hydroxyl ions constant at 5.0 M EtOH and pH 13, the total hemin concentration was varied from 0.338 μM up to 2.35 μM and the resulting optical density measured at 402 mμ using cuvettes of 5.0 cm optical pathlength. The hemin concentration was further increased from 2.35 μM up to 17.25 μM and D_{402} measured in 1.0 cm cuvettes. From these data, a plot according to eqn. (3) was made. A straight line with the slope of 1.0 was located to give the best fit for the experimental data. The meaning of the formulas is explained in the text.

Magnetic susceptibility

The magnetic susceptibility of free hemins and hematins has been measured by several groups of workers. Hartree [17] has written an excellent review on the subject in 1946 and included magnetic data on hemoproteins. The magnetic measurements reported here were made in cooperation with A. Ehrenberg of the Nobel Medical Institute, using the highly sensitive Gouy balance of Theorell and Ehrenberg [5]. A stock solution of protohemin was prepared by dissolving 6.49 mg of the hemin in 0.60 ml of 0.03 N NaOH and adding 1.40 ml of ethanol to give 1.96 ml total solution of 5.08 mM protohemin. Of this stock solution 0.35 ml was added to 0.80 ml of 0.13 N H_2SO_4 in 67 % EtOH (v/v), and 0.35 ml to 0.80 ml of aqueous 67 % EtOH (v/v). The final concentration of hemin was thus 1.55 mM in each case. The molar magnetic susceptibility in the acid solution was found to be 12 400 ($\pm$250) $\times$ 10^{-6} c.g.s. e.m.u. at 20.5°. The alkaline solution gave 13 450 ($\pm$300) $\times$ 10^{-6} c.g.s. e.m.u. at 20.5°. These values correspond to 5.41 and 5.64 Bohr magnetons respectively and indicate an essentially ionic bond type with 5 unpaired electrons. The theoretical value for 5 unpaired electrons is 5.92 Bohr magnetons.

Alcohol compounds of deuterohemin

Deuterohemin IX, which differs from protohemin IX by the absence of the two vinyl groups in positions 2 and 4 of the porphyrin ring, gives compounds with ethanol very similar to those of protohemin. Spectrophotometric studies on deuterohemin are facilitated by the stability of its alkaline solutions. The study of alcohol binding was performed at two selected pH regions, pH 1 (0.1 N H_2SO_4) and pH 12 (0.01 N NaOH). The acid and alkaline alcohol compounds formed show distinct spectra, reproduced in Fig. 8. The alcohol compounds at intermediate pH values show either one or the other of these spectra as is the case with protohemin. The pH region at which the acid ethanol compound of deuterohemin changes into the alkaline one has not yet been ascertained because of complications brought about by the pronounced changes of the spectrum of deuterohemin in aqueous solution in the neutral pH region.

The titration data of deuterohemin at pH 1 and pH 12 show that in both cases 2 moles of EtOH are entering the hemin molecule, and that the dissociation constant is nearly the same, namely 0.46 M at pH 12 and 0.57 M at pH 1.

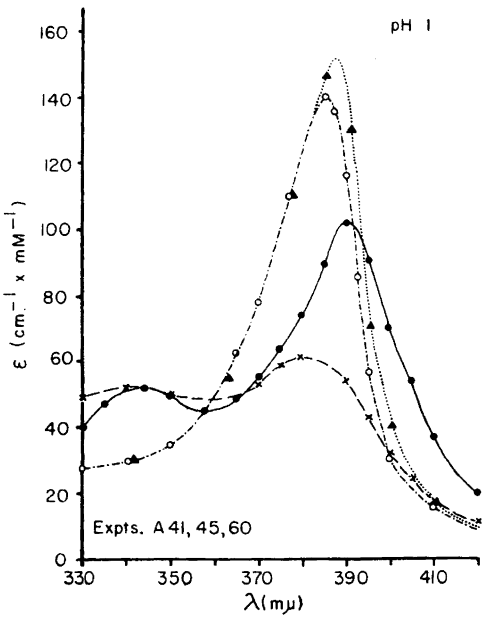

Fig. 8. The Soret spectra of deuterohemin and its alcohol compounds at pH 1 and pH 12. Small amounts of deuterohemin dissolved in 0.01 N NaOH and added to the solutions listed below gave the following spectra plotted in the figure:

O--O--O in 0.1 N H_2SO_4 of pH 1
▲···▲···▲ in 0.1 N H_2SO_4 containing 50 % EtOH
X---X---X in 0.01 N NaOH of pH 12
●—●—● in 0.01 N NaOH containing 50 % EtOH

The deuterohemin concentrations used were of the order of 10^{-5} M.

Table 1. Spectra and equilibrium constants of hemins in alcohol.

Hemin[a]	Alcohol[b]	pH[c]	λ(mμ)	ε[d]	λ(mμ)	ε[d]	λ(mμ)	ε[d]	pK[e]
Proto-	EtOH	1.0	398	131	504	6.0	627	2.5	−0.40
Proto-	EtOH	7.0	400	74	482	7.4	597	5.4	−0.75
Deutero-	EtOH	1.0	386	171	—	—	—	—	−0.59
Deutero-	EtOH	12.0	390	96	478	11.7	582	7.8	−0.46
Proto-	MeOH	7.0	396	73	—	—	—	—	−1.03

a) All hemins were of type 9.
b) EtOH stands for ethanol; MeOH för methanol.
c) The pH of the aqueous solution before adding alcohol.
d) All extinction coefficients were calculated from 50 % alcoholic solutions and have the dimension $cm^{-1}mM^{-1}$
e) The negative logarithm of the alcohol concentration (in Moles x $liter^{-1}$) at which half of the spectral change was observed.

Since the reproducibility of these constants was not better than 0.05 M, this difference can not be regarded as significant.

Table 1 gives a summary of the data on the alcohol compounds of protohemin and deuterohemin presented in this paper.

DISCUSSION *

Evidence for hemin alcohol compounds

The evidence for the formation of true alcohol compounds of hemin can be analyzed as follows: (i) The absorption spectrum of protohemin undergoes a pronounced change on the addition of 50 % ethanol. This suggests the formation of alcohol compounds of the hemin, though a change in the state of aggregation due to the change in solvent can not be excluded. (ii) At all pH values except in a critical neutral range, 2 moles of alcohol are needed to bring about the spectral change. Within the neutral pH range more than 2 alcohol molecules are needed per mole of hemin to convert them into alcohol compounds. Apparently the alcohol compounds can be formed only after some large aggregates of hemin molecules have been dissociated by the alcohol. (iii) The strict adherence to the deviations of Beer's law to a proposed mechanism of dimer splitting suggests that a stoichiometric reaction is involved. (iv) The possibility that an impurity in the alcohol might be the reacting species is excluded by the observation that methanol gives similar, but not identical compounds as ethanol, and that the use of ethanol from different sources gives identical results. (v) The fact that ethanol does not change the spectrum of aqueous hemin-dicyanide appreciably seems to indicate that the CN ions compete for the binding sites of the ethanol molecules. The magnetic data show clearly that the bond type of hematin in ethanol (5.64 B.M.) is different from that measured by Rawlinson [18] (3.62 B.M.) and by Hartree [17] (3.23 B.M.)

* The results of the preceding paper[3] are included in the discussion.

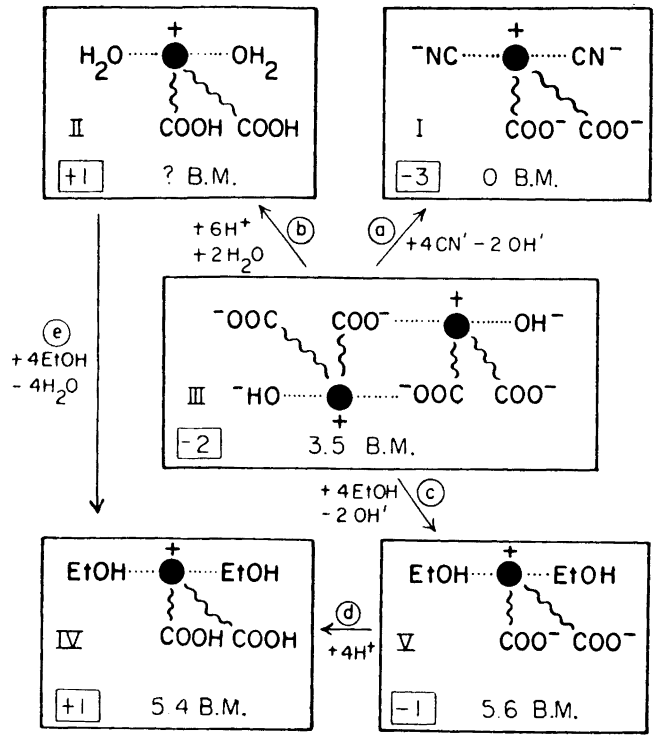

Fig. 9. The proposed reaction mechanism of protohemin with ethanol, cyanide and hydroxyl ions. The compounds are labeled thus (EtOH stands for ethanol):

I protohemin-dicyanide *
II protohemin compound B (acid hemin, *cf.* (3)) *
III protohematin (dimer)
IV acid protohemin-ethanol *
V alkaline protohemin-ethanol *

The hemin molecule is not shown as such. Only the central iron atom, marked by a solid circle, 2 of the total of 6 co-ordination places (4 are taken up by the 4 pyrrol nitrogens), and the 2 carboxyl groups of the propionyl sidechains appear in the formulae. The postulated overall charge is shown inside a small box. The paramagnetic susceptibility where known, is given in Bohr Magnetons (B.M.). The individual reactions are marked with small letters inside a circle. The iron remains in the trivalent state throughout.

of protohemin in aqueous NaOH. (vii) The fact that glycerol or sucrose do not change the spectrum of aqueous hemin solutions shows that the alcohol is not merely influencing the hydratation of the hemin molecule.

The dimer theory

The alcohol binding data lend further support to the theory that hematin forms a dimer in aqueous solution, since the deviation from Beer's law can be

* Two moles (to fit the stoichiometric relationships).

quantitatively explained on the basis of this assumption. The splitting of the dimer by alcohol is quite akin to the action of cyanide observed by Hogness *et al*[16]. The spectrophotometric observations of Davies [11] also fit the dimer theory.

The structure of the dimer as drawn in Fig. 9 (Compound III) was proposed by Lemberg and Legge [19]. It is assumed that the iron atom of each hemin molecule interacts with one of the propionyl groups of the other hemin molecule, thus leaving one of the six coordination places of each iron free for the binding of a hydroxyl ion. We constructed models of two hemin molecules, using the correct bond angles and degrees of freedom of the $-CH_2-CH_2-CO-O$-chain and found that a strainfree structure linking two molecules in the fashion discussed above could be obtained, with the porphyrin "disks" oriented in parallel planes. An additional bond between the iron atom of one hemin and the second propionyl group of the other hemin is sterically impossible.

The scheme outlined in Fig. 9 is suggested for the reactions of ferric protoporphyrin with ethanol, cyanide ion, and hydroxyl ion, although one must keep in mind that absolute proof for dimerization is still lacking.

The structure of hemin alcohol compounds

The suggested structure of alkaline hemin-ethanol (V of Fig. 9) is subject to some doubt due to the electrophoretic experiments of Haurowitz [9] which suggest a negative overall charge for the unesterified form of V. In order to account for it one can consider heptacoordination as suggested by Coryell and Stitt [20].

The transition from the alkaline to the acid form of hemin-ethanol seems to take place at around pH 5, though accurate measurements could so far not be achieved. The carboxyl ions of the propionyl side chains are the only obvious sites for the reception of hydrogen ions, unless heptacoordination is adhered to. This would also explain why only one spectral change could be observed within the pH range from 1 to 13.

Acid hemin compounds

Fig. 9 shows the formation of an acid hemin compound in aqueous solution (reaction b) where 3 protons and 1 H_2O are taken up by the hemin molecule. This overall reaction is composed of at least 2, but probably 3 or 4, steps. Starting from the alkaline range, the first change of spectrum and redox potential occurs between pH 7 and 8 (Mori [21] and Shack and Clark [1]).

The large spectral change taking place at around pH 1.5 has been described in the preceding paper [3], where it was also shown that this reaction does not involve the vinyl groups and that no removal of iron takes place. The compound B formed at very low pH by sulfuric, perchloric, or nitric acid reacts with halogen ions [3]. It incorporates one Cl′, the equilibrium being independent of the H^+ concentration, at least between pH 1—3 [3]. This reaction differs from that of acid cytochrome c, where Boeri *et al.*[22] had found that 2 Cl′ are taken up simultaneously and that the dissociation constant increases with

decreasing pH. The authors postulated that the Cl′ ions form a "bridge" between the positively charged Fe atom of the hemin and the —NH-groups of the imidazole rings that are believed to participate in the binding of the hemin to the apoprotein of cytochrome c. A similar effect in free hemin would only be possible if polymerization of the hemin molecules with the help of Cl′ bridges is assumed. The observed collapse of the high Soret band of acid hemins in the presence of increasing Cl′ concentrations makes this assumption not improbable.

The data so far obtained strengthen the hypothesis of Erdman and Corwin [23] that compound B represents the free ionized form of acid hemin, in contrast to "neutral" hemin, where negative ions of small radius (especially F′, Cl′, Br′, I′) are thought to move into one of the co-ordination places of the iron and are not dissociated appreciably in aqueous solutions. Erdman and Corwin could show that the spectra of hemin-chloride, -bromide, and -iodide in dioxane are not identical and that these compounds are essentially undissociated *.

There remains one phenomenon that is unexplained. It is not readily evident how the complexing of protohemin with ethanol is able to prevent the spontaneous changes that have been shown to occur in aqueous solutions. The experimental data show that the vinyl groups must be involved in the reaction, since the spectrum of deuterohemin in aqueous solution remains unaltered. It was also demonstrated that the process requires oxygen. It can be postulated that hemin catalyses its own oxydation and that it is the solvent action of alcohol that prevents this process.

Acknowledgements. The authors are indebted to Professor B. Chance and Professor Hugo Theorell for their interest and encouragement. The able assistance of Mrs. Inger Sörbo, Miss N. M. Rumen, and Mr. Henry Altschuller during various phases of this work is gratefully acknowledged. One of us (A.C.M.) wants to express his gratitude for grants from the *U.S. Public Health Service, Divisions of Grants and Fellowships*, the *Swedish Medical Research Council* and the *Swiss Academy of Medical Sciences.*

REFERENCES

1. Shack, J. and Clark, W. M. *J. Biol. Chem.* **171** (1947) 143.
2. Blyumenfeldt, L. A. *Doklady Akad. Nauk. S.S.S.R.* **85** (1952) 1111.
3. Maehly, A. C. *Acta Chem. Scand.* **12** (1958) 1247.
4. Theorell, H. and Åkeson, Å. *Ann. Acad. Sci. Fennicae, Ser. A II Chem.* **60** (1955) 303.
5. Theorell, H. and Ehrenberg, A. *Arkiv Fysik* **3** (1951) No. 16.
6. Keilin, J. *Biochem. J.* **37** (1943) 281.
7. Maehly, A. C., Smith, Lucile, and Graham Jr., J. D. *Science* **122** (1955) 767.
8. Dhéré, Ch. and Vegezzi, G. *Compt. rend.* **163** (1916) 18.
9. Haurowitz, F. *Z. physiol. Chem. Hoppe-Seyler* **169** (1927) 235.
10. Hicks, C. S. and Holden, H. F. *Austral. J. Exptl. Biol. Med. Sci.* **6** (1929) 175.
11. Davies, T. H. *J. Biol. Chem.* **135** (1940) 597.
12. Hamsík, A. *Z. physiol. Chem. Hoppe-Seyler* **200** (1930) 199.
13. Estabrook, R. W. and Mackler, B. *J. Biol. Chem.* **224** (1957) 637.
14. Sinsheimer, R. L., Scott, J. F. and Loofbourow, J. R. *J. Biol. Chem.* **187** (1950) 299.

* More recently, U. J. Lewis (*J. Biol. Chem. 206* (1954) 109) has shown that the spectra of protohemin 9-chloride and -sulfate differ appreciably in acetone.

15. Keilin, D. and Hartree, E. F. *Nature* **164** (1949) 254.
16. Hogness, T. R., Zscheile, Jr. F. P., Sidwell, Jr. A. E. and Barron, E. S. G. *J. Biol. Chem.* **118** (1937) 1.
17. Hartree, E. F. *Ann. Repts, on Progr. Chem. (Chem. Soc. London)* **43** (1946) 287.
18. Rawlinson, W. A. *Austral. J. Exptl. Biol. Med. Sci.* **18** (1940) 185.
19. Lemberg, R. and Legge, J. W. *Hematin Compounds and Bile Pigments*, Interscience, New York and London 1949.
20. Coryell, C. D. and Stitt, F. *J. Am. Chem. Soc.* **62** (1940) 2942.
21. Mori, T. *Science (Japan)* **17** (1947) 334.
22. Boeri, E., Ehrenberg, A., Paul, K. G. and Theorell, H. *Biochim. et Biophys. Acta* **12** (1953) 273.
23. Erdman, J. G. and Corwin, A. H. *J. Am. Chem. Soc.* **69** (1947) 750.

Received April 10, 1958.

ACTA CHEMICA SCANDINAVICA 12 (1958) 1274—1278

Substituted Diphenyl-(2-pyridyl)-methanes

KURT RUBINSTEIN and JYTTE CHRISTIANSEN

Aktieselskabet Pharmacia, Research Division, Copenhagen — Vanløse, Denmark

In order to gain further insight into the relationship between chemical structure and laxative activity three substituted diphenyl-(2-pyridyl)-methanes were prepared by condensing *p*-methoxyphenyl-2-pyridyl carbinol with phenol, *m*-cresol and *m*-chlorophenol, respectively.

In another approach to the synthesis of diphenyl-(2-pyridyl)-methanes from *bis*-(*p*-methoxyphenyl)-2-pyridyl carbinol the reactions took an unexpected course with the production of a new red-brown compound, the structure of which is discussed.

In the course of investigations on the relationship between chemical structure and laxative activity, Schmidt and Seeger [1] found the grouping I to be of particular importance for the attainment of laxative effect (*cf.* Ref.[2]). Recently, the substituted diphenyl-(2-pyridyl)-methanes, II—IV, were synthesized [3–6]; pharmacological evaluation demonstrated II and III to be very potent laxatives [1,2]. Again, laxative activity was reported for IV[3], yet without presentation of pharmacological data.

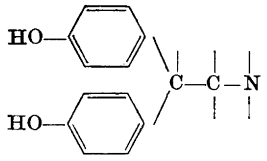

I

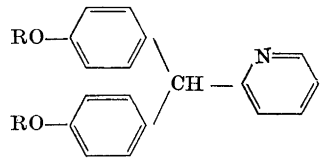

II, R = H
III, R = $COCH_3$
IV, R = CH_3

The dimethoxy compound IV has been reported as an oil [3,6]. In our hands, however, a sample of IV crystallized after having been stored in a closed vessel for some time. After recrystallization from petroleum ether the pure substance melted at 62—63°. Pharmacological evaluation showed IV to possess a laxative effect comparable to that of III.

Schultz and Geller [6,7] lately reported the surprising observation that IV on standing in an open flask at room temperature suffers hydrolytic cleavage to pyridine and *p,p'*-dimethoxybenzhydrol (V) (no m.p. or analytical data were presented), the latter claimed to possess high laxative activity. We have

not been able to detect any laxative activity of authentic V (m.p. 70—71°). The similarity in melting points of IV and V, however, leaves the identity of Schultz and Geller's active product open to discussion *.

In order to gain further insight into the relationship between chemical structure and laxative activity, a series of *p*-hydroxy-*p*'-methoxy-diphenyl-(2-pyridyl)-methanes were synthesized and pharmacologically evaluated. Previously reported methods for preparing substituted diphenyl-(2-pyridyl)-methanes [3–6] are limited to yielding compounds with identical substituents in the benzene rings. The present paper, however, reports a synthetic route to diphenyl-(2-pyridyl)-methanes, VII—IX, dissimilarly substituted in the two aromatic rings, *viz.* the condensation of *p*-methoxyphenyl-2-pyridyl carbinol (VI) with various phenols **.

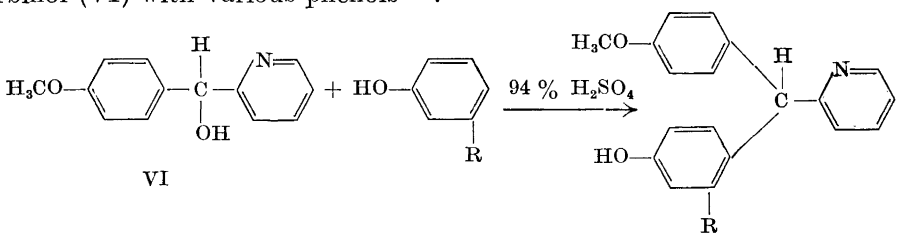

VI

VII, R = H
VIII, R = Cl
IX, R = CH_3

When R = H it was found, as expected, that condensation took place at the *p*-position to the aromatic hydroxy group. This course of reaction was proved by transforming VII into the known *bis*-(*p*-hydroxyphenyl)-(2-pyridyl)-methane (II), which was, in turn, acetylated to its known diacetyl derivative *bis*-(*p*-acetoxyphenyl)-(2-pyridyl)-methane (III). In those cases where R = Cl and R = CH_3 it is believed that condensation proceeds analogously at the position located *para* to the hydroxy grouping.

The synthesis of VI from anisaldehyde and 2-bromopyridine by the Grignard reaction has been previously described [8]. It was found advantageous, however, to employ 2-pyridinealdehyde and *p*-bromoanisole as reactants in the Grignard synthesis, which under these conditions proceeded to give VI in a yield of 82 %.

In another approach to the synthesis of diphenyl-(2-pyridyl)-methanes *bis*-(*p*-methoxyphenyl)-2-pyridyl carbinol (X), formerly synthesized from 2-pyridyl lithium and *p,p*'-dimethoxybenzophenone [9], was prepared from ethyl picolinate and *p*-bromoanisole by Grignard reaction. Attempted reduction of X with formic acid to give IV (*cf.* the synthesis of triphenyl methane by formic acid reduction of triphenyl carbinol [10]) resulted in the production of a red-brown compound (XI), m.p. 146°. Similarly, XI was obtained on attempted dealkylation of X with anhydrous aluminium chloride in carbon disulphide.

* *Note added in proof:* Schultz, O. E. and Schnekenburger, J. (*Arch. Pharm.* **291/63** (1958) 356) now report that the cleavage of IV to pyridine and V could not be reproduced. The product obtained was crystalline IV (m.p. 63—63.5°).

** Patent pending.

The observed diamagnetic properties of XI excluded its free radical character.

The alternative possibility of XI representing the 'double' molecule, 1,1,2,2-*tetrakis*-(*p*-methoxyphenyl)-1,2-*bis*-(2-pyridyl)-ethane, is ruled out by its colour as well as by a comparison of its infrared spectrum with that of IV. The absorption patterns indicate that the methoxysubstituted aromatic rings are retained in the coloured product whereas the pyridine moiety seems to be involved in the formation of a quinoid system. On basis of the available evidence a structure such as XII appears to be a likely proposal, compatible also with the cryscopically determined molecular weight. No further attempts have been made to substantiate the structure XII.

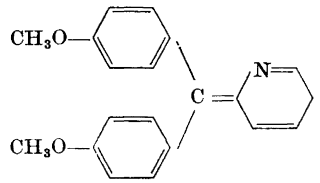

XII

EXPERIMENTAL *

bis-(p-*Methoxyphenyl*)-(*2-pyridyl*)-*methane (IV)*. IV was prepared according to Schultz and Geller [6]. After having been stored in a closed vessel for some time, IV crystallized. After recrystallization from petroleum ether the m. p. of IV was 62—63°. (Found: C 78.8; H 6.2; N 4.7. Calc. for $C_{20}H_{19}NO_2$ (305.4): C 78.7; H 6.3; N 4.6.)

p,p'-*Dimethoxybenzhydrol (V)*. V was prepared according to Bergmann and Hervey[11]. The m. p. of V was 70—71° (previously reported [11] 70—72°). (Found: C 74.0; H 6.6; OCH_3 25.4. Calc. for $C_{15}H_{16}O_3$ (244.3): C 73.8; H 6.6; OCH_3 24.9.)

p-*Methoxyphenyl-2-pyridyl carbinol (VI)*. Magnesium turnings (97.2 g, 4.0 moles) were placed in a 10 l three-necked flask fitted with a stirrer, dropping funnel and a reflux condenser protected by a calcium chloride tube. *p*-Bromoanisole (936 g, 5.0 moles), dissolved in anhydrous ether (2.4 l), was added in small portions until the reaction started and then, at such a rate (1.5 h) that gentle reflux was maintained. The reaction mixture was further heated under reflux for 2 h and cooled in an ice-salt mixture whereupon 2-pyridinealdehyde (214 g, 2.0 moles), dissolved in anhydrous ether (400 ml), was gradually added in the course of 1 h. Stirring was continued for another hour at room temperature. 4 N Hydrochloric acid (2.4 l), followed by conc. hydrochloric acid (800 ml), were added during 1 h to the cooled solution. The reaction mixture was left standing overnight, and the ether layer removed. The aqueous layer was further extracted with ether (2 × 800 ml) and then made alkaline by adding 15 % aqueous ammonia under cooling. The precipitate formed was removed by filtration and dried. The yield was 401 g (93 %) of crude VI, m. p. 128—131°. Crystallization from ethanol (3 l) gave 353 g (82 %) of VI as colourless crystals, m. p. 132—134° (previously reported [8] 133—134°).

p-*Hydroxy*-p'-*methoxy-diphenyl-(2-pyridyl)-methane (VII)*. VI (300 g, 1.4 moles) and phenol (329 g, 3.5 moles) were placed in a three-necked flask provided with stirrer and reflux condenser protected by a calcium chloride tube. Under cooling in an ice bath, 94 % sulphuric acid (210 g) was added with stirring. The reaction mixture was kept in

* All melting points are uncorrected. Microanalyses have been performed by Mr. P. Hansen, The Chemical Laboratory of the University of Copenhagen, and by Mr. W. H. Kirsten, University of Uppsala, Sweden.

the ice bath for 30 min, then at room temperature for 1.5 h and finally at 100° for 30 min. After cooling, 30 % sodium hydroxide (1.5 l) was added followed by water to at total volume of 8 l, whereby a clear solution was obtained. After extraction with ether (3 × 700 ml), the aqueous layer was neutralized with 50 % acetic acid. The precipitate formed was removed by filtration, washed with water, dried, and crystallized first from *iso*propyl alcohol (1 750 ml) and then from ethyl acetate (1 500 ml). The yield was 217 g (64 %) of VII (colourless crystals, m. p. 149—150°). (Found: C 78.2; H 5.8; N 4.8. Calc. for $C_{19}H_{17}NO_2$ (291.3): C 78.3; H 5.9; N 4.8.)

bis-(p-*Acetoxyphenyl*)-*(2-pyridyl)-methane (III)*. VII (1.94 g) was dissolved in a 35 % solution (15 ml) of hydrogen bromide in 90 % acetic acid and the reaction mixture heated under reflux for 3 h. After cooling, water was added and the reaction mixture neutralized under cooling with 2 N sodium hydroxide. An oil was formed, which soon crystallized. Filtration, washing and drying gave 1.82 g (98 %) of crude *bis*-(*p*-hydroxyphenyl)-(2-pyridyl)-methane (II) which, without further purification, was dissolved in a mixture of acetic anhydride (9.1 ml) and pyridine (3.6 ml). The reaction mixture was heated under reflux for 15 min, cooled and poured into water (90 ml). An oil was formed which soon crystallized. After filtration, the product was stirred with ice-cold 3 % sodium hydroxide, removed by filtration, washed with water and dried. The yield was 2.22 g (94 %) of crude III (m. p. 132—133°). Crystallization from ethanol (10 ml) gave 2.00 g (84 %) of III (almost colourless crystals, m. p. 133—134°, previously reported [6] 135—136°). The mixed m. p. of III and a specimen of *bis*-(*p*-acetoxyphenyl)-(2-pyridyl)-methane, prepared according to Schultz and Geller [6] (m. p. 131—132°), was 131—133°.

p-*Hydroxy*-o-*chloro*-p'-*methoxy-diphenyl-(2-pyridyl)-methane (VIII)*. VI (5.0) and *m*-chlorophenol (7.5 g) were condensed in 94 % sulphuric acid (3.5 g) for 2 h as described above for the preparation of VII. The crude product was crystallized twice from aqueous dimethyl formamide. The yield was 4.8 g (38 %) of VIII (colourless crystals, m. p. 220—222°). (Found: C 70.0; H 5.1; N 4.5; Cl 10.8. Calc. for $C_{19}H_{16}ClNO_2$ (325.8): C 70.1; H 4.9; N 4.3; Cl 10.8.)

p-*Hydroxy*-o-*methyl*-p'-*methoxy-diphenyl-(2-pyridyl)-methane (IX)*. VI (5.0 g) and *m*-cresol (6.3 g) were condensed in 94 % sulphuric acid (3.5 g) for 30 min as described above for the preparation of VII. The crude reaction product was boiled with ethanol (200 ml). After filtration, the filtrate was evaporated and the residue recrystallized from aqueous dimethyl formamide. Another crystallization from methanol gave 2.5 g (35 %) of IX as colourless crystals with m. p. 205—207°. (Found: C 78.0; H 6.5; N 4.5. Calc. for $C_{20}N_{19}NO_2$ (305.4): C 78.7; H 6.3; N 4.6.)

bis-(p-*Methoxyphenyl*)-*2-pyridyl carbinol (X)*. Magnesium turnings (19.3 g, 0.80 moles) were placed in a three-necked flask fitted with a stirrer, a dropping funnel and a reflux condenser with a calcium chloride tube, and a stream of dry, oxygen-free nitrogen was passed through the apparatus. *p*-Bromoanisole (148 g, 0.80 moles), dissolved in anhydrous ether (310 ml), was added during 1 h and the reaction mixture was then heated under reflux for 1 h. After cooling in an ice bath, ethyl picolinate (20.0 g, 0.13 moles) dissolved in anhydrous ether (60 ml) was added during 1.25 h, and the reaction mixture was allowed to stand at room temperature for 1 h. After cooling in an ice bath, 4 N hydrochloric acid (650 ml) was slowly added, the mixture was filtered, and the aqueous layer separated, washed with ether (2 × 100 ml) and made alkaline by adding 10 % aqueous ammonia. An oil separated which was extracted with a chloroform-ether mixture, the extract was dried with magnesium sulphate and evaporated in a vacuum. The oily residue (41.6 g) was dissolved in hot methanol (50 ml). Cooling and addition of a little water gave 27.7 g of crude X. After crystallization from methanol (50 ml) the yield was 20.9 g (49 %) of colourless crystals with m. p. 90—92° (previously reported [9] 90—91°).

XI. A mixture of X (1.00 g) and 99 % formic acid (15 g) was heated under reflux for 3 h. After cooling, water (15 ml) was added and the reaction mixture made alkaline by 2 N sodium hydroxide. A black oil formed which was extracted with benzene. After washing with water and drying with magnesium sulphate the benzene was distilled off in a vacuum and the residue (0.93 g) recrystallized from aqueous *iso*propyl alcohol. The yield was 0.75 g (79 %) of XI (red-brown crystals, m. p. 145—147°). Two further crystallizations from aqueous *iso*propyl alcohol furnished red-brown crystals, m. p. 146—147°. (Found: C 78.7; H 5.7; N 4.5; OCH_3 19.8. Calc. for $C_{20}H_{19}NO_2$ (305.4): C 78.7; H 6.3; N 4.6; OCH_3 20.4.)

XI was also obtained in the following experiment. A mixture of X (0.70 g), anhydrous carbon disulphide (20 ml) and anhydrous aluminium chloride (0.61 g) was heated under reflux for 7 h. After cooling, the reaction mixture was shaken with water and the organic layer dried with magnesium sulphate and evaporated in a vacuum. The residue (0.48 g) was recrystallized from aqueous *iso*propyl alcohol to yield 0.26 g (39 %) of XI as red-brown crystals, m. p. 145–147°. Two further crystallizations from the same solvent gave red-brown crystals, m. p. 146–148°. (Found: C 79.0; H 5.8; N 4.6; OCH_3 20.1.)

Magnetic measurements. On basis of determination of the magnetic susceptibility of XI at four different field intensities it was concluded that the compound was diamagnetic, a result excluding its character as a free radical.

Infrared spectra. The infrared spectra of XI and IV were determined in the solid state (KBr pellets) on a Perkin-Elmer double-beam spectrophotometer (Model 21 B).

The C–H stretching modes of the aromatic rings (3 040 cm^{-1}) and the CH_3O-groupings (2 840 and 2 950 cm^{-1}) were detectable in both compounds. Again, bands attributable to the aromatic ether C–O vibration (1 250 cm^{-1}) and the corresponding aliphatic stretching mode (1 025 cm^{-1}) were conspicuously present in XI and IV, yet possibly masked by pyridine bands in the latter compound. A strong C=C absorption band in IV at 1 608 cm^{-1} was substituted with a band at 1 620 cm^{-1} in XI, possibly assignable to a C=N stretching vibration such as would be expected from the structure XII. In the C–H-deformation vibration region the band complex at 750 cm^{-1}, expected from a 2-substituted pyridine moiety, was present in IV but lacking in XI. Both compounds displayed strong absorption around 800 cm^{-1} attributable to *para*-substituted aromatic rings.

Molecular weight determination. The molecular weight of XI was determined in camphor by the usual Rast method. (Found: 228. Calc.: 305.4.)

*Pharmacology.** III, IV, V, VII, VIII, IX and XI were evaluated orally in rats for laxative activity following a technique similar to that used by Schmidt [2]. In doses of 11 mg/kg/day, III, IV and VII displayed strong laxative effect. IX was less active, and even in doses of 76 mg/kg/day the effect was not maximal. VIII was without appreciable effect in doses of 76 mg/kg/day. V was found devoid of laxative activity in a dose of 126 mg/kg/day. XI was found without laxative effect in a dose of 45 mg/kg/day. On a dose of approximately 70 mg/kg/day the rats fed with XI died in 4–5 days.

Acknowledgment. We are grateful to prof. B. Bak and prof. A. Kjær, both of the Chemical Laboratory of the University of Copenhagen, for the recording and interpretation of the infrared spectra, and to Dr. B. Nygaard, of the same laboratory, for the magnetic measurements.

REFERENCES

1. Schmidt, L. and Seeger, E. *Arzneimittel-Forsch.* **6** (1956) 22.
2. Schmidt, L. *Arzneimittel-Forsch.* **3** (1953) 19.
3. Seeger, E. and Kottler, A. *German Patent 951, 987.*
4. Seeger, E. and Kottler, A. *German Patent 956, 043.*
5. Seeger, E. and Kottler, A. *German Patent 956, 755.*
6. Schultz, O. E. and Geller, L. *Arch. Pharm.* **288/60** (1955) 234.
7. Schultz, O. E. and Geller, L. *Arch. Pharm.* **287/59** (1954) 582.
8. Sperber, N., Papa, D., Schwenk, E. and Sherlock, M. *J. Am. Chem. Soc.* **71** (1949) 887.
9. McCarty, F. J., Tilford, C. H. and van Campen, M. G. *J. Am. Chem. Soc.* **79** (1957) 472.
10. Kovache, A. *Ann. chim.* 9, **10** (1918) 184.
11. Bergmann, E. and Hervey, J. *Ber.* **62** (1929) 893.

Received April 2, 1958.

* We are indebted to Dr. J. G. A. Pedersen of our Biological Department for the pharmacological evaluation.

ACTA CHEMICA SCANDINAVICA 12 (1958) 1279—1285

The Equilibrium Constant of the System Ethanol, Aldehyde, DPN^+, DPNH and H^+

KARL-INGEMAR BÄCKLIN

Nobel Medical Institute, Biochemical Department, Stockholm, Sweden

The equilibrium constant for the ethylalcohol + DPN^+ ⇌ acetaldehyde + DPNH + H^+ reaction has been determined at different pH's, temperatures and ionic strengths, using yeast ADH as catalyst. At 20°C and ionic strength 0.1, K is found to be $0.801 \pm 0.014 \times 10^{-11}$ M in the pH range 7—10. The free-energy change for the reduction of DPN has been calculated by combining the experimental values with reliable free-energy data for alcohol and acetaldehyde. At 25°C and zero ionic strength, $\Delta F^\circ = 5.47$ kcal mole^{-1}. Calculation of the oxidation-reduction potential for the DPN—DPNH system gives $E'_o = -0.326$ V at pH 7, 25°C and zero ionic strength, which is in good agreement with recent data in the literature.

Some values have been reported previously for the equilibrium constant of the enzyme catalysed reaction

$$CH_3CH_2OH + DPN^+ \underset{ADH}{\rightleftharpoons} CH_3CHO + DPNH + H^+$$

By using a crude enzyme preparation from Lebedew juice, von Euler *et al.*[1] found the inverse equilibrium constant,

$$k = \frac{[DPN]\,[CH_3CH_2OH]}{[DPNH]\,[CH_3CHO]}$$

to have the value 0.73×10^4 at pH 7.6. As could be expected from the reaction formula, this constant was found to be strongly dependent on pH. Negelein and Wulff[2] using a crystalline preparation of yeast ADH, found the same constant to have the value 1.35×10^3 at pH 7.9 and 20°C. For the overall equilibrium constant

$$K = [DPNH]\,[CH_3CHO]\,[H^+]/[DPN^+]\,[CH_3CH_2OH]$$

Racker[3] found $K = 1.15 \times 10^{-11}$ at 25°C, the value being independent of pH throughout the range investigated. Theorell and Bonnichsen[4] determined K at low concentrations of liver ADH and found, on an average, $K = 0.86 \times 10^{-11}$ at 20°C over the pH range 7 to 10.

Because of the discrepancies between the values, which could be due to the influence of temperature and ionic strength, the value of K for the yeast ADH catalysed reaction has been determined at 20°C for the pH range 7—10 with $\mu = 0.1$; at different ionic strengths at pH 7 and 20°C and at different temperatures in the pH range 7 to 9 with $\mu = 0.1$. The effect of sodium chloride on K has also been determined.

MATERIALS AND METHODS

Yeast ADH was prepared according to the method of Racker [3] and recrystallized several times. Before use the enzyme was dialysed against the buffer. At pH 10, some loss of activity could not be avoided.

A commercial sample of DPN from the Sigma Chemical Company which was found to be 84 % pure was used.

All buffers ($\mu = 0.1$) were stabilized with Versene (0.001 M), phosphate being used at pH 7 and 8 and glycine-NaOH at pH 9 and 10.

The experiments were carried out in 1 cm Beckman cuvettes (3 ml), the temperature being controlled by water circulated from a thermostat through coils on both sides of the cell compartment of a Beckman DU spectrophotometer.

To a cuvette containing 2.8 ml of buffer, 0.1 ml of a dilute alcohol solution and 0.1 ml of a DPN solution, 5—10 μl of the enzyme solution were added with rapid stirring. The concentration of DPNH at equilibrium was determined by measuring the light absorption at 340 mμ. The molecular extinction coefficient [5] for reduced DPN was taken as 6.22×10^6 cm^2/mole.

The temperature dependence of K was determined by measuring the light absorption at 340 mμ and hence K first at 15°C, and then for each 5°C rise in temperature. It was thus possible to determine K in one and the same reaction mixture at all the temperatures. In order to prevent evaporation of the acetaldehyde, the cuvettes had to be covered with lids.

Corrections were made for the pH dependence on temperature of the different buffers [6]. These were checked in separate experiments.

The method unaccountably failed at pH 10, but gave good results from pH 7 to 9.

EXPERIMENTAL RESULTS

Varying pH. Temperature and ionic strength constant. Some of the experimental results for the pH range 7 to 10 (20°C, $\mu = 0.1$) are collected in Tables

Table 1. Equilibria at 20°C, pH 7.0 and $\mu = 0.1$.

[ADH] × 10^4	[EtOH] × 10^4	$[DPN]_{tot}$ × 10^4	% Red	$K \times 10^{11}$
0.0043	5 470	0.29	72.8	0.846
0.0043	1 087	0.53	33.8	0.778
0.0045	547	0.49	24.3	0.623
0.0086	1 087	0.53	33.1	0.760
0.0215	1 087	0.53	33.1	0.747
0.0223	1 090	0.49	35.1	0.760
0.0356	5 470	0.50	65.9	0.940
0.0416	1 050	0.51	34.6	0.812
0.0430	5 470	0.33	71.8	0.912
0.0430	1 087	0.53	34.4	0.798
0.0864	1 090	0.33	42.3	0.793
0.1296	109	0.52	13.1	0.770
			Mean:	0.795

Table 2. Equilibria at 20°C, pH 8.0 and $\mu = 0.1$.

[ADH] × 10^4	[EtOH] × 10^4	$[DPN]_{tot}$ × 10^4	% Red	K × 10^{11}
0.0043	1 087	0.53	69.7	0.790
0.0045	1 090	0.50	63.8	0.782
0.0086	543	0.53	57.5	0.768
0.0215	543	0.53	59.5	0.856
0.0223	109	0.50	29.2	0.840
0.0356	547	0.49	52.7	0.835
0.0534	109	0.49	29.4	0.878
0.0712	54.7	0.49	22.3	0.908
0.1120	547	0.49	55.8	0.848
0.1680	547	0.49	56.7	0.896
			Mean:	0.840

Table 3. Equilibria at 20°C, pH 9.0 and $\mu = 0.1$.

[ADH] × 10^4	[EtOH] × 10^4	$[DPN]_{tot}$ × 10^4	% Red	K × 10^{11}
0.0020	51.8	0.49	60.0	0.822
0.0020	55.0	0.53	62.1	0.820
0.0045	109.0	0.53	82.0	0.871
0.0045	10.7	0.53	43.3	0.775
0.0080	109.0	0.53	73.0	0.806
0.0200	109.0	0.53	73.4	0.826
0.0200	10.7	0.53	38.2	0.777
0.0400	54.0	0.53	60.3	0.757
0.0600	54.0	0.53	61.6	0.808
			Mean:	0.807

Table 4. Equilibria at 20°C, pH 10.0 and $\mu = 0.1$

[ADH] × 10^4	[EtOH] × 10^4	$[DPN]_{tot}$ × 10^4	% Red	K × 10^{11}
0.0037	2.74	0.51	39.1	0.710
0.0183	5.47	0.51	50.9	0.722
0.0356	10.90	0.50	61.7	0.829
0.0356	5.47	0.50	51.3	0.813
0.0367	10.90	0.53	66.3	0.881
0.0533	2.74	0.50	38.3	0.733
0.0712	5.47	0.50	49.7	0.830
0.0712	2.74	0.50	38.9	0.764
0.0712	2.74	0.50	38.3	0.830
			Mean:	0.795

1—4. As stated previously, K is seen to be independent of pH. An average value of $K_{20°, \mu=0.1} = 0.801 \pm 0.014 \times 10^{-11}$ M has been calculated from a larger number of experiments.

Varying ionic strength. pH and temperature constant. The results of these experiments, carried out in phosphate buffer (pH 7, 20°C) are summarized

Table 5. Equilibria at 20°C. Phosphate buffers of different ionic strengths at pH 7.0 and added sodium chloride.

[ADH] $\times 10^{-4}$	[EtOH] $\times 10^{-4}$	$[DPN]_{tot} \times 10^{-4}$	% Red	[NaCl]	μ	$K \times 10^{11}$
0.0062	1 062	0.398	35.2	—	0.096	0.801
0.0062	5 393	0.398	63.8	—	0.096	0.813
0.0062	5 393	0.398	59.8	—	0.050	0.736
0.0062	5 393	0.398	69.8	—	0.189	0.927
0.0062	5 393	0.398	74.2	—	0.376	0.997
0.0062	5 393	0.398	57.8	0.167	0.259	0.925
0.0062	5 393	0.398	56.6	0.333	0.423	1.047
0.0062	5 393	0.398	52.3	0.667	0.749	1.184

in Table 5. Fig. 1, where for a temperature of 20°C log K has been plotted against $\sqrt{\mu}$, shows that an increase of ionic strength causes an increase of K. Addition of sodium chloride also increases K in the same manner. Perhaps the increase of K is due to the effect of ionic strength on the activity coefficients of the reactants. Similar results have been reported by Burton and Wilson [7] for the malic dehydrogenase system.

Statistical analysis gave a regression line with a slope of 0.315 and an intercept of log $K + 12 = 0.8085$ at $\sqrt{\mu} = 0$, which corresponds to a value of $K_{20°, \mu=0} = 0.646 \times 10^{-11}$ M.

Varying temperature and pH. Ionic strength constant. The experimental results for the temperature dependence of K at different pH's when $\mu = 0.1$ are shown in Fig. 2, where $K_{\mu=0.1}$ has been plotted against $1/T$. The equation for the regression line is log $K = (1554/T) - 5.80$.

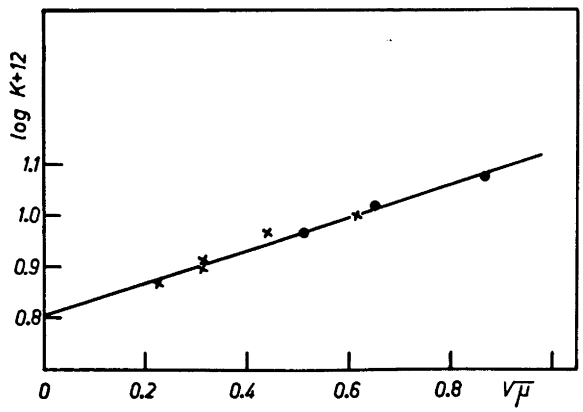

Fig. 1. Equilibrium constant, K, at varied ionic strength. Temp. 20°C; log $K + 12$ plotted *versus* $\sqrt{\mu}$; × phosphate buffers pH 7; ● added NaCl.

Table 6. $K \times 10^{11}$ at different temperatures, ($\mu = 0.1$), and the related thermodynamic constants

pH	Slope of the line	15°C	20°C	25°C	30°C	35°C	$\Delta H°$ kcal/mole	$\Delta S°$ cal/mole · degr.
7.0	−1.55	0.646	0.800	0.977	1.202	1.445	7.09	−26.6
8.0	−1.52	0.642	0.795	0.966	1.175	1.413	6.96	−27.1
9.0	−1.60	0.635	0.794	0.972	1.200	1.454	7.32	−25.8
Mean:	−1.55	0.641 ±0.005	0.796 ±0.004	0.972 ±0.006	1.192 ±0.020	1.437 ±0.020	7.13 ±0.20	−26.5 ± 0.7
$\Delta F°$ kcal/mole		14.76	14.89	15.02	15.16	15.29		

Table 6 gives the mean value of $K_{\mu=0.1}$ for different temperatures and pH's and the corresponding thermodynamic constants, obtained by applying the general formulas

$$\frac{d(\log K)}{d(1/T)} = -\frac{\Delta H°}{R \ln 10}; \quad \Delta F° + RT \ln K = 0; \quad \Delta H° = \Delta F° + T \Delta S°$$

from which

$\Delta H° = 7.13 \pm 0.20$ kcal mole^{-1} at $\mu = 0.1$
$\Delta S° = -26.5$ cal mole^{-1} degree^{-1} at $\mu = 0.1$
$\Delta F° = 14.89$ kcal mole^{-1} at 20°C (15.02 kcal mole^{-1} at 25°C) and $\mu = 0.1$

Extrapolation to zero ionic strength gives $\Delta F° = 15.01$ kcal mole^{-1} at 20°C (15.15 kcal mole^{-1} at 25°C).

Burton [8] has calculated that for the reaction

$$CH_3CHO\ (aq) + H_2\ (g) \rightleftharpoons CH_3CH_2OH\ (aq)$$

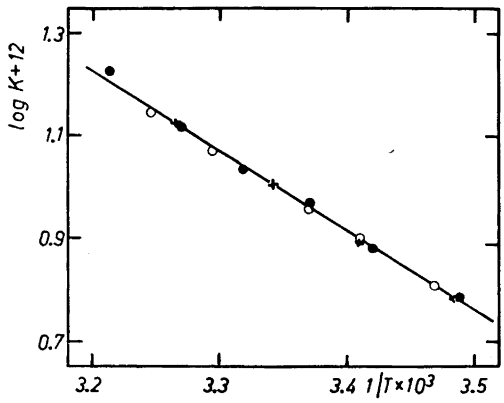

Fig. 2. Equilibrium constant, K, at different temperatures and pH's; $\mu = 0.1$. $\log K + 12$ plotted *versus* $1/T \times 10^3$; ● pH = 7; ○ pH = 8; × pH = 9.

$\Delta F^\circ = -9.68 \pm 0.4$ kcal mole^{-1} at 25°C. Combining this value of ΔF° with the above value of $\Delta F^\circ = 15.15$ kcal mole^{-1} gives for the reaction

$$DPN^+ + H_2 \rightleftharpoons DPNH + H^+$$

$\Delta F^\circ = 5.47$ kcal mole^{-1} ($\pm$ 0.4 kcal mole^{-1} according to Burton [8]) at 25°C and $\mu = 0$. This in turn gives $E'_0 = -0.326$ V ($\pm$ 0.008 V) as the value of the oxidation-reduction potential for the DPN — DPNH system at pH 7, 25°C and $\mu = 0$, calculated by using the formula

$$E'_0 = -\frac{\Delta F^\circ}{2F} - \frac{RT \ln 10 \text{ pH}}{2F}$$

DISCUSSION

Recalculating the value of the equilibrium constant reported by Negelein and Wulff [2] and correcting for the erronous molecular weight of DPN (N. and W. used 700 instead of 663) and molecular extinction coefficient of DPNH ($\varepsilon = 7.7 \times 10^6$ instead of 6.22×10^6 cm^2/mole), gives for a 50 % reduction of DPN, $K = 0.896 \times 10^{-11}$ M at pH 7.9 and 20°C. This value agrees with ours if they worked at an ionic strength of $\mu = 0.20$.

When recalculating the value reported by von Euler *et al.*[1], K is found to be $= 0.342 \times 10^{-11}$ M at pH 7.6. No temperature data are reported, but this value is certainly too low and would be still lower if recalculated [5] with $\varepsilon = 6.22 \times 10^6$ cm^2/mole instead of the value 4.05×10^6 cm^2/mole used by von Euler *et al.* The low value could be due to the crude enzyme preparation used.

Under the conditions of ionic strength (0.04) and temperature (25°C) used by Racker [3], K as calculated from our values should be $= 0.92 \times 10^{-11}$ M, the assumption being made that the influence of ionic strength on K is constant in the temperature interval 20—25°C. The value of $K = 1.15 \times 10^{-11}$ M reported by Racker [3] therefore seems to be too high, particularly as he used the higher value for the molecular extinction coefficient of reduced DPN ($\varepsilon = 6.28 \times 10^6$ cm^2/mole) reported by Ohlmeyer [9].

The value of $K = 0.86 \times 10^{-11}$ M at 20°C and $\mu = 0.1$ reported by Theorell and Bonnichsen [4] should be corrected for the protein concentration. If 50 % reduction of the 40 μM DPN used at a protein concentration of 0.004×10^{-4} M ($= 0.8$ μN) is assumed, $K = 0.83 \times 10^{-11}$ M which is close to the value found in this investigation.

The value reported here for the oxidation-reduction potential of the DPN—DPNH system is in good agreement with the value $E'_0 = -0.320$ V at pH 7 and 25°C recently reported by Burton [8] from investigations of the *iso*propanol-DPN-acetone system. Rodkey [10] has found, by potentiometric titration, the value $E'_0 = -0.318 \pm 0.001$ V at pH 7 and 30°C. The formerly accepted value for the DPN-DPNH potential (—0.282 V at pH 7 and 30°C) reported by Borsook [11] thus again seems to be too high.

Grateful acknowledgement is made to Professor Hugo Theorell for suggesting the present investigation and for his kind advice and criticism in connection with the work. The author is indebted to *Institutet för Maltdrycksforskning* for financial support.

REFERENCES

1. v. Euler, H., Adler, E. and Hellström, H. *Hoppe-Seyler's Z. physiol. Chem.* **241** (1936) 239.
2. Negelein, E. and Wulff, H. J. *Biochem. Z.* **293** (1937) 351.
3. Racker, E. *J. Biol. Chem.* **184** (1950) 313.
4. Theorell, H. and Bonnichsen, R. *Acta Chem. Scand.* **5** (1951) 1105.
5. Horecker, B. L. and Kornberg, A. *J. Biol. Chem.* **175** (1948) 385.
6. Clark, W. M. *The Determination of Hydrogen Ions*, London 1927.
7. Burton, K. and Wilson, T. H. *Biochem. J.* **54** (1953) 86.
8. Burton, K. *Biochim. et Biophys. Acta* **8** (1952) 114.
9. Ohlmeyer, P. *Biochem. Z.* **297** (1938) 66.
10. Rodkey, F. L. *J. Biol. Chem.* **213** (1955) 777.
11. Borsook, H. *J. Biol. Chem.* **133** (1940) 629.

Received April 17, 1958.

ACTA CHEMICA SCANDINAVICA 12 (1958) 1286—1291

Enzymatic Hydrolysis of Organophosphorus Compounds

VIII. Effect of Anions

KLAS-BERTIL AUGUSTINSSON

Institute of Organic Chemistry and Biochemistry, University, Stockholm, Sweden

Molybdate and tungstate are markedly active in increasing the spontaneous hydrolysis of tabun. Among the 25 anions tested, chromate, metavanadate, perborate and selenite are also active in this respect, but less so than molybdate and tungstate. None of the anions influence the enzymatic hydrolysis of tabun by phosphorylphosphatase (prepared from human serum), except fluoride which is an inhibitor. The degradation products formed after treatment of tabun with molybdate do not inactivate cholinesterase. This enzyme is protected from inactivation by tabun when mixed with molybdate prior to addition of tabun.

The effect of metallic ions on phosphorylphosphatases was reported in a recent paper of this series [1]. The present report deals with the results obtained in studies of the effect of a variety of anions on both the enzymatic and spontaneous hydrolysis of dimethylamido-ethoxy-phosphoryl cyanide (tabun).

METHODS AND MATERIAL

The determination of hydrolysis rates, spontaneous as well as enzymatic, was carried out in a 0.04 M $NaHCO_3-CO_2$ buffer by the Warburg manometric technique at 25°C and pH 7.6 [2]. Hydrolysis rates were expressed in μl CO_2 evolved (b_{30}) or μmoles of substrate hydrolysed in 30 min. Tabun was used as substrate, and its concentration in the reaction mixture (total volume, 2.00 ml) was 5.3×10^{-3} M (*i. e.* 10.6 μmoles of tabun present).

The phosphorylphosphatase preparation was prepared from human serum, dissolved in the bicarbonate buffer, and dialysed free from other ions. The cholinesterase preparation was purified from human serum and was free from phosphorylphosphatase activity. Cholinesterase activity was determined in a Ringer bicarbonate buffer by the Warburg technique with acetylcholine iodide (3.3×10^{-3} M) as substrate.

In testing the effects of various anions, sodium and ammonium salts were used in most cases; the salt concentration in the reaction mixture during hydrolysis rate determinations was 1.0×10^{-3} M. The phosphorylphosphatase was incubated 50 min with the ions before the substrate (tabun) was added. The same incubation time was employed in iactivation experiments with cholinesterase, except as otherwise stated.

RESULTS

Effect of anions on the spontaneous hydrolysis of tabun. The effects of a number of anions on the rate of spontaneous hydrolysis of tabun are illustrated in Table 1. Most anions did not influence the hydrolysis rate in the concentration range tested. Perborate, selenite and thiocyanate increased the rate of hydrolysis, and still more active were chromate and metavanadate. Especially active in increasing the rate of spontaneous hydrolysis were tungstate and molybdate. The effect of molybdate ($Na_2MoO_4.2H_2O$) was such that the time required for 50 % hydrolysis of 10.6 μmoles of tabun under the experimental conditions used was decreased from 3h 40 min to 15 min by 20 μmoles of molybdate, and to 2 min by 100 μmoles.

Fig. 1 illustrates the effect of molybdate on tabun hydrolysis as a function of molybdate concentration, and Fig. 2 the graphical evaluation of first order reaction constants for the reactions in the absence and presence respectively of molybdate.

Table 1. Effect of anions (1.0 mM) on the spontaneous (non-enzymatic) and enzymatic hydrolysis of tabun. Enzyme: purified phosphorylphosphatase of human serum. Sodium salts used, unless otherwise stated.

Ion	% Activation (a) or Inhibition (i)	
	Non-enzymatic	Enzymatic
$HCOO^-$	0	10 a
$C_2O_4^{2-}$	0	0
CN^-	0	0
NO_3^-	0	0
$H_2PO_2^-$	0	0
$P_2O_7^{4-}-HP_2O_7^{3-}$	0	5 a
$BO_2^- - H_2BO_3^-$	0	0
BO_3^- *	20 a	0
$B_4O_7^{2-}$	0	12 a
SO_3^{2-}	0	0
SO_4^{2-}	0	0
$S_2O_3^{2-}$	0	0
$S_2O_8^{2-}$	0	8 a
SH^-	0	12 i
SCN^-	11 a	8 i
SeO_3^{2-}	20 a	0
AsO_3^{3-}	0	5 a
VO_3^- **	81 a	0
CrO_4^{2-}	52 a	0
MoO_4^{2-}	175 a	0
MoO_4^{2-} **	175 a	0
$[Mo(MoO_4)_6]^{6-}$ **	1 190 a	0
WO_4^{2-}	159 a	0
F^-	100 i	54 i
ClO^-	< 10 a	0
ClO_3^-	0	0
ClO_4^- (10^{-4} M) ***	0	0

* active ion, probably HO_2^-; ** NH_4-salt; *** Ca-salt.

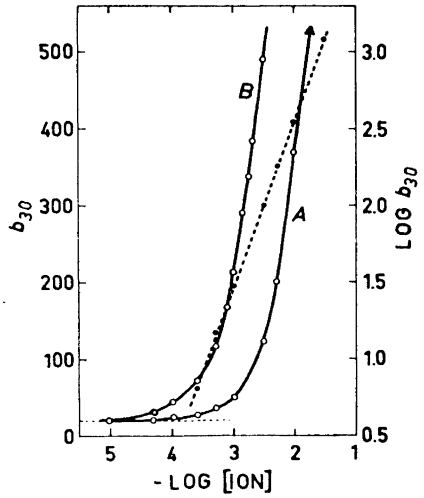

Fig. 1. Effect of molybdate on the spontaneous initial hydrolysis rate of tabun. Molar concentrations of anion are those in the reaction mixture (2.00 ml) during rate determination. A: $Na_2MoO_4 \cdot 2H_2O$; B: $(NH_4)_6[Mo(MoO_4)_6] \cdot 4H_2O$. The log curve (dotted line) refers to the effect of Na_2MoO_4 (log μl CO_2/30 min), corrections made for blank (no molybdate present).

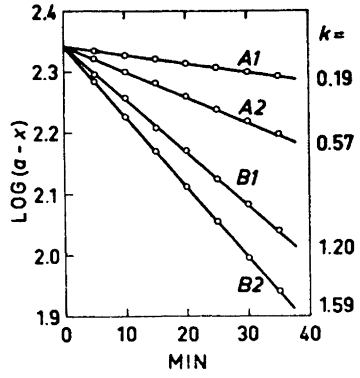

Fig. 2. Graphical evaluation of first order reaction constants for the spontaneous (A) and enzymatic (B) hydrolysis of tabun, in the absence (1) and presence (2) of 1.0 mM Na_2MoO_4. Note that the differences between the rate constants for the reactions taken part in the absence and presence of molybdate are the same (0.38 and 0.39 h^{-1} respectively).

It was found in previous reports that copper(II) salts accelerate the spontaneous hydrolysis of tabun [1] and di*iso*propoxy-phosphoryl fluoride [4]. Under the experimental conditions of the present investigation, 4 μmoles of $CuCl_2$ increased the initial rate of tabun hydrolysis by a factor of 2, in both the absence and presence of molybdate (Table 2). The effects revealed by Cu^{2+} and molybdate are therefore assumed to be purely additive, and a copper complex which might be particularly active, was not formed. Mixtures of $CuCl_2$ and molybdate with other ratios than that used in Table 2 gave similar results.

The spontaneous hydrolysis of tabun was inhibited by fluoride (Table 1). It was of interest to find out whether this effect was reflected in the cholinesterase inactivating effect of a tabun solution "stabilized" with fluoride. The

Table 2. Hydrolysis of tabun in the presence of mo ybdate and copper(II) chloride. Initial reaction rate expressed as μmoles of tabun/10 min.

10.6 μmoles tabun	0.3
+ 15 μmoles Na_2MoO_4	2.6
+ 4 μmoles $CuCl_2$	0.7
+ 15 μmoles Na_2MoO_4 + 4 μmoles $CuCl_2$	5.2
+ 2 μmoles ammonium molybdate	2.7
+ 2 μmoles ammonium molybdate + 4 μmoles $CuCl_2$	5.0

Table 3. Effect of fluoride on the cholinesterase inactivating effect of tabun. Tabun was incubated for 24 h in bicarbonate solutions with and without NaF (1 mM) at room temperature. The inactivating effect of these solutions was then measured and expressed in pI_{50} values [8]. A freshly prepared tabun solution was used as control ("No incubation"). Other experimental conditions, as in Table 4.

Incubation medium	No incubation	HCO_3^-	$HCO_3^- + F^-$
pI_{50}	7.80	6.35	6.95

experimental results of Table 3 show that this is the case. A solution of tabun in a bicarbonate buffer containing NaF was more powerful in inactivating cholinesterase than a bicarbonate solution without fluoride. The stabilization, however, was far from complete in this experiment, but the effect of fluoride in this respect was obvious.

Effect of anions on the enzymatic hydrolysis of tabun. Most of the anions studied did not influence the enzymatic hydrolysis of tabun by a purified phosphorylphosphatase preparation of human serum (Table 1). The results obtained with molybdate are illustrated in Fig. 2. Fluoride was an inhibitor, and weak inhibiting effects were obtained with hydrosulphide and thiocyanate. There was no marked acceleration of the enzymatic reaction in any case when the anions (2 μmoles) were added to the reaction mixture. The weak increase in the rate of enzymatic hydrolysis observed with borate, formate, persulphate, etc. may be due to complex formation with some enzyme inhibitor present in the preparation used.

The study was broadened with phosphorylphosphatases of other sources (swine kidney and liver). Anions did not have any significant effect on these enzymes either, except for calcium perchlorate which was a strong inhibitor of the kidney enzyme (93 % inhibition by 10^{-4} M $Ca(ClO_4)_2$).

Effect of molybdate on the cholinesterase inactivation by tabun. With the observation of strong increase in the spontaneous hydrolysis rate of tabun by molybdate, the effect of this and some other anions on the cholinesterase inactivation by tabun was studied. The results obtained are summarized in Table 4. Molybdate, in the concentrations used, did not influence the cholinesterase activity (Column 4). When cholinesterase was inactivated 85—95 % by tabun and molybdate was then added, no reactivation of enzyme activity was observed (Column 3). A tabun solution which had been treated for 30 min with molybdate prior to adding to the enzyme solution, did not inhibit cholinesterase (Column 6). It was also observed that the enzyme could be "protected" from inactivation by tabun when the enzyme was mixed with molybdate prior to addition of tabun (Column 5); compared with controls, complete protection was not achieved in the experimental series of Table 4. Complete protection, however, was obtained by using higher molybdate concentration. Similar results were obtained with ammonium molybdate. Sodium perborate which showed an accelerating effect on tabun hydrolysis (Table 1),

Table 4. Effect of molybdate and perborate on the cholinesterase (ChE) inactivation by tabun. Inactivator (tabun), 1.0×10^{-8} M (during incubation of ChE). Concentration values refer to the reaction mixture during enzyme activity determination, unless otherwise stated. Incubation time 30 min for reagents in brackets, followed by another 50 min incubation with salt or/and inactivator before addition of substrate. Activity expressed in b_{30} values.

		1	2	3	4	5	6
Salt	M	Control	(ChE + Tabun)	(ChE + Tabun) + Salt	(ChE + Salt)	(ChE + Salt) + Tabun	(ChE + (Tabun + Salt)
$Na_2MoO_4 \cdot 2H_2O$	1.0×10^{-3}	134	11.5	10.5	136.5	66	135
	5.0×10^{-3}	156	20.5	27.5	151.5	132.5	156.5
$(NH_4)_6[Mo(MoO_4)_6] \cdot 4H_2O$	7.5×10^{-4}	150.5	26	23	146.5	81	150
$NaBO_2$	1.0×10^{-4}	150	2.5	3	146	—	67

but less so than molybdate, also gave similar results vis-à-vis cholinesterase inactivation.

Effect of anions on the hydrolysis of sarin. Similar studies of spontaneous hydrolysis as those described for tabun were performed by Larsson [5] with sarin (methyl-*iso*propoxy-phosphoryl fluoride). Among the salts tested as catalysts with the gasometric technique, sodium perborate, sodium molybdate and calcium hypochlorite markedly accelerated the hydrolysis of sarin. Calcium hypochlorite was also active on some sarin analogoues and on parathion. The effect of calcium hypochlorite on the tabun hydrolysis was much lower. Generally, various organophosphorus compounds show differences as to the catalytic effect of various inorganic agents, cations as well as anions, on spontaneous hydrolysis.

DISCUSSION

An interpretation of the catalysing effect of a salt on the spontaneous hydrolysis of tabun (and other organophosphorus compounds as well) may be the formation of a labile complex with the organophosphorus compound. This likely is the explanation of the activation of hydrolysis rates caused by molybdate and tungstate, the complex formed being of unknown nature. The formation of such complexes with molybdate and other organophosphorus compounds [7] has been discussed.

The hydrolysis products of tabun do not inhibit cholinesterase [6,8] when present in concentrations lower than 10^{-3} M. The products formed in the molybdate catalysed reaction are also inactive as cholinesterase inhibitors, as demonstrated above. The fact that cholinesterase mixed with molybdate is protected from inactivation by tabun, the capacity of protection being dependent on the molybdate concentration, makes it likely that molybdate reacts directly with the phosphorus atom which is the site of the inhibiting compound that reacts with the active group of the enzyme molecule. The more this

atom is in the cationic state, dependent on the electrophilic strenght of the acid constituent of the molecule (CN in the case of tabun), the higher affinity does it have for the enzyme and also for molybdate. It is reasonable to regard the formation of an organophosphorusmolybdate complex as a sort of "model" reaction for that of the substrate-enzyme complex (*cf.* Ref.[4]).

In contrast to certain metallic ions [1], anions do not influence the enzymatic hydrolysis of tabun by phosphorylphosphatase. The enzyme activity is probably not dependent on the presence of SH-groups, for those agents which react with these groups do not inhibit the activity. The inhibiting effect observed with fluoride is probably due to a shift in equilibrium of the reactions in which cyanide is set free, the base-catalysed spontaneous reaction as well as the enzymatic hydrolysis reaction.

The kind interest shown this investigation by Professor Gustaf Ljunggren, Chief of the Research Institute of National Defence, Department 1, is gratefully acknowledged.

REFERENCES

1. Augustinsson, K.-B. and Heimbürger, G. *Acta Chem. Scand.* **9** (1955) 383.
2. Augustinsson, K.-B. and Heimbürger, G. *Acta Chem. Scand.* **8** (1954) 753.
3. Augustinsson, K.-B. *Methods Biochem. Anal.* **5** (1957) 1.
4. Wagner-Jauregg, T., Hackley, B. E. Jr., Lies, T. A., Owens, O. O. and Proper, R. *J. Am. Chem. Soc.* **77** (1955) 922.
5. Larsson, L. *Acta Chem. Scand.* **12** (1958) 1226.
6. Larsson, L. *Acta Chem. Scand.* **7** (1953) 306.
7. Weil-Malherbe, H. *Biochem. J* **55** (1953) 741.
8. Augustinsson, K.-B. and Heimbürger, G. *Acta Chem. Scand.* **8** (1954) 762.

Received March 14, 1958.

ACTA CHEMICA SCANDINAVICA 12 (1958) 1292—1296

A Group Separation Method for Gamma Spectrometry of Complex Radionuclide Mixtures — with Special Application to Stainless Steel and its Corrosion Products

K. SAMSAHL

Nuclear Chemistry Laboratory, AB Atomenergi, Stockholm, Sweden

Short anion exchange columns coupled in series and saturated with chloride, citrate and hydroxide ions have been used for simple and very rapid separations of common elements in water solutions as a pretreatment for subsequent analysis with gamma spectrometry. A method was developed for the analysis of stainless steel, its corrosion products, and other elements, present as impurities in a water cooled nuclear reactor. Practical examples are described in detail.

With this method it seems possible to measure continuously water corrosion rates of individual or small groups of stainless steel elements.

Since the use of scintillation counters for gamma radiation was originally described by Bell and Cassidy [1], it has been shown that gamma spectrometry makes possible the identification and quantitative determination of gamma emitters in mixtures of radionuclides [2,3].

As most elements form radioactive gamma emitting isotopes on irradiation with thermal neutrons in an atomic reactor, gamma spectrometry has become a modern analytical tool of increasing importance.

Gamma spectrometric analysis of simple radionuclide mixtures can in many cases be carried out successfully without prior chemical separation of individual constituents. However, a coarse separation of the present elements in groups is often necessary or preferable. The presence in a sample of only minute amounts of common elements with extremely high activation cross section and hard gamma radiation, like sodium and manganese, giving rise to $^{24}_{11}$Na and $^{56}_{25}$Mn, can by Compton distribution partly or completely mask the activity of other elements. In many analyses the alkalies and alkaline earths constitute only interferring impurities without interest. A rapid and accurate anion exchange method for separating them from, as it seems, all other elements has been worked out. The method simultaneously allows the latter elements to be gathered in groups suitable for gamma spectrometry.

Samuelson and Schram [4] used an anion exchange column (as citrate) for separating alkali salts from various cations in a water solution. The use of anion exchange resins as solid precipitants and filters was suggested by Glueckauf and Roberts [5]. The present method makes use of these principles. The behaviour of different cations has been studied by flowing neutral water solutions through short anion exchange columns in the citrate- and the hydroxide form. An anion exchanger in the chloride form was also studied, in as much as metals like tungsten and molybdenum can be easily separated from many other elements as negatively charged ions by the chloride form after an initial HCl-H_2O_2 standard treatment of irradiated samples.

EXPERIMENTAL

The experiments were performed with irradiated metallic chromium, molybdenum and tungsten, and furthermore salts of the cations, Na^+, Mn^{2+}, Fe^{2+}, Co^{2+}, Ni^{2+}, Cu^+, Zn^{2+} and Sr^{2+}. The samples were individually brought into solution with hot 1:1 HCl containing a few drops of H_2O_2 and taken to dryness on a water bath. Subsequently they were dissolved in water and diluted to a suitable strength of gamma activity. Carriers were added in amounts of about 5 mg of the appropriate cation per 100 ml of solution. No carriers were added to the solutions of tungsten and molybdenum. Then 20 ml portions of a single gamma emitter solution were added to four ion exchange columns consisting of Dowex 2, 200—400 mesh in the citrate, chloride- and hydroxide form, and Dowex 50, 200—400 mesh in the hydrogen form. Each column consisted of 10 ml in water sedimented resin contained in a 2.5 cm diameter glass filter crucible. The active solutions were sucked through at a rate of about 4 ml/min and the columns washed with two five ml portions of water and drained by suction. Finally the crucibles were placed directly at definite geometry on the top of a gamma scintillation detector, and the activity assayed with a single channel pulse analyzer.

The activity of the Dowex 50 resin was measured and used as a standard for the estimation of the per cent absorbtion on the others. The eluate was controlled for possible gamma activity.

RESULTS AND DISCUSSION

The behaviour of the different ions on the ion exchange columns is summarized in Table 1.

The first column of the table illustrates the oxidation states of the elements after the initial HCl-H_2O_2 treatment.

The behaviour of hydrogen peroxide in acid medium can be advantageously utilized for the analysis of stainless steel elements, which is shown by a practical example further on. Besides its powerful solving and oxidizing action on many elements it will for example reduce possible higher valences of manganese to the divalent state and does not effect oxidation of trivalent chromium in hydrochloric acid. As a result chromium, if not initially present as chromate, and manganese can easily be quantitatively separated from other elements.

The molybdates and tungstates obtained by solution of the metals consist of many complicated compounds which do not seem to be very well known. Their partly retention on the Dowex 50 resin is probably due to the precipatation of the corresponding acids, as additional experiments showed that they were not or only to a very small extent adsorbed on a cation exchanger in Na^+ form.

Table 1.

Cation	% adsorbtion		Error < 5 %	
	Dowex 2 chloride	Dowex 2 citrate	Dowex 2 hydroxide	Dowex 50 hydrogen
Na^+	0	0	0	100
Mn^{2+}	0	0	100	100
Fe^{3+}	0	100	100	100
Co^{2+}	0	100	100	100
Ni^{2+}	0	100	100	100
Cu^{2+}	0	100	100	100
Zn^{2+}	0	50—70	100	100
Sr^{2+}	0	0	0	100
Cr^{3+}	0	0	100	100
Molybdates	100	100	100	30—70
Tungstates	100	100	100	30—70

The retention of Zn^{2+} on the citrate form was found to be 90 % if the final washing procedure with two 5 ml portions of water was omitted. Washing with about 100 ml of water caused a quantitative break through of the zinc activity.

PRACTICAL EXAMPLES

1. Stainless steel analysis

According to Table 1 a separation into three groups of common steel components is achieved by passing a water solution of the irradiated sample through three Dowex 2 columns subsequently in chloride-, citrate- and hydroxide form. Molybdenum and tungsten are quantitatively retained on the chloride form. Other elements pass through to the citrate resin, where iron, cobalt and nickel are adsorbed as complexed ions. Manganese and chromium, however, still pass through and are finally precipitated on the hydroxide form.

The practical arrangement is shown in Fig. 1. It consists of three identical glass filter crucibles attached to each other and to a suction flask by means of rubber rings.

Carriers of Ni^{2+}, Co^{2+}, Mn^{2+} and Cr^{3+} are added to the sample solution. An even flow rate of the active solution is obtained if the crucibles are filled with water before being attached to each other.

After drainage of the active solution the upper crucible is washed with water and removed for counting. The next one is then drained and treated in the same way, and so on.

Separation speed. The various resin forms are kept on stock under distilled water, and the whole separation procedure is finished about one hour after removal of the sample from the pile. The gamma spectrometric measurements of the first resin column in the series can start about 20 min earlier. However, a few experiments with stainless steel has been carried out by converting the sample to water soluble sulphates with a H_2SO_4-H_2O_2 treatment before irradia-

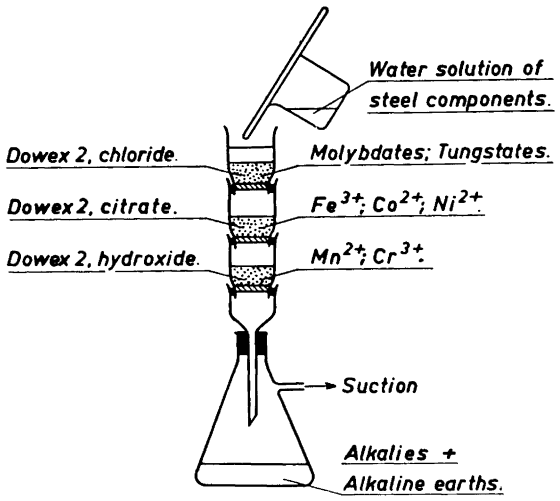

Fig. 1.

tion. The active material was directly dissolved in water and passed through the resin columns. The activity measurements could then start about 10 min after the end of irradiation. In this way it may be possible to analyze elements with short lived isotopes, like vanadium in steel and magnesium in aluminium alloys. However, the possible interferring influence on the separation of Szilard-Chalmers reactions has not been studied in detail.

Gamma spectrometric measurements. The single channel pulse analyzer used for the analysis has previously been standardized against known amounts of the various elements. The measurements are carried out in the usual way by writing spectra and following decays.

The separation procedure as now described is, however, not ideal for the gamma spectrometry of cobalt-containing steel. Because of the similar gamma radiation emitted from $^{60}_{27}$Co and $^{59}_{26}$Fe, which both are retained on the citrate form of the resin, their individual determination is difficult. The problem can, however, be easily solved by eluting the resin, extracting the iron with ether and again adsorbing the cobalt activity on an ion exchanger for comparative measurements.

The determination of small amounts of molybdenum in the presence of tungsten is best done after some days decay of the 24 hours $^{187}_{74}$W. Chromium in the presence of manganese is easily determined about one day after the end of irradiation.

2. Corrosion measurements

Some measurements of corrosion products in the heavy water of the Swedish R1 reactor has been carried out. 20 ml portions of D_2O were passed without pretreatment and addition of carriers through the same arrangement of resin

forms as used for the steel analysis, except that an additional Dowex 50 column in the hydrogen form was coupled after the resin in the hydroxide form for the control of the adsorbtion efficiency of the others.

About 20 ml of each resin form were used and the D_2O samples passed through at a rate of about 3 ml/min, owing to the extremely small salt concentration in the heavy water, which is continuously demineralized in the external reactor system.

The measurements started 30 min after the end of irradiation. $^{187}_{74}W$ was found only on the chloride form and $^{56}_{25}Mn$ on the hydroxide form, just as in steel analysis. $^{64}_{29}Cu$ had been quantitatively retained on the citrate form. The cation exchanger, ending the series, showed only a clean $^{24}_{11}Na$ spectrum. The eluate was inactive. Although in all cases the separation of various elements seemed to be quantitative, this is difficult to state definitely, due to the very small amounts of activities present in a sample. However, there is reason to believe that the separation method described may be of some value for the continuous control of individual- or groups of water corrosion products in a nuclear reactor, and for material testing experiments.

CONCLUSIONS

From the practical examples given, in addition to a lot of other cases, it appears that the present group separation method used in connection with gamma spectrometry, is very helpful for the identification and quantitative determination of many elements. Because of the simplicity of the method, and also its rapidity it has been adopted as a routine procedure in this laboratory. However, it may also exist many possibilities to prepare the anion exchange resin in other forms, *e.g.* sulphide, sulphate, carbonate, fluoride *etc.* to allow more advantageous separations in many practical cases.

REFERENCES

1. Bell, P. and Cassidy, J. *Phys. Rev.* **79** (1950) 173.
2. Connally, R. E. and Leboeuf, M. B. *Anal. Chem.* **25** (1953) 1095.
3. Salmon, L. *A. E. R. E.*, C/M 206 (1954).
4. Samuelson, O. *Ion Exchangers in Analytical Chemistry*, Almqvist and Wiksell AB, Stockholm 1952.
5. Glueckauf, E. and Roberts, P.J.P. *A.E.R.E.*, C/R 1443 (1955).

Received March 27, 1958.

ACTA CHEMICA SCANDINAVICA 12 (1958) 1297—1304

The Structure of Hexagonal Mercury(II)oxide

KARIN AURIVILLIUS and INGA-BRITT CARLSSON

Institute of Inorganic and Physical Chemistry, University of Stockholm, Stockholm, Sweden; Joint Establishment for Nuclear Energy Research, Kjeller, Norway

The crystal structure of hexagonal mercury(II)oxide has been determined by means of X-ray and neutron diffraction methods. The symmetry is $P3_121$ (No. 152) or the enantiomorphous symmetry $P3_221$ (No. 154). The structure is built up of infinite spiral chains $(-O-Hg-)_n$ running parallel to the c axis of the hexagonal unit cell. Within the chains, the Hg-O distance is 2.03 ± 0.02 Å and the angles O—Hg—O and Hg—O—Hg are 176° ± 3° and 108° ± 2°, respectively. The structure is analogous to that of hexagonal mercury (II) sulphide (cinnabar).

In addition to the well-known orthorhombic modification of mercury(II) oxide, the structure of which was reported in a previous article [1], another form of hexagonal symmetry was recently described by Laruelle [2]. The crystal structure of the latter has now been determined by means of X-ray and neutron diffraction methods.

PREPARATION AND ANALYSIS

The hexagonal modification of mercury(II)oxide was synthesized according to Laruelle[2] by adding sodium hydroxide to a solution of K_2HgI_4, containing an excess of KI. The experimental conditions, such as concentrations and temperature, were varied within wide limits. The best method for preparing a pure sample of hexagonal mercury(II) oxide was to mix one part of 0.1 M K_2HgI_4, containing an excess of 0.025 M KI, with two parts of 5.5 M NaOH or KOH at about 50°C and to keep the solution at this temperature for about 100 h. The purity of the sample was checked by means of X-ray powder photographs. Identical preparations were also obtained by substituting rubidium or caesium for the potassium or sodium ions. It was, however, not possible to prepare hexagonal HgO from a solution of Li_2HgI_4, LiI and LiOH, probably because of the relatively low solubility of LiOH. The hexagonal modification mostly crystallized in spherical conglomerates of extremely small red crystals but sometimes it sedimented as a yellow powder. The preparations were not always pure but were sometimes mixed with orthorhombic mercury(II)oxide or with other phases probably containing alkali. Occasionally, red transparent plates appeared. They were always found to be built up of both hexagonal and orthorhombic mercury(II)oxide.

The pure sample described above was analysed for Hg, Na, K, I and H_2O and was found to contain neither alkali, iodine nor water. The result of the mercury analysis performed using electrolysis was 92.1 % in fair agreement with the value of 92.6 % calculated for HgO.

CELL DIMENSIONS AND SYMMETRY

The powder photographs were taken in a Guinier focussing camera of 80 mm diameter using monochromatic Cu$K\alpha_1$ radiation and potassium chloride (a = 6.2930 Å) [3] as an internal standard. The powder pattern is given in Table 1. Amply exposed photographs (3 h) did not show any lines that were

Table 1. Powder photograph of HgO. Cu$K\alpha_1$ radiation.

hkl	$\sin^2\Theta_{obs}$	$\sin^2\Theta_{calc}$	I_{obs}
100	0.0618	0.0618	m
101	0.0697	0.0697	vst
003	0.0708	0.0709	m+
102	0.0934	0.0933	vst
103	0.1327	0.1327	w
110	0.1854	0.1855	m
104	0.1879	0.1878	m
111	0.1932	0.1934	m
112	0.2169	0.2170	w
200	0.2475	0.2473	vvw
201	0.2564	0.2552	st
113		0.2563	
105	0.2588	0.2587	m
202	0.2788	0.2788	m
006	0.2833	0.2834	w
114	0.3115	0.3115	vw
203	0.3181	0.3182	vw
106	0.3454	0.3453	vvw
204	0.3733	0.3733	w
115	0.3823	0.3823	vw
210	0.4330	0.4328	w+
211	0.4408	0.4407	vw
205	0.4441	0.4441	vw

not visible in normally exposed ones (1 h). The powder pattern could be interpreted by means of a hexagonal unit cell with the cell dimensions:

$$a = 3.577 \text{ Å} \qquad c = 8.681 \text{ Å} \qquad V = 96.2 \text{ Å}^3$$

The observed density 11.0 indicates a cell content of 3 formula units of HgO (calculated density 11.2).

The only crystals that were large enough for single crystal studies with the equipment available were obtained from samples containing both forms of the oxide. Several crystals were investigated and found to be composed of individuals of both modifications. However, a Weissenberg photograph was finally taken, registering both the reflexions $h0l$ of hexagonal HgO and $hk0$ of orthorhombic HgO.

The only systematic extinction found in the powder and Weissenberg diagrams of hexagonal HgO was $00l$ absent for $l \neq 3n$, which is characteristic of the space groups $P3_112$ (No. 151), $P3_121$ (No. 152), $P3_212$ (No. 153) and $P3_221$ (No. 154). Because the unit cell contains 3 formula units of HgO, both the mercury and oxygen atoms must occupy threefold point positions 3(a) and/or 3(b). Since the (a) and (b) point positions only differ with respect

Table 2. Observed X-ray intensities *hkl* from the powder sample of HgO examined with a Geiger-Mueller diffractometer. The intensities are calculated: I) for the mercury atoms only, neglecting the influence of the oxygen atoms; II) for both the mercury and oxygen atoms. In each case, I_{calc} was normalized so as to give the best agreement with I_{obs}. A correction factor for each reflexion was taken from a curve where log I_{obs}/I_{calc} was plotted against $\sin^2\Theta$.

hkl	I_{obs}	$(I_{calc})_I$	$(I_{calc})_{II}$	*hkl*	I_{obs}	$(I_{calc})_I$	$(I_{calc})_{II}$
100	29	41	33	106 $10\bar{6}$	3	4	3
101 $10\bar{1}$ 003	395	350	376	204 $20\bar{4}$ 115	14	21	20
102 $10\bar{2}$	157	202	204	210 211 $21\bar{1}$			
103 $10\bar{3}$	25	25	28	205 $20\bar{5}$	58	43	42
110 104 $10\bar{4}$	127	131	129	107 $10\bar{7}$			
111 112	13	21	18	212 $21\bar{2}$ 116	18	21	19
200 201 $20\bar{1}$ 113 105 $10\bar{5}$	110	114	106	213 300 214 $21\bar{4}$ 301 $30\bar{1}$	15 31	18 23	16 21
202 $20\bar{2}$ 006	57	37	36	108 $10\bar{8}$ 117			
114 203 $20\bar{3}$	15	15	15				

to the choice of origin, 3(*a*) was arbitrarily chosen as the site of the mercury atoms. For these point positions, the two groups with enantiomorphous symmetry ($P3_121$ and $P3_221$) and ($P3_112$ and $P3_212$) differ with respect to the structure amplitudes of the reflexions *h*0*l* and *h*0$\bar{l}$, which are different for the former but assume identical values for the latter space-groups. Actually the intensities I_{h0l} differed from $I_{h0\bar{l}}$, as judged from the Weissenberg diagram, which suggested the symmetry to be $P3_121$ (or $P3_221$) in accordance with the data given by Laruelle [2]. Due to the composite character of the crystal, which was likely to give rise to serious absorption effects, this observation could not be considered conclusive. By means of neutron diffraction data (*v. infra*), however, it was possible to confirm the symmetry.

THE POSITIONS OF THE MERCURY ATOMS

Accurate values for the intensities of the X-ray powder reflexions were obtained by means of a Hilger Y 115 G.M. diffractometer, using Cu$K\alpha$ radiation. The sample was carefully ground and mounted in a cavity in an aluminium holder and the specimen was adjusted to the reflexion position. The intensities of the diffraction peaks were measured at counter intervals of 1°/60 scattering angle. The observed intensities obtained by measuring the areas under the peaks are given in Table 2. For overlapping reflexions, the sum of the intensities is given.

In the following the structure will be discussed in terms of the symmetry $P3_121$. The parameter value x for the mercury atoms in 3(a) was derived by trial and error, the best accordance between calculated and observed intensities being obtained for $x = 0.745$ (*cf.* Table 2).

THE POSITIONS OF THE OXYGEN ATOMS

The difference between mercury and oxygen in their scattering power for X-rays is considerable and this made it impossible to locate the latter from the observed intensity data. The relative scattering powers of the two elements for neutrons are much more favourable.

	Scattering amplitude[4] *(10^{-12} cm)*	
	Neutron	X-ray ($\Theta = 0°$)
Hg	1.31	22.5
O	0.58	2.25

The amplitude values for neutrons are independent of the scattering angle, while those for X-rays decrease with Θ and relatively more so for oxygen than for mercury.

The neutron diffraction work was carried out on a powder sample in a flat aluminium container. The reactor was run at a level of 450 kW. The diffracted intensity was measured at intervals of 0.2° scattering angle, counts being taken during the time necessary for accumulating 200 000 neutron counts from the monitor in the incident monochromator neutron beam. The appearance of the curve obtained by plotting the counts against the angles is given in Fig. 1. The observed intensities, obtained by measuring the areas under the peaks with a planimeter and corrected for the small contribution of the intensities of the aluminium reflexions 111 and 200 from the container, are given in Table 3. Due to serious overlapping, the intensities of reflexions at higher Θ angles could not be evaluated.

From space considerations, it was found that both mercury and oxygen atoms cannot occupy the same point position (3(a)) since this would give mercury-oxygen distances shorter than $a/2 \sim 1.8$ Å. The only point position left for the oxygen atoms is thus 3(b). Systematic variation of the parameter for the oxygen atom position gave the best agreement between observed and calculated intensities when x_o was equal to 0.46 (Table 3). The neutron intensities of the reflexions were calculated according to Bacon[4], the temperature factor, however, being neglected. (The R index for the data given in Table 3 was found to be 0.7 %. This means, of course, that the agreement is good

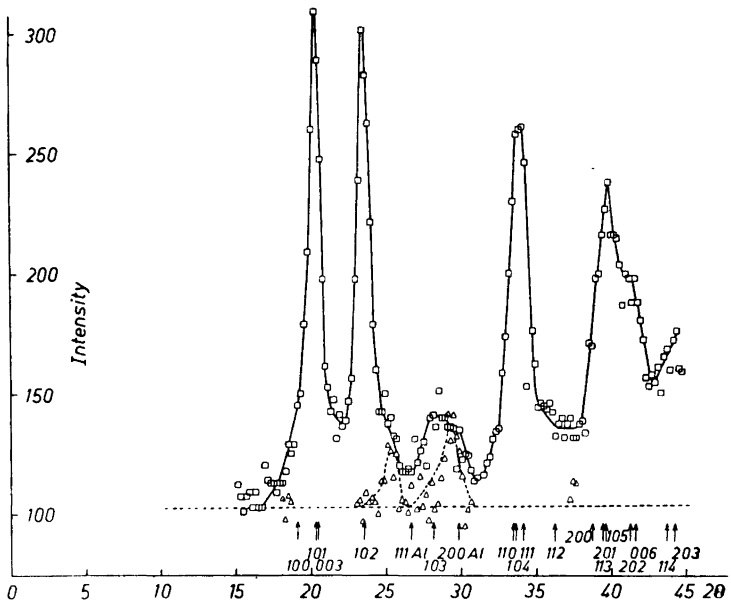

Fig. 1. Neutron diffraction powder diagram of a sample of hexagonal mercury(II) oxide in an aluminium container.

Table 3. Observed neutron intensities from a powdered sample of HgO in a flat aluminium container. The reflexions 102 and 103 are corrected for the small contributions of the aluminium reflexions 111 and 200. The calculations are made according to Bacon [4]. No correction was made for thermal vibrations. The value μt was found by measurement to be 1.23. The intensities are calculated: I) for the mercury atoms only, neglecting the influence of the oxygen atoms; II) for both the mercury and oxygen atoms. In each case I_{calc} was normalized so as to give the best agreement with I_{obs}.

hkl	I_{obs}	$(I_{calc})_I$	$(I_{calc})_{II}$
100			
101	324	497	321
$10\bar{1}$			
003			
102	331	251	334
$10\bar{2}$			
103	74	39	73
$10\bar{3}$			
110			
104			
$10\bar{4}$	375	318	374
111			
112			

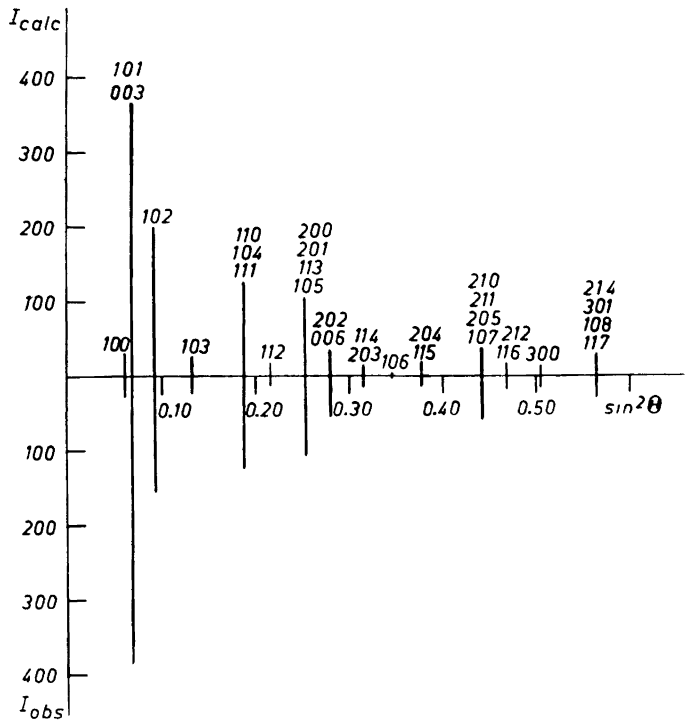

Fig. 2. Comparison between observed and calculated X-ray intensities of the reflexions *hkl* registered in a powder diffractogram of hexagonal mercury(II) oxide.

but the small number of reflexions implies that the R index is lacking in statistical significance.)

The X-ray intensities of the reflexions *hkl* were now recalculated, the influence of the oxygen atoms being also taken into account (*cf.* Table 2 and Fig. 2). In this way the agreement between calculated and observed intensities was improved. (The R index for the data given in Table 2 was thus found to decrease from 16.3 % to 13.0 %.)

DESCRIPTION OF THE STRUCTURE

The following structure for the hexagonal modification of mercury(II) oxide has been arrived at:

Cell content: 3 HgO.
Symmetry: $P3_121$, No. 152 or $P3_221$, No. 154.
Space-group $P3_121$; 3 Hg in 3(*a*): $x0\frac{1}{3}$; $0x\frac{2}{3}$; $\bar{x}\bar{x}0$ $\quad x = 0.745$
3 O in 3(*b*): $x0\frac{5}{6}$; $0x\frac{1}{6}$; $\bar{x}\bar{x}\frac{1}{2}$ $\quad x = 0.46$

The structure is built up of infinite spiral chains, $(—O—Hg—)_n$, running parallel to the c axis of the hexagonal unit cell (*cf.* Figs. 3 and 4).

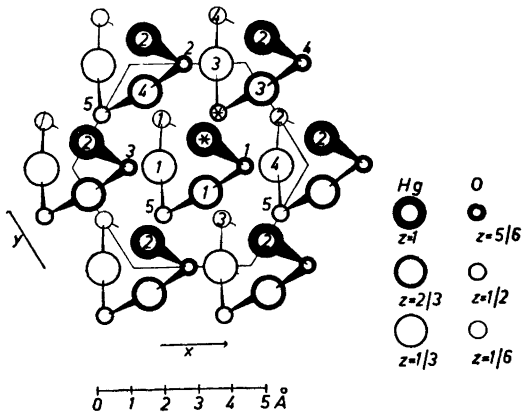

Fig. 3. Projection parallel to [00*l*] of the structure of hexagonal mercury(II) oxide. The diagram shows the coordination of the atoms. The large circles indicate mercury atoms and the smaller ones oxygen atoms.

Every mercury atom (*e.g.* Hg *, $(\bar{x}\bar{x}0)$ in Fig. 3) is surrounded by:

2	O	(1)	at 2.03 ± 0.02 Å
2	O	(2)	2.79 ± 0.02 Å
2	O	(3)	2.90 ± 0.03 Å
2	Hg	(1)	3.30 ± 0.02 Å
6	Hg	(2)	3.58 Å = a
4	Hg	(3,4)	3.72 ± 0.02 Å

The oxygen atoms around each mercury form a greatly distorted octahedron.
Every oxygen atom (*e.g.* O *, $(\bar{x}\bar{x}\frac{1}{2})$ in Fig. 3) is surrounded by:

2	Hg	(3)	at 2.03 ± 0.02 Å
2	Hg	(4)	2.79 ± 0.02 Å
2	Hg	(1)	2.90 ± 0.02 Å
2	O	(4)	4.06 ± 0.04 Å
6	O	(5)	3.58 Å = a
4	O	(1,2)	3.41 ± 0.02 Å

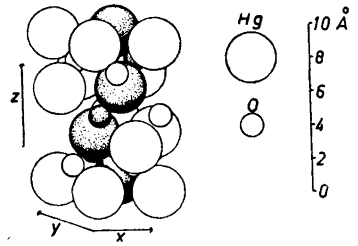

Fig. 4. Diagram showing the spiral chain $(-Hg-O-)_n$ which extends parallel to the *c* axis of hexagonal mercury(II)oxide.

The angles within the chains are:

Hg — O — Hg	108° ± 2°
O — Hg — O	176° ± 3°

The Hg—O distance found within the chain and the bond angles are nearly the same as those found in the planar zig-zag chain of orthorhombic mercury(II) oxide [1]. Thus, for the hexagonal modification, it can also be suggested that the bond between the Hg and O atoms within the chain is mainly homopolar. The forces between the chains are far weaker since the interatomic distances are considerably larger than those within the chains. It is probable that the chains support each other by means of these Hg—O contacts.

A comparison between the structures of hexagonal mercury(II)oxide and hexagonal mercury(II)sulphide (cinnabar [5]) indicates that these compounds are isostructural.

These studies form part of a research program on metal oxides and fluorides financially supported by the *Swedish Natural Science Research Council.*

The authors wish to thank Professor A. Ölander for his kind interest in this work. The authors are also much indebted to Dr. A. Magnéli for very valuable discussions. Thanks are also due to Dr. J. A. Goedkoop, head of the Neutron Physics Department of the *Joint Establishment for Nuclear Energy Research*, Kjeller, Norway, for his kind hospitality and for very valuable help in the neutron diffraction work. The Hilger Y 115 G.M. diffractometer was kindly placed at our disposal by Messrs. Bergman and Beving AB, Stockholm.

REFERENCES

1. Aurivillius, K. *Acta Chem. Scand.* **10** (1956) 852.
2. Laruelle, M. P. *Compt. rend.* **241** (1955) 802.
3. Hambling, P. G. *Acta Cryst.* **6** (1953) 98.
4. Bacon, G. E. *Neutron Diffraction*, Oxford 1955.
5. Aurivillius, K. *Acta Chem. Scand.* **4** (1950) 1413.

Received April 21, 1958.

ACTA CHEMICA SCANDINAVICA 12 (1958) 1305—1311

The Ionization Constant, Solubility Product and Solubility of Lauric and Myristic Acid

VERA NYRÉN and ERNST BACK

Paper Technology Department, Swedish Forest Products Research Laboratory, Stockholm, Sweden

The ionization constant (K_S), solubility product (K_L) and solubility of lauric and myristic acid at 20°C have been determined simultaneously from potentiometric titrations of their aqueous sodium salt solutions according to the method of Back and Steenberg. Measurements were carried out at soap anion concentrations ranging from below the concentration of limited ion association to above the critical concentration for micelle formation. The data obtained support the conception of Ekwall that limited soap anion association starts at a well defined concentration.

Below this concentration of limited ion association the following electrolytic constants were obtained. For lauric acid: $pK_S = 5.3$; $pK_L = 10.0$, and L, the solubility of unionized acid, $= 2.3 \times 10^{-5}$ moles/litre. For myristic acid: $pK_S \leq 6.3$; $pK_L = 11.5$, and $L \leq 0.6 \times 10^{-5}$ moles/litre.

Data published on the ionization constant and the solubility in water of higher fatty acids are scarce and of insufficient mutual agreement. This is due to experimental difficulties arising in consequence of both the low solubility of these acids and the low concentration at which their anions start to associate.

Ionization constants of fatty acids have been obtained by extrapolation from lower, more soluble homologues [1,2], by recalculation of pH measurements in water-ethanole mixtures [3,4] and by pH measurements in dilute solutions of neutral sodium salts [5]. In a recent review Ekwall [6], referring to unpublished measurements, has indicated the apparent change in the ionization constant of lauric acid with soap concentration due to ion association and thereupon following micelle formation. Reported solubilities of fatty acids have been determined using conductivity measurements [7] or conductometric titration [8,9] of fatty acids in saturated water solutions.

Here the method of Back and Steenberg [10] for simultaneous determination of both the ionization constant, the solubility product and the solubility of the unionized protolyte by single potentiometric titrations has been used. Measurements were carried out with sodium laurate and sodium myristate

solutions at concentrations ranging from above the critical concentration for micelle formation (CMC) to below the concentration of limited ion association (LAC).

EXPERIMENTAL

Purissimum Lauric acid (of St. Just) with a melting point of 42.4°C and myristic acid (of Eastman Kodak) with a melting point of 52.5°C have been used. Sodium salt solutions were prepared by dissolving the acid under nitrogene atmosphere in 0.1 N sodium hydroxide, added in an excess of about 3–5 %. Distilled water and sodium hydroxide solutions had been freed from carbon dioxide by passing a weak anion exchange resin column. After dilution the soap solutions were titrated with 0.02 and 0.002 N hydrochloric acid under nitrogene atmosphere using a magnetic stirrer and a low alkaline error glass electrode, a saturated calomel electrode and a vacuum tube voltmeter. The pH meter was calibrated at pH values 4.00, 6.88 and 9.22 using freshly prepared standard buffers of respectively, potassium hydrogene phtalate [11], an equimolar mixture of monopotassium phosphate- and disodium phosphate [12] and sodium tetraborate [13]. All titrations were carried forward beyond the second equivalence point. To prevent interference of carbon dioxide, the soap solutions prepared had to be transferred rapidly into the titration vessel. Thus, it was decided to determine the total amount of sodium soap titrated from the two equivalence points of the titration curve. These equivalence points were determined using the method of Gran [14]. At checking points during the titration, at which a fresh liquid junction was desirable at the saturated potassium chloride and the soap solution interface, the calomel electrode was removed before releasing some potassium chloride. Measurements were performed at 20° ± 1°C.

Activity coefficients of soap anions were estimated according to the simplified Debye-Hückel equation, and were used in the calculation of ionization constants and solubility products. For calculation of the ionization constant only titration points down to a pH value corresponding to the solubility limit of unionized acid were employed. A few titration points close to the equivalence point also were disregarded because of the very low buffering capacity at these points. Yet within a single titration there appeared a slight downward trend in the ionization constants calculated, when carrying forward the titration with hydrochloric acid. Thus in Figs. 1 and 2 most titrations are represented by a line connecting the lowest and highest value of the ionization constant calculated.

At very low soap concentrations the accuracy of the titration method naturally falls off. Thus only soap solutions exceeding 0.0004 M were employed. At concentrations considerably exceeding the critical concentration for micelle formation, the equilibrium pH was reached extremely slowly, thus lowering the accuracy of the results.

RESULTS

The ionization constant, K_s, the solubility product, K_L, and the solubility of unionized acid, L, all are calculated according to the method of Back and Steenberg [10] assuming the simple equilibrium conditions

$$K_s = \frac{a_{H_3O^+} \cdot a_{A^-}}{a_{HA}} \tag{1}$$

and

$$K_L = a_{H_3O^+} \cdot a_{A^-} \tag{2}$$

to be valid. The fatty acid anion activity $a_{A^-} = f_{A^-}\, c_{A^-}$ is calculated from the total concentration, c_a, of titrand HA and A^- and from the concentration of titrator added in excess of the neutralization point, c_s, according to

$$c_{A^-} = c_a + c_{H_3O^+} - c_s - c_{OH^-} \tag{3}$$

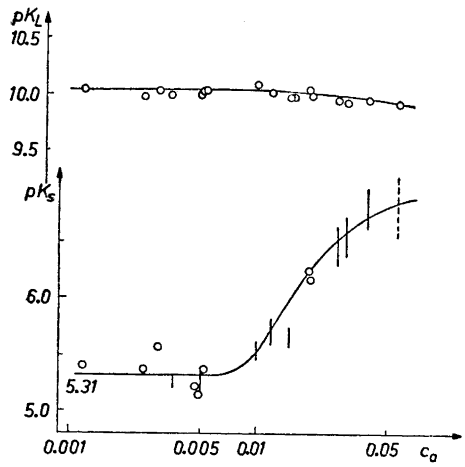

Fig. 1. pK_s and pK_L of lauric acid at 20°C *versus* the total titrand (soap) concentration c_a in moles/litre at the neutralization point.

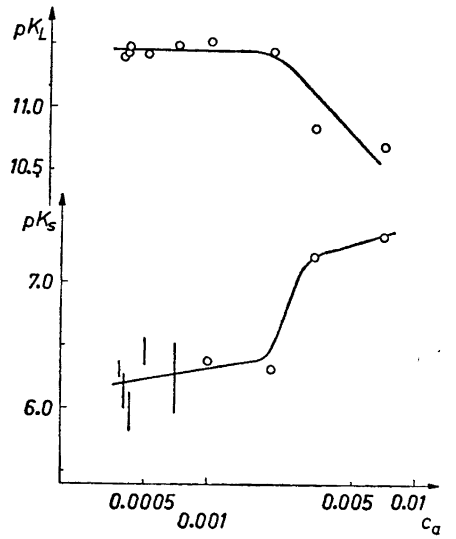

Fig. 2. pK_s and pK_L of myristic acid at 20°C *versus* the total titrand (soap) concentration c_a in moles/litre at the neutralization point.

Correspondingly c_{HA} is obtained as

$$c_{HA} = c_s + c_{OH^-} - c_{H_3O^+} \quad (4)$$

If due to formation of micelles or associated ions eqns. (3) and (4) or eqn. (2) are not valid, the constants calculated naturally represent pseudoconstants only.

Ionization constants. The lower part of Figs. 1 and 2 presents the pK_s values *versus* the total titrand concentration c_a at the neutralization point, using a logarithmic scale.

A general agreement exists between these results for fatty acids and those of Ekwall, Rosendal and Löfman for bile acids [15] as well as the preliminary data of Ekwall for lauric acid [6]. As obvious from the data in Fig. 1 for lauric acid, the pK_s values are independent of the total titrand concentration at the neutralization point as long as this concentration is low enough. The slight upward trend in pK_s within a single titration, which might indicate complex formation between fatty acid anion, and unionized fatty acid here also appears negligible. It seems justifiable to consider the corresponding pK_s value of 5.3 as given in Table 1 with its 90 % confidence range, as the true ionization constant for lauric acid. For myristic acid it was not possible to perform reliable potentiometric titrations at concentrations low enough to finally secure this true ionization constant. Only a lower limit for the ionization constant, *i.e.* $pK_s \leq 6.3$, appears from the measurements.

At an intermediate concentration range, within which Ekwall and coworkers by the use of several other methods have demonstrated a limited association

Table 1. Ionization constants of some fatty acids in water.

Fatty Acid	Temp. °C	pK_s with 90 % confidence range	Method
Lauric	20°	5.31 ± 0.08	pH measurements, titration in
Myristic	20°	≤ 6.3	water, (this work)
Lauric	20°	4.9—5.0	(3) pH measurements
Myristic	20°	4.9—5.0	(3) in
Palmitic	25°	5.06	(4) water-ethanol
Oleic	25°	5.02	(4) mixture
Lauric	25°	4.8	(5) pH measurements in sodium
Myristic	25°	5.7	soap water solutions
Lauric	20°	5.5	(6) measurements in water *
Lauric	25°	4.82	(2) extrapolated from lower homologues

* extrapolated from data presented.

of laurate ions [16,17,18], the pKs values calculated increase with total titrand concentration, again levelling off to constant values at the critical concentration for micelle formation. This change in the apparent ionization constants is to be interpreted as a decrease in activity a_{HA} of unionized acid due to complex formation and provides another indication of beginning ion association.

At higher concentrations the corresponding pseudoconstant again shows up as mainly concentration independant, indicating the size of the micelles to be essentially constant.

Table 1 gives a comparison between the true pK_s values obtained here and those obtained by other methods. Obviously the direct method as used in this work gives higher pK_s values, *i.e.* lower ionization constants, than an extrapolation from lower fatty acid homologues or a recalculation from titrations in water-ethanol mixtures.

Solubility products. When the potentiometric titration of the soap solution is carried forward at low titrand concentrations, the free fatty acid is precipitated and coagulated near the neutralization point, as expected. If ion association would not occur this precipitation point should move towards the neutralization point at higher titrand concentrations. But obviously this is not the case. Fig. 3 shows a titration starting with a total titrand concentration at the neutralization point of 0.019 moles/litre. When adding hydrochloric acid after this point, the solution slowly turns slightly turbid. Yet precipitation does not occur until late in the titration curve, in connection with a pronounced discontinuity in this curve. The upper part of Fig. 3 presents the solubility product calculated assuming eqns. (2) and (3) to be valid all over the titration curve. Obviously only after the precipitation point has been reached, a constant pK_L-value occurs, indicating a solubility product to be valid within the later part of the titration curve. This means that a solid phase of unionized acid here seems to exist, while in the earlier part of the titration curve unionized

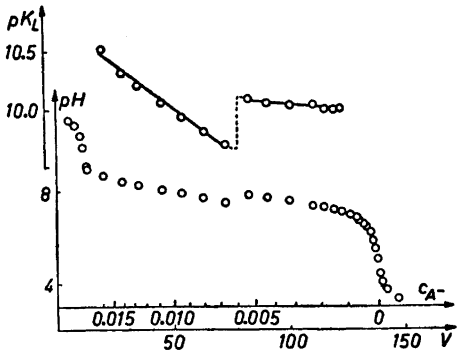

Fig. 3. Titration curve for a 0.019 M sodium laurate solution and the corresponding pK_L values calculated. Abscissa expressed in V ml 0.0216 N HCl added in excess of the neutralization point as well as in overall concentration of untitrated laurate anions, c_{A^-}, in moles/litre.

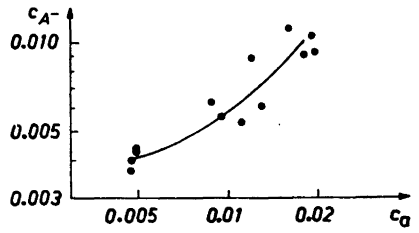

Fig. 4. Overall concentration c_{A^-} of laurate anion at the titration curve discontinuity point, *versus* the corresponding total titrand concentration, c_a, both in moles/litre.

fatty acid is associated to fatty acid anions and thus held in solution. When checking these results by a retitration from the acid to the alkaline side, the discontinuity in the titration curve was less obvious but the change in pK_L as shown in Fig. 3 still was apparent.

The upper part of Figs. 1 and 2 presents the solubility product obtained *versus* the total titrand concentration at the neutralization point. It is obvious from these data that a true solubility product exists at low total titrand concentrations, and that this solubility product is valid also above the concentration of limited ion association (LAC) as soon as a solid phase of free acid has formed. The solubility products with their 90 % confidence range thus obtained are:

for lauric acid 9.98 ± 0.03; for myristic acid 11.45 ± 0.01

Ekwall and coworkers have pointed out that within the concentration range of limited ion association unionized fatty acid molecules are associated with fatty acid anions. This is evident also from the data in Fig. 3 typical for this concentration range, showing the precipitation of free fatty acid to be delayed. Further proof is given in Fig. 4 showing that the residual concentration of untitrated fatty acid anions at the point of precipitation is approximately equal to this concentration of limited ion association. The slight upward trend of residual anion concentration with increasing total titrand concentration at the neutralization point indicates that after the precipitation point and the formation of a solid fatty acid phase, residual fatty acid anions still occur to some extent in associated form.

Solubility of unionized fatty acid and total solubility. According to the method af Back and Steenberg [10] the solubility of unionized fatty acid, L, is obtained as the quotient of the solubility product and the corresponding ionization

Table 2. Solubility of some fatty acids in water.

Fatty acid	Temp. °C	Solubility of unionized acid		Total solubility		Reference
		in moles/litre × 10^5	in mg/litre	in moles/litre × 10^5	in mg/litre	
Lauric	20°	2.3	4.6	3.4	6.8	
(90 % confidence range)		1.8 −3.0	3.6 −5.9	2.6 −4.4	5.2−8.8	This Work
Myristic	20°	≤ 0.6	≤ 1.4	≤ 0.8	≤ 1.8	
Lauric	25°	1.19	2.4	2.4	4.8	John and Mc Bain [7]
	50°	3.5	7.0	5.5	11.0	
	40°	—	—	3.9	7.8	Eggenberger *et al.*[8]
	50°	—	—	4.6	9.2	
Myristic	25°	0.09−0.11	0.21−0.25	0.42−0.51	1.0−1.2	John and Mc Bain [7]
	50°	0.34	0.78	0.97	2.2	
	50°	—	—	1.84	4.2	Eggenberger *et al.*[8]

constant. Table 2 gives the data thus obtained together with their 90 % confidence limits. Also given are the total solubilities of these fatty acids in a saturated water solution, *i.e.* the total solubilities at the acid equivalence point, at which $a_{H_3O^+} = a_{A^-}$. For comparison other published data also are given. The total solubilities established in this work are lower than those of Eggenberger *et al.* [8] obtained by conductometric titration of with fatty acid saturated water solutions when rechecking earlier data of their own.

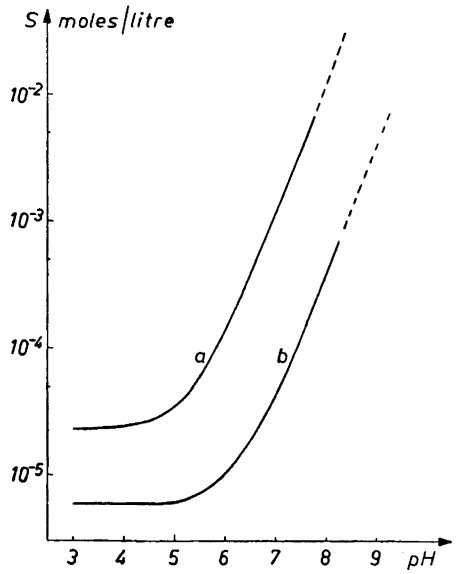

Fig. 5. Total solubility, *S*, in moles/litre as a function of pH, for a) lauric acid, b) myristic acid.

On the other hand our data are in reasonable agreement with those of John and Mc Bain [7], obtained from conductivity measurements using earlier data on the equivalence conductance of soap ions and selecting as the ionization constant for these fatty acids, the one of acetic acid.

To give a complete picture of the solubility of these fatty acids, Fig. 5 shows our values for the total solubility as a function of the pH, (adding the solubility of unionized acid to that of the fatty acid anion determined by the solubility product). Naturally, this solubility product is valid only as long as the fatty acid anion concentration does not exceed the LAC. After the LAC is reached the total solubility increases more rapidly due to solubilization of fatty acid by fatty acid anions. The dotted lines in Fig. 5 within this later region thus present a minimum total solubility only. Naturally, in mixtures of fatty acid the total solubility as calculated for each fatty acid separately, will be exceeded when mixed associate soap anions or mixed micelles begin to form.

Acknowledgement. Financial support of this work by *Stiftelsen Pappersbrukens Forskningsinstitut (The Research Foundation of the Swedish Paper Mills)* is gratefully acknowledged.

REFERENCES

1. Dippy, J. F. J. *Chem. Rev.* **25** (1939) 151.
2. Gregory, N. W. and Tartar, H. V. *J. Am. Chem. Soc.* **70** (1948) 1992.
3. Jukes, T. H. and Schmidt, C. L. A. *J. Biol. Chem.* **110** (1935) 9.
4. White, J. R. *J. Am. Chem. Soc.* **72** (1950) 1859.
5. Stainsby, G. and Alexander, A. E. *Trans. Faraday Soc.* **45** (1949) 585.
6. Ekvall, P. *J. Colloid Sci. Suppl.* **1** (1954) 66.
7. John, L. M. and McBain, J. W. *J. Am. Oil Chemists' Soc.* **25** (1948) 40.
8. Eggenberger, D. N., Broome, F. K., Ralston, A. W. and Harwood, H. J. *J. Org. Chem.* **14** (1949) 1108.
9. Ralston, A. W. and Hoerr, C. W. *J. Org. Chem.* **7** (1942) 546.
10. Back, E. and Steenberg, B. *Acta Chem. Scand.* **4** (1950) 810.
11. Manov, G. G. *Am. Soc. Testing Materials Tech. Publ.* **73** (1946) 31 Symp.
12. Manov, G. G. *J. Assoc. Offic. Agr. Chemists* **30** (1947) 500.
13. Manov, G. G., DeLollis, N. J., Lindvall, P. W. and Acree, S. F. *J. Research Natl. Bur. Standards* **36** (1946) 543.
14. Gran, G. *Acta Chem. Scand.* **4** (1950) 559.
15. Ekvall, P., Rosendahl, T. and Löfman, N. *Acta Chem. Scand.* **11** (1957) 590.
16. Ekvall, P. and Harva, O. *Finska Kemistsamfundets Medd.* **1943** 257.
17. Ekvall, P. *Nord. Kemistmötet, Berättelse och Föredrag. 6th Meeting,* Lund **1947**, p. 179.
18. Ekvall, P. and Danielsson, I. *Acta Chem. Scand.* **5** (1951) 973.

Received February 20, 1958.

ACTA CHEMICA SCANDINAVICA 12 (1958) 1312—1318

Die Isolierung von Meerrettichperoxydase

K. G. PAUL

Medicinska Nobelinstitutet, Biokemiska avdelningen, Stockholm, Schweden

Eine vereinfachte Methode zur Isolierung von Meerrettichperoxydase wird beschrieben. Die Ausbeute an Aktivität, mit der Mesidinmethode gemessen, ist höher als 40 % des Rohauszuges. Durch Chromatographie auf Karboxymethylzellulose kann das Enzym in vier Komponenten aufgetrennt werden.

Meerrettichperoxydase (MRP) interessiert als Häminproteid und ist auch ein praktisch verwendbares Mittel für gewisse Oxydationen. Sie wird ebenfalls als zuverlässige Vergleichsubstanz benutzt, wenn man vor der Frage steht, ob ein beobachteter Stoffwechselvorgang möglicherweise durch Peroxydase katalysiert werden kann. In diesen Fällen und für die Aufklärung des Peroxydasemechanismus ist es notwendig, reinste Enzympräparate zu verwenden. So fanden z.B. Paul und Avi-Dor [1] in Versuchen über Harnsäureoxydation, dass Allantoin nicht nachzuweisen war, wenn MRP, die etwa 1 % Hämin enthielt, verwendet wurde. Der Nachweis gelang nur mit der kristallisierten Peroxydase mit 1.26 % Hämin.

MRP wurde zum erstenmal von Theorell [2] kristallisiert. Diese Methode ist jedoch etwas mühsam, und verschiedene Autoren [3-5] haben andere Darstellungsverfahren angegeben, die vom Verfasser nachgeprüft wurden. Die Ergebnisse gehen aus dem folgenden hervor.

METHODEN UND MATERIALIEN

Die Aktivitätsbestimmungen wurden nach der Mesidinmethode [6] ausgeführt. Die unten in Molen angegebenen Peroxydasemengen sind also auf ältere Aktivitätsbestimmungen mit "reinen" Präparaten bezogen. Die Guajacolmethode [7] wurde ebenfalls versucht, erwies sich aber in den ersten Stufen der Reinigung ebensowenig zuverlässig wie die Purpurogallinmethode — Ausbeuten über 100 % kamen vor. Mit steigender Reinheit der Peroxydase normalisierten sich die Ausbeuten. Man sieht bei den Aktivitätsbestimmungen an Rohauszügen, dass die zunächst auftretende Farbe bald verschwindet; dies kann nicht die Folge einer Peroxydasehemmung sein, offenbar findet auch eine Entfärbung des Oxydationsproduktes durch die Verunreinigungen in den Rohauszugen statt.

Bei den Häminbestimmungen [8] wurde der Wert $\beta = 8{,}0 \times 10^7$ cm^2 × Mole^{-1} für den molaren Absorptionskoeffizienten des α-Bandes des Pyridinhämochromogens benutzt *.

* $\beta = \frac{1}{c} \times \frac{1}{d} \times \ln \frac{I_0}{I}$ wo c = Konzentration in Molen pro cm^3, d = Schichtdicke der Küvette in cm.

Stickstoff wurde nach Kjeldahl bestimmt. Zur Bestimmung des Trockengewichts wurde 6 Std auf 105° und zur Aschenbestimmung 1 Std auf 500°C erhitzt.

Das Verhältnis Q zwischen den Extinktionen bei 403 mμ (Maximum der Häminbande) und etwa 280 mμ (Maximum der Eiweissbande) wurde ebenfalls bestimmt. Die zu untersuchende Lösung wurde, wenn nötig, mit 0,1 M Phosphatpuffer von pH 7 verdünnt.

ARBEITSGANG

1. Extraktion und erste Ammoniumsulfatfällung

Fein zerteilter Meerrettich (26,2 kg) wurde zweimal mit 39,3 und einmal mit 19,7 l destilliertem Wasser, jedesmal wenigstens vier Stunden unter gelegentlichem Umrühren oder über Nacht, bei Zimmertemperature extrahiert. Die Extrakte wurden vom Rückstand mittels Gaze getrennt und ohne weitere Behandlung bis auf etwa das halbe Volumen in Vacuum eingeengt. Der scharfe Meerrettichgeruch verschwand dabei. Der Extrakt wurde in Glaszylindern im Kältezimmer einige Stunden oder über Nacht stehengelassen. Die Flüssigkeit, die noch trübe, aber von grossen Partikeln frei war, wurde abgehebert, der Bodensatz mit etwas Wasser ausgewaschen und zentrifugiert. Die vereinigten Lösungen wurden mit Ammoniumsulfat auf 40 %-ige Sättigung gebracht (230 g Ammoniumsulfat pro Liter Flüssigkeit, +4°C). Der Niederschlag, der nur wenig Aktivität enthielt, wurde abzentrifugiert und ohne erneute Extraktion verworfen. Das Gesamtvolumen des nicht ganz klaren Extraktes war dann 39,6 l. Nach der Aktivitätsbestimmung enthielt es 30,0 μMole MRP.

Die Beobachtung [3,9], dass die Menge einer mit Wasser extrahierbaren Substanz, wahrscheinlich von Kohlenhydratnatur, mit der Jahreszeit schwankt, wurde bestätigt; die Schwierigkeiten, die mit der Aufarbeitung von herbstgeernteten Wurzeln verknüpft sind, wurden jedoch durch die zweistufige Ammoniumsulfatbehandlung (2. Stufe, siehe unten) beseitigt. Bei unmittelbarer Sättigung des Rohextraktes mit Ammoniumsulfat fällt zwar MRP aus, die Trennung des Niederschlags und der Mutterlauge ist aber schwierig, was auch bei den früheren Methoden anscheinend der Fall war.

Die Behandlung des Rohextraktes mit Alkohol-Chloroform [4] wurde zweimal versucht. Es wurden keine Verluste beobachtet (Ausbeute 98 und 104 %, Mesidinmethode), der Reinigungseffekt war aber mässig (1,22 und 1,18). Diese Behandlung wurde daher nicht weiter ausgeführt.

Ein aus praktischen Gründen wichtiger Befund war, dass die Dauer der Extraktion kritisch ist. Bei der kürzeren Extraktionszeit von z.B. dreimal dreissig Minuten ist zwar die Ausbeute an Peroxydaseaktivität fast unverändert, aber der Niederschlag nach dem zweiten Alkoholzusatz (siehe unten) kann nur mit Schwierigkeit in Lösung gebracht werden. Die darauf folgende Ammoniumsulfatfällung gibt einen sehr klebrigen Niederschlag, was auch von Keilin und Hartree [3] gefunden wurde. Die Behandlung mit Dowex-2 bewirkt nur eine unbedeutende Reinigung.

Während der Extraktion färbt sich allmählich der Meerrettichbrei graubraun. Extrakte aus solchen verfärbten Breien sind meistens leicht zu reinigen. Auch wenn ein Kausalitätszusammenhang zwischen der Verfärbung und der Leichtigkeit, mit der der Brei aufzuarbeiten ist, vielleicht nicht besteht, ist doch die "Reife" des Breies Voraussetzung für eine einfache Reindarstellung der Peroxydase.

Es ist zweckmässig, die Wurzeln während 2—4 Tagen in fliessendem Leitungswasser liegen zu lassen. Dadurch wird die Ausbeute erhöht und das Zerkleinern erleichtert. Physiologische Kochsalzlösung [5] als Extraktionsmittel für solche mit Wasser behandelte Wurzeln hat gegenüber dem Wasser keine besonderen Vorteile.

2. Ausfällung mit Ammoniumsulfat

Die 39,6 l MRP-Lösung, die schon an Ammoniumsulfat zu 40 % gesättigt war, wurden mit weiteren 12,0 kg Salz versetzt, wodurch 85 % Sättigung erreicht wurde. Der Niederschlag war leicht abzuzentrifugieren. Die völlig inaktive Mutterlauge wurde verworfen. Der Niederschlag wurde in etwas 0,01 M Phosphatpuffer von pH 7 aufgelöst und im Kältezimmer bis zur Sulfatfreiheit gegen Wasser dialysiert und weiter über Nacht gegen 0,04 M Acetatpuffer (K-Salz) von pH 5. Die MRP-Lösung wurde in der Kälte zentrifugiert und der graue Bodensatz einmal mit Acetatpuffer gewaschen. Die vereinigten Lösungen ergaben 1 210 ml, die 22 μMole MRP enthielten. $Q = 0{,}21$. Trockengewicht 13,3 und Asche 0,3 mg/ml.

Die Dialyse wurde die ganze Zeit über in ziemlich kleinen Glasgefässen mit oft erneuertem Wasser durchgeführt, da rohe Peroxydasepräparate Zellophan angreifen, wodurch die Schläuche zerbrechlich werden. Zur Sicherheit wurde auch bei *jeder* Präparation nach einigen Stunden die Innenflüssigkeit in frische Schläuche übergeführt.

3. Alkoholfällung

Anderthalb Volumen (1,8 l) von 96 %-igem Aethylalkohol von —13°C wurden langsam unter mechanischem Umrühren der eiskalten MRP-Lösung zugesetzt. Der graue Niederschlag wurde in der Kälte abzentrifugiert, in etwas Wasser aufgelöst, mit Alkohol umgefällt und der Niederschlag verworfen. Die vereinigten Lösungen wurden mit 2,5 Volumen kaltem Alkohol (3,2 l) versetzt. Der braune MRP-Niederschlag wurde auf der Zentrifuge gesammelt, in einer minimalen Menge Wasser aufgelöst und gegen Wasser dialysiert. Nach zwei Tagen wurde die Lösung scharf zentrifugiert, der graue Niederschlag mit etwas Wasser gewaschen und verworfen. Das Volumen der MRP-Lösung war dann 147 ml mit einem Trockengewicht von 11.30, Asche 0,50 und Hämin 0,090 mg pro ml. Die Gesamtmenge MRP betrug nach der Aktivitätsmessung 21,0 nach dem Hämingehalt 20,4 μMole. $Q = 1{,}72$. Die Lösung wurde durch Gefriertrockung auf etwa 50 ml konzentriert.

Nach der Alkoholbehandlung wurden Schwankungen im Reinheitsgrad von $Q = 0{,}9-1{,}7$ und im Hämingehalt von 0,53—0,80 % in verschiedenen Präparationen gefunden. Es ist gelegentlich notwendig, einige Tropfen gesättigter KCl-Lösung zuzusetzen, um die Koagulation des Kolloids nach dem zweiten Alkoholzusatz zu beschleunigen.

Die Abtrennung des Niederschlags nach dem zweiten Alkoholzusatz kann bei grossen Mengen von Meerrettich zeitraubend werden. Das folgende Verfahren kann dabei benutzt werden. Die MRP-Lösung, die mit 0,04 M Acetatpuffer von pH 5 im Gleichgewicht steht, wird wie oben beschrieben mit 1,5 Volumen Alkohol versetzt und der Niederschlag abzentrifugiert. MRP in der Mutterlauge wird dann auf Karboxymethylzellulose (siehe unten) adsorbiert, entweder durch Rühren oder in einer Säule. MRP wird mit 0,1 M Acetatpuffer von pH 5 in Abwesenheit von Alkohol eluiert. Die Wahl zwischen dem erstgenannten Verfahren mit vier Volumen Alkohol und der Zellulosemethode wird von den zugänglichen Zentrifugen bestimmt. Der erste Weg wird vom Verfasser empfohlen.

4. Behandlung mit Anionenaustauscher

Vorbehandlung des Ionenaustauschers. Käufliches "Dowex-2, 8—10 % cross linking, 200—400 mesh", wurde mit dem zehnfachen Volumen von etwa molarer Salzsäure bis zum Aufhören der Gasentwicklung (etwa 24 Std) gerührt,

Tabelle 1. Reinigung der Meerrettichperoxydase mit Dowex 2. Für Einzelheiten siehe Text.

Fraktion	Volumen ml	Q	% vom Ansatz nach der Lichtabsorption bei 403 mμ
I 1	22	2,45	41
I 2	42	2,49	46
I 3	7	2,21	10
			97
II 1	26	2,48	78
II 2	19	2,18	15
II 3	12	1,87	2
			95
III 1	32	2,62	4
III 2	35	2,68	78
III 3	19	2,47	14
III 4	23	1,83	4
			100

mehrmals mit Wasser gewaschen, abgenutscht und endlich in 0,05 M Tris HCl-Puffer von pH 8,6 aufgerührt. Das Chromatographierohr wird mit Puffer beschickt, die Austauschersuspension eingegossen und die Säule bis zum pH-Gleichgewicht mit dem Puffer gewaschen.

Dieselbe Säule kann mehrmals benutzt werden, wenn sie mit dem Puffer jedesmal nach der Verwendung bis zur Lichtabsorptionsfreiheit bei 280 mμ gewaschen wird. Es ist jedoch vorzuziehen vor dem Waschen das oberste Zehntel der Säule zu entfernen und die entsprechende Menge frischer Dowex einzufüllen.

Die MRP-Lösung wurde mit dem Tris-Puffer ohne Dialyse auf 147 ml verdünnt und in drei Portionen (I 50, II 50, III 47 ml) durch eine Säule (60 × 2,7 cm) von Dowex-2 mit einer Geschwindigkeit von 22—26 ml pro Stunde filtriert. Fraktionen wurden manuell gesammelt, wenn sich das Eluat braun zu färben begann (Tabelle 1). Die Fraktionen I 1—2, II 1—2 und III 1—3 wurden vereinigt. Das Gesamtvolumen war nach dem Waschen 201 ml mit Q 2,56. Nach der Aktivitätsbestimmung enthielt die Lösung 17,2 μMole MRP.

Die Bedingungen für die Reinigung der Peroxydase mittels Dowex-2 sind nicht kritisch. Der Puffer kann innerhalb der Grenzen 0,02—0,10 M Tris und pH 7,6—8,6 variieren. Die Präparatmenge kann ohne Verschlechterung des Q-Werts hoch gehalten werden (<2 mg pro cm^3 der Säule), ebenso die Durchlaufgeschwindigkeit (<5 ml pro cm^2/Stunde). Bei grösseren Ansätzen oder schnellerem Filtrieren werden zwar die Begleitpigmente zurückgehalten, eine farblose Verunreinigung wird aber nicht entfernt.

5. Ammoniumsulfatfällung

182 ml der obengenannten Lösung wurden mit festem Ammoniumsulfat versetzt (41,8 g, 40 % Sättigung). Ein kleiner, jedoch inaktiver Niederschlag wurde auf der Zentrifuge abgeschieden, und die Mutterlauge mit 69,2 g Ammonium-

sulfat versetzt (88 % Sättigung). Nach einigen Stunden im Kühlschrank wurde scharf zentrifugiert, die Peroxydase in 0,01 M Phosphatpuffer von pH 7 aufgelöst und gegen Wasser einige Tage lang dialysiert.

Analyse: Volumen 18,5 ml, Q 3,03. Trockengewicht 33,80 mg, Asche 0,05 mg, Hämin 0,404 mg und Eisen 33,4 μg, alles pro ml. Der Stickstoffgehalt war 13,3 %. Die Aktivitätsbestimmung gab die Gesamtmenge von 10,5 μMolen MRP *.

Bei vorsichtigem Zusatz von Ammoniumsulfat kristallisiert MRP zum Teil. Es ist aber zu empfehlen, die Peroxydase mittels Ammoniumsulfat quantitativ auszufällen und in diesem Zustand in geschlossenen Gefässen im Eisschrank aufzubewahren. Die Aktivität bleibt dabei jahrelang nahezu unverändert, und die Peroxydase kann bei Bedarf weitergereinigt werden.

6. Chromatographie auf Karboxymethylzellulose (CMC)

Vorbehandlung des Ionenaustauschers. Zellulose ("Whatman cellulose powder, standard grade"), die nach Peterson und Sober [10] karboxyliert ist, wird mit Puffer (30 ml 1 M Essigsäure + 15 ml 1 M NaOH + Wasser auf 1 l) im Kältezimmer bis zum Gleichgewicht gerührt. Das Rohr wird mit Puffer gefüllt, die Karboxymethylzellulose eingegeben, und man lässt sie ohne Druck bis zu konstantem Volumen sedimentieren. Danach wird die Säule einige Stunden lang mit kaltem Wasser gewaschen.

Grössere Ansätze als 8 mg Substanz pro cm³ Säule wurden nicht untersucht, wählt man jedoch Mengen bis zu dieser Konzentration, so werden die Chromatogramme identisch. Fig. 1 zeigt ein Beispiel für das Verfahren. Die gegen Wasser dialysierte MRP-Lösung wird verwendet, und man beginnt die

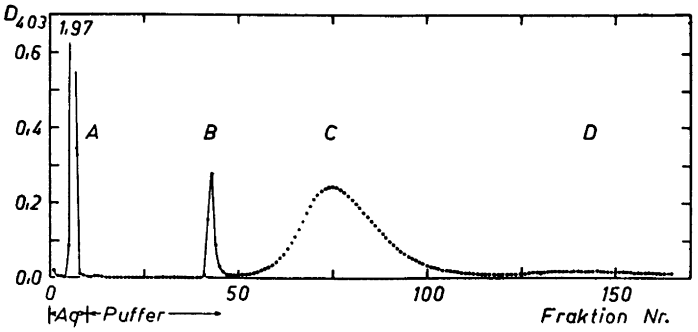

Fig. 1. Chromatographie von Meerrettichperoxydase auf Karboxymethylzellulose. Ausgangsmaterial: 0,50 ml einer gegen Wasser dialysierten Lösung mit log (I_0/I) = 29,5 bei 403 mμ, Q = 2,44. Ansatz etwa 8 mg. Säule 210 × 9 mm. Durchlaufgeschwindigkeit 5,9 ml pro cm² pro Stunde. 20 Min. pro Fraktion. Sämtliche Fraktionen ohne Verdünnung in Beckman DU-Spektrophotometer gemessen.

* Wegen Unfall ging hier in dieser Preparation etwa ein Drittel verloren. Diese Stufe ist sonst praktisch ohne Verluste.

Tabelle 2. Analysen der vier Meerrettichperoxydasen.

	A	B	C	D
Hämin [1]	1,04	1,28	1,44	1,36
Asche [2]	7,1	2,9	1,8	2,4
Stickstoff [1]	11,07	13,41	13,24	13,06
Q	3,53	2,92	3,31	3,13
Aktivität nach				
der Guaiacolprobe [3]	0,019	0,080	0,075	0,077
der Mesidinprobe [4]	0,48	1,28	1,25	1,25

Elution mit Wasser. Etwa ein Viertel des Enzyms wird nicht zurückgehalten, wandert aber schnell abwärts. Diese Fraktion, als MRP A bezeichnet, wird gegen Wasser dialysiert und im gefrorenen Zustand getrocknet. Das Eluat bleibt dann farblos, und die MRP-Bande im obersten Teil der Säule bewegt sich nicht.

Das Chromatogramm wird dann mit dem oben beschriebenen Acetatpuffer weitereleuiert, wobei drei Fraktionen MRP B, C und D erhalten werden. Sie werden gegen Wasser über Nacht dialysiert und danach, zwecks Konzentrierung, auf drei Säulen adsorbiert (wie oben CMC in Puffer, mit Wasser ausgewaschen). Diese Säulen können klein sein, z.B. für 500 mg MRP C in 1 200 ml 50 × 9 mm. Nach Adsorption und Waschen mit Wasser wird mit Acetatpuffer (30 ml 1 M Essigsäure + 20 ml 1 M NaOH + Wasser auf 1 l) eluiert, die Peroxydasen gegen Wasser dialysiert und endlich analysiert

Die Aschenwerte sind auffallend hoch. MRP A und C wurden elektrophoretisch untersucht und zeigten dabei eine Verunreinigung, die noch bei pH 4.6 anodisch wanderte. Sie machte in A einen Drittel, in C weniger als zehn Prozent aus. Versuche, die saure Fraktion, die von Kohlenhydratnatur sein dürfte, chromatographisch, auch auf Dowex 2-Borat, abzutrennen, sind bisher nicht erfolgreich geworden. Es ist von Interesse, dass Paraperoxydase aus MRP A bei pH über 9, besonders in Boratbuffer, leicht gebildet wird, aus den anderen Peroxydasen aber nicht. Peroxydase und Paraperoxydase waren auf Dowex-2 bei pH 7, Phosphatpuffer, leicht zu trennen. Paraperoxydase bewegte sich dabei etwas langsamer.

Der Befund von Jermyn und Thomas [11] über die Uneinheitlichkeit der Meerrettichperoxydase ist somit bestätigt worden. Die vier Peroxydasen A, B, C und D werden am besten innerhalb der pH-Grenzen 4,2—4,9 getrennt. Bei niedrigerem pH bewegen sich C und D kaum, bei höherem pH wandern B, C und D als eine Fraktion. Wenn die Säule nicht mit Wasser gewaschen wird, bleibt A unverändert, B kommt aber als eine zwar gut begrenzte und fast symmetrische aber weit ausgedehnte Bande heraus.

Drei MRP-Präparationen aus herbstgeernteten Wurzeln gaben nahezu konstante Mengenverhältnisse zwischen den vier Peroxydasen und zwar verhielt sich A:B:C:D wie 2:1:4:1. Die relativen Q-Werte der vier Peroxydasen sind auch ziemlich konstant. A hat

[1] In % des aschefreien Trockengewichtes.

[2] In % des Gesamttrockengewichtes.

[3] In $1/t$ min^{-1}, wo t = Zeit fur die Steigerung des D_{470} mit 0.050. 6.9×10^{-6} μMole von MRP-Hämin in der Kuvette.

[4] In $1/t$ min^{-1}, wo t = die Zeit, in der $D_{490} = 0.450$ erreicht wird. 10^{-4} μMole von MRP-Hämin in der Kuvette.

immer den höchsten und B den niedrigsten Q-Wert. Das Spektrum von A variiert stark mit dem pH und Q-Werte über 4,5 sind für Lösungen in Acetatpuffer beobachtet worden. Wenn die Zellulosesäule mit grossen Mengen beladen war, konnte zweimal eine kleine und sehr ausgedehnte, aber deutlich begrenzte Fraktion E beobachtet werden. Es wurde kein Versuch gemacht, sie zu isolieren.

Diese Arbeit wurde von *Statens naturvetenskapliga forskningsråd* unterstützt. Fräulein A. Hartkoorn sei sehr wertvolle Assistanz gedankt.

LITERATUR

1. Paul, K. G. und Avi-Dor, Y. *Acta Chem. Scand.* **8** (1954) 637.
2. Theorell, H. *Arkiv Kemi, Mineral. Geol.* **16** *A* (1942) No. 2.
3. Keilin, D. und Hartree, E. F. *Biochem. J.* **49** (1951) 88.
4. Kenten, R. H. und Mann, P. J. G. *Biochem. J.* **57** (1954) 347.
5. Boman, H. G. und Westlund, L. E. *Arch. Biochem. Biophys.* **64** (1956) 217.
6. Paul, K. G. und Avi-Dor, Y. *Acta Chem. Scand.* **8** (1954) 649.
7. Georg, P. *J. Biol. Chem.* **201** (1953) 413.
8. Paul, K. G., Theorell, H. und Åkeson, Å. *Acta Chem. Scand.* **7** (1953) 1284.
9. Theorell, H. und Åkeson, Å. *Persönliche Mitteilung.*
10. Peterson, E. A. und Sober, H. A. *J. Am. Chem. Soc.* **78** (1956) 751.
11. Jermyn, M. A. und Thomas, R. *Biochem. J.* **56** (1954) 631.

Eingegangen am 4. Februar 1958.

ACTA CHEMICA SCANDINAVICA 12 (1958) 1319—1322

The Constituents of Conifer Needles

I. Low Molecular Weight Carbohydrates in the Needles of *Pinus silvestris*

ANDERS ASSARSSON and OLOF THEANDER

Träkemiska avdelningen, Svenska Träforskningsinstitutet, Stockholm, Sweden

An investigation has been made of the low-molecular weight carbohydrates in needles collected from *Pinus silvestris*. Glucose, fructose, sucrose, melibiose, raffinose, *myo*-inositol and pinitol, the principal carbohydrates, were isolated together with smaller amounts of cellobiose, laminaribiose, a glucopyranosyl-fructose and a glucopyranosyl-mannose. Oligosaccharides were found which contained residues of glucose, galactose and fructose. Paper chromatography indicated the presence also of small amounts of galactose, arabinose and xylose.

In the present investigation a study has been made of the low-molecular weight carbohydrates present in the needles of *Pinus silvestris*, which had been collected in October. Glucose, fructose, sucrose, raffinose and pinitol were previously found [1,2] in conifer needles and the present investigation was made to get information on their amounts and on other components, some of which might be of interest in connection with the biosynthesis of polysaccharides.

By treating the needles successively with ethanol and methanol, a mixture of neutral carbohydrates was obtained. It was fractionated on carbon columns and sub-fractionated by chromatography and by electrophoresis on thick filter paper. The values for the monosaccharides were determined quantitatively following paper chromatographic separation while the other values are for these substances which were isolated in a pure state (See Table 1).

Myo-inositol, pinitol, melibiose, sucrose and raffinose crystallised. From a mixture containing glucose, fructose and some of the pinitol, the two monosaccharides were isolated as their *iso*propylidene derivatives. Smaller amounts were isolated of four disaccharides and of two higher oligosaccharides; the latter two gave glucose, galactose and fructose on hydrolysis. Galactose, arabinose and xylose were detected on paper chromatograms and also smaller amounts of compounds having higher R_F-values.

The four minor disaccharides were investigated by paper chromatography and electrophoresis and by studying the products obtained, both when they were hydrolysed and when they were reduced with borohydride prior to hyd-

Table 1. Low-molecular weight carbohydrates in the needles of *Pinus silvestris*. The amounts are given as the percentages of the dry weight of the needles.

Arabinose	0.06
Xylose	0.02
Fructose	2.5
Galactose	0.03
Glucose	2.2
Melibiose	0.3
Sucrose	1.7
Raffinose	0.8
Other oligosaccharides	< 0.1
Myo-inositol	0.3
Pinitol	2.0

rolysis. By these methods two of the disaccharides were shown to be indistinguishable from laminaribiose and cellobiose. The other two were found to be reducing, and it was concluded that they were a glucopyranosyl-mannose and a glucopyranosyl-fructose.

It was possible that a portion of the sugars might have been formed from higher oligosaccharides by hydrolysis during either the extraction or the purification. To determine whether or not this was the case, a sample of the purified extract, which had not been passed through a carbon column, was examined on chromatograms. There it was compared with samples of non-purified extracts obtained by treating needles immediately after their removal from the same tree. In one case, cold ethanol was used to minimise the possibility of acid hydrolysis and, in the other, boiling ethanol was used to inactivate the enzyme systems as rapidly as possible. Those two extracts were similar; glucose, fructose, sucrose, melibiose and raffinose were present as the principal sugars. Glucopyranosyl-fructose was also shown to be present in those extracts as, when they were concentrated on the chromatograms the disaccharide gave an intense red spot on treatment with resorcinol in acid. There were slight indications of reactions with *p*-anisidine hydrochloride at those positions on the chromatogram where the other, and minor, disaccharides might be. On the other hand the examination showed that, under the mild conditions used for extraction and purification, some of the sucrose and raffinose had been hydrolysed.

The investigation will be repeated on a larger scale to obtain further informations on certain of the substances present.

EXPERIMENTAL

All melting points were corrected. Solvents were removed either by distillation, carried out under reduced pressure (bath temperature under 40°), or by lyophilisation. Whatman No. 1 filter paper was normally used for paper chromatography and electrophoresis, but large scale separations were carried out on Whatman No. 3 MM paper, which had previously been thoroughly washed with water. Reagents used for the detection of substances on chromatograms and electrophoretograms were silver nitrate-ethanolic sodium hydroxide, *p*-anisidine hydrochloride and resorcinol-hydrochloric acid.

The chromatographic solvents and the buffer used in the electrophoresis were:

A — Ethyl acetate — acetic acid — water, 3:1:3 (the upper phase).
B — Butanol — ethanol — water, 10:3:5.
C — Butanol — pyridine — water, 6:2:3.
D — Borate buffer [3] pH 10.0, 0.1 M.

5-Hydroxymethylfurfural was used to enable correction to be made for electroendosmotic movement. This compound is readily detected with all the sprays used in this investigation.

The needles were collected at the end of October from all parts of the branches. The age of the tree was about 20 years. The fresh needles (540 g, corresponding to a dry weight of 230 g) within a few hours of their having been collected were cut into pieces (*ca.* 1 cm) and were boiled with ethanol (5 l) for 30 min. The mixture, when cold, was filtered and the residue washed with ethanol. The residual material was air-dried, disintegrated in a Wiley-mill and then treated with methanol (3 × 24 h) in a Soxhlet extractor. The final extract, which was almost colourless, yielded only 1.9 g of material on removal of the solvent. The ethanolic extracts, the wash liquids and the three methanolic extracts were examined chromatographically and found to be similar. They were combined and concentrated to *ca.* 400 ml. Water (200 ml) was added and the solution was shaken with successive volumes (400 ml) of chloroform. After removal of the solvent from an aliquot of the aqueous layer, the total soluble non-volatile material was found to be 44 g. The aqueous layer was deionised by passing it through columns containing Amberlite IR 120 and IR 4B. The eluate was evaporated to about 500 ml and to the solution there was added ethanol to give a final concentration of 50 % with respect to the ethanol. This solution was shaken for 16 h with a mixture of charcoal and Celite (1:1; 150 g). After filtration and washing of the residues, the filtrate and washings were concentrated and yielded a colourless product (32.1 g). Part of this product was separated on paper chromatograms (Solvents A and C) and the monosaccharides were quantitatively determined by the method of Saeman *et al.*[4] *Glucose* and *fructose* were the principal sugars and there were smaller amounts of *galactose*, *arabinose* and *xylose* (see Table 1). The products were examined on paper chromatograms and there compared with the components in two other extracts from the needles of the same tree. One of those extracts was obtained by treating the needles with cold ethanol for a day at room temperature, the other, by boiling the needles with ethanol for 30 min. The extracts were not purified. Appropriate volumes of the two solutions were concentrated directly on the starting-line of the chromatogram by a stream of cold air.

The main part of the purified product (31.8 g) was fractionated on a carbon-Celite column (50 × 6 cm), using the gradient-elution technique (ethanol: 0—20 %, 15 l, and 50 %, 10 l). The fractions, after examination on paper chromatograms, were then grouped and combined to give two main fractions. Fraction I contained most of the monosaccharides and inositols (17.8 g) while fraction II contained mainly oligosaccharides (9.8 g). Fraction II was refractionated on the same column (water, 4 l; ethanol 0.30 %, 14 l; and ethanol 50 %, 6 l). The first sub-fractions (1.33 g) from it contained monosaccharides and inositols and they were combined with fraction I. The later sub-fractions from fraction II on chromatographic and electrophoretic examination were found to contain compounds indistinguishable from melibiose, sucrose and raffinose (stated in the order in which they emerged from the column). A portion of each of these sugars was crystallised from aqueous ethanol; each sugar was crystallised from that fraction in which it was present in its highest concentration. In order to estimate the total amounts of the individual sugars the mother liquors and fractions containing smaller sugar concentration, or aliquots of them, were evaporated to dryness, and the material redissolved and separated on thick filter papers using solvent A. The various sugars were eluted from the papers, the eluate evaporated to dryness, and the residue weighed. Two disaccharides (I and II), which had been eluted from the carbon column together with melibiose, and two (III and IV), which had been eluted together with sucrose, were separated by pairs on the paper chromatograms. Smaller amounts of two other oligosaccharides (*ca.* 25 mg of each), probably a tetra- and pentasaccharide, were also separated on the chromatograms. They gave galactose, glucose and fructose on hydrolysis with N sulphuric acid (100°, 2 h).

Pure fractions of the four disaccharides (about 10—30 mg of each) were obtained by electrophoresis of the individual pairs of disaccharides on thick filter papers. The sugars were eluted from the papers with N acetic acid and, after having deionised the eluate, it was evaporated to dryness. Each of the disaccharides would appear to have a glycosidically-linked pyranose residue as they were all but little affected by those hydrolysis conditions which led to complete hydrolysis of sucrose, that is, by treatment with 0.1 N hydrochloric acid at 100° for 5 min.

The disaccharides I and III, on hydrolysis with N sulphuric acid (100°, 2 h) yielded

glucose only. They were indistinguishable from *laminaribiose* and *cellobiose*, respectively, on both paper chromatograms and electrophoretograms, but were distinguishable from nigerose, maltose, *iso*maltose and gentiobiose.

Disaccharide II ($M_{G^3} = 0.52$) on hydrolysis yielded approximatively equimolar amounts of glucose and mannose. Reduction with borohydride, and hydrolysis of the reduction product yielded glucose as the only reducing sugar. The results obtained indicated that it was a *glucopyranosyl-mannose*.

Disaccharide IV ($M_{G^3} = 0.62$) on hydrolysis yielded approximately equimolar amounts of glucose and fructose. It was reduced and hydrolysed as above and then gave glucose as the only reducing sugar. The results obtained indicated that disaccharide IV was a *glucopyranosyl-fructose*. It was distinguishable both chromatographically and electrophoretically from turanose.

The disaccharide II had the following $R_{Glucose}$ -values: 0.48 (A), 0.49 (B) and 0.57 (C) and the disaccharide IV: 0.30 (A), 0.29 (B) and 0.34 (C).

Melibiose (0.40 g) crystallised as the dihydrate (m. p. 75—76°) and was characterised as melibiitol, obtained by borohydride reduction. It had $[\alpha]_D^{22}$ +111 (*c*, 2 in water) and m. p. 173—175°, not depressed on admixture with an authentic sample.

Sucrose (2.82 g) was recrystallised from aqueous ethanol. It had $[\alpha]_D^{22}$ +66 (*c*, 2 in water) and m. p. 183—185°.

Raffinose (1.38 g) was recrystallised from aqueous ethanol. It had $[\alpha]_D^{21}$ +106 (*c*, 2 in water; literature: raffinose pentahydrate $[\alpha]_D^{20}$ +105), m. p. 135—139°, as had both an authentic sample of raffinose pentahydrate and a mixture of the two samples. Examination in polarised light revealed that the material lost its crystalline properties at 76—80° due to dehydration. The shape of the material, however, remained unaltered until the solid collapsed at 135—138°. Hydrolysis with 0.1 N hydrochloric acid (100°, 5 min) gave melibiose and fructose.

From the combined fractions containing the monosaccharides and inositols (19.33 g), a sample (4.00 g) was taken and fractionated on a smaller carbon-Celite column (32 × 4 cm) using the gradient-elution technique (water, 3 l; ethanol 0.5 %, 4 l, and 50 %, 3 l).

Myo-inositol (0.16 g) was obtained from the first fractions. It was chromatographically and electrophoretically indistinguishable from an authentic sample and after recrystallisation from aqueous ethanol it had m. p. and mixed m. p. 228—231°.

By paper chromatography and electrophoresis certain of the fractions were shown to contain glucose, fructose and pinitol, as principal components, and smaller amounts of *myo*-inositol, galactose, arabinose and xylose. Those combined fractions were taken to dryness and the residues dissolved in aqueous ethanol. Part of the *pinitol* (0.72 g) crystallised and after recrystallisation from the same solvent it had m. p. and mixed m. p. 189—190° and $[\alpha]_D^{22}$ +64 (*c*, 2, water). The material in the mother liquors was treated with acetone and sulphuric acid to convert the sugars to their di-*iso*propylidene derivatives while leaving the remaining pinitol unaffected. A further crop of crystalline pinitol was obtained (0.21 g) and by following the partial hydrolysis technique of Bell [5], crystalline *iso*propylidene derivatives of glucose and fructose were also isolated. *1,2*-O-iso*propylidene-glucofuranoside*, on recrystallisation from ethyl acetate, had m. p. 160—161° (lit. 161—162.5) and *2,3-4,5-di (*O-iso*propylidene)-fructo-pyranoside*, on recrystallisation from petrol ether, had m. p. 95—96° (lit. 95—96).

The authors are indebted to Dr. S. A. Barker (Birmingham University) and Dr. W. J. Whelan (Lister Institute, London) for a gift of reference specimens.

REFERENCES

1. Neish, A. C. *Can. J. Biochem. Physiol.* **35** (1957) 161.
2. Plouvier, V. *Compt. rend.* **234** (1952) 362.
3. Foster, A. B. *J. Chem. Soc.* **1953** 982.
4. Saeman, J. F., Moore, W. E., Mitchell, R. L. and Millett, M. A. *Tappi* **37** (1954) 336.
5. Bell, D. J. *Moderne Methoden der Pflanzenanalyse*, edited by Peach, K. and Tracey, M. V., Springer-Verlag Berlin 1955, Vol. II, p. 32.

Received March 17, 1958.

ACTA CHEMICA SCANDINAVICA 12 (1958) 1323—1329

A Cryoscopic Study of Ionic Association in Bivalent Metal Sulphates using Saturated Aqueous Solutions

JOUKO KENTTÄMAA

Institute of Chemistry, University of Helsinki, Helsinki, Finland

The classical dissociation constants of a number of bivalent metal sulphates have been determined at three ionic strengths by the method previously used by the author. The dependence of pk values on ionic strength has been expressed with the aid of the Debye-Hückel formula and the thermodynamic dissociation constants have been extrapolated.

A considerable amount of work has been done in the field of incomplete dissociation of higher charge type electrolytes in water. Spectrophotometric methods have frequently been used but in most cases the evaluation of the degree of association has been based on deviations from the Debye-Hückel theory or other theories based on similar models. This type of procedure always includes some arbitrary assumptions, *e.g.* about the activities or conductivities of the ions or associated molecules. These theories give reliable approximations for the changes in the activity or conductivity of ions only in very dilute solutions in which the degree of association often is very slight. Very accurate measurements are needed but still leave some doubt about the interpretation of the results. However, most investigations support the existence of association in higher charge type electrolytes and give association constants of the same order of magnitude. Nevertheless, this ionic association has not been generally accepted and papers have frequently been published, in which complete dissociation has been assumed in conditions where it is certainly not valid. Further work is required in this field to draw attention to these phenomena and to provide additional information. In particular, there is a need for the development of methods that do not involve arbitrary assumptions about ion activities and allied properties.

METHOD

The approach employed in this paper is based on the behaviour of a mixture of ice and water saturated with an electrolyte like a one component solvent [1–6] in cryoscopic measurements. The author [6] has previously introduced the use of such "solvent" in the study of the incomplete dissociation of

some bivalent metal sulphates at one ionic strength. This paper describes the extension of this study to three ionic strengths. These "solvents" themselves contain a certain concentration of ions, dependent on the saturating electrolyte, and the activity factors of the ions in them will therefore change only slightly or will remain almost constant when considerable amounts of some other electrolyte are added, provided that the saturating electrolyte is soluble to raise the ionic strength, about up to 0.05 or more. The depression of the freezing point of this kind of "solvent"-ice mixture is therefore almost directly proportional to the sum of the concentrations of ions, and associated ions, other than those arising from the saturating electrolyte. Hence the method provides a means of estimating the sum of the concentrations of these. When these and the corresponding stoichiometric concentrations of an electrolyte are known, it is possible to find the dissociation constant for this electrolyte by extrapolation. Data obtained from solutions containing relatively high concentrations of the electrolyte being studied and showing a relatively large effect due to the ionic association can be used for the extrapolation. This method has been applied here to the study of 2—2 type electrolytes but, it can be used to study the association of any type of electrolyte.

For a water-ice mixture saturated with an electrolyte, the dependence of the freezing point depression ΔT, on Σm_i, the sum of the concentrations of the ions and molecules that are not common with those arising from the saturating electrolyte is given by

$$\Sigma(dm_i + m_i d\ln f_i) = d(\Delta T)/K^\circ_f \quad (1)$$

When the changes in activity coefficients are small the expression

$$\Sigma m_i \simeq \Sigma \bar{m}_i \equiv \Delta T/K^\circ_f \quad (2)$$

gives a good approximation, $\Sigma\bar{m}_i$, for Σm_i. However, from eqn. (1) it is essential, that

$$\lim_{m_s \to 0} \Sigma\bar{m}_i = \Sigma m_i \quad (3)$$

where m_s is the stoichiometric concentration of added electrolyte.

The molar depression of the freezing point of a saturated solution, K°_f, is best derived from the freezing point depressions of 1—1 electrolytes for which the association is negligible. Extrapolation of the values given by

$$K_f \equiv \Delta T/2m_s \quad (4)$$

to infinite dilution for the added 1—1 electrolyte gives the value of K°_f.

In solutions of a bivalent metal sulphate MSO_4, there may be MSO_4 molecules and $M(SO_4)_2^{2-}$ ions present due to ion-pair formation in addition to M^{2+} and SO_4^{2-} ions. If the dissociation constants are

$$k_1 = [M^{2+}]\,[SO_4^{2-}] \,/\, [MSO_4] \quad (5)$$

and

$$k_2 = [MSO_4]\,[SO_4^{2-}] \,/\, [M(SO_4)_4^{2-}] \quad (6)$$

it can be shown that[6]

$$\varphi = 2m_s - \Sigma m_i/(\Sigma m_i - m_s)^2 = 1/k_1 + \Sigma m_i/k_1 k_2 \quad (7)$$

Replacement of Σm_i by $\Sigma \bar{m}_i$ obtained from measurements according to eqn. (2) gives an approximate value $\bar{\varphi}$ for φ. The value of $\bar{\varphi}$ equals the value of φ when extrapolated to infinite dilution of the added electrolyte, as can be seen from eqns. (3) and (7). For the electrolytes studied in this investigation the variation of $\bar{\varphi}$ with $\Sigma \bar{m}_i$ in all cases is linear within the limits of the experimental error. The intercept of these lines on the y-axis gives the value $\bar{\varphi} = 1/k_1$. The slope of these lines gives at most only a rough approximation for $1/k_1k_2$ due to the changes in activity coefficient. In addition the ions of the saturating electrolyte may also participate in ion-pair formation. The effect of this on $\bar{\varphi}$ can be assumed to be slight. It may be pointed out that the same method could be applied using pure water as a solvent but the variation of $\bar{\varphi}$ with $\Sigma \bar{m}_i$ would not be linear, and here again some arbitrary assumptions about the ion activities would be necessary for the extrapolation of $1/k_1$. The method will, of course, give classical dissociation constants at the ionic strengt of the saturating electrolyte.

RESULTS

The author has previously studied [6] the ion association of cupric sulphate, zinc sulphate, nickel sulphate and magnesium sulphate in saturated potassium perchlorate solutions. The same dissociation constants have now been determined in saturated potassium chlorate and potassium nitrate solutions. The freezing point depressions were measured using the method of Richards [7]. The apparatus used, consisting of two Dewar vessels, propeller driven water circulator and ten-junction thermocouples, and the method have been described previously [5,6]. The accuracy in temperature measurements was about 0.0003°C. The concentrations of copper, zinc, nickel and magnesium were determined by complexometric methods. All reagens were of A.R. grade.

The molar depressions of the eutectic points of these solutions in equlibrium with ice were determined using nitric acid in the case of potassium chlorate and hydrochloric acid in the case of potassium nitrate. As before [6], an empirical equation

$$K_f \equiv \Delta T/2m_s = K^\circ_f + a \cdot m_s \qquad (8)$$

was found suitable for the extrapolation of K°_f values. The following equations were derived using the method of least squares:

$$K_f = 1.803 - 0.106\ m_{HNO_3} \qquad (9)$$

for potassium chlorate solutions and

$$K_f = 1.693 - 0.141\ m_{HCl} \qquad (10)$$

for potassium nitrate solutions. All concentrations are expressed in moles per kg of water. The eutectic point for saturated potassium chlorate solution in equilibrium with ice was found to be —0.800°C and the saturation concentration at this temperature was 0.258 molal, for saturated potassium nitrate solution these values were —2.831°C and 1.150 moles per kg of water, respecti-

Tables 1 and 2. Eutectic point depressions for saturated potassium chlorate (1) and potassium nitrate (2) solutions produced by various sulphates and dissociation constants calculated from these data.

Table 1.

m_s	ΔT	$\Sigma\bar{m}_i$	$\bar{\varphi}$	k_1
		$CuSO_4$		
0.0221	0.0681	0.0378	26.0	0.051
0.0433	0.1222	0.0678	31.3	
0.0641	0.1695	0.0940	38.3	
0.0837	0.2142	0.1188	39.4	
0.1027	0.2566	0.1423	40.2	
0.1210	0.2919	0.1619	47.9	
0.1386	0.3267	0.1812	52.9	
		$ZnSO_4$		
0.0330	0.0977	0.0542	26.3	0.049
0.0655	0.1788	0.0922	28.0	
0.0954	0.2467	0.1368	31.5	
0.1247	0.3078	0.1707	37.3	
0.1457	0.3548	0.1968	36.2	
0.1730	0.4078	0.2262	42.3	
		$NiSO_4$		
0.0213	0.0660	0.0366	25.6	0.054
0.0418	0.1185	0.0657	31.3	
0.0618	0.1658	0.0920	34.6	
0.0816	0.2087	0.1157	40.8	
0.1003	0.2470	0.1370	47.2	
0.1173	0.2846	0.1578	46.8	
0.1364	0.3210	0.1780	54.8	
		$MgSO_4$		
0.0286	0.0905	0.0502	15.0	0.087
0.0569	0.1632	0.0905	20.6	
0.0820	0.2251	0.1248	21.4	
0.1083	0.2839	0.1575	24.4	
0.1332	0.3379	0.1874	26.9	
0.1565	0.3878	0.2151	28.5	
0.1797	0.4354	0.2415	30.9	

vely. The results of measurements made with the different sulphates are given in Tables 1 and 2. These gave the expressions

$$\begin{aligned} \bar{\varphi}_{CuSO_4} &= 18.5 + 185\Sigma\bar{m}_i \\ \bar{\varphi}_{ZnSO_4} &= 21.0 + 85\Sigma\bar{m}_i \\ \bar{\varphi}_{NiSO_4} &= 18.5 + 190\Sigma\bar{m}_i \\ \bar{\varphi}_{MgSO_4} &= 11.7 + 80\Sigma\bar{m}_i \end{aligned} \qquad (11)$$

for saturated potassium chlorate solutions and

$$\begin{aligned} \bar{\varphi}_{CuSO_4} &= 5.3 + 31\Sigma\bar{m}_i \\ \bar{\varphi}_{ZnSO_4} &= 4.6 + 36\Sigma\bar{m}_i \\ \bar{\varphi}_{NiSO_4} &= 4.9 + 34\Sigma\bar{m}_i \\ \bar{\varphi}_{MgSO_4} &= 2.4 + 15\Sigma\bar{m}_i \end{aligned} \qquad (12)$$

Table 2.

m_s	ΔT	$\Sigma\bar{m}_i$	$\bar{\varphi}$	k_1
		$CuSO_4$		
0.0148	0.0485	0.0286	5.3	0.19
0.0295	0.0924	0.0546	7.0	
0.0442	0.1331	0.0786	8.3	
0.0580	0.1704	0.1006	8.5	
0.0712	0.2038	0.1204	9.1	
0.0857	0.2390	0.1412	9.8	
0.0998	0.2730	0.1612	10.2	
		$ZnSO_4$		
0.0190	0.0613	0.0362	6.1	0.22
0.0378	0.1172	0.0692	6.5	
0.0565	0.1670	0.0986	8.1	
0.0750	0.2137	0.1262	9.1	
0.0933	0.2576	0.1521	10.0	
0.1103	0.2967	0.1752	10.8	
		$NiSO_4$		
0.0154	0.0501	0.0296	6.0	0.20
0.0300	0.0940	0.0555	6.9	
0.0444	0.1349	0.0797	7.3	
0.0590	0.1738	0.1026	8.1	
0.0734	0.2090	0.1234	9.3	
0.0873	0.2435	0.1438	9.7	
0.1008	0.2753	0.1626	10.2	
		$MgSO_4$		
0.0322	0.1036	0.0612	3.8	0.42
0.0643	0.1947	0.1150	5.3	
0.0966	0.2774	0.1638	6.5	
0.1279	0.3507	0.2071	7.8	
0.1598	0.4248	0.2509	8.3	

for saturated potassium nitrate solutions. For saturated potassium perchlorate solutions the author earlier [6] obtained the equations:

$$\begin{aligned} \bar{\varphi}_{CuSO_4} &= 49.3 + 359\Sigma\bar{m}_i \\ \bar{\varphi}_{ZnSO_4} &= 51.1 + 238\Sigma\bar{m}_i \\ \bar{\varphi}_{NiSO_4} &= 50.5 + 161\Sigma\bar{m}_i \\ \bar{\varphi}_{MgSO_4} &= 36.3 + 157\Sigma\bar{m}_i \end{aligned} \qquad (13)$$

In all cases the variation of φ with $\Sigma\bar{m}_i$ is linear within the limits of experimental error. This is an empirical assumption, and much more accurate measurements are required to show whether it is really valid. In any case the relationship between $\bar{\varphi}$ and $\Sigma\bar{m}_i$ is so nearly linear that even where it is more complicated the linear extrapolation will not lead to any large error in k_1. There can hardly be any unexpected variations in $\bar{\varphi}$ between the points of intersection and the first points measured at such relatively high ionic strengths. The variations in the values of k_1 obtained from eqns. (11), (12)

and (13) with ionic strength have been expressed by means of the Debye-Hückel equation

$$pk_1 = pk^\circ_1 - 3.9\sqrt{I}/(1 + a\sqrt{I}) + BI \qquad (14)$$

The values obtained for pk°_1, a and B and the values of pk_1 at different ionic strengths are shown in Table 3. The values of k_1 for each ionic strength were measured at several temperatures for solutions of different saturating electrolytes and, strictly speaking, eqn. (14) is not applicable as such to the experiments. The effect of the temperature on k_1 can be estimated according to the Bjerrum theory of ion-pair formation[8]. For instance, for the pk_1 value 2.300 at 0°C this gives a theoretical value of 2.293 at —3°C. The effects of temperature differences are, therefore probably within the limits of the experimental error and have been ignored. The characteristic salt effects of the different saturating electrolytes on the pk_1 values can similarly be assumed to be negligible. The dissociation constants for these sulphates have been reported frequently before [9–14]. Although the values obtained depend on various assumptions on activity factors of ions, they agree, being mostly of a magnitude of 0.003—0.008, remarkably well with each other and the values in Table 3. Näsänen [15] has obtained spectrophotometrically for cupric sulphate

$$pk_1 = 2.099 - 4.05\ \sqrt{I}/(1 + 1.618\ \sqrt{I}) + 0.0521I \qquad (15)$$

Table 3. Values of pk_1, pk°_1, a, and B for some bivalent metal sulphates.

	t°C	$\sqrt{I}$	$CuSO_4$	$ZnSO_4$	$NiSO_4$	$MgSO_4$
pk_1, KNO_3 sol.	−2.831	1.073	0.724	0.663	0.690	0.380
pk_1, $KClO_3$ sol.	−0.800	0.508	1.290	1.312	1.267	1.061
pk_1, $KClO_4$ sol.	−0.163	0.220	1.692	1.708	1.703	1.561
pk°_1, water	0.000	0.000	2.259	2.256	2.294	2.186
a	—	—	2.55	2.90	2.22	1.87
B	—	—	−0.36	−0.50	−0.32	−0.36

According to this the variation of pk_1 values with ionic strength is similar to that obtained by the author at low values of ionic strength. At higher ionic strengths some differences appear due to the abnormally large B-values obtained in this work. The fact that the optical method of Näsänen gives values for k°_1 about one and a half times as large as those given by e.m.f., conductance and cryoscopic methods [16] raises again the question whether all such ion-pairs formed by electrostatic forces, which can be detected by the latter methods, undergo any changes in optical properties. For cupric sulphate Fronæus [17,18] obtained spectrophotometrically $k_1 = 0.2$ and potentiometrically $k_1 = 0.1$ at I = 1. The former value is in excellent agreement with the corresponding value, $k_1 = 0.200$, obtained in this paper.

REFERENCES

1. Lewis, G. N. and Randall, M. *Thermodynamics*, N.Y. 1923, p. 240, Exercise 3.
2. Jahr, K. F. and Brechlin, A. *Z. anorg. Chem.* **270** (1952) 257.
3. Souchay, P. *Bull. soc. chim. France* **15** (1948) 143.

4. Müller, H. J. *Ann. chim. Paris* **8** (1937) 143.
5. Kenttämaa, J. *Ann. Acad. Sci. Fennicæ A II*, **67** (1955).
6. Kenttämaa, J. *Suomen Kemistilehti* **B 29** (1956) 59.
7. Richards, J. *Z. physik. Chem.* **44** (1903) 563.
8. Bjerrum, N. *Kgl. Danske Videnskab. Selskab., Mat. fys. Medd.* **7** (1926) No. 9.
9. Jones, H. W. and Monk, C. B. *Trans. Faraday Soc.* **48** (1952) 929.
10. Wyatt, P. A. H. *Trans. Faraday Soc.* **47** (1951) 656.
11. Owen, B. B. and Curry, W. *J. Am. Chem. Soc.* **60** (1938) 3074.
12. Davies, C. W. *Trans. Faraday Soc.* **23** (1927) 351.
13. Brown, G. M. and Prue, J. E. *Proc. Roy. Soc. London* **A 232** (1955) 320.
14. Dunsmore, H. S. and James, J. C. *J. Chem. Soc.* **1951** 2925.
15. Näsänen, R. *Acta Chem. Scand.* **3** (1949) 179.
16. Robinson, R. A. and Stokes, R. H. *Electrolyte Solutions*, London 1955, p. 395.
17. Fronæus, S. Diss., Lund (1948).
18. Fronæus, S. *Acta Chem. Scand.* **4** (1950) 72.

Received March 25, 1958.

ACTA CHEMICA SCANDINAVICA 12 (1958) 1330—1348

Short Communications

Factor 3 and 6-Selenoctic Acid

KLAUS SCHWARZ and CALVIN M FOLTZ

National Institute of Arthritis and Metabolic Diseases, National Institutes of Health, Bethesda 14, Maryland, U.S.A.
and
GÖRAN BERGSON

Chemical Institute, University of Uppsala, Sweden

Factor 3 was recognized as a nutritional agent *per se* in 1951 by Schwarz [1]. It protects against dietary liver necrosis in the rat and the pig [2], multiple necrotic degeneration (heart, liver, kidney, and muscle necrosis) in the mouse [3], as well as against exudative diathesis in the chick [4,5] and the turkey. Factor 3 has been shown to be an organic compound of high biological potency which contains the element selenium as an essential constituent [6]. Recently G. Bergson described the synthesis of 6-selenoctic acid, the selenium analogue of 6-thioctic acid; the author stated that "the hypothesis may be advanced that Factor 3 is identical with or related to 6-selenotic acid" [7]. This assumption can be eliminated for the following reasons:

(a) The possible involvement of thioctic acid or of compounds with similar physicochemical properties was excluded in 1951, in the course of extensive unpublished fractionation studies on Factor 3 carried out at Bethesda. Various procedures which separated thioctic acid from Factor 3 were applied to prepurified Factor 3 fractions from enzymatic casein digests and other sources. For instance, continuous extractions at a low pH with solvents such as benzene removed thioctic acid readily, but failed to remove the Factor 3-activity from the aqueous phase *.

(b) Following the discovery of selenium as an integral part of the Factor 3 molecule, a large variety of organic selenium compounds has been tested for Factor 3 activity, using the quantitative assay against dietary necrotic liver degeneration in the rat. An appreciable degree of chemical specificity was detected [8,9]. Several types of selenium compounds are inactive, while others prevent liver necrosis. The majority of the compounds tested, including selenate, selenite, and also the selenium analogues of cystine, cystathionine and methionine, was found to afford 50 % protection at dose levels which supply 2—3 μg of selenium per 100 g of diet (ED_{50} = 2—3 μg % Se). A purified preparation of α-Factor 3 from pork kidney powder was more potent than any other compound investigated. The fraction was accurately analyzed for selenium by radio activation analysis; its ED_{50} was established to be 0.7 μg % Se.

Animal assays for Factor 3 potency, at Bethesda, with 6-selenoctic acid from Uppsala have resulted in a value of 3.8 μg % Se for 50 % protection (Table 1) * §. Comparison of this ED_{50} value to that for α-Factor 3 clearly indicates that the latter is different from 6-selenoctic acid. The potency of the thioctic acid analogue is only 1/5 of that of the α-Factor 3 preparation, and somewhat less than that of selenite, selenocystine, etc. At present, the structure of the organic part of the Factor 3 molecule remains to be established.

Experimental. Synthesis and properties of 6-selenoctic acid have been described in this journal [7]. For the animal tests, the substance was dissolved in ethanol and added to the basal diet. Details of the standardized procedure

* Schwarz, K. *Unpublished results.*

* The authors wish to express their appreciation to Dr. B. Sjögren, Astra Research Laboratories, Södertälje, for advice.

§ A test with 6-selenoctic acid in chicks on an exudative diathesis producing diet (30 % *Torula* yeast, 28 % purified soy protein, 4% vitamin E free lard), carried out by J. G. Bieri, showed that 15 μg % of selenium in form of this compound protected all animals against the disease, while 7 out of 8 controls succumbed to the deficiency.

Table 1. Factor 3-activity of 6-selenoctic acid

Amount in diet		No. of animals	No. of dead animals *	Protection %	ED_{50}
Compound I μg %	Selenium μg %				μg Se/100 g diet
0	0	30	27		
3.8	2	20	17	16	
5.7	3	10	6	43	3.8
7.6	4	10	5	57	
11.4	6	10	2	83	
19	10	10	0	100	

* The experiments were terminated on the 30th day.

of the Factor 3 assay using a vitamin E and Factor 3-free 30 % *Torula* yeast ration [10], and weanling, inbred Fischer 344 rats [11] have been specified elsewhere. For evaluation of the results, the average velocity of death from liver necrosis (V_{st}) was calculated from individual survival times [12]. The effects were expressed in "% protection", *i.e.*, in per cent reduction of the velocity as compared to that of the control groups (% protection = 100 — 100 × V_{st} exp./V_{st} contr.). Weighted averages were used, and the ED_{50} was computed from those results which fell on the ascending part of the dose response curve (between 15 and 85 % protection). The assay method, set up twice weekly with 10—15 groups of 10 rats each, yields very consistent ED_{50}'s for selenite, Factor 3 and other compounds tested.

1. Schwarz, K. *Proc. Soc. Exptl. Biol.Med.* **78** (1951) 852.
2. Eggert, R. G., Patterson, E., Akers, W. T. and Stokstad, E. L. R. *J. Animal Science* **16** (1957) 1037.
3. DeWitt, W. B. and Schwarz, K. *Experientia* **14** (1958) 28.
4. Schwarz, K., Bieri, J. G., Briggs, G. M. and Scott, M. L. *Proc. Soc. Exptl. Biol. Med.* **95** (1957) 621.
5. Patterson, E. L., Milatroy, R. and Stokstad, E. L. R. *Proc. Soc. Exp. Biol. and Med.* **95** (1957) 621.
6. Schwarz, K. and Foltz, C. M. *J. Am. Chem. Soc.* **79** (1957) 3292.
7. Bergson, G. *Acta Chem. Scand.* **11** (1957) 1607.
8. Schwarz, K. and Foltz, C. M. *Federation Proc.* **17** (1958) 492.
9. Schwarz, K. and Foltz, C. M. *J. Biol. Chem. In press.*
10. Schwarz, K. *Proc. Soc. Exptl. Biol. Med.* **77** (1951) 818.
11. Jay, G. E., Jr., National Vitamin Foundation: *Rat Quality, A Consideration of Heredity, Diet and Disease*, New York, (1953) p. 98.
12. Schwarz, K. *Proc. Soc. Exptl. Biol. Med.* **80** (1952) 319.

Received June 13, 1958.

Preparation of Monoperphthalic Acid

S. LINHOLTER and P. SØRENSEN

Department of Organic Chemistry, University of Technology, Copenhagen, Denmark

The method for preparing monoperphthalic acid by oxidising phthalic anhydride with an alkaline solution of hydrogen peroxide, first suggested by Böhme [1], gives according to *Organic Syntheses* [2] normally 65—70 % yield. We found, however, this reaction to be somewhat capricious, sometimes giving only 40—50 % yield. By slightly modifying the procedure we succeeded in eliminating the capriciousness, and at the same time the yield was raised to 90—95 %.

The essential problem is to keep the solution sufficiently cool during the reaction. Operating the same charge as indicated in *Organic Syntheses* we cooled the solution in a carbon dioxide-acetone mixture and maintained a temperature below —5° during the whole reaction. At this temperature a crystal-layer will cover the walls of the reaction vessel, thus preventing the transmission of the heat of reaction to the cooling mixture. It is, therefore, necessary constantly to scrape down the crystals from the walls, which may easily be effected when using a beaker as reaction vessel instead of a flask. Using this procedure no foaming is observed and practically no phthalic acid was formed.

After the addition of sulphuric acid the temperature is allowed to rise to 0° and enough water is added to dissolve the inorganic material. The solution is extracted 5 times with ether, the ether-solution washed 3 times with ammoniumsulphate solution and dried over magnesiumsulphate.

The yield, ranging from 90 to 95 %, was estimated iodometrically as indicated in *Organic Syntheses*.

1. Böhme, H. *Ber.* **70** (1937) 379.
2. Böhme, H. *Org. Syntheses* **20** (1940) 70; Coll. Vol. **3** (1955) 619.

Received July 2, 1958.

Table 1. Factor 3-activity of 6-selenoctic acid

Amount in diet		No. of animals	No. of dead animals *	Protection %	ED_{50}
Compound I μg %	Selenium μg %				μg Se/100 g diet
0	0	30	27		
3.8	2	20	17	16	
5.7	3	10	6	43	3.8
7.6	4	10	5	57	
11.4	6	10	2	83	
19	10	10	0	100	

* The experiments were terminated on the 30th day.

of the Factor 3 assay using a vitamin E and Factor 3-free 30 % *Torula* yeast ration [10], and weanling, inbred Fischer 344 rats [11] have been specified elsewhere. For evaluation of the results, the average velocity of death from liver necrosis (V_{st}) was calculated from individual survival times [12]. The effects were expressed in "% protection", *i.e.*, in per cent reduction of the velocity as compared to that of the control groups (% protection = 100 — 100 × V_{st} exp./V_{st} contr.). Weighted averages were used, and the ED_{50} was computed from those results which fell on the ascending part of the dose response curve (between 15 and 85 % protection). The assay method, set up twice weekly with 10—15 groups of 10 rats each, yields very consistent ED_{50}'s for selenite, Factor 3 and other compounds tested.

1. Schwarz, K. *Proc. Soc. Exptl. Biol.Med.* **78** (1951) 852.
2. Eggert, R. G., Patterson, E., Akers, W. T. and Stokstad, E. L. R. *J. Animal Science* **16** (1957) 1037.
3. DeWitt, W. B. and Schwarz, K. *Experientia* **14** (1958) 28.
4. Schwarz, K., Bieri, J. G., Briggs, G. M. and Scott, M. L. *Proc. Soc. Exptl. Biol. Med.* **95** (1957) 621.
5. Patterson, E. L., Milatroy, R. and Stokstad, E. L. R. *Proc. Soc. Exp. Biol. and Med.* **95** (1957) 621.
6. Schwarz, K. and Foltz, C. M. *J. Am. Chem. Soc.* **79** (1957) 3292.
7. Bergson, G. *Acta Chem. Scand.* **11** (1957) 1607.
8. Schwarz, K. and Foltz, C. M. *Federation Proc.* **17** (1958) 492.
9. Schwarz, K. and Foltz, C. M. *J. Biol. Chem. In press.*
10. Schwarz, K. *Proc. Soc. Exptl. Biol. Med.* **77** (1951) 818.
11. Jay, G. E., Jr., National Vitamin Foundation: *Rat Quality, A Consideration of Heredity, Diet and Disease*, New York, (1953) p. 98.
12. Schwarz, K. *Proc. Soc. Exptl. Biol. Med.* **80** (1952) 319.

Received June 13, 1958.

Preparation of Monoperphthalic Acid

S. LINHOLTER and P. SØRENSEN

Department of Organic Chemistry, University of Technology, Copenhagen, Denmark

The method for preparing monoperphthalic acid by oxidising phthalic anhydride with an alkaline solution of hydrogen peroxide, first suggested by Böhme [1], gives according to *Organic Syntheses* [2] normally 65—70 % yield. We found, however, this reaction to be somewhat capricious, sometimes giving only 40—50 % yield. By slightly modifying the procedure we succeeded in eliminating the capriciousness, and at the same time the yield was raised to 90—95 %.

The essential problem is to keep the solution sufficiently cool during the reaction. Operating the same charge as indicated in *Organic Syntheses* we cooled the solution in a carbon dioxide-acetone mixture and maintained a temperature below —5° during the whole reaction. At this temperature a crystal-layer will cover the walls of the reaction vessel, thus preventing the transmission of the heat of reaction to the cooling mixture. It is, therefore, necessary constantly to scrape down the crystals from the walls, which may easily be effected when using a beaker as reaction vessel instead of a flask. Using this procedure no foaming is observed and practically no phthalic acid was formed.

After the addition of sulphuric acid the temperature is allowed to rise to 0° and enough water is added to dissolve the inorganic material. The solution is extracted 5 times with ether, the ether-solution washed 3 times with ammoniumsulphate solution and dried over magnesiumsulphate.

The yield, ranging from 90 to 95 %, was estimated iodometrically as indicated in *Organic Syntheses*.

1. Böhme, H. *Ber.* **70** (1937) 379.
2. Böhme, H. *Org. Syntheses* **20** (1940) 70; Coll. Vol. **3** (1955) 619.

Received July 2, 1958.

Zur Bestimmung von γ-Aminobuttersäure und Glutaminsäure in biologischem Material mit Hilfe von Hochspannungselektrophorese

ARNE HANSON und WILFRIED v. STUDNITZ

Chemisches Zentrallaboratorium d. Allg. Krankenhauses, Malmö, Schweden

Bei Untersuchungen im hiesigen Laboratorium über die Glutaminsäure-dekarboxylase im Gehirn ist die Bestimmung von γ-Aminobuttersäure (γ-ABS) und Glutaminsäure (GLTS) aktuell geworden. Die bisher vorliegenden Methoden beruhen entweder auf der Säulenchromatographie oder der Papierchromatographie. Beide Methoden sind relativ zeitraubend und bei einer quantitativen Bestimmung gibt letztere keine zufriedenstellenden Resultate. So waren wir interessiert eine Methode zu finden, die es ermöglicht γ-ABS und GLTS *gleichzeitig* und mit relativer Genauigkeit in kurzer Zeit zu bestimmen. Wichtig war es auch für uns mit relativ kleinen Mengen Ausgangsmaterial auszukommen, da wir als solches Gehirnextrakt verwandten. — So arbeiteten wir eine Methode aus, die mit Hilfe der Hochspannungselektrophorese die von uns gewünschten Kriterien erfüllte.

Methode. Hochspannungselektrophorese nach Wieland und Pfleiderer [1]. Als Träger diente Papier von Macherey & Nagel Nr. 214. Pufferlösung: konz. Ameisenäure: Eisessig : Wasser (15:10:75) v/v. Elektrophoresedauer 75 Min bei einem Spannungsgefälle von 2 100 Volt zwischen den Elektroden (55 Volt/cm). Auftragsstelle 8 cm von der Anode. Wir trugen 0.005—0.03 ml Gewebeextrakt auf (alkoholischer Extrakt eines sauren Gewebeinkubates). Ein Entsalzen fällt bei den hier verwandten Spannungen weg. Nach einer Elektrophoresezeit von 75 Min ist die GLTS 10.5 cm und die γ-ABS 15.8 cm kathodenwärts gewandert. (Siehe Bild 1.) Nach Trennung wird das Papier bei 75° im Trockenschrank eine halbe Stunde getrocknet, wobei sich die Pufferlösung verflüchtigt. Anschliessend wird das Pherogramm mit einer 0.5 % Ninhydrinlösung in *n*-Butanol, der mit einer Mischung von Pyridin:Eisessig:Wasser (10:1:95) pH 6, gesättigt ist, besprüht. Dann wird das Papier für 20 Min vor einem Ventilator bei ca. 40° getrocknet und der Farbentwicklung im Trockenschrank bei 65° für 20 Min überlassen. Nun wird die gebildete Ninhydrinfarbe nach Kawerau und Wieland [2] in einen Kupferkomplex überführt. Es wurde das Kupferreagens in der Modifikation nach Fischer und Dörfel [3] verwandt. Die gebildeten roten Farbflecke werden nach Trocknem im kalten Luftstrom mit einer bestimmten Menge (in unseren Versuchen 4 ml) Methanol eluiert und nach 20 Min im Beckman-Spektrophotometer B bei 504 mμ in 1 cm-Küvetten gemessen. — Zur Errechnung des Leerwertes wird ein entsprechend grosses Papierstück, das auf die gleiche Art behandelt wurde, eluiert und der erhaltene Extinktionswert von den anderen abgezogen. — Eine bekannte Standardlösung von γ-ABS und GLTS wird — am besten in 3 verschiedenen Konzentrationen — mit pherographiert und entsprechend behandelt. Mit Hilfe der von den Standardlö-

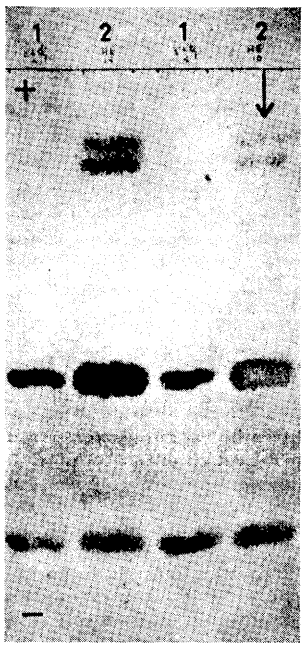

Abb. 1. Elektropherogramm einer Standardlösung von γ-Aminobuttersäure und Glutaminsäure (1) und Gehirnextrakt (2). Siehe Text.

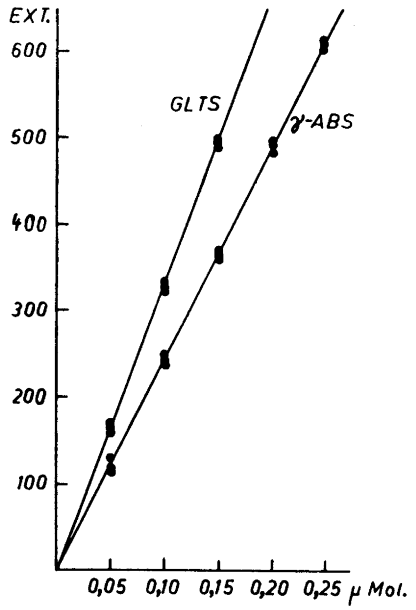

Abb. 2.

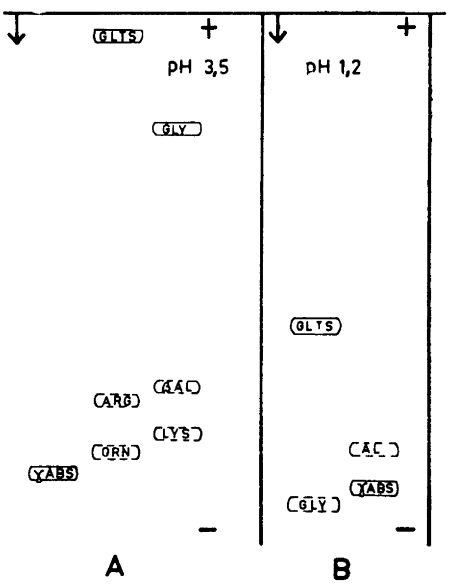

Abb. 3, A und B.

sungen erhaltenen Extinktionen (nach Korrektion mit dem Leerwert) werden Eichkurven angefertigt und so die Konzentration an γ-ABS und GLTS in der zu untersuchenden Lösung rechnerisch ermittelt. Beispiel siehe Bild 2. — Sollten in dem zu untersuchenden Material (z.B. Serumextrakt) grössere Mengen Glycin auftreten, so kann es vorkommen, dass in Folge eines "Overloading"-Effektes die γ-ABS nicht klar vom Glycin zu trennen ist. Letzteres hat eine etwas grössere Mobilität als γ-ABS. (Siehe Bild 3 A.) Hier kann man sich weiter helfen in dem man in einem Puffermilieu von pH 3,5 arbeitet. (Puffer: Eisessig:Pyridin:Wasser, 15:1:89, v/v.) Bei gleichen Versuchsbedingungen wie oben erhält man ein Trennungsbild wie im Bild 3 B; Auftragsstelle 12 cm von der Anode. γABS wandert 15 und Glycin nur 5 cm zur Kathode. Auch GLTS ist in diesem Milieu gut zu bestimmen und wird bei ihrer kurzen Wanderungsstrecke (1 cm) nicht von anderen Aminosäuren überlagert.

Die Untersuchungen wurden vom *Schwedischen Medizinischen Forschungsrat* unterstützt.

1. Wieland, Th. und Pfleiderer, G. *Angew. Chem.* **67** (1955) 257.
2. Kawerau, E. und Wieland, Th. *Nature* **168** (1951) 77.
3. Fischer, F. G. und Dörfel, H. *Biochem. Z.* **324** (1953) 544.

Eingegangen am 16. Juni 1958.

On Light-Induced Phosphorylation in *Rhodospirillum rubrum*

HERRICK BALTSCHEFFSKY and MARGARETA BALTSCHEFFSKY

Wenner-Gren Institute, University of Stockholm, Sweden

Light-induced phosphorylation (LIP) was described in 1954 by Arnon, Allen and Whatley [1] for plant and by Frenkel [2] for bacterial systems. Among the concepts about its mechanism are: (1) the phosphorylation reactions are coupled to an electron carrier chain, which recombines the photochemical oxidant (OH) and the

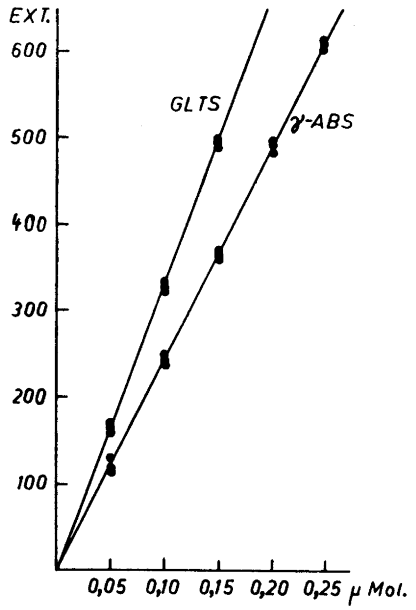

Abb. 2.

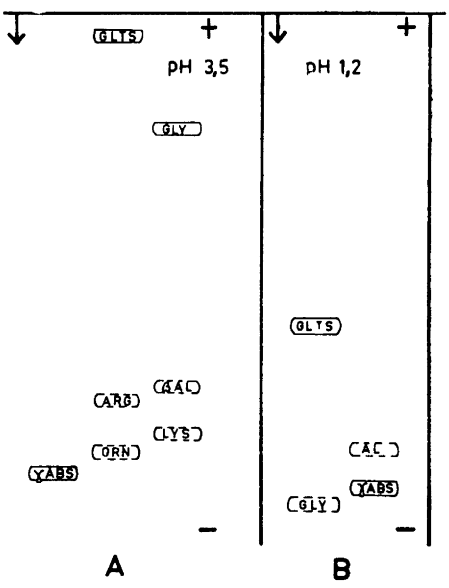

Abb. 3, A und B.

sungen erhaltenen Extinktionen (nach Korrektion mit dem Leerwert) werden Eichkurven angefertigt und so die Konzentration an γ-ABS und GLTS in der zu untersuchenden Lösung rechnerisch ermittelt. Beispiel siehe Bild 2. — Sollten in dem zu untersuchenden Material (z.B. Serumextrakt) grössere Mengen Glycin auftreten, so kann es vorkommen, dass in Folge eines "Overloading"-Effektes die γ-ABS nicht klar vom Glycin zu trennen ist. Letzteres hat eine etwas grössere Mobilität als γ-ABS. (Siehe Bild 3 A.) Hier kann man sich weiter helfen in dem man in einem Puffermilieu von pH 3,5 arbeitet. (Puffer: Eisessig:Pyridin:Wasser, 15:1:89, v/v.) Bei gleichen Versuchsbedingungen wie oben erhält man ein Trennungsbild wie im Bild 3 B; Auftragsstelle 12 cm von der Anode. γABS wandert 15 und Glycin nur 5 cm zur Kathode. Auch GLTS ist in diesem Milieu gut zu bestimmen und wird bei ihrer kurzen Wanderungsstrecke (1 cm) nicht von anderen Aminosäuren überlagert.

Die Untersuchungen wurden vom *Schwedischen Medizinischen Forschungsrat* unterstützt.

1. Wieland, Th. und Pfleiderer, G. *Angew. Chem.* **67** (1955) 257.
2. Kawerau, E. und Wieland, Th. *Nature* **168** (1951) 77.
3. Fischer, F. G. und Dörfel, H. *Biochem. Z.* **324** (1953) 544.

Eingegangen am 16. Juni 1958.

On Light-Induced Phosphorylation in *Rhodospirillum rubrum*

HERRICK BALTSCHEFFSKY and MARGARETA BALTSCHEFFSKY

Wenner-Gren Institute, University of Stockholm, Sweden

Light-induced phosphorylation (LIP) was described in 1954 by Arnon, Allen and Whatley [1] for plant and by Frenkel [2] for bacterial systems. Among the concepts about its mechanism are: (1) the phosphorylation reactions are coupled to an electron carrier chain, which recombines the photochemical oxidant (OH) and the

photochemical reductant (H) from the Hill reaction, or its equivalent in bacteria, to H_2O, and (2) P + ADP = ATP * is the net chemical reaction in LIP. Molecular oxygen is not involved in the process. Arnon, Whatley and Allen [3] have suggested that FMN, vitamin K and ascorbate are three of the components in the postulated carrier chain in isolated spinach chloroplasts. Recently, however, they have included TPN and excluded ascorbate and postulated that vitamin K and FMN participate in "alternative pathways for cyclic photophosphorylation" [4], in agreement with the hypothesis of Wessels. [5] Smith and Baltscheffsky [6] have shown that a substance with an absorption spectrum peak at 434 mμ appears to be involved in LIP in extracts of *Rhodospirillum rubrum*. It very probably is identical with the hemoprotein isolated by Vernon and Kamen [7] and recently described by Bartsch and Kamen [8]. Phenazine methosulfate stimulates the phosphorylation in *R. rubrum* [9] and in isolated chloroplasts [10]. The mechanism of the phosphorylation reactions is unknown.

This preliminary communication about LIP in cell-free extracts of *R. rubrum* deals with inhibitor effects, the action of phenazine methosulfate, ATP-ase and ^{32}P-ATP-exchange reactions. The bacteria were grown anaerobically at 30°C in light from incandescent lamps, in essentially the medium of Gest, Kamen and Bregoff [11]. After one washing of the harvested bacteria with distilled water and one with 0.02 M glycylglycine, pH 7.4, the extracts were prepared by grinding with alumina [6] and securing the supernatant from a 10 min centrifugation at 10 000 × *g*. The phosphorylation experiments were performed at saturating light intensities and 30°C. Phosphate was measured according to Lindberg and Ernster [12].

Table 1 shows the effect of some inhibitors on our system. In agreement with earlier data by Smith and Baltscheffsky [13] the inhibitors of mitochondrial respiration, KCN and NaN_3 did not influence LIP, whereas the uncoupler of oxidative phosphorylation dicoumarol had a strong effect. The observations of Smith and Baltscheffsky [6] that HOQNO and of Geller and Gregory [9] that antimycin A inhibit LIP are confirmed. Both inhibit electron transport between cytochrome b and cytochrome c_1 in mitochondria [14], thus it would seem logical to assume that the point of action is the same in LIP as in mitochondria. The absence of an effect of KCN and NaN_3 on LIP is in line with the fact that the hemoprotein, which Bartsch and Kamen [8] described and which very probably is the compound suggested by Smith and Baltscheffsky [6] to take part in LIP, does not form addition compounds with KCN and NaN_3. We consider the possibility that this hemoprotein, assumed by Chance and Smith [15] and by Bartsch and Kamen [8] to be a terminal oxidase for *R. rubrum*, reacts in LIP with oxidizing equivalent produced by the bacterial equivalent of the Hill reaction.

Table 1. Effect of different inhibitors on LIP. Medium: 2 ml 0.2 M glycylglycine pH 7.4, 20 μmoles K_2HPO_4, 10 μmoles ADP, 35 μmoles $MgCl_2$, 30 μmoles NaF, diluted to a final volume of 3.0 ml.

Inhibitor	Final concentration of inhibitor M	% Inhibition
KCN	10^{-3}	0
NaN_3	10^{-3}	0
Dicoumarol	10^{-4}	> 90
HOQNO	2×10^{-6}	> 95
Antimycin A	3×10^{-6}	> 95
Atebrin	7×10^{-3}	about 25

Table 2 shows a typical stimulation of the LIP obtained by 0.02 % phenazine

Table 2. Effect of HOQNO and phenazine methosulfate on LIP. Medium: as in Table 1. Where added: 2×10^{-6} M HOQNO and 0.01 % phenazine methosulfate, final concentrations.

Addition	μmoles P/hour/"OD_{800}" *
—	22
HOQNO	0
Phenazine methosulfate	180
HOQNO + phenazine methosulfate	130

* Abbreviations: P, orthophosphate; ADP, adenosine diphosphate; ATP, adenosine triphosphate; ATP-ase, adenosine triphosphatase; TPN, triphosphopyridine nucleotide; FMN, flavin mononucleotide; HOQNO, 2-*n*-heptyl-4-hydroxyquinoline-N-oxide; M, moles per liter.

* "OD_{800}" stands for the optical density of the absorption spectrum peak near 800 mμ of the bound chlorophyll (compare with Frenkel [17]).

methosulfate and the effect of HOQNO in the absence and the presence of phenazine methosulfate. Similar effects as with HOQNO are obtained with antimycin A and dicoumarol. Geller [16] assumes that phenazine methosulfate serves as a fast "by-pass" around the site which is rate limiting in the system. Our data indicate that a site which is inhibited by antimycin A and HOQNO is "by-passed" by phenazine methosulfate. The point at which dicoumarol acts, which is also "by-passed" may or may not be the same as is acted upon by antimycin A and HOQNO.

Frenkel [17] has reported that an active ATP-ase is present in his "crude" preparation of *R. rubrum*. In our system both a Mg++-stimulated ATP-ase and a ^{32}P-ATP-exchange reaction are present. The ATP-ase activity was inhibited to more than 90 % and the ^{32}P-ATP-exchange activity to about 80 % by 7 mM atebrin, which Löw [18] has shown to inhibit respiration, ATP-ase and ^{32}P-ATP-exchange reactions in liver mitochondria. The possible relation between these reactions and LIP is under investigation.

1. Arnon, D. I., Allen, M. B. and Whatley, F. R. *Nature* **174** (1954) 394.
2. Frenkel, A. W. *J. Am. Chem. Soc.* **76** (1954) 5568.
3. Arnon, D. I., Whatley, F. R. and Allen, M. B. *Biochim. et Biophys. Acta* **16** (1955) 607.
4. Arnon, D. I., Whatley, F. R. and Allen, M. B. *Science* **127** (1958) 1026.
5. Wessels, J. S. C. *Biochim. et Biophys. Acta* **25** (1957) 97.
6. Smith, L. and Baltscheffsky, M. *Federation Proc.* **15** (1956) 357.
7. Vernon, L. P. and Kamen M. D. *J. Biol. Chem.* **211** (1954) 643.
8. Bartsch, R. G. and Kamen, M. D. *J. Biol. Chem.* **230** (1958) 41.
9. Geller, D. M. and Gregory, J. D. *Federation Proc.* **15** (1956) 260.
10. Jagendorf, A. T. and Avron, M. *J. Biol. Chem.* **231** (1958) 277.
11. Gest, H., Kamen, M. D. and Bregoff, H. M. *J. Biol. Chem.* **182** (1950) 153.
12. Lindberg, O. and Ernster, L. in Glick, D. *Methods of Biochemical Analysis*, Interscience Pulishers, New York 1956, Vol. 3 p. 1.
13. Smith, L. and Baltscheffsky, M. *To be published.*
14. Chance, B. in Colowick, S. P. and Kaplan, N. O. *Methods in Enzymology*, Academic Press, New York 1957, Vol. IV, p. 273.
15. Chance, B. and Smith, L. *Nature* **175** (1955) 803.
16. Geller, D. M. *Dissertation* (quoted from Ref.[4]).
17. Frenkel, A. W. *J. Biol. Chem.* **222** (1956) 823.
18. Löw, H. *Biochim. et Biophys. Acta, In press.*

Received June 16, 1958.

Chromatography of Tropolones on Paper Impregnated with Ethylenediaminetetraacetic Acid and Dimethyl Sulphoxide

CARL AXEL WACHTMEISTER and BÖRJE WICKBERG

Institutionen för organisk kemi, Kungl. Tekniska Högskolan, Stockholm, Sweden

Tropolones have recently been found in a number of conifer heartwoods and their identification by paper chromatography is therefore a matter of considerable interest. Conventional methods for the identification of phenols have been tried but give bad results due to tailing of the spots. This disadvantage was successfully eliminated by Zavarin and Anderson [1] by using paper impregnated with phosphoric acid and toluene — *iso*octane as mobile phase. In a search for a chemically less agressive stationary phase, which would also be suitable for preparative work, the use of dimethyl sulphoxide was investigated. Although highly polar, this is a good solvent for most lipophilic compounds and has been used with advantage in paper chromatography of sugar acetates and related compounds [2].

Preliminary experiments using dimethyl sulphoxide impregnated paper with light petroleum as mobile phase indicated favourable R_F-values although the spots were still very elongated, extending from the starting line. The length of the spots was dependent on the amount of substance applied but the distance travelled by the lower edge of the spot reached a limit when the amount of tropolone was increased. These results point to an irreversible adsorption of the tropolones.

Tropolones are known to form stable chelates with a number of multivalent cations and an obvious explanation of their

methosulfate and the effect of HOQNO in the absence and the presence of phenazine methosulfate. Similar effects as with HOQNO are obtained with antimycin A and dicoumarol. Geller [16] assumes that phenazine methosulfate serves as a fast "by-pass" around the site which is rate limiting in the system. Our data indicate that a site which is inhibited by antimycin A and HOQNO is "by-passed" by phenazine methosulfate. The point at which dicoumarol acts, which is also "by-passed" may or may not be the same as is acted upon by antimycin A and HOQNO.

Frenkel [17] has reported that an active ATP-ase is present in his "crude" preparation of *R. rubrum*. In our system both a Mg++-stimulated ATP-ase and a ^{32}P-ATP-exchange reaction are present. The ATP-ase activity was inhibited to more than 90 % and the ^{32}P-ATP-exchange activity to about 80 % by 7 mM atebrin, which Löw [18] has shown to inhibit respiration, ATP-ase and ^{32}P-ATP-exchange reactions in liver mitochondria. The possible relation between these reactions and LIP is under investigation.

1. Arnon, D. I., Allen, M. B. and Whatley, F. R. *Nature* **174** (1954) 394.
2. Frenkel, A. W. *J. Am. Chem. Soc.* **76** (1954) 5568.
3. Arnon, D. I., Whatley, F. R. and Allen, M. B. *Biochim. et Biophys. Acta* **16** (1955) 607.
4. Arnon, D. I., Whatley, F. R. and Allen, M. B. *Science* **127** (1958) 1026.
5. Wessels, J. S. C. *Biochim. et Biophys. Acta* **25** (1957) 97.
6. Smith, L. and Baltscheffsky, M. *Federation Proc.* **15** (1956) 357.
7. Vernon, L. P. and Kamen M. D. *J. Biol. Chem.* **211** (1954) 643.
8. Bartsch, R. G. and Kamen, M. D. *J. Biol. Chem.* **230** (1958) 41.
9. Geller, D. M. and Gregory, J. D. *Federation Proc.* **15** (1956) 260.
10. Jagendorf, A. T. and Avron, M. *J. Biol. Chem.* **231** (1958) 277.
11. Gest, H., Kamen, M. D. and Bregoff, H. M. *J. Biol. Chem.* **182** (1950) 153.
12. Lindberg, O. and Ernster, L. in Glick, D. *Methods of Biochemical Analysis*, Interscience Pulishers, New York 1956, Vol. 3 p. 1.
13. Smith, L. and Baltscheffsky, M. *To be published.*
14. Chance, B. in Colowick, S. P. and Kaplan, N. O. *Methods in Enzymology*, Academic Press, New York 1957, Vol. IV, p. 273.
15. Chance, B. and Smith, L. *Nature* **175** (1955) 803.
16. Geller, D. M. *Dissertation* (quoted from Ref.[4]).
17. Frenkel, A. W. *J. Biol. Chem.* **222** (1956) 823.
18. Löw, H. *Biochim. et Biophys. Acta, In press.*

Received June 16, 1958.

Chromatography of Tropolones on Paper Impregnated with Ethylenediaminetetraacetic Acid and Dimethyl Sulphoxide

CARL AXEL WACHTMEISTER and BÖRJE WICKBERG

Institutionen för organisk kemi, Kungl. Tekniska Högskolan, Stockholm, Sweden

Tropolones have recently been found in a number of conifer heartwoods and their identification by paper chromatography is therefore a matter of considerable interest. Conventional methods for the identification of phenols have been tried but give bad results due to tailing of the spots. This disadvantage was successfully eliminated by Zavarin and Anderson [1] by using paper impregnated with phosphoric acid and toluene — *iso*octane as mobile phase. In a search for a chemically less agressive stationary phase, which would also be suitable for preparative work, the use of dimethyl sulphoxide was investigated. Although highly polar, this is a good solvent for most lipophilic compounds and has been used with advantage in paper chromatography of sugar acetates and related compounds [2].

Preliminary experiments using dimethyl sulphoxide impregnated paper with light petroleum as mobile phase indicated favourable R_F-values although the spots were still very elongated, extending from the starting line. The length of the spots was dependent on the amount of substance applied but the distance travelled by the lower edge of the spot reached a limit when the amount of tropolone was increased. These results point to an irreversible adsorption of the tropolones.

Tropolones are known to form stable chelates with a number of multivalent cations and an obvious explanation of their

tailing would be complex formation between the tropolone molecules and cations adsorbed on the cellulose surface. The ion exchange properties of cellulose due to its content of carboxyl groups is well known [3] and the influence of adsorbed metal ions on the tailing of ionisable compounds in paper chromatography has been discussed [3,4].

In view of these considerations it appeared possible to eliminate the tailing of the tropolone spots simply by adding an excess of a competing chelating agent. This was successfully achieved by chromatography on paper impregnated with partly neutralised solutions of ethylenediaminetetraacetic acid (EDTA) before impregnation with dimethyl sulphoxide. Under slightly acidic conditions which gave the best results, the tropolones investigated gave well-defined, almost circular spots. Light petroleum, *cyclo*-hexane and di-*iso*propylether were used as mobile phases, and the chromatograms were run in an atmosphere of low moisture content. The first two solvents gave a satisfactory separation of β- and γ-thujaplicins which have very similar properties. The R_F-values observed are given in Table 1. Within the range 5—200 μg these values were largely independent of the amount of substance applied. The R_F-values were fairly reproducible if care was taken to carry out the impregnation under identical conditions.

It is obvious that the use of paper impregnated with EDTA may be of a general value in eliminating tailing caused by adsorbed inorganic ions. The use of other chelating agents would also be possible; the phosphoric acid used by Zavarin and Anderson [2] is probably also an example of this.

Table 1. R_F-values of tropolones on paper impregnated with EDTA and dimethyl sulphoxide.

Mobile phase	Light petroleum B.p. 60—71°	*Cyclo*-hexane	Di-*iso*propyl ether
Tropolone	0.08	0.10	0.30
7-Hydroxy-4-*iso*propyl-tropolone	0.15	0.18	0.40
γ-Thujaplicin	0.32	0.38	0.55
β-Thujaplicin	0.40	0.45	0.60
α-Thujaplicin	0.62	0.65	0.75
Nootkatin	0.72	0.75	0.82

Experimental. The strips of paper (46 × 12 cm, Whatman No. 1) were soaked in an aqueous solution containing 0.015 moles of the disodium salt of EDTA and 0.005 moles of EDTA per litre. After drying in air, the strips were impregnated twice with a 25 % v/v solution of dimethyl sulphoxide in toluene as described previously [2]. The solvents were of reagent grade and were used without drying. The moisture content of the air in the tanks containing hydrocarbon solvents was kept low with anhydrous silica gel.

The tropolones (5—200 μg) were applied as 1—5 % solution in chloroform and the strips were protected from contact with air by covering with glass slides [2]. The chromatograms were developed by the descending technique, the solvent front reaching 30 cm from the starting line in 1—3 h. After short drying in air, the strips were sprayed with a 1 % solution of iron (III) chloride to give spots of red or, in case of 7-hydroxy-4-*iso*propyltropolone, violet colours. The tropolones could also be located under the ultra-violet lamp as dark spots which after spraying with alkali showed a greenish or yellowish fluorescence. They gave red or yellow spots on treatment of the chromatograms with a solution of *bis*-diazotised benzidine [5] followed by spraying with a sodium carbonate solution.

Acknowledgement. The authors are indebted to Dr. H. Fernholz and Dr. J. A. F. Gardner for generous gifts of tropolone and 7-hydroxy-4-*iso*propyltropolone, respectively, to *Statens Naturvetenskapliga Forskningsråd* for financial support and to Dr. B. Thomas for checking the English.

1. Zavarin, E. and Anderson, A. B. *J. Org. Chem.* **21** (1956) 332.
2. Wickberg. B. *Acta Chem. Scand.* **12** (1958) 615.
3. Schröder, K. H. *Chemiker-Ztg.* **81** (1957) 558.
4. Hanes, C. S. and Isherwood, F.A. *Nature* **164** (1949) 1107.
5. Koch, J. E. and Krieg, W. *Chemiker-Ztg.* **62** (1938) 140.

Received June 18, 1958,

Crystal Data on Salts of Hexathionic Acid

OLAV FOSS and KARSTEN H. PALMORK

Chemical Institute, University of Bergen, Bergen, Norway

The existence of hexathionic acid, $H_2S_6O_6$, was first established by Weitz and Achterberg [1] in 1928, through the isolation of the potassium salt from the reaction of potassium thiosulphate and potassium nitrite with hydrochloric acid. Although the polythionate series extends far higher, up to and including the hydrophilic Odén's sulphur sols which appear to be sodium polythionates $Na_2S_xO_6$ with $50 < x < 100$, hexathionates are the highest polythionates which have been isolated in a pure state and not as mixtures with higher and lower homologues [2-5].

The present authors have made a preparative and X-ray crystallographic study of salts of hexathionic acid, for subsequent attempts at structure analyses, and the results are given below. Unit cell and space group data have been obtained for two salts the crystals of which are, in view of the rather unstable nature and poor crystallization power of hexationates, surprisingly well developed and stable. The salts are, *trans*-dichloribis(ethylenediamine)cobalt(III) hexathionate, first prepared by Weitz and Achterberg [1], and a potassium barium double salt found in the present work. As starting material for their preparation served the potassium salt, prepared by Weitz and Achterberg's procedure [1] as slightly modified by Stamm, Seipold and Goehring [6].

The X-ray data were derived from oscillation and Weissenberg photographs of single-crystal specimens, using CuK radiation, $\lambda(\alpha) = 1.542$ Å, and for the cobalts salts FeK radiation, $\lambda(\alpha) = 1.937$ Å. The axial lengths were calibrated against potassium chloride powder lines superimposed on zero-layer Weissenberg photographs, and are believed to be accurate to within 0.5 %. Density determinations were made by flotation in bromoform-carbon tetrachloride mixtures.

Potassium hexathionate, $K_2S_6O_6$. The salt crystallizes in small, very thin plates [1,2], and only in one sample was a crystal found large enough for some photographs to be taken. The crystals are triclinic, with $a = 7.37$ Å, $b = 7.43$ Å (from layer-line separations on oscillation photographs), $d_{100} = 7.07$ Å, $d_{010} = 7.15$ Å, $d_{001} = 10.42$ Å, $\alpha^* = 74\frac{1}{2}°$, $\beta^* = 73\frac{1}{2}°$ (from zero-layer Weissenberg photographs about the a and b axes). The a and b axes lie in the plane of the plate and make an angle of about 90° with each other. This gives a cell volume of about 570 Å^3 and a density of about 2.13 g/cm^3 for two formula units per unit cell; found, 2.15 g/cm^3.

trans-*Dichlorobis(ethylenediamine)cobalt(III)hexathionate*, $[Coen_2Cl_2]_2S_6O_6 \cdot H_2O$. Green, long, orthorhomic prisms {110}, with $a = 12.12$ Å, $b = 19.13$ Å, $c = 6.43$ Å, and two formula units per unit cell; density, calc. 1.80, found 1.80 g/cm^3. Systematic absences, $0kl$ when k is odd, $h0l$ when h is odd. Of the two space groups compatible with these absences, C_{2v}^8 —*Pba*2 is probably the correct one; it requires that the hexathionate ion lies on a twofold axis of symmetry. The other possible place group, D_{2h}^9—*Pbam*, would require the symmetry 2/m for the ion, which is quite improbable. The space group *Pba*2 appears to be rare, no example being listed by Donnay and Nowacki [7] (1954).

Although no mentioning of water of crystallization was made by Weitz and co-workers [1,2], the density and the analytical data point to the presence of one mole of crystal water in the salt. The water molecule would lie on the second set of twofold positions (twofold axes) of the space group. In a vacuum over phosphorus pentoxide the finely powdered salt lost 1.3 % weight in the course of three weeks; calc. for monohydrate, 2.2 %.

The salt was prepared from equal volumes of about 0.2 M aqueous *trans*-dichlorobis(ethylenediamine)cobalt(III) chloride and about 0.13 M potassium hexathionate in 0.5 N hydrochloric acid, by mixing at about 50°C, and cooling. For analysis, 0.6055 g was dissolved in water, and the solution run through a 'Zeo-Karb' 225 ion exchange column (acid form) and then made up to 250 ml in a volumetric flask. Four 25 ml samples were pipetted out and analyzed for hexathionate by means of the sulphite method [8]: 22.98±0.02 ml of 0.00982 N iodine; calc. for monohydrate, 22.94 ml. Cobalt and total sulphur were determined gravimetrically in separate samples, sulphur as barium sulphate, and cobalt as sulphate after ignition of the substance and treatment of the residue with sulphuric acid, in both cases as described by Weitz and Spohn [2]. (Found:

S 23.81, Co 14.62. Calc. for monohydrate, S 23.86, Co 14.62.)

Potassium barium hexathionate, $K_2Ba(S_6O_6)_2$. Monoclinic prismatic, $a = 11.58$ Å, $b = 10.81$ Å, $c = 9.14$ Å, $\beta = 112°$. There are two formula units per unit cell; density, calc. 2.48, found 2.49 g/cm³. The space group is C_{2h}^4-$P2/c$, which requires that the barium ions lie in special, twofold positions.

The salt crystallized, very slowly, as well developed prisms extended along the c axis, bounded by {100} (dominant) and {110} and terminated by {$\bar{1}$11}. It has a faint yellowish colour, discernible only in the larger crystals.

The crystal structure has been solved [9], through Fourier projections along the b and c axes by use of the heavy atom technique in the first stages. All the cations lie in special, twofold positions, the barium ion and one of the potassium ions on a twofold axis at $0,y,\frac{1}{4}$ with $y = 0$ and $y = 0.45$, respectively, and the other potassium ion in a symmetry centre at $\frac{1}{2},0,0$. The hexathionate ions occupy general, fourfold positions. The sulphur chain of the hexathionate ion is unbranched and nonplanar, and the configuration of the chain is *cis-cis*, *i. e.*, as in the S_8 ring of orthorhombic sulphur.

Crystals of the salt, admixed with crystals of barium chloride, were first observed in an attempt to prepare barium hexathionate from crude potassium hexathionate, containing potassium chloride, through metathesis with barium perchlorate. A subsequent experiment using pure, recrystallized potassium hexathionate (5 g) and half the equimolar amount (2.66 g) of barium perchlorate trihydrate, in which, after addition of methanol, and standing, 1.4 g of potassium hexathionate first crystallized and then 0.35 g of the double salt, led to the following procedure: 3.6 g of potassium hexathionate was dissolved in 6 ml of 0.5 N hydrochloric acid at about 50°C, and the solution added to 2.66 g of barium perchlorate trihydrate in 1 ml of water. The mixture was cooled and the potassium perchlorate filtered off, and 5 ml of methanol was added to the filtrate. Yield, after two days in a refrigerator, 0.9 g of the double salt.

Barium was determined gravimetrically as sulphate, and potassium as tetraphenylborate. 0.1242 g substance gave 0.0372 g $BaSO_4$ and 0.1110 g $KB(C_6H_5)_4$ (Found: Ba 17.6, K 9.75. Calc. for $K_2Ba(S_6O_6)_2$: Ba 17.3, K 9.87.) Polythionate analysis was made by the sulphite method: One fifth of 0.1307 g substance gave 19.85 ml of 0.01 N iodine; calc. 19.79 ml.

In the course of the work, unit cell and space group data were obtained also for three pentathionates.

Sodium pentathionate dihydrate, $Na_2S_5O_6 \cdot 2H_2O$. Orthorhombic prisms extended along the c axis, with $a = 8.94$ Å, $b = 22.86$ Å, $c = 5.53$ Å. There are four formula units per unit cell; density, calc. 1.99, found 2.05 g/cm³. Systematic absences, $0kl$ when $k+l$ is odd, $h0l$ when l is odd. In view of the shortness of the c axis and the known configuration and dimensions of the pentathionate ion, the existence of a mirror plane normal to the c axis appears unlikely, so that the space group is probably $C_{2v}^6 - Pnc2$.

The salt was prepared from potassium pentathionate through metathesis with sodium perchlorate. It was described as a dihydrate by Kurtenacker and Laszlo [10], and as a trihydrate by Deines and Christoph [11]. Iodometric analysis of the X-ray sample by the sulphite method indicated two moles of water, and in a vacuum over phosphorus pentoxide the sample lost 9.5 % weight; calc. for dihydrate, 10,6 %.

Ammonium pentathionate hemitrihydrate, $(NH_4)_2S_5O_6 \cdot 1\frac{1}{2}H_2O$. Orthorhombic bipyramidal, $a = 20.59$ Å, $b = 9.33$ Å, $c = 12.61$ Å. The space group, from systematic absences, is $D_{2h}^{14} - Pbcn$. These X-ray data indicate that the salt is isomorphous with a series of pentathionate, selenopentathionate and telluropentathionate hemitrihydrates described earlier [12]. They contain eight formula units per unit cell. Iodometric analysis by the sulphite method gave a formula weight agreeing with that of a hemitrihydrate.

The salt was obtained as long prisms by recrystallization from 2 N hydrochloric acid of a sample of ammonium hexathionate (containing about 35 mole % of pentathionate) prepared from benzidinium hexathionate as described by Weitz and Spohn [2]. It appears that the '*überraschend gut ausgebildete, bis zu 1 cm lange Stäbchen*' of alleged ammonium hexathionate obtained in the same way by Weitz and Spohn [2] may have been the pentathionate.

trans-*Dichlorobis(ethylenediamine)cobalt(III) pentathionate*, $[Co\ en_2Cl_2]_2S_5O_6$. Green, monoclinic prisms extended along the c axis, with $a = 23.30$ Å, $b = 18.46$ Å, $c = 6.53$ Å, $\beta = 97°$, and four formula units per unit cell; density, calc. 1.80,

found 1.80 g/cm³. The systematic absences, $0k0$ when k is odd, indicate that the space group is $C_2^2-P2_1$ or $C_{2h}^2-P2_1/m$. No molecular symmetry is required in either case.

The crystals are thus different from those of the corresponding hexathionate, described above. From hexathionate upwards to about nonathionate, mixed crystals of *trans*-dichlorobis(ethylenediamine)cobalt(III) polythionates, indicating isomorphism, appear to exist [2].

1. Weitz, E. and Achterberg, F. *Ber.* **61** (1928) 399.
2. Weitz, E. and Spohn, K. *Chem. Ber.* **89** (1956) 2332.
3. Weitz, E., Becker, F. and Gieles, K. *Chem. Ber.* **89** (1956) 2345.
4. Weitz, E., Becker, F., Gieles, K. and Alt, B. *Chem. Ber.* **89** (1956) 2353.
5. Weitz, E., Gieles, K., Singer, J. and Alt, B. *Chem. Ber.* **89** (1956) 2365.
6. Stamm, H., Seipold, O. and Goehring, M. *Z. anorg. allgem. Chem.* **267** (1941) 277.
7. Donnay, J. D. H. and Nowacki, W. *Crystal Data*. The Geological Society of America Memoir 60, New York, 1954.
8. Kurtenacker, A. *Analytische Chemie der Sauerstoffsäuren des Schwefels*, Ferdinand Enke, Stuttgart 1938.
9. Foss, O., Hordvik, A. and Palmork, K. H. *Acta Chem. Scand.* **12** (1958) 1339.
10. Kurtenacker, A. and Laszlo, G. *Z. anorg. allgem. Chem.* **237** (1938) 359.
11. Deines, O. and Christoph, E. *Z. anorg. allgem. Chem.* **213** (1933) 209.
12. Foss, O. and Jahr, J. *Acta Chem. Scand.* **4** (1950) 1560.

Received June 18, 1958.

Structure of the Hexathionate Ion in a Potassium Barium Salt

OLAV FOSS, ASBJØRN HORDVIK and KARSTEN H. PALMORK

Chemical Institute, University of Bergen, Bergen, Norway

The tetra- and pentathionate ions are built up of unbranched and non-planar sulphur chains, with three oxygen atoms bonded to each of the terminal sulphur atoms, according to crystal structure determinations of barium tetrathionate dihydrate [1], orthorhombic and triclinic barium pentathionate dihydrate [2,3], barium pentathionate hydrate acetonate [4], and sodium tetrathionate dihydrate [5,6]. The present note reports the preliminary results of a structure analysis of a salt of hexathionic acid.

In a preceding note [7], crystal data were given for a potassium barium hexathionate, $K_2Ba(S_6O_6)_2$. The crystals are monoclinic, with $a = 11.58$ Å, $b = 10.81$ Å, $c = 9.14$ Å, $\beta = 112°$, and two formula units per unit cell. The systematic absences, $h0l$ when l is odd, together with the monoclinic-prismatic morphology of the crystals, indicated that the space group is C_{2h}^4-P2/c. This space group has, beside the fourfold general positions, six set of special, twofold positions, two on twofold axes and four on symmetry centres; the latter are in the glide plane c at $y = 0$ and $\frac{1}{2}$, and atoms in these positions do not contribute to hkl reflections with l odd. It was observed on oscillation photographs about the c axis that reflections on odd layer lines were, particularly for large scattering angles, weak relative to those on even layer lines, and it was therefore proceeded on the assumption that the barium ions lie in symmetry centres of the space group C_{2h}^4-P2/c.

The intensities of the $h0l$ and $hk0$ reflections were estimated visually from zero-layer Weissenberg photographs taken with CuK radiation, and were converted to relative structure amplitudes in the usual way. The signs of the larger terms (74 out of 114 observed $h0l$ reflections and 70 out of 141 observed $hk0$ reflections) were then put positive and Fourier syntheses made. The resulting maps gave the positions of the sulphur atoms, and also showed that the potassium ions lie in two sets of twofold positions, and that the barium ion lies, not in a symmetry centre but on a twofold axis with y equal to or very close to zero. Structure factor calculations including the potassium and sulphur contributions and next also the oxygen contributions led to more refined electron density maps, one of which is shown in Fig. 1. Of the 141 $hk0$ reflections included in the synthesis of this map, only 7 very weak ones have negative signs.

The cations are in the following twofold positions of the space group C_{2h}^4-P2/c: The barium ion and one of the potassium ions on a twofold axis at $0,y,\frac{1}{4}$ with $y = 0$

found 1.80 g/cm³. The systematic absences, $0k0$ when k is odd, indicate that the space group is $C_2^2-P2_1$ or $C_{2h}^2-P2_1/m$. No molecular symmetry is required in either case.

The crystals are thus different from those of the corresponding hexathionate, described above. From hexathionate upwards to about nonathionate, mixed crystals of *trans*-dichlorobis(ethylenediamine)cobalt(III) polythionates, indicating isomorphism, appear to exist [2].

1. Weitz, E. and Achterberg, F. *Ber.* **61** (1928) 399.
2. Weitz, E. and Spohn, K. *Chem. Ber.* **89** (1956) 2332.
3. Weitz, E., Becker, F. and Gieles, K. *Chem. Ber.* **89** (1956) 2345.
4. Weitz, E., Becker, F., Gieles, K. and Alt, B. *Chem. Ber.* **89** (1956) 2353.
5. Weitz, E., Gieles, K., Singer, J. and Alt, B. *Chem. Ber.* **89** (1956) 2365.
6. Stamm, H., Seipold, O. and Goehring, M. *Z. anorg. allgem. Chem.* **267** (1941) 277.
7. Donnay, J. D. H. and Nowacki, W. *Crystal Data*. The Geological Society of America Memoir 60, New York, 1954.
8. Kurtenacker, A. *Analytische Chemie der Sauerstoffsäuren des Schwefels*, Ferdinand Enke, Stuttgart 1938.
9. Foss, O., Hordvik, A. and Palmork, K. H. *Acta Chem. Scand.* **12** (1958) 1339.
10. Kurtenacker, A. and Laszlo, G. *Z. anorg. allgem. Chem.* **237** (1938) 359.
11. Deines, O. and Christoph, E. *Z. anorg. allgem. Chem.* **213** (1933) 209.
12. Foss, O. and Jahr, J. *Acta Chem. Scand.* **4** (1950) 1560.

Received June 18, 1958.

Structure of the Hexathionate Ion in a Potassium Barium Salt

OLAV FOSS, ASBJØRN HORDVIK and KARSTEN H. PALMORK

Chemical Institute, University of Bergen, Bergen, Norway

The tetra- and pentathionate ions are built up of unbranched and non-planar sulphur chains, with three oxygen atoms bonded to each of the terminal sulphur atoms, according to crystal structure determinations of barium tetrathionate dihydrate [1], orthorhombic and triclinic barium pentathionate dihydrate [2,3], barium pentathionate hydrate acetonate [4], and sodium tetrathionate dihydrate [5,6]. The present note reports the preliminary results of a structure analysis of a salt of hexathionic acid.

In a preceding note [7], crystal data were given for a potassium barium hexathionate, $K_2Ba(S_6O_6)_2$. The crystals are monoclinic, with $a = 11.58$ Å, $b = 10.81$ Å, $c = 9.14$ Å, $\beta = 112°$, and two formula units per unit cell. The systematic absences, $h0l$ when l is odd, together with the monoclinic-prismatic morphology of the crystals, indicated that the space group is C_{2h}^4-P2/c. This space group has, beside the fourfold general positions, six set of special, twofold positions, two on twofold axes and four on symmetry centres; the latter are in the glide plane c at $y = 0$ and $\frac{1}{2}$, and atoms in these positions do not contribute to hkl reflections with l odd. It was observed on oscillation photographs about the c axis that reflections on odd layer lines were, particularly for large scattering angles, weak relative to those on even layer lines, and it was therefore proceeded on the assumption that the barium ions lie in symmetry centres of the space group C_{2h}^4-P2/c.

The intensities of the $h0l$ and $hk0$ reflections were estimated visually from zero-layer Weissenberg photographs taken with CuK radiation, and were converted to relative structure amplitudes in the usual way. The signs of the larger terms (74 out of 114 observed $h0l$ reflections and 70 out of 141 observed $hk0$ reflections) were then put positive and Fourier syntheses made. The resulting maps gave the positions of the sulphur atoms, and also showed that the potassium ions lie in two sets of twofold positions, and that the barium ion lies, not in a symmetry centre but on a twofold axis with y equal to or very close to zero. Structure factor calculations including the potassium and sulphur contributions and next also the oxygen contributions led to more refined electron density maps, one of which is shown in Fig. 1. Of the 141 $hk0$ reflections included in the synthesis of this map, only 7 very weak ones have negative signs.

The cations are in the following twofold positions of the space group C_{2h}^4-P2/c: The barium ion and one of the potassium ions on a twofold axis at $0,y,\frac{1}{4}$ with $y = 0$

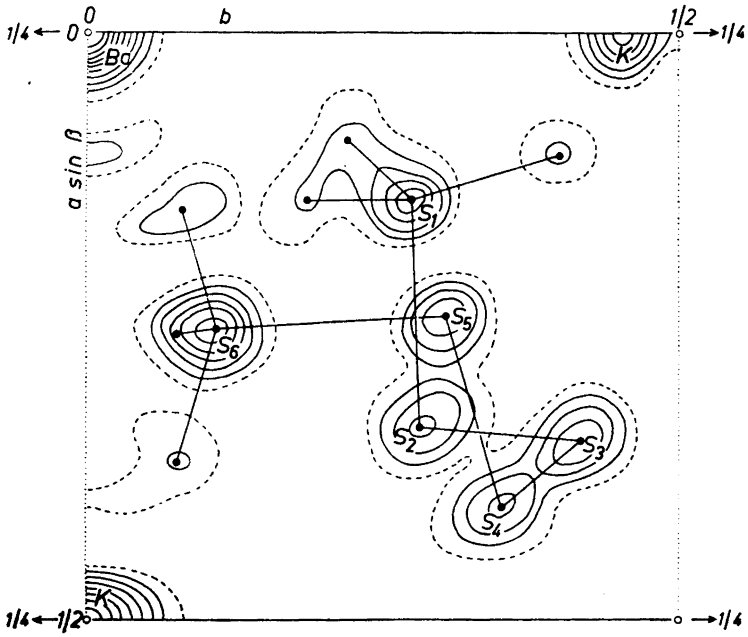

Fig. 1. Electron density projection of potassium barium hexathionate, $K_2Ba(S_6O_6)_2$, along the c axis. The 7-electron line is dashed, and contours are at intervals of 20 e · Å^{-2} for the barium peak and 5 e · Å^{-2} for the other atoms.

and $y = 0.45$, respectively, and the other potassium ion in a symmetry centre at ½,0,0. The sulphur coordinates are at present as listed in Table 1. The reliability index *R*, with approximate oxygen contributions and temperature corrections included in the calculated structure factors, is 14 % for the *hk*0 reflections. Refinement of the structure is in progress.

In elemental sulphur and in sulphur chain compounds, a dihedral angle of about 90° occurs between successive planes through three and three sulphur atoms. Given a chain of four, a fifth sulphur atom may occupy a *cis* or a *trans* position relative to the first. This leads to two possible rotational-isomeric forms of the pentathionate ion [8], one *cis* form in which the first and fifth sulphur atoms are on the same side of the plane through the three middle ones, and a *trans* form in which they are on opposite sides. In the three barium pentathionates referred to above [2-4], the *cis* form occurs. For the hexathionate ion, with a sulphur chain of six, three forms should be possible, one *cis-cis* in which the fifth and sixth atoms are in *cis* positions relative to the first and second, respectively, one *cis-trans* or *trans-cis*, and one *trans-trans*. All three forms may be right- or left-handed; a *cis-trans* form is the mirror-image of a *trans-cis*. The *cis-cis* form represents a segment of the S_8 ring of orthorhombic sulphur, and the *trans-trans* form corresponds to the helical chains of fibrous sulphur and hexagonal selenium and tellurium; these two forms of the six-membered chain possess a twofold axis of symmetry provided that

Table 1. Sulphur coordinates, in fractions of monoclinic cell edges. Origin at a centre of symmetry.

	x	*y*	*z*
S_1	0.141	0.273	0.055
S_2	0.335	0.281	0.169
S_3	0.348	0.416	0.321
S_4	0.404	0.350	0.548
S_5	0.242	0.303	0.581
S_6	0.252	0.108	0.590

bond lengths and angles are equal in the two halves.

In the crystals of potassium barium hexathionate the configuration of the sulphur chain is *cis-cis*. Thus, in the pentathionates and the one hexathionate for which structural data so far are available, the sulphur chain has the same configuration as in orthorhombic sulphur. Whether or not this is the preferred form of the ions, or due in some measure to the presence of oxygen-coordinating barium ions in the crystals, must await a study of other salts. A *trans* five-membered sulphur chain occurs in sulphur dimethanethiosulphonate [9], and a *trans-trans* six-membered one in cesium hexasulphide [10].

1. Foss, O., Furberg, S. and Zachariasen, H. *Acta Chem. Scand.* **8** (1954) 459.
2. Foss, O. and Zachariasen, H. *Acta Scand.* **8** (1954) 473.
3. Foss, O. and Tjomsland, O. *Acta Chem. Scand.* **10** (1956) 288.
4. Foss, O. and Tjomsland, O. *Acta Chem. Scand.* **12** (1958) 44.
5. Foss, O. *Acta Chem. Scand.* **6** (1952) 802.
6. Foss, O. and Hordvik, A. *To be published.*
7. Foss, O. and Palmork, K. H. *Acta Chem. Scand.* **12** (1958) 1337.
8. Foss, O, *Acta Chem. Scand.* **7** (1953) 1221.
9. Foss, O., Furberg, S. and Hadler, E. *Acta Chem. Scand.* **5** (1951) 1417.
10. Abrahams, S. C. and Grison, E. *Acta Cryst.* **6** (1953) 206.

Received June 18, 1958.

Preliminary Note on the Solubility of Oxygen in α-Zirconium

BO HOLMBERG and ARNE MAGNÉLI

Institute of Inorganic and Physical Chemistry, University of Stockholm, Stockholm, Sweden

In the course of studies on the crystal chemistry of titanium and vanadium oxides at elevated temperatures which are being carried out at this Institute with the sponsorship of the Office, Chief of Research and Development, U.S. Department of Army, through its European Office, ordered phases have been found to occur in the solid solubility range of oxygen in α-titanium [1]. In connection with these studies an investigation has also been started of the corresponding region of the zirconium-oxygen system.

The solubility limit for samples heat-treated at 800°C has been found to be close to the composition $ZrO_{0.40}$ in agreement with data reported by previous authors [2]. The length of the a axis reaches a maximum at the approximate composition $ZrO_{0.25}$ (a(Zr) = 3.232 Å[3]), $a(ZrO_{0.25})$ = 3.256 Å, $a(ZrO_{0.40})$ = 3.245 Å), while the length of the c axis increases with increasing oxygen content over the whole solubility range (c(Zr) = 5.148 Å[3]), $c(ZrO_{0.25})$ = 5.188 Å, $c(ZrO_{0.40})$ = 5.207 Å). The behaviour is similar to that observed for the titanium-oxygen system [4].

When annealed at 800°C the sample $ZrO_{0.30}$ gives X-ray powder photographs which show the oxygen atoms to be distributed at random in the interstices of the zirconium lattice. The preparation $ZrO_{0.35}$, similarly heat-treated, gives a powder pattern essentially corresponding to a structure of *anti*-$Cd(OH)_2$ type. The oxygen atoms should thus occur only in every second layer of octahedral holes extending normally to the c axis. About 30 % of these holes must thus be vacant. The metal atoms are slightly forced apart by the interstitial atoms. The z parameter of the zirconium atoms thus acquires the value of 0.26 as compared to 0.25 for the ideal structure. There are, however, also indications of the vacancies in the oxygen positions being ordered. Research on this matter will be continued.

1. Andersson, S., Åsbrink, S. Holmberg, B. and Magnéli, A. *Symposium on Crystal Physics, National Institute of Sciences (India), Gulmarg, Kashmere, June 1958.*
2. Domagala, R. F. and McPherson, D. J. *J. Metals* **6** Trans. (1954) 238.
3. Treco, R. M. *J. Metals* **5** Trans. (1953) 344.
4. Andersson, S., Collén, B., Kuylenstierna, U., and Magnéli, A. *Acta Chem. Scand.* **11** (1957) 1641.

Received July 17, 1958.

bond lengths and angles are equal in the two halves.

In the crystals of potassium barium hexathionate the configuration of the sulphur chain is *cis-cis*. Thus, in the pentathionates and the one hexathionate for which structural data so far are available, the sulphur chain has the same configuration as in orthorhombic sulphur. Whether or not this is the preferred form of the ions, or due in some measure to the presence of oxygen-coordinating barium ions in the crystals, must await a study of other salts. A *trans* five-membered sulphur chain occurs in sulphur dimethanethiosulphonate [9], and a *trans-trans* six-membered one in cesium hexasulphide [10].

1. Foss, O., Furberg, S. and Zachariasen, H. *Acta Chem. Scand.* **8** (1954) 459.
2. Foss, O. and Zachariasen, H. *Acta Scand.* **8** (1954) 473.
3. Foss, O. and Tjomsland, O. *Acta Chem. Scand.* **10** (1956) 288.
4. Foss, O. and Tjomsland, O. *Acta Chem. Scand.* **12** (1958) 44.
5. Foss, O. *Acta Chem. Scand.* **6** (1952) 802.
6. Foss, O. and Hordvik, A. *To be published.*
7. Foss, O. and Palmork, K. H. *Acta Chem. Scand.* **12** (1958) 1337.
8. Foss, O, *Acta Chem. Scand.* **7** (1953) 1221.
9. Foss, O., Furberg, S. and Hadler, E. *Acta Chem. Scand.* **5** (1951) 1417.
10. Abrahams, S. C. and Grison, E. *Acta Cryst.* **6** (1953) 206.

Received June 18, 1958.

Preliminary Note on the Solubility of Oxygen in α-Zirconium

BO HOLMBERG and ARNE MAGNÉLI

Institute of Inorganic and Physical Chemistry, University of Stockholm, Stockholm, Sweden

In the course of studies on the crystal chemistry of titanium and vanadium oxides at elevated temperatures which are being carried out at this Institute with the sponsorship of the Office, Chief of Research and Development, U.S. Department of Army, through its European Office, ordered phases have been found to occur in the solid solubility range of oxygen in α-titanium [1]. In connection with these studies an investigation has also been started of the corresponding region of the zirconium-oxygen system.

The solubility limit for samples heat-treated at 800°C has been found to be close to the composition $ZrO_{0.40}$ in agreement with data reported by previous authors [2]. The length of the a axis reaches a maximum at the approximate composition $ZrO_{0.25}$ (a(Zr) = 3.232 Å[3]), $a(ZrO_{0.25})$ = 3.256 Å, $a(ZrO_{0.40})$ = 3.245 Å), while the length of the c axis increases with increasing oxygen content over the whole solubility range (c(Zr) = 5.148 Å[3]), $c(ZrO_{0.25})$ = 5.188 Å, $c(ZrO_{0.40})$ = 5.207 Å). The behaviour is similar to that observed for the titanium-oxygen system [4].

When annealed at 800°C the sample $ZrO_{0.30}$ gives X-ray powder photographs which show the oxygen atoms to be distributed at random in the interstices of the zirconium lattice. The preparation $ZrO_{0.35}$, similarly heat-treated, gives a powder pattern essentially corresponding to a structure of *anti*-$Cd(OH)_2$ type. The oxygen atoms should thus occur only in every second layer of octahedral holes extending normally to the c axis. About 30 % of these holes must thus be vacant. The metal atoms are slightly forced apart by the interstitial atoms. The z parameter of the zirconium atoms thus acquires the value of 0.26 as compared to 0.25 for the ideal structure. There are, however, also indications of the vacancies in the oxygen positions being ordered. Research on this matter will be continued.

1. Andersson, S., Åsbrink, S. Holmberg, B. and Magnéli, A. *Symposium on Crystal Physics, National Institute of Sciences (India), Gulmarg, Kashmere, June 1958.*
2. Domagala, R. F. and McPherson, D. J. *J. Metals* **6** Trans. (1954) 238.
3. Treco, R. M. *J. Metals* **5** Trans. (1953) 344.
4. Andersson, S., Collén, B., Kuylenstierna, U., and Magnéli, A. *Acta Chem. Scand.* **11** (1957) 1641.

Received July 17, 1958.

Syntheses of Some Hydroquinone Derivatives

ULF ULFVARSON

Organisk-kemiska Institutionen, Kungl. Tekniska Högskolan, Stockholm, Sweden

Work has been in progress in this laboratory for some time on the synthesis of a number of substituted phenyl- and benzoylalkanes. A Friedel-Crafts reaction on adipoyl chloride and hydroquinone dimethylether gave 1,4-bis(2,5-dimethoxybenzoyl)butane and δ-(2,5-dimethoxybenzoyl)valeric acid. The ratio of the two reaction products depended on the proportion of adipoyl chloride to hydroquinone dimethylether.

Reduction and demethylation of 1,4-bis(2,5-dimethoxybenzoyl)butane gave 1,6-bis(2,5-dihydroxyphenyl)hexane. Oxidation of this hydroquinone gave the corresponding quinone.

Until recently the only attempt that had been made to prepare these types of substances was that of Bruce *et al.* [1] who obtained δ-(2,5-dihydroxybenzoyl)valeric acid in poor yield from hydroquinone and adipic acid using an $AlCl_3$-NaCl melt. No other products were isolated. Okuma and Tamura [2] have now prepared some of these substances by other methods for use as antioxidants.

Experimental. (Melting points were determined with a Koefler apparatus.)

δ-(2,5-Dimethoxybenzoyl)valeric acid and 1,4-bis(2,5-dimethoxybenzoyl) butane. Hydroquinone dimethylether (70 g, 0.5 mole) and adipoyl chloride (183 g, 1.0 mole) were dissolved in dry carbondisulfide (300 g) and finely ground $AlCl_3$ (266 g, 2.0 mole) was added with stirring. The temperature was not allowed to exceed 10°C. After the addition of $AlCl_3$ was complete the solvent was decanted from the orange-red syrup, and this was decomposed with ice. The reaction products were shaken out with chloroform and the acid fraction was separated by shaking with $NaHCO_3$-solution. δ-(2,5-Dimethoxybenzoyl)valeric acid was precipitated with hydrochloric acid, dried and recrystallised from benzene-light petroleum, white prisms, m.p. 80.5—82°C (65 g). (Found: C 63.55; H 6.69; OCH_3 22.7. $C_{14}H_{18}O_5$ requires C 63.14; H 6.81; OCH_3 23.3.)

The neutral chloroform solution was dried and evaporated and the 1,4-bis (2,5-dimethoxybenzoyl) butane was recrystallised from 95 % ethanol, white needles, m.p. 112—113°C (10 g) (Found: C 68.50; H 6.63; $C_{22}H_{26}O_6$ requires C 68.37; H 6.78.)

δ-(2,5-Dihydroxybenzoyl)valeric acid. δ-(2,5-Dimethoxybenzoyl) valeric acid (5 g) was demethylated by refluxing for 1 h in a mixture of hydrobromic acid (48 %, 40 ml) and acetic acid (100 ml). The acetic acid was evaporated and the δ-(2,5-dihydroxybenzoyl) valeric acid was precipitated by cooling and recrystallised from water, yellow leaves m.p. 130—131.5°C (Bruce *et al.*[1]: 130°C) (3 g).

The crystalline acid chloride of δ-(2,5-dimethoxybenzoyl)valeric acid was prepared in good yield with oxalyl chloride in dry benzene at room temperature by the method of Adams[3]. It gave 1,4-bis (2,5-dimethoxybenzoyl) butane by reaction with hydroquinone dimethylether and aluminium chloride as above.

1,6-Bis (2,5-dimethoxyphenyl) hexane. 1,4-Bis(2,5-dimethoxybenzoyl)butane (10 g) suspended in absolute ethanol (300 ml) was hydrogenated over a 5 % Pd on charcoal catalyst (2 g) (Theilacker [4]). 2 400 ml of hydrogen (760 torr) was adsorbed in 120 min. The reduced product was soluble in ethanol; the catalyst was filtered off and the solvent evaporated giving 1,6-bis (2,5-dimethoxyphenyl) hexane (7.5 g) which was recrystallised from light petroleum, white needles, m.p. 55—56°C. (Found: C 73.38; H 8.33. $C_{22}H_{30}O_4$ requires C 73.71; H 8.44.)

1,6-Bis (2,5-dihydroxyphenyl) hexane. 1,6-Bis (2,5-dimethoxyphenyl)hexane (5 g) was mixed with pyridine hydrochloride (20 g) and heated to 200°C in oil bath for 2 h by the method of Prey [5]. After cooling, 150 ml of water was added to the reaction mixture. The oil which separated crystallised on standing and was recrystallised from acetonitrile, white needles, m.p. 160.5—162°C (3 g). (Found: C 70.61; H 7.18; $C_{18}H_{22}O_4$ requires C 71.50; H 7.34.)

1,6-Bis(p-benzoquinoyl)hexane. 1,6-Bis (2,5-dihydroxyphenyl) hexane (400 mg) dissolved in acetic acid (50 ml) was heated to about 50°C, and a 10 % solution of CrO_3 in water (2 ml) was added. The quinone which separated was filtered after cooling and recrystallised from acetonitrile, yellow leaves m.p. 153.5—155.5°C. (Found: C 72.15; H 6.10. $C_{18}H_{18}O_4$ requires C 72.47; H 6.08.)

ε-(2,5-Dimethoxyphenyl)hexanoic acid. δ-(2,5-Dimethoxybenzoyl)valeric acid was reduced in the same way as the 1,4-bis (2,5-dimethoxybenzoyl)butane; white crystals, m.p. approx. 40°C. It was difficult to purify and was characterised by its *p*-toluidide: ε-(2,5-

Dimethoxyphenyl) hexanoyl chloride (1 g), prepared with oxalyl chloride in the same way as δ-(2,5-dimethoxybenzoyl)valeroyl chloride, was refluxed with *p*-toluidine (2 g) in dry benzene (50 ml) for 15 min. After cooling the solution was washed with water, dilute hydrochloric acid and bicarbonate solution. The solution was dried and evaporated and the residue was recrystallised from benzene--light petroleum and gave white needles m.p. 103.5—105°C. (Found: C 73.26; H 7.98; N N 3.79. $C_{21}H_{27}O_3N$ requires C 73.86; H 7.97; N 4.10.)

1,4-Bis(2-hydroxy-5-methoxybenzoyl) butane. 1,4-Bis(2,5-dimethoxybenzoyl)butane (3 g) was dissolved in a cooled solution of $AlCl_3$ (12 g) in nitrobenzene (150 ml). After 45 h at room temperature the mixture was decomposed with ice and the nitrobenzene was removed by steam distillation. The solid product was dissolved in chloroform and shaken with sodium hydroxide solution (1 N). The alkaline solution was acidified with hydrochloric acid and the crystals which separated were dissolved in chloroform. After drying the chloroform solution was run through a silica gel column and evaporated. A small amount of pure 1,4-bis(2-hydroxy-5-methoxybenzoyl)butane was obtained. It was recrystallised from ethanol-benzene, yellow prisms, m.p. 157—158°C. It gave a violet colour with $FeCl_3$ in methanol. (Found: C 66.49; H 6.22; OCH_3 15.9. $C_{20}H_{22}O_6$ requires C 67.03; H 6.19; OCH_3 16.1.)

An attempt to prepare this substance from adipoyl chloride, hydroquinone monomethylether and aluminium chloride using the same conditions as in the preparation of 1,4-bis (2,5-dimethoxybenzoyl)butane gave the bis-*p*-methoxyphenylester of adipic acid, white needles from ethanol, m.p. 126—127°C. (Found: C 67.13; H 6.04. $C_{20}H_{22}O_6$ requires C 67.02, H 6.19.)

Infrared spectrum of 1,4-bis(2-hydroxy-5-methoxybenzoyl)butane indicated that the demethylation took place in the *ortho* positions to the carbonylgroups. There was no absorption attributable to a hydroxyl group in the 3 500—2 500 cm^{-1} region. The same is true for *o*-hydroxyacetophenone which is attributed to intramolecular hydrogen bonding by Hergert [6].

The carbonyl frequency of 1,4-bis(2,5-dimethoxybenzoyl) butane was measured to 1 665 cm^{-1} and that of 1,4-bis(2-hydroxy-5-methoxybenzoyl) butane to 1 650 cm^{-1}. The difference is 15 cm^{-1}. The difference between the carbonyl frequencies of *o*-methoxyacetophenone and *o*-hydroxyacetophenone [6] is 14 cm^{-1}, from 1 649 cm^{-1} to 1 635 cm^{-1}.

The low carbonyl frequency of 1,4-bis(2-hydroxy-5-methoxybenzoyl)butane may be explained if a conjugated chelate system as in *o*-hydroxyacetophenone [6] is assumed.

The author is greatly indebted to AB Casco, Stockholm, for financial support.

1. Bruce, D. B., Sorrie, A. J. S. and Thomson, R. H. *J. Chem. Soc.* **1953** 2403.
2. Okuma, K. and Tamura, S. *Nippon Nôgeikagaku Kaishi* **28** (1954) 28; *Chem. Abstracts* **51** (1957) 14617h.
3. Adams, R. and Ulich, L. H. *J. Am. Chem. Soc.* **42** (1920) 599.
4. Theilacker, W. and Drössler, H.-G. *Ber.* **87** (1954) 1676.
5. Prey, V. *Ber.* **74B** (1941) 1219.
6. Hergert, H. L. and Kurth, E. F. *J. Am. Chem. Soc.* **75** (1953) 1622.

Received July 10, 1958.

Metal-Metal Bonding in a Mixed Chromium Molybdenum Oxide Phase of Rutile Structure

ANITA SUNDHOLM, STEN ANDERSSON, ARNE MAGNÉLI, and BENGT-OLOV MARINDER

Institute of Inorganic and Physical Chemistry, University of Stockholm, Stockholm, Sweden

Mixed chromium molybdenum oxide $(Cr,Mo)O_2$ of rutile type has been prepared by heating mixtures of chromium(III)-oxide, molybdenum(IV)oxide and molybdenum (VI)oxide ($Cr_2O_3 + aMoO_2 + MoO_3$) in sealed, evacuated silica tubes and keeping the temperature at about 1 000°C for several days. For values of a of 3 – 7.5 the X-ray powder patterns showed that the products only contained the rutile type phase. The width of the homogeneity range was not determined. No indications were observed of the metal atoms being ordered. The following unit cell dimensions were obtained:

	a	c	V
$Cr_{0.33}Mo_{0.67}O_2$	4.696 Å	2.886 Å	63.64 Å^3
$Cr_{0.22}Mo_{0.78}O_2$	4.749	2.858	64.44
$Cr_{0.19}Mo_{0.81}O_2$	4.760	2.848	64.53

The increase of the unit cell volume with the molybdenum content is in accordance

Dimethoxyphenyl) hexanoyl chloride (1 g), prepared with oxalyl chloride in the same way as δ-(2,5-dimethoxybenzoyl)valeroyl chloride, was refluxed with *p*-toluidine (2 g) in dry benzene (50 ml) for 15 min. After cooling the solution was washed with water, dilute hydrochloric acid and bicarbonate solution. The solution was dried and evaporated and the residue was recrystallised from benzene--light petroleum and gave white needles m.p. 103.5—105°C. (Found: C 73.26; H 7.98; N N 3.79. $C_{21}H_{27}O_3N$ requires C 73.86; H 7.97; N 4.10.)

1,4-Bis(2-hydroxy-5-methoxybenzoyl) butane. 1,4-Bis(2,5-dimethoxybenzoyl)butane (3 g) was dissolved in a cooled solution of $AlCl_3$ (12 g) in nitrobenzene (150 ml). After 45 h at room temperature the mixture was decomposed with ice and the nitrobenzene was removed by steam distillation. The solid product was dissolved in chloroform and shaken with sodium hydroxide solution (1 N). The alkaline solution was acidified with hydrochloric acid and the crystals which separated were dissolved in chloroform. After drying the chloroform solution was run through a silica gel column and evaporated. A small amount of pure 1,4-bis(2-hydroxy-5-methoxybenzoyl)butane was obtained. It was recrystallised from ethanol-benzene, yellow prisms, m.p. 157—158°C. It gave a violet colour with $FeCl_3$ in methanol. (Found: C 66.49; H 6.22; OCH_3 15.9. $C_{20}H_{22}O_6$ requires C 67.03; H 6.19; OCH_3 16.1.)

An attempt to prepare this substance from adipoyl chloride, hydroquinone monomethylether and aluminium chloride using the same conditions as in the preparation of 1,4-bis (2,5-dimethoxybenzoyl)butane gave the bis-*p*-methoxyphenylester of adipic acid, white needles from ethanol, m.p. 126—127°C. (Found: C 67.13; H 6.04. $C_{20}H_{22}O_6$ requires C 67.02, H 6.19.)

Infrared spectrum of 1,4-bis(2-hydroxy-5-methoxybenzoyl)butane indicated that the demethylation took place in the *ortho* positions to the carbonylgroups. There was no absorption attributable to a hydroxyl group in the 3 500—2 500 cm^{-1} region. The same is true for *o*-hydroxyacetophenone which is attributed to intramolecular hydrogen bonding by Hergert [6].

The carbonyl frequency of 1,4-bis(2,5-dimethoxybenzoyl) butane was measured to 1 665 cm^{-1} and that of 1,4-bis(2-hydroxy-5-methoxybenzoyl) butane to 1 650 cm^{-1}. The difference is 15 cm^{-1}. The difference between the carbonyl frequencies of *o*-methoxyacetophenone and *o*-hydroxyacetophenone [6] is 14 cm^{-1}, from 1 649 cm^{-1} to 1 635 cm^{-1}.

The low carbonyl frequency of 1,4-bis(2-hydroxy-5-methoxybenzoyl)butane may be explained if a conjugated chelate system as in *o*-hydroxyacetophenone [6] is assumed.

The author is greatly indebted to AB Casco, Stockholm, for financial support.

1. Bruce, D. B., Sorrie, A. J. S. and Thomson, R. H. *J. Chem. Soc.* **1953** 2403.
2. Okuma, K. and Tamura, S. *Nippon Nôgeikagaku Kaishi* **28** (1954) 28; *Chem. Abstracts* **51** (1957) 14617h.
3. Adams, R. and Ulich, L. H. *J. Am. Chem. Soc.* **42** (1920) 599.
4. Theilacker, W. and Drössler, H.-G. *Ber.* **87** (1954) 1676.
5. Prey, V. *Ber.* **74B** (1941) 1219.
6. Hergert, H. L. and Kurth, E. F. *J. Am. Chem. Soc.* **75** (1953) 1622.

Received July 10, 1958.

Metal-Metal Bonding in a Mixed Chromium Molybdenum Oxide Phase of Rutile Structure

ANITA SUNDHOLM, STEN ANDERSSON, ARNE MAGNÉLI, and BENGT-OLOV MARINDER

Institute of Inorganic and Physical Chemistry, University of Stockholm, Stockholm, Sweden

Mixed chromium molybdenum oxide $(Cr,Mo)O_2$ of rutile type has been prepared by heating mixtures of chromium(III)-oxide, molybdenum(IV)oxide and molybdenum (VI)oxide ($Cr_2O_3 + aMoO_2 + MoO_3$) in sealed, evacuated silica tubes and keeping the temperature at about 1 000°C for several days. For values of a of 3 – 7.5 the X-ray powder patterns showed that the products only contained the rutile type phase. The width of the homogeneity range was not determined. No indications were observed of the metal atoms being ordered. The following unit cell dimensions were obtained:

	a	c	V
$Cr_{0.33}Mo_{0.67}O_2$	4.696 Å	2.886 Å	63.64 Å^3
$Cr_{0.22}Mo_{0.78}O_2$	4.749	2.858	64.44
$Cr_{0.19}Mo_{0.81}O_2$	4.760	2.848	64.53

The increase of the unit cell volume with the molybdenum content is in accordance

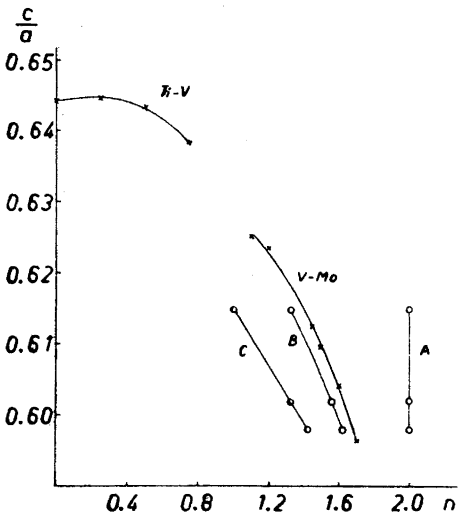

Fig. 1.

with the corresponding data for chromium dioxide (V = 57.06 Å^3 for rutile type cell [1]) and molybdenum dioxide (V = 65.03 Å^3 for subcell of distorted rutile type [2]). The decrease, with the molybdenum content, of the c axis (*i.e.* the shortest metal-metal distance of the structure) is the reverse of what would be expected from the relative sizes of the component atoms. This is taken as an indication of bonding forces acting between the neighbouring metal atoms of the mixed oxide as has previously been found for molybdenum dioxide (shortest metal-metal distance = 2.50 Å[2,3]) and several other compounds of transition metals when in valency states lower than their maximum ones [4]. The long metal-metal distance in chromium dioxide (c = 2.917 Å) [1] shows that no such bonding is present in this substance. This interpretation of the meaning of the intermetallic distances is supported by the magnetic data reported for the chromium and molybdenum dioxides [5]. It is also of interest to note that the metal atoms are "non-bonding" in the $Cr_2Cl_9^{3-}$ ion [6] while structural and magnetic data indicate bond formation in the $W_2Cl_9^{3-}$ ion [7,8].

It was shown in a previous article [4] that the axial ratio c/a provides an acceptable "normalized" measure of the metal-metal distance and this makes possible a comparison of rutile structures containing atoms of different sizes. On plotting the axial ratio against the number of excess valency electrons available per close metal-metal contact (n) (*i.e.* the number of valency electrons of the transition metal atoms which are not engaged in metal oxygen bonding) smooth curves are obtained.

Fig. 1 shows the curves thus derived for rutile type phases occurring in the systems (Ti,V)O_2 and (V,Mo)O_2. A few rutile type preparations in the systems (V,Re)O_2, (V,Mo,Re)O_2 and (Nb,Mo)O_2 give further data in fair agreement with the (V,Mo)O_2 curve or its extrapolation towards higher n values. For the (Cr,Mo)O_2 preparations, the following alternatives are indicated in the figure:

A. The excess valency electrons of both chromium and molybdenum are available for the formation of metal-metal bonds.

B. The excess chromium electrons are "non-bonding". All the metal atoms are tetravalent.

C. The excess chromium electrons are "non-bonding". The chromium atoms are trivalent and the corresponding proportion of the molybdenum atoms pentavalent or hexavalent.

It appears that curve *B* is in the best agreement with the data for other rutile phases containing molybdenum. This may be taken as an indication that the excess chromium electrons do not contribute to the metal-metal bonding and that the chromium atoms are probably in a tetravalent state.

This investigation forms part of a research program on metal oxides and related compounds financially supported by the *Swedish Natural Science Research Council*.

1. Wilhelmi, K.-A. *Acta Chem. Scand. In print.*
2. Magnéli, A. *Arkiv Kemi, Mineral. Geol.* **A24** (1946) No. 2.
3. Magnéli, A. and Andersson, G. *Acta Chem. Scand.* **9** (1955) 1348.
4. Marinder, B.-O. and Magnéli, A. *Acta Chem. Scand.* **11** (1957) 1635.
5. Selwood, P. W. *Magnetochemistry*, 2nd Ed., New York 1956, pp. 315 and 336.
6. Wessel, G. J. and IJdo, D. J. W. *Acta Cryst.* **10** (1957) 466.
7. Brosset, C. *Arkiv Kemi, Mineral. Geol.* **12A** (1935) No. 4.
8. Pauling, L. *Chem. Eng. News* **25** (1947) 2970.

Received July 17, 1958.

Rutile-Type Phases in Some Systems of Mixed Transition Metal Dioxides

BENGT-OLOV MARINDER and ARNE MAGNÉLI

Institute of Inorganic and Physical Chemistry, University of Stockholm, Stockholm, Sweden

It has previously been pointed out that, in some dioxides of transition metals, very short metal-metal distances are present, indicating the existence of bonds between the metal atoms. This is the case for the dioxides of MoO_2-type [1] and for orthorhombic rhenium dioxide [2]. In the search for further substances exhibiting such bonds, one pseudo-ternary and several pseudo-binary systems of transition metal dioxides have been studied. Since the intention was principally to find the metal-metal distances, it was natural to concentrate the interest on the occurrence of phases of rutile type, where the intermetallic distances are simply connected with the unit cell dimensions. A comprehensive knowledge of the phase relations in the various systems was not aimed at. This article presents the findings obtained during these studies. Discussions of the occurrence of metal-metal bonds in the various systems have been given elsewhere [3-5].

The samples investigated comprised mixed dioxides of titanium, vanadium, niobium, chromium, molybdenum, wolfram and rhenium. The starting materials were all of high purity. The samples were generally prepared by heating appropriate mixtures of oxides and sometimes also metals in sealed, evacuated silica tubes and keeping the temperature at about 1 000°C for several days. This treatment was with few exceptions found satisfactory for the attainment of equilibrium conditions.

The preparations were studied by means of X-ray powder photographs obtained in a Guinier focusing camera with strictly monochromatized Cu$K\alpha_1$ radiation. Potassium chloride ($a = 6.2919$ Å at 20°C) [6] was always added to the powder specimens as an internal standard. The results of the phase analysis are summarized in Table 1 which also includes some data reported by Schönberg [7].

A noticeable feature of several of the systems investigated is the occurrence of rutile-type phases (r) existing over wide ranges of composition (*cf.* Fig. 1). This

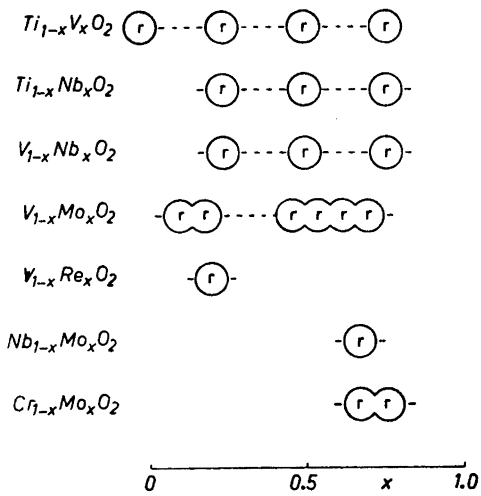

Fig. 1.

is the case not only in systems containing a component of rutile structure (*i.e.* the systems with titanium dioxide). Systems formed with components of other crystal structures, including vanadium and molybdenum dioxide (MoO_2-structure) [1], niobium dioxide (superstructure of distorted rutile) [5] and rhenium dioxide (orthorhombic ReO_2-type) [2] also show intermediary regions of ideal rutile type. These results evidently add further examples to the data given by Brandt [8], of the pronounced adaptability of the rutile structure to a variety of metal atom species.

In no case were indications observed of superstructures like those reported by Byström, Hök and Mason [9] for the large group of mixed oxides of ordered trirutile type. No attempts were made in this study to find out if such ordering occurs at lower temperatures.

The occurrence at an intermediary composition in the molybdenum dioxide-wolfram dioxide system of a MoO_2-type phase (which may extend over the entire range of composition) is evidently rather exceptional. Probably a mixed MoO_2-type structure will form over a wide range of composition only if the structures of the two components are similar.

This investigation forms part of a research program on metal oxides and related com-

Table 1. Methods of preparation and results of phase analyses.

System	Starting materials	Composition of sample	X-Ray evidence	Unit cell dimension of rutile type phase		Ref.
				a Å	*c* Å	
TiO_2-VO_2	TiO_2(anatase), V_2O_5, V or TiO_2(anatase), V_2O_5, V_2O_3	TiO_2 $Ti_{0.75}V_{0.25}O_2$ $Ti_{0.50}V_{0.50}O_2$ $Ti_{0.25}V_{0.75}O_2$ $Ti_{0.20}V_{0.80}O_2$	Rutile Rutile Rutile Rutile Orthorhombic phase	4.593 4.581 4.566 4.550	2.959 2.954 2.938 2.905	10
TiO_2-NbO_2	TiO_2(anatase), Nb_2O_5, Nb	TiO_2 $Ti_{0.75}Nb_{0.25}O_2$ $Ti_{0.50}Nb_{0.50}O_2$ $Ti_{0.25}Nb_{0.75}O_2$	Rutile Rutile Rutile Rutile	4.593 4.659 4.719 4.778	2.959 2.986 2.997 2.999	10
TiO_2-TaO_2			Rutile			7
TiO_2-MoO_2	TiO_2(anatase), MoO_3, Mo		Low solubility of MoO_2 in TiO_2 (rutile)			
TiO_2-ReO_2	TiO_2(anatase), ReO_3, Re		Low solubility of ReO_2 in TiO_2 (rutile)			
VO_2-NbO_2	V_2O_5, V_2O_3, Nb_2O_5, Nb	$V_{0.25}Nb_{0.75}O_2$ $V_{0.50}Nb_{0.50}O_2$ $V_{0.75}Nb_{0.25}O_2$	Rutile Rutile Rutile	4.759 4.692 4.602	3.018 3.033 2.956	
VO_2-TaO_2			Rather low solubility of VO_2 in TaO_2(rutile type)			7
VO_2-MoO_2	V_2O_5, V_2O_3, MoO_3, Mo	$V_{0.90}Mo_{0.10}O_2$ $V_{0.80}Mo_{0.20}O_2$ $V_{0.55}Mo_{0.45}O_2$ $V_{0.50}Mo_{0.50}O_2$ $V_{0.40}Mo_{0.60}O_2$ $V_{0.30}Mo_{0.70}O_2$	Rutile Rutile Rutile Rutile Rutile Rutile	4.573 4.591 4.664 4.680 4.709 4.747	2.860 2.864 2.857 2.854 2.845 2.831	
VO_2-MoO_2-ReO_2	MoO_3, V_2O_3, Re	$V_{0.33}Mo_{0.50}Re_{0.17}O_2$	Rutile	4.742	2.818	
VO_2-ReO_2	V_2O_5, Re	$V_{0.80}Re_{0.20}O_2$	Rutile	4.612	2.835	
NbO_2-MoO_2	MoO_3, Nb	$Nb_{0.33}Mo_{0.67}O_2$	Rutile	4.855	2.883	
CrO_2-MoO_2	Cr_2O_3, MoO_2, MoO_3	$Cr_{0.33}Mo_{0.67}O_2$ $Cr_{0.22}Mo_{0.78}O_2$	Rutile Rutile	4.696 4.749	2.886 2.858	4
MoO_2-WO_2	MoO_3, Mo, WO_3, W	$Mo_{0.50}W_{0.50}O_2$	Deformed rutile (MoO_2-type)			

pounds financially supported by the *Swedish Natural Science Research Council.*

1. Magnéli, A. and Andersson, G. *Acta Chem. Scand.* **9** (1955) 1378.
2. Magnéli, A. *Acta Chem. Scand.* **11** (1957) 28.
3. Marinder, B.-O. and Magnéli, A. *Acta Chem. Scand.* **11** (1957) 1635.
4. Sundholm, A., Andersson, S., Magnéli, A. and Marinder, B.-O. *Acta Chem. Scand* **12** (1958) 1343.
5. Marinder, B.-O. *To be published.*
6. Hambling, P. G. *Acta Cryst.* **6** (1953) 98.
7. Schönberg, N. *Acta Chem. Scand.* **8** (1954) 244.
8. Brandt, K. *Arkiv Kemi, Mineral. Geol.* **17A** (1943) No. 15.
9. Byström, A., Hök, B. and Mason, B. *Arkiv Kemi, Mineral. Geol.* **15B** (1941) No. 4.
10. Andersson, S., Collén, B., Kuylenstierna, U. and Magnéli, A. *Acta Chem. Scand.* **11** (1957) 1641.

Received July 7, 1958.

The Preparation of Some Naphthylselen-carboxylic Acids

BERNDT SJÖBERG and STEFAN HERDEVALL

Chemical Institute, University of Uppsala, Uppsala, Sweden

In connection with the studies on synthetic plant growth regulators going on at this institute some naphthylsulphide-carboxylic acids have previously been prepared [1,2] and the plant growth regulating activity has been investigated by Professor B. Åberg at the Royal Agricultural College, Uppsala [3]. We have now extended these studies to some naphthylselen-carboxylic acids.

Some phenylselenacetic acids and 1-naphthylselenacetic acid have previously been prepared by reacting the Grignard reagents with selenium and then adding dilute alkali solution and bromoacetic acid [4]. As bromobenzene and 1-bromonaphthalene are readily available this method seems to be convenient for the preparation of phenylselen-carboxylic acids and for 1-naphthylselen-carboxylic acids. For the syntheses of the 2-naphthylselen-carboxylic acids we have tried three methods:

Acid	Method	Yield	M.p.
1-Naphthylselen-acetic	2	50	66—67°*
2-Naphthylselen-acetic	1	26	89—90°
2-Naphthylselen-acetic	2	20	89—90°
2-Naphthylselen-acetic	3	75	89—90°
α-(2-Naphthylselen)-propionic	1	20	118—119°
α-(2-Naphthylselen)-propionic	2	15	118—119°
α-(2-Naphthylselen)-propionic	3	77	118—119°
β-(2-Naphthylselen)-propionic	2	14	105—106°

* Morgan and Porritt reported m.p. 54°.

1. Hydrolysis of 2-naphthylselenocyanate [5] and direct reaction with different bromosubstituted acids.
2. Reaction of selenium with the Grignard reagent of 2-iodonaphthalene and further reaction with halogen substituted acids.
3. Reduction with sodiumborohydride of 2,2'-dinaphthyldiselenide dissolved in a benzene-alcohol mixture followed by reaction with haloesters.

As can be seen in the table above, method 1 has given a somewhat higher yield (counted on 2-naphthylselenocyanate) than method 2 (counted on 2-iodonaphthalene). However, 2-iodonaphthalene is much easier to prepare than 2-naphthylselenocyanate, and so method 2 is to be preferred. Both in method 1 and 2 some diselenide is formed from which the acids can be obtained in very good yield. If the diselenide is accessible, this method is certainly the best.

Experimental. Method 1. 2-Naphthylselenocyanate was prepared according to Loevenich, Fremdling and Föhr [5]. The naphthylselenocyanate was dissolved in hot alcohol, some glucose and excess of concentrated potassium hydroxide solution were added and the mixture boiled until a homogeneous phase had been obtained. The mixture was cooled and the neutralised bromosubstituted acid was added. After standing in a closed bottle for 12 h warm water was added, the mixture filtered and the solution acidified with hydrochloric acid.

pounds financially supported by the *Swedish Natural Science Research Council.*

1. Magnéli, A. and Andersson, G. *Acta Chem. Scand.* **9** (1955) 1378.
2. Magnéli, A. *Acta Chem. Scand.* **11** (1957) 28.
3. Marinder, B.-O. and Magnéli, A. *Acta Chem. Scand.* **11** (1957) 1635.
4. Sundholm, A., Andersson, S., Magnéli, A. and Marinder, B.-O. *Acta Chem. Scand* **12** (1958) 1343.
5. Marinder, B.-O. *To be published.*
6. Hambling, P. G. *Acta Cryst.* **6** (1953) 98.
7. Schönberg, N. *Acta Chem. Scand.* **8** (1954) 244.
8. Brandt, K. *Arkiv Kemi, Mineral. Geol.* **17A** (1943) No. 15.
9. Byström, A., Hök, B. and Mason, B. *Arkiv Kemi, Mineral. Geol.* **15B** (1941) No. 4.
10. Andersson, S., Collén, B., Kuylenstierna, U. and Magnéli, A. *Acta Chem. Scand.* **11** (1957) 1641.

Received July 7, 1958.

The Preparation of Some Naphthylselen-carboxylic Acids

BERNDT SJÖBERG and STEFAN HERDEVALL

Chemical Institute, University of Uppsala, Uppsala, Sweden

In connection with the studies on synthetic plant growth regulators going on at this institute some naphthylsulphide-carboxylic acids have previously been prepared [1,2] and the plant growth regulating activity has been investigated by Professor B. Åberg at the Royal Agricultural College, Uppsala [3]. We have now extended these studies to some naphthylselen-carboxylic acids.

Some phenylselenacetic acids and 1-naphthylselenacetic acid have previously been prepared by reacting the Grignard reagents with selenium and then adding dilute alkali solution and bromoacetic acid [4]. As bromobenzene and 1-bromonaphthalene are readily available this method seems to be convenient for the preparation of phenylselen-carboxylic acids and for 1-naphthylselen-carboxylic acids. For the syntheses of the 2-naphthylselen-carboxylic acids we have tried three methods:

Acid	Method	Yield	M.p.
1-Naphthylselen-acetic	2	50	66—67°*
2-Naphthylselen-acetic	1	26	89—90°
2-Naphthylselen-acetic	2	20	89—90°
2-Naphthylselen-acetic	3	75	89—90°
α-(2-Naphthylselen)-propionic	1	20	118—119°
α-(2-Naphthylselen)-propionic	2	15	118—119°
α-(2-Naphthylselen)-propionic	3	77	118—119°
β-(2-Naphthylselen)-propionic	2	14	105—106°

* Morgan and Porritt reported m.p. 54°.

1. Hydrolysis of 2-naphthylselenocyanate [5] and direct reaction with different bromosubstituted acids.
2. Reaction of selenium with the Grignard reagent of 2-iodonaphthalene and further reaction with halogen substituted acids.
3. Reduction with sodiumborohydride of 2,2'-dinaphthyldiselenide dissolved in a benzene-alcohol mixture followed by reaction with haloesters.

As can be seen in the table above, method 1 has given a somewhat higher yield (counted on 2-naphthylselenocyanate) than method 2 (counted on 2-iodonaphthalene). However, 2-iodonaphthalene is much easier to prepare than 2-naphthylselenocyanate, and so method 2 is to be preferred. Both in method 1 and 2 some diselenide is formed from which the acids can be obtained in very good yield. If the diselenide is accessible, this method is certainly the best.

Experimental. Method 1. 2-Naphthylselenocyanate was prepared according to Loevenich, Fremdling and Föhr [5]. The naphthylselenocyanate was dissolved in hot alcohol, some glucose and excess of concentrated potassium hydroxide solution were added and the mixture boiled until a homogeneous phase had been obtained. The mixture was cooled and the neutralised bromosubstituted acid was added. After standing in a closed bottle for 12 h warm water was added, the mixture filtered and the solution acidified with hydrochloric acid.

Method 2. 2-Iodonaphthalene was prepared in the usual way [6]. However, the yield and the quality of the product were improved when excess of nitrous acid was removed by potassium permanganate and the diazotized solution filtered before it was treated with potassium iodide [7].

The Grignard reagent of 0.2 mole 2-iodonaphthalene was prepared in a nitrogen atmosphere using a mixture of dry ether and benzene as solvent. Selenium (0.18 g-atom) was added and the mixture refluxed for 2 h. The flask was then cooled and 200 ml of about 3 M potassium hydroxide was added. A neutralised solution of the bromosubstituted acid was added with vigorous stirring. The stirring was continued for 12 h, the mixture was then treated with hydrochloric acid. The organic phase was extracted with ammonia and the naphthylselen-carboxylic acid was precipitated with hydrochloric acid. From the ether-benzene phase about 8 g of 2,2'-dinaphthyldiselenide was isolated.

Method 3. The diselenide was dissolved in boiling benzene and alcohol was added until starting turbidity. Sodiumborohydride was added until the solution was almost colourless. After addition of excess of haloester the mixture was refluxed for 2 h, potassium hydroxide solution was added and the alcohol and the benzene were distilled off. The alkaline solution was extracted with ether and then acidified.

All the naphthylselen-carboxylic acids were recrystallised from carbon tetrachloride and from formic acid. Yield and melting points are given in the table above.

1. Fredga, A. *Arkiv Kemi* **3** (1951) 123.
2. Fredga, A. *Arkiv Kemi* **5** (1953) 223.
3. Åberg, B. *Kgl. Lantbruks-Högsk. Ann.* **20** (1953) 241.
4. Morgan, G. T. and Porritt, W. H. *J. Chem. Soc.* **127** (1925) 1755.
5. Loevenich, J., Fremdling, H. and Föhr, M. *Ber.* **62** (1929) 2862.
6. Schmidlin, J. and Huber, M. *Ber.* **43** (1910) 2829.
7. Gies, H. and Pfeil, E. *Ann.* **578** (1952) 11.

Received July 22, 1958.

ACTA CHEMICA SCANDINAVICA 12 (1958) 1349—1358

Proceedings of the Swedish Biochemical Society

Papers read at the meeting in Uppsala, June 6—7, 1958

Mass Spectrometric Studies on Bile Acids and Other Steroid Derivatives

Sune Bergström*

Institute of Physiological Chemistry, University of Lund, Lund, Sweden

Ragnar Ryhage

Laboratory for mass spectrometry, Kemiska Institutionen I, Karolinska Institutet, Stockholm, Sweden

and Einar Stenhagen

Department of Medical Biochemistry, Institute of Medical Chemistry, University of Uppsala, Uppsala, Sweden

The mass spectra of the methyl esters of the bile acids show several characteristic features which render them useful for analytical purposes. The methyl ester of cholanic acid shows an intense peak of *m/e* 374 corresponding to the unfragmented ionized molecule $C_{25}H_{42}O_2^+$. This peak is the largest in the spectrum. When the sterol nucleus carries one or more hydroxyl groups the molecular peaks ("parent peaks") are either very small or absent because the hydroxyl groups are easily eliminated as water with the formation of double bonds. The side chain is also readily split off and in the mass spectrum there occurs a peak corresponding to the ionized unsaturated nucleus. For methyl esters of monohydroxycholanic acids such as 3-hydroxycholanic (lithocholic) acid this peak occurs at *m/e* 257. For 3,7,12-trihydroxycholanic (cholic) acid the "nuclear peak" is at *m/e* 253. For a saturated bile acid the nuclear peak thus indicates the number of hydroxyl groups present in the sterol ring system.

If the ring system contains both hydroxyl groups and double bonds the nuclear peak indicates their sum. Thus stigmasterol and β-sitosterol, which both have one hydroxyl group and one double bond in the ring system, give a characteristic nuclear peak at *m/e* 255.

The saturated monohydroxy tetracyclic triterpene tetrahydrodammaradienol [1] which possesses a trimethyl-substituted steroid nucleus gives a nuclear peak at *m/e* 299 = (257 + 3 × 14).

Peaks due to methoxycarbonyl-containing fragments are less prominent in the spectra of methyl esters of bile acids than they are in the spectra of methyl esters of aliphatic acids [2], but the intensity distribution among these peaks depends on the structure of the side chain in a manner analogous to that found in the case of methyl esters of branched chain aliphatic acids.

Positional isomers such as 3-hydroxy- and 12-hydroxycholanic acid give very different mass spectra.

The methyl ester of triacetoxycholic acid gives a very good spectrum in which the last peak observed is a strong peak at *m/e* 428 = (M—120). This fragment has evidently been formed by the elimination of two of the three acetyl groups in the form of acetic acid. The acetic acid is indicated by its strong molecular peak at *m/e* 60.

* Address from July 1, 1958: Kemiska Institutionen I, Karolinska Institutet, Stockholm.

1. Asselineau, C. and Asselineau, J. *Bull. soc. chim.* **1957** 1359.
2. Asselineau, J., Ryhage, R. and Stenhagen, E. *Acta Chem. Scand.* **11** (1957) 196.

On the Mechanism of Deoxycholic Acid Formation

S. Bergström, S. Lindstedt and B. Samuelsson

Department of Physiological Chemistry, University of Lund, Lund, Sweden

Recent work has shown that deoxycholic acid is formed from cholic acid by the action of intestinal microorganisms [1-3]. The aim of the present investigation was to study the reaction mechanisms of this transformation with the aid of cholic acid labelled with tritium in the 7β-position. The acid was prepared by reduction of 3α, 12α-dihydroxy-7-ketocholanic acid with sodium borohydride earlier exposed to tritium gas for 6 days. This compound was first administered together with cholic acid-24-^{14}C to rabbits. A bile fistula was made after two days. Practically all of the cholic acid had then been transformed into deoxycholic acid. The ratios of isotopes (^{3}H/^{14}C) in this acid and in the administered cholic acid were determined and found to be equal, thus demonstrating complete retention of the 7β-hydrogen during the elimination of the 7α-hydroxyl group.

The doubly labelled cholic acid was then given to rats and allowed to take part in the enterohepatic circulation for 1—7 days. Determinations of isotope ratios in the cholic acid samples isolated from the animals showed that a progressive loss of tritium had occurred.

It is known that in the rat deoxycholic acid is hydroxylated to cholic acid in the liver [4] and it was assumed that the loss of the 7β-^{3}H had taken place during the reaction sequence: cholic acid → deoxycholic acid → cholic acid. Norman and Sjövall [3] have isolated labelled deoxycholic and 3α, 12α-dihydroxy-7-ketocholanic acid from feces of rats that had received labelled cholic acid, and have further shown that the keto acid can be transformed into deoxycholic acid in the gut. If the 7-keto acid was an obligatory intermediate in the reaction cholic acid → deoxyholic acid this would explain the loss of the 7β-^{3}H. To clarify this point doubly labelled cholic acid was injected into the coecum of rats with a bile fistula and deoxycholic acid isolated from the feces. This acid retained 80 % of the tritium activity indicating that 3α,12α-dihyroxy-7-ketocholanic acid is only of minor importance as an intermediate in the formation of deoxycholic acid, the main path probably leading *via* the stereospecific elimination of water with the formation of an unsaturated acid as an intermediate.

The loss of tritium activity might also have occurred in the step deoxycholic acid → cholic acid which occurs in the liver. The doubly labelled deoxycholic acid obtained in the aforementioned experiments was therefore injected intraperitoneally into rats with a bile fistula. The ratio of T/^{14}C in the isolated cholic acid was then found to be less than 4 % of that in the injected deoxycholic acid.

The 7α-hydroxylation of cholesterol and the 11α- and 11β-hydroxylation in the pregnane-3,20-dione series have been found to proceed by direct replacement of the 7α-, 11α- and 11β-hydrogen, resp.[5-7] and it seems plausible that the 7α-hydroxylation of deoxycholic acid proceeds by a similar reaction, in which the 7β-hydrogen would not be labelized.

One explanation of these results is that the 7-hydrogen of the possible unsaturated intermediate formed by the elimination of water is brought into the 7α-position at the reduction of the double bond.

1. Lindstedt, S. and Sjövall, J. *Acta Chem. Scand.* **11** (1957) 417.
2. Lindstedt, S. *Arkiv Kemi* **11** (1957) 145.
3. Norman, A. and Sjövall, J. *To be published.*
4. Bergström, S., Rottenberg, M. and Sjövall, J. *Hoppe Seyler's Z. physiol. Chem.* **295** (1953) 278.
5. Bergström, S., Lindstedt, S., Samuelsson, B., Corey, E. J. and Gregoriou, G. A. *J. Am. Chem Soc. In press.*
6. Corey, E. J., Gregoriou, G. A., Peterson, D. H. and Sebek, O. K. *J. Am. Chem. Soc. In press.*
7. Hayano, M. and Gut, M. *Private communication.*

Determination of the Position of Carbon-Carbon Double Bonds by Mass Spectrometry

Nguyen Dinh-Nguyen

Department of Medical Biochemistry, University of Gothenburg, Sweden

The position of the double bond in methyl oleate may be determined by comparing the mass spectra of methyl stearate and methyl 9,10-dideuterostearate. The latter compound was prepared by reduction of methyl oleate with deutero-hydrazine.

The extension of the method to poly-unsaturated fatty esters is under investigation.

The Effect of Parathyroid Extract on Oxidative Phosphorylation

Carl-Henric de Verdier

Institute of Medical Chemistry, University of Uppsala, Sweden

In a previous communication the *in vivo* effect of a parathyroid extract was studied on the incorporation of ^{32}P labelled phosphate into different phosphorus compounds in rat kidney and liver [1]. Additional experiments have been made with kidney slices and liver mitochondria *in vitro*. The kidney slices were incubated in a medium containing different ions (Ca^{++} 2.5 mM) and glucose as a substrate. In this system parathormone (Lilly) in a concentration of 0.2 U. S. P. units per ml partly inhibited the incorporation of labelled phosphate into some nucleotides and phosphorylthreonine isolated from phosphoprotein. The effect on oxidative phosphorylation has been tested in a system of liver mitochondria similar to that of Dawson and Jones [2] by working on the assumption that although kidney and bone are the main target organs, the action of the hormone must be demonstrable in most cells. The mitochondrial suspension was obtained after homogenization in 0.25 M sucrose containing 0.001 M EDTA followed by centrifugations; the final two washings were performed in sucrose without EDTA. The result of a typical experiment is shown in Table 1.

Table 1. Effect of parathormone on oxidative phosphorylation in rat liver mitochondria. Each sample contained mitochondria from 0.5 g wet weight liver, 40 μmoles potassium orthophosphate, 5 μmoles ATP, 17 μmoles $MgCl_2$, 30 μmoles pyruvate, 0.04 μmoles cytochrome c, 295 μmoles sucrose, 60 μmoles glucose and hexokinase, pH 7.4. About 0.1 mC ^{32}P per flask. Final volume 3.0 ml. Incubation in open vessels with shaking at 30°C.

Hormone concentration units per ml	Ca^{++} concentration mM	Organic phosphate formed % of total labelled phosphate 7 min	18 min
0	0	42	98
0	0.33	40	98
0.025	0.33	32	77
0.05	0.33	31	72
0.10	0.33	30	69
0.20	0.33	30	55

The effect is obtained only when Ca^{++} is present in a concentration of about 3×10^{-4} M. The necessary presence of calcium ions seems to indicate that the hormone exerts its effect *via* these ions. Their inhibitory effect on oxidative phosphorylation in different mitochondrial systems is well-known[3]. Experiments with $^{45}Ca^{++}$, however, did not reveal any significant effect of the extract on the distribution of calcium ions between intra- and extramitochondrial space.

1. de Verdier, C.-H. *Acta Physiol. Scand.* **39** (1957) 1.
2. Dawson, J. and Jones, E. A. *International Congress on Clinical Chemistry*, Stockholm 1957. Summaries and Abstracts p. 86.
3. Mc Murray, W. C., Maley, G. F. and Lardy, H. A. *J. Biol. Chem.* **230** (1958) 219.

On the Use of Gas Chromatography and Mass Spectrometry in the Analysis of the Fatty Acids Found in Butter and Margarine

B. Hallgren and S. Stenhagen

Department of Medical Chemistry, University of Gothenburg, Gothenburg

R. Ryhage

Laboratory for Mass Spectrometry, Kemiska Institutionen I, Karolinska Institutet, Stockholm, Sweden

Under standardized operational conditions in gas chromatography the retention volume or retention time is characteristic of a certain component. When investigating mixtures of several components it is, however, necessary to use additional identification methods. In analysing mixtures of esters of fatty acids we have submitted them to both gas chromatography and mass spectrometry. If the gas chromatograms and the mass spectra of the mixtures are compared it is sometimes possible to identify the components. The mass spectrum of a mixture of many components will, however, become too complex. We have then collected fractions coming out from the gas chromatography column and identified the components of the fractions by a mass spectrometer run.

Using these methods we have analysed the complex mixtures of fatty acids present in butter and margarine.

The Isolation of Phosphorylhexosamine from the Rest Protein Fraction of *Escherichia coli* B

Gunnar Ågren

Institute of Medical Chemistry, University of Uppsala, Sweden

In earlier communications [1,2] it has been shown that acid hydrolysates of the Schneider rest protein fractions from mammalian organs contain O-phosphorylserine and O-phosphorylthreonine. Phosphorylserine has also been isolated from the corresponding fraction of yeast [3]. In other microorganisms phosphorylated hydroxy-amino acids of different composition seem to dominate in the acid hydrolysates. From *L. casei* O-phosphorylmuramic acid has recently been isolated [4], and from *E. coli* in the same way O-phosphorylethanolamine [5].

It has now been possible to isolate chromatographically pure phosphorylhexosamine from the acid hydrolysate of the rest protein of *E. coli*. Previously published methods for cultivation and isolation have been followed[6]. The bacteria were harvested at the end of the lag phase. They had been cultivated for about 2 h on a medium containing 1 mC ^{32}P per liter to facilitate the identification of phosphorus compounds. After lyophilization the cells were disrupted in a Raytheon 50-watt 9 kc magnetostriction oscillator during continuous cooling. The cell walls were separated by fractionated centrifugation [6]. The elution curve of the acid hydrolysate of cell walls passing through a Dowex 50-column was given in a previous paper [5].

By paper ionophoretic analysis it was found that the material from peak No. III on the curve was a mixture of at least three ninhydrin-positive compounds which at pH 5 migrated slower than phosphorylserine or phosporylthreonine. Sufficient amounts of material for analysis of peak No. III was obtained by mixing radioactive bacteria with large amounts of unlabeled cells. For large scale cultivation the bacteria were incubated in a 1 000 liter tank on the same medium for about 20 h. The usual yield of fresh bacteria from a single cultivation was about 2.5 kg. Material from two cultivations was used in this study. The hydrolysates of the rest protein fractions were separated on 10 Dowex-50 columns. Column dimensions were 6.5 × 55 cm.

Preparative paper ionophoresis of all material from peak No. III was carried out for 4 h in a 0.1 N pyridine-acetate buffer of pH 5 using Whatman paper No. 3. Two large ninhydrin-positive spots were found close to each other and well separated from a weaker spot with a more rapid migration. The phosphorus contents were 2.7 %, 0.71 %, and 0.16 %, respectively. Material from the slowest moving spot with the highest phosphorus content was eluted from the paper with water and purified by chromatography first on a small Dowex-50 column as a single peak with 0.01 N HCl and then on a small (0.9 cm × 25 cm) Dowex-1 formate column where the material could be eluted with water. Two rather well separated peaks were observed. Only a few mg were obtained from the first fraction with a phosphorus content of 6.0 %. The second peak had a phosphorus content of 11.6 %. In all about 40 mg of material was obtained from 5 kg of fresh bacteria.

The identity of this material with phosphorylhexosamine was verified by paper ionophoresis at pH 5 and paper chromatography in two solvent systems[1] where the compound moved as a single green-coloured ninhydrin-positive spot parallel with glucosamine-6-phosphate. This was prepared by incubating a yeast hexokinase preparation with equimolar amounts of glucosamine and radioactive ATP followed by purification on Dowex-1 formate column. Elementary analysis of the compound from *E. coli* gave the following values (Found: C 27.5; H 5.8; N 5.2; P 11.6. Calc. for $C_6H_{14}O_8NP$ (259): C 27.8; H 5.5; N 5.4; P 11.9). The position of the phosphate group must probably be in the primary alcoholic group. Only a phosphate group attached here would seem to resist the acid hydrolysis used in the isolation procedure [7].

Phosphorylhexosamine may not be present only in the cell walls. Water soluble fractions of proteins were obtained after centrifugation of the vibrated bacteria at 105100 *g* for 30 min at 0°C and precipitation with ethanol or acetone [6]. The acid hydrolysates of these purified fractions also gave the same types of elution curves on Dowex-50 columns with peaks in the same column volumes as No. III from the hydrolyzed cell walls. The function of phosphorylhexosamine in bacterial phosphoproteins is not clear. It could connect some peptide chains by diester bonds as in casein or pepsin [8], or possibly represent the active site in a transphosphorylating mechanism. A preliminary note has been published that galactosaminephosphate should be present in the hydrolysate of bone tissue [9].

This investigation was supported by the *Swedish Medical Research Council.*

1. Ågren, G., de Verdier, C-H. and Glomset, J. *Acta Chem. Scand.* **8** (1954) 1570.
2. Ågren, G., de Verdier, C-H. and Glomset, J. *Acta Chem. Scand.* **9** (1954) 1041.
3. Engström, L. and Ågren, G. *Acta Chem. Scand.* **10** (1956) 877.
4. Ågren, G. and de Verdier, C-H. *To be published.*
5. de Verdier, C-H. and Ågren, G. *Acta Chem. Scand.* **12** (1958). *In press.*
6. Ågren, G. *Acta Chem. Scand.* **10** (1956) 152.
7. Leloir, L. F. and Cardini, C. E. in Colowick and Caplan *Methods of Enzymology Vol. III* (1957) 840.
8. Perlmann, G. E. *Advances Protein Chem.* **10** (1955) 1.
9. Di Stefano, V., Neuman, W. F. and Rouser, G. *Arch. Biochem. Biophys.* **47** (1953) 218.

Mass Spectrometric Studies on Amino Acid and Peptide Derivatives

Carl-Ove Andersson

Department of Medical Biochemistry, Institute of Medical Chemistry, University of Uppsala, Uppsala, Sweden, and Laboratory for Mass Spectrometry, Kemiska Institutionen I, Karolinska Institutet, Stockholm, Sweden

In the mass spectrum of a methyl ester of the type RCH_2COOCH_3 the most prominent peak is normally found at *m/e* 74 and is due to a rearranged fragment $^1C_3H_6O_2^+$. A prominent peak due to the alkyl fragment R^+ is only observed when carbon atom 3 is quaternary. The mass spectrum of the methyl ester of an *α*-amino acid $RCHNH_2COOCH_3$ shows, on the other hand, a very large peak due to the ionized fragment $RCHNH_2^+$. The mass number of this fragment is different for all amino-acids except the isomeric valines and leucines.

The parent peaks are small but in the cases so far examined allow a direct determination of the molecular weight of the esters. A further prominent peak occurs at *m/e* 88 corresponding to the fragment $-CHNH_2COOCH_3^+$.

Although several free amino-acids and simple peptides can be brought into the gas phase without decomposition [2] compounds with the zwitterion structure have been found less suitable for mass spectrometric analysis than compounds in which either the amino group or the carboxyl is protected. It has been found possible to analyze peptides with protected amino- and carboxyl groups. Thus N-trifluoroacetyl-L-alanyl-L-phenylalanine methyl ester [3] gives an excellent mass spectrum with a parent peak at *m/e* 346 (calculated molecular weight 346.3).

The high-mass, high-resolution mass spectrometer thus seems to offer interesting possibilities in the analysis of amino-acids and peptides.

It is intended to extend this work to other amino-acid derivatives and to study the possibility of analyzing mixtures. As carried out at present one analysis requires about 100 micrograms of material.

1. Asselineau, J., Ryhage, R., and Stenhagen, E. *Acta Chem. Scand.* **11** (1957) 196.
2. Gross, D. and Grodsky, G. *J. Am. Chem. Soc.* **77** (1955) 1678.
3. Weygand, F., Geiger, R. and Swodenk, W. *Angew. Chem.* **68** (1956) 307.

Infrared-spectroscopic Studies on Bile Acids

I. Fischmeister

Department of Medical Biochemistry, Institute of Medical Chemistry, University of Uppsala, Sweden

The poor solubility of the bile acids in the nonpolar solvents required for infrared spectroscopy prevents their investigation in solution. We have therefore examined the spectra of the solid substances pressed in potassium bromide pellets. In the case of the bile acid esters which can be examined both in solution and in the solid state, the solid state spectra are found to be more distinct, owing to the fixed positions of the molecules in the crystal.

The spectra are sufficiently specific to allow identification of each bile acid by infrared spectroscopy. They are especially sensitive to the number and position of the hydroxyl groups in the skeleton. This is shown for the series of cholanic acid and its hydroxy derivatives, for coprostanic acid and its 3,7- and 3,7,12-hydroxy derivatives as well as for peptide conjugates of cholanic acid and its hydroxy derivatives with glycine and taurine. The length of the side chain affects not only the CH_2-vibrations but also those of the hydroxyl- and carboxyl group, indicating differences in the hydrogen bond pattern and/or different degree of hydrogen bonding in the crystallized compounds with different side chains.

This investigation was supported by the *Swedish Medical Research Council.*

1. Ågren, G., de Verdier, C-H. and Glomset, J. *Acta Chem. Scand.* **8** (1954) 1570.
2. Ågren, G., de Verdier, C-H. and Glomset, J. *Acta Chem. Scand.* **9** (1954) 1041.
3. Engström, L. and Ågren, G. *Acta Chem. Scand.* **10** (1956) 877.
4. Ågren, G. and de Verdier, C-H. *To be published.*
5. de Verdier, C-H. and Ågren, G. *Acta Chem. Scand.* **12** (1958). *In press.*
6. Ågren, G. *Acta Chem. Scand.* **10** (1956) 152.
7. Leloir, L. F. and Cardini, C. E. in Colowick and Caplan *Methods of Enzymology Vol. III* (1957) 840.
8. Perlmann, G. E. *Advances Protein Chem.* **10** (1955) 1.
9. Di Stefano, V., Neuman, W. F. and Rouser, G. *Arch. Biochem. Biophys.* **47** (1953) 218.

Mass Spectrometric Studies on Amino Acid and Peptide Derivatives

Carl-Ove Andersson

Department of Medical Biochemistry, Institute of Medical Chemistry, University of Uppsala, Uppsala, Sweden, and Laboratory for Mass Spectrometry, Kemiska Institutionen I, Karolinska Institutet, Stockholm, Sweden

In the mass spectrum of a methyl ester of the type RCH_2COOCH_3 the most prominent peak is normally found at *m/e* 74 and is due to a rearranged fragment $^1C_3H_6O_2^+$. A prominent peak due to the alkyl fragment R^+ is only observed when carbon atom 3 is quaternary. The mass spectrum of the methyl ester of an *α*-amino acid $RCHNH_2COOCH_3$ shows, on the other hand, a very large peak due to the ionized fragment $RCHNH_2^+$. The mass number of this fragment is different for all amino-acids except the isomeric valines and leucines.

The parent peaks are small but in the cases so far examined allow a direct determination of the molecular weight of the esters. A further prominent peak occurs at *m/e* 88 corresponding to the fragment $-CHNH_2COOCH_3^+$.

Although several free amino-acids and simple peptides can be brought into the gas phase without decomposition [2] compounds with the zwitterion structure have been found less suitable for mass spectrometric analysis than compounds in which either the amino group or the carboxyl is protected. It has been found possible to analyze peptides with protected amino- and carboxyl groups. Thus N-trifluoroacetyl-L-alanyl-L-phenylalanine methyl ester [3] gives an excellent mass spectrum with a parent peak at *m/e* 346 (calculated molecular weight 346.3).

The high-mass, high-resolution mass spectrometer thus seems to offer interesting possibilities in the analysis of amino-acids and peptides.

It is intended to extend this work to other amino-acid derivatives and to study the possibility of analyzing mixtures. As carried out at present one analysis requires about 100 micrograms of material.

1. Asselineau, J., Ryhage, R., and Stenhagen, E. *Acta Chem. Scand.* **11** (1957) 196.
2. Gross, D. and Grodsky, G. *J. Am. Chem. Soc.* **77** (1955) 1678.
3. Weygand, F., Geiger, R. and Swodenk, W. *Angew. Chem.* **68** (1956) 307.

Infrared-spectroscopic Studies on Bile Acids

I. Fischmeister

Department of Medical Biochemistry, Institute of Medical Chemistry, University of Uppsala, Sweden

The poor solubility of the bile acids in the nonpolar solvents required for infrared spectroscopy prevents their investigation in solution. We have therefore examined the spectra of the solid substances pressed in potassium bromide pellets. In the case of the bile acid esters which can be examined both in solution and in the solid state, the solid state spectra are found to be more distinct, owing to the fixed positions of the molecules in the crystal.

The spectra are sufficiently specific to allow identification of each bile acid by infrared spectroscopy. They are especially sensitive to the number and position of the hydroxyl groups in the skeleton. This is shown for the series of cholanic acid and its hydroxy derivatives, for coprostanic acid and its 3,7- and 3,7,12-hydroxy derivatives as well as for peptide conjugates of cholanic acid and its hydroxy derivatives with glycine and taurine. The length of the side chain affects not only the CH_2-vibrations but also those of the hydroxyl- and carboxyl group, indicating differences in the hydrogen bond pattern and/or different degree of hydrogen bonding in the crystallized compounds with different side chains.

Cellular Localisation and Specificity of Intestinal Invertase

Bengt Borgström and Arne Dahlqvist

Department of Physiological Chemistry, University of Lund, Lund, Sweden

In homogenates from intestinal mucosa (swine), invertase has been found exclusively localized in the microsome fraction, obtained by differential centrifugation. By treating the microsomes with a solution of desoxycholate the invertase activity was obtained in a clear solution which, however, did not prove to be a true solution, as dialysis lead to a recovery of the enzyme in the particulate form.

When isolated microsomes were digested by trypsin, invertase was rapidly inactivated parallel with the hydrolysis of proteins. In the beginning of this reaction, a solubilisation of invertase was observed. Phosphate buffer was found to protect invertase against the inactivation by trypsin, without affecting its solubilisation. In the presence of desoxycholate, it is therefore possible to use trypsin digestion for preparation of soluble invertase.

The relation of invertase to other α-glucosidases of intestinal mucosa is not known. According to the theory of Weidenhagen [1], the animal intestine should contain only one α-glucosidase, hydrolyzing maltose, sucrose, and other α-D-glucopyranosides. Enzyme preparations from animal intestine have, however, no action upon α-methylglucoside [2] and recently two α-glucosides have been demonstrated to be hydrolyzed by enzymes different from maltase, namely *iso*maltose and nigerose [3,4].

During the further purification of solubilized invertase, we have found that the trehalase activity is rapidly lost during ethanol fractionation while invertase and maltase activity are not affected during this procedure. Intestinal trehalase must therefore be an enzyme separate form maltase and invertase.

The further separation of invertase and maltase activity is explored by the use of DEAE-cellulose columns and these results will be discussed.

1. Weidenhagen, R. in Nord F. F. und Weidenhagen, R. *Handbuch der Enzymologie.* Vol. 1, Lepzig, 1940.
2. Myrbäck, K. and Myrbäck, S. *Svensk Kem. Tidskr.* **48** (1936) 64.
3. Larner, J. and McNickle, C. M. *J. Biol. Chem.* **215** (1955) 723.
4. Larner, J. and Gillespie, R. E. *J. Am. Chem. Soc.* **78** (1956) 882.

Fractionation of Enzymes from Ringhals Venom

Walter Björk and Hans G. Boman

Institute of Biochemistry, University of Uppsala, Uppsala, Sweden

Venom from the South African ringhals cobra *(Hemachatus haemachates)* has been studied by anion exchange chromatography and column electrophoresis.

Early results showed considerable differences in the chromatograms for different batches of venom and it was found that storage and autoincubation of the venom would alter the chromatographic behaviour of especially the phosphodiesterase. These results indicated that the procedure for the collection of the venom might be of significant importance for a successful fractionation. We have later by the kind cooperation of Dr. J. H. Mason at The South African Institute for Medical Research, been able to compare venom collected in the ordinary way (dried at room temperature) and venom "milked" down in a container cooled by dry ice and immediately freeze-dried. The chromatograms of these two materials showed that the main part of the phosphodiesterase is present in different forms depending on the collection procedure and that chromatography of the freeze-dried venom gives about 7 times better purification for the phosphodiesterase than obtained for venom collected in the ordinary way. It has also been found that the successful chromatographic separation of the diesterase is dependent on a sort of double fronting of the developing agent. The phosphodiesterase was separated from lecithinase A and cholinesterase, but the chromatography so far used did not separate the two latter enzymes from each other. However, column electrophoresis at pH 5.5 effects a complete separation of cholinesterase from both lecithinase A and phosphodiesterase. It thus appears that a combination of chromatography and electrophoresis may offer possibilities for an efficient purification of all three enzymes.

Recent Studies on Sialic Acid

Gunnar Blix

Institute of Medical Chemistry, University of Uppsala, Sweden

Inhibition of DNA-Synthesis by Deoxyadenosine

Hans Klenow and Lorna Langer

The Fibiger-Laboratory, University of Copenhagen, Denmark

The effect of some purine derivatives on the incorporation of ^{14}C-formate into DNA (deoxyribonucleic acid) and of ^{32}P-orthophosphate into DNA and RNA (ribonucleic acid) of ascites tumor cells *in vitro* has been investigated.

When Ehrlich's ascites tumor cells were incubated *in vitro* with ^{14}C-formate it was found that adenine, adenosine and deoxyinosine had some stimulatory effect or no effect on the incorporation of ^{14}C into DNA-thymine (measured a specific activity) when these compounds were added in concentrations of 2.3—3.9 μmoles per ml cell suspension. In the presence of added deoxyadenosine, however, the specific activity of DNA-thymine was only 6—15 % of that of the control. This effect was found both in the presence and in the absence of added deoxycytidine or deoxycytidylic acid. The total radioactivity of the pooled acid-soluble thymine compounds from cells incubated in the presence of ^{14}C-formate and deoxyadenosine for about 3 h, was about twice as high as that of the control experiment without added deoxyadenosine. The specific radioactivity of these thymine compounds were, however, about the same in the two cases. It is likely, therefore, that deoxyadenosine inhibits the biosynthesis of DNA and that this inhibition is not due to a block of the biosynthesis of the thymine part of DNA.

Experiments with ^{32}P-orthophosphate have shown a similar inhibitory effect by deoxyadenosine on the incorporation of ^{32}P into DNA. Fifty per cent inhibition was obtained with about 1 μmole of deoxyadenosine per ml cell suspension. Incorporation of ^{32}P into RNA was slightly increased under these conditions.

Experiments with suspensions of Yoshida's ascites tumor cells showed that addition of deoxyadenosine in concentrations of 3.5—3.9 μmoles per ml cell suspension had only a modest inhibitory effect in incorporation of ^{14}C-formate into DNA-thymine, while deoxyinosine showed a consistent stimulation of this incorporation, suggesting that the rate of DNA-synthesis is increased by about 50 %.

Table 1. Rate of incorporation of ^{32}P-orthophosphate into RNA and DNA of Ehrlich's ascites tumor cells.

Each vessel contained 0.4 g packed cells, suspended in 1.2 ml Tyrode's solution, deoxycytidine 5 μmoles, $H_2^{32}PO_4^-$ 12 μC, glucose 55 μmoles, and sodium succinate 37 μmoles. To the experimental vessels were further added 5 μmoles of adenine compounds as indicated; final volume 2.25 ml. Incubated at 37°C with shaking. The figures are averages of two experiments.

Additions	Rate of incorporation in per cent of the control	
	RNA	DNA
Adenine	99	105
Adenosine	105	122
Deoxyadenosine	94	14

Mass Spectrometric Studies on Esters of Rosin Acids

Henrik H. Bruun

Institute of Wood Chemistry, Åbo Akademi, Åbo, Finland

Ragnar Ryhage

Laboratory for mass spectrometry, Kemiska Institutionen I, Karolinska Institutet, Stockholm

and Einar Stenhagen

Department of Medical Biochemistry, Institute of Medical Chemistry, University of Uppsala, Uppsala, Sweden

A mass spectrometric study has been performed on the methyl esters of the following rosin acids: *d*-pimaric, levopimaric, *iso*-*d*-pimaric, podocarpic, palustric, abietic, neoabietic, dihydroabietic, tetrahydroabietic and dehydroabietic (nomenclature of Simonsen and Barton [1], as well as on the related hydrocarbons fichtelite and retene.

All the methyl esters give excellent mass spectra showing a very strong peak due to the ionized unfragmented molecule. All the spectra differ markedly from each other and a rosin acid may be readily identified by the mass spectrum of its methyl ester. Methyl tetrahydroabietate and fichtelite have several strong peaks in common, a feature to be expected as the hydrocarbon skeleton of tetrahydroabietic acid is identical with that of fichtelite.

1. Simonsen, Sir J. *The terpenes.* Vol. III, 2nd Ed., Cambridge 1952.

The Vitamin B_{12}-Content of Human Fetal Tissues

Johan Killander

Department of Microbiology, Institute of Medical Chemistry, University of Uppsala, Sweden

Deficiency of B_{12} during fetal life has been suggested to cause malformation or death of the fetus [1]. Moreover the fetal erythroblasts have been considered to be related to the megaloblasts occurring in anemias caused by B_{12} deficiency. It was therefore of interest to study the B_{12}-content of fetal tissues.

Method. 25—500 mg of tissue was homogenised; crude papain and sodium cyanide were added. The volume was made up to 25 ml with phosphate-citric acid buffer, pH 5.0. One hour's digestion at + 60°C was followed by heating at 100°C for 15 min. After filtration or centrifugation the B_{12} content of the extract was assayed microbiologically using *Euglena gracilis* z[2]. The recovery of added B_{12}-^{60}Co was nearly complete as determined by both radioactivity and microbiological measurements. Extracts of liver and muscle from a hog previously injected with B_{12}-^{60}Co contained close to 100 % of the radioactivity of the organ.

Material. Liver, spleen, kidney, adrenals, heart, lung, thymus, brain, spinal cord and muscle from 28 fetuses of 6—25 cm length were analysed. *Results*, See Table 1.

Conclusions. No changes in B_{12} concentration of fetal organs were observed over the period of life investigated except for brain and spinal cord in which the vitamin was found to decrease with age. The data on fetuses will be compared with those on prematures, children and adults.

Table 1. Mean and range of the vit. B_{12} content of human fetal tissues in mμg/g fresh weight.

Tissue	Fetal length 6—15 cm No. of observations		Fetal length 16—25 cm No. of observations	
Liver	17	360 (250—490)	6	340 (230—530)
Spleen	6	59 (48—79)	11	50 (37—72)
Kidney	14	140 (115—170)	7	130 (75—230)
Adrenals	15	180 (120—270)	7	180 (130—260)
Lung	2	77 (55—99)	2	87 (82—92)
Heart	17	45 (39—62)	8	41 (32—54)
Thymus			4	23 (14—30)
Brain	14	25 (13—38)	8	9,7 (5,3—15)
Spinal cord	14	63 (36—106)	11	36 (14—51)
Muscle	13	39 (23—44)	6	29 (21—35)

1. Thiersch, J. B. *Am. J. Obstet. Gynecol.* 63 (1952) 1298.
2. Ross, G. I. M. und Mollin, D. L. in Heinrich, H. C. *Vitamin B_{12} und Intrinsic Factor*, Ferdinand Enke Verlag, Stuttgart 1957, p. 437.

A Twin Microscope for the Perkin-Elmer Model 21 Infra-red Double-Beam Spectrophotometer

Fredrik Möhl

Department of Medical Biochemistry, Institute of Medical Chemistry, University of Uppsala, Uppsala, Sweden

In our laboratory a Perkin-Elmer 21 infra-red double-beam spectrophotometer is employed. As the need arose for a microscope attachment to it, we began constructing such a device in the autumn of 1956.

The instrument now completed consists of 2 parallel microscopes lying horizontally directly in the beams. Each microscope has 10 mm reflecting Schwarzschild aplanats for objective and condenser. A lamp was built into the monochromator of the spectrometer to project its entrance slit upon the sample. The latter is observed through a retractable viewer with a semi-reflecting right-angle prism.

The stage is vertical, it has right-angle slides and moves axially for focusing. It can also be swung upwards-outwards for attention.

The whole microscope attachment forms a unit. It is easily removed and replaced with accuracy, being secured in position by two pins.

It is, however, still our opinion that no satisfactory device for infra-red double-beam microspectrophotometry has yet been made [1,2]. In our microscope too much energy is lost at the entrance. Had this not been the case, an excessive heating of the sample would have been unavoidable.

The remedy should be to reverse the beam path by interchanging the energy source and the detector of the spectrometer. Thus the sample would be placed in a monochromatic beam causing little heat. We have, however, not been able to solve this problem practically. It seems a task for the makers.

1. *Cf.* Ford, M. A., Price, W. C., Seeds, W. E. and Wilkenson, G. R. *J. Opt. Soc. Am.* **48** (1958) 249, for a discussion of this subject.
2. *Cf.*, however, Ref. 1, p. 250.

The Nucleophilic Reactivity of Biological Thiols with Respect to Thiol-Disulphide Exchange Reactions *

Alexander Pihl, Lorentz Eldjarn and Karl F. Nakken

Norsk Hydro's Institute for Cancer Research, The Norwegian Radium Hospital, Oslo, Norway

The biological significance of thiols can to a considerable extent be explained by the nucleophilic reactivity of their thiol group. It has generally been felt that in most of the nucleophilic exchange reactions of thiols the mercaptide ion is the active molecular species. Recently this mechanism has been proven in the case of thiol-disulphide exchange reactions [1,2]. At pH 7.4 the concentrations of the ionized forms of the physiological thiols are not inconsiderable as their pK values prove to be much lower than previously realized [3,4].

In the present investigation the relative nucleophilic reactivity of a series of biologically important thiols has been studied. The initial rate of interaction of the thiols (cysteine, glutathione, homocysteine, cysteamine, diethylcysteamine, and penicillamine) with cystine at pH 7.4 and 37°C was measured using ^{35}S-labeled cystine followed by paper electrophoretic separation of the reaction products [5]. The unexpected observation was made that the observed initial reaction rates (k_{SH}) were approximately equal in spite of the very large differences in the concentrations of the ionized thiols (pK varied from 7.7 to 9.75). The rate constants for the respective ionized thiols (k_{S^-}) were found to obey the Brönsted equation with the following parameters:

$$\log k_{S^-} = 0.73\ pK_{SH} - 1.88$$

The above k values (expressed in liter $\times$ moles^{-1} $\times$ min^{-1}) refer to the interaction of the thiols with the one of the sulphur atoms of cystine. Since cystine contains two symmetrical sulphur groups which are equivalent in these exchange reactions, the observed rates were actually twice the one given in the equation. The above presentation was preferred for thermodynamic reasons.

Several thiols tested did not obey the above equation but reacted at distinctly slower rates. This was the case with certain N-acyl derivatives (N-acetylcysteamine, aletheine, and coenzyme A). Compounds where the ionized thiol is part of a resonating system (thiocyanide, *o*-aminothiophenol, ergothionine, thiolhistidine, *etc.*) did not interact at all with cystine.

Thiol-disulphide exchange reactions play an important part in the enzymatic reduction of disulphides [6] and similar reactions may be envisaged to occur in the establishment and the splitting of disulphide cross linkages in proteins. The fact that a series of thiols obey the above equation strongly indicates that in such reactions the pK value of the attacking thiol is of minor significance with regard to the reaction rates. This finding may be interpreted to mean that with increasing pK_{SH} value the decrease in the concentration of the ionized thiol at a given pH is effectively counteracted by a concurrent increase in the nucleophilic reactivity of the ionized thiol.

* Supported by *The Norwegian Cancer Society.*

1. Eldjarn, L. and Pihl, A. *J. Biol. Chem.* **225** (1957) 499.
2. Fava, A., Iliceto, A. and Camera, E. *J. Am. Chem. Soc.* **79** (1957) 833.
3. Calvin, M. in *Glutathione*, Academic Press, Inc. New York 1954, p. 3.
4. Benesch, R. E. and Benesch, R. *J. Am. Chem. Soc.* **77** (1955) 5877.
5. Eldjarn, L. and Pihl, A. *J. Am. Chem. Soc.* **79** (1957) 4589.
6. Pihl, A., Eldjarn, L. and Bremer, J. *J. Biol. Chem.* **227** (1957) 339.

The Vitamin B_{12}-Content of Human Fetal Tissues

Johan Killander

Department of Microbiology, Institute of Medical Chemistry, University of Uppsala, Sweden

Deficiency of B_{12} during fetal life has been suggested to cause malformation or death of the fetus [1]. Moreover the fetal erythroblasts have been considered to be related to the megaloblasts occurring in anemias caused by B_{12} deficiency. It was therefore of interest to study the B_{12}-content of fetal tissues.

Method. 25—500 mg of tissue was homogenised; crude papain and sodium cyanide were added. The volume was made up to 25 ml with phosphate-citric acid buffer, pH 5.0. One hour's digestion at + 60°C was followed by heating at 100°C for 15 min. After filtration or centrifugation the B_{12} content of the extract was assayed microbiologically using *Euglena gracilis* z[2]. The recovery of added B_{12}-^{60}Co was nearly complete as determined by both radioactivity and microbiological measurements. Extracts of liver and muscle from a hog previously injected with B_{12}-^{60}Co contained close to 100 % of the radioactivity of the organ.

Material. Liver, spleen, kidney, adrenals, heart, lung, thymus, brain, spinal cord and muscle from 28 fetuses of 6—25 cm length were analysed. *Results*, See Table 1.

Conclusions. No changes in B_{12} concentration of fetal organs were observed over the period of life investigated except for brain and spinal cord in which the vitamin was found to decrease with age. The data on fetuses will be compared with those on prematures, children and adults.

Table 1. Mean and range of the vit. B_{12} content of human fetal tissues in mμg/g fresh weight.

Tissue	Fetal length 6—15 cm No. of observations		Fetal length 16—25 cm No. of observations	
Liver	17	360 (250—490)	6	340 (230—530)
Spleen	6	59 (48—79)	11	50 (37—72)
Kidney	14	140 (115—170)	7	130 (75—230)
Adrenals	15	180 (120—270)	7	180 (130—260)
Lung	2	77 (55—99)	2	87 (82—92)
Heart	17	45 (39—62)	8	41 (32—54)
Thymus			4	23 (14—30)
Brain	14	25 (13—38)	8	9,7 (5,3—15)
Spinal cord	14	63 (36—106)	11	36 (14—51)
Muscle	13	39 (23—44)	6	29 (21—35)

1. Thiersch, J. B. *Am. J. Obstet. Gynecol.* 63 (1952) 1298.
2. Ross, G. I. M. und Mollin, D. L. in Heinrich, H. C. *Vitamin B_{12} und Intrinsic Factor*, Ferdinand Enke Verlag, Stuttgart 1957, p. 437.

A Twin Microscope for the Perkin-Elmer Model 21 Infra-red Double-Beam Spectrophotometer

Fredrik Möhl

Department of Medical Biochemistry, Institute of Medical Chemistry, University of Uppsala, Uppsala, Sweden

In our laboratory a Perkin-Elmer 21 infra-red double-beam spectrophotometer is employed. As the need arose for a microscope attachment to it, we began constructing such a device in the autumn of 1956.

The instrument now completed consists of 2 parallel microscopes lying horizontally directly in the beams. Each microscope has 10 mm reflecting Schwarzschild aplanats for objective and condenser. A lamp was built into the monochromator of the spectrometer to project its entrance slit upon the sample. The latter is observed through a retractable viewer with a semi-reflecting right-angle prism.

The stage is vertical, it has right-angle slides and moves axially for focusing. It can also be swung upwards-outwards for attention.

The whole microscope attachment forms a unit. It is easily removed and replaced with accuracy, being secured in position by two pins.

It is, however, still our opinion that no satisfactory device for infra-red double-beam microspectrophotometry has yet been made [1,2]. In our microscope too much energy is lost at the entrance. Had this not been the case, an excessive heating of the sample would have been unavoidable.

The remedy should be to reverse the beam path by interchanging the energy source and the detector of the spectrometer. Thus the sample would be placed in a monochromatic beam causing little heat. We have, however, not been able to solve this problem practically. It seems a task for the makers.

1. *Cf.* Ford, M. A., Price, W. C., Seeds, W. E. and Wilkenson, G. R. *J. Opt. Soc. Am.* **48** (1958) 249, for a discussion of this subject.
2. *Cf.*, however, Ref. 1, p. 250.

The Nucleophilic Reactivity of Biological Thiols with Respect to Thiol-Disulphide Exchange Reactions *

Alexander Pihl, Lorentz Eldjarn and Karl F. Nakken

Norsk Hydro's Institute for Cancer Research, The Norwegian Radium Hospital, Oslo, Norway

The biological significance of thiols can to a considerable extent be explained by the nucleophilic reactivity of their thiol group. It has generally been felt that in most of the nucleophilic exchange reactions of thiols the mercaptide ion is the active molecular species. Recently this mechanism has been proven in the case of thiol-disulphide exchange reactions [1,2]. At pH 7.4 the concentrations of the ionized forms of the physiological thiols are not inconsiderable as their pK values prove to be much lower than previously realized [3,4].

In the present investigation the relative nucleophilic reactivity of a series of biologically important thiols has been studied. The initial rate of interaction of the thiols (cysteine, glutathione, homocysteine, cysteamine, diethylcysteamine, and penicillamine) with cystine at pH 7.4 and 37°C was measured using ^{35}S-labeled cystine followed by paper electrophoretic separation of the reaction products [5]. The unexpected observation was made that the observed initial reaction rates (k_{SH}) were approximately equal in spite of the very large differences in the concentrations of the ionized thiols (pK varied from 7.7 to 9.75). The rate constants for the respective ionized thiols (k_{S^-}) were found to obey the Brönsted equation with the following parameters:

$$\log k_{S^-} = 0.73\ pK_{SH} - 1.88$$

The above k values (expressed in liter $\times$ moles^{-1} $\times$ min^{-1}) refer to the interaction of the thiols with the one of the sulphur atoms of cystine. Since cystine contains two symmetrical sulphur groups which are equivalent in these exchange reactions, the observed rates were actually twice the one given in the equation. The above presentation was preferred for thermodynamic reasons.

Several thiols tested did not obey the above equation but reacted at distinctly slower rates. This was the case with certain N-acyl derivatives (N-acetylcysteamine, aletheine, and coenzyme A). Compounds where the ionized thiol is part of a resonating system (thiocyanide, *o*-aminothiophenol, ergothionine, thiolhistidine, *etc.*) did not interact at all with cystine.

Thiol-disulphide exchange reactions play an important part in the enzymatic reduction of disulphides [6] and similar reactions may be envisaged to occur in the establishment and the splitting of disulphide cross linkages in proteins. The fact that a series of thiols obey the above equation strongly indicates that in such reactions the pK value of the attacking thiol is of minor significance with regard to the reaction rates. This finding may be interpreted to mean that with increasing pK_{SH} value the decrease in the concentration of the ionized thiol at a given pH is effectively counteracted by a concurrent increase in the nucleophilic reactivity of the ionized thiol.

* Supported by *The Norwegian Cancer Society.*

1. Eldjarn, L. and Pihl, A. *J. Biol. Chem.* **225** (1957) 499.
2. Fava, A., Iliceto, A. and Camera, E. *J. Am. Chem. Soc.* **79** (1957) 833.
3. Calvin, M. in *Glutathione*, Academic Press, Inc. New York 1954, p. 3.
4. Benesch, R. E. and Benesch, R. *J. Am. Chem. Soc.* **77** (1955) 5877.
5. Eldjarn, L. and Pihl, A. *J. Am. Chem. Soc.* **79** (1957) 4589.
6. Pihl, A., Eldjarn, L. and Bremer, J. *J. Biol. Chem.* **227** (1957) 339.

On the Metabolism of Thiosulfate Esters

Bo Sörbo

Research Institute of National Defence, Dept. 1, Sundbyberg, and Nobel Medical Institute, Biochemical Dept., Stockholm, Sweden

When sodium sulfocysteine [$NaS_2O_3CH_2CH(NH_2)COOH$] or aminoethylthiosulfuric acid [$NH_2C_2H_4S_2O_3H$] were incubated with rat liver homogenates under aerobic conditions, sulfate was formed. Under anaerobic conditions sulfite was formed instead of sulfate, but sulfite is oxidized to sulfate in the presence of oxygen by the action of sulfite oxidase [1]. The formation of sulfite was a non-enzymic reaction involving protein-bound sulfhydryl groups. The other reaction product was a protein-bound mixed disulfide. As the protective properties of certain sulfur compounds against ionizing radiation have been attributed to their capacity to form mixed disulfides [2], the possibility was considered that thiosulfate esters should also protect against ionizing radiation. This has been experimentally verified in the case of aminoethylthiosulfuric acid [3]. The presence of an enzyme in rat liver, which forms thiosulfate from sulfocysteine (but not from aminoethylthiosulfuric acid) was also found and this supports earlier work of Cavallini and Stirpe [4], who observed an increased excretion of thiosulfate in rats injected with sulfocysteine.

1. Heimberg, M., Fridovich, I. and Handler, P. *J. Biol. Chem.* **204** (1953) 913.
2. Eldjarn, L. and Pihl, A. *J. Biol. Chem.* **223** (1956) 341.
3. Holmberg, B. and Sörbo, B. *To be published.*
4. Cavallini, D. and Stirpe, F. *Atti accad. nazl. Lincei, Rend. Classe sci. fis. mat. e nat.* **20** (1956) 378.

ACTA CHEMICA SCANDINAVICA 12 (1958) 1359—1363

Pyrazole Studies

XI.* Oxidation by Air of 1:4-Disubstituted Pyrazolidine-3:5-diones

STIG VEIBEL, S. LINHOLTER and P. SØRENSEN

Department of Organic Chemistry, University of Technology, Copenhagen, Denmark

Previously reported studies on the triethylaminecatalysed oxidation by air of 4-alkylsubstituted pyrazol-5-ones have been extended to embrace 1:4-disubstituted pyrazolidine-3:5-diones. These substances are oxidised to the corresponding 4-hydroxysubstituted compounds considerably faster than the pyrazolones, and the scheme followed is another, no triethylamine oxide being formed simultaneously and further oxidation to unidentified products taking place more readily than in the case of the pyrazolones.

The identity of a substance mentioned by Gagnon *et al.* as 1:4-diphenylpyrazolidine-3:5-dione with phenylacetic acid phenylhydrazide has been suggested and the genuine 1:4-diphenylpyrazolidine-3:5-dione has been prepared.

In a previous communication [1] we were able to show that 4-alkylsubstituted pyrazol-5-ones in methanolic solution are oxidised by air to 4-alkyl-4-hydroxysubstituted pyrazol-5-ones, this oxidation, in the presence of triethylamine in excess and at constant concentration of oxygen, following a first order scheme, one molecule of oxygen being absorbed per molecule of pyrazolone and one molecule of triethylamine oxide being formed simultaneously.

In view of the growing significance of substituted pyrazolidine-3:5-diones we decided to investigate the oxidation of these substances under conditions similar to those being in force in the investigations mentioned. We found that the pyrazolidine-3:5-diones are oxidised extremely readily under these conditions, but the scheme is not so clear-cut as in the instance of the pyrazol-5-ones where a first order scheme was followed usually at least up to 80 % completion and the hydroxy-compound could be isolated in 95—100 % yield. With the pyrazolidine-3:5-diones the absorption of oxygen usually comes to an end when about 66—75 % of the calculated volume of oxygen has been absorbed, presuming the absorption of one mole of oxygen per mole of pyrazolidinedione. The velocity with which oxygen is absorbed is considerably greater

* X: *Acta Chem. Scand.* **9** (1955) 970.

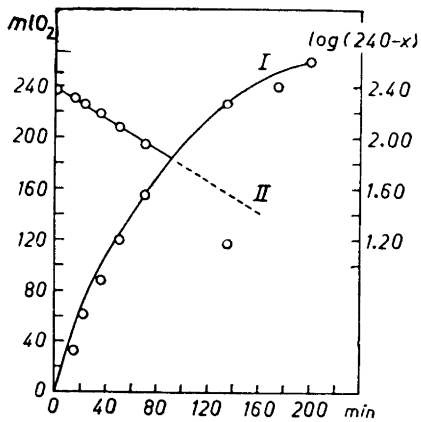

Fig. 1. Oxidation of a 0.02 M solution of 4-butylpyrazolidine-3:5-dione.
Curve I (ordinates left): Uptake of oxygen.
Curve II (ordinates right): log(240—x).

in the case of the pyrazolidinediones than in the case of the pyrazolones, and no triethylamine oxide can be isolated from the reaction products.

This means that only one *atom* of oxygen per molecule of pyrazolidinedione is demanded for the oxidation to the hydroxy compound, and the total consumption of oxygen is thus somewhat greater than calculated. As, however, the yield of hydroxy compound isolated is only some 50—75 %, and as the formation of oily products is always observed, we are of the opinion that the formation of the hydroxy compound is followed by a hydrolytic cleavage of the pyrazolidine-nucleus and possibly an oxidation of the substituted tartronic acid monophenylhydrazide formed (compare the following paper), this oxidation being responsible for the excess of oxygen consumed. As seen from Fig. 1, which is representative for all the oxidations, a first order scheme is followed up to some 60 % oxidation, presuming that only 1 atom of oxygen is used per molecule. This means that we here as in the case of the pyrazolones may compare the velocities of oxidation by indicating the time necessary for the absorption of 50 % of the calculated volume of oxygen.

A possible sequence of reactions might be:

$$\mathrm{PyRH} + (\mathrm{C_2H_5})_3\mathrm{N} \rightleftharpoons \mathrm{PyR^-} + (\mathrm{C_2H_5})_3\mathrm{NH^+}$$

$$\mathrm{PyR^-} + \mathrm{O_2} \rightleftharpoons \mathrm{PyROO^-}$$

$$\mathrm{PyROO^-} + \mathrm{PyR^-} \longrightarrow 2\ \mathrm{PyRO^-},$$

PyRH meaning a 4-substituted pyrazolidine-3:5-dione.

The difference between the oxidation of pyrazolones and pyrazolidinediones should, thus, depend on the oxidation potentials of the pyrazolone anion, the triethylammonium ion and the pyrazolidinedione anion, decreasing in this order if the explanation given here is the correct one.

Table 1. Oxidation of different pyrazolones and pyrazolidine-diones with oxygen.

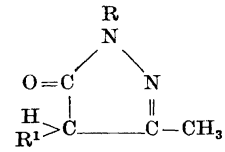

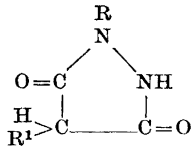

R	R^1	Time for 50 % oxidation	R	R^1	Time for 50 % oxidation
C_6H_5	CH_3	26 h	C_6H_5	CH_3	2 min
C_6H_5	C_2H_5	20 h	C_6H_5	C_2H_5	2.5 min
C_6H_5	C_3H_7*iso*	22.5 h	C_6H_5	C_3H_7*iso*	14 min
C_6H_5	C_4H_9	32 h	C_6H_5	C_4H_9	50 min
C_6H_5	C_6H_{11}	9 h	C_6H_5	C_6H_{11}	60 min
C_6H_5	$C_6H_5CH_2$	72 h	C_6H_5	$C_6H_5CH_2$	14 min
			C_6H_5	C_6H_5	4 min
			C_6H_5	$(C_6H_5)_3C$	—

The technique applied was that described previously [1]. Table 1 summarises the results obtained and gives a comparison of oxidation rates for corresponding pyrazol-5-ones and pyrazolidine-3:5-diones.

It is seen from Table 1 that we extended the investigation to the oxidation by air of 1:4-diphenylpyrazolidine-3:5-dione and of 1-phenyl-4-triphenylmethylpyrazolidine-3:5-dione. The former of these two substances was oxidised readily, the latter was not oxidised at all.

A comparison of columns 3 and 6 of Table 1 shows that not only are the rates of oxidation much higher for the pyrazolidinediones than for the pyrazolones, but the influence of the substituent present at C^4 is quite different in the two series. The 4-*cyclo*hexylpyrazolone is the one most rapidly oxidised, whereas the 4-*cyclo*hexylpyrazolidinedione is the one most slowly oxidised in the series of pyrazolidinediones investigated. So far, we have found no explanation covering this difference, but the mechanism followed in the two series is, as mentioned, quite different.

The presence of a phenyl group (or possibly also other substituents) at N^1 seems to be essential for the oxidisability of the pyrazolidinediones. 4-Benzylpyrazolidine-3:5-dione was not oxidised when the usual technique was applied. By addition of some crystals of cupric acetate, however, the absorption of oxygen was started and some 60 % of the volume calculated for the formation of the hydroxy compound was absorbed during 2 h. We did not succeed in isolating a definite oxidationproduct. Evidently an oxidative degradation of the cyclic compound takes place.

On the other hand, we succeeded, when oxidising 4-benzylpyrazolidine-3:5-dione in the absence of triethylamine, in isolating after 13 h, when 1 mole of oxygen per mole of pyrazolidinedione had been absorbed, a small quantity of a substance with m.p. 159—161° which contained 9.33 % of nitrogen, calculated for the 4-hydroperoxide of the pyrazolidinedione 9.28 % N. The main product was, however, an oil which was not further investigated but which,

in analogy to results obtained with butazolidine (see the following paper) might be impure benzyltartronic acid monophenylhydrazide or the free benzyltartronic acid.

EXPERIMENTAL PART *

The pyrazolidine-3:5-diones were prepared by current methods [2,3]. The yields obtained and the m. p.'s found as well as those indicated in the literature are tabulated in Table 2, whereas Table 3 contains the corresponding figures for the 4-hydroxypyrazolidine-3:5-diones.

Table 2. 1-Phenyl-4-alkyl-pyrazolidine-3:5-diones.

	Alkyl	Yield %	M. p.	M. p. Literature		C %	H %	N %
I	CH_3	70	168–170°	—	calc.	63.15	5.26	14.73
					found	62.90	5.42	14.76
II	C_2H_5	75	108–109°	108° [4,5]		—	—	—
III	C_3H_7*iso*	70	114–115°	110° [6]		—	—	—
IV	C_4H_9	75	94–95°	94° [5]		—	—	—
V	C_6H_{11}	80	154–156°	—	calc.	69.76	7.00	10.85
					found	69.70	6.99	10.75
VI	$C_6H_5CH_2$	75	183–185°	—	calc.	72.14	5.26	10.45
					found	72.95	5.37	10.44
VII	$(C_6H_5)_3C$	90	225–235°	—	calc.	80.00	5.42	6.89
					found	79.55	5.54	6.48
VIII	C_6H_5	*ca.* 5	218–220°	—	calc.	71.43	4.71	11.11
					found	70.80	5.14	10.95

Table 3. 1-Phenyl-4-alkyl-4-hydroxypyrazolidine-3:5-diones.

	Alkyl	Yield %	M. p.		C %	H %	N %
I	CH_3	70	207–208°	calc.	58.25	4.89	13.58
				found	58.15	4.92	13.48
II	C_2H_5	50	175–176°	calc.	60.00	5.49	12.72
				found	60.20	5.73	12.56
III	C_3H_7*iso*	50	175°	calc.	61.54	6.00	11.95
				found	61.81	6.21	12.12
IV	C_4H_9	75	174–175°	calc.	62.90	6.41	11.30
				found	62.70	6.39	11.39
V	C_6H_{11}	75	148°	calc.	65.70	6.61	10.21
				found	65.95	6.86	10.36
VI	$C_6H_5CH_2$	75	225°	calc.	68.09	5.00	10.00
				found	68.10	5.20	9.80
VIII	C_6H_5	75	210–212°	calc.	67.10	4.47	10.40
				found	66.90	4.38	10.26

The substance VII, 1-phenyl-4-triphenylmethylpyrazolidine-3:5-dione, was prepared in analogy to 1-phenyl-3-methyl-4-triphenylmethylpyrazol-5-one [7] by refluxing 1.95 g of triphenylcarbinol and 1.50 g of 1-phenylpyrazolidine-3:5-dione dissolved in 10 ml of glacial acetic acid and 3 drops of concentrated hydrochloric acid. After 45 min refluxing a substance precipitated which was not redissolved by addition of glacial acetic acid. After cooling some ml of water were added and the substance was isolated by suction, washed on the filter with methanol and dried.

* All microanalyses by Mr. Preben Hansen, Department of Organic Chemistry, University of Copenhagen.

In preparing VIII the yield was very poor, only some few (5) % of a substance with m. p. 218—220° and the composition calculated for 1:4-diphenylpyrazolidine-3:5-dione, $C_{15}H_{12}O_2N_2$ (252.3) as indicated in Table 2. This substance is soluble in alkali, leaving behind a substance insoluble in alkali. The alkali-insoluble substance was recrystallised from ethanol and isolated in a yield of 90 % with m. p. 166—167° (uncorr.). It was recognised as phenylacetic acid phenylhydrazide, $C_6H_5CH_2CONHNHC_6H_5$, $C_{14}H_{14}ON_2$ (226.3). (Found C 74.10; H 6.40; N 12.42. Calc. C 74.34; H 6.22; N 12.40.) The hydrazide has been prepared by Schott [8] who indicates m. p. 168—170°. Gagnon *et al.*[9] report the preparation of 1:4-diphenylpyrazolidine-3:5-dione which they describe as an alkali-insoluble substance with m. p. 172—173°, containing 11.60 % N. We think it reasonable to regard this substance as the phenylhydrazide, the cyclisation evidently taking place less readily in this instance than in the instance of alkylsubstituted malonic esters.

The formation of minor amounts of alkaliinsoluble substances was observed in the preparation of most of the substances I—IV. In one instance we isolated the alkali-insoluble substance which showed a composition in accordance with the corresponding phenylhydrazide, the formation of which may be explained by the scheme:

$$RCH{<}^{COOE}_{COOE} + C_6H_5NHNH_2 \longrightarrow RCH{<}^{CONHNHC_6H_5}_{COOE} \xrightarrow{NaOE}$$

$$RCH{<}^{CONHNHC_6H_5}_{COONa} + EOH \xrightarrow{HCl} RCH_2CONHNHC_6H_5 + CO_2 + EOH + NaCl.$$

Accordingly, we observed a slight liberation of carbon dioxide upon acidification of the reaction mixture when alkylmalonic esters were reacted with phenylhydrazine, but in the case of phenylmalonic ester the liberation of carbon dioxide was much stronger than usually.

Thanks are due to *Det Teknisk-Videnskabelige Forskningsråd* for a research-fellowship (P. S.).

REFERENCES

1. Veibel, S. and Linholt, S. C. *Acta Chem. Scand.* **8** (1954) 1007.
2. Ammann, J. U. *Diss.*, E. T. H. Zürich 1952.
3. Büchi, J., Ammann, J., Lieberherr, R. and Eichenberger, E. *Helv. Chim. Acta* **36** (1953) 75.
4. Michaelis, A. and Schenk, K. *Ber.* **41** (1908) 3865.
5. Dox, A. W. *J. Am. Chem. Soc.* **54** (1932) 3674.
6. Stenzl, H., Staub, A., Simon, Ch. and Baumann, W. *Helv. Chim. Acta* **33** (1950) 1183.
7. Ginsburg, O. F. *Zhur. Obshchei Khim.* **23** (1953) 1890.
8. Schott, H. *Ber.* **29** (1896) 1985.
9. Gagnon, P. E., Boivin, J. L. and Tremblay, M. *Can. J. Chem.* **31** (1953) 673.

Received May 8, 1958.

ACTA CHEMICA SCANDINAVICA 12 (1958) 1364—1366

Pyrazole Studies

XII.* The Hydrazobenzene-catalysed Oxidation of 1:2-Diphenyl-4-butylpyrazolidine-3:5-dione (Butazolidine)

STIG VEIBEL, S. LINHOLTER and P. SØRENSEN

Department of Organic Chemistry, University of Technology, Copenhagen, Denmark

The oxidation by air of alkaline-ethanolic solutions containing 1:2-diphenyl-4-butylpyrazolidine-3:5-dione and hydrazobenzene has been studied. The oxidation products were found to be butyltartronic acid mono-(N:N'-diphenyl)hydrazide and azobenzene. No 4-hydroxybutazolidine could be isolated.

It was found that the oxidation of butazolidine and of hydrazobenzene proceed simultaneously.

In previous papers the oxidation by air of 4-substituted pyrazol-5-ones [1,2] and 1:4-disubstituted pyrazolidine-3:5-diones [3] was studied. We found that triethylamine or sodium ethylate are catalysts for the oxidation, the result of which is the formation of 4-hydroxysubstituted pyrazolones or pyrazolidinediones.

Recently Sokolova and Magidson [4] announced that during the preparation of butazolidine from hydrazobenzene and ethyl butylmalonate a by-product was formed which they identified as 1:2-diphenyl-4-butyl-4-hydroxypyrazolidine-3:5-dione. This substance, they state, can be prepared, in a rather poor yield though, by dissolving butazolidine and hydrazobenzene (equimolar quantities) in ethanol, adding 1 equiv. of sodium ethylate and slowly distilling off the ethanol, passing a stream of air through the solution during the distillation. From the residue 60 % of butazolidine were recovered and the 4-hydroxy compound was isolated in a 9 % yield.

The hydroxy compound is very easily hydrolysed by aqueous bases to butyltartronic acid mono-(N:N'-diphenyl)hydrazide.

We tried to reproduce this result, following as exactly as possible the directions given by Sokolova and Magidson. We did not succeed, however, unchanged butazolidine, hydrazobenzene and azobenzene being the only crystalline products obtained by us.

Using the oxidation-technique described previously [1] we were, on the other hand, able to establish the absorption of one molecule of oxygen per

* Part XI: Preceding paper.

molecule of butazolidine when a solution of this substance and hydrazobenzene in absolute ethanol containing sodium ethylate is agitated in an oxygen atmosphere. The oxidation proceeds extremely slowly at room temperature, 6 days and nights being necessary for the absorption of the calculated volume of oxygen. This means that both the butazolidine and the hydrazobenzene must be oxidised during the absorption of oxygen, and we were able to establish that the two oxidations proceed simultaneously, as we in an experiment discontinued the oxidation after the absorption of 70 % of the volume calculated and isolated from the reaction mixture 30 % unchanged butazolidine and 70 % azobenzene.

Even with the technique employed here we were not able to isolate the hydroxybutazolidine, but only the hydrolysed substance, butyltartronic acid mono-(N:N'-diphenyl)hydrazide which was identified by its m.p. and by electrometric titration with sodium hydroxide.

The overall reaction thus is represented by the equation:

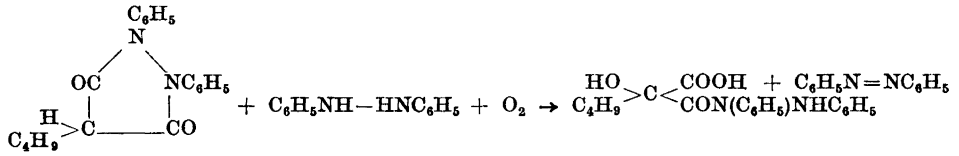

Realising that the amine-catalysed oxidation proceeds through the formation of peroxides a possible sequence might be:

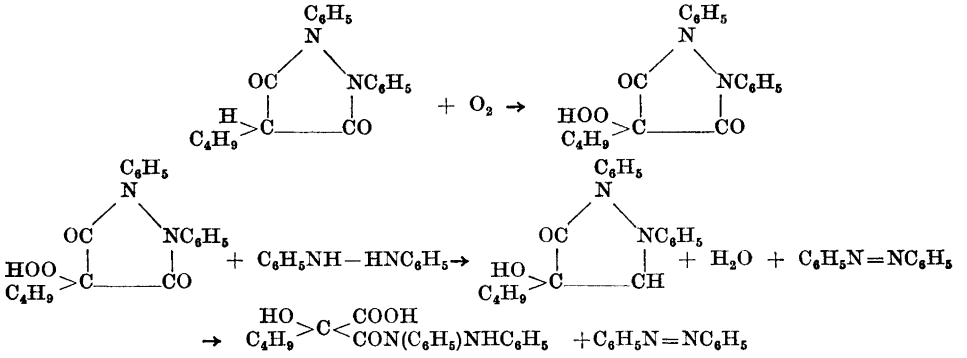

As, however, no oxidation takes place in the absence of hydrazobenzene, not even when azobenzene is added, the oxidation possibly starts with the formation of a hydroperoxide of hydrazobenzene so that the sequence might be:

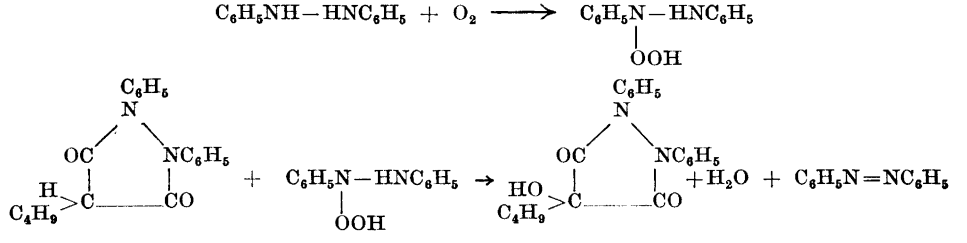

It is seen that during the reaction sufficient water is formed to permit the hydrolysis of the hydroxybutazolidine. Sokolova and Magidson do not state how they have been able to suppress the hydrolysis but they mention that the hydroxy compound is extremely readily hydrolysed in alkaline solution.

EXPERIMENTAL PART

A solution of sodium ethylate was prepared from 0.75 g of sodium and 100 ml of absolute ethanol. In this solution 10 g of butazolidine (0.033 mole) and 6 g of hydrazobenzene (0.033 mole) were dissolved and the solvent slowly removed by distillation (5 h), a stream of air passing through the solution. From the residue 8.5 g of butazolidine, 1 g of azobenzene and 4.5 g of hydrazobenzene were recovered. If any, only an insignificant oxidation of butazolidine has thus taken place.

A similar solution was placed in a flask connected to an oxygen-reservoir, enabling the reading of the volume of oxygen absorbed. After 6 days and nights no more oxygen was absorbed, the total volume absorbed being 800 ml (at 20°) or 0.032 mole. The solution was diluted with 500 ml of water, precipitating azobenzene and hydrazobenzene if this substance remains unoxidised. The filtrate was acidified and the substance precipitated filtered off and dried.

The substance precipitated by water was dissolved in light petroleum and recrystallised by slowly evaporating the solvent. Different crops of crystals (*in toto* 5.1 g) were collected. They had the colour of azobenzene and m. p. 65° (azobenzene 68°). In this case practically quantitative oxidation of hydrazobenzene to azobenzene had taken place.

The substance precipitated by acid (9 g) had m. p. 128—132° (uncorr.). Sokolova and Magidson indicate for 4-hydroxybutazolidine m. p. 132—133°. Recrystallised from 50 % methanol, however, the m. p. of our substance was raised to 143—144° (corr.), whereas Sokolova and Magidson indicate the m. p. 145° for butyltartronic acid mono-(N:N′-diphenyl)hydrazide. 0.8600 g consumed (electrometric titration) 24.96 ml of 0.1029 N NaOH. Equiv. wt. found 335, calc. for the hydrazide 342.

In another experiment the reaction was interrupted when 70 % of the calculated volume of oxygen had been consumed. From the solution was recovered 3 g = 30 % of butazolidine, and a mixture of azo- and hydrazobenzene containing 4 g = 70 % of azobenzene was isolated. Besides, butyltartronic acid mono-(N:N′-diphenyl) hydrazide was isolated in a yield of 40 %. It is thus seen that the oxidation of butazolidine is coupled to the oxidation of hydrazobenzene.

Finally we tried to oxidise butazolidine with *tert*-butylhydroperoxide. 0.05 mole of butazolidine, 30 ml of 2 N sodium ethylate solution (0.06 mole) and 7.5 ml of *tert*-butylhydroperoxide (0.08 mole) were dissolved in 75 ml of *tert*-butylalcohol. After 20 min the experiment was discontinued. From the solution a solid was isolated, m. p. 145—46°, equiv. wt 330, titrated with sodium hydroxide (phenolphthalein). Here, again, the only oxidation product isolated was the butyltartronic acid mono-(N:N′-diphenyl)hydrazide.

Thanks are due to *Det Teknisk-Videnskabelige Forskningsråd* for a research-fellowship (P.S.) and to A. G. Geigy, for a gift of butazolidine generously placed at our disposal.

REFERENCES

1. Veibel, S. and Linholt, S. C. *Acta Chem. Scand.* **8** (1954) 1007.
2. Veibel, S. and Linholt, S. C. *Acta Chem. Scand.* **9** (1955) 970.
3. Veibel, S., Linholter, S. and Sørensen, P. *Preceding paper.*
4. Sokolova, V. N. and Magidson, O. J. *Zhur Obshchei Khim.* **26** (1956) 604.

Received May 8, 1958.

ACTA CHEMICA SCANDINAVICA 12 (1958) 1367—1372

Viscosity of Binary Mixtures

THOR A. BAK and KNUD ANDERSEN

Universitetets Fysisk-Kemiske Institut, København, Denmark

The viscosities of the mixtures CCl_4—$CHCl_3$, C_6H_6—$CH_2(C_6H_5)_2$ and C_7H_{16}—$C_{16}H_{34}$ have been measured in an ordinary Ostwald viscometer. The deviation from linearity in the fluidity is positive in the first case, negative in the last two. The first case is discussed using the theorem of corresponding states, and it is shown that the dipole interaction is responsible for the asymmetry in the "excess fluidity".

In recent years the theory of liquid mixtures has reached a high degree of perfection. Using the average potential model of Prigogine and coworkers [1] one can predict, at least semi-quantitatively, the thermodynamic functions for mixtures when one knows the properties of the pure components.

With regard to a property like the viscosity of mixtures the situation is less satisfactory. The only workable theory of which we are aware is that of Eyring and coworkers [2] and its extensions by Grunberg [3]. This theory, however, contains an empirical correction term of appreciable magnitude, and in our opinion it can therefore primarily be considered as a convenient way of classifying experimental results.

The difficulty in setting up a theory for viscosity of mixtures is that one does not have a good theory for viscosity of pure liquids. A more promising way of attacking the problem for the time being is therefore to make a semi-phenomenological theory in which one uses the properties of the pure liquids without trying to account for them by means of a molecular model. The natural vehicle for such work is the theory of corresponding states, since the fluidity of a liquid can be described using only two parameters, *viz.* $\Phi = A \exp(-E/RT)$.

Such a development was suggested by K. Meyer [4] as early as 1909, but it was not until the idea of an average potential in liquid mixtures had been developed that it actually became possible.

The method we use has been developed by Thomaes [5] and used successfully on the mixture CCl_4—$C(CH_3)_4$. In order to test the method further we have measured the viscosity of a mixture where dipolar effects are predominant, namely CCl_4—$CHCl_3$ and two mixtures for which size effects dominate, namely C_6H_6—$CH_2(C_6H_5)$ and C_7H_{16}—$C_{16}H_{34}$. The ordinary thermodynamic properties of these mixtures are well known, and the surface tensions of the mixtures have recently been measured in this laboratory [6].

EXPERIMENTAL

The liquids were purified as described by Koefoed and Villadsen [6]. The viscosities were measured in an ordinary Ostwald viscometer which in each case was standardized on one of the pure liquids. The values for the viscosity of the pure liquids (CCl_4, C_6H_6 and C_7H_{16}) were taken from the book by Timmermans [7]. Table 1 gives the results obtained for the fluidity and its deviation from the linearly interpolated fluidity.

Table 1.

1. CCl_4-CHCl_3. (X is the mole-fraction of $CHCl_3$). $T = 25.01°C$.

X	Φ cp^{-1}	$\Phi-\Phi_{lin}$ cp^{-1}
0.000	1.103	0.000
0.151	1.226	0.011
0.328	1.367	0.020
0.610	1.580	0.024
0.803	1.716	0.017
1.000	1.845	0.000

2. $C_6H_6-CH_2(C_6H_5)_2$. (X is mole-fraction of diphenylmethane.) $T = 29.70°C$.

X	Φ cp^{-1}	$\Phi-\Phi_{lin}$ cp^{-1}
0.000	1.773	0.000
0.113	1.364	−0.253
0.204	1.140	−0.350
0.288	0.975	−0.398
0.523	0.666	−0.382
0.686	0.534	−0.285
0.801	0.469	−0.192
0.893	0.427	−0.106
1.000	0.383	0.000

3. $C_7H_{16}-C_{16}H_{34}$. (X is mole-fraction of $C_{16}H_{34}$.)

X	Φ cp^{-1} $T = 20.02°C$	$\Phi-\Phi_{lin}$ cp^{-1} $T = 20.02°C$	Φ cp^{-1} $T = 30.00°C$	$\Phi-\Phi_{lin}$ cp^{-1} $T = 30.00°C$
0.000	2.445	0.000	2.747	0.000
0.097	1.808	−0.429	2.062	−0.455
0.195	1.370	−0.655	1.582	−0.705
0.492	0.678	−0.707	0.811	−0.767
0.785	0.385	−0.371	0.481	−0.404
1.000	0.291	0.000	0.370	0.000

It should perhaps be remarked that in the last two cases, for which the 'excess fluidity" is negative, the "excess viscosity" is positive, as it is also in the case of CCl_4-CHCl_3.

THEORY

We want to treat the fluidity of mixtures by the method of corresponding states, *i.e.*, we want to get a dimensionless fluidity by multiplying it with a suitable combination of the molecular mass and the parameters which charac-

terize the intermolecular potential, ε and r. The dimension of fluidity is g^{-1} cm sec, and it is therefore reduced by multiplication with $(m\varepsilon)^{1/2} r^{-2}$. We shall neglect the pressure dependence of the viscosity, so that we can assume that two liquids at the same reduced temperature are at corresponding states as long as we only consider their viscosity.

For a mixture, ideal with respect to fluidity [2], we have

$$\Phi = X_1\Phi_{11} + X_2\Phi_{22}$$

where Φ_{11} and Φ_{22} are the fluidities of the pure components, and X_1 and X_2 are the mole-fractions. For a non-ideal solution we therefore set

$$\Phi = X_1\Phi_1 + X_2\Phi_2$$

where Φ_1 and Φ_2 are quantities to be determined.

Formally we have:

$$\Phi_{11}(T_1) = \frac{r^2_{11}}{(m_{11}\varepsilon_{11})^{1/2}}\,\widetilde{\Phi}(T_1)$$

$$\Phi_1(T) = \frac{r^2_1}{(m_1\varepsilon_1)^{1/2}}\,\widetilde{\Phi}(T)$$

where $\widetilde{\Phi}(T)$ denotes a reduced fluidity at the (non-reduced) temperature T, T_1 is an undetermined temperature, and T is the temperature of the mixture. Assuming that $m_1 = m_{11}$, that is, assuming that the effective mass of species 1 in the flow process is independent of the mole-fraction we have

$$\Phi_1(T) = \Phi_{11}(T_1)\left(\frac{\varepsilon_{11}}{\varepsilon_1}\right)^{1/2}\left(\frac{r_1}{r_{11}}\right)^2 \frac{\widetilde{\Phi}(T)}{\widetilde{\Phi}(T_1)}$$

If in this expression we choose $\widetilde{T}_1 = \widetilde{T}$, *i.e.*, $T_1 = T\,\frac{\varepsilon_{11}}{\varepsilon_1}$ the two reduced fluidities cancel, and we therefore can express $\Phi_1(T)$ in terms of the pure compound at another temperature:

$$\Phi_1(T) = \Phi_{11}\left(T\,\frac{\varepsilon_{11}}{\varepsilon_1}\right)\left(\frac{\varepsilon_{11}}{\varepsilon_1}\right)^{1/2}\left(\frac{r_1}{r_{11}}\right)^2$$

An analogous expression is found for Φ_2.

The quantities ε_1 and r_1 which we have introduced in this way are assumed to be "average potentials" and "average distances" in the liquid mixture, *i.e.*,

$$\varepsilon_1 = X_1\varepsilon_{11} + X_2\varepsilon_{12}$$

where ε_{11} is the maximum interaction energy between two 1-molecules, and ε_{12} is the maximum interaction energy between a 1-molecule and a 2-molecule. Analogous expressions are used for r_1, ε_2 and r_2. For r_{12} we take, as long as dipolar effects can be neglected $r_{12} = \frac{1}{2}(r_{11} + r_{22})$, and for ε_{12} we take, when no other information can be obtained,

$$\varepsilon_{12} = (\varepsilon_{11}\varepsilon_{22})^{1/2}$$

For the mixture CCl_4—$CHCl_3$ we have, when dipolar effects are neglected, $\varepsilon_{11} = \varepsilon_{22}$, $r_{11} \neq r_{22}$, but $|r_{11} - r_{22}| << r_{11} + r_{22}$. We shall therefore first investigate this case where the only differences which can cause non-ideal behaviour is a difference in size.

We set $2\,\frac{r_{22} - r_{11}}{r_{11} + r_{22}} = \varrho$ and have

$$\Phi_1 = \Phi_{11}(1 - \varrho X_2)$$
$$\Phi_2 = \Phi_{22}(1 + \varrho X_1)$$

neglecting higher powers of ϱ. Therefore

$$\Phi = X_1\Phi_1 + X_2\Phi_2 = X_1\Phi_{11} + X_2\Phi_{22} + (\Phi_{11} - \Phi_{22})\varrho X_1 X_2$$

The deviation from linearity is positive when $\Phi_{11} - \Phi_{22}$ has the same sign as ϱ, which is the most common thing. Its maximum value is $\frac{1}{4}\varrho(\Phi_{11} - \Phi_{22})$. For the mixture we consider $r_{11} = 6.62$ Å and $r_{22} = 6.10$ Å, so that $\varrho = -0.082$. The maximum deviation is then 0.015 cp^{-1}.

It is known, however, that for CCl_4 — $CHCl_3$ dipolar effects are predominant. From the measurements of McGlashan, Prue and Sainsbury [8] and Cheesman and Whitaker [9] one finds, for $X_1 = X_2 = \frac{1}{2}$, $h^E/g^E = 2.14$, where h^E stands for the excess molar enthalpy of mixing and g^E for the excess molar Gibbs function of mixing, and this almost satisfies the relation of Pople [10], $g^E = Ts^E = \frac{1}{2}h^E$, valid for mixtures where dipolar effects are predominant and differences in polarizability between the two species can be neglected.

To treat the dipolar effects we set

$$\varepsilon_{ij} = \varepsilon^0{}_{ij}(1 + \psi_{ij})$$
and
$$r_{ij} = r^0{}_{ij}\ (1 + \varphi_{ij})$$

where ψ_{ij} and φ_{ij} are small perturbations which stem from the dipole interaction. For details on this method, we refer to chapter 14 in the book by Prigogine [1].

Using the technique described there, we find

$$\psi_{11} = \psi_1 = \varphi_{11} = \varphi_1 = 0$$
$$\psi_{22} = \tfrac{2}{3}\Gamma \qquad \varphi_{22} = -\tfrac{1}{18}\Gamma$$
$$\psi_2 = \tfrac{2}{3}X_2\,(1 + 3\varrho X_1)\Gamma$$
$$\varphi_2 = \tfrac{1}{18}X_2\,(1 + 3\varrho X_1)\Gamma$$

with $\Gamma = \dfrac{\mu^4{}_2}{r^6{}_{22}\varepsilon_{22}kT}$ where μ_2 is the dipole moment of $CHCl_3$.

Therefore we have

$$\Phi_1 = \Phi_{11}\left(\frac{r_1}{r_{11}}\right)^2$$

$$\Phi_2 = \Phi_{22}\,(T + \tfrac{2}{3}\vartheta T)\left(\frac{r_2}{r_{22}}\right)^2(1 + \tfrac{4}{9}\vartheta)$$

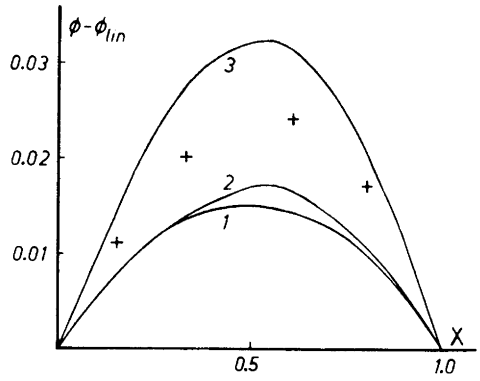

Fig. 1. Excess fluidity in reciprocal centipoise for the system CCl_4—$CHCl_3$. 1 size effect, 2 dipolar effect, 3 sum of 1 and 2, + experimental points.

with $\vartheta = (1 - X_2 + 3\varrho X_1 X_2)\Gamma$; $\Gamma = 0.013$ at 25°C. Here we have again neglected higher powers of ϱ and ϑ, and we shall therefore also expand Φ_{22} in a Taylor series from T retaining only the linear term. We then have

$$\Phi_2 = \Phi_{22}(T)\left(\frac{r_2}{r_{22}}\right)^2\left[1 + \vartheta\left(\tfrac{2}{3}\frac{T\Phi'_{22}}{\Phi_{22}} + \tfrac{4}{9}\right)\right]$$

$$= \Phi_{22}\left(\frac{r_2}{r_{22}}\right)^2 (1 + 2.47\ \vartheta)$$

at 25°C, using data from the book by Timmermans [7]. Substituting this into the expression for Φ we have $\Phi = \Phi_{\text{lin}} + 0.061\ X_1X_2 + 0.059\ X_2(1 - X_2 + 0.25\ X_1X_2)$

Within this approximation we see that the size effect and the dipolar effect simply add. Fig. 1 shows the experimental values of $\Phi - \Phi_{\text{lin}}$ and the curves for the size effect, the dipole effect and the sum of the two. Although the curve for the sum overshoots the mark considerably, it is seen that qualitatively it has all the right features including the asymmetry.

For the other two mixtures we have not so far been able to give a satisfactory theoretical development along these lines, but we hope to return to this problem in a later publication.

We are indebted to Dr. G. Thomaes for valuable discussions and for letting us see his paper before its publication.

REFERENCES

1. Prigogine, I. *The molecular Theory of Solutions*, Amsterdam 1957.
2. Glasstone, S., Laidler, K. J. and Eyring, H. *The Theory of Rate Processes*, New York 1941.
3. Grunberg, L. *Trans. Faraday Soc.* **50** (1954) 1293.
4. Meyer, K. *Temperaturbegrebets Udvikling gennem Tiderne*, København 1909.

5. Thomaes, G. *To be published.*
6. Koefoed, J. and Villadsen, J. V. *Acta Chem. Scand.* **12** (1958) 1124.
7. Timmermans, J. *Physico-chemical constants of pure organic compounds*, Amsterdam 1950.
8. McGlashan, M. L., Prue, J. E. and Sainsbury, I. E. J. *Trans. Faraday Soc.* **50** (1954) 1284.
9. Cheesman, G. H. and Whitaker, A. M. B. *Proc. Roy. Soc. London* **A 212** (1952) 406.
10. Pople, J. A. *Trans Faraday Soc.* **49** (1953) 591.

Received May 14, 1958.

ACTA CHEMICA SCANDINAVICA 12 (1958) 1373—1385

Chemistry of Arylboric Acids VIII. The Relationship between Physico-chemical Properties and Activity in Plants

KURT TORSSELL, JOHN H. McCLENDON
and G. FRED SOMERS

Biochemical Institute, University of Stockholm, Stockholm, Sweden and Department of Agricultural Chemistry, University of Delaware, Newark, Delaware, U.S.A.

Ionization constants for a number of arylboric acids and their complexes with sugars have been measured. Further, the effect of arylboric acids on retrogradation of starch and viscosity of borax-galactomannan solutions have been investigated. Results of these physico-chemical investigations have been compared with the root cell elongation effect of the compounds in order to validate a hypothesis on the mode of action of arylboric acids in plants. Evidence is presented for a correlation between root growth promoting effect and ability of the compounds to form complexes with polyols.

It has been known for a long time that polyhydroxy compounds enhance the acidity of boric acid through complex formation [1,2]. The following equilibria are involved:

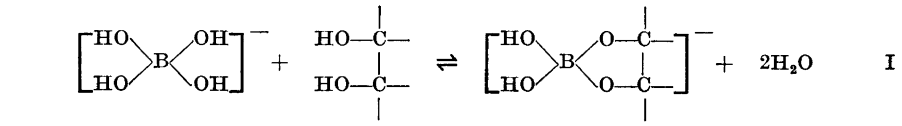

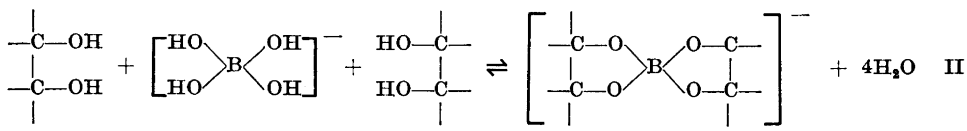

It is obvious that if compound I is a stronger acid than boric acid, the acidity must increase when the polyalcohol is added to a boric acid solution. For steric reasons compound II must be completely dissociated.

Phenylboric acid behaves in the same manner but can bind only one polyalcohol [3].

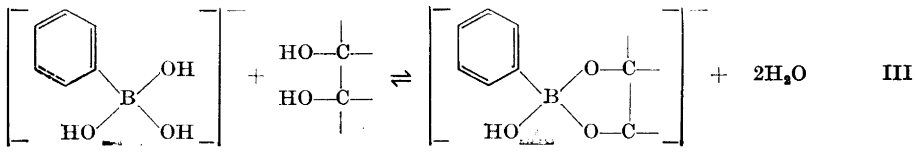

III

Boric acid can also interact with other functional groups, *i.a.* an amino group:

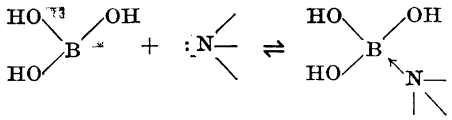

but in comparison to the B—O bond the B—N bond is much weaker [4].

From a chemical point of view it seems, therefore, reasonable to associate the plant physiological effects of boric acid and arylboric acids with an effect on hydroxyl-rich compounds. Thus we can expect that boric acid or arylboric acids may act upon: a) an enzyme system where either the coenzyme or the substrate contains a polyhydroxyl compound; b) the polysaccharide chains in the cell wall; Schmucker [5], Torssell [6], Odnoff [7] and O'Kelley [8*]; c) translocation of sugars; Gauch and Dugger [9].

a. *Effect of boric acid and phenylboric acid on enzymes.* The effect of boric acid on various enzymes has been tested by several workers (Ref.[10], reviews). As a general rule it may be said that boric acid has no or very little effect at low concentrations but inhibits enzyme activity at higher concentrations *in vitro*.

The action of phenylboric acid on the enzymes tested shows the same general picture but the inhibiting effect seems to be stronger than that of boric acid [11]. It was found that the activity of invertase, α-amylase and phosphorylase *in vitro* and the fermentation activity of baker's and brewer's yeast were not affected by phenylboric acid at concentrations less than 5×10^{-3} M. In the present paper three other enzymes have been tested: pectinase, pectin esterase and the "Zwischenferment" with its coenzyme TPN. Pectins presumably play a prominent role as cell wall constituents and as the boric acids seem to regulate the cell stretching it was of interest to test whether or not phenylboric acid has an influence on enzymes controlling the breakdown and de-esterification of pectins. In the first two enzyme systems phenylboric acid can couple with the substrate and in the third with both the coenzyme and the substrate, glucose-6-phosphate.

b. *Effect of boric acid and arylboric acids on the cell wall.* Schmucker [5] found that boron is essential for the germination of pollen and growth of the pollen tube and attributed this to an effect of the boric acid — polyalcohol complexes on cell wall formation. Boron deficiency symptoms appear first in meristematic tissues, root tips and buds, *i.e.* parts of the plant characterized

* *Added in proof.* Recently A. R. Spurr, *Am. J. Bot.* **44** (1957) 637, also hypothesized that boron affects the carbohydrate deposition into the cell wall.

by rapid growth rate. By discontinuous addition of boric acid to boron deficient bean plants, Odnoff [7] has shown the role of boron in the stretching process of the roots. On the basis of experiments with arylboric acids on wheat roots, Torssell [6] proposed the hypothesis that arylboric acids and boric acid control the deposition and orientation of polysaccharides in the cell wall through complex formation and thereby also regulate the stretching of the cell. More evidence for such a view is presented in the present work.

It has already been pointed out that the effects of arylboric acids on plants probably are not associated with an auxin effect [6]. The activity of synthetic auxin or antiauxin compounds strongly depends upon what kind of nuclear substituents they have and on the general structure of the molecule whereas this is of less importance in the arylboric acid series.

It is more likely that the effects of arylboric acids are associated with the properties of the dioxyboron group than with an overall effect of the molecule. The paper chromatographic experiments show, however, that an adsorption of arylboric acids on polysaccharides also may play a role. In order to explain the action of arylboric acids on amylose retrogradation, we have to take into consideration both complex formation and adsorption.

If now the arylboric acid-polyalcohol complexes play the proposed role in cell wall formation and in a wider sense in the cell stretching, we would expect to find a correlation between the plant physiological activity of different arylboric acids and their ability of form sugar complexes. The delaying effect of arylboric acids on amylose retrogradation [6] that served as a model experiment for the aging process of the polysaccharide chains in the cell wall, should further parallel their activity in plants.

In proposing this working hypothesis, however, we should not neglect two other factors that can greatly affect the activity of the compounds in plant. The uptake and translocation may be different with compounds that have the same intrinsic effect at the site of action. Secondly, the toxicity of some derivatives may be so high that side reactions completely counteract the cell elongation effect.

We have been looking for other model experiments more closely related to the proposed stabilization mechanism and have investigated the effect of arylboric acids on borax-galactomannan gels [12]. Galactomannan is a polysaccharide, consisting of a chain of 1,4′ linked D-mannopyranose units with single side units of D-galactopyranose linked 1,6′ to every other D-mannose unit [13]. The addition of borax to dilute solutions of this polysaccharide gives rise to an increased viscosity.

c. *Effect of boric acid and arylboric acid on sugar translocation.* Gauch *et al.*[9,14] have postulated that boric acid plays a role in the translocation of sugars in plants. There is evidence in favor of this hypothesis but other evidence is not in accord with it. McIlrath and Palser [15] found that in roots of boron deficient cotton plants, where no phloem necrosis was observed, the total sugar content was equal to that of normal plants and in the leaves it was lower. Spraying of buds with sucrose solution did not inhibit the boron deficiency symptoms. Odnoff [7] reported that the sugar level in the roots of boron deficient young bean plants was higher than in normal control plants.

Provided that the mechanism of action of arylboric acids and boric acid is the same, it is not possible to explain their cell stretching effect only on basis of an increased sugar translocation [14]. We probably have to account for several modes of action of boron in plants, of which the translocation effect may be one.

EXPERIMENTAL

Determination of enzyme activities in the presence of phenylboric acid

1. *Pectinase.* The effect of phenylboric acid on pectinase was tested viscosimetrically and by measurement of reducing groups produced.

a. *Viscosimetrically.* The following solutions were prepared: (I) sodium pectate, 1 %, (Sunkist Growers, Inc., Ontario, Calif., U.S.A.), buffered to pH 4.0 with acetate, 0.05 M. (II) Pectinase, 0.01 % (Nutritional Biochemicals Corp., Cleveland, Ohio). The crude pectinase was first purified by ultra filtration according to McClendon and Somers [16]. (III) Phenylboric acid 7.0×10^{-2}, 7.0×10^{-3} and 7.0×10^{-4} M. To 20 ml (I) + 2 ml (III) (or 2 ml water in the control run) equilibrated at 30° in a water bath were added 2 ml enzyme solution (II). The mixture was shaken rapidly. The time of efflux was measured at intervals with an Ostwald viscosimeter. In one experiment the enzyme was first incubated with 3.5×10^{-2} M phenylboric acid for 1.5 h and then added to the pectin solution. Fig. 1 shows the efflux time (extent of degradation) as a function of time.

b. *Measurement of reducing groups.* To 50 ml of sodium pectate (I) and 20 ml phenylboric acid (III) equilibrated at 30° 2 ml of 0.1 % enzyme solution was added. The time was noted and 10 ml aliquots were removed at various times and analyzed for reducing groups according to Willstätter and Schudel [17]. Fig. 2 shows the I_2 consumption (liberated reducing groups) as a function of time.

2. *Pectinesterase.* (Pectin from Nutritional Biochemicals Corp., Cleveland, Ohio and Pectinesterase from Worthington Biochemical Sales Co., Freehold, New Jersey.) The enzyme activity was tested according to the procedure of Kertesz [18]. Fifty ml of 1 % pectin solution containing 0.1 M NaCl and a suitable amount of phenylboric acid was equilibrated at 30° and adjusted to pH 6. Two ml of 0.01 % enzyme solution was added; followed by thorough mixing. Sodium hydroxide (0.01 M) was added at a rate to keep the pH constant at 6. In Fig. 3 the alkali consumption is plotted against time.

3. *Glucose-6-phosphate dehydrogenase (Zwischenferment).* The assay method, described by Kornberg and Horecker [19] was employed. The reduction of the coenzyme in presence of various phenylboric acid and boric acid concentrations was followed (Fig. 4) by measuring at various times the intensity of the absorption band (at 340 mμ) of the reduced form. (Zwischenferment from Sigma Chemical Co., St. Louis, Mo.; TPN, Nutritional Biochemicals Corp., Cleveland, Ohio). Veronal buffer pH 7.5 was used instead of glycylglycin.

Complex constant measurements

Complex constants of arylboric acids with fructose, maltose, starch (Lintner, potato) and galactomannan were measured. The method, described in an earlier paper [3], was employed with the difference that a saturated calomel electrode was used and the measurements were carried out in pure water instead of 0.1 M KCl. The constants in Table 1 are mean values from two or more runs. The arylboric acids tested were synthesized according to Torssell [20].

Effect of arylboric acids on amylose retrogradation

Because identically prepared amylose solutions may retrograde with different velocity, all substances were tested [6] at the same time with the same amylose solution in order to get comparable values of their inhibiting effect. Into 5 ml of 4×10^{-2} M arylboric acid

were pipetted 15 ml 0.5 % maize amylose containing 0.02 M buffer (pH 5.0 acetate; pH 6.5 and 6.9 phosphate; and pH 7.9 veronal). The final arylboric acid concentration was 10^{-2} M. Because of insolubility of some compounds (*p*-nitro-phenylboric acid, 3-nitro-4-carbomethoxy-phenylboric acid) they were tested at a concentration of 5×10^{-3} M. Intensity of the scattered light was measured at various times with a *Leifo*-photometer. The experiments were duplicated at various pH's.

Effect of arylboric acids on the viscosity of borax-galactomannan solutions

Galactomannan from guar seed (Stein Hall, New York, U.S.A.; trade name Jaguar A-20-D) was reprecipitated once [21] and 1.6 g of the dry ground product was dispersed in 400 ml vigorously stirred hot water (*ca.* 80°). After standing overnight the solution was heated to boiling for 10 min, filtered hot with suction through porous filter paper and was buffered to pH 8.9 with glycine buffer (0.02 M).

Four series of solutions were prepared: a) 10 ml galactomannan (I) + 10 ml borax of various concentrations ($10^{-3}-10^{-2}$ M); b) 10 ml (I) + 10 ml phenylboric acid (half neutralized in order to minimize pH changes) in various concentrations ($10^{-3}-10^{-2}$ M); c) 10 ml (I) + 10 ml of a mixture in various proportions of borax (10^{-2} M) + phenylboric acid (10^{-2} M); d) 10 ml (I) + 5 ml borax (3.0×10^{-3} M, final concn.) + 5 ml of various arylboric acids (half neutralized, 1.2×10^{-3} M, final concn.). The mixtures were shaken vigorously and equilibrated for 2 h at 25°. Their viscosity was measured with an Ostwald viscometer. Efflux times are shown for series a–c in Table 5. The decrease in efflux time (viscosity) caused by addition of various arylboric acids to the borax-galactomannan solution, series d, has been calculated as percent of the viscosity increase caused by borax alone, when added to the galactomannan solution, Table 1.

Paper chromatography

A technique, elaborated by Rockland and Dunn [22] was employed. R_F-values refer to pure water as solvent. The arylboric acids (0.3 % water-methanol solution) were placed upon the paper, W 52, by means of a drawn out melting point capillary. Colors were developed with 0.4 % alcoholic curcuma solution, which gives brown-red spots with boron on a yellow background when the paper strips were left to dry for 5 min in an oven at 90° [27].

RESULTS AND DISCUSSION

Effects on enzymes. Presence of phenylboric acid does not affect the time course of pectic acid degradation by pectinase when followed viscosimetrically (Fig. 1) but a slight inhibition (*ca.* 10 % after 20 h, 10^{-3} M) could be detected by measuring reducing groups, (Fig. 2). Rather high concentrations of phenylboric acid (10^{-2} M) must be used before the inhibiting effect on pectinesterase is significant (Fig. 3). Glucose-6-phosphate dehydrogenase is also left unaffected by phenylboric acid in concentrations $<10^{-3}$ M. Boric acid is less active (Fig. 4). Thus when summing up results from the enzymatic work carried out in previous [11] and present papers we find, with one exception — cholinesterase [11] (which, however, does not occur in plant tissues) — that phenylboric acid at concentrations $<10^{-3} - 5 \times 10^{-3}$ M has no effect on the tested enzymes and at higher concentrations acts as an inhibitor.

According to Eliasson [23] phenylboric acid has no effect on the respiration of excised wheat roots.

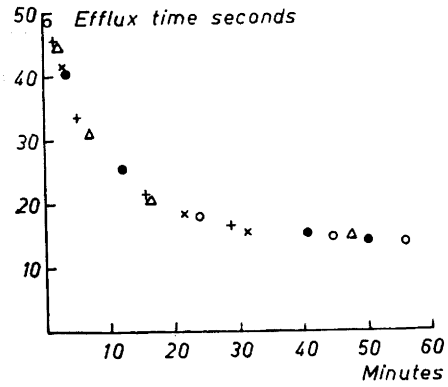

Fig. 1. Effect of phenylboric acid on the activity of pectinase. O Control, + 0.58 × 10^{-4} M phenylboric acid, × 0.58 × 10^{-3} M PhBA, ● 0.58 × 10^{-2} M PhBA, △ Enzyme incubated for 1.5 h with 0.58 × 10^{-2} M PhBA. The degradation of pectin is measured viscosimetrically.

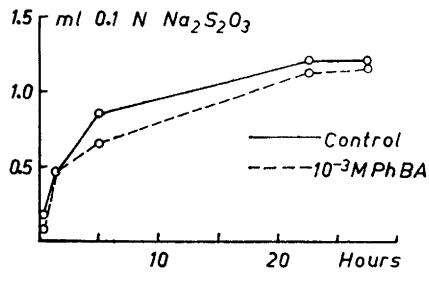

Fig. 2. Effect of phenylboric acid on the activity of pectinase. Degradation is followed by measurements of reducing groups, (equivalent to ml $Na_2S_2O_3$).

The effects of phenylboric acid on enzymes are in no cases striking and it seems to be difficult to draw any conclusions about relationships between the action of phenylboric acid on enzyme systems and its cell stretching effect in plants. However, the possibility may not be excluded that boric acid might be a constituent of an enzyme or act in some way *via* an enzyme.

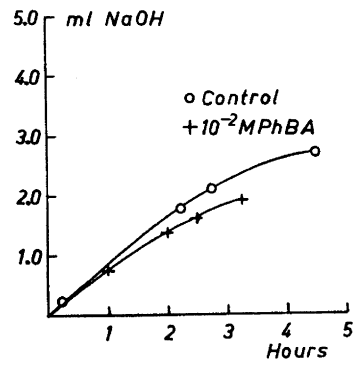

Fig. 3. Effect of phenylboric acid on the activity of pectinmethylesterase.

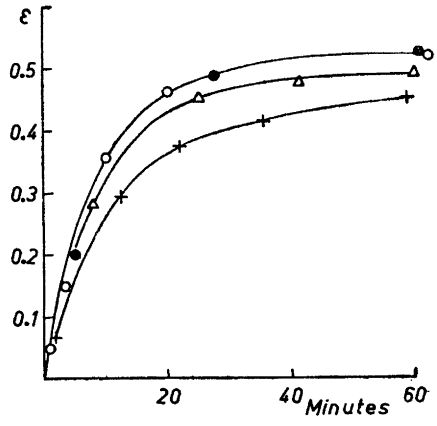

Fig. 4. Effect of phenylboric acid and boric acid on glucose-6-phosphate dehydrogenase. O Control, ● 2.3 × 10^{-3} M H_3BO_3, △ 2.5 × 10^{-3} M phenylboric acid, + 0.92 × 10^{-2} M phenylboric acid.

Table 1. Ionization constants for arylboric acids and their complexes with fructose; root growth promoting effect of arylboric acids and their effect on the viscosity of galactomannan-borax solutions. PhBA = Phenylboric acid.

	Compound	Ionization constant k_s $RBH \rightleftharpoons RB^- + H^+$ at 25°; $\times 10^9$	Complex constant k_1 $D + RB^- \rightleftharpoons RBD^-$ at 25°; $\times 10^{-3}$	$k_s \times k_1 \times 10^6$ $D + RBH \rightleftharpoons RBD^- + H^+$	Reduction of viscosity; per cent	Activity in plants
1	Boric acid	0.653 a)	0.69 ($k_2 = 0.83 \times 10^5$)	0.45	—	— b)
2	Phenylboric acid	1.37 c)	5.18 d)	7.10	55	+++
3	4-NO_2-PhBA	70.7	2.49	176	86	+++
4	3-NO_2-PhBA	50.0	2.50	125	73	++
5	2-NO_2-PhBA	~3	~1.5	~4.5	—	++
6	3-CHO-PhBA	16.0	3.00	48.0	57	+(+)
7	2-CHO-PhBA	48.6	0.837	40.7	62	+
8	2-CH_2OH-PhBA	41.5	0.832	34.5	76	0
9	4-OCH_3-PhBA	0.482	5.76	2.78	26	+++
10	2-NO_2-5-NH_2-PhBA	0.101	1.54	0.156	0	0
11	2-NO_2-4-NH_2-PhBA	0.230	2.73	0.63	32	0
12	2-NO_2-4-$COOCH_3$-PhBA	4.35	1.67	7.26	46	0(+)
13	4-NHAc-PhBA	1.87	5.35	10.0	54	+(+)
14	2-CH_3-3,5-diNO_2-PhBA	125	3.70	462	89	++
15	4-CH_3-PhBA	—	—	—	32	++
16	4-NO_2-phenol	—	—	—	24	0

a) Torssell, K. *Arkiv Kemi* 3 (1952) 571. b) Ref.[6] c) Ref.[24] d) Ref.[3]

Relationship between complex constants, $k_s \times k_1$ and growth promoting effect. Ionization constants, k_s:

$$k_s = \frac{[RBH]}{[H^+]\,[RB^-]}$$

and complex constants [3] k_1 (arylboric acid — fructose):

$$k_1 = \frac{[RBD^-]}{[RB^-]\,[D]} = \frac{([H^+] + [Na^+]) \cdot [H^+] - k_s\,[RBH]}{k_s\,[RBH]\,[D]}$$

Table 2. Complex constants for some arylboric acids with different polyalcohols. The complex constants for fructose, mannose and starch have been calculated on the basis that only one complex can be formed per molecule and for galactomannan that one complex can be formed per sugar unit. Temp. 25° C.

Compound	Fructose $k_1 \times 10^{-3}$	Maltose $k_1 \times 10^{-3}$	Starch (Lintner) $k_1 \times 10^{-3}$	Galactomannan $k_1 \times 10^{-3}$
Phenylboric acid	5.18	0.0410	0.072	0.0082
3-NO_2-PhBA	2.50	0.0259	—	—
2-CH_2OH—PhBA	0.832	0.0165	—	—

(RBH = Phenylboric acid; RB^- = ionized acid; D = polyalcohol) have been measured for a number of arylboric acids which show various degrees of cell stretching effect (Table 1). When comparing the complex formation ability of arylboric acids ($k_s \times k_1$) with their action in plants, the assumption has to be made that the relative magnitude of complex constants for one sugar, in this case fructose, is about the same for another polyalcohol. This has been proved to be true for maltose, which forms much weaker complexes than fructose (Table 2). The systems, Lintner starch-phenylboric acid and galactomannan-phenylboric acid have also been investigated. Calculation of complex constants can be only very approximate as the units within the chain differ in complex forming ability. Galactose residues do not form as strong complexes as the mannose units of galactomannan. Also at end groups or at groups where branching occurs, the conditions for complex formation are different. As a first approach toward an investigation of the nature of these complexes, an end group determination (reducing groups) was carried out according to Willstätter and Schudel. This gives some idea concerning the average molecular weight (lower limit). It was found with starch that the concentration of the complex always was less than the reducing group concentration and calculation of the complex constant on the basis of reducing group concentration gave a more constant value than a calculation on a basis that every glucose unit takes part in complex formation to the same degree. The fact that methyl glucoside [1] gives very weak complexes with boric acid in comparison with glucose favors the idea that in starch the end groups preferentially combine with phenylboric acid. The complex constant for the starch-phenylboric acid system when only end groups are taken into consideration is of the same magnitude as that of the maltose-phenylboric acid system, in which the formation of a complex containing two phenylboric acid per maltose seems to be negligible, Table 2. It may therefore be assumed that complex formation between starch and phenylboric acid preferably takes place at the end groups and that to some extent weaker complexes are formed with the other units of the chain. Willstätter-Schudel end-group determination of starch usually gives too high values. According to the analysis, the starch molecule contains on an average 15—20 units, which seems to be too low for this kind of starch (Lintner potato starch). A lower end group concentration gives a higher complex constant k_1 but on the other hand a formation of weak complexes between phenylboric acid and some of the units in the chain has the opposite effect on k_1.

In the galactomannan-phenylboric acid system it was found that the complex formation is higher than the amount of reducing groups, *i.e.* the units in the chain are as important as the end groups for complex formation. This is to be expected from steric reasons; mannose and galactose have adjacent *cis*-hydroxyl groups at carbon atoms 2,3 and 3,4 respectively, which favors complex formation while the hydroxyl groups of the glucose unit in starch are all *trans* and only the end group has adjacent *cis*-hydroxyls (in 1,2 position). Table 3 shows some of the original measurements and in column 7 the concentration of the complex is calculated. A Willstätter-Schudel end group determination gave a polymerization degree of about 30, a value that for this kind of polysaccharide is too low. From the last row of column 7,

Table 3. 40.00 ml of a galactomannan-phenylboric acid solution is titrated with 0.1668 N NaOH. (D_{tot}) is the concentration of sugar residues = molecular concentration x degree of polymerization. Temp. 25° C.

ml NaOH	$[Na^+]$ $\times 10^2$	$[RBH_{tot}]$ $\times 10^2$	$[RBH]$ $\times 10^2$	$[D_{tot}]$ $\times 10^2$	$[D]$ $\times 10^2$	$[RBD^-]$ $\times 10^2$	pH	$[H^+]$ $\times 10^8$	k_1
—	—	2.18	2.18	1.50	1.50	—	5.75	178	—
1.20	0.486	2.12	1.63	1.46	1.42	0.041	8.30	0.501	6.5
2.20	0.869	2.07	1.20	1.42	1.34	0.084	8.68	0.209	8.0
3.47	1.332	2.01	0.68	1.38	1.25	0.130	9.11	0.0775	8.7

however, we find that the concentration of the complex is 0.130×10^{-2} M which is about one tenth of the total sugar concentration in the solution. That means that, as an average, every tenth sugar unit has formed a complex with phenylboric acid at this pH and we must therefore have more than one complex per molecule. The complex constant for galactomannan, Table 2, has been calculated on the assumption that every chain unit gives equally strong complexes and that already formed complexes do not affect the formation of adjacent ones. The complex constants for starch and galactomannan are not comparable as they are calculated on basis of different assumptions. In order to get an idea about their relative magnitude the galactomannan constant has to be multiplied by the polymerization number of galactomannan.

In the last column of Table 1 the activities of the compounds are tabulated according to an arbitrary scale: +++ means a root elongating effect of 175 % or more, ++ = 150—175 %, + = 125—150 % and 0 = 100 % (none) — 125 %. The values are taken from a previous paper [6] and by the gradation the position of the maximum (concentration at which maximum occurs) has been considered.

The active acids 3, 4, 6 and 14 (see Table 1 for identification) all have high ionization constants, k_s, and also high complex formation ability, $k_s \times k_1$, in comparison with the inactive acids 10, 11 and 12. The $k_s \times k_1$ values of the highly active 2, 5 and 9 are higher than that of the inactive 10 and 11 but of the same magnitude as 12. Numbers 7 and 8 also are strongly dissociated and have high $k_s \times k_1$ values and we would therefore expect that they should be active in plants which, however, is not the case. A closer examination of their activity curves shows that they are more toxic to the roots, than the other compounds. Number 8, for example, inhibits the root growth completely at a concentration of 10^{-5} M whereas 10, 11 and 12 at 10^{-4} M do not show any inhibiting effect. *o*-Hydroxymethyl-phenylboric acid, 8, shows in comparison with other tested arylboric acids a strong bacteriostatic effect [11]. Therefore, it is probable that they actually are active, but their toxicity reverses the cell elongating effect by disturbing other essential reactions of importance for root growth. It has already been pointed out in the introduction that uptake and translocation may influence the activity of the compounds. When these factors are of the same magnitude for different compounds the complex constant alone ought to determine the activity in plants. Isomeric compounds as the *o*-, *m*- and *p*-nitrophenylboric acids are probably affected

equally by the mentioned factors and we find that complex constants $k_s \times k_1$ and root growth promoting activity (Ref.[6], Fig. 1) increases in the same order:

$$o\text{-}NO_2 < m\text{-}NO_2 < p\text{-}NO_2\text{-phenylboric acid}$$

Thus, it may be concluded that a correlation exists between plant physiological action of arylboric acids and their ability to form complexes with polyalcohols.

Relation between retrogradation effect, degelation effect and growth promoting effect. The inhibiting effect of arylboric acids on amylose retrogradation decreases in the following order:

$$3\text{-}NO_2 > 4\text{-}OCH_3 > 2\text{-}CH_2OH > \text{-}H \geq 2\text{-}NO_2\text{-}5\text{-}NH_2 > 2\text{-}NO_2 \geq 2\text{-}CHO > H_3BO_3$$

Relative order for some compounds may slightly change from experiment to experiment; the main order, however, is the same. The sequence above represents an average obtained from several runs at various pH's. Some compounds were tested in 0.005 M solution (4-NO_2- and 2-NO_2-4-$COOCH_3$-phenylboric acid) as they precipitated at higher concentrations. Their activity decreased in the following order:

$$4\text{-}NO_2 > 2\text{-}NO_2\text{-}5\text{-}NH_2 > 2\text{-}NO_2\text{-}4\text{-}COOCH_3$$

In Fig. 5 the effect of phenylboric acid at various concentrations is demonstrated.

It is obvious that complex formation alone cannot be responsible for the retrogradation inhibiting effect, because 4-methoxy-phenylboric acid and phenylboric acid show stronger inhibitions than 2-formyl-phenylboric acid that has a higher complex constant $k_s \times k_1$. Adsorption of arylboric acids on the growing amylose aggregates probably plays a role. Therefore a similarly built aromatic compound, 3-nitrophenol, (inactive in plants) was tested and found to have the same activity as phenylboric acid; aniline, 0.01 M, has no activity.

The measurements of starch complexes show further that units in the chain form only very weak complexes and that phenylboric acid is mainly linked to the end groups, which explains the fact that correlation between complex constants and the effect on retrogradation is not good. Even if the compounds most active in root growth are found in the beginning of the sequences above, the value of the retrogradation experiment as a true model for deposition of cell wall material is decreased, because of the fact that other compounds inactive in plants, *e.g.* nitrophenol, also hamper the retrogradation.

The chromatographic behavior of arylboric acids demonstrates clearly the importance of adsorption effects. It is possible to separate arylboric acids on paper with pure water as eluent. R_F values of different derivatives are shown in Table 4.

Table 4. R_F values of arylboric acids. Water as solvent. Whatman 52. The numbers refer to compounds in Table 1.

Compound	1	2	3	4	5	7	8	9	10	11	12	15	16
R_F	~1	0.74	0.56	0.58	0.57	0.87	0.66	0.62	0.64	0.70	0.79	0.67	0.70

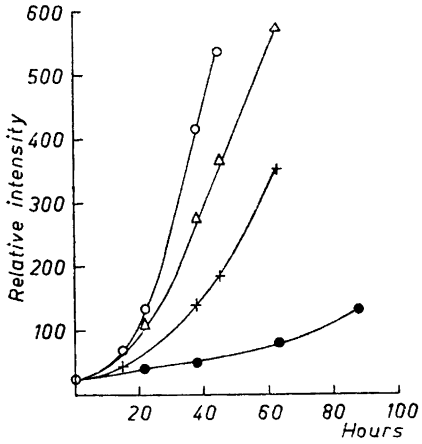

Fig. 5. Effect of various phenylboric acid concentrations on the retrogradation rate of maize amylose at pH 6.90—6.96. O Control, △ 2×10^{-3} M PhBA, + 10^{-2} M PhBA, ● 4×10^{-2} M PhBA.

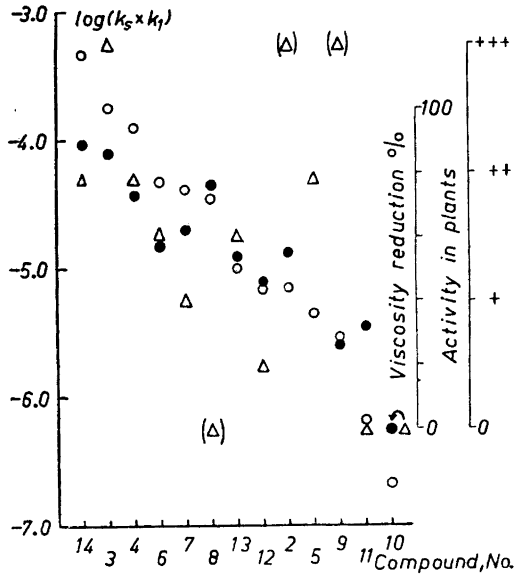

Fig. 6. Comparison of complex constants for arylboric acids, O, with their effect in plants, △, and on the viscosity of galactomannan-borax solutions, ●.

Borax forms gels with galactomannans; in dilute solution a viscosity increase takes place. Repeated cross linkages between galactomannan and and boric acid causes increased chain length and molecular weight, which results in an increased viscosity or, finally, in a gel formation [12]. Arylboric acids reduce the viscosity; probably in the following way. When an arylboric acid and boric acid are present in the polysaccharide solution at the same time, they will compete for the favorably oriented hydroxyl groups of the chain. As arylboric acids are not able to combine with more than one sugar residue, the formation of such complexes will decrease the chain length. The negatively charged arylboric acid-polysaccharide complexes have furthermore a repelling effect on other charged chains, which make it more difficult for boric acid to link them together.

Table 5. Effect of boric and phenylboric acids on the viscosity of galactomannan solutions (~ 0.15 %) pH 8.95.

Boric acid concn. M	—	2×10^{-3}	5×10^{-3}	10^{-2}	—	2×10^{-3}	5×10^{-3}
Phenylboric acid conc. M	—	—	—	—	10^{-2}	2×10^{-3}	2×10^{-3}
Efflux time, sec	37.2	43.2	248	∞	38.0	41.5	120

The galactomannan-boric acid-phenylboric acid system illustrates the proposed role of boric acid as a regulator of deposition and orientation of cell wall material and the role of arylboric acids as an inhibition in this process. Tables 1 and 5 show the effect of arylboric acids in decreasing the viscosity of a borax-galactomannan solution. Derivatives with high complex constant reduce the viscosity strongly and compounds low in complex forming ability have less effect (see also Fig. 6). Thus the degelation effect parallels complex formation and consequently the root growth promoting effect. Nitrophenol was also tested but showed here little effect in comparison with active compounds.

In order to clarify the relationship between complex constants of arylboric acids, their action on the viscosity of borax-galactomannan solutions and their activity in plants, the compounds have been arranged along the x-axis of Fig. 6 in the order of their ability to form complexes. log ($k_s \times k_1$) is plotted along the y-axis, open rings. Also along the y-axis are plotted: 1) The reduction in viscosity due to arylboric acids in the borax-galactomannan mixtures (as percent of the viscosity increase caused by borax alone, filled rings); 2) The cell elongating effect of the compounds (triangles). Results from the viscosity measurements parallel fairly well the complex constants. With three exceptions (triangles in parenthesis) the points for the cell elongating effect follow the pathway or the other two sets of data. The deviation of number 8 has already been discussed. 2 and 9, phenylboric acid and *p*-methoxy-phenylboric acid have in comparison with their complex constants, a very high action on roots. But here, as is pointed out earlier, uptake, transport and toxicity can play a role. The activity curves of these two compounds have a very broad maximum in comparison to the other tested compounds [6].

Note on the ionization constants of some arylboric acids

Ionization constants of a number of arylboric acids have been measured earlier and the results discussed on the basis of negativities and resonances of the groups involved [24-26]. Additional data for some new derivatives are presented here. From negativity and resonance interaction of the formyl group with the benzene ring it is to be expected that the *o*-compound should be a stronger acid than the *m*-compound and both of them stronger than phenylboric acid; this is the case (Table 1). The anomalous weakness of *o*-nitrophenylboric acid is ascribed to formation of a ring structure imposing a negative charge on the boron atom [25], a phenomenon which appears also with the three

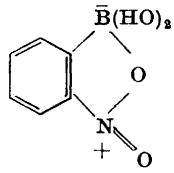

other nitroderivatives 10, 11 and 12. As expected, the 3,5-dinitro compound is a strong acid in comparison with phenylboric acid — about 100 times stronger.

The k_s for *o*-amino-phenylboric acid has not been measured but it ought to be considerably weaker than phenylboric acid because of resonance interaction between the nitrogen and boron atoms. Its acetyl derivative, however, has a k_s value very slightly greater than that of phenylboric acid, which means that the free electrons at the nitrogen atom are completely neutralized by the carbonyl group. We can find the same general trend in the benzoic acid series.

Acknowledgments. This work has been supported by grants from *Statens Naturvetenskapliga Forskningsråd*, Sweden and Mr. Thomas Brittingham. We are indebted to Dr. G. Neumüller for a sample of maize amylose.

REFERENCES

1. Boeseken, J. *Advances in Carbohydrate Chem.* **4** (1949) 189.
2. Zittle, C. A. *Advances in Enzymol.* **12** (1951) 493.
3. Torssell, K. *Arkiv Kemi* **10** (1957) 541.
4. Brown, H. C. and Fletcher, E. A. *J. Am. Chem. Soc.* **73** (1951) 2808.
5. Schmucker, T. *Planta* **23** (1934) 264.
6. Torssell, K. *Physiol. Plantarum* **9** (1956) 652.
7. Odnoff, C. *Ibid.* **10** (1957) 984.
8. O'Kelley, J. C. *Am. J. Botany* **44** (1956) 239.
9. Gauch, H. G. and Dugger Jr., W. M. *Plant Physiol.* **28** (1953) 457.
10. Gauch, H. G. and Dugger Jr., W. M. *Bull. A-80 Agric. Exptl. Station*, College Park, Maryland, 1954.
11. Torssell, K. *Arkiv Kemi* **10** (1957) 529.
12. Deuel, H. and Neukom, H. *Makromol. Chem.* **3** (1949) 13.
13. Ahmed, Z. F. and Whistler, R. L. *J. Am. Chem. Soc.* **72** (1951) 2524.
14. Sisler, E. C., Dugger, W. M. and Gauch, H. G. *Plant Physiol.* **31** (1956) 11.
15. McIlrath, W. J. and Palser, B. F. *Bot. Gaz.* **118** (1956) 43.
16. McClendon, J. H. and Somers, G. F. *Plant Physiol.* **30** (1955) 485.
17. Willstätter, R. und Schudel, G. *Ber.* **51** (1918) 788.
18. Kertesz, Z. I. in Colowick, S. P. and Kaplan, N. O. *Methods in Enzymology I.* p. 159. Academic Press Inc., New York 1955.
19. Kornberg, A. and Horecker, B. L. in Colowick, S. P. and Kaplan, N. O. *Methods in Enzymology I.* p. 323. Academic Press Inc., New York 1955.
20. Torssell, K. *Arkiv Kemi* **10** (1957) 473, 497, 507, 513.
21. Moe, O. A., Miller, S. E. and Iwen, M. H. *J. Am. Chem. Soc.* **69** (1947) 2621.
22. Rockland, L. B. and Dunn, M. S. *Science* **109** (1949) 539.
23. Eliasson, L. *Private communication.*
24. Branch, G. E. K., Yabroff, D. L. and Bettman, B. *J. Am. Chem. Soc.* **56** (1934) 937.
25. Yabroff, D. L., Branch, G. E. K. and Bettman, B. *Ibid.* **56** (1934) 1850.
26. Bettman, B., Branch, G. E. K. and Yabroff, D. L. *Ibid.* **56** (1934) 1865.
27. Caujolle, F., Gayrel, P., Meynier, D. and Huynh-Ngoc-Anh, *Toulouse Pharmaceutique.* **1** (1954) 25.

Received March 27, 1958.

ACTA CHEMICA SCANDINAVICA 12 (1958) 1386—1394

The Distribution of Polyalcohols between Organic Ion Exchangers and Water

MALTE MATTISSON and OLOF SAMUELSON

Department of Engineering Chemistry, Chalmers Tekniska Högskola, Göteborg, Sweden

The distribution of glycol, glycerol and sorbitol between an aqueous solution and different types of ion exchange resin has been studied. It has been found that the concentration is lower in the resin phase than in the outer solutions. The counter ions and the degree of cross-linking of the resin have a considerable influence. The application of the Gibbs-Donnan theory is discussed.

The distribution of non-electrolytes between an ion exchanger and an aqueous solution has been dealt with by many authors. Polyalcohols have been subjected to investigations with respect to their sorption as borate complexes on anion exchangers [1-3], and their distribution between ion exchangers and solutions in pure water has also been studied [4,5]. The aim of the present work is to give an idea of the factors which influence the distribution, through a more detailed investigation of a small number of compounds, namely ethylene glycol, glycerol and sorbitol using water as solvent.

EXPERIMENTAL PART

The ion exchanger was shaken with the solution for a time, long enough to attain equilibrium. The two phases were then separated by centrifugation and analysed. Experiments were performed with a single polyalcohol in the solution, not with mixtures of them.

Ion Exchange Resins. The anion exchanger Dowex 2 and the cation exchanger Dowex 50 were used. Of the latter, resins with varying degrees of cross-linking (X), 0.5, 1, 2 and 8 % DVB (divinylbenzene) were studied. In order to obtain as good reproducibility of centrifugation as possible, spherical resin particles were used. The anion exchanger and the cation exchanger, X8, with a normal degree of cross-linking had the particle size 0.2—0.4 mm (40/70 mesh) in an air-dried state and the other resins 0.14—0.29 mm (50/100 mesh). Very fine particles were washed out with water. The cation exchangers were washed with hydrochloric acid and the anion exchanger alternately with hydrochloric acid and sodium hydroxide solutions. The resins were transformed into their ionic states and air-dried in the usual way [6].

Equilibration. The equilibrium experiments were performed in 50 ml test tubes. The solutions of polyalcohols were freshly prepared from c.p. chemicals by dilution with

boiled-out distilled water. On prolonged storage at room temperature the solutions are liable to microbial destruction. In each experiment 40 ml solution and 0.5 – 2 g air-dried resin were added, the lower amount being used for the resins which swell most. The test tubes were rotated slowly in an air thermostat kept at 25.0 ± 0.1°C. The time of contact had to be chosen long enough to obtain equilibrium, but not so long that the polyalcohols were destroyed by microbes. Other authors have reported as short times as a few minutes for obtaining equilibrium between ion exchangers and aqueous solutions of non-electrolytes [4], but in the present work some systems were found to require longer times. The potassium form of normally cross-linked Dowex 50 and a solution of sorbitol attained equilibrium within one hour. The corresponding value for the perchlorate form of Dowex 2 was 10 h. The differences between various systems may be explained by differences in the molecular size of the solutes and in the swelling of the resins. To secure equilibrium the contact time was chosen as long as 40 h.

Separation of the Resin. After equilibration the resin was transferred to a weighed centrifuge basket, made of stainless steel and fitted with a bottom of wire-netting. The solution was collected in a 50 ml conical flask and stored in a refrigerator until analysed. The basket with the resin was placed in a centrifuge tube, closed with a rubber cap, and subjected to centrifugation for 40 min at 2 000 r/min, corresponding to a centrifugal acceleration of about 600 *g*. After the run, the basket with resin was weighed in a closed weighing bottle. Subsequently the resin was transferred by washing to a column of 10 mm diameter and 120 mm height fitted with glass filter bottom. The polyalcohol was eluted with water until the volume of the eluate was 100 ml. The solution was kept in a refrigerator until analysis could be performed.

Analyses. The concentration of glycol, glycerol and sorbitol in the equilibrium solution and in the eluate was determined by oxidation with periodic acid [*cf.* Ref.[7]]. Samples containing less than 30 mg ethylene glycol, 20 mg glycerol or 15 mg sorbitol were mixed in conical flasks with 25 ml of a solution of periodic acid, made by dissolving 5 g $HIO_4 . 2H_2O$ in 200 ml distilled water and filling up to one litre with glacial acetic acid. Fresh solution was made every day. The flasks were shaken vigorously and then kept well closed at room temperature. After 30 min, 10 ml potassium iodide solution (270 g/l) was added, and the liberated iodine was titrated with 0.1 N sodium thiosulfate solution. In order to obtain as good accuracy as possible, a 10 ml burette fitted with a 40 ml pipette on the top was used. As an indicator, 10 ml starch solution (2 g/l) was added. The discoloration was best observed in the light from a blue bulb. On each solution 2 or 3 determinations were made, and 4 to 7 blanks were run in each series of 17 to 25 titrations in all. For the calculation of the concentration of polyalcohol from the sodium thiosulfate consumption, factors taken from the literature were used [8]. These factors deviated only slightly from the theoretical ones. A control showed that they gave satisfactory results.

After the experiment, the resin was treated in the following manner: The cation exchangers were transformed into the hydrogen form and washed. The hydrogen ions were eluted with sodium chloride solution and titrated with 0.1 N sodium hydroxide solution to the color change of phenolphthalein. After being washed with water, the resin was transferred to a glass filter crucible and, after being dried for 6 days at 60 – 70°C over magnesium perchlorate under vacuum, the crucible and contents were weighed. In all cases the determinations of dry weight and capacity were checked by calculating the equivalent weight of the resin. The dry weight was recalculated to the actual ionic form.

The anion exchangers were transformed into the chloride form, washed and eluted with sodium nitrate solution. The chloride ions were determined by titration with silver nitrate solution according to Mohr [9]. After being washed, the resins were again transformed into the chloride form, washed, dried and weighed.

List of Symbols

x mole fraction of polyalcohol in the solution
x_r mole fraction of polyalcohol in the resin phase (ion exchanger not included)
K^* distribution coefficient ($= x_r/x$)
m molality of polyalcohol in the solution

m_r molality of polyalcohol in the resin phase
f practical activity coefficient of polyalcohol in the solution
f_r practical activity coefficient of polyalcohol in the resin phase
π swelling pressure of the resin, atmospheres
$\bar{v}$ partial molal volume of polyalcohol, ml
$\bar{v}_o$ partial molal volume of polyalcohol in an infinitely diluted aqueous solution at atmospheric pressure, ml
R gas constant, ml-atmospheres per degree per mole
T absolute temperature, degrees
k_s salting out parameter
n_r normality of resinate, equiv./1 000 ml water

RESULTS AND DISCUSSION

The experimental data are presented in Tables 1—3. The polyalcohol concentration in the solution and in the resin phase is given as mole fractions x and x_r. In the calculation of x_r the ion exchanger has not been included but only water and polyalcohol. The distribution coefficient K^*, *i.e.* the ratio x_r/x, is also given in the tables. Furthermore, figures are given for the total swelling, expressed in grams of water plus polyalcohol per equivalent of ion exchange resin, and for the water content and the polyalcohol content of the resin phase in moles per equivalent of resin. The water content is calculated by the difference.

Table 1. Distribution of ethylene glycol between various forms of Dowex 50 or Dowex 2 and water.

Resin	$x \times 10^2$	$x_r \times 10^2$	K^*	Total swelling g/equiv. resin	Mole H_2O / equiv. resin	Mole glycol / equiv. resin
Dowex 50 Li^+	0.901	0.617	0.68	204.0	11.09	0.0688
	2.67	1.99	0.75	204.4	10.60	0.216
Dowex 50 Na^+	0.910	0.677	0.74	179.2	9.72	0.0662
	2.69	2.00	0.74	179.5	9.31	0.190
Dowex 50 K^+	0.899	0.663	0.74	155.6	8.44	0.0563
	2.67	2.05	0.77	156.9	8.13	0.170
Dowex 2 SO_4^{2-}	0.337	0.242	0.72	270.4	14.88	0.0361
	1.51	1.22	0.81	270.9	14.42	0.178
	3.28	2.61	0.80	273.6	13.90	0.373
	0.338	0.275	0.81	238.5	13.11	0.0362
Dowex 2 Cl^-	1.51	1.35	0.89	234.6	12.44	0.170
	3.27	2.79	0.85	242.7	12.26	0.352
	0.459	0.440	0.96	99.0	5.41	0.0239
Dowex 2 ClO_4^-	1.50	1.40	0.93	94.2	4.99	0.0707
	3.25	3.17	0.97	93.3	4.66	0.152

Table 2. Distribution of glycerol between various forms of Dowex 50 or Dowex 2 and water.

Resin	$x \times 10^2$	$x_r \times 10^2$	K *	Total swelling g/equiv. resin	Mole H_2O / equiv. resin	Mole glycerol / equiv. resin
	0.367	0.209	0.57	201.2	11.05	0.0232
Dowex 50 Li^+	1.43	0.845	0.59	206.8	11.0	0.0938
	3.00	1.86	0.62	206.7	10.46	0.198
	0.360	0.323	0.90	767.5	41.90	0.136
Dowex 50 X2 Li^+	1.52	1.35	0.89	778.1	40.37	0.553
	3.39	3.02	0.89	788.4	37.75	1.18
	0.360	0.351	0.97	1 804	98.37	0.346
Dowex 50 X1 Li^+	1.51	1.44	0.95	1 806	93.30	1.36
	3.39	3.24	0.95	1 830	86.72	2.90
	0.359	0.352	0.98	2 317	126.35	0.447
Dowex 50 X 0.5 Li^+	1.51	1.47	0.98	2 343	120.84	1.80
	3.37	3.34	0.99	2 335	110.15	3.80
	0.370	0.212	0.57	181.7	9.97	0.0212
Dowex 50 Na^+	1.43	0.836	0.59	182.2	9.70	0.0818
	3.01	1.86	0.62	182.2	9.22	0.175
	0.368	0.236	0.64	159.0	8.72	0.0206
Dowex 50 K^+	1.42	0.939	0.66	158.6	8.40	0.0796
	2.98	2.00	0.67	158.8	7.98	0.163
	0.361	0.329	0.91	678.7	37.04	0.122
Dowex 50 X2 K^+	1.52	1.39	0.91	678.4	35.12	0.495
	3.39	3.11	0.92	686.9	32.76	1.05
	0.360	0.352	0.98	1 687	91.95	0.325
Dowex 50 X1 K^+	1.51	1.48	0.98	1 703	87.77	1.32
	3.37	3.29	0.98	1 708	80.78	2.75
	0.358	0.358	1.00	2 208	120.33	0.433
Dowex 50 X0.5 K^+	1.50	1.49	0.99	2 234	115.11	1.74
	3.39	3.33	0.98	2 261	106.70	3.68
	0.334	0.234	0.70	270.8	14.85	0.0349
Dowex 2 SO_4^{2-}	1.52	1.11	0.73	271.7	14.26	0.160
	3.38	2.49	0.74	277.0	13.60	0.347
	0.336	0.242	0.72	248.2	13.61	0.0330
Dowex 2 Cl^-	1.52	1.11	0.74	251.5	13.20	0.149
	3.37	2.50	0.74	257.8	12.65	0.324
Dowex 2 ClO_4^-	1.51	1.02	0.67	99.0	5.22	0.0536
	3.36	2.28	0.68	95.3	4.73	0.110

The distribution coefficient is a function of solute concentration [4], but from the data given in Tables 1—3 it is evident that within the examined range of concentration — up to 3.5 mole per cent in the outer solution — this dependence is small. For the normally cross-linked cation exchange resins the

Table 3. Distribution of sorbitol between various forms of Dowex 50 or Dowex 2 and water.

Resin	$x \times 10^2$	$x_r \times 10^2$	K^*	Total swelling g/equiv. resin	Mole H_2O / equiv. resin	Mole sorbitol / equiv. resin
Dowex 50 Li+	0.262	0.0948	0.36	206.9	11.38	0.0108
	1.15	0.432	0.37	209.3	11.13	0.0483
	2.67	1.06	0.40	213.2	10.68	0.114
Dowex 50 X2 Li+	0.357	0.280	0.78	776.8	41.93	0.118
	1.52	1.21	0.79	794.5	39.25	0.480
	3.54	2.80	0.79	824.4	35.45	1.02
Dowex 50 X1 Li+	0.355	0.323	0.91	1 798	96.63	0.314
	1.51	1.39	0.92	1 837	89.21	1.26
	3.56	3.22	0.91	1 884	78.24	2.61
Dowex 50 Na+	0.260	0.113	0.43	182.9	10.04	0.0114
	1.15	0.522	0.45	184.5	9.73	0.0510
	2.65	1.22	0.46	188.1	9.29	0.114
Dowex 50 K+	0.260	0.134	0.52	157.7	8.64	0.0116
	1.15	0.601	0.52	159.5	8.34	0.0504
	2.64	1.42	0.54	163.1	7.90	0.114
Dowex 50 X2 K+	0.358	0.319	0.89	675.7	36.33	0.116
	1.53	1.35	0.88	704.8	34.37	0.470
	3.48	3.13	0.90	723.0	30.25	0.977
Dowex 50 X1 K+	0.352	0.342	0.97	1 699	91.15	0.313
	1.50	1.45	0.96	1 752	84.69	1.24
	3.52	3.34	0.95	1 824	75.01	2.59
Dowex 50 X0.5 K+	0.350	0.351	1.00	2 225	119.27	0.420
	1.51	1.48	0.98	2 274	109.58	1.65
	3.53	3.40	0.97	2 355	96.38	3.40
Dowex 2 SO_4^{2-}	0.258	0.158	0.61	271.4	14.83	0.0234
	1.14	0.683	0.60	276.6	14.36	0.0987
	2.64	1.59	0.60	285.3	13.61	0.220
Dowex 2 Cl^-	0.259	0.136	0.53	239.1	13.09	0.0178
	1.16	0.601	0.52	240.3	12.57	0.0760
	2.67	1.41	0.53	246.1	11.94	0.170
Dowex 2 ClO_4^-	0.258	0.095	0.37	91.5	5.03	0.0048
	1.14	0.471	0.41	87.0	4.61	0.0218
	2.63	1.03	0.39	89.1	4.47	0.0466

distribution coefficient increases slightly with increased concentration, but for the anion exchange resins and for the weakly cross-linked cation exchanger the variations are probably within the limits of experimental errors.

As may be seen, the concentration in the resin phase is in all cases lower than that in the outer solution. Thus the net effect may be considered as a salting out of the polyalcohol from the resin phase.

It may be of interest to apply the Gibbs-Donnan theory [10] to the distribution of the non-electrolyte between the two phases. Different approaches have recently been reviewed by Holm [11]. The distribution can be approximately represented by the following equation [cf. Ref. [11c] p. 464—465].

$$\ln \frac{m \cdot f}{m_r \cdot f_r} = \frac{\pi \cdot \bar{v}}{RT} \quad (1)$$

If the concentration of non-electrolyte is low in both phases, we may put m/m_r equal to x/x_r and $f = 1$. Consequently, the equation may be written

$$-\log K^* = \frac{\pi \bar{v}}{2.303\ RT} + \log f_r \quad (2)$$

The first term on the right-hand side of eqn. (2) (the pressure term) accounts for the influence of the swelling pressure upon the distribution, whereas the second term (the interaction term) accounts for the interaction between the non-electrolyte and a hypothetical strain-less ion exchanger. The salting-out effect on non-electrolytes in common electrolyte solutions can, as a good approximation, be represented by the following eqn. (12)

$$\log f_i = k_s\ m_s \quad (3)$$

where f_i is the practical activity coefficient of the non-electrolyte, k_s a salting-out parameter and m_s the molal concentration of the salt. This equation is valid only at fairly low concentrations of the non-electrolyte. If eqn. (3) is applied to our problem, eqn. (2) may be written:

$$-\log K^* = \frac{\pi \bar{v}}{2.303\ RT} + k_s \cdot n_r \quad (4)$$

The distribution coefficient, K^*, is obtained in the experiments. The swelling pressure, π, may be obtained from isopiestic measurements [13,14] and data for Dowex 50X8 have been taken from the paper by Boyd and Soldano [14]. A few isopiestic measurements were made with the resin (Li-form) used in the present work and it was observed that the calculated osmotic pressure was somewhat lower than the data given by these authors. The deviations were less than 10 %. The non-electrolyte has within the actual range of concentration only a slight influence upon the swelling, and so the swelling pressures determined for pure water can be used.

The partial molal volume, $(\bar{v}_o)$, in aqueous solution at infinite dilution is reported by Riiber, Sörensen and Thorkelsen to be 54.28 ml per mole for glycol, 70.59 ml per mole for glycerol and 117.86 ml per mole for sorbitol [15]. As no data are available for the calculation of the partial molal volume, $(\bar{v})$, in the resin, the values, $\bar{v}_o$, for pure aqueous solutions at atmospheric pressure have been inserted in eqn. (2).

From these data f_r has been calculated according to eqn. (2). The calculation is based upon the values for K^* obtained at the lowest concentration under investigation. The results are given in Table 4. Although several objections might be raised to the calculations, this approach may serve as a basis for a discussion of the results obtained in the present work. First of all, it may be

Table 4. The magnitude of the pressure term and the interaction term.

	π	$-\log K^*$	$\frac{\pi \cdot \bar{v}_0}{2.303\ RT}$	$\log f_r$	k_s
Li^+, glycol	150	0.1675	0.1445	0.0230	0.005
Li^+, glycerol	150	0.2441	0.1880	0.0561	0.011
Li^+, sorbitol	150	0.4437	0.3138	0.1299	0.027
Na^+, glycol	124	0.1308	0.1195	0.0113	0.002
Na^+, glycerol	124	0.2441	0.1554	0.0887	0.016
Na^+, sorbitol	124	0.3665	0.2594	0.1071	0.019
K^+, glycol	99	0.1308	0.0956	0.0352	0.005
K^+, glycerol	99	0.1938	0.1243	0.0695	0.011
K^+, sorbitol	99	0.2840	0.2075	0.0765	0.012

pointed out that the pressure term has a predominating influence upon the distribution coefficient for the non-electrolytes studied in the present work, whereas in ion exchange equilibria the influence of the pressure term upon the equilibrium distribution is fairly small [13].

For resins with lower degrees of cross-linking the swelling pressure is much lower than for the X8 resin, and for this reason the pressure term will have lower values for these resins. On the other hand it must be expected that the interaction term is also lower for these resins. Because of the experimental difficulties involved in the determination of the swelling pressure for these resins the data published by different authors are contradictory. An attempt has been made to calculate the pressure term for the X2 resin. This calculation, which is based upon isopiestic measurements by Boyd [16], indicates that the relative magnitude of the pressure term is fairly large for this resin also. As the probable errors are considerable, these calculations are not included in the table.

From eqn. (2) it may be predicted that, if the interaction term is small or of the same order of magnitude for different non-electrolytes, the distribution coefficient will decrease for an increase in molecular size. It might therefore be expected that for all forms of the resin the distribution coefficient should increase according to the following sequence

$$\text{sorbitol} < \text{glycerol} < \text{glycol}$$

This is in agreement with the experimental results.

The influence of the degree of cross-linking can be predicted from eqn. (4). The pressure term decreases rapidly for a decrease in the degree of cross-linking. At the same time there is an increase in swelling, which means that n_r decreases. Consequently, it must be expected that for strongly polar non-electrolytes K^* is increased and approaches the value of unity at low degrees of cross-linking. This is in agreement with the experimental results given in Tables 2 and 3. In this connection it may be mentioned that also for less polar solutes (acetic acid and butyric acid), where, because of a van der Waals' adsorption on the resin matrix, K^* is larger than unity, the distribution coef-

ficient has been shown to be equal to unity for resins with a low degree of cross-linking [17,18].

From Tables 2 and 3 it may also be seen that the degree of cross-linking does not affect the order of the effects of different counter ions upon the distribution of glycerol and sorbitol.

The influence of different counter ions upon the distribution coefficient compared at a constant degree of cross-linking is a more complicated matter. The swelling of the resin is dependent on the counter ions, which means that both π and n_r are affected. At a constant degree of cross-linking a higher swelling means an increase in swelling pressure but a decrease in inside concentration (n_r). This means that the pressure term and the interaction term are affected in opposite directions. Furthermore, it must be expected that, as in the case of normal electrolytes, the parameter, k_s, is different for different ions and also varies considerably for various non-electrolytes. Thus it might be expected that the effect of the counter ions upon the distribution coefficient might be different for different polar solutes. This is in agreement with the experimental data presented in the tables. This effect is most clearly demonstrated in the experiments with anion exchangers, where a reversed order between the counter ions is obtained for glycol and sorbitol.

It may be of interest to compare the results obtained in the present work with the data given in an earlier paper [19] on the distribution of glucose between different forms of the resins and an outer aqueous solution. The experimental technique was the same in both investigations and the results are comparable. It is found that the order of the different counter ions is the same for glucose as for sorbitol. For both solutes the distribution coefficients increase according to the following series:

For Dowex 50: $Li^+ < Na^+ < K^+$
For Dowex 2: $ClO_4^- < Cl^- < SO_4^{2-}$

For the cation exchanger the sequence is in agreement with the order which can be calculated from the swelling pressure according to the method used in the present work, whereas for the anion exchanger a reversed order has been observed. This shows that it is not permissible to neglect the interaction term even if it is only desired to make predictions of a qualitative kind.

Some conclusions about the possibilities of adopting ion exchange resins for the separation of glycol, glycerol and sorbitol in aqueous solution can be drawn from the data given in the present paper. The ratio between the distribution coefficients has a predominating influence upon the separation [cf. Ref.[20]]. For the anion exchanger in the perchlorate form this ratio (the separation factor) is 1.4 for glycol/glycerol and 1.6 for glycerol/sorbitol indicating that a good separation can be obtained provided that the flow rate is not too high. It may also be concluded that the forms of the cation exchanger used in the present work will be less suitable, but from the data given for different degrees of cross-linking it may be anticipated that an increase in the degree of cross-linking would give more favorable results.

The financial support of *The State Technical Research Council (Statens Tekniska Forskningsråd)* is gratefully acknowledged.

REFERENCES

1. Zager, S. E. and Doody, T. C. *Ind. Eng. Chem.* **43** (1951) 1070.
2. Costa, G. and Camus, A. M. *Ann. chim. (Rome)* **45** (1955) 598.
3. Sargent, R. and Rieman, W. *J. Phys. Chem.* **60** (1956) 1370.
4. Wheaton, R. M. and Bauman, W. C. *Ann. N.Y. Acad. Sci.* **57** (1953) 159.
5. Asher, D. R. and Simpson, D. W. *J. Phys. Chem.* **60** (1956) 518.
6. Samuelson, O. *Ion Exchangers in Analytical Chemistry*, Stockholm 1952 and New York 1953.
7. Pohle, W. D., Mehlenbacher, V. C. and Cook, J. H. *Oil & Soap* **22** (1945) 115.
8. Miner, C. S. and Dalton, N. N. *Glycerol. Am. Chem. Soc. Monograph No. 117*, New York 1953.
9. Kolthoff, I. M. and Sandell, E. B. *Textbook of Quantitative Inorganic Analysis*, New York 1948.
10. Donnan, F. G. and Guggenheim, E. A. *Z. physik. Chem.* **162A** (1932) 346.
11 a. Holm, L. W. *Arkiv Kemi* **10** (1956) 151.
11 b. Holm, L. W. *Ibid.* **10** (1956) 445.
11 c. Holm, L. W. *Ibid.* **10** (1956) 461.
12. Long, F. A. and McDevit, W. F. *Chem. Revs.* **51** (1952) 119.
13. Glueckauf, E. *Proc. Roy. Soc. London* **214A** (1952) 207.
14. Boyd, G. E. and Soldano, B. A. *Z. Elektrochem.* **57** (1953) 162.
15. Riiber, C. N., Sörensen, T. and Thorkelsen, K. *Ber.* **58B** (1925) 964.
16. Calmon, C. and Kressman, T. R. E. *Ion exchangers in organic and biochemistry*, New York 1957, p. 45–46.
17. Samuelson, O. *Diss.* Tekn. Högskolan, Stockholm 1944.
18. Reichenberg, D. and Wall, W. F. *J. Chem. Soc.* **1956** 3364.
19. Rückert, H. and Samuelson, O. *Acta Chem. Scand.* **11** (1957) 315.
20. Glueckauf, E. *Ion exchange and its applications*, Soc. of Chemical Industry, London 1954, p. 27.

Received May 2, 1958.

ACTA CHEMICA SCANDINAVICA 12 (1958) 1395—1404

The Sorption of Polyalcohols from Aqueous Alcohol by Cation Exchange Resins

MALTE MATTISSON and OLOF SAMUELSON

Department of Engineering Chemistry, Chalmers Tekniska Högskola, Göteborg, Sweden

The rate of sorption and the equilibrium distribution of glycol, glycerol, sorbitol and mannitol between aqueous alcohol and cation exchange resins has been studied. It has been found that the alcohol concentration has a predominating influence upon the rate of uptake. The equilibrium uptake increases considerably for an increase in alcohol concentration, but also the counter ions and the degree of cross-linking have an effect.

In earlier papers [1-3] it has been shown that sugars, dissolved in a mixture of water and ethyl alcohol, can be taken up by means of ion exchange resins. It was found that considerable amounts could be sorbed especially at low water concentrations in the solution. In the present work these investigations have been extended to include another group of polar non-electrolytes, namely polyalcohols, and it is shown that these behave in a similar manner. Because of the poor solubility of sugars in ethyl alcohol the earlier investigations were restricted to systems with a considerable water content. The higher solubility of certain polyalcohols has made it possible to study the uptake also from an almost water-free medium. As mentioned in a preliminary report, the sorption of polyalcohols is much larger in nearly water-free solutions than in solutions more rich in water [4]. Also, the rate of sorption is highly dependent on the water concentration.

EXPERIMENTAL PART

Preparation of ion exchange resins. The experiments were performed with the cation exchanger Dowex 50. The normally cross-linked resin (X8) with 8 % divinylbenzene as well as a resin (X2) with 2 % divinylbenzene were used. Most experiments were made with Dowex 50 X8 with a particle size of 0.2—0.4 mm obtained by grinding and screening in an air-dried condition (sodium form). In one experimental series (Table 1) the influence of the particle size upon the rate of sorption has been studied and in this case spherical beads of both types of resin have been used.

Before the experiments the resin was immersed in water and very fine particles removed by decantation. The resin was washed with hydrochloric acid and sodium hydr-

oxide solutions several times. The sodium state of the resin was air-dried and stored in tight bottles. When other ionic forms were needed the sodium form of the resin was weighed out and subsequently converted into the desired ionic form.

The exchange capacity was determined titrimetrically by treating the hydrogen form of the resin with potassium chloride solution and subsequently titrating with alkali [5].

In the experiments, samples of the air-dried ion exchanger (usually 7.80 mequiv.) were brought into equilibrium with aqueous alcohol of the same composition as that used as solvent. This equilibration was performed in columns of about 5 ml volume, by passing the aqueous alcohol through the resin. The apparatus used in the experiments with absolute ethanol permitted the ethanol to be supplied intermittently and the eluate collected without contamination by atmospheric humidity. Once or twice every day about 5 ml of ethanol was fed to each column until 100 ml effluent had been collected. Analysis of the effluent showed that its water content was about 3 % higher than it should be when calculated from the water content of the resin as determined by drying the resin over magnesium perchlorate at 60°C in vacuum. This would indicate that the last traces of moisture are not removed during the drying but there is also a possibility that — despite the precautions taken — water has been taken up from the atmosphere.

In the experiments presented in Table 1 the technique was altered in some respects. The ion exchangers were converted into the potassium form and air-dried samples weighed out in this state. Also in this series 7.8 mequiv. were transferred to each column, but all columns were treated simultaneously with absolute alcohol in a special apparatus. The time required to remove the water was around 40 days, but the treatment was continued for 60 days in order to make sure that all the samples were in equilibrium with the solvent.

Absolute alcohol was prepared from 99.5 % ethanol by treatment with magnesium powder [6].

The sorption of polyalcohol. After equilibration with the solvent, dried air was sucked gently through the columns at 30—40°C in order to remove the interstitial solution and to make it possible to empty the columns. The resin was transferred into 50 ml test tubes fitted with ground in stoppers. The empty columns were also placed in the test tubes in order to avoid any loss of resin. Into each test tube 40 ml of polyalcohol solutions were pipetted. The tubes were closed and rotated slowly in an air thermostat at 25.0 ± 0.1°C. After the desired contact time, the test tubes were taken out of the thermostat, and the solution was passed through a fritted glass filter, which had previously been dried.

Analyses. The water concentration in the solution was determined according to a modified Karl-Fischer method [7]. The concentration is expressed in weight per cent and all data given below refer to the solution after the contact with the resin.

The concentration of polyalcohol in the solution, before and after the experiments, was determined by oxidation with periodic acid [8]. The amount of sorbed polyalcohol was calculated from the decrease in solution concentration. No correction was applied for the change in volume of the solution.

RESULTS AND DISCUSSION

The sorption is characterized by the ratio m_r/m, where m_r is the amount of polyalcohol in the resin phase expressed in mmoles per equiv. ion exchanger and m is the concentration of polyalcohol in the solution in mmoles per 1 000 g solvent. Where equilibrium has been established, this ratio, which will be called the sorption coefficient (K_e), can be used to characterize the equilibrium distribution. The original concentration of the solution is denoted by m_o.

Rate of sorption. In order to establish the time required for obtaining equilibrium some kinetic experiments have been carried out. Fig. 1 demonstrates the rate of uptake of glycerol using the lithium form of Dowex 50. Similar curves for the potassium form of the resin are shown in Fig. 2. The glycerol concentration in the original solutions (20 mmole/1 000 g solvent) was the same in all experiments incorporated in Figs. 1 and 2. It may be seen that the rate of uptake depends markedly on the alcohol concentration. This is in

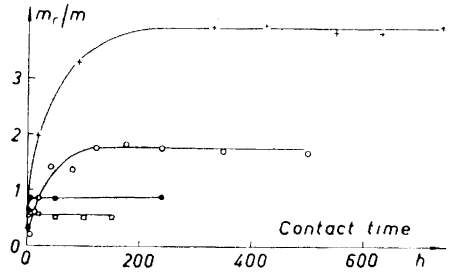

Fig. 1. The rate of glycerol sorption by the Li^+-form of Dowex 50 from various ethanol-water mixtures. % water at equilibrium 0.06 0.6 7.5 12.6
+ ○ ● □

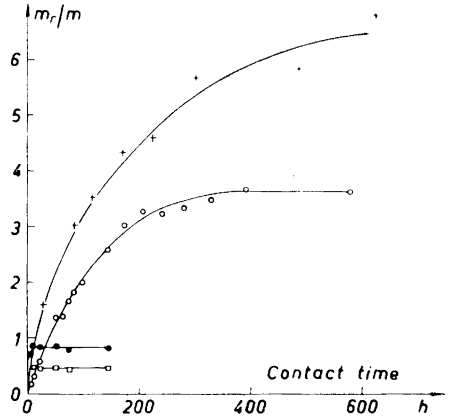

Fig. 2. The rate of glycerol sorption on the K^+-form of Dowex 50 from various ethanol-water mixtures. % water at equilibrium 0.06 0.6 7.5 12.6
+ ○ ● □

agreement with earlier observations on the sorption of sugars [2]. At the highest water concentration in the solution (12.6 %) equilibrium is reached within one hour, whereas several hundred hours are required in the experiments at the lowest water concentration. A comparison between Figs. 1 and 2 shows that the lithium form of the resin reacts more rapidly than the potassium form. In ethyl alcohol, as well as in water, lithium ions cause a higher swelling of the resin than potassium ions [9], and in general ion exchange reactions occur at a faster rate the higher the swelling. This is ascribed to differences in diffusion velocity inside the particles. If the particle diffusion is the rate determining step, this explains the difference between the two forms of the resin. Experiments with solutions of glycerol in alcohol containing 7.5 % water showed that within wide limits (20—1 200 mmole/1 000 g solvent) the concentration of glycerol had only slight influence upon the time required for equilibrium. This is an indication that the influence of the film diffusion step can be neglected in these systems.

It is interesting to note that the rate of glycerol uptake decreases to a marked extent when the water content of the solution is lowered from 0.6 % to 0.06 %. For this reason it was deemed to be of interest to study in more detail the rate of uptake in an almost water-free system. The results obtained with a resin in the potassium form are presented in Table 1. In agreement with the results presented in Fig. 2 it has been found that the time required to reach equilibrium is extremely long. This is true not only for the normal cation exchanger but also for the weakly cross-linked resin (X2). The uptake obtained after 1 198 h has been considered as the equilibrium uptake. As the rate of uptake is extremely slow the film diffusion step cannot be rate determining.

Table 1. The rate of glycerol sorption by the K^+-form of Dowex 50. 7.80 mequiv. resin + 40 ml alcohol (0.02 % water). Initial concentration: 2.018 mg glycerol per g solution.

Time of reaction h	Glycerol uptake, mg per 7.80 mequiv. resin			
	X2 0.037—0.074 mm	X2 0.14—0.29 mm	X8 0.300—0.385 mm	X8 0.75—1.02 mm
1	22.12	3.21	2.65	1.50
5	33.73	7.65	6.49	5.55
12	34.22	12.35	9.51	8.70
25	36.35	15.77	12.73	11.69
45	36.90	20.29	16.07	14.71
70	36.56	23.11	18.35	16.66
110	36.90	25.00	22.58	20.28
185	36.94	28.72	25.09	24.08
1 198	37.10	38.68	37.74	37.17
1 198	37.21	39.64	36.59	37.07

Consequently, either the diffusion within the particle or the sorption mechanism or these two factors together must determine the rate of uptake. From Table 1 it is evident that the particle size has a marked influence upon the rate of uptake, which excludes the possibility that the sorption mechanism is the rate determining step. This effect is most clearly demonstrated by the results obtained with the weakly cross-linked resin (X2), whereas with the normal resin (X8) this effect is surprisingly small. The explanation for the different behavior of the two types of resin is given by the micrographs presented in Fig. 3. It may be seen that the weakly cross-linked resin consists of intact spheres, whereas the normal resin contains a large number of cracked particles. Consequently, the sorbed molecules may have about the same way to diffuse within the particles of the two samples of the X8 resin.

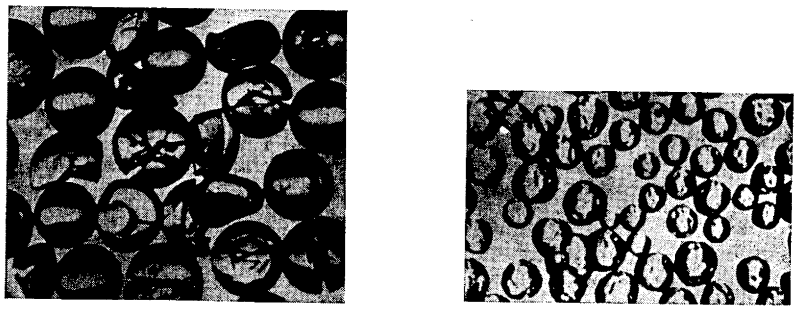

Fig. 3. Micrographs of the resins used in the kinetic experiment reported in Table 1. Magnification 25 times.
A: Normally cross-linked resin.
B: Weakly cross-linked resin.

An attempt has been made to apply the theory of particle diffusion according to Boyd, Adamson and Myers [10]. In the present case the solute concentration was not constant throughout the experiment, therefore it may be expected that the equation given by these authors can be applied only to the first part of the reaction. The particle size was not uniform, which has made it necessary to make the calculation for small fractions of each sample. The particle size distribution of the samples has been determined microscopically and the weight distribution curve has been calculated. The diffusion coefficient obtained in this way is around 10^{-10} — 10^{-11} cm^2/sec for both samples of the X2 resin. For a comparison it may be mentioned that the diffusion constant for glycerol in 96 % ethyl alcohol [11] is $5.3 \cdot 10^{-6}$ cm^2/sec. The results support the conclusion that the particle diffusion is the rate determining step.

As mentioned above, the differences in the rate of uptake between resins in different ionic forms can be explained by differences in swelling. The lowered swelling, which occurs when the water concentration is lowered, may to some extent explain the decrease in rate for a decrease in water concentration. However, the decrease in swelling corresponding to a change in the water concentration from 0.6 % to 0.06 % is so small that it can hardly be determined experimentally (less than 2 %). Consequently, the influence of the water concentration upon the swelling does not give the whole explanation of the differences in the rate of sorption in different solvent mixtures. It must be observed that the water content given in Figs. 1 and 2 refers to the outer solution. Within this range of concentration the water content in the resin phase is considerably higher [9]. From available data it can be roughly estimated that, at an outer concentration of 0.6 % water, the inside concentration is about 13 %, whereas for 0.06 % in the outer solution, the corresponding inside concentration is around 4 %. It is likely that this change in composition of the inside solution may also contribute to a decrease in the rate of diffusion inside the resin particles. A change in composition may have a considerable effect upon the structure of the inside solution. According to Sutra [12,13] the radii of the solvated alkali metal ions in ethyl alcohol are more than twice their size in water. It is known that in a mixture of alcohol and water the solvate sheaths of the alkali metal cations consist of both water and alcohol, water being held preferentially in the solvate sheath. When the alcohol concentration is increased a resolvation must occur, which in the case of ion exchange resins must result in a considerable decrease in the volume of the "free" inner solution. Probably this factor may contribute to a decrease in the rate of diffusion inside the resin particles, which would explain the lowered rate of sorption at extremely low water contents in the solution. It may also be pointed out that some of the glycerol molecules which diffuse into the resin phase must enter the solvate sheath, and that this resolvation may in some way have an influence upon the rate of uptake.

Equilibrium distribution. From Figs. 1 and 2 it is obvious that the solvent composition has a large effect upon the equilibrium. In agreement with earlier observations for sugar [2,3], the uptake of glycerol is found to increase when the relative amount of water in the solvent is decreased. It is interesting to note that the uptake is changed by a factor of about two, when the water content in the solvent is lowered from 0.6 % to 0.06 %. Also with glycol and sorbitol

Table 2. The effect of the counter ions and the degree of cross-linking upon the distribution equilibrium.

Polyalcohol	Water conc. %	m_o	%DVB in the resin	K_e						
				H^+	Li^+	Na^+	K^+	Rb^+	Cs^+	NH_4^+
Sorbitol	0.03–0.06	7.65	8	1.17	87	83	169	221	222	30.1
Glycerol	0.06	21.12	8	0.28	3.4	10.5	6.85	5.97	4.86	1.39
Glycerol	0.03–0.04	20.57	2	0.40	1.37	8.51	5.80	4.92	4.13	1.12
Glycol	0.04–0.08	13.87	8	0.23	1.32	2.35	1.36	0.84	0.86	0.51
Glycerol	7.5	12.00	8	0.24	0.89	1.11	0.95	0.87	0.79	0.62

it has been found that the uptake increases considerably for a decrease in water concentration in the solvent (*cf.* Tables 2 and 3). In pure water the net effect is a salting out, *i.e.* the concentration of polyalcohol in the resin phase is lower than in the outer solution [8].

The influence of the solute concentration upon the equilibrium distribution for glycerol in solutions with 7.7 % water is shown in Figs. 4 and 5. Fig. 4 also illustrates the uptake of glycerol from an almost water-free medium. All isotherms are convex, *i.e.* the sorption coefficient decreases for an increase in concentration. The effect of the solute concentration upon the sorption coefficient is largest in almost water-free solutions. This dependence on concentration must be remembered when comparing the sorption by different ionic states of a resin or by resins of different degrees of cross-linking. The rigorous method would be to make the comparison at constant equilibrium concentration in the outer solution. This would require measurements at different concentrations and such measurements have only been made in a few systems. Measurements are available, which permit a comparison between the effects of Li^+, Na^+ and K^+ upon the uptake of glycerol from a solution containing 7.7 % water. The data given in Fig. 4 show that at low solute concentrations the highest sorption is obtained with the Na^+-resin and the least sorption with the K^+-resin, whereas the Li^+-resin takes an intermediate

Table 3. The sorption of various polyalcohols on the K^+-form of Dowex 50.

Polyalcohol	m_o	m	m_r	% sorbed	K_e
Glycol	9.18	8.64	2.10	5.9	0.24
		8.76	1.83	4.6	0.21
Glycerol	9.05	8.06	4.18	12.3	0.52
Mannitol	9.29	4.84	19.64	47.9	4.06
		4.82	19.56	48.1	4.06
Sorbitol	9.30	3.90	23.71	58.1	6.08
		3.93	23.72	57.7	6.04

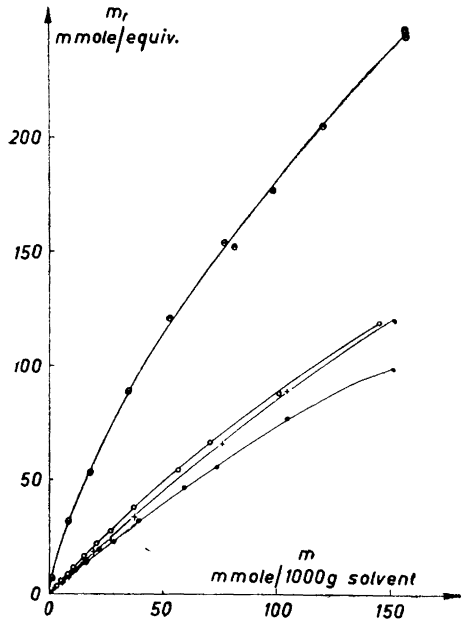

Fig. 4. The glycerol sorption by alkali metal forms of Dowex 50.
⊖ Li^+, 0.02—0.06 % water, 720 h
○ Li^+
\+ Na^+ } 7.7 % water, 170 h
● K^+

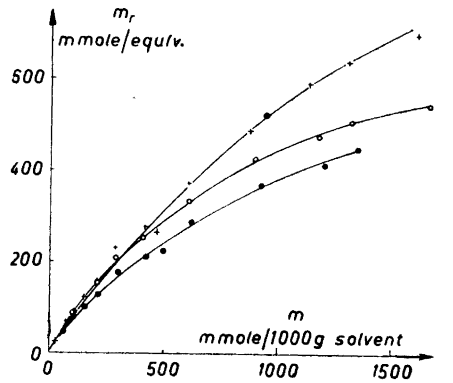

Fig. 5. The glycerol sorption by alkali metal forms of Dowex 50 from solutions with 7.7 % water. Contact time 170 h.
\+ Li^+
○ Na^+
● K^+

position. From Fig. 5 it may be seen that the order of the Li^+-resin and the Na^+-resin is reversed, *i.e.* the sorption isotherms for these two forms of the resin cross each other.

A reversed order of the effects of different counter ions can be obtained also when the relative amount of water in the solvent is changed. A comparison between Fig. 1 and Fig. 2 confirms that at higher water concentrations (7.5 and 12.6 %) the lithium form is a more effective sorbent than the potassium form. At low water concentrations (0.06 and 0.6 %) the order is reversed and the sorption is much higher for the potassium form.

In Table 2 further data are collected showing the influence of the counter ions upon the equilibrium uptake of different polyalcohols. The data refer to the solute concentration given in the table and, as already mentioned, the sorption coefficients are affected by changes in the solute concentration. Among the alkali metal resins the sodium form is the most effective sorbent for glycol and glycerol at the concentrations investigated. On the other hand, sorbitol is sorbed more strongly by the resin saturated with potassium ions and particularly with rubidium and cesium ions. In this respect sorbitol behaves like glucose [2]. The hydrogen and ammonium forms of the resin

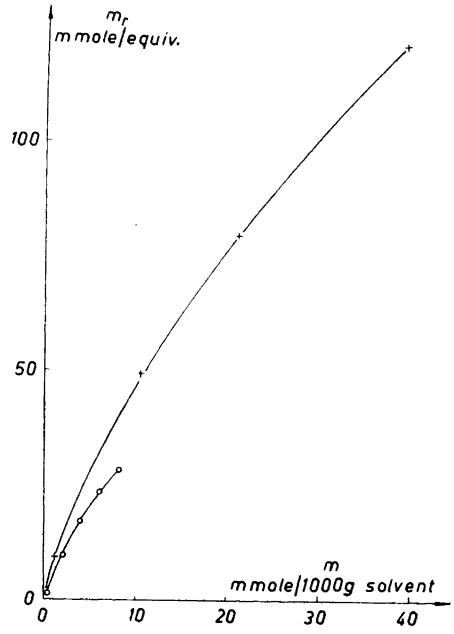

Fig. 6. The sorption of sorbitol and mannitol by the K^+-form of Dowex 50 from solutions with 12.5 % water. Contact time 48 h.
+ sorbitol
O mannitol

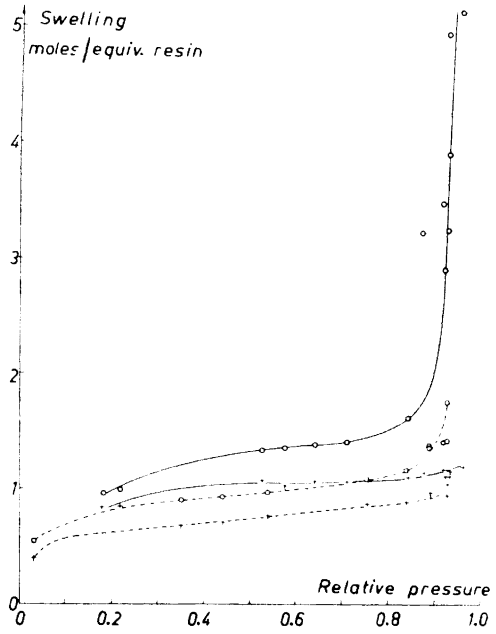

Fig. 7. Uptake of ethyl alcohol vapor.
Continuous lines: desorption.
Dotted lines: sorption.
+ Dowex 50 X8
O Dowex 50 X0.5

sorb less than the alkali metal forms, which is in agreement with the results obtained with glucose.

The experiments with glycerol presented in Table 2 indicate that the degree of cross-linking has an influence upon the sorption. However, this factor is less important than the effect of the ionic form of the resin. This is in agreement with the results obtained with glucose [3].

The sorption differs considerably for various polyalcohols. Table 3, which contains data for the sorption from a solution with 12.5 % water shows that the uptake increases according to the following series: glycol < glycerol < mannitol < sorbitol. In an almost water-free medium only glycol, glycerol and sorbitol have been investigated and it has been found that the sorption increases according to this sequence. In water the sequence is reversed [8]. Evidently the number of hydroxyl groups in the sorbed molecule has a marked effect upon the distribution coefficient. The uptake of mannitol and sorbitol at various solute concentrations is demonstrated in Fig. 6. The two polyalcohols have the same number of hydroxyl groups in the molecule, but sorbitol is held more strongly than mannitol. Consequently, small differences in the structure between different solutes may have a considerable influence upon the sorption.

In a previous work on the distribution of polyalcohols between an aqueous solution and an ion exchange resin an attempt was made to split up the distribution coefficient into two parts, a pressure term and an interaction term [8]. The calculation was based upon the Gibbs-Donnan theory. It was found that both terms have a considerable influence upon the distribution. Because of the lack of data, *e.g.* swelling pressure data, no attempts will be made to perform such calculations for the uptake from the solvents used in the present work. However, some remarks of a qualitative kind may be made.

In aqueous solutions the distribution coefficient (K^*) is less than unity, which means that the concentration of polyalcohol is lower in the resin than in the outer solution. This net effect is explained by the contributions of the pressure term and the interaction term, which both have an influence in the same direction. The pressure term will always act in this direction and therefore it may be concluded that for solutions in ethanol, where the net effect is a considerable sorption, the pressure term is small compared with the interaction term. The pressure term has a larger influence upon large molecules than upon small ones, but despite this fact the larger molecules are, in alcohol solution, sorbed more strongly by the resin. This can only be explained if the interaction term has a higher numerical value for the larger molecules.

The interaction term accounts for the interaction between the solute and the ion exchanger and between the solute and the solvent. The interaction between the solute and pure solvent mixtures can be accounted for if the activity coefficients for the solute are known at different solvent compositions. Data, which show the solvent composition inside the resin as a function of the outer concentration, are given in an earlier paper [9]. Within the range of alcohol concentrations studied in the present work the water concentration inside the resin is higher than in the outer solution and therefore the polar solutes, preferring the better solvent, will accumulate in the resin phase. Based upon solubility measurements, an attempt was made in an earlier paper to estimate the relative magnitude of the solute-solvent interaction and the solute-resin interaction for glucose in aqueous alcohol. It was shown that both factors have to be taken into consideration. As to the solute-resin interaction it has been demonstrated that for sugars the interaction between the ions inside the resin and the solute is a more important factor than the interaction between the resin matrix and the solute [2,3]. For less polar solutes, *e.g.* acetic acid, the latter factor may predominate [5].

As demonstrated in earlier papers the uptake of polar non-electrolytes from aqueous alcohol can be used for analytical separations. Under suitable conditions non-electrolytes can be separated according to the chromatographic technique [4,1]. From the present work it is obvious that the separation factors, *i.e.* the ratio between the sorption coefficients (or distribution coefficients), differ much more in aqueous alcohol than in pure water [*cf.* Ref.[8]]. An increase in alcohol concentration causes an increased separation factor. For this reason it is advantageous to use a high alcohol concentration for chromatographic separations of polar non-electrolytes. As observed earlier for sugars [1,2] and confirmed in the present work for polyalcohols, the reaction equilibrium is reached slowly in aqueous alcohol and as demonstrated above the rate of reaction is extremely low in an almost water-free medium. This is a consider-

able disadvantage as far as chromatographic work is concerned, and for practical purposes the concentration cannot be chosen too high.

In this connection it may be mentioned that glycol, glycerol and sorbitol can be easily separated, *e.g.* by elution with 95 % ethyl alcohol from a column with the sodium form of Dowex 50 [4]. Glycol and glycerol appear as sharp peaks and sorbitol, which is bound much more strongly, appears as a broad band of low concentration. After glycol and glycerol have been eluted, sorbitol can be displaced quickly by means of water. The resin swells much more in water than in aqueous alcohol and so it might be necessary to break up the resin bed after the addition of water. Because of the influence of solvent composition upon the swelling, gradient elution based upon a gradient in solvent composition cannot be used as the changes in swelling causes channelling or even plugging in the column [14].

APPENDIX

An attempt was made to determine the swelling pressure of Dowex 50 in ethyl alcohol according to the isopiestic method [15,16]. Isotherms of the same shape as for water were obtained. The weakly cross-linked resin X0.5 sorbed considerably more than the normally cross-linked resin. The sequence of the ionic forms of the resin was the same as for water sorption, *i. e.* the lithium form sorbed more than the sodium form, which showed a stronger sorption than the potassium form. The order is the same as obtained for the swelling in alcohol solutions [9].

Considerable experimental difficulties arose in these experiments and only the results obtained with the sodium form of the resin will be given in the present paper. The isotherms are given in Fig. 7. The time of reaction in these experiments has been 3—6 days and no significant differences have been observed for different times of reaction. The isotherms for the sorption and desorption do not coincide, and for this reason it seems improbable that a true equilibrium has been reached. Furthermore, it is very difficult to prevent traces of water vapor from entering the system, so no swelling pressure data will be given here. It may only be mentioned that the lithium resin gave data of the same order of magnitude as for water [15,16], whereas higher pressures were calculated for the sodium and potassium forms of the resin.

The financial support of *The State Technical Research Council (Statens Tekniska Forskningsråd)* is gratefully acknowledged.

REFERENCES

1. Samuelson, O. and Sjöström, E. *Svensk Kem. Tidskr.* **64** (1952) 305.
2. Rückert, H. and Samuelson, O. *Svensk Kem. Tidskr.* **66** (1954) 337.
3. Rückert, H. and Samuelson, O. *Acta Chem. Scand.* **11** (1957) 315.
4. Samuelson, O. *9. Nordiske Kemikermöde i Aarhus*, August 1956, p. 105.
5. Samuelson, O. *Diss.* Tekniska Högskolan, Stockholm 1944.
6. Vogel, A. I. *A Textbook of Practical Organic Chemistry*, London, New York and Toronto 1948, p. 165.
7. Johansson, A. *Svensk Papperstidn.* **50**, No. 11 B (Jubilee Vol. E. Hägglund) (1947) 124.
8. Mattisson, M. and Samuelson, O. *Acta Chem. Scand.* **12** (1958) 1386.
9. Rückert, H. and Samuelson, O. *Acta Chem. Scand.* **11** (1957) 303.
10. Boyd, G. E., Adamson, A. W. and Myers, L. S. *J. Am. Chem. Soc.* **69** (1947) 2836.
11. Öholm, L. W. *Medd. Vetenskapsakad. Nobelinst.* **2** (1912) No. 24.
12. Sutra, G. *J. chim. phys.* **43** (1946) 189.
13. Sutra, G. *J. chim. phys.* **43** (1946) 279.
14. Samuelson, O. and Appelgren, L. *Unpublished.*
15. Boyd, G. E. and Soldano, B. A. *Z. Elektrochem.* **57** (1953) 162.
16. Glueckauf, E. *Proc. Roy. Soc. London* **214A** (1952) 207.

Received May 2, 1958.

ACTA CHEMICA SCANDINAVICA 12 (1958) 1405–1410

Synthesis of Potential Hypnotics

POUL NEDENSKOV*, WILLIAM TAUB and DAVID GINSBURG

Department of Chemistry, Israel Institute of Technology, Haifa, Israel

Several 2,2-disubstituted *cyclo*hexanones were prepared and a number of their corresponding oximes was subjected to Beckmann rearrangement in order to obtain ε,ε-disubstituted caprolactams believed to possess hypnotic activity.

It was believed that lactams containing a quaternary carbon atom adjacent to the lactam moiety, *i.e.* the grouping —CO—NH—CRR'— within a cyclic system, might possess hypnotic activity. Such compounds would be available from 2,2-dialkyl-*cyclo*hexanones, for example, through Beckmann rearrangement of the corresponding oximes.

It has been shown [1] that such rearrangement leads exclusively to the above grouping rather than to the isomeric (—CRR'—CO—NH—) one. It was also expected [2] that the disubstituted caprolactams would be less prone to polymerization than caprolactam itself. However, this expectation was not realized. In fact, although some of the products synthesized did indeed possess hypnotic activity, polymerization occurred so readily that preparation of this type of compound was abandoned as impractical.

The difficulties in preparing 2,2-disubstituted *cyclo*hexanones in one step are well known. However, the availability of Stork's excellent method for the synthesis of monoalkyl*cyclo*hexanones [3] afforded the possibility of alkylating the latter derivative in the presence of sodium hydride in reasonable overall yield. The purification of the liquid products was effected by distillation through the efficient column described by Clauson-Kaas and Limborg [4].

The oximes were prepared in high yield by the pyridine procedure [5] and were rearranged by means of polyphosphoric acid [6]. The disubstituted caprolactams thus obtained polymerized very readily during distillation or even upon standing. Purification with lower loss of material could be effected chromatographically.

In the attempt to prepare 6,6-dialkylpyridones from the corresponding oximes of 2,2-disubstituted *cyclo*pentanones, the following approach was attempted but failed.

* Calanda Foundation fellow, 1956.

Table 1. 2,2-Disubstituted

2,2-Disubstituted *cyclohexanone*	Yield %	B. p. °C	B. p. mm	n_D^{30}	C=O I.R. ν cm^{-1}	Empirical formula	Analysis Calc. C	Analysis Calc. H	Analysis Calc. O
Et, Et	61	83— 85	12	1.4560	1 708	$C_{10}H_{18}O$	77.9	11.8	10.4
Et, Allyl	76	115—124	19	1.4694	1708	$C_{11}H_{18}O$	79,5	10.9	9.6
Et, *i*-Pr	41	110—112	20	1.4559	1 700	$C_{11}H_{20}O$	78.5	12.0	9.5
Et, *n*-Bu	49	123—125	20	1.4568	1 695	$C_{12}H_{22}O$	79.1	12.2	8.8
Et, *i*-Bu	61	118—120	20	1.4560	1 695	$C_{12}H_{22}O$	79.1	12.2	8.8
Et, Ph	80	99—105	0.2	1.5305	1 705	$C_{14}H_{18}O$	83.1	9.0	7.9
Me, *n*-Bu	62	96	12	1.4525	1 698	$C_{11}H_{20}O$	78.5	12.0	9.5
Allyl, *i*-Pr	56	120—124	20	1.4725	1 695	$C_{12}H_{20}O$	79.9	11.2	8.9

Chlorination of 2-ethyl*cyclo*pentanone with sulfuryl chloride afforded 2-chloro-2-ethyl*cyclo*pentanone. Treatment of the latter with diethyl cadmium indeed effected alkylation by replacement of the chlorine atom with an ethyl group without attack of the carbonyl group but unfortunately this cadmium alkyl was a sufficiently strong base so as to effect dehydrochlorination and 2-ethyl-*cyclo*pent-2-enone was formed concomitantly. Perhaps a different metal alkyl might be employed successfully but this was not pursued further.

EXPERIMENTAL PART *

*2-Ethyl*cyclo*hexanone.* A mixture of freshly distilled *cyclo*hexanone (108 g, 1.1 mole), pyrrolidine (156 g, 2.1 mole) and dry thiophene-free benzene (500 ml) was heated and stirred in a nitrogen atmosphere [7]. The water formed during the preparation of the enamine was collected in a calibrated moisture trap. Most of the benzene and excess pyrrolidine were removed at atmospheric pressure and the rest at the water pump. The flask containing the residual yellow oil was cooled to room temperature and ethyl iodide (187 g, 1.2 mole) was slowly added, causing a strong exothermic reaction. When stirring became difficult due to the thickness of the reaction mixture, absolute ethanol (125 ml) was added. After addition of the ethyl iodide was complete the mixture was heated under reflux overnight (under nitrogen).

The ethanol was removed at reduced pressure and the resulting crystalline mass was heated under reflux with water (200 ml) for 3 h. After cooling and separation of the oily phase, the aqueous phase was extracted twice with ether. The aqueous phase was then subjected to steam distillation; the distillate was saturated with sodium chloride and was extracted several times with ether. The oil and combined ether extracts were dried

* M.p.'s and b.p.'s are uncorrected. Infrared spectra were measured in chloroform solution with a Perkin Elmer Model 21 Spectrophotometer using sodium chloride optics.

ketones and their oximes.

Found			Oxime m.p. or b. p. (°C)	Empirical Formula	Analysis					
					Calc.			Found		
C	H	O			C	H	N	C	H	N
77.2	12.1	10.6	46—48	$C_{10}H_{19}ON$	71.0	11.3	8.3	70.8	11.2	8.0
79.6	10.7	9.7	100—103/0.2	$C_{11}H_{19}ON$	72.9	10.6	7.7	72.6	10.4	7.7
78.3	11.8	10.0	90—94/0.1	$C_{11}H_{21}ON$	72.1	11.6	7.6	71.7	11.1	7.7
78.7	12.2	9.1	48—49; 98—103/0.2	$C_{12}H_{23}ON$	73.0	11.8	7.1	73.0	11.6	7.0
78.4	12.0	9.2	80; 100—105/0.01	$C_{12}H_{23}ON$	73.0	11.8	7.1	72.7	11.7	7.0
82.9	8.9	7.8	149—150	$C_{14}H_{19}ON$	77.4	8.8	6.5	77.8	8.9	6.5
78.4	12.2	9.8	40—41; 85—88/0.05	$C_{11}H_{21}ON$	72.1	11.6	—	72.1	11.4	—
79.6	11.5	9.1	76—77	$C_{12}H_{21}ON$	73.8	10.8	7.2	73.6	10.6	7.1

(magnesium sulfate) and the ether was removed, leaving a brownish oil (140 ml) which when distilled through an efficient column [4] afforded 2-ethyl*cyclo*hexanone as a colorless oil, b. p. 88°/50 mm, n_D^{30} 1.4464 (71 g, 63 % based on unrecovered *cyclo*hexanone). Lit.[8] reports b. p. 67°/12 mm, n_D^{15} 1.4543.

*2-Allyl*cyclo*hexanone.* This ketone was similarly prepared from *cyclo*hexanone (49 g, 0.5 mole), pyrrolidine (71 g, 1 mole) in dry benzene (500 ml) and freshly distilled allyl bromide (73 g, 0.6 mole). Dry *n*-butanol was used instead of ethanol. The ketone had b. p. 90—98°/20 mm, n_D^{30} 1.4647 (42 g, 60 %). Lit.[9] reports b. p. 91—94°/12 mm.

*2-n-Butyl-2-methyl*cyclo*hexanone.* In a 1-liter 3-necked flask equipped with mechanical stirrer, reflux condenser and dropping funnel, a mixture of 2-methyl*cyclo*hexanone (56 g, 0.5 mole), dry toluene (500 ml) and sodium hydride (13.2 g, 0.55 mole) was heated and stirred under reflux for 15 h under nitrogen. The suspension of sodio-derivative was then cooled and *n*-butyl bromide (67.5 g, 0.5 mole) was added with stirring during 10 min and then heated under reflux for 2—3 h. After cooling to *ca.* 50°, the precipitated sodium bromide was removed by filtration and the salt was washed with two portions (50 ml) of dry ether. The solvents were removed at the water pump from the combined filtrates. The light yellow residue (*ca.* 90 ml) was distilled through an efficient column [4] affording 2-*n*-butyl-2-methyl*cyclo*hexanone, b. p. 96°/12 mm) n_D^{30} 1.4525 (52 g, 62 %) and 2,6-di-*n*-butyl-2-methyl*cyclo*hexanone, b. p. 144—145°/12 mm, n_D^{30} 1.4560 (9.0 g, 8 %). (Found: C 80.2; H 12.3; O 7.5. Calc. for $C_{15}H_{28}O$: C 80.3; H 12.6; O 7.1.)

The disubstituted ketone gave an orange 2,4-dinitrophenylhydrazone, m. p. 144—145° (from ethanol-ethyl acetate). (Found: C 58.5; H 6.9; N 16.6. Calc. for $C_{17}H_{24}O_4N_4$: C 58.6; H 6.9; N 16.1.) The trisubstituted ketone did not form the analogous derivative, presumably for steric reasons.

Other 2,2-disubstituted cyclo*hexanones.* These were prepared analogously employing the corresponding 2-substituted *cyclo*hexanone and alkyl bromide or iodide. The 2-ethyl-, 2-allyl- and 2-methyl-compounds served as starting materials except in the case of the preparation of 2-ethyl-2-phenyl*cyclo*hexanone, when 2-phenyl*cyclo*hexanone was alkylated as described above, with ethyl bromide. 2-Allyl-2-ethyl*cyclo*hexanone was prepared by alkylation of 2-allyl*cyclo*hexanone with ethyl iodide.

Oximes. The pyridine procedure was used. The ketone was heated under reflux with an equal weight of hydroxylamine hydrochloride in pyridine-absolute ethanol [5] for 3 h. The crystalline oximes were recrystallized from aqueous methanol and the liquid oximes were distilled in a high vacuum. They were obtained pure in at least 70 – 80 % yield.

The data pertinent to the ketones and oximes are summarized in Table 1.

ε,ε-Disubstituted caprolactams. It was found in this case that 85 % sulfuric acid and boron trifluoride [10] were inferior to polyphosphoric acid [6] as catalysts for Beckmann rearrangement of the oximes. The best experimental conditions found were the following.

In a 3-necked flask provided with a teflon-blade stirrer, calcium chloride tube and a flask with a connecting rubber sleeve containing phosphorus pentoxide (30 g) was placed orthophosphoric acid (85 %, 30 g). The solid pentoxide was added in small portions with vigorous stirring during 15 min. Its container was then replaced by a thermometer. The polyphosphoric acid thus prepared was heated in an oil bath to 100° and the oxime (2 g) was added, causing the temperature to rise to *ca.* 115° during the first minute after addition. When the temperature had dropped to 105°, the reaction mixture was heated to 115° and thus maintained for 10 min. After cooling to 90°, the slightly yellow mixture was poured on to cracked ice (150 g). The resulting turbid solution was cooled to −10° in an ice-salt bath and aqueous potassium hydroxide (40 %, 100 ml) was added dropwise with vigorous stirring, keeping the temperature below −5°. The pH was then *ca.* 6.5 and the lactam was readily extracted with chloroform-ethyl acetate (10:1; 150 ml + 100 ml). The bright yellow solution was dried (magnesium sulfate) under nitrogen in the refrigerator. A change of color to red indicates occurrence of polymerization. The solvents were removed at water pump pressure under nitrogen and the residual oil was dissolved in carbon tetrachloride in order to remove any insoluble polymer which may have formed. Removal of the solvent from the filtrate under nitrogen at water pump pressure usually affords a dark oil which can be further purified either by distillation of small portions (2 g) in a high vacuum or by chromatography. In the latter case a solution of the lactam in carbon tetrachloride is poured on to a column of florex-celite (5:1) with successive elution by carbon tetrachloride-benzene and chloroform. Analytically pure lactam is present in the chloroform fractions.

Table 2 records the data pertinent to the lactams.

Table 2. ε,ε-Disubstituted caprolactams.

Lactam	Yield	B. p. °C	B. p. mm	C=O I.R. ν(cm^{-1})	Emperical Formula	Analysis Calc. C	Calc. H	Calc. N	Found C	Found H	Found N
Et, Et	29	101 – 104	0.05	1 650	$C_{10}H_{19}ON$	71.0	11.3	8.3	71.6	11.0	7.9
Et, *n*-Bu	33	115 – 117	0.01	1 650	$C_{12}H_{23}ON$	73.0	11.8	7.1	72.3	11.3	7.3
Et, *i*-Bu	17	120 – 132	0.01	1 670	$C_{12}H_{23}ON$	73.0	11.8	7.1	72.8	11.6	7.2
Et, Ph	62	150 – 160	0.01	1 665	$C_{14}H_{19}ON$	77.4	8.8	6.5	77.0	8.6	6.4

6-Ethyl-6-phenyl-2-piperidone. This compound was prepared *via* the following reaction scheme:[11]

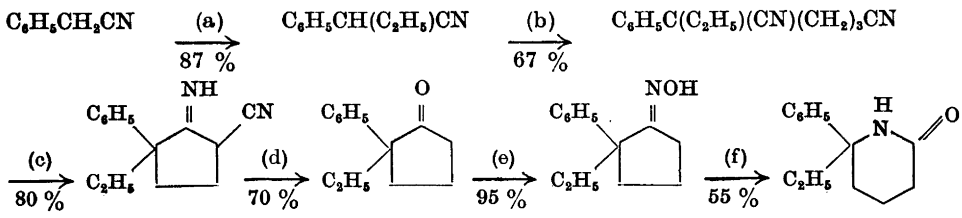

(a) The procedure was exactly analogous to the synthesis of the corresponding methyl derivative [11]. The product had b. p. 115—120°/12 mm.

(b) The alkylation was carried out with γ-iodobutyronitrile (b. p. 72—73°/0.5 mm, n_D^{30} 1.5180), prepared from the γ-bromocompound [11].

The product was obtained after a forerun (b. p. 70—134°/0.01 mm), as an oil, b. p. 135.5—138°/0.01 mm, n_D^{30} 1.5040. (Found: C 78.7; H 7.5. Calc. for $C_{14}H_{16}N_2$: C 79.2; H 7.6.)

(c) Cyclization was effected by means of sodamide in dry benzene [11]. The major portion of the crystalline imine had m. p. 122° but an additional small amount of light brown crystals from the mother liquor, m. p. 112—116°, was sufficiently pure for further work. (Found: C 78.7; H 7.5; N 12.9. Calc. for $C_{14}H_{16}N_2$: C 79.2; H 7.6; N 13.2.)

(d) Hydrolysis of the imine (12.1 g) was effected by heating under reflux with acetic acid (100 ml), concentrated sulfuric acid (6 ml) and water (6 ml) for 4 h [11]. After dilution with water (120 ml), extraction with benzene and distillation, 2-ethyl-2-phenyl*cyclo*pentanone was obtained as an oil (7.5 g), b. p. 79—81°/0.01 mm, n_D^{30} 1.5283.

(e) A mixture of the above ketone (6.8 g), hydroxylamine hydrochloride (5 g), pyridine (20 ml) and absolute ethanol (20 ml) was heated under reflux for 4 h. After the usual workup, the colorless crystalline oxime (7.0 g) was obtained, m. p. 84—85° (from aqueous methanol). (Found: C 76.6; H 8.2; N 6.7. Calc. for $C_{13}H_{17}ON$: C 76.8; H 8.4; N 6.9.)

(f) Beckmann rearrangement with polyphosphoric acid (see above) gave the desired pyridone as a slightly yellow unstable oil, b. p. 120—125°/0.1 mm. It was best stored in the refrigerator under nitrogen. (Found: C 76.1; H 7.8; N 6.3. Calc. for $C_{13}H_{17}ON$: C 76.8; H 8.4; N 6.9.)

Attempted preparation of 2,2-diethylcyclopentanone. (a) To a solution of 2-ethyl*cyclo*pentanone [12] (22.4 g) in dry carbon tetrachloride (100 ml) was added a solution of sulfuryl chloride (18 ml) in dry carbon tetrachloride (30 ml) during 1 h. Stirring was continued for an additional 2 h and then the mixture was kept in the dark overnight. The solvent was removed at water pump pressure and the desired 2-chloro-2-ethyl*cyclo*pentanone was obtained as a colorless oil (22 g, 73 %), b. p. 78—82/20 mm, n_D^{30} 1.4658, which soon turned yellow. It was used immediately after distillation.

(b) Diethyl cadmium was prepared in the usual way by treating ethyl magnesium bromide (from ethyl bromide (32.7 g, 0.3 mole), magnesium (6.1 g, 0.25 g.atom) in dry ether (200 ml)) with anhydrous cadmium chloride (23.8 g, 0.13 mole). To this solution was added during 10 min a solution of freshly distilled 2-chloro-2-ethyl*cyclo*pentanone (15.1 g) in dry ether (80 ml). After stirring for 10 min at 0°, the dark gray suspension appeared greenish-white. Stirring at ice-bath temperature was continued for an additional 2 h and then the mixture was stirred overnight at room temperature. It was finally heated under reflux for 1 h. Ammonium chloride solution (0.5 M, 100 ml) was added with stirring at 0° followed by hydrochloric acid (10 %, 50 ml). The yellow ether layer was separated and the aqueous phase was extracted with several portions of ether. The combined ether extracts were washed with saturated sodium bicarbonate solution and dried (magnesium sulfate). Distillation gave a mixture of the desired but impure 2,2-diethyl*cyclo*pentanone (66 g), b. p. 82—92°/20 mm, after a forerun of 2-ethyl-*cyclo*pent-2-enone (2.8 g), b. p. 74—82°/20 mm, and higher boiling material (6 g).

Each of the first two fractions was treated with 2,4-dinitrophenylhydrazine. Chromatography of the benzene solutions on basic alumina showed that the first fraction consists mainly of the unsaturated ketone, whose red 2,4-dinitrophenylhydrazone had m. p. 200° (from ethanol-ethyl acetate). (Found: C 53.6; H 4.6; N 19.2. Calc. for $C_{13}H_{14}O_4N_4$: C 53.8; H. 4.9; N. 19.3.) However, this was accompanied by an orange-red 2,4-dinitrophenylhydrazone which formed the main component in the mixture of hydrazones obtained from the second fraction. This was the derivative of 2,2-diethyl*cyclo*pentanone and had m. p. 205° (from ethanol-ethyl acetate). (Found: C 56.2; H 6.2; N 17.5. Calc. for $C_{15}H_{20}O_4N_4$: C 56.2; H 6.3; N 17.5.)

This procedure is therefore impractical for obtaining the pure disubstituted ketone as dehydrochlorination of the starting material accompanied the desired alkylation reaction.

REFERENCES

1. Pailer, M. and Allmer, I. *Monatsh.* **86** (1955) 824.
2. Ziegenbein, W., Schäffler, A. and Kaufhold, R. *Chem. Ber.* **88** (1955) 1906.
3. Stork, G., Terrell, R. and Szmuszkovicz, J. *J. Am. Chem. Soc.* **76** (1954) 2029.
4. Clauson-Kaas, N. and Limborg, F. *Acta Chem. Scand.* **8** (1954) 1579.
5. Shriner and Fuson, *Identification of Organic Compounds*, Wiley, New York, 1948, p. 202.
6. Horning, E. C. and Stromberg, V. L. *J. Am. Chem. Soc.* **74** (1952) 2680.
7. *Cf.* Ref.[3]
8. Conia, J. M. *Bull. soc. chim. France* **1950** 538.
9. Ref. 8, p. 539.
10. Hoffenberg, D. S. and Hauser, C. R. *J. Org. Chem.* **20** (1955) 1496.
11. Newman, M. S. and Closson, R. D. *J. Am. Chem. Soc.* **66** (1944) 1553.
12. Case, F. H. and Reid, E. E. *J. Am. Chem. Soc.* **50** (1928) 3062.

Received April 28, 1958.

ACTA CHEMICA SCANDINAVICA 12 (1958) 1411—1414

Fungus Pigments

IX.* Some Further Constituents of *Hydnum aurantiacum* Batsch

JARL GRIPENBERG

Department of Chemistry, Finland Institute of Technology, Helsingfors, Finland

Two further constituents of the fungus *Hydnum aurantiacum* Batsch have been isolated and identified as 1,2,4,5-tetrakis(benzoyloxy)-3,6-bis(*p*-hydroxyphenyl)benzene (dihydroaurantiacin dibenzoate) (II) and thelephoric acid.

The isolation of aurantiacin (I), the pigment of the fungus *Hydnum aurantiacum* Batsch has been described in a previous paper[1]. Another crystalline component has now been isolated from the same extract. This compound is colourless, and was finally shown to have the composition $C_{46}H_{30}O_{10}$, although it was at first difficult to get consistent analytical results owing to its great tendency to retain solvent of crystallisation. It was most conveniently recrystallised from dioxan which could be completely removed only by prolonged heating at 150°/0.01 mm.

When warmed with dilute alkali the compound dissolved and the solution eventually became dark brown. Acidification yielded a mixture of benzoic acid and atromentin. This together with the lack of colour indicated that the compound was a hydrogenated derivative of aurantiacin.

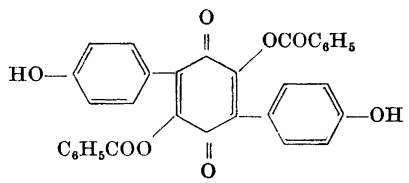

I

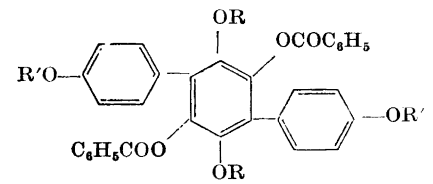

II R = COC_6H_5; R′ = H
III R = COC_6H_5; R′ = $COCH_3$
IV R = R′ = $COCH_3$
V R = R′ = H

* Part VIII, *Acta Chem. Scand.* 12 (1958) 603.

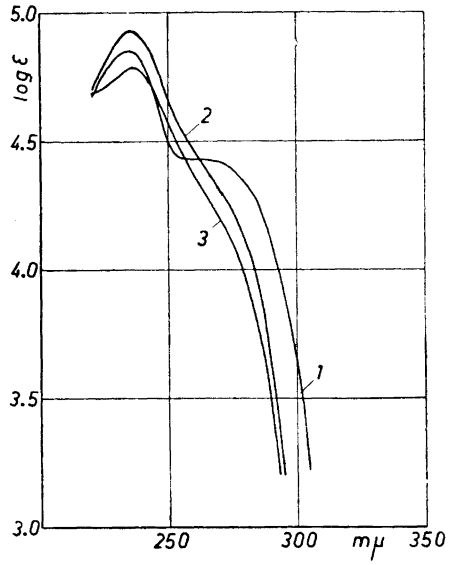

Fig. 1. Absorption spectra of: *1.* 1,2,4,5-Tetrakis(benzoyloxy)-3,6-bis(*p*-hydroxyphenyl)benzene (II) (in dioxan), *2.* 1,2,4,5-Tetrakis(benzoyloxy)-3,6-bis(*p*-acetoxyphenyl)benzene (III) (in dioxan) and *3.* aurantiacin leuco-acetate (IV) (in alcohol).

The composition $C_{46}H_{30}O_{10}$ corresponds to a dibenzoate of dihydro-aurantiacin. That the compound has free phenolic hydroxyl groups can be seen from the UV and IR spectra. The former (Fig. 1; curve. 1) has a strong inflexion at 270 mμ and the latter a strong peak at 3 420 cm^{-1}; both disappear on acetylation. The UV spetrum of the diacetate thus obtained (Fig. 1; curve. 2) is very close to that of aurantiacin leuco-acetate [1] (IV) (Fig. 1; curve 3).

The compound $C_{46}H_{30}O_{10}$ is very stable, but dihydroaurantiacin (V), prepared from aurantiacin by catalytic hydrogenation shows a great tendency to revert to aurantiacin by aerial oxidation. This indicates that the compound $C_{46}H_{30}O_{10}$ has no hydroquinone grouping. It should therefore be II (assuming that the two benzoyl groups are symmetrically situated). This view was confirmed by synthesis of III from aurantiacin diacetate by hydrogenation followed by benzoylation. This was identical with the acetate of the compound $C_{46}H_{30}O_{10}$ referred to above.

The presence of this leucobenzoate of aurantiacin together with aurantiacin recalls the simultaneous occurrence of leucomelone and its leucoacetate in *Polyporus leucomelas* Pers. ex Fries [2]. There are also a number of cases known where a quinone occurs in fungi together with the corresponding hydroquinone, sometimes forming a quinhydrone [3-5]. It is possible that the occurrence of the dihydroderivative either free or acylated, together with the corresponding quinone is more common than is usually appreciated because the dihydroderivatives which are usually colourless are easily overlooked.

Extraction of the ether-extracted fungus material with acetone gave a small amount of thelephoric acid. The occurrence of thelephoric acid is by no means surprising, since its presence in a number of *Hydnum* species has been reported before [6,7].

EXPERIMENTAL

(The analyses were carried out by Dr. A. Bernhardt, Mülheim, and the IR spectra were taken by Mr. B. C. Fogelberg, AB Centrallaboratorium, Helsingfors.)

*Isolation of 1,2,4,5-tetrakis (benzoyloxy)-3,6-bis (*p*-hydroxyphenyl)benzene* (II). The mother liquor from which aurantiacin had been filtered off [1] was evaporated under vacuum. The residue was extracted with benzene and then with a small amount of acetone. The grey insoluble powder was repeatedly recrystallised from dioxan giving 1,2,4,5-tetrakis(benzoyloxy)-3,6-(*p*-hydroxyphenyl)benzene as clusters of colourless needles, m. p. 305—307°. (Found: C 74.47; H 4.07; O 21.83. $C_{46}H_{30}O_{10}$ requires C 74.38; H 4.07; O 21.55 %.) The benzene and acetone solutions were evaporated to dryness under vacuum and repeated treatment with benzene and acetone gave further amounts of the same compound.

Further amounts of the compound were obtained by purification of aurantiacin by chromatography [1]. It was obtained by evaporation of the fraction just preceding aurantiacin. It was slightly contaminated with aurantiacin which could be removed by crystallisation from dioxan.

*Hydrolysis of 1,2,4,5-tetrakis (benzoyloxy)-3,6-bis (*p*-hydroxyphenyl)benzene.* The compound (30 mg) on warming with 2 N sodium hydroxide (5 ml) for a few minutes dissolved completely. The dark brown solution was acidified and extracted with ether. The ether was evaporated and the residue extracted with a little benzene. Evaporation of the benzene solution gave benzoic acid (12 mg) identified by mixed m. p. The dark brown benzene-insoluble material was acetylated with acetic anhydride and pyridine giving yellow needles, m. p. 242—244°/290—295°, unchanged by admixture of atromentin tetra-acetate.

*1,2,4,5-Tetrakis (benzoyloxy)-3,6-bis (*p*-acetoxyphenyl)benzene* (III) a). From 1,2,4,5-tetrakis(benzoyloxy)-3,6-bis(*p*-hydroxyphenyl)benzene. The compound was suspended in acetic anhydride, a drop of pyridine was added and the mixture was warmed to give a clear solution. On cooling the acetate crystallised out and was recrystallised from dioxan giving glass-like crystals which turned opaque on standing in air, m. p. 317—321°. (Found C 72.66; H 4.29; O 22.89. $C_{50}H_{34}O_{12}$ requires C 72.63; H 4.15; O 23.22 %.)

b) From aurantiacin. Aurantiacin diacetate [1] (220 mg) was suspended in alcohol and hydrogenated over PtO_2 catalyst. The originally yellow crystals turned slowly colourless, without ever completely dissolving. The consumption of hydrogen was about 10 ml (theor. 8 ml). The crystals and the catalyst were filtered off and the crystals were dissolved in pyridine. Excess of benzoyl chloride was added and the mixture allowed to stand for three days. It was then poured into water giving a colourless precipitate. Ether was added to the suspension and the precipitate was then filtered off and recrystallised from dioxan. The crystals were identical in appearance with those obtained according to b), m. p. 320—324°, mixed m. p. undepressed. The IR spectra of the two preparations were identical

Dihydroaurantiacin (V). Aurantiacin (50 mg) was hydrogenated over a prereduced Adams catalyst in dioxan. The uptake of hydrogen was 2.1 ml (theor: 2.1 ml) and the solution turned colourless. It was evaporated under vacuum at room temperature to give slightly yellow crystals of dihydroaurantiacin, m. p. 310—312°. On attempted recrystallisation from dioxan they turned much darker in colour, apparently re-oxidising to aurantiacin. The substance was not analysed.

Isolation of thelephoric acid. The ether extracted fungus material was further extracted with acetone in a Soxhlet apparatus giving a violet-red solution in which a small amount of grey precipitate formed during the extraction. This was removed and the solution allowed to stand. A dark blue precipitate gradually formed, which was almost insoluble in all organic solvents except pyridine in which it dissolved with a wine-red colour. Dilution with water gave a blue solution, from which a blue precipitate slowly formed. This had no m. p. but gradually decomposed above 350°. Acetylation with acetic anhydride and pyridine gave an orange-red acetate, which was recrystallised from dimethyl

succinate m. p. 330—335° (decomp.). Reductive acetylation with zinc, acetic anhydride and pyridine gave a colourless leuco-acetate, after recrystallisation from nitrobenzene m. p. 370—380° (decomp.). All these properties agree well with those given for thelephoric acid [7-9].

This investigation has been supported by a grant from *Statens Naturvetenskapliga Kommission*, which is gratefully acknowledged.

REFERENCES

1. Gripenberg, J. *Acta Chem. Scand.* **10** (1956) 1111.
2. Akagi, M. *J. Pharm. Soc. Japan* **62** (1942) 129; *Chem. Abstracts* **45** (1951) 2898.
3. Anslow, W. K. and Raistrick, H. *Biochem. J.* **32** (1938) 687.
4. Engel, B. G. and Brzeski, W. *Helv. Chim. Acta* **30** (1947) 1472.
5. Brian, P. W., Curtis, P. J., Howland, S. R., Jeffrys, E. G. and Raudnitz, H. *Experientia* **7** (1951) 266.
6. Zellner, J. *Monatsh.* **36** (1915) 611.
7. Sawada, M. *J. Japan. Forestry Soc.* **34** (1952) 110; *Chem. Abstracts* **47** (1953) 4436.
8. Kögl, F., Erxleben, H. and Jänecke, L. *Ann.* **482** (1930) 105.
9. Asahina, Y. and Shibata, S. *Ber.* **72** (1939) 1531.

Received April 24, 1958.

ACTA CHEMICA SCANDINAVICA 12 (1958) 1415—1426

An X-Ray Study on the System Cu-S

SEVED DJURLE

Institute of Chemistry, University of Uppsala, Uppsala, Sweden

The phase relations in the system Cu—S have been investigated by X-ray diffraction methods. Phases of the following (approximate) compositions were found to exist:

Cu_2S, $Cu_{1.96}$ S, $Cu_{1.8}$ S and CuS.

All of these phases except CuS undergo one or more transitions at higher temperatures. Each ultimately transforms into a face-centred cubic phase which probably exists at least over the composition range Cu_2S to $Cu_{1.8}S$.

The previously unknown sulphide $Cu_{1.96}S$ seems to be low-symmetric at room temperature. A high-temperature modification of this sulphide is tetragonal and can be preserved as a metastable phase at room temperature, where its body-centred unit cell has the dimensions:

$a = 4.008$ Å, $c = 11.268$ Å.

The low-temperature modification of $Cu_{1.8}$ S is the only phase with a homogeneity range. The range seems to extend at least from the composition $Cu_{1.80}S$ to $Cu_{1.73}S$.

The following sulphides of copper are known as minerals: Cu_2S (chalcocite), $Cu_{1.8}S$ (digenite), CuS (covellite).

The binary system Cu-S has been the object of several studies. References to the earlier investigations are found in the bibliography of Haughton and Prince [1]. Different controversial opinions about the system have been put forward.

Buerger [2,3] studied the system Cu_2S—CuS with a controlled-temperature camera and found the compound $Cu_{1.8}S$, in addition to the earlier known Cu_2S and CuS. According to Buerger, $Cu_{1.8}S$ below approximately 78°C should have the ideal composition Cu_9S_5, and above 78°C have a range of homogeneity with both sulphur excess and sulphur deficit. Concerning Cu_2S, Buerger states that above 105°C it has a hexagonal basic structure and below 105°C an orthorhombic superstructure. The relations between the unit cells of the modifications and their probable space groups are given. According to Buerger the superstructure phase is capable of dissolving sulphur up to eight atomic per cent CuS, while the basic structure dissolves only up to two atomic per cent CuS.

Rühl [4] has also studied the system Cu_2S—CuS with a high-temperature camera. Contrary to Buerger, he found that $Cu_{1.8}S$ at room temperature has the homogeneity range $Cu_{1.81}S$—$Cu_{1.77}S$, and that at higher temperatures, the solid solution region is very much broadened, but only towards the copper side. He observed that the diffraction pattern of $Cu_{1.8}S$ at room temperature and up to about 75°C had superstructure lines. The phase in equilibrium with $Cu_{1.8}S$ was not Cu_2S, but a phase whose diffraction pattern had the strongest lines in places similar to Cu_2S. He thought it probable that Cu_2S had a small range of homogeneity (up to two atomic per cent CuS).

Jensen [5] has studied Cu_2S by differential thermal analysis and found a maximum melting temperature of 1 129°C for the composition $Cu_{1.989}S$. He could not observe the limits of solubility of sulphur in Cu_2S, nor any transformations in the solid state between 404°C and the melting points in the composition range 77.00 to 82.00 weight per cent copper.

Hirahara [6] has determined several physical properties of Cu_2S as a function of temperature and found two transition points, the lower one at about 110°C and the upper one at about 470°C.

X-Ray and thermal studies on the phase transitions of Cu_2S, performed by Ueda [7], gave results in good agreement with those of Hirahara. For the modification of Cu_2S above 470°C, Ueda could observe only two diffraction lines. He pointed out the similarity of the places of the lines with the strongest ones of high-temperature $Cu_{1.8}S$.

Further contributions to the knowledge of the electrical conductivity of the copper sulphides, together with X-ray work, has been given by Kamaigaichi [8].

Attempts to solve the structure of hexagonal Cu_2S have been made by Ueda [7], using powder data, and also by Belov and Butuzov [9]. The last two used the single crystal data given by Buerger and Buerger [10]. It seems to the present author that none of them has come to any quite satisfactory agreement between observed and calculated intensities, and hence the structure determination cannot be regarded as settled. For CuS, the structure has been determined by Oftedal [11], and later confirmed by Berry [12].

EXPERIMENTAL

Finely powdered Cu (electrolytically precipitated, E. Merck, Darmstadt) and S (sublimated sulphur, T. Schuchardt, Goerlitz) of better than 99.9 % purity were used as starting materials.

Samples were prepared by carefully mixing weighed amounts of the elements, pressing the mixtures to pellets at a pressure of up to 16 ton/cm² and sintering in evacuated Supremax or silica tubes at a temperature of 320 or 470°C. The heating time varied between 1 and 7 days. The samples were either quenched in cold water from the sintering temperature or allowed to cool slowly, within 24 h, in the furnace.

Visual examination or X-ray analysis indicated that some samples were heterogeneous after this treatment. They were then finely powdered, pressed into pellets and annealed in evacuated tubes for times up to 1 month.

No signs of contamination of the samples from the Supremax or silica tubes were detected.

In order to see if the preparation technique was satisfactory, selected samples were chemically analyzed. The sample was dissolved in fuming HNO_3 and the solution was evaporated to dryness on a steam bath. HNO_3 was removed by repeated evaporations

with HCl, and then the sample was diluted to 100 ml. SO_4 and Cu were determined in aliquote parts, the former gravimetrically as $BaSO_4$ and the latter by titration with 0.01 M EDTA with murexide as an indicator. The composition, calculated from the weighed amounts of the elements, was in good agreement with the chemical analysis. The deviation amounted to 0.5 weight per cent for copper and 0.2 weight per cent for sulphur.

The samples were investigated by taking X-ray powder photographs in Guinier type focusing cameras with quartsmonochromatized Cu-$K\alpha$ radiation (sometimes with Cr-$K\alpha$ radiation). KCl or CaF_2 were used as internal standards. The following constants of wavelengths and standards were used:

Cu$K\alpha$ = 1.5418 Å	$a_{KCl}21°$ = 6.29215 Å
Cr$K\alpha$ = 2.2909 Å	$a_{CaF_2}21°$ = 5.46300 Å

In order to investigate samples at higher temperatures in most cases from room temperature up to 500°C, X-ray measurements were made with an one-sided Debye-Scherrer heating camera of 4.55 cm film radius, registering reflexions between 2Θ = 26.456° and 2Θ = 157.15°. The radiation used was Cu-$K\alpha$ filtered with a Ni-foil. The camera and the X-ray technique used has been described by Fischmeister [13]. The thermocuple of the camera was calibrated against known melting points [14].

The temperature fluctuation limits were:

± 2°C below	300°C
± 3°C between	300°C and 400°C
± 4°C above	400°C

The samples, in the form of very fine powder, were mounted in thin-walled capillary tubes. The tubes used were of Pyrex glass, had an outside diameter of about 0.3 mm and walls about 0.01 mm thick. The capillaries were either sealed after evacuation to prevent decomposition of the samples when heated, or continually evacuated through the camera. In order to be sure that no abnormal changes took place during heating, room temperature powder patterns before and after the heat treatment were included in each run.

RESULTS

The present study has revealed the existence of several previously unknown phases in the system Cu—S. Table 1 summarizes the result of the analysis with the high-temperature camera. The modifications have been labelled with Roman numerals (I for the one which exists above the highest transition temperature). As will be shown later, all the I-modifications probably belong to the same high-temperature phase.

The approximate composition of the phases which could be preserved at room temperature was determined by means of Guinier photographs. The X-ray analyses showed that many of the samples were not in equilibrium. In spite of different heat treatment, this could often not be completely remedied. The result of the phase analysis of two groups of samples, one annealed at 400°C and the other at 75°C during one month is summarized in Table 2, in which the denomination of the phases is the one arrived at after the high-temperature studies had been made.

Data from powder photographs of the different phases are collected in Table 3. The crystallographic results are discussed in the following.

Table 1. The sulphides of copper.

Compound	Approximate range of existence *	Crystal system
Cu_2S III	<110°C	Orthorhombic
Cu_2S II	110°C–470°C	Hexagonal
Cu_2S I	>470°C	Cubic F.C.
$Cu_{1.96}S$ III	<100°C	"Low-symmetric"
$Cu_{1.96}S$ II	Metastable?	Tetragonal
$Cu_{1.96}S$ I	>100°C	Cubic F.C.
$Cu_{1.8}S$ II	<78°C	
$Cu_{1.8}S$ I	>78°C	Cubic F.C.
CuS	<500°C	Hexagonal

* Range of investigation 20–500°C.

Table 2. Results of the phase analysis of two groups of copper sulphide samples.

Composition of the samples	Temperature of annealing before quenching	
	400°C	75°C
	Phases observed *	Phases observed *
$Cu_{1.00}S$	CuS	
1.50	» + $Cu_{1.8}$SII	
1.63	$Cu_{1.8}$SII + (CuS)	
1.70	»	
1.74	»	
1.78	»	$Cu_{1.8}$SII
1.80	»	»
1.82	» + ($Cu_{1.96}$SIII)	»
1.84	» + ($Cu_{1.96}$SII) + ($Cu_{1.96}$SIII)	» + ($Cu_{1.96}$SIII)
1.86	» + (») + ((»))	» + (»)
1.88	$Cu_{1.96}$SII + $Cu_{1.8}$SII + ((»))	$Cu_{1.96}$SIII + $Cu_{1.8}$SII
1.90	» + » + ((»))	» + (») + (($Cu_{1.96}$SII))
1.92	» + (») + (»)	» + (») + ((»))
1.94	» + ($Cu_{1.96}$SIII) + (($Cu_{1.8}$SII))	» + (») + ((»))
1.95	» + (») ((»))	
1.96	» + (»)	$Cu_{1.96}$SIII + (($Cu_{1.96}$SII))
1.97	» + (») + ((Cu_2SIII))	
1.98	Cu_2SIII + ($Cu_{1.96}$SII) + (($Cu_{1.96}$SIII))	Cu_2SIII + ($Cu_{1.96}$SIII) + (($CuSII_{1.96}$))
1.99	» + (»)	» + (») + ((»))
2.00	»	»
2.03	»	
2.13	» + (Cu)	

* No parenthesis = large amount, one parenthesis = small amount, two parentheses = trace amount.

The phases occurring at the composition Cu_2S

The high temperature X-ray analysis has revealed two transitions. The lower one takes place gradually at about 110°C in agreement with data published earlier [3,6], and the upper one occurs at 465 to 475°C, in agreement with the temperature reported by Hirahara [6].

Cu_2S III

Minerals of chalcocite (gratefully received from the Institute of Mineralogy and Geology in Uppsala) were examined by means of powder photographs, and a single crystal was selected from a sample giving the same diffraction lines as synthetic samples. The Weissenberg photographs gave an A-centred orthorhombic cell, and after indexing the powder photograph the cell dimensions were determined as:

$$a = 11.881 \pm 0.004 \text{ Å}, \qquad b = 27.323 \pm 0.008 \text{ Å},$$
$$c = 13.491 \pm 0.004 \text{ Å}.$$

The result is in good agreement with the works of Ueda [7], Buerger and Buerger [10] and Oftedal [11]. Buerger and Buerger give the lattice parameters:

$$a = 11.90 \text{ Å}, \qquad b = 27.28 \text{ Å}, \qquad c = 13.41 \text{ Å}$$

with an accuracy of about 1 %.

The method of Ueda to determine the c-axis from rotation photographs and the a- and b-axis from the reflexions |6.0.0| and |3.4.6.| is unsatisfactory, since with Cu-radiation the reflexion |6.0.0| cannot be separated from |3.12.0| and |3.4.6| is inseparable from |0.8.6|.

Cu_2S II

The powder photographs of Cu_2S II could be indexed with a hexagonal unit cell. The dimensions at different temperatures are:

152°	$a = 3.961$	$c = 6.722$		$c/c = 1.697$
300°	$a = 3.981$	$c = 6.761$		$c/a = 1.698$
460°	$a = 4.005$	$c = 6.806$		$c/a = 1.699$

± 0.004 Å $\qquad \pm 0.007$ Å

This is in fairly good agreement with the value of B. and B.[10], $a = 3.89$ Å, $c = 6.68$ Å, $c/a = 1.717$ at 112°C (accuracy 1 %) and the diagram of Ueda [7] (his Fig. 4).

Cu_2S I

The powder photograph of this modification has been indexed as the pattern of a face-centred cubic lattice with the cell edge at

465°C	$a = 5.725$	± 0.010 Å
500°C	$a = 5.735$	

A cell content of 4 Cu_2S is consistent with the cube edge.

The phases occurring around the composition $Cu_{1.96}S$

The photographs of samples of this composition have revealed that three modifications exist.

$Cu_{1.96}S$ III is stable up to at least 75°C and $Cu_{1.96}S$ II is a high temperature modification, metastable at room temperature. When heating pure $Cu_{1.96}S$ III in the high temperature camera it begins at about 100°C to transform slowly into $Cu_{1.96}S$ I. The transition from $Cu_{1.96}S$ III to $Cu_{1.96}S$ II has not been observed.

$Cu_{1.96}S$ II is formed together with $Cu_{1.96}S$ III when quenching samples of the right composition from above a temperature of at least 320°C. From Table 2 it seems that $Cu_{1.96}S$ II is metastable at room temperature and up to at least 75°C. In the high-temperature camera, its powder pattern can only be observed below 150°C. Owing to the sluggish transitions, the patterns taken in the high temperature camera probably do not correspond to equilibrium.

$Cu_{1.96}S$ III

The diffraction pattern of this phase has not been indexed. Its complexity indicates a low symmetry.

$Cu_{1.96}S$ II

The Guinier photograph, taken at room temperature corresponds to a primitive tetragonal lattice with a cell content of 4 $Cu_{1.96}S$ and with the dimensions:

$$a = 4.008 \pm 0.002 \text{ Å}$$
$$c = 11.268 \pm 0.006 \text{ Å}.$$

$Cu_{1.96}S$ I

This modification is cubic, and has a face-centred unit lattice with the cube edge $a = 5.707 \pm 0.006$ Å at 500°C and a cell content of 4 $Cu_{1.96}S$. The unit cells of $Cu_{1.96}S$ II and $Cu_{1.96}S$ I have the following relations:

$$a_{II} \approx 1/\sqrt{2} \times a_I; \qquad c_{II} \approx 2 \times a_I$$

The phases occurring around the composition $Cu_{1.8}S$

The high temperature investigation has established a transition at 78°C in agreement with the work of Rühl [4].

$Cu_{1.8}S$ II

The Guinier powder photographs of four samples with the composition $Cu_{1.82}S$, $Cu_{1.78}S$, $Cu_{1.74}S$ and $Cu_{1.70}S$ are listed in Table 3. It appears that line displacements occur for variation in the composition. As the displacements are regular and the lines, except for some very weak ones, can be followed through the series of samples, it seems that the most probable interpretation

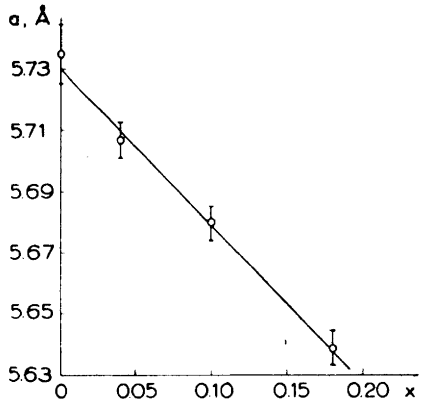

Fig. 1. Cube edge of $Cu_{2-x}S$ at 500°C as a function of x.

of the data implies the existence of a single phase, called $Cu_{1.8}S$ II, having a homogeneity range. The range extends surely from $Cu_{1.80}S$ to $Cu_{1.73}S$, and possibly from $Cu_{1.82}S$ to $Cu_{1.70}S$. The uncertainty is due to possible errors in the measurements.

Attempts to find a common indexing of the four photographs of $Cu_{1.8}S$ II have not been successful. However, most of the strongest lines of the photographs seem to correspond to a face-centred cubic basic lattice. The basic cube edge for the various compositions are:

$Cu_{1.82}S$	$Cu_{1.78}S$	$Cu_{1.74}S$	$Cu_{1.70}S$
$a = 5.570$	$a = 5.564$	$a = 5.556$	$a = 5.551 \pm 0.003$ Å

The displacements of most of the other lines when the composition is varied shows, however, that the real lattice cannot be cubic.

$Cu_{1.8}S$ I

The unit cell of this modification is face-centred cubic and is evidently closely related to the basic cell of $Cu_{1.8}S$ II. At the composition $Cu_{1.82}S$, it has the following cell constants,

at	80°C	$a = 5.577$	± 0.006 Å
	152°C	$a = 5.593$	
	300°C	$a = 5.610$	
	500°C	$a = 5.639$	

A cell content of 4 $Cu_{1.8}S$ is compatible with the cube edge.

Table 3. X-Ray diffraction data of the phases Cu_2S, $Cu_{1.96}S$ and $Cu_{1.8}S$.

Cu_2S III 20°C Cr-*Ka*

hkl	*I*rel	$\sin^2\theta$ Obs.	$\sin^2\theta$ Calc.	*hkl*	*I*rel	$\sin^2\theta$ Obs.	$\sin^2\theta$ Calc.
111	vw	0.0181	0.0183	373			0.2347
131	w	0.0319	0.0323	235	w	0.2337	0.2332
231	w	0.0604	0.0602	155			0.2335
151			0.0604	471	m	0.2419	0.2420
240	vw	0.0648	0.0653	2.10.2			0.2418
013	vw	0.0675	0.0666	480			0.2612
222	w	0.0728	0.0730	502	m	0.2611	0.2612
251	w	0.0882	0.0883	255			0.2613
133	vw	0.0899	0.0900	404	vw	0.2639	0.2641
062	w	0.0920	0.0921	315			0.2656
242	m	0.0940	0.0941	075	vw	0.2667	0.2664
162	m	0.1013	0.1014	026			0.2666
053	vw	0.1082	0.1088	522	m	0.2690	0.2682
080	vw	0.1123	0.1125	106			0.2688
233	w	0.1179	0.1179	126	w	0.2758	0.2759
153			0.1181	1.11.3	vw	0.2874	0.2868
322	m	0.1193	0.1195	046			0.2877
024	m	0.1223	0.1224	444	w	0.2924	0.2922
262	m	0.1292	0.1293	533	vw	0.3133	0.3131
351	vw	0.1347	0.1348	2.12.2	w	0.3192	0.3191
342	m	0.1404	0.1406	562	w	0.3247	0.3245
280	w	0.1496	0.1497	246			0.3248
400			0.1487	464	w	0.3274	0.3273
182	m	0.1505	0.1506	415	vw	0.3308	0.3307
204	m	0.1526	0.1525	195	vw	0.3322	0.3319
144			0.1528	166			0.3321
411	m	0.1576	0.1577	600	m	0.3346	0.3346
173	w	0.1597	0.1603	3.12.0	st	0.3368	0.3367
224			0.1596	553	vw	0.3415	0.3412
333	w	0.1645	0.1644	580	m	0.3447	0.3448
431	m	0.1716	0.1717	435			0.3447
362	m	0.1757	0.1758	306			0.3432
440	m	0.1768	0.1768	631	vw	0.3571	0.3576
244	w	0.1803	0.1806	493			0.3560
422	m	0.1847	0.1846	266	w	0.3598	0.3600
291	w	0.1879	0.1868	3.12.2	w	0.3653	0.3656
164			0.1879	117			0.3643
115	m	0.1912	0.1913	346	st	0.3714	0.3713
353			0.1925	086			0.3720
451	w	0.1998	0.1999	582	w	0.3734	0.3737
0.10.2	m	0.2046	0.2046	455			0.3729
442	m	0.2055	0.2057	137	vw	0.3783	0.3784
135			0.2053	651	vw	0.3858	0.3858
1.10 2	m	0.2139	0.2139	366	w	0.4060	0.4065
413	m	0.2154	0.2154	237			0.4062
193			0.2165	157			0.4065
215	w	0.2194	0.2192	2.12.4			0.4056
344	st	0.2272	0.2271	2.14.2	w	0.4106	0.4105
084	st	0.2280	0.2278	564			0.4110
433	w	0.2293	0.2294	633	w	0.4140	0.4153
				475			0.4151
				515			0.4144

Cu_2S III 20°C Cr-Kα

hkl	*I*rel	$\sin^2\Theta$ Obs.	$\sin^2\Theta$ Calc.
4.11.3	w	0.4263	0.4263
257	vw	0.4340	0.4344
0.10.6			0.4353
593	w	0.4396	0.4396
4.10.4			0.4398
317			0.4387
077			0.4394
653	vw	0.4438	0.4434
3.13.3	vw	0.4447	0.4456
177	w	0.4497	0.4487
604			0.4499
3.12.4	w	0.4519	0.4521
624	vw	0.4565	0.4570
555			0.4565
584	w	0.4612	0.4602
008			0.4614
1.15.3	w	0.4690	0.4696
1.14.4			0.4691
028			0.4684
466			0.4715
682	w	0.4756	0.4759
0.16.2	w	0.4786	0.4788
277			0.4765
128			0.4777
722	w	0.4903	0.4913
048			0.4895

$Cu_{1.96}S$ III 20°C Cu-Kα

$\sin^2\Theta$ Obs.	I_{rel}	$\sin^2\Theta$ Obs.	I_{rel}
0.0323	w	0.0906	w
0.0392	w	0.0936	w
0.0422	m	0.0968	w
0.0462	w	0.1017	w
0.0519	m	0.1040	st
0.0553	w	0.1106	w
0.0583	w	0.1131	w
0.0617	w	0.1157	w
0.0644	w	0.1292	w
0.0655	w	0.1336	w
0.0676	w	0.1385	w
0.0687	w	0.1416	w
0.0710	w	0.1539	m
0.0714	w	0.1550	m
0.0723	w	0.1697	st
0.0740	w	0.1771	w
0.0750	w	0.2077	m
0.0765	w	0.2102	w
0.0821	w	0.2591	w
0.0843	w	0.3659	m
0.0878	w	0.4732	w

$Cu_{1.96}S$ II 20°C Cu-Kα

hkl	I_{rel}	$\sin^2\Theta$ Obs.	$\sin^2\Theta$ Calc.
101	w	0.0419	0.0417
003			0.0421
102	w	0.0559	0.0557
110	w	0.0741	0.0740
004	vw	0.0750	0.0749
103	st	0.0789	0.0791
111			0.0789
194	st	0.1117	0.1119
113	w	0.1161	0.1161
200	m	0.1486	0.1480
114			0.1489
201	m	0.1529	0.1527
202	w	0.1666	0.1667
203	w	0.1900	0.1901
211			0.1898
212	w+	0.2037	0.2037
106	vw	0.2055	0.2055
213	w	0.2273	0.2271
214	vw	0.2598	0.2599
107	w	0.2664	0.2663
215	m	0.3014	0.3020
221			0.3007
108	w	0.3368	0.3365
301			0.3377
223			0.3381
312	w	0.3888	0.3887
217	w	0.4143	0.4143

Cu_2S II 460°C Cu-Kα

hkl	I_{rel}	$\sin^2\Theta$ Obs.	$\sin^2\Theta$ Calc.
102	m	0.1004	0.1007
110	st	0.1481	0.1482
103	st	0.1651	0.1649
112	w	0.1992	0.1995
201	vw	0.2109	0.2104

Cu_2S I 500°C Cu-Kα

hkl	I_{rel}	$\sin^2\Theta$ obs.	$\sin^2\Theta$ Calc.
111	w	0.0544	0.0542
200	w+	0.0722	0.0723
220	st	0.1445	0.1446
311	m	0.1991	0.1988

Phase $Cu_{1.8}S$ II 20°C Cu-$K\alpha$

hkl	Composition							
	$Cu_{1.82}S$		$Cu_{1.78}S$		$Cu_{1.74}S$		$Cu_{1.70}S$	
	$\sin^2\Theta$ Obs.	I_{rel}	$\sin^2\Theta$ Obs.	I_{rel}	$\sin^2\Theta$ Obs.	I_{rel}	$\sin^2\Theta$ Obs.	I_{rel}
	0.0512	vw	0.0515	vw			0.0516	vw
	0.0528	w	0.0527	vw	0.0528	vw	0.0526	vw
							0.0557	vw
111	0.0576	m+	0.0576	m+	0.0578	m	0.0579	m
	0.0656	m	0.0652	m	0.0647	w	0.0643	w
200	0.0767	m+	0.0769	m+	0.0770	m	0.0771	m
	0.0784	vw	0.0794	vw			0.0828	vw
	0.0909	w	0.0919	vw	0.0929	vw	0.0949	vw
	0.1084	w	0.1070				0.1020	vw
							0.1172	vw
	0.1291	m	0.1284	m	0.1273	w	0.1257	w
					0.1297	vw	0.1303	vw
					0.1358	vw	0.1368	vw
220	0.1530	st	0.1536	st	0.1539	st	0.1543	st
	0.1802	vw	0.1791	vw			0.1760	vw
	0.1930	w	0.1918	w	0.1897	w	0.1876	w
							0.1914	vw
	0.2058	vw	0.2060	vw			0.2058	vw
311	0.2109	m	0.2113	m	0.2117	m	0.2124	m
222	0.2297	w	0.2301	w	0.2304	vw	0.2310	w
	0.2440	vw	0.2460	vw				
	0.2825	w	0.2817	w	0.2812	vw	0.2799	vw
400	0.3065	w	0.3071	w+	0.3081	w	0.3088	w
	0.3464	w	0.3455	w	0.3441	vw	0.3420	vw
	0.3592	vw	0.3598	vw			0.3604	vw
	0.3640	vw	0.3640	vw			0.3670	vw
	0.3716	vw	0.3721	vw			0.3730	vw
	0.3980	vw	0.3979	vw	0.3993	vw	0.4037	vw
	0.4106	vw	0.4094	vw				
	0.4352	vw	0.4348	vw			0.4347	vw
422	0.4597	m	0.4605	m	0.4623	m	0.4632	m

$Cu_{1.8}S$ I 500°C Cu-$K\alpha$

Composition $Cu_{1.82}S$.			
hkl	I_{rel}	$\sin^2\Theta$ Obs.	$\sin^2\Theta$ Calc.
111	m−	0.0561	0.0561
200	m	0.0748	0.0748
220	st	0.1496	0.1495
311	w+	0.2057	0.2056
222	vw		
400	w	0.2984	0.2990
422	vw	0.4489	0.4486
511	vw	0.5048	0.5046
333			

$Cu_{1.96}S$ I 500°C Cu-$K\alpha$

hkl	I_{rel}	$\sin^2\Theta$ Obs.	$\sin^2\Theta$ Calc.
111	w	0.0548	0.0547
200	m	0.0729	0.0729
220	st	0.1459	0.1460
311	m	0.2005	0.2007

vw = strong
m = medium
w = weak
vw = very weak

The phase CuS

The powder photograph of this phase gave, for the hexagonal unit cell, the dimensions:

$$a = 3.794 \pm 0.003 \text{ Å}$$
$$c = 16.332 \pm 0.010 \text{ Å}$$

in close agreement with the values of Oftedal [11] and Berry [12]

$$\left.\begin{matrix} a = 3.80 \text{ Å} \\ c = 16.4 \text{ Å} \end{matrix}\right\} \text{ and } \left.\begin{matrix} a = 3.796 \text{ Å} \\ c = 16.36 \text{ Å} \end{matrix}\right\} \text{ respectively}$$

From the above it is evident that all the compounds, except CuS, have cubic, face-centred high-temperature modifications, whose diffraction lines show nearly the same relative intensity.

This points to a common high-temperature phase $Cu_{2-x}S$, where x can vary from 0 to at least 0.18 ($x > 0.18$ was not investigated). The variation of the unit cell edge of $Cu_{2-x}S$ with the composition at 500°C, as shown in Fig. 1, supports this view.

DISCUSSION

The results of the present study are contradictory to the phase diagram reported by Buerger [2,3].

The fact that Buerger's results do not agree with those of the present author is not surprising because of the way Buerger's samples were prepared. According to Buerger, chalcocite and synthetic CuS powders were compacted, placed in an *open* glass tube and heated at a temperature of about 110°C for at least 12 h. This treatment is so much more astonishing as Buerger himself, later in his paper, states: "When chalcocite is heated in direct contact with air, it begins to convert to digenite", and "It appears, then, that oxygen can proxy for sulphur".

The data reported by Rühl [4] are in good agreement with those of the present author. Thus he observed the diffraction pattern of Cu_2S only in the range Cu_2S—$Cu_{1.98}S$ (compare Table 2): and his Cu_2S-similar phase probably is the phase $Cu_{1.96}S$ III. The largest divergence between the work of Rühl and that of the present author concerns the homogeneity range of $Cu_{1.8}S$.

More work is needed to establish the composition-temperature phase diagram. Particular attention ought to be called to establishing the range of existence of the modifications of $Cu_{1.96}S$.

Acknowledgements. The author wishes to thank Professor G. Hägg for his encouraging interest in this investigation and Mr. H. Fischmeister and Mr. S. Rundqvist for stimulating discussions and valuable advice.

REFERENCES

1. Haugton, J. L. and Prince, A. *The constitutional diagrams of alloys: A Bibliography. Institute of Metals Monograph and Report Series* No. 2, 1956.
2. Buerger, N. W. *Am. Mineralogist* **27** (1942) 712.
3. Buerger, N. W. *Econ. Geol.* **36** (1941) 19.
4. Rühl, W. *Diplomarbeit. Röntgenuntersuchung des Phasendiagramms Cu_2S—CuS*, Physikal-Inst. d. Univ. Erlangen 1952. *Private communication.*

5. Jensen, E. Avh. *Norske Videnskabs-Akad. Oslo I Math.-Nat. Kl.* No. **6** (1947).
6. Hirahara, E. *J. Phys. Soc. Japan* **6** (1951) 422.
7. Ueda, R. *J. Phys. Soc. Japan* **4** (1949) 287.
8. Kamaigaichi, T. *J. Sci. Hiroshima Univ. A* **16** (1952) 325.
9. Belov, N. V. and Butuzov, V. P. *C. R. Acad. Sci. USSR* **54** (1946) 717.
10. Buerger, M. J. and Buerger, N. W. *Am. Mineralogist* **29** (1944) 55.
11. Oftedal, I. *Z. Krist.* **83** (1932) 9.
12. Berry, L. G. *Am. Mineralogist* **39** (1954) 504.
13. Fischmeister, H. F. *J. Inorg. & Nuclear. Chem.* **3** (1956) 182.
14. Fischmeister, H. F. *Acta Cryst.* **9** (1956) 416.

Received May 5, 1958.

ACTA CHEMICA SCANDINAVICA 12 (1958) 1427—1436

An X-Ray Study on the System Ag-Cu-S

SEVED DJURLE

Institute of Chemistry, University of Uppsala, Uppsala, Sweden

The phase relations in the ternary system Ag-Cu-S have been investigated by X-ray diffraction methods. Ternary phases of the following approximate compositions were found to exist:

$Ag_{1.55}Cu_{0.45}S$ (α), corresponding to the mineral jalpaite

$Ag_{1.2}Cu_{0.8}S$ (β) and

$Ag_{0.93}Cu_{1.07}S$ (γ), corresponding to the mineral stromeyerite.

At room temperature the α phase is tetragonal and its body-centred unit cell has the dimensions:

$a = 8.673$ Å, $c = 11.756$ Å.

It transforms at 112°C into a body-centred cubic lattice, which transforms at about 300°C into a face-centred cubic lattice.

The β phase has two transition temperatures, the lower one at about 97°C and the upper one at about 130°C. Attempts to index its powder pattern have not been successful. At room temperature the γ phase is orthorhombic but transforms at 90°C into a hexagonal lattice. A second transition occurs at about 180°C.

Present evidence indicates that the modifications above the highest transition temperatures all belong to a face-centred cubic phase $(Ag,Cu)_2S$.

Previous investigators of the ternary system Ag-Cu-S have restricted themselves to the study of the "quasi-binary" system Ag_2S—Cu_2S.

Schwartz [1] examined the relations of chalcocite (Cu_2S)-stromeyerite (AgCuS)-argentite (Ag_2S), using both microscopic and X-ray techniques. He found the ternary compound AgCuS, which had a transition at a temperature of 93°C. He also stated that there was "considerable solubility of Ag_2S in Cu_2S and of Cu_2S in Ag_2S". The melting points of samples of various proportions of Ag_2S and Cu_2S followed a smooth curve, indicating complete solid solubility at high temperatures.

Suhr [2], contrary to Schwartz, could not find any extensive solid solution regions at room temperature. He found, in addition to Ag_2S, the compound AgCuS, the compound jalpaite, Ag_3CuS_2, and two unknown compounds, one silver-rich, which he thought was off the Ag_2S—Cu_2S join, and the other copper-rich, which was not Cu_2S.

Using a natural crystal of stromeyerite, AgCuS, Suhr found the unit cell to be orthorhombic with the cell dimensions:

$$a = 4.06, \qquad b = 6.66, \qquad c = 7.99 \text{ Å}.$$

A crystal structure determination of stromeyerite has been made by Frueh [3].

EXPERIMENTAL

The preparative methods and the X-ray technique used in this study were the same as in a preceding paper on copper sulphides [4].

As the third component of the system finely powdered Ag ("Finsilver", Grave, Stockholm) of better than 99.9 % purity was used.

The sintering temperature was 320, 470 or 500°C.

Selected samples were chemically analyzed. After the sample had been dissolved in fuming HNO_3 and the solution evaporated to dryness, the sample was dissolved in dilute HNO_3 and Ag was determined potentiometrically by titration with 0.1 M NaCl. The AgCl precipitate was filtered off and SO_4 and Cu were then determined as previously described [4].

The composition, calculated from the weighed amounts of the elements, was in good agreement with the chemical analysis. The maximum deviation for each element was ±0.5 atomic per cent.

RESULTS

The present study has revealed the existence of ternary phases at the approximate compositions

$Ag_{1.55}Cu_{0.45}S = \alpha$ phase (composition corresponding to the mineral jalpaite)
$Ag_{1.2}Cu_{0.8}S = \beta$ phase
$Ag_{0.93}Cu_{1.07}S = \gamma$ phase (composition corresponding to the mineral stromeyerite)

which all contain 33 1/3 atomic per cent sulphur *i. e.* lie on the "quasi-binary" line Ag_2S—Cu_2S of the ternary diagram. At each of these three compositions three different modifications appear when the temperature is raised from room temperature. These modifications are denoted by Roman numerals (I for the one existing above the highest transition temperature observed). All phases of the general formula $Ag_{2-x}Cu_xS$ ($0 \leq x \leq 2$) are listed in Table 1.

Diffraction lines of the high temperature modifications of the ternary phases were only observed at elevated temperatures in the heating camera. Quenched specimens only showed lines of the III modifications at room temperature, which shows that the high temperature modifications transform too rapidly to be preserved by quenching. Data from powder photographs of the different phases are collected in Table 2.

The section of the phase diagram at 20°C which is given in Fig. 1 is based on Guinier powder photographs taken at room temperature of a great number of samples. All triangles of the diagram are three-phase regions except the one with the corners γ, $Cu_{1.80}S$ and $Cu_{1.73}S$, which represents a two-phase region. In his work on the system Cu—S the author[4] has found that the phase denoted as $Cu_{1.8}S$ has a homogeneity range at least existing between the compositions $Cu_{1.80}S$ and $Cu_{1.73}S$.

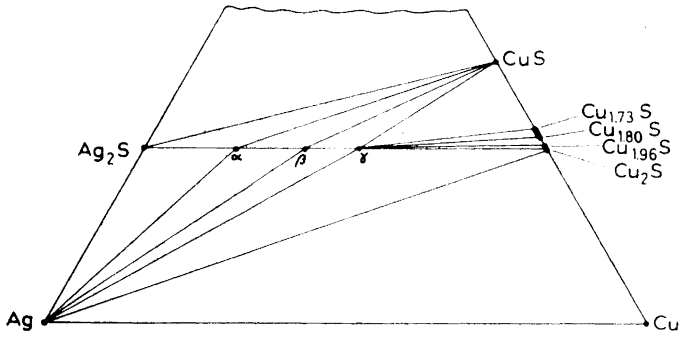

Fig. 1. The phase diagram of Ag-Cu-S. Isothermal section at 20°C.

The α phases

The two transition temperatures observed are: the lower one 112°C, and the upper one 290—310°C.

α III

This modification is tetragonal and has a body-centred unit cell with the dimensions, at room temperature:

$$a = 8.673 \pm 0.004 \text{ Å} \qquad c = 11.756 \pm 0.006 \text{ Å} \qquad c/a = 1.355$$

Table 1. The sulphides of the general formula $Ag_{2-x}Cu_xS$ $(0 \leqq x \leqq 2)$.

Compound	Composition (At.-%)			Approximate range of existence *	Crystal system
	Ag	Cu	S		
Ag_2S III	66.2/3	0	33.1/3	<177°C	Monoclinic
Ag_2S II				177—600	Cubic B.C.
Ag_2S I				>600	Cubic F.C.
α III	51.2/3	15	33.1/3	<112	Tetragonal
α II				112—300	Cubic B.C.
α I				>300	Cubic F.C.
β III	40	26.2/3	33.1/3	< 97	(Low-symmetric)
β II				97—130	
β I				>130	Cubic F.C.
γ III	31	35.2/3	33.1/3	< 90	Orthorhombic
γ II				90—180	Hexagonal
γ I				>180	Cubic F.C.
Cu_2S III	0	66.2/3	33.1/3	<110	Orthorhombic
Cu_2S II				110—470	Hexagonal
Cu_2S I				>470	Cubic F.C.

* Range of investigation 20—500°C, except for Ag_2S.

A Debye-Scherrer photograph taken at 105°C gave the values

$$a = 8.725 \pm 0.009 \text{ Å} \quad \text{and} \quad c = 11.74 \pm 0.01 \text{ Å}.$$

The fact that the a-axis expands and the c-axis contracts on heating, allows an unequivocal indexing.

The density, calculated from the cell constants, assuming 16 $Ag_{1.55}Cu_{0.45}S$ per unit cell, is 6.8 g/cm^3. Measuring of the density gave 6.9 g/cm^3.

α II

The diffraction pattern of this modification has been indexed as body-centred cubic. The cell constant measured at different temperatures is,

$$\left.\begin{array}{lll} \text{at} & 116°C & a = 4.825 \\ & 152°C & a = 4.836 \\ & 300°C & a = 4.870 \end{array}\right\} \pm 0.005 \text{ Å}$$

The cell volume is 1/8 of that of modification III, indicating 2 $Ag_{1.55}Cu_{0.45}S$ as the cell contents.

α I

Due to the high background blackening, only two lines of the pattern of this modification could be discerned.

As will be shown below, the highest temperature modifications between Ag_2S I and Cu_2S I can all be indexed on the basis of a face-centred cubic cell, giving a straight line relationship between cell edge and composition.

The two lines of α I have therefore been given indices consistent with a face-centred cubic lattice.

The cube edge at three different temperatures is as follows:

$$\left.\begin{array}{ll} 300°C & a = 6.110 \\ 400°C & a = 6.123 \\ 500°C & a = 6.140 \end{array}\right\} \pm 0.006 \text{ Å}$$

A cell content of 4 $Ag_{1.55}Cu_{0.45}S$ is consistent with the cell constants.

The β phases

Two transition temperatures have been observed, The lower one occurs at 95 to 99°C and the upper one at 120 to 143°C. No satisfactory indexing of the diffraction patterns of the modifications β III and β II has been found.

β I

The pattern of β I was indexed as derived from a face-centred cubic lattice. The edge of the unit cube was found to be,

$$\left.\begin{array}{lll} \text{at} & 151°C & a = 5.999 \\ & 300°C & a = 6.015 \\ & 500°C & a = 6.042 \end{array}\right\} \pm 0.006 \text{ Å}$$

This is consistent with a cell content of 4 $Ag_{1.2}Cu_{0.8}S$.

The γ phases

The examination has revealed two transition temperatures, the lower one at 90°C and the upper one at about 180°C.

The value of the lower transition temperature is in good agreement with the value 93°C given by Schwartz [1].

γ III

The Guinier photograph taken at room temperature gives an orthorhombic cell with the cell constants:

$$\begin{aligned} a &= 4.066 \pm 0.002 \text{ Å} \\ b &= 6.628 \pm 0.003 \text{ Å} \\ c &= 7.972 \pm 0.004 \text{ Å} \end{aligned}$$

as compared with the values reported by Suhr [2]

$$a = 4.06 \qquad b = 6.66 \qquad c = 7.99 \text{ Å}$$

γ II

This modification has been indexed hexagonally, giving a unit cell with a cell content of 2 $Ag_{0.93}Cu_{1.07}S$ and the dimensions

$$\left.\begin{array}{lll} \text{at} & 100°C & a = 4.138 \pm 0.004 \text{ Å} \\ & & c = 7.105 \pm 0.007 \text{ Å} \end{array}\right\} \quad c/a = 1.983$$

and at

$$\left.\begin{array}{ll} 152°C & a = 4.158 \pm 0.004 \text{ Å} \\ & c = 7.068 \pm 0.007 \text{ Å} \end{array}\right\} \quad c/a = 1.963$$

γ I

With the indexing chosen, the unit cell is face-centred cubic, has a cell content of 4 $Ag_{0.93}Cu_{1.07}S$ and the following cell constant,

$$\left.\begin{array}{lll} \text{at} & 196°C & a = 5.961 \\ & 300°C & a = 5.973 \\ & 500°C & a = 5.993 \end{array}\right\} \pm 0.009 \text{ Å}$$

The phases occurring at the composition Ag_2S

The transition temperatures as found in the present study are in complete agreement with the work of Kracek [5]. He states that there exist three modifications, the lower transition from Ag_2S III to Ag_2S II occurring between

176 and 178°C, the upper transition from Ag_2S II to Ag_2S I at a temperature of 586 ± 3°C in the presence of excess silver, and of 622 ± 3°C when sulphur is in excess.

Ag_2S III

The indexed Guinier photograph at room temperature gives a monoclinic unit cell with the following lattice parameters:

$$\left.\begin{array}{l} a = 9.531 \\ b = 6.925 \\ c = 8.278 \end{array}\right\} \pm 0.005 \text{ Å}$$
$$\beta = 123.85 \pm 0.10°$$

in fair agreement with the values of Ramsdell [6]

$$a = 9.47 \text{ Å}, \qquad b = 6.92 \text{ Å}, \qquad c = 8.28 \text{ Å}, \qquad \beta = 124°$$

Ag_2S II

Powder photographs of Ag_2S II were taken with the high-temperature camera, and the patterns have been indexed as belonging to a body-centred cube in accord with the work of Rahlfs [7]. Only the three strongest lines of the patterns have been used for evaluating the cell edge. This is,

$$\left.\begin{array}{lll} \text{at} & 189°C & a = 4.870 \\ & 300°C & a = 4.890 \\ & 500°C & a = 4.926 \end{array}\right\} \pm 0.008 \text{ Å}$$

The cell dimensions are in good agreement with the value 4.88 Å at 250°C given by Rahlfs.

Ag_2S I

A powder photograph of this modification was taken at 600°C. Due to the very high background blackening, only one line of the pattern could be seen With regard to the suspected isomorphism of the highest temperature modifications, discussed below, and the fact that all the I modifications have /220/ as their strongest diffraction line, this line has been indexed as /220/ of a face-centred cubic lattice, with the cube edge $a = 6.269 \pm 0.020$ Å.

The I-modifications

As has been mentioned above, and as can be seen from Tables 1 and 2 all the I-modifications of the sulphides on the "quasi-binary" line Ag_2S—Cu_2S give X-ray diffraction patterns which can be indexed with a face-centred cubic

Table 2. X-Ray diffraction data of the phases Ag_2S, α, β and γ.

α III 20° Cu-$K\alpha$

hkl	I_{rel}	$\sin^2\Theta$ Obs.	$\sin^2\Theta$ Calc.
101	w	0.0124	0.0122
200	m	0.0318	0.0316
211	w	0.0440	0.0438
103	w	0.0467	0.0466
202	w	0.0490	0.0488
301	st	0.0755	0.0754
213	st	0.0783	0.0782
312	m	0.0963	0.0962
204	st	0.1004	0.1004
321	st	0.1072	0.1070
303	w	0.1098	0.1098
105	w	0.1153	0.1154
400	w	0.1266	0.1264
224	m	0.1319	0.1320
215	w	0.1467	0.1470
332	vw	0.1593	0.1594
116	vw	0.1706	0.1706
404	w	0.1952	0.1952
501	vw	0.2020	0.2018
334	vw	0.2109	0.2110
503	vw	0.2357	0.2362
415	vw	0.2417	0.2418
523	w	0.2677	0.2678
514	vw	0.2743	0.2742
532	w	0.2854	0.2858
611	w	0.2968	0.2966
336			0.2970
435	w	0.3049	0.3050
327	vw	0.3134	0.3134
534	w	0.3370	0.3374
525			0.3366
631	vw	0.3598	0.3598
516			0.3602
512	vw	0.4205	0.4201
329	vw	0.4515	0.4510

Ag_2S II 300°C Cu-$K\alpha$

hkl	I_{rel}	$\sin^2\Theta$ Obs.	$\sin^2\Theta$ Calc.
200	st	0.0992	0.0994
211	m	0.1491	0.1491
220	w	0.1989	0.1988

Ag_2S I 600°C Cu-$K\alpha$

hkl	$\sin^2\Theta$ Obs.
220	0.1210

Ag_2S III 20°C Cu-$K\alpha$

hkl	I_{rel}	$\sin^2\Theta$ Obs.	$\sin^2\Theta$ Calc.
$10\bar{2}$	vw	0.0355	0.0355
200	w	0.0379	0.0380
111	vw	0.0466	0.0466
002	m	0.0503	0.0503
210			
$21\bar{2}$	w	0.0519	0.0520
012	m	0.0627	0.0627
$31\bar{1}$	m	0.0738	0.0738
121	m	0.0838	0.0838
220	st	0.0875	0.0875
$22\bar{2}$	m	0.0891	0.0891
$11\bar{3}$	w	0.0986	0.0986
022	m	0.0999	0.0999
$31\bar{3}$	w	0.1014	0.1014
$40\bar{2}$	m	0.1047	0.1047
$13\bar{1}$	w	0.1214	0.1214
$12\bar{3}$	vw	0.1355	0.1357
202	m	0.1370	0.1369
$32\bar{3}$	vw	0.1387	0.1386
$20\bar{4}$	w	0.1418	0.1418
212	w	0.1494	0.1493
230			0.1495
$21\bar{4}$	w	0.1542	0.1542
032	vw	0.1621	0.1618
410	w	0.1643	0.1642
$41\bar{4}$	w	0.1708	0.1707
040	vw	0.1982	0.1983
$51\bar{1}$	w	0.2014	0.2012
420			0.2014
$14\bar{1}$	vw	0.2082	0.2082
240	vw	0.2363	0.2362
332	vw	0.2459	0.2460
024	vw	0.2509	0.2508
$34\bar{1}$	vw	0.2597	0.2597
$13\bar{3}$	vw	0.2706	0.2707
$11\bar{5}$	vw	0.2754	0.2754
$55\bar{3}$	vw	0.2794	0.2793
$14\bar{3}$	vw	0.2846	0.2844
$51\bar{1}$	vw	0.3235	0.3230
$33\bar{5}$	vw	0.3288	0.3287
242	vw	0.3354	0.3352
600	vw	0.3420	0.3415
214	vw	0.3490	0.3489
422			0.3490

α II 152°C Cu-*Kα*

hkl	I_{rel}	$\sin^2\Theta$ Obs.	$\sin^2\Theta$ Calc.
200	m	0.1016	0.1016
211	st	0.1524	0.1525
220	w	0.2033	0.2033
400	vw	0.4067	0.4066

α I 500°C Cu-*Kα*

hkl	I_{rel}	$\sin^2\Theta$ Obs.	$\sin^2\Theta$ Calc.
220	st	0.1259	0.1261
311	w	0.1736	0.1734

β III 20°C Cu-*Kα*

$\sin^2\Theta$ Obs.	I_{rel}
0.0371	w
0.0394	w
0.0484	m
0.0636	m
0.0725	m
0.0851	w
0.0873	st
0.0903	w
0.0933	w
0.0950	vw
0.1025	m
0.1114	m
0.1240	w
0.1267	w
0.1359	w
0.1386	m
0.1471	w
0.1567	m

β II 99°C Cu-*Kα*

$\sin^2\Theta$ Obs.	I_{rel}
0.0920	w
0.1311	w
0.1384	st
0.1434	w
0.1512	st
0.1611	m

β I 151°C Cu-*Kα*

hkl	I_{rel}	$\sin^2\Theta$ Obs.	$\sin^2\Theta$ Calc.
200	w	0.0660	0.0660
220	st	0.1322	0.1321
311	m	0.1816	0.1816
222	vw	0.1975	0.1981

γ II 100°C Cu-*Kα*

hkl	I_{rel}	$\sin^2\Theta$ Obs.	$\sin^2\Theta$ Calc.
102	st	0.0933	0.0934
110	st	0.1388	0.1388
103	st	0.1521	0.1521
200 }	w	0.1856	0.1852
112 }			0.1859
004	w	0.1888	0.1883
201	w	0.1967	0.1970

γ I 500°C Cu-*Kα*

hkl	I_{rel}	$\sin^2\Theta$ Obs.	$\sin^2\Theta$ Calc.
220	st	0.1319	0.1324
311	w	0.1825	0.1820

st = strong
m = medium
w = weak
vw = very weak

γ III 20°C Cu-$K\alpha$

hkl	I_{rel}	$\sin^2\Theta$ Obs.	$\sin^2\Theta$ Calc.	*hkl*	I_{rel}	$\sin^2\Theta$ Obs.	$\sin^2\Theta$ Calc.
002	vw	0.0375	0.0374	024	w	0.2033	0.2036
101	vw	0.0451	0.0453	221	w	0.2071	0.2073
110	m	0.0496	0.0495	222	w	0.2352	0.2353
020	m	0.0542	0.0541	213	w	0.2417	0.2414
021	w	0.0635	0.0635	133			0.2418
112	st	0.0868	0.0868	233	w	0.2819	0.2820
022	m	0.0915	0.0915	204	m	0.2934	0.2932
113	vw	0.1333	0.1335	224	w	0.3476	0.3474
023	w	0.1382	0.1382	312	w	0.3747	0.3744
200	m	0.1438	0.1438	150			0.3742
004	m	0.1494	0.1494	116	w	0.3863	0.3857
131	m	0.1670	0.1671	321			0.3870
211			0.1667	026			0.3904
132	m	0.1949	0.1951	135	w	0.3912	0.3912
212			0.1947	215			0.3908
220	w	0.1975	0.1979	331	vw	0.4551	0.4547
114	w	0.1986	0.1989				

unit cell. They also have comparable line intensities. The values of the cube edge, extrapolated to 600°C from values at different temperatures in order to be comparable, are as follows:

x in $Ag_{2-x}Cu_xS$	a, Å
0	6.269 ± 0.020
0.45	6.153 ± 0.006
0.80	6.055 ± 0.006
1.07	6.000 ± 0.009
2.00	5.752 ± 0.010

The value for Cu_2S I is extrapolated from measurements reported in Ref.[4]

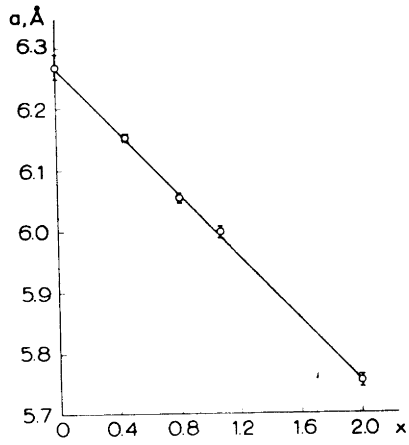

Fig. 2. Variation of cube edge of $Ag_{2-x}Cu_xS$ with x.

The values of the cell edge are plotted against the composition in Fig. 2, and within the errors of measurement, a straight line is obtained for the variation of the cell edge with the composition.

This indication of isomorphous phases with complete solid solubility is in accord with the melting point curve determined by Schwartz [1].

From the present investigation it thus seems probable that in the system Ag_2S—Cu_2S there is only one common highest temperature modification $Ag_{2-x}Cu_xS$, $0 \leq x \leq 2$.

With regard to the face-centred cubic phase $Cu_{2-y}S$, where y varies from 0 to at least 0.18, in the system Cu—S[4], there is a possibility, not investigated, that the ternary phase $Ag_{2-x}Cu_xS$ could also exist with a small deficit of copper and/or silver atoms.

Acknowledgements. The author wishes to express his sincere gratitude to Professor G. Hägg and Dr. H. Fischmeister for their encouraging interest in this investigation.

REFERENCES

1. Schwartz, G. M. *Econ. Geol.* **30** (1935) 128.
2. Suhr, N. *Econ. Geol.* **50** (1955) 347.
3. Frueh, Jr. A. J. *Z. Krist.* **106** (1955) 299.
4. Djurle, S. *Acta Chem. Scand.* **12** (1958) 1415.
5. Kracek, F. C. *Trans. Am. Geophys. Union* **27** (1946) 364.
6. Ramsdell, L. S. *Am. Mineralogist* **28** (1943) 401.
7. Rahlfs, P. *Z. physik. Chem.* **B 31** (1935) 157.

Received May 5, 1958.

ACTA CHEMICA SCANDINAVICA 12 (1958) 1437—1443

The Chemistry of Dicarboxylic Acids

I. A New Method for Quantitative Determination of Malonic Acid

AAGE JART

Danish Fat Research Institute, Copenhagen, Denmark

Malonic acid interacts with acetic acid anhydride to form a coloured compound on which it has proved possible to base a method for quantitative determination of the acid. A description is given of an analytical method depending on the absorption exhibited at 345 mμ by the compound produced. The influence of the presence of oxalic acid, succinic acid and citric acid on the reaction has been examined. In addition the ultraviolet and infrared spectra of the coloured compound formed are given.

Malonic acid can be determined quantitatively by direct titration; gravimetrically after precipitation of its barium salt [1]; by oxidation in sulphuric acid solution by means of potassium permanganate [2], sodium dichromate [3] or ceric sulphate [4]; and by measuring the areas of the coloured spots resulting from paper chromatography either of the acid or its salts.

The object of the present investigation is to develop a spectrophotometric method — as far as possible a method specific to malonic acid and enabling quantitative determination of the acid even when present in relatively small quantities. The interest in determining malonic acid arises in connection with ozonolysis of unsaturated fatty acid methyl esters. As in natural fatty acids the double bonds are often placed with a distance of three carbon atoms the ozonolysis gives rise to formation of malonic acid as an end product in the oxidation processes. The amount of malonic acid produced corresponds to the content of fatty acids with this configuration. A suitable chemical reaction on which to base the analytical method was found in the interaction between malonic acid and acetic acid anhydride which results in the appearance of a yellowish-green to yellowish-brown colour which — especially on dilution with glacial acetic acid — shows strong fluorescence [5].

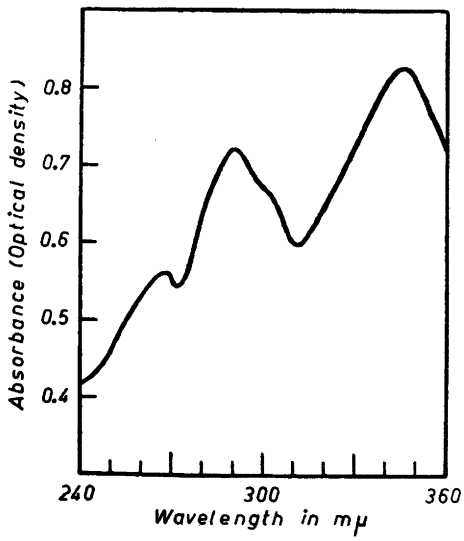

Fig. 1. The ultraviolet spectrum of "malonic colour".

PRELIMINARY INVESTIGATIONS

The ultraviolet spectrum of the coloured compound formed when crystalline malonic acid is heated with acetic acid anhydride shows a distinct absorption maximum at 290 mμ and likewise at 345 mμ (Fig. 1). The peak at 345 mμ is the highest and also the most stable, for which reason it was chosen as the basis of the present work. If D is the optical density measured in a 1 cm layer and c the corresponding concentration in mg/ml of the malonic acid used for the experiment, the reaction coefficient, α, is defined by the equation

$$\alpha = \frac{D}{c} \tag{1}$$

In order to examine the influence of the reaction time on α, a series of eight experiments at different but constant temperatures was made. The temperatures and quantities of malonic acid used appear from Table 1.

The reaction vessel used was a 250 ml round-bottom flask with a stoppered opening for drawing samples and with a reflux condenser, through which a thermometer was passed into the flask. The flask was completely immersed in a thermostat consisting of a 5 l beaker with oil and a contact thermometer with relay, heating element (150 W) and magnetic stirrer; the beaker was insulated by means of a 1 cm layer of cotton fabric.

To start the experiment 50 ml acetic anhydride (analytical grade, Merck) was transferred by means of a pipette to the preheated reaction flask. After a period of 20 min (15—20 min were necessary to establish constant temperature) the sample of crystalline malonic acid (analytical grade, Merck) was introduced by means of a 1 ml weighing cup, and the flask was swirled slightly to effect rapid solution of the sample. One minute after the introduction of the sample the thermometer reading was 0.5°C below the reaction

Table 1. Summary of the experiments at eight different temperatures (*cf.* Fig. 2).

Experiment	Temperature, °C	Malonic acid, mg
A	69.9	78.5
B	79.7	58.5
C	89.2	43.1
D	99.5	33.9
E	111.6	20.3
F	120.2	25.0
G	129.3	16.4
H	138.3	12.2

temperature, and after altogether 10 min the temperature had again reached the desired level.

During the individual experiments about 20 samples were drawn and, after dilution with glacial acetic acid (analytical grade, Merck), measured against corresponding mixtures of acetic acid anhydride and glacial acetic acid in a Beckman spectrophotometer model DU.

The reaction coefficient was calculated for the individual samples, and the results of the eight experiments are represented graphically in Fig. 2. It appears from the figure that the intensity of the absorption at 345 mμ increases with increasing temperature and reaction time. The only exception from this observation is graph H at which the temperature is 138.3°C. The reason is

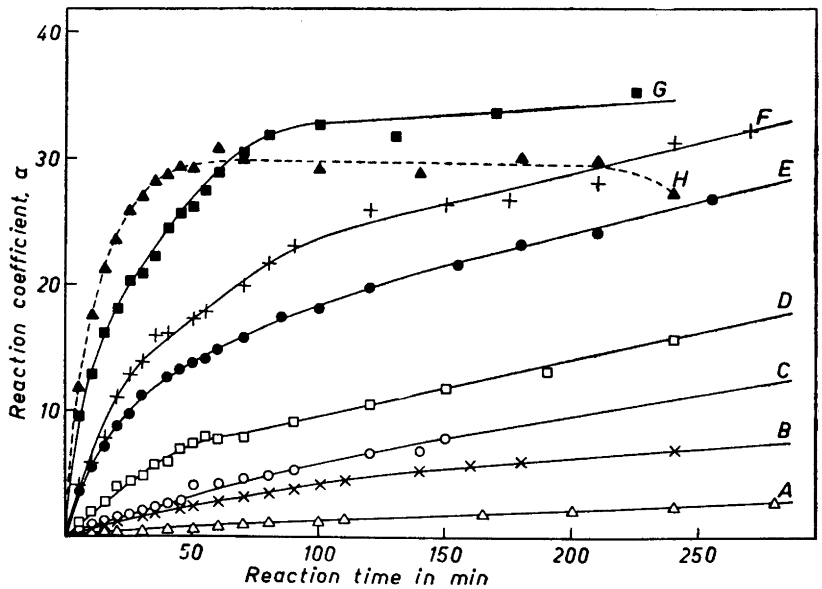

Fig. 2. The influence of the reaction time on the reaction coefficient at different temperatures (*cf.* Table 1).

that malonic acid decomposes at high temperatures to form acetic acid and carbon dioxide. The pure acid decomposes when heated to its melting point (135.6°C), while in solution the reaction often occurs at a lower temperature.

DEVELOPMENT OF ANALYTICAL METHOD

The object of the first experiments was to ascertain whether reproducible reaction coefficient values could be obtained at 100.0°C, 110.0°C, and 125.0°C.

The thermostat consisted of an enamelled tank, thoroughly insulated with glass wool and containing about 17 litres of oil. It was fitted with a stirrer, a contact thermometer with relay and an adjustable heating element. The heating element operated for about two thirds of the time, and the temperature was kept constant within ±0.1°C. The thermostat was arranged to hold four reaction vessels (test tubes).

By means of a pipette 5 ml acetic acid anhydride was transferred to each of the tubes, and after a preheating period of 20 min malonic acid was introduced by means of a little weighing cup into three of the vessels, the fourth serving as a blank. The reaction was allowed to proceed for 60 min and was then stopped by transferring the reaction vessels to a beaker with ice water. The four samples were now transferred quantitatively into 100 ml volumetric flasks by means of glacial acetic acid (the samples which had been kept at 125.0°C were further diluted five times) and measured in a Beckman spectrophotometer model DU (wavelength: 345 mμ, slit width: 0.18 mm with hydrogen lamp, and a 1 cm cuvette).

According to this procedure each experimental series provides three analytical results, and in Table 2 three series of this kind are given for each of the temperatures chosen. It will be seen that reproducibility is best at 110.0°C, the individual experimental series resulting in identical reaction coefficient values, although the thermostat used was not sufficiently stable to ensure that results obtained from day to day were in complete agreement. At 125.0°C the tendency of malonic acid to decarboxylation seems to be so pronounced that it is impossible to obtain reliable results, even though the relatively high value of the reaction coefficient, α, would enable a greater accuracy when

Table 2. Values of the reaction coefficient α at 100.0°C, 110.0°C and 125.0°C.

No.	100.0°		110.0°		125.0°	
	Malonic acid mg	α	Malonic acid mg	α	Malonic acid mg	α
1	10.5	3.77	11.6	6.43	13.1	18.6
2	14.2	3.95	13.2	6.39	10.8	18.9
3	11.3	4.15	8.6	6.38	10.2	18.0
4	12.3	3.97	14.6	6.73	11.3	17.0
5	11.5	4.02	11.1	6.77	12.9	17.5
6	11.4	3.96	12.7	6.69	12.1	19.0
7	11.4	3.66	13.6	6.54	6.8	17.7
8	12.6	3.66	11.4	6.60	11.9	17.3
9	13.0	4.22	11.6	6.57	10.5	18.7

working with small quantities of malonic acid. The lack of reproducibility of the results obtained at 100.0°C is due to the fact that at this temperature the viscosity of the thermostat oil is so high as to prevent sufficiently uniform transmission of heat to the four reaction vessels — this resulted in highly varying α values even within the same experimental series.

The conclusion to be drawn from this is that it is possible to perform the analysis at 110°C but that in case the thermostat available is not an extremely good one, it is necessary to include a control sample with malonic acid in each experimental series.

The influence of other compounds on the reaction

It is necessary to know whether other compounds which may be present in the sample to be analyzed have any influence on the reaction producing the coloured compound. It was examined whether the presence of oxalic acid and succinic acid, impurities which occur frequently together with malonic acid (for instance after chromatographic separation) will result in variations in the reaction coefficient values found. Table 3 shows that small quantities of these compounds (analytical grade, Merck) do not interfere in the malonic acid determination.

Table 3. The influence of the presence of oxalic acid and succinic acid on the malonic acid determination.

No.	Oxalic acid mg	Malonic acid mg	Succinic acid mg	α
1	2.9	11.2	1.55	7.14
2	—	10.3	—	7.10
3	5.1	9.7	4.4	7.01

In another experiment 11.7 mg citric acid monohydrate (analytical grade, Merck) was treated according to the described analytical method. This gave rise to a uniform absorption (D = about 0.1) between 240 mμ and 360 mμ, while a mixture of equal parts of citric acid and malonic acid resulted in a smaller absorption throughout the range 240—360 mμ than that produced by malonic acid alone. It is thus impossible to determine malonic acid in mixtures of malonic acid and citric acid without a preliminary separation, and samples to be analyzed must therefore in each individual case be examined to find out whether such a separation is necessary prior to the malonic acid analysis. The control sample should as far as possible be of the same composition as the mixture in which the content of malonic acid is to be determined.

THE RECOMMENDED ANALYTICAL METHOD

Use a thermostat with vigorous stirring and containing a liquid with good heat transmission characteristics. Adjust the temperature at 110°C and maintain this temperature within $\pm$0.1°C. As reaction vessels use three or

Table 4. Two series of malonic acid determinations. (Samples diluted to 100 ml before the measurement.)

Malonic acid mg	Optical density, D	α	Malonic acid found, mg
11.0	0.814	—	10.9
11.1	0.828	7.46	—
10.4	0.777	—	10.4
10.9	0.791	—	10.9
11.0	0.797	7.25	—
9.7	0.698	—	9.6

more absolutely identical test tubes (length 12 cm, external diameter 2 cm, Pyrex glass), and keep the test tubes half-way immersed in the thermostat liquid during the process.

By means of a pipette transfer 5 ml acetic acid anhydride, analytical grade, to each test tube. Place the test tubes in the thermostat at 0.5 min intervals. After a preheating period of 20 min transfer, by means of small weighing cups, the weighed samples (plus one standard sample with a known content of malonic acid) to the test tubes. One test tube is used for a blank determination, and in this test tube a weighing cup without malonic acid is placed. Exactly 60 min after the introduction of the samples into the reaction vessels remove the latter from the thermostat and place in a beaker with ice water. Allow the solutions to cool down to room temperature, and then dilute with sufficient glacial acetic acid, analytical grade, to produce solutions suitable for measurement in a spectrophotometer at 345 mμ. On the basis of the known content of malonic acid in the standard sample determine the reaction coefficient, α, using this coefficient and (1) for the subsequent calculation of the malonic acid content in the samples examined (*cf.* Table 4).

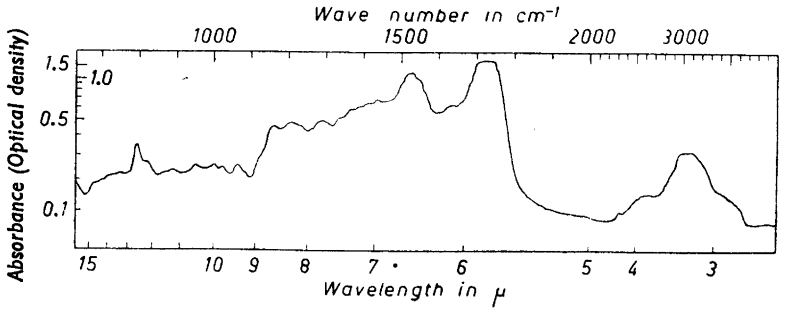

Fig. 3. The infrared spectrum of "malonic colour".

SPECTRA OF THE "MALONIC COLOUR"

The ultraviolet spectrum (Fig. 1) was obtained by means of a recording spectrophotometer (Beckman, DK-2, scanning time: 6—7 minutes); the material used being 12.2 mg malonic acid treated according to the above analytical method. After the peak at 345 mμ the absorption decreases uniformly with increasing wavelength ($D_{400\ m\mu} = 0.10$, $D_{450\ m\mu} = 0.02$, and $D_{500\ m\mu} = 0.00$). When the coloured solution is allowed to stand (after dilution with glacial acetic acid) the peak at 345 mμ becomes gradually smaller, but the change produced in the course of 24 h is hardly measurable; the reaction is not materially influenced by daylight.

The infrared spectrum (Fig. 3) was obtained from 1.1 mg "malonic colour" in 300 mg potassium bromide (Perkin-Elmer spectrophotometer, model 21).

The "malonic colour" was prepared by treating 1 g malonic acid with 50 ml acetic acid anhydride for 60 min at 110°C. The acetic acid anhydride was distilled off in vacuum, and the residue was dissolved in methyl acetate, filtered and evaporated to dryness in vacuum at a temperature not higher than 70°C, the treatment of the residue being repeated once.

The spectrum shows that the compound in question is a polymer with a considerable number of C=O bonds; it seems moreover to contain acid and ester groups, while the presence of more or less modified aromatic rings is likely.

REFERENCES

1. Coutelle, C. *J. prakt. Chem. (2)* **73** (1906) 49, p. 76.
2. Durand, E. *Ann. chim. anal. et chim. appl.* **8** (1903) 330. (Cited from *Chem. Zentr.* **74** (1903 II) 968.)
3. Launer, H. F. and Tomimatsu, Y. *Anal. Chem.* **25** (1953) 1767.
4. Willard, H. H. and Young, P. *J. Am. Chem. Soc.* **52** (1930) 132.
5. Kleemann, S. *Ber.* **19** (1886) 2030.

Received May 22, 1958.

ACTA CHEMICA SCANDINAVICA 12 (1958) 1444—1450

Electroörganic Preparations

V. On the Polarographic Determination of Phenols after Treatment with Nitrous Acid

HENNING LUND

Leo Pharmaceutical Products, Copenhagen, Denmark

It is shown that the polarographic wave obtained in the wellknown determination of morphine and other *p*-substituted phenolic compounds after treatment with nitrous acid is due to a nitro derivative rather than a nitroso derivative.

A number of *p*-substituted phenolic compounds and derivatives thereof which are not, themselves, reducible at the dropping mercury electrode can be determined polarographically after treatment with nitrous acid; such compounds are, *e. g.*, morphine [1], codeine [2], cephaeline [3], estrone [4,5], and estrogenic compounds [4,5]. The reaction has generally been formulated as a nitrosation of the phenolic compound to an *o*-nitroso derivative.

The reaction of phenolic compounds with nitrous acid [6] or nitric acid [7] has been applied to the colorimetric determination of phenols and the coloured compound obtained in alkaline solution has been regarded as a salt of the quinone oxime.

Ochiai and Nakamura [8], however, reported that the compound obtained by Wieland and Kapelmeier [9] on treatment of morphine with N_2O_3 was not 2-nitrosomorphine but 2-nitromorphine. Most recently Baggesgaard Rasmussen and Boll [10] have published results which strongly favour the formulation of the compound as 2-nitromorphine.

The formation of a nitro derivative is in agreement with the results of Philpot and Small [11] who examined the action of nitrous acid on *p*-cresol and tyrosine and found, that unless the nitroso compound was trapped as the stable copper derivative, very little of it accumulated, since it was rapidly transformed further. The products of further reaction was found to depend on the concentration of nitrous acid and phenols and on the temperature. At high concentrations of nitrous acid the formation of nitro compounds was suggested, whereas diazo derivatives were formed at somewhat lower concentrations of nitrous acid.

The purpose of the present investigation was to determine the nature of the derivative responsible for the polarographic wave obtained from morphine after treatment with nitrous acid. The investigation consists of a polarographic examination of "2-nitrosomorphine" and related compounds, and a preparative reduction at controlled potential of some of these compounds.

POLAROGRAPHIC INVESTIGATION

In Table 1 are listed the half-wave potentials at a few pH-values of 4-hydroxy-3-nitro-toluene, 4-hydroxy-3-nitroso-toluene, 3-hydroxy-6-nitro-toluene, 3-hydroxy-6-nitroso-toluene, "2-nitroso-morphine", prepared according to Wieland and Kappelmeier [9], and 4-nitro-estrone.

Table 1. Half-wave potentials (*vs.* S.C.E.) at different pH-values of "2-nitroso-morphine" and some reference compounds.

	4-Hydroxy-3-nitro-toluene	4-Hydroxy-3-nitroso-toluene	3-Hydroxy-6-nitro-toluene	3-Hydroxy-6-nitroso-toluene	"2-Nitroso-morphine"	4-Nitro-estrone
pH	0.78	1.32	0.81	0.96	0.80	1.02
$E_{\frac{1}{2}}$	0.14_5	$\begin{cases}+0.22\\-0.09\end{cases}$	0.23	+0.20	0.14	0.15
pH	3.00	3.05	2.93	3.00	3.13	3.63
$E_{\frac{1}{2}}$	0.25_5	$\begin{cases}+0.09_5\\-0.35\end{cases}$	0.39_5	+0.04	0.24	0.31_5
pH	4.65	4.62	4.65	4.58	4.92	5.15
$E_{\frac{1}{2}}$	0.35	$\begin{cases}-0.00_5\\-0.9\end{cases}$	0.51	−0.08	0.34	0.40_5
pH	6.88	6.88	6.90	6.84	7.07	7.44
$E_{\frac{1}{2}}$	0.45	0.15	0.60	0.21	0.52_5	0.52
pH	8.86	9.01	8.89	8.89	9.13	10.0
$E_{\frac{1}{2}}$	0.58	0.28_5	0.79	0.34	0.59_5	0.63
pH	13	13	13	13	13	13
$E_{\frac{1}{2}}$	0.80_5	0.54_5	$\begin{cases}0.99\\1.40\end{cases}$	0.59	0.82_5	0.86_5

The polarographic behaviour of 4-hydroxy-3-nitro-toluene in the medium used was similar to that of *o*-nitrophenol found by Stocesova [12]. The wave obtained in acid and alkaline solution corresponded to a 6 electron reduction, which was verified by a controlled potential reduction at pH 1.5 and 10. This is in disagreement with the results of Astle *et al.*[13] who from the wave height in acid solution reported that 4 electrons were consumed in acid solution. In a pH interval around pH 5 the height of the wave corresponded to a consumption of less than 6 electrons (between 4 and 5) and the main wave was mostly succeeded by a drawn out wave. The sum of the waves nearly corresponded to a 6 electron reduction. The reason for this behaviour, according to Stocesova, is that the *o*-hydroxyphenylhydroxylamine which is primarily formed by a 4 electron reduction is converted to the quinoneimine, which is reduced by a 2

electron reduction. The conversion is acid-base catalyzed, and in a pH-interval around 5 the height of the wave is determined by the rate of the conversion.

The 4-hydroxy-3-nitroso-toluene showed at pH-values higher than 8 a single wave corresponding to a 4 electron reduction, which was verified by a controlled potential reduction at pH 10. In acid solution 2 waves occurred. The height of the first wave corresponded to between 2.5 and 3 electrons and the second one to about 1 electron. The second wave became more and more drawn out at higher pH values and disappeared almost at pH 6. The half-wave potential of the first wave was in the whole pH region 0.25—0.3 V more positive than that of the nitro compound.

The polarographic behaviour of 3-hydroxy-6-nitro-toluene was somewhat different from that of 4-hydroxy-3-nitro-toluene. The compound showed a single wave at pH-values lower than 7 corresponding to a 6 electron reduction, which was verified by a controlled potential reduction at pH 4. At pH 7 the wave was somewhat drawn out and in a small interval about pH 8 the wave split up in 2 waves. From pH 9 to 10 a single 6 electron wave again was found, but at higher pH values the wave split up in two waves. The height of these waves were dependent upon pH, but the nature of the phenomenon was not investigated further.

3-Hydroxy-6-nitroso-toluene was reduced in a single step at pH values higher than 7 and the wave corresponded to a 4 electron reduction, which was verified by a controlled potential reduction at pH 10. In an interval around pH 5 the height of the main wave decreased somewhat and a drawn out, second wave appeared.

"2-Nitroso-morphine" was reduced polarographically very similarly to 4-hydroxy-3-nitro-toluene. At pH-values higher than 7 a single wave was obtained, whereas the main wave decreased somewhat in a pH interval about pH 4 and a second wave appeared, which became more and more drawn out at higher pH-values. The difference between the half-wave potential of 4-hydroxy-3-nitro-toluene and that of "2-nitroso-morphine" was, except at pH about 6, less than 0.02 V.

4-Nitro-estrone was reduced in a single 6 electron wave in the whole pH region, except in a small interval about pH 5. The diminishing of the wave was not very pronounced.

Another series of experiments were performed in which morphine, estrone and a few of their derivatives together with some model compounds were treated with nitrous acid under the conditions used by Baggesgaard Rasmussen *et al.*[1] for the determination of morphine (N HCl, method A) and those described by Gry[4] for the determination of estrone (acetate buffer pH 3.2, method B). After treatment with nitrous acid excess of potassium hydroxide (method A) or ammonium hydroxide (method B) was added. In some cases no nitrite was present. The results are summarized in Table 2, where only the half-wave potentials of the main wave(s) is given.

Morphine treated with nitrite (method A) and "2-nitroso-morphine" without nitrite behaved very similarly; morphine only differed from "2-nitroso-morphine" by a small second wave succeeding the main wave. The height of this wave was about 5 % of the height of the main wave; the half-wave potential was about 1.0 V. The nature of this wave was not investigated further.

Table 2. Half-wave potentials of the main wave(s) obtained on treatment of some phenolic compounds with nitrous acid.

Compound	Method	Nitrite	pH	$E_{\frac{1}{2}}$ V
Morphine	A	+	14	0.84
"2-Nitroso-morphine"	A	–	14	0.84
p-Cresol	A	+	14	0.82_5
p-Cresol	B	+	10	0.76
4-Hydroxy-3-nitroso-toluene	A	–	14	0.56
4-Hydroxy-3-nitroso-toluene	B	–	10	0.36
4-Hydroxy-3-nitroso-toluene	B	+	10	0.75
4-Hydroxy-3-nitro-toluene	A	–	14	0.81
4-Hydroxy-3-nitro-toluene	B	–	10	0.75_5
4-Hydroxy-3-amino-toluene	B	+	10	0.54 1.02
Estrone	B	+	10	0.65
4-Nitro-estrone	B	–	10	0.64_5
m-Cresol	B	+	10	0.44 0.81 1.00
3-Hydroxy-6-nitroso-toluene	B	–	10	0.43
3-Hydroxy-6-nitroso-toluene	B	+	10	0.99
3-Hydroxy-6-nitro-toluene	B	–	10	0.98_5
2,4-Dinitro-phenol	B	–	10	0.69 0.97

Treatment (method A) of *p*-cresol with nitrite yielded a main wave very much like that of 4-hydroxy-3-nitro-toluene under the same conditions without nitrite, but different from the wave of 4-hydroxy-3-nitroso-toluene without nitrite. The main wave of the "nitrosated" *p*-cresol was preceded by a small wave (wave height about 5 % of the height of the main wave) with a half-wave potential about 0.47 V. This wave might have been due to the nitroso derivative or the "diazo-derivative" [11].

Estrone with nitrite in acetate buffer (method B) produced a wave similar to that of 4-nitro-estrone without nitrite.

p-Cresol nitrosated (method B) with potassium nitrite or amyl nitrite, 4-hydroxy-3-nitroso-toluene with nitrite and 4-hydroxy-3-nitro-toluene without nitrite showed very similar waves, which were different from the wave of 4-hydroxy-3-nitroso-toluene under the same conditions without nitrite.

m-Cresol on the same treatment produced 3 waves, a small wave at the same potential as did 3-hydroxy-6-nitroso-toluene without nitrite and a main wave at the same potential as that of 3-hydroxy-6-nitro-toluene. The nature of the third wave at a potential between the other two waves is not known. 3-Hydroxy-6-nitroso-toluene produced on treatment with nitrous acid a wave at the same potential as that of the nitro derivative; only a small part remained as the nitroso compound.

The spectra of the solutions used for polarography (method B) showed, that other compounds besides the nitro derivative were formed from *p*-cresol on treatment with nitrous acid. 4-Hydroxy-3-nitro-toluene showed under

these conditions (pH 10) an absorption maximum about 437 mμ, 4-hydroxy-3-nitroso-toluene (without nitrite) a maximum about 454 mμ and the maximum of the "nitrosated" *p*-cresol varied around 420 mμ.

PREPARATIVE REDUCTIONS

4-Hydroxy-3-nitro-toluene was reduced at pH 1.5 and 10. At pH 1.5 a small second wave was found on the polarograms taken in the strong solutions (5×10^{-2} M) used for the preparative reductions indicating that the rate of the conversion of the primarily formed phenylhydroxylamine derivative was not sufficiently high to secure a single 6 electron wave under these conditions. As the reduction, however, consumed 5.9 ± 0.1 electrons the intermediate formed product must be transformed in the bulk of the solution to a species reducible at the potential used, which is considerably more positive than the half-wave potential of the second wave. Some coloured compounds were formed during the reduction, but apparently not enough to influence the electron consumption to any appreciable degree. At pH 10 6.0 electrons were consumed, and in both cases the expected 4-hydroxy-3-amino-toluene was isolated. The same compound was obtained by the reduction at pH 10 of 4-hydroxy-3-nitroso-toluene. The reduction required 4 electrons. 3-Hydroxy-6-nitro-toluene was reduced at pH 4 consuming 6 electrons and 3-hydroxy-6-nitroso-toluene at pH 10 requiring 4 electrons for the reduction.

"2-Nitroso-morphine" was reduced at pH 10 at —0.85 V. The reduction consumed 5.95 ± 0.1 electrons and an aromatic amine could be detected in the reaction mixture.

DISCUSSION

The polarographic data presented in Tables 1 and 2 substantiate the assumption that *p*-substituted phenols on treatment with excess of nitrous acid form mononitro derivatives as a main product. The reaction, however, is not clean and various amounts of other phenolic derivatives are formed. The importance of these side reactions depends among other things on the structure of the phenolic compound; tyrosine, for instance, forms much more material of unidentified structure than does *p*-cresol under the same conditions. A special method, therefore, has to be developed for a given phenol, if a polarographic determination of the compound is to be worked out.

The question whether the nitro compounds are formed by a direct attack of N_2O_4 on the phenol or by an oxidation of a primarily formed nitroso derivative cannot be answered conclusively, although it can be pointed out, that both 4-hydroxy-3-nitroso-toluene and 3-hydroxy-6-nitroso-toluene on treatment with nitrous acid yield, more or less completely, the nitro derivative.

The investigation of Baggesgaard Rasmussen *et al.*[1] and the data presented here point to the conclusion that the wave obtained on treatment of morphine with nitrous acid is due to the compound formulated by Wieland and Kappelmeier as "2-nitroso-morphine". The reduction wave of this compound is found to represent a 6 electron reduction under conditions, where 4-hydroxy-

3-nitro-toluene consumed 6 electrons and 4-hydroxy-3-nitroso-toluene was reduced by 4 electrons per molecule. As it seems very unlikely that other parts of the molecule than the substituent in the 2 position are involved in the reduction the presented data are taken as strong evidence in favour of the formulation [8,10] of the compound obtained by Wieland *et al.* as 2-nitro-morphine.

The result of the present investigation is that the main polarographic wave obtained on treatment of morphine [1], estrone [4], or *p*-cresol with excess of nitrous acid is due to the reduction of the mononitro derivative rather than the mononitroso derivative.

EXPERIMENTAL

The polarograph was a recording polarograph Radiometer Type PO 3a. The capillary delivered 3.24 mg of mercury per second at a corrected mercury height of 48.5 cm; the drop time 5.82 sec (H_2O, open circuit); the capillary constant $m^{2/3}t^{1/6} = 2.94$ $mg^{2/3}sec^{-1/2}$.

The reference electrode, the buffer solutions and the apparatus used for the controlled potential reductions were the same as described in Part I [14] and III [15]. The medium used in the polarographic investigation was aqueous N KCl, except for the nitroestrone, where the solution contained 40 % alcohol.

4-Hydroxy-3-nitroso-toluene was made according to Philpot and Small [11]. It was recrystallized from petrol ether (b. p. 60°—80°) by cooling in a carbon dioxide-acetone cooling bath, m. p. 56°—58°.

"2-Nitroso-morphine" was prepared according to Wieland *et al.*[9] and the potassium salt purified after recrystallization from alcohol by chromatography [10]. The potassium salt was converted to the hydrochloride. (Found: C 49.75; H 5.94; N 6.90; Cl 9.38. Calc. for $C_{17}H_{19}N_2O_5$, 2 ½ H_2O: C 49.62; H 5.89; N 6.81; Cl 8.63.)

Reduction of "2-nitroso-morphine". 400 mg of the hydrochloride of "2-nitroso-morphine" was dissolved in 120 ml N NaCl containing 5 % sodium bicarbonate and 5 % sodium carbonate, which was deaerated and purified by electrolysis beforehand. The compound was reduced at −0.85 V (*vs* S.C.E.). The reduction was followed polarographically. It required 5.9_5 electrons. After completion of the reduction a small part of the reaction mixture was made acid and treated with sodium nitrite. After destruction of excess of nitrous acid with ammonium sulfamate, naphthylethylenediamine was added, and a violet colour slowly developed indicating the presence of an aromatic amine in the reduction medium. 2-Amino-morphine was found by Wieland *et al.* to couple slowly after diazotation. Attempts to isolate the diamine were not succesful.

REFERENCES

1. Baggesgaard Rasmussen, H., Hahn, C. and Ilver, K. *Dansk Tidskr. Farm.* **19** (1945) 41.
2. Brezina, M. and Zuman, P. *Die Polarographie in der Medizin, Biochemie und Pharmazie*, Akademische Verlag Leipzig 1956, p. 338.
3. Jindra, A., Junger, V. and Zyka, J. *Ceskoslov. Farm.* **1** (1952) 177.
4. Gry, O. *Dansk Tidskr. Farm.* **23** (1949) 139.
5. Heusghem, C. *J. pharm. Belg.* **5** (1950) 3.
6. Lykken, L., Treseder, R. S. and Zahn, V. *Ind. Eng. Chem., Anal. Ed.* **18** (1946) 103.
7. Stoughton, R. W. *J. Biol. Chem.* **115** (1936) 293.
8. Ochiai, E. and Nakamura, T. *Proc. Imp. Acad. (Tokyo)* **14** (1938) 134; *Chem. Abstr.* **32** (1938) 5843.

9. Wieland, H. and Kappelmeier, P. *Ann.* **382** (1911) 306.
10. Baggesgaard Rasmussen, H. and Boll, P. *Acta Chem. Scand.* **12** (1958) 885.
11. Philpot, J. St. L. and Small, P. A. *Biochem. J.* **321** (1938) 534.
12. Stocesova, D. *Collection Czechoslov. Chem. Communs.* **14** (1949) 615.
13. Astle, M. J. and Cropper, W. P. *J. Am. Chem. Soc.* **65** (1943) 2395.
14. Lund, H. *Acta Chem. Scand.* **11** (1957) 283.
15. Lund, H. *Acta Chem. Scand.* **11** (1957) 990.

Received May 27, 1958.

ACTA CHEMICA SCANDINAVICA 12 (1958) 1451—1455

Localization of the C=S and the C—S Group Frequencies in Carboxymethyl Dithioesters

BØRGE BAK, LISE HANSEN-NYGAARD and CHRISTIAN PEDERSEN

Chemical Laboratory of the University of Copenhagen, Copenhagen, Denmark

Twenty-one carboxymethyl dithioesters were investigated spectrophotometrically in the infrared (400—4 000 cm^{-1}). Almost without exceptions intense bands were observed at 1 350—1 365, 1 290—1 325, 1 190—1 225, and 640—670 cm^{-1}. The bands close to 1 200 and 660 cm^{-1} were assigned to the C=S and the C—S stretching frequency modes.

The location of the C=S and the C—S group frequencies in organosulphur compounds has been a matter of considerable discussion. The literature concerned with this problem has lately been reviewed by Bellamy [1]. Both group frequencies are difficult to localize because they, unlike *e. g.* the characteristic C—H, C=N, and C=O frequencies, fall in a spectral region where "fingerprint frequencies" are numerous. Valuable guidance as to their approximate position may, however, be obtained by a simplified force-constant calculation. From this it follows, that the two frequencies must be looked for in the vicinity of 1 200 cm^{-1} (C=S) and 700 cm^{-1} (C—S). Probably, therefore, the somewhat meager literature on the localization of the latter frequency is caused by the fact that the usual rock-salt optics does not allow observations below *ca.* 700 cm^{-1}. Since a number (21) of new carboxymethyl dithioesters were prepared in this laboratory [2] we decided to determine their infrared absorption spectra. All dithioesters should possess the two group frequencies we are looking for. Recently, Brader *et al.*[3] have studied infrared spectra of a few (7) alkyl dithioesters. Tentatively they assigned the C=S frequency to 1 170—1 195 cm^{-1} for dithioesters but they were unable to identify the C—S frequency because of lack of KBr-optics. Felumb [6] located the C=S group frequency in dixanthogenes to the 1 210—1 230 cm^{-1} region. Schotte [7] has found the C—S group frequency in a series of dithiolane derivatives. Also, the paper by Mecke [8] on thiocarbonyl compounds discusses the position of the C=S band.

Table 1. Schematic representation of infrared absorption spectra of 21 carboxymethyl
Ordinate in mm = 1/10 of observed optical density per

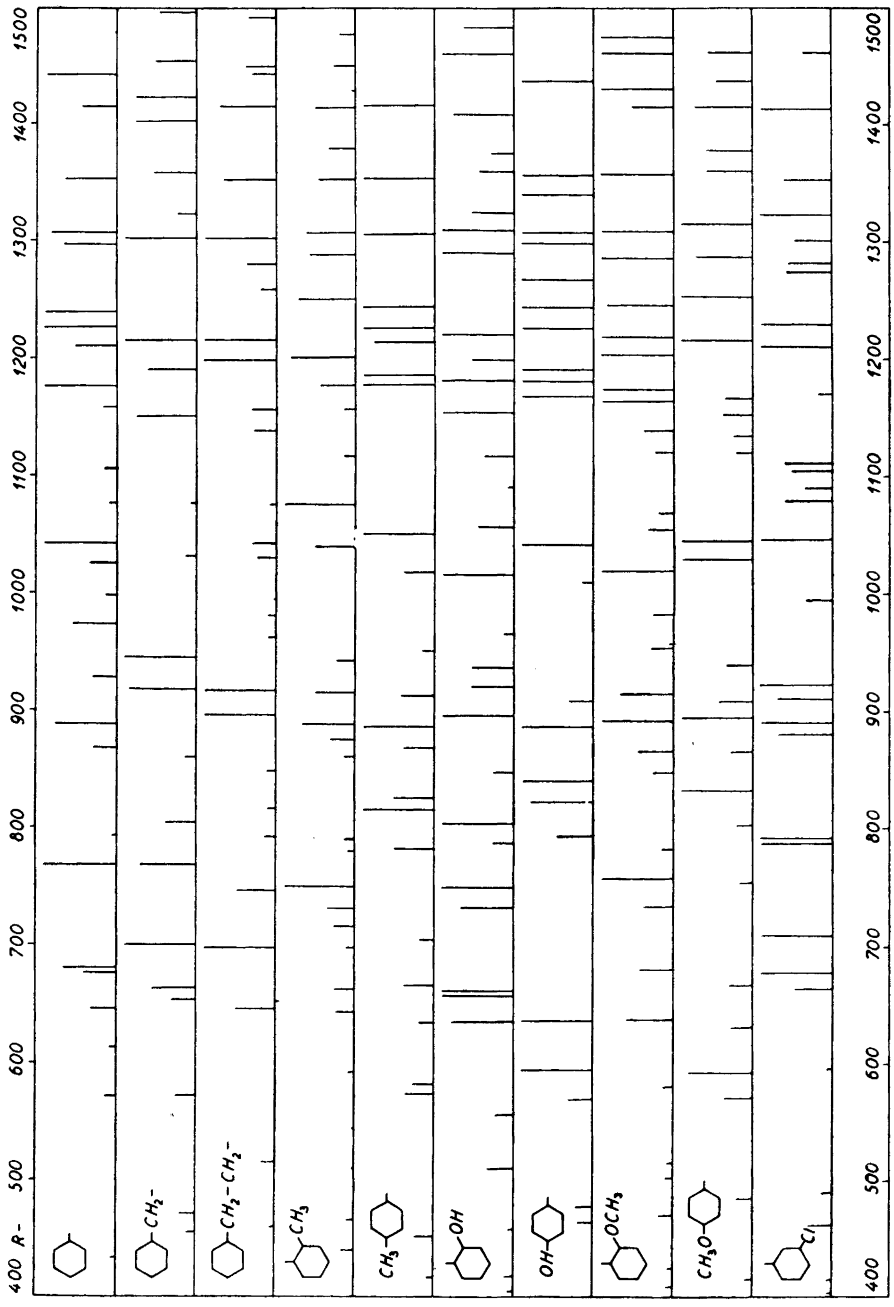

Table 1 (a)

dithioesters ($R-CSSCH_2COOH$). Abscissa: wavenumber of radiation (400—1 500 cm^{-1}). millimole if less than 100. Higher densities recorded as 10 mm.

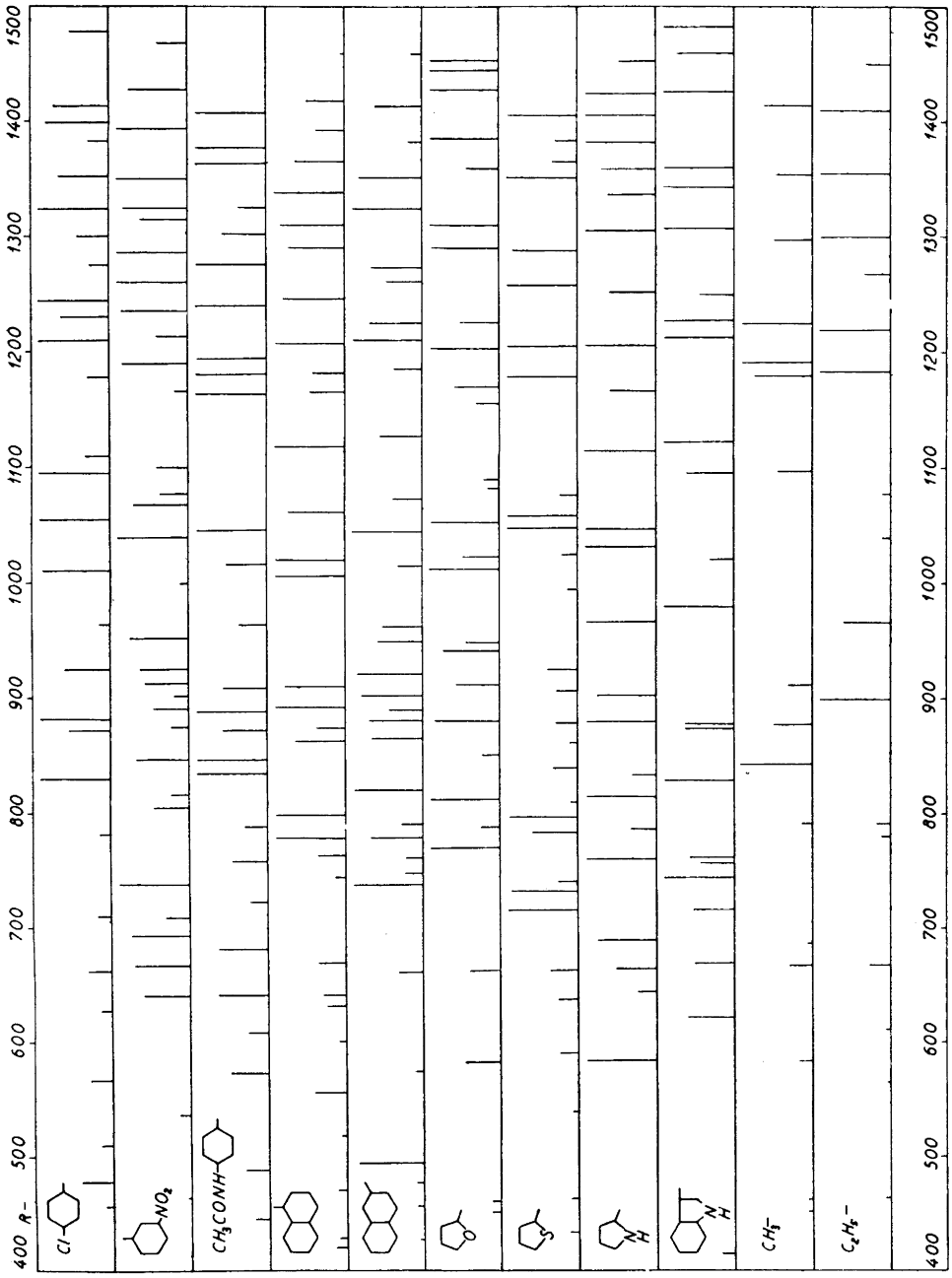

Table 1 (b)

EXPERIMENTAL

The spectra were obtained employing a Perkin-Elmer model 21 double beam infrared spectrophotometer equipped with NaCl, KBr, and CaF_2 optics. Since the compounds investigated are solids, KBr disk technique was applied (300 mg KBr mixed with 0.4—1.8 mg sample). The error in the frequency measurements is thought to be less than 2 cm^{-1}. For convenience the main features of the observed spectra are recorded graphically in Table 1. Although all the spectra were examined in the 400—4 000 cm^{-1} region it was not found useful to include more than the 400—1 500 cm^{-1} interval in Table 1. The spectra of all the compounds in question show, of course, the very broad and intense carboxyl band in the 2 400—3 400 cm^{-1} region and the intense carbonyl band at 1 700—1 725 cm^{-1}, these bands are of little diagnostic value.

DISCUSSION

The analysis was started by localizing a number of group frequencies that must be present in the spectra of these compounds according to their composition (*e. g.* the CH_3-, the CH_2-, the C_6H_5-, and the OH-group frequencies). It was, *i. a.*, noted that the two low-frequency COOH-bands appeared rather persistently in the 1 400—1 425 cm^{-1} and the 880—945 cm^{-1} intervals.

Two other bands of rather constant frequency throughout the series were observed, *viz.* bands at 1 350—1 365 and 1 290—1 325 cm^{-1}. The present spectroscopic material is insufficient for an identification of the mechanical

Table 2. Observed optical densities per mmole (D_{obs}) for C=S and C—S group frequencies.

Radical R—	C=S		C—S			
	D_{obs} per mmole	Frequency	D_{obs} per mmole		Frequency	
Phenyl-	113	1 226	45		667	
Benzyl-	210	1 215	62		663	
a-Phenylethyl-	240	1 215	56		661	
o-Tolyl-	89	1 200	31		662	
p-Tolyl-	110	1 225	44		666	
o-Hydroxyphenyl-	210	1 219	118		662	
p-Hydroxyphenyl-	350	1 225				
o-Methoxyphenyl-	260	1 218	13		670	
p-Methoxyphenyl-	132	1 215	36		667	
m-Chlorophenyl-	130	1 210	54		664	
p-Chlorophenyl-	115	1 210	33		662	
m-Nitrophenyl-	94	1 190	66	(79)	640	(667)
p-Acetamidophenyl-	230	1 194	71	(71)	640	(682)
a-Naphthyl-	110	1 207	41		670	
β-Naphthyl-	120	1 210	37		662	
2-Furyl-	175	1 203	46		663	
2-Thenyl-	112	1 205	42		664	
2-Pyrryl-	200	1 206	60		665	
3-Indolyl-	294	1 213	57		670	
Methyl-	130	1 225	34		668	
Ethyl-	100	1 220	31		668	

character of these modes of vibration. They must, however, somehow be characteristic for the —$CSSCH_2COOH$ grouping since the radicals attached to the group are rather different. Neither of the two bands can be attributed to the C=S stretching vibration because of their position at too high a frequency.

Table 2 gives the observed optical density (D_{obs}) per mmole substance for bands in the 1 190—1 225 cm^{-1} interval finally assigned as the C=S stretching frequency, and for bands in the 640—670 cm^{-1} interval assigned as the C—S stretching frequency.

The result fits well with the assignment given by Mecke and Spiesecke for CH_3CSSH [4]. They found ν (C=S) = 1 216 cm^{-1}. Also there is substantial agreement with Sheppards paper [5] in which "primary" mercaptans, sulphides and disulphides all were shown to absorb in the 630—660 cm^{-1} region.

The C—S band is, therefore, unobservable by means of the ordinary NaCl optics.

Acknowledgment. We are indebted to professor K. A. Jensen of this laboratory for making the dithioesters investigated here available to us.

REFERENCES

1. Bellamy, L. J. *The Infrared Spectra of Complex Molecules*, Methuen, London; Wiley, New York 1954, p. 288.
2. Jensen, K. A. and Pedersen, Chr. *Acta Chem. Scand. To be published.*
3. Marvel, C. S., De Radzitzky, P. and Brader, J. J. *J. Am. Chem. Soc.* **77** (1955) 5997.
4. Mecke, R. and Spiesecke, H. *Ber.* **89** (1956) 1110.
5. Sheppard, N. *J. Chem. Phys.* **17** (1949) 79.
6. Felumb, R. *Bull. soc. chim. France* **1957** 890.
7. Schotte, L. *Arkiv Kemi* **9** (1956) 441.
8. Mecke, R. et al. *Ber.* **90** (1957) 975.

Received May 21, 1958.

ACTA CHEMICA SCANDINAVICA 12 (1958) 1456—1475

Kristallviolett. Eine quantitative Untersuchung über die Protolysenverhältnisse in Wasserlösungen

RUNE CIGÉN

Abteilung für anorganische und physikalische Chemie des Chemischen Instituts der Universität Lund, Schweden

Die Protolysenreaktionen des Kristallviolett, KV, wurden quantitativ untersucht. KV bildet eine Reihe gefärbte Formen, die in Protonengleichgewicht miteinander stehen. Diese gefärbten Formen stehen in Hydratationsgleichgewicht mit einer Reihe farbloser Formen, die ihrerseits miteinander in Protonengleichgewicht stehen. Die Protonengleichgewichte stellen sich momentan ein, während die Hydratationsgleichgewichte messbare Zeit brauchen, um sich einzustellen. Ein Protolysenschema wurde aufgestellt, und die in diesem Schema enthaltenen 5 Dissoziations-, 4 Hydratations- und 8 Geschwindigkeitskonstanten wurden bestimmt. Ferner wurden die Absorptionskurven der drei gefärbten Formen des KV bestimmt.

Die Messungen wurden spektrophotometrisch bei 20°C und mit konstanter Ionenstärke = 0,5 M durchgeführt.

Von den zahlreichen Untersuchungen über basische Triphenylmethanfarbstoffe, die in den letzten fünfzig Jahren durchgeführt worden sind, behandeln nur wenige ihre Protolysenverhältnisse quantitativ. Vor kurzem publizierte Cigén [1] eine Dissertation, in der die Protolysenverhältnisse von zehn basischen Triphenylmethanfarbstoffen mit zwei reaktiven Aminogruppen genau untersucht worden waren. Sämtliche untersuchte Farbstoffe folgten demselben Reaktionsschema, und die zum Protolysenschema gehörenden Dissoziations-, Hydratations- und Geschwindigkeitskonstanten konnten bestimmt werden. Als eine Fortsetzung dieser Arbeiten ist nun das Kristallviolett, das drei reaktive Aminogruppen hat, untersucht worden. Das Kristallviolett wird in der Folge KV geschrieben. Das Perchlorat hat die Formel $[(CH_3)_2NC_6H_4]_3C\,ClO_4$.

Adams und Rosenstein [2] haben einen Versuch gemacht, Dissoziationsgleichgewichte und Reaktionsgeschwindigkeiten von KV zu bestimmen. Die Zahlenwerte, die diese erhalten haben, sind zwar wegen mangelhafter Methodik im grossen und ganzen irreführend und unterscheiden sich, in den wenigen Fällen, wo ein Vergleich möglich ist, stark von denen, die in dieser Arbeit vorgelegt werden.

Es ist schon lange bekannt, dass Farbstoffe, die zu dem jetzt untersuchten Typus gehören, in einer Reihe gefärbter und einer Reihe farbloser Formen auftreten können, wobei das pH der Lösung die Verteilung unter die verschiedenen Komponenten bestimmt. Man kann schematisch die Reaktionen auf folgende Weise schreiben: $R = [(CH_3)_2NC_6H_4]_3C$

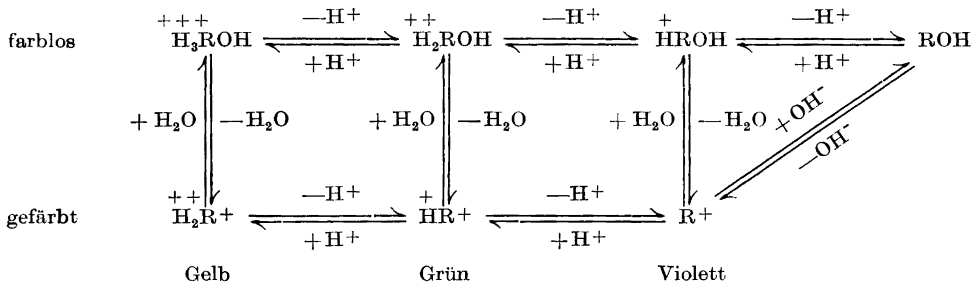

Das aufgestellte Schema ist das denkbar einfachste. Es berücksichtigt nicht die Isomeriemöglichkeiten [3] oder den Umstand, dass die Reaktionen sicher über Zwischenformen gehen. Frühere Untersuchungen [1] über Farbstoffe mit zwei reagierenden Aminogruppen zeigten, dass die Protonengleichgewichte sich "momentan", d.h. mit nicht messbarer Geschwindigkeit, einstellen, während die Zeitreaktionen im Bereich $pH<10$ Hydratationen sind, deren wirkliche Geschwindigkeitskonstanten unabhängig von dem pH sind. Für $pH > 10$ bekommt man Zeitreaktionen, deren Geschwindigkeiten zeigen, dass OH^--Ionen an der Protolyse teilnehmen.

Man kann annehmen, dass KV ein Protolysenschema hat, welches im Prinzip dem gleicht, das früher für die nahe verwandten Farbstoffe aufgestellt worden ist (Cigén [1]). Wir nehmen demnach an, dass KV eine Reihe von gefärbten Formen bilden kann, die durch rasche Protonenaufnahme oder Protonenabspaltung ineinander übergehen, und eine Reihe von farblosen Formen, die auch in sich schnell einstellenden Protonengleichgewichten miteinander stehen. Zwischen den drei farblosen Salzen und den drei gefärbten Formen herrschen Hydratationsgleichgewichte, deren Zustandekommen eine gewisse messbare Zeit beansprucht. Zwischen dem farblosen nicht geladenen Carbinol und der violetten Form herrscht bei hohem pH ein OH^--Gleichgewicht, das, um sich einzustellen, eine messbare Zeit beansprucht.

Wenn man die Protolysenreaktionen quantitativ untersuchen will, muss man mathematische Beziehungen zwischen Reaktionsgeschwindigkeiten, Farbennuancen, Farbenintensitäten und pH ableiten. Um solche Ableitungen bequemer zu erzielen, werden folgende Bezeichnungen und Kürzungen eingeführt:

$$ROH = C, \quad \overset{+}{H}ROH = S_1, \quad \overset{++}{H_2}ROH = S_2, \quad \overset{+++}{H_3}ROH = S_3$$

$$R^+ = B, \quad \overset{+}{H}R+ = G, \quad \overset{++}{H_2}R+ = Y, \quad [H^+] = h, \quad [OH^-] = oh$$

Ferner werden folgende Konstanten definiert:

a) Dissoziationskonstanten: $K_1 = \frac{h[G]}{[Y]}$, $K_2 = \frac{h[B]}{[G]}$,

$K'_1 = \frac{h[S_2]}{[S_3]}$, $K'_2 = \frac{h[S_1]}{[S_2]}$, $K'_3 = \frac{h[C]}{[S_1]}$

b) Hydratationskonstanten (Gleichgewichtskonstanten):

$K_4 = \frac{[S_3]_\infty}{[Y]_\infty}$, $K_5 = \frac{[S_2]_\infty}{[G]_\infty}$, $K_6 = \frac{[S_1]_\infty}{[B]_\infty}$

c) Geschwindigkeitskonstanten (Gk):

k_1 = die Gk der Reaktion $Y + H_2O \rightarrow S_3$
k_2 = » » » » $S_3 \rightarrow Y + H_2O$
k_3 = » » » » $G + H_2O \rightarrow S_2$
k_4 = » » » » $S_2 \rightarrow G + H_2O$
k_5 = » » » » $B + H_2O \rightarrow S_1$
k_6 = » » » » $S_1 \rightarrow B + H_2O$
k_7 = » » » » $B + OH^- \rightarrow C$
k_8 = » » » » $C \rightarrow B + OH^-$

Die Untersuchungen wurden mit einem Spektrophotometer durchgeführt, weshalb spezifische Extinktionen benutzt wurden, um die Konzentrationen der verschiedenen Farbstoffskomponenten auszudrücken. Hierbei bedeuten:

ε_B,	ε_G,	ε_Y	die molekularen Extinktionskoeffizienten für B, G und Y.
e_o,	e_t,	e_∞	die spezifische Extinktion einer Lösung bei der Zeit 0 und t und bei Gleichgewicht (die Schichtdicke $d = 1$ cm).
E_o,	E_t,	E_∞	die abgelesenen Extinktionen, wenn $d \neq 1$.
e_B,	e_G,	e_Y	die spezifischen Extinktionen für B, G und Y.

ABLEITUNG VON NÖTIGEN FORMELN

Vorbereitende Untersuchungen über KV zeigten, dass KV im pH-Gebiete 5—6 bei Gleichgewicht in Form von B bis sehr nahe an 100 % vorliegt. Dies bedeutet, dass das Gleichgewicht $B + H_2O \rightleftharpoons S_1$ gegen das gefärbte B stark verschoben ist. Dagegen ist das Gleichgewicht $Y + H_2O \rightleftharpoons S_3$ stark gegen das farblose S_3 verschoden, und eine Lösung mit einem pH < 1 ist bei Gleichgewicht nahezu völlig entfärbt. Das Gleichgewicht $G + H_2O \rightleftharpoons S_2$ nimmt eine Zwischenstellung ein, und die vorbereitenden Untersuchungen deuteten an, dass es relativ stark gegen das gefärbte G verschoben ist. Alkalische Lösungen, mit pH > 11, sind nahezu entfärbt wegen des entstandenen farblosen Carbinols, C.

Die Bestimmung von K_1 und K_2. Man geht von einer Wasserstammlösung des KV, pH ~ 5, aus, wo [B] = die Totalkonzentration, C_M, des Farbstoffes. Diese Stammlösung wird mit Puffern von HCl + KCl von verschiedenem pH gemischt. Hierbei stellen sich die Gleichgewichte zwischen den verschiedenen

gefärbten Formen B, G und Y "momentan" ein. Wir bekommen, wenn sich diese schnellen Gleichgewichte eingestellt haben, bei $t = 0$

$$C_M = [B]_o + [G]_o + [Y]_o \tag{1}$$

$$e_o = [B]_o\varepsilon_B + [G]_o\varepsilon_G + [Y]_o\varepsilon_Y \tag{2}$$

Aber

$$C_M = [B]_o\left(1 + \frac{h}{K_2} + \frac{h^2}{K_1K_2}\right) \tag{3}$$

und

$$e_o = [B]_o\left(\varepsilon_B + \frac{h}{K_2}\varepsilon_G + \frac{h^2}{K_1K_2}\varepsilon_Y\right) \tag{4}$$

Nun ist $C_M\varepsilon_B = e_B$, $C_M\varepsilon_G = e_G$, $C_M\varepsilon_Y = e_Y$, und wir können also schreiben

$$e_o = \frac{e_B + \frac{h}{K_2}e_G + \frac{h^2}{K_1K_2}e_Y}{1 + \frac{h}{K_2} + \frac{h^2}{K_1K_2}} \tag{5}$$

(5) kann man folgendermassen schreiben

$$\frac{h}{e_o - e_B} = \frac{K_2 + h\left(1 + \frac{h}{K_1}\right)}{e_G + \frac{h}{K_1}e_Y - e_B\left(1 + \frac{h}{K_1}\right)} \tag{6}$$

Anfangs kann man in der Gleichung (6) nur h und e_B bestimmen. Man bekommt e_B, indem man eine Absorptionskurve für KV in Wasserlösung, pH $\sim$ 5, aufnimmt. e_G und e_Y können nicht unmittelbar bestimmt werden. Man kann aber eine Auffassung von der Grössenordnung des e_Y bei verschiedenen Wellenlängen bekommen, wenn man eine Absorptionskurve für KV in stark saurer Lösung aufnimmt, wo der Farbstoff bei Gleichgewicht hauptsächlich in Form von Y und S_3 vorliegt. Um K_2 zu bestimmen, wählt man eine Wellenlänge, wo $\varepsilon_Y << \varepsilon_B$. Man kann dabei $\frac{h}{K_1} \cdot \varepsilon_Y$ im Nenner der Gleichung (6) vernachlässigen. Die Messungen werden ferner bei solchen pH-Werten durchgeführt, dass $h < K_1$. In einem Diagramm trägt man $\frac{h}{e_o - e_B}$ als Funktion von h auf und bekommt so eine schwach gebogene Linie, deren Abschnitt auf der Ordinatenachse, y, und deren Winkelkoeffizient, l, wenn $h \to 0$, die Gleichungen $y = \frac{K_2}{e_G - e_B}$ und $l = \frac{1}{e_G - e_B}$ ergeben. Man bekommt also $K_2 = y/l$ und $e_G = 1/l + e_B$. Danach kann man K_1 entweder algebraisch oder graphisch bestimmen. Im ersten Falle löst man K_1 aus der Gleichung (5) heraus

$$K_1 = \frac{h^2(e_o - e_Y)}{K_2(e_B - e_o) + h\,(e_G - e_o)} \tag{7}$$

Im zweiten Falle verfährt man folgenderweise. Die Messungen werden für $h \geq K_1$ durchgeführt und bei einer Wellenlänge λ, wo e_B bedeutend kleiner als e_G ist und wo e_Y an der Seite von e_o vernachlässigt werden kann. Wenn $K_1 > 10 \cdot K_2$, kann man $K_2(e_B - e_o)$ im Nenner der Gleichung (7) vernachlässigen, die sich danach als

$$\frac{1}{e_o} = \frac{h}{K_1 e_G} + \frac{1}{e_G} \tag{8}$$

schreiben lässt. Falls die vorgenommenen Approximationen erlaubt sind, bekommt man eine Gerade, wenn man $1/e_o$ als Funktion von h aufträgt. Man erhält $e_G = 1/y$ und $K_1 = y/l$.

Die Farbintensität, die man durch Mischung der Stammlösung mit (HCl + KCl)-Puffern erhält, nimmt mit der Zeit ab. Die Farbe verbleicht, weil sowohl G als Y sich zu den farblosen S_2 und S_3 hydratisieren. Um die e_o zu bestimmen, aus welchen man K_1 und K_2 erhält, muss man also der Verbleichung kinetisch folgen und aus den Kinetikmessungen e_o durch Extrapolation der Extinktion zu der Zeit $t = 0$ bestimmen. Der Kontrolle wegen sollen die Messungen von e_o wenn möglich bei einigen verschiedenen Wellenlängen durchgeführt werden.

Die Bestimmung von K_4, K_5 und K_6. Diese Konstanten sind Gleichgewichtskonstanten und werden aus Lösungen bestimmt, die Gleichgewicht erreicht haben. Man hat dann

$$C_M = [B]_\infty + [S_1]_\infty + [C]_\infty + [G]_\infty + [S_2]_\infty + [Y]_\infty + [S_3]_\infty \tag{9}$$

$$= [B]_\infty \left[1 + K_6 + \frac{K_6 K_3'}{h} + \frac{h}{K_2}(1 + K_5) + \frac{h^2}{K_1 K_2}(1 + K_4) \right] \tag{10}$$

$$e_\infty = [B]_\infty \cdot \varepsilon_B + [G]_\infty \cdot \varepsilon_G + [Y]_\infty \cdot \varepsilon_Y \tag{11}$$

$$= [B]_\infty \left(\varepsilon_B + \frac{h}{K_2} \varepsilon_G + \frac{h^2}{K_1 K_2} \varepsilon_Y \right) \tag{12}$$

Aus (10) und (12) erhält man, da $C_M \cdot \varepsilon_B = e_B$ etc., die Gleichgewichtsextinktion e_∞

$$e_\infty = \frac{e_B + \frac{h}{K_2} e_G + \frac{h^2}{K_1 K_2} e_Y}{1 + K_6 + \frac{K_6 K_3'}{h} + \frac{h}{K_2}(1 + K_5) + \frac{h^2}{K_1 K_2}(1 + K_4)} \tag{13}$$

Aus (13) können K_4, K_5 und K_6 nur unter speziellen Voraussetzungen aufgelöst werden. In alkalischen Lösungen hat man bei Gleichgewicht das KV nur in Form von B, S_1 und C. Man kann da alle Glieder in (13), die K_1 und K_2 enthalten, vernachlässigen, und man bekommt

$$e_\infty = \frac{e_B}{1 + K_6 + \frac{K_6 K_3'}{h}} \tag{14}$$

(14) wird umgeformt zu

$$\frac{h}{e_\infty} = \frac{h(1 + K_6)}{e_B} + \frac{K_6 K_3'}{e_B} \tag{15}$$

Man bekommt eine Gerade, wenn man h/e_∞ als Funktion von h aufträgt. Der Abschnitt auf der Ordinatenachse $y = K_6 K_3'/e_B$ und der Winkelkoeffizient $l = (1 + K_6)/e_B$. Wir haben früher gesagt, dass bei pH $\sim$ 4—6 das KV nur in Form von B vorliegt, und wir können e_B aus einer Absorptionskurve, aufgenommen bei pH 4—6, erhalten. Aber hieraus folgt, dass $K_6 \ll 1$, und wir können also K_6 aus $l = (1 + K_6)/e_B$ nicht bestimmen. Dagegen können wir aus l eine Kontrolle unseres früher bestimmten Wertes von e_B erhalten, da $e_B \simeq 1/l$. Aus $y = K_6 K_3'/e_B$ bekommen wir nur $K_6 K_3' = y \cdot e_B$.

In stark sauren Lösungen kann man in erster Linie in der Gleichung (13) K_6 und $K_6 K_3'/h$ vernachlässigen. Wenn wir λ so wählen, dass e_Y neben e_B und e_G vernachlässigbar ist und K_4 auflöst, dann bekommen wir

$$K_4 = \frac{e_B + \frac{h}{K_2} \cdot e_G - e_\infty \left[1 + \frac{h}{K_2}(1 + K_5)\right]}{e_\infty \cdot h^2/K_1 K_2} - 1 \tag{16}$$

Die vorbereitenden Untersuchungen zeigten, dass das Gleichgewicht $G + H_2O \rightleftharpoons S_2$ verhältnismässig stark gegen das gefärbte G verschoben ist, weshalb es wahrscheinlich wirkt, dass $K_5 < 0{,}1$ ist. K_5 hat deshalb den Charakter eines Korrektionsgliedes in (16). In stark sauren Lösungen kann man K_4 berechnen, ohne einen genaueren Wert von K_5 zu kennen, als dass $K_5 < 0{,}1$ ist. In schwach sauren Lösungen kann man verschiedene Werte von K_5 versuchen, um zu prüfen, ob man einen konstanten K_4-Wert erhalten kann, der mit dem in stark sauren Lösungen gewonnenen K_4-Wert übereinstimmt. Auf diese Weise kann man einen approximativen Wert von K_5 berechnen.

Wenn man K_5 und K_6 genau bestimmen will, muss man ganz andere Methoden als die bisher durchgegangene ergreifen, nämlich Methoden, die sich auf die pH-Abhängigkeit der Reaktionsgeschwindigkeiten gründen. Dabei kann man auch die Geschwindigkeitskonstanten k_1—k_8 bestimmen.

ABLEITUNG VON KINETIKFORMELN

Frühere Untersuchungen über nahe verwandte Farbstoffe [1] zeigten, dass die Geschwindigkeitskonstanten bei den Hydratationen in dem Reaktionsschema unabhängig von dem pH sind. Dagegen wird die Geschwindigkeit, mit der eine Lösung ihre Farbintensität ändert, wegen des komplizierten Reaktionsschemas von dem pH abhängig. Wenn man annimmt, dass dasselbe auch für das KV gilt, kann man folgende Beziehungen zwischen Geschwindigkeits-, Hydratations-, Dissoziationskonstanten und $[H^+]$ ableiten. Man muss aber daran denken, dass das aufgeschriebene Schema den geschwindigkeitsbestimmenden Bruttoverlauf angibt. Der Reaktionsmechanismus ist komplizierter als was aus dem Schema hervorgeht.

Wir leiten Kinetikformeln ab, die für das ganze pH-Intervall 1—13 gelten. Die Reaktionen verlaufen als pseudomonomolekulare, da die Totalkonzentration des Farbstoffes $C_M \leq 10^{-5}$ M ist und Pufferlösungen bei den Messungen benutzt werden.

Wenn man die oben eingeführten Bezeichnungen verwendet, kann man die Bildungsgeschwindigkeit für B + G + Y folgendermassen schreiben

$$\frac{d([B] + [G] + [Y])}{dt} = k_2[S_3] - k_1[Y] + k_4[S_2] - k_3[G] + k_6[S_1] - \\ - k_5[B] + k_8[C] - k_7[B]oh \qquad (17)$$

oder

$$\left(1 + \frac{h}{K_2} + \frac{h^2}{K_1K_2}\right)\frac{d[B]}{dt} = \left(k_2 + k_4 \cdot \frac{K_1'}{h} + k_6 \cdot \frac{K_1'K_2'}{h^2} + k_8 \cdot \frac{K_1'K_2'K_3'}{h^3}\right)[S_3] - \\ - \left(k_1 \cdot \frac{h^2}{K_1K_2} + k_3 \cdot \frac{h}{K_2} + k_5 + k_7 \cdot oh\right)[B] \qquad (18)$$

die

$$\frac{d[B]}{dt} = k'[S_3] - k''[B] \qquad (19)$$

geschrieben werden kann.

Nun ist

$$C_M = [B] + [G] + [Y] + [S_3] + [S_2] + [S_1] + [C] \qquad (20)$$

und man kann

$$C_M = \left(1 + \frac{h}{K_2} + \frac{h^2}{K_1K_2}\right)[B] + \left(1 + \frac{K_1'}{h} + \frac{K_1'K_2'}{h^2} + \frac{K_1'K_2'K_3'}{h^3}\right)[S_3] \qquad (21)$$

schreiben, und bekommt also

$$[S_3] = \frac{C_M - \left(1 + \frac{h}{K_2} + \frac{h^2}{K_1K_2}\right)[B]}{1 + \frac{K_1'}{h} + \frac{K_1'K_2'}{h^2} + \frac{K_1'K_2'K_3'}{h^3}} = \frac{C_M - A[B]}{R} \qquad (22)$$

Aus (19) und (22) erhält man

$$\frac{d[B]}{dt} = \frac{k'A + k''R}{R}\left(\frac{k'C_M}{k'A + k''R} - [B]\right) = k(a - [B]) \qquad (23)$$

Integration von (23) ergibt

$$\ln(a - [B]_t) = -k\ t + I \qquad (24)$$

Für $t = 0$ ist $[B] = [B]_o$ und also $I = \ln(a - [B]_o)$

Bei Gleichgewicht ist $d[B]/dt = 0$ und aus (23) erhält man dann $a = [B]_\infty$. Dies ergibt schliesslich

$$k = \frac{1}{t} \ln \frac{[B]_\infty - [B]_o}{[B]_\infty - [B]_t} \tag{25}$$

Aus (18), (19), (22), (23) und (25) bekommen wir nach Vereinfachung die zusammenfassende Kinetikformel

$$k = \frac{h^3 k_2 + h^2 k_4 K_1' + h k_6 K_1' K_2' + k_8 K_1' K_2' K_3'}{h^3 + h^2 K_1' + h K_1' K_2' + K_1' K_2' K_3'} + \frac{h^2 k_1 + h k_3 K_1 + k_5 K_1 K_2 + k_7 K_1 K_2 \cdot oh}{h^2 + h K_1 + K_1 K_2} = \frac{1}{t} \ln \frac{[B]_\infty - [B]_o}{[B]_\infty - [B]_t} \tag{26}$$

Man kann zeigen, dass $\frac{[B]_\infty - [B]_o}{[B]_\infty - [B]_t} = \frac{[G]_\infty - [G]_o}{[G]_\infty - [G]_t} = \frac{[S_3]_\infty - [S_3]_o}{[S_3]_\infty - [S_3]_t}$ etc.

$$= \frac{e_\infty - e_o}{e_\infty - e_t}$$

. Bei den Messungen setzt man deshalb

$$k = \frac{1}{t} \ln \frac{e_\infty - e_o}{e_\infty - e_t} \text{ oder } k = \frac{1}{t} \ln \frac{e_o - e_\infty}{e_t - e_\infty} \tag{27}$$

In einem Diagramm trägt man z.B. $\log(e_t - e_\infty)$ als Funktion von t auf. Hierbei erhält man eine Gerade, deren Winkelkoeffizient $= -k \cdot \log e$, und k kann berechnet werden. Da k davon unabhängig ist, bei welcher Wellenlänge man die Messungen durchführt, wählt man die Wellenlänge, die am besten in das pH-Gebiet passt, in dem man sich gerade befindet.

Bei Gleichgewicht ist $[Y]_\infty k_1 = [S_3]_\infty k_2$, $[G]_\infty k_3 = [S_2]_\infty k_4$, $[B]_\infty k_5 = [S_1]_\infty k_6$ und $[B]_\infty oh k_7 = [C]_\infty k_8$. Wie man S. 1458 sieht wird $k_1 = k_2 K_4$, $k_3 = k_4 K_5$, $k_5 = k_6 K_6$ und $k_7 = k_8 K_6 K_3'/K_w$. (28)

Um sämtliche zu dem Protolysenschema gehörende Konstanten aus (26) und (28) zusammen mit den früher abgeleiteten (5) und (13) bestimmen zu können, ist es notwendig, dass man die Gleichung (26) approximieren kann. Im Zusammenhang mit der Beschreibung des experimentellen Verfahrens werden eine Anzahl verschiedener Approximationen behandelt.

EXPERIMENTELLES

Chemikalien und Lösungen. Kristallviolett: Das Handelspräparat in Form von Hydrochlorid (Merck's Reagenzien) wurde in das entsprechende schwerlösliche Perchlorat übergeführt, das dreimal aus Eisessig und einmal aus Wasser umkristallisiert wurde. Weitere Umkristallisation war wirkungslos, was sich dadurch feststellen liess dass eine Absorptionskurve nach jedem Schritt des Prozesses aufgenommen wurde.

Zu Pufferlösungen wurden *Salzsäure, Natriumacetat, Dinatriumhydrogenphosphat, Kaliumdihydrogenphosphat, Borsäure* und *Natriumhydroxyd*, die sämtliche von pro Analysi Qualitet waren, verwendet.

Man kann kaum thermodynamische Konstanten in einem so komplizierten Reaktionsschema wie das von KV bestimmen. Darum wählen wir die Methode, Konzentrationskonstanten zu bestimmen, die bei der Ionenstärke 0,5 M gelten, und mit Kaliumchlorid p.a., als Neutralsalz. Durch Zusatz von Neutralsalz kann man die Aktivitätskoeffizienten der an den Reaktionen teilnehmenden verschiedenen Arten von Ionen und Molekylen konstant halten, so lange ihre Konzentration im Verhältnis zur Ionenstärke klein ist.

Von dem KV wurden Stammlösungen durch Abwiegen des Perchlorates bereitet, das danach im Wasser aufgelöst wurde. Die Totalkonzentration des Farbstoffes war $(1-2) \times 10^{-5}$ M. Aus konzentrierteren Lösungen kristallisiert allmählich das Perchlorat des KV. Die Stammlösungen wurden in Polyäthylenflaschen aufbewahrt, die zuerst mit der Farbstofflösung mehrmals gespült worden waren.

Wie schon u.a. Turgeon und LaMer [4] hervorheben, hat das KV eine ausserordentlich grosse Neigung, sich an den Wänden der benutzten Gefässe zu adsorbieren. Um die Adsorption, die bei genauen Messungen sehr lästig ist, zu eliminieren oder wenigstens zu verringern, wurden folgende Methoden ergriffen. Nur Quarzküvetten bester Qualität wurden gebraucht. Wenn es experimentell möglich war, konnte man die Küvettenwände vor den Messungen mit dem KV "sättigen", indem man die Messlösung in der Küvette einige Minuten stehen liess, wonach die Messlösung mit einer neuen Portion davon ersetzt wurde. Die Adsorption ist in neutralen und schwach alkalischen Lösungen am lästigsten, wo das äusserst schwerlösliche Carbinol des KV sehr stark adsorbiert wird. Alle benutzten Glasgefässe waren aus Pyrexglas. Die Küvetten und Glasgefässe wurden äusserst genau gereinigt.

Apparatur. Bei den Extinktionsmessungen wurde ein Beckman Quarzspektrophotometer Modell DU benutzt, das umgebaut worden war, um die Temperatur im Küvettenhaus mit grösserer Genauigkeit konstant zu halten, als was mit dem Standardmodell möglich war. Der Apparat war in einem Zimmer aufgestellt, dessen Temperatur auf (20,0 ± 0,5)°C gehalten wurde, während temperiertes Wasser von (20,00 ± 0,02)°C durch die Wände des Küvettenhauses gepumpt wurde. Alle Messungen wurden bei 20°C durchgeführt.

Die $[H^+]$-Bestimmungen wurden titrimetrisch oder potentiometrisch ausgeführt. Bei den potentiometrischen Messungen wurde als Referenzlösung eine Lösung der Zusammensetzung 10 mM HCl + 490 mM KCl benutzt, deren pH gleich 2 gesetzt wurde. In vorliegender Arbeit bedeutet pH immer $-\log [H^+]$ und nicht $-\log a_{H^+}$. Als Elektroden wurden für pH <8 vergoldete Platinbleche und Chinhydron verwendet, Reproduzierbarkeit 0,1 mV. Für pH > 8 wurden Wasserstoffgaselektroden benutzt, Reproduzierbarkeit ~0,3 mV.

MESSUNGEN UND ERGEBNISSE

Die Bestimmung der verschiedenen Konstanten

Zuerst wurden drei Absorptionskurven von der blauen Form B des KV in Acetatpuffern, pH = 5, aufgenommen. $C_M = 1 \times 10^{-5}$, 8×10^{-6} bzw. 4×10^{-6} M. Dieselben ε-Werte wurden bei den verschiedenen C_M erzielt. Kurve B in Fig. 1. B hat ein Absorptionsmaximum für $\lambda = 590$ mμ. In einer Reihe von Lösungen wurde die Stammlösung mit Acetat- und Phosphatpuffern gemischt, wonach ein genauer Wert von ε_B bei 590 mμ bestimmt wurde. Das Resultat war $\varepsilon_B = (1{,}000 \pm 0{,}002) \times 10^5$.

Danach wurde eine Reihe von Boratpuffern mit der Farbstoffsstammlösung so gemischt, dass in den Messlösungen $C_M = 2 \times 10^{-6}$ M war. Die Lösungen verblassten langsam wegen der Carbinolbildung. Die Gleichgewichtsextinktionen $E_\infty = 2\, e_\infty$ wurden nach zwei Tagen abgelesen, $\lambda = 590$ mμ. Man kann die Messungen bei solchem pH, dass $[C]_\infty > 0{,}5 \times C_M$, nicht durchführen, weil das Carbinol so schwerlöslich ist, dass es ausfällt. Verringert man anderseits C_M, um die Gefahr der Ausfällung von Carbinol zu mindern, be-

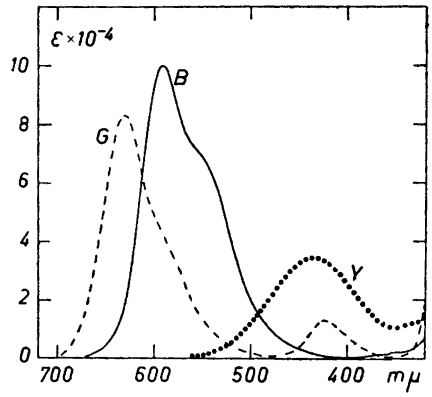

Fig. 1. Absorptionskurven von Kristallviolett in Wasserlösungen. Kurve B entspricht dem violetten Ion $[(CH_3)_2NC_6H_4]_3\overset{+}{C}$, Kurve G dem grünen $[(CH_3)NC_6H_4]_2\overset{+}{C}C_6H_4N\overset{+}{H}(CH_3)_2$, Kurve Y dem gelben $(CH_3)_2NC_6H_4\overset{+}{C}[C_6H_4N\overset{+}{H}(CH_3)_2]_2$.

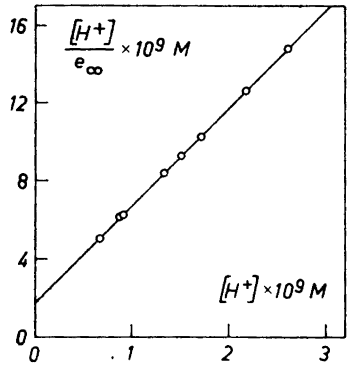

Fig. 2. $[H^+]/e_\infty$ als Funktion von $[H^+]$ für die Bestimmung von K_6K_3' und ε_B. $\lambda = 590$ mμ.

kommt man eine grössere Ungenauigkeit in den Messungen, indem die prozentuelle Adsorption von Farbstoff mit dessen Verdünnung steigt. In Fig. 2 ist $[H^+]/e_\infty$ der Gleichung (15) gemäss als Funktion von $[H^+]$ aufgetragen. Aus der erhaltenen Geraden bekommt man $y = K_6K_3'/e_B = 1{,}72 \times 10^{-9}$ und $l = (1 + K_6)/e_B = 5{,}00$. Man findet, da $K_6 \ll 1$, also $e_B = 0{,}200$, was $\varepsilon_B = 1{,}00 \times 10^5$ ergibt. Die Übereinstimmung mit dem früher erhaltenen $\varepsilon_B = 1{,}000 \times 10^5$ ist folglich sehr gut. Dies zeigt, dass $K_6 \ll 1$, denn falls K_6 nicht $\ll 1$, kann man zeigen, dass das graphisch erhaltene $e_B = (1 + K_6)/l$ grösser wird, als das e_B', das man aus einer Absorptionskurve, in Acetatpuffer aufgenommen, bekommt, wo $[S_1]$ und $[S_2]$ bei Gleichgewicht neben [B] nicht vernachlässigbar sind. Man kann also K_6 nicht aus diesen Messungen bestimmen, aber die Kenntnis davon dass $K_6 \ll 1$ ist, wird im folgender benutzt. Dagegen geben die Messungen $K_6K_3' = 3{,}44 \times 10^{-10}$.

Die Bestimmung von K_1 und K_2. Zwischen pH 3 und pH 2 schlägt die Farbe des KV von blauviolett in grün um, wegen der Reaktion $B + H^+ \rightleftharpoons G$. Aus Absorptionskurven, bei pH ~ 2 aufgenommen, findet man, dass die grüne Form G ein Absorptionsmaximum für etwa $\lambda = 635$ mμ und eines für etwa $\lambda = 420$ mμ hat. Zwischen pH 1 und pH 0 schlägt die Farbe des KV von grün in gelb um, wegen der Reaktion $G + H^+ \rightleftharpoons Y$. Eine Absorptionskurve, in 2 M HCl aufgenommen, zeigt, dass die gelbe Form Y ein Absorptionsmaximum für $\lambda = 434$ mμ hat.

Um K_1 und K_2 genau bestimmen zu können, führt man die Messungen bei solchen Wellenlängen aus, wo der Unterschied zwischen ε_B, ε_G und ε_Y so gross wie möglich ist. Es zeigte sich als zweckmässig, K_2 bei $\lambda = 635$ mμ $= \lambda_{G\ max}$

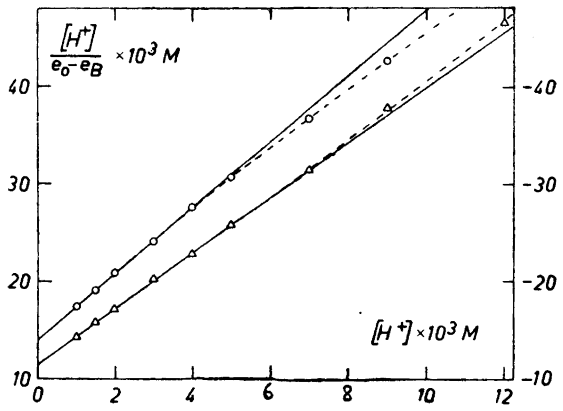

Fig. 3. $[H^+]/(e_0-e_B)$ als Funktion von $[H^+]$ für die Bestimmung von K_2, ε_B und ε_G. ○ $\lambda = 590$ mμ, Ordinate rechts, und △ $\lambda = 635$ mμ.

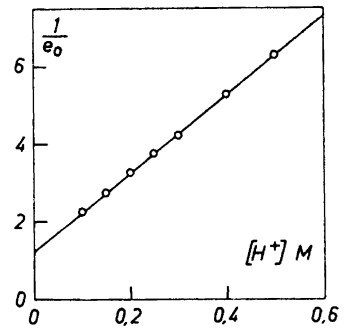

Fig. 4. $1/e_0$ als Funktion von $[H^+]$ für die Bestimmung von K_1 und ε_G. λ = 635 mμ.

und $\lambda = 590$ mμ $= \lambda_{B\ max}$ und K_1 bei $\lambda = 635$ mμ zu bestimmen. Da ε_B für $\lambda = 590$ mμ schon bekannt war und ε_B für $\lambda = 635$ mμ auf entsprechende Weise bestimmt werden konnte, wurde die Gleichung (6) verwendet.

Eine Reihe Messlösungen wurde dadurch bereitet, dass die Farbstammlösung mit verschiedenen Pufferlösungen von HCl + KCl schnell in Y-geformten Mischröhren gemischt wurde. Die Extinktionen wurden zur Zeit $t = 0$ extrapoliert. Für die Messlösungen war $C_M = 5 \times 10^{-6}$ M, $d = 2$ cm und $[H^+] =$ 1—12 mM. In Fig. 3 ist $[H^+]/(e_0-e_B)$ als Funktion von $[H^+]$ aufgetragen. Man erhält für $\lambda = 590$ mμ: $y = -0{,}0139$ M und $l = -3{,}40$ und für $\lambda = 635$ mμ: $y = 0{,}0115$ M und $l = 2{,}85$. Dies ergibt für 590 mμ: $K_2 = \mathbf{0{,}00409}$, $e_G = 0{,}206$, $\varepsilon_G = 4{,}12 \times 10^4$ und für 635 nμ: $K_2 = \mathbf{0{,}00404}$, $e_G = 0{,}409$, $\varepsilon_G = 8{,}18 \times 10^4$.

Die Absorptionskurve von B hat einen sehr steilen Verlauf um $\lambda = 635$ mμ, und dasselbe gilt für G um 590 mμ. Man muss deshalb alle Messungen bei der einen Wellenlänge zu Ende führen, bevor man die Messungen bei der anderen beginnt, da auch kleine Differenzen der Einstellung von λ grosse Fehler in den Berechnungen veranlassen können.

K_1 wurde für $\lambda = 635$ mμ bestimmt, wo $\varepsilon_Y \ll \varepsilon_G$ und ε_B ist. $C_M = 1 \times 10^{-5}$ M, $d = 2$—5 cm, $[H^+] = 100$—500 mM. In Fig. 4 ist $1/e_0$ als Funktion von $[H^+]$ der Gleichung (8) gemäss aufgetragen. Man bekommt $y = 1{,}23$ und $l = 10{,}10$ woraus $K_1 = \mathbf{0{,}122}$, $e_G = 0{,}813$, $\varepsilon_G = 8{,}13 \times 10^4$. Die Übereinstimmung mit dem ε_G, das oben in schwach sauren Lösungen bei $\lambda = 635$ mμ bestimmt wurde, ist folglich gut.

Die Bestimmung von K_4 und K_5. Gleichung (16) wurde benutzt. Eine Reihe Lösungen von KV in HCl + KCl standen so lange, bis sie nach 1—12 Stunden Gleichgewicht erreichten. Das C_M war $(0{,}5—1) \times 10^{-5}$ M. Die Messungen wurden durchgeführt, teils für $[H^+] = 1$—15 mM bei $\lambda = 590$ mμ, wo e_B und e_G aus $\varepsilon_B = 9{,}98 \times 10^4$ und $\varepsilon_G = 4{,}12 \times 10^4$ berechnet wurden, und teils

Tabelle 1. Berechnung von K_4.

$\lambda = 590$ mμ, $C_M = 5 \times 10^{-6}$ M

[H$^+$] mM	E_∞ (d = 2 cm)	K_4
1	0,774	79
1,5	0,652	82
2	0,553	80
3	0,407	77
4	0,307	78
5	0,239	78
7	0,157	81
9	0,116	79
	$C_M = 1 \times 10^{-5}$ M	
12	0,159	81
15	0,120	81

$\lambda = 635$ mμ, $C_M = 1 \times 10^{-5}$ M

[H$^+$] mM	E_∞ (d = 5 cm)	K_4
12	0,458	80
15	0,383	78
20	0,295	78
25	0,238	79
30	0,200	79
40	0,150	80
50	0,121	79
60	0,105	77
80	0,078	78
100	0,064	76
150	0,042	77
200	0,032	76
250	0,025	78
300	0,021	78

Mittelwert $K_4 = 79$

für [H$^+$] = 12—300 mM bei $\lambda = 635$ mμ, wo $\varepsilon_B = 1{,}17 \times 10^4$ und $\varepsilon_G = 8{,}16 \times 10^4$ sind.

Da die vorbereitenden Untersuchungen darauf deuteten, dass $K_5 < 1$ und möglicherweise $\ll 1$ ist, wurde versuchsweise $K_5 = 0{,}05$ gesetzt. Die Resultate sind in Tabelle 1 zusammengestellt. Man bekommt eine gute Konstanz für K_4. Der Mittelwert wird $K_4 = 79$. Für die sauersten Lösungen ist die Messgenauigkeit weniger gut, wegen der niedrigen Gleichgewichtsextinktionen. Der Wert des K_5 ist äusserst approximativ. Einen genaueren Wert für K_5 bekommt man aus den folgenden Kinetikmessungen.

KINETIKMESSUNGEN

In stark alkalischen Lösungen findet die Reaktion B + OH$^-$ $\rightleftharpoons$ C statt. Diese Reaktion, deren Gleichgewicht in stark alkalischen Lösungen fast vollständig gegen das farblose Carbinol, C, verschoben ist, ist von mehrere Forschern [4-8] für KV und andere basische Triphenylmethanfarbstoffe untersucht worden. Die Bleichungsgeschwindigkeit der Reaktion ist eine lineare Funktion von [OH$^-$]. In einer Reihe von Versuchen wurde die Farbstammlösung mit NaOH + KCl gemischt, und die Bleichung wurde kinetisch verfolgt. $C_M = 5 \times 10^{-6}$ M, $\lambda = 590$ mμ, [OH$^-$] = 25—250 mM. Die Entfärbung geschieht schnell und vollständig in stark alkalischen Lösungen. Mit Kenntnis von $K_6 K_3'$ kann man e_∞ berechnen, das in den am stärksten alkalischen Lösungen ganz vernachlässigbar ist. Wenn $C_M = 5 \times 10^{-6}$ M ist, fällt das Carbinol nicht augenblicklich aus, sondern man kann die Entfärbung wenigstens etwa 15 Minuten kinetisch verfolgen, was genügt, obwohl die Lösung hinsichtlich

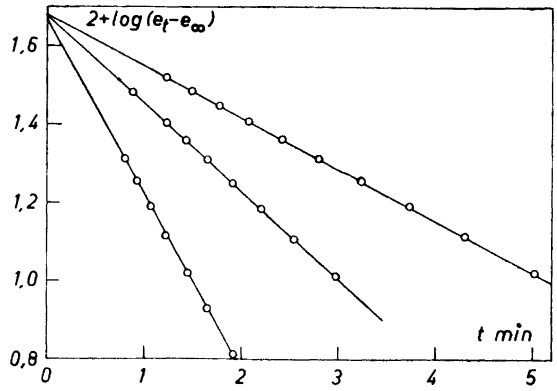

Fig. 5. Kinetikmessungen in NaOH + KCl, λ = 590 mμ, T = 20.0°C. [OH⁻] ist von oben nach unten 75, 125 und 250 mM.

des Carbinols übersättigt wird. In Fig. 5 ist $\log(e_t - e_\infty)$ als Funktion von t bei drei verschiedenen [OH⁻] aufgetragen. Man erhält Gerade, deren Winkelkoeffizienten, l, $-k \cdot \log e$ ergeben, wo k = die Geschwindigkeitskonstante der pseudomonomolekularen Reaktion ist. In stark alkalischen Lösungen kann die Gleichung (26) folgendermassen approximiert werden

$$k = k_8 + k_5 + k_7 \cdot \mathrm{oh} \tag{29}$$

In Fig. 6 ist k als Funktion von [OH⁻] bei fünf verschiedenen [OH⁻] aufgetragen. Man bekommt in Übereinstimmung mit (29) eine Gerade. Diese geht aber approximativ durch Origo, weshalb man $k_5 + k_8$ nicht aus dem Abschnitt auf der Ordinatenachse bestimmen kann. Dagegen erhält man $k_7 = \mathbf{4.12\ min^{-1}}$ aus dem Winkelkoeffizient der Gerade.

k_8 kann man folgenderweise bestimmen: Bei Gleichgewicht gilt

$$k_7 \cdot \mathrm{oh}\ [\mathrm{B}]_\infty = k_8\ [\mathrm{C}]_\infty \tag{30}$$

Aber $\mathrm{h}[\mathrm{C}]_\infty = K_3'[\mathrm{S}_1]_\infty$ und $[\mathrm{S}_1]_\infty = K_6[\mathrm{B}]_\infty$ weshalb $k_8 = k_7 K_w / K_6 K_3'$, wo K_w das Ionenprodukt des Wassers ist. Durch Messungen mit Wasserstoffgaselektroden in Lösungen vom Typus x mM NaOH + (500-x) mM KCl wurde K_w zu $1{,}24 \times 10^{-14}$ bestimmt. Man erhält $k_8 = \mathbf{0{,}000148\ min^{-1}}$.

Um k_5 zu bestimmen, kann man in schwach alkalischen Lösungen die Gleichung (26) zu

$$k = \frac{\mathrm{h} \cdot k_6 + k_8 K_3'}{\mathrm{h} + K_3'} + k_5 + k_7 \cdot \mathrm{oh} \tag{31}$$

approximieren. Wenn man annimmt, dass K_3' von derselben Grössenordnung, 10^{-6}, ist, wie die entsprechenden Diss.konstanten der früher untersuchten basischen Triphenylmethanfarbstoffe [1], kann man das h im Nenner vernach-

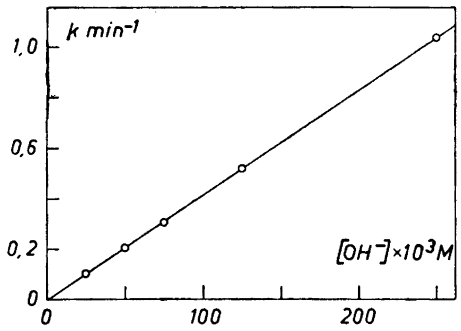

Fig. 6. Die Geschwindigkeitskonstante k als Funktion von $[OH^-]$ für $[OH^-]$ = 25—250 mM.

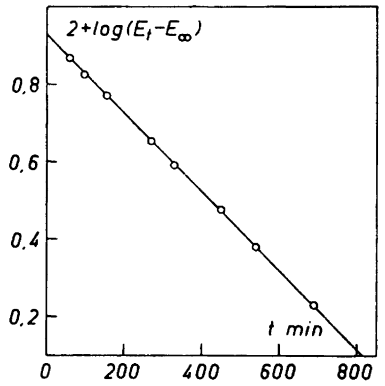

Fig. 7. Eine Kinetikreihe in Boratpuffer pH = 8,77. λ = 590 mμ, $C_M = 1 \times 10^{-6}$ M, d = 5 cm, T = 20.0°C.

lässigen, wenn pH > 8.5 ist. Ferner gilt ja bei Gleichgewicht $k_5[B]_\infty = k_6[S_1]_\infty$ und $[S_1]_\infty = K_6[B]_\infty$. Man kann dann (31) folgendermassen schreiben:

$$k = k_5(h/K_6K_3' + 1) + k_8 + k_7 \cdot oh \qquad (32)$$

Aus (32) kann k_5 durch Kinetikmessungen in geeigneten Boratpuffern bestimmt werden. Hier entsteht die experimentelle Schwierigkeit, dass wenn eine Farbstammlösung mit Boratpuffer, pH 9—10, gemischt wird, die Lösung sehr langsam verbleicht, und das schwerlösliche Carbinol ausfällt. Wenn man dies verhindern will, indem man das C_M genügend vermindert, bekommt man statt dessen grosse Unsicherkeit wegen der Adsorption. Man wählt zweckmässigerweise ein pH, wo nur ein kleinerer Teil von B zu C übergeführt wird. Zwar wird die Änderung der Extinktion klein, aber die Reaktion geht so langsam, dass man für jeden Messpunkt zu vielen Ablesungen Zeit hat. Man erreicht ausserdem, dass das Glied $k_7 \cdot oh$ den Charakter eines Korrektionsgliedes bekommt. Fig. 7 zeigt eine Kinetikreihe für pH 8,77, die k = 0,00236 min^{-1} ergibt, und aus (32) bekommt man danach $k_5 = 0{,}000367$ min^{-1}. Die Reproduzierbarkeit der Kinetikgerade war gut.

Um k_1 und k_2 zu bestimmen, wird (26) in stark sauren Lösungen folgenderweise approximiert

$$k = k_2 + \frac{k_1 \cdot h}{h + K_1} \qquad (33)$$

Nun ist $k_1[Y]_\infty = k_2[S_3]_\infty$ und $[S_3]_\infty = K_4[Y]_\infty$, weshalb man (33)

$$k = k_1\left(\frac{h}{h + K_1} + \frac{1}{K_4}\right) \qquad (34)$$

schreiben kann.

In Tabelle 2 ist k_1 aus (34) durch Kinetikmessungen mit $[H^+]$ = 100—300 mM berechnet. Der Wert von k_1 steigt etwas, wenn $[H^+]$ sinkt. Dies beruht

Tabelle 2. Approximative Berechnung von k_1.

[H+] mM	k min^{-1}	k_1 min^{-1}
100	0,0589	0,127
150	708	126
200	771	121
250	821	120
300	853	118

teils darauf, dass (33) eine immer schlechtere Approximation wird, je niedriger [H$^+$] wird, und teils möglicherweise darauf, dass das Ionenmedium sich merkbar verändert, wenn KCl in höherem Grade von HCl ersetzt wird. Aus Gründen, die sich im folgenden ergeben, wurde der Wert $k_1 = 0{,}117$ min^{-1} gewählt; dabei wird $k_2 = 0{,}00148$ min^{-1}. In Fig. 8 sind als Beispiel sechs Kinetikreihen eingezeichnet. $C_M = 1 \times 10^{-5}$ M, $\lambda = 635$ mμ, [H$^+$] = 80—300 mM, $d = 2$ cm.

Die restlichen Konstanten des Protolysenschemas sind wesentlich schwieriger zu bestimmen als die schon bestimmten. Man kann keine einfache und gleichzeitig gute Approximation von (26) in schwach und sehr schwach sauren Lösungen erzielen. Als eine grobe Approximation kann man um pH 5 schreiben

$$k = \frac{hK_6K_2'}{h^2 + hK_2' + K_2'K_3'} + k_5 \qquad (35)$$

Durch Derivierung von (35) hinsichtlich [H$^+$] findet man, dass die Reaktionsgeschwindigkeit durch ein Maximum geht, wenn $h^2 = K_2'K_3'$. Man kann danach mit verschiedenen Werten von K_3' probieren, wobei man K_6 aus dem schon

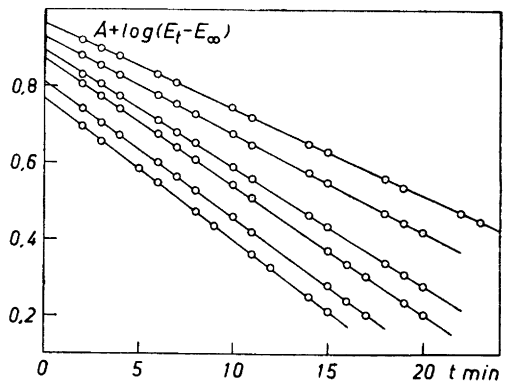

Fig. 8. Kinetikmessungen in HCl + KCl, $\lambda = 635$ mμ, $C_M = 1 \times 10^{-5}$ M, $d = 2$ cm, $T = 20$°C. Von oben nach unten sind die zusammengehörigen Werte für [H+] und A in A + log($E_t - E_\infty$):

[H+]	80	100	150	200	250	300 mM
A	1	1	1,05	1,1	1,1	1,1

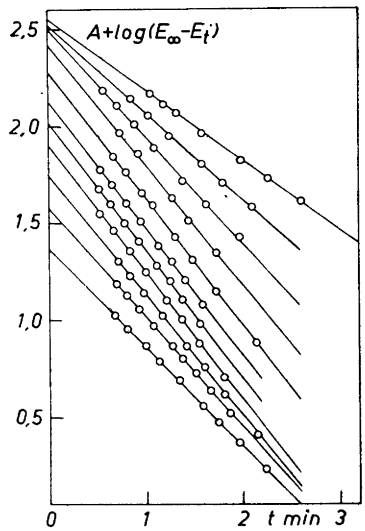

Fig. 9. Kinetikmessungen in Acetatpuffern, $\lambda = 590$ mμ, $C_M = (1-5) \times 10^{-6}$ M, $d = 1-5$ cm, T = 20°C. Von oben nach unten sind pH und A

pH	5,94	5,77	5,59	5,45	5,35	5,26	5,18	5.11	4,98	4,88	4,78
A	3,1	3,1	3,1	3,0	2,8	2,6	2,5	2,5	2,2	2	1,8

bekannten $K_6'K_3'$ und k_6 aus $k_6 = k_5/K_6$ bekommt. Ausserdem gilt dem Reaktionsschema gemäss

$$K_5K_2' = K_6K_2 \text{ und } K_4K_1' = K_5K_1 \qquad (36)$$

weshalb man approximative Werte von K_5 und K_1' erhält, wenn man K_3' festgelegt hat. Da $k_3 = k_4K_5$, vgl. (28), kann man dann durch Kinetikmessungen bei pH 1—3 approximative Werte für k_3 und k_4 aus (26) bestimmen.

In experimenteller Hinsicht verfährt man folgenderweise: Man bereitet eine Stammlösung von KV in 20 mM HCl. Eine solche Lösung wird wegen der Reaktionen $G + H_2O \rightleftharpoons S_2$ und $Y + H_2O \rightleftharpoons S_3$ bis zu $e_o/10$ entfärbt. Diese schwach gefärbte Stammlösung wird dann mit einer Reihe von Acetat- oder Phosphatpuffern gemischt, deren Zusammensetzungen so sind, dass man pH 3.2—6.3 bekommt. Hierbei wird B mit einer Geschwindigkeit, die k in der Gleichung (26) ergibt, wiedergebildet. Bei höherem pH wird im Mischungsaugenblick Carbinol in so hohem Grade gebildet, dass seine Schwerlöslichkeit die Messungen schwerreproduzierbar und unsicher macht. Eine andere Schwierigkeit liegt darin, dass die Reaktionsgeschwindigkeit um pH 5 so gross ist, dass sich die Kinetikmessungen nur schwer ausführen lassen. Bei k_{max} verläuft die Reaktion bis 50 % in nur 30 Sek. Trotzdem kann man gute Kinetikgeraden erhalten, was aus Fig. 9 hervorgeht, die eine Reihe von Kinetikmessungen, pH 4.78—5.94, zeigt. Indem man mehrere Kinetikreihen für jedes benutzte pH aufnimmt, kann man die Genauigkeit von k erhöhen. Bei den Messungen war $C_M = 1 \times 10^{-6}$ M für die meisten Messlösungen und 5×10^{-6} M für einige. $\lambda = 590$ mμ. Im Gebiete pH 1—3 wurde die Ge-

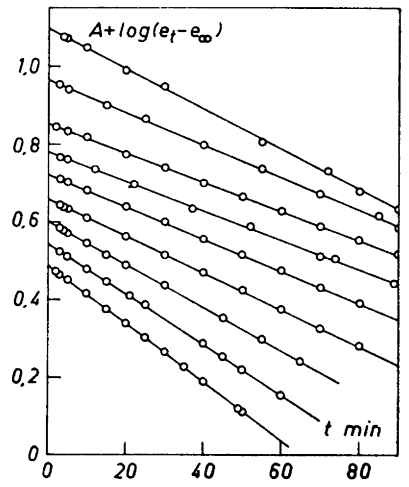

Fig. 10. Kinetikmessungen in HCl + KCl, $\lambda = 590$ mμ, $C_M = 1 \times 10^{-5}$, $d = 1$ cm, $T = 20°C$. Von oben nach unten sind [H$^+$] und A:

[H$^+$]	1,5	2	3	4	5	7	9	12	15 mM
A	1,9	1,6	1,35	1,2	1,1	1	0,95	0,9	0,85

schwindigkeit der Bleichung gemessen, die stattfindet, wenn die ursprüngliche Farbstammlösung, deren [B] = C_M, mit Lösungen von HCl + KCl gemischt wird. Die Messlösungen hatten $C_M = 1 \times 10^{-5}$ M, $\lambda = 590$ mμ. Fig. 10 gibt eine Reihe Kinetikgeraden für [H$^+$] = 1.5—15 mM.

In Fig. 11 und Fig. 12 sind die aus den Kinetikmessungen erhaltenen k-Werte als Funktion von pH aufgetragen. Die Kinetikmessungen wurden bei 48 verschiedenen [H$^+$] durchgeführt. Für jedes [H$^+$] wurden 2—4 Kinetikreihen durchgeführt, wonach man Mittelwerte für k erhielt. Die Bedeutung der verschiedenen Zeichen geht aus den Figurtexten hervor. Die ausgezogenen Kurven sind aus der Gleichung (26) berechnet, wobei die Konstanten benutzt wurden, die man auf direktem Wege bestimmen kann, und die Konstanten, die man durch sukzessive Approximationen bekommt. Nachdem man, S. 1471 gemäss, approximative Werte von K_3', K_2', K_1', K_5, k_3 und k_4 bestimmt hat, kann man diese Konstanten in (26) verwenden und sie justieren, bis man die denkbar beste Übereinstimmung bekommt zwischen den in Fig. 11 und Fig. 12 experimentell gefundenen k-Werten und den aus (26) berechneten. Die ausgezogenen Kurven wurden also aus der nicht approximierten Gleichung (26) berechnet.

Folgende Konstantwerte wurden benutzt:

$K_1 = 0{,}122$	$K_2 = 0{,}00406$			M
$K_1' = 4{,}86 \times 10^{-5}$	$K_2' = 1{,}78 \times 10^{-5}$	$K_3' = 2{,}46 \times 10^{-6}$		M
$K_4 = 79$	$K_5 = 0{,}0319$	$K_6 = 1{,}4 \times 10^{-4}$		
$k_1 = 0{,}117$	$k_3 = 0{,}00660$	$k_5 = 0{,}000367$	$k_7 = 4{,}12$	min^{-1}
$k_2 = 0{,}00148$	$k_4 = 0{,}207$	$k_6 = 2{,}62$	$k_8 = 0{,}000148$	min^{-1}

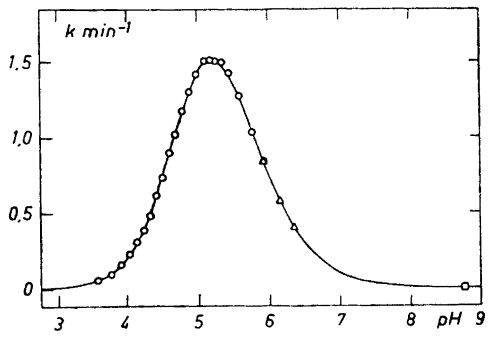

Fig. 11. Kinetikmessungen in Acetat- O, Phosphat- △ und Boratpuffern □. $\lambda = 590$ mμ, $C_M = 1 \times 10^{-6}$ M und 5×10^{-6} M, $d = 1$ und 5 cm, T = 20°C. Die Geschwindigkeitskonstante als Funktion von pH. Die ausgezogene Kurve wurde aus der Gleichung (26) berechnet.

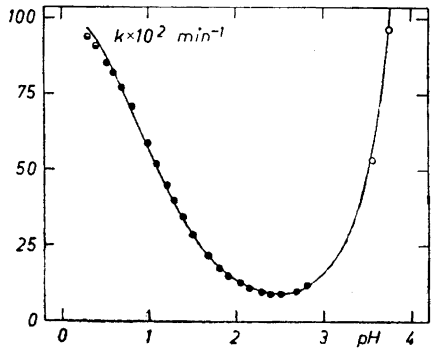

Fig. 12. Kinetikmessungen in Acetatpuffern O und in HCl + KCl ● und ◒. $\lambda = 635$, 590 und 434 mμ, $C_M = 5 \times 10^{-6}$ M und 1×10^{-5} M, $d = 1$, 2 und 5 cm, $T = 20$°C. Die Geschwindigkeitskonstante als Funktion von pH. Die ausgezogene Kurve wurde aus (26) berechnet.

Diese Konstanten satisfieren teils die Gleichung (26) und teils die Beziehungen, die in den Gleichungen (28) und (36) zusammengestellt sind.

Die Übereinstimmung zwischen experimentell gefundener und aus der Gleichung (26) berechneter Reaktionsgeschwindigkeit ist sehr gut. Versuche wurden unternommen, die ausgezogene Kurve unter Verwendung anderer Konstantenwerte als die oben gegebenen zu berechnen, aber schon die Änderung von einigen Prozenten in einem Konstant führt entweder dazu, dass die Kurve die experimentellen Punkte verlässt, oder dazu, dass die Beziehungen von (28) und (36) nicht erfüllt werden. Die Genauigkeit der bestimmten Konstanten variiert und lässt sich nur schwer exakt schätzen, sie liegt aber zwischen 1 und 5 %.

Absorptionskurven von G und Y sind auch in Fig. 1 eingezeichnet. Sie wurden folgendermassen berechnet: ε_G und ε_Y wurden für gewisse Wellenlängen, durch Extrapolation der Extinktion auf $t = 0$, aus der Gleichung (5) bestimmt. Danach wurden Absorptionskurven bei Gleichgewicht in schwach sauren Lösungen aufgenommen, nämlich $[H^+] \sim 4$ mM für die Bestimmung der Absorptionskurve von G, wobei e_G und ε_G aus (13) berechnet wurden, wo man ε_B im Gebiet $\lambda = 320$—700 mμ aus Kurve B in Fig. 1 kennt und ε_Y vernachlässigen kann. Danach wurde die Absorptionskurve von Y durch Messungen in stark sauren Lösungen auf entsprechende Weise bestimmt, nämlich $[H^+] \sim 250$ mM und ähnliche Berechnung aus (13), wo man nun sowohl e_B als e_G kennt.

G hat ein Absorptionsmaximum für $\lambda = 631$ mμ, $\varepsilon_G = 8{,}3 \times 10^4$, und eines für $\lambda = 424$ mμ, $\varepsilon_G = 1{,}40 \times 10^4$. Y hat ein Absorptionsmaximum für $\lambda = 434$ mμ, $\varepsilon_Y = 3{,}5 \times 10^4$.

DISKUSSION DER ERGEBNISSE

Die früher von Adams und Rosenstein [2] unternommenen Versuche, Ionisationskonstanten für KV zu bestimmen, ergaben u.a., dass die Absorptionskurve von G eine höhere Extinktion in Abs.max. hat als die Absorptionskurve von B in Abs.max. $\varepsilon_{G\ max} = 11{,}3 \times 10^4$, $\lambda_{G\ max} = 635$ mμ, $\varepsilon_{B\ max} = 8{,}8 \times 10^4$, $\lambda_{B\ max} = 590$ mμ. Die Lagen der Maxima stimmen mit denen dieser Untersuchung überein, aber die von Adams und Rosenstein erhaltenen ε sind unwahrscheinlich. G soll nämlich eine Absorptionskurve haben, deren Abs.max. niedriger ist als die von B. Die Absorptionskurve von G soll der des primären gefärbten Ions von Malachitgrün, $[(CH_3)_2NC_6H_4]_2\overset{+}{C}C_6H_5$, ähnlich sein, und dasselbe gilt in noch höherem Grade für das entsprechende Farbion des Methylgrün, $[(CH_3)_2NC_6H_4]_2\overset{+}{C}C_6H_4N(CH_3)_3\overset{+}{C}lO_4^-$. Von meinen früheren Untersuchungen und den nun durchgeführten findet man für

	λ_{max}	ε_{max}	λ_{max}	ε_{max}
KV sekundäres Farbion G	631 mμ	$8{,}3 \times 10^4$	424 mμ	$1{,}40 \times 10^4$
Methylgrün primäres Farbion	633 »	$9{,}0 \times 10^4$	422 »	$1{,}85 \times 10^4$
Malachitgrün » »	618 »	$8{,}6 \times 10^4$	430 »	$1{,}8 \times 10^4$

Die Lagen der Maxima für G und das primäre Farbion des Methylgrün stimmen also nahe überein.

Die Ergebnisse von Adams und Rosenstein beruhen auf ihrer mangelhaften Methodik. Deshalb sind ihre Ergebnisse betreffs der Ionisationskonstanten und Reaktionsvorgänge nicht nur unvollständig, sondern auch quantitativ

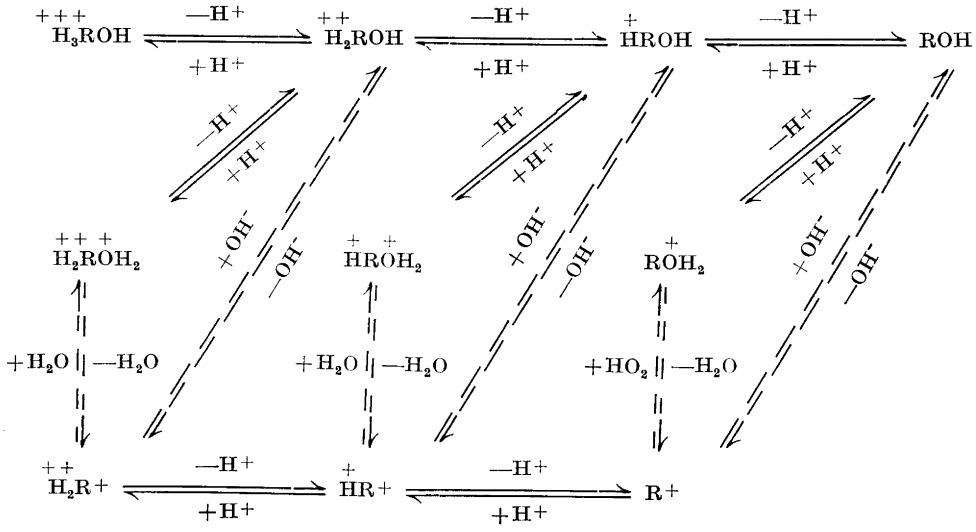

Ausgezogene Pfeile bedeuten, dass die Reaktionen sehr rasch, "momentan", verlaufen, während gestrichelte Pfeile bedeuten, dass die Reaktionen mit messbarer Geschwindigkeit verlaufen.

irreführend. Man kann daher ihre Ergebnisse nicht mit den jetzt publizierten Ergebnissen für Kristallviolett vergleichen.

Zu Beginn wurde hervorgehoben, dass das jetzt für KV aufgestellte Protolysenschema als ein vereinfachtes Reaktionsschema zu betrachten ist, das nur den Bruttoverlauf und die geschwindigkeitsbestimmenden Reaktionen angibt. Hier folgt ein Protolysenschema, das die wahrscheinlichen Reaktionswege besser deckt.

Wenn dem Carbinol, ROH, ein Proton hinzugefügt wird, kann es entweder zum Stickstoff in einer Aminogruppe, $\overset{+}{\mathrm{H}}\mathrm{ROH}$ treten, oder zum Sauerstoff in der OH-Gruppe bei dem zentralen Kohlenstoffatom, $\mathrm{R}\overset{+}{\mathrm{O}}\mathrm{H}_2$. Im letzteren Falle kann ein $\mathrm{H_2O}$ abgespaltet werden, und wir erhalten das gefärbte R^+. $\overset{+}{\mathrm{H}}\mathrm{ROH}$ dürfte OH^- abspalten und $\overset{+}{\mathrm{H}}\mathrm{R}^+$ bilden können, gleich wie R^+ aus ROH gebildet werden kann. Wie aus dem Schema hervorgeht, soll dasselbe Reaktionsprinzip für das ganze Schema gelten. In neutralen und sauren Lösungen erfolgt zwar die Abspaltung des OH^- von $\overset{+}{\mathrm{H}}\mathrm{ROH}$ und $\mathrm{H_2}\overset{++}{\mathrm{R}}\mathrm{OH}$ so langsam, dass die Hydratations- und Dehydratationsgeschwindigkeiten geschwindigkeitsbestimmend werden. Nur in stark alkalischen Lösungen werden die Reaktionen, die OH^- mit einbegreifen, die Reaktionsgeschwindigkeit dominieren.

Da die Messungen mit der Ionenstärke 0.5 M durchgeführt wurden, wurden keine quantitativen Messungen in z.B. konz. $\mathrm{H_2SO_4}$ unternommen, wo KV wahrscheinlich das Ion $\mathrm{H_3}\overset{+++}{\mathrm{R}}^+$ bilden kann.

REFERENZEN

1. Cigén, R. *Protolysengleichgewichte und Reaktionsgeschwindigkeiten einiger basischer Triphenylmethanfarbstoffe* (Diss.), Universität Lund 1956.
2. Adams, E. Q. und Rosenstein, L. *J. Am. Chem. Soc.* **36** (1914) 1452.
3. Lewis, G. N., Magel, T. und Lipkin, D. *J. Am. Chem. Soc.* **64** (1942) 1774.
4. Turgeon, J. C. und LaMer, V. K. *J. Am. Chem. Soc.* **74** (1952) 5988.
5. Sidgwick, N. V. und Moore, T. S. *Z. physik. Chem.* **58** (1907) 385.
6. Biddle, H. C. und Porter, C. W. *J. Am. Chem. Soc.* **37** (1915) 1571.
7. Hochberg, S. und LaMer, V. K. *J. Am. Chem. Soc.* **63** (1941) 3110.
8. Langvad, T. *Acta Chem. Scand.* **4** (1950) 300.
9. Bodforss, S., Ahrland, S. und Cigén, R. *Z. physik. Chem.* **203** (1954) 73.

Eingegangen am 21. Mai, 1958.

ACTA CHEMICA SCANDINAVICA 12 (1958) 1476—1480

The Effect of Boron on the Formation of σ-FeCr at 700° C

B. ARONSSON and J. ÅSELIUS

Institute of Chemistry, University of Uppsala, Uppsala, Sweden

Iron-chromium-boron alloys with the atomic ratio Fe/Cr = 54/46 and containing varying amounts of boron (0—26 at %) have been melted twice in an arc-furnace and subsequently annealed for 40—48 days at 700°C in evacuated silica tubes. It has been found that chromium is concentrated in the $(Cr, Fe)_2B$ phase, thereby lowering the amount of Cr available for the formation of σ-FeCr. In the presence of >8 at % B no sigma phase is found in the samples. The solubility of boron in σ-FeCr is probably very small. Thus, the influence of boron on the formation of σ-FeCr is analogous to that of carbon and nitrogen.

It has been assumed[1,2] that the bonding strength between a transition metal (Me) and one of the nonmetals boron, carbon or nitrogen (X) decreases with increasing atomic number of the transition metal in a given transition period. This assumption has been useful when systematizing general features and properties of systems containing the mentioned elements. The decreasing stability of the binary borides, carbides and nitrides of the transition metals with increasing group number of the metal is in accordance with this assumption as are the observations that in Me_1—Me_2—X systems (Me_1 and Me_2 from the same transition period) the lower atomic number metal is always concentrated in the phase richest in nonmetal [3-6].

The influence of carbon on the formation of σ-FeCr is one example of this general behaviour. In the metal rich part of the Fe-Cr-C system (15—43 weight % Cr). Shortsleave and Nicholson [7] found that Cr-rich $(Cr, Fe)_{23}C_6$ carbide is formed, thereby lowering the amount of chromium available for sigma formation. The higher the carbon content of the Fe-Cr-C alloy, the higher the *total* chromium content which is necessary for σ-FeCr to be found. The effect of nitrogen on sigma formation in Fe-Cr-Ni steels is quite analogous, Cr-rich nitrides being formed [8].

The present investigation has been undertaken in order to study if the effect of boron on the formation of σ-FeCr could be explained as depending on higher affinity of B for Cr than for Fe. We also wanted to know if boron, like silicon [9,10], could be dissolved in σ-FeCr to any considerable extent.

EXPERIMENTAL

The metals used in this investigation had a claimed purity of 99.7 %. The boron was analysed and found to contain 94 % B. 2—3 g samples were melted twice in an arc furnace. The samples contained 0, 4.0, 8.5, 13.2, 16.9, 22.5 and 26.0 atomic % B, and within 2 % the Fe/Cr atomic ratio was 54/46 in all of them. The melts were cold worked by hammering with a sledge and subsequently annealed in evacuated silica tubes for 40 days at 700°C and quenched in oil. After this annealing time the powder photographs showed sharp lines and no changes were observed after annealing another 8 days. Filings of the samples were recovered for 1—2 h at 600°C in vacuum. X-Ray photographs were taken in a Guinier type powder camera using Cr$K\alpha$ radiation and NaCl as calibration standard. (a_{NaCl} has been assumed to be = 5.6400$_6$ Å at 21°C.) Measurements of the cube edge of the α-phase could be reproduced within ± 0.01 %. The accuracy of the l.p. (lattice parameters) of the other phases present is estimated to be 0.02—0.03 %.

The samples were chemically analysed for B, Fe and Cr. After dissolving in HCl (under reflux) boron was determined by titration with sodium hydroxide after addition of D-mannitol. Iron and chromium were determined with standard volumetric methods. The result of the chemical analyses (in weight %) is given in Table 1.

Table 1.

Sample No.	% B	% Fe	% Cr	Σ
0		55.2	43.2	98.4
1	0.82	54.8	43.1	98.7
2	1.83	53.5	42.6	97.9
3	2.92	53.1	42.5	98.5
4	3.85	52.9	41.3	98.0
5	5.40	51.5	41.1	98.0
6	6.40	50.5	40.9	97.8

In order to identify the expected boron-rich phases, some alloys in the Cr—B system ($\leq$ 33 at % B) were prepared by arc-melting. They were investigated with X-ray powder methods both in the unannealed state and after annealing in vacuum for 3—4 weeks at 1150°C.

RESULTS

I. *The Cr-B system.* Only one intermediate phase was observed in the region 0—33 at % B. Its composition was approximately Cr_2B. The positions and intensities of all the X-ray powder lines could be explained assuming the crystal structure to be isomorphous with that of Mn_4B[11]. Sufficiently small single crystals gave very nice Weissenberg photographs which definitely showed that the Cr_2B phase in our samples had the Mn_4B structure. "Our" Cr_2B is evidently identical with the Cr_4B phase reported by Bertaut and Blum [12] but as we found the composition to be much nearer to $CrB_{0.50}$ than to $CrB_{0.25}$ it will be referred to as Cr_2B in the following. Two additional phases with the composition Cr_2B have earlier been reported, namely one orthorhombic [13] (space group *A b m m* or *A b m* 2) and one having the $CuAl_2$ structure [12]. Neither of these phases were observed in this investigation.

II. Except the ferrite (α) and sigma phases, only Cr_2B (with some dissolved Fe) was found in the Fe-Cr-B alloys. (Two or three very weak lines from samples 1, 2 and 3 probably originate from impurities.) The phases observed in the different samples and the l.p. of the α and Cr_2B phases are collected in

Table 2.

Sample	at % B	obs. phases	Lattice parameters in Å				at % Cr in α-phase
			Cr_2B			α	
Fe	—	α				2.8662	
Cr	—	α				2.8857	
0	—	σ				—	
1	4.0	α +σ+Cr_2B				2.8736	29
2	8.6	α+Cr_2B	a= 14.63	b = 7.37	c = 4.23	2.8731	24
3	13.2	α+Cr_2B	14.63	7.36	4.23	2.8729	22
4	16.9	α+Cr_2B	14.61	7.36	4.22	2.8721	16
5	22.5	α+Cr_2B	14.60	7.34	4.22	2.8697	7
6	26.0	α+Cr_2B	14.58	7.33	4.21	2.8681	3
Cr_2B	33	Cr_2B	14.71	7.41	4.25		

Table 2. The l. p. of the Fe and Cr used in the preparation of the samples 0—6 and those of pure Cr_2B are also given in the table.

The variation of the l. p. of the α-phase with the Cr content has been determined by Preston [14] (Fig. 1). From Fig. 1 the Cr content of the α-phase of the different samples has been determined and is given in Table 2.

The following observations should be made. With no boron present only the sigma phase is found in the 54/46 (Fe/Cr) sample; with 4 at % B present so much Cr has been bound in the Cr_2B boride that both ferrite (α) and sigma are found. At higher boron concentrations too little Cr is available for any sigma phase to be formed at all, and the α-phase is gradually depleted of Cr with further increasing boron content. The composition of the α-phase at the $\alpha/(\alpha + \sigma)$ boundary (700°C) obtained from sample 1 is 29 at. % Cr in good agree-

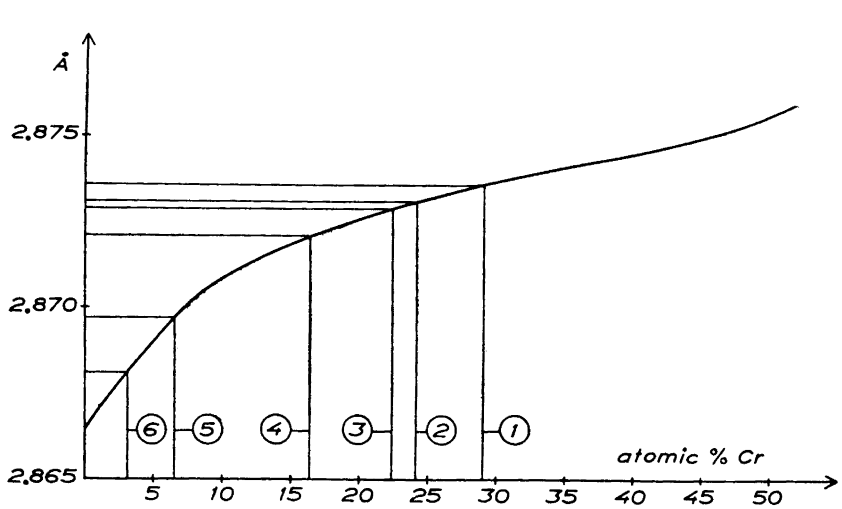

Fig. 1. Cube edge of α-phase as function of Cr content [14]. The numbers in circles refer to samples.

ment with the value of 31 at. % Cr which Cook and Jones [15] give for the binary Fe-Cr system. Thus, boron seems to have very little influence on the position of this boundary. In the samples 2—6 the l. p. of the (Cr, $Fe)_2B$ phase are smaller than those of pure Cr_2B showing that considerable amounts of Fe are dissolved in this phase. The atomic ratio Cr/(Cr + Fe) is estimated to be about three times as great in Cr_2B as in the α-phase.

If there is any appreciable solubility of boron in σ-FeCr it should influence the l. p. of this phase, and a closer study of these parameters is appropriate. The l. p. of the sigma phases in the samples 0 and 1 together with those earlier given by Lundström and Aronsson [10] are collected in Table 3.

Table 3.

Sample	Composition	l.p. of the sigma phase	
	$Fe_{0.504}$ $Cr_{0.496}$	a = 8.798 Å	c = 4.558 Å
0	$Fe_{0.551}$ $Cr_{0.449}$	a = 8.787 Å	c = 4.560 Å
1	$Fe_{0.56}$ $Cr_{0.44}$	a = 8.784 Å	c = 4.562 Å

The compositions have been obtained from chemical analyses except for sample 1. Cook and Jones [15] have found that the Fe-rich $\sigma/(\sigma + \alpha)$ limit in the Fe-Cr system occurs at 43.5—44 at % Cr (700°C). We have assumed that the composition of the sigma phase of sample 1 (containing both ferrite and sigma) is the same as at the $\sigma/(\sigma + \alpha)$ boundary of the binary Fe-Cr system.

The l. p. of the different sigma phases show that the a-axis of σ-FeCr decreases and the c-axis increases with increasing Fe content. The l. p. vary in the same directions when Si is dissolved in σ-FeCr[10]. These similarities are not unexpected as it has been assumed the Si and Fe are similarly distributed in the sigma structure. We think that the differences in l. p. of the sigma phases are entirely explained by the variations in Fe content and that they are not due to the solubility of boron in σ-FeCr. This solubility is likely to be very small.

CONCLUSIONS

We have found that the influence of boron on the formation of σ-FeCr is similar to that of carbon and nitrogen. With increasing boron content of a Fe-Cr-B alloy (the atomic ratio Fe/Cr = 54/46), increasing amounts of Cr-rich $(Cr, Fe)_2B$ are formed and less Cr is available for sigma formation. We have found no evidence that there is any appreciable solubility of boron in σ-FeCr.

Acknowledgements. We want to thank professor G. Hägg for his kind interest. We are much indebted to the Analytical Department of Fagersta Bruks AB, where the chemical analyses were carried out. Financial support from *Statens Tekniska Forskningsråd* is gratefully acknowledged.

REFERENCES

1. Hägg, G. *Z. physik. Chem.* **6 B** (1929) 221.
2. Ehrlich, P. *Z. anorg. Chem.* **259** (1949) 1.
3. Goldschmidt, H. J. *J. Iron Steel Inst. London* **160** (1948) 345.
4. Hultgren, A. and Kuo, K. *Jernkontorets Ann.* **135** (1951) 449.

5. Hägg, G. *Ibid.* **135** (1951) 493 (discussion).
6. Hägg, G. and Kiessling, R. *J. Inst. Metals* **81** (1951–52) 57.
7. Shortsleave, F. J. and Nicholson, M. E. *Trans. Am. Soc. Metals* **43** (1951) 142.
8. Tisinai, G. F., Stanley, J. K. and Samans, C. H. *Trans. Am. Inst. Min. Met. Eng.* **200** (1954) 1259.
9. Andersen, A. G. H. and Jette, E. R. *Trans. Am. Soc. Metals* **24** (1936) 375.
10. Aronsson, B. and Lundström, T. *Acta Chem. Scand.* **11** (1957) 365.
11. Kiessling, R. *Ibid.* **4** (1950) 146.
12. Bertaut, F. and Blum, P. *Compt. rend.* **236** (1953) 1055.
13. Andersson, L. H. and Kiessling, R. *Acta Chem. Scand.* **4** (1950) 160.
14. Preston, G. P. *J. Iron Steel Inst. London* **124** (1931) 141.
15. Cook, A. J. and Jones, F. W. *Ibid.* **148 II** (1943) 217.

Received May 21, 1958.

ACTA CHEMICA SCANDINAVICA 12 (1958) 1481—1491

Hydrolysis of Carboxylic Acid Esters of Thiocholine and its Analogues

1. Acid Hydrolysis

EDITH HEILBRONN

Research Institute of National Defence, Dept. 1, Sundbyberg 4, Sweden

The hydrolysis of thiocholine esters, α-methylthiocholine esters and β-methylthiocholine esters was studied by a colorimetric method at pH-values 1.07, 1.65 and 2.20. First and second order rate constants are given. The temperature dependence of the hydrolysis was studied at 55°C, 75°C and 90°C at pH 1.2. The constants in Arrhenius' equation and activation energies are given.

The products of hydrolysis were studied by means of paper chromatography. Cleavage between the sulphur atom and the carbonyl group was found for all the esters investigated. R_F-values for choline and its analogues, choline esters, thiocholine and its analogues, thiocholine esters and the oxidation products of thiocholine and its analogues are given.

The results are discussed and a possible reaction mechanism for the hydrolysis of thioesters is given.

In the course of investigations, in this institute, concerning the relationship between the structure and cholinesterase affinity of substrates and inhibitors, series of carboxylic acid esters of thiocholine, α-methylthiocholine and β-methylthiocholine were synthesized [1,2].

Before a study of any enzyme kinetics or pharmacology with these compounds, it was considered necessary to study the dependence of their acid and alkaline hydrolysis on pH and temperature. Since up till now there has been relatively little known about the mechanism of hydrolysis of thioesters, it also seemed to be of interest to compare the hydrolysis of the thiocholine esters with the hydrolysis of the corresponding choline esters [3].

Earlier data reported on the hydrolysis of thioesters seem mostly to refer to studies carried out in water-acetone or water-dioxan solutions. Morse and Tarbell [4] describe the hydrolysis in hydrochloric acid in 62 % acetone of allyl, benzyl and trityl thioacetates. They found cleavage between the carbonyl group and the sulphur atom with allyl and benzyl thioacetates, but cleavage between the alkyl group and the sulphur atom with trityl thioacetate. Noda

et al. [5], Rylander and Tarbell [6] and Schaefgen [7] have investigated the hydrolysis of several thioacetates, among them *n*-butyl, *iso*butyl, *n*-amyl and *iso*amyl, in hydrochloric acid. They found the hydrolysis to be first order with respect to ester concentration and hydronium ion concentration. However, Böhme and Schran [8], who have studied the hydrolysis of some thioesters in water-dioxan and found a cleavage between acyl and sulphur, report catalysis by the hydronium ion which was not first order with respect to hydronium ion concentration, but dependent upon the type of acid used.

The dependence on pH and temperature of the hydrolysis of thiocholine and methylthiocholine esters reported in this paper was studied in acid buffer solutions. The products of hydrolysis were analyzed after hydrolysis in 0.1 M hydrochloric acid in a nitrogen atmosphere.

EXPERIMENTAL

Materials. Thiocholine, thiocholine esters, α-methylthiocholine esters and β-methylthiocholine esters were synthesized by Hansen [1,2]. Choline, β-methylcholine and acetyl-α-methylcholine were synthesized according to a method described by Tammelin [9] for the synthesis of acetylcholine and acetyl-β-methylcholine. The esters were iodides or bromides. The thioacetic acid was commercial (Fluka A.G.).

Paper chromatography. Five solvents were used for the chromatography of the products of hydrolysis and their reference substances. The compositions of these solvents were

1) *n*-butanol saturated with water [10],
2) *n*-butanol:ethanol:acetic acid:water (8:2:1:3) [11],
3) *n*-propanol:1 M acetic acid (3:1) [12],
4) diethylene glycol:*n*-butanol:water (1:4:1) [13],
5) 2 M ammonium hydroxide:*iso*propanol (1:3) [14].

Solvents 2—4 were used in descending technique, 1 and 5 in ascending technique. The filter paper used was Whatman No. 1. With the aid of a micropipette, 10—50 μl of the solutions were placed in small portions on the filterpaper, which was dried between each addition. Duplicate spots were run. The reference substances were dissolved in water to determine their R_F-values and in 0.1 M hydrochloric acid, when they accompanied the hydrolysates. Mixtures of hydrolysate and reference substance were also run.

The esters were hydrolyzed in sealed tubes containing 0.1 M hydrochloric acid in a nitrogen atmosphere at 35°C for several days. Hydrolysates were analysed by chromatography. A hydrolysis where the solutions were kept at 80°C in a nitrogen atmosphere was followed by determining the amount of unhydrolyzed ester as iron-hydroxamate complex [15].

The investigation of the spots was carried out by inserting the sheets into a chamber of iodine vapour in order to find the spots. Quaternary ammonium compounds were identified by spraying the chromatograms with dipicrylamine (DPA) [16] which gave yellow spots or by immersing the chromatograms in a solution of phosphomolybdic acid with subsequent reduction with stannous chloride (PMA) [13] which gave blue spots. Unhydrolyzed esters and thioacids were found as iron-hydroxamate complexes [17]. Thiols and also sometimes disulphides could be located with N-ethyl maleinimide (NEM) [18], which gave red spots. This reagent reacted also with the unhydrolysed esters, which apparently were hydrolysed by the reagent. Hydroxyl groups usually gave yellow-coloured spots.

Kinetic measurements. Acid hydrolysis was studied in Clark and Lubs standard buffer solutions [19] at 55°C, 75°C and 90°C. The pH-values of the solutions were determined with a Radiometer pH-meter 23, type PHM 23C, and are given in Table 6. A saturated calomel electrode and a glass electrode, G302A, were used for measurements at high temperature. The instrument was standardised against a citrate buffer, pH 2.75 ± 0.02 (55°C) (P-H Tamm, Svenska Finkemikalier).

Table 1. Chromatogram following oxidation of thiocholine, acetyl-α-methylthiocholine and acetyl-β-methylthiocholine. Solvent No. 4. Solvents are described in the experimental part.

Time (h) after oxidation start	Oxidised compound								
	Thiocholine			Acetyl-α-methylthiocholine			Acetyl-β-methylthiocholine		
	R_F	colour with	indicating	R_F	colour with	indicating	R_F	colour with	indicating
0	0.60 (0.22)	PMA, NEM PMA, NEM	thiocholine (oxidised thiocholine)	0.72	PMA, NEM	(acetyl-)α-methyl-thiocholine	0.62	PMA, NEM	(acetyl-)β-methyl-thiocholine
4	0.60 (0.22)	PMA, NEM PMA, NEM	thiocholine (oxidised thiocholine)	0.72 (0.24)	PMA, NEM PMA	(acetyl-)α-methyl-thiocholine (oxidised α-methyl-thiocholine)	0.62 (0.29)	PMA, NEM PMA	(acetyl-)β-methyl-thiocholine (oxidised β-methyl-thiocholine)
22	0.22	PMA, NEM	oxidised thiocholine	0.24	PMA (NEM)	oxidised α-methyl-thiocholine	0.29	PMA	oxidised β-methyl-thiocholine
60	0.22	PMA, NEM	oxidised thiocholine	0.24	PMA	oxidised α-methyl-thiocholine	0.29	PMA	oxidised β-methyl-thiocholine

4.0×10^{-3} M solutions of the compounds were hydrolysed in a thermostat. The pH of the solution was measured at the beginning and at the end of each kinetic experiment. The ester concentration in solutions was determined as iron-hydroxamate complex [15] and measured with a Beckman B spectrophotometer at 540 mμ.

Preparation of disulphide compounds. Bis (trimethyl ammonium ethyl) disulphide (oxidised thiocholine): 100 mg of thiocholine iodide were dissolved in 25 ml of 48 % hydrogen bromide, *d* 1.49. The solution was refluxed at the boiling point and a stream of oxygen was led in. The progress of the oxidation was followed with hydroxamate-$FeCl_3$ and also by chromatography. In this way it was made clear which spot was the thiol and which was the disulphide. After 60 h all the thiocholine was oxidised. Bis(trimethyl ammonium 2-methyl ethyl) disulphide, oxidised α-methylthiocholine, and bis(trimethyl ammonium 1-methyl ethyl) disulphide, oxidised β-methylthiocholine, were prepared in the same way, but here the starting material was the corresponding acetyl ester. Chromatograms are shown in Table 1.

RESULTS

Products of hydrolysis

The hydrolysis of thiocholine and its analogues can be expected to proceed according to one of the following reaction schemes:

$$R_1\overset{\overset{O}{\|}}{C}-SR_2 + H_2O \longrightarrow R_1\overset{\overset{O}{\|}}{C}-OH + HSR_2 \qquad (1)$$

or

$$R_1\overset{\overset{O}{\|}}{C}-SR_2 + H_2O \longrightarrow R_1\overset{\overset{O}{\|}}{C}-SH + HOR_2 \qquad (2)$$

where R_1 = alkyl or phenyl and

$$R_2 = -CH_2-CH_2-N^+(CH_3)_3,\ -CH_2-\underset{\displaystyle CH_3}{\underset{|}{CH}}-N^+(CH_3)_3 \text{ or } -\underset{\displaystyle CH_3}{\underset{|}{CH}}-CH_2-N^+(CH_3)_3$$

$$R_1\overset{\displaystyle O}{\overset{\|}{C}}-SH \text{ in acid medium splits into } R_1\overset{\displaystyle O}{\overset{\|}{C}}-OH \text{ and } H_2S, \text{ but } HSR_2N^+(CH_3)_3$$

probably is stable at least at moderate temperatures, the hydrolysates were analysed with respect to choline and thiocholine or their analogues.

Table 2. R_F—values for several quaternary ammonium compounds and thioacetic acid in 5 different solvents, described in the experimental part.

Compound	R_F in solvent					Spots developed with
	1	2	3	4	5	
Choline chloride	0.09	0.25	0.40	0.39	—	I_2, PMA, DPA
Choline bromide	0.12	0.27	0.43	0.41	—	I_2, PMA, DPA
Choline iodide	0.18	0.34	0.52	0.51	—	I_2, PMA, DPA
β-Methylcholine iodide	0.27	0.44	0.61	0.60	—	I_2, PMA, DPA, FeH
Acetylcholine iodide	0.22	0.39	0.56	0.56	—	I_2, PMA, DPA, FeH
Acetyl-α-methylcholine iodide	0.30	0.45	0.60	0.60	—	I_2, PMA, DPA, FeH
Acetyl-β-methylcholine iodide	0.35	0.47	0.66	0.67	—	I_2, PMA, DPA, FeH
Thiocholine iodide	0.25	0.43	0.55	0.62	—	I_2, PMA, DPA, Nem
Acetylthiocholine bromide	0.24	0.41	0.52	0.60	—	I_2, PMA, DPA, FeH, Nem
Acetylthiocholine iodide	0.28	0.43	0.59	0.65	—	I_2, PMA, DPA, FeH, Nem
Acetyl-α-methylthiocholine bromide	0.32	0.50	0.60	0.71	—	I_2, PMA, DPA, FeH, Nem
Acetyl-α-methylthiocholine iodide	—	—	0.70	0.78	—	I_2, PMA, DPA, FeH, Nem
Acetyl-β-methylthiocholine bromide	0.29	0.47	0.61	0.62	—	I_2, PMA, DPA, FeH, Nem
Acetyl-β-methylthiocholine iodide	0.30	0.47	0.64	0.66	—	I_2, PMA, DPA, FeH, Nem
Valeryl-β-methylthiocholine iodide	—	0.72	—	—	—	I_2, PMA, DPA, FeH, Nem
Bis(tri-methyl ammonium ethyl) disulphide, oxidized thiocholine	0.04	0.19	0.26	0.23	—	I_2, PMA, DPA, (Nem)
Bis(tri-methyl ammonium 1-methyl ethyl) disulphide, oxidized β-methylthiocholine	0.08	0.20	0.31	0.29	—	I_2, PMA, DPA, (Nem)
Bis(tri-methyl ammonium 2-methyl ethyl) disulphide, oxidised α-methylthiocholine	0.06 0.17	0.18 0.34	0.33	0.32 0.24	—	I_2, PMA, DPA, (Nem)
Thioacetic acid	—	—	0.92	—	0.58	Nem, FeH

Table 3. Chromatogram showing hydrolysis of acetylthiocholine at 80°C in 0.1 M HCl.

Time in h	R_F	Colour with	Indicating
0	0.66 (0.62)	PMA, Nem, FeH PMA, Nem	acetylthiocholine (thiocholine)
0.1	0.66 (0.62)	PMA, Nem, FeH PMA, Nem	acetylthiocholine (thiocholine)
1.0	0.66 0.62	PMA, Nem, FeH PMA, Nem	acetylthiocholine thiocholine
2.5	0.66 0.62	PMA, Nem, FeH PMA, Nem	acetylthiocholine thiocholine
4.5	(0.66) 0.62 0.21	PMA, Nem, FeH PMA, Nem PMA	(acetylthiocholine) thiocholine oxidised thiocholine
22	0.62 0.21	PMA, Nem PMA, Nem	thiocholine oxidised thiocholine
28	0.62 0.21	PMA, Nem PMA, Nem	thiocholine oxidised thiocholine
48	0.62 0.21	PMA, Nem PMA, Nem	thiocholine oxidised thiocholine

Before starting the chromatograms of the products of hydrolysis, the R_F-values for the expected reference substances were determined. Values are given in Table 2. Observed variation of R_F-values in different runs was about $\pm$ 10 %. It is seen that R_F-values for thioesters increase in the order chlorides, bromides, iodides. This has also been observed for quaternary ammonium compounds by Sheppars *et al.*[20].

A chromatogram following hydrolysis of acetylthiocholine iodide is shown in Table 3. Blue colour with phosphomolybdic acid and stannous chloride

Table 4. Chromatogram of hydrolysate of acetyl-β-methylthiocholine after hydrolysis in 0.1 M HCl in sealed tubes filled with nitrogen.

Solvent	R_F	Colour with	Indicating
1	0.27 (0.04)	PMA, Nem PMA	β-methylthiocholine (oxidised β-methyl- thiocholine)
2	0.39 (0.15)	PMA, Nem PMA	β-methylthiocholine (oxidised β-methyl- thiocholine)
3	0.52 (0.32)	PMA, Nem PMA	β-methylthiocholine (oxidised β-methyl- thiocholine)
4	0.61 (0.31)	PMA, Nem	β-methylthiocholine (oxidised β-methyl- thiocholine)

Table 5. Chromatogram of hydrolysate of acetyl-α-methylthiocholine after hydrolysis in 0.1 M HCl in sealed tubes filled with nitrogen.

Solvent	R_F	Colour with	Indicating
1	0.31 (0.09 + 0.17)	PMA, Nem PMA	α-methylthiocholine (oxidised α-methyl-thiocholine)
2	0.45 (0.21 + 0.34)	PMA, Nem PMA	α-methylthiocholine (oxidised α-methyl-thiocholine)
3	0.53 (0.45)	PMA, Nem PMA	α-methylthiocholine (oxidised α-methyl-thiocholine)
4	0.64 (0.31)	PMA, Nem PMA	α-methylthiocholine (oxidised α-methyl-thiocholine)

(PMA) indicates a quaternary ammonium group or a tertiary amino group. For the esters analysed the identification of a quaternary ammonium group was accepted. The iron-hydroxamate complex (FeH) indicates an ester linkage and a colour reaction with N-ethyl-maleinimide (NEM) indicates a thio group. However, in a few cases red colour with NEM was observed also with the disulphide compounds. The colour of the spots and their R_F-values identify them as acetylthiocholine (R_F 0.66), thiocholine (R_F 0.62) and probably oxidised thiocholine (R_F 0.21).

The hydrolysates of acetyl-β-methylthiocholine bromide gave, after 3 days at 55°C, β-methylthiocholine and very small amounts of oxidised β-methyl-thiocholine, as seen in Table 4. In the same way hydrolysis of acetyl-α-methylthiocholine bromide was shown to give α-methylthiocholine and small amounts of oxidised α-methyl-thiocholine, as seen in Table 5. For some unknown reason oxidised α-methyl-thiocholine often gave two spots.

Thus chromatograms of the products of acid hydrolysis of acetylthiocholine, acetyl-α-methylthiocholine and acetyl-β-methylthiocholine show that, for all three types of esters, cleavage occurs between the carbonyl group and the sulphur atom. This was also shown to be true for the other thioesters analysed, including the benzoyl thioesters.

Rate of hydrolysis

The rate of hydrolysis for thiocholine esters and their analogues was determined in buffer solutions at pH—values 1.07, 1.65 and 2.20 at 55°C. The ionic strengths (μ) of the solutions were estimated to be 0.142 at pH 1.07, 0.077 at pH 1.65 and 0.057 at pH 2.20. Straight lines were obtained when the logarithm of the ester concentration at constant pH was plotted against time as is seen

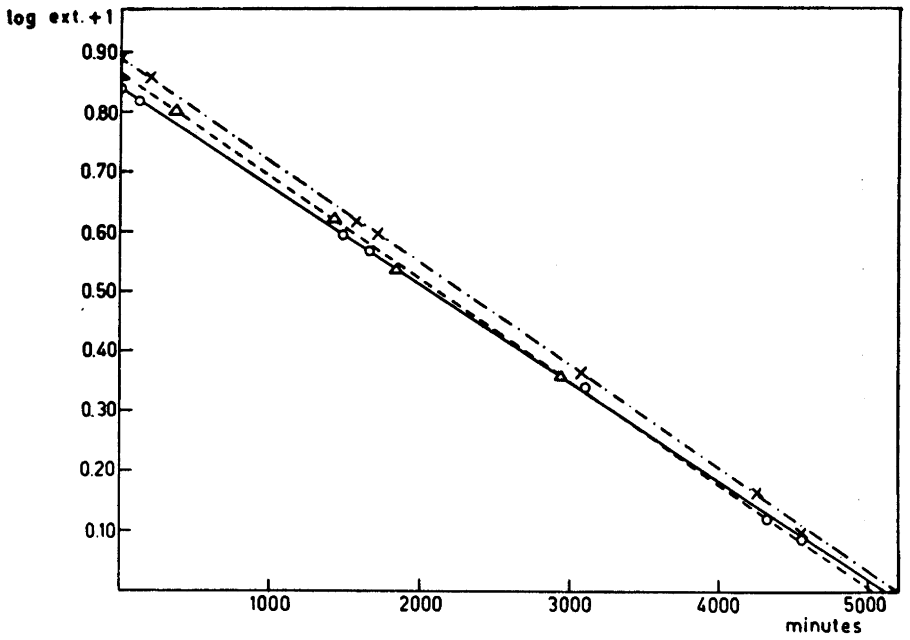

Fig. 1. Hydrolysis at pH 1.07. Logarithm of ester concentration, expressed as logarithm of optical density of iron-hydroxamate complex, plotted against time. × = acetylthiocholine, O = acetyl-α-methylthiocholine, △ = acetyl-β-methylthiocholine.

in Fig. 1, indicating a first order reaction. First order rate constants in minutes were calculated according to equation

$$k_1 = \frac{1}{t} \ln \frac{c_0}{c}$$

where c_0 and c are the optical densities at zero time and time t, respectively. It was shown earlier [15] that Lambert-Beer's law is obeyed. Second order rate constants in $1 \cdot \text{mole}^{-1} \cdot \text{min}^{-1}$ were calculated according to equation

$$k_2 \cdot a_{H^+} = k_1$$

as the catalysis by hydroxyl ions can be neglected at the pH—values investigated. Second order rate constants at ionic strength = 0 were not calculated, as Nilsson (Olered) [21,22] has shown that the ionic strength does not seem to influence the rate of the acid hydrolysis of choline esters.

Rate constants given in Table 6 show that the rate is proportional to hydrogen ion activity with a slight tendency to increase at the highest pH used.

Table 6. Pseudo first order rate constants and second order rate constants for several carboxylic acid esters of thiocholine, α-methylthiocholine and β-methylthiocholine, determined at pH 1—2.2, $t = 55°C$.

R_1 \ R_2		$-CH_2-CH_2-N^+(CH_3)_3$			$-CH_2-CH(CH_3)-N^+(CH_3)_3$			$-CH(CH_3)-CH_2-N^+(CH_3)_3$		
CH_3-	pH	1.07	1.65	2.22	1.07	1.65	2.20	1.07	1.65	2.20
	k_1 min^{-1} × 10^4	4.04	1.18	0.407	3.09	0.805	0.305	3.95	1.03	0.400
	k_2 l × mole^{-1} × min^{-1} × 10^3	4.8	5.2	6.8	3.5	3.6	4.8	4.7	4.6	6.3
CH_3CH_2-	pH	1.03	1.65	2.23	1.03	1.62	2.22	1.00	1.60	2.26
	k_1 min^{-1} × 10^4	3.45	0.776	0.313	2.84	0.810	0.190	3.49	0.922	0.189
	k_2 l × mole^{-1} × min^{-1} × 10^3	3.7	3.5	5.3	3.0	3.4	3.2	3.5	3.6	3.4
$CH_3CH_2CH_2$-	pH	1.05	1.62	2.25	1.05	1.62	2.21	1.00	1.65	2.26
	k_1 min^{-1} × 10^4	1.99	0.486	0.204	1.38	0.503	0.103	2.25	0.410	0.147
	k_2 l × mole^{-1} × min^{-1} × 10^3	2.2	2.0	3.6	1.6	2.0	1.7	2.3	1.8	2.7
$(CH_3)_2CH_2$-	pH	1.07	1.65	2.20						
	k_1 min^{-1} × 10^4	1.55	0.422	0.131	—	—	—	—	—	—
	k_2 l × mole^{-1} × min^{-1} × 10^3	1.8	1.9	2.1	—	—	—	—	—	—
$CH_3CH_2CH_2CH_2$-	pH	1.05	1.65	2.25	1.05	1.62	2.21	1.00	1.65	2.26
	k_1 min^{-1} × 10^4	1.96	0.473	0.200	1.38	0.501	0.154	1.96	0.434	0.184
	k_2 l × mole^{-1} × min^{-1} × 10^3	2.2	2.1	3.6	1.5	2.1	2.5	2.0	2.0	3.4
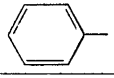	pH	1.05			1.07			1.07		
	k_1 min^{-1} × 10^4	0.138	—	—	0.072	—	—	0.148	—	—
	k_2 l × mole^{-1} × min^{-1} × 10^3	0.2			0.1			0.2		

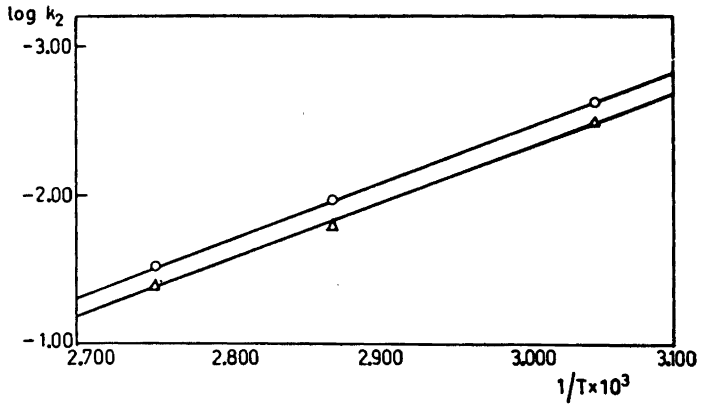

Fig. 2. Temperature dependence of hydrolysis. Second order rate constants in $1 \times \text{mole}^{-1} \times \text{min}^{-1}$ plotted against $1/T$. Lines calculated by method of least squares. △ = acetylthiocholine, ○ = acetyl-α-methylthiocholine.

Temperature dependence

Temperature dependence of the acid hydrolysis was determined for four esters of each of the thiols at pH 1.2 at 55°C, 75°C and 90°C. Difficulties in the determination of the exact pH at the high temperatures which were necessary to speed up hydrolysis, influence the accuracy of the calculated values. The logarithms for second order rate constants in $1 \cdot \text{mole}^{-1} \cdot \text{min}^{-1}$ were calculated as described earlier and plotted against $1/T$ as seen in Fig 2. The line

$$\log k_2 = A_H+ + B_H+/T$$

representing Arrhenius' equation, was calculated by means of the method of least squares, and the activation energies were calculated. The logarithm for the collision factor, PZ, is equal to A_H+ · Arrhenius' constants and activation energies are shown in Table 7.

Table 7. Constants in Arrhenius' equation and activation energies for several carboxylic acid esters of thiocholine, α-methylthiocholine and β-methylthiocholine at pH 1.2.

R_1 \ R_2	$-CH_2-CH_2-N^+(CH_3)_3$			$-CH_2-\underset{\displaystyle CH_3}{\underset{\vert}{CH}}-N^+(CH_3)_3$			$-\underset{\displaystyle CH_3}{\underset{\vert}{CH}}-CH_2-N^+(CH_3)_3$		
	A_H+	B_H+	*E* kcal	A_H+	B_H+	*E* kcal	A_H+	B_H+	*E* kcal
CH_3-	8.8	3 590	16.4	8.7	3 440	15.7	8.5	3 610	16.5
$CH_3-CH_2-CH_2$-	8.8	3 710	17.0	9.4	3 980	18.2	8.6	3 660	16.7
$(CH_3)_2CH_2$-	8.8	3 740	17.1	9.5	4 130	18.9	—	—	—
	9.3	4 270	19.5	9.6	4 450	20.4	9.4	4 370	20.0

DISCUSSION

The rate of hydrolysis of the thioesters studied is rather low compared with the rate of the corresponding choline esters, determined in the same medium by Larsson [3]. The thiocholine esters hydrolyse at 75°C about 3 times slower than their choline analogues. The same phenomenon has been found by other authors [7], who have compared the rate of hydrolysis of thioesters with that of the corresponding oxygen esters. Sulphur is considered to be less negative than oxygen, which results in a less positive carbon in the C—S bond than in the C—O bond. This would retard the water attack on the carbon, supposed to be the rate determining step in acid hydrolysis. Even hydrogen ion attack on the sulphur would be slower than on the oxygen.

A comparison of activation energies found for thiocholine esters with those found for choline esters [3] shows no difference in these values, indicating that the two types of ester may hydrolyse by the same mechanism.

The effect of the substituent on the thiol on the rate of hydrolysis is not great. The esters of the unsubstituted thiocholines hydrolyse fastest, immediately followed by β-methyl substituted esters. The α-methyl substituted esters show the slowest rate of hydrolysis. No steric effect of the β-methyl group could be observed. The reason for this may be the length of the C—S—C bond, according to Pauling 2.58 Å. A methyl group in the β-position to the ammonium group in the thiol would be far enough away from the attacked carbon atom to have little chance of hindering the water molecule from reaching the carbon. Also the small hydrogen ion would easily reach the sulphur atom for an attack in the second step of the hydrolysis.

It is more difficult to explain the small but obvious retardation of hydrolysis found for the α-substituted esters. Several anomalies in the behaviour of these esters were observed. They were found to be the least water-soluble esters and they showed a different behaviour in chromatography from that of the choline esters. Thus it was found that the R_F-values for choline esters increase in the order unsubstitued, α-methyl substituted, β-methyl substituted ester, but for the thiocholine esters the order was found to be unsubstituted, β-methyl substituted, α-methyl substituted ester. This indicates that α-methyl substituted thiocholine esters have a lower affinity for water than the other thioesters and would be in agreement with the observed lower rate of hydrolysis.

The substituent on the carboxy group of the thioesters seems to be important for the rate of hydrolysis of the esters. The rate decreases as the carbon chain grows longer, and bulky substituents retard hydrolysis more than their straight analogues. Thus the rate of hydrolysis for the *iso*butyryl substituted thioester is lower than for *n*-butyryl substituted thioester. It is remarkable that the benzoyl thioester is practically not hydrolysed at all at 55°C. The effect of these substituents may be explained as a steric as well as an inductive and mesomeric (*e.g.* phenyl) effect. If the attack of water at the carbonyl carbon is the rate determining step, bulky substituents on this atom should retard the hydrolysis and thus have a greater influence upon the reaction rate than substituents at the thiol, which is in agreement with the experimental results. The electron releasing effect of the substituents increases with the length

of their carbon chain, leaving the carbonyl carbon less positive, thus retarding the attack of water at this atom.

From the observed data on the rate and products of hydrolysis of thiocholine esters and their analogues it seems probable that the mechanism for their hydrolysis is the same as for choline esters and for esters in general and thus can be described by

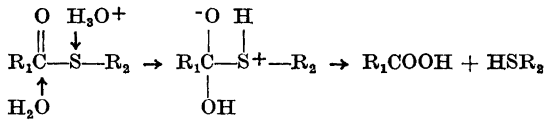

REFERENCES

1. Hansen, B. *Acta Chem. Scand.* **11** (1957) 537.
2. Hansen, B. *Acta Chem. Scand.* (1958) *In press.*
3. Larsson, L. *Acta Chem. Scand.* **8** (1954) 1017.
4. Morse, B. K. and Tarbell, D. S. *J. Am. Chem. Soc.* **74** (1952) 416.
5. Noda, L. H., Kuby, S. A. and Lardy, H. A. *J. Am. Chem. Soc.* **75** (1953) 913.
6. Rylander, P. N. and Tarbell, D. S. *J. Am. Chem. Soc.* **72** (1950) 3021.
7. Schaefgen, J. R. *J. Am. Chem. Soc.* **70** (1948) 1304.
8. Böhme, H. and Schran, H. *Chem. Ber.* **82** (1949) 453.
9. Tammelin, L.-E. *Acta Chem. Scand.* **10** (1956) 145.
10. Whittaker, V. P. and Wijesundera, S. *Biochem. J.* **51** (1952) 348.
11. Augustinsson, K. B. and Grahn, M. *Acta Chem. Scand.* **7** (1953) 906.
12. Ames, B. N. and Mitchell, H. K. *J. Am. Chem. Soc.* **74** (1952) 252.
13. Levine, C. and Chargaff, E. *J. Biol. Chem.* **192** (1951) 465.
14. Isherwood, F. A. and Hanes, C. *Biochem. J.* **55** (1953) 824.
15. Heilbronn, E. *Acta Chem. Scand.* **10** (1956) 337.
16. Malyoth, G. and Stein, H. W. *Biochem. Z.* **323** (1952) 265.
17. Whittaker, V. P. *Biochem. J.* **51** (1952) 348.
18. Benesch, R., Benesch, R. E., Gutcho, M. and Laufer, L. *Science* **123** (1956) 981.
19. Clark and Lubs in Kolthoff, I. M. *Säure-Basen-Indikatoren*, Springer Verlag, Berlin, 1932, p. 246.
20. Sheppars, H. and Sachs D'Asaro, B. *Nature* **177** (1956) 1089.
21. Nilsson, R. *Svensk Kem. Tidskr.* **65** (1953) 213.
22. Olered, R. *Svensk Kem. Tidskr.* **68** (1956) 90.

Received April 25, 1958.

ACTA CHEMICA SCANDINAVICA 12 (1958) 1492—1506

Hydrolysis of Carboxylic Acid Esters of Thiocholine and its Analogues

2. Alkaline Hydrolysis

EDITH HEILBRONN

Research Institute of National Defence, Dept. 1, Sundbyberg 4, Sweden

The hydrolysis of thiocholine esters, α-methylthiocholine esters and β-methylthiocholine esters was studied with an automatic recording titrator at pH values 9.00, 9.50, 9.75 and 10.00 at 35°C and with a colorimetric method at pH 6.0, 7.0 and 8.0 at 55°C. First and second order rate constants are given.

The dependence of the hydrolysis rate on temperature was studied at 25°C, 30°C, and 35°C at pH 10.00. Arrhenius' constants and activation energies are given. The products of hydrolysis were studied by means of paper chromatography and paper ionophoresis and found to be fairly complex. Cleavage between the sulphur atom and the carbonyl group was found.

The hydrolysis of acetylcholine, acetyl-α-methylcholine and acetyl-β-methylcholine was studied with an automatic titrator at pH 9.00, 9.50 and 10.00 at 35°C. First and second order rate constants, Arrhenius' constants and activation energies are given. The results and possible reaction mechanisms are discussed.

Previous studies on the alkaline hydrolysis of thioesters [1-7] refer mostly to hydrolysis in various amounts of sodium hydroxide. Most experiments were carried out under conditions, to which the mathematical treatment of second order kinetics could be applied. Some experiments [3, 5, 6] were, however, carried out in large excess of hydroxyl ion, thus keeping the pH approximately constant. The authors have found agreement with the theory for second order reactions up to 60—80 % completion of hydrolysis. Cleavage between acyl and sulphur was found in all cases. However, Morse and Tarbell [4] found after hydrolysis of tritylthioacetate certain amounts of triphenylcarbinol, but this seems to be a secondary product, as mainly material of disulphide type, among others probably ditrityl disulphide, was obtained.

The only papers known to the present author and treating hydrolysis of thioesters at lower, exactly defined pH-values are by Koningsberger and Overbeek [8-11]. They studied the hydrolysis of ethyl thioacetate between pH 8

and 12 in 0.2 M borate buffer and found that the rate of hydrolysis was directly proportional to the hydroxyl ion concentration up to pH 8.6, as is usually the case with oxygen esters. Above this pH the second order rate constant started to decrease rapidly down to about 10 % of its original value, thereafter proportionality to hydroxyl ion concentration was again observed. They explained this observation by assuming two competitive reactions, a hydroxyl ion catalysed hydrolysis prevailing at high pH and another type of hydrolysis, prevailing at lower pH. Several ways were proposed for the latter type of hydrolysis.

In the preceding paper [12] the acid hydrolysis of carboxylic acid esters of thiocholine and two methylthiocholines is described. The study of the alkaline hydrolysis of these compounds was started with the methods [12] already described. However, complications occurred when the hydroxamate-$FeCl_3$ method [13] was used for kinetic measurement at higher pH-values and so it was decided to use an automatic recording titrator [14]. The dependence of the reaction rate on pH and temperature was also measured for some corresponding choline esters.

EXPERIMENTAL

Materials. The same preparations as for the study on acid hydrolysis [12] were used.

Paper chromatography. Solvents, paper and technique as described earlier [12].

The esters were hydrolysed in excess of 0.1 M sodium hydroxide in an atmosphere of nitrogen previous to chromatography with procedure as described earlier [12]. Hydrolysates from titrations at pH 9.0 were also subject to chromatographic analysis. The hydrolysates were acidified to prevent oxidation during chromatography.

High voltage paper ionophoresis. Hydrolysates from kinetic measurements were used. Paper ionophoresis was carried out with an apparatus according to Foster [15] on Whatman paper No. 1 at a voltage of 2 000 V, 40 V/cm. A 0.1 M borate buffer solution of pH 10.0 was used. Spots were placed on dry paper with a micropipette. After being air dried the papers were immersed in the buffer solution. Excess buffer solution was removed with filter papers. After ionophoresis the papers were air dried and the spots were developed as described earlier for paper chromatography [12].

Kinetic measurements. The alkaline hydrolysis was at first studied in modified Clark and Lubs standard buffer solutions [16] at 55°C. The pH-values of the solutions were determined against a standard buffer of pH 6.95 ± 0.02 (55°C) (P-H Tamm) as described earlier [12].

Automatic titration at constant pH was carried out at constant ionic strength in 0.1 M potassium chloride. The titrator was a 0.098 M solution of sodium hydroxide. The glass electrode used was a Radiometer G 202B and the reference electrode was a saturated calomel electrode, Radiometer K 300. In most experiments 2.77×10^{-5} moles of thiocholine esters were titrated. The same method was used for the determination of the rate constants of some corresponding choline esters. 5.54×10^{-5} moles of these compounds were titrated.

In a few experiments at pH 9.00 and 35°C the titrator was used to keep the pH constant and the amount of unhydrolysed ester was determined as iron-hydroxamate complex [13] in a Beckman apparatus at 540 mμ. In these experiments the concentration of the esters was 2.77×10^{-4} M and the titrator was 0.502 M sodium hydroxide.

RESULTS

Products of hydrolysis

The following reaction schemes are possible for the alkaline hydrolysis of thiocholine esters and analogues at high pH:

(1)

or

(2a)

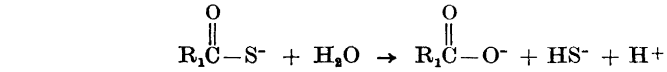

(2b)

where R_1 = alkyl or phenyl and

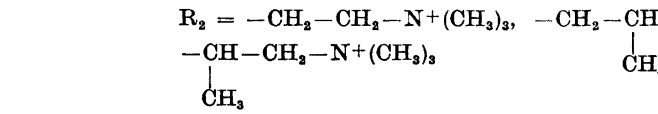

In the first reaction two moles of alkali for each mole of hydrolysed ester would be consumed. In the second reaction one mole of alkali would be used in step a. The reaction described in step b has been found to be incomplete [18] and would thus consume less than one mole of alkali.

It was shown by titration that the esters hydrolysed at pH 10.00 used 2 moles of alkali. However, at pH 9.00 this could not be shown to be true for β-methylthiocholine esters, which used somewhat less than two moles of alkali. Because of the low rate of hydrolysis at this pH, the exact amount of sodium hydroxide used could not be determined.

The hydrolysates were analysed with respect to choline and thiocholine or their analogues. The reference substances described earlier [12] accompanied the chromatograms. The results of the chromatograms of the hydrolysates of acetylthiocholine and acetyl-α-methylthiocholine are given in Table 1. A chromatogram of valeryl-β-methylthiocholine after hydrolysis at pH 9.00 is also given in Table 1. An attempt to identify the source of the unknown spots in these chromatograms was made by studying the products of thiocholine after storage for 4 days in 0.1 M sodium hydroxide at 35°C. The results of this chromatogram are given in Table 2. Acidification by hydrochloric acid after the 4 days of storage gave traces of hydrogen sulphide.

The paper chromatograms were too complex to allow complete identification of the products of hydrolysis. It was, *e.g.*, not possible to decide if any choline compounds were formed as the R_F-values of choline and thiocholine and of their analogues are close to each other [12], which would make it possible for the thio compounds to "mask" spots of the corresponding oxygen compounds.

Table 1. Chromatograms after hydrolysis of acetylthiocholine and acetyl-α-methylthiocholine at 35°C in excess of alkali and after hydrolysis of valeryl-β-methylthiocholine at pH 9.00 and 35°C.

Solvent	R_F	Colour with	Indicating
1[23]	0.18	PMA, (NEM)	?
	0.27	PMA, NEM	thiocholine
2[24]	0.39	PMA	?
	0.45	PMA, NEM	thiocholine
3[25]	0.52	PMA	?
	0.58	PMA, NEM	thiocholine
4[26]	0.37	PMA, (NEM)	?
	0.60	PMA, NEM	thiocholine
3[25]	0.34	PMA	oxidised α-methylthiocholine
	0.42	PMA, (NEM)	?
	0.61	PMA, NEM	α-methylthiocholine
2[24]	0.48	PMA, NEM	β-methylthiocholine
	0.65	PMA, (NEM)	?
	(0.72)	PMA, NEM	valeryl-β-methylthiocholine

Table 2. Chromatogram of solution of 100 mg of thiocholine after 4 days in 0.1 M sodium hydroxide at 35°C.

Solvent	R_F	Colour with	Indicating
1[24]	0.03	PMA	oxidised thiocholine
	0.18	PMA	choline ?
	0.27	PMA, NEM	thiocholine
	0.45	PMA, NEM	?
2[25]	0.26	PMA	choline ?
	0.43	PMA, NEM	thiocholine
	0.55	PMA, NEM	?
3[26]	0.44	PMA	choline ?
	0.57	PMA, NEM	thiocholine
	0.69	PMA, NEM	?
4[27]	0.36	PMA	choline ?
	0.60	PMA, NEM	thiocholine
	0.76	PMA, NEM	?

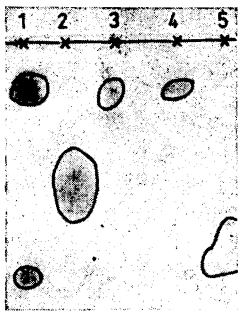

Fig. 1. Ionophoretogram of hydrolysate of valeryl-β-methylthiocholine. 1 = mixture of β-methylthiocholine and oxidised β-methylthiocholine (colour with NEM, PMA), 2 = valeryl-β-methylthiocholine (NEM, PMA), 3 and 4 = hydrolysate (NEM, PMA), 5 = β-methylcholine (PMA).

To determine the products of hydrolysis it was decided to use high voltage paper ionophoresis at a pH above the pK'_a of thiocholine and methylthiocholine. The pK'_a of thiocholine was found to be ~ 7.7 by titration at ionic strength $\mu = 0.1$ with an automatic recording titrator [14]. The values for the other two compounds had to be approximated from the pK'_a-values of analogous dimethylamino compounds. They were found by Hansen [17] to be 7.84 for dimethylamino ethanthiol, 7.59 for dimethylamino-α-methylethanthiol and 7.62 for dimethylamino-β-methylethanthiol.

It was therefore decided that a borate buffer solution of pH 10 should be used. At this pH it can be expected that thiocholine and its analogues will be dissociated and, owing to their state of "Zwitterion", $^-SRN^+(CH_3)_3$, will not move far from the starting point of the ionophoresis, but choline and its analogues, which are not dissociated at this pH, will move rapidly towards the negative pole because of their positive charge, $HORN^+(CH_3)_3$. Secondary oxidation products, having two positive charges, can also be expected to move rapidly towards the negative pole.

The results of the ionophoresis of the products of hydrolysis are given for valeryl-β-methylthiocholine in Fig. 1. It is clearly seen that no β-methylcholine is obtained, whereas β-methylthiocholine is. Hydrolysates of thiocholine esters and α-methylthiocholine esters showed spots indicating thiocholine and α-methylthiocholine, respectively. A spot of unknown origin was sometimes obtained between spots of unhydrolysed ester and thiol. It thus seems that cleavage between the sulphur atom and the carbonyl group occurs in alkaline hydrolysis, but that the products are somewhat complex even when oxidation is prevented during hydrolysis.

Rate of hydrolysis

The rate of hydrolysis for choline and thiocholine esters and their analogues was determined at the pH-values 9.00, 9.50, 9.75 (only α-methyl and β-methylthiocholine esters) and 10.00 at 35°C and at constant ionic strength, $\mu = 0.1$. The pseudo first order rate constant in min^{-1} was calculated according to the method of Guggenheim [19] except for β-methylthiocholine esters at pH 9.00. Second order rate constants were calculated according to the equation

$$k_2 \cdot a_{OH^-} = k_1 \qquad (3)$$

Table 3. Pseudo first order rate constants, second order rate constants, and second order rate constants at ionic strength = 0 for acetylcholine, acetyl-α-methylcholine and acetyl-β-methylcholine.

	R_2	$-CH_2-CH_2-N^+(CH_3)_3$			$-CH_2-CH(CH_3)-N^+(CH_3)_3$			$-CH(CH_3)-CH_2-N^+(CH_3)_3$		
R_1	pH	9.00	9.50	10.00	9.00	9.50	10.00	9.00	9.50	10.00
CH_3-	k_1 $min^{-1} \times 10^3$	4.75	13.9	46.9	4.05	12.4	41.3	1.10	3.40	11.4
	k_2 $l \times mole^{-1} \times min^{-1}$	220±8			193±5			52.9±1.7		
	k_2° $l \times mole^{-1} \times min^{-1}$	302±12			269±7			72.4±3.2		

and k_2° was calculated according to

$$\log k_2 + \log f_{OH} = \log k_2^\circ + z_a z_b \sqrt{\mu} - 0.6 z_a z_b \mu \quad (4)$$

where z_a and z_b are the charges of the reacting ions and 0.6 is a constant found and used by Olered [20] and shown by him to be valid for acetylcholine and some of its analogues. The value for log f_{OH^-} used in the equations was estimated to be — 0.12. The error in k_2, given in Table 3, is a maximum error.

Choline esters. The constant values of k_2 obtained for choline esters and their analogues and given in Table 3, show that the rate of hydrolysis of these esters depends only upon hydroxyl ion activity. The use of eqn. (3) is thus justified for these esters.

Thiocholine esters. Table 4 shows k_2 for thiocholine esters and their analogues. It is seen that k_2 for thiocholine esters is practically constant, though there seems to be a very slight tendency towards a higher value at lower pH. The logarithm of ester concentration, calculated from the amount of sodium hydroxide consumed, plotted against time, shows a straight line, indicating a pseudo first order reaction. Thus it is justified to use eqn. (3) also for these esters.

α-Methylthiocholine esters. The "k_2" values found for α-methylthiocholine esters, given in Table 4, show a tendency to decrease at lower pH. Plots of log c against time show no perfectly straight lines. It is questionable if the method of Guggenheim can be used for calculations of these reaction rates.

β-Methylthiocholine esters. The "k_2" values for β-methylthiocholine esters increase with decreasing pH. A check of the assumed pseudo first order rate of hydrolysis at constant pH, again done by plotting log c against time (Fig. 2), showed no straight line for any β-methylthiocholine ester at pH below 9.50. The method of Guggenheim could thus not be used for calculating the reaction

Table 4. Pseudo first order rate constants, "second order rate constants", and "second order rate constants" at ionic strength = 0 for several carboxylic acid esters of thiocholine, α-methylthiocholine and β-methylthiocholine, determined at pH 9—10, $t = 35°C$.

R_1 \ R_2		$-CH_2-CH_2-N^+(CH_3)_3$			$-CH_2-CH(CH_3)-N^+(CH_3)_3$				$-CH(CH_3)-CH_2-N^+(CH_3)_3$		
R_1	pH	9.00	9.50	10.00	9.00	9.50	9.75	10.00	9.50	9.75	10.00
CH_3-	k_1 min^{-1} × 10^3	3.05	9.55	27.9	2.55	6.77	14.7	22.1	9.17	15.7	24.9
	"k_2" l × mole^{-1} × min^{-1}	146	145	134	122	103	125	105	139	134	119
	"k_2°" l × mole^{-1} × min^{-1}	200	198	186	168	142	173	145	191	185	164
CH_3-CH_2-	k_1 min^{-1} × 10^3	2.92	8.97	26.7	1.20	5.43	10.8	20.7	8.54	14.7	23.7
	"k_2" l × mole^{-1} × min^{-1}	140	136	128	56.9	80.2	92.3	98.9	129	125	114
	"k_2°" l × mole^{-1} × min^{-1}	195	186	178	78.6	112	126	138	178	173	157
$CH_3-CH_2-CH_2-$	k_1 min^{-1} × 10^3	1.69	4.84	14.7	0.802	3.77	5.73	11.2	4.74	8.31	13.8
	"k_2" l × mole^{-1} × min^{-1}	80.9	73.3	70.3	38.4	57.0	48.8	53.5	71.8	69.8	66.1
	"k_2°" l × mole^{-1} × min^{-1}	112	102	97.7	53.0	78.6	67.4	73.8	99.1	96.3	91.3
$(CH_3)_2CH-$	k_1 min^{-1} × 10^3	1.38	4.34	12.7				8.50			
	"k_2" l × mole^{-1} × min^{-1}	66.1	65.8	60.8				40.6			
	"k_2°" l × mole^{-1} × min^{-1}	91.2	91.2	83.2				56.0			
$CH_3-CH_2-CH_2-CH_2-$	k_1 min^{-1} × 10^3	1.67	4.95	14.7	0.854	2.32	4.98	10.9	5.08	8.16	12.8
	"k_2" l × mole^{-1} × min^{-1}	80.0	75.0	70.3	40.8	35.2	42.4	52.1	76.9	69.5	61.2
	"k_2°" l × mole^{-1} × min^{-1}	110	105	97.7	56.2	48.4	58.5	71.9	106	96.0	84.4
	k_1 min^{-1} × 10^3	1.44	4.17	13.3	0.640	2.06	4.67	7.78	4.00	7.26	11.6
	"k_2" l × mole^{-1} × min^{-1}	68.9	63.5	63.7	30.5	31.1	39.7	37.2	60.5	61.8	55.6
	"k_2°" l × mole^{-1} × min^{-1}	95.5	87.1	87.1	42.1	42.9	54.9	51.3	83.5	85.2	76.6

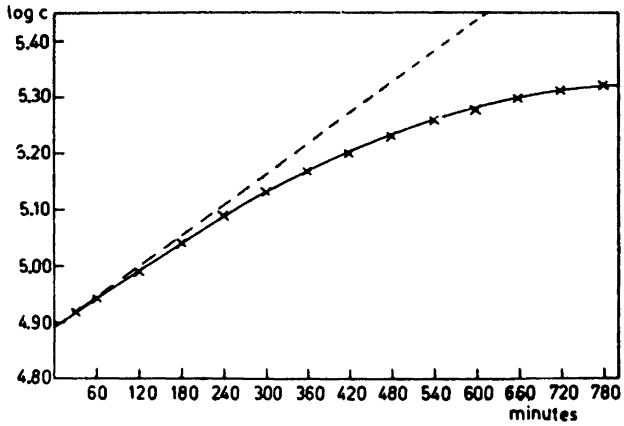

Fig. 2. Hydrolysis at pH 9.00. Logarithm of ester concentration for acetyl-β-methylthiocholine, calculated from consumed amount of sodium hydroxide, plotted against time. Dotted line shows, how ester concentration should decrease, if the reaction was pseudo first order. $t = 35°C$.

rates of these compounds at pH 9.00. The other values are shown in Table 4. The observed deviation from pseudo first order kinetics may depend upon another type of hydrolysis or upon secondary reactions, disturbing in the chosen method of analysis. To see if the hydrolysis of β-methylthiocholine esters at pH 9.00 proceeded as a first order reaction with respect to ester concentration,

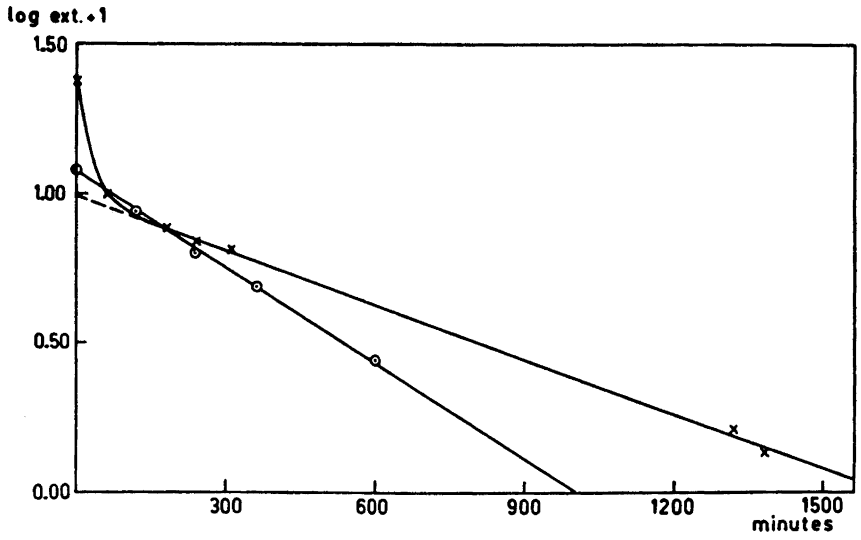

Fig. 3. Hydrolysis at pH 9.00. Logarithm of ester concentration for acetyl-β-methylthiocholine (⊙) and butyryl-β-methylthiocholine (×), expressed as logarithm of optical density of iron-hydroxamate complex, plotted against time. $t = 35°C$.

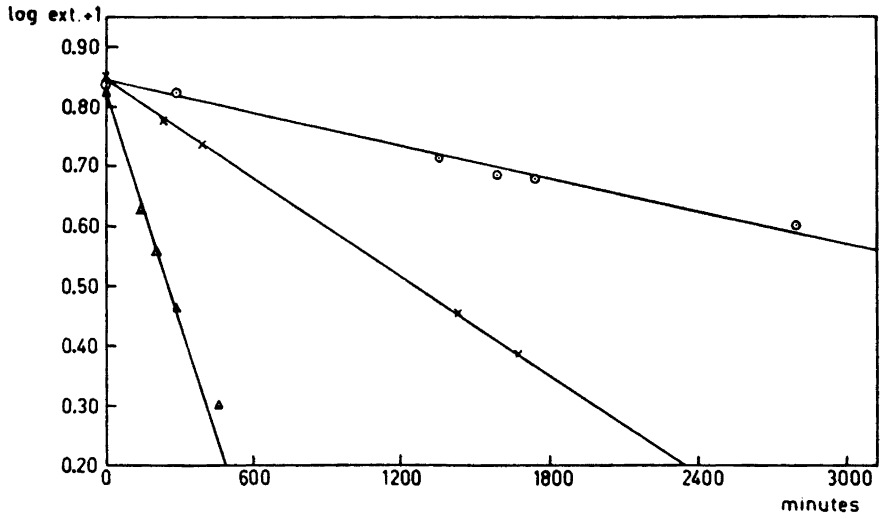

Fig. 4. Hydrolysis at pH 6 (⊙), 7 (×) and 8 (△). Logarithm of ester concentration of acetyl-α-methylthiocholine, expressed as logarithm of optical density of iron-hydroxamate complex, plotted against time. $t = 55°C$.

the automatic recording titrator was used to keep the pH constant and the amount of unhydrolysed ester was measured as iron-hydroxamate complex. The initial concentration of the ester had to be higher than in earlier experiments because of the unsensitivity of the colorimetric method. As Fig. 3 shows, the pseudo first order rate constant for acetyl-β-methylthiocholine was in this case 0.00248 min^{-1}, which would be the expected value, if the hydrolysis was dependent only upon hydroxyl ion activity. The hydrolysis seems to be first order with respect to ester concentration. The pseudo first order rate constant for butyryl-β-methylthiocholine was, by the same method, found to be 0.00137 min^{-1}. The bend at the beginning of the curve may indicate that the sample, which was slightly hydroscopic, was not pure. The same type of curve was obtained with valeryl-β-methylthiocholine.

Hydrolysis of the thioesters at lower pH. The rate of hydrolysis of thiocholine esters and their analogous was also determined in phosphate buffers at pH 6.0, 7.0 and 8.0 at 55°C. These buffer solutions could not keep the pH completely constant during hydrolysis. Owing to the acid character of the hydrolysis products a decrease of 0.10—0.15 pH units was observed. It is seen in Fig. 4 that the hydrolysis was first order with respect to ester concentration. First order rate constants, "second order rate constants", calculated according to eqn. (3), and "k_2^o" calculated according to eqn. (4), are given in Table 5. The ionic strenth is calculated from logarithm diagrams and the values were ~ 0.12 at pH 6, ~ 0.20 at 7 and ~ 0.31 at pH 8. The value used for pK_w was 13.13. It is seen that proportionality to hydroxyl ion activity is not obtained: k_2^o increases as pH decreases.

Table 5. Pseudo first order rate constants, "second order rate constants" and "second order rate constants" at ionic strength = 0 for several carboxylic acid esters of thiocholine, α-methylthiocholine and β-methylthiocholine determined at pH 6—8, $t = 55°C$.

R_1 \ R_2		$-CH_2-CH_2-N^+(CH_3)_3$			$-CH_2-\underset{\displaystyle CH_3}{\underset{\vert}{CH}}-N^+(CH_3)_3$			$-\underset{\displaystyle CH_3}{\underset{\vert}{CH}}-CH_2-N^+(CH_3)_3$		
	pH	5.98	6.95	7.90	5.98	6.92	8.00	5.92	6.86	7.90
CH_3-	k_1 $min^{-1} \times 10^4$	2.86	12.2	35.3	1.92	6.95	32.0	1.89	8.69	31.0
	$"k_2"$ $l \times mole^{-1} \times min^{-1}$	4 170	1 870	620	2 750	1 150	440	3 120	1 640	540
	$"k_2^\circ"$ $l \times mole^{-1} \times min^{-1}$	5 750	2 750	960	3 800	1 700	680	4 370	2 460	830
CH_3-CH_2-	pH	5.99	6.96	8.00			7.93			
	k_1 $min^{-1} \times 10^4$	2.35	9.43	36.6			20.4			
	$"k_2"$ $l \times mole^{-1} \times min^{-1}$	3 370	1 450	510			330			
	$"k_2^\circ"$ $l \times mole^{-1} \times min^{-1}$	4 570	2 090	780			510			
$CH_3-CH_2-CH_2-$	pH	5.99	6.92	8.00			7.89			
	k_1 $min^{-1} \times 10^4$	1.25	4.92	24.2			11.4			
	$"k_2"$ $l \times mole^{-1} \times min^{-1}$	1 770	810	330			200			
	$"k_2^\circ"$ $l \times mole^{-1} \times min^{-1}$	2 510	1 200	510			320			
$CH_3-CH_2-CH_2-CH_2-$	pH	5.95	6.98	8.00			7.93			
	k_1 $min^{-1} \times 10^4$	1.32	4.47	22.2			10.7			
	$"k_2"$ $l \times mole^{-1} \times min^{-1}$	1 910	640	300			170			
	$"k_2^\circ"$ $l \times mole^{-1} \times min^{-1}$	2 820	960	480			270			
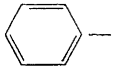	pH	5.97	6.96	8.00						
	k_1 $min^{-1} \times 10^4$	1.11	3.86	21.2						
	$"k_2"$ $l \times mole^{-1} \times min^{-1}$	1 590	580	290						
	$"k_2^\circ"$ $l \times mole^{-1} \times min^{-1}$	2 240	870	460						

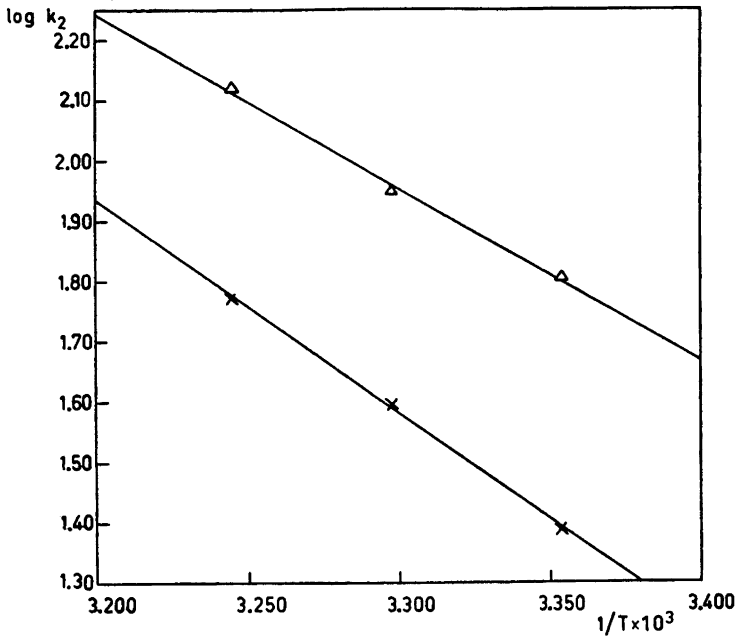

Fig. 5. Temperature dependence of hydrolysis. Second order rate constant in $l \times mole^{-1} \times min^{-1}$ plotted against $1/T$. Line calculated by method of least squares. △ = acetylthiocholine, × = acetyl-β-methylcholine. pH = 10.00.

Temperature dependence

The temperature dependence of the rate of hydrolysis for choline and thiocholine esters and methyl substituted analogues of both was determined at pH 10.00 at 25°C, 30°C and 35°C. The logarithms of the second order rate constants, calculated as described earlier, were plotted against $1/T$ as shown in Fig. 5. The line

$$\log k_2 = A_{OH^-} + B_{OH^-}/T \qquad (3)$$

Table 6. Arrhenius' constants and activation energies for acetylcholine, acetyl-α-methylcholine and acetyl-β-methylcholine. pH = 10.00.

R_2	$-CH_2-CH_2-N^+(CH_3)_3$			$-CH_2-\underset{\displaystyle CH_3}{\underset{\vert}{CH}}-N^+(CH_3)_3$			$-\underset{\displaystyle CH_3}{\underset{\vert}{CH}}-CH_2-N^+(CH_3)_3$		
R_1	A_{OH^-}	B_{OH^-}	E kcal	A_{OH^-}	B_{OH^-}	E kcal	A_{OH^-}	B_{OH^-}	E kcal
CH_3-	11.4±0.8	2780±260	12.7	11.2±0.6	2730±180	12.5	13.3±0.2	3550±150	16.2

Table 7. Arrhenius' constants and activation energies for several carboxylic acid esters of thiocholine, α-methylthiocholine and β-methylthiocholine. The error is calculated by regression analysis. No error given means only 3 determinations. pH = 10.00.

R_1 \ R_2	$-CH_2-CH_2-N^+(CH_3)_3$			$-CH_2-CH(CH_3)-N^+(CH_3)_3$			$-CH(CH_3)-CH_2-N^+(CH_3)_3$		
	A_{OH^-}	B_{OH^-}	*E* kcal	A_{OH^-}	B_{OH^-}	*E* kcal	A_{OH^-}	B_{OH^-}	*E* kcal
CH_3-	11.5±0.6	2760±350	12.6	11.0	2 760	12.6	10.7	2 660	12.1
CH_3-CH_2-	11.1±1.5	2780±450	12.7	10.8±0.6	2720±240	12.4	10.7±0.5	2670±140	12.1
$CH_3-CH_2-CH_2-$	11.2±0.6	2870±170	13.1	11.3±2.3	2830±650	12.9	10.8±0.9	2729±280	12.4
$(CH_3)_2CH-$	12.7±0.7	3360±220	15.4						
$CH_3-CH_2-CH_2-CH_2-$	11.6±0.9	3020±260	13.8	11.2	2930	13.4	10.9±0.9	2810±290	12.9
	13.0±0.8	3450±230	15.9	11.6	3 070	14.0	11.3±0.5	2960±160	13.5

representing the Arrhenius' equation, was calculated by means of the method of least squares. The activation energy was also calculated. The logarithm for the collision factor, PZ, is equal to A_{OH^-}. The following values for pK_w were used: pK_w 25°C = 14.00, pK_w 30°C = 13.83 and pK_w 35°C = 13.68. The constants in the Arrhenius' equation and the activation energies are given in Tables 6 and 7.

DISCUSSION

Only a slight difference in the rate of hydrolysis of the thiocholine esters and the two methylthiocholine esters was found at pH 10.00 as long as the acid residue of the esters was the same. The unbranched thiocholine esters were found to hydrolyse fastest, followed by β-methyl substituted esters. Slowest hydrolysis showed the α-methyl substituted esters. Even activation energies and PZ factors were found to be almost equal for the three types of esters. This is obviously different from the corresponding choline esters. The hydrolysis of unsubstituted and α-methyl substituted choline esters was found to proceed faster than that of β-methylcholine esters. This is also indicated by the activation energies of the choline esters, which were found to be about 12.6 kcal/mole for unsubstituted and α-methyl substituted esters, but 16.2 kcal/mole for β-methylsubstituted esters. The reason for this difference may be found in the steric effect of the β-methyl group. The radius of the oxygen atom, according to Pauling 0.66 Å, and the resulting length of the

C—O—C bridge (2.20 Å) seems to make it possible for the β-methyl group to provide a screen against an approaching hydroxyl ion, but the bigger sulphur atom, according to the same author 1.04 Å, and giving rise to a greater length of the C—S—C bridge (2.58 Å) leaves more space for the attack of the approaching hydroxyl ion at the carbonyl carbon and seems to counteract the effect of the β-methyl group. The observed influence of the substituents of the acid residue upon the rate of hydrolysis is greater than the effect of the substituents of the thiol residue. The reaction rate decreases with the length of the carbon chain, methyl and ethyl showing nearly the same rate, and then the reaction rate falling to about 50 % of the value found for methyl, when the substituents are propyl or butyl; phenyl and *iso*propyl substituted esters showing a still smaller rate of reaction. These observations may be explained by the combined steric (*e.g.*, *iso*propyl) and inductive (*e.g.*, phenyl) effects of the substituents upon the attacked carbonyl carbon.

The observed deviations at lower pH, especially with the β-methyl-thiocholine esters, from pseudo first order kinetics in experiments with the automatic recording titrator seem to depend upon secondary reactions, probably by the products of hydrolysis. This is indicated by the unknown spots in the paper chromatograms and ionophoretograms of the hydrolysates. A possible reaction would be

$$HS-\underset{\displaystyle CH_3}{\underset{|}{CH}}-CH_2-N^+(CH_3)_3 \rightarrow CH_3-S-\underset{\displaystyle CH_3}{\underset{|}{CH}}-CH_2N(CH_3)_2 + H^+ \rightleftharpoons$$

$$\rightleftharpoons CH_3-S-\underset{\displaystyle CH_3}{\underset{|}{CH}}-\overset{\displaystyle H}{\overset{|}{CH_2N^+}}(CH_3)_2$$

The pK_a of the latter compound is probably more than 9, which would offer an explanation of the smaller amount of alkali used by β-methyl-thiocholine esters for complete hydrolysis at pH 9.

The found activation energies for choline esters and thiocholine esters are near the activation energies found by other workers [1,3] for other thioesters. Together with the found pseudo first order hydrolysis and the found products of hydrolysis this indicates, that the mechanism of the alkaline hydrolysis of the studied esters may be described by the Lowry mechanism for ordinary ester hydrolysis, *viz.*

$$R_1-\underset{\displaystyle \uparrow OH^-}{\overset{\displaystyle O}{\overset{\displaystyle \|}{C}}}-\overset{\displaystyle \downarrow H_2O}{S}-R_2 \rightarrow R_1-\underset{\displaystyle OH}{\overset{\displaystyle O^-H}{\overset{|}{C}}}-S^+-R_2 + OH^- \rightarrow R_1COOH + HSR_2 \qquad (5)$$

However, the bond S- - -HOH should be weaker[21] than O- - -HOH, so perhaps solvation is less influential for thioesters. In this case the mechanism of alkaline hydrolysis could perhaps be described by

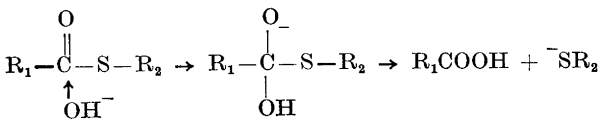

(6)

Such a mechanism would make it still easier to understand the nonexistent steric effect of the β-methyl group in the thiol.

The increasing value for "k_2^o" observed in rate reactions in phosphate buffer solutions may indicate catalysis by phosphate ions. In earlier studies on choline esters, performed with the same methods and in the same medium by Larsson [22], this effect was not observed. However, there is a factor of about two between the rate constants for choline esters found by Larsson and those found now with the automatic titrator, which supports the possibility of a catalysis by phosphate ions. In that case the catalytic activity comes from the ions $H_2PO_4^-$ and HPO_4^{2-} and their effect seems to be greater upon thioesters than upon oxygen esters. There is also the possibility of explaining the increasing "k_2^o" values by assuming two competitive reactions, each with a reaction rate proportional to ester concentration. These reactions could for instance be hydrolysis according to eqns. (5) and (6) described earlier, where reaction (6) would prevail at higher pH-values.

My sincere thanks are due to the Director of the Research Institute of National Defence, Dept 1, Professor G. Ljunggren, to Professor A. Tiselius, Director of the Institute of Biochemistry, University of Uppsala, for their kind interest in this work, and to Professor A. Fredga, Director of the Institute of Organic Chemistry, University of Uppsala, for instructive discussions.

REFERENCES

1. Schaefgen, J. R. *J. Am. Chem. Soc.* **70** (1948) 1308.
2. Böhme, H. and Schran, H. *Chem. Ber.* **82** (1949) 453.
3. Rylander, P. N. and Tarbell, D. S. *J. Am. Chem. Soc.* **72** (1950) 3021.
4. Morse, B. K. and Tarbell, D. S. *J. Am. Chem. Soc.* **74** (1952) 416.
5. Noda, L. H., Kuby, S. A. and Lardy, H. A. *J. Am. Chem. Soc.* **75** (1953) 913.
6. Hawkins, P. J. and Tarbell, D. S. *J. Am. Chem. Soc.* **75** (1953) 2982.
7. Tarbell, D. S. and Cameron, D. P. *J. Am. Chem. Soc.* **78** (1956) 2731.
8. Overbeek, J. Th. G. and Koningsberger, V. V. *Koninkl. Ned. Akad. Wetenschap. Proc.* **B 57** (1954) 81.
9. Overbeek, J. Th. G. and Koningsberger, V. V. *Koninkl. Ned. Akad. Wetenschap. Proc.* **B 57** (1954) 311.
10. Overbeek, J. Th. G. and Koningsberger, V. V. *Koninkl. Ned. Akad. Wetenschap. Proc.* **B 58** (1955) 266.
11. Koningsberger, V. V. *A reaction kinetic study on two models of the biosynthesis of the peptide bond* (Diss.) University, Utrecht 1955.
12. Heilbronn, E. *Acta Chem. Scand.* **12** (1958) 1481.
13. Heilbronn, E. *Acta Chem. Scand.* **10** (1956) 337.
14. Larsson, L. and Hansen, B. *Svensk Kem. Tidskr.* **68** (1956) 521.
15. Foster, A. B. *Chem. & Ind. London* **1952** 1050.
16. Clark and Lubs in Kolthoff, J. M. *Säure-Basen-Indicatoren.* Springer Verlag, Berlin 1932, p. 246.
17. Hansen, B. *Acta Chem. Scand.* **12** (1958) 324.

18. Tarbell, D. S. and Harnish, D. P. *Chem. Rev.* **49** (1951) 45.
19. Guggenheim, E. A. *Phil. Mag.* **2** (1926) 538.
20. Olered, R. *Svensk Kem. Tidskr.* **68** (1956) 90.
21. Lassettre, E. N. *Chem. Revs.* **20** (1937) 267.
22. Larsson, L. *Acta Chem. Scand.* **8** (1954) 1017.
23. Whittaker, V. P. and Wijesundera, S. *Biochem. J.* **51** (1952) 348.
24. Augustinsson, K. B. and Grahn, M. *Acta Chem. Scand.* **7** (1953) 906.
25. Ames, B. N. and Mitchell, H. K. *J. Am. Chem. Soc.* **74** (1952) 252.
26. Levine, C. and Chargaff, E. *J. Biol. Chem.* **192** (1951) 465.

Received April 25, 1958.

ACTA CHEMICA SCANDINAVICA 12 (1958) 1507—1511

The Oxidation of Glycosides

VI. Oxidation of Methyl 4,6-*O*-Ethylidene-β-D-glucopyranoside with Chromium Trioxide

ANDERS ASSARSSON and OLOF THEANDER

Organisk-kemiska Institutionen, Kungl. Tekniska Högskolan and Träkemiska avdelningen, Svenska Träforskningsinstitutet, Stockholm, Sweden

Methyl 4,6-*O*-ethylidene-β-D-glucopyranoside was oxidised with chromium trioxide in acetone and, after removal of the ethylidene groups, oxo-glucosides were isolated; the principal one being the 3-oxo-glucoside. Fractionation on a charcoal column yielded, *inter alia*, methyl 2-oxo-glucoside admixed with methyl glucoside. Those components were separated by chromatography on a carbon column using an irrigant containing sodium hydrogen sulphite. Small amounts of D-arabinose, D-erythrose and D-erythrono-γ-lactone were also isolated. The oxidation of methyl β-D-glucopyranoside was studied in an analogous experiment.

Amongst the products formed on the oxidation of the anomers of methyl 6-*O*-trityl-glucopyranosides with chromium trioxide are the corresponding 2-oxo-, 3-oxo- and 4-oxo-derivatives (Part V[1]). The present investigation was undertaken to simplify the preparation of methyl β-D-2-oxo-glucopyranoside and of methyl β-D-3-oxo-glucopyranoside. The hydroxyl group at C-4 and that at C-6 were protected by an ethylidene group prior to the oxidation. After removal of the ethylidene groups the mixtures of neutral oxidation products were fractionated on carbon columns and subfractionated by chromatography and by electrophoresis on thick filter papers. When 1.5 moles of oxidant per mole of sugar were used, the yield of 3-oxo-glucoside (5.4 %) was only slightly higher than that obtained (4.7 %) under similar conditions from methyl 6-*O*-trityl-β-D-glucopyranoside. The ethylidene derivative is prepared more easily than is the trityl derivative and the former gives a less complex mixture of products (in the present work no 4-oxo- or 6-oxo-glucosides were detected). The present procedure is then to be preferred to that used earlier. The yield of oxo-glucosides was not increased when a higher proportion of oxidant to sugar was used.

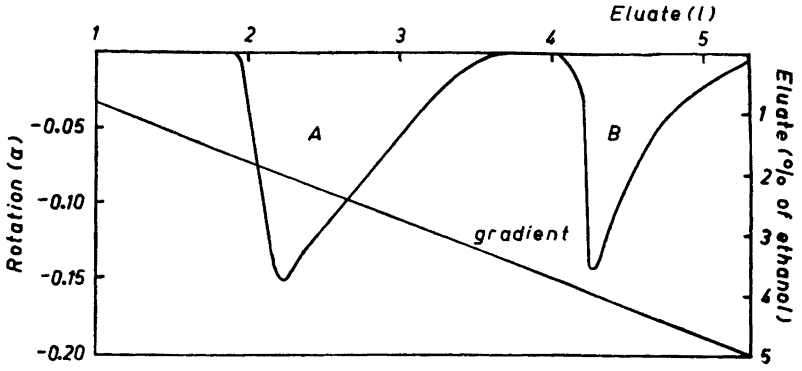

Fig. 1. Separation of methyl β-D-2-oxo-glucopyranoside (A) from methyl β-D-glucopyranoside on a carbon-Celite column using an irrigant containing sodium hydrogen sulphite.

The 2-oxo-glucoside was eluted from the carbon column together with the methyl glucoside. These two substances are easily separated by paper electrophoresis in sulphite buffer [3]. Barker *et al.*[4] used an irrigant containing borate for the carbon column chromatography of some sugars which were difficult to separate by ordinary carbon column chromatography, but which had different electrophoretic mobilities in borate buffer. In the present work the analogous use of sodium hydrogen sulphite in the irrigant resulted in the separation of methyl glucoside and methyl 2-oxo-glucoside (1.2 %) (see Fig. 1).

Many other components were chromatographically indicated to be present and the principal ones were isolated. They included D-glucose (principally from the hydrolysis of part of the methyl glucoside), D-arabinose (0.05 %), D-erythrose (0.13 %) and D-erythrono-γ-lactone (0.20 %) and a trace of a compound chromatographically indistinguishable from ribulose. Small amounts of a neutral and reducing compound (A) were isolated, which gave colour reactions with *p*-anisidine hydrogen chloride and with resorcinol-hydrochloric acid. It had a high electrophoretic mobility in hydrogen sulphite and on reduction with borohydride it gave mainly erythritol.

Another compound (B) giving a characteristic red-violet coloration with resorcinol was isolated. Some properties are given in the experimental part. A compound having similar properties was formed when methyl β-glucoside or its 6-*O*-trityl ether [1,2] was oxidised.

The arabinose and erythrose may have been formed *via* oxoaldonic acids. Whistler *et al.* recently showed that D-erythrono-γ-lactone was formed in relatively large amount when starch was oxidised with hypochlorite [5,6].

Methyl-β-glucoside on oxidation by dichromate in the presence of oxalic acid, yielded 6-oxo- and 3-oxo-glucosides as the principal neutral products [2]. In the present work methyl-β-glucopyranoside was oxidised with trioxide using conditions similar to those above and the following substances were isolated: arabinose (0.1 %), glucose (0.25 %) and the 2-oxo- (0.5 %), 3-oxo- (3.3 %), 4-oxo- (0.3 %) and 6-oxo- (1.3 %) derivatives of methyl glucoside.

Those results were unlike those obtained when an aqueous solution of chromate and oxalic acid was used as the oxidant [2]. In that case there was obtained a larger amount of aldehydo-glucoside than of keto-glucosides. The final yields will of course depend not only on the rate of formation of oxo-groups, but also upon any secondary reactions. The results obtained in the present and in an earlier investigation [1] showed that the 3-oxo-glucoside is the predominating neutral product obtained on oxidation with chromium trioxide. It is unlikely that under the oxidation conditions used one oxo-compound could be transformed into another by enolisation. No chromatographically detectable formation of 3-oxo-glucoside from 2-oxo-glucoside took place during the treatment of the oxidation products prior to fractionation. Recrystallisation of 2-oxo-glucoside from hot *n*-propanol, however, resulted in the formation of 3-oxo-glucoside and of unidentified compounds.

A small amount of methyl glucoside and, in a separate experiment, of methyl 4,6-ethylidene glucoside were oxidised with *t*.-butyl chromate in a mixture of acetone and *t*.-butanol. The yields of oxo-glucosides were lower, and that of the acids higher, than when chromium trioxide in acetone was used as oxidant.

EXPERIMENTAL

Melting points are corrected. All distillations were carried out under reduced pressure (bath temperature $<40°$) or by lyophilisation. Papers and spray-reagents used in the paper chromatography and electrophoresis were as given in Part. V[1].

Irrigants and buffers used:

A. Ethyl acetate-acetic acid-water, 3:1:3 (the upper phase).
B. Butanol-pyridine-water, 3:1:1.5.
C. Hydrogen sulphite buffer pH 4.7, 0.1 M[3].
D. Borate buffer pH 10.0, 0.1 M.

Oxidation of methyl 4,6-*O*-ethylidene-β-D-glucopyranoside with chromium trioxide and fractionation of the product

The methyl 4,6-*O*-ethylidene-β-D-glucopyranoside was made by a slight modification of the method of Helferich and Appel [7].

The oxidation and fractionation procedures were essentially as described in Part V[1] and accordingly only an abbreviated description is given. The percentage yields quoted are based upon the original weight of the starting-material calculated as methyl-β-glucoside.

Methyl 4,6-ethylidene-glucoside (80.0 g) was oxidised by boiling it under reflux, for 30 min, with acetone (4 l) and chromium trioxide (55.0 g). The brown chromium oxides were filtered off from the oxidation mixture and boiled with successive volumes of acetone with intermediate filtrations. During the evaporation of the combined filtrate, crystals of pure starting-material (31.0 g, m. p. 187—188°) separated and were filtered off. To the filtrate there were added ethanol (100 ml) and dilute sulphuric acid to give an 0.3 N solution (600 ml). The solution was kept at 100° for 30 min and then extracted with chloroform. The acidity was reduced to pH 5 by the addition of barium carbonate, the mixture being stirred and the temperature kept below 10°. After filtration, the solution was deionised and the solvent distilled off. The product, a light-yellow syrup (20.2 g), was fractionated on a carbon-Celite column (48 × 6 cm) using the linear-gradient elution technique (ethanol: 0—15 %, 10 l and 50 % 4 l). The following main fractions were obtained:

Fraction I (1.8 g) contained glucose and smaller amounts of other components. The material was sub-fractionated by paper chromatography and electrophoresis on thick filter papers, and the following components were obtained: D-erythrono-γ-lactone (0.20 %), D-arabinose (0.05 %), D-ribulose (<0.02 %), D-erythrose (0.13 %) and an unidentified compound A (0.1 %). The first three were chromatographically and electrophoretically indistinguishable from reference substances. The compound A was neutral and was rapidly oxidised by the alkaline silver reagent and also gave a yellow coloration with *p*-anisidine hydrogen chloride and a faint pink coloration with resorcinol-hydrochloric acid. Compound A had: $R_{Glucose}$ = 2.03 (irrigant A), $R_{Glucose}$ = 1.28 (irrigantB), M_V [3] (buffer C at 50°) = 1.70 and M_G (buffer D) = 0.66. On reduction with borohydride it gave erythritol which had m. p. and mixed m. p. 119—120°.

D-*Erythrose*. The amorphous sugar had $[\alpha]_D^{22}$ −14° (*c*, 2.2 in water), $R_{Glucose}$ = 2.35 (irrigant A), M_V = 0.18 (Buffer C at 50°) and M_G = 0.80 (buffer D). A sample of the sugar was reduced with borohydride. After deionisation and recrystallisation of the product from ethanol it had m. p. 120—120.5°, not depressed on admixture with erythritol. It was paper chromatographically and electrophoretically indistinguishable from erythritol. It was acetylated in the usual way and the product, after recrystallisation from ethanol, had m. p. 84—85°, not depressed on admixture with erythritol tetra-acetate.

D-*Arabinose*. The specific rotation of the amorphous sugar was $[\alpha]_D^{22}$ −100 (*c*, 0.8 in water).

D-*Erythrono-γ-lactone*. It was recrystallised from ethyl acetate and had m. p. 104—105° (*Lit.*[5] 104—105°) and $[\alpha]_D^{21}$ −74° (*c*, ? in water), *Lit.*[5] −72). The equivalent weight by titration was 114 (calc. 116).

Fraction II (11.5 g) consisted mainly of methyl β-glucoside and methyl 2-oxo-glucoside. After recrystallisation from aqueous ethanol, pure methyl glucoside (8.7 g) was obtained. The components in the mother liquor were fractionated on a carbon-Celite column (40 × 3 cm) using aqueous ethanol (0—10 %, 4 l and 50 %, 2 l) to remove both traces of glucose and of products which had been formed in small amounts from the labile 2-oxo-glucoside during the crystallisation of the methyl glucoside. A mixture (2.15 g) of methyl 2-oxo-glucoside and methyl glucoside was eluted with *ca.* 4 % aqueous ethanol. It was refractionated on the same column which had been thoroughly washed with 0.1 M sodium hydrogen sulphite. The column was irrigated with 0—5 % ethanol (5 l) using 0.1 M aqueous sodium hydrogen sulphite solution instead of water. The fractionation was followed polarimetrically (2 dm tube, Fig. 1) and by electrophoretic examination using buffer D. The methyl 2-oxo-glucoside was completely separated from the methyl glucoside and, after deionisation and evaporation of the solutions, the two components (0.85 g and 0.96 g, respectively) were obtained chromatographically and electrophoretically pure. Part of the 2-oxo-glucoside crystallised (for data *cf.* part V[1]). Paper chromatographic examination of the mother liquor showed that some rearrangement had taken place during the crystallisation.

Fraction III (4.0 g) consisted mainly of 3-oxo-glucoside which crystallised on removal of the solvent. It was recrystallised from *n*-propanol and had m. p. 130—131°, $[\alpha]_D^3$ −63 (*c*, 2 in water), The yield of this material plus that recovered from the mother liquors was 5.3 %.

Fraction IV (1.6 g) contained an unidentified neutral compound (B), isolated in amorphous state (0.2 %). It gave a distinctive red-violet coloration with resorcinol-hydrochloric acid, a yellow coloration with *p*-anisidine hydrogen chloride and was acid sensitive but alkali-stable. It had $R_{Glucose}$ = 2.98 (irrigant A) and 1.48 (irrigant B), M_V = 0 (Buffer C) and M_G = 0.42 (buffer D). It had OCH_3 *ca.* 14 % and $[\alpha]_D^{21}$ −29° (*c*, 1.4 in water).

The fraction also contained other components most of which could be chromatographically correlated to substances obtained in the previous fractions, while others were probably condensation products formed from the oxo-glucosides.

Oxidation of methyl β-D-glucopyranoside with chromium trioxide and fractionation of the product

The oxidation and fractionation procedures were essentially as described previously, but the reduction of the chromium compounds in aqueous solution by the ethanol was carried out at room temperature and after slight acidification with sulphuric acid. Methyl β-glucoside (20.2 g) was oxidised with chromium trioxide (15.6 g) in acetone (1.20 l) and the product was fractionated on a carbon-Celite column. After sub-fractionation by chromatography and electrophoresis on thick filter paper the following substances were obtained: arabinose (0.1 %), glucose (0.25 %) and the 2-oxo- (0.5 %), 3-oxo- (3.3 %), 4-oxo- (0.3 %) and 6-oxo- (1.3 %) derivatives of methyl β-glucoside. The substance B (see earlier) was obtained in 0.15 % yield.

The authors are indebted to *Statens Tekniska Forskningsråd* for financial support.

REFERENCES

1. Theander, O. *Acta Chem. Scand.* **11** (1957) 1557.
2. Lindberg, B. and Theander, O. *Acta Chem. Scand.* **8** (1954) 1870.
3. Theander, O. *Acta Chem. Scand.* **11** (1957) 717.
4. Barker, S. A., Bourne, E. J. and Theander, O. *J. Chem. Soc.* **1955** 4276.
5. Whistler, R. L., Linke, E. G. and Kazeniac, S. *J. Am. Chem. Soc.* **78** (1956) 4704.
6. Whistler, R. L. and Schweiger, R. *J. Am. Chem. Soc.* **79** (1957) 6460.
7. Helferich, B. and Appel, H. *Chem. wer.* **64** (1931) 1841.

Received June 4, 1958.

ACTA CHEMICA SCANDINAVICA 12 (1958) 1512—1515

Birch Wood Constituents

I. Carbohydrates of Low Molecular Weight

BENGT LINDBERG and LARS SELLEBY

Institutionen för Träkemi, Kungliga Tekniska Högskolan and Träkemiska avdelningen, Svenska Träforskningsinstitutet, Stockholm, Sweden

Myo-inositol, glucose, fructose, sucrose, raffinose, stachyose and verbascose have been isolated from birch wood *(Betula verrucosa)*. The presence of two higher oligosaccharides, probably belonging to the same series as verbascose, was also indicated.

During recent years hardwood has attracted considerable interest as pulp wood. In the Scandinavian countries the birches *(Betula verrucosa* and *B. pubescens)* are the only hardwoods sufficiently abundant to be of general importance. A chemical investigation of the constituents in birch wood is therefore warranted and has been started at this institute. The present communication reports studies on the low molecular weight carbohydrates in the wood of birch *(B. verrucosa)*. The two species *(B. verrucosa* and *B. pubescens)* are closely related and major differences in their chemical composition would not be expected.

A tree was felled in January 1958, and a log cut from it was chopped and milled. The product was treated with acetone as rapidly as possible to inactivate the enzyme systems and thereby to minimise post-mortem changes. The milled wood was then treated with various solvents and the extracts dealt with as described in the experimental part. The carbohydrate fraction was subfractionated by chromatography on carbon-Celite columns and the following substances were isolated (they are listed in the order in which they emerged from one of the columns).

	% of dry wood
Myo-inostiol	0.02
Fructose }	0.56
Glucose }	
Sucrose	0.62
Raffinose	0.04
Stachyose	0.03
Verbascose	0.02

The yields reported are approximate and should be regarded as representative only of the tree in question at the time when it was felled.

Glucose and fructose were not isolated but were identified by their paper chromatographic and electrophoretic behaviour. The other sugars, with the exception of verbascose, were isolated in the crystalline states. Verbascose was obtained as an amorphous powder and was chromatographically and electrophoretically indistinguishable from an authentic sample, and had a specific rotation, +146°, which agreed well with the value recorded in the literature [1].

The three highest oligosaccharides all possessed the structure: *O*-α-D-galactopyranosyl-(1→6)-[*O*-α-D-galactopyranosyl-(1→6)-]$_{n-3}$-*O*-α-D-glucopyranosyl-(1→2)-β-D-fructofuranoside. (In verbascose n = 5.) The chemistry of such oligosaccharides has recently been summarized by French [2] and by Wickström [3]. The two next higher members of the series (n = 6 and n = 7) were chromatographically indicated to be present in a fraction eluted from the column after the verbascose.

All of the oligosaccharides possessed a fructofuranosidic linkage, known to be very easily hydrolysed either by enzymes or by acids. Small amounts of melibiose, manninotriose and verbascotetraose were chromatographically indicated to be present and may have arisen from post-mortem reactions. Their presence does not necessarily imply that they were present in significant amounts in the living tree.

In addition to the carbohydrates described above, a fraction containing a mixture of phenolic substances was obtained, and is now under investigation.

EXPERIMENTAL

Paper chromatography was carried out on Whatman No. 1 filter paper using the follwing solvent systems (v/v): A. Ethyl acetate-acetic acid-water (3:1:3, upper layer); B. *n*-Butanol-ethanol-water (10:3:5); C. Ethyl acetate-pyridine-water (2:1:2, upper layer).

The chromatograms were developed with one of the following spray reagents: silver nitrate in acetone and ethanolic sodium hydroxide, or *p*-anisidine hydrochloride in butanol or resorcinol in hydrochloric acid.

Electrophoresis was carried out on Whatman No. 3 MM filter paper in borate buffer solution (pH 10).

A birch, about 40 years old, was felled and from the trunk a log (100 × 20 cm) was sawn, 1 1/2 – 2 1/2 m from the root end. After one day in the cold, the bark of the log was stripped off. The wood was cut into chips, milled and the wood meal (>30 mesh) covered with acetone and kept at 40°. After 20 h the acetone extract was decanted off and taken to dryness. The residue was dissolved in water (200 ml) and extracted with ether (3 × 100 ml) and the ether layer was taken to dryness. The aqueous layer contained a yellow-brown bulky precipitate, which was centrifuged off. The clear solution was decanted and the precipitate in the centrifuge bottle was washed with water. The aqueous solutions were combined and concentrated to a small volume under reduced pressure at 35°. This solution contained compounds with chromatographic characteristics similar to those of phenols. It was subjected to countercurrent extraction between water and ethyl-methyl-ketone. The extraction was performed in 6 steps with a ratio of water to ethyl-methyl-ketone of 1:3 (v/v). The first two aqueous phases (80 ml) contained most of the carbohydrates. After concentration to dryness it yielded a syrup (20 g), which on chromatograms gave no spots on spraying the papers with diazotised sulphanilic acid.

The airdried wood-meal (2 520 g) from the acetone treatment was continuously extracted in a Soxhlet-type apparatus for 3 days with ether and thereafter once again dried in

the air, and the residue extracted in a similar way with methanol for 4 days. The extract was withdrawn and replaced with fresh methanol every day to minimise the hydrolysis of the extracted carbohydrates. The methanolic extracts were combined and taken to dryness under reduced pressure and the residue after dissolution in water (150 ml), was extracted with chloroform (3 × 50 ml). The chloroform solution contained only traces of material and was discarded. The aqueous phase was centrifuged and the then clear solution on concentration gave a yellow syrup (16 g) which was chromatographically free of phenolic compounds.

Separation of carbohydrates on carbon-Celite columns

The carbohydrate fractions from the acetone and the methanolic extracts were combined (36 g) and, after dissolution in water (150 ml) were added to the top of a carbon-Celite (1:1) column (65 × 7.0 cm). The column was irrigated with the following solvents using the gradient-elution technique:

Water		20 l
Aqueous ethanol	1 %	6 l
» »	1→ 8 %	20 l
» »	8→25 %	20 l
» »	25→35 %	12 l

Fractions (225 ml) were collected automatically and examined on paper chromatograms. Those fractions which were similar were combined and taken to dryness.

Fraction No. 1 (270 mg) contained *myo*-inositol, which crystallised when the solvent was removed. By crystallisation from aqueous ethanol pure *myo*-inositol was obtained. It had m. p. and mixed m. p. 230—233°.

Fraction No. 2 (9.21 g) contained most of the glucose and fructose and a small amount of *myo*-inositol.

Fraction No. 3 (3.35 g) contained glucose and fructose only.

Fraction No. 4 (14.1 g) contained sucrose and traces of melibiose. Crystallisations from aqueous ethanol yielded pure sucrose, $[\alpha]_D^{25}$ +66.6° (*c*, 2.0 in water) and m. p. and mixed m. p. 191—192°.

Fraction No. 5 (187 mg) contained sucrose, raffinose and traces of manninotriose.

Fraction No. 6 (1.43 g) contained raffinose, stachyose and traces of sucrose. This fraction was sub-fractionated on a smaller carbon-Celite (2:1) column (40 × 3.8 cm). The syrup was dissolved in water (50 ml) and added to the top of the column. The column was irrigated with aqueous ethanol the concentration of which was linearly increased from 7 to 15 % (6 l). Fractions (50 ml) were collected and treated as above. Two compounds, later identified as raffinose and stachyose, were obtained in the crystalline state. The former (320 mg) crystallised as the pentahydrate from aqueous ethanol and had $[\alpha]_D^{25}$ +104° (*c*, 1.8 in water). On heating it lost its crystalline properties at 75.5—80°, due to dehydration. The shape of the material was unaffected but examination in polarised light revealed that the material was no longer crystalline; the solid residue collapsed at *ca.* 135°. Authentic raffinose pentahydrate behaved in the same way and no depression was observed on admixture of the two samples. A saturated solution of the other major component in aqueous ethanol on nucleation with crystalline stachyose deposited crystals (240 mg) having $[\alpha]_D^{27}$ +132° (*c*, 1.9 in water) and m. p. and mixed m. p. 153—158°.

Fraction No. 7 (758 mg) contained verbascose, stachyose and raffinose.

Fraction No. 8 (880 mg) contained mainly verbascose and stachyose. This fraction was sub-fractionated on a small carbon-Celite (1:1) column (22 × 3.2 cm). The column was irrigated with aqueous ethanol (9→15 %; 4 l) and fractions (25 ml) were collected and treated as previously described. In this way a compound (217 mg) was obtained which was chromatographically and electrophoretically indistinguishable from verbascose. It was a white, anhydrous, powder which had $[\alpha]_D^{25}$ +146° (*c*, 2.1 in water). The product

was at first believed to be crystalline, but an investigation under the polarizing microscope revealed it to be amorphous. The substance has previously been obtained as a crystalline pentahydrate [1].

This separation also yielded chromatographically pure verbascotetraose (314 mg) which may possibly have been formed from verbascose by hydrolysis by traces of acid on the column. The substance failed to crystallise and was precipitated from an aqueous solution with absolute ethanol. It yielded a white amorphous powder which had $[\alpha]_D^{25}$ +161° (c, 2.0 in water).

Fraction No. 9 (160 mg) contained verbascose and traces of two compounds with lower R_F-values which gave the same colour reactions as did verbascose.

The authors are indebted to Docent A. Wickström, Farmasøytisk Institutt, Oslo, for gifts of authentic stachyose and verbascose.

REFERENCES

1. Herissey, H., Fleury, P., Wickström, A., Courtois, J. E. and de Dizet, P. *Bull. soc. chim. biol.* 36 (1954) 1507.
2. French, D. *Advances in Carbohydrate Chem.* 9 (1954) 149.
3. Wickström, A. *Medd. Norsk Farm. Selskap* 8 (1956) 129.

Received May 29, 1958.

ACTA CHEMICA SCANDINAVICA 12 (1958) 1516—1520

The Ionization Constant, Solubility Product and Solubility of Abietic and Dehydroabietic Acid

VERA NYRÉN and ERNST BACK

Paper Technology Department, Swedish Forest Products Research Laboratory, Stockholm Ö, Sweden

The ionization constant (K_S), solubility product (K_L) and solubility in water of abietic and dehydroabietic acid at 20°C have been determined simultaneously from potentiometric titrations of their aqueous salt solutions within soap concentrations ranging from below the concentration of limited ion association to above the critical concentration for micelle formation resulting in:

For abietic acid: $pK_S = 6.4$; $pK_L = 11.3$ and L, the solubility of unionized acid: $= 1.2 \times 10^{-5}$ mole/litre.

For dehydroabietic acid: $pK_S = 5.7$; $pK_L = 10.5$ and $L = 1.62 \times 10^{-5}$ mole/litre. Total solubilities at 20°C are presented as a function of pH.

True ionization constants can be determined only below the concentration of limited ion association. This concentration of limited ion association for these acids was estimated from the ionization data.

As our measurements on lauric and myristic acid [1] and those of Ekwall [2] on bile acids have shown that a true ionization constant has to be determined below the limited concentration of ion association, it was decided to reinvestigate data of Back and Steenberg [3] on the electrolytic constants of abietic acid. Dehydroabietic acid was then included in this investigation as it has been indicated that this acid is significantly stronger and more water soluble [4,5].

The method of Back and Steenberg for simultaneous evaluation of the ionization constant, the solubility product and the solubility of the unionized protolyte from single potentiometric titrations has been employed.

EXPERIMENTAL

High purity abietic acid ($[\alpha]_D^{20} = -105.5°$) was prepared by recrystallization as butylamine abietate as described earlier [3]. Dehydroabietic acid of at least 98 % purity ($[\alpha]_D^{20} = 63.0°$) was kindly provided by Hercules Powder Co. The experiments were carried out using the equipment and experimental technique described in the paper on lauric and myristic acid [1], which may be referred to for details. In order to obtain a rapid dissolution of resin acid crystals, sodium resinate solutions for potentiometric titrations had to be prepared with a sodium hydroxide excess of about 10 %.

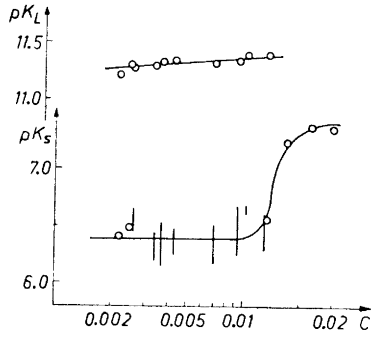

Fig. 1. pK_s and pK_L of abietic acid at 20°C as a function of the total resinate and resin acid concentration, C, in mole/litre at the neutralization point.

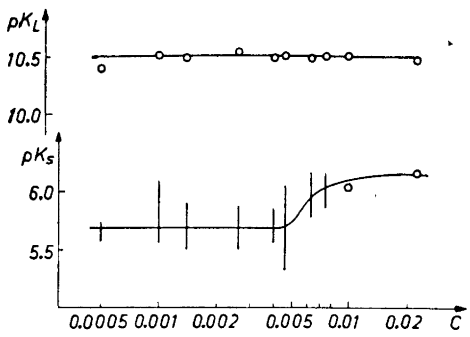

Fig. 2. pK_s and pK_L of dehydroabietic acid at 20°C as a function of the total resinate and resin acid concentration, C, in mole/litre at the neutralization point.

RESULTS

The ionization constant, K_s, the solubility product, K_L, and the solubility of unionized acid, L, were all calculated from single potentiometric titrations and corrected for activity coefficients as earlier described [1,3]. If, due to formation of micelles or associated ions, the presumptions made in these calculations are not valid, the constants calculated naturally represent pseudo-constants only, probably of little interest.

Ionization constants

The ionization constants of abietic and dehydroabietic acid, calculated from the measurements performed, are presented as pK_s values in the lower part of Figs. 1 and 2 as a function of the total resinate and resin acid concentration at the neutralization point. Where necessary, the range of pK_s values within each single titration is indicated by a line.

In agreement with the results obtained for fatty acids [1] and bile acids [2] the data for abietic acid and dehydroabietic acid show true concentration independent ionization constants to be obtained at low resinate concentrations only. The mean values, given together with their 90 % confidence limits, are at 20°C

for abietic acid: $pK_s = 6.4 \pm 0.1$ (6.39 ± 0.08)

$$K_s = 4.1 \times 10^{-7} \text{ mole/litre } (3.4 \times 10^{-7} \text{ to } 4.9 \times 10^{-7})$$

for dehydroabietic acid: $pK_s = 5.7 \pm 0.1$ (5.71 ± 0.05)

$$K_s = 2.0 \times 10^{-6} \text{ mole/litre } (1.7 \times 10^{-6} \text{ to } 2.2 \times 10^{-6})$$

Bruun [5] from monolayer measurements obtained a pK_s value for dehydroabietic acid of 5.84 in good agreement with these direct measurements.

At higher resinate concentrations a pseudo-ionization constant is obtained because of ion association and following micelle formation, not accountable for in evaluating the primary data [1]. Thus, as is seen from Figs 1 and 2 the apparent pK_s value is increasing within a certain concentration range, dominated by limited ion association. Unfortunately the measurements of Back and Steenberg [3] on the ionization constant of abietic acid were carried out within this intermediate concentration range, not accounting for the then little known occurrence of ion association below the critical concentration for micelle formation.

As was also shown for fatty acids [1] and bile acids [2], the pseudo-constant levels off to a constant value, after ion association has reached the stage of micelle formation. Thus, the data of Figs. 1 and 2 permit an estimation of the concentration at which limited ion association becomes obvious, namely

for the abietate anion	10^{-2} mole/litre
for the dehydroabietate anion	6×10^{-3} »

Solubility

The solubility products obtained for abietic and dehydroabietic acid are plotted in the upper part of Figs. 1 and 2 as pK_L values against the total resinate and resin acid concentration at the neutralization point. In both cases the pK_L value obtained can be regarded as independent of concentration (although for abietic acid a very slight change of pK_L with concentration shows up). Also, as pointed out for fatty acids, constant pK_L values occurred, once the acid had coagulated within the system. The following mean solubility products with their 90 % confidence ranges are obtained

for abietic acid	11.31 ± 0.03
for dehydroabietic acid	10.50 ± 0.03

Back and Steenberg earlier obtained within a limited concentration range the pK_L value of 11.4, in reasonable agreement with these data.

The solubility of unionized acids, L, obtained as the quotient of the solubility product and corresponding ionization constant [1,3], given with its 90 % confidence limits, is at 20°C

for abietic acid	1.2×10^{-5} mole/litre	($0{,}9 \times 10^{-5}$ to 1.6×10^{-5})
	3.6 mg/litre	(3 to 5 mg/litre)
for dehydroabietic acid	1.6×10^{-5} mole/litre	(1.4×10^{-5} to 2.0×10^{-5})
	4.9 mg/litre	(4 to 6 mg/litre)

The total solubility, i.e. the sum of the solubilities of ionized and unionized acid at 20°C, determined by L and K_L, respectively, is presented in Fig. 3 as a function of pH. At the equivalence point defined by $a_{H_3O^+} = a_{A^-}$, *i.e.* in a saturated water solution, the mean total solubilities are at 20°C

for abietic acid	1.4×10^{-5} mole/litre = 4.3 mg/litre
for dehydroabietic acid	2.2×10^{-5} mole/litre = 6.6 mg/litre

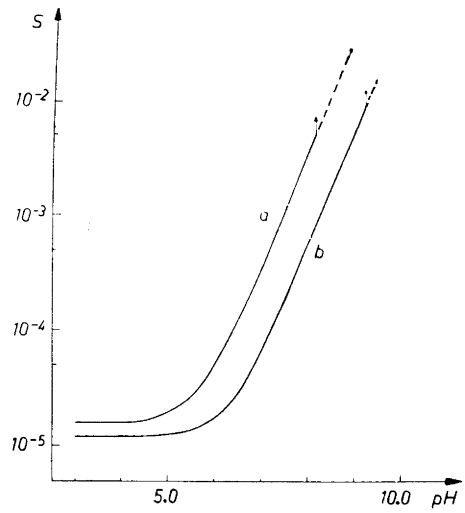

Fig. 3. Total solubility, S, in mole/litre as a function of pH for a) abietic acid b) dehydroabietic acid.

Obviously there is a significant difference in the total solubility of abietic and dehydroabietic acid, which has already found technical applications in the separation of resin acids by fractional acidification [4]. Solubility data, as here presented, make possible more detailed calculations on the efficiency of such a separation.

The solubility curves of Fig. 3 are valid only until the concentration of limited ion association has been reached. Thereafter, the true total solubility might exceed the one to be calculated. In Fig. 3 the corresponding point in the curve is indicated by an arrow. In the following part of the curves calculated dashed lines have been employed to indicate a minimum solubility. The curves are discontinued at a pH-value, where for available anions the critical concentration of micelle formation has been reached. Above this concentration, due to formation of mixed resin acid — resinate ion micelles, a rather rapid increase in total resin acid solubility will occur.

It might be pointed out that in mixtures of several resin acids or of resin and fatty acids the apparent solubility effects mentioned above will all occur at still lower single resinate anion concentrations because of the formation of mixed resinate and soap anion micelles [6], and of mixed associated ions.

Abietic acid *versus* dehydroabietic acid

The differences in solubility between abietic and dehydroabietic acid are in the direction expected. Dehydroabietic acid containing an aromatic ring is more hydrophilic and more water soluble than abietic acid containing a conjugated double bond only. The significant increase in ionization constant

occurring on aromatization of this B-ring (containing the *iso*propylgroup) might be due to steric effects.

Differences obviously also occur in ion association and micelle formation. The ratio of the true ionization constant to the pseudo-constant after micelle formation is considerably larger for abietic acid than for dehydroabietic acid, while limited ion association occurs within a more narrow concentration range. Such differences in micelle formation have also been indicated in the work of Corrin, Klevens and Harkins [7].

Acknowledgement. We are indebted to Hercules Powder Company, Research Dept., for providing a sample of dehydroabietic acid and to *Stiftelsen Pappersbrukens Forsknings-institut (The Research Foundation of the Swedish Paper Mills)* for financial support.

REFERENCES

1. Nyrén, V. and Back, E. *Acta Chem. Scand.* **12** (1958) 1305.
2. Ekwall, P. *J. Colloid Sci. Suppl.* **1** (1954) 66.
3. Back, E. and Steenberg, B. *Acta Chem. Scand.* **4** (1950) 810.
4. Zeiss, H. H. *US Patent 2.580.495*, of Jan. 1, 1952.
5. Bruun, H. H. *Acta Chem. Scand.* **6** (1952) 955.
6. Harva, O. *Diss., Åbo, Finland 1951.*
7. Corrin, M., Klevens, H. and Harkins, W. *J. Chem. Phys.* **14** (1946) 480.

Received May 8, 1958.

ACTA CHEMICA SCANDINAVICA 12 (1958) 1521—1527

Elution of Alkaloids from Cation Exchangers

A. BERGGREN, C. O. BJÖRLING and B. WILLMAN-JOHNSON

Research Laboratories of Pharmacia Ltd., Uppsala, Sweden

Elution of tertiary and quaternary amines of a high molecular weight from a strong cation exchanger can be performed with 1 N hydrochloric acid if a resin with a very low degree of crosslinking is used. Usually alcohol will considerably improve the elution rate and for some compounds is in fact necessary.

Organic cations of high molecular weight, *e.g.* alkaloidal ions, can usually be adsorbed on strong cation exchange resins. However, once the amines are adsorbed they are often difficult to elute. Bregman [1] states that molecular adsorption is negligible for all univalent organic cations for Dowex 50, all active sites of the exchanger thus being available.

For organic bases the situation is more complicated. Some authors have been able to elute tertiary alkaloidal ions with alcoholic ammonia and Büchi and Furrer [2] also tried aqueous 10 % hydrochloric acid for the elution of quinine but very large eluates were necessary. The difficulties of the elution can be avoided by using an inorganic ion exchanger, *e.g.* Decalso, as suggested by the present authors [3]. Although this method gives good results it is somewhat inconvenient because of the low capacity.

When working on resins with cations of high molecular weight the importance of the degree of crosslinking has been emphasized by Moore and Stein [4], Davey [5], Balenović and Štefanac [6], Jacobs, Work and Kressman [7], Büchi and Furrer [2], van Etten [8], Kunin and Myers [9], Sjöström and Nykänen [10] and Hale, Packham and Pepper [11]. Briefly it may be stated that with a low degree of crosslinking the resin swells to a higher extent and becomes more porous. This causes the resin to take up and give off big ions more easily.

Most experiments performed on ions of moderate size have been restricted to aqueous solutions but with bigger ions it would seem necessary to modify the solvent. Bodamer and Kunin [12] have shown that ion-exchange in non-aqueous media is possible although the rate of the exchange is lower than in water. The main condition is that the resin swells to such an extent that the pores can hold the ions. Gemant [13] investigated ion exchange in hydrocarbons and Drèze and Reith [14] used 20 % alcohol as a solvent. Rückert and Samuelson [15] studied the influence of alcohol on the shrinkage and showed that more glucose is adsorbed from alcohol than from water. Sjöström and Nykänen [10] used alcoholic media at the elution from anion exchangers.

Table 1. Compounds eluted with 1 N hydrochloric acid in 25 ml eluate.

Per cent recovery for varying strengths of alcohol

Compound	Per cent alcohol	0			30			50			70			90		
	Eluate	1st	2nd	sum	1st	2nd	sum	1st	2nd	sum	1st	2nd	sum	1st	2nd	sum
Papaverine ethyltosylate		0	0	0				100.5 99.9		100.5 99.9				102.7		102.7
Ethyl quinolinium bromide		95.5	4.5	100.0							99.7 101.4	0.6 0.0	100.3 101.4			
Hyoscine methylnitrate		98.6 98.6 101.8 104.3		98.6 98.6 101.8 104.3												
Oxaditon / [1]		99.6		99.6							103.1		103.1			
Quinine ethiodide		20	20	40							99.3 98.7	0.0 0.0	99.3 98.7			
Codeine ethiodide		85.5 97.8	11.3 2.4	96.8 100.2				95.4 98.3	1.9 2.3	97.3 100.6	100.7 100.7	0.0 1.5	100.7 102.2			
Berberine sulphate											100.0 99.8	0.0 0.0	100.0 99.8			
Strychnine ethiodide		69.3 59.2	22.5 30.4	91.8 89.6							99.2 99.6	0.0 0.0	99.2 99.6	98.3 98.1		98.3 98.1
Benzethonium chloride [2]		0		0							99.6 97.2	1.7 1.7	101.3 98.9	99.9 99.3	0 0.9	99.9 100.2
DMABF		0	0	0 at80°	11.5	20.3	31.8 [3]	91.0 92.9	7.6 5.3	98.6 98.2	99.2 99.2	1.2 0.9	100.4 100.1	98.5	3.2	101.7

[1] N,N,N,N^1-tetraethyl-N^1,N^1-dimethyl-3-oxapentane-1,5-diammonium dimonohydrogen tartrate

[2] the elution was performed with 1 N sulphuric acid in 10 ml eluate

[3] the elution was performed with 2 N hydrochloric acid

Previously we [16] have found that both tertiary and quaternary amines can easily be eluted with acids if *i.* the degree of crosslinking of the resin is low, *ii.* the solvent contains ethanol, methanol, or acetone in varying amounts.

It was found that 5—50 μ equiv. of the compounds investigated were quantitatively retained by Dowex 50 X1 in a column 20—30 × 4 mm and could not be eluted by the usual solvents. In Table 1 the elution of different substances has been made with 1 N hydrochloric acid in water or alcohol of different strengths. Although some compounds may be eluted with aqueous acid this medium is without effect for papaverine ethyltosylate, benzethonium chloride and DMABF [9-(4-dimethylamino-benzylidene)-fluorene ethyltosylate]. If the acid is made alcoholic its elution capacity is increased. 50—70 % of alcohol seems to be sufficient and generally 15—20 ml eluates gave quantitative recoveries. By taking small eluates of 5 ml this phenomenon can be demonstrated and some typical curves are shown in Fig. 1 and 2. The effect of alcohol is not correlated to the molecular weight of the substance. It is interesting to note that DMABF which is soluble in hot water cannot be eluted by aqueous hydrochloric acid even at 80°.

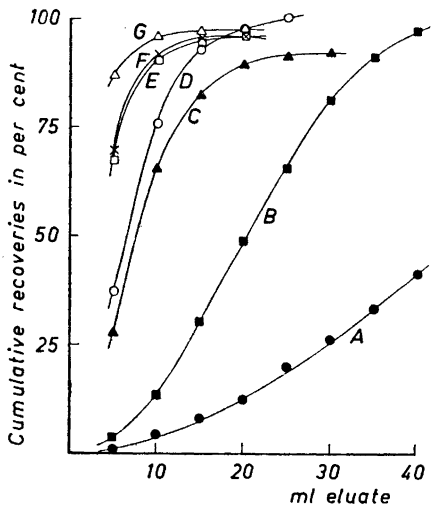

Fig. 1. Elution at different alcohol strengths with 1 N hydrochloric acid.

A Quinine ethiodide in water
B Strychnine ethiodide in water
C DMABF in 50 % alcohol
D Quinine ethiodide in 70 % alcohol
E DMABF in 70 % alcohol
F DMABF in 90 % alcohol
G Strychnine ethiodide in 70 % alcohol

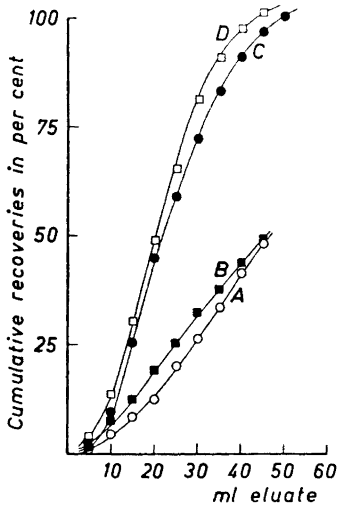

Fig. 2. Elution of tertiary amines and their corresponding quaternary compounds with 1 N hydrochloric acid in water.

A Quinine ethiodide
B Quinine sulphate
C Strychnine nitrate
D Strychnine ethiodide

From Fig. 2 may be seen that there is hardly any difference between the tertiary alkaloid and the corresponding quaternary compound in the two cases investigated. The elution curves were obtained with aqueous 1 N hydrochloric acid as alcoholic acids eluted both types of compounds too rapidly to obtain any reliable values.

Table 2. DMABF eluted with perchloric acid of different concentrations in alcohol of varying strengths.

Acid concentration	Per cent recovery for varying concentrations of perchloric acid											
	0.2 N			0.5 N			1 N			2 N		
Eluate	1st	2nd	sum	1st	2nd	sum	1st	2nd	sum	1st	2nd	sum
Alcohol % 30	0	0	0	18.7	21.0	39.7	27.7	28.3	56.0	93.6	3.6	97.2
» » 50	82.0	14.8	96.8	96.8	2.0	98.8	98.6	0.9	99.5	92.9	7.1	100 0
» » 70	95.3	1.1	96.4	98.5	0	98.5	98.8	0	98.8	99.9	0	99.9
» » 90	95.0	1.5	96.5	98.8	0	98.8	99.0	0	99.0			

Table 3. The effect of the degree of crosslinking on adsorption and elution.

Ion exchanger	Per cent recovery													
	Ethyl quinolinium bromide Elution with 1 N hydrochloric acid in 70 % alcohol in 25 ml eluate					Benzetonium chloride Elution with 1 N sulphuric acid in 70 % alcohol in 10 ml eluate					DMABF Elution with 1 N hydrochloric acid in 70 % alcohol in 25 ml eluate				
	not adsorbed	Eluate No.				not adsorbed	Eluate No.				not adsorbed	Eluate No.			
		1	2	3	Sum		1	2	3	Sum		1	2	3	Sum
50 X1	0.0	99.7	0.6		100.3	0.3	99.6	1.7		101.6	0.0	99.2	0.9		100.1
						0.0	97.2	1.7		98.9	0.0	99.2	1.2		100.4
50 X2	0.0	97.5	0.7	0.0	98.2	3.0	96.0	0.0		99.0	0.0	87.8	8.4	0.7	96.9
						0.0	99.8	0.0		99.8	0.0	85.7	11.4	1.7	98.8
50 X4	0.0	99.3	0.0	0.0	99.3	8.4	83.3	9.7	0.0	101.4	0.0	48.3	26.4	12.8	87.5
						0.0	95.2	4.9	0.0	100.1	0.0	52.6	24.2	11.5	88.3
50 X8	0.0	92.5	7.0	0.0	99.5	83.8	12.0	4.4	0.0	100.3	0.0	35.9	13.8	9.8	59.5
						59.9	22.4	11.0	5.2	98.5	0.0	45.5	12.5	8.1	66.4
50 X12	0.0	85.1	8.4	2.6	96.1	96.1	3.8	0.0		99.8	0.0	64.1	12.6	5.2	81.9
						88.5	7.7	3.9	0.0	99.9	0.0	74.0	9.3	2.8	86.1
50 X16	0.0	79.0	12.2	6.3	97.5	95.1	5.0	0.0		100.1	0.0	73.8	10.8	2.8	87.3
						86.7	10.0	2.6	0.0	99.3	0.0	66.6	11.4	4.8	82.8

In Table 2 perchloric acid solutions of different concentrations and of various alcoholic strengths have been tested for their elution capacity towards DMABF. If the acid concentration is higher than 0.5 N and the alcohol strength more than 50 % the elution is quantitative with 25 ml. Other experiments have shown that hydrochloric acid is somewhat inferior to perchloric acid and that sulphuric acid has a markedly lower elution power. As alcoholic solutions of perchloric acid are disagreable we have chosen 1 N hydrochloric acid as the general elutriant.

Substitution of ethanol for methanol or acetone gave for DMABF the same result. Thus, elution with 1 N hydrochloric acid in 70 % methanol gave 100.6 % recovery in 25 ml eluate and in 70 % acetone 100.3 % recovery.

For a few compounds alcoholic potassium hydroxide is a good elutriant. Thus 0.5 N potassium hydroxide in 90 and 50 % alcohol, respectively, gave quantitative recoveries of papaverine ethyltosylate in 25 ml eluate. On the other hand 1.0 and 0.5 N potassium hydroxide in 70 % alcohol gave only about 70 % recoveries in 25 ml eluate. As many compounds are unstable in alkaline medium and as column blanks are liable to become high these media were not further investigated.

Some experiments have been made with alcoholic solutions of sodium bromide, calcium chloride, barium bromide, and aluminium chloride. In 0.5 M solutions in 50—70 % alcohol the salts will elute DMABF but the elution is rather slow and seems generally to be inferior to that of hydrochloric acid.

In order to investigate the effect of crosslinking, cation exchangers from the same manufacturer with varying degrees of crosslinking were used in the same manner as before. Table 3 shows the results obtained on three different compounds. Of these molecules the ethyl quinolinium bromide is comparati-

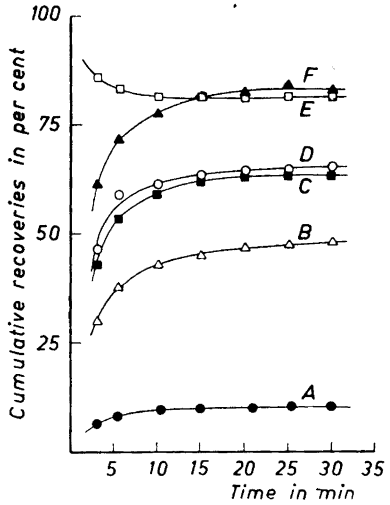

Fig. 3. Equilibrium between DMABF and Dowex 50 X1 at varying concentrations of alcohol and hydrochloric acid.

A 0.05 N hydrochloric acid in 30 % alcohol
B 0.05 N hydrochloric acid in 50 % alcohol
C 0.05 N hydrochloric acid in 70 % alcohol
D 0.05 N hydrochloric acid in 90 % alcohol
E 0.1 N hydrochloric acid in 70 % alcohol
F 0.1 N hydrochloric acid in 70 % alcohol

ABCD and F: Dowex 50 X1 with DMABF adsorbed was shaken with the corresponding acid.
E: Dowex 50 X1 was shaken with DMABF dissolved in the corresponding acid.

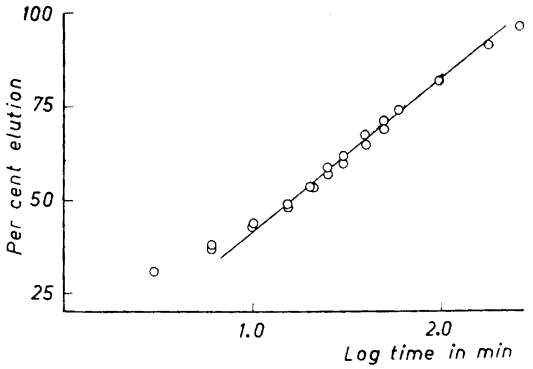

Fig. 4. Equilibrium between DMABF and Dowex 50 X1 with 0.5 M sodium bromide in 70 % alcohol.

vely small, the benzethonium chloride contains a fairly long chain, and the DMABF is rather large. The long-chained benzethonium ion could not be completely adsorbed on ion exchangers with more than 4 % crosslinking. On the ion exchangers X12 and X16 the adsorption from water was very small. Further, there is a tendency towards a slower elution of the amount adsorbed on the more crosslinked resins. For all crosslinkings tried both the small ethyl quinolinium ion and the large DMABF ion are completely adsorbed. The elution rate is, however, greatly decreased if the crosslinking is increased. Further, the large DMABF ion is more strongly retained than the smaller ethyl quinolinium ion. It is interesting to note that the elution rate of DMABF has a pronounced minimum at X8 where the rate is only about 40 % of that of X1 and 60 % of that of X12 and X16.

In Fig. 3 the influence of the concentrations of alcohol and acid is clearly demonstrated from experiments on the equilibrium between DMABF and Dowex 50 X1. The equilibrium is rapidly attained with alcoholic hydrochloric acid. Therefore, the column experiments were most likely performed under equilibrium conditions. With 0.1 N hydrochloric acid in 70 % alcohol the equilibrium was reached from both sides, thus showing that it is a true one. With 0.5 M sodium bromide in 70 % alcohol the process is much slower and here it is possible to apply Langmuir's adsorption isotherm. This is shown in Fig. 4, where the desorption is directly proportional to the logarithm of the time.

EXPERIMENTAL

Column experiments

The ion exchangers (200—400 mesh) used were washed with ammonium citrate solution to remove traces of heavy metals and were then alternately treated several times with aqueous and alcoholic solutions of sodium hydroxide and hydrochloric acid. By this treatment the blanks became negligible.

Unless otherwise stated Dowex 50 X1 in the hydrogen form was used. The columns were 20—30 × 4 mm and could adsorb 15 to 20 mg of substance. When working with resins with a low degree of crosslinking the swelling and shrinking are often cumbersome but with the method used in this work no troubles were encountered. When changing solvents in the columns bubbles are easily formed. They can be avoided by using freshly boiled solvents. The flow rate was kept at about 1 ml/min.

The reagents were of analytical grade and the compounds investigated were of the highest quality available and recrystallized from alcohol and water. Most of the quaternary compounds were synthetized by standard methods and recrystallized from alcohol and water. The equivalent weights and elementary analyses were in good agreement with theory.

For most of the substances a standard curve was drawn at the maximum characteristic for the compound in question in the ultraviolet region and the concentrations of the solutions assayed with its aid. The solvent was usually water or alcohol-water. If acetone was used at the elution it had to be evaporated and the residue dissolved in the appropriate solvent for the final assay. Benzethonium chloride was titrated according to Carkhuff and Boyd [17] and hyoscine methylnitrate was determined either according to Berggren and Nordberg [18] or colorimetrically using bromothymol blue [19].

Procedure 1 to 2 mg of the substance to be investigated — of benzethonium chloride, however, 10 mg and of hyoscine methylnitrate 10—15 mg — dissolved in 10 ml of water or alcohol-water was allowed to flow through the column which was then washed three times with 5 ml of the solvent. The liquids were collected and assayed. The substances on the column were eluted with different solutions, the eluates diluted to the appropriate volume, and assayed. Blanks were always run but their values were usually negligible.

Equilibrium experiments

50 ml of Dowex 50 X1 was mecanically stirred in 400 ml of 50 % alcohol and from a burette a solution of 207.4 mg DMABF in 100 ml of 50 % alcohol was slowly added during 2 h. The resin was transferred to a column and thoroughly washed with 50 % alcohol and finally dried at 50° over night. The resin so prepared contained 4.9 % of moisture determined by the Karl Fischer method.

The resin was assayed by elution with 1 N perchloric acid in 70 % alcohol. Three determinations gave 53.6, 53.1, and 53.9 mg of DMABF per g of resin.

Prior to all experiments an accurately weighed amount, about 50 mg, of the resin was allowed to swell over night in 10.00 ml of water. The rest of the elutriant, about 90.00 g, was added and the mixture shaken. At known intervals 5.00 ml was withdrawn in such a manner that no resin was removed and assayed spectrophotometrically. No special attempts were made to keep the temperature constant.

REFERENCES

1. Bregman, J. I. *Ann. N.Y. Acad. Sci.* **57** (1953) 125.
2. Büchi, J. and Furrer, F. *Arzneimittel-Forsch.* **3** (1953) 1.
3. Björling, C. O. and Berggren, A. *J. Pharm. and Pharmacol.* **5** (1953) 169, 615; Björling, C. O. and Berggren, A. *Acta Chem. Scand.* **9** (1955) 567.
4. Moore, S. and Stein, W. H. *J. Biol. Chem.* **211** (1954) 893.
5. Davey, C. L. *Nature* **179** (1957) 209.
6. Balenović, K. and Štefanac, Z. *Chem. & Ind. London* **1956** 23.
7. Jacobs, S., Work, T. S. and Kressman, T. R. E. *Chem. & Ind. London* **1955** 117.
8. van Etten, C. H. *Anal. Chem.* **27** (1955) 954.
9. Kunin, R. and Myers, R. J. *Discussions Faraday Soc.* **7** (1949) 114.
10. Sjöström, E. and Nykänen, L. *Suomen Kemistilehti B* **29** (1956) 23.
11. Hale, D. K., Packham, D. I. and Pepper, K. W. *J. Chem. Soc.* **1953** 844.
12. Bodamer, G. W. and Kunin, R. *Ind. Eng. Chem.* **45** (1953) 2577.
13. Gemant, A. *J. Inst. Petrol.* **40** (1954) 50.
14. Drèze, A. and Reith, W. S. *Biochem. J.* **63** (1956) 21 P.
15. Rückert, H. and Samuelson, O. *Acta Chem. Scand.* **11** (1957) 303, 315.
16. Berggren A. and Björling, C. O. *Acta Chem. Scand.* **11** (1957) 179.
17. Carkhuff, E. D. and Boyd, W. F. *J. Am. Pharm. Assoc. Sci. Ed.* **43** (1954) 240.
18. Berggren, A. and Nordberg, M. *Farm. Revy* **51** (1952) 177.
19. Björling, C. O. and Berggren, A. *To be published.*

Received May 20, 1958.

ACTA CHEMICA SCANDINAVICA 12 (1958) 1528—1548

Short Communications

Hydantoins from Chalcone Oxides

CARL ENEBÄCK

Department of Chemistry, Institute of Technology, Helsingfors, Finland

5-Phenyl-5-benzylhydantoin has been obtained in fair yield by boiling chalcone oxide with ethanolic potassium hydroxide in the presence of urea. This reaction involves a rearrangement of the carbon skeleton of the initial molecule. A range of substituted chalcone oxides has been subjected to the same treatment, and the isolated, weakly acidic reaction products are characterized, by analogy, as the corresponding hydantoins.

It is known that chalcone oxides under similar conditions but without urea yield phenylbenzylglycolic acids, a reaction proceeding *via* the isomeric α-diketone which then undergoes a rearrangement of the benzilic acid type [1]. Recently, Dunnavant and James [2] have presented convincing evidence in favour of a reaction mechanism of the benzilic acid rearrangement type in the well-known formation [3] of 5,5-diphenylhydantoin from benzil with alkali and urea, as well. In conformity with this view *o*-methoxyl groups in the aroyl nucleus of the chalcone oxide should hinder the genesis of a hydantoin about as strongly as they, in the absence of urea, hinder the formation of an α-hydroxy acid through a rearrangement of the benzilic acid type. This seems to be the case judging from the relevant yields of the present work.

Experimental. (All analyses are microanalyses, performed by Dr. A. Bernhardt, Mühlheim, Germany).

3,4-Dimethoxychalcone oxide. To 3,4-dimethoxychalcone (2.68 g) in methanol (25 ml) were added hydrogen peroxide (15 %, 4 ml) and 2 N sodium hydroxide (2.5 ml). The mixture was stirred for 3 h and then cooled in a refrigerator. The crystals separated by filtration were recrystallised from methanol and from chloroform-light petroleum. Yield 2.3 g (81 %), m.p. 89—90°. (Found: C 72.34; H 5.49; $C_{17}H_{16}O_4$ requires C 71.82; H 5.67).

3,3',4,4'-Tetranethoxychalcone oxide. Finely powdered 3,3',4,4'-tetramethoxychalcone, (3.28 g, m.p. 111°), was stirred for 6 h together with a solution of hydrogen peroxide (15 %, 5 ml) and 6 N potassium hydroxide (0.83 ml) in methanol (30 ml). Dissolution came about only partly. Filtration of the reacted mixture gave an almost white powder which was recrystallised from methanol and from chloroform-light petroleum to give 2.75 g (80 %) of the epoxide, m.p. 150—151°. (Found: C 66.44; H 5.91; $C_{19}H_{20}O_6$ requires C 66.27; H 5.85).

5-Phenyl-5-benzylhydantoin. The solution of chalcone oxide (2.24 g, 0.01 mole) in ethanol (20 ml) was kept boiling under reflux. In one operation was added a hot solution of potassium hydroxide (1.23 g, 0.022 mole) and urea (1.32 g, 0.022 mole) in ethanol (20 ml). The refluxing was continued for 2 h and the reaction mixture was then poured into water (400 ml). A tiny precipitate was removed and after that the water solution was saturated with carbon dioxide. The obtained precipitate was collected and recrystallised from dilute ethanol. Yield 2.0 g (75 %), m.p. 210°. Mixing with 5-phenyl-5-benzylhydantoin [4], m.p. 210°, obtained [5] by treating desoxybenzoin with potassium cyanide and ammonium carbonate in dilute ethanol at 60°, did not depress the m.p.

In the same way were obtained:

5-Phenyl-5-(4-methoxybenzyl)-hydantoin, yield 2.55 g (86 %), m.p. 206—208°, (Found: C 68.95; H 5.86; N 9.48; $C_{17}H_{16}O_3N_2$ requires C 68.90; H 5.44; N 9.45) from 4-methoxychalcone oxide (2.54 g), and

5-Phenyl-5-(3,4-dimethoxybenzyl)-hydantoin, yield 2.85 g (87 %), m.p. 211—212°, (Found: C 65.61; H 5.44; N 8.66; $C_{18}H_{18}O_4N_2$ requires C 66.24; H 5.56; N 8.66) from 3,4-dimethoxychalcone oxide (2.84 g).

5-(3,4-Dimethoxyphenyl) -5- (3,4-dimethoxybenzyl)-hydantoin, yield 2.8 g (72 %), m.p. 212—213°, (Found- C 62.05; H 5.84; N 7.48;

$C_{20}H_{22}O_6N_2$ requires C 62.16; H 5.74; N 7.25) was obtained from 3,3',4,4'-tetramethoxychalcone oxide (3.44 g) in the same way with the exception that the main part of the epoxide remained undissolved in the initial boiling ethanolic mixture.

5-Phenyl-5-(1-phenylethyl)-hydantoin. The boiling solution of 2.38 g of dypnone oxide [6], (the crude epoxide containing both of the isomers may be used), in ethanol (20 ml) was treated with ethanolic potassium hydroxide and urea as above. The precipitation of a voluminous potassium salt followed close on the addition of the reagents. After refluxing the mixture for 2 h the precipitate was separated by filtration and washed with a small amount of ethanol. It was then dissolved in water (200 ml) by heating and adding a little sodium hydroxide. The solution thus obtained was saturated with carbon dioxide and the precipitated mass collected and recrystallised from ethanol. Yield 1.0 g (36 %), m.p. 305—307°. (Found: C 72.82; H 5.82; N 10.07; $C_{17}H_{16}O_2N_2$ requires C 72.84; H 5.75; N 9.99). The filtrate from the insoluble potassium salt was poured into water (400 ml). The solution was clarified by filtration and was then saturated with carbon dioxide. The obtained precipitate was collected and recrystallised from ethanol. Yield 1.1 g (39 %) of m.p. 265—266°, (Found: C 72.69; H 5.80; N 10.05; $C_{17}H_{16}O_2N_2$ requires C 72.84; H 5.75; N 9.99). The two products of this preparation are presumably the diastereoisomers of 5-phenyl-5-(1-phenylethyl)-hydantoin.

5-(2-Methoxyphenyl)-5-benzylhydantoin. 2'-Methoxychalcone oxide [7] (2.54 g) was treated with ethanolic potassium hydroxide and urea analogously with the model preparation above. After pouring the reaction mixture in water, the solution, however, was extracted with ether instead of being filtered, by reason of the stickiness of the cloudy precipitate. Saturation of the water phase, from which all the ether had been removed, with carbon dioxide, and repeated recrystallisation of the obtained precipitate from dilute ethanol gave 0.3 g (10 %) of m.p. 224°, (Found: C 69.11; H 5.87; N 9.44; $C_{17}H_{16}O_3N_2$ requires C 68.90; H 5.44; N 9.45).

Benzyl-(2-methoxyphenyl)-glycolic acid. The above procedure was repeated but without urea. The filtrate after precipitating α-hydroxy-2'-methoxychalcone with carbon dioxide was acidified with dilute sulphuric acid and the obtained precipitate recrystallised from dilute ethanol, yielding 0.35 g (13 %) of m.p. 183—184°, (Found: C 70.44; H 5.84; $C_{16}H_{16}O_4$ requires C 70.57; H 5.92).

α-Hydroxy-2',4',6'-trimethoxychalcone[7] but no hydantoin or hydroxy acid was obtained when 2',4',6'-trimethoxychalcone oxide was subjected to the described treatment with or without urea.

Work is in progress to find out suitable conditions for hydrolysis of the present hydantoins.

The author is indebted to *Svenska Vetenskapliga Centralrådet*, Helsingfors, for a grant.

1. Jörlander, H. *Ber.* **50** (1917) 406.
2. Dunnavant, W. R. and James, F. L. *J. Am. Chem. Soc.* **78** (1956) 2740.
3. Biltz, H. *Ber.* **41** (1908) 1379.
4. Slotta, K. H., Behnisch, R. and Szyszka, G. *Ber.* **67B** (1934) 1529.
5. Henze, H. R. and Speer, R. J. *J. Am. Chem. Soc.* **64** (1938) 522.
6. Stevens, C. L., Church, R. J. and Traynelis, V. J. *J. Org. Chem.* **19** (1954) 522.
7. Enebäck, C. and Gripenberg, J. *Acta Chem. Scand.* **11** (1957) 866.

Received July 21, 1958.

A Contribution to the Principles of Electrodiffusion

STIG LJUNGGREN

The Royal Institute of Technology, Division of Physical Chemistry, Stockholm, Sweden

Electrodiffusion was suggested by Mysels [1] and Lamm [2] as a method for studying the equilibrium kinetics of certain reactions involving ions. The term refers to the increased diffusion which occurs on the superposition of an electric field in the diffusion direction. The magnitude of this effect is related to the field characteristics and to the kinetics of the system studied. More recently, Giddings [3-5] and Bak and Kauman [6] have contributed to the theory of electrodiffusion.

The theory of Mysels and that of Bak and Kauman refer (although this is not explicitely stated) to the case of selfdiffusion or to the case where a large excess of an electrolyte, which does not partake in the kinetic equilibrium, is added in order to maintain a constant field throughout the diffusion column. In this case the

$C_{20}H_{22}O_6N_2$ requires C 62.16; H 5.74; N 7.25) was obtained from 3,3',4,4'-tetramethoxychalcone oxide (3.44 g) in the same way with the exception that the main part of the epoxide remained undissolved in the initial boiling ethanolic mixture.

5-Phenyl-5-(1-phenylethyl)-hydantoin. The boiling solution of 2.38 g of dypnone oxide [6], (the crude epoxide containing both of the isomers may be used), in ethanol (20 ml) was treated with ethanolic potassium hydroxide and urea as above. The precipitation of a voluminous potassium salt followed close on the addition of the reagents. After refluxing the mixture for 2 h the precipitate was separated by filtration and washed with a small amount of ethanol. It was then dissolved in water (200 ml) by heating and adding a little sodium hydroxide. The solution thus obtained was saturated with carbon dioxide and the precipitated mass collected and recrystallised from ethanol. Yield 1.0 g (36 %), m.p. 305—307°. (Found: C 72.82; H 5.82; N 10.07; $C_{17}H_{16}O_2N_2$ requires C 72.84; H 5.75; N 9.99). The filtrate from the insoluble potassium salt was poured into water (400 ml). The solution was clarified by filtration and was then saturated with carbon dioxide. The obtained precipitate was collected and recrystallised from ethanol. Yield 1.1 g (39 %) of m.p. 265—266°, (Found: C 72.69; H 5.80; N 10.05; $C_{17}H_{16}O_2N_2$ requires C 72.84; H 5.75; N 9.99). The two products of this preparation are presumably the diastereoisomers of 5-phenyl-5-(1-phenylethyl)-hydantoin.

5-(2-Methoxyphenyl)-5-benzylhydantoin. 2'-Methoxychalcone oxide [7] (2.54 g) was treated with ethanolic potassium hydroxide and urea analogously with the model preparation above. After pouring the reaction mixture in water, the solution, however, was extracted with ether instead of being filtered, by reason of the stickiness of the cloudy precipitate. Saturation of the water phase, from which all the ether had been removed, with carbon dioxide, and repeated recrystallisation of the obtained precipitate from dilute ethanol gave 0.3 g (10 %) of m.p. 224°, (Found: C 69.11; H 5.87; N 9.44; $C_{17}H_{16}O_3N_2$ requires C 68.90; H 5.44; N 9.45).

Benzyl-(2-methoxyphenyl)-glycolic acid. The above procedure was repeated but without urea. The filtrate after precipitating α-hydroxy-2'-methoxychalcone with carbon dioxide was acidified with dilute sulphuric acid and the obtained precipitate recrystallised from dilute ethanol, yielding 0.35 g (13 %) of m.p. 183—184°, (Found: C 70.44; H 5.84; $C_{16}H_{16}O_4$ requires C 70.57; H 5.92).

α-Hydroxy-2',4',6'-trimethoxychalcone[7] but no hydantoin or hydroxy acid was obtained when 2',4',6'-trimethoxychalcone oxide was subjected to the described treatment with or without urea.

Work is in progress to find out suitable conditions for hydrolysis of the present hydantoins.

The author is indebted to *Svenska Vetenskapliga Centralrådet*, Helsingfors, for a grant.

1. Jörlander, H. *Ber.* **50** (1917) 406.
2. Dunnavant, W. R. and James, F. L. *J. Am. Chem. Soc.* **78** (1956) 2740.
3. Biltz, H. *Ber.* **41** (1908) 1379.
4. Slotta, K. H., Behnisch, R. and Szyszka, G. *Ber.* **67B** (1934) 1529.
5. Henze, H. R. and Speer, R. J. *J. Am. Chem. Soc.* **64** (1938) 522.
6. Stevens, C. L., Church, R. J. and Traynelis, V. J. *J. Org. Chem.* **19** (1954) 522.
7. Enebäck, C. and Gripenberg, J. *Acta Chem. Scand.* **11** (1957) 866.

Received July 21, 1958.

A Contribution to the Principles of Electrodiffusion

STIG LJUNGGREN

The Royal Institute of Technology, Division of Physical Chemistry, Stockholm, Sweden

Electrodiffusion was suggested by Mysels [1] and Lamm [2] as a method for studying the equilibrium kinetics of certain reactions involving ions. The term refers to the increased diffusion which occurs on the superposition of an electric field in the diffusion direction. The magnitude of this effect is related to the field characteristics and to the kinetics of the system studied. More recently, Giddings [3-5] and Bak and Kauman [6] have contributed to the theory of electrodiffusion.

The theory of Mysels and that of Bak and Kauman refer (although this is not explicitely stated) to the case of selfdiffusion or to the case where a large excess of an electrolyte, which does not partake in the kinetic equilibrium, is added in order to maintain a constant field throughout the diffusion column. In this case the

Joule heat evolved in the cell may render experiments difficult because of the convection danger. It was evidently this fact which led Lamm [2] to study the possibility of obtaining an electrodiffusion effect of a mutual type with the system

$$\begin{array}{ccccc} AB & \rightleftharpoons & A^+ & + & B^- \\ C(1-a) & & Ca & & Ca \end{array}$$

The theory overlooks, however, the fact that, due to the lack of divergence of the electric current, such an effect will not be obtained in a system that contains only those components which are involved in the dynamic equilibrium. In such a case each ion will migrate with a velocity proportional to its mobility and carry a constant proportion (equal to the transfer number) of the electric current. The latter being constant *, the velocities and also the step-lengths of the ions will be inversely proportional to the ionic concentration, C.

Now, ordinary (mutual) diffusion is the result of an assymmetrical initial condition and a random walk which attempts to smooth out the initial condition. It can, however, be shown that in the case mentioned the variation of the step-lengths has the effect of compensating the skewness of the initial condition. This is most easily realized in the case where a is small. In this case the migration rates are proportional to $1/Ca$. But the "lifetime" of the ions, $T^{\pm}$, is also proportional to $1/Ca$. Hence, the step-lengths are proportional to $1/(Ca)^2$:

$$l \sim 1/C^2a^2$$

Now, according to the law of mass action,

$$Ca^2(1-a) = K$$

so that for small a

$$l \sim 1/C^2a^2 \approx 1/KC$$

i. e. the step-lengths are inversely proportional to the total concentration. In cases where the migration rates of the positive and negative ions are equal, we obtain a simple visualization of electrodiffusion by regarding AB as concentrated in thin layers at a mutual distance equal to the step-length. Each layer will then contain an equal quantity of AB. This is essential, since we may now regard electrodiffusion simply as a random walk of ions, A^+ or B^-, from layer to layer. Hence the ions will change places with one-another giving rise to self-diffusion but not to "ordinary" diffusion, the number of ions and molecules in the layers being unaffected by the random walk. If a is not small, the simple visualization breaks down and the argument becomes more complicated, but the final conclusion still holds.

It should perhaps be stressed that the lack of divergence which is responsible for the difficulties mentioned is a characteristic property of the electric current. In the chromatographic dispersion case treated by Giddings [4] we do not have this difficulty, which can be eliminated by the addition of KCl or some other electrolyte as will be more closely outlined below.

The formulae derived by Lamm [2] for the electrodiffusion coefficient of the positive and negative ions respectively, *i.e.* D^+ and D^-, are good approximations to the truth if the relative concentration change in the cell is small (differential diffusion). However, as already mentioned, the small variation of D^+ and D^- is sufficient to prevent any mutual diffusion from taking place. Since we thus have a case of pure self-diffusion it is obviously without meaning to speak of the diffusion of AB as a whole. Now, by adding a second electrolyte component, it is indeed possible to obtain a sort of mutual type diffusion in which, however, the presence of the additional electrolyte allows A^+ and B^- to diffuse more or less independently of one another.

Generally it will be necessary to use two components also from other reasons, *e. g.* to provide a suitable pH. If the quantity of the second electrolyte component is not too large the Joule heat evolved can be maintained within reasonable limits. It seems possible, in this way, to effect Lamm's original idea of a mutual type electrodiffusion. Another way is, of course, to measure the selfdiffusion of A^+ or B^- in the presence of a mutual gradient between AB and the medium.

Equations valid also for systems of this kind are given below (*cf.* Ref. [6]).

Symbols

a = degree of dissociation.
n = total number of species.
c_j = concentration of the species j in electrochemical equivalents per ml with the sign of the charge included.

* *i. e.* constant with respect to x but not with respect to t.

(If the species is uncharged the sign may be chosen at will).
u_j = ionic mobility of j with the sign of the ionic charge included.
D_j = individual diffusion coefficient of j.
$\varkappa$ = specific conductivity (a function of time and position).
t = time.
t_j = transfer number of j.
x = height coordinate in diffusion cell.
$\mathbf{i}$ = current density (vector). ($\mathbf{i} = \mathbf{i}(t)$).
i = current density in one-dimensional case. ($i = i(t)$).
$\mathbf{X}$ = strength of superposed electric field (vector).
F = Faraday's constant.
$\mathbf{v}_j$ = velocity of the ion j (vector).
$\mathbf{J}_j$ = (electrophoretical) flow of the ionic species j (vector).
J_j = flow of j in one-dimensional case.
Q_j = net reaction rate.

Equations

The current density equals the product of the conductivity and the field strength:

$$\mathbf{i} = \varkappa \mathbf{X} \tag{1}$$

The condition of electroneutrality reads

$$\sum_m c_m = 0 \tag{2}$$

where m denotes summation over ionic species only.
For the conductivity we have

$$\varkappa = F \sum_m c_m u_m \tag{3}$$

The ionic velocity equals the product of the mobility and the field strength

$$\mathbf{v}_j = u_j \mathbf{X} = u_j \mathbf{i}/\varkappa \tag{4}$$

Hence we have for the electrophoretical flow

$$\mathbf{J}_j = c_j \mathbf{v}_j = c_j u_j \mathbf{X} = c_j u_j \mathbf{i}/\varkappa = \frac{\mathbf{i}}{F} \frac{c_j u_j}{\sum_m c_m u_m} \tag{5}$$

Leaving out the terms relating to ordinary diffusion we have

$$(\partial c_j/\partial t) = -\operatorname{div} \mathbf{J}_j + Q_j(c_1, c_2, \cdots, c_n) \tag{6}$$

where Q_j represents the purely chemical rate law, *e. g.*

$$Q_j = \sum_p k_{jp}\, c_1^{r_{1p}} c_2^{r_{2p}} \cdots c_n^{r_{np}}$$

In the one-dimensional case we have

$$J_j = i c_j u_j / F \sum_m c_m u_m \tag{7}$$

and

$$\frac{\partial c_j}{\partial t} = Q_j(c_1, \cdots, c_n) - \frac{i}{F} \frac{\partial}{\partial x} \left(\frac{c_j u_j}{\sum_m c_m u_m} \right) \tag{8}$$

Including additional terms arising from ordinary diffusion, the equation reads

$$\frac{\partial c_j}{\partial t} = Q_j(c_1, \cdots, c_n) - \frac{i}{F} \frac{\partial}{\partial x} \left(\frac{c_j u_j}{\sum_m c_m u_m} \right) + D_j \frac{\partial^2 c_j}{\partial x^2} - \frac{\partial}{\partial x} (c_j u_j X') \tag{9}$$

where

$$X' = \frac{\sum_m D_m (\partial c_m/\partial x)}{\sum_m c_m u_m} \tag{10}$$

is the Nernst ("internal") potential gradient, which depends exclusively on the concentrations and the concentration gradients but not directly on the superposed field.

The quasilinear system (8) of first order partial differential equations will give a complete description of electrodiffusion in all kinds of systems. It may be regarded as a combination of Kohlrausch's differential equation known from electrophoresis with the well-known chemical rate laws. It should not be overlooked that the mathematical difficulties involved in solving these equations may be considerable.

Finally it should be pointed out that the absence of an effect in the case AB follows in a very easy way from these equations. If no other electrolyte is added we have

$$\frac{\partial}{\partial x} \left(\frac{c_j u_j}{\sum_m c_m u_m} \right) = \frac{\partial t_j}{\partial x} = 0$$

where t_j denotes the transfer number.

The financial support of the *Swedish Natural Science Research Council* is gratefully acknowledged.

1. Mysels, K. J. *J. Chem. Phys.* **24** (1956) 371.
2. Lamm, O. *Acta Chem. Scand.* **10** (1956) 1132.
3. Giddings, J. C. and Eyring, H. *J. Phys. Chem.* **59** (1955) 416.
4. Giddings, J. C. *J. Chem. Phys.* **26** (1957) 169.
5. Giddings, J. C. *J. Chem. Phys.* **26** (1957) 1755.
6. Bak, T. A. and Kauman, W. G. *J. Chem. Phys.* **27** (1958) 509.

Received August 6, 1958.

Note on the Crystal Structure of Ferromagnetic Chromium Dioxide

KARL-AXEL WILHELMI and
OLA JONSSON

Institute of Inorganic and Physical Chemistry, University of Stockholm, Stockholm, Sweden

The formula CrO_2 for the ferromagnetic chromium oxide was established by Michel and Bénard in 1935 [1,2]. They found that this phase is of a rutile type. The compound has subsequently been studied by several investigators [3-6].

The following methods have been used for preparing chromium dioxide:

A) thermal decomposition of CrO_2Cl_2 [1,2,5]
B) thermal decomposition of pure CrO_3 under oxygen pressure [3,4]
C) thermal decomposition of aqueous CrO_3-solution under oxygen pressure [6]

Method A) seems to give a product which is contaminated with Cr_2O_3 and method B) a product contaminated with higher chromium oxides [3] or Cr_2O_3 [3,4]. In Ref.[6] the product (method C) is characterized as "X-ray pure" but no analytical data are given.

Bhatnagar [7] has reported a normal paramagnetic susceptibility corresponding to two unpaired electrons per Cr atom for a substance said to be CrO_2. On the other hand, the ferromagnetism of CrO_2 has been recently confirmed by Glemser [5] and by Ariya *et al.*[4]

This paper gives the results of an X-ray diffraction study of an oxide sample obtained by thermal decomposition of pure CrO_3 (Baker's analyzed, dried over P_2O_5) at 350°C under oxygen pressure (60 atm). The material so obtained consisted of opaque, black, strongly magnetic crystalline aggregates. The sample was dissolved in hot concentrated sulphuric acid and the chromium content determined using Mohr's salt and standard permanganate solution after oxidation by peroxodisulphate in the presence of silver ions. The composition of the sample was found to be $CrO_{2.14}$.

Table 1 lists results reported by previous authors and those obtained in this investigation. The unit cell dimensions of the rutile-type structure were in all cases derived from X-ray powder patterns. Our data were obtained from a Guinier powder photograph taken with CuKa_1 radiation using potassium chloride (a = 6.2919 Å) as an internal standard (*cf.* Table 2). The back-ground fogging caused by the fluorescence radiation from chromium was effectively depressed by means of an aluminium foil (35 μ) covering the photographic film. Even in amply exposed photographs it was not possible to find indications of a doubling of the c axis as

Table 1.

Reference	Mean composition of sample	a Å	c Å	Density
2	$CrO_{1.8}$	4.41	2.86	—
3	—	4.43 *	2.92 *	—
4	$CrO_{1.98}$	4.394	5.77	4.90
5	$CrO_{1.9}$	4.41	2.91	4.80
6	—	4.421	2.916	—
This investigation	$CrO_{2.14}$	4.423	2.917	4.83

* Calculated from the d-values given in Ref.[3]

Table 2. X-Ray powder pattern of a sample with the mean composition $CrO_{2.14}$

hkl	I_{obs}	$\sin^2\theta_{obs}$	$\sin^2\theta_{calc}$
—	w *	0.05568	—
110	v st	0.06066	0.06067
101	v st	0.10002	0.10003
200	v w	0.12133	0.12137
111	m	0.13036	0.13038
210	v w	0.15166	0.15167
211	v st	0.22135	0.22137
220	m	0.24266	0.24255
002	w	0.27876	0.27869
310	w	0.30332	0.30330
102	—	—	0.30910
221	—	—	0.31235
112	w	0.33943	0.33931
301	w	0.34268	0.34269
311	—	—	0.37301
320	—	—	0.39432
202	—	—	0.40009
212	—	—	0.43042
321	v w	0.46401	0.46399

* The presence of this line suggests that the excess oxygen content of the sample over the composition CrO_2 is due to a contamination by the phase $CrO_{2.5}$, the strongest reflexion of which occurs at $\sin^2\theta$ = 0.0558 as calculated from the data given by Schwartz *et al.*[3]

reported by Ariya *et al.*[4] The observed density is in good agreement with the value of 4.89 g/cm³ calculated for a cell content of two formula units of CrO_2.

The axial ratio of chromium dioxide ($c/a = 0.660$) corresponds to a relatively long distance between adjacent Cr atoms and indicates that no attracting forces are acting between these metal atoms in contrast to what is the case in several other compounds of transitions metals with valency states lower than their maximum ones [8]. Of particular interest in this connection is the rutile type phase $(Cr, Mo)O_2$ with its considerably lower values of c/a (down to 0.60) which have been interpreted as caused by the presence of metalmetal bonding [9].

This study forms part of research programs on metal oxides and on chromates and related compounds financially supported by the *Swedish Natural Science Research Council.*

The authors wish to thank Dr. Arne Magnéli for valuable discussions.

1. Michel, A. and Bénard, J. *Compt. rend.* **200** (1935) 1316.
2. Michel, A. and Bénard, J. *Bull. soc. chim. France* **10** (1943) 315.
3. Schwartz, R. S., Fankuchen, I. and Ward, R. *J. Am. Chem. Soc.* **74** (1952) 1676.
4. Ariya, S. M., Shchukarev, S. A. and Glushkova, V. B. *Zhur. Obshchei Khim.* **23** (1953) 1241—5.
5. Glemser, O., Hauschild, U. and Trüpel, F. *Z. anorg. u. allgem. Chem.* **277** (1954) 113.
6. Thamer, B. J., Douglass, R. M. and Staritzky, E. *J. Am. Chem. Soc.* **79** (1957) 547.
7. Bhatnagar, S. S., Prakash, B. and Hamid, A. *J. Chem. Soc. 1938, 1428.*
8. Marinder, B.-O. and Magnéli, A. *Acta Chem. Scand.* **11** (1957) 1635.
9. Sundholm, A., Andersson, S., Magnéli, A. and Marinder, B.-O. *To be published.*

Received August 8, 1958.

Chemical Synthesis of Oleyl Adenylate

BENGT BORGSTRÖM

Department of Physiological Chemistry, University of Lund, Lund, Sweden

Mixed anhydrides of adenylic acid with short and middle chain fatty acids have been proposed as intermediates in the enzymatic activation of these acids to their CoA derivatives [1-5]. Chemical synthesis of these adenylates has been reported using three different methods: 1) coupling of silver adenylate with the acid chloride (acetyladenylate [1]), 2) the reaction of the acid anhydride with adenylic acid in aqueous pyridine (buturyl and hexanoyl adenylate [2,5]), and 3) the condensation of fatty acid and adenylic acid in the presence of carbodiimides (buturyl adenylate [5]).

For an attempted synthesis of long chain fatty acid adenylates method 2 did not seem practical due to the low solubility of the long chain anhydrides. Of the two other methods the carbodiimide method was found to be the most practical and to give the best yields.

This paper will describe the synthesis of oleyl adenylate by the condensation of oleic acid with adenylic acid in the presence of di*cyclo*hexylcarbodiimide and also includes experiments to show the metabolic activity of this compound with rat liver mitochondria *in vitro*.

EXPERIMENTAL

Materials. Adenylic acid (AMP) was obtained from Sigma Chemical Company and di*cyclo*hexylcarbodiimide (DCC) from Fluka A.G.

Methods. Oleyl adenylate was estimated by the hydroxamic acid-$FeCl_3$ method modified for the acid insoluble hydroxamates of oleic acid [6]. A sample containing approximately 1 mg adenylate in 0.1—0.5 ml was added with 1 ml of a freshly prepared solution of equal volumes of 28 % hydroxylamine and 14 % sodium hydroxide. After 5 min 3 ml of 7 % perchloric acid was added and the insoluble hydroxamates filtered off on a paper filter (Munktell No. 8, diam. 5.5 cm) and washed on the filter two times with each 3 ml of the perchloric acid solution. The hydroxamates were then extracted from the filter with 3 ml of a dilution of Hill's reagent 1:20 in ethanol and the extinction of the solution measured at 530 mμ. With this method 1 μmole hydroxamate gives an extinction of 0.28, the molecular extinction of hydroxamates being around 1 000.

Synthesis of oleyl adenylate. 1 g adenylic acid (= 2.74 mmole) was dissolved in 40 ml pyridine and 8 ml water and 10 ml oleic acid (= 30 mmole) added. This solution was cooled to 0° and was added to an icecold solution of 10 g DCC in 20 ml pyridine. The reaction mixture was allowed to stand for 6 h in an ice-bath and was then added with 32 ml ice-cold

reported by Ariya *et al.*[4] The observed density is in good agreement with the value of 4.89 g/cm³ calculated for a cell content of two formula units of CrO_2.

The axial ratio of chromium dioxide ($c/a = 0.660$) corresponds to a relatively long distance between adjacent Cr atoms and indicates that no attracting forces are acting between these metal atoms in contrast to what is the case in several other compounds of transitions metals with valency states lower than their maximum ones [8]. Of particular interest in this connection is the rutile type phase $(Cr, Mo)O_2$ with its considerably lower values of c/a (down to 0.60) which have been interpreted as caused by the presence of metalmetal bonding [9].

This study forms part of research programs on metal oxides and on chromates and related compounds financially supported by the *Swedish Natural Science Research Council.*

The authors wish to thank Dr. Arne Magnéli for valuable discussions.

1. Michel, A. and Bénard, J. *Compt. rend.* **200** (1935) 1316.
2. Michel, A. and Bénard, J. *Bull. soc. chim. France* **10** (1943) 315.
3. Schwartz, R. S., Fankuchen, I. and Ward, R. *J. Am. Chem. Soc.* **74** (1952) 1676.
4. Ariya, S. M., Shchukarev, S. A. and Glushkova, V. B. *Zhur. Obshchei Khim.* **23** (1953) 1241—5.
5. Glemser, O., Hauschild, U. and Trüpel, F. *Z. anorg. u. allgem. Chem.* **277** (1954) 113.
6. Thamer, B. J., Douglass, R. M. and Staritzky, E. *J. Am. Chem. Soc.* **79** (1957) 547.
7. Bhatnagar, S. S., Prakash, B. and Hamid, A. *J. Chem. Soc. 1938, 1428.*
8. Marinder, B.-O. and Magnéli, A. *Acta Chem. Scand.* **11** (1957) 1635.
9. Sundholm, A., Andersson, S., Magnéli, A. and Marinder, B.-O. *To be published.*

Received August 8, 1958.

Chemical Synthesis of Oleyl Adenylate

BENGT BORGSTRÖM

Department of Physiological Chemistry, University of Lund, Lund, Sweden

Mixed anhydrides of adenylic acid with short and middle chain fatty acids have been proposed as intermediates in the enzymatic activation of these acids to their CoA derivatives [1-5]. Chemical synthesis of these adenylates has been reported using three different methods: 1) coupling of silver adenylate with the acid chloride (acetyladenylate [1]), 2) the reaction of the acid anhydride with adenylic acid in aqueous pyridine (buturyl and hexanoyl adenylate [2,5]), and 3) the condensation of fatty acid and adenylic acid in the presence of carbodiimides (buturyl adenylate [5]).

For an attempted synthesis of long chain fatty acid adenylates method 2 did not seem practical due to the low solubility of the long chain anhydrides. Of the two other methods the carbodiimide method was found to be the most practical and to give the best yields.

This paper will describe the synthesis of oleyl adenylate by the condensation of oleic acid with adenylic acid in the presence of di*cyclo*hexylcarbodiimide and also includes experiments to show the metabolic activity of this compound with rat liver mitochondria *in vitro*.

EXPERIMENTAL

Materials. Adenylic acid (AMP) was obtained from Sigma Chemical Company and di*cyclo*hexylcarbodiimide (DCC) from Fluka A.G.

Methods. Oleyl adenylate was estimated by the hydroxamic acid-$FeCl_3$ method modified for the acid insoluble hydroxamates of oleic acid [6]. A sample containing approximately 1 mg adenylate in 0.1—0.5 ml was added with 1 ml of a freshly prepared solution of equal volumes of 28 % hydroxylamine and 14 % sodium hydroxide. After 5 min 3 ml of 7 % perchloric acid was added and the insoluble hydroxamates filtered off on a paper filter (Munktell No. 8, diam. 5.5 cm) and washed on the filter two times with each 3 ml of the perchloric acid solution. The hydroxamates were then extracted from the filter with 3 ml of a dilution of Hill's reagent 1:20 in ethanol and the extinction of the solution measured at 530 mμ. With this method 1 μmole hydroxamate gives an extinction of 0.28, the molecular extinction of hydroxamates being around 1 000.

Synthesis of oleyl adenylate. 1 g adenylic acid (= 2.74 mmole) was dissolved in 40 ml pyridine and 8 ml water and 10 ml oleic acid (= 30 mmole) added. This solution was cooled to 0° and was added to an icecold solution of 10 g DCC in 20 ml pyridine. The reaction mixture was allowed to stand for 6 h in an ice-bath and was then added with 32 ml ice-cold

solution containing 66 mg lithium hydroxide (= 2.74 mmole). After 5 min the di-*cyclo*hexylurea was filtered off on a glassfilter and the clear solution extracted with 3 times 200 ml ether to remove excess oleic acid and pyridine. The water phase containing the adenylate was lyophilized and 1.40 g of a slightly yellow powder obtained. When assayed with the hydroxamic acid method this powder contained 1.26 μmoles adenylate per mg corresponding to 0.80 mg oleyl adenylate. The yield was 64 %, calculated on the AMP, and the purity around 80 %. This preparation was further purified by chromatography on a column of Whatman No. 1 paper powder (coarse grade) using *iso*propanol:water 70:30 as solvent [5]. For the purification of 200 mg of the crude preparation a column was prepared from 90 g paper powder (diam. 34 cm). The column was washed with *iso*propanol:water until the effluent was free from substances adsorbing at 259 mμ. 200 mg of the adenylate mixture was dissolved in 10 ml of the 70 % *iso*propanol and applied to the column which was developed with the same solvent. 20 ml fractions were collected and their optical density at 259 mμ determined. A pea kwas obtained between 160 and 240 ml of effluent. These 80 ml were added with 48 ml water and 130 ml ether to extract the *iso*propanol from the water phase and the latter lyophilized. The ultraviolet adsorption spectrum of a solution of this powder showed a single peak at 259 mμ with an optical density at this wavelength of 23.0 per mg as compared to a theoretical figure of 24.4 assuming the oleyl adenylate to have the same molar extinction coefficient as AMP (= 15.4×10^3). The ratio between activated fatty acid as determined by the hydroxamic acid method and the AMP content as derived from the optical density at 259 mμ was 0.96.

A study of the effect of fatty acid to AMP ratio on the yield of adenylate showed that 1, 3 and 9 moles of oleic acid per mole of AMP gave a yield of 45, 69 and 82 %, respectively, of adenylate calculated on the AMP of the reaction. To get the best yield calculated on the fatty acid moiety, as desired in the synthesis of fatty acid labeled adenylate, therefore equimolar amount of AMP and fatty acid should be used.

The method described gave low yields for the synthesis of adenylates with palmitic and stearic acid due to the low solubility of these acids in the solvent mixture used at 0°. If the reaction was allowed to take place at room temperature to facilitate the solution of these acids, the yield of hydroxamic acid forming substances was low most probably due to the formation of polyacylated compounds [5].

Table 1. Oxidation of oleyl adenylate and oleic acid with rat liver mitochondria. The Warburg vessels contained final concentration of 0.01 M phosphate buffer pH 7.4, 0.05 M KCl, 0.005 M $MgCl_2$, 0.0005 M succinate as priming substrate and 10^{-5} M cytochrome c. Mitochondria added in 0.15 M KCl suspension corresponding to 1.5 g liver. Additions according to table. Final volume 2.0 ml; gas phase air. Incubated at 30°: equilibration time 10 min.

Additions	O_2 uptake, μl, 0—20 min.
None	12.8
Oleyl adenylate 0.25 μmole	54.8
» » 0.50 »	58.9
» » 1.0 »	31.6
» » 2.0 »	11.1
ATP 2 μmole	32.8
» 2 + oleic acid 0.25 μmole	65.9
» 2 » » 0.50 »	—
» 2 » » 1.0 »	60.3
» 2 » » 2.0 »	7.2

From Table 1 it appears that rat liver mitochondria can oxidize oleyl adenylate at the same rate as oleic acid in the presence of adenosine triphosphate (ATP) and thus can replace the ATP requirement for the oxidation of oleic acid [7]. The optimal concentration for the oxidation of adenylate in this system is the same as for oleic acid, *i.e.* 2.5×10^{-4} M. At higher substrate concentration both adenylate and oleic acid inhibit respiration.

1. Berg, P. *J. Biol. Chem.* **222** (1956) 1010.
2. Lee Peng, C. H. *Biochim. et Biophys. Acta* **22** (1956) 42.
3. Whitehouse, M., Moeksi, H. and Gurin, S. *J. Biol. Chem.* **226** (1957) 813.
4. Jencks, W. P. and Lipmann, F. *J. Biol. Chem.* **225** (1957) 207.
5. Talbert, P. T. and Huennekens, F. M. *J. Am. Chem. Soc.* **78** (1956) 4671.
6. Kornberg, A. and Pricer, W. E. *J. Biol. Chem.* **204** (1953) 329.
7. Kennedy, E. P. and Lehninger, A. L. *J. Biol. Chem.* **185** (1950) 275.

Received August 27, 1958.

Diphenyl-picrylhydrazyl as a Standard in Electron Spin Resonance

JOHAN J. LOTHE and GUNNAR EIA

The Central Institute for Industrial Research, Blindern, Oslo, Norway

In the study of free radicals by electron spin resonance α,α-diphenyl-β-picrylhydrazyl (DPH) is widely used as a standard for estimating the number of unpaired electrons present. Recently DPH has become commercially available through Fluka AG. Investigating two separate samples of DPH from this company it was found, that the maximum resonance intensity from one sample was only about one third of that from the other, the line being at the same time correspondingly broader. Subsequent analyses of the samples indicated the presence of substantial amounts of benzene. In view of the importance of DPH as a standard it was thought desireable to investigate the observed effect in some more detail, and especially to ascertain if recrystallization from benzene was responsible for the broadening of the resonance line.

The electron spin resonance spectra were obtained at a frequency of 31.5 Mc/s using a Pound and Knight type spectrometer [1]. The magnetic field produced by a pair of Helmholtz coils was modulated at a frequency of 415 cps, and the signals were displayed on a recorder using a phase-sensitive detector. This technique permits the graphic presentation of the first derivative of the absorption as a function of field. The ordinate in the published spectra was calibrated in number of spin centers according to the resonance intensity from a sample of DPH recrystallized from carbon disulfide.

The existence of a stable (1:1) addition complex between DPH and benzene has been mentioned twice in the literature [2, 3]. We prepared the complex both by recrystallization from a mixture of 3 parts benzene and 2 parts *cyclo*hexane, and by slowly evaporating the solvent at room temperature from a solution of DPH in benzene. Microchemical analysis indicated that the ratio of DPH to benzene in the sample used for the investigation was as 1:0.8.

The resonance line of the DPH-benzene complex (Fig. 1) was extremely broad with a total width of 4.6 ørsted between inflection points of the absorption curve. The peak to peak intensity was only about 1/30th of that observed in a sample of DPH recrystallized from carbon disulfide (Fig. 2), which showed a total width of 0.85 ørsted between inflection points.

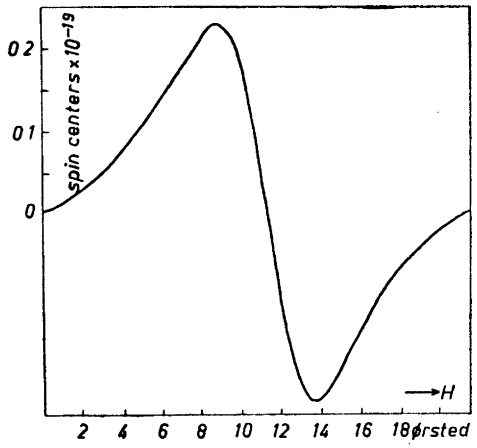

Fig. 1. Electron spin resonance of 60 mg crystalline DPH-benzene complex. (Ordinate is calibrated in spin centers according to resonance intensity from a sample of DPH recrystallized from carbon disulfide.)

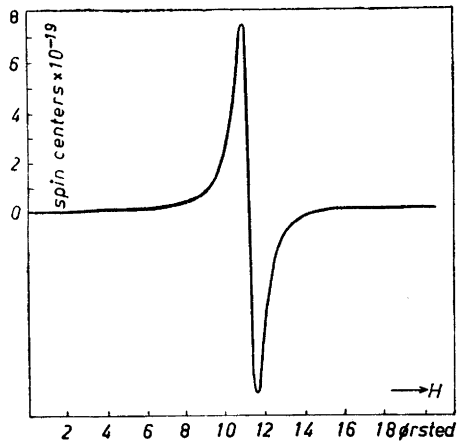

Fig. 2. Electron spin resonance of 50 mg crystalline DPH recrystallized from carbon disulfide.

In accordance with the findings by Müller [3] benzene is only very slowly driven away from the complex. Evacuation of the sample for 24 h at 0.1 mm Hg at room temperature had no effect on the spectrum, and after 10 h of vacuum treatment at 60° the peak-to-peak intensity had increased only by a factor of three. It is interesting to note, however, the ease with which the benzene apparently is dispelled by other organic liquids. Only 2 min after the addition of a small amount of *cyclo*hexane to the DPH-benzene complex the peak-to-peak intensity had increased by a factor of five.

Electron spin resonance spectra of solid free radicals are usually characterized by very narrow absorption lines with a half width of less than 10 ørsted. Large intermolecular exchange interaction of the unpaired electrons is mainly responsible for the sharpening of the lines. Some overlapping of the orbitals should occur in order to have exchange narrowing operating. When the distance between the free radicals in the crystal is increased, one may consequently expect, that the exchange effect will be reduced. It seems likely, that the broadening of the resonance line of the molecular addition complex between DPH and benzene may be ascribed to reduced exchange narrowing. A somewhat similar effect has already been observed by Holden and Kittel [4] in the resonance spectra of di-*p*-anisyl nitric oxide. The resonance lines from this compound was found to have a half width of 15.7 ørsted, whereas a crystalline material in which one part of di-*p*-anisyl nitric oxide was diluted with ten parts of the isomorphous *p,p'*-dimethoxy benzophenone gave a half width of 29.6 ørsted.

It has been pointed out [5], that the line shape, when exchange narrowing is operating should be of the Lorentzian type, whereas for the case of negligible exchange effects a Gaussian line shape is expected. Weidner and Whitmer [6] have previously found a Lorentz type resonance line for DPH. Analysis of the resonance line from the DPH-benzene complex showed, that the line could also in this case be closely reproduced by a Lorentz curve. Even though the line of the DPH-benzene complex is considerably broader than in the sample of DPH recrystallized from carbon disulfide, the line shape indicates thus that the line is still sharpened by exchange narrowing. This is not surprising as according to Holden and Kittel [4], the line width in DPH calculated on the basis of dipole-dipole interaction only should be of the order of 100 ørsted.

Table 1.

Sample	a) ΔH_i ørsted	b) I_p	c) A	d) A
DPH recrystallized from CS_2	0.85	1	1	1
DPH-benzene complex	4.6	0.031	0.9	0.6

a) Distance between inflection points on absorption curve.

b) Peak-to-peak intensity of derivated curve in arbitrary units.

c) Area under absorption curve in arbitrary units, calculated from $(\Delta H_i)^2 \times I_p$.

d) Area under absorption curve in arbitrary units, calculated from the product of the line width and the area under the derivated curve.

It is actually the area under the absorption curve, that is a measure of the number of unpaired electrons present in a sample. This area may be estimated either from the product of the square of the line width and the peak-to-peak intensity, or from the line width times the area under the derivated curve. It is seen from Table 1, that using the first method the areas under the absorption curves of the two samples were found to be nearly equal. The lower results on the DPH-benzene complex obtained using the second method of calculation, is probably due to neglect of the area beyond the limits of integration.

A search was made for a suitable solvent for the recrystallization of DPH. It turned out, that the solvent had a pronounced effect on the resonance line. The highest peak-to-peak intensity in the derivated resonance spectrum was obtained from a sample of DPH recrystallized from carbon disulfide. These observations emphasize that great care should be exercised when using DPH as a standard for estimating the number of unpaired electrons present in a system. DPH should preferably be recrystallized from carbon disulfide, and only the area under the absorption curve should be used for the estimate.

So far the observations on the electron spin resonance spectrum of the DPH-

benzene molecular addition complex have been restricted to the radiofrequency region. It is our hope in the near future to extend the work to the microwave region. Work is in progress on the electron spin resonance spectra of other molecular addition complexes of DPH.

The authors wish to express their gratitude to Mr. H. Hognestad, who constructed the electron spin resonance spectrometer. The microchemical analyses were carried out by Dr. Kirsten, University of Uppsala.

1. Pound, R. V. and Knight, W. D. *Rev. Sci. Instr.* **21** (1950) 219.
2. Müller, E., Müller-Rodloff, I. and Bunge, W. *Ann.* **520** (1935) 244.
3. Lyons, J. A. and Watson, W. F. *J. Polymer Sci.* **18** (1955) 141.
4. Holden, A. N., Kittel, C., Merritt, F. R. and Yager, W. A. *Phys. Rev.* **77** (1950) 147.
5. Anderson, P. W. and Weiss, P. R. *Revs. Modern Phys.* **25** (1953) 269.
6. Weidner, R. T. and Whitmer, C. A. *Phys. Rev.* **91** (1953) 1279.

Received July 30, 1958.

Ligand Field Spectrum of Vanadium(II) Hexaquo Ions

CHR. KLIXBÜLL JØRGENSEN

Chemistry Department A, Technical University of Denmark, Copenhagen, Denmark

The absorption spectra of hexaquo ions of divalent metals in the first transition group has been one of the most common subjects for ligand field theory. Cr(II)[1,2], Mn(II)[3], Fe(II)[4,5], Co(II)[6], Ni(II)[7,8] complexes have all been rather much studied. Only the study of vanadium(II) has been very little performed, due to the strongly reducing character of this oxidation state and the interfering colours of the probable vanadium(III) impurities. Kato [9] photographed bands at 820, 760, 560, and 540 mμ of a solution in 3 M HCl. However, measurements on a Cary MS-11 recording spectrophotometer has not confirmed the doublet structure in the green, and it is known that the highly varying sensitivity of most photographic plates in this region may produce spurious maxima. Therefore, Ballhausen and the present author concluded [10] that the three spin-allowed transitions from $^4\Gamma_2$ to $^4\Gamma_5$, $^4\Gamma_4$(F), and $^4\Gamma_4$(P) occur at 820, 555, and 378 mμ, respectively. Similar conclusions were drawn previously by Holmes and McClure [11], but only published recently.

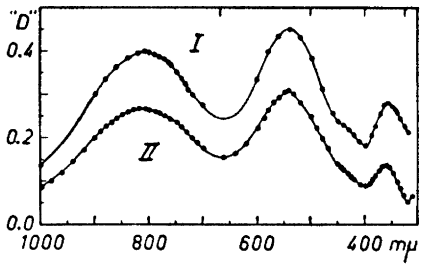

Fig. 1. Reflection spectra of vanadium(II), zinc(II) Tutton salt.

Fig. 1 gives the reflection spectra (as measured on a Beckman DU) of two samples of $(NH_4)_2[Zn(H_2O)_6](SO_4)_2$ into which vanadium(II) is included isomorphically. This happens to be a method of evading the presence of vanadium(III) in the substance. The salt was also dissolved in 2 M H_2SO_4 and measured on the Cary. The band maxima (and shoulders in parentheses) occur at the wavelengths in mμ:

Sample I	Sample II	Solution
810	810	>810
(765)	(760?)	(778)
540	542	563
(430)	(434)	—
355	362	368

The solution has higher wavelengths of all its bands, compared to the solid samples. This may be caused by the presence of sulphate complexes (even though this has relatively little influence on the spectra of other divalent ions), or by partly oxidation to +3 (of which the spectral characteristics is discussed in Ref.[12] p. 79). However, another explanation may be found in the phenomenon [8] that $Ni(H_2O)_6^{++}$ has smaller wavelengths when imbedded in $(NH_4)_2[Ni(H_2O)_6](SO_4)_2$ than in other salts or in solution. Further, the lattice constants of the zinc Tutton salt are so small that $V(H_2O)_6^{++}$ may be compressed to some extent [13].

benzene molecular addition complex have been restricted to the radiofrequency region. It is our hope in the near future to extend the work to the microwave region. Work is in progress on the electron spin resonance spectra of other molecular addition complexes of DPH.

The authors wish to express their gratitude to Mr. H. Hognestad, who constructed the electron spin resonance spectrometer. The microchemical analyses were carried out by Dr. Kirsten, University of Uppsala.

1. Pound, R. V. and Knight, W. D. *Rev. Sci. Instr.* **21** (1950) 219.
2. Müller, E., Müller-Rodloff, I. and Bunge, W. *Ann.* **520** (1935) 244.
3. Lyons, J. A. and Watson, W. F. *J. Polymer Sci.* **18** (1955) 141.
4. Holden, A. N., Kittel, C., Merritt, F. R. and Yager, W. A. *Phys. Rev.* **77** (1950) 147.
5. Anderson, P. W. and Weiss, P. R. *Revs. Modern Phys.* **25** (1953) 269.
6. Weidner, R. T. and Whitmer, C. A. *Phys. Rev.* **91** (1953) 1279.

Received July 30, 1958.

Ligand Field Spectrum of Vanadium(II) Hexaquo Ions

CHR. KLIXBÜLL JØRGENSEN

Chemistry Department A, Technical University of Denmark, Copenhagen, Denmark

The absorption spectra of hexaquo ions of divalent metals in the first transition group has been one of the most common subjects for ligand field theory. Cr(II)[1,2], Mn(II)[3], Fe(II)[4,5], Co(II)[6], Ni(II)[7,8] complexes have all been rather much studied. Only the study of vanadium(II) has been very little performed, due to the strongly reducing character of this oxidation state and the interfering colours of the probable vanadium(III) impurities. Kato [9] photographed bands at 820, 760, 560, and 540 mμ of a solution in 3 M HCl. However, measurements on a Cary MS-11 recording spectrophotometer has not confirmed the doublet structure in the green, and it is known that the highly varying sensitivity of most photographic plates in this region may produce spurious maxima. Therefore, Ballhausen and the present author concluded [10] that the three spin-allowed transitions from $^4\Gamma_2$ to $^4\Gamma_5$, $^4\Gamma_4$(F), and $^4\Gamma_4$(P) occur at 820, 555, and 378 mμ, respectively. Similar conclusions were drawn previously by Holmes and McClure [11], but only published recently.

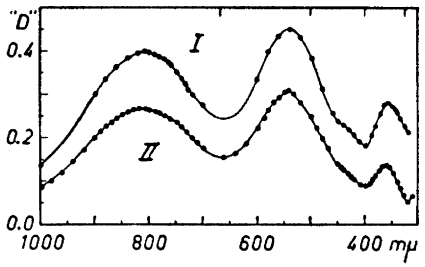

Fig. 1. Reflection spectra of vanadium(II), zinc(II) Tutton salt.

Fig. 1 gives the reflection spectra (as measured on a Beckman DU) of two samples of $(NH_4)_2[Zn(H_2O)_6](SO_4)_2$ into which vanadium(II) is included isomorphically. This happens to be a method of evading the presence of vanadium(III) in the substance. The salt was also dissolved in 2 M H_2SO_4 and measured on the Cary. The band maxima (and shoulders in parentheses) occur at the wavelengths in mμ:

Sample I	Sample II	Solution
810	810	>810
(765)	(760?)	(778)
540	542	563
(430)	(434)	—
355	362	368

The solution has higher wavelengths of all its bands, compared to the solid samples. This may be caused by the presence of sulphate complexes (even though this has relatively little influence on the spectra of other divalent ions), or by partly oxidation to +3 (of which the spectral characteristics is discussed in Ref.[12] p. 79). However, another explanation may be found in the phenomenon [8] that $Ni(H_2O)_6^{++}$ has smaller wavelengths when imbedded in $(NH_4)_2[Ni(H_2O)_6](SO_4)_2$ than in other salts or in solution. Further, the lattice constants of the zinc Tutton salt are so small that $V(H_2O)_6^{++}$ may be compressed to some extent [13].

From the average values of the two solid samples, Δ is seen to be 12 350 K (= cm^{-1}). The parameter of interelectronic repulsion B can be found by the same way [7,8] as in Ni(II), *viz.* from the wavenumbers of all three spin-allowed bands $15B = 18\,500 + 27\,950 - 3 \times 12\,350 = 9\,400$ K, while $15B = 11\,260$ K in gaseous V^{++}. However, as pointed out by Schäffer [13] for the isoelectronic $Cr(H_2O)_6^{+++}$, the third band has undoubtedly too low wavenumber, and it is reasonable to calculate the interelectronic repulsion parameters from the positions of the two first bands alone. In this way, the comparison with isoelectronic species as Mn(IV) in MnF_6^{--} or Mo(III) in $MoCl_6^{-3}$ is also facilitated. From this assumption, $15B$ is found = 10 300 K. The ratio $\beta = 0.92$ between this value and the value for the gaseous V^{++} is comparable with $\beta = 0.93$ in $Mn(H_2O)_6^{++}$ and 0.89 in $Ni(H_2O)_6^{++}$, demonstrating an early position in the nephelauxetic series of central ions (while $\beta = 0.79$ for $Cr(H_2O)_6^{+3}$ and 0.76 for $Fe(H_2O)_6^{+3}$).

For systematical reasons, it would be very valuable, if the spinforbidden transitions from $^4\Gamma_2$ to $^2\Gamma_3$ and $^2\Gamma_4$ (degenerate for pure d-electrons with the sub-shell configuration γ_5^3) could be detected. Even though water has a weak absorption range 740—790 mμ, it is believed that the shoulder $\sim$ 770 mμ actually is this transition (ζ_{3d} is only 169 K in V^{++}, and correspondingly, the spin-forbidden transitions are very weak), which occurs between 700 and 650 mμ in most chromium(III) complexes. The shoulder at 430 mμ in the solid samples may be another spin-forbidden band, or it may be due to superficial oxidation to $V(H_2O)_5OH^{++}$, which has an enormous absorption there [14] (perhaps, it is a dimer $(H_2O)_5\,VOV(H_2O)_5^{+4}$).

It was hoped to prepare other vanadium(II) complexes by dissolving the salt in different complexing agents. Thus, a solution in concentrated aqueous ammonia exhibit bands at $\sim$ 690 and 476 mμ. However, oxidation by traces of air produces a precipitate of $V(OH)_3$, and the possible experiments with other ligands have not yet been successful.

Experimental. 11.7 g (0.1 mole) NH_4VO_3 was mixed with 150 ml water, and 50 ml concentrated sulphuric acid added. The red-brown solution was reduced by zinc foil (Merck p.a.) over dark blue and dark green intermediate colours (of VO^{++} and V(III) sulphato complexes) until a violet solution was formed. This was quickly added to strong solutions (nearly saturated) of $(NH_4)_2SO_4$ in water, and a precipitate was formed of the mixed vanadium(II) and zinc(II) Tutton salt, could be sucked dry on a Büchner funnel. The salt can be kept several months in air without oxidation.

Acknowledgment. This research was supported by the *European Research Office, U. S. Department of Army* (Frankfurt/Main), under contract No. DA-91-508-EUC-247.

1. Pecsok, R. L. and Bjerrum, J. *Acta Chem. Scand.* **11** (1957) 1419.
2. Schläfer, H. L. and Skoludek, H. *Z. physik. Chem.* **11** (1957) 277.
3. Jørgensen, C. Klixbüll *Acta Chem. Scand.* **11** (1957) 53.
4. Jørgensen, C. Klixbüll *Acta Chem. Scand.* **8** (1954) 1502.
5. Furlani, C. *Gazz. chim. ital.* **87** (1957) 371.
6. Ballhausen, C. J. and Jørgensen, C. Klixbüll *Acta Chem. Scand.* **9** (1955) 399.
7. Jørgensen, C. Klixbüll *Acta Chem. Scand.* **9** (1955) 1362; **10** (1956) 887.
8. Bostrup, O. and Jørgensen, C. Klixbüll *Acta Chem. Scand.* **11** (1957) 1223.
9. Kato, S. *Sci. Papers Inst. Phys. Chem. Research, Tokyo* **13** (1930) 49.
10. Ballhausen, C. J. and Jørgensen, C. Klixbüll *Kgl. Danske Videnskab. Selskab, Mat.-fys. Medd.* **29** (1955) No. 14.
11. Holmes, O. G. and McClure, D. S. *J. Chem. Phys.* **26** (1957) 1686.
12. Jørgensen, C. Klixbüll *Acta Chem. Scand.* **11** (1957) 73.
13. Schäffer, C. E. *International Symposium on Coordination Compounds. Suppl. Ricerca Scientifica* **28** (1958) 149.
14. Furman, S. C. and Garner, C. S. *J. Am. Chem. Soc.* **72** (1950) 1785.

Received August 23, 1958.

Ligand Field Bands of Hexafluoro Manganate(IV) and Predictions of Band Positions of Transition Group Fluorides

CHR. KLIXBÜLL JØRGENSEN

Chemistry Department A, Technical University of Denmark, Copenhagen, Denmark

Ligand field theory describes the energy levels of central ions with partly filled d-shells in octahedral (O_h) complexes in terms of two parameters: the energy difference Δ (also called $(E_1 - E_2)$ or 10 Dq) between the two equivalent γ_3-orbitals and the three equivalent γ_5-orbitals; and the ratio β between the interelectronic repulsion parameters in the complex and in the corresponding gaseous ion. Even though these parameters are determined by rather unknown mixtures of electrostatic and covalent bonding [1], they are very useful for an empirical classification of the complexes, and Δ (the spectrochemical series) and β (the nephelauxetic series [2]) as function of central ions and of ligands behave very regularly. It is evident, *e.g.* from the many nickel(II) complexes studied [3,4], that the absorption spectrum of an unknown complex often can be precisely interpolated from other, known spectra, even though the parameters of ligand field theory are not accessible for an *a priori* calculation. The present note will discuss the possibilities of predicting the spectra of fluoride complexes which are interesting for many reasons: they are even less nephelauxetic than aquo ions (corresponding to weaker tendency towards covalent bonding) and they represent high and often unusual oxidation states of the metals involved. Further, the Laporte-forbidden ligand field transitions are not so often masked by Laporte-allowed electron transfer bands as in most other complexes. Unfortunately, these fluoride complexes are generally so reactive with glass and with moisture that no reflection spectra have been published (nor absorption spectra of the gaseous fluorides; solutions are not liable to be made in any solvent). It is hoped that this note will draw attention to the spectra and encourage somebody to surmount the large experimental difficulties. It can be remarked that ligand field theory is not especially applicable to fluoride complexes, because they are the least covalent (and therefore the most "electrostatic") complexes of a given central ion; a similar series of predictions might equally well be given for the relatively more covalent chloride or bromide complexes.

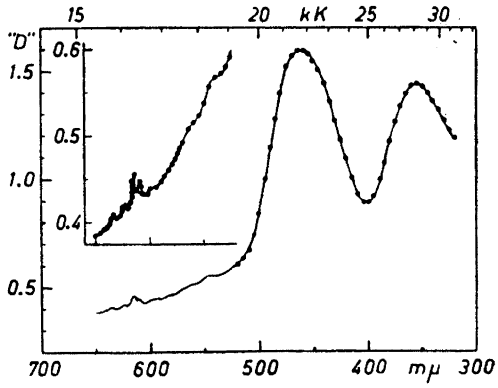

Fig. 1. Reflection spectrum of K_2MnF_6. The optical density "*D*" is indicated on larger scale for the small bands in the red.

The actual knowledge of ligand field parameters of fluoride complexes is mainly derived from CrF_6^{---}, extensively studied by Dr. Claus Schäffer, and from FeF_6^{---}. The latter ion [2] has Δ = 13.9 kK (1 kK = 1 000 cm^{-1}) and β = 0.79, as compared with $Fe(H_2O)_6^{+++}$ Δ = 14.2 kK and β = 0.76. Fig. 1 indicates the reflection spectrum of K_2MnF_6, prepared according to Weinland and Lauenstein [5]. The two spin-allowed bands with maxima at 460 mμ (= 21.75 kK) and 355 mμ (= 28.2 kK) imply Δ = 21.75 kK and the interelectronic repulsion parameter B = 600 K. Since B = 985 K in [6] gaseous Mn^{+4}, β = 0.61 for MnF_6^{--}. This is a surprisingly small value for a fluoride complex, showing that Mn(IV) is placed in the nephelauxetic series of metals even after Rh(III) and Co(III). Previously, it has not been possible to determine β of a Mn(IV) complex, because only the first spin-allowed band of the heteropoly molybdate was observed [7] at 21.4 kK. The latter complex has a narrow, spin-forbidden band at 14.3 kK, as also Mn(IV) heteropolywolframate [8] at 14.5 kK. This is nearly the same position as the transitions from $^4\Gamma_2$ to $^2\Gamma_3$ and $^2\Gamma_4$ in chromium(III) complexes. Kröger [9] found narrow phosphorescence lines of Mn(IV),

surrounded octahedrally by six oxygen atoms, at 15.26 and 15.32 kK. This effect corresponds to the opposite influence on the interelectronic repulsion parameters of increasing ionic charge and increasing covalency, which nearly cancel each other in Mn(II) and Fe(III) complexes [2,10]. Actually, Fig. 1 shows four weak, narrow bands * at 610, 614.5, 622 and 632 mμ. The wavenumbers 15.8—16.4 kK are some 8 % larger than in the oxo complexes of Mn(IV) (corresponding to the larger nephelauxetic effect of O^{--} than of F^-) and indicates a value of $\beta \sim 0.8$. In the molecular orbital theory [11] the wavenumber of $^4\Gamma_2 \rightarrow {}^2\Gamma_3$ is 3K(4,5), representing the interaction between two γ_5-electrons, while the energy difference between $^4\Gamma_5$ and $^4\Gamma_4$ is J(3,4)—J(1,4)—K(3,4) + K(1,4), representing interactions between a γ_5- and a γ_3-electron. If the γ_3-electrons are delocalized more by σ-bonding than the γ_5-electrons are by π-bonding, this difference is intelligible. However, configuration interaction in the complex may disturb this description rather much.

In Table 1 are indicated the positions of ligand field bands of octahedral fluoride complexes, predicted from the general behaviour of Δ and β as function of oxidation state. A few such predicted values have previously been given [12]. Wheeler, Perros and Naeser [14] indicate that PtF_6^{--} has bands at 31.4 and 36.4 kK. Dr. Perros, George Washington University, Wash. D.C., has kindly informed me that these two bands have $\varepsilon = 33$ and 24, respectively, while two weak bands are observed at 22.5 and 24.5 kK with $\varepsilon \sim 4$ and 5. Thus, the spectrum resembles very much that [16] of $IrCl_6^{-3}$, and the excited levels can be identified as $^3\Gamma_4$, $^3\Gamma_5$, $^1\Gamma_4$, and $^1\Gamma_5$. Hepworth, Robinson, and Westland [15] give a band at 31.6 kK of IrF_6^{--}. Since it is known from the chloro complexes of $4d^5$ Ru(III) and $4d^6$ Rh(III) [16] that the first spin-allowed ligand field band occurs nearly at the same wavenumber, a similar analogy may exist between Ir(IV) and Pt(IV). Thus, RhF_6^{--} is expected to have a band $\sim$ 350 mμ. The d^4-systems with $S = 3/2$ might be studied as fluoro complexes for finding the ligand field bands, which are as yet not known [16]. OsF_6^{--} has a band [15] at 32.5 kK, which is expected to be found in IrF_6^- at 36 and in RuF_6^{--} at 29 kK.

Table 1. Predicted positions of ligand field bands of fluoro complexes in kK (= 1 000 cm^{-1}).

d^3-systems	$^4\Gamma_2 \rightarrow {}^2\Gamma_{3,4}$	$^2\Gamma_5$	$^4\Gamma_5$	$^4\Gamma_4$
MnF_6^{--} obs.	16.2	—	21.75	28.2
MoF_6^{---}	11	16	24.5	30
TcF_6^{--}	10.5	15	28	34
RuF_6^-	10	14.5	31	36.5
RhF_6	9.5	14	33	38
ReF_6^{--}	10	15, 16.5	32	38
OsF_6^-	9.5	14.5, 16.5	35	40
IrF_6	9.5	14, 16	37	41.5

d^6-systems	$^1\Gamma_1 \rightarrow {}^1\Gamma_4$	$^1\Gamma_5$
NiF_6^{--}	20	28
RhF_6^{---}	24.5	32
PdF_6^{--}	27	34
IrF_6^{---}	28	34
PtF_6^{--} obs.	31.5	36.4
(CoF_6^{---}	$^5\Gamma_5 \rightarrow {}^5\Gamma_3$ 17)	

d^8-systems	$^3\Gamma_2 \rightarrow {}^1\Gamma_3$	$^3\Gamma_5$	$^3\Gamma_4$(F)	$^3\Gamma_4$(P)
CuF_6^{---}	13	15	22	35

There is no doubt that the quinque- and sexavalent metals have very late places in the nephelauxetic series, corresponding to a certain principle of electroneutrality [10]. The parameters of interelectronic repulsion will probably have the same magnitude as in gaseous ions with charges +1 or +2. Further, the orbital energy differences such as Δ assume large values, corresponding to the diamagnetism of NiF_6^{--} and low-spin behaviour of all the $4d^n$- and $5d^n$-fluorides. Nevertheless, a confirmation by measurements would be very valuable, and especially the numerical values of the nephelauxetic effect very interesting. Finally, an interesting stereochemical problem exists by comparison of the green gas RuF_5 with RuF_6^-. If the former is not a double-bridged dimer Ru_2F_{10}, it is one

* When K_2MnF_6 is dissolved in saturated aqueous NH_4F, relatively broad bands are observed in the red at 600, 660, and 702 mμ. Since these bands do not have the same positions as the narrow bands of the solid compound, it must be concluded that it decomposes to hydroxo- or perhaps polymeric oxo-complexes, and a slow evolution of the spectrum is also seen in some ten minutes, before the solution is too opaque of precipitated MnO_2. That hydrolysis products of halide complexes of d^3-systems often have the narrow, spin-forbidden bands highly broadened and somewhat intensified, is known from rhenium(IV)[13]. The bridged compound $W_2Cl_9^{-3}$ has also anomalously high, broad bands in the red at 13.2 and 16.3 kK[12].

of the very rare cases [12] of a d^3-system deviating from octahedral symmetry, and any information about its absorption spectrum will be highly desirable.

Acknowledgments. I thank Dr. Claus E. Schäffer much for many valuable discussions on ligand field theory and its applications. This research was supported by the *European Research Office, U.S. Department of Army* (Frankfurt / Main) under contract no. DA-91-508-EUC-247.

1. Jørgensen, C. Klixbüll, *Energy Levels of Complexes and Gaseous Ions.* Gjellerups Forlag, Copenhagen 1957.
2. Schäffer, C. E. and Jørgensen, C. Klixbüll, *International Symposium on the Chemistry of the Coordination Compounds. Suppl. Ricerca Scientifica* **28** (1958) 143; *Acta Chem. Scand. To be published.*
3. Jørgensen, C. Klixbüll, *Acta Chem. Scand.* **9** (1955) 1362; **10** (1956) 887.
4. Bostrup, O. and Jørgensen, C. Klixbüll, *Acta Chem. Scand.* **11** (1957) 1223.
5. Weinland, R. F. and Lauenstein, O. *Z. anorg. Chem.* **20** (1899) 40.
6. Moore, C. E. *Atomic Energy Levels. Natl. Bur. Standards Circ. No. 467, Vol.* I, II, III (1949, 1952, 1958).
7. Shimura, Y., Ito, H. and Tsuchida, R. *J. Chem. Soc. Japan* **75** (1954) 560.
8. Shimura, Y. and Tsuchida, R. *Bull. Chem. Soc. Japan* **30** (1957) 502.
9. Kröger, F. A. *Some Aspects of the Luminiscence of Solids.* Elsevier Publishing Company Amsterdam 1948, p. 74.
10. Jørgensen, C. Klixbüll, *Discussions Faraday Soc. No.* **26** (1958).
11. Jørgensen, C. Klixbüll, *Acta Chem. Scand.* **12** (1958) 903.
12. Jørgensen, C. Klixbüll, *Quelques Problèmes de Chimie Minérale, X Conseil de Chimie Solvay.* R. Stoops, Bruxelles 1956, p. 355.
13. Maun, E. K. and Davidson, N. *J. Am. Chem. Soc.* **72** (1950) 2254.
14. Wheeler, T. E., Perros, T. P. and Naeser, C. R. *J. Am. Chem. Soc.* **77** (1955) 3488.
15. Hepworth, M. A., Robinson, P. L. and Westland, G. J. *J. Chem. Soc.* **1958** 611.
16. Jørgensen, C. Klixbüll, *Acta Chem. Scand.* **10** (1956) 500, 518.

Received August 23, 1958.

Some Observations on Betaine-Homocysteine-Methyl-Transferases

L.-E. ERICSON

Division of Food Chemistry, Royal Institute of Technology, Stockholm 70, Sweden

Experiments carried out in our laboratory suggest that enzymes capable of synthesizing methionine by means of a transfer of a methyl group from betaine (carboxymethyl-trimethyl-ammonium chloride) to homocysteine, are present in appreciable amounts only in the livers of vertebrate animals. Attempts to find such enzymes in microorganisms, plants or invertebrates have so far failed [1]. The apparent pH-optima of the betaine-homocysteine-methyltransferases of all the vertebrate livers tested occur between 7.0 and 7.8. These transferases are strongly inhibited by dimethylglycine, which besides methionine is a product of the enzymic reaction [1,2]. Choline can not replace betaine as the methyl donor with purified enzyme preparations nor does choline act as an inhibitor of the transferases.

In order to study the characteristics of this type of methyl group transfer in more detail, a procedure for the purification of the betaine-homocysteine-methyl-transferase of pig liver was worked out. It comprises the following steps:

1. One part of fresh pig liver is homogenized in three parts of water in a Waring blender. The pH of the homogenate is adjusted to 5.1 at 0°C and the thick "brei" obtained immediately centrifuged at 44 000 $\times$ g for 30 min.

2. The supernatant fluid is adjusted to a pH-value of 7.7 and poured into a series of test tubes which are then placed in a water bath at 80°C for 90 sec. An inactive precipitate is formed and is removed by centrifuging at 44 000 $\times$ g for 30 min.

3. The enzyme which is contained in the supernatant fluid from step 2, is adsorbed on calcium phosphate gel prepared according to Keilin and Hartree [3]. The enzyme is eluted from the gel by means of 0.15 M orthophosphate and 0.1 M pyrophosphate.

4. The eluates from step 3 are pooled and the pH adjusted to 7.2. Acetone is added to a final concentration of 50 %. The precipitate that forms is collected by centrifuging at 5 000 $\times$ g for 10 min, dissolved in water and dialysed against water at pH 8.5.

of the very rare cases [12] of a d^3-system deviating from octahedral symmetry, and any information about its absorption spectrum will be highly desirable.

Acknowledgments. I thank Dr. Claus E. Schäffer much for many valuable discussions on ligand field theory and its applications. This research was supported by the *European Research Office, U.S. Department of Army* (Frankfurt / Main) under contract no. DA-91-508-EUC-247.

1. Jørgensen, C. Klixbüll, *Energy Levels of Complexes and Gaseous Ions.* Gjellerups Forlag, Copenhagen 1957.
2. Schäffer, C. E. and Jørgensen, C. Klixbüll, *International Symposium on the Chemistry of the Coordination Compounds. Suppl. Ricerca Scientifica* **28** (1958) 143; *Acta Chem. Scand. To be published.*
3. Jørgensen, C. Klixbüll, *Acta Chem. Scand.* **9** (1955) 1362; **10** (1956) 887.
4. Bostrup, O. and Jørgensen, C. Klixbüll, *Acta Chem. Scand.* **11** (1957) 1223.
5. Weinland, R. F. and Lauenstein, O. *Z. anorg. Chem.* **20** (1899) 40.
6. Moore, C. E. *Atomic Energy Levels. Natl. Bur. Standards Circ. No. 467, Vol.* I, II, III (1949, 1952, 1958).
7. Shimura, Y., Ito, H. and Tsuchida, R. *J. Chem. Soc. Japan* **75** (1954) 560.
8. Shimura, Y. and Tsuchida, R. *Bull. Chem. Soc. Japan* **30** (1957) 502.
9. Kröger, F. A. *Some Aspects of the Luminiscence of Solids.* Elsevier Publishing Company Amsterdam 1948, p. 74.
10. Jørgensen, C. Klixbüll, *Discussions Faraday Soc. No.* **26** (1958).
11. Jørgensen, C. Klixbüll, *Acta Chem. Scand.* **12** (1958) 903.
12. Jørgensen, C. Klixbüll, *Quelques Problèmes de Chimie Minérale, X Conseil de Chimie Solvay.* R. Stoops, Bruxelles 1956, p. 355.
13. Maun, E. K. and Davidson, N. *J. Am. Chem. Soc.* **72** (1950) 2254.
14. Wheeler, T. E., Perros, T. P. and Naeser, C. R. *J. Am. Chem. Soc.* **77** (1955) 3488.
15. Hepworth, M. A., Robinson, P. L. and Westland, G. J. *J. Chem. Soc.* **1958** 611.
16. Jørgensen, C. Klixbüll, *Acta Chem. Scand.* **10** (1956) 500, 518.

Received August 23, 1958.

Some Observations on Betaine-Homocysteine-Methyl-Transferases

L.-E. ERICSON

Division of Food Chemistry, Royal Institute of Technology, Stockholm 70, Sweden

Experiments carried out in our laboratory suggest that enzymes capable of synthesizing methionine by means of a transfer of a methyl group from betaine (carboxymethyl-trimethyl-ammonium chloride) to homocysteine, are present in appreciable amounts only in the livers of vertebrate animals. Attempts to find such enzymes in microorganisms, plants or invertebrates have so far failed [1]. The apparent pH-optima of the betaine-homocysteine-methyltransferases of all the vertebrate livers tested occur between 7.0 and 7.8. These transferases are strongly inhibited by dimethylglycine, which besides methionine is a product of the enzymic reaction [1,2]. Choline can not replace betaine as the methyl donor with purified enzyme preparations nor does choline act as an inhibitor of the transferases.

In order to study the characteristics of this type of methyl group transfer in more detail, a procedure for the purification of the betaine-homocysteine-methyl-transferase of pig liver was worked out. It comprises the following steps:

1. One part of fresh pig liver is homogenized in three parts of water in a Waring blender. The pH of the homogenate is adjusted to 5.1 at 0°C and the thick "brei" obtained immediately centrifuged at 44 000 $\times$ g for 30 min.

2. The supernatant fluid is adjusted to a pH-value of 7.7 and poured into a series of test tubes which are then placed in a water bath at 80°C for 90 sec. An inactive precipitate is formed and is removed by centrifuging at 44 000 $\times$ g for 30 min.

3. The enzyme which is contained in the supernatant fluid from step 2, is adsorbed on calcium phosphate gel prepared according to Keilin and Hartree [3]. The enzyme is eluted from the gel by means of 0.15 M orthophosphate and 0.1 M pyrophosphate.

4. The eluates from step 3 are pooled and the pH adjusted to 7.2. Acetone is added to a final concentration of 50 %. The precipitate that forms is collected by centrifuging at 5 000 $\times$ g for 10 min, dissolved in water and dialysed against water at pH 8.5.

5. The pH of the dialysed enzyme preparation is adjusted to 7.50 and acetone is added to a concentration of 50 %. The precipitate is collected by centrifuging at 20 000 × *g* for 10 min and dissolved in 0.005 M phosphate buffer. The pH is adjusted to 6.5 and the solution centrifuged at 20 000 × *g* for 2 min. The supernatant fluid contains the enzyme. The enzyme preparation thus obtained is coloured and has a specific activity approximately 100 times that of the homogenate. The overall yield is of the order of 35 %.

Further purification has been attempted in many different ways. Preparative electrophoresis at pH 9.2 in a density gradient [4] separates the coloured material present in the step 5-preparation from the transferase. Experiments of this type suggest that 60—70 % of the total protein content of the step 5-preparation constitutes an enzyme which is electrophoretically homogeneous at alkaline pH-values. This enzyme can use dimethylpropiothetin as the methyl donor in place of betaine.

Colourless enzyme preparations with a high specific activity have also been obtained using ion-exchange chromatography on triethylaminoethyl cellulose according to Porath [5]. This purification method has also failed to separate betaine-homocysteine-methyl-transferase from material having "thetin homocysteine methylpherase" [6] activity.

Fractionation of the enzyme preparation from step 5 with ethanol has occasionally resulted in crystalline material with a specific activity of about 150 times that of the liver homogenate. Dimethylpropiothetin can replace betaine as the methyl donor both with the crystalline and all other active ethanol fractions obtained. The ratio between the amount of methionine formed with propiothetin and the amount formed with betaine is approximatively ten for these fractions.

If a solution of purified betaine-homocysteine-methyl-transferase is kept at 80°C its ability to transfer methyl groups from betaine is lost at the same rate as its ability to transfer methyl groups from dimethylpropiothetin. — Dimethylglycine, which interferes with the utilization of betaine as the methyl donor also inhibits the methyl transfer from porpiothetin.

A number of compounds were synthesized [7] and tested for their ability to replace betaine as the methyl donor. It was found that the methyl donor specificity of betaine-homocysteine-methyl-transferase is by no means absolute. Not only dimethylpropiothetin and dimethylacetothetin but also carboxymethyl-dimethylethyl-ammonium chloride, carboxymethyl-diethylmethyl-ammonium chloride, 1-carboxyethyl-trimethyl-ammonium chloride and the methyl ester of betaine can more or less efficiently replace betaine as the methyl donor at pH 7.8 in phosphate buffer. However, the enzyme does not seem to be able to transfer ethyl groups.

An interesting property of the purified enzyme is that it is stimulated by some commonly occurring metabolites and inhibited by others. This phenomenon will only be exemplified here with a few remarks on the stimulation by oxalate. An approximately 10 % increase in the activity of the enzyme, as measured by the amount of methionine formed per hour can be obtained with potassium oxalate concentrations of 0.1 mM. The stimulation increases with increasing oxalate concentrations up to about 10 mM. The activity of the stimulated enzyme is then approximately 50 % above that of the control. At still higher concentrations of oxalate the stimulation decreases. Stimulation of the enzyme activity by oxalate is more marked at saturation than at subsaturation levels of either of the substrates. The enzymic formation of methionine is increased by the addition of oxalate also when dimethylpropiothetin serves as the donor of the methyl group.

A full account of the work reported here will be published shortly.

The financial support of the *Swedish Medical Research Council* is gratefully acknowledged.

1. Ericson, L.-E. *IV. International Congress of Biochemistry*, Vienna (1958), *Abstracts of Communications, 4-58*, p. 45.
2. Muntz, J. A. *J. Biol. Chem.* **182** (1950) 489.
3. Colowick, S. P. in Colowick, S. P. and Kaplan, N. O. *Methods in Enzymology* **1** (1955) 90—98. Academic Press Inc., Publishers, New York.
4. Svensson, H., Hagdahl, L. and Lerner, K.-D. *Science Tools* **4** (1957) 1.
5. Porath, J. *Arkiv Kemi* **11** (1957) 97.
6. Durell, J., Anderson, D. G. and Cantoni, G. L. *Biochem. et Biophys. Acta* **25** (1957) 270.
7. Walde, N. Division of Organic Chemistry, Royal Institute of Technology, Stockholm, kindly prepared most of the compounds tested.

Received September 1, 1958.

A Shadow Schlieren Method for the Study of Diffusion Boundary Layers at Electrodes

GOSTA WRANGLÉN

Division of Applied Electrochemistry, Royal Institute of Technology, Stockholm 70, Sweden

The Schlieren method described below corresponds to the method developed by Schmidt [1] for the study of temperature boundary layers. It so far seems to have been seldom used for the investigation of concentration boundary layers [2]. Like all Schlieren methods, it is based on the fact that light rays passing through a medium with a continuously changing refractive index are deviated into the optically denser parts of the medium. Since in this case the image is formed by the projection of a shadow without the use of lenses the designation "shadow Schlieren method" seems appropriate [3].

A microscope lamp (Fig. 1) with a small spiral (2 × 2 mm) acts as a point source of light. It is placed at the focus of a condensor lens with a small focal length. This lens gives a beam of approximately parallel light. A high degree of parallelity is achieved by placing two slits at a large distance from each other in the light path. The slits 1 and 2 are 2—3 mm wide and the distance between them is 10 m which means that the deviation from parallelity can be neglected. For qualitative purposes, as in lecture experiments, the distance between the slits can be reduced to about 1 m. The electrolysis cell, consisting of planoparallel plates of optical glass, is placed behind slit 2 in the light path. The light beam passes along and parallel to a copper plate, 1 mm thick, occupying the whole cross section of the cell. A shadow image is obtained on a screen or photographic plate. When no current is flowing, a photograph like the one in Fig. 2 a is obtained.

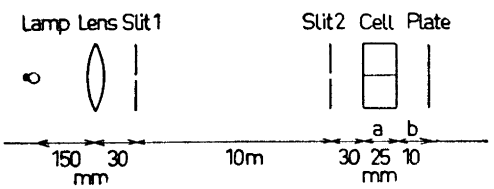

Fig. 1. Optical arrangement for the study of electrode films, viewed from above.

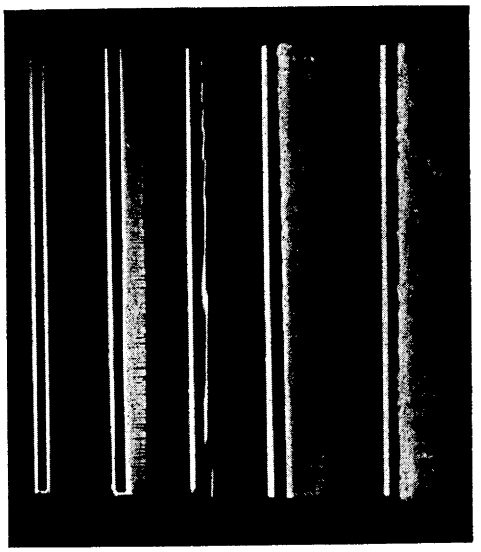

a b c d e

Fig. 2. a) Current shut off b) Cathode with 2 A/dm² on right side c) Anode with 2 A/dm² on right side d) Transition from laminar to turbulent flow at 1.5 A/dm² e) Fully developed turbulence at 4 A/dm². With a), b) and c) slit 2 was 2 mm wide and a = 25 mm, b = 7 mm. With d) and e) slit 2 was 3 mm wide and a = 45 mm, b = 10 mm. In exps. d) and e), the total cathode height was 180 mm, but only the height between 80 and 140 mm from the lower end of the cathode was photographed.

Upon electrolysing, the concentration gradients produced will manifest themselves on the image. In all the cases shown in the photographs here, the electrolyte consisted of 1 M $CuSO_4$ and the temperature was 20°C. If a cathodic current is applied on one side of the copper plate, the photograph in Fig. 2 b is obtained. In the cathode diffusion layer (cathode film), the concentration and refractive index are lower than those in the bulk solution. The light beam is therefore deviated away from the electrode. The deviation is proportional to the refractive index gradient. Since the gradient is greatest close to the cathode surface, the light

rays that enter the solution near the cathode surface will undergo the greatest deviation. The width of the bright band is, therefore, a measure of the concentration gradient on the cathode surface. The deviation may be expected to be proportional to the current density and to the width of the electrode, *i.e.* the length of the light path within the cell. However, this seems to be valid only up to a certain c.d. and electrode width, above which the deviation is constant. This is probably due to the fact that the cathode film is so thin (about 0.5 mm) that the light ray soon enters the bulk solution in which its path is rectilinear. Besides the bright band, a broadening of the cathode shadow is observed, obviously because the light is deviated out of the cathode film. The thickness of this film can therefore be estimated. In the upper part of Fig. 2 b, it seems to be about 0.4 mm.

For photographic purposes, the distance b between the cell and the plate should not be greater than 10 mm, otherwise the shadow image of the cathode will not be sharp. For accuracy in measurement however, this distance should preferably be increased to 100 mm which gives a corresponding increase in the displacement on the screen.

The shadow Schlieren method is less valuable for the investigation of the anode film. The light passing through the boundary layer will be deviated towards and deflected by the electrode. This will result in a broadening of the electrode shadow. There is, however, also an opposing effect, which results in a narrowing of the shadow, due to the light passing close to the rear edge of the electrode. Both these effects seem to appear in Fig. 2 c.

The free convective flow [4] caused by the difference in gravity between the electrode film and the bulk solution is also revealed by the method described, particularly at the cathode. In the case corresponding to Fig. 2 b, horizontal dark lines can be seen in the bright band adjacent to the cathode shadow. These lines move upwards with an increasing speed which seems to correspond to the vertically accelerated laminar flow in the cathode film. Since the velocity of this flow increases with the current density and with the electrode height, the flow will turn turbulent if these variables are increased. The transition from laminar to turbulent flow at a certain distance from the lower edge of the cathode is shown in Fig. 2 d. The diffuse bright band at the upper part of the cathode in Fig. 2 d appears to the naked eye much like the flickering of a flame, obviously due to the formation of eddies. Finally, Fig. 2 e shows fully developed turbulence due to a higher c.d.

While useful information is obtained by this simple method without lenses, it would be of interest to analyse the whole concentration profile in the boundary layer. According to Lamm [5], this could be done by the addition of lenses to the apparatus so as to correspond to Lamm's slit method [6]. The investigation will be continued.

Thanks are due to Civ.ing. Stig Ljunggren for valuable discussions.

1. Schmidt, E. *Forsch. Gebiete Ingenieurw.* **3** (1932) 181.
2. Ibl, N. *CITCE, Proc. 7th Meeting* (1955) 112.
3. Wolter, H. *Handbuch der Physik*, Springer-Verlag 1956, Vol. **24**, p. 565.
4. Wranglén, G. *Acta Chem. Scand.* **12** (1958) 1143.
5. Lamm, O. *Personal communication.*
6. Jost, W. *Diffusion*, New York 1952, p. 452.

Received August 27, 1958.

Isotope Effect in the Decomposition of Grignard Compounds by Ordinary Phenol and a Sterically Hindered Phenol

LARS OLOF ASSARSSON

Nobel Institute of Chemistry, Stockholm 50, Sweden

Measurements of the hydrogen isotope effect in the hydrolysis and methanolysis of a number of Grignard compounds in different solvents and under different conditions have been reported in earlier papers [1-4]. Decomposition of Grignard compounds by tritiated phenols has now been carried out. In a series of experiments methylmagnesium iodide and *sec*-butylmagnesium bromide have been decomposed by ordinary phenol, C_6H_5OH, in which tritium has been partially introduced into the hydroxylic position. In another series of experiments the same Grignard compounds have been decomposed by a phenol with steric hindrance, 2,6-di-*tert*-butyl-4-methyl-phenol (called "lonol"), in which tritium has also been partially introduced into the hydroxylic group.

As it seems possible that the reaction mechanism should include a coordination of the hydroxylic compound to the magnesium atom in the Grignard compound (analogous to the coordination of ethers to Grignard compounds), the idea with the present experiments has been to investigate the effect of steric hindrance on this coordination. It is known from v. Braun and Kirschbaum [5] that steric hindrance can render some Grignard reactions impossible. These investigators state that the Grignard compound of [β-chloroethyl] methyl-aniline does not react with ketones though very well with aldehydes. On the other hand a Grignard compound of [γ-halogenopropyl]-methyl-aniline reacts with ketones as well as with aldehydes.

From its reactions it is obvious that 2,6-di-*tert*-butyl-4-methyl-phenol with its branched alkyl groups in the positions *ortho* to the hydroxylic group will offer strong steric hindrance to reactions concerning the latter. For example the compound is not soluble in aqueous sodium hydroxide or potassium hydroxide and it does not give the colour with ferric chloride solution characteristic of phenols [6]. Esterification is also retarded [6]. On the other hand it reacts with Zerewitinoff reagent (methylmagnesium iodide) in the usual manner with formation of methane [6].

The isotope effect in the decompositions by ordinary phenol, given in Table 1, is of the same order of magnitude as those obtained in the hydrolysis and methanolysis.

The isotope effect in the corresponding reactions with lonol, as shown in Table 2, deviates considerably from those obtained with ordinary phenol, methanol and water, but they are not of the same order of magnitude as a "full" hydrogen isotope effect.

The rather large values of k_T/k_H, obtained in the decompositions by phenol, methanol and water, could be explained by a reaction mechanism consisting of a slow coordination of the hydroxylic compound to the Grignard compound followed by a rapid proton transfer with formation of a hydrocarbon (*cf.* Wiberg [7]).

Lonol, on the other hand, could be expected not to be able to be coordinated to the Grignard compounds for steric reasons. If, nevertheless, the coordination takes place, it must be slower than the coordination of ordinary phenol and must consequently give larger ratios k_T/k_H than in the case of ordinary phenol. Actually the experiments give smaller ratios in the case of the phenol with steric hindrance. Therefore the mechanism discussed above can be eliminated, at least for the hindered reaction.

The fact that the reactions with the sterically hindered phenol take place at all (giving about the same ratio k_T/k_H with methylmagnesium iodide and with *sec*-butylmagnesium bromide) indicates, that they are at least partly of dissociative nature. Conseqently the phenol must dissociate off its hydroxylic proton, which in some way later reacts with the Grignard compound or with an alkyl carbanion derived from the Grignard compound with formation of the corresponding hydrocarbon. This seems to be in accordance with one of the mechanisms mentioned by Wiberg [7], who, however, obtained ratios k_D/k_H larger than unity in his methanolysis experiments. If the cleavage of the hydroxylic oxygen-hydrogen bond is supposed to be partly rate determining, it seems natural that the isotope effect should be more pronounced in the case of the hindered phenol than in the ordinary one, since the cleavage is likely to be slower

Table 1. Decomposition of Grignard compounds with phenol-t in *n*-butyl ether at 20°C.

Grignard compound	k_T/k_H	Number of parallel determinations of tritium in combustion water	Mean value (including error in determination of tritium in combustion water from the phenol)
Methyl-Mg iodide	0.757	2	0.78 ± 0.06
	0.814	1	
	0.734	1	
	0.810	2	
Sec-butyl-Mg bromide	0.738	1	0.79 ± 0.06
	0.822	1	
	0.795	1	

and hence more strongly rate-determining in the case of the former.

The Grignard reagents used in the experiments were solutions of the appropriate Grignard compounds in *n*-butyl ether. In the case of *sec*-butylmagnesium bromide part of the solvent plus the "false" butane was distilled off under reduced pressure immediately prior to every decomposition with the phenols[4]. The *n*-butyl ether used as solvent was dried by refluxing over and distillation from metallic sodium. The tritiated phenols were prepared by addition of tritiated water to a solution of the appropriate phenol in an organic solvent. In the case of phenol-t the tritiated water, ethyl ether and ordinary phenol were mixed after which the tritiated phenol was isolated by distilling under reduced pressure. Lonol-t was prepared in an analogous manner with the difference that a mixture of ethyl ether and ethanol was used as solvent, because the tritiated water used in this case had a smaller specific activity than that used in the phenol-t preparation, for which reason a larger amount of water must be used and consequently also a solvent being able to dissolve more water. The lonol-t was isolated by distilling off the solvent and water in vacuum.

As it is known that an exchange between hydrogen in the hydroxylic group and hydrogen in the benzene ring occurs with phenols,

Table 2. Decomposition of Grignard compounds with lonol-t in *n*-butyl ether at 20°C.

Grignard compound	k_T/k_H	Number of parallel determinations of tritium in combustion water	Mean value (including error in determination of tritium in combustion water from the lonol)
Methyl-Mg iodide	0.307	1	0.29 ± 0.03
	0.299	1	
	0.274	1	
Sec.-butyl-Mg bromide	0.306	1	0.33 ± 0.04
	0.322	1	
	0.347	1	

especially at higher temperatures [8], it was necessary to investigate whether and to what extent such an exchange had taken place in the preparations of phenol-t and lonol-t. The possible transition of tritium from the hydroxylic group to the benzene ring should of course give too small tritium activities in the hydrocarbons evolved with the Grignard compounds.

The check of this exchange proceeded in the same manner as described by Kukhtenko [9]. Tritium in the hydroxylic group of the ordinary phenol was washed off by dissolving the phenol in a large volume of 2 % aqueous sodium hydroxide. The phenolate solution was acidified and the phenol was extracted by benzene. The extract was dried with anhydrous calcium chloride and distilled for isolation of phenol free from tritium in the hydroxylic group. In the case of lonol-t, which is not soluble in sodium hydroxide, the method was modified. The tritiated lonol was dissolved in 96 % ethanol, after which ordinary water was added in portions while shaking the mixture until lonol began to precipitate. The precipitated crystals were carefully washed with much water and dried.

The phenols free from hydroxylic tritium were burned over cupric oxide like the initial tritiated phenols, and the radioactivity of the combustion water after reduction to hydrogen was determined by means of a Geiger-Müller counter. The activities thus obtained indicate that the tritiated phenols are practically free from tritium in the benzene rings.

The technique of the Grignard decompositions was the same as the one used earlier, *i. e.* the Grignard reagent in *n*-butyl ether solution was added by means of an injection syringe to a solution of the phenol in the same solvent. The phenols were present in excess over the Grignard compounds.

The tritiated phenols and the hydrocarbons formed in the decompositions were burned over cupric oxide and the radioactivity of the combustion water was determined (after reduction to hydrogen) in the same manner as in the case of the detritiated phenols.

The ratios k_T/k_H in the tables have not been corrected for the change in the isotopic composition of the phenols taking place during the reaction.

1. Assarsson, L. O. *Acta Chem. Scand.* **9** (1955) 1399.
2. Assarsson, L. O. *Acta Chem. Scand.* **10** (1956) 1509.
3. Assarsson, L. O. *Acta Chem. Scand.* **11** (1957) 1283.
4. Assarsson, L. O. *Acta Chem. Scand.* **12** (1958) 1547.
5. v. Braun, J. and Kirschbaum, G. *Chem. Ber.* **52** (1919) 1725.
6. Stillson, G. H., Sawyer, D. W. and Hunt, C. K. *J. Am. Chem. Soc.* **67** (1945) 303.
7. Wiberg, K. B. *J. Am. Chem. Soc.* **77** (1955) 5987.
8. Ingold, C. K., Raisin, C. G. and Wilson, C. L. *J. Chem. Soc.* **1936** 1637.
9. Kukhtenko, I. I. *Doklady Akad. Nauk. SSSR* **93** (1953) 487.

Received September 12, 1958.

Isotope Effect in the Methanolysis of *n*-Butylmagnesium Bromide. A Reinvestigation

LARS OLOF ASSARSSON

Nobel Institute of Chemistry, Stockholm 50, Sweden

In a previous preliminary paper [1] measurements of the hydrogen isotope effect in the methanolysis of *n*-butylmagnesium bromide have been reported. The ratios k_T/k_H obtained in those experiments diverge considerably, the ratio obtained with the freshly prepared Grignard reagent being larger than those obtained with an

Table 1. Results in the decomposition of *n*-butylmagnesium bromide with methanol in *n*-butyl ether at 20°C.

k_T/k_H	Number of parallel determinations of tritium in combustion water	Mean value (including error in determination of tritium in combustion water from the methanol)
1.014	1	
1.002	1	1.00 ± 0.03
1.006	2	
0.978	1	

especially at higher temperatures [8], it was necessary to investigate whether and to what extent such an exchange had taken place in the preparations of phenol-t and lonol-t. The possible transition of tritium from the hydroxylic group to the benzene ring should of course give too small tritium activities in the hydrocarbons evolved with the Grignard compounds.

The check of this exchange proceeded in the same manner as described by Kukhtenko [9]. Tritium in the hydroxylic group of the ordinary phenol was washed off by dissolving the phenol in a large volume of 2 % aqueous sodium hydroxide. The phenolate solution was acidified and the phenol was extracted by benzene. The extract was dried with anhydrous calcium chloride and distilled for isolation of phenol free from tritium in the hydroxylic group. In the case of lonol-t, which is not soluble in sodium hydroxide, the method was modified. The tritiated lonol was dissolved in 96 % ethanol, after which ordinary water was added in portions while shaking the mixture until lonol began to precipitate. The precipitated crystals were carefully washed with much water and dried.

The phenols free from hydroxylic tritium were burned over cupric oxide like the initial tritiated phenols, and the radioactivity of the combustion water after reduction to hydrogen was determined by means of a Geiger-Müller counter. The activities thus obtained indicate that the tritiated phenols are practically free from tritium in the benzene rings.

The technique of the Grignard decompositions was the same as the one used earlier, *i. e.* the Grignard reagent in *n*-butyl ether solution was added by means of an injection syringe to a solution of the phenol in the same solvent. The phenols were present in excess over the Grignard compounds.

The tritiated phenols and the hydrocarbons formed in the decompositions were burned over cupric oxide and the radioactivity of the combustion water was determined (after reduction to hydrogen) in the same manner as in the case of the detritiated phenols.

The ratios k_T/k_H in the tables have not been corrected for the change in the isotopic composition of the phenols taking place during the reaction.

1. Assarsson, L. O. *Acta Chem. Scand.* **9** (1955) 1399.
2. Assarsson, L. O. *Acta Chem. Scand.* **10** (1956) 1509.
3. Assarsson, L. O. *Acta Chem. Scand.* **11** (1957) 1283.
4. Assarsson, L. O. *Acta Chem. Scand.* **12** (1958) 1547.
5. v. Braun, J. and Kirschbaum, G. *Chem. Ber.* **52** (1919) 1725.
6. Stillson, G. H., Sawyer, D. W. and Hunt, C. K. *J. Am. Chem. Soc.* **67** (1945) 303.
7. Wiberg, K. B. *J. Am. Chem. Soc.* **77** (1955) 5987.
8. Ingold, C. K., Raisin, C. G. and Wilson, C. L. *J. Chem. Soc.* **1936** 1637.
9. Kukhtenko, I. I. *Doklady Akad. Nauk. SSSR* **93** (1953) 487.

Received September 12, 1958.

Isotope Effect in the Methanolysis of *n*-Butylmagnesium Bromide. A Reinvestigation

LARS OLOF ASSARSSON

Nobel Institute of Chemistry, Stockholm 50, Sweden

In a previous preliminary paper [1] measurements of the hydrogen isotope effect in the methanolysis of *n*-butylmagnesium bromide have been reported. The ratios k_T/k_H obtained in those experiments diverge considerably, the ratio obtained with the freshly prepared Grignard reagent being larger than those obtained with an

Table 1. Results in the decomposition of *n*-butylmagnesium bromide with methanol in *n*-butyl ether at 20°C.

k_T/k_H	Number of parallel determinations of tritium in combustion water	Mean value (including error in determination of tritium in combustion water from the methanol)
1.014	1	
1.002	1	1.00 ± 0.03
1.006	2	
0.978	1	

older reagent. This fact was supposed to be due to small amounts of moisture gradually entering the flask containing the Grignard reagent and forming inactive butane. This "false" butane, staying dissolved in the solvent, possibly might also be supposed to be formed by other reactions of the Grignard reagent.

In order to eliminate the "false" butane, part of the solvent *n*-butyl ether was distilled off in vacuum immediately prior to every methanolysis. Owing to the high volatility of butane, its absence then seems warranted. The ratios k_T/k_H obtained in the present experiments show very good reproducibility.

As k_T/k_H is equal to unity the isotopic composition of the methanol does not change during the reaction and hence no correction of the ratio is necessary.

It is interesting to note that the inverse isotope effect obtained by Wiberg [2] has not been confirmed by the present experiments, using tritium instead of deuterium.

1. Assarsson, L. O. *Acta Chem. Scand.* **11** (1957) 1283.
2. Wiberg, K. B. *J. Am. Chem. Soc.* **77** (1955) 5987.

Received September 12, 1958.

ACTA CHEMICA SCANDINAVICA 12 (1958) 1549—1553

The Acid-soluble Nucleotides of *Polyporus squamosus* and *Amanita muscaria*

ROLF BERGKVIST

Institute of Biochemistry, University of Lund, Sweden

The acid-soluble nucleotides of *Polyporus squamosus* and *Amanita muscaria* have been isolated and fractionated by ion exchange chromatography. These substances have been identified by ultraviolet absorption measurements, their chromatographic and ionophoretic behaviour both before and after hydrolysis, and by chemical and enzymic analyses.

In a previous publication from this laboratory [1] a method has been presented for the isolation and analysis of the acid-soluble nucleotides from plant tissues. Methods have also been described for the separation and quantitative analysis of varying amounts of nucleotides using paper chromatography and ionophoresis [2–4], and their application to the nucleotides in wheat, oats and barley [1,5]. It is the purpose of the present paper to extend the previous work on this subject to include the analysis of the acid-soluble nucleotides of two different mushrooms.

The acid-soluble nucleotides were isolated from *P. squamosus* and *A. muscaria* by homogenizing the fruiting bodies in cold perchloric acid. The nucleotides were then freed from interfering substances according to the procedure already described [1]. The separation and quantitative analysis of the nucleotide mixtures were accomplished by ion exchange chromatography on a Dowex 1 column (formate form) as described in the preceding papers. The elution of the nucleotides was followed by the changes in optical densities of the eluate. Figs. 1 and 2 show the effluent curves that were obtained. Since the nucleotide content of both mushrooms were quite similar, the analysis of the two materials are described together.

The eluate fractions from the Dowex column falling under the same peaks were pooled and concentrated by adsorption on charcoal and subsequently eluted with ethanol-ammonia. The isolated nucleotides were identified by their chromatographic and ionophoretic behaviour, both before and after hydrolysis, as compared with authentic nucleotides. The purified samples were then further characterized by the following criteria: (a) ultraviolet ab-

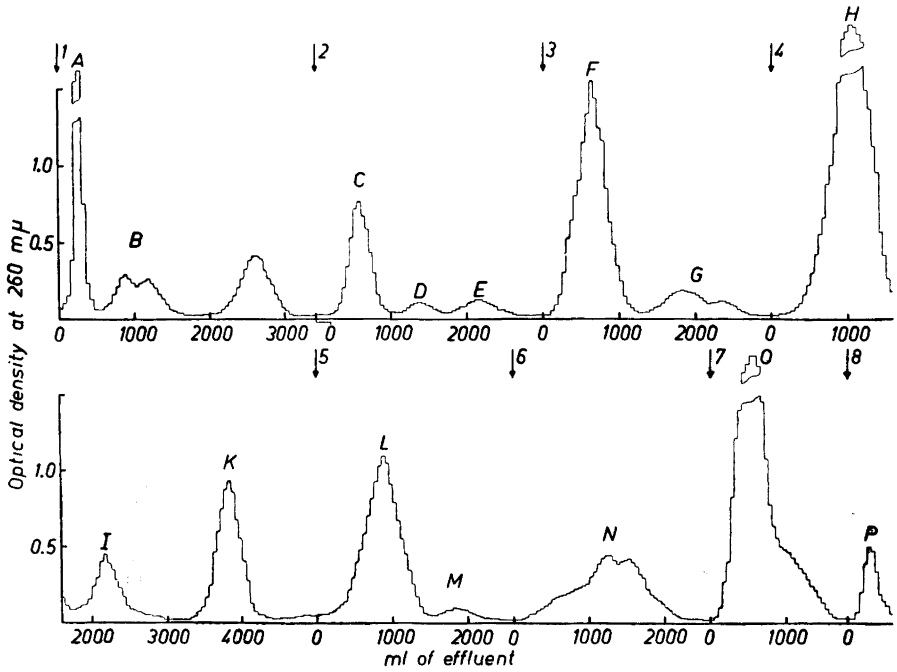

Fig. 1. Ion exchange chromatogram of acid-soluble nucleotides from 1 000 g of *P. squamosus*. The unmarked peaks contained no nucleotides. Exchanger: Dowex 1, X-10, 200 to 400 mesh, 2.4 × 70 cm, formate form; flow rate 2.0 ml/min.

Eluting agents:

1) 0.02 M formic acid
2) 0.1 M » »
3) 0.1 M » » + 0.05 M sodium formate
4) 0.1 M » » + 0.3 M » »
5) 0.1 M » » + 0.4 M » »
6) 0.1 M » » + 0.6 M » »
7) 0.2 M » » + 0.8 M » »
8) 0.5 M » » + 1.0 M » »

Identity of peaks:

A) Bases, uridine and DPN
B) 2′- and 3′-CMP
C) 5′-AMP
D) CMP-peptide
E) 2′-AMP
F) 5′-UMP
G) 2′- and 3′-UMP
2′- and 3′-GMP
TPN and CDP
H) UDPAG
I) UDPG
K) UDP
L) ADP
M) CTP
N) GDP, UTP and ATP derivative
O) ATP
P) GTP

sorption spectra in acid and alkali; (b) total and acid-labile phosphorus content; (c) sugar content; (d) paper chromatographic identification of the sugar components; and (e) ultraviolet absorption curves of the bases obtained after acid hydrolysis. The position of the phosphate groups was confirmed by the action of rattle snake venom and by oxidation with periodate.

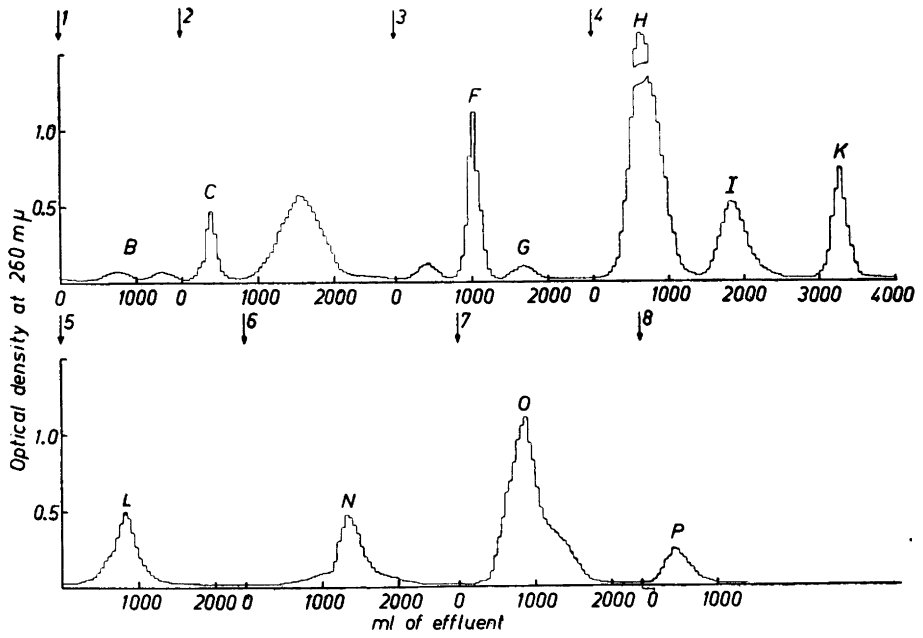

Fig. 2. Ion exchange chromatogram of acid-soluble nucleotides from 500 g of *A. muscaria*. The unmarked peaks contained no nucleotides. Exchanger: Dowex 1, X-10, 200 to 400 mesh, 1.6 × 50 cm, formate form; flow rate 1.5 ml/min. The eluting agents and identity of the peaks are the same as in Fig. 1.

The quantities of the nucleotides in the various column fractions were calculated by using the molecular extinction coefficients previously reported [1]. The results of the analysis are summarized in Table 1.

Peak A was obtained in the wash water or immediately after starting the elution with 0.02 M formic acid. This peak contained non-nucleotide material as the major component in addition to bases, uridine and DPN *.

Among the acid-soluble nucleotides of *P. squamosus*, a cytosine nucleotide is eluted from the resin after 5'-AMP. This compound has been identified as a cytidylic acid-peptide complex [6].

The different nucleotides were obtained as separate fractions with the exception of the peaks G and N. These fractions could be separated by either paper chromatography or ionophoresis. The separation could be made on a larger scale by applying the mixture to the paper as a streak instead of a spot, or by using continuous ionophoresis [5]. Fraction N from *P. squamosus* contained, in addition to the nucleotides, large amounts of a phosphorus-free sub-

* Abbreviations used: A, adenosine; G, guanosine; U, uridine; C, cytidine; MP, monophosphate; DP, diphosphate; TP, triphosphate; UDPG, uridine diphosphate glucose; UDPAG, uridine diphosphate acetylglucosamine; DPN, diphosphopyridine nucleotide; TPN, triphosphopyridine nucleotide.

Table 1. The nucleotide content of *Polyporus squamosus* and *Amanita muscaria*. Concentration in μmoles per 1 000 g fresh weight.

Compound	Identity	*P. squamosus*	*A. muscaria*
B	2′- and 3′-CMP	25.3	8.1
C	5′-AMP	17.3	6.2
D	CMP-peptide	6.8	
E	2′-AMP	4.5	
F	5′-UMP	68.3	42.0
G	2′- and 3′-UMP	10.5	5.0
G	2′- and 3′-GMP	1.5	0.5
G	TPN	0.8	1.0
G	CDP	2.6	2.0
H	UDPAG	187.0	212.5
I	UDPG	13.5	48.5
K	UDP	32.5	37.0
L	ADP	37.5	30.9
M	CTP	4.0	
N	GDP	7.6	4.2
N	ATP derivative	1.5	13.5
N	UTP	2.6	1.8
O	ATP	122.0	114.5
P	GTP	13.0	6.0
Adenosine 5′-phosphates		178.3	165.1
Uridine 5′-phosphates		303.9	341.8
Guanosine 5′-phosphates		20.6	10.2
Cytidine 5′-phosphates		6.6	2.0

stance with an absorption maximum at 262 mμ. Peak N, from both materials, contained GDP, UTP and an adenosine derivative. The latter compound had an absorption spectrum that was typical for adenosine, but behaved both chromatographically and ionophoretically differently from known adenosine derivatives. The base liberated on acid hydrolysis was adenine, as determined by paper chromatography and spectrophotometry. Three phosphate groups per molecule of adenosine were found, only one of which was acid-labile and could be hydrolyzed in 10 min with 1 N hydrochloric acid at 100°C. Two pentose residues per adenosine were found. No periodate was consumed when the substance was tested by the method of Dixon and Lipkin [7]. The amount of material was not sufficient for a more detailed study of the structure of this adenosine triphosphate.

The chromatography of the nucleotides from these plant materials produced several non-nucleotide peaks. From *A. muscaria* two peaks appeared before the 5′-AMP peak, and from *P. squamosus* a single peak occurred after the 5′-AMP peak.

In addition to the 15 to 18 different nucleotides identified from the acid-soluble nucleotide fraction of these fungi, there are indications of many other nucleotides present in such small concentration that their identifications were not possible.

EXPERIMENTAL

Isolation and separation of acid-soluble nucleotides. Only the fruiting bodies of the mushrooms occurring out of doors under natural field conditions were investigated. 1 000 g of fresh material were homogenized in 1 000 ml of ice cold 10 % perchloric acid in a Waring Blendor and after reextraction with 1 000 ml of 5 % perchloric acid the nucleotides were isolated and freed from disturbing substances according to the method previously reported [1].

Fractionation of the isolated nucleotide mixture was carried out by ion exchange chromatography using Dowex 1, X-10, 200 to 400 mesh, in the formate form. Details about these separations are seen from Figs. 1 and 2. The nucleotides were recovered from the pooled fractions by norite adsorption and elution with 50 % aqueous ethanol containing 0.5 % ammonia.

Analytical methods. The analysis of the different nucleotides has been made using the same methods as described earlier and the same solvent systems have been used for the paper chromatographic identifications [1,5].

The one-dimensional paper ionophoretic separations were carried out with an acetate buffer of ionic strength 0.1 and pH 4.15. For continuous separations the ionic strength was decreased to 0.033. The details of these methods and the apparatus used have been reported in preceding papers [2,3].

The nucleotides used as standard substances were obtained from Sigma Chemical Company or isolated in our laboratory.

This work has been supported by a grant from the *Swedish Natural Science Research Council.*

REFERENCES

1. Bergkvist, R. *Acta Chem. Scand.* **10** (1956) 1303.
2. Bergkvist, R. *Acta Chem. Scand.* **11** (1957) 1465.
3. Bergkvist, R. *Acta Chem. Scand.* **12** (1958) 752.
4. Bergkvist, R. *Acta Chem. Scand.* **12** (1958) 555.
5. Bergkvist, R. *Acta Chem. Scand.* **11** (1957) 1457.
6. Bergkvist, R. *Acta Chem. Scand.* **12** (1958) 364.
7. Dixon, J. S. and Lipkin, D. *Anal. Chem.* **26** (1954) 1092.

Received June 23, 1958.

ACTA CHEMICA SCANDINAVICA 12 (1958) 1554—1558

The Acid-soluble Nucleotides of Different Mushrooms

ROLF BERGKVIST

Institute of Biochemistry, University of Lund, Sweden

The acid-soluble nucleotides of eight different mushrooms have been separated and their concentrations determined by a combination of ionophoresis and chromatography on paper.

During the development of a scheme for the analysis of the acid-soluble nucleotides of plant materials, different methods have been developed for nucleotide separations. When large amounts of material are available, the use of ion exchange chromatography is most suitable for obtaining a complete resolution and a quantitative recovery of the various components of the nucleotide mixture [1]. Other less time-consuming methods have also been developed. Ionophoresis at pH 4.15 has been found to produce a sufficiently different separation from that obtained with paper chromatography for it to be used in combination with the latter. The nucleotides are fractionated into groups by paper chromatography and then completely separated by one-dimensional ionophoresis [2], or by continuous ionophoresis [3], depending on the quantities to be separated. Preliminary analyses of nucleotide mixtures were carried out by two-dimensional fractionation on a single sheet of filter paper using a combination of ionophoresis and chromatography [4]. This method is especially suitable when only small amounts of material are available, and these analyses can be completed in 24 h.

The latter method has been used for the analysis of the acid-soluble nucleotides of eight different species of mushrooms. The same types of apparatus which have been described earlier were used [4]. For the detailed description of the apparatus and the performance of the analyses the reader is referred to the preceding references.

An aliquot of a concentrated solution of the nucleotide mixture containing about 3 μmoles of nucleotides (calculated from the optical density at 260 mμ) was subjected to paper ionophoresis in a sodium acetate buffer of pH 4.15 and of ionic strength 0.1. The ionophoresis was carried out on a large sheet of Whatman No. 1 paper at 1 000 V for 10 h. The paper was dried at room temperature and then the separation in the second direction was achieved by paper chromatography. The previously described solvent system consisting

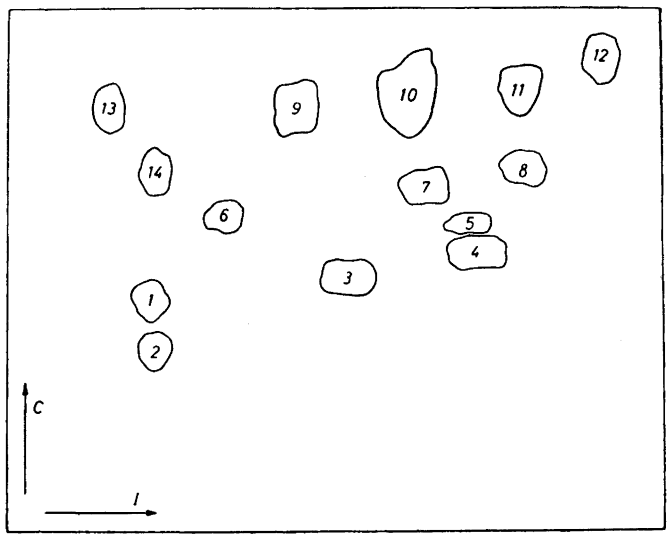

Fig. 1. Diagram of the locations of the nucleotides resolved by combined ionophoretic (I) and chromatographic (C) separations.

1) 5′-AMP
2) 2′-AMP
3) ADP
4) ATP
5) ATP derivative
6) GMP
7) GDP
8) GTP
9) UMP
10) UDPG and UDPAG
11) UDP
12) UTP
13) CMP
14) CMPX

of saturated ammonium sulphate solution-*n*-butanol-water (79:0.5:19) was used to get an almost complete separation of the different nucleotides. The various nucleotides were located on the paper photographically in ultraviolet light of 254 mμ, and prints were made with various exposure times to detect components of lower concentration. The spots were cut out from the paper and eluted with 0.1 N hydrochloric acid, and then the concentrations were calculated from the optical densities measured against the appropriate blanks. The uridine diphosphate derivatives, UDPG * and UDPAG, were obtained together as a single spot. To determine the concentrations of these two components an aliquot of the original nucleotide mixture was chromatographed in a solvent composed of 7.5 volumes of 95 % ethanol and 3 volumes of 1 M ammonium acetate of pH 7.5. This solvent separates these nucleotides from each other and from the main bulk of the nucleotide mixture.

To obtain a quantitative indication of the efficiency of this method, the acid-soluble nucleotides of *Polyporus squamosus* and of *Amanita muscaria* were analysed both by this method and by ion exchange chromatography.

* Abbreviations used: A, adenosine; G, guanosine; U, uridine; C, cytidine; MP, monophosphate; DP, diphosphate; TP, triphosphate; UDPG, uridine diphosphate glucose; UDPAG, uridine diphosphate acetylglucosamine; CMPX, cytidylic acid — peptide complex; TPN, triphosphopyridin nucleotide.

Table 1. Analysis of the acid-soluble nucleotides of *Polyporus squamosus* and *Amanita muscaria* by ion exchange chromatography (Ion ex.) and by combination of ionophoresis and paper chromatography (Combi.). Concentration in μmoles per 1 000 g fresh weight.

Compound	*P. squamosus*		*A. muscaria*	
	Ion ex.	Combi.	Ion ex.	Combi.
5′-AMP	17.3	17.0	6.2	6.5
2′-AMP	4.5	6.2		
ADP	37.5	37.9	30.9	30.8
ATP	122.0	122.0	114.5	113.0
ATP derivative	1.5		13.5	13.4
TPN	0.8		1.0	
2′- and 3′-GMP	1.5	2.0	0.5	
GDP	7.6	9.5	4.2	4.8
GTP	13.0	11.5	6.0	6.6
UMP	78.8	78.0	47.0	50.0
UDP	32.5	31.5	37.0	36.6
UTP	2.6		1.8	
UDPG and UDPAG	200.5	199.0	261.0	267.0
2′- and 3′-CMP	25.3	29.0	8.1	8.2
CDP	2.6		2.0	
CTP	4.0			
CMPX	6.8	5.2		

The separation and analysis of the nucleotides of these mushrooms by ion exchange chromatography are described in detail in the preceding paper [5]. Fig. 1 shows a map of the positions taken by the various nucleotides after a two-dimensional separation. The results of the analyses are summarized in Table 1.

The amount of each component that could be separated and detected on the filter paper was 0.01—0.50 μmoles. The great variations in the concentration of the different nucleotides in the mixture made the analyses more difficult. High recoveries were obtained for the substances present in high concentrations, while the recovery of nucleotides occurring in lower concentrations was less quantitative. The different monophosphates of the two pyrimidine nucleotides were isolated together, since they are not sufficiently separated by this method. The results of these analyses show that the method is useful for obtaining preliminary analyses of nucleotide mixtures. For more exact analyses of the components present in the lower concentrations, the other methods described must be used [1,2].

The acid-soluble nucleotides of eight different mushrooms were analysed with the method outlined above. The results of these analyses for the various

Table 2. Nucleotide content of eight species of mushroom. Concentration in μmoles per 1 000 g fresh weight.

Compound	*Polyporus squamosus*	*Amanita muscaria*	*Lycoperdon pratense*	*Hypholoma capnoides*	*Armillaria mellea*	*Pholiota squarrosa*	*Lactarius vellereus*	*Lactarius turpis*
5′AMP	17.0	6.5	10.5	13.0	3.0	3.5	11.8	8.3
2′-AMP	6.2							
ADP	37.9	30.8	50.2	76.7	27.3	86.3	54.8	15.5
ATP	122.0	113.0	113.5	105.5	138.5	115.0	158.0	95.0
ATP derivative		13.4						
TPN				6.5			1.9	6.7.
GMP	2.5		8.8					
GDP	9.5	4.8	15.5	19.5	4.0	8.6	10.9	
GTP	11.5	6.6	14.8	17.5	6.9	4.8	16.4	
UMP	78.0	50.0	72.0	54.7	22.5	48.4	43.7	26.5
UDP	31.5	36.6	46.0	62.9	48.5	11.3	31.6	6.2
UTP			11.0	5.0	14.5	4.2	15.4	2.0
UDPG + UDPAG	199.0	267.0	178.0	206.0	229.5	164.5	226.0	131.0
CMP	29.2	8.2	4.4	3.7				
CDP								
CTP				5.6			3.7	
CMPX	5.2							
UDPG	13.5	18.5	18.0	38.0	55.5	33.0	55.3	25.5
UDPAG	185.5	248.5	160.0	168.0	174.0	131.5	170.7	105.5
A derivatives	183.1	163.7	174.2	195.2	168.5	204.8	224.6	118.8
G derivatives	23.5	11.4	39.1	37.0	10.9	13.4	27.3	
U derivatives	308.5	353.6	307.0	328.6	315.0	228.4	316.7	165.7
C derivatives	34.4	8.2	4.4	9.3			3.7	

species are shown in Table 2. Since the uridine diphosphate sugar compounds were obtained as a single spot by the two-dimensional separation described above, they have been further separated by paper chromatography and the results of these analyses are also included in the same table.

There is a striking species variation of the relative nucleotide concentrations among the mushrooms. In all of the species studied the major nucleotide

components are the uridine and adenosine derivatives, as was also observed for wheat, oats and barley. In the mushrooms, however, UDPAG greatly predominates over UDPG while in the cereals UDPG is found in greater amounts than UDPAG.

EXPERIMENTAL

Isolation of acid-soluble nucleotides. The fruiting bodies of the mushrooms occurring out of doors under natural field conditions were investigated. 1 000 g of fresh material were homogenized in 1 000 ml of ice cold 10 % perchloric acid in a Waring Blendor and after reextraction with 1 000 ml of 5 % perchloric acid, the nucleotides were isolated and freed from disturbing substances according to the method previously reported [1].

The nucleotides were readsorbed on norite in order to free them from interfering salts and were eluted by repeated shaking with small volumes of 50 % aqueous ethanol containing 0.5 % ammonia. The combined eluents were neutralized and the volumes reduced to a small volume by blowing air through them.

Analytical methods. The nucleotides were analysed using the apparatus previously described [2,4]. The separations were carried out on Whatman No. 1 paper purified by washing with 1 N hydrochloric acid and water. The mixture to be separated was applied as a line to the dry paper and then the paper was impregnated with sodium acetate buffer of pH 4.15 and of ionic strength 0.1. After an ionophoretic separation at 1 000 V for 10 h, the paper was unfolded and dried at room temperature. The chromatographic separation was made after cutting away the extraneous parts of the paper sheet. Complete separation was obtained in 10 h by descending chromatography with the above mentioned solvent. Spectrophotometric determinations of the different substances were made with a Beckman DU spectrophotometer adapted for use with a volume of 0.6 ml in silica cells with a 10 mm light path.

This work has been supported by a grant from the *Swedish Natural Science Research Council.*

REFERENCES

1. Bergkvist, R. *Acta Chem. Scand.* **10** (1956) 1303.
2. Bergkvist, R. *Acta Chem. Scand.* **11** (1957) 1465.
3. Bergkvist, R. *Acta Chem. Scand.* **12** (1958) 555.
4. Bergkvist, R. *Acta Chem. Scand.* **12** (1958) 752.
5. Bergkvist, R. *Acta Chem. Scand.* **12** (1958) 1549.

Received June 23, 1958.

ACTA CHEMICA SCANDINAVICA 12 (1958) 1559—1563

On the Glycogen in *Escherichia coli B*; Variations in Molecular Weight during Growth. II

T. HOLME, T. LAURENT and H. PALMSTIERNA

Bacteriological Department and Chemical Department I, Karolinska Institutet, Stockholm, Sweden

Previous investigations have shown that the molecular weight of glycogen from *E. coli B* changes during growth. The glycogen has now been fractionated in different molecular weight fractions. It was found that the glycogen consisted mainly of two fractions, one of high molecular weight, $40-90 \times 10^6$, and one of low molecular weight, $<2 \times 10^6$. The high molecular weight fraction is more active in metabolism than is the low molecular one. The changes in the overall molecular weight observed during growth are mainly attributable to changes in this fraction.

In earlier experiments the synthesis and breakdown of the glycogen in cells of *Escherichia coli B* has been investigated [1-3]. Isotopic techniques have been employed in some of these experiments [2]. By the use of these techniques it has been shown that the glycogen was not homogeneous with respect to its metabolic activity. In later experiments variations in the molecular weight of the glycogen were shown to be correlated to the physiological state of the bacterial cells [3].

This paper reports the additional information obtained by the application of isotopic techniques to the study of the metabolic activity of the different molecular weight fractions obtained by ultracentrifugal fractionation of the glycogen.

METHODS

Bacteriological methods. A medium with glucose as the carbon source and ammonium chloride as the sole nitrogen source was used [4] with appropriate modifications for one-factor-starvation [1]. In the nitrogen-deficient media the ammonium chloride concentration was 200 mg/l giving a population density of approximately 380 mg of dry cells per litre of culture upon exhaustion of the nitrogen source.

The cells were cultivated as described earlier [1] in a nitrogen-deficient medium and allowed to enter the "starvation phase" at which time isotopic carbon was added (uniformly labelled ^{14}C-glucose). After this addition, the cells were allowed to metabolize for 45 min. The culture was then rapidly cooled and the cells quantitatively recovered by

Table 1. Isotopic incorporation and molecular weight of glycogen isolated from cells of *E. coli B* during different conditions of growth. For an explanation of the symbols, see the text.

	Glycogen, per cent of dry weight of bacteria	Counts per min per μg glycogen-glucose	Weight average molecular weight of soluble glycogen
Experiment E			
I	9.9	—	24×10^6
II	13.7	129	50×10^6
III	11.4	36	44×10^6
Experiment F			
I	9.2	—	40×10^6
II	10.2	133	51×10^6
III	7.2	27	42×10^6

centrifugation. The cells were resuspended in a carbon-free medium, which contained the nitrogen source in excess. After 90 min additional incubation, the cells were spun down. Three samples were taken for analysis; one immediately before the addition of the isotopic carbon (I), the second 45 min after this addition (II), and the third 90 min after the resuspension in the carbon-free, nitrogen-containing medium (III). The dry weight of the cells per litre of culture and their nitrogen and glycogen in per cent of the dry weight was determined.

Chemical methods. The glycogen was isolated as previously described [3]. Light-scattering was used for the molecular weight determinations [3].

Before the molecular weight was determined, the glycogen was fractionated in five fractions by means of centrifugation. The first fraction was obtained as a precipitate after centrifugation in a common laboratory centrifuge at about 2 000 r.p.m. This fraction was insoluble in water and accounted for 10—20 % of the total glycogen. It contained silicate impurities and therefore no estimation of the molecular weight could be made. Three fractions were obtained as precipitates after ultracentrifugation in a Spinco preparative ultracentrifuge at 20 000, 40 000 and 105 000 × *g*. The fifth fraction was the supernatant remaining after these centrifugations.

For the measurements of radioactivity, the samples were spread on aluminium planchets and counted at infinite thinness in a windowless gas flow counter, flushed with a helium-*iso*butane mixture. Since the layer of material did not exceed 0.05 mg per cm^2 no correction was made for self-absorption.

A modification of Dische's carbazol method was used for the quantitative determinations of glucose [5].

RESULTS

The results reported in earlier communications have been confirmed [2, 3]. During a phase in which *E. coli B* cells accumulated glycogen, the molecular weight of the glycogen increased. During a subsequent utilization of the accumulated glycogen, the molecular weight decreased (Table 1).

The results of the fractionation experiments are given in Table 2. On account of the different centrifugation times the experiments E and F are not strictly comparable. In both cases, however, the soluble glycogen was divided into four fractions of quite distinct molecular weight. About 50 % of the soluble glycogen has a very high molecular weight, 40—90 × 10^6. Between 25—40 % was found in the low molecular weight, "supernatant fraction" ($< 2 \times 10^6$). The fractions between these extremes contained a

Table 2. Distribution of glycogen in different molecular weight fractions and the specific activity of these fractions. In experiment E the time of each centrifugation was 60 min, while in experiment F the time of centrifugation was 20 min.

Sample	Fraction	Per cent of total soluble glycogen	Counts per min per μg glycogen-glucose	Molecular weight × 10^{-6}
Experiment E				
I	Insoluble	—	—	—
	Precipitated at			
	20 000 *g*	50.5	—	40
	40 000 *g*	17.2	—	20
	105 000 *g*	5.3	—	8
	Supernatant	27.0	—	< 1.5
II	Insoluble	—	140	—
	Precipitated at			
	20 000 *g*	57.8	106	83
	40 000 *g*	2.3	102	18
	105 000 *g*	11.1	97	10
	Supernatant	28.9	93	< 1.5
III	Insoluble	—	40	—
	Precipitated at			
	20 000 *g*	52.0	21	82
	40 000 *g*	0.7	19	<35
	105 000 *g*	7.3	19	10
	Supernatant	39.9	27	< 1.5
Experiment F				
I	Insoluble	—	—	—
	Precipitated at			
	20 000 *g*	53.0	—	67
	40 000 *g*	5.3	—	45
	105 000 *g*	11.6	—	10
	Supernatant	30.1	—	< 1.4
II	Insoluble	—	146	—
	Precipitated at			
	20 000 *g*	49.2	120	92
	40 000 *g*	12.9	(187)	35
	105 000 *g*	15.8	105	10
	Supernatant	22.1	55	< 1.5
III	Insoluble	—	(not measured)	—
	Precipitated at			
	20 000 *g*	48.4	24	80
	40 000 *g*	8.2	24	21
	105 000 *g*	9.1	25	10
	Supernatant	34.3	37	< 1.9

rather small portion of the total glycogen. The high molecular weight fraction was the one having the highest specific activity at the end of the glycogen accumulation phase (the nitrogen starvation phase). At this time the specific activity in the low molecular weight fraction was considerably lower. At the end of the carbon starvation period the specific activity in the high molecular weight fraction was low. The low molecular weight fraction retained its specific activity to a higher extent than the high molecular one.

DISCUSSION

The results given in Table 1 are in good agreement with our earlier observations [2, 3]. The specific activity of the glucose incorporated in the glycogen during accumulation was the same as that of the medium, indicating that no large pool of intermediary metabolites was present in the bacterial cells. During a subsequent growth period, when the cells had been transferred to a nitrogen-containing and carbon-free medium, the glycogen concentration decreased. Mainly the labelled glucose residues were split off. These facts have been interpreted as depending upon a formation of a peripheral tier of labelled glucose around the glycogen molecules during the starvation phase. This tier was the first one to be split off, when the glycogen was utilized [2]. Furthermore the results might be explained by differing metabolic activities in different glycogen fractions. The present experiments have been performed to determine whether different molecular weight fractions have different metabolic activity.

The fraction with a molecular weight of $40—90 \times 10^6$ contained in all samples about 50 % of the total soluble glycogen. The low molecular weight fraction contained 20—40 % (molecular weight $< 2 \times 10^6$). Thus, the two fractions in between contained only small quantities of glycogen. The polydispersity of the glycogen has thus no Gaussian distribution. Instead there seems to be two different kinds of glycogen, one low molecular weight species and one high molecular weight species.

In an earlier report [3] the weight average molecular weight of the total soluble glycogen was followed during growth. It was found to increase during glycogen synthesis and to decrease during glycogen utilization. For comparison the over all weight average molecular weights were calculated from data in Table 2. They are given in Table 1. These data confirm the earlier results, and it is now obvious that the changes occur mainly in the high molecular weight fraction (Table 2).

The specific activity of the glycogen after nitrogen starvation was higher in the insoluble fraction than in any of the others. In the soluble glycogen the metabolic activity was greater in the high molecular weight fractions than in the low molecular weight ones. During the subsequent breakdown of the glycogen more of the labelled glucose was split off from the highest labelled fractions than from the less labelled fractions. This shows that of the soluble glycogen the high molecular weight fraction had the highest metabolic activity. This result may seem surprising in view of the relatively smaller surface of the large molecules.

Metabolic inhomogeneity of the same kind has been found in rabbit muscle glycogen, but in rat liver the low molecular fraction showed a higher metabolic activity [6].

The authors are grateful for the skilled technical assistance given by Mr. R. Eliasson and Mrs. Berit Edling.

REFERENCES

1. Holme, T. and Palmstierna, H. *Acta Chem. Scand.* **10** (1956) 578.
2. Holme, T. and Palmstierna, H. *Acta Chem. Scand.* **10** (1956) 1557.
3. Holme, T., Laurent, T. and Palmstierna, H. *Acta Chem. Scand.* **11** (1957) 757.
4. Hook, A. E., Beard, D., Taylor, A. R., Sharp, D. G. and Beard, J. W. *J. Biol. Chem.* **165** (1946) 241.
5. Gurin, S. and Hood, D. B. *J. Biol. Chem.* **131** (1939) 211.
6. Stetten, H. R., Katzen, H. M. and Stetten, D. J. *J. Biol. Chem.* **222** (1956) 587.

Received June 4, 1958.

ACTA CHEMICA SCANDINAVICA 12 (1958) 1564—1567

On the Glycogen in *Escherichia coli B*; Variations in Molecular Weight during Growth. III

T. HOLME

Bacteriological Department, Karolinska Institutet, Stockholm, Sweden

The glycogen formed by *Escherichia coli B*, cultivated in continuous culture at different growth rates, has been isolated. This glycogen has been subjected to ultracentrifugal fractionation and the molecular weight of the different fractions has been determined. Of the total glycogen isolated the rapidly dividing cells contained a high percentage of a *low* molecular weight fraction. Slowly dividing cells contained a high percentage of a *high* molecular weight fraction.

In experiments reported in a preceding article ultracentrifugal fractionation was used to obtain fractions of glycogen with different molecular weights [1]. In the present report this method has been applied to glycogen isolated from cells of *E. coli B* grown in continuous culture at different growth rates.

METHODS

The continuous culture methods used have been described earlier [2]. Nitrogen-deficient synthetic medium with sodium lactate as the carbon source was used [3]. The concentration of ammonium chloride (the sole nitrogen source) was 4×10^{-3} M. The data of the experiment reported here are given in Table 1.

Glycogen was isolated from the cells as described earlier [4]. Light-scattering was used for the molecular weight determinations [4]. Fractionation was effected by centrifugation in a Spinco preparative ultracentrifuge. Two fractions were obtained as precipitates after subsequent runs of 20 min at 20 000 *g* and at 105 000 *g*. The supernatant remaining after the last run constituted a third fraction.

A modification of Dische's carbazol method was used for the quantitative determinations of glucose [5].

RESULTS

The molecular weights of the fractions obtained by ultracentrifugal fractionation of the glycogen samples are given in Table 2. Of the three fractions prepared the low molecular weight fraction and the intermediate fraction showed small variations between the different samples. The high molecular weight fraction showed an increase in the molecular weight in rapidly dividing cells.

Table 1.

Dilution rate (h^{-1})	Number of cells per ml $\times 10^{-9}$	Dry weight of cells per litre of culture (mg)	Glycogen-glucose, % of dry weight	Total nitrogen, % of dry weight	Bacterial nitrogen per litre of culture (mg)	Synthetic rate of glycogen
0.09	2.5	401.7	18.6	11.7	47.0	14.3
0.09	2.5	428.5	19.5	11.2	48.0	15.6
0.14	2.5	415.7	15.0	11.5	48.8	18.2
0.14	2.5	423.9	15.4	11.7	49.6	18.4
0.27	2.3	399.0	12.1	12.6	50.3	25.9
0.36	2.2	384.7	6.8	13.4	51.5	18.3
0.36	2.0	382.1	6.7	13.3	50.8	18.1
0.47	1.9	378.9	4.7	13.6	51.5	16.2
0.68	1.8	356.9	2.4	14.1	50.3	11.6

Nitrogen-limited continuous culture of *E. coli B*. Input concentration of ammonium nitrogen: 56 mg/l.

In a continuous culture steady-state growth can be maintained for long periods of time and the growth rate of the bacteria controlled by the rate of addition of new medium. This "rate of addition" is called the *dilution rate*, defined as f/v, where f is the flow rate of the medium and v is the culture volume. The values given in the last column represent the amount of glycogen synthesized in 1 h per 100 mg bacterial nitrogen.

The glycogen content of these cells was low however, and a large amount of cell material had to be hydrolyzed to obtain the required amount of glycogen. Impurities might have been responsible for the increased molecular weight in these samples.

In Fig. 1 the distribution of glycogen between the different molecular weight fractions is shown. The values are expressed in per cent of the total glycogen of the cells. These values are given in Table 3.

In rapidly dividing cells, at a dilution rate of 0.68 h^{-1}, the amount of glycogen found in the low molecular weight fraction was 50 % of the total glycogen, the high molecular weight fraction contained 45 % and the remainder was found in the intermediate fraction. The glycogen content of these cells was 2.4 % of the dry weight (Table 1).

As reported earlier, the glycogen content of cells cultivated at different growth rates is not uniform [2]. Rapidly dividing cells have a low glycogen content while the reverse is true of slowly dividing cells.

Table 2. Molecular weight of different fractions of glycogen obtained by ultracentrifugal fractionation.

Dilution rate (h^{-1})	Molecular weight $\times 10^{-6}$ 20 000 *g*	105 000 *g*	supernatant
0.09	51	15	<2.1
0.14	67	16	<1.6
0.27	91	16	<1.4
0.36	109	21	<0.9
0.47	149	18	<1.1
0.68	262	17	<1.2

Table 3. Distribution of glycogen between different molecular weight fractions.

Dilution rate (h^{-1})	Per cent of total glycogen		
	20 000 *g*	105 000 *g*	supernatant
0.09	61.9	16.3	21.8
0.14	57.4	18.4	24.2
0.27	59.5	14.6	25.9
0.36	58.2	8.7	33.1
0.47	57.7	6.6	35.7
0.68	44.9	5.2	49.9

At a reduced growth rate of the cells, the percentage of glycogen found in the low molecular weight fraction decreased, while the percentage of it in both of the other two fractions increased (Fig. 1). At a dilution rate of 0.09 h^{-1} the low molecular weight fraction accounted for about 22 % of the total glycogen, the intermediate fraction for about 16 % and the high molecular weight fraction for about 62 %. The glycogen content of these cells was about 19 % of the dry weight (Table 1).

DISCUSSION

In the earlier reported experiments [1,4,6] concerned with the synthesis and breakdown of glycogen in *E. coli B*, a special cultivation technique was used involving complete nitrogen starvation. During periods of such starvation, glycogen accumulated in the cells. In the continuous culture, however, nitrogen limitation may be used as a rate-regulating factor and the growth rate of the cells can be varied within a wide range.

As shown earlier [2], the rate of glycogen synthesis increases when the growth rate of the cells is reduced in the nitrogen-limited continuous culture. In the

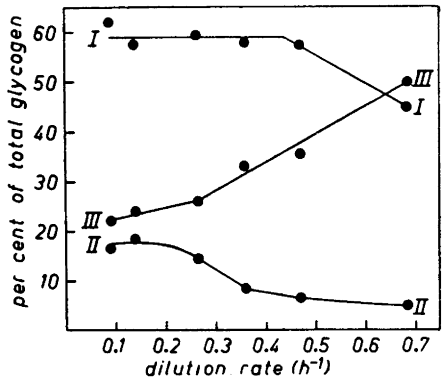

Fig. 1. Distribution of glycogen between different molecular weight fractions. Glycogen samples from *E. coli B* cells grown at different growth rates in continuous culture.

I: high molecular weight fraction.
II: intermediate fraction.
III: low molecular weight fraction.

last column of Table 1 this is confirmed; it can be seen that the rate of glycogen synthesis increases to a maximum at a dilution rate of 0.27 h^{-1}. At lower rates, however, a decrease is noted. This decrease may be the result of such a high content of glycogen in the cells that further formation is inhibited.

In the preceding communication [1] it was shown that there seems to exist two main fractions of glycogen in *E. coli B*, one with a high molecular weight (40—90 $\times$ 10^6) and one with a low molecular weight ($< 2 \times 10^6$). Corresponding fractions are found in the glycogen obtained from continuously cultivated cells, the intermediate fraction never exceeding 20 % of the total glycogen.

From the experiments reported here it can be concluded that the main part of the glycogen that accumulates in slow-growing cells, when their content of glycogen is high, is found in the high molecular weight fraction. When the cells grow at a higher rate, the glycogen content of the cells decreases and at the same time there is an alteration of the distribution ratio of the different molecular weight fractions; half of the total glycogen in these cells may be found in the low molecular weight fraction.

The results are of interest for studies of glycogen metabolism in *Escherichia coli B* since it was previously shown [1], that the different molecular weight fractions have different metabolic activities.

The author is grateful for the skilled technical assistance given by Mr. R. Eliasson and Mrs. Berit Edling. The work has been supported by a grant from the *State Medical Research Council.*

REFERENCES

1. Holme, T., Laurent, T. and Palmstierna, H. *Acta Chem. Scand.* **12** (1958) 1559.
2. Holme, T. *Acta Chem. Scand.* **11** (1957) 763.
3. Friedlein, F. *Biochem. Z.* **164** (1928) 273.
4. Holme, T., Laurent, T. and Palmstierna, H. *Acta Chem. Scand.* **11** (1957) 757.
5. Gurin, S. and Hood, D. B. *J. Biol. Chem.* **131** (1939) 211.
6. Holme, T. and Palmstierna, H. *Acta Chem. Scand.* **10** (1956) 1557.

Received June 4, 1958.

ACTA CHEMICA SCANDINAVICA 12 (1958) 1568—1574

A Combined X-Ray and Neutron Diffraction Investigation of Mercuric Cyanide

JAN HVOSLEF

Universitetets Kjemiske Institutt, Blindern-Oslo, Norway,
Joint Establishment for Nuclear Energy Research, Kjeller, Norway

The precise position of the Hg atom in $Hg(CN)_2$ was found by X-ray methods, while the CN group was localized by means of neutron data. The Hg-C distance is 1.986 ± 0.016 Å and the C-N triple bond is 1.186 ± 0.024 Å. The angle C-Hg-C is 171 ± 2°, while the Hg-C-N angle is 173 ± 2°. The distance between the Hg atom and two N atoms in neighbouring molecules is 2.70 Å. This indicates the existence of an interaction between them.

The space group and approximate Hg positions in $Hg(CN)_2$ were first established by Hassel [1] (1926). Although the light atoms were not detected, he concluded that the lattice must be built up of molecules, and not of separate Hg^{++} and CN^- ions. Later, Hanawolt *et al.*[2] confirmed the proposed structure, and in 1944, Zhdanov and Shugam [3] gave trial parameters for the light atoms, based upon the experimental data of Hanawolt. In a study by infrared spectra of solid $Hg(CN)_2$, Jones [4] was able to confirm the generally accepted opinion that the cyanide group was bound to the Hg atom through the C atom.

The structure was not, however, considered to be firmly established due to the uncertainty of the light atom positions. This uncertainty arises from the dominating influence of Hg *versus* C and N on the scattering of X-rays. For neutron diffraction no such difficulty occurs, as the coherent scattering amplitudes have the following values: $b_{Hg} = 1.30 \times 10^{-12}$ cm, $b_C = 0.66 \times 10^{-12}$ cm, $b_N = 0.94 \times 10^{-12}$ cm.

As no Hg-C distances have been accurately determined it seemed of interest to establish this distance with some precision by means of a neutron diffraction study.

EXPERIMENTAL

Mercuric cyanide crystallizes in the tetragonal space group No. 122 (International tables [5]) D_{2d}^{12}—$I\bar{4}2d$ with eight molecules in the unit cell. The CN groups are in the general 16-fold positions, while the Hg atoms are situated in the 8-fold position (*d*) with one degree of freedom only.

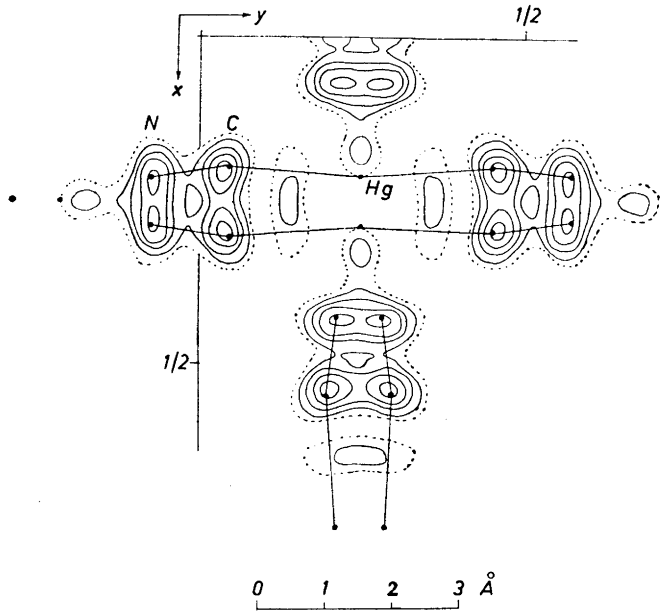

Fig. 1. Fourier projection on (001) of the electron density of the cyanide group in $Hg(CN)_2$, resulting from a synthesis of the coefficients $\{F_{obs}-F_c(Hg)\}$. Final coordinates are indicated by dots. Intervals at arbitrary scale.

The axial lengths were remeasured and found to be $a = 9.643$ Å and $c = 8.880$ Å. Hassel's values were 9.67 Å and 8.92 Å, respectively.

For the X-ray investigation a very small specimen was chosen. The data were recorded on Weissenberg diagrams, using Cu radiation. Multiple film technique and visual estimation was used to obtain the intensities in the $hk0$ zone. No $0kl$ data were recorded.

For the neutron work, a crystal with the dimensions 4.2 × 3.3 × 1.8 mm^3 was grown from aqueous solution. The crystal was mounted on the goniometer

Table 1. Parameters found by X-rays and neutrons. Values for C and N atoms given for X-rays are found from $(F^X_{obs}-F^X_{calc})$ synthesis.

		Hg			C			N		
		x	y	z	x	y	z	x	y	z
Previous Work	Hassel	0.21	1/4	1/8	—	—	—	—	—	—
	Zhdanov and Shugam	0.21	1/4	1/8	0.21	0.03	0.18	0.21	−0.08	0.21
This invest.	X-ray data	0.2125	1/4	1/8	0.205	0.040	—	0.221	−0.068	—
	Neutron data	0.2125	1/4	1/8	0.197	0.047	0.159	0.212	−0.073	0.183

Table 2. Calculated and observed structure factors for X-rays, F^X and neutrons, F^n. Observed X-ray amplitudes believed to be suffering from extinction are marked with asterisks.

(*hkl*)	F^X_{calc}	F^X_{obs}	F^n_{calc}	F^n_{obs}	(*hkl*)	F^n_{calc}	F^n_{obs}
200	565	317 *	11.6	11.3	004	16.4	15.0
400	422	341	13.1	12.6	008	2.3	2.1
600	255	260	11.3	12.0			
800	78	88	10.0	9.9	011	1.1	1.5
1 000	32	46			013	11.2	11.3
1 200	6	0			015	7.1	7.4
					017	5.2	5.2
310	80	62	5.8	5.4			
510	140	141	3.7	4.3	022	14.5	14.8
710	181	209	1.5	0	024	8.4	8.9
910	228	295			026	3.1	2.6
1 110	202	202					
					031	12.4	14.2
220	400	240 *	5.5	5.8	033	5.1	5.9
420	338	229	3.8	5.4	035	6.3	7.1
620	230	211	11.7	11.1	037	2.3	0
820	86	95	0.2	0			
1 020	41	47			042	1.5	0
					044	8.1	7.3
530	67	67	2.0	1.9	046	3.7	0
730	133	138	0	0			
930	183	198			051	14.5	13.9
1 130	175	185			053	6.1	7.3
					055	6.4	5.7
440	248	209 *	4.5	4.4	057	1.1	0.9
640	140	121	5.9	6.3			
840	31	0			062	8.3	10.8
1 040	13	0			064	4.1	3.6
					066	1.2	0
750	77	68					
950	120	115			071	8.4	7.1
1 150	125	106			073	11.9	12.1
					075	1.8	0
660	51	44	2.1	2.2			
860	22	0			082	2.9	2.0
1 060	68	57			084	1.2	0
970	40	37					
880	56	53					

described by Barstad and Andresen [6]. The neutron source was the Kjeller reactor JEEP, using monochromatic beam with wavelength 1.132 Å. Data for the *hk*0 and 0*kl* zones were recorded.

X-RAY WORK

A very accurate value for the parameter of Hg was derived from the X-ray data by means of Fourier methods. Due to the dominating influence of this atom in the X-ray spectra, a temperature parameter $B_{Hg} = 1.1$ Å^2 could be

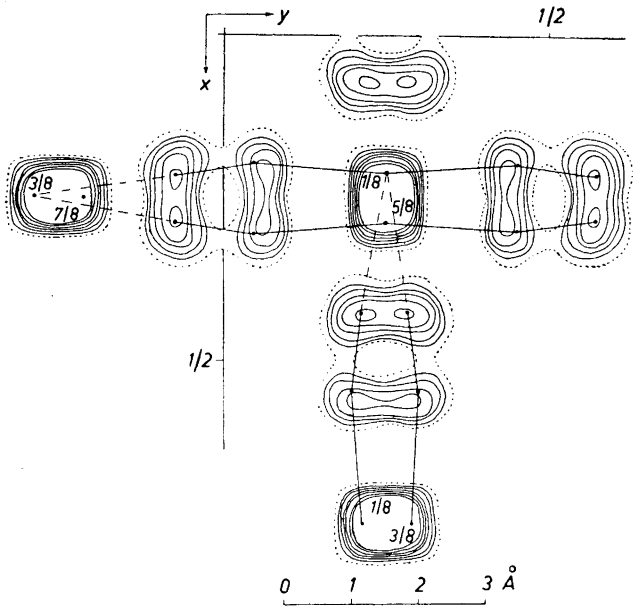

Fig. 2. Fourier projection on (001) by neutron data. Final coordinates are indicated by dots, and *z*-parameters of Hg are given as fractions of the cell edge. Broken lines indicate the Hg..N interactions. Contours are drawn at intervals of 0.33 × 10^{-12} cm/Å^2. The zero level is dotted.

assigned to this atom without knowledge of the precise light atom positions. Hence a difference synthesis with the coefficients (F_{obs}—$F(Hg)_{calc}$) could be made. In the Fourier map (Fig. 1) the light atoms show up, indicating a slight deviation from linearity in the molecule. The parameters are listed in Table 1, and observed and calculated absolute values of the amplitudes are given in Table 2. The *R* index for the X-ray data with final parameters was 8.1 % when reflexions believed to be seriously affected by extinction were omitted.

Significant deviation from linearity in the molecule could, however, not be claimed from the X-ray data.

TREATMENT OF NEUTRON DATA

The approximate light atom positions formed the basis for further work with the neutron data. From the *hk*0 data it became evident that the linear model must be rejected. The Fourier map in Fig. 2 also indicates this, although it suffers severely from series termination errors. Successive (F_o—F_c) syntheses finally lead to the parameters given in Table 2. The *B* value for C and N in this zone was 1.7 Å^2.

In the projection along the *a* axis, the *z* parameters are determined from the inclination of N—C—Hg—C—N with the *c* axis. For this angle, Zhdanov

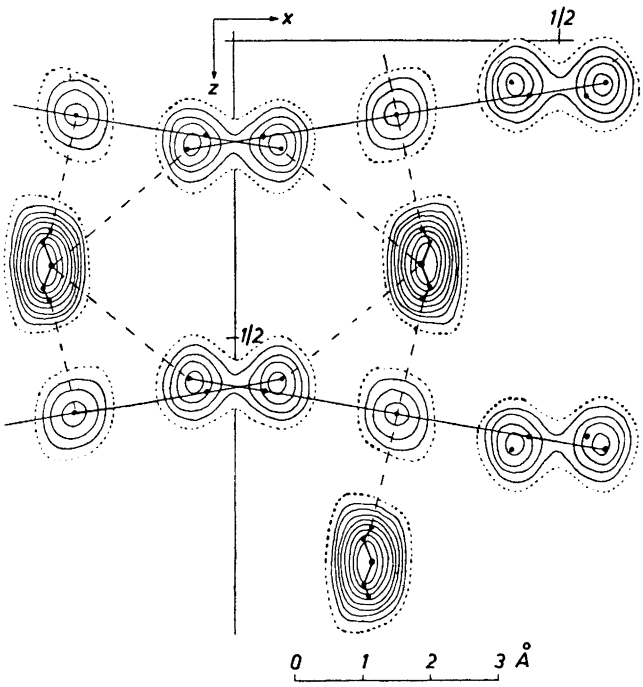

Fig. 3. Fourier projection on (100) by neutron data. Contour intervals are now drawn at intervals of 0.66×10^{-12} cm/Å^2. The interaction between Hg and neighbouring N atoms form zig-zag chains through the lattice, as shown by the broken lines.

and Shugam [3] suggest 76.5° while Jones [4] finds 73°. The treatment of the neutron data for this projection finally lead to the Fourier map shown in Fig. 3. It is unfortunate that most atoms overlap, but as the x and y parameters were known, the z parameters could be determined by a combination of trial-and-error methods and (F_o—F_c) syntheses. During this procedure, the parameters finally converged to the values listed in Table 1. It appeared from these values that the inclination of the molecule to the c axis was 81.2°.

Larger values for the temperature amplitudes were found in this projection. No attempt was made to correct for anisotropy, but it is believed that the higher B values ($B_{Hg} = 2.8$ Å^2, $B_{CN} = 3.3$ Å^2) are significant, indicating higher amplitudes along the c axis.

The over-all R index for the neutron data was 8.9 %, the zero observed reflexions omitted. Absolute values of the neutron amplitudes are listed in Table 2.

RESULTS AND DISCUSSION

The intramolecular distances and their estimated standard deviations (Cruickshank [7] 1949) are as follows: Hg—C = 1.986 ± 0.016 Å, C—N =

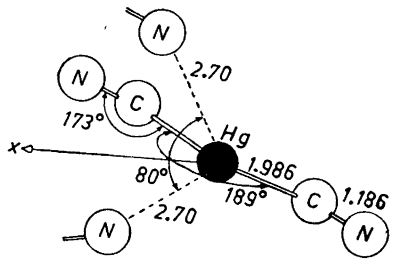

Fig. 4. The atomic arrangement around a Hg atom. The N...Hg...N plane is at an angle of 92° to the plane through the $Hg(CN)_2$ molecule, and the direction from a Hg atom along the x-direction bisects the N..Hg..N and C-Hg-C angles.

1.186 ± 0.024 Å. The angles are: C—Hg—C = 171 ± 2°, Hg—C—N = 173 ± 2°.

From the e.s.d. it must be concluded that the deviation from linearity in N—C—Hg—C—N is significant. In this connection, it is interesting to note that the distance from a mercury atom to two crystallographically equivalent N atoms in neighbouring molecules is 2.70 Å, *i. e.* 0.3—0.4 Å shorter than the van der Waals distance. The N...N distance is 3.44 Å, and the plane N...Hg...N is almost normal to C—Hg—C. Fig. 4 illustrates the atomic arrangement around a Hg atom. All other intermolecular distances have normal values.

These relationships indicate an interaction between Hg and the neighbouring cyanide groups which may be interpreted as due to electrostatic attraction. This attraction is thought to arise from the strong polar properties of the CN group, leaving a small positive charge at the Hg atom and a negative charge at the N atoms. This possibility has also been pointed out by Zhdanov and Shugam, but their N...Hg distance was only 2.52 Å, which would imply a stronger interaction.

Considering the N...Hg interaction as a bond, the $Hg(CN)_2$ molecules are linked together in endless zig-zag chains through the lattice. This is illustrated in Fig. 3.

This investigation was suggested by Dr. G. C. A. Schuit of the Koninklijke/Shell Laboratory, Amsterdam, in connection with the work in progress there in the structure of HgX_4^{--} ions.

The author wants to express his gratitude to Professor O. Hassel, Oslo and to Dr. J. A. Goedkoop, Kjeller for their kind help and many illuminating discussions. *Norges almenvitenskapelige forskningsråd* is acknowledged for financial aid.

REFERENCES

1. Hassel, O. *Z. Krist.* **64** (1926) 218.
2. Hanawolt, I. D., Rinn, H. W. and Fervel, L. N. *Ind. Eng. Chem. Anal. Ed.* **10** (1938) 457.

3. Zhdanov, G. S. and Shugam, E. A. *Compt. rend. acad. sci. URSS* **45** (1944) 295.
4. Jones, L. H. *J. Chem. Phys.* **27** (1957) 665.
5. *International Tables for X-ray Crystallography* (1952) Birmingham, England.
6. Barstad, G. E. B. and Andresen, A. F. *Rev. Sci. Instr.* **28** (1957) 916.
7. Cruickshank, D. W. J. *Acta Cryst.* **2** (1949) 55.

Received June 4, 1958.

ACTA CHEMICA SCANDINAVICA 12 (1958) 1575—1584

Degradation of ^{14}C-Labelled Carolic and Carlosic Acids from *Penicillium Charlesii* G. Smith

SIGVAR LYBING and LEMBITU REIO

Department of Physiological Chemistry, The Wenner-Gren Institute, University of Stockholm, Sweden

From cultures of *Penicillium Charlesii* G. Smith, grown on glucose and ^{14}C-carboxyl-labelled acetate as an additional carbon source, labelled carlosic and carolic acid have been isolated. Itaconic acid, not earlier reported for this species, has also been isolated. Degradation procedures for the two tetronic acids have been worked out and on the basis of the observed isotopic distribution, the synthesis of the tetronic acids is suggested to take place as a condensation between a high labelled 6-carbon unit of β-keto acid type derived directly from acetate by head-to-tail coupling and a low labelled 4-carbon member of the citric acid cycle, the latter being comparatively more diluted by unlabelled carbon from glucose during the incorporation of the acetate added.

It is known from the work of Raistrick and his collaborators [1,2] that *Penicillium Charlesii*, when grown on glucose, produces five closely related acids of the tetronic acid type: carolic, carlosic, carolinic, carlic and γ-methyltetronic acid. From other *Penicillium* species and molds in general a vast number of different organic compounds have been isolated and structurally determined, to a great extent by the work of the Raistrick school, but relatively little is known about the metabolic pathways which lead to the synthesis of these substances. The use of radioactive isotopes, added to the culture medium in the form of labelled glucose, acetate or other intermediary metabolites, is here, as has been the case in the studies on bacterial metabolism, one way of approaching the problem of mold biosynthesis. Among the increasing number of investigations of this kind, the papers by Arnstein and Bentley [3] on the formation of kojic acid, the work by Bentley and Thiessen [4] on itaconic acid biosynthesis and Birch's [5] studies on the synthesis of aromatic compounds can be mentioned.

The study of *Penicillium Charlesii* was suggested by Professor G. Ehrensvärd * as an interesting parallel to a more extensive investigation on the

* Now Professor of Biochemistry, University of Lund, Sweden.

production of phenols and phenol-carbonic acids by *Penicillium* molds belonging to the species *brevi-compactum*, *griseo-fulvum*, *patulum*, *urticae* and *Daleae*. The biosynthesis of aromatic seven- and eight-carbon compounds from glucose by *P. urticae* is discussed in a paper by Ehrensvärd [6].

In order to get a more detailed picture of the metabolic production pattern of *Penicillium Charlesii*, a systematic search for substances in the culture medium was made, using a chromatographic method specially worked out at the laboratory for the study of mold metabolites [7]. With this method new substances could be detected and chromatographically defined, even though their structures were not known.

From the medium of younger cultures grown on glucose (14 days) itaconic acid, not earlier reported for this species, could be isolated in fairly large amounts (0.5 g from six cultures). In older cultures itaconic acid was present in much smaller amounts, for example, only 0.4 g could be isolated from forty-five cultures grown on glucose for a period of 47 days. This suggested that itaconic acid during the incubation period was taken up again from the medium and might be used as an intermediary metabolite in the synthesis of the tetronic acids. To test this possibility ^{14}C-carboxyl-labelled acetate was added to culture medium containing glucose with the expectation of obtaining ^{14}C-labelled itaconic acid. The labelled acid was then intended to be used as an additional carbon source in cultures of the same age as those from which it was to be isolated in order to study its eventual incorporation in the tetronic acids. After two weeks, however, itaconic acid could only be found in very small amounts, while on the other hand carolic and carlosic acid could be isolated, yielding about 0.25 g of each acid from five cultures. The labelled acetate was incorporated in itaconic acid as well as in the two tetronic acids. Addition of acetate apparently increased the formation rate of the tetronic acids, which normally could not be isolated from 2 weeks old cultures.

As itaconic acid could not be isolated in amounts sufficient either for addition to growing cultures, or to permit a complete degradation, no conclusions as to its role in tetronic acid synthesis could be drawn. The purpose of this paper will be to present degradation procedures for carolic and carlosic acid and to report the results of these degradations.

EXPERIMENTAL

Cultivation: Penicillium Charlesii P146, obtained by the courtesy of Professor H. Raistrick at the London School of Hygiene and Medicine, was grown at a temperature of 24°C on a modified Czapek-Dox solution of the following composition: glucose 50.0 g, $NaNO_3$ 2.0 g, KH_2PO_4 1.0 g, KCl 0.5 g, $MgSO_4 . 7H_2O$ 0.5 g, $FeSO_4 . 7H_2O$ 0.005 g, distilled water 1 000 ml and $ZnSO_4 . 7H_2O$ added to give a final concentration of 10^{-6} M of the Zn^{2+}-ion. 1 liter, flat bottom culture flasks, containing 500 ml of the modified Czapek-Dox solution, were inoculated with a spore suspension of about 2×10^6 spores per flask.

In the isotope experiment 50 mg of ^{14}C-carboxyl-labelled sodium acetate was added on the 3rd and 5th days after inoculation. Altogether 100 mg of labelled acetate (214 000 counts/min/mg carbon in the carboxyl group) was added to each of five culture flasks.

Isolation: After a growing period of two weeks, the culture medium was separated from the mycelium by filtration through cotton wool. The solution from five flasks, about 3 l including 500 ml distilled water used for washing of the mycelia, was evaporated

in vacuo to 200 ml. The solution was then, after acidification with 8 ml of concentrated hydrochloric acid, shaken 5 times with a total of 500 ml ethyl acetate. This extract was evaporated *in vacuo* to 50 ml and upon standing for a couple of days the solution solidified into a sticky mass of dark brown crystals, weighing 7.6 g. From this crude mixture of substances carolic and carlosic acid were isolated according to the procedure outlined in Table 1.

Table 1.

Table 1. Isolation of carolic and carlosic acid.

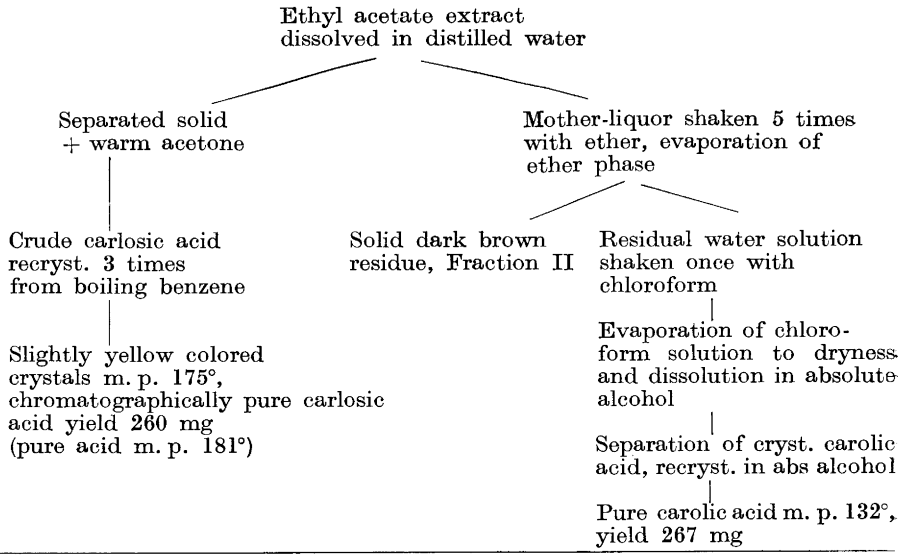

Both acids were chromatographically tested in six different systems [7], and were found to give R_F values identical with those of the corresponding acids obtained from Professor Raistrick's laboratory and also isolated here from larger cultures.

Chromatography of different fractions during the isolation procedure did reveal the presence of itaconic acid only in the crude mixture called fraction II in Table 1.

This fraction was further purified by repeated crystallisation from chloroform, giving 100 mg of a crystalline substance, by chromatography test found to be a mixture of carlosic and itaconic acids. 50 mg of this mixture was run on a silicic acid column and eluted with chloroform and 5—15 % solutions of butanol in chloroform, according to the scheme worked out by Marvel and Rands [8]. The effluent peak volumes for carlosic and itaconic acid were 200 ml and 290 ml, respectively, identical with the values obtained for a test mixture of the same substances. The eluent was collected in 10 ml fractions, which were titrated with 0.2 N NaOH using phenol red as an indicator. The fractions containing itaconic acid were evaporated to dryness but could not be separated from the indicator substance without losing most of the acid at the same time. The remaining 50 mg of the ^{14}C-labelled carlosic-itaconic acid mixture was run on a silicic acid column in exactly the same way as the first portion with the exception that the collected fractions were not titrated. The fractions known to contain itaconic acid were evaporated to dryness, giving 11.8 mg of practically pure itaconic acid.

Degradation: Hydrolysis of the tetronic acids in 2 N sulphuric acid is known [2] to break up the ring to give carbon dioxide and acetoin, one molecule of each, and a third molecule of a 4-carbon compound formed by the side chain attached to the α-position of the ring.

The side chains of carolic and carlosic acid give one molecule of γ-butyrolactone and butyric acid, respectively.

The common procedure for the different steps worked out for the degradation of carolic and carlosic acid is outlined in the following.

1 mmole of the acid is hydrolyzed for 24 h in 10 ml of 2 N sulphuric acid at a temperature of 140°C. A stream of CO_2-free nitrogen is passed through the hydrolysis solution into a flask with saturated $Ba(OH)_2$ solution to take up the CO_2 formed, on its way passing another flask with 2,4-dinitrophenylhydrazine to trap any acetoin leaving the solution. The CO_2 coming from the ring is easily split off during the first three hours of hydrolysis, while on the other hand the second molecule of CO_2 from the carboxy-methyl group in the γ-position of carlosic acid is more slowly released. By prolonged hydrolysis for 23 h about 60 % of this carboxyl group is recovered as $BaCO_3$ as seen from the values in Table 2. Another 6 h of hydrolysis does not increase the yield. The hydrolysis flask is supplied with an efficient reflux-condenser to decrease the amount of acetoin carried along with the nitrogen stream.

The hydrolysate was then neutralized (to phenolphthalein) with a 33 % solution of NaOH and steam distilled in order to blow over the acetoin. 100 ml of distillate was collected, a large enough volume for all the acetoin to be carried over. The acetoin solution was further treated, according to the method of Clutterbuck and Reuter [9], with 10 ml of 2 N H_2SO_4 and 300 mg (1.3 mmole) of potassium periodate for the oxidation of acetoin to acetaldehyde and acetic acid. Merely keeping the mixture at room temperature for 23 h, as suggested by Clutterbuck and Reuter, was in this case not very effective. A more complete splitting of the molecule was obtained by keeping the solution at 60°C for about 70 h. During this time nitrogen was continuously bubbled through the solution and the acetaldehyde formed was passed *via* an alkaline trap (2 ml 0.01 N NaOH) to take up any acetic acid carried along, into a chromic acid solution (6 N H_2SO_4 + 0.8 N CrO_3) kept at 70°C. The chromic acid solution was later steam distilled and the acetic acid (from acetaldehyde) was titrated with 0.2 N NaOH and put aside for further degradation.

In order to recover the acetic acid split off from acetoin, the reaction mixture was neutralized, evaporated to about 10 ml and after acidification with H_2SO_4 solid sodium sulphite was added in amounts just enough to reduce all the iodine to iodide. The solution could then be steam-distilled and the acetic acid titrated and stored for later Schmidt degradation.

The neutralized hydrolysate contained after steam-distillation sodium butyrate or sodium γ-hydroxybutyrate, depending upon whether carlosic or carolic acid was degraded. Alkaline titration of butyrolactone at a temperature of 80 – 90° did within about 2 h lead to the complete opening of the lactone ring and the formation of sodium γ-hydroxybutyrate. Butyrolactone and butyric acid were separated from the neutralized hydrolysis mixture by steam-distillation after acidification with conc. H_2SO_4.

Butyric acid was after titration with 0.2 N NaOH and evaporation to dryness ready for Schmidt degradation. Butyrolactone on the other hand, or rather Na-γ-hydroxybutyrate obtained after alkaline titration, had to be reduced to butyric acid. This could be done in one operation by heating the sodium γ-hydroxybutyrate (about 0.5 mmole) in a bomb tube containing 1 ml of hydriodic acid, d 1.96, for 5 h at a temperature of 230°C. At this temperature the γ-iodo-butyric acid, formed already at lower temperatures [10], was further converted to butyric acid. The acid was separated from the reaction mixture after dilution to about 20 ml with distilled water and addition of solid sodium sulphite until all the iodine was reduced to iodide. 3 g of silver sulphate dissolved in 3 ml of 85 % H_2SO_4 was then added in order to precipitate the iodide-ions as silver iodide. The precipitate was filtered off, the filtrate steam-distilled and the distillate, containing butyric acid, titrated and evaporated to dryness.

In this manner all the degradation products from carolic and carlosic acid, with the exception of the CO_2 formed during hydrolysis, were obtained in the form of fatty acids suitable for further degradation by the Schmidt procedure [11].

The total ^{14}C-content of the labelled substances was determined by combustion to CO_2 in a stream of oxygen passed through a quartz tube over a platinum gauze heated to 800°C.

RESULTS

The results of the degradations are presented in Tables 2 and 3 and Fig. 1. 1 mmole of each acid was taken for hydrolysis. Carlosic acid was mixed with non-active acid in the proportion 1:1, while carolic acid was degraded without being diluted. The CO_2 formed, either by hydrolysis, by Schmidt degradation or by total combustion, was trapped in a saturated barium hydroxide solution as $BaCO_3$. The ^{14}C-content was determined on 15 mg samples of uniform layers or $BaCO_3$ on 1 cm^2 discs under standard conditions, using a Tracergraph Geiger counter with an automatic sample changer. The ^{14}C-content is given in counts per min per mg carbon counted as $BaCO_3$. The ^{14}C-values of the different carbon atoms of carlosic acid are multiplied by two in order to get values comparable to those obtained for undiluted carolic acid.

Table 2. Degradation of carlosic acid.

Substance formed	time after start of hydrolysis	mmole of CO_2 collected during the diff. time intervals	^{14}C-content counts/min/ mg carbon	amounts in mmole of the degradation products
CO_2:	35 min	0.25	1 600	0.25
	1 h 10 min	0.35	1 564	0.60
	1 h 45 min	0.18	1 598	0.78
	2 h 20 min	0.09	1 278	0.87
	3 h 10 min	0.11	1 080	0.98
	11 h 40 min	0.43	560	1.41
	22 h 55 min	0.17	488	1.58
Acetoin:				
acetaldehyde → acetic acid (tot. combust.)			70	0.61
COOH-group			137	0.28
CH_3-group			22	0.23
acetic acid (total combustion)			72	0.69
COOH-group			130	0.43
CH_3-group			8	0.05 *
Butyric acid: (total combustion)			830 **	0.95
COOH-group			1 674	0.83
propionic acid			—	0.79
COOH-group			72	0.48
acetic acid			—	0.38
COOH-group			1 688	0.31
CH_3-group			16	0.23
Total combustion of carlosic acid			680	

* As this amount of $BaCO_3$ was not sufficient for the 1 cm^2 disc, the activity was measured on a uniform layer of 4 mg of $BaCO_3$ in a 0.4 cm^2 disc, giving values 1/3 of those obtained with discs of standard size.

** This value refers to the isotope content of CO_2 from total combustion of butyric acid obtained by hydrolysis of 0.1 mmole of undiluted carlosic acid.

Table 3. Degradation of carolic acid.

Substance formed	time after start of hydrolysis	mmole of CO_2 collected during the diff. time intervals	^{14}C-content counts/min/mg carbon	amounts in mmole of the degradation products
CO_2:	1 h	0.60	1 617	0.60
	3 h	0.34	1 650	0.94
	3 h 30 min	0.03	—	0.97
Acetoin:				
acetaldehyde → acetic acid				0.67
0.15 mmole for total combustion			55	(0.52)
COOH-group			179	0.38
CH_3-group			13	0.32
acetic acid (total combustion)			75	0.65
COOH-group			158	0.34
CH_3-group			11	0.43
Butyrolactone:				
(0.42 mmole * → 0.32 mmole butyric acid)				
butyric acid			—	0.32
COOH-group			1 299	0.24
propionic acid			—	0.20
COOH-group			101	0.14
acetic acid			—	0.16
COOH-group			909	0.08
CH_3-group			23	0.13
Total combustion of carolic acid			550	

* About 0.5 mmole of the butyrolactone was used in order to try the Schmidt degradation on sodium γ-hydroxybutyrate without previous reduction to butyric acid. The yield of the degradation was, however, only about 15 %.

The isotope content of the CO_2 split off from the tetronic acid ring is in the case of carolic acid a mean value of the two determinations made, in the case of carlosic acid a mean value of the first three determinations, containing undiluted CO_2 from the ring. The following fractions, obtained from carlosic acid, have a continuously decreasing isotope content depending upon a mixing with low labeled CO_2 from the carboxy-methyl group at the γ-position. The ^{14}C-content given for this carboxyl carbon might be regarded as a maximum value due to contamination by heavily labelled CO_2 from the ring.

In the above-mentioned paper by Clutterbuck and Reuter [9] it is indicated that by periodate oxidation of acetoin the carbonyl carbon and its adjacent methyl group yield acetic acid and the carbinol group and its adjacent methyl group are split off as acetaldehyde. Whether the symmetrical labelling found for acetoin corresponds to the original isotopic distribution between the β- and γ-carbon atoms in the tetronic acid ring (see Fig. 1) is doubtful. The asymmetrical carbon atom in the carbinol group in the γ-position is responsible for the optical activity of the tetronic acids. As hydrolysis of an ester linkage

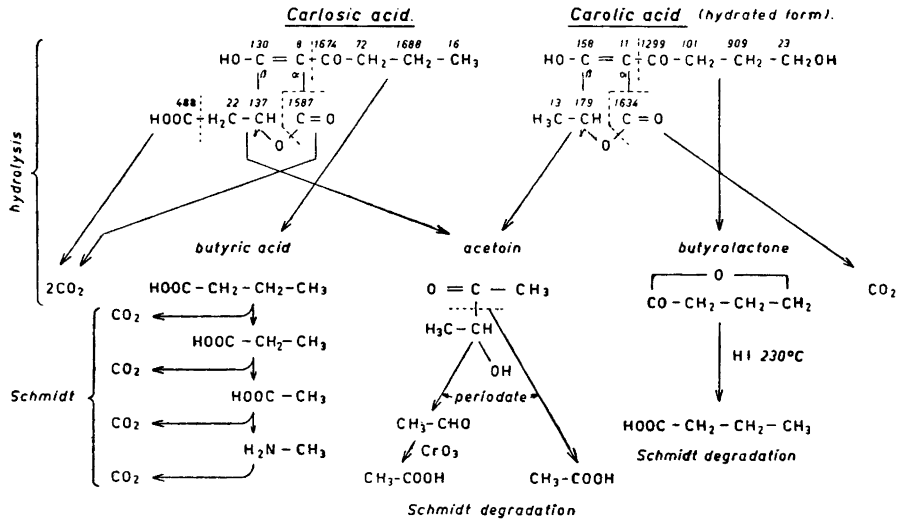

Fig. 1. Degradation scheme for carlosic and carolic acid. The values refer to the isotope content in counts/min/mg C, showing the incorporation of $CH_3{}^{14}COOH$ (214 000 counts/min/mg C in the carboxyl group).

normally does not lead to the rupture of the bond between the carbon atom and the attached hydroxyl group of a secondary alcohol [12], the acetoin formed by hydrolysis would be expected to show optical rotation. The fact that the optical activity of the solutions of carolic and carlosic acid dropped to zero during the hydrolysis, shows, however, that there must have been a change in the configuration of acetoin. As this change is probably not just a stereochemical alteration within the carbinol group [12], an exchange of substituents between the carbinol and carbonyl groups must be assumed to have taken place, with a mixing of the isotope contents as a consequence.

The isotope content found for the β- and γ-carbon atoms might then originally have been built into either one of these two carbon atoms.

It has also been shown by Juni [13] that in unevenly labelled acetoin, produced by yeast, there occurs some mixing between the carbon atoms, for example by alkaline steam-distillation. In the present investigation it was not necessary to avoid alkaline steam-distillation for the separation of acetoin from the hydrolysis mixture, as at this stage acetoin was already optically inactive.

The only certain information about the ^{14}C-incorporation in itaconic acid was obtained by total combustion. Two determinations gave a mean value of 225 counts/min/mg carbon.

DISCUSSION

From the results of the incorporation of ^{14}C-labelled acetic acid in carolic and carlosic acid it is evident that, in the synthesis of the two acids, a common plan is followed. Considering carlosic acid, the distribution of the ^{14}C-isotope

indicates that the molecule can be regarded to be composed of two differently labelled parts, one 6-carbon and one 4-carbon unit, the former about 10 times as heavily labelled as the latter. The 6-carbon chain seems to be more directly built up from acetyl groups, whereas the lower isotope content of the other part points to a greater dilution with carbon from unlabelled glucose, probably over the citric acid cycle.

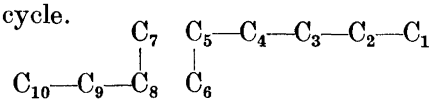

If this 4-carbon part, represented by the carbon atoms C_7 to C_{10} in the schematic formula given above (arbitrarily numbered), should at all be considered as a ^{14}C-labelled member of the citric acid cycle, it should have its ^{14}C-carbon mainly in C_7 and C_{10} corresponding to the carboxyl groups of one of the four dicarboxylic acids. The diverging results obtained, *i. e.* an equal distribution of the isotope between C_7 and C_8, can be accounted for, as was discussed earlier, by a change in the configuration of the acetoin molecule formed in the course of the hydrolytic breakdown of the tetronic acids. The isotope content of these two carbon atoms can thus be thought of as originating from C_7. The isotope content of this carbon is thereby increased to 267 counts/min (337 counts/min in the case of carolic acid), a value of the same order of magnitude as that of C_{10}, 488 counts/min.

If the total ^{14}C-content, $5 \times 225 = 1\ 125$ counts/min, obtained for itaconic acid, is assumed to be equally distributed between the two carboxyl groups, a distribution found in itaconic acid from *Aspergillus terreus*, fed carboxyl-labelled acetate [4], the ^{14}C-content of each group will be about 500 counts/min. This value is comparable in magnitude to the isotope contents of C_7 and C_{10}, supposed to originate from the carboxyl groups of a dicarboxylic acid, thus suggesting that itaconic acid in *Penicillium Charlesii* might also be formed over the citric acid cycle.

Even if the results do not suggest a definite scheme for the synthesis of the tetronic acids, they seem, however, to exclude a few pathways along which the acids probably not are formed.

A similar formation mechanism for ascorbic acid and the tetronic acid ring might be anticipated from the structural relationship between the two compounds. The tetronic acid ring would then in accordance with ascorbic acid be synthesized from glucose [14], so that the carbon sequence 6—1 in the glucose molecule would correspond to the carbon sequence 6, 5, 7, 8, 9, 10 in the schematic formula shown above. In glucose labelled by the incorporation of ^{14}C-carboxyl acetate the isotope will appear [15] in carbon atoms 3 and 4. Tetronic acid formed in this way from glucose would thus be labelled in C_7 and C_8. This is in accordance with the results, but the labelling of C_{10} and the high isotope content of C_6 cannot be accounted for by this scheme.

Another route for the formation of the tetronic acids would be a synthetic pathway over acetoin as an intermediary step. Such a mechanism is, however, not consistent with the results obtained, as it does not explain either the origin of the heavily labelled carbon in the carbonyl group in C_6 or the presence of the carboxyl group in C_{10}. Acetoin was furthermore never chromatographically detected in any of the isolated fractions.

Although tracer studies of this kind have their limitations, especially when a number of alternative pathways can be considered for the formation of a certain metabolite, the following speculations on tetronic acid synthesis are cautiously presented as consistent with the observed isotopic distribution.

The formation of the tetronic acids is thought to take place as a condensation between a 6-carbon chain, β-keto-caproyl-coenzyme A, formed *via* acetyl groups in fatty acid synthesis, and a 4-carbon compound of the citric acid cycle. If placed in the schematic formula shown above the β-keto acid will have its carboxyl group in C_6 and the carboxyl groups of the dicarboxylic acid will be in C_7 and C_{10}. The most suitable configuration of the dicarboxylic acid would be that of malic acid with the carbinol group in C_8 and a CoA-linked carboxyl group in C_7. The latter might then take part in a condensation reaction with the methylene group in C_5, activated and having a tendency to give off protons due to the influence of the adjacent carbonyl group and the CoA-linked carboxyl group. The hydroxyl group at C_7 would be formed by enolization, which also would give the double bond between C_5 and C_7. To complete the ring an ester linkage is then assumed to form between C_6 and C_8. Some support for the idea of malic acid as the 4-carbon unit is given by the findings of Larsen and Eimhjellen [16] that malic acid is accumulated with exclusion of itaconic acid in cultures of *Aspergillus terreus*, when the pH of the medium is increased by addition of $CaCO_3$. Whether an increase of the pH-value during the growth period is responsible for the observed accumulation of tetronic acids in preference to itaconic acid in younger cultures of *Penicillium Charlesii* cannot be settled. The pH-value of the culture medium was found to be almost the same before and after an incubation period of 14 days, 4.4 and 4.3 pH-units, respectively. Whatever the cause of the changed production pattern, the accumulation of tetronic acids with the exclusion of itaconic acid might be favored by an increased formation of malic acid. The assumption that malic acid would be present in a CoA-linked form is purely speculative.

The condensation might also take place between β-keto-caproyl-CoA and succinyl-CoA as the activated form of the dicarboxylic acid. It is known that succinyl-CoA by the action of the enzyme thiophorase preferentially gives off its coenzyme A to β-keto acids [17]. For the case that the β-keto acid already is activated by coenzyme A it seems not impossible that a condensation can take place instead. Once the 4-carbon part is attached to the methylene group in C_5, it might then be oxidized and hydrated in order to get a hydroxyl group in C_8, required for an ester linkage to be formed between C_6 and C_8.

Carlosic acid synthesized in this way by condensation of 6-carbon and 4-carbon units might then by decarboxylation of the carboxyl group in C_{10} and oxidation of the methyl group in C_1 to a hydroxy-methyl group be transformed to carolic acid. Oxidation of C_1 in carlosic acid to a hydroxy-methyl group would give carlic acid; decarboxylation of C_{10} together with an oxidation of C_1 to a carboxyl group would lead to the formation of carolinic acid. γ-Methyl-tetronic acid, finally, might be formed by hydrolysis of the bond between C_4 and C_5 from any of the other four tetronic acids, in the case of carlosic and carlic acid a decarboxylation of the carboxyl group in C_{10} would also be required.

γ-Methyltetronic acid might also be considered as the parent substance synthesized by a condensation of acetyl-CoA and activated malic acid or succinyl-CoA.

The authors wish to express their thanks to Professor G. Ehrensvärd for his stimulating interest in this work.

REFERENCES

1. Clutterbuck, P. W., Haworth, W. N., Raistrick, H., Smith, G. and Stacey, M. *Biochem. J.* **28** (1934) 94.
2. Clutterbuck, P. W., Raistrick, H. and Reuter, F. *Biochem. J.* **29** (1935) 300, 871, 1300.
3. Arnstein, H. R. V. and Bentley, R. *Biochem. J.* **54** (1953) 508; **62** (1956) 403.
4. Bentley, R. and Thiessen, C. P. *J. Biol. Chem.* **226** (1957) 673, 689, 703.
5. Birch, A. J. *Progress in the chemistry of organic natural products*, Springer, Wien 1957, Vol. 14, p. 186.
6. Ehrensvärd, G. *Exptl. Cell Research* Suppl. **3** (1955) 102.
7. Reio, L. *J. Chromatogr.* **1** (1958) 338.
8. Marvel, C. S. and Rands, Jr, R. D. *J. Am. Chem. Soc.* **72** (1950) 2642.
9. Clutterbuck, P. W. and Reuter, F. *J. Chem. Soc.* **1935** 1467.
10. Henry, L. *Compt. rend.* **102** (1886) 368.
11. Mosbach, E. H., Phares, E. F. and Carson, S. F. *Arch. Biochem. Biophys.* **33** (1951) 179.
12. Hermans, P. H. *Introduction to theoretical organic chemistry*, Elsevier Publishing Co. Amsterdam 1954, p. 330.
13. Juni, E. *J. Biol. Chem.* **195** (1952) 727.
14. Mapson, L. W. *Vitamins and Hormones* **13** (1955) 71.
15. Wood, H. G. *Cold Spring Harbor Symposia Quant. Biol.* **13** (1948) 201.
16. Larsen, H. and Eimhjellen, K. E. *Biochem. J.* **60** (1955) 135.
17. Stern, J. R., Coon, M. J. and Del Campillo, A. *J. Biol. Chem.* **221** (1956) 1, 15.

Received June 17, 1958.

ACTA CHEMICA SCANDINAVICA 12 (1958) 1585—1588

Duodenal Glucuronide Synthesis

I. Identification of Estradiol Glucuronide as a Conjugation Product of Estradiol by the Rat Duodenal Mucosa. Qualitative Studies

ANITA LEHTINEN, V. NURMIKKO and K. HARTIALA

Department of Physiology, University of Turku, Finland

Upon incubating estradiol with slices of duodenum taken from 5 rats a product with the properties of estradiol glucuronide is formed. This product which is extractable from acid solution by ethylacetate gives after hydrolysis with β-glucuronidase chromatographically a qualitative reaction for estradiol and glucuronic acid.

Previous studies by one of us [1,2] have shown that in addition to the liver also mucosal specimens taken from various regions of the gastrointestinal tract are able to conjugate glucuronides *(in vitro)* in the presence of *o*-aminophenol. According to these observations the intestinal glucuronide synthesis participates in the detoxication processes of the organism.

Feeding of another glucurogenic substance, cinchophen, to a dog leads to increased glucuronide contents of portal blood also under conditions when the bile flow into the intestine is prevented [3]. Recently we have also been able to identify phenolphthalein-glucuronide as a conjugation product of the duodenal mucosa [4].

In the present work estradiol is used as the substrate. Its conjugation to a glucuronide by the duodenal mucosa *in vitro* has been demonstrated.

MATERIAL AND METHODS

Tissue specimens. Rats were used in these experiments. The animals were killed by a blow on the head. The tissue specimens were removed immediately, the size of specimens kept equal by means of a starsis. The samples were first placed into the ice cold incubation mixture.

Estradiol. Chrystallized estradiol (Sigma Co., 4.9 mg) was dissolved in 2 ml of propyleneglycol [5].

Incubation. This was carried out in the Warburg apparatus at 37°C over a period of 90 min. The incubation solution (Krebs-Ringer) contained 100 mg glucose and 112 mg sodium lactate per 50 ml of the mixture. Into each Warburg flask were transferred 2.9 ml of this Ringer solution, 0.1 ml of the estradiol propyleneglycol solution (0.9 μmole estradiol) and after this the tissue specimens (approximate dry weight 8—10 mg). Gas phase was 5 % carbon dioxide in oxygen. As controls parallel runs were made with the incubation solution without tissue slices and also with tissue slices but without estradiol.

Sampling. After incubation the contents of 2 Warburg flasks were combined to make one sample for further concentration and chromatographic analysis. The tissue slices were removed from the incubation media and washed with 2 ml Ringer solution (6 ml + 2 ml).

Deproteinization. The incubation mixture was heated at 60°C for 3 min and centrifuged thereafter.

Extraction of free estradiol [5]. The clear protein-free supernatant was extracted with 10 ml of benzene (3 × 10 min). The precipitate left after the previous centrifugation was washed with absolute alcohol (1 ml), centrifuged and the alcohol supernatant added to the benzene solution. This was then evaporated in vacuum.

Extraction of estradiol glucuronide. The water phase left after benzene extraction was made 2 N with HCl and the glucuronide was extracted with ethylacetate (10 ml, 3 × 10 min). The ethylacetate was removed in vacuum.

Hydrolysis. To the ethylacetate residue were added acetate buffer (2 ml, 0.1 M, pH 4.5) and β-glucuronidase enzyme preparation (2 mg, Worthington Biochem. Corp.). The hydrolysis was carried out over a period of 24 h at 37°C.

Extraction of the estradiol liberated by hydrolysis. After the hydrolysis with β-glucuronidase the incubation solution was reextracted with benzene (7 ml, 3 × 10 min). Benzene was removed in vacuum as usual.

Glucuronic acid. The glucuronic acid made free by hydrolysis and after extraction with benzene is left in the water phase. This was evaporated to dryness and subjected for further analysis.

Paper chromatography. 1 ml of a solvent (ethylacetate/benzene) was added to each residue and the solutions were used for chromatographic analyses. These were carried out according to the descending chromatography method. A mixture of butanol, glacial acetic acid and water was used as an irrigant; 24 h, Paper Whatman No. 1. Estradiol spots were identified on the paper by a saturated aqueous solution of *p*-nitrobenzene-azodimethoxy-aniline (Fast Black Salt K, Heftman, 1950). Glucuronic acid was identified with the $AgNO_3$-ammonia reagent (1 vol. 0.1 N $AgNO_3$, 1 vol. 5.0 N NH_3-solution. 1 vol. 2 N NaOH).

RESULTS

From the acidified incubation mixture a compound was extracted with ethylacetate which, on hydrolysis with β-glucuronidase, gave spots for free estradiol and glucuronic acid.

Estradiol glucuronide. The nonhydrolyzed residue after evaporation of the ethylacetate extract failed to give a violet spot on the paper after fixation with Fast Black Salt K (Fig. 2. H, I, J,). This reagent is known to produce such colour with free estradiol [6]. This finding indicates that the estradiol is in a conjugated form in the ethylacetate extract. Spots F and G in Fig. 2 were obtained using 100 μg and 150 μg pure estradiol. From the nonhydrolyzed residue no dark brown spot characteristic for glucuronic acid was formed with the ammonia silver nitrate solution (Fig. 3. A, B, C). The small spots seen at A, B and C are probably caused by some carbohydrate impurities reacting with the potent silver nitrate reagent. The R_F-values of these are distinct from those given by pure glucuronic acid. Spot D corresponds to 150 μg of pure glucuronic acid.

Estradiol and glucuronic acid liberated by hydrolysis. After the hydrolysis a compound dissolved in benzene which on the chromatogram appeared to be estradiol (Fig. 2. A, B, C and D). Spots for pure estradiol are also shown in the same figure (F, G).

Fixation with the ammonia-silver nitrate reagent produced from the hydrolyzed samples spots characteristic for glucuronic acid (Fig. 3. E and F).

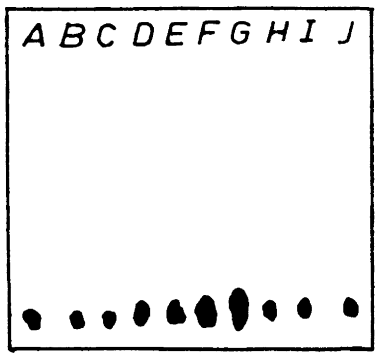

Fig. 1. Unconjugated estradiol. A, B, C, D, H, I, J spots of estradiol left unconjugated during the incubation (in the benzene-alcohol extract). Stained with Fast Black Salt K. G. control solution. E with 100 μg and F with 150 μg of estradiol.

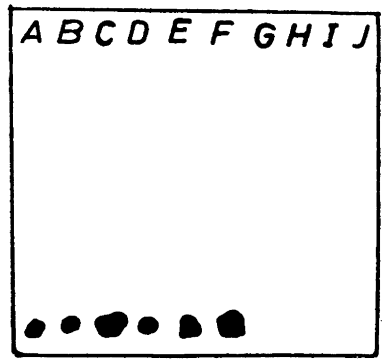

Fig. 2. Estradiol glucuronide. No dark spots characteristic for free estradiol could be obtained from the nonhydrolyzed ethylacetate residue after staining with Fast Black Salt K. (G, H, I, J). Free estradiol. A, B, C, D free estradiol spots after hydrolysis with β-glucuronidase. E and F obtained with 100 μg and 150 μg estradiol.

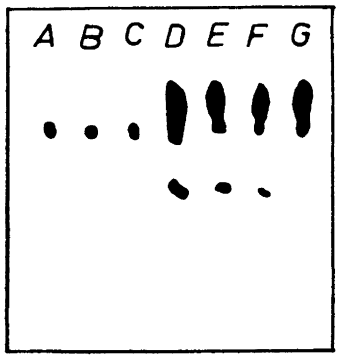

Fig. 3. Free glucuronic acid. E, F, G obtained by hydrolysis with β-glucuronidase; staining with the $AgNO_3$-ammonia reagent. A, B, C nonhydrolyzed samples. D with 100 μg of glucuronic acid.

A spot developed from pure glucuronic acid is shown in the same picture (D). It is to be noted that the spot obtained from the hydrolyzed samples lies higher on the paper than that of pure glucuronic acid. Since this observation was familiar from our previous trials 50 μg pure glucuronic acid was added to the samples of the nonhydrolyzed residue. After the development of the chromatogram the dark spot (Fig. 3. G) appeared at the same point as in the original hydrolyzed samples (Fig. 3. E and F).

Since the spots are formed also with pure glucuronic acid the compound indicated by them apparently is formed during the run. They do not correspond to the R_F-values obtained with glucuronic acid lactone. One possibility is that they are esters formed from glucuronic acid and butanol. The presence of these additional spots does not invalidate the fact that spots representing free glucuronic acid are also produced by hydrolysis of the ethylacetate extract.

Unbound estradiol. The part of the estradiol which remained unconjugated during the incubation and which was extracted with the benzene alcohol extracts appeared very nicely as violet spots in the chromatograms (Fig. 1, A, B, C, D, H, I, J). These were, however, strikingly smaller and weaker than those in the control solutions (Fig. 1, G) in which the incubation procedures were made without any tissue slices. The comparison of spots A, B, C, D, H, I, J with G indicates that pure estradiol has been bound during the incubation. Spots E and F correspond to 100 μg and 150 μg pure estradiol.

Tissue specimens. In order to secure that no agents reacting in the chromatogram similar to estradiol were excreted from the tissue itself during the incubation the following control analyses were performed. Tissue slices were incubated in the usual manner but without the presence of estradiol. The chromatograms produced after this revealed no such spots either from the alcohol-benzene extracts, from the unhydrolyzed samples or from the hydrolysed samples. As a control 100 μg of pure estradiol was run on the same paper.

DISCUSSION

These experimental results indicate that the rat duodenum is capable to conjugate estradiol to the corresponding glucuronide *in vitro*. This conjugate can be hydrolyzed after extraction from acid incubation medium with ethylacetate. These components produced by hydrolysis are estradiol and glucuronic acid. So far these studies have demonstrated only the qualitative formation of estradiol glucuronide. The incubation solution contained 0.9 μmole of estradiol per 8—10 mg of tissue dry weight and a portion of the estradiol has apparently remained unconjugated. Although the exact amounts will be calculated in our later quantitative studies, it seems likely that perhaps some 40—50 % of the estradiol are bound to glucuronic acid. It is worth mentioning that the incubation was performed in a solution in which also sulphate ions were present. It is therefore possible that in addition to the glucuronide conjugation the estradiol has also reacted with sulphate.

These observations are taken as a further evidence to support the previous studies of Hartiala (1954 and 1955) in which *o*-aminophenol under similar conditions as above — with the exception that the incubation solution did not contain sulphate ions — was found to yield a conjugate similar to the *o*-aminophenolglucuronide produced by the liver.

These studies have been supported by the *State Council of Natural Sciences* and *Sigrid Jusélius Stiftelse*, Finland.

REFERENCES

1. Hartiala, K. *Acta Physiol. Scand.* **31** (1954). Suppl. 114, 20.
2. Hartiala, K. *Ann. Med. Exptl. Biol. Fenniæ Helsinki* **33** (1955) 239.
3. Hartiala, K. J. W., Leikkola, P. and Savola, P. *Acta Physiol. Scand.* **42** (1957) 36.
4. Lehtinen, A., Savola, P., Pulkkinen, M. and Hartiala, K. *Acta Chem. Scand.* **12** (1958) 1592.
5. Sie, H-G. and Fishman, W. H. *J. Biol. Chem.* **225** (1957) 451.
6. Heftman, E. *Science* **111** (1950) 571.

Received June 12, 1958.

ACTA CHEMICA SCANDINAVICA 12 (1958) 1589—1591

Duodenal Glucuronide Synthesis

II. Identification of Estradiol Glucuronide as a Conjugation Product of Estradiol by the Rat Duodenal Mucosa. Quantitative Studies

ANITA LEHTINEN, K. HARTIALA and V. NURMIKKO

Department of Physiology, University of Turku, Finland

Estradiol was incubated in the presence of duodenal mucosal specimens. Free estradiol was extracted with benzene. Thereafter the product, extractable from the supernatant by ethylacetate, was hydrolyzed by β-glucuronidase. The product liberated was then extracted with benzene. Analyses of this product with the Kober reagent revealed that 53 % of the original estradiol appeared as a glucuronide formed during the incubation with duodenal mucosa.

As has been indicated in previous studies [1] estradiol, when incubated with surviving duodenal tissue slices, is conjugated to a compound identified by paper chromatography as estradiol glucuronide. In order to produce further evidence quantitative studies have been performed.

EXPERIMENTAL

The incubation procedures were exactly the same as described in the first part of these experiments. Also the extraction procedures were the same. In order to obtain conditions, comparable to the previous chromatographic procedures, incubates from 2 Warburg flasks were first combined.

First the free estradiol was extracted with benzene. After extraction of the conjugated estradiol-compound with ethylacetate this product was hydrolyzed with β-glucuronidase. The liberated estradiol was then extracted with benzene, the extract was evaporated to dryness and the residue was then transferred to absolute ethanol. From the mixture proteins were removed by centrifugation and the supernatant was transferred to Kober-tubes. The ethanol was then evaporated.

Quantitative estimation of estradiol. This was performed according to the method described by Brown[2], making use of the Kober reaction. To the evaporated residue were added 3 ml of the Kober reagent (2 g chinol/100 ml 60 % H_2SO_4, allowed to stand in the dark for one day before use). The tubes were heated on a boiling water bath for 20 min and brought to room temperature; 0.2 ml aq. dest. was added and the tubes were rewarmed for 10 min and cooled again. The mixture was then diluted for the photometric reading. The brown-yellow colour was read in a spectrophotometer at 518 mμ which was found to be the absorption maximum for pure estradiol and for the experimental samples.

Table 1. Quantitative determination of the amount of estradiol conjugated by duodenal mucosa and hydrolysable by β-glucuronidase. Original amount of free estradiol in the incubation mixture 490 μg.

Samples (1–4) during different runs (I–V)	Tissue dry weight mg	Estradiol conjugated μg	Estradiol conjugated per 10 mg tissue μg
I			
1	10.6	265	251
2	10.8	270	248
3	12.8	285	222
4	13.8	*	
II			
1	11.6	255	220
2	8.2	*	
3	7.0	285	305
4	8.3	275	330
III			
1	11.2	265	238
2	9.2	275	288
3	12.0	*	
4	7.4	262	353
IV			
1	13.5	263	195
2	14.6	*	
3	11.1	270	243
4	9.6	*	
V			
1	11.2	*	
2	9.2	*	
3	12.0	262	218
4	7.4	*	

* Specimens stained brown after the addition of the Kober reagent.

The extinction curve was obtained by preparing a stock solution from estradiol (5 mg/10 ml) and a series of dilutions (containing 15–55 μg estradiol/ml). The colour produced from these samples with the Kober reagent was rectilinear in the 25–50 μg range. According to this a 1:10 dilution was necessary for the later incubation samples. Estradiol was incubated in the Ringer solution but without the tissue slices. This mixture was then treated in the same way as the actual samples. After extraction and hydrolysis these samples should be free of estradiol and serve well as blanks for the Kober reagent readings. The slight colour developed by the blanks was subtracted in the final calculations.

RESULTS

Table 1 presents the results obtained in 5 parallel experiments. The results are expressed as μg of estradiol conjugated per 10 mg of duodenal tissue. The maximum was 353 μg and the minimum 195, mean 256 μg. The amount of estradiol of two Warburg incubates was 490 μg. It appears then that a maximum of 71 and a minimum of 40 % of estradiol was conjugated to glucuronide. Excluding the extreme values the conjugated estradiol amounts to 53 % of the total steroid material.

DISCUSSION

These studies support our previous observations that the duodenal mucosa possesses the ability to carry out active glucuronide synthesis in the presence of suitable material. The chromatographic studies showed no signs of free estradiol in the ethylacetate extract. The present quantitative analyses on the other hand gave high readings for estradiol after hydrolysis of the extracted material with an enzyme specific for the β-glucuronides.

The quantitative studies meet with some technical difficulties. The Kober reaction involves the use of H_2SO_4 which causes a darkening of the samples in the presence of some organic compounds. Therefore the presence of, *e. g.*, glucuronic acid in the conjugated samples does not allow analyses of the non-hydrolyzed material by this method. The results are, however, in good agreement with some of our other similar studies. As shown with phenolphthalein which can be detected by relatively simple chemical means the amount conjugated under similar experimental conditions amounts to 60 % [3].

These studies do not reveal in what form the remaining portion of the original material after the incubation is. Since the incubation mixture contains sulphate ions it is also possible that a certain amount of estradiol-sulphate is formed.

This study has been supported by *The State Council of Natural Sciences* and *Sigrid Jusélius Stiftelse*, Finland.

REFERENCES

1. Lehtinen, A., Nurmikko, V. and Hartiala, K. *Acta Chem. Scand.* **12** (1958) 1585.
2. Brown, J. B. *Biochem. J.* **60** (1955) 185.
3. Lehtinen, A., Savola, P., Pulkkinen, M. and Hartiala, K. *Acta Chem. Scand.* **12** (1958) 1592.

Received June 12, 1958.

ACTA CHEMICA SCANDINAVICA 12 (1958) 1592—1594

Duodenal Glucuronide Synthesis

III. Identification of Phenolphthalein Glucuronide as a Conjugation Product of Phenolphthalein in the Intestinal Tract in Rat

ANITA LEHTINEN, P. SAVOLA, M. PULKKINEN and K. HARTIALA

Department of Physiology, University of Turku, Finland

Incubation of phenolphthalein in the presence of surviving duodenal slices resulted in the partial disappearance of the free phenolphthalein from the incubation mixture. The treatment with β-glucuronidase of the ethylacetate extract made from the mixture revealed that some 66 % of the original phenolphthalein appeared as a glucuronide hydrolysable by this enzyme.

Recent studies have indicated that the mucous membrane of the gastrointestinal tract posesses its own defence mechanism against harmful chemical substances. It has been found that the glucuronide conjugation is *in vitro* carried out not only by the liver and the kidney, but also by the gastrointestinal mucous membrane. These observations were made by incubation of the tissue specimens in the presence of *o*-aminophenol [1,2]. This phenomenon has been verified by others using *o*-aminobenzoic acid and *p*-aminobenzoic acid [3]. Most recently we have been able to demonstrate that estradiol glucuronide is formed upon incubation of estradiol with duodenal mucosa in rat [4] and also that the feeding of a glucurogenic substance, cinchophen, leads to increased glucuronide contents in the portal blood in dog [6].

In the present study another glucurogenic substance has been used to confirm these earlier observations. Phenolphthalein was considered to be suitable for this purpose. It is known to be converted into a glucuronide in the organisms, in which form it also is excreted in urine [7]. Phenolphthalein glucuronide is widely used in connection with quantitative determination of β-glucuronidase. This enzyme hydrolyzes the conjugate readily in a linear course to phenolphthalein and glucuronic acid. The quantitative measurement of free phenolphthalein is a simple procedure [8].

MATERIAL AND METHODS

Albino rats (Wistar breed) were used in the experiments.

Incubation. The incubation of free phenolphthalein with duodenal mucosa slices was performed in the Warburg apparatus at 37°C for 90 min. The experimental procedure has been described in detail in previous papers [9,10].

Phenolphthalein concentrations. A stock solution of phenolphthalein was made by dissolving 200 mg of phenolphthalein (Fluka, pro anal.) in 1 ml 10 % NaOH. From this solution 0.02 ml was taken and transferred to 50 ml of the Ringer solution. Thus, this contained 4 mg/50 ml of phenolphthalein or 0.72 mg/9 ml. This 9 ml sample was made by putting the contents of 3 Warburg flasks together, each containing 3 ml of the incubation mixture. The tissue slices from these 3 flasks were removed after the incubation, washed with 1 ml of pure Ringer solution and dried on glass plates for later weighing. The washing solution was added to the combined 9 ml incubation mixture.

Deproteinization. The incubation mixture (10 ml) was made 2 N with hydrochloric acid. By using 4.44 N HCl, the amount used for this was 8.2 ml. This mixture was then heated at 60°C for 2 min and the protein precipitate was separated by centrifugation. The clear supernatant was transferred to an extraction funnel and shaken with 13 ml ethylacetate (2 × 15 min). The precipitant left after the centrifugation was washed with ethanol (1 ml), centrifuged and the alcohol supernatant added to the ethylacetate solution. The ethylacetate was removed in vacuum. The residue was dissolved in 2 ml of an acetate buffer (pH 4.5).

Hydrolysis of phenolphthalein conjugate. 2 mg of β-glucuronidase (Worthington Co) was added to the buffered solution of the residue and this was then incubated together with the separate control samples without β-glucuronidase at 37°C for 4 h. The proteins were removed by heating the mixture at 60°C for 2 min and centrifuging thereafter. The clear supernatant was diluted with 3 ml of distilled water and made alkaline with 3 ml glycine-sodium hydroxide buffer (pH 10.45–10.7). By this means the optimum pH

Table 1. Duodenal glucuronide synthesis. I, II, and III different Warburg runs. C control analysis made from the mixture incubated without the tissue slice. + β, hydrolysed sample, − β, unhydrolysed sample. BF: bound phenolphthalein calculated from the difference of the control and nonhydrolysed values. FG, phenolphthalein present as a glucuronide. Calculated from the difference of the hydrolysed and nonhydrolysed values. Δ "lost amount", difference of BF and FG.

		Phenolphthalein recovered				Tissue dry weight, mg	Phenolphthalein, mg/100 mg tissue dry wt		
		mg	BF mg	FG mg	Δ		BF	FG	Δ
I.		0.78							
	1+β	0.58		0.39	0.20	24.9		1.5 (6)	0.8 (0)
	2+β	0.62		0.43	0.16	26.2		1.8 (5)	0.6 (1)
	3−β	0.19	0.59			23.5	2.5 (4)		
II.		−0.76							
	1+β	0.56		0.39	0.20	25.0		1.5 (6)	0.8 (0)
	2+β	0.54		0.37	0.22	24.8		1.5 (0)	0.8 (9)
	3−β	0.17	0.59			23.5	2.5 (4)		
III.		−0.79							
	1+β	0.58		0.40	0.21	26.0		1.5 (6)	0.8 (2)
	2+β	0.60		0.42	0.19	28.0		1.5 (1)	0.6 (8)
	3+β	0.59		0.41	0.20	21.4		1.8 (8)	0.9 (2)
	4−β	0.18	0.61			20.1	3.0 (5)		
	Mean		0.60	0.40	0.20				

for the stability of the colour given by phenolphthalein was maintained. After this the mixture was centrifuged. The colour intensity of the clear solutions was measured with a Beckman DU spectrophotometer (540 mμ). This method is a modified Fishman method, originally designed for the determination of β-glucuronidase activity [11]. In our procedure the unknown factor was the amount of free phenolphthalein produced from the conjugate during the incubation with β-glucuronidase.

Calibration curve. This was made by preparing a dilution 0.005 ml/2 ml in 10 % NaOH from the phenolphthalein stock solution and making a dilution series (in Ringer solution) from this. The colour intensity was then measured after mixing the samples with the glycine-sodium hydroxide buffer (3 ml buffer + 3 ml H_2O).

RESULTS AND DISCUSSION

The results are listed in Table 1. First the methodical accuracy can be checked from the values. The measured amount of phenolphthalein in the original incubation mixture was 0.72 mg. The recovery in the triplicate control samples was 0.78, 0.76 and 0.79, mean 0.78. No loss of the original phenolphthalein is indicated. By studying the results it is apparent that a great part of the phenolphthalein present in the mixture is not found in free form after incubation with surviving duodenal tissue. It is also evident that a major portion of this bound glucuronide can be liberated by β-glucuronidase. The calculations indicate that 66 % of the ethylacetate extractable bound phenolphthalein was converted into the glucuronide. The nature of the remaining part (Δ) has not been identified in these studies. There are several possibilities. It might include material conjugated to sulphate and it might also be bound to the protein present in the original mixture.

These studies add to the previous evidence that the duodenal mucosa is able to carry out active glucuronide synthesis. The physiological meaning of this intestinal function is still obscure. In the liver this conjugation serves the purpose of active detoxication. In the intestine it might also serve as a part of the selective absorption mechanism. Our studies now in progress aim at elucidation of some of these points.

This study has been supported by grants from the *State Council for Natural Sciences (Valtion Luonnontieteellinen Toimikunta)* and from the *Sigrid Jusélius Stiftelse.*

REFERENCES

1. Hartiala, K. J. W. *Acta Physiol. Scand.* **31** (1954) suppl. 114, 20.
2. Hartiala, K. J. W. *Ann. Med. Exptl. Fenniæ Helsinki* **33** (1955) 239.
3. Shiray, Y. and Ohkubo, T. *J. Biochem. (Tokyo)* **4** (1954 b) 341.
4. Lehtinen, A., Nurmikko, V. and Hartiala, K. *Acta Chem. Scand.* **12** (1958) 1585.
5. Lehtinen, A., Hartiala, K. and Nurmikko, V. *Acta Chem. Scand.* **12** (1958) 1589.
6. Hartiala, K. J. W., Leikkola, P. and Savola, P. *Acta Physiol. Scand.* **42** (1958) 36.
7. Fleig, C. *J. Pharm. Chem.* **29** (1909) 55.
8. Talalay, P., Fishman, W. H. and Huggins, C. *J. Biol. Chem.* **166** (1946) 757.
9. Levvy, G. A. and Storey, I. D. E. *Biochem. J.* **44** (1949) 295.
10. Hartiala, K. J. W. and Sirkku Rontu *Ann. Med. Exptl. Fenniæ Helsinki* **33** (1955) 213.
11. Fishman, W. H., Springer, N. and Brunetti, R. *J. Biol. Chem.* **173** (1948) 449.

Received June 12, 1958.

ACTA CHEMICA SCANDINAVICA 12 (1958) 1595—1604

The Stability of Metal Halide Complexes in Aqueous Solution

IV. The Fluoride and Chloride Complexes of the Vanadyl Ion, VO^{2+}

STEN AHRLAND and BERTIL NORÉN

Department of Inorganic and Physical Chemistry, Chemical Institute, University of Lund, Lund, Sweden

The stability constants of the fluoride and chloride complexes of the vanadyl ion, VO^{2+}, have been determined. As could be predicted from the position of vanadium in the Periodic Table, the fluoride complexes are much stronger than the chloride ones which are very weak. They are also much stronger than the fluoride complexes formed by divalent ions of similar size but higher symmetry. This is due to the increase of effective charge on the metal atom induced by the strongly electronegative oxygen. On the other hand they are perceptibly weaker than the fluoride complexes of the uranyl ion, UO_2^{2+}, where two oxygen atoms co-operate in increasing the charge on the central uranium atom.

Vanadium is one of the few elements outside the actinide series forming well-established "yl"-ions in acid solutions, *i. e.* ions where a central metal atom is linked to one or two oxygen atoms by strong bonds of a pronouncedly covalent character (*cf.* Refs.[1,2] and refs. quoted therein). Vanadium(IV) thus forms the vanadyl ion, VO^{2+}, and vanadium(V) the vanidol[1] ion, VO_2^+. In connexion with the work on metal halide complexes at present in progress in this laboratory, it seemed worth-while to investigate the tendency of these ions towards halide complex formation, in order to compare them in this respect with the actinide "yl"-ions and also with di- and monovalent ions of higher symmetry.

From the general trends found for the formation of halide complexes by central ions of different positions in the Periodic Table [3], it can be predicted that the stability of the complexes of VO^{2+} and VO_2^+ will decrease in the sequence $F^- \gg Cl^- > Br^- > I^-$. Moreover the complexes formed by the three heavier halides are expected to be very weak, and therefore it might only be possible to determine very approximate values of their stability constants. The fluoride systems therefore seemed to present the most profitable task.

As to experimental methods, the obvious one for the system VO^{2+}—F^- was measurement of $[H^+]$ in acid fluoride solutions by means of the quinhydrone electrode, provided that the electrode functions satisfactorily in the presence of VO^{2+}. This method has been used before for the investigation of several fluoride systems, and a full description of the calculation of stability constants from such data is given in the work [4] on the rather similar system of UO_2^{2+}, *cf.* also Ref.[5] As stated there, the conditions might be complicated by the existence of hydroxo [2] and/or polynuclear complexes in solution besides the postulated simple series of mononuclear fluoride complexes of VO^{2+}; complexes containing HF_2^- as ligand are also conceivable. Such complexes will, however, cause the ligand number $\bar{n}_M$ to be a function not only of the free ligand concentration*, [A], but also of $[H^+]$ and/or the free central ion concentration, [M]. By varying $[H^+]$ and [M], which is brought about by varying the total concentrations of acid and central ion, C_H and C_M, it is therefore possible to decide whether such complexes exist or not [4].

As to VO_2^+, its fluoride complexes cannot be investigated by measurements involving the quinhydrone electrode, as quinhydrone is certainly oxidized by vanadium (V).

Once the constants of the fluoride system of VO^{2+} are known, the weaker complexes of the heavier halides can be investigated by the method of ligand displacement [6]. This has been carried out in the case of chloride.

The measurements were performed at 20°C in a medium of ionic strength 1 M, with $NaClO_4$ as the supplementary salt.

EXPERIMENTAL

Chemicals. Vanadium (IV) perchlorate solutions were prepared in a way similar to that described in Ref.[2] Vanadium(IV) was determined by titration with cerium(IV). The titration was carried out both potentiometrically and with ferroin as indicator. Provided the concentration of sulphuric acid in the solution was kept as low as about 0.5 M, the indication with ferroin was acceptable and gave the same result as was found potentiometrically (*cf.* Ref.[7]). The concentration of V(IV) in the stock solution was 471 mM. In the preparation of the perchlorate solution a slight oxidation to V(V) occurred the amount of which was determined in two ways. First it was calculated from the difference of emf measured in the potentiometric titrations between the solution which was half oxidized and the original solution, before any Ce(IV) had been added. Secondly it was determined by titrating a solution which had previously been completely reduced by SO_2 (the excess of which was removed by boiling the solution). Both methods gave the same value of the amount of V(V), $\approx$0.4 % of that of V(IV). This contamination was considered to be of no importance.

In order to avoid hydrolysis the stock solution was prepared with an excess of free perchloric acid (*cf.* Ref.[2]). The concentration of free acid was determined potentiometrically in the way described for uranyl perchlorate [4]. As certain difficulties (discussed below) were encountered when quinhydrone electrodes were used in vanadium perchlorate solution of low $[H^+]$, glass electrodes were used in this determination. The concentration of perchloric acid in the stock solution was 143 mM.

Sodium fluoride. A stock solution with C_A = 600 mM was prepared from "Merck" *p. a.* material, and sodium perchlorate was added to bring the total ionic strength to 1 M. In order to determine the small amount of foreign basic impurity usually found in fluoride

* Unless stated otherwise, the same symbols are used as in the paper on uranyl fluoride [4].

solutions [4], a small amount of perchloric acid was added to the stock solution which was then titrated with alkali. The present preparation also contained this impurity, buffering around pH = 7 where the hydrofluoric acid was practically neutralized. Its concentration was estimated to about 0.2 % of that of the fluoride. From earlier experience [4] it was evident that this foreign base would have to be suppressed before the fluoride solution could be used in the measurements on complex halides. This was achieved by adjustment of the pH of the solution from the original value of 7.2 to about 6.3. At this lower pH the basic impurity is converted into the corresponding acid while the fluoride ion is still practically unaffected.

Stock solutions close to 1 M were prepared from analytical grade *perchloric acid* and *sodium chloride*. *Sodium perchlorate* was prepared by neutralization of perchloric acid as described before [8].

The behaviour of the quinhydrone electrode in solutions of vanadyl perchlorate. The function of the quinhydrone electrode in the presence of vanadium was checked by measuring the emfs of cells of the type

+ Au	C_H mM $HClO_4$ I = 1 M ($NaClO_4$) quinhydrone(s.)	1 M $NaClO_4$	C_H mM $HClO_4$ C_M mM $VO(ClO_4)_2$ I = 1 M ($NaClO_4$) quinhydrone (s.)	Au —

The measurements were arranged as titrations where C_M was varied and C_H kept constant within a certain series. Series were carried out with C_H = 10, 30 and 100 mM. In this range of pH the hydrolysis of V(IV) is negligible for all values of C_M used [2] and thus $C_H = [H^+]$. If the electrode is working ideally the emf measured should therefore always be = 0. As seen from Table 1, this is very nearly the case for C_H = 30 mM, at least up to C_M = 50 mM. The deviation is also slight for C_H = 100 mM. Its direction and order of magnitude resembles that found for the quinhydrone electrode in uranyl perchlorate solution [9] and the cause might be the same in both cases. For C_H = 10 mM on the other hand, the deviation is much greater and, moreover, goes in the other direction. The potentials at C_H = 10 mM are also much less reproducible than those measured at higher C_H.

Thus, in order to secure an acceptable measurement of $[H^+]$ in vanadyl perchlorate solutions up to a value of C_M = 50 mM by means of the quinhydrone electrode, C_H must be at least 25 mM. The question then arises if the electrode gives the right response for $C_H \geqq 25$ mM also in the presence of fluoride. This was tested by performing the fluoride measurements with several different values of C_H and C_M, *i. e.* by varying those quantities which evidently determine the behaviour of the electrode. The calculation of identical complex formation functions (and hence identical stability constants) from all the experimental values of C_H and C_M implies that the underlying determination of $[H^+]$ was correct and the electrode thus functioning normally.

Table 1. The behaviour of the quinhydrone electrode in vanadyl perchlorate solutions.

$[H^+]\rightarrow$ mM	100	30	10
C_M mM	E mV		
2	0	0	0.7
5	−0.1	0	1.3
10	−0.2	0.2	2.2
20	−0.8	0.3	3.5
30	−1.5	0.4	
50	−3.0	0.4	

As pointed out above such a variation of C_H and C_M was also necessary in order to reveal if the solution contains other complexes than the simple mononuclear series $VOF_n^{(n-2)-}$. Therefore, if no variation with C_H or C_M is found for the complex formation function, this means not only that those other complexes do not exist but also that the determination of the constants of the complexes $VOF_n^{(n-2)-}$ is not impaired by faulty electrode function.

Procedure of the main measurements. The measurements were all arranged as titrations. A cell similar to that written above was connected. The specially prepared fluoride stock solution and an acid perchlorate solution were then added from individual burettes to the right-hand solution so that C_H and C_M were both kept constant during each titration. A plastic vessel was used for this half-cell which had to accomodate acid fluoride solutions. The left hand half-cell, serving as a reference electrode, always had $C_H = 10$ mM in the halide measurements.

In the chloride measurements, the solution of the right-hand cell also contained a certain total chloride concentration C_{Cl} which was also kept constant during a titration.

In the halide titrations, the value of E_H could as a rule be reproduced within ± 0.2 mV. The potentials attained equilibrium practically at once and were stable for hours.

RESULTS

The fluoride system. Corresponding values of [A] and the ligand number $\bar{n}_M$ were calculated according to the equations listed as (1) and (2) of Ref.[5], *i. e.* by using the constants δ_1 and δ_2 of the hydrogen fluoride system. In particular the value of δ_2 is fairly sensitive to the presence of basic impurities in the sodium fluoride solution [4]. As a new stock solution of fluoride, prepared from salt of another source, was used in the present measurements, it seemed advisable to redetermine the constants δ_1 and δ_2. This was done by titrations similar to those described in Ref.[4] Higher values of C_H were however chosen, *viz.* $C_H = 25$, 50 and 100 mM, because the measurements on vanadyl solutions had to be performed at these values of C_H. The present titrations gave $\delta_1 = 850 \pm 30$ M^{-1}, $\delta_2 = 2\,300 \pm 300$ M^{-2}, in good agreement with the values found for the second fluoride preparation used previously.

In order to find E_H of eqn. (1), Ref.[5], it is necessary to know the liquid junctions potentials of the cells used (*cf.* Ref.[4], eqns. (1) and (2). On the reasonable assumption that these potentials depend only on $[H^+]$ they have been previously determined in separate experiments up to $[H^+] = 35$ mM, with reference to the usual quinhydrone electrode of $[H^+]_0 = 10$ mM and $I = 1$ M (Ref.[4], Table 1). For the present investigation the determination of E_d had to be extended to $[H^+] = 100$ mM, Table 2. At such high values of $[H^+]$, E_d is a very substantial correction to the measured values of E.

Table 2. The liquid junction potential E_d as a function of E (and $[H^+]$). $[H^+]_0 = 10$ mM.

E mV	−35	−40	−45	−50	−55
E_d mV	2.3	3.0	4.0	5.3	6.9
$[H^+]$ mM	44	55	70	90	115

Table 3. Determination of $\bar{n}_M$ as a function of [A] for $C_H = 25$ mM, $C_M = 25$ mM.

C_A mM	E_H mV	[A] mM	$\bar{n}_M$
22.9	8.6	0.48	0.60
43.6	22.4	1.70	1.09
62.6	39.3	4.40	1.52
80.0	55.9	9.43	1.91
96.0	69.2	16.5	2.20
110.9	79.6	24.8	2.42
137.1	93.8	42.2	2.71
160.0	103.6	60.0	2.86
180.0	110.0	74.8	3.04
206.0	118.0	97.8	3.11

In the measurements on vanadyl solutions, titrations with $C_H = 100$ and 50 mM were performed with two different values of C_M, *viz.* 50 and 25 mM, while only one value of C_M, 25 mM, was used with $C_H = 25$ mM. The results are given in Tables 3—5, and the complex formation functions giving $\bar{n}_M$ as a function of log [A] are plotted in Fig. 1. Evidently all the combinations of C_H and C_M give identical functions. Thus neither polynuclear complexes nor complexes with HF_2^- as ligand seem to exist in these solutions. Above all no hydrolysis occurs, in spite of the fact that values of pH are reached where the hydrolysis is quite substantial in non-complex perchlorate solutions [2]. Evidently the complex formation with fluoride effectively prevents the formation of soluble hydroxo complexes of V (IV) (*cf.* Ref.[4], p. 706; Ref.[10]). On the other hand the absence of hydrolytic reactions also means that fluoride ions do not displace the oxygen of VO^{2+} within the present range of pH contrary to what

Table 4. Determination of $\bar{n}_M$ as a function of [A] for $C_H = 50$ mM, $C_M = 25$ and 50 mM.

C_A mM	25			50		
	E_H mV	[A] mM	$\bar{n}_M$	E_H mV	[A] mM	$\bar{n}_M$
22.9	6.2	0.33	0.46	3.9	0.20	0.31
43.6	14.6	0.93	0.81	8.4	0.47	0.57
62.6	25.4	2.06	1.14	14.3	0.91	0.79
80.0	38.0	4.12	1.44	20.8	1.52	1.01
96.0	51.2	7.67	1.75	28.1	2.43	1.19
110.9	63.6	13.08	2.01	35.7	3.67	1.33
137.1	80.8	26.0	2.38	50.4	7.40	1.70
160.0	92.7	40.6	2.62	63.5	13.04	1.99
180.0	101.2	55.2	2.76	74.1	19.98	2.20
206.0	110.0	74.8	2.91	86.0	31.7	2.44
240.0	118.9	100.6	3.12	99.2	51.4	2.65
266.2				107.7	69.0	2.78
288.0				113.4	84.0	2.89

Table 5. Determination of $\bar{n}_M$ as a function of [A] for $C_H = 100$ mM, $C_M = 25$ and 50 mM.

25				50			
C_A mM	E_H mV	[A] mM	$\bar{n}_M$	C_A mM	E_H mV	[A] mM	$\bar{n}_M$
22.9	4.0	0.20	0.32	17.3	2.4	0.12	0.16
43.6	8.7	0.49	0.52	33.4	4.9	0.26	0.31
62.6	13.8	0.87	0.75	48.2	7.5	0.41	0.42
80.0	19.6	1.40	0.95	62.0	10.1	0.59	0.55
96.0	26.0	2.14	1.16	75.0	13.0	0.80	0.66
110.9	33.3	3.23	1.31	87.2	16.0	1.05	0.76
137.1	48.4	6.77	1.69	109.0	21.9	1.64	0.97
160.0	62.6	12.54	2.10	128.6	28.6	2.50	1.14
180.0	74.7	20.48	2.34	145.8	35.1	3.55	1.30
206.0	87.8	33.9	2.65	168.8	44.5	5.65	1.54
240.0	101.1	55.0	2.92	200.0	59.3	10.92	1.92
266.4	109.4	73.3	3.04	225.0	70.8	17.67	2.17
288.0	115.1	88.8	3.17	245.5	79.9	25.1	2.37
				276.7	91.9	39.4	2.59
				300.0	99.5	52.0	2.72
				317.8	104.6	62.0	2.84

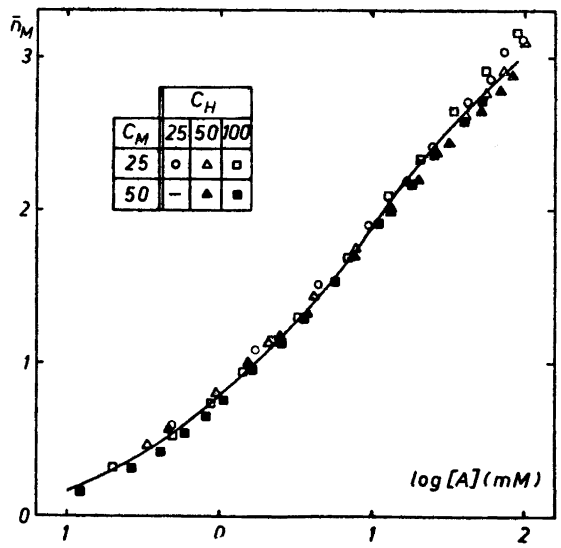

Fig. 1. The complex formation function of the vanadyl fluoride system. The points refer to titrations with different values of C_M and C_H, as indicated by the scheme given in the figure. The curve is calculated from the constants β_n finally found.

has recently * been believed [11]. It might finally also be concluded that the quinhydrone electrode works satisfactorily under the prevailing conditions.

As pointed out in the paper [4] on uranyl fluoride the way of calculating [A] and $\bar{n}_M$ from δ_1 and δ_2 might produce figures at high values of C_A, which are too low for [A] and hence too high for $\bar{n}_M$. A method giving better values of [A] and $\bar{n}_M$ in this region was given and it has also been tried in the present case. However it does not work quite satisfactorily here as $[H^+]$ is so large relative to [HA] and $[HA_2]$ that eqn. (18) of Ref.[4] is no longer a sufficiently close approximation. It can be estimated however that the complex formation curve will only be slightly displaced downwards if calculated according to this method. For the uppermost points at [A] = 100 mM, the difference would be about 0.2 units in $\bar{n}_M$ and it would then decrease rapidly with [A], completely disappearing at [A] $\approx$ 20 mM.

When [A] reached a value of $\approx$100 mM at C_M = 25 mM and $\approx$80 mM at C_M = 50 mM, a precipitate was formed and simultaneously the emf started drifting. The titration series had then to be interrupted. Unfortunately the complex formation curve (Fig. 1) is still steeply rising at these values of [A] and therefore the present measurements could give no reliable information about the coordination number, N, of the vanadyl ion.

For analysis, a larger quantity of the precipitate was prepared in a separate experiment. The filtered substance was washed with small portions of cold water (it is perceptibly soluble) and then dried at 105°C. It could then be heated for 5 h at 180°C without changing its weight. For the determination of vanadium, samples were dissolved in 2 M sulphuric acid and titrated potentiometrically as described above. For the determination of fluorine, another sample was dissolved in 0.05 M hydrochloric acid and the fluoride then precipitated as PbClF (*cf.* Vogel [12], p. 261). In order to achieve a complete precipitation, pH must be kept between 3 and 4. In such a solution, however, the hydrolysis of vanadium(IV) is quite marked, resulting in a coprecipitation of hydrolysed vanadium species. The filtered and washed precipitate therefore cannot be weighed as PbClF. Instead it was dissolved in nitric acid and titrated according to Volhard. At this procedure, no disturbance was observed from the slight amount of vanadium present. Found: V 22.3, 22.0 %, F 40.8 %. Calc. for Na_3VOF_5: V 22.1 %, F 41.1 % (Calc. for Na_2VOF_4: V 27.0 %, F 40.2 %; for Na_4VOF_6: V 18.7 %; F 41.8 %). From the vanadium analysis it thus seems certain that the compound is Na_3VOF_5. The fluorine analysis is in accordance with this, although it cannot decide between several conceivable alternatives with almost the same fluorine content. The ammonium analogue of Na_3VOF_5 has been known since long ago [13]. Unfortunately, neither the structure of this compound, nor that of any other complex vanadyl fluoride seems ever to have been determined. From these solid phases no evidence can therefore be derived about the co-ordination number of the vanadyl ion in its fluoride complexes. As stated above, the complex formation function, valid for aqueous solution, was also inconclusive on this point. The question must therefore be left open for the present.

From the experimental complex formation function the stability constants β_1, β_2 and β_3 of the first three complexes $VOF_n^{(n-2)-}$ are calculated in the usual

* The findings of Ducret [11] might be explained by his use of glass electrodes (and probably glass vessels) for acid fluoride solutions.

Table 6. Computation of the stability constants of the vanadyl fluoride system.

$\beta_1 = 2\,000 \pm 100$ M^{-1} $\quad \beta_2 = (2.9 \pm 0.3) \times 10^5$ M^{-2} $\quad \beta_3 = (1.4 \pm 0.2) \times 10^7$ M^{-3}

$\beta_4 = 3 \times 10^7$ M^{-4}

$b_1 = \beta_1$ $\quad b_2 = 150$ M^{-1} $\quad b_3 = 50$ M^{-1}

$b_1/b_2 = 13$ $\quad b_2/b_3 = 3$

[A] mM	$\frac{X([A])}{X(10^{-4})}$	$X_{1M} \times 10^{-3}$ M^{-1}	$X_{2M} \times 10^{-5}$ M^{-2}	$X_{3M} \times 10^{-7}$ M^{-3}	$X_{4M} \times 10^{-7}$ M^{-4}
0	*0.827*	*2.0*	*2.9*	*1.4*	*3*
0.1	1.000	2.10			
0.2	1.174	2.10			
0.3	1.349	2.10			
0.4	1.522	2.10			
0.5	1.699	2.11			
0.6	1.881	2.12			
0.8	2.256	2.18			
1	2.654	2.21			
2	5.032	2.54	2.72		
3	8.114	2.94	3.12		
4	11.93	3.36	3.39		
5	16.54	3.80	3.60	1.4	
6	22.06	4.28	3.80	1.5	
8	36.09	5.33	4.17	1.59	
10	54.21	6.46	4.46	1.56	
15	120.1	9.61	5.07	1.45	
20	223.6	13.47	5.73	1.42	
30	585	23.55	7.19	1.43	
40	1 220	36.85	8.72	1.46	
50	2 221	53.7	10.34	1.49	
60	3 707	74.7	12.11	1.54	
80	8 656	130.9	16.11	1.65	3.1
100	17 160	207.5	20.55	1.77	3.7

way [14], with a lower integration limit $[A]_0 = 0.1$ mM, Table 6. A very tentative value of β_4 is also given. From these constants the complex formation curve and the composition of the system is calculated according to eqns. (2) and (8) of Ref.[14] The formation curve, fulldrawn in Fig. 1, fits the experimental points well. The composition is presented graphically in Fig. 3.

The Chloride System. As the chloride system could be expected to be weak, a high concentration of chloride $C_{Cl} = 400$ mM was used. The values of δ_1 and δ_2 are however likely to change when such a large amount of the perchlorate is exchanged for chloride. These constants must therefore be determined in the chloride medium also. This was done by titrations at $C_H = 50$ and 100 mM and resulted in $\delta_1 = 800 \pm 30$ M^{-1}; $\delta_2 = 3\,100 \pm 300$ M^{-2}.

Fluoride titrations were then performed with a solution having a vanadium(IV) concentration $C_M = 30$ mM, $C_H = 50$ mM and $C_{Cl} = 400$ mM. The function $\bar{n}_M/[A]$ of the fluoride system obtained from these measurements was very close to that found above for pure fluoride solutions, Fig. 2. An addition of $C_{Cl} = 400$ mM was thus able to repress the complex formation of fluoride only very little, on account of the extreme weakness of the chloride complexes. In fact it was no use to try lower values of C_{Cl}, as these would have

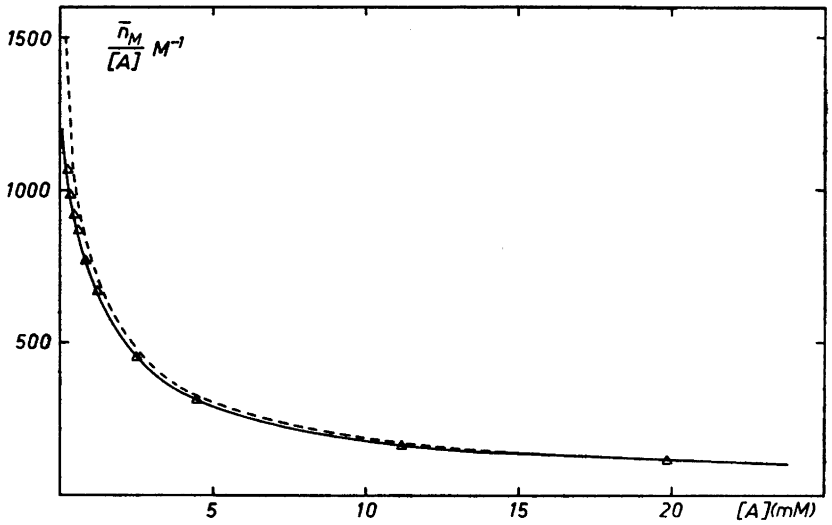

Fig. 2. The function $\bar{n}_M/[A]$ for the vanadyl fluoride system at $I = 1$ M a) in pure perchlorate medium: dashed curve, and b) in the presence of a chloride concentration $C_{Cl} = 400$ mM: triangles, fulldrawn curve.

given functions not significantly separated from the function of $C_{Cl} = 0$. The constant, β_1, of the first chloride complex is therefore calculated from this single value of C_{Cl} under the reasonable assumption that no higher complexes have yet been formed. Using [6] a value of $b = 0.018$ M, the integral $\ln X\,(0.4) = \int_0^b \frac{\bar{n}_M}{[A]} \cdot d[A]$ is graphically found to be $= 0.3625$ giving $\beta_1 = 1.1$ M^{-1}. On account of the possible influence of medium effects *etc.* on the slight difference found between the $\bar{n}_M/[A]$-curves, this value of β_1 can only be considered as showing the order of magnitude. In Fig. 3, the partition of vanadium between VO^{2+} and $VOCl^+$ is shown graphically.

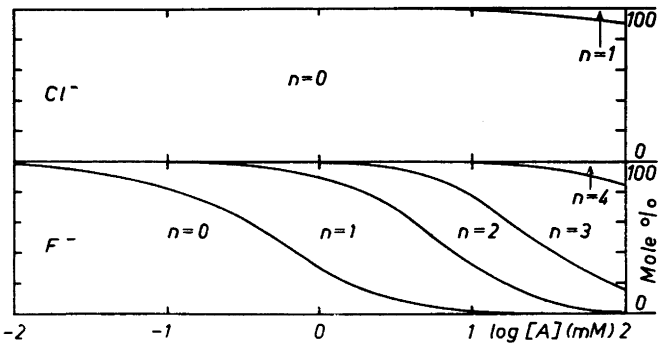

Fig. 3. The distribution of vanadium between the different complexes as a function of log [A].

DISCUSSION

As could be predicted from the position of vanadium in the Periodic Table, the fluoride complexes of VO^{2+} are much stronger than the chloride ones. VO^{2+} is a typical class (a) acceptor [15] and its complex formation with halide ions is thus governed essentially by electrostatic forces [3].

The fluoride complexes of VO^{2+} are much stronger than those of divalent central ions of a similar size, possessing higher symmetry [5], *e. g.* Ni^{2+}, Cu^{2+}, Zn^{2+}. Obviously the effective charge on vanadium in VO^{2+} is greater than +2 due to the high electronegativity of the attached oxygen. On the other hand the fluoride complexes of VO^{2+} is markedly weaker than those [4] of UO_2^{2+}. Certainly two oxygen atoms induce a higher effective charge on uranium in UO_2^{2+} than does one oxygen on vanadium in VO^{2+}. This increase of charge is evidently only partly compensated by the increase of ionic size and the result is a net increase of electrostatic attraction.

A grant from *Statens Naturvetenskapliga Forskningsråd (Swedish Natural Science Research Council)* is gratefully acknowledged. We are further indebted to Dr George Gamlen, I.C.I. Dyestuffs Division, Blackley, Manchester, for his careful linguistic revision of our manuscript.

REFERENCES

1. Carpenter, J. E. *J. Am. Chem. Soc.* **56** (1934) 1847.
2. Rossotti, F. J. C. and Rossotti, H. S. *Acta Chem. Scand.* **9** (1955) 1177.
3. Ahrland, S. *Acta Chem. Scand.* **10** (1956) 723.
4. Ahrland, S., Larsson, R. and Rosengren, K. *Acta Chem. Scand.* **10** (1956) 705.
5. Ahrland, S. and Rosengren, K. *Acta Chem. Scand.* **10** (1956) 727.
6. Fronæus, S. *Acta Chem. Scand.* **4** (1950) 72.
7. Walden, G. H., Hammett, L. P. and Edmonds, S. M. *J. Am. Chem. Soc.* **56** (1934) 57.
8. Ahrland, S. and Grenthe, I. *Acta Chem. Scand.* **11** (1957) 1111.
9. Ahrland, S. *Acta Chem. Scand.* **3** (1949) 374.
10. Ahrland, S. *Acta Chem. Scand.* **5** (1951) 199.
11. Ducret, L.-P. *Ann. Chim.* **6** (1957) 705.
12. Vogel, A. I. *Quantitative Inorganic Analysis*, 2. Ed. Longmans, Green and Co., London 1951.
13. Simons, J. H. (Ed.) *Fluorine Chemistry*, Academic Press Inc. New York 1954, Vol. II, p. 21.
14. Ahrland, S. *Acta Chem. Scand.* **3** (1949) 783.
15. Ahrland, S., Davies, N. R. and Chatt, J. *Quart. Rev.* **1958** (In press).

Received June 5, 1958.

ACTA CHEMICA SCANDINAVICA 12 (1958) 1605–1610

Aminosugars and Related Compounds

Part V.* 2-Amino-1:6-Anhydro-2-Deoxy-β-D-altropyranose hydrochloride**

A. B. FOSTER, M. STACEY and S. V. VARDHEIM***

Chemistry Department, The University, Edgbaston, Birmingham, England

Treatment of methyl 2:3-anhydro-4:6-*O*-benzylidene-α-D-allopyranoside (IV) with methanolic ammonia (followed by acetylation) yields, as the major product, methyl 2-acetamido-4:6-*O*-benzylidene-2-deoxy-α-D-altropyranoside monohydrate (II) the structure of which is proved. Graded and total acidic hydrolysis of the latter compound yields respectively methyl 2-acetamido-2-deoxy-α-D-altropyranoside and 2-amino-1:6-anhydro-2-deoxy-β-D-altropyranose hydrochloride. The latter compound serves to characterise the parent aminosugar.

Until 1945 the only aminosugars which had been isolated from natural sources were 2-amino-2-deoxy-D-glucose [1] and 2-amino-2-deoxy-D-galactose [2]. Since then a number of other naturally occurring aminosugars have been recognized † and interest in their synthesis has been stimulated ††. In addition to these aminosugars a number of *N*-methylamino [15] and *N*:*N*-dimethylamino sugars [16] are now known. This paper describes work aimed at the synthesis of 2-amino-2-deoxy-D-altrose.

An obvious starting point for a synthesis of 2-amino-2-deoxy-D-altrose is the compound methyl 2-acetamido-3-*O*-acetyl-4:6-*O*-benzylidene-2-deoxy-α-D-altropyranoside (I) reported by Peat and Wiggins [17] to be the major product of the action of methanolic ammonia (followed by acetylation) on methyl 2:3-

---

* Part IV. *J. Chem. Soc.* **1958** 2218.

** A brief report of this work appeared in *Nature* **180** (1957) 247.

*** Present address (S.V.V.): Papirindustriens Forskningsinstitutt, Boks 250, Vinderen, Oslo, Norway.

† Muramic acid[3], 3-amino-3-deoxy-D-ribose[4], 2-amino-2-deoxy-D-fucose[5], 2-amino-2-deoxy-D-gulose[6], 2-amino-2-deoxy-D-talose[7] and 2-amino-2-deoxy-D-mannose[8].

†† The following D-aminosugars have been synthesized: 2-amino-2-deoxy-D-allose[9], 2-amino-2-deoxy-D-galactose[10], 2-amino-2-deoxy-D-glucose[11], 2-amino-2-deoxy-D-gulose[12], 2-amino-2-deoxy-D-mannose[13] and 2-amino-2-deoxy-D-talose[14], usually isolated as the hydrochloride or *N*-acetate.

anhydro-4:6-*O*-benzylidene-α-D-allopyranoside (IV). Whilst the minor product of this reaction, methyl 3-acetamido-2-*O*-acetyl-4:6-*O*-benzylidene-3-deoxy-α-D-glucopyranoside, was studied in detail [17] the major product apparently was not further examined.

Reinvestigation of this reaction gave methyl 3-acetamido-2-*O*-acetyl-4:6-*O*-benzylidene-3-deoxy-α-D-glucopyranoside in 4.2 % yield with physical constants (m. p. 271°, $[\alpha]_D$ +44.1° in chloroform) in good agreement with those reported [17] (m. p. 270°, $[\alpha]_D$ +44.6° in chloroform) by Peat and Wiggins. The major product *A* (45.7 %) of the reaction was initially assumed to be methyl 2-acetamido-3-*O*-acetyl-4:6-*O*-benzylidene-2-deoxy-α-D-altropyranoside(I) although the physical constants (m. p. 188°, $[M]_D$ +218° in chloroform) were slightly different from those (m. p. 184°, $[M]_D$ +179° in chloroform) reported [17] for this compound. However, failure to release acetate ions by treatment of compound *A* with alkali suggested the absence of *O*-acetyl groups and this was proved by the fact that the infra-red spectrum of compound *A* showed strong absorptions (1 541 and 1 651 cm^{-1}) characteristic [18] of *N*-acetyl groups but no absorption in the region 1 725—1 749 cm^{-1} characteristic [18] of *O*-acetyl groups. The identity of Peat and Wiggins' compound, of which a specimen survived in the chemical collection of the University of Birmingham Chemistry Department, was confirmed when its infra-red spectrum was found to contain strong absorptions at 1 531 and 1 649 cm^{-1} (*N*-acetyl) and at 1 729 cm^{-1} (*O*-acetyl) and on Zemplén deacetylation it gave compound *A*. The latter compound is thus shown to be methyl 2-acetamido-4:6-*O*-benzylidene-2-deoxy-α-D-altropyranoside (II) (isolated as a monohydrate). The infra-red spectra of a series of sugar derivatives containing *O*-acetyl and/or *N*-acetyl groups revealed the range 1 726—1 748 cm^{-1} for *O*-acetyl absorptions and the ranges 1 531—1 555 and 1 634—1 665 cm^{-1} for *N*-acetyl absorptions.

The absence of an *O*-acetyl group from compound *A* is surprising, especially since the minor product isolated from the same reaction mixture was *O*-acetylated. Attempts to *O*-acetylate compound *A* with pyridine and acetic anhydride or acetyl chloride were unsuccessful. The *O*-acetyl group in methyl 2-acetamido-3-*O*-acetyl-4:6-*O*-benzylidene-2-deoxy-α-D-altropyranoside (the product anticipated on *O*-acetylation of compound *A*) was not abnormally labile in that recrystallization could be effected without change under the usual conditions. Since Peat and Wiggins [17] did not give full experimental details further comparison is not possible.

Other evidence was accumulated which substantiated the structure of compound *A*. The presence of a free hydroxyl group was confirmed on treatment of compound *A* with toluene-*p*-sulphonyl chloride in pyridine when methyl 2-acetamido-4:6-*O*-benzylidene-2-deoxy-3-*O*-toluene-*p*-sulphonyl-α-D-altropyranoside (III) was obtained in good yield.

Graded acidic hydrolysis of compound *A* removed the benzylidene residue and yielded methyl 2-acetamido-2-deoxy-α-D-altropyranoside. The ready consumption of approximately one mole of metaperiodate by this latter compound under the usual conditions [19] indicates the presence of a vicinal glycol group and confirms the location of the acetamido residue at C_2 in compound *A*. Assuming normal cleavage of the epoxide ring in methyl 2:3-anhydro-4:6-*O*-benzylidene-α-D-allopyranoside under the action of methanolic ammonia

to give diaxial substituents (Fürst-Platner rule [20]) then compound *A* and the compounds subsequently derived from it must have the D-altrose configuration. The presence of vicinal *cis*-hydroxyl groups in methyl 2-acetamido-2-deoxy-α-D-altropyranoside is indicated by the more rapid consumption of oxidant than in the case of methyl 2-acetamido-2-deoxy-D-glucopyranoside which contains vicinal *trans*-hydroxyl groups.

Total acidic hydrolysis of methyl 2-acetamido-2-deoxy-α-D-altropyranoside or its 4:6-*O*-benzylidene derivative (II) yielded 2-amino-1:6-anhydro-2-deoxy-β-D-altropyranose hydrochloride (V) in low yield (28 % and 33 %, respectively). The highly crystalline nature of this compound recommends it for characterization of the parent aminosugar. That 2-amino-2-deoxy-D-altrose was also produced in the hydrolysis was indicated by the reducing power of the hydrolysate since the 1:6-anhydro compound itself is non-reducing. Examination of the hydrolysate by paper chromatography using the organic phase of a butanol-water-acetic acid (4:5:1) solvent system revealed only a single component. However with the *t*-butanol-water-acetic acid (2:1:1) solvent system [21] two components were observed which had R_F values and chemical properties similar to those of 2-amino-2-deoxy-D-gulose and 2-amino-1:6-anhydro-2-deoxy-β-D-gulopyranose [6]. Attempts to isolate the 2-amino-2-deoxy-D-altrose failed to yield a crystalline product.

The formation of a mixture of the free amino sugar and its 1:6-anhydride on acidic hydrolysis of methyl 2-acetamido-2-deoxy-α-D-altropyranoside and its 4:6-*O*-benzylidene derivative (II) is not surprising since the action of acid on D-altrose is well known [22] to yield an equilibrium mixture of approximately equal proportions of D-altrose and 1:6-anhydro-D-altrose. The $[M]_D$ value —315° (water) of 2-amino-1:6-anhydro-2-deoxy-β-D-altropyranose hydrochloride is similar to those, —339° and —348°, respectively, of 3-amino-1:6-anhydro-3-deoxy-β-D-altropyranose hydrochloride [23] and 1:6-anhydro-β-D-altropyranose [22].

Like 2-amino-1:6-anhydro-2-deoxy-β-D-gulopyranose hydrochloride [6], 2-amino-1:6-anhydro-2-deoxy-β-D-altropyranose hydrochloride readily consumed 2 moles of periodate.

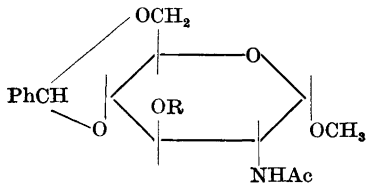

I R = $CH_3 \cdot CO$—
II R = H—
III R = $CH_3 \cdot C_6H_4 \cdot SO_2$—

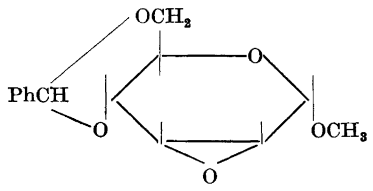

IV

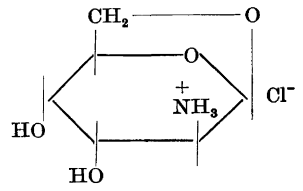

V

EXPERIMENTAL

All m. p. s are uncorrected. Dry pyridine connotes pyridine which has been distilled repeatedly from phosphorus pentoxide.

Action of methanolic ammonia on methyl 2:3-anhydro-4:6-*O*-benzylidene-α-D-allopyranoside

Methyl 2:3-anhydro-4:6-*O*-benzylidene-α-D-allopyranoside [m. p. 198°, $[\alpha]_D$ +140.2° (*c*, 1.0 in $CHCl_3$)] was prepared from methyl 4:6-*O*-benzylidene-2:3-di-*O*-toluene-*p*-sulphonyl-α-D-glucopyranoside by the method of Richtmyer and Hudson [24].

The alloside (5 g) was treated, in a Carius tube, with a cooled (0°) mixture of methanol (60 ml, dried over calcium oxide) and liquid ammonia (21 ml). The tube and contents were cooled in liquid air, the tube sealed and then heated at 140° for 3 days. After cooling in liquid air the tube was opened, the solvents were evaporated at 40° (bath)/14—16 mm, and the residue dried over phosphorus pentoxide *in vacuo*. Acetylation of the residue was effected by addition of dry pyridine (50 ml) and acetic anhydride (7.5 ml). After 12 h the mixture was evaporated at 30° (bath)/0.1 mm, the residue was washed with water then dissolved in chloroform (5 ml) and diluted with ether. On cooling (methanol-solid carbon dioxide mixture) methyl 3-acetamido-4:6-*O*-benzylidene-3-deoxy-α-D-glucopyranoside separated which after recrystallization from chloroform-ether afforded a product (0.3 g, 4.2 %) m. p. 271°, $[\alpha]_D$ +44.1° (*c*, 1.0 in chloroform). (Peat and Wiggins [17] record m. p. 270°, $[\alpha]_D$ +44.6° for this compound). The infra-red spectrum (KBr disc) of this compound showed strong absorptions characteristic of *O*-acetyl (1 726 cm^{-1}) and *N*-acetyl (1 549 and 1 634 cm^{-1}).

From the mother liquors a second product separated and after recrystallization from aqueous-methanol *methyl 2-acetamido-4:6-O-benzylidene-2-deoxy-α-D-altropyranoside hydrate* (2.8 g, 45.7 %) m. p. 188°, $[\alpha]_D$ +64° (*c*, 1.0 in chloroform) was obtained. (Found: C 55.8; H 6.7; N 4.1. $C_{16}H_{20}O_6N \cdot H_2O$ requires C 56.3; H 6.7; N 4.1), $[M]_D$ +218°. The infra-red spectrum (KBr disc) showed strong absorptions characteristic of the *N*-acetyl group (1 541 and 1 651 cm^{-1}) but not for *O*-acetyl.

Attempted *O*-acetylation of the foregoing compound using dry pyridine and acetyl chloride or acetic anhydride was unsuccessful; starting material was recovered unchanged.

Methyl 2-acetamido-4:6-*O*-benzylidene-2-deoxy-3-*O*-toluene-*p*-sulphonyl-α-D-altropyranoside

A solution of methyl 2-acetamido-4:6-*O*-benzylidene-2-deoxy-α-D-altropyranoside (2 g) in dry pyridine (12 ml) was treated with toluene-*p*-sulphonyl chloride (3 g) at 30° for 48 h. On dilution of the reaction mixture with ice water and recrystallization of the precipitate from aqueous-acetone the *product* (1.4 g, 50 %) was obtained m. p. 174° (decomp.), $[\alpha]_D$ +62° (*c*, 1.0 in acetone), $[M]_D$ +296°. (Found: C 58.0; H 5.6; N 3.0; S 7.2. $C_{23}H_{27}O_8NS$ requires C 57.8; H 5.7; N 2.9; S 6.8.)

Acidic hydrolysis of methyl 2-acetamido-4:6-*O*-benzylidene-2-deoxy-α-D-altropyranoside

(a) A solution of methyl 2-acetamido 4:6-*O*-benzylidene-2-deoxy-α-D-altropyranoside (1 g) in 2 N hydrochloric acid (10 ml) was boiled under reflux for 3.5 h. After two extractions with light petroleum (60—80°) the hydrolysate was neutralised with methyl di-*n*-octylamine [25] and then freeze dried. Dissolution of the syrupy residue in 2 *N* hydrochloric acid and dilution with acetone gave *2-amino-1:6-anhydro-2-deoxy-β-D-altropyranose hydrochloride* (0.19 g, 33 % after recrystallization from the same solvent system) which was non-reducing towards Fehling's solution and had m. p. 350° (decomp.), $[\alpha]_D$ −160° (*c*, 0.5 in water) $[M]_D$ −315°. (Found: C 35.7; H 6.0. $C_6H_{10}O_4N \cdot HCl$ requires C 36.4; H 6.1.)

The hydrolysate from which the foregoing compound was isolated was strongly reducing towards Fehling's solution. Examination of the neutralised hydrolysate by paper chromatography using the organic phase of a butanol-water-acetic acid (4:5:1) solvent system gave apparently a single spot which reacted strongly with ninhydrin, aniline hydrogen phthalate [26] and ammoniacal silver nitrate [27]. However with a *t*-butanol-water-acetic acid (2:1:1) solvent system [21] two spots were obtained with mobilities similar to those of 2-amino-2-deoxy-D-gulose and 2-amino-1:6-anhydro-2-deoxy-β-D-gulose [6]. In each case the faster moving component reacted with ninhydrin only and the slower moving component reacted with both ninhydrin and aniline hydrogen phthalate [26]. Attempts to isolate the 2-amino-2-deoxy-D-altrose, presumed present in the hydrolysate, by preparative scale paper chromatography did not yield a crystalline product.

(b) A solution of the altroside (1 g) in 0.5 % methanolic hydrogen chloride (10 ml) was boiled under reflux for 2 h. After two extractions with light petroleum (60 – 80°) the solution was diluted with water and deacidified with methyl di-*n*-octylamine [25] and then evaporated at 30° (bath)/0.1 mm. Methyl 2-acetamido-2-deoxy-α-D-altropyranoside (0.672 g, 92.5 %) was obtained as a syrup showing $[\alpha]_D$ +16.3° (*c*, 1.3 in water), $[M]_D$ +94°.

A solution of methyl 2-acetamido-2-deoxy-α-D-altropyranoside (0.0672 g) in water (5 ml) was treated with 0.25 M sodium metaperiodate solution (15 ml) and the volume rapidly adjusted to 50 ml. The consumption of oxidant was determined by the standard arsenite procedure on aliquots withdrawn at suitable time intervals. In a separate experiment methyl 2-acetamido-2-deoxy-α-D-glucopyranoside (0.0672 g) was oxidised under identical conditions. The consumption of oxidant (moles per mole) was as follows:

Time (h)	0.5	1.0	2.0	3.0	4.5
altroside	0.915	0.950	0.950	0.950	0.950
glucoside	0.710	0.915	0.950	0.994	0.994

A solution of methyl 2-acetamido-2-deoxy-α-D-altropyranoside (0.5 g) in 2 N-hydrochloric acid (10 ml) was boiled under reflux for 3 h. 2-Amino-1:6-anhydro-2-deoxy-β-D-altropyranose hydrochloride (0.118 g, 28 %), m. p. 350° (decomp.), $[\alpha]_D$ −160° (*c*, 0.5 in water) was subsequently isolated as in the foregoing hydrolysis (a).

Periodate oxidation of 2-amino-1:6-anhydro-2-deoxy-β-D-altropyranose hydrochloride

The aminosugar derivative (25 mg) was subjected to periodate oxidation in a manner similar to that described earlier. The consumption of oxidant was as follows:

30 min. 1.85 moles; 1 h. 2.02 moles (final constant value).

Deacetylation of methyl 2-acetamido-3-*O*-acetyl-4:6-*O*-benzylidene-2-deoxy-α-D-altropyranoside

A solution of the altroside derivative [17] (50 mg) in dry methanol (20 ml) was treated with a few mg of metallic sodium. After 12 h the solution was neutralised with carbon dioxide, evaporated and the residue recrystallized from aqueous methanol to yield a product m.p. 188° alone or in admixture with the methyl 2-acetamido-4:6-*O*-benzylidene-2-deoxy-α-D-altropyranoside hydrate described above.

The infra-red spectrum (KBr disc) of methyl 2-acetamido-3-*O*-acetyl-4:6-*O*-benzylidene 2-deoxy-α-D-atropyranoside showed strong absorptions characteristic of *O*-acetyl (1 729 cm^{-1}) and *N*-acetyl (1 531 and 1 649 cm^{-1}).

Acknowledgment. The authors thank Professor E. van Tamelen for samples of 2-amino-2-deoxy-D-gulose and its 1:6-anhydride, and Dr. D. H. Whiffen for the infra-red spectra measurements and for discussion. One of them (S.V.V.) thanks *Papirindustriens Forskningsinstitutt*, Oslo, Norway for a grant.

REFERENCES

1. Ledderhose, G. *Z. physiol. Chem. Hoppe-Seyler* **2** (1878) 213.
2. Levene, P. A. and LaForge, F. B. *J. Biol. Chem.* **18** (1914) 123.
3. Parks, J. T. *J. Biol. Chem.* **194** (1952) 885.
4. Walker, C. W., Fryth, P. W., Hutchings, B. L. and Williams, J. H. *J. Am. Chem. Soc.* **75** (1953) 2025.
5. Davies, D. A. L. *Biochem. J.* **59** (1955) 696.
6. van Tamelen, E. E., Dyer, J. R., Carter, H. E., Pierce, J. V. and Daniels, E. E. *J. Am. Chem. Soc.* **78** (1956) 4817.
7. Crumpton, M. J. *Nature* **180** (1957) 605; *cf.* Muir, H. *Biochem. J.* **65** (1957) 33P.
8. Comb, D. G. and Roseman, S. *J. Am. Chem. Soc.* **80** (1958) 497.
9. Jeanloz, R. W. *Ibid.* **79** (1957) 2591.
10. James, S. P., Smith, F., Stacey, M. and Wiggins, L. F. *J. Chem. Soc.* **1946** 625.
11. Fischer, E. and Leuchs, H. *Ber.* **35** (1902) 3787; **36** (1903) 24; Haworth, W. N., Lake, W. H. G. and Peat, S. *J. Chem. Soc.* **1939** 271.
12. Tarasiejsha, Z. and Jeanloz, R. W. *J. Am. Chem. Soc.* **79** (1957) 2660.
13. Levene, P. A. *J. Biol. Chem.* **39** (1919) 69.
14. Kuhn, R. and Fischer, H. *Ann.* **612** (1958) 65.
15. Kuehl, F. A., Flynn, E. H., Holly, F. W., Mozingo, R. and Folkers, K. *J. Am. Chem. Soc.* **68** (1946) 536.
16. For a review see Stoll, A. and Jucker, E., in *Encyclopedia of Plant Physiology*, Springer, Berlin 1958, p. 534.
17. Peat, S. and Wiggins, L. F. *J. Chem. Soc.* **1938** 1810.
18. Bellamy, L. F. *Infra-red spectra of Complex Molecules*, Methuen, London 1956.
19. Jackson, E. L. *Org. Reactions* **2** (1944) 341; Bobbitt, J. M. *Advances in Carbohydrate Chem.* **11** (1956) 1.
20. Overend, W. G. and Vaughan, G. *Chem. & Ind. London* **1955** 995, and references cited therein.
21. van Tamelen, E. E. *Personal communication.*
22. Richtmyer, N. K. and Hudson, C. S. *J. Am. Chem. Soc.* **61** (1939) 214.
23. Wiggins, L. F. *J. Chem. Soc.* **1947** 18.
24. Richtmyer, N. K. and Hudson, C. S. *J. Am. Chem. Soc.* **63** (1941) 1727.
25. Lester Smith, E. and Page, J. E. *J. Soc. Chem. Ind.* **67** (1948) 48.
26. Partridge, S. M. *Nature* **164** (1949) 443.
27. Hough, L. *Ibid.* **165** (1950) 400; Trevelyan, W. E., Proctor, D. P. and Harrison, J. S. *Ibid.* **166** (1950) 444.

Received May 30, 1958.

ACTA CHEMICA SCANDINAVICA 12 (1958) 1611—1621

Die Darstellung von reinen Häminen

K. G. PAUL

Medicinska Nobelinstitutet, Biokemiska avdelningen,
und Wallenbergstiftelsens laboratorium för fysiologisk kemi, Stockholm, Schweden

Drei Methoden für Hämindarstellung werden mit dem Hämochromogenspektrum als Reinheitsprobe verglichen.

1. Rohporphyrin-Porphyrinester-reines Porhyrin-Hämin. Manchmal werden Produkte erhalten, deren Hämochromogenspektra eine erhöhte Absorption im Rot besitzen.

2. Rohporphyrin-Porphyrinester-Häminester-Hämin. Die Hämochromogenspektra der Häminester wiesen auch manchmal die Rotabsorption auf. Der dafür verantwortliche Abkömmling kann durch Chromatographie auf sekundärem Natriumphosphat weggenommen werden. Die molaren Absorptionskoeffizienten für solche Hämine, die nach Verfahren 3. nicht gereinigt werden können, sind dadurch bestimmbar.

3. Kuppelung eines Hämins mit dem Apoprotein eines Häminproteides und Chromatographie auf Anionenaustauscher. Die Hämochromogenspektra der so erhaltenen Häminproteide sind einwandfrei. Auf diesem Weg können 6,7-dikarboxylige Hämine gereinigt werden, möglicherweise auch Monokarboxyhämine.

Bei der Darstellung von Häminen * werden meistens die entsprechenden Porphyrine über ihre Methylester gereinigt. Nach Hydrolyse des Esters wird Eisen in die Porphyrine eingeführt. Die Reinheit der Hämine wird durch Elementaranalyse, Chromatographie auf Säule oder Papier und Spektrophotometrie geprüft. Auf Grund des Darstellungsverfahrens sind als wahrscheinlichste Verunreinigung Abkömmlinge des gewünschten Hämins zu erwarten. Die Elementaranalyse ist daher als Reinheitsprobe nur von beschränktem Wert. Für die spektrophotometrische Reinheitsprüfung muss das Hämin in eine Form gebracht werden, in der die Abkömmlinge gut hervortreten. Bei Häminproteiden kommen bisweilen eine nicht umkehrbare Inaktivierung und eine erhöhte Lichtabsorption im Rot zusammen vor. Diese Erhöhung, die bei Reduktion mit Dithionit in Gegenwart von hämochromogenbildenden Stoffen, z. B. CO, nicht verschwindet (vgl. Hämoglobin-Choleglobin), ist spektrophotometrisch leicht nachweisbar. Weil die Veränderungen in den Hämin-

* Hämin bedeutet in der vorliegenden Arbeit eine Eisen-Porphyrin-Verbindung im allgemeinen. Bluthämin wird Protohämin genannt.

abkömmlingen wahrscheinlich mit denen in den Häminproteiden verwandt sind, dürfte das Hämochromogen eine geeignete Form der Hämine für die spektrophotometrische Reinheitsprüfung sein. Es wurde bald gefunden, dass ein Hämochromogenspektrum ein Plateau oder sogar ein schwaches Maximum bei 600—620 mμ besitzen könnte, ohne dass das Hämin eine Uneinheitlichkeit im Papierchromatogram aufwiese. Messungen des Hämochromogenspektrums wurden deshalb für die zuverlässigste Reinheitsprobe gehalten.

MATERIALIEN UND METHODEN

Alle molaren Lichtabsorptionskoeffizienten (β^*) sind auf Eisenbestimmungen mit Sulphosalicylsäure [1,2] gegründet. Bei unzureichender Verbrennungszeit mit Schwefelsäure-Wasserstoffperoxyd zeigt die Blindprobe eine gelbe Nuance, die der von Eisen verursachten Farbe ähnelt und Werte bis zu $D_{424} = 0{,}1$ gibt. Bei der Verbrennung muss wenigstens 10 Min nach dem letzten Peroxydzusatz gekocht werden [2]. Die Einführung des Eisens in die Porphyrine geschah nach den gewöhnlichen Methoden [3,4].

Für Papierchromatogramme wurde 2,6-Lutidin/Wasser 100/20, Whatman-Papier No. 1 und Zimmertemperatur verwendet, aber kein Ammoniakdampf im Gefäss [5,6].

Die Hämochromogene der freien Hämine mit Pyridin als Base wurden wie gewöhnlich [7] erhalten (Pyridin/0,1 M NaOH 1/3 + Dithionit). Die Häminester wurden in über KOH destilliertem Pyridin gelöst und die Lösung mit einem Volumen von 0,2 M NaOH versetzt.

Meerrettichperoxydase war mit Dowex-2 gereinigt, nicht aber auf Karboxymethylcellulose chromatographiert [8]. Für die Spaltung wurde die Lösung mit 0,2 Vol. von 5 % NaCl und 0,1 M HCl bis an pH 2 versetzt und nach 5 Min in 10 Vol. Azeton von −13° unter Umrühren langsam gegossen. Das Eiweiss wurde in der Kälte abzentrifugiert, ohne Waschen in Wasser aufgelöst und über Nacht gegen kaltes Wasser dialysiert. Ein ähnliches Verfahren ohne Neutralisation wurde früher für Cytochrom c verwendet [9]. Die Peroxydaseaktivität in der Mesidinprobe war mit Protohämin vollständig wiederherstellbar.

Myoglobin I (Mb), von Herrn Å. Åkeson erhalten, wurde wie früher beschrieben [11] gespalten.

Bluthämin wurde nach Chu und Chu [12] oder Fischer [13] erhalten (Tabelle 1). Koproporphyrin III wurde aus *Corynebact. diphteriae*-Bouillon (von Dr. G. Norlin erhalten) isoliert [14] (Fp. des Esters 153 und 178°, korr.). Koproporphyrin I, eine Gabe von Dr. J. J. Scott, enthielt nach Scott höchstens 5 % Koproporphyrin III. Mesoporphyrin I-Ester wurde aus der Fischer-Sammlung durch Professor S. Goldschmidt erhalten. Die übrigen Porphyrine wurden nach Fischer-Orth [15] dargestellt. Zweimal krystallisiertes Cytochrom c wurde von Doz. S. Paléus erhalten.

Tabelle 1. Ausbeute an Protohämin (mg/100 ml Blut) und molare Absorptionskoeffizienten der α-Bande des Pyridinhämochromogens ohne Umkristallisierung.

Darstellung nach Fischer		Darstellung nach Chu und Chu	
Ausbeute	$\beta \times 10^{-7}$	Ausbeute	$\beta \times 10^{-7}$
210	6,45	440	7,68
470	7,38	300	7,79 **
360		350	7,72
		460	7,96

* $\beta = \frac{1}{c} \times \frac{1}{d} \times \ln \frac{I_0}{I}$; wo c = Konzentration in Mole × cm^{-3}, d = Schichtdicke in cm

** Nach Umkristallisierung 7,60.

ERGEBNISSE

Drei Wege für die Darstellung von reinen Häminen wurden probiert. Die Ergebnisse sind in Tabelle 2 gesammelt.

Tabelle 2. Molare Absorptionskoeffizienten der Hämochromogene für Hämine die nach den drei Methoden erhalten sind. Alle Wellenlängen mittels Beckman DU Spektrophotometer erhalten. "Rot" bedeutet die Wellenlänge 50 mμ rotwärts der α-Bande.

Hämin	Methode	α-Bande		Minimum		β-Bande		Rot
		λ	β	λ	β	λ	β	β
PH	1 [1]	556	7,44	540	2,05	525	3,65	0,18
PH	1 [2]	557	7,68	540	2,05	525	3,73	0,13
PH	1 [3]	557	7,60	540	2,11	525	3,79	0,24
Hämoglobin	[4]	558	8,04	541	2,18	526	3,96	0,09
PH	3	557	7,83	541	2,03	526	3,70	0,11
MH	1	547	7,50	532	2,05	517	4,30	0,28
MH-Ester	2	546	7,80	532	2,01	514	4,39	0,20
MH	3	547	7,84	532	2,09	517	4,47	0,16
MH I	1	547	6,64	531	2,02	515	4,03	0,36
HH	1	550	5,71	535	2,40	519	3,79	0,55
HH	3	547	7,64	532	2,09	517	4,41	0,21
Zytochrom c	[5]	551	7,18	537	2,01	522	4,28	0,18
DH	1	544	6,14	530	1,98	514	4,25	0,27
DH	1 [3]	544	6,46	530	2,00	514	4,42	0,24
DH-Ester	2	545	6,40	530	1,91	514	4,35	0,08
DH	2 [6]	544	6,03	530	1,90	515	4,21	0,25
DH	3	544	6,27	530	1,91	515	4,27	0,13
DiAcDH	1	574	3,22	555	2,12	539	2,40	0,32
DiAcDH	3	575	3,80	556	2,37	542	2,82	0,09
KH III	1	548	6,68	532	1,93	517	4,02	0,26
KH I	1	548	6,36	530	1,93	517	3,92	0,28
KH I-Ester	2	548	6,16	533	1,94	518	4,04	0,13

[1] Nach Fischer. [2] Nach Chu und Chu. [3] Dasselbe Präparat umkristallisiert. [4] Gewaschene Erythrozyten. [5] In Pyridin-Lauge. [6] Freies Deuterohämin nach Verf. 2 und Verseifung (2,2 μMole, S. 1616).

1. Rohporphyrin — Porphyrinester — reines Porphyrin — Hämin

Mesohämin wird als Beispiel gegeben.

Mesoporphyrin wurde mit Methanol-HCl verestert und durch Chromatographie (Aluminiumoxyd Merck, nach Brockmann, Grad IV, 125 mM Methanol in Chloroform [16]) und Kristallisation bis zum konstanten Schmelzpunkt (216°) gereinigt. Der Ester wurde mit 4 M HCl bei Zimmertemperatur während 48 St verseift und das Porphyrin in Äther getrieben. Es wurde mit 0,02 M HCl gewaschen (geringe Ausbeute, verworfen) und das Porphyrin mit 0,15 M HCl herausgenommen. Gegenstromverteilung [17] zeigte Einheitlichkeit. Der Äther wurde *in vacuo* verjagt, das Porphyrin ausgeflockt, gewaschen, getrocknet und in Hämin überführt.

Ohwohl das Porphyrin also bestimmt rein gewesen war, zeigte das Hämochromogenspektrum erhöhte Absorption bei 600—640 mμ (Abb. 1). Eisen, als

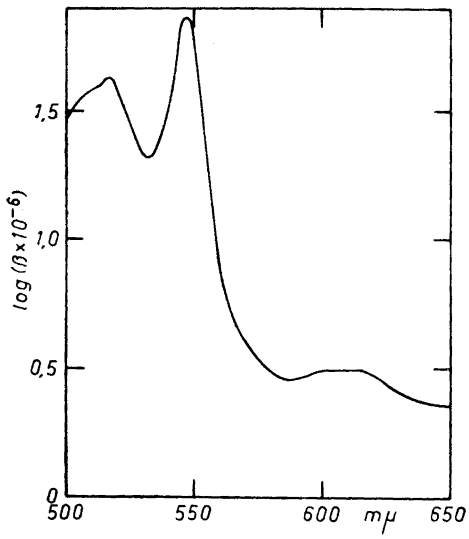

Abb. 1. Pyridinhämochromogen des Mesohämins nach Verfahren 1 erhalten.

Eisen(II)Acetat, gab unter den Bedingungen der Hämochromogenbestimmung $\beta_{600} = 0{,}02 \times 10^7$ cm^2 × Mole^{-1} und ist also als Ursache der Absorption auszuschliessen. Umkristallisation des Hämins aus Pyridin-Eisessig oder einfache Fällung aus alkalischer Lösung mit Überschuss an Säure reduzierte nicht die Absorption im Rot. Freies Porphyrin war in den Mutterlaugen nicht nachweisbar. Versuche, die erhöhte Absorption im Rot zu vermeiden durch Eiseneinführung in N_2- oder CO_2-Atmosphäre mit nachfolgender Oxydation des Ferroeisens mit Cerisulfat oder grossem Überschuss an Ferrichlorid blieben erfolglos. Die erhöhte Absorption im Rot trat auch hier öfters auf.

2. Rohporphyrin — Porphyrinester — Häminester — Hämin

Auch bei Eiseneinführung in Porphyrinester trat die erhöhte Absorption im Rot auf. Die Trennung von reinen Häminestern und ihren Abkömmlingen ging durch Chromatographie auf sekundärem Phosphat [18] glatt.

Deuterohäminester wurde aus Protohämin über Deuteroporphyrinester (Reinigung wie beim Mesoester, Fp. 218°) erhalten und aus Chloroform-Eisessig kristallisiert (Fp. 242—244°). Nach Trocknen *in vacuo* über KOH wurde auf $Na_2HPO_4 \cdot 2H_2O$ / Chloroform (13 × 1 cm) chromatographiert. Der Ester (4,8 μMole nach der Eisenbestimmung) wurde in Chloroform aufgetragen. 15 mM Methanol in Chloroform eluierte eine rote, gut begrenzte Fraktion (3,7 μMole), die sich bei wiederholtem Chromatographieren mit 10 mM Methanol nicht aufteilen liess. Deuterohäminester (Fp. 251°) kristallisierte aus Chloroform und kochsalzgesättigtem Eisessig. Aus der Säule war mit 70 mM Methanol nichts, mit reinem Methanol 0,4 μMole eluierbar; dabei sinterte die Säule.

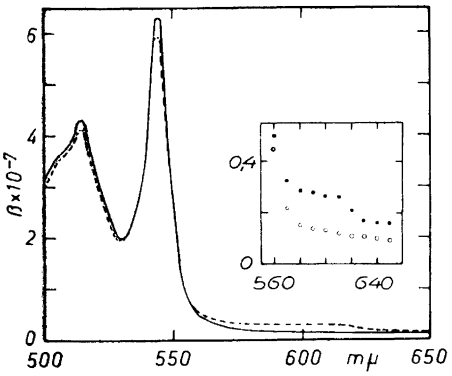

Abb. 2. Pyridinhämochromogen des Deuterohämoinesters vor (----) und nach (——) Chromatographie auf $Na_2HPO_4 \cdot 2H_2O$.

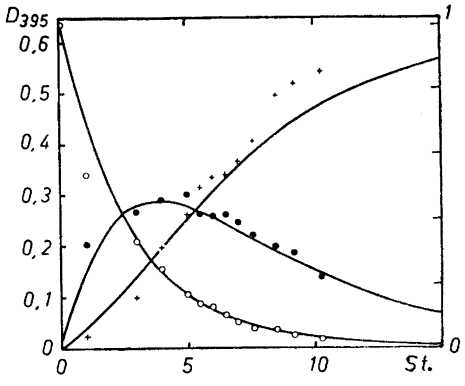

Abb. 3. Verseifung von Mesohämindimethylester mit HCl in Azeton. ○● + bedeuten Absorption der Flecke mit R_F-Werten entsprechend Diester, Monoester und freies Hämin (Ordinate links). Kurven bedeuten Molbrüche (Ordinate rechts), für $k_1 = 0{,}360$ und $k_2 = 0{,}193$ St^{-1} berechnet.

Bei Umchromatographieren mit Gemischen von Chloroform und Methanol erwies sich diese Fraktion als uneinheitlich. Die Hämochromogenspektra des Ausgangsmateriales und der roten Fraktions sind in Abb. 2 gegeben.

In der nachfolgenden Verseifung des Häminesters waren alkalische Lösungen wegen Gefahr der Häminzersetzung zu vermeiden. Die Wahl des Lösungsmittels war bei der sauren Verseifung durch die Anwesenheit von sowohl Ester als freiem Hämin beschränkt. Für Hydrolyse bei Zimmertemperatur, z. B. für die Isolierung des Monoesters, war über Zinn(II)Chlorid gereinigtes Dioxan brauchbar. Bei Temperaturen über 40° trat aber allmählich merkbare Porphyrinfreisetzung und Bildung von Häminabkömmlingen mit niedrigen R_F-Werten auf. Aceton wurde bei mässigen Temperaturen verwandt. Die Geschwindigkeitskonstanten k_1 und k_2 der Verseifung wurden in einem Versuch experimentell bestimmt.

$$\text{Diester} \xrightarrow{k_1} \text{Monoester} \xrightarrow{k_2} \text{freies Hämin}$$

Während einer Verseifung (Abb. 3) wurden Proben entnommen, auf Papier chromatographiert, die Flecke ausgeschnitten und mit kochendem Eisessig eluiert. Die R_F-Werte waren 0,92 (0,87—0,96), 0,80 (0,74—0,84) und 0,68 (0,61—0,77). Diester und freies Hämin als Vergleichungsstoffe gaben den ersten bzw. letzten Wert. Die Konstanten k_1 und k_2 wurden berechnet [19] aus

$\text{Diester}_{t_1} = \text{Diester}_{t_0} \times e^{-k_1 t_1}$

Freies Hämin $= 2\ (1 - e^{-k_2 t_1}) - (1 - e^{-k_1 t_1})$

Diester + Monoester + freies Hämin = 1

Die Molbrüche wurden aus den Lichtabsorptionen erhalten, z. B.

$$\text{Diester} = \frac{\text{Abs. d. Fleckes mit } R_F = 0{,}92}{\text{Summe Abs. d. drei Flecke}}$$

k_1 wurde als 0,360 St^{-1} gefunden. k_2 wurde aus den Messwerten für sowohl freies Hämin als auch Monoester berechnet; beide Möglichkeiten gaben den Wert 0,193 St^{-1}. Wenn Dioxan-10 M HCl, 2:1, für die Verseifung verwendet wurde verschwand der Diester bei 100, 50 und 20° mit den Geschwindigkeiten $t_{\frac{1}{2}}$ 0, 8, 40 und 1 200 Min, was eine scheinbare Aktivierungsenergie von 21 000 cal/Mol entspricht.

4,2 μMole von Deuterohäminester, die auf sekundärem Phosphat (15 mM Methanol in Chloroform) gereinigt waren, wurden bei 50° während 4 St in geschmolzenem Rohr mit 0,8 ml 8 M HCl in 4 ml Aceton verseift. Die Lösung wurde dann mit Chloroform verdünnt und mit Wasser bis zur Neutralität gewaschen. Das dabei ausgefallene freie Hämin (2,2 μMole) war papierchromatographisch einheitlich. Sein Hämochromogen zeigte aber im Vergleich mit dem des Esters erhöhte Absorption im Rot mit einem Maximum bei 602 mμ. Ein Teil der Chloroformlösung wurde getrocknet (Tabelle 2) und auf einer Phosphatsäule ($Na_2HPO_4 \cdot 2\ H_2O/NaH_2PO_4 \cdot 2\ H_2O$ 1/10, 10 × 1 cm, rein Chloroform) chromatographiert, erwies sich aber als uneinheitlich mit niedrigem Quotient α-Bande/Minimum.

3. Kuppelung an das Apoprotein eines Häminproteides und Isolierung des widergebildeten Häminproteides

Eine dritte Möglichkeit wäre, ein Hämin, z. B. nach Methode 1 erhalten, mit einem Ionenaustauscher reagieren zu lassen, aus dem die Abkömmlinge durch reines Hämin völlig verdrängt werden. Ein Ionenaustauscher mit solchen Eigenschaften wäre möglicherweise im Apoprotein eines Häminproteides zu erwarten. Der Arbeitsgang würde demnach, das Apoprotein mit einem — nach dem Gewicht oder der Eisenmenge — so grossen Überschuss an Hämin reagieren zu lassen, dass das molare Verhältnis 1:1 zwischen reinem Hämin und Apoprotein überschritten würde. Der Überschuss an reinem Hämin und die Abkömmlinge wären dann mit einem unspezifischen, starken Anionenaustauscher wegzunehmen.

Meerrettichperoxydase, Pferdeleberkatalase, Methämoglobin, Karboxyhämoglobin, Metmyoglobin und Karboxymyoglobin wanderten auf Dowex-2 (200—400 mesh, 8 % Querbindung, pH 7,4, 0,03—0,15 M Phosphat) mit R_F-Werten $>0{,}9$. Bei niedriger Durchlaufgeschwindigkeit der Flüssigkeit wurde freies Hämin als eine braune Zone am obersten Teil der Säule adsorbiert, bei hoher Geschwindigkeit aber verfärbte sich die ganze Säule braun. Die Reaktion zwischen Hämin * und Austauscher war also nicht momentan. Bei konstanter Durchlaufgeschwindigkeit war die Länge der braunen Zone dem Häminüberschuss proportional. Für die Vermeidung von freiem Hämin im Eluat wurde immer das Chromatographieren während etwa einer halben Stunde unterbrochen sobald die Lösung in der Säule gesunken war; erst dann wurde das Häminproteid eluiert.

Aus Protohämin und Peroxydaseapoprotein rekombinierte Peroxydase war von ungespaltener Peroxydase auf Dowex-2 nicht zu trennen. In qualitativen

* In NaOH-Phosphat, s. unten.

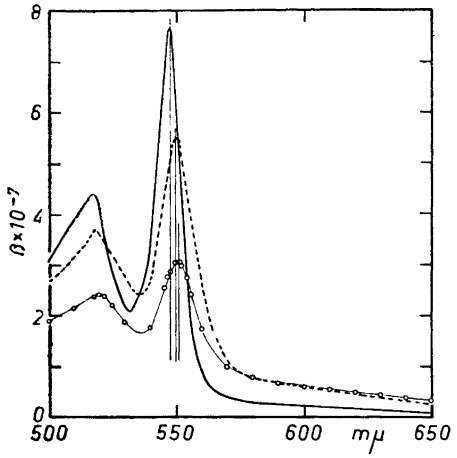

Abb. 4. Pyridinhämochromogen des Hämatohämins vor (---) und nach (———) Kuppelung an Apomyoglobin und Chromatographie auf Dowex-2. —o— ist das Hämochromogenspektrum der mit 1 M HCl eluierten Fraktion. Die Säule war nach der Eluierung mit der Säure nicht häminfrei, weswegen die Kurven nicht ohne weiteres addiert werden können.

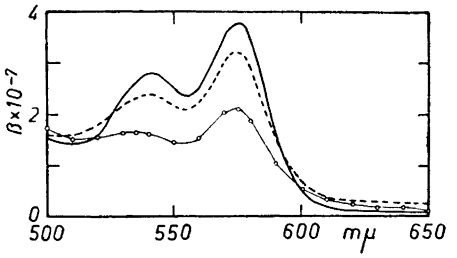

Abb. 5. Pyridinhämochromogen des Diacetyldeuterohämins. Symbolen vgl. Abb. 4.

Versuchen mit einigen Häminen zeigten die Hämochromogenspektra der rekombinierten und chromatographierten Peroxydasen in Vergleich mit den der Ausgangshämine gesteigerte Verhältnisse zwischen Maxima und Minima und Verschwinden der Erhöhung im Rot. Apoprotein "wählt" also reines Hämin aus. Kuppelung ohne Chromatographie von Apoperoxydase mit einer nach dem Eisengehalt äquivalenten Häminmenge beeinflusste nicht das Hämochromogenspektrum.

Bei der Bestimmung der molaren Absorptionskoeffizienten der verschiedenen Hämochromogene wurde wegen des grossen Materialverbrauches in den Eisenbestimmungen Myoglobin I statt Peroxydase verwendet. Rekombiniertes Hämoglobin dürfte mit ungespaltenem Hämoglobin nicht identisch sein [20]. Rekombiniertes und ungespaltenes Myoglobin I zeigen identische Kristallformen, Spektra und elektrophoretische Eigenschaften [11], auch waren sie auf Dowex-2 nicht zu trennen. Es dürfte deshalb gestattet sein, Myoglobin-Apoprotein als "Ionenaustauscher" zu verwenden obwohl die gasbindende Wirkung hier nicht geprüft wurde.

Für jede Kuppelung wurde abgemessen

Mb-Apoprotein	(0,58 μMole/ml)	3,0 ml
Phosphatpuffer	(0,03 M, pH 7,3)	0,2 ml
Hämin	(in M/30 NaOH, NaOH : Hämin = 5)	0,5 ml
Hämin/Protein = 2		

Nach 55 St im Kühlschrank wurden die Lösungen chromatographiert (Dowex-2, 15 × 1 cm, 0,03 M Phosphat, pH 7,3) und Hämochromogen und

Eisen in den Eluaten bestimmt. Die Reinigungen von Hämatohämin und Diacetyldeuterohämin werden als Beispiele gegeben (Abb. 4, 5).

Ausser Apoperoxydase und Apomyoglobin wurde Serumalbumin für die Reinigung probiert. Bei dem Verhältnis 1:1 zwischen Protohämin und Albumin wurde das Hämin von der Säule quantitativ aufgenommen. Bei derselben Durchlaufgeschwindigkeit zog sich aber die braune Farbe weiter hinunter als in Abwesenheit von Eiweiss. Je grösser das Verhältnis von Albumin zu Hämin war je weiter färbte sich die Säule braun, und Hämin trat zuletzt im Eluat auf. Keine Reinigung des Hämins wurde dabei beobachtet. Durch Alter völlig inaktivierte Apoperoxydase verhielt sich wie Serumalbumin.

Verfahren 3 wurde auf einigen anderen Porphyrinverbindungen als 6,7-Dikarboxyl-Häminen geprüft. Apomyoglobin und die oben (S. 1617) gegebenen Bedingungen wurde benutzt. Mesohämin I (6,8-diCOOH) wurde bei dem Verhältnis Hämin/Protein 1:1 von dem Anionenaustauscher zurückgehalten und zwar so, dass der oberste Teil der Säule am stärksten gefärbt wurde mit abwärts abnehmender Verfärbung ohne getrennten Fraktionen. Mit Überschuss an Eiweiss oder schnellem Chromatographieren wurde die ganze Säule braun. Koprohämin III (2,4,6,7-tetraCOOH) gab einen ähnlichen Befund aber ausgeprägter, so dass das Hämin am Anfang der Säule eine scharfe Bande bildete.

Tabelle 3. Chromatogramme auf Dowex-2 Häminisomeren nach Kuppelung an Apoperoxydase. Apoenzym (0,40 ml = 0,72 mg N) und Hämin (0,60 = 0,01 mg N, Hämin:Eiweiss 2,5) während 10 St bei Zimmertemperatur gelassen. Alle Lösungen und Puffern pH 7,6, 0,03 M Phosphat. 0,80 ml der Gemische wurden für Chromatographie genommen. Säulen: Dowex-2, 16 × 0,9 cm.

Hämin	Gesamt-N im Eluat mg	$\frac{D_{400}}{D_{280}}$ im Eluat
MH IX	0,50	2,67
MH I	0,52	1,98
KH III	0,52	0,40
KH I	0,55	0,24
Apoperoxydase	0,54	0,02

Koprohämin I (2,4,6,8-tetraCOOH) benahm sich genau wie sein Isomer. Aus Tabelle 3 geht hervor, dass das Eiweiss bei den drei Häminen fast quantitativ eluiert wurde. Bei Pyrrohämin (7-monoCOOH) war der Befund wegen der niedrigen Lösligkeit dieser Verbindung in Lauge nicht ganz klar. Eine freie, wandernde Bande war aber gut wahrnehmbar; bei Umchromatographieren auf Dowex zeigte sie Einheitlichkeit. Mesoporphyrin IX (6,7-diCOOH) zeigte zwar eine Spektrumänderung bei Zusatz von Apomyoglobin oder Serumalbumin, bei Chromatographieren auf Dowex-2 wurde es aber zurückgehalten, und das Eiweiss trat im Eluat allein auf. Kobalt (III) Mesoporphyrin IX gab denselben Befund wie die 6,7-Dikarboxyl-Hämine. Es wird auch hier daran erinnert, dass die geprüften Eisen(II)Protoporphyrin-Protein-Verbindungen ohne Zerlegung wanderten. Karboxyhämoglobin wanderte schneller als Methämoglobin und Paraperoxydase schneller als Peroxydase; in beiden Fällen waren die relativen R_F-Werte etwa 1:0,9. Diese Beobachtungen stimmen mit denen bei elektrophoretischen Untersuchungen überein.

DISKUSSION

Das übliche Verfahren für Hämindarstellung, hier als Methode 1 bezeichnet, gibt zwar bisweilen Präparate, deren Pyridinhämochromogenspektra niedrige Absorption im Rot zeigen. Meistens aber werden Spektra erhalten, die im Vergleich mit den Hämochromogenspektra von z. B. Erythrocyten oder Cytochrom c gesteigerte Absorption im Rot zeigen. Niedrige Absorption gibt auch aus Blut isoliertes Protohämin. Mit dem beschriebenen Verfahren für die Reinigung von Mesoporphyrin ist es sicher, dass das Porphyrin rein war. Das deutet auf die Eiseneinführung, wahrscheinlicherweise die mit den Redoxverläufen verbundene Bildung von freien Radikalen, als das schädigende Moment. Der geringe Wert [7] der Umkristallisierung aus Pyridin-Eisessig als Reinigungsmethode für schon kristallisierte Hämine wurde bestätigt.

Auch wenn es nicht gelungen ist die Verseifung des Häminesters ohne Nebenreaktionen durchzuführen sind doch die molaren Absorptionskoeffizienten des Hämochromogens des freien Hämins mittels dem Ester erreichbar. Bei der Berechnung der Geschwindigkeitskonstanten k_1 und k_2 der Verseifung wurde dieselbe molare Absorption in Eisessig für Diester, Monoester und freies Hämin angenommen. Dies mag nur annähernd richtig sein, weil eine Auflösung von freiem Hämin in Eisessig nicht stabil ist, und ein Zuwachs der Gesamtabsorption von etwa 10 % während der Verseifung (Abb. 3) wurde in der Tat beobachtet. Dies erklärt warum k_2 etwas grösser als $k_1/2$ gefunden wurde. Die k-Werte zeigen, dass die beiden Karboxylgruppen von einander unabhängig verseift werden.

Die Reinigung mittels Apoprotein gelang bei Proto-, Meso-, Hämato-, Deutero- und Diacetyldeuterohämin, die alle zwei Karboxylgruppen, in 6- und 7-Stellung, besitzen. Die Hämochromogenspektra der vier erstgenannten sind einander sehr ähnlich mit einer engen α-Bande. Aus Abb. 4 geht hervor, dass die Hämatohäminabkömmlinge nicht nur flachere sondern auch langwelligere Hämochromogenbanden als das reine Hämin besitzen. Es war darum von Interesse zu finden, dass Diacetyldeuterohämin, trotz der Ausdehnung und Rotverschiebung seines Hämochromogenspektrums, durch Kuppelung und Anionenaustauscherchromatographie gereinigt werden konnte (Abb. 5). Die relativen Affinitäten der fünf Dikarboxyl-Hämine zu Apoproteinen werden in einer späteren Arbeit näher untersucht; hier wird nur vorläufig erwähnt, dass die Proto-, Meso- und Hämatohäminperoxydasen dieselbe Aktivität in der Mesidinprobe zeigen; Diacetyldeuterohämin dagegen ist völlig inaktiv.

Die fünf genannten 6,7-Dikarboxyl-Hämine (Eisen(III)Porphyrine) ebensowie Kobalt(III)Mesoporphyrin, Eisen(II)Protoporphyrin und Pyrrohämin wanderten, nach Kuppelung an Apoeiweiss, wie gut begrenzte Banden abwärts auf der Säule. Das Eluat konnte mehrmals ohne Aufteilung umchromatographiert werden. Alle anderen geprüften Hämine und Mesoporphyrin IX wurden trotz »Kuppelung» von der Säule adsorbiert. Die Versuche mit verschiedenen Eiweisskörpern — zwei nativen Apoproteinen und zwei unspezifischen Substanzen (Serumalbumin und gealterte Apoperoxydase) — zeigen, dass eine bestimmte Konfiguration im Träger vorhanden sein muss. Es mag angenommen werden, dass die Konfiguration zwei Gruppen umfasst, die imstande sind mit den Häminkarboxylgruppen 6 und 7, oder mit an-

deren Säuregruppen, die ebensoweit von einander getrennt sind, zu reagieren. Gekuppeltes Mesohämin I bekomme dadurch eine freie Karboxylgruppe, die mit Dowex reagieren könnte. Nach dem Befund mit Pyrrohämin genügen Eisen + eine Karboxyäthylgruppe um eine einheitlich wandernde Verbindung zu schaffen. Mesoporphyrin IX zeigt, dass die Karboxylgruppen nicht allein die Bindung Wirkungsgruppe-Eiweiss vermitteln können. Bei pH 7,3 sind die pyrrolischen Stickstoffatomen ungeladen [21], und man muss deshalb schliessen, dass bei den Karboxylgruppen in Mesoporphyrin IX das Apoeiweiss von dem Dowex ersetzt wird. In Kobaltmesoporphyrin gibt es noch eine Bindungsmöglichkeit.

Der Befund bei Koprohämin III wäre verständlich wenn das Hämin, ausser dem Eisen, mit nur einer Karboxylgruppe oder einem "falschen" Paar (2—4, 4—6 oder 2—7, nicht aber 6—7) an dem Eiweiss gebunden wäre oder sonst die Bindung Hämin-Anionenaustauscher stärker als die Bindung Hämin und Protein wäre. Die Frage kann nicht beantwortet werden, weil die möglichen Abstände zwischen Eisen und Karboxylgruppen und die Reihenfolge der vier Dissoziationen unbekannt sind. Aus dem Versuch mit Koprohämin I kann nur geschlossen werden, dass die beiden isomeren Porphyrinen als Hämine unter den hier benutzten Bedingungen nicht zu trennen sind. Bei allen Häminen besteht die Möglichkeit, dass Eisen und Karboxylgruppen in der Bildung von Häminaggregaten teilnehmen. Es ist aber nicht klar warum sich die Koprohämine von den dikarboxyligen Häminen unterscheiden sollten.

Die Stickstoffatome in Dowex sind bei pH 7 positiv geladen, und eine Eisen-Stickstoff-Bindung ist deshalb sehr unwahrscheinlich [22]. Dowex-2 besitzt eine alkoholische Hydroxylgruppe, und Alkohole bilden mit Hämin Komplexe [15]. Eine Esterbildung ist aber unter den gegebenen Bedingungen bei günstigen sterischen Verhältnissen möglich. Es ist auffallend, dass die Reaktion zwischen Dowex und Hämin so viel Zeit braucht und auch, dass adsorbiertes Hämin mit hohen Eiweisskonzentrationen nicht zu eluieren ist.

Die Beobachtung, dass die Abkömmlinge lockerer als die entsprechenden nativen Hämine gebunden sind, steht in Übereinstimmung mit der Auffassung, dass der Hämoglobinabbau am Häminteil beginnt. Die Bindung an Globin würde dabei aufgelockert werden, und die prosthetische Gruppe könnte von anderen Trägern übernommen werden.

Für die freundliche Überlassung von Präparaten werden gedankt Herrn Å. Åkeson (Myoglobin I) und Doz. S. Paléus (Cytochrom c), Medicinska Nobelinstitutets biokemiska avdelning, Stockholm, Dr. G. Norlin (*Corynebact. diphteriae*-Bouillon), Statens bakteriologiska Laboratorium, Stockholm, Prof. S. Goldschmidt (Mesoporphyrin I-Ester), Organisch-chemisches Institut, München und Dr. J. J. Scott (Koproporphyrin I-Ester) National Institute for Medical Research, London.

Fräulein A. Harthoorn hat sehr wertfolle Assistanz geliefert. Die Untersuchung wurde von *Statens naturvetenskapliga forskningsråd* unterstützt.

LITERATUR

1. Lorber, F. *Biochem. Z.* **181** (1927) 391.
2. Paul, K. G. *Acta Chem. Scand.* **2** (1948) 430.
3. Warburg, O. und Negelein, R. *Biochem. Z.* **244** (1932) 239.

4. Erdman, J. G. und Corwin, A. H. *J. Am. Chem. Soc.* **69** (1947) 750.
5. Rimington, C. und Nicholas, R. E. H. *Scand. J. Clin. Lab. Invest.* **1** (1949) 12.
6. Kehl, R. und Stich, W. *Z. physiol. Chem.* **289** (1951) 6.
7. Paul, K. G., Theorell, H. und Åkeson, Å. *Acta Chem. Scand.* **7** (1953) 1284.
8. Paul, K. G. *Acta Chem. Scand.* **12** (1958) 1312.
9. Paul, K. G. *Acta Chem. Scand.* **5** (1951) 379.
10. Paul, K. G. und Avi-Dor, Y. *Acta Chem. Scand.* **8** (1954) 649.
11. Theorell, H. und Åkeson, Å. *Ann. Acad. Sci. Fennicæ* **A 60** (1955) *(Festschrift Virtanen)*.
12. Chu, T. C. und Chu, E. J.-H. *J. Biol. Chem.* **212** (1955) 1.
13. Fischer, H. *Org. Syntheses* **31** (1941) 53.
14. Gray, C. H. und Holt, L. B. *Biochem. J.* **43** (1948) 191.
15. Fischer, H. und Orth, H. *Die Chemie des Pyrrols*, Leipzig 1937.
16. Nicholas, R. E. H. *Biochem. J.* **48** (1951) 309.
17. Paul, K. G. *Scand. J. Clin. Lab Invest.* **5** (1953) 212.
18. Paul, K. G. *Unveröffentlicht.*
19. Getman, F. H. und Daniels, F. *Outlines of Physical Chemistry*, Ed. 7, John Wiley & Sons, New York und London 1941.
20. Wyman, J. Jr. *Advances in Protein Chem.* **4** (1948) 406.
21. Neuberger, A. und Scott, J. J. *Proc. Roy. Soc. London* **A 213** (1952) 307.
22. Cowgill, R. W. und Clark, W, M. *J. Biol. Chem.* **198** (1952) 33.

Eingegangen am 13. Juni 1958.

ACTA CHEMICA SCANDINAVICA 12 (1958) 1622—1633

Studies on Bile Acid Salt Solutions

II. The Solubility of Cholic Acid in Sodium Cholate Solutions and that of Desoxycholic Acid in Sodium Desoxycholate Solutions

PER EKWALL, TORSTEN ROSENDAHL and A. STEN

Institute of Physical Chemistry, Åbo Akademi, Åbo, Finland

The solubility of cholic acid in sodium cholate solutions and that of desoxycholic acid in sodium desoxycholate solutions has been determined by potentiometric titration of solutions of their sodium salts and by measuring the changes in the refractive indexes when the solutions have been saturated with the acids. The former method was found suitable for the determination of the solubilities in dilute solutions where no association has yet occurred; the latter method was more appropriate for solutions containing micellar substance. The solubility product exponent of cholic acid at 20°C was found to be $pK_L = 8.72$ and that of desoxycholic acid $pK_L = 9.15$.

From bile salt solutions saturated with the corresponding acids, the acids separate in pure form. No acid salts were detected in the precipitates. The activity of undissociated cholic acid in sodium cholate solutions saturated with the acid was found to be $a_{HA} = 1.8 \times 10^{-4}$ M. Knowing this value, it has been possible to evaluate the activity of the cholate anion from the pH values of the solutions. The results obtained show that no association takes place in the cholate solutions below a cholate concentration of about 0.01 M. From this concentration up to about 0.03 M, a partial association is observed, but above the latter concentration all the added cholate ions become associated. The activity of undissociated desoxycholic acid in solutions of its sodium salt saturated with the acid is 1.05×10^{-4} M. The evaluation of the activity of the desoxycholate anion in these solutions showed that no association occurs up to a desoxycholate concentration of 0.005—0.006 M. Above the latter concentration a partial association takes place which seems to become complete at least when the desoxycholate concentration exceeds about 0.01 M.

As soon as association sets in, the bile salt solutions begin to dissolve the respective bile acids. The solubilizing power increases stepwise which shows that the micelles have different properties in different concentration ranges. The concentrations delimiting these ranges in solutions saturated with bile acids have been determined.

When an attempt is made to elucidate the structures of aqueous bile salt solutions it is desirable to have exact information about the solubilities of the respective acids in these salt solutions.

As far as the solubilities of bile acids in water are concerned, it is known that the unconjugated acids are sparingly soluble and that their solubilities increase with the number of hydroxyl groups in the molecule. Gillert [1] has reported the solubility of desoxycholic acid as 0.24 g/l and that of cholic acid as 0.28 g/l at 15°C. Also the bile acids conjugated with glycine have relatively low solubilities, whereas the taurine conjugate of desoxycholic acid and especially that of cholic acid are very soluble in water.

The bile acids have a tendency to remain in the colloidal state in solution. Josephson [2] found that when strong acid is slowly added to aqueous bile salt solutions a colloidal solution often results from which the liberated bile acid begins to crystallize out only after some time, frequently after several days. The excess of mineral acid that can be added to solutions of the same concentration of different bile salts before the crystallization begins is observed to vary with the nature of the bile acid. Also foreign salts present in the solution influence the separation of the bile acid. Ekwall and coworkers have confirmed some of these observations [3-5] and have also reported preliminary values for the solubilities of cholic and desoxycholic acids in their respective salt solutions. They have further shown that the solubility increases with the degree of micelle formation.

We have now performed a more detailed investigation of the solubility of cholic acid in sodium cholate solutions and that of desoxycholic acid in sodium desoxycholate solutions. The solubilities have been calculated from the results of potentiometric titrations of the bile salt solutions with hydrochloric acid or have been determined directly by measuring the changes in refractive indices of the saturated solutions. In addition the solubility of cholic acid in pure water has been evaluated.

The bile salts were prepared from the same acids as were employed in the experiments in Part I of this series [5].

THE SOLUBILITY OF CHOLIC ACID IN WATER

The solubility of cholic acid was determined as follows. An excess of cholic acid was added to a volume of boiling conductance water exceeding 2 litres. The resulting mixture was then allowed to stand in a closed flask at 20°C and was shaken from time to time during a period of one week. The undissolved acid was then separated from the solution by filtration and two one-litre aliquots of the solution were evaporated separately to dryness in platinum dishes. The solubilities were found to be 91.9 and 91.4 mg of cholic acid per litre.

Another determination was carried out without heating. The water and excess of cholic acid were mixed in a rocking machine at about 20°C for one week and the mixture was then allowed to stand at 20°C for a further three days. The solubility value was 92.2 mg of cholic acid per litre.

The mean of these three solubility values is 91.8 mg per litre. This value is appreciably lower than the value reported by Gillert.

POTENTIOMETRIC DETERMINATION OF THE SOLUBILITIES OF BILE ACIDS IN BILE SALT SOLUTION

Back and Steenberg [6] have shown that it is possible to determine the solubility of a sparingly soluble weak acid and hence the corresponding solubility product K_L by a potentiometric titration of the solution of the salt of the acid with a strong mineral acid up to a point slightly past that where the acid begins to precipitate. The solubility is calculated directly from the amount of strong acid added and the pH of the solution at the precipitation point where the following equation is in force.

$$L_{HA} = c'_S + c'_{OH^-} - c'_{H_3O^+} \tag{1}$$

In the solution saturated with the weak acid (HA):

$$a_{H_3O^+} \cdot a_{A^-} = K_A \cdot a_{HA} = \text{constant} = K_L \tag{2}$$

$$a_{A^-} = (c_{tot} - c_S - c_{OH^-} + c_{H_3O^+})\, f_{A^-} \tag{3}$$

$$pK_L = pH - \log(c_{tot} - c_S - c_{OH^-} + c_{H_3O^+}) + \frac{0.5\sqrt{\mu}}{1+\sqrt{\mu}} \tag{4}$$

In the equations c_{tot} is the initial salt concentration recalculated with respect to the changed volume of the titration solution, c_S the concentration of free weak acid liberated by adding hydrochloric acid. The primed concentrations, c', refer to those at the precipitation point.

$$L_{HA} = \frac{K_L}{K_A} \cdot \frac{1}{f_{HA}} \simeq \frac{K_L}{K_A} \tag{5}$$

Whereas the calculations based on eqn. 1 should always yield correct values, this is the case for the calculations based on eqns. 4 and 5 only when the activity of the anion of the weak acid can be computed from eqn. 3. In the case of association colloids, *e.g.* bile acid salts, the latter is true only when no micelle formation has taken place. After micelles have been formed eqn. 3 must be replaced by eqn. 3 a.

$$a_{A^-} = (c_{tot} - c_S - c_{OH^-} + c_{H_3O^+} - c_{mic}) \cdot f_{A^-} \tag{3 a}$$

where c_{mic} is the concentration of acid anions bound in the micelles.

If the micelle formation is disregarded, the values obtained for K_L will be too high. As long as the extent of micelle formation is unknown the above method of evaluating the solubility product will not be valid when the salt concentration is so high that micelles are present in the solution. Furthermore, as soon as micelles are formed, the bile acid will be solubilized in the solution; eqn. 5, however, gives only the concentration of unsolubilized bile acid and can hence be applied only when solubilization does not occur. Thus, when micelle formation and solubilization does occur, it is necessary to calculate the solubility with the aid of eqn. 1.

The theory presumes, of course, that the precipitate that separates from the solution when hydrochloric acid is added is actually the weak acid itself and not an acid salt. In order to confirm this in the case of bile acid salts, the precipitates formed on titration of these salts were examined under the

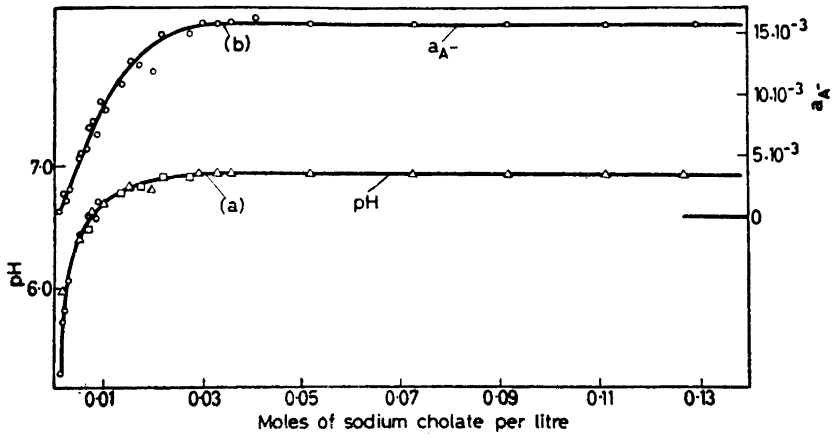

Fig. 1. pH values (curve a) and cholate anion activities, a_{A^-},(curve b) in sodium cholate solutions saturated with cholic acid at 20°C.

microscope, their melting points were determined, and, in a few doubtful cases, an analysis was carried out. All these investigations revealed that the precipitate forming during the titrations consisted only of the bile acid in question.

In titrations of bile salt solutions the applicability and reliability of the potentiometric method are limited by experimental difficulties. It may happen that supersaturated solutions of bile acids in solutions of their salts are readily formed. Sometimes the supersaturation continues also after the appearance of an opalescence or turbidity in the solution or even in solutions containing macroscopically dispersed bile acid precipitate. The calculation of the solubility and solubility product based on pH values for such supersaturated solutions will naturally lead to too high values.

In some cases it may be possible to break off the supersaturation whereupon the pH of the solution will rise abruptly to an appreciably higher value than previously. Probably this higher pH value is the theoretical value for the bile salt solution saturated with bile acid at the point in question in the titration. When no micelle formation has occurred in the solution, the experimental data for this equilibrium state can be used to calculate the solubility product from eqn. 4. It will, however, be less appropriate to use data for such a titration curve to calculate the solubility from eqn. 1 because there will be difficulties in determining at which point in the titration precipitation should have occurred if no supersaturation had taken place. (It is, of course, possible to extend the horizontal part of the curve after the abrupt rise in pH to the left to intersect the descending part of the curve (see Ref.[5], Fig. 1) and consider that part of the curve which is below the horizontal line as being due to supersaturation and to take the point of intersection to represent the saturation point. The solubility value obtained in this way will,

Table 1. The solubility and solubility product of cholic acid in sodium cholate solutions at 20°C.

Sodium cholate mole/l	pH of solution saturated with cholic acid	$pK_{I'}$	Mean $pK_{I'}$	$L_{HA} = \frac{K_{I'}}{K_A}$
0.00049	5.34	8.67		
0.00137	5.73	8.61		
0.00293	6.06	8.62		
0.00480	6.40	8.73		
0.00509	6.43	8.77		
0.00674	6.47	8.69		
0.00682	6.43	8.64		
0.00688	6.47	8.67	8.72 S.D. 0.07	$1.82 \cdot 10^{-4}$ mole/l 77.6 mg/l undissociated acid
0.00690	6.60	8.80		
0.00750	6.62	8.79		
0.00847	6.57	8.69		
0.00862	6.71	8.82		
0.0100	6.69	8.74		
0.0133	6.77	8.77		
0.0151	6.84	8.72		

however, be in error and the magnitude of the error will increase with the solubility.)

When calculating the solubilities of the bile acids we have used in addition to the experimental data previously collected in our earlier determination of the dissociation constants of cholic and desoxycholic acids data obtained in new titrations which were continued until precipitation occurred. In the titration of dilute desoxycholate solutions it was in many cases possible to avoid supersaturation and the data could be used directly in the calculation

Table 2. The solubility and solubility product of desoxycholic acid in sodium desoxycholate solutions at 20°C.

Sodium desoxy-cholate mole/l	pH of solutions saturated with desoxy-cholic acid	$pK_{I'}$	Mean $pK_{I'}$	$L_{HA} = \frac{K_{I'}}{K_A}$	Solubility at the precipitation point	
					L_{HA}	Mean L_{HA}
0.000849	6.04	9.12			$9.5 \cdot 10^{-5}$	
0.000850	6.04	9.13			$9.4 \cdot 10^{-5}$	
0.00180	6.40	9.17			$9.25 \cdot 10^{-5}$	
0.00181	6.40	9.16			$8.60 \cdot 10^{-5}$	
0.00273	6.54	9.13	9.15	$1.05 \cdot 10^{-4}$ mole/l	$10.5 \cdot 10^{-5}$	$1.05 \cdot 10^{-4}$ mole/l
0.00274	6.58	9.17	SD. 0.025		$10.4 \cdot 10^{-5}$	
0.00275	6.58	9.19		43.1 mg/l	$10.3 \cdot 10^{-5}$	43.1 mg/l
0.00367	6.65	9.12		undissociated	$10.8 \cdot 10^{-5}$	undissociated
0.00368	6.70	9.16		acid	$11.1 \cdot 10^{-5}$	acid
0.00369	6.70	9.16			$10.7 \cdot 10^{-5}$	

of the solubility and solubility product. More concentrated desoxycholate solutions containing micelles often yielded highly viscous, supersaturated systems in which the supersaturation could not be broken off and thus the solubility could not be evaluated. In the titration of cholate solutions a supersaturated state usually resulted which, however, could be broken off; in many of these cases the data could be used to calculate the solubility product.

The data obtained are presented in Tables 1 and 2. In the calculation of solubility products only values for solutions in which no micelle formation had occurred were employed. The solubility product exponent (pK_L) for cholic acid in 0.001—0.015 M sodium cholate solutions was found to be 8.72, S.D. 0.07 and that for desoxycholic acid in 0.001—0.004 M sodium descoxycholate solutions 9.15, S.D. 0.025. Using eqn. 5 and the previously determined values of the dissociation constants (cholic acid, $pK_A = 4.98$; desoxycholic acid, $pK_A = 5.17$) the following solubility values were calculated: 77.6 mg of undissociated cholic acid per litre and 43.1 mg of undissociated desoxycholic acid per litre. By direct measurement of pH at the point where precipitation begins and substitution of this value in eqn. 1, the solubility of desoxycholic acid in the above concentration range was found to be 43.1 mg per litre.

The titration method leads to higher solubility values at higher salt concentrations than the above- mentioned. These values are, however, not reliable. Nevertheless, they show that micelle formation and solubilization take plase in these solutions.

DISCUSSION

The solubility products of the bile acids. The value of the solubility of cholic acid in pure water, 91.9 mg/l or 2.15×10^{-4} mole/l, refers to both undissociated and dissociated cholic acid. When the dissociation of the acid is taken into account, the value $K_L = 1.84 \times 10^{-9}$ ($pK_L = 8.73$) is obtained for the solubility product of the acid at 20°C and the value 1.78×10^{-4} M for the activity, a_{HA}, of the undissociated acid in its saturated aqueous solution. When calculating these values it has been assumed that the dissociation equilibrium is not influenced by dissolved carbon dioxide.

This value of the solubility product is in excellent agreement with the mean value, $pK_L = 8.72$, obtained by the potentiometric method. The latter value gives for the activity of undissociated cholic acid in its saturated aqueous solution the value 1.82×10^{-4} M.

The solubility product K_L of desoxycholic acid at 20°C computed from data obtained by potentiometric titration is 7.08×10^{-10} ($pK_L = 9.15$) from which the activity a_{HA} of the undissociated acid in its saturated aqueous solutions is found to be 1.05×10^{-4} M. The direct determination of the solubility from the titrimetric data yielded the same value.

The structure of bile salt solutions saturated with bile acid. Despite the occurrence of micelle formation and solubilization the activity of cholic acid in all sodium cholate solutions saturated with cholic acid should remain constant and equal to 1.82×10^{-4} M. It should therefore be possible to calculate the activity of the cholate ion in these solutions from the data provided by the potentiometric titrations.

Table 1 contains pH values for 0.005—0.015 M cholate solutions at the points in the titration where a precipitate began to form and after equilibrium was attained. As already mentioned, above this point in the titration the titration curve runs parallel to the horizontal axis for some distance. The same is the case also in more concentrated cholate concentrations. Curve a in Fig. 1 shows how the pH at this point and on the horizontal part of the curve varies with the cholate concentration (the abscissa gives the actual cholate concentration at the point in question). In dilute solutions the pH increases with cholate concentration, remains practically constant at the value 6.94 in the 0.03—0.175 M concentration range, but tends to decrease slightly at still higher concentrations (0.3 M, pH 6.88; 0.4 M, pH 6.82; 0.8 M, pH 6.70). The constant value of the pH implies that the activity of the cholate anion is also constant.

The activity of the cholate ion in cholate solutions saturated with cholic acid has been computed from the pH values with the aid of eqns. 2 or 2 a.

$$\log a_{A^-} = \mathrm{pH} - \mathrm{p}K_{\mathrm{I}} \qquad (2\,\mathrm{a})$$

The values of the activity are plotted in curve b of Fig. 1. In the concentration range where the pH is constant the cholate ion activity is 1.57×10^{-2} M. This shows that the major proportion of the cholate ions are bound in micelles at concentrations above 0.03 M. At low concentrations up to approximately 0.01 M cholate the cholate ion activity increases linearly with the cholate concentration, and the activity values are only slightly lower than the concentration values. Between 0.01 and 0.031 M the cholate ion activity increases more slowly as the concentration approaches the upper value. These data show that all the cholate is present in form of single ions up to a concentration of about 0.01 M, but that above this concentration the ions begin to associate more and more until in solutions above 0.03 M in cholate all the added cholate is completely bound to micelles.

The data can also be used to calculate the concentration of unassociated cholate ions and the concentration of the cholate ions bound in the micelles. These calculations, which can be carried out in different ways, are subject to the uncertainties involved when calculating the activity coefficients of ions in solutions where micelle formation has taken place. Our procedure has been as follows. When data obtained for micellar solutions are substituted in eqn. 4 values $\mathrm{p}K_{\mathrm{I,\,exp}}$ are obtained, which differ from the correct values $\mathrm{p}K_{\mathrm{I,\,theor}}$. The correct value $\mathrm{p}K_{\mathrm{I,\,theor}}$ is in these cases obtained only when eqn. 4 is modified by taking into account eqn. 3 a. By combining both these modifications of eqn. 4, eqn. 6 is obtained which permits the calculation of the concentration of micellar substance in the solution.

$$c_{\mathrm{mic}} = (c_{\mathrm{tot}} - c_{\mathrm{S}} - c_{\mathrm{OH^-}} + c_{\mathrm{H_3O^+}}) \left(1 - \frac{K_{\mathrm{I,\,theor}}}{K_{\mathrm{I,\,exp}}} \right) \qquad (6)$$

The results of the calculation are given by the points of curve a in Fig. 2. Micelle formation is seen to begin at the 0.015 M cholate concentration and increases rapidly in extent. (The values in the region immediately above 0.015 M are erratic and it may be that they are slightly too high.)

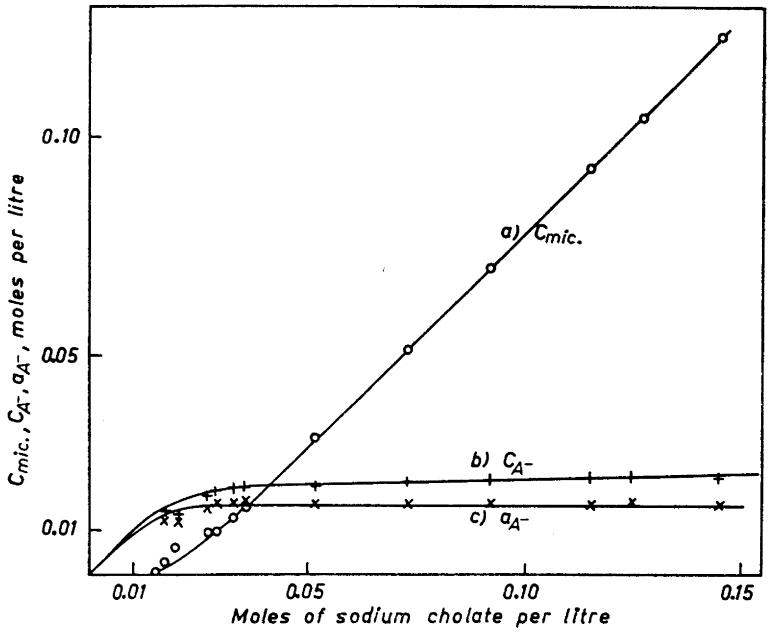

Fig. 2. Micelle formation in sodium cholate solutions saturated with cholic acid at 20°C. The concentration of micellar cholate (a) and of molecular cholate (b), and cholate anion activity (c). The points marked o, × and + have been calculated with the aid of eqn. 6, the curves are based on the activity values given in Fig. 1 b.

On the basis of these values the concentrations of unassociated cholate ions (the points on curve b) and the activity of free cholate ions (the points on curve c) have been calculated (the continuons curves a, b and c have been drawn using values calculated from the activity values in Fig. 1 b). Also these calculations show that the micelle formation begins above 0.01 M (concentration limit 1) is incomplete between 0.01 and 0.03 M, and that all added cholate forms micelles above the latter concentration (concentration limit 2). They give the constant value 1.62×10^{-2} M for the cholate ion activity in the concentration range above about 0.03 M; this value is only slightly higher value than that previously mentioned.

In sodium desoxycholate solutions saturated with desoxycholic acid, also in solutions containing micelles, the activity, a_{HA}, of desoxycholic acid is $1.05 \times 10^{4-}$ M. Using the pK_I value 9.15 we have, as above, calculated the activities of the desoxycholate anion from the pH values of desoxycholate solutions titrated to the precipitation point. It was possible, however, to carry out these calculations with satisfactory accuracy only up to a desoxycholate concentration of about 0.005 M. (At higher desoxycholate concentrations the solutions, as mentioned above, become supersaturated with respect to the acid during the titration and it was not possible to break off the supersaturation; hence exact pH values could not be determined for the saturated solutions.)

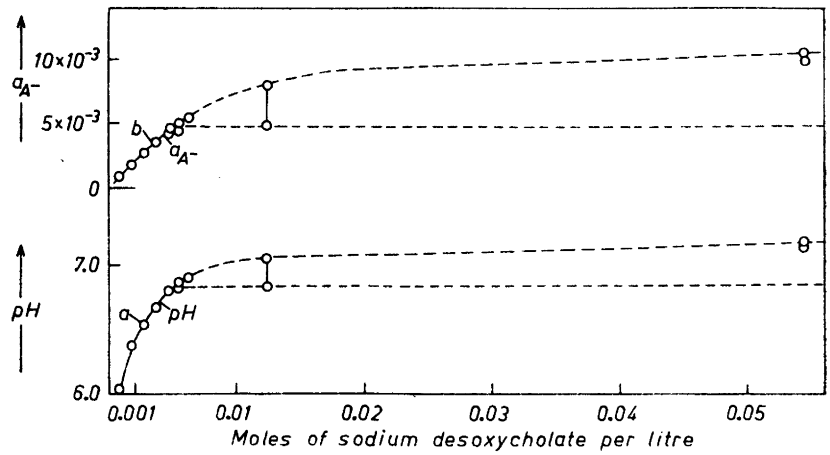

Fig. 3. pH values (curve a) and desoxycholate anion activities, a_{A^-}, (curve b) in sodium desoxycholate solutions saturated with desoxycholic acid at 20°C. In the concentration range above 0.005 M desoxycholate only approximate values lying between the two dashed curves were obtained.

The measured pH values and the respective anion activities are given by curves a and b in Fig. 3. It is possible to state with certainty only that the activity of the desoxycholate anion increases linearly up to a desoxycholate concentration of 0.005 M and that the activities are only slightly lower than the concentration values. This shows that no association takes place up to the mentioned concentration. Above this concentration (concentration limit 1) the activity of the desoxycholate anion seems to remain practically constant or to increase slowly with increasing concentration. In the 0.075 M desoxycholate solution saturated with desoxycholic acid, the anion activity does not seem to be higher than 1.1×10^{-2} M. Association hence begins at the 0.005 M desoxycholate concentration and increases rapidly to such an extent that, at least in solutions above 0.01 M, all the added desoxycholate forms micelles.

DIRECT DETERMINATION OF THE SOLUBILITIES IN BILE SALT SOLUTIONS

In order to obtain reliable information on the solubilities of bile acids in solutions of their salts at concentrations where micelles are formed we have performed a series of direct solubility measurements. In these experiments known weights of cholic and desoxycholic acids were added to measured volumes of solutions of the respective sodium salts in ampoules. After the ampoules had been sealed by fusing, they were placed in a thermostat at 40°C, in some cases at 20°C, and shaken for 5—7 days, during which time either the acid dissolved or the solution became saturated with the acid. The changes in refractive index of the solutions caused by the dissolved acid were measured with a Zeiss — Löwe liquid interferometer. As soon as the solution

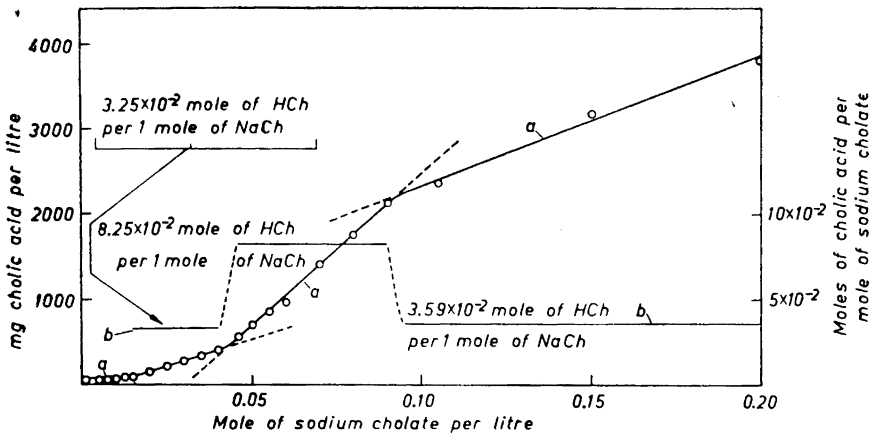

Fig. 4. The solubility of cholic acid in sodium cholate solutions at 40°C determined with the aid of liquid interferometer measurements. The solubility in mg of cholic acid per litre of sodium cholate solution (curve a). The solubility in moles of cholic acid per mole of sodium cholate in the micellar state, *i. e.* the saturation capacity of the cholate micelles (curve b).

became saturated with the acid, no further change in the refractive index was observed. At low bile salt concentrations, where very little acid dissolved, the solubility values were erratic (the maximum deviations from the mean were as large as ± 10 %. With increasing salt concentration and acid solubility more reproducible values (maximum deviations from the mean less

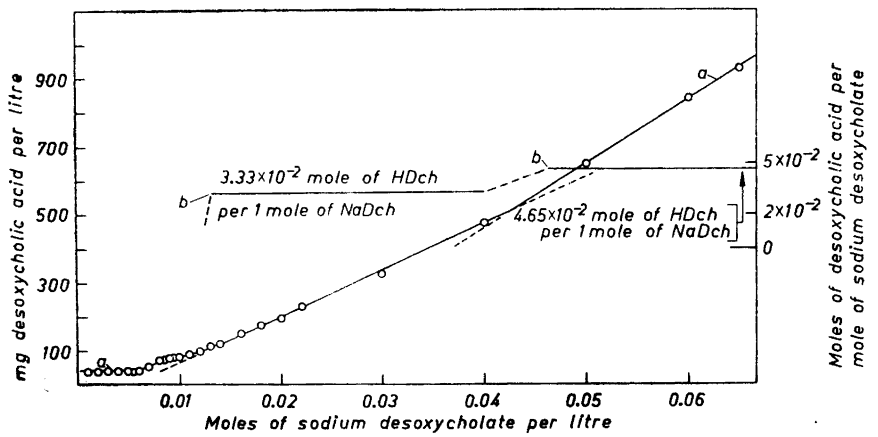

Fig. 5. The solubility of desoxycholic acid in sodium desoxycholate solutions at 40°C determined by the aid of liquid interferometer measurements. The solubility in mg of desoxycholic acid per liter of sodium desoxycholate solution (curve a). The solubility in moles of desoxycholic acid per mole of sodium desoxycholate in the micellar state, *i. e.* the saturation capacity of the desoxycholate micelles (curve b).

than ± 2 %) were recorded. The direct method is thus less suitable for measurement of the solubility in very dilute bile salt solutions than the titration method. In this concentration range the direct method gave somewhat lower solubility values (although they were measured at 40°C) than the titration method. (The values of the solubility products of the bile acids calculated from these values were: for cholic acid in 0.003—0.009 M sodium cholate solutions $pK_L = 8.90$ and in 0.010—0.015 M solutions $pK_L = 8.74—8.69$; for desoxycholic acid in 0.001—0.0055 M sodium desoxycholate solutions $pK_L = 9.23—9.24$.) In bile salt solutions where micelle formation and solubilization occurs the direct method yields more reliable solubility values than the titration method. The results obtained are shown in Figs. 4 and 5, curves a.

SOLUBILIZATION OF BILE ACIDS AND THE PROPERTIES OF THE MICELLES

In sodium cholate solutions (Fig. 4 a) up to 0.015 M in cholate (concentration limit 1) no solubilization of cholic acid could be detected; the solubility in this range is practically constant. Above limit 1 the solubility increases linearly until the cholate concentration rises to 0.04—0.045 M (concentration limit 2). Above this second limit the solubility also increases linearly but more rapidly. Above a cholate concentration of 0.09—0.10 M (limit 3) the increase of the solubility continues but less rapidly than between limits 2 and 3. The ability of cholate to solubilize cholic acid thus varies in different concentration ranges.

It should be noted that the solutions in question were not supersaturated but equilibrium systems in which the cholic acid is solubilized by cholate micelles; thus, they are thermodynamically stable, colloidal systems. Supersaturated solutions may contain appreciably larger amounts of dissolved acid than solutions in which only solubilization occurs. In the potentiometric titrations we have, for instance, encountered clear 0.012 M sodium cholate solutions containing up to 800 mg of cholic acid in one litre (no solubilized acid) and clear 0.03 M cholate solutions containing up to 3 000 mg of the acid per litre (only about 230 mg of cholic acid is solubilized). Also in these cases the cholic acid is colloidally dissolved, but the colloid formed is for the most part unstable and the excess acid will separate from the system sooner or later.

From the solubility curve we have computed the saturation capacity of the micellar cholate, *e.g.* the solubilizing power of the cholate micelles expressed in moles of cholic acid per mole of micellar cholate.

Above concentration limit 2, where all added cholate forms micelles, the slope of the solubility curve directly gives the saturation capacity per mole of micellar substance. Between limits 1 and 2, where all added cholate does not form micelles, we have computed the real saturation capacity of the micellar substance using our previous calculated values of the content of cholate anions in micellar form. The curve b in Fig. 4 shows that the power of the cholate micelles to solubilize cholic acid changes abruptly at the concentration limits but is constant in the concentration ranges between the limits. This implies

that the association leads to the formation of micelles with different properties in the different ranges and that the concentration limits represent cholate concentrations where new types of micelles begin to form in sodium cholate solutions saturated with cholic acid.

In sodium desoxycholate solutions up to about 0.006 M (limit 1) no solubilization of desoxycholic acid could be observed (Fig. 5, curve a); the solubility is practically constant in this range. Above limit 1 the solubility of desoxycholic acid increases rapidly at first, but then somewhat more slowly. Above the 0.010—0.012 M concentration (limit 2) the solubility again increases rapidly, but now practically linearly, up to 0.04—0.05 M concentration (limit 3) above which the solubility curve rises even more rapidly with increasing desoxycholate concentration.

We have shown above that all added desoxycholate forms micelles from the concentration 0.01 M upwards. Above this concentration, the slope of the solubility curve thus gives the saturation capacity of the micellar desoxycholate for desoxycholic acid (curve b in Fig. 5). (Between limits 1 and 2 it is impossible to evaluate the saturation capacity of the micellar substance with certainty because the extent of the micelle formation is not known.) Our calculations show that the solubilization power of the desoxycholate micelles changes at the concentration limits 2 and 3 but remains constant between these limits and in the range above limit 3. Hence micelles with different properties and of different types exist in different concentration ranges also in desoxycholate solutions saturated with desoxycholic acid.

We have previously come to similar conclusions with respect to association and micelle properties in cholate and desoxycholate solutions not saturated with the respective bile acids. The bile acids seem, however, to shift the limits slightly to lower concentrations.

REFERENCES

1. Gillert, X. *Z. ges. exptl. Med.* **48** (1926) 255.
2. Josephson, B. A. *Biochem. Z.* **263** (1933) 428.
3. Ekwall, P., Lindström, E. V. and Setälä, K. *Acta Chem. Scand.* **5** (1951) 990.
4. Ekwall, P. *Koninkl. Vlaamse Acad. v. Wetenschap v. Belgie, Intern. Conference on Biochemical Problems of Lipids*, Brüssel 1953, p. 103.
5. Ekwall, P., Rosendahl, T. and Löfman, N. *Acta Chem. Scand.* **11** (1957) 590.
6. Back, E. and Steenberg, B. *Acta Chem. Scand.* **4** (1950) 810.
7. Ekwall, P. *Acta Acad. Aboensis. Math. Phys.* **XVII** (1951) 8.
8. Ekwall, P., Fontell, K. and Sten, A. *Proc. 2nd Intern. Congress of Surface Activity, Gas/Liquid and Liquid/Liquid Interface*, p. 357. Butterworths, London 1957.

Received May 12, 1958.

ACTA CHEMICA SCANDINAVICA 12 (1958) 1634—1642

The First Step in the Swelling of Gelatin with Water. III

CHR. WINTHER

Photochemical Laboratory, Technical University of Denmark, Copenhagen, Denmark

The normal content of water in air dried gelatin is shown to be present as a solution of soluble gelatin. On this basis it is possible to give a detailed account of the progress of the watering of the gelatin.

In some earlier treatises [1] I have examined the speed of swelling of the Christensen-interference plate [2] with water. About five different plates were treated with water, each of them going through three successive treatments. It was thereby observed that after drying of the plates the edges of the extinction bands as a whole had shifted towards lower wavelengths.

In order to examine this peculiar phenomenon closer nine other plates were treated with water and dried, each one three separate times, in a single case four times, and the speeds of swelling and of the subsequent drying were examined. Thereby the said phenomenon was confirmed in all cases.

1. THEORY OF THE PHENOMENON

The wavelengths of the two edges of the extinction band (BB) are determined by the formula

$$\lambda_{I} = 263 \left(n_{A} \frac{v_{A}}{100} + n_{G} \right) \tag{1}$$

for the upper edge, and

$$\lambda_{II} = 265 \left(n'_{A} \frac{v'_{A}}{100} + n'_{G} \right) \tag{1a}$$

for the lower edge [3]. Here 263 and 265 are the thicknesses of the gelatin layer plus chromic oxide, n_A and n'_A the indices of refraction for silver bromide, n_G and n'_G the the same values for gelatin, and v_A and v'_A the percentage by volume of silver bromide.

Now, the falling off of the wavelength by subsequent treatment with water cannot be due to a loss of silver bromide as the solubility of this substance is extremely low. As the subsequent calculations show, the loss cannot be due to inorganic components (ashes) because then the found connections between the different amounts of water during the swelling process would be quite meaningless. Therefore the observed falling off must be due to a loss of gelatin.

2. EARLIER MEASUREMENTS

Pouradier [4] has found — using two homogeneous samples of gelatin — that up to 0.13 % of gelatin can be dissolved in cold water without any reduction of the molecular weight. It must be remarked that the examined samples of gelatin had been washed beforehand to remove impurities. Unlike Pouradier earlier investigators [5] had found that the high molecular gelatin had to be split up in smaller molecules in order to be soluble.

The loss of gelatin which I have found is of an entirely different nature. Each watering during two or three days caused a certain loss, and after drying renewed watering resulted in a further, but somewhat smaller, loss, tending against a maximal amount which cannot be exceeded. These maximal values lie between 2.8 and 5.7 % by volume of gelatin.

3. DIRECT MEASUREMENTS

About 1.5 g of Nelson I emulsion gelatin were dried to constant weight over calcium chloride and then for a total of ten days treated with cold water, which was renewed every second day. After removal of the water and spontaneous evaporation for some days the remainder was dried to constant weight over calcium chloride. Thereby were found losses of 16.4 and 16.8 % by volume, on an average 16.6 %.

As the values of G′, the percentage by volume of unhardened gelatin in the interference plates, lie between 31.4 and 22.2 for, respectively, the upper and the lower edge of the BB the values for the interference plates should lie between 3.7 and 5.2 if the densities are the same for the soluble and the insoluble parts of the gelatin.

It is commonly known that commercial gelatin must be regarded as a mixture of molecules of varying size, *e.g.* from 5 000 to 100 000. It may reasonably be taken for granted that only the smallest molecules are directly soluble, whereas the big molecules just swell with water, with the exception of the very small percentage of soluble gelatin which is found among the big molecules, as mentioned before.

4. THE WATER CONTENT OF THE GELATIN

It is commonly known [6] that commercial gelatin contains 10—20 % by weight of water, or 13.6—26.2 % by volume, if the density of completely dry gelatin is taken as 1.42 (see below).

In the course of the swelling experiments the amounts of water, V, which were absorbed during all series of watering were calculated for all values g of dissolved gelatin, from $g = 0$ to $g = g_\infty$. The differences V_0 to V_∞ for the 9 examined plates (18 values) lie between 12.0 and 24.0 % by volume. This leads to the conclusion that the soluble gelatin in air dried gelatin is present as a solution. As the quotient $(V_\infty - V_0):g_\infty$ for the 18 cases varies irregularly between 3.8 and 4.5, average 4.1, the said solution must contain about 25 volumes of gelatin to 100 volumes of water.

The mean value of the 18 values measured here is 17.3. As the mean of 13.6 and 26.2 is a little higher (19.9) I have taken the value 18 as a general mean. The earlier [7] found value of d_G, the density of air dried gelatin, 1.32, consequently must apply to this water content. Therefore, the value of d_G for absolutely dry gelatin and for gelatin with other water contents can be calculated. The results are shown in Table 1.

Table 1.

Water	d_G
0	1.42
12	1.35
18	1.32
24	1.30

The same considerations apply to the values of n_G, the indices of refraction for gelatin, which I have measured on an earlier occasion [7]. Through use of the formula

$$\frac{n_G - 1}{d_G} = \frac{(n_v - 1)\frac{v}{100}}{1} + \frac{(n'_G - 1)\frac{100 - v}{100}}{1.42}$$

where n_v, n_G and n'_G are the indices of refraction for water, gelatin with 18 % by volume of water, and for pure gelatin, respectively, it is possible to calculate the indices of refraction for pure gelatin and afterwards for gelatin with different contents of water. Table 2 shows the results.

Table 2. n_G for different water contents.

λ	0	3	6	9	12	15	18	21	24
700	1.580	1.569	1.558	1.547	1.539	1.529	1.518	1.511	1.504
650	1.585	1.574	1.563	1.552	1.542	1.533	1.525	1.517	1.510
600	1.590	1.579	1.568	1.557	1.547	1.537	1.527	1.520	1.514
500	1.600	1.589	1.578	1.567	1.555	1.546	1.536	1.530	1.524

5. THE LOSS OF GELATIN BY WATERING OF THE INTERFERENCE PLATE

It is now possible to calculate the loss of gelatin. To this end the formula 1 must be altered in the following way:

$$\lambda_I = \left(263—253\,\frac{g}{100}\right)\left(n_A\,\frac{v_A}{100} + n_G\,\frac{100—g}{100}\right)$$

and formula 1a is altered in the same way. Here g is the percent loss of gelatin after each treatment with water for 2 or 3 days, and the number 253 is the thickness of the pure gelatin layer [8]. The values of g are found in Table 3 where the first column shows the number of the plate. Each plate of the size 9 × 12 cm was divided into small pieces, and the small index figure denotes the number of the examined piece of the particular plate. The figures I and II denote the upper and lower edges of the BB. The second column shows the number of days, D, during which the plate was treated with water, the third the successive values of the wavelengths, the fourth the values of v_A, the percentage by volume of silver bromide, the fifth the observed wavelengths after watering for 2 or 3 days. These wavelengths were found to be practically constant for each individual plate and edge. The values here quoted are the averages of the individual measured values. The sixth column shows the values of g.

6. THE MECHANISM OF THE ABSORPTION OF WATER

In the second paper in this series [9] I have found that the first absorption of water, v_0, takes place very rapidly. In the said paper I have also found that the speed of this first diffusion through the plate is 0.69 sec for each μ of thickness. The nine plates now examined have thicknesses from 9.6 to 12.0 μ, and the time for the first diffusion therefore varies from 6.6 to 8.3 sec, a quite negligible value compared with the much longer spaces of time for the following periods of watering.

As the new measurements show the subsequent absorption of water can be divided in two periods, both of which are first order. The first of these periods is ended in about 30 min, whereas the second takes 2 or 3 days.

Assuming, as said before, that the soluble gelatin is present as a series of solutions, situated between the higher molecular gelatin molecules, it is probable that some of these solutions are directly accessible, whereas others are protected by the big molecules. The first ones must therefore be diluted by the water and must hereby give the water the possibility to penetrate into the adjacent cavities between the big molecules. This process then takes about 30 min. Thereafter the dissolved gelatin has to diffuse out into the outer water, and the water in the layer has to force its way between gelatin and silver bromide, and then to fill all accessible cavities. These latter processes are very slow and take a total of about 2 or 3 days.

Furthermore, during the drying the whole network has the possibility of rearranging so that new regions of gelatin solution are made accessible to the next ingress of water. This is going on as long as there is any soluble gelatin available.

Table 3.

Plate No.	D	λ	v_A	λ_∞	g	v_0	v_1	V	Δ V	$\frac{\partial g}{\partial V}$	k_1	k_2	k_g
196,I	0	628	38.5	552	0	81	—	136	20.0	—	—	—	0.074
	3	606			2.1	106	100	144.5		4.0	0.055	0.073	
	2	597			3.0	120	121	148		3.9	0.056	0.128	
	3	596			3.4	—	135	151		4.0	0.074	0.172	
	∞	—			5.0	—	—	156		4.0			
196,II	0	566	26.0	541	0	90	—	147.6	12.4	—	—	—	0.068
	3	550			1.5	115.5	112	153		4.1	0.040	0.069	
	2	544			2.1	128.5	131	155		3.8	0.044	0.123	
	3	536			2.9	—	139	158		4.0	0.067	0.129	
	∞	—			4.0	—	—	162		4.0			
196_{11}I	0	565	26.2	556	0	97	—	158	12.0	—	—	—	0.149
	2	548			1.5	110	120	164		3.9	0.051	0.095	
	2	544			2.1	136	129	165.5		4.0	0.056	0.066	
	2	538			2.7	—	150	167		4.0	0.057	0.154	
	∞	—			3.0	—	—	170		4.0			
196_{11}II	0	527	19.4	542	0	102	—	159.5	14.5	—	—	—	0.153
	2	510			1.6	113	126	166		4.1	0.049	0.090	
	2	506			1.9	139	130	167		3.9	0.064	0.076	
	2	499			2.6	—	157.5	170		4.0	0.103	0.084	
	∞	—			3.1	—	—	174		4.0			
196_8I	0	546	24.2	546	0	82	—	156.5	20.0	—	—	—	0.062
	2	533			1.5	119	117	162.5		4.0	0.044	0.120	
	3	525			2.4	143	141.5	166.5		4.1	0.077	0.119	
	3	514			3.7	—	151	172		4.2			
	∞	—			4.9	—	—	176.5		4.1			
196_8II	0	511	18.0	534	0	85	—	158.5	20.0	—	—	—	0.122
	2	494			2.1	123	125	167		4.0	0.049	0.069	
	3	483			3.2	148	142	173		4.5	0.061	0.114	
	3	481			3.3	—	158	174		4.7			
	∞	—			4.5	—	—	178.5		4.4			
216_9I	0	632	39.1	516	0	69	—	113	20.5	—	—	—	0.067
	3	600			3.0	83	87	125		4.0	0.057	0.116	
	2	600			3.0	98	94	125		3.9	0.066	0.061	
	3	596			3.4	115	111	126.7		4.0	0.066	0.115	
	2	591			3.9	—	122.5	128.5		4.0	0.054	0.158	
	∞	—			5.1	—	—	133.5		4.0			
216_9II	0	571	30.0	501	0	81	—	121.5	22.2	—	—	—	0.059
	3	551			2.0	94.5	98	130		4.2	0.048	0.112	
	2	546			2.5	110	106	132		4.1	0.074	0.114	
	3	537			3.5	120	121	136		4.0	0.050	0.080	
	2	537			3.5	—	128.5	136		4.0	0.058	0.181	
	∞	—			5.4	—	—	143.7		4.1			
216_{12}I	0	575	28.6	503	0	74.5	—	122.5	14.6	—	—	—	0.139
	2	558			1.7	97.5	94	129.3		4.0	0.073	0.105	
	2	549			2.6	118.5	111	133.2		4.1	0.072	0.138	
	3	548			2.7	—	128.5	134		4.2	0.076	0.211	
	∞	—			3.6	—	—	137		4.1			
216_{12}II	0	547	22.6	486	0	75	—	120	12.0	—	—	—	0.122
	2	538			0.8	92	91	123		4.0	0.080	0.119	
	2	524			2.3	115	108	129		3.9	0.067	0.132	
	3	524			2.3	—	126	129		3.9	0.062	0.246	
	∞	—			2.8	—	—	132		3.9			

Table 3 (continued)

47_3I	0	605	33.8	492	0	62	—	107.5	14.5	—	—	—	0.074
	2	—			1.4	—	74.5	111.5		4.0	0.048	0.060	
	(3)	580			2.6	87	—	117.5		3.9	—	—	
	2	571			3.4	105	108	121		3.9	0.039	0.103	
	2	569			3.6	—	112	122		3.9	0.067	0.105	
		—			3.6	—	—	122		3.9			
47_3II	0	547	22.8	459	0	65.5	—	104	12.2	—	—	—	0.088
	2	—			1.1	—	80.5	107.8		3.8	0.050	0.057	
	(3)	524			2.3	88	—	112.7		3.8	—	—	
	2	516			3.2	102	101	115.5		3.8	0.053	0.155	
	2	516			3.2	—	110	115.5		3.8	0.064	0.166	
		—			3.5	—	—	116.2		3.8			
47_{10}I	0	555	24.6	454	0	58	—	99.5	12.4	—	—	—	0.121
	2	543			1.3	79.5	74	105		4.2	0.051	0.093	
	2	537			2.0	94.5	91	107		3.8	0.052	0.085	
	2	532			2.6	—	98.5	109		3.6	0.046	0.208	
		—			3.1	—	—	112		3.9			
47_{10}II	0	508	16.0	434	0	60	—	100.5	12.3	—	—	—	0.108
	2	494			1.1	79	74	105		4.1	0.068	0.115	
	2	487			1.8	94	88	107.4		3.8	0.081	0.122	
	2	483			2.3	—	100	109		3.7	0.050	0.151	
		—			2.9	—	—	110		3.9			
212_{10}I	0	615	36.7	568	0	101	—	149	24.0	—	—	—	0.072
	2	—			1.5	—	124	156		4.4	0.067	0.112	
	(3)	582			3.3	120	—	163		4.4	—	—	
	2	580			3.6	138	138	165		4.4	0.042	0.081	
	2	572			4.3	—	155.5	168		4.4	0.039	0.156	
		—			5.5	—	—	173		4.4			
212_{10}II	0	559	26.0	553	0	110	—	157	22.4	—	—	—	0.092
	2	—			1.5	—	135	163		4.0	0.050	0.145	
	(3)	530			3.7	128	—	171.4		3.9	—	—	
	2	526			4.2	146	145	174.6		4.2	0.057	0.097	
	2	522			4.6	—	163	176		4.2	0.046	0.156	
		—			5.3	—	—	179.4		4.1			
212_{11}I	0	638	40.3	583	0	—	—	152	20.3	—	—	—	0.158
	2	614			2.3	116	116	162		4.4	—	0.103	
	2	602			3.4	139	135	167.8		4.6	0.064	0.100	
	2	597			4.0	—	150	170		4.5	0.058	0.107	
		—			4.5	—	—	172		4.5			
212_{11}II	0	576	28.9	560	0	—	—	155	21.3	—	—	—	0.108
	2	555			1.9	122	127	163		4.2	—	0.082	
	2	545			3.1	142	142	168.5		4.4	0.069	0.132	
	2	537			3.8	—	155	171.5		4.4	0.062	0.172	
		—			4.9	—	—	176.3		4.3			

7. CALCULATION OF THE AMOUNT OF WATER

The results of the treatment with water were measured spectrographically after 1, 2, 4, 8, 15, 30, 60, 90 and 120 min, and then after 2 or 3 days. Prolonged watering had no further effect.

The wavelengths observed during the treatment with water are all of the second order. In order to convert these values into the corresponding

wavelengths of the first order, I have calculated, with the aid of the indices of refraction for gelatin (with 18 % by volume of water), water and silver bromide, a series of curves which indicate the factor by which the observed wavelength has to be multiplied, for a series of different percentages by volume of water. In each case a probable value is found by a preliminary calculation, and if the finally calculated value for v_v differs too much from the supposed value the calculation is repeated until the supposed and the finally calculated values are practically the same.

The formula for the calculation for the upper edge of the BB is

$$\lambda_v = \left(263—253\frac{g}{100}\right)\left(n_A \frac{v_A}{100} + n_G \frac{100\text{-}g}{100} + n_v v_v\right)$$

and similarly for the lower edge.

For the first series of measurements of the individual plate the value of g is at first zero. During the further treatment with water the available amount of soluble gelatin, g, is dissolved and removed. The final value V therefore must be calculated with this value of g inserted in the formula. The same is the case for all the values in the third period — from 30 min to 2—3 days — when the solution of gelatin is diluted and removed.

I have, therefore, calculated two series of values of v_v, the first one for $g = 0$, the second for $g = g_1$. These two curves are practically parallel. Then I have drawn a curve from the beginning of the lower curve to the upper one in such a way that it coincides with the upper one after about 30 min and thereafter follows this curve to the end. For the next following treatments with water the two curves are calculated for $g = g_1$ and $g = g_2$, and so on.

The results are given in Table 3, where the 7th column contains the values of v_0, the momentary absorption of water, the 8th column the values of v_1, the second step, and the 9th column the values of V, the final amount of water. The 10th column shows the difference $V_\infty—V_0$, which indicates the amount of water in the air dried plate, the 11th column the quotient $\Delta V: \Delta g$ and the 12th and 13th column the two reaction constants of the first order, where the time factors denote minutes and hours, respectively.

The table shows some irregularities. The plates 47_3 and 212_{10} were at first watered as usual. Then they were placed in water for 2 days without measuring the wavelength, only to find the speed of drying. After the drying they were measured again in the normal way during the following treatment with water. For No. 212_{11} it was impossible to measure the values up to 15 min on account of a technical hindrance. Therefore the values of v_0 could not be found in this case.

8. THE VALUES OF g_∞ AND V_∞

These values can be found in two different ways, either graphically, as points of intersection between the two curves which show the variation of

v_0 or v_1 with g, and of V with g, or by calculating the values of g as if varying after the first order, the time factor denoting days, and thereafter calculating the corresponding values of V_∞ as

$$\frac{V_\infty - V_0}{g_\infty - g_0} = 4.1$$

The values of k_g are to be found in Table 3, column 14.

9. THE VALUES OF v_0 AND v_1

If the theory here advanced is correct the values of v_0 must be a little higher than the immediately preceding values of v_1. The values of v_0 have been increased by the cavities, which were made free at the preceding treatment by removal of the soluble gelatin. Furthermore, this soluble gelatin itself has a certain volume, which has to be added to v_1 to give the next value of v_0.

The individual measurements are not accurate enough to allow a test of this kind. The only way is to examine the question in a statistical way. A total of 34 corresponding pairs of v_0 and v_1 have been measured. 22 of them give positive values of the difference $v_0 - v_1$, all of them together making 89.7. The other 12 give negative values, totalling 44.7. The total positive amount is 45.0, on the average 1.32.

The corresponding values of Δg for the 34 cases average 1.26. The two figures are identical.

10. THE SPONTANEOUS DRYING OF THE WET PLATE

In the last paper in this series [10] I have found that the spontaneous drying of the wet interference plate follows the equation

$$v_v = V_\infty \cdot 10^{-k_5 t/D}$$

where D is the thickness of the plate in μ. The thickness of the coating was measured as previously [11] by counting the number of interference lines. The piece of plate glass which was laid on to the edge of the coating was very small, and the distance from the scratched line to the edge of the plate was only 4.4 mm. It was illuminated with the yellow sodium line (589 mμ). Table 4

Table 4.

Plate No.	196_7	196_{11}	196_8	216_9	216_{12}	47_3	47_{10}	212_{10}	212_{11}	mean
D	11.5	11.7	11.0	9.6	12.0	10.3	9.6	10.6	10.6	
k_5 upper	2.33	2.59	2.60	2.51	2.88	2.57	2.27	2.24	2.45	2.48
k_5 lower	2.36	2.65	2.66	2.18	2.55	2.41	2.44	2.37	2.26	2.43

contains the results for the 9 examined plates. The first line of values for k_5 corresponds to the upper edge, the second one to the lower edge of the BB.

The total mean is then 2.46. In the earlier experiments the mean value 2.38 was found for 5 other plates. These two values must be regarded as identical.

11. CONCLUSIONS

1. It is found that by watering of the interference plates some per cent of gelatin is removed. After drying and renewed watering a further, but smaller, portion is removed, and so on, up to a certain limit.

2. The soluble gelatin is shown to be present in the air dried gelatin in the form of a solution of about 25 volumes of gelatin in 100 volumes of water.

3. By the aid of a simple model of the interference plate it is possible to divide the amount of swelling water into three parts which are absorbed with different speeds. It is possible to give a probable explanation of this phenomenon.

REFERENCES

1. Winther, Chr. *Trans. Danish Acad. Tech. Sci.* **1953** No. 6; *Acta Chem. Scand.* **7** (1954) 1053; **10** (1956) 1124.
2. Winther, Chr. *Trans. Danish Acad. Techn. Sci.* **1953** No. 5.
3. Winther, Chr. *Trans. Danish Acad. Techn. Sci.* 1953 No. 5, 33.
4. Pouradier, J. *Compt. rend.* **230** (1950) 1466.
5. References by Pouradier [4].
6. Mees, *The theory of the photogr. process*, 2d ed. 1954, p. 60.
7. Winther, Chr. *Trans. Danish Acad. Techn. Sci.* **1953** No. 5, 12.
8. Winther, Chr. *Trans. Danish Acad. Techn. Sci.* **1953** No. 5, 39.
9. Winther, Chr. *Acta Chem. Scand.* **10** (1956) 1124.
10. Winther, Chr. *Acta Chem. Scand.* **10** (1956) 1130.
11. Winther, Chr. *Trans. Danish Acad. Techn. Sci.* **1953** No. 5, 7.

Received June 23, 1958.

ACTA CHEMICA SCANDINAVICA 12 (1958) 1643—1651

The First Step in the Swelling of Gelatin with Water. IV

CHR. WINTHER

Photochemical Laboratory, Technical University of Denmark, Copenhagen, Denmark

By the aid of a simple model of the constitution of the interference plate it is possible to explain the peculiar phenomenon that the lower edge of the extinction band by aftertreatment in some cases takes up more silver bromide than the upper edge. The same model makes it possible to calculate the diameter of the gelatin molecule.

1. AFTERTREATMENT OF THE PLATE

In spite of the very detailed recipe which the late civil engineer Herman Christensen has given for the preparation of his interference gelatin plate [1], and in spite of the practice which I have afterwards developed during the preparation of some 250 plates, it still is a rather delicate job to prepare a really first class plate. Especially the colour is very often too weak.

To overcome this difficulty I have tried to give the finished plates an aftertreatment with silver nitrate and potassium bromide, exactly in the same way as during the original preparation, and it is in this way possible to arrive at much stronger colours and, by varying the concentration of the silver nitrate solution, to obtain any desired colour and, finally, through repetition of the procedure, nearly opaque plates.

By this procedure the concentration of silver bromide is of course increased and, by repeated aftertreatment, the percentage by volume can reach values higher than 60.

In order to get the greatest possible material the original plates (9 × 12 cm) were cut in small pieces (18 × 20 mm) which were indicated by small index figures, *e.g.* 47_3, and examined separately. In this way a total of 30 pieces of 6 different plates have been aftertreated, 13 of them two times and 5 three times, 57 measurements in all of both the upper and the lower edge of the broad band.

The silver nitrate solutions had the concentrations 25:100, 11:100 and 5:100. The first one was applied for 3 or 1 1/4 min with identical results, the second one for 3 min and the third one for 6 min. 24 pieces were treated with the strongest solution, 9 with the intermediate one and 6 with the most diluted solution. The results are shown in Tables 1, 2 and 3.

Table 1. First aftertreatment.

$AgNO_3$ 25:100, 3 min.				
	I		II	
Plate No.	v_A	Δv_A	v_A	Δv_A
181_3	37.3	9.9	30.0	11.0
212_3	34.8	9.4	24.0	9.9
216_8	30.1	8.2	20.8	10.9
50_{11}	30.1	11.6	20.3	8.6
47_1	29.3	11.5	20.4	8.4
216_{12}	28.6	12.9	22.6	8.4
50_8	28.4	12.9	18.7	8.0
50_5	27.9	12.0	19.2	9.1
47_4	27.2	13.6	18.3	9.7
47_9	26.9	13.3	17.0	10.0
196_7	25.0	13.5	15.4	10.6
196_5	24.6	12.6	16.0	9.9
196_9	23.7	13.0	15.4	11.0

$AgNO_3$ 25:100, 1 1/4 min.				
	I		II	
Plate No.	v_A	Δv_A	v_A	Δv_A
181_2	36.9	13.7	30.4	13.6
212_{10}	36.7	14.6	26.0	15.5
212_4	34.8	8.7	22.8	11.3
216_4	31.0	8.3	21.5	10.7
47_5	29.1	13.1	18.7	11.6
47_2	27.7	13.4	19.3	10.1
47_8	27.2	13.8	18.1	9.3
47_{10}	24.6	16.1	16.0	9.9
196_{10}	24.6	13.7	16.2	10.7
196_2	24.3	11.0	16.2	8.4
196_8	24.2	12.9	18.0	9.1

$AgNO_3$ 11:100, 3 min.				
	I		II	
Plate No.	v_A	Δv_A	v_A	Δv_A
181_4	37.4	4.6	29.5	7.6
212_5	34.8	6.6	22.8	8.6
216_9	31.0	8.1	21.1	8.4
47_7	29.1	7.3	19.6	5.4
50_{14}	28.3	8.0	19.2	5.8
50_{13}	27.7	7.3	18.5	5.3
47_3	27.2	6.6	18.1	4.7
196_6	24.6	5.5	16.3	5.4
196_4	23.9	5.8	15.8	5.7

$AgNO_3$ 5:100, 6 min.				
	I		II	
Plate No.	v_A	Δv_A	v_A	Δv_A
181_7	37.7	5.3	31.7	7.2
212_{11}	35.2	4.5	22.8	4.6
216_{10}	30.8	4.5	21.5	5.2
50_4	28.9	5.0	17.8	4.2
47_6	26.5	4.8	16.9	3.7
196_{11}	22.7	3.5	15.6	4.7

The figures I and II refer to the upper and the lower edge of the broad band. The first column gives the number of the plate, the second the value of v_A, the percentage by volume of silver bromide, and the third the increase in v_A by the aftertreatment.

2. RESULTS OF THE AFTERTREATMENT

With exception of the plates, which have in advance been watered, the increase in v_A is, for each concentration of silver nitrate, independent of the original value of v_A.

Table 2. Second aftertreatment.

$AgNO_3$ 25:100, 3 min.				
	I		II	
Plate No.	v_A	Δv_A	v_A	Δv_A
47_1	40.8	4.7	28.8	5.7
216_{12}	41.5	7.6	31.0	11.0
47_4	40.8	6.0	28.0	2.1
47_9	40.2	7.3	27.0	2.1
196_5	37.2	8.8	25.9	7.5
196_9	36.7	7.1	26.4	8.2

$AgNO_3$ 25:100, 1 1/4 min.				
	I		II	
Plate No.	v_A	Δv_A	v_A	Δv_A
212_{10}	51.3	11.0	41.5	11.0
47_5	42.2	9.2	30.3	9.2
47_2	41.1	4.5	29.4	3.8
47_8	41.0	4.9	27.4	4.2
47_{10}	40.7	12.3	25.9	8.6
196_{10}	38.3	6.7	26.9	7.5
196_8	37.1	10.7	27.1	8.4

$AgNO_3$ 11:100, 3 min.				
	I		II	
Plate No.	v_A	Δv_A	v_A	Δv_A
212_5	41.4	3.0	31.4	5.7
216_9	39.1	7.0	29.5	3.0
47_3	33.8	9.4	22.8	4.6

$AgNO_3$ 5:100, 6 min.				
	I		II	
Plate No.	v_A	Δv_A	v_A	Δv_A
212_{11}	40.3	1.9	27.4	2.6
47_6	31.3	0.7	20.6	0.7
196_{11}	26.2	2.6	20.3	0.9

In most cases the increases in v_A are higher for the upper than for the lower edge of the broad band, as could be expected. This is the case for the No. 47 (10 cases), 50 (6 cases), 196 (8 cases and 1 exception), whereas No. 181 (4 cases), 212 (4 cases and 1 exception) and 216 (5 cases) show the opposite phenomenon.

As explained earlier [2] the broad band originates from a series of layers whose percentages by volume of silver bromide are so great and lie

Table 3. Third aftertreatment.

$AgNO_3$ 11:100, 3 min.				
	I		II	
Plate No.	v_A	Δv_A	v_A	Δv_A
216_9	46.1	2.8	32.5	6.8
47_3	43.2	6.7	27.4	4.3

$AgNO_3$ 5:100, 6 min.				
	I		II	
Plate No.	v_A	Δv_A	v_A	Δv_A
212_{11}	42.2	2.7	30.0	4.8
196_{11}	28.8	2.6	21.2	4.8

so near each other, that the individual interference bands merge into one broad band. These layers go from the air side of the coating and into about 2/3 of the whole thickness of the coating. In the next following part of the coating the concentration of silver bromide decreases rapidly so that the individual bands are separated from each other and thereby constitute the so-called fringes.

It appears from this, that v_A is always lower at the lower than at the upper end of the broad band. The most probable explanation why the increase of v_A in a number of cases nevertheless is higher at the lower edge than at the upper edge seems to be that the silver bromide is dispersed in the form of grains, and that these grains at the lower edge are so much smaller than those at the upper edge that the larger surface of these smaller grains more than compensates for the lower concentration.

However, the further development of this explanation leads to great difficulties, especially in respect of the understanding of the different steps of the swelling process [3]. On the other hand, it is possible on the basis of a simple model of the constitution of the plate to give an entirely different explanation of these peculiarities.

3. THE CONSTITUTION OF THE PLATE

In a previous paper [4] I have assumed that the polar groups of the gelatin molecule are found on one side of the molecule, which is therefore hydrophilic, whereas the non-polar groups are found on the other side, which is therefore hydrophobic. The silver bromide is situated between two adjacent hydrophilic surfaces, and the corresponding percentage by volume, G', of unhardened gelatin is therefore divided in two halves.

4. THE COURSE OF THE AFTERTREATMENT

By aftertreatment with silver nitrate, which is terminated already after 1 1/4 min, the solution must at once fill the space v_0 between the adjacent hydrophobic surfaces but has no time for diluting the solutions of soluble gelatin [5], which are distributed throughout the network of gelatin molecules. On the other hand, the silver ions have the possibility of being adsorbed on the already present surfaces of silver bromide.

By the subsequent treatment with potassium bromide (20:100), the silver nitrate, which fills the space v_0, must immediately be converted into silver bromide, and the same is the case with some of the adsorbed silver ions on the surface of the silver bromide.

During the following treatment (6 min) with the mixed solution of potassium bromide and potassium metabisulphite the rest of the adsorbed silver ions are converted into silver bromide, and the molecular silver bromide in the volume v_0 is dissolved by the metabisulphite and then transported to and adsorbed on the surface of the layer of silver bromide, which thereby thickens.

Table 4.

$AgNO_3$ 25:100							
Plate No.	number of pieces	I				II	
		Δv_A mean	v_o mean	ΔS	ΔA	Δv_A mean	ΔA
47	7	13.2	61	2.6	10.6	9.7	7.1
196	6	12.8	90	3.8	9.0	9.8	6.0
212	2	9.0	107	4.5	4.5	10.8	6.3
216	2	8.2	75	3.2	5.0	10.8	7.6

Table 5.

$AgNO_3$ 11:100						
Plate No.	number of pieces	I			II	
		Δv_A mean	ΔS	ΔA	Δv_A mean	ΔA
47	2	7.4	1.3	6.1	5.4	4.3
196	2	5.6	1.9	4.7	5.6	3.7
212	1	6.6	2.2	4.4	8.6	6.4
216	1	8.1	1.6	6.5	8.4	6.8

Table 6.

$AgNO_3$ 5:100						
Plate No.	number of pieces	I			II	
		Δv_A	ΔS	ΔA	Δv_A	ΔA
47	1	4.8	0.5	4.3	3.7	3.2
196	1	3.5	0.8	2.7	4.7	3.9
212	1	5.1	0.9	4.2	4.6	3.7
216	1	4.5	0.7	3.8	5.2	4.5

The increase in v_A through the aftertreatment is therefore made up of two parts, the directly adsorbed quantity ΔA, and the quantity ΔS subsequently transported from v_o.

1. For the silver nitrate solution 25:100 one volume corresponds to the following volume of silver bromide:

$$\frac{25 \times 1.194 \times 1.14}{125 \times 6.46} = 0.0422$$

where 1.194 is the density of the solution, 1.14 the previously [6] found value of the quotient $AgBr:AgNO_3$, and 6.46 the density of silver bromide.

For the solutions 11:100 and 5:100 the figures are 0.0209 and 0.0088, respectively.

2. For the four plates whose values of v_o are experimentally determined [7] the data are collected in Tables 4, 5 and 6.

For the second and third aftertreatment there are fewer observations, and the results therefore are not very exact. See Tables 7 to 11.

Table 7. Second aftertreatment.

$AgNO_3$ 25:100					
		I		II	
Plate No.	number of pieces	Δv_A mean	ΔA	Δv_A mean	ΔA
47	6	6.6	4.0	5.1	2.5
196	4	8.2	4.4	7.9	4.1
212	1	—	—	11.0	6.5
216	1	7.6	4.4	11.0	7.8

Table 8.

$AgNO_3$ 11:100					
		I		II	
Plate No.	number of pieces	Δv_A	ΔA	Δv_A	ΔA
47	1	7.0	5.7	4.6	3.3
212	1	3.0	0.8	5.7	3.5
216	1	7.0	5.4	3.0	1.4

Table 9.

$AgNO_3$ 5:100					
		I		II	
Plate No.	number of pieces	Δv_A	ΔA	Δv_A	ΔA
47	1	0.7	0.2	0.7	0.2
196	1	2.6	1.8	0.9	0.1
212	1	1.9	1.0	2.6	1.7

Table 10. Third aftertreatment.

$AgNO_3$ 11:100					
		I		II	
Plate No.	number of pieces	Δv_A	ΔA	Δv_A	ΔA
47	1	6.7	5.4	4.3	3.0
216	1	2.8	1.2	6.8	5.2

Table 11.

$AgNO_3$ 5:100					
		I		II	
Plate No.	number of pieces	Δv_A	ΔA	Δv_A	ΔA
196	1	2.6	1.8	4.8	4.0
212	1	2.7	1.8	3.1	2.2

The adsorbed amount of silver bromide ΔA is supposed to form a compact layer the thickness of which can be either the total length of a molecule of silver bromide or — on the average — half this value, if the layer consists of only single silver or bromide ions. The total length of the silver bromide molecule is known to be 0.64 mμ, and it is consequently to be expected that the thickness of the layer is either 0.32 or 0.64 mμ.

If the value of G′, the percentage by volume of unhardened gelatin, is known it must therefore be possible to calculate the diameter of the gelatin molecule because

$$\frac{G'}{2d_G} = \frac{\Delta A}{0.64} \quad \text{or} \quad \frac{G'}{d_G} = \frac{\Delta A}{0.32}$$

where d_G is the diameter of the gelatin molecule. It is multiplied by 2 because the silver bromide is situated between two surfaces of unhardened gelatin, and therefore corresponds to two diameters of gelatin molecules.

From earlier measurements [8] it is known that the values of G′ for the upper edge of the broad band vary from 30.2 to 34.2, with the mean value 31.4, for the lower edge from 21.9 to 22.2 mean 22.2. I assume that these values also are valid for the new measurements. By inserting these values in the equation above we find for the first aftertreatment with the strongest solution of silver nitrate the following values of d_G. (See Table 12).

Table 12.

	I		II		
Plate No.	d_{AgBr}	d_G	d_{AgBr}	d_G	d_G mean
47	0.64	0.93	0.64	0.91	0.92
196	0.64	1.12	0.64	1.18	1.15
212	0.32	1.11	0.64	1.13	1.12
216	0.32	1.00	0.64	0.94	0.97

The table shows that no intermediary values are possible between 0.32 and 0.64, and this fact seems to be the real cause of the peculiar phenomenon that v_A for some plates (212,216) are greater for the lower edge than for the upper edge of the broad band.

The calculated values of d_G agree well with the values 0.8—0.9 mμ which Sheppard, Lambert and Swinehart [9] have assumed earlier.

For the more diluted solutions of silver nitrate and for the second and third aftertreatment the results are scant and not very exact. By using the now known values for d_G we find the corresponding values for the thickness of the silver bromide layer, which are collected in Tables 13 to 15.

Table 13.

Plate No.	$AgNO_3$ 25:100			
	I		II	
	aftertr.		aftertr.	
	1	2	1	2
47	0.64	0.23	0.64	0.21
196	0.64	0.32	0.64	0.42
212	0.32	—	0.64	0.65
216	0.32	0.27	0.64	0.68

Table 14.

Plate No.	$AgNO_3$ 11:100					
	I			II		
	aftertr.			aftertr.		
	1	2	3	1	2	3
47	0.36	0.33	0.32	0.36	0.27	0.25
196	0.34	—	—	0.38	—	—
212	0.31	0.06	—	0.64	0.35	—
216	0.40	0.33	0.07	0.60	0.12	0.45

Table 15.

Plate No.	$AgNO_3$ 5:100					
	I			II		
	aftertr.			aftertr.		
	1	2	3	1	2	3
47	0.25	0.01	—	0.27	0.02	—
196	0.20	0.13	0.13	0.40	0.00	0.42
212	0.30	0.07	0.13	0.37	0.17	0.22
216	0.24	—	—	0.39	—	—

The figures I and II refer to the upper and the lower edge of the broad band. Column 1 shows the number of the plate, and the following columns the calculated thicknesses of the silver bromide layer for the first, the second and the third aftertreatment, if any.

For the first aftertreatment the values 0.32 and 0.64 seem to be valid for all concentrations of silver nitrate. It is worth noting that also for the concentration 11:100 the lower edge takes up more silver bromide than the upper edge, in the same two cases as before.

The measurements of the following aftertreatments are too scant and uncertain to permit any conclusions.

REFERENCES

1. Winther, Chr. *Trans. Danish Acad. Techn. Sci.* **1953** No. 5, 7.
2. *Ibid.* 41.
3. Winther, Chr. *Acta Chem. Scand.* **12** (1958) 1634.

4. Winther, Chr. *Ibid.* **10** (1956) 1125.
5. Winther, Chr. *Ibid.* **12** (1958) 1652.
6. Winther, Chr. *Trans. Danish Acad. Techn. Sci.* **1953** No. 5, 19.
7. Winther, Chr. *Acta Chem. Scand.* **12** (1958) 1634.
8. Winther, Chr. *Ibid.* **10** (1956) 1125.
9. Sheppard, S. E., Lambert, R. H. and Swinehart, D. *J. Chem. Phys.* **13** (1945) 372.

Received June 23, 1958.

ACTA CHEMICA SCANDINAVICA 12 (1958) 1652—1656

The First Step in the Swelling of Gelatin with Water. V

CHR. WINTHER

Photochemical Laboratory, Technical University of Denmark, Copenhagen, Denmark

By the aid of a simple model of the constitution of the interference plate it is possible to calculate the thickness of the silver bromide layer and the swelling factor of the gelatin.

In the preceding paper of this series [1] it was shown that the amount of silver bromide which was taken up during the aftertreatment of the interference plate was due to two sources, namely 1) the adsorbed amount of silver ions, and 2) the solution of silver nitrate.

When the original chromated gelatin plate, after exposure, is bathed in the solution of silver nitrate (25:100) a certain amount of silver ions are directly adsorbed [2], and at the same time the solution is filling the network of gelatin molecules for which reason the said amount is determined by 1) the swelling factor f, and 2) the percentage by volume of unhardened gelatin, G′.

1. THE ADSORPTION.

As shown before [3], the adsorption is expressed by the formula

$$\text{ads.} = 0.64 \frac{G'}{2d_G} \qquad (1)$$

where d_G is the diameter of the gelatin molecule.

Table 1 contains, 1) the numbers of the plates, 2) the mean values of v_A, the percentage by volume of silver bromide, for the upper (I) and the lower (II) edge of the broad band. No. 47 comprises 10 cases, No. 196 9, No. 212 5 and No. 216 5 cases. The values of d_G are known from an earlier paper [4], the mean values of G′ are taken as 31.4 and 22.2, respectively [5]. The third column contains the calculated amount of adsorbed silver bromide (ads) and the fourth column the quotients ads:v_A.

From previous measurements [6] it is possible to calculate this quotient for different values of G′, which are taken from Table 7 of the paper just quoted. Table 2 contains the results for three different values of G′, which correspond to the three last values in the said Table 7.

Table 1.

Plate No.	v_A	ads.	ads:v_A	exp.
47 I	27.7	10.9	0.39	0.32
47 II	18.4	7.7	0.42	0.38
196 I	24.7	8.7	0.35	0.32
196 II	16.0	6.2	0.39	0.38
212 I	35.1	9.0	0.26	0.32
212 II	23.6	6.3	0.37	0.38
216 I	30.4	10.4	0.39	0.32
216 II	21.2	7.3	0.42	0.38

The first column shows the number of days which have passed between the coating and the exposure of the plate, the second and the third column show the adsorbed and the total amounts of silver nitrate, and the fourth column the quotient ads: total.

It appears that the behaviour of the plates which have remained only 2 days before the exposure is different from that of plates which have remained 4, 7 or 11 days before the exposure. For these three groups of plates the quotient for each individual value of G′ is nearly constant and markedly greater than for the plates which have had 2 days rest.

All the newly examined plates have only remained 2 days between coating and exposure. It is therefore possible to interpolate graphically the values for G′ = 31.4 and 22.2. These values are shown in Table 1, column 5 under the desingnation exp.

Table 3 contains the corresponding values for the older plates [7].

As the same sort of gelatin (Stoess hard) was used as for No. 212, the value 1.12 for d_G was used for the calculation.

Both Tables 1 and 3 show that the calculated and the experimentally found values of the quotient agree well.

Table 2.

	G′								
	53.0			28.3			3.2		
Days	ads.	total	ads : total	ads.	total	ads : total	ads.	total	ads : total
2	2.4	11.6	0.21	2.9	8.3	0.35	3.3	7.0	0.47
4	3.5	10.6	0.33	3.8	8.3	0.46	4.4	7.7	0.57
7	3.5	10.4	0.34	3.5	8.2	0.43	3.9	7.1	0.55
11	4.8	11.2	0.43	2.7	8.4	0.49	4.3	7.6	0.57
			0.37			0.44			0.56

Table 3.

Plate No.	Days	v_A	G′	ads.	ads : v_A	exp.
14a I	2	26.4	30.2	8.6	0.33	0.34
14a II	2	17.3	22.2	6.3	0.37	0.38
2 I	3	27.0	30.6	8.7	0.32	0.33
2 II	3	17.3	22.2	6.3	0.36	0.38
9 I	9	22.9	30.9	8.8	0.39	0.44
9 II	9	14.9	22.2	6.3	0.42	0.48
28 I	9	23.3	34.2	9.8	0.42	0.43
28 II	9	14.2	21.9	6.2	0.44	0.48

2. THE ABSORPTION OF SILVER NITRATE SOLUTION

In order to calculate the amount of silver nitrate solution which is absorbed by the exposed chromated gelatin plate it is necessary to know the swelling factor f. Earlier measurements [8] have been interpreted under the assumption that — for each sort of gelatin — f should be a constant, independent of the exposure, when it was calculated for 100 % unhardened gelatin. By closer examination of the results this assumption does not seem to hold good. On the contrary, there seems to be an approximate proportionality between f and the amount of swelling water, so that $f = 0.093$ V. It appears from this, that the value of f must be higher at the upper than at the lower edge of the broad band.

The formula for the absorption is now

$$((f—v_o)\frac{G'}{100} + v_o) \times 0.0422$$

or

$$\left[f\frac{G'}{100} + v_o\left(1— \frac{'G'}{100}\right)\right] \times 0.0422 \qquad (2)$$

where v_o is the volume which is filled momentarily with water (or solution), and 0.0422 the volume of silver bromide which corresponds to one volume of silver nitrate solution 25:100.

The experimentally found values of the quotient ads:v_A are only valid for a certain sort of gelatin. They cannot therefore be used for calculating v_A for plates made with other sorts of gelatin. The only possible expedient therefore is to use the experimentally found values of v_A and from them calculate the values of f with the aid of the formulae (1) and (2). Table 4 contains the results for the mean values of the new plates, and Table 5 for the previously examined plates.

3. THE THICKNESS OF THE SILVER BROMIDE LAYER

The silver bromide v_A has one of its surfaces in common with half of the unhardened gelatin G′. Therefore

$$\frac{G'}{2d_G} = \frac{V_A}{d_{AgBr}}$$

Table 4.

Plate No.	v_A	v_o	d_G	ads.	diff.	G′	f
47 I	27.7	61	0.92	10.9	16.8	31.4	11.4
47 II	18.4	61	0.92	7.7	10.7	22.2	9.3
196 I	24.7	90	1.15	8.7	16.0	31.4	10.2
196 II	16.0	90	1.15	6.2	9.8	22.2	7.3
212 I	35.1	106	1.12	9.0	26.1	31.4	17.5
212 II	23.6	106	1.12	6.3	17.3	22.2	14.8
216 I	30.4	75	0.97	10.4	20.0	31.4	13.5
216 II	21.2	75	0.97	7.3	13.9	22.2	12.3

Table 5.

$v_o = 64$ $d_G = 1.12$					
Plate No.	v_A	ads.	diff.	G′	f
14a I	26.4	8.6	17.8	30.2	12.5
14a II	17.3	6.3	11.0	22.2	9.5
2 I	27.0	8.7	18.3	30.6	12.7
2 II	17.3	6.3	11.0	22.2	9.5
9 I	22.9	8.8	14.1	30.9	9.4
9 II	14.9	6.3	8.6	22.2	7.0
28 I	23.3	9.8	13.5	34.2	8.4
28 II	14.2	6.2	8.0	21.9	6.4

where d_{AgBr} is the thickness of the silver bromide layer. The thicknesses d_G of the gelatin molecule are taken from Table 12 in the previous paper in this series [9]. The results are collected in Table 6.

All the values of dAgBr for the lower edge of the broad band are lower than for the upper edge. This is explained by the fact [10] that during the drying of the plate after bathing in silver nitrate solution some of the silver nitrate diffuses deeper into the coating where it constitutes the fringes. This loss is of course greater at the lower than at the upper edge.

4. THE PREPARATION OF THE INTERFERENCE PLATE

This preparation has been thoroughly described in a previous paper [11]. Through the results of the latest experiments it is possible to give some further hints about the procedure.

1. The gelatin should be characterised by the greatest possible swelling factor.

2. After coating the plate should be laid on a plate glass which can be cooled by cold water.

3. The time between the coating and the exposure should not exceed 2 days.

Table 6.

Plate No.	v_A	d_G	G′	d_{AgBr}
47 I	27.7	0.92	31.4	1.62
47 II	18.4	0.92	22.2	1.52
196 I	24.7	1.15	31.4	1.82
196 II	16.6	1.15	22.2	1.66
212 I	35.1	1.12	31.4	2.52
212 II	23.6	1.12	22.2	2.38
216 I	30.4	0.97	31.4	1.88
216 II	22.2	0.97	22.2	1.84

4. The drying of the plate treated with silver nitrate should be accelerated as much as the coating can stand without melting.

5. The treatment with the potassium bromide solution (20:100) which takes about 10—15 sec should be prolonged until the plate shows faint signs of opacity.

5. CONCLUSIONS

1. A scheme for the adsorption and absorption of silver nitrate in the exposed chromated gelatin plate is proposed.

2. The swelling factor f is nearly proportional to the amount of water taken up by the chromated gelatin plate.

3. The calculated values of the quotient ads:v_A agree very well with the experimentally found values.

4. When v_o, the amount of water momentarily absorbed, and d_G, the diameter of the gelatin molecule, are known, it is possible to calculate the swelling factor f.

5. The calculated values of f are smaller when the plate is stored longer than two days between coating and exposure.

6. From the values of unhardened gelatin G′ and of the thickness of the gelatin molecule it is possible to calculate the thickness of the silver bromide layer.

7. The results of the new experiments can give some hints about the preparation of the interference plates.

REFERENCES

1. Winther, Chr. *Acta Chem. Scand.* **12** (1958) 1634.
2. Winther, Chr. *Trans. Danish Acad. Techn. Sci.* **1953** No. 5, 18—19
3. Winther, Chr. *Acta Chem. Scand.* **12** (1958) 1643.
4. Winther, Chr. *Ibid.* Table 12.
5. Winther, Chr. *Ibid.*
6. Winther, Chr. *Trans. Danish Acad. Techn. Sci.* **1953** No. 5, 17.
7. Winther, Chr. *Acta Chem. Scand.* **10** (1956) 1125.
8. Winther, Chr. *Trans. Danish Acad. Techn. Sci.* **1953** No. 5, 18, 21.
9. Winther, Chr. *Acta Chem. Scand.* **12** (1958) 1643.
10. Winther, Chr. *Trans. Danish Acad. Techn. Sci.* **1953** No. 5, 41.
11. Winther, Chr. *Ibid.* 7.

Received June 23, 1958.

ACTA CHEMICA SCANDINAVICA 12 (1958) 1657—1670

On the Kinetics of the Decomposition of Cyanic Acid

MOGENS BALLUND JENSEN

The Royal Danish School of Pharmacy, Copenhagen, Denmark

The decomposition of cyanic acid and cyanate into ammonia and carbon dioxide has been investigated kinetically in dilute aqueous solution over the pH-range 0—7 and in strongly basic medium. The experimental results indicate that the decomposition takes place according to three simultaneous reactions, *viz.* $OCNH + H_3O^+ \rightarrow NH_4^+ + CO_2$ (I), $OCNH + H_2O \rightarrow NH_3 + CO_2$ (II), and $OCN^- + 2H_2O \rightarrow NH_3 + HCO_3^-$ (III). The velocity constants for the reactions I and II were found to be 3.61 (l mole^{-1} min^{-1}) and 0.047 (min^{-1}), respectively, at 18°C. The energy of activation was found to be 15.1 kcal mole^{-1} for reaction I and 19.9 kcal mole^{-1} for reaction II. The velocity constant for reaction III was found to be 0.0017 (min^{-1}) at 94°C with an energy of activation of 23.9 kcal mole^{-1}.

Bicarbonate was found to act catalytically on the decomposition.

The acidic dissociation constant of cyanic acid was found to be $10^{-3.54}$ at 18°C.

1. The velocity for the decomposition of cyanate into ammonia and carbon dioxide in aqueous medium has been studied in several cases [1-5]. Most of the investigations have been carried out in strongly acid or basic solution, whereas measurements of the velocity in moderately and weakly acid solution are rather limited.

The present investigation deals with the decomposition of cyanate (meaning cyanic acid and cyanate ion) in dilute solution over the pH range 0—7 and in strongly basic medium.

2. Solutions of potassium cyanate were in most cases prepared by shaking silver cyanate with a solution containing the equivalent amount of potassium iodide. Silver cyanate was prepared by heating 120 g of urea and 68 g of silver nitrate dissolved in about 1 l of water. The needles of silver cyanate, gradually precipitated, were filtered off from time to time and washed until the wash water was almost free from silver ion. The silver cyanate was dried at 60° and stored in a desiccator containing silica gel.

In some experiments solutions prepared from Sodium Cyanate pure (Hopkin and Williams, Ltd.) were used.

Table 1. 20.00 ml 0.1004 M KNCO + 0.1 N $AgNO_3$

Final solution		ml 0.1 N $AgNO_3$ pr. 200 ml	c_{KNCO} found
c_{CH_3COOH}	c_{CH_3COONa}		
0	0	25.00	0.0996
0	0	25.00	0.0994
0	0	50.00	0.1001
0	0	50.00	0.1004
0.025	0.075	50.00	0.0999
0.050	0.050	50.00	0.0993
0.075	0.025	50.00	0.0982

3. The experiments were, unless otherwise stated, carried out in such a way that equal volumes of solutions of potassium cyanate and buffers of the temperature in question were mixed and placed in a thermostat. After an appropriate lapse of time the mixture or a sample of the mixture was brought to pH = approx. 5.5 by the addition of sodium acetate or acetic acid and immediately analysed for cyanate or ammonia.

The method of analysis was in the case of cyanate a procedure analogous to the determination of chloride according to Volhard. The cyanate was precipitated as silver cyanate by the addition of silver nitrate whereupon the excess of silver nitrate was titrated back with ammonium thiocyanate in a quota part of the filtrate acidified with nitric acid.

In Table 1 are listed some determinations of the concentration of cyanate in 20.00 ml of a solution of potassium cyanate prepared by shaking a 0.1004 M solution of potassium iodide with silver cyanate, *i.e.* the concentration of cyanate being 0.1004. The cyanate was precipitated with excess silver nitrate in neutral or in weakly acid medium the total volume being 200 ml.

It is seen from Table 1 that a relative great excess of silver nitrate is required in order to precipitate the cyanate quantitatively. It is furthermore seen that if the pH of the solution is less than approx. 5, more or less cyanate remains unprecipitated.

In the case of ammonia the analysis was carried out in such a manner that the cyanate was precipitated as silver cyanate and the content of ammonia in the filtrate was determined in the usual way by distilling off the ammonia.

4. The velocity constants were calculated on the basis of Napierian logarithms and refer to molar concentrations, the unit of time being the minute. The activity coefficient, f, for a monovalent ion was calculated from the expression of Bjerrum: $-\log f = 0.3 \sqrt[3]{c_{ion}}$.

It should be noted that $c_{cyanate}$ means the total concentration of cyanate, *i.e.* the sum of the concentrations of cyanic acid and of cyanate ion.

5. The values 1.44×10^{-3} and 1.82×10^{-5} for the acidic dissociation constants of chloroacetic acid [6] and acetic acid [7], respectively, and the value 4.01×10^{-7} for the first acidic dissociation constant of carbonic acid [8] were used in the calculations at 18°C.

The solubility of carbon dioxide in water at 18°C and at a pressure of 1 atmosphere was calculated from the data of Harned and Davis [8].

In the case of cyanic acid a calculation of the acidic dissociation constant, K_{OCNH}, was carried out on the basis of determinations of the hydrogen ion activity in solutions containing both cyanic acid and cyanate ion. The solutions were prepared by mixing a solution of sodium cyanate with an appropriate

Table 2. Determination of the acidic dissociation constant of cyanic acid. 18°C.

c_{OCNH}	c_{OCN^-}	c_{ion}	Minutes after mixing	pH	$\frac{\Delta pH}{\Delta t}$	pH extrapol.	K_{OCNH}
0.0501	0.0474	0.10	1.5	3.52		3.38	$10^{-3.54}$
			2.5	3.61	0.09		
			3.5	3.70	0.09		
			4.5	3.77	0.07		
0.0334	0.0966	0.13	1.0	3.96		3.84	$10^{-3.53}$
			2.0	4.08	0.12		
			3.0	4.20	0.12		
			4.0	4.31	0.11		
			5.0	4.39	0.08		
0.0167	0.0483	0.065	1.0	3.99		3.88	$10^{-3.54}$
			2.0	4.08	0.09		
			3.0	4.15	0.07		
			4.0	4.20	0.05		
0.0167	0.0483	0.20	1.5	3.94		3.83	$10^{-3.55}$
			2.5	4.01	0.07		
			3.5	4.08	0.07		
			4.5	4.15	0.07		

Mean value of K_{OCNH} $10^{-3.54}$

Table 3. The velocity constant for the reaction $OCNH + H_3O^+ \rightarrow NH_4^+ + CO_2$. 18°C.

Run	Initial solution				Min.	% cyanate	k	k mean	c_{H^+} mean
	c_{H^+}	$c_{NO_3^-}$	c_{K^+}	$c_{cyanate}$					
4	0.472	0.48	0.02	0.0195	0.5	41.3	1.77	1.75	0.467
					1.0	17.1	1.76		
					1.5	7.2	1.75		
					2.0	3.2	1.72		
3	0.207	0.23	0.02	0.0198	0.5	67.2	0.794	0.797	0.198
					1.0	45.8	0.781		
					1.5	30.7	0.785		
					2.0	20.7	0.787		
					2.5	13.3	0.806		
					3.0	8.5	0.824		
2	0.098	0.12	0.02	0.0201	1.0	68.8	0.375	0.373	0.090
					1.5	57.2	0.373		
					2.0	47.3	0.375		
					2.5	39.0	0.378		
					3.0	33.5	0.364		
					4.0	23.1	0.366		
6	0.100	0.14	0.04	0.0383	1.0	68.9	0.373	0.371	0.089
					1.5	57.2	0.373		
					2.0	48.1	0.366		
					40	0			
7	0.098	0.22	0.12	0.0182	1.0	66.0	0.414	0.408	0.092
					1.5	54.0	0.410		
					2.0	44.7	0.403		
					3.0	30.7	0.398		
8	0.098	0.32	0.22	0.0182	1.0	67.4	0.394	0.398	0.092
					1.5	53.4	0.419		
					2.0	46.2	0.387		
					3.0	31.0	0.391		
9	0.098	1.12	1.02	0.0182	1.0	67.6	0.391	0.389	0.092
					2.0	46.0	0.389		
					3.0	31.0	0.389		
1	0.066	0.09	0.02	0.0199	0.9	79.8	0.251	0.251	0.059
					2.0	61.0	0.246		
					3.0	46.5	0.256		
					4.0	36.3	0.253		
					5.0	29.0	0.249		
					30	0.6			

$k_{OCNH \cdot H_3O^+} = 3.61.$

Table 4. The velocity constant for the reaction $OCNH + H_3O^+ \rightarrow NH_4^+ + CO_2$. 18°C.

Run	Initial solution			Min.	% cyanate	% CO_2	% NH_4^+	k	k mean	c_{H^+} mean
	c_{H^+}	c_{K^+}	$c_{cyanate}$							
10	0.098[1]	0.02	0.0196	1.0	67.4			0.394	0.385	0.090
				1.5	56.3			0.382		
				2.0	46.8			0.380		
				3.0	31.5			0.385		
				4.0	21.5			0.382		
11	0.098[2]	0.02	0.0196	1.0	66.4			0.410	0.394	0.091
				2.0	45.9			0.389		
				3.0	32.1			0.380		
12	0.096[3]	0.02	0.0205	1.0		30.9		0.368	0.382	0.087
				2.0		54.5		0.394		
				3.0		66.2		0.362		
				4.0		78.2		0.380		
				5.0		87.0		0.408		
13	0.098[3]	0.02	0.0198	1.05			32.8	0.380	0.385	0.090
				2.0			54.3	0.391		
				3.0			68.2	0.382		
				4.0			78.4	0.382		

[1] $c_{ClO_4^-} = 0.12$
[2] $c_{Cl^-} = 0.12$
[3] $c_{NO_3^-} = 0.12$

$k_{OCNH \cdot H_3O^+} = 3.61$

volume of hydrochloric acid which in some cases contained sodium nitrate. The temperature of both solutions was 18°C.

By means of a glass electrode the pH of the solution was determined at intervals of one minute and on the basis of the quantity $\Delta pH/\Delta t$ an extrapolation to zero time was made.

In Table 2 are listed the composition of the solutions and the measured and extrapolated values of pH together with the values of K_{OCNH} calculated from the expression

$$K_{OCNH} = \frac{a_{H^+} \cdot a_{OCN^-}}{a_{OCNH}} = \frac{a_{H^+} \cdot c_{OCN^-} \cdot f}{c_{OCNH}}$$

The mean value of K_{OCNH} obtained in this way is $10^{-3.54}$ at 18°C.

ON THE REACTION: $OCNH + H_3O^+ \rightarrow NH_4^+ + CO_2$

In Tables 3 and 4 are listed the experiments which were carried out in strongly acid solutions at 18°C. In most cases nitric acid was used for the experiments just as some of the solutions contained potassium nitrate.

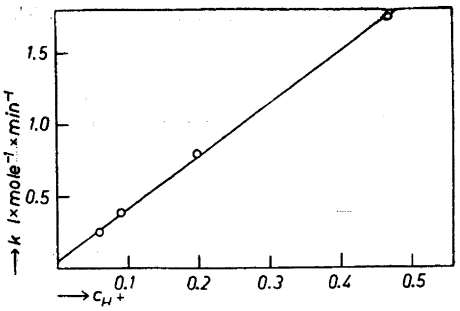

Fig. 1. Velocity constants for the reaction: "cyanic acid → $NH_4^+ + CO_2$" as a function of the hydrogen ion concentration. 18°C.

In runs 10 and 11 perchloric acid and hydrochloric acid, respectively, was used.

It is seen from Table 4 that nitric acid, perchloric acid and hydrochloric acid yield practically the same results.

In run 11 the method of analysis was modified in the following manner. The chloride and the cyanate were precipitated as silver salts at pH = 5.5 upon addition of silver nitrate. The silver chloride and silver cyanate were filtered off, washed, and boiled with excess of 0.1 N hydrochloric acid whereby: $AgNCO + 2HCl + H_2O = AgCl + CO_2 + NH_4Cl$, and back-titration was carried out with 0.1 N sodium hydroxide.

In runs 12 and 13 the decomposition was followed not by determining the concentration of cyanate but by determining the concentration of carbon dioxide and ammonia, respectively. In the case of carbon dioxide the analysis was carried out in such a manner that sodium hydroxide and barium chloride were added and the barium carbonate precipitated was then determined by acidimetric titration.

It is seen from Tables 3 and 4 that good agreement exists between the content of ammonia and carbon dioxide and the content of cyanate the sum being virtually constant, meaning that cyanate decomposes quantitatively into ammonia and carbon dioxide in strongly acid medium.

Tables 3 and 4 also list the velocity constants calculated from the unimolecular expression: $kt = \ln a/a-x$. It is seen that the velocity constants are almost proportional to the hydrogen ion concentration the mean values of which also are listed in Tables 3 and 4. This indicates a bimolecular reaction between cyanic acid and hydrogen ion.

In Fig. 1 the velocity constants listed in Tables 3 and 4 are plotted against the mean values of the hydrogen ion concentration and a straight line is drawn. The slope of this line is 3.61, meaning that the velocity constant, $k_{OCNH \cdot H_3O^+}$, for the reaction:

$$OCNH + H_3O^+ \rightarrow NH_4^+ + CO_2$$

is equal to 3.61 at 18°C. This value is in good agreement with the value 3.75, which was calculated at an ionic strength of 1.0 from the data reported by Lister [3].

Table 5. The temperature dependence of $k_{OCNH \cdot H_3O^+}$

Run	°C	Initial solution				Min.	% cyanate	k	k mean	c_{H^+} mean	$k_{OCNH \cdot H_3O^+}$
		c_{H^+}	$c_{NO_3^-}$	c_{K^+}	$c_{cyanate}$						
56	10.0	0.181	0.20	0.02	0.0197	1.0	73.4	0.311	0.311	0.173	1.71
						2.0	53.8	0.311			
						3.0	39.2	0.313			
						5.0	21.2	0.309			
55	4.0	0.181	0.20	0.02	0.0197	1.0	84.1	0.173	0.173	0.173	0.986
						2.0	70.6	0.175			
						5.0	42.2	0.172			
						9.0	21.2	0.173			

From Fig. 1 can be seen that the straight line intersects the ordinate axis at 0.05 indicating that also another reaction is taking place, *viz.* a reaction between cyanic acid and water, see next section.

In Table 5 are listed some experiments on the temperature dependence of $k_{OCNH \cdot H_3O^+}$. Table 5 contains the velocity constants, k, calculated from the unimolecular expression. k represents a sum of $k_{OCNH \cdot H_3O^+}$ multiplied with the hydrogen ion concentration and k_{OCNH} (see next section), although the contribution of k_{OCNH} to k is small (about 2—5 %). The value of $k_{OCNH \cdot H_3O^+}$ was obtained dividing the difference between k and k_{OCNH} by the mean value of the hydrogen ion concentration. The values of $k_{OCNH \cdot H_3O^+}$ are 1.71 and 0.986 at 10°C and 4°C, respectively. These values give an average of 15.1 kcal . mole^{-1} for the energy of activation, calculated on the basis of the value of $k_{OCNH \cdot H_3O^+}$ at 18°C. Lister [3] has found the energy of activation to be 14.5 kcal mole^{-1}.

ON THE REACTION: $OCNH + H_2O \rightarrow NH_3 + CO_2$

In Table 6 are listed the experiments which were carried out at 18°C in solutions initially being 0.04 N with respect to nitric acid.

The decomposition takes place through the two simultaneous reactions:

$$OCNH + H_3O^+ \rightarrow NH_4^+ + CO_2 \quad (I)$$

and

$$OCNH + H_2O \rightarrow NH_3 + CO_2 \quad (II)$$

fololwed by the instantaneous reaction $NH_3 + H^+ = NH_4^+$. In more acid solution reaction I predominates but in the less acid solutions listed in Table 6 the velocity of reaction II is about a third of that for reaction I.

The velocity constant for reaction II is denoted k_{OCNH}.

Table 6. The velocity constant for the reaction $OCNH + H_2O \rightarrow NH_3 + CO_2$. 18°C.

Run	Initial solution				Min.	$c_{cyanate}$	k_{OCNH}	k_{OCNH} mean
	c_{H^+}	$c_{NO_3^-}$	c_{K^+}	$c_{cyanate}$				
5	0.0386	0.06	0.02	0.0198	2.0	0.0141	0.0414	0.0414
					4.0	0.0106	0.0345	
					6.0	0.0079	0.0391	
					10.0	0.0046	0.0414	
					15.0	0.0023	0.0461	
14	0.0396	0.06	0.02	0.0196	1.0	0.0164	0.0368	0.0414
					2.0	0.0138	0.0414	
					4.0	0.0101	0.0414	
					6.0	0.0076	0.0414	
					10.0	0.0043	0.0437	
					15.0	0.0021	0.0484	

$k_{OCNH} = 0.0414$

The concentration of hydrogen ion varies from approx. 0.04 to 0.02 meaning that practically all of the cyanate exists as cyanic acid and the amount being present as cyanate ion has been neglected in the calculations.

Let a denote the initial concentration of cyanic acid and x the amount decomposed at the time t. The initial concentration of hydrogen ion is denoted b. k_1 stands for $k_{OCNH \cdot H_2O^+}$ and k_2 for k_{OCNH}. For the decomposition of the cyanic acid we have: $dx/dt = (k_1 \cdot c_{H^+} + k_2)(a-x)$.

Introducing $c_{H^+} = b-x$ and integrating we get:

$$k_2 = 1/t \left[\ln \frac{a}{a-x} + \ln \frac{k_1(b-x) + k_2}{k_1 b + k_2} \right] - k_1(b-a).$$

Table 7. The temperature dependence of k_{OCNH}

Run	°C	Initial solution				Min.	$c_{cyanate}$	k_{OCNH}	k_{OCNH} mean
		c_{H^+}	$c_{NO_3^-}$	c_{K^+}	$c_{cyanate}$				
57	10.0	0.0412	0.06	0.02	0.0197	5.0	0.0132	0.0159	0.0157
						10.0	0.0092	0.0161	
						15.0	0.0068	0.0152	
58	4.0	0.0412	0.06	0.02	0.0197	7.0	0.0150	0.0025	0.003
						15.0	0.0113	0.0021	
						30.0	0.0067	0.0044	

The values for k_{OCNH} calculated from the above mentioned expression are also listed in Table 6.

In both experiments the mean value 0.041 for k_{OCNH} was obtained at 18°C. This value is in good agreement with the value 0.05 which was found from Fig. 1.

In Table 7 are listed a few experiments on the temperature dependence of k_{OCNH}, the value of which was calculated from the above mentioned expression inserting the value of $k_{OCNH\cdot H_3O^+}$ at the temperature in question. The value of k_{OCNH} is 0.0157 at 10°C corresponding to an anergy of activation of 19.9 kcal mole^{-1}. The value 0.003 found at 4°C is not very accurate since reaction I is by far the predominant at this temperature.

Further experiments on the determination of k_{OCNH} at 18°C were carried out in less acid solutions buffered with a weak acid and its salt. The ionic strength was adjusted to 0.2 by means of sodium nitrate and the samples were analysed for cyanate and ammonia.

For the rate of formation of ammonia we have:

$$dc_{ammonia}/dt = (k_{OCNH\cdot H_3O^+} \cdot c_{H^+} + k_{OCNH}) \cdot c_{OCNH}$$

Introducing $c_{OCNH} = c_{cyanate}/(1 + K_{OCNH}/a_{H^+} \cdot f)$ and $c_{H^+} = a_{H^+}/f$ we get:

$$\frac{dc_{ammonia}}{dt} = \frac{k_{OCNH\cdot H_3O^+} \cdot a_{H^+}/f + k_{OCNH}}{1 + K_{OCNH}/a_{H^+} \cdot f} \cdot c_{cyanate} = k \cdot c_{cyanate}$$

k_{OCNH} was calculated from the experimental value of k inserting the mean value of the hydrogen ion activity and the values 3.61 and $10^{-3.54}$ for $k_{OCNH\cdot H_3O^+}$ and K_{OCNH}, respectively.

The hydrogen ion activity was calculated from the expression $a_{H^+} = K_a/f \cdot c_{HA}/c_{A^-}$, where c_{HA} and c_{A^-} denote the mean value of the concentration of the weak acid and its corresponding base, respectively. K_a is the acidic dissociation constant.

The experiments which were carried out in solutions containing chloroacetic acid and sodium chloroacetate are listed in Table 8. It is seen (runs 15 and 16) that the velocity of the decomposition is practically independent of the total amount of chloroacetic acid if the solutions have the same pH-value, *i.e.* chloroacetic acid shows no appreciable catalytic effect on the decomposition.

It is furthermore observed from Table 8 that the percentages of cyanate and ammonia do not correspond, the sum being less than 100 although the deviations are rather limited. This is probably due to a polymerisation of cyanic acid, *cf.* that a more concentrated solution of sodium cyanate upon addition of acetic acid yields a precipitate of a polymer.

Since the sum of cyanate and ammonia was not constant the value of k could not be calculated from the unimolecular expression but was obtained from $\Delta c_{ammonia} / \Delta t = k \cdot \bar{c}_{cyanate}$, where $\Delta c_{ammonia}$ is the increase in the concentration of ammonia in the time interval Δt and $\bar{c}_{cyanate}$ is the mean value of the cyanate concentration in that interval. In Table 8 are listed the values of k calculated in this way. There is some decrease in the values of

Table 8. The decomposition of cyanate at pH = 2.3—3.0. c_{ion} = 0.2. 18°C.

Run	Initial solution		$c_{cyanate}$	Min.	% cyanate	% ammonia	k	k mean	pH initial	pH mean	k_{OCNH}
	c_{HA} [1]	c_{A^-} [2]									
17	0.15	0.02	0.02	2.0	87.4	14.5	0.077	0.067	2.17	2.25	0.0414
				4.0	75.3	23.4	0.055				
				6.0	65.0	33.6	0.073				
				15.0	35.0	61.7	0.062				
15	0.10	0.10	0.02	3.0	84.7	15.0	0.054	0.048	2.63	2.69	0.0484
				6.0	71.7	27.2	0.052				
				10.0	58.2	38.4	0.043				
				15.0	44.4	50.7	0.048				
				25.0	27.7	66.5	0.044				
16	0.06	0.06	0.02	3.0	85.4	15.5	0.056	0.046	2.62	2.70	0.0461
				6.0	73.0	25.5	0.042				
				10.0	60.4	36.7	0.042				
				15.0	47.4	48.6	0.044				
18	0.07	0.13	0.02	5.0	79.6	17.7	0.039	0.035	2.97	3.04	0.0461
				10.0	64.2	30.6	0.036				
				15.0	52.8	40.7	0.035				
				31.0	28.8	60.5	0.030				

[1]) HA ~ $CH_2ClCOOH$
[2]) A^- ~ CH_2ClCOO^-

k during a run but this is probably mainly due to the variation in the hydrogen ion activity.

Table 8 also lists the values of k_{OCNH} calculated from the mean values of k.

It should be noted that the velocity of reaction II in the experiments listed in Table 8 is 1.5 to 10 times greater than the velocity of reaction I.

In Table 9 are listed some quite analogous experiments carried out in solutions containing acetic acid and sodium acetate. Also in this case no appreciable catalytic effect of the buffer was observed (runs 19 and 20). The discrepancy between the percentage of cyanate and ammonia is a little more pronounced than in the experiments carried out at pH = 2.3—3.1. The values for k_{OCNH} listed in Table 9 were calculated in the same manner as for those listed in Table 8.

It should be noted that the velocity of reaction I in the experiments listed in Table 9 is less than 1 % of the velocity of reaction II.

Table 10 shows the experiments which were carried out at 18°C with solutions containing sodium cyanate and sodium bicarbonate saturated with carbon dioxide at a pressure of 1 atmosphere. If there was no catalytic effect of the buffer, the rate of the decomposition should be proportional to the hydrogen

Table 9. The decomposition of cyanate at pH = 4.1—4.8. c_{ion} = 0.2. 18°C.

Run	Initial solution			Min.	% cyanate	% ammonia	k	k mean	pH initial	pH mean	k_{OCNH}
	c_{HA} [1]	c_{A^-} [2]	$c_{cyanate}$								
26	0.15	0.05	0.02	10	90.2	6.7	0.0070	0.0062	4.12	4.18	0.0437
				20	83.2	12.2	0.0063				
				40	70.3	22.2	0.0065				
				60	60.8	28.7	0.0049				
19	0.10	0.10	0.02	20	92.2	6.7	0.0035	0.0026	4.57	4.67	0.0553
				40	85.3	11.6	0.0027				
				58	81.0	15.9	0.0029				
				99	70.6	23.6	0.0025				
				174	56.4	34.9	0.0024				
				297	41.6	46.8	0.0020				
				557	23.0	64.3	0.0021				
				4 132	0						
20	0.06	0.06	0.02	20	92.3	[3]			4.56	4.67	
				57	80.9						
				98	72.7						
				179	58.9						
22	0.07	0.13	0.02	30	92.7	5.3	0.0018	0.0014	4.83	4.89	0.0484
				60	87.1	9.7	0.0016				
				139	74.1	17.4	0.0012				
				242	62.5	26.1	0.0012				
				279	59.0	28.5	0.0011				

[1]) HA ~ CH_3COOH
[2]) A^- ~ CH_3COO^-
[3]) This run has not been analysed for ammonia.

ion activity, *i.e.* inverse proportional to the concentration of bicarbonate (the concentration of carbon dioxide is constant). The results in Table 10 show that the rate increases with increasing concentration of bicarbonate, *i.e.* bicarbonate acts catalytically on the decomposition of cyanate. The following rate expression is proposed:

$$dc_{cyanate}/dt = -(k' \cdot c_{HCO_3^-} \cdot c_{OCN^-} + k_{OCNH \cdot H_3O^+} \cdot c_{H^+} \cdot c_{OCNH} + k_{OCNH} \cdot c_{OCNH})$$

where k' is the velocity constant for the process catalyzed by bicarbonate.

Introducing $c_{OCNH} = 1/(1 + K_{OCNH}/a_{H^+} \cdot f) \cdot c_{cyanate} \sim a_{H^+} \cdot f/K_{OCNH} \cdot c_{cyanate}$ and neglecting the term $k_{OCNH \cdot H_3O^+} \cdot c_{H^+} \cdot c_{OCNH}$ which plays practically no part in this case, we get:

$$dc_{cyanate}/dt = -(k' \cdot c_{HCO_3^-} + k_{OCNH} \cdot a_{H^+} \cdot f/K_{OCNH}) \cdot c_{cyanate} = -k \cdot c_{cyanate}, \text{ or}$$

$$k \cdot K_{OCNH}/a_{H^+} \cdot f = (k' \cdot K_{OCNH}/a_{H^+} \cdot f) \cdot c_{HCO_3^-} + k_{OCNH} \cdot$$

Table 10. The decomposition of cyanate in carbon dioxide-bicarbonate buffer. pH = 6.5—6.9. c_{ion} = 0.2. 18°C.

Run	Initial solution				Min.	% cyanate	% ammonia	k	k mean	pH mean	$c_{HCO_3^-}$ mean
	pH	c_{CO_2}	$c_{HCO_3^-}$	$c_{cyanate}$							
42	6.38	0.04	0.06	0.02	1 648	86.7	14.0	0.000091	0.000093	6.47	0.075
					3 270	67.9	25.4	0.000091			
					7 232	45.6	44.4	0.000084			
					10 077	32.7	56.0	0.000104			
					12 836	24.3	63.5	0.000095			
40	6.60	0.04	0.10	0.02	1 386	84.7	12.2	0.000095	0.000100	6.66	0.115
					3 107	69.7	25.4	0.000100			
					4 620	58.8	35.8	0.000107			
					5 977	50.7	43.2	0.000099			
					8 454	37.1	54.7	0.000106			
					11 666	26.8	65.5	0.000095			
44	6.82	0.04	0.16	0.02	1 526	82.9	15.4	0.000110	0.000124	6.86	0.178
					2 989	65.7	28.1	0.000117			
					4 581	55.9	41.4	0.000138			
					6 900	40.7	55.2	0.000123			
					9 770	27.8	67.1	0.000117			
					12 657	19.0	76.4	0.000137			

If the quantity $k \cdot K_{OCNH}/a_{H^+} \cdot f$ is plotted against the quantity $(K_{OCNH}/a_{H^+} \cdot f) \cdot c_{HCO_3^-}$ using mean values for the hydrogen ion activity and the bicarbonate ion concentration a straight line can be drawn. The slope of this line gives k' = approx. 0.00060. The line intersects the ordinate axis at 0.062, *i.e.* the value of k_{OCNH} determined in this way is 0.062 which is in relatively good agreement with the value obtained in more acid solution.

It is seen from Table 10 (run 44) that the discrepancy between the percentages of cyanate and ammonia is not so pronounced as in the experiments at pH = 4.1—5.0. The values of k listed in Table 10 were calculated in the same manner as for those listed in Table 8.

The velocity constant, k_{OCNH}, for the reaction:

$$OCNH + H_2O \rightarrow NH_3 + CO_2$$

is 0.047 at 18°, which is the mean value for the determinations in this section.

THE DECOMPOSITION OF CYANATE IN STRONGLY BASIC MEDIUM

In Table 11 are listed the experiments which were carried out with solutions containing sodium cyanate and sodium hydroxide. Upon addition of sodium nitrate the initial ionic strength was adjusted to 0.2.

It is seen from Table 11 that the rate of the decomposition is independent of the hydroxyl ion concentration and identical with the rate of formation of ammonia.

Table 11. The decomposition of cyanate at pH = approx. 13. $c_{ion} = 0.2$.

Run	°C	Initial solution		Min.	% cyanate	% ammonia	k_{OCN^-}	k_{OCN^-} mean
		c_{NaOH}	$c_{cyanate}$					
49	94	0.18	0.018	66	89.0		0.00176	
				121	81.6		0.00169	
				212	70.4		0.00166	0.00171
				285	61.4		0.00171	
				420	48.2		0.00174	
				503	42.1		0.00172	
50	94	0.10	0.019	120	81.9		0.00166	
				301	60.2		0.00169	
				514	42.6		0.00166	0.00169
				617	34.5		0.00172	
				662	32.3		0.00171	
52	94	0.10	0.018	91		14.5	0.00172	
				242		34.4	0.00175	0.00170
				436		51.5	0.00166	
				571		61.8	0.00169	
54	82	0.10	0.020	277	85.3		0.000580	
				578	72.4		0.000562	
				1 346	45.9		0.000578	0.000571
				2 001	31.8		0.000573	
				2 773	20.8		0.000566	
53	70	0.10	0.019	531	91.4		0.000169	
				1 285	80.4		0.000170	
				2 049	71.6		0.000164	0.000170
				2 996	59.4		0.000174	
				4 247	47.8		0.000174	

Table 11 also lists the velocity constant, k_{OCN^-}, for the gross reaction:

$$OCN^- + 2H_2O \rightarrow NH_3 + HCO_3^- \quad \text{(III)}$$

calculated from the expression for an unimolecular reaction. The mean value of k_{OCN^-} is 0.00170 at 94°C, 0.000571 at 82°C and 0.000170 at 70°C.

The mean value of the energy of activation for the reaction is 23.9 kcal mole^{-1} calculated on the basis of the value of k_{OCN^-} at 94°C. The value determined by Lister [3] is 23.4 kcal mole^{-1}.

By extrapolation the value $10^{-6.48}$ for k_{OCN^-} is obtained at 18°C.

It should be added that the reactions I and II are too slow to take any appreciable part in the decomposition in strongly basic medium. On the other hand reaction III can be neglected in the more acid solutions investigated in the preceding sections.

The author wishes to express his sincere thanks to Professor Carl Faurholt, Head of the Department of Inorganic Chemistry, for valuable discussion and advice.

REFERENCES

1. Taufel, K., Wagner, C. and Dunwald, H. *Z. Electrochem.* **34** (1928) 115.
2. Masson, O. and Masson, I. *Z. physik. Chem.* **70** (1910) 290.
3. Lister, M. W. *Can. J. Chem.* **33** (1955) 426.
4. Amell, A. R. *J. Am. Chem. Soc.* **78** (1956) 6234.
5. Kemp, I. A. and Kohnstam, G. *J. Chem. Soc.* **1956** 900.
6. Wright, D. D. *J. Am. Chem. Soc.* **56** (1934) 314.
7. Noyes, A. A., Kato, Y. and Sosman, R. B. *Z. physik. Chem.* **73** (1910) 1.
8. Harned, H. S. and Davis, R. *J. Am. Chem. Soc.* **65** (1943) 2030.

Received June 21, 1958.

ACTA CHEMICA SCANDINAVICA 12 (1958) 1671—1674

Electron Diffraction Studies of 2,2′-Dithienyl Vapour

A. ALMENNINGEN, O. BASTIANSEN and P. SVENDSÅS

Universitetets Kjemiske Institutt, Blindern-Oslo, Norway;
Institutt for teoretisk kjemi, NTH, Trandheim, Norway

Electron diffraction studies based upon the sector method have been carried out on 2,2′-dithienyl. The obtained structure parameters of the thienyl ring are in good agreement with values obtained by micro-wave investigations for thiophene. The molecule as a whole does not seem to be planar. The angle of twist is found to be 34°.

In a series of earlier papers structure investigations have been carried out on molecules composed of ring systems linked together with single bonds [1-6]. As a member of this series of molecules 2,2′-dithienyl has been included, and an electron diffraction study based upon the sector method has been undertaken.

The sample used in the present investigation was prepared by Siv. Ing. Oddrun Holmboe at the Institute of Organic Chemistry at the Technical University of Norway. The electron diffraction diagrams were taken with the Oslo apparatus at a temperature of 130°C. The photometer curves were read off at an interval of 0.25 s units. Reproducible intensity data were obtained in the s interval ranging from 1.25 Å^{-1} to approximately 45 Å^{-1}. The photometer curves were subjected to the necessary corrections as for the photographic plates, sector corrections, *etc.*[7] To obtain intensity values suited for Fourier transformations the background due to atomic and incoherent scattering has to be subtracted. The theoretical background fitted the experimental intensity curve very well except for a small deviation in the s region beyond $s = 20$ Å^{-1}, where a minor correction had to be made. Difference curves between experimental intensity curves and the background were calculated and multiplied by an artificial damping factor $\exp(-ks^2)$. Radial distribution curves were calculated using k values of 0.0009 and 0.0036. A preliminary model from these curves was used for calculating a theoretical radial distribution curve and the corresponding intensity curve. Experiences thus obtained were used for further corrections of the background. A final intensity curve ready for Fourier transformation is given in Fig. 1. The curve has been multiplied by $\exp(-0.0036\, s^2)$. The upper curve of Fig. 2 is the corresponding Fourier transformation after the subtraction of the envelope [7]. This curve was well suited for the study of the interplanar twist in the molecule.

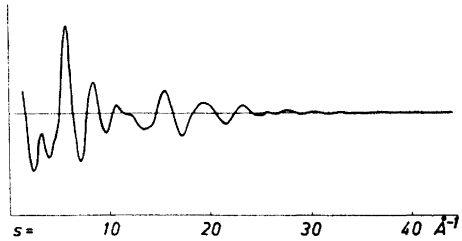

Fig. 1. Experimental intensity curve for Fourier transformation. (k = 0.0036).

A new model was obtained from this improved radial distribution curve. From the position of the peaks corresponding to the distances S—S and C_2—S_{10} (see Fig. 3) it could immediately be concluded that a planar model was improbable. An interplanar angle of approximately 30° had to be assumed.

The new model was used as the starting model for a least square procedure. The structure parameters, listed in the second column of Table 1, are the result of two successive approximations combined with further studies of the radial distribution curve. These values were obtained entirely from our experiment, and it is very satisfactory to compare them with those obtained by Bak *et al.* for thiophene by the micro-wave method [8]. For comparison Bak's two alternative sets of parameters are given in the third and fourth columns of Table 1. It should be pointed out that our values were calculated under the assumption of planar thienyl rings and mirror symmetry in the rings. We have also assumed that the bridge bond between the two rings is in the plane of each of them.

In order to obtain further improvements in the determination of the angle of twist, Bak's parameters for thiophene were used in the thienyl rings. If Bak's model I were used, it would be possible to determine the three additional parameters necessary for elucidating the structure of the 2,2′-dithienyl molecule, namely C_1—C_6, $\angle C_1$—C_6—S_{10}, and the angle of twist φ. The least square

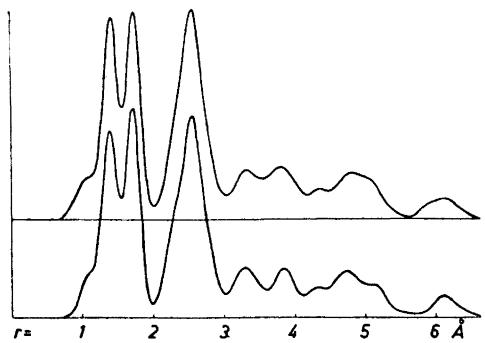

Fig. 2. Upper curve experimental and lower curve theoretical radial distribution curve. (k = 0.0036.)

Table 1. Structure parameters of 2.2'-dithienyl obtained from electron diffraction studies (present work) and structure parameters of thiophene obtained from micro-wave studies (Bak *et al.*[8]).

	E. D. data for 2.2'-dithienyl	M. W. data for thiophene (Bak *et al.*[8]) I	M. W. data for thiophene (Bak *et al.*[8]) II		
C_4-H_4 }	1.08 Å	1.085 Å	1.079 Å		
C_2-H_2 }		1.073 Å	1.079 Å		
C_1-S_5	1.717 Å	1.718 Å	1.723 Å		
C_1-C_2	1.357 Å	1.352 Å	1.360 Å		
C_2-C_3	1.433 Å	1.455 Å	1.430 Å		
$C_1-S_5-C_4$	92.02°	91.30°	91.67°		
C_1-C_6	1.480 Å			1.501 Å	1.476 Å
$C_1-C_6-S_{10}$	120.1°			119.4°	120.0°
	33.8°			34.2°	34.3°

procedure gave as a result for the three additional parameters the values listed in the fifth column of Table 1. In the sixth column the corresponding values obtained from Bak's model II are listed.

The obtained angle of twist of approximately 34° can no doubt be explained by steric difficulties. In the case of a planar molecule the distance between an S atom and the nearest H atom is approximately 2.92 Å. At an angle of 34° the distance increases to 3.09 Å which value should be compared with the van der Waals distance between sulphur and hydrogen of approximately 3.10 Å.

Unfortunately the angle of twist, φ, is not at all determined with an accuracy corresponding to the three values of Table 1. An error estimate based upon least square calculation will lead to a too optimistic result. A more realistic estimate of errors can be carried out by a discussion of the radial distribution curve, including the effects of anharmonic oscillation about the equilibrium angle. In spite of all the sources of error and the small effect upon the decisive distances for the φ determination at small φ values, we feel that the rigid planar model can be excluded. It seems, however, difficult to exclude a more or less free rotation through a certain angle interval. From steric considerations it seems for instance probable that the molecule has a practically free rotation from a φ value corresponding to a contact between H_2 and S_{10} (φ approximately 34°) up to a φ value corresponding to contact in a *cis* like molecule (φ approximately 85°). It is not unlikely that there exist two minima on the energy curve at approximately 34° and 85° with a flat maximum in between. As a matter of fact a better agreement between experimental and theoretical

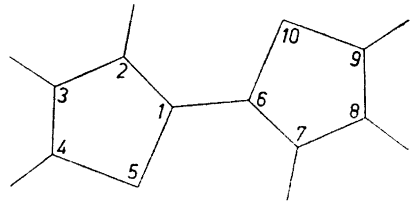

Fig. 3. Numbering of the atoms in the 2,2'-dithienyl molecule.

distribution curves can be obtained if the constancy of φ is abandoned. If, in addition to the molecules with a φ value equal to 34°, there are included a number of other molecules with φ values larger than this value, according to a certain distribution, a nearly complete correspondence can be obtained. Theoretically one might along this line obtain information about the molecular population at various φ values. This is, however, omitted in the present work, as such calculations do not seem to be justified by the present experimental material.

REFERENCES

1. Bastiansen, O. *Acta Chem. Scand.* **3** (1949) 408.
2. Bastiansen, O. *Acta Chem. Scand.* **4** (1950) 926.
3. Bastiansen, O. *Acta Chem. Scand.* **6** (1952) 205.
4. Bastiansen, O. and Smedvik, L. *Acta Chem. Scand.* **8** (1954) 1593.
5. Almenningen, A. and Bastiansen, O. *Kgl. Norske Videnskab. Selskabs Skrifter. In press.*
6. Almenningen, A., Bastiansen, O. and Skancke, P. *Acta Chem. Scand.* **12** (1958) 1215.
7. Almenningen, A. and Bastiansen, O. *Acta Chem. Scand.* **9** (1955) 815.
8. Bak, B., Christensen, C., Rastrup-Andersen, J. and Tannenbaum, E. *J. Chem. Phys.* **25** (1956) 892.

Received June 9, 1958.

ACTA CHEMICA SCANDINAVICA 12 (1958) 1675—1689

High Molecular Weight Enzyme Inhibitors

III. Polyestradiol Phosphate (P.E.P.), a Long-acting Estrogen

O. FERNÖ, H. FEX, B. HÖGBERG, T. LINDEROT, S. VEIGE

Research Department, AB Leo, Hälsingborg, Sweden, and

E. DICZFALUSY

Hormone Laboratory of the Department of Women's Diseases, Karolinska Sjukhuset, Stockholm, Sweden

The preparation and some of the chemical and pharmacological properties of polyestradiol phosphate, a long-acting water soluble estrogen are described. Data are presented indicating that polyestradiol phosphate is a powerful inhibitor of several enzymes, such as acid and alkaline phosphatases and hyaluronidase.

The preparation of a large number of polymeric phosphoric acid esters and amides of polyphenols, aromatic polyamines and aminophenols has been reported previously [1,2]. These compounds have been found to exert a strong inhibitory effect on certain enzymes, *e.g.* hyaluronidase and acid and alkaline phosphatases. The present investigation deals with the preparation of high molecular weight polyesters of estradiol-17β and phosphoric acid as well as with a study of some chemical and biological properties of these polymers.

PREPARATION AND CHEMICAL PROPERTIES OF P.E.P.

In the Experimental Part a typical experiment on the preparation of polyestradiol phosphate (P.E.P. Standard) is described. The phosporylation was carried out in dry pyridine with phosphoryl chloride (1.1 mole) as phosphorylating agent. This product showed a greatly prolonged duration of estrogenic action, when administered parenterally to spayed mice [15].

In the determination of the molecular weight of P.E.P. Standard (ultracentrifuge) a value of 26 000 was obtained (see Experimental Part) indicating that the molecule contains approximately 80 estradiol moieties. The viscomet-

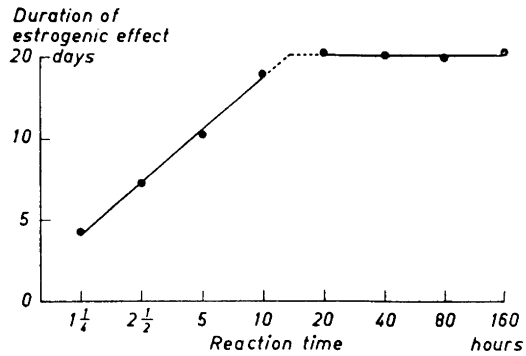

Fig. 1. Correlation between polymerisation time and duration of estrogenic effect of a single subcutaneous injection of 10 μg of polyestradiol phosphate (P.E.P.). Prolonged estrogenic effect was measured by the duration of cornified vaginal smears in spayed mice. The scales are logarithmic but are graduated in true units. Each point corresponds to 30 animals.

ric behavior of this substance is typical for linear polyelectrolytes [3]. The low value of intrinsic viscosity ($[\eta] = 0.04$) may be explained by the hydrophobic character of the estradiol moieties [4].

In order to follow the course of polymerisation, samples were withdrawn at different intervals and the products isolated. After dialysis the non-dialyzable material was investigated. From the data shown in Fig. 1, it appears

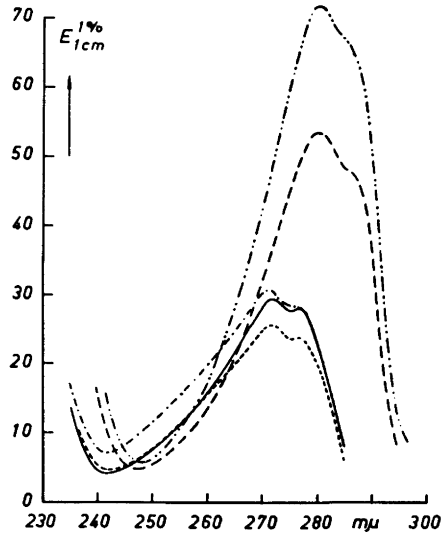

Fig. 2. Ultraviolet absorption spectra of estradiol (—..—..—), estradiol-17-phosphate (— — —), estradiol-3-phosphate (————), estradiol-3,17-diphosphate (. . . . .) and P.E.P. Standard (—.—.—) in 75 % aqueous ethanol.

Table 1. Influence of polymerisation time on the properties of polyestradiol phosphate (P.E.P.).

P.E.P. [a]	Reaction time, hours	% Non-dialyzable $P_{org.}$	% P[b]	% C[b]	% H[bc]	Molar P/Estradiol[d]	% Free hydroxyl groups[e]	λmax.[f] (mμ)
I	1 1/4	37[g]	8.2	—	—	—	26	279
II	2 1/2	42[g]	8.7	—	—	—	22	278
III	5	53[i]	8.8	61.3	7.30	1.00	12	278
III B[h]	5	44[i]	10.9	56.3	6.88	1.35	0	271
IV	10	66	9.3	—	—	—	9	272
V	20	81	9.4	60.4	7.05	1.08	4	272
VI	40	87	9.6	61.7	6.93	1.08	0	271
VII	80	88	9.6	—	—	—	0	271
VIII	160	90	9.5	60.1	6.98	1.10	0	271
P.E.P.-Standard	70	88—90	9.5	62.2	6.88	1.06	0	271

a) In these experiments the samples were hydrolyzed and worked up in the same way as P.E.P. Standard with the exception that the precipitation with HCl was made without ethanol.
b) Calculated on P.E.P., free from moisture, pyridine and chlorine.
c) % H somewhat higher than the value, which can be calculated (from % C, % free hydroxyl groups and % acid groups) possibly due to small amounts of firmly bound water.
d) Estradiol calculated from % C.
e) According to B. Baggett *et al.*[20] Calculated as % of 'estradiol oxygens'.
f) In 75 % ethanol. P.E.P. was dissolved in a small amount of 0.1 N NaOH, ethanol added, and then neutralized with 0.1 N HCl. Immediate reading.
g) Dialyzed in the presence of pyridine in order to avoid precipitation.
h) "Rephosphorylated" with excess $POCl_3$ in pyridine before hydrolysis and dialysis.
i) If % non-dialyzable is calculated on estradiol, the corresponding figures are, 54 % (III), and 52 % (III B).

that a reaction time of 20 h or more will yield polymers exhibiting maximal duration of estrogenic effect. Likewise it appears from Table 1 that after a reaction time of about 20 h the reaction is nearly complete. After this time practically no free hydroxyl groups could be demonstrated in the non-dialyzable material, while for instance after 75 min, 25 % of the hydroxyl groups originally present were free. In an attempt to assess the relative proportions between free 3-hydroxyl and free 17-hydroxyl groups in the polymer, the ultraviolet absorption spectra were studied.

The ultraviolet absorption spectra of estradiol, estradiol-3-phosphate, estradiol-17-phosphate, estradiol-3,17-diphosphate as well as that of the P.E.P. Standard are given in Fig. 2. When estradiol-3,17-diphosphate and estradiol-17-phosphate were mixed in such a proportion as to give the same percentage of free hydroxyl groups as found in the different polyestradiol phosphates (Table 1), practically identical ultraviolet absorption curves were obtained, indicating that the free hydroxyl groups are predominantly in the 3-position.

In order to investigate the stability of P.E.P., hydrolysis experiments were carried out in aqueous solution at 98° and at various pH values. The rate of hydrolysis was followed by determining the amount of inorganic phosphorus (P_o) liberated. The formation of P_o was most rapid at pH values between

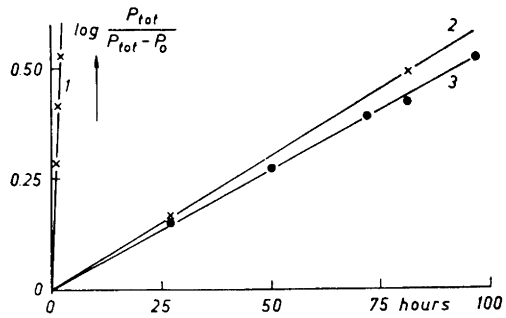

Fig. 3. Hydrolysis of estradiol phosphates in 0.1 M acetate buffer at pH 5.2 (98°). Rates of hydrolysis determined by analysis for liberated phosphoric acid (P_o). 1: Estradiol-3-phosphate ($k = 0.64$ h^{-1}). 2: Estradiol-17-phosphate ($k = 0.014$ h^{-1}). 3: P.E.P. Standard ($k = 0.013$ h^{-1}). As to P.E.P. Standard, 29 % of its phosphorus content is calculated as P_{tot}.

5 and 6; after 50 h 13.5 % of the phosphorus originally present was split off (Fig. 3). In 0.2 N sodium hydroxide solution the formation of P_o took place very slowly (< 1 % P_o, 81 h, 98°).

Furthermore it was found that following hydrolysis at different pH-values (98°, 81 h) the antihyaluronidase activity was practically unchanged within the investigated range (from pH 3.1 to 0.2 N sodium hydroxide solution). In another experiment, using the same conditions (pH 7.1), the duration of estrogenic effect was not changed significantly (potency: 88 % of that of P.E.P. Standard, with fiducial limits ($P = 0.05$) at 75 and 103 %). Under these conditions no free estradiol could be found, not even after a hydrolysis time of 270 h at pH 5.2.

We have also studied the rate of hydrolysis of the different monomeric estradiol phosphates (Fig. 3). In all cases the hydrolysis was found to follow a first order reaction. The period of half life (pH 5.2; 98°) for estradiol-3-phosphate was found to be 1.1 h and for estradiol-17-phosphate 50 h. In case of estradiol-3,17-diphosphate the experimental values were identical with those calculated from the 3- and 17-monophosphate values. The diphosphate is practically stable in 0.1 N sodium hydroxide solution (81 h, 98°) and similarly to the P.E.P. Standard, it has a maximal rate of hydrolysis between pH 5 and 6.

The fact that no free estradiol was found during the hydrolysis of P.E.P. seems to indicate that the liberated P_o is formed from endstanding, primary phosphoric acid esters only.

Even after a very long time (270 h, 98°, pH 5.2) only 28—30 % P_o was found. From Fig. 3 it is evident that the hydrolysis of P.E.P. follows the same course as that of estradiol-17-phosphate. It seems also that the percentage of primary 17-phosphate in P.E.P. lies between 25 and 28 and that the proportion of primary 3-phosphate is small.

From what is said above and from the fact that the free hydroxyl groups found at the beginning of the phosphorylation seem to be in the 3-position,

it seems likely that the first reaction step involves predominantly phosphorylation of the 17-hydroxyl groups yielding estradiol-17-dichlorophosphinate, and thus the polymerisation will take part mainly *via* the 3-hydroxyl groups. In order to confirm this assumption, a phosphorylation was carried out in the same way as described for the P.E.P. Standard, and the reaction mixture hydrolysed after 5 min. The pyridine was removed *in vacuo* (alkalization) and the resulting solution precipitated with hydrochloric acid without dialysis. Analysis of the precipitate and of the filtrate, respectively, showed that 84 % (0.84 mole) of the estradiol had reacted with 79 % (0.87 mole) of the phosphoryl chloride. In titration experiments only primary esters could be demonstrated. The rate of hydrolysis (pH 5.2; 98°) was the same as that of estradiol-17-phosphate. It seems thus very likely that the first step involves a phosphorylation of the 17-hydroxyl group.

Titration experiments with P.E.P. Standard (see Experimental Part) indicate the occurrence of 30 % monoester, 60 % diester and 10 % triester. This latter fact also points to a certain branching of the polymer. The value of 30 % monoester agrees well with that (28—30 %) found in the hydrolysis experiments.

EXPERIMENTAL

A. Preparation of estradiol phosphates

1. Preparation of polyestradiol phosphate. Estradiol-17β (27.2 g) was dissolved in dry pyridine (600 ml) in a flask fitted with a mechanical stirrer, a thermometer, a dropping funnel and a $CaCl_2$-tube. The flask was surrounded by an ice and salt mixture and when the temperature reached $-10°$ to $-12°$ a solution of phosphoryl chloride (10.1 ml) in dry pyridine (80 ml) was added in the course of 25 min. The temperature of the reaction mixture was then allowed to rise to room temperature. The stirring was stopped and the reaction mixture kept at room temperature for another 70 h. (After 30 to 50 h standing the solution may change into a jelly.) 250 g of crushed ice was then added with vigorous stirring and the mixture allowed to stand over night. 2 N NaOH (225 ml) was added and most of the pyridine evaporated *in vacuo*. The rest was made up to a volume of 2 000 ml by water and the pH adjusted to 7.0 to 7.5. The solution was dialyzed against dist. water (cellophane tube, several days). To the content of the tube containing 90 % of the phosphorus originally present, the same volume of ethanol was added and the solution poured with stirring into a mixture of 5 N HCl (200 ml) and ethanol (400 ml). The resulting white precipitate was then filtered and washed with 30 % aqueous ethanol and finally with water. Yield (after drying *in vacuo* over phosphorus pentoxide) about 30 g. Melting range 195—202°. A number of different batches, prepared according to the above mentioned procedure were mixed and the resulting mixture is referred to as P.E.P. Standard *.

Analysis: (P.E.P. Standard)

Moisture: (*in vacuo* 100°) 3.9 %.

Pyridine: (determined spectrophotometrically after alkalization and distillation) 0.3 %.

Chlorine: None.

Phosphorus: (calculated on dried and pyridine free sample) 9.5 %. $[[\alpha]_D = +40°$ ($c = 1$, in pyridine-water 1:1).]

* Samples of this have been distributed to different centra as a reference standard for the bioassay of long-acting estrogens. Such standards can be obtained on request from the Steroid Reference Collection, Postgraduate Medical School, London W 12, and from AB Leo, Hälsingborg, Sweden.

P.E.P. is very soluble in aqueous pyridine, soluble in aqueous alkali and very slightly soluble in ethanol, ethanol-water (1:1), water, dioxane, acetone and chloroform.

Molecular weight. This has been determined on the sodium salt of P.E.P. at pH 7.5 in 0.5 M NaCl solution. The sedimentation constant, determined in a Spinco ultracentrifuge model E with a synthetic boundary cell was found to have the same value at P.E.P. concentrations 1 and 0.5 %, $S_{20} = 2.16 \times 10^{-13}$ *.

The diffusion coefficient (moving boundary method using area and height of diffusion curves) was found to be $D_{20} = 5.8 \times 10^{-7}$ and the partial specific volume $V_{20} = 0.65$. The molecular weight was calculated to be about 26 000.

Viscosity measurements. These were made in an Ubbelohde viscometer at 25° ± 0.01°. The intrinsic viscosity $[\eta]$ has been determined in 0.25 M NaCl solution at pH 7.5. The value of $[\eta] = 0.04$ has been obtained by extrapolating η_{sp}/c to infinite dilution (c in g/100 ml).

Potentiometric titration. P.E.P. Standard was dissolved in an excess of 0.1 N NaOH in the presence of 0.1 M NaCl and titrated with 0.1 N HCl. Inflexion points were found at pH 9.4 and 5.5 respectively. The titrations show 0.90 strongly acid groups and a total number of 1.20 acid groups per phosphorus atom.

The different monomeric estradiol phosphates were dissolved in ethanol-water (1:1) and titrated with 0.02 N NaOH.

2. Preparation of estradiol-3-phosphate. Estradiol-17-acetate (1.5 g) was dissolved in dry pyridine and the solution was added drop by drop with shaking to a solution of phosphorus oxychloride (1.3 ml) in dry pyridine at −10°. After standing for one hour at this temperature the reaction mixture was hydrolyzed with crushed ice. Most of the pyridine was evaporated *in vacuo*. In order to hydrolyze the 17-acetate, 2 N NaOH (50 ml) was added. After standing for 1 h at room temperature the remaining pyridine was removed by shaking several times with ether and the solution poured with stirring into 5 N HCl (50 ml). The resulting precipitate was filtered, washed with 0.2 N HCl and finally with a small quantity of water. Yield after drying in vacuo: 1.6 g. M. p. 212–214°. Found: P 8.9; equiv. wt 177 (as a monobasic acid) and 174 (as a dibasic acid). Calc. for $C_{18}H_{25}O_5$ P: P 8.8; equiv. wt 176.]

3. Estradiol-17-phosphate was prepared in the same way as the 3-phosphate from estradiol-3-acetate (1.5 g). Yield 1.6 g. M. p. 181–183°. [Found: P 9.0; equiv. wt 174 (as a monobasic acid) and 170 (as a dibasic acid). Calc. for $C_{18}H_{25}O_5$ P: P 8.8; equiv. wt 176.]

4. Estradiol-3,17-diphosphate was prepared as above from estradiol (2.5 g) and phosphorus oxychloride (7.5 ml). After 1 h at −10° the mixture was maintained at room temperature for another 3 h. Yield 2.7 g. M. p. 179–181°. [Found: P 13.6; equiv. wt 118 (as a dibasic acid) and 115 (as a tetrabasic acid). Calc. for $C_{18}H_{26}O_8P_2$: P 14.3; equiv. wt 108.] Discrepancy probably due to firmly bound water.

B. Antienzymic properties

The enzymes studied were acid phosphatase, alkaline phosphatase and hyaluronidase.

1. *Acid phosphatase* **. Human seminal acid phosphatase was selected for the purposes of this study in view of its high enzymic activity.

Enzyme. A pool of human seminal fluid was used without purification. Semen was used in a dilution of 1:2 000.

Substrates. a. Phenyl phosphate and *b. p*-nitrophenyl phosphate were used.

Analytical methods. a. Phenol was estimated by Folin's reagent as described by Buch and Buch [5]. Inorganic phosphate was determined according to the method of Martin and Doty [6].

---

* These measurements have been carried out in the Carlsberg Laboratories, Copenhagen, by the courtesy of Professor K. Linderstrøm-Lang.

** The experiments with acid phosphatase using phenyl phosphate as substrate have been carried out in collaboration with Dr. C.-G. Beling. A detailed report of the kinetics and inhibition of this enzyme by different polymeric phosphates will be published elsewhere.

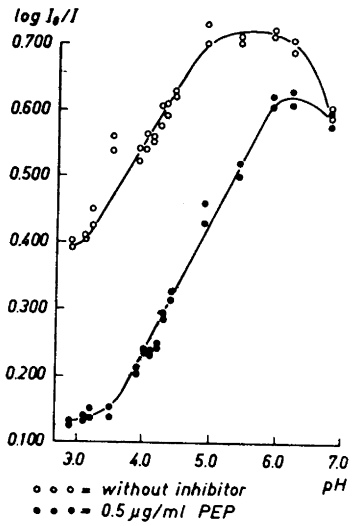

Fig. 4. Relationship between pH and inhibition of human seminal acid phosphatase by 0.5 µg/ml polyestradiol phosphate. 0.15 M acetate buffer, 37°, 8 min. incubation. Substrate: 2×10^{-3} M phenyl phosphate.

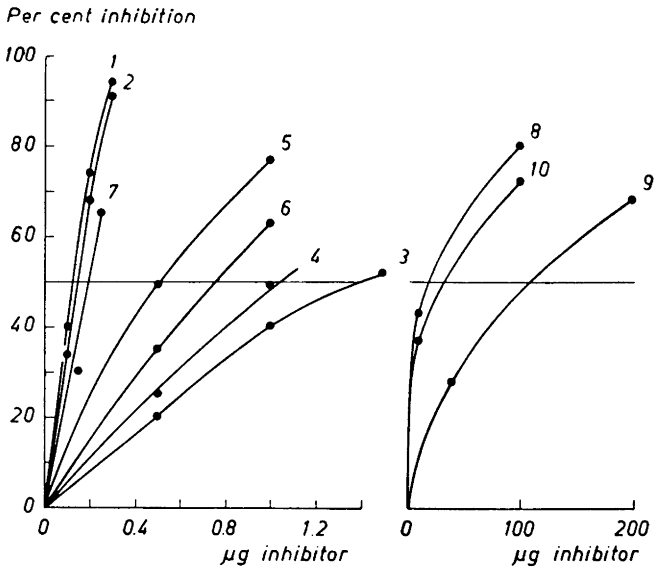

Fig. 5. Inhibition of seminal acid phosphatase by different batches of phosphorylated estradiol at pH 4.5 (acetate buffer). Substrate, *p*-nitrophenyl phosphate. Incubation time 30 min. at 37.5°. 1. P.E.P. Standard, 2. P.E.P. VI + P.E.P. VII (1:1), 3. P.E.P. I, 4. P.E.P. II, 5. P.E.P. III, 6. P.E.P. III B, 7. P.E.P. Standard after hydrolysis (81 h, pH 5.2, 98°), 8. Estradiol-3,17-diphosphate, 9. Estradiol-17-phosphate, 10. Estradiol-3-phosphate.

For further particulars consult Table 1.

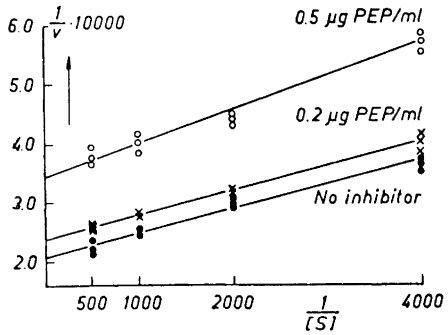

Fig. 6. Relation between acid phosphatase activity and substrate concentration in the presence and absence of polyestradiol phosphate. Activity is expressed as the reciprocal of the amount of phenol liberated in 8 min at 37°. 0.15 M acetate buffer. Substrate: phenyl phosphate, pH 4.5.

b. The method devised by Bessey, Lowry and Brock [7], for the determination of serum alkaline phosphatase was used. The *p*-nitrophenol was determined directly in a spectrophotometer (absorption maximum: 410 mμ).

Conditions of enzyme experiments. a. Enzyme activity was generally estimated within the pH range 3.0 to 6.8, using a 0.15 M acetate buffer, a substrate concentration of 2×10^{-3} M, and a short incubation time (generally 4 or 8 min at 37°).

b. Determinations were carried out at pH 4.5. Reaction volume 1.5 ml (0.5 ml 0.3 M acetate buffer, 0.5 ml 16 mM disodium *p*-nitrophenyl phosphate *, 0.1 ml enzyme). Incubation time 30 min at 37.5°.

Results. The inhibition of seminal acid phosphatase by P.E.P., is shown in Fig. 4. It appears from this figure that the inhibition is most marked on the acid side of the pH-optimum, and that no inhibition occurs at pH 6.8. The inhibition of acid phosphatase at pH 4.5, by different batches of P.E.P. as well as by estradiol-3-phosphate, estradiol-17-phosphate and estradiol-3,17-diphosphate is presented in Fig. 5. It appears from the data of Fig. 5 that estradiol monophosphates and also the diphosphate are much weaker inhibitors than the different P.E.P. preparations.

Reversibility. The enzyme inhibition by P.E.P. could be reversed by small amounts of basic proteins, *e. g.* protamine sulphate.

Type of inhibition. In order to study the type of inhibition, the concentrations of the substrate and inhibitor (P.E.P.) were varied at constant concentration of the enzyme. The typical Lineweaver plots obtained [8] are shown in Fig. 6. The data indicate that the inhibition is not substrate competitive. The same type of inhibition was obtained when *p*-nitrophenyl phosphate was used as a substrate.

2. *Alkaline phosphatase.* Alkaline phosphatase was measured by the method of Bessey, Lowry and Brock [7], using *p*-nitrophenyl phosphate as substrate.

Enzyme. The enzyme was the purified commercial product of Sigma Chemical Co. (St. Louis).

Reagents. 16 mM disodium *p*-nitrophenyl phosphate (Sigma Chemical Co.) in 0.001 N HCl. 0.1 M glycine buffer **. This was prepared from 7.50 g of glycine, 95 mg (0.001 M) of $MgCl_2$, about 80 ml of 1 N NaOH and water to 1 l. Buffered substrate: This consists of equal volumes of the two reagents.

Conditions of enzyme experiments. Determinations were mainly carried out at pH 9.3. The inhibition by the P.E.P. Standard was also investigated within the pH range 7.0—

* This is a 0.42 % solution of the Sigma 104 phosphatase substrate.

** Since it has been suggested that the use of glycine as buffer inhibits the enzyme activity [22], parallel experiments were run using glycine and 2-amino-2-methyl-1-propanol (1 M), respectively. Under our experimental conditions the use of these two buffers gave identical results.

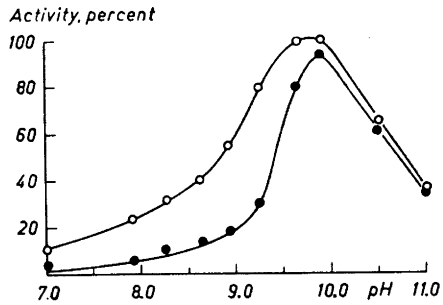

Fig. 7. Relationship between pH and inhibition of the enzymic hydrolysis of *p*-nitrophenyl phosphate by polyestradiol phosphate at 37.5°. 30 min incubation. Substrate concentration 3.3 × 10^{-4} M. Alkaline phosphatase concentration 13.3 μg per ml. O——O——O without inhibitor, ●——●——● 15 μg P.E.P. Standard per ml.

11.0. Reaction volume 1.5 ml (1 ml of the buffered substrate, 0.1 ml enzyme), incubation time 30 min at 37.5°. Enzyme concentration 13.3 μg per ml.

Results. From the relationship between pH and inhibition of the enzymic hydrolysis of *p*-nitrophenyl phosphate by P.E.P., it appears (Fig. 7), that inhibition occurs on the acid side of the pH-optimum only. A similar type of inhibition of alkaline phosphatase by estradiol-3,17-diphosphate, or by polyphloretin phosphate has been reported previously [1,9].

The inhibition of alkaline phosphatase at pH 9.3 by different batches of P.E.P. as well as by estradiol-3-phosphate, estradiol-17-phosphate and estradiol-3,17-diphosphate is presented in Fig. 8. A comparison of the data of Figs. 5 and 8 reveals that estradiol-3,17-diphosphate is a much stronger inhibitor of alkaline phosphatase than of acid phosphatase.

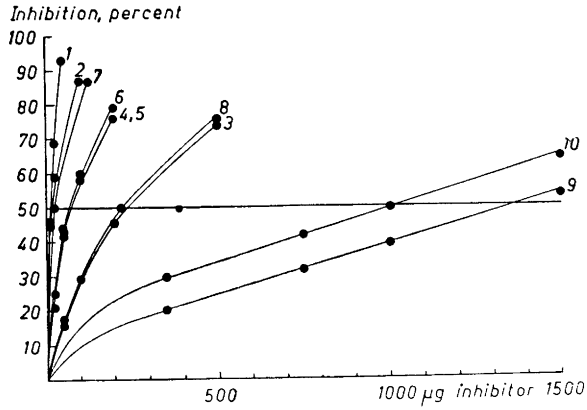

Fig. 8. Per cent inhibition of alkaline phosphatase by different batches of phosphorylated estradiol at pH 9.3. Enzyme concentration 13.3 μg per ml. Substrate, *p*-nitrophenyl phosphate. Glycine buffer with $MgCl_2$, pH 9.3. Incubation time 30 min at 37.5°. 1. P.E.P. Standard. 2. P.E.P. VI + P.E.P. VII (1:1). 3. P.E.P. I. 4. P.E.P. II. 5. P.E.P. III. 6. P.E.P. III B. 7. P.E.P. Standard after hydrolysis. 8. Estradiol-3,17-disphosphate. 9. Estradiol-17-phosphate. 10. Estradiol-3-phosphate.

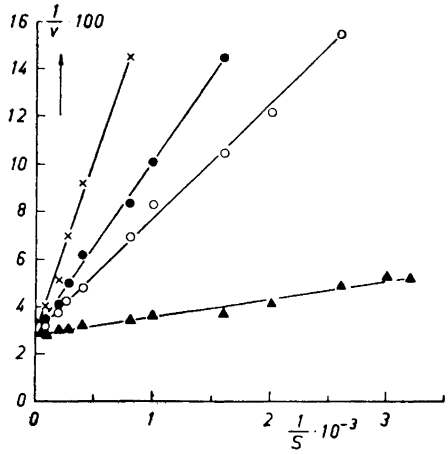

Fig. 9. A double reciprocal plot of the effect of polyestradiol phosphate (P.E.P. Standard) upon the velocity of alkaline phosphatase action at various substrate concentrations. The effect of 3.3 μg (○), 6.6 μg (●), and 10 μg of Polyestradiol phosphate [P.E.P. Standard] (×) upon the action of 13.3 μg alkaline phosphatase at pH 9.3 and 37.5° for 30 min. in the presence of various amounts of *p*-nitrophenyl phosphate. Filled triangles (▲) indicate enzyme activity in the absence of inhibitor.

Reversibility. Similarly to the case of acid phosphatase, the inhibition of alkaline phosphatase could also completely be reversed by basic proteins.

Type of inhibition. 3.3, 6.6 and 10 μg of P.E.P. Standard were added to solutions containing 13.3 μg of enzyme, and 0.27—27 μ moles/ml of *p*-nitrophenyl phosphate. A double reciprocal plot of velocity *versus* substrate concentration is shown in Fig. 9. It appears from the figure that the inhibition is of a competitive nature.

These findings are different from previous observations on polyphloretin phosphate [1], which study, however, was carried out at a lower pH (7.5). Experiments were therefore

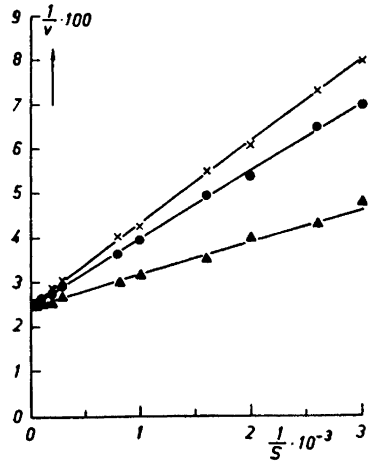

Fig. 10. A double reciprocal plot of the effect of polyphloretin phosphate (P.P.P). upon the velocity of alkaline phosphatase action at various substrate concentrations. The effect of 3.3 μg (●), and 16.7 μg (×) of P.P.P. upon the action of 13.3 μg alkaline phosphatase at pH 9.3 and 37.5° for 30 min. in the presence of various amounts of *p*-nitrophenyl phosphate. Filled triangles (▲) indicate enzyme activity in the absence of inhibitor.

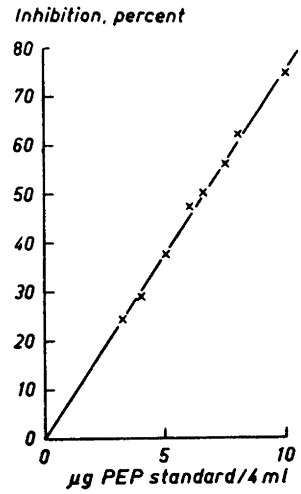

Fig. 11. Inhibition of hyaluronidase by polyestradiol phosphate (P.E.P. Standard). The effect of various amounts of inhibitor upon the action of 5 I.U. hyaluronidase per 4 ml at pH 7.0 and 37.5°.

carried out with polyphloretin phosphate at pH 9.3 and with *p*-nitrophenyl phosphate as substrate. It appears (Fig. 10) that the inhibition under these conditions is substrate-competitive. Further data on this problem will be reported in a forthcoming publication, dealing with polystilboestrol phosphate.

3. *Hyaluronidase.*

Bovine testicular hyaluronidase. The highly purified enzyme was prepared from bull testes according to Högberg [10] and assayed 90 000 I.U./mg nitrogen. Before use the enzyme was dissolved in water and the solution was stabilized with 2 µg methylgelatine (Leo) per I.U. of enzyme. 5 I.U. enzyme was used for the test.

Hyaluronic acid. The substrate, hyaluronic acid, was prepared from human umbilical cords and contained 3.39 % N, 10.3 % acetyl, 42.9 % glucosamine and 46.0 % glucuronic acid. Mc Ilvaine citrate-phosphate buffer, pH 7.0, containing sodium chloride was used

Table 2. The effect of polymerisation time upon the inhibition of phosphatases and of hyaluronidase by different batches of phosphorylated estradiol.

Inhibitor	No. in Figs. 5 and 8	Rel. amount of inhibitor necessary for 50 % inhibition		
		Hyaluronidase	Alkaline phosphatase	Acid phosphatase
P.E.P. Standard	1	1.0	1.0	1.0
P.E.P. Standard *	7	1.0	1.7	1.5
P.E.P. I	3	12	15.5	10.8
P.E.P. II	4	5.0	4.8	8.1
P.E.P. III	5	3.1	4.4	3.8
P.E.P. III B	6	4.0	4.3	5.8
P.E.P. VI+VII (1:1)	2	1.0	1.0	1.2
Estradiol-3,17-diphosphate	8	225	14.5	154
Estradiol-17-phosphate	9	225	90	810
Estradiol-3-phosphate	10	225	67	270

* P.E.P. Standard after hydrolysis (81 h, pH 5.2, 98°).

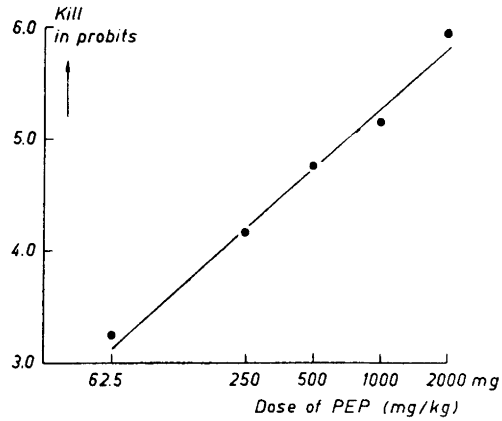

Fig. 12. Relationship between log dose of polyestradiol phosphate and kill (in probits) in a 60-days chronic toxicity test. Each point represents 25 adult male mice.

to dissolve hyaluronic acid (Na_2HPO_4 2 H_2O 16.1 g; citric acid. 2.02 g; NaCl 3.05 g; water to 1 000 ml). The concentration of the substrate was chosen to give a relative viscosity of 4.

Inhibitors. The inhibitors studied were shaken with the buffer and then diluted with buffer to a concentration of 0.1 mg per ml.

Conditions of enzyme experiments. The determination of the antihyaluronidase activity was carried out exactly according to the scheme described previously [1].

Results. Fig. 11 illustrates the inhibition of hyaluronidase at different concentrations of P.E.P. Standard. The influence of polymerisation time on the inhibitory activity of phosphorylated estradiol is demonstrated in Table 2. The inhibition is increased by increased polymerisation time, indicating that the inhibition is depending on the molecular size. An increase in the number of acidic groups (rephosphorylation) or a decrease (hydrolysis) does not change the magnitude of the inhibition (Table 2).

C. Pharmacological properties

Toxicity. The acute toxicity of P.E.P. was estimated in adult male mice. 48 h following a single intravenous injection the L.D.50 was found to be 240 mg/kg, with 95% fiducial limits of error at 212 and 272 mg/kg. It is realized, that in the absence of a toxicity reference standard the calculation of fiducial limits has a rather limited significance.

Chronic toxicity was estimated as follows: groups of 25 adult male mice were injected subcutaneously with P.E.P. in water on every 10th day. On the 60th day of experiment the number of survivors in each group was recorded. No correction has been made for spontaneous mortality. The correlation between the logarithm of dose and mortality in probits [21] is shown in Fig. 12. It appears from the data that under these conditions the L.D.50 is 700 mg/kg. Confidence limits (P = 0.95) were calculated as 350 and 1 400 mg/kg.

Biological activity. The duration of action of P.E.P. depends on the polymerisation time, as demonstrated in Fig. 1. From these data it appears that a polymerisation time less than 20 h will yield P.E.P. preparations with a relatively poor duration of action.

When different preparations of P.E.P. were administered to spayed mice it was found that the logarithm of dose was linearly related to the logarithm of duration of estrogenic action (in days) [11]. On basis of this observation a method of bioassay of long-acting estrogens was worked out [12]. When a mixture of P.E.P. preparations VI and VII (Table 1) was assayed by this method against the P.E.P. Standard, a relative potency of

103 % was obtained (fiducial limits of error: 91 and 117 %, respectively). The index of precision (estimated as Gaddum's λ-criterion [13]) was 0.09, indicating a very satisfactory precision.

It also appears from the data of Table 1 that following "rephosphorylation" with excess $POCl_3$ in pyridine before hydrolysis and dialysis, a P.E.P. preparation (III. B) could be obtained, in which no 'free' hydroxyl groups, but a great number of primary phosphate groups were present. Polymerisation time was only 5 h, which — according to the data of Fig. 1 — is too short for obtaining preparations with an optimal duration of action. When this "rephosphorylated" preparation was bioassayed against the P.E.P. standard, its potency was only 34 % of that of the Standard. This estimate of potency agrees very closely with that (30 %) of another preparation obtained following the same reaction time without "rephosphorylation" (prep. III). It is concluded therefore that the duration of estrogenic effect of P.E.P. does not depend on the relative proportion of acid groups present, but rather on the degree of polymerisation. It is also of interest, that when tested at the dose levels of 7 and 14 μg, respectively, estradiol-3,17-diphosphate did not show any prolonged estrogenic activity. In the same experiment the P.E.P. Standard exhibited a mean duration of 17.9 days (7 μg) and 24.6 days (14 μg), respectively. Finally, when as much as 100 μg of P.E.P. Standard were administered orally to each of 15 spayed mice, in all but one of the animals only negative smears could be obtained, indicating that P.E.P. is inactive when given orally.

DISCUSSION

Assuming that in the P.E.P. molecule the estradiol moieties are linked together by -OPO-bridges and that no free estradiol hydroxyl groups are present, the maximum phosphorus content and some other data can be calculated. The highest possible value of the phosphorus content of a polyestradiol phosphate molecule is dependent on the number of estradiol moieties only and not on possible branchings (one phosphorus being attached to three estradiol moieties). Thus, if the number of estradiol moieties (R) is n, it follows from the formula

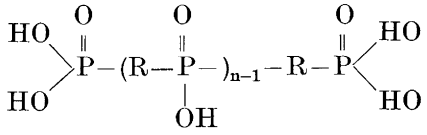

that the phosphorus content (per cent) of this molecule is

$$100 \cdot \frac{31\ (n+1)}{334\,n+98} = 9.28 \cdot \frac{n+1}{n+0.29}$$

that the corresponding estradiol (HRH) content is $81.4 \cdot \frac{n}{n+0.29}$

and that the number of acid groups per phosphorus $= \frac{n+3}{n+1}$.

If the molecular weight of P.E.P. Standard is accepted to be 26 000, the n value will be about 80. In the formula above the theoretical percentage of phosphorus will be 9.36 and that of estradiol 81.1. The number of acid groups per phosphorus can be calculated as 1.03. P.E.P. Standard contains 9.5 % phosphorus, 78.2 % estradiol and 1.2 acid groups per phosphorus.

The small discrepancy in the phosphorus and estradiol values may be due to a relatively small proportion of pyrophosphate linkages (formed from small amounts of water in the reaction mixture). The high ratio acid groups to phosphorus, however, seems to speak in favour of a lower molecular weight, as does the low percentage of tertiary phosphate, which does not agree with the amount of primary phosphoric acid esters found. Assuming the molecular weight to lie between 3 000 and 5 000, the high ratio of acid groups to phosphorus as well as the low percentage of tertiary phosphate are easily explained, and if so the ultracentrifuge values may be due to a strong association.

The enzyme experiments reported in this paper indicate that P.E.P. — like most compounds in these series of polymeric phosphates — is a powerful inhibitor of several enzymes.

The results recorded in Tables 1 and 2 seem to indicate that an increase or a decrease in the number of acidic groups present in the inhibitor does not markedly influence the inhibitory effect. From the results obtained with products of different polymerisation time as well as with the monomeric esters, it appears that the degree of condensation is of greater importance.

Interesting is the relatively strong inhibitory effect of estradiol-3, 17-diphosphate upon alkaline phosphatase, as compared to the weak effect of this compound on the other enzymes studied. These findings are in agreement with the results reported previously [9], and indicate that alkaline phosphatases are inhibited by estradiol-3,17-diphosphate. Thus the previous suspicion [15] that the inhibition of kidney alkaline phosphatase by estradiol-3,17-disphosphate might have been due in part to a contamination of this compound by polymeric estradiol phosphates is not supported by the present data.

P.E.P. as well as polyphloretin phosphate have also been found [14] to exert a strong inhibitory effect on the disruption of mast cells produced by compound 48/80 or phospholipase A.

As far as its biological action is concerned, polyestradiol phosphate is a long-acting estrogen when administered parenterally to spayed mice [15], or to human beings [16, 17]. Since P.E.P. is rather resistant to acid or alkaline hydrolysis, as well as to the effect of different phosphatases, it would seem justifiable to assume, that its prolonged duration of action depends on a slow liberation of estradiol in the organism. In fact, experiments, in which P.E.P. labelled with radioactive phosphorus was administered to spayed mice [11] indicate that a definite relationship exists between circulating blood levels and log dose of P.E.P. administered, as well as between the duration of estrous smears and log dose of P.E.P. These correlations suggest that the circulating amount of P.E.P. may be instrumental in maintaining a prolonged estrogenic activity through its slow degradation into estradiol. Furthermore, evidence is also on record indicating that in the human organism substantial amounts of estradiol are liberated from the administered P.E.P. molecule and that this estradiol is metabolized and excreted in the same way as the body's own estrogen. Following the administration of P.E.P. to surgically castrated women, estrone, estradiol-17β and estriol were isolated and identified in their urine [16].

Finally, it is also of interest to note that P.E.P. has found an application in the treatment of prostatic carcinoma [18,19].

REFERENCES

1. Diczfalusy, E., Fernö, O., Fex, H., Högberg, B., Linderot, T. and Rosenberg, T. *Acta Chem. Scand.* **7** (1953) 913.
2. Fernö, O., Fex, H., Högberg, B., Linderot, T. and Rosenberg, T. *Acta Chem. Scand.* **7** (1953) 921.
3. Strauss, U. and Fouss, R. *Die Physik der Hochpolymeren* vol. II, p. 695 (Edited by Stuart) Berlin Springer 1953.
4. Ferry, J., Vdy, D., Feng Chi Wu, Heckler, G. and Fordyce, D. *J. Colloid Sci.* **6** (1951) 429.
5. Buch, I. and Buch, H. *Acta Med. Scand.* **101** (1939) 211.
6. Martin, J. B. and Doty, D. M. *Anal. Chem.* **21** (1949) 965.
7. Bessey, O. A., Lowry, O. H. and Brock, M. J. *Biol. Chem.* **164** (1946) 321.
8. Lineweaver, H. and Burk, D. *J. Am. Chem. Soc.* **56** (1934) 658.
9. Aldman, B., Diczfalusy, E., Högberg, B. and Rosenberg, T. *Biochem. J.* **49** (1951) 218.
10. Högberg, B. *Acta Chem. Scand.* **8** (1954) 1098.
11. Diczfalusy, E., Borell, U., Magnusson, A.-M. and Westman, A. *Acta Endocrinol. Suppl.* **24** (1956) 1.
12. Diczfalusy, E., Magnusson, A.-M., Nilsson, L. and Westman, A. *Endocrinology* **60** (1957) 581.
13. Gaddum, J. H. *Spec. Rep. Ser. med. Res. Council* London **1933** No. 183.
14. Högberg, B. and Uvnäs, B. *Acta Physiol. Scand.* **41** (1957) 345.
15. Diczfalusy, E. *Endocrinology* **54** (1954) 471.
16. Diczfalusy, E. and Westman, A. *Acta Endocrinol.* **21** (1956) 321.
17. Tillinger, K.-G. and Westman, A. *Acta Endocrinol.* **25** (1957) 113.
18. Goodhope, C. D. *J. Urol.* **77** (1957) 312.
19. Jönsson, G., Röhl, L. and Wiegner, K. *Acta Chir. Scand.* **113** (1957) 68.
20. Baggett, B., Engel, L. and Fielding, L. *J. Biol. Chem.* **213** (1955) 87.
21. Finney, D. J. *Probit Analysis: A statistical treatment of the sigmoid response curve,* Cambridge University Press, London 1952.
22. Lowry, H., Roberts, N. R., Wu, M.-L., Hixon, W. S. and Crawford, E. J. *J. Biol. Chem.* **207** (1954) 19.

Received March 13, 1958.

ACTA CHEMICA SCANDINAVICA 12 (1958) 1690—1700

Short Communications

On the Biological Methylation of Histamine

KERSTIN M. LINDAHL

Institute of Zoophysiology, University of Uppsala, Sweden

For some time histamine has been known to be methylated and oxidatively deaminated prior to excretion [1]. Recently the postulated intermediary metabolite 1-methyl-4-(β-aminoethyl) imidazole, hereafter referred to as methylhistamine, has been shown to appear in the urine following administration of an amine oxidase inhibitor [2].

In vitro experiments have also demonstrated that the methylation process precedes the deamination [3,4] and may be separated from the following reaction steps [5].

In the above mentioned *in vitro* experiments methionine was added to the enzyme extracts on the assumption that the methyl group is derived from methionine as in many other biological transmethylations. The experiments reported in this communication were undertaken in order to test this hypothesis.

A mouse liver extract, described previously [5] in which methylation of histamine takes place but not deamination, was incubated from 1 to 24 h with nonisotopic histamine and methionine containing radiocarbon in the methyl group. The extract was dialysed prior to use.

Samples were withdrawn at the beginning and the end of the incubation, and analyzed for radioactive methylhistamine according to the isotope dilution method developed by Schayer and co-workers (for a description see Lindell and Schayer [6]).

The method briefly consists of the following steps: carrier methylhistamine * is added to the sample, extracted with chloroform after protein precipitation, and the picrate is recrystallized from water-ethanol using alternately different charcoal adsorbents until constant radioactivity is attained.

The zero-time samples were entirely inactive after two crystallizations, whereas the incubated ones retained a constant activity from the 2nd through the 4th crystallization.

* Methylhistamine was obtained from Dr. R. W. Schayer, Merck Institute for Therapeutic Research, which is hereby gratefully acknowledged.

Table 1.

	15.5 μg ^{14}C histamine, 1.48 mC/mM; 100 μg nonisotopic methionine	100 μg ^{14}C methionine 2.49 mC/mM; 15.5 μg nonisotopic histamine
^{14}C methylhistamine after 2 h incubation, cpm[1]	2 376	1 122
^{14}C histamine at zerotime, cpm	5 816	—
^{14}C histamine after 2h incubation, cpm	3 464	—

[1] The samples were counted in a windowless flow counter, Tracerlab, SC-16, which was made available through the courtesy of Prof. A. Tiselius, Institute of Biochemistry, Uppsala.

In the same manner simultaneous incubates containing only enzyme extract and ^{14}C methionine were assayed for methylhistamine. Now the carrier contained no radioactivity after only two crystallizations. It was thus concluded that carrier methylhistamine can, by repeated crystallization of the dipicrate, be completely freed from contamination by ^{14}C methionine and its possible metabolites.

The destruction of histamine and the formation of methylhistamine was followed by simultaneous incubation of the crude enzyme extract with radiocarbon histamine labelled in the imidazole nucleus. At the end of the incubation remaining histamine and methylhistamine were assayed by isotope dilution technique. It has been shown that by repeated crystallization of the dipicrate carrier amounts of methylhistamine can be freed from contamination by ^{14}C histamine or its metabolic products. By conversion of carrier histamine to its pipsyl derivative the contaminating methylhistamine can be removed [7]. Therefore constant activity of the samples during three successive crystallizations was considered as a sufficient criterion of the purity.

The essential figures from an experiment are given in Table 1. It has been concluded from these results that the methyl group of methylhistamine can be transferred from methionine. Whether methionine is the immediate precursor of the methyl group or an intermediate step is involved cannot be concluded from this type of experiment.

1. Schayer, R. W. *Brit. J. Pharmacol.* **11** (1956) 472.
2. Rothschild, Z. and Schayer, R. W. *Federation Proc.* **17** (1958) 300.
3. Kobayashi, Y. and Schayer, R. W. *Arch. Biochem. Biophys.* **63** (1956) 480.
4. Lindahl, K. M. *Acta Physiol. Scand.* **43** (1958) 254.
5. Lindahl, K. M. *Arkiv Kemi* **13** (1958) 149.
6. Lindell, S.-E. and Schayer, R. W. *Brit. J. Pharmacol.* **13** (1958) 44.
7. Schayer, R. W., Cooper, J. A. D., Smiley, R. L. and Davis, K. J. *J. Appl. Physiol.* **9** (1956) 481.

Received September 18, 1958.

Phosphorus-32 Pentasulfide: Preparation by Isotopic Exchange and Conversion to Thiophosphoryl-32 Chloride and Phosphorus-32 Trichloride

JOHN E. CASIDA*

Department of Entomology, University of Wisconsin, Madison 6, Wisconsin, USA

Certain triesters of phosphoric and thiophosphoric acids are important as pesticides and potential chemical warfare agents. Adequate studies on the metabolism and mode of action of these organophosphorus compounds require their synthesis from high specific activity radiolabeled inorganic intermediates such as phosphorus pentasulfide (P_2S_5), thiophosphoryl chloride ($PSCl_3$), phosphorus trichloride (PCl_3), and phosphoryl chloride ($POCl_3$).

$^{32}POCl_3$ can be readily prepared in high specific activity from the reaction of $H_3{}^{32}PO_4$ with phosphorus pentachloride (PCl_5)[1]. Neutron irradiation is commonly employed to label certain of the other inorganic phosphorus intermediates [2-5]. This method is often inconvenient and the specific activity of the organophosphorus compounds prepared from these irradiated intermediates is usually not greater than 5 mC/g. $^{32}PSCl_3$ can also be prepared from $H_3{}^{32}PO_4$ *via* $^{32}POCl_3$ and $^{32}PCl_3$[6,7] or by an inefficient isotope exchange reaction [8].

Various procedures were tried to achieve isotope exchange between $H_3{}^{32}PO_4$ or $Na_2H{}^{32}PO_4$ and red phosphorus, $PSCl_3$ or P_2S_5. The products from each attempt were reacted with ethanol [9] or converted to other known organic derivatives [4] and then separated by paper and ion-exchange chromatography [10] to determine the degree of exchange. After correction for the radioactivity remaining on the glassware, the

* Current address: Institute of Organic Chemistry and Biochemistry, University of Stockholm, Stockholm, Sweden.

In the same manner simultaneous incubates containing only enzyme extract and ^{14}C methionine were assayed for methylhistamine. Now the carrier contained no radioactivity after only two crystallizations. It was thus concluded that carrier methylhistamine can, by repeated crystallization of the dipicrate, be completely freed from contamination by ^{14}C methionine and its possible metabolites.

The destruction of histamine and the formation of methylhistamine was followed by simultaneous incubation of the crude enzyme extract with radiocarbon histamine labelled in the imidazole nucleus. At the end of the incubation remaining histamine and methylhistamine were assayed by isotope dilution technique. It has been shown that by repeated crystallization of the dipicrate carrier amounts of methylhistamine can be freed from contamination by ^{14}C histamine or its metabolic products. By conversion of carrier histamine to its pipsyl derivative the contaminating methylhistamine can be removed [7]. Therefore constant activity of the samples during three successive crystallizations was considered as a sufficient criterion of the purity.

The essential figures from an experiment are given in Table 1. It has been concluded from these results that the methyl group of methylhistamine can be transferred from methionine. Whether methionine is the immediate precursor of the methyl group or an intermediate step is involved cannot be concluded from this type of experiment.

1. Schayer, R. W. *Brit. J. Pharmacol.* **11** (1956) 472.
2. Rothschild, Z. and Schayer, R. W. *Federation Proc.* **17** (1958) 300.
3. Kobayashi, Y. and Schayer, R. W. *Arch. Biochem. Biophys.* **63** (1956) 480.
4. Lindahl, K. M. *Acta Physiol. Scand.* **43** (1958) 254.
5. Lindahl, K. M. *Arkiv Kemi* **13** (1958) 149.
6. Lindell, S.-E. and Schayer, R. W. *Brit. J. Pharmacol.* **13** (1958) 44.
7. Schayer, R. W., Cooper, J. A. D., Smiley, R. L. and Davis, K. J. *J. Appl. Physiol.* **9** (1956) 481.

Received September 18, 1958.

Phosphorus-32 Pentasulfide: Preparation by Isotopic Exchange and Conversion to Thiophosphoryl-32 Chloride and Phosphorus-32 Trichloride

JOHN E. CASIDA*

Department of Entomology, University of Wisconsin, Madison 6, Wisconsin, USA

Certain triesters of phosphoric and thiophosphoric acids are important as pesticides and potential chemical warfare agents. Adequate studies on the metabolism and mode of action of these organophosphorus compounds require their synthesis from high specific activity radiolabeled inorganic intermediates such as phosphorus pentasulfide (P_2S_5), thiophosphoryl chloride ($PSCl_3$), phosphorus trichloride (PCl_3), and phosphoryl chloride ($POCl_3$).

$^{32}POCl_3$ can be readily prepared in high specific activity from the reaction of $H_3{}^{32}PO_4$ with phosphorus pentachloride (PCl_5)[1]. Neutron irradiation is commonly employed to label certain of the other inorganic phosphorus intermediates [2-5]. This method is often inconvenient and the specific activity of the organophosphorus compounds prepared from these irradiated intermediates is usually not greater than 5 mC/g. $^{32}PSCl_3$ can also be prepared from $H_3{}^{32}PO_4$ *via* $^{32}POCl_3$ and $^{32}PCl_3$[6,7] or by an inefficient isotope exchange reaction [8].

Various procedures were tried to achieve isotope exchange between $H_3{}^{32}PO_4$ or $Na_2H{}^{32}PO_4$ and red phosphorus, $PSCl_3$ or P_2S_5. The products from each attempt were reacted with ethanol [9] or converted to other known organic derivatives [4] and then separated by paper and ion-exchange chromatography [10] to determine the degree of exchange. After correction for the radioactivity remaining on the glassware, the

* Current address: Institute of Organic Chemistry and Biochemistry, University of Stockholm, Stockholm, Sweden.

only significant exchange occurred with the sulfur-containing compounds. The percentage exchange was low with $PSCl_3$ but almost complete with P_2S_5.

For preparation of $^{32}P_2S_5$, carrier-free $H_3{}^{32}PO_4$ or $Na_2H{}^{32}PO_4$ was evaporated in a reaction flask. The acid was preferable when the residue after evaporation was high and the salt when the residue was no more than a few milligrams. Red phosphorus and sulfur were then added in a 2 to 5 molar ratio with a combined weight of 0.20 to 2.0 g. While gassing the flask with dry carbon dioxide, the mixture was heated in one spot with a weak flame to initiate the vigorous reaction [11] that liquified the mixture and formed P_2S_5. When the mixture was then boiled for 10 min the exchange reaction was over 98 % complete. Similar exchange (95—98 %) resulted by slowly melting P_2S_5 in a reaction flask and then boiling for 10 min while gassing with carbon dioxide, and by heating the P_2S_5 for 2 h at 300—500°C in sealed ampules. The specific activity of the $^{32}P_2S_5$ thusly formed remained constant through repeated recrystallizations from carbon disulfide. When this $H_3{}^{32}PO_4$—P_2S_5 exchange reaction was run in the presence of varying amounts of non-labeled H_3PO_4, the percentage of the radioactivity recovered as $H_3{}^{32}PO_4$ closely approximated the percentage of the total phosphorus in the reaction mixture contributed by the H_3PO_4.

$^{32}PSCl_3$ was prepared in 73 % yield from $^{32}P_2S_5$ by reaction with 3 molar equivalents of PCl_5 [12,13] in the presence of anhydrous aluminium chloride comparable to 1.5 times the weight of the sulfur. The reaction was carried out in a closed all-glass system for 1.5 h at 160°C. $^{32}PCl_3$ was then formed in 91 % yield by reaction of the $^{32}PSCl_3$ with 1.1 molar equivalents of triphenyl phosphine at 130—140°C for 2 h according to a known type reaction [14] for obtaining sulfur migration from $PSCl_3$.

$^{32}P_2S_5$ prepared by this isotope exchange reaction has been used in the preparation of 15 different organic phosphate and phosphorothioate insecticides. Yields of the chromatographically-pure insecticides varied from 20—90 % based both on total phosphorus and radioactivity. The specific activities ranged from 2 to 340 mC/g. A more detailed report on the conversion of the $^{32}P_2S_5$ to various labeled insecticides and the characterization of the radioactive products will be published elsewhere.

Approved for publication by the Director of the Wisconsin Agricultural Experiment Station. This investigation was supported in part by a research contract with the *U. S. Atomic Energy Commission* (Contract No. AT (11—1)-64, Project No. 14). The author gratefully acknowledges the kind advice of Drs. G. Schrader and R. Mühlmann of *Farbenfabriken Bayer*, Elberfeld, Germany, and Dr. C. Simon of *J. R. Geigy*, Basle, Switzerland, and the skilled technical assistance of Mr. T. K. Knoke and Mr. K. Bürgin.

1. Kalinsky, J. L. and Weinstein, A. *J. Am. Chem. Soc.* **76** (1954) 5882.
2. Hein, R. E. and McFarland, R. H. *J. Am. Chem. Soc.* **74** (1952) 1856.
3. Louloudes, S. J., Kaplanis, J. N. and Roan, C. C. *J. Org. Chem.* **21** (1956) 685.
4. Mühlmann, R. and Schrader, G. *Z. Naturforsch.* **12b** (1957) 196.
5. Casida, J. E. *Unpublished results.*
6. Murray, D. H. and Spinks, J. W. *Can. J. Chem.* **30** (1952) 497.
7. Vigne, J. P., Tabau, R. L. and Fondarai, J. *Bull. soc. chim. France* **23** (1956) 459.
8. Vigne, J. P. and Tabau, R. L. *Bull. soc. pharm. Marseille* **5** (1956) 321.
9. Kosolapoff, G. M. *Organophosphorus Compounds*, John Wiley and Sons, New York 1950, pp. 180, 211, 217 and 236.
10. Plapp, F. W. and Casida, J. E. *Anal. Chem.* **30** (1958) *In press.*
11. Schrader, G. *Personal communication.*
12. Thorpe, T. E. *Chem. News* and *J. Phys. Sci.* **24** (1871) 135.
13. Lockau, V. S. and Lüdicke, M. *Z. Naturforsch.* **7b** (1952) 389.
14. Gottlieb, H. B. *J. Am. Chem. Soc.* **54** (1932) 748.

Received September 19, 1958.

*iso*Thiocyanates XXXIII. * An *iso*Thiocyanate Glucoside (Glucobarbarin) of *Reseda luteola* L.

ANDERS KJÆR and ROLF GMELIN

Organic Chemical Laboratory of The Royal Veterinary and Agricultural College, Copenhagen V, Denmark

Phylogenists are agreed that the family *Resedaceae*, comprising six genera and about 70 species, belongs in the order *Rhoeadales*. Within the latter its close affinity to the *Cruciferae* and, particularly, the *Capparidaceae* has been generally accepted. Hence, it is not surprising that several literature references can be found to the occurrence of mustard oils in species of the genus *Reseda*.

Reseda luteola L. (dyer's weed, weld) was once grown as a source of the flavonoid dye luteolin. In 1871, Hirschberg [1] reported on the appearance of a smell similar to that of horse-radish in disintegrated root material of *R. luteola* and *R. odorata*. This observation was confirmed by Spatzier [2] who further demonstrated the presence of myrosinase in seeds and epidermic tissue of various *Reseda* species.

Pietschmann [3] later adduced microchemical evidence for the occurrence of an unidentified mustard oil in the leaf, stem, root and seed of *R.luteola*. In their paper-chromatographic survey of *iso*thiocyanate glucosides in numerous plants, Schultz and Gmelin [4] recorded the presence in roots, as well as other parts of fresh plants, of *R. luteola* of a single, unidentified glucoside travelling on paper at a rate (R_F 0.20) considerably lower than that of glucotropaeolin (R_F 0.31), the glucoside of *Tropaeolum majus*.

A closer study of the mustard oil glucoside in leaves and inflorescences of *Reseda luteola* L. has now resulted in the isolation of (−)-5-phenyl-2-oxazolidinethione as a product of enzymic fission. Paper chromatography in two solvent systems revealed the presence of only one glucoside in the employed material, migrating at a rate similar to that of glucotropaeolin.

Leaves and inflorescences of *Reseda luteola* (fresh weight 300 g) were added to hot methanol (3 l) and the mixture was refluxed for 1 h. After filtration, the pressed filter cake was extracted with hot 50 % methanol (3 l) and the filtrate collected and combined with the first extract. The solution was stripped of methanol, and water (1 l) was added to the residue. The precipitate was removed by filtration through Celite and 10 % lead acetate solution was added to the filtrate until no further precipitation took place. Excess lead ions were removed as lead phosphate by adding excess of 1/15 M phosphate buffer (pH 6.5) to the filtrate. After filtration, a cell-free myrosinase preparation (10 ml) was added and the buffered mixture set aside at room temperature for 3 h. The solution was then extracted with three 200 ml portions of chloroform. The chloroform extract was washed thrice with a 5 % $NaHCO_3$-solution and then shaken with about 10 g of acid-washed alumina in order to remove traces of flavonoid impurities. On evaporation of the dried chloroform extract a crystalline fraction remained which was recrystallized from ethyl acetate to give well-formed prisms. An additional recrystallization from 70 % ethanol afforded a pure specimen of colourless material (496 mg), m. p. 126—127° (capillary tube, uncorrected), $[\alpha]_D^{23}$ −69.3° ± 1.5° (c=2.0, MeOH).

The identity of the isolated compound with (−)-5-phenyl-2-oxazolidinethione (I) was suggested through the above physical constants and established beyond doubt upon comparison with an authentic specimen of the latter, previously synthesized in this laboratory [5]. Undepressed mixed melting point along with coinciding infra-red spectra served to establish the identity of the compound isolated from *Reseda luteola* and (I).

The formation of (I) upon enzymic hydrolysis suggests the presence in *R. luteola* of glucobarbarin, formerly encountered in seeds of *Barbarea vulgaris* R.Br.[5] As briefly pointed out previously [5], (I) depicts the absolute configuration of the naturally derived, *levo*rotatory heterocyclic compound as a consequence of its synthesis from (−)-2-amino-1-phenylethanol, accomplished in the following way.

(−)-2-Amino-1-phenylethanol (2.0 g) (m. p. 62—3°, $[\alpha]_D^{23}$ −43.5° (c = 2.0, abs. EtOH)), prepared by $LiAlH_4$ reduction of (−)-mandelamide as described by Pratesi and Grassi [6], was dissolved in anhydrous dioxane (6 ml), con-

* Part XXXII of this series: *Acta Chem. Scand.* **12** (1958) *(In press.)*

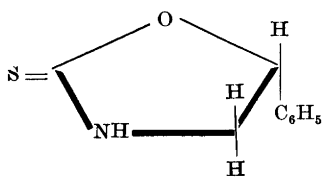

I

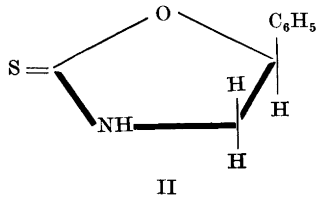

II

taining triethylamine (1.55 g), and the solution was cooled to —10°. CS_2 (0.90 ml) was added with stirring, and the solution was allowed to come to room temperature. After cooling again to —10°, ethyl chloroformate (1.78 g) was introduced, resulting in separation of triethylammonium chloride. Chloroform (12 ml) and triethylamine (1.50) were added and the stirred reaction mixture was allowed to come to room temperature. After the evolution of COS had ceased, HCl (1 N) was added to acid reaction, and the aqueous phase was extracted thrice with chloroform. On evaporation of the dried chloroform solution a partly crystalline product resulted, which could be recrystallized from a mixture of ethyl acetate and hexane to give prisms of (—)-5-phenyl-2-oxazolidinethione (I) (1.48 g), m. p. 125°. An analytical specimen was produced by two additional recrystallizations from 50 % ethanol as colourless prisms, m. p. 126° (uncorr.), $[\alpha]_D^{23}$ —71.0° ± 1.5° (c = 2.0, MeOH). (Found: C 60.10; H 4.84; N 7.68. Calc. for C_9H_9NOS: C 60.31; H 5.06; N 7.82).

Similarly processed, (+)-2-amino-1-phenylethanol (m. p. 63°, $[\alpha]_D^{23}$ +44.2° (c = 2.0, abs. EtOH)) afforded the enantiomeric (+)-5-phenyl-2-oxazolidinethione (II), m. p. 126° (uncorr.), $[\alpha]_D^{23}$ +71° ± 1.5° (c = 2.0, MeOH) (Found: C 60.00; H 5.00; N 7.66).

A solution of equal amounts of the antipodes in hot aqueous ethanol crystallized on cooling and seeding as the racemic compound, m. p. 139° (uncorr.), undepressed on admixture with an authentic specimen [5].

The employed synthesis procedure represents an extension of the method developed by Hodgkins and Ettlinger [7] for the synthesis of *iso*thiocyanates *.

Glucobarbarin appears to be a glucoside of the general structural type [8], containing a 2-hydroxy-2-phenylethyl-side chain. The configuration of the latter is likely to be the same as that established above for (—)-5-phenyl-2-oxazolidinethione (I), which results from spontaneous cyclization of the primarily formed 2-hydroxy-2-phenylethyl *iso*thiocyanate without participation of bonds extending from the asymmetric carbon atom.

Paper chromatography and spectrophometric assays have disclosed the presence of glucobarbarin also in seeds of *R. luteola* L. The results of further investigations of *Resedaceae* species will form the subject of a forthcoming communication.

The work is part of investigations supported by *The Danish State Research Foundation* and *The Carlsberg Foundation*. A special grant from *Kai Hansen's Fond* is gratefully acknowledged.

1. Hirschberg. Foot note in: Vollrath, A. *Arch. Pharm.* **198** (1871) 156.
2. Spatzier, W. *Jahrb. wiss. Botan.* **25** (1893) 39.
3. Pietschmann, A. *Mikrochemie* **2** (1924) 34.
4. Schultz, O.-E. and Gmelin, R. *Z. Naturforsch.* **7b** (1952) 500.
5. Kjær, A. and Gmelin, R. *Acta Chem. Scand.* **11** (1957) 906.
6. Pratesi, P. and Grassi, M. *Farm. sci. e tec. (Pavia)* **8** (1953) 86.
7. Hodgkins, J. E. and Ettlinger, M. *J. Org. Chem.* **21** (1956) 404.
8. Ettlinger, M. G. and Lundeen, A. J. *J. Am. Chem. Soc.* **78** (1956) 4172.

* Applied similarly by Dr. Ettlinger for the synthesis of (±)-4-vinyl-2-oxazolidinethione (private communication).

Received September 4, 1958.

A Note on the Substrate Specificity of Horse Liver Alcohol Dehydrogenase

ALFRED D. WINER*

Biochemical Department, Nobel Medical Institute, Stockholm, Sweden

During the course of a kinetic study of various aldehydes on the DPNH–ADH** compound with the aid of a fluorescence recorder [1], it was found that several hitherto unreported aldehydes and alcohols would function as substrates for horse liver ADH. The substrate specificity of ADH has been previously studied by several investigators [2-4]. Lutwak-Mann using impure ADH found that the relative order of reactivity was ethanol>propanol> amyl alcohol>methanol. Zatman with ADH prepared according to Lutwak-Mann found methanol to be oxidized at about one ninth of the rate for ethanol. Theorell and Bonnichsen using pure ADH found that the Michaelis constants of some higher aliphatic alcohols (allyl, *n*-propanol and *n*-butanol) were lower than for ethanol and stated that higher homologues of ethanol are substrates if they contain the group $-C-CH_2OH$. Bliss [5] has reported that Vitamin A alcohol is converted to retinene using an enzyme prepared according to Bonnichsen and Wassén [6], and Bonnichsen and Hubbard [7] confirmed this observation with pure ADH + DPNH + retinene. In the present study it was found that not only do a number of aliphatic aldehydes and alcohols show greater initial reaction velocities than the physiological substrates acetaldehyde and ethanol under the experimental conditions employed but also that benzyl alcohol, furfuryl alcohol and *cyclo*hexanol are reversibly oxidized by pure ADH.

Experimental part. Pure crystalline ADH was prepared by a modification procedure of Bonnichsen and Brink [8] as described by Dalziel [9]. All final determinations were made with the main component of the resolved enzyme as obtained by chromatography on carboxymethylcellulose. DPN and DPNH were commercial products from Sigma Chemical Company. Yeast ADH was a C. F. Boehringer Company product. All substrates were reagent grade chemicals further purified by distillation under suitable pressures. Rate determinations of the oxido-reduction of DPN(H) were made either in phosphate buffer, ionic strength 0.1, pH 6.95 or in glycine-NaOH buffer, 0.1 M, pH 9.50, at 23.5°, and initial velocities are expressed as moles per liter per min per mole of ADH ***. Details of the fluorescence characteristics of DPNH have been previously described [11,12].

Discussion. ADH appears to have a very broad specificity toward aliphatic carbinol compounds and acts as well on some aromatic and cyclic alcohols and aldehydes (see Table 1). As previously reported by Theorell and Bonnichsen [4], and confirmed in the present studies, pure ADH does not react with methanol + DPN to any observable extent, nor do the alcohols *tert*-butanol, *tert*-amyl or *iso*propyl. Methanol, furthermore, does not effect the activity toward ethanol or other alcohols. That Merritt [13], employing a rat liver acetone powder preparation, found *cyclo*hexanol to be reversibly oxidized to *cyclo*hexanone is probably due to the ADH present in the preparation. The K_m for *cyclo*hexanol was determined to be 1.3×10^{-3} M and for furfuryl alcohol 1.4×10^{-4} M (K_m for ethanol 5.3×10^{-4} M). Furfural was found to have a K_m of 7.7×10^{-6} M and *cyclo*hexanone of 1.9×10^{-3} M (K_m for acetaldehyde 2.1×10^{-4} M) ****. It is easily possible in the case of some alcohols and aldehydes listed in Table 1 to determine quantitative amounts of these substrates in concentrations of 10^{-7} M.

The reactivity of these substrates on yeast ADH are, however, quite different. *Cyclo*hexanol and *cyclo*hexanone will not react with the yeast enzyme and furfural acts at about one sixth of the rate for acetaldehyde while furfuryl alcohol reacts at about one-two hundredth of the rate for ethanol.

---

* U.S. Public Health Service Research Fellow of the National Institute of Neurological Diseases and Blindness.

** Abbreviations. DPNH: reduced, and DPN: oxidized diphosphopyridine nucleotide; ADH: 1/2 molecule of liver alcohol dehydrogenase.

*** The molecular weight was taken as 84 000 and the absorbancy index at 280 mμ as 0.42×10^5 cm per mole per liter [10].

**** See Table 1 for the coenzyme concentrations used to determine these constants.

Table 1. The influence of chain length and substitution on the ability of alcohols and aldehydes to serve as substrates for liver ADH.

Alcohol *	initial velocity (M/L/min/mole ADH)	Aldehyde **	initial velocity (M/L/min/mole ADH)
n-Butanol	215	*n*-Butyraldehyde	510
Allyl	192	Cinnamaldehyde	350
2-Phenylethanol	184	Furfural	236
n-Hexanol	170	*Iso*valeraldehyde	208
*Iso*amyl	167	Benzaldehyde	55
Amyl	160	Acetaldehyde	30
n-Propanol	146	Formaldehyde	7
Ethanol	135	*Cyclo*hexanone	5
*Cyclo*hexanol	135	DL-Glyceraldehyde	2
n-Octanol	135	Glyoxal	0
Benzyl	118	Methylethylketone	0
Methyl*cyclo*hexanol	108	Acetone	0
Furfuryl	108		
3-Phenyl-1-propanol	46		
3-Hexanol	35		
Methanol	0		
tert-Butanol	0		
tert-Amyl	0		
*Iso*propyl	0		

* The alcohols were tested at a concentration of 1.0×10^{-3} M; DPN, 1.20×10^{-4} M; ADH, 1.44×10^{-8} M. Glycine-NaOH buffer, 0.1 M, pH 9.50.

** The aldehydes (or ketones) were tested at a concentration of 5.0×10^{-5} M; DPNH, 3.21×10^{-6} M; ADH, 4.84×10^{-9} M. Phosphate buffer, ionic strength 0.1, pH 6.95.

The complete data will be given in a forthcoming paper in this journal.

Acknowledgments. The author wishes to thank Dr. Keith Dalziel and Mr. O. Eriksson for the purified ADH preparation and Professor Hugo Theorell for his kind interest shown during the course of this investigation. Thanks are due to *Svenska Maltdrycksforskningsinstitutet* for financial support.

1. Theorell, H. and Nygaard, A. P. *Acta Chem. Scand.* **8** (1954) 877.
2. Lutwak-Mann, C. *Biochem. J.* **32** (1938) 1364.
3. Zatman, L. J. *Biochem. J.* **40** (1946) LXVII.
4. Theorell, H. and Bonnichsen, R. *Acta Chem. Scand.* **5** (1951) 1105.
5. Bliss, A. *Biol. Bull.* **97** (1949) 221.
6. Bonnichsen, R. and Wassén, A. M. *Arch. Biochem.* **18** (1948) 361.
7. *Personal communication.*
8. Bonnichsen, R. and Brink, N. G. in Colowick, S. P. and Kaplan, N. O. *Methods in Enzymology*, Vol. I, p. 495, Academic Press, New York 1955.
9. Dalziel, K. *Acta Chem. Scand.* **12** (1958) 275.
10. Ehrenberg, A. and Dalziel, K. *Acta Chem. Scand.* **12** (1958) 465.
11. Theorell, H., Nygaard, A. P. and Bonnichsen, R. *Acta Chem. Scand.* **9** (1955) 1148.
12. Winer, A. D. and Schwert, G. W. *Biochim. et Biophys. Acta* **29** (1958) 424.
13. Merritt, A. D. *Federation Proc.* **17** (1958) 275.

Received September 22, 1958.

Formation of Particulate Ribonucleoprotein with Enzymatic Activities *in vitro*

AGNAR P. NYGAARD

Johan Throne Holst's Institutt for Ernæringsforskning, University of Oslo, Norway

During the purification of lactic dehydrogenase from baker's yeast [1] a particulate ribonucleoprotein was observed to be formed in a soluble preparation of proteins and ribonucleic acid. The solution was obtained from the mechanically extracted cells by acetone precipitation, calcium phosphate adsorption/elution and ammonium sulfate precipitation. The nucleoprotein precipitated on storage at 6°C from the saltfree solution which had been concentrated by lyophilization.

The precipitate contained about equal amounts of nucleic acid and protein. Adenine, guanine, cytosine and uracil were all present. The nucleoprotein (nucleic acid and protein) was insoluble in water and in different salt solutions (*e. g.* 1 M sodium chloride), but dissolved in 0.04 M sodium hydroxide. In some preparations the particles settled easily in a low centrifugal field, in others a clear solution was not obtained even after 30 min centrifugation at 30 000 × *g*.

The original solution contained 10 % ribonucleic acid, 5—10 % each of lactic-, malic-, alcohol- and triosephosphate dehydrogenase, and had proteolytic and nucleolytic activities. The well-washed particles had malic dehydrogenase activity. None of the other dehydrogenases were present. The particles digested the particulate ribonucleic acid. Thus, on incubation in phosphate buffer purine and pyrimidine material appeared in the supernatent. This material was not liberated by boiling of the particulate ribonucleoprotein.

Malic dehydrogenase was measured spectrophotometrically at 340 mμ, with oxalacetic acid and DPNH at pH 8.4, with malic acid and DPN at pH 9.6. The rate was 40 μmoles oxalacetic acid reduced per mg particulate protein per hour. Highly purified malic dehydrogenase has been obtained from the original ammonium sulfate precipitate by zone electrophoresis on cellulose. This soluble preparation did not contain ribonucleic acid and had an activity of 8 500 μmoles oxalacetic acid reduced per mg protein per hour.

The results indicate that particulate ribonucleoproteins isolated from bacterial cells may not necessarily represent original particles of the cell. Particles may be formed in a haphazard manner during extraction and purification.

1. Nygaard, A. P. *Biochim. et Biophys. Acta. In press.*

Received September 23, 1958.

Standard Deviations of Interatomic Distances in Completely Deuterated Benzene

S. J. CYVIN

Institutt for teoretisk kjemi, Norges tekniske høgskole, Trondheim, Norway

In a previous communication the calculation of standard deviations of interatomic distances in the benzene molecule has been reported [1]. The calculated values have been compared with values obtained from electron diffraction data [2].

Similar calculations from spectroscopic data have been performed for the benzene-d_6 molecule with the result given in Table 1. The experimental fundamental

Table 1. Standard deviations for interatomic distances in benzene-d_6.

Distance	Calculated standard deviations in Å units $T = 0$	273.16	298.16	323.16
C_1—D_1	0.0660	0.0660	0.0660	0.0660
C_2—D_1	0.0889	0.0895	0.0898	0.0902
C_3—D_1	0.0835	0.0845	0.0848	0.0952
C_4—D_1	0.0821	0.0834	0.0839	0.0844
C_1—C_2	0.0455	0.0456	0.0457	0.0458
C_1—C_3	0.0529	0.0539	0.0543	0.0546
C_1—C_4	0.0570	0.0587	0.0593	0.0599
D_1—D_2	0.1277	0.1290	0.1296	0.1303
D_1—D_3	0.1095	0.1107	0.1112	0.1117
D_1—D_4	0.1012	0.1024	0.1028	0.1033

frequencies given by Brodersen and Langseth [3] have been applied. To the knowledge of the author, the molecule has not been investigated by electron diffraction.

1. Cyvin, S. J. *Acta Chem. Scand.* **11** (1957) 1499.

2. Bastiansen, O. and Cyvin, S. J. *Nature* **180** (1957) 980.
3. Brodersen, S. and Langseth, A. *Kgl. Danske Videnskab. Selskab, Mat. Fys. Skrifter* **1** (1956) No. 1.

Received September 17, 1958.

Two New Naturally Occurring Methoxyl-Containing Carotenoids

SYNNØVE LIAAEN JENSEN

Institutt for Organisk Kjemi, Norges tekniske høgskole, Trondheim, Norway

Methoxyl-containing carotenoids have so far been restricted to the photosynthetic bacteria. Carotenoids hitherto known to contain methoxyl groups are:

1) Spirilloxanthin, isolated by van Niel *et al.*[1] in 1935 from old cultures of *Rhodospirillum rubrum*, and shown by comparision of analythical data [2] to be identical with rhodoviolascin, isolated the same year by Karrer *et al.*[3] from mixed cultures of *Rhodovibrio* species. Karrer *et al.* have proposed the formula for spirilloxanthin [4].

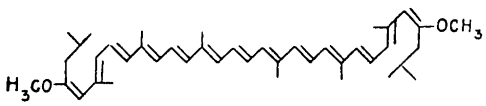

2) Pigment Y (Yellow) and Pigment R (Red), isolated from *Rhodopseudomonas spheroides*, and both shown by Goodwin *et al.*[5] to contain one methoxyl group. For Pigment R Goodwin *et al.* have proposed the formula

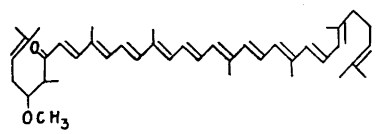

and renamed it spheroidenone [5].

Kinetic experiments performed by Stanier *et al*[6]. to establish the route of carotenoid synthesis in the photosynthetic, nonsulphur purple bacterium *Rhodospirillum rubrum*, showed that the following transformation occurs quantitatively during growth:

lycopene → P481 → spirilloxanthin
OH-lycopene → OH-P481 → OH-spirilloxanthin

The structures of the carotenoids P481 and OH-P481 are not known. The designation Pigment 481 was given by Goodwin *et al.*[7] from the main absorption band in petroleum ether.

During endogenous carotenoid synthesis (anaerobically in light) washed cells of *Rhodospirillum rubrum* previously grown in the presence of diphenylamine, produced considerable amounts of P481 and OH-P481, whereas only a limited synthesis of spirilloxanthin normally was observed. This observation led to the assumption that P481 and OH-P481 were carotenoids with the same C_{40} skeleton as lycopene, and that lack of intracellular methyl donators limited the endogenous spirilloxanthin synthesis [8].

In the investigation now reported the presence of methoxyl groups in crystalline, chromatographically pure P481 and OH-P481 was indicated by IR-absorption bands at 1 078 cm^{-1} (KBr discs).

Quantitative methoxyl determinations were carried out according to the modified method of Inglis [8], and gave the following results:

Carotenoid	% OCH_3 found	% OCH_3 calculated	based on formula
P481	5.51	5.48	$C_{40}H_{55}(OCH_3)$
OH-P481	5.33	5.31	$C_{40}H_{54}(OH)(OCH_3)$

These results establish the presence of one methoxyl group in both P481 and OH-P481.

The fact that P481 and OH-P481 are C_{41} compounds is not in accordance with our previous suggestion. However, this finding fits well the role that has been ascribed to these two carotenoids as biosynthetic intermediates between lycopene ($C_{40}H_{56}$) and spirilloxanthin ($C_{42}H_{60}O_2$)[6].

Work on the chemical structure of P481 and OH-P481 is in progress.

The author is indebted to prof. R. Y. Stanier, Dept. of Bacteriology, University of California, Berkeley, for providing facilities for the cultivation of mass cultures of *Rhodospirillum rubrum* in his laboratory, to Mr. Charles E. Spotts for skilled assistance, and to prof. N. A. Sørensen, NTH, for inspiring interest in this work.

Formation of Particulate Ribonucleoprotein with Enzymatic Activities *in vitro*

AGNAR P. NYGAARD

Johan Throne Holst's Institutt for Ernæringsforskning, University of Oslo, Norway

During the purification of lactic dehydrogenase from baker's yeast [1] a particulate ribonucleoprotein was observed to be formed in a soluble preparation of proteins and ribonucleic acid. The solution was obtained from the mechanically extracted cells by acetone precipitation, calcium phosphate adsorption/elution and ammonium sulfate precipitation. The nucleoprotein precipitated on storage at 6°C from the saltfree solution which had been concentrated by lyophilization.

The precipitate contained about equal amounts of nucleic acid and protein. Adenine, guanine, cytosine and uracil were all present. The nucleoprotein (nucleic acid and protein) was insoluble in water and in different salt solutions (*e. g.* 1 M sodium chloride), but dissolved in 0.04 M sodium hydroxide. In some preparations the particles settled easily in a low centrifugal field, in others a clear solution was not obtained even after 30 min centrifugation at 30 000 × *g*.

The original solution contained 10 % ribonucleic acid, 5—10 % each of lactic-, malic-, alcohol- and triosephosphate dehydrogenase, and had proteolytic and nucleolytic activities. The well-washed particles had malic dehydrogenase activity. None of the other dehydrogenases were present. The particles digested the particulate ribonucleic acid. Thus, on incubation in phosphate buffer purine and pyrimidine material appeared in the supernatent. This material was not liberated by boiling of the particulate ribonucleoprotein.

Malic dehydrogenase was measured spectrophotometrically at 340 mμ, with oxalacetic acid and DPNH at pH 8.4, with malic acid and DPN at pH 9.6. The rate was 40 μmoles oxalacetic acid reduced per mg particulate protein per hour. Highly purified malic dehydrogenase has been obtained from the original ammonium sulfate precipitate by zone electrophoresis on cellulose. This soluble preparation did not contain ribonucleic acid and had an activity of 8 500 μmoles oxalacetic acid reduced per mg protein per hour.

The results indicate that particulate ribonucleoproteins isolated from bacterial cells may not necessarily represent original particles of the cell. Particles may be formed in a haphazard manner during extraction and purification.

1. Nygaard, A. P. *Biochim. et Biophys. Acta. In press.*

Received September 23, 1958.

Standard Deviations of Interatomic Distances in Completely Deuterated Benzene

S. J. CYVIN

Institutt for teoretisk kjemi, Norges tekniske høgskole, Trondheim, Norway

In a previous communication the calculation of standard deviations of interatomic distances in the benzene molecule has been reported [1]. The calculated values have been compared with values obtained from electron diffraction data [2].

Similar calculations from spectroscopic data have been performed for the benzene-d_6 molecule with the result given in Table 1. The experimental fundamental

Table 1. Standard deviations for interatomic distances in benzene-d_6.

Distance	Calculated standard deviations in Å units $T = 0$	273.16	298.16	323.16
C_1—D_1	0.0660	0.0660	0.0660	0.0660
C_2—D_1	0.0889	0.0895	0.0898	0.0902
C_3—D_1	0.0835	0.0845	0.0848	0.0952
C_4—D_1	0.0821	0.0834	0.0839	0.0844
C_1—C_2	0.0455	0.0456	0.0457	0.0458
C_1—C_3	0.0529	0.0539	0.0543	0.0546
C_1—C_4	0.0570	0.0587	0.0593	0.0599
D_1—D_2	0.1277	0.1290	0.1296	0.1303
D_1—D_3	0.1095	0.1107	0.1112	0.1117
D_1—D_4	0.1012	0.1024	0.1028	0.1033

frequencies given by Brodersen and Langseth [3] have been applied. To the knowledge of the author, the molecule has not been investigated by electron diffraction.

1. Cyvin, S. J. *Acta Chem. Scand.* **11** (1957) 1499.

2. Bastiansen, O. and Cyvin, S. J. *Nature* **180** (1957) 980.
3. Brodersen, S. and Langseth, A. *Kgl. Danske Videnskab. Selskab, Mat. Fys. Skrifter* **1** (1956) No. 1.

Received September 17, 1958.

Two New Naturally Occurring Methoxyl-Containing Carotenoids

SYNNØVE LIAAEN JENSEN

Institutt for Organisk Kjemi, Norges tekniske høgskole, Trondheim, Norway

Methoxyl-containing carotenoids have so far been restricted to the photosynthetic bacteria. Carotenoids hitherto known to contain methoxyl groups are:

1) Spirilloxanthin, isolated by van Niel *et al.*[1] in 1935 from old cultures of *Rhodospirillum rubrum*, and shown by comparision of analythical data [2] to be identical with rhodoviolascin, isolated the same year by Karrer *et al.*[3] from mixed cultures of *Rhodovibrio* species. Karrer *et al.* have proposed the formula for spirilloxanthin [4].

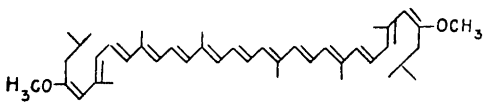

2) Pigment Y (Yellow) and Pigment R (Red), isolated from *Rhodopseudomonas spheroides*, and both shown by Goodwin *et al.*[5] to contain one methoxyl group. For Pigment R Goodwin *et al.* have proposed the formula

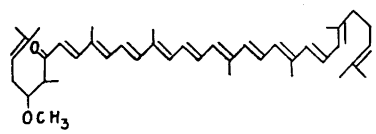

and renamed it spheroidenone [5].

Kinetic experiments performed by Stanier *et al*[6]. to establish the route of carotenoid synthesis in the photosynthetic, nonsulphur purple bacterium *Rhodospirillum rubrum*, showed that the following transformation occurs quantitatively during growth:

lycopene → P481 → spirilloxanthin
OH-lycopene → OH-P481 → OH-spirilloxanthin

The structures of the carotenoids P481 and OH-P481 are not known. The designation Pigment 481 was given by Goodwin *et al.*[7] from the main absorption band in petroleum ether.

During endogenous carotenoid synthesis (anaerobically in light) washed cells of *Rhodospirillum rubrum* previously grown in the presence of diphenylamine, produced considerable amounts of P481 and OH-P481, whereas only a limited synthesis of spirilloxanthin normally was observed. This observation led to the assumption that P481 and OH-P481 were carotenoids with the same C_{40} skeleton as lycopene, and that lack of intracellular methyl donators limited the endogenous spirilloxanthin synthesis [8].

In the investigation now reported the presence of methoxyl groups in crystalline, chromatographically pure P481 and OH-P481 was indicated by IR-absorption bands at 1 078 cm^{-1} (KBr discs).

Quantitative methoxyl determinations were carried out according to the modified method of Inglis [8], and gave the following results:

Carotenoid	% OCH_3 found	% OCH_3 calculated	based on formula
P481	5.51	5.48	$C_{40}H_{55}(OCH_3)$
OH-P481	5.33	5.31	$C_{40}H_{54}(OH)(OCH_3)$

These results establish the presence of one methoxyl group in both P481 and OH-P481.

The fact that P481 and OH-P481 are C_{41} compounds is not in accordance with our previous suggestion. However, this finding fits well the role that has been ascribed to these two carotenoids as biosynthetic intermediates between lycopene ($C_{40}H_{56}$) and spirilloxanthin ($C_{42}H_{60}O_2$)[6].

Work on the chemical structure of P481 and OH-P481 is in progress.

The author is indebted to prof. R. Y. Stanier, Dept. of Bacteriology, University of California, Berkeley, for providing facilities for the cultivation of mass cultures of *Rhodospirillum rubrum* in his laboratory, to Mr. Charles E. Spotts for skilled assistance, and to prof. N. A. Sørensen, NTH, for inspiring interest in this work.

This work was partly performed at University of California, Berkeley, with a Haakon Styri Fellowship, and partly at Norges tekniske høgskole with a grant from the latter institution.

1. van Niel, C. B. and Smith, J. H. C. *Arch. Microbiol.* **6** (1935) 219.
2. Polgàr, A., van Niel, C. B. and Zechmeister, L. *Arch. Biochem.* **5** (1944) 243.
3. Karrer, P. and Solmssen, U. *Helv. Chim. Acta* **18** (1935) 1306.
4. Karrer, P. and Koenig, H. *Helv. Chim. Acta* **23** (1940) 460.
5. Goodwin, T. W., Land, D. G. and Sissins, M. E. *Biochem. J.* **64** (1956) 486.
6. Liaaen Jensen, S., Cohen-Bazire, G., Nakayama, T. O. M. and Stanier, R. Y. *Biochem. et Biophys. Acta* **29** (1958) 477.
7. Goodwin, T. W. and Land, D. G. *Arch. Microbiol.* **24** (1956) 305.
8. Inglis, A. S. *Microchimica Acta* **1957** 677.

Received September 22, 1958.

Notiz über α-Phenoxyhydrozimtsäure

H. SEBELIUS*

Vor etwa vierzig Jahren hat der Verf. am Chemischen Institut der Universität Lund auf Veranlassung von Professor J. M. Lovén die α-Phenoxyhydrozimtsäure mit Hilfe der aktiven α-Phenäthylamine [1] in ihre optisch aktiven Komponenten gespalten und einige vorläufige Ergebnisse darüber publiziert [2]. Ehe die Untersuchung für andere Arbeiten unterbrochen wurde, lagen noch einige Resultate vor, die sich unter anderem auf die Säureamide bezogen. Für ihre Darstellung wurde ein Verfahren erprobt, das einfach und mit vorzüglicher Ausbeute zu so gut wie analysenreinen Substanzen direkt führte und wahrscheinlich auch für andere α-Phenoxykarbonsäuren verwendbar ist. Verschiedene Derivate dieser Säuren haben ja in der letzten Zeit als Pflanzenwachstumsregulatoren bedeutendes Interesse erreicht, und in diesem Zusammenhang verdienen die hierauf bezüglichen Säureamide Aufmerksamkeit.

Das Verfahren zur Darstellung der Säureamide war folgendes: Die Äthylester der Säuren wurden in der etwa zehnfachen Menge mit Ammoniak bei −10°C gesättigten Äthylalkohols aufgelöst und in gut verschlossenen, starkwändigen Gefässen rund zehn Tage bei Zimmertemperatur aufbewahrt. Nach dieser Zeit hatten sich die gebildeten Amide in centimeterlange, gut entwickelte Prismen ausgeschieden.

Das Amid der Racemsäure schmolz bei 145°C und war in Wasser, Alkohol und Aether schwer löslich. Stickstoffbestimmung nach Kjeldahl gab 5,7 % N, ber. 5,8 %.

Der für die Darstellung des Amids der linksdrehenden α-Phenoxyhydrozimtsäure verwendete Äthylester hatte bei 14 mm Hg den Siedepunkt 198°C und die spezifische Drehung in Alkohol $[\alpha]_D^{18}$ −20°, in Chloroform $[\alpha]_D^{18}$ −24°. Das nach dem oben angegebenen Verfahren erhaltene Amid kristallisierte sehr schön, gab bei der Analyse den berechneten Stickstoffgehalt von 5,8 % N und schmolz bei 147°C, also unbedeutend höher als das Amid der Racemsäure. Wegen der Schwerlöslichkeit des Amids in Alkohol wurde die Drehung in Aceton bestimmt: $[\alpha]_D^{18}$ −11°. Auffallenderweise zeigte es in Chloroform entgegengesetzte Drehungsrichtung, $[\alpha]_D^{18}$ +26°. Die Drehungsveränderung wurde damals als Resultat einer relativ festen Anlagerung von Chloroform an die Amidgruppe gedeutet. In Eisessig, wo man eine derartige selektive Solvatisierung vermuten konnte, war die Drehung ebenfalls positiv, nämlich $[\alpha]_D^{18}$ rund +11°. Die Drehungsmessungen wurden mit einem alten, wenig empfindlichen Polarimeter und ziemlich bescheidenen Substanzmengen ausgeführt und machen daher keinen Anspruch auf Präcision.

* Adresse: Statens Lantbrukskemiska Kontrollanstalt, Stockholm 50, Schweden.

1. Lovén, J. M. *J. prakt. Chem.* (2) **72** (1905) 307.
2. Sebelius, H. *Festskrift utgiven av Kem.-Min. fören. Lund* (1918) 87.

Eingegangen am 3. Oktober 1958.

This work was partly performed at University of California, Berkeley, with a Haakon Styri Fellowship, and partly at Norges tekniske høgskole with a grant from the latter institution.

1. van Niel, C. B. and Smith, J. H. C. *Arch. Microbiol.* **6** (1935) 219.
2. Polgàr, A., van Niel, C. B. and Zechmeister, L. *Arch. Biochem.* **5** (1944) 243.
3. Karrer, P. and Solmssen, U. *Helv. Chim. Acta* **18** (1935) 1306.
4. Karrer, P. and Koenig, H. *Helv. Chim. Acta* **23** (1940) 460.
5. Goodwin, T. W., Land, D. G. and Sissins, M. E. *Biochem. J.* **64** (1956) 486.
6. Liaaen Jensen, S., Cohen-Bazire, G., Nakayama, T. O. M. and Stanier, R. Y. *Biochem. et Biophys. Acta* **29** (1958) 477.
7. Goodwin, T. W. and Land, D. G. *Arch. Microbiol.* **24** (1956) 305.
8. Inglis, A. S. *Microchimica Acta* **1957** 677.

Received September 22, 1958.

Notiz über α-Phenoxyhydrozimtsäure

H. SEBELIUS*

Vor etwa vierzig Jahren hat der Verf. am Chemischen Institut der Universität Lund auf Veranlassung von Professor J. M. Lovén die α-Phenoxyhydrozimtsäure mit Hilfe der aktiven α-Phenäthylamine [1] in ihre optisch aktiven Komponenten gespalten und einige vorläufige Ergebnisse darüber publiziert [2]. Ehe die Untersuchung für andere Arbeiten unterbrochen wurde, lagen noch einige Resultate vor, die sich unter anderem auf die Säureamide bezogen. Für ihre Darstellung wurde ein Verfahren erprobt, das einfach und mit vorzüglicher Ausbeute zu so gut wie analysenreinen Substanzen direkt führte und wahrscheinlich auch für andere α-Phenoxykarbonsäuren verwendbar ist. Verschiedene Derivate dieser Säuren haben ja in der letzten Zeit als Pflanzenwachstumsregulatoren bedeutendes Interesse erreicht, und in diesem Zusammenhang verdienen die hierauf bezüglichen Säureamide Aufmerksamkeit.

Das Verfahren zur Darstellung der Säureamide war folgendes: Die Äthylester der Säuren wurden in der etwa zehnfachen Menge mit Ammoniak bei −10°C gesättigten Äthylalkohols aufgelöst und in gut verschlossenen, starkwändigen Gefässen rund zehn Tage bei Zimmertemperatur aufbewahrt. Nach dieser Zeit hatten sich die gebildeten Amide in centimeterlange, gut entwickelte Prismen ausgeschieden.

Das Amid der Racemsäure schmolz bei 145°C und war in Wasser, Alkohol und Aether schwer löslich. Stickstoffbestimmung nach Kjeldahl gab 5,7 % N, ber. 5,8 %.

Der für die Darstellung des Amids der linksdrehenden α-Phenoxyhydrozimtsäure verwendete Äthylester hatte bei 14 mm Hg den Siedepunkt 198°C und die spezifische Drehung in Alkohol $[\alpha]_D^{18}$ −20°, in Chloroform $[\alpha]_D^{18}$ −24°. Das nach dem oben angegebenen Verfahren erhaltene Amid kristallisierte sehr schön, gab bei der Analyse den berechneten Stickstoffgehalt von 5,8 % N und schmolz bei 147°C, also unbedeutend höher als das Amid der Racemsäure. Wegen der Schwerlöslichkeit des Amids in Alkohol wurde die Drehung in Aceton bestimmt: $[\alpha]_D^{18}$ −11°. Auffallenderweise zeigte es in Chloroform entgegengesetzte Drehungsrichtung, $[\alpha]_D^{18}$ +26°. Die Drehungsveränderung wurde damals als Resultat einer relativ festen Anlagerung von Chloroform an die Amidgruppe gedeutet. In Eisessig, wo man eine derartige selektive Solvatisierung vermuten konnte, war die Drehung ebenfalls positiv, nämlich $[\alpha]_D^{18}$ rund +11°. Die Drehungsmessungen wurden mit einem alten, wenig empfindlichen Polarimeter und ziemlich bescheidenen Substanzmengen ausgeführt und machen daher keinen Anspruch auf Präcision.

* Adresse: Statens Lantbrukskemiska Kontrollanstalt, Stockholm 50, Schweden.

1. Lovén, J. M. *J. prakt. Chem.* (2) **72** (1905) 307.
2. Sebelius, H. *Festskrift utgiven av Kem.-Min. fören. Lund* (1918) 87.

Eingegangen am 3. Oktober 1958.

Structure of the Tetrathionate Ion in the Sodium Salt

OLAV FOSS and ASBJØRN HORDVIK

Chemical Institute, University of Bergen, Bergen, Norway

A crystal structure analysis of barium tetrathionate dihydrate five years ago [1] led to an unbranched, non-planar structure for the sulphur chain of the tetrathionate ion, and gave the following values (±0.03 Å and ± 2°) for bond lengths and angles: $S_1-S_2 = 2.10$ Å, $S_2-S_3 = 2.02$ Å, $S_3-S_4 = 2.13$ Å, $\angle S_1-S_2-S_3 = 104°$, $\angle S_2-S_3-S_4 = 102°$. The dihedral angle, $S_1S_2S_3/S_2S_3S_4$, was found to be 90°. These results have now been confirmed through a more accurate structure analysis of sodium tetrathionate dihydrate, $Na_2S_4O_6 \cdot 2H_2O$.

This salt is monoclinic [2], with $a = 14.50$ Å, $b = 6.37$ Å, $c = 5.47$ Å, $\beta = 105.6°$, and two formula units per unit cell. The space group is C_2^3-C2, which requires that the tetrathionate ion lies on a twofold axis of symmetry. The b and c-axis projections were solved through Patterson and Fourier syntheses and refined through repeated difference syntheses, based on 81 observed $h0l$ reflections and 56 observed $hk0$ reflections out of 90 and 61, respectively, accessible with Cu$K\alpha$ radiation. The intensities were estimated visually from zero-layer Weissenberg photographs of an approximately spherical crystal with a diameter of 0.12 mm. Individual temperature corrections, anisotropic for some atoms, were applied in calculating $h0l$ structure factors, whereas an overall, isotropic temperature correction was used for the $hk0$ data. The final atomic coordinates are listed in Table 1; the reliability index R is 0.076 for both zones.

Table 1. Atomic coordinates for sodium tetrathionate dihydrate, in fractions of monoclinic cell edges. Origin on a twofold axis.

	x	y	z
S_2	0.0234	0	0.342
S_1	0.1340	0.227	0.420
O_1	0.090	0.435	0.379
O_2	0.180	0.169	0.223
O_3	0.192	0.193	0.678
Na	0.271	0.406	0.020
H_2O	0.123	0.619	—0.088

These coordinates give a length of 2.019 Å for the middle S—S bond across the twofold axis, and 2.116 Å for the end S—S bonds, with estimated standard deviations of 0.01 Å. There is thus no doubt that the middle bond, between the two divalent sulphur atoms of the tetrathionate ion, is shorter than the two other S—S bonds. The S—S—S bond angles are 103.8° ± 0.5° and the dihedral angle SSS/SSS is 90.4° ± 1°.

The SO_3 groups have trigonal symmetry within the accuracy of the analysis, with S—O bond lengths of 1.45, 1.46 and 1.46 Å (± 0.02 Å) and O—S—O angles of 112.6°, 113.5° and 114.8° (± 1.5°). The axis of the trigonal pyramid does not coincide with the direction of the O_3S-S bond, the O—S—S angles being 108.1°, 98.6° and 107.6° (± 1°).

Details of the structure will be published later.

1. Foss, O., Furberg, S. and Zachariasen, H. *Acta Chem. Scand.* **8** (1954) 459.
2. Foss, O. *Acta Chem. Scand.* **6** (1952) 802.

Received September 20, 1958.

ACTA CHEMICA SCANDINAVICA 12 (1958) 1701—1714

The Crystal Structure of $Mo(OH)_3PO_4$

PEDER KIERKEGAARD

Institute of Inorganic and Physical Chemistry, University of Stockholm, Stockholm, Sweden

$Mo(OH)_3PO_4$ has a monoclinic unit cell containing two formula units and with the dimensions

$a = (6.731 \pm 0.005)$ Å
$b = (6.319 \pm 0.005)$ Å
$c = (7.034 \pm 0.005)$ Å
$\beta = (110.16 \pm 0.05)°$
$V = 280._8$ Å^3

A structure is proposed with atomic positions in the space group No. 11, $P2_1/m$. The positions of the molybdenum and phosphorus atoms in the unit cell were determined by Fourier methods. The parameters of the oxygen atoms were determined partly from electron density projections and partly from geometrical considerations, interatomic distances from previously determined structures being used. The crystals are built up of double chains parallel to the y-axis and formed by MoO_6 octahedra, coupled together by PO_4 groups so that every MoO_6 octahedron is sharing edges with three phosphate tetrahedra and every PO_4 tetrahedron with three MoO_6 octahedra. The double chains are then held together by the hydrogen atoms situated between adjacent oxygen atoms from different chains.

In connection with an X-ray investigation of oxygen-phosphorus compounds of molybdenum and wolfram undertaken at this institute a crystal structure determination of a molybdenum(VI)-phosphate, $2\ MoO_3 \cdot P_2O_5 \cdot 3\ H_2O$, has been made. The existence of a crystalline compound of this composition was reported by Schulz [1]. The crystals were described as slightly soluble in cold water but dissolving easily in warm water, giving a strongly acid solution, yellow when warm but colourless at room temperature. The compound did not lose water until it was heated to a temperature above 225°C and, as a water-free final product $2\ MoO_3 \cdot P_2O_5$ was formed. From this and some other experiments it was concluded by Schulz that the first compound was an orthophosphate with the formula $MoO_2HPO_4 \cdot H_2O$ and the second was a pyrophosphate, $(MoO_2)_2P_2O_7$. A structure determination of the latter has been started but here we shall deal only with the first-mentioned compound.

PREPARATION OF THE CRYSTALS

A viscous solution of MoO_3 (15 g) in concentrated (14.5 M) H_3PO_4 (45 ml) was prepared at about 180°C. On cooling the solution was diluted with 400 ml of concentrated (15.5 M) HNO_3 and then evaporated, during which time small crystals were obtained. The evaporation was continued to a volume of 200 ml after which the crystals were filtered off, washed with cold water and dried in air. (The method according to Schulz [1].)

The crystals were small colourless rods. However, the yield was low and the crystals obtained were too small for X-ray work and therefore the synthesis was repeated several times, resulting in sufficient amounts of the small crystals. The biggest single crystal obtained after growth in hot solution was one of about 0.1 mm in length and 0.03 mm in diameter.

Analysis. A sample was dissolved in hot water. From an ammoniacal solution the *phosphorus* was precipitated (according to Kolthoff and Sandell [2]) with a magnesium solution. The precipitate of magnesium phosphate was filtered off, washed with water, dissolved in hot 1 M HNO_3 and from this solution the phosphorus finally was precipitated with ammonium molybdate and weighed as $(NH_4)_3PO_4 \cdot 12\ MoO_3$. The amount of *molybdenum* in the filtrate was determined gravimetrically by precipitation with 8-hydroxyquinoline [3,4] from a solution slightly acid with acetic acid. The precipitate was filtered off, washed with water, dried at 140°C and weighed as molybdenum hydroxyquinolate. The *water* was determined by Hartwig-Bendig's [5] modification of Brush's [6] and Penfield's [7] methods.

The *density* of the crystals was determined from the apparent loss of weight in benzene.

	Calculated for $2\ MoO_3 \cdot P_2O_5 \cdot 3\ H_2O$	Found
% MoO_3	59.48	59.7
% P_2O_5	29.35	29.5
% H_2O	11.17	10.7
Density	2.862	2.82

The density is calculated for one formula unit per unit cell.

UNIT CELL AND SPACE GROUP

From rotation photographs (around [010] and [100]) and the corresponding Weissenberg photographs (zero, first and second layer lines), taken with CuK radiation it was concluded that the crystals are monoclinic with $a = 6.8$ Å, $b = 6.4$ Å, $c = 7.1$ Å and $\beta = 110°$ (the b-axis coincides with the needle axis of the crystal).

The reflections were recorded photographically with multiple film techniques and the relative intensities were estimated visually by comparison with an intensity scale obtained by photographing a reflection with different exposure times. However, the accuracy in the intensity estimations was rather low since the photographs were fairly poor owing to the smallness of the crystals prepared. The values of F^2 were then calculated from the relative intensities using the polarization and Lorentz' factor given by Lu[8]. No correction was applied for absorption.

More accurate values for the unit cell dimensions were calculated from a powder photograph taken with monochromatized Cu$K\alpha_1$ radiation in a focusing camera of Guinier type. KCl was used as an internal standard substance (see Table 1).

$$a = (6.731 \pm 0.005)\ \text{Å}$$
$$b = (6.319 \pm 0.005)\ \text{Å}$$
$$c = (7.034 \pm 0.005)\ \text{Å}$$
$$\beta = (110.1_6 \pm 0.05)^\circ$$
$$V = 280._8\ \text{Å}^3$$

The value (2.82) found for the density gives $0.99 \approx 1$ formula unit in the unit cell.

The reflections systematically absent are

$$0k0 \text{ with } k = \text{odd}$$

This is characteristic of the two space groups No. 4, $P2_1$, and No. 11, $P2_1/m$. The investigation was started by examining whether the structure was consistent with the latter space group, having the highest symmetry. In No. 11, $P2_1/m$, the following point positions are possible.

$2(a)$: 000; $0\frac{1}{2}0$; $2(b)$: $\frac{1}{2}00$; $\frac{1}{2}\frac{1}{2}0$; $2(c)$: $00\frac{1}{2}$;$0\frac{1}{2}\frac{1}{2}$
$2(d)$: $\frac{1}{2}0\frac{1}{2}$; $\frac{1}{2}\frac{1}{2}\frac{1}{2}$; $2(e)$: $\pm(x\frac{1}{4}z)$
$4(f)$: $\pm(xyz)$; $\pm(x,\frac{1}{2}\text{-}y,z)$

Table 1. Powder photograph of $Mo(OH)_3PO_4$. CuK_{α_1}-radiation. $\lambda_{CuK_{\alpha_1}} = 1.54050$ Å.

$h\ k\ l$	$10^4\sin^2\Theta$ calc	$10^4\sin^2\Theta$ obs	pF^2 calc	I obs	$h\ k\ l$	$10^4\sin^2\Theta$ calc	$10^4\sin^2\Theta$ obs	pF^2 calc	I obs
0 0 1	136	136	6	w	1 1 2	1036	1033	25	w
1 0 0	149	149	4	w	2 1 1	1074	—	1	—
1 0 $\bar{1}$	187	187	62	vst	1 0 $\bar{3}$	1079	—	0	—
0 1 1	284	289	36	m	1 2 $\bar{2}$	1087	—	0	—
1 1 0	296	296	21	w	2 2 $\bar{1}$	1125	1122	15	vw
1 1 $\bar{1}$	334	334	36	m	0 2 2	1134	1134	5	vvw
1 0 1	383	382	40	st	3 0 $\bar{1}$	1180	1182	14	vw
1 0 $\bar{2}$	497	497	10	vw	2 2 0	1184		18	
1 1 1	530	530	19	w	0 0 3	1225	1222	43	m
2 0 $\bar{1}$	535	533	28	w	1 1 $\bar{3}$	1227		26	
0 0 2	544	543	16	w	2 0 $\bar{3}$	1231	—	12	—
0 2 0	590	592	85	vvst	3 0 $\bar{2}$	1294	1289	64	w
2 0 0	594		31		3 1 $\bar{1}$	1327	1323	36	vw
1 1 $\bar{2}$	644	—	0	—	2 2 $\bar{2}$	1337	1332	1	vvw
2 1 $\bar{1}$	682	681	12	vvw	3 0 0			11	
0 1 2	692	690	62	st	0 1 3	1372	1368	9	vvw
0 2 1	726	—	1	—	2 1 $\bar{3}$	1379	—	8	—
1 2 0	739	739	2	vvw	3 1 $\bar{2}$	1441	—	1	—
2 1 0	742	—	0	—	0 3 1	1464	1464	30	w
2 0 $\bar{2}$	747	744	3	vvw	1 3 0	1476	1476	25	w
1 2 $\bar{1}$	777	778	29	m	1 2 2	1479	—	1	—
1 0 2	889	891	4	vvw	3 1 0	1485	—	15	—
2 1 $\bar{2}$	894		10		1 3 $\bar{1}$	1514	1515	26	w
2 0 1	927	—	1	—	2 2 1	1516		1	
1 2 1	973	972	14	vw	2 0 2	1531	1528	14	vvw

The powder photograph was measured and interpreted to $\sin^2\Theta = 0.41$.
Reflections systematically absent in space group $P2_1/m$ have been omitted.
KCl ($a = 6.2930$ Å) has been used as an internal standard substance.

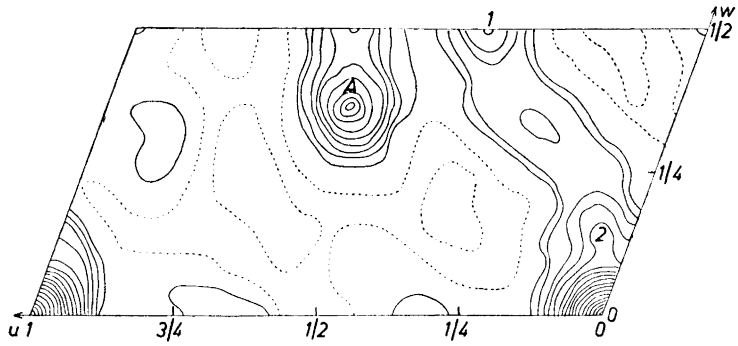

Fig. 1. The Patterson function $P(upw)$ for $Mo(OH)_3PO_4$. Dashed lines indicate negative values.

POSITIONS OF THE MOLYBDENUM AND PHOSPHORUS ATOMS

In order to find the positions of the two molybdenum atoms the Patterson projections, $P(upw)$ and $P(pvw)$, were calculated (Figs. 1 and 2). Those atoms must occupy one of the twofold positions, *i.e.* 2(*a*)—(*e*). Now, in the Patterson projections on the *uw* and *vw* plane there are high peaks (besides the origin maxima) at $u = 0.57_0$, $w = 0.36_2$ in $P(upw)$ (A in Fig. 1), and at $v = \frac{1}{2}$, $w = 0.35_2$ in $P(pvw)$ (B in Fig. 2). (All maxima have been located by the interpolation table given by Booth [9].) Thus, in the half-cell there is a high peak at $u = 0.57$, $v = \frac{1}{2}$, $w = 0.36$ and this maximum certainly corresponds to the Mo—Mo vector. The molybdenum atoms thus must occupy the point position 2(*e*), as the other twofold point positions would require the Mo—Mo vector to have the specialized coordinates $u = \frac{1}{2}$, $v = 0$, $w = \frac{1}{2}$. From the coordinates given above we get

2 Mo in $P2_1/m$ 2(*e*) with $x \approx 0.285$, $y = 1/4$, $z \approx 0.180$

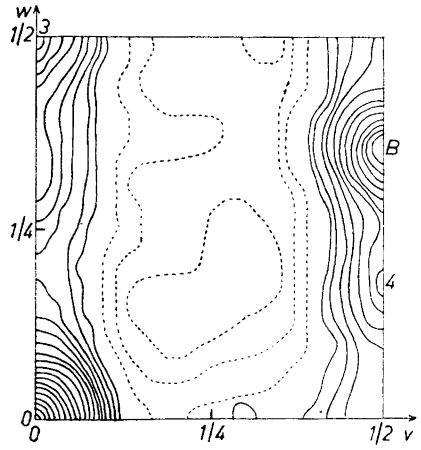

Fig. 2. The Patterson function $P(pvw)$ for $Mo(OH)_3PO_4$. Dashed lines indicate negative values.

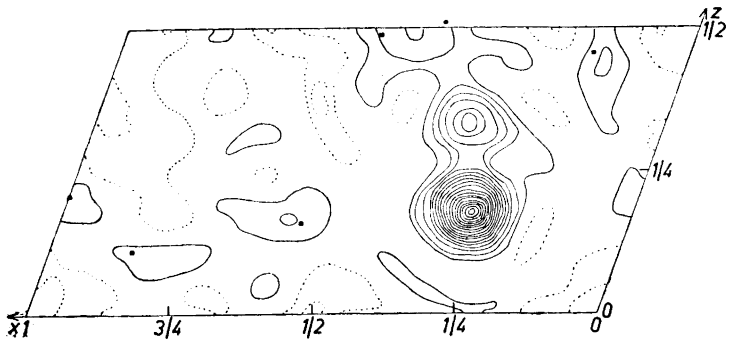

Fig. 3. Electron density of $Mo(OH)_3PO_4$ projected on the *xz* plane. The positions of the oxygen atoms O_2-O_6 (■) have been marked. Dashed lines indicate negative values.

In addition to the peak corresponding to the Mo—Mo vector the Patterson projections also show maxima, the heights of which suggest that they can be ascribed to the Mo—P distances. Thus, the peaks 1 ($u = 0.38$, $w = 0.50$) and 2 ($u = 0.06$, $w = 0.15$) in $P(upw)$ (Fig. 1) and 3 ($v = 0$, $w = 0.50$) and 4 ($v = \frac{1}{2}$, $w = 0.16$) in $P(pvw)$ (Fig. 2) define two maxima in the Patterson function, *viz.* at $u = 0.38$, $v = 0$, $w = 0.50$ and at $u = 0.06$, $v = \frac{1}{2}$, $w = 0.15$. These Mo—P vectors are only in accordance with the two phosphorus atoms occupying the point position 2(*e*) with the approximate coordinates

$$x_P = x_{Mo} + 0.38 = 0.67$$
$$y_P = 1/4$$
$$z_P = z_{Mo} + 0.50 = 0.68$$

POSITIONS OF THE OXYGEN ATOMS

Electron density projections. In order to obtain more accurate values of the molybdenum and phosphorus coordinates the electron density projec-

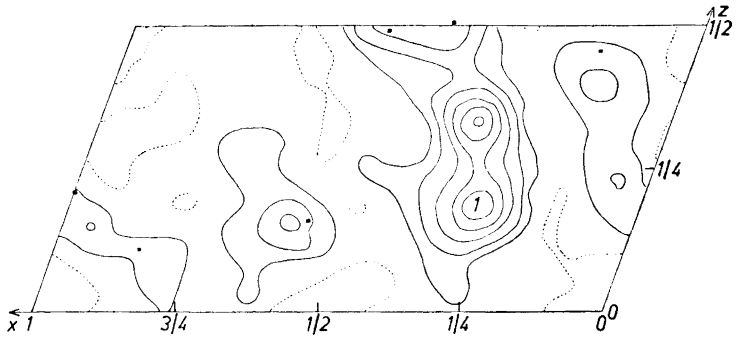

Fig. 4. Electron density of $Mo(OH)_3PO_4$ projected on the *xz* plane and with the molybdenum atom substracted. The positions of the oxygen atoms have been indicated as in Fig. 3. Dashed lines indicate negative values.

tion on the *xz* and *yz* planes were calculated. The signs of all structure factors $F(h0l)$ and $F(0kl)$ were determined from the contributions given by the molybdenum atoms. The results are given in Figs. 3 and 5.

From Fig. 3 we see that the molybdenum and the phosphorus atoms are clearly indicated at $x = 0.282$, $z = 0.176$ and at $x = 0.34$, $z = 0.34$. However, the "phosphorus" peak might be a little displaced from the correct phosphorus position by diffraction effects caused by the heavy molybdenum atom. In order to get, probably more reliable, coordinates for the phosphorus atoms the molybdenum atom was subtracted from the Fourier image in Fig. 3. — The contributions of the Mo atoms to the structure factors were multiplied by a "temperature" factor of $10^{-0.315 \sin^2\Theta}$, obtained in the ordinary way for the determination of temperature factors.

From Fig. 4, which shows this new electron density projection, we see the phosphorus atom at $x = 0.32_7$, $z = 0.33_8$. However, there is yet another maximum (1 in Fig. 4, with $x = 0.28_7$, $z = 0.18_8$) with nearly the same positions as the molybdenum atom. The height of the peak is about the same as the maximum corresponding to the phosphorus position and if it is a real one the only atoms which could give a maximum of this height are two overlapping oxygen atoms, which will occur if four oxygen atoms occupy the point position 4(*f*). Now, from Fig. 5 showing the electron density projected on the *yz* plane, we see that there are two peaks (1') outside (*i.e.* $y = 0.54$ and 0.96) the mirror planes ($y = \pm 1/4$) and with the *z* parameter ($z = 0.18_9$) in close agreement with the *z* parameter found above for peak 1 in Fig. 4. It seems therefore very probable that peak 1 is a real maximum and that four oxygen atoms are situated in the point position 4(*f*). (The accuracy of the *x*-coordinate of these oxygen atoms might be reduced owing to inadequate subtraction of the overlapping Mo atom [10].)

The molybdenum and phosphorus atoms stand out very clearly in $\varrho(pyz)$ (Fig. 5), the molybdenum at $y = 1/4$, $z = 0.177$ and the phosphorus at $y = 3/4$,

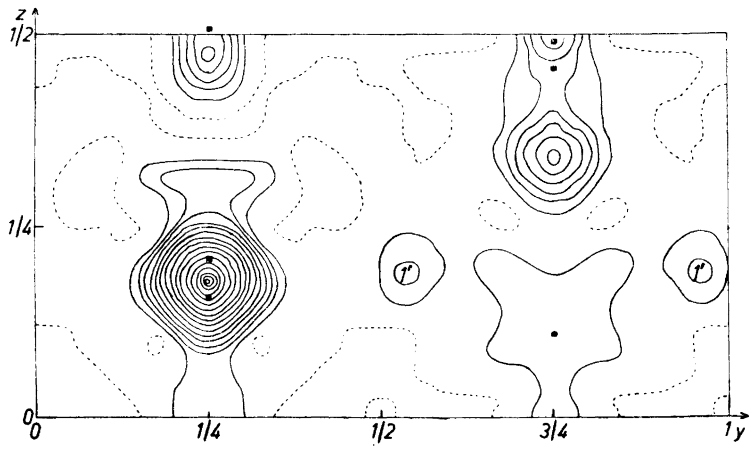

Fig. 5. Electron density of $Mo(OH)_3PO_4$ projected on the *yz* plane. The positions of the oxygen atoms have been indicated as in Fig. 3. Dashed lines indicate negative values.

$z = 0.34_0$, the z parameters being in good agreement with those obtained from $\varrho(xpz)$. The values obtained from $\varrho(xpz)$ should, however, be more correct, since in the calculation of this projection more F-values were used. Thus from the electron density projections the following parameters could be obtained:

2 Mo	in	$P2_1/m$	2(*e*)	with:	$x = 0.282$,	$y = 1/4$,	$z = 0.176$
2 P	in	»	»	»	$x = 0.67_3$,	$y = 1/4$,	$z = 0.66_2$
4 O_1	in	»	4(*f*)	»	$x = 0.71_3$,	$y = 0.46_0$	$z = 0.81_1$

The remaining maxima in the electron density projections were, at this state of the investigation, not considered as they are rather diffuse and of about the same height as the false maxima [11]. However, as will be seen (see p. 1708) they were found to correspond to oxygen positions.

Geometrical considerations. The four oxygen atoms (O_1), the positions of which have been found from the electron density projections, are situated close to phosphorus atoms with the distances P—2 $O_1 = 1.6_5$ Å. These distances are in good agreement with P—O distances found in previously described structures [12–14] (*viz.* P—O = 1.4_5—1.6_5 Å). Assuming that the coordination figure around the phosphorus atoms is a fairly regular tetrahedron, which seems to be very probable, it is then possible to calculate the parameters of the remaining oxygen atoms (O_2 and O_3) in the PO_4 tetrahedron. If we assume the bond lengths P—O_2 = P—O_3 = 1.5_5 Å and O_2—O_3 = 2.5_3 Å (these distances are mean values of those published [12–14]) the coordinates of the oxygen atoms O_2 and O_3 follow immediately. Thus we obtain

2 O_2	in	$P2_1/m$	2(*e*)	with:	$x = 0.44_3$,	$y = 1/4$,	$z = 0.50_9$
2 O_3	in	»	»	»	$x = 0.83_0$,	$y = 1/4$,	$z = 0.54_4$

Now we have to find the positions of the remaining six oxygen atoms in the unit cell. They must occupy three of the twofold or one of the twofold and one of the fourfold positions, if the arrangement of these atoms also has the symmetry $P2_1/m$. Assuming that the distances between these oxygen atoms and the oxygens already located (*i.e.* O_1—O_3) are not less than 2.6_0 Å, the twofold positions 2(*a*)—2(*d*) can at once be eliminated and thus the remaining oxygen atoms are situated in 4 × 2(*e*) or 2(*e*) + 4(*f*). Of these point positions, 4(*f*) seems to be improbable since nothing indicates this in the electron density projections. (Figs. 3—5.) Moreover, with the oxygen parameters found above, we have three oxygen atoms (2 O_1 and O_2) in contact with one molybdenum atom (*viz.* Mo—2 $O_1 = 1.8_3$ Å and Mo—$O_2 = 2.2_2$ Å, in good agreement with Mo—O distances found in previously determined structures of oxygen compounds of molybdenum [15–18] and these four atoms are situated in the same plane. Now, if we have four oxygens in 4(*f*) these oxygens cannot be in contact with the molybdenum atoms since all O—O distances ought to be $\geq 2.6_0$ Å and thus we would obtain a very improbable coordination, quite different from previously known arrangements [16–18]. For these reasons we conclude that the remaining six oxygen atoms must occupy the point positions 2(*e*).

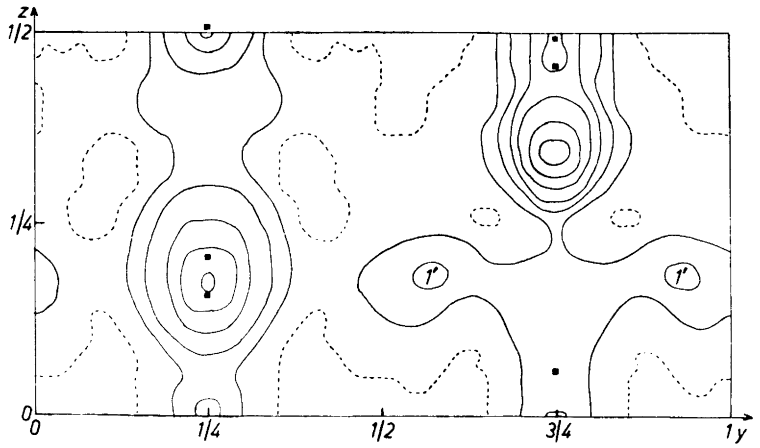

Fig. 6. Electron density of $Mo(OH)_3PO_4$ projected on the *yz* plane and with the molybdenum atom substracted. The positions of the oxygen atoms have been indicated as in Fig. 3. Dashed lines indicate negative values.

Now, with the assumption made above for the O—O distances and assuming the distance Mo—O to be not less than that found [15] in MoO_3, *i.e.* 1.8_0 Å, reasonable interatomic distances were only obtained assuming

2 O_4	in	$P2_1/m$	2(*e*)	with	$x = 0.15_0$,	$y = 1/4$,	$z = 0.89_0$
2 O_5	»	»	»	»	$x = 0.57_3$,	$y = 1/4$,	$z = 0.15_8$
2 O_6	»	»	»	»	$x = 0.99_6$,	$y = 1/4$,	$z = 0.20_8$

When the coordinates of all oxygen atoms have been determined the positions of these atoms were checked against the electron density projections (Figs. 3—5). The positions of the oxygen atoms O_2—O_6 have been denoted in these figures and, as we see, they are situated in positive areas and in most cases nearly coinciding with small peaks. However, these maxima are spread over a rather wide area, probably because of inadequate intensity material owing to the smallness of the crystal, so it is not possible to obtain any coordinates from the positions of these peaks. From Fig. 5 we see that the oxygen atoms O_5 and O_6 coincide with the molybdenum atom in this projection. In order to check if these oxygen atoms can be distinguished, the molybdenum atom was also subtracted from this Fourier image (in the same way as with Fig. 3, see p. 1706). The result is given in Fig. 6 and we see the phosphorus and oxygen (1') peaks with the same positions as in Fig. 5. The remaining maxima in Fig. 6 are well explained since they correspond to oxygen positions.

ARRANGEMENT OF THE HYDROGEN ATOMS

In the unit cell there are also six hydrogen atoms, which should be situated close to some of the oxygen atoms. Now, the oxygen atoms are not all equivalent in the sense that they have not the same environment. Thus the oxygen

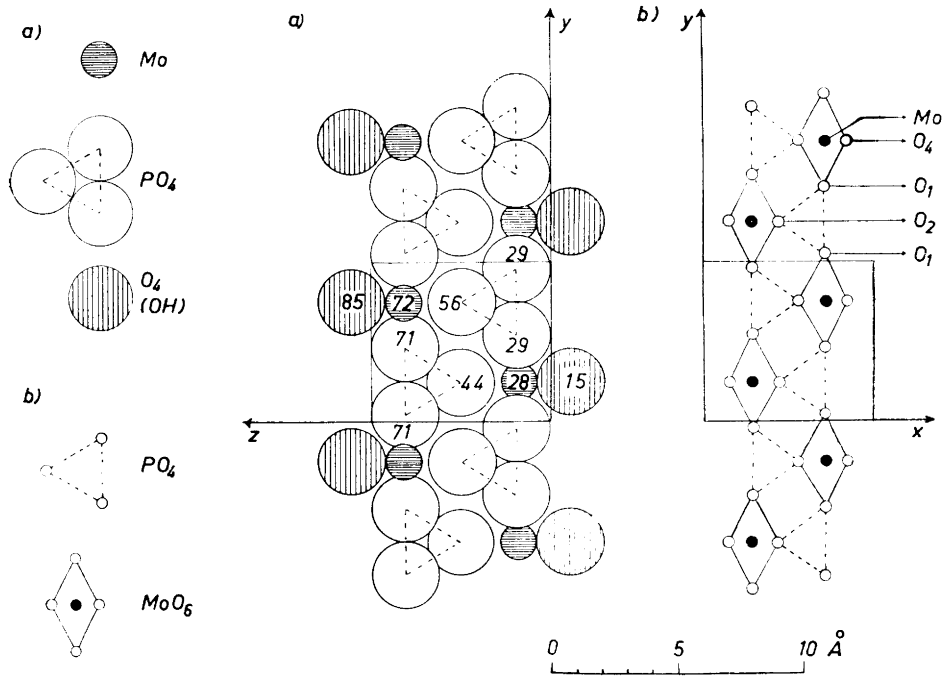

Fig. 7. The contacts between MoO_6-octahedra and PO_4-tetrahedra showing the double chains in $Mo(OH)_3PO_4$. The oxygen atoms O_5 and O_6 in the MoO_6-octahedra are situated over or below the molybdenum atoms and have not been indicated. a) Projection of the *yz* plane. The figures denote the height of the atoms in percentages of *a*. b) Projection of the *xy* plane.

atoms O_1 and O_2 are in contact with phosphorus and also with molybdenum atoms, while the oxygen atom O_3 is in contact only with one phosphorus atom and the oxygen atoms O_4—O_6 only with one molybdenum atom (*cf.* Fig. 7). It seems therefore much more probable that the hydrogen atoms are situated close to six of the oxygen atoms O_3—O_6. Now, as the proton affinity of O^{2-} is greater than that of PO_4^{3-}, it seems much more likely that the hydrogen atoms are situated close to all or some of the oxygen atoms O_4—O_6 than to the phosphate oxygen atom O_3 and some of the oxygen O_4—O_6. Thus, the six oxygen atoms O_4—O_6 exist either as six OH^- or as three O^{2-} and three H_2O, of which the first alternative seems to be the most plausible. As the interatomic distances between the oxygen atoms O_4—O_6 and neighbouring oxygen atoms are about 2.7_5 Å, the hydroxyl ions almost certainly form hydroxyl bonds (Ref.[13], p. 413) with neighbouring oxygen atoms. However, in this investigation it has not been possible to determine the parameters of the hydrogen atoms.

With the arrangement proposed for the hydrogen atoms there are no water molecules present in the crystals — which may also be supported by

the fact that the crystals do not lose water until it is heated to above 225°C [1] — but they contain three hydroxyl groups for one molybdenum atom. Their formula should then be written $Mo(OH)_3PO_4$ rather than $2\ MoO_3 \cdot P_2O_5 \cdot 3\ H_2O$ or $MoO_2HPO_4H_2O$.

FINAL STRUCTURE PROPOSITION

The following structure is thus proposed for $Mo(OH)_3PO_4$. Space group: No. 11, $P2_1/m$. Two formula units per unit cell.

		x	y	z
2 Mo	in 2(*e*)	0.282 ± 0.003	1/4	0.176 ± 0.003
2 P	in 2(*e*)	0.673 ± 0.006	1/4	0.662 ± 0.006
4 O_1	in 4(*f*)	0.71	0.46	0.81
2 O_2	in 2(*e*)	0.44	1/4	0.51
2 O_3	in 2(*e*)	0.83	1/4	0.54
2 O_4	in 2(*e*)	0.15	1/4	0.89
2 O_5	in 2(*e*)	0.57	1/4	0.16
2 O_6	in 2(*e*)	0.00	1/4	0.21

2(*e*): $\pm(x,\ 1/4,\ z)$
4(*f*): $\pm(x,y,z);\ \pm(x,\frac{1}{2}-y,z)$

The accuracy of the oxygen parameters is estimated to be about ±0.01. The structure factors were calculated with these parameters, multiplied by the exponential factor $10^{-0.315\ \sin^2\Theta}$ (*cf.* above) and compared with the observed structure factors from the corresponding Weissenberg photographs (Table 2). Taking into account that, particularly in 0*kl* and 1*kl* dependent on the shape of the crystals, there is an absorption effect [11] in the reflections, the agreement between observed and calculated intensities is quite good. The reliability index, *R*, valculated according to Booth (*cf.* Ref.[9], p. 101), was found to be 0.17 for *h*0*l* and 0.19 for 0*kl* (absent reflections not included).

DESCRIPTION OF STRUCTURE

In the structure, the molybdenum atoms are surrounded by six oxygen atoms in an octahedral arrangement. These MoO_6 octahedra are linked together by phosphate tetrahedra so that every molybdenum atom is in contact with three PO_4 tetrahedra and every PO_4 tetrahedron with three molybdenum atoms so that the cyrstals are built up of double chains extending to [010] and containing alternately MoO_6 and PO_4 groups (*cf.* Fig. 7). These double chains with the composition $(Mo_2O_6(PO_4)_2^{6-})_n$ are then held together by the hydrogen atoms, situated between adjacent oxygen atoms (O_3—O_6) from different chains.

The *xz* projection of the structure is shown in Fig. 8.

The distances between adjacent atoms in the structure will be (*in* Å)

Table 2. Comparison between calculated and observed structure factors from Weissenberg photographs of $Mo(OH)_3PO_4$. Cu*K*-radiation.

h k l	*F* calc	|*F*| obs	*h k l*	*F* calc	|*F*| obs	*h k l*	*F* calc	|*F*| obs	*h k l*	*F* calc	|*F*| obs
1 0 8	−3	—	2 0 4	18	25	0 0 $\bar{1}$	33	27	4 1 5	−7	—
0 0 8	−31	32	1 0 4	57	58	1 0 $\bar{1}$	111	114	3 1 5	22	24
1 0 $\bar{8}$	11	15	0 0 $\bar{4}$	−19	24	2 0 $\bar{1}$	−75	91	2 1 5	−4	—
2 0 $\bar{8}$	34	35	1 0 $\bar{4}$	−49	53	3 0 $\bar{1}$	−53	25	1 1 5	−31	23
3 0 $\bar{8}$	−36	38	2 0 $\bar{4}$	25	28	4 0 $\bar{1}$	80	82	0 1 5	26	24
4 0 $\bar{8}$	−15	—	3 0 $\bar{4}$	38	35	5 0 $\bar{1}$	−2	—	1 1 $\bar{5}$	−24	25
5 0 $\bar{8}$	38	29	4 0 $\bar{4}$	−26	22	6 0 $\bar{1}$	−52	38	2 1 $\bar{5}$	35	37
6 0 $\bar{8}$	−9	—	5 0 $\bar{4}$	−5	—	7 0 $\bar{1}$	23	26	3 1 $\bar{5}$	37	29
			6 0 $\bar{4}$	37	31	8 0 $\bar{1}$	29	—	4 1 $\bar{5}$	−50	45
2 0 7	11	—	7 0 $\bar{4}$	3	—				5 1 $\bar{5}$	1	—
1 0 7	−46	36	8 0 $\bar{4}$	−36	30	8 0 0	−11	—	6 1 $\bar{5}$	37	29
0 0 7	−11	—				7 0 0	47	23	7 1 $\bar{5}$	−24	22
1 0 $\bar{7}$	51	45	6 0 3	10	21	6 0 0	1	—	8 1 $\bar{5}$	−14	14
2 0 $\bar{7}$	−15	22	5 0 3	23	34	5 0 0	−40	43			
3 0 $\bar{7}$	−46	33	4 0 3	−32	27	4 0 0	36	29	5 1 4	−24	25
4 0 $\bar{7}$	35	36	3 0 3	−17	27	3 0 0	46	47	4 1 4	23	29
5 0 $\bar{7}$	8	—	2 0 3	33	29	2 0 0	−79	104	3 1 4	19	19
6 0 $\bar{7}$	−45	33	1 0 3	28	37	1 0 0	−29	35	2 1 4	−20	37
7 0 $\bar{7}$	3	—	0 0 3	−92	92				1 1 4	−3	—
			1 0 $\bar{3}$	−7	—	1 1 8	26	17	0 1 $\bar{4}$	65	68
4 0 6	8	—	2 0 $\bar{3}$	50	46	0 1 8	−30	26	1 1 $\bar{4}$	21	23
3 0 6	37	37	3 0 $\bar{3}$	−7	—	1 1 $\bar{8}$	8	—	2 1 $\bar{4}$	58	44
2 0 6	−23	23	4 0 $\bar{3}$	−53	54	2 1 $\bar{8}$	−29	28	3 1 $\bar{4}$	−61	51
1 0 6	−40	41	5 0 $\bar{3}$	19	13	3 1 $\bar{8}$	−13	18	4 1 $\bar{4}$	−21	13
0 0 6	59	51	6 0 $\bar{3}$	40	25	4 1 $\bar{8}$	20	20	5 1 $\bar{4}$	34	28
1 0 $\bar{6}$	−4	—	7 0 $\bar{3}$	−49	36	5 1 $\bar{8}$	−5	—	6 1 $\bar{4}$	−2	—
2 0 $\bar{6}$	−55	40	8 0 $\bar{3}$	−9	—	6 1 $\bar{8}$	−15	13	7 1 $\bar{4}$	−39	29
3 0 $\bar{6}$	24	28							8 1 $\bar{4}$	17	—
4 0 $\bar{6}$	42	36	7 0 2	−6	—	2 1 7	23	29			
5 0 $\bar{6}$	−26	28	6 0 2	29	31	1 1 7	−4	—	6 1 3	−25	26
6 0 $\bar{6}$	−29	23	5 0 2	−3	—	0 1 7	−25	26	5 1 3	10	—
7 0 $\bar{6}$	29	20	4 0 2	−53	49	1 1 $\bar{7}$	−9	—	4 1 3	42	39
8 0 $\bar{6}$	−1	—	3 0 2	0	—	2 1 $\bar{7}$	−18	23	3 1 3	−34	38
			2 0 2	52	61	3 1 $\bar{7}$	23	26	2 1 3	−39	34
5 0 5	−12	—	1 0 2	−29	20	4 1 $\bar{7}$	7	—	1 1 3	67	68
4 0 5	55	37	0 0 2	−56	76	5 1 $\bar{7}$	−15	22	0 1 3	30	28
3 0 5	0	—	1 0 $\bar{2}$	44	43	6 1 $\bar{7}$	−17	14	1 1 $\bar{3}$	51	55
2 0 5	−46	38	2 0 $\bar{2}$	23	37	7 1 $\bar{7}$	26	28	2 1 $\bar{3}$	−29	17
1 0 5	35	34	3 0 $\bar{2}$	−113	131				3 1 $\bar{3}$	−41	32
0 0 5	30	36	4 0 $\bar{2}$	2	25	3 1 6	20	20	4 1 $\bar{3}$	45	35
1 0 $\bar{5}$	−42	34	5 0 $\bar{2}$	67	66	2 1 6	13	17	5 1 $\bar{3}$	14	20
2 0 $\bar{5}$	−6	—	6 0 $\bar{2}$	−25	25	1 1 6	−23	19	6 1 $\bar{3}$	−48	32
3 0 $\bar{5}$	66	56	7 0 $\bar{2}$	−40	33	0 1 6	−20	24	7 1 $\bar{3}$	−6	—
4 0 $\bar{5}$	−5	—	8 0 $\bar{2}$	25	21	1 1 $\bar{6}$	−13	—	8 1 $\bar{3}$	18	16
5 0 $\bar{5}$	−33	24				2 1 $\bar{6}$	−1	—			
6 0 $\bar{5}$	13	—	7 0 1	16	19	3 1 $\bar{6}$	31	36	7 1 2	−26	14
7 0 $\bar{5}$	24	27	6 0 1	24	29	4 1 $\bar{6}$	−6	—	6 1 2	−8	—
8 0 $\bar{5}$	−8	—	5 0 1	−28	27	5 1 $\bar{6}$	−32	37	5 1 2	33	46
			4 0 1	−37	35	6 1 $\bar{6}$	28	27	4 1 2	−8	—
5 0 4	30	26	3 0 1	75	72	7 1 $\bar{6}$	26	22	3 1 2	−69	69
4 0 4	20	15	2 0 1	13	—				2 1 2	41	58
3 0 4	−53	52	1 0 1	−89	97	5 1 5	−13	—	1 1 2	50	37

Table 2.
(cont.)

h k l	*F* calc	|*F*| obs	*h k l*	*F* calc	|*F*| obs	*h k l*	*F* calc	|*F*| obs	*h k l*	*F* calc	|*F*| obs
0 1 2	−79	85	0 5 1	−22	27	1 3 7	1	—	1 3 3	−66	61
1 1 $\bar{2}$	0	—	0 6 1	−9	—	1 2 7	35	35	1 2 $\bar{3}$	−10	—
2 1 $\bar{2}$	−32	29	0 7 1	29	16	1 2 $\bar{7}$	−36	31	1 2 $\bar{3}$	1	—
3 1 $\bar{2}$	7	—	0 8 1	6	—	1 3 $\bar{7}$	7	—	1 3 $\bar{3}$	−58	54
4 1 $\bar{2}$	44	34				1 4 $\bar{7}$	39	28	1 4 $\bar{3}$	−4	—
5 1 $\bar{2}$	−20	22	0 2 2	22	27				1 5 $\bar{3}$	32	38
6 1 $\bar{2}$	−16	21	0 3 2	71	75	1 5 6	−15	15	1 6 $\bar{3}$	2	—
7 1 $\bar{2}$	18	21	0 4 2	−33	28	1 4 6	−29	31	1 7 $\bar{3}$	−37	36
8 1 $\bar{2}$	9	22	0 5 2	−42	35	1 3 6	24	29			
			0 6 2	22	16	1 2 6	26	36	1 7 2	−29	20
7 1 1	−34	27	0 7 2	40	30	1 2 $\bar{6}$	12	—	1 6 2	9	—
6 1 1	33	37				1 3 $\bar{6}$	18	23	1 5 2	25	22
5 1 1	24	21	0 2 3	51	50	1 4 $\bar{6}$	−4	—	1 4 2	−15	18
4 1 1	−59	52	0 3 3	−27	31	1 5 $\bar{6}$	−8	—	1 3 2	−50	49
3 1 1	7	—	0 4 3	−53	40				1 2 2	7	—
2 1 1	12	20	0 5 3	14	—	1 6 5	−22	25	1 2 $\bar{2}$	−7	—
1 1 1	−44	52	0 6 3	35	28	1 5 5	−19	—	1 3 $\bar{2}$	−9	—
0 1 1	−60	60	0 7 3	−14	—	1 4 5	28	32	1 4 $\bar{2}$	25	18
1 1 $\bar{1}$	−60	62				1 3 5	35	33	1 5 $\bar{2}$	−2	—
2 1 $\bar{1}$	−33	35	0 2 4	18	13	1 2 5	31	44	1 6 $\bar{2}$	−16	17
3 1 $\bar{1}$	60	61	0 3 4	−66	49	1 2 $\bar{5}$	29	31	1 7 $\bar{2}$	−6	—
4 1 $\bar{1}$	19	21	0 4 4	−15	—	1 3 $\bar{5}$	30	38			
			0 5 4	40	37	1 4 $\bar{5}$	−32	31	1 7 1	20	21
5 1 $\bar{1}$	−5	—	0 6 4	12	—	1 5 $\bar{5}$	−15	—	1 6 1	34	43
6 1 $\bar{1}$	−11	—	0 7 4	−40	23	1 6 $\bar{5}$	24	26	1 5 1	−24	33
7 1 $\bar{1}$	28	29							1 4 1	−50	47
8 1 $\bar{1}$	−7	—	0 2 5	−11	—	1 7 4	3	—	1 3 1	36	40
			0 3 5	−26	—	1 6 4	−28	25	1 2 1	37	47
7 1 0	15	—	0 4 5	21	13	1 5 4	−1	—	1 2 $\bar{1}$	−54	69
6 1 0	35	30	0 5 5	17	—	1 4 4	40	35	1 3 $\bar{1}$	51	62
5 1 0	−30	50	0 6 5	14	—	1 3 4	5	—	1 4 $\bar{1}$	59	49
4 1 0	−19	19				1 2 4	−33	37	1 5 $\bar{1}$	−27	26
3 1 0	39	45	0 2 6	−45	45	1 2 $\bar{4}$	21	32	1 6 $\bar{1}$	−40	44
2 1 0	6	—	0 3 6	22	—	1 3 $\bar{4}$	−21	22	1 7 $\bar{1}$	27	19
1 1 0	−46	46	0 4 6	46	39	1 4 $\bar{4}$	−31	22			
0 2 0	−130	187	0 5 6	−11	—	1 5 $\bar{4}$	14	—	1 8 0	−8	—
0 4 0	103	120				1 6 $\bar{4}$	20	24	1 7 0	27	34
0 6 0	−68	53	0 2 7	6	—	1 7 $\bar{4}$	−13	—	1 6 0	12	—
0 8 0	45	23	0 3 7	28	30				1 5 0	−19	21
			0 4 7	−8	—	1 7 3	−40	27	1 4 0	−17	26
0 2 1	−8	13				1 6 3	−9	—	1 3 0	50	54
0 3 1	55	66	0 2 8	20	16	1 5 3	41	41	1 2 0	15	16
0 4 1	14	—	1 2 $\bar{8}$	−8	—	1 4 3	16	—			

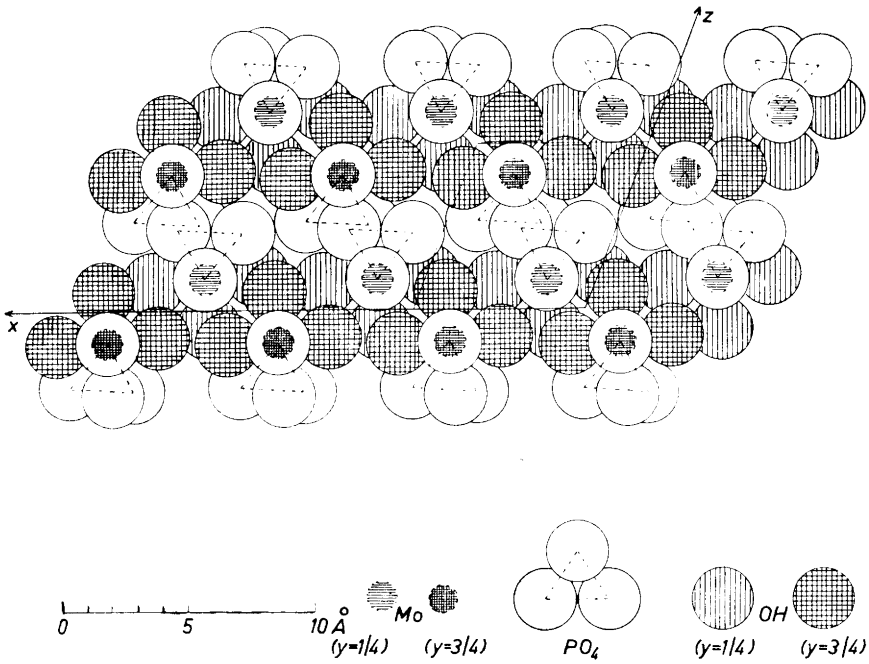

Fig. 8. Projection on the *xz* plane of the structure of $Mo(OH)_3PO_4$.

Mo—2 O_1;	O_1—Mo	$= 1.8_3$	O_1—O_5;	O_5—2 O_1	$= 2.7_2$
Mo—O_2 ;	O_2—Mo	$= 2.2_2$	O_1—2 O_6;	O_6—4 O_1	$= 2.7_2$; 3.1_0
Mo—O_4 ;	O_4—Mo	$= 1.9_0$	O_2—2 O_2		$= 3.2_6$
Mo—O_5 ;	O_5—Mo	$= 2.0_0$	O_2—O_3;	O_3—O_2	$= 2.5_3$
Mo—O_6 ;	O_6—Mo	$= 2.0_1$	O_2—O_5;	O_5—O_2	$= 2.8_9$
P —2 O_1;	O_1—P	$= 1.6_5$	O_2—O_6;	O_6—O_2	$= 3.0_2$
P —O_2 ;	O_2—P	$= 1.5_5$	O_3—O_4;	O_4—O_3	$= 2.6_4$
P —O_3 ;	O_3—P	$= 1.5_5$	O_3—O_5;	O_5—O_3	$= 2.6_7$
O_1—O_1		$= 2.6_5$	O_3—O_6;	O_6—O_3	$= 3.0_8$
O_1—2 O_2;	O_2—4 O_1	$= 2.7_0$; 2.8_1	O_4—O_5;	O_5—O_4	$= 2.8_2$
O_1—O_3 ;	O_3—2 O_1	$= 2.6_3$	O_4—2 O_6;	O_6— $2O_4$	$= 2.7_7$; 3.4_5
O_1—2 O_4;	O_4—4 O_1	$= 2.7_0$; 3.1_0	O_5—O_6;	O_6—O_5	$= 2.7_4$

The O—O distances are all within the normal range, showing that the lattice is also supported by O—O contacts. However, the distances may be in error by a few tenths of an Ångström unit, because the oxygen positions could not be determined very accurately.

This investigation forms part of a research program on metal oxides and related compounds supported by the *Swedish Natural Science Research Council.*

The author wishes to thank Professor Arne Ölander for his kind interest and Dr. Arne Magnéli for his encouraging interest and for many valuable discussions. The author is also indebted to Fil.lic. Georg Lundgren for his helpful interest and to Mr. Rolf Norin for valuable help with the preparation work and for drawing some of the figures. Thanks are also due to the Swedish Board for Computing Machinery for making the Calculator BESK available for considerable part of the calculating work involved in this investigation.

REFERENCES

1. Schulz, I. *Z. anorg. u. allgem. Chem.* **281** (1955) 99.
2. Kolthoff, I. M. and Sandell, E. B. *Textbook of Quantitative Inorganic Analysis*, 3rd Ed., New York, 1952, p. 382.
3. Balanescu, G. *Ann. chim. appl.* 2 **12** (1930) 259.
4. Niericker, R. and Treadwell, W. D. *Helv. Chim. Acta* **29** (1946) 1472.
5. Hartwig-Bendig, M. *Z. angew. Mineral.* **3** (1941) 195.
6. Brush, G. J. *Am. J. Sci.* **460** (1868) 240.
7. Penfield, S. L. *Am. J. Sci.* 3 **48** (1894) 30.
8. Lu, C. S. *Rev. Sci. Instr.* **14** (1943) 331.
9. Booth, A. D. *Fourier Technique in X-ray Organic Structure Analysis*, Cambridge 1948, p. 64.
10. Burns, D. M. *Acta Cryst.* **11** (1958) 88.
11. Wells, A. F. *Z. Krist.* **96** (1937) 451.
12. Pauling, L. *The Nature of the Chemical Bond*, 2nd Ed., New York 1940, p. 240.
13. Wells, A. F. *Structural Inorganic Chemistry*, 2nd Ed., Oxford 1950, p. 487.
14. Mac Arthur, D. M. and Beevers, C. A. *Acta Cryst.* **10** (1957) 428.
15. Andersson, G. and Magnéli, A. *Acta Chem. Scand.* **4** (1950) 793.
16. Magnéli, A. *Nova Acta Regiae Soc. Sci. Upsaliensis* **4 14** (1950) No. 8.
17. Hägg, G. and Magnéli, A. *Rev. Pure Appl. Chem. (Australia)* **4** (1954) 235.
18. Magnéli, A. *J. Inorg. & Nuclear Chem.* **2** (1956) 330.

Received June 7, 1958.

ACTA CHEMICA SCANDINAVICA 12 (1958) 1715—1729

The Crystal Structure of WOP_2O_7

PEDER KIERKEGAARD

Institute of Inorganic and Physical Chemistry, University of Stockholm, Stockholm, Sweden

WOP_2O_7 has a monoclinic unit cell containing four formula units and with the dimensions

$$a = (15.170 \pm 0.005)\ \text{Å}$$
$$b = (5.162 \pm 0.005)\ \text{Å}$$
$$c = (6.917 \pm 0.005)\ \text{Å}$$
$$\beta = (102.41 \pm 0.05)^\circ$$
$$V = 547.9\ \text{Å}^3$$

A structure is proposed with the symmetry No. 12, $C2/m$. The positions of the wolfram and phosphorus atoms in the unit cell were determined by Fourier methods. The parameters of the oxygen atoms were derived partly from electron density projections and partly from geometrical considerations, interatomic P—O and O—O distances from previously determined structures being used. The crystals are built up of layers parallel to the yz plane and formed of fairly regular WO_6 octahedra coupled together by P_2O_7 groups. The layers are held together by van der Waals' forces and the crystals show pronounced basal cleavage resulting from this layer structure.

In the system WO_3—P_2O_5 the existence of two crystalline compounds with the compositions $2WO_3 \cdot P_2O_5$ and $WO_3 \cdot P_2O_5$ was reported by Schulz [1]. The crystals were insoluble in water, acids and dilute ammonia and difficultly soluble in hot dilute sodium hydroxide. In solutions of $WO_3 \cdot P_2O_5$ only ortho- and diphosphate ion could be proved. Polyphosphate ions were not found. In connection with an X-ray investigation of oxides undertaken at this institute a crystal structure determination of these compounds was started and this paper gives the structure of $WO_3 \cdot P_2O_5$.

PREPARATION OF THE CRYSTALS

A mixture of 4 g WO_3 and 4.8 g P_2O_5, in a platinum crucible, was heated in an autoclave at 550°C for about a week, when crystals good for X-ray work were obtained. (The method according to Schulz [1].) After being cooled the crystals were washed with hot water and dried in air. Under the microscope they showed to be colourless, elongated plates, which cleft very easily into long, thin plates of various widths.

Analysis. A sample was fused with sodium potassium carbonate in a platinum crucible and the cake dissolved in boiling water. From an ammoniacal solution the *phosphorus*

was precipitated (according to Kolthoff and Sandell [2]) with a magnesium solution. The precipitate was filtered off, washed with water, dissolved in hot 1 M HNO_3 and from this solution the phosphorus was finally precipitated with ammonium molybdate and weighed as $(NH_4)_3PO_4 \cdot 12MoO_3$. The amount of *wolfram* in the filtrate — made neutral — was determined gravimetrically by precipitation with mercury(I)nitrate according to Cumming and Kay [3] and weighed, after ignition, as WO_3. The methods of analysis were tested carefully on samples with known various compositions and this examination showed very low errors.

The *density* of the crystals was determined from the apparent loss of weight in benzene.

	Calculated for $WO_3 \cdot P_2O_5$	Found
% WO_3	62.02	62.0 ± 0.2
% P_2O_5	37.98	38.0 ± 0.2
Density	4.54	4.46 ± 0.01

The density is calculated for 4 formula units per cell.

UNIT CELL AND SPACE GROUP

Two small single crystals of different shape were split from larger ones. For the taking of rotation and Weissenberg photographs (zero, first and second layer) with CuK radiation, one, a needle about 0.2 mm in length and about 0.01 mm in diameter, was rotated around the needle axis [010] and the other, a plate only about 0.04 mm thick, 0.03 mm wide, and 0.2 mm long, was rotated round a diagonal in the plane of the plate [001]. It was concluded that the crystals are monoclinic and that the dimensions of the unit cell are about 15.7_4 Å, 5.0_9 Å, 6.8_4 Å and the monoclinic angle is about 102°.

The reflections were recorded photographically with the multiple film technique and the relative intensities were estimated visually by comparison with an intensity scale obtained by photographing a reflection with different exposure times. The F^2 values were then calculated using the polarization and Lorentz' factor given by Lu [4]. No correction was applied for the absorption.

More accurate values for the unit cell dimensions were calculated from a powder photograph, taken with strictly monochromatized Cu$K\alpha_1$ radiation in a focusing camera of Guinier type. KCl was used as an internal standard substance (see Table 1).

$$a = (15.710 \pm 0.005)\ \text{Å} \qquad \beta = (102.41 \pm 0.05)^\circ$$
$$b = (5.162 \pm 0.005)\ \text{Å} \qquad V = 547.9\ \text{Å}^3$$
$$c = (6.917 \pm 0.005)\ \text{Å}$$

The value (4.46) found for the density gives 3.93 ≈ 4 formula units in the unit cell.

The reflections systematically absent are

hkl	with	$h+k$	= odd
$h0l$	»	h	= odd
$0k0$	»	k	= odd

This is characteristic of the three space groups No. 5,$C2$, No. 8,Cm and No. 12,$C2/m$. The investigation was started by examining whether the

Table 1. Powder photograph of WOP_2O_7. CuKa_1-radiation. $\lambda_{CuKa_1} = 1.54050$ Å.

hkl	$10^4\sin^2\Theta$ calc	$10^4\sin^2\Theta$ obs	pF^2 calc	*I* obs	*hkl*	$10^4\sin^2\Theta$ calc	$10^4\sin^2\Theta$ obs	pF^2 calc	*I* obs
200	101	—	0	—	600	907	—	35	vvw
001	130	129	5	vw	220	992	—	0	—
$20\bar{1}$	182	181	61	st	021	1021	—	3	—
110	248	248	77	vst	$22\bar{1}$	1072	1073	48	vw
201	280	279	88	m	511	1106	1105	48	vvw
$11\bar{1}$	353	353	35	w	312	1117	1117	67	vw
111	403	402	159	vvst	402	1120		37	
400			146		$20\bar{3}$	1123	—	13	—
$40\bar{1}$	435	435	58	w	$51\bar{2}$	1127	1131	77	w
310	449	447	4	vvw	$60\bar{2}$	1132		39	
$31\bar{1}$	506	506	213	st	003	1170	1171	20	w
002	520	520	35	w	221	1171		72	
$20\bar{2}$	522	523	21	vw	601	1185	1187	74	vw
401	632	—	11	—	$40\bar{3}$	1278	1276	37	vvw
311	653	652	79	vw	420	1294	—	42	—
202	719	720	0	vvst	$42\bar{1}$	1326	1327	52	vvw
$11\bar{2}$			361		$11\bar{3}$	1344	—	2	—
$40\bar{2}$	726	—	0	—	$31\bar{3}$	1398	1401	85	vw
112	817	—	4		022	1411	1414	130	m
$31\bar{2}$	822	—	0		$22\bar{2}$	1413		100	
510	853	852	135	vvw	$71\bar{1}$	1415		121	
$51\bar{1}$	860	—	0	—	203	1418		17	
$60\bar{1}$	890	891	14	m	710	1458	—	36	—
020	891		134		113	1492	1493	98	w

Reflections systematically absent in space group $C2/m$ have been omitted.
KCl ($a = 6.2930$ Å) has been used as an internal standard substance.

structure was consistent with the last space-group, that having the highest symmetry.

In No. 12,$C2/m$ the following point positions are possible

$$(000,\ \tfrac{1}{2}\tfrac{1}{2}0) +$$

2(a): 000; 2(b): $0\frac{1}{2}0$; 2(c): $00\frac{1}{2}$; 2(d): $0\frac{1}{2}\frac{1}{2}$
4(e): $\frac{1}{4}\frac{1}{4}0$; $\frac{1}{4}\frac{3}{4}0$; 4(f): $\frac{1}{4}\frac{1}{4}\frac{1}{2}$; $\frac{1}{4}\frac{3}{4}\frac{1}{2}$
4(g): $\pm(0,y,0)$; 4(h): $\pm(0,y,\frac{1}{2})$; 4(i): $\pm(x,0,z)$
8(j): $\pm(x,y,z)$; $\pm(x,\bar{y},z)$

POSITIONS OF THE WOLFRAM ATOMS

In order to find the four wolfram positions, the Patterson projections $P(uvp)$ and $P(upw)$ were calculated (Figs. 1 and 2).

The four wolfram atoms in the unit cell must occupy two of the twofold, or one of the fourfold, positions. Now $P(upw)$ has no maximum at $u = 0$, $w = \frac{1}{2}$ or at $u = \frac{1}{2}$, $w = \frac{1}{2}$ and $P(uvp)$ has no maximum at $u = 0$, $v = \frac{1}{2}$ or at $u = \frac{1}{2}$, $v = 0$ so this will exclude the possibility of the wolfram atoms being situated in combinations of the twofold positions or in 4(e)—(h). Thus the

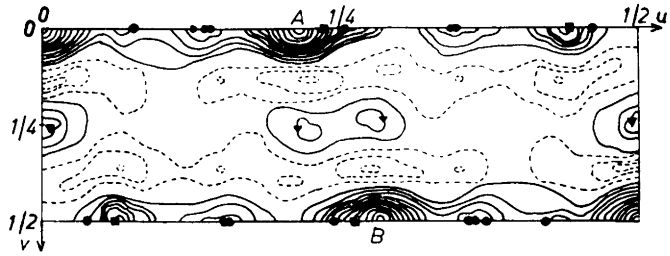

Fig. 1. The Patterson function $P(uvp)$. The W—P (■), W—O_{1-2} (▲) and W—O_{3-6} (●) vectors have been indicated. For the largest maxima (00) and ($\frac{1}{2}\frac{1}{2}$), only every second contour has been marked. Dashed lines indicate negative values.

wolfram atoms must be situated in 4(*i*) and the W—W distances should be

$$\pm(\tfrac{1}{2},\tfrac{1}{2},0); \qquad \pm(2x,0,2z); \qquad \pm(\tfrac{1}{2}+2x\,\tfrac{1}{2},2z)$$

The Patterson projections on the *uv* and *uw* plane should therefore show (besides the origin maxima) the following maxima

in the *uv* plane		in the *uw* plane	
I. $(\frac{1}{2},\frac{1}{2})$	weight 4	IV. $(\frac{1}{2},0)$	weight 4
II. $\pm(2x,0)$	weight 2	V. $\pm(2x,2z)$	weight 2
III. $\pm(\frac{1}{2}+2x,\frac{1}{2})$	weight 2	VI. $\pm(\frac{1}{2}+2x,2z)$	weight 2

There are two high peaks in $P(uvp)$ at $u = 0.21_2$, $v = 0$ (A in Fig. 1) and at $u = 0.28_8$, $v = \frac{1}{2}$ (B in Fig. 1) and one peak at $u = \frac{1}{2}$, $v = \frac{1}{2}$, whose height is about double that of the other two. (All maxima have been located by the interpolation table given by Booth [5].) These maxima certainly correspond to the W—W vectors I, II, and III so that peak A corresponds to the vector II above (and B to III) and thus we get $x_W = 0.10_6$. (It is sufficient to consider the range $0 \leq x \leq 1/4$, $0 \leq z \leq \frac{1}{2}$.)

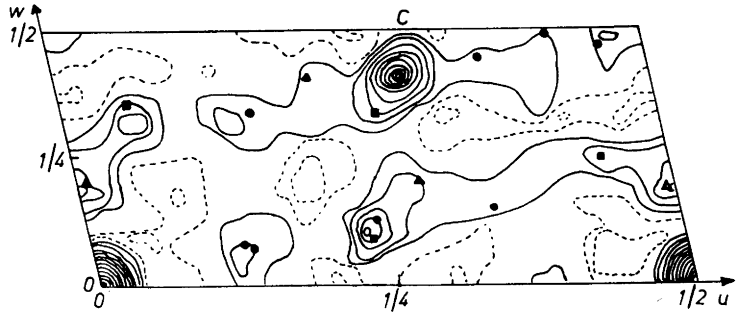

Fig. 2. The Patterson function $P(upw)$. The positions of the vectors have been marked as in Fig. 1. For the largest maxima (00) and ($\frac{1}{2}$0), only every second contour has been marked. Dashed lines indicate negative values.

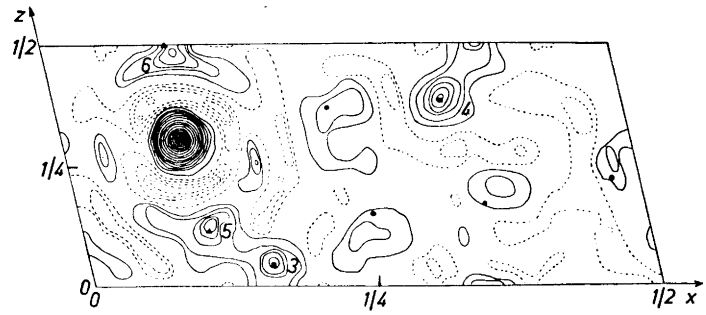

Fig. 3. Electron density projected on the *xz* plane. The positions of the phosphorus atoms (■), oxygen atoms O_{1-2} (▲) and oxygen atoms O_{3-6} (●) have been marked. In the wolfram peak only every second contour has been marked. Dashed lines indicate negative values.

The projection $P(upw)$ should therefore have one high peak at $u = \frac{1}{2}$, $w = 0$ (corresponding to the vector IV above) and two peaks with the u coordinates equal to $\pm 0.21_2$ and ± 0.712 (corresponding to the vectors V and VI above). Now the projection $P(upw)$ has a pronounced peak at $u = \frac{1}{2}$, $w = 0$ and two peaks (the heights of which are about half that of the first one) at $u = 0.20_8$, $w = 0.60_0$ and at $u = 0.29_2$, $w = 0.40_0$ (C in Fig. 2). Since the height and positions of these peaks correspond to the calculated values we conclude:

4 W in $C2/m$ $4(i)$ with $x = 0.10_5$, $y = 0$, $z = 0.30_0$.

POSITIONS OF THE LIGHT ATOMS

Electron density projections. In the Patterson projections in Figs. 1 and 2 there are, in addition to peaks corresponding to the W—W vectors, several lower maxima which perhaps could be ascribed to the W—P, and maybe also to some W—O, distances. From these small maxima, if real, it would be possible to determine the positions of the phosphorus atoms in the unit

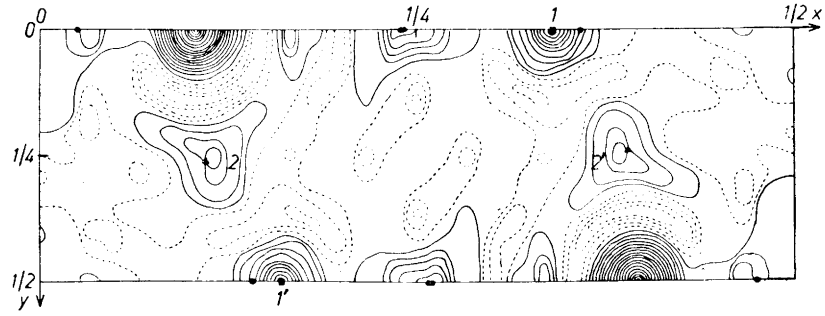

Fig. 4. Electron density projected on the *xy* plane. The positions of the atoms have been indicated as in Fig. 3. In the wolfram peak only every second contour has been marked. Dashed lines indicate negative values.

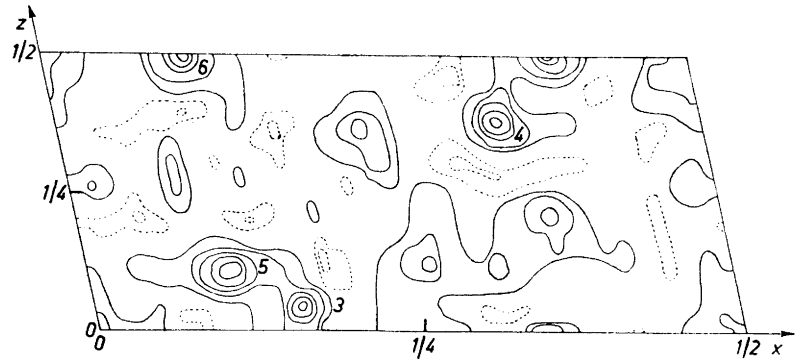

Fig. 5. Electron density projected on the *xz* plane with the wolfram atom subtracted. Dashed lines indicate negative values.

cell. It would, however, be more favourable to determine their sites from a map giving electron density, as such a map gives maxima that are sharper and less in number than those of the corresponding vector map.

For a compound of this type the electron density projections can easily be calculated since the signs of all the F-values can be determined from the contributions given by the wolfram atoms because of their dominant scattering factors. In this way $\varrho\ (xpz)$ and $\varrho\ (xyp)$ were calculated and the results are given in Figs. 3 and 4. We see that the wolfram atoms are clearly indicated at $x = 0.103$, $z = 0.295$ in $\varrho(xpz)$ (Fig. 3) and at $x = 0.103$, $y = 0$ in $\varrho\ (xyp)$ (Fig. 4) and from these values we thus obtain the final parameters of the wolfram atoms: $x = 0.103$, $y = 0$, $z = 0.295$.

Besides the very high wolfram peaks in the calculated electron density projections there are lower peaks in $\varrho\ (xyp)$ (Fig. 4) at $x = 0.34$ (0.16), $y = 0$ ($\frac{1}{2}$) (1 and 1' in Fig. 4) and at $x = 0.11$ (0.39), $y = 0.25$ (2 and 2' in Fig. 4). The electron density projected on the *xz* plane (Fig. 3) also shows lower maxima (all of about the same heights) with the following sets of parameters

3.	$x = 0.16$	$z = 0.05$
4.	$x = 0.34$	$z = 0.38$
5.	$x = 0.11$	$z = 0.12$
6.	$x = 0.11$	$z = 0.47$

If these lower peaks in the projections are real maxima, and not false ones formed by errors — diffraction effects or errors in the observed intensities due to absorption within the crystal [6] — the only atoms, which could give peaks of this height are the phosphorus atoms or overlapping oxygen atoms.

In order to find out if the lower maxima from $\varrho\ (xpz)$ and $\varrho\ (xyp)$ really correspond to atom positions in the unit cell, the wolfram atoms were subtracted from these projections and the results are given in Figs. 5 and 6. (The effect of the temperature factor, calculated by the ordinary procedure was found to be negligible; probably it roughly cancels out with the absorption effect.)

From Fig. 5, which shows ϱ (xpz) with the wolfram atoms subtracted, we see that we still have four distinct maxima of about the same height and with the following sets of parameters

3.	$x = 0.160$	$z = 0.044$
4.	$x = 0.340$	$z = 0.380$
5.	$x = 0.111$	$z = 0.113$
6.	$x = 0.109$	$z = 0.499$

from which it should be possible to get the positions of the phosphorus atoms. Now, in the unit cell we have eight phosphorus and thirty-two oxygen atoms. In the xz projection never more than two oxygen atoms can overlap (the b-axis is only 5.16 Å). Since the parameters given above are not special, the eight phosphorus atoms must occupy the point positions 8(j) or 4(i). Moreover, if they are situated in 8(j) two phosphorus maxima should overlap in the xz projection and thus we should get only one pronounced maximum in the quadrant of the projection represented in Fig. 5, and the height of this peak should have been at least double that of the other maxima in this quadrant. Now, as mentioned above, we have four distinct maxima, which all have nearly the same height. So we conclude that the phosphorus atoms are situated in two point positions 4(i), which will give two peaks in ϱ (xpz). The remaining two maxima should correspond to two sets of oxygen atoms in point positions 8(j) each giving a maximum from two superimposed oxygen atoms.

From Fig. 6, which shows ϱ (xyp) with the wolfram atoms subtracted, we see that the wolfram atoms and most of their diffraction effects have disappeared but there are, however, two pronounced maxima at $x = 0.339$ (0.161), $y = 0$ ($\frac{1}{2}$) (1 and 1′ in Fig. 6) and two small peaks at $x = 0.11_3$, $y = 0.24_0$ and at $x = 0.38_7$, $y = 0.26_0$ (2 and 2′ in Fig. 6). According to the conclusions given above the first two maxima (1 and 1′) correspond to the phosphorus positions and the peaks 2 and 2′ will correspond to the oxygen positions in the point position 8(j). Thus we conclude that the maxima 3 and 4 in Fig. 5 will give the parameters of the phosphorus atoms and with these coordinates we find that two phosphorus maxima overlap in the xy-projection. This is in good agreement with observed heights in this projection. Finally the posi-

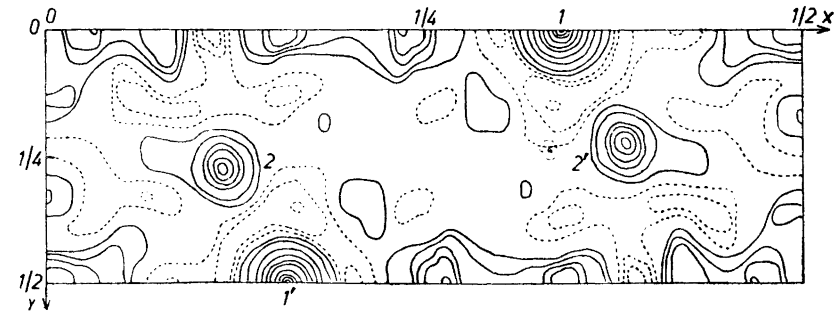

Fig. 6. Electron density projected on the xy plane with the wolfram atoms subtracted. Dashed lines indicate negative values.

tions of the sixteen oxygen atoms in the position 8(*j*) follow immediately from the maxima 5 and 6 in Fig. 5 and 2 and 2' in Fig. 6. The values obtained from ϱ (*xpz*) should be more correct, since in the calculation of this projection more *F*-values were used.

Thus, from the electron density projections the following parameters could be obtained:

4	W	in	*C*2/*m*	4(*i*)	with	$x = 0.103$	$y = 0$ $z = 0.295$
4	P_1	»	»	»	»	$x = 0.34_0$	$y = 0$ $z = 0.38_0$
4	P_2	»	»	»	»	$x = 0.34_0$	$y = 0$ $z = 0.95_6$
8	O_1	»	»	8(*j*)	»	$x = 0.39_0$	$y = 0.24_0$ $z = 0.50_1$
8	O_2	»	»	»	»	$x = 0.39_0$	$y = 0.24_0$ $z = 0.88_7$

Using these parameters W—P and W—O distances were calculated and the maxima in the Patterson projections (Figs. 1—2) were compared with these W—P and W—O vectors. All of these vectors were found to correspond to maxima (*cf.* Figs. 1 and 2) in *P*(*uvp*) and *P*(*upw*) and moreover the heights of the peaks also corresponded to the calculated weights.

The remaining maxima in the Patterson and electron density projections may correspond to W—O vectors or oxygen atom positions but at this stage of the investigation they were not considered, since these peaks are of about the same height as the false maxima [6].

Geometrical considerations. The sixteen oxygen atoms, the positions of which have been found from electron density projections, are situated close to phosphorus atoms with the distances P_1—2 $O_1 = 1.6_0$ Å and P_2—2 $O_2 = 1.6_0$ Å. These distances are in good agreement with P—O distances in previously described structures [7-9] (*i.e.* P—O = 1.45—1.65 Å). Assuming that the coordination figure around the phosphorus atoms is a tetrahedron, which seems to be very probable, it is then possible to calculate the parameters of the remaining oxygen atoms in the PO_4 tetrahedra. If we assume the bond lengths P—O = 1.5_5 Å and O—O = 2.5_3 Å (these distances are mean values of those published [7-9]) the coordinates of the oxygen atoms O_3—O_5 follow immediately. Thus we obtain

4	O_3	in	*C*2/*m*	4(*i*)	with	$x = 0.24_0$	$y = 0$ $z = 0.36_5$
4	O_4	»	»	»	»	$x = 0.35_8$	$y = 0$ $z = 0.16_8$
4	O_5	»	»	»	»	$x = 0.24_2$	$y = 0$ $z = 0.85_2$

Now we have to find the position of the remaining four oxygen atoms in the unit cell. They must occupy two of the twofold, or one of the fourfold, positions. Assuming that the distances between these oxygen atoms and the oxygens already located (*i.e.* O_1—O_5) are not less than 2.6_0 Å, the twofold (2(*a*)—(*d*)) and the fourfold (4(*e*)—(*h*)) point positions at once can be eliminated and thus we must have four oxygen atoms (O_6) in 4(*i*). In order to determine the coordinates, the section $y = 0$ in the unit cell was drawn and regions forbidden to oxygen atoms were marked out (Fig. 7). From the figure we see that there are only very small areas left free for the centres of these oxygen atoms. The coordinates of the oxygen atoms O_6 would then be

4 O_6 in *C*2/*m* 4(*i*) with $x = 0.97_5$ $y = 0$ $z = 0.21_7$

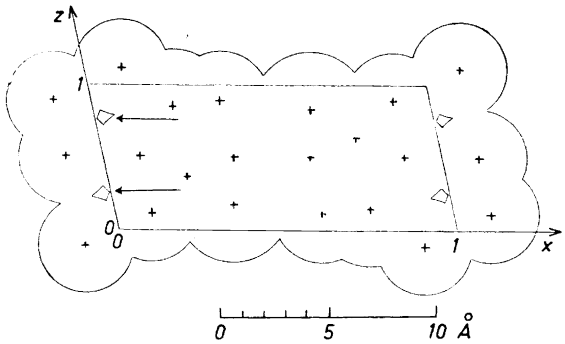

Fig. 7. Section at $y = 0$ through the unit cell showing the areas forbidden to the oxygen atoms, O_6, in this plane. The circles enclose domains forbidden around the oxygen atoms O_{1-5}. The arrows point out the only areas left free for the centres of O_6. + = centre of oxygen.

Using these oxygen coordinates the remaining W—O distances were calculated and these vectors have been indicated in Figs. 1 and 2. The positions of the oxygen atoms O_3—O_6 have also been marked in the electron density projections (Figs. 3—4). From the figures we see that these vectors or oxygen positions are situated in positive areas and, in fact, in most cases they coincide fairly well with small peaks in the Patterson and electron density projections. This seems to indicate the coordinate values to be plausible. Moreover with the coordinates found above we obtain contacts W—6O with a coordination figure, within the errors, a regular octahedron, which has been found in previously determined crystal structures of wolfram compounds [11–13]. For the coordination figure around the phosphorus we have presumed a tetrahedron with two P—O distances equal to 1.5_5 Å and one O—O distance equal to 2.5_3 Å. This will give P_2O_7-groups (*i.e.* two PO_4 tetrahedra sharing an oxygen) with a P—O—P angle at the central oxygen of 142°, which can be compared with 134° found in $Na_4P_2O_7.10H_2O$ [9] and 180° found in the curious series of SiP_2O_7 and related compounds [14]. Thus, the assumptions made above to get the coordinates, give an arrangement of the atoms, which seems to be very probable.

FINAL STRUCTURE PROPOSITION

The following structure is thus proposed for $WO_3.P_2O_5$. Space group: No. 12, $C2/m$. 4 formula units per unit cell

		x	y	z
4 W	in 4(*i*)	0.103 ± 0.003	0	0.295 ± 0.003
4 P_1	» 4(*i*)	0.340 ± 0.006	0	0.380 ± 0.006
4 P_2	» 4(*i*)	0.340 ± 0.006	0	0.956 ± 0.006
8 O_1	» 8(*j*)	0.390 ± 0.006	0.24 ± 0.01	0.501 ± 0.006
8 O_2	» 8(*j*)	0.390 ± 0.006	0.24 ± 0.01	0.887 ± 0.006
4 O_3	» 4(*i*)	0.24	0	0.36
4 O_4	» 4(*i*)	0.36	0	0.17
4 O_5	» 4(*i*)	0.24	0	0.85
4 O_6	» 4(*i*)	0.98	0	0.22

(000; $\frac{1}{2}\frac{1}{2}$0) ±

4 (*i*): (*x*0*z*)
8 (*j*): (*xyz*); ($x\bar{y}z$)

Table 2. Comparison between calculated and observed structure factors from Weissenberg photographs of WOP_2O_7. CuK radiation.

$h\,k\,l$	F calc	F obs	$h\,k\,l$	F calc	F obs	$h\,k\,l$	F calc	F obs	$h\,k\,l$	F calc	F obs
4 0 8	3	—	16 0 $\bar{5}$	21	—	4 0 $\bar{2}$	−1	—	3 1 7	−69	62
2 0 8	−69	61	18 0 $\bar{5}$	−74	57	6 0 $\bar{2}$	88	110	1 1 7	56	58
0 0 8	−27	30				8 0 $\bar{2}$	26	41	1 1 $\bar{7}$	62	91
2 0 $\bar{8}$	37	38	14 0 4	−67	52	10 0 $\bar{2}$	−104	122	3 1 $\bar{7}$	−7	—
4 0 $\bar{8}$	61	53	12 0 4	−74	66	12 0 $\bar{2}$	−40	41	5 1 $\bar{7}$	−64	64
6 0 $\bar{8}$	−8	—	10 0 4	34	42	14 0 $\bar{2}$	51	55	7 1 $\bar{7}$	−53	66
8 0 $\bar{8}$	−47	41	8 0 4	64	71	16 0 $\bar{2}$	55	41	9 1 $\bar{7}$	36	45
10 0 $\bar{8}$	−35	35	6 0 4	37	54	18 0 $\bar{2}$	−2	—	11 1 $\bar{7}$	93	83
12 0 $\bar{8}$	55	35				20 0 $\bar{2}$	−33	36	13 1 $\bar{7}$	−16	—
			4 0 4	−71	71						
8 0 7	32	17	2 0 4	−81	84	18 0 1	38	40	11 1 6	67	37
6 0 7	−42	42	0 0 4	24	33	16 0 1	81	79	9 1 6	−27	45
4 0 7	−54	39	2 0 $\bar{4}$	160	167	14 0 1	8	—	7 1 6	−72	71
2 0 7	−18	—	4 0 $\bar{4}$	−2	—	12 0 1	−95	93	5 1 6	−18	—
0 0 7	55	64	6 0 $\bar{4}$	−95	119	10 0 1	−53	58	3 1 6	82	85
2 0 $\bar{7}$	57	86	8 0 $\bar{4}$	−52	63	8 0 1	105	96	1 1 6	49	61
4 0 $\bar{7}$	−56	68	10 0 $\bar{4}$	76	80	6 0 1	122	110	1 1 $\bar{6}$	−39	51
6 0 $\bar{7}$	−80	86	12 0 $\bar{4}$	61	73	4 0 1	−46	45	3 1 $\bar{6}$	−96	124
8 0 $\bar{7}$	27	28	14 0 $\bar{4}$	12	—	2 0 1	−133	117	5 1 $\bar{6}$	5	—
10 0 $\bar{7}$	58	62	16 0 $\bar{4}$	−82	70	0 0 1	−31	34	7 1 $\bar{6}$	64	73
12 0 $\bar{7}$	21	17	18 0 $\bar{4}$	−40	38	2 0 $\bar{1}$	110	102	9 1 $\bar{6}$	48	52
14 0 $\bar{7}$	−25	—				4 0 $\bar{1}$	108	100	11 1 $\bar{6}$	−60	50
			16 0 3	−77	74	6 0 $\bar{1}$	−53	61	13 1 $\bar{6}$	−65	55
10 0 6	26	32	14 0 3	−26	26	8 0 $\bar{1}$	−142	139	15 1 $\bar{6}$	−3	—
8 0 6	−52	54	12 0 3	72	60	10 0 $\bar{1}$	−19	—			
6 0 6	−76	76	10 0 3	43	48	12 0 $\bar{1}$	100	102	13 1 5	23	26
4 0 6	39	34	8 0 3	−44	41	14 0 $\bar{1}$	47	48	11 1 5	−74	69
2 0 6	89	97	6 0 3	−69	68	16 0 $\bar{1}$	−64	61	9 1 5	−40	41
0 0 6	23	—	4 0 3	−27	23	18 0 $\bar{1}$	−71	71	7 1 6	33	—
2 0 $\bar{6}$	−98	86	2 0 3	59	71	20 0 $\bar{1}$	11	11	5 1 5	64	68
4 0 $\bar{6}$	−68	73	0 0 3	63	80				3 1 5	46	52
6 0 $\bar{6}$	48	56	2 0 $\bar{3}$	−50	63	18 0 0	66	67	1 1 5	−63	82
8 0 $\bar{6}$	92	81	4 0 $\bar{3}$	−86	90	16 0 0	−67	45	1 1 $\bar{5}$	−91	112
10 0 $\bar{6}$	−13	—	6 0 $\bar{3}$	11	—	14 0 0	−104	86	3 1 $\bar{5}$	62	82
12 0 $\bar{6}$	−96	82	8 0 $\bar{3}$	62	75	12 0 0	29	29	5 1 $\bar{5}$	115	111
14 0 $\bar{6}$	−36	27	10 0 $\bar{3}$	48	50	10 0 0	79	87	7 1 $\bar{5}$	−28	41
16 0 $\bar{6}$	59	61	12 0 $\bar{3}$	−16	—	8 0 0	96	113	9 1 $\bar{5}$	−83	82
			14 0 $\bar{3}$	−65	73	6 0 0	−84	80	11 1 $\bar{5}$	−28	—
12 0 5	12	—	16 0 $\bar{3}$	−13	—	4 0 0	−171	159	13 1 $\bar{5}$	33	—
10 0 5	−92	66	18 0 $\bar{3}$	80	73	2 0 0	8	—	15 1 $\bar{5}$	58	61
8 0 5	−58	56							17 1 $\bar{5}$	5	—
6 0 5	105	86	18 0 2	−29	21	3 1 8	−42	26			
4 0 5	105	90	16 0 2	12	—	1 1 $\bar{8}$	−66	53	15 1 4	−3	—
2 0 5	−67	77	14 0 2	63	41	1 1 $\bar{8}$	−12	—	13 1 4	−78	50
0 0 5	−93	94	12 0 2	37	42	3 1 $\bar{8}$	81	78	11 1 4	−42	24
2 0 $\bar{5}$	0	—	10 0 2	−45	54	5 1 $\bar{8}$	42	49	9 1 4	58	68
4 0 $\bar{5}$	82	75	8 0 2	−96	106	7 1 $\bar{8}$	−46	37	7 1 4	96	90
6 0 $\bar{5}$	79	79	6 0 2	52	54	9 1 $\bar{8}$	−62	45	5 1 4	−58	66
8 0 $\bar{5}$	−41	57	4 0 2	86	99	11 1 $\bar{8}$	18	—	3 1 4	−94	90
10 0 $\bar{5}$	−130	115	2 0 2	−10	38				1 1 4	2	—
12 0 $\bar{5}$	5	—	0 0 2	−84	72	7 1 7	30	36	1 1 $\bar{4}$	91	69
14 0 $\bar{5}$	112	104	2 0 $\bar{2}$	−65	68	5 1 7	−79	80	3 1 $\bar{4}$	58	70

h k l	*F* calc	*F* obs	*h k l*	*F* calc	*F* obs	*h k l*	*F* calc	*F* obs	*h k l*	*F* calc	*F* obs
5 1 $\bar{4}$	−18	—	13 1 1	−56	55	2 4 0	10	—	3 3 $\bar{1}$	114	114
7 1 $\bar{4}$	−89	78	11 1 1	−67	74	4 4 0	−105	114	5 3 $\bar{1}$	2	—
9 1 $\bar{4}$	−17	—	9 1 1	20	—	6 4 0	−54	53	7 3 $\bar{1}$	−93	97
11 1 $\bar{4}$	105	102	7 1 1	104	82	8 4 0	62	57	9 3 $\bar{1}$	−58	46
13 1 $\bar{4}$	49	43	5 1 1	69	59	10 4 0	63	41	11 3 $\bar{1}$	37	37
15 1 $\bar{4}$	−63	55	3 1 1	−89	95	12 4 0	23	22	13 3 $\bar{1}$	69	80
17 1 $\bar{4}$	−67	58	1 1 1	−126	121				15 3 $\bar{1}$	3	—
19 1 $\bar{4}$	19	—	1 1 $\bar{1}$	59	68	14 4 0	−87	80	17 3 $\bar{1}$	−75	89
			3 1 $\bar{1}$	146	114						
15 1 3	−55	50	5 1 $\bar{1}$	−3	—	1 5 0	51	56	14 4 1	5	—
13 1 3	−1	—	7 1 $\bar{1}$	−110	90	3 5 0	4	—	12 4 1	−79	63
11 1 3	76	74	9 1 $\bar{1}$	−66	66	5 5 0	−76	84	10 4 1	−42	30
9 1 3	45	63	11 1 $\bar{1}$	39	51	7 5 0	−37	31	8 4 1	78	56
7 1 3	−89	88	13 1 $\bar{1}$	73	93	9 5 0	89	55	6 4 1	86	69
5 1 3	−101	91	15 1 $\bar{1}$	4	—	11 5 0	45	37			
3 1 3	45	52	17 1 $\bar{1}$	−79	85				4 4 1	−31	33
1 1 3	99	130	19 1 $\bar{1}$	−42	37	0 6 0	98	86	2 4 1	−88	102
1 1 $\bar{3}$	15	18				2 6 0	4	—	0 4 $\bar{1}$	−22	28
3 1 $\bar{3}$	−92	83	19 1 0	41	41	4 6 0	−55	46	2 4 $\bar{1}$	73	93
5 1 $\bar{3}$	−83	86	17 1 0	10	—	6 6 0	−29	16	4 4 $\bar{1}$	72	95
7 1 $\bar{3}$	50	66	15 1 0	−73	59				6 4 $\bar{1}$	−37	44
9 1 $\bar{3}$	120	93	13 1 0	−67	55	18 2 1	39	39	8 4 $\bar{1}$	−103	112
11 1 $\bar{3}$	−2	—	11 1 0	59	60	16 2 1	68	72	10 4 $\bar{1}$	−14	—
13 1 $\bar{3}$	−91	90	9 1 0	130	120	14 2 1	−1	—	12 4 $\bar{1}$	82	75
15 1 $\bar{3}$	−24	—	7 1 0	−60	51	12 2 1	−80	82	14 4 $\bar{1}$	40	32
17 1 $\bar{3}$	55	55	5 1 0	−116	118	10 2 1	−35	33			
19 1 $\bar{3}$	54	45	3 1 0	20	29	8 2 1	87	60	11 5 1	−53	49
			1 1 0	88	113	6 2 1	84	72	9 5 1	16	—
17 1 2	−50	78				4 2 1	−39	48	7 5 1	73	63
15 1 2	68	55	0 2 0	164	185	2 2 1	−85	85	5 5 1	40	31
13 1 2	89	78	2 2 0	−6	—	0 2 1	−17	25	3 5 1	−59	71
11 1 2	−41	58	4 2 0	−65	65	2 2 $\bar{1}$	69	82	1 5 1	−74	93
9 1 2	−69	64	6 2 0	−35	43	4 2 $\bar{1}$	73	89	1 5 $\bar{1}$	34	37
7 1 2	−43	49	8 2 0	38	37	6 2 $\bar{1}$	−32	34	3 5 $\bar{1}$	87	109
5 1 2	78	71	10 2 0	33	40	8 2 $\bar{1}$	−107	94	5 5 $\bar{1}$	3	—
3 1 2	82	78	12 2 0	46	53	10 2 $\bar{1}$	−22	16	7 5 $\bar{1}$	−73	69
1 1 2	−19	19	14 2 0	−62	73	12 2 $\bar{1}$	79	81	9 5 $\bar{1}$	−48	25
1 1 $\bar{2}$	−190	170	16 2 0	−67	63	14 2 $\bar{1}$	43	47	11 5 $\bar{1}$	31	35
3 1 $\bar{2}$	1	—	18 2 0	32	50	16 2 $\bar{1}$	−49	49	13 5 $\bar{1}$	59	65
5 1 $\bar{2}$	88	78	1 3 0	76	91	18 2 $\bar{1}$	−64	74			
7 1 $\bar{2}$	62	61	3 3 0	3	—				6 6 1	60	37
9 1 $\bar{2}$	−63	73	5 3 0	−103	129	15 3 1	39	43	4 6 1	−24	16
11 1 $\bar{2}$	−67	71	7 3 0	−46	46	13 3 1	−52	47	2 6 1	−61	61
13 1 $\bar{2}$	−32	51	9 3 0	119	121	11 3 1	−64	68	0 6 1	−14	13
15 1 $\bar{2}$	93	106	11 3 0	55	43	9 3 1	17	—	2 6 $\bar{1}$	50	49
17 1 $\bar{2}$	56	53	13 3 0	−65	65	7 3 1	91	77	4 6 $\bar{1}$	51	49
19 1 $\bar{2}$	−58	55	15 3 0	−70	55	5 3 1	55	57	6 6 $\bar{1}$	−24	14
			17 3 0	12	16	3 3 1	−74	93	8 6 $\bar{1}$	−74	49
17 1 1	78	68				1 3 1	−98	106			
15 1 1	40	49	0 4 0	170	212	1 3 $\bar{1}$	45	55			

The accuracy of the parameters of the oxygen atoms O_3—O_6 is estimated to be about $\pm$ 0.01.

Table 3. Comparison between calculated and observed structure factors of some reflections from Weissenberg photographs of WOP_2O_7. CuK radiation.

$h\,k\,l$	F_W calc	F_P calc	$F_W + F_P$ calc	F_O calc	F_{tot} calc	F obs
3 3 0	−38	+32	−6	+9	+3	—
7 3 0	−17	−20	−37	−9	−46	46
9 3 0	+81	+25	+106	+13	+119	121
7 5 0	−15	−16	−31	−6	−37	31
8 0 $\bar{7}$	+6	+22	+28	−1	+27	28
10 0 $\bar{5}$	−83	−23	−106	−24	−130	115
2 0 $\bar{4}$	+105	+19	+124	+36	+160	167
4 0 $\bar{3}$	−114	−15	−129	+43	−86	90
13 1 $\bar{3}$	−84	−15	−99	+8	−91	90
4 0 $\bar{2}$	+56	−38	+18	−19	−1	—
5 1 $\bar{2}$	+106	+22	+128	−40	+88	78
7 1 $\bar{2}$	+75	−30	+45	+17	+62	61
9 1 0	+93	+29	+122	+8	+130	120
2 2 0	+33	−17	+16	−22	−6	—
4 2 0	−98	−24	−122	+57	−65	65
1 1 2	−44	+17	−27	+8	−19	19
3 1 2	+96	+20	+116	−34	+82	78
5 1 2	+87	−30	+57	+21	+78	71
6 0 3	−102	+20	−82	+13	−69	68
10 0 3	+76	−14	+62	−19	+43	48
8 0 5	−24	−21	−45	−13	−58	56
5 1 5	+87	−24	+63	+1	+64	68
9 1 5	−65	+17	−48	+8	−40	41

Using these parameters the F values were calculated for the reflexions and compared with the observed ones. They are given in Table 2 for $hk0$, $h0l$, $hk1$ and $h1l$. Table 3 gives the details for some reflexions which have more pronounced phosphorus and oxygen contributions to the magnitudes of the structure factors. The reliability index, R, calculated according to Booth (see Ref.[5], p. 101), was found to be 0.14 for $hk0$ and 0.13 for $h0l$ (absent reflexions not included) and 0.34 or 0.24 for the same reflexions calculated *without* the phosphorus and oxygen atoms, and 0.24 or 0.19 calculated without the oxygen atoms, showing that the structure should be essentially correct as regards the heavy atoms and also indicating that the proposed coordinates of the phosphorus and the oxygen atoms will give much better agreement between observed and calculated intensities.

In the structure determination described above we have assumed that the structure is consistent with the space group $C2/m$ having the highest symmetry. This will give that the y coordinates for W, P, O_3—O_6 must be equal to 0 or $\frac{1}{2}$. From the Patterson projection $P(uvp)$ we see that these atoms at least will be situated close to these planes. In fact it does not seem possible to get any essential difference for the atom arrangement even if the less symmetrical space groups are considered but this will increase the errors in the parameters, as most of the coordinates will be obtained from overlapping peaks [10]. Moreover, since the electron density projections show distinct

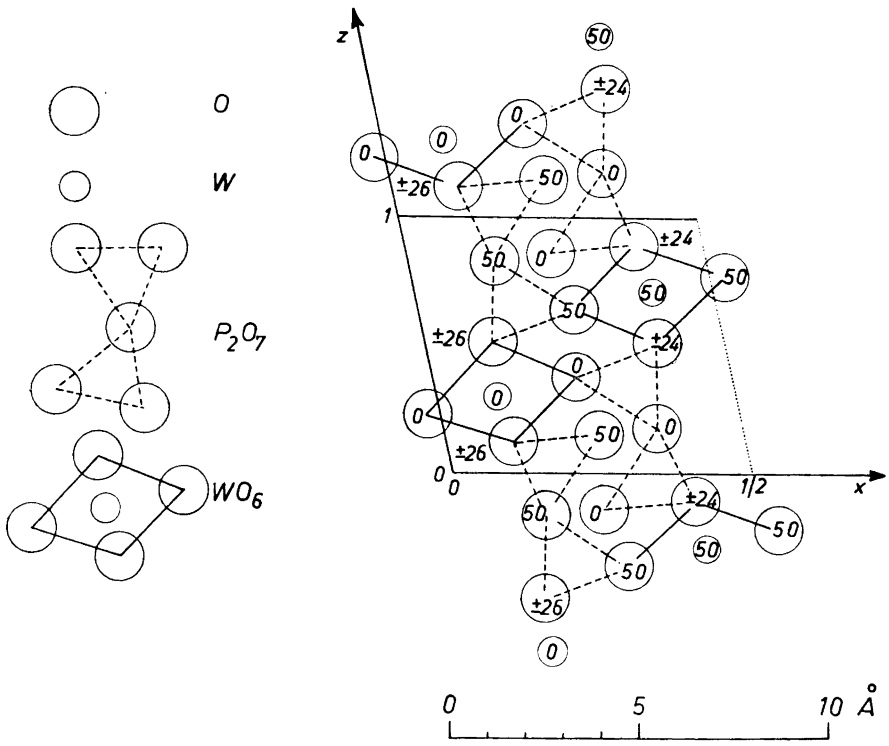

Fig. 8. The layer of WOP_2O_7. Only one layer has been indicated (*i. e.* wolfram and oxygen atoms with x parameters within the limits $-0.02 \leq x \leq 0.52$). The figures denote the height of the atoms in percentages of b.

maxima and the electron density projected on two different planes (xy and xz) show mutual agreement, it seems very probable that the atoms belong to the space group $C2/m$.

DESCRIPTION OF THE STRUCTURE

The structure of $WO_3.P_2O_5$ may be described as built up of WO_6-octahedra and P_2O_7-groups. Every wolfram atom is in contact with five P_2O_7-groups and every P_2O_7-group with five wolfram atoms. Every wolfram atom is also in contact with one oxygen atom (O_6), which is bonded only to this wolfram atom, so that the crystals are built up of WOP_2O_7-layers parallel to the yz plane (Fig. 8). The layers are thus electrically neutral, so that in the crystals there are only feeble attractive forces between neighbouring layers, which will explain the pronounced basal cleavage along the yz plane. The building principle might be expressed by the formula WOP_2O_7 and the compound should then be written according to this rather than $WO_3.P_2O_5$.

The xz projection of the structure is shown in Fig. 9.

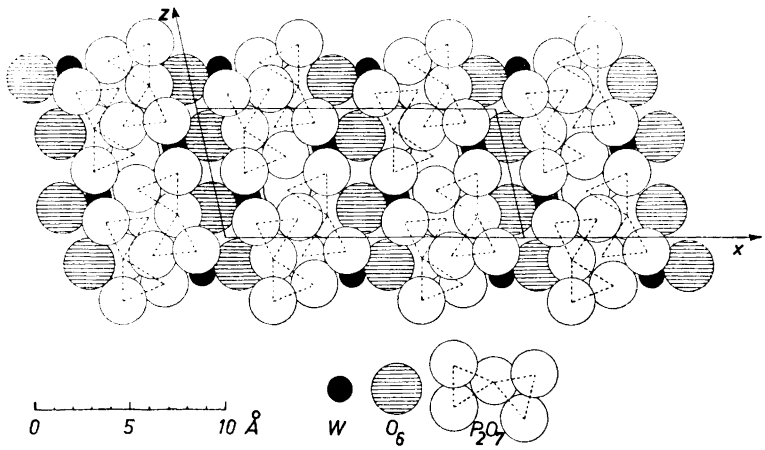

Fig. 9. Projection on the *xz* plane of the structure of WOP_2O_7.

The distances between neighbouring atoms in WOP_2O_7 will be (in Å)

W—2 O_1;	O_1—W	$= 1.9_6$
W—2 O_2;	O_2—W	$= 1.8_9$
W—O_3 ;	O_3—W	$= 2.1_0$
W—O_6 ;	O_6—W	$= 1.9_7$
P_1—2 O_1;	O_1—P	$= 1.6_0$
P_1—O_3 ;	O_3—P_1	$= 1.5_5$ *
P_1—O_4 ;	O_4—2 $P_{1,2}$	$= 1.5_5$ *
P_2—O_2 ;	O_2—P_2	$= 1.5_9$
P_2—O_4 ;	O_4—2 $P_{1,2}$	$= 1.5_5$ *
P_2—O_5 ;	O_5—P_2	$= 1.5_5$ *
O_1—3 O_1		$= 2.4_8$; 2.6_8; 3.4_6
O_1—O_2 ;	O_2—O_1	$= 2.6_7$
O_1—2 O_3;	O_3—2 O_1	$= 2 \times 2.6_5$; $2 \times 2.7_6$
O_1—O_4 ;	O_4—2 O_1	$= 2.5_7$
O_1—O_5 ;	O_5—2 O_1	$= 3.1_4$
O_1—2 O_6;	O_6—4 O_1	$= 2 \times 2.8_8$; $2 \times 2.9_3$
O_2—3 O_2		$= 2.4_8$; 2.6_8; 3.4_7
O_2—O_3 ;	O_3—2 O_2	$= 2.7_3$
O_2—O_4 ;	O_4—2 O_2	$= 2.4_5$
O_2—2 O_5;	O_5—2 O_2	$= 2 \times 2.6_0$; $2 \times 3.3_2$
O_2—2 O_6;	O_6—4 O_2	$= 2 \times 2.7_3$; $2 \times 2.7_4$
O_3—O_3		$= 3.1_6$
O_3—O_4 ;	O_4—O_3	$= 2.5_3$ *
O_3—3 O_5;	O_5—3 O_3	$= 3.0_3$; 3.3_6 (3.5_6)
O_4—2 O_5;	O_5—2 O_4	$= 2.5_3$ *; 3.0_1
O_4—O_6 ;	O_6—O_4	$= 3.1_4$
O_5—O_6 ;	O_6—O_5	$= 3.3_4$
O_6—O_6		$= 3.2_6$

* These distances were taken from previously determined structures and used directly in the determination of the oxygen positions.

The O—O distances are all within the normal range — the shortest O—O distances 2.4_5 Å are within the P_2O_7 group — showing that the lattice is also supported by O—O contacts. However, they may be in error by a few tenths of an Ångström unit.

The author wishes to thank Professor Arne Ölander for his kind interest and Dr. Arne Magnéli and Fil.lic. Georg Lundgren for valuable discussions in connection with this work. This investigation forms part of a research program on metal oxides and related compounds supported by the *Swedish Natural Science Research Council.*

REFERENCES

1. Schulz, I. *Z. anorg. u. allgem. Chem.* **281** (1955) 99.
2. Kolthoff, I. M. and Sandell, E. B. *Textbook of Quantitative Inorganic Analysis*, 3rd Ed., New York 1952, p. 382.
3. Cumming, A. C. and Kay, S. A. *Quantitative Chemical Analysis*, 9th Ed., Edinburgh 1945, p. 367.
4. Lu, C. S. *Rev. Sci. Instr.* **14** (1943) 331.
5. Booth, A. D. *Fourier Technique in X-Ray Organic Structure Analysis*, Cambridge 1948, p. 64.
6. Wells, A. F. *Z. Krist.* **96** (1937) 451.
7. Pauling, L. *The Nature of the Chemical Bond*, 2nd Ed., New York 1940, p. 240.
8. Wells, A. F. *Structural Inorganic Chemistry*, 2nd Ed., Oxford 1950, p. 487.
9. MacArthur, D. M. and Beevers, C. A. *Acta Cryst.* **10** (1957) 428.
10. Burns, D. M. *Acta Cryst.* **11** (1958) 88.
11. Magnéli, A. *Nova Acta Regiae Soc. Sci. Upsaliensis (IV)*, **14** (1950) No 8.
12. Hägg, G. and Magnéli, A. *Revs. Pure Appl. Chem. (Australia)* **4** (1954) 235.
13. Magnéli, A. *J. Inorg. & Nuclear. Chem.* **2** (1956) 330.
14. Levi, G. R. and Peyronel, G. *Z. Krist.* **92** (1935) 190.

Received June 7, 1958.

ACTA CHEMICA SCANDINAVICA 12 (1958) 1730—1745

On the Determination of Thiosulphate by the Silver Thiocyanate Method

NILS-HERMAN SCHÖÖN

Department of Engineering Chemistry, Chalmers Tekniska Högskola, Göteborg, Sweden

The silver thiocyanate method for the colorimetric determination of thiosulphate has been studied. The relation between the amount of thiosulphate added and the amount of silver thiocyanate dissolved was calculated at the ionic strengths, $I = 0$ and $I = 4$, with the aid of available data on silver thiosulphate complexes. The influence of hydrogen sulphite was also calculated.

Experiments were performed at 20°C for the thiosulphate concentration interval $2.5 \times 10^{-5} - 1.5 \times 10^{-3}$ M and for the sulphite concentrations 0.01 M and 0.1 M. The amount of silver thiocyanate dissolved was determined both colorimetrically and by measuring the radioactivity of the solution, ^{110}Ag being used as tracer. In the colorimetric method, the absorbance gives the total thiocyanate concentration in the solution since complexes of silver and thiocyanate and mixed complexes of silver, thiosulphate and thiocyanate can be neglected.

The dissolved amount of silver thiocyanate was shown to be constant when shaking for 10—40 min. With longer reaction times, the concentration of thiocyanate increased owing to the formation of silver sulphide.

At low ionic strengths, the relationship between thiosulphate added and silver thiocyanate dissolved was linear for $c_{S_2O_3} > 2 \times 10^{-4}$, while, for lower thiosulphate concentrations, a nonlinear relationship was valid. An addition of 0.1 M hydrogen sulphite did not increase the solubility of the silver thiocyanate.

At $I = 4$, the relationship between thiosulphate added and silver thiocyanate dissolved was linear within the whole range of concentration investigated ($c_{S_2O_3} < 5 \times 10^{-4}$). It was found that hydrogen sulphite decreased the solubility of silver thiocyanate at this ionic strength. This decrease was almost completely eliminated by the addition of an excess of formaldehyde.

The use of silver azide instead of silver thiocyanate for the determination of thiosulphate in coloured solutions was also studied.

If a solution of thiosulphate is shaken with a solid silver halogenide, the halogenide is dissolved owing to the formation of stable complexes containing silver and thiosulphate ions. This phenomenon is well-known from the

photographic fixing process and many investigations have been published on the dissolution of silver halogenides in complex-forming solutions. On the basis of the photographic fixing reaction, Utsumi [1] has worked out a colorimetric method for the determination of thiosulphate. According to Utsumi, the thiosulphate solution is shaken for some minutes with an excess of solid silver thiocyanate. After separating the solid phase, the amount of thiocyanate dissolved is colorimetrically determined as iron(III)thiocyanate. Utsumi observed that, within the concentration range examined (3×10^{-6}—1.8×10^{-4} M thiosulphate), the relationship between the thiocyanate and thiosulphate concentrations was linear. Utsumi supposed that the dissolution occurred according to the reaction

$$3\ S_2O_3^{2-} + 2\ AgSCN_{(s)} \rightleftharpoons Ag_2(S_2O_3)_3^{4-} + 2\ SCN^-$$

In the present paper, this method has been studied more particularly with regard to the determination of thiosulphate in solutions containing hydrogen sulphite. The method is especially designed for analysing thiosulphate in spent liquor from sulphite cellulose cooking. The determination of thiosulphate can be done, in this case, either before or after the separation of high polymer compounds by ion exchange. In the latter case, the low polymer anions are eluted from the anion exchanger with a large amount of 4 M sodium perchlorate. For this reason, the dissolution of silver thiocyanate in thiosulphate has been investigated both for solutions at low ionic strength and for solutions containing 4 M sodium perchlorate.

From investigations published on the thiosulphate in sulphite spent liquor [2], it can be seen that the thiosulphate concentration amounts to about 10^{-3} M. In the present paper, the silver thiocyanate method has, therefore, been primarily tested for a corresponding concentration range. In solutions containing 4 M sodium perchlorate, a lower concentration range has, however, been of greater interest.

EXPERIMENTAL

Chemicals. Part of the investigation was performed with silver thiocyanate containing ^{110}Ag. The neutron radiation of a silver wire (puriss) was carried out by AB Atomenergi. The chemicals used were of analytical quality, except for iron(III)nitrate which was puriss grade.

Shaking- and filtration procedure. The solution was vigorously shaken (15 min at about 1 500 shakes per min) at (20 ± 0.5)°C with a laboratory "Microid flaskshaker" from Griffin & George Ltd. In the experiments with a longer time of reaction (8—9 h), the solution was rotated (25 r.p.m.) in an air thermostat. When inactive silver thiocyanate was used, 70 mg precipitate was added to 30 ml solution. In the experiments with radioactive silver thiocyanate, the precipitate was dispersed in water or in 4 M sodium perchlorate. A certain volume, 10 or 15 ml, of this mixture was added to the solution. The amount of radioactive precipitate was 15—20 mg per 30 ml solution shaken. The shaking, as well as the other operations, was performed in dark coloured flasks. After shaking, the solutions were immediately filtered through an ultra colloid filter according to Zsigmondy (average pore size 150 mμ) under a pressure of 2—3 atm nitrogen in a Thiessen apparatus.

The colorimetric determination. In the experiments at high ionic strength ($I = 4$), 5 ml iron(III)nitrate solution containing 0.5 M iron(III)nitrate and 0.5 M nitric acid was added to 10 ml of the filtrate. In the experiments at the same ionic strength but in the

presence of hydrogen sulphite, 5 ml 1 M formaldehyde and 5 ml iron(III)nitrate solution were added to 15 ml of the filtrate. The formaldehyde was added in order to bind the hydrogen sulphite. In the experiments at low ionic strengths, the procedure was for $c_{S_2O_3} < 2 \times 10^{-4}$ the same as that described above, while, for a thiosulphate concentration of $2 \times 10^{-4} - 1.5 \times 10^{-3}$ M, 5 ml iron(III)nitrate solution was added to 10 ml of the filtrate. This latter solution was diluted to 50 ml before the colorimetric determination. In the experiments with hydrogen sulphite, 10 ml 1 M formaldehyde was added before the dilution. The concentration of the iron(III)thiocyanate complexes formed was determined at the wavelength 460 mμ using a spectrophotometer Beckman Model DU. The slit width was 0.02–0.03 mm and a 1 cm cell was used. In each series of experiments, a calibration was performed with potassium thiocyanate in order to determine the relationship between the absorbance and the concentration of thiocyanate. Sodium thiocyanate was used in solutions containing 4 M sodium perchlorate.

The flame photometric measurements. In some of the experiments at low ionic strengths, the concentration of sodium was determined by means of a spectrophotometer Beckman Model DU with a flame photometry attachment. The intensity of flame emission was measured at 589 mμ.

The radioactivity determination. The activity of 10 ml filtrate was measured with a G.M. tube for liquids, supplied by Mullard Ltd. The radioactivity of the silver thiocyanate was chosen to give about 700 c.p.m./10^{-4} M silver. Corrections had to be applied for the difference between the radioactive absorptions of solutions of low and high ionic strengths and for the radioactive decay. The scaler was an Electronic Counter PW 4035 from Philips.

The potentiometric measurements. The silver electrode was made according to Brown [3], but with thicker platinum wires in order to obtain larger electrode surfaces. A mercury-(I)sulphate electrode, consisting of a 4 M sodium perchlorate solution saturated with mercury(I)sulphate, served as reference electrode. The potentiometer equipment was obtained from Rubicon Co., Philadelphia and the galvanometer from Leeds & Northrup Co. The measurements were carried out at (20 ± 0.05)°C.

THEORY

For the quantitative analysis it is of interest to calculate the relation between the total concentrations of thiosulphate and thiocyanate. This calculation has been done on the assumption that solid silver thiocyanate is in equilibrium with the silver thiosulphate complexes in the solution. At the ionic strength $I = 0$, the calculation has only been performed for mononuclear complexes since no constants for polynuclear complexes are available in the literature at this ionic strength. The influence of hydrogen sulphite has also been studied. At the ionic strength $I = 4$, the calculations can be done more exactly since, in this case, the constants for the polynuclear complexes are known. At this ionic strength, the calculation is divided into two cases. In the first case, the solution is assumed to be supersaturated with $NaAgS_2O_3 \cdot H_2O$ whereas, in the second case, this salt is presumed to be in equilibrium with the solution. Whether $NaAgS_2O_3 \cdot H_2O$ could precipitate at the lower ionic strength cannot be decided from the literature data [4].

Solubility of silver thiocyanate at $I = 0$

Chateau and Pouradier [5] determined potentiometrically the mononuclear dissociation constants at 20°C for silver thiosulphate complexes. The constants

were recalculated by the authors to the ionic strength $I = 0$. From these values, the following complexity constants can be obtained

$$\beta_{1,1} = 6.7 \times 10^8,\ \beta_{1,2} = 2.9 \times 10^{13} \text{ and } \beta_{1,3} = 1.4 \times 10^{14}.$$

The constants are defined as

$$\beta_{1,n} = \frac{[Ag(S_2O_3)_n^{(2n-1)-}]}{[Ag^+]\ [S_2O_3^{2-}]^n}$$

(All concentrations in the present article are given in mole/litre).

Silver sulphite complexes were studied potentiometrically at 25°C by Chateau, Duranté and Hervier [6]. At the ionic strength $I = 0$, the complexity constants can be calculated to be $\gamma_{1,1} = 4 \times 10^5$, $\gamma_{1,2} = 4.8 \times 10^8$ and $\gamma_{1,3} = 10^9$. Chateau *et al.* also showed that the formation of silver sulphite complexes was low in a hydrogen sulphite solution owing to the low concentration of free sulphite. Consequently, all complexes except $AgSO_3^-$ can be neglected even in a rather concentrated hydrogen sulphite solution. From the constants for the silver thiosulphate complexes, it is clear that the complex with three ligands is not formed within the actual concentration range $c_{S_2O_3} < 1.5 \times 10^{-3}$. The concentration of uncomplexed silver ion and the concentrations of silver thiocyanate complexes [7], mixed silver thiosulphate-thiocyanate complexes (*cf.* under F), the ion pair $NaS_2O_3^-$ and $HS_2O_3^-$ can also be neglected [8]. All these ions can in addition be neglected in the calculations for the ionic strength $I = 4$. For the solubility product $L_R = [Ag^+][SCN^-]$, the value 1.08×10^{-12} has been used [9].

With these simplifications, the total thiosulphate content is

$$c_{S_2O_3} = [S_2O_3^{2-}] + [Ag^+]\ (\beta_{1,1}[S_2O_3^{2-}] + 2\beta_{1,2}[S_2O_3^{2-}]^2) \tag{1}$$

and the total sulphite content

$$c_{SO_3} = [SO_3^{2-}] + \frac{[H^+][SO_3^{2-}]}{k_2} + \frac{[H^+]^2[SO_3^{2-}]}{k_1 k_2} + [Ag^+]\,\gamma_{1,1}[SO_3^{2-}] \tag{2}$$

where

$$k_1 = \frac{[H^+]\ [HSO_3^-]}{[H_2SO_3]} \text{ and } k_2 = \frac{[H^+]\ [SO_3^{2-}]}{[HSO_3^-]}$$

The total thiocyanate content is

$$c_{SCN} = c_{Ag} = [Ag^+]\ (\beta_{1,1}[S_2O_3^{2-}] + \beta_{1,2}[S_2O_3^{2-}]^2 + \gamma_{1,1}[SO_3^{2-}]) \tag{3}$$

Since $c_{SCN} = [SCN^-]$, the following relations can be derived from eqns. (1) and (3)

$$c_{S_2O_3} = 2[SCN^-] - \frac{2\gamma_{1,1}L_R}{[SCN^-]}\ [SO_3^{2-}] + \left(1 - \frac{L_R\beta_{1,1}}{[SCN^-]}\right)\left\{\left[\left(\frac{\beta_{1,1}}{2\beta_{1,2}}\right)^2 + \right.\right.$$
$$\left.\left. + \frac{1}{\beta_{1,2}}\left(\frac{[SCN^-]^2}{L_R} - \gamma_{1,1}[SO_3^{2-}]\right)\right]^{\frac{1}{2}} - \frac{\beta_{1,1}}{2\beta_{1,2}}\right\} \tag{4}$$

and from (2)

$$[SO_3^{2-}] = \frac{c_{SO_3}}{1 + \frac{[H^+]}{k_2} + \frac{[H^+]^2}{k_1 k_2} + \gamma_{1,1} \frac{L_R}{[SCN^-]}} \quad (5)$$

On inserting the values of the constants, eqn. (4) becomes

$$c_{S_2O_3} = 2[SCN^-] - 8.64 \times 10^{-7} \frac{[SO_3^{2-}]}{[SCN^-]} + \left(1 - \frac{7.24 \times 10^{-4}}{[SCN^-]}\right)[(1.33 \times 10^{-10} + 0.0319\ [SCN^-]^2 - 1.38 \times 10^{-8}\ [SO_3^{2-}])^{\frac{1}{2}} - 1.16 \times 10^{-5}] \quad (6)$$

The relation $[SCN^-] = f(c_{S_2O_3})$, which is of interest here, was calculated numerically from eqn. (6) (*cf.* Fig. 2). It will be discussed later in connection with the results of the experiments. The solubility function was also calculated for the ionic strengths $I = 10^{-3}$ and $I = 10^{-4}$. It was found that the solubility at these ionic strengths was only a little higher than that at $I = 0$. For this calculation, a correction was introduced for the activity factors. The activity factors were calculated according to Debye-Hückel's approximation $-\log f_i = \frac{0.5\ z_i^2 \sqrt{I}}{1 + \sqrt{I}}$.

The influence of hydrogen sulphite was also estimated from eqn. (6). An addition of 0.1 M hydrogen sulphite, which corresponds to $[SO_3^{2-}] \sim 10^{-4}$, was found not to increase the solubility at the thiosulphate concentration 10^{-3} M while, at 10^{-4} M, the increase in the solubility amounted to 0.7 %. The comparison is made at the same ionic strength. However, if the increase in ionic strength is taken into consideration, then it is found that the solubility will be decreased by the addition of 0.1 M hydrogen sulphite.

Solubility of silver thiocyanate at $I = 4$

The dissolution of silver thiocyanate in thiosulphate, with 4 M sodium perchlorate as an additional salt, is somewhat different to that at the ionic strength $I = 0$, because of the formation of insoluble $NaAgS_2O_3 \cdot H_2O$. In a solution saturated with $NaAgS_2O_3 \cdot H_2O$, Nilsson [10] found the product $L_T = [Ag^+]\,[S_2O_3^{2-}] = 5.7 \times 10^{-14}$ at $I = 4$. At this ionic strength, the solubility product of silver thiocyanate is $L_R = 7.76 \times 10^{-13}$ according to Leden and Nilsson [9]. A comparison of these values shows that sodium silver thiosulphate is the more insoluble one. It can, however, be seen from Nilsson's work that $NaAgS_2O_3 \cdot H_2O$ precipitates slowly and therefore the calculations must also include the case in which a supersaturated solution is obtained.

No formation of $NaAgS_2O_3 \cdot H_2O$

The complexity constants for silver thiosulphate ions were determined by Nilsson [11] at $I = 4$ and 25°C. He found that the measurements could not be explained only by the formation of the mononuclear complexes $Ag(S_2O_3)_n^{(2n-1)-}$

but also the formation of polynuclear complexes had to be taken into consideration. The best agreement with the experimental results was obtained if the complexes $Ag_2(S_2O_3)_4^{6-}$ and $Ag_{3z}(S_2O_3)_{3z+2}^{(3z+4)-}$ were assumed to exist. From the complexity constants $\beta_{m,n}$ given by Nilsson (*cf.* Ref.[11], Table 5), it can be calculated that the ions Ag^+, $Ag(S_2O_3)_3^{5-}$, $Ag_2(S_2O_3)_4^{6-}$ and $Ag_3(S_2O_3)_5^{7-}$ can be neglected in the concentration range studied here ($c_{S_2O_3} < 5 \times 10^{-4}$). The concentration of $AgS_2O_3^-$ is also low but this ion can only be neglected in the upper part of the interval.

If the solution is supersaturated with $NaAgS_2O_3 \cdot H_2O$, then, using the above simplifications, the total silver and thiosulphate contents of the solution can be written:

$$c_{Ag} = [Ag^+] \sum_{n=1}^{2} \beta_{1,n} [S_2O_3^{2-}]^n + \sum_{z=2}^{\infty} 3z\beta_{3z,3z+2}[Ag^+]^{3z} [S_2O_3^{2-}]^{(3z+2)} \quad (7)$$

$$c_{S_2O_3} = [S_2O_3^{2-}] + [Ag^+] \sum_{n=1}^{2} n\beta_{1,n}[S_2O_3^{2-}]^n + \sum_{z=2}^{\infty} (3z+2)\beta_{3z,3z+2}[Ag^+]^{3z}[S_2O_3^{2-}]^{(3z+2)} \quad (8)$$

Since the sum of the polynuclear terms converges very slowly, the whole series must be summed. This summation was performed in Ref.[11] [*cf.* particularly eqns. (48)—(54)] where the constants h_0 and h where also defined. Upon summation, eqns. (7) and (8) become:

$$c_{Ag} = \beta_{1,1} [Ag^+] [S_2O_3^{2-}] + \beta_{1,2} [Ag^+] [S_2O_3^{2-}]^2 + \beta_{6,8} [Ag^+]^6 [S_2O_3^{2-}]^8 \times$$
$$\times \left[6 + h_0 \beta_{3,5} [Ag^+]^3 [S_2O_3^{2-}]^3 \frac{(9 - 6h \beta_{3,5} [Ag^+]^3 [S_2O_3^{2-}]^3)}{(1 - h \beta_{3,5} [Ag^+]^3 [S_2O_3^{2-}]^3)^2} \right] \quad (9)$$

$$c_{S_2O_3} = [S_2O_3^{2-}] + \beta_{1,1} [Ag^+] [S_2O_3^{2-}] + 2\beta_{1,2} [Ag^+] [S_2O_3^{2-}]^2 + \beta_{6,8} [Ag^+]^6 [S_2O_3^{2-}]^8 \times$$
$$\times \left[8 + h_0 \beta_{3,5} [Ag^+]^3 [S_2O_3^{2-}]^3 \frac{(11 - 8h \beta_{3,5} [Ag^+]^3 [S_2O_3^{2-}]^3)}{(1 - h \beta_{3,5} [Ag^+]^3 [S_2O_3^{2-}]^3)^2} \right] \quad (10)$$

Since the complexes are in equilibrium with solid silver thiocyanate, the concentration of free silver ions is $[Ag^+] = L_R [SCN^-]^{-1}$. For the thiocyanate, it is also valid that $c_{SCN} = [SCN^-] = c_{Ag}$. The function $[SCN^-] = f(c_{S_2O_3})$ can be calculated from these four relations by the trial and error method. The results of this calculation are given in Fig. 4 and are discussed below in connection with the results of the experiments.

Formation of $NaAgS_2O_3 \cdot H_2O$

If $NaAgS_2O_3 \cdot H_2O$ precipitates and if this salt is in equilibrium with the solution, then the system will be described by the following two material balances:

$$c_{Ag} = [SCN^-] = [Ag^+] \sum_{n=0}^{3} \beta_{1,n} [S_2O_3^{2-}]^n + 2\beta_{2,4} [Ag^+]^2 [S_2O_3^{2-}]^4 + \\ + 3\beta_{3,5} [Ag^+]^3 [S_2O_3^{2-}]^5 + \sum_{z=2}^{\infty} 3z\, \beta_{3z,3z+2} [Ag^+]^{3z} [S_2O_3^{2-}]^{(3z+2)} + c_s \qquad (11)$$

$$c_{S_2O_3} = [S_2O_3^{2-}] + [Ag^+] \sum_{n=1}^{3} n\beta_{1,n} [S_2O_3^{2-}]^n + 4\beta_{2,4} [Ag^+]^2 [S_2O_3^{2-}]^4 + \\ + 5\beta_{3,5} [Ag^+]^3 [S_2O_3^{2-}]^5 + \sum_{z=2}^{\infty} (3z+2)\, \beta_{3z,3z+2} [Ag^+]^{3z} [S_2O_3^{2-}]^{(3z+2)} + c_s \qquad (12)$$

Since in this case a general function $c_{S_2O_3} = f([SCN^-])$ can easily be derived, the equations will not be simplified as in the calculation for the supersaturated solution. In eqns. (11) and (12), c_s denotes the amount of $NaAgS_2O_3 \cdot H_2O$ formed by the reaction. Since the solution is in equilibrium with both solid silver thiocyanate and solid sodium silver thiosulphate, the concentration of free silver is $[Ag^+] = L_R[SCN^-]^{-1} = L_T[S_2O_3^{2-}]^{-1}$ and the concentration of free thiosulphate is $[S_2O_3^{2-}] = L_T\, L_R^{-1}\, [SCN^-]$.

After summation and elimination of c_s, $[Ag^+]$ and $[S_2O_3^{2-}]$, the following relation is obtained

$$c_{S_2O_3} = \left(1 + \frac{L_T}{L_R} + \beta_{1,2} \frac{L_T^2}{L_R} - \frac{L_R}{[SCN^-]^2}\right) [SCN^-] + 2\left(\frac{L_T}{L_R}\right)^2 \left[\beta_{1,3}\, L_T + \beta_{2,4}\, L_T^2 + \right. \\ \left. + \beta_{3,5}\, L_T^3 + \beta_{6,8}\, L_T^6 \left(1 + \frac{h_0 \beta_{3,5}\, L_T^3}{1 - h\, \beta_{3,5}\, L_T^3}\right)\right] [SCN^-]^2 \qquad (13)$$

and, on inserting the values of the constants:

$$c_{S_2O_3} = 0.0429\, [SCN^-]^2 + 1.096\, [SCN^-] - \frac{7.76 \times 10^{-13}}{[SCN^-]}$$

For the concentration range studied, the first and third term can be neglected and the simple relation $[SCN^-] = 0.91\, c_{S_2O_3}$ is obtained.

Whether an addition of hydrogen sulphite will increase the solubility of silver thiocyanate at $I = 4$ has not been calculated since no complexity constants for this system are available. The influence of this addition was very small at low ionic strengths and is assumed to be of the same order at high ionic strengths.

RESULTS AND DISCUSSION

A. *Stability of the colour.* On adding the acidic iron(III)solution to the filtrate, there is a risk that the silver thiosulphate complexes will decompose and hence silver thiocyanate will precipitate again. This problem has been studied by measuring the absorbance as a function of time. To 10 ml filtrate ($c_{S_2O_3} \sim 5 \times 10^{-4}$), 10 ml iron(III)solution was added. The solution was diluted to 50 ml before the colorimetric determination was performed.

Table 1. Stability of the colour.

Sample	Absorbance, after			
	10 min	30 min	50 min	90 min
$I \sim 0$	0.232	0.233	0.233	—
$I = 4$	0.250	0.250	0.250	0.253

The time values in Table 1 refer to the time passed since the addition of the iron(III)solution. As can be seen from the table, the colour is sufficiently stable to allow a reliable determination of the absorbance. After about 2—3 h, the colour intensity becomes smaller and the solution turns gradually turbid. In solutions containing hydrogen sulphite, a stable colour can only be obtained after the addition of an excess of formaldehyde.

In the following experiments it has been studied whether the measured absorbance really corresponds to the total thiocyanate content in the solution. Two solutions were investigated in this case. One of these consisted of 10 ml silver thiosulphate solution (containing 0.5 mM silver and 1 mM thiosulphate) and 10 ml 0.45 mM potassium thiocyanate, while in the other solution the silver thiosulphate was replaced by 10 ml water. To both solutions 10 ml iron(III)nitrate solution was added. The solutions were diluted to 50 ml and the absorbance was measured. The result of these measurements showed that the absorbance was exactly the same for the two solutions. This means that the colorimetric method gives the total thiocyanate content of the solutions, *i.e.* complexes of silver and thiocyanate and mixed complexes of silver, thiosulphate and thiocyanate can be neglected.

B. *Influence of the shaking time.* The influence of the shaking time has been studied by shaking 10^{-4} M thiosulphate with inactive silver thiocyanate. The results of these experiments (Fig. 1) show that the dissolved amount of thiocyanate remains constant in an interval from 10 to 40 min. Further shaking gives an increased dissolution and, after 8—9 h of rotation, the concentration of thiocyanate reaches a limit $c_{SCN} = 2\ c_{S_2O_3}$.

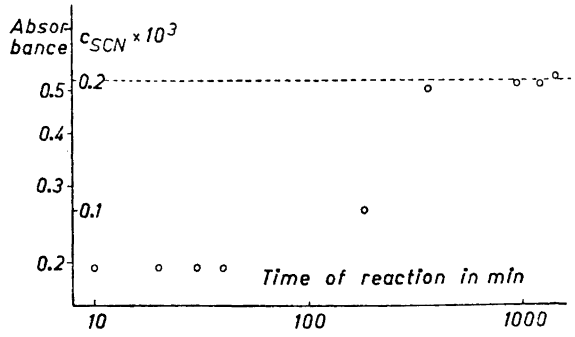

Fig. 1. Dissolution of silver thiocyanate as a function of time of reaction.

The precipitate turns gradually dark during the rotation, indicating a formation of silver sulphide. The dissolution reaction can in this case be written: $2\ AgSCN_{(s)} + S_2O_3^{2-} + H_2O \rightarrow Ag_2S_{(s)} + SO_4^{2-} + 2SCN^- + 2H^+$. Whether the experimentally found relation $c_{SCN} = 2c_{S_2O_3}$ is due to a complete transformation of thiosulphate into sulphide and sulphate according to this reaction has not yet been studied. — Similar observations were made by Dickinson [12], and by Chateau and Pouradier [13] for the dissolution of silver bromide in sodium thiosulphate. — From an analytical point of view, the sample can either be shaken for 10—40 min or rotated for about 8 h. In the latter case, a higher absorbance is obtained and, also, it is probable that the dissolution can be better reproduced. As will be reported in a forthcoming paper [14], this long time of reaction is not suitable for the determination of thiosulphate in solutions containing polythionates.

C. *Formation of* $NaAgS_2O_3 \cdot H_2O$ *at* $I \sim 0$. The precipitation of $NaAgS_2O_3 \cdot H_2O$ at $I \sim 0$ was investigated by measuring the sodium content before and after shaking. The determination of sodium was made flame photometrically. The experiments were carried out with 2×10^{-4} M thiosulphate. Parallel determinations of the thiocyanate concentration were performed colorimetrically.

Table 2. Determination of sodium content. Measuring-conditions: O_2-pressure 15 psi, C_2H_2-pressure 4 psi. Slit width 0.01 mm, sensitivity 3.

Time of shaking min	Sodium concentration		Thiocyanate concentration	
	Scale divisions	10^{-3} M	Absorbance	10^{-3} M
0	2.80	0.40	—	—
10	2.75	0.39	0.377	0.142
20	2.63	0.38	0.377	0.142
30	2.56	0.37	0.380	0.144
40	2.60	0.37	0.377	0.142

As is seen from Table 2, the sodium concentration decreases when the reaction time is increased from 10 to 40 min. This decrease cannot be due to an increased formation of $NaAgS_2O_3 \cdot H_2O$ since the thiocyanate concentration is constant during this interval of time. The sodium concentration of the filtrate is about 5 % less than that of the original solution. Because this decrease is probably partly caused by an adsorption of sodium ions on the solid silver thiocyanate, the formation of $NaAgS_2O_3 \cdot H_2O$ can be considered to be very small. Hence the dissolution of silver thiocyanate at this ionic strength must be due to a formation of complexes with silver ions.

D. *Determination of thiosulphate at low ionic strengths.* The investigations were performed for the thiosulphate concentration interval 2.5×10^{-5}—1.5×10^{-3} M. In Figs. 2 a and 2 b, the results with inactive silver and active silver are compared. The calculated relation $[SCN^-] = f(c_{S_2O_3})$ is also given in both figures. Fig. 2 a shows the solubility for $c_{S_2O_3} < 1.5 \times 10^{-3}$ while, in Fig. 2 b,

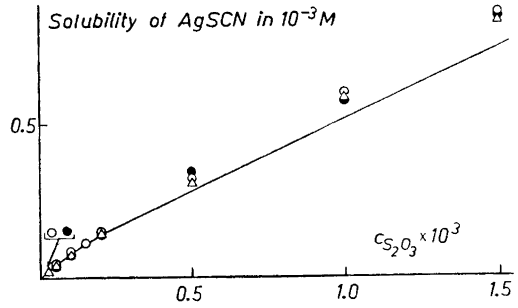

Fig. 2 a. Solubility of silver thiocyanate at low ionic strengths.
O c_{SCN}, inactive silver thiocyanate
● c_{SCN}, radioactive silver thiocyanate
△ c_{Ag}
— calculated solubility

the solubility for $c_{S_2O_3} < 2 \times 10^{-4}$ is shown on an enlarged scale. From Fig. 2 a, it is seen that both the calculated and found relationships between the thiocyanate content and the thiosulphate content are linear within a large interval. This linearity does not, however, extend over the whole concentration range investigated.

It can furthermore be seen from the figures that the experiments with inactive and active silver gave the same results despite the fact that these experiments were performed with different amounts of silver thiocyanate. This means that the method is reproducible even if the amount of silver thiocyanate added is varied. This result, as well as the fact that the solubility is independent of the time of shaking, shows that the solid phase is in equilib-

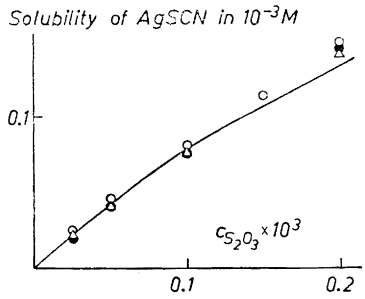

Fig. 2 b. Solubility of silver thiocyanate at low ionic strengths.
O c_{SCN}, inactive silver thiocyanate
● c_{SCN}, radioactive silver thiocyanate
△ c_{Ag}
— calculated solubility

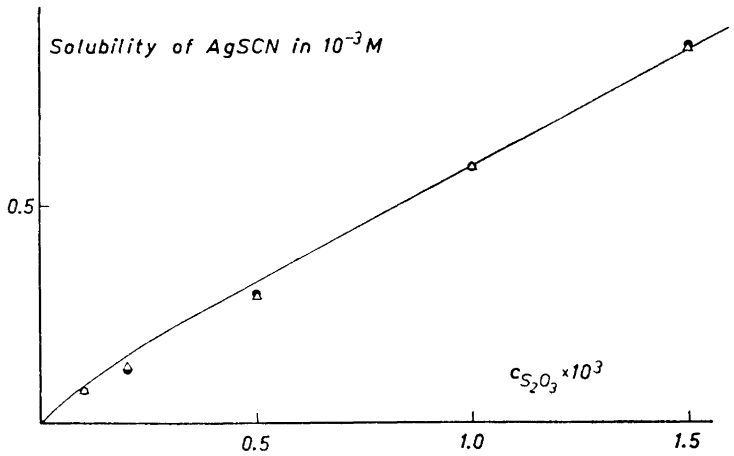

Fig. 3. Solubility of silver thiocyanate in thiosulphate solutions containing 0.1 M hydrogen sulphite.
● c_{SCN}
△ c_{Ag}
—solubility determined experimentally in solutions without hydrogen sulphite

rium with the solution. It is also seen that the silver content is equal to the thiocyanate content, which indicates that no solid phase containing silver is formed. The experimentally found curve deviates from the calculated one for $c_{S_2O_3} > 1.5 \times 10^{-4}$ (*cf.* Fig. 2 b). The calculated values are lower than those found experimentally and the deviation amounts to about 10 %. This deviation is probably due to the formation of polynuclear complexes. These complexes are partly included in the calculated function since the mononuclear dissociation constants [5] were determined without any corrections for polynuclear complexes.

Fig. 3 shows the results of the shaking experiments with thiosulphate and 0.1 M hydrogen sulphite. The curve obtained from the experiments without an addition of hydrogen sulphite is also drawn. It can be seen that the addition of hydrogen sulphite has only a slight influence, as already predicted by the theory. The solubility of silver thiocyanate in a neutral or alkaline sulphite solution is on the other hand considerable. This can be seen from Table 3 which contains the results of the experiments with solutions containing only sulphite.

Table 3. Solubility of silver thiocyanate in sulphite solutions.

c_{SO_3}	c_{Ag}
0.1	1.2×10^{-3}
0.01	4.7×10^{-4}

Summarizing this examination of the silver thiocyanate method at low ionic strengths, it can be said that thiosulphate can be determined in solutions with an excess of hydrogen sulphite but cannot be determined in solutions containing alkaline sulphite. The determination can be performed either colorimetrically or with a method using active silver thiocyanate. For the concentration interval $c_{S_2O_3} > 2 \times 10^{-4}$ the standard curve $[SCN^-] = f(c_{S_2O_3})$ can be approximated by the straight line $[SCN^-] = 0.53\ c_{S_2O_3} + 0.05 \times 10^{-3}$ which means that the solubility of silver thiocyanate does not increase proportional to the concentration of thiosulphate. For $c_{S_2O_3} < 2 \times 10^{-4}$ the standard curve deviates considerably from this straight line.

E. *Determination of thiosulphate at high ionic strengths.* A calculation of the function $[SCN^-] = f(c_{S_2O_3})$ at ionic strengths up to $I = 0.1$ indicates that the solubility decreases with increasing ionic strengths. The calculation of this function at higher ionic strengths is, however, difficult with the data available at the present for the complexity constants. In order to investigate the circumstances at various ionic strengths, some experiments with 10^{-3} M thiosulphate were performed. Sodium perchlorate was added to the thiosulphate solution in order to obtain the desired ionic strength (Table 4).

Table 4. Solubility of silver thiocyanate at various ionic strengths.

I	$c_{Ag} \times 10^3$	$c_{SCN} \times 10^3$
0.001	0.58	0.57
0.01	0.59	0.57
0.1	0.60	0.58
1	0.59	0.59

Contrary to the calculated results, the values found experimentally show that the solubility is independent of the ionic strength up to $I = 1$.

Particular interest is given in this paper to the course of the dissolution at $I = 4$. The investigation at this ionic strength was confined to the concentration range $c_{S_2O_3} < 5 \times 10^{-4}$. As in the investigations at the low ionic

Table 5. Solubility of silver thiocyanate at $I \sim 4$.

$c_{S_2O_3} \times 10^3$	$c_{SO_3} \times 10^3$	$c_{HCHO} \times 10^3$	$c_{Ag} \times 10^3$	$c_{SCN} \times 10^3$	Absorption coefficient
0.100	—	—	0.062	0.065	4.58
0.200	—	—	0.114	0.127	4.58
0.500	—	—	0.272	0.307	4.46
0.100	10	—	0.036	0.048	4.00
0.200	10	—	0.092	0.110	4.00
0.500	10	—	0.263	0.286	4.25
0.100	10	200	0.056	0.065	4.00
0.200	10	200	0.109	0.125	4.00

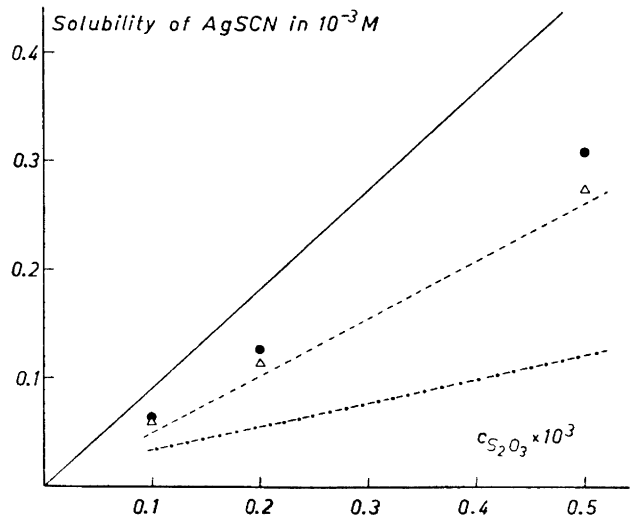

Fig. 4. Solubility of silver thiocyanate at $I = 4$.

● c_{SCN}
△ c_{Ag}
— c_{SCN}, calculated. The solution is assumed to be saturated with $NaAgS_2O_3 \cdot H_2O$
---- calculated solubility. The solution is assumed to be supersaturated with $NaAgS_2O_3 \cdot H_2O$.
----- calculated concentration of silver bound as mononuclear complexes in the supersaturated solution.

strength the influence of hydrogen sulphite was also studied. The results obtained from these investigations are given in Table 5. The table also contains the absorption coefficients obtained from the experiments with sodium thiocyanate solutions. The unit for the absorption coefficient values is $10^3\,M^{-1}\,cm^{-1}$. The results in Table 5 obtained without hydrogen sulphite are plotted in Fig. 4. As is seen from the results, the solubility of silver thiocyanate is considerably decreased by an addition of hydrogen sulphite. This effect can almost be eliminated by adding an excess of formaldehyde. For the analytical application, however, it must be pointed out that, in this case, the relation between the absorbance and the concentration of thiocyanate is not the same as that obtained for solutions without hydrogen sulphite and formaldehyde since a large excess of formaldehyde must be added before the colorimetric determination in order to obtain a stable colour. A corresponding change in the relationship between the absorbance and concentration of thiocyanate is also obtained at low ionic strengths.

In Fig. 4, the calculated solubility functions $[SCN^-] = f(c_{S_2O_3})$ are shown. The corresponding relation for the amount of silver, bound as mononuclear complexes in the supersaturated solution, is also presented in the figure. From this relation it can be seen that the amount of silver, bound as polynuclear complexes, is about 50 % of the total silver content. In solutions

saturated with $NaAgS_2O_3 \cdot H_2O$, the silver content is on the other hand very low and follows the equation, $c_{Ag} = 0.02\ c_{S_2O_3} + 1.3 \times 10^{-6}$, when $c_{S_2O_3} < 5 \times 10^{-4}$. All the silver is in this case bound as mononuclear complexes. The calculated solubility function, for saturated and supersaturated solutions, can in both cases be approximated by straight lines in the concentration range in question. As already shown in the theory, the relation $[SCN^-] = 0.91\ c_{S_2O_3}$ holds for the saturated solution.

A comparison between the experimentally found values and the calculated ones indicates that the solution is supersaturated with $NaAgS_2O_3 \cdot H_2O$. A small amount of precipitate is, however, formed since the silver content is lower than the thiocyanate content. The agreement between the calculated values and the experimental ones is considered to be acceptable. The calculated values are somewhat lower than the found ones. The experimentally found values also show that the solubility of silver thiocyanate is proportional to the concentration of thiosulphate which can also be seen from the results given in Table 6.

F. *Formation of mixed complexes.* In the investigations reported in literature, the dissolution of silver halogenides in thiosulphate solutions is assumed to occur by the formation of mononuclear silver thiosulphate complexes with various numbers of ligand ions. Yatsimirskii and Panova [15], however, are of the opinion that the formation of $AgS_2O_3^-$ and $Ag(S_2O_3)_2^{3-}$ is not so probable. They discuss the problem on the basis of experiments performed by Valenta [16] and consider that the results indicate the formation of the complex $AgXS_2O_3^{2-}$, where X is the halogenide. Valenta's experiments have also been discussed by Chateau and Pouradier [5]. They determined the mononuclear dissociation constants for $Ag(S_2O_3)_n^{(2n-1)-}$ and showed, with the aid of these values, that the solubility of the silver halogenides investigated by Valenta is mainly due to the formation of $Ag(S_2O_3)_2^{3-}$ and $Ag(S_2O_3)_3^{5-}$. Whether or not mixed complexes are formed is not discussed by Chateau and Pouradier.

From the results given under A in this work, it is seen that the formation of complexes between silver, thiosulphate and thiocyanate is negligible in solutions containing a large excess of iron(III)ion. The question whether mixed complexes exist in the filtrates from the shaking experiments (before the addition of iron(III)nitrate) has been studied in the present work by measuring the concentration of free silver ion $[Ag^+]$ and the total content of thiocyanate. The experiments were performed at the ionic strength $I = 4$ using inactive silver thiocyanate. For the potentiometric determination of the concentration of free silver ion, the cell can be written:

$$- \text{Ag} \mid \underset{I=4}{\text{filtrate}} \mid 4\ \text{M}\ NaClO_4 \mid Hg_2SO_4,\ \text{Hg} +$$

The emf (in mV) of this cell is at 20°C

$$E = E_0 - 58.17\ \log\ [Ag^+] = -81.3 - 58.17\ \log\ [Ag^+]$$

The value of E_0 was determined in a cell where the filtrate was replaced by silver perchlorate solutions of known concentrations. Sodium perchlorate was added to these solutions to make ionic strength $I = 4$. This determination

also gave a check that the electrodes followed Nernst's law. No corrections for the diffusion potentials were made since the ionic mobilities of the complexes formed were not known. The results are given in Table 6. Two series are reported — in the first, the experiments were performed with an aged precipitate while, in the latter, the precipitate was freshly prepared.

Table 6. Determination of [Ag+].

$c_{S_2O_3} \times 10^4$	$c_{SCN} \times 10^4$	E	$[Ag^+] \times 10^9$	$[Ag^+]\, c_{SCN} \times 10^{13}$	$c_{SCN} / c_{S_2O_3}$
1.00	0.59	375.5	14.0	8.3	0.59
2.00	1.17	397.1	5.97	7.0	0.59
5.00	2.97	423.8	2.08	6.2	0.59
1.00	0.61	376.9	13.3	8.1	0.61
2.00	1.17	398.1	5.74	6.7	0.59
3.50	2.11	414.9	2.95	6.2	0.60

If mixed complexes exist in the filtrate the product $c_{SCN}\,[Ag^+]$ will be higher than the solubility product of silver thiocyanate. The product $c_{SCN}[Ag^+]$ will in addition increase with the concentration of thiosulphate and thiocyanate, since the formation of the mixed complexes also increase. From Table 6 it is seen that the calculated product decreases with increasing thiosulphate concentration. In comparison with the value for the solubility product $L_R = 7.76 \times 10^{-13}$ given by Leden and Nilsson, all the calculated values are too low except those for the lowest concentration of thiosulphate. Consequently it cannot be shown by these experiments whether or not mixed complexes are formed. On the other hand, the potentiometric measurements and the experiments performed with radioactive silver indicate that the concentration of mixed complexes in the filtrate is considerably lower than predicted by Yatsimirskii and Panova.

From Table 6 it is seen that the dissolution is independent of the age of the precipitate. The calculated ratio $c_{SCN}/c_{S_2O_3}$ shows the linearity of the dissolution function.

G. *Determination of thiosulphate using other insoluble salts than silver thiocyanate.* The determination of thiosulphate as reported above is not limited to the use of silver thiocyanate. Utsumi [17] has also used copper(I)thiocyanate for the determination. In this case, Utsumi suggests an addition of 0.3 ml 6 N nitric acid to 10 ml of the sample before the shaking procedure in order to obtain a higher solubility. In the present investigation it was shown that, with such an addition, the solubility was very high even without the addition of thiosulphate. In a neutral thiosulphate solution, the solubility of the copper(I)thiocyanate was found to be lower than the solubility of silver thiocyanate at a corresponding thiosulphate concentration.

By using radioactive silver salts, the analytical method is not limited to those compounds where the solubility can be determined colorimetrically. Silver chloride, bromide and iodide can be employed. The solubility of silver

iodide is, however, too low from an analytical point of view. For dark coloured solutions, the method with radioactive silver is of course the only suitable one. In certain cases, a colorimetric method is available for dark coloured solutions if silver azide is used as solid salt. In this case, the filtrate is steam distilled in a Parnas [18] apparatus after addition of sulphuric acid. The volatile hydrazoic acid is driven off by the distillation and is subsequently absorbed in a receiver containing acidic iron(III)nitrate solution. Like thiocyanate, the azide ion forms coloured complexes with the iron(III)ion. These complexes have an absorption maximum at the wave-length 460 mμ. Since the hydrazoic acid is a weak acid ($K_s = 2.6 \times 10^{-5}$) and since the silver azide is comparatively soluble ($L = 2.6 \times 10^{-9}$), the use of silver azide is limited to weakly alkaline solutions which do not contain sulphite. The distillation procedure was tested in the present work. It was found that hydrazoic acid was completely driven off by passing 50 g steam through 30 ml 1 mM azide solution to which 2 ml 5 N sulphuric acid had been added. The relationship between added thiosulphate and dissolved silver azide was found to be nonlinear.

The author wishes to thank Docent I. Leden and Dr. R. O. Nilsson for valuable discussions and Mr. E. Seyfarth for assistance with the laboratory work. *Statens Tekniska Forskningsråd* and *Chalmerska Forskningsfonden* have supported the research financially, which support is gratefully acknowledged.

REFERENCES

1. Utsumi, S. *J. Chem. Soc. Japan, Pure Chem. Sect.* **74** (1953) 358.
2. Samuelson, O. and Westlin, A. *Svensk Papperstidn.* **50**, No. 11 B (1947) 149.
3. Brown, A. S. *J. Am. Chem. Soc.* **56** (1934) 646.
4. Basset, H. and Lemon, J. T. *J. Chem. Soc.* **1933** 1423.
5. Chateau, H. and Pouradier, J. *Sci. et inds. phot.* **24** (1953) 129.
6. Chateau, H., Duranté, M. and Hervier, B. *Sci. et inds. phot.* **27** (1956) 81, 257.
7. Leden, I. and Nilsson, R. O. *Z. Naturforsch.* **10a** (1955) 67.
8. Gimblett, F. G. R. and Monk, C. B. *Trans. Faraday Soc.* **51** (1955) 793.
9. Leden, I. and Nilsson, R. O. *Svensk Kem. Tidskr.* **66** (1954) 126.
10. Nilsson, R. O. *Arkiv Kemi* **12** (1958) 219.
11. Nilsson, R. O. *Arkiv Kemi* **12** (1958) 337.
12. Dickinson, H. O. *Sci. et inds. phot.* **28** (1957) 43.
13. Chateau, H. and Pouradier, J. *Sci. et inds. phot.* **25** (1954) 305; **27** (1956) 465.
14. Schöön, N.-H. *To be published.*
15. Yatsimirskiĭ, K. B. and Panova, V. E. *Zhur. Obshcheĭ Khim.* **22** (1952) 1284.
16. Valenta, E. *Sitz.-Ber. Akad. Wiss. Wien* 103, II. B, see also quotation by Cohen, E. *Z. physik. Chem.* **18** (1895) 61.
17. Utsumi, S. *J. Chem. Soc. Japan, Pure Chem. Sect.* **74** (1953) 526.
18. Parnas, J. K. *Z. anal. Chem.* **114** (1938) 261.

Received June 9, 1958.

ACTA CHEMICA SCANDINAVICA 12 (1958) 1746—1758

*iso*Thiocyanates XXXII.* Synthesis and Reactions of 3-Benzoyloxypropyl *iso*Thiocyanate, Enzymically Liberated from Glucomalcolmiin, and some Compounds of Related Structure

ANDERS KJÆR and ROALD BOE JENSEN

Organic Chemical Laboratory, Royal Veterinary and Agricultural College, Copenhagen, Denmark

Observations resulting in the discovery of a new mustard oil glucoside, *glucomalcolmiin*, in seeds of *Malcolmia maritima* R. Br. *(Cruciferae)* are discussed. Preliminarily reported evidence [1] for the structure of the corresponding *iso*thiocyanate, *malcolmiin*, has been supplemented by unequivocal proof of its structure. 3-Benzoyloxypropyl *iso*thiocyanate has been synthesized and its identity with malcolmiin definitely established. A structural expression for glucomalcolmiin is proposed.

The additional presence in *M. maritima* seeds of glucocheirolin is rigorously proved.

The complex picture observed on ammonia treatment of an enzymically hydrolyzed seed extract of *M. maritima* has been interpreted and the formation of tetrahydro-1,3-oxazine-2-thione corroborated by synthesis. Additional representatives of this little known class of heterocyclic compounds have been synthesized by base-induced ring-closure of the corresponding 3-hydroxyalkyl *iso*thiocyanates. The diminished cyclization tendency of these relative to the 2-hydroxyalkyl mustard oils is pointed out. The biogenesis of glucomalcolmiin is briefly discussed.

A preliminary communication of this series [1] announced the detection in Nature of a new *iso*thiocyanate glucoside, *glucomalcolmiin*, characterized by undergoing enzymic hydrolysis to glucose, sulphate and a mustard oil, tentatively formulated as 3-benzoyloxypropyl *iso*thiocyanate. It is the purpose of the present paper to describe in more detail the experimental data supporting the proposed structure, including the synthesis of the new mustard oil, as well as to expand on the chemistry of some structurally related compounds.

* Part XXXI of this series: *Botan. Tidsskr.* **54** (1958) 36.

The cruciferous genus *Malcolmia* comprises about 25 herbaceous species indigenous to the Mediterranean region. A few of these have attained horticultural significance, *e.g. Malcolmia maritima* (L.) R.Br.* which is easily procurable as seed material from commercial sources **. It is only recently, however, that its contents of *iso*thiocyanate-producing glucosides has been recognized. Thus, an earlier paper of this series [2], surveying the results of paperchromatographic analyses of volatile mustard oils in numerous seed samples, listed *Cheiranthus maritimus* as a species furnishing methyl *iso*thiocyanate on enzymic hydrolysis. This assignment proved untenable when authentic methyl mustard oil glucoside (glucocapparin) was encountered in our laboratory as a natural compound, occurring in several species belonging to the family *Capparidaceae* [3,4]. Schultz and Wagner [5,6], in a communication on paperchromatographic analysis of mustard oil glucosides in numerous plant species, reported the occurrence in seeds of *M. maritima* R.Br. of three partly unidentified glucosides, one of which was found to be present in small amounts only. Essentially the same pattern was observed independently in our laboratory on chromatography of the glucosides in a crude methanolic seed extract [1]. Conspicuous spots, possessing R_B-values [5] of 0.34 and 1.36, were noticed on chromatograms run with the upper layer of the solvent system: *n*-butanol: ethanol: water (4:1:4) as the mobile phase, whereas a minor, and still unidentified glucoside appeared as a weak spot with an R_B-value of 1.03.

Enzymic hydrolysis of a homogeneous preparation of the fastest moving glucoside (R_B 1.36), provided by elution of the appropriate zone from a band paper chromatogram with phosphate buffer, furnished a mustard oil possessing absorption characteristics in the ultra-violet region indicative of aromatic structure. A high-extinction maximum at 232 mμ, together with an auxiliary band of much lower intensity at about 270 mμ, suggested the presence in the *iso*thiocyanate of a conjugated aromatic system, possibly of the benzoyl-type. This pattern, in conjunction with the R_B-value of the parent glucoside, clearly demonstrated this to be different from all heretofore recorded mustard oil glucosides. In accord with common usage within this field the designation *glucomalcolmiin* was therefore introduced for the new natural product [1], affording the corresponding *iso*thiocyanate, *malcolmiin*, on enzymic hydrolysis.

Efforts were first directed towards the isolation of a crystalline thiourea-derivative of malcolmiin. When a purified glucoside extract, prepared from a larger amount of *Malcolmia maritima* seeds, was subjected to enzymic hydrolysis in a buffered solution at pH 6.8, an ether-soluble, optically inactive mustard oil fraction was produced. Subsequent treatment of this with methanolic ammonia resulted in the formation of crystalline malcolmiin-thiourea, $C_{11}H_{14}O_2N_2S$, devoid of optical activity and displaying UV-data in alcoholic solution [1] interpretable as ordinary thiourea-absorption (λ_{max}^{EtOH} 243 mμ) superimposed upon a benzoyl pattern (λ_{max}^{EtOH} 228 mμ, 270—280 mμ). Infrared absorption data [1] provided further evidence for the presence of a benzoate grouping in the thiourea, eventually established beyond doubt by the isola-

* *Nomen conservandum* over *Cheiranthus maritimus* L.

** The seed material employed in the present investigations was obtained from the company *J. E. Ohlsen's Enke*, Copenhagen K., Denmark.

tion of benzoic acid subsequent to alkaline hydrolysis. In water-saturated chloroform malcolmiin-thiourea migrated at a rate corresponding to an R_{Ph}-value [7] of 1.07. Several structural possibilities for malcolmiin, $C_6H_5COO(C_3H_6)NCS$, were discussed in the preliminary paper [1] and evidence adduced in favour of 3-benzoyloxypropyl *iso*thiocyanate, $C_6H_5COO(CH_2)_3NCS$, being the correct formulation.

This conclusion has now been verified by various synthetic approaches. Thus, malcolmiin (I) reacted with benzylamine to give the crystalline benzylthiourea (II) which could be smoothly transformed into the corresponding benzylurea (III) on treatment with a solution of silver nitrate in aqueous ethanol. The identity of (III) as 1-(3-benzoyloxypropyl)-3-benzylurea was ascertained by an unequivocal synthesis of the latter starting with 3-aminopropanol (IV).

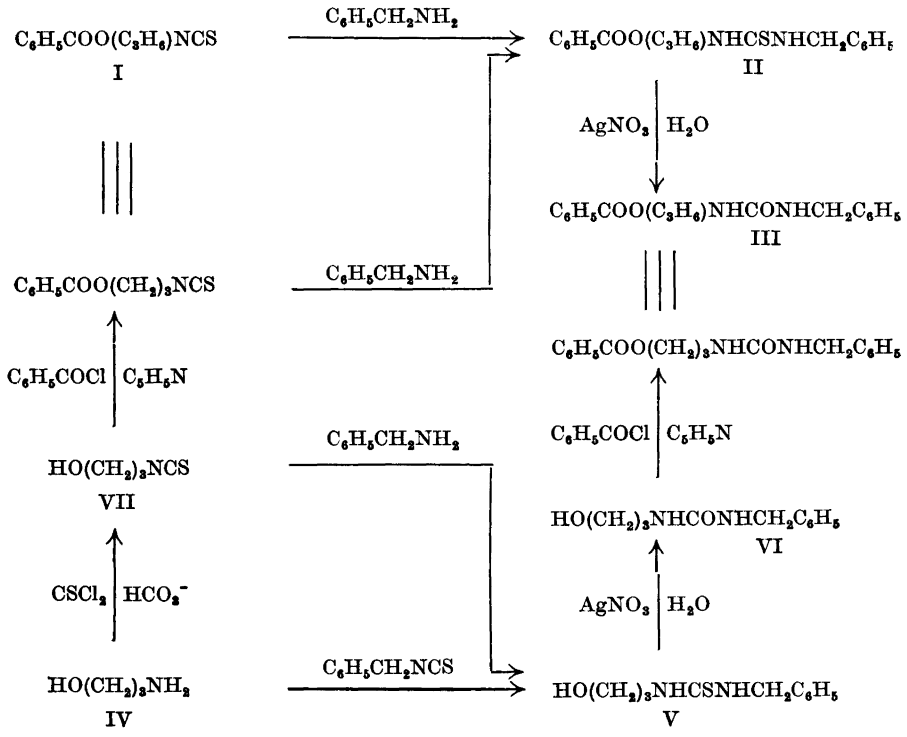

Reaction of this amino-alcohol with one molecular equivalent of benzyl *iso*thiocyanate afforded 1-benzyl-3-(3-hydroxypropyl)-thiourea (V), smoothly transformed by means of silver nitrate into the corresponding, syrupy benzylurea (VI). When benzoylated in pyridine solution the latter yielded 1-(3-benzoyloxypropyl)-3-benzylurea which proved identical with (III) on critical comparison.

A more direct structure proof for malcolmiin (I) was achieved by its synthesis. After several alternative routes had been unsuccessfully explored it was found that the bifunctional 3-aminopropanol (IV) on treatment with thiocarbonyl chloride in bicarbonate solution afforded a moderate yield of the distillable 3-hydroxypropyl *iso*thiocyanate (VII), the identity of which appeared from its reaction with benzylamine to give a benzylthiourea (V) indistinguishable from the specimen prepared as described above. Benzoylation of (VII) in pyridine solution proceeded easily to give 3-benzoyloxypropyl *iso*thiocyanate as a distillable, colourless oil with correct analytical figures. The identity of the synthetic mustard oil and malcolmiin (I) appeared from the fact that the former reacted with benzylamine to give 1-(3-benzoyloxypropyl)-3-benzylthiourea (II), identical with the benzylthiourea derivative of malcolmiin.

Glucomalcolmiin is a mustard oil glucoside of the ordinary type, furnishing glucose and sulphate in addition to malcolmiin on enzymic hydrolysis. Liberation of sulphate was demonstrated by reaction with barium ions, whereas the formation of glucose was established by paper chromatography in two solvent systems. Again, strong acid treatment of glucomalcolmiin produced hydroxylamine, a characteristic fission product as pointed out by Ettlinger and Lundeen [8] in support of the revised general structure for the *iso*thiocyanate glucosides advanced by these authors. Although conclusive evidence for the stereochemical details are lacking in the present case, it appears very likely that the glucomalcolmiin ion possesses the following structure:

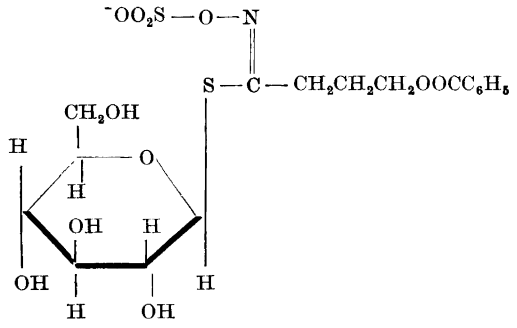

The accessibility of the new mustard oil (I) by synthesis prompted a closer study of its behaviour towards ammonia. The ester linkage and *iso*thiocyanate-grouping both constitute possible sites for nucleophilic attack by the base. In fact, several reaction products were encountered resulting from competing reactions at the vulnerable centers. The following scheme represents the predictable reaction products, the mutual relationships of which were established by paper chromatography.

Upon treatment of synthetic malcolmiin (VIII) with 0.5 N ethanolic ammonia for 40 min. at room temperature, a maximum yield of the corresponding 1-(3-benzoyloxypropyl)-thiourea (IX) was produced together with

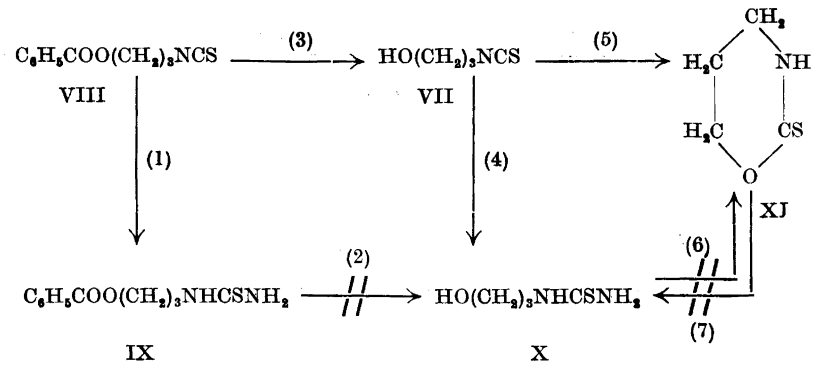

traces of 1-(3-hydroxypropyl)-thiourea (X). Prolonged exposure of (VIII) to ammonia resulted in an increase of the relative amounts of (X), whereas the benzoate-thiourea (IX) proved almost inert towards ammonia under the same conditions. Hence, the route (3)-(4) is the preferred path of reaction rather than (1)-(2) under the present circumstances, indicating an enhanced susceptibility to ammonolysis of the ester mustard oil compared to the ester thiourea. A solution of (VIII), which had been treated for 24 h with ammonia, afforded on paper chromatography in water-saturated chloroform a weak spot with a violet-blue Grote-reaction in addition to those of the thioureas (IX) and (X) and located intermediate between these. The same spot appeared, yet to a much larger extent and supplementary to the expected spot of (X), upon treatment of 3-hydroxypropyl mustard oil (VII) with ammonia. It therefore seemed reasonable to consider the unexpected by-product to be tetrahydro-1,3-oxazine-2-thione (XI), competitively formed by base-induced cyclization of (VII). This assumption was further strengthened by a synthesis of the previously unknown ring-compound (XI)[1] which on paper chromatography afforded a spot indistinguishable from that observed in the ammonia-treated reaction mixture. That the ring compound was produced by the direct route (5) rather than *via* the path (4)-(6) followed from the established inertness of (X) to excess ammonia. Again, the remote possibility of (X) being formed *via* the heterocyclic compound was ruled out on basis of the established stability of (XI) towards ammonia under the conditions employed.

The above conclusions provide a logical interpretation of the complex pattern observed on paper chromatography of crude thiourea fractions of enzymically hydrolyzed seed extracts of *Malcolmia maritima*, as presented and discussed in a preliminary communication [1].

Appropriate processing of a larger seed portion of *M. maritima* disclosed its content of a substantial amount of glucocheirolin, enzymically hydrolyzed to cheirolin (3-methylsulphonylpropyl *iso*thiocyanate) which was characterized as crystalline derivatives formed upon reaction with aniline and benzylamine [1]. The finding of glucocheirolin in *M.maritima* is not surprising in view of the long established occurrence of this glucoside in several *Cheiranthus* species (for a review *cf.* Ref.[9]), closely related botanically to the genus *Malcolmia*. As pointed out previously [1] one of the two spots reported by Schultz and

Wagner [5,6] in thiourea-chromatograms of *M.maritima* extracts was correctly attributed to cheirolin-thiourea whereas the second component, assigned by the same authors to a new, naturally occurring mustard oil, undoubtedly represents 1-(3-hydroxypropyl)-thiourea (X) the artifact character of which in the present case was demonstrated in our preliminary note [1].

The unexpected appearance of the heterocyclic compound (XI) during the present studies rendered a closer investigation of this ring-system desirable. Only one tetrahydro-1,3-oxazine-2-thione seems to have been previously recorded, *viz.* the 4,4,6-trimethyl-derivative prepared by Rosen [10] from 4-amino-4-methyl-2-pentanol. In the course of the current studies (±)-6-methyl- (XII) and 6,6-dimethyl-tetrahydro-1,3-oxazine-2-thione (XIII) were synthesized by treating the appropriate γ-amino-alcohols, *viz.* (±)-4-amino-2-butanol and 4-amino-2-methyl-2-butanol, respectively, with thiocarbonyl chloride in bicarbonate solution to give the corresponding (±)-3-hydroxybutyl (XIV) and 3-methyl-3-hydroxybutyl *iso*thiocyanate (XV) both of which could be cyclized in alkaline solution to the ring compounds (XII) and (XIII), respectively. The distillable mustard oils, (XIV) and (XV), were further characterized as crystalline thioureas formed on reaction with ammonia in chloroform solution. In addition, the benzylthiourea derivative of (XV) was prepared by reaction of 4-amino-2-methyl-2-butanol with benzyl *iso*thiocyanate.

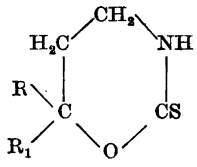

$R = H$, $R_1 = CH_3$: XII
$R = R_1 = CH_3$: XIII

$CH_3CHOHCH_2CH_2NCS$ XIV

$(CH_3)_2C(OH)CH_2CH_2NCS$ XV

In general, it appears that 3-hydroxysubstituted *iso*thiocyanates readily undergo intramolecular cyclization to tetrahydro-1,3-oxazine-2-thiones in alkaline solution, a reaction which is comparable to the analogous and well-established cyclization of 2-hydroxy-alkyl mustard oils to 2-oxazolidinethiones (XVI) [10–15] *. In connexion with the present studies a new representative of the latter class of heterocyclic compounds was synthesized, *viz.* (±)-5-ethyl-5-methyl-2-oxazolidinethione (XVII) derivable from (±)-1-amino-2-methyl-2-butanol which was, in turn, produced by reduction of 2-hydroxy-2-methyl-butyronitrile with lithium aluminium hydride.

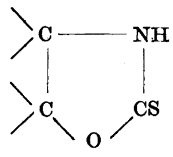

XVI

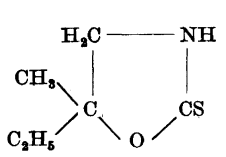

XVII

* For references to earlier papers *cf.* Ref.[11]

Infra-red spectra of the six-membered heterocyclic compounds, (XI)—(XIII), in the solid state or neutral solutions, indicated their character of tetrahydrooxazinethiones rather than dihydrooxazinethiols. In a detailed study, Ettlinger [16] formerly demonstrated several representative compounds of the five-membered class (XVI) to exist entirely in the thione form under comparable conditions.

Contrary to γ-hydroxysubstituted *iso*thiocyanates the tetrahydro-1,3-oxazine-2-thiones, (XI)—(XIII), exert a high-extinction band at 243 mμ in aqueous solution, displaced to 250 mμ in 96 % ethanol. Apart from a minor hyperchromic shift virtually no change of the absorption pattern occurs on addition of alkali provided prolonged exposure to strong base is avoided; if not, a slow but irreversible cleavage of the ring system takes place. Hence, spectrophotometric assays provide a convenient means of following the intramolecular cyclization under varying conditions. From such experiments it was concluded that: (i) a very rapid ring-closure occurs at pH 12 or above in ethanol solution, whereas at pH 10 or below the cyclization is extremely slow, (ii) hydrogen ions are without any promoting effect on the cyclization rate, (iii) a slow ring-closure occurs in boiling ethanol, and (iv) heating to a temperature as high as 125° without solvent does not result in appreciable ring formation. A less striking, but definite promoting effect was demonstrable with triethylamine although paperchromatographic controls indicated that with this base the ring-closure did not proceed to completion. Under standardized conditions there seemed to be a slight increase in the cyclization rate parallel to the increasing number of carbon atoms in the mustard oils. The above observations are consistent with the view that cyclization proceeds by nucleophilic attack of the deprotonized hydroxy substituent on the carbon atom of the *iso*thiocyanate grouping. Hence, the acid strength of the hydroxy-group as well as the intrinsic cyclization tendency may be expected to influence the over-all reaction rate, which, however, appears to be generally less than that prevailing in the corresponding 2-hydroxysubstituted *iso*thiocyanates under comparable conditions. Thus far, all syntheses designed to yield the latter compounds have invariably resulted in cyclized products.

Although no experimental evidence is yet available it appears reasonable to envisage glucomalcolmiin as biogenetically derived from *des*benzoylglucomalcolmiin containing the 3-hydroxypropyl-side chain. Furthermore, it may be of interest to consider a possible generic relationship of the latter with other well-established glucosides containing a 3-carbon unit in their side-chains, such as sinigrin, with the allyl-grouping, and glucoibervirin [17] possessing the methylthiopropyl radical as its side-chain. Glucoiberin and glucocheirolin may tentatively be regarded as secondarily formed oxidation products of glucoibervirin. Several examples of enzymic transformations between analogously substituted compounds can be adduced from modern biochemistry and suggest a common biogenetic pathway for these glucosides, a possibility which will be submitted to experimental trial in forthcoming studies.

EXPERIMENTAL

Melting points are uncorrected and determined in capillary tubes in a slowly heated bath. Analytical specimens have been dried *in vacuo* over calcium chloride at room temperature.

Most of the synthetic compounds described in the sequel have been prepared with no special view to establishing the optimal conditions for the reactions involved. Hence, in many cases the reported yields most likely can be improved considerably.

Spectroscopic detection of glucomalcolmiin. A concentrated methanolic extract of finely ground seeds of *Malcolmia maritima* was applied as a narrow band to the starting line of a 15 cm broad strip of prewashed Whatman paper No. 1. After descending chromatography for 24 h with the upper layer of the system *n*-BuOH:EtOH:H_2O (4:1:4) as the mobile phase, two edge cuts were employed for locating the band of the fastest moving glucoside by means of a silver nitrate spray. The appropriate area of the paper was cut out, eluted with dilute phosphate buffer (pH 6.8), and the resulting solution subjected to enzymic hydrolysis on addition of a drop of a cell-free myrosinase preparation [18]. After extraction of the liberated mustard oil (malcolmiin) with ether and displacement of the solvent by water, the ultra-violet absorption spectrum was determined. A sharp peak at 232 mμ and an inflexion of much lower extinction near 275 mμ were characteristic features, suggesting aromatic character of malcolmiin.

Isolation of malcolmiin and cheirolin as thiourea-derivatives. Finely ground seeds (500 g) of *M. maritima* were defatted with a total of 4 l of boiling carbon tetrachloride and then thoroughly extracted with 70 % methanol (2.5 l). After removal of the solvent *in vacuo*, the residue was taken up in water, treated with excess lead acetate and the white precipitate filtered off and discarded. Lead ions in the filtrate were precipitated by hydrogen sulphide and after repeated filtrations the solution was buffered with phosphates to pH 6.8, adjusted to a total volume of 2 l with water and subjected to enzymic hydrolysis by addition of a cell-free myrosinase preparation (15 ml). At the end of 12 h the mixture was extracted, first with three 300-ml portions of ether and then thrice with the same volumes of chloroform. In order to remove some coloured impurities both extracts were briefly washed with cold 1 N NaOH and then with water. The dried and concentrated extracts were now processed separately.

The chloroform fraction was treated with benzylamine (1 ml), resulting in the separation of a crystalline product (470 mg). Two recrystallizations from 10 % ethanol afforded *1-benzyl-3-(3-methylsulphonylpropyl)-thiourea* (cheirolin-benzylthiourea) (390 mg) as colourless, rhombic plates, m. p. 116°, identified on comparison with an authentic, synthetic specimen (m. p. 116°), prepared from cheirolin [19] and benzylamine (analyses previously published [1]).

The ether extract was divided into two halves. To the first was added aniline (1 ml), and the resulting crystalline precipitate (84 mg) was recrystallized twice from water to yield *1-(3-methylsulphonylpropyl)-3-phenylthiourea* (cheirolin-phenylthiourea) (54 mg), m. p. 138°, undepressed on admixture with a previously prepared synthetic specimen [19].

The remaining half of the ether extract was kept overnight in ammonia-containing methanol. Next day, the solvent was removed and the residue treated with hot ethyl acetate, leaving a slight amount of cheirolin-thiourea undissolved. Concentration of the filtrate resulted in separation of an oily fraction, paperchromatographically proved to be a mixture of 3-hydroxypropylthiourea (X) and tetrahydro-1,3-oxazine-2-thione (XI). Further concentration of the supernatant yielded a solid product which proved homogeneous on paper chromatography after one recrystallization from aqueous methanol (78 mg), m. p. 159°. Additional recrystallizations, first from ethyl acetate and then from 30 % ethanol, afforded *malcolmiin-thiourea* (23 mg) as colourless, dense, optically inactive crystals, m. p. 162° (analyses, UV- and IR-data as well as the R_{Ph}-value have been previously published [1]), undepressed on admixture with a specimen of synthetic 1-(3-benzoyloxypropyl)-thiourea (IX) described in the following.

A separate preparation of an ether extract, procured as just described, was treated with benzylamine to yield crystalline *malcolmiin-benzylthiourea* (101 mg), separating from a mixture of ethyl acetate and hexane as colourless crystals, m. p. 80.5°. Mixed melting point determination and coinciding infra-red spectra served to establish the identity of this derivative with a synthetic sample of 1-benzyl-3-(3-benzoyloxypropyl)-thiourea described in the sequel.

Desulphurization of malcolmiin-benzylthiourea (II). The benzylthiourea of natural malcolmiin (II) (100 mg), dissolved in 90 % ethanol (2 ml), was treated with silver nitrate (214 mg) in water (2 ml), and the solution was heated on a water-bath for 0.5 h. pH was kept at 7 by gradual addition of 0.5 N NaOH during the heating process. Precipitated Ag_2S was filtered off and the reaction product (15 mg) caused to separate by addition of water. Three recrystallizations from 80 % ethanol yielded a pure specimen (3 mg) of a compound, m. p. 145°, identified as 1-(3-benzoyloxypropyl)-3-benzyl-urea (III). No depression of the melting point was observed on admixture with an authentic specimen of the latter, prepared as described below. Furthermore, coinciding infra-red spectra served to confirm the identity.

Degradation of malcolmiin-thiourea. A sample of partly purified malcolmiin-thiourea (73 mg), secured as described above, was dissolved in ethanol containing excess of 0.1 N NaOH and left at room temperature for 48 h. The acidified solution was then extracted with ether and the extract concentrated to dryness. The residue (40 mg) was treated with charcoal in hot hexane, recrystallized once from water and finally sublimed to give pure benzoic acid (17 mg), m. p. 123°, undepressed on admixture with an authentic sample.

The aqueous solution was concentrated to dryness, dissolved in a few drops of water and chromatographed on paper, both in water-saturated chloroform and *n*-butanol: ethanol:water, together with synthetic 3-hydroxypropylthiourea *(vide infra)* from which it could not be distinguished. Both remained on the starting line in chloroform but travelled corresponding to an R_F-value of *ca.* 0.52 in the alcoholic system.

Degradation of glucomalcolmiin. A glucomalcolmiin fraction, prepared by elution of the appropriate zones from several band chromatograms, was subjected to enzymic cleavage in the usual way. After removal of malcolmiin by ether extraction, the concentrated aqueous phase was assayed for glucose by paper chromatography in *n*-butanol-ethanol:water (4:1:4) and pyridine:amyl alcohol:water (35:30:30). R_F-values of 0.16 and 0.34 were determined, respectively, the same as for simultaneously run reference samples of authentic D-glucose.

A separate sample of the aqueous phase yielded a positive sulphate reaction when tested with barium chloride. In both cases, appropriate blanks were checked in order to exclude positive reactions from possible trace constituents of the paper or enzyme preparation.

The dry residue from a similarly prepared solution of glucomalcolmiin was left overnight with excess of conc. HCl at room temperature. The liberation of hydroxylamine was demonstrated paperchromatographically by the method employed by Ettlinger and Lundeen [8].

1-Benzyl-3-(3-hydroxypropyl)-thiourea (V). 3-Aminopropanol (1.0 g) and benzyl *iso*thiocyanate (2.0 g) were mixed in ether (25 ml) and left at room temperature for 24 h. After removal of the solvent, the crystalline product was recrystallized twice from aqueous ethanol to yield the pure thiourea (2.84 g), m. p. 99° (Found: C 58.90; H 7.06; N 12.41. Calc. for $C_{11}H_{16}N_2OS$: C 58.89; H 7.19; N 12.49).

1-Benzyl-3-(3-hydroxypropyl)-urea (VI). The above thiourea (V) (2.0 g) was dissolved in ethanol (35 ml) and a solution of silver nitrate (3.0 g) in water (5 ml) was added. The mixture was heated on a water-bath for 20 min., and 0.5 N NaOH was gradually added to maintain pH 7. The solvents were removed in vacuum after filtration, and the reaction product dissolved in abs. ethanol and thus separated from $NaNO_3$. On concentration a colourless syrup separated which showed no signs of crystallization by various treatments.

1-(3-Benzoyloxypropyl)-3-benzyl-urea (III). To a solution of the syrupy urea (VI) (1.76 g) in dry pyridine (20 ml) freshly distilled benzoyl chloride (1.30 g) was added, and the mixture was set aside for 24 h. The brown solution was then diluted with ice-water (50 ml) when the oily precipitate readily crystallized. Three recrystallizations from 80 % ethanol afforded a pure specimen (686 mg) of the benzoylurea as glistening needles, m. p. 146°, alone or in admixture with the preparation above, derived from 'natural' malcolmiin-benzylthiourea. (Found: C 69.10; H 6.60; N 8.89. Calc. for $C_{18}H_{20}N_2O_3$: C 69.20; H 6.45; N 8.97). The infra-red spectrum (in KBr) displayed a strong benzoate C=O-band at 1 722 cm^{-1}.

3-Hydroxypropyl iso*thiocyanate* (VII). A mixture of 3-aminopropanol (16 g) in 5 % $NaHCO_3$-solution (270 ml) and thiocarbonyl chloride (25 g) in chloroform (350 ml) was vigorously stirred until the thiophosgene colour had disappeared. The dried chloroform

solution was concentrated and the yellow, pungent oil was distilled *in vacuo*. A small fore-run was followed by a constant boiling fraction (6.5 g), b. p. 80°/2 mm, of almost colourless 3-hydroxypropyl mustard oil, n_D^{25} 1.5432. A center-cut sample was analyzed. (Found: C 41.20; H 6.08; N 11.90. Calc. for C_4H_7NOS: C 40.98; H 6.02; N 11.95). A residue (2—3 g) of a very viscous product remained in the distilling flask. After a few weeks a distilled sample had changed into a similar product, probably of polymeric nature (polythiourethanes).

In order to prove the identity of the distilled mustard oil, a small sample was allowed to react with benzylamine in ether to give a quantitative yield of 1-benzyl-3-(3-hydroxypropyl)-thiourea (V) which, recrystallized from aqueous ethanol, had the m. p. 99°, undepressed on admixture with the product described above, prepared from 3-aminopropanol and benzyl *iso*thiocyanate.

3-Benzoyloxypropyl iso*thiocyanate (malcolmiin)* (I). In a typical experiment freshly distilled 3-hydroxypropyl mustard oil (1.56 g) was dissolved in dry pyridine (7 ml) and freshly distilled benzoyl chloride (2.5 g) was added. After 14 h at room temperature excess dilute HCl was added. When all benzoyl chloride was hydrolyzed, the solution was extracted with ether. The organic layer was washed with 5 % $NaHCO_3$-solution and water, and dried. The new *iso*thiocyanate distilled as a colourless oil (1.20 g), b. p. 144°/0.4 mm, n_D^{25} 1.5687. (Found: C 59.60; H 4.93; N 6.43. Calc. for $C_{11}H_{11}NO_2S$: C 59.73; H 5.01; N 6.33.)

1-(3-Benzoyloxypropyl)-thiourea (IX). Synthetic malcolmiin (150 mg) was dissolved in abs. ethanol (10 ml) and a 6 N solution of ammonia in the same solvent (1 ml) was added. After 40 min. at room temperature, the solvent and excess ammonia was removed *in vacuo*, leaving the thiourea (156 mg) as a colourless solid. This was recrystallized once from 30 % ethanol and once from ethyl acetate to give pure malcolmiin-thiourea (76 mg), m. p. 162°. Mixed melting point determination and coinciding infra-red spectra served to establish the identity of the product with the thiourea prepared from 'natural' malcolmiin and described above.

1-(3-Benzoyloxypropyl)-3-benzyl-thiourea (II). When synthetic malcolmiin (150 mg) was mixed with benzylamine (150 mg) in ether (5 ml), and the solution left overnight at room temperature, (II) (210 mg) crystallized on removal of the solvent and trituration of the residue with a few drops of dilute acid. Recrystallization, first from aqueous ethanol and thence from a mixture of ethyl acetate and hexane, afforded a colourless specimen for analysis, m. p. 80.5°, alone or in admixture with the above preparation from 'natural' malcolmiin. (Found: C 65.80; H 6.10; N 8.39. Calc. for $C_{18}H_{20}N_2O_2S$: C 65.82; H 6.14; N 8.53.)

1-(3-Hydroxypropyl)-thiourea (X). A solution of freshly distilled 3-hydroxypropyl *iso*thiocyanate (VII) (600 mg) in chloroform (100 ml), saturated with dry ammonia, deposited after 12 h at room temperature a crop (572 mg) of colourless crystals. An analytical specimen was produced by three recrystallizations from nitromethane, m. p. 131°. (Found: C 35.70; H 7.47; N 20.82. Calc. for $C_4H_{10}N_2OS$: C 35.80; H 7.51; N 20.89.) The thiourea (X) travels on paper chromatography in *n*-butanol-ethanol:water (4:1:4) at a rate corresponding to an R_F-value of 0.52.

Tetrahydro-1,3-oxazine-2-thione (XI). 3-Aminopropanol was subjected to mustard oil synthesis under non-aqueous conditions, according to the directions given by Hodgkins and Ettlinger [20]. The solution of the reaction product in triethylamine-containing chloroform was concentrated to a small volume, acidified with HCl and thoroughly extracted with ether. The turbid, dry ether extract contained a greenish oil which was refluxed in benzene solution for 0.5 h. Evaporation of the solvent resulted in the separation of a partly crystalline product which was purified by charcoal treatment in chloroform solution. Two recrystallizations from chloroform-pentane mixtures yielded the pure ring-compound as colourless plates, m. p. 129°. (Analyses previously published [1].) Yields were of the order of 20 % but could undoubtedly be improved. The ultra-violet spectrum in 96 % ethanol had λ_{max} 250 mμ (ε 14 200), in water: λ_{max} 243 mμ (ε 13 700). Addition of NaOH resulted in an increased molecular extinction (ε 16 300), yet at the same wavelength.

The infra-red spectrum (in KBr), though reminiscent of that of 2-oxazolidinethione, possessed several characteristic, individual features. Conspicuous bands were observed

at: 765 (m, broad), 810 (s), 914 (s), 964 (s), 1 052 (vs), 1 130 (s), 1 168 (vs), 1 210 (m), 1 238 (vs), 1 315 (vs), 1 374 (m), 1 478 (m), 1 578 (vs) and 3 200 (s) cm^{-1}.

In water-saturated chloroform the heterocyclic compound travelled at a rate corresponding to an R_{Ph}-value of 0.78.

(±)-3-Hydroxybutyronitrile. Propylene chlorohydrin (200 g), prepared from propylene oxide and HCl[21], was refluxed for 5 h with slightly more than one molecular equivalent of KCN dissolved in ethanol, and a trace of KI. The solvent was then distilled off and the residue fractionated *in vacuo* to give racemic 3-hydroxybutyronitrile (185 g) as a colourless liquid, b. p. 103°/13 mm. A similar procedure has been previously employed by Bruylants and Castille [22].

(±)-4-Amino-2-butanol. This amino-alcohol has previously been synthesized either by aluminium amalgam reduction of 2-hydroxybutyraldoxime [23,24] or, in 48 % over-all yield, by a two-step process from 1,3-butanediol cyclic sulphate [25]. In the present work, however, reduction of 3-hydroxybutyronitrile (8.5 g) with lithium aluminium hydride (10 g) in dry ether (300 ml), carried out in the usual way, proceeded satisfactorily to give 5.4 g of distilled amino-alcohol, b. p. 74—82°/10 mm. The broad boiling point range, noticed also by other workers [25], is undoubtedly ascribable to hydrate formation. The picrate melted at 122° (literature values [23,25] 122°.)

(±)-3-Hydroxybutyl iso*thiocyanate* (XIV). The above amine (3.6 g), dissolved in saturated $NaHCO_3$-solution (150 ml), was vigorously stirred with a solution of thiocarbonyl chloride (4.73 g) in chloroform (100 ml), until the red colour had disappeared. The chloroform layer was washed with dilute HCl and water, dried and distilled to remove the solvent. The residual oil was fractionated *in vacuo* to give a pure preparation (1.08 g) of the almost colourless mustard oil, b. p. 89°/0.5 mm, n_D^{25} 1.5267. (Found: C 45.95; H 6.96; N 10.50. Calc. for C_5H_9NOS: C 45.77; H 6.92; N 10.68.)

(±)-1-(3-Hydroxybutyl)-thiourea. A solution of the mustard oil (XIV) (150 mg) was kept in ammonia-saturated chloroform (75 ml) for 12 h. Removal of the solvent left a syrup which crystallized in contact with nitromethane to give the colourless thiourea (37 mg), which was recrystallized from the same solvent before analysis, m. p. 115°. (Found: C 40.49; H 8.09; N 18.80. Calc. for $C_5H_{12}N_2OS$: C 40.53. H 8.17; N 18.91.) In *n*-butanol-ethanol:water (4:1:4) the thiourea travels with an R_F-value of 0.64.

(±)-6-Methyl-tetrahydro-1,3-oxazine-2-thione (XII). A chloroform solution of 3-hydroxybutyl mustard oil, prepared from 3.78 g of 4-amino-2-butanol, as described above, was stirred with 1 N NaOH for 2 h at room temperature. After acidification, the organic phase was separated, dried and concentrated to yield a crystalline crop, embedded in an oil. The latter was removed by ether treatment and subsequently demonstrated to consist essentially of non-cyclized mustard oil.

The crystalline fraction (1.15 g) was purified by repeated recrystallizations from chloroform-pentane mixtures to give colourless needles, m. p. 142°. (Found: C 45.55; H 6.85; N 10.50. Calc. for C_5H_9NOS: C 45.77; H 6.92; N 10.68.) λ_{max}^{EtOH} 250 mμ (ε 15 500). The ring-compound travels in chloroform with an R_F-value of 0.82 (R_{Ph} 1.05).

3-Hydroxy-3-methyl-butyronitrile. 1-Chloro-2-methyl-2-propanol [26] (33 g) was dissolved in ethanol and placed together with excess NaCN in a round-bottomed flask, equipped with a reflux condenser, and heated locally to start an exothermic reaction. After this had ceased the mixture was gently refluxed for 1 h. The solvent was then removed, water was added and the reaction products extracted with ether. Distillation gave the pure cyanohydrin (21 g), b. p. 114°/30 mm, n_D^{25} 1.4277. (Found: C 60.80; H 9.08; N 13.90. Calc. for C_5H_9NO: C 60.59; H 9.15; N 14.14.)

The hydroxynitrile has been previously reported, yet with a deviating b. p., *viz.* 130—132°/30 mm (n_D 1.42911) [27].

4-Amino-2-methyl-2-butanol. Reduction of the above hydroxynitrile (10 g) with $LiAlH_4$ (7.6 g) in the usual way gave, after two distillations, the colourless amine as a viscous oil (5.3 g), b. p. 71.5°/10 mm, n_D^{25} 1.4484. (Found: C 58.20; H 12.65; N 13.63. Calc. for $C_5H_{13}NO$: C 58.19; H 12.70; N 13.58.)

A poorly characterized specimen of the same amine was reported by Barger and White [28] as a hydrolysis product of hydroxydihydrogalegin and also as a product resulting from the reaction between 4-amino-2-methyl-2-butene and dilute sulphuric acid.

1-Benzyl-3-(3-hydroxy-3-methyl-butyl)-thiourea. A solution of the above amine (300 mg) and benzyl *iso*thiocyanate (420 mg) in dry ether (20 ml) deposited after 0.5 h at room temperature a crop (594 mg) of almost pure thiourea. An analytical specimen was secured by two recrystallizations from aqueous ethanol, m. p. 127°. (Found: C 61.93; H 7.86; N 10.92. Calc. for $C_{13}H_{20}N_2OS$: C 61.86; H 7.99; N 11.05.)

3-Hydroxy-3-methyl-butyl iso*thiocyanate* (XV). 4-Amino-2-methyl-2-butanol (3.10 g) was treated with thiocarbonyl chloride (3.45 g) in bicarbonate solution exactly as described above for the lower homologue, to give 1.73 g of redistilled mustard oil, b. p. 77°/0.3 mm, n_D^{25} 1.5220. (Found: C 49.70; H 7.49; N 9.58. Calc. for $C_6H_{11}NOS$: C 49.63; H 7.64; N 9.65.)

1-(3-Hydroxy-3-methyl-butyl)-thiourea. This derivative was prepared from the above mustard oil (200 mg) and ammonia-saturated chloroform as described above for the lower homologue. The pure thiourea (150 mg) was obtained after two recrystallizations from nitromethane, m. p. 99°. (Found: C 44.54; H 8.60; N 17.14. Calc. for $C_6H_{14}N_2OS$: C 44.39; H 8.69; N 17.26.) On paper chromatography in *n*-butanol:ethanol:water (4:1:4) the R_F-value 0.69 was determined.

6,6-Dimethyl-tetrahydro-1,3-oxazine-2-thione (XIII). When 3-hydroxy-3-methyl-butyl *iso*thiocyanate (200 mg) was treated for 15 min. in ethanol (2 ml) with 0.1 N NaOH (15 ml) and then brought to pH 7 with acid, ether extraction yielded the cyclized product in crystalline form. An analytical specimen (40 mg) separated from ethyl acetate-hexane mixtures as colourless, nacreous plates, m. p. 136°. (Found: C 49.56; H 7.69; N 9.56. Calc. for $C_6H_{11}NOS$: C 49.63; H 7.64; N 9.65.) λ_{max}^{EtOH} 251 mμ (ε 14 500). R_F in chloroform 0.90 (R_{Ph} 1.15).

(±)-1-Amino-2-methyl-2-butanol. Methyl ethyl ketone cyanohydrin (7.6 g) was smoothly reduced with lithium aluminium hydride (5.3 g) in anhydrous ether (200 ml) under the usual conditions. The resulting amino-alcohol was obtained after distillation as a viscous, colourless oil (3.2 g), b. p. 69°/12 mm. It was characterized as the *neutral oxalate*, separating from hot ethanol in nacreous plates, m. p. 193°. (Found: C 48.58; H 9.50; N 9.43. Calc. for 2 $C_5H_{13}ON$, $C_2H_2O_4$: C 48.62; H 9.52; N 9.45.)

The amino-alcohol has formerly been characterized as its nitrate [30] and its hygroscopic hydrochloride, the latter though with varying melting points [29,30].

(±)-5-Ethyl-5-methyl-2-oxazolidinethione (XVII). The above amine (2.5 g) was subjected to the general conditions designed by Hodgkins and Ettlinger [20] for mustard oil synthesis under non-aqueous conditions. The oily reaction product crystallized in a desiccator to the cyclic compound (1.20 g) of which an analytical specimen separated slowly from water as compact, colourless rhombs, m. p. 52–53°. (Found: C 49.15; H 7.57; N 9.58. Calc. for $C_6H_{11}NOS$: C 49.63; H 7.64; N 9.65.)

The valuable assistance of Dr. R. Gmelin in the preliminary phases of the present work is gratefully acknowledged. Microanalyses have been performed by Mr. P. Hansen at the Chemical Laboratory of the University of Copenhagen.

The work is part of investigations supported by *Statens Almindelige Videnskabsfond (The Danish State Research Foundation)* and *Carlsbergfondet (The Carlsberg Foundation)*. A special grant from *Kai Hansen's Fond* is also gratefully acknowledged.

REFERENCES

1. Kjær, A. and Gmelin, R. *Acta Chem. Scand.* **10** (1956) 1193.
2. Kjær, A., Conti, J. and Larsen, I. *Acta Chem. Scand.* **7** (1953) 1276.
3. Kjær, A., Gmelin, R. and Larsen, I. *Acta Chem. Scand.* **9** (1955) 857.
4. Kjær, A. and Gmelin, R. *Acta Chem. Scand.* **10** (1956) 335.
5. Schultz, O.-E. and Wagner, W. *Z. Naturforsch.* **11b** (1956) 73.
6. Wagner, W. *Papierchromatographische Analyse der Senfölglucoside, präparative Darstellung ihrer Acetylderivate und ein Beitrag zu ihrer allgemeinen Struktur* (Diss.) University, Tübingen 1956.
7. Kjær, A. and Rubinstein, K. *Acta Chem. Scand.* **7** (1953) 528.
8. Ettlinger, M. G. and Lundeen, A. J. *J. Am. Chem. Soc.* **78** (1956) 4172.

9. Kjær, A. *Encyclopedia of Plant Physiology*, Springer-Verlag, Berlin-Göttingen-Heidelberg, 1958, vol. IX, p. 71.
10. Rosen, A. A. *J. Am. Chem. Soc.* **74** (1952) 2994.
11. Kjær, A., Gmelin, R. and Boe Jensen, R. *Acta Chem. Scand.* **10** (1956) 432.
12. Ettlinger, M. G. *J. Am. Chem. Soc.* **72** (1950) 4792.
13. Viscontini, M. and Adank, K. *Helv. Chim. Acta* **33** (1950) 2251.
14. Bergmann, E. D. and Herman, D. F. *J. Appl. Chem. (London)* **3** (1953) 42.
15. Kjær, A. and Gmelin, R. *Acta Chem. Scand.* **11** (1957) 906.
16. Ettlinger, M. G. *J. Am. Chem. Soc.* **72** (1950) 4699.
17. Kjær, A., Gmelin, R. and Larsen, I. *Acta Chem. Scand.* **9** (1955) 1143.
18. Neuberg, C. and Wagner, J. *Biochem. Z.* **174** (1926) 457.
19. Kjær, A., Marcus, F. and Conti, J. *Acta Chem. Scand.* **7** (1953) 1370.
20. Hodgkins, J. E. and Ettlinger, M. G. *J. Org. Chem.* **21** (1956) 404.
21. Michael, A. *Ber.* **39** (1906) 2785.
22. Bruylants, P. and Castille, A. *Bull. soc. chim. Belges* **34** (1925) 261.
23. Robinson, R. and Suginome, H. *J. Chem. Soc.* **1932** 304.
24. Sasaki, S. and Ri, S. *Bul. Sci. Fak. Terkult. Kyushu Imp. Univ. Fukuoka, Japan* **11** (1944) 86; *cf. Chem. Abstracts* **43** (1949) 5367.
25. Lichtenberger, J. and Lichtenberger, R. *Bull. soc. chim. France* **1948** 1002.
26. Burgin, J., Hearne, G. and Rust, F. *Ind. Eng. Chem.* **33** (1941) 385.
27. Lemaire, J. *Rec. trav. chim.* **29** (1910) 22, p. 59.
28. Barger, G. and White, F. D. *Biochem. J.* **17** (1923) 827.
29. Fourneau, E. *J. pharm. chim.* [7] **2** (1910) 56, 109; *cf. Chem. Zentr. 1910*, II, 1365.
30. Barbière, J. *Bull. soc. chim. France* **11** (1944) 470.

Received July 5, 1958.

ACTA CHEMICA SCANDINAVICA 12 (1958) 1759—1761

Approximate Calculations of Mean Amplitudes of Vibration

S. J. CYVIN and J. BAKKEN

Institutt for teoretisk kjemi, Norges tekniske høgskole, Trondheim, Norway

The mean amplitudes of vibration for the interatomic distances in several four-atomic molecules are calculated by an approximate method, and the results are compared to the rigorously calculated values. The method is based on a four-constant approximation for the hyperbolic cotangent and gives the mean amplitudes with about 1/2 percent accuracy.

Morino *et al.*[1] have developed an approximate formula for calculating mean square amplitudes of vibration, assuming $\coth t = 1/t + t/4$. This approximation is applicable only for frequencies below 1 200 cm^{-1} and may give as much as 4 % error in the mean amplitude. In the present investigation, a four-constant approximation, *viz.*

$$\coth t = -\Theta_{-3}t^{-3} + \Theta_{-1}t^{-1} + \Theta_1 t - \Theta_3 t^3$$

has been applied. The resulting formula for the mean square amplitude may be written

$$\overline{R_i^2} = -\delta\ (\mathrm{FGF})^{-1}_{ii} + \gamma\ \mathrm{F}^{-1}_{ii} + \alpha\ \mathrm{G}_{ii} - \beta\ (\mathrm{GFG})_{ii}$$

where F and G denote the energy matrices introduced by Wilson [2], and

$$\alpha = h^2\Theta_1/16\pi^2 kT;\quad \beta = h^4\Theta_3/256\pi^4(kT)^3$$

$$\gamma = \Theta_{-1}kT\ :\quad \delta = 16\Theta_{-3}\pi^2(kT)^3/h^2$$

The contants Θ may be adjusted by a least-squares technique for a given interval of t. It has been possible to construct functions with at the most about 1 % deviation from the hyperbolic cotangent in the following intervals:

I	$t = 0.5$—4.0	(207—1 658 cm^{-1})
II	$t = 1.0$—5.5	(414—2 279 cm^{-1})
III	$t = 1.5$—6.5	(622—2 694 cm^{-1})
IV	$t = 2.0$—7.5	(829—3 108 cm^{-1})

Table 1. Calculated mean square amplitudes.

Molecule	Distance	Mean square amplitude ($Å^2$) *	Range of frequencies (cm^{-1})	Ref.
P_4	P–P	$0.06457a - 0.009531\beta + 0.4961\gamma - 4.3079\delta$	363 – 606	3
ND_3	N–D	$0.5679a - 2.1116\beta + 0.1536\gamma - 0.04243\delta$	749 – 2 555	3
	D–D	$0.9930a - 2.3322\beta + 0.8355\gamma - 1.3597\delta$		
NH_3	N–H	$1.0636a - 7.1948\beta + 0.1575\gamma - 0.02344\delta$	950 – 3 337	3
	H–H	$1.9844a - 9.1025\beta + 0.8699\gamma - 0.8296\delta$		
PH_3	P–H	$1.0243a - 3.2640\beta + 0.3215\gamma - 0.1010\delta$	992 – 2 328	4; 5
	H–H	$1.9841a - 3.8743\beta + 1.7552\gamma - 2.2467\delta$		
AsH_3	As–H	$1.0054a - 2.6630\beta + 0.3796\gamma - 0.1434\delta$	906 – 2 123	6; 5
	H–H	$1.9841a - 3.2054\beta + 2.1525\gamma - 3.3872\delta$		
SbH_3	Sb–H	$1.0003a - 2.1112\beta + 0.4739\gamma - 0.2246\delta$	782 – 1 894	7; 5
	H–H	$1.9841a - 2.5041\beta + 2.9850\gamma - 6.5533\delta$		
CH_2O	C–H	$1.0753a - 5.1578\beta + 0.2253\gamma - 0.04783\delta$	1 280 – 2 874	
	C–O	$0.1458a - 0.2705\beta + 0.08365\gamma - 0.04955\delta$	1 503 – 2 780	3
	H–H	$1.9841a - 7.5236\beta + 0.6839\gamma - 0.3247\delta$	1 503 – 2 780	
	O–H	$1.0546a - 3.4850\beta + 0.5137\gamma - 0.3781\delta$	1 280 – 2 874	

* Based upon the atomic weight units for masses and mdyne/Å for force constants.

The proper one of the alternatives I to IV should be selected according to the magnitude of the fundamentals contributing to the desired mean amplitude. The corresponding intervals of frequencies, referring to the temperature 298 °K, are included above. Thus the present formula will give not more than

Table 2. Mean amplitudes of vibration in Å units at 298 °K.

Molecule	Distance	Approximation I	II	III	IV	Rigorous
P_4	P–P	0.0534				0.0533 [8]
ND_3	N–D			0.0619		0.0618
	D–D			0.1042		0.1040
PH_3	P–H			0.0866	0.0862	0.0862 [8]
	H–H			0.1512	0.1514	0.1521 [8]
AsH_3	As–H		0.0896	0.0899	0.0893	0.0894 [8]
	H–H		0.1587	0.1598	0.1596	0.1597 [8]
SbH_3	Sb–H		0.0950	0.0946		0.0944 [8]
	H–H		0.1734	0.1745		0.1736 [8]
CH_3O	C–H				0.0798	0.0801 [8]
	C–O				0.0375	0.0372 [8]
	H–H				0.1201	0.1170 [8]
	O–H				0.0944	0.0912 [8]

about 0.5 % error in the mean amplitude for vibrational frequencies within the indicated intervals.

The method has been applied to several molecules with the results given in Table 1, which also includes the actual intervals of frequencies with references to the experimental data. The mean amplitudes calculated by the approximate method are given in Table 2. In accordance with the prediction, it is seen that most of the present results deviate less than 0.5 % from the rigorously calculated values. The mean amplitudes for NH_3 are not included in Table 2, because the extremely high frequency 3 337 cm^{-1} falls outside the chosen intervals. The approximation IV gives 0.0715 Å for N—H and 0.1227 Å for the H—H mean amplitude. When compared with the rigorously calculated values 0.0727 and 0.1236 Å, the errors 1.7 and 0.7 % are found for the N—H and H—H amplitudes, respectively.

Further details concerning the method and development of the formula is to be published later.

REFERENCES

1. Morino, Y., Kuchitsu, K., Takahashi, A. and Maeda, K. *J. Chem. Phys.* **21** (1953) 1927.
2. Wilson, E. B. Jr. *J. Chem. Phys.* **7** (1939) 1047; **9** (1941) 76.
3. Herzberg, G. *Infrared and Raman Spectra of Polyatomic Molecules*, N. Y. 1945.
4. McConaghie, V. M. and Nielsen, H. H. *J. Chem. Phys.* **21** (1953) 1836.
5. Loomis, C. C. and Strandberg, M. W. P. *Phys. Rev.* **81** (1951) 798.
6. McConaghie, V. M. and Nielsen, H. H. *Phys. Rev.* **75** (1949) 663.
7. Haynie, W. H. and Nielsen, H. H. *J. Chem. Phys.* **21** (1953) 1839.
8. Bakken, J. *Acta Chem. Scand.* **12** (1958) 594.

Received August 5, 1958.

ACTA CHEMICA SCANDINAVICA 12 (1958) 1762—1767

Fungus Pigments

X.* The Ultra-violet Absorption of Some Substituted 2,5-Diphenylbenzoquinones and their Leucoacetates

JARL GRIPENBERG

Department of Chemistry, Finland Institute of Technology, Helsingfors, Finland

The ultra-violet absorption spectra of a number of substituted 2,5-diphenylbenzoquinones and their leucoacetates have been determined. These spectra and their significance in structure determination are discussed.

During the investigation of aurantiacin, the most recently isolated member of the diphenylbenzoquinone pigments found in fungi, the ultra-violet absorption spectrum was of considerable help in the structure determination [1].

It was felt that a knowledge of the spectra of other substituted diphenylbenzoquinones might be of value in future work. The spectra of a number of such compounds were therefore measured in dioxan solution and the results are given in Table 1.

Dioxan was selected because it is the only suitable solvent which is not too polar in which all the compounds are sufficiently soluble. The spectrum of 2,5-diphenylbenzoquinone (I) in carbon tetrachloride has been published by Flaig *et al.*[2] and it agrees well with that obtained here. Murray [3] reported maxima at 388 and 494 mμ for polyporic acid (II) in pyridine; in this solvent, however, polyporic acid is present at least partly as an anion, and the absorption is therefore not comparable with the data given here.

All the spectra have two maxima, that at shorter wave-length being always the stronger. The spectra are divided clearly into two distinct groups by the position of the second maximum. In the first, substances I—VIII, this maximum lies between 330 and 350 mμ. In substances IX—XVI forming the second group, this maximum is at 380—405 mμ. On inspecting the structural features of the compounds in the two groups, it is obvious, that in all those belonging to the first group, R is either hydrogen or an acylated hydroxyl, while in the second group R is hydroxyl or methoxyl. The nature of the substituent

* IX *Acta Chem. Scand.* 12 (1958) 1411.

Table 1.

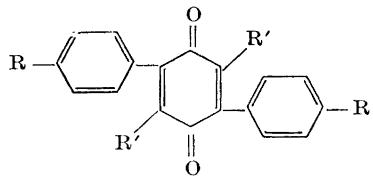

			max$_1$		max$_2$	
			mμ	log ε	mμ	log ε
I	R = H;	R′ = H	240	4.37	338	3.94
II	R = H;	R′ = OH	261	4.45	332	3.86
III	R = H;	R′ = $OCOCH_3$	240	4.33	336	3.78
IV	R = $OCOCH_3$;	R′ = H	246	4.49	346	4.02
V	R = $OCOCH_3$;	R′ = $OCOCH_3$	247	4.46	347	3.82
VI	R = $OCOCH_3$;	R′ = $OCOC_6H_5$	244	4.67	350	3.81
VII	R = $OCOC_6H_5$;	R′ = $OCOC_6H_5$	244	4.82	351	3.89
VIII	R = $OCOC_6H_5$;	R′ = OCH_3	242 *	4.66	337	3.82
IX	R = OH;	R′ = H	252	4.48	393	4.03
X	R = OCH_3;	R′ = H	251	4.43	390	3.98
XI	R = OH;	R′ = OH	268	4.55	385	3.66
XII	R = OH;	R′ = OCH_3	256	4.34	386	3.64
XIII	R = OCH_3	R′ = OH	268	4.55	382	3.66
XIV	R = OCH_3;	R′ = OCH_3	257	4.45	385	3.70
XV	R = OH;	R′ = $OCOC_6H_5$	240	4.63	405	3.82
XVI	R = OCH_3;	R′ = $OCOC_6H_5$	242	4.65	404	3.80

* In addition an inflexion at 260 mμ (4.45)

R′, on the other hand, seems to be much less important because both types of substituents occur in both groups.

A hydroxyl or methoxyl group in the *p*-position of the aromatic ring thus has a bathochromic effect, which disappears on acylation. A hydroxyl or methoxyl group attached directly to the quinone ring has no such effect and in fact a slight hypsochromic effect can be observed (Compare: II with I; VIII with VII; XI, XII, XIII and XIV with IX and X).

The effect of different substituents on the short wave maximum is more difficult to determine because in the substances with a benzoyl group the absorption of this group will appear in the same region and may thus mask the absorption of the parent substance. The contribution of the benzoyl group to the absorption is seen clearly in the higher extinction coefficient for the benzoates. The substance VIII forms a special case. In addition to the maximum at 242 mμ there is an inflexion at ~ 260 mμ (The complete absorption curve of this substance is reproduced in Part IV [1]). It is assumed that the maximum at 242 mμ is due to the benzoyl group and that the absorption of the other part of the molecule is responsible for the inflexion.

Hydroxyl or methoxyl groups in the *p*-positions have a bathochromic effect as is shown by comparison of IX and X with I and of XI and XIII with II. An apparent exception is formed by XV and XVI which show no bathochromic shift in the short-wave band in spite of a hydroxyl or methoxyl group in

the *p*-position. This is probably the result of overlapping of the absorption referred to above.

Hydroxyl groups and to a lesser extent methoxyl groups in the quinone ring have a definite bathochromic affect on the short-wave band as is readily seen by a comparison of II with I, and of XI, XII, XIII and XIV with IX and X. The inflexion in VIII will also be due to such an effect. This bathochromic effect is at least partly removed by acylation (see III, XV and XVI).

The effect of the substituents in the *p*-positions on the long wave absorption maximum is readily understood, on the assumption that this absorption is the result of an electronic transition leading to excited forms such as A and B

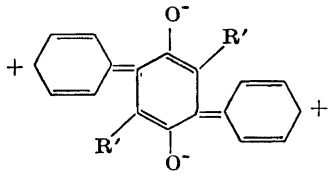

A

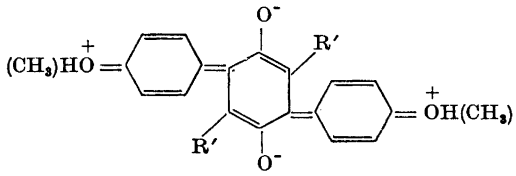

B

that is, that the chromophore is composed of two benzylideneketone systems.

Table 2.

	max_1		max_2	
	mμ	log ε	mμ	log ε
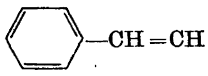	220.5	4.08	286	4.37
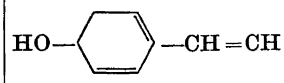	234	4.01	323	4.37
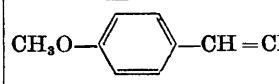	232	4.02	318	4.39
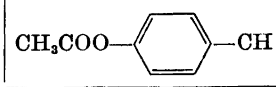	223	4.06	290	4.36

As can be seen from the figures reported in Table 2, which are taken from the work of Wilds *et al.*[4], the effect of a substituent in the aromatic ring in benzylideneacetone on the second maximum is of the same relative magnitude as in the diphenylbenzoquinones. The fact that the maximum in the diphenylbenzoquinones is at much longer waver-lengths than in similarly substituted benzylideneacetones shows clearly that the two benzylideneketone systems

which formally exist in the diphenylbenzoquinones are not independent of another, although they are neither conjugated nor cross-conjugated in the ordinary sense [5]. They are, however, both cross-conjugated with the same vinylketone system forming a kind of double cross-conjugated system, similar to that found for instance in benzil and vinylogous benzils [6,7].

A possible explanation for the slight hypsochromic shift of the long-wave maximum observed when R′ is hydroxyl or methoxyl is given below.

For the maximum at shorter wavelenghts there are two obvious explanations: it may correspond either to the shortwave absorption of the benzylideneketone system or to that of the quinone ring. As can be seen from Table 2, the effect of the substitutes in the *p*-position on this band in the benzylideneacetones is the same as on the long-wave band, just as is observed in the diphenylbenzoquinones. It should, however, be noted that the shortwave maximum in the benzylideneacetones is weaker than the long-wave maximum, while the opposite is true for the diphenylbenzoquinones. Further the observed bathochromic effect of the hydroxyl or methoxyl groups in the quinone ring finds no obvious explanation in this way.

The second possibility referred to above, however, offer a ready explanation of this. According to Braude [8] the short-wave band of benzoquinone has its origin in an electronic transition leading to an excited state, which in the present cases would be C and D with a consequent bathochromic shift

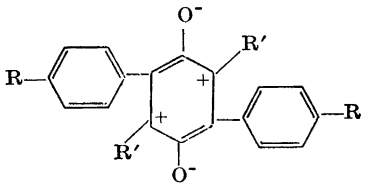

C

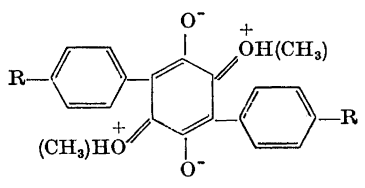

D

when R′ is hydroxyl or methoxyl. Actually the bathochromic shift is smaller than expected on this assumption. For instance 2,5-dihydroxybenzoquinone has maxima at ~277 and 285 mμ and 2,5-dihydroxythymoquinone has a maximum at ~295 mμ [2]. One explanation for this would be that the electronic transition leading to D is in the opposite direction to that leading to A and B and may thus require more energy than in 2,5-dihydroxybenzoquinone and its homologues.

The bathochromic shift when R is hydroxyl or methoxyl is not readily explained in this way; the opposite effect, due to the counteraction of the two systems, would have been expected.

This counteraction of the two systems could, however, explain the hypsochromic effect on the second maximum, which is observed when R′ is hydroxyl or methoxyl.

It is obvious that neither of the two alternative explanations alone is quite satisfactory, and it may well be that both contribute to the formation of the short-wave band.

Brockmann and Budde [9] have devised a method by which the parent ring system of a polycyclic quinone is fixed by comparison of the UV-spectrum of the acetylated hydroquinone with that of the corresponding hydrocarbon. These usually differ only by a small bathochromic shift caused by the acetoxyl groups. It was of interest to see whether this method was applicable also to the diphenylbenzoquinones.

Table 3.

		max	
	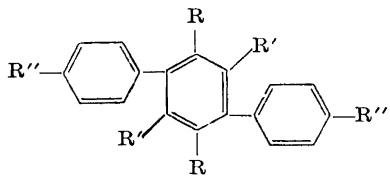	mμ	log ε
XVII	R = $OCOCH_3$; R′ = R″ = H	260	4.40
XVIII	R = $OCOCH_3$; R′ = H; R″ = $OCOCH_3$	263	4.40
XIX	R = R′ = $OCOCH_3$; R″ = H	245	4.27
XX	R = R′ = R″ = $OCOCH_3$	249	4.35

Table 3 gives absorption maxima of the leuco-acetates of some of the diphenylbenzoquinones listed in Table 1. They are all at shorter wavelengths than that of terphenyl [10] (276 mμ). This hypsochromic shift instead of the expected bathochromic shift is by no means surprising. It is well known that substituents *ortho* to the central bond in diphenyl have a hypsochromic effect which has been attributed to non-coplanarity of the two rings due to steric hindrance [11]. Even a single methyl group is enough to produce this effect [12]. The same should also apply to derivatives of terphenyl, although very little is known about their spectra. Erdtman *et al.*[13] have shown that the spectrum of 2,5,2′,5′,2″,5″-hexa-acetoxy-*p*-terphenyl, an isomer of (XX), has a strong inflexion at ~250 mμ, and is thus in good agreement with that of XX, although this has a definite maximum.

The difference between those substances having only a single substituent adjacent to the connecting bonds between the aromatic rings and those having two substituents is also clerly revealed by the figures of Table 3.

In the spectra of aurantiacin leuco-acetate and the acetate of dihydroaurantiacin dibenzoate, recorded in a previous paper [14], the maximum due to the terphenyl system is covered by the strong absorption of the benzoyl group and occurs only as a weak inflexion at 260—270 mμ.

When allowance is made for this hypsochromic effect due to restricted rotation, it should be possible to identify diphenylbenzoquinones by the spectra of their leuco-acetates, and it is definitely possible to distinguish them from quinones derived from condensed hydrocarbons.

EXPERIMENTAL

All the quinones used in this investigation have been described before. The compounds V, VI, VII, VIII, XI, XV and XVI were obtained during work on the structure of aurantiacin [1]. XII, XIII and XIV were obtained from atromentin (XI) according to Kögl and Becker[15]. I, IX and X were synthesised according to the method of Pummerer and Prell[16] and II according to Frank and coworkers [17]. III and IV were obtained by acetylation of II and IX, respectively. All substances prepared in the present work had m. p. s in agreement with those given in the literature, except 3,6-dibromo-2,5-diphenylbenzoquinone, used as an intermediate in the synthesis of polyporic acid (II). Our sample had m. p. 232–233°, whereas Frank *et al.*[17] as well as Schildneck and Adams [18] report 223–224°. Dr. Frank has kindly informed us that the m. p. of his sample, determined now, is 233–234° and that he regards the earlier statement as a misprint.

The leuco-acetates were prepared by reductive acetylation of the corresponding quinones in the presence of pyridine. XVIII and XX have been described before [1,16]. XVII had m. p. 193–194°. (Found: C 76.28; H 5.24. $C_{22}H_{18}O_4$ requires C 75.85; H 5.29 %) and XIX m. p. 266–267°. (Found: C 66.60; H 4.72. $C_{26}H_{22}O_8$ requires C 67.52; H 4.80 %.) Both substances were recrystallised from acetic acid.

The spectra were measured with a Beckman Model DU Spectrophotometer. The dioxan, used as solvent, was purified by distillation over sodium.

The author wishes to thank Prof. R. Adams and Dr. R. L. Frank for their help in settling the reason for the differences in m. p. referred to above.

REFERENCES

1. Gripenberg, J. *Acta Chem. Scand.* **10** (1956) 1111.
2. Flaig, W., Ploetz, T. and Küllmer, A. *Z. Naturforsch.* **10 b** (1955) 668.
3. Murray, J. *J. Chem. Soc.* **1952** 1345.
4. Wilds, A. L., Beck, L. W., Close, W. J., Djerassi, C., Johnson Jr., J. A., Johnson, T. L. and Shunk, C. H. *J. Am. Chem. Soc.* **69** (1947) 1985.
5. Allen, C. F. H. and Blatt, A. H. in Gilman, H. (editor) *Organic Chemistry* 2nd Edit., Wiley & Sons, New York 1945, Vol. I. p. 689.
6. Karrer, P. and Cochand, C. *Helv. Chim. Acta.* **28** (1945) 1181.
7. Leonard, N. J. and Robinson, G. C. *J. Am. Chem. Soc.* **75** (1953) 2714.
8. Braude, E. A. *J. Chem. Soc.* **1945** 490.
9. Brockmaun, H. and Budde, G. *Chem. Ber.* **86** (1953) 432.
10. Gillam, A. E. and Hey, D. H. *J. Chem. Soc.* **1939** 1170.
11. Braude, E. A. and Waight, E. S. in Klyne, W. (editor) *Progress in Stereochemistry*, Butterworths, London 1954, Part I, p. 126.
12. Braude, E. A. and Forbes, W. F. *J. Chem. Soc.* **1955** 3776.
13. Erdtman, H., Granath, M. and Schultz, G. *Acta Chem. Scand.* **8** (1954) 1442.
14. Gripenberg, J. *Acta Chem. Scand.* **12** (1958) 1411.
15. Kögl, F. and Becker, H. *Ann.* **465** (1928) 211.
16. Pummerer, R. and Prell, E. *Ber.* **55** (1922) 3105.
17. Frank, R. L., Clark, G. R. and Coker, J. N. *J. Am. Chem. Soc.* **72** (1950) 1824.
18. Schildneck, P. R. and Adams, R. *J. Am. Chem. Soc.* **53** (1931) 2373.

Received July 9, 1958.

ACTA CHEMICA SCANDINAVICA 12 (1958) 1768—1776

The Crystal Structure of Acetaldehyde-ammonia

EINAR WANG LUND

Kjemisk Institutt, Universitetet i Oslo, Blindern, Norway

In the solid state acetaldehyde-ammonia is found to be the trihydrate of trimethyl-hexahydrotriazine. The methyl groups are bonded equatorially to the carbon atoms of the hydrogenated triazine ring. The C—C and C—N distances are normal. Oxygen atoms of the waters of crystallization are interconnected by hydrogen bonds of length 2.70 Å to form a six-membered puckered ring. Hydrogen bonds probably exist between oxygen atoms and nitrogen atoms of adjacent rings.

In a previous short communication [1] a preliminary account of the crystal structure of acetaldehyde-ammonia has been given. This article is a more complete description of the structure.

The general tendency of aldehydes to polymerize has led several authors to the assumption that acetaldehyde-ammonia is a trimer. Among others Delépine [2] presented the idea that acetaldehyde-ammonia in the solid state actually is a trihydrate of 2,4,6-trimethyl-hexahydro-1,3,5-triazine. Delépine based this assumption mainly on the fact that the compound is easily dehydrated *in vacuo* over concentrated sulphuric acid. The anhydrous product formed under such conditions has been found by the author to cyrstallize in the cubic space group $Pa3$ with the lattice constant $a = 14.56$ Å.

The molecular structure proposed by Delépine was also the main result of an X-ray crystallographic determination made by Moerman [3]. The structure reported by Moerman was, however, rather improbable with respect to interatomic distances and bond angles. Therefore a re-investigation of the structure using Fourier methods has been carried out.

Crystals of acetaldehyde-ammonia in the form of rhombohedra were obtained by adding gaseous ammonia to an ice-cold solution of acetaldehyde in dry ether. Rotation and Weissenberg photographs showed that the Laue symmetry of the crystals is $D3d$- $3m$ and that the unit cell with hexagonal axes has the dimensions: $a = 11.29$ Å, $c = 15.87$ Å. With the value of the density reported by Moerman $d = 1.06$ gcm^{-3} these dimensions led to a number of 18 units of $CH_3CHO{\cdot}NH_3$ in the hexagonal unit cell. Inspection of Weissenberg diagrams showed no systematic extinctions of reflexions other than those given by a rhombohedral structure based on a hexagonal

unit cell. Therefore the possible space groups are D_{3d}^5—$R\bar{3}m$, D_3^7—$R32$ or C_{3v}^5—$R3m$. Of these only D_{3v}^5—$R\bar{3}m$ contains a center of symmetry.

The first X-ray study of acetaldehyde-ammonia was made by Hassel and Mark [4] who determined the cell dimensions and the space group. They based the space group determination on the statement made by Groth [5] that acetaldehyde-ammonia belongs to the ditrigonal scalenohedral class D_{3d}—$\bar{3}m$. Hassel and Mark found therefore unambigously from the sets of reflexions present that the only possible space group is D_{3d}^5—$R\bar{3}m$.

In order to support the crystal class determination, investigation was made for the presence of piezoelectricity. This was kindly undertaken by Mr. Erik Blomgren at the Chemistry Department of the University of Uppsala, Sweden. Mr. Blomgren could state very positively that no piezoeffect was present. This negative result together with the statement of Groth and the fact that the space group $R\bar{3}m$ is the only of the three groups mentioned that has a 36-fold general position led to the choice of this space group as the most probable. The final result is considered to be a confirmation of the correctness of this choice.

The arrangement of symmetry elements in this space group is such that any Fourier projection will give considerable amount of overlap of nonequivalent atoms and no resolved peaks suitable for determination of atomic coordinates. Therefore the computation of a Fourier section was considered necessary in order to get details of the structure. The asymmetric part of the "monomer" contains (apart from the hydrogen atoms) two carbon atoms, one nitrogen atom and one oxygen atom which have to be placed in one of the special 18-fold positions. The only possible one from steric considerations is that which involves a plane of symmetry. This plane with the equation $y = -x$ then contains all the important atoms in the asymmetric unit and is therefore highly suitable as the plane for a Fourier section.

In order to obtain the necessary intensities double sets of equi-inclination Weissenberg photographs were taken with Cu-K radiation. With rotation about c sets of photographs were from $l = 0$ to $l = 7$ and with rotation about a sets were taken for $h = 0$ to $h = 3$. Intensities of reflexions were estimated visually using a standard scale with known relative values. After correction for Lorentz and polarization factors the intensities were interrelated and brought to the same relative scale. Later the observed values of the structure factors were normalized to the set of calculated values.

The trial structure used in order to obtain signs of the structure factors was partly based on the main features of the structure of Moerman, *viz.* a hydrogenated, methyl substituted triazine ring with center in (0,0,z), the nitrogen atoms of the ring being loosely connected to oxygen atoms by means of hydrogen bonds. A satisfactory agreement between absolute values of observed and calculated structure factors was obtained with the parameter z having a value about 1/4 and oxygen atoms forming a puckered six-membered ring with center in $z = \frac{1}{2}$.

After some refinement, including the introduction of the effect of hydrogen atoms in the calculated structure factors, a final Fourier map was obtained which is reproduced in Fig. 1. In this map contour lines are drawn for arbitrary equidistant values of the function ϱ (x,$\bar{x}$,z). The peaks corresponding

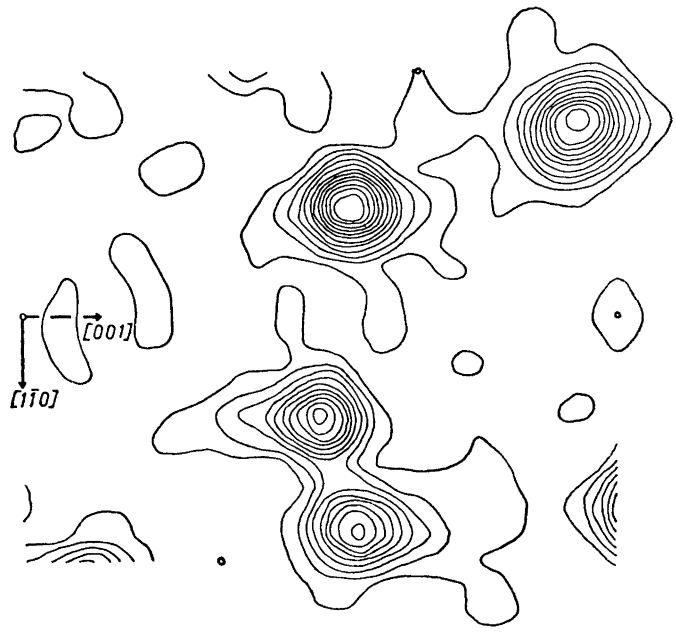

Fig. 1. Fourier section in the plane $y = -x$. Contour lines are drawn at arbitrary equidistant values of the function $\varrho\ (x,\bar{x},z)$.

to nitrogen, oxygen and two carbon atoms are well resolved and the positions of the maxima are assumed to determine atomic coordinates of these atoms which are listed in Table 1.

The main features of the structure formed by carbon, nitrogen and oxygen atoms can be described as follows. Alternating carbon and nitrogen atoms form a six-membered puckered ring of the *cyclo*hexane type. The N—C distance is found to be 1.47 Å. The angles in the ring, ∠NCN and ∠CNC are 114.6° and 109.0°, respectively. To each carbon atom of the ring is linked a methyl group in equatorial position. The C—C distance found is 1.53 Å. The angle between the C—C direction and the threefold axis (negative *c*-axis for the molecule in question) is found to be 109.1° whereas the angle ∠NCC amounts to 109.5°. The oxygen atoms closest to the substituted triazine ring are situated at a distance 2.87 Å from the nitrogen atoms. A hydrogen bond is probably established between these atoms. The angle between the N—O direction and the threefold axis is 115.5°. The N—O direction is thus not far from that corresponding to a bond directed equatorially away from the nitrogen atom.

Oxygen atoms more distant from the triazine ring in question lie at 3.20Å from the nitrogen atoms in a direction making 19° with the threefold axis. These oxygen atoms are, however, at the shorter distance of 2.87 Å from nitrogen atoms of other substituted triazine rings. On account of the symmetry

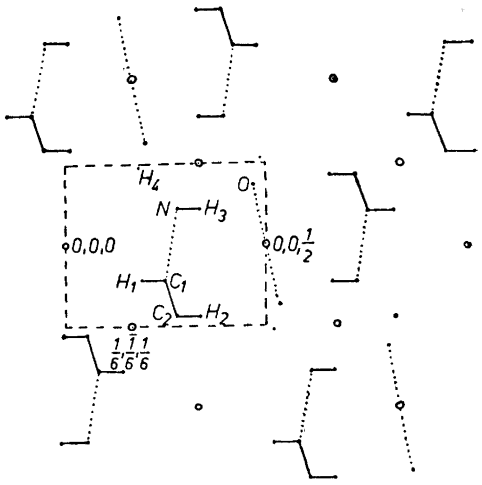

Fig. 2. General survey of positions of atoms and symmetry centers in the plane of the Fourier section. C—C, C—H and N—H bonds lying in the plane are shown by full lines. Nitrogen and carbon atoms belonging to the same hydrotriazine ring are interconnected by dotted lines; the same applies to oxygen atoms of one oxygen ring. The asymmetric unit of Fig. 1 is outlined by a broken line.

six oxygen atoms form a puckered ring. In this ring the O—O distance found is 2.70 Å and the angle ∠OOO is 106.3°. These oxygen atoms are therefore assumed to be interconnected by hydrogen bonds.

Introduction of hydrogen atoms in the calculation of structure factors improved the correspondence with the observed values. The positions of the hydrogen atoms were chosen from chemical facts using reasonable bond distances and valency angles. In spite of the trimerization of the molecule it is highly reasonable that the arrangement $CH_3 \cdot CH \cdot NH$ is retained whereas the remaining two hydrogen atoms of the monomer are probably connected to oxygen. For the methyl groups there are two equilibrium positions consistent with the presence of a symmetry plane through the C—C bond. The one which makes van der Waals' distances most favourable has a C—H bond parallel to the threefold axis. For steric reasons free rotation of methyl groups is improbable. The hydrogen atoms connected to carbon and nitrogen atoms of the ring are assumed to be in axial positions with C—H and N—H distances equal to 1.09 Å and 1.00 Å, respectively. These two hydrogen atoms and one of the methyl hydrogen atoms are thus assumed to lie in the plane of the Fourier section and the extensions of the peaks may indicate their presence.

Between two adjacent oxygen atoms of the oxygen ring one hydrogen atom is assumed to be located. The space group symmetry requires this hydrogen atom either to be located half way between the oxygen atoms or to be disor-

Table 1. Atomic coordinates determined from the Fourier section.

	x	z
C_1	0.071	0.250
C_2	0.145	0.281
N	−0.073	0.277
O	−0.128	0.467

Table 2. Assumed coordinates of hydrogen atoms.

	x	y	z
H_1	0.071		0.181
H_2	0.145		0.350
H_3	−0.073		0.346
H_4	−0.159		0.181
H_5	0.093	−0.251	0.258
H_6	0.037	−0.173	0.509

derly distributed over two symmetrically located positions equidistant from the two oxygen atoms. The latter alternative was chosen, with O—H distance equal to 0.96 Å. For the calculation of structure factors this arrangement corresponds to placing half a hydrogen atoms in a general 36-fold position.

The position of the other hydrogen atom connected to oxygen was assumed to be equatorial to the oxygen ring with an angle ∠OOH equal to 109°. This hydrogen atom will then be located about 0.7 Å from the line of length 2.87 Å connecting the oxygen atom and the nearest nitrogen atom.

The coordinates thus chosen for hydrogen atoms and used in the calculation of structure factors are listed in Table 2. In Fig. 2 is shown the arrangement of atoms and symmetry centers over a greater area of the plane of the Fourier section with the inclusion of hydrogen atoms.

The atomic scattering factors used for carbon, nitrogen and oxygen are those calculated by Berghuis *et al* [6]. For hydrogen the scattering factor given by McWeeny [7] was applied. The calculated structure factors were corrected with an isotropic temperature factor $\exp(-B \sin^2\Theta/\lambda^2)$ with $B = 4.14$ Å^2. A test for an expected anisotropic vibration with the trigonal axis as a preferred direction had no positive result.

In Table 3 a list of observed and calculated structure factors is given. Calculated values for all 415 reflexions with $\sin\Theta/\lambda$ less than 0.6 are included. That only 136 reflecions are observed is partly due to too short exposure of Weissenberg diagrams of higher layer lines. Of the observed structure factors 96 % have a value greater than 10. It is assumed that the value 8 is an average lower limit of the values of structure factors which are observable from the diagrams taken. For unobserved reflexions only that part of a calculated structure factor which exceeds 8 is considered as an error in computing the R-factor.

The over all R-factor with the limit of 8 as observable is found to be 0.24. To this value the contribution from five of the strongest reflexions with $|F_{calc}| > 90$ is 0.04. These strongest reflexions are assumed to be affected by extinction and to be less accurately observed due to the difficulty in estimating their intensities visually. The R-factor for $hk0$-reflexions only is 0.10, for $0kl$-reflexions 0.24. To the latter value the strong reflexions mentioned contribute 0.07. The R-factor including only reflexions with $F_{obs} \neq 0$ is 0.16.

It is believed that the structure is more accurate than an over all R-factor of 0.24 generally would imply. The reasons for this are the difficulty in obtain-

Table 3. Observed and calculated structure factors.

hkl	F_o	F_c	*hkl*	F_o	F_c	*hkl*	F_o	F_c
110	40	39	762		− 6	1.10.3		1
220	63	55	402	18	11	204	81	−93
330	37	36	512	18	13	314		− 8
440	40	36	622	20	−22	424		− 6
550	60	58	732		− 7	534		−11
660		3	842		0	644	26	24
300	99	−99	702	17	18	754		− 8
410	63	−53	812	30	29	504	19	21
520	17	−20	922		− 1	614		− 6
630	20	11	10.0.2	11	8	724		2
740		1	11.1.2		0	834		3
850	11	−12	022	53	−68	804	14	− 6
600	32	−23	132	68	65	914	22	−22
710	9	8	242	37	33	10.2.4		3
820	15	−12	352	38	−35	11.0.4		−10
930		2	462	21	−18	014	124	189
900	18	−16	572		2	124	22	17
10.1.0	6	− 8	052	56	54	234		17
201	6	−13	162		1	344	25	26
311	24	23	272		4	454	48	45
421	24	−25	382		−10	564	18	20
531		10	492	13	13	674		0
641		−11	082	21	26	044	106	−131
751		− 2	192		3	154	64	−63
501	58	56	2.10.2		4	264		9
611		− 4	0.11.2		4	374		−11
721	15	16	003		−13	484		− 6
831		5	113	22	23	074	12	12
941		4	223		−13	184		0
801	26	−33	333	26	−30	294		− 4
911		0	443	23	23	0.10.4		1
10.2.1		− 7	553		− 3	105	66	−90
11.0.1		10	663		− 2	215	43	43
011	59	−73	303	71	80	325	35	−36
121	60	61	413	48	−45	435		6
231	76	−73	523	36	40	545	16	−18
341	23	17	633		8	655		− 9
451	15	−13	743		2	765		3
561		− 6	853		4	405	40	42
671		3	603	14	−10	515		− 4
041	10	− 5	713		− 9	625		20
151	27	24	823		− 8	735		0
261		9	933		− 3	845		5
371		2	903		0	705	17	−21
481		5	10.1.3		3	815		2
071	22	−22	033	49	−43	925		− 4
181		− 1	143	18	13	10.0.5		17
291		2	253	19	−22	025	6	6
0.10.1		9	363		12	135	18	−13
1.11.1		− 4	473		− 3	245		9
102	88	−137	583		− 1	355	16	− 4
212	40	−40	063	26	25	465		−11
322	54	54	173		−12	575		3
432	22	−15	283		14	055	62	70
542	56	−50	393		3	165		1
652		3	093	16	−22	275		4

Table 3. (Continued.)

hkl	F_o	F_c	*hkl*	F_o	F_c	*hkl*	F_o	F_c
385		9	487		− 5	20.10	14	−19
085		− 7	077		9	31.10		−18
195		5	187		− 3	42.10		− 4
2.10.5		− 5	297		10	53.10		−12
0.11.5		− 5	0.10.7		−13	64.10		− 6
006	73	−68	108	23	24	50.10		5
116	37	−34	218	21	−30	61.10		3
226	19	16	328		− 3	72.10		− 3
336		15	438		−11	83.10		7
446	26	−24	548		9	80.10		7
556		−15	658		2	91.10		11
666		− 1	408	29	30	01.10	33	−24
306	48	−63	518		19	12.10	15	16
416		2	628		−10	23.10		7
526		−16	738		15	34.10		− 2
636	23	−25	848		− 1	45.10		− 3
746		4	708		− 7	56.10		− 9
606	14	14	818		−11	04.10	38	38
716		8	928		− 1	15.10		8
826		12	10.0.8	19	−20	26.10		8
936		1	028	64	73	37.10		− 5
906	29	26	138	22	−17	07.10		2
10.1.6		0	248		− 3	18.10		− 9
036	57	58	358	33	32	0.10.10		2
146	49	44	468		8	10.11	50	45
256		2	578		7	21.11		6
366		− 2	058	65	−79	32.11		22
476		− 9	168		− 3	43.11		5
066	17	6	278		− 6	54.11		20
176		7	388		− 8	65.11		5
286		− 9	088		6	40.11		− 1
396		4	198		6	51.11		− 7
096		− 4	009	53	−71	62.11		6
1.10.6		5	119	15	−10	73.11		− 7
207	51	69	229		− 8	70.11		9
317		13	339		4	81.11		−11
427		1	449		−19	10.0.11	7	− 8
537	27	33	559		−12	02.11	13	−27
647		6	309	25	37	13.11	23	−23
757		4	419		−12	24.11		− 7
507	42	−45	529		11	35.11		− 6
617		9	639		−12	46.11		10
727		−11	749		−11	05.11	35	−31
837		− 7	609	20	−25	16.11		− 3
807		− 7	719		7	27.11		− 3
917		− 7	829		− 4	08.11		12
017	36	27	909	22	20	19.11		3
127	37	−38	039	12	−12	00.12	13	−22
237		− 1	149	42	42	11.12		11
347		−14	259		− 7	22.12		−18
457		18	369		−11	33.12		−13
567		− 2	479		4	44.12		4
047	32	−26	069	18	21	55.12		− 5
157		− 5	179		− 1	30.12		2
267		−13	289		6	41.12		20
377		10	099		− 1	52.12		− 1

hkl	F_o	F_c	*hkl*	F_o	F_c	*hkl*	F_o	F_c
63.12		6	07.13		3	03.15	10	−17
60.12		11	18.13		− 1	14.15	27	−20
71.12		−10	10.14		− 7	25.15		− 3
90.12	12	−12	21.14		0	06.15	14	−12
03.12	15	24	32.14		− 6	20.16		10
14.12	27	−23	43.14		− 2	31.16		1
25.12		17	54.14		2	42.16		0
36.12		6	40.14		− 9	50.16		11
06.12		−17	51.14		0	01.16		−10
17.12		− 4	62.14		− 1	12.16		5
09.12		10	70.14		3	23.16		−16
20.13		7	02.14		2	34.16		2
31.12		− 6	13.14		10	04.16		4
42.13		3	24.14		− 3	15.16		3
53.13		− 3	35.14		5	10.17		5
50.13	20	−31	05.14	13	13	21.17		− 5
61.13		− 4	16.14		5	32.17		5
72.12		− 1	00.15	23	28	40.17	15	−20
80.13	15	18	11.15		0	02.17		− 6
01.13	16	−12	22.15		6	13.17		11
12.13		−10	33.15		8	05.17	11	11
23.13		17	44.15		1	00.18		− 1
34.12		− 7	30.15		− 1	11.18		0
45.13		−10	41.15		14	22.18		1
04.13	30	32	52.15		− 3	30.18		2
15.13		16	60.15		5	03.18		− 1
26.13		− 5						

ing reliable estimated values of intensities for higher layer lines, too short exposure time for some of the diagrams and extinction effects on five of the strongest reflexions.

The values of interatomic distances and bond angles given above and listed in Table 4 are assumed to be accurate to about one per cent. It is seen that the C—C and C—N bond lengths found are normal. The O—O distance and the shortest N—O distance are assumed to correspond to hydrogen bonds. In comparison with an ideal *cyclo*hexane ring the hydrotriazine ring does not have a center of symmetry geometrically, the angles at N and at C being somewhat different.

It may be of interest to point out that the six-membered ring formed by oxygen atoms in this structure is very similar to the structure element in

Table 4. Interatomic distances and bond angles.

C—C	1.53 Å	∠NCN	(ring)	114.6°
C—N	1.47 Å	∠CNC	(ring)	109.0°
N—O	2.87 Å	$\angle NC_1C_2$		109.5°
N—O′	3.20 Å	∠OOO		106.3°
O—O	2.70 Å			
methyl-methyl	3.74 Å			

hexagonal ice. In ice the O—O distance is about 2 % longer and there are no centers of symmetry whereas in acetaldehyde-ammonia a center of symmetry of the space group is the mid-point of the six-membered ring of oxygen atoms.

The author wishes to acknowledge a grant from *Axel Auberts fond.*

REFERENCES

1. Lund, E. W. *Acta Chem. Scand.* **5** (1951) 678.
2. Delépine, M. *Bull. soc. chim. France* **19** (1898) 15.
3. Moerman, N. F. *Z. Krist.* **98** (1938) 447.
4. Hassel, O. and Mark, H. *Z. physik. Chem.* **111** (1924) 357.
5. Groth, P. *Elemente der physikalischen und chemischen Krystallographie*, München und Berlin 1921, p. 242.
6. Berghuis, J., Haanappel, I-M., Potters, M., Loopstra, B. O., MacGillavry, C. H. and Veenendaal, A. L. *Acta Cryst.* **8** (1955) 478.
7. McWeeny, R. *Acta Cryst.* **4** (1951) 513.

Received August 13, 1958.

ACTA CHEMICA SCANDINAVICA 12 (1958) 1777—1781

Intra- and Intermolecular Hydrogen Bonds in Nitro- and Nitrosophenols

PER M. BOLL

Department of Organic Chemistry, The Royal Danish School of Pharmacy, Copenhagen, Denmark

Nitro- and nitrosophenols are examined in the infrared part of the spectrum in the solid state as well as in solution in order to gain information on the relationship between molecular structure and intra- and intermolecular hydrogen bond formation.

2-Nitrophenols show intramolecular hydrogen bonding, whereas 3- and 4-nitrophenols show intermolecular hydrogen bonding, which is ruptured by solution. 2-Nitrosophenols (4-nitrosoresorcinol, 1-nitroso-2-naphthol) lack fundamental bands of hydroxyl absorption indicating that these compounds exist exclusively in the condition of a completely chelated system.

Additional evidence of the derivative formed by reacting morphine hydrochloride with nitrous fumes being 2-nitromorphine hydrochloride is given.

There has been some doubt about the derivative prepared when reacting morphine hydrochloride with nitrous fumes was a *nitroso* or a *nitro* compound. By chemical means Baggesgaard Rasmussen and Boll [1] found the compound to be 2-*nitro*morphine. Spectroscopically, in the infrared part of the spectrum a *nitroso* compound (N←→O) is characterized by only one absorption band whereas a *nitro* compound due to both symmetrical stretching (—N(→O)↙) and unsymmetrical stretching (N(→O)↖) is characterized by two absorption bands. All these bands have to be strong. The spectrum of the compound considered to be 2-*nitro*morphine hydrochloride has indeed such two bands at 1 525 and 1 530 cm^{-1}. These frequencies correspond closely to the frequencies expected for a *nitro* compound. A *nitroso* compound, on the other hand, should have given one band at 1 525 cm^{-1}.

The present work was planned in order to gain information on the relationship between molecular structure and intra- and intermolecular hydrogen formation in *nitro* and *nitroso*phenols. It was hoped that such information should give conclusive spectroscopic evidence of the aforementioned compound being 2-*nitro*morphine hydrochloride.

Since the infrared spectrum affords a picture of the molecule in its ground state it seemed that the infrared examination of the strength of chelation in *nitro*- and *nitroso*phenols through the hydroxyl band shift might afford the desired information. The hydroxyl bands in the 3 000—3 500 cm^{-1} region have been measured for some *nitro*- and *nitroso*phenols in solid state and in chloroform solution. The high frequency band is due to the free hydroxyl group and the low frequency band is due to the bonded hydroxyl group.

DISCUSSION

It has been known for a long time that 2-*nitro*phenol differs from its 3- and 4-isomers in many of its physical properties. The explanation has been that the former compound is chelated and not associated. The vibration corresponding essentially to the hydroxyl bond stretching for molecules containing this group gives absorption in the 3 000—3 500 cm^{-1} region and its

Table 1. Fundamental bands of hydroxyl and amine absorption in the infrared part of the spectrum.

Compound	Hydroxyl and Amine Band (cm^{-1}) Solid (KBr)	In $CHCl_3$	Conc.	Interpretation
2-Nitrophenol	3 200	3 200	0.025 M	intramolecular H-bond
3-Nitrophenol	3 330	3 520	0.025 M	intermolecular H-bond
4-Nitrophenol	3 325	3 530	0.025 M	intermolecular H-bond
4-Nitrosophenol	3 170	3 500	0.025 M	intermolecular H-bond
1-Nitro-2-naphthol	no absorpt.	3 200 (weak)	0.025 M	intramolecular H-bond
1-Nitroso-2-naphthol	no absorpt.	no absorpt.	0.025 M	completely chelated
4-Nitroresorcinol	3 225 3 340	broad band 3 580	 saturat.	intramolecular H-bond intermolecular H-bond
4-Nitrosoresorcinol	no absorpt. 3 270	no absorpt. 3 580	 0.0125 M	completely chelated intermolecular H-bond
2-Nitromorphine hydrochloride	3 220 3 360 3 450 (NH)	3 220 3 540 3 620 (NH)	 0.01 M	intramolecular H-bond intermolecular H-bond intermolecular H-bond
Morphine hydrochloride	3 340 (broad) 3 510 (NH)	3 560 3 620 (NH)	 0.01 M	intermolecular H-bond intermolecular H-bond
2,4-Dinitrophenol	3 250	3 250	0.025 M	intramolecular H-bond
2,4,6-Trinitrophenol	broad band	3 190 (weak)	0.025 M	intramolecular H-bond
1-Methyl-4,6-dinitrophenol	3 240	3 240	0.025 M	intramolecular H-bond

first overtone is found at about 7 000 cm^{-1}. Hilbert *et al.*[2] have studied the hydrogen bonding in the 7 000 cm^{-1} region for a large number of compounds containing phenolic hydroxyl groups and found that such a group forms a strong hydrogen bond with an oxygen atom of an adjacent *nitro* group. For example, 2-*nitro*phenol does not absorb radiation in this region indicating that the steric conditions for forming strong hydrogen bonds are satisfied, whereas 3-*nitro*phenol as well as 4-*nitro*phenol present strong absorption indicating absence of intramolecular hydrogen bonding.

The same conclusion can be drawn from Table 1. The position of the hydroxyl band of 2-*nitro*phenol does not shift by dissolving the compound, whereas those of both 3- and 4-*nitro*phenol shift. This observation can only be explained by intramolecular hydrogen bonding in 2-*nitro*phenol. The values recorded for 3-and 4-*nitro*phenol are close to the values given by Ginetti [3] who for both compounds found the hydroxyl band at 3 330 cm^{-1} and 3 520 cm^{-1} in chloroform and in solid state, respectively.

Furthermore, the finding of Amstutz *et al.*[4] that the fundamental band of hydroxyl absorption is lacking for 1-*nitroso*-2-naphthol, whereas 1-*nitro*-2-naphthol has a definite, although weak, band at approximately 3 250 cm^{-1}, has been confirmed. Besides, it was found that 4-*nitroso*-resorcinol only showed one band of hydroxyl absorption at 3 270 cm^{-1} corresponding to an intermolecular type of hydrogen bonding which was ruptured by solution and shifted to 3 580 cm^{-1}. 4-*Nitro*resorcinol, on the other hand, gave two bands of hydroxyl absorption corresponding to intermolecular as well as intramolecular hydrogen bonding. The lack of a fundamental band of hydroxyl absorption for 1-*nitroso*-2-naphthol and the presence of only one band of hydroxyl absorption for 4-*nitroso*resorcinol corresponding to intermolecular hydrogen bonding appears to be conclusive evidence that the phenolic hydroxyl group adjacent to the nitroso group is not free. This lack of hydroxyl absorption indicates that 1-*nitroso*-2-naphthol exists exclusively in the condition of a completely chelated system, whereas 4-*nitroso*resorcinol, besides possessing a completely chelated system, also is di- or polymerized. The existence of a resonance possibility with the corresponding quinone monoxime only tends to stabilize the chelated system:

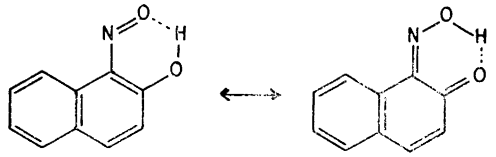

Fig. 1.

From the above mentioned observations it should now be possible to give additional evidence of the derivative prepared by reacting morphine hydrochloride with nitrous fumes being in fact 2-*nitro*morphine hydrochloride. If the compound had been 2-*nitroso*morphine hydrochloride, the infrared spectrum of the compound should only give two bands, namely from the alcoholic hydroxyl group and the substituted amino group, respectively. On the other hand, the infrared spectrum of 2-*nitro*morphine hydrochloride should, besides

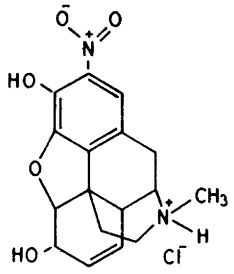

2-Nitromorphine hydrochloride

Fig. 2.

showing the two aforementioned absorption bands, give a third band originating from a not completely chelated system consisting of the *ortho*-situated *nitro* and phenolic hydroxyl groups. From Table 1 is clearly seen that the compound which is thought to be 2-*nitro*morphine hydrochloride, indeed gives the three expected absorption bands. At this place it has to be mentioned that this conclusion is only valid if it be assumed that the alcoholic hydroxyl group and the substituted amino group in 2-*nitro*morphine hydrochloride each only gives one band of absorption.

Finally it can be seen from Table 1 that a *para*-substituted *nitroso*phenol gave the same type of intermolecular hydrogen bonding as the *para*-substituted *nitro*phenol, just as three different poly*nitro*phenols with the phenolic hydroxyl group *ortho* to the *nitro* group all showed intramolecular hydrogen bonding.

EXPERIMENTAL

The measurements were carried out with a Perkin-Elmer model 21 double beam spectrophotometer equipped with a rock salt prism.

For the bands due to unassociated molecules, solutions were made up to 0.025 M in chloroform *Merck* grade *pro analysi*. However, in some cases the components were not soluble to this extent and saturated solutions of the compounds in chloroform were used. The solutions were measured in 1 mm cells. In the reference beam chloroform was placed to compensate for the bands originating from the solvent.

Commercially available chemicals recrystallized from ethanol-water mixtures were used with the exception of the following compounds:

1-Nitro-*2-naphthol*. 1-*Nitroso*-2-naphthol was oxidized with nitric acid following the procedure of Fierz-David and Ischer [5]. Subjected to distillation with superheated steam the compound distilled over as orange-yellow crystals, which after recrystallization melted at 100—102°C (Lit. value [5] 102°C).

4-Nitroso*resorcinol*. Resorcinol was reacted with *iso*amyl nitrite in alkaline alcoholic solution according to Henrich [6]. After recrystallization from water the compound began to decompose at 110°C and turned black at 145°C.

4-Nitro*resorcinol*. The potassium salt of 4-*nitroso*resorcinol was oxidized with 3 % hydrogen peroxide according to Gilbert *et al.*[7] The reaction mixture was acidified and extracted with ethyl ether. After evaporation of the ether, the compound was recrystallized from water. Its melting point, after quick dehydration, was 112—115°C (Lit. value [7] 115°C).

2-Nitro*morphine hydrochloride*. Morphine hydrochloride was reacted with nitrous fumes at −2 to −3°C using the modified procedure described by Baggesgaard Rasmussen and Boll [1]. The compound was recrystallized from N hydrochloric acid.

Acknowledgement. My sincere thanks are due to Professor Børge Bak, University of Copenhagen, for valuable advice.

REFERENCES

1. Baggesgaard Rasmussen, H. and Boll, P. M. *Acta Chem. Scand.* **12** (1958) 885.
2. Hilbert, G. E., Wulf, O. R., Hendricks, S. B. and Liddel, U. *Nature* **135** (1935) 147.
3. Ginetti, Y. *Naturwiss.* **41** (1954) 333.
4. Amstutz, E. D., Hunsberger, I. M. and Chessich, J. J. *J. Am. Chem. Soc.* **73** (1951) 1220.
5. Fierz-David, H. E. and Ischer, H. *Helv. Chim. Acta* **21** (1938) 680.
6. Henrich, F. *Ber.* **35** (1902) 4192.
7. Gilbert, F. L., Laxton, F. C. and Prideaux, E. B. R. *J. Chem. Soc.* **1927** 2301.

Received August 14, 1958.

ACTA CHEMICA SCANDINAVICA 12 (1958) 1782—1798

The Constitution of the Formamidinium Disulphide Ion, from the Crystal Structures of the Diiodide and Dibromide

OLAV FOSS, JONAS JOHNSEN and OLE TVEDTEN

Chemical Institute, University of Bergen, Bergen, Norway

The unit cells of formamidinium disulphide diiodide (I) and dibromide (II) monohydrates, $[(H_2N)_2C-S-S-C(NH_2)_2]X_2 \cdot H_2O$, are: I, $a = 5.15$ Å, $b = 16.52$ Å, $c = 13.39$ Å; space group, D_{2h}^{10}-$Pccn$ with $Z = 4$. II, $a = 8.61$ Å, $b = 5.12$ Å, $c = 12.40$ Å, $\beta = 99\frac{1}{2}°$; space group, $C_{2h}^{4}-P2/c$ with $Z = 2$. The structures have been determined by two-dimensional X-ray methods.

The crystals are built up of formamidinium disulphide cations and halide anions, and water of crystallization; the cation possesses, by space group requirements, a twofold axis of symmetry in both salts. The disulphide group has normal configuration and dimensions, with S—S = 2.04 Å, and ∠S—S—C = 99° and 104°, CSS/SSC dihedral angle = 105° and 89°, in I and II, respectively. The dimensions of the thiourea groups are as in the thiourea molecule before oxidation to formamidinium disulphide cation, but for a slight lengthening of the C—S bond. There is a small but not significant deviation from planarity of the thiourea groups, and no significant difference between the lengths of the two C—N bonds of a group. In both salts the water molecules lie on twofold axes, and each participates in hydrogen bonds with two halide ions and two nitrogen atoms.

Salts of formamidinium disulphide are formed from thiourea by the action of oxidizing agents such as chlorine [1], bromine [1–5], iodine [6–13], cupric ion [14,15], hydrogen peroxide [7,11,15,16], peroxydisulphate ion [8], peroxyacetic acid [15], sulphonyl chlorides [6], sulphuryl chloride [10], permanganate [7], and by anodic oxidation [17,18]:

$$2\ (H_2N)_2CS = [(H_2N)_2C—S—S—C(NH_2)_2]^{++} + 2\ e \qquad (1)$$

Conversely, the disulphide may be reduced to thiourea by means of sodium amalgam [1], hydrogen sulphide [2], nascent hydrogen [10], or cathodically [18]. The reaction of thiourea with iodine:

$$2\ (H_2N)_2CS + I_3^- = [(H_2N)_2C—S—S—C(NH_2)_2]^{++} + 3\ I^- \qquad (2)$$

leads to an equilibrium which can be readily approached from either side [6–13]. Thus, in dilute solutions thiourea may be titrated quantitatively with iodine [9], whereas on dissolving crystals of formamidinium disulphide diiodide in water [6,8,10], on addition of potassium iodide to a solution of the dichloride or other salts [6,8,10], or on addition of solvents of low ionizing power such as methanol, ethanol or acetone to an aqueous solution of the diiodide [8,10,13], iodine is liberated. From potentiometric measurements, Preisler and Berger [16] found the oxidation-reduction potential of the reversible thiourea-formamidinium disulphide system (1) to be 0.42 V at 30°C, referred to the normal hydrogen electrode, for solutions at constant ionic strength containing 0.05 N to 1 N hydrochloric acid. The results of Preisler and Berger have later been confirmed by Freedman and Corwin [19]. Together with the potential, 0.54 V, of the iodide-triiodide system, this gives $K = 10^4$ for the equilibrium constant of reaction (2), in close agreement with the value obtained by Mahr [12] from spectrophotometric measurements of iodine concentration in equilibrium mixtures.

A number of salts of formamidinium disulphide have been isolated and characterized. The sparingly soluble dinitrate [5-8,10,11,17] separates on addition of nitric acid or nitrates to solutions of other salts, or on oxidation of thiourea in presence of nitrate ions.

The salts show normal disulphide reactivity. Typical heterolytic cleavage of the S–S bond takes place in the reaction with cysteine (RSH) to produce [11] in the first step a mixed disulphide:

$$[(H_2N)_2C-S-S-C(NH_2)_2]^{++} + RS^- = [RS-S-C(NH_2)_2]^+ + (H_2N)_2CS \qquad (3)$$

and in the second step cystine:

$$[RS-S-C(NH_2)_2]^+ + RS^- = RS-SR + (H_2N)_2CS \qquad (4)$$

The hydrolysis of the disulphide [1,6], to give thiourea, sulphur and cyanamide, has been formulated thus [11]:

$$[(H_2N)_2C-S-S-C(NH_2)_2]^{++} + OH^- = [(H_2N)_2C-S-OH]^+ + (H_2N)_2CS \qquad (5)$$

with subsequent decomposition of the sulphenyl hydroxide, although it appears that an alternative mechanism involving a nucleophilic attack on carbon instead of sulphur cannot be excluded. Likewise, the reaction with cyanide ion [2], which leads to the same products as the hydrolysis reaction except for the formation of thiocyanate ion instead of sulphur, may be interpreted in terms of a nucleophilic attack of cyanide ion on sulphur, to give the species

$$[(H_2N)_2C-SCN]^+$$

as an intermediate. Heterolytic fission of the disulphide link has been considered [20] as a possible first step in the reaction of the disulphide with secondary and primary amines. The reaction of the disulphide with acetone and other ketones to give substituted 2-aminothiazoles [4] is likely to involve a first step analogous to halogenation reactions of ketones, to produce

$$[(H_2N)_2C-S-CH_2-\underset{\underset{O}{\|}}{C}-CH_3]^+$$

with subsequent ring closure under elimination of water.

The tetramethyl analogue of formamidinium disulphide has been isolated as the perchlorate by Lecher *et al.*[21], from the reaction of tetramethylthiourea with bromine. Sahasrabudhey [22,23] prepared also the chloride and bromide, and demonstrated the reactions:

$$[(Me_2N)_2C-S-S-C(NMe_2)_2]^{++} + 2\ S_2O_3^{--} = (S_2O_3)_2^{--} + 2\ (Me_2N)_2CS \qquad (6)$$

$$[(Me_2N)_2C-S-S-C(NMe_2)_2]^{++} + 2\ (H_2N)_2CS = [(H_2N)_2C-S-S-C(NH_2)_2]^{++} + 2\ (Me_2N)_2CS \qquad (7)$$

Eqn. (7) represents a readily displaceable equilibrium. Although quite different explanations are implicit in Sahasrabudhey's arguments, reactions (6) and (7) have the appearance of typical two-step nucleophilic displacements, involving heterolysis of the S—S bond of the original disulphide in the first step, and of the S—S bond of a mixed disulphide in the second step, like the two steps of the formamidinium disulphide-cysteine reaction given by Eqs. (3) and (4) above.

The disulphide nature of the salts is well established, and has indeed not been questioned until Sahasrabudhey [5,13,22,23] in 1951—53 argued that they were not disulphides, but monomeric compounds derived from a single thiourea molecule. His experimental results, of which some are referred to above, are in fact in complete accord with the disulphide formula, but were by Sahasrabudhey construed to imply a "rather unusual type of link" [23] between the oxidized thiourea residue and the anion, something like "a free radical, Weitz's or Wurster's salt" structure. His cryscopic measurements in glacial acetic acid [22,23] gave values of 190—220 for the molecular weight of the tetramethyl derivative of the dibromide, as compared with 212 required for the monomeric formula Me_2NCSBr; however, the results agree equally well with the double formula for a salt composed of three ions.

The present X-ray crystallographic work serves to establish the disulphide nature of the salts in the crystalline state. There should be no reason to suspect that the disulphide bond is not preserved in solution, insofar as cleavage through ordinary chemical interactions does not take place.

CRYSTAL DATA

Unit cell and space group data were derived from oscillation and Weissenberg photographs of single-crystal specimens. The axial lengths are based on $\lambda(\mathrm{Cu}K\alpha) = 1.542$ Å and are probably accurate to within 0.5 %. Densities were determined by flotation in mixtures of carbon tetrachloride with benzene or bromoform.

Formamidinium disulphide dichloride, $[(H_2N)_2CS]_2Cl_2$. Orthorhombic bipyramidal, $a = 10.54$ Å, $b = 19.75$ Å, $c = 8.85$ Å. There are eight formula units per unit cell; density, calc. 1.61, found 1.57 g/cm³. The space group, from systematic absences, is $D_{2h}^{15} - Pbca$. The crystals occurred as long prisms {021}.

Formamidinium disulphide dibromide monohydrate, $[(H_2N)_2CS]_2Br_2 \cdot H_2O$. Monoclinic, $a = 8.61$ Å, $b = 5.12$ Å, $c = 12.40$ Å, $\beta = 99\frac{1}{2}°$. Two formula units per unit cell; density, calc. 2.04, found 2.04 g/cm³. Systematic absences, $h0l$ when l is odd. These are characteristic of the space groups, $C_{2h}^4 - P2/c$ and $C_s^2 - P/c$, of which the former would require that the formamidinium disulphide ion possess a centre or a twofold axis of symmetry.

The crystals were obtained as plates {100}, or as flat prisms bounded by {100} and, less developed, {001}.

Formamidinium disulphide diiodide monohydrate, $[(H_2N)_2CS]_2I_2 \cdot H_2O$. Orthorhombic bipyramidal, $a = 5.15$ Å, $b = 16.52$ Å, $c = 13.39$ Å. Four formula units per unit cell; density, calc. 2.47, found 2.47 g/cm³. The space group, from systematic absences, is $D_{2h}^{10} - Pccn$, which has eightfold general positions, and centres of symmetry and twofold axes as special, fourfold positions.

The crystals were well developed prisms, elongated along the *a* axis and in most cases flattened along the *c* axis.

The diiodide (I) and later the dibromide (II) were chosen for further study. The results on II indicate that the centrosymmetric space group, C_{2h}^4 — $P2/c$, is the correct one. Twofold symmetry of the disulphide ion is thereby crystallographically required in both salts; of the two possibilities the molecular symmetry element was found to be a twofold axis and not a symmetry centre. The latter would have led to a planar, *trans* disulphide group; the only planar disulphide group yet found is the *cis* group occurring in thiuret hydroiodide [24].

A preliminary account of the structure of the diiodide has been published [25].

EXPERIMENTAL

The dichloride was prepared from thiourea in hydrochloric acid solution by oxidation with hydrogen peroxide as described by Preisler and Berger [16], the dibromide by slowly adding the equivalent amount of bromine to a 20 % aqueous solution of thiourea, under cooling in ice water, and the diiodide as described by Marshall [8], by gradually adding 5 parts of iodine crystals to 3 parts of powdered thiourea in 25 parts of water, and subsequent cooling.

The measured densities as compared with the X-ray densities, and the occurrence of peaks of reasonable height on the twofold axes in the electron density maps, leave no doubt that the crystals of I and II are monohydrates, although no mentioning of water of crystallization in these salts is found in literature. However, the analyses by McGowan [6] and Werner [10] of I and by Hunter and Jones [3] of II agree better with monohydrates than anhydrous salts. Boeseken [15] obtained the dichloride as a pentahydrate, whereas the present crystals, and preparations analyzed by earlier workers [6,18], were anhydrous.

For the structure determinations, the intensities of the $0kl$ and $hk0$ reflections of I and the $h0l$ and $0kl$ reflections of II were estimated visually from zero-layer Weissenberg photographs. Copper radiation was used, and crystals with cross-sections of 0.04 × 0.05 mm and 0.07 × 0.05 mm, respectively, for the *a*- and *c*-axis photographs of I, and 0.11 × 0.09 mm and about 0.1 × 0.1 mm, respectively, for the *b*- and *a*-axis photographs of II. The absorption coefficient for Cu$K\alpha$ radiation is 499 and 130 cm^{-1} for I and II, respectively. No corrections for absorption were made, and absorption effects are undoubtedly reflected in the temperature corrections later applied to the calculated structure factors. In the case of I, 98 out of 144 $0kl$ reflections and 48 out of 60 $hk0$ reflections within the range $\sin\Theta < 0.985$ were recorded with measurable intensity, the corresponding figures for II being 124 out of 130 $h0l$ reflections and 71 out of 81 $0kl$ reflections. They were converted to relative structure amplitudes in the usual way, and eventually put to an approximately absolute scale by comparison with the calculated values.

Viervoll and Ögrim's [26] atomic scattering curve for sulphur was used in the calculation of structure factors, and the curves of Berghuis *et al.*[27] for oxygen, nitrogen and carbon. The hydrogen contributions were ignored in both structures. For the iodide and bromide ions, curves were constructed based on the Thomas-Fermi values for xenon and krypton, respectively, at small scattering angles and for electroneutral iodine and bromine at intermediate and larger scattering angles.

Summations were made by means of Beevers-Lipson strips, at 12° intervals along the *a* axis of I and the *a* and *b* axes of II, and at 6° intervals along the other axes.

THE STRUCTURE ANALYSES

The structures were solved by use of the heavy atom method, the positions of the iodide and bromide ions being found from Patterson projections. Although the vector maps gave also the position of the one sulphur atom of the asymmetric unit, the signs used in the first F_o synthesis were in each case

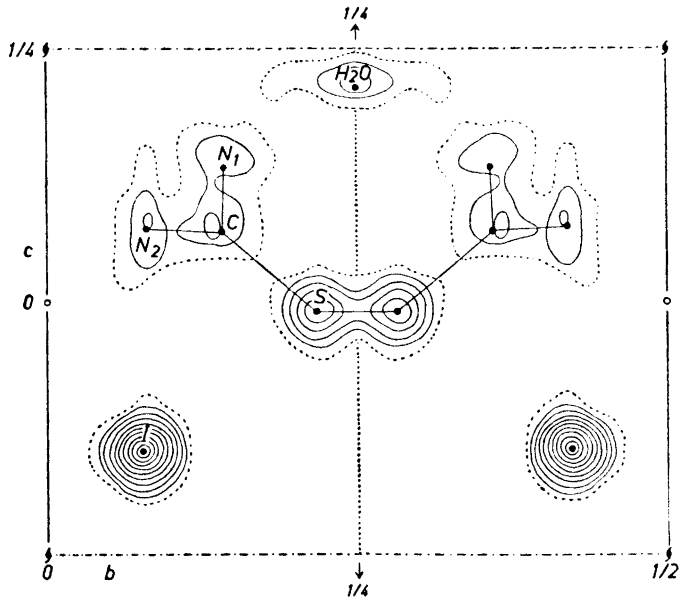

Fig. 1. Electron density projection of formamidinium disulphide diiodide monohydrate (I) along the *a* axis. The figure shows two asymmetric units. Contours at intervals of 10 e · Å^{-2} for the iodide ion, 5 e · Å^{-2} for sulphur, 4 e · Å^{-2} for oxygen and 3 e · Å^{-2} for the carbon and nitrogen atoms. The 3-electron line is dashed. The final atomic positions are marked with dots, and lines drawn to indicate the outline of the disulphide cation.

based on the contributions of the heavy atom alone, and the location of the sulphur peak appearing in the first electron density map was then checked against the coordinates derived from the vector map. In the projec-

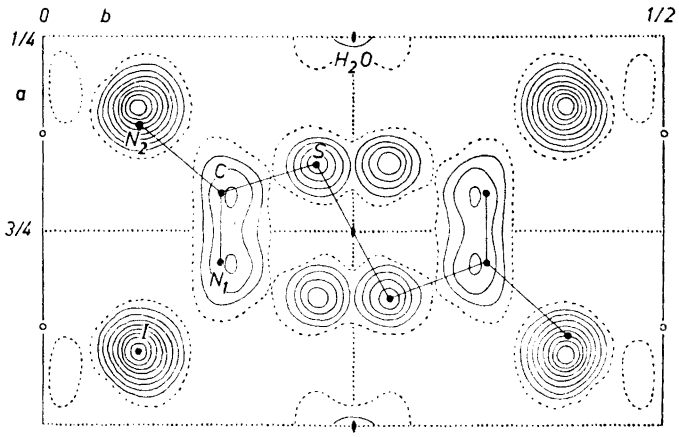

Fig. 2. Electron density projection of I along the *c* axis, showing four asymmetric units. The 6-electron line is dashed, and contours are at intervals of 10 e · Å^{-2} for the iodide ion and 5 e · Å^{-2} for the other atoms.

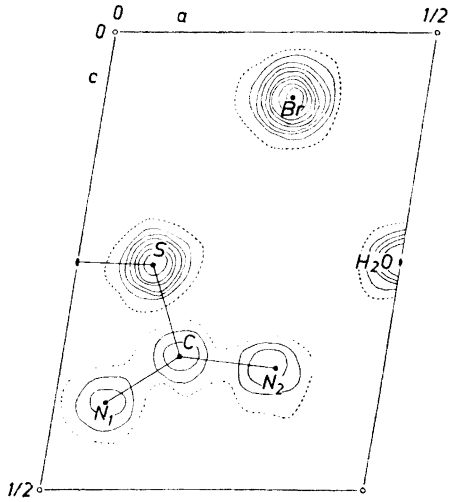

Fig. 3. Electron density projection of the asymmetric unit of formamidinium disulphide dibromide monohydrate (II) along the *b* axis. The 3-electron line is dashed, and contours are at intervals of 6 e · Å^{-2} for the bromide ion, 3 e · Å^{-2} for sulphur and oxygen and 2 e · Å^{-2} for carbon and nitrogen. The final atomic positions are marked with dots, and the outline of one thiourea group is drawn; the other thiourea group (not shown) of the disulphide cation lies on the other side of the twofold axis.

tion along the short axis of each salt, the approximate positions of also the lighter atoms could be determined from the first electron density map, whereas in the projection along the second longest axis, overlapping occurred, of iodine and nitrogen and of carbon and nitrogen in the *c*-axis projection of I, and of carbon and nitrogen and of sulphur and oxygen in the *a*-axis projection of II. The *y* coordinates in the case of I, and *z* coordinates in the case of II, of the overlapped lighter atoms were at first put equal to those determined from the better resolved short-axis projections, and preliminary *x* and *y* coordinates, respectively, were assigned on the basis of assumed bond lengths and angles. When F_o refinement had led to the determination of the sign of all but a few very weak reflections of a zone, further refinement was carried out by means of repeated $(F_o - F_c)$ syntheses.

The two electron density projections of the diiodide are shown in Figs. 1 and 2, and those of the dibromide in Figs. 3 and 4. The atomic coordinates are given in Tables 1 and 2. In the case of II, Table 2, the coordinates used for the last structure-factor calculations were corrected on the basis of the gradients still present at some atomic positions in the last difference map for each zone. Two sets of *z* coordinates for II were obtained, one from each zone; where the corrected values differed the final value was taken as the mean of the two, weighted according to their apparent reliability. The two sets of *y* coordinates for I, used together with the *x* and *z* coordinates of Table 1 for the last structure-factor calculations, were: $y(\mathrm{I}) = 0.0782$ and 0.0785, $y(\mathrm{S}) = 0.2195$ and 0.2185, $y(\mathrm{C}) = 0.139$ and 0.144, $y(\mathrm{N_1}) = 0.140$ and 0.145, $y(\mathrm{N_2}) = 0.080$

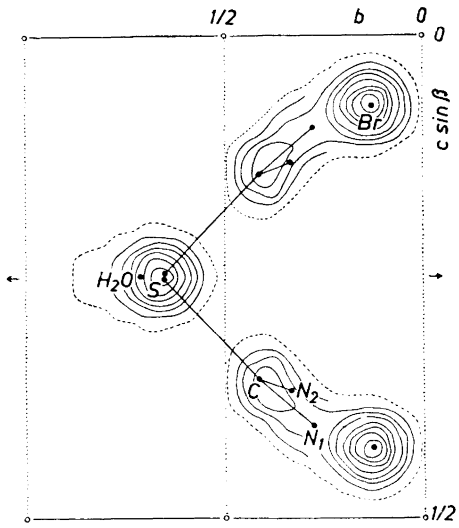

Fig. 4. Electron density projection of II along the *a* axis. One disulphide cation (two asymmetric units) is shown. The 6-electron line is dashed, and contours are at intervals of 6 e . Å^{-2} for bromine, sulphur and oxygen, and 3 e . Å^{-2} for carbon and nitrogen. The map shows that the final atomic positions (marked with dots) correspond to not quite planar thiourea groups, and that the best plane of a group is nearly parallel to the projection axis.

and 0.079, from the 0*kl* and *hk*0 data, respectively. The *y* values of Table 1 are in the case of C, N_1 and N_2 from the 0*kl* data; for I and S they are weighted means.

Table 1. Atomic coordinates for formamidinium disulphide diiodide monohydrate, in fractions of cell edges. Origin at a centre of symmetry.

	x	*y*	*z*
I	0.428	0.0783	0.3547
S	0.578	0.2192	−0.008
C	0.665	0.139	0.071
N_1	0.850	0.140	0.136
N_2	0.481	0.080	0.076
H_2O	0.250	0.250	0.214

In Tables 3 and 4, observed and calculated structure factors are listed for the 0*kl* zone of I and the *h*0*l* zone of II. In the temperature factor exp $[-B(\sin^2\Theta/\lambda^2)]$ applied to the calculated structure factors, the final values of B were chosen on the basis of the difference maps, and were as follows, in Å^2 units: In the 0*kl* zone of I, $B = 2.4$ for iodine, 2.2 for sulphur, and 2.6 for the lighter atoms, while in the *hk*0 zone, $B = 2.0$ for sulphur, 2.8 for the lighter atoms, and $2.4 + 1.4 \cos^2\varphi$ for iodine, where φ is the angle between the normal of the reflectiong plane and the direction of maximum

vibration of the atom, the a axis. In the $h0l$ zone of II, $B = 3.2$ for all atoms except bromine, where $B = 3.0 + 0.8 \cos^2\varphi$. Here, the direction of maximum vibration made an angle of about 44° with the a axis in the acute angle. In the $0kl$ zone of II, $B = 4.5$ for bromine, 2.0 for carbon and 4.0 for the other atoms.

The strong reflections, 060 of I and 200 and 302 of II have $|F_o|$ values markedly lower than the calculated ones. The two last reflections were omitted from the difference syntheses and the calculations of scale factor for the zone while the first one was, rather arbitrarily, included in the difference syntheses with half weight.

Table 2. Atomic coordinates for formamidinium disulphide dibromide monohydrate, in fractions of monoclinic cell edges. Origin at a centre of symmetry.

Coordinates used for final structure-factor calculations.

	($h0l$)		($0kl$)	
	x	z	y	z
Br	0.2925	0.0733	0.1310	0.0730
S	0.1200	0.2550	0.6500	0.2550
C	0.186	0.356	0.414	0.358
N_1	0.083	0.407	0.276	0.407
N_2	0.334	0.369	0.327	0.369
H_2O	0.500	0.250	0.706	0.250

Coordinates used to calculate interatomic distances and angles.

	x	y	z
Br	0.2925	0.1307	0.0727
S	0.1197	0.6502	0.2550
C	0.185	0.410	0.356
N_1	0.083	0.277	0.405
N_2	0.334	0.332	0.368
H_2O	0.500	0.711	0.250

The reliability index, $R = \Sigma||F_o| - |F_c||/\Sigma|F_o|$, with non-observed reflections included when $|F_c|$ exceeds the observable limit, is 0.089 and 0.097, respectively, for the $0kl$ and $hk0$ zones of the diiodide, and 0.068 for the $h0l$ zone (0.076 if the above-mentioned 200 and 302 reflections with low observed values are included) and 0.098 for the $0kl$ zone of the dibromide.

In the space group $Pccn$ of the diiodide, there is an uncertainty of $z = \frac{1}{4}$ with respect to location of symmetry centres which cannot be resolved from projections alone. That is because in the projection along the a as well as the b axis, symmetry centres, and twofold screw axes parallel to the projection axis and thus apparent symmetry centres, alternate at $c/4$ intervals along the c axis. Another uncertainty is that, once a set of coordinates for atoms of the disulphide cation has been chosen, there are two symmetry-related possibilities for the third coordinate of an iodide ion chosen in one projection. Both ambiguities can be resolved only by reference to hkl reflections with l

Table 3. Observed and calculated 0*kl* structure factors for formamidinium disulphide diiodide monohydrate.

k	F_o	F_c
	0*k*0	
2	75	+ 98
4	126	−143
6	304	−381
8	157	−156
10	34	+ 30
12	170	+159
14	202	+190
16	41	− 27
18	91	− 87
20	90	− 89
	0*k*2	
0	38	+ 33
1	105	+ 96
2	117	−116
3	239	+290
4	62	+ 53
5	220	+243
6	43	+ 53
7	64	− 60
8	36	+ 34
9	240	−250
10	< 26	+ 16
11	137	−130
12	85	− 78
13	< 32	+ 27
14	< 33	+ 17
15	116	+110
16	36	− 36
17	82	+ 77
18	45	+ 42
19	< 25	+ 21
20	< 20	− 2
	0*k*4	
0	269	−266
1	70	− 78
2	270	−262
3	215	−234
4	226	+217
5	82	− 72
6	191	+198
7	43	+ 34
8	148	+147
9	126	+121
10	< 28	− 12
11	83	+ 80
12	172	−163
13	< 33	− 6
14	104	− 92
15	69	− 66
16	< 32	− 26
17	54	− 58
18	94	+100
19	< 23	+ 1
20	40	+ 47
	0*k*6	
0	240	+228
1	86	− 86
2	45	+ 40
3	207	−199
4	< 23	− 13
5	145	−138
6	181	−163
7	60	+ 58
8	109	− 98
9	136	+137
10	34	+ 42
11	114	+110
12	73	+ 65
13	38	− 31
14	96	+ 96
15	64	− 62
16	< 30	− 26
17	73	− 72
18	< 24	− 22
19	< 19	+ 1
	0*k*8	
0	170	+157
1	149	+130
2	< 26	+ 14
3	173	+170
4	< 27	− 7
5	154	+144
6	118	−105
7	68	− 62
8	66	− 59
9	150	−142
10	< 33	+ 26
11	90	− 99
12	46	+ 37
13	< 33	+ 9
14	68	+ 70
15	85	+ 87
16	26	− 22
17	50	+ 62
18	< 18	− 12
	0,*k*,10	
0	159	−145
1	66	+ 47
2	149	−138
3	58	+ 55
4	117	+107
5	41	+ 44
6	134	+128
7	< 33	− 16
8	100	+ 99
9	45	− 55
10	< 33	− 13
11	< 32	− 21
12	101	−110
13	< 29	− 9
14	59	− 64
15	46	+ 34
16	< 20	− 15
17	< 14	+ 12
	0,*k*,12	
0	< 33	+ 26
1	< 33	− 32
2	< 33	− 20
3	147	−162
4	< 33	+ 10
5	74	− 82
6	< 33	− 10
7	< 33	+ 26
8	< 32	− 6
9	94	+114
10	< 30	+ 14
11	68	+ 77
12	< 26	− 14
13	< 33	− 24
14	22	+ 17
	0,*k*,14	
0	149	+156
1	< 30	+ 31
2	< 30	+ 38
3	< 30	+ 7
4	< 30	− 36
5	< 29	+ 18
6	94	−107
7	< 27	− 10
8	50	− 55
9	< 24	− 14
10	< 22	+ 12
11	< 18	− 6
	0,*k*,16	
0	28	− 20
1	32	+ 39
2	< 22	− 32
3	39	+ 55
4	< 21	+ 15
5	< 21	+ 15
5	49	+ 55
6	22	+ 31
7	< 15	− 18

Table 4. Observed and calculated *h0l* structure factors for formamidinium disulphide dibromide monohydrate.

h	F_o	F_c
	*h*00	
1	10	+ 11
2	80	− 98
3	41	+ 43
4	4	+ 2
5	102	− 99
6	9	+ 7
7	44	+ 38
8	10	− 9
9	7	− 8
10	21	+ 22
	*h*02	
0	10	+ 10
1	71	− 79
2	12	− 7
3	114	+137
4	< 2	+ 3
5	37	− 35
6	44	+ 39
7	12	+ 11
8	52	− 52
9	6	− 7
10	10	+ 12
	*h*0$\bar{2}$	
1	4	+ 6
2	122	−128
3	12	+ 12
4	94	+ 91
5	7	+ 6
6	51	− 50
7	25	+ 22
8	< 3	+ 2
9	30	− 29
10	< 3	+ 1
	*h*04	
0	21	− 21
1	78	− 78
2	87	+ 88
3	11	+ 14
4	69	− 68
5	11	− 10
6	42	+ 38
7	12	− 10
8	< 3	− 2
9	26	+ 22
	*h*0$\bar{4}$	
1	112	+121
2	8	− 8
3	118	−119
4	31	+ 31
5	< 3	0
6	56	− 55
7	17	+ 17
8	55	+ 54
9	5	− 5
10	7	− 7
	*h*06	
0	123	−117
1	50	− 45
2	60	+ 58
3	8	− 5
4	26	− 26
5	64	+ 62
6	15	+ 14
7	39	− 38
8	4	− 4
9	13	+ 13
	*h*0$\bar{6}$	
1	47	+ 40
2	18	+ 19
3	52	− 47
4	20	+ 19
5	79	+ 77
6	3	− 2
7	23	− 22
8	6	+ 4
9	3	− 21
10	20	− 21
	*h*08	
0	13	− 11
1	59	+ 48
2	18	+ 15
3	73	− 69
4	20	− 20
5	17	+ 18
6	8	− 7
7	7	− 8
8	26	+ 24
	*h*0$\bar{8}$	
1	5	− 6
2	71	+ 69
3	15	− 14
4	49	− 50
5	16	+ 14
6	17	+ 17
7	32	− 34
8	6	+ 7
9	24	+ 25
10	3	− 4
	h,0,10	
0	26	− 26
1	42	+ 43
2	12	− 14
3	12	− 13
4	36	+ 36
5	9	+ 9
6	28	− 28
	h,0,$\bar{1}\bar{0}$	
1	54	− 54
2	26	+ 27
3	38	+ 38
4	24	− 23
5	8	+ 12
6	23	+ 23
7	14	− 16
8	18	− 21
9	5	+ 5
	h,0,12	
0	32	+ 35
1	16	+ 17
2	22	− 25
3	8	− 8
4	13	+ 16
5	11	− 13
	h,0,$\bar{1}\bar{2}$	
1	10	− 9
2	< 3	+ 1
3	16	+ 15
4	17	− 18
5	30	− 36
6	7	+ 7
7	11	+ 11
8	5	− 6
	h,0,14	
0	12	+ 13
1	9	− 11
2	9	− 11
3	17	+ 23
	h,0,$\bar{1}\bar{4}$	
1	8	− 9
2	26	− 31
3	8	+ 12
4	14	+ 16
5	4	− 6
6	2	+ 4

odd. In each case a choise was first made on the basis of calculated I—I and I—S distances, and the choise was later confirmed through comparison of calculated structure factors with rough intensity observations for a few representative *hkl* reflections.

ESTIMATE OF ERRORS

The standard deviations of atomic coordinates were estimated from the root-mean-square gradient of the difference maps and the curvature of the electron density peaks [28,29]. Where overlapping occurred, the s.d. was taken as about twice that which would otherwise have applied. In this way the following s.d. were obtained. In the diiodide, $\sigma(x) = 0.005$ Å, $\sigma(y) = \sigma(z) = 0.002$ Å for iodine; $\sigma(x) = \sigma(y) = \sigma(z) = 0.010$—0.012 Å for sulphur; $\sigma(x) = 0.04$—0.05 Å, $\sigma(y) = \sigma(z) = 0.02$—0.03 Å for carbon and nitrogen. In the dibromide, $\sigma(x) = \sigma(y) = 0.002$ Å, $\sigma(z) = 0.003$ Å for bromine; $\sigma(x) = \sigma(z) = 0.005$ Å, $\sigma(y) = 0.01$ Å for sulphur; $\sigma(x) = \sigma(z) = 0.015$—0.020 Å, $\sigma(y) = 0.03$—0.04 Å for carbon and nitrogen.

These values give standard deviations of 0.01 Å for the S—S bond length in the dibromide, and about 0.03 Å for S—C and C—N bond lengths. In the diiodide the corresponding figures are 0.02 Å and about 0.04 Å, respectively. For the S—S—C bond angle, $\sigma = 1°$ and 1—2°, and for S—C—N and N—C—N bond angles, about 2° and 3°, in the dibromide and diiodide, respectively. In both salts the S—S bond lies across a twofold axis, and the length is independent of the sulphur coordinate along the axis.

THE FORMAMIDINIUM DISULPHIDE ION

The salts are built up of disulphide cations and halide anions, and water of crystallization. The dimensions of the cation are listed in Table 5.

Table 5. Bond lengths and angles in the formamidinium disulphide ion.

	Diiodide	Dibromide		Diiodide	Dibromide
S—S	2.044 Å	2.044 Å	∠S—S—C	98.9°	104.0°
S—C	1.75	1.78	∠S—C—N_1	122.9°	121.2°
C—N_1	1.33	1.33	∠S—C—N_2	113.1°	118.3°
C—N_2	1.36	1.33	∠N_1—C—N_2	116.3°	119.0°
			Dihedral angle CSS/SSC	104.8°	89.2°

The S—S bond length is the same as in four other open-chain disulphides X—S—S—X for which data of comparable accuracy are available, namely 2.05 ± 0.02 Å in hydrogen disulphide [30], 2.04 ± 0.03 Å in dimethyl disulphide [30], 2.05 ± 0.02 Å in *bis*(trifluoromethyl) disulphide [31] and 2.04 ± 0.005 Å in N,N'-diglycyl-L-cystine dihydrate [32]. Also, the sulphur valency angle and the dihedral angle of the disulphide group lie in the normal range, *cf.* the recent review by Abrahams [33].

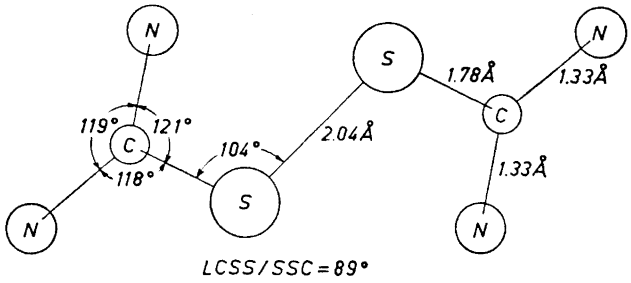

Fig. 5. The formamidinium disulphide cation as seen along the *b* axis of the dibromide.

The thiourea groups are planar within the accuracy of the atomic coordinates. Least squares planes through the four atoms of the group, with the sulphur coordinates given three times the weight of the carbon and nitrogen coordinates, have the equations

$$0.5340\ X - 0.4554\ Y - 0.7124\ Z = 0.023 \quad \text{(Diiodide)}$$
$$0.0573\ X + 0.6852\ Y + 0.7261\ Z = 4.582 \quad \text{(Dibromide)}$$

where X, Y and Z are in Å, in the case of the dibromide not referring to the axes of the monoclinic unit cell but to orthogonal axes a, b and c' where c' is normal to a and b. The planes pass at shortest distances of —0.006 Å from S, +0.083 Å from C, —0.036 Å from N_1 and —0.027 Å from N_2 in the diiodide, and at —0.007 Å from S, +0.068 Å from C, —0.022 Å from N_1 and —0.020 Å from N_2 in the dibromide. In view of the relatively large standard deviations of the coordinates of the lighter atoms, the displacements of the atoms from the planes can hardly be considered significant. On the other hand, it is known [34] that packing forces in crystals may cause distortions from planarity, of molecules or groups otherwise planar. As pointed out by Wheatley [35] with reference to ethylenethiourea, "distortions by crystal forces of molecules placed in unsymmetrical surroundings should be quite common". A decision is not possible in the present cases, although in the diiodide there is an indication that the distortion is real: As discussed later, the CN_1N_2 plane, $0.5548\ X - 0.6803\ Y - 0.5953\ Z = 0.001$, passes nearly equidistant between two iodide ions, and appears to allow a more reasonable location of amino hydrogen atoms than does the least-squares thiourea plane.

The two C—N bonds of a thiourea group have the same length, the slightly larger value for C—N_2 (1.36 Å) in the diiodide relative to the three other values of 1.33 Å being well within the experimental uncertainty. In fact, the thiourea groups are as in the thiourea molecule before oxidation of formamidinium disulphide, but for a slight but probably significant lengthening of the C—S bond relative to thiourea. According to a recent redetermination of the crystal structure of thiourea by Truter[36] the thiourea molecule is planar, with C—S = 1.710 ± 0.01 Å, C—N = 1.332 ± 0.01 Å, and ∠ N—C—N = 115°. The C and S atoms lie in a mirror plane which passes midway between the N atoms. Wheatley [35] found the same length, 1.708 ± 0.01 Å, for the C—S bond in

ethylenethiourea, and deduced a value of 22 % double-bond character for a C—S bond of this length. Abrahams' bond length-bond order curve [33], based on 1.61 Å for a double and 1.82 Å for a single C—S bond, gives about 65 %. Although thus the bond order data are conflicting it seems certain that the C—S bond of thiourea possesses a considerable degree of double-bond character; whether or not some is retained in formamidinium disulphide cannot be decided on the basis of the rather inaccurate values of 1.75 Å and 1.78 Å for the bond, but appears probable since interaction of the lone electrons of sulphur (a $p\pi$ pair or one of two sp^3 π pairs) with the $p\pi$ orbital of the sp^2-hybridized carbon atom is still possible. The concerned sulphur and carbon π orbitals are approximately parallel, the normal of the SSC plane making an angle of 14° with the normal of the least-squares plane of the thiourea group in the diiodide, and 6° in the dibromide.

The relative orientation of the two thiourea groups of a formamidinium disulphide cation is slightly different in the two salts. Such differences may be expected to arise, from different packing forces in the crystals, and they manifest themselves in three ways: The sulphur valency angle is 99 ± 1—2° in the diiodide and 104 ± 1° in the dibromide. Although on the basis of the standard deviations the difference may not be real, the statistically more accurate S—S—G angles, where G is the centre of gravity of the thiourea group (the sulphur coordinates given three times the weight of those of the lighter atoms) are also different, namely 101° in the diiodide and 104° in the dibromide. Furthermore, a difference in the degree of rotation about the

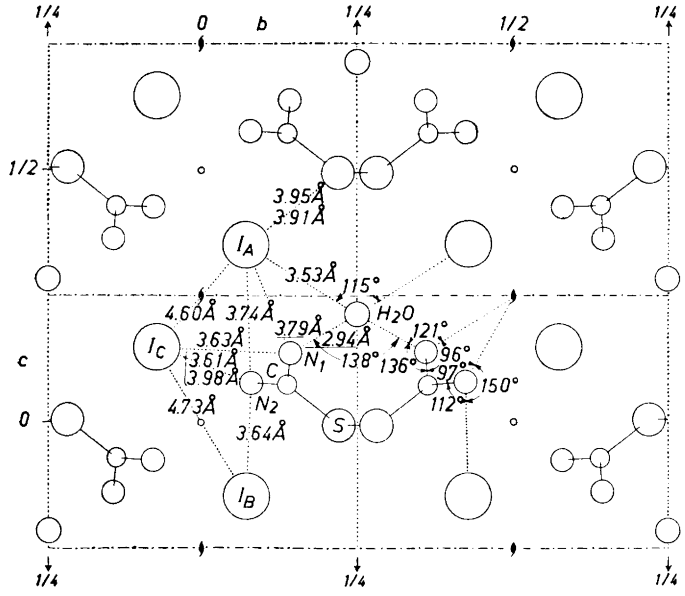

Fig. 6. The atomic arrangement in formamidinium disulphide diiodide monohydrate as seen along the *a* axis. Some non-bonded approaches and distances and angles relevant to the location of the hydrogen atoms are indicated.

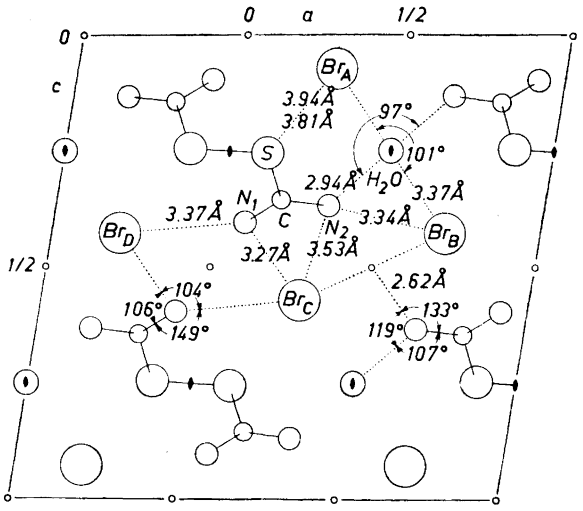

Fig. 7. A view along the *b* axis of the dibromide (one and a half unit cell) with interatomic approaches indicated as in Fig. 6.

S—S bond occurs, as expressed in the dihedral angles CSS/SSC which are 105° in the diiodide and 89° in the dibromide. Third, the sulphur atom of one thiourea group lies 0.48 Å from the least-squares plane of the other thiourea group in the diiodide and 0.22 Å in the dibromide, corresponding to different degrees of rotation, about the S—C bond, of the sulphur atom out of the plane.

THE PACKING IN THE CRYSTALS

The standard deviations of electron density, evaluated as the root-mean-square of the figures in the difference maps, are 0.46 and 0.65 e.Å^{-2}, respectively, for the *h*0*l* and 0*kl* zones of the dibromide, and 0.84 and 1.5 e.Å^{-2}, respectively, for the 0*kl* and *hk*0 zones of the diiodide. Any peak in the difference maps which might indicate positions of hydrogen atoms would therefore not be significant. In the following, the amino hydrogen atoms are assumed to be located in or not too far from positions corresponding to planar sp^2-hybridized nitrogen, as in urea and thiourea. They will be discussed with reference to the least-squares plane of the thiourea group in the dibromide, and to the CN_1N_2 plane in the diiodide, since this leads to slightly more reasonable hydrogen positions is some cases.

The atomic arrangements as seen along the shortest axis of each crystal are shown in Figs. 6 and 7.

Diiodide. The water molecule, located on a twofold axis at $\frac{1}{4},\frac{1}{4},z$ with $z = 0.214$, lies 3.53 Å from iodide ion I_A and the corresponding iodide ion on the other side of the twofold axis. The angle I—H_2O—I is 115°, and it seems probable that the water molecule forms hydrogen bonds to these iodide ions. Jellinek [37] reports a length of 3.57 Å for a O—H···I hydrogen bond in

muscarine iodide. The same water molecule participates with its two lone electron pairs in N—H···O hydrogen bonding from two nitrogen atoms, at a distance of 2.94 Å and a N—H_2O—N angle of 138°. These nitrogen atoms are $N_{1(\bar{1}00)}$, in an adjacent unit cell along the a axis, and N_1', in the same unit cell but on the other side of the twofold axis, and belong to different formamidinium disulphide cations. This leads to the occurrence in the crystal of infinite helical chains parallel to the a axis, of alternating formamidinium disulphide cations and water molecules, with one of each per turn of the helix, and $a = 5.15$ Å as repeat distance. The C—N—H_2O angle is 136° and the oxygen atom lies 10°, as seen from the nitrogen atom, out of the CN_1N_2 plane. Each oxygen atom thus participates in four hydrogen bonds, with atoms which form a distorted tetrahedron about it; two of the relevant angles are given above and the other four are I—H_2O—N_1' = 120°, I—H_2O—$N_{1(\bar{1}00)}$ = 71°, and a corresponding pair on the other side of the twofold axis.

Each of the two iodide ions forms, in directions 87° and 67° away from the water molecule, close contacts (3.91 Å and 3.95 Å) with two sulphur atoms ($\angle$S—I—S = 82°) of an adjacent helix, related to the first through the operation of the glide plane c normal to the a axis. The sulphur atoms belong to different disulphide cations, in adjacent unit cell along the a axis. Four such I—S contacts occur per turn of the helix, one of each length on each side of the twofold axis. Each iodide ion also forms two fairly close contacts with other iodide ions, in directions away from the helixes, namely 4.60 Å over the nearest screw axis parallel to the a axis, and 4.73 Å over the nearest symmetry centre.

One of the four amino hydrogen atoms of each thiourea group has so far been accounted for, through hydrogen bonding to water. There are short approaches between the nitrogen atoms and the iodide ions I_A and I_C (at $\frac{1}{2} + x, \bar{y}, \frac{1}{2}-z$; related to I_A through the operation of the screw axis at $x,0,\frac{1}{4}$): N_1—I_A = 3.79 Å, N_1—I_C = 3.63 Å, N_2—I_A = 3.74 Å, N_2—I_C = 3.61 Å. Expected length of a N—H···I hydrogen bond would be in this range, judging from values listed for N—H···Cl bonds [38]. However, I_A lies — 2.36 Å and I_C lies + 2.24 Å out of the CN_1N_2 plane, so that linear hydrogen bonds are improbable *. Now, the line joining I_A and I_C is normal to the CN_1N_2 plane (I_A—I_C = 4.60 Å), and the midpoint P between I_A and I_C, on the screw axis, is only —0.06 Å out of the plane, and 2.91 Å from N_1 and 2.86 Å from N_2. It appears likely that one N_1—H and one N_2—H bond are directed, not towards I_A or I_C but towards their midpoint, or nearly so. The relevant angles at N_1 and N_2 are: C—N_1—P = 96°, $H_2O_{(100)}$—N_1—P = 121°, C—N_2—P = 97°. With a N—H bond length of 1.0 Å the hydrogen atoms would lie 2.9—3.0 Å from the iodide ions, each hydrogen atom forming two such contacts.

It remains to account for one N_2 hydrogen atom. N_2 lies 3.64 Å from I_B (at $\frac{1}{2}-x, y, z-\frac{1}{2}$, related to I_A through the glide plane c at $x = \frac{1}{4}$) and 3.98 Å from $I_{C(\bar{1}00)}$. These two iodide ions are 4.73 Å apart, and are related through the symmetry centre at the origin. Both lie 0.62 Å out of the CN_1N_2 plane, their midpoint Q (the origin) lies in the plane and 2.99 Å from N_2. There are

* The distances from I_A and I_C to the least-squares plane of the thiourea group are —2.82 Å and +1.73 Å. The midpoint between I_A and I_C lies —0.54 Å out of the least-squares plane.

then two directions of the second N_2—H bond to consider, namely, towards I_B or towards the midpoint Q between I_B and $I_{C(\bar{1}\,0\,0)}$. The angles, C—N_2—I_B = 112°, P—N_2—I_B = 150°, C—N_2—Q = 112°. It appears that a direction intermediate between these two would give reasonable valency angles at N_2.

Dibromide. The expected lengths of N—H···Br and O—H···Br hydrogen bonds, from analogous bonds involving chloride, are about 3.3 Å.

The environment of the water molecule is as in the diiodide. The molecule lies on a twofold axis, at $\frac{1}{2},y,\frac{1}{4}$ with $y = 0.711$, and participates in hydrogen bonding to two bromide ions, above, and from two amino nitrogen atoms, below as seen down the twofold axis, one of each kind on each side of the axis, and in an approximately tetrahedral arrangement. The bromide ions are $Br_{A(010)}$, in an adjacent cell along the *b* axis, and $Br_{B(010)}$, related to the first through the twofold axis. The coordinates of Br_A are those listed in Table 2. The distances O—H···Br = 3.37 Å and N_2—H···O = 2.94 Å, and the angles, Br—H_2O—Br = 101°, N_2—H_2O—N_2 = 97°, $Br_{A(010)}$-H_2O-N_2 = 120° and $Br_{B(010)}$—H_2O—N_2 = 110°. The angle C—N_2—H_2O is 107°, and the water molecule is 0.35 Å out of the least-squares plane of the thiourea group, or 7° as seen from N_2. Again the N—H···O hydrogen bonds lead to the occurrence of an infinite chain, parallel to the *a* axis, of alternating water molecules and formamidinium disulphide cations. The water molecules and the sulphur atoms of the cations lie approximately on a straight line, at $y = 0.65$—0.71 and $z = \frac{1}{4}$, with the N_2 atoms below at $y = 0.332$ and the bromide ions above at $y = 1.131$, on both sides of $z = \frac{1}{4}$. The distances from Br_A and $Br_{A(010)}$ to the sulphur atom of the thiourea group to which N_2 belongs are 3.94 Å and 3.81 Å, respectively.

The nitrogen atom N_2 lies 3.34 Å and 3.53 Å, respectively, from the bromide ions Br_B and Br_C, these two ions are 4.46 Å apart and are related through the symmetry centre P at $\frac{1}{2},0,\frac{1}{2}$, they lie —0.03 Å and + 0.12 Å, respectively, out of the least-squares plane of the thiourea group. The geometry is, however, not favourable for N—H···Br hydrogen bonding, the angle C—N_2—Br_B being 173°, H_2O—N_2—Br_B = 77°, C—N_2—Br_C = 94° and H_2O—N_2—Br_C = 156°. The symmetry centre P, midway between the bromide ions, is 2.62 Å from N_2 and 0.05 Å out of the least-squares plane, and the angle C—N_2—P = 133° and H_2O—N_2—P = 119°. It appears probable that a N_2—H bond is directed towards the symmetry centre, the hydrogen atom would then lie about 2.75 Å from both bromide ions.

The other nitrogen atom of the thiourea group, N_1, lies 3.27 Å and 3.37 Å, respectively, from the bromide ions Br_C and Br_D, related to each other through a symmetry centre at $0,0,\frac{1}{2}$. They are 0.12 Å and — 0.54 Å, respectively, out of the least-squares plane, or 2° and 9° as seen from N_1. The angles, C—N_1—Br_C = 106°, Br_C—N_1—Br_D = 104°, C—N_1—Br_D = 150°, are not quite satisfactory for hydrogen bonding; the valency angles at N_1 would become more equal if the two N_1—H bonds are directed not towards the bromide ions but slightly aside of the ions.

A hydrate structure analogous to the two present ones occurs in adenine hydrochloride hemihydrate [39], where the water molecule lies on a twofold axis with two chloride ions (O—H···Cl = 3.12 Å) and two nitrogen atoms (O···H—N = 2.87 Å) in a distorted tetrahedral arrangement about it.

REFERENCES

1. Claus, A. *Ann.* **179** (1875) 135.
2. McGowan, G. *J. Chem. Soc.* **51** (1887) 378.
3. Hunter, R. F. and Jones, J. W. T. *J. Chem. Soc.* **1930** 2190.
4. King, L. C. and Ryden, I. *J. Am. Chem. Soc.* **69** (1947) 1813.
5. Sahasrabudhey, R. H. *J. Indian Chem. Soc.* **28** (1951) 309.
6. McGowan, G. *J. Chem. Soc.* **49** (1886) 190.
7. Storch, L. *Monatsh.* **11** (1890) 452.
8. Marshall, H. *Proc. Roy. Soc. Edinburgh* **24** (1902) 233.
9. Reynolds, J. E. and Werner, E. A. *J. Chem. Soc.* **83** (1903) 1.
10. Werner, E. A. *J. Chem. Soc.* **101** (1912) 2166.
11. Toennies, G. *J. Biol. Chem.* **120** (1937) 297.
12. Mahr, C. *Z. anal. Chem.* **117** (1939) 91.
13. Sahasrabudhey, R. H. *J. Indian Chem. Soc.* **30** (1953) 64.
14. Rathke, B. *Ber.* **17** (1884) 297.
15. Boeseken, J. *Proc. Koninkl. Akad. Wetenschap. Amsterdam* **39** (1936) 717.
16. Preisler, P. W. and Berger, L. *J. Am. Chem. Soc.* **69** (1947) 322.
17. Fichter, F. and Wenk, W. *Ber.* **45** (1912) 1373.
18. Fichter, F. and Braun, F. *Ber.* **47** (1914) 1526.
19. Freedman, L. D. and Corwin, A. H. *J. Biol. Chem.* **181** (1949) 601.
20. Heyns, K., Walter, W. and Bebenburg, W. *Angew. Chem.* **68** (1956) 415.
21. Lecher, H., Graf, F., Heuck, C., Köberle, K., Gnädinger, F. and Heydweiller, F *Ann.* **445** (1925) 35.
22. Sahasrabudhey, R. H. *J. Indian Chem. Soc.* **28** (1951) 341.
23. Sahasrabudhey, R. H. and Sheshadri, K. R. *J. Indian Chem. Soc.* **29** (1952) 901.
24. Foss, O. and Tjomsland, O. *Acta Chem. Scand.* **10** (1956) 869.
25. Foss, O. and Johnsen, J. *Acta Chem.* Scand. **11** (1957) 189.
26. Viervoll, H. and Ögrim, O. *Acta Cryst.* **2** (1949) 277.
27. Berghuis, J., Haanappel, I. M., Potters, M., Loopstra, B. O., MacGillavry, C. H. and Veenendaal, A. L. *Acta Cryst.* **8** (1955) 478.
28. Cruickshank, D. W. *Acta Cryst.* **2** (1949) 65.
29. Cochran, W. *Acta Cryst.* **4** (1951) 81.
30. Stevenson, D. P. and Beach, J. Y. *J. Am. Chem. Soc.* **60** (1938) 2872.
31. Bowen, H. J. M. *Trans. Faraday Soc.* **50** (1954) 452.
32. Yakel, H. L. and Hughes, E. W. *Acta Cryst.* **7** (1954) 291.
33. Abrahams, S. C. *Quart. Revs. London* **10** (1956) 407.
34. Wheatley, P. J. *Ann. Rev. Phys. Chem.* **8** (1957) 373.
35. Wheatley, P. J. *Acta Cryst.* **6** (1953) 369.
36. Truter, M. R. *Acta Cryst.* **10** (1957) 785.
37. Jellinek, F. *Acta Cryst.* **10** (1957) 277.
38. Donohue, J. *J. Phys. Chem.* **56** (1952) 502.
39. Broomhead, J. M. *Acta Cryst.* **1** (1948) 324.

Received August 12, 1958.

ACTA CHEMICA SCANDINAVICA 12 (1958) 1799—1809

The Crystal and Molecular Structure of Thiuret Hydroiodide

OLAV FOSS and OLAV TJOMSLAND

Chemical Institute, University of Bergen, Bergen, Norway

The crystal structure of the five-membered cyclic disulphide, thiuret hydroiodide, a 3,5-diamino derivative of 1,2,4-dithiazole, has been determined by two-dimensional X-ray methods. The disulphide group lies across a crystallographic mirror plane and is therefore planar, and the thiuret ion as a whole is planar or nearly so.

The crystals have four $[S_2(C-NH_2)_2N]I$ units in a cell based on the space group, D_{2h}^{16}-*Pnma*, with $a = 5.38$ Å, $b = 9.24$ Å, $c = 13.98$ Å. The dimensions of the thiuret ring were found to be, S—S = 2.09 ± 0.012 Å, S—C = 1.73 ± 0.03 Å, C—N = 1.31 ± 0.03 Å, ∠S—S—C = 92.4 ± 1°, ∠S—C—N = 118 ± 2°, ∠C—N—C = 117 ± 2°, and the exocyclic C—NH_2 bond, 1.36 ± 0.03 Å. Within the experimental accuracy the carbon valencies are trigonal planar.

Thiourea reacts with numerous oxidizing agents to give salts of formamidinium disulphide, which according to recent crystal structure determinations of the diiodide and dibromide monohydrates [1], contains a normal, non-planar disulphide group. Similarly, the formal condensation product of two moles of thiourea, dithiobiuret, undergoes reversible oxidation by such reagents as hydrogen peroxide, iodine, ceric salts, thallic salts, or formamidinium disulphide salts, to give compounds which are regarded as salts of the base, thiuret, or 3,5-diimino-1,2,4-dithiazolidine [2–5]. This is a five-membered cyclic disulphide.

Fromm [6] in 1893 first assigned the name, thiuret, and a disulphide formula, to an oxidation product of a dithiobiuret. Although a number of derivatives of dithiobiuret and thiuret were studied by Fromm and later workers [5], the synthesis of dithiobiuret itself was not achieved until 1943 [7], and its oxidation product (thiuret hydrochloride and hydroiodide) described in 1947 [2,3]. In this year, Preisler and Bateman [2] published a potentiometric study of the reversible dithiobiuret-thiuret system:

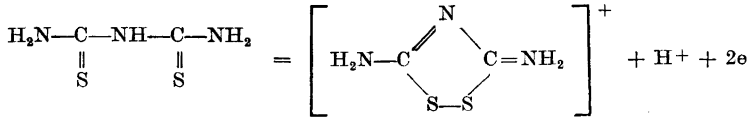

They found a value of + 0.25 V for the oxidation-reduction potential at pH = 0 and 30°C, referred to the normal hydrogen electrode, as compared with + 0.42 V for the potential of the thiourea-formamidinium disulphide system measured earlier by Preisler and Berger [8]:

$$2\ (H_2N)_2CS = [(H_2N)_2C—S—S—C(NH_2)_2]^{++} + 2e$$

Dithiobiuret is thus a markedly stronger reducing agent than thiourea. The acid dissociation constant of the monovalent thiuret cation was measured [2] as 4×10^{-8}. The free thiuret base has not been isolated, the salts being rapidly decomposed by alkalies with elimination of sulphur.

A survey [9] of unit cells and space groups of some 1,2,4-dithiazolidine derivatives, including thiuret hydrohalides, indicated the occurrence in the hydroiodide of a molecular mirror plane of symmetry and thereby of a planar *cis* disulphide group. This would be the first example of a planar disulphide group, all previous structure determinations of compounds of the type X—S—S—X having given a dihedral angle XSS/SSX of about 90°. The barrier towards rotation about the S—S bond, through the planar *cis* form with zero dihedral angle, has been estimated [10,11] as 10—14 kcal/mole. A preliminary account of the crystal structure of the hydroiodide was published at the same time [12].

CRYSTAL DATA

The salt was prepared by addition of an excess of aqueous potassium iodide to a warm aqueous solution of thiuret hydrochloride, and was recrystallized from water. The crystals are faintly yellow, m. p. (reported [3]) 247°C. They occurred as prisms extended along the *a* axis and bounded by {001} and {011}. There is perfect cleavage along the *c* plane, and a rather pronounced tendency of irregular growth and twinning, but crystals were found which gave satisfactory intensity photographs.

The crystals are orthorhombic, with the unit cell dimensions [9]: $a = 5.38$ Å, $b = 9.24$ Å, $c = 13.98$ Å (± 0.5 %). There are four $[S_2(C—NH_2)_2N]I$ units in the cell; density, calc. 2.50, found 2.49 g/cm^3. From the systematic absences, $0kl$ when $k + l$ is odd and $hk0$ when h is odd, and the subsequent structure analysis, the space group is D_{2h}^{16} — *Pnma*. The iodide ion and the ring nitrogen atom of the cation lie in the mirror plane of this space group, the other atoms are in general, eightfold positions. There are thus 13 positional parameters to be determined, excluding the hydrogen atoms.

THE STRUCTURE ANALYSIS

The intensities of the reflections of the three principal zones were estimated visually from zero-layer Weissenberg photographs. Copper radiation was used ($\mu = 438$ cm^{-1}) and crystals with cross-sections of 0.07 × 0.07 mm for the $0kl$ and $hk0$ zones and 0.07 × 0.03 mm for the $h0l$ zone. Out of 88 $0kl$, 93 $h0l$ and 33 $hk0$ reflections within the range $\sin \Theta < 0.985$, 83, 86 and 29, respectively, were observed and measured. The intensities were corrected for the Lorenz and polarization factors in the usual way, but not for absorp-

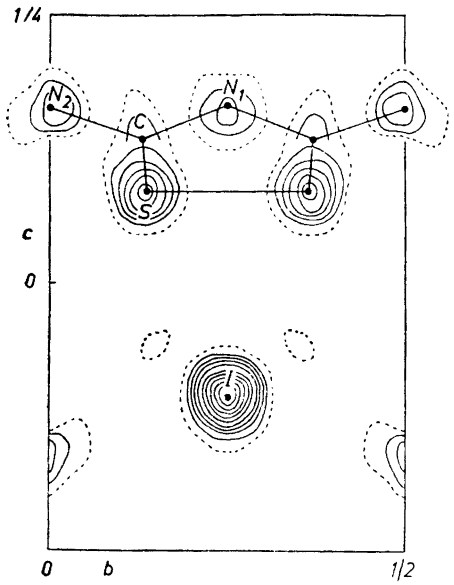

Fig. 1. Electron density projection of thiuret hydroiodide along the *a* axis. Contours at intervals of 10 e · Å^{-2} for iodine, 4 e · Å^{-2} for sulphur, 2 e · Å^{-2} for carbon and nitrogen, beginning with 4 e · Å^{-2} (dashed). The mirror plane is normal to the plane of the paper and passes through I and N_1.

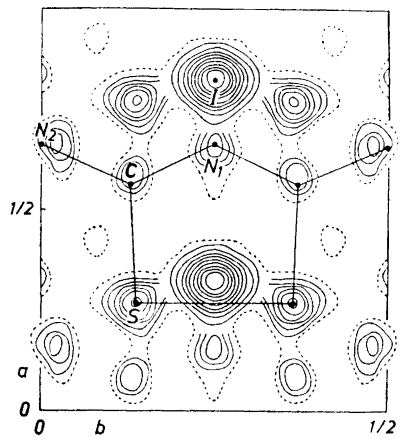

Fig. 2. Electron density projection of thiuret hydroiodide along the *c* axis. The contour interval is 3 e · Å^{-2} for carbon and nitrogen, and the 8-electron line is dashed; otherwise as in Fig. 1.

tion, and were converted to relative structure amplitudes and ultimately brought to an approximately absolute scale by comparison with the calculated values.

The coordinates of the iodide ion were found from Patterson projections, and the structure was solved by use of the heavy atom method and refined through successive Fourier and Fourier difference syntheses. Summations were made by means of Beevers-Lipson strips, at 12° intervals along the *a* axis and 6° intervals along the *b* and *c* axes. The 0*kl* zone was refined first, and the *h*0*l* zone next considered, but here extensive overlapping occurred, so that attention was shifted to the *hk*0 zone. The five *x* coordinates are thus based on the 29 observed *hk*0 reflections; together with the five thermal parameters employed for this zone the number of variables is fairly large relative to the number of observations.

The 0*kl* and *hk*0 electron density maps are shown in Figs. 1 and 2, and the final atomic coordinates are listed in Table 1. The positions corresponding to these coordinates are marked with dots in Figs. 1 and 2. It is seen that particularly in the *hk*0 projection the maxima of the electron density peaks differ markedly from the final positions, apparently because of series termination effects corrected for through the difference refinement.

Table 1. Atomic coordinates for thiuret hydroiodide, in fractions of cell edges. Origin at a centre of symmetry.

	x	y	z
I	0.8235	0.250	−0.1075
N_1	0.665	0.250	0.165
S	0.270	0.1370	0.0845
C	0.565	0.129	0.134
N_2	0.662	0.000	0.163

The observed and calculated values of the 0*kl* and *hk*0 structure factors are listed in Table 2. The calculated values are based on the atomic scattering curves of Berghuis *et al.*[13] for carbon and nitrogen, of Viervoll and Ögrim [14] for sulphur, and an iodine curve constructed from the Thomas-Fermi values for xenon at small scattering angles and electroneutral iodine at intermediate and large angles. In the temperature factor exp $[-B(\sin^2\Theta/\lambda^2)]$ the following values of B were finally adopted, mainly on the basis of the difference maps: In the 0*kl* zone, $B = (2.3 + 0.8 \cos^2\varphi)$ Å^2 for iodine, where φ is the angle between the normal of the reflecting plane and the c axis, and $B = 2.6$ Å for the other atoms. In the *hk*0 zone, $B = (2.0 + 0.5 \cos^2\varphi)$ Å^2 for iodine and $(1.8 + 0.8 \cos^2\varphi)$ Å^2 for sulphur, where φ is the angle between the normal of the reflecting plane and the b axis, and $B = 2.3$ Å^2 for carbon and nitrogen. No significance in terms of anisotropic thermal vibrations should be attached to the B values, as they may reflect absorption and other errors in the observed structure factors.

In the case of the C and N_2 atoms the y coordinates used for the final structure factor calculations were, $y(C) = 0.126$ and 0.132, $y(N_2) = -0.002$ and $+0.002$, respectively, for the 0*kl* and *hk*0 zones. The values of Table 1 are weighted means.

The reliability index, $R = \Sigma||F_o| - |F_c||/\Sigma|F_o|$, with non-observed reflections included when $|F_c|$ is larger than the observable limit, is 0.073 for the 0*kl* zone and 0.061 for the *hk*0 zone. The strong reflections 004 and 033 have calculated values relatively much larger than the observed ones, and were omitted from the calculation of R index and scale factors for the zone, and from the difference syntheses. A calculation of structure factors for the *h*0*l* zone, using the x and z coordinates derived from the 0*kl* and *hk*0 zones and an approximate temperature correction with $B = 4.0$ Å^2, gave a R index of 0.15 for this zone.

ASSESSMENT OF ACCURACY

The standard deviation of electron density, evaluated from the difference maps, is 0.7 e.Å^{-2} for the 0*kl* zone and 1.2 e.Å^{-2} for the *hk*0 zone. The s.d. of the atomic coordinates were estimated from the root-mean-square of the gradients in the difference maps and the curvatures of the electron density peaks [15,16], and the following values were found: $\sigma(x) = 0.003$ Å, $\sigma(z) = 0.002$ Å for iodine, $\sigma(x) = 0.010$ Å, $\sigma(y) = 0.006$ Å, $\sigma(z) = 0.009$ Å for sulphur, and $\sigma = 0.02$ Å for the carbon and nitrogen coordinates, except $\sigma(z)$ for carbon

Table 2. Observed and calculated 0*kl* and *hk*0 structure factors for thiuret hydroiodide.

l	F_o	F_c	*l*	F_o	F_c	*l*	F_o	F_c
	0*kl* zone			04*l*			0,10,*l*	
	00*l*		14	57	− 60	2	21	− 21
2	53	+ 57	16	15	− 3	4	51	+ 51
4	244	−275				6	43	+ 44
6	100	−103		05*l*		8	17	− 20
8	48	+ 46	1	112	−108			
10	83	+ 82	3	156	−165		0,11,*l*	
12	31	+ 30	5	8	+ 5	1	25	+ 26
14	32	− 35	7	134	+121	3	33	+ 38
16	21	− 24	9	46	+ 43	5	9	− 9
			11	46	− 45			
	01*l*		13	35	− 34		*hk*0 zone	
1	34	− 37	15	< 6	+ 4	*k*	0*k*0	
3	70	− 76				2	179	−186
5	31	+ 32		06*l*		4	108	+103
7	111	+107	0	78	− 77	6	81	− 71
9	< 8	− 8	2	18	− 16	8	131	+131
11	90	− 89	4	80	+ 72	10	67	− 67
13	22	− 23	6	45	+ 41			
15	39	+ 48	8	63	− 54		2*k*0	
17	22	+ 33	10	54	− 48	0	197	−182
			12	25	+ 26	1	104	+113
	02*l*		14	37	+ 39	2	92	+ 94
0	172	−183				3	98	−100
2	55	− 57		07*l*		4	45	− 47
4	127	+141	1	44	+ 39	5	73	+ 73
6	104	+106	3	70	+ 63	6	30	+ 36
8	70	− 67	5	12	− 11	7	60	− 57
10	87	− 85	7	74	− 67	8	65	− 68
12	13	+ 16	9	10	− 10	9	45	+ 42
14	43	+ 46	11	47	+ 48	10	41	+ 39
16	< 6	+ 6	13	17	+ 20	11	26	− 29
	03*l*			08*l*			4*k*0	
1	115	+127	0	130	+132	0	< 9	+ 3
3	167	+191	2	23	+ 22	1	130	−114
5	16	− 16	4	96	− 95	2	14	+ 15
7	137	−140	6	51	− 48	3	62	+ 61
9	38	− 35	8	25	+ 25	4	67	− 66
11	66	+ 61	10	39	+ 41	5	36	− 41
13	37	+ 33	12	10	+ 11	6	23	+ 27
15	8	− 13				7	50	+ 58
17	13	− 17		09*l*		8	< 8	− 1
			1	14	− 18	9	44	− 50
	04*l*		3	22	− 23			
0	100	+102	5	14	+ 19		6*k*0	
2	24	− 18	7	35	+ 37	0	36	+ 36
4	90	− 88	9	13	− 10	1	30	+ 32
6	17	+ 8	11	35	− 40	2	46	− 42
8	69	+ 61				3	< 7	− 11
10	49	+ 39		0,10,*l*		4	76	+ 74
12	27	− 26	0	65	− 67	5	< 5	+ 4

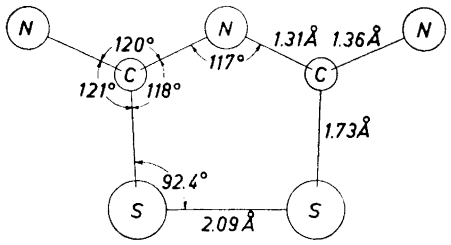

Fig. 3. The thiuret ion, with bond lengths and angles.

which is larger because of overlapping. y for iodine and N_1 are fixed by symmetry relations. This gives $\sigma = 0.012$ Å for the S—S bond length across the mirror plane, about 0.03 Å for S—C and C—N bond lengths, 1° for the S—S—C angle and 2° for other bond angles in the cation.

THE THIURET ION

The bond lengths, as calculated from the atomic coordinates of Table 1, are as follows: S—S = 2.088 Å, S—C = 1.73 Å, C—N_1 (cyclic) = 1.31 Å, C—N_2 (exocyclic) = 1.36 Å, and the angles, S—S—C = 92.4°, S—C—N_1 = 118.1°, C—N_1—C = 116.9°, N_2—C—S = 120.5°, N_2—C—N_1 = 119.5°. The cation as seen in projection along the c crystal axis is shown in Fig. 3.

The S—S bond appears to be significantly longer than 2.04—2.05 Å normally found in non-cyclic disulphides, *e.g.*, 2.044 ± 0.01 Å in formamidinium disulphide dibromide monohydrate [1]. Within the accuracy of the results the carbon valencies are trigonal planar, and although the rather large s.d. do not permit definite conclusions, the found lengths for the three bonds from carbon indicate that they possess some double-bond character. If the lengths of single and double bonds between the atoms in the appropriate hybridization states are taken to be [17-19], C—N = 1.47 Å, C=N = 1.27 Å, C—S = 1.80 Å, C=S = 1.60 Å, Pauling's expression relating bond length and bond order [20] gives about 55 % double-bond character for the C—N_1 bond, 30 % for the C—N_2 bond and 15 % for the C—S bond. Although to discuss bond orders when the experimental uncertainty is 0.03 Å seems rather naive, the results are reasonable.

The shortness of the ring C—N bond thus indicates that the ring N_1 atom has a π orbital available for overlap with the carbon π orbital. Since mirror plane symmetry of the thiuret ion is crystallographically required, it follows that of the four hydrogen atoms of the ion, two are bonded to each of the exocyclic N_2 nitrogen atoms. The other mirror plane-symmetric alternative, one hydrogen atom on each N_2 atom and two on the ring N_1 atom, would make N_1 quaternary and leave no available π orbital. The C—N_1 bond should then be expected to be considerably longer than the C—N_2 bond, and the C—N_1—C angle should be closer to tetrahedral. The found value for the angle (117°) is in agreement with the observation [21,22] that in heterocyclic rings containing nitrogen atoms, the bond angle of the (mainly sp^2-hybridized) nitrogen is less than 120°. A diamino as contrasted with a diimino structure

should correspond to higher stability as a result of conjugation across the ring nitrogen atom, of the two sp^2-hybridized carbon atoms. A similar nitrogen bridge between carbon atoms each bonded to an amino group occurs in melamine, 2,4,6-triamino-*s*-triazine [23].

The N_2—C—N_1—C—N_2 grouping is planar. A least-squares plane through the atoms:

$$0.6209\ X - 0.7839\ Z = 0.419$$

(X and Z in Å) passes through C and at —0.006 Å from N_1 and +0.006 Å from N_2. This plane makes an angle of 15° with the C—S—S—C plane. A least-squares plane through all the atoms of the cation, with the sulphur coordinates given three times the weight of the carbon and nitrogen coordinates:

$$0.4544\ X - 0.8908\ Z = -0.384$$

passes at a shortest distance of —0.008 Å from S, +0.097 Å from C, —0.046 Å from N_1 and —0.027 Å from N_2. The distances are particularly dependent on the z coordinates, and since the z coordinate of C probably has a larger s.d. than the other light atom coordinates (0.02 Å) the apparent deviation from planarity of the thiuret ion as a whole can hardly be considered significant. However, distortions from planarity do sometimes occur in crystals of molecules which on the basis of hybridization and resonance considerations should be expected to be planar [17,24].

The thiuret ion contains two thiourea groups, and is formally derived from the formamidinium disulphide ion through ring closure under elimination of an ammonium ion. Neither in the structure analyses of formamidinium disulphide diiodide and dibromide monohydrates [1] do the experimental results permit a decision whether the thiourea groups are quite planar or not. The difference between the C—S bond lengths in the dibromide [1] (1.78 Å) and in thiuret hydroiodide (1.73 Å) is within the limits of error. Thiourea itself is planar in the crystals [25], with C—S = 1.71 ± 0.01 Å.

THE PLANARITY OF THE DISULPHIDE GROUP

The disulphide group lies across a crystallographic mirror plane. Therefore, unless the mirror plane symmetry is statistical, the disulphide group is exactly planar. Such groups are normally non-planar, with a dihedral angle of about 90° between the planes of the valencies of the two sulphur atoms [19], there being a barrier of 10—14 kcal/mole [10,11] towards rotation about the S—S bond, through the planar *cis* and *trans* forms. This barrier can be explained [26,27] as arising principally from the mutual repulsion of the unshared $p\pi$ electron pairs, one on each sulphur atom. The σ-bonding orbitals of sulphur are thereby assumed to be nearly pure p in character. The possibility exists that extra stability is conferred upon the S—S bond in the non-planar form with about 90° dihedral angle, through overlap of the sulphur $p\pi$ electron pair with an available d orbital of the bond partner; the S—S bond would then have some pd π-bond character. The S—S bond of about 2.04 Å in non-cyclic

disulphides and the short bonds of the same length in the tetra- and pentathionate ions would, on the basis of the present knowledge about length-order relations for S—S bonds [19,28], correspond to about 20 % π-bonding.

In the relatively stable thiuret hydroiodide, with planar disulphide group, the S—S rotation barrier, if it exists also there, must be compensated through other effects, such as favourable lattice conditions in the mirror-plane arrangement, and through resonance stabilization of the ring. The most probable resonance forms of the supposedly correct tautomer of the thiuret ion are

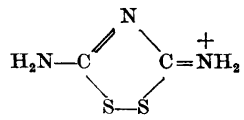

(A)

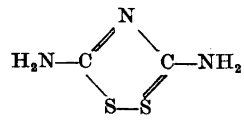

(B)

and their mirror images. Form A would seem to be the more important one, and confer considerable stability on the ion. Form B involves a π electron pair of sulphur.

The incorporation of the disulphide group in a five-membered ring will, for strain reasons, not allow a normal dihedral angle of about 90°; however, in the saturated five-membered cyclic disulphide, 1,2-dithiolane-4-carboxylic acid [29,30], the dihedral angle is not zero but 27 $\pm$ 1°, and the dithiolane ring is rather unstable. It appears that the unsaturated character of the thiuret ring system is responsible for the planarity of the disulphide group and the stability of the ion. The presence of an unsaturated carbon atom (sp^2-hybridized, with an available $p\pi$ orbital) adjacent to each sulphur atom is not a sufficient requisite for planarity of a disulphide group; in the non-cyclic formamidinium disulphide ion, where the carbon atoms are in the same state of hybridization as in the thiuret ion and also there bonded to a sulphur and two nitrogen atoms, the disulphide group is non-planar, with a dihedral angle of 105° in the diiodide and 89° in the dibromide [1]. The question arises whether the planarity of the disulphide group in unsaturated cyclic disulphides of the thiuret type is due in some degree to π-electron conjugation over the ring as a whole, with participation of sulphur π orbitals; in cyclic conjugated systems such as thiophen and thiazole, a sulphur atom replaces a —CH=CH— group and contributes two π electrons to the aromatic sextet. From the observed S—S bond length in thiuret hydroiodide, conjugation across the S—S bond does not appear to be very strong. In a crystal structure analysis of another unsaturated five-membered cyclic disulphide, 4-methyl-1,2-dithia-4-*cyclo*pentene-3-thione, Kehl and Jeffrey [31] have found that the molecule lies approximately in a plane. They state that "From the observed bond lengths the five-membered ring has some aromatic character. — This π-bonding does not, however, appear to include the S_1—S_2 link, which has a normal single bond length (2.03 Å)." The bond is thus shorter than the S—S bond in thiuret hydroiodide; on the basis of the available length-order data [19,28] the length does indicate 20—30 % π character. It is noteworthy that the ring atoms in the thiuret ion have a sextet of π electrons, as have the ring atoms in the tri-

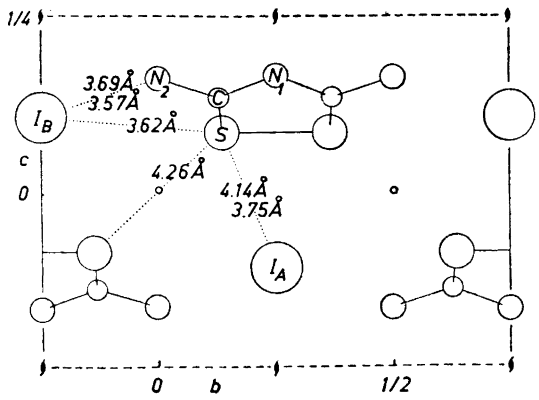

Fig. 4. The ionic arrangement as seen along the *a* axis. Half a unit cell is shown.

thiones of which the above 4-methyl derivative is an example. Lüttringhaus [32,33] has emphasized the aromatic, thiophen-like character of the trithione ring in the thiocarbonyl polarized form, and pointed out that in this ring system the planar form of the disulphide group appears to be stable.

THE IONIC ENVIRONMENT

The arrangement of thiuret ions and iodide ions as seen along the *a* crystal axis is shown in Fig. 4.

The crystals have a layer structure, there being no bonds and only weak non-bonded contacts across the glide plane *a* normal to the *c* axis at $z = \frac{1}{4}$ and $-\frac{1}{4}$. This accounts for the perfect cleavage along the *c* plane. The shortest distances across the glide plane are, N_1—N_1 = 3.55 Å, N_2—N_2 = 3.63 Å, N_2—N_1 = 4.30 and 4.31 Å, N_2—I = 3.95 Å and I—I = 4.81 Å. The N—N approaches are not close enough for van der Waals contacts or hydrogen bonds between the atoms, and the I—I distance is longer than twice the ionic radius of iodine, 2.16 Å [20]. If the hydrogen atoms are trigonally bonded to N_2 and lie in or not too far removed from the least-squares plane of the thiuret ion, then one of the N_2—H bonds is directed approximately toward the related nitrogen atom (N_2') across the glide plane, at an angle of about 60° with the plane of the thiuret ion to which N_2' belongs. N_2' lies 15° out of the plane of the first thiuret ion, as seen from N_2, and the C—N_2—N_2' angle is 119°. With a N—H bond length of 1.0 Å and van der Waals radii for hydrogen and nitrogen of 1.2 and 1.5 Å, respectively [20], the N_2—N_2' distance of 3.63 Å may indicate a weak contact between hydrogen and N_2'.

There are several close non-bonded approaches within a layer. In Fig. 4, the iodide ion I_B is related to I_A through the symmetry centre in $\frac{1}{2}$,0,0; the coordinates of I_A are those listed in Table 1. N_2 lies 3.57 Å from I_B and 3.69 Å from $I_{B(100)}$; these iodide ions are —0.52 Å and + 1.92 Å, respectively, out of the plane of the thiuret ion. A trigonal N_2—H bond located in this plane

would be directed about 20° away from I_B, as seen from N_2, and the hydrogen atom would lie about 2.8 Å from I_B.

Each sulphur atom forms close contacts with two iodide ions and a weaker one with a third. If the coordinates of the reference sulphur atom are those listed in Table 1, the contacts are S—I_A = 4.14 Å, S—$I_{A(\bar{1}00)}$ = 3.75 Å and S—I_B = 3.62 Å. In formamidinium disulphide diiodide monohydrate [1] the closest S—I approaches are 3.91 and 3.95 Å, and in 2,2′-diiododiethyltrisulphide [34], with covalent iodine, 3.74, 3.80 and 3.85 Å. It appears that the value, 1.60 Å proposed by Donohue [34] for the van der Waals radius of sulphur fits the experimental data, at least for S—I contacts, better than does the Pauling value [20] of 1.85 Å.

The environment of an iodide ion is as follows. Located in a mirror plane, it has on each side of the plane two nitrogen atoms at 3.57 and 3.69 Å and three sulphur atoms at 3.62, 3.75 and 4.14 Å, and in the plane a nitrogen atom at 3.90 Å; these approaches are all within the layer. In the adjacent layer there is a nitrogen atom at 3.95 Å on each side of the mirror plane, and two iodide ions in the plane, both at 4.81 Å.

The shortest non-bonded S—S distance in the crystals is 4.26 Å over a centre of symmetry.

The work has been supported financially by *Norges Almenvitenskapelige Forskningsråd*. A sample of thiuret hydrochloride was generously provided by American Cyanamid Company, New York.

REFERENCES

1. Foss, O., Johnsen, J. and Tvedten, O. *Acta Chem. Scand.* **12** (1958) 1782.
2. Preisler, P. W. and Bateman, M. M. *J. Am. Chem. Soc.* **69** (1947) 2632.
3. American Cyanamid Co. *Dithiobiuret, Technical Data Sheet*, New York, 1947.
4. American Cyanamid Co. *New Product Bulletin*, Collective Vol. I, New York 1952 p. 54.
5. Kurzer, F. *Chem. Revs.* **56** (1956) 95.
6. Fromm, E. *Ann.* **275** (1893) 20.
7. Sperry, R. L. *U. S. patent* 2 371 112; *Chem. Abstracts* **39** (1945) 3556.
8. Preisler, P. W. and Berger, L. *J. Am. Chem. Soc.* **69** (1947) 322.
9. Foss, O. *Acta Chem. Scand.* **10** (1956) 868.
10. Scott, D. W., Finke, H. L., Gross, M. E., Guthrie, G. B. and Huffman, H. M. *J. Am. Chem. Soc.* **72** (1950) 2424.
11. Scott, D. W., Finke, H. L., McCullough, J. P., Gross, M. E., Pennington, R. E. and Waddington, G. *J. Am. Chem. Soc.* **74** (1952) 2478.
12. Foss, O. and Tjomsland, O. *Acta Chem. Scand.* **10** (1956) 869.
13. Berghuis, J., Haanappel, I. M., Potters, M., Loopstra, B. O., MacGillavry, C. H. and Veenendaal, A. L. *Acta Cryst.* **8** (1955) 478.
14. Viervoll, H. and Ögrim, O. *Acta Cryst.* **2** (1949) 277.
15. Cruickshank, D. W. *Acta Cryst.* **2** (1949) 65.
16. Cochran, W. *Acta Cryst.* **4** (1951) 81.
17. Wheatley, P. J. *Acta Cryst.* **6** (1953) 369.
18. Donohue, J., Lavine, L. R. and Rollett, J. S. *Acta Cryst.* **9** (1956) 655.
19. Abrahams, S. C. *Quart. Revs. London* **10** (1956) 407.
20. Pauling, L. *The Nature of the Chemical Bond*, Cornell University Press, Ithaca, N. Y. 1945.
21. Bertinotti, F., Giacomello, G. and Liquori, A. M. *Acta Cryst.* **9** (1956) 510.
22. Wheatley, P. J. *Acta Cryst.* **10** (1957) 182.
23. Hughes, E. W. *J. Am. Chem. Soc.* **63** (1941) 1737.

24. Wheatley, P. J. *Ann. Rev. Phys. Chem.* **8** (1957) 373.
25. Truter, M. R. *Acta Cryst.* **10** (1957) 785.
26. Pauling, L. *Proc. Natl. Acad. Sci. U. S.* **35** (1949) 495.
27. Bergson, G. *Arkiv Kemi* **12** (1958) No. 24.
28. Foss, O. and Tjomsland, O. *Acta Chem. Scand.* **12** (1958) 44.
29. Foss, O. and Tjomsland, O. *Acta Chem. Scand.* **11** (1957) 1426.
30. Bergson, G. and Schotte, L. *Acta Chem. Scand.* **12** (1958) 367.
31. Kehl, W. L. and Jeffrey, G. A. *Acta Cryst.* **10** (1957) 807.
32. Lüttringhaus, A. *Angew. Chem.* **59** (1947) 244.
33. Lüttringhaus, A. and Hägele, K. *Angew. Chem.* **67** (1955) 304.
34. Donohue, J. *J. Am. Chem. Soc.* **72** (1950) 2701.

Received August 12, 1958.

ACTA CHEMICA SCANDINAVICA 12 (1958) 1810—1818

The Crystal and Molecular Structure of 1,2-Dithiolane-4-carboxylic Acid

OLAV FOSS and OLAV TJOMSLAND

Chemical Institute, University of Bergen, Bergen, Norway

The crystals of 1,2-dithiolane-4-carboxylic acid are triclinic, with $a = 5.34$ Å, $b = 5.85$ Å, $c = 10.75$ Å, $\alpha = 93\frac{1}{2}°$, $\beta = 89\frac{1}{2}°$, $\gamma = 109\frac{1}{2}°$, and two molecules per unit cell. The space group is $C_i^1-P\bar{1}$. A structure analysis based on 268 observed $0kl$ and $h0l$ reflections has shown that the 1,2-dithiolane ring is not planar, the dihedral angle CSS/SSC being $26.6 \pm 1°$.

The bond lengths in the ring were found to be, $S_1-S_2 = 2.096 \pm 0.009$ Å, $S_2-C_3 = 1.85$ Å, $C_3-C_4 = 1.48$ Å, $C_4-C_5 = 1.55$ Å, $C_5-S_1 = 1.83$ Å, and the angles, $C_5-S_1-S_2 = 92.6 \pm 0.7°$, $S_1-S_2-C_3 = 96.6 \pm 0.6°$, $S_2-C_3-C_4 = 111°$, $C_3-C_4-C_5 = 114°$, $C_4-C_5-S_1 = 104°$. The carboxyl group is planar and has normal dimensions. The molecules are arranged into dimers about centres of symmetry, through O—H···O hydrogen bonds between carboxyl groups.

The 1,2-dithiolane ring has attracted considerable interest in the later years [1-4] because of its presence in 6-thioctic acid (α-lipoic acid) [5]. From a viewpoint of sulphur stereochemistry the importance of the 1,2-dithiolane ring lies in the circumstance that, due to the geometrical requirements of the five-membered ring, the disulphide group cannot maintain the normal dihedral angle of about 90° [6-9] between the planes of the valencies of the sulphur atoms.

1,2-Dithiolane itself is an unstable yellow substance which readily undergoes polymerization [1,4,10], but beside 6-thioctic acid, some substituted 1,2-dithiolanes have been prepared which are more stable, *e.g.*, the 4,4′-dimethyl, 4,4′-dihydroxymethyl, 3,3′-dimethyl and 3,3′,5,5′-tetramethyl derivatives [11,12,4] and the 3,5-dicarboxylic [13] and 3- and 4-carboxylic [14,15] acids. The crystal structure of the last acid is described in this paper.

1,2-Dithiolane-4-carboxylic acid was first isolated by Schotte and Ström [15] in 1956, as yellow prisms with m.p. 76.5—77.5°C, although the corresponding dithiol, β,β'-dithiol*iso*butyric acid, was obtained in 1948 by Jansen [16] on reduction of a sulphur-containing polymeric material isolated from asparagus juice. The UV absorption was measured by Schotte [3] and found to be closely related to that of 1,2-dithiolane itself [1,10]. The unit cell and space group has been published [17], and also a preliminary report on the crystal structure [18].

CRYSTAL DATA

From oscillation and Weissenberg photographs about the three axes and about [1$\bar{1}$0] (of length 6.46 Å) the lattice parameters are, to within 0.5 %: $a = 5.34$ Å, $b = 5.85$ Å, $c = 10.75$ Å, $\alpha = 93\frac{1}{2}°$, $\beta = 89\frac{1}{2}°$, $\gamma = 109\frac{1}{2}°$. There are two molecules per unit cell; density, calc. 1.58, found 1.54 g/cm^3. On the basis of the subsequent structure analysis, the space group is C_i^1—$P\bar{1}$. The asymmetric unit is thus one molecule.

The intensities of the 0*kl* and *h*0*l* reflections were estimated visually from zero-layer Weissenberg photographs taken with copper radiation. The crystals used for the photographs had cross-sections of about 0.1 × 0.1 mm or smaller. During the exposures they changed slowly, from the surface inwards, into an oily, presumably polymeric material. Out of 146 0*kl* reflections within the range sin $\Theta < 0.985$, 136 were observed, the corresponding figures for the *h*0*l* zone being 132 out of 137. Although the absorption is not negligible ($\mu = 70$ cm^{-1} for Cu$K\alpha$ X-rays) no correction was applied. The intensities were corrected for the Lorentz and polarization factors and converted into relative structure amplitudes in the usual way.

DETERMINATION AND REFINEMENT OF THE STRUCTURE

The approximate y and z coordinates of the sulphur atoms ($y = 0.224$, $z = 0.107$ for S_1 and $y = 0.576$, $z = 0.165$ for S_2) were determined from a Patterson projection along the a axis. A subsequent Fourier synthesis of 77 of the strongest 0*kl* reflections, with signs based on the sulphur contributions, gave the approximate positions of the lighter atoms and allowed refinement by Fourier and Fourier difference methods to be carried out. The b-axis projection was afterwards solved and refined in the same way. Nine cycles

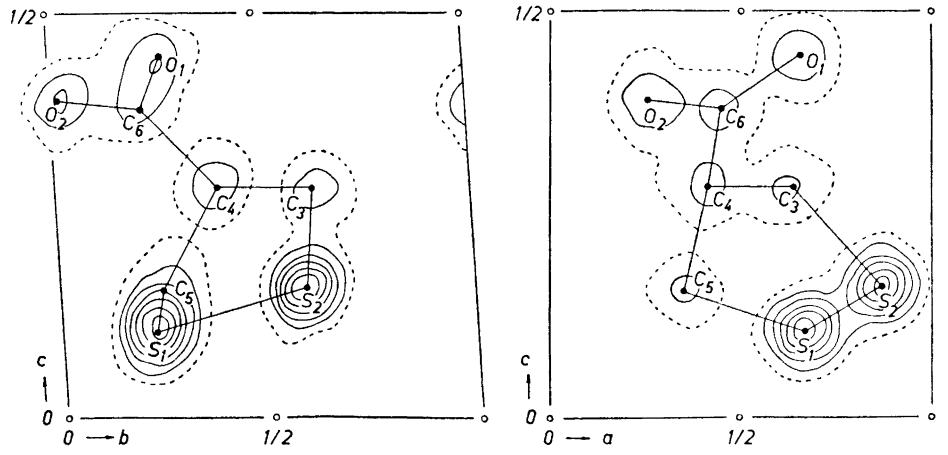

Figs. 1 and 2. Electron density projection of 1,2-dithiolane-4-carboxylic acid along the a axis (left) and along the b axis (right). Contours at intervals of 3 e · Å^{-2}, beginning with 3 e · Å^{-2} (dashed). The final atomic positions are marked with dots.

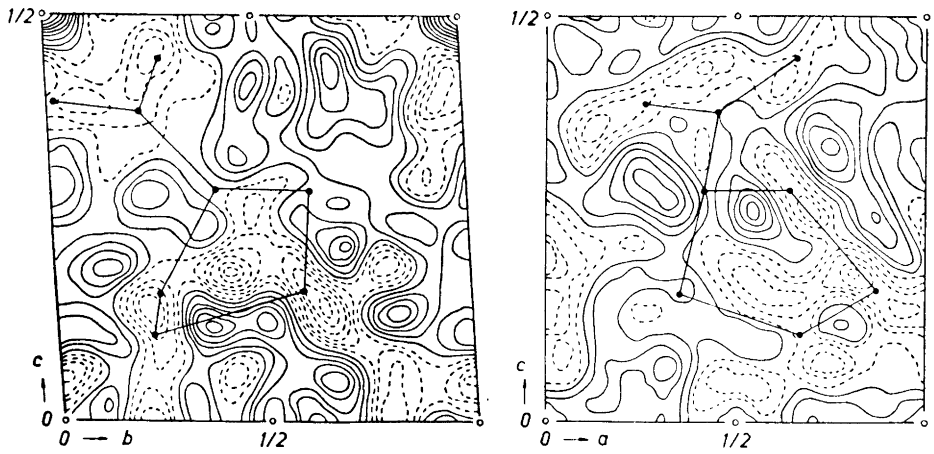

Figs. 3 and 4. Difference projection along the *a* axis (left) and along the *b* axis (right). Contours at intervals of 0.15 e · Å^{-2}, with negative dashed, zero and positive fully drawn. The final atomic positions are marked with dots.

of difference refinement were made for the 0*kl* zone and six for the *h*0*l* zone. The summations were made by means of Beevers-Lipson strips, using axial subdivisions equal to *a*/30 (0.18 Å), *b*/30 (0.20 Å) and *c*/60 (0.18 Å).

The electron density projections along the *a* and *b* axes are shown in Figs. 1 and 2, and the final difference maps in Figs. 3 and 4. The atomic coordinates are listed in Table 1. The two independent sets of *z* coordinates obtained, one from each zone, differed for the following atoms: $z(S_1) = 0.1060$ and 0.1055, $z(S_2) = 0.1610$ and 0.1605, $z(C_3) = 0.284$ and 0.283, $z(C_4) = 0.286$ and 0.284, $z(C_5) = 0.157$ and 0.156, from the 0*kl* and *h*0*l* data, respectively.

Table 1. Atomic coordinates for 1,2-dithiolane-4-carboxylic acid, in fractions of the triclinic axes, and relating to a centre of symmetry.

	x	*y*	*z*
S_1	0.669	0.228	0.1057
S_2	0.871	0.593	0.1608
C_3	0.638	0.621	0.284
C_4	0.412	0.392	0.285
C_5	0.349	0.248	0.157
C_6	0.448	0.217	0.381
O_1	0.658	0.270	0.446
O_2	0.254	0.012	0.392

The observed and calculated values of the 0*kl* and *h*0*l* structure factors are listed in Table 2. The calculated values are based on the atomic scattering curve of Viervoll and Ögrim for sulphur [19] and of Berghuis *et al.*[20] for carbon and oxygen. It was not thought worth while to attempt a location of the hydrogen atoms from the X-ray data, although some of the peaks in the

Table 2. Observed and calculated $0kl$ and $h0l$ structure factors for 1,2-dithiolane-4-carboxylic acid.

l	F_o	F_c	l	F_o	F_c	l	F_o	F_c
	$0kl$ zone		7	2.7	− 1.1	4	3.2	− 2.1
	$00l$		8	6.9	− 7.7	5	2.6	+ 2.4
1	5.4	+ 5.8	9	8.0	− 9.7	6	5.1	− 6.5
2	13.4	−13.0	10	2.8	+ 1.4	7	7.5	− 8.9
3	24.2	−24.9	11	< 2.2	− 1.0	8	2.9	+ 0.1
4	37.0	−37.5	12	1.8	+ 1.8	9	2.3	+ 3.7
5	7.1	− 5.0				10	2.5	+ 2.2
6	2.0	− 1.4		$0\bar{2}l$				
7	17.2	+17.4	1	12.3	+11.5		$0\bar{4}l$	
8	5.4	+ 3.4	2	6.3	+ 5.4			
9	5.9	− 7.3	3	16.7	+17.9	1	2.4	− 0.3
10	2.2	+ 1.7	4	< 1.8	+ 1.6	2	12.3	+12.2
11	4.8	+ 5.3	5	< 2.0	− 0.4	3	2.8	− 3.4
12	1.4	− 0.5	6	9.0	+ 5.9	4	18.1	−18.2
13	1.6	+ 2.3	7	2.7	+ 1.0	5	3.2	− 1.8
			8	4.2	+ 3.5	6	7.0	− 7.0
	$01l$		9	8.0	− 7.7	7	2.6	+ 2.5
0	20.7	−19.4	10	5.2	− 4.8	8	9.1	+ 8.1
1	36.1	−38.7	11	4.7	− 4.8	9	6.9	+ 6.7
2	16.3	+20.8	12	2.2	+ 0.8	10	2.1	+ 1.1
3	19.5	−18.8	13	2.2	+ 2.6	11	4.0	− 3.3
4	9.5	− 9.2						
5	4.2	+ 4.2		$03l$			$05l$	
6	2.5	− 4.4	0	8.6	+ 7.7	0	13.3	+14.7
7	5.1	+ 0.5	1	13.5	+15.1	1	2.8	− 1.6
8	14.4	+14.5	2	15.7	+16.5	2	5.3	− 6.2
9	6.5	+ 6.5	3	17.2	+18.6	3	7.5	− 7.9
10	3.2	+ 2.3	4	4.7	− 6.9	4	6.3	− 6.5
11	6.2	− 6.5	5	5.8	− 6.4	5	2.8	− 0.9
12	4.1	− 4.2	6	6.3	− 7.5	6	2.6	+ 3.3
13	1.6	− 0.9	7	3.5	+ 4.3	7	4.2	+ 5.2
			8	2.6	− 0.2	8	2.9	+ 2.2
	$0\bar{1}l$		9	2.5	− 2.0			
1	6.9	+ 7.4	10	2.6	− 2.5		$0\bar{5}l$	
2	24.6	+24.9	11	2.0	− 1.4	1	7.8	+ 9.2
3	45.7	+49.8				2	5.0	− 2.9
4	6.7	− 8.6		$0\bar{3}l$		3	3.6	+ 3.3
5	11.4	+12.6	1	32.8	−33.4	4	6.9	− 7.0
6	21.9	−22.6	2	24.3	−24.1	5	2.8	− 1.4
7	23.0	−23.3	3	13.5	−15.0	6	< 2.5	− 2.0
8	3.3	− 3.2	4	14.7	+13.9	7	< 2.3	+ 0.5
9	4.2	+ 4.8	5	13.8	+14.7	8	2.4	+ 1.0
10	6.5	+ 6.1	6	9.5	+10.0	9	4.5	− 4.2
11	4.2	+ 2.9	7	3.0	+ 4.1	10	1.8	+ 1.4
12	2.9	+ 1.8	8	4.3	− 4.4			
13	1.9	− 0.5	9	6.4	− 6.4			
			10	2.4	+ 1.3			
	$02l$		11	2.5	+ 1.6		$06l$	
0	21.3	−22.1	12	1.7	− 1.2	0	6.1	− 7.7
1	26.5	−27.4				1	4.8	− 4.7
2	25.2	−27.3		$04l$		2	< 2.2	+ 1.9
3	3.3	+ 4.5	0	6.9	+ 7.5	3	< 2.1	+ 2.0
4	15.5	+15.8	1	4.3	− 3.2	4	< 2.0	+ 1.1
5	21.4	+24.8	2	8.1	+ 9.3	5	< 1.7	+ 2.3
6	7.4	+ 8.0	3	3.1	+ 0.3	6	< 1.4	− 2.0

l	F_o	F_c
	$0\bar{6}l$	
1	2.3	− 2.5
2	2.7	+ 2.0
3	7.4	+ 7.9
4	4.4	+ 5.2
5	2.0	+ 0.9
6	1.8	− 1.4
7	5.5	− 6.0
8	1.4	− 0.9
	$h0l$ zone	
	$00l$	
1	5.0	+ 6.4
2	12.3	−12.5
3	22.2	−24.8
4	34.0	−36.2
5	6.5	− 5.0
6	1.8	− 2.0
7	15.8	+15.7
8	4.9	+ 3.5
9	5.4	− 5.8
10	2.0	+ 1.1
11	4.4	+ 4.2
12	1.3	+ 0.1
13	1.5	+ 1.5
	$10l$	
0	32.0	−32.5
1	29.3	+30.7
2	31.1	+32.6
3	1.3	− 1.9
4	1.7	− 0.3
5	11.4	+11.3
6	3.8	− 4.7
7	< 1.4	+ 1.5
8	9.5	− 7.5
9	3.3	− 3.8
10	2.3	− 3.6
11	2.7	− 3.0
12	5.9	+ 5.9
13	1.6	+ 2.0
	$\bar{1}0l$	
1	4.5	− 4.8
2	33.5	−37.0
3	23.4	−23.7
4	3.5	+ 2.7
5	11.5	+ 9.8
6	29.7	+30.8
7	1.3	− 2.8
8	1.5	+ 1.4
9	3.0	− 2.6
10	5.9	− 5.2
11	2.4	− 1.5
12	1.3	− 0.1
13	1.1	+ 0.1

l	F_o	F_c
	$20l$	
0	22.1	−19.8
1	7.6	+ 7.5
2	1.2	+ 0.7
3	5.5	− 4.4
4	2.3	− 3.0
5	14.4	−15.3
6	10.7	+11.6
7	7.5	+ 8.1
8	11.9	+11.3
9	1.6	+ 1.6
10	5.4	− 5.7
11	4.3	− 4.7
12	3.9	− 3.9
	$\bar{2}0l$	
1	13.0	−11.3
2	12.6	−13.4
3	17.0	+17.7
4	22.9	+22.3
5	19.2	+18.8
6	4.0	− 3.4
7	11.5	−11.2
8	13.4	−14.1
9	6.4	− 6.0
10	3.7	+ 2.9
11	4.5	+ 4.3
12	4.2	+ 3.4
13	< 0.8	0
	$30l$	
0	12.3	+12.7
1	7.1	+ 6.6
2	9.0	+ 8.7
3	2.9	+ 3.0
4	8.8	− 8.2
5	11.9	−14.5
6	7.2	− 8.5
7	2.3	+ 2.8
8	2.4	+ 3.9
9	5.5	+ 5.8
10	1.7	+ 2.3
11	1.1	+ 0.2
	$\bar{3}0l$	
1	3.8	− 3.2
2	2.7	+ 2.6
3	4.0	− 4.5
4	5.2	+ 5.1
5	8.1	− 7.5
6	9.0	− 9.6
7	2.1	− 1.0
8	1.6	− 1.6
9	5.7	+ 5.5
10	4.4	+ 3.6
11	3.9	+ 3.1
12	1.0	− 0.6

l	F_o	F_c
	$40l$	
0	12.6	−13.1
1	2.0	− 1.0
2	4.6	+ 5.0
3	16.0	+14.3
4	4.2	+ 5.5
5	4.4	+ 5.4
6	5.6	− 6.9
7	7.2	− 8.8
8	1.4	− 0.8
9	< 1.2	+ 0.4
10	1.6	+ 1.3
	$\bar{4}0l$	
1	13.3	−12.9
2	3.3	+ 3.7
3	4.2	+ 3.3
4	< 1.6	− 0.6
5	2.5	+ 2.2
6	1.6	0
7	1.5	− 1.3
8	3.4	+ 3.5
9	3.2	+ 2.2
10	1.5	+ 1.6
	$50l$	
0	3.9	− 3.6
1	9.1	− 9.7
2	2.1	− 2.2
3	1.6	− 0.6
4	3.7	+ 4.1
5	< 1.4	+ 1.0
6	1.2	+ 1.2
7	1.4	+ 1.4
8	0.8	− 0.8
	$\bar{5}0l$	
1	3.3	+ 4.0
2	1.6	+ 0.3
3	7.9	+ 8.2
4	2.7	+ 2.9
5	1.8	− 1.0
6	2.3	− 2.6
7	1.8	− 1.9
8	1.0	+ 0.3
	$60l$	
0	1.8	− 2.5
1	1.1	+ 1.0
2	1.9	− 2.3
3	1.6	− 2.2
4	0.8	+ 0.1
	$\bar{6}0l$	
1	3.4	+ 3.3
2	3.5	+ 3.7
3	1.8	− 2.1
4	2.8	− 2.7

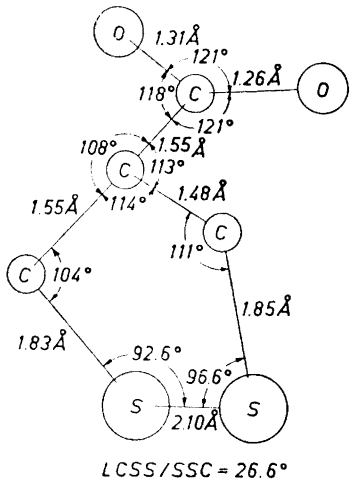

Fig. 5. 1,2-Dithiolane-4-carboxylic acid as seen along the *b* axis.

difference maps (the standard deviation of electron density is about 0.3 e.$Å^{-2}$ for both zones) are in the approximate positions expected for hydrogen atoms. In the temperature factor exp $[-B(\sin^2\Theta/\lambda^2)]$ applied in the calculation of structure factors, B (in $Å^2$) is 4.5 for sulphur and oxygen and 3.5 for carbon in the $0kl$ zone, and 5.2 for sulphur, 5.5 for oxygen and 4.8 for carbon in the $h0l$ zone. The reliability index $R = \Sigma||F_o|-|F_c||/\Sigma|F_o|$, with non-observed reflections included when $|F_c|$ exceeds the observeable limit, is 0.122 for the $0kl$ zone and 0.105 for the $h0l$ zone.

Standard deviations of atomic coordinates were estimated from the root-mean-square gradients in the final difference maps and the curvatures of the peaks in the electron density maps [21,22]. Where overlapping occurred, the s.d. was taken as up to twice that which would otherwise have applied. In this way the following values were obtained and used for calculation of the s.d. of bond lengths and angles: For the sulphur coordinates $\sigma = 0.005$ Å except $\sigma(y)$ for S_1 which was put equal to 0.008 Å. For the light atoms $\sigma = 0.015$ Å for x of C_5 and O_1, y of C_3 and C_4 and z of C_3, C_4 and C_5; 0.02 Å for x of C_3, C_4 and O_2 and for y and z of C_6, O_1 and O_2; 0.025 Å for x of C_6 and 0.03 Å for y of C_5.

CONFIGURATION AND DIMENSIONS OF THE 1,2-DITHIOLANE RING

The bond lengths and angles in the molecule, calculated from the coordinates of Table 1, are listed in Table 3, together with estimated standard deviations. A drawing of the molecule as seen in projection along the *b* crystal axis is shown in Fig. 5.

The data show that the disulphide group differs from non-cyclic disulphides in three distinct ways: The bond angles are smaller and the S—S bond slightly longer, and there is a large decrease in dihedral angle.

Table 3. Dimensions of 1,2-dithiolane-4-carboxylic acid.

$S_1-S_2 = 2.096 \pm 0.009$ Å	$\angle S_1-S_2-C_3 = 96.6 \pm 0.6°$
$S_1-C_5 = 1.83 \pm 0.02$	$\angle S_2-S_1-C_5 = 92.6 \pm 0.7$
$S_2-C_3 = 1.85 \pm 0.02$	$\angle S_1-C_5-C_4 = 104.2 \pm 1.3$
$C_3-C_4 = 1.48 \pm 0.025$	$\angle S_2-C_3-C_4 = 110.6 \pm 1.2$
$C_4-C_5 = 1.55 \pm 0.03$	$\angle C_3-C_4-C_5 = 114.1 \pm 1.6$
$C_4-C_6 = 1.55$ $C_6-O_1 = 1.26$ } ± 0.03 Å $C_6-O_2 = 1.31$	$\angle O_1-C_6-O_2 = 121.0$ $\angle C_4-C_6-O_1 = 121.2$ } $\pm 2°$ $\angle C_4-C_6-O_2 = 117.8$
$\angle C_5-C_4-C_6 = 107.5 \pm 1.5°$	$\angle C_3-C_4-C_6 = 113.1 \pm 1.5°$

Dihedral angle $C_5S_1S_2/S_1S_2C_3 = 26.6 \pm 1°$

The bond angles of the two sulphur atoms, although they appear to differ significantly, are both smaller than the angle of 107 ± 3° in dimethyl disulphide [23], 105.4 ± 3° in *bis*(trifluoromethyl) disulphide [24], 103 ± 1° in N,N'-diglycyl-L-cystine dihydrate [25], and 104 ± 1° and 99 ± 2°, respectively, in formamidinium disulphide dibromide and diiodide monohydrates [26]. For all but the last example the angles lie in the range 103—107°.

The observed S—C and C—C bond lengths do not differ significantly from the normal single-bond lengths, 1.82 Å [8] and 1.54 Å. The S—S bond appears to be significantly longer than in non-cyclic disulphides. In the five examples referred to above the mean of the observed lengths is 2.044 Å, with an average deviation of 0.004 Å. In orthorhombic sulphur [27], S—S = 2.037 ± 0.005 Å. The longest bonds between two divalent sulphur atoms, measured with any accuracy, appear to be the two long bonds of 2.10 and 2.13 ± 0.03 Å in cesium hexasulphide [28], and that of 2.088 ± 0.012 Å in the planar thiuret ion, an unsaturated five-membered cyclic disulphide [29]. It has been suggested [8,28,30] that the bonds of length about 2.04 Å possess some double-bond character, and that the single-bond length is in the neighbourhood of 2.08—2.10 Å, as found here. Another view [31] is that the observed variations in S—S bond lengths are due to different degrees of *s* and *p* character in the hybrid σ-bond orbitals of sulphur. A smaller bond angle at sulphur would then lead to less *s* character and a longer bond.

The major change in the disulphide group induced by the geometrical requirements of the ring is the decrease in dihedral angle, from the normal value [8] of about 90° to 26.6 ± 1° in the 1,2-dithiolane ring. The barrier to rotation about the bond between two divalent sulphur atoms, through the planar *cis* and *trans* forms with zero and 180° dihedral angles, has been estimated as 10—14 kcal/mole [32,33]. With the barrier a twofold cosine type the observed dihedral angle in 1,2-dithiolane-4-carboxylic acid corresponds to a S—S torsion energy equal to 80 % of the barrier height. A smaller dihedral angle occurs in thiuret hydroiodide [29] where the angle is zero, and probably in 4-methyl-1,2-dithia-4-*cyclo*pentene-3-thione which according to a short report [34] is approximately planar; these are five-membered cyclic disulphides, but conditions are presumably different because of the unsaturated character of the rings. It appears likely that the decrease in dihedral angle has a bearing on

the increase in S—S bond length, through the increased repulsion between the unshared $p\pi$ electron pairs of sulphur which are thought to be the principal cause of the barrier [6,9], and possibly through less favourable conditions for pd π-bonding.

The 1,2-dithiolane ring is not symmetrical about the disulphide group. Of the bond angles at carbon, that at C_5 appears to be significantly smaller than tetrahedral, and that at C_4 is larger, but not significantly. Here, at C_4, a widening of the angle would result from torsion and bending strain in the disulphide group, the distance between the carbon atoms C_3 and C_5 bonded to sulphur being about 0.2 Å larger in non-cyclic disulphides than the distance, 3.54 Å, observed here. The dihedral angles in the ring, beside that of the disulphide group, are $S_1S_2C_3/S_2C_3C_4 = 20°$, $S_2C_3C_4/C_3C_4C_5 = 26°$, $C_3C_4C_5/C_4C_5S_1 = 54°$, $C_4C_5S_1/C_5S_1S_2 = 49°$. The two large dihedral angles are associated with the carbon atom, C_5, which has the smallest bond angle.

Bergson and Schotte have [35], on the basis of the present structural data, made a conformation analysis of the 1,2-dithiolane ring, and concluded that the total strain in the ring is at least 16 kcal/mole.

The 4-carboxyl group is planar, the maximum deviation of an atom from the least-squares plane through the group being 0.002 Å, in the case of C_6. This carbon atom lies 3.17 Å from S_1 and 3.57 Å from S_2. The dimensions of the group agree reasonably well with values reported for other aliphatic carboxylic acids [36,37]. The carboxyl group is directed towards the symmetry centre at $\frac{1}{2},0,\frac{1}{2}$, which lies 0.11 Å from the plane of the group. Two molecules, one on each side of the symmetry centre, are arranged into dimers through O—H···O hydrogen bonds of length 2.61 Å between the carboxyl groups. This is the structure normally found in monocarboxylic acids [38,39].

A van der Waals contact of length 3.41 Å occurs between two S_1 sulphur atoms across the symmetry centre at $\frac{1}{2},0,0$. In orthorhombic sulphur [27] the shortest intermolecular contact is 3.69 Å and thus longer, but a van der Waals radius for sulphur of about 1.60 Å is indicated in two compounds containing iodine [28,39].

The authors are indebted to Docent Lennart Schotte, University of Uppsala, for providing the sample of 1,2-dithiolane-4-carboxylic acid used in this study. A grant from *L. Meltzers Høyskolefond* to one of us (O. F.) is gratefully acknowledged.

REFERENCES

1. Barltrop, J. A., Hayes, P. M. and Calvin, M. *J. Am. Chem. Soc.* **76** (1954) 4348.
2. Sunner, S. *Nature* **176** (1955) 217; *Svensk Kem. Tidsskr.* **67** (1955) 513.
3. Schotte, L. *Arkiv Kemi* **9** (1956) No. 37.
4. Schöberl, A. and Gräfje, H. *Ann.* **614** (1958) 66.
5. For a review see the article by Reed, L. J. *Advances in Enzymol.* **18** (1957) 319.
6. Pauling, L. *Proc. Natl. Acad. Sci. U. S.* **35** (1949) 495.
7. Foss, O. *Acta Chem. Scand.* **8** (1954) 469.
8. Abrahams, S. C. *Quart. Revs. London* **10** (1956) 407.
9. Bergson, G. *Arkiv Kemi* **12** (1958) No. 24.
10. Bergson, G. and Claeson, G. *Acta Chem. Scand.* **11** (1957) 911.
11. Backer, H. J. and Tamsma, A. F. *Rec. trav. chim.* **57** (1938) 1183.
12. Schotte, L. *Arkiv Kemi* **9** (1956) No. 24.

13. Schotte, L. *Acta Chem. Scand.* **8** (1954) 130; *Arkiv Kemi* **9** (1956) No. 36.
14. Claeson, G. *Acta Chem. Scand.* **9** (1955) 178.
15. Schotte, L. and Ström, H. *Acta Chem. Scand.* **10** (1956) 687.
16. Jansen, E. F. *J. Biol. Chem.* **176** (1948) 657.
17. Foss, O. and Schotte, L. *Acta Chem. Scand.* **11** (1957) 1424.
18. Foss, O. and Tjomsland, O. *Acta Chem. Scand.* **11** (1957) 1426.
19. Viervoll, H. and Ögrim, O. *Acta Cryst.* **2** (1949) 277.
20. Berghuis, J., Haanappel, I. M., Potters, M., Loopstra, B. O., MacGillavry, C. H. and Veenendaal, A. L. *Acta Cryst.* **8** (1955) 478.
21. Cruickshank, D. W. *Acta Cryst.* **2** (1949) 65.
22. Cochran, W. *Acta Cryst.* **4** (1951) 81.
23. Stevenson, D. P. and Beach, J. Y. *J. Am. Chem. Soc.* **60** (1938) 2872.
24. Bowen, H. J. M. *Trans. Faraday Soc.* **50** (1954) 452.
25. Yakel, H. L. and Hughes, E. W. *Acta Cryst.* **7** (1954) 291.
26. Foss, O., Johnsen, J. and Tvedten, O. *Acta Chem. Scand.* **12** (1958) 1782.
27. Abrahams, S. C. *Acta Cryst.* **8** (1955) 661.
28. Abrahams, S. C. and Grison, E. *Acta Cryst.* **6** (1953) 206.
29. Foss, O. and Tjomsland, O. *Acta Chem. Scand.* **12** (1958) 1799.
30. Foss, O. and Tjomsland, O. *Acta Chem. Scand.* **12** (1958) 44.
31. Lindquist, I. *J. Inorg. & Nuclear Chem.* **6** (1958) 159.
32. Scott, D. W., Finke, H. L., Gross, M. E., Guthrie, G. B. and Huffman, H. M. *J. Am. Chem. Soc.* **72** (1950) 2424.
33. Scott, D. W., Finke, H. L., McCullough, J. P., Gross, M. E., Pennington, R. E. and Waddington, G. *J. Am. Chem. Soc.* **74** (1952) 2478.
34. Kehl, W. L. and Jeffrey, G. A. *Acta Cryst.* **10** (1957) 807.
35. Bergson, G. and Schotte, L. *Acta Chem. Scand.* **12** (1958) 367.
36. Vaughan, P. and Donohue, J. *Acta Cryst.* **5** (1952) 530.
37. Ahmed, F. R. and Cruickshank, D. W. J. *Acta Cryst.* **6** (1953) 385.
38. Ubbelohde, A. R. and Gallagher, K. J. *Acta Cryst.* **8** (1955) 71.
39. Donohue, J. *J. Phys. Chem.* **56** (1952) 502.
40. Donohue, J. *J. Am. Chem. Soc.* **72** (1950) 2701.

Received August 12, 1958.

ACTA CHEMICA SCANDINAVICA 12 (1958) 1819—1824

The Action of Alkali on Methyl 2:3-Anhydro-α-D-allopyranoside and 1:5-Anhydro-2-deoxy-3-*O*-toluene-*p*-sulphonyl-D-arabinohexitol

A. B. FOSTER, M. STACEY and S. V. VARDHEIM*

Chemistry Department, The University, Edgbaston, Birmingham, England

Treatment of methyl 2:3-anhydro-α-D-allopyranoside with alkali yields methyl 3:6-anhydro-α-D-glucopyranoside as the only isolable product. Under similar reaction conditions 1:5-anhydro-2-deoxy-3-*O*-toluene-*p*-sulphonyl-D-*arabino*hexitol (the synthesis of which is described) rapidly loses the toluene-*p*-sulphonyloxy residue apparently without the formation of a 3:6-anhydro derivative. The relationship of these observations to those noted by Peat and Wiggins [1], following the treatment of methyl 2:4:6-tri-*O*-acetyl-3-*O*-toluene-*p*-sulphonyl-β-D-glucopyranoside with alkali, is discussed.

The action of alkali on methyl 2:4:6-tri-*O*-acetyl-3-*O*-toluene-*p*-sulphonyl-β-D-glucopyranoside has been found[1] to yield a mixture of methyl 2:3-anhydro- and 3:4-anhydro-β-D-allopyranosides and methyl 3:6-anhydro-β-D-glucopyranoside. These compounds were isolated as derivatives in which the anhydro-rings were preserved; the sensitivity of the latter compound towards acidic reagents resulted in its conversion to methyl 3:6-anhydro-β-D-glucofuranoside during the isolation procedure [2]. Initially it was thought that the methyl 3:6-anhydro-β-D-glucopyranoside had arisen by direct intramolecular attack of the C_6-hydroxyl group on the C_3-toluene-*p*-sulphonyloxy residue but it was later realised [3] that the first products of reaction were the two epoxide derivatives and that the 3:6-anhydro-compound resulted from intramolecular attack of the C_6-hydroxyl group on C_3in either or both of the 2:3- and 3:4-anhydro compounds. That the 2:3-anhydrocompound was involved in such a reaction was suggested by Ohle *et al.*[3], presumably on analogy with reactions in the furanose series [3]; the formation of a 3:4-anhydro-compound is, however, precluded in this case. No experimental evidence has been obtained which would indicate the true course of reaction.

Methyl 2:3-anhydro- and 3:4-anhydro-α- and β-D-allopyranoside would be expected [4] to adopt half-chair in preference to half-boat conformations.

* Present address (S.V.V.): Papirindustriens Forskningsinstitutt, Boks 250, Vinderen, Oslo, Norway.

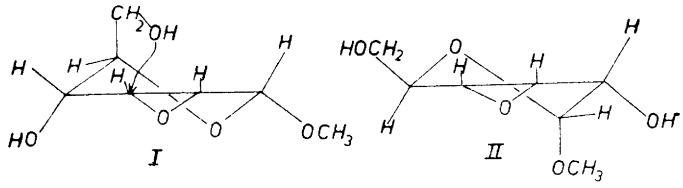

(The presence of the epoxide ring requires that C_1:C_2:C_3:C_4 and C_2:C_3:C_4:C_5 be coplanar in the 2:3- and 3:4-epoxide compounds, respectively). An examination of accurate scale models reveals that in the half-chair conformation (I) of methyl 2:3-anhydro-α-D-allopyranoside the C_6-hydroxyl group is well situated for nucleophilic attack on C_3 to yield a 3:6-anhydro-D-glucopyranoside and that this is not the case in either of the half-chair conformations (*e.g.* II) of methyl 3:4-anhydro-α-D-allopyranoside. Normal scission of the epoxide ring would be predicted in the latter case. Experimental evidence has been obtained which confirms these predictions.

Graded acidic hydrolysis of methyl 4:6-*O*-benzylidene-2:3-anhydro-α-D-allopyranoside [5] yielded methyl 2:3-anhydro-α-D-allopyranoside (III) in good yield. The latter compound was only slowly attacked ($[\alpha]_D$ + 149° → + 142.5° in 6 days) on treatment with N sodium hydroxide at room temperature. Elevation of the temperature to 50° resulted in completion of reaction within 3 days. ($[\alpha]_D$ + 142.5° → + 37.8°). Quantitative analysis of the reaction products was not possible because of the occurrence of some decomposition but methyl 3:6-anhydro-α-D-glucopyranoside (IV) was the only isolable compound. Although some decomposition occurred the fall in $[\alpha]_D$ during the reaction indicated that methyl 3:6-anhydro-α-D-glucopyranoside was the major, if not the sole product since the alternative products (methyl α-D-glucopyranoside and methyl α-D-altropyranoside) which would result from normal scission of the epoxide are strongly dextrorotatory ($[\alpha]_D$ + 158° and + 125°, respectively). These compounds could not be detected in the products of reaction. The known [2] sensitivity of methyl 3:6-anhydro-α-D-glucopyranoside towards acid is further illustrated by its conversion to methyl 3:6-anhydro-α-D-glucofuranoside on short contact with the resin Amberlite IR-120 (H^+ form).

The slow conversion of methyl 2:3-anhydro-α-D-allopyranoside to methyl 3:6-anhydro-α-D-glucopyranoside probably accounts for the low yield of 3:6-anhydro compound isolated in the reaction studied by Peat and Wiggins [1]. Further, a close analogy may be drawn with the conversion [6] of 1:2-anhydro-α-D-glucopyranose to 1:6-anhydro-β-D-glucopyranose under similar reaction conditions.

Since methyl 3:4-anhydro-α or β-D-allopyranoside is apparently unknown and inaccessible a synthesis of a suitable 3:4-epoxide derived from 1:5-anhydro-2-deoxy-D-*arabino*hexitol (V) (1:2-dideoxy-D-"glucose") was examined. 1:5-Anhydro-2-deoxy-D-*arabino*hexitol (V) was obtained by sequential application of platinum catalysed hydrogenation and saponification to 3:4:6-tri-*O*-acetyl-D-glucal. Reaction of 1:5-anhydro-2-deoxy-D-*arabino*hexitol (V) with benzaldehyde at 115° yielded a 4:6-*O*-benzylidene derivative (VI) which was readily converted to 1:5-anhydro-4:6-*O*-benzylidene-2-deoxy-3-*O*-toluene-*p*-

sulphonyl-D-*arabino*hexitol (VII). Graded acidic hydrolysis of the latter compound yielded 1:5-anhydro-2-deoxy-3-*O*-toluene-*p*-sulphonyl-D-*arabino*hexitol (VIII) (3-*O*-toluene-*p*-sulphonyl-1:2-dideoxy-D-"glucose"). Allocation of structures to these compounds was based on the following arguments. The 3-*O*-toluene-*p*-sulphonate (VIII) was different to the mono-*O*-toluene-*p*-sulphonate obtained by selective toluene-*p*-sulphonylation of 1:5-anhydro-2-deoxy-D-*arabino*hexitol (III). The structure of the latter compound was shown to be 1:5-anhydro-2-deoxy-6-*O*-toluene-*p*-sulphonyl-D-*arabino*hexitol (IX) by its ready consumption of approximately 1 mol. of metaperiodate. The formation of a seven membered 3:6-*O*-benzylidene ring in the reaction of 1:5-anhydro-2-deoxy-D-*arabino*hexitol (III) with benzaldehyde would seem very improbable in view of the fact that an alternative product is the six-membered 4:6-*O*-benzylidene compound the structure of which is related to *trans*-decalin. Whilst 3:6-*O*-benzylidene-D-glucopyranose derivatives are unknown a wealth of examples of 4:6-*O*-benzylidene-D-glucopyranose derivatives is provided in carbohydrate chemistry. Seven-membered alkylidene rings, however, have been observed [7], thus D-mannitol reacts with acetaldehyde to yield 1:3-2:5-4:6-tri-*O*-ethylidene-D-mannitol. Although this example is not strictly analogous to the case being considered it may be noted that formation of the 1:3- and 4:6-rings precedes formation of the 2:5-ring and that the six-membered cyclic acetals are more stable towards acid than the seven-membered cyclic acetal [8]. Thus compound (VI) is allocated the structure 1:5-anhydro-4:6-*O*-benzylidene-2-deoxy-D-*arabino*hexitol.

Treatment of 1:5-anhydro-2-deoxy-3-*O*-toluene-*p*-sulphonyl-D-*arabino*hexitol (VIII) with sodium hydroxide at 50° resulted in ready elimination of the toluene-*p*-sulphonyloxy group. Direct hydrolysis of the 3-*O*-toluene-*p*-sulphonate is ruled out since Peat has pointed out [9] that, unless anhydro ring formation can occur, direct hydrolysis of carbohydrate toluene-*p*-sulphonates occurs slowly. Examination of the products of reaction revealed that the major product(s) were susceptible to attack by periodate. Further, on zone electrophoresis (ionophoresis) on paper in a borate buffer (pH 10) using the enclosed strip technique [10], two components, detectable by the periodate-permanganate reagent [11] were observed. The major component had an M_G value [10] and properties identical with those of 1:5-anhydro-2-deoxy-D-*arabino*hexitol (III); the minor component had a higher M_G value. These observations are entirely consistent with the formation and reaction of 1:5-2:3-dianhydro-2-deoxy-D-*ribo*hexitol (X) to yield a mixture of 1:5-anhydro-2-deoxy-D-*arabo* (III) and D-*xylo*hexitols (XI) following the action of alkali on 1:5-anhydro-2-deoxy-3-*O*-toluene-*p*-sulphonyl-D-*arabino*hexitol. Since the above products (III) and (XI) are susceptible to attack by metaperiodate and because 3:6-anhydro-D-glucopyranosides are resistant, it may be inferred that 1:5-3:6-dianhydro-2-deoxy-D-*arabino*hexitol must be formed to an insignificant extent, if at all, as a consequence of the action of alkali on 1:5-anhydro-2-deoxy-3-*O*-toluene-*p*-sulphonyl-D-*arabino*hexitol.

Thus in the original experiments of Peat and Wiggins [1] it is most probable that of methyl 2:3-anhydro-β-D-allopyranoside and methyl 3:4-anhydro-β-D-allopyranoside, the first products of the action of alkali on methyl 2:4:6-tri-*O*-acetyl-3-*O*-toluene-*p*-sulphonyl β-D-glucopyranoside, the former but not

the latter yields methyl 3:6-anhydro-β-D-glucopyranoside on further action of alkali.

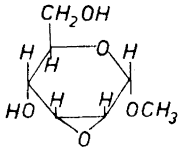

III

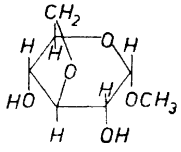

IV

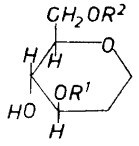

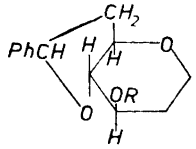

V $R^1 = R^2 = H$

VI $R = H$

VIII $R^1 = CH_3 . C_6H_4 . SO_2$, $R^2 = H$

VII $R = CH_3 . C_6H_4 . SO_2$

IX $R^1 = H$, $R^2 = CH_3 . C_6H_4 . SO_2$

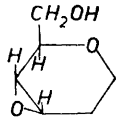

X

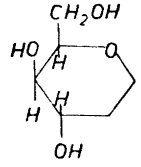

XI

EXPERIMENTAL

Methyl 2:3-anhydro-α-D-allopyranoside. The method adopted was a modification of that reported by Gut and Prins [12].

A solution of methyl 2:3-anhydro-4:6-*O*-benzylidene-α-D-allopyranoside [5] (1.75 g, m. p. 198°, $[\alpha]_D$ +140.2° in chloroform) in 0.05 N hydrochloric acid (20 ml) and methanol (70 ml) was boiled under reflux for 2 h. After cooling and dilution with water (50 ml) the solution was concentrated at 35°, (bath)/16 mm, and deacidified with methyl di-*n*-octylamine [13]. After extraction with ether the neutral hydrolysate was concentrated at 60° (bath)/14—16 mm and the residue decolorized by dissolution in ethanol and treatment with charcoal. Concentration of the solution gave methyl 2:3-anhydro-α-D-allopyranoside (0.9 g, 77.5 %), m. p. 105°, $[\alpha]_D$ + 152° (*c*, 1.0 in methanol). Gut and Prins [12] quote m. p. 104—107°, $[\alpha]_D$ + 152° in methanol.

Action of alkali on methyl 2:3-anhydro-α-D-allopyranoside. (a) A solution of methyl 2:3-anhydro-α-D-allopyranoside (0.5 g) in N sodium hydroxide (5 ml) was stored at room temperature; $[\alpha]_D$ changed from 149° → 142.5° during 6 days. Elevation of the temperature to 50° caused a change in $[\alpha]_D$ +142.5° → +37.8° (final constant value) during 3 days. Some decomposition occurred during this process. Calculated final value for complete conversion to methyl 3:6-anhydro-α-D-glucopyranoside was *ca.* +55°. After neutralisation of the reaction mixture with carbon dioxide and evaporation at 60°, (bath)/14—16 mm, the residue was extracted with boiling acetone during 30 min (acidic hydrolysis of the residue produced no substances reducing toward Fehling's solution). The extract was decolorized with charcoal and evaporated at 40° (bath)/14—16 mm. Crystallization of the residue from ethyl acetate gave methyl 3:6-anhydro-α-D-glucopyranoside (0.28 g, 56 %) m. p. 108°, $[\alpha]_D$ +56.5° (*c*, 0.5 in water). Haworth *et al.*[2] record m. p. 108°, $[\alpha]_D$ +56° in water for this compound.

(b) In a second experiment methyl 2:3-anhydro-*α*-D-allopyranoside (0.3 g) was treated with alkali at 50° as described in (a). The reaction mixture was freed from cations by passage down a column of Amberlite IR-120 (H^+ form). Evaporation of the eluate at 60°, (bath)/14 — 16 mm, gave a syrupy residue which crystallized slowly. Methyl 3:6-anhydro-*α*-D-glucofuranoside (0.16 g, 53.3 %) was subsequently isolated with m. p. 67°, $[\alpha]_D$ +164.5° (*c*, 0.5 in water). Haworth *et al.*[2] record m. p. 68°, $[\alpha]_D$ +164° in water for this compound. The infra-red spectrum (KBr disc) of the furanoside showed absorptions at 795 and 882 cm^{-1} indicative [14] of the furanose structure.

Treatment of an aqueous solution of methyl 3:6-anhydro-*α*-D-glucopyranoside with sodium metaperiodate using the conditions described elsewhere [15] resulted in zero consumption of oxidant during 24 h.

1:5-Anhydro-2-deoxy-D-arabino*hexitol (1:2-dideoxy*-D-*"glucose")*. A solution of amorphous 3:4:6-tri-*O*-acetyl-1:5-anhydro-2-deoxy-D-*arabino*hexitol (15 g, prepared by hydrogenation of an ethanolic solution of 3:4:6-tri-*O*-acetyl-D-glucal [16] in the presence of platinum oxide [17]) in dry methanol (50 ml) was treated with a small amount of metallic sodium. [18] After 12 h the solution was diluted with water (10 ml) concentrated to small volume (*ca.* 5 — 10 ml) and then deionized by passage down a column of Amberlite IR-120 (H^+ form). Evaporation of the eluate and recrystallization of the residue from chloroform-light petroleum (60 — 80°) gave 1:5-anhydro-2-deoxy-D-*arabino*hexitol (6.1 g, 75 %) m. p. 88°, $[\alpha]_D$ +16° (*c*, 2.0 in water). Fischer[16] records m. p. 86 — 87°, $[\alpha]_D$ +16.3° in water for the same compound prepared by a different method.

*1:5-Anhydro-4:6-*O*-benzylidene-2-deoxy*-D-arabino*hexitol (4:6-*O*-benzylidene-1:2-dideoxy*-D-*"glucose")*. A solution of 1:5-anhydro-2-deoxy-D-*arabino*hexitol (1 g) in freshly distilled benzaldehyde (5 ml) was maintained at 115° for 45 min [19], a stream of carbon dioxide being passed continuously through the mixture during this period. The cooled mixture was diluted with light petroleum (60 — 80°) and the crude product collected and washed with light petroleum (60 — 80°). Recrystallization from ether-light petroleum (60 — 80°) afforded *1:5-anhydro-4:6-*O*-benzylidene-2-deoxy*-D-arabino*hexitol* (1.1 g, 69 %) m. p. 98°, $[\alpha]_D$ −54.6° (*c*, 0.4 in ethanol). (Found: C 66.0; H 6.8. $C_{13}H_{16}O_4$ requires C 66.1; H 6.8.)

*1:5-Anhydro-4:6-*O*-benzylidene-2-deoxy-3-*O*-toluene*-p-*sulphonyl*-D-arabino*hexitol (4:6-*O*-benzylidene-3-*O*-toluene*-p-*sulphonyl-1:2-dideoxy*-D-*"glucose")*. A solution of 1:5-anhydro-4:6-*O*-benzylidene-2-deoxy-D-*arabino*hexitol (2 g) in dry pyridine (10 ml) was treated with a solution of toluene-*p*-sulphonyl chloride (2 g) also in dry pyridine (5 ml) at 35° for 48 h. The crude product which separated on dilution of the reaction mixture with water was collected, washed with water and recrystallized from ethanol to yield *1:5-anhydro-4:6-*O*-benzylidene-2-deoxy-3-*O*-toluene*-p-*sulphonyl*-D-arabino*hexitol* (2.2 g, 66.5 %), m. p. 167°, $[\alpha]_D$ −31.7° (*c*, 0.44 in chloroform). (Found: C 61.55; H 5.6; S 8.4. $C_{20}H_{22}O_6S$ requires C 61.5; H 5.6; S 8.2).

*1:5-Anhydro-2-deoxy-3-*O*-toluene*-p-*sulphonyl*-D-arabino*hexitol (3-*O*-toluene*-p-*sulphonyl-1:2-dideoxy*-D-*"glucose")*. A solution of 1:5-anhydro-4:6-*O*-benzylidene-2-deoxy-3-*O*-toluene-*p*-sulphonyl-D-*arabino*hexitol (1 g) in methanolic hydrogen chloride (5 ml, 0.5 % w/v) was boiled under reflux for 2 h. After cooling and dilution with water (10 ml) the solution was neutralised with sodium hydrogen carbonate, concentrated to small volume at 40°, (bath)/14 — 16 mm, and finally freeze-dried. Recrystallization of the residue from chloroform-light petroleum (60 — 80°) afforded *1:5-anhydro-2-deoxy-3-*O*-toluene*-p-*sulphonyl*-D-arabino*hexitol* (0.51 g, 65.8 %), m. p. 111°, $[\alpha]_D$ +23.4° (*c*, 0.51 in chloroform). (Found: C 51.7; H 6.3; S 10.6. $C_{13}H_{18}O_6S$ requires C 51.65; H 6.0; S 10.6).

*Action of alkali on 1:5-anhydro-2-deoxy-3-*O*-toluene*-p-*sulphonyl*-D-arabino*hexitol.* (a) A solution of 1:5-anhydro-2-deoxy-3-*O*-toluene-*p*-sulphonyl-D-*arabino*hexitol (60.4 mg, 0.2 mmole) in ethanol (2.5 ml) and N sodium hydroxide (5 ml) was stirred at 50° for 3 days. After neutralisation with N hydrochloric acid, aqueous sodium metaperiodate solution (15 ml, 0.25 M) was added and the volume rapidly adjusted to 50 ml. The consumption of periodate was determined by the standard procedure [20] of addition of excess arsenite solution and back titration with standard iodine solution using the appropriate blank solutions. A final constant uptake of 0.955 mole of periodate was observed after 30 min.

(b) A solution of 1:5-anhydro-2-deoxy-3-*O*-toluene-*p*-sulphonyl-D-*arabino*hexitol (0.15 g) in ethanol (5 ml) and N sodium hydroxide (10 ml) was stored at 50° for 3 days, and then deionized by passage successively through Amberlite resins IR-120 (H^+ form) and CG-400 (HO^- form). After concentration of the eluate to small volume (*ca.* 1 ml)

zone electrophoresis (ionophoresis) was carried out on Whatman No. 3 paper, using a borate buffer [21] (pH 10) and the enclosed strip technique [10] at a potential gradient of 20 —25 V/cm for 1.5 h. Using the periodate-permanganate reagent [11] for detection, two zones were located; the major zone had a mobility and detection properties identical with that of 1:5-anhydro 2-deoxy-D-*arabino*hexitol whilst the minor zone had a higher mobility.

*1:5-Anhydro-2-deoxy-6-*O*-toluene*-p-*sulphonyl*-D-arabino*hexitol (6-*O*-toluene*-p-*sulphonyl-1:2-dideoxy*-D-*"glucose")*. To a cooled (0°) solution of 1:5-anhydro-2-deoxy-D-*arabino*hexitol (1 g) in dry pyridine (20 ml) a solution of toluene-*p*-sulphonyl chloride (1.3 g) also in dry pyridine (3 ml) was added. After storage at 0° for 2 h and then at room temperature overnight the mixture was diluted with water (50 ml) and extracted with chloroform (4 × 25 ml). The combined and dried ($MgSO_4$) extracts were concentrated at 35°, (bath)/14—16 mm, and, after drying over P_2O_5 *in vacuo*, the residue was dissolved in the minimum volume of chloroform and diluted with continual stirring with light petroleum (60—80°) to turbidity. *1:5-Anhydro-2-deoxy-6-*O*-toluene*-p-*sulphonyl*-D-arabino*hexitol* (1.1 g, 54 %), m. p. 104°, $[\alpha]_D$ +8.5° (*c*, 1.0 in chloroform) was obtained. (Found: C 51.6; H 6.0; S 10.5. $C_{13}H_{18}O_6S$ requires C 51.65; H 6.0; S 10.6.)

A solution of the above compound (60.4 mg, 0.2 mmole) in water (15 ml) was treated with aqueous sodium periodate (15 ml, 0.25 M) and the solution rapidly adjusted to 50 ml. The consumption of periodate was determined as described above and was as follows:

Time (h)	0.5	1.0	2.5	4.0	5.0
Oxidant consumed (mole)	0.816	0.864	0.912	0.960	0.960

One of the authors (S.V.V.) thanks *Papirindustriens Forskningsinstitutt*, Oslo, Norway for a grant.

REFERENCES

1. Peat, S. and Wiggins, L. F. *J. Chem. Soc.* **1938** 1088.
2. Haworth, W. N., Owen, L. N. and Smith, F. *Ibid.* **1941** 88.
3. Ohle, H., Wilcke, H. and Tessmar, K. *Chem. Ber.* **71** (1938) 2316.
4. Barton, D. H. R. and Cookson, R. C. *Quart. Rev.* **10** (1956) 44.
5. Richtmyer, N. K. and Hudson, C. S. *J. Am. Chem. Soc.* **63** (1941) 1727.
6. Bardolph, M. P. and Coleman, G. H. *J. Org. Chem.* **15** (1950) 169.
7. Bourne, E. J., Bruce, G. T. and Wiggins, L. F. *J. Chem. Soc.* **1951** 2708.
8. Barker, S. A. and Bourne, E. J. *Advances in Carbohydrate Chem.* **7** (1952) 137.
9. Peat, S. *Advances in Carbohydrate Chem.* **2** (1946) 37.
10. Foster, A. B. *Chem. & Ind. London* **1952** 1050; *Advances in Carbohydrate Chem.* **12** (1957) 81.
11. Lemieux, R. U. and Bauer, H. F. *Anal. Chem.* **26** (1954) 920.
12. Gut, M. and Prins, D. A. *Helv. Chim. Acta* **30** (1947) 1223.
13. Lester Smith, E. and Page, J. E. *J. Soc. Chem. Ind.* **67** (1948) 48.
14. Barker, S. A. and Stephens, R. *J. Chem. Soc.* **1954** 4550.
15. Foster, A. B., Stacey, M. and Vardheim, S. V. *Acta Chem. Scand.* **12** (1958) 1605.
16. Fischer, E. *Chem. Ber.* **47** (1914) 196.
17. *cf.* Gatterman, L. *Laboratory Methods of Organic Chemistry*, Macmillan, London 1943, p. 379.
18. Zemplén, G. and Pacsu, E. *Chem. Ber.* **62** (1929) 1613.
19. Oldham, M. A. and Honeyman, J. *J. Chem. Soc.* **1946** 986.
20. Bobbitt, J. M. *Advances in Carbohydrate Chem.* **11** (1956) 1.
21. Foster, A. B., Newton-Hearn, P. A. and Stacey, M. *J. Chem. Soc.* **1956** 30.

Received June 27, 1958.

ACTA CHEMICA SCANDINAVICA 12 (1958) 1825—1829

Adsorption of Plasminogen Activator to Fibrin

MOGENS LASSEN

From the Biological Institute of the Carlsberg Foundation and the University Institute of Physical Chemistry, Copenhagen, Denmark

The plasminogen activator formed by reaction between streptokinase and human proactivator is quantitatively adsorbed on human fibrin clots. Separation of fibrin from adsorbed activator was not accomplished, but dilute neutral solutions suitable for estimation of activator could be prepared. The proactivator obtained by heat inactivation of acid solutions of fibrin and adsorbed activator was separated from the fibrin. It was extremely labile in neutralized solutions.

According to present knowledge [1,2], the effect of streptokinase in the activation of fibrinolysis can be described by the following schemes:

$$\text{streptokinase} + \text{proactivator} \rightleftharpoons \text{activator}$$

$$\text{plasminogen} \xrightarrow{\text{activator}} \text{plasmin}$$

A purified preparation of the plasminogen activator would be of interest for many reasons. Its properties could be studied and it could be compared with other components of the fibrinolytic system. It would also be valuable in clinical research. Müllertz [3,4] has found the activator to be adsorbed on fibrin. The present work describes the preparation of acid solutions of fibrin containing adsorbed activator, and the estimation of the content of activator in such solutions. With the procedure described, the yield of activator was nearly quantitative.

MATERIALS AND METHODS

Barbital buffer. Diethyl barbiturate (Michaelis), pH 7.8, to which was added NaCl to give a final ionic strength of 0.15.

Phosphate buffer (Sørensen) pH 7.6.

Streptokinase. "Varidase" was kindly supplied by the Lederle Laboratories Division, American Cyanamid Company. The units are those stated on the packages and determined according to Christensen [5].

Proactivator. Human plasma obtained from out-dated citrated bank blood was used without further purification.

Thrombin. A preparation of bovine thrombin containing about 20 000 NIH units (National Institute of Health) per g was kindly supplied by Løvens kemiske Fabrik, Copenhagen.

Measuring methods: Activator and proactivator were determined by the modified lysis time method described by Lassen [6].

RESULTS

1. *Adsorption of activator to fibrin.* The following procedure was found to give the best yield:

Streptokinase dissolved in 1 ml of phosphate buffer, pH 7.6, 0.1 mg of thrombin dissolved in 50 μl of the same buffer, and 1 ml of human plasma were cooled in an ice bath and mixed in the order mentioned. In general, 5 000 units of streptokinase were used, since this amount was found to be nearly equivalent to the content of proactivator in 1 ml human plasma, and thus ensured the best utilization of both precursors. After standing for 4 h at 0° the clot was finely divided with a glass rod and collected by centrifuging for 10 min in a high speed centrifuge (20 000 rev/min) at 0°. The precipitate was washed thoroughly with 5 ml of icecold phosphate buffer and again centrifuged. This washing procedure was repeated twice, first with buffer as before, and then with 5 ml of icecold distilled water. Finally, the fibrin was dissolved at 0° in 2 ml 0.05 M acetic acid, and cleared by centrifuging. It is important to keep the temperature at 0°, since even at this temperature the activator was found to deteriorate in acid solutions (5 — 10 % were lost per hour and the temperature coefficient was high).

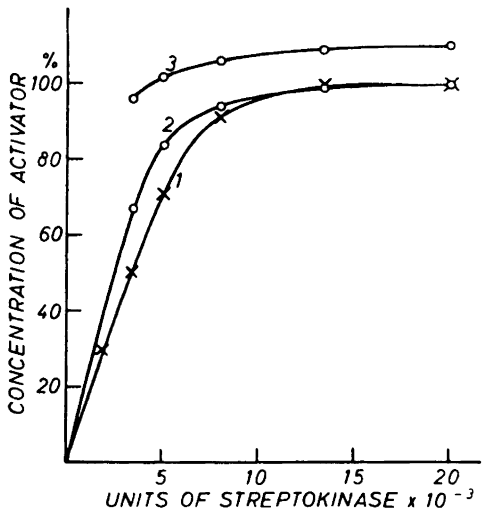

Fig. 1. Adsorption of activator to fibrin. 1 ml of streptokinase solutions in phosphate buffer, pH 7.6, containing the amounts of streptokinase stated on the abscissa were mixed with 50 μl thrombin solution at 0°. 1 ml plasma was then added and the clotted mixtures were stored overnight at 0°. Acid solutions of fibrin were then prepared as described in the text. The activator was estimated in the following solutions: Curve 2, 50 μl fibrin solution + 10 ml barbital buffer. Curve 3, 50 μl fibrin solution + 10 ml barbital buffer containing 500 units of streptokinase. Curve 1, the original mixtures of streptokinase and plasma were prepared without addition of thrombin and incubated for 10 min at room temperature. The activator was then estimated in 50 μl of these solutions diluted with 10 ml barbital buffer.

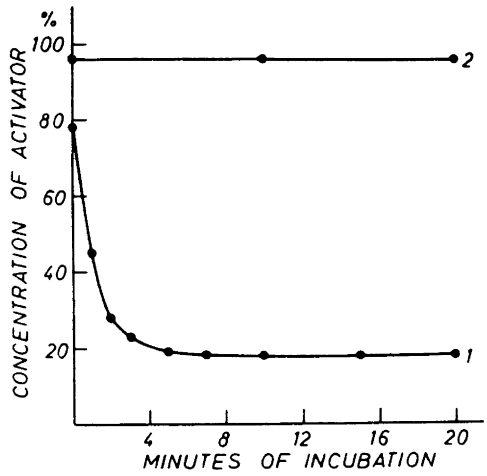

Fig. 2. Inactivation of activator at acid reaction. A solution of fibrin and activator in 0.05 M acetic acid, pH 3.5, was prepared as described. The solution was incubated at 37° and the activator (curve 1) and the sum of activator and proactivator (curve 2) were determined at different times. For the estimations of activator 50 μl of the acid solution were diluted with 10 ml of barbital buffer. For the estimations of activator + proactivator 250 units of streptokinase were added. 1 000 units of streptokinase dissolved in 1 ml of the heated solution of fibrin was found to be stable for 2 h at 37°.

After diluting 50 μl of the acid solution with 10 ml barbital buffer the activator could be measured as described [6]. This was possible since precipitation of fibrin is a very slow process at this high dilution. In four experiments in which 5 000 units of streptokinase per ml of plasma were used, the amounts of activator obtained constituted 110, 135, 140 and 150 %, respectively, of the amounts obtained when the same amount of streptokinase and proactivator (human plasma) were incubated for 10 min at room temperature. In all experiments the amount of activator which remained in serum constituted less than 0.5 %. The apparent excess over 100 % in "yields" can perhaps be ascribed to an influence of fibrin on the formation and stability of the activator.

In many experiments it was found more convenient to leave the clotted solutions overnight at 0°. This was investigated in the next experiment with different concentrations of streptokinase (Fig. 1, curve 2). Curve 1 shows the amounts of activator formed after incubation of the unclotted streptokinase-plasma mixtures for 10 min at room temperature. This curve is in full agreement with the results obtained by Müllertz [2] on the basis of which the reaction between streptokinase and proactivator was proposed to be stoichiometric. The similarity between curves 1 and 2 shows the adsorption of the activator to be nearly quantitative for all concentrations of streptokinase employed. Furthermore, the sum of activator and proactivator in the acid solutions of fibrin was estimated by adding an excess of streptokinase to the buffer used for the dilution (curve 3). The higher values obtained in curve 3 as compared

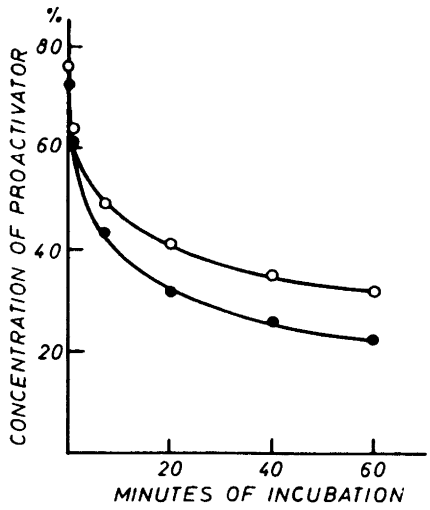

Fig. 3. Lability of proactivator prepared from two different solutions of fibrin plus activator. These solutions were stored overnight at −20°, thawed and centrifuged. The supernatants were neutralized at room temperature with equal volumes of 0.2 M Na_2HPO_4 and the proactivator was estimated at different time intervals.

with curve 2 indicate the presence of an excess of proactivator in the acid solutions of fibrin.

Attempts at separating fibrin and activator have been performed as follows: Precipitation with sodium chloride, or with ethanol at low temperature, or with sodium tungstate, or by neutralization in the presence of phosphate buffer at different concentrations and in the presence of L-lysine ethylester, benzoyl-L-arginine ethylester, amino acids, proteins (including casein, gelatin, Witte peptone, or bovine fibrin hydrolysed with trypsin or chymotrypsin), nucleic acid, sodium sulphosalicylate or sodium tungstate. The best yield (5 %) was obtained with bovine fibrin hydrolysed by trypsin. By precipitation at neutral reaction most of the activator was recovered in the fibrin, while the precipitations at acid reactions were accompanied by deterioration of activator. Furthermore, selective adsorption to barium sulphate and Amberlite IRC 50 from the acid solutions was studied, but these procedures caused either inactivation or irreversible adsorption of activator. An attempt to hydrolyse fibrin in acid solution with pepsin resulted in rapid inactivation of activator. Fibrin made by thrombin coagulation of the citrated plasma used was found to be insoluble in dilute acetic acid. An attempt was made to produce insoluble fibrin from the mixture of plasma and streptokinase by centrifuging immediately after formation of the clot, but some of the fibrin dissolved and the yield of activator was low.

2. *Inactivation of activator in acid solutions.* Troll and Sherry [1] inactivated the activator at acid pH under rather drastic conditions (100° for 15 min at pH 2). They found that most of the original amount of proactivator was

still present in the heated solutions, since reactivation could be obtained by addition of streptokinase to the neutralized solutions. They assumed the acid inactivation to result from destruction of streptokinase and concluded that the activator was formed through a reversible reaction between streptokinase and proactivator:

$$\text{Streptokinase} + \text{proactivator} \rightleftharpoons \text{activator}$$

The inactivation at acid reaction was explained by a displacement of this reaction towards the left, due to removal of streptokinase. The activator present in the acid solution of fibrin (pH about 3.5) was found to be extremely labile at 37°, as well as at room temperature, although complete inactivation could never be achieved (Fig. 2, curve 1). During inactivation equivalent amounts of proactivator were apparently formed (Fig. 2, curve 2). These results are in accordance with Troll and Sherry [1]. However, streptokinase was found to be stable under the experimental conditions (legend to Fig. 2). The assumption that the inactivation of activator at acid reaction is caused by destruction of the orginal streptokinase therefore appears questionable.

3. *Separation of proactivator and fibrin.* Several attempts to isolate the proactivator produced by acid inactivation have been made. Of many experiments the following procedure was found to give the nearest approach to a separation: Acid solutions of fibrin and adsorbed activator were prepared as described. The solutions were placed overnight at —20° and thawed the next day. This procedure caused irreversible precipitation of the fibrin. The centrifuged solutions contained very little activator and about 75 % of the theoretical amount of proactivator. However, proactivator produced in this manner was found to be extremely labile in the neutralized solutions (Fig. 3). In this respect this "proactivator" apparently differs from the genuine proactivator.

Acknowledgements. The author is indebted to Dr. Tage Astrup for his interest and helpful advice. The investigation was made possible by a grant from *Statens almindelige Videnskabsfond*, Denmark. It forms part of the investigations on fibrinolysis for which Dr. Astrup receives support from *The Josiah Macy, Jr. Foundation*, New York, and the *National Danish Association against Rheumatic Diseases*.

REFERENCES

1. Troll, W. and Sherry, S. *J. Biol. Chem.* **213** (1955) 881.
2. Müllertz, S. *Biochem. J.* **61** (1955) 424.
3. Müllertz, S. *Acta Physiol. Scand.* **28** (1953) 29.
4. Müllertz, S. *Mechanism of activation and effect of plasmin in blood* (Diss.) p. 44. *Acta Physiol. Scand.* **38** (1956), Suppl. No. 130.
5. Christensen, L. R. *J. Clin. Invest.* **28** (1949) 163.
6. Lassen, M. *Scand. J. Clin. Lab. Invest.* **10** (1958) 384.

Received July 3, 1958.

ACTA CHEMICA SCANDINAVICA 12 (1958) 1830—1833

Synthesis of Compounds Related to Muscarufin

IV.* 2,5-Bis-(2-carbomethoxyphenyl)-veratraldehyde

MARTIN NILSSON

Organisk-kemiska Institutionen, Kungl. Tekniska Högskolan, Stockholm, Sweden

The preparation of the title compound (II) from 2,5-di-iodovanillin is reported.

Recently Bohlmann and Kritzler [1] described an approach to the synthesis of muscarufin starting with the preparation of 3-(4-carboxy-$\Delta^{1,3}$-butadienyl)-6-methoxybenzoquinone-(1,4) from *iso*vanillin. However, due to the poor solubility of the quinone they were unable to attach the 2-carboxyphenyl residues.

A somewhat similar approach has been investigated in this laboratory aimed at the preparation of a *p*-terphenylaldehyde, the aldehyde group of which could be the starting point for the attachment of a side chain by methods similar to those of Bohlmann and Kritzler.

The Ullmann reaction is often a convenient route to *p*-terphenyl derivatives [2,3] and as the aldehyde group might be difficult to introduce at a later stage a di-iodoaldehyde was chosen as the starting material. Aldehyde groups generally survive under the conditions of the Ullmann reaction (*cf.* review by Fanta [4]), but preliminary experiments on the reactions of 2-iodo- and 5-iodoveratraldehydes with copper indicated that some oxidation was likely to occur in the first case.

Acetalisation was therefore chosen for protection of the aldehyde group. No acetal of vanillin appears to be described in literature and early comments [5] indicate that *o*- and *p*-hydroxybenzaldehydes fail to give acetals under standard conditions.

Vanillin when treated with ethylene glycol and boron trifluoride at room temperature gave a blue solution, from which only starting material was recovered. 2,5-Di-iodovanillin [6] under the same treatment gave a colourless solution from which 2,5-di-iodovanillin ethylene acetal was obtained (30—40

* Part III. *Acta Chem. Scand.* **12** (1958) 537.

% yield); a faint pink coloration appeared at the very beginning but soon faded. Better yield (64 %) was obtained when the reaction was carried out at higher temperature with continuous removal of water.

The failure of vanillin to give an acetal may be ascribed to the stability of the "quinoid" vanillin-boron trifluoride complex. As judged from the faint colour the corresponding complex of 2,5-di-iodovanillin is not as stable and this is presumably due to steric interference of the iodine atom(s).

Treatment of 2,5-di-iodovanillin ethylene acetal with diazomethane gave 2,5-di-iodoveratraldehyde ethylene acetal in good yield. The alkaline methylation of 2,5-di-iodovanillin gave poor yields.

The Ullmann reaction with 2,5-di-iodoveratraldehyde ethylene acetal and methyl 2-bromobenzoate gave 2,5-bis-(2-carbomethoxyphenyl)-veratraldehyde ethylene acetal (I) in fair yield.

Mild acid hydrolysis of I gave 2,5-bis-(2-carbomethoxyphenyl)-veratraldehyde (II) which, however, did not give crystalline derivatives.

Demethylation of II (or I) with hydrobromic acid gave a high-melting, sparingly soluble product, which was difficult to purify and gave a poor analysis. Its resemblance to the stable dilactones described in previous communications [2,3] and infrared data indicate it to be the dilactone of 2,5-bis-(2-carboxyphenyl)-protocatechualdehyde (III).

Attempts to use the Reformatsky reaction with methyl γ-bromocrotonate [1,7], the Wittig reaction using the triphenylphosphonium salt from the same ester [7], and the acid-catalysed condensation with diethyl ethylidenemalonate [8] for the introduction of the muscarufin side-chain on 2,5-(2-carbomethoxyphenyl)-veratraldehyde (II) have so far been unsuccessful.

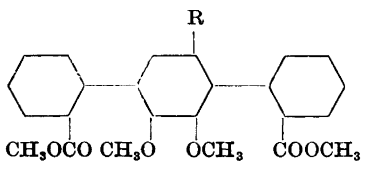

I R = —CH(O)(O)

II R = — CHO

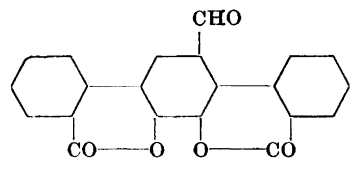

III

EXPERIMENTAL

The melting points were determined on a Kofler block. The infrared spectra (potassium bromide discs) were recorded on a Perkin Elmer No. 21 instrument with a sodium chloride prism.

Ullmann coupling of iodoveratraldehydes. 2-Iodoveratraldehyde [6] (0.8 g) and copper bronze (2 g) were mixed in a test tube and heated to 250° for 15 min. The cooled mixture was extracted with chloroform, the opaque greenish solution was evaporated and the residue was distilled at 10 mm to give an oil (0.2 g, 45 %), which solidified and was recrystallised from methanol to give *5,5',6,6'-tetramethoxy-2,2'-diformyldiphenyl* as prisms, m. p. 136—137°. (Found: C 65.1; H 5.6. Calc. for $C_{18}H_{18}O_6$: C 65.4; H 5.5.)

5-Iodoveratraldehyde [9] by the same procedure gave *5,5',6,6'-tetramethoxy-3,3'-diformyldiphenyl* (65 %), m. p. 138–140°, undepressed by the product obtained by methylation of "dehydrodivanillin" [10] (*cf.* Ref.[9]). There were no obvious signs of oxidation in this experiment.

The mixed m. p. of the synthetic products gave a marked depression (115–135°).

2,5-Di-iodovanillin ethylene acetal. 2,5-Di-iodovanillin (45 g) prepared in 35 % overall yield from vanillin [6], ethylene glycol (40 ml) and boron trifluoride-ether complex (47 %, 10 ml) were heated in trichloroethylene (250 ml) under reflux with continuous removal of water from the condensate for 16 h. After cooling the glycol phase was separated and extracted with trichloroethylene. The combined trichloroethylene solution was washed quickly with water and sodium hydrogen carbonate solution and dried over sodium sulphate. Evaporation of the solvent gave a solid (32 g, 64 %, m. p. 110–125°), which was recrystallised from dry methyl *cyclo*hexane to give 2,5-di-iodovanillin ethylene acetal as elongated plates, m. p. 127–128°, occasionally resolidifying and finally melting at 135–137°. (Found: C 27.1; H 2.1; I 56.4. Calc. for $C_{10}H_{10}I_2O_4$: C 26.8; H 2.3; I 56.7.) The acetal was rather sensitive to water; recrystallisation from ethanol-water mixtures and even from moist light petroleum caused extensive hydrolysis.

2,5-Di-iodoveratraldehyde ethylene acetal. Crude 2,5-di-iodovanillin ethylene acetal was suspended in ether and treated with a moderate excess of diazomethane. After 1 h the nitrogen evolution ceased, the solvent was removed and the solid product was recrystallised from small volumes of methanol, m. p. 80–81° (70 % yield). (Found: C 28.2; H 2.6; 55.1. Calc. for $C_{11}H_{12}I_2O_4$: C 28.6; H 2.6; I 54.9.)

2,5-Bis-(2-carbomethoxyphenyl)-veratraldehyde ethylene acetal (I). 2,5-Di-iodoveratraldehyde ethylene acetal (4.3 g, 0.009 mole), methyl 2-bromobenzoate (17 g, 0.08 mole) and copper bronze (50 g) were allowed to react at 250°. The oil obtained by extraction with chloroform was distilled giving methyl benzoate, dimethyl diphenate and a fraction, b. p. 240–260°, 1 mm (2.5 g, yellow oil), which was dissolved in benzene and passed through a column of alumina. The solvent was removed and the residue was dissolved in a small volume of methanol and after keeping in the refrigerator gave I as compact prisms, m. p. 124–126° (1.0 g). (Found: C 67.9; H 5.8. Calc. for $C_{27}H_{26}O_8$: C 67.8; H 5.5.)

The infrared spectrum showed an ester carbonyl band at 1 730 cm^{-1}.

Mild acid hydrolysis of the material in the mother liquors gave a further quantity of crystalline material (II, 0.5 g, m. p. 135–137°; see below) bringing the total yield for the Ullmann coupling to 35 %.

2,5-Bis-(2-carbomethoxyphenyl)-veratraldehyde (II). The acetal I was heated on the water bath for 0.5 h in aqueous acetic acid containing a trace of *p*-toluenesulphonic acid. On cooling the aldehyde II separated in quantitative yield and was recrystallised from methanol to give prisms, m. p. 140–141°. (Found: C 68.8; H 5.3. Calc. for $C_{25}H_{22}O_7$: C 69.1; H 5.1.)

The infrared spectrum showed ester carbonyl (1 730 cm^{-1}), aldehyde carbonyl (1 695 cm^{-1}) and aldehyde C–H stretching band (2 760 cm^{-1}).

Attempts to prepare the 2,4-dinitrophenylhydrazone and the semicarbazone gave only amorphous material.

Demethylation. The aldehyde II (0.20 g), hydrobromic acid (*d* 1.48, 1 ml) and acetic acid (2 ml) were heated under reflux for 0.5 h. After cooling the precipitate was collected and was recrystallised from large volumes of acetic acid to give small needles, which were always somewhat brownish, m. p. *ca.* 360° (decomp.). (Found: C 72.8; H 2.9. Calc. for $C_{21}H_{10}O_5$: C 73.7; H 2.9.)

The infrared spectrum showed a very strong band at 1 755 cm^{-1}, which may be ascribed to a six-membered ring lactone, and bands due to an aldehyde group (1 695 and 2 760 cm^{-1}). The dilactone of 2,5-dihydroxy-1,4-bis-(2-carboxyphenyl)-benzene [2] gave a very strong band at 1 750 cm^{-1}.

The author is indebted to *Statens Tekniska Forskningsråd* for a fellowship and to Dr. B. R. Thomas for linguistic criticism.

REFERENCES

1. Bohlmann, F. and Kritzler, H. *Chem. Ber.* **90** (1957) 1512.
2. Erdtman, H. and Nilsson, M. *Acta Chem. Scand.* **10** (1956) 735.
3. Nilsson, M. *Acta Chem. Scand.* **10** (1956) 1377.
4. Fanta, P. *Chem. Revs.* **38** (1946) 139.
5. Fischer, E. and Giebe, G. *Ber.* **30** (1897) 3053.
6. Raiford, L. C. and Wells, E. H. *J. Am. Chem. Soc.* **57** (1935) 2500.
7. Bohlmann, F. *Chem. Ber.* **90** (1957) 1519.
8. Higginbotham, L. and Lapworth, A. *J. Chem. Soc.* **121** (1922) 2823.
9. Erdtman, H. *Svensk Kem. Tidskr.* **47** (1935) 223.
10. Elbs, K. and Lerch, H. *J. prakt. Chem.* [2] **93** (1916) 2.

Received June 28, 1958.

ACTA CHEMICA SCANDINAVICA 12 (1958) 1834—1850

A Relaxation Method for the Determination of Moderately Rapid Reaction Rates near Chemical Equilibrium

STIG LJUNGGREN and OLE LAMM

The Royal Institute of Technology, Division of Physical Chemistry, Stockholm 70, Sweden

A new relaxation method, based on the equilibrium displacement produced by a *rapid pressure rise*, is described. Using the present technique, the pressure was raised from 1 to 150 atmospheres in about one twentieth of a second. The relaxation to equilibrium was followed by a continuous registration of the conductivity of the sample solution. This technique was employed to study the kinetics near equilibrium of the carbon dioxide-water system. It was also found possible to calculate the true dissociation constant of carbonic acid.

SYMBOLS

b_{rs} = constants defined in text
C_p = specific heat
C = total concentration
c^o = equilibrium concentration
c_o = concentration of undissociated constituent
c_+ = concentration of positive ion
c_- = concentration of negative ion
H^o = partial molar enthalpy of standard state (referred to infinite dilution)
J = cell constant
K = equilibrium constant in general
K_s = true dissociation constant of CO_2
K_h = hydration constant of CO_2
K_{sh} = apparent dissociation constant of CO_2
k_f = forward rate constant
k_r = reverse rate constant
l = eqivalent ionic conductance
p = pressure; algebraic expression defined in the text
q = algebraic expression defined in the text
R = gas constant; cell resistance
S = entropy
T = absolute temperature

t = time
V° = partial molar volume of standard state (referred to infinite dilution)
$V^{\neq}$ = partial molar volume of activated state
y = recorder deflexion
α = degree of dissociation
α_0 = equilibrium degree of dissociation
β = relative change in K on compression from p_1 to p_2
γ = volume compression ratio
Δ = finite difference operator; perturbation from equilibrium concentration
ε = constant of integration
Θ = perturbation measure
$\varkappa$ = specific conductance of solution
λ = eigenvalues of matrix
τ = relaxation time

INTRODUCTION

In connection with other investigations at this Institute there arose a need for a method suitable for the study of the kinetics of certain reactions with half-times ranging from 0.05 sec up to a few minutes. All reactions which were studied involved ionic species. For this reason it seemed most convenient to utilize the conductivity of the solutions. Of the existing methods [1] for studying fast reactions, only the rapid flow method of Hartridge and Roughton [2] seemed to be applicable in the region of rates mentioned. An estimation showed, however, that it would be difficult to adapt the flow method successfully to conductivity registration without sacrificing the low liquid consumption which is characteristic of certain modifications of this method. From the point of view of general experimental simplicity, a relaxation method seemed most attractive. This led the authors to the development of what might be called *a pressure jump method.* By recording the variation of conductivity following the application of a rapid pressure rise, the rate at which the new equilibrium was approached could be studied. There is a simple relation between the relaxation time (time lag) and the reaction rates (*cf.* Refs.[3,4]). A rather similar method, the temperature jump method, has been indicated by Eigen [5].

A still simpler relaxation method, which to the authors' knowledge, has not been tried as yet, would be a rapid dilution of the sample solution followed by, for example, conductivity registration.

The pressure jump method is not confined to solutions having an electric conductivity. The variation of colour, temperature or dielectric constant of the solution may be used as well. In addition to the relaxation process, the pressure dependence of the equilibrium constant can be studied by the same experimental arrangement.

The original flow method[2,2a] requires large quantities of liquid. In later modifications [2], *e. g. the stopped flow and accelerated flow methods,* this drawback has been overcome. The flow method has hitherto been applied mainly to biological systems, *e. g.* enzyme reactions. The rate of hydration and dehydration of carbon dioxide and the rate of the conversion $Cr_2O_7^{2-} - HCrO_4^-$ have, however, also been determined in this way[6].

Relaxation methods[1] have attracted much attention in recent years. In addition to the *pressure jump method* described in this paper and the *remperature jump method* already mentioned, we have, for example, the method utilizing the equilibrium displacement caused by a strong electric field, the so called *dissociation field effect* (or second Wien effect) [1,3]. Owing to the enormous production of Joule heat per unit time, this method can only be used for very fast reactions. The same thing is true for the *sound absorption method* [1].

Proton magnetic resonance has been applied, for example, to the study of the extremely rapid protolysis of ammonia and various amines [1,7].

A *dielectric dispersion method* has recently been used to study the dissociation rate of boric acid [8].

Polarographic and related methods [9-14] are applicable in cases where the electrode process is preceded by the reaction to be studied. As an example of a successful application of this technique, the determination of the dissociation rate of the complex ion $[Cd(CN)_4]^{2-}$ may be mentioned [15].

BASIC THEORY

The effects of pressure on the conductivity of an electrolyte are twofold. First, the ionic mobilities are changed, due in the first place to the change in viscosity of the solvent. Second, there is a displacement of the equilibrium position (*i.e.* a change in the equilibrium degree of dissociation) which we utilize to study the rate of approach to the new equilibrium at the higher pressure. The equilibrium perturbation is to be ascribed partly to the change in the equilibrium constant and partly to the pure volume effect, *i.e.* the increase of the concentrations due to the volume compression.

1. The pressure effect on the equilibrium constant

For the variation of the equilibrium constant, K, with pressure, p, under adiabatic conditions we have

$$(\partial \ \ln K/\partial p)_S = (\partial \ \ln K/\partial p)_T + (\partial \ \ln K/\partial T)_p \ \ (\partial T/\partial p)_S ,$$

where T is the absolute temperature and S the entropy of the solution. Now, from thermodynamics we know that

$$(\partial \ \ln K/\partial p)_T = -\Delta V^\circ/RT$$

$$(\partial \ \ln K/\partial T)_p = \Delta H^\circ/RT^2$$

$$(\partial T/\partial p)_S = T(\partial V/\partial T)_p/C_p$$

where V° and H° are the volume and enthalpy of the standard states (referred to infinite dilution).

$$(\partial \ \ln K/\partial p)_S = \frac{1}{RT} \cdot \left[-\Delta V^\circ + \Delta H^\circ \ (\partial V/\partial T)_p/C_p \right]$$

Realizing that

$$\ln \ (K_2/K_1) = \int_{p_1}^{p_2} (\partial \ \ln K/\partial p)_S \mathrm{d}p$$

and introducing the ratio

$$\beta = K_2/K_1$$

we have

$$\beta = \exp\left[\int_{p_1}^{p_2} (\partial \ln K/\partial p)_S \mathrm{d}p\right] =$$

$$= \exp\left[\int_{p_1}^{p_2} \frac{-\Delta V^\circ + \Delta H^\circ (\partial V/\partial T)_p/C_p}{RT} \cdot \mathrm{d}p\right]$$

When working with dilute aqueous solutions, we may disregard the second term within the bracket in the expression for $(\partial \ln K/\partial p)_S$ since $(\partial V/\partial T)_p$ is very small for water at room temperature (and zero at the temperature of maximum density). If the equilibrium involves ionic species, the change in K is accompanied by a corresponding change in the conductivity of the solution.

As to the magnitude of the pressure effect, we find that if $\Delta V^\circ = 1$ cm^3 per mole, then a change of p from 1 to 100 atm will produce a change in K of 4×10^{-3}. This is sufficient to permit registration of the relaxation process.

2. The volume effect

The volume effect is of course much smaller in a solution than in a gas mixture, but it is comparable in magnitude to the change in K (*i.e.* β) given above. As an example let us study the dissociation equilibrium

$$\underset{c_0}{AB} \rightleftharpoons \underset{c_+}{A^+} + \underset{c_-}{B^-}$$

According to the law of mass action we have

$$c_+ c_-/c_0 = K$$

If, now, the pressure is rapidly raised, say, from 1 to 100 atm, all concentrations are instantaneously increased in the same ratio, γ, as the volume decrease of the solution.

$$c_0' = \gamma c_0$$

$$c_+' = \gamma c_+$$

$$c_-' = \gamma c_-$$

γ can be calculated if the compressibility of the solution is known. As c changes to c', K will simultaneously change to K'

$$K' = \beta K$$

where β can be calculated using the equation deduced in the foregoing section.

The equilibrium is perturbed as a result of the changes in c and K. As a measure for the perturbation, we introduce a quantity Θ, defined by the relation

$$c_+' c_-'/c_o' = (1 + \Theta)\ K'$$

Thus

$$\gamma c_+ \gamma c_-/\gamma c_o = (1 + \Theta)\beta K$$

i.e.

$$\Theta = (\gamma - \beta)/\beta$$

Obviously, the two effects, γ and β, may occasionally cancel. On the other hand, it is possible to obtain a measurable effect even in such cases where β is very small or equal to zero. It is hard to make any predictions since ΔV° varies appreciably from case to case. (*cf.* Ref.[16]).

3. The change in the ionic mobilities

As discussed by Bridgman [17], the ionic mobilities are themselves functions of the pressure. However, this effect, being instantaneous, has no influence on the relaxation time.

4. The relaxation

In order to get an idea of the relaxation process we will study the case of a weak binary electrolyte * which dissociates according to the formula

$$AB \underset{k_r}{\overset{k_f}{\rightleftharpoons}} A^+ + B^-$$

$$C(1-\alpha) \qquad C\alpha \qquad C\alpha$$

Then

$$\frac{C\,\alpha_o^2}{1-\alpha_o} = K$$

where α_o is the equilibrium degree of dissociation and α the actual degree of dissociation. k_f and k_r are the forward and reverse rate constants respectively. The rate equation of the system is

$$\frac{d\alpha}{dt} = k_f\left(1-\alpha-\frac{C\alpha^2}{K}\right)$$

On integration (*cf.* Ref.[4]) at constant K and k_f we obtain

$$\frac{\alpha-\alpha_o}{\alpha+\dfrac{\alpha_o}{1-\alpha_o}} = \varepsilon e^{-t/\tau}$$

* An example of a more complicated case will be encountered below in connection with the system carbon dioxide-water.

where s is a constant and

$$\tau = \frac{1-\alpha_o}{k_r C(2-\alpha_o)\alpha_o}$$

τ is the so-called Langevin time lag. The expression may be rewritten in the form

$$\tau = \frac{\alpha_o}{k_f (2-\alpha_o)}$$

If $\alpha-\alpha_o = \Delta\alpha$ is small in comparison with α_o, the integrated rate equation becomes approximately

$$\Delta \alpha = (\Delta\alpha)_o \, e^{-t/\tau}$$

where $(\Delta\alpha)_o$ refers to $t = 0$.

The specific conductance of the relaxing solution is proportional to α:

$$\varkappa = 10^{-3} \, C\alpha \, (l_{A+} + l_{B-})$$

where l_{A+} and l_{B-} denote the equivalent conductances of A^+ and B^- respectively at the elevated pressure.

Hence

$$\Delta\varkappa = (\Delta\varkappa)_o e^{-t/\tau}$$

Using this expression, τ may be determined by following the variation of $\varkappa$.

The expression for τ shows that it depends on α_o. Since α_o depends in turn on C and K, a suitable *concentration* range must be chosen in each particular case in order that τ may assume a value suitable for measurement.

Having determined τ, the question arises as to whether the value obtained agrees with the reaction rate at atmospheric pressure. For the variation of the rate constants with pressure we have [18]

$$\left(\frac{\partial \ln k}{\partial p}\right)_T = \frac{\Delta V^{\neq}}{RT}$$

where $\Delta V^{\neq}$ refers to the activated state. Obviously this effect is of the same order of magnitude as the change in K, *i.e.* about 1 % for a pressure variation of 100 atm. As a rule this is within the limit of errors in the determination of τ and k.

THE APPARATUS

A conductivity cell, two types of which are shown in Figs. 1 and 2 *, was enclosed in a pressure vessel of stainless steel, Fig. 3. The pressure was transmitted from the pressure medium (water or paraffin oil) to the solution in the cell by means of a flexible polythene tube, Fig. 1. This simple arrangement proved completely satisfactory in practice. When water was used as pressure

* The cell in Fig. 2 has the advantage of giving a constant current density in every part of the electrode surfaces.

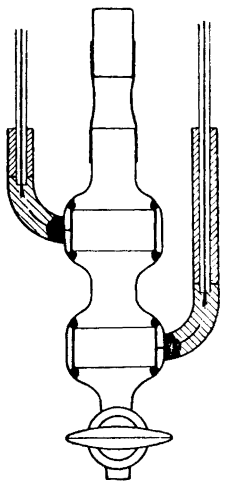

Fig. 1. Conductivity cell. The polythene tube on top of the cell transmits the pressure.

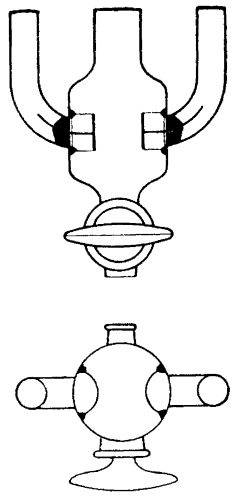

Fig. 2. Conductivity cell. The electrodes are curved (harmonic circles) so that the current density is nearly constant over the whole electrode surface.

medium, the knurled screws inside the vessel and the connections to the insulated leads were completely embedded in picein in order to avoid conduction through the water. The rapid pressure rise was achieved simply by connecting the pressure vessel to a 150 atm nitrogen cylinder and rapidly opening the

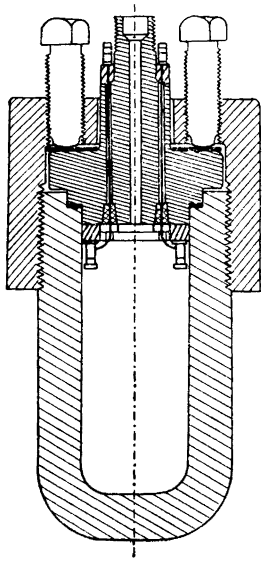

Fig. 3. Pressure vessel. The electrode leads pass through teflon cones tightening according to the "principle of the unsupported area" [17].

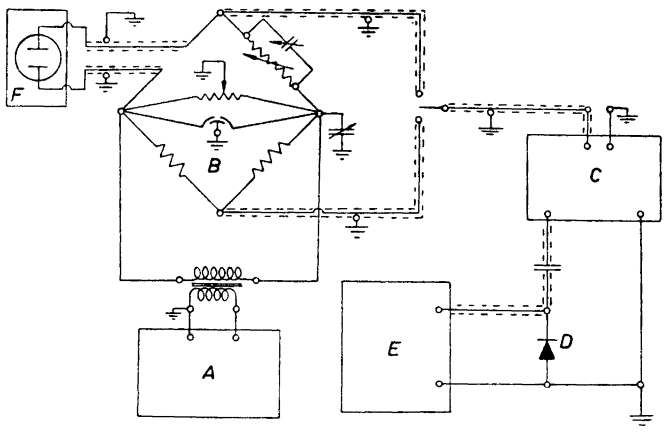

Fig. 4. Recording system. A, oscillator; B, Wheatstone bridge (separately balanced against earth); C, amplifier; D, rectifier; E, recorder; F, conductivity cell.

stopcock. In this way the pressure variation could be obtained without shock or vibration in less than one twentieth of a second. This sets the lower limit to the range of time-lags that can be determined. However, it should possible to improve the present form of the method.

The recording system is shown schematically in Fig. 4. The cell, the isolated leads of which passed through the cover of the pressure vessel, forms one branch of a Wheatstone bridge fed from an audio frequency oscillator *. The detector signal, which at low degress of unbalance is approximately proportional to the relative variation of the resistance of the cell, was amplified ** and rectified. The DC voltage from the copper rectifier was then recorded ***. The working conditions have to be chosen in such a way that, as far as possible, the recording system is linear in the whole range used.

Fig. 5 shows an actual registration with 0.01 M KCl in the cell and *paraffin oil* as pressure medium. In this case, the whole of the change in conductivity is due to the change in ionic mobilities and to the pure volume effect.

Fig. 6 shows a registration from an experiment with a carbon dioxide solution. The instantaneous change, AB, is due to the same reasons as those for KCl and also to a displacement of the rapid equilibrium: $H_2CO_3 \rightleftharpoons H^+ + HCO^-_3$. The slow change, BC, on the other hand, reflects the relaxation of the hydration reaction of CO_2. The theory of this will be given below.

* At frequencies above 5 000 cycles/sec, the mass of the recorder galvanometer prevents the superimposed AC component (ripple) from being recorded.

** In order to avoid transient distortion (from the building-up process), the band width of the amplifier must not be too small. (*cf.* Ref.[18a]). For this reason, an untuned amplifier was used.

*** A direct writing recorder, the Mingograph, manufactured by the Elema Co., Stockholm, Sweden, was used. The ink is sprayed on to the recording paper by a small, light nozzle. This eliminates the friction between pen and paper and enables rapid processes to be recorded on ordinary paper. The instrument was originally designed for medical purposes.

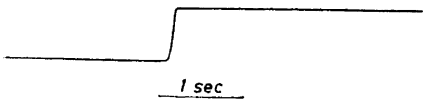

Fig. 5. Record obtained with 0.01 M KCl.

Fig. 6. Record obtained with a CO_2 solution. AB, rapid change; BC, slow change (relaxation curve).

Fig. 6 also illustrates the method of evaluation used. We have

$$y = y_0 \, e^{-t/\tau}$$

Hence, if y is plotted in a logarithmic scale *versus* time, then $-1/\tau$ is obtained as the slope of the line.

Theoretically there should be no *lower* limit for the rates of reactions which can be determined by the method. The following facts have, however, to be considered. On compression to a hundred atmospheres, the temperature of the *medium* may rise by several degrees.* Thus heat is slowly transferred to the conductivity vessel, changing the conductivity of the electrolyte. This may mask the change in conductivity if the reaction studied is slow (large τ)**. If the reaction is fast the heat of the compression is less disturbing ***. However, the advantage of using a pressure medium at the temperature of its density maximum (if it has one), *e.g.* water at 4°C, becomes apparent. For fast

* The adiabatic heat of compression obeys the equation already stated:

$$(\partial T/\partial p)_S = (T/C_p)(\partial V/\partial T)_p$$

Assuming that $(\partial T/\partial p)_S$ remains constant, we may easily calculate the temperature rise on compression to a hundred atmospheres. Approximate values for some common substances are (at room temperature):

Substance	*Temperature rise (°C/100 atm)*	
Pentane	3.5	
Ethyl ether	3.15	
Benzene	2.45	
Rubber	0.84	
Paraffin	0.84	
Glycerol	0.49	
Mercury	0.28	
2.5 % KCl in aq.	0.16	
Water	0.07	(20°C)
»	0	(4°C)
Brass	0.10	
Glass	0.03	
Porcelain	0.007	
Nitrogen gas	77.5	(calcd. in a different way)

** In experiments with solutions having a high conductivity, the Joule heat evolved in the cell must also be considered.

*** For such rapid reactions where the heat conduction can be neglected, the *temperature jump method* may have an advantage over the present one, since it permits a more rapid application of the perturbation. However, the rate of application of the pressure might be considerably increased using, for example, »a bursting membrane» technique (compare *e.g.* [19,20]).

processes, paraffin oil is superior since the turbulence resulting from the application of pressure is damped much more rapidly in paraffin oil than in water. In addition, paraffin oil is a superior electrical insulator. It was found practical to use *agar* in the water to increase its viscosity to approximately that of paraffin oil.

The electrodes of the cell were treated with HNO_3/HCl and then carefully washed before each run. In the experiments with carbon dioxide solutions, unplatinized electrodes were used in order to prevent adsorption on the electrode surfaces.

THE SYSTEM CARBON DIOXIDE-WATER

a. *Relaxation time.* The system carbon dioxide-water is an example of a case which is more complicated than the simple binary electrolyte case treated above. In this system, there is an intermediate stage, the hydration of CO_2, so that the dissociation proceeds according to the formula

$$CO_2 + H_2O \underset{k_2}{\overset{k_1}{\rightleftharpoons}} H_2CO_3 \underset{k_4}{\overset{k_3}{\rightleftharpoons}} H^+ + HCO^-_3$$

There is also a competing reaction path

$$CO_2 + OH^- \rightleftharpoons HCO^-_3$$

which, however, does not become important unless p H$>$8 (*cf.* Ref.[21]). Hence, the system will obey the following rate equations

$$\begin{cases} \dfrac{dc_{CO_2}}{dt} = -k_1 c_{CO_2} + k_2 c_{H_2CO_3} \\ \dfrac{dc_{H_2CO_3}}{dt} = k_1 c_{CO_2} - k_2 c_{H_2CO_3} - k_3 c_{H_2CO_3} + k_4 c_{\pm}^2 \\ \dfrac{dc_{\pm}}{dt} = k_3 c_{H_2CO_3} - k_4 c_{\pm}^2 \end{cases}$$

where

$$c_{\pm} = c_{H^+} = c_{HCO^-_3}$$

We will now introduce

$$\begin{cases} c_{CO_2} = c^\circ_{CO_2} + \Delta_1 \\ c_{H_2CO_3} = c^\circ_{H_2C_3O} + \Delta_2 \\ c_{\pm} = c^\circ_{\pm} + \Delta_3 \end{cases}$$

where Δ_1, Δ_2, and Δ_3 denote small deviations from the equilibrium concentrations (denoted c°).

$$\begin{cases} 0 = k_1 c^\circ_{CO_2} + k_2 c^\circ_{H_2CO_3} \\ 0 = k_1 c^\circ_{CO_2} - k_2 c^\circ_{H_2CO_3} - k_3 c^\circ_{H_2CO_3} + k_4 (c^\circ_{\pm})^2 \\ 0 = k_3 c^\circ_{H_2CO_3} - k_4 (c^\circ_{\pm})^2 \end{cases}$$

For small Δ we may put

$$c_{\pm}^2 \approx (c_{\pm}^\circ)^2 + 2c_{\pm}^\circ \Delta_3 = (c_{\pm}^\circ)^2 + k_5\Delta_3/k_4$$

where $k_5 = 2c_{\pm}^\circ k_4$
In this case there results

$$\begin{cases} \dfrac{d\Delta_1}{dt} = -k_1\Delta_1 + k_2\Delta_2 \\ \dfrac{d\Delta_2}{dt} = k_1\Delta_1 - k_2\Delta_2 - k_3\Delta_2 + k_5\Delta_3 \\ \dfrac{d\Delta_3}{dt} = k_3\Delta_2 - k_5\Delta_3 \end{cases}$$

or written in matrix notation

$$\frac{d\Delta}{dt} + A\Delta = 0$$

where

$$A = \begin{pmatrix} k_1 & -k_2 & 0 \\ -k_1 & k_2 + k_5 & -k_5 \\ 0 & -k_3 & k_5 \end{pmatrix}; \quad \Delta = \begin{pmatrix} \Delta_1 \\ \Delta_2 \\ \Delta_3 \end{pmatrix}$$

The general solution of this system, which is easily obtained on diagonalization of the matrix (*cf. e.g.* Frost and Pearson [22] or Matsen and Franklin [23]), can be written as linear combinations of exponential functions

$$\Delta = e^{-At}\,\Delta_0 \quad \text{or} \quad \Delta_r = \sum_{s=1}^{3} b_{rs}\, e^{-\lambda_s}$$

where b_{rs} are constants (components of the eigenvectors) and λ_s are the eigenvalues of the matrix, or solutions of the secular equation:

$$\begin{vmatrix} k_1 - \lambda & -k_2 & 0 \\ -k_1 & k_2 + k_3 - \lambda & -k_5 \\ 0 & -k_3 & k_5 - \lambda \end{vmatrix} = 0$$

This equation has three solutions

$$\lambda_1 = 0$$
$$\lambda_2 = \tfrac{1}{2}(p+q)$$
$$\lambda_3 = \tfrac{1}{2}(p-q)$$

where

$$p = k_1 + k_2 + k_3 + k_5$$
$$q = [p^2 - 4(k_1k_3 + k_2k_5 + k_1k_5)]^{1/2}$$

Now $\lim_{t\to\infty} \Delta_r = 0, \qquad r = 1,2,3.$

Hence $b_{r1} = 0, \qquad r = 1,2,3.$

The second term in the expression for Δ_r, *i.e.* $b_{r2}\ e^{-\lambda_2 t}$, becomes negligible very quickly since λ_2 is large ($k_3,k_5 \rangle\rangle k_1,k_2$). Thus the relaxation is approximately described by

$$\Delta_r = b_{r3}\ e^{-\lambda_3 t}$$

and we have for the relaxation time

$$\tau = 1/\lambda_3$$

or, since $(k_1k_3 + k_2k_5 + k_1k_5) \langle\langle\ p^2$, we may approximate

$$\frac{1}{\tau} = \lambda_3 = \tfrac{1}{2}\ p\left(1 - \sqrt{1 - 4\cdot\frac{k_1k_3 + k_2k_5 + k_1k_5}{p^2}}\right) \approx$$
$$\approx \frac{k_1k_3 + k_2k_5 + k_1k_5}{p} = \frac{k_1k_3 + k_2k_5 + k_1k_5}{k_1 + k_2 + k_3 + k_5}$$

Utilizing the fact that $k_1,k_2 \langle\langle k_3,k_5$, we may approximate further

$$\frac{1}{\tau} \approx \frac{k_1k_3 + k_2k_5 + k_1k_5}{k_3 + k_5} = k_1 + \frac{k_2k_5}{k_3 + k_5}$$

Resubstituting

$$k_5 = 2k_4c_\pm^\circ$$

we obtain

$$\frac{1}{\tau} \approx k_1 + \frac{2k_4c_\pm^\circ k_2}{2k_4c_\pm^\circ + k_3}$$

Denoting the true dissociation constant of H_2CO_3 by $K_s = k_3/k_4$, we finally obtain

$$\frac{1}{\tau} \approx k_1 + \frac{2c_\pm^\circ k_2}{2c_\pm^\circ + K_s}$$

This expression agrees asymptotically with those given by Eigen [24] for the two limiting cases *, $2c_\pm^\circ \rangle\rangle\ K_s$ and $2c_\pm^\circ \rangle\rangle\ K_s$. The former is equivalent to the simple case treated in the preceding section.

* $2c_\pm^\circ \langle\langle K_s$ means that the dissociation of H_2CO_3 is practically complete, *i. e.* we are concerned with the reaction: $CO_2 + H_2O \rightleftharpoons H^+ + HCO_3^-$. In this case we have

$$1/\tau = k_1 + 2k_2c_\pm/K_s.$$

$2c_\pm^\circ \rangle\rangle K_s$ means that the dissociation of H_2CO_3 is very small, *i. e.* we would have the reaction $CO_2 + H_2O \rightleftharpoons H_2CO_3$, with the rate of relaxation determined by $1/\tau = k_1 + k_2$.

b. Experimental. In view of the theoretical considerations given above, it is now possible by carrying out experiments at various concentrations to determine the rate constants k_1, k_2 and the true dissociation constant K_s as well as the hydration constant K_h. For, utilizing the fact known from earlier investigations that $k_1 \ll k_2$ *, the equation

$$\frac{1}{\tau} = k_1 + \frac{2c_{\pm}^{\circ} k_2}{2c_{\pm}^{\circ} + K_s}$$

may in our case be replaced by

$$\tau = \frac{1}{k_2}\left(1 + \frac{K_s}{2c_{\pm}^{\circ}}\right)$$

Denoting the equivalent ionic conductances by l, we have for the conductivity (neglecting the difference between the actual equivalent conductivities and those at infinite dilution):

$$\varkappa = 10^{-3} c_{\pm}^{\circ} \; (l_{H+}^{\circ} + l_{HCO_3^-}^{\circ})$$

Now

$$J = R \; \varkappa$$

where J is the cell constant and R the resistance of the cell. Hence

$$1/c_{\pm}^{\circ} = 10^{-3} \; (l_{\pm+}^{\circ} + l_{HCO_3^-}^{\circ}) \; R/J$$

If this is inserted in the expression for τ we obtain

$$\tau = 1/k_2 + 10^{-3} K_s \; (l_{H+}^{\circ} + l_{HCO_3^-}^{\circ}) \; R/2Jk_2$$

Consequently we may plot τ *versus* R to obtain a straight line.

The results of the experiments are given in Table 1 and shown in Fig. 7.

Table 1. Chemical relaxation time for aqueous solutions ** of CO_2 at 4°C and 150 atm pressure.

R	R_{corr} ***	τ
5.24 kΩ	5.20 kΩ	0.76 sec
5.24	5.20	0.77
5.98	5.93	0.62
5.98	5.93	0.61
9.13	9.06	0.75
9.13	9.06	0.72
9.13	9.06	0.83
13.7	13.6	0.92
13.7	13.6	0.95
16.4	16.2	1.30
16.4	16.2	1.19

* *cf.* Table 2.

** The carbon dioxide solutions were prepared by bubbling CO_2 through conductivity water and then diluting to the desired concentration. Since losses of CO_2 were difficult to avoid, it is more reliable to use the conductivity for the concentration determination throughout.

*** R_{corr} denotes the values corrected for the volume change on compression to 150 atm.

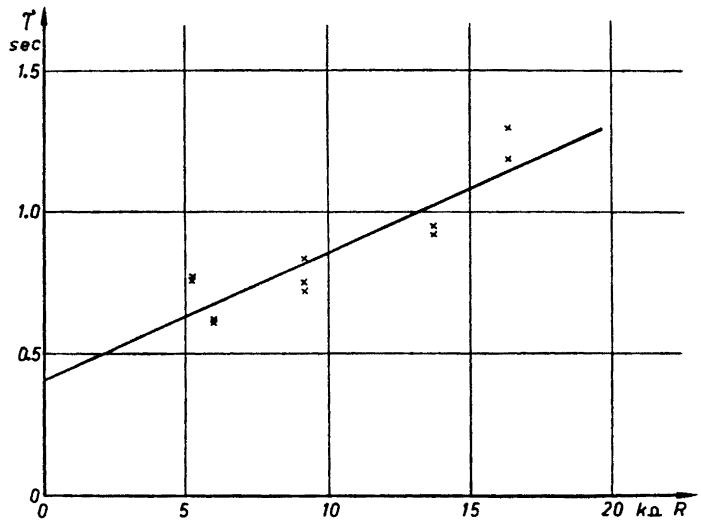

Fig. 7. Plot of τ *versus* R from experiments with CO_2-H_2O at 4°C.

A straight line has been fitted to the points in Fig. 7 using the method of least squares. The equation of this line is

$$\tau = aR + b$$

where

$$a = (0.045 \pm 0.006)10^{-3} \text{ sec ohm}^{-1}$$

$$b = (0.409 \pm 0.025)\text{sec}$$

Thus

$$k_2 = 1/b = 2.4 \text{ sec}^{-1}$$

and with

$$K_s = 2 \times 10^3 \, Jk_2a/(l^{\circ}_{H+} + l^{\circ}_{HCO_3^-})$$

insertion of the various quantities yields

$$K_s = 1.6 \times 10^{-4}$$

In these experiments, a cell with $J = 0.21$ cm^{-1} was used.

If we denote the hydration constant of carbon dioxide by K_h:

$$K_h = c_{H_2CO_3}/c_{CO_2} = k_1/k_2$$

and the apparent primary dissociation constant of carbonic acid by K_{sh}:

$$K_{sh} = \frac{c_{H+} \cdot c_{HCO_3^-}}{c_{CO_2} + c_{H_2CO_3}}$$

it is well known that

$$K_{sh} = \frac{K_s K_h}{1 + K_h}$$

Inserting our values for K_s and k_2 and the known [25] value of K_{sh} (interpolation yields $K_{sh} \approx 2.94 \times 10^{-7}$ at 4°C) we obtain

$$K_h = 1.8 \times 10^{-3}$$
$$k_1 = 4.4 \times 10^{-3} \text{ sec}^{-1} \text{ mole}^{-1} \text{ l}$$

c. *Discussion.* The results of our present investigation at 4°C and 150 atm are *

$k_1 = 4.4 \times 10^{-3}$ sec^{-1} mole^{-1} l
$k_2 = 2.4$ sec^{-1}
$K_h = 1.8 \times 10^{-3}$
$K_s = 1.6 \times 10^{-4}$

Some previous results are given in Table 2 for comparison.

Table 2. Previous results for k_1, k_2, K_s and K_h.

Ref.	Investigator	Method	k_1	k_2	K_s	K_h	temp. °C
26	Saal 1928	flow method, conductivity		8			13.5
26	» 1928	» » hydrogen electrode		10.2			20
27	Roughton 1935	» » rapid thermal		12.1			19.7
27	» 1936	» » photoelectric		9.5			15
28	Roughton 1941	» » rapid thermal		1.97	2.5×10^{-4}		0
28	» 1941	» » » »		19			14
28	» 1941	» » » »		30			27
29	» 1949	» » » »	0.002	2.0		1/1 000	0
29	» 1949	» » » »	0.013	11.0		1/ 826	15
29	» 1949	» » » »	0.033	26.6		1/ 807	25
29	» 1949	» » » »	0.110	89.0		1/ 818	38
30	Wissburn et. al. 1954	high field conductivity			1.56×10^{-4}	1.95×10^{-3}	5
30	» 1954	» » »			1.76×10^{-4}	2.16×10^{-3}	15
30	» 1954	» » »			1.72×10^{-4}	2.59×10^{-3}	25
30	» 1954	» » »			1.67×10^{-4}	2.94×10^{-3}	35
30	» 1954	» » »			1.59×10^{-4}	3.15×10^{-3}	38
30	» 1954	» » »			1.60×10^{-4}	3.23×10^{-3}	45
31	Meier & Schwarzenbach 1957	flow method, glass-electrode (ionic strength = 0.1)	0.025	10	$10^{-3,58}$		20

* It was observed that curves corresponding to a much shorter relaxation time were obtained at 18°C consistent with the temperature dependence of the rate constants. However, no quantitative experiments were carried out at this temperature.

By carrying out experiments at two different temperatures, it would, however, be possible to determine the activation energies of the various steps of the reaction between CO_2 and water.

The dispersion of the points in Fig. 7 indicates that the precision of the method is not yet very great. There are two imperfections in the electric circuit which should be mentioned. One is the deviation from linearity of the rectifier. Although the recording system was calibrated before each run, a certain loss of accuracy is always obtained. The other is the "overshoot" effect produced by the resonance compensating arrangement of the recorder. This imperfection is present in all mechanical oscillographs and cannot be avoided unless very particular measures are taken. These systematic erros together with the accidental errors of the recording system and errors in the evaluation of the relaxation curves cause an error in the τ values obtained of an order of magnitude from 10 % to 20 % in unfavourable cases. It seems however that, using more elaborate components in the electric system, it will be possible to increase the accuracy.

The low ionic concentrations in the experiments with the volatile CO_2-water system makes these determinations particularly difficult.

In the experiments it was observed that the balancing capacitance of the cell had to be changed when the pressure was applied. This was considered to be without influence on the determinations. It would be possible, by the use of a phase sensitive rectifier, to study this effect which is, at least in part, of a purely mechanical nature (a change in the capacitance of the leads).

Acknowledgement. A pressure method for the determination of micelle formation rates was independently proposed several years ago by G. Aniansson of this Institute.

The financial support of *Statens Naturvetenskapliga Forskningsråd* is most gratefully acknowledged.

REFERENCES

1. *Discussions Faraday Soc.* **17** (1954) 114 f.f.
2. Weissberger, A. *Technique of Organic Chemistry*, vol. VIII, Ch. X, New York 1953.
2a. DuBois, D. *J. Biol. Chem.* **137** (1941) 123.
3. Onsager, L. *J. Chem. Phys.* **2** (1934) 599.
4. Harned, H. S. and Owen, B. B. *The physical chemistry of electrolytic solutions*, 3rd ed., New York 1958, p. 96.
5. *Discussions Faraday Soc.* **17** (1954) 202.
6. La Mer, V. K. and Read, C. L. *J. Am. Chem. Soc.* **52** (1930) 3098.
7. Loewenstein, A. *J. Chem. Phys.* **27** (1957) 1067.
8. Gilkersson, W. R. *J. Chem. Phys.* **27** (1957) 914.
9. Delahay, P. *J. Am. Chem. Soc.* **73** (1951) 4944.
10. Henke, K. H. and Hans, W. *Z. Elektrochem.* **57** (1953) 591, 595.
11. Vetter, K. J. *Z. physik. Chem.* **194** (1950) 199, 284.
12. Gerischer, H. and Vetter, K. J. *Z. physik. Chem.* **197** (1951) 92.
13. Gierst, L. and Juliard, A. *J. Phys. Chem.* **57** (1953) 701.
14. Delahay, P. and Berzius, T. *J. Am. Chem. Soc.* **75** (1953) 2486, 4205.
15. Gerischer, H. *Z. physik. Chem.* **2 (1/2)** (1954) 79.
16. Hamman, S. D., and Linn, S. C. *Australian J. Chem.* **7** (1954) 329.
17. Bridgman, P. W. *The physics of high pressure*, London 1949.
18. Glasstone, S. Laidler, K. and Eyring, H. *The theory of rate processes*, New York 1941, p. 470.
18a. Van Santen, G. W. *Introduction to a Study of Mechanical Vibration*, 2nd ed., Eindhoven 1958, p. 52.
19. Carrington, T. and Davidson, N. *J. Phys. Chem.* **57** (1953) 418.
20. *Discussions Faraday Soc.* **17** (1954) 58.
21. Pinsent, B. and Roughton, F. *Trans. Faraday Soc.* **47** (1951) 263.

22. Frost, A. A. and Pearson, R. G. *Kinetics and mechanism*, New York 1953.
23. Matsen and Franklin *J. Am. Chem. Soc.* **72** (1950) 3337.
24. Eigen, M. *Z. physik. Chem.* **1 (3/4)** (1954) 176.
25. Shedlovsky, T. and Mc Innes, D. *J. Am. Chem. Soc.* **57** (1935) 1705.
26. Saal *Rec. trav. chim.* **47** (1928) 264.
27. Roughton, F. and Millikan *Proc. Roy. Soc. London* **A 155** (1936) 272.
28. Roughton, F. *J. Am. Chem. Soc.* **63** (1941) 2930.
29. Pinsent, B. and Roughton, F. *Intern. Congr. Biochem., Abstrs of Communs*, 1st Congr., Cambridge, England, 1949, p. 375.
30. Wissburn, K. F. et al. *J. Phys. Chem.* **58** (1954) 693.
31. Meier, J. and Schwarzenbach, G. *Helv. Chim. Acta* **40** (4) (1957) 907.

Received July 9, 1958.

ACTA CHEMICA SCANDINAVICA 12 (1958) 1851—1868

Electrophoretic and Ultracentrifugal Study of Plaice Myogen

J. W. JEBSEN* and G. HAMOIR**

Laboratory of General Biology, University of Liège, Belgium

The protein composition of water extracts and myogen of plaice muscle has been investigated by electrophoresis and ultracentrifugation. Plaice myogen has been fractionated with neutral ammonium sulphate in the whole range of saturation and the different fractions analysed by both methods. The salting-out range of the various electrophoretic and ultracentrifugal gradients has been determined. Usually the components precipitating at a higher salt concentration sediment more slowly and migrate more rapidly in the electrical field. Some properties of two crystalline albumins have been described. The isolation of a third component by preparative electrophoresis has allowed to show that the protein of abnormal amino acid composition discovered in carp myogen also occurs in plaice. Although the muscle extracts of low ionic strength present a high specificity from the electrophoretic point of view, their more detailed study will make the common properties of their protein constituents more conspicuous.

Fish muscle extracts of low ionic strength have been investigated electrophoretically in several laboratories. Carp [1–7] and cod [8,9] have been examined fairly extensively while general surveys of about 25 species including *Gadidae*, *Pleuronectidae*, *Selachii* and fresh-water fishes have been carried out by *Connell* [10] and by Nikkilä and Linko [11]. These surveys have, however, been limited to the electrophoretic analysis of whole extracts. A fractionation scheme with ethanol at low temperature has been described [11] but applied only on a small scale and to pike muscle extracts, the fractions obtained being characterized by paper electrophoresis. The separation of the albumins and globulins of the whole extracts by dialysis against water and the electrophoretic analysis of the myogens isolated in this way have been carried out on cod [8], carp [1–4] and plaice [12]. The fractionation of the carp myogen with neutral ammonium sulphate has been investigated in Liège by Henrotte [5–7] who crystallized two carp albumins and described some of their properties (*cf.* also Hamoir [13]). Preliminary experiments have also been done on plaice myogen resulting in the crystallization of another muscle albumin [12,14].

* Norwegian Fisheries Research Institute, Bergen, Norway.
** Associé du Fonds National de la Recherche Scientifique.

A systematic study of the fractionation of fish myogens is thus still lacking. We have thought it therefore of interest to investigate more completely the electrophoretic and ultracentrifugal behaviour of plaice muscle extracts of low ionic strength, of plaice myogen and of fractions isolated from it with neutral ammonium sulphate in the whole range of saturation. A preliminary report of a part of this work has already been published [15].

METHODS

Plaice *(Pleuronectes platessa* L.) was caught on the Belgian coast, immediately eviscerated and kept in ice for about 20 h before filleting. The muscles are cut into small blocks and stored at −20°C for 1 to 30 days in closed containers in order to avoid evaporation. All operations are carried out at 0°C. Muscles fragments are cut in slices 40 μ thick with an automatic freezing microtome [16]. The muscle pulp is mixed with one volume of water and gently stirred for one hour. The extract is sometimes dialyzed for 48 h against 2 l of a phosphate buffer of μ 0.05 and pH 7.5 renewed once (0.0156 M Na_2HPO_4 + 0.0035 M KH_2PO_4). The precipitate formed is spun down and the supernatant examined by electrophoresis or ultracentrifugation. Usually the dialysis is carried out against the same volume of distilled water renewed several times for three days in order to remove completely the globulins. The myogen is then fractionated with neutral ammonium sulphate or dialyzed against the usual buffer of μ 0.05 and pH 7.5 before electrophoretic or ultracentrifugal analysis.

For fractionation, a mixture of solid ammonium sulphate and disodium phosphate (0.71 g $Na_2HPO_4 \cdot 12\ H_2O$/100 g ammonium sulphate) is added to the rapidly stirred solution. The precipitate formed is removed immediately except in the case of the last fraction (90 − 100 % saturation) which is left overnight in the cold room before centrifugation. In the calculation of the degree of saturation, we have admitted that the total amount of salt added correspond only to ammonium sulphate and we have taken account of the variations of volume occurring: the degree of saturation used corresponds to the percentage of the salt concentration of the saturated solution at 0°C (*cf.* Brenner-Holzach and Staehelin [17]). After dialysis the protein content of the solutions is determined with a dipping refractometer. Samples of the protein solution and of the dialysis fluid are placed in a water bath of constant temperature (25°C) and illuminated with a sodium lamp (589 mμ). The refractive increment corresponding to a concentration of 1 g/100 ml has been taken equal to 182×10^{-5} according to determinations by Hamoir [3] on carp myogen.

Electrophoresis is conducted at 1°C in a Tiselius apparatus slightly modified [18], the recording of the patterns beeing made according to the Longsworth's procedure [19,20]. The mobilities are calculated from the mean conductivity of the buffer and the protein solution and from the maximum ordinate of the gradients. At the low ionic strength used, the ascending mobilities notably exceed the descending ones and depend on the protein concentration. A correction according to Longsworth and Mac-Innes [21] has however not been applied. We will thus consider mainly the descending values. The relative concentrations of the different gradients have been determined according to the perpendicular extrapolation method of Tiselius and Kabat [22]. At the low ionic strength used, an overestimation of the quick gradients at the expense of the slow ones may occur particularly on the ascending side [23]. Our surface determinations did not, however, disclose notable discrepancies between the ascending and the descending values (*cf.* Table 3). This anomaly appears thus usually not very pronounced here. A further check of its importance by use of higher ionic strength has not been made.

The ultracentrifugations are carried out with an ultracentrifuge Spinco Model E in the department of Physical Chemistry (Prof. V. Desreux). The rates of sedimentation are corrected for water and 20°C, use being made of the mean partial specific volume given in Svedberg and Pedersen's [24] Appendix II. The relative concentrations are also calculated according to Tiselius and Kabat [22]. No account is taken of the decrease of concentration of the slower components occurring at the different boundaries observed which lead to an overestimation of the slow components at the expense of the quick ones [25].

Some measurements of absorption in the ultraviolet have been made with a D. U. Beckman spectrophotometer.

RESULTS

A. The protein composition of whole extracts and myogen

a) *Content in albumins and globulins.* The amounts of proteins isolated after one or several extractions with water and subsequent dialysis against a phosphate buffer of μ 0.05 and pH 7.5 or water are given in Table 1. Although each extract was made from about 10 fishes, notable variations occur from one extraction to the other reminiscent of those observed on the carp [3]. The amounts of globulin X and myogen obtained after exhaustive extraction are definitely lower than the values given for the carp [3]. The content of myogen of plaice muscle is lower than the ones of carp white or red muscles; if one assumes a protein content of 16 %, it would represent only 13 % of the muscle proteins. In the case of globulin X, the difference is perhaps not significant owing to the lower ionic strength used in the present experiments.

b) *Electrophoretic analysis.* The electrophoretic pattern of the whole extract at μ 0.05 and pH 7.5 is given in Fig. 1 a. Its peaks are numbered according to Connell's nomenclature. Four gradients are visible on the ascending side. The quickest small ascending peak of Connell [10] is not observable here. It is not always present in the electrophoretic patterns. The quickest fraction of Fig. 1 a is heterogeneous and corresponds to the component 1 a of Connell [10]. Peak 2 is well defined on the ascending and descending sides; it is separated

Table 1. Content in albumins and globulin X of plaice muscles (g protein/100 g fresh muscle).

Expt. No.	A			B		
	$Q_{sol.}$ at μ 0.05 pH 7.5	$Q_{sol.}$ at μ 0	% globulin X	$Q_{sol.}$ at μ 0.05 pH 7.5	$Q_{sol.}$ at μ 0	% globulin X
1	2.00	1.44	28			
2	1.70	1.06	38			
3	1.81	1.43	21	2.53	1.98	22
4	1.95	1.58	19	2.50	1.97	21
5	1.87	1.44	23			
6	2.19	1.61	26			
7				3.32	2.26	32
8				3.18	1.92	40
9				3.28	2.08	37
Mean	1.92	1.43	25	3.26 *	2.04	36
Carp white muscles. Mean (from Hamoir [3]).				3.82	2.70	29

A Extraction with one vol. of water and subsequent dialysis against μ 0.05 of pH 7.5 or water.

B Successive extractions with one, two and one vol. of water and subsequent dialysis against μ 0.05 of pH 7.5 or water.

* Mean of experiments 7, 8 and 9. The lower values of experiments 3 and 4 are apparently due to a partial extraction of the globulins.

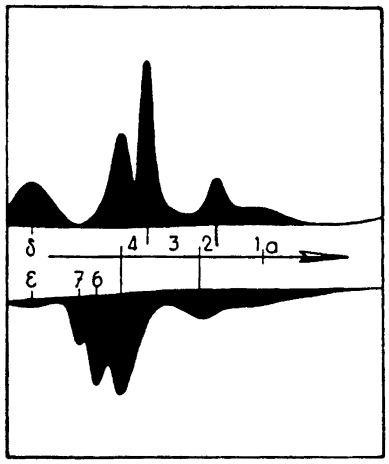

a

Fig. 1 a. Electrophoretic pattern of a water extract of plaice muscle dialysed at μ 0.05 and pH 7.5. Upper diagram: ascending limb. Lower diagram: descending limb. Migration to the right. Conditions of electrophoresis: conc. 1.54 %; μ 0.05; pH 7.5; electrical field 6.6 V/cm; duration: 125 min.

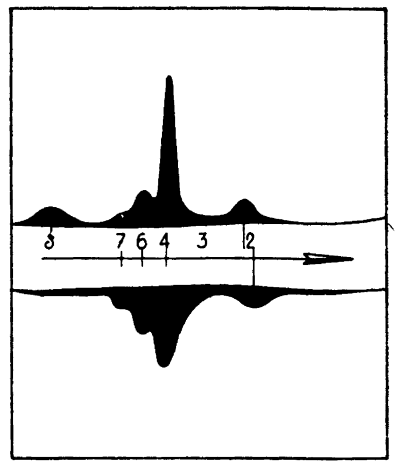

b

Fig. 1 b. Electrophoretic pattern of the myogen fraction of a water extract of plaice muscle. Upper diagram: ascending limb. Lower diagram: descending limb. Migration to the right. Conditions of electrophoresis: conc. 0.96 %; μ 0.05; pH 7.5; electrical field field 6.6 V/cm; duration: 130 min.

from the main peak 4 by a heterogeneous fraction numbered 3. The slowest ascending gradient appears fairly symmetrical; prolonged electrophoresis reveals, however, that it splits into two gradients on the descending side. As some fractionations have shown that a component of intermediate mobility occurs between gradient 4 and this slow peak, it has been represented by the numbers 6 and 7 instead of 5 and 6 previously used [10].

If the extract of Fig. 1 a is dialysed against water, the globulin X fraction precipitates. The supernatant obtained after centrifugation gives a somewhat different electrophoretic pattern (Fig. 1 b). The components 1 and 1 a disappear. The relative proportion of peak 4 increases definitely. The following slow ascending peak is notably reduced and the two gradients corresponding to numbers 6 and 7 separate now clearly on both limbs.

The mobilities of these different gradients are given in Table 2 together with the data obtained by Connell [10] in a single experiment. Connell's values are much lower. In view of the larger number of experiments and of the good agreement of our results, our data are probably more correct. The percentages of the different gradients are given in Table 3. They are similar to the ones given earlier [10]. The measurements made on myogen and the determinations of the proportion of globulin X in these extracts allow to estimate the amount of globulin X corresponding to each peak (*cf.* Table 1). As the total content in globulins varies notably from one extract to the other (*cf.* Table 1), these evaluations are approximate. They show nevertheless that the peaks 3 and 4

Table 2. Electrophoretic mobilities ($\times 10^5$) of plaice muscle extracts of low ionic strength, of the corresponding albumin fraction and of the fractions isolated from plaice myogen with neutral ammonium sulphate at μ 0.05 (phosphate) and pH 7.5.

Protein comp.	Number of electroph.	Prot. conc. in %		Components							
				1	1 a	2	3	4	5	6	7
Whole extract (myogen + globulin x)	3	1.75 ± 0.2	D	8.5	—	6.66	—	3.73	—	2.86	2.26
Connell's data	1	—		9.45	6.55	5.4	4.3	3.05	—	2.35	1.60
Myogen	5	1.11 ± 0.15	D	—	—	6.74	—	3.75	—	2.86	2.13
Myogen fractions precipitated between:											
0—40 % saturation	2	1.5	A	7.74 *	7.17	—	—	4.61	3.76 (1)	3.16 (1)	—
			D	7.55 *	6.95 (1)	—	—	3.87	3.08 (1)	2.46 (1)	—
40—55 » »	3	1.5	A	10.44 ± 0.55 (2)	8.55 ± 0.8 (2)	—	—	4.40	4.07	3.63	—
			D	9.2 ± 0.4 (2)	7.0 ± 0.3 (2)	—	—	3.66	2.86		
40—48 » »	3	1.5	A	—	—	7.13 (2)	—	4.38	—	3.56	—
			D	—	—	6.40 (2)	—	3.57	—	2.77	—
48—55 » »	3	1.5	A	9.3	—	—	—	4.47	3.98	3.67	—
			D	8.37 (1)	—	6.75 (2)	—	3.72	3.0		—
55—65 » »	3	1.5	A	—	8.46 (1)	6.78 (2)	4.93 (1)	4.42	3.74	3.49	2.84 (2)
			D	—	—	6.38 (2)	—	3.62	2.80		2.16 (2)
70—80 » »	3	1.5	A	—	—	7.14	—	4.54	—	3.48	2.77
			D	—	—	6.68	—	3.68	—	2.81	2.10
80—90 » »	3	1.5	A	—	—	7.19	5.0 (1)	4.49	—	3.56	2.70
			D	—	—	6.78	—	3.63	—	2.78	2.07
90—100 » »	3	1.5	A	—	—	7.75	—	4.89	4.12 (1)	3.67	2.73
			D	—	—	6.55	—	3.47	2.71 (1)	2.46	2.0

* Mobility intermediate between 1 and 1 a.
When a small gradient is not regularly present, the number of electrophoresis in which it occurs, is given between brackets.
A = Ascending values
D = Descending values

Table 3. Electrophoretic analysis of plaice muscle extracts of low ionic strength, of the corresponding albumin fraction and of the fractions isolated from plaice myogen with neutral ammonium sulphate at μ 0.05 (phosphate) and pH 7.5.

Protein comp.	Number of electroph.	Prot. conc. in %		Components							
				1	1a	2	3	4	5	6	7
Whole extract (myogen + globulin X)	3	1.75 ± 0.2	A	8.7		12.0	4.3	39.7	35.2		
			D	8.6		14.6	6.0	38.7	24.0		8.0
Connell's data		—	A	4.5	6.6	10.8	5.7	32.8	39.6		
			D	7.2	13	12.2	7.8	32.4	16.6		10.8
Myogen	4	1.11 ± 0.15	A	—	—	14.5	6.6	51.9	20.6		6.0
			D	—	—	14.4	7.6	50.5	20.6		6.6
Myogen fractions precipitated between:											
0—40 % saturation	1	1.5	A	—	4.6	5.4		76.7	9.6	3.8 *	—
			D	—	6.3	7.5		69.6	11.1	5.6	—
40—48 » »	2	1.5	A	—	—	—	—	—	—	—	—
			D	—	—	9.5	11.8	68.1	—	10.5	—
48—55 » »	2	1.5	A	4.9 *	8.1 *			44.0	30.3	12.6	—
			D	6.9 *	9.0 *			47.8	36.2		—
55—65 » »	2	1.5	A	—	8.0	15 *	5.9 *	25.0	16.0	30.1	—
			D	—	5.5	14.6 *	2 *	29.4	46.4		2.1
70—80 » »	2	1.5	A	—	—	5.2 *	12.1 *	65.6	—	5.6	11.6
			D	—	—	7	9.9 *	65.7	—	7.5 *	10.9
80—90 » »	2	1.5	A	—	—	14.4	3.3	53.4	—	11.8	17.0
			D	—	—	13.4	5.6 *	51.7	—	12.9 *	16.4
90—100 » »	3	1.5	A	—	—	44.2	2.5 *	23.7	5.3	18.6	9.5
			D	—	—	37.6	0.8	26.9	—	26.5	8.3

A = Ascending values
D = Descending values

* = heterogeneous

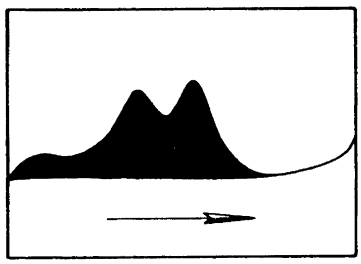

a

Fig. 2 a. Ultracentrifugal pattern of a water extract of plaice muscle dialysed at μ 0.05 and pH 7.5. Direction of migration: from left to right. Protein conc. 1 %; μ 0.05; pH 7.5. Duration of the ultracentrifugation: 56 min.

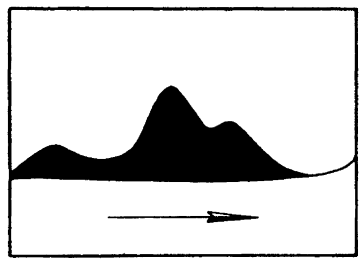

b

Fig. 2 b. Ultracentrifugal pattern of the myogen fraction of a water extract of plaice muscle. Direction of migration from left to right. Protein conc. 1 %; μ 0.05; pH 7.5. Duration of the ultracentrifugation: 64 min.

of whole extracts are entirely soluble in water while a partial precipitation of peak 2 occurs. Globulin X is formed mainly by the slow moving components 5, 6 and 7 and by the quick ones 1 and 1 a.

c) *Ultracentrifugal analysis.* Two ultracentrifugations of plaice myogen made by Henrotte [12] have shown that the three components sedimenting with rates of about 7, 5 and 1.5 *S* observed in carp myogen [3,4] are also present in this case. We have carried out further experiments on myogen and have examined whole extracts similar to those analysed by electrophoresis too.

The whole extract (Fig. 2 a) does not differ qualitatively from myogen (Fig. 2 b); it includes the three peaks already mentioned. Their corrected rates of sedimentation and relative concentrations are given in Table 4, together with similar data relative to the myogen. Notable variations occur in the rate of sedimentation of each peak. Two of the experiments of myogen carried out on two different concentrations and the surface measurements show that these variations cannot be due to changes in concentration. They also obviously exceed the experimental errors, particularly in the case of the slow and the median peaks. Several components of close rates of sedimentation are present in these two gradients. The comparison of the surface determinations relative to whole extracts and myogen allows also to estimate the amount of globulins occurring in each peak of the whole extract. After dialysis against water the slow peak remains entirely in solution, the medium one precipitates in the proportion of about 25 % (*cf.* Table 1) and the third one about 50 %. Fish muscle extracts of low ionic strength appear thus to behave very similarly in the ultracentrifuge. They seem to contain generally the slow sedimenting components first observed by Deuticke [26] on frog muscle extracts which do not occur in rabbit muscles and therefore not in muscles of warm-blooded animals. They differ only from each other in the proportions of the different gradients observed.

Table 4. Ultracentrifugal analysis of plaice muscle extracts of low ionic strength, of the corresponding albumin fraction and of the fractions isolated from plaice myogen with neutral ammonium sulphate at μ 0.05 (phosphate) and pH 7.5.

Protein comp.	Total conc. in % protein	Number of ultracent.	Corrected rate of sedimentation			Composition in % of the total area		
			Slow peak	Median peak	Quick peak	Slow peak	Median peak	Quick peak
Whole extract	1	2	1.53 ± 0.31	4.97 ± 0.01	7.08 ± 0.03	11.6 ± 0.7	43.2 ± 3.3	45.3 ± 2.2
(myogen + globulin_X)	0.71	1	1.47	5.10	7.24	13.3	47.1	39.6
Myogen	1	3	1.39	5.07	7.23	20.6	50.8	28.3
	0.5	2	1.55	5.28	7.55	22.6	51.1	26.3
Myogen of carp	1.32 [a]	3	1.45 [a]	4.85 [a]	7.10 [a]	48 [a]	39 [a]	13 [a]
Myogen fractions precipitated between								
0— 40 % sat.	1	1	1.58	5.96	8.03	4.1	7.3	88.5
0— 48 » »	1	1	1.97	5.53	7.76	8.6	7.3	84.2
	0.5 [b]	1	2.14	5.72	8.09			
40— 48 » »	1	1	—	—	7.64	5	10.7	84.3
48— 55 » »	1	1	—	5.63	7.52	0	15.9	84.1
55— 65 » »	1	1	—	5.32	7.05—9.29 [c]	0	63.1	23.1—13.8 [c]
70— 80 » »	1	2	—	4.73	—	8.3 [d]	84.8	6.8
	0.5 [b]	1	—	4.91	—	0	92.6	7.4
80—100 » »	1	1	1.15	5.36	6.99	50.2	34.5	15.3
	0.5 [b]	1	1.23	5.38	—			
90—100 » »	1	1	1.29	—	7.07			
	0.5 [b]	1	1.42	4.10	7.18	58.4	17.5	24.1

[a] Mean of three ultracentr. at 1.07, 1.1 and 1.8 %. [b] Preparation obtained by dilution of the preceding one of 1 %. [c] Component moving ahead of the quick component not apparent in whole myogen. [d] Heterogeneous.

B. The fractionation of myogen with neutral ammonium sulphate

The range of salt fractionation up to 65 % has already been briefly examined by Henrotte [12,14]. He has considered the fractions corresponding to 0—40, 40—48, 48—55 and 55—65 % of saturation at pH 6.5 and analysed the fractions 40—48 and 48—55 by ultracentrifugation. The first one sediments as a single peak of about 7 *S*; the second one is a mixture of the previous component and of another one of about 5 *S* which could be crystallized [12,14].

We have fractionated plaice myogen at neutral pH in the whole range of saturation. In order to avoid arbitrariness in the determination of the zones of fractionation, a salting-out curve has first been measured by ultraviolet absorption up to 65 % saturation. The precipitation starts at 35 % saturation and increases progressively without definite break of the curve. There was therefore no reason to change the earlier zones of fractionation. The main fractions examined are 0—40, 40—48, 48—55, 55—65, 70—80, 80—90 and 90—100 %. The amount of protein isolated in each of these fractions is given in Table 5. Two major ranges of precipitation appear clearly separated by the small zone 65—70 % of lower precipitation.

a) *Electrophoretic analysis of the fractions.* All the fractions considered except fraction 65—70 % have been isolated several times in order to check the reproducibility of the electrophoretic results. Many overlapping fractions have also been considered such as 40—55, 48—65, 65—80, 70—100, 80—100 whose results are mainly confirmatory of the previous ones and will therefore usually not be described here. The relative positions of some peaks pertaining to different fractions have been controlled by mixing some fractions and examining the elctrophoretic pattern of the mixture. The results obtained are summarized in Fig. 3.

The fractionation discloses some new peaks which are not observed in plaice myogen. Small quick heterogeneous gradients are visible on the ascending side in the fractions isolated up to 65 % saturation (Fig. 3a, b, c, d); the only ones which appear more or less homogeneous migrate at the level of 1a in fractions 0—40 and 55—65 %. Component 2 remains soluble up to

Table 5. Partition of myogen by ammonium sulphate fractionation at neutral pH.

Zone of saturation		0—40	40—48	48—55	55—65	65—70	70—80	80—90	90—100
% of myogen precipitated	a)	4.5	8.05	11.15	10.7	2.0	28.4	26.5	8.8
	b)	4.2	6.0	10.5	11.8	3.0	32.2	22.4	8.7
	c)	4.1	6.9	14.3	13.8	2.4	25.6	25.1	8.1
Mean		4.3	7.0	12.0	12.1	2.5	28.7	24.7	8.5
Content in g/100 g fresh muscle *		0.09	0.14	0.24	0.25	0.05	0.59	0.50	0.17

* Assuming the myogen content of 2.04 g/100 g fresh muscle of Table 1.

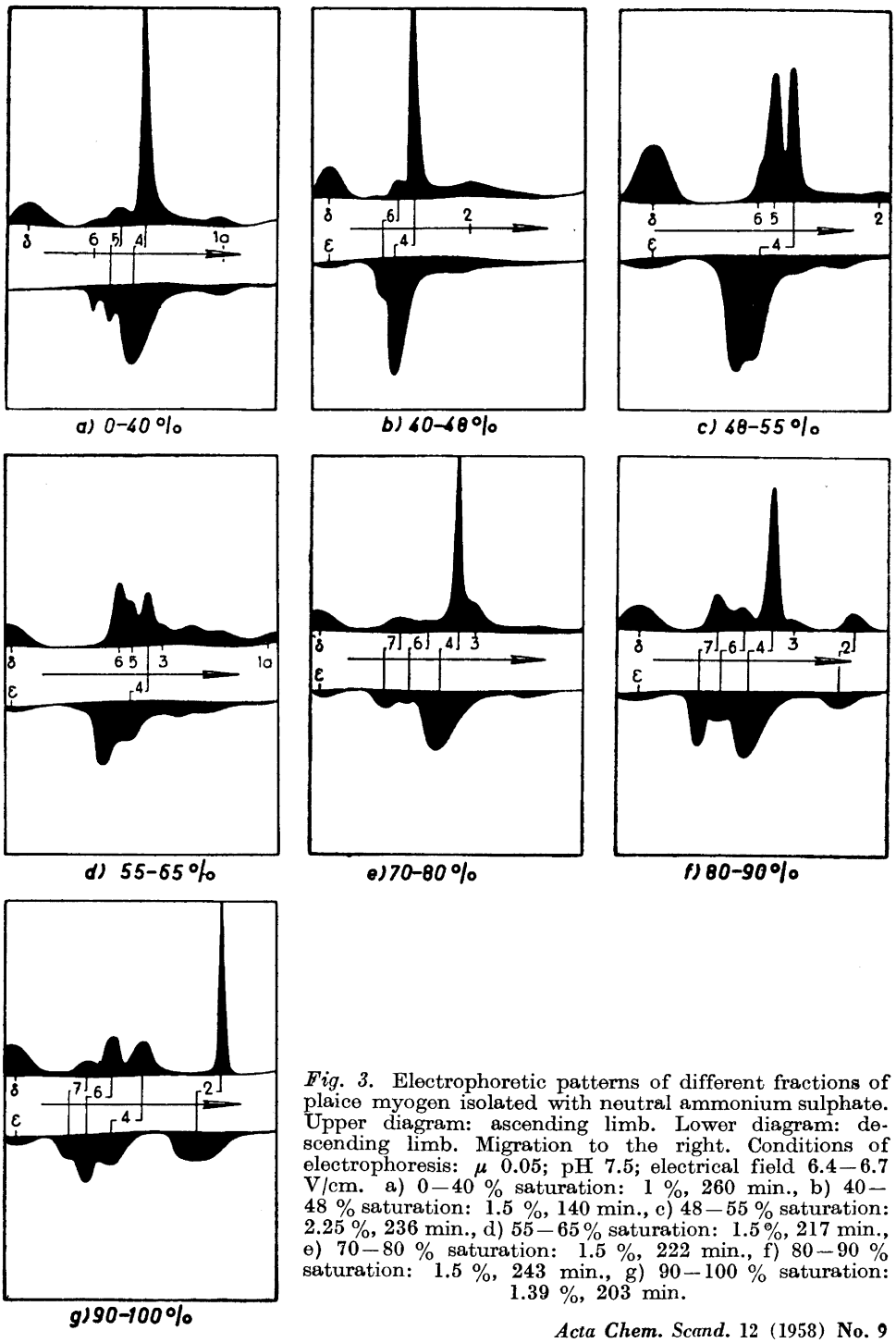

Fig. 3. Electrophoretic patterns of different fractions of plaice myogen isolated with neutral ammonium sulphate. Upper diagram: ascending limb. Lower diagram: descending limb. Migration to the right. Conditions of electrophoresis: μ 0.05; pH 7.5; electrical field 6.4—6.7 V/cm. a) 0—40 % saturation: 1 %, 260 min., b) 40—48 % saturation: 1.5 %, 140 min., c) 48—55 % saturation: 2.25 %, 236 min., d) 55—65 % saturation: 1.5 %, 217 min., e) 70—80 % saturation: 1.5 %, 222 min., f) 80—90 % saturation: 1.5 %, 243 min., g) 90—100 % saturation: 1.39 %, 203 min.

70 % saturation; it precipitates mainly in the fractions 80—90 % and 90—100 %. Component 3 which does not appear clearly in whole myogen is somewhat better defined in Fig. 3d, e and f. The proportion of component 4 in the different fractions varies suprisingly: it decreases up to 55—65 % and increases again in fractions 70—80 and 80—90 %. This behaviour suggests that this peak corresponds to at least two components of different solubilities. Component 5 separates from component 6 after prolonged electrophoresis on the ascending side in fractions 48—55 and 55—65 % (Fig. 3c and d) as a sometimes important peak although it is not visible in myogen. It corresponds probably to a rapid portion of the gradient 6 of myogen which does not clearly resolve from this gradient because of its low concentration in myogen. Component 7 is fairly soluble and precipitates in the range 70—100 % (Fig. 3e, f, g). The analysis of these electrophoretic patterns is given in Tables 2 and 3.

Our results differ somewhat from those obtained by fractionation of pike muscle extracts with ethanol [11]. It was found in this case that the solubility of the various components increases with the electrophoretic mobility. The

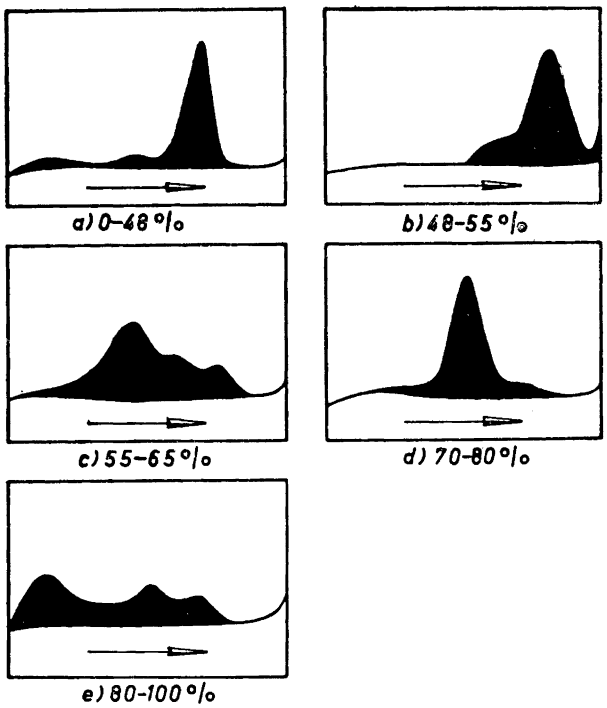

Fig. 4. Ultracentrifugal patterns of some fractions of plaice myogen isolated with neutral ammonium sulphate. Direction of migration: from left to right. Protein conc. 1 %; μ 0.05; pH 7.5. a) 0—48 % saturation, 56 min., b) 48—55 % saturation, 48 min., c) 55—65 % saturation, 56 min., d) 70—80 % saturation, 64 min., e) 80—100 % saturation, 76 min.

behaviour of components 7 and 4 of plaice myogen are in disagreement with these results. The quicker electrophoretic components are apparently generally more soluble but it is clear that this regularity has many exceptions.

b) *Ultracentrifugal analysis of the fractions.* Henrotte [12,14] has already shown that a single component of about 7 *S* is present in fraction 40—48 % while two of about 5 and 7 *S* are observed in the fraction 48—55 %. We have extended this analytical work to the various fractions described in the preceding paragraph. The main results obtained are summarized in Fig. 4.

The three ultracentrifugal gradients of plaice myogen precipitate on ammonium sulphate fractionation in very different ranges. The fractions 0—40 and 40—48 % contain nearly exclusively the quick peak (Fig. 4a). The median ones begin to precipitate in significant amounts in the range 48—55 % (Fig. 4b *) and occur as a single peak in the fraction 70—80 (Fig. 4d) with sometimes a slight admixture of the quick peak. The intermediate fraction 55—65 % is a mixture of the quick and the median components. It reveals also the occurrence of a new gradient sedimenting more quickly than the quick one of whole myogen. The slow gradient is present as an impurity in fraction 0—48 % and is the major component of the fraction 80—100 %. A nearly complete isolation of the quick and the median gradients and a considerable increase in concentration of the slow gradient are thus obtained by ammonium sulphate fractionation at neutral pH. The corrected rates of sedimentation and the relative amounts of the different peaks are given in Table 4. The surface determinations are somewhat inaccurate because of the difficulty in determining the exact position of the base line. In the case of the small gradients, a quick spreading is also usually observed which makes the determinations of the rates of sedimentation less precise. Some conclusions are nevertheless possible. The slow peak of plaice myogen precipitates in a small proportion in the range 35—48 % and mainly in the range 80—100 %. The two other peaks are more heterogeneous; they precipitate in the whole range. The rates of sedimentation are of the same order of magnitude for the fractions as for the total myogen. The higher variations observed are apparently due to the quick spreading of some gradients and to changes in concentration except perhaps for the quick peak which shows a progressive decrease of the rate when higher salting-out ranges are considered.

The comparison of the ultracentrifugal results with the electrophoretic patterns obtained with the same preparations is very instructive. It shows that the main parts of the fractions 0—48 % and 70—80 % which sediment so differently, migrate with the mobility of peak 4. The wide range of precipitation of this peak is due to the successive salting-out of two different types of molecules. The electrophoresis of a fraction 70—80 % which appeared pure by ultracentrifugation has shown that few percent of the median ultracentrifugal gradient migrate in the electrical field more slowly than peak 4.

The major part of the slow sedimenting component of plaice myogen precipitates in the range 80—100 % as the electrophoretic gradient 2. This gradient isolated by preparative electrophoresis sediments effectively at the rate of

* The apparently higher rates of sedimentation observed in this picture are due to the incomplete filling of the cell.

about 1.5 *S* (*cf.* following paragraph). The higher proportion of the slow ultracentrifugal peak (*cf.* Tables 3 and 4) in fraction 80—100 % suggests however the occurrence in this peak of proteins migrating more slowly in the electrical field.

C. Isolation of some components

The electrophoretic and ultracentrifugal analyses just described have shown the occurrence of some fractions which are fairly homogeneous under the conditions of our experiments. The precipitates which separate between 0—48 % and between 70—80 % contain relatively low percentages of impurities. Further experiments would, however, be necessary to determine their degree of homogeneity. A first step has been made in this direction by isolating crystalline components sedimenting with the rate of these two fractions. Henrotte and Dresse [14] have crystallized from plaice myogen a component of a rate of sedimentation of about 5 *S*. We have reproduced these results and made a preliminary examination of two other components.

1. *Crystalline component of 5.5 S.* Our method of preparation differs somewhat from the one described earlier [12,14]. Myogen is brought to 48 % saturation and about pH 6.5 by addition of solid ammonium sulphate. A saturated solution of ammonium sulphate at neutral pH is then added up to 55 % saturation. This second precipitate is also removed. The fraction precipitating between 55 % and 62 % saturation is redissolved in a minimum amount of water. Rhombohedra similar to those obtained by Henrotte [12,14] separate usually within a day (Fig. 5). They have also been prepared from fractions precipitating with neutral saturated ammonium sulphate in the range of 59—65 or 65—70 % saturation. The slight acidity of 6.5 recommended by Henrotte probably favours the crystallization but seems not very critical.

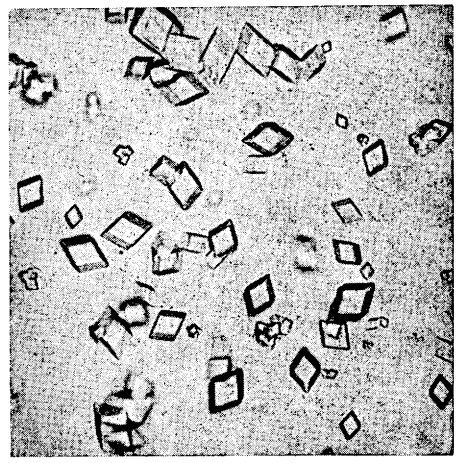

Fig. 5. Crystalline component of 5.5 *S*. Magnification: × 190.

Fig. 6. Crystalline component of 7.1 *S*. Magnification: × 1 800.

Three preparations have been examined by ultracentrifugation. An impurity sedimenting more quickly than the main peak and amounting to less than 5 % of the total protein content is observed. The corrected rates of sedimentation of the main peak at a concentration of 1 % are of 5.48 *S*, 5.48 *S* and 5.46 *S* and at 0.5 % of 5.54 *S* (one determination). The corresponding values of the impurity have been measured on a single preparation at a total concentration of 1 and 0.5 %; they are, respectively, of 8.11 and 8.31 *S*. The values for the main peak are in agreement with the determinations made on the corresponding fractions (Table 4). They are somewhat higher than the rates of the median peak of myogen. This crystalline component seems to correspond to a quick fraction of this median peak. In the electrical field, this crystalline material migrates at μ 0.05 and pH 7.5 as a single peak, moving at the rate of peak 4. A good degree of purity has therefore been achieved in this preparation.

2. *Crystalline component of 7.1 S.* In the course of the previous preparation, another crystalline material could be isolated. This result was first observed by Henrotte [12]. The method of preparation of this new type of crystals differs only slightly from the preceding one. The same fraction 55—62 % redissolved in a minimum amount of water sometimes gives rise to bunches of needles instead of rhombohedra. An important amorphous precipitate appears also at about the same speed. The aspect of the preparations is shown in the Fig. 6. Needles could also been obtained from precipitates isolated in the ranges 48—53 and 53—59 %. We have also been able recently to prepare these crystals in an easier way: myogen has been precipitated at neutral pH with our usual mixture of solid ammonium sulphate and disodium phosphate up to 55 % saturation. The precipitate is partially redissolved with water and the supernatent is separated by centrifugation. Bunches of needles soon appear in the solution together with an amorphous precipitate. The formation

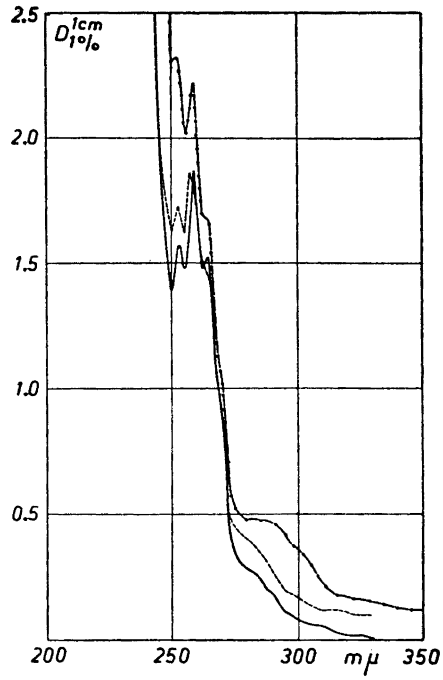

Fig. 7. Ultraviolet absorption spectra of the component of 1.5 *S* at neutral pH (——) and in presence of 0.1 N NaOH (—·—·—) and 0.1 N HCl (— — —).

of these crystals occurs therefore at neutral pH. This protein has a lower range of precipitation than the preceding one. The mixture of crystals and amorphous material shown in Fig. 6 has been separated by centrifugation, redissolved and examined by ultracentrifugation. A single peak has been observed on four different preparations sedimenting at a concentration of 1 % with corrected rates of 6.92 *S*, 7.24 *S*, 7.1 *S* and 7.17 *S*. The last preparation has also been examined at a concentration of 0.5 %; a somewhat higher corrected rate of 7.37 *S* was observed. These values are in agreement with those obtained for the quick component of myogen (Table 4) but somewhat smaller than those of the corresponding fractions.

A preliminary electrophoresis on the other hand suggests that this mixture of crystals and amorphous material is still fairly heterogeneous. A further fractionation should be necessary to isolate this crystalline material in a satisfactory degree of purity.

3. *Component of 1.5 S.* The myogens of cold-vertebrates appear to contain generally a fraction sedimenting very slowly in the ultracentrifuge. A crystalline component of this fraction has been isolated from carp muscles [7]. It precipitates with ammonium sulphate at very high salt concentration, contains about 15 % phenylalanine and no tyrosine and tryptophane [7,13]. This abnormal amino acid composition allowed to determine if a similar protein exists also in plaice myogen. In the fraction precipitating with neutral ammonium sulphate between 90 and 100 % saturation, a sharp ascending peak

(*cf.* Fig. 3g) migrates much quicker than the other gradients. We have been unable to isolate this component by zone electrophoresis on starch columns but small amounts could be obtained by preparative electrophoresis. They have been examined by ultracentrifugation and spectrophotometry. A preliminary report on this part of our work has already been published [15].

a. *Ultracentrifugal behaviour:* A single peak is observed which sediments with a corrected rate of 1.4—1.5 *S*. The values obtained with three different preparations are 1.45 *S* at 0.88 %, 1.52 *S* at 0.5 % and 1.43 *S* at 0.4 %. They do not differ essentially from those obtained previously for the slow peak (Table 4).

b. *Ultraviolet spectrum:* This component presents the abnormal amino acid composition of the corresponding component of carp muscle. Several preparations have been examined at pH 7.5. The three maxima of phenylalanine at 252, 257 and 263 mμ are observed at 253, 259 and 265 mμ and a small absorption which varies from one preparation to the other occurs at higher wave length suggesting the presence of an impurity containing tyrosine, tryptophane or cystine (Fig. 7). In presence of 0.1 N NaOH, the absorption due to this impurity is notably increased. We are therefore not dealing with tryptophane but possibly with tyrosine or cystine. The absence of a definite maximum at about 295 mμ suggests the presence of cystine. In 0.1 N HCl, the spectrum does not differ notably from the one observed at neutral pH.

The content in phenylalanine has been evaluated spectrophotometrically: if the absorption at 259 mμ is attributed exclusively to phenylalanine and if use is made of Fromageot and Schneck's data [27] for the absorption of this amino acid, it amounts to 16 % and is therefore approximatively equal to the one of the carp component. The comparison of the electrophoretic data on the other hand suggests a notable difference in charge: its descending mobility at μ 0.05 and pH 7.5 is -6.5×10^{-5} cm^2 volt^{-1} sec^{-1} while that of the carp protein at μ 0.075 (0.05 phosphate and 0.025 NaCl) and pH 7.3, is -3.2×10^{-5} cm^2 volt^{-1} sec^{-1}. The content in basic and acid amino acids appears thus variable according to the origin.

DISCUSSION

The present investigation has attempted a general survey of the protein composition of plaice myogen by electrophoresis and ultracentrifugation. In order to increase the resolution, the electrophoresis has been carried out at low ionic strength. The resulting improvement of the qualitative analysis, however, increases the boundary anomalies and decreases the precision of the quantitative data. Although myogen contains about 50 different enzymes according to several authors [28,29], the resolution obtained by electrophoresis at pH 7.5 is particularly poor in this case. Five components are observed in the whole extracts instead of 7 in the cod [8] and 6 in the carp [12] and the major one represents a particularly high percentage of the total amount: 50 to 55 % instead of about 40 % in the two other fishes. Electrophoresis carried out at different pH values would perhaps give a better separation but this point has not been investigated. On the other hand, the resolution obtained by

ultracentrifugation is small and similar to the one previously obtained with the carp [3,4].

The fractionation of plaice myogen with neutral ammonium sulphate has made possible an improvement of this analysis: peaks could be observed which were initially too small to be visible and some components could be separated. The examination of the different fractions by electrophoresis und ultracentrifugation shows the occurrence of a general trend: when the degree of saturation of the range considered increases, the electrophoretic mobilities of the components isolated increase and the ultracentrifugal ones decrease. A similar electrophoretic result has already been observed after ethanol fractionation of a pike muscle extract [11]. The range of fractionation suitable to the isolation of a component identified by ultracentrifugation or electrophoresis can thus bee foreseen. This paper shows, however, that discrepancies are not uncommon neither from the electrophoretic nor from the ultracentrifugal point of view.

The comparative electrophoretic studies of Connell [10] and Nikkilä and Linko [11] have shown the great heterogeneity of fish muscle extracts of low ionic strength. This heterogeneity has not been observed so far by ultracentrifugation. Furthermore, when a protein such as the component of S 1.5 can be characterized by some peculiar properties, it seems to occur generally but with different electrophoretic mobilities according to its origin. The charge of these proteins seems to play a secondary role and not to be related to their function in the cell. The further comparative study of the muscle albumins will certainly show more clearly the properties of these proteins which are directly related to their enzymatic functions and must not differ according to their origin.

We are much indebted to *Fiskeribedriftens Forskningsfond*, Norway (J. W. Jebsen) and to the *Fonds National de la Recherche Scientifique* (G. Hamoir) for financial support of this investigation, and wish to thank Prof. Dubuisson and Desreux for facilities put at our disposal. One of us (J. W. J.) expresses his sincere gratitude to Prof. Dubuisson for his kind hospitality, and to Director Eirik Heen, *Norwegian Fisheries Research Institute*, for making this study possible.

REFERENCES

1. Hamoir, G. *Biochem. Soc. Symposia*, Cambridge, Engl. *No.* **6** (1951) 8.
2. Hamoir, G. *Symposia on Cured and Frozen Fish Technology*, Svenska Inst. för Konserveringsforskning, Göteborg (1954).
3. Hamoir, G. *Arch. intern. physiol. et biochimie* **63** (1955) Suppl.
4. Hamoir, G. *Advances Protein Chem.* **10** (1955) 227.
5. Henrotte, J. G. *Nature* **169** (1952) 968.
6. Henrotte, J. G. *Arch. internat. physiol.* **62** (1954) 14.
7. Henrotte, J. G. *Nature* **176** (1955) 1221.
8. Connell, J. J. *Biochem. J.* **54** (1953) 119.
9. Dingle, J. R., Eagles, D. E. and Neelin, J. M. *J. Fisheries Research Board Can.* **12** (1955) 75.
10. Connell, J. J. *Biochem. J.* **55** (1953) 378.
11. Nikkilä, O. E. and Linko, R. R. *Biochem. J.* **60** (1955) 242.
12. Henrotte, J. G. *To be published.*
13. Hamoir, G. *Biochem. J.* **66** (1957) 29 P.
14. Henrotte, J. G. and Dresse, F. *3rd Internat. Congr. Biochem. Brussels* (1955) 81.
15. Jebsen, J. W. and Hamoir, G. *Acta Chem. Scand.* **12** (1958) 351.

16. Dubuisson, M. *Experientia* **3** (1947) 372.
17. Brenner-Holzach, O. and Staehelin, M. *Helv. Physiol. et Pharmacol. Acta* **11** (1953) 212.
18. Dubuisson, M., Disteche, A. and Debot, A. *Biochim. et Biophys. Acta* **6** (1950) 97.
19. Longsworth, L. G. *J. Am. Chem. Soc.* **61** (1939) 529.
20. Longsworth, L. G., Shedlowsky, T. and MacInnes, D. A. *J. exptl. Med.* **70** (1939) 399.
21. Longsworth, L. G. and MacInnes, D.M. *J. Am. Chem. Soc.* **62** (1940) 705.
22. Tiselius, A. and Kabat, E. A. *J. exptl. Med.* **69** (1939) 119.
23. Svensson, H. *Arkiv Kemi, Mineral. Geol.* **17 A** (1940) No. 14.
24. Svedberg, T. and Pedersen, K. O. *The Ultracentrifuge*, Clarendon Press, Oxford 1940.
25. Johnston, J. P. and Ogston, A. G. *Trans. Faraday Soc.* **42** (1946) 789.
26. Deuticke, H. J. *Z. physiol. Chem. Hoppe-Seyler* **224** (1934) 216.
27. Fromageot, Ch. and Schneck, G. *Biochim. et Biophys. Acta* **6** (1950) 113.
28. Dubuisson, M. *Biol. Revs. Cambridge Phil. Soc.* **25** (1950) 46.
29. Perry, S. V. *Physiol. Revs.* **36** (1956) 1.

Received February 28, 1958.

ACTA CHEMICA SCANDINAVICA 12 (1958) 1869—1872

Hexosamine and Ester Sulphate Content of the Human *Nucleus Pulposus* at Different Ages

ANUND HALLÉN

Chemistry Department II, Karolinska Institutet, Stockholm, Sweden

The hexosamine and sulphate content of adult human *nucleus pulposus* (central part of the intervertebral disc) has been determined. Equimolar quantities of hexosamine and ester sulphate were found. An increase could be noted in the ratio of glucosamine/galactosamine, from about 0.5 at 15 years of age to 1.5 at 90 years. It is concluded that, with rising age, a change takes place in the mucopolysaccharide pattern, in the form of an increase in the ratio of keratosulphate/chondroitin sulphate.

The *nucleus pulposus* (*N.P.*), the central part of the intervertebral disc, is a form of connective tissue that contains unusually large quantities of carbohydrate. It has been shown to contain chondroitin sulphate by Malmgren and Sylvén [1], and keratosulphate by Gardell and Rastgeldi [2]. A method for partial separation of the two polysaccharides has been described by Gardell [3].

The object of the present investigation was to determine whether there are any age differences in the mucopolysaccharide pattern of *N.P.*, and whether it has a high hyaluronic acid content, as claimed by Meyer [4] and by Hall *et al.*[5] Since keratosulphate contains equimolar quantities of glucosamine and ester sulphate, chondroitin sulphate equimolar quantities of galactosamine and ester sulphate, and hyaluronic acid hexosamine but no sulphate, this can be done by comparing the quantities of the hexosamines and ester sulphates at different ages.

EXPERIMENTAL

Non-pathologic lumbar and lower thoracic intervertebral discs were taken from autopsy cases. The *N. P.* was dissected free from the surrounding *annulus fibrosus*, freeze-dried and ground in a mortar. About 4 mg were analyzed for amino sugars according to Gardell [6]. Hydrolysis was performed in sealed tubes with 0.5 ml of 6 N hydrochloric acid for 8 h in a boiling water bath. After desiccation the hydrolysate was put on the top of a Dowex-50 column; the hexosamines were eluted with 0.3 N hydrochloric acid, and determined with the Elson-Morgan method.

About 50—100 mg of the *N. P.* powder were taken for determination of the sulphate content. The powder was hydrolyzed in 4 ml of 6 N hydrochloric acid for 4 h in a boiling

Table 1. Hexosamine and sulphate-sulphur content of freeze-dried *N. P.* from subjects of different ages.

Age, years	% Hexosamine	% Sulphur	Mole hexosamine / Mole sulphur
19	11.3	2.85	0.7
22	10.5	2.48	0.7
27	12.2	2.72	0.8
38	10.0	2.44	0.7
43	8.1	1.13	1.3
50	12.0	2.07	1.0
60	8.5	1.84	0.8
68	7.0	0.98	1.3
74	5.5	1.01	1.0
79	5.5	1.77	0.6
86	6.4	1.07	1.1

water bath, and filtered. Barium sulphate was precipitated from hot solution by the addition of barium chloride. On the following morning, the precipitate was collected on a platinum-iridium Gooch filter, dried and weighed.

To remove free sulphate ions, which might have interfered to some extent with the ester sulphate determinations, the *N. P.* was digested with proteolytic enzymes according to Gardell [7], and run down an anion exchange column according to Boström and Månsson [8]. One g of *N. P.*, both from subjects aged 20—60 years and aged 70 years, was denatured in boiling water; the pH was adjusted to 8.5, and glycerol extracts from pig pancreas and intestinal mucosa were added. The mixtures were digested at 40°C for 2—3 weeks, the pH being controlled and, when necessary, adjusted by the addition of dilute sodium hydroxide. After some particles had been centrifuged off and discarded, the solutions were allowed to pass Dowex-2×8 20—40 mesh columns in chloride form. No barium sulphate opalescence could then be detected on addition of barium chloride. The materials were freeze-dried, and about 10 mg were taken for hexosamine determination and 100—150 mg for sulphate determination.

RESULTS

The results of the analyses are presented in Tables 1—3. As can be seen in Table 1, the hexosamine and sulphate content of dry *N.P.* decreases with rising age. The values were only roughly reproducible, since the powders were not sufficiently homogenized. The values are, however, of the order of magnitude expected for equimolar quantities of hexosamine and ester sulphate being present

Table 2. Hexosamine and sulphate-sulphur content of *N. P.* digested with proteolytic enzymes and devoid of free sulphate ions.

N. P.	% Hexosamine *	% Sulphur	Mole hexosamine / Mole sulphur
20—60 years	6.1	1.24	0.9
70 years	3.5	0.72	0.9

* The ratio of glucosamine/galactosamine remained essentially unchanged during digestion; 0.9 for subjects aged 20—60 years, and 1.2 for 70 years.

Table 3. Hexosamine content and ratio of glucosamine/galactosamine of freeze-dried *N. P.* from subjects of different ages.

Age years	No. of cases	% Hexosamine Mean	Range	% Glucosamine Mean	Range	% Galactosamine Mean	Range	Glucosamine / Galactosamine Mean	Range
11–20	6	14.7	11.3–16.8	4.8	4.3–5.6	9.9	6.9–12.0	0.50	0.41–0.64
21–30	6	11.2	10.3–12.7	4.5	3.2–5.3	6.4	5.4– 8.0	0.75	0.60–0.90
31–40	4	10.6	9.5–11.9	5.2	4.6–6.3	5.4	4.9– 5.9	0.96	0.89–1.13
41–50	4	9.5	7.6–12.0	4.4	3.8–5.5	5.1	3.8– 6.5	0.89	0.66–1.05
51–60	12	8.3	6.1–11.0	4.0	2.8–5.5	4.3	2.8– 5.6	0.96	0.69–1.33
61–70	9	7.8	4.2–11.5	4.1	2.4–5.9	3.7	1.7– 6.1	1.13	0.90–1.38
71–80	5	6.7	5.5– 8.1	3.7	3.1–4.2	3.0	2.4– 3.8	1.25	1.10–1.45
81–90	3	6.6	6.4– 6.8	3.8	3.6–3.9	2.9	2.5– 3.1	1.42	1.17–1.53
91–	1	3.3	–	2.1	–	1.2	–	1.79	–

Table 2 shows the hexosamine and sulphate content of freeze-dried *N.P.*, digested with proteolytic enzymes and devoid of free sulphates. Within errors of method equimolar quantities of hexosamine and ester sulphate were found with no excess of hexosamine. The figures are lower than could be expected from the values in Table 1, probably depending on a higher water content.

It can be inferred from Table 3 that a fairly consistent change in the hexosamine pattern of *N.P.* takes place during aging. Not only does the hexosamine content decrease from about 14 % of dry weight at 15 years of age to 6 % at 90 years, but the ratio of glycosamine/galactosamine increases from about 0.5 to 1.5.

DISCUSSION

The presence of equimolar quantities of hexosamine and ester sulphate suggests that hyaluronic acid contributes very little to the amount of the human *N.P.* mucopolysaccharides. This is in agreement with the findings of Gardell and Rastgeldi [2], who concluded that the glucosamine in *N.P.* belongs to keratosulphate and the galactosamine to chondroitin sulphate. The changes observed in the hexosamine pattern of *N.P.* with age thus reflect an increase in the ratio keratosulphate/chondroitin sulphate.

Hirsch *et al.*[9] studied the sulphate content of human *N.P.* They found that although in the dry substance it diminished with age, as also observed in the present investigation, it was practically constant per volume native tissue.

It is probable that a similar change in the mucopolysaccharide pattern with rising age occurs in other tissues as well. Hass [10] studied the reducing power and sulphate content of dried costal cartilage, and noted a slight increase up to the third and fourth decades of life, and a slight decrease thereafter. Loewi [11] found equimolar amounts of hexosamine, as determined with the Elson-Morgan method, and ester sulphate. With age the values slightly decreased. Shetlar and Masters [12], on the other hand, who determined uronic acid with the carbazole method of Dische, and hexosamine with the Elson-Morgan

method, found that uronic acid had a maximal value at birth and then diminished markedly. Moreover, with increasing age, there was much more hexosamine than could be expected from the uronic acid content. Kuhn and Leppelmann [13] studied the hexosamines of joint cartilage, using paper chromatography for the separation of glucosamine and galactosamine, and found that the ratio of glucosamine/galactosamine increased with rising age, in a similar manner as found for *N.P.* in the present investigation.

Acknowledgements. Iam greatly indebted to Professor Erik Jorpes and Docent Sven Gardell for valuable discussions, and to Docent Harry Boström and Docent Lennart Rodén for help with the ester sulphate determinations.

The investigation has been aided by grants from *Karolinska Institutets reservationsanslag.*

REFERENCES

1. Malmgren, H. and Sylvén, B. *Biochim. et Biophys. Acta* **9** (1952) 706.
2. Gardell, S. and Rastgeldi, S. *Acta Chem. Scand.* **8** (1954) 362.
3. Gardell, S. *Acta Chem. Scand.* **9** (1955) 1035; **11** (1957) 668.
4. Meyer, K. Modern trends in Ophthalmology, London 1948 p. 71.
5. Hall, D. A., Lloyd, P. F., Happey, F., Horton, W. G. and Naylor, A. *Nature* **179** (1957) 1078.
6. Gardell, S. *Acta Chem. Scand.* **7** (1953) 207.
7. Gardell, S. *Arkiv Kemi* **4** (1952) 449.
8. Boström, H. and Månsson, B. *J. Biol. Chem.* **196** (1952) 483.
9. Hirsch, C., Paulson, S., Sylvén, B. and Snellman, O. *Acta Orthopaed. Scand.* **22** (1952) 175.
10. Hass, G. M. *A. M. A. Arch. Pathol.* **35** (1943) 275.
11. Loewi, G. *J. Pathol. Bacteriol.* **65** (1953) 381.
12. Shetlar, M. R. and Masters, Y. F. *Proc. Soc. Exptl. Biol. Med.* **90** (1955) 31.
13. Kuhn, R. and Leppelmann, H. J. *Ann* **611** (1958) 254.

Received June 30, 1958.

ACTA CHEMICA SCANDINAVICA 12 (1958) 1873—1886

Short Communications

Zur Strahlenschutzwirkung eines SH-haltigen Vitamin B_6-Derivates

RUPRECHT KOCH*

Radiologisches Institut der Universität Freiburg/Brsg., Deutschland; Institut für Organische Chemie und Biochemie der Universität Stockholm, Schweden

Vor kurzem beschrieben wir den Strahlenschutzeffekt eines sulfhydrylhaltigen Pyridoxinderivates bei der Maus [1]. Der Beobachtung kommt insofern sowohl praktische als auch theoretische Bedeutung zu, als wir selbst früher ausführlich dargestellt haben [2-4], dass offenbar nur Sulfhydrylkörper der sogenannten Cystein-Cysteaminreihe beim Tier in der Lage seien gegen eine Einwirkung energiereicher Strahlen zu schützen. Die Körper dieser Reihe haben die allgemeine Struktur:

$$HS-(CH_2)_x-N\begin{matrix}R_1\\R_2\end{matrix}$$

dazu gehören alle entsprechenden α-Aminosäuren. Auf die Bedeutung von x, R_1 und R_2 soll hier nicht eingegangen werden; wir verweisen auf unsere früheren Arbeiten. Unter cyclischen Verbindungen mit freier SH-Gruppe sind mit Sicherheit bisher keine strahlenschützenden gefunden worden. Das sulfhydrylhaltige Pyridoxinderivat stellt die erste Ausnahme dar. Es handelt sich um das 3-Mercaptomethyl-4-hydroxymethyl-5-hydroxy-6-methylpyridin **, ein echtes Derivat (I) des Vitamin B_6 (kurz B_6-SH genannt):

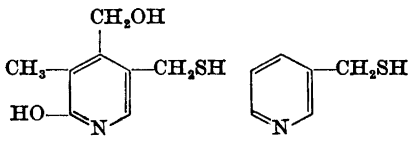

I II

Es lassen sich, wie wir früher ausgeführt haben [1], keine Unterlagen gewinnen, dass Pyridoxin selbst in der Lage ist eine Strahlenschutzwirkung zu entfalten. — Wie im Falle anderer Schutzstoffe [5,6] ist zu prüfen, ob auch nach peroraler Applikation ein Effekt zu erzielen ist. Ferner interessiert, ob die Wirkung an das unversehrte Mercapto-Pyridoxinmolekül gebunden ist.

Experimenteller Teil. Material und Methode: Weibliche 120—150 g schwere Ratten im Falle des B_6-SH-Fütterungsversuches und weibliche 20 g schwere Mäuse bei der Prüfung des 3-Mercaptomethylpyridins werden einer Röntgenganzkörperbestrahlung unterworfen. Beide Tierarten entstammen institutseigenen Inzuchtstämmen. Die Fütterung erfolgt bei den Ratten mit Latz-Rattenkeksen und Wasser *ad libitum*, bei den Mäusen mit Hafer/Weizen und einem Milchgriespudding. B_6-SH wird morgens nach 12 stündigem Fasten 100 mg/120 g Ratte per Schlundsonde und 60 min vor der Bestrahlung als wässrige Lösung appliziert. Diese B_6-SH-Dosis wird sehr gut vertragen. Wir richten uns in der Dosierung nach anderen Versuchen mit Homocysteinthiolacton [5] und β-Aminoäthyl-isothiuronium-Br-HBr (AET)[6]. — Die Mäuse erhalten 5 min vor dem Strahleninsult 3 mg 3-Mercaptomethylpyridin (wiss. Abt. Fa. E. Merck A.G./Darmstadt)/20 g Maus intraperitoneal. Es handelt sich ebenfalls um eine wässrige Lösung. Die Dosis entspricht etwa dem in früheren Versuchen injizierten B_6-SH und wird von den Mäusen gerade noch vertragen. D.h. es treten keine Todesfälle auf, jedoch schon die ersten Intoxikationserscheinungen.

---

* Herrn Professor Philipp/Freiburg zum 65. Geburtstag gewidmet.

** Die Substanz, die von der Fa. E. Merck A.G./Darmstadt (Deutschland) zum Patent angemeldet ist, wurde uns von dieser in liebenswürdigerweise zur Verfügung gestellt. Herrn Dr. O. Zima danken wir für seine Hilfe.

Die Bestrahlungsbedingungen sind folgende: Apparatur der Fa. C. H. F. Müller/Hamburg, M.G. 300, 200 kV, 15 mA, HWS: 0,57 mm Cu, 306 r/min, Fokus-Tierabstand 30 cm. Jeweils 3 Ratten bzw. 6 Mäuse werden in einem dafür konstruierten Celluloidbehälter bestrahlt. Kontrolltiere erhalten nur eine Röntgenbestrahlung und keinerlei Behandlung.

Die Ergebnisse des B_6-SH-Versuches sind in Tabelle 1 zusammengestellt. Hieraus ergibt

Tabelle 1.

Dosis in r	Zahl d. Tiere B_6—SH	Prozent tot	Zahl d. Tiere Kontrolle	Prozent tot
300	—	—	50	10
400	25	4	50	22
500	50	12	50	58
550	75	21,3	150	47,4
600	50	32	50	80
700	75	84	—	—

sich nach der Probit-Analyse die Regressionsgleichung für:

B_6—SH: $y = 13{,}34\ x - 32{,}27$
Kontrolle: $y = 5{,}91\ x - 11{,}04$
DL 50 = 622,1 ± 20,1 r
DL 50 = 517,6 ± 29,6 r

Zwischen den beiden DL 50-Werten besteht eine gesicherte Differenz (P = 0,01—0,001). In Figur 1 sind die Regressionslinien aufgezeichnet. Sie vermitteln uns deutlich das Bild des Schutzeffektes.

Durch die verschiedenartige Neigung beider Kurven ist der Unterschied im Bereich der höheren Strahlendosen nicht so ausgeprägt wie bei niederen, z. B. 300 r, 400 r oder 500 r. Eine eventuelle Parallelität beider Kurven kann ausgeschlossen werden (P = <0,001).

Nachdem sowohl nach parenteraler als peroraler Applikation des B_6-SH ein Strahlenschutzeffekt bei Maus und Ratte auftritt, erhebt sich die Frage, ob derselbe streng an die Pyridoxinkonfiguration gebunden ist. Wir untersuchen daher entsprechend unseren ersten B_6-SH-Versuchen die Wirkung des 3-Mercaptomethylpyridins (II), eines Körpers, dem 3 Substituenten des Pyridinringes im Vergleich zum Pyridoxin fehlen. Die Ergebnisse sind in Tabelle 2 zusammengestellt.

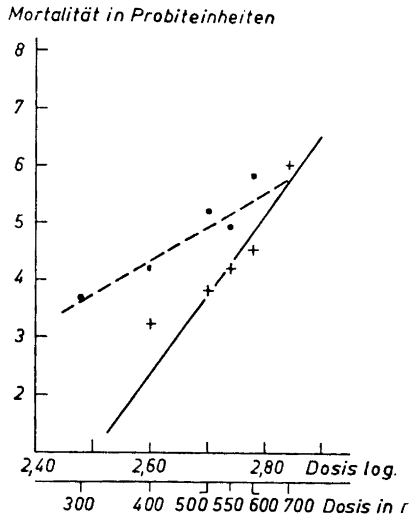

Fig. 1. Dosis-Wirkungskungskurve bei Ganzkörperbestrahlung.
•———• : Kontrollen
+——+ : B_6—S
Abszisse: log. der in r gemessenen Dosis, darunter die regelrechten r-Werte.
Ordinate: Prozent der gestorbenen Tiere in Probiteinheiten.

Tabelle 2.

Dosis in r	Zahl d. Tiere Mercaptomethylpyridin	Prozent tot	Zahl d. Tiere Kontrolle	Prozent tot
500	50	18	50	8
550	50	22	—	—
575	—	—	50	22
600	50	74	—	—
620	—	—	50	64
700	50	94	50	92

Aus ihnen ergeben sich die Regressionsgleichungen für:

3-Mercaptomethylpyridin:
$y = 18{,}31\ x - 45{,}54$; DL 50 = 575,7 ± 14,8 r

Kontrolle:
$y = 20{,}19\ x - 51{,}16$; DL 50 = 604,8 ± 7,2 r

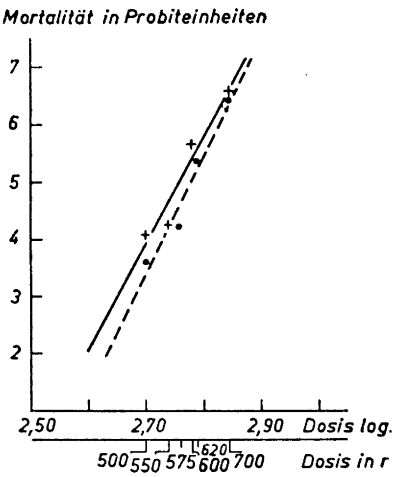

Fig. 2. Dosis-Wirkungskurven bei Ganzkörperbestrahlung.
•———•: Kontrollen.
+——+: 3-Mercaptomethylpyridin.
Abszisse: log. der in r gemessener Dosen, darunter die regelrechten r-Werte.
Ordinate: Prozent der gestorbenen Tiere in Probiteinheiten.

Zwischen den beiden DL 50-Werten besteht keine gesicherte Differenz (P = 0,8—0,9). Eine weitere Prüfung gibt die Gewähr, dass beide Regressionslinien parallel verlaufen (für Nicht-Parallelität: P = 0,9—0,8). Figur 2 zeigt die Verhältnisse graphisch. Die leichte Linksverschiebung der 3-Mercaptomethylpyridin-Kurve ist sehr wahrscheinlich auf eine gewisse Giftwirkung des Mercaptans zu beziehen und auf keinen Fall im Sinne einer Sensibilisierung zu deuten.

Diskussion. Die vorliegenden Ergebnisse bestätigen unsere ersten Beobachtungen, dass im Mercapto-Pyridoxin ein Schutzköper gegenüber energiereichen Strahlen vorliegt. Derselbe tritt sowohl nach parenteraler als auch peroraler Applikation auf und entspricht damit den Schutzstoffen der Cystein-Cysteaminreihe. Der perorale Schutz lässt sich mit dem nach Homocysteinthiolacton oder AET vergleichen. Mit diesem Befund lässt sich die Vorstellung einer spezifischen Strahlenschutzwirkung der Sulfhydrylkörper der Cystein-Cysteaminreihe nicht mehr aufrecht erhalten.

Entsprechend unseren Untersuchungen im Bereich der Cysteaminreihe prüfen wir auch beim Mercapto-Pyridoxin, welche Bedeutung den einzelenen Substituenten des Pyridinringes zukommt. Dabei zeigt sich, dass das einfache 3-Mercaptomethylpyridin vollkommen unwirksam ist.

Wie im Falle der Schutzwirkung der Cystein-Cysteaminkörper ist auch im vorliegenden eine Deutung des Schutzmechanismus nicht möglich.

Die Untersuchungen wurden mit Unterstützung der Deutschen Forschungsgemeinschaft ausgeführt.

1. Koch, R. und Langendorff, M. *Strahlentherapie* **107** (1958) 121.
2. Koch, R. *Fortschr. Gebiete Röntgenstrahlen u. Nuklearmed.* **86** (1956) 767.
3. Langendorff, H. und Koch, R. *Strahlentherapie* **99** (1956) 567.
4. Langendorff, H., Koch, R. und Hagen, U. *Strahlentherapie* **100** (1956) 137.
5. Langendorff, M. und Koch, R. *Strahlentherapie* **106** (1958) 451.
6. Langendorff, H. und Koch, R. *Naturwiss.* **43** (1956) 524.

Eingegangen am 27. September, 1958.

On the Significance of the Release of two Different Peptides from Fibrinogen during Clotting

TORVARD C. LAURENT and BIRGER BLOMBÄCK

Department of Chemistry, Karolinska Institutet, Stockholm, Sweden

The first step in the clotting process when fibrinogen is incubated with thrombin is a release of two different peptides, A and B [1,2]. It has been shown that clotting also occurs after incubation with reptilase when only peptide A is released [3,4]. This raises the question of the biological significance of the release of peptide B.

The second step in the clotting process with thrombin has been shown to be a formation of an intermediate polymer with a varying length and a width corresponding to two parallel fibrinogen molecules [5]. Casassa [6] showed that it is possible by means of light-scattering to obtain the ratio of the molecular weight and molecular length (M/L) of this polymer. The second

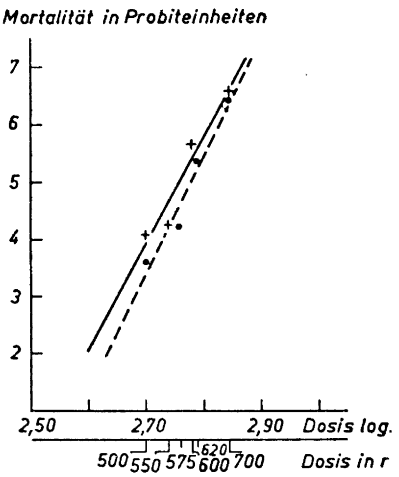

Fig. 2. Dosis-Wirkungskurven bei Ganzkörperbestrahlung.
•———•: Kontrollen.
+——+: 3-Mercaptomethylpyridin.
Abszisse: log. der in r gemessener Dosen, darunter die regelrechten r-Werte.
Ordinate: Prozent der gestorbenen Tiere in Probiteinheiten.

Zwischen den beiden DL 50-Werten besteht keine gesicherte Differenz (P = 0,8—0,9). Eine weitere Prüfung gibt die Gewähr, dass beide Regressionslinien parallel verlaufen (für Nicht-Parallelität: P = 0,9—0,8). Figur 2 zeigt die Verhältnisse graphisch. Die leichte Linksverschiebung der 3-Mercaptomethylpyridin-Kurve ist sehr wahrscheinlich auf eine gewisse Giftwirkung des Mercaptans zu beziehen und auf keinen Fall im Sinne einer Sensibilisierung zu deuten.

Diskussion. Die vorliegenden Ergebnisse bestätigen unsere ersten Beobachtungen, dass im Mercapto-Pyridoxin ein Schutzköper gegenüber energiereichen Strahlen vorliegt. Derselbe tritt sowohl nach parenteraler als auch peroraler Applikation auf und entspricht damit den Schutzstoffen der Cystein-Cysteaminreihe. Der perorale Schutz lässt sich mit dem nach Homocysteinthiolacton oder AET vergleichen. Mit diesem Befund lässt sich die Vorstellung einer spezifischen Strahlenschutzwirkung der Sulfhydrylkörper der Cystein-Cysteaminreihe nicht mehr aufrecht erhalten.

Entsprechend unseren Untersuchungen im Bereich der Cysteaminreihe prüfen wir auch beim Mercapto-Pyridoxin, welche Bedeutung den einzelenen Substituenten des Pyridinringes zukommt. Dabei zeigt sich, dass das einfache 3-Mercaptomethylpyridin vollkommen unwirksam ist.

Wie im Falle der Schutzwirkung der Cystein-Cysteaminkörper ist auch im vorliegenden eine Deutung des Schutzmechanismus nicht möglich.

Die Untersuchungen wurden mit Unterstützung der Deutschen Forschungsgemeinschaft ausgeführt.

1. Koch, R. und Langendorff, M. *Strahlentherapie* **107** (1958) 121.
2. Koch, R. *Fortschr. Gebiete Röntgenstrahlen u. Nuklearmed.* **86** (1956) 767.
3. Langendorff, H. und Koch, R. *Strahlentherapie* **99** (1956) 567.
4. Langendorff, H., Koch, R. und Hagen, U. *Strahlentherapie* **100** (1956) 137.
5. Langendorff, M. und Koch, R. *Strahlentherapie* **106** (1958) 451.
6. Langendorff, H. und Koch, R. *Naturwiss.* **43** (1956) 524.

Eingegangen am 27. September, 1958.

On the Significance of the Release of two Different Peptides from Fibrinogen during Clotting

TORVARD C. LAURENT and BIRGER BLOMBÄCK

Department of Chemistry, Karolinska Institutet, Stockholm, Sweden

The first step in the clotting process when fibrinogen is incubated with thrombin is a release of two different peptides, A and B [1,2]. It has been shown that clotting also occurs after incubation with reptilase when only peptide A is released [3,4]. This raises the question of the biological significance of the release of peptide B.

The second step in the clotting process with thrombin has been shown to be a formation of an intermediate polymer with a varying length and a width corresponding to two parallel fibrinogen molecules [5]. Casassa [6] showed that it is possible by means of light-scattering to obtain the ratio of the molecular weight and molecular length (M/L) of this polymer. The second

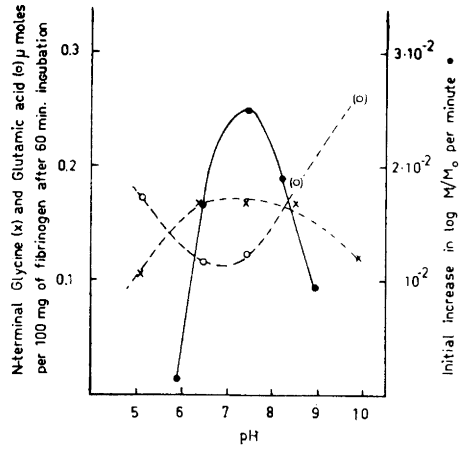

Fig. 1. N-Terminal analysis on glycine and glutamic acid after incubation of 0.17 % fibrinogen with 0.024 NIH-units/ml of reptilase for 60 min. The initial polymerization rate of the protein has been plotted for comparison. M is the weight-average molecular weight of the polymer and M_0 is the molecular weight of fibrinogen.

step of the clotting can conveniently be studied in urea solutions, where step three, the visible clotting, is inhibited [7].

The aim of the present investigation, of which this is a preliminary report, was to see whether an intermediate polymer could be formed even by reptilase as the coagulating agent.

The first experiment was planned to determine the pH-optimum of the action of reptilase as well as to assure that only peptide A was split off within the working range of the pH. The experimental conditions were described earlier [4]. N-Terminal glycine, glutamic acid and tyrosine were determined after incubation of fibrinogen with reptilase for 1 h and 17.5 h at room temperature. The protein concentration was 0.17 %, the reptilase concentration 0.024 NIH-units/ml and the medium was tris-imidazole buffer and sodium chloride, ionic strength 0.2. The values for glycine and glutamic acid were corrected with respect to the tyrosine values [8]. The initial polymerization rate was followed by light-scattering [4]. Fig. 1 shows that the decrease of glutamic acid, the increase of glycine and the initial polymerization rate all had pH-optima at pH 6—8. Within the error of the method, the disappearance of one N-terminal glutamic acid corresponded to the appearance of one N-terminal glycine. After 17.5 h incubation the ratio of N-terminal glycine to N-terminal tyrosine (Table 1) was, within the experimental errors, 1:1, indicating that most of the fibrinogen had been transformed to fibrin at all pH's studied and that only one peptide, A, had been split off.

Table 1. Ratio of N-terminal glycine and tyrosine after incubation of fibrinogen with reptilase for 17.5 h. The experimental conditions are described in the text.

pH	5.1	6.35	7.4	8.5	9.9
Glycine / Tyrosine	1.12	0.81	0.97	0.97	0.95

In the second experiment, thrombin and reptilase were added in a concentration of 0.03 NIH-units/ml to different solutions of 1 % fibrinogen containing 0.02 M tris-imidazole buffer pH 6.35 and 0.38 M sodium chloride. The solutions were incubated in dialysis bags for 9 h at 37°C. The clots formed were then dissolved by dialysis for 6 h against 2 M urea containing 0.01 M tris-imidazole buffer pH 7.45 and 0.22 M

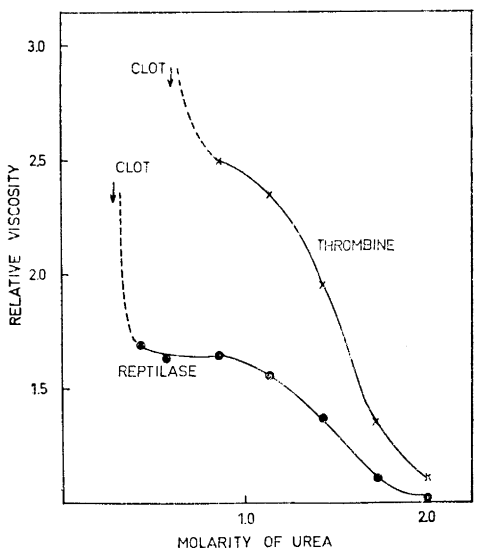

Fig. 2. Relative viscosity at different urea concentrations of fibrin formed by the action of thrombin and reptilase. Protein concentration 0.14 %.

sodium chloride. The solutions were diluted, the protein concentration being 0.14 %, keeping the ionic concentration constant, at varying urea concentrations. The viscosities of the solutions were measured in an Ostwald viscometer at 20°C, 18—24 h after dilution. No correction for non-Newtonian flow was applied. The result is shown in Fig. 2. The increase in the range of 0.4—2 M urea of the viscosity of fibrin formed by reptilase and in the range of 0.7—2 M urea of the viscosity of fibrin formed by thrombin is most probably an indication of the formation of urea soluble fibrin polymers.

In order to compare the two intermediate polymers by light-scattering a third experiment was performed identical with the second except that the enzyme concentration was now kept at 0.06 NIH-units/ml in the original incubation mixture and the incubation time was 18 h. The N-terminal analysis in the first experiment indicates that during this incubation time, all

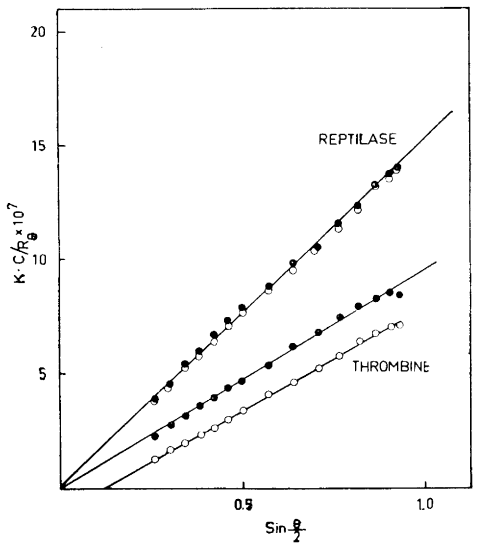

Fig. 3. Evaluation of light-scattering data according to Casassa. ($K = 2\pi^2 n^2 (dn/dc)^2 / N\lambda^4$, where n is the refractive index of the solvent; dn/dc the refractive increment, 0.197 ml/g; N, Avogadros number and λ the wavelength of the light. c is the concentration of protein in g/ml and R_Θ is the reduced angular intensity measured at the angle Θ.) ● = protein concentration 0.07 %; ○ = protein concentration 0.14 %.

fibrinogen is converted to fibrin. The intermediate polymers formed were studied in 1 M urea at protein concentrations of 0.07 and 0.14 % 18—24 h after the dilutions were made. The angular distribution of the scattered light at a wavelength of 4 360 Å was measured at 35°—135° in a Brice-Phoenix light-scattering photometer using a cylindrical glasscell [8]. The solutions had been cleaned from dust in the usual way [4]. The results were evaluated according to Casassa [5] (Fig. 3). The slope of the line $K \cdot c/R_\Theta$ *vs.* sin $\Theta/2$ is related to the weight-average of M/L. For reptilase formed fibrin at 0.14 % concentration, the slope in four experiments was $1.50 - 1.78 \times 10^{-6}$ and for thrombin formed fibrin $0.87 - 1.16 \times 10^{-6}$. The averages correspond to M/L values of 0.73×10^{11} and 1.16×10^{11}, respectively. If calculated according to Casassa, this should mean polymers 1.1 and 1.8 times wider than fibrinogen. At l ast at the present conditions, it seems as if reptilase formed fibrin was polymerized mainly end-to-end while thrombin formed fibrin had a tendency for lateral aggregation.

Note added in proof. The reptilase was obtained from AB Pentapharm, Basel. A new batch of this enzyme, obtained from the same firm, after this note was submitted for publication, had the same activity as thrombin, *i.e.* it splitted off both peptide A and B. Light-scattering data of fibrin obtained with this enzyme were identical with data of thrombin formed fibrin. This is in agreement with the observation that a lateral aggregation occurs when peptide B is split off. The reason for the different activities of the two reptilase batches is unknown.

1. Bettelheim, F. R. and Bailey, K. *Biochim. et Biophys. Acta* **9** (1952) 578.
2. Blombäck, B. and Vestermark, A. *Arkiv Kemi* **12** (1958) 173.
3. Blombäck, B. *Arkiv Kemi* **12** (1958) 321.
4. Blombäck, B. and Laurent, T. C. *Arkiv Kemi* **12** (1958) 137.
5. For references see, *e. g.*, Scheraga, H. A. and Laskowski Jr. M. *Advances in Protein Chem.* **12** (1957) 1.
6. Casassa, E. F., *J. Am. Chem. Soc.* **78** (1956) 3980.
7. Ehrlich, P., Schulman, S. and Ferry, J. D. *J. Am. Chem. Soc.* **74** (1952) 2258.
8. Stacey, K. A. *Light-scattering in Physical Chemistry*, Butterworths Scientific Publications, London 1956.

Received September 23, 1958.

Note on the Purification of Human Antihemophilic Globulin

BIRGER BLOMBÄCK, MARGARETA BLOMBÄCK and INGA MARIE NILSSON

Chemistry Department II, Karolinska Institutet, Stockholm, Sweden

Purification of the antihemophilic globulin in Cohn's fraction I (human) by different procedures in the presence of glycine has been reported earlier [1,2]. A fraction, denoted as I-1-A, was obtained by these procedures. The yield of antihemophilic globulin in this fraction was about 80 % of that in fraction I, and the activity per mg of protein was about 200 times that of plasma. The antihemophilic factor of fraction I-1-A probably forms a complex with fibrinogen. Approximately two-thirds of the fraction are coagulable with thrombin. Attempts to dissociate this complex by fractionation with organic solvents were unsuccessful.

It was, however, found that in contrast to the behaviour of the antihemophilic activity in plasma (*cf.* Ref.[3]), the antihemophilic activity in the purified fraction I-1-A could easily be adsorbed on barium sulphate, aluminium oxide and calcium phosphate (di- and tribasic) as well as on kaolin and bentonite. Barium sulphate adsorbed (from a 0.05 M sodium citrate solution) not only the antihemophilic activity, but also considerable amounts of fibrinogen. The other salts adsorbed more or less selectively the antihemophilic activity, leaving fibrinogen and other proteins in the supernatant. Attempts to elute the activity from all these salts were unsuccessful.

It was also found that the antihemophilic activity could conveniently be adsorbed on tricalcium citrate. Thus, 25 mg of tricalcium citrate adsorbed about 90 % of the antihemophilic factor from 1 ml of a 0.3 % protein solution of fraction I-1-A dissolved in 0.05 M sodium citrate, pH 6.8. After centrifugation and washing of the precipitate with 0.05 M sodium citrate, pH 6.8, the activity could be eluted by dissolving the tricalcium citrate precipitate in 2.0 ml of 0.1 M sodium-EDTA, pH 6.8.

Table 1.

Fraction	Protein		Activity	
	total, mg	yield, % of fr. I-1-A	yield, % of fr. I-1-A	relative, per mg prot.
I-1-A (10 ml)	33.1	100	100	1.0
Supernatant	30.0	90.6	7.3	0.08
			3.9 *	—
EDTA-eluate	3.0	8.5	99.0	11.0
			106.0	

* Values obtained in another experiment, using a different sample of fr. I-1-A.

It can be inferred from Table 1 that less than 10 % of the total protein in the solution of fraction I-1-A is adsorbed on tricalcium citrate. The fibrinogen in fraction I-1-A remained in the supernatant after adsorbtion. As judged by the protein determination procedure used [4], the antihemophilic activity per mg protein in the EDTA eluate is about 10 times higher than in the original fraction. Thus, purification of the antihemophilic factor as compared with plasma is about 2000 times on the protein basis.

Work is now in progress to recover and further study the antihemophilic factor in the EDTA solution. A complete report will be given in *Arkiv Kemi*.

1. Blombäck, B. and Blombäck, M. *Arkiv Kemi* **10** (1956) 415.
2. Blombäck, M. *Arkiv Kemi* **12** (1958) 387.
3. Wagner, R. H., and Thelin, G.M. *Hemophilia and Hemophilioid Diseases*, Chapel Hill, Ed. Brinkhous, 1957.
4. Lowry, O. H., Rosebrough, N. J., Farr, A. L. and Randall, R. J. *J. Biol. Chem.* **193** (1951) 265.

Received October 16, 1958.

The pS-Activity Curve of a Serum Fraction IV-6-3 Studied with Butyrylcholine at pS above 3

EDITH HEILBRONN

Research Institute of National Defence, Dept. 1, Sundbyberg 4, Sweden

Studies on the butyrylcholinesterase (BuChE) catalyzed hydrolysis of thiocholine esters [1] performed in 0.1 M potassium chloride, with the aid of an automatic recording titrator [2] and using fraction IV-6-3 obtained from retroplacentar serum (AB Kabi, Stockholm), gave results, which apparently did not follow the Michaelis-Menten law. In no case could straight lines be obtained when, for example, according to Hofstee's [3] variation of the Michaelis-Menten equation

$$v = -\frac{v}{S} \times K_M + V_m \qquad (1)$$

enzyme activity (v) was plotted against v/S (S = conc. of the substrate). All pS-activity curves showed a kind of S-shape, but the activity did not approach zero around substrate concentrations of 0.5×10^{-3} M, as one would expect. The unexpected high reaction velocities at low substrate concentrations were shown not to depend upon spontaneous hydrolysis of the substrates or upon accelerating effects of potassium iodide (Fig. 1).

In order to find out, if the reason for the deviation from the Michaelis-Menten law was to be found in the enzyme preparation, it was decided to study a pS-activity curve with the same enzyme preparation and a wellknown substrate such as butyrylcholine iodide (BuChI). This was done at constant ionic strength $\mu = 0.20$, pH = 8.00 and 25°C. By means of introducing a second syringe in the automatic recording titrator, driven synchronously with the syringe containing the titrator (sodium hydroxide) and containing a BuChI solution of exactly the same concentration as the titrator (each mole of hydrolysed BuChI consumes one mole of sodium hydroxide), it was possible to keep the substrate concentration constant during the course of hydrolysis and thus to change a pseudo-first order reaction to a pseudo-zero order reaction. This method allowed studies of the hydrolysis down to about 10^{-6} M solutions of substrate. The small amounts of solutions from the syringes caused only insignificant changes in the ionic strength of the solution during the course of hydrolysis.

Enzyme: 25 mg of serumfraction IV-6-3 were dissolved in 100 ml of 0.1 M potassium chloride. *Titrator:* 0.025 M sodium hydroxide. *Substrate solution:* The second syringe contained a 0.025 M solution of butyrylcholine iodide in distilled water. *Substrate concentration and ionic strength*: A substrate concentration range from 10^{-1} M to 10^{-6} M (in final solution) was studied. The ionic strength of the final

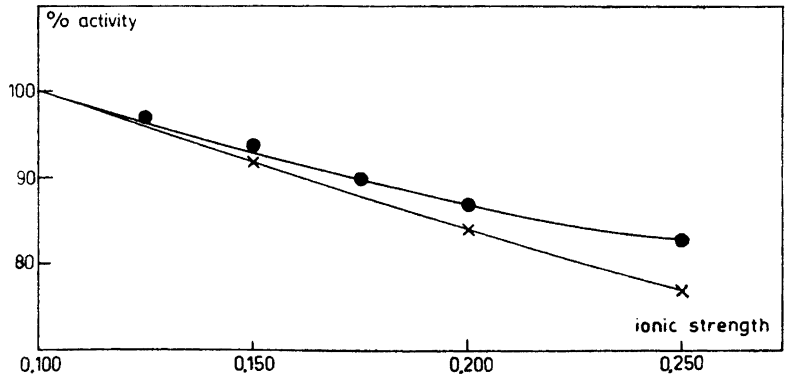

Fig. 1. Dependence of enzyme activity on ionic strength for the system potassium chloride —IV-6-3—acetylthiocholine iodide (●) and potassium iodide—IV-6-3—acetylthiocholine iodide (×). Concentration of acetylthiocholine iodide 0.001 M.

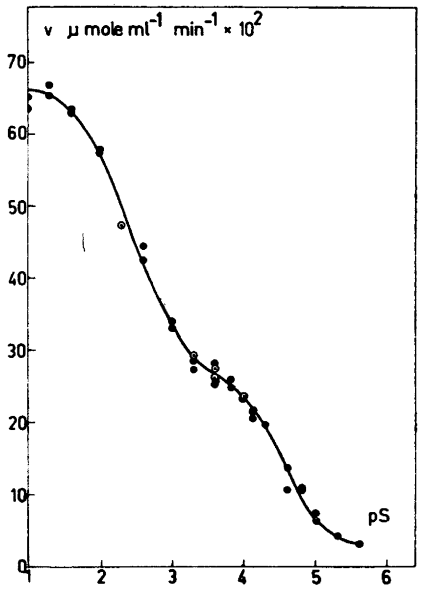

Fig. 2. pS-Activity curve for the system serum fraction IV-6-3—BuChI at $t = 25°C$, ionic strength $\mu = 0.20$, pH = 8.00. Substrate concentration kept constant by means of "double syringe" method.

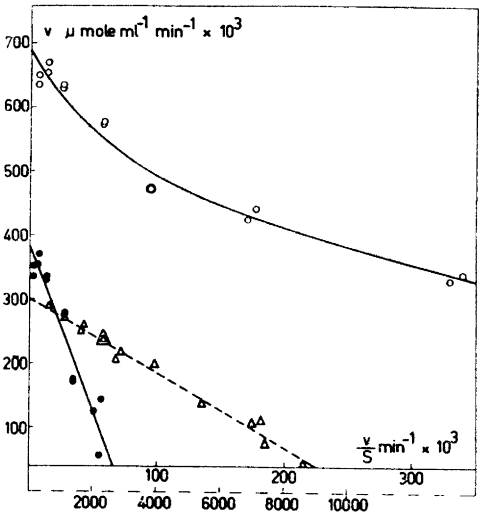

Fig. 3. Michaelis-Menten plot according to Hofstee. O, experimentally obtained curve; ●, first part of the curve minus maximum activity for the second part of the curve; △, second part of the curve. Straight lines calculated by method of least squares.

solutions was kept at 0.20 by dissolving additional amounts of potassium iodide. *Method:* 37 ml of 0.10 M potassium chloride were added to the vessel. Substrate and potassium iodide were dissolved in this solution. The syringe containing the titrator was put into place and pH was adjusted to 8.00. 3 ml of enzyme solution were administered and pH was immediately again adjusted to 8.00. The second syringe was put into place and hydrolysis was recorded during about 10 min. Initial values were used for calculations.

Fig. 2 shows the curve obtained which gives the impression of 2 enzymes able to split BuChI. The second enzyme seems to have a very low substrate maximum, about 0.5×10^{-3} M. Assuming that the second enzyme is of the BuChE type, thus not inhibited by excess of substrate, it was possible to obtain two straight lines, according to Hofstee's equation, as shown in Fig. 3. The lines were calculated by the method of least squares. From the line representing the second enzyme, the maximum activity for the second enzyme, 0.3 μmole ml^{-1} min^{-1}, was calculated. This value was subtracted from the activity values of the first part of the experimentally obtained pS-activity curve. The last values belonging to the first part of this curve were subtracted by 0.29 μmole ml^{-1} min^{-1}, as maximum activity does not seem to be reached at this point.

The possibility of two enzymes occurring in the preparation used is also indicated by earlier electrophoretic and chromatographic studies[4] on fraction IV-6-3. Chromatograms on calcium phosphate showed always two peaks with cholinesterase activity.

My sincere thanks are due to Professor G. Ljunggren, Director of the Research Institute of National Defence, Dept. 1, for his kind interest in this work.

1. Heilbronn, E. *Acta Chem. Scand.* In press.
2. Larsson, L. and Hansen, B. *Svensk Kem. Tidskr.* **68** (1956) 521.
3. Hofstee, B. H. J. *Science* **116** (1952) 329
4. Malmström, B. G., Levin, Ö. and Boman, H. G. *Acta Chem. Scand.* **10** (1956) 1077.

Received October 22, 1958.

Alkaline Incineration of Iodine-Containing Organic Material

GÖSTA WIDSTRÖM and MONICA BJÖRKMAN

Clinical Laboratories, Centrallasarettet, Stocksund, Sweden

Methods for alkaline incineration of organic material have been extensively studied as an important step in the estimation of iodine content. Alkaline incineration for analysis of protein-bound iodine, as suggested by Barker, Humphrey and Soley[1], has become generally accepted as a very useful method for estimation of circulating thyroid hormone.

In order to obtain reproducible results, all conditions in the several steps of this analysis must be kept constant within narrow limits. One reason is that it is difficult to avoid considerable losses of iodine during the ashing procedure. Difficulties are encountered both in keeping this loss constant, and in compensating for it. In experiments with radioactive iodine, van Middlesworth [2] found the recovery of iodine with the method of Barker *et al.* to range from 68 to 86 %. Skanse and Hedenskog,[3] using a slightly modified technique, claimed a recovery of not better than 86 %. Since the iodine recovery is evidently unsatisfactory with the incineration method in question, an attempt to reduce the losses is motivated. In the present experiments, the iodine losses were studied on dry ashing of iodine-containing substances, both protein-bound and in the iodide form, labelled with ^{131}I.

General procedure. A working solution of $Na^{131}I$, with an activity of about 0.06 μC/ml was prepared by 500-fold dilution of a stock solution of $Na^{131}I$ in very dilute sulphite. Dilution was performed with 0.04 N NaOH, and NaI added as a carrier to a concentration of 20 μg/100 ml.

Protein-bound ^{131}I ($PB^{131}I$) was obtained from patients treated for thyroid disease. The $PB^{131}I$ serum was diluted with normal serum to an activity convenient for measurements and treated with small charges of Dowex 2 × 8, 40 mesh, for elimination of inorganic iodine.

One ml of either of these dilute solutions and various amounts of other substances were collected in Pyrex tubes, dried overnight at 100°C, and ashed in a muffle furnace at 600°C for 3 h.

Table 1. Recovery of iodine in % after incineration at 600°C for 3 and 24 h, respectively, with various amounts of different alkalis added to the incineration mixture. Each value is the mean of 2—5 experiments.

Alkali added	Without Somogyi's reagent $Na^{131}I$		$PB^{131}I$		With Somogyi's reagent $Na^{131}I$		Precipitated with Somogyi's reagent $PB^{131}I$
	3 h	24 h	3 h	24 h	3 h	24 h	3 h
1 ml 4 N K_2CO_3	99	92	95	88	100	96	96
1 ml 4 N Na_2CO_3	95	93	82	56	97	94	76 Barker's meth.
2 ml 4 N Na_2CO_3	95	94	95	78	97	95	93
1 ml 4 N NaOH + Zn	78	93	89	61	89	84	80
1 ml 4 N Na_2CO_3 + S	82	66	68	39	73	19	60
1 ml 4 N NaOH + 1 ml 20 % $Na_2S_2O_5$	89	85	98	70	87	91	96
1 ml 4 N NaOH + 1 ml 5 % $Na_2S_2O_5$	94	95	88	63	97	89	91
1 ml 4 N NaOH + 1 ml 1 % $Na_2S_2O_5$	90	72	90	49	94	69	86
2 ml 4 N $CaAc_2$	13	9	18			11	2
2 ml 4 N $BaAc_2$	51	9	46		60	12	40

Table 2. Recovery of iodine in % after incineration of $Na^{131}I$ in nickel crucibles with addition of alkali acetate.

Acetate added	Metal iodide m.p.°C	b.p.°C	Recovery, % 1 h	2 h	6 h	24 h
1 ml 4 N KAc	723	1 420	—	78	68	60
1 ml 4 N NaAc	651	1 300	70	66	38	20
2 ml 4 N $BaAc_2$	740 d		15	8	1	0
2 ml 4 N $CaAc_2$	575	718	5	2	0	0

After incineration and cooling, the ashes were dissolved in 5 ml of 1 N HCl by stirring with a glass rod, and the tubes centrifuged. Three ml of each centrifugate were taken for activity measurements, and compared with the activity of the corresponding working solution or $PB^{131}I$ serum. An LKB scintillation counter was used for the measurements, and the activity of the samples was adjusted to give about 10 000 counts/min.

Results. Experiments in which inorganic ^{131}I and protein-bound ^{131}I, respectively, were incinerated with and without Somogyi's reagent are recorded in Table 1. When the serum protein-bound ^{131}I was incinerated together with Somogyi's reagent and 1 ml of 4 N Na_2CO_3 (method of Barker *et al.*), the mean recovery was 76 %. When K_2CO_3 was used instead of Na_2CO_3, the recovery increased to 96 %. Substitution of K_2CO_3 for Na_2CO_3 in the incineration mixture therefore seems to be a practical means of reducing the losses of iodine during incineration *.

Table 1 shows large differences in the recovery of added iodine on incineration with various alkalis. An explanation might be provided by taking into account the melting and boiling points of the corresponding iodides. They decrease in the following order: K,Na,Ba and Ca. It is, however, difficult to predict the vapour pressure of the iodides in these somewhat complicated mixtures of salts.

The following experiments were made to demonstrate the correlation between losses of iodides and their melting points on alkaline incineration. Nickel crucibles were each charged with 1 ml of $Na^{131}I$ working solution, after which an equimolar amount of the alkali acetate of K, Na, Ca and Ba, respectively, was added. The crucibles were dried at 100°C for 24 h, and then incinerated at 600°C for 1, 2, 6 and 24 h, respectively. The ashes were brought into solution, and their activity measured as described. The results are summarized in Table 2. The correlation between the physical constants of the iodides and the losses on incineration, increasing with time, is clearly apparent.

A similar experiment, recorded in Table 3, confirms the considerable reduction in these losses when K_2CO_3 is substituted for Na_2CO_3, as used in the alkaline incineration method of Barker *et al.* It is also fully evident that the losses were much greater in the wideopen crucibles than in the test tubes heated in an almost horizontal position.

The practical consequences of the large loss of iodide on incineration with Ca must also be taken into account. This is because the presence of Ca in normal serum might decrease the iodide recovery on incineration with Na_2CO_3 or even with K_2CO_3. The following experiment was therefore made. One ml of $Na^{131}I$ working solution was mixed in Pyrex tubes with 1 ml of 2 N Na_2CO_3 or K_2CO_3, and 1 ml of $CaAc_2$ solution in various concentrations was added, as shown in Table 4. All the tubes were dried at 100°C for 24 h, and then incinerated at 600°C for 3 h. It can be inferred from the table that the amount of Ca present in normal serum may influence the iodide loss. The losses were considerably smaller in the K_2CO_3 than in the Na_2CO_3 series. The effect of Ca was found to be

* Vilkki (pers. comm. and Ref.[4]) has published a modification of Baker and Humphrey's method using KOH instead of Na_2CO_3 for the incineration, as the experience is that KOH is better than NaOH for collecting iodine in the distillation procedure. Kingsley *et al.*[5] has substituted Na_2CO_3 for K_2CO_3 in the B. & H. incineration method because of the better purity of the potassium reagent (pers. comm.).

Table 3. Recovery of iodine in % after incineration of $Na^{131}I$ with addition of alkali carbonate.

Carbonate added	Vessel	Iodide m.p.°C	Iodide b.p.°C	Recovery, % 1 h	2 h	6 h	24 h
1 ml 4 N K_2CO_3	Ni crucible	723	1 420	—	92	79	71
1 ml 4 N Na_2CO_3	do.	651	1 300	81	75	70	49
1 ml 4 N K_2CO_3	Pyrex tube	723	1 420	98	92	87	87
1 ml 4 N Na_2CO_3	do.	651	1 300	100	92	87	64

Table 4. Effect of calcium on iodine recovery in % after alkaline incineration of $Na^{131}I$.

Ca conc. mg/100 ml	K_2CO_3 incineration Batch 1		K_2CO_3 incineration Batch 2	Na_2CO_3 incineration Batch 1		Na_2CO_3 incineration Batch 2
15 800	94	92	96	70	72	85
158	82	84	79	43	42	55
15.8	88	85	82	81	81	75
1.58	90	91	88	89	89	81
0	94	96	97	90	88	87

about the same in the physiologic range, but in higher concentrations the loss was much more pronounced in the Na_2CO_3 series.

It is obvious that the presence of greater concentrations of cations, the iodides of which have low meltingpoints, may result in considerable errors in the quantitative determination of iodine in organic material. The use of K_2CO_3 instead of Na_2CO_3 on incineration will result in a more complete recovery of iodine.

1. Barker, S. B., Humphrey, M. J. and Soley, M. H. *J. Clin. Invest.* **30** (1951) 55.
2. van Middlesworth *Federation Proc.* **12** (1953) 147.
3. Skanse, B. and Hedenskog, J. *Scand. J. Clin. & Lab. Invest.* **7** (1955) 291.
4. Vilkki, P. *Scand. J. Clin. & Lab. Invest.* **10** (1958) 272.
5. Kingsley, G. R. *et al. Standard Methods of Clin. Chemistry* **2** (1958) 147.

Received October 28, 1958.

The Oxidation of Glycosides

X.* Reduction of Some Methyl D-Oxo-glucopyranosides

OLOF THEANDER

Träkemiska Avdelningen, Svenska Träforskningsinstitutet, Stockholm, Sweden

The reduction of oxo-*cyclo*-hexane ring compounds has been widely studied and it is well known that the proportion of axial to equatorial hydroxyl groups formed is dependent upon the type of reduction, and that hindered oxo groups afford axial alcohols. The effect of hindrance is particularly strong in catalytic hydrogenation (for summary and references see Barton[1]). There is usually considered to be good conformational analogy between pyrane- and *cyclo*-hexane-rings. Reymond recently[2] reported the results of borohydride reduction of *myo*-inosose-2 (I) and *epi*-inosose-2 (II) and compared the ratio of the inositol isomers formed with the results previously obtained by Posternak, using catalytic hydrogenation (Pt-catalyst) and reduction

* Part IX. *Acta Chem. Scand.* **12** (1958) 1887.

Table 3. Recovery of iodine in % after incineration of $Na^{131}I$ with addition of alkali carbonate.

Carbonate added	Vessel	Iodide m.p.°C	Iodide b.p.°C	Recovery, % 1 h	2 h	6 h	24 h
1 ml 4 N K_2CO_3	Ni crucible	723	1 420	—	92	79	71
1 ml 4 N Na_2CO_3	do.	651	1 300	81	75	70	49
1 ml 4 N K_2CO_3	Pyrex tube	723	1 420	98	92	87	87
1 ml 4 N Na_2CO_3	do.	651	1 300	100	92	87	64

Table 4. Effect of calcium on iodine recovery in % after alkaline incineration of $Na^{131}I$.

Ca conc. mg/100 ml	K_2CO_3 incineration Batch 1		K_2CO_3 incineration Batch 2	Na_2CO_3 incineration Batch 1		Na_2CO_3 incineration Batch 2
15 800	94	92	96	70	72	85
158	82	84	79	43	42	55
15.8	88	85	82	81	81	75
1.58	90	91	88	89	89	81
0	94	96	97	90	88	87

about the same in the physiologic range, but in higher concentrations the loss was much more pronounced in the Na_2CO_3 series.

It is obvious that the presence of greater concentrations of cations, the iodides of which have low meltingpoints, may result in considerable errors in the quantitative determination of iodine in organic material. The use of K_2CO_3 instead of Na_2CO_3 on incineration will result in a more complete recovery of iodine.

1. Barker, S. B., Humphrey, M. J. and Soley, M. H. *J. Clin. Invest.* **30** (1951) 55.
2. van Middlesworth *Federation Proc.* **12** (1953) 147.
3. Skanse, B. and Hedenskog, J. *Scand. J. Clin. & Lab. Invest.* **7** (1955) 291.
4. Vilkki, P. *Scand. J. Clin. & Lab. Invest.* **10** (1958) 272.
5. Kingsley, G. R. *et al. Standard Methods of Clin. Chemistry* **2** (1958) 147.

Received October 28, 1958.

The Oxidation of Glycosides

X.* Reduction of Some Methyl D-Oxo-glucopyranosides

OLOF THEANDER

Träkemiska Avdelningen, Svenska Träforskningsinstitutet, Stockholm, Sweden

The reduction of oxo-*cyclo*-hexane ring compounds has been widely studied and it is well known that the proportion of axial to equatorial hydroxyl groups formed is dependent upon the type of reduction, and that hindered oxo groups afford axial alcohols. The effect of hindrance is particularly strong in catalytic hydrogenation (for summary and references see Barton[1]). There is usually considered to be good conformational analogy between pyrane- and *cyclo*-hexane-rings. Reymond recently[2] reported the results of borohydride reduction of *myo*-inosose-2 (I) and *epi*-inosose-2 (II) and compared the ratio of the inositol isomers formed with the results previously obtained by Posternak, using catalytic hydrogenation (Pt-catalyst) and reduction

* Part IX. *Acta Chem. Scand.* **12** (1958) 1887.

Table 1. Reduction of methyl D-oxo-glucopyranosides (Percentage of equatorial (glucoside) and axial (mannoside, alloside) epimers formed).

Method of reduction	Methyl β-2--oxo-glucoside		Methyl β-3--oxo-glucoside		Methyl α-3--oxo-glucoside	
	glucoside	mannoside	glucoside	alloside	glucoside	alloside
H_2/Pt (*ca.* pH 6 and room temperature)	6	94	23	77	14	86
Raney nickel (*ca.* pH 6 and 78°)	26	74	38 *	62 *	9	91
Sodium amalgam (pH 6 and room temperature)	47	53	34	66	37	63
Borohydride (pH 9.5 and room temperature)	35 **	65 **	51 **	49 **	4	96

* A 500 mg-scale experiment gave an 85 % yield of sugars, containing glucose (35 %), allose (57 %) and 1,6-anhydro-allose (8 %).

** These figures are more accurate than those previously [4] given.

with sodium amalgam. The *myo*-inosose-2, having no axial hydroxyl groups, gave a large proportion of the axial epimer on catalytic hydrogenation, and a ratio of axial to equatorial epimers of about 4:3 on reduction with borohydride and sodium amalgam. The second compound (II), in which the oxo group is hindered by an axial hydroxyl group in β-position, gave the axial epimer only, on catalytic hydrogenation or borohydride reduction and an axial to equatorial ratio of about 6:2 on reduction with sodium amalgam. The results obtained with compound II show that the axial hydroxyl group β to the oxo group has a considerable effect on the approach of the borohydride ion.

In the present investigation methyl β-D-2-oxo-glucopyranoside (III), methyl β-D-3-oxo-glucopyranoside (IV) and methyl α-D-3-oxo-glucopyranoside (V) were reduced catalytically with Pt- and Raney nickel-catalyst, with sodium amalgam and with borohydride and the proportions of the methyl glycosides obtained were estimated. It was shown by paper chromatography that the resulting glycosides contained only small amounts of unreacted oxo-glucoside and only traces of other compounds. The ratios of epimeric glycosides obtained were determined by quantitative analysis of the sugars obtained on hydrolysis of the reduction product. The analytical figures (Table 1) were corrected for sugar decomposition during hydrolysis and for the formation of 1,6-anhydro-D-allose [3].

In comparing the four types of reducing agents, it must be borne in mind that one of them (Raney nickel) was used at a higher temperature and one (borohydride) at a higher pH than the others. As in the case of the two inososes none of these reducing agents gave products in which the most stable, equatorial isomer (the methyl glucoside) predominated. In general the effect of hindrance was most marked in the Pt-catalysed reduction and least using sodium amalgam. The reduction with Raney nickel catalyst gave ratios of the methyl glycoside epimers closer to those obtained with sodium amalgam and borohydride than to those obtained using H_2/Pt. Methyl α-3-oxo-glucoside (V), with an axial, bulky methoxyl group β to the oxo-group, was similar to *epi*-inosose-2, and gave a large proportion of the axial isomer on reduction with borohydride, as was expected, and also with Raney nickel.

Experimental. The oxo-glucosides were prepared as described previously [5,6] and 20 mg samples of the compounds were reduced in 1 % solution. Reduction over platinum catalyst was done in unbuffered aqueous solution at pH 6 for 4 h using Adams catalyst and with Raney nickel according to the procedure of Karabinos

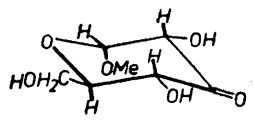

Methyl-α-D-3-oxo-glucopyranoside.

and Ballun [7], by refluxing the oxo-glucoside for 3 h in unbuffered aqueous ethanol (30 % water) at pH 6. They were reduced with sodium amalgam (2.5 % sodium) for 4 h in aqueous solution buffered to pH 6. The amalgam was added at intervals over 4 h and the pH was kept at 6 by the addition of small amounts of acetic acid, the product was then deionised. The borohydride reduction was done in aqueous solution buffered to pH 9.5 for 5 h and the product was then deionised.

The reduction products were hydrolysed with 0.5 N sulphuric acid for 16 h at 100°, neutralised with Amberlite IR-4B (free base) and the solution obtained was concentrated. The sugars were separated by paper chromatography and a quantitative quadruple estimation was made using the procedure of Saeman *et al.*[8]. Schleicher and Schüll No. 2043a papers were used and the chromatograms were eluted with ethyl acetate-acetic acid-water, 3:1:3 (upper phase).

1. Barton, D. H. R. *J. Chem. Soc.* **1953** 1027.
2. Reymond, D. *Helv. Chim. Acta* **40** (1957) 492.
3. Pratt, J. W. and Richtmyer, N. K. *J. Am. Chem. Soc.* **77** (1955) 1906.
4. Lindberg, B. and Theander, O. *Acta Chem. Scand.* **11** (1957) 1355.
5. Theander, O. *Acta Chem. Scand.* **11** (1957) 1557.
6. Assarsson, A. and Theander, O. *Acta Chem. Scand.* **12** (1958) 1507.
7. Karabinos, J. V. and Ballun, A. T. *J. Am. Chem. Soc.* **75** (1953) 4501.
8. Saeman, J. F., Moore, W. E., Mitchell, R. L. and Millett, M. A. *Tappi* **37** (1954) 336.

Received November 17, 1958.

Some Remarks about the Shape of Gaussian Error Curve of Absorption Bands

LECH STOLARCZYK

Chemistry Department A, Technical University of Denmark, Copenhagen; Electrochemical Department, Institute of Physical Chemistry, Polish Academy of Science, Warsaw, Poland

As it is well known in literature, the Gaussian error curve is often a good approximation of absorption band shape for transition group complexes [1]. In the theory of electronic transitions in molecules [2] this behaviour can be understood as the projection of the (squared) vibrational wavefunction of the electronic groundstate on the potential curve of the excited electronic state. If the electronic groundstate has a parabolic potential curve as function of the internuclear distance, and if the temperature is so low that only the groundstate ($n=0$ in $E=(n+{}^1/_2)h\nu_0$) of the harmonic oscillator is populated, the Gaussian shaped wavefunction will produce a nearly Gaussian shaped absorption band (by projection on a linear potential curve of the excited electronic state) viz.

$$\varepsilon = \frac{\sigma}{\sigma_s}\,\varepsilon_0 \exp\left[-\frac{(\sigma-\sigma_0)^2}{\delta^2}\right] \ln 2 \qquad (I)$$

where the indices zero on the wavenumber σ and extinction coefficient ε refer to a point near to the band maximum. The factor $\frac{\sigma}{\sigma_0}$ explains partly that fact [1] that $\delta(-)<\delta<\delta(+)$, where $\delta(-)$ and $\delta(+)$ are the halfwidths of two halves of non-corrected Gaussian curves towards smaller and larger σ. Dr. Klixbüll Jørgensen has pointed out that in this approximation, the maximum occurs at $\sigma = \sigma_0 + \frac{\delta^2}{\sigma_0 2\ln 2}$ and the ratio between the two half-widths is $\frac{\delta(+)}{\delta(-)} \simeq 1 + \frac{\delta}{\sigma_0 \ln 2}$. Reasonable values for the slope of the excited state's potential curve, as implied from ligand field theory [3-5], agree well with the observed values of δ.

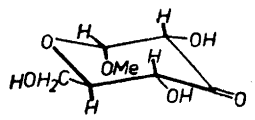

Methyl-α-D-3-oxo-glucopyranoside.

and Ballun [7], by refluxing the oxo-glucoside for 3 h in unbuffered aqueous ethanol (30 % water) at pH 6. They were reduced with sodium amalgam (2.5 % sodium) for 4 h in aqueous solution buffered to pH 6. The amalgam was added at intervals over 4 h and the pH was kept at 6 by the addition of small amounts of acetic acid, the product was then deionised. The borohydride reduction was done in aqueous solution buffered to pH 9.5 for 5 h and the product was then deionised.

The reduction products were hydrolysed with 0.5 N sulphuric acid for 16 h at 100°, neutralised with Amberlite IR-4B (free base) and the solution obtained was concentrated. The sugars were separated by paper chromatography and a quantitative quadruple estimation was made using the procedure of Saeman *et al.*[8]. Schleicher and Schüll No. 2043a papers were used and the chromatograms were eluted with ethyl acetate-acetic acid-water, 3:1:3 (upper phase).

1. Barton, D. H. R. *J. Chem. Soc.* **1953** 1027.
2. Reymond, D. *Helv. Chim. Acta* **40** (1957) 492.
3. Pratt, J. W. and Richtmyer, N. K. *J. Am. Chem. Soc.* **77** (1955) 1906.
4. Lindberg, B. and Theander, O. *Acta Chem. Scand.* **11** (1957) 1355.
5. Theander, O. *Acta Chem. Scand.* **11** (1957) 1557.
6. Assarsson, A. and Theander, O. *Acta Chem. Scand.* **12** (1958) 1507.
7. Karabinos, J. V. and Ballun, A. T. *J. Am. Chem. Soc.* **75** (1953) 4501.
8. Saeman, J. F., Moore, W. E., Mitchell, R. L. and Millett, M. A. *Tappi* **37** (1954) 336.

Received November 17, 1958.

Some Remarks about the Shape of Gaussian Error Curve of Absorption Bands

LECH STOLARCZYK

Chemistry Department A, Technical University of Denmark, Copenhagen; Electrochemical Department, Institute of Physical Chemistry, Polish Academy of Science, Warsaw, Poland

As it is well known in literature, the Gaussian error curve is often a good approximation of absorption band shape for transition group complexes [1]. In the theory of electronic transitions in molecules [2] this behaviour can be understood as the projection of the (squared) vibrational wavefunction of the electronic groundstate on the potential curve of the excited electronic state. If the electronic groundstate has a parabolic potential curve as function of the internuclear distance, and if the temperature is so low that only the groundstate ($n=0$ in $E=(n+{}^1/_2)h\nu_0$) of the harmonic oscillator is populated, the Gaussian shaped wavefunction will produce a nearly Gaussian shaped absorption band (by projection on a linear potential curve of the excited electronic state) viz.

$$\varepsilon = \frac{\sigma}{\sigma_s}\,\varepsilon_0 \exp\left[-\frac{(\sigma-\sigma_0)^2}{\delta^2}\right] \ln 2 \qquad (I)$$

where the indices zero on the wavenumber σ and extinction coefficient ε refer to a point near to the band maximum. The factor $\frac{\sigma}{\sigma_0}$ explains partly that fact [1] that $\delta(-)<\delta<\delta(+)$, where $\delta(-)$ and $\delta(+)$ are the halfwidths of two halves of non-corrected Gaussian curves towards smaller and larger σ. Dr. Klixbüll Jørgensen has pointed out that in this approximation, the maximum occurs at $\sigma = \sigma_0 + \frac{\delta^2}{\sigma_0 2\ln 2}$ and the ratio between the two half-widths is $\frac{\delta(+)}{\delta(-)} \simeq 1 + \frac{\delta}{\sigma_0 \ln 2}$. Reasonable values for the slope of the excited state's potential curve, as implied from ligand field theory [3-5], agree well with the observed values of δ.

It is obvious that for a mixture, where the electronic groundstate is populated *e.g.* ~75 % ($n=0$), 20 % ($n=1$), 4 % ($n=2$), 1 % ($n=3$), a Gaussian shape cannot be obtained of the absorption band. On the other hand, the present note will draw attention to the fact that high temperature and Maxwell-Boltzmann distribution also produces a Gaussian probability distribution in the harmonic oscillator, and thus, a nearly Gaussian-shaped band (I) will also be expected here. We have three cases, which can be experimentally distinguished, *viz*:

1. $kT \ll h\nu_0$ Nearly Gaussian-shaped band, independent of T for a small heating, δ proportional to $(fm)^{-1/4}$, f is the force constant and m the effective mass.
2. $kT \sim h\nu_0$ The band is not Gaussian-shaped to any good approximation.
3. $kT \gg h\nu_0$ Nearly Gaussian-shaped band, proportional to $\sqrt{T}$ and to $f^{-1/4}$, independent of m.

The proof of the third case is the following: The Maxwell-Boltzmann probability of oscillation with amplitude from a to $a + da$ in a system of harmonic oscillators is given by

$$P_{(a,da)} = \frac{f}{kT} \exp\left(-\frac{fa^2}{2kT}\right) a\, da$$

Probability of finding a classical harmonic oscillator vibrating with the amplitude a in a position from x to $x + dx$ is given by:

$$P_{a(x,dx)} = \frac{dx}{\pi \sqrt{a^2 - x^2}}$$

Total probability of position from x to $x + dx$ in a system of oscillators vibrating with various amplitudes in thermal equilibrium is given by:

$$P_{(x,dx)} = \int_{a=x}^{\infty} P_{(a,da)}\, P_{a(x,dx)} =$$

$$= \frac{f}{\pi kT}\, dx \int_{a=x}^{\infty} \frac{\exp\left(-\frac{fa^2}{2kT}\right)}{\sqrt{a^2 - x^2}}\, a\, da = \quad \text{(II)}$$

$$= \frac{\sqrt{f}}{\sqrt{2\pi kT}} \exp\left(-\frac{fx^2}{2kT}\right) dx$$

It is seen from (II) that the half width for Gaussian error curve based on the assumption of ligands high vibrational excitement should be proportional to $\sqrt{f/T}$ and unrelated to mass of ligands. Measurements seem to show the half width of absorption bands being nearly unchanged by exchange of ligands in spite of great differences in their masses. Small effects can easily be related to force constants. In such a manner the assumption of high vibrational excitement seems to be more probable. Further confirmations are to be searched by examining the temperature dependande of absorption band half width.

1. Jørgensen, C. Klixbüll *Acta Chem. Scand.* **8** (1954) 1495.
2. Herzberg, G. *Molecular Spextra and Molecular Structure I. Spectra of Diatomic Molecules.* 2. Ed. 1950, p. 392.
3. Stolarczyk, L. *Résumés des Communications de XVI^e Congrés International de Chimie Pure et Appliquée*, Tome I, Divisions de Chimie Physique et de Chimie Minérale, Paris 1957, p. 114.
4. Stolarczyk, L. *Roczniki Chem.* **31** (1957) 1273.
5. Jørgensen, C. Klixbüll *Acta Chem. Scand.* **11** (1957) 53.

Received October 28, 1958.

ACTA CHEMICA SCANDINAVICA 12 (1958) 1887—1896

The Oxidation of Glycosides

VIII.* The Degradation of Methyl α-D-3-oxo-glucopyranoside, Methyl β-D-3-oxo-glucopyranoside and Methyl β-D-2-oxo-glucopyranoside by Lime-water **

OLOF THEANDER

Träkemiska avdelningen, Svenska Träforskningsinstitutet, Stockholm, Sweden

On treatment with lime-water methyl α-D-3-oxo-glucopyranoside, methyl β-D-3-oxo-glucopyranoside and methyl β-D-2-oxo-glucopyranoside were very rapidly degraded. The principal route involved the elimination of the methoxyl group and, in all cases, led initially to the formation of a dicarbonyl intermediate which then gave acids. The dicarbonyl intermediate was proved to be 1,5-anhydro-2,3-dioxo-D-glucitol. On reduction it gave all four expected 1,5-anhydro-D-glycitols including the hitherto unknown 1,5-anhydro-D-allitol.

It is commonly believed that the pronounced sensitivity of oxidised cellulose to alkali depends upon the presence of oxo-glucose residues. The alkaline degradation of carbohydrates to saccharinic acids has recently been reviewed by Sowden [1]. A probable ionic mechanism for those transformations, which has been advanced by Isbell [2], involves the following successive steps: (i) the formation and ionisation of an enediol; (ii) the β-elimination of a hydroxyl, alkoxyl or glycosyl group; (iii) a rearrangement to an α-dicarbonyl intermediate; and (iv) a benzilic acid type of rearrangement to give a saccharinic acid. In Fig. 1 this mechanism is shown applied to the alkaline degradation of those oxo-glucosides studied in the present investigation. Haskins and Hogsed [3] were the first to suggest that it was probable that the alkaline degradation of oxidised cellulose involved the scission of β-glucosylcarbonylresidues.

Oxo-glucosides are now available [4,5] and these were used as models simulating oxo-glucose residues in oxidised cellulose or in oxidised starch. Alkaline treatment with lime-water was used to enable a comparison to be made with the results obtained by Kenner *et al.*[1], who used oxygen-free, saturated lime-

* Part VII. *Svensk Papperstidning* **61** (1958) 581.

** A preliminary report was given at the XVth International Congress of Pure and Applied Chemistry, Paris, in July 1957.

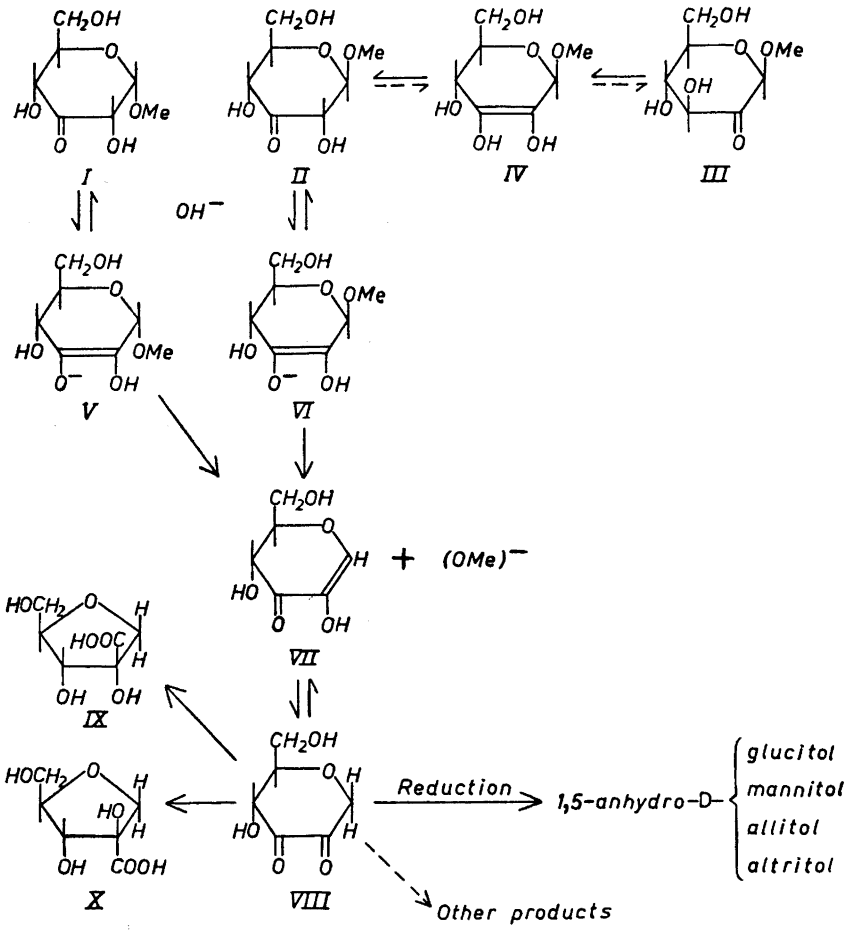

Fig. 1. Treatment of methyl α-3-oxo-glucoside (I), methyl β-3-oxo-glucoside (II) and methyl β-2-oxo-glucoside (III) with lime-water and reduction of 1,5-anhydro-2,3-dioxo-glucitol(VIII).

water (at 25°) in their extensive studies of the role played by substituents during the alkaline degradation of monosaccharides, oligosaccharides or polysaccharides.

When methyl β-D-3-oxo-glucopyranoside (II) was treated with saturated lime-water (at 25°) the optical rotation altered very rapidly from a negative to a high positive value. Fractions were withdrawn after short periods of treatment and immediately acidified and then examined on paper chromatograms. It was found that, associated with a rapid decrease of II, there was an increase in the amounts of the acids. A considerable quantity of a compound, giving distinctive colorations with the various spray reagents, was

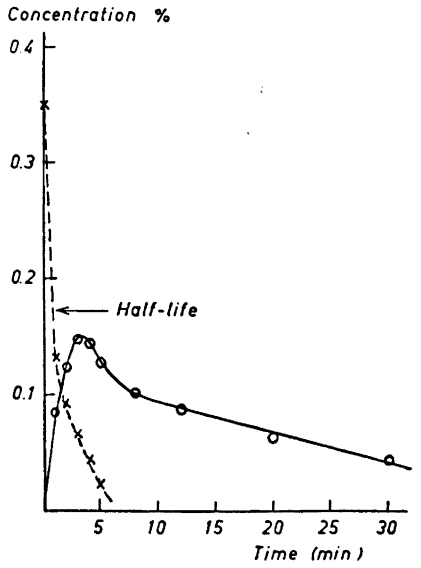

Fig. 2. Formation of 1,5-anhydro-2,3-dioxo-glucitol (—O—O—) on treatment of methyl β-3-oxo-glucoside (– – × – – × – –) with lime-water (0.042 N) at 25°.

observed. It was shown to be the α-dicarbonyl intermediate (VIII) that would be expected to be formed if the degradation involved scission of the glycosidic ether linkage. Both II and VIII were semi-quantitatively determined throughout the reaction period (Fig. 2). The extremely short half-life of II (about one minute) is roughly one hundreth of those of the most alkali-labile sugars previously studied (laminaribiose and turanose [6]) and is about 2 000 times less than that of cellobiose [7].

Dilute lime-water (0.02 N) was used to enable the optical rotation to be followed during the degradation of methyl α-D-3-oxo-glucopyranoside (I), methyl β-D-3-oxo-glucopyranoside (II) and methyl β-D-2-oxo-glucopyranoside (III). All three oxo-glucosides gave a maximum positive rotation which was correlated, by paper chromatographic examination, with the presence of the principal component (compound VIII). The 2-oxo-glucoside (III) was degraded more slowly than were the two anomers of 3-oxo-glucoside, and by the paper chromatographic examination, it was shown that it was first transformed into a compound having the same R_F-values as II. There was also a component present which gave a pink spot with resorcinol, and which had an R_F-value between those of the two oxo-glucosides. This spot may have been due to the enediol IV. But no epimerisation of II to III was detected when the former was treated with alkali (Fig. 3).

In several experiments compound VIII (prepared from II) was isolated. The amorphous product, in aqueous solution at pH 5, had $[\alpha]_D^{22}$ + 155° and ε_{max} 3 100 at 293 mμ (methyl β-3-oxo-glucoside: $\varepsilon_{max.}$ 90 at 285 mμ). Small amounts were obtained crystalline (m.p. 53—55°). The amorphous and crystalline products gave single clearly defined spots which were both chromatographically and electrophoretically indistinguishable from one another.

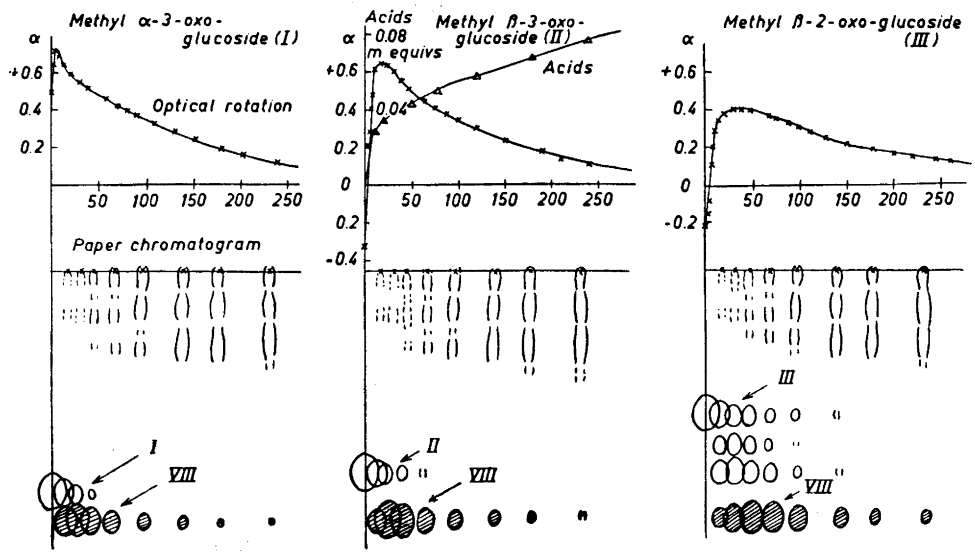

Fig. 3. Diagram of paper chromatograms (irrigant B) showing spots observed and relating them to the fall in optical rotation when methyl α-3-oxo-glucoside, methyl β-3-oxo-glucoside and methyl β-2-oxo-glucoside were separately treated with lime-water (0.02 N) at 22°. Abscissa = time in minutes.

The dicarbonyl compound rapidly formed a precipitate with 2,4-dinitrophenylhydrazine, but did not give a satisfactory crystalline derivative with this reagent or with *o*-phenylenediamine. It carried no methoxyl group, but carbonyl determination, by the borohydride method, indicated the presence of two carbonyl groups (assuming M.W. 160).

The mixture of products obtained on the reduction of the dicarbonyl intermediate with Raney nickel or with borohydride was separated. The four products obtained were: amorphous 1,5-anhydro-D-altritol (characterised as its crystalline tetra-acetate) and crystalline 1,5-anhydro-D-glucitol, 1,5-anhydro-D-mannitol and a substance having m.p. 147—148°, $[\alpha]_D^{22}$ + 26° (in water). This last substance gave an analysis consistent with the formula $C_6H_{12}O_5$ and, from the evidence presented below, it was concluded to be 1,5-anhydro-D-allitol. Its specific rotation, +26°, accords reasonably well with those calculated from the specific rotations of methyl β-D-alloside and the methyl β-D-glycosides and 1,5-anhydro-D-glycitol derivatives of glucose, altrose and gulose ($[\alpha]_D$ = +20°, 22° and 28°). The values calculated from the rotations of the corresponding derivatives of mannose and galactose however were markedly different. Foster [8] has shown that 1,5-anhydro-glycitols and the corresponding methyl-glycosides behave similarly on electrophoresis. The M_G value of the above unknown compound was similar to that of methyl β-alloside (Table 1); a strong indication of the former being 1,5-anhydro-D-allitol. No 1,5-anhydro-galactitol could be detected among the reduction products.

Table 1. Paper electrophoretic mobilities in borate (M_G-values) of methyl D-glycopyranosides and 1,5-anhydro-D-glycitols.

	M_G
Methyl β-alloside	0.49
1,5-Anhydro-allitol	0.48
1,5-Anhydro-altritol	0.63
Methyl α-glucoside	0.10
Methyl β-glucoside	0.16
1,5-Anhydro-glucitol	0.18
Methyl α-mannoside	0.39
Methyl β-mannoside	0.30
1,5-Anhydro-mannitol	0.38
Methyl α-galactoside	0.35
Methyl β-galactoside	0.37
1,5-Anhydro-galactitol	0.36

It is of interest to note that the proportions of the four reduction products varied with the choice of reducing conditions. When Raney nickel was used (at pH 5) there was a much higher yield of anhydro-mannitol than of anhydro-glucitol but this order was reversed when borohydride was used (at pH 9.5). There was no marked difference in the relative yields of anhydro-allitol, but that of anhydro-altritol decreased to traces when borohydride was used. The difference might be due both to the nature of the reductants as such, and to a preferential formation of the dioxo form (VIII) at pH 5 and of the enolic form (VII) at pH 9.5. At pH 5, the dicarbonyl intermediate gave no coloration with ferric chloride. UV spectroscopic studies at different pH values strongly indicate that at pH 9.5 a keto-enol equilibrium exists (Fig. 4). At that pH the UV absorption is compounded of a contribution given by the absorption peak noted at 290 mμ at pH 5 and of the peak noted at *ca.* 340 mμ at pH 12 (a ketone having an αβ-ethylenic bond exhibits an absorption peak at *ca.* 330 mμ [9]). A compatible observation was made when II was treated with lime-water and the reaction stopped, by acidification of the mixture, at that time at which VIII was present in maximum amount. The peak initially observed in the UV spectra at 320 mμ then vanished and a new peak appeared at 280 mμ; simultaneously the optical rotation fell by about 50 %. The UV absorption reverted to the former type on making the solution alkaline.

The isolation of the four 1,5-anhydro-glycitols (in the relatively high yield of 60 %) proves that the structure of the intermediate is 1,5-anhydro-2,3-dioxo-D-glucitol. This is the first case reported of isolation and identification of a dicarbonyl intermediate in the alkaline degradation of carbohydrates.

Recently Blears, Machell and Richards [10] reported that when 4-*O*-substituted glucose derivatives were degraded by dilute sodium hydroxide solution, an intermediate was formed which was believed to be a dicarbonyl derivative. It was not pure, although it gave a crystalline osazone. Evidence was also obtained of the presence of fragmentation products, possibly formed from dicarbonyl intermediates.

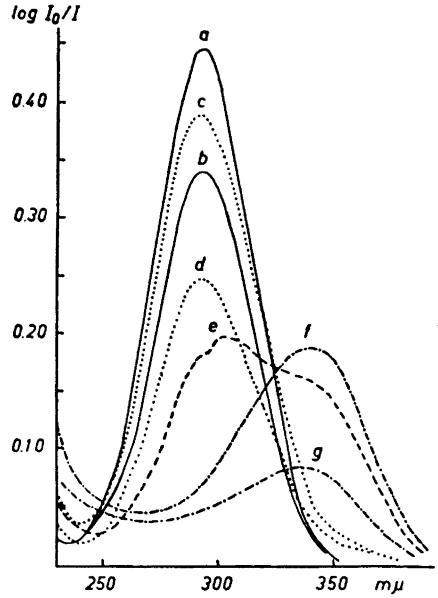

Fig. 4. Ultraviolet absorption spectra of 1,5-anhydro-2,3-dioxo-glucitol in aqueous solutions at different pH-values at 22°. (All four solutions were made from the same stock solution by diluting it to $1.5 \cdot 10^{-4}$ M).

pH 5.0 (0.05 M acetate buffer):	*a*, directly		after	pH	adjustment
	b, 1 day		»	»	»
pH 7.5 (0.05 M phosphate buffer):	*c*, 10—30	min.	»	»	»
	d, 130—150	»	»	»	»
pH 9.5 (0.05 M borate buffer):	*e*, 10—30	»	»	»	»
pH 12.1 (0.02 N lime-water):	*f*, 35—50	»	»	»	»
	g, 110—125	»	»	»	»

From the reaction-mixture produced when methyl 3-oxo-glucoside was treated with lime-water the various neutral products were isolated at that time at which the product VIII was present in maximum amount. The overall yield of neutral products was 65 % and of this three fifths were VIII, one fifth was unreacted methyl 3-oxo-glucoside and one fifth a complex mixture of components. Scission of a carbon-oxygen bond could take place at three sites in β-position to the oxo-group, namely at the two ring-oxygen linkages or at the glycosidic link (see Fig. 1). It is apparent that the reaction proceeded, to a very large extent by elimination of the glycosidic methoxyl to give the intermediate VIII. This view is supported by the fact that the acids were present in roughly the same proportions as were those obtained when a sample of VIII was treated with lime-water; in both cases the mixtures of acids were electrophoretically similar. They have not yet been studied in detail. On treatment of VIII with lime-water also some neutral products were formed. The dicarbonyl compound VIII was unstable over the entire pH range investi-

gated (1.5—12) but most labile on the alkaline side. The reaction-mixtures were studied by paper chromatography and by UV spectroscopy (Fig. 4). These studies indicated that different types of reactions take place under acidic and under basic conditions.

The mixture of neutral products obtained on treating II with lime-water would be expected to be highly complex as numerous reactions will have taken place. In addition to the principal reaction discussed, there may be, for instance, reactions involving epimerisation, molecular fragmentation or the scission of ring-oxygen linkage. From the mixture small amounts of a compound were isolated, which were chromatographically and electrophoretically indistinguishable from methyl β-D-4-oxo-glucopyranoside. On reduction and subsequent hydrolysis it gave glucose and galactose, indicating that epimerisation had taken place at C_4. Two other compounds were isolated having higher R_F-values than VIII. One had a methoxyl group, while the other did not. The latter compound crystallised (m.p. 157—159°) and gave a violet coloration with ferric chloride.

Investigations are continuing on the alkaline degradation of oxo-glucosides. Experiments now in progress show that the degradation of II and III via VIII is of importance even under slightly acidic conditions.

EXPERIMENTAL

Melting points are corrected. The ultraviolet spectra were determined in aqueous solution with a Beckman DU instrument. All solvents were removed by distillation under reduced pressure. Whatman No. 1 paper was normally used for paper chromatography and electrophoresis. Preparative separations were carried out on Whatman No. 3 MM or 31 paper. The following reagents were used in sprays: (a) silver nitrate-sodium hydroxide, (b) *p*-anisidine hydrogen chloride, (c) resorcinol-hydrochloric acid, (d) bromocresol green and (e) ferric chloride.

The irrigants and buffers used were:
A. Ethyl acetate-acetic acid-water, 3:1:3 (upper phase).
B. Butanol-ethanol-water, 10:3:5.
C. Hydrogen sulphite buffer pH 4.7, 0.1 M. (used at 50°) [11].
D. Borate buffer pH 10.0, 0.1 M.
E. Acetate buffer pH 4.0, 0.1 M.

Kinetic studies of the action of lime-water on methyl α-D-3-oxo-glucopyranoside (I), methyl β-D-3-oxo-glucopyranoside (II) and methyl β-D-2-oxo-glucopyranoside (III)

The oxo-glucosides were prepared as previously [4,5] described. The lime-water used was freed from oxygen by bubbling a stream of nitrogen through it.

A sample (35 mg) of II was treated with saturated lime-water (50 ml; 0.042 N; pH 12.3) at 25°. The pH remained practically constant throughout the treatment and fractions were withdrawn at short intervals and immediately shaken with an excess of Amberlite resin IR-120 (H^+) to form the free acids from the calcium salts of the reaction products. Samples of the fractions were placed, with cold air drying of the solutions, on paper chromatograms, some of which were then run in irrigant A and some in irrigant B. One paper of each was treated with spray *a* and one with spray *c* and quantitative estimations were made by visual comparison of the area of the spots produced with those, produced by a series of reference spots corresponding to known amounts of II and of VIII. The

average values obtained are given in Fig. 2. The sample of VIII used for the preparation of the reference solution was freshly isolated from a pure fraction on thick paper chromatograms. The concentration in an aliquot of the stock solution was determined gravimetrically following evaporation of the solvent. The amount of contaminating decomposition products formed between the time of elution of VIII and that of its application to the chromatograms was probably < 5 %.

In another series of experiments samples (63 mg of each) of I, II and III were treated with dilute lime-water (25 ml; 0.019 N, pH 12.1) at 22°. The change in optical rotation was noted (2 dm tube) and samples were withdrawn from time to time and, after acidification (by treatment with Amberlite IR-120, see above), were examined on paper chromatograms. The number of equivalents of acids formed during the alkaline treatment of II was estimated in a separate experiment by back-titration after the addition of an excess of sulphuric acid. The results are given in Fig. 3.

In all three cases the solution became pale yellow and turned cloudy shortly after the maximum optical rotations were observed. This cloudiness may have been due to sparingly soluble calcium salts. The precipitated material was filtered off and nitrogen again passed through the solution. The optical rotations taken before and after the development of the cloudiness all lay on a smooth continuous curve.

Action of lime-water on methyl β-D-3-oxo-glucopyranoside (II) and fractionation of the products

Methyl β-3-oxo-glucoside was treated batchwise (0.2—1.0 g) with oxygen-free lime-water (40 ml 0.02 N/0.1 g of II) at 25° and the products were then fractionated. The course of the reaction was followed polarimetrically and when the maximum rotation was observed the degradation was normally stopped by acidification as previously, giving a pH of *ca.* 4. In a few cases before paper chromatographic separation the solution was rapidly passed through a column containing an excess of Amberlite IR-4 B (free base) from which the acids could then be recovered as ammonium salts. It was found that a better yield of VIII could be obtained if the last ion exchange step was omitted. The acidic products accounted for 25 % and the neutral products for 65 % of the starting material. The solution was concentrated to a volume small enough to be suitable for application to chromatographic papers (the last step of this concentration was by lyophilisation). The separation was carried out on Whatman No. 31 papers by irrigating them with A for 1 3/4 h. After drying the sheets, the positions of the various components were determined in the usual way and they were then eluted. The total time for those procedures was *ca.* 1 h. Four fractions were obtained:

A. A complex mixture of compounds, principally acids, having R_F-values less than that of II.
B. Unreacted II (*ca.* 20 % of the neutral products).
C. Chromatographically pure VIII (*ca.* 60 % of the neutral products).
D. A mixture of compounds having R_F-values higher than that of VIII and containing two major components. (Two minor components giving brown spots were noted on unsprayed chromatograms on which this fraction was examined.)

From fraction A a small amount of a component, indistinguishable from methyl β-D-4-oxo-glucopyranoside, was separated by paper chromatography (irrigant A). On reduction with borohydride and subsequent hydrolysis it gave compounds chromatographically indistinguishable from glucose and galactose.

From fraction D the two principal neutral products were chromatographically separated (each representing about 5 % of the starting II) on Whatman No. 3 MM paper (irrigant A). One of them, which contained no methoxyl gave a strong violet coloration with spray *e*, crystallised (m.p. 157—159°) from aqueous ethanol and the other contained *ca.* 15 % OCH_3.

Characterisation and properties of 1,5-anhydro-2,3-dioxo-D-glucitol (VIII)

Fraction C was slightly contaminated by traces of acetic acid (pH of solution 3—4). Generally the solution was used directly in order to minimize the danger of decomposition. The concentration was determined gravimetrically after evaporating the solvent from an aliquot and drying the amorphous material over P_2O_5. The optical rotations and UV-absorptions of the fresh eluates were determined in several cases (the pH was adjusted to 5). The average values obtained were $[\alpha]_D^{22}$ +155° and $\varepsilon_{max.}$ 3 100 at 293 mμ. In three experiments the solutions were lyophilised in a flask externally cooled to −10°. The syrup obtained, partly crystallised. By treatment of aqueous slurries of this material with either acetone, *n*-propanol or methyl ethyl ketone and acetic acid, small amounts of chromatographically and electrophoretically pure crystalline material (m.p. 53—55°) were obtained. The compound decomposed so readily that it was not possible to crystallise it in the usual way from warmed solvents (even at 0° the crystals decomposed).

Assuming the molecular weight of VIII to be 160, the compound was estimated, by borohydride reduction [12], to contain 1.84 carbonyl groups. It had no methoxyl groups. On paper chromatographic examination it was found to react with silver nitrate, even in the absence of sodium hydroxide, and to give distinctive yellow spots with sprays *b* or *c* but no coloration with sprays *d* or *e*. The compound has $R_{Glucose}$ 4.42 and 2.31 (irrigants A and B, resp.); M_V, 1.62 (buffer C); M_G, 0.63 and 0 (buffers D and E, resp.).

The results of UV-studies on VIII at different pH-values are given in Fig. 4. Products formed from VIII on treating it for various times and at different pH-values (1.5—12) were examined paper chromatographically. A sample of VIII was treated for 30 min with lime-water (0.02 N) and the ammonium salts of the acids formed were compared on electrophoretograms (buffer E) with the ammonium salts mentioned earlier (those obtained on the alkaline treatment of II). The two mixtures were electrophoretically similar, and contained one component which predominated in each case and which had $M_{Gluconic\ acid}$, 1.30.

Reduction of 1,5-anhydro-2,3-dioxo-D-glucitol and fractionation of the products

Samples of VIII (present in freshly isolated eluates) were reduced either by boiling them under reflux with Raney nickel in 70 % ethanol (pH 5) for 3 h, or by treating them with borohydride (pH 9.5) at room temperature for 6 h. After deionisation and evaporation of the solvents the products were chromatographically fractionated (irrigant A) on Whatman No. 3 MM paper (previously washed with water).

Two fractions (1 and 2) were obtained (60 % yield from VIII). The first one was subfractionated by chromatography (irrigant A) and the second one by electrophoresis in borate buffer to give four fractions (1a, 1b, 2a and 2b).

Fraction 1a was treated with charcoal and then crystallised from aqueous ethanol. It was chromatographically and electrophoretically indistinguishable from 1,5-anhydro-D-glucitol and had m.p. and mixed m.p. 141—142° and $[\alpha]_D^{22}$ +43° (*c*, 0.5 in water).

Fraction 1b was crystallised in the same way as above. The product was chromatographically and electrophoretically indistinguishable from 1,5-anhydro-D-mannitol and had m.p. and mixed m.p. 156—157° and $[\alpha]_D^{22}$ −54° (*c*, 0.5 in water).

Fraction 2a was amorphous. The product was chromatographically and electrophoretically indistinguishable from 1,5-anhydro-D-altritol. It had $[\alpha]_D^{22}$ +25 (*c*, 0.5 in water) (Ref.[13] +28.4). The product was acetylated and then gave 2,3,4,6-tetra-*O*-acetyl-1,5-anhydro-D-altritol which had m.p. and mixed m.p. 102—103°.

Fraction 2b was crystallised from aqueous ethanol. The product had m.p. 147—148° $[\alpha]_D^{22}$ +26 (*c*, 0.5 in water) and C 43.8; H 7.28. Calc. for $C_6H_{12}O_5$: C 43.9; H 7.37.

The author is indebted to Mr. A. Assarsson for his skilful assistance and to Dr. N. K. Richtmyer, Bethesda, U.S.A., for a gift of 1,5-anhydro-D-altritol and of 1,5-anhydro-D-galactitol.

REFERENCES

1. Sowden, J. C. *Advances in Carbohydrate Chem.* **12** (1957) 35.
2. Isbell, H. S. *J. Research Natl. Bur. Standards* **82** (1944) 45.
3. Haskins, J. F. and Hogsed, M. I. *J. Org. Chem.* **15** (1950) 1264.
4. Theander, O. *Acta Chem. Scand.* **11** (1957) 1557.
5. Assarsson, A. and Theander, O. *Acta Chem. Scand.* **12** (1958) 1507.
6. Corbett, W. M. and Kenner, J. *J. Chem. Soc. 1954* 5365.
7. Corbett, W. M. and Kenner, J. *J. Chem. Soc. 1955* 5885.
8. Foster, A. B. *Advances in Carbohydrate Chem.* **12** (1957) 81.
9. Mohler, H. *Helv. Chim. Acta* **20** (1937) 289.
10. Blears, M. J., Machell, G. and Richards, G. N. *Chem. & Ind. London* **1957** 1150.
11. Theander, O. *Acta Chem. Scand.* **11** (1957) 717.
12. Lidman-Safwat, S. and Theander, O. *Svensk Papperstidning* **61** (1958) 42.
13. Zissis, E. and Richtmyer, N. K. *J. Am. Chem. Soc.* **77** (1955) 5154.

Received August 7, 1958.

ACTA CHEMICA SCANDINAVICA 12 (1958) 1897—1905

The Oxidation of Glycosides

IX. Acidic and Alkaline Degradation of Methyl β-D-2-Oxo-glucopyranoside and Methyl β-D-3-Oxo-glucopyranoside

OLOF THEANDER

Träkemiska avdelningen, Svenska Träforskningsinstitutet, Stockholm, Sweden

An investigation has been made of the acidic and alkaline degradation of methyl β-D-2-oxo-glucopyranoside (I) and methyl β-D-3-oxo-glucopyranoside (II). Under acidic conditions both gave reductic acid while I also gave D-glucosone and II gave D-ribulose. The degradation of I and II in aqueous solution at pH 4 and pH 7 at 100° was rapid and followed the alkaline type of degradation with elimination of the methoxyl group and formation of the dicarbonyl intermediate, 1,5-anhydro-2,3-dioxo-D-glucitol. The reaction products of I also contained II and D-ribulose. No fundamental differences in the type and pattern of the reaction products from those obtained by degradation of II with either lime-water or sodium hydroxide were detected but the rate of reaction of the dicarbonyl intermediate was much slower when sodium hydroxide was used.

Part VIII [1] described the degradation of some oxo-glucosides by lime-water. The present investigation was undertaken to study the degradation of methyl β-D-2-oxo-glucopyranoside (I) and of methyl β-D-3-oxo-glucopyranoside (II) at other pH values and to compare the effect of using sodium hydroxide as the base instead of lime-water.

When the oxo-glucosides were treated with sulphuric acid (0.5 N at 100°) the solution rapidly developed a yellow coloration, then gradually turned brownish and formed a dark coloured precipitate. The hydrolysate had a smell similar to that of furfural. Under similar conditions methyl β-D-glucopyranoside turned only slightly yellow. A semi-quantitative determination (Fig. 1) showed that the rates of hydrolysis of I, II and the unsubstituted methyl glucoside were rather similar and followed the sequence: methyl 3-oxo-glucoside > methyl 2-oxo-glucoside > methyl glucoside. The dioxo sugars formed by hydrolysis of I and II would be expected to be much more reactive than glucose. The oxo-glucosides were not hydrolysable with β-glucosidase.

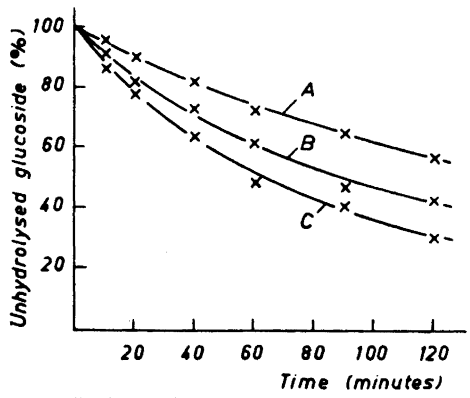

Fig. 1. Treatment of methyl β-D-glucopyranoside (A), methyl β-D-2-oxo-glucopyranoside (B) and methyl β-D-3-oxo-glucopyranoside (C) with 0.5 N sulphuric acid at 100°.

Under hydrolytic conditions that gave mostly glucose and only small amounts of further degradation products from methyl β-glucoside, there was formed from the oxo-glucosides a very complex mixture of compounds that gave positive and very characteristic reactions with silver nitrate-sodium hydroxide, *p*-anisidine hydrochloride, resorcinol-hydrochloric acid and 2,4-dinitrophenylhydrazine reagents. Electrophoresis in hydrogen sulphite buffer [2] was found to be particularly useful in studying the products and gave good separations and round, well-defined spots. Some compounds were present in the hydrolysates from both I and II, some were present only when shorter reaction times were used.

From the degradation of both I and II there was isolated an acidic, strongly reducing crystalline compound that was shown to be reductic acid (III). This substance was obtained by Reichstein and Oppenauer [3] by acid treatment of monomeric uronic acids or polyuronides in a yield of 7 % and in small amounts from xylose. Sohn [4] has recorded its formation in small amount on acid treatment of oxidised cellulose. The acid treatment of oxo-glucosides in the present investigation seems to give a higher yield of this substance than has been obtained previously from other carbohydrates and in this case it is probably an intermediate in the main path of degradation. It was isolated in 22 % yield from the degradation of methyl 3-oxo-glucoside. Other compounds that were obviously associated with the occurrence of reductic acid were also present such as furfural which was isolated in small amounts and has previously[3] been shown to be formed by acid treatment of III, oxidation products of the easily oxidisable III and a product that did not migrate an electrophoresis in hydrogen sulphite but gave the same characteristic reactions as III with several different reagents.

A liquid compound was formed from both I and II (ca. 5 %) which had a relatively high mobility in electrophoresis in hydrogen sulphite ($M_{Vanillin}$ = 1.70), did not reduce a neutral silver solution, gave a characteristic colour reaction with *p*-anisidine hydrochloride and with resorcinol-hydrochloric acid and rapidly gave a precipitate with 2,4-dinitrophenylhydrazine. In addition

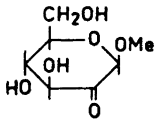
I

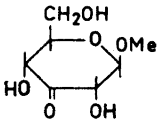
II

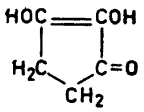
III

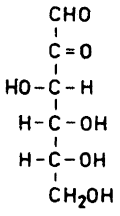
IV

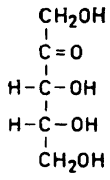
V

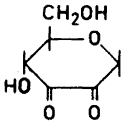
VI

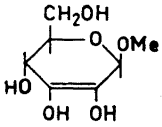
VII

to these compounds there were a few other very minor components that were present in the products from both I and II.

D-Glucosone (IV) was isolated in about 20 % yield from the product obtained from I*. Attempts to isolate a corresponding 3-oxo-glucose from the product from II were unsuccessful. This sugar is probably more reactive than IV. However a small amount of D-ribulose (V, 1.5 %) which might have arisen from cleavage of 3-oxo-glucose was isolated from a hydrolysate of II. Ribulose could not be detected in the hydrolysate from I.

In the preceding paper [1] it was shown that both I and II are degraded very rapidly at room temperature by lime-water and that the principal course of the degradation involves elimination of the methoxyl group and the formation of 1,5-anhydro-2,3-dioxo-D-glucitol (VI) which then gives rise to acids, probably by a benzilic acid type rearrangement. Blears, Machell and Richards [5] have reported that the alkaline degradation of 4-*O*-substituted glucose derivatives gives greater amounts of the dicarbonyl intermediate and that the fragmentation of this intermediate was favoured at the expense of saccharinic acid formation when dilute sodium hydroxide solution was used instead of lime-water. In the present investigation a comparison was made of the results of treatment of methyl β-3-oxo-glucoside (II) with lime water and with sodium

* *Addeed in proof:* No reductic acid was detected on treatment of D-glucosone under acid conditions in the same way as methyl 2-oxo-glucoside (I). This indicates that formation of the five-membered ring might not be preceded by hydrolysis of I.

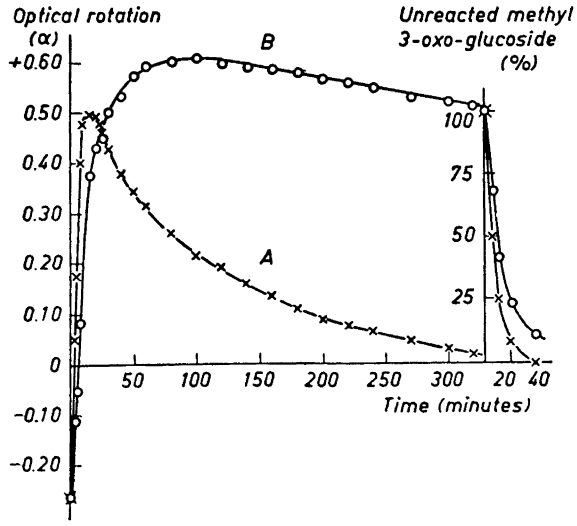

Fig. 2. Treatment of methyl β-D-3-oxo-glucopyranoside with A. lime water (— × — × —) and B sodium hydroxide (—O—O—), 0.018 N at 23°.

hydroxide. The degradation was followed by the optical rotation, by semi-quantitative determination of II (Fig. 2) and by paper chromatographic examination. The dicarbonyl intermediate (VI) reacted much more slowly in sodium hydroxide solutions than in lime-water; II was also degraded somewhat more slowly by sodium hydroxide. The only difference which was detected between samples taken from the two reaction mixtures when the rotation was a maximum was a somewhat lower amount of II and a larger amount of VI in the sodium hydroxide product. No other difference was detected in either the neutral or the acid products which could indicate that the reactions with sodium hydroxide were any different from those with lime-water.

The stability of the oxo-glucosides at the neutral point and at a pH value (pH 4) near that at which carbohydrates are known to be most stable was also of interest.

On treatment of either I or II at pH 7 (at 100°) the solution turned yellow in a few minutes just as in alkaline treatment at room temperature paper chromatographic examination showed that they underwent the same degradation *via* the dicarbonyl intermediate VI as when treated with alkali. In a large scale experiment with the methyl 2-oxo-glucoside (I) at pH 7 for 10 min, methyl 3-oxo-glucoside (18 %) and D-ribulose (3 %) were isolated; most of the remainder of the product was made up of compounds similar to those formed in the alkaline degradation. No methyl 3-oxo-mannoside (an epimerisation product that would be expected together with II) could be isolated and if present it was probably only in much smaller amount than II.

In a large scale experiment with the methyl 3-oxo-glucoside (II) at pH 7 the dicarbonyl intermediate VI and the neutral, unidentified crystalline com-

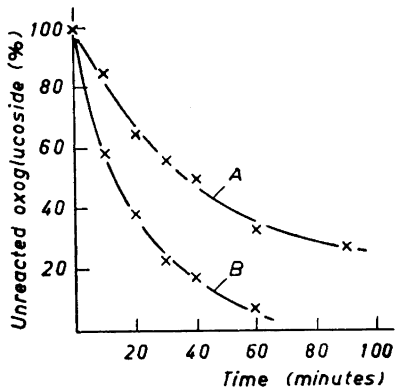

Fig. 3. Treatment of methyl β-D-2-oxo-glucopyranoside and methyl β-D-3-oxo-glucopyranoside at pH 4 and 100°. A. Methyl 3-oxo-glucoside. B. Methyl 2-oxo-glucoside.

pound that had been obtained by alkaline treatment were isolated; traces of I were also detected. The acids obtained showed a similar paper electrophoretic pattern to those from the product of alkaline treatment.

The principal neutral products obtained at pH 4 were the same as those obtained at pH 7 but the rate of degradation was slower. Semi-quantitative determinations of I and II were made throughout the course of the reaction (Fig. 3). The 2-oxo-glucoside was rapidly converted to the 3-oxo-glucoside which then underwent a further change *via* VI. This compound was isolated and identified chromatographically and was shown electrophoretically to give the expected products on reduction with Raney nickel and with borohydride. These results show that the mechanism of the alkaline degradation of oxo-glucosides involving epimerisation, the elimination of the methoxyl group and the formation of a dicarbonyl intermediate is also operative under slightly acid conditions. Whether the further transformation of the dicarbonyl intermediate follows the benzilic acid type rearrangement at this low pH value is, however, uncertain since preliminary results have shown [1] that VI is transformed in different ways at low and high pH values.

Among the products obtained by treatment of I and II at pH 4 there was found in small amount a compound with the same chromatographic behaviour and giving the same reactions with the reagents used as the possible enediol VII, that was suggested [1] as an intermediate in the formation of II on alkaline treatmetnt of I.

In an aqueous solution of methyl β-2-oxo-glucoside in contact with an excess of a weakly basic resin (Amberlite IR-4B: free base) for 4 h at room temperature there was formed about 10 % of methyl β-3-oxo-glucoside. However, when the latter was treated in the same way only traces of transformation products were detected. The 3-oxo-glucoside as well as the possible enediol (VII) mentioned above were detected in a solution of the 2-oxo-glucoside in distilled water after keeping at 4° for a few months but no transformation products were found in a solution of the 3-oxo-glucoside kept under similar conditions.

EXPERIMENTAL

Melting points are corrected. All solvents were removed either by distillation under reduced pressure or by lyophilisation. Paper chromatograms were normally run on Schleicher and Schüll No. 2043 a paper; preparative chromatographic separations were done on Whatman 3MM (after thorough washing) or 31 papers; paper electrophoreses were run on Whatman 3MM paper.

The spray reagents used were: (a) silver nitrate-sodium hydroxide, (b) *p*-anisidine hydrochloride, (c) resorcinol-hydrochloric acid, (d) 2,4-dinitrophenylhydrazine-hydrochloric acid and (e) ferric chloride.

The eluting solvents and buffers used were:

A Ethyl acetate-acetic acid-water, 3:1:3 (upper phase)
B Butanol-ethanol-water, 10:3:5
C Hydrogen sulphite buffer pH 4.7, 0.1 M[2] (used at 50°, M_V = migration relative to that of vanillin)
D Borate buffer, pH 10.0, 0.1 M
E Acetate buffer pH 4.0, 0.1 M
F Phosphate buffer pH 7.0, 0.1 M

Reaction of methyl β-2-oxo-glucopyranoside (I) and methyl β-3-oxo-glucopyranoside (II) with sulphuric acid

Solutions of I, II (prepared as previously [6] described) and methyl β-D-glucopyranoside (0.5 ml, 1 %) in 0.5 N sulphuric acid in sealed glass tubes were kept in a water bath at 100° for different times. After cooling, water (1 ml) was added and the pH was adjusted to 5 by the addition of dry Amberlite resin IR 4B (free base). Aliquots of these solutions were paper chromatographed using solvent A and semi-quantitative determinations were made of the components present by visual estimation on three runs as described previously [1]. For comparison, the amounts of unhydrolysed glucoside in the products from the methyl glucoside were calculated from determinations of glucose by the method of Saeman [7]; the two methods gave good agreement. The kinetic results are shown in Fig. 1.

Paper chromatographic and electrophoretic (buffer C) studies showed that the products obtained from I and II were quite complicated mixtures but there were only a few main components.

Separation of the degradation products obtained from II. In a preliminary large scale experiment, a solution of II (1.00 g) in sulphuric acid (100 ml, 0.5 N) was kept in a water bath at 100° for 2 h. The brownish hydrolysate after cooling was filtered to remove the small amounts of brown precipitate and then extracted continuously with ether for 24 h. The semi-solid dark brown product obtained on evaporation of the ethereal solution contained two main components, A and B, with M_V-values of 1.07 and 1.70 respectively (buffer C) and a considerable amount of material which did not migrate in this buffer. Some minor products were also present which had high migration values in buffers E and F. The product was distilled in a vacuum (ca. 0.06 mm of Hg). A colourless oil distilled at 85° which contained largely B together with traces of other compounds. At 125° a colourless product sublimed which was found to be pure A. It was recrystallised from methanol-methyl ethyl ketone and identified as reductic acid (III). The principal component remaining in the ether-extracted aqueous solution was unchanged II (0.228 g).

Since the hydrolysates from the kinetic investigation showed that some components of the products of the degradation were more rapidly destroyed than others, a solution of II (0.50 g) in 0.5 N sulphuric acid was heated in a water bath at 100° for only 30 min. Chromatography on thick filter paper gave about 60 per cent of II together with a mixture containing principally A and B and, in addition, small amounts (1.5 %) of a compound which was isolated and shown to be D-ribulose (V).

To give a better idea of the proportions of the different components present a further large scale run was made omitting the somewhat drastic distillation step. II (1.00 g) was heated in 0.5 N sulphuric acid (100 ml) for 3 h in a water bath at 100°. The hydrolysate (which had a smell of furfural) was diluted with water (100 ml) and distilled at ordinary pressure until 100 ml had been distilled off. Furfural only was detected in this fraction (by electrophoresis using buffer C); estimation by colorometric analysis showed that 15 mg was present. The hydrolysate, which was now free of the smell of furfural, was continuously extracted with ether for 4 days. The aqueous phase was treated with barium carbonate, deionised on Amberlite IR-120 (H^+) and taken to dryness (0.24 g). The ether extract was evaporated (0.43 g) and on crystallisation gave reductic acid (85 mg) in an electrophoretically pure state; the mother liquor was fractionated by electrophoresis on thick filter paper using buffer C. The strips containing separate fractions were eluted with water and the resultant solutions treated with barium carbonate to a pH 5—6, filtered, passed through an Amberlite IR-4B (free base) column and taken to dryness by lyophilisation. Before evaporation the fraction containing reductic acid was given a short treatment with hydrogen sulphide to reduce any tri-oxo-pentane which might have been present [8]. The material not extracted by ether contained some B but only small amounts of reductic acid; it was fractionated by paper chromatography on thick filter paper using solvent A. The two fractionations gave unreacted II (165 mg) reductic acid (90 mg) and B (45 mg).

Separation of the degradation products from I. Methyl β-2-oxo-glucoside (I, 200 mg) was heated in sulphuric acid solution (0.5 N, 20 ml) for 3 h in a water bath at 100°. Chromatography on thick filter paper (solvent A) gave: unreacted I (35 mg), D-glucosone (30 mg) and reductic acid (20 mg). The substance B that had been isolated from the product of acid treatment of II was present but no trace of ribulose could be detected.

Reductic acid (II). Recrystallisation from a methanol-methyl ethyl ketone mixture gave reductic acid, m.p. 211—212°, undepressed on admixture with an authentic sample, $R_F = 0.65$ (solvent A), $M_V = 1.07$ (buffer C). The infrared spectrum was identical with that of authentic material. It reduced a neutral silver solution immediately at room temperature and gave a characteristic green-yellow coloration with spray reagent *b*. These two characteristic spray reactions were also given by small amounts of material with $M_V = 0$ on an electrophoretogram (buffer C) of the ether extract from II. The product of oxidation of the reductic acid with iodine, as described by Reichstein and Oppenauer [8] in their preparation of trioxo-pentane from reductic acid, gave two spots on electrophoretograms (buffer C) with M_V-values 2.03 and 2.12, respectively, and a single elongated spot $R_F = 0.31$ on paper chromatograms (solvent A). These spots were detected by reduction of a neutral silver solution at room temperature or by a red brown coloration with spray reagent *b*. It was found that the same substances were also present in smaller amounts in the ether extract from II and were formed in a few days when the easily oxidisable reductic acid was kept in aqueous solution at room temperature.

Furfural. It was electrophoretically shown to be indistinguishable from an authentic sample and characterised as its 2,4-dinitro-phenylhydrazone, m.p. and mixed m.p. 228°.

Compound B. This was not identified. It distilled at 85—90°/ca 0.06 mm; $R_F = 0.56$ (solvent A), $M_V = 1.70$ (buffer C), $M_V = 0$ (buffer F). It reduced alkaline silver solution immediately, gave on orange colour with spray reagent *b* and pink colour with spray reagent *c*. It gave an orange precipitate immediately with 2,4-dihitrophenylhydrazine. It did not give reductic acid on acid treatment.

D-*Ribulose* (V). The amorphous compound, $[\alpha]_D^{24}$ ca. −15°, (*c*, 0.5 in water), paper chromatographically and electrophoretically indinstinguishable from authentic material. The gray colour with spray reagent *c* was particularly characteristic and sensitive. Part of the product was converted to the *o*-nitrophenylhydrazone, m.p. and mixed m.p. 167—168°. Part of the product was reduced with borohydride, deionised and acetylated (acetic anhydride-pyridine). The two acetates obtained were indistinguishable from the authentic acetates of ribitol and D-arabitol by paper chromatography using the method of Wickberg [9] with formamide + dimethyl formamide as stationary phase and eluting with light petroleum (b.p. 60—70°).

D-*Glucosone* (IV). The amorphous compound was paper chromatographically and electrophoretically (buffer C; M_V = 1.24) indistinguishable from authentic D-glucosone. It was characterised by the formation at room temperature of D-glucose phenylosazone, m.p. and mixed m.p. 205–207°.

Reaction of methyl β-D-3-oxo-glucopyranoside (II) with lime-water and with sodium hydroxide

Two series of experiments were made on the reactions of II (50 mg) in lime-water (25 ml, 0.018 N) and in aqueous sodium hydroxide solution (25 ml, 0.018 N) at 23°. At intervals the change in optical rotation was determined and samples were withdrawn, acidified with Amberlite IR-120 and examined by paper chromatography and electrophoresis; a semi-quantitative estimation of the amount of unreacted II present was also made using the method previously[1] described. The results are shown in Fig. 2. Oxygen was removed from the basic solutions by bubbling nitrogen through the solutions, but later experiments showed that degradation proceeded at the same rate without this treatment.

Reaction of methyl β-D-2-oxo-glucopyranoside (I) and methyl β-D-3-oxo-glucopyranoside (II) at pH 7

Methyl β-3-oxo-glucoside (II, 500 mg) in 0.2 N phosphate buffer (50 ml) was kept in a water bath at 100° for 30 min. A yellow colour appeared after a few minutes and gradually increased in strength. After cooling the solution was stirred with Amberlite IR-120 (H+) and then with Amberlite IR-4B (free base), the pH was adjusted to 5 and the solution was concentrated to a small volume and separated on Whatman No. 31 paper (solvent A). The neutral product (240 mg) gave unreacted II (85 mg), 1,5-anhydro-2,3-dioxo-D-glucitol (VI) (65 mg) and the unidentified crystalline compound previously[1] obtained from the alkaline treatment of II (5 mg), m.p. and mixed m.p. 156–158°. Traces of I were detected but no ribulose was present. The acids were recovered as the ammonium salts from the Amberlite IR-4B resin; electrophoresis showed a similar pattern to that given by the corresponding product from the alkaline treatment.

Methyl β-2-oxo-glucoside (I, 250 mg) was treated in the same way as above for 10 min. After deionisation the product was fractionated on a carbon-Celite column (2.5 × 22 cm) using gradient elution and gave unreacted I (20 mg), D-ribulose (15 mg) and II (70 mg); other minor compounds were also present. D-Ribulose was characterised as above. The methyl β-3-oxo-glucoside (II), m.p. and mixed m.p. 130–131°, $[\alpha]_D^{22}$ −61° (*c*, 2 in water) was chromatographically and electrophoretically identical with an authentic sample.

Treatment of methyl β-D-2-oxo-glucopyranoside (I) and methyl β-D-3-oxo-glucopyranoside (II) at pH 4

Two series of experiments were made with I and II, respectively. Solutions of the substance in 0.2 N acetate buffer (0.5 ml, 1 %) in sealed glass tubes were kept in a water bath at 100° for different times. After cooling. the samples were diluted with water (1 ml), excess Amberlite IR-120 (H+) was added and semi-quantitative determinations were made of unreacted I and II present as described previously. The results are shown in Fig. 2.

In one experiment, II (250 mg) in 0.2 N acetate buffer (25 ml) was kept in a water bath at 100° for 45 min. After cooling and deionisation the product was separated on Whatman No. 31 paper (solvent A) giving: unreacted II (90 mg), VI (15 mg); the unidentified crystalline product (m.p. 156–158°) mentioned above was detected by paper chromatography. A part of VI was reduced with borohydride and with Raney nickel and the four 1,5-anhydroglycitols obtained were characterised by paper electrophoresis (buffer D) as described previously[1].

The author is indebted to Mr. A. Assarsson for his skilful assistance and to Professor T. Reichstein, Basel, Switzerland, for a gift of reductic acid.

REFERENCES

1. Theander, O. *Acta Chem. Scand.* **12** (1958) 1887.
2. Theander, O. *Acta Chem. Scand.* **11** (1957) 717.
3. Reichstein, T. and Oppenauer, R. *Helv. Chim. Acta* **16** (1933) 988.
4. Sohn, W. A. *Angew. Chem.* **60** (1948) 284.
5. Blears, M. J., Machell, G. and Richards, G. N. *Chem. & Ind. London* **1957** 1150.
6. Assarsson, A. and Theander, O. *Acta Chem. Scand.* **12** (1958) 1507.
7. Saeman, J. F., Moore, W. E. Mitchell, R. L. and Millett, M. A. *Tappi* **37** (1954) 336.
8. Reichstein, T. and Oppenauer, R. *Helv. Chim. Acta* **17** (1934) 390.
9. Wickberg, B. *Acta Chem. Scand.* **12** (1958) 615.

Received September 17, 1958.

ACTA CHEMICA SCANDINAVICA 12 (1958) 1906—1910

On the Reaction between Substituted Cyanoacetic Esters and Methylene Bromide. The Preparation of α,α′-Di-(*tert.*-butyl)-glutaric Acid

LENNART EBERSON

Department of Organic Chemistry, Chemical Institute, University of Lund, Sweden

Ethyl methyl-, ethyl-, *iso*propyl-, and *tert.*-butylcyanoacetate, in the form of their sodium compounds, react with methylene bromide with the formation of 1,3-dialkyl-1-carbethoxyglutaronitriles, *i.e.*, one carbethoxy group is eliminated during the reaction. These compounds on hydrolysis and decarboxylation give the diastereoisomers of the corresponding α,α′-dialkylsubstituted glutaric acids.

A monoalkylsubstituted malonic ester, in the form of its sodium compound, reacts with methylene bromide with the formation of a 1,3-dialkyl-1,1,3-tricarbethoxypropane [1,2]. One carbethoxy group is eliminated as diethyl carbonate. The yields of the products were dependent on the nature of the alkyl substituent in the way shown in Table 1.

Table 1. Yields of 1,3-dialkyl-1,1,3-tricarbethoxypropanes.

Alkyl group	Yield of product in %
CH_3 [1]	83
C_2H_5 [1]	61
n-C_3H_7 [1]	68
iso-C_3H_7 [1]	39 [a]
n-C_4H_9 [1]	74
iso-C_4H_9 [1]	51
tert.-C_4H_9 [1]	0 [a,b]
n-C_5H_{11} [1]	77
neo-C_5H_{11} [1]	0 [c]
$(CH_3)_3SiCH_2$ [2]	62
$C_6H_5CH_2$ [1]	77

a. The reaction was carried out in ethanol-toluene solution to attain an increased reflux temperature. b. Only unchanged starting material was obtained. c. The product was mainly ethyl α-*neo*pentylacrylate.

Thus branching at the α- or β-position in the alkyl group retards or, as for the *tert.*-butyl and *neo*pentyl derivatives, completely inhibits the reaction. It was suggested that the unreactivity of diethyl *tert.*-butylmalonate was due to its considerably reduced CH-acidity rather than the presence of the bulky *tert.*-butyl group. For the *neo*pentyl derivative the situation is another, as this compound is readily alkylated with alkyl halogenides in ethanolic solution [3] and apparently has an acidity comparable with that of *n*-alkylmalonic esters. In the reaction with methylene bromide diethyl bromomethyl-*neo*pentylmalonate consequently is formed and then split by sodium ethoxide into ethyl α-*neo*pentylacrylate, diethyl carbonate, and sodium bromide. This acrylic ester has been found to be very resistant to addition reagents and thus the reaction will stop at this stage. The unreactivity probably depends on the steric influence of the *neo*pentyl group. The difference between the rates of bromine addition to *tert.*-butylethylene and *neo*pentylethylene has been explained in the same way [4]. The great difference between the *neo*pentyl group and its silicon analogue, the trimethylsilylmethyl group [5], also manifests itself in this reaction.

As the cyano group is known to have a greater acid-strengthening effect than the carbethoxy group, the reaction between ethyl *tert.*-butylcyanoacetate and methylene bromide was studied in order to test the above hypothesis. In fact the reaction product consisted of I, R = *tert.*-butyl, formed according to the formula:

$$2\ \mathrm{R.CH(CN)COOEt} + \mathrm{CH_2Br_2} + 2\ \mathrm{OEt^-} \longrightarrow$$

$$\mathrm{R.C(CN)COOEt}\ (\mathrm{R.CH.CN}\ \text{—}\ \mathrm{CH_2}) + \mathrm{EtOH} + (\mathrm{EtO})_2\mathrm{CO} + 2\ \mathrm{Br^-}$$

I

with the elimination of one carbethoxy group, in close analogy with the behaviour of monosubstituted malonic esters. In ethanolic solution the yield was 19 %, whereas addition of toluene to the reaction mixture in order to increase the reflux temperature gave 52 % yield. Ethyl methyl-, ethyl-, and *iso*propylcyanoacetate in ethanolic solution similarly gave I, R = CH_3, C_2H_5, and *iso*-C_3H_7 in 70, 77, and 58 % yield, respectively.

I, R = *tert.*-C_4H_9 was purified by distillation *in vacuo* and then solidified on standing, m.p. 75—80°. Recrystallization from 80 % methanol gave m.p. 79—81°. The small change in m.p. indicates that the substance which is capable of existing in two diastereoisomeric forms either is produced in preponderantly one form or that the solid consists of the eutectic mixture. The formation of both forms of α,α'-di-(*tert.*-butyl)-glutaric acid is no conclusive evidence, as the drastic conditions necessary for hydrolysis are likely to affect the asymmetric centra. Recrystallization from several solvents and solvent pairs had no effect upon the m.p.

Zelinsky [6] and Auwers and Thorpe [7] carried out the same reaction with ethyl methylcyanoacetate and methylene iodide and claimed that 1,3-dimethyl-

1,3-dicarbethoxyglutaronitrile was formed in about 50 % yield. However, as their analyses did not agree well with this formula and the substance was stated to be difficult to purify owing to decomposition during distillation, it seems probable that their compound actually was I, R = CH_3. This is also indicated by the b.p. reported, 165—170°/12 mm. For comparison it should be mentioned that 1,3-dicarbethoxyglutaronitrile has b.p. 195°/20 mm [8].

I, R = *tert.*-C_4H_9, was very resistant to hydrolysis in acid or alkaline solution. Sulphuric acid of various strengths was either without effect or caused decomposition due to oxidation. Boiling ethanolic potassium hydroxide also left the substance unchanged. However, boiling with excess potassium hydroxide in ethylene glycol containing some water (boiling temperature about 175°) converted it into a mixture of the monoamides of α,α'-di-(*tert.*-butyl)-glutaric acid, which could be separated by fractionated crystallization from acetic acid, m.p. 242—243° and 214—216°, respectively. Apparently the carbethoxy group (or one of the cyano groups) was eliminated directly during this procedure, as evidenced by the evolution of large amounts of carbon dioxide on acidification. In order to hydrolyze the remaining amide group the monoamides were dissolved in a mixture of concentrated hydrochloric acid and acetic acid and treated with sodium nitrite. This method gave the two forms of α,α'-di-(*tert.*-butyl)-glutaric acid in almost quantitative yields, m.p. 221—222° and 213—214°. The eutectic m.p. was 189°. The amide with m.p. 242—243° corresponded to the acid with m.p. 213—214°.

1,3-Dimethyl-, 1,3-diethyl-, and 1,3-di*iso*propyl-1-carbethoxyglutaronitrile (I, R = CH_3, C_2H_5, and *iso*-C_3H_7) were hydrolyzed and decarboxylated in acid media as described in the experimental part. The acid mixtures obtained were separated into diastereoisomers according to known procedures. [1,9,10]

EXPERIMENTAL

The preparation of 1,3-di-(tert.-*butyl*)*-1-carbethoxyglutaronitrile (I, R =* tert.-C_4H_9*) in ethanolic solution.* Sodium, 4.6 g (0.2 mole), was dissolved in 70 ml of absolute ethanol, and 33.8 g (0.2 mole) of ethyl *tert.*-butylcyanoacetate were added followed by 17.4 g (0.1 mole) of methylene bromide. The reaction mixture was allowed to boil for 24 h after which time it reacted almost neutrally. After neutralization with acetic acid the ethanol was distilled off and the residue treated with water. The organic layer was taken up in ether and the ether solution washed with water and finally dried with anhydrous magnesium sulphate. Fractionation yielded besides unchanged starting material 5.7 g of I, R = *tert.*-C_4H_9, b.p. 113—114°/1 mm, which solidified upon standing, m.p. 75—80°. After recrystallization from 80 % aqueous methanol 5.2 g of the pure compound were obtained, m.p. 79—81°. Further recrystallizations from 80 % aqueous methanol, 80 % aqueous ethanol, petroleum ether, benzene-petroleum ether, or ethyl acetate-petroleum ether did not change the m.p. (Found: C 68.9; H 9.3; N 10.0. Calc. for $C_{16}H_{26}O_2N_2$: C 69.0; H 9.4; N 10.1). The yield was 19 %.

The preparation of I, R = tert.-C_4H_9*, in ethanol-toluene solution.* Sodium, 11.5 g (0.5 mole), was heated under 200 ml of toluene until the metal had melted. A mixture of 40 ml of absolute ethanol and 84.5 g (0.5 mole) of ethyl *tert.*-butylcyanoacetate was added during a period of 10 min whereby a vigorous reaction occurred. To the resulting yellow solution were added 43.5 g (0.25 mole) of methylene bromide, and the mixture was kept at reflux temperature for 36 h, after which time it reacted neutrally. Water was added and the product was isolated and purified as above, b.p. 150—152°/4 mm, m.p. after recrystallization from 80 % aqueous methanol 79—81°. The yield was 29.8 g (52 %), based on unrecovered starting material (69.3 g).

The monoamides of a,a'-di-(tert.-*butyl*)-*glutaric acid.* 1,3-di-(*tert.*-butyl)-1-carbethoxyglutaronitrile, 13.9 g (0.05 mole), was slowly heated together with 28.0 g (0.5 mole) of potassium hydroxide, 80 ml of ethylene glycol, and 5 ml of water. A vigorous reaction occurred, and when it had subsided the solution was refluxed for 20 h. After cooling it was poured into 150 ml of water. On acidification with concentrated hydrochloric acid large amounts of carbon dioxide were evolved and a solid was obtained. The latter was very difficult to filter owing to contamination with silicon dioxide from the reaction vessel. After drying it weighed 15.7 g. A small amount was treated with boiling ethyl acetate, filtered from insoluble matter, and the solution allowed to cool slowly. Crystals with m.p. 235—240° separated, m.p. after another recrystallization from ethyl acetate 242—243°. The mother liquor from the first filtration was freed from solvent and the residue recrystallized twice from aqueous acetic acid, m.p. 214—216°. (Found for the monoamide with m.p. 242—243°: C 64.0; H 10.2; N 5.8; equiv. wt. 243.5. Found for the monomide with m.p. 214—216°: C 64.2; H 10.4; N 5.8; equiv. wt. 242.3. Calc. for $C_{13}H_{25}O_3N$: C 64.2; H 10.4; N 5.8; equiv. wt. 243.3).

a,a'-Di-(tert.-*butyl*)-*glutaric acid.* Crude mixture of the monoamides, 3.0 g, was dissolved in 50 ml of glacial acetic acid and filtered from insoluble matter. Concentrated hydrochloric acid, 10 ml, was added and the solution cooled in an ice-bath. When the temperature was below 5°, a solution of 3.0 g of sodium nitrite in a few ml of water was added slowly. The mixture was cautiously heated in a water-bath whereby evolution of nitrogen began at about 40°. When the gas evolution had ceased, the solution was boiled for 10 min and then diluted with 300 ml of water. The solid was filtered and dried (1.4 g). It was dissolved in a mixture of ethyl acetate and benzene (1:1) and the solution allowed to cool. The crystals were filtered, m.p. 220—222°, and recrystallized once from glacial acetic acid, m.p. 221—222° (0.5 g). The mother liquor was evaporated to dryness and the residue recrystallized twice from aqueous acetic acid, m.p. 213—214° (0.45 g). The eutectic mixture melted at 189°. (Found for the acid with m.p. 221—222°: C 63.8; H 9.9; equiv. wt. 121.8. Found for the acid with m.p. 213—214°: C 63.7; H 9.9: equiv. wt. 122.7. Calc. for $C_{13}H_{24}O_4$: C 63.9; H 9.9; equiv. wt. 122.2).

When small amounts of the pure monoamides were treated in the same way, almost quantitative yields of the respective acids were obtained. The amide with m.p. 242—243° corresponded to the acid with m.p. 213—214°.

1,3-Dimethyl-1-carbethoxyglutaronitrile (*I*, $R = CH_3$). This compound was prepared from 0.2 mole of sodium dissolved in 70 ml of ethanol, 0.2 mole of ethyl methylcyanoacetate, and 0.1 mole of methylene bromide. The reflux time was 24 h. The product was isolated as above, b.p. 137—138°/4 mm, n_D^{20} 1.4438, d_4^{20} 1.0354, yield 70 %. (Found: C 61.4; H 7.3; N 14.0; r_D 0.2564. Calc. for $C_{10}H_{14}O_2N_2$: C 61.8; H 7.3; N 14.4; r_D 0.2560).

a,a'-Dimethylglutaric acid. 1,3-Dimethyl-1-carbethoxyglutaronitrile was hydrolyzed and decarboxylated by boiling with concentrated hydrochloric acid for 20 h. The yield of crude acid mixture was almost quantitative and it was separated into the diastereoisomers according to Möller [9], m.p. 140—141° and 125—127°, respectively.

1,3-Diethyl-1-carbethoxyglutaronitrile (*I*, $R = C_2H_5$). This compound was prepared in the same way as the methyl derivative in a 0.2 mole run, b.p. 151—153°/4 mm, n_D^{20} 1.4468, d_4^{20} 1.0088, yield 77 %. (Found: C 64.6; H 8.1; N 12.5; r_D 0.2648. Calc. for $C_{12}H_{18}O_2N_2$: C 64.8; H 8.2; N 12.6; r_D 0.2655).

a,a'-Diethylglutaric acid. 1,3-Diethyl-1-carbethoxyglutaronitrile was hydrolyzed and decarboxylated by boiling with 50 % sulphuric acid for 12 h. The yield of crude acid mixture was almost quantitative and it was separated into the diastereoisomers according to Berner and Landmark [10], m.p. 119—121° and 92—94°, respectively.

*1,3-Di*iso*propyl-1-carbethoxyglutaronitrile* (*I*, R = iso-C_3H_7). This compound was prepared in the same way as the methyl derivative in a 0.5 mole run, b.p. 136—142°/2 mm, n_D^{20} 1.4523, d_4^{20} 0.9992, yield 58 %. (Found: C 67.0; H 8.9; N 11.3; r_D 0.2701. Calc. for $C_{14}H_{22}O_2N_2$: C 67.2; H 8.9; N 11.2; r_D 0.2728).

*a,a'-Di*iso*propylglutaric acid.* 1,3-Di*iso*propyl-1-carbethoxyglutaronitrile was hydrolyzed and decarboxylated by boiling with 80 % sulphuric acid for 20 min. The yield of crude acid mixture was 90 %, and it was separated into diastereoisomers according to Eberson [1], m.p. 141—142° and 119—120°, respectively.

The author wishes to express his sincere gratitude to Professor Erik Larsson for his kind interest in this work. A grant from the *Kungliga Fysiografiska Sällskapet* is gratefully acknowledged.

REFERENCES

1. Eberson, L. *Acta Chem. Scand.* **12** (1958) 314.
2. Eberson, L. *Acta Chem. Scand.* **9** (1955) 1711.
3. Brändström, A. *Private communication.*
4. Newman, M. S. *Steric Effects in Organic Chemistry.* John Wiley & Sons, Inc. New York 1956, p. 244.
5. Whitmore, F. C. and Sommer, L. H. *J. Am. Chem. Soc.* **68** (1946) 481.
6. Zelinsky, N. *Ber.* **22** (1889) 2823.
7. Auwers, K. and Thorpe, J. F. *Ann.* **285** (1895) 310.
8. Higson, A. and Thorpe, J. F. *J. Chem. Soc.* **89** (1906) 1458.
9. Möller, E. *Kgl. Fysiograf. Sällskap. Lund. Förh.* **30** (1918) Ns. 6.
10. Berner, E. and Landmark, L. H. *Acta Chem. Scand.* **7** (1953) 1347.

Received July 23, 1958.

ACTA CHEMICA SCANDINAVICA 12 (1958) 1911—1918

Studies on Hemicelluloses from Pine (*Pinus silvestris* L.)

HANS MEIER

Wood Chemistry Department, Swedish Forest Products Research Laboratory, Stockholm Ö, Sweden

A number of glucomannan fractions and an araboxylan fraction have been isolated from pine (*Pinus silvestris* L.) holocellulose. The ratio glucose:mannose varied from 1:3.1 to 1:3.7 in the different glucomannans. All fractions contained a few per cent of galactose residues and the possible presence of galactoglucomannans cannot be excluded. The ratio arabinose:xylose in the isolated araboxylan was 1:7.4 and the uronic acid content 18.6 %.

The average degree of polymerisation ($\overline{DP}_n$) increased from about 70 for the most easily extractable glucomannan fractions up to about 115 for the most resistant. The $\overline{DP}_n$ value for the araboxylan was 121.

It seems probable that the glucomannans in a holocellulose are partly bound to the remaining lignin even when the holocellulose in question has a very low Klason-lignin content.

Studies were earlier reported [1] on the physical properties of glucomannans from Norwegian spruce (*Picea Abies* Karst.). Similar investigations have now been carried out on glucomannans and on an araboxylan from pine (*Pinus silvestris* L.).

ISOLATION OF THE CRUDE HEMICELLULOSES

The crude hemicelluloses were isolated by successive treatments of a chlorite-holocellulose with dimethyl sulphoxide, hot water, potassium hydroxide and finally with potassium hydroxide and boric acid. The xylans were practically completely extracted, but about 25 % of the glucomannans present in the holocellulose were resistant to those treatments. They could, however, be extracted, in part at least, after having destroyed the cellular structure of the residue by dissolving it in cupri-ethylene diamine and regenerating it by reprecipitation with acetic acid.

Table 1. Carbohydrate analyses of the crude hemicellulose extracts and of the residues.

Sample		Yield g	Galactose/Glucose %		Mannose %	Arabinose %	Xylose %
K_2	Holocellulose (yield with respect to acetone-treated wood: 69 %. Klason-lignin: 1 %)	147.1	1.6	71.8	15.6	1.7	9.3
$K_2GM_1X_1$	$(CH_3)_2SO$-extract	1.1	26.7		16.4	6.8	50.0
$K_2GM_2X_2$	H_2O-extract	2.9	24.4		72.6	1.2	1.8
$K_2GM_3X_3$	14 % KOH-extract	22.1	15.5		28.0	6.8	49.8
$K_2GM_4X_4$	(14 % KOH+3 % H_3BO_3)-extract	3.5	23.0		63.5	2.5	11.0
$K_2GM_5X_5$	(24 % KOH+3 % H_3BO_3)-extract	2.3	24.7		70.3	2.3	2.7
K_3	Residue after the previous extractions		92.9		7.1	trace	trace
$K_3GM_6X_6$	(24 % KOH+3 % H_3BO_3)-extract from the cupri-ethylene diamine-regenerate of K_3	2.5	29.0		65.3	2.1	3.6
K_4	Residue after the extraction of the cupri-ethylene diamine-regenerate of K_3		95.1		4.9	trace	trace

The composition of the different fractions is shown in Table 1. The dimethyl sulphoxide extracted principally xylans but only in small amounts. Hot water extracts contained an almost pure glucomannan having only 1.8 % of xylose residues while two samples of spruce holocellulose under similar conditions contained 16.5 and 11 % of xylose residues [1]. About a quarter of the material extracted by 14 % potassium hydroxide consisted of mannose residues while the rest of the fraction contained most of the xylans that could be extracted from the holocellulose. Relatively pure glucomannans were isolated in later extractions by a solution of potassium hydroxide and boric acid.

FRACTIONATION AND PURIFICATION OF THE CRUDE HEMICELLULOSES

The hemicelluloses extracted by hot water and by potassium hydroxide and boric acid contained primarily glucose and mannose residues. The contaminating araboxylans could to a large extent be removed by fractionation of the samples with Fehling's solution and then with barium hydroxide. Barium hydroxide has been shown [2] to be a good reagent for the selective precipitation of polysaccharides containing mannose residues. Xylans do not precipitate under the conditions employed, but in certain cases do so at higher concentrations of barium hydroxide. As will be seen in Table 2, glucomannans were obtained having only 1.2 to 2.8 % of xylose residues. Unlike the glucomannans isolated from spruce [1] they contained 2.8 to 4.7 % of galactose residues and normally also a low proportion of arabinose residues.

Table 2. Carbohydrate analyses and degree of polymerisation of the glucomannans and of an araboxylan obtained by fractionation using Fehling's solution and barium hydroxide.

Sample	Origin (*cf.* Table 1)	Galactose %	Glucose %	Mannose %	Arabinose %	Xylose %	Glucose: Mannose	$[\alpha]_D^{20}$ [a]	$\overline{DP}_n$	$\overline{DP}_w$	Nitrogen[b] %
K_2GM_2	from $K_2GM_2X_2$	4.7	19.9	73.8	trace	1.6	1:3.7	—37	70.8	40.0	12.65
K_2GM_3		3.9	22.6	63.1	1.8	8.6	1:2.8	—31	89.9	50.1	12.33
K_2GM_3*	from $K_2GM_3X_3$	5.2	22.4	70.0	trace	2.4	1:3.1	—33	—	—	—
K_2X_3		2.7	3.6	1.2	11.0	81.5	—	—63	121.0	—	—
K_2GM_4	from $K_2GM_4X_4$	2.8	20.0	73.5	0.9	2.8	1:3.7	—33	90.6	59.3	12.17
K_2GM_5	from $K_2GM_5X_5$	2.8	21.7	71.6	2.0	1.9	1:3.3	—27	92.5	61.2	12.25
K_3GM_6	from $K_4GM_6X_6$	3.1	22.4	72.1	1.2	1.2	1:3.2	—34	115.8	78.3	11.75

[a] In 2.5 N NaOH.
[b] Nitrogen content of the nitrated samples used in DP-determinations.

The material extracted by 14 % potassium hydroxide was sub-fractionated from an aqueous alkaline solution by the addition of Fehling's solution and then yielded a precipitate (A) enriched in glucomannan, and a supernatant (B) enriched in xylan. No significant reduction in the proportion of xylose residues in the glucomannan-rich fraction (A) was obtained when the material was again treated with Fehling's solution, but the xylose residues were reduced from 19.6 to 8.3 % in the precipitate obtained when barium hydroxide was added to a solution of the material (K_2GM_3, Table 2). The xylan-rich supernatant (B) contained 10.8 % of mannose residues but this was reduced to 1.2 % by the preferential precipitation with barium hydroxide solution of a fraction enriched in mannose residues. In this way an araboxylan (K_2X_3, Table 2) was obtained having a uronic acid content of 18.6 % and a ratio of arabinose to xylose residues of 1:7.4. (This ratio refers only to those xylose residues in the xylan which have no uronic acid residues bound to them since the latter, under the hydrolytic conditions used, are present in aldobiuronic acids.)

Although cetyltrimethylammonium bromide (CTA-Br) has been used [3] to separate acidic and neutral polysaccharides, its use in the present work did not result in any significant reduction in the proportion of xylose residues in fraction K_2GM_3.

Table 3. Carbohydrate- and lignin-analyses of two fractions from K_2GM_3 precipitated with cetavlon hydroxide in the presence of boric acid. (Carbohydrate content is assumed to be 100 %.)

Sample	Lignin %	Galactose %	Glucose %	Mannose %	Arabinose %	Xylose %
F_2	5.8	4.2	18.9	64.0	2.3	10.6
F_4	trace	2.5	18.5	77.0	trace	2.0

Finally K_2GM_3 was divided into five fractions (F_{1-5}) by adding boric acid and then making successive additons of cetyltrimethylammonium hydroxide (CTA-OH). This method has been used at this laboratory [4] to fractionate arabogalactans. The first three fractions (F_{1-3}), which accounted for about 80 % of the recovered material, were similar to one another but were still heterogeneous (*cf.* Table 3). The next two fractions ($F_{4,5}$), on the other hand, contained glucose and mannose residues almost exclusively.

Recent studies by Lindgren[5] strongly indicate that in coniferous woods the hemicelluloses are in part chemically bound to lignin. It is, therefore, possible that the major component, F_{1-3}, is a hemicellulose-lignin complex with one or more types of hemicelluloses bound to lignin. By spectral analysis the lignin content in F_{1-3} was determined to be about 6 %; F_4 and F_5, on the other hand, contained no lignin (the Klason-lignin in the starting holocellulose was less than 1 %). On electrophoresis of a sample of F_2 on glass-fibre sheets wet with 0.05 N sodium hydroxide, it gave a single spot with a migration distinct from that of the glucomannan sample F_5. This indicated that in F_2 there was no glucomannan similar to that in F_5 and that the mannose residues present in the former fraction must either have been present in a different type of molecule, or be in a glucomannan chemically bound to some other species. There were two items indicating that a lignin-hemicellulose complex was present. Firstly, Lindgren [5] has noted that when lignin-free hemicelluloses are chromatographed on glass-fibre paper, using 0.05 N sodium hydroxide as irrigant, then the hemicelluloses migrate with the solvent front; lignin-hemicellulose complexes, on the other hand, have R_F values below 1. F_2 and F_5 had R_F 0.3—0.4 and 1, respectively, indicating that the former was a lignin-hemicellulose complex. Secondly, a sample of K_2GM_3 (lignin content 5 %) was delignified by chlorination and by extraction with ethanolic ethanolamine, and the product, in solution, was afterwards treated with barium hydroxide. The precipitate then obtained (K_2GM_3*) contained a much smaller amount of xylose residues than did K_2GM_3 (see Table 2). This indicated that, prior to delignification, the xylose residues had been present in some molecular species other than the glucomannan but that both species were probably bound to lignin molecules. The mobility of K_2GM_3* on an electrophoretogram was similar to that of the glucomannan F_5.

The samples K_2X_3, K_2GM_4 and K_2GM_6 contained, respectively, 1.1, 3.6 and 5 % lignin. By chromatographic examination on glass-fibre paper a sample of K_2X_3 was found to contain two components; one having an R_F of 0.3, the other of 1, indicative, it is believed, of their having been produced by a hemicellulose-lignin complex and a hemicellulose, respectively. The spot produced by the former was very weak, and that by the latter strong, while K_2GM_4 and K_2GM_6 gave two spots each of about equal intensity. It seems, therefore, that in the latter two samples also a considerable part of the glucomannan was bound to the lignin.

DP-DETERMINATIONS

The degrees of polymerisation based on number-average molecular weights ($\overline{DP}_n$), were determined osmometrically on the nitrates in butyl acetate [1]. The results are shown in Table 2. The $\overline{DP}_n$ value for the glucomannan extracted by water was *ca.* 70 and was practically identical to that of the corresponding fraction from spruce holocellulose [1]. The value for K_2GM_3 was relatively high (89.9) probably due to the presence, as a contaminant, of an araboxylan of higher molecular weight. The fractions that had been extracted with potassium hydroxide/boric acid differed but little from one another. The fraction extracted from the regenerated cellulose (K_2GM_6) had a $\overline{DP}_n$ of *ca.* 115, a value rather lower than that given by the corresponding fraction from spruce [1].

The $\overline{DP}_n$ value of the sodium salt of the acidic araboxylan (K_2X_3) was determined in 0.1 N sodium chloride (*cf.* Ref.[7]) to be *ca.* 120.

The problem had to be considered of whether these $\overline{DP}_n$ values related to hemicelluloses or to lignin-hemicellulose complexes. Lignin was, however, found to be absent from the nitrated samples, and this indicated that delignification had taken place during nitration and that, in consequence, the $\overline{DP}_n$ values were those of hemicelluloses and not of lignin-hemicellulose complexes.

The degrees of polymerisation based on weight-average molecular weight ($\overline{DP}_w$), were determined viscometrically on the nitrates in butyl acetate. $K\eta$ in the equation of Schulz and Blaschke

$$Z\eta = \frac{\eta_{sp}}{c(1 + K_\eta \cdot \eta_{sp})}$$

was determined to be 0.29 and the $\overline{DP}_w$ values were then obtained by application of the equation derived by Marx [8]:

$$Z_{\eta \text{ acetone}} = 1.5 \times 10^{-3} \overline{DP}_w{}^{0.9}$$

In a separate experiment $Z_{\eta \text{ butyl acetate}}$ was determined to be $1.13 \times Z_{\eta \text{ acetone}}$.

The derivation of Marx' equation was based on measurements carried out on cellulose nitrates which contained *ca.* 13.6 % nitrogen. The calculation of the $\overline{DP}_w$ values of the nitrated glucomannans was based on the average weight of the residues, allowance being made for their incomplete nitration. It must, however, be stressed that the $\overline{DP}_w$ values in Table 2 are of necessity highly uncertain as it is very doubtful if the formula of Marx can legitimately be applied to nitrated glucomannans of low molecular weight. The $\overline{DP}_n$ and $\overline{DP}_w$ values of the various fractions both increase in the same order; the lowest values being given by the most readily extracted glucomannans and the highest values by those most difficult to extract. This indicates that all of the molecular species probably possess a similar degree of branching.

DISCUSSION

The mannose residues in the holocellulose of *Pinus silverstris* are present in glucomannans as was also earlier found in work on *Picea Abies* [1]. The ratio of glucose to mannose appears, however, to be rather higher in the former (*ca.* 1:3.5 as compared to *ca.* 1:4 in *Picea Abies*).

From the various fractions glucomannans were precipitated by the addition of Fehling's solution and those precipitates were dissolved in water and fractionated by the addition of barium hydroxide. The glucomannan then precipitated generally contained about 2 % xylose, 2 % arabinose, and up to 4.2 % galactose residues. The material extracted by the 14 % potassium hydroxide ($K_2GM_3X_3$) did not yield a similar polysaccharide when treated in like manner but from its mannose-rich sub-fraction, K_2GM_3, by fractional precipitation with cetavlon hydroxide and boric acid there was obtained a small amount of a polysaccharide containing principally glucose and mannose residues. The major part of the K_2GM_3 sub-fraction contained xylose and galactose residues in addition to glucose and mannose residues. As the xylose residues could largely be removed after delignification of the material, it seems probable that they and the glucomannan were bound independently to the lignin. It is uncertain whether or not the galactose residues were present as part of the glucomannan. The galactose residues may be present in contaminating polysaccharides as arabogalactans or pectic galactans.

The various glucomannans had optical rotations differing relatively widely from one another. This variation may have been due to varying amounts of lignin and to differences in the proportions of the different sugar residues.

The $\overline{DP}_n$ values of the different purified glucomannans were similar to those given by the corresponding fractions from spruce. The araboxylan K_2X_3 had a $\overline{DP}_n$ of 121, that is a value even higher than that given by the least readily extracted glucomannan (K_2GM_6).

EXPERIMENTAL

Quantitative paper chromatography. The hydrolyses and the quantitative sugar analyses of the hemicelluloses were carried out by the method of Saeman *et al.*[9] using the chromatographic irrigants ethyl acetate — acetic acid — water (3:1:3), and, for the separation of glucose and galactose, ethyl acetate — pyridine — water (2:1:2).

Electrophoresis. The electrophoresis was carried out on glass-fibre sheets [5]. The spray-reagent was a mixture of *a*-naphthol (1 g), conc. sulfuric acid (5 ml) and *n*-butanol (100 ml).

Fractional extraction of the hemicellulose. Wood meal (18—35 mesh) of *Pinus silvestris* L. was treated in a Soxhlet-type extractor with acetone and the residue was then delignified by the chlorite method [10]. The product remaining after delignification was 68.9 % of the acetone-treated wood. The holocellulose (147 g) was thoroughly washed with water and was then mechanically shaken, at room temperature, with dimethyl sulphoxide (1.5 l) in an atmosphere of nitrogen. Three such treatments were carried out over a total period of 24 h. Then the residual material was washed with cold water. The combined extracts were slightly acidified by the addition of a little hydrochloric acid and the hemicelluloses were precipitated from the solution by the addition of twice its volume of ethanol. The precipitate was centrifuged down and, after washing with *ca.* 65 % aqueous ethanol, was suspended in water. The remaining ethanol was distilled off, and the solution then freezedried. The residual material from the dimethyl sulphoxide

treatment was then treated successively, and in a similar way, with boiling water (giving extract $K_2GM_2X_2$), 14 % potassium hydroxide (giving extract $K_2GM_3X_3$), 14 % potassium hydroxide and 3 % boric acid (giving extract $K_2GM_5X_5$), and 24 % potassium hydroxide and 3 % boric acid (giving extract $K_2GM_4X_4$). In all cases a total of 4.5 l of liquid was employed over three treatments. A sample of the final residue (K_3) was dissolved in cupriethylene diamine and precipitation was effected by the addition of acetic acid. The precipitate was treated once with 24 % potassium hydroxide + 3 % boric acid (giving extract $K_2GM_6X_6$). All extractions were carried out in an atmosphere of nitrogen. The extracts were sligthly acidified and the hemicelluloses precipitated, washed, and dried as described earlier. Those precipitates contaminated by borate were washed also with warm methanol to remove the boric salts.

Isolation and purification of the glucomannans and of an araboxylan. The various crude hemicellulose fractions were suspended in fifty times their weight of water and the mixture was homogenized in a Turmix blender. After boiling the mixture for a few minutes, then cooling, it remained turbid, but complete dissolution was effected on the addition of a little dilute sodium hydroxide. To these solutions Fehling's solution was added, and the resultant precipitate was centrifuged down and washed once with water. The centrifugate from the $K_2GM_3X_3$ fraction, after acidification with hydrochloric acid, was passed through a column of cation-exchange resin (IR 120). The hemicelluloses were then precipitated by the addition of ethanol and the precipitates, after washing, were dried. As this product still contained *ca.* 10 % mannose residues it was redissolved in water and was treated with barium hydroxide and the precipitate centrifuged down. The centrifugate, after acidification with acetic acid, was treated with ethanol and a relatively pure araboxylan (K_2X_3) was obtained.

Those precipitates that had been obtained from the crude hemicelluloses with Fehling's solution were dissolved in N hydrochloric acid and glucomannans were precipitated by the addition of ethanol. The precipitates were separated and washed until neutral. They were then suspended in water, and, after distilling off the remaining ethanol, were freeze-dried. As some samples were still obviously heterogeneous all were redissolved in water and were precipitated by the addition of saturated barium hydroxide solution. The precipitates were dissolved in either 2 N acetic acid or in N hydrochloric acid. The glucomannans were precipitated with ethanol, then washed and dried.

Fractionation of the sample K_2GM_3 *with cetyltrimethylammonium hydroxide* (CTA-OH). A sample (500 mg) of the K_2GM_3 fraction was dissolved in water (25 ml) and CTA-OH (0.3 mmole) was added. The precipitate was separated and dissolved in N sodium chloride. From this solution the CTA was precipitated by potassium iodide and was centrifuged down and washed with potassium iodide solution. The centrifugate and the washings were combined and acidified and the hemicelluloses, after precipitation with ethanol, were washed and dried (yield 175 mg). The material was hydrolysed and the hydrolysate examined chromatographically. The sugars were all present in amounts similar to those found in a hydrolysate of the starting material. The hemicelluloses, left in the supernatant after the cetavlon precipitation, were precipitated by the addition of ethanol. This material (180 mg) on hydrolysis was found to contain all of the sugars noted in the hydrolysate of the previous precipitate, but the galactose and xylose were present in somewhat lower amounts.

In another experiment a sample (1 g) of K_2GM_3 was dissolved in water (100 ml) and boric acid (6.2 mmole) was added. To this solution there were added four successive portions of both sodium hydroxide and cetavlon hydroxide with intermediate separation of the precipitate formed on each addition (fractions: F_{1-4}). A total of 4 mmole of each reagent was added. The precipitates were dissolved in 6 % acetic acid and the hemicelluloses precipitated by the addition of ten times the volume of ethanol. After centrifugation the samples were washed and dried. The solution remaining after the final precipitation was passed successively through columns of cation-, and anion-exchange resins (IR 120 and IR 4B), then the solvent was distilled off from the eluate and a further fraction (F_5) was obtained. Samples of the first three fractions (F_{1-3}), after hydrolysis, were found to contain similar amounts of the same sugars as found in the hydrolysate of the non-fractionated material. F_4 and F_5 accounted for about 20 % of the weight of F_{1-5} and contained glucose and mannose residues almost exclusively.

Delignification of K_2GM_3. A 1 % aqueous solution of K_2GM_3 was treated with chlorine by passing the gas for 5 min through the solution which was kept at 6° [11]. The hemicellu-

loses were then precipitated by the addition of four times the volume of ethanol. After washing the precipitate, it was suspended in a 3 % solution of ethanolamine in ethanol and the mixture was boiled for 5 min. The residue was separated and, after treating it again in the same way with ethanolic ethanolamine, it was redissolved in water and the above procedure repeated twice from the chlorination stage. By those treatments the amount of lignin was reduced from *ca.* 5 % in K_2GM_3 to 0.4 % in K_2GM_3*.

Lignin analyses. Samples (0.5 g/l) of the hemicellulose fractions were dissolved in 0.5 N sodium hydroxide and the absorption curves from 250—320 mμ were determined with a Beckman spectrophotometer. A lignin-free ivory nut mannan was used as reference substance. Those samples which contained lignin had a sharp absorption maximum at 280—285 mμ (*cf.* Ref.[6]) whereas in the chlorinated sample the corresponding maximum was at *ca.* 295 mμ. From the height of the maximum the lignin content was calculated using the equation:

$$\log \frac{I_o}{I} = \varepsilon \cdot c \cdot d$$

in which $\log \frac{I_o}{I}$ is the determined absorption value. ε is the "molar" extinction coefficient, c is the "molar" concentration of lignin, and d is the thickness of the liquid layer in cm. The "molarity" of lignin solutions is arbitrarily based upon the methoxyl content of the lignin, which, is taken to be 15 %. A "molar" solution of lignin then contains 206 g (*i.e.* $\frac{1 \text{ mole } OCH_3}{15} \times 100$ g) of lignin per litre. The value of ε used, *viz.* 3 200, was that determined for native lignin by Aulin-Erdtman [6]. Our determinations are therefore only valid if we are justified in assuming that no changes took place in the lignin structure during the various treatments.

Osmotic determinations. The osmotic determinations were carried out on the nitrated glucomannans as described in an earlier paper [1].

An aqueous solution of the acidic araboxylan (K_2X_3) was passed through a column of the cation-exchange resin IR 120 (Na^+) and the osmotic pressure was then determined on the sodium salt of the araboxylan dissolved in 0.1 N sodium chloride (cf. Ref[7].). The semipermeable membranes used were "Ultracellafilter allerfeinst" supplied by "Membranfiltergesellschaft Göttingen".

Viscometric determinations. The relative viscosity was determined on the nitrated samples in butyl acetate in an Ostwald viscometer at 25°.

Acknowledgement. The author wishes to express his thanks to Miss Barbro Enström for her skilful assistance.

REFERENCES

1. Lindberg, B. and Meier, H. *Svensk Papperstidn.* **60** (1957) 785.
2. Meier, H. *Acta Chem. Scand.* **12** (1958) 144.
3. Scott, J. E. *Chem. & Ind. London* **1955** 168.
4. Bouveng, H. O. and Lindberg, B. *Acta Chem. Scand.* **12** (1958) 1977.
5. Lindgren, B. O. *Acta Chem. Scand.* **12** (1958) 447.
6. Aulin-Erdtman, G. *Svensk Papperstidn.* **57** (1954) 745.
7. Pals, D. T. F. and Hermans, J. J. *Rec. trav. chim.* **71** (1952) 458.
8. Marx, M. *Das Papier* **10** (1956) 135.
9. Saeman, J. F., Moore, W. E., Mitchell, R. L. and Millett, M. A. *Tappi.* **38** (1954) 336.
10. Wise, L. E., Murphy, M. and D'Addieco, A. A. *Paper Trade J.* **122** (1946). No. 2, p. 35.
11. Van Beckum, W. G. and Ritter, G. J. *Paper Trade J.* **105** (1937). No. 18, p. 127.

Received July 17, 1958.

ACTA CHEMICA SCANDINAVICA 12 (1958) 1919—1922

Effect of Benzoic Acid on the Metabolic Conjugations of *p*-Aminobenzoic Acid in the Rat

MARTTI KOIVUSALO, TAPANI LUUKKAINEN, TATU MIETTINEN and JAAKKO PISPA

Department of Medical Chemistry, University of Helsinki, Finland

The excretion of *p*-aminobenzoic acid and its conjugates is determined by the counter current distribution technique in rat urine after the administration of *p*-aminobenzoic acid alone and with the addition of benzoate.

It has been found that *p*-aminobenzoic acid is excreted also in rat urine as glucuronide in addition to acetyl and glycine conjugates.

After administration of benzoate with *p*-aminobenzoic acid the amounts of glycine and glucuronide conjugates decreased whereas the amount of acetyl-*p*-aminobenzoic acid increased.

Only a small fraction of the administered *p*-aminobenzoic acid was excreted as such and this was unaffected by benzoate.

Most of the administered *p*-aminobenzoic acid is rapidly excreted by the mammal in the urine as different conjugates and only a small part is excreted as free *p*-aminobenzoic acid [1–3]. In man most of the administered *p*-aminobenzoic acid is conjugated with glycine to *p*-aminohippurate, but also appreciable amounts of acetyl-*p*-aminobenzoate and of the glucuronides of *p*-aminobenzoic acid and acetyl-*p*-aminobenzoic acid are excreted with small amounts of free *p*-aminobenzoic acid and acetyl-*p*-aminohippurate [3,4]. Similar results have been obtained in rabbits [5–7]. In rat urine Riggs and Christensen [8] found *p*-aminohippurate, *p*-aminobenzoate and their acetyl derivatives after administration of *p*-aminobenzoic acid. Simultaneous administration of benzoic acid increased the amount of acetyl-*p*-aminobenzoate and decreased the amount of glycine conjugates excreted [8].

In the present paper results are reported from studies by the counter current distribution technique on the excretion pattern of *p*-aminobenzoic acid and its metabolites in rat urine. It was found that also in rats there was an appreciable excretion of glucuronide conjugates, as had been found earlier in man and in rabbits. Simultaneous administration of benzoic acid abolished almost totally the excretion of conjugates other than acetyl-*p*-aminobenzoate whose excretion increased correspondingly. The excretion of unconjugated *p*-aminobenzoate was unaffected by the administration of benzoate.

EXPERIMENTAL

The experimental animals were 40 white rats of Wistar strain weighing 180—220 g. The diet during the experiments was the usual stock diet of this Department.

The dosage of *p*-aminobenzoic acid was 15 μmoles per rat and it was given in 5 ml of water by stomach tube. Urine was collected without preservative during a period of 4 h after the administration of *p*-aminobenzoic acid and the urine samples of all rats were pooled. After five days the same rats were given 300 μmoles of sodium benzoate and 15 μmoles of *p*-aminobenzoic acid in 5 ml of water and the urines collected as above.

The counter current distribution technique of Craig [9] was used. The solvent system was amyl alcohol and 0.1 M acetate buffer pH 3.4, 24 transfers were made in an all-glass apparatus.

The glucuronides were determined in the aqueous phase by the modified naphthoresorcinol method of Miettinen *et al.*[10] Before analysis the samples were extracted three times with ether to remove the traces of amyl alcohol present.

The diazotisable amines were determined by the method of Bratton and Marshall [11] before and after acid hydrolysis. The determinations were made from both phases. *p*-Aminobenzoic acid and its derivatives were extracted from the organic phase with 0.1 N NaOH.

The distribution coefficients of authentic samples of *p*-aminobenzoic acid, *p*-aminohippuric acid and acetyl-*p*-aminobenzoic acid were determined in the solvent system used, and compared with those obtained from the peaks of the experimental distribution curves uring the formula presented by Rauen and Stamm [12]. These values are presented in Table 1 and the identification of the peaks in the distribution curves is based on them.

Table 1. Distribution coefficients of *p*-aminobenzoic acid and its conjugates in amyl alcohol/acetate buffer.

	Determined	Calculated from the curves
p-Aminobenzoic acid	10.80	11.00
Acetyl-*p*-aminobenzoic acid	14.00	15.67
p-Aminohippuric acid	0.36	0.35
Acetyl-*p*-aminohippuric acid	—	1.00

RESULTS AND DISCUSSION

The results are presented in Fig. 1 and 2. It is seen from Fig. 1 that in the normal rat most of the *p*-aminobenzoic acid excreted in the urine is conjugated with glycine to form *p*-aminohippurate and acetyl-*p*-aminohippurate. An appreciable amount of acetyl-*p*-aminobenzoate is also excreted but the amount of free *p*-aminobenzoate is rather small. The *p*-aminobenzoic acid glucuronides excreted are mostly unconjugated as regards the amino group, only negligible amounts of acetyl-*p*-aminobenzoic acid glucuronide were found. The glucuronide peak apparently contains also other glucuronides besides those of *p*-aminobenzoic acid and its derivatives, as is seen when the total amount of amines in the first plates is compared with the amount of total glucuronide in the same plates.

Conversely, when benzoate was also administered, the excretion of the glycine conjugates of *p*-aminobenzoic acid fell to very low values, but was not totally abolished. No acetyl-*p*-aminobenzoic acid glucuronide was found and the amount of *p*-aminobenzoic acid glucuronide was also much diminished. The

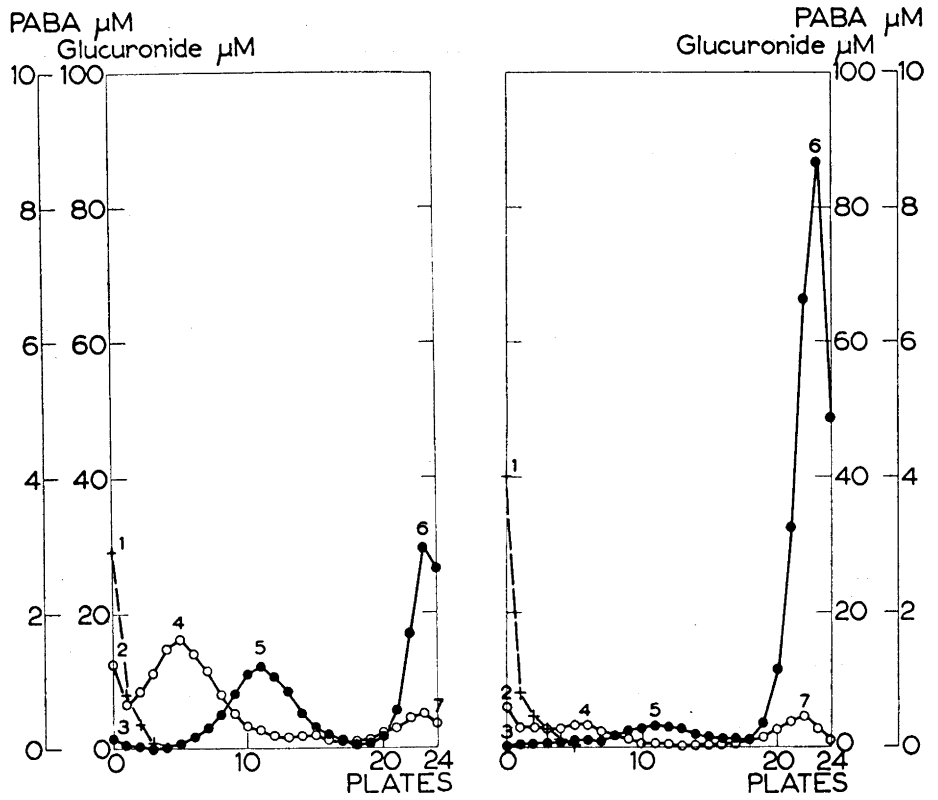

Fig. 1. Excretion pattern of *p*-aminobenzoic acid and its conjugates in rat urine.
+——+ Glucuronide O——O Diazotisable amines
●——● Undiazotisable amines

1. Total glucuronide. 2. *p*-Aminobenzoic acid glucuronide. 3. Acetyl-*p*-aminobenzoic acid glucuronide. 4. *p*-Aminohippurate. 5. Acetyl-*p*-aminohippurate. 6. Acetyl-*p*-aminobenzoate. 7. *p*-Aminobenzoate.

Fig. 2. Excretion pattern of *p*-aminobenzoic acid and its conjugates after simultaneous administration of benzoate.
The curves and peak numbers as in Fig. 1.

total amount of glucuronides was increased probably due to the excretion of benzoic acid glucuronide. The excretion of acetyl-*p*-aminobenzoic acid was correspondingly increased, it was in fact the only metabolite of *p*-aminobenzoic acid excreted in the urine in noteworthy amounts after administration of benzoate. The low excretion of unconjugated *p*-aminobenzoic acid was not affected by benzoate.

The appreciable amounts of *p*-aminobenzoic acid glucuronides excreted by the rat makes it necessary to determine also these conjugates in addition to

glycine and acetyl conjugates when the pattern of the *p*-aminobenzoic acid conjugates is determined in the urine. If this is not done, the amounts of free *p*-aminobenzoic acid and *p*-aminohippuric acid in particular will be estimated too high.

The relative amount of acetyl conjugates calculated as a percentage of the total *p*-aminobenzoic acid excretion increased after administration of benzoate from 53 to 85%. This rise is not due to any activation of the acetylation processes but presumably to the inhibition of the glycine conjugation, which in turn leads to diminished excretion of total *p*-aminobenzoic acid as shown by the experiments on the acetylation of aromatic amines by Luukkainen [13].

An interesting observation is that, although the excretion pattern of all the conjugates is changed after the administration of benzoate, the amount of unconjugated *p*-aminobenzoic acid excreted remained constant.

REFERENCES

1. Beyer, K. H., Tillson, E. K., Runo, H. F., Schuchardt, G. S. and Pitt, A. A. *Federation Proc.* **11** (1952) 13.
2. Lustig, B., Goldfarb, A. R. and Gerstl, G. *Arch. Biochem.* **5** (1944) 59.
3. Tabor, C. W., Freeman, M. F., Baily, J. and Smith, P. K. *J.Pharmacol. Exptl. Therap.* **102** (1951) 98.
4. Mandel, H. G., Yen, C. and Smith, P. K. *Federation Proc.* **11** (1952) 372.
5. Bray, H. G., Lake, H. J., Neale, F. C., Thorpe, W. V. and Wood, P. B. *Biochem. J.* **42** (1948) 434.
6. Umeda, Y. *Fukuoka-Igaku-Zasshi* **48** (1957) 299; *Chem. Abstracts* **52** (1958) 2228.
7. Venkataraman, P. R., Venkataraman, A. and Lewis H. B. *Arch. Biochem. Biophys.* **26** (1950) 173.
8. Riggs, T. R. and Christensen, H. N. *J.Biol.Chem.* **193** (1951) 675.
9. Craig, L. C. *J.Biol.Chem.* **155** (1944) 519.
10. Miettinen, T., Ryhänen, V. and Salomaa, H. *Ann. Med. exptl. et Biol. Fenniae, Helsinki* **35** (1957) 173.
11. Bratton, A. C. and Marshall, E. K., Jr. *J.Biol.Chem.* **128** (1939) 537.
12. Rauen, H. M. and Stamm, W. *Gegenstromverteilung*, Springer-Verlag, Würzburg 1953, p. 46.
13. Luukkainen, T. *Acta Physiol. Scand.* **45** (1956) Suppl. 154.

Received August 28, 1958.

ACTA CHEMICA SCANDINAVICA 12 (1958) 1923—1926

Electrophoretic Behaviour of Pea Formic Dehydrogenase

MARTTI KOIVUSALO and JAAKKO PISPA

Department of Medical Chemistry, University of Helsinki, Finland

Zone electrophoresis of partially purified formic dehydrogenase from green peas was carried out in polyvinyl chloride resin blocks.

The enzyme activity moved as a single symmetrical peak in all the preparations and was located between the two principal protein peaks, which presumably were vicilin and legumin. When normal human serum was run in the same block with formic dehydrogenase, the enzyme activity was found to have approximately the same mobility as the β-globulins.

A plant formic dehydrogenase was first discovered by Thunberg [1-3] in bean seeds. Pea seeds contain the same enzyme, which differs from the bacterial formic dehydrogenase requiring diphosphopyridine nucleotide as coenzyme [4-7]. The enzyme has been partially purified from peas and beans but has resisted many efforts for further purification [8-10]. During attempts in this laboratory to develop a reliable and sensitive enzymic micromethod for the determination of formic acid in blood and other biological materials, the pea formic dehydrogenase was taken under further study. In the present paper the results of studies on the electrophoretic behaviour of green pea formic dehydrogenase during various stages of purification are reported. Both the enzymic activity and the protein content of the electrophoretic fractions of the partially purified preparations were determined.

METHODS

The source of the enzyme preparations was green pea seeds (*Pisum sativum*, var. *Celvedon*).

The purification of the formic dehydrogenase was made principally by the methods of Nason and Little [10] and Davison [9] with only minor modifications. The purification steps mentioned in the present paper refer to the steps of Nason and Little [10].

Diphosphopyridine nucleotide was purchased from Boehringer und Söhne (DPN, reinst). Calcium phosphate gel and alumina C_γ gel were prepared after instructions given by Colowick [11].

The preparative zone electrophoresis * was carried out using a rectangular perspex trough packed with polyvinyl chloride resin, Geon 426 (G. F. Goodrich Co.) moistened

* We are grateful to Dr. Rainer Pesola from this Institute for introducing this technique to us.

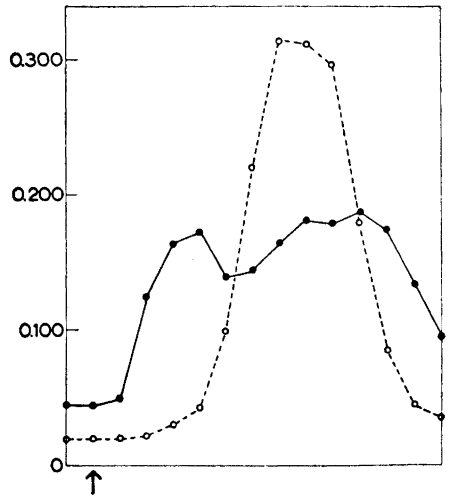

Fig. 1. Electropherogram of pea formic dehydrogenase preparation. Step 7. O———O enzyme activity, ●———● protein. Fractions of 0.8 cm. Place of application marked with arrow.

with barbital buffer, pH 8.6, ionic strength 0.05. To prevent evaporation melted paraffin was poured on the block and allowed to solidify. The substance under analysis was applied to the block trough a narrow cut in the paraffin cover. The contact to the buffer vessels was effected from the ends of the block with strips of filter paper. During the run the block was in a vertical position in a perspex chamber [12].

The time of electrophoresis ranged from 48 to 72 h; a voltage of 400 V and a current of 10 mA were used per block. After the run the resin block was cut in 0.4 or 0.8 cm fractions, and each fraction was divided into two parts, from which the enzyme activity and the protein content, respectively, were determined.

The protein content of the fractions was determined by the method of Kunkel and Tiselius [13] after elution by shaking for 30 min with 3 ml of 0.1 N NaOH.

The other part of each fraction was eluted with 3 ml of 0.5 M potassium phosphate buffer pH 6.5 and the formic dehydrogenase activity of the eluates was assayed in the following system: 1 ml of eluate, 1 ml of 0.5 M potassium phosphate buffer, pH 6.5, and 1 ml of assay mixture. The assay mixture consisted of 30 ml of 0.5 sodium formate, neutralised with hydrochloric acid, 10 ml of diphosphopyridine nucleotide solution (2 mg per ml) and 0.5 M potassium phosphate buffer pH 6.5 and 100 ml. The assay was carried out in test tubes which were held at room temperature for 2 h, after which the optical densities were read with a Beckman DU spectrophotometer at 340 mμ in 1 cm silica cuvettes.

Paper electrophoresis was run in the conventional apparatus using Whatman No. 1 filter paper strips. The time of the run was 6 h using a voltage of 500 V. Barbital buffer pH 8.6 and ionic strength 0.05 was used. After the run the proteins were stained with Lissamin Green and the papers were cut in fragments of 3 mm, which were eluted with 4 ml of 0.1 N NaOH each. The optical densities of the eluates were determined with Beckman B spectrophotometer at 635 mμ.

The free electrophoresis was carried out in the conventional Tiselius apparatus at pH 8.6.

RESULTS AND DISCUSSION

Typical electrophoresis curves obtained are presented in Figs. 1 and 2.

The protein curve did not change much during the purification of the enzyme. There were two main peaks in all the curves obtained in various

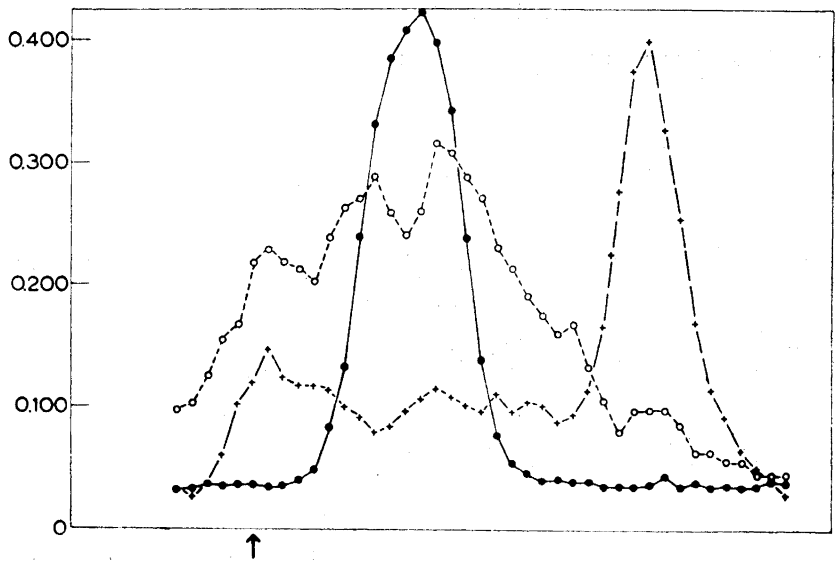

Fig. 2. Electropherograms of pea formic dehydrogenase and human serum run in the same block. +----+ serum protein. O----O enzyme protein, ●----● enzyme activity. Step 7. Place of application marked with arrow.

stages of purification. These peaks are most probably due to the two pea globulins, legumin and vicilin. Legumin and vicilin are two proteins differing in sulphur content, amino acid composition and molecular weight as determined by ultracentrifugation, and probably function principally as reserve proteins [14–19].

With free Tiselius electrophoresis and paper electrophoresis similar protein curves with two peaks were also obtained.

The enzyme activity moved as a single symmetrical peak in all the electrophoretic runs made. It was always localised between the two protein peaks, a little nearer to the faster moving one. No clear peak was found in the protein curves to correspond to the enzyme activity even at the later stages of purification. However, all the preparations used were still rather crude.

To obtain some information of the relative electrophoretic mobility of formic dehydrogenase, normal human serum was run in the same block. When the curves obtained (Fig. 2) are compared, it is seen that the pea formic dehydrogenase activity has about the same mobility as the β-globulins.

Further purification was attempted with a technique in which the active fractions from several electrophoretic runs were pooled and lyophilised and submitted once again to electrophoresis. No increase in the purification was achieved, however, due to partial inactivation of the enzyme during lyophilisation.

REFERENCES

1. Thunberg, T. *Arch.intern.physiol.* **18** (1922) 601.
2. Thunberg, T. *Biochem.Z.* **206** (1929) 109.
3. Thunberg, T. *Skand.Arch.Physiol.* **74** (1936) 16.
4. Fodor, A. and Frankenthal, L. *Fermentforschung* **15** (1936) 44.
5. Lichtenstein, N. *Fermentforschung* **15** (1936) 44.
6. Andersson, B. *Z.physiol.Chem. Hoppe-Seyler.* **225** (1934) 57.
7. Adler, E. and Sreenivasaya, M. *Z.physiol.Chem.Hoppe-Seyler.* **249** (1937) 24.
8. Mathews, M. B. and Vennesland, B. *J.Biol.Chem.* **186** (1950) 667.
9. Davison, D. C. *Biochem.J.* **49** (1951) 520.
10. Nason, A. and Little, H. N. in Colowick, S. P. and Kaplan, N. O. *Methods in Enzymology*, Academic Press, New York, 1955, Vol. I, p. 536.
11. Colowick, S. P. In Colowick, S. P. and Kaplan, N. O. *Methods in Enzymology*, Academic Press New York, 1955, Vol. I, p. 90.
12. Nikkilä, E., Haahti, E. and Pesola, R. *Acta Chem.Scand.* **7** (1953) 1222.
13. Kunkel, H. G. and Tiselius, A. *J.Cen.Physiol.* **35** (1951) 89.
14. Osborne, T. B. *J.Am.Chem.Soc.* **20** (1898) 348.
15. Osborne, T. B. and Cambell, G. F. *J.Am.Chem.Soc.* **20** (1898) 410.
16. Danielsson, C-E. *Biochem. J.* **44** (1949) 387.
17. Danielsson, C-E. *Acta Chem.Scand.* **3** (1949) 41.
18. Danielsson, C-E. *Acta Chem.Scand.* **4** (1950) 762.
19. Danielsson, C-E. and Lis, H. *Acta Chem.Scand.* **6** (1952) 139.

Received August 28, 1958.

ACTA CHEMICA SCANDINAVICA 12 (1958) 1927—1936

The Isolation of Protein-Bound Phosphorylmuramic Acid from *Lactobacillus casei*

GUNNAR ÅGREN and CARL-HENRIC DE VERDIER

Institute of Medical Chemistry, University of Uppsala, Sweden

A new phosphorylated amino acid has been isolated from a hydrolysate of the protein residue of *L. casei*. It has been identified as phosphorylated muramic acid. The position of the phosphate group must probably be in the primary alcoholic group. The yield of crystalline material was about 150 mg from 1 kg fresh bacteria.

In earlier communications it was demonstrated that acid hydrolysates of protein from *L. casei* mainly contained a phosphorylated amino acid [1,2] which was not identical with the phosphorylated amino acids isolated with a similar procedure from animal proteins [3]. The amino acid contained one nitrogen atom per phosphoryl group and ionophoretically behaved as a neutral amino acid. The rate of ^{32}P-incorporation into this amino acid was compared with that of other phosphorus compounds such as free and RNA-bond nucleotides. By preparing large amounts of the phosphorylated compound it could be shown that it contained about 50 % oxygen and behaved as an amino sugar. Later, the dephosphorylated compound was found to be identical with 3-O-α-carboxyethyl-D-glucosamine [4] which also has been named muramic acid (Mur)*.

PREPARATION OF PHOSPHORYLMURAMIC ACID

Lactobacillus casei (7461) was cultivated in a medium with the following composition: 10 g of Dextropur **, 10 g of $NaOCOCH_3 \cdot 3\ H_2O$, 10 g of Bactopeptone ***, 1 g of yeast extract ****, 25.4 ml of liver extract §, 0.5 ml of

* The following abbreviations are used: Mur = muramic acid; MurP = O-phosphorylmuramic acid; SerP = O-phosphorylserine.

** Glucose manufactured by Corn Products Co., New York.

*** Parke, Davis and Co.

**** Difco Laboratories.

§ 100 g of Difco Liver was dissolved in 1 330 ml water and kept at 50°C for one hour and subsequently at 80° for 5 min. After filtration and concentration the filtrate was lyophilized This material was dissolved to contain 15 mg per ml.

salt mixture * per 1 000 ml of medium at pH 6.8. For large scale cultivation (90 l) the necessary ingredients were first dissolved in 5 l water and heated at 100°C for about 15 min. After cooling a dark precipitate was removed by filtration. The filtrate was evenly distributed in thirty 6 liter Erlenmayer flasks and subsequently water was added to a final volume of 3 l per flask. After adjusting the pH to 6.8 sterilization was accomplished by autoclaving the flasks 15 min at 118°C.

Inocula for large scale cultivations was prepared by transferring a small amount of growth from a stab culture [5] to two 10 ml flasks, each containing 5 ml of medium. The amount of inocula was increased in the four subsequent steps (2, 3, 4, and 5) according to Table 1. 300 ml of suspension from step

Table 1. Increase of inocula for large scale cultivation.

Step No.	Ml of inocula to ml of culture		Incubation time, h
1	0.1	2 × 5	24
2	8 × 0.5	8 × 5	24
3	30 × 1	30 × 20	17
4	30 × 20	30 × 100	17
5	30 × 100	30 × 300	17
6	30 × 300	30 × 3 000	

5 was then added to each 6 l flask containing 3 l sterilized medium. 1 mC radioactive phosphate per liter medium was added at the same time. Previously it had been shown that the presence of as much as 100 mC per liter had no demonstrable effect on growth or acid production over a period of 72 h [6]. Incubation was carried out in an air incubator for 17 h at 37°C. In order to increase the utilization of ^{32}P added to the medium inorganic phosphate was excluded from the salt mixture, since preliminary experiments had shown that the phosphorus present in Bactopeptone and liver furnished sufficient total phosphorus (0.003 %) for normal growth.

At the end of the cultivation the bacteria were separated from the medium in Sharples centrifuges. The usual yield of fresh bacteria from a single cultivation of 90 l was about 400—500 g. This material was washed two times with cold 10 % TCA. Lipids were extracted by treatment two times with a mixture of ethanol and ether in the ratio 3:1 at 40 to 50°C for 15 min and then with ether. Nucleic acids were extracted according to Schneider [7] for 15 min at 90°C with 5 % TCA. The residue was then treated with ethanol-ether (3:1) and ether and taken as the Schneider protein fraction. The normal yield was between 75—90 g.

After hydrolysis with 10 volumes of 2 N HCl per g dry protein for 20 h at 100°C insoluble humin was removed by centrifugation. The centrifugate was evaporated to dryness *in vacuo* three times with intermittent addition of water. The dissolved hydrolysate was usually mixed with the hydrolyzed

* 4 g of $MgSO_4 \cdot H_2O$, 1 g $FeSO_4 \cdot 7\ H_2O$, 1 g of NaCl, 0.1 g of $MnSO_4 \cdot H_2O$ were dissolved to 100 ml.

protein from an unlabeled batch of cells. Each half of the mixed hydrolysates was applied to a Dowex 50 column. The diameter was 6.5 and column length about 50 cm. Elution was carried out with 0.01 N HCl. A typical elution curve is given in a previous paper [1]. Irrespective of column dimensions MurP was obtained in the third column volume of eluate.

Excess of HCl was removed as described above and the residue, about 0.5 g by weight, was dissolved in a small volume of water and applied to a Dowex 1 formate (2 % DVB) column. (Dimensions 2 cm × 45 cm). Elution was carried out with a gradient 0→1 M formic acid and with a volume of 200 ml in the mixer. When the acidity in the eluate reached a value which corresponded to 0.60 M formic acid MurP appeared. For rechromatography a constant concentration of 0.5 M formic acid was sometimes used. With this system MurP appeared after 4.0 column volumes when it was chromatographed in a 1.0 cm × 43 cm column of Dowex 1. The usual yield of MurP from the two batches of cells was about 150 mg. For the following analysis about 1 g of MurP was prepared.

Dephosphorylation of MurP was at first performed in sealed glasstubes with 2 N HCl at 120°C and for 20 h. In this procedure a considerable part of Mur was destructed. It was found that MurP like O-phosphorylserine was hydrolyzed by prostate phosphatase. For that purpose an enzyme was used which had been purified according to Boman [8]. The digestion was performed in a 1.6 % solution of the substrate after pH was adjusted to 5.0 with trimethylamine. The reaction was followed by ionophoresis runs at pH 5 in a 0.1 M solution of pyridine-acetic acid. With the amounts of enzyme used it was found to be complete after 5 h of digestion at room temperature.

Crystalline phosphorylmuramic acid was obtained by slow evaporation of water solutions and from ethanol-water solutions as small needleshaped crystals. It was not possible to get crystals large enough for single crystal X-ray analysis. Under similar conditions Mur gave relatively large rods.

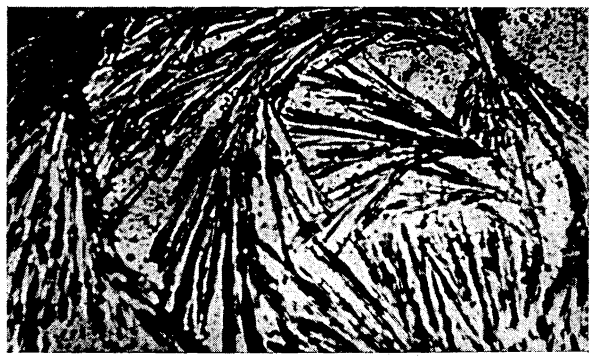

Fig. 1. A photograph of phosphorylmuramic acid isolated from the "protein fraction" of *L. casei*. Crystallized from a weak formic acid solution.

IDENTIFICATION AND CHARACTERIZATION

The elementary analysis first obtained showed that the compound must be a carbohydrate derivative containing nine carbon atoms. Sialic acid [9] and muramic acid are the most well known compounds with such a constitution. Different colour reactions described below were in favour of muramic acid. Against identity with sialic acid also was the high acid stability of our isolated compound. The following different methods were used for identification of the compound with muramic acid.

Elementary analysis

The data obtained are given in Table 2. The determinations of C, H, O, N were made by Mr. W. Kirsten at this institute and by Dr. A. Bernhardt, Mikroanalytisches Laboratorium im Max-Planck-Institut für Kohlenforschung, Mühlheim (Ruhr), Western Germany. Phosphorus was analysed according to a modification of Martin and Doty [10].

Table 2. Elementary analyses of the phosphorylated and dephosphorylated compound.

MurP:									
$C_9H_{18}O_{10}NP \cdot H_2O$ (349)	Calc.	C	30.95	H	5.77	O 50.40	N	4.01	P 8.87
	Found	1.						4.02	
								4.01	
		2.	30.55		5.94			3.94	
		3.							9.43
Mur:									
$C_9H_{17}O_7N$ (251)	Calc.	C	43.02	H	6.82	O 44.60	N	5.58	
	Found	1.	42.43		6.61	44.28		5.82	
		2.	41.44		7.09	—		5.76	
		3.	41.86		6.74	—		5.55	

Paper ionophoresis and paper chromatography

For ionophoresis Whatman paper No. 3 was used and for chromatography mostly No. 1. The ionophoretic migration of MurP in comparison to SerP is shown in Table 3. The dephosphorylated compound showed the same mobility as glycine by ionophoresis at pH 5. The solvents for the paper chromatographic identification of this compound are listed in the preceding paper [1]. The second solvent mentioned there was not used. Fig. 2 is a photograph of

Table 3. The ionophoretic mobility of MurP at pH 3 and 5 compared with SerP. + and − indicate that the substances move toward the anode and the cathode, respectively. Figures are given in cm.

	MurP	SerP
Sodium citrate − citric acid, pH 3	−4.0	+1.8
Pyridine acetate − acetic acid, pH 5	+14.0	+18.3

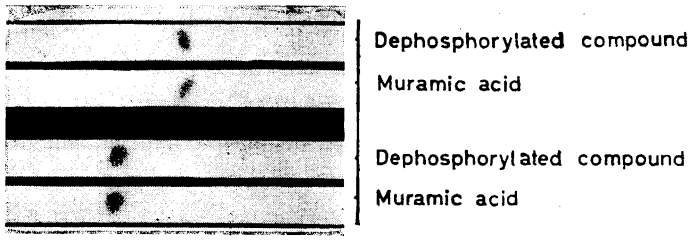

Fig. 2. Two one-dimensional chromatograms run with *iso*-butyric acid-NH_3-water (below) and *n*-butanol-acetic acid-water (above) showing that the dephosphorylated compound gives a spot identical with muramic acid.

a chromatogram with the dephosphorylated compound and Mur * running parallely. In the four solvents identical R_F values for the two compounds were obtained.

X-Ray diffraction studies

X-Ray powder diagram of MurP was obtained with a Debye-Scherrer camera but for the dephosphorylated compound a Guinier camera was used. Single crystal studies of Mur was done at the Department of Inorganic Chemistry, University of Uppsala **. The diagram of Mur supplied by Dr. Dark was identical with that obtained by enzymatic dephosphorylation of the phosphorus compound from the rest protein fraction (Fig. 3).

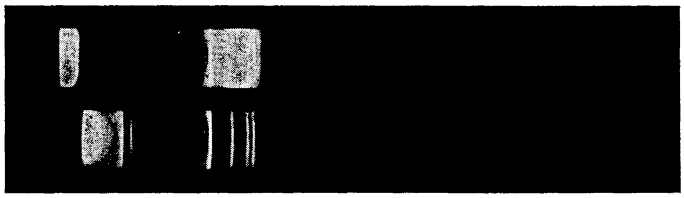

Fig. 3. X-Ray powder diagram of the dephosphorylated compound (below) is identical with that of muramic acid (above). (Some impurity in muramic acid has given a few additional weak bands.)

The density of the small crystals obtained was determined with the flotation method. Table 4 gives the spacings obtained for the phosphorylated and dephorsphorylated substances. The crystals of Mur belonged to the orthorhombic system with the cell dimensions: $a = 5.406$ Å; $b = 10.40$ Å, $c = 20.48$ Å. The density was 1.41. Calculated for four molecules per unit cell the formula weight will be 244.5 (calc. for $C_9H_{17}O_7N$ 251.24).

* The authors want to express their gratitude to Dr. F. A. Dark, the Microbiological Research Establishment, Porton, England, for the gift of a sample of muramic acid.

** The authors want to express their thanks to Dr. Abrahamsson who carried out this study.

Table 4. X-Ray diffraction data obtained from the phosphorylated and dephosphorylated compound.

Phosphorylmuramic acid		Muramic acid			
observed spacings		observed spacings		calculated spacings	
intensity	Å	intensity	Å	Å	index
v.w.	3.20	s	10.21	10.21	002
w	3.38	s	9.35	9.28	011
w	3.53	s	5.24	5.20	020
s	4.11	s	4.69	4.67	111
s	4.68	s	4.35	4.34	112
w	5.43	s	4.24	4.24	103
m	6.03	v.w.	4.19	—	—
w	6.73	m	3.93	3.92	113
v.w.	10.43	s	3.72	3.72	104
m	12.22	m	3.51	3.50	114
		w	3.46	—	—
		w	3.41	3.41	006
		v.w.	3.32	—	—
		v.w.	3.24	3.24	016
		m	3.04	3.02	124
		v.w.	2.89	2.89	131
				2.89	106
		w	2.85	2.85	026
		w	2.71	2.70	200
		v.w.	2.78	2.78	116
		w	2.67	—	—
		w	2.66	—	—
		w	2.56	2.56	008
		w	2.45	—	—
		v.w.	2.41	—	—
		v.w.	2.39	2.39	204
		v.w.	2.34	2.34	222

s = strong, m = medium, w = weak, v.w. very weak

Electrometric titration

The dissociation constants of MurP were determined by titration with 1.0 N sodium hydroxide added with an Agla micro burette. pH was measured with a direct reading pH meter (Electronic Instruments Ltd, Richmond, England Model 23 A). 38.05 mg MurP was titrated. The pK_s-values for the different steps can be seen from the following formula (Fig. 4). The corresponding values for L-O-phosphorylserine and L-O-phosphorylthreonine were 2.1; 5.7; 9.7; and 2.8; 6.1; 10.1. The dissociation constants of DL-phosphorylserine were determined by Österberg [11] with somewhat divergent values. The titration gives a molecular weight of 355 for MurP.

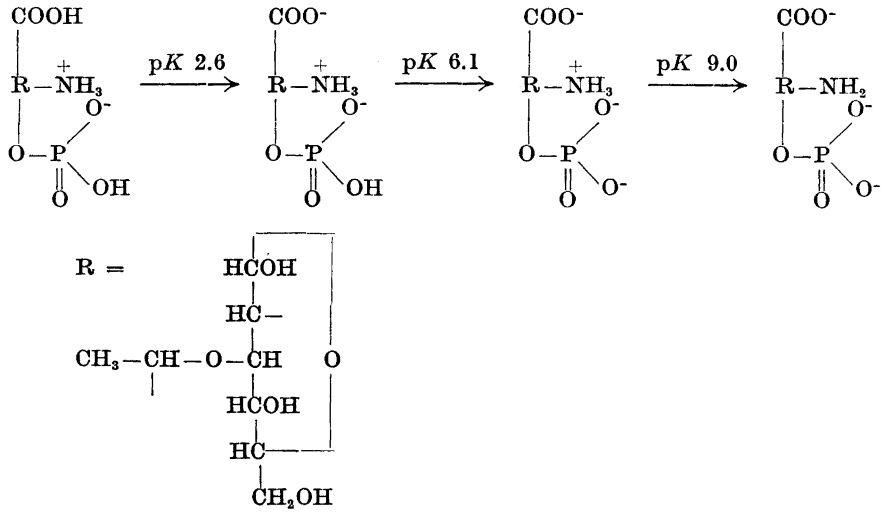

Fig. 4. The different steps of the protolysis of phosphorylated muramic acid.

Optical rotation

For MurP the following value was obtained: $\alpha_D^{25} + 3.43°$ (water; *l*,1; *c*, 4.21) which corresponds to

$$[\alpha]_D^{25} + 81.5°; [M]_D^{25} + 285°$$

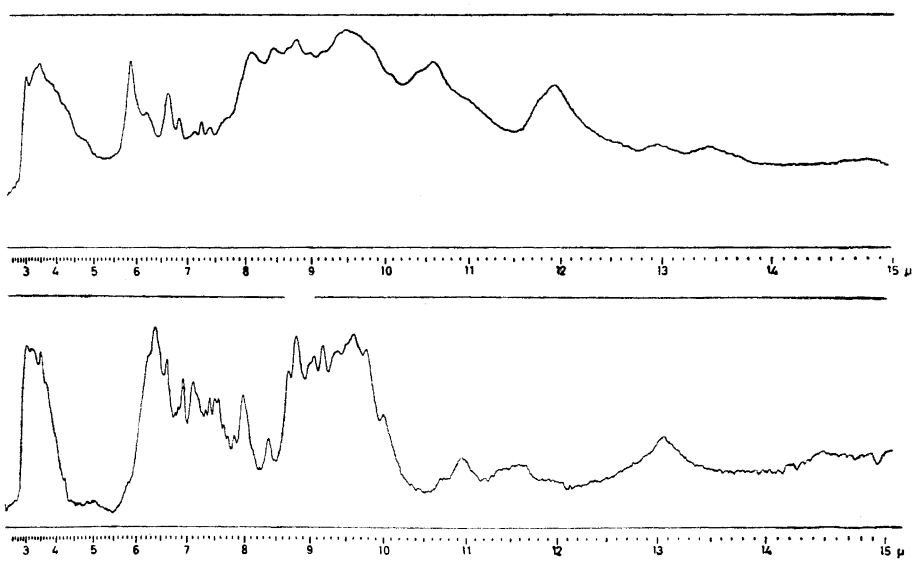

Fig. 5. Infrared absorption curves for MurP (above) and Mur.

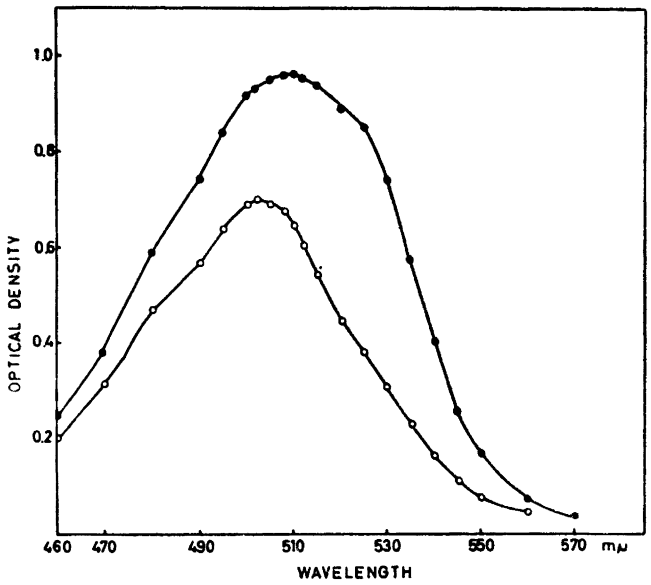

Fig. 6. Absorption curves of the colours obtained from Mur and MurP with the Elson-Morgan reaction. For -●-●- 1.94 μmole of MurP, for -O-O- 2.8 μmoles of Mur.

Infrared absorption analyses of the dephosphorylated compound and Mur were performed and showed identity. The absorption curves of Mur and MurP are shown in Fig. 5 *.

Colour reactions

The Elson-Morgan reaction was performed according to Blix' modification [12]. Absorption curves were drawn for both Mur and MurP after determinations with a Beckman DU spectrophotometer (Fig. 6). The displacement of the absorption maximum below 510 mμ is characteristic for a 3-substituted hexosamine [13]. On paper chromatograms MurP gave a positive reaction with ammoniacal $AgNO_3$ and also with anilinhydrogenphthalate a positive reaction was obtained [14]. Likewise on paper chromatograms both MurP and Mur were detected in very small amounts (2 and 1 μg, respectively) with ninhydrin reagent, 0.4 % solution in *iso*propanol-water (10:90).

DISCUSSION

To our knowledge protein-bound or free MurP has not been described. The exact position of the phosphorus linkage in MurP has not been certainly proved but according to all observations described in the previous sections

* The authors are indebted to Dr. Ingrid Fischmeister at this Institute for these analyses.

(acid stability and ninhydrin reaction) the phosphorus ought to be bound to the sixth carbon atom of the glucosamine moiety. The half life times of glucose-1-phosphate and glucosamine-1-phosphate in 1 N HCl at 100°C are about 1 and 4 min, respectively. For glucose-6-phosphate the corresponding figure is 1 300 min [15].

Mur is a major constituent of the bacterial cell wall [16] and according to theories put forward by Park and Strominger [17], uridine diphosphate-Mur and uridine diphosphate-Mur-peptides accumulate in consequences of the interference by penicillin with the biosynthesis of the cell wall. An alternative hypothesis has been put forward by Trucco and Pardee[18]. It was suggested that penicillin causes formation of an enzyme that attacks the cell membrane rather than the cell wall and that disruption of the membrane results in the escape of the cell content.

The observations of Park and Strominger were carried out with *Staphylococcus aureus* and in the microorganism an uridine diphosphate-Mur-peptide had the same amino acid composition as the cell wall. In *L. casei* the amino acid pattern is more complicated [16]. Possibly in line with this observation we have found a series of uridine diphosphate-Mur-peptides from *L. casei* inhibited by penicillin. These will be described in a following paper where the isolation of some Mur-P-peptides from the protein residue also will be given.

Regarding the role of MurP phosphorus in the phosphoproteins of *L. casei* it is possible that it has the structural function to cross-link peptide chains. Mur may also represent the active site in transphosphorylating enzymes [19] located either to cell plasma or cell walls. The relatively low turnover reported earlier makes it probable that most of the phosphorus atoms have a structural function. The mechanism for the synthesis of protein bound MurP has not been investigated more closely. It has so far not been possible to isolate free MurP. It cannot be excluded that uridine diphosphate-MurP may be an intermediate in the biosynthesis of protein-bound MurP. In this connection it must be mentioned that Strominger [20] recently isolated uridine diphosphate acetylglucosamine phosphate from oviduct of laying hen. He also suggested that uridine nucleotides of similar types may be activated intermediates in the biosynthesis of glycoproteins and mucopolysaccharides. A preliminary note has been published that galactosamine phosphate should be present in the hydrolysate of bone tissue [21]. More recently hexosamine phosphate has also been isolated in the hydrolysate of protein residue form *E. coli* [22].

REFERENCES

1. Ågren, G., de Verdier, D.-H. and Glomset, J. *Acta Soc. Med. Upsaliensis* **60** (1955) 30.
2. Ågren, G., de Verdier, C.-H. and Glomset, J. *Rev. Fermentations et inds. aliment.* **11** (1956) 234.
3. Ågren, G., de Verdier, C.-H. and Glomset, J. *Acta Chem. Scand.* **8** (1954) 1570.
4. Kent, L. H. *Biochem. J.* **67** (1957) 5P.
5. Ågren, G. *Acta Physiol. Scand.* **17** (1949) 55.
6. Ågren, G., Verdier, C.-H. and Glomset, J. *Acta Chem. Scand.* **9** (1955) 196.
7. Schneider, W. C. *J. Biol. Chem.* **161** (1945) 293.
8. Boman, H. G. *Biochim. et Biophys. Acta* **16** (1955) 295.
9. Blix, G., Lindberg, E., Odin, L. and Werner, I. *Acta Soc. Med. Upsaliensis* **61** (1956) 1.

10. Martin, J. B. and Doty, D. M. *Anal. Chem.* **21** (1953) 965.
11. Osterberg, R. *Nature* **179** (1957) 476.
12. Blix, G. *Acta Chem. Scand.* **2** (1948) 467.
13. Cifonelle, J. A. and Dorfman, A. *J. Biol. Chem.* **228** (1957) 547.
14. Cramer F. *Papierchromatographie*, Verlag Chemie, Weinheim 1953.
15. Leloir, L. F. and Cardini, C. E. in Colowick S. P. and Kaplan, N. O. *Methods of Enzymology*. Acad. Press, New York 1955, Vol. I p. 51,
16. Cummins, C. S. and Harris, H. *J. Gen. Microbiol.* **14** (1956) 583.
17. Park, J. T. and Strominger, J. L. *Science* **125** (1957) 99.
18. Trucco, R. E. and Pardee, A. B. *J. Biol. Chem.* **230** (1958) 434.
19. Ågren, G. *Acta Univ. Upsaliensis* **1958**, No. 5.
20. Strominger, J. L. *Biochim. et Biophys. Acta* **17** (1955) 283.
21. DiStefano, V., Neuman, W. F. and Rouser, G. *Arch. Biochem. Biophys.* **47** (1953 218.
22. Ågren, G. *Acta Chem. Scand.* **12** (1958) 1352.

Received July 18, 1958.

ACTA CHEMICA SCANDINAVICA 12 (1958) 1937—1954

On the Complex Chemistry of the Tervalent Rare Earth Ions

II. The Acetate Systems of Praseodymium, Samarium, Dysprosium, Holmium, Erbium and Ytterbium

ARTUR SONESSON

Department of Inorganic and Physical Chemistry, Chemical Institute, University of Lund, Lund, Sweden

Six rare earth acetate systems have been examined potentiometrically and one of these moreover extinctiometrically. The complexity constants are listed in Table 13 and the stability constants in Table 14 (together with four systems reported in Part I [1]). All measurements have been performed in perchlorate medium of ionic strength 2 M at 20°C.

The extinctiometric investigation of the $Er^{3+}-Ac^{-}-$ system* shows that the formation of the acetate complexes is accompanied by the appearance of new peaks close to the original absorption bands at about 380 mμ and 525 mμ. The new peaks, one at every band, have a somewhat shorter wavelength than the original peaks. The agreement between the potentiometrically and the extinctiometrically obtained complexity constants is good.

The stability constant of the first complex, b_1, increases with the atomic number from La to Sm. Then it decreases for Gd and Dy and remains approximately constant for Dy, Ho, Er and Yb. To begin with, b_2 and b_3 also increase with the atomic number of the rare earth. For the heaviest rare earths, however, b_2 and b_3 decrease slightly.

The heavier rare earths (Gd—Yb) seem to form polynuclear complexes which, however, are rather weak.

In Part I[1] the complexity constants of the acetate systems of La, Ce, Nd, and Gd were reported. The first three ions belong to the lightest rare earths, whilst Gd is situated in the middle of the series. In the present paper the investigation of the acetate systems of two light rare earths (Pr and Sm) and four heavy ones (Dy, Ho, Er, and Yb) is reported.

* Ac^{-} = acetate ion.

CHEMICALS USED

Rare earth perchlorates. Praseodymium and samarium perchlorates were prepared from the nitrates (> 98 % pure) by repeated evaporations with perchloric acid. In the preparations of the other rare earth perchlorates oxides with purity > 99 % were dissolved in perchloric acid.

The concentrations of the stock solutions were determined by gravimetric analysis. Pr and Sm were precipitated as oxalates, Dy, Ho, Er, and Yb as hydroxides. Moreover, the concentrations of the stock solutions were controlled by means of a cation exchanger column.

The concentration of free perchloric acid of the stock solutions was determined by electrometric titration with sodium hydroxide.

The *other chemicals* used were of analytical grade as in Part I. The concentrations of the stock solutions of NaAc and $NaClO_4$ were checked by means of a cation exchanger column.

A. THE POTENTIOMETRIC INVESTIGATION

Notations and general formulae (for deductions of the formulae the reader is referred to Part I and to Fronæus [2]).

$[H^+]'$, $[H^+]$ = the hydrogen ion concentration of the buffer solution and the complex solution, respectively.

C_H° = the concentration of free perchloric acid of the rare earth perchlorate solution before buffer is added. Thus $C_H^\circ = \nu \cdot C_M^\circ$, ν being a constant and C_M° the starting concentration of the rare earth perchlorate.

C_H = $\nu . C_M$, C_M being the total concentration of rare earth of the complex solution.

C'_{HA}, C'_A = the stoichiometric concentrations of acid HA and salt NaA, calculated from the amount of buffer added to the complex solution.

δ = C'_{HA}/C'_A

C_A = the actual total concentration of the ligand A, thus $C_A = C'_A + [H^+] - C_H$.

[M], [A] = the concentrations of free central ion and free ligand respectively.

E_A = $E' - E$ = the difference between the emfs (in mV) of two elements according to I(15)*, which have $C_M = 0$ and $C_M \neq 0$, respectively.

ΔE_A = a correction term applied to E_A to correct for the increase of emf caused by the reduction of the ionic strength through the complex formation. ΔE_A is computed according to the eqns. I(16) and I(17).

β_n, β'_n = the complexity constants of the mononuclear and the dinuclear complexes, respectively.

b_n = the stability constants: $b_1 = \beta_1$, $b_n = \beta_n/\beta_{n-1}$ $(n = 2, 3, \ldots)$.

$\bar{n}$ = the ligand number.

$\bar{n}_I$ = the ligand number of the mononuclear complexes.

$\bar{n}_c$ = the ligand number of the mononuclear complexes, calculated by means of the complexity constants.

$$\beta_n = \frac{[MA_n]}{[M] \cdot [A]^n} \tag{1a}$$

$$\beta'_n = \frac{[M_2A_n]}{[M]^2 \cdot [A]^n} \tag{1b}$$

* Formulae in Part I are referred to in this way.

$$[A] = \frac{[H^+]'}{[H^+]} \cdot \frac{(C_A' + [H^+]')\ (\delta C_A' + C_H - [H^+])}{\delta C_A' - [H^+]'} \tag{2}$$

$$E_A - \Delta E_A = 58.16 \log \frac{[H^+]}{[H^+]'} \tag{3}$$

$$\bar{n} = \frac{C_A' + [H^+] - C_H - [A]}{C_M} \tag{4}$$

$$\bar{n}_I = [A] \cdot \frac{X'}{X} = \frac{\sum_{n=1}^{N} n\beta_n[A]^n}{1 + \sum_{n=1}^{N} \beta_n[A]^n} \tag{4a}$$ *

$$X = 1 + \sum_{n=1}^{N} \beta_n \cdot [A]^n \tag{5}$$

$$X = \frac{C_M}{[M]}\text{, if only mononuclear complexes are formed} \tag{5a}$$

$$Y = \sum_{n=1}^{L} \beta_n' \cdot [A]^n \tag{6}$$

$$\ln X([A]_j) = \int_0^{[A]_j} \frac{\bar{n}_I}{[A]} \cdot d[A] \tag{7}$$

$$X_1 = (X-1)/[A]\ ;\ X_n = (X_{n-1} - \beta_{n-1})/[A]\ (n = 2, 3, \ldots) \tag{8}$$

Experimental. The experimental procedure has been the same as that described in Part I. The quinhydrone elements measured have had the composition shown in I(15).

As was shown in Part I, the hydrolysis of the lower rare earths caused by the addition of acetate buffer can be neglected. However, the hydrolysis increases considerably with the atomic number of the rare earth, and therefore the $Yb^{3+}-Ac^-$—system has been examined by use of buffers with different concentrations of acetic acid (δ = 0.5, 2.0 and 5.0; C_M = 25 mM). As seen in Table 8A—C and Fig. 2 the buffer ½HAc:1 NaAc gives somewhat higher values of $\bar{n}/[A]$ at low [A] than the other buffers. This indicates formation of OH-complexes. Hydrolytic reactions, *e.g.*

$$Yb(H_2O)_n^{3+} + H_2O \rightarrow Yb(OH)(H_2O)_{n-1}^{2+} + H_3O^+$$

$$Yb(Ac)(H_2O)_m^{2+} + H_2O \rightarrow Yb(Ac)(OH)(H_2O)_{m-1}^{1+} + H_3O^+$$

produce hydrogen ions, which then combine with acetate ions ($H_3O^+ + Ac^- \rightleftharpoons HAc + H_2O$) until equilibrium has been reached. The result will be a decrease of $[Ac^-]$ in the same way as if rare earth acetate complexes were formed, and the ligand number $\bar{n}$ obtained by the potentiometric measurements will include also the OH-complexes.

* This formula is a correction of eqn. I (7), which has been written in an erroneous form.

However, the hydroxide complexes are formed in competition with the acetate complexes and therefore the tendency of forming hydroxide complexes must decrease when the acetate concentration is increased. Moreover, the hydrolytic reactions must be depressed if the hydrogen ion concentration of the complex solution is increased, *i.e.* if a more acid buffer solution is used.

From the investigation of the Yb^{3+}—Ac^-—system it is evident that the hydrolysis of the ytterbium ions is rather weak, as the $\bar{n}$/[A]-functions obtained with the different buffers approach each other rapidly when [A] is increased. Besides, the buffers with $\delta = 2$ and 5 give approximately the same $\bar{n}$/[A]-functions even at the lowest values of [A]. Therefore it seems certain that the formation of Yb^{3+}—OH^-—complexes by the addition of the buffer 2 HAc:1 NaAc is so slight that it can be neglected.

In the discussion above the possibility of complex formation between Yb^{3+} and unprotolyzed HAc has been excluded, as extinctiometric measurements have shown that two solutions with the composition

80 mM $Ho(ClO_4)_3$ + 100 mM $HClO_4$ + 1420 mM $NaClO_4$ + x mM HAc

and having $x = 0$ and 990, respectively, show the same extinction curve within the limits of the random errors.

THE SYSTEMS INVESTIGATED

The praseodymium acetate system. The E_A-values obtained experimentally and the values of [A] and $\bar{n}$/[A], calculated by means of eqns. (2)—(4), are collected in Table 1. The coincidence between the two $\bar{n}$/[A]-functions is so good that formation of polynuclear complexes to a detectable amount can be excluded.

The complexity constants have been computed by means of eqns. (5), (7) and (8). The X-functions of the system are to be found in Table 3A.

Table 1. The corresponding values of [A] and $\bar{n}$/[A] for the praseodymium acetate system.

$C_M = C_M^\circ (1 - C_A' \times 10^{-3})$ mM							
C_M° = 20.2 mM $C_H = 3.27 \times 10^{-2} \times C_M$ mM δ = 2				C_M° = 40.2 mM $C_H = 1 \times 10^{-3} \times C_M$ mM δ = 2			
C_A' mM	$E_A - \Delta E_A$ mV	[A] mM	$\frac{\bar{n}}{[A]}$ M^{-1}	C_A' mM	$E_A - \Delta E_A$ mV	[A] mM	$\frac{\bar{n}}{[A]}$ M^{-1}
3.323	27.7	1.222	62.4	6.62	31.0—0.1	1.953	60.8
9.90	20.9—0.1	4.50	53.7	13.16	29.3—0.2	4.165	54.8
19.61	17.6—0.1	9.98	45.8	29.13	26.0—0.3	10.62	44.8
38.5	13.9—0.2	22.55	35.0	47.6	22.7—0.4	19.71	37.0
56.6	11.5—0.3	36.5	28.0	65.4	20.1—0.5	30.1	31.2
74.1	9.9—0.3	50.9	23.8	90.9	17.0—0.6	47.5	25.0
107.1	7.9—0.4	79.9	18.5	122.8	14.1—0.7	72.3	19.8
166.7	5.6—0.4	135.9	13.2	189.2	10.5—0.8	128.9	14.3
230.7	4.3—0.4	198.0	10.5	285.5	7.3—0.8	220.9	10.2
333	3.1—0.4	299.5	8.2	375	5.5—0.7	310	8.3
412	2.4—0.3	379	7.2	444	4.4—0.7	384	7.0
474	1.9—0.3	445	6.0	500	3.6—0.6	444	6.3
546	1.6—0.3	519	5.7	583	2.8—0.5	532	5.7

Table 2. The corresponding values of [A] and $\bar{n}$/[A] for the samarium acetate system.

$C_M = C_M^\circ (1 - C_A' \times 10^{-3})$ mM										
	C_M° = 25.0 mM C_H = 4.3 × 10^{-3} × C_M mM δ = ½			C_M° = 50.0 mM C_H = 4.3 × 10^{-3} × C_M mM δ = ½			C_M° = 75.0 mM C_H = 4.3 × 10^{-3} × C_M mM δ = 2			
C_A' mM	$E_A - \Delta E_A$ mV	[A] mM	$\frac{\bar{n}}{[A]}$ M^{-1}	$E_A - \Delta E_A$ mV	[A] mM	$\frac{\bar{n}}{[A]}$ M^{-1}	C_A' mM	$E_A - \Delta E_A$ mV	[A] mM	$\frac{\bar{n}}{[A]}$ M^{-1}
9.90	29.3 − 0.1	3.18	84.1	45.1 − 0.1	1.729	93.6	9.90	53.3 − 0.2	1.220	95.2
19.61	26.0 − 0.2	7.13	70.8	41.8 − 0.2	3.85	82.6	19.61	51.3 − 0.3	2.617	87.9
29.13	23.1 − 0.2	11.85	59.7	39.3 − 0.4	6.33	73.8	38.5	47.3 − 0.5	6.05	74.1
47.6	18.7 − 0.3	23.09	44.5	34.5 − 0.5	12.49	58.8	56.6	43.6 − 0.7	10.38	62.7
74.1	14.6 − 0.4	42.3	32.3	28.8 − 0.7	24.48	43.6	74.1	40.1 − 0.9	15.72	53.3
107.1	11.2 − 0.5	70.3	23.5	23.2 − 0.9	44.5	31.5	90.9	36.8 − 1.0	22.07	45.6
137.9	9.2 − 0.5	97.9	18.9	19.4 − 1.0	66.8	24.7	122.8	31.2 − 1.2	37.5	34.5
166.7	7.9 − 0.5	124.5	16.3	16.7 − 1.0	89.7	20.5	152.5	26.9 − 1.3	55.4	27.5
230.7	5.8 − 0.5	187.2	12.0	12.4 − 1.0	147.1	14.7	193.5	22.2 − 1.4	85.0	21.1
333	4.0 − 0.5	290.4	8.9	8.3 − 1.0	249.9	10.0	285.5	14.9 − 1.4	167.5	13.1
412	3.0 − 0.4	372	7.3	6.2 − 0.9	334	7.9	375	10.6 − 1.3	259.6	9.5
500	2.3 − 0.4	464	6.2	4.7 − 0.7	427	6.8	444	8.4 − 1.2	334	7.9
546	2.0 − 0.3	510	6.1	4.0 − 0.7	479	6.1	546	5.9 − 1.0	449	6.3

The samarium acetate system. The results obtained for this complexity system are collected in Tables 2 and 3B. Also for this system the formation of polynuclear complexes can be excluded.

The dysprosium acetate system. As seen in Table 4 and Fig. 1 the $\bar{n}$/[A]-value's increase with C_M at low [A]. This indicates the presence of polynuclear

Table 3. The X-functions of the praseodymium and the samarium acetate systems.

[A] mM	A Praseodymium acetate system					B Samarium acetate system				
	X ([A])	X_1 M^{-1}	X_2 M^{-2}	X_3 M^{-3}	X_4 M^{-4}	X ([A])	X_1 M^{-1}	X_2 M^{-2}	X_3 M^{-3}	X_4 M^{-4}
0	1	*64.6*	*645*	*1 940*	*2 300*	1	*102.8*	*1 810*	*7 100*	*6 500*
2	1.1325	66.2				1.2128	106.4			
6	1.411	68.6				1.683	113.9			
12	1.869	72.5				2.508	125.5	1 900		
20	2.567	78.3	685			3.845	142.2	1 970		
30	3.59	86.3	723			5.93	164	2 045		
50	6.15	103.0	768			11.64	212.5	2 200		
70	9.50	121.5	813			19.75	268	2 360		
100	16.33	153.5	887			37.3	363	2 600		
140	29.4	203	990			73.4	517	2 960	8 180	
200	59.5	292.5	1 140	2 475		162	805	3 510	8 460	6 800
300	150.3	498	1 445	2 665	2 380	440	1 460	4 530	9 050	6 500
400	316.5	789	1 810	2 915	2 410	960	2 400	5 730	9 800	6 800
500	590	1 178	2 225	3 160	2 420	1 820	3 650	7 090	10 560	6 900

Table 4. The corresponding values of [A] and $\bar{n}/[A]$ for the dysprosium acetate system.

	C_M = 25.0 mM (constant) C_H = 0.225 mM δ = 2. Sign ○			C_M = 50.0 mM (constant) C_H = 0.485 mM δ = 2. Sign □			C_M = 73.0 mM (constant) C_H = 0.723 mM δ = 2. Sign △			
C_A' mM	$E_A - \Delta E_A$ mV	[A] mM	$\frac{\bar{n}}{[A]}$ M^{-1}	$E_A - \Delta E_A$ mV	[A] mM	$\frac{\bar{n}}{[A]}$ M^{-1}	C_A' mM	$E_A - \Delta E_A$ mV	[A] mM	$\frac{\bar{n}}{[A]}$ M^{-1}
3.98	21.5	1.753	47.5	34.8	1.063	48.1	3.88	44.6	0.720	49.8
9.90	20.2 − 0.1	4.52	46.2	32.4 − 0.1	2.82	47.5	9.65	41.0 − 0.1	1.978	49.2
19.61	19.2 − 0.2	9.30	43.7	31.2 − 0.2	5.82	46.1	28.4	38.7 − 0.3	6.29	46.9
38.5	17.9 − 0.3	19.23	39.7	29.9 − 0.4	12.04	43.3	46.4	37.7 − 0.6	10.77	44.6
56.6	16.6 − 0.4	29.9	35.6	28.7 − 0.6	18.69	40.1	63.8	36.6 − 0.8	15.55	42.0
90.9	14.2 − 0.5	52.9	28.6	26.4 − 0.8	33.1	34.7	88.6	35.3 − 1.0	22.9	39.0
122.8	12.3 − 0.6	77.3	23.4	24.0 − 1.0	49.5	29.4	134.5	32.4 − 1.3	39.4	32.9
166.7	10.4 − 0.6	113.2	18.9	21.1 − 1.2	76.0	23.8	188.7	28.8 − 1.7	64.7	26.1
230.7	8.4 − 0.6	169.5	14.4	17.6 − 1.3	121.2	18.1	325	21.8 − 2.0	148.6	16.2
333	6.6 − 0.7	264	10.5	13.8 − 1.4	204.2	12.6	365.5	20.1 − 2.1	179.5	14.1
412	5.7 − 0.7	338	8.7	11.9 − 1.4	271.9	10.3	433	17.7 − 2.1	234	11.6
500	4.9 − 0.7	424	7.2	10.3 − 1.5	353	8.3	532	15.1 − 2.2	319.5	9.1
583	4.4 − 0.8	506	6.1	9.2 − 1.5	430	7.1	600	13.9 − 2.2	378	8.0

complexes. When both mono- and dinuclear complexes are formed, the connection between $\bar{n}/[A]$ and [M] is given by the equation

$$\frac{\bar{n}}{[A]} = \frac{X' + [M] \cdot Y'}{X + 2[M] \cdot Y} \tag{9}$$

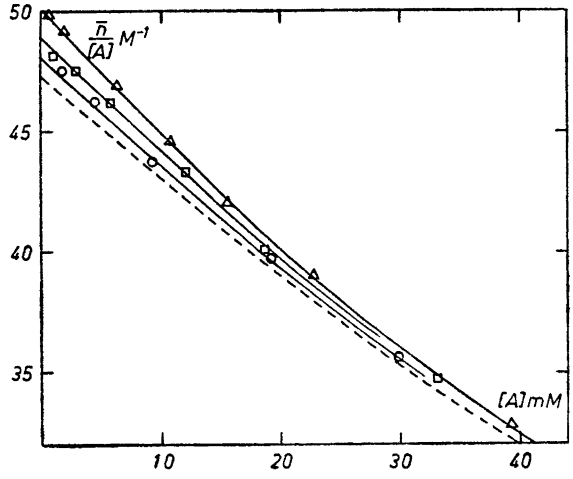

Fig. 1. The function $\frac{\bar{n}}{[A]} = f([A])$ of the dysprosium acetate system. The signs refer to the different values of C_M given in Table 4. The broken curve is the function obtained by extrapolation to $C_M = 0$.

(*cf. eqn.* I(8)). From the theory given by Fronæus [2] and confirmed experimentally, it appears that the $\bar{n}$/[A]-functions of series with different C_M will approach each other when [A] is increased. Finally the functions will meet at a point, and after that they will diverge again but in the reversed order. For the Dy^{3+}-Ac^--system the $\bar{n}$/[A]-curves meet at [A] ≈ 60 mM, but the curves seem to coincide at higher [A]-values.

As [M] = 0 at $C_M = 0$ we can deduce from (9)

$$\lim_{C_M \to 0} \frac{\bar{n}}{[A]} = \left(\frac{\bar{n}}{[A]}\right)_{C_M=0} = \frac{X'}{X} = \frac{\bar{n}_I}{[A]} \tag{10}$$

The function $(\bar{n}/[A])_{C_M=0} = f([A])$ is listed in Table 6A and represented by the broken curve in Fig. 1. The function has been used for the computation of the X-functions in Table 6A according to eqns. (7) and (8). In this way it is possible to calculate the complexity constants of the mononuclear complexes.

From eqn. (9) it can be deduced

$$\lim_{C_A \to 0} \frac{\bar{n}}{[A]} = \beta_1 + C_M \cdot \beta_1' \tag{11}$$

According to this formula $\beta_1' \approx 40$ M^{-2}.

The holmium acetate system. The results of the measurements on the Ho^{3+}-Ac^--system are shown in Tables 5 and 6B. Also for this system the series with $C_M = 40$ mM gives somewhat higher $\bar{n}$/[A] at low [A] than the series with $C_M = 20$ mM. In calculating the X-functions in Table 6B the $\bar{n}$/[A]-curve was drawn in accordance to the values of $(\bar{n}/[A])_{C_M=0}$ given in Table 6B.

Table 5. The corresponding values of [A] and $\bar{n}$/[A] for the holmium acetate system.

C_M = 20.0 mM (constant) C_H = 0.225 mM δ = 2				C_M = 40.0 mM (constant) C_H = 0.450 mM δ = 2			
C_A' mM	$E_A - \Delta E_A$ mV	[A] mM	$\frac{\bar{n}}{[A]}$ M^{-1}	C_A' mM	$E_A - \Delta E_A$ mV	[A] mM	$\frac{\bar{n}}{[A]}$ M^{-1}
3.323	18.0	1.693	43.4	6.62	27.4	2.315	42.7
9.90	16.0 − 0.1	5.35	41.0	13.16	25.9 − 0.1	4.82	41.4
19.61	15.1 − 0.1	10.90	39.2	29.13	24.7 − 0.3	11.18	39.3
38.5	14.0 − 0.3	22.44	35.3	47.6	23.6 − 0.4	19.10	36.8
56.6	13.0 − 0.3	34.3	32.2	65.4	22.6 − 0.6	27.5	34.1
74.1	12.0 − 0.4	46.9	28.8	90.9	21.0 − 0.7	40.8	30.5
107.1	10.5 − 0.5	72.2	24.1	122.8	19.0 − 0.9	60.1	25.9
166.7	8.2 − 0.5	123.0	17.7	189.2	15.4 − 1.0	107.1	19.1
230.7	6.7 − 0.6	181.4	13.5	285.5	11.9 − 1.1	186.5	13.2
333	5.2 − 0.6	278	9.9	375	9.8 − 1.2	267	10.1
412	4.4 − 0.6	354	8.1	444	8.5 − 1.2	333	8.3
474	4.0 − 0.6	414	7.2	500	7.9 − 1.2	384	7.5
546	3.6 − 0.6	485	6.3	583	7.1 − 1.2	462	6.5
615	3.3 − 0.6	553	5.6	667	6.4 − 1.2	543	5.7

Table 6. The X-functions of the dysprosium and the holmium acetate systems.

[A] mM	A Dysprosium acetate system						B Holmium acetate system					
	$\left(\frac{\bar{n}}{[A]}\right)_{C_M=0}$	X([A])	X_1 M^{-1}	X_2 M^{-2}	X_3 M^{-3}	X_4 M^{-4}	$\left(\frac{\bar{n}}{[A]}\right)_{C_M=0}$	X([A])	X_1 M^{-1}	X_2 M^{-2}	X_3 M^{-3}	X_4 M^{-4}
0	*47.3*	1	*47.1*	*930*	*6 100*	*7 800*	*43.4*	1	*43.3*	*725*	*5 600*	*3 800*
2	46.4	1.0983	49.1				42.5	1.0898	44.9			
6	44.7	1.318	53.0				40.8	1.2875	47.9			
10	43.0	1.571	57.1	1 000			39.2	1.511	51.1	780		
20	39.0	2.367	68.4	1 065			35.9	2.200	60.0	835		
30	35.3	3.432	81.1	1 133			33.0	3.107	70.2	897		
50	29.1	6.52	110.5	1 265			28.0	5.71	94.3	1 020		
70	24.9	11.16	145	1 400			24.2	9.61	123.0	1 140	5 910	
100	20.4	21.9	209	1 620	6 900		20.1	18.60	176	1 325	6 020	
140	16.5	45.6	318.5	1 935	7 190		16.2	38.2	266	1 590	6 170	
200	12.9	108.5	538	2 455	7 630	7 650	12.5	89.6	443	2 000	6 370	3 830
300	9.5	326.5	1 085	3 460	8 430	7 760	9.2	261	866	2 740	6 730	3 760
400	7.6	763	1 905	4 640	9 280	7 950	7.4	593	1 480	3 590	7 170	3 930
500	6.2	1 510	3 020	5 940	10 020	7 840	6.1	1 165	2 330	4 570	7 700	4 200

The erbium acetate system. From the $\bar{n}$/[A]-values in Table 7 it must be inferred that polynuclear complexes are present also in this system. β_1' can be estimated to $\approx$ 30 M^{-2}. In the computation of the X-functions in Table 9A, the values of $(\bar{n}/[A])_{C_M=0}$ have been used.

Table 7. The corresponding values of [A] and $\bar{n}$/[A] for the erbium acetate system.

	C_M = 25.0 mM (constant) C_H = 0.295 mM δ = 2			C_M = 50.0 mM (constant) C_H = 0.590 mM δ = 2			C_M = 75.2 mM (constant) C_H = 1.013 mM δ = 2			
C_A' mM	E_A—ΔE_A mV	[A] mM	$\frac{\bar{n}}{[A]}$ M^{-1}	E_A—ΔE_A mV	[A] mM	$\frac{\bar{n}}{[A]}$ M^{-1}	C_A' mM	E_A—ΔE_A mV	[A] mM	$\frac{\bar{n}}{[A]}$ M^{-1}
6.62	18.9	3.21	39.6	30.6	2.059	39.6	6.62	40.7	1.418	40.8
9.90	18.3—0.1	4.90	39.0	29.6—0.1	3.17	39.4	13.16	37.8—0.1	3.07	40.0
19.61	17.4—0.2	10.01	37.5	28.4—0.2	6.52	38.7	29.13	36.0—0.3	7.21	38.8
38.5	16.2—0.3	20.59	34.3	27.2—0.4	13.42	36.6	47.6	35.0—0.5	12.28	37.3
56.6	15.3—0.4	31.5	31.6	26.3—0.6	20.57	34.5	65.4	34.1—0.7	17.57	35.5
74.1	14.2—0.4	43.0	28.7	25.3—0.7	28.1	32.4	90.9	33.0—1.0	25.75	33.4
107.1	12.6—0.6	66.7	24.1	23.6—0.9	43.7	28.8	122.8	31.4—1.2	37.3	30.2
166.7	10.1—0.6	114.6	18.1	20.2—1.2	78.7	22.2	189.2	27.9—1.6	67.0	24.1
230.7	8.3—0.7	170.9	13.9	17.2—1.3	123.1	17.4	285.5	22.9—2.0	125.1	17.0
333	6.4—0.7	266.1	10.1	13.6—1.4	205.8	12.3	375	19.4—2.1	189.3	13.0
412	5.6—0.7	339	8.5	11.7—1.5	275.2	9.9	444	17.1—2.2	246.7	10.6
500	4.9—0.7	424	7.2	10.1—1.5	356	8.1	546	14.8—2.2	332	8.5
583	4.5—0.7	502	6.4	9.1—1.5	432	7.0	615	13.5—2.3	395	7.4

Table 8. The corresponding values of [A] and $\bar{n}/[A]$ for the ytterbium acetate system.

	A C_M = 25.0 mM (constant) C_H = 0.280 mM δ = ½. Sign +			B C_M = 25.0 mM (constant) C_H = 0.280 mM δ = 2. Sign ○			C C_M = 25.0 mM (constant) C_H = 0.280 mM δ = 5. Sign ●		
C'_A mM	$E_A - \Delta E_A$ mV	[A] mM	$\frac{\bar{n}}{[A]}$ M^{-1}	$E_A - \Delta E_A$ mV	[A] mM	$\frac{\bar{n}}{[A]}$ M^{-1}	$E_A - \Delta E_A$ mV	[A] mM	$\frac{\bar{n}}{[A]}$ M^{-1}
3.323	25.1	1.433	45.5	21.5	1.494	43.5	20.4	1.534	43.8
6.62	21.8	3.025	44.1	19.9	3.082	43.2	19.5	3.115	43.6
13.16	19.7 − 0.1	6.31	41.7	18.5 − 0.1	6.43	40.6	18.4 − 0.1	6.43	41.1
29.1	17.6 − 0.2	14.91	37.4	17.0 − 0.2	15.06	36.8	17.0 − 0.2	15.04	37.1
47.6	15.9 − 0.3	26.0	32.9	15.5 − 0.3	26.2	32.4	15.6 − 0.3	26.05	32.9
65.4	14.6 − 0.4	37.6	29.3	14.4 − 0.4	37.7	29.2	14.5 − 0.4	37.5	29.6
90.9	13.1 − 0.5	55.6	25.3	12.9 − 0.5	55.7	25.1	12.9 − 0.5	55.7	25.1
122.8	11.5 − 0.6	80.2	21.2	11.4 − 0.6	80.2	21.1	11.4 − 0.6	80.2	21.2
189.2	9.1 − 0.7	136.1	15.5	9.0 − 0.7	136.4	15.4	9.0 − 0.7	136.3	15.5
285.5	7.1 − 0.7	222.2	11.4	7.0 − 0.7	222.8	11.3	7.0 − 0.7	222.7	11.3
375	5.8 − 0.7	307	8.8	5.8 − 0.7	307	8.9	5.8 − 0.7	307	8.9
444	5.2 − 0.7	372	7.7	5.2 − 0.7	372	7.8	5.2 − 0.7	372	7.8
546	4.6 − 0.7	468	6.6	4.6 − 0.7	468	6.6	4.6 − 0.7	468	6.7
615	4.2 − 0.7	536	5.9	4.2 − 0.7	536	5.9	4.3 − 0.7	534	6.1

	D C_M = 50.0 mM (constant) C_H = 0.560 mM δ = 2. Sign □			E C_M = 75.0 mM (constant) C_H = 0.840 mM δ = 2. Sign △		
C'_A mM	$E_A - \Delta E_A$ mV	[A] mM	$\frac{\bar{n}}{[A]}$ M^{-1}	$E_A - \Delta E_A$ mV	[A] mM	$\frac{\bar{n}}{[A]}$ M^{-1}
6.62	32.3	1.920	44.3	41.8	1.340	45.8
9.90	31.2 − 0.1	2.971	43.6	40.3 − 0.1	2.097	45.3
19.61	29.6 − 0.2	6.21	41.7	38.3 − 0.2	4.43	43.6
38.5	27.8 − 0.4	13.10	38.0	36.6 − 0.4	9.27	41.0
56.6	26.5 − 0.6	20.40	35.0	35.3 − 0.6	14.43	38.3
74.1	25.2 − 0.7	28.2	32.2	34.1 − 0.8	19.93	35.7
107.1	23.0 − 0.9	44.8	27.6	32.1 − 1.1	31.5	31.7
142.9	20.8 − 1.1	65.6	23.4	29.9 − 1.4	46.4	27.5
230.7	16.3 − 1.3	127.6	16.1	24.8 − 1.8	93.0	19.6
333	12.9 − 1.4	211.5	11.5	20.1 − 2.1	163.7	13.7
412	11.2 − 1.5	281	9.3	17.5 − 2.2	225	11.0
500	9.7 − 1.5	362	7.6	15.3 − 2.2	298	9.0
583	8.7 − 1.5	439	6.6	13.7 − 2.2	370	7.7
667	8.0 − 1.5	516	5.8	12.5 − 2.3	446	6.6

The ytterbium acetate system. As mentioned before the hydrolysis of Yb^{3+} has been examined by means of acetate buffers with different δ. Table 8A—C and Fig. 2 show that the hydrolysis can be neglected when the buffer 2 HAc: 1 NaAc is added.

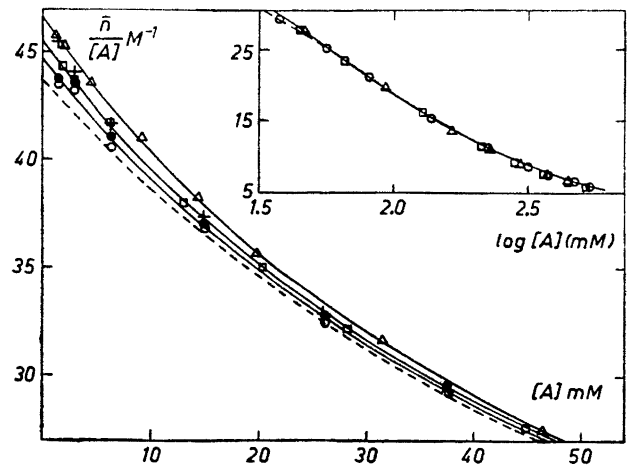

Fig. 2. $\frac{\bar{n}}{[A]}$ as a function of [A] for the ytterbium acetate system at different values of C_M and δ, according to the titration series in Table 8. The broken curve is obtained by extrapolation to $C_M = 0$.

It is seen from Table 8B, D, E and Fig. 2 that polynuclear complexes probably are formed. β_1' can be estimated to about 30 M^{-2}. The X-functions in Table 9B are computed from $(\bar{n}/[A])_{C_M=0}$.

Table 9. The X-functions of the erbium and the ytterbium acetate systems.

	A Erbium acetate system						B Ytterbium acetate system					
[A] mM	$\left(\frac{\bar{n}}{[A]}\right)_{C_M=0}$	$X([A])$	X_1 M^{-1}	X_2 M^{-2}	X_3 M^{-3}	X_4 M^{-4}	$\left(\frac{\bar{n}}{[A]}\right)_{C_M=0}$	$X([A])$	X_1 M^{-1}	X_2 M^{-2}	X_3 M^{-3}	X_4 M^{-4}
0	*40.1*	1	*40.1*	*678*	*4 520*	*4 300*	*43.8*	1	*43.7*	*680*	*3 500*	*4 200*
2	39.5	1.0831	41.5				42.7	1.0904	45.2			
6	38.4	1.2665	44.4				40.5	1.288	48.0			
10	37.3	1.474	47.4	725			38.7	1.509	50.9	720		
20	34.4	2.110	55.5	770			34.6	2.175	58.8	752		
30	31.8	2.938	64.6	817			31.2	3.022	67.4	790		
50	27.2	5.29	85.8	915	4 740		26.2	5.345	86.9	864	3 680	
70	23.6	8.78	111.2	1 015	4 810		22.7	8.71	110.1	949	3 840	
100	19.7	16.75	157.5	1 175	4 970		18.8	16.17	151.7	1 080	4 000	
140	15.9	34.0	236	1 400	5 160		15.3	31.8	220	1 260	4 150	
200	12.5	79.3	391	1 760	5 400	4 380	12.1	71.9	354.5	1 555	4 380	4 400
300	9.4	232.5	771	2 440	5 870	4 500	9.1	205	680	2 120	4 810	4 350
400	7.6	540	1 350	3 270	6 480	4 890	7.4	464	1 160	2 790	5 260	4 400
500	6.5	1 098	2 195	4 310	7 260	5 480	6.4	920	1 840	3 590	5 810	4 600

B. THE EXTINCTIOMETRIC INVESTIGATION

In order to check the potentiometrically determined complexity constants of the acetate systems of the higher rare earths, an extinctiometric examination of the erbium acetate system has been performed. This method of investigation has been examined theoretically by Fronæus [2,p. 87], who has shown that only systems of exclusively mononuclear complexes are suitable for extinctiometric investigation. However, we can in favourable cases get an approximate value of at least β_1 also for systems with dinuclear complexes (*cf.* the extinctiometric investigation of the copper(II) acetate system performed by Fronæus [2]).

As to the erbium acetate system it is indicated by the potentiometric investigation that polynuclear complexes are probably formed ($\beta_1' \approx 30$ M^{-2}, if the presence of only mono- and dinuclear complexes is assumed). However, the concentration of the first dinuclear complex, calculated from β_1', is very low (*cf.* Table 10), and it might therefore be possible to get at least some idea of the constants of the mononuclear complexes by extinctiometric measurements.

Calculation of the complexity constants from extinctiometric data

In addition to the notations already given, it is denoted by

E the total extinction of the solution, measured with water in the reference cell,

d the thickness of the absorbing layer in cm,

e the quotient E/d,

ε_M°, ε_A° the molar extinctions of M and A,

ε_n, ε_n' the molar extinctions of the mononuclear complexes MA_n and the dinuclear complexes M_2A_n, respectively.

In the case where both mono- and dinuclear complexes are formed, the following is valid

$$e = \varepsilon_M^\circ \cdot [M] + \sum_{n=1}^{N} \varepsilon_n \cdot [MA_n] + \sum_{n=1}^{L} \varepsilon_n' \cdot [M_2A_n] + \varepsilon_A^\circ \cdot [A] \qquad (12)$$

Table 10. The concentrations of the first dinuclear (a) and the first mononuclear (b) erbium acetate complexes at some values of C_M and [A], chosen from the extinctiometric measurements. The potentiometrically obtained values of β_1 and β_1' have been used in the calculations.

C_M mM	37.3	36.6	35.8	14.9	14.8	14.6	7.5	7.4	7.3
[Ac^-] mM	2	10	20	2	10	20	2	10	20
a mM	0.07	0.18	0.17	0.011	0.03	0.03	0.003	0.008	0.007
b mM	2.8	9.9	13.6	1.1	4.0	5.6	0.56	2.0	2.8
$\frac{a}{b} \cdot 10^{+2}$	2.5	1.8	1.3	1.0	0.8	0.5	0.5	0.4	0.3

After having expressed $[MA_n]$ and $[M_2A_n]$ by means of [A], β_n and β_n', and introduced the abbreviations

$$\varepsilon = \frac{e - \varepsilon_M^\circ \cdot C_M - \varepsilon_A^\circ \cdot C_A}{C_M}$$

$$\xi = \sum_{n=1}^{N} (\varepsilon_n - \varepsilon_M^\circ - n \cdot \varepsilon_A^\circ)\, \beta_n [A]^n$$

$$\eta = \sum_{n=1}^{L} (\varepsilon_n' - 2\varepsilon_M^\circ - n\varepsilon_A^\circ)\, \beta_n' [A]^n$$

we get the expression

$$\varepsilon = \frac{\xi + [M] \cdot \eta}{X + 2[M] \cdot Y} \tag{13}$$

$\varepsilon = \xi/X$ in the case where *only mononuclear* complexes are formed, as $\eta = 0$ and $Y = 0$. Thus $\varepsilon = f([A])$, independent of [M], and consequently solutions with the same value of ε must have the same value of [A]. In this case we have

$$\left(\frac{\partial C_A}{\partial C_M}\right)_\varepsilon = \bar{n}_I \text{ (Constant } \varepsilon) \tag{14}$$

By extrapolating the straight line $(C_A)_\varepsilon = [A] + \bar{n}_I \times (C_M)_\varepsilon$ obtained from eqn. (14) to $C_M = 0$, we get [A] of all solutions with the same value of ε.

If *both mono- and dinuclear* complexes are present, eqn. (14) is not valid, as $\varepsilon = f([A], [M])$. However, using eqn. (13) (ε being constant) and the expressions of C_M and C_A at the bottom of page 167 in Part I, we can deduce for $C_M = 0$

$$\left(\frac{\partial C_A}{\partial C_M}\right)_{\substack{\varepsilon \\ C_M=0}} = k_\varepsilon = \bar{n}_I + \frac{2\,Y \cdot \xi - X \cdot \eta}{X(X \cdot \xi' - X' \cdot \xi)} \tag{15}$$

The determination of k_ε can be performed in the following way. The function $\varepsilon = f(C_A)$ is determined experimentally for some values of C_M. By cutting the curves with lines ε = constant, we obtain the pairs of corresponding values $(C_A, C_M)_\varepsilon$. Then, k_ε for every value of ε is determined from the slope of the function $(C_A)_\varepsilon = f(C_M)_\varepsilon$ at $C_M = 0$. This function, however, is not necessarily a straight line as seen from eqn. (15), and therefore the calculation of k_ε can be rather uncertain.

For the Er^{3+}-Ac^--system, $[M_2A_n]$ is very low and decreases much more rapidly than $[MA_n]$ when $[M] \to 0$, as seen in Table 10 (calculated with the use of eqns. 1a, 1b, 5 and 5a). Therefore it is probable that the values of $(C_A)_{C_M=0} = [A]$, obtained by extrapolations of the function $(C_A)_\varepsilon = f(C_M)_\varepsilon$ to $C_M = 0$, represent approximately the concentration of free ligand also in solutions with low $C_M \neq 0$. Therefore, the function $(C_A)_\varepsilon = f(C_M)_\varepsilon$

ought to be a straight line at low values of C_M, indicating that $k_\varepsilon \approx \bar{n}_I$ at low C_M. Then, if the second term of eqn. (15) can be neglected, we can compute the complexity constants of the mononuclear complexes by use of $k_\varepsilon/[A]$ and eqn. (7). However, the constants may contain a systematic error that we cannot estimate.

From eqn. (15) it can be deduced

$$\lim_{[A]\to 0} \frac{k_\varepsilon}{[A]} = \beta_1 - \frac{\Delta\varepsilon_1'\cdot\beta_1'}{\Delta\varepsilon_1\cdot\beta_1}, \text{ with } \begin{cases}\Delta\varepsilon_1' = \varepsilon_1' - 2\varepsilon_M^\circ - \varepsilon_A^\circ \\ \Delta\varepsilon_1 = \varepsilon_1 - \varepsilon_M^\circ - \varepsilon_A^\circ\end{cases} \quad (16)$$

Thus, we get directly an approximate value of β_1 if we can compute k_ε at so low [A] that it is possible to extrapolate $k_\varepsilon/[A]$ to $[A] = 0$, and if the last term of (16) can be neglected.

Measurements

The extinctiometric measurements have been carried out at 20°C with a Beckman Recording Quartz Spectrophotometer Model DK 1. Except in obtaining the survey in Fig. 3, the spectrophotometer was constantly adjusted to the wavelength 378 mμ. As the absorption bands are very narrow, it is necessary to use a very narrow band width. Therefore the apparatus was set at a high sensitivity (80), which resulted in a very narrow slit and an effective band width of only ≈ 5 Å.

According the Fronæus [2,p.95] the experimental error caused by the imperfect monochromaticity of the light is reduced if the measurements are carried out in a wavelength range where the extinction curve has a horizontal tangent. This is not possible in the case of the Er^{3+}-Ac^--system, owing to the narrow peaks and to the fact that the positions of the peaks are shifted when the complexes are formed. At 378 mμ, however, the extinction curve has about the same slope at all values of $[Ac^-]$.

Another systematic error is caused by the partial reflection of the light at the end plates of the absorption cells. This error is reduced if the corresponding solutions, used at the calculation of k_ε (*i.e.*, solutions with the same ε), have the same value of E. This condition is fulfilled approximately if solutions with the same value of C_A' also have the same value of $d.C_M$ (*cf.* Table 11).

The solutions measured have been prepared by mixing different volumes of two solutions,

S_1: $\frac{75}{d}$ mM $Er(ClO_4)_3$ + (2 000 − 6.$\frac{75}{d}$) mM $NaClO_4$

S_2: 2 000 mM HAc + 1 000 mM NaAc + 1 000 mM $NaClO_4$

Thus, the connection between C_M and C_A' is

$$C_M = \frac{75}{d}(1 - C_A' \times 10^{-3}), \; C_M \text{ and } C_A' \text{ in mM} \quad (17)$$

In the calculation of the true ligand concentration $C_A = C_A' + [H^+] - C_H$ of the complex solution, the potentiometrically obtained values of the correction terms $[H^+]$ and C_H have been used.

As one absorption cell has been filled with the complex solution and the other with a buffer solution with the same C_A', the value of $E - d \cdot \varepsilon_A^\circ \cdot C_A'$ has been determined directly.

It was controlled that Beer's law is valid for erbium perchlorate solutions with low C_M. At 378 mμ it was found $\varepsilon_M^\circ = 2.15 \pm 0.03$ for $C_M \leq 40$ mM.

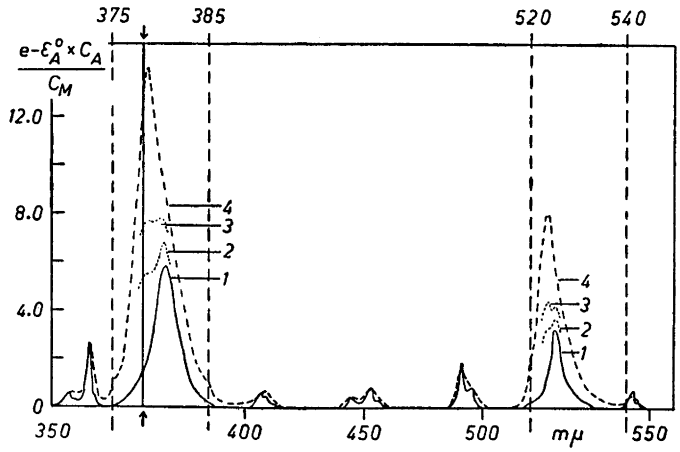

Fig. 3. Extinction curves of one erbium perchlorate solution (curve 1) and three erbium perchlorate solutions with various amounts of the buffer 2 HAc:1 NaAc; $\bar{n} \approx 0.9$ (curve 2), $\bar{n} \approx 1.4$ (curve 3) and $\bar{n} \approx 4$ (curve 4), $\bar{n}$ according to the potentiometric measurements. The arrows and the line indicate the wavelength 378 mμ at which the extinctiometric investigation has been performed. - - - - The erbium ion has still another absorption band in the visible range at about 660 mμ. The height of the peak is nearly independent of C_{Ac} ($\varepsilon_M^0 \approx 1.5$). — — — The two ranges 375—385 mμ and 520—540 mμ have been enlarged.

Fig. 3 shows the extinction curves of one erbium perchlorate solution and three complex solutions with different values of [A]. The addition of acetate buffer results in the appearance of a new peak of somewhat shorter wavelength in the band at 380 mμ as also in the band at 525 mμ. At high acetate concentration the new peak dominates and incorporates the original peak. It is evident that ε of the new peak is a function of [A]. Otherwise, of course, the extinc-

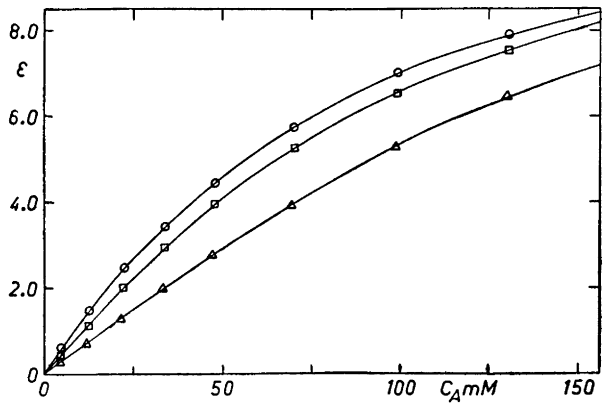

Fig. 4. ε of the erbium acetate system as a function of C_{Ac} - for three different values of the factor $\frac{75}{d}$ of eqn. (17). O : d = 10 cm; □ : d = 5 cm; △ : d = 2 cm.

Table 11. Determination of the corresponding values of [A] and k_ε for the erbium acetate system and a comparison between k_ε/[A] and the potentiometrically obtained values of $\bar{n}_I$/[A].

ε	d = 2 cm		d = 5 cm		d = 10 cm		C_M=0 [A] mM	k_ε	$\frac{k_\varepsilon}{[A]}$	$\frac{\bar{n}_I}{[A]}$ pot.
	C_A mM	C_M mM	C_A mM	C_M mM	C_A mM	C_M mM				
1.5	25.6	36.6	16.6	14.8	13.0	7.4	10.2	0.42	41.5	37.5
2.0	33.8	36.2	22.3	14.7	17.8	7.4	14.0	0.55	39	36.5
2.5	42.4	35.9	28.2	14.6	23.0	7.3	18.2	0.68	37.5	35
3.0	51.5	35.6	34.4	14.5	28.6	7.3	22.8	0.81	35.5	34
3.5	60.5	35.2	40.8	14.4	34.6	7.2	28.0	0.93	33	32.5
4.0	70.0	34.8	48.5	14.3	41.0	7.2	33.5	1.05	31.5	31
4.5	80.5	34.5	56.0	14.2	48.0	7.1	39.5	1.18	30	29.5
5.0	91.5	34.1	65.0	14.0	56.0	7.1	46.5	1.32	28.5	28
5.5	103	33.6	74.5	13.9	65.0	7.0	55.0	1.45	26.5	26
6.0	116.5	33.1	85.5	13.7	75	6.9	64.0	1.59	25	24.5
6.5	131	32.6	98	13.5	86.5	6.8	74.5	1.73	23	23
7.0	148	32.0	112	13.3	99.5	6.8	86.5	1.92	22	21.5
7.5	167	31.2	129	13.1	115	6.6	102	2.1	20.5	19.5
8.0	190	30.4	148	12.8	134	6.5	120	2.2	18	17.5

tiometric method of investigation of the complexity system were not applicable. The peak at 380 mμ has been chosen for the measurements as solutions with lower C_M can be used.

Complex rare earth systems have been examined extinctiometrically before, *e.g.*, by Moeller and Brantley [3] and by Vickery [4], who have examined solutions of the EDTA-complexes. They, too, observed that in some cases the dominating bands of the rare earth were split when the complexing agent was added. However, no attempts of computing the complexity constants of the systems were made.

The function $\varepsilon = f(C_A)$ of three series with different C_M is shown in Fig. 4. Table 11 gives the corresponding values of C_A and C_M at some values of ε. The function $(C_A)_\varepsilon = f(C_M)_\varepsilon$ proves to be approximately linear for $\varepsilon > 2.0$. Thus it is possible to extrapolate the function to $C_M = 0$ and to calculate

Table 12. The X-functions of the erbium acetate system calculated from the extinctiometric measurements.

[A] mM	X ([A])	X_1 M^{-1}	X_2 M^{-2}	X_3 M^{-3}
0	1	*45*	*770*	*4 500*
10	1.535	53.5		
15	1.87	58		
25	2.69	67.5	900	
40	4.35	84	975	
60	7.57	110	1 080	5 100
80	12.2	140	1 200	5 300
100	18.7	177	1 320	5 500

Table 13. The complexity constants with the random errors of the systems investigated.

Systems	β_1 M^{-1}	β_2 M^{-2}	β_3 M^{-3}	β_4 M^{-4}	β_1' M^{-2}
A. Potentiometric investigation.					
Pr^{3+} $-Ac^-$	65 ± 2	650 ± 60	1 900 ± 300	~2 000	—
Sm^{3+} $-Ac^-$	103 ± 3	1 810 ± 180	7 100 ± 1 200	~7 000	—
Dy^{3+} $-Ac^-$	47 ± 2	930 ± 90	6 100 ± 1 000	~8 000	40 ± 20
Ho^{3+} $-Ac^-$	43 ± 2	730 ± 70	5 600 ± 800	~4 000	—
Er^{3+} $-Ac^-$	40 ± 2	680 ± 70	4 500 ± 700	~4 000	30 ± 20
Yb^{3+} $-Ac^-$	44 ± 2	680 ± 70	3 500 ± 600	~4 000	30 ± 20
B. Extinctiometric investigation.					
Er^{3+} $-Ac^-$	45 ± 5	750 ± 150	~5 000	—	—

the values of k_ε and [A] given in Table 11. As seen in the table the agreement between $k_\varepsilon/[A]$ and $\bar{n}_I/[A]$, potentiometrically obtained, is surprisingly good, especially for $[A] > 25$ mM.

The function $k_\varepsilon/[A] = f([A])$ has been extrapolated to $[A] = 0$ and after that the complexity constants have been computed in the same way as before (Table 12). The constants obtained extinctiometrically are in good agreement with those determined potentiometrically (Table 13). Therefore it seems plausible to assume that the approximations made are permissible, *i.e.*, that the concentration of polynuclear complexes in erbium acetate solutions with low C_M is so low that $k_\varepsilon \approx \bar{n}_I$.

Table 14. The stability constants of the rare earth acetate systems reported in Parts I and II, the ionic radii and the numbers of electrons in the 4f-orbitals of the tervalent rare earth ions.

Rare earth	Atomic number	Ionic radius* in A	Number of electrons in the 4f-orbitals	$b_1 = \beta_1$	b_2	b_3	b_4	$\frac{b_1}{b_2}$	$\frac{b_2}{b_3}$	$\frac{b_3}{b_4}$
La	57	1.06	0	36	8.3	3.2	0.9	4.3	2.6	4
Ce	58	1.03	1	48	10.2	2.8	1.1	4.7	3.6	3
Pr	59	1.01	2	65	10.0	2.9	1.0	6.5	3.5	3
Nd	60	1.00	3	80	12.8	2.8	1.2	6.3	4.6	2
Sm	62	0.96	5	103	17.6	3.9	1.0	5.9	4.5	4
Gd	64	0.94	7	69	19.1	3.9	1.0	3.6	4.9	4
Dy	66	0.91	9	47	19.8	6.6	1.3	2.4	3.0	5
Ho	67	0.89	10	43	17.0	7.7	0.7	2.5	2.2	11
Er	68	0.88	11	40	17.0	6.6	0.9	2.4	2.6	7
Yb	70	0.86	13	44	15.5	5.1	1.1	2.8	3.0	5

* Templeton, D. H. and Dauben, C. H. *J. Am. Chem. Soc.* **76** (1954) 5237.

At low [A], k_ε/[A] seems to be somewhat higher than $\bar{n}_I$/[A]. As seen in eqn. (16) this is possible if $\Delta\varepsilon_1 < 0$, or, perhaps more likely, if $\Delta\varepsilon_1' < 0$. When [A] < 15 mM, [A] and k_ε will be very uncertain, as the values of $(C_A, C_M)_\varepsilon$ no longer represent a straight line.

DISCUSSION OF THE RESULTS

As seen in Table 14, the stability constant b_1 of the first mononuclear complex increase strongly from La to Sm. This increase is expected as the ionic radius decreases in the same direction. However, from Sm to Dy b_1 decreases strongly and then b_1 remains approximately constant at Dy, Ho, Er and Yb, although the ionic radius decreases incessantly. Thus it seems as if the possibility of forming the first acetate complex is rendered more difficult after the 4f-orbitals have been half-filled with electrons.

To begin with, the stability constant of the second complex increases when the ionic radius of the rare earth decreases, but from Dy to Yb also b_2 shows a decided tendency to decrease. The maximum stability of the third complex is reached at Ho. Thus the tendency to form higher complexes does not decrease as rapidly as the tendency to form the first complex.

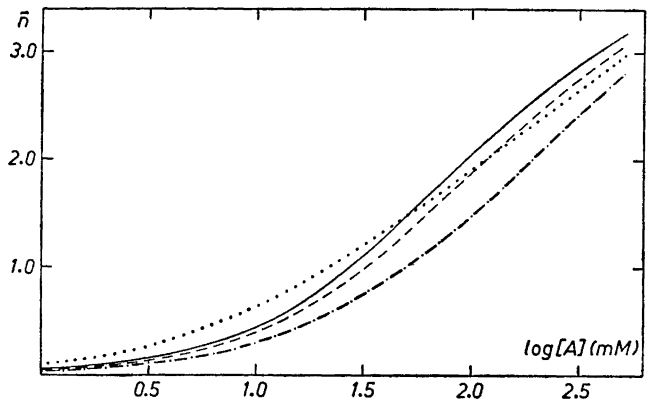

Fig. 5. The complex formation curves of some rare earth acetate systems: ——— the Dy^{3+}-Ac^--system; — — — the Yb^{3+}-Ac^--system; · · · · · the Sm^{3+}-Ac^--system; — · — · — the La^{3+}-Ac^--system.

Fig. 5 shows how the ligand number $\bar{n}_I$ of some rare earth acetate systems varies with the concentration of free ligand of the solution.

As was discussed in Part I, it is doubtful whether the fourth complexity constant has a real meaning, as anionic acetate complexes of the rare earths cannot be proved by anion exchange experiments (Fronæus [5]).

As to the formation of polynuclear complexes, β_1' is 30 à 40 M^{-2} for Gd, Dy, Er and Yb and probably also for Ho. For the acetate systems of the

lighter rare earths the presence of polynuclear complexes is not so evident (perhaps because the $\bar{n}$/[A]-curves are rather steep at the lowest values of [A]).

Finally I wish to express my gratitude to Professor Sven Bodforss for the facilities he has kindly placed at my disposal.

My thanks are also due to Professor Sture Fronæus and Dr. Sten Ahrland for kind advice and criticism.

This work is a part of an investigation supported by *Statens Naturvetenskapliga Forskningsråd (Swedish Natural Science Research Council)*.

REFERENCES

1. Sonesson, A. *Acta Chem. Scand.* **12** (1958) 165.
2. Fronæus, S. *Komplexsystem hos koppar* (Diss.) Lund 1948.
3. Moeller, Th. and Brantley, J. C. *J. Am. Chem. Soc.* **72** (1950) 5447.
4. Vickery, R. C. *J. Chem. Soc.* **1952** 421.
5. Fronæus, S. *Svensk Kem. Tidskr.* 65 (1953) 19.

Received July 9, 1958.

ACTA CHEMICA SCANDINAVICA 12 (1958) 1955—1964

Studies on Histidyl Peptides. I

Imidazole Protected Histidine in the Synthesis of C-Terminal and N-Terminal Histidyl Peptides

DIMITRIOS THEODOROPOULOS* and GEORG FÖLSCH

Department of Medical Biochemistry, University of Gothenburg, Sweden

Carbobenzoxy-*im*.benzyl-L-histidine and *im*.benzyl-L-histidine benzyl ester have been used as starting materials in the synthesis of C-terminal and N-terminal histidyl peptides.

It has been suggested during the last few years that histidine probably constitutes a portion of the active center of various hydrolytic enzymes. This suggestion is strongly supported by the evidence that photo-oxidation of the residues of histidine in ribonuclease, trypsin, lysozyme, etc., is accompanied by the loss of enzymic activity. The esteratic properties of various imidazole compounds have been extensively studied [1], but whether the histidine residue is the primary site of reaction of the various organophosphorus enzyme inhibitors, remains a subject of intense controversy [2–4]. The tempting hypothesis that a phosphoryl group is transferred from the imidazole group of histidine to a hydroxyl group of an adjacent residue of serine, needs to be established on the basis of experimental evidence.

We therefore consider it worth while to undertake the synthesis of various peptides containing histidine and serine for two reasons. Primarily to study their behavior towards organophosphorus enzyme inhibitors, and secondly, to study the sensitivity of various proteolytic enzymes towards these peptides when phosphorylated at different functional groups. This is a part of the study of the biological importance of phosphorylated peptides [5,6] which is carried out in this laboratory.

A report of the synthesis of such peptides, involving the sequences histidylserine and serylhistidine, as well as several other C-terminal and N-terminal histidyl peptides will be presented in this paper. During this synthetic work, the recently reported procedure [7] *, employing imidazole-benzyl-L-histidine,

* *Footnote added in proof.* A preliminary note appeared in *J. Org. Chem.* **21** (1956) 1550 and it is noteworthy that Schwyzer has successfully employed imidazole protected histidine in the recent synthesis of a pentapeptide, [*Nature* **182** (1958) 1669].

was exclusively used. The potentialities of this procedure have also been investigated in detail in the course of this work.

DISCUSSION AND RESULTS

The use of carbobenzoxy-*im*.benzyl-L-histidine in the synthesis of N-terminal histidyl peptides.

The basic nature of the imidazole group of histidine has presented formidable problems during the incorporation of an histidine residue into synthetic polypeptides.

Recently, Katchalski *et al.*[8] reported the synthesis of 1,N-dicarbobenzoxy-L-histidine, but it has since been noted, that this compound decarbobenzoxylates readily to produce N-carbobenzoxy-L-histidine.

Akabori *et al.*[9], employing 1,N-dicarbobenzoxy-L-histidine as starting material, have synthesized a number of histidyl dipeptide ester derivatives. It is, however, evident from the work of Katchalski, that any attempt to extend the peptide chain of these dicarbobenzoxy histidyl peptide esters on either the carboxyl or the amino end, will be complicated due to the elimination of the 1-carbobenzoxy group.

It is noteworthy that although a number of synthetic procedures are currently available for the synthesis of histidyl peptides [9–11], no synthesis of dipeptide L-histidyl-L-histidine in optically pure form has yet been reported.

Fischer and Suzuki [12] in 1905 prepared histidyl-histidine by alkaline hydrolysis of L-histidine anhydride, but this hydrolysis was accompanied by racemization. Almost thirty years later, Abderhalden and Leinert [13] hydrolysed L-histidine anhydride with acid, thinking that they could avoid racemization, but no product was isolated.

In this connection, we have succeeded in producing an unequivocal synthesis of an L-histidyl-L-histidine derivative by employing *im*.benzyl-L-histidine [14] as starting material.

Coupling *im*.benzyl-L-histidine with one mole of benzyl chloroformate [15] in aqueous solution at 0°, at pH alkaline by addition of lithium hydroxide *, followed by acidification, resulted in the synthesis of carbobenzoxy-*im*. benzyl-L-histidine [7]. This compound is sparingly soluble in various organic solvents, such as chloroform, dioxane, ethylacetate, tetrahydrofuran, *etc.*, a fact which appeared to be a stumbling block in its usefulness in peptide synthesis. An attempt to convert carbobenzoxy-*im*.benzyl-L-histidine into its chloride hydrochloride on treatment with thionyl chloride, resulted in a crystalline product. Further work is in progress to identify the composition of this product.

Although the condensation of carbobenzoxy-*im*.benzyl-L-histidine with amino acid and peptide esters, employing the tetraethyl pyrophosphite procedure [16], holds promise due to its well established capacity to deal with

* Lithium hydroxide was chosen instead of sodium or potassium hydroxide since the latter forms less soluble salts with carbobenzoxy-*im*. benzyl-L-histidine which precipitated during the coupling, thus forming a mass.

amino acid and peptide derivatives of low solubility [17], we did not persist in pursuing this procedure since the carbodiimide method [18] operated with excellent results in our case.

A slight modification was, however, enforced due to the afore mentioned solubility properties of carbobenzoxy-*im*.benzyl-L-histidine in organic solvents. Carbobenzoxy-*im*.benzyl-L-histidine was therefore dissolved in dimethylformamide upon heating, and when the solution standing at room temperature had cooled to 40—50°, it was mixed with amino acid esters and carbodiimide. Condensation of carbobenzoxy-*im*.benzyl-L-histidine, with *im*.benzyl-L-histidine benzyl ester thus resulted in the production of carbobenzoxy-*im*.benzyl-L-histidyl-*im*.benzyl-L-histidine benzyl ester.

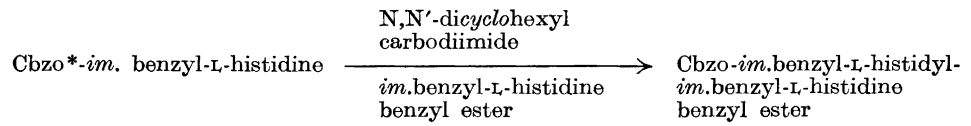

The conversion of the latter in to L-histidyl-L-histidine will be reported in a later communication.

In the investigated cases, reported below, the peptide ester derivatives thus formed were easily isolated in crystalline form from the dimethylformamide solution by addition of water.

Carbobenzoxy-*im*.benzyl-L-histidyl peptide esters can be extended on either the carboxyl or the amino end by hydrolysis of the ester group, or selective splitting of the N-carbobenzoxy group by hydrogen bromide [16,19] or catalytic hydrogenation [15].

The use of *im*.benzyl-L-histidine benzyl ester in the synthesis of histidine peptides

All the amino acid benzyl esters used in the course of this work were prepared in accordance with the directions of Cipera and Nicholls [20]. Following their method, we also conveniently esterified *im*.benzyl-L-histidine to give the *im*.benzyl-L-histidine benzyl ester dibenzenesulfonate. The latter ester was obtained in crystalline form in about 80 % yield. It can readily recrystallize and remain unchanged for several days in the open. In contrast, *im*.benzyl-L-histidine methyl ester dihydrochloride[7], obtained by the Fischer procedure, appears to be extremely hygroscopic.

Condensation of carbobenzoxy-L-phenylalanine with L-histidine methyl ester employing the carboxylic-carbonic anhydride procedure has been recently reported [21]. This procedure, however, does not always produce satisfactory results, probably due to the undesired side-reaction with the imidazole group of histidine.

When carbobenzoxy amino acids were condensed with *im*.benzyl-L-histidine benzyl ester *via* the mixed carboxylic-carbonic anhydride [22,23] or the

* Cbzo stands for Carbobenzoxy.

carbodiimide procedure for peptide bond formation, the desired derivatives were obtained in good yield and in crystalline form. Carbobenzoxy-L-serine [24] was thus coupled with *im*.benzyl-L-histidine benzyl ester, employing the carbodiimide prodedure to give the product carbobenzoxy-L-seryl-*im*.benzyl-L-histidine benzyl ester * in crystalline form.

Merrifield and Woolley [25], during their synthetic studies with peptides possessing strepogeny activity, attempted the synthesis of carbobenzoxy-L-seryl-L-histidine methyl ester, to this end employing the azide and carbodiimide methods to condense carbobenzoxy-L-serine with histidine methyl ester. As the authors state, the oily product obtained was not homogeneous, and crystallized only after it had been purified by countercurrent distribution.

When carbobenzoxy-L-phenylalanine was condensed with *im*.benzyl-L-histidine benzyl ester by either of the aforementioned condensing methods, the product carbobenzoxy-L-phenylalanyl-*im*.benzyl-L-histidine benzyl ester (I) was obtained in good yield. Compound (I) was saponified, with no difficulty, with the equivalent amount of sodium hydroxide, and upon acidification with acetic acid, carbobenzoxy-L-phenylalanyl-*im*.benzyl-L-histidine (II) was obtained, after recrystallization, at a 72 % yield.

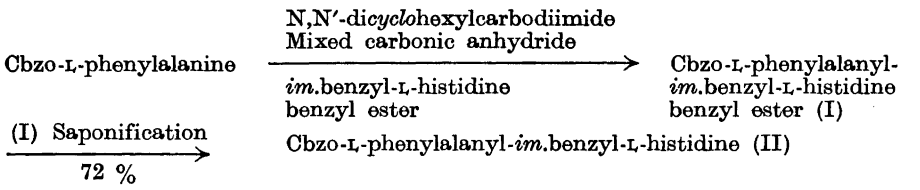

Hydrolysis of the ester (I) provides the carboxyl group of the *im*.benzyl-L-histidine residue free to link with other amino acids and peptides. Compound (II) was consequently condensed with L-leucine benzyl ester and L-aspartic acid dibenzyl ester by the carbodiimide procedure to produce carbobenzoxy-L-phenylalanyl-*im*.benzyl-L-histidyl-L-leucine benzyl ester (III) as well as the corresponding aspartate derivative.

Unreacted compound (II) was separated from (III), not by the usual procedure consisting in extraction with sodium or potassium bicarbonate solution [26]. Compound (II) and the corresponding derivatives reported here, form sparingly soluble salts in water with alkalies, triethylamine, dimethylamine, and ammonia.

Taking advantage of the widely different solubilities of (II) and (III) in ethylacetate, we were able to separate them by dissolving the residue in the above-mentioned solvent. Compound (II) is sparingly soluble in ethylacetate, precipitates and can be removed by filtration. Complete removal of (II) is accomplished by washing the ethylacetate layer thoroughly with 5 % sodium carbonate solution.

---

* The sequence serylhistidine has been identified in the B chain of insulin [Ryle A., Sanger F., Smith L. and Kitai R. *Biochem. J.* **60** (1955) 541] and it is rather interesting to note that the reverse sequence histidylserine occurs in glucagon [Bromer W., Sinn L. and Behrens O. *J. Am. Chem. Soc.* **79** (1957) 2807].

Compound (III) upon saponification, followed by acidification with acetic acid, produced carbobenzoxy-L-phenylalanyl-*im*.benzyl-L-histidyl-L-leucine (IV) in good yield.

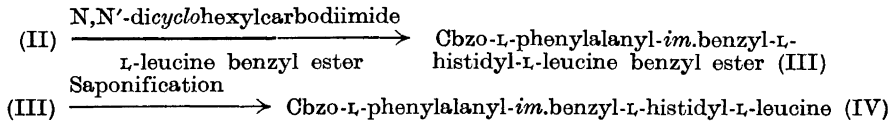

Condensation of carbobenzoxy-L-phenylalanyl-*im*.benzyl-L-histidine azide with leucine benzyl ester does not always give satisfactory results due to the tendency of the azide to rearrange. A similar tendency has been observed in the case of carbobenzoxy-L-seryl-L-histidine azide by Merrifield and Wolley [25].

Compound (IV), dissolved in absolute ethanol, was selectively decarbobenzoxylated by catalytic hydrogenation in the presence of palladium black. The so formed L-phenylalanyl-*im*.benzyl-L-histidyl-L-leucine(V), being insoluble in absolute ethanol, precipitates during the hydrogenation. Selective splitting of the N-carbobenzoxy group frees the amino end for extension of the peptide chain, using conventional methods.

Compound (IV), dissolved in 50 % ethanol and hydrogenated for 24 h in the presence of palladium black, afforded the peptide L-phenylalanyl-L-histidyl-L-leucine with an $[\alpha]_D^{24}$ value of +30.5° as a 1.08 % solution in glacial acetic acid.

Since it is a well-known fact that *im*.benzyl-L-histidine easily splits by reduction with sodium in liquid ammonia [14] to produce free histidine, compound (IV) was reduced by this procedure. The tripeptide L-phenylalanyl-L-histidyl-L-leucine * thus obtained showed an optical rotation of $[\alpha]_D^{24}$ +29.5° as a 1 % solution in glacial acetic acid.

EXPERIMENTAL

Carbobenzoxy-im.*benzyl-L-histidine*. A solution of 1.22 g (0.005 mole) of *im*.benzyl-L-histidine in 5 ml of N LiOH was cooled in an ice-bath, and 1 ml of carbobenzoxy chloride, diluted in 3 ml of dioxane, was added in four portions while stirring. During the addition of the carbobenzoxy chloride the solution was kept alkaline by addition of N LiOH. When the last portion of the carbobenzoxy chloride was added, the solution was permitted to remain at room temperature for about 15 min. Addition of 20—30 ml of water, and acidification with acetic acid, caused the desired product to precipitate. It was then filtered off, washed well with water and finally with ether. It was recrystallized by dissolving in dimethylformamide and precipitating with ether. Yield 1.3 g (70 %), m.p. 210—213° (reported [7] 210—213°), $[\alpha]_D^{21}$ + 5.2° (*c* 5 in glacial acetic acid).

im.*Benzyl-L-histidine benzyl ester dibenzenesulfonate*. Into a 150 ml round-bottomed flask were placed 2.45 g (0.01 mole) of *im*.benzyl-L-histidine, 3.87 g (10 % excess) of benzenesulfonic acid monohydrate, 10 ml of benzyl alcohol and 20 ml of carbon tetrachloride. The mixture was then heated under reflux, the liberated water being removed azeotropically. A clear solution was obtained after reflux began. When water no longer

* The C-terminal sequence in valine-hypertensin has been shown to be phenylalanylhistidyl-leucine [Elliot, D. and Peart, W. *Nature* **177** (1956) 527].

distilled off (about the seventh addition of carbon tetrachloride), the reaction mixture was permitted to cool down to room temperature. Through addition of dry ether, the ester precipitated. It was then filtered and washed several times with ether, after which it was dried in a desiccator and then recrystallized by dissolving in *iso*propyl alcohol or dioxane, and precipitating by ether, yield 5.1 g (80 %), m.p. 174—177°, $[\alpha]_D^{18}$ + 8.0° (*c* 1.5 in dimethylformamide). (Found: N 6.50. Calc.for $C_{32}H_{33}O_8N_3S_2$: N 6.45).

Carbobenzoxy-im.*benzyl*-L-*histidyl*-L-*serine benzyl ester.* A suspension of 1.89 g (0.005 mole) of carbobenzoxy-*im*.benzyl-L-histidine in 30 ml of dimethylformamide was dissolved upon heating and then left to cool to 40—45°. This solution was mixed with a previously prepared solution of 1.76 g (0.005 mole) of L-serine benzyl ester benzenesulfonate, and 0.5 g (0.005 mole) of triethylamine in 10 ml of dimethylformamide. Di*cyclo*hexyl-carbodiimide (0.98 g, 0.005 mole) was immediately added and the solution was stirred overnight at room temperature. Di*cyclo*hexylurea was removed by filtration, and the solution was diluted by with 400—500 ml of water *. The ensuing oil crystallized upon scratching with a glass rod. It was cooled, filtered and washed several times with water, then recrystallized by dissolving in ethanol and precipitating with ether. Yield 1.7 g (60 %), m.p. 149—151°, $[\alpha]_D^{21}$ + 2.9° (*c* 5.8 in glacial acetic acid). When recrystallized again from ethylacetate, the m.p. remained the same. (Found: C 66.70; H 5.98; N 10.05. Calc. for $C_{31}H_{32}O_6N_4$: C 66.89; H 5.79; N 10.07).

Carbobenzoxy-im.*benzyl*-L-*histidyl*-im.*benzyl*-L-*histidine benzyl ester.* To 10 ml of dimethylformamide were added 3.25 g (0.005 mole of *im*.benzyl-L-histidine benzyl ester dibenzenesulfonate and 1.01 g (0.01 mole) of triethylamine. This solution was mixed with 1.86 g (0.005 mole) of cbzo-*im*.benzyl-L-histidine, dissolved in 30 ml of dimethylformamide (heated at 40—45°) and 1 g (about 0.005 mole) of di*cyclo*hexylcarbodiimide. The solution was stirred overninght at room temperature. The di*cyclo*hexylurea was then filtered off, washed twice with tetrahydrofuran, and the combined filtrates were diluted with 400 ml of water. Upon cooling and scratching with a glass rod, the desired product crystallized. It was filtered off, washed with water several times, and recrystallized from ethanol-ether. Yield 1.9 g (54 %) m.p. 137°, $[\alpha]_D^{21}$ —22.3° (*c* 5.3 in glacial acetic acid). A further 200 mg of the compound was obtained from the mother-liquor on addition of petroleum ether, m.p. 135°. (Found: C 70.50; H 5.77; N 11.95. Calc for $C_{51}H_{50}O_5N_6$: C 70.68; H 5.78; N 12.06).

Carbobenzoxy-im.*benzyl*-L-*histidylglycine benzyl ester.* A solution of 1.68 g (0.005 mole) of glycine benzyl ester *p*-toluenesulfonate in 10 ml of dimethylformamide was neutralized by addition of 0.5 g (0.005 mole) of triethylamine. It was then mixed with a hot solution (40—45°) of 1.86 g (0.005 mole) of cbzo-*im*.benzyl-L-histidine in 30 ml of dimethylformamide, and 0.98 g (0.005 mole) of di*cyclo*hexylcarbodiimide. The mixture was stirred overnight at room temperature. Di*cyclo*hexylurea was removed by filtration, and the solution was diluted by addition of 500 ml of water. On standing in the refrigerator, the oily product crystallized. It was recrystallized from ethanol-ether, yield 1.1 g (40 %), m.p. 111—112°. (Found: N 10.71. Calc. for $C_{30}H_{30}O_5N_4$: N 10.64).

Carbobenzoxy-im.*benzyl*-L-*histidylglycine.* To a solution of 1 g of the above ester in 15 ml of acetone, 2 ml of N NaOH was added. 5 min later, the product that far saponified, precipitated. Water (5 ml) was then added, and the precipitate was completely dissolved. The solution thus obtained was then allowed to remain for another 15 min at room temperature, and was then diluted with 150 ml of water. Acidification with acetic acid made the desired product precipitate, yield 0.75 g (90 %), m.p. 235—240°, $[\alpha]_D^{20}$ —5.5° (*c* 2.1 in glacial acetic acid). (Found: C 62.80; H 5.85; N 12.75. Calc. for $C_{23}H_{24}O_5N_4$: C 63.20; H 5.54; N 12.85).

Carbobenzoxy-im.*benzyl*-L-*histidyl*-L-*glutamic acid dibenzyl ester.* A solution of 2.49 g (0.005 mole) of L-glutamic acid dibenzyl ester *p*-toluenesulfonate and 0.5 g (0.005 mole) of triethylamine in 10 ml of dimethylformamide was mixed with a solution of 1.89 g

* Alternatively the dimethylformamide was distilled off *in vacuo* (1 mm pressure) at 50° and the remaining residue taken up in ethylacetate or chloroform. The solution was then washed successively with 5 % lithium carbonate and water, and dried over sodium sulphate. The solvent was evaporated *in vacuo*, and the remaining residue was treated as above.

(0.005 mole) of cbzo-*im*.benzyl-L-histidine pro-heated at 40—45°. Di*cyclo*hexylcarbodiimide (0.98 g, 0.005 mole) was immediately added, and the solution was stirred overnight at room temperature. Then di*cyclo*hexylurea was filtered off, and the solution was diluted with 400—500 ml of water. On standing overnight in the refrigerator, the desired product crystallized. Yield 2.8 g. It was recrystallized from ethylacetate-ether, yield 1.8 g (50 %), m.p. 89—91°. (Found: N 8.24. Calc. for $C_{40}H_{40}O_7N_4$: N 8.13).

Carbobenzoxy-im.*benzyl*-L-*histidyl*-L-*glutamic acid.* A solution of 1.72 g (2.5 mmole) of the above ester, and 5 ml of N NaOH in 10 ml of acetone, was stirred for 30 min at room temperature. At the end of that time, 10 ml of water was added, and the solution was filtered and diluted with further 200 ml of water. Upon acidification with acetic acid and cooling in the refrigerator, the product precipitated. Yield 1.15 g (90 %), m.p. 95—97° (recrystallized from ethanol-water). (Found: N 11.10. Calc for $C_{26}H_{28}O_7N_4$: N 11.19).

Carbobenzoxy-L-*phenylalanyl*-im.*benzyl*-L-*histidine. A. By the mixed anhydride procedure.* A solution containing 1.48 g (0.005 mole) of carbobenzoxy-L-phenylalanine, 10 ml of tetrahydrofuran and 0.5 g (0.005 mole) of triethylamine, was cooled to 0°, and 0.5 g (0.005 mole) of ethylchlorocarbonate was then added. After 5 min, 3.25 g (0.005 mole) of *im*.benzyl-L-histidine benzyl ester dibenzenesulfonate and 1.01 g. (0.01 mole) of triethylamine, dissolved in 20 ml of tetrahydrofuran, were added. Coupling was ensured by evolution of carbon dioxide. After 30 min the reaction mixture was diluted with 250—300 ml of water and the desired ester precipitated. The ester was filtered off, washed several times with bicarbonate solution and finally with water. It was then recrystallized by dissolving in ethanol and precipitating with ether, yield 1.9 g (61 %), m.p. 106—107°. (Found: N 8.90. Calc. for $C_{37}H_{36}O_5N_4$: N 9.08).

B. By the carbodiimide method. To a solution of 10 ml of tetrahydrofuran were added 3.25 g (0.005 mole) of *im*.benzyl-L-histidine benzyl ester dibenzenesulfonate, 1.01 g (0.01 mole) of triethylamine, 1.48 g (0.005 mole) of carbobenzoxy-L-phenylalanine and 0.98 g (0.005 mole) of di*cyclo*hexylcarbodiimide. After 15 min di*cyclo*hexylurea began to precipitate. The mixture was stirred at room temperature for 5—6 h and then acidified with a few drops of acetic acid. After 30 min the di*cyclo*hexylurea was removed by filtration, and the solution was diluted with water as described above. Alternatively, the tetrahydrofuran was evaporated *in vacuo* at 40° and the residue was taken up in chloroform. The chloroform layer was washed successively with bicarbonate solution and water. It was dried over sodium sulphate, and the solvent evaporated *in vacuo*. The solid residue was recrystallized from ethanol-ether in a manner similar to that described above, yield 2.1 g (70 %), m.p. 106—107°.

Saponification of the ester. The above ester (6.16 g, 0.01 mole) was dissolved in 20 ml of acetone, 11 ml (10 % excess) of N NaOH was added and the mixture was stirred at room temperature for 30 min. The thus formed sodium salt of the dipeptide derivative which precipitated in the meantime, was dissolved upon gentle heating, and the solution was quickly filtered and diluted with 300 ml of water. This made the slightly soluble sodium salt of the dipeptide precipitate and form a white mass. Upon acidification with acetic acid, the desired compound crystallized. After cooling, the product was filtered, washed several times with water and recrystallized by dissolving in 80 % ethanol, and precipitating with ether. Yield 3.7 g (72 %), m.p. 139—140° (reported [7] 140—141°), $[\alpha]_D^{12}$ + 28° (*c* 1 in glacial acetic acid).

Carbobenzoxy-L-*phenylalanyl*-im.*benzyl*-L-*histidyl*-L-*aspartic acid.* A solution of 1.21 g (2.5 mmole) of L-aspartic acid dibenzyl ester *p*-toluenesulfonate in 10 ml of dimethylformamide was neutralized by addition of 0.25 g (250 mmole) of triethylamine. This solution was mixed with 1.31 g (250 mmole) of cbzo-L-phenylalanyl-*im*.benzyl-L-histidine, and when the latter was completely dissolved, 0.49 g (2.5 mmole) of di*cyclo*hexylcarbodiimide was added. Di*cyclo*hexylurea was filtered off 6 h later and the solvent was evaporated to dryness at 1 mm pressure at 50°. Ethylacetate was added to the residue and concentrated *in vacuo*. This process was repeated four times. The residue was then taken up in ethylacetate (50 ml), cooled for one hour, and filtered. Afterwards the filtrate was washed twice with 5 % sodium carbonate solution, and dried over sodium sulphate. The solvent was evaporated *in vacuo* and the remaining residue solidified upon treatment with ether. Yield 1.5 g. The ester thus obtained was further saponified as follows:

The ester (2.04 g, 2.5 mmole) was suspended in 20 ml of acetone-ethanol (1:1) and 5 ml of N NaOH were added. Stirring for 30 min at room temperature, with gentle

heating at the end of this period, brought about the solution of the hydrolyzed ester. The solution was immediately filtered to remove traces of insoluble compound and then diluted with 200 ml of water, when the tripeptide sodium salt precipitated. The precipitate was acidified with acetic acid, filtered, washed several times with water and recrystallized from 60 % ethanol. Yield 1.2 g (80 %), m.p. 193—196° (reported [7] 193—196°), $[\alpha]_D^{12}$ +20° (*c* 1 in glacial acetic acid).

*Carbobenzoxy-*L*-phenylalanyl-*im.*benzyl-*L*-histidyl-*L*-leucine.* This compound was prepared in a manner similar to that used in the synthesis of the carbobenzoxy-L-phenylalanyl-*im.*benzyl-L-histidyl-L-aspartic acid. When carbobenzoxy-L-phenylalanyl-*im.*benzyl-L-histidine was coupled with leucine methyl or benzyl esters, an oily product was obtained. Saponification produced the desired product in an overall yield of 50 %, m.p. 96°. A sample of the product was recrystallized by dissolution in *iso*propyl alcohol and by precipitation with *iso*propyl ether, m.p. 160—165° (not sharp, reported [7] 163—165°).

L-*Phenylalanyl-*im.*benzyl-*L*-histidyl-*L*-leucine.* A solution of 1.55 g (2.5 mmole) of carbobenzoxy-L-phenylalanyl-*im.*benzyl-L-leucine (m.p. 96°) in absolute ethanol was hydrogenated in the presence of 300 mg of palladium black. Hydrogenation was carride out for half-an-hour during which time the desired product precipitated. The precipitate was dissolved by addition of water and heating. The catalyst was filtered off and the solution evaporated to dryness *in vacuo*. The residue was filtered by addition of ether, yield 1.09 g (90 %). Paper chromatography revealed besides the main product another faint ninhydrin-positive spot at the region of the free peptide phenylalanylhistidylleucine. Recrystallization from 50 % alcohol gave a homogeneous product, as was indicated by paper chromatography and paper electrophoresis, m.p. 162—164° (decomp.), $[\alpha]_D^{21}$ +23.3°; (*c* 1.03 in glacial acetic acid). (Found: C 66.10; H 6.80. Calc. for $C_{28}H_{35}O_4N_5$: C 66.51° H 6.97).

L-*Phenylalanyl-*L*-histidyl-*L*-leucine.* Carbobenzoxy-L-phenylalanyl-*im.*benzyl-L-histidyl-L-leucine (1.59 g, 2.5 mmole) was suspended in 50 ml of liquid ammonia and 0.34 g (100 % excess) of sodium was added in pieces. The blue color remained for about 20 min and then the excess of sodium was neutralized by addition of ammonium acetate. Ammonia was allowed to evaporate and the residue was taken up in 15 ml of water. The water layer was washed twice with ether and evaporated *in vacuo* at 40°. To the residue 5 ml of water was added and the solution reconcentrated. This process was repeated several times. At the end, the residue was treated with 3 ml of water and cooled in the refrigerator. The precipitated peptide was filtered off and washed with 1 ml of cold water. Yield 0.5 g (50 %), $[\alpha]_D^{24}$ +29.5° (*c* 1 in glacial acetic acid), [reported [7] $[\alpha]_D^{24}$ +30.5° (*c* 1.08 in glacial acetic acid)].

*Carbobenzoxy-*L*-seryl-*im.*benzyl-*L*-histidine benzyl ester.* A suspension of 3.25 g (0.005 mole) of *im.*benzyl-L-histidine benzyl ester dibenzenesulfonate in 30 ml of tetrahydrofuran was neutralized by addition of 1.01 g (0.01 mole) of triethylamine. 5 min later 1.19 g (0.005 mole) of carbobenzoxy-L-serine and 0.98 g (0.005 mole) of di*cyclo*hexylcarbodiimide were added while stirring. The mixture was permitted to remain overnight at room temperature and di*cyclo*hexylurea was then removed by filtration. The solution was diluted with 300 ml of water, causing the desired product to precipitate. The product was filtered off, washed several times with water, and purified by dissolution in hot ethylacetate and precipitated by addition of petroleum ether. Yield 2.2 g. Further recrystallization from ethanol-ether gave a product with a sharp m.p. 138.5—139.5°, yield 1.6 g (57 %), $[\alpha]_D^{21}$ −26.3° (*c* 8.4 in glacial acetic acid). (Found: C 66.70; H 5.92; N 10.01. Calc. for $C_{31}H_{32}O_6N_4$: C 66.89; H 5.79; N 10.07).

*N-Tritylglycyl-*im.*benzyl-*L*-histidine.* Coupling of tritylglycine [27] with *im.*benzyl-L-histidine benzyl ester was accomplished either by the mixed carboxylic-carbonic anhydride procedure, or the carbodiimide method, in a manner similar to that described for the preparation of carbobenzoxy-L-phenylalanyl-*im.*benzyl-L-histidine. At the end of the reaction the tetrahydrofuran was evaporated *in vacuo* and the residue was taken up in ethylacetate. The ethylacetate layer was then washed thoroughly with 5 % sodium carbonate solution and water. It was dried over sodium sulphate and the solvent evaporated *in vacuo*. No attempt was made to crystallize the remaining residue which was further hydrolyzed in the same way as described for the carbobenzoxy-L-phenylalanyl-*im.*benzyl-

L-histidine derivative. The product was recrystallized from ethanol-water, yield 60 %, $[\alpha]_D^{21}$ +24.2° (*c* 2.7 in tetrahydrofuran), m.p. 198—201° (reported [7] 198—201°).

*Carbobenzoxy-L-isoleucyl-*im.*benzyl-L-histidine benzyl ester.* This compound was prepared in a manner similar to that used in the synthesis of carbobenzoxy-L-phenylalanyl-*im.* benzyl-L-histidine. Thus 2.65 g (0.01 mole) of carbobenzoxy-L-*iso*leucine [21] was coupled with *im.*benzyl-L-histidine benzyl ester, employing either the mixed carboxylic-carbonic anhydride procedure or the carbodiimide method. After recrystallization from 70 % ethanol, 3.5 g (60 %), and 4 g (70 %), respectively, were obtained, m.p. 132—134°, $[\alpha]_D^{21}$ −21.8° (*c* 10.1 in glacial acetic acid). (Found: N 9.76. Calc. for $C_{34}H_{38}O_5N_4$: N 9.61).

im.*Benzyl-L-histidine methyl ester dihydrochloride.* A fast stream of hydrogen chloride was bubbled for 15 min into a suspension of 2.45 g (0.01 mole) of *im.*benzyl-L-histidine in 20 ml of absolute methanol. The obtained solution was then evaporated *in vacuo* and the residue dissolved by addition of a new portion of methanol. Hydrogen chloride was bubbled in again. After removal of the solvent *in vacuo*, the remaining oily residue was dried *in vacuo* for 3—4 h at 40°, making thus the oily product solidify. The product (3.1 g), being extremely hygroscopic, was further dried before use in a desiccator (P_2O_5) for 24 h. The ester obtained is pure enough for peptide synthesis. A sample of it was dissolved in the minimal amount of methanol, concentrated with hydrogen chloride, and upon addition of dry ether precipitated. The solvent was decanted and the precipitate was washed with ether and dried in a desiccator (P_2O_5). The thus recrystallized ester melted at 111—115°, (reported [7] 111—115°), when heated quickly.

*Carbobenzoxy-L-phenylalanyl-*im.*benzyl-L-histidine hydrazide.* A solution containing 2.99 g (0.01 mole) of carbobenzoxy-L-phenylalanine and 1.01 g (0.01 mole) of triethylamine in 20 ml of chloroform was cooled to 5° and treated with 1.08 g (0.01 mole) of ethylchlorocarbonate. After 5 min it was mixed with a solution of 3.30 g (0.01 mole) of *im.*benzyl-L-histidine methyl ester dihydrochloride, and 2.02 g (0.02 mole) of triethylamine in 30 ml of chloroform. Coupling was ensured by evolution of carbon dioxide. After 30 min the solution was washed with dilute bicarbonate solution and water. It was then dried over sodium sulphate and the solvent evaporated *in vacuo* at 40°. To the residue ethanol was added and concentrated again. The remaining oily residue (3.8 g, 70 %) was dissolved in 20 ml of hot ethanol and mixed with 1 g (200 % excess) of hydrazine monohydrate. The mixture was kept overnight at room temperature, and by addition of water the hydrazide precipitated completely. It was filtered off and recrystallized from 80 % ethanol, yield 2.8 g (75 %), m.p. 183—186° (reported [7] 183—186°).

Acknowledgements. The authors wish to express their sincere thanks to Professor Olof Mellander for his support in this work.

Aid from the *Medical Faculty of the University of Gothenburg* and *AB. Marabou, Sundbyberg*, for a research fellowship to one of us (D. Th.) is gratefully acknowledged.

Thanks are also due to *Hässle-Tika AB.* for placing laboratory facilities at our disposal.

The work was supported by grants from the *Swedish Medical Research Council* to Professor Olof Mellander.

REFERENCES

1. Bruice, T. and Schmir, G. *J. Am. Chem. Soc.* **79** (1957) 1663; **80** (1958) 148.
2. Wagner-Jauregg, T. and Hackley, B. *J. Am. Shem. Soc.* **75** (1953) 2125.
3. Müller, Th., Rathlev, T. and Rosenberg, Th. *Biochim. et Biophys. Acta* **19** (1956) 563.
4. Dixon, G. and Neurath, H. *Biochim. et Biophys. Acta* **20** (1956) 572.
5. Mellander, O. *Upsala Läkareförens. Förh.* **52** (1947) 107.
6. Fölsch. G. *Acta Chem. Scand.* **12** (1958) 561.
7. Theodoropoulos, D. *J. Org. Chem.* **21** (1956) 1550.
8. Patchornik, A., Berger, A. and Katchalski, E. *J. Am. Chem. Soc.* **79** (1957) 6416.
9. Akabori, S., Okawa, K. and Sakiyama, F. *Nature* **181** (1958) 772.
10. Holley, R. and Sondheimer, E. *J. Am. Chem. Soc.* **79** (1954) 1326.
11. Fischer, R. and Whetstone, R. *J. Am. Chem. Soc.* **76** (1954) 5076.
12. Fischer, E. and Suzuki, U. *Ber. (1905)* 4173.
13. Abderhalden, E. and Leinert, F. *Fermentforschung* **15** (1937) 324.

14. du Vigneaud, V. and Behrens, O. *J. Biol. Chem.* **117** (1937) 27.
15. Bergmann, M. and Zervas, L. *Ber.* **62** (1932) 1192.
16. Anderson, G. Blodinger, J. and Welcher, A. *J. Am. Chem. Soc.* **74** (1952) 5309.
17. du Vigneaud, V. Ressler, C. Swan, J. Roberts, W. Katsoyannis, P. and Gordons, S. *J. Am. Chem. Soc.* **75** (1953) 4879.
18. Sheehan, J. and Hess, G. *J. Am. Chem. Soc.* **77** (1955) 1067.
19. Ben-Ishai, and Berger, A. *J. Org. Chem.* **17** (1952) 1564.
20. Cipera, J. and Nicholls, R. *Chem. & Ind.* London **16** (1955).
21. Theodoropoulos, D. and Craig, L. C. *J. Org. Chem.* **20** (1955) 1169.
22. Vaughan, J. and Osato, R. *J. Am. Chem. Soc.* **78** (1951) 553.
23. Boissonas, R. *Helv. Chem. Acta* **34** (1951) 874.
24. Baer, E. and Maurukas, J. *J. Biol. Chim.* **212** (1955) 25.
25. Merrifield, R. and Woolley, D. *J. Am. Chem. Soc.* **78** (1956) 4646.
26. Fruton J. *Advances in Protein Chem.* **5** (1949) 28.
27. Zervas, L. and Theodoropoulos, D. *J. Am. Chem. Soc.* **78** (1956) 1359.

Received July 23, 1958.

ACTA CHEMICA SCANDINAVICA 12 (1958) 1965—1976

The Crystal Structure of KCr_3O_8

KARL-AXEL WILHELMI

Institute of Inorganic and Physical Chemistry, University of Stockholm, Stockholm, Sweden

KCr_3O_8 crystallizes in the monoclinic system, space group No. 12 $C2/m$, with the unit-cell dimensions $a = 8.593$ Å, $b = 5.466$ Å, $c = 7.641$ Å, $\beta = 96°39'$ and two formula units in the unit cell. The structure is formed by CrO_6 octahedra and CrO_4 tetrahedra arranged in layers by sharing corners. The layers are held together by K ions. The bond distances are briefly compared with those found in some other chromium compounds. KCr_3O_8 is stoichiometric. The structure differs considerably in character from those of the non-stoichiometric vanadium and wolfram bronzes of similar composition.

In connection with work on the thermal decomposition of CrO_3, the compound KCr_3O_8 was obtained by melting CrO_3 with $K_2Cr_2O_7$ [1]. The same procedure was described by Suchow *et al.*[2] for preparing compounds MCr_3O_8 (M = Li, Na, K, Rb). The X-ray study performed by these authors indicated that two of the six chromium atoms in the unit cell occupy positions which are not equivalent to the positions occupied by the other four. This suggested the possibility of the former chromium atoms being trivalent and the latter hexavalent.

EXPERIMENTAL

A complete elucidation of the crystal structure had to be based on single-crystal data. The previous investigators failed in preparing material for such techniques. A satisfactory procedure for obtaining good crystals was, however, to heat a mixture of composition $K_2Cr_2O_7 + 2\ CrO_3$ at 350°C at oxygen pressures up to 55 atm for 2 h.

The reagents used were potassium dichromate (analytical grade, Hopkins and Williams Ltd.) and chromium trioxide (Baker's analyzed, dried over P_2O_5). The materials were powdered, intimately mixed and transferred to a silica crucible. The crucible was then placed in an autoclave consisting of a thickwalled steel tube welded at one end. A lid, containing a small copper tube attached to an oxygen cylinder, was bolted to the open end, a silver gasket being placed between the tube and the lid. A commercial pressure-reducing valve was used to measure the pressure. The autoclave was flushed several

times with oxygen before heating it in an electrical oven. After 2 h the autoclave was allowed to cool slowly.

The excess potassium dichromate was extracted with water, leaving a residue of rod-shaped prisms. After drying in an oven at 120°C, the sample was dissolved in hot concentrated sulphuric acid and the chromium determined using Mohr's salt and standard permanganate solution after oxidation by peroxodisulphate in the presence of silver ions. The potassium was determined gravimetrically as potassium perchlorate in samples dissolved in hot 65 % perchloric acid [3]. The reproducibility of the analyses was found to be good and the results in fair agreement with the values calculated for KCr_3O_8.

Chromium, %		Potassium, %	
Found	Calcd	Found	Calcd
48.30 ± 0.05	48.29	12.0 ± 0.2	12.10

The density of the crystals was determined from the loss of weight in benzene (*cf.* Table 1).

A single crystal (*ca.* 0.1 × 0.05 × 0.03 mm^3) was selected. Rotation photographs around [010] and [100] and Weissenberg photographs (*h*0*l*, *h*1*l*, *h*2*l*, *h*3*l* and 0*kl*) were taken with Cu-*K* radiation. The crystals proved to be monoclinic with the *b*-axis along the prism axis and with unit cell dimensions in good agreement with the values given by Suchow *et al.*[2]. More accurate values for the lattice parameters were calculated from a powder photograph obtained in a Guinier type focusing camera of 80 mm diameter (transmission position) with strictly monochromatized Cu$K\alpha_1$ radiation. Potassium chloride (Analar, British Drug Houses, a = 6.2919 Å at 20°C [4]) was added to the specimen as an internal standard (Table 2). The measurement of the reflexions was made on the very sharp high-angle edge of the lines, a procedure introduced by Österlöf [5].

The only reflexions systematically absent were *hkl* with $h+k$ odd, which is characteristic of the space groups No. 12 $C2/m$, No. 8 Cm and No. 5 $C2$. Since it was found possible to derive a plausible structure assuming the highest symmetry $C2/m$, the space groups Cm and $C2$ were not considered. A test for piezoelectricity accordingly did not show any effect. (Experiment carried out by J. Baecklund, University of Uppsala.) Suchow *et al.* on prolonged exposure obtained several weak extra powder lines, incompatible with the unit cell and symmetry found here. Such lines were not observed in the present investigation even after ample exposure nor did they show up in the Weissenberg photographs. In this connection it is worth mentioning that the density, 3.15, found by Suchow *et al.* differs considerably from the calculated value, 3.01, which might indicate that the preparation studied by them is not identical with the one used in the present investigation.

The crystallographic data obtained in this investigation are summarized in Table 1.

The Weissenberg reflexions were recorded photographically using multiple film techniques and their intensities were estimated visually. The F^2 values were then calculated using nomograms given by Lu [6]. No correction was applied for absorption. The maxima in the Fourier syntheses were located by an interpolation table given by Booth [7]. The analytical representation of atomic scattering factors given by Vand, Eiland and Pepinsky [8] for chromium, potassium and oxygen atoms were used when calculating the F values.

Table 1. Crystallographic data for KCr_3O_8.

Laue symmetry: $2/m$.
Unit-cell dimensions: a = 8.593 ± 0.001 Å
b = 5.466 ± 0.001 Å
c = 7.641 ± 0.001 Å
β = 96°39′ ± 20′.

Absent spectra: hkl with $h+k \neq 2n$
Space group: No. 12 $C2/m$
Density: 3.02 (observed)
Density: 3.01 (calculated for $K_2Cr_6O_{16}$)

DERIVATION OF THE STRUCTURE

In $C2/m$ the following point positions exist:

$(0,0,0;\ \frac{1}{2},\frac{1}{2},0)+$
$2(a)$: $(0,0,0)$; $2(b)$: $(0,\frac{1}{2},0)$; $2(c)$: $(0,0,\frac{1}{2})$; $2(d)$: $(0,\frac{1}{2},\frac{1}{2})$
$4(e)$: $(\frac{1}{4},\frac{1}{4},0;\ \frac{1}{4},\frac{3}{4},0)$; $4(f)$: $(\frac{1}{4},\frac{1}{4},\frac{1}{2};\ \frac{1}{4},\frac{3}{4},\frac{1}{2})$
$4(g)$: $(0,y,0;\ 0,\bar{y},0)$; $4(h)$: $(0,y,\frac{1}{2};\ 0,\bar{y},\frac{1}{2})$; $4(i)$: $(x,0,z;\ \bar{x},0,\bar{z})$
$8(j)$: $(x,y,z;\ x,\bar{y},z;\ \bar{x},y,\bar{z};\ \bar{x},\bar{y},\bar{z})$

The two potassium atoms may be assumed arbitrarily to occupy the twofold position $2(a)$.

In order to determine the positions of the six chromium atoms, the projection $P(upw)$ of the Patterson function was calculated (Fig. 1). All the chromium atoms cannot occupy two-fold positions as this would require maxima in this function only at $u = 0$ or $\frac{1}{2}$ and $w = 0$ or $\frac{1}{2}$. Actually $P(upw)$ in addition to such maxima (A and B of Fig. 1) also shows three further high maxima (C, D and E). Of the six chromium atoms, two must thus be accomodated in a two-fold position and four in a four-fold position. The position $2(b)$ is not probable since it would give the far too short K-Cr distance of $b/2 = 2.733$ Å. The positions $4(e)$—$4(h)$ would only require maxima at $u = 0$ or $\frac{1}{4}$ and $w = 0$ or $\frac{1}{2}$. Thus it is concluded that the six chromium atoms occupy $2(c)$ or $2(d)$ and $4(i)$. To decide between $2(c)$ and $2(d)$, the linear Harker section $P(0v\frac{1}{2})$

Table 2. Powder photograph of KCr_3O_8. CuKa_1 radiation. Reflexions systematically absent in space group $C2/m$ have been omitted. The intensities were calculated from the expression $\frac{p}{100}(F_{calc})^2$ where p is the number of equivalent reflexions.

hkl	$10^5\sin^2\Theta$ calc	$10^5\sin^2\Theta$ obs	I_{calc}	I_{obs}	hkl	$10^5\sin^2\Theta$ calc	$10^5\sin^2\Theta$ obs	I_{calc}	I_{obs}
001	01 030	01 033	65	st	$22\bar{4}$	26 340	26 333	361	m
110	02 800	—	2	—	422	26 438	26 444	484	m
200	03 258	03 258	115	st	331	26 737	—	17	—
$11\bar{1}$	03 663	03 664	228	vvst	$40\bar{4}$	26 827	—	15	—
$20\bar{1}$	03 952	03 951	123	st	$20\bar{5}$	27 330	—	7	—

111	03 998	04 000	189	st	13$\bar{3}$	27 455	—	28	—
002	04 120	—	0.2	—	11$\bar{5}$	27 711	—	16	—
201	04 624	04 628	220	vst	314	27 810	27 824	297	vw
11$\bar{2}$	06 585	06 591	553	vvst	512	28 146	—	23	—
20$\bar{2}$	06 707	—	4	—	42$\bar{3}$	28 214	28 240	1	vw
112	07 256	07 255	184	st	33$\bar{2}$	28 317	—	7	—
020	07 944	07 941	302	vst	133	28 461	—	37	—
202	08 049	08 057	18	vvw	224	29 024	—	2	—
021	08 974	08 990	1	vvw	51$\bar{3}$	29 101	—	7	—
003	09 270	09 312	71	vvst	600	29 321	—	74	—
310	09 316		265		60$\bar{1}$	29 344	29 392	8	vw
31$\bar{1}$	09 843	09 853	20	vw	115	29 389		100	
311	10 850	10 864	65	vw	332	30 331	—	1	—
220	11 202	11 193	6	vvw	205	30 686	—	6	—
20$\bar{3}$	11 521	11 567	7	vw	601	31 358	—	18	—
11$\bar{3}$	11 567		56		60$\bar{2}$	31 428	31 430	50	vvw
22$\bar{1}$	11 896	11 905	225	st	040	31 775	31 762	366	w
022	12 064	12 072	54	vw	404	32 196	—	8	—
31$\bar{2}$	12 429	12 433	42	vvw	423	32 259	32 259	148	vvw
221	12 567	12 569	55	w	31$\bar{5}$	32 550	32 563	73	vvw
113	12 574		32		041	32 805	32 810	15	vvw
400	13 032	13 050	34	vvw	33$\bar{3}$	32 964	32 968	103	vvw
40$\bar{1}$	13 390	—	1	—	025	33 694	33 676	27	vvw
203	13 535	13 544	128	vw	513	34 135	34 121	69	vvw
312	14 443	—	4	—	13$\bar{4}$	34 497	—	1	—
22$\bar{2}$	14 651	14 651	120	vw	42$\bar{4}$	34 771	—	—	—
401	14 733	—	18	—	240	35 033	35 032	39	vvw
40$\bar{2}$	15 809	15 819	51	vw	22$\bar{5}$	35 274	—	31	—
222	15 993	15 998	169	w	40$\bar{5}$	35 426	—	15	—
004	16 480	16 488	77	vw	602	35 455	—	1	—
31$\bar{3}$	17 076	17 073	164	vw	51$\bar{4}$	35 472	35 481	421	vw
023	17 214	—	4	—	60$\bar{3}$	35 571	—	18	—
20$\bar{4}$	18 395	18 430	286	m	24$\bar{1}$	35 727	—	80	—
402	18 493	18 508	300	w	134	35 839	35 863	107	vw
11$\bar{4}$	18 609	—	8	—	042	35 895	—	1	—
130	18 688	—	1	—	333	35 984	35 977	10	vvw
22$\bar{3}$	19 465	19 481	87	vw	241	36 399	36 412	148	vw
13$\bar{1}$	19 550	19 555	110	vw	006	37 080	—	47	—
131	19 886	19 873	93	vw	620	37 265	—	16	—
114	19 952	19 953	203	vw	62$\bar{1}$	37 288	37 305	71	vvw
313	20 096	—	18	—	31$\bar{5}$	37 583	37 578	75	vvw
40$\bar{3}$	20 288	—	27	—	20$\bar{6}$	38 324	—	7	—
420	20 975	20 979	7	vvw	24$\bar{2}$	38 482	—	—	—
204	21 080	—	4	—	225	38 630	—	8	—
42$\bar{1}$	21 334	—	10	—	11$\bar{6}$	38 874	38 855	296	vw
223	21 479	—	1	—	621	39 302	39 364	61	w
13$\bar{2}$	22 472	22 465	347	m	62$\bar{2}$	39 371		93	
51$\bar{1}$	22 539	—	1	—	33$\bar{4}$	39 670	—	2	—
421	22 677	—	38	—	242	39 824	—	43	—
132	23 144	23 153	163	vw	424	40 140	40 116	82	vvw
42$\bar{2}$	23 753	23 747	129	m	116	40 887	—	3	—
511	24 217	24 223	62	vw	043	41 045	41 006	26	vvw
403	24 315	—	3	—	603	41 612	—	3	—
024	24 424	24 421	76	vw	60$\bar{4}$	41 774	—	6	—
51$\bar{2}$	24 790	—	10	—	405	42 138	—	15	—
330	25 204	25 194	174	m	206	42 352	42 359	231	vw
33$\bar{1}$	25 730	25 740	27	vw	24$\bar{3}$	43 296	—	1	—
005	25 750		158						

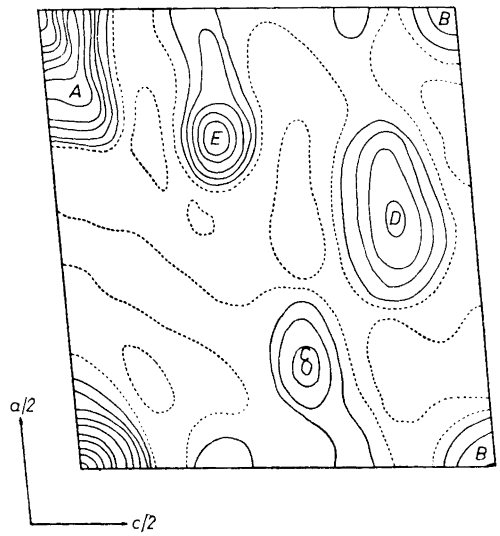

Fig. 1. Projection of the Patterson function *P(upw)*. Dashed lines indicate negative values.

was calculated and found to have only one high maximum, *viz.* at $v = 0$. This locates these two chromium atoms at the point position 2(*c*) and thus we conclude the following arrangement of the metal atoms: 2 K in 2(*a*), 2 Cr_I in 2(*c*) and 4 Cr_{II} in 4(*i*).

The projections in *P(upw)* of the interatomic vectors corresponding to the metal atoms are given in Table 3 (*cf.* Fig. 1). Reasonable Cr_I—Cr_{II} distances are only obtained if it is assumed that the maximum C is caused by a K—Cr_{II} vector $(\frac{1}{2}+x,z)$ and thus the x and z parameters for the Cr_{II} atoms are 0.62 and 0.29, respectively. These values require further peaks in *P(upw)* in perfect agreement with the observed data (*cf.* Table 3 and Fig. 1).

Table 3. Observed and calculated metal-metal peaks in *P(upw)*.

Vector groups		Weight	Maximum calc		Maximum obs		Max. in *(Pupw)*
			u	*w*	*u*	*w*	
K—K	$\frac{1}{2}$, 0	1	$\frac{1}{2}$	0	0.50	0.00	A
K—Cr_1	0, $\frac{1}{2}$	1	0	$\frac{1}{2}$	0.00	0.50	B
	$\frac{1}{2}$, $\frac{1}{2}$	1	$\frac{1}{2}$	$\frac{1}{2}$	0.50	0.50	B
K—Cr_2	$\pm(x,z)$; $\pm(\frac{1}{2}+x,z)$	1	0.12	0.28	0.12	0.28	C
Cr_1—Cr_1	$\frac{1}{2}$, 0	1	$\frac{1}{2}$	0	0.50	0.00	A
Cr_2—Cr_2	$\pm(2x,2z)$; $\pm(\frac{1}{2}+2x,2z)$	1	0.26	0.42	0.28	0.42	D
	$\frac{1}{2}$, 0	2	$\frac{1}{2}$	0	0.50	0	A
Cr_1—Cr_2	$\pm(\frac{1}{2}+x, \frac{1}{2}+z)$; $\pm(x,\frac{1}{2}+z)$	1	0.38	0.21	0.38	0.20	E

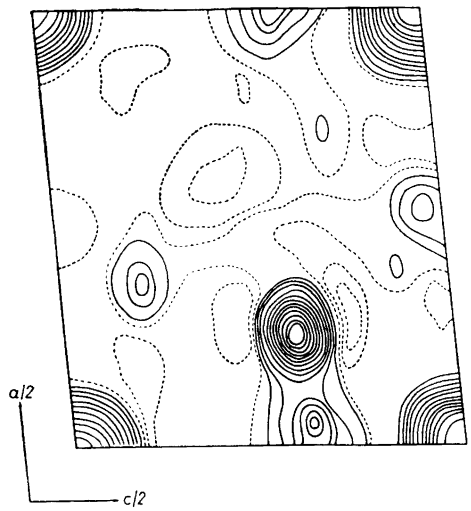

Fig. 2a. Electron density projection $\varrho_2(xpz)$. Dashed lines indicate negative values.

Since the *b* axis is rather short, the *xz* projection of the electron density should show little or no overlapping. At first this projection was calculated using only those *F* values whose signs could be derived from the potassium and chromium contributions. Three pronounced maxima were found giving the positions of the potassium (height 1 165) and chromium atoms (height

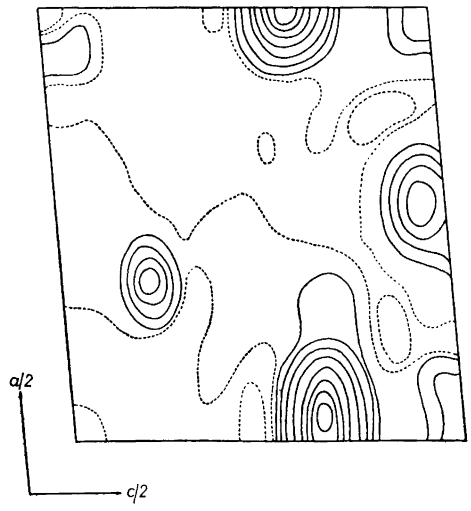

Fig. 2b. Electron density projection $\varrho_3(xpz)$ with the potassium and chromium atoms (Cr_1 and Cr_2) subtracted. Dashed lines indicate negative values.

1 230 and 1 350). (The heights are given on an arbitrary scale.) In addition there were five further maxima:

I.	$x = 0$,	$z = 0.33$	(Height 470);
II.	$x = 0.25$,	$z = 0.50$	(» 270);
III.	$x = 0.18$,	$z = 0.08$	(» 180);
IV.	$x = 0.13$,	$z = 0.47$	(» 180);
V.	$x = 0.22$,	$z = 0.25$	(» 130);

Of these maxima, I and II were assumed to correspond to oxygen atoms in the positions 8(*j*) and 4(*i*) in conformity with their relative heights.

The electron density projection obtained after including these twelve oxygen atoms in the calculations (Fig. 2a) showed no displacements of the positions of the potassium and chromium atoms. The oxygen maxima (I) and (II) had moved and were considerably sharpened and their relative heights were in better agreement with the K and Cr maxima. The maxima IV and V had vanished while III now appeared with the same height as II indicating maximum III to correspond to the remaining four oxygen atoms in a fourfold position 4(*i*). Including all the atoms in the calculations improved the agreement between observed and calculated F values but did not change the sign of any structure factor. Fig. 2b shows the appearance of the projection $\varrho(xpz)$ after subtracting the metal atom contributions. The parameter values thus derived are given in Table 4.

There was only one y parameter to be determined, *viz.* that of the O_{III} atom. In order to find it, the electron density projection $\varrho(pyz)$ was calculated (Fig. 3). Here the potassium and chromium atoms appear very distinctly. The value obtained for $z(Cr_{II})$ is 0.292, in almost perfect agreement with the value found above. The O_I atom is overlapped by Cr_I. The z parameter of the O_{II} atom is somewhat changed from the value obtained from $\varrho(xpz)$. The latter should, however, be more reliable since more F values were used in the calculation of this projection. Also the close vicinity to the high maximum in 0,0 might have contributed to this displacement.

The remaining maximum in $\varrho(pyz)$ is due to two superimposed O_{II} atoms and gives the parameter values $y = 0.250$ and $z = 0.317$, the latter being in fair agreement with the value obtained above.

A careful inspection of the Weissenberg photographs shows a very close agreement between all pairs of structure factors $F(h1l)$ and $F(h3l)$, which supports the reliability of the values for the y parameters.

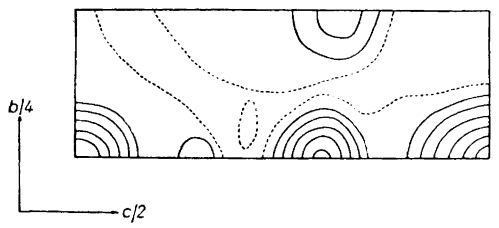

Fig. 3. Electron density projection $\varrho(pyz)$. Dashed lines indicate negative values.

Table 4. Atomic parameters for KCr_3O_8.

(Space-group No. 12 $C2/m$)

Atoms	Point position	x	y	z
2 K	2(*a*)	0	0	0
2 Cr_I	2(*c*)	0	0	½
4 Cr_{II}	4(*i*)	0.625	0	0.293
4 O_I	4(*i*)	0.225	0	0.551
4 O_{II}	4(*i*)	0.682	0	0.108
8 O_{III}	8(*j*)	0.024	0.250	0.315

DESCRIPTION AND DISCUSSION OF THE STRUCTURE

The atomic arrangement thus derived for KCr_3O_8 is summarized in Table 4

Using these parameters, the F values were calculated for the reflexions $h0l$, $h1l$ (identical with $h3l$) and $0kl$ and compared with the observed ones (Table 5). The F_{calc} values were modified by an isotropic temperature factor $B = 0.35$ Å^2 obtained experimentally for $F(h0l)$, $F(h1l)$ and $F(0kl)$. The "reliability" index R calculated according to Booth (1948) was found to be 0.14 for $h0l$, 0.12 for $h1l$ and 0.15 for $0kl$, when the reflexions with vanishingly small amplitudes were taken as having structure amplitudes equal to half the minimum value that it was found possible to observe at the corresponding angle. If only observed reflexions were considered, then the index values for the three groups of reflexions were 0.12, 0.12 and 0.15, respectively. The good agreement between observed and calculated structure factors and the low R values suggest that the coordinates proposed above are essentially correct. The accuracy of the parameters is estimated to be $\pm$ 0.002 for Cr_{II} and $\pm$ 0.004 for the oxygen atoms.

The structure of KCr_3O_8 is shown in Fig. 4 in which it can be seen that the chromium coordination is of two kinds. The first type (Cr_I) forms six bonds with oxygen atoms, *viz.* four with O_{III} atoms and two with O_I atoms. The arrangement of these oxygen atoms is very nearly perfectly octahedral. On the other hand, the coordination around the Cr_{II} atoms consists of a tetrahedron of four oxygen atoms, *viz.* one O_I atom, one O_{II} atom and two O_{III} atoms. The octahedra and tetrahedra are linked together by having corners in common forming continuous layers || the *ab*-plane. All the oxygen atoms except O_{II} belong simultaneously to one CrO_6 octahedron and one CrO_4 tetrahedron. The O_{II} atoms belong only to CrO_4 tetrahedra. The layers are held together by K ions which have ten nearest oxygen neighbours.

Interatomic distances and bond angles are given in Table 6. The accuracy of the Cr-O distance is estimated to be $\pm$ 0.04 Å, while the K-O and O-O distances may be in error by $\pm$ 0.10 Å and $\pm$ 0.10 Å respectively. The distances are of reasonable length throughout.

There is a significant difference between the Cr_I-O and Cr_{II}-O distances. The average of the former (1.97 Å) coincides with that recently found by Douglass [9] in $HCrO_2$ (average value of six Cr^{3+}-O distances 1.97 $\pm$ 0.04 Å).

Table 5. Comparison between calulated and observed structure factors from Weissenberg photographs of KCr_3O_8. Cu$K\alpha$-radiation. Intensities only observed as β-reflexions are marked with an asterisk.

hkl	F_c	F_o	*hkl*	F_c	F_o	*hkl*	F_c	F_o
200	81	77	$40\bar{5}$	24	18	$91\bar{2}$	57	55
400	38	42	$60\bar{5}$	− 36	26	913	− 31	34
600	55	56	$80\bar{5}$	− 26	31	713	2	< 6
800	61	64	806	29	34	513	36	30
1 000	23	22	606	4	< 8	313	− 22	17
1 001	− 26	33	406	36	35	113	− 32	29
801	− 35	28	206	92	98	$11\bar{3}$	− 40	33
601	26	21	006	41	46	$31\bar{3}$	60	59
401	− 31	25	$20\bar{6}$	9	< 5	$51\bar{3}$	− 6	5
201	−118	115	$40\bar{6}$	33	25	$71\bar{3}$	− 38	36
001	− 64	59	$60\bar{6}$	54	57	$91\bar{3}$	− 5	< 8
$20\bar{1}$	83	78	$80\bar{6}$	15	19	914	13	18
$40\bar{1}$	− 9	15	607	3	< 9	714	−	< 7
$60\bar{1}$	− 20	25	407	− 36	41	514	22	16
$80\bar{1}$	− 6	13	207	− 11	10	314	77	69
1 $00\bar{1}$	24	20	$00\bar{7}$	35	31	114	56	59
1 002	35	30	$20\bar{7}$	3	< 6	$11\bar{4}$	12	17
802	8	< 7	$40\bar{7}$	− 10	< 7	$31\bar{4}$	4	< 4
602	4	< 5	$60\bar{7}$	− 9	13	$51\bar{4}$	90	86
402	116	123	$80\bar{7}$	26	20	$71\bar{4}$	28	23
202	32	33	408	19	24	$91\bar{4}$	−	< 9
$00\bar{2}$	− 7	< 1	208	− 4	< 8	715	6	< 8
$20\bar{2}$	− 16	9	008	− 5	< 7	515	− 19	15
$40\bar{2}$	48	53	$20\bar{8}$	33	35	315	− 42	41
$60\bar{2}$	44	49	$40\bar{8}$	25	32	115	44	41
$80\bar{2}$	− 14	16	$60\bar{8}$	−	< 9	$11\bar{5}$	14	14
1 $00\bar{2}$	−	< 9	209	13	13	$31\bar{5}$	− 41	36
1 003	19	20	$00\bar{9}$	− 4	11	$51\bar{5}$	− 23	23
803	19	11	$20\bar{9}$	− 25	26	$71\bar{5}$	23	17
603	− 14	12	$40\bar{9}$	14	11	$91\bar{5}$	5	< 10
403	− 13	14	110	8	< 4	716	31	33
203	79	86	310	115	117	516	44	45
003	59	64	510	74	74	316	12	8
$20\bar{3}$	9	8	710	−	< 5	116	− 8	3
$40\bar{3}$	− 36	41	910	13	< 7	$11\bar{6}$	75	72
$60\bar{3}$	26	27	911	14	12	$31\bar{6}$	45	41
$80\bar{3}$	26	28	711	− 10	12	$51\bar{6}$	10	< 6
1 $00\bar{3}$	− 27	31	511	− 65	64	$71\bar{6}$	6	< 8
804	32	30	311	38	34	$91\bar{6}$	24	23
604	32	31	$11\bar{1}$	71	72	517	14	< 9
404	18	14	$11\bar{1}$	− 86	80	317	18	14
204	− 15	14	$31\bar{1}$	− 28	27	117	− 18	14
004	60	68	$51\bar{1}$	−	< 4	$11\bar{7}$	− 30	29
$20\bar{4}$	114	110	$71\bar{1}$	31	29	$31\bar{7}$	11	< 7
$40\bar{4}$	23	13	$91\bar{1}$	− 16	19	$51\bar{7}$	17	12
$60\bar{4}$	13	< 5	912	27	24	$71\bar{7}$	− 9	< 9
$80\bar{4}$	49	43	712	66	64	518	− 6	< 11
1 $00\bar{4}$	43	36	512	21	18	318	32	33
805	22	27	312	− 3	< 3	118	39	37
605	1	< 7	112	86	80	$11\bar{8}$	22	25
405	17	15	$11\bar{2}$	127	127	$31\bar{8}$	−	< 8
205	− 18	20	$31\bar{2}$	30	29	$51\bar{8}$	19	18
005	− 84	92	$51\bar{2}$	13	< 4	$71\bar{8}$	39	~ 36*
$20\bar{5}$	− 19	15	$71\bar{2}$	24	18	319	− 20	22

hkl	F_c	F_o	*hkl*	F_c	F_o	*hkl*	F_c	F_o
119	− 5	6	022	49	58	045	− 50	39
11$\bar{9}$	17	19	042	− 3	< 5	065	− 20	15
31$\bar{9}$	2	< 10	062	14	< 10	026	13	5
51$\bar{9}$	− 22	~ 16*	023	− 17	9	046	27	32
020	128	110	043	29	29	027	25	26
040	121	114	063	1	< 10	047	24	23
060	47	41	024	55	50	028	17	10
021	− 11	17	044	39	32	048	− 2	~ 10*
041	− 26	28	064	28	23	029	− 12	16
061	− 5	< 10	025	− 35	33			

The Cr_{II}-O distances of 1.55—1.65 Å agree well with values around 1.60 Å reported for the $Cr^{6+}O_4$ groups in K_2CrO_4 [10], $CaCrO_4$ [11], Na_2CrO_4 [12] and $CuCrO_4$ [13]. Thus the coordination numbers as well as the interatomic distances indicate that the Cr_I atoms are essentially trivalent and the Cr_{II} atoms hexavalent. While the unsymmetrical Cr_I^{3+}—O—Cr_{II}^{6+} bridges of KCr_3O_8 thus differ completely from the symmetrical bridges Cr^{6+}—O—Cr^{6+} in CrO_3 [14] and $(NH_4)_2Cr_2O_7$ [15] with Cr-O distances of 1.8_0 and 1.9_0 Å, respectively, the

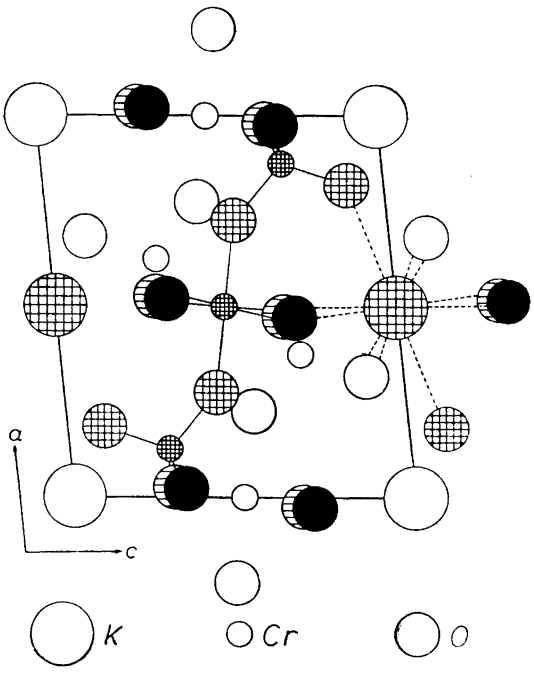

Fig. 4. The unit cell content of KCr_3O_8 projected on (010). Atoms at $y = 0$ open circles, atoms at $y = \frac{1}{4}$ shaded horizontally, atoms at $y = \frac{1}{2}$ shaded horizontally and vertically and atoms at $y = \frac{3}{4}$ black. Bonds between the atoms in a $Cr_3O_8^-$ unit with the chromium atoms at $y = \frac{1}{2}$ are shown with lines. The broken lines represent the K—O bonds.

Table 6. Interatomic distances and bond angles in KCr_3O_8.

Cr_I — 2 O_I	1.93 Å	K — 4 O_{II}	3.21 Å
Cr_I — 4 O_{III}	1.99 Å	O_I — 2 O_{II}	2.89 Å
Cr_{II} — O_I	1.65 Å	O_I — O_{II}	2.64 Å
Cr_{II} — O_{II}	1.55 Å	O_I — 2 O_{III}	2.66 Å, 2.72 Å
Cr_{II} — 2 O_{III}	1.64 Å	O_{II} — 2 O_{III}	2.59 Å
K — 4 O_{III}	2.80 Å	O_{III} — 2 O_{III}	2.73 Å, 2.90 Å
K — 2 O_{II}	2.94 Å	Cr_I — Cr_{II}	3.39 Å, 3.42 Å
Cr_I — O_{III} — Cr_{II}	138°	2(O_{III} — Cr_I — O_{III})	94°
Cr_I — O_I — Cr_{II}	146°	2(O_I — Cr_{II} — O_{III})	108°
O_I — Cr_I — O_I	180°	O_I — Cr_{II} — O_{II}	111°
2(O_{III} — Cr_I — O_{III})	86°	O_{II} — Cr_{II} — O_{III}	109°

bond angles Cr—O—Cr have similar values in all three substances, *viz.* 138° and 146° (KCr_3O_8), 136° (CrO_3) and 115° ($(NH_4)_2Cr_2O_7$). The O_2 atom which belongs to one Cr atom only (Cr^{6+}) is in slightly closer contact with the latter than are the shared O atoms.

Wadsley recently determined the structures of two vanadium compounds with formulae similar to that of KCr_3O_8, *viz.* the so-called vanadium bronzes $Na_{2-x}V_6O_{15}$ [16] and $Li_{1+x}V_3O_8$ [17]. These phases are intensely coloured, chemically very inert and electric semiconductors as are also the earlier well known wolfram bronzes [18–20]. The present investigation has revealed a fundamental difference in structural character between KCr_3O_8 and these compounds. In the bronzes, all vanadium or wolfram atoms occupy positions which are energetically equivalent or probably nearly so. This is likely to facilitate an electron transfer between the metal atoms which is reflected in the considerable electric conductivity of these compounds. In KCr_3O_8, on the other hand, the chromium atoms of fourfold and sixfold coordination must differ very much in energy and hence electron transport between these atoms must be considerably hindered. This view is supported by the recent observation by Wadsley (private communication) that KCr_3O_8 has a very high electrical resistance. The black colour of KCr_3O_8 might possibly indicate a very slight electron transfer between the Cr^{3+} and Cr^{6+} atoms but it might also be caused by the character of the Cr—O bonds. Accurate determinations of Cr—O distances in other chromates would be of great interest. Determinations of the structures of $Rb_2Cr_2O_7$ ($C2/c$ and $P2_1/n$) are in progress and will be published elsewhere. It is planned to reinvestigate the crystal structure of $(NH_4)_2Cr_3O_{10}$ [21].

A comparison between the structures of KCr_3O_8 and $KAl(SO_4)_2$ [22] reveals a certain structural relationship between these compounds, a fact which was first suggested by Professor J. Zemann (Göttingen).

Acknowledgement. This investigation forms part of a research programme on the crystal chemistry of chromium compounds, which is financially supported by the *Swedish Natural Science Research Council.* Part of the calculations involved in this structure determination has been carried out on the BESK, for the use of which the author is indebted to the *Swedish Board for Computing Machinery.*

The author is indebted to the head of this Institute, Professor Arne Ölander, for his kind interest and for the provision of laboratory facilities. Thanks are also due to Dr. Arne Magnéli for stimulating discussions and criticism in connection with this work, to Dr. A. D. Wadsley (C.S.I.R.O., Melbourne) for helpful discussion and permission to quote data as yet unpublished, and to Dr. J. Baecklund for carrying out the piezoelectric test.

REFERENCES

1. Wilhelmi, K.-A. *Naturwiss.* **44** (1957) 580.
2. Suchow, L., Fankuchen, I. and Ward, R. *J. Am. Chem. Soc.* **74** (1952) 1678.
3. Charlot, G. and Bézier, D. *Quantitative Inorganic Analysis.* Methuen & Co. Ltd., Frome and London 1957.
4. Hambling, P. G. *Acta Cryst.* **6** (1953) 98.
5. Österlöf, J. *To be published. Cf.* also Westman, S. and Magnéli, A. *Acta Chem. Scand.* **11** (1957) 1587.
6. Lu, C. S. *Rev. Sci. Instr.* **14** (1943) 331.
7. Booth, A. D. *Fourier Technique in X-ray Organic Structure Analysis.* Cambridge 1948.
8. Vand, V., Eiland, P. E. and Pepinsky, R. *Acta Cryst.* **10** (1957) 303.
9. Douglass, R. M. *Acta Cryst.* **10** (1957) 423.
10. Zachariasen, W. H. and Ziegler, G. E. *Z. Krist.* **80** (1931) 164.
11. Clouse, J. H. *Z. Krist.* **83** (1932) 161.
12. Miller, J. J. *Z. Krist.* **94** (1936) 131.
13. Brandt, K. *Arkiv Kemi, Mineral. Geol.* **A17** (1943) No. 15.
14. Byström, A. and Wilhelmi, K.-A. *Acta Chem. Scand.* **4** (1950) 1131.
15. Byström, A. and Wilhelmi, K.-A. *Acta Chem. Scand.* **5** (1951) 1003.
16. Wadsley, A. D. *Acta Cryst.* **8** (1955) 695.
17. Wadsley, A. D. *Acta Cryst.* **10** (1957) 261.
18. Hägg, G. *Z. physik. Chem.* **B29** (1935) 192.
19. Magnéli, A and Blomberg, B. *Acta Chem. Scand.* **5** (1951) 372.
20. Hägg, G. and Magnéli, A. *Revs Pure and Appl. Chem.* (Australia) **4** (1954) 235.
21. Seiter, E. D. *Diss.* Rutgers Univ., New Brunswick, New Jersey 1956.
22. Vegard, L. and Maurstad, A. *Skrifter Norske Videnskaps-Akad. Oslo. I. Mat. Natur. Klasse* (1928) No. 7.

Received August 7, 1958.

ACTA CHEMICA SCANDINAVICA 12 (1958) 1977—1984

Studies on Arabogalactans

II. Fractionation of the Arabogalactan from *Larix occidentalis* Nutt. A Methylation Study of one of the Components

HANS O. BOUVENG and BENGT LINDBERG

Träkemiska Institutionen, Kungl. Tekniska Högskolan, Stockholm, Sweden

The arabogalactan from Western Larch (*Larix occidentalis* Nutt.) heartwood has been separated into two components by fractional precipitation of their borate complexes with cetyl-trimethylammoniumhydroxide. These differ in electrophoretic mobility in borate buffer and in sedimentation velocity but have about the same composition and optical rotation. Methylation and hydrolysis of the component with the higher molecular weight afforded 2-*O*-methyl-D-galactose, 2,4-di-*O*-methyl-D-galactose, 2,6-di-*O*-methyl-D-galactose, 2,3,4-tri-*O*-methyl-D-galatose, 2,4,6-tri-*O*-methyl-D-galactose, 2,3,4,6-tetra-*O*-methyl-D-galactose, 2,5-di-*O*-methyl-L-arabinose, 2,3,4-tri-*O*-methyl-L-arabinose and 2,3,5-tri-*O*-methyl-L-arabinose, which were separated, characterised and estimated quantitatively.

FRACTIONATION OF THE ARABOGALACTAN

The homogeneity of the arabogalactans from the *Larix* genus has long been under discussion. In ultracentrifuge studies of a larchwood arabogalactan (species not stated) Mosimann and Svedberg [1] found two components with approximate molecular weights of 16 000 and 100 000. In Western Larch arabogalactan Lystad-Borgin [2] found only one component in the heartwood but two in the sapwood. The molecular weight of these components seemed to be of the same order as those calculated by Mosimann and Svedberg, the heartwood component having the higher molecular weight. Fractional precipitation of the polysaccharide, either directly or after methylation or acetylation has given opposite results (*cf.* Ref.[3]). In a recent publication Aspinall *et al.*[4] concluded that the arabogalactan from European Larch, *L. decidua* Miller, was homogeneous, since no proof of heterogeneity could be found. The heterogeneity of the arabogalactan from Western Larch (*L. occidentalis* Nutt.) heartwood which was left undecided in a previous communication [5] has now been investigated. Electrophoresis of the polysaccharide on glass fibre sheets using borate buffer showed the presence of two components (A and B), which gave two distinct spots on development of the electrophoretograms.

Cetyl-trimethylammonium bromide and similar quaternary ammonium salts have been used succesfully by Scott [6] and others for the fractionation of acidic polysaccharides. Barker *et al.*[7] recently showed that the method could also be applied to neutral polysaccharides capable of forming borate complexes. When this method was used for the fractionation of larch arabogalactan, only part of one component (A), the more mobile on electrophoresis, could be precipitated. The incompleteness of the fractionation was probably caused by to high an ionic strength in the solution. The method was therefore modified by using the corresponding base, cetyl-trimethylammoniumhydroxide, together with boric acid and this gave almost complete precipitation of the polysaccharide. The addition of a small amount of sodium hydroxide had a favourable coagulating effect. The fractionations were made in 4—5 steps at pH 7—8; usually only one of the fractions contained both components. As the mixed fractions were easily refractionated by the same procedure, the original material could be separated completely into the two components.

The proportion of A to B was about 2:1. A, $[\alpha]_D^{20}$ +7° (in water), contained 19 % (molar) arabinose and B, $[\alpha]_D^{20}$ +10°, 21 % arabinose. Sedimentation analysis, made by courtesy of Prof. S. Claesson, Dept. of Physical Chemistry, Uppsala University, gave sedimentation constants 4.3 and 1.4, resp., for A and B in good agreement with the values previously reported [1,2]; the components appeared in the approximate proportion of 2:1. The molecular weights of A and B are therefore of the same magnitude, 100 000 and 16 000, as those calculated for the two components in the sample studied by Mosimann and Svedberg.

A METHYLATION STUDY OF ARABOGALACTAN A

Arabogalactan A was methylated first with methyl sulphate and sodium hydroxide and then with methyl iodide and silver oxide in dimethyl formamide. The latter procedure, devised by Kuhn *et al.*[8] for carbohydrates of low molecular weight, proved to be valuable for polysaccharides also. It was, however, necessary to modify the method of isolation of the methylated product in order to improve the yield. After four methylations in dimethyl formamide the product had a methoxyl content of 44.4 % (theoretical value 44.7 %). The usual methods of estimating the completeness of the methylation of a polysaccharide are not unambiguous; those using methoxyl analyses and infrared spectrophotometry are both open to criticism. Besides the methoxyl analysis a good criterion of the completeness of methylation in the present case was also found in the absence of even traces of unmethylated monomers in the hydrolysate of the methylated polysaccharide.

The hydrolysate from the methylated polysaccharide was fractionated by chromatography on carbon and cellulose columns and on thick filter papers. Carbon columns, in some cases combined with filter paper chromatography, proved most satisfactory for the separation of ethers with at least one free alcoholic hydroxyl; separation on cellulose columns gave better results for highly methylated ethers. The results from the fractionation of the hydrolysate are summarised in Table 1. The ethers were either obtained crystalline or characterised as crystalline derivatives.

Table 1. Galactose and arabinose methyl ethers isolated from the hydrolysate of 0.96 g of methylated arabogalactan A.

Methyl Ethers	mmoles	molar %
2-Methylgalactose	0.14	3.7
2,4-Dimethylgalactose	1.42	37.5
2,6-Dimethylgalactose	0.11	2.9
2,3,4-Trimethylgalactose	0.52	13.7
2,4,6-Trimethylgalactose	0.16	4.2
2,3,4,6-Tetramethylgalactose 2,3,5-Trimethylarabinose	1.22	32.2
2,5-Dimethylarabinose	0.12	3.2
2,3,4-Trimethylarabinose	0.10	2.6

As is often found in this type of investigation, the number of end groups, represented by the tetramethyl galactose and trimethyl arabinose, was smaller than that required by the number of branching points as determined by the amount of mono- and dimethyl galactoses. Incomplete methylation, possibly demethylation during the acid hydrolysis and losses due to the volatility of the fully methylated monomers will all contribute to this discrepancy. A recent publication of Gardiner and Percival [9] has emphasised the last possibility. In the present investigation it was found that about 5 % of a sample of tetramethyl galactose was lost on concentration of an aqueous solution under the conditions used in the quantitative estimation of the ether. Further, if 2,3,4-tri-*O*-methyl-L-arabinose and 2,5-di-*O*-methyl-L-arabinose are derived entirely from 3-*O*-β-L-arabopyranosyl-L-arabofuranose units [10,5], the difference in the amounts of these ethers gives a measure of the deficiences of the methods used.

It is difficult to decide whether the occurrence of 2-*O*-methyl-D-galactose and 2,6-di-*O*-methyl-D-galactose has any structural significance as an indication of the presence of 1,4-linkages. As the hydroxyl group at $C_{(4)}$ in a galactose residue is axial, it is presumably less reactive in the methylation (*cf.* Ref.[11]). The results of a partial methylation of 6-trityl-β-methyl-D-galactoside also indicated that this hydroxyl group is less reactive [12]; in this case, however, steric interaction from the trityl group might be of some importance. If 2-*O*-methyl-D-galactose and 2,6-di-*O*-methyl-D-galactose were the results of demethylation of 2,4-di-*O*-methyl-D-galactose and 2,4,6-tri-*O*-methyl-D-galactose or incomplete methylation of residues, corresponding to these ethers, it would be expected that these pairs of methyl ethers would be formed in about same proportion. However, the proportions actually found are 1.3:1 and 8.8:1. Therefore, and in view of the virtual absence of other monomethyl and dimethyl ethers of galactose, this strongly supports the structural significance of 2-*O*-methyl-D-galactose and 2,6-di-*O*-methyl-D-galactose.

2,3,5-Tri-*O*-methyl-L-arabinose and 2,3,4,6-tetra-*O*-methyl-D-galactose did not separate on the carbon column; separation of the corresponding fraction on thick filter paper afforded the arabinose ether but this was impure and in insufficient quantity for proper characterisation. A larger amount of methylated polysaccharide was therefore subjected to a mild hydrolysis and the low-molecular part of the hydrolysate was hydrolysed further and then frac-

tionated on a cellulose column. The first fraction afforded 4.5 % (molar) of pure 2,3,5-tri-*O*-methyl-L-arabinose; a further quantity of this ether appeared in the following fraction which contained mainly 2,3,4,6-tetra-*O*-methyl-D-galactose. As the hydrolysis of the arabinose residues was not taken to completion, this figure does not represent the total amount of terminal arabofuranosidic units.

It was therefore not possible to make a quantitative estimation of the relative amounts of 2,3,5-tri-*O*-methyl-L-arabinose and 2,3,4,6-tetra-*O*-methyl-D-galactose. In view of the proportion of arabinose to 3-*O*-β-L-arabopyranosyl-L-arabinose (5.9:2) formed on partial hydrolysis [5], it seems reasonable to assume that about 2/3 of the arabinose is present as terminal arabofuranose units and 1/3 as 3-*O*-β-L-arabopyranosyl-L-arabofuranose. Therefore, taking the values for 2,5-di-*O*-methyl-L-arabinose and 2,3,4-tri-*O*-methyl-L-arabinose also into consideration, the arabinose content of the original polysaccharide could be estimated as 18—19 % (molar), in good agreement with the value 18.7 %, found by quantitative paper chromatography.

The relatively low percentage of galactose trimethyl ethers indicates that the arabogalactan A has a more branched structure than previously investigated polysaccharides of similar type; the isolation of 2-*O*-methyl-D-galactose suggests a small number of doubly branched units. The galactose residues are substituted in the 3- and 6-positions to about the same extent with linkages of the β-pyranoside type. A small number of 1,4-linkages seems to be present. There is 18—19 % (molar) of arabinose, about one third of which is combined as 3-*O*-β-L-arabopyranosyl-L-arabofuranose and the remainder as terminal L-arabofuranose residues.

The results previously reported of a partial hydrolysis of the arabogalactan strongly indicated the presence of galactofuranosidic residues in the polysaccharide. An additional, chromatographic investigation of A and B separately revealed no fundamental differences between the two components in this respect. However, no furanoside methyl ethers of galactose were found in the present investigation. This does not necessarily imply that galactofuranosidic residues are not present in arabogalactan A, since the experimental methods used were inadequate for the isolation of the corresponding ethers in the presence of large amounts of other ethers. This problem therefore requires further examination.

A comparison of the results of the present investigation with those of previous studies of related polysaccharides is of interest but must await the structure investigation of arabogalactan B.

EXPERIMENTAL

Melting points are corrected. All evaporations were carried out under reduced pressure.

Chromatography. Papers: Whatman No. 1 and 3 MM and Schleicher and Schüll 602 hP. Solvent: Butanol, ethanol, water, 10:3:5. Developer: Anisidine hydrochloride.

Paper electrophoresis. Paper: Schleicher and Schüll Glass Fibre Paper. Developer: α-Naphthol/sulphuric acid in butanol.

Preparation of larch arabogalactan. The polysaccharide was prepared mainly as described in part I[5]. It was purified further by filtering through ion exchange columns

(Amberlite IR-120 and IR-4B) and treatment with Floridin before being concentrated. It was obtained as a light-coloured powder on precipitation from ethanol. The arabinose content was 16.3 %, determined according to Saeman *et al* [13].

Electrophoresis of arabogalactan. The electrophoretograms (14 × 50 cm) were run in borate buffer at pH 10 for 30—45 min at 2 000 V and 30—50 mA. To allow for electroosmosis, which is very pronounced on glass fibre papers, the non-complexforming ω-hydroxymethylfurfural was used as reference substance. On development the electrophoretograms gave two distinct spots, the denser one (A) moving about 30 % faster than the other (B).

Sedimentation analysis of arabogalactan. Sedimentation analysis revealed two components with sedimentation constants (S_{20}) of 4.3 (A) and 1.4 (B) in the proportion 2:1. Determination on the pure components, prepared as described below, gave the same sedimentation constants (4.3 and 1.4). Both components showed considerable polymolecularity but were found to be essentially free of the other component.

Fractionation of arabogalactan. In a typical experiment the polysaccharide (40 g = 0.25 mole anhydrosugar) was dissolved in water (1 000 ml) and 0.6 M boric acid (415 ml). Cetyltrimethylammonium hydroxide (CTA-OH) was prepared by filtering an aqueous solution of the corresponding bromide through a hydroxyl-saturated column of Dowex 2 ion exchange resin. A portion of this solution (0.095 N) was added to the polysaccharide solution which became cloudy but formed no precipitate until a small amount of sodium hydroxide was added. The sticky precipitate thus obtained was collected on a glass filter and washed thoroughly with water. A further portion of CTA-OH and of sodium hydroxide was added to the filtrate and the fresh precipitate collected. The residual solution was deionised, concentrated and the remaining boric acid was removed by evaporation with methanol, giving a small quantity of polysaccharide which was isolated in the usual manner by precipitation with ethanol. To regenerate the polysaccharides, the precipitates obtained above were dissolved in the miniumum amount of 6 % acetic acid and poured into ethanol; the different fractions were obtained as white powders after filtering and drying. The results of the fractionation are summarised in Table 2. The mixed fraction was dissolved in water (500 ml) and 0.6 M boric acid (120 ml); 0.095 N CTA-OH (52 ml) and 0.5 N sodium hydroxide (5 ml) were added, the precipitate formed was collected and the polysaccharide was isolated as desribed above. 8.0 g of pure arabogalactan A was obtained; the residual solution afforded 3.2 g of mixed material. The arabogalactan fractions thus obtained were electrophoretically pure.

Table 2. Fractionation of 40 g of larch arabogalactan.

0.095 N CTA-OH added (ml)	0.50 N NaOH added (ml)	Weight of fraction (g)	Components
105	5	14.6	A
105	10	11.6	A + B
105	10	5.9	B
52	20	1.5	B
Residue	—	2.1	B

Methylation of arabogalactan A. The polysaccharide (5.70 g) was dissolved in 22.5 % sodium hydroxide (60 ml) under a nitrogen atmosphere. Methyl sulphate (30 ml) was added in small portions over 6 h while the solution was stirred vigorously and cooled with ice water. After a further 2 h the reaction mixture was neutralised with dilute sulphuric acid, dialysed over night against running tap water and then de-ionised by filtering through columns of Amberlite resins IR-120 and IR-4B. After concentration to dryness, the polysaccharide was dissolved in chloroform and precipitated in light petroleum. Yield 6.07 g (93 %); OCH_3 = 26.7 %.

The premethylated polysaccharide (6.05 g) was dissolved in 60 ml of freshly distilled dimethyl formamide (DMFA) and dry methyl iodide (25 ml). The solution was stirred vigorously and cooled while silver oxide (20 g) was added in portions over one hour. After

a reaction time of 20 h the polysaccharide was isolated as described by Kuhn *et al.*[9] for the isolation of fully methylated low-molecular weight carbohydrates. Precipitation in light petroleum gave 5.39 g (82 %), OCH_3 = 41.7 %.

This product (5.29 g) was methylated 20 h with methyl iodide (8 ml) and silver oxide (6 g) in DMFA (50 ml). The reaction mixture was centrifuged and the solid material was thoroughly washed with DMFA and chloroform. The combined centrifugates were concentrated almost to dryness and benzene (150 ml) was added. The precipitated silver salts were filtered off. The precipitate was treated with a small volume of hot DMFA, poured into benzene and filtered. The combined filtrates were concentrated and, if necessary, filtered again. The product was isolated either as a glass or by precipitation in light petroleum as a yellowish powder. This methylation was repeated twice. The final methylation gave 4.15 g of methylated arabogalactan A; OCH_3 = 44.4 % (theoretical value 44.7 %), $[\alpha]_D^{20}$ −37° (*c*, 1.0 in ethanol). The average yield for each methylation was thus 92 %. No trace was found of unmethylated arabinose and galactose on hydrolysis of the methylated polysaccharide.

Separation of methyl ethers from hydrolysed, methylated arabogalactan A. Methylated arabogalactan A (0.96 g) was heated in formic acid (60 ml) at 100° for 6 h. The formyl esters obtained on concentration were hydrolysed by heating in hydrochloric acid (100 ml, 0.5 N) at 100° for 10 h. After neutralising by filtration through an ion exchange column (IR-4B) and concentration of the solution, the hydrolysate was added to the top of a carbon-Celite column (3.5 × 43 cm) and eluted, using the gradient elution technique[14], with 5 l 6—24 % ethanol + 2.5 l 24—50 % ethanol + 1 l 60 % acetone. Table 3 shows how the fractions (25 ml each) were combined; the amount of sugar present was estimated by hypoiodite oxidation[15] and weighing.

A similar preparative separation was made using 2.0 g of methylated polysaccharide and gave crystalline 2-*O*-methyl-D-galactose, 2,4-di-*O*-methyl-D-galactose and 2,6-di-*O*-methyl-D-galactose; the other ethers, except 2,3,5-tri-*O*-methyl-L-arabinose were obtained in quantities sufficient for the preparation of derivatives. Except for the identifications, this separation will not be described in detail.

Fractions 146—159 contained about 50 % each of 2,3,4-trimethylgalactose and 2,5-dimethylarabinose, as estimated by paper chromatograms. Fractions 95—106, 107—119

Table 3. Fractionation of hydrolysed, methylated arabogalactan A.

Fract. No.	Amount of red. sugars as determined by hypoiodite oxid. mmoles	hypoiodite oxid. mg	weighing mg	Principal sugars present
27— 37	0.137	27	29	2-methylgalactose
53— 94	1.385	288	295	2,4-dimethylgalactose
95—106	0.094	19	20	2,4-dimethylgalactose 2,6-dimethylgalactose
107—119	0.540	117 *	118	2,3,4-trimethylgalactose 2,3,4-trimethylarabinose
120—145	0.195	40 *	41	2,3,4-trimethylgalactose 2,5-dimethylarabinose
146—159	0.046	10	14	2,3,4-trimethylgalactose 2,5-dimethylarabinose
160—192	0.162	36	39	2,4,6-trimethylgalactose
217—285	1.102	253 **	256	2,3,4,6-tetramethylgalactose 2,3,5-trimethylarabinose
60 % acetone eluate	0.120	28 **	30	2,3,4,6-tetramethylgalactose 2,3,5-trimethylarabinose

* Calculated from values given below. ** Calc. as 2,3,4,6-tetramethylgalactose.

Table 4.

Fract. No	Sugars	Equiv. in ml. 0.01 N $Na_2S_2O_3$	%	mmoles
95—106	2,4-dimethylgalactose	0.81	20	0.019
(0.094 mmoles)	2,6-dimethylgalactose	3.18	80	0.075
107—119	2,4-dimethylgalactose	0.09	1.9	0.010
(0.540 mmoles)	2,6-dimethylgalactose	0.19	4.0	0.022
	2,3,4-trimethylgalactose	3.60	75.8	0.409
	2,3,4-trimethylarabinose	0.87	18.3	0.099
120—145	2,4,-dimethylgalactose	0.11	4.0	0.008
(0.195 mmoles)	2,6-dimethylgalactose	0.14	5.0	0.010
	2,3,4-trimethylgalactose	1.19	42.7	0.083
	2,5-dimethylarabinose	1.35	48.3	0.094

and 120—145 were analysed in the following way. A suitable quantity (7—9 mg) of each fraction was separated on thick filter paper (Schleicher and Schüll 602 hP). The substances were located in the usual way, eluted from the corresponding strips with water and a quantitative estimation was made by hypoiodite oxidation. The following results were obtained (Table 4). Combination of these analytical data gives the values shown in Table 1.

Partial hydrolysis of methylated arabogalactan A. Exhaustively methylated polysaccharide (6.3 g) was boiled for six days in 0.02 N sulphuric acid containing 30 % ethanol. The solution was neutralised with barium carbonate and concentrated to dryness; the hydrolysate was dissolved in benzene, precipitated in light petroleum and filtered. The solid material was re-precipitated twice and the combined filtrates concentrated to a lightcoloured syrup (1.74 g), which was further hydrolysed in 0.5 N hydrochloric acid to split the methylated oligosaccharides present.

*Isolation of 2,3,5-tri-O-methyl-*L*-arabinose.* This product was added to the top of a cellulose column and eluted with butanol saturated with water. The top fraction afforded 282 mg of 2,3,5-tri-*O*-methyl-L-arabinose (4.5 % calculated on the original material). The following fraction contained mainly 2,3,4,6-tetra-*O*-methyl-D-galactose and a lesser quantity of the arabinose ether.

Characterisation of the methyl ethers

*2-O-Methyl-*D*-galactose.* The ether was crystallised from ethanol, m.p. and mixed m.p. 150—152°. On chromatography and electrophoresis, the ether was indistinguishable from an authentic sample of 2-*O*-methyl-D-galactose.

*2,4-Di-O-methyl-*D*-galactose.* The ether was crystallised from moist ethyl acetate, m.p. 103°, sintering at 80°; m.p. of the corresponding aniline derivative 216—219°. The ether was converted to the osazone, m.p. 146—149°, undepressed on admixture with an authentic sample of 4-*O*-methyl-D-galactosazone. On electrophoresis in borate buffer the ether, as expected, was immobile.

*2,6-Di-O-methyl-*D*-galactose.* The ether was recrystallised from ethyl acetate, m.p. 120—122°, undepressed on admixture with a synthetic sample. On electrophoresis in borate buffer, it moved somewhat more slowly than 2-*O*-methyl-D-galactose but decidedly faster than 4-*O*-methyl-D-galactose, as would be expected for a galactose derivative, capable of forming a complex only between $C_{(3)}$ and $C_{(4)}$ [12].

*2,3,4-Tri-O-methyl-*D*-galactose.* The ether was converted to the aniline derivative, m.p. 170—171°, undepressed on admixture with an authentic specimen.

*2,4,6-Tri-O-methyl-*D*-galactose.* The ether was converted to the aniline derivative, m.p. 179—180°. For further characterisation, a portion of the ether was reduced with

sodium borohydride. The trimethylgalactitol thus obtained consumed no periodate. This is in agreement with a 2,4,6-tri-*O*-methyl-D-galactose structure for the original ether which is the only pyranosidic trimethylgalactose of which the corresponding galactitol derivative is not oxidised by periodate.

2,3,4,6-Tetra-O-methyl-D-galactose. The ether was converted to the aniline derivative, m.p. 198—200°, undepressed on admixture with an authentic sample.

2,5-Di-O-methyl-L-arabinose. This was somewhat faster on paper chromatogram than 2,3,4-tri-*O*-methyl-L-arabinose and yielded arabinose only on demethylation. It was converted to the corresponding amide, m.p. 132—133°, in good agreement with values previously reported [16].

2,3,4-Tri-O-methyl-L-arabinose. The ether was converted to the corresponding phenylhydrazide, m.p. 157—158°, undepressed on admixture with an authentic specimen.

2,3,5-Tri-O-methyl-L-arabinose. The ether was faster on paper chromatogram than 2,3,4,6-tetra-*O*-methyl-D-galactose and gave arabinose on demethylation. It was converted to the corresponding arabonamide, m.p. 139—140°, in good agreement with values previously reported [16].

The authors are indebted to Miss Rose-Marie Karlsson and Miss Anita Myhrman for skilful assistance and to *Fonden för Skoglig Forskning* for financial support.

REFERENCES

1. Mosimann, H. and Svedberg, T. *Kolloid-Zeitschr.* **100** (1942) 99.
2. Lystad-Borgin, G. *J. Am. Chem. Soc.* **71** (1949) 2247.
3. Whistler, R. W. and Smart, C. L. *Polysaccharide Chemistry*, New York 1953, p. 203.
4. Aspinall, G. O., Hirst, E. L. and Ramstad, E. *J. Chem. Soc.* **1958** 593.
5. Bouveng, H. and Lindberg, B. *Acta Chem. Scand.* **10** (1956) 1515.
6. Scott, J. E. *Chem. and. Ind.* **1955** 168.
7. Barker, S. A., Stacey, M. and Zweifel, G. *Chem. and Ind.* **1957** 332.
8. Kuhn, R., Trischmann, H. and Löw, I. *Angew. Chem.* **67** (1955) 32.
9. Gardiner, J. G. and Percival, E. *J. Chem. Soc.* **1958** 1414.
10. Jones, J. K. N. *J. Chem. Soc.* **1953** 1672.
11. Dauben, W. G. and Pitzer, K. S. in Newman, M. S. *Steric Effects in Organic Chemistry*, New York 1956, p. 47.
12. Bouveng, H. and Lindberg, B. *Acta Chem. Scand.* **10** (1956) 1283.
13. Saeman, J. F., Moore, W. E., Mitchell, R. L. and Millet, M. A. *TAPPI* **37** (1954) 336.
14. Lindberg, B. and Wickberg, B. *Acta Chem. Scand.* **8** (1954) 569.
15. Hirst, E. L., Hough, L. and Jones, J. K. N. *J. Chem. Soc.* **1949** 57.
16. Maher, G. G. *Advances in Carbohydrate Chem.* **10** (1955) 263.

Received July 26, 1958.

ACTA CHEMICA SCANDINAVICA 12 (1958) 1985—1989

Incorporation of ^{14}C-Acetate in the Phenolic Substances in *Penicillium Islandicum* Sopp

STEN GATENBECK

Institute of Biochemistry, University of Lund, Sweden

The ^{14}C-distribution in 3-hydroxyphthalic acid, isolated from *P. islandicum*, grown on $CH_3{}^{14}COONa$, has been investigated. It was shown that the phthalic acid molecule is built up according to the acetate hypothesis. A new phenolic metabolite was studied and the anthraquinone content of the mycelium investigated which resulted in the identification of catenarin and emodin and the isolation of islandicin.

From previous studies [1,2] it is well known that acetate is the starting material for the formation of several aromatic compounds. The anthraquinone, emodin, belongs to those [3] and the present work will give evidence for an acetate coupling in other anthraquinones too.

In order to study the biosynthesis of anthraquinones a UV-mutant of *Penicillium islandicum*, strain N.R.R.L. 1036, was used, and the incorporation of ^{14}C-labelled acetate in the phenolic substances produced has been studied in the hope to find a precursor to the anthraquinone molecule among them. This special mutant shows a larger production of 3-hydroxyphthalic acid [4] and islandicin [5] than the wild type and it does not produce erythroskyrine [6] which in the wild type disturbs the localization of the anthraquinones on the paper chromatogram.

The culture medium contained very few appreciably labelled compounds. By developing an ether extract of the culture medium on paper chromatogram only three radioactive peaks could be detected by scanning the paper chromatogram with a G.M.-counter (Fig. 1). Two of these peaks were identified by chemical reagents as 3-hydroxyphthalic acid and a mixture of anthraquinones.

3-Hydroxyphthalic acid was isolated and its ^{14}C distribution investigated according to Fig. 2. The radioactive pattern of 3-hydroxyphthalic acid shows a strict conformity to the acetate theory.

The third radioactive peak contained a phenolic substance that has not previously been shown in *P. islandicum*. This substance which for the sake of brevity will be called compound A was isolated and its chemical properties

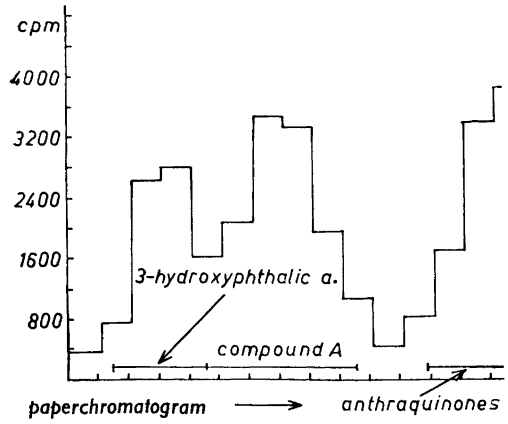

Fig. 1.

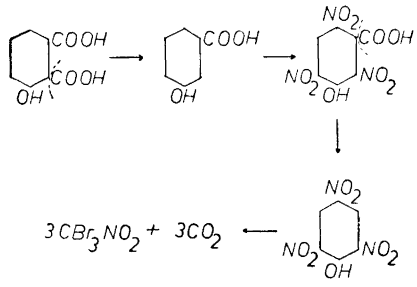

Fig. 2.

studied. It is very soluble in ethanol and acetone, slightly soluble in ether and water. It dissolves readily in 0.5 N $NaHCO_3$ with a slight yellow color and gives a gray brown coloration with ferric chloride solution. It has a strong reducing power indicating a hydroquinone structure. An interesting property of compound A is its behavior in concentrated sulfuric acid. By gentle warming it forms a new compound which shows all the reactions of an anthraquinone. It is orange in color and sublimes at 155—160°C in vacuum. It dissolves readily in 1 N NaOH and in 1 N Na_2CO_3 with a blue violet color. A pure blue color is obtained with alcoholic magnesium acetate. The anthraquinone has the following absorption maxima in ethanol, λ_{max} (mμ): 237.5, 258, 284, 301, 490, 515, 463—468 (inflexion). The solubility of the anthraquinone in 1 N Na_2CO_3 indicates that it has a β-hydroxyl group and the absorption spectrum points to a 1,4-position of two hydroxyl groups. The small amount of the sample has not allowed further analysis of the anthraquinone.

The compound A has a very sharp decomposition point at 212°C and shows no optical activity. Dithionite solution does not alter the compound and no anthraquinone is formed by thermal decomposition excluding any relationship to the hydrated anthraquinones rubroskyrin [6] and luteoskyrin [7].

The radioactive compound A was added to spores from *P. islandicum* suspended in a Czapek-Dox-agar medium. The culture was harvested after fourteen days. It was extracted with acetone and the extract put on a thick paper chromatogram. Two radioactive peaks were obtained by scanning the paper chromatogram with a G.M.-counter. One of them represented the unaltered compound A, the other one a yellow pigment with no anthraquinone properties. This pigment has not been further investigated.

The radioactive 3-hydroxyphthalic acid was tested in the same way as above in a spore suspension. No radioactive substance other than 3-hydroxyphthalic acid could be detected on the paper chromatogram under the experimental conditions employed.

The mycelium, cultivated on labelled acetate, was extracted with chloroform and the chloroform extract fractionated on a silica gel column. From one fraction, orange in UV-light, islandicin was isolated. The specific radioactivity of islandicin was compared with that of 3-hydroxyphthalic acid. The following values were obtained: islandicin, 10.1×10^4 counts min^{-1} $mmole^{-1}$ C-$atom^{-1}$; 3-hydroxyphthalic acid, 9.6×10^4 counts min^{-1} $mmole^{-1}$ C-$atom^{-1}$; *i. e.* they have about the same specific radioactivity indicating a similar acetate coupling in islandicin as there is in 3-hydroxyphthalic acid.

From a second fraction, violet in UV-light, small amounts of two further anthraquinones could be isolated after repeated running on thick paper chromatogram. One of them was catenarin which has recently been found by Shibata *et al.*[7] in *P. islandicum*. It was identified by the absorption spectrum and the melting point 246°C. The other anthraquinone was emodin, which was recognized by its R_F value on the paper chromatogram. Extraction of the emodin from the paper and adding unlabelled emodin as a carrier to the extract resulted in substantial amount of this compound. It could then be recrystallized to constant radioactivity. Emodin has earlier been found in higher plants and in higher fungi.

EXPERIMENTAL

Culture conditions. Four flasks, each containing 500 ml of Czapek-Dox medium, were cultivated according to Howard and Raistrick [5] for thirteen days. At that time a solution of 1 mC of $CH_3{}^{14}COONa$ was equally distributed to the four flasks and the growth was allowed to continue for further eight days. The mycelium was filtered off and washed with distilled water.

Culture medium. The culture medium was neutralized with solid Na_2CO_3 and concentrated in vacuum to about 600 ml. It was acidified with concentrated HCl and extracted four times with ether. The ether phases were extracted with 0.5 N $NaHCO_3$. The ether solution did not contain any radioactivity after the extraction. The hydrogen carbonate solution was acidified with HCl and extracted with ether. After drying the ether solution with anhydrous Na_2SO_4 it was evaporated to a small volume. The residue was placed on Whatman paper No. 3 and the chromatogram developed in a solvent containing chloroform-methanol-formic acid (4 %) (10 : 1 : 1). The 3-hydroxyphthalic acid (R_F about 0.15) was cut out and eluted with ethanol. The strongly colored ethanol extract was put on a silica gel column with water as the solvent. The 3-hydroxyphthalic acid fraction was collected and extracted with ether. The ether extract was then further purified by paper chromatography as described above. The ethanol solution was concentrated in vacuum and the concentrate evaporated to dryness at room temperature and atmospheric pressure. The substance isolated melted at 155—157°C and the melting point was not depressed on admixture with authe tic 3-hydroxyphthalic acid.

The compound A that was detected by its aborption in UV-light was cut out of the paper chromatogram and purified in the same way as 3-hydroxyphtalic acid.

Degradation of 3-hydroxyphthalic acid. (All radioactive measurements are listed in Table 1.) 311 mg of unlabelled, synthetic 3-hydroxyphthalic acid were added to the radioactive 3-hydroxyphthalic acid, isolated from the culture medium, and the mixture dissolved in acetone. The acetone solution was evaporated to dryness at room temperature. A portion of the substance was totally combusted according to van Slyke and Folch [8]. The carbon dioxide was trapped in a barium hydroxide solution. The barium carbonate was isolated and its radioactivity measured. Throughout the work the same amount of barium carbonate (15 mg) has been used for the measurements of the radioactivity and with the same apparatus as reported earlier.

Decarboxylation of 3-hydroxyphtalic acid. 100.9 mg of 3-hydroxyphthalic acid were dissolved in 20 ml of diluted H_2SO_4 (1:1). The solution was refluxed for 25 min. The

Table 1. ^{14}C-Distribution in 3-hydroxyphthalic acid.

Material	Number of C-atoms from 3-hydroxy-phthalic acid	Radio-activity counts/min	Total radio-activity of the material counts/min.	Numbers of COOH-groups according to the acetate theory	
				Found	Calculated
1	2	3	4	5	6
3-Hydroxyphthalic acid (total comb.)	8	739	5 912	3.96	4
COOH-Group (2-position)	1	1 495	1 495	1	1
m-Hydroxybenzoic acid (total comb.)	7	644	4 508	3.01	3
COOH-Group (1-position)	1	79	79	0.05	0
Picric acid (total) comb.)	6	734	4 404	2.95	3
Bromopicrin (C-atoms from 2,4,6-positions)	3	2	6	0	0
CO_2 from the hypo-bromite degradation (C-atoms from 1,3,5-positions)	3	1 361	4 083	2.74	3

The numbers of the COOH-groups in column 5 are obtained by taking the radioactivity of the COOH-group from 2-position as the basis for the calculations. This COOH-group is supposed to derive directly from the COOH-group in acetic acid.

top of the condensor was connected with a barium hydroxide solution. A stream of carbon dioxide free nitrogen was flushed through the system to force the evolved carbon dioxide into the barium hydroxide solution. The barium carbonate was isolated and its radioactivity measured. The sulfuric acid solution was diluted with water and then extracted four times with ether. The residue from the ether extract was recrystallized twice from water yielding 52.7 mg of *m*-hydroxybenzoic acid, m. p. 200°C. A part of the *m*-hydroxybenzoic acid was combusted as above while the remaining acid was diluted 5.22 times with nonradioactive *m*-hydroxybenzoic acid by recrystallization from 3.5 ml of water. All radioactive values listed have been corrected to correspond to the most diluted state.

Nitration of m-hydroxybenzoic acid. The nitration was made according to Wolffenstein and Paar [9]. 0.78 ml of HNO_3 (*d* 1.52) was added to 208 mg of *m*-hydroxybenzoic acid and the mixture evaporated to dryness on a steam bath. This procedure was repeated with the same amount of HNO_3. After extracting the residue three times with boiling benzene, 2,4,6-trinitro-*m*-hydroxybenzoic acid crystallized from the benzene solution. Yield 203 mg, m. p. 180°C.

Decarboxylation of 2,4,6-trinitro-m-*hydroxybenzoic acid.* 203 mg of trinitro-*m*-hydroxybenzoic acid were suspended in 5 ml of glycerol and the mixture refluxed for 20 min. The carbon dioxide was trapped in barium hydroxide solution and the radioactivity measured as above. The glycerol solution was diluted with water, acidified with HCl and extracted five times with ether. The ether solution was evaporated to dryness and the picric acid recrystallized from diluted sulfuric acid. Yield 130 mg, m. p. 120°C. About 10 mg of the picric acid were combusted and the radioactivity measured.

Hypobromite degradation of picric acid. 70 mg of picric acid were added at 0°C to a carbonate free solution of barium hypobromite (from 2.8 mg of barium hydroxide and 0.38 ml of bromine in 60 ml of water). After keeping the mixture at room temperature for 30 min, the bromopicrin was isolated by steam distillation, washed with diluted HCl and water, combusted as above and the radioactivity of the barium carbonate measured. The barium carbonate formed during the reaction was filtered off and washed with water. It was purified by recycling the carbon dioxide into a fresh solution of barium hydroxide. The barium carbonate was isolated and the radioactivity measured.

The mycelium. The mycelium was air dried and extracted with chloroform in a Soxhlet apparatus. The chloroform solution was concentrated to a small volume on the steam bath and then dried at room temperature. Islandicin, catenarin and emodin were isolated as described above. After sublimation and recrystallization from glacial acetic acid the yield of islandicin was 600 mg, m. p. 218°C.

The fractions from the silica gel column containing catenarin and emodin were developed on paper chromatogram (Whatman No. 3) in a solvent consisting of benzene-formic acid (2 %) (10 : 1). Catenarin has R_F 0.45 and emodin R_F 0.50. The anthraquinones were extracted from the paper with acetone and identified as already mentioned in this paper.

The author wishes to thank Professor G. Ehrensvärd for many helpful discussions. Thanks are also due to Cand.Mag. P. Barbesgaard for preparing the mutant used in this work.

REFERENCES

1. Birch, A. J., Massy-Westropp, R. A. and Moye, C. J. *Australian J. Chem.* **8** (1955) 539.
2. Birch, A. J., Massy-Westropp, R. A., Rickards, R. W. and Smith, H. *J. Chem. Soc.* **1958** 360.
3. Gatenbeck, S. *Acta Chem. Scand.* **12** (1958) 1211.
4. Gatenbeck, S. *Acta Chem. Scand.* **11** (1957) 555.
5. Howard, B. H. and Raistrick, H. *Biochem. J.* **44** (1949) 227.
6. Howard, B. H. and Raistrick, H. *Biochem. J.* **57** (1954) 212.
7. Shibata, S., Takido, M. and Nakajima, T. *Pharm. Bull. Tokyo* **3** (1955) 286.
8. *Cf.* Calvin, Heidelberg, Reid, Tolbert and Yankwich, *Isotopic Carbon*, Wiley, New York 1949, p. 92.
9. Wolffenstein, R. and Paar, W. *Ber.* **46** (1918) 598.

Received August 27, 1958.

ACTA CHEMICA SCANDINAVICA 12 (1958) 1990—1996

On the Metabolism of Thiosulfate Esters

BO SÖRBO

Research Institute of National Defense, Medical Dept., and Nobel Medical Institute, Biochemical Dept., Stockholm, Sweden

An enzyme has been demonstrated in rat liver, which converts sulfocysteine to thiosulfate, ammonia and pyruvate. No thiosulfate is formed from aminoethylthiosulfuric acid. Sulfite is formed from both these thiosulfate esters when they are incubated with liver homogenate under anaerobic conditions, and the reaction is augmented by heat denaturation of the homogenate. The reaction is attributed to a nonenzymic reaction with protein bound thiol groups. A possible use of thiosulfate esters as protective substances against ionizing radiation is suggested.

Thiosulfate esters have so far not attracted much interest from a biochemical point of view. One ester, sulfocysteine * [$COOHCH(NH_2)CH_2S_2O_3H$], was demonstrated by Clarke [1] to be a reaction product from cystine and sulfite, but was apparently not considered as a possible normal metabolite. Later work with mould mutants [3,4] has, however, suggested that in these moulds, sulfocysteine may be an intermediate in the metabolic pathway leading from sulfate to cysteine. Recently Cavallini and Stirpe [5] administered sulfocysteine to rats and observed an increased excretion of thiosulfate. They suggested that the compound was deminated to ammonia, pyruvate and thiosulfate and that sulfocysteine was a precursor of the thiosulfate normally excreted in the urine from higher animals.

The present work was undertaken in order to study possible transformations of sulfocysteine and its decarboxylated analogue, β-aminoethylthiosulfuric acid (AETA) in the presence of rat liver and rat kidney. These two compounds were chosen for study as they are more stable than simple aliphatic thiosulfate esters. A preliminary report of the present work has appeared in this journal [6].

* Clarke originally proposed the name cysteine-S-sulfonate, but this could erroneously imply a thiosulfonate structure (RSO_2SH) instead of a thiosulfate ester structure (RS_2O_3H) for the compound. Recently [2] the name S-sulfocysteine has been suggested and it is used in the present paper.

MATERIALS

Attempts were first made to prepare sodium sulfocysteine according to Clarke [1], but in confirmation of the original report it was found that the product obtained was contaminated with copper ions. These could not be removed by cation exchangers; presumeably the copper ions were complexed by sulfocysteine. Attempts to remove the copper by treating the sample with H_2S led to immediate decomposition of the sulfocysteine. The following improved method for the preparation of the compound, giving a copper free product, was then worked out. To 2.4 g cystine (10 mmole) dissolved in 80 ml water and 5 ml 25 % ammonia was added 12.6 g $Na_2SO_3 \cdot 7H_2O$ (50 mmole) and the solution left for 1 h. 30 % H_2O_2 was then added dropwise with efficient stirring until no free cysteine could be detected with phosphotungstic acid [7]. About 3 ml H_2O_2 were required. The solution was then neutralized with 2.4 ml anhydrous acetic acid, and 15 ml 2 M barium acetate solution was added. Barium sulfate was centrifuged off and the supernatant taken to dryness *in vacuo*. The residue was treated successively with 50, 25 and 15 ml hot 95 % ethanol in order to remove sodium acetate, and the ethanol insoluble residue was then dissolved in 6 ml H_2O. By addition of one volume of 95 % ethanol the sodium sulfocysteine was precipitated as crystals which were collected after one night in the refrigerator. 1.74 g of the compound (containing 3 moles of water per 2 moles of salt [1]) was obtained, corresponding to 34 % of the theoretical yield. Recrystallization from ethanol-water (1:1) gave 1.54 g of pure product.

AETA [8] was a gift from Dr. B. Hansen.

METHODS

Thiosulfate was determined colorimetrically as previously described [9]. Sulfate was determined by a turbidimetric method modified from that of Gassner and Friedel [10]. To 3 ml of the sample was added 0.3 ml 2 M trichloroacetic acid and 5.7 ml water, and precipitated proteins centrifuged off. To 3 ml of supernatant was then added 0.4 ml gelatine reagent followed by 0.4 ml of barium chloride reagent [10]. The turbidity was measured in a 1 cm cuvette at 400 mμ against a blank, obtained by adding 0.8 ml gelatine reagent to another 3 ml aliquot of the supernatant. Sulfite was determined by a colorimetric procedure, based on that of West and Gaeke [11]. To the sample was added an equal volume of 0.2 M $HgCl_2$ and the precipitate was centrifuged off. To 0.5 ml of supernatant was then added 2.0 ml of 0.04 % *p*-rosaniline hydrochloride in 0.72 M HCl and 2.0 ml of 0.2 % formaldehyde, and after 3—7 min. the absorbance of 570 mμ was determined. A blank value was obtained by adding $HgCl_2$ to the test system before the thiosulfate ester. Pyruvic acid and ammonia were determined in trichloroacetic acid filtrates, the former according to Friedemann and Haugen [12] and the latter by nesslerization following aeration.

Paper chromatography was carried out with ascending development on Whatman paper No. 1 and either 75 % acetone-water or 80 % phenol-water as solvents. The samples were deproteinized either by trichloroacetic acid or by heating at 100°C for 2 min. The chromatograms were sprayed with ninhydrine or iodoplatinate [13] (the latter reagent demonstrated compounds containing oxidizable sulfur). The presence of disulfides on the chromatograms was in some cases verified by spraying with phosphotungstic acid-sulfite [14]. The identity of the pyruvate formed from sulfocysteine was also established by paper chromatography according to Wieland and Fisher [15].

RESULTS

When sulfocysteine was incubated with rat liver or kidney slices, small amounts of thiosulfate were formed (Table 1). With a rat liver homogenate instead of slices, the yield of thiosulfate was increased. The formation of thiosulfate was not dependent upon the presence of oxygen and the active system was heat labile (Table 1). No thiosulfate was formed from AETA under otherwise similar conditions. Further experiments demonstrated that the formation

Table 1. Thiosulfate formation from sulfocysteine. Sulfocysteine 0.01 M, pH 7.9, slices or homogenate corresponding to 50 mg of rat tissue per ml. Incubated 1 h in Warburg vessels with shaking at 37°. Experiments with slices were made in Ringer phosphate solution, experiments with homogenate in 0.025 M phosphate buffer.

Preparation	Gas phase	S_2O_3 formed μmole/ml
Liver slices	Air	0.18
Kidney »	»	0.13
Liver homogenate	»	0.64
» »	N_2	0.72
heated 2 min. at 100°C	Air	0

of thiosulfate from sulfocysteine was a zero order reaction (under the conditions indicated in Table 1). Active extracts could be prepared from acetone dried rat liver powder and they were not significantly inactivated by dialysis against 0.01 M sodium acetate at 4°C. When such dialyzed extracts were incubated with sulfocysteine the formation of pyruvate and ammonia besides thiosulfate could be easily demonstrated. When the three reaction products were quantitatively determined the results shown in Table 2 were obtained. The somewhat low yields of pyruvate and ammonia can be attributed to a conversion of these compounds to other products by the liver extract [16], and consequently the stoichiometry of the reaction is best represented by

$$-S_2O_3CH_2 \cdot CHNH_2 \cdot COOH + H_2O \rightarrow CH_3 \cdot CO \cdot COO^- + S_2O_3^{2-} + NH_4^+ + H^+$$

However, not only thiosulfate, but also sulfate was formed, when a rat liver homogenate was incubated with sulfocysteine while about the same amount of sulfate was obtained when sulfocysteine was replaced by AETA (Table 3). The responsible system was heat labile. As no sulfate was formed under anaerobic conditions a simple hydrolysis of the thiosulfate ester to sulfate could be excluded and it was then suspected that sulfate was formed through oxidation of another primary reaction product. (The possibility that thiosulfate was this primary product in case of sulfocysteine was excluded by the fact that thiosulfate is not oxidized to sulfate by liver homogenates [17]). A possible sulfate precursor would be sulfite, and this was in fact formed, when sulfocysteine or AETA was incubated with liver homogenates under

Table 2. Products from sulfocysteine. Test system contained 0.01 M sulfocysteine, 0.025 M phosphate and dialyzed acetone powder extract corresponding to 15 mg dry weight/ml. Incubated 1 h at 37° in air.

Experiment No.	S_2O_3 formed μmole/ml	NH_3 formed μmole/ml	Pyruvate formed μmole/ml
1	0.77	0.69	0.57
2	1.36	1.28	1.00
3	1.16	0.98	0.72

Table 3. Sulfate formation from thiosulfate esters. Substrate concentration 0.01 M, phosphate 0.025 M, pH 7.4, homogenate corresponding to 50 mg rat liver per ml. Incubated 1 h at 37°.

Substrate	Homogenate	Gas phase	SO_4 formed μmole/ml
Sulfocysteine	Unheated	Air	0.48
»	»	N_2	0
»	Heated 2 min. at 100°C	Air	0.04
AETA	Unheated	»	0.51
»	Heated 2 min. at 100°C	»	0.04

anaerobic conditions. No sulfite could be detected when the incubation was carried out in air as the sulfite was rapidly oxidized to sulfate, presumably through the action of the sulfite oxidase system [18]. It was somewhat unexpectedly found that heating of the homogenate did not destroy, but on the contrary stimulated sulfite formation (Table 4) and this could only in part be attributed to an inactivation of the heat labile sulfite oxidase, as this "activation" was observed also under anaerobic conditions (Table 4). Further experiments demonstrated that the sulfite formation was completely inhibited by 0.001 M *p*-chloromercuribenzoate, a sulfhydryl group reagent, which suggested that sulfite was formed through a reaction between the thiosulfate ester and a sulfhydryl group. As it is well known that heat denaturation liberates "masked" sulfhydryl groups in proteins, the effect of heat treatment on the homogenate indicated that the active sulfhydryl groups were mainly protein bound. This was also supported by the fact that dialysis of a heat denatured homogenate gave only a 25 % decrease of the sulfite forming activity. (The dialysis was carried out in a nitrogen atmosphere, as otherwise a large decrease of activity was obtained.) Of interest was also that sulfite was formed from sulfocysteine and heat denatured ovalbumin, a protein containing SH-groups, but not from sulfocysteine and the native protein. The

Table 4. Sulfite formation from thiosulfate esters. Conditions as in Table 3 except that the reaction time was only 10 min.

Substrate	Homogenate	Gas phase	SO_3 formed μmole/ml
Sulfocysteine	Unheated	Air	0
»	»	N_2	0.18
»	Heated 2 min. at 100°C	Air	0.38
»	»	N_2	0.55
AETA	Unheated	Air	0
»	»	N_2	0.23
»	Heated 2 min. at 100°C	Air	0.41
»	»	N_2	0.53

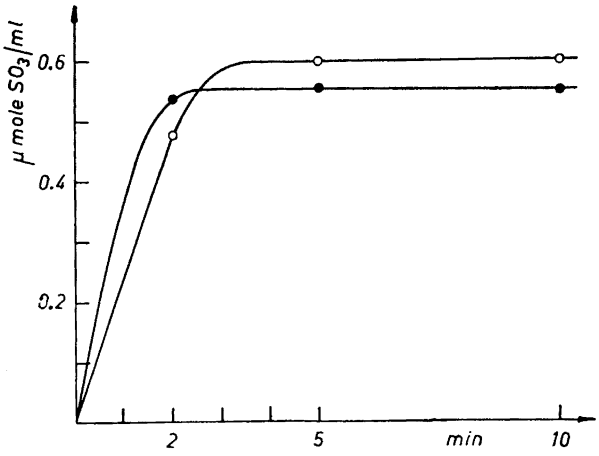

Fig. 1. Relation between glutathione and thiosulfate esters. Thiosulfate ester conc. 0.01 M, glutathione 1 μmole/ml, pH 7.4 and temp. 20°C.
○ ○ ○ Sulfocysteine ● ● ● AETA

reaction between a thiosulfate ester and a sulfhydryl compound gives sulfite and a mixed disulfide according to Ref.[2]

$$R_1SSO_3H + R_2SH \rightarrow R_1SSR_2 + H_2SO_3$$

In the present case the mixed disulfide should be protein bound. Indirect evidence for a formation of a protein bound disulfide from the thiosulfate ester and liver homogenate could in fact be obtained. When the reaction mixtures were deproteinized with trichloroacetic acid, paper chromatography did not reveal any reaction products containing amino groups or sulfur in the supernatant (except thiosulfate in the case of sulfocysteine), but when deproteinization was carried out by heat denaturation, cystine and cystamine were detected in the sulfocysteine and AETA system, respectively. The formation of these symmetrical disulfides could be attributed to a rearrangement of the primary formed mixed disulfide by the heating steps according to 2 PSSR → $(PS)_2 + (RS)_2$ (where P indicates protein).

The formation of sulfite with a simple sulfhydryl compound, glutathione, was also studied for comparative purposes (Fig. 1). It is evident that the reaction stops, when an equilibrium point is reached, as already demonstrated by Stricks and Kolthoff [19] in similar systems by a polarographic technique. The reaction between the thiosulfate esters and inorganic sulfide was also studied, but in this case the reaction was more complicated, as not only sulfide but also thiosulfate was formed. The time course of these reactions in shown in Fig. 2. The results can be explained by a primary formation of sulfite and a persulfide, followed by a slower transsulfuration according to

$$RSSO_3^- + HS^- \rightarrow RSSH + SO_3^{2-} \rightarrow RSH + S_2O_3^{2-}$$

as already suggested by Gutman [20]. Under the reaction conditions used in

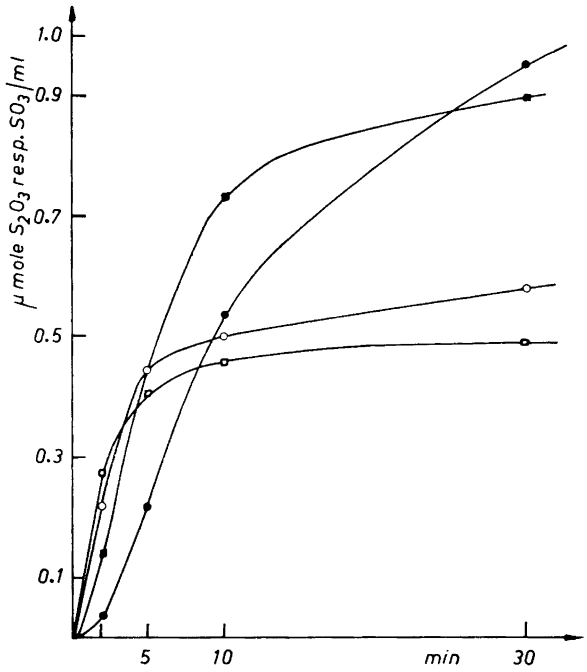

Fig. 2. Relation between inorganic sulfide and thiosulfate esters. Conditions as in Fig. I except that glutathione was replaced by Na_2S, 0.99 μmole/ml.

● ● ● ● Thiosulfate formed from sulfocysteine
■ ■ ■ ■ Thiosulfate from AETA
○ ○ ○ ○ Sulfite from sulfocysteine
□ □ □ □ Sulfite from AETA

this work the thiosulfate ester was present in excess, and consequently the following reaction also occurred

$$RSSO_3^- + RSH \rightarrow (RS)_2 + HSO_3^-$$

as is evident from the fact that the molar yield of sulfite plus thiosulfate was in excess over the sulfide added to the system (*cf.* Fig. 2). The formation of cystine and cystamine, respectively, in the systems was confirmed by paper chromatography, but no persulfide was detected, presumably due to the instability of the latter. The results obtained have a certain resemblance to those obtained in a study of the reaction between a thiosulfonate ester (disulfoxide) and inorganic sulfide [21]. The reaction products were here found to be sulfinate, as expected, but a disulfide and thiosulfonate instead of the expected persulfide.

DISCUSSION

The present work has demonstrated an enzymic formation of thiosulfate from sulfocysteine, with pyruvate and ammonia as the other reaction products, thus confirming the suggestion of Cavallini and Stirpe [5]. This reaction shows a resemblance to the cysteine desulfhydrase reaction [22], where hydrogen sulfide,

pyruvate and ammonia are formed from cysteine, when the latter is incubated with liver. As sulfocysteine is structurally related to cysteine, the same enzyme system may be responsible for both these reactions. It is of interest here that the thiosulfate formation from sulfocysteine in the presence of liver homogenate was strongly inhibited by semicarbazide (87 % inhibition at 0.001 M inhibitor conc.) and thus also in this respect similar to cysteine desulfhydrase [21]. Concerning the possibility that sulfocysteine is a precursor for thiosulfate in higher animals, the available data do not indicate that sulfocysteine is of importance in this respect. It was previously [2] demonstrated that thiosulfate is rapidly formed from β-mercaptopyruvate and sulfite in the presence of liver, and the ability of a liver homogenate to form thiosulfate by this reaction is about 10^4 times higher than its catalytic activity on sulfocysteine.

The ability of thiosulfate esters to form mixed disulfides is of interest in connection with chemical protection against ionizing radiation. Eldjarn and Pihl [23] have attributed the protecting properties of certain sulfhydryl and disulfide compounds (for instance cysteamine) to their ability to form mixed disulfides with proteins. If this theory is valid one should expect that also thiosulfate esters have radiation protective properties and this has, as a matter of fact, been experimentally verified for AETA in connection with the present work [24]. Experiments with other thiosulfate esters are now in progress.

The valuable technical assistance of Mrs. E. Ekblom is gratefully acknowledged.

REFERENCES

1. Clarke, H. T. *J. Biol. Chem.* **97** (1932) 235.
2. Swan, J. M. *Nature* **180** (1957) 643.
3. Hockenhull, D. J. D. *Biochim. et Biophys. Acta* **3** (1949) 326.
4. Shepherd, C. J. *J. Gen. Microbiol.* **15** (1956) 29.
5. Cavallini, D. and Stirpe, F. *Atti accad. nazl. Lincei, Rend. Classe sci. fis. mat. e nat.* **20** (1956) 378.
6. Sörbo, B. *Acta Chem. Scand.* **12** (1958) 1358.
7. Folin, O. *J. Biol. Chem.* **106** (1934) 311.
8. Bretschneider, H. *Österr. Akad. Wiss. Math.-naturw. Kl. Sitz. ber. Abt. IIb* **159** (1950) 372.
9. Sörbo, B. *Biochim. et Biophys. Acta* **24** (1957) 324.
10. Gassner, K. and Friedel, H. *Z. anal. Chem.* **152** (1956) 420.
11. West, P. W. and Gaeke, G. C. *Anal. Chem.* **28** (1956) 1816.
12. Friedemann, T. E. and Haugen, G. E. *J. Biol. Chem.* **148** (1943) 415.
13. Toennies, G. and Kolb, P. *Anal. Chem.* **23** (1951) 823.
14. Cavallini, P., de Marco, C. and Mondovi, B. *Ricerca Sci.* **25** (1955) 2901.
15. Wieland, T. and Fischer, E. *Naturwiss.* **36** (1949) 219.
16. Smythe, C. V. *J. Biol. Chem.* **142** (1942) 387.
17. Pirie, N. W. *Biochem. J.* **38** (1934) 1063.
18. Heimberg, M., Fridovich, I. and Handler, P. *J. Biol. Chem.* **204** (1953) 913.
19. Stıicks, W. and Kolthoff, I. M. *J. Am. Chem. Soc.* **73** (1951) 4569.
20. Gutmann, H. *Chem. Ber.* **48** (1915) 1162.
21. Sörbo, B. *Biochim. et Biophys. Acta* **22** (1956) 570.
22. Fromageot, Cl. in Sumner, J. B. and Myrbäck, K. *The Enzymes* **Vol. I** Academic Press, Inc., New York 1951, p. 1237.
23. Eldjarn, L. and Pihl, A. *J. Biol. Chem.* **223** (1956) 341.
24. Holmberg, B. and Sörbo, B. *To be published.*

Received September 1, 1958.

ACTA CHEMICA SCANDINAVICA 12 (1958) 1997—2006

Cellular Localisation, Solubilization and Separation of Intestinal Glycosidases

BENGT BORGSTRÖM and ARNE DAHLQVIST

Department of Physiological Chemistry, University of Lund, Lund, Sweden

Invertase, maltase and trehalase activities of hog small intestinal mucosa are localized in the microsome fraction obtained from a homogenate on differential centrifugation.

Trypsin causes a solubilization of the glycosidases from the microsomes. During specified conditions the invertase and maltase activities are not affected by trypsin, and trehalase activity only to a minor extent. A method for preparation of soluble glycosidases based on this finding is described.

Trehalase activity of this soluble preparation in contrast to invertase and maltase activities, is destroyed by exposure to ethanol at +4°C. Intestinal trehalase, therefore, must be an enzyme separate from maltase and invertase.

Trehalase activity is also obtained as a separate peak by column chromatography on substituted cellulose (DEAE-cellulose), while invertase and maltase activities could not be completely separated. A change in the ratio of maltase to invertase activity during elution from 1.0 to 6.4, however, indicates the separate identity also of these two enzymes.

The disaccharide hydrolases of mammalian intestine are usually described as maltase, invertase and lactase. According to the specificity theory of Weidenhagen, intestinal invertase and maltase should only be two activities of one and the same enzyme, an α-D-glucopyranosidase, capable of hydrolyzing all α-D-glucopyranosides [1]. With the same nomenclature, lactase, which is well known to be a separate enzyme [2], should be a β-D-galactopyranosidase.

That intestinal extracts from certain mammals are also able to hydrolyze trehalose (1-*O*-α-D-glucopyranosyl-α-D-glucopyranoside) has been known for a long time [3], but it has never been shown if intestinal trehalase is a separate enzyme, or if it is identical with the α-D-glucopyranosidase supposed by Weidenhagen. In many lower organisms, trehalase has been found to be a special enzyme, separable from maltase [3].

Experimental results have been reported, which make the assumption of one single intestinal α-D-glucopyranosidase questionable. Intestinal extracts cannot hydrolyze methyl-α-D-glucopyranoside, which shows that not all α-D-

glucopyranosides can be hydrolyzed [4,5]. Recently it has been reported that activities against nigerose (3-*O*-α-D-glucopyranosyl-D-glucose) and *iso*maltose (6-*O*-α-D-glucopyranosyl-D-glucose) in intestinal extracts from swine have been partially separated from maltase activity [6–8]. All α-D-glucopyranosides which can be hydrolyzed by intestinal enzyme preparations therefore do not seem to be hydrolyzed by the same enzyme.

In the present paper are reported studies of glycosidases from swine small intestinal mucosa: invertase, maltase, trehalase and lactase. These glycosidase activities were found to be particle-bound in intestinal mucosa preparations, and their solubilization from the particles has been studied. Chromatography of the solubilized enzyme solution on substituted cellulose (DEAE-cellulose) according to Peterson and Sober [9] has indicated the presence therein of three separate α-D-glucopyranosidases, *i. e.* trehalase, invertase and maltase.

RESULTS AND DISCUSSION

Differential centrifugation of mucosa homogenate. Freshly prepared intestinal mucosa from swine was homogenized with 4 parts (volume/weight) of 0.25 M sucrose, previously chilled to prevent its enzymatic hydrolysis. In the first experiments a homogenizer of the Potter-Elvehjem type [10] with a plastic pestle was used. This was, however, found to give incomplete homogenization, with a great part of the enzymes remaining in intact cells. Later an "Ultra Turrax" homogenizer was used with a homogenization time of 2 min and a volume of about 100 ml. After homogenization, the sample was centrifuged at 600 *g* for 10 min to remove whole cells and nuclei. The supernatant from this centrifugation is henceforth named total homogenate.

In the experiments where the "Ultra Turrax" homogenizer was used, the total homogenate was more enzyme-rich, but both homogenization techniques gave the same results in the subsequent fractionation.

The total homogenate obtained contained 20—30 units of invertase per ml. The other glycosidases were determined in homogenates made with buffer instead of sucrose solution, or in homogenates from which the sucrose had been removed by dialysis against distilled water (this procedure does not affect the glycosidase activity). The ratios of the other glycosidase activities to invertase activity were relatively constant, being about 2.0 for maltase, 0.5 for trehalase, and 0.2 for lactase.

The total homogenate was fractionated in a "Spinco" preparative ultracentrifuge [11]. The mitochondria were first sedimented at 7 000 *g* for 20 min (rotor 40, 10 000 RPM). The sediment was resuspended in 0.25 M sucrose and centrifuged once more at 7 000 *g*. The combined supernatants were centrifuged at 100 000 *g* for 45 min (rotor 40, 40 000 RPM) to give the microsome fraction and the particle-free supernatant. The invertase activity was found to be mainly localized in the microsome fraction (Table 1).

The microsomes were washed with distilled water, and the remaining sucrose removed by dialysis before determination of maltase, trehalase, and lactase activities. The microsomes were found to have the same ratios of action upon maltose, trehalose, and lactose as the total homogenate. These activities

Table 1. Differential centrifugation of homogenate from intestinal mucosa. Homogenized with "Ultra Turrax" homogenizer in 4 parts (v/w) of 0.25 M sucrose. Volume of the homogenate 10 ml.

Fraction	Units of invertase	Invertase % of total	Milligrams of protein	Specific invertase activity
Total homogenate	330	(100)	315.0	1.05
Mitochondria (7 000 *g* for 20 min.)	21	6.4	28.5	0.74
Microsomes (100 000 *g* for 45 min.)	276	83.7	72.0	3.83
Particle-free supernatant	36	10.9	210.0	0.17

must therefore also be localized in the microsomes. (Of the small amounts of amylase present, less than 25 % was localized in the microsome fraction.)

Solubilization of the glycosidases from the microsome fraction. Different methods were tried to solubilize the glycosidases. Treatment with distilled water or repeated freezing and thawing, which has been found to release some particle-bound enzymes [12], were without effect in the present case. Larner and Gillespie, who had found intestinal maltase and oligo-1,6-glucosidase localized in the microsomes, used acetone powder extracts for fractionation [13]. They have not, however, reported any criterion that the enzymes really were brought into solution by the acetone treatment. We have found the glycosidase activities in acetone powder extracts from intestinal mucosa readily sedimentable in the ultracentrifuge at 100 000 *g* for 45 min (rotor 40, 40 000 RPM), which shows that no solubilization occurs with this method. Treatment with *n*-butanol according to Morton [12], resulted in a partial inactivation of the enzymes, without any solubilization. Nor did snake venom [14] give any solubilization (0.2 mg *Crotalus adamanteus* venom/ml in 0.1 M acetate buffer pH 6.5, incubated for 5 h at 37°C).

Sodium desoxycholate has been found to solubilize most of the proteins from isolated liver microsomes [15]. When intestinal microsomes were treated with 0.5 % sodium desoxycholate in 0.1 M phosphate buffer pH 7.5, the glycosidases remained in a perfectly clear supernatant upon centrifugation at 100 000 *g* for 45 min. Together with the glycosidases about 80 % of the microsome protein remained in the supernatant. In spite of this, it could however be demonstrated in different ways that the glycosidases still were particulate:

1) The desoxycholate extract was dialyzed against phosphate buffer pH 7.5 to remove the desoxycholate. The effect of the dialysis was controlled by isotope-carbon-labelled desoxycholate, added to give 13 620 c.p.m. per ml. After dialysis for 72 h less than 0.5 % of the radioactivity remained. When now centrifuged at 100 000 *g*, the glycosidases slowly sedimented into a transparent, yellow pellet. If sodium desoxycholate was added to the sample before centrifugation, the glycosidases again remained in the supernatant.

2) When a desoxycholate extract was brought to pH 5.0 by the addition of acetate buffer, it became turbid, and the glycosidases sedimented readily in

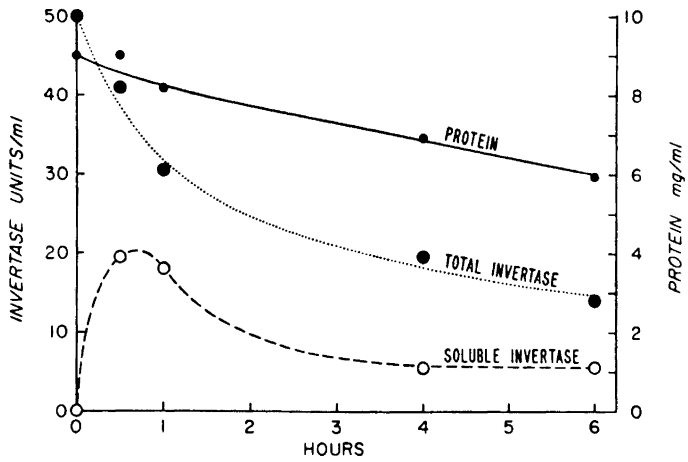

Fig. 1. Digestion of intestinal microsomes by trypsin in the absence of buffer. A suspension of microsomes in distilled water was added with 1 mg of trypsine per ml and incubated at 37°C. Soluble invertase was determined after ethyl alcohol precipitation (see the text) and (undigested) protein after precipitation with 5 % trichloroacetic acid.

an ordinary laboratory centrifuge (Wifug, 4 000 RPM for 10 min). This seems to be caused by agglutination of the particles at pH 5.0, a phenomenon which is well known [16].

3) When a desoxycholate extract was precipitated with ethyl alcohol in the cold, and the precipitate suspended in distilled water, all the invertase, maltase, and lactase activities were retained in the suspension (but the trehalase was partly inactivated by exposure to ethyl alcohol). When then centrifuged in Wifug at 4 000 RPM for 30 min, the glycosidases sedimented. The effect of ethyl alcohol precipitation seems to be the removal of desoxycholate, as the addition of desoxycholate after suspension of the precipitate retained the glycosidases in the supernatant.

When isolated microsomes were suspended in distilled water and incubated with trypsin, the glycosidases were inactivated parallel with the digestion of protein (Fig. 1). In the beginning of the reaction a solubilization of the glycosidases was, however, found to occur.

In the presence of phosphate buffer pH 7.5, the course of the reaction was found to be different (Fig. 2). In spite of the rapid digestion of protein, the invertase and maltase activities were unaffected even in a strong trypsin solution, and the enzymatic activity obtained in solution. The maltase activity indeed increased somewhat during the solubilization. The trehalase and lactase activities, on the other hand, decreased slightly during trypsin digestion. However, even in a solution containing 2 mg of trypsin per ml, incubated at 37°C for 4 h, less than 50 % of the lactase and trehalase activities were inactivated in the presence of phosphate.

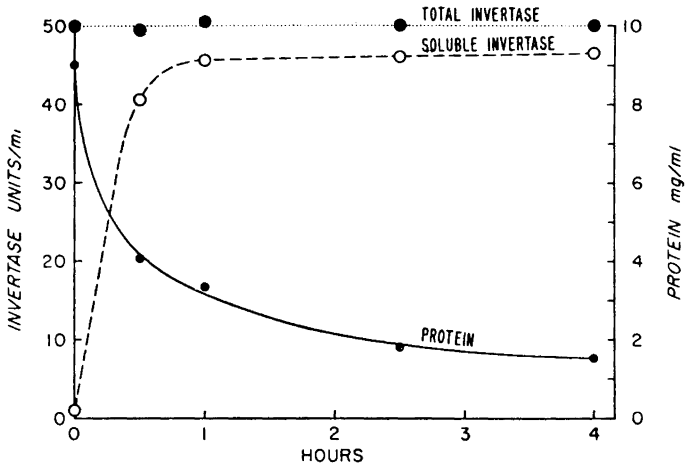

Fig. 2. Digestion of intestinal microsomes by trypsin in the presence of phosphate buffer. The same conditions as described in Fig. 1, but in the presence of 0.1 M phosphate buffer pH 7.5.

The influence of phosphate is not clearly understood. It was found that phosphate could be replaced by some other buffers as borate or tris-(hydroxymethyl) aminomethane but not by veronal buffer. Phosphate is not the only factor that is needed for protection of the glycosidases against trypsin digestion. When a solubilized glycosidase preparation, purified by ethyl alcohol precipitation, containing 5 mg of protein and 100 units of invertase per ml was incubated with 2 mg of trypsin per ml in 0.1 M phosphate buffer pH 7.5 at 37°C for 4 h, less than 10 % of the invertase and maltase activities remained. When, however, a boiled suspension of intestinal microsomes, with a protein content about equal to the purified glycosidase preparation, was added to the reaction mixture, 100 % of the maltase and 75 % of the invertase activities survived digestion under the same conditions.

The degree of solubilization of the glycosidases was measured after ethyl alcohol precipitation. A sample was precipitated in the cold with 5 parts of ethyl alcohol. After centrifugation, the sediment was suspended in distilled water to the original volume of the sample. The total glycosidases were determined on a sample of the suspension, and the rest was centrifuged in Wifug at 4 000 RPM for 20 min. The clear supernatant contained the soluble glycosidases, while the particle-bound glycosidases were found in the sediment.

Glycosidases from hog small intestinal contents. Intestinal contents from hog, obtained by gentle milking out by hand from an excised piece of intestine immediately after the slaughter, was found to contain rather much invertase (50—60 units per ml) and the same proportions of maltase, trehalase, and lactase as in the intestinal mucosa.

The glycosidases in intestinal contents seem to be in real solution. They are not sedimentable in the ultracentrifuge even after prolonged dialysis, they

Table 2. Comparison of the properties of invertase in the intestinal microsomes and the intestinal contents from swine.

	Intestinal microsomes	Intestinal contents
Optimum pH for sucrose hydrolysis	6.3–6.8	6.3–6.8
Optimum pH for melezitose hydrolysis	6.3–6.8	6.3–6.8
K_S for sucrose hydrolysis	2.5×10^{-2}	2.5×10^{-2}
K_S for melezitose hydrolysis	2.6×10^{-1}	2.8×10^{-1}
Action on melezitose *	0.002	0.002
Action on sucrose		
Action on raffinose	0	0

* Number of totally hydrolyzed melezitose molecules [22], divided with number of hydrolyzed sucrose molecules in 0.1460 M substrate concentration (5.0 % sucrose, 7.89 % melezitose . $2H_2O$) at pH 6.5 and temperature 37°C.

do not sediment in a centrifuge at pH 5.0, and they are readily soluble in distilled water after precipitation with ethyl alcohol.

To investigate if the glycosidases in the intestinal contents were identical with those obtained from the intestinal mucosa, some properties of the invertase from the two sources were compared (Table 2). The good agreement seems to show, that the enzyme preparations obtained from the two sources are identical.

When isolated microsomes were incubated with intestinal contents, a rapid solubilization of the glycosidases from the microsomes was found to occur.

Preparation of soluble intestinal glycosidases. The richest source for preparation of intestinal glycosidases was the material obtained by hard manual pressure or by pressing between two rolls pieces of the upper small intestine of hog. This material consists of the intestinal contents together with part of the intestinal mucosa and has an invertase activity of 100—150 units and a protein content of 50—60 mg/ml. If this material was frozen immediately, and thawed just before analysis, over 50 % of the invertase could be demonstrated to be in particular form, and in most cases it contained enough proteolytic enzymes to solubilize the glycosidases within 1—2 h at room temperature.

After storage for a few hours at room temperature, the material was chilled to 0°C and precipitated with 2 volumes of ethyl alcohol, previously chilled to —14°C. After centrifugation at 600 *g* for 10 min (International Refrigerated Centrifuge 2 000 RPM) the clear green supernatant was discarded, and the sediment suspended in its original volume of distilled water. By another centrifugation at 600 *g* a thick sediment, containing 2/3 of the protein, was obtained, while all glycosidase activity remained in the opalescent supernatant. The supernatant was then centrifuged in the Spinco ultracentrifuge at 35 000 *g* for 20 min (rotor 30, 20 000 RPM) to give a light yellow, clear supernatant. This supernatant was precipitated with 2 volumes of chilled ethyl alcohol and again centrifuged at 600 *g*. The sediment was yellow-stained, gelatinous, and

dissolved instantaneously in a small volume of distilled water to give a clear, yellow solution. The remaining ethyl alcohol was removed by dialysis against distilled water.

The solution thus obtained contained all the invertase, maltase, and lactase activities of the original material. The trehalase activity was found to be partly destroyed by exposure to ethyl alcohol at low temperature (Table 3), which clearly demonstrates that intestinal trehalase is an enzyme separate from maltase, invertase, and lactase. By keeping the solutions well chilled and avoiding unnecessarily long exposure to ethyl alcohol, about 50 % of the original trehalase activity could be obtained in the final solution.

The preparation obtained had a specific invertase activity of 55—60 units per mg of protein, which is about 50 times that in homogenates from intestinal mucosa.

Table 3. Action of ethyl alcohol on intestinal glycosidases. After ethanol treatment, the glycosidases are sedimented by centrifugation, and the sediment dissolved in water to the original volume. Invertase, maltase, and lactase activities are not affected by ethyl alcohol, but the trehalase activity is inactivated.

	Activity before treatment with ethyl alcohol units/ml	Activity after treatment with 60 vol. % ethyl days at +4°C units/ml	Per cent of activity remaining after ethyl alcohol treatment
Invertase	214	218	102
Maltase	325	324	99.5
Trehalase	78.5	5	6.5
Lactase	30	30	100

Separation of intestinal glycosidases on DEAE-cellulose. Columns of 0.5 g of DEAE-cellulose (dry weight) equilibrated with 0.01 M phosphate buffer pH 6.0 were used. A solution of solubilized glycosidases, containing 1 500 units of invertase, 3 000 units of maltase, 200 units of lactase, 400 units of trehalase, and 31 mg of protein, was dialyzed against 0.01 M phosphate buffer pH 6.0 and then applied to the column. The chromatogram was then developed with phosphate buffer pH 6.0 with a molarity continuously increasing from 0.01 to 0.16 M (Fig. 3). The rate of flow was 9 ml/h, and each fraction was collected over a 30 min interval.

1/4 of the total protein came out in the first three fractions, before any rise in molarity had occurred in the outcoming buffer. In this peak none of the glycosidases investigated could be detected. Already at 0.015 M phosphate the trehalase activity began to appear in the effluent. The lactase activity began to come out at 0.06 M phosphate and the invertase and maltase activities at 0.08 M phosphate. Thus trehalase, lactase, and invertase activities were clearly separated from each other. The maltase and invertase activities came out within the same interval, but the ratio of maltase activity to invertase activity increased from 1.0 at the beginning of the peak to 6.4 at its end (Table 4).

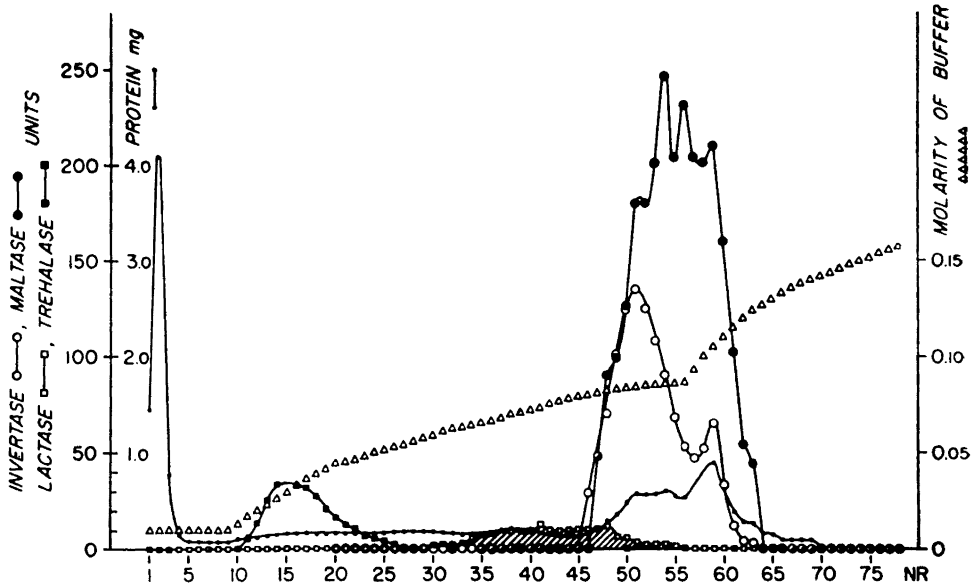

Fig. 3. Separation of intestinal glycosidases on DEAE-cellulose in phosphate buffer pH 6.0. The molarity of the effluent was determined by conductometry. The irregularity of the gradient around tube 52 is caused by a technical manipulation. For practical purposes all zero values for enzymatic activity are not shown in the figure.

It therefore seems probable that these activities are not caused by one single enzyme, as proposed by Weidenhagen [1] but that two different enzymes are involved in the hydrolysis of these sugars. It is, however, not possible at present, to say if there is one specific maltase and one specific invertase, or if

Table 4. Ratio maltase/invertase in fractions from the chromatography shown in Fig. 3.

Fraction No.	Invertase units/ml	Maltase units/ml	Ratio $\frac{\text{Maltase}}{\text{Invertase}}$
47	16.0	16.0	1.0
48	23.6	30.0	1.3
49	33.6	33.0	1.0
50	41.2	42.0	1.0
51	44.8	60.0	1.3
52	41.6	60.0	1.4
53	36.0	67.0	1.7
54	30.0	82.0	2.7
55	22.4	68.0	3.0
56	17.0	77.0	4.5
57	15.6	68.0	4.4
58	17.2	67.0	3.9
59	20.8	67.0	3.2
60	8.0	51.0	6.4

there are two enzymes with different relative activities against these two sugars. Chromatography of the enzymes on DEAE-cellulose at other pH values (from 5.0 to 8.5) did not give any better separation of the maltase and invertase activities. These enzymes were not absorbed to CM-cellulose.

In the most purified invertase fractions, the specific invertase activity was 250 units per mg of protein, which is 250 times that of intestinal mucosa, and 5 times that of the enzyme preparation applied on the column. The specific maltase activity reached 400 units per mg of protein, which is 200 times that of intestinal mucosa and 4 times that of the enzyme solution applied on the column.

MATERIALS AND METHODS

Intestinal mucosa. Pieces of hog intestine were chilled with crushed ice immediately after the slaughter. The pieces were cut from the upper part of the jejunum. The intestines were cut open, washed with tap water to remove the intestinal contents, and gently blotted with a piece of cloth. The mucosa was scraped off with a glass slide. The yield was 25—30 g of mucosa per meter of intestine.

Substrates. Sucrose and lactose were obtained from J. T. Baker Co., maltose from Merck A. G. (Germ.), *α,α*-trehalose and melezitose from Pfanstiehl Chemical Co. The trehalose was recrystallized from 80 % ethanol before use to remove traces of reducing substances. All the substrates used were chromatographically pure.

Assay of enzymatic activity. The reaction mixture was generally contained in 2.0 ml with 0.1388 M substrate concentration (4.75 % sucrose, 5.0 % maltose . H_2O, 5.0 % lactose . H_2O, and 5.25 % trehalose . $2H_2O$) in 0.05 M maleate buffer at optimum pH (6.5 for invertase and maltase, 6.0 for trehalase, and 5.6 for lactase). Toluene was used as preservative. The reaction mixture was incubated at 37°C for 60 min. With the non-reducing substrates (sucrose and trehalose) the degree of hydrolysis was determined with the 3,5-dinitrosalicylic acid method of Sumner [17] using a Beckman B spectrophotometer [18]. With the reducing substrates the method of Tauber and Kleiner [19] was used. Precipitation of proteins was made with the zinc-bariumreagent of Somogyi [20].

The hydrolysis followed a zero order reaction with a rate proportional to the amount of enzyme present up to over 10 % hydrolysis in 1 h. One unit of enzyme causes 1 % hydrolysis (= 1 mg of monohexoses produced) in 2.0 ml of reaction mixture at 37°C in 1 h.

Protein. Protein was determined with the method of Lowry *et al.*[21] A standard curve was made with human serum albumin (kindly supplied by A. B. Kabi).

Snake venom. Crotalus adamanteus venom was obtained from Ross Allen's Reptile Institute.

Sodium desoxycholate. Sodium desoxycholate (twice recrystallized) was kindly supplied by A. Norman.

Isotope-carbon labelled desoxycholic acid. 24-^{14}C-desoxycholic acid was a gift from S. Bergström. The activity was determined with a Tracerlab flow-counter.

Trypsin. Crystalline trypsin (Trypure Novo) was a gift from A.B. Ferrosan.

DEAE-cellulose. Diethylaminoethyl-cellulose was prepared from Whatman cellulose powder by the method of Peterson and Sober [9].

Conductivity measurements were with a Philips conductometer type PR 9500.

K_S *for the hydrolysis of sucrose and melezitose* were determined as described elsewhere [22].

Acknowledgement. This work has been supported by grants from *Statens Medicinska Forskningsråd* and the *Medical Faculty of the University of Lund.* Mrs. K. Hagebris is acknowledged for valuable technical assistance.

REFERENCES

1. Weidenhagen, R. *Ergeb. Enzymforsch.* **1** (1932) 168.
2. Bailey, C. B., Kitts, W. D. and Wood, A. J. *Can. J. Agr. Sci.* **36** (1956) 51.
3. Myrbäck, K. *Ergeb. Enzymforsch.* **10** (1949) 168.
4. Myrbäck, K. and Myrbäck, S. *Svensk Kem. Tidskr.* **48** (1936) 64.
5. Steensholt, G. and Veibel, S. *Acta Physiol. Scand.* **6** (1943) 62.
6. Larner, J. and McNickle, C. M. *J. Am. Chem. Soc.* **76** (1954) 4747.
7. Larner, J. and McNickle, C. M. *J. Biol. Chem.* **215** (1955) 723.
8. Larner, J. and Gillespie, R. E. *J. Am. Chem. Soc.* **78** (1956) 882.
9. Peterson, E. A. and Sober, H. A. *J. Am. Chem. Soc.* **78** (1956) 751.
10. Potter, V. R. and Elvehjem, C. A. *J. Biol. Chem.* **114** (1936) 495.
11. Hogeboom, G. H. in Colowick, S. P. and Kaplan, N. O. *Methods in Enzymology*, Vol. I., New York 1955.
12. Morton, R. K. in Colowick, S. P. and Kaplan, N. O. *Methods in Enzymology*, Vol. I., New York 1955.
13. Larner, J. and Gillespie, R. E. *J. Biol. Chem.* **223** (1956) 709.
14. Strittmatter, Ph. and Velick, S. F. *J. Biol. Chem.* **228** (1957) 785.
15. Palade, G. E. in *Enzymes, Units of Biological Structure and Function*, Henry Ford Hospital International Symposium, New York 1956.
16. Claude, A. *J. Exptl. Med.* **84** (1946) 61.
17. Sumner, J. B. and Howell, S. F. *J. Biol. Chem.* **108** (1935) 51.
18. Hostettler, F., Borel, E. and Deuel, H. *Helv. Chim. Acta* **34** (1951) 2132.
19. Tauber, H. and Kleiner, I. S. *J. Biol. Chem.* **99** (1932) 249.
20. Somogyi, M. *J. Biol. Chem.* **160** (1945) 69.
21. Lowry, O. H., Rosebrough, N. J., Farr, A. L. and Randall, R. J. *J. Biol. Chem.* **193** (1951) 265.
22. Dahlqvist, A. *Acta Chem. Scand.* **12** (1958) 2012.

Received August 27, 1958.

ACTA CHEMICA SCANDINAVICA 12 (1958) 2007—2011

Conjugate Additions of Grignard Reagents to alpha,beta-Unsaturated Esters

III. Additions of Methylmagnesium Bromide

JON MUNCH-PETERSEN

Organisk-kemisk Laboratorium, Polyteknisk Læreanstalt, Copenhagen, Denmark

The cuprous chloride catalyzed additions of methylmagnesium bromide to *sec*-butyl and ethyl esters of crotonic, tiglic and cinnamic acids and to *sec*-butyl β,β-dimethylacrylate are described. The crotonic esters give simple 1,4-addition products (*iso*valeric esters), whereas the other esters form saturated methyl ketones, resulting from both 1,4-addition and one 1,2-addition. The general features of additions of Grignard reagents to α,β-unsaturated esters are considered.

In principle, addition of a Grignard reagent to an α,β-unsaturated ester may lead to five different products, as the result of one 1,4- and one or two 1,2-additions. From crotonic ester and a methylmagnesium halide the following compounds could thus be formed:

$$CH_3CH=CH-COOR \xrightarrow{CH_3MgX} \begin{cases} CH_3CH=CH-CO-CH_3 & \text{I (1,2)} \\ CH_3CH=CH-C(OH)(CH_3)_2 & \text{II (1,2 + 1,2)} \\ (CH_3)_2CH-CH_2COOR & \text{III (1,4)} \\ (CH_3)_2CH-CH_2CO-CH_3 & \text{IV (1,4 + 1,2)} \\ (CH_3)_2CH-CH_2C(OH)(CH_3)_2 & \text{V (1,4 + 1,2 + 1,2)} \end{cases}$$

Methylmagnesium halides are, according to literature, usually added mainly to the carbonyl group of α,β-unsaturated carbonyl compounds, tertiary alcohols (type II) being produced [1–5], although the formation of small amounts of compounds resulting from 1,4-addition has also been reported, *e.g.* ethyl *iso*valerate (type III) (besides crotyldimethylcarbinol) from ethyl crotonate [4] and 3-methylpentanone-2 (type IV) (besides *iso*propenyldimethylcarbinol) from ethyl methacrylate [5].

In 1941, Kharasch and Tawney [6] demonstrated, that, in the case of the α,β-unsaturated cyclic ketone *iso*phorone, they were able to change the direction of addition of methylmagnesium bromide drastically from predominantly 1,2- to almost exclusively 1,4-addition by adding a catalytic amount of cup-

rous chloride. Such an effect of cuprous chloride has more recently been verified by other workers (for further references, see Ref.[3]).

As described in the first paper in this series [3], it was found that when cuprous chloride was present, *sec*-butyl *iso*valerate (III) was formed in 45 % yield by the conjugate addition of methylmagnesium bromide to *sec*-butyl crotonate, and with *sec*-butyl cinnamate this Grignard reagent gave a 40 % yield of 4-phenylpentanone-2 (VI) as a result of both 1,4- and 1,2-addition (*cf.* IV, above). In the second paper [7], however, in which the uncatalyzed 1,4-additions of higher Grignard reagents to *sec*-butyl crotonate and tiglate are described, it was stated that methylmagnesium bromide gives mixtures of compounds which are of little preparative value.

The present paper reports a number of addition reactions of methylmagnesium bromide with some α,β-unsaturated esters. It has been established that a catalyst, such as cuprous chloride must be present in order to secure any great degree of conjugate addition. When *sec*-butyl crotonate or cinnamate react with methylmagnesium bromide under conditions [7] which in the case of higher Grignard reagents lead to good yields of simple 1,4-addition compounds, well-defined substances can not be easily isolated by fractional distillation. The reaction products are mixtures, probably of several of the compounds corresponding to types I—V, as well as the below-mentioned high-boiling condensation-addition compounds and non-distillable polymerisation products from the unsaturated esters. When, however, the addition reactions are carried out in the presence of catalytic amounts of cuprous chloride under cooling in an ice-salt freezing mixture, there are obtained fair to good yields of products (Table 1), which in the case of crotonic ester is the simple 1,4-addition product (III, *iso*valeric ester), but in the case of cinnamic ester, is the above-mentioned saturated methyl ketone (VI), resulting from both 1,4- and 1,2-addition:

$$C_6H_5CH=CH-COO\text{-}sec\text{-}C_4H_9 \xrightarrow{CH_3MgBr} C_6H_5CH(CH_3)CH_2COCH_3 \qquad VI$$

Similarly, *sec*-butyl tiglate and *sec*-butyl β,β-dimethylacrylate give the saturated methyl ketones, 3,4-dimethylpentanone-2 (VII) and 4,4-dimethylpentanone-2 (methyl *neo*pentyl ketone, VIII), respectively.

It has further been found that, in this reaction, the ethyl esters give the same products in the same yields as do the *sec*-butyl esters (in the case of crotonic ester, of course, ethyl *iso*-valerate instead of the *sec*-butyl ester is formed).

As mentioned above, the reaction leading to products of type IV consists of one 1,4- and one 1,2-addition, and the question could be asked, as to which one of the two additions takes place first [5,2]. No answer, however, could be given on the basis of the experiments here described, since, in each case, only one of the possible products has been obtained. Probably this sequence differs from case to case, depending on the structure of the ester (and of the Grignard reagent), and the whole problem is thus intimately connected with the influence of the structure on the course of the addition. Investigations of this relationship are in progress.

Table 1. Additions of methylmagnesium bromide to α,β-unsaturated esters in the presence of cuprous chloride.

Ester	Product	Yield %	b. p., °C found	b. p., °C lit.	n_D^{25} found	n_D^{25} lit.
sec-butyl crotonate	*sec*-butyl *iso*valerate [a]	51	57/15 mm	100/98 mm [3]	1.4043	1.4075 [3]
ethyl crotonate	ethyl *iso*valerate	54	134	133.8 [8]	1.3967	1.3975 [8]
sec-butyl tiglate	3,4-dimethyl-pentanone-2, VII [b,g]	63	133—134	136—138 [9]	1.4088 n_D^{14}	1.4129 [9]
ethyl tiglate	3,4-dimethyl-pentanone-2, VII	64				
sec-butyl β,β-dimethyl acrylate	4,4-dimethyl-pentanone-2, VIII [c,g]	33 [d]	124	124—125 [10]	1.4037	1.4018 [10]
sec-butyl cinnamate [3]	4-phenyl-pentanone-2, VI	40 [e]	88.5/1.7 mm		1.5102	
ethyl cinnamate	4-phenyl-pentanone-2, VI [f,g]	77	69/0.8 mm		1.5071	

[a] III (R = *sec*-butyl); calc. for $C_9H_{18}O_2$ (158.23): sap.equiv. 158.2. Found: 158.1. [b] Calc. for $C_7H_{14}O$ (114.18): C 73.63; H 12.36. Found: C 73.75; H 12.48. [c] Calc. for $C_7H_{14}O$ (114.18): C 73.63; H 12.36. Found: C 73.40; H 12.32. [d] This yield could probably be increased by leaving the reaction mixture over-night in stead of for only 1—2 h, since a large amount (30 %) of unreacted ester was recovered in spite of a great excess of Grignard reagent. [e] This yield could probably be increased, since actually too little Grignard reagent (1.5 equiv.) was used, and a considerable amount (20 %) of unreacted ester was recovered (se Ref. [3]). [f] Calcd. for $C_{11}H_{14}O$ (162.22): C 81.44; H 8.70. Found: C 81.30; H 8.63. [g] Infra-red spectrum shows the presence of a ketone group, and the absence of hydroxyl groups and double bonds.

The experimental facts here described, together with the previously reported [3,7] results, seem to indicate the following general picture of the addition of Grignard reagents to α,β-unsaturated esters:

a. Adding ethyl esters to Grignard reagents without special precautions (as Grignard reactions are ordinarily carried out) results mainly in 1,2-additions (to the carbonyl group), tertiary alcohols (of type II) being formed *.

b. By the use of esters with large alcohol moieties, such as *sec*-butyl esters [3], instead of ethyl esters, 1,2-addition is largely prevented (except with certain Grignard reagents, e.g. methylmagnesium halides). Instead, 1,4-addition takes place, but if special conditions (*c*, below) are not fulfilled, the ester first, to a large extent, dimerizes by a Michael-type condensation to an α-alkylidene-

* One exception is the reaction between ethyl cinnamate and phenylmagnesium bromide, giving predominantly 1,4-addition (β,β-diphenylpropionic ester) [1].

glutaric ester. The Grignard reagent then adds to the α,β-carbon-carbon double bond of this latter ester, so that a high-boiling saturated, substituted glutaric ester is produced:

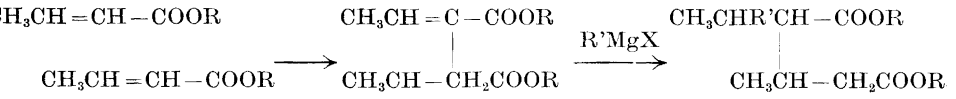

Only minor amounts of the simple conjugate addition product (type III) are formed.

c. The formation of the high-boiling condensation-addition product is suppressed by 1) cooling the Grignard solution during the addition of the ester, 2) diluting the ester solution (with ether) and 3) adding the ester solution slowly. Ordinary Grignard reagents, with the exception af methylmagnesium halides, may in this way give good yields of simple 1,4-addition products (saturated esters of type III) [7]. The reaction thus provides a practical route to 3-methyl-, 2,3-dimethyl- and 3-phenyl-substituted alkanoic acids.

d. The precautions mentioned under *c* do not prevent 1,2-addition in those cases where such addition takes place in spite of the use of *sec*-butyl esters, *e.g.* the Grignard reagent being a methylmagnesium halide.

e. Cuprous chloride has a definitely established effect in promoting 1,4-addition in favor of 1,2-addition.

f. Cuprous chloride has little, if any, effect in preventing the formation of the high-boiling condensation-addition compound [7].

The mode of action of cuprous chloride is still obscure, although it appears likely that some kind of Lewis-acid effect could operate, activating the carbon-carbon double bond [3].

The above-mentioned points *c* and *e* suggest that the combination of the conditions mentioned under *c* with the presence of cuprous chloride should make possible the use of ethyl esters in stead of *sec*-butyl esters in the simple 1,4-addition process. Preliminary experiments have shown, that *n*-butylmagnesium bromide with ethyl crotonate in the presence of cuprous chloride gives the 1,4-addition product ethyl 3-methylheptanoate in the same yield (about 70 %) as is obtained with *sec*-butyl crotonate without catalyst. With ethyl tiglate and cinnamate, however, much lower yields have been obtained. The results of this investigation will be published in a forthcoming paper.

EXPERIMENTAL

Microanalyses are by Mr. Preben Hansen, Microanalytical Division, The Chemical Laboratory, University of Copenhagen. Infra-red spectra were recorded in this laboratory by Mrs. Susanne Refn, M. Sc. Fractional distillations were through a simple 45 cm × 8 mm Podbielniak-type column with a tantalum wire spiral, heated jacket and partial reflux head.

sec-*Butyl esters* were prepared as previously described [3]. *Ethyl crotonate* and *tiglate* were prepared in 80 % yield by the conventional esterification procedure: boiling the acid with excess of ethanol in the presence of concentrated sulfuric acid. *Ethyl cinnamate* was obtained by the condensation of benzaldehyde with ethyl acetate.

Methyl bromide was either a commercial c. p. product (Fluka, purum) or a technical product (from a steel cylinder), which was purified by passing the gas through sodium hydroxide solution and concentrated sulfuric acid, followed by liquefaction. For weighing it was dissolved in ice-cold ether.

The cuprous chloride catalyzed additions of methylmagnesium bromide were carried out as previously described [3], except that a greater excess of Grignard reagent and a longer addition time for the ester were used. Effective stirring was applied throughout. The methylmagnesium bromide was usually prepared from 6.3 g (0.26 g-atom) of magnesium turnings and 28 to 32 g (about 0.3 mole) of methyl bromide in about 160 ml of ether. The clear solution, after being heated under reflux for 15 min, was cooled in ice-salt for 15 min; 0.25 g of cuprous chloride was added in one portion, and then 0.1 mole of the ester, dissolved in 100 ml of ether, was added dropwise from a graduated dropping funnel during about 1.5 h. During this period the temperature of cooling bath usually rose from about $-18°$ to about $-5°$. Stirring was continued for an additional 10—15 min at this temperature, then at room temperature for 1 to 2 h. (In the case of tiglic ester this period at room temperature was prolonged overnight, and this should probably also be done with β,β-dimethylacrylic ester in order to obtain maximum yield, *cf.* note[d], Table 1). The reaction mixture was finally poured onto ice and hydrochloric acid and worked up in the conventional way [3].

REFERENCES

1. Kohler, E. P. and Heritage, G. *Am. Chem. J.* **33** (1905) 21, 153 [*Chem. Zentr.* **1905** *I*, 521, 824].
2. Kohler, E. P. *Am. Chem. J.* **36** (1906) 529 [*Chem. Zentr.* **1907** *I*, 559].
3. Munch-Petersen, J. *J. Org. Chem.* **22** (1957) 170.
4. Van Keersbilck, N. *Bull. soc. chim. Belges* **38** (1929) 205 [*Chem. Zentr.* **1929** *II*, 2036].
5. Blaise, E.-E. and Courtot, A. *Compt. rend.* **140** (1905) 370 [*Chem. Zentr.* **1905** *I*, 726].
6. Kharasch, M. S. and Tawney, P. O. *J. Am. Chem. Soc.* **63** (1941) 2308.
7. Munch-Petersen, J. *Acta Chem. Scand.* **12** (1958) 967.
8. Munch, J. C. *J. Am. Chem. Soc.* **48** (1926) 994.
9. Colonge, J. and Mostafavi, K. *Bull. soc. chim. France* [5] **6** (1939) 346; *cf.* Adams, J. T., Abramovitch, B. and Hauser, C. R. *J. Am. Chem. Soc.* **65** (1943) 552.
10. Mosher, W. A. and Cox, J. C. *J. Am. Chem. Soc.* **72** (1950) 3701.

Received August 23, 1958.

ACTA CHEMICA SCANDINAVICA 12 (1958) 2012—2020

Characterization of Intestinal Invertase as a Glucosido-Invertase

I. Action on Different Substrates

ARNE DAHLQVIST

Department of Physiological Chemistry, University of Lund, Lund, Sweden

The basis for classification of intestinal invertase as a glucosido-invertase is discussed.

The action of a preparation of intestinal glycosidases on some di- and trisaccharides, related to sucrose, has been studied.

No action upon raffinose [*O*-α-D-galactopyranosyl-(1→6)-*O*-α-D-glucopyranosyl-(1→2)-β-D-fructofuranoside] or gal-sucrose (α-D-galactopyranosyl-β-D-fructofuranoside) could be detected. Intestinal invertase can therefore not hydrolyze these sugars. This supports the view that intestinal invertase has a great specificity for the glucopyranoside part of the sucrose molecule.

Melezitose [*O*-α-D-glucopyranosyl-(1→3)-*O*-β-D-fructofuranosyl-(2→1)-α-D-glucopyranoside] was hydrolyzed, but at a very slow rate. The substitution in the fructofuranoside part of the sucrose molecule must therefore have a marked influence on the action of intestinal invertase. At present, however, we do not know, if sucrose and melezitose really are hydrolyzed by the same enzyme.

An attempt to demonstrate, if the sucrose linkage in melezitose can be hydrolyzed before the turanose linkage, had no success. This failure was explained by the slow rate of melezitose hydrolysis.

The results indicate that intestinal invertase has a very high degree of specificity for the glucopyranosyl part of sucrose, but that also alterations in the fructofuranosyl part of the molecule interfere strongly with the action of the enzyme. Further specificity studies require more purified enzyme preparations.

The division of invertases into glucosido- and fructosidoinvertase was first made by Kuhn, grounded on their inhibition by glucose or fructose, respectively [1–3]. Such inhibitions, however, show many irregularities [4–6], and are therefore no practical ground for the classification of invertases.

Later Kuhn *et al.* proposed the use of raffinose [*O*-α-D-galactopyranosyl-(1→6)-*O*-α-D-glucopyranosyl-(1→2)-β-D-fructofuranoside] and melezitose [*O*-α-D-glucopyranosyl-(1→3)-*O*-β-D-fructofuranosyl(2→1)-α-D-glucopyranoside] for the characterization of invertases [6]. These sugars are regarded as sucrose, where the glucosyl or the fructosyl parts, respectively, are substituted with a

third sugar. Glucosido-invertases should be able to hydrolyze melezitose and fructosido-invertases raffinose (into fructose and melibiose) in addition to sucrose.

That intestinal invertase cannot hydrolyze raffinose was observed by Bierry [7] already in 1912. Recent reports support this statement [8].

The behavior of intestinal invertase against melezitose has never been investigated, although the interest for such an investigation has been expressed [9].

Recently has been reported the synthesis of a new disaccharide, gal-sucrose (α-D-galactopyranosyl-β-D-fructofuranoside), which is a sucrose where the glucose has been replaced by galactose [10]. The only structural difference from an ordinary sucrose molecule is therefore that the hydrogen and the hydroxyl at the fourth carbon atom of the glucosyl part have shifted place. This substance seems very interesting for testing the specificity demands of invertases for the glucopyranosyl part of sucrose.

In the present paper are reported some experiments on the action of an intestinal glycosidase preparation upon raffinose, melezitose, and gal-sucrose. Turanose (3-*O*-α-D-glucopyranosyl-D-fructose) is also included, because it is a part of the melezitose molecule. For the substrates hydrolyzed, the optimum pH, relative rate of hydrolysis, K_s, and v_{max} have been determined.

As source of enzyme was selected swine intestinal mucosa. In this material invertase (together with maltase, lactase, and trehalase) has been found localized in the microsome fraction [11], obtained by differential centrifugation. The enzymes were extracted from the microsomes by sodium desoxycholate.

MATERIALS AND METHODS

Substrates. A sample of gal-sucrose was kindly supplied by D. Feingold, G. Avigad, and S. Hestrin, who recently reported the synthesis of this sugar [10]. The other substrates were commercial preparations of analytical grade purity, sucrose from J. T. Baker Co., raffinose and melezitose from Pfanstiehl Chemical Co., and turanose from Nutritional Biochemicals Corporation.

Glycosidase preparation. Pieces of swine intestine were taken from the slaughterhouse immediately after the slaughter, and chilled with ice during the transport to the laboratory. The pieces were cut from the proximal jejunum, because this part seems to be richest in invertase [12]. The mucosa was scraped off, homogenized in 0.25 M sucrose (previously chilled to 0° to prevent hydrolysis), and the microsomes were isolated by differential centrifugation [11]. The glycosidases were eluted from the microsomes with 0.5 % sodium desoxycholate (kindly supplied by A. Norman). The desoxycholate and the remaining sucrose were removed by dialysis against phosphate buffer pH 7.5, and then the buffer was removed by dialysis against distilled water. The suspension thus obtained contained 80—90 % of the invertase present in the original homogenate, and corresponding amounts of maltase, lactase, and trehalase [11].

Determination of enzymatic activity. Samples of enzyme solution were mixed at 37°C with buffered substrate solutions, to give a concentration of 0.1 M buffer (acetate or phosphate) and, when not otherwise noted, 0.1460 M substrate (5 % sucrose or turanose, 7.89 % melezitose . $2H_2O$, or 8.65 % raffinose . $5H_2O$). Toluene was used as preservative. The degree of hydrolysis was not allowed to exceed 5 % per hour. During these conditions, the reaction was found to be of zero order up to at least 10 % hydrolysis, and the (initial) reaction velocity was found to be proportional to the amount of enzyme present.

Gal-sucrose, of which only a total amount of 2 mg was available, was used in lower concentration as described later.

The degree of hydrolysis was determined by different methods, depending of the properties of the substrates.

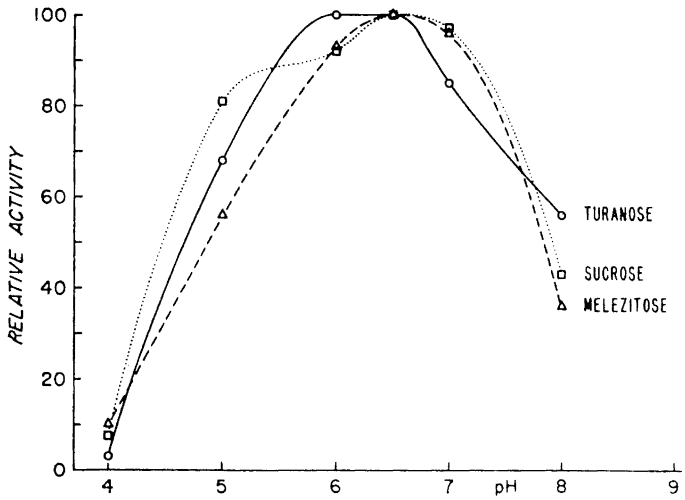

Fig. 1. Influence of pH on the hydrolysis of sucrose, melezitose and turanose. Buffers: 0.1 M acetate pH 4.0—5.0, 0.1 M phosphate pH 6.0—8.0. Temperature 37°C. Substrate concentration 0.1460 M.

1) Sucrose, raffinose, and melezitose are nonreducing. For determination of the monosaccharides produced from these sugars was used a modification of the 3,5-dinitrosalicylic acid method of Sumner [13,14], with spectrophotometric reading of the obtained colour [15]. No protein precipitation is necessary with this reagent.

2) Gal-sucrose is also nonreducing, but because this sugar was used in a very dilute solution, the highly sensitive method of Somogyi and Nelson [16,17] was used, after previous precipitation of proteins with Zn-Ba reagent [18].

3) Turanose is a reducing disaccharide. The liberated glucose was determined by the specific enzymatic method of Keilin and Hartree [19].

Samples of 0.4 ml of the reaction mixture were added 1.6 ml of 0.1 M acetate buffer pH 5.0, and the glycosidase action was interrupted by boiling in water-bath for 2 min. (The addition of acid buffer before boiling was found to be essential since turanose is a very alkali-labile sugar, and if it is boiled at a pH higher than 6.0, part of the turanose will be decomposed, leaving free glucose. This buffer will not interfere with the following enzymatic determination of glucose.) 1.0 ml of this solution was transferred to a Warburg flask (without central cylinder). 2.0 ml of a 0.1 M acetate buffer pH 5.6, containing 0.1 ml of catalase solution (Catalase, sterile solution, Worthington) and 0.02 ml of 99.5 % ethanol per 2 ml, were added. In the side arm of the flask was placed 0.5 ml of a 10 % glucose oxidase solution (Glucose oxidase, crude, Sigma). This contains no enzyme acting upon turanose (but it contains maltase) and might therefore in this case be used without further purification. After equilibration at 25°C, the tap was closed and the flask tipped. When no more oxygen was absorbed (after 30—45 min) the readings of the manometers were recorded. 124.4 mm^3 of oxygen absorbed corresponds to 1.0 mg of glucose oxidized.

Paper chromatography of sugars was performed by the ascending technique on 30 cm long pieces of paper (Whatman No. 1). A roll of equal breadth, containing about 120 cm of filter paper was placed on the top to absorb the solvent. The chromatograms were developed for 24 h with ethyl acetate:acetic acid:water 9:2:2 v/v. The sugar spots were detected with aniline hydrogen phthalate [20].

RESULTS

Sucrose was rapidly hydrolyzed by the enzyme solution, with an optimum pH between 6.3 and 6.8 (Fig. 1). The amount of invert sugar produced per

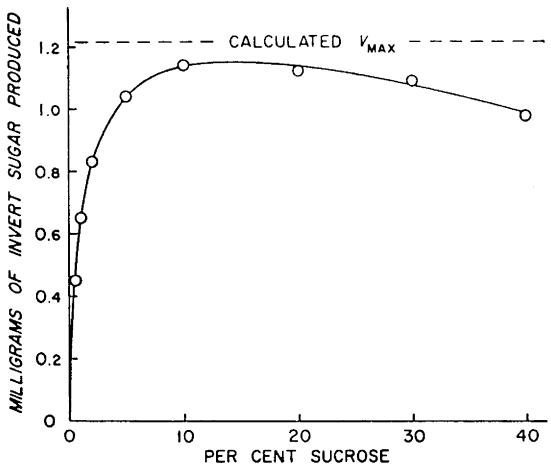

Fig. 2. Influence of substrate concentration upon the hydrolysis of sucrose. Reaction volume 2.0 ml in 0.1 M phosphate buffer pH 6.5. Incubated for 1 h at 37°C. Mg of produced invert sugar determined by the 3,5-dinitrosalicylic acid method. For calculation of v_{max} see Fig. 3.

time unit increased with increasing substrate concentration up to 10 % (0.2920 M) sucrose, but at higher substrate concentration the amount of invert sugar produced (as measured with the 3,5-dinitrosalicylic acid method) decreased somewhat (Fig. 2). This decrease may be caused by transglycosidation, which is marked at concentrations higher than 10 % sucrose, but hardly detectable at 5 % [21]. From the values obtained at substrate concentrations below 10 % the theoretical v_{max} for infinite substrate concentration and the K_s (*i. e.* the substrate concentration at which the initial rate of hydrolysis is half of the v_{max}) were calculated by the graphical method of Lineweaver and Burk [22] as modified by Dixon [23] (Fig. 3). The v_{max} was found to be 1.2 times the rate of reaction in 0.1460 M sucrose, and the K_s was calculated to 2.5×10^{-2} M sucrose.

No action upon raffinose could be detected. A solution of raffinose was mixed with enzyme solution to give a concentration of 0.1460 M raffinose in 0.1 M phosphate buffer pH 6.5. No reducing sugars could be detected after 72 h at 37°C, and only raffinose was found on a paper chromatogram. During the conditions used, a hydrolysis at a rate only 1/1000 of that of sucrose hydrolysis would have been easily detected.

Gal-sucrose (α-D-galactopyranosyl-β-D-fructofuranoside) was available only in a minute quantity (2 mg), and was therefore used in a considerably more diluted solution than the other substrates. For comparison of the results, it was therefore necessary to study the rate of hydrolysis in an equally diluted sucrose solution (Table 1). It is seen, that even in a 0.05 % solution of sucrose, this sugar is rapidly hydrolyzed. Corresponding experiments were then performed with weighed amounts of gal-sucrose (Table 2). As blanks were used

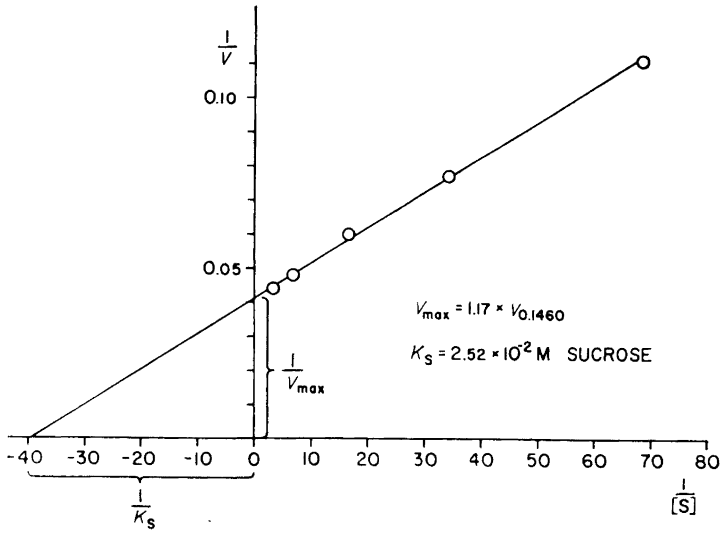

Fig. 3. Graphical determination of v_{max} and K_S for invertase. Temperature 37°C. 0.1 M phosphate buffer pH 6.5.

mixtures of enzyme and buffer, without sugar, incubated in the thermostat for the same time. It was also found necessary to correct the values obtained with gal-sucrose for a small amount of reducing sugar present as a contamination in this sugar (Table 2). No hydrolysis of gal-sucrose could be detected. During the conditions used a hydrolysis at a rate of only 1/500 of that of sucrose would have been easily demonstrated.

Table 1. Hydrolysis of a dilute sucrose solution by intestinal invertase. Sucrose solution, 1 mg/ml in 0.2 M phosphate buffer pH 6.5, is mixed with an equal volume of enzyme solution. After incubation at 37°C, the protein is precipitated with Zn-Ba-reagent, and reducing sugars are determined by the method of Somogyi and Nelson. The sucrose is rapidly hydrolyzed.

	Time of incubation	*D* 500	*D* 660	Reduction power (expressed as μg of invert sugar per 2 ml	% hydrolysis
Blank without sugar	0	0.038	0.160	(24)	—
» » »	3 h	0.050	0.190	(32)	—
1 mg of sucrose	0	0.040	0.161	24	(0)
1 » » »	10 min	0.360	1.225	212	20.3
1 » » »	1 h	1.200	(>2.5)	740	70.5
1 » » »	3 h	1.530	(>2.5)	950	87.5

Table 2. Incubation of gal-sucrose with intestinal invertase. Weighed amounts of gal-sucrose were dissolved in 1.0 ml of 0.2 M phosphate buffer pH 6.5. 1.0 ml of enzyme solution was added, and the sample was incubated in water-bath at 37°C. Reducing sugars were determined by the method of Somogyi and Nelson. No hydrolysis could be detected.

	D 660	% hydrolysis
Expt. 1.		
0.460 mg of gal-sucrose without enzyme (reducing contaminants in gal-sucrose)	0.063	—
Expt. 2.		
0.820 mg of gal-sucrose incubated for 4 h	0.267	0
Blank without sugar, incubated for 4 h	0.200	
Reduction by 0.820 mg of gal-sucrose *	0.057	
Blank value:	0.257	
Expt. 3.		
0.640 mg of gal-sucrose incubated for 4 h	0.242	0
Blank without sugar, incubated for 4 h	0.191	
Reduction by 0.640 mg of gal-sucrose *	0.044	
Blank value:	0.235	
* calculated from Expt. 1		

Turanose was hydrolyzed with optimum pH between 6.0 and 6.5 (Fig. 1). The initial rate of hydrolysis in 0.1460 M turanose at pH 6.5 and a temperature of 37°C was 0.15 times the rate of sucrose hydrolysis during the same conditions. The K_s was calculated to 2.8×10^{-2} M turanose, and the v_{max} to 1.2 times the rate at 0.1460 M substrate concentration. By paper chromatography turanose was shown to be completely hydrolyzed into glucose and fructose.

Melezitose was also hydrolyzed by the enzyme solution, with an optimum pH equal to that for sucrose hydrolysis (Fig. 1). The rate of melezitose hydrolysis was, however, very low. At 0.1460 M melezitose concentration, pH 6.5, and a temperature of 37°C, the amount of hexoses produced was only 0.003 times the amount produced from sucrose under the same conditions. Calculated as the number of glucosidic linkages split per time unit, the rate of melezitose hydrolysis is 0.004 times the rate of sucrose hydrolysis. The hydrolysis of melezitose proceeds to completion.

In order to find out which of the two glycosidic linkages in melezitose that is hydrolyzed first, the reaction was followed on repeated paper chromatograms, but none of the two possible intermediate disaccharides (sucrose or turanose) could be demonstrated at any stage of the reaction. This is apparently caused by the fact, that these disaccharides are hydrolyzed at a rate so great, compared with melezitose, that whichever of the linkages in the trisaccharide that is hydrolyzed first, the liberated disaccharide is almost instantaneously split. In calculating the rate of melezitose hydrolysis, it must therefore be more correct to compare the number of *completely* hydrolyzed

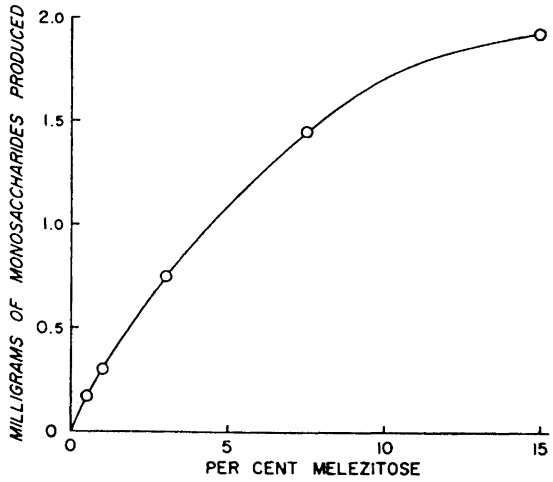

Fig. 4. Influence of the substrate concentration of the hydrolysis of melezitose. Reaction volume 2.0 ml in 0.1 M phosphate buffer pH 6.5. Incubated for 24 h at 37°C. Mg of produced monosaccharides determined by the 3,5-dinitrosalicylic acid method.

melezitose molecules with the number of hydrolyzed sucrose molecules. Calculated in this way, the rate of melezitose hydrolysis is only 0.002 times the rate of sucrose hydrolysis during the conditions used.

The rate of melezitose hydrolysis is rather much increased by increasing the substrate concentration, indicating that the enzyme has a low affinity for melezitose (Fig. 4). The K_s was calculated to 2.6×10^{-1} M melezitose and the v_{max} to 2.8 times the rate at 0.1460 M melezitose concentration.

It is not proven, if sucrose and melezitose really are hydrolyzed by the same enzyme. Both activities are inhibited by tris(hydroxymethyl)-aminomethane (buffer grade, Sigma) at alkaline pH (Fig. 5). This inhibition is caused by competition with the substrate for the enzyme. However, this inhibition seems to be common for several glycosidases, since Larner *et al.*[24] have found that both oligo-1,6-glucosidase and maltase (which they have separated from each other) are inhibited by tris(hydroxymethyl)aminomethane.

DISCUSSION

The findings of Bierry [7], that intestinal invertase has no action upon raffinose, was confirmed. Furthermore, it was found that the new disaccharide gal-sucrose was not hydrolyzed. These facts demonstrate, that intestinal invertase has a very high degree of specificity for the α-D-glucopyranosyl part of sucrose.

Melezitose, on the other hand, was hydrolyzed by the enzyme preparation used, but at a very slow rate as compared with sucrose. At 0.1460 M substrate concentration the hydrolysis of melezitose proceeded with a rate that was only

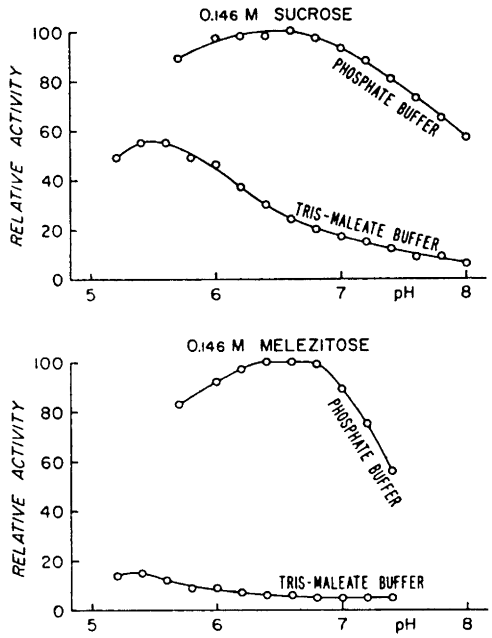

Fig. 5. Inhibition of the hydrolysis of sucrose and melezitose by tris(hydroxymethyl)-aminomethane at alkaline pH. Buffers: 0.05 M phosphate or maleate, respectively, with 0.05 M tris(hydroxymethyl)aminomethane. Maleate buffer without tris(hydroxymethyl)-aminomethane gave the same values as phosphate buffer.

0.002 times the rate for sucrose hydrolysis during the same conditions. The K_s for melezitose hydrolysis is about ten times greater than the K_s for sucrose hydrolysis, which indicates that the slow hydrolysis of melezitose is partly caused by a low affinity for this substrate. By comparing the v_{max} for the two substrates, however, one can see that the most important factor is a slow formation of the hydrolysis products from the enzyme-melezitose complex.

These calculations are valid only for the first hydrolyzed link in melezitose. Because melezitose is hydrolyzed so slowly, compared with sucrose or turanose, it was not possible to determine which of the linkages in the trisaccharide that was hydrolyzed first.

The calculations also presume that melezitose and sucrose are hydrolyzed by the same enzyme. At present no proof for this has been obtained. Conclusions must therefore be drawn with care. The action of purified preparations of intestinal invertase upon melezitose and turanose is under investigation.

It can, however, be stated, that, even if the substitution in the fructofuranosyl part of sucrose does not totally prevent the action of invertase, it interferes strongly with the reaction. It seems therefore probable that intestinal invertase has a marked specificity also for the fructofuranosyl part of the sucrose molecule.

This is in accordance with the recently observed multiple nature of intestinal glycosidases, which contests the view of Weidenhagen, who thought that mammalian intestine contains one single α-D-glucopyranosidase, hydrolyzing maltose, sucrose, and other α-D-glucopyranosides [25,26]. It has been shown that intestinal glycosidase preparations are without action upon α-methylglucoside [27–29]. The activities against *iso*maltose (6-*O*-α-D-glucopyranosyl-D-glucose) and nigerose (3-*O*-α-D-glucopyranosyl-D-glucose) have been partially separated from maltase activity [30–32]. The trehalase activity of intestinal mucosa has been totally separated from invertase and maltase activities, and the invertase and maltase activities partially separated from each other [11]. For a further study of the specificity demands of intestinal invertase, it is therefore necessary to separate the enzyme from the other glycosidases.

Acknowledgment. This work has been supported by a grant from the *Medical Faculty of the University of Lund.*

REFERENCES

1. Gottschalk, A. in Sumner, J. B. and Myrbäck, K. *The Enzymes*, Vol. I., part 1, New York 1950.
2. Pigman, W. W. and Goepp, R. W. *Chemistry of the Carbohydrates*, New York 1948.
3. Kuhn, R. *Z. physiol. Chem. Hoppe-Seyler* **129** (1923) 57.
4. Neuberg, C. and Mandl, I. in Sumner, J. B. and Myrbäck, K. *The Enzymes*, Vol. I., part 1, New York 1950.
5. Kuhn, R. und Münch, K. *Z. physiol. Chem. Hoppe-Seyler* **150** (1925) 221.
6. Kuhn, R. und Münch, K. *Z. physiol. Chem. Hoppe-Seyler* **163** (1927) 1.
7. Bierry, H. *Biochem. Z.* **44** (1912) 426.
8. Courtois, J. E., Anagnostopoulos, C. and Petek, F. *Bull. soc. chim. biol.* **35** (1953) 731.
9. Weidenhagen, R. in Bamann, E. und Myrbäck, K. *Die Methoden der Fermentforschung*, Vol. I., p. 1758, Leipzig 1941.
10. Feingold, D. S., Avigad, G. and Hestrin, S. *J. Biol. Chem.* **224** (1957) 295.
11. Borgström, B. and Dahlqvist, A. *Acta Chem. Scand.* **12** (1958) 1997.
12. von Euler, H. und Svanberg, O. *Z. physiol. Chem. Hoppe-Seyler* **115** (1921) 43.
13. Sumner, J. B. and Graham, V. A. *J. Biol. Chem.* **47** (1921) 5.
14. Sumner, J. B. and Howell, S. F. *J. Biol. Chem.* **108** (1935) 51.
15. Hostettler, F., Borel, E. und Deuel, H. *Helv. Chim. Acta* **34** (1951) 2132.
16. Somogyi, M. *J. Biol. Chem.* **195** (1952) 19.
17. Nelson, N. *J. Biol. Chem.* **153** (1944) 375.
18. Somogyi, M. *J. Biol. Chem.* **160** (1945) 69.
19. Keilin, D. and Hartree, E. F. *Biochem. J.* **42** (1948) 230.
20. Partridge, S. M. *Nature* **164** (1949) 443.
21. Dahlqvist, A. *To be published.*
22. Lineweaver, H. and Burk, D. *J. Am. Chem. Soc.* **56** (1934) 658.
23. Dixon, M. *Biochem. J.* **55** (1953) 170.
24. Larner, J. and Gillespie, R. E. *J. Biol. Chem.* **223** (1956) 709.
25. Weidenhagen, R. *Ergeb. Enzymforsch.* **1** (1932) 168.
26. Weidenhagen, R. in Nord, F. F. und Weidenhagen, R. *Handbuch der Enzymologie*, Vol. I., Leipzig 1940.
27. Myrbäck, K. *Z. physiol. Chem. Hoppe-Seyler* **198** (1931) 196.
28. Myrbäck, K. och Myrbäck, S. *Svensk Kem. Tidskr.* **48** (1936) 64.
29. Steensholt, G. and Veibel, S. *Acta Physiol. Scand.* **6** (1943) 62.
30. Larner, J. and McNickle, C. M. *J. Am. Chem. Soc.* **76** (1954) 4747.
31. Larner, J. and McNickle, C. M. *J. Biol. Chem.* **215** (1955) 723.
32. Larner, J. and Gillespie, R. E. *J. Am. Chem. Soc.* **78** (1956) 882.

Received September 3, 1958.

ACTA CHEMICA SCANDINAVICA 12 (1958) 2021—2027

Preparation and Infrared Spectra of 1 D-, 2 D-, 1,2 D_2-, and 1,2,2′ D_3- Ethyl Fluorides and Bromides

BØRGE BAK, DANIEL H. CHRISTENSEN, JØRGEN MØLLER and SNEGULKA DETONI*

Chemical Laboratory of the University of Copenhagen, Copenhagen, Denmark

1 D-, 2 D-, 1,2 D_2-, and 1,2,2′ D_3-ethyl fluorides and bromides were prepared. Infrared absorption curves were recorded. In the spectra of the bromides the existence of rotational isomers is demonstrated.

In connection with a microwave determination of the structure of ethyl fluoride, the five isotopic species CH_3CH_2F (I), CH_2DCH_2F (II), CH_2CHDF (III), CH_2DCHDF (IV) and CHD_2CHDF (V) (b. p. —32°C), were prepared. A brief record of their preparation is given here together with the infrared absorption curves of the five intermediates, CH_3CH_2Br (I′), CH_2DCH_2Br (II′), CH_3CHDBr (III′), $CH_2DCHDBr$ (IV′) and CHD_2CHDBr (V′) (b. p. +38°C), referring to the substances in the liquid and the gas phase, and the infrared absorption curves of I—V, referring to the substances in the gas phase.

EXPERIMENTAL

A. Preparations. Henne [1] prepared ethyl fluoride from ethyl bromide and HgF_2. Later, he suggested [2] the use of the more easily available HgF which can be applied at the cost of yield. All five fluorides were prepared by us by the latter procedure, modified, for sake of simplicity, by using sealed-off glass ampullae instead of metal vessels. After twenty experiments in which the temperature, the reaction period, and the C_2H_5Br/HgF ratio were systematically varied it was found most advantageous to work at 110°C for 20 h with a 1:2 ratio between ethyl bromide and mercurous fluoride. Usually, ½—1 ml ethyl bromide was treated in a 50 ml pyrex glass ampulla. Occasional shaking proved to be very important for the magnitude of the yield which was 25—30 % of theory based on ethyl bromide. This amount of purified material was obtained after a crude distillation *in vacuo* from solid reaction products and subsequent gaschromatographical separation on a dry silica-gel column (length 150 mm, diameter 10 mm, temperature 82°C). The infrared spectrum of (I) (gas-phase) was identical with the spectrum published by Nielsen *et al.*[3] Its boiling point was correct (—32°C).

* On leave of absence from the University of Ljubljana, Yugoslavia.

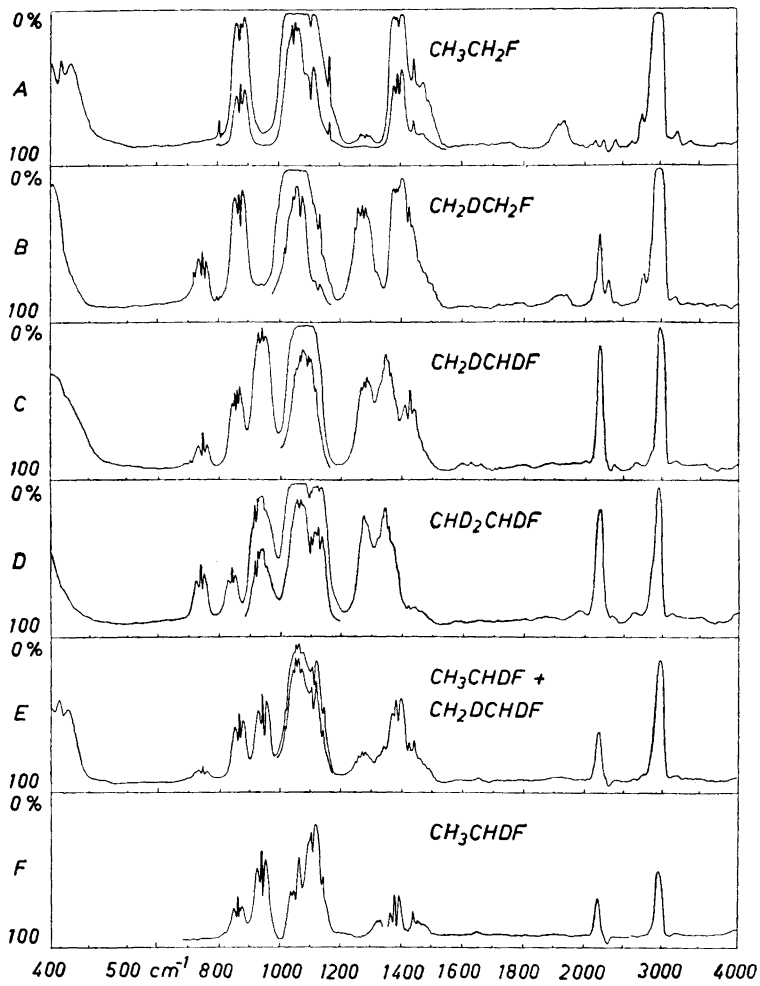

Fig. 1. Infrared spectra of gaseous ethyl flouride (A) and deuterated species (B)–(F) at room temperature. Pressure 150 mm unless otherwise stated. The spectrum (F) is the spectrum of the mixture $CH_3CHDF + CH_2DCH_2F$ (p = 75 mm), run against CH_2DCH_2F (p = 37 mm) in a reference cell (length 10 cm).
Ordinate: percent transmission at 10 cm path length.
Abscissa: wave numbers in cm^{-1}.

(II′)–(V′) were prepared by the reactions:

$$H_2C=CH_2 + DBr \rightarrow CH_2DCH_2Br \qquad (\alpha)$$

$$\left.\begin{array}{l} HC\equiv CH + 2DBr \rightarrow CHDBrCHDBr \ ^{4,5} \\ CHDBrCHDBr \rightarrow CHD = CHD \ ^{4,5} \\ CHD=CHD + HBr \rightarrow CH_2DCHDBr \end{array}\right\} \qquad (\beta)$$

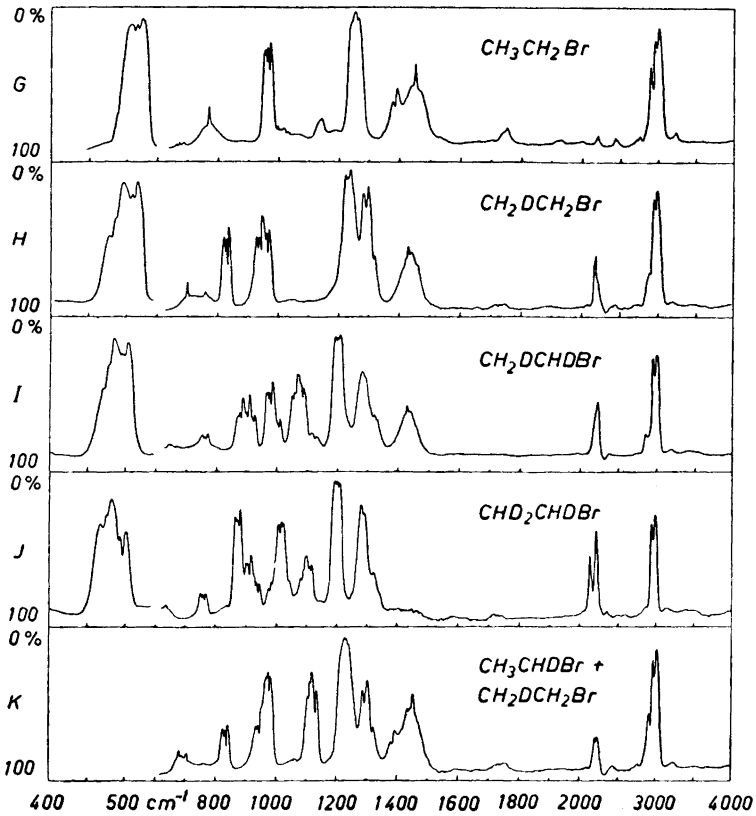

Fig. 2. Infrared spectra of gaseous ethyl bromide (G) and deuterated species (H)—(K) at room temperature. Pressure 70 mm Hg unless otherwise stated. The spectrum (K) is the spectrum of the mixture $CH_3CHDBr + CH_2DCH_2Br$. Because of a mishap, (K) was not run in the 400—600 cm^{-1} region.
Ordinate and abscissa as in Fig. 1.

(III′) was only obtained as a 50 % mixture with (II′):

$$\left.\begin{array}{l} CH_2{=}CHBr + DBr \rightarrow CH_2BrCHDBr \\ CH_2BrCHDBr \rightarrow CH_2 = CHD \ ^{4,5} \\ 2\ CH_2 = CHD + 2\ HBr \rightarrow (II') + CH_3CHDBr \end{array}\right\} \quad (\gamma)$$

$$\left.\begin{array}{l} HC{\equiv}CH + 2\ DBr \rightarrow CHDBrCHDBr \ ^{4,5} \\ CHDBrCHDBr \rightarrow CHD = CHD \ ^{4,5} \\ CHD = CHD + DBr \rightarrow CHD_2CHDBr \end{array}\right\} \quad (\delta)$$

The yield at the processes (α)—(δ) was 90 %. As shown by the infrared absorption spectra no undesired exchange took place. In all cases (including ethylene) the addition of HBr (DBr) took place under ultraviolet irradiation.

B. Infrared spectra. Infrared spectra of (I), (II), (III), (IV) and (V) in the gas phase were recorded on a Perkin-Elmer 21 double beam instrument at room temperature.

Table 1. Raman data [6] and infrared spectra of ethyl bromide and four deuterated species (liquids). Temperature 25°C. Infrared spectra were recorded in the 400—1 500 cm^{-1} region. Cell thickness 0.03 mm. In parenthesis, optical density at peak. The accuracy of the infrared measurements is ± 2 cm^{-1}.

CH_3CH_2Br (I′)		CH_2DCH_2Br (II′)		CH_3CHDBr (III′)		$CH_2DCHDBr$ (VI′)	CHD_2CHDBr (V′)
Infrared	Raman	Infrared	Raman	Infrared	Raman	Infrared	Infrared
—	290.4(6)	—	280.8(5)	—	290.6(5)	—	523(>1)
562(>1)	560.4(10)	—	287.0(3)	548(>1)	549.0(10)	526(0.62)	542(0.70)
765(0.80)	—	534(0.75)	536.7(7)	673(0.50)	678.4(½)	543(>1)	605(0.25)
954(>1)	959.3(2)	555(>1)	557.5(10)	802(0.18)	807.7(1)	640(0.41)	625(0. 26)
—	1 022 (½)	699(0.50)	703.8(½)	966(>1)	971 (2)	671(0.28)	636(0.28)
1 060(0.15)	1 062.0(3)	758(0.35)	—	1 048(0.22)	1 054 (3)	758(0.34)	753(0.34)
1 120(0.15)	—	822(>1)	826.4(2)	1 090(0.40)	—	792(0.12)	817(0.11)
1 238(>1)	1 241.5(2)	—	896.8(½)	1 110(>1)	1 117 (2)	821(0.13)	863(> 1)
1 250(>1)	1 250 (½)	—	912.0(½)	1 210(>1)	1 214.0(3)	874(0.86)	901(0.80)
—	1 255 (1)	930(>1)	935.2(2)	—	1 311 (½)	894(0.44)	929(0.36)
—	1 348.5(½)	957(>1)	960.8(1.5)	1 375(0.70)	1 378 (1)	914(0.92)	955(0.13)
1 375(>1)	1 378.5(1)	1 025(0.12)	1 031.0(1.5)	1 440(>1)	1 443.7(2)	966(>1)	978(0.29)
1 442(>1)	1 443.3(2)	1 042(0.13)	1 046.4(1)	—	1 453 (1)	1 002(0.69)	1 008(0.98)
1 447(>1)	1 453 (1)	1 112(0.18)	—			1 052(>1)	1 027(0.32)
		1 182(0.36)	1 181 (½)			1 078(>1)	1 080(0.54)
		—	1 189 (½)			1 112(0.34)	1 102(0.54)
		1 227(>1)	1 231.2(3)			1 194(>1)	1 136(0.13)
		—	1 247 (½)			1 275(>1)	1 192(>1)
		—	1 260 (0.6)			1 312(0.62)	1 232(0.22)
		1 282(>1)	1 286.3(2)			1 422(0. 84)	1 276(>1)
		1 307(0.86)	1 309.9(0.8)			1 438(0.59)	1 307(0. 41)
		—	1 347 (½)				1 327(0.23)
		1 423(0.86)	1 424.5(1)				
		—	1 437 (½)				
		1 442(0.90)	1 444.5(2)				
			1 453 (1)				
Number of rotational isomers:							
1		2		1		3	3
Number of diff. bands in I.R. and Raman							
14 (theory 13)		26 (theory 26)		13 (theory 13)		20* (theory 39)	22* (theory 39)

* Not comparable with the numbers 14, 26 and 13 since no Raman data are available.

A cell thickness of 10 cm was applied throughout. Due to the usual band-spread in the spectra of gases a reliable normal vibration analysis on this basis is not possible. Since the spectra of (I)—(V) in the liquid phase were not obtained we shall refrain from extending Nielsen's work [3] on ethyl fluoride, but the spectra are nevertheless given because of their documentary value (Fig. 1).

Infrared spectra of the bromides (I′), (II′), (II′ + III′), (IV′) and (V′) in the liquid phase at room temperature were also taken. The absorption line frequencies are given in Table 1. We have attempted to subtract the lines originating from (II′) in the spectrum of (II′ + III′). For sake of comparison we have included the Raman observations made

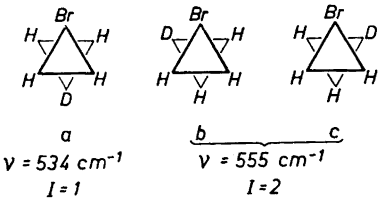

Fig. 3. Rotational isomers (*a*), (*b*) and (*c*) of CH_2DCH_2Br. Since (*b*) and (*c*) are mirror images they are spectroscopically indistinguishable. ν = frequency, I = relative intensity of observed bands.

by Langseth and Bak [6]. These are, *e. g.*, of special value in the identification of the (III′)-lines since Langseth and Bak prepared (III′) by the different process

$$CH_3CHN_2 + DBr \rightarrow CH_3CHDBr,$$

giving a sample not contaminated with CH_2DCH_2Br.

DISCUSSION

The default that no Raman data have been published for (IV′) and (V′) may tentatively be removed by the argument supported by columns 1—6 of Table 1, that the *total* number of different lines observed, either in the infrared or in the Raman spectrum, is approximately equal to the number of observed lines + 4n when n is the number of rotational isomers. Estimated in this way, the number of different bands from (IV′) or (V′) would be, respectively, 20 + 12 = 32 and 22 + 12 = 34. This is probably an upper limit so that for both (IV′) and (V′) we are so far from the number of theoretically observable lines, 39, that it is hard to avoid the conclusion that two of the rotational isomers have many coinciding bands. In fact we believe that these isomers can be pointed out.

In the spectrum of (II′) (Table 1. Two rotational isomers in a 1:2 ratio) it is seen that the rotational isomers absorb near 540 cm^{-1} (C—Br stretching frequencies). Fig. 3 illustrates the situation.

Now, the three spectroscopically distinguishable isomers (IV′) are, in fact, deuterium derivatives of the species in Fig. 3.

According to the Rayleigh rule, which it is legitimate to apply here because of the relatively isolated position of the C—Br band in question (*cf.* Table 1),

$$\nu \text{ (}e \text{ and } f\text{)} \leq 534 \text{ cm}^{-1}$$
$$\nu \text{ (}g \text{ and } h\text{)} \leq 555 \text{ cm}^{-1}$$
$$\nu \text{ (}i \text{ and } j\text{)} \leq 555 \text{ cm}^{-1}.$$

Now, two lines were observed at 526 and 543 cm^{-1}, their intensity ratio being about 1:2. The only solution is that

$$\nu \text{ (}e \text{ and } f\text{)} = 526 \text{ cm}^{-1}$$

$$\nu \text{ (}g \text{ and } h\text{)} \sim \nu \text{ (}i \text{ and } j\text{)} = 543 \text{ cm}^{-1}.$$

Therefore, the C—Br stretching frequencies coincide for the isomers (*g*, *h*) and (*i*, *j*).

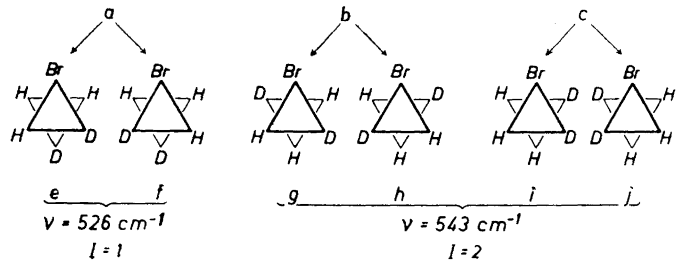

Fig. 4. Rotational isomers of $CH_2DCHDBr$. Since (*e*) and (*f*), (*g*) and (*h*), (*i*) and (*j*) are mirror images there are only three spectroscopically distinguishable isomers.

We can argue in a similar way considering (V′) as a deuterium derivative of (IV′). Selecting (*e*), (*g*), and (*i*) as suitable representatives we get the isomers (*k*), (*l*), (*m*), (*n*), (*o*) and (*p*) (Fig. 5).

According to the Rayleigh rule:

$\nu\ (k) \leq 526\ \text{cm}^{-1}$, $\nu\ (o) \leq 543\ \text{cm}^{-1}$. Since $(k) \equiv (o)$, $\nu\ (o) \leq 526\ \text{cm}^{-1}$
$\nu\ (l) \leq 526\ \text{cm}^{-1}$, $\nu\ (n) \leq 543\ \text{cm}^{-1}$. Since $(l) \equiv (n)$, $\nu\ (n) \leq 526\ \text{cm}^{-1}$.

Also

$$\nu\ (m) \leq 543\ \text{cm}^{-1},\ \nu\ (p) \leq 543\ \text{cm}^{-1}.$$

Again, two lines were observed at 542 and 523 cm^{-1} with an intensity ratio of 1:2. The only solution is that

$$\nu\ (k) \sim \nu\ (l) = 523\ \text{cm}^{-1}$$
$$\nu\ (m) = 542\ \text{cm}^{-1}.$$

It follows from the low number of observed lines in the spectra of (IV′) and (V′) that some coincidence of spectral lines must take place. Since the C—Br stretching frequencies coincide in the spectra of the rotational isomers (*g*) and (*i*), respectively (*k*) and (*l*), the remaining parts of these spectra may also be very similar.

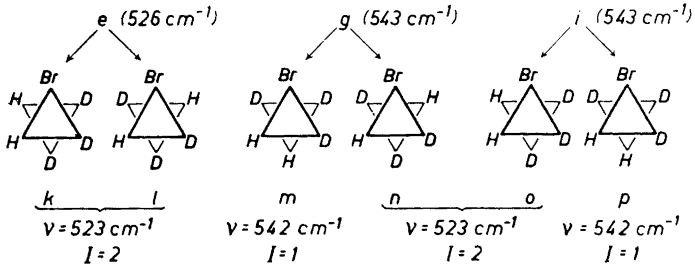

Fig. 5. Rotational isomers of CHD_2CHDBr. Here $(k) \equiv (o)$, $(m) \equiv (p)$, and $(l) \equiv (n)$.

Table 2. Comparison between infrared absorption frequencies of the C—Br stretching vibration of $CH_2DCHDBr$ (IV′) and CHD_2CHDBr (V′) in the liquid and gaseous states. Frequencies in cm^{-1}. In parenthesis, relative intensity.

	$CH_2DCHDBr$			CHD_2CHDBr		
Liquid	526(1)	543(2)		523(2)	542(1)	
Vapour	538.8(1)	556.6(1)	559.2(1)	536.0(1)	536.0(1)	554.7(1)

This postulated closer similarity is in harmony with the fact that (*k*) and (*l*) are identical molecules with respect to the grouping about one carbon atom and mirror images with respect to the grouping about the second carbon atom whereas no such simple relationship exists between (*k*) and (*m*).

In order to see whether the C—Br stretching frequencies of the rotational isomers (*g*) and (*i*), respectively (*k*) and (*l*), are at all separated, spectra of (IV′) and (V′) in the gas phase were run, using a Beckman IR3 spectrograph with a somewhat higher resolution than the Perkin-Elmer instrument. The path length was 10 cm and the pressure 150 mm Hg. In Table 2 the results are summarized and compared with the data for the liquid state.

As seen from Table 2, three distinct Q-branches were observed only in the case of the rotational isomers (*e*), (*g*) and (*i*) with the common formula $CH_2DCHDBr$.

Acknowledgement. We are grateful to Dr. F. A. Andersen for taking the spectra on the Beckman instrument. One of us (S.D.) wants to express her thanks for a Danish Government scholarship.

REFERENCES

1. Henne, A. L. and Midgley, T. *J. Am. Chem. Soc.* **58** (1936) 884.
2. Henne, A. L. and Renoll, M. W. *J. Am. Chem. Soc.* **60** (1938) 1060.
3. Smith, D. C., Saunders, R. A., Nielsen, J. R. and Ferguson E. E. *J. Chem. Phys.* **20** (1952) 847.
4. Jungers, I. C. and Verhulst, J. J. *Acad. roy. Belg. Classe sci.* Mem. 2. ser. **23** (1949) 44.
5. Leitch, L. C. and Morse, A. T. *Can. J. Chem.* **30** (1952) 924.
6. Langseth, A. and Bak, B. *Kgl. Danske Videnskab. Selskab Mat. Fys. Medd.* **24** (1947) No. 3.

Received September 17, 1958.

ACTA CHEMICA SCANDINAVICA 12 (1958) 2028—2033

The Use of Half Width and Position of the Lines in the X-Ray Diffractograms of Native Cellulose to Characterize the Structural Properties of the Samples

JON GJØNNES and NICOLAI NORMAN

Central Institute for Industrial Research, Oslo, Norway

Measurements of the position and half width of the (002)-reflexion for different samples of cellulose I (native) have been carried out. The values of the half widths have been compared with the degree of amorphity determined from a separation of the observed intensity into an amorphous and a crystalline part, and it is shown that this factor increases monotonically with the half width. The structural interpretation of the half width parameter is ambiguous, but its value should be related to the diameter and state of order of the microfibrils.

In a previous paper [1] it has been demonstrated that the X-ray diffractograms of cellulose I (native) to a fair degree of approximation can be interpreted as a superposition of broad crystalline reflexions, each reflexion having the shape of a Cauchy distribution. The normalized intensity distribution can thus be written

$$I(s) = \sum K_j \frac{\alpha_j}{\alpha_j^2 + (s - s_{oj})^2} \qquad (1)$$

where

$s = \frac{4\pi}{\lambda} \sin \Theta$

s_{oj} = peak position
$2\alpha_j$ = half width of the j'th reflexion
K_j = constant depending on the structure factor of the j'th reflexion

Each sample of cellulose I is in this way characterized by the parameters in equation (1). Of these the α_j and s_{oj} can be measured from the diffractograms.

The intensity distribution below $s = 2$ is dominated by the four reflexions (101), (10$\bar{1}$), (02$\bar{1}$) and (002). (101), (10$\bar{1}$) and (002) are of special interest as

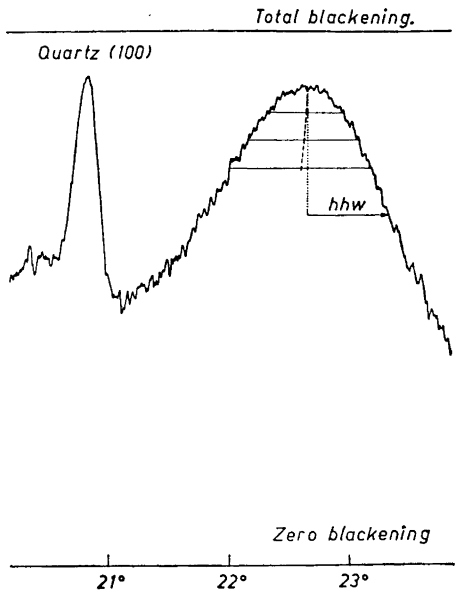

Fig. 1. Part of microphotometer curve. Residue of H_2SO_4 treated surgical cotton.

they give informations about dimensions and lattice distortions in directions normal to the fibre axis. As an accurate determination of the position and half width of (101) and (10$\bar{1}$) is impeded by the superposition of the two peaks, the investigations were restricted to the measurement of the peak position and half width of the (002)-reflexion.

EXPERIMENTAL PROCEDURE

Powder patterns of the investigated samples were prepared in a Guinier vacuum camera using Cu $K\alpha$-radiation. For accurate determination of the (002) peak position the samples were mixed with quartz (15 % by weight) and pressed into thin sheets in a briquetting machine. From the diffractograms film density curves were obtained by means of a recording microphotometer, the angular scale of the diffractograms being determined from the zero mark and the position of the quartz reflexions.

Fig. 1 shows a typical microphotometer curve. The peak abscissa was determined by bisecting horizontal cords and extrapolating to the peak level, as indicated in the figure. The half half-width was measured from the peak abscissa towards the high-angle side of the peak, as the low-angle side is strongly influenced by the (021)-reflexion, especially for samples with low order. The ordinates were read from zero film blackening, *i. e.* no coherent or incoherent background was subtracted.

RESULTS

11 different qualities of cellulose I were investigated. Half widths and peak positions were measured for five samples of each quality, and the mean values are listed in Table 1.

Table 1. (002)-peak position and half width for samples of cellulose I. Degree of amorphity determined by the method of Ellefsen *et al.*[2]

	Samples	Peak position $2\Theta°$	Half width in degrees	Degree of amorphity
1.	Surgical cotton	22.72	1.54	
2.	» » treated with H_2SO_4, residuum	22.71	1.32	0.37
3.	» » » » » peptized	22.68	1.40	0.36
4.	Cotton linters	22.71	1.40	0.41
5.	Acetate grade wood pulp	22.55	2.12	0.49
6.	Super cord grade wood pulp	22.52	2.44	0.53
7.	Viscose grade wood pulp	22.48	2.52	0.52
8.	Bleached sulfite pulp	22.40	2.80	0.56
9.	Surgical cotton ground in agate ball mill 1 h	20.2	8.8	
10.	» » » » » » » 3 »	19.9	9.8	
11.	» » » » » » » 8 »	19.8	11.0	1.00 *

* by definition

Based on the 40 diffractograms for samples 1—8, the standard deviation in peak position and half width for the average values in Table 1 were found to be 0.015° and 0.03°, respectively. For the ground samples the errors are appreciably higher.

DISCUSSION

Owing to the overlap of the reflexions, the correct values of the parameters α and s_0 can only be obtained when the line profile is corrected for neighbouring peaks and the structure independent scattering. In order to carry out such corrections the intensity distribution would have to be normalized, and more thorough considerations be made about line shapes. As the corrections will involve a considerable amount of work and in no case alter the sequence in which the samples can be placed on the basis of half width or peak position, such corrections were omitted. The error in the measured width was estimated from eqn. (1) using the parameters from the previous article [1]. The widths in Table 1 were found to be 5 % and 8 % too high for the cotton and acetate pulp samples, respectively.

The results in Table 1 seem to be in consistency with the technological knowledge of the cotton and pulps involved. A narrow width corresponds to a well crystalline material, a broad peak to a sample of less order, herein included small particle size.

In order to compare the results with other measurements, the Degree of amorphity determined by the method of Ellefsen, Wang Lund, Tønnesen and Øien [2] was calculated for 7 of the samples. The numbers are given in the last column in Table 1. In Fig. 2 the Degree of amorphity is plotted *versus* measured half width, and it can be seen that it increases monotonically with the half width. This result is by no means surprising since the calculated Degree of amorphity is proportional to the normalized intensity at $s = 1.32$ ($2\Theta = 18.6°$) where the adjusted intensity curve for the amorphous material touches

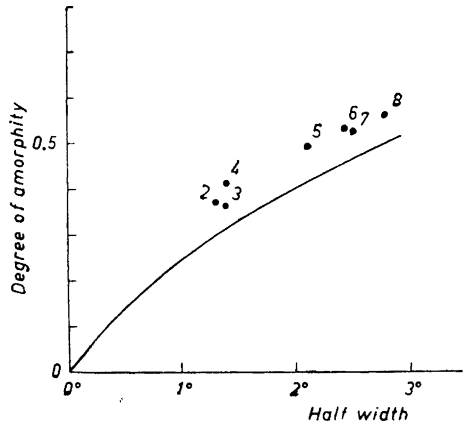

Fig. 2. Degree of amorphity *versus* half width for samples of cellulose I. The numbers correspond to the sample numbers in Table 1. The full drawn curve is based on the calculated intensity from eqn. (1) at $s = 1.32$.

the total intensity curve. Assuming eqn. (1) to be valid and the widths of the four significant (101), (10$\bar{1}$), (021) and (002) peaks to be interdependent in accordance with earlier results [1], an estimate of the total intensity at $s = 1.32$ can be made. The calculations led to the values of the Degree of amorphity represented by the full-line curve in Fig. 2, and it is seen that the plotted values in the same figure follow the trend of this curve.

The data in Table 1 seem to indicate a connection between half width and peak position, an observation which is illustrated in the graphical plot in Fig. 3. The reason for the almost linear decrease in the position of the (002)

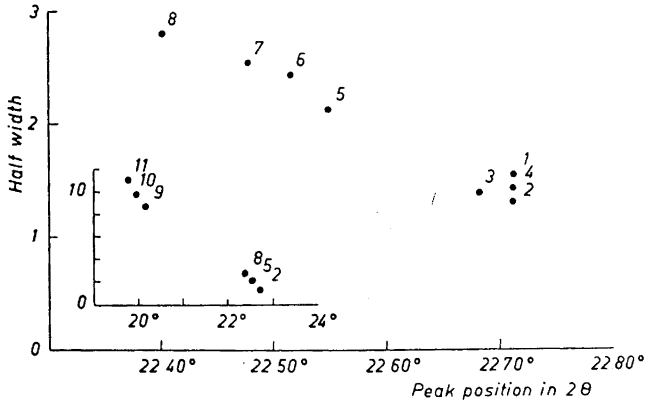

Fig. 3. Half width and position of the (002)-peak for samples of cellulose I. The numbers correspond to the sample numbers in Table 1.

peak with increasing half width may be found in an increase in the average interplanar spacing, though such a conclusion is highly uncertain since shifts in the position of the peak of the observed magnitude may be due to the influence of the other crystalline reflexions.

It is a question whether the measured half width can be associated more directly with structural parameters like the dimensions and intrinsic order of the microfibrils. Also here it is necessary to be cautious as the interpretation of line widths to a certain extent is arbitrary when only one order of the reflexions from a set of lattice planes can be measured. If the broadening of the line is attributed to small particle size only, calculations give a mean particle diameter of 60 Å for cotton and 30 Å for sulfite pulp. These dimensions should be taken as lower limits.

Finally the influence of the experimental technique should be considered. In pressing the samples the fibres are preferentially oriented with their axes in the plane of the sheet. This will for instance lead to a much higher intensity of the (021) peak compared with the (101), (10$\bar{1}$) and (002) peaks in a diffractogram of a sample in a symmetrical transmission set up than in a symmetrical reflexion set up. The position and half width of the (002)-reflexion from some pressed samples were therefore also measured in the Bragg-Brentano focusing set up with a proportional counter. The determination of half widths was further carried out on unoriented samples in the Guinier camera. For the counter measurements it was found a systematic shift of magnitude 0.05° towards higher angles in the peak position, and the half widths decreased 5 to 10 %. The half width determined from the film diffractograms of the unoriented samples led to values between the counter readings and the data in Table 1. When different samples are compared, the same technique should therefore be used in order to obtain the best result.

CONCLUSION

The present X-ray method gives an expedient and accurate prodecure to describe differences in the structural properties of samples of cellulose I. For measuring half widths it is not necessary to add a standard substance, and the line width can be read directly from a microphotometer trace or a counter diffractogram. The interpretation of the half width is somewhat arbitrary, but its value depends on the dimensions and lateral order of the microfibrils.

When the specimen also contains cellulose II, the influence of the new reflexions has to be considered. Further work on cellulose II and of mixtures of cellulose I and II is in progress.

The authors are indebted to cand.real. Ø. Ellefsen for supplying the samples, and they also want to thank Mrs. L. Bryn and Miss T. L. Arstal for their help in preparing the diffractograms. This investigation is part of a research program on the structure of cellulose carried out at the Central Institute for Industrial Research and The Norwegian Pulp and Paper Research Institute. Financial support from the *Royal Norwegian Council for Industrial Research* is gratefully acknowledged. One of the authors (J.G.) is indebted to the *Norwegian Research Council for Science and the Humanities* for financial support.

REFERENCES

1. Gjønnes, J., Norman, N. and Viervoll, H. *Acta Chem. Scand.* **12** (1958) 489.
2. Ellefsen, Ø., Wang Lund, E., Tønnesen, B. A. and and Øien, K. *Norsk Skogindustri* **11** (1957) 349. Part II.

Received August 22, 1958.

ACTA CHEMICA SCANDINAVICA 12 (1958) 2034—2042

Immunologic Studies of the Old Yellow Enzyme. A Comparison between the Enzyme and Its Apoprotein

STEN KISTNER

Biochemical Department, Nobel Medical Institute, Stockholm, Sweden

To achieve immunization rabbits were injected with preparations of Warburg's Old Yellow Enzyme (OYE) and its apoprotein. This resulted in the appearance of precipitating antibodies. The antigen-antibody reaction was studied by means of quantitative precipitin reactions and agar gel diffusion experiments. Crude enzyme preparations were found to contain several antigenic components, one of which was identical with the crystalline enzyme. The precipitin reaction between crystalline OYE and antiserum showed a regular behaviour in excess antibody and equivalence zones, and after diffusion in agar gel one single precipitin line was formed. A comparison between OYE and its apoprotein showed an immunologic identity of the two proteins. The coenzyme, flavin mono-nucleotide, did not have hapten activity. The biologic significance of these findings is discussed.

Enzymes, being proteins, may act as antigens. The resulting antibodies, in their reaction with the specific antigen, are often inhibitors of the catalytic activity. The inhibition of enzyme activity by antibodies is a mechanism of considerable biological interest, and has been the subject of a great number of investigations. Recent reviews have been published by Sevag [1,2], Marrack [3] and Cinader [4]. The importance of the catalytic sites on the enzyme molecule in these antigen-antibody reactions has been emphasized. If these sites are identical with the sites of antigenic activity, the binding of antibody takes place here. Another possibility of inhibition arises when the antibodies couple to other parts of the enzyme molecule, causing steric blocking of the catalytic sites. In some instances precipitating antibodies with little effect on the enzyme activity *in vitro* have been obtained [5]. However, such antibodies may afford protection against the catalytic activity *in vivo*, probably because the antigen-antibody complexes are rapidly removed from the circulation [3,5,6].

In many enzymes the catalytic activity is centered in a prosthetic or coenzyme group. These groups are often identical in widely different species. Antibodies formed to fit such groups might then cross-react with enzyme sys-

tems in the immunized organism, causing a non-desirable condition of auto-immunization. It does not appear, however, that antibodies are produced against such structures, but rather against the species specific protein part of the molecule [7,8]. One would therefore not expect these coenzyme groups to act as haptens [1].

Although much work has been done in this field, the role of the catalytic sites in different enzyme — antienzyme* systems has not yet been finally settled. Many difficulties prevent the study of the eventual participation of coenzyme groups as antigenic determinants. In most cases the interaction between coenzyme and the corresponding apoprotein is unknown, in other cases the reversibility of this reaction makes the immunologic studies erratic. The present work is a study of Warburg's »Old Yellow Enzyme» (OYE) using immunologic methods. This enzyme offers certain advantages for such an investigation. It can be prepared in a crystalline form [9], and it has a molecular weight [10] of about 104 000, suggesting good antigenic properties. The coenzyme group is flavin-mononucleotide (FMN), an *iso*alloxazin derivate, which may have the properties of a hapten. OYE contains 2 FMN molecules per mole [9], which can easily be split off [11], and thus the apoprotein is formed. The reaction

$$\text{coenzyme} + \text{apoprotein} \rightleftharpoons \text{enzyme}$$

has been extensively studied by Theorell and Nygaard by fluorescence measurements [12–14]. The equilibrium is shifted far to the right, and thus the enzyme is rather stable, as well as the apoprotein in the absence of FMN.

MATERIALS AND METHODS

1. Preparation of OYE and apoprotein

OYE was prepared from brewer's bottom yeast **, using the method described by Theorell and Åkeson [9]. The light absorption spectrum of crystalline OYE was in good agreement with that found by these authors. The enzyme was stored at 4°C under 80 % saturated ammonium sulphate solution until used. To determine the amount of enzyme and the degree of purity in the different fractions, the light absorption at 464 mμ was measured in a Beckman DU spectrophotometer. Using the value β_{464} for FMN = 2.43×10^7 cm²/mole and FMN-content in OYE = 0.877 %, the amount OYE corresponding to this absorption could easily be calculated. Dry weight determinations were done on the same sample. The degree of purity was expressed as the ratio

$$\frac{\text{amount enzyme found by light absorption}}{\text{amount enzyme found by dry weight determination.}}$$

For the crystalline OYE this "purity index" was 1.00 ± 0.05.

Apoprotein was obtained after dissociation of the enzyme by the procedure of Warburg and Christian [11]. The solutions of apoprotein showed no light absorption corresponding to the 383 mμ or 464 mμ peaks of OYE or the 445 mμ peak of FMN. The activity could be controlled and the concentration determined in a recording fluorescence meter by measuring the ability of the apoprotein to quench the fluorescence of FMN, as described

* In this paper the word »anti-enzyme» is used in the meaning: antibody against enzyme.
** Kindly supplied by Hamburgerbryggeriet, Stockholm.

by Theorell and Nygaard [12]. In all experiments where OYE and apoprotein were compared, the apoprotein was first prepared by cleaving the enzyme. The concentration was determined on a small aliquot of the solution. The rest was divided into two equal parts. FMN, slightly exceeding the equivalence, was added to one part, and a buffer blank to the other. Excess FMN was removed by dialysis. OYE thus obtained by dissociation and reassociation with FMN, showed the characteristic light absorption of the enzyme. The other solution contained an equivalent amount of apoprotein. All experiments were carried out in 0.15 M sodium phosphate buffer, pH 7.4. The "titration" of apoprotein with FMN was done at room temperature.

FMN-solutions were made up from a commercial preparation (Sigma Chemical Company). A fresh solution was prepared the same day as the experiments were carried out and kept in the dark and the cold until used. The concentration was determined by measuring the light absorption [9], using the value β_{445} for FMN = 2.81×10^7 cm²/mole *.

2. Immunization

Four male albino rabbits, 6 months old, weighing 2.5—3 kg, were used for immunization. Rabbit No. 1 received 3 weekly i. m. injections of an enzyme preparation with purity index 0.20. Each injection contained 60 mg substance, as determined by dry weight, corresponding to 12 mg of pure enzyme. For the other rabbits a Freund's adjuvant [15,16] as described by Cohn [17] was used. About 2/3 of the antigen were given in the first injection. Three weeks later the rest was injected i. m. without adjuvant as a booster dose. Rabbit No. 2 received 32 mg of a preparation with purity index 0.70 (corresponding to 22 mg of pure enzyme). For the last two rabbits an enzyme preparation with purity index 0.56 was used. The enzyme was dissociated, and one part of it reassociated with FMN. Each part contained 54 mg (corresponding to 30 mg of pure enzyme or the equivalent amount of apoprotein, respectively). Rabbit No. 3 received the OYE, and No. 4 the apoprotein.

Blood samples were collected by puncturing the central artery of the ear. Before immunization 10—12 ml of blood were taken from each animal to obtain serum for control experiments. 7—10 days after the last injection the rabbits were anaesthetized and a cannula inserted into the left carotid artery. In this way 50—100 ml of blood were collected from each rabbit. The blood was allowed to clot at room temperature, and the clot retraction accomplished by incubation at 37°C for 30 min. Serum was sucked off and stored at —15°C in small aliquots. When used for experiments it was 1—3 months old.

3. Precipitin reactions

The appearance of precipitating antibodies in the immune-sera was checked by ring tests [18]. Quantitative precipitin reaction [19] was performed, using ultraviolet absorption spectroscopy to measure the precipitate [20,21]. Antigen solution in 0.15 M sodium phosphate buffer pH 7.4 was mixed with 1 ml serum. The volume was kept constant at 2.5 ml. The incubation time was 60 min at 37°C, followed by 48 h at 4°C. The precipitates were washed twice in saline in the cold and dissolved in 0.25 M acetic acid [21] to a volume of 3.0 ml. The absorption was read in a Beckman DU spectrophotometer at 277 mμ, where antigen as well as precipitate in acetic acid solution had a maximum. The extinction coefficient of the antigen had previously been determined. In excess antibody and equivalence zones the optical density of the antibody could be obtained by subtracting the optical density of antigen from that of the precipitate [21].

Control experiments were run, using serum from the immunized animals, but collected before immunization.

---

* FMN Sigma contains some impuriries [12]. The apoprotein reacts, however, preferentially with the component identical with FMN from OYE [12-14]. With FMN in excess, the OYE obtained in these association reactions could therefore be expected to be identical with the product obtained, when FMN from OYE is used.

4. Electrophoresis

Paper electrophoresis was performed, using Durrum's technique [22], in barbiturate buffer pH 8.6, ionic strength 0.075, for 16 h at 100 V, on 30 cm long Whatman No. 1 paper strips. Staining of proteins was done for 16 h in 0.01 % bromophenol blue, the fractions were cut out, eluted in 0.01 N NaOH, and the absorption read at 590 mμ[22]. To correct for different uptake of stain by albumins and globulins, the values obtained for globulins were multiplied by 1.3.

5. Antigen-antibody reactions in agar gel

The technique described by Ouchterlony was used [23]. The gel contained 1.5 % agar, 0.15 M sodium phosphate buffer pH 7.4, and merthiolat 1:10 000. The reactions were performed in sealed Petri dishes. A 50 × 50 mm glass plate was placed in the bottom of each dish under the agar [24]. Antigen and antibody were added in concentrations close to their equivalence ratio. Incubation was done at 4°C, room temperature, or 37°C for different periods of time. In some experiments the basins were refilled 2 or 3 times, each filling consisting of 0.15—0.20 ml. After the reactions were completed, the gel was washed in saline, distilled water, and finally dehydrated with ethyl alcohol [24]. The gel was cut along the sides of the glass plate and allowed to dry at room temperature [25]. In this way a thin film containing the precipitin lines was obtained on the glass plate. These preparations were stained for 20—30 min in a solution of azocarmine B containing 10 % acetic acid and 50 % methyl alcohol. Excess stain was removed by washing the film in the solvent. After this procedure the precipitin lines showed a strong red colour, whereas the rest of the film was practically without colour.

Buffer solutions of OYE and apoprotein were used as antigens. They were tested against sera from the immunized animals, collected before and after immunization. 1/10 volume EDTA-solution (1 g sequestrene-Na_2 and 0.7 g NaCl per 100 ml solution) was added to all sera. In absorption experiments different amounts of OYE or apoprotein were added in the basins containing serum. Absorbed sera were tested against OYE and apoprotein solutions. All experiments were run in duplicate.

RESULTS

Precipitating antibodies were found in the serum of all animals on the 4th week of immunization. In rabbits receiving adjuvant, antibodies appeared even before the booster-dose was given. Paper electrophoresis of the sera showed a relative decrease of the albumin fraction and increase of globulin fractions, especially β and γ, following immunization in all animals. These changes were essentially the same, regardless of the technique of immunization, and whether OYE or apoprotein was used as antigen.

Quantitative studies of the precipitin reaction showed a regular behavior of the OYE-anti-OYE system in excess antibody and equivalence zones. Plotting the amount of antigen added against the amount of precipitate formed gave a parabolic curve. When, according to the equation of Heidelberger and Kendall [19], the amount of antigen added was plotted against the ratio

$$\frac{\text{antibody precipatated}}{\text{antigen precipitated}} \quad (R)$$

a straight line was obtained. Curve A of Fig. 1 shows the results, when a crystalline preparation of OYE was tested against an anti-OYE serum. In excess antigen zone there is a rather slow decline of the curve. Even in large

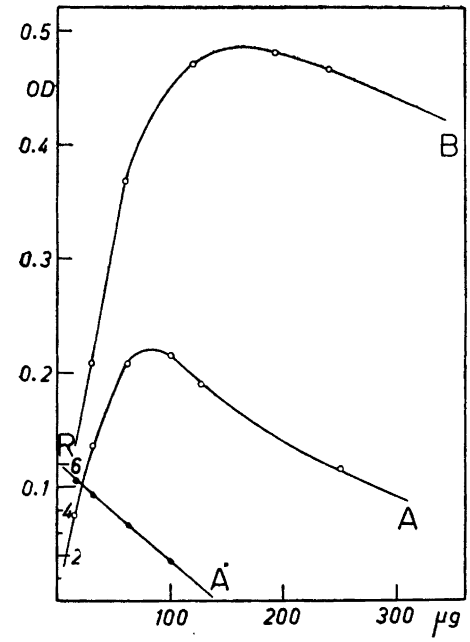

Fig. 1. Quantitative precipitin reaction. Anti-OYE serum from a rabbit, immunized with a total of 54 mg of an enzyme preparation with purity index 0.56 (No. 3). Curve A shows the reaction with crystalline OYE, purity index 0.97, as antigen. A′ is the corresponding line, obtained by plotting the amount of antigen added against $R\left(\frac{\text{antibody precipitated}}{\text{antigen precipitated}}\right)$. In B the antigen is an enzyme preparation with purity index 0.52. See text.

excess antigen, *i.e.* 5 times as much as the amount needed to reach the equivalence zone, there was a small precipitate formed. This behaviour of the system will be further commented on in the discussion. The reaction did not show the same regularity when an impure enzyme preparation was tested against the same serum. Also, the equivalence point was moved towards higher concentrations of antigen, (Curve B, Fig. 1). The antigen in this case contained about 50 % OYE, and about twice as much as of crystalline OYE was needed to reach the equivalence point. This did not, however, indicate that OYE was the only reacting antigen, since the precipitate formed was much larger [26]. In this latter case the decline of the curve in the antigen excess area was even less pronounced than in the reaction, where crystalline enzyme was used as antigen.

Hapten reactions [18] were performed in the equivalence zone, using crystalline OYE as antigen. The antiserum was incubated with FMN before adding the enzyme. The concentration of FMN was determined on the basis of the amount of OYE taking part in the reaction. Thus, in different experiments incubation with 1 to 20 moles of FMN per mole of OYE was tried. In no case did the presence of FMN reduce the formed precipitate significantly nor was a precipitate formed when FMN alone was incubated with antiserum.

When crystalline OYE reacted with anti-OYE serum after diffusion in agar gel, only one precipitine line was formed, whereas impure preparations caused the appearance of several lines. The two antigen solutions were tested simultaneously against the same serum, using agar plates with 3 basins, as

Fig. 2. Antigen-antibody reaction in agar gel. The gel contained 3 basins, arranged as described in Ref.[23]. Antigens and antiserum were the same as in the experiments illustrated in Fig. 1. The upper left basin contained the crystalline OYE, 0.1 mg/ml, the upper right contained the impure enzyme, 0.2 mg/ml, and the lower basin contained the anti-OYE serum. The basins were filled 4 times. Incubation at 37°C. Lines appeared after 24–36 h. Note the fusion of the single line on the left side, representing the reaction between the crystalline OYE and antiserum, into one of the 4 lines on the right side (crossing the first and completely fusing into the second line from the left).

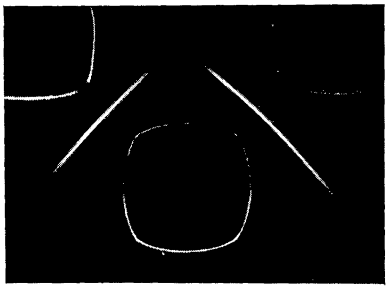

Fig. 3. Antigen-antibody reaction in agar gel. Anti-OYE serum in the lower basin tested against an OYE-preparation (purity index 0.60, 0.15 mg/ml) in the upper left basin and the equivalent apoprotein solution in the upper right. The basins were filled three times. Incubation at 37°C. Three lines appeared on each side of the serum basin after 24–36 h, forming a symmetric pattern, with the lines on one side fusing into those on the other side.

described in Ref [23]. Crystalline OYE was added in one basin, a crude enzyme preparation in another, and antiserum in the middle. The line formed between the crystalline enzyme and antiserum fused into one of the lines formed between the crude enzyme and serum. Fig. 2 is a photograph of such an experiment, where antigens and antiserum tested were the same as those in the quantitative precipitin reactions illustrated in Fig. 1. Similar results were obtained with all anti-OYE sera. Incubation at lower temperatures did not alter the results, although a longer time was necessary for the lines to develop. Leaving the plates at 4°C for several weeks did not result in the appearance of more precipitin lines. Negative results were consistently obtained in these experiments when sera from the immunizied animals, collected before immunization, were tested.

Different preparations of OYE were compared with corresponding apoprotein solutions (see Material and Methods, 1) in similar experiments. The pattern of lines between OYE and anti-OYE serum was identical with that between apoprotein and the same serum, and the lines on one side fused into those on the other side (Fig. 3). When crystalline OYE and apoprotein, obtained after cleaving the crystalline enzyme, were tested, one line was formed on each side of the serum basin (Fig. 4). When the same experiments were repeated using anti-apoprotein serum, the results were identical with those obtained with anti-OYE serum.

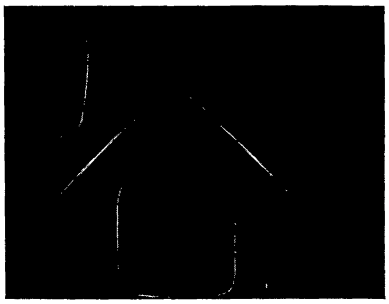

Fig. 4. Antigen-antibody reaction in agar gel. Anti-OYE serum in the lower basin tested against a solution of crystalline OYE, 0.1 mg/ml, in the upper left basin, and an equivalent solution of apoprotein in the upper right. The basins were filled 4 times. Incubation at 37°C. The lines appeared after 24 h. An identical result was obtained when the same antigens were tested against an anti-apoprotein serum.

A rough estimation of the sensitivity of the agar gel diffusion technique was done when 10 μg of crystalline OYE were tested against the equivalent amount of serum, as found by quantitative precipitin reaction. A clearly visible line was obtained.

Anti-OYE and anti-apoprotein serum from rabbits Nos 3 and 4 were tested after absorption with antigen. Only crystalline OYE and apoprotein from crystalline OYE, respectively, were used in these experiments. The equivalence point of each serum with the homologous antigen was determined. Serum and the equivalent amount of antigen were mixed in one basin in an agar plate and tested against OYE and apoprotein. Antigens, used for absorption, were then reversed, *i.e.* anti-OYE serum was absorbed with apoprotein and vice versa. In no experiment did the absorbed serum retain the ability to react with either OYE or apoprotein. The two antigens seemed able to replace each other, and to absorb homologous as well as heterologous serum.

DISCUSSION

Attempts to immunize rabbits with preparations of OYE have previously been made by Várterész and Kesztyüs [27]. The antigen used was a crude enzyme preparation. These workers found no precipitating or complement fixating antibodies, nor was the activity of the enzyme inhibited by the antiserum. Their conclusion was that OYE lacks antigenic properties, possibly due to identical structure in different species. This opinion clearly differs from the common concept of protein specificity, and has also been criticized [1,28]. Considering later investigations it appeared even more probable that antibodies against OYE could be obtained, since immunization with crystalline yeast enzymes had been successful [29,30]. Results of the present work show that crude preparations of OYE contain several antigenic components. One of these is evidently identical with the crystalline OYE.

When crystalline OYE reacted with anti-OYE serum, a precipitate was formed. Quantitative studies showed a regularity of this reaction in excess antibody and equivalence zones, suggesting a single antigen-antibody system [26]. There was still a precipitate formed in rather large excess antigen. This may be an indication of impurities in the antigen, or of cross-reactions with several antibodies. Certain antigens, however, although of somewhat different type,

have been described to cause this type of reaction (see Ref [26]). Also, in this particular case the method employed influenced the curve. At the wave length where the precipitates were measured, the extinction coefficent of crystalline OYE is higher than that found for different rabbit antibodies [21]. Precipitates formed in excess antigen thus caused a relatively high absorption. — A careful analysis of the quantitative precipitin reaction was not done because of the shortage of material. It was mainly employed to determine optimum reaction conditions for other experiments.

The reaction between crystalline OYE and anti-OYE serum in agar gel diffusion experiments resulted in a single precipitin line. This is an indication of antigenic homogeneity of the material. Also it appeared that the precipitate was the result of the reaction between enzyme and specific antibody. A cross reaction with some other yeast protein antibodies was not likely, since the precipitin line fused into an identical line on the site of reaction between antiserum and crude enzyme, which contained the same concentration of pure OYE as did the crystalline preparation (Fig. 2). The existence of an eventual homologous antigen in this area would have prevented a cross reaction to occur here [31,32], and the line between the crystalline enzyme and serum on the left side would probably have shown partial coalescence [33] into the line representing the reaction between the homologous antigen and serum on the right side. The complete fusion of the two lines into an arc that now occurred is evidence of identical antigen on both sides [23,33]. The same antigen diffused from the basins containing crystalline and crude enzyme.

OYE and apoprotein showed same reactivity with anti-OYE as well as anti-apoprotein serum. Both sera were equally absorbed with any one of these antigens. Also, FMN did not have the effect of a hapten. The enzyme and its apoprotein were identical from the immunologic point of view. The coenzyme group was apparently not engaged in the antigenic active part of the enzyme molecule or in the binding to antibody.

It may be asked whether injection of OYE and apoprotein into the animals actually ment the introduction of two different antigens. Injected OYE could hardly have dissociated to any great extent because of the firm association between FMN and apoprotein*. On the other hand, it may be postulated that injected apoprotein associates with free FMN *in vivo* to form flavoprotein. If this is true, apoprotein, for all practical purposes, is immunologically identical with OYE. Such an association could not be assumed to take place in the *in vitro* experiments. The assumption that the coenzyme group does not take part in the immunologic active part of the enzyme molecule therefore appears to be valid. The biologic importance of this finding has already been discussed in the introduction. Production of antibodies reacting with structures common to the immunized organism, does not seem beneficial. Antibodies against the

* The equilibrium constant in the dissociation reaction of OYE has been determined by Theorell and Nygaard. It was found to be around 0.7×10^{-8} in a buffer of pH 5.75, containing 0.25 M Na-phosphate and 0.4 M NaCl [12]. At pH around 7 and lower Cl^- the constant is considerably decreased [13]. It is therefore very unlikely that injected OYE dissociated to any notable extent. At least this could not be true in rabbit No. 1, which was immunized with injections of enzyme without adjuvant, and results with immune serum from this rabbit were in good agreement with those obtained with serum from the other animals.

enzyme may still inhibit the activity. This problem is presently under investigation. It is possible, however, that replacement of the coenzyme group with some structually related compound, as perhaps happens in chemotherapy [34], may alter the antigenic behaviour of the enzyme.

Acknowledgement. The author wishes to express his thanks to Professor Hugo Theorell and coworkers at the Department of Biochemistry, Nobel Medical Institute, for valuable discussions and advices during the course of this work.

REFERENCES

1. Sevag, M. G. *Immuno-Catalysis*, Charles C. Thomas Publ., Springfield 1945.
2. Sevag, M. G. *Ergeb. Hyg. Bakteriol. Immunitätsforsch. u. Exptl. Therap.* **28** (1954) 424.
3. Marrack, J. R. in Sumner, J. B. and Myrbäck, K. *The Enzymes*, Vol. I, Part 1, Academic Press Inc., New York 1950, p. 343.
4. Cinader, B. *Ann. Rev. Microbiol.* **11** (1957) 371.
5. Kirk, J. S. *J. Biol. Chem.* **100** (1933) 667.
6. Kirk, J. S. and Sumner, J. B. *J. Biol. Chem.* **94** (1931) 21.
7. Heidelberger, M. and Landsteiner, K. *J. Exptl. Med.* **38** (1923) 561.
8. Bonnichsen, R. K. *Arch. Biochem.* **12** (1947) 83.
9. Theorell, H. and Åkeson, Å. *Arch. Biochem. Biophys.* **65** (1956) 439.
10. Ehrenberg, A. *Acta Chem. Scand.* **11** (1957) 1257.
11. Warburg, O. and Christian, W. *Biochem. Z.* **298** (1938) 368.
12. Theorell, H. and Nygaard, A. *Acta Chem. Scand.* **8** (1954) 877.
13. Theorell, H. and Nygaard, A. *Acta Chem. Scand.* **8** (1954) 1649.
14. Nygaard, A. and Theorell, H. *Acta Chem. Scand.* **9** (1955) 1587.
15. Freund, J. and McDermott, K. *Proc. Soc. Exptl. Biol. Med.* **49** (1942) 548.
16. Freund, J. and Walter, W. W. *Proc. Soc. Exptl. Biol. Med.* **56** (1944) 47.
17. Cohn, M. in *Methods in Medical Research Vol. 5*, p. 271, The Year Book Publ. Inc., Chicago 1952.
18. Kabat, E. A. and Mayer, M. M. *Experimental Immunochemistry*, Charles G. Thomas, Springfield 1948.
19. Heidelberger, M. and Kendall, F. E. *J. Exptl. Med.* **61** (1935) 563.
20. Eisen, H. N. *J. Immunol.* **60** (1948) 77.
21. Gitlin, D. *J. Immunol.* **62** (1949) 437.
22. Block, R. J., Durrum, E. L. and Zweig, G. *A Manual of Paper Chromatography and Paper Electrophoresis*, 2nd Ed. Academic Press Inc. New York 1958.
23. Ouchterlony, Ö. *Arkiv Kemi, Mineral. Geol.* **26B** (1948) No. 14.
24. Perlman, P. and D'Amelio, V. D. *Nature* **181** (1958) 491.
25. Uriel, J. and Grabar, O. *Ann. inst. Pasteur* **90** (1956) 427.
26. Cohn, M. in *Methods in Medical Research Vol. 5*, p. 301, The Year Book Publ. Inc., Chicago 1952.
27. Várterész, W. and Kesztyüs, L. *Z. Immunitätsforsch.* **99** (1941) 211.
28. Landsteiner, K. *The Specificity of Serological Reactions*, Harvard University Press, Cambridge 1947.
29. Najjar, V. A. and Fisher, J. *Science* **122** (1955) 1272.
30. Antoni, F. and Keleti, T. *Nature* **179** (1957) 1020.
31. Mayer, M. and Heidelberger, M. *J. Biol. Chem.* **143** (1942) 567.
32. Cohn, M. and Torriani, A. M. *J. Immunol.* **69** (1952) 471.
33. Oudin, J. in *Methods in Medical Research, Vol. 5*, p. 335, The Year Book Publ. Inc. Chicago 1952.
34. Haas, E. *J. Biol. Chem.* **155** (1944) 321.

Received August 22, 1958.

ACTA CHEMICA SCANDINAVICA 12 (1958) 2043—2054

Short Communications

Studies on Histidyl Peptides

II. The Synthesis of L-Histidyl-L-Leucine and its Optical Homogeneity

DIMITRIOS THEODOROPOULOS*

Department of Medical Biochemistry, University of Gothenburg, Sweden

The potentialities of the new procedure [1] for the incorporation of an histidine residue into synthetic peptides have been demonstrated during the synthesis of several histidine and histidyl peptides [2]. The latter were obtained through condensation of carbobenzoxy-*im*.benzyl-L-histidine (I) with amino acid esters for which purpose the carbodiimide method [3] for the peptide bond formation was employed. Owing to the slight solubility of (I) in various organic solvents and especially in cold, its condensation was accomplished in dimethylformamide solution although at a higher temperature than that customarily used. This alteration naturally raises speculations regarding the optical homogeneity of peptides thus produced. It has also been reported recently from two different laboratories [4,5] that, as a condensing agent, carbodiimide yields partly racemized peptides in certain cases. Among the factors which influence racemization, it has been found that temperature and solvents predominate.

Consequently, it was considered desirable to reveal whether racemization takes place while (I) is being coupled with amino acid esters under the experimental conditions previously described [2], and if possible, to eliminate such a risk by carrying out the reaction at a lower temperature.

When (I) was coupled with L-leucine benzyl ester in the same way as previously reported [2], the product, carbobenzoxy-*im*. benzyl-L-histidyl-L-leucine benzyl ester (IIa) showed an $[\alpha]^{22}D$ value of $-13.4°$ (*c* 3.6 in glacial acetic acid).

Alternatively, the same product was synthesized by mixing (I) with the equivalent amount of triethylamine in dimethylformamide or methylene chloride, thus causing the carbobenzoxy derivative to dissolve, followed by addition of the equivalent amount of L-leucine benzyl ester *p*-toluenesulfonate [6] and carbodiimide. The above modification not only facilitates the condensation of (I) at room temperature but more-over, produces better yields. Carbobenzoxy-*im*.benzyl-L-histidyl-L-leucine benzyl ester (IIb) was thus obtained at a rate of 65 % as against 50 % yield produced by the previously described procedure [2].

It is signifficant that compounds (IIa) and (IIb) showed identical optical rotations and melting points.

This evidence, however, does by no means exclude the possibility that compounds (IIa) and (IIb) have suffered racemization to the same extent during their syntheses. Carbobenzoxy-*im*.benzyl-L-histidyl-L-leucine benzyl ester, prepared by either of the two above mentioned processes, was therefore converted into free peptide L-histidyl-L-leucine, and the optical value of the latter was compared to that reported by Holley and Sondheimer [7]. These authors synthesized L-histidyl-L-leucine by he azide procedure which, up to the present, has been believed to cause no racemization.

Carbobenzoxy-*im*.benzyl-L-histidyl-L-leucine benzyl ester was hydrogenated in the presence of palladium black or reduced by sodium in liquid amonnia [8], to produce L-histidyl-L-leucine.

* Research Fellow at the University of Gothenburg under funds defrayed by A. B. Marabou.

The obtained peptide, L-histidyl-L-leucine, showed and $[\alpha]^{22}D$ value of 45.2° as a 1 % solution in 0.10 N sodium hydroxide, practically identical with the reported $[\alpha]^{22}D$ value of 43.5° as a 1 % solution in 0.10 N sodium hydroxide. This finding emphasizes the capability of the new procedure [1] in producing optically active histidyl peptides.

EXPERIMENTAL

Carbobenzoxy-im.*benzyl*-L-*histidyl*-L-*leucine benzyl ester. A. Modified procedure.* To a suspension of 1.89 (0.005 mole) of carbobenzoxy-*im*.benzyl-L-histidine in 30 ml of dimethylformamide, 0.5 g (0.005 mole) of triethylamine was added. This caused the carbobenzoxy derivative to dissolve almost completely. A solution of 1.89 g (0.005 mole) of L-leucine benzyl ester *p*-toluenesulfonate in 10 ml dimethylformamide was then added, followed by the addition of 1.1 g of carbodiimide. The mixture was stirred overnight at room temperature, and di*cyclo*hexylurea was subsequently removed by filtration. The solution was treated in the manner described below and the peptide derivative thus obtained at 65 % yield, melted at 112—114° and showed an optical rotation of $[\alpha]^{22}D$ —13.8° (*c*, 3.5 in glacial acetic acid). (Found: C 70.2; H 6.80; N 9.80. Calc. for $C_{34}H_{38}O_5N_4$: C 70.08; H 6.57; N 9.61.) B. Carbobenzoxy-*im*.benzyl-L-histidine (0.005 mole) was treated with L-leucine benzyl ester (0.005 mole) and 1.1 g of carbodiimide as previously described [2]. Di*cyclo*hexylurea was filtered and the solution diluted with 500 ml of water. The precipitating product was recrystallized by dissolving in ethylacetate followed by addition of petroleum ether. Yield 1.4 g (50 %), needles, m. p. 112—114°, $[\alpha]^{22}D$ —13.4° (*c*, 3.6 in glacial acetic acid).

Carbobenzoxy - im.*benzyl* - L - *histidyl* - im.*benzyl* - L - *histidine benzyl ester.* Carbobenzoxy-*im*.benzyl-L-histidine (1.89 g) was dissolved in 30 ml of methylene chloride by addition of 1.01 g of triethylamine. To this solution 3.4 g of *im*.benzyl-L-histidine benzyl ester di-*p*-toluenesulfonate dissolved in 5 ml of methylene chloride and 1.1 g of di*cyclo*hexylcarbodiimide were then added. After 12 h the di*cyclo*hexylurea was filtered and the solution washed with water. It was then dried over Na_2SO_4 and the solvent evaporated *in vacuo*. The residue was crystallized by addition of ether. It was recrystallized from ethylacetate-petroleum ether. Yield 2.2 g (65 %), small needles, m. p. 137°, (reported [2] 137°), $[\alpha]^{22}D$ —23.3° (*c*, 4.5 in glacial acetic acid), reported $[\alpha]^{22}D$ —22.3° (*c*, 5.3 in glacial acetic acid).

L-*Histidyl*-L-*leucine. By catalytic hydrogenation.* A solution of 1.48 g of carbobenzoxy-*im*.benzyl-L-histidyl-L-leucine benzyl ester in 25 ml of dimethylformamide-water (1:1) was hydrogenated in the presence of 200 mg of palladium black. Half an h later a thick mass was formed and then an equal portion of 50 % ethanol followed by 500 mg of palladium on charcoal were added. Since no more CO_2 was evolved, the hydrogenation continued in a closed apparatus for 24 h. At that time all the precipitate was redissolved. The catalyst was filtered, washed with 50 % ethanol and the combined filtrates evaporated *in vacuo*. The product was recrystallized in accordance with the directions of Holley and Sondheimer [7]. Yield 300 mg (70 %), m. p. 220—222° (reported [7] 214—217°), $[\alpha]^{22}D$ —45.2° (*c*, 1 in 0.10 N NaOH), reported [7] $[\alpha]^{22}D$ —43.5° (*c*, 1 in 0.10 N NaOH).

im.*Benzyl* - L - *histidine benzyl ester di-p-toluenesulfonate.* This compound was prepared in the same way as described for the corresponding dibenzenesulfonate derivative [2]. The product was obtained in 80 % yield when recrystallized by dissolving in *iso*propyl alcohol and precipitating by addition of ether, m. p. 176—177°. (Found: N 6.05. Calc. for $C_{34}H_{39}O_8N_3S_2$: N 6.16.)

Acknowledgement. To Professor Olof Mellander my gratitude is due for his encouragement and support in this work. The work was partly supported by grants from the *Swedish Medical Research Council* to Professor Olof Mellander.

1. Theodoropoulos, D. *J. Org. Chem.* **21** (1956) 1550.
2. Theodoropoulos, D. and Fölsch, G. **12** (1958) 1955.
3. Sheehan, J. and Hess, G. *J. Am. Chem. Soc.* **77** (1955) 1067.
4. Hofmann, K., Woolner, M., Spühler, G. and Schwartz, E. *Ibid.* **80** (1958) 1486.
5. Anderson, G. and Callahan, F. *Ibid.* **80** (1958) 2902.
6. Zervas, L., Winitz, M. and Greenstein, J. *J. Org. Chem.* **22** (1957) 1515.
7. Holley, R. and Sondheimer, E. *J. Am. Chem. Soc.* **76** (1954) 1326.
8. du Vigneaud, V. and Behrens, O. *J. Biol. Chem.* **117** (1937) 27.

Received October 9, 1958.

A Simple Apparatus for Making Holes in Agar Plates

DANLEY A. CALLIERI

Royal Institute of Technology, Division of Food Chemistry, Stockholm, Sweden

The cup-plate method for vitamin and antibiotic assays is nowadays widely used because of its simple technique and the satisfactory results obtained. Nevertheless, when the number of samples is very large considerable time is taken to make the numerous holes in the agar plates by means of the cork-borer technique. Some mechanical apparatuses combined with suction have been tested, but without satisfactory results as the holes produced are not sufficiently sharp-edged and clean-cut. Moreover, the agar surrounding the holes is often lifted from the bottom of the plate due to the suction.

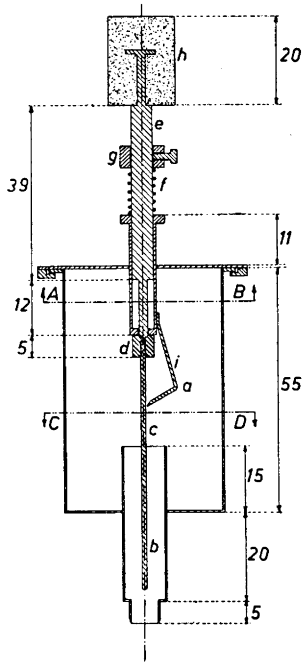

Fig. 1.

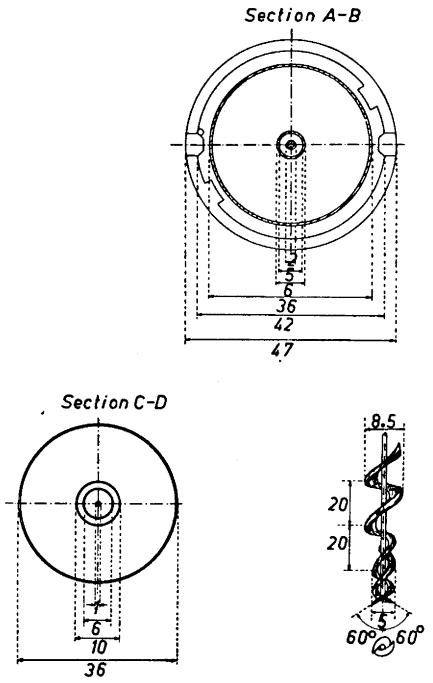

Fig. 2.

The apparatus described below does not require any suction, has a simple design, makes sharpedged and clean holes. It is easy to keep clean and does not need the help of any other device, which provides a high degree of independence in its use. The best material for the construction of this apparatus is stainless steel.

Description. The apparatus consists of two separable parts, part I and part II.

Part I. The shape and the dimensions (in mm) can be seen in Fig. 1. This part consists of the cylinder (a) in which the pieces of agar are collected as they are taken up from the plate, and the cylinder (b) which cuts the agar and brings the pieces of agar into the cylinder (a) by means of a helical conveyer. For the sake of simplicity the helical conveyer does not appear in Fig. 1 but is seen in detail in Fig. 2.

Part II consists of the lid and the following parts attached to it:

(c) Shaft of the helical conveyer.
(d) Device to join the shaft in such a way that the shaft or helical conveyer

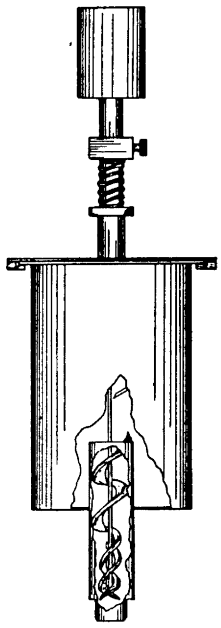

Fig. 3.

can be changed if it breaks or becomes defected during use. Part (d) acts also as a stop for the piston on its way up.

(e) Piston.

(f) Spring which brings the piston up automatically, once the hole has been made. This movement allows a more perfect function of the apparatus because it cleans the terminal and narrowest part of the cylinder (b).

(g) Movable part (attached to the piston by a screw) which acts as a stop for the piston on its way down. It permits adjustment of the effective length of the piston thereby bringing the ends of the helical conveyer into the most favourable working position.

(h) Knob.

(i) Wiper to remove the pieces of agar attached to the shaft by making them fall into cylinder (a).

Procedure. The apparatus is placed on the agar plate and pushed down vertically to cut the agar. The piston is pushed down and turned simply by rotating the knob between the thumb and the forefinger. In this way the pice of agar is taken up by the helical conveyer. On releasing the downward pressure on the screw-cap the piston readily slides up into its initial position.

Capacity. 100–120 holes/min.

Received November 12, 1958.

Conjugate Additions of Grignard Reagents to alpha, beta-Unsaturated Esters IV. Cuprous Chloride Catalysed Additions to Ethyl Esters

JON MUNCH-PETERSEN

Organisk-Kemisk Laboratorium, Polyteknisk Læreanstalt, Copenhagen, Denmark

Additions of Grignard reagents to *sec*-butyl esters of α,β-unsaturated acids, such as crotonic, tiglic and cinnamic acids, have been found to usually take place at the double bond (1,4-addition) [1] whereas, in general, additions to the corresponding ethyl esters take place predominantly at the carbonyl group (1,2-addition). However, in certain cases 1,4-addition to *sec*-butyl esters does not occur to any appreciable extent. This is for instance the case in some recently described [2] additions of methylmagnesium bromide, but it was found [2,3] that the presence of cuprous chloride during the addition of the esters to the Grignard reagent would secure fair to good yields of 1,4-addition products. It was further found that these yields were obtained not only with *sec*-butyl esters but also with ethyl esters. Crotonic esters thus gave the corresponding *iso*valeric esters, whereas tiglic and cinnamic esters gave saturated ketones as results of both 1,4- and 1,2-addition.

The present investigation was carried out as a consequence of the above-mentioned findings in order to establish if 1,4-addition products would also with higher Grignard reagents be the major products from ethyl esters in the presence of cuprous chloride, thus avoiding the use of *sec*-butyl esters. As model reactions the additions

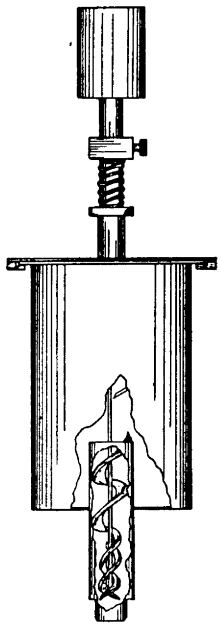

Fig. 3.

can be changed if it breaks or becomes defected during use. Part (d) acts also as a stop for the piston on its way up.

(e) Piston.

(f) Spring which brings the piston up automatically, once the hole has been made. This movement allows a more perfect function of the apparatus because it cleans the terminal and narrowest part of the cylinder (b).

(g) Movable part (attached to the piston by a screw) which acts as a stop for the piston on its way down. It permits adjustment of the effective length of the piston thereby bringing the ends of the helical conveyer into the most favourable working position.

(h) Knob.

(i) Wiper to remove the pieces of agar attached to the shaft by making them fall into cylinder (a).

Procedure. The apparatus is placed on the agar plate and pushed down vertically to cut the agar. The piston is pushed down and turned simply by rotating the knob between the thumb and the forefinger. In this way the pice of agar is taken up by the helical conveyer. On releasing the downward pressure on the screw-cap the piston readily slides up into its initial position.

Capacity. 100 – 120 holes/min.

Received November 12, 1958.

Conjugate Additions of Grignard Reagents to alpha, beta-Unsaturated Esters IV. Cuprous Chloride Catalysed Additions to Ethyl Esters

JON MUNCH-PETERSEN

Organisk-Kemisk Laboratorium, Polyteknisk Læreanstalt, Copenhagen, Denmark

Additions of Grignard reagents to *sec*-butyl esters of α,β-unsaturated acids, such as crotonic, tiglic and cinnamic acids, have been found to usually take place at the double bond (1,4-addition) [1] whereas, in general, additions to the corresponding ethyl esters take place predominantly at the carbonyl group (1,2-addition). However, in certain cases 1,4-addition to *sec*-butyl esters does not occur to any appreciable extent. This is for instance the case in some recently described [2] additions of methylmagnesium bromide, but it was found [2,3] that the presence of cuprous chloride during the addition of the esters to the Grignard reagent would secure fair to good yields of 1,4-addition products. It was further found that these yields were obtained not only with *sec*-butyl esters but also with ethyl esters. Crotonic esters thus gave the corresponding *iso*valeric esters, whereas tiglic and cinnamic esters gave saturated ketones as results of both 1,4- and 1,2-addition.

The present investigation was carried out as a consequence of the above-mentioned findings in order to establish if 1,4-addition products would also with higher Grignard reagents be the major products from ethyl esters in the presence of cuprous chloride, thus avoiding the use of *sec*-butyl esters. As model reactions the additions

of *n*-butylmagnesium bromide to ethyl crotonate, tiglate and cinnamate have been tried. The results are given in Table 1.

In the case of crotonic esters a good yield of simple 1,4-addition product was indeed obtained, and it appears as if in this case the two alternative procedures to prepare β-methylsubstituted fatty acids are equally good. In fact, when the conditions of the procedure previously described [1,2] were otherwise observed, it was found that no particular precautions with respect to the quality of cuprous chloride and the cooling of the reaction mixture were necessary: cooling in ice-water and the use of commercial cuprous chloride (Merck, p.a., without any previous reduction or drying) were sufficient to secure the same yield as was obtained in the non-catalyzed reaction with *sec*-butyl crotonate.

Methyl crotonate, with *n*-butylmagnesium bromide in the presence of cuprous chloride, has previously [3] been found to give 1,4-addition, although, in this case, the primarily produced ester self-condensed to give an acetoacetic ester.

When no cuprous chloride is used, ethyl crotonate has been found to give a mixture of different compounds, including large amounts of high-boiling material.

In the case of the cuprous chloride catalyzed reaction with ethyl tiglate, the simple 1,4-addition product (α,β-dimethyl-substituted ester) was not formed, but the saturated ketone (resulting from both 1,4- and 1,2-addition) was produced, as was the case when methylmagnesium bromide [2] was used. Only a 45 % yield was obtained.

With ethyl cinnamate and *n*-butylmagnesium bromide a 15 % yield of the simple 1,4-addition product, 3-phenylbutyric ester, was obtained.

It may be concluded that, as a practical procedure for preparing substituted fatty acids from α,β-unsaturated acids (by the conjugate addition of Grignard reagents), the cuprous chloride catalyzed reaction with ethyl esters is not as generally applicable as the use of *sec*-butyl esters; although 3-methyl-substituted acids (from crotonic esters) do arise in equally good yields by the two methods.

Table 1. Additions of *n*-butylmagnesium bromide to ethyl esters of α,β-unsaturated acids.

Ethyl ester	Product	Yield %	b. p. °C	Refractive index
Crotonic	ethyl 3-methylheptanoate [a]	70—74	89— 90/20 mm 81/15 »	n_D^{20} 1.4186
Tiglic	6,7-dimethylundecanone-5 [b]	45	118—119/15 »	n_D^{25} 1.4370
Cinnamic	ethyl 3-phenylheptanoate [c]	15	113°/1 mm	n_D^{25} 1.4879

[a] Calc. for $C_{10}H_{20}O_2$ (172.26): Sap.equiv. 172.26. Found: 172.0.

[b] Calc. for $C_{13}H_{26}O$ (198.34): C 78.72; H 13.21. Found: C 78.15; H 13.14 (microanalysis by Mr. Preben Hansen, The Chemical Laboratory, University of Copenhagen). Infra-red spectrum (recorded in this laboratory by Mrs. Susanne Refn, M.Sc.) shows the presence of a ketone group and the absence of hydroxyl groups.

[c] Calc. for $C_{15}H_{22}O_2$ (234.33): Sap.equiv. 234.33. Found 234.2.

1. Munch-Petersen, J. *Acta Chem. Scand.* **12** (1958) 967.
2. Munch-Petersen, J. *Acta Chem. Scand.* **12** (1958) 2007.
3. Munch-Petersen, J. *J. Org. Chem.* **22** (1957) 170.

Received November 15, 1958.

Chromatographic Separations of Cytosine Containing Compounds

PETER REICHARD

Department of Chemistry I, Karolinska Institutet, Stockholm, Sweden

During work on the biological formation of deoxyribosidic compounds it became important to separate deoxyribosides and deoxyribotides from the corresponding ribosides and ribotides. The present note describes the separation of different cytosine containing compounds by a simple procedure involving chromatography on Dowex 50 (H+-form, 200–400 mesh). Fig. 1 shows a complete separation of cytidine-5′-phosphate, deoxycytidine-5′-phosphate, cytidine, deoxycytidine and cytosine on such a column. Cytidine-2′ (and -3′)-phosphate moved as the deoxyribotide. The recovery of all substances was 95–100 %. The compounds may be recovered quantitatively by simple evaporation *in vacuo* of the solvent.

The compounds could also be separated by paper chromatography with a borate containing solvent (20 ml of 5 M ammonium acetate, pH 9.5, 80 ml of saturated sodium tetraborate, 220 ml ethanol and 0.5 ml of 0.5 M versene). This solvent is a modification of the one originally described by Plesner [1]. The following R_F values were obtained: Cytidine-5′-phosphate = 0.06; deoxycytidine-5′-phosphate = 0.12; cytidine = 0.27; cytosine = 0.68; and deoxycytidine = 0.76. The R_F values changed considerably in different experiments but the relative positions of the substances remained the same. The same solvent could also be used for a similar separation of uracil or thymine containing compounds.

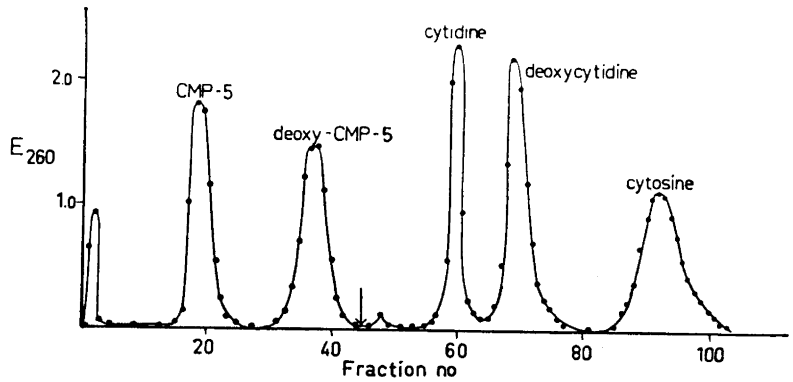

Fig. 1. Separation of 4—5 μmoles each of cytidine-5′-phosphate, deoxycytidine-5′-phosphate, cytidine, deoxycytidine, and cytosine on Dowex 50 (H+-form, length 10 cm, diam. 0.9 cm). Fraction size: 4—5 ml per 30 min. The chromatogram was first developed with 0.2 N acetic acid; at the arrow elution was started with N HCl. The first peak represents uracil containing compounds present as impurities in the commercial cytosine derivatives.

These methods have been used for the preparation of deoxycytidine and deoxycytidine-5′-phosphate from *in vitro* experiments [2].

1. Plesner, P. *Acta Chem. Scand.* **9** (1955) 197.
2. Reichard, P. *Biochim. et Biophys. Acta* **27** (1958) 434.

Received November 25, 1958.

The Solubility Curve for the System Adipic acid—*p*-Dioxane

GUNNAR B. LINDSTRÖM

Division of Physical Chemistry, Royal Institute of Technology, Stockholm, Sweden

A figure for the solubility of adipic acid in *p*-dioxane was required for the preparation of tritium labelled dioctyl-adipate. The determination was performed in a 100 ml test tube with a thermometer (graduated to 1/10°C) and a stirrer inserted through the cork. 50 ml *p*-dioxane (m. p. 11.3°C, b. p. 100—101.5°C) was pipetted into the tube and the adipic acid (m. p. 151—153°C) subsequently added in small portions. The tube was heated in a water bath until the acid had completely dissolved. It was then cooled and the temperature, at which the first inhomogeneities were observed, was recorded. The cooling was performed in a water-filled Dewar vessel kept at a temperature about 5°C below the expected temperature for the phase separation. Three readings were taken for each concentration.

Table 1. Phase separation temperature for adipic acid — *p*-dioxane mixtures.

Amount of adipic acid per 50 ml (= 50.18 g) *p*-dioxane		Temperature for phase separation (mean of three determinations)
g	mole %	°C
0.00	0.00	11.3
1.00	1.18	10.7
2.21	2.48	9.9
3.39	3.91	11.5
4.63	5.27	25.3
6.13	6.85	34.7
10.30	11.01	53.5
12.47	13.03	61.0
14.53	14.86	67.4
20.62	19.92	77.6
26.69	24.27	88.5
33.42	28.65	96.5

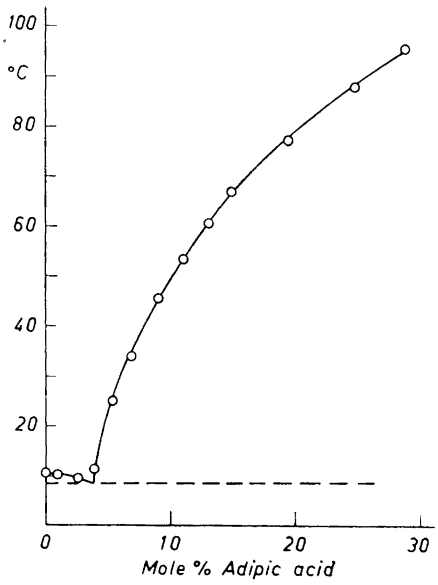

Fig. 1. Solubility curve for the system adipic acid — *p*-dioxane.

The results show that the system behaves like an ordinary binary mixture. At 2.9 mole % adipic acid, the curve has a eutectic point, the extrapolated temperature of which is 9.5°C. The readings at high temperatures do not agree exactly with those at low temperatures. This was probably due to the fact that some dioxane evaporated at the high temperatures, causing the actual concentrations of adipic acid to be higher than the calculated ones.

Received November 26, 1958.

On the Biological Methylation of Histamine. 3

KERSTIN M. LINDAHL

Institute of Zoophysiology, University of Uppsala, Uppsala, Sweden

It is well known that many biological transmethylation reactions require methionine [1]. However, in the case of guanidinoacetate and nicotinamide it has been shown by Cantoni and co-workers [2] that the active methylating agent is S-adenosylmethionine.

In an earlier study [3] it was demonstrated that radioactive methylhistamine was formed, when methionine labelled with ^{14}C in the methyl group was incubated with histamine, enzyme extract from mouse liver, and appropriate cofactors. It was thus concluded that the methyl group of methionine can be utilized for the methylation of histamine.

In this communication it is demonstrated that the histamine methylating enzyme in mouse liver utilizes with great efficiency S-adenosyl-methionine as methyl donor.

Methods. Enzyme extract. Fresh mouse liver was ground in a blendor with 3 volumes of cold 0.1 M sodium acetate buffer pH 5.6. The homogenate was centrifuged for 30 min at 25 000 *g* in the cold. The supernatant liquid was heated to 47°C for 10 min, centrifuged, and dialyzed for 2 h against 0.05 M sodium acetate buffer pH 6.0 [3,4].

Determination of histamine according to Schayer and co-workers [5,6]. Histamine dihydrochloride was added to the sample as carrier. After removal of the proteins, the pipsyl derivative was prepared, and recrystallized until the radioactivity count was unchanged for at least three successive crystallizations. The average value of the constant samples was used.

Determination of methylhistamine. Carrier methylhistamine * was added to the sample, extracted with chloroform [7] after protein precipitation, and converted into the picrate which was recrystallized until constant radioactivity was attained. The activity was considered constant, if three successive values coincided within experimental errors.

S-adenosylmethionine was isolated from yeast according to Schlenk and De Palma [8]. A chromatographically pure product was obtained by extraction with $HClO_4$, chromatography on Dowex 50, and precipitation with phosphotungstic acid.

Results. Histamine-2-^{14}C-dihydrochloride was incubated with the enzyme extract obtained from mouse liver for 1 h at 37°C. The incubation mixture was analyzed for histamine and its N-methylated metabolite, 1-methyl-4-(β-aminoethyl) imidazole (methylhistamine), according to the isotope dilution method, developed by Schayer and co-workers [5-7] (see under Methods).

It was found that nearly all histamine remained intact after 1 h incubation, and that very little methylhistamine was formed. However, when S-adenosylmethionine was added to the incubation mixture, virtually all histamine had disappeared after 1 h, and the radioactivity was recovered as methylhistamine.

The essential figures from an experiment are given in Table 1. From these results, in comparison with earlier studies [3,4] it is obvious that the soluble fraction of mouse liver contains a histamine methylating enzyme which utilizes S-adenosylmethionine as methyl donor with great

Table 1. The complete system contained 0.5 ml of the enzyme preparation, 15.5 μg ^{14}C histamine dihydrochloride, 1.5 μmole S-adenosylmethionine, and Tris 0.5 M, pH 7.4, to make 1 ml. The calculated maximal radioactivity count is denoted as 100 % *.

	% of radioactivity recovered as	
	Histamine	Methyl-histamine
No enzyme	97	—
No S-adenosylmethionine	92	4
Complete system	0.6	100

* Methylhistamine was obtained from Dr. R. W. Schayer, Rahway, N. J. which is gratefully acknowledged.

* The samples were counted in a windowless flow counter, Tracerlab. SC—16, which was made available through the courtesy of Prof. A. Tiselius, Institute of Biochemistry, Uppsala.

efficiency. The metabolization of histamine corresponds to at least 110 μg/h/g fresh liver.

1. Challenger, F. *Quart. Revs. London* **9** (1955) 255.
2. Cantoni, G. L. in Colowick, S. P. and Kaplan, N. O. *Methods in Enzymology* Academic Press Inc. N. Y. 1955, Vol. 2, p. 257.
3. Lindahl, K. M. *Acta Chem. Scand.* **12** (1958) 1690.
4. Lindahl, K. M. *Arkiv Kemi* **13** (1958) 149.
5. Schayer, R. W. and Cooper, J. A. D. *J. Appl. Physiol.* **9** (1956) 481.
6. Schayer, R. W. and Karjala, S. A. *J. Biol. Chem.***221** (1956) 307.
7. Rothschild, Z. and Schayer, R. W. *Biochim. et Biophys. Acta. In press.*
8. Schlenk, F. and De Palma, R. E. *J. Biol. Chem.* **229** (1957) 1051.

Received November 27, 1958.

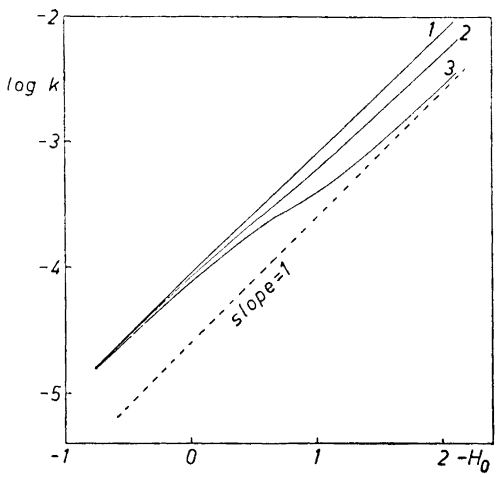

Fig. 1. A plot of log k against $-H_0$ for competing uni- and bimolecular reactions. Aqueous hydrochloric acid solutions, 25°C. In dilute acid the bimolecular reaction assumes 25 % (*curve 1*), 50 % (*curve 2*), and 75 % (*curve 3*) of the overall reaction.

On the Applicability of the H_0 Acidity Function to the Case of Two Competing Mechanisms

PENTTI SALOMAA and RAILI LINNANTIE

Department of Chemistry, University of Turku, Turku, Finland

The H_0 acidity function has become the subject of a great number of studies on the mechanisms of acid catalysis [1,2], although cases have been also reported in which this function is of a limited applicability [2]. Apart from the fundamental restrictions involved in assuming certain activity coefficient terms to remain constant in different media, there is the following particular case, in which the use of the acidity function may lead, at least partly, to fallacious conclusions.

Let us consider an acid-catalysed hydrolysis reaction in which the unimolecular and bimolecular mechanisms are in competition. The overall rate coefficient k, which can be measured experimentally, is then made up of the two individual rate coefficients, k_1 and k_2, which refer to the different mechanisms. If the Zucker-Hammett hypothesis is valid, k_2 should be proportional to the acid concentration, whereas $\log k_1$ should vary similarly as the value of $-H_0$ of the solution. Fig. 1 shows some examples calculated for the dependence of $\log k$ on $-H_0$ in such cases. The H_0 values of aqueous hydrochloric acid solutions used in the calculations are those revised by Paul and Long [3].

The most striking feature is that the contribution of the bimolecular mechanism becomes largely masked by the unimolecular mechanism, when higher acidities are approached. Thus the curves are experimentally indistinguishable from a straight line of a slope of nearly unity, which would correspond to a purely unimolecular reaction, except that case where the bimolecular mechanism is the prominent in dilute acid; here the curve shows a clearly notable point of inflexion. Such a behaviour is thus highly characteristic of competing mechanisms which depend on the acidity of the solution in a different way.

An example of the masking of a mixed unimolecular and bimolecular reaction by

efficiency. The metabolization of histamine corresponds to at least 110 μg/h/g fresh liver.

1. Challenger, F. *Quart. Revs. London* **9** (1955) 255.
2. Cantoni, G. L. in Colowick, S. P. and Kaplan, N. O. *Methods in Enzymology* Academic Press Inc. N. Y. 1955, Vol. 2, p. 257.
3. Lindahl, K. M. *Acta Chem. Scand.* **12** (1958) 1690.
4. Lindahl, K. M. *Arkiv Kemi* **13** (1958) 149.
5. Schayer, R. W. and Cooper, J. A. D. *J. Appl. Physiol.* **9** (1956) 481.
6. Schayer, R. W. and Karjala, S. A. *J. Biol. Chem.***221** (1956) 307.
7. Rothschild, Z. and Schayer, R. W. *Biochim. et Biophys. Acta. In press.*
8. Schlenk, F. and De Palma, R. E. *J. Biol. Chem.* **229** (1957) 1051.

Received November 27, 1958.

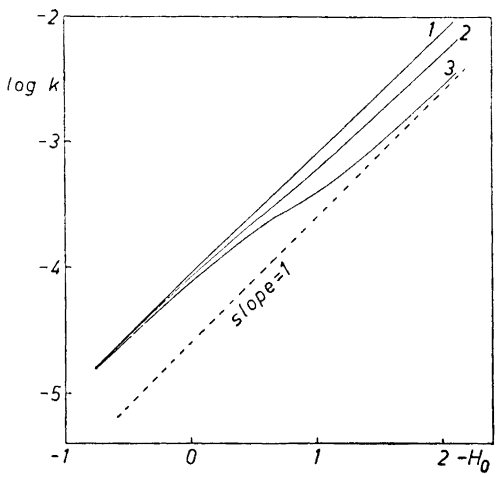

Fig. 1. A plot of log k against $-H_0$ for competing uni- and bimolecular reactions. Aqueous hydrochloric acid solutions, 25°C. In dilute acid the bimolecular reaction assumes 25 % (*curve 1*), 50 % (*curve 2*), and 75 % (*curve 3*) of the overall reaction.

On the Applicability of the H_0 Acidity Function to the Case of Two Competing Mechanisms

PENTTI SALOMAA and RAILI LINNANTIE

Department of Chemistry, University of Turku, Turku, Finland

The H_0 acidity function has become the subject of a great number of studies on the mechanisms of acid catalysis [1,2], although cases have been also reported in which this function is of a limited applicability [2]. Apart from the fundamental restrictions involved in assuming certain activity coefficient terms to remain constant in different media, there is the following particular case, in which the use of the acidity function may lead, at least partly, to fallacious conclusions.

Let us consider an acid-catalysed hydrolysis reaction in which the unimolecular and bimolecular mechanisms are in competition. The overall rate coefficient k, which can be measured experimentally, is then made up of the two individual rate coefficients, k_1 and k_2, which refer to the different mechanisms. If the Zucker-Hammett hypothesis is valid, k_2 should be proportional to the acid concentration, whereas $\log k_1$ should vary similarly as the value of $-H_0$ of the solution. Fig. 1 shows some examples calculated for the dependence of $\log k$ on $-H_0$ in such cases. The H_0 values of aqueous hydrochloric acid solutions used in the calculations are those revised by Paul and Long [3].

The most striking feature is that the contribution of the bimolecular mechanism becomes largely masked by the unimolecular mechanism, when higher acidities are approached. Thus the curves are experimentally indistinguishable from a straight line of a slope of nearly unity, which would correspond to a purely unimolecular reaction, except that case where the bimolecular mechanism is the prominent in dilute acid; here the curve shows a clearly notable point of inflexion. Such a behaviour is thus highly characteristic of competing mechanisms which depend on the acidity of the solution in a different way.

An example of the masking of a mixed unimolecular and bimolecular reaction by

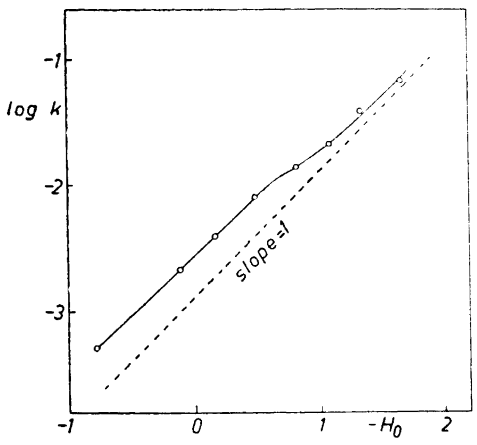

Fig. 2. A plot of log k against $-H_0$ for the hydrolysis of β-chloroethoxymethyl formate in aqueous hydrochloric acid solutions at 25°C.

the prominent unimolecular reaction is furnished by the hydrolysis of methoxymethyl formate, reported earlier [4]. On the other hand, a curve showing a point of inflexion was observed in the hydrolysis of β-chloroethoxymethyl formate (Fig. 2).

In cases like that of Fig. 2, an accurate determination of the rates of the individual reactions should require the use of more specialised kinetic methods. If, however, such methods are not available, the relative contributions may be roughly estimated, as described below. The most essential limitation in these calculations is that the value of k_2 is usually not strictly proportional to the acid concentration, and that the slope of the plot of log k_1 against $-H_0$ may slightly differ from unity, and therefore the results should be regarded as very approximate.

It may be found that the position of the point of inflexion depends on the relative rates of the competing reactions. If R denotes the ratio of the rate of the unimolecular reaction to that of the bimolecular reaction in dilute hydrochloric acid, it can be calculated that the following numerical relation holds for the H_0 value of the point of inflexion:

$$R = 10^{H_0}\left(\frac{1-2.35\ H_0 + 1.17\ H_0^2}{-0.93-1.27\ H_0 + 4.60\ H_0^2}\right)$$

This equation was derived by representing the concentration of hydrochloric acid in 0.1—6.0 M solutions as a polynomial of H_0 of the second power, the coefficients of which were calculated by the method of least squares using weighed values of c_{HCl} (the weights were chosen as inversely proportional to the values of the acid concentration). The H_0 data given by Paul and Long [3] were used.

The method of iteration may be also applied, taking into account that it is the unimolecular reaction that predominates at high acidities, and thus the value of k in these media gives the value of k_1 as a first approximation, from which the values of k_1 for dilute acids may be calculated with the use of the respective H_0 values. These give first approximations for the values of k_2 in dilute acid solutions ($k_2 = k - k_1$), from which, in turn, the values of k_2 for the higher acid concentrations may be calculated.

In the example shown in Fig. 2, the point of inflexion lies at a H_0 value of -0.67 ± 0.10, from which it is estimated that in dilute acid the unimolecular reaction assumes 27 ± 9 % of the overall reaction. Calculations by the iteration method gave a corresponding estimate of 39 ± 7 %. These percentages correspond to a value of 0.0022 ± 0.0005 l mole^{-1} s^{-1} for the rate coefficient of the bimolecular reaction at 25°C, which is a very reasonable value, as the rate coefficients reported for the bimolecular $A_{AC}2$ hydrolysis of alkyl formates are of the same magnitude under similar conditions [5,6].

A full account of the experimental details and examples of other similar reactions will be published shortly.

The financial support of the *Valtion Luonnontieteellinen Toimikunta* is gratefully acknowledged.

1. Long, F. A. and Paul, M. A. *Chem. Revs.* **57** (1957) 935.
2. Taft Jr., R. W., Deno, N. C. and Skell, P. S. *Ann. Rev. Phys. Chem.* **9** (1958) 303.
3. Paul, M. A. and Long, F. A. *Chem. Revs.* **57** (1957) 1.
4. Salomaa, P. *Acta Chem. Scand.* **11** (1957) 132.
5. Salmi, E. J. *Ann. Univ. Turkuensis, Ser.* **A** III (1932) No. 3.
6. Tommila, E. and Hella, A. *Ann. Acad. Sci. Fennicae, Ser.* **A** II (1954) No. 53.

Received November 26, 1958.

The Reaction between *p*-Benzoquinone and Ethyl Acetoacetate

ERLING BERNATEK and TORE LEDAAL

Universitetets Kjemiske Institutt, Blindern-Oslo, Norway

This reaction has since its discovery by v. Pechmann [1] and Ikuta [2] evoked only sporadic interest. Graebe and Levy [3] extended the synthesis to include toluquinone and one of the present authors has in several articles [4-8] treated this and analogous reactions. Recently Grinev and collaborators [9,10] have published some results which are the occasion for this article.

The first step in the reaction is believed to be the formation of a quinol (I).

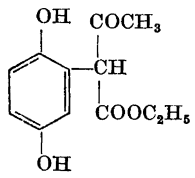

I

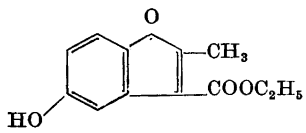

II

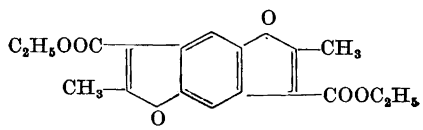

III

Quinols of the type I have not been isolated, but indirect evidence for their existence has been furnished [4]. This primary quinol can react in two ways: It can be cyclised to a benzofuran (II) or be oxidised to its corresponding quinone by unreacted benzoquinone. Further this newformed quinone can add a second molecule of ethyl acetoacetate forming a disubstituted quinol which in turn will be cyclised to a benzodifuran (III). Normally there is formed a mixture of II and III, the ratio of the amounts being determined by the competition between oxidation and cyclisation of I.

In synthetic practice it has for several reasons been an object to obtain a good yield of II and suppress the formation of III. Grinev reports a yield of 98 % of II in a procedure where a mixture of anhydrous ethanol and ether is used as solvent and the reaction performed in an extraction apparatus with benzoquinone in the thimble. This technique was adopted in order to ensure a slow addition of benzoquinone, the reaction requiring 27 h. We have repeated Grinev's experiments but in no case obtained the yields claimed by him. The amounts of II fell far short of 98 % and appreciable amounts of III were formed. Further it is our experience that alcohols are not ideal as solvents in this reaction as dark substances are formed which contaminate the product.

It is well known that the potentials of reduction-oxidation systems of quinols and quinones are very sensitive to changes in the proton activity. A possible mode of displacing the benzofuran-benzodifuran ratio could therefore be to change the acidity of the reaction mixture. Two reduction-oxidation systems are present: [Quinol-benzoquinone] and [the quinol I — the corresponding quinone]. *A priori* it is impossible to say how changes in the proton activity will alter the potentials of the two systems relative to each other in the very special solvent employed (acetone-ethyl acetoacetate-zinc chloride). Actually it was found that the addition of small amounts of strong bases and acids was very detrimental to the overall yield and in some cases benzodifuran was formed almost exclusively. Acetic acid, however, proved to be a suitable additive, a fair amount of very pure II being obtained while only traces of III were observed. (The effect of acetic acid may also include a kinetic contribution, *e. g.* catalysis of the ring-closure of I.) On this basis a reliable procedure has been worked out in which acetone has been adopted as solvent as originally proposed by Graebe and Levy. The main advantage of our procedure is that it furnishes II free from III rather than a high overall yield as it is difficult to separate the two compounds without heavy losses.

Experimental. Ethyl 2-methyl-5-hydroxybenzofuran-3-carboxylate. *p*-Benzoquinone (27 g) was dissolved in a mixture of ethyl acetoacetate (100 ml) and acetone (100 ml) at

room temperature. This mixture was added during 10 h to a solution of anhydrous zinc chloride (35 g) in acetone (50 ml) and acetic acid (2.5 ml). The reaction mixture was kept at 75° and stirred mechanically. Afterwards it was kept overnight in an open beaker, cooled well in ice and filtered by suction. The light brownish product was washed with small amounts of ice-cold methanol thus becoming white. M. p. 138°. The substance gave a clean purple colour with hot concentrated sulphuric acid. (The benzodifuran III gives a blue colour with this reagent and even a small contamination of II with III changes the colour to violet.) Yield 33 g (60 %, calculated on the basis of benzoquinone).

1. v. Pechmann, H. *Ber.* **21** (1888) 3005.
2. Ikuta, M. *J. prakt. Chem.* [2] **45** (1892) 65.
3. Graebe, C. and Levy, S. *Ann.* **283** (1894) 245.
4. Bernatek, E. *Acta Chem. Scand.* **7** (1953) 677.
5. Bernatek, E. and Ramstad, S. *Acta Chem. Scand.* **7** (1953) 1351.
6. Bernatek, E. and Thoresen, F. *Acta Chem. Scand.* **9** (1955) 743.
7. Bernatek, E. *Acta Chem. Scand.* **10** (1956) 273.
8. Bernatek, E. and Bø, I. *Acta Chem. Scand. In press.*
9. Grinev, A. N., Bon-Khvar, P. and Terent'ev. A. P. *Zhur. Obshchei Khim.* **26** (1956) 2928.
10. Grinev, A. N., Bon-Khvar, P. and Terent'ev, A. P. *Zhur. Obshchei Khim.* **27** (1957) 1087.

Received November 27, 1958.